
TRANSACTIONS

of The American Society of Mechanical Engineers

Effect of Fillets on Wing-Fuselage Interference (AER-56-1)	<i>A. L. Klein</i>	1
Field Welds in Pressure Pipe Lines of Steam Systems (FSP-56-1)	<i>H. N. Boetcher</i>	11
Roller-Bearing Service in Locomotive, Passenger, and Freight Equipment (RR-56-1) . . .	<i>T. V. Buckwalter</i>	23
Dry Film Gluing in Plywood Manufacture (WDL-56-1)	<i>Ray Sorensen</i>	37

JANUARY, 1934

VOL. 56, NO. 1

U OF I
LIBRARY

Published by The American Society of Mechanical Engineers
29 West Thirty-Ninth Street, New York, N. Y.

TRANSACTIONS

of The American Society of Mechanical Engineers

Published on the tenth of each month

Publication Office, 20th and Northampton Streets, Easton, Pa.
Editorial Department at the Headquarters of the Society, 29 West Thirty-Ninth Street, New York, N. Y.

Includes Applied Mechanics and Aeronautical Engineering

Members of Council, 1933-1934

PRESIDENT

PAUL DOTY

VICE-PRESIDENTS

Terms expire December, 1934

HAROLD V. COES
JAMES D. CUNNINGHAM
C. F. HIRSHFELD

PAST-PRESIDENTS

Terms expire December

WILLIAM L. ABBOTT 1934
CHARLES M. SCHWAB 1935
ROY V. WRIGHT 1936
CONRAD N. LAUER 1937
A. A. POTTER 1938

VICE-PRESIDENTS

Terms expire December, 1935

WILLIAM L. BATT
H. L. DOOLITTLE
ELY C. HUTCHINSON
ELLIOTT H. WHITLOCK

MANAGERS

Terms expire December, 1934

ALEXANDER J. DICKIE
EUGENE W. O'BRIEN
HARRY R. WESTCOTT

Terms expire December, 1935

R. L. SACKETT
ALEX D. BAILEY
JOHN A. HUNTER

Terms expire December, 1936

JAMES A. HALL
ERNEST L. OHLE
JAMES M. TODD

TREASURER

ERIK OBERG

SECRETARY

CALVIN W. RICE

EXECUTIVE SECRETARY, C. E. DAVIES

Chairmen of Standing Committees of Council

AWARDS, F. L. EIDMANN
CONSTITUTION AND BY-LAWS, R. S. NEAL
EDUCATION AND TRAINING FOR THE INDUSTRIES (TO BE APPOINTED)
FINANCE, JOHN H. LAWRENCE
LIBRARY, W. M. KEENAN
LOCAL SECTIONS, JILES W. HANEY
MEETINGS AND PROGRAM, C. P. BLISS
MEMBERSHIP, O. E. GOLDSCHMIDT

POWER TEST CODES, F. R. LOW
PROFESSIONAL CONDUCT, H. S. PHILBRICK
PROFESSIONAL DIVISIONS, C. B. PECK
PUBLICATIONS, L. C. MORROW
RELATIONS WITH COLLEGES, E. F. CHURCH, JR.
RESEARCH, ALEX D. BAILEY
SAFETY, T. A. WALSH, JR.
STANDARDIZATION, E. BUCKINGHAM

Committee on Publications

L. C. MORROW, *Chairman*
S. F. VOORHEES
S. W. DUDLEY
W. F. RYAN
M. H. ROBERTS

Advisory Members

E. H. OHLE, ST. LOUIS, MO.
E. B. NORRIS, BLACKSBURG, VA.
A. J. DICKIE, SAN FRANCISCO, CALIF.

EDITOR: GEORGE A. STETSON

BY-LAW: The Society shall not be responsible for statements or opinions advanced in papers or . . . printed in its publications (B2, Par. 3).

Entered as second-class matter March 2, 1928, at the Post Office at Easton, Pa., under the Act of August 24, 1912. Price \$1.50 a copy, \$12.00 a year; to members and affiliates, \$1.00 a copy, \$7.50 a year. Changes of address must be received two weeks before they are to be effective on our mailing list. Please send old, as well as new, address.

Copyrighted, 1934, by THE AMERICAN SOCIETY OF MECHANICAL ENGINEERS

Effect of Fillets on Wing-Fuselage Interference

By A. L. KLEIN,¹ PASADENA, CALIF.

Mutual interference of wing and fuselage has been the subject of many previous investigations, but these have been on a very small scale. A comprehensive investigation into the case of a low-wing monoplane was thought to have important possibilities, especially as this type of airplane was known to have some aerodynamical peculiarities. In a preceding investigation it had been found that the addition of large fillets to the intersection of wing and fuselage would cause a great improvement and it was decided to extend these tests and to include the case of a high-wing monoplane for comparison.



NUMEROUS investigations have been made on the mutual interference of wings and fuselages, but much of the preceding work has been done on a very small scale (ref. 1).² It was thought that a comprehensive investigation into the case of the low-wing monoplane might be of importance, especially as this type of airplane was known to have some aerodynamical peculiarities. In a preceding investigation it had been found that the addition of large fillets to

the wing-fuselage intersection would cause a great improvement; it was therefore decided to extend these tests and to include the case of the high-wing monoplane for comparison.

The model used for the investigation was a $1/8$ -scale model of the Northrop "Alpha," a Wasp-engined transport plane of approximately 5000 lb gross weight. The model had a span of 7 ft and a length of 52 in. The airfoil section was 18 per cent Clark-Y at the root and 12 per cent at the tip. The wing area of the model was 8.33 sq ft, and the root chord of the wing was 16.67 in. The wing was mounted with reference to the fuselage as shown in Fig. 5. The model as used consisted of a wing and fuselage only. This model was presented to the laboratory by the Northrop Aircraft Corporation, a unit of United Aircraft and Transport Company.

EXPERIMENTAL METHODS

The investigation was carried on by two distinct methods. The set-up for force measurements was identical with that described in ref. 2, while in addition three combs of pitot tubes were mounted behind the model for exploration of the wake behind the wing. These combs can be seen in Fig. 1, and also some of the pitot tubes can be seen in Figs. 6 and 7. The total pressure orifices were made of $1/8$ -in. brass tubing mounted on a steel tube. For static-pressure measurements, jackets containing side orifices were slipped over the total-pressure tubes. These tubes were

¹ Assistant Professor of Aeronautics, California Institute of Technology. Mr. Klein received his B.S. from California Institute of Technology in 1921, M.S. in 1924, and Ph.D. in 1925. He was Teaching Fellow in Physics, California Institute of Technology, 1921-1925; Research Fellow in Physics and in Aeronautics, 1927-1929; and has been Assistant Professor since 1929.

² See list of references at end of paper.

Contributed by the Aeronautic Division and presented at the Pacific Coast Aeronautics Meeting, Berkeley, Calif., June 9 and 10, 1932, of THE AMERICAN SOCIETY OF MECHANICAL ENGINEERS.

NOTE: Statements and opinions advanced in papers are to be understood as individual expressions of their authors, and not those of the Society.

connected to the multiple manometer, and observations were made of the wake distribution behind the set-up for various angles of attack. Records of the wake observations were made by taking shadowgraphs of the manometer on ozalid paper. These records were then reduced by plotting curves showing the loss of total head as percentage of the total head in the free stream. Figs. 2, 3, and 10 show curves of this type, and also show the relative position of the model and the combs. The position of the stabilizer and elevator for each angle of attack is indicated on the curves. The fillets used in the investigation were built up from physicists' soft wax, a compound of beeswax, Venice turpentine, and rosin, and modeled to templates. It was found that an almost glasslike surface could be given this wax by rubbing it with sandpaper dipped in kerosene.

WAKE OBSERVATIONS

Fig. 2 shows the wake losses behind the wing tested alone. Noting first the wake losses in row 1, it is seen that as the angle of attack increases, the center of the wake moves downward, as one would expect. When the wing reaches an angle of attack of 15 deg, the center of the wake has reached its lowest point, near which it remains until the angle increases to 16.5 deg, after which the wake moves noticeably upward. If one now looks at the force-measurement curves for the wing alone (Fig. 8), one sees that the angle for maximum lift is 16.5 deg. In row 2 the behavior is similar to row 1; the downwash causes the wake to go downward until the angle of maximum lift is reached, after which the wake moves upward. In the case of row 3 an anomaly occurs; the downwash does not reach the maximum value at 16.5 deg, but continues to increase, and apparently stalling does not occur at this section of the wing until an angle of attack of approximately 20.5 deg is reached. The wake curves for small angles in rows 2 and 3 are omitted because the wake was smaller than the distance between the pitot tubes, so that no deductions could be drawn as to its magnitude and shape.

Below on the same figure is a similar set of observations for the model assembled as a low-wing monoplane with no fillet at the intersection between the wing and the fuselage. The maximum diameter of the fuselage was 9.5 in. Pitot comb 1 was mounted approximately halfway between comb 2 and the wing tip. The positions of the stabilizer and elevator are drawn in on the successive curves. It will be noticed that the wake curves for row 1 differ completely from those for the wing alone, while the wake curves in rows 2 and 3 are hardly distinguishable from those for the wing alone. The wake curves in row 1 are not only larger in area than those for the wing alone, but also the position of their center line indicates a much smaller downwash. It will be noticed that the center line of the wake never goes below the chord line, while for the case of the wing alone the center of the wake moves down below the chord line at small angles and remains there. These two conditions represent the limiting cases of the present investigation, the wing alone giving the condition for zero interference and the wing and fuselage with no fillet the case of maximum interference.

Now consider the case of a fillet that partly remedies the interference effect. Fig. 3 shows the wake distribution for what will be called the "wrong fillet." Fig. 4 is a photograph of this fillet, and its lines are shown in Fig. 5. In the case of the "wrong fillet," the wake curves in row 1 are similar to those for the wing alone up to an angle of 6 deg, but at and above an angle of 9 deg the wakes

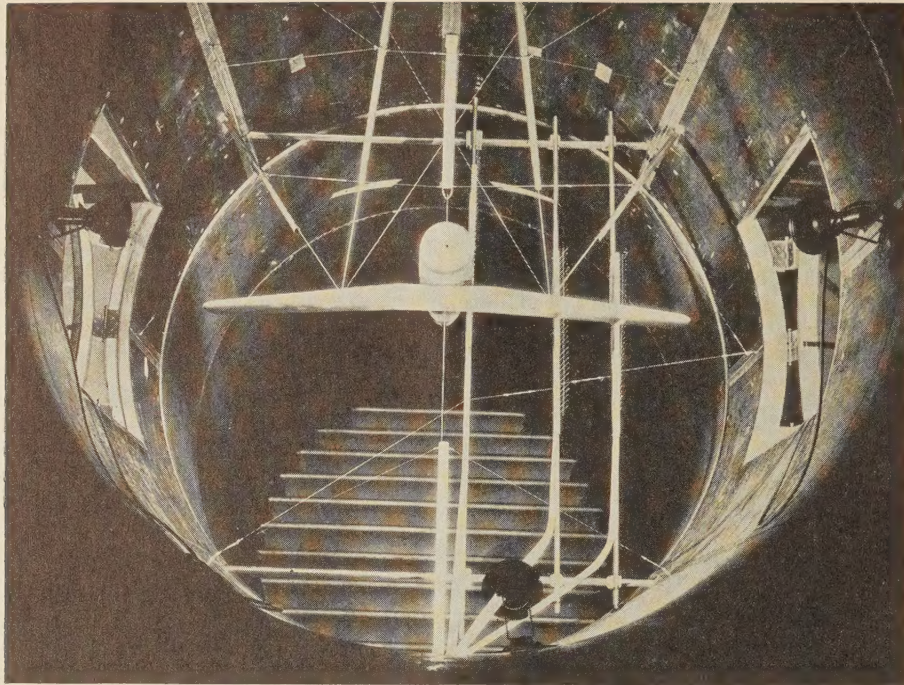


FIG. 1 VIEW OF MODEL AS A HIGH-WING MONOPLANE IN THE TUNNEL
(The three pitot-tube combs can be seen in the background.)

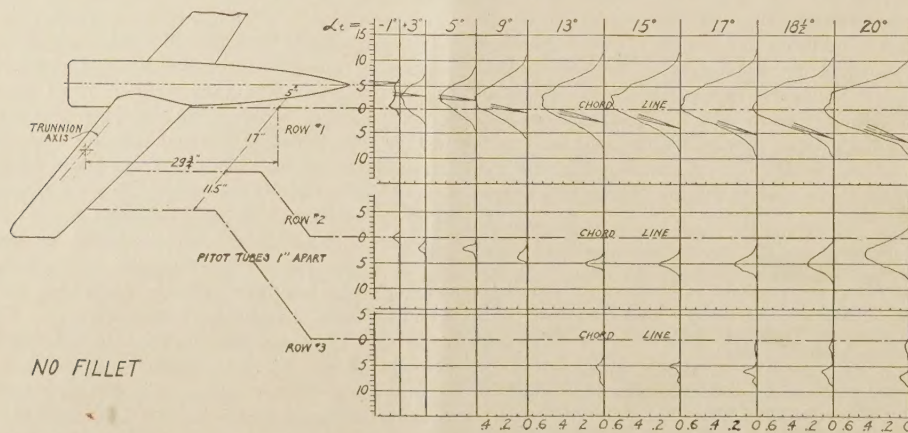
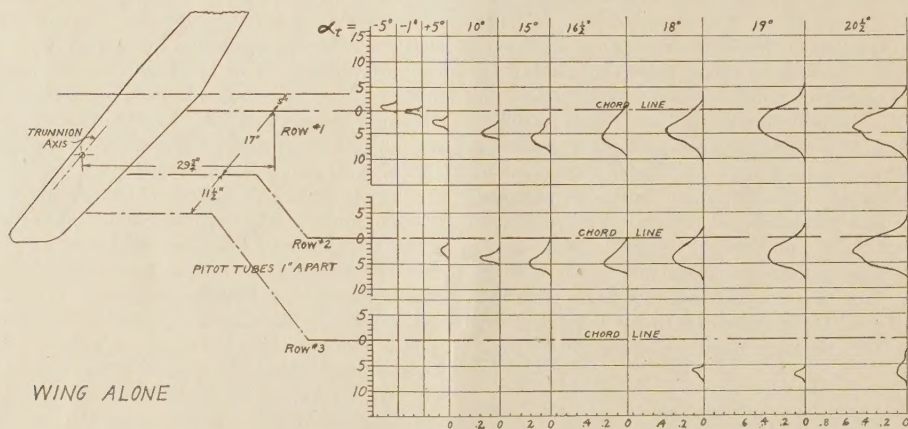


FIG. 2 WAKE DISTRIBUTION BEHIND THE WING ALONE AND THE WING AND FUSELAGE WITH NO FILLET
(The area between the vertical lines represents the energy lost.)

in this row are similar to those for the wing and fuselage with no fillet. The fact that this behavior is not observed at rows 2 and 3 indicates once more that the effect is largely localized in the region of the intersection of wing and fuselage. The force-measurement curves (Fig. 8) discussed later show that at the angle of 7 deg something happens to the flow. The change in the flow pattern from the wing-alone type to the no-fillet type is completely discontinuous. An observer watching the multiple manometer when the model is set at this critical angle sees either one pattern or the other, and the change from one to the other is sudden and complete. At this angle the manometer is in a very unsteady condition. The smaller flow pattern for the downwash and the larger for the trailing vortex replace each other rapidly on the tubes. There are no intermediate stable states; either the manometer is showing one pattern or the other, or it is changing rapidly. The method of watching the multiple manometer for the change in pattern was found to be extremely sensitive, as improvements could be made and the critical angle checked visually with an accuracy of $1/4$ deg. This made an exceedingly rapid method of observing the effect of modifications, as no computations were necessary, and all that was needed was to start the tunnel and to run the model through a range of angles of attack. The critical angles obtained in this manner checked very accurately with the breaks in the polar, lift, and moment curves. Fig. 3 shows the wake curves for a fillet of the optimum type. The critical angle in this case was 15.7 deg. The lines of this fillet are shown in Fig. 5, and it is illustrated in Fig. 7.

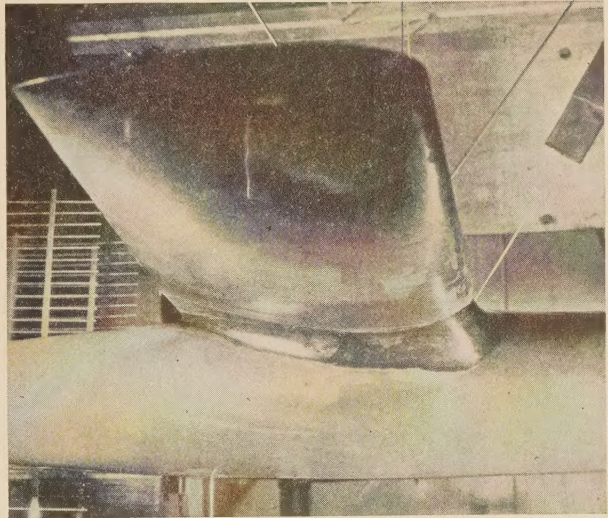


FIG. 4 THE WRONG FILLET NO. 2

(Note that the model is inverted and the pitot tubes can be seen in the background.)

FORCE MEASUREMENTS

The force measurements were made with the normal three-

component set-up. The tests were run at a water head of 39.24 cm, and as the root chord of the model was 42.35 cm, the Reynolds number for the tests was approximately 2,100,000. The accuracy of the tests can be judged from the points shown on the enlarged section of the polar (Fig. 14). It is not believed that variations in the maximum-lift coefficient of the order of 2 or 3 per cent are of any significance, as it was found that almost imperceptible changes in the surface condition of the model would cause this much variation. This variation is in line with that found by the N.A.C.A. in large-scale tests (ref. 3).

Before beginning the investigation on the effect of fillets, lift, drag, and pitching moment, tests were run of the wing alone. These results furnish a convenient basis for the subsequent discussion.

NORMAL LOW-WING CONFIGURATION

Results of three component tests on the normal low-wing arrangement are shown in Fig. 8. Considering the curves in the case of no fillet, it is observed that at a CL of 0.6 the polar starts breaking over sharply, the CL against α -curve

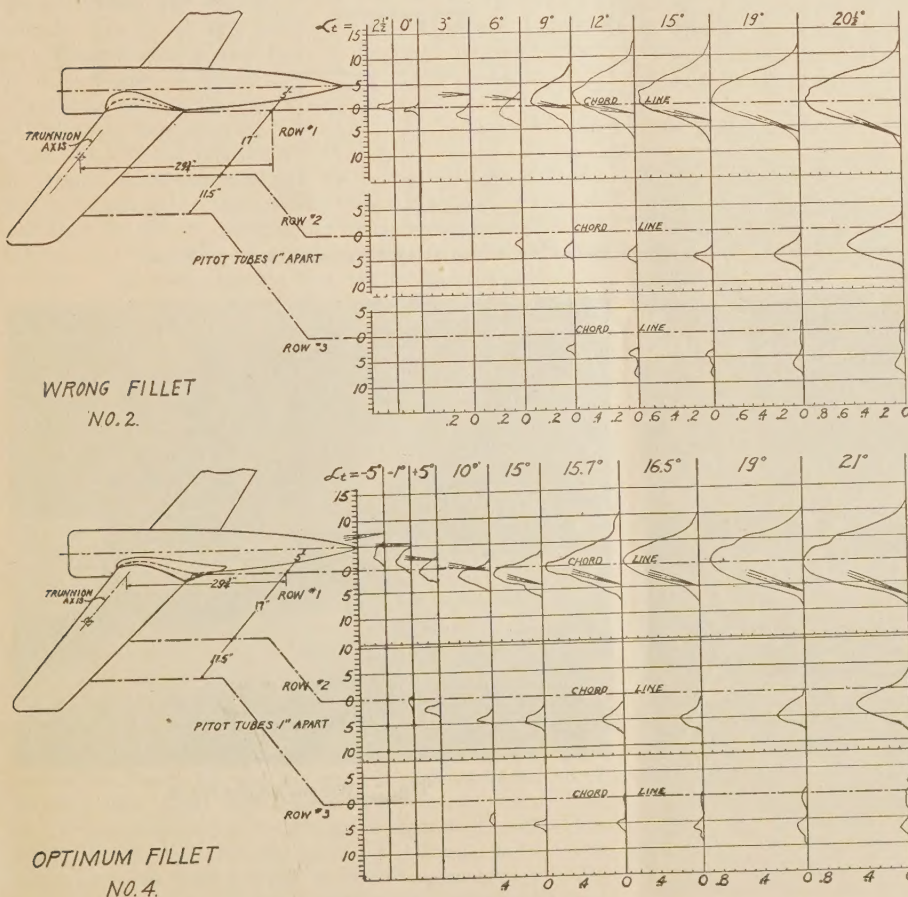


FIG. 3 WAKE DISTRIBUTION BEHIND FILLET NO. 2 (WRONG FILLET) AND OPTIMUM FILLET NO. 4

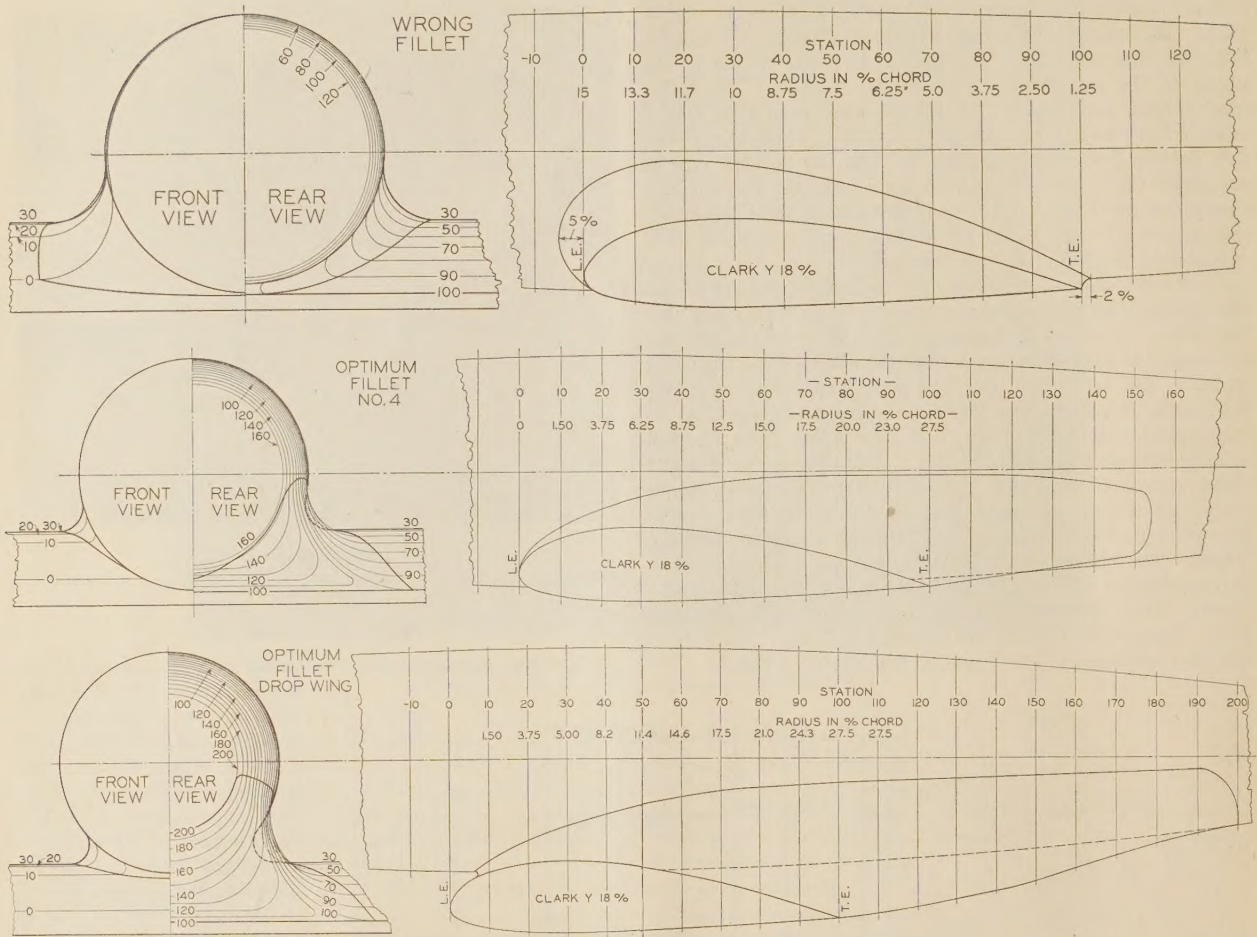


FIG. 5 LINES OF THE WRONG FILLET NO. 2, OPTIMUM FILLET NO. 4, AND FILLET D OF THE DROPPED WING

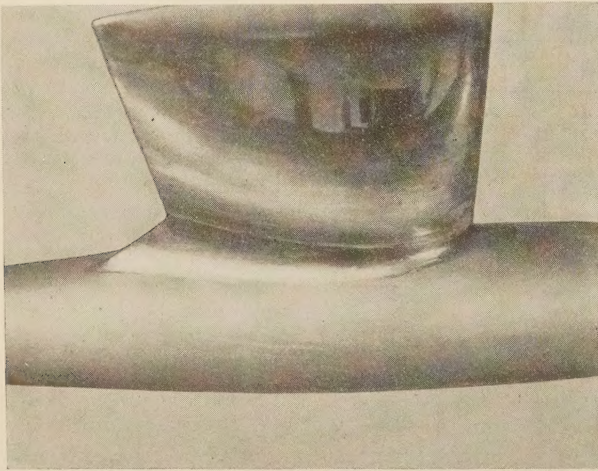


FIG. 6 FILLET NO. 3

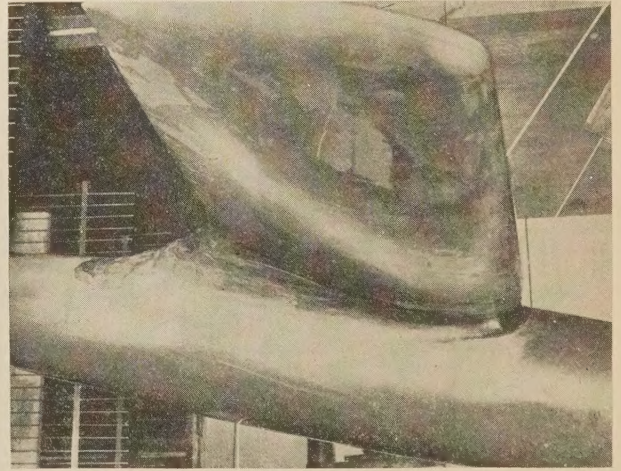


FIG. 7 WRONG FILLET NO. 4

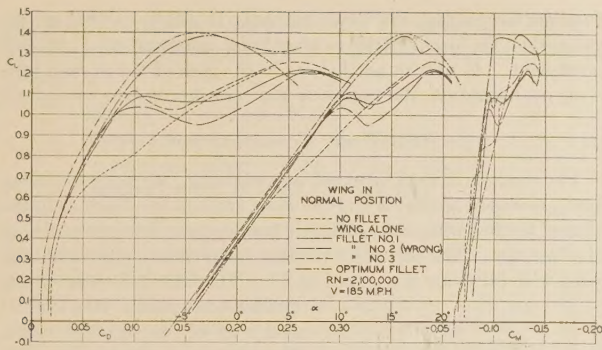


FIG. 8 NORMAL LOW-WING CONFIGURATION

takes up a new slope, and the moment curve becomes irregular. Now referring to the wake-loss diagrams, it is seen that for an angle of 5 deg the downwash is much smaller for the wing and fuselage than for the wing alone. The wing-alone polar parallels the induced-drag parabola (aspect ratio 5.97). The polar curve of the wing-fuselage arrangement parallels the wing-only polar up to a C_L of 0.45, and then starts deviating from it. If one attempts to fit an induced-drag polar to this curve in the region from a lift coefficient of 1.0 to 1.2, one needs

an aspect ratio of approximately 2.5, or somewhat less than one-half the aspect ratio of the complete wing. This leads one to suspect that the wing is acting as two monoplates separated by the fuselage and that there is a trailing vortex on each side of the fuselage. The wake diagrams lead one to the same conclusion, as from them one sees that the downwash is practically the same at rows 2 and 3 as for the wing alone, while in row 1 the downwash has practically disappeared for all positive angles. It will then be assumed as a working hypothesis that the foregoing is correct and that the interference corresponds to the breaking up of the horseshoe lifting vortex into two side-by-side horseshoe vortices.

This aerodynamic picture enables one to account for the peculiar shapes of the various curves, and also shows why the minimum drag is not subject to much improvement.

Three fillets were then tested to determine the best type. These fillets all had a radius of 15 per cent of the root chord. Fillet 1 was a uniform fillet of this radius throughout. Fillet 2 (wrong) had a 15 per cent radius at the nose and tapered aft; its lines are shown in Fig. 5. Fillet 3 had a small nose and a radius of 15 per cent at the trailing edge, and was of the same type as the optimum fillet shown in Fig. 5. A photograph of fillet 3 is shown in Fig. 6. All three of these fillets were a marked improvement over the unfilleted condition, fillet 3 having the greatest maximum lift and the greatest slope of its lift curve. As all of these fillets were a great improvement over no fillet, an elaborate program was undertaken to develop fillets of various types. It soon appeared that fillets 1 and 2 could not be much improved, while fillet 3 could be developed with considerable success. Numerous variations of this type were constructed, and the following rules were deduced from the tests:

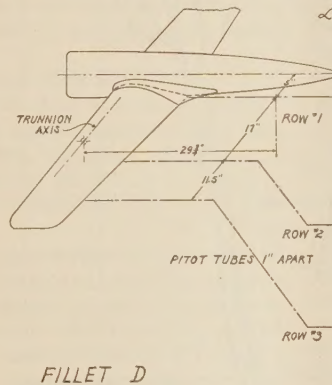


FIG. 9 DROPPED-WING CONFIGURATION

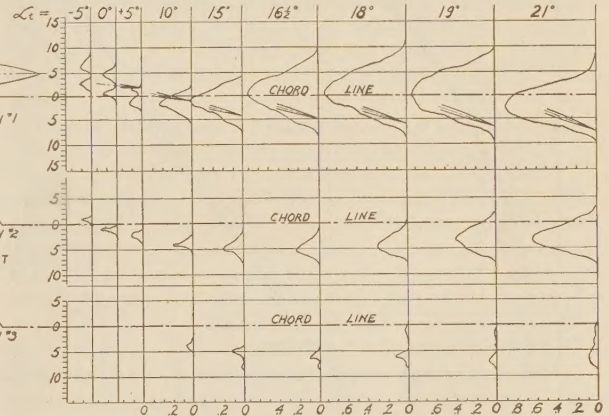


FIG. 10 WAKE DIAGRAM FOR OPTIMUM FILLET D

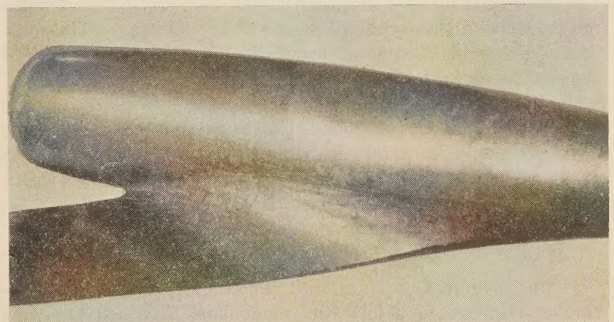


FIG. 11 OPTIMUM FILLET D (WING LOWERED)

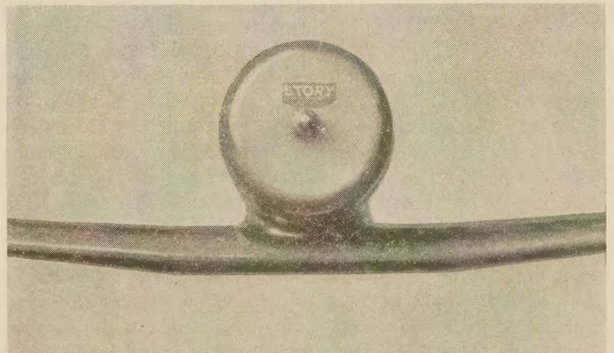


FIG. 12 OPTIMUM FILLET D (WING LOWERED)

- 1 Increasing the trailing-edge radius improves the maximum lift and prevents induced-drag losses at medium-lift coefficients; excessive trailing-edge radii increase the drag
- 2 Increasing the radius at the nose increases the drag and decreases the maximum lift
- 3 The fillet should taper as uniformly as possible from the nose to the trailing edge, and its maximum size should be as close to the trailing edge as possible
- 4 The fillet should be washed out smoothly to the fuselage.

Fillet 4 is an optimum design of this type. Maximum lift has

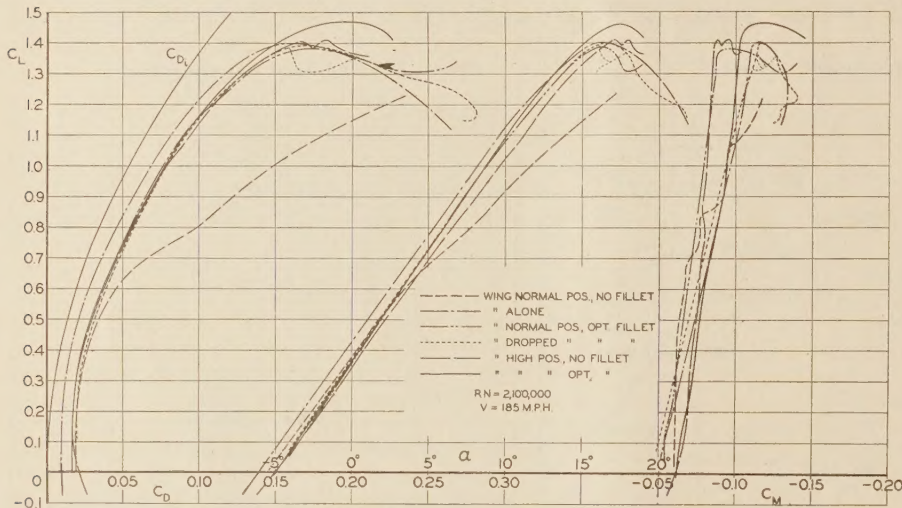


FIG. 13 CURVES FOR VARIOUS CONFIGURATIONS

been sacrificed for low drag, and it will be noticed that there is only a trace of the former ill effects of the fuselage. The wake diagrams for this fillet are shown in Fig. 3, and it will be noticed that the break in the downwash does not occur until over 15 deg, while in fillet 3 the break occurred at 10 deg. It will be noticed also that with fillet 4 the slope of the lift curve is steeper than the corresponding curves for the wing alone. This effect can be easily explained, as in this case the fuselage contributes some lift, and the coefficients are calculated neglecting this effect.

LOW-WING CONFIGURATION, WING LOWERED

It was suggested by an aircraft constructor that an investigation of the case of a low-wing monoplane in which the wing passes entirely below the cabin floor would be of great interest. Accordingly, a block 2 in. thick was made and placed between the wing and the fuselage. This corresponded to lowering the wing 1 ft at full scale. It was impossible to take any observations of the unfilleted condition for this arrangement. The first fillet put on in this configuration had a 20 per cent chord trailing-edge radius and had the nose of the wing faired forward and up to the fuselage. The results are plotted as fillet *a* in Fig. 9. Fillet *b* in the same figure corresponds to a similar fillet with the leading edge cut back. The fillet was then enlarged to 27.5 per cent trailing-edge radius and the nose was undercut still more. The lines of this fillet *D* are given in Fig. 5. Fillet *D* was found to be the optimum for this configuration. Fillet *e* was an endeavor to secure still greater improvement. The fillet was hollowed out by decreasing the radii in front of the trailing edge of the wing. This hoped-for improvement was not realized, but the curve is included in the figure. The curves for case *D* and for the wing alone illustrate how perfectly the pernicious effect of the wing-

fuselage intersection can be eliminated; it will be noticed on the polar that the profile drag is practically independent of the lift coefficient. It was found that, as in the case of the normal low-wing configuration, the radius at the nose should be a minimum.

HIGH-WING CONFIGURATION

The model was next arranged as a high-wing airplane, the wing being mounted so that it had the same angle of incidence as in the case of the low wing and so that its trailing edge was just touching the fuselage. The curves for the high wing with no fillet and high wing with fillets are shown in Fig. 13. The fillet had quite a large

trailing-edge radius (20 per cent) and was of the tapered type. The lift obtained with this fillet was the highest found, but was associated with a slight increase in drag. Fillets of intermediate radius and of various types, large at the front, small at the rear, constant radii, etc., caused very little change. The curves for intermediate radii, and in fact for all of the other variations, lie between the two curves mentioned. The most remarkable point in this group is the behavior of the polar of the no-fillet case in the vicinity of zero lift. It will be noticed that this curve departs markedly from the wing-only polar in the same manner, for negative angles, as does the low-wing no-fillet polar

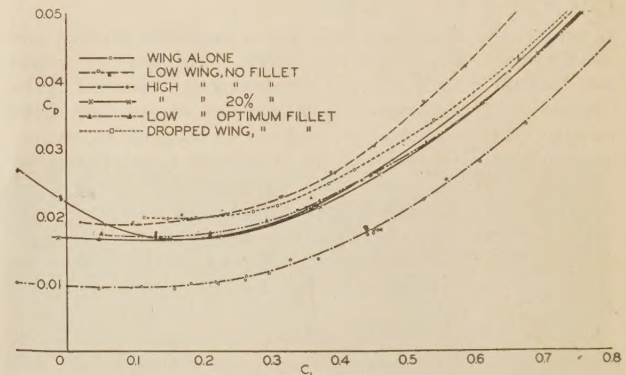


FIG. 14 COMPARISON OF VARIOUS CONFIGURATIONS IN THE HIGH-SPEED REGION SHOWING THE EXPERIMENTAL SCATTER

at small positive angles. This illustrates the extreme sensitivity of the suction side of the wing.

GENERAL DISCUSSION

It has been seen from the foregoing that the aerodynamic disadvantages of the low-wing monoplane can be almost completely eliminated by proper design of the wing-fuselage intersection. The maximum-lift coefficient of the wing alone can be attained with either a high-wing or a low-wing configuration. The differences in drag between the high wing and the normal low wing are inappreciable.

In the case of the dropped low wing there is found to be some drag increase, but it is thought that this difference could be

reduced by further investigation. The size of the optimum fillet in the case of a low-wing design can be decreased by the following means:

- 1 Making the fuselage small
- 2 Keeping the distance of the trailing edge of the wing below the bottom of the fuselage small
- 3 Using an airfoil of small top camber.

The minimum drag of the fuselage-wing combination can be best decreased by making the fillet at the leading edge of the wing as small as possible.

Buffeting. For the purposes of discussion, buffeting will be defined as follows: Buffeting is a violent shaking of the airplane and tail surfaces by aerodynamic forces at angles below the stall. Buffeting in this sense has been observed in the case of almost all low-wing monoplanes. If one considers the wake measurements and notices the critical angles, there is no difficulty in seeking what occurs.

The buffeting seems to be due to these three causes: first, the lift over the center section of the wing disappears, causing a decrease in the total lift available; second, the wake jumps from one side of the stabilizer to the other; and third, the stabilizer is then in the trailing vortex formed at the side of the fuselage. The position of the stabilizer is indicated on each of the wake drawings.

Mr. H. J. Steiger (ref. 4) has suggested that buffeting could be eliminated by cutting away the wing root and reducing the angle of attack at the fuselage. It is dubious if any such attempt would be satisfactory, as it would inevitably result in trailing vortices forming near the fuselage, and these vortices might cause a dangerous or uncomfortable tail vibration, in addition to their pernicious effect on the induced drag. It is easily seen that for a properly designed junction between the wing and the fuselage the lift must carry entirely across the span, since if there were no lift over that portion of the wing covered by the fuselage, the polar curve for the wing and fuselage would of necessity differ more from that of the wing alone than it actually does.

ACKNOWLEDGMENTS

The author wishes to acknowledge his gratitude to the entire staff of the laboratory for their assistance in performing the tests and in preparing this report. He is especially indebted to Dr. C. B. Millikan, Mr. W. H. Bowen, Mr. W. B. Oswald, and Mr. N. B. Moore for their efforts.

REFERENCES

- 1 Parkin, Klein, Coates, and Roberts, "The Interference Between the Body and Wings of Aircraft," Engineering Research Bulletin, University of Toronto, Bull. No. 8, 1928, Section No. 9. "The Influence of Superstructure on the Upper Surface of a Wing on Its Aerodynamics Characteristics," Transactions of the Central Aerohydrodynamic Institute, U.S.S.R., 86. Muttray, H., "Investigation of the Effect of the Fuselage on the Wing of a Low-Wing Monoplane," N.A.C.A. Technical Memorandum 517, 1929 (from "Luftfahrtforschung," June 11, 1928). Perring, W. G. A., and Calen, C., "Drag and Interference of a Nacelle When Installed on the Upper Surface of a Wing," British Aeronautical Research Committee, Reports and Memoranda 1414 (1930). Ward, Kenneth E., "Interference Effects and Drag of Struts on a Monoplane Wing," N.A.C.A. Technical Note 365 (1931). Ryan, Wm. Carleton, and Wieben, Hermann C., "Effect of Fillets Between Wings and Fuselage," New York University Report. Ober, Shatswell, "Some Studies on the Aerodynamic Effect of the Gap Between Airplane Wings and Fuses-lages," N.A.C.A. Technical Note 327 (1929).
- 2 Clark B. Millikan and Arthur L. Klein, "Description and Calibration of 10-Ft Wind Tunnel at California Institute of Technology."
- 3 R. F. Anderson, "The Aerodynamic Characteristics of Airfoils at Negative Angles of Attack," N.A.C.A. Technical Note 412.
- 4 H. J. Steiger, address before the Royal Aeronautical Society, April 7, 1932.

Discussion

E. Ower.³ The author's results entirely confirm the ideas formed from some similar, although not so comprehensive, work for which the writer was responsible some time ago. An account of this work was given in a lecture read to the Royal Aeronautical Society in January, 1932,⁴ and the writer thinks that the explanation he then put forward of the type of interference for which fillets are found to be beneficial is worth repeating. He suggested that this interference occurs when the air stream has to expand at more than a certain rate if it is to remain in contact with the body and wing surfaces. A certain rate of expansion can be tolerated, but if the surfaces diverge from one another too rapidly, the flow detaches itself from them and a region of turbulence is set up which leads to a loss of lift and an increase of drag. A well-known analogous case is that of the outlet cone of a venturi tube—if the angle of this cone is too great, it does not "run full;" that is, the flow breaks away from the walls, with the resulting loss of efficiency of reconversion of the kinetic energy into static pressure.

This hypothesis was confirmed by the various tests made to investigate its truth, and it explains the author's results with fillets. For in his case the geometry was such, as indeed it is in most practical body-wing combinations, that the rate of expansion increased progressively from the maximum camber of the wing toward the trailing edge. Hence, as the author found, the best fillet increases in radius toward the rear of the wing. The writer's experiments were made with fillets of constant radius, but he did in fact predict that fillets of increasing radius toward the trailing edge would be preferable. The same line of reasoning indicates why fillets on the under surface of a high-wing combination are found to have very little effect; the divergence between the surfaces of the body and the wing is much less in such a combination than it is in low-wing positions. Moreover, in the high-wing position the pressure gradient along the lower wing surface is such as slightly to assist the flow to adhere to the surfaces, whereas in the low-wing position the pressure gradient on the upper surface tends powerfully in the opposite direction.

The author mentions the importance of preserving as far as possible the normal lift distribution along the span of the wing. This again agrees with views that the writer has expressed. This principle, together with that of avoiding regions of divergent flow, will be found to be of the utmost importance to the designer in his efforts to build high-performance aircraft. The designer is always more interested in direct proof than in speculation, and the author has provided such proof, whereas the writer, mainly through lack of time, was content to put forward ideas which needed corroboration by facts before they could be accepted with complete confidence.

RICHARD M. MOCK.⁵ This is believed to be the most interesting piece of aerodynamic research in America published during 1932, outside of that of the N.A.C.A. It is unfortunate that the tests were not made with a running model propeller, as it is possible and likely that the slipstream affects the flow around the fuselage and especially over the wing-fuselage intersection. Therefore it is believed that the comparative drag figures are somewhat questionable. During take-off and climb with high angles of attack, the same would be true as affecting the lift coefficients,

³ Aerodynamics Department, National Physical Laboratory, Teddington, Middlesex, England.

⁴ See *Jour. Royal Aero. Soc.*, 1932, vol. 36, p. 531. Also, Reports and Memoranda no. 1480 of the Aeronautical Research Committee, E. Ower, "Some Aspects of the Mutual Interference Between Parts of Aircraft."

⁵ Aeronautical Engineer, A. H. G. Fokker, New York, N. Y. Jun. A.S.M.E.

while for landing the propeller effect is negligible. The comparative maximum lift coefficients, without propeller, are very valuable, as this is applicable to the landing condition.

The writer differs from the author regarding his comparison with the high-wing monoplane. The high-wing monoplane which he used as a comparison showed almost 6 per cent more maximum lift and about 3 to 4 per cent less drag than the best low-wing arrangement. However, the writer is under the impression that a high-wing design, rather than have the wing resting on top of the fuselage with its trailing edge just touching the fuselage, will have less drag if the wing is sunk into the fuselage, so that the top of the fuselage meets the top of the wing about one-third or one-half chord back from the wing leading edge and the combination is carefully filleted. The top of the fuselage might be lowered in front of the wing to allow a clean leading edge, and the portion of the fuselage above the rear portion of the wing might have fillets of very large radius. This should reduce the frontal area and the drag still below that of the combination used, and if the leading edge is carefully faired, should not affect the lift other than increase it by directing the flow from the fuselage over the upper surface.

Regarding the best position for the low wing, it would be interesting to raise the wing, as on the Gee Bee racer, rather than lower it as was done. As the fuselage decreases in width near the bottom and the wing is cambered on top, a pocket or cavity is formed between upper surface of the wing, just in front of the trailing edge, and the lower surface of the fuselage. The air passing over the wing and over the fuselage must fill this pocket, causing eddies and consequently drag. Therefore it is logical that by fairing over this cavity, as the author has done, the drag of the combination will be reduced. This could also be done by raising the wing slightly to where the fuselage is wider and then using a fillet, and also perhaps by changing the fuselage cross-section slightly so that an excessive fillet will not be necessary. Another means would be to have the wing, in front view, curve upward at the root, meeting the fuselage side at a right angle.

Of course, if the landing gear is attached to the wing, the wheel supports will be longer if the wing is raised. The increased length means slightly greater weight, and if the undercarriage is not retractable, the frontal area and consequently the drag will be increased. Lowering the wing from the optimum (filleted) low-wing position to the optimum (also filleted) dropped-wing position (Fig. 14) means an increase in drag of approximately 17 per cent. With a fixed external landing gear, the two shorter wheel supports with the dropped-wing position might partially offset the increased wing-fuselage drag. With a fully retractable landing gear, the landing-gear resistance could be neglected, and only the best wing-fuselage arrangement considered, with the tail location and fillet varied to eliminate buffeting.

The effect of lift-increasing trailing-edge flaps on buffeting would be interesting.

The writer would appreciate having the author's opinion of the meaning of the double curve near the maximum-lift coefficient of the dropped-wing combination with optimum fillet *D*. He also would appreciate an opinion of the double wake behind the fuselage at -5 deg, zero, and $+5$ deg for the same wing-fuselage combination. Another pilot combination between 1 and 2 and still within the stabilizer span would have been interesting. The writer would like to know the drag coefficient of the fuselage at the various angles of attack so that it can be added to the drag of the wing alone and compared with the drag of the combination.

G. J. KLEIN.⁶ The early investigations into body-wing interference were, it is true, conducted at rather low values of Reyn-

⁶ Junior Research Physicist, National Research Council, Ottawa, Ont., Canada. Jun. A.S.M.E.

olds' number. However, they disclosed very interesting results, particularly in the case of the low-wing monoplane, and certainly showed the need for further research at higher Reynolds' number. In this connection, the present paper, together with an extensive series of experiments at the N.P.L. (R. & M. 1480 and R. & M. 1300), form a valuable extension and show that the general conclusions reached in the earlier work still hold at much higher values of Reynolds' numbers. When we consider all these researches together, we get a fairly accurate picture of the subject.

It is now definitely established that detrimental interference is due to burbling caused by an attempt to expand the airstream too rapidly in the angle between the side of the body and the surface of the wing. It is true that the presence of the body does change the lift grading of the wing and thus increases the induced drag, but unless this burbling occurs, this effect is very small. Actually the wings so modify the flow about the body that the body contributes appreciably to the total lift of the combination, and the resulting lift grading is not very different from the lift grading of the wing alone.

For the foregoing reasons it is sufficient to confine this discussion to the case where burbling occurs and to consider the factors involved. Obviously, the worst case would be a low-wing monoplane without fillets, having a highly cambered wing root and a body of small fineness ratio and of such a cross-sectional shape that the angle between the side of the body and the upper surface of the wing is small compared with 90 deg. This combination forms a pocket between the body and the wing near the trailing edge of the latter, into which the airstream cannot expand, even at the zero lift angle of attack of the combination. Increasing the angle of attack increases the difficulties in expanding the airstream, thus causing increased burbling. There are several methods of suppressing this burbling:

(1) The wing can be raised to a higher position on the body to eliminate the pocket effect.

(2) The body can be given flat sides, making an angle of 90 deg with the wing surface, as was done in the Schneider Trophy Racer S5.

(3) A fillet of increasing radius toward the trailing edge can be employed, as was done in the present paper.

In short, anything that eliminates this pocket effect over the useful range of angle of attack will result in a combination of body and wing that will be free of any undesirable interference effects.

An interesting result brought out by the paper is that the "double stalls" found in the earlier work at low values of Reynolds' number are still present at much higher values. Undoubtedly the recovery from the first stall is due to a decrease in the extent of the burbling caused by the downwash from the nose of the body.

Probably the most important point brought out by the paper is that a properly designed low-wing monoplane can be just as efficient as a high-wing monoplane.

AUTHOR'S CLOSURE

Replying to Mr. Ower, the low-wing fillet described was first developed in our wind tunnel in May, 1931, and test-flown in June of the same year. The second Northrop Beta and all succeeding Northrop ships have carried this device. The author agrees entirely with Mr. Ower's statements as to the necessity of eliminating most of the expansion of the wing fuselage intersection, as was first pointed out by Muttray (*loc. cit.*).

Replying to Mr. Mock, as he says, it is unfortunate that the tests were not made with a running propeller. The laboratory has under development a fuselage, in which is included an electric motor with complete dynamometer, for repeating the pre-

ceding investigation with a slipstream. The model when finished will have the proper scale horsepower and the proper ratio of propeller diameter to span. However, the author does not believe that the drag differences will be large in the case with slipstream and without, as the laboratory has been rather successful in predicting the performance and especially the high speed of the airplanes which it has tested. In a paper by Drs. Th. von Kármán and Clark B. Millikan⁷ there are described the methods used by this laboratory in estimating the performance of the actual airplane. Due to the successful checks which have been secured, it is not very probable that the discrepancies in drag between power off and power on will be large.

Since the investigation of the fillet was undertaken as an engineering study rather than as a scientific investigation into the configuration for minimum drag of the wing and fuselage alone, we did not consider several of the cases mentioned by Mr. Mock, as the lowering of the wing in the case of a high-wing monoplane or the raising of it in the case of a low-wing monoplane would require a larger fuselage in order to maintain the headroom in the cabin.

The reduction in frontal area in the cases mentioned by Mr. Mock would be more apparent than real, as it would necessitate, if his suggestions were carried out, the enlarging of the fuselage in order to accommodate the passengers or other loads. The raising of the wing any great distance was impossible in this particular case as it would bring the floor level too high. The consolidation of a stressed-skin wing into beams in order to enable the passengers to place their feet below the top surface of the wing is exceedingly extravagant of weight, and it also causes the cabin to be encumbered with structural members which interfere with the free circulation of passengers or the stowing of freight.

The author does not believe that the position of the wing with reference to the fuselage is a vital matter, as what is gained in one place is lost in another. In the multimotor transport field there is a very interesting case. There are two modern low-wing bimotor transports of the same power loading and span loading, one with the wing passing completely below the cabin floor and the other with the wing beams passing through the cabin. The airplane with the wing completely below the cabin floor is much faster, in the neighborhood of 25 mph, than its competitor. The difficulties of designing a retractable landing gear increase with at least the square of the length of the members as does also its weight. The raising of a wing 6 in. or 8 in. farther above the ground will often make a satisfactory retractable landing gear almost impossible. The addition of lower surface flaps has been found in this laboratory to have no effect on the buffeting of a well-filleted airplane. The author believes that the double peak of the curve for the optimum fillet D is probably due either to asymmetries of the model or to asymmetries of the air stream. The model was known to have developed some aerodynamic twist. This twist raised the angle of attack of one side of the model above that of the other, and consequently one side stalled in advance of the other. This effect has also been found in the laboratory a number of times in rolling-moment tests. The author believes that the two peaks in the wake diagrams shown in Fig. 10, at -5 deg. and $+5$ deg., can be explained as follows: The upper one is probably the wake of the fuselage and the lower one that of the wing. When the downwash becomes large, the fuselage wake becomes merged into that of the wing. The drag coefficient of the fuselage has never been measured separately, so that Mr. Mock's question on this point cannot be answered.

Replying to Mr. G. J. Klein, he is completely correct in his statement as to the three methods of eliminating the burbling in

the wing-fuselage intersection. However, in the case of a straight-sided fuselage, the burble is not completely absent. The author would like to cite Fig. 15 as evidence in this case. The results in this figure were obtained with the Douglas transport fuselage, which is straight-sided in the region in contact with the wing and for a considerable distance aft of the trailing edge. The wing

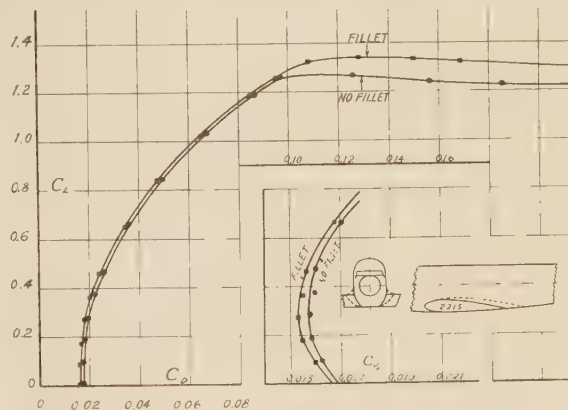


FIG. 15 LIFT AND DRAG POLAR CURVES FOR THE CASE OF A FUSELAGE WING COMBINATION IN WHICH THE FUSELAGE IS STRAIGHT SIDED

(Note: The separation in drag between the curves on the larger plot has been increased to permit satisfactory reproduction. The real separation is shown on the smaller plot.)

section used in this transport is the N.A.C.A. 2215. This section is of only 15 per cent thickness, has a very small camber (2 per cent), and furthermore the point of maximum camber is only 20 per cent aft from the leading edge. This wing has therefore probably the smallest top camber of any section in common use.

Nevertheless, in the tests shown, the difference between fillet and no fillet is quite perceptible. The model was tested with tail surfaces but less nacelles. The separation between the two curves shown on the larger plot in the figure has been exaggerated in the region of low lift coefficient in order to enable the two curves to appear separately on the reproduction. The smaller plot shows the experimental points in their true separation. In the low drag region the addition of the fillet reduced the minimum drag for the model approximately 1.8 per cent and raised the maximum lift coefficient as shown from 1.27 to 1.34. For very high angles not shown in the plot, the curves cross each other, an effect the author is unable to explain, but at all usable angles of attack the filleted case is superior to that of the unfilleted.

The discussion of why some of the lift curves have double peaks has been included in the reply to Mr. Mock. However, the double stalls in the other sense, i.e., of curves that come to a maximum and then go on to a further maximum, are apparently due to the local burbling of the wing in the center, while outboard portions of the wing do not stall as soon, but continue to work at larger and larger angles of attack. These restricted portions of the span can then go to larger lift coefficients, as it is well known that wings of small aspect ratio can reach larger lift coefficients than normal wings. It has been found in our laboratory that the characteristic sharp break in the lift curve can be explained as an effect of this kind. We always find the sharp break in untapered wings. Tapered wings usually show the rounding top which we think means that the center of the wing stalls before the outboard portions. Evidence for this can be seen in Fig. 2 on the wake diagrams for the wing alone. In one very interesting case the laboratory found that this sharp drop-off of the lift curve was obtained with a tapered wing in which an auxiliary

⁷ Th. von Kármán and Clark B. Millikan, "The Use of the Wind Tunnel in Connection With Aircraft Design Problems," *Aeronautical Engineering*, 1933.

airfoil was used only over a part of the center section. In this case the sharp drop in the lift curve was obtained, not only in the laboratory but also in flight, while the airplane without the auxiliary airfoil stalled in the more usual manner. We therefore think that in this case the auxiliary airfoil held the flow on the center section to a higher lift coefficient than that which it would normally reach, and when it stalled, the entire wing stalled at once.

Since the foregoing paper was written, two confirmations^{8,9} have been published of the results, and numerous airplanes have been designed and flown with these devices.

⁸ Biechteler, Curt, "Versuche zur Beseitigung von Leitwerk-schütteln," Z.F.M., vol. 24, no. 1, Jan. 14, 1933.

⁹ Hood, Manley J. and White, James A., "Full-Scale Wind-Tunnel Research on Tail Buffeting and Wing-Fuselage Interference of a Low-Wing Monoplane," Technical Note no. 460, May, 1933.

Field Welds in Pressure Pipe Lines of Steam Systems

By H. N. BOETCHER,¹ BALTIMORE, MD.

Fusion welding has in these later years come to be an important method of making all types of joints in construction work. The paper is confined to welding as it is done in the field on pipe lines to be operated under high pressures and temperatures. Based on the author's tests and investigations, as well as on service experience extending over many years and on published and unpublished data obtained elsewhere, it is indicated that oxyacetylene welding fills the requirements in regard to soundness and adaptation to service conditions better than electric-arc welding, although it is not intended to claim any superiority of gas over electric-arc welding.



FUSION welding, which for many years has been looked upon as a patch-up type of work for repairs or for fixing up faulty castings, has during these later years come to be a quite important method of making all types of joints in construction work. As frequently happens with quickly progressing methods, design features and technique have received more attention than the fundamental characteristics of welds. Even though many points to be brought out

apply equally well to other types of welding work, this paper will be confined to welding as it is done in the field on pipe lines to be operated under high pressures and temperatures.

STRESSES IN PIPING

Since it is a fundamental principle of engineering that requirements should be closely correlated with the service stresses to which the equipment is subjected, a review of such stresses as are present in piping is advisable.

The inner pressure results mainly in tensile stresses. The temperature gradient across the thickness of the metal causes an additional stress, which is usually very small in a heat-insulated pipe line under normal conditions. However, investigations, some of which have been published recently, indicate

that this stress may be very high at starting conditions when a large amount of steam is suddenly admitted to a cold pipe line, especially with heavy pipe walls. The third factor concerns stresses resulting from axial expansion and contraction of the pipe on heating and cooling. This stress depends greatly on the skill of the designer and on conditions of space limitations.

The combination of pressure and temperature gradient effects a slight elastic expansion of the pipe, which in turn results in a concentration of stresses at the inner surface. This concentration grows rapidly with increasing wall thickness, and therefore necessitates the use of as thin a material as possible to avoid excessive stresses at the inner surface. In considering the stresses, it should be noted that the starting stresses caused by the temporarily high temperature gradient constitute repeated stress peaks which may lead to fatigue conditions. Similarly, axial expansion and contraction exert fatigue stresses.

Inasmuch as both technical and economical considerations demand the use of as thin-walled piping as it is safe to use, the weld must be such that uncertainty in regard to its quality does not necessitate the use of thicker pipe metal.

Turning to the welds, it is necessary to consider three phases: the properties of the welds, including the steel affected by the welding; the stresses introduced by the welding; and the connection between the properties of the welded joint and the operating stresses.

CHARACTERISTICS OF WELDS

Since the characteristics of a weld are largely determined by the welding method used, it is necessary to go somewhat into the metallurgy of welds. It has been pointed out often that a weld is nothing but a steel casting. Though this is true, there are certain important differences which make it possible to obtain the excellent properties associated with present-day welds. There are the methods of pouring in and puddling of the liquid metal, factors depending on the type of welding. Furthermore, only a small amount of metal is cast into a large more or less rigid metallic "mold" to which it firmly adheres, a fact which introduces hot and cold working on account of shrinkage taking place during cooling. This working is an important factor in determining the properties of the weld.

OXYACETYLENE WELDS

Application of heat and the introduction of the welding metal are separate functions in the oxyacetylene-welding process. Since, therefore, the steel can be preheated to a temperature at which the surface is molten, it is not necessary to heat the rod metal far above the melting point. The welder has complete control over temperature conditions and the amount of metal to be fused in at any period of the operation. This control makes it possible to work out slag and other impurities from the metal, and eventually to remelt sections appearing faulty. It furthermore aids considerably in making welds in difficult positions, as overhead, and gives an experienced welder good control over penetration and fusion at the root of the weld. The constant uniform heating, with the presence of a large amount of hot metal at all periods of the welding, results in a gradual slow cooling and in a homogeneous structure of the welding metal.

¹ Assistant to Superintendent of Steam Stations, Consolidated Gas, Electric Light, and Power Company of Baltimore. H. N. Boetcher was born in 1898 in Altona, Germany. After war service, he attended the Technische Hochschule at Hannover, from which he was graduated in 1922. He was connected with Nordwest-deutsche Kraftwerke A.G., formerly Siemens Elektrische Betriebe A.G., as assistant mechanical engineer and assistant to the president, working in connection with the operation of several power plants and transmission systems and with design and construction of extensions to plants and of a new power station. In 1924 he came to the United States. He has been connected with the Consolidated Company since early in 1925, working in connection with the operation of steam-power and heating plants, development work with powdered-coal equipment and feed control at Gould Street Station, and with engineering materials, especially metals.

Presented before a meeting of the Boston Local Section, Boston, Mass., September 21, 1932, of THE AMERICAN SOCIETY OF MECHANICAL ENGINEERS.

NOTE: Statements and opinions advanced in papers are to be understood as individual expressions of their authors, and not those of the Society.

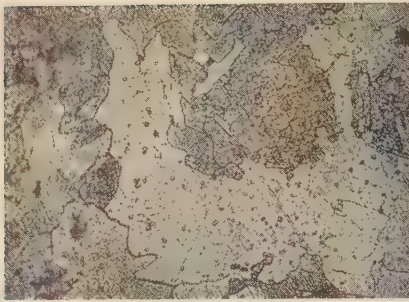


Fig. 1

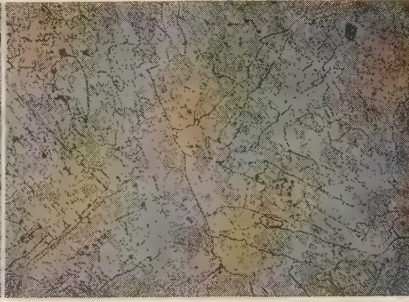


Fig. 2

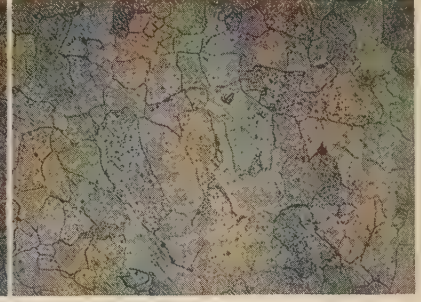


Fig. 3

FIGS. 1 TO 3 MICROPHOTOGRAPHS OF STRUCTURE OF OXYACETYLENE HEAD WELDS $\times 100$

(Fig. 1, extreme outside; Fig. 2, center; Fig. 3, root.)

Only at the starting point of the weld the structure frequently is different, due to reheating of the first flowed-in metal and accelerated cooling of the finishing point.

Figs. 1 to 3 show the microstructure of head welds which were used to fasten a plate to the dead end of a pipe. Excepting the immediate outside, the structure is uniform, showing fairly large regular grains and indicating a very low carbon content as a result of the burning out of carbon during welding.



FIG. 4 LAPS IN OXYACETYLENE WELDS

(a and b, laps caused by lack of care in remelting the surface; c, an extreme case.)

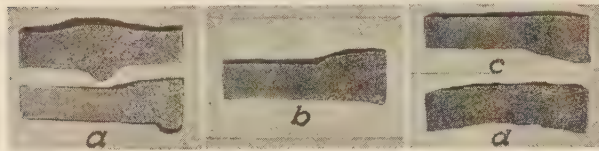


FIG. 5 CROSS-SECTIONS OF 6-IN. STANDARD-PIPE OXYACETYLENE BUTT WELD

(a, random transverse sections; b, transverse section, top of pipe; c, transverse section, bottom of pipe; d, longitudinal section.)

"Laps" in gas welds, though by no means unavoidable, are quite frequent. Fig. 4, in a and b, shows this condition, which is caused by lack of care in remelting the surface of solidified welding metal before more metal is fused on. Even when no visible cracks are present at the dividing lines between layers, the weld is weakened, because the layers have a tendency to slip on each other on deformation. However, some cracks will usually be found on closer examination. Fig. 4c shows an extreme case.

The characteristics of gas welding make it possible to obtain welds with good penetration throughout, which show practically no voids or inclusions without fine polishing and a magnifying glass; Fig. 5 is a good example.

Fig. 6 shows the structure of a butt weld of 6-in. standard pipe. This is the structure of the butt weld shown by Fig. 5.

The examination of a weld would be incomplete if the effect on the adjacent steel were neglected. A sharply defined division line between flowed-in and pipe metal is rare in a good gas weld. Usually, a zone of transition, with a combination of the two

metals, will be found. The prolonged heating necessarily connected with gas welding affects the base metal to a large distance from the weld. For instance, with a 6-in. standard pipe, the structure was found to have been changed to a distance of about $\frac{3}{4}$ in. from the edge of the weld. A 4-in., B.w.g. No. 8 boiler tube showed a change of structure to a distance of $1\frac{1}{4}$ in. from the weld. In detail, the structural changes and the extent of the affected zone depend on the type of steel and on the welding conditions (Figs. 7 and 8).

The structure of gas welds is indicative of their mechanical properties. With sound metal and uniform structure, changes in strength may be judged fairly accurately from Rockwell hardness tests. These show a hardness of the flowed-in metal and the adjacent steel, which is highly heated during welding, higher than that of the original pipe steel, a gradual decrease below this level in a softened zone comprising both structurally changed and unchanged steel, and a return to the original hardness at a distance from the weld at which the metal was heated to less than 1000 to 1100 F. The tensile strength of the flowed-in metal is usually close to that of the pipe steel. The ductility is uniformly high throughout the weld. A striking example is presented by Fig. 9 showing butt welds of 4-in. boiler tubes flattened between parallel plates until the distance between the plates was $\frac{1}{2}$ in. Afterward, on hydrostatic pressure, the flattened section was reexpanded to nearly 3 in., at 600 lb per sq in., before a crack occurred in the base metal adjacent to the weld. A specimen of unwelded boiler tube subjected to a test under the same conditions cracked at a pressure of 700 lb per sq in., with a reexpansion to $3\frac{1}{8}$ in. The ductility of the weld metal was quite remarkable when it is considered that the thickness of the weld was approximately $\frac{1}{4}$ in., compared with a tube thickness of $\frac{5}{32}$ in., a difference which caused a much more severe bending of the welding metal than of the boiler-tube steel.

ELECTRIC-ARC FUSION WELDS

Electric-arc fusion welding with metal electrodes has characteristics quite different from oxyacetylene welding. The electric arc heats base and wire metal rapidly, almost instantaneously, to a very high temperature, at which it has a high fluidity, and is in part even in a gaseous condition. At this temperature the metal reacts readily with the oxygen and nitrogen of the air. The resulting nitrides make the metal hard and brittle. Part of the oxides react with the carbon of the welding wire to form carbon-monoxide gas, which is entrapped in bubbles by the metal, making the weld porous. It is evident that the conditions can be improved very much by maintaining an atmosphere of neutral gases surrounding the arc and the weld. Of the various methods devised to accomplish this, only the coating of

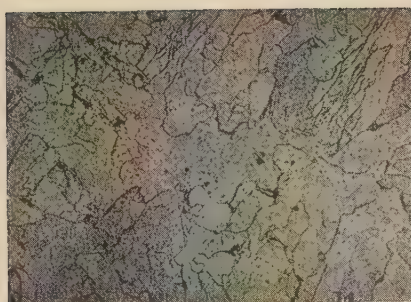


Fig. 6

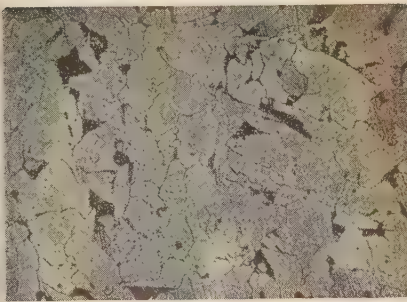


Fig. 7

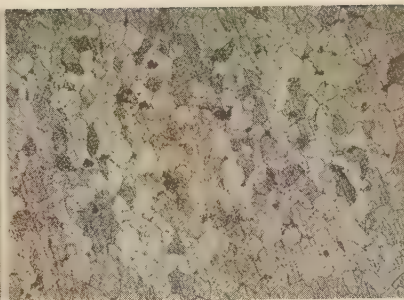


Fig. 8

FIGS. 6 TO 8 MICROPHOTOGRAPHS OF OXYACETYLENE WELDS $\times 100$

(Fig. 6, structure of butt weld shown by Fig. 5; Fig. 7, structure of unwelded pipe; Fig. 8, structure of pipe metal $\frac{1}{16}$ in. from weld.)

the electrodes with a material which develops inert gases on heating has achieved commercial importance so far in the field welding of pipe lines, and has as a matter of fact resulted in producing welds of high quality. In addition to eliminating oxidization, nitriding, and the burning out of the carbon to a large extent, the inert atmosphere apparently has a heat-insulating effect resulting in a higher heat input into the weld. A beneficial effect of this condition is an improved distribution of heating stresses at the weld. On the other hand, some undercutting along the edges of the welds has not been eliminated entirely, and the higher heat concentration causes a high fluidity of the metal as flowed into the weld, which makes it very difficult to obtain good overhead welds. The attempt to overcome this trouble by applying numerous thin layers which solidify immediately at the surface of the previously flowed-in metal has yielded promising results, even though it still has disadvantages in regard to uniformity of structure and probability of slag inclusions.

Heating and flowing-in of metal are simultaneous and interconnected operations in arc welding. If a sound weld is needed, it is necessary, therefore, to clean the surfaces of base metal or previously flowed-in metal very carefully, since any slag or other impurity left will be included in the weld and cannot be worked

out during welding. Such inclusions, accordingly, are found more frequently in electric-arc welds than in gas welds. One finds a similar condition in regard to penetration and fusion at the root of the weld. If the weld metal is not fused to the base metal at the root immediately or if the electrode metal which flows in in drops and slugs rather than in a continuous stream bridges over the root section, poor penetration results. Fig. 10 shows that the penetration is not certain to be good throughout the weld. Lately, backing strips have been used to secure more uniform penetration, care being taken to have the arc go from the welding electrode to the backing strip. The method which has been taken over from the welding of pressure vessels promises good results in pipe-line



FIG. 9 FLATTENING TEST
(Of 4-in. boiler-tube oxy-acetylene butt weld.)

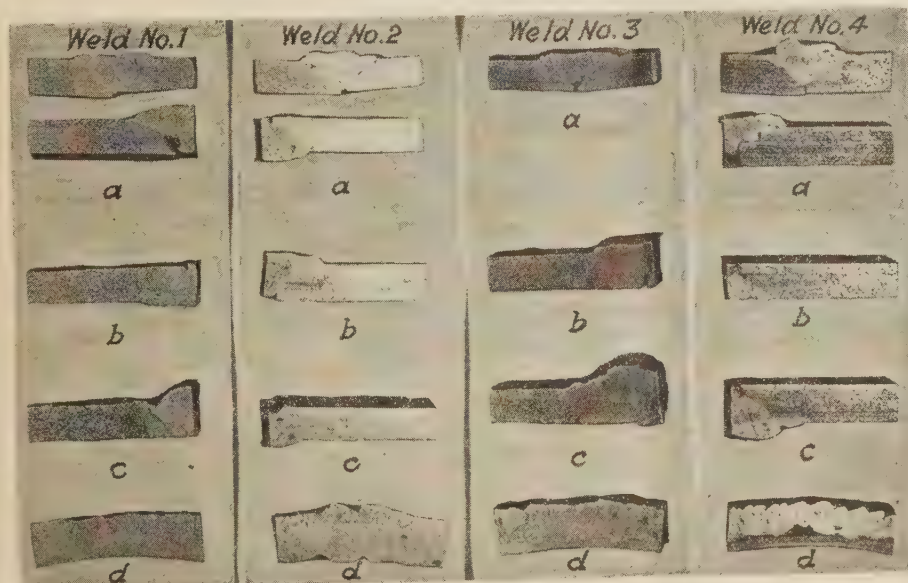


FIG. 10 CROSS-SECTIONS OF ELECTRIC-ARC FUSION BUTT WELDS, COATED WIRE, 6-IN. STANDARD PIPE
(a, random transverse sections; b, transverse sections, top of pipe; c, transverse sections, bottom of pipe; d, longitudinal sections.)

welding, though more attention should be paid to shaping the backing strips to suit flow conditions in the pipes.

Structural features of the welds are of course the result of the welding conditions. In electric-arc welding, the temperature of the weld metal is very high, while the total heat input is low, compared with gas welding, on account of the short duration of the welding action. Accordingly, the average total temperature of the joint is low during welding, and tends to chill the fused-in metal, which freezes rapidly in needles or columns of grains radiating from the colder surfaces. The heat liberated by the arc and by the freezing and cooling of the molten metal increases the temperature of the parent metal or of pre-

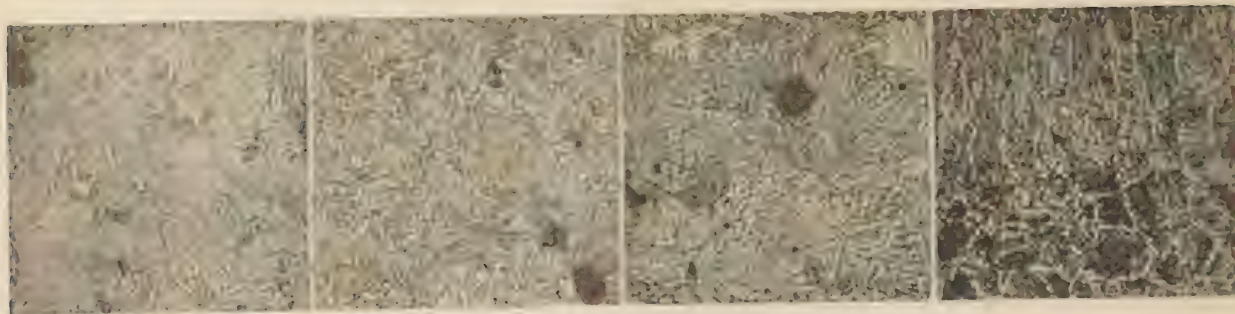


Fig. 11

Fig. 12

Fig. 13

Fig. 14

FIGS. 11 TO 14 MICROPHOTOGRAPHS OF ELECTRIC-ARC WELDS, BARE WIRE $\times 100$

(Fig. 11, one-layer weld; Fig. 12, same layer after second layer was applied; Fig. 13, second layer; Fig. 14, fusion line.)



Fig. 15

Fig. 16

Fig. 17

FIGS. 15 TO 17 MICROPHOTOGRAPHS OF ELECTRIC-ARC WELDS, COATED WIRE $\times 100$

(Figs. 15 and 16, structure of outer layer; Fig. 17, structure of inner layer.)



Fig. 18

Fig. 19

Fig. 20

FIGS. 18 TO 20 MICROPHOTOGRAPHS OF ELECTRIC-ARC WELDS, COATED WIRE $\times 100$

(Fig. 18, transition between inner and outer layer; Fig. 19, fusion line at outer layer; Fig. 20, transition line between inner and outer layer, no grain growth.)

viously flowed-in metal to the critical point at which it recrystallizes to a refined structure. Immediately adjacent to the weld, the temperature usually is kept up sufficiently long to effect a slight grain growth. At a very short distance from the weld, the duration of the heating is already so short that only partial recrystallization results along the boundary lines of ferrite grains and in the pearlite.

The result is the presence of two very different types of metal structure. The last layer flowed on and any sections of previous layers not recrystallized, due to insufficient heat input during the flowing-in of the succeeding layer, have a dendritic metal. The remainder of the flowed-in metal and the steel adjacent to the weld have a highly refined structure. The grain refinement in the base steel does not usually extend to a distance from the weld exceeding $\frac{3}{32}$ in. from the edge at the surface. Toward the root, the width of the affected zone increases; this increase, however, is less than the decrease in the width of the weld with the usual 45-deg bevel. Absence of the intermediate zone of larger grains between the two types of metal mentioned before indicates a condition similar to those of "laps" in gas welding and may be the result of an interruption in the welding of a layer when the metal on restarting is not fused to the last fused-in metal. (See Fig. 10, weld No. 2, *d*.) The conditions are illustrated by Figs. 11 to 22.

The ratio of the thickness of the two layers is of importance for the overall properties of the weld. It depends, of course, on the number of passes or layers employed, the relative amount of refined metal being increased with an increase in the

number of layers. Two-layer welds usually show the thickness of the outer layer to be about 50 per cent of the throat line, the volume being 50 to 70 per cent. With more layers, this relative thickness decreases, in general, though there are cases in which we have found the total thickness of unrefined metal to be 67 per cent in a three-layer weld, on account of insufficient recrystallization due to the use of thin layers with low heat input.

The determination of the properties of an electric-arc weld by means of tensile tests frequently disregards the fact that the usual tensile specimen contains a much smaller percentage of fibrous dendritic metal than the actual weld, and is therefore not representative. Welds made by bare-wire welding shall be excluded from further consideration, since their properties make them unsuited for use at high pressures and temperatures. The mechanical properties of the dendritic metal are influenced by the directional grain arrangement. The recrystallized weld metal usually has high strength and ductility.

Bending tests offer conclusions in regard to the differences in ductility between the layers. If the outside of an unmachined weld is at the outside of the bend, the fracture usually runs through the outer layer at an angle of 90 deg to the surface, parallel to the direction of the fibers. It often changes its direction at the separating line between outer and inner layer, following the softened zone between chilled and refined metal, sometimes even splitting to both sides of the original fracture. The ductility of the inner layer is generally high. When bending tests are made for determination of the ductility of a weld, removal of the reinforcement keeps the specimen from being truly representative of the weld. In our experience, sideways bending of specimens about $\frac{3}{16}$ in. thick gives a better idea of the ductility of a weld than the usual bending test, especially since all sections of the weld are subjected to uniform amounts of stretching.

As with gas welds, Rockwell hardness tests can give a fair idea of the relative strength of the various types of metal of an electric-arc weld made with coated wire. The hardness ratio between chilled and refined metal varies. The steel close to the weld shows large changes, the metal adjacent to the weld being decidedly harder than the original steel. The transition zone from increased to normal hardness is frequently so small that it is indicated only by its behavior during bending tests.

WELDING STRESSES

During welding, first an expansion of the parent metal occurs on heating, and is followed by a contraction of the solidified weld metal and the heated base steel during cooling. As far as expansion and contraction cannot be taken up by free movement of the material or by deformation, they result in cracks, or at least in residual stresses, lowering the resistance of the metal to stresses imposed from the outside. It is surprising that designers of welded structures often do not realize the importance of this simple mechanical process.

Roughly, welding stresses may be either general or local. General stresses are those resulting from the expansion or contraction of the weld as a unit. It is evident that these stresses increase with the amount of flowed-in metal per inch of weld. Accordingly, the weld should be not larger than necessary to obtain good penetration. A double-V weld is preferable in this respect to the single-V wherever the size of the equipment permits welding from both sides. With single-V welds, a decrease in flowed-in metal and heat input may be obtained with heavy wall thicknesses by decreasing the angle of the bevel, and accordingly the width of the weld.

General stresses are lowest in circumferential welds, which are the most frequent type of pipefield joints. The expansion merely causes a slight increase in diameter, the contraction a decrease, part of which is balanced by the preceding expansion. The residual stresses remaining after contraction are smallest with oxyacetylene

welds, since the plasticity of the large amount of heated steel is higher than of the cooler steel close to electric-arc welds; accordingly, it can take up a greater amount of deformation close to the weld and distributes the contraction stresses over a longer length of the pipe. With heavy wall thicknesses, the residual stresses in a weld may be higher as a result of the greater stiffness of the pipe. The influence of the factor of rigidity suggests that the size of residual inner stresses may be determined by the combination of diameter and wall thickness rather than by the thickness alone.

Other types of welds do not always offer as favorable possibilities of deformation as circumferential welds. This is true not only with T-welds and angle welds, but also with all methods so far suggested and used for strengthening circumferential pipe welds by welding on reinforcing members. If sleeves are used which cover the butt weld and are fixed to the pipe by circumferential fillet welds, the sleeve and the section of the pipe between fillet welds are usually too rigid to take up the contraction stresses of the welds by deformation. The situation is still less

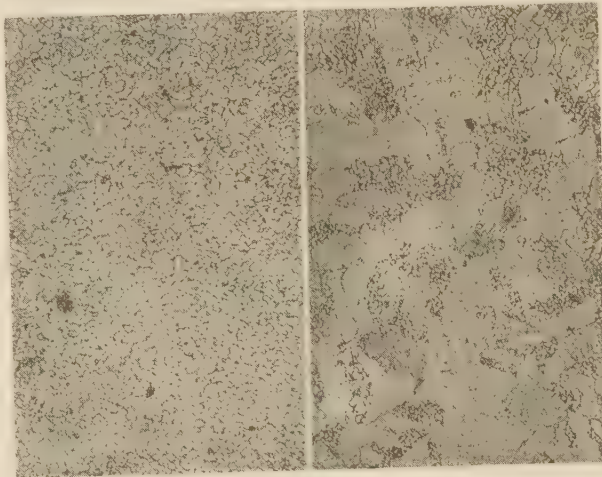


Fig. 21

Fig. 22

FIGS. 21 AND 22 MICROPHOTOGRAPHS OF ELECTRIC-ARC WELDS, COATED WIRE $\times 100$

(Figs. 21 and 22, changes in steel near weld.)

favorable if heavy longitudinal straps are used as reinforcements. Such straps are attached to the pipe by fillet welds, either all around or along the longitudinal edges, excepting at the pipe butt weld. The material between fillet welds is extremely stiff, and the cooling contraction of flowed-in and heated metal results in high stresses within weld, pipe, and strap. Since, in addition to welding stresses, operating conditions impose stresses caused by temperature differences between pipe and reinforcements, the value of such safeguards is doubtful, and it seems certain that they weaken the joint rather than strengthen it.

Local stresses are caused by uneven cooling within the weld and can be aggravated by lever action, especially at the start of a thin metal weld, since the slower heat transfer to the air

TABLE 1 ROCKWELL HARDNESS TESTS OF OXYACETYLENE WELDS

Material and heat treatment	Hardness			Difference from unheated steel—		
	Steel Not affected by welding	Steel Close to weld	Weld metal	Steel Not affected by welding	Steel Close to weld	Weld metal
Boiler-tube butt welds:						
As welded	B61.0	...	B61.5	0	+ 0.5
Annealed at 1700 F.	B56.1	...	B61.5	- 4.9	+ 0.5
6-in. std. pipe butt welds:						
As welded	B81.7	B82.1	B85.0	0	+ 0.4	+ 3.3
Annealed	B64.1	B70.1	B73.6	-17.6	-11.6	- 8.1
Annealed at 1100 F.	B61.1	B61.1	B67.6	-20.1	-20.6	-14.1
Annealed at 1650 F.						



Fig. 23

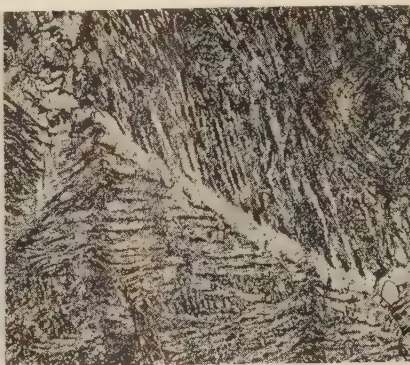


Fig. 24

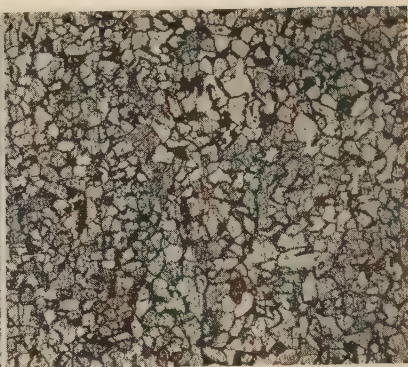


Fig. 25

FIGS. 23 TO 25 MICROPHOTOGRAPHS OF BOILER-TUBE METAL $\times 100$
(Fig. 23, unwelded boiler tube; Figs. 24 and 25, boiler-tube metal $\frac{1}{4}$ in. from butt weld before and after anneal at 1700 F.)



FIG. 26 MICROPHOTOGRAPH OF SHARP-EDGED INCLUSION $\times 100$
(At transition between inner and outer layers of coated-wire electric-arc weld.)

keeps the starting point softened longer than the adjacent metal, which is cooled by heat transfer to the metal. These stresses can be equalized only by sufficient ductility of the metal.

If the residual stresses in a weld joint are large, whether general or local, it is probable that the metal has been stretched to nearly the limit of its ductility. As a result, only small additional stresses, especially impact or repeated stresses, are likely to cause local or general failure. The ductility of such

metal, unless cracks actually have been formed, can be restored by heating, which in addition relieves the stresses.

Experience and tests indicate that residual stresses in a circumferential joint made by oxyacetylene welding are usually very small, due to the characteristics mentioned before. Annealing is therefore likely to weaken the weld rather than strengthen it, and may even increase the difference in properties between pipe and weld metal, due to the difference in reaction under recrystallization. Table 1 suggests the advisability of investigation in every single case warranting especial care. In the case of the boiler tube which was not weakened seriously by the annealing treatment, a comparison of Figs. 23 to 25 indicates that the structure should be normalized.

The conditions are different with electric-arc welds in which localized heating to high temperatures results in high unrelieved stresses and plastic hot and cold deformation. Annealing treatment of bare-wire welds is not practicable, and may even result in weakening of the weld—a condition which has been attributed to the growth of nitride needles on slow cooling and to the presence of nitrogen in solid solution with the iron on quick cooling. As far as welds made with coated electrodes are concerned, the effect of annealing on the pipe metal should be determined and should be considered in the calculation of permissible fiber stresses. The increased differences in hardness between pipe and weld metal after annealing, shown in Table 2, are not necessarily detrimental, since the ductility of each metal is increased by the annealing. Heating above the critical point is required for removal of the columnar structure in the outer layer and for equalizing the properties within the base metal and within the flowed-in metal.

STRESS CONDITIONS AT WELDS

The final point to be considered is the influence of the properties of welds on the behavior under operating stresses. This point will be better understood after a short review of some actions of metals under stress.

Whenever the unit stress in a metal exceeds the yield point, stretching takes place until the work hardening has increased

TABLE 2 ROCKWELL HARDNESS TESTS OF ELECTRIC-ARC WELDS WITH FLUX-COATED WIRE

Material and heat treatment	Hardness				Difference from unheated steel			
	Steel Not affected by welding	Steel Close to weld	Weld metal Outer layer	Weld metal Inner layer	Steel Not affected by welding	Steel Close to weld	Weld metal Outer layer	Weld metal Inner layer
6-in. std. pipe butt welds:								
As welded.....	B81.7	B85.4	B89.4	B92.2	0	+ 3.7	+7.7	+10.5
Annealed at 1100 F.....	B84.1	B71.4	B89.0	B86.0	-17.6	-10.3	+7.3	+ 4.3
Annealed at 1650 F.....	B61.6	B61.7	B76.0	B76.3	-20.1	-20.0	-5.7	- 5.4
1/2-in. low-carbon steel-plate double-V welds:								
Annealed at 1100 F.....	B68.9	B73.4	B82.2	B77.6	Hardness of unwelded steel not known			
Annealed at 1680 F.....	B71.3	B71.3	B78.9	B75.2				

the yield point to the unit stress. If the overload is confined to part of the cross-section, the local deformation affords an additional relief by distributing the stress over a larger cross-section area. The maximum amount of local stress concentration to be taken up is limited by the ductility of the metal.

Below the yield point, failure can be caused by repeated stresses to a point above the "fatigue limit." Close to the fatigue limit, failure is caused by millions of stress reversals; with increasing load, the number of stress repetitions required to cause a fracture decreases rapidly. Stress concentrations are especially dangerous, since deformation does not take place, and therefore ductility cannot give relief. If large residual stresses are present in the metal, even small operating stresses may lead to fatigue conditions.

The detrimental effect of voids or inclusions is due largely to the stress concentrations in the metal next to them; these are highest at sharp corners (Fig. 26). The stress concentration at inclusions is sometimes indicated by cracking during cooling (Fig. 27). An especially serious form of voids is presented by poor penetration or by lack of fusion at the root of the weld, since the wedge effect causes high stress concentration at a point of maximum operating stress. Fig. 28 shows inclusions and poor penetration of head welds; the weld shown by Fig. 28c appeared to be very good until it was cut.

The influence of structural differences on stress conditions is best demonstrated by an examination of the bending fracture, a sketch of which is shown by Fig. 29. The weld was a double-V butt weld, made in a shop and stress relieved at 1100 F for removal of contraction stresses. The fracture occurred in accordance with the structural properties, with a rough break

parallel to the fibers in the outer layers, smooth silky surfaces in the inner layers, and changes of direction in the transition zones. Evidence of stresses caused by structural differences is offered by the branching crack in one of the transition zones. Before bending, this section was found to be sound. If the crack were the result of bending alone, in the absence of inner stresses, it would be widest at its mouth and would have a sharp root. The size of the inner stresses is indicated by the fact that splitting occurred even before the bending had proceeded far enough to cause grain deformation of the inner layer (Figs. 30 and 31).

Just as lack of ductility of the metal may lead to local stress concentrations and failures, rigidity of the weld within the pipe causes stress concentrations in weld and adjacent pipe metal. In this connection, high ultimate elongation of the weld metal is of little importance if the welded pipe would fail under a pressure imposing a unit stress on the weld metal far below the

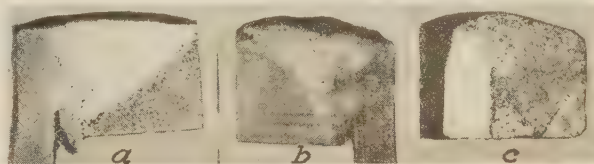


FIG. 28 HEAD WELDS SHOWING POOR PENETRATION AND VOIDS (a and b, faults showing on inner surface; c, fault disclosed by cutting.)

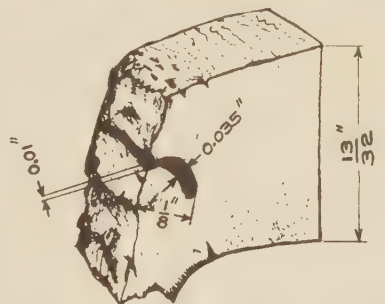


FIG. 29 FRACTURE OF BENDING TEST (Electric-arc double-V butt weld. See Figs. 30 and 31.)

ultimate strength or even below any other stress causing appreciable deformation. High tensile strength of weld metal and reinforcement contribute to rigidity of the weld. The aim should be to obtain a weld as similar in all properties to the pipe as possible and not to get weld metal as high in tensile strength and ductility as possible.

Selecting covered-wire electric-arc welds as representatives of high-strength welds and oxyacetylene welds to represent flexible welds, a comparison of both elastic and plastic deformation is offered by the following two tests.

Fig. 32 shows the stress-strain relationship of the two types of welds. As a result of the reinforcement, the oxyacetylene weld does not follow the expansion of the pipe as readily as it would, according to the close similarity of the properties of the two metals—shown by Fig. 33. The electric-arc weld, however, has a much higher rigidity, even though in this case poor penetration has cut down the stress-carrying cross-section area.

The behavior of the two types of welds under plastic deformation is evident from Fig. 34. The rigidity of the electric-arc welds—i.e., the butt welds of Nos. 1, 2, and 4 and the head welds of No. 4—resulted in stress concentrations at the welds which caused splits originating in the pipe to continue through the butt welds or close to the head welds. The greater plasticity of the oxyacetylene welds served to distribute the stresses more evenly,



FIG. 27 MICROPHOTOGRAPH OF INCIPIENT CRACK $\times 100$ (Caused by stress concentration at inclusion during cooling.)

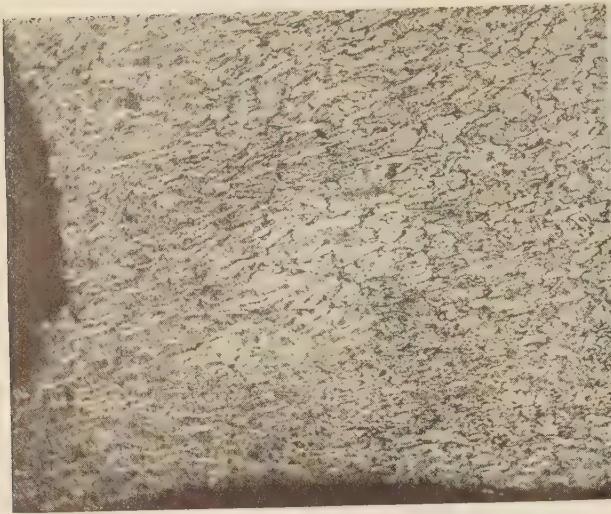


Fig. 30

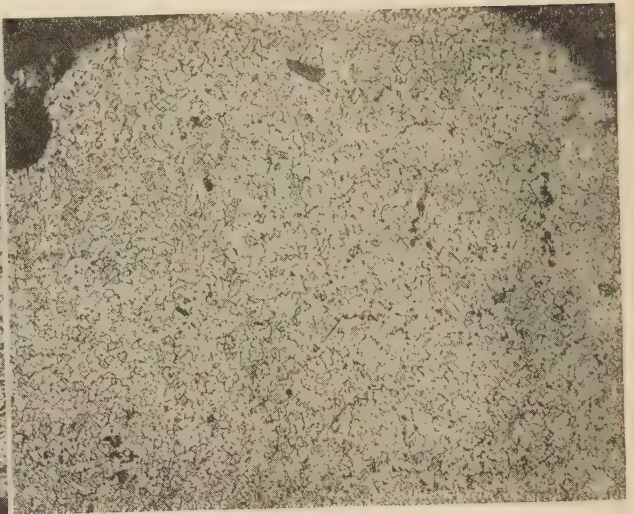


Fig. 31

FIGS. 30 AND 31 MICROPHOTOGRAPHS AFTER BENDING TEST OF SPECIMEN OF MACHINED ELECTRIC-ARC DOUBLE-V BUTT WELD, FLUX-COATED WIRE $\times 100$

(This is of test shown in Fig. 29. Structure at either side of mouth of branching crack.)

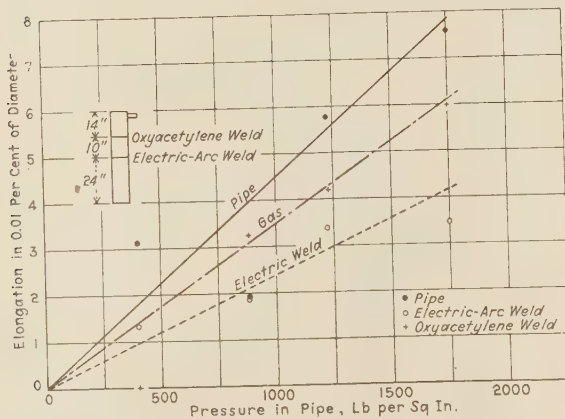


FIG. 32 EXPANSION TEST OF 8-IN.-PIPE BUTT WELD

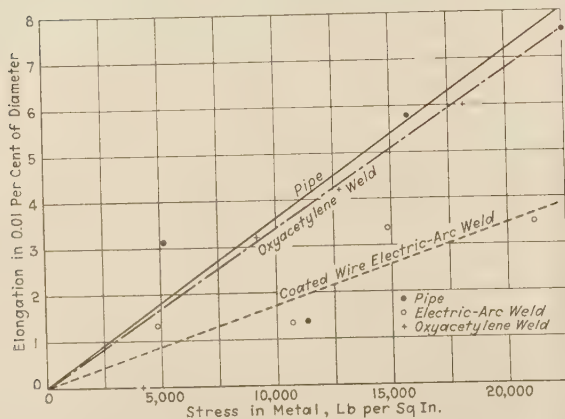


FIG. 33 APPROXIMATE STRESS-STRAIN CURVES OF 8-IN. PIPE AND UNMACHINED BUTT WELDS

a condition which limited the extension of the fracture, permitted a uniform rate of expansion (as shown by Table 3), and increased the bursting strength of the specimen. This result

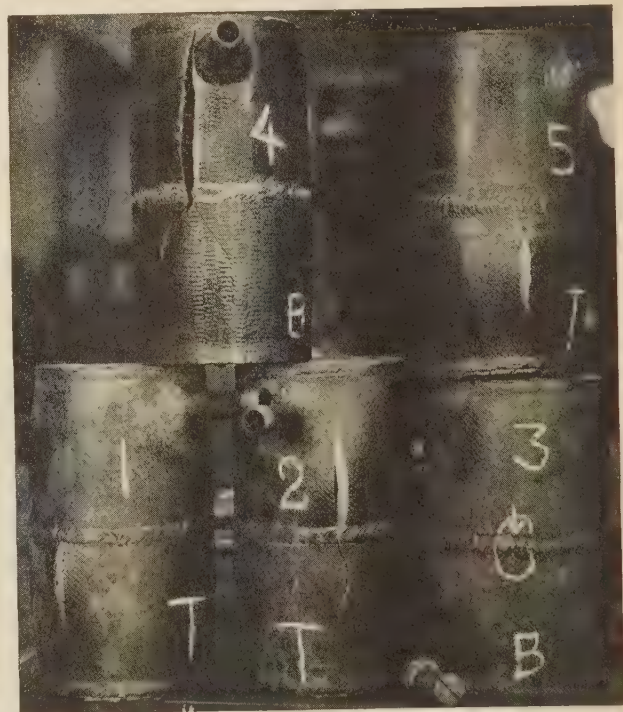


FIG. 34 SPECIMENS OF 6-IN. STANDARD-PIPE BUTT WELDS BROKEN BY INTERNAL HYDRAULIC PRESSURE

was obtained in spite of the fact that the tensile strength of the electric-arc weld metal was 10 per cent higher than that of the oxyacetylene-weld metal. The importance of the stress concentration is indicated by the fact that the breaking stress of the electric-arc metal was less than 70 per cent of its tensile strength, if the stress concentration is disregarded.

TABLE 3 MAXIMUM EXPANSION OF PIPE AND BUTT WELD OF SPECIMENS SHOWN BY FIG. 39

	Pipe	Weld
Electric-arc welds, per cent.....	12.5	8.3
Oxyacetylene weld, per cent.....	11.3	11.1

CONCLUSIONS

If these investigations, which have been based on our own tests as well as on service experiences extending over many years and on some published and unpublished data obtained elsewhere, indicate that in this case oxyacetylene welding fills the requirements in regard to soundness and adaptation to service conditions better than electric-arc welding, it is not intended to claim any general superiority of gas over electric-arc welding. Investigations of other types of welded joints have indicated that in many cases the properties of electric-arc welds made with covered wire, or sometimes even with bare wire, may be better suited to the particular conditions and requirements.

Discussion

GEORGE C. EATON.² The author's conclusion is that the oxyacetylene method at present offers more certainty of a thoroughly sound weld than electric-arc welding, but the writer believes that the day is not far off when electric welds made in the field will be far superior to the other type. This company has used welding of pressure pipe lines for over eight years. The first use of any magnitude was during the building of the first section of Edgar Station in North Weymouth. Oxyacetylene seal welding of Sargol joints on steam piping was used extensively. No butt welds of any type of piping were made at this time. Sargol joints have since been used for both steam and feedwater piping in the high-pressure additions to the station.

In practise the use of oxyacetylene welding for resealing the Sargol joints, after breaking for maintenance work, has not been continued. We use electric welding instead for this reason: When breaking the weld, it is necessary to chip away the weld metal, and in doing so it is impossible not to remove part of the joint lips. After several breaks and rewelds of one joint, a failure of the pipe metal was found at the flange due to the heating by the oxyacetylene-welding procedure. Since that time we have used the electric-arc method, which enables us to readily build up the lips without endangering the pipe metal.

It may be interesting to know that we have also substituted a thin soft-iron gasket for the seal weld on a number of joints with consistent success. Our operators and repair foreman are strongly in favor of electric-arc welding over oxyacetylene for all purposes except brazing of thin metal and cutting.

In the addition to Edgar Station in 1927, we have used butt-welded pipe lines for water up to 30 lb per sq in. pressure and steam piping up to 120 lb per sq in. pressure and 525 F. No trouble with these welds as made by the oxyacetylene method has developed.

At our Kneeland Street Steam Heating Station in Boston, butt-welded boiler-feed lines up to 325 lb per sq in. have been used successfully since the first installation in 1930. The oxyacetylene-welding method was used in this case because of the portability of the equipment.

In the steam-heating distribution system all joints of the recent additions built for 200 lb per sq in. have been oxyacetylene welded. The joints of one of the earlier welded jobs were annealed, as it was then felt worth while. Subsequently this practise was given up because it was not considered that the cost of the annealing justified the results obtained. The largest pipes yet welded have been 16 in. in diameter. It is believed that annealing of welds on pipes over 24 in. in diameter when installed will be economically justified in the light of present practise.

F. P. FAIRCHILD.³ The use of welded joints for pipe work in power-station practise is relatively new. Our company has recently completed two installations for the Public Service Electric and Gas Company in which all the line joints are welded. One of these installations is for a pressure of 700 lb per sq in. and a total temperature of 850 F, and the other for 375 lb pressure and 750 F temperature. To as great an extent as possible pipe joints were made in the fabricator's shop by the electric-arc-weld process, using coated wire. Field welds were made by the oxyacetylene process. The welders were qualified for the work by demonstrating their ability to make sample welds to meet requirements as to ductility, tensile strength, grain structure, porosity, fusion, penetration, and absence of slag inclusions. The actual welding work in the field is also witnessed by a qualified inspector.

A large number of samples tested showed failure of the welds to penetrate to the bottom of the V, and some trouble has been experienced with deposits of welding material inside the pipe. Both of these difficulties can be largely overcome by the exercise of sufficient care on the part of the welder. However, in order to eliminate the human element as far as possible, the practise has been adopted of inserting a 1/16-in. by 1-in. ring of metal inside the pipe under the weld. The ring is tack welded to one of the pipes before putting the ends together. It acts as a base for starting the weld and permits the welder to get full penetration without the formation of stalactites inside the pipe. At Burlington Generating Station the inside rings were not used, but reinforcing strips were placed longitudinally on the outside of the high-pressure pipe. On the installation at Kearny Generating Station, the rings were used on the most recent work, and the reinforcing strips were omitted except on field nozzle welds, where the reinforcing strips are still thought advisable.

Field welds are annealed by heating to approximately 1200 F. In order to assure slow cooling, a special removable box packed with asbestos is placed over the joint before heating and the pipe ends are closed to prevent inside air circulation.

Valves up to 10 in. in size have been welded into the line. The larger valves are the screwed-end type, with short pipe nipples screwed and electric arc welded into each end in the manufacturer's shop. The field welds are then only an ordinary pipe weld between the nipples and the pipe. On smaller valves, 2 in. and under, the valve body is machined down to pipe size and welded directly into the line. By using the proper tips the temperature of the valve body never exceeds 750 F, and there is no danger of warping of the valve seat or disk due to excessive heating. Small water-cooling jackets were at first provided to insure against exceeding this temperature, but later were found to be unnecessary. The stresses which can be transmitted to the valve during welding are materially reduced by the pipe nipples on the large valves. On the small valves the relatively thin part of the valve body, where it has been machined down to pipe size, serves the same purpose.

Because of the human element involved in making welds, the tests of finished work must be extra rigid. Samples of welders' work can only indicate their ability and conscientiousness and do not absolutely insure against faulty work. Installations of this kind should be hydraulically tested to at least twice the working pressure and be hammered while under pressure as heavily as the thickness of the material permits.

There is little doubt that eventually the electric method of welding will develop to a point such that it can be used for field work, except perhaps for special cases, and will give more satisfactory results than the gas method. However, we are in agree-

² Mechanical Technical Engineer, Generating Department, Edison Electric Illuminating Company, Boston, Mass. Jun. A.S.M.E.

³ United Engineers and Constructors, Inc., Philadelphia, Pa. Mem. A.S.M.E.

ment with the author of the paper that this state of the art has not yet been reached.

O. A. TILTON.⁴ Fortunately there is a considerable volume of published data of a reliable nature available indicating the characteristics of welds. Today there is no excuse for the designing engineer who approaches the subject with an open mind not knowing exactly what he has to work with in using welds. Such organizations as the American Welding Society and the A.S.M.E. have established Tentative Codes for Pressure Piping which have set forth the conditions that must be met by suppliers of raw materials and the performance characteristics that may be demanded of the finished weld. These factors are thereby established as the essential elements to permit of the use of welding in such work. Manufacturers of electrode wire have readily met these requirements and have been spurred on by the healthy element of competition to provide complete tabulated physical characteristics of welded joints producible with their electrodes, basing their results on standard test specimens and methods, which standards have likewise been established by the national bodies interested in this work.

The standard joint for arc-welded pipe is of the single-V type. The following is from a specification used by the General Electric Company for field-welded joints of pipe from 2 in. to 18 in. diameter, inclusive: "The pipe ends shall be beveled to an angle of 45 deg and with a width of flat at the end of the pipe of $\frac{1}{32}$ in. plus or minus $\frac{1}{32}$ in. The angle of bevel shall be measured from a line drawn perpendicular to the axis of the pipe."

Experience has shown that good quality weld metal and penetration at the bottom of a V are obtained when chill rings are used. On pipe sizes up to and including 4 in. in diameter they are not necessary, but on sizes greater than 4 in. in diameter it has become standard practise with our company to use chill rings, thus insuring a joint of 100 per cent cross-section of good weld metal. In heavy walled piping where several passes are necessary each pass is limited to not over $\frac{5}{32}$ in. in thickness per layer. Stress relief is accomplished in several ways. In some cases this is done by peening each layer thoroughly. In the great majority of cases, however, the pipe wall is relatively so thin that stresses set up by welding are negligible. Each subsequent layer of weld metal partially strain-relieves the previous layer and refines its structure. It is therefore a standard element of the American Welding Society's tentative welding specifications that the top of the next to last bead of a weld shall be $\frac{1}{16}$ in. above the surface of the parent metal. This insures a joint of 100 per cent thickness of refined and strain-relieved weld metal.

The statement is made that oxyacetylene welding has proceeded to a stage where its success depends entirely upon the judgment, skill, and carefulness of the welder, whereas electric-arc welding has not proceeded this far. It is a mistake to assume that either process is entirely dependent upon these factors. In our opinion these are but three of the important factors and may be summed up into one term—namely, "proper qualification of the welder." Other equally important factors are rigid adherence to design specifications for material and joints, engineering specifications as to electrode diameter, welding current, arc voltage, thickness of layers, speed of welding, and technique. These factors are all controlled by systematic supervision and inspection, by the consistent testing of specimens cut from the work, and by proper qualification tests of operators before employment, as well as periodical checking of this qualification from time to time as the work progresses. Electric-arc welding most certainly has progressed to the point where its success is

definitely predictable and is dependent less on the human element than on correct engineering and intelligent supervision. It is therefore entitled to recognition as an exact science available as a construction tool.

Another statement is made that a weld can be considered reliable even when certain deficiencies are present to a limited extent and that the gradual elimination of such defects should be required of the welder. This is hardly admissible in present-day practise in welding. We ourselves consider piping generally to come under the classification of "class II pressure vessels," as described in the A.S.M.E. Boiler Construction Code for Unfired Pressure Vessels. This code differentiates between class I and class II vessels mainly in that class I vessels can and must be X-rayed, whereas class II vessels need not be. The other physical property requirements are equally as rigid. Welders who cannot meet these requirements consistently should not be, and are not, permitted to engage in such work. Experience has shown that with the arc-welding materials and procedure as they are known today such qualification of welders is not too rigid and there is no need for accepting any lower quality of workmanship.

Reference to the presence of small voids, air and gas pockets, and inclusion of oxides, slag, and other foreign matter in welds leads the writer to assume that the author believes these are still necessarily met in the arc-welding materials and procedure of today. Such imperfections were common in the welds made with bare or lightly coated electrodes of a few years ago, but such materials are no longer used in this class of work. Heavily coated electrodes are now used exclusively for pipe-line systems.

The General Electric Company is now installing a 14-in.-in-diameter, $\frac{1}{2}$ -in.-wall arc-welded steam pipe line at its plant in Schenectady. This line is designed for operation at 400 lb pressure and 750 F. The following results are taken from qualification tests made by two of the welders: Average tensile, 64,033 lb per sq in.; average elongation (free bend), 50.6 per cent. In this particular project we are perhaps a little ruthless in our methods of testing the welders. Each man is required to weld a set of qualification test samples after every 20 joints, and is not permitted to continue until these are tested and his work is found to be of required quality. In addition one completed joint is cut out of the line at random from every 20 completed joints and is subjected to a complete set of tests.

Although oil pipe lines are not strictly comparable with steam and water lines, it is interesting to note that a survey made by the American Gas Association showed that there are 5000 miles of this kind of welded pipe lines in the country today, with no reports of serious failures of any of the welded joints. A large refiner in Pennsylvania has just completed a 200-mile gasoline transmission line of seamless-steel tubing of 6 in. and 8 in. diameters. All joints were welded and with electrodes of the heavily coated type.

In the new factory of the Cleveland Wire Works of the General Electric Company the entire piping system for steam, water, and process gases has been installed by arc welding, using the heavily coated type of electrode.

It will be interesting to note the relative effect of corrosion on arc welds of the type mentioned and on the parent metal. Test welds made on A.S.M.E. specification S1 steel boiler plate have been immersed in a 50 per cent solution of hydrochloric acid at room temperature for 86 hours, and show no greater corrosion of the weld than of the plate itself. Welds made with ordinary bare or lightly coated electrodes, when subjected to this test, show a very spongy appearance of the weld, due to the unrefined metal and the inclusion of oxides and nitrides which are quickly attacked by the acid.

It is commonly believed by some, and stated by this author,

⁴ Industrial Engineering Department, General Electric Company, Schenectady, N. Y.

that an inherent characteristic of welds made with the heavily coated electrodes is an undercutting at the edges of the weld. Our experience has shown that this is an erroneous idea. If an electrode is of the proper design and used by a competent operator, there is no excuse for undercutting.

The writer is in agreement with the author's statements as a whole, and although it has been indicated that arc welding is considerably more advanced than the paper would lead one to believe, this discussion should be considered as completing the story rather than unduly criticising it.

ALBERT SAUVEUR.⁵ In his critical review of the features of the electric-arc welding and of the oxyacetylene welding of pipes in field work, the author seems to favor the latter method. Only the metallurgical side of these operations comes within the writer's province. In arc welding, the possibility exists of obtaining the weld metal in a fine-grained condition, owing to the refining influence of each layer or bead on the preceding layer upon which it is deposited. The first layer is rapidly cooled, and therefore becomes somewhat martensitic in structure. This implies hardness and lack of ductility. Upon the deposition on this layer of a second layer, the former is reheated above its thermal critical temperature. Recrystallization takes place, resulting in a fine-grained ductile structure. Each layer in this fashion refines the layer upon which it is deposited. In gas welding, on the contrary, owing to the preheating of the base metal, the liquid steel cools relatively slowly and acquires a coarse structure which it would seem must lack the ductility and probably the strength of a fine-grained structure.

It has often been said, and rightly so, that the metal deposited in welding is necessarily in a cast condition. In arc welding, however, this casting may be annealed during the process of welding, whereas in gas welding such a possibility does not exist.

C. A. ADAMS.⁶ The average gas weld is for some purposes superior to the average bare-electrode arc weld, particularly when ductility is important. On the other hand, arc welds with heavily covered electrodes are regularly being made in the commercial production of class I pressure vessels that are superior to the best gas welds. However, some of these electrode coverings are of such a nature as to make overhead welding difficult, if not impractical. With one type of covered electrode, it is possible to make overhead welds of high quality, but for field work such as described in the paper it is probably true that one is more likely to get satisfactory results from gas welding than from electric-arc welding on the overhead part of the job, although it is entirely possible to do equally satisfactory work with the proper type of covered electrode.

The major purpose served by an electrode covering is the protection of the molten and hot metal from contamination by the atmosphere, since both oxygen and nitrogen would otherwise be absorbed by the molten metal in passing across the arc and seriously affect the quality of the deposited weld metal. The oxides and nitrides in such quantities as appear in bare-electrode arc welds do not detract from the tensile strength, but do detract seriously from the ductility of the weld.

In a gas weld made with a proper mixture of acetylene and oxygen, the hot metal is protected by a considerable envelope of the products of combustion which are normally neutral.

There are two principal types of electrode covering: one a slag covering, which is quite unsuited for overhead welding; the other is a covering of carbohydrate material with some combus-

tion retarder such as sodium silicate or water glass. In this case the covering is largely converted into a protective reducing gas envelope by combustion, and there is a negligible amount of slag. With this type of electrode covering it is possible to make good overhead welds, although considerable skill is required. The purpose in presenting this discussion is to prevent a possible misinterpretation of the author's conclusions, which are, within the field covered by the paper, substantially correct.

AUTHOR'S CLOSURE

Without going into a detailed analysis of the conditions, the author would say that electric-arc welding should be superior to oxyacetylene welding in the sealing of Sargol joints, as mentioned by Mr. Eaton. This particular type of work does not require any flexibility or a weld completely free from inclusions, while the greater heat input of oxyacetylene welding is detrimental, especially if the joint is occasionally broken.

The use of reinforcements in the case of nozzle welds, mentioned by Mr. Fairchild, is justified only by the weakening of the pipe; in other words, the pipe is reinforced, not the weld itself. The suggestion made in the paper that the stress concentrations necessarily resulting from the use of reinforcing straps may weaken the welded joint has been substantiated by fatigue tests carried out at the instigation of the German State Railroads. Such tests showed failure of joints reinforced by straps after less than one-third of the reversals needed to cause failure of joints not reinforced.⁷ The reinforcements, accordingly, tended to weaken the joint rather than to strengthen it. The use of backing strips is much more desirable, both for oxyacetylene and electric-arc welds, especially if the cross-sectional shape is adapted to flow conditions in the pipe.

The statement quoted in the fifth paragraph of Mr. Tilton's comments related, of course, to deficiencies such as were discussed at that particular section of the paper, not to deficiencies as defined by the various codes. It should be kept in mind that, though the code has raised the standard of welds by making higher minimum requirements, compliance with the code does not relieve the user from the responsibility of analyzing the particular conditions of any one problem and of taking into account factors which are not covered by the code. Failure to realize this condition is responsible for the tendency found so frequently to overrate especially the importance of the tensile properties of the weld metal. A weld may be a weak point of any structure, in spite of very high tensile strength and ductility of the weld metal, if it causes stress concentrations by its shape or by relative rigidity resulting from its very strength.

Mr. Tilton's company kindly made an overhead weld for us to examine. While the weld was the best electric-arc overhead weld we have had an opportunity to test and while it filled all code requirements relating to strength and ductility of the metal, it failed to come up to the requirements regarding shape of reinforcement and relative freedom from voids or inclusions. The shape of the reinforcement, which in this case had its greatest thickness close to the edges, is detrimental whenever fatigue stresses appear in service. This condition is aggravated by undercutting; though this is not believed to be an inherent characteristic of electric-arc welds, it has been found generally or at localized spots in all extended welding jobs that the author has seen so far and to a slight degree even in the test weld mentioned. Inclusions and voids were the deficiencies to which the statement quoted by Mr. Tilton referred. Micrographs of some of the inclusions found in the test weld have been used in the paper to

⁵ Gordon McKay, Professor of Metallurgy and Metallography, Harvard University, Cambridge, Mass.

⁶ Lawrence Professor of Engineering, Harvard University, Cambridge, Mass. Mem. A.S.M.E.

⁷ "Dauerfestigkeit von Schweissverbindungen bei verschiedener Formgebung," by Prof. Dr. A. Thum, *V.D.I.*, vol. 77, no. 19, May 13, 1933. "Die Dauerfestigkeit der Schweissverbindungen," by G. Schaper, *V.D.I.*, vol. 77, no. 21, May 27, 1933.

supplement the illustrations of defects. The test weld, in general, corroborated the statements made in the paper.

Professor Sauveur touches on a problem which has occupied the author's attention at various times. Tensile and bending tests actually do show a ductility of the coarse-grained oxyacetylene weld metal equal or superior to that of the small-grained recrystallized electric-arc weld metal. The ductility of the unrefined layers of electric-arc welds is sometimes quite inferior, due not only to martensitic constituents, but also largely to the columnar grain arrangement. It is believed that the high ductility of the oxyacetylene weld metal is to be credited to the low residual stresses and, metallurgically, to the low carbon content resulting from the higher loss of carbon during welding, as compared with covered-wire electric-arc welding. While the low carbon content counteracts the effect of grain size in regard to ductility, there is a possibility that coarseness of the structure lowers the impact strength of the weld metal. Since there have been indications pointing to this condition in some instances, an investigation by notched-bar tests would be of value and is suggested to laboratories which have suitable testing equipment.

The necessity of using several layers in electric-arc welding has advantages from the metallurgical point of view, as pointed out by Professor Sauveur. The disadvantage, especially in field

welding, is that pieces not only of slag, but of oxide scale, are entrapped by subsequent layers. Before electric-arc welding can be considered entirely satisfactory in field welding involving the service factors considered in the paper, it will be necessary to find ways that will positively insure the removal of all slag and scale on the surfaces of intermediate layers. The choice of a covering in accordance with Professor Adams' suggestions is one step in this direction. It is necessary, furthermore, to develop electrodes and welding procedure to a stage at which overhead and any other type of field welding can be done successfully by a good welder, without unduly high demands on skill or precautions.

The opinion was variously advanced or indicated during the discussion that electric-arc welding would soon or ultimately be superior to oxyacetylene welding. The author believes "superiority" to be a relative term inasmuch as he is aware of many types of welds for which even now he considers electric-arc welding "superior." Progress in further insurance of soundness, reduction of residual welding stresses, increase of weld flexibility by improved control over weld metal properties, and better realization of the factors influencing fatigue resistance are points to which the paper was intended to direct attention for the benefit of power piping welding and, perhaps, of many other applications of welding in general.

Roller-Bearing Service in Locomotive, Passenger, and Freight Equipment

By T. V. BUCKWALTER,¹ CANTON, OHIO

Modern civilization is based on transportation, and the fundamental prime mover in transportation is the steam locomotive. Improvements in the steam locomotive affecting its efficiency and reliability are reflected in a corresponding manner in the entire transportation industry. The loads and stresses developed in locomotive service on bearings are exceptionally severe, and the consequences of failure are far reaching, and these conditions together have militated against rapid introduction of the roller bearing in locomotive service. The application of the roller bearing in passenger service has progressed in an encouraging manner over a period of years, but efforts to interest railroad men in application of roller bearings to a complete locomotive were unsuccessful, and finally convinced the Timken company of the desirability of building a locomotive equipped on all wheels with roller bearings and loaning it for an extended period of service to the railroads of the United States. The Timken locomotive



THE Timken locomotive was designed for application of Timken bearings on all of the drivers, engine-truck, trailer, and tender-truck wheels, on the Franklin booster, and on various elements of the control mechanism. The introduction of roller bearings on the drivers permits of higher rotative speeds, as the bearings surround the drivers completely, and eliminates pounds within the bearing boxes. Heating is eliminated, as the temperature rise does not exceed 25

deg above atmosphere. The wheel diameter was therefore selected between that prevailing for modern high-speed freight locomotives, averaging 70 in., and high-speed passenger locomotives, with 80-in. drivers. The economy in friction, estimated at 12 to 15 per cent, was utilized in increasing the diameter of the drivers over that of the modern freight locomotive, and developing through the saving in friction a drawbar capacity equivalent to the latter.

The 73-in. wheel was therefore selected. Careful proportioning of reciprocating parts and rods permits of operating the 73-in. driver at speeds sufficiently high to handle the existing American passenger-train schedules.

¹ Vice-President, Timken Roller Bearing Company. Mem. A.S.-M.E. Mr. Buckwalter entered the employ of the Pennsylvania Railroad at the Altoona Works in 1900, and after six years of shop experience was transferred to the motive power engineering department, continuing work on automotive engineering matters until 1916. He developed the electric baggage, mail, and express trucks generally used at railway terminals throughout the world. He was Chief Engineer of the Timken Roller Bearing Company from 1916 to 1922 and Vice-President since 1923.

Contributed by the Railroad Division and presented at the Semi-Annual Meeting, Bigwin Inn, Lake of Bays, Ontario, Canada, June 27 to July 1, 1932, of THE AMERICAN SOCIETY OF MECHANICAL ENGINEERS.

NOTE: Statements and opinions advanced in papers are to be understood as individual expressions of their authors, and not those of the Society.

was designed for application of Timken bearings on all of the drivers, engine-truck, trailer, and tender-truck wheels, on the Franklin booster, and on various elements of the control mechanism. The introduction of roller bearings on the drivers permits of higher rotative speeds, as the bearings surround the drivers completely, and eliminates pounds within the bearing boxes. Heating is eliminated, as the temperature rise does not exceed 25 deg above atmosphere. The wheel diameter was therefore selected between that prevailing for modern high-speed freight locomotives, averaging 70 in., and high-speed passenger locomotives, with 80-in. drivers. The economy in friction, estimated at 12 to 15 per cent, was utilized in increasing the diameter of the drivers over that of the modern freight locomotive, and developing through the saving in friction a drawbar capacity equivalent to the latter. The 73-in. wheel was therefore selected. The 4-8-4 wheel arrangement with four-wheel trailer truck was favored.

The weight was held within the limits imposed on certain American roads, namely, 61,000 lb per driving axle, but in order to compare reasonably with much heavier freight power on other roads a duplex steam pressure was utilized in connection with the weight transfer between the drivers and trucks, making available a weight of 66,000 lb per driver and a steam pressure of 250 lb on roads permitting of the heavier axle loads. The supporting of the large boiler capable of developing maximum power at high speeds favored the adoption of the 4-8-4 wheel arrangement with four-wheel trailer truck.

LOCOMOTIVE SPECIFICATIONS

The locomotive companies, the motive-power departments of the railroad companies, and the specialty companies assisted wholeheartedly in the selection of specifications for the locomotive and made available their enormous funds of information and data on locomotive design. The locomotive is a composite of specifications of a number of trunk-line railroads and was built as large and powerful as the clearance limitations of the principal railroads of the United States would permit. Specifications are as follows:

Owner, Timken Roller Bearing Company	
Builder, American Locomotive Company	
Type of locomotive, 4-8-4	
Service, freight and passenger	
Maximum rated tractive force (boiler pressure, 235 lb), lb.....	59,900
Rated tractive force of booster (boiler pressure, 235 lb), lb.....	12,000
Tractive force at starting (boiler pressure, 235 lb), lb.....	71,900
Maximum rated tractive force (boiler pressure, 250 lb), lb.....	63,700
Rated tractive force of booster (boiler pressure, 250 lb), lb.....	12,800
Tractive force at starting (boiler pressure, 235 lb).....	76,500
Weight on drivers ÷ tractive force (boiler pressure, 235 lb).....	4.10
Weight on drivers ÷ tractive force (boiler pressure, 250 lb).....	4.14
Cylinders, diameter and stroke, in.....	27 × 30
Valve gear, Walschaert type; valves, piston type, size, in.....	12
Maximum travel, in.....	8 1/2
Steam lap, in.....	1 1/2
Exhaust clearance, in.....	1/4
Lead, in.....	1/4
Cut-off in full gear, per cent.....	85
Weights in working order (boiler pressure, 235 lb):	
On drivers, lb.....	246,000
On trailing truck, front, lb.....	48,500
On trailing truck, rear, lb.....	55,500
On front truck, lb.....	67,500
Total engine, lb.....	417,500

Weights in working order (boiler pressure, 250 lb):

On drivers, lb.	264,000
On trailing truck, front, lb.	34,500
On trailing truck, rear, lb.	59,000
On front truck, lb.	60,000
Total engine, lb.	417,500
Total tender, lb.	294,000
Total engine and tender, lb.	711,500

Wheelbases:

Driving, ft.	19 ³ / ₁₂
Driving, rigid, ft.	12 ¹⁰ / ₁₂
Total engine, ft.	45 ¹⁰ / ₁₂
Total engine and tender, ft.	89 ⁹ / ₁₂

Wheels, diameter outside tires:

Driving, in.	73
Trailing truck, front, in.	36
Trailing truck, rear, in.	44
Front truck, in.	33

Journals, nominal diameter:

Driving, main, in.	11 ¹ / ₂
Driving, others, in.	11 ¹ / ₂
Trailing truck, front, in.	7 × 14
Trailing truck, rear, in.	9 × 14
Front truck, in.	7 × 12

Boiler (extended wagon-top type):

Steam pressure (weight on drivers, 246,000 lb), lb.	235
Steam pressure (weight on drivers, 264,000 lb), lb.	250
Diameter, first ring, inside, in.	84 ¹ / ₄
Tubes, 66 in number, diameter, in.	2 ¹ / ₄
Flues, 194 in number, diameter, in.	3 ¹ / ₂
Length over tube sheets, ft.	21 ¹ / ₂
Grate area, sq ft.	88.3

Heating surfaces:

Firebox and combustion chamber, sq ft.	360
Arch tubes, sq ft.	18
Thermic siphons, sq ft.	105
Tubes and flues, sq ft.	4637
Total evaporation, sq ft.	5120
Superheating, sq ft.	2157
Combined evaporation and superheating, sq ft.	7277

Tender:

Water capacity, gal.	14,200
Fuel capacity, tons.	31
Wheels, diameter, in.	23
Journals, normal diameter and length, in.	6 × 11

Weight proportions (boiler pressure, 235 lb):

Weight on drivers ÷ total engine weight per cent.	59
Weight on drivers ÷ tractive force.	4.10
Total weight engine ÷ comb. heating surface.	57.4

Boiler proportions (boiler pressure, 235 lb):

Tractive force ÷ comb. heating surface.	8.24
Tractive force × diam. drivers ÷ comb. heating surface.	602
Firebox heating surface ÷ grate area.	5.47
Firebox heating surface per cent of evap. heating surface.	9.44
Combined heating surface ÷ grate area.	82.4

Weight proportions (boiler pressure, 250 lb):

Weight on drivers ÷ total engine weight per cent.	63.4
Weight on drivers ÷ tractive force.	4.14
Boiler proportions:	
Tractive force ÷ comb. heating surface.	8.77
Tractive force × diam. drivers ÷ comb. heating surface.	639

ROLLER-BEARING APPLICATIONS

The driver application was made without adjustable mechanism. Hardened steel trunnion guides are mounted on the bearing housings centrally pivoted to permit of the housing following track irregularities while maintaining full surface contact with the hardened steel liners on locomotive frame.

The forces due to piston thrust, therefore, are transmitted and absorbed in a complete train of moving parts composed of hardened steel. These comprise the pedestal liner, trunnion guide, hardened wear plates on the bearing housing, and the inner and outer races of the bearing, together with the rolls. The mounting construction is shown in greater detail on the elevations and cross-sections of the locomotive (Figs. 1 and 2). The accessibility of the bearings for inspection at major shopping periods is illustrated by a view of the axle assembly (Fig. 3).

The complete housing of the driver axles and the use of bearings restraining the axle on a complete circle of 360 deg eliminate pounding while under steam and while coasting, and, together with careful proportioning of reciprocating parts, permit of operation of 73-in. drivers at speeds of 85 mph.

The engine truck follows in general the construction of the driver. It utilizes the integral split housing, the trunnion guides, and one bearing for each wheel. The trailer trucks are designed for direct replacement of plain bearings, making no change in trucks, pedestals, or springs. The trailer is an outboard application and requires the double-bearing construction. The tender truck is likewise designed for direct replacement, using tender trucks, pedestals, equalizers, and springs designed for A.R.A. plain bearings.

The booster was applied on the locomotive to increase the

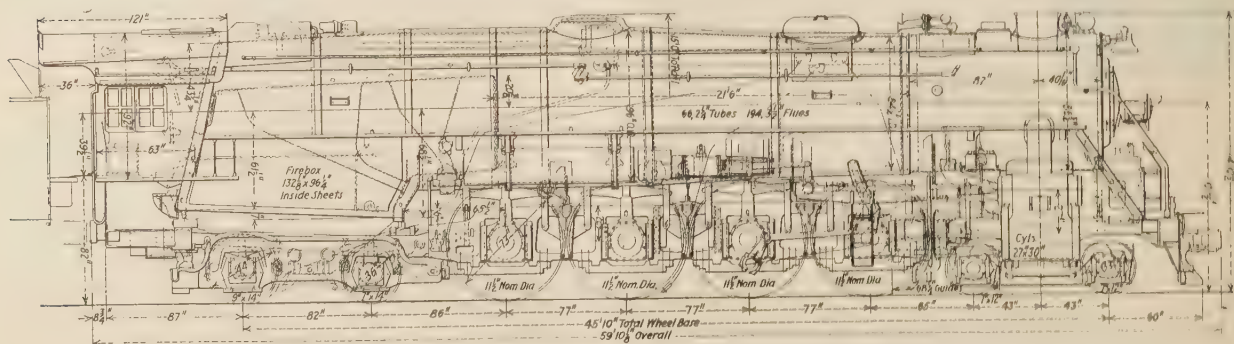


FIG. 1 ELEVATION OF THE TIMKEN LOCOMOTIVE

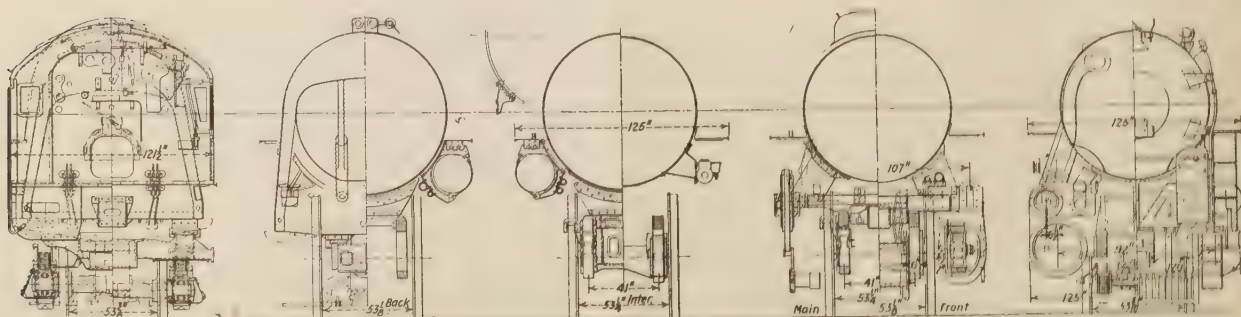


FIG. 2 CROSS-SECTIONS OF THE TIMKEN LOCOMOTIVE

acceleration, to increase the starting power and utilize the full boiler capacity in starting, and to handle heavy trains without helpers over ruling grades, especially where stops must be made on these grades. The booster has been found especially valuable in handling heavy passenger trains in mountainous territory without helper service. The booster is equipped on the crankshaft with two double bearings, and the idler gear is equipped with the Timken quad bearing. The application of roller bearings to the booster permits of its operation at higher speeds, and experience has confirmed the practise of dropping in the booster on adverse grades at speeds of 22 mph, holding approximately this speed over the top. The booster bearings have been examined periodically when trailer wheels were removed for attention to tires and have been found in perfect condition.

The lateral motion of Alco design and construction is applied on No. 1 driver. The lateral motion involves no change in bearing housing, but the trunnion guide is provided with $1\frac{1}{4}$ -in. total lateral freedom, with respect to the pedestal liner, whereas the lateral freedom on drivers 2, 3, and 4 is $\frac{1}{4}$ to $\frac{5}{16}$ in. The lateral motion device on the front driver permits of free operation over 20-deg curves and limits the rigid wheelbase to 12 ft 10 in. It is of interest to note that the lateral freedom on all drivers after two years' operation measures the same (within 0.0020 to 0.0037 in.) as when the locomotive left the shop. This is an indication that the desired lateral freedom in drivers having been ascertained, this freedom can be built into roller-bearing housing construction with the expectation that it will not be subject to change over a period of years of service.

Crosshead guides and valve link operate in open atmosphere and are subject to the lapping action of dust and grit. An effort was made to reduce the wear of these parts by making the crosshead guides and the valve links of Timken bearing steel. This steel has a tough core with approximately 6 per cent alloy and is cased approximately $\frac{1}{4}$ in. deep to eutectoid to develop a surface material of exceptional wear-resistant characteristics. The crosshead slipper is lined with tin, as this permits atmospheric dust to imbed in the soft tin and avoid cutting the crosshead guide, and in addition the guide is of sufficiently hard material so that atmospheric dust and grit, composed largely of silica, does not wear and abrade the guide. The experience of two years indicates the soundness of this selection of materials, as the crosshead guides show very little evidence of wear and have taken on an exceedingly high polish of great hardness.

The link and link block of the same material and treatment have about 0.010 in. looseness after two years and have not received any attention and do not now require any. It is of interest to note that the crosshead slipper operates at a temperature of 20 to 30 deg above atmosphere.

The side-rod bearings are of the floating bushing type. The main and main side-rod floating bushings are of the conventional type. Pins 1, 3, and 4 have hardened bearing-steel bushings pressed in the rods. These bushings have a spherical bore of a radius approximately equal to the distance between wheels. A floating bronze bushing operates between the pins and the fixed steel bushing and has parallel bore and o.d. crowned approximately the same as the spherical bore of the steel bushings. This results in an equal distribution of wear on the pins and may have assisted in prolonging the life of the pin bearings.

Reciprocating parts were given special thought and were reduced in weight in accordance with the best American practise. The specifications given the builder, the American Locomotive Company, was a speed of 85 mph with a dynamic augment not exceeding 10,000 lb. This is 12 miles in excess of diameter speed and was made available by the use of low-carbon-nickel steel, as per specifications of the International Nickel Company in the main rod, side rods and pins, and the use of the hollow

piston-rod, heat-treated steel castings for crossheads, of composition developed by Union Steel Castings Company. The total reduction in reciprocating parts per side under conventional practise of locomotives of similar capacity is 460 lb.

The balancing system is of the cross-balance type, involving distribution of approximately one-half the overbalance on the main drivers and the other half of the overbalance distributed on pins 1, 3, and 4.

The detailed attention given to reciprocating parts and balancing system, together with the complete housing of the axles of the roller bearings, has produced a locomotive of exceptionally smooth operating characteristics. The operation in the 70's is exceptionally smooth, and vibration is not excessive at 85 mph.



FIG. 3 DRIVER MOUNTING TAPER BEARINGS AND LOWER HALF HOUSING IN POSITION
(Far view of assembled housing.)

Lubrication of the drivers and of truck wheels is accomplished by immersing the bearings in a bath of oil. The oil level is approximately $\frac{1}{2}$ in. below the enclosure level, permitting the rolls to dip into lubricant at each revolution. The straight-line elements of the taper roller bearing permit of close running clearances between the axle sleeves and the enclosure. These close clearances fill up with heavy ends of the lubricant and form an effective seal. The lubricant has been changed but three times in two years' operation, and the added lubricant between changes has been slight.

ROLLER-BEARING INFLUENCE ON LOCOMOTIVE DESIGN

The introduction of the roller bearing modifies in a number of ways the characteristics of the locomotive, which can be briefly enumerated.

Thrust plates are eliminated entirely. The thrust reactions due to curvature or flange thrust from any cause are taken on the roller-bearing surfaces of the tapered bearings, and no provision need be made anywhere in the locomotive for thrust plates. Maintenance due to the presence of thrust plates is eliminated entirely.

The engine-truck wheels do not require the large hub surface on the inside, and wheels of symmetrical design, having hub diameters the same on both sides of the web similar to those used in tender service, provide the best construction for roller, bearing engine trucks. This method provides a stronger wheel inasmuch as the heat treatment is more uniform, the cost is reduced, and likewise the unsprung weight. The four years' experience with the engine-truck wheels indicates an increase in life. The life of the wheel is limited by tread wear only. The heat rise of the bearings is about 15 deg, and consequently checking of the thrust surfaces of plain bearings is entirely eliminated. A number of engine trucks have operated in excess of 400,000 miles without wheel replacements.

Axles can be selected for stress and deflection only; no provi-

TABLE 1 STARTING EFFORT OVER 72,000 POUNDS FROM ERIE TEST

Test No.	Mile post	Drawbar dyn. car roll	Grade correction	Actual effort	Factor adhesion	Ton in train
134-A.....	167	80,640	+6072	86,812	3.72	2348
134-B.....	64	75,000	-2508	72,492	4.46	2603
135-B.....	255	77,200	-1650	75,550	4.27	2137
136-A.....	206	82,520	+5428	87,948	3.68	2697
137-B.....	201.75	76,100	-264	75,836	4.26	2107
132-A.....	238.2	71,500	+4554	76,054	4.25	...
132-A.....	284	73,200	+990	74,190	4.35	...
132-A.....	239.1	72,500	+3432	75,732	4.27	...
129-A.....	164.75	72,500	72,500	4.45	2602

NOTE: Total weight on driver plus weight on rear booster axle = 264,000 + 59,000 = 323,000 lb. Factor of adhesion equals total weight divided by starting effort. Booster used in all of the starting efforts.

sion need be made for wear. The temperature rise varies from 15 deg at the front end of the engine to 40 or 50 deg under the tender. No provision need be made in the axle as regards increased diameter to provide for wear. Use of the roller bearing

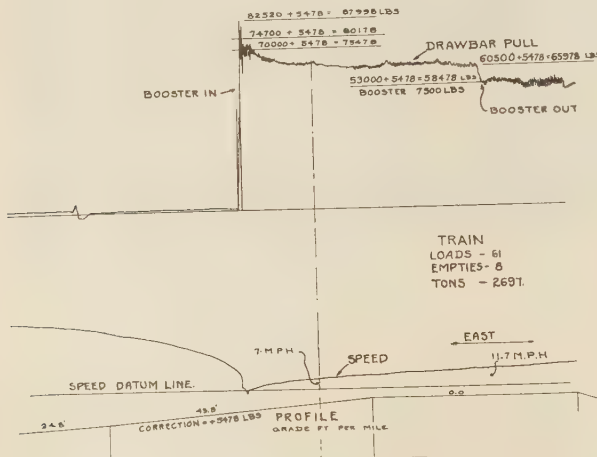


FIG. 4 TIMKEN LOCOMOTIVE, STARTING DRAWBAR PULL, CURVE 1
(Erie test 136-A, Kent to Meadville east.)

will permit of the axle to be made of alloy steel with treatment to develop the superior physical properties of alloy steel, the reason being that the axles are not subject to heat checks due to daily cycles of high temperature and ultimate cooling. The axles on the Timken engine are composed of carbon-vanadium normalized steel. The driver axles were of uniform diameter, 11 1/2 in. This reduced the diameter of the main from 1 to 1 1/2 in. under corresponding plain-bearing original equipment.

The bearing housings are provided with separate oil pockets for each bearing on the engine truck and drivers. This avoids the flow of lubricant from one side to the other on tracks of high super-elevation.

The reduction in vibration following the use of roller bearings indicates a reduced maintenance expense on account of the noticeable absence of loose bolts and loosened clamps and broken pipe connections, these features being frequently commented upon by railroad men servicing the locomotive.

The factor of adhesion is modified in certain respects with the introduction of the roller bearing on drivers. A higher percentage of the piston thrust

is communicated to the drivers at point of contact with the rail, and consequently the power "input" to the locomotive for given "drawbar pull" is reduced. A saving in friction can be conservatively estimated at 12 per cent. The reductions following this modification would be that the adhesion factor should be slightly higher if the locomotive was not modified in any other respect, and on the other hand, the experience to date would indicate that the cylinder capacity could be reduced in accordance with the saving in friction. Probably the best compromise would be to split the saving in power and put one-half of it in reduced cylinder capacity and the other half in reduced factor of adhesion. The adhesion factor of the Timken locomotive is 4.14. This gives uniformly good service, but comment has been made of slipperiness under bad rail conditions.

The subject has been carefully studied, and the opinions of experts on the subject have been sought. The opinion of one

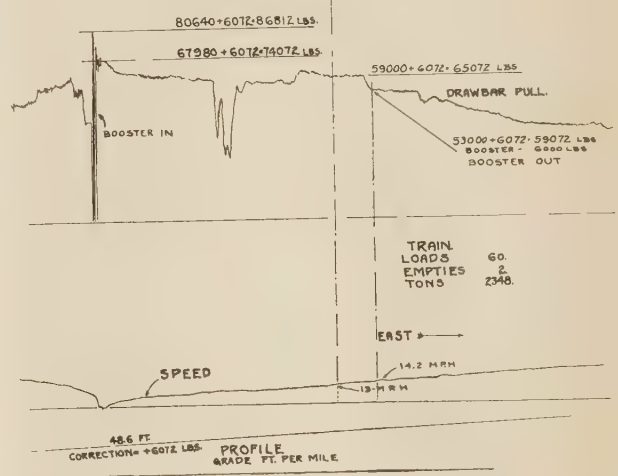


FIG. 5 TIMKEN LOCOMOTIVE, STARTING DRAWBAR PULL, CURVE 2
(Erie test 134-A, Marion to Kent east.)

locomotive expert was that locomotives have always slipped and always will slip under certain conditions, even though the factor be made 100 to 1. The fact that the roller-bearing engine is new has made it a target for criticism on any point that is even slightly different from conventional practise, and if a slip would occur it would be blamed on the roller bearings even though plain-bearing engines had slipped over identical track for one-hundred years under certain atmospheric conditions. On an observation on one railroad over a distance of more than 450 miles, with full tonnage train, there was noted only a slip of half a

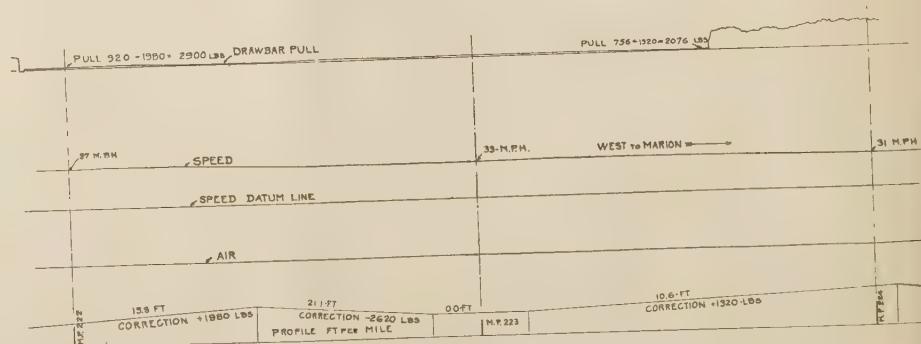


FIG. 6 TIMKEN LOCOMOTIVE, DRIFTING PULL, CURVE 3
(Erie test 133-B, Kent to Marion west.)

dozen revolutions on poorly maintained curved track at the ladder of a yard.

The starting characteristics of the locomotive on roller bearings is materially changed. The Timken engine has a normal starting drawbar pull of 63,700 lb, based on conventional formula. It has been frequently observed to develop starting power of 68,000 to 69,000 lb. Table 1 from Erie tests gives the data on a number of starts in excess of 72,000 lb with booster; some of these starts are in excess of 80,000 lb, the maximum being 87,998 lb. Two starts, curve 1 (Fig. 4) and curve 2 (Fig. 5), on Erie test at m.p. 206 and m.p. 267 indicate speed, grade, and test conditions and illustrate the high momentary surge at starting. The sustained power in starting is over 80,000 lb and illustrates also the effect of drawbar pull at the point of cutting off the booster. The added starting power contributed by the roller bearing is of particular value and adds to the capacity of the locomotive in handling heavy trains.

The free coasting is another of the outstanding features of the roller-bearing locomotive. Free coasting is of particular value in eliminating surges in passenger trains when the throttle is closed. The coasting characteristics of the engine are about equivalent to the free running of the train, and closing the throttle does not result in the bunching of the train on the engine and the consequent taking up of slack when the throttle is opened. The freedom from train surging with the roller-bearing locomotive has been frequently commented upon in passenger service. The curve 3 (Fig. 6) illustrates a drifting test on the Erie. The locomotive in drifting on a 21-ft grade at a speed of 33 mph developed a drawbar pull of 2900 lb on the dynamometer car. The pull of the locomotive on the train continued on an ascending grade of 10.6 ft to the mile, with a gradual decrease in train speed from 37 to 29 mph, at which point the throttle was opened. The train had 6 loads and 68 empties, a total of 2128 tons. The reduction in wear and tear of couplers and draft equipment on account of the continuous stretching of either freight or passenger trains is a valuable feature of the roller-bearing locomotive.

PERFORMANCE RECORD

The performance record has been ably presented in the trade publications. The locomotive performed with equal efficiency in passenger and freight service, and of the 119,586 miles, 51,655 miles were in freight service (43 per cent) and 67,931 miles were in passenger service (57 per cent).

Passenger service includes operation on some of the fastest American trains, among which are the 20-hour mail trains on the

Pennsylvania in New York-Chicago service, the mail trains on the same road in New York-St. Louis service, the "Sportsman" on the Chesapeake & Ohio, the "Erie Limited" the "Merchants Limited" on the New Haven, 109 runs on the Lackawanna in passenger service between Scranton, Pa., and Hoboken, N. J.,

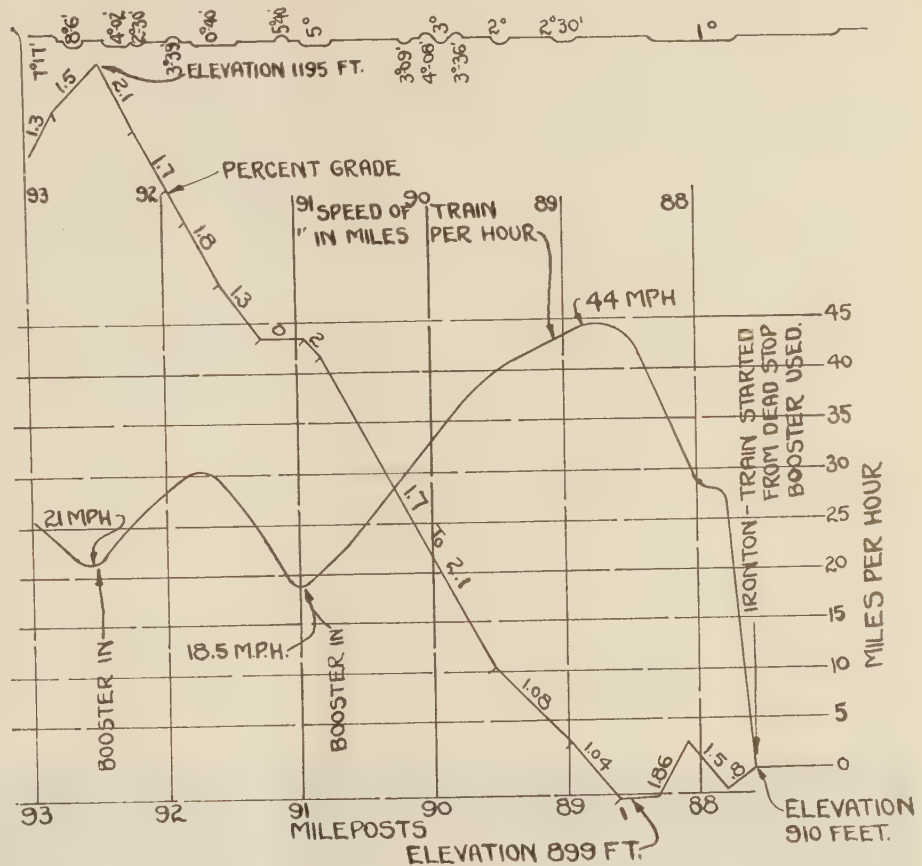


FIG. 7 CURVE OF ACTUAL SPEED OF TIMKEN LOCOMOTIVE

(Pulling 18 passenger cars, of which 13 were Pullmans; total 1260 tons; passenger train No. 17, over critical Ozark Mountain grade between Ironton and Tipton on run between St. Louis and Poplar Bluff, over Missouri Pacific Railroad.)

the "Lehigh Limited," the "Sunshine Special" on the Missouri Pacific, the "Aristocrat" and "Overland Limited" on the Chicago, Burlington & Quincy between Lincoln, Neb., and Denver, Colo., and four months of hauling the "North Coast Limited" on the 906-mile run over three ranges of the Rocky Mountains between Missoula, Mont., and Jamestown, N. D.

The locomotive has handled all varieties of freight service, the heaviest being a 9960-ton coal train on the Chesapeake & Ohio. The outstanding freight service is the handling of heavy fast-freight trains at high speed on the New York Central, Pennsylvania, Erie, Boston & Maine, Lehigh Valley, Nickel Plate, Missouri Pacific, Chicago, Burlington & Quincy, and Northern Pacific.

OUTSTANDING RUNS

A non-stop run, Altoona to Enola on the Pennsylvania, 124 miles, with 115 cars weighing 8625 tons, was at an average speed of 25.7 and evaporated 8.33 lb of water per pound of coal. This trip was at a work rate of 221,427 gtm per train-hour, exclusive of locomotive.

A merchandise train was hauled between Crestline and Ft.

Wayne, on the Pennsylvania, consisting of 102 cars of 3986 tons, a distance of 131 miles, at a rate of 41.5 mph, at an evaporative rate of 8.2 and work rate of 165,457 gtm per train-hour.

Twelve passenger-equipment cars were handled unassisted on the east slope of the Alleghenies over a uniform mountain grade of 1.9 per cent, compensated.

Pennsylvania train No. 52, "New Yorker," Chicago to Crestline, made the 280 miles in 274 min running time.

The heaviest train hauled was on the Chesapeake & Ohio and comprised 134 coal cars, weighing with locomotive 10,219 tons. The run was made at the rate of 212,000 gtm per train hour.

The "Erie Limited" was handled between Hornell, N. Y., and Salamanca, N. Y., making up 25 minutes in a distance of 82 miles at an average speed of 59 mph.

The assignment on the Boston & Maine, a total of 35 runs being made, involved operation at temperatures of 20 deg below zero. An outstanding run was a train of 86 cars, 2040 tons, hauled 112 miles at a rate of 33.7 mph in sub-zero weather.

The passenger service on the Lackawanna was outstanding, involving 109 runs between Scranton, Pa., and Hoboken, N. J. This includes the Pocono mountain grade and long grades over the hills of northern New Jersey. A Lackawanna run working the engine to the limit was train No. 12, March 11, 1931, 11 cars, which left Scranton 56 min late, was detained 13 min at Stroudsburg, and made up the 69 min lost time in 112 miles running. The run over the division was made with 9 tons of coal. Speeds of 78 mph were attained on ascending 0.4 per cent grades.

The average speed of 54.8 mph in passenger service on the Lehigh Valley is outstanding. This involves running for long distances at speeds in excess of 70 mph.

On a Lehigh Valley freight run, Manchester to Sayre, 2410 tons, 67 cars, 89 miles were made in 1 hour and 52 min.

An interesting passenger run, which was repeated twice, was that of hauling of 18 passenger-equipment cars, including 13 Pullmans, over the Ozark Mountain grades on the Missouri

Pacific between St. Louis and Poplar Bluff. These runs encountered maximum grades of 2.1, and the practise followed was to approach the grades at speeds of 50 mph, and as the speed fell the booster was dropped in at 22 mph, and in the three runs the train was handled over Tip Top grade at speeds of 15, 17, and 19 mph. These trains average 1260 to 1290 tons, and indicate with booster a tractive capacity approximating 80,000 lb. The chart (Fig. 7) shows the profile and speed which this train made, as taken from the valve pilot record.

An outstanding passenger-service record was on the Northern Pacific, where the "North Coast Limited" was hauled between Jamestown, N. D., and Missoula, Mont., a distance of 906 miles, which includes three Rocky Mountain ranges with grades of 2.2 and several grades of the Black Hills between Glendive, Mont., and Mandan, N. D. There were 19 trips made on this run, which developed and showed the adaptability of the roller-bearing equipment for long continuous service.

OPERATING TEMPERATURES

The normal temperature rise of the bearings varies from 15-deg rise on the engine truck to 40-deg to 50-deg rise on the tender, the interesting feature being that the temperature rise of the drivers is only 15 to 20 deg above atmosphere. The normal condition of bearing housings in zero weather is with frost adhering to the bearing housings and the end of the axles. The photograph (Fig. 8) illustrates the condition of frost adhering to the engine truck and the driver axles and to trailer and tender boxes.

MAINTENANCE

The maintenance work consists of the normal engine-house attention, including replacement of rod bearings, brake shoes, etc. The entire demonstration of two years' time, 120,000 miles, over every condition of topography and temperature, with mid-winter assignments on the Boston & Maine and Northern Pacific and

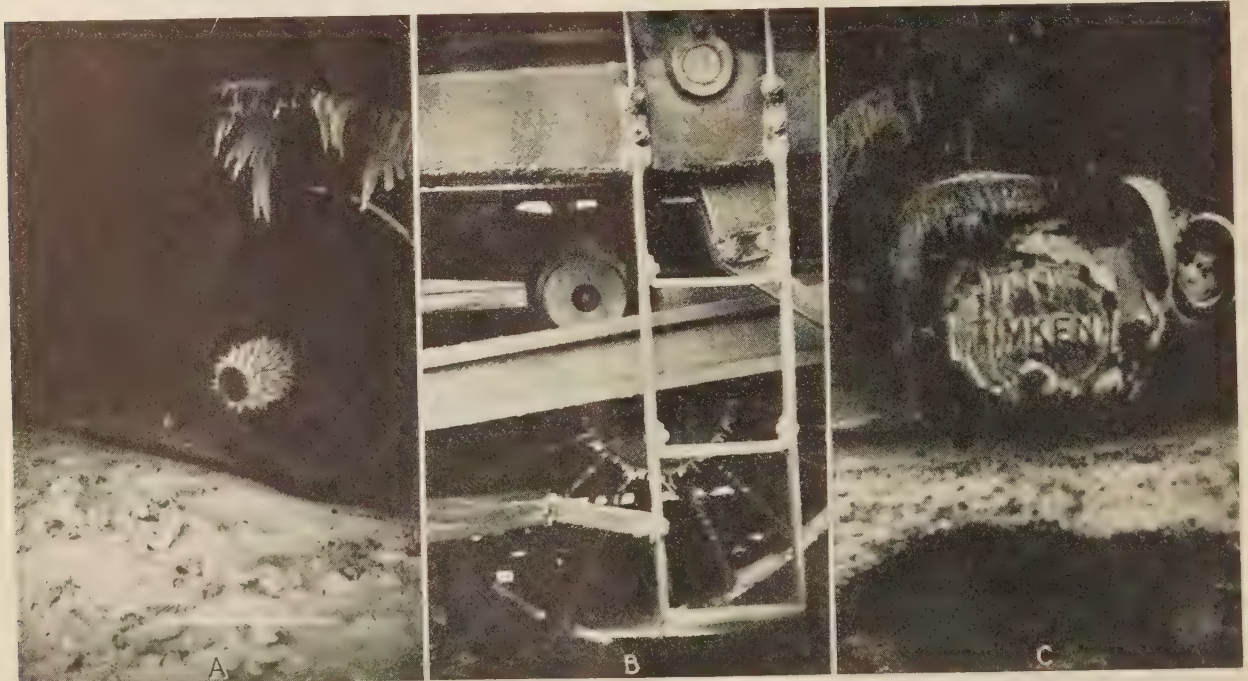


FIG. 8 ENGINE TRUCK, DRIVER, AND TRAILER AT COMPLETION OF 900-MILE RUN
(A, engine truck; B, driver; C, trailer.)

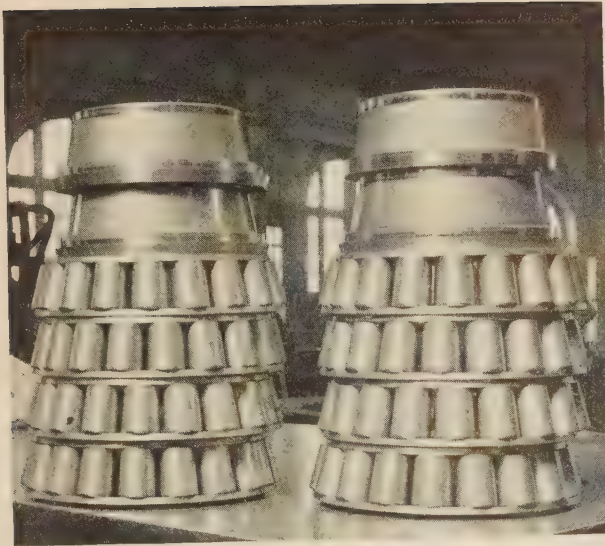


FIG. 9 TIMKEN LOCOMOTIVE DRIVER BEARINGS
(In perfect condition at 119,600 miles, or two years' work.)

mid-summer on the Missouri Pacific, was made without development of roller-bearing troubles on any of the wheels.

A looseness developed on the main driver on the Burlington, which was taken up by pressing on each wheel center an additional $\frac{1}{32}$ of an inch. The looseness was due to seating of the bearing in the housing; this has been corrected on subsequent designs by increasing the backing of the bearings.

TABLE 2 PERFORMANCE OF MAIN AND SIDE-ROD BUSHINGS

Mileage	Right	Left	Right	Left	Right	Left	Right	Left	Right	Left
146					(1)				(1)	
1,462	(2)				(3)					
2,098					(4)				(4)	
6,582					(5)				(5)	
42,010					(6)				(6)	
64,653	(5B)	(5A)	(5B)	(5A)						
64,740	(7)		(7X)							
66,112	(8)				(5)				(5)	
69,129	(9)		(5)		(6)				(6)	
69,651			(9)							
73,516	(9)		(10)							
80,146	(12)	(11A)	(11A)	(11A)						
83,145		(11)		(13)						
109,963					(5)				(6)	
110,867					(5)				(14)	
116,291		(9)			(15)				(15)	
119,586		(16)	(16)		(16)				(16)	

NOTE: Maximum mileages for any one bushing application: 63,191, 64,653, 69,042, 64,653, 62,547, 35,428, 58,071, 62,547, 62,547, 62,547.

Reasons for renewing rod bushings at the mileages indicated in the table:

- (1) Rods were out of tram.
- (2) Bushing was thought tight on o.d.; was rebored and then found loose.
- (3) Not enough lateral.
- (4) Changed from solid to three-piece floating bushing with crown.
- (5) Diameter wear.
- (5A) Diameter wear and changed from floating to three-piece bushing with crown.
- (5B) Diameter wear and changed from floating to three-piece bushing with crown.
- (6) Broken bushing.
- (7) Experimental bushing.
- (7X) Experimental bushing defective, but replaced; removed at 64,653 miles.
- (8) Defective casting.
- (9) Cracked bushing.
- (10) Crankpin rough and was reground.
- (11) Replaced with solid floating bushing.
- (11A) Replaced with solid floating bushing, as it was damaged when main crankpin broke.
- (12) Rebored to fit new pin after right main crankpin broke.
- (13) Bushing rough.
- (14) Bushings applied at 109,963 miles; did not have sufficient stock.
- (15) Steel bushings were loose; new steel and brass bushings were applied.
- (16) Bushings damaged account of accident.

TABLE 3 SUMMARY OF ALL RUNS IN FREIGHT SERVICE

	New York, Chicago & St. Louis	Chicago, Burlington & Quincy	Missouri Pacific	Northern Pacific	Totals and averages
Number of runs, mph.	12	50	15	22	328
Average running speed, mph.	31.70	34.27	33.64	28.0	29.80
Locomotive-miles	175.8	123.0	261.1	122.0	152.0
Train-miles	174.2	122.0	232.8	110.1	126.9
No. of cars	76.0	77.8	79.8	60.0	83.4
Tons per trip	913	1,198	2,885.7	1,323	27,356
Total tons	383,570	383,570	2,885.7	2,879	3,160
Coal, tons	15,141	17,877	2,885.7	2,879	3,160
Water, gal	181,690	265,155	3,240.7	3,034	1,036,393
Car miles	470,401	710,810	43,286	58,934	1,153,257
G.t.m. per trip	594,865	795,610	48,611	15,078	14,364
G.t.m. total	5,644,821	10,296,268	48,611	15,078	144,425,533
Aver. lb coal per 1000 gtm	68.43	68.43	68.43	68.43	66.15
Running time, hr	77.32	77.32	77.32	77.32	77.32
Train-hours	76.21	76.21	76.21	76.21	76.21
Gross ton-miles per train-hour	103.78	103.78	103.78	103.78	103.78
Evaporation, lb water per lb of coal	69.07	69.07	69.07	69.07	69.07
	95.65	95.65	95.65	95.65	95.65
	61,032	61,032	61,032	61,032	61,032
	7.02	7.02	7.02	7.02	7.02
	6.50	6.50	6.50	6.50	6.50
	7.39	7.39	7.39	7.39	7.39
	7.56	7.56	7.56	7.56	7.56
	7.41	7.41	7.41	7.41	7.41
	7.10	7.10	7.10	7.10	7.10
	7.36	7.36	7.36	7.36	7.36
	6.88	6.88	6.88	6.88	6.88

NOTE: The Delaware, Lackawanna & Western, with 834 locomotive-miles, and the Chicago & Alton with 158 locomotive-miles in freight service, are omitted from the table, as performance details are not available. The mileages, however, are included in the total.

TABLE 4 SUMMARY OF ALL RUNS IN PASSENGER SERVICE

	Pennsylvania	Chesapeake & Ohio	Erie	New York, New Haven & Hartford	Delaware, Lackawanna & Western	Lehigh Valley	Missouri Pacific	Chicago, Burlington & Quincy	Northern Pacific	Totals and averages
Number of runs.....	23	20	28	2	109	11	14	3	52	262
Average running speed, mph	45.89	38.73	41.56	48.01	39.39	54.83	41.88	45.16	43.6	42.5
Locomotive-miles { Trip....	342	339	105	180	138.9	258.1	253	323	518	267
{ Total....	7,871	7,128	3,058	360	15,140	3,017	3,448	970	26,933	67,931
Train miles { Trip....	341	343	98.5	180	136.7	253.5	243	967	26,815	66,713
{ Total....	7,846	6,872	2,760	360	14,901	2,788.6	3,403.5	13.3	11	10.7
Number of Cars { Trip....	12.5	8.8	9.8	14	10	11.5	14.5	40	520	2,781
{ Total....	289	177	275	28	1,121	127	204	20.5	30.7	15.67
Coal, tons { Trip....	16	14	5.7	7.5	8.7	12.7	15.7	61.5	1,901.9	41,037
{ Total....	370	283.5	160.5	15	952	139.5	219.25	31,100	49,088	24,109
Water, gal. { Trip....	31,651	26,891	11,218	15,550	13,500.6	22,707	24,180	93,300	2,552,576	6,316,377
{ Total....	727,993	537,830	314,120	31,100	1,471,567	249,776	338,515	4,135	5,003	2,621
Car miles { Trip....	4,119	2,890	997	2,198	1,384.8	2,887	3,328	12,405	260,169	686,731
{ Total....	94,744	57,795	27,934	4,396	150,945	31,757	46,586	9.91	14.62	11.9
Average lb coal per car-mile.	7.77	9.68	11.43	6.82	12.57	8.78	9.41	7.13	9.89	5.98
Running time, hr { Trip....	7.43	8.88	2.37	3.20	3.47	4.63	5.71	21.39	614.6	1567.57
{ Total....	170.92	177.62	66.55	6.40	379.18	51.00	79.91	8.45	13.86	6.28
Train hours { Trip....	8.61	9.57	3.56	3.78	6.42	25.37	720.83	1645.5
{ Total....	198.10	191.53	7.13	412.69	89.95	6.82	5.59	6.4
Average lb water per lb coal	8.24	8.00	8.20	8.63	6.46	7.46	6.43

BEARING LIFE EXPECTANCY

The trailer and tender bearings have been examined from time to time when servicing wheels. A few hairlines have developed on one roll of the trailer bearing and which has continued without change for six months. It does not require replacement or renewal.

The driver bearings were removed and minutely examined at the conclusion of the demonstration period. The cups (outer races) and rolls showed no evidence whatever of wear. The driver cones (inner races) showed very slight wear, visible only under a microscope. As a matter of experiment the removal of 0.0005 in. of metal in regrinding removed the microscopic evi-

that the wheel bearings, with the exception of driver*cones, should have a normal life expectancy of 1,000,000 miles, the driver cones having a life expectancy of one-half that figure. This presumption is further borne out by the study of the condition of the engine-truck bearings after 400,000 miles' service, which show no appreciable evidence of wear, and is supplemented further by the study of the original roller-bearing applications on the Milwaukee Road, many of which have now crossed 1,000,000 miles, and which have been studied in detail over the past seven years.

An axle assembly of engine-truck bearings removed from a Michigan Central engine, having run 303,756 miles, is illustrated in Fig. 9. The disassembly was made on account of wheel

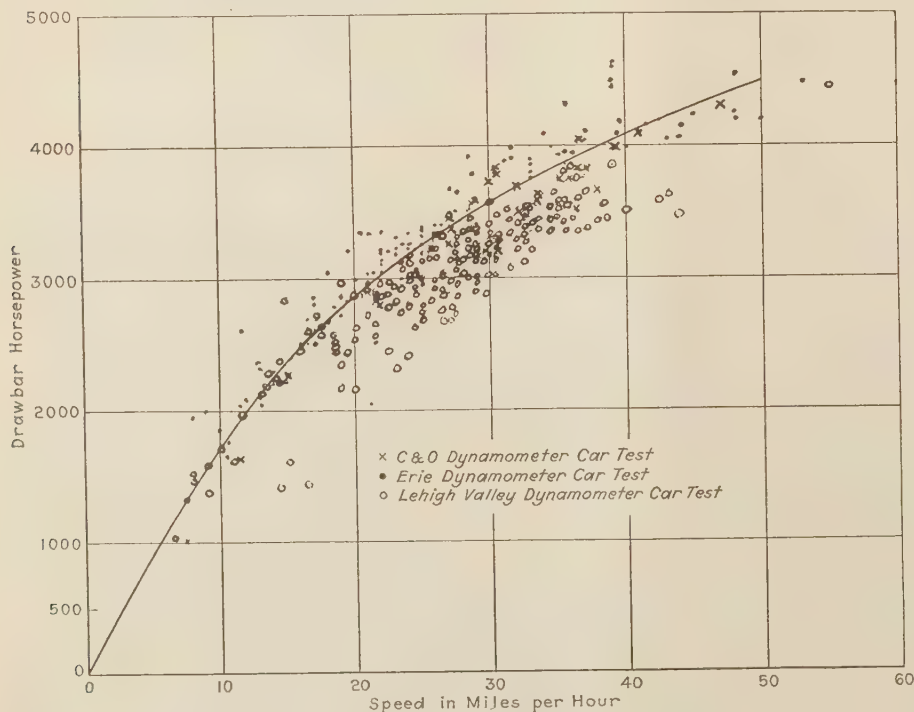


FIG. 10 TIMKEN LOCOMOTIVE DRAWBAR HORSEPOWER, CURVE 4

dences of wear. The cones have been returned to service without other modifications (some of the cones were not touched) to study further the development of wear. The indications from the study of the bearings at the conclusion of the demonstration period, visualized against the accumulative available information on service of roller bearings in all kinds of industries, would indicate

The availability is definitely increased by the roller bearings. The operation for two years in a wide variety of services without any bearing trouble whatever, and which for long periods of time involved the dispatchment of four divisional trips each 24 hours, is an indication that the use of the roller bearing increases the availability of the locomotive by 50 per cent.

change and developed the perfect condition of the bearings after two complete shopping periods, approximating 153,000 miles each. These bearings did not show sufficient wear to indicate any reasonable percentage of life expectancy, having been given up in service. A number of engine-truck bearings have been examined with similar results at mileages between 400,000 to 500,000.

The rod-bearing life is apparently increased while operating on roller-bearing drivers, as is evidenced by Table 2, which shows the replacement of rod bearings. A number of the bushings on each of the main-rod and side-rod applications have operated in excess of 60,000 miles, which is about double the average life expectancy of these bearings. The probability is that rod bearing life is increased on account of the greater accuracy of alignment of driver axles in the roller bearings.

FUEL ECONOMY

The record of fuel and water consumption is indicated in the summaries of freight runs (Table 3) and passenger runs (Table 4). The lowest average was on the Chesapeake & Ohio, of 38.3 lb of coal per 1000 gtm, but individual runs on this road were as low as 26 lb of coal per 1000 gtm.

Favorable loads and favorable grades favor low coal consumption. A fair average is that of 53.6 and 55.5 lb of coal per 1000 gtm on the New York Central and the Pennsylvania, which average covers a wide variety of service over typical trunk-line roads. A tendency is noted for fuel consumption to increase on the Western roads. Much of this is due to the lower fuel value of the coals available to the Western roads, this being particularly true of the Montana coals and some of the coals available on the Burlington and the Missouri Pacific. The coal consumption on the Erie of 91.6 is on account of operating in the rolling country between Meadville, Pa., and Marion, Ohio, against frequent ruling grades of 1 per cent.

An exact comparison with comparable locomotives in identical service was not made available during the demonstration, but the study of such records as are available would indicate that the roller-bearing locomotive operated at rates of 10 to 30 lb per 1000 gtm below that of the plain-bearing locomotives. The fuel consumption is in general one-half of that published by the Interstate Commerce Commission, which, however, is not strictly comparable on account of the latter records including all service and all power.

The locomotive was, in general, operated at full capacity and frequently ran for long distances at cut-offs longer than 60 per cent. This was made possible on account of the free-steaming characteristics of the Timken locomotive boiler and which encouraged road foremen and enginemen to work the locomotive at full capacity. The fuel consumption could have been greatly improved provided effort had been made to operate the cut-offs not in excess of 50 per cent, with the particular object in view of fuel economy records. The attitude of the owners of the locomotive, however, was to encourage the railroad people to work the locomotive to the limit so as to develop the capabilities of roller bearings, and therefore the only efforts at fuel economy were voluntary on the part of engine crews and road foremen.

In consideration of the wide variety of services encountered and generally with strange crews, totaling approximately 840, unfamiliar with the locomotive, and the prevailing attitude of attempting to work the new machine to the limit, taken all together the performance record of fuel and water is truly remarkable and is an indication of the economy records possible with completely equipped roller-bearing locomotives, where economy in fuel rather than demonstration of bearings is the prime object of the test.

The tender is built on a General Steel Casting tender bed and has a capacity of 21 tons of coal and 14,000 gal of water. It is equipped with a cupola for the accommodation of the owners' observer. The operation of the locomotive and the fuel performance have been modified adversely by the water capacity

of the tender, particularly in view of the high steaming capacity of the boiler. The survey of American roads indicated the presence of a number of 90-ft turntables at critical points, over which it was desired to operate the locomotive, which by limiting the overall wheelbase to slightly less than 90 ft, placed decided limita-

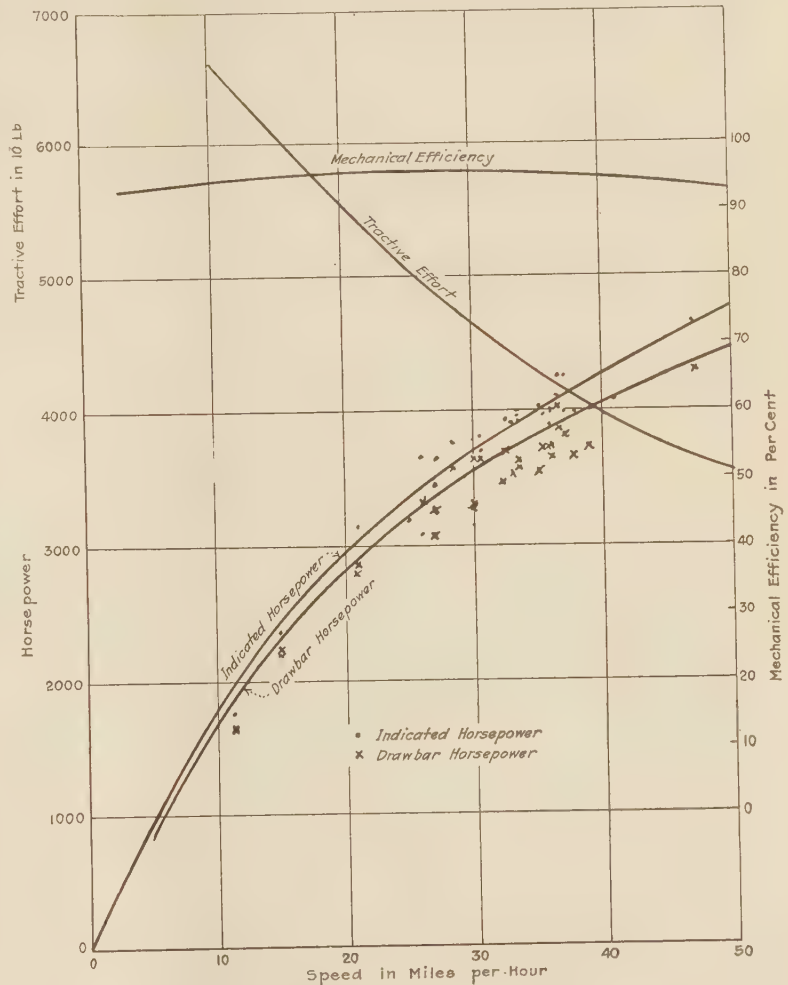


FIG. 11 POWER PERFORMANCE, TIMKEN LOCOMOTIVE, LEHIGH TEST, CURVE 5

tions on tender capacity. The performance of the locomotive as regards increased average speed and fuel economy would have been materially improved had the tender capacity for water been increased to 21,000 gal.

MECHANICAL EFFICIENCY

Dynamometer-car tests were made on the Chesapeake & Ohio, Erie, Lehigh Valley, Nickel Plate, and Northern Pacific. A number of readings of the Chesapeake & Ohio, Erie, and Lehigh Valley tests have been plotted. In addition to the dynamometer-car record, a limited number of indicator-card tests were available—the Lehigh Valley from both cylinders and the Northern Pacific on one side.

The drawbar horsepower readings, taken from the Chesapeake & Ohio, Erie, and Lehigh Valley tests, with the locomotive working to capacity or nearly so, are indicated on curve 4, Fig. 10. High readings were available on the Erie on account of the frequent 1 per cent grades with tonnage trains. The C. & O. read-

ings were made with heavy coal trains on a water-level division. The Lehigh Valley tests were made on the Seneca division over rolling country. The outstanding feature of this diagram is the

ECONOMIC VALUE OF ROLLER BEARINGS

The value of the roller bearing in locomotive construction is reflected in a number of ways. Some of these advantages can be

evaluated, and while others are present and recognized, the definition of value is more difficult to determine. The advantages are as follows:

- 1 Reduction in maintenance
- 2 Reduction in consumption of lubricants
- 3 Reduction in consumption of fuel
- 4 Reduction in consumption of water
- 5 Increased development of power, a conservative figure being 10 per cent
- 6 Increased availability, about 50 per cent.

These advantages are subject to evaluation and can be capitalized; and in addition the following conditions are present, but are more difficult to evaluate:

- 1 Increased permissible speed
- 2 Engine-house force reduction
- 3 Elimination of axle failure due to heat checks
- 4 Reduction in rod maintenance

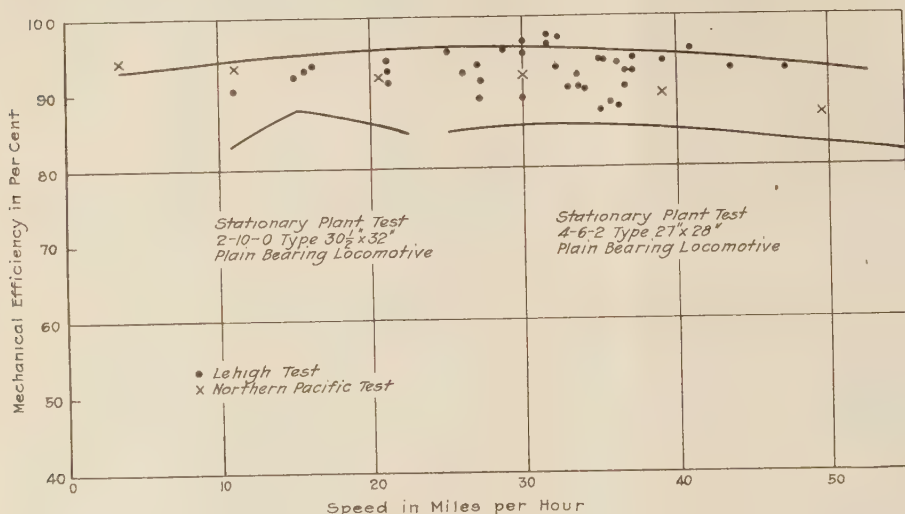


FIG. 12 TIMKEN LOCOMOTIVE DYNAMOMETER CAR TEST, CURVE 6
(Plotted points indicate efficiency from Lehigh and Northern Pacific test.)

development of 4000 drawbar horsepower at speeds in excess of 36 mph under favorable train and grade conditions.

The power performance showing mechanical efficiency is indicated on curve 5, Fig. 11. This is compiled from readings of the Lehigh Valley and the Northern Pacific. The mechanical efficiency varies from 90 to 96 per cent, although a reading is available at 97½ per cent. The high efficiency, as indicated on the tests, is confirmed by the low temperature rise of the wheel bearings, particularly the driver bearings, this average being 15 to 20 deg above atmosphere.

The mechanical efficiency of roller-bearing and plain-bearing locomotives is shown on curve 6, Fig. 12. The roller-bearing curve is transferred from curve 5, Fig. 11. The plain-bearing curve is taken from the stationary plant test of a 2-10-0 freight locomotive for the lower speed range and a 4-6-2 passenger locomotive for the higher speed range. The stationary plant readings for the plain-bearing locomotive omits the effect of windage and track resistance. Strictly comparable tests would tend to increase the spread between the roller-bearing and plain-bearing curves.

The increased capacity of the roller bearings, as applied to the locomotive, is indicated on curve 7, Fig. 13, which is combined from curves 5 and 6 and is plotted to show the increased locomotive performance resulting from the roller bearing. This increased capacity for work varies from 10 to 13 per cent, averaging 12 per cent. A conservative assumption is that the roller-bearing locomotive can be reduced in size 10 per cent to perform equally with plain-bearing locomotives, or, conversely, locomotives identical with a roller-bearing locomotive could be expected to produce an increase of 10 to 12 per cent with roller bearings.

The service performance record confirms the test data in that the roller-bearing locomotive consistently exceeded the performance of similar-sized plain-bearing locomotives with identical cylinders and pressure and equaled, and at times exceeded, the performance of engines having 1 in. to 1½ in. increased cylinder diameter. The plain-bearing cylinder capacity in some cases was 20 per cent in excess of the Timken engine 1111.

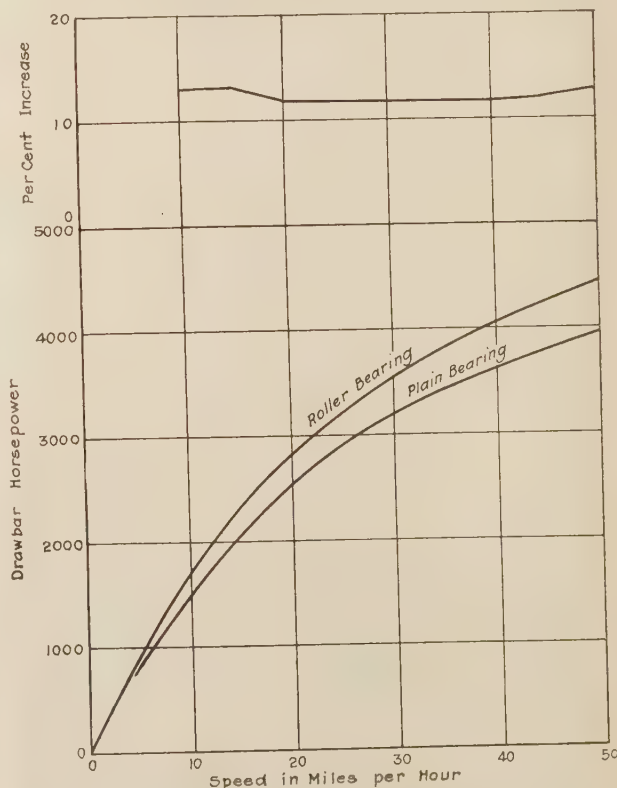


FIG. 13 DRAWBAR HORSEPOWER, ROLLER-BEARING AND PLAIN-BEARING LOCOMOTIVE, CURVE 7
(Based on mechanical efficiency, for roller-bearing locomotive, Lehigh test, and plain-bearing stationary test.)

The approximate cost of roller-bearing equipment, including bearings and housings and application parts for the 4-8-4 locomotive, not including tender, is \$8000.

The bearing-replacement charges on the basis of an annual mileage of 168,000 and a life expectancy of wheel bearings, except driver cones, of 1,000,000 miles, and driver cones 500,000 miles, would be \$1500 per year.

Saving in maintenance and lubrication, based on data accumulated during the roller-bearing-locomotive demonstration period, would vary from \$3900 per locomotive year for territory with light grades to \$6700 per locomotive year in heavy service in mountainous territory. This is on the basis of:

- 1 Attention during running
- 2 Maintenance at terminals
- 3 Semi-monthly inspection
- 4 Replacement of bearing brasses
- 5 Replacement of hub liners
- 6 Saving in lubrication:

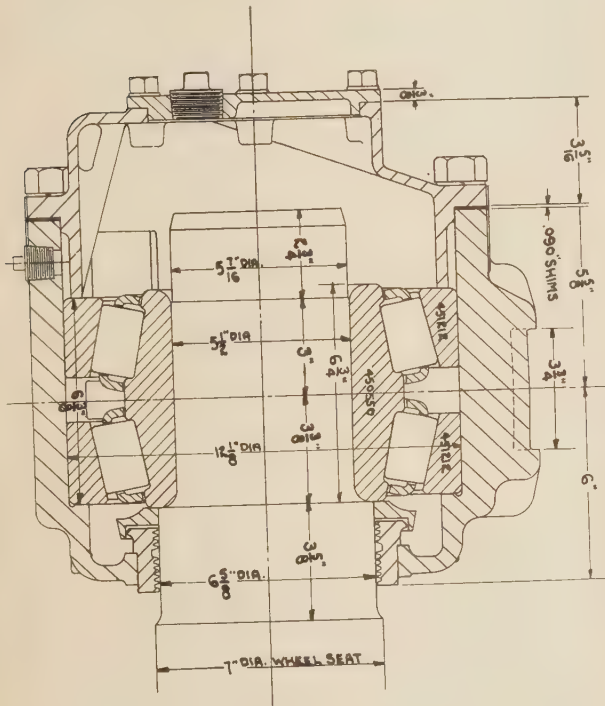


FIG. 14 PASSENGER-EQUIPMENT ROLLER-BEARING LAYOUT (Wide-pedestal type, 5 1/2 by 10 in.)

The net maintenance saving, after deducting the bearing-replacement charges, would vary from \$2400 to \$5200 per year.

Fuel economy, based on average machine efficiency of 86 per cent for the plain-bearing locomotive and 93 per cent for the roller-bearing locomotive, would vary from 750 tons to 1200 tons per year, this representing an annual saving of \$1500 in the lighter service to \$2000 in the heavier service.

The locomotive operating cost would therefore be reduced in amounts from \$3900 annually in light service to \$7200 in mountainous service, corresponding with direct returns on investment of 49 per cent and 90 per cent, respectively, the high return corresponding with the greater severity of service.

The return of bearing investment, in addition to economy in operation due to savings in maintenance, fuel, and lubrication would also include a factor on account of increased availability

of the roller-bearing locomotive and an account of increase in power, averaging 12 per cent—in conservative figures, 10 per cent.

An increase in availability of 50 per cent on an investment of \$80,000 is equivalent to \$40,000 to be written off in the life of, say, 20 years, or \$2000 a year.

An increase in power of 10 per cent on an investment of \$80,000 can be evaluated at \$8000, which in a life of 20 years is worth \$400 annually.

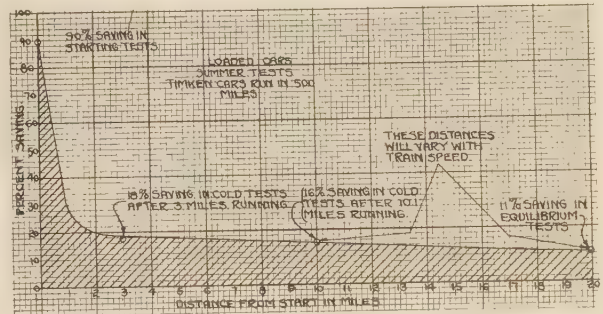


FIG. 15 TESTS IN SUMMER OF 1930 ON LOADED CARS (Per cent of saving, with distance operated, Timken cars run in 500 miles.)

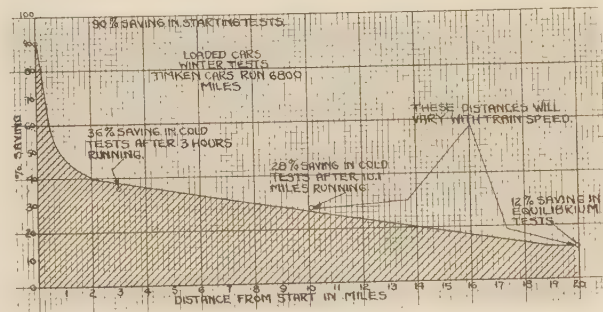


FIG. 16 TESTS IN WINTER OF 1931 ON LOADED CARS (Per cent of saving, with distance operated, Timken cars run in 6800 miles.)

The increased value of the roller bearings in locomotives on account of increased power development and increased availability would be worth approximately \$10,000 or considerably in excess of the purchase price of the roller-bearing equipment.

ROLLER-BEARING ROD APPLICATIONS

Considerable study has been devoted to the application of roller bearings to main and side rods, and methods have been developed that will permit of the application of roller bearings to these parts.

A unique device avoids the transmission of twisting and extraneous loads, incident to locomotive operation, to the bearings. The application avoids an increase in rotating parts carried on the pins, as compared to plain bearings, on the basis of using carbon steels in the rods. The advantages of the roller bearing, involving long continuous runs, reduction in maintenance, and economy in lubrication, are available without sacrificing maximum speed performance or increasing dynamic blow on rails.

An interesting feature of the roller-bearing study is that the main and side rods have practically uniform sections and permit and facilitate the use of alloy steels, developing higher physical properties. The roller-bearing application on the basis of using alloy steels effects reductions of 25 per cent in reciprocating and rotating parts and permits of increase of speed of 12 to 15 per

cent with the development of dynamic augment corresponding with plain bearings with diameter speed.

This increase in permissible speed has a high economic value and improves the position of the railroads as regards meeting competition of other forms of transportation. The higher speeds will permit of reducing train schedules to the extent of 10 to 15 per cent and will place the railroads in a position more in keeping with present-day economic demands for high speed.

PASSENGER-EQUIPMENT APPLICATIONS

The improved service and advantages resulting from the use of roller bearings in locomotives apply with equal force in passen-

total mileage in Pennsylvania service is in excess of 47,000,000 miles, and it is an interesting example of durability and reliability that in this mileage a train detention has never been charged to Timken bearings.

Freedom from hot boxes is a general characteristic of the tapered roller bearing in passenger service.

Greater availability follows the use of the roller bearing, inasmuch as inspection is only necessary at monthly intervals, and equipment can therefore be dispatched with no delays at terminals on account of bearing inspection and maintenance.

An absence of surging is particularly noticeable on complete roller-bearing trains, this resulting from a uniformly low rolling

resistance of the roller bearing, and particularly the low resistance at starting.

Reduced cost of maintenance on equipment generally follows the use of the roller bearing on account of the absence of surging in service, and in particularly the reduced blow to draft gears, couplers, and sub-frames in starting.

FREIGHT-EQUIPMENT APPLICATION

Freight-train equipment presents a field for the application of roller bearings which in value to the railroads should rank next to the successful application to the locomotive. The development of the freight-car application has been slow. The great surplus of freight equipment has practically stopped the purchase of new freight rolling stock, but notwithstanding these conditions, the Timken Company has continued the development of

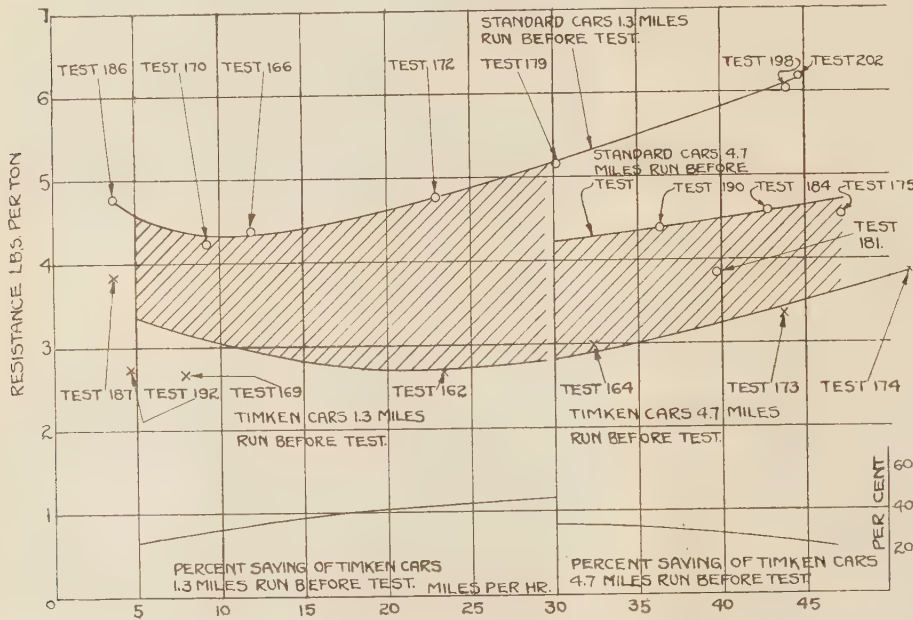


FIG. 17 COLD TEST, LOADED CARS, WINTER OF 1931
(Timken cars run in 6800 miles.)

ger equipment, and as a consequence the tapered bearings are generally used in this service. A distinguishing feature of the passenger mountings is the outboard construction, using double bearings in pedestal mounting with increased width of pedestal opening.

A typical installation is shown in Fig. 14—a 5½-in. by 10-in. application as adapted to General Steel Casting four- or six-wheel trucks.

MILWAUKEE INSTALLATION

The Milwaukee Road made the first large passenger installation on Timken bearings. This involved the complete equipment of the "Pioneer Limited," for service between Chicago and Twin Cities, and the "Olympian," operating between Chicago and Seattle. The original equipment, numbering 127 cars, was placed in service in 1927. The Milwaukee Road has since extended the installation of roller bearings to 153 cars, which include coaches, Pullmans, and diners. The accumulative mileage of these cars to June, 1932, is 116,000,000 miles, the average mileage per car being in excess of 1,000,000 miles.

PENNSYLVANIA TIMKEN PASSENGER EQUIPMENT

The Pennsylvania has 304 passenger-equipment cars in main-line coaches, dining cars, gas-mechanical, and multiple-unit electric cars, the original installations being made in 1927. The

the application of roller bearings to the freight car in the belief that ultimately the value of the development will be recognized, and with the return to more nearly normal business conditions utilizing the reserve of rolling stock, the purchase of new freight cars would initiate the gradual introduction of roller bearings in freight service.

Freight-car roller-bearing development has involved the construction, testing, and arrangement for operation of equipment in capacities of 40, 50, 70, and 100 tons. These cars were built singly or in groups of two or three to develop the characteristics of specific constructions.

The 100-car train has been tested as regards service for a total of 3,000,000 car miles, and in complete trains or in single cars has been tested under the following conditions, in comparison with plain-bearing cars of identical capacity. These tests comprise running resistance tests, both in summer and winter conditions, empty and loaded. The tests were made starting cold and after obtaining equilibrium temperature. There were starting tests for complete trains, starting tests for single cars, acceleration tests for complete trains, and tonnage rating tests for complete trains.

The data, as regards running tests and starting test of single cars in addition to the accumulated service of the 100 cars over a period of three years, permit of drawing reasonable deductions as to the value of roller-bearing equipment in railroad service.

The freight service improvement by roller bearings, from the data derived from the tests, supplemented by service records, can be listed under the following headings:

The break-away resistance of the roller-bearing cars, as developed in 115 tests, was slightly in excess of the low-speed rolling resistance, as compared with the break-away resistance of the plain-bearing cars, which is ten or more times the lowest rolling resistance. This characteristic should be reflected in reduction of wear and tear in couplers, draft gear, and car bodies, and in reducing the strain on locomotives in starting.

The running-resistance tests indicate a reduction in rolling resistance of the roller bearing throughout the entire speed range. The reduction is considerable in starting cold trains amounting to approximately 40 per cent.

A reduction of 16 to 28 per cent, varying with weather conditions, is indicated after ten miles of operation.

The reduction at equilibrium point, attained after approximately 20 miles of running where the temperature of the plain bearing ceases to rise, averages 11 per cent. The reduction in rolling friction with loaded cars under summer and winter conditions, at starting, after running 3 miles, 10 miles, and 20 miles, is indicated on two curves shown in Figs. 15 and 16. The four points are a general average of 170 running tests and 115 starting tests. The shape of the curve between the points, particularly between 0 and 3 miles operation, is conjectural. The normal resistance as controlled by load and temperature conditions, and which control the shape of the curve between the 0 and 3-mile points, is probably attained in the first few hundred feet of operation.

The winter tests are more nearly representative of the compari-

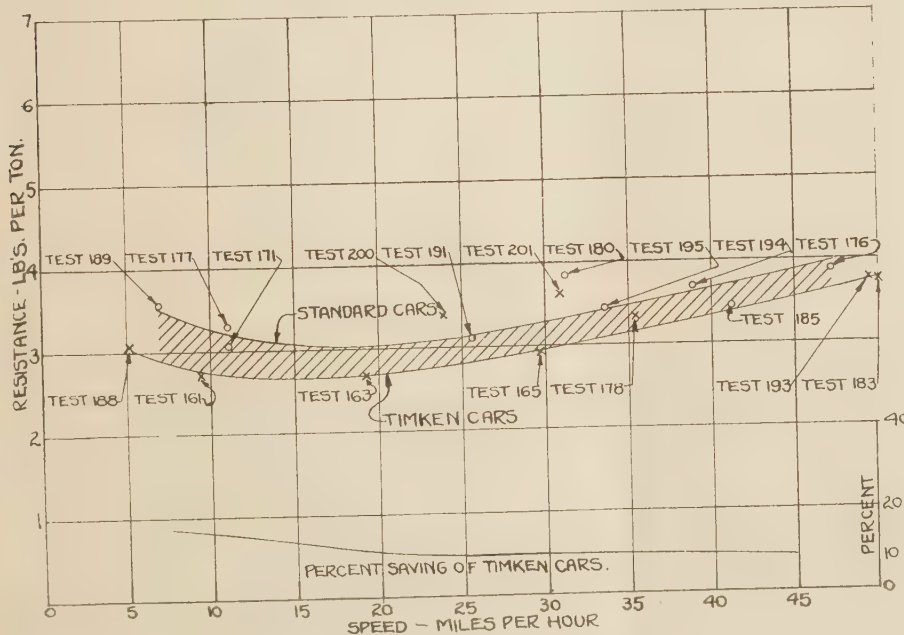


FIG. 18 EQUILIBRIUM TESTS, LOADED CARS, WINTER OF 1931
(Timken cars run in 6800 miles.)

son in rolling friction of the plain and roller bearings, as these tests were made with plain-bearing cars well run-in after several years of service and with roller-bearing cars after one year of service, averaging 6800 miles.

The comparative frictional resistance of loaded cars under winter conditions, after running 3 to 10 miles, is indicated on the curve in Fig. 17.

The equilibrium test on a loaded car is the best indication available of the comparative rolling resistance of cars with the two types of bearings. A general reduction of the roller bearing, ranging from 18 per cent at 10 mph to 9 per cent at 45 mph, is in-

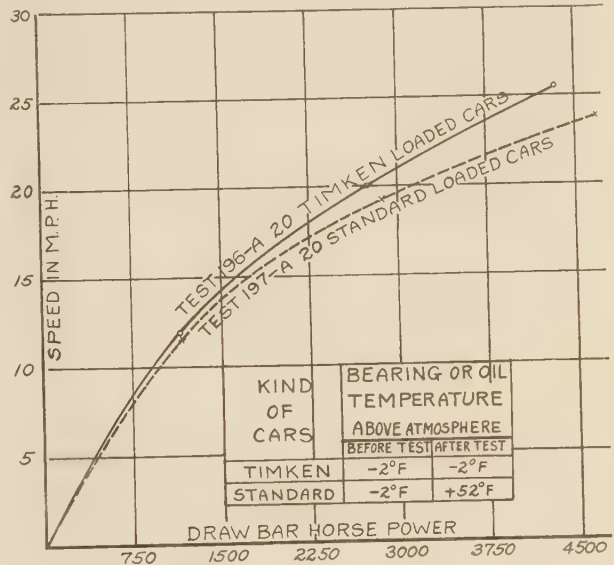


FIG. 19 FIRST ACCELERATION TEST
(Relation between drawbar horsepower and speed.)

indicated in Fig. 18. It will be noted that on account of the wide varying of conditions affecting rolling resistance, in addition to the roller bearing friction, a number of the tests show results slightly above or below the average. This is indicative of the need for a much greater number of tests before definite conclusions can be drawn. The 170 tests, spread over a wide variety of conditions, do not give any points to locate a curve representing specific conditions; however, it is the best data available. A fair check is provided by plotting the curve through points at various speeds from 10 to 50 mph, and where nearly all of these points show a logical curve, the influence of the erratic tests in locating the curve can be considerably reduced.

The test data and the experience available with roller bear-

ings indicate a wide divergence at starting, and the comparable rolling resistance of the plain and roller bearings converge at approximately 25 mph with a parallelism of the curves above that speed. The data available in the comparison of plain and roller bearings in steel-mill service indicate greater divergence and more important economies, while other data available for higher speeds and heavy loads, available in the copper-rolling industry,

indicate still further economies in favor of the roller bearing.

Acceleration tests, while limited in number, furnished indications that roller-bearing trains can be accelerated to predetermined speeds in less time or with less power, and given the same power, will attain a certain speed in a shorter distance. Curves showing acceleration tests are shown in Figs. 19 to 22. The curve in Fig. 20, representing relation between drawbar horsepower and speed, is of interest in showing a temperature rise in attaining a speed of $25\frac{1}{2}$ mph for the roller bearing of zero, whereas the temperature rise of the plain bearing in attaining a speed of 24 mph is 54 deg.

Starting tests on complete trains, made in limited numbers, gave indications that trains of equal weight can be started with plain or roller bearings, with trains having full slack, and 0.3 per cent grades.

The increase in the size of the stretched train that could be started with identical locomotive on roller bearings was 76 per cent. A total of 76 cars were started with either type of bearing in a slack train, but with a stretched train 65 roller-bearing cars

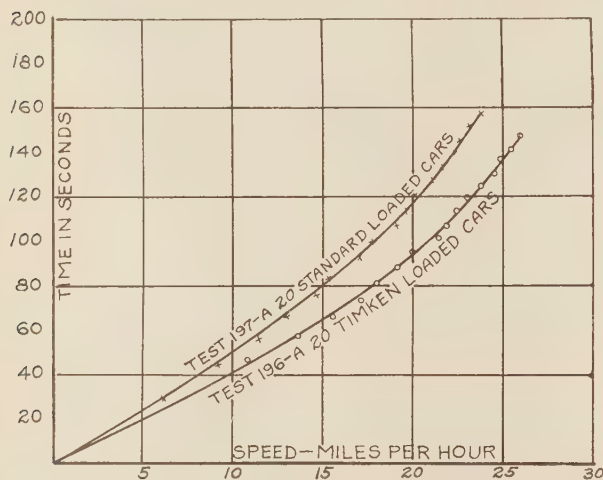


FIG. 20 FIRST ACCELERATION TEST
(Relation between time and speed.)

and 37 plain-bearing cars developed the full capacity of the identical locomotive.

Hot boxes, based on experience from October, 1925, on the first cars built and including the experience of the 100-car roller-bearing train, indicate that hot boxes are eliminated as a factor in railroad operation by the roller bearing. There have been no hot boxes to date.

Reduction in car maintenance is indicated by the experience with the 100 cars, with over 3,000,000 car miles without repairs to bearings or related parts and without a recorded repair to car bodies. While the experience is limited, a reduction in maintenance with roller bearings is indicated.

Increased speed of transportation should result with use of roller bearings. Speed limitation, as imposed by plain bearings, is eliminated entirely. It was found that 50 mph was the maximum permitted speed of the loaded 70-ton equipment as used in the running tests. The roller-bearing cars were operated at the top speed of the freight locomotive, namely 65 mph, without appreciable heat rise, but the plain-bearing cars developed hot boxes with such frequency at speeds of 50 mph as to cause the abandonment of the test program with plain bearings at the higher speeds. Higher speeds than 50 mph are operated on

plain bearings in passenger service and in general freight commodity service, but with reduced axle loads. It is expected that increased truck competition will force higher railroad speeds.

Economy in fuel should follow the reduction in rolling friction throughout the entire speed range from 5 to 50 mph. An economy of 10 per cent on level track would be equivalent to a 3 per cent saving on a normal heavy tonnage grade of 0.3 per cent and would be equivalent to $1\frac{1}{2}$ per cent on a 1 per cent grade.

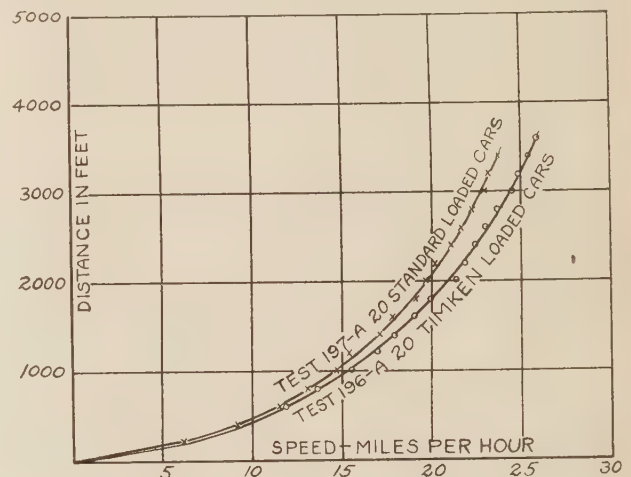


FIG. 21 FIRST ACCELERATION TEST
(Relation between distance and speed.)

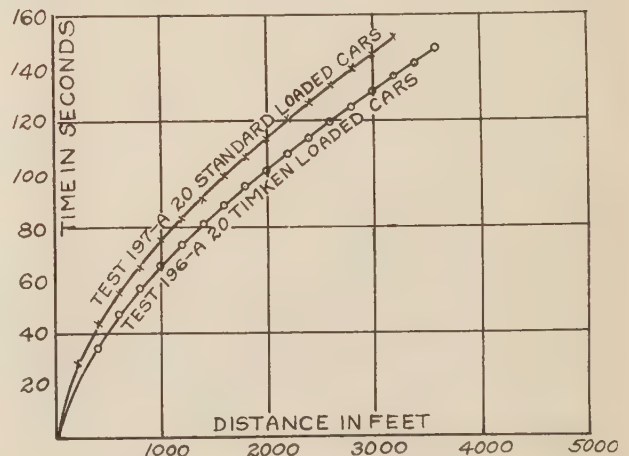


FIG. 22 FIRST ACCELERATION TEST
(Relation between time and distance.)

Fuel saving is affected by many other variables, but a general average could be expected.

Improvement in coupler and draft-gear service should follow the use of roller bearings on account of the 90 per cent reduction in effort required in break-away and the 75 per cent reduction in starting a stretched train.

An increased capacity of locomotives to haul larger trains or to haul equivalent trains at faster speeds is a natural corollary in the reduction of rolling friction.

The weight reduction is a factor of importance, amounting to 4400 lb per 70-ton car, which, with the identical rail load, increases the value of the car for hauling commodities.

Dry Film Gluing in Plywood Manufacture

By RAY SORENSEN,¹ LOUISVILLE, KY.

BETTER PLYWOOD ADHESIVES NEEDED

THE limitations of recognized plywood adhesives have been a severe handicap to the veneer and plywood industries, seriously retarding their development of known and promising plywood types and products. The recognized commercial wood adhesives in the United States, until within the last two years, might be termed *wet glues*, and consist chiefly of either animal or vegetable matter. All of these fluid glues, animal, vegetable, casein, albumin, soya bean, and their combinations, have been found inadequate to meet the wonderful opportunities in the plywood fields immediately ahead.

Partly for this reason, and partly because of inefficient promotion, the veneer and plywood industries have been severely restricted in their growth, while the metal and synthetic sheet material industries, with broader vision, have made big inroads into the well-recognized woodworking fields. It is a truism that an inferior but well-promoted product will often be accepted in place of an intrinsically better product that is not well presented. It is seldom possible to find new uses or new fields for plywood products because of the lack of proper adhesives and the dearth of necessary industrial research. It has been well said that plywood is no stronger than its glue line, and a glue of limited scope is a severe handicap in every way.

It is a fact that today, and for some time to come, the facilities for producing plywood are far in excess of the demand, and unless new uses and new fields are found, the industry faces a drastic curtailment of volume. Consequently it is incumbent on the industry to carefully analyze and evaluate all new materials offered to determine to what extent the old limitations are overcome.

PLYWOOD PROGRESS ASSURED BY DRY GLUE FILM

The ideal wood adhesive is one which is of a uniform quality, which can be laid or spread in an even coating, which gives a perfect glue bond, and which can be applied economically. *Dry glue film* stands ready to meet all of these conditions in an efficient way. The dry glue film process eliminates many complications that beset the manufacturers of fine veneered work because dry glue film is simpler to apply than wet glues; in fact, all of the untidy and unpleasant mixing and spreading operations in wet gluing are wholly removed from the plywood factory by the use of dry glue film. Properly manufactured glue film contains in each square foot of surface precisely the same quantity of glue, of equal quality, of uniform composition, of exactly the same bond strength, and of the same standard thickness.

The entire industry is certain to benefit greatly by the introduction of dry glue films for the fabrication of veneers, non-porous substances, and insulating materials into a new and wider range of plied-up combinations. The extent of the benefit to the industry will depend upon the degree that this dry glue film overcomes the known limitations of the commonly used wet glues.

PROBLEM OF WOOD MOISTURE IN PLYWOOD GLUING

The industry has long known that warping, winding, and twisting in plywood is greatly influenced by the *moisture content* of the

wood. It is also true that the strength of plywood varies widely with its moisture content. Only when properly dried wood is used can an acceptable product be obtained. It is much easier to dry the individual plies before gluing, such as lumber cores, veneer cores, or outer veneers, by an efficient and reliable drying process, than it is to dry the jointed, glued, and veneered plywood.

When using fluid glues containing a high percentage of water, which we have termed wet glues, these problems will be particularly great. The percentage of water contained in glues cannot be kept uniform nor can it be kept within certain limits. There is no possibility of regulating the influence of moisture on the glued plies. How deep the glue moisture penetrates into the plies to be glued depends greatly on the structure, dryness, thickness, density, and temperature of the wood, as well as on the consistency and composition of the glue. It is of prime importance in gluing to have not only even spreading, but also standard quality and predetermined consistency of the glue. It is known that many variations occur when glue is mixed in a plywood factory, regardless of the care exercised in its preparation.

The industry has been aware of the many disadvantages of wet glues and has tried to find or to perfect ways of evaporating part of the glue moisture after spreading and pressing, but with only mediocre success. These endeavors have inevitably opened the field to the development of the dry glue film.

EARLY DEVELOPMENT OF DRY GLUE FILM

In the early development of *dry glue film* it was discovered that it was impractical to produce a dry glue film having as a base the ordinary wood adhesives. The possibilities of dry glue films have had the attention of various individuals for a number of years, and as a result a dry glue film has been gradually developed, improved, and finally marketed.

The adhesive power to wood of phenol-formaldehyde condensation products has long been known, but their general use or commercial application has been prevented because of the expense or cost.

The qualities offered by phenolic resin as a wood adhesive were quickly recognized, and attention was then turned to the application of the resin product, whether as a colloidal solution, dry film, or powder. Many attempts were made by industries, both in this country and in Europe. About nine years ago a German research and chemical manufacturing company set out to perfect the use of phenolic resin as a commercial wood adhesive, which meant bringing it to the simplest form of application and within a cost range for general adoption by the plywood industry. The final result, after seven years of research, was the development of a phenolic resin dry glue film. Dry glue films have proved to be very simple, clean and quick in their application, and to eliminate many of the disadvantages unavoidably involved in the wet glues of today.

Because it is the first scientifically manufactured form of adhesive which at all times has the correct quantity and quality of glue, and sets up for the first time a scientific method of plywood manufacturing, it presents a distinctly new method which promises to revolutionize the present form of applying and using wood adhesives. There being but one dry glue film commercially recognized and used today, it may be considered typical of a class that is in the development stage.

As mentioned before, the industry has long felt the need of

¹ Formerly Secretary, Tego Gluefilm, Inc.; present address, 131 North Western Parkway, Louisville, Ky.

Contributed by the Wood Industries Division and presented at the Semi-Annual Meeting, Chicago, Ill., June 26 to July 1, 1933, of the AMERICAN SOCIETY OF MECHANICAL ENGINEERS.

better adhesives which would permit it to seek new uses and new fields for its products. It has been repeatedly shown that many new outlets for plywood are necessary in order to enable the industry to continue its sturdy progress. The newly developed dry glue film answers this need and permits the industry to proceed to enter these new markets.

TYPES AND GRADES OF DRY GLUE FILM

The dry glue film, as marketed today, might well be termed a sheeted synthetic or phenolic resin film because, as mentioned, it is a phenol-formaldehyde condensation product. The film is to be had in various weights, to meet a wide range of requirements. For example, what is termed a standard film which meets all ordinary conditions as an adhesive for plywood, is a 60-gram film. This means that over a given area the film contains by weight 40 grams of resin and 20 grams of paper, which is the carrier required in producing the film. This paper or carrier must be thin, porous, and fibrous, so as to permit a uniform impregnation of adhesive on both sides. It must be tough enough not to break in handling and so porous that under the influence of heat and pressure the adhesive will thoroughly penetrate the carrier and eliminate any tendency for the glue joint to separate. Film can be furnished with a greater or less amount of resin, according to the requirements demanded as an adhesive and the type of materials to be laminated. The shear values resulting from such variations are shown in Table 1.

TABLE 1 SHEAR VALUE OF TEGO GLUE FILM BOND

(In pounds per sq in. as influenced by different proportions of resin on the same carrier)

Pressure: Mahogany 142, and Birch 284 lb per sq in.

Time in Press: 10 min

Temperature: 130° C

Moisture Content of Veneer: Approximately 10%

Resin-coating per sq meter, gr	Mahogany 3-ply, 1/4 in.		Birch 3-ply, 1/4 in.	
	Dry	Wet	Dry	Wet
21	154	107	261	193
23	182	123	312	237
26	209	145	336	228
28	222	162	321	239
32	253	204	325	239
40	308	266	396	330

The standard glue film, described as 60 grams, is the last in the table, having 40 grams of resin and 20 grams of paper carrier.

TABLE 2 SHEAR VALUE OF SINGLE AND DOUBLE LAYERS OF TEGO GLUE FILM BOND

(In pounds per square inch)

3/16 in., 3-ply, All Birch

Pressure: 284 lb per sq in.

Time in press: 10 min

Temperature: 130° C

Moisture Content of Veneer: 10%

Resin coating per sq meter, gr	Single layer	Double layer	Increase, %
21	248	312	26
40	298	445	49

In case more than 40-gram coating is required, as in gluing metal to wood, it is practicable to use two sheets of dry film glue in each joint. While this does not double the bond strength, still it does result in a substantial increase, as shown in Table 2. It is frequently advisable to use double layers where the surfaces are rough, requiring more glue bulk, or where veneers vary slightly in thickness.

The standard width is 51 in., but can be made up to 82 in. Rolls will average over 3900 ft in length, and a 51 in. X 3900-ft roll will weigh 225 lb crated, containing approximately 17,000 sq ft.

APPLICATION OF DRY FILM GLUES

The assembling of veneer into plywood with dry glue film methods demands an entirely different technique than that which

has been commonly employed with the usual wet glues. The dry film glue, being a phenolic resin, is thermoplastic and thermo-setting, which now permits the fabricating of plywoods without the introduction of water into the carefully dried veneers, as is necessary with the wet glues.

The film glue being thermoplastic and thermo-setting, the bond is accomplished with heat and pressure, requiring a hy-

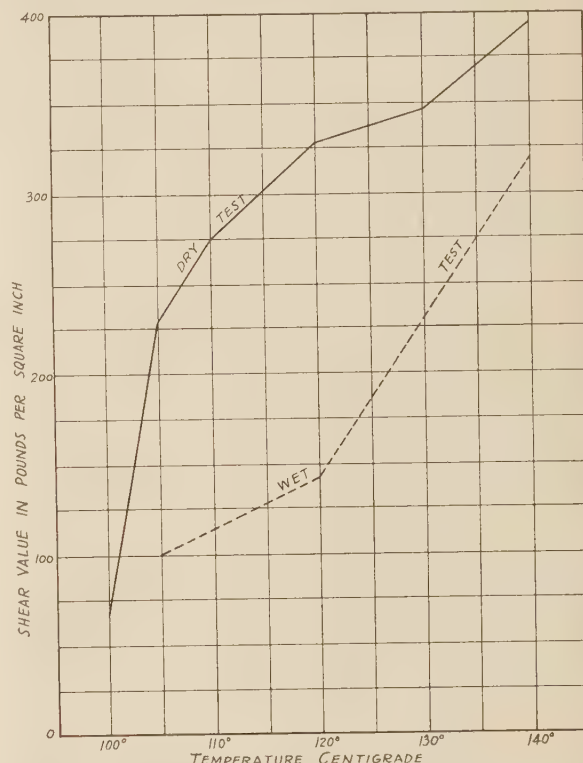


CHART 1 INFLUENCE OF TEMPERATURE ON GLUE FILM JOINTS
3/16 IN., 3-PLY BIRCH

(Glued at 10% moisture content in 10 min time, with 284 lb per sq in. Dotted line is test after immersion. Full line is dry test before immersion.)

draulic hot plate press. With the application of both heat and pressure at the same time, as is had uniformly with the modern type of hydraulic hot plate presses, the resin film polymerizes and becomes both insoluble in water and chemically inert. This method of producing a bond with the dry film glue might be termed "vulcanizing," and has for the first time set up a laminated panel in which the fibers of the adjacent plies are brought directly in contact with one another. In fact, the adjacent plies might be said to be welded to each other. Thus the bond obtained has in reality converted the several original plies into an ultimate panel of solid material, and this has been done without the internal stress and strain which is often so troublesome.

The dry glue film process eliminates the expensive redrying methods which have to follow gluing with wet glues. The industry has spent a great deal of time and money to set up proper methods for this subsequent redrying necessary to remove the glue moisture. Woods vary in their structure and density, making it impossible to accurately control the drying process, which is often the cause of distorted plywood and checked faces.

Inasmuch as the dry glue film is only 0.005 in. thick, entirely new demands must be made as to the pressure required. The hydraulic hot plate presses must be designed and built to new

standards of accuracy as to the deflection of its members. The maintenance of proper temperatures on the entire surface of the plates is of extreme importance.

RELATION OF HEAT, MOISTURE, PRESSURE, AND TIME

When gluing with dry glue film there are four variables to be considered, namely, *temperature* or heat, *moisture*, *pressure*, and *time*. All are closely related to one another in producing a satisfactory bond with resin adhesives, but it is best to consider the influence of each factor separately. The strength value of each of these variables in relation to the others has been accurately determined and charted. The accompanying charts 1, 2, 3, 4 show definitely the strength of the bond obtained when varying the factors and prove conclusively that the laminating of plywood with dry glue film may be considered a scientifically controlled process. A careful study of the series of charts will readily show that when the same combinations of variables are repeated, the value or strength of the bond obtained comes within close limits, if the same or similar woods are used.

1 *Influence of Temperature or Heat.* The dry glue film, being a phenolic resin and thermoplastic, requires a definite amount of heat and a predetermined time to set up or produce polymerization.

Chart 1 clearly indicates the influence of heat for a given period of time, and demonstrates the greater shear values of the bond as the temperature is increased. In preparing these charts it will be noted that certain standard time, pressure, moisture, and heat factors have been established, to show relative comparative values with one another. The construction of the

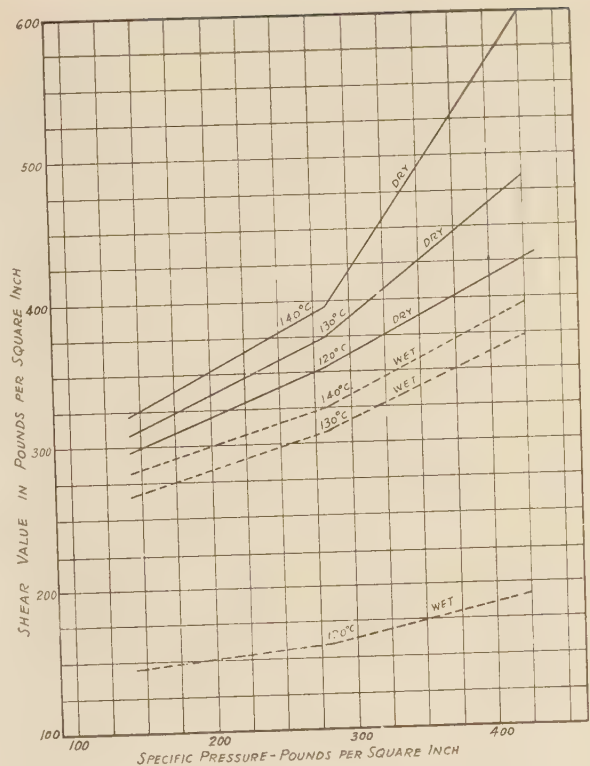


CHART 3 INFLUENCE OF PRESSURE ON GLUE FILM
3/16 IN., 3-PLY BIRCH

(Glued in 10 min time, with 10% moisture content in veneer. Dotted lines are tests after immersion. Full lines are dry tests before immersion.)

plywood used is a 3-ply panel, 3/16 in. thick, all plies 1/16 in. birch.

The solid line indicates the strength of the bond when testing the plywood in a dry state, having an average moisture content of 7 to 8 per cent. The dotted line indicates the strength after soaking in water at room temperature for 48 hr. It will be noted that while the value obtained when testing the bond after soaking is somewhat lower than the dry test, this does not mean that the glue line has weakened to this extent, but rather that the tensile strength of the fibers of wood are lower in a wet state. It is also a fact that the shear value of the dry glue film bond always increased when redried after soaking.

In studying this chart it will be readily observed that the increase of temperature in a given time materially increases the strength of the glue bond. For instance, a panel glued at a temperature of 100 C for 10 min at a pressure of 284 lb per sq in. and with a moisture content of 10 per cent, has a shear value of 66 lb per square inch. With all other factors remaining the same and the heat increased to 140 C, the shear value increases to 396 lb per sq in. The same increase is proportional to a lesser extent in the wet test. Increase of heat in a given period of time always produces a better glue bond.

In the manufacture of dry glue film the resin has been prepared to a definite point, and it will be observed on all the charts that a temperature no higher than 140 C has been shown. Tests have proved that no material increase in the bond is found at temperatures beyond 140 C, but any increased temperature above this has no detrimental effect upon the curing of the resin. The wood itself is the item that must be kept in mind when employing high temperatures. The gluing temperature of 140 C

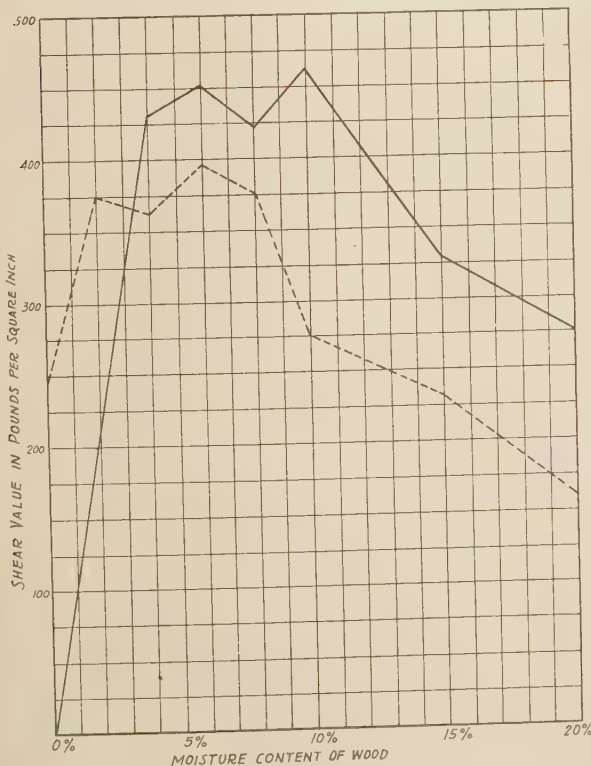


CHART 2 INFLUENCE OF MOISTURE CONTENT OF WOOD ON GLUE FILM JOINTS
3/16 IN., 3-PLY BIRCH

(Glued at 130 C, 284 lb per sq in., 10 min time. Dotted line is film 14 days old. Full line is film one year old.)

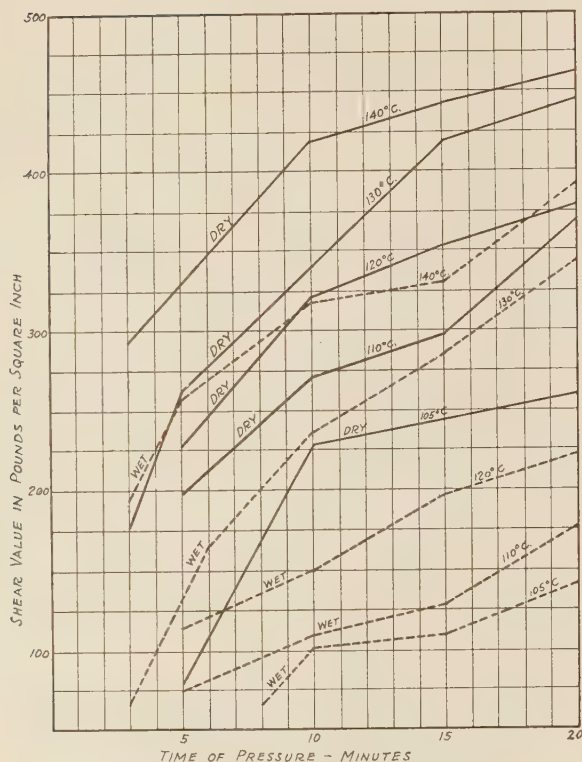


CHART 4 INFLUENCE OF TIME OF PRESSURE ON GLUE FILM JOINTS
3/16 IN., 3-PLY BIRCH

(Glued at 284 lb per sq in., and 10% moisture content. Full line is dry plywood test. Dotted line is plywood test after 48 hr immersion. All temperatures are given in Centigrade.)

required for dry glue film does not damage the quality of the wood.

This has been proved by a number of tests, especially those of Professor Dr. Otto Gerngross of the Technical University of Berlin, as shown in Table 3. While the table refers only to birch and fir, these are taken as typical of the hardwoods (deciduous) and the softwoods (coniferous). It is to be noted that both species have a strength increment of more than 10 per cent due to simultaneous heat and pressure. The heat alone on the birch does not alter the strength value, but heat alone on the fir will carry the strength value to that of combined heat and pressure. This is due to the natural rosin content of the coniferous wood that is equalized and hardened by the heat.

TABLE 3 EFFECT OF HEAT, WITH AND WITHOUT PRESSURE, ON TENSILE STRENGTH OF SINGLE-PLY VENEER

Specimens tested: 1 1/8 in. X 4 in. X 5/64 in. Birch and Fir veneer
Temperature: 140 C
Pressures and tensile strength given in lb per sq in.

Species	Specific pressures	Time, min	Tensile Strength Before heat	After heat
Deciduous (Hardwoods)				
Birch.....	0	45	7892	7864
Birch.....	142	15	8788	8674
Coniferous (Softwoods)				
Fir.....	0	45	5631	6897
Fir.....	142	20	6541	6826

Adapted from article in "Sperrholtz," 1930 (S-382) by Prof. Otto Gerngross, of Berlin, Germany.

When gluing with dry film glue it is always safer to employ the higher temperatures, but seldom over 140 C. This usually depends on the type of material to be laminated.

2 Influence of Moisture Content in Wood. Methods of

gluing with dry glue film differ from those of ordinary wet gluing because the natural moisture in the wood is not increased by glue water. Experiments have shown that, regardless of the type of glue used, warping and wavy surfaces in lumber core plywood are not only caused by irregular thickness and resistance against compression by the core, but that they also occur if the moisture content of the core exceeds 5 to 6 per cent. This limit of moisture content, however, does not apply to cross-banding and outer veneers.

It will be noted from chart 2 that the shear value or bond strength depends to a great extent on the moisture content of the veneers. A careful study of the chart shows the bond that can be obtained when using a dry glue film that is several months old, which is the average age of the film when used. This is indicated by the solid line, while the dotted line represents the bond obtained when using a freshly manufactured film about ten to fourteen days old.

A certain amount of moisture is necessary to plasticize the resin, and this moisture may come either from a freshly made glue film or from the veneer. Consequently it is important to regulate the moisture of the veneer within safe operating limits. The chart indicates that freshly made glue film must be used where veneers are substantially less than 4 per cent moisture content, but that even better joint strength is obtainable from aged glue film when the veneer is between 4 and 12 per cent m.c., which is the normal condition found in veneer as stored in the average warehouses. It is obvious that this eliminates the ordinary redrying required prior to wet gluing.

Experience has proved that the most useful medium for the moisture necessary in plasticizing dry glue film is the cross-banding in 5-ply construction. This is so situated in the assembling operation as to supply the required moisture to the dry glue film adjacent to both the core and face. It has been pointed out that excessive moisture in a lumber core is dangerous, and it is apparent that surplus moisture in face veneer may result in open joints or hair lines and checks.

It might be mentioned that in gluing very fragile face veneers, such as highly figured crotches and burls, tests have shown a moisture content of about 6 per cent to be the most satisfactory.

3 *Influence of Specific Pressure.* The pressure applied on the surface of the plywood is the *specific gluing* pressure, or, as it is frequently called, the *platen* pressure in pounds per square inch and should not be confused with the higher pump pressure that is required. The application of pressure with dry glue film is no different than when gluing with wet glues, except that wet gluing usually requires 75 to 150 lb specific pressure, while dry gluing ranges from 150 to 250 lb and in some instances up to 300 lb per sq in. The amount of pressure exerted on a panel depends on the density of the wood and the construction of the plywood.

It is also indicated on chart 3 that the strength of the glue line increases with additional pressure. The maximum pressure depends upon the compression loss in plywood thickness that can be allowed. Some woods and synthetic boards will crush under 50 lb, while denser woods and non-porous synthetic products will permit greater pressure. Consequently the adhesion on the softer products will not be as great as on the harder materials. The average compression percentages on the commoner woods are given in Table 4.

4 *Influence of Time of Pressure.* The time required to complete the bond, which is often referred to as *gluing time*, is generally understood to be the time that elapses after obtaining the correct specific pressure and until the reopening of the press. It is also essential that the temperature of the plates is secured before closing the press. The gluing time depends chiefly upon the time necessary for the heat to penetrate from the steam-

heated platens through the aluminum cauls, the outer veneer and crossbanding, or to the film farthest from the source of heat.

Mention has been made of using aluminum cauls. They retard the penetration of heat but a very few seconds and are used to facilitate the handling of the stock in and out of the press.

Chart 4 readily indicates that a strong bond can be obtained in 3 min when employing temperatures in excess of 130 C. The ordinary $1\frac{3}{16}$ -in., 5-ply construction as is commonly manufactured for tops, requires an average of 12 min to complete the bond. It will be noticed from this chart that the increase of time materially increases the strength of the glue line.

TABLE 4 COMPRESSION FACTORS IN PLYWOOD

Species wood	Plywood thickness	Construction: 3-ply Time of Pressing: 10 min Temperature: 130 C Moisture: 10% Pressure: Lb per sq in.	
		Specific pressure	Compression, per cent
Mahogany.....	$1\frac{3}{8}$ "	142	6.2
		213	6.8
		284	32.0
Fir.....	$1\frac{3}{8}$ "	142	9.5
		213	15.3
		284	39.0
Alder.....	$3\frac{3}{32}$ "	142	2.4
		213	3.1
		284	9.3
Beech.....	$3\frac{5}{16}$ "	142	7.8
		213	9.1
		284	15.2
Birch.....	$1\frac{1}{16}$ "	142	4.5
		213	4.5
		284	13.3

Again it is shown that the waterproofness of the glue line increases with the gluing temperature and elapsed time the material remains under pressure.

HYDRAULIC HOT PLATE PRESS

The hydraulic hot plate press is not a recent development. Its origins, as adapted to plywood, date back some fifty years in Europe. The modern hot plate press is the result of the progressive development of the plywood industry based on scientific and practical research. The comparatively recent development of dry glue film has revolutionized this press industry in the United States, since the low unit pressure of wet gluing processes permitted a comparatively light-weight press, while dry gluing requires higher pressures and sturdier presses.

1 *Plate Design.* The modern hydraulic hot plate press for high pressure is fitted with plates of special alloy steel having good heat conductivity and high compressive strength. The steam channels, bored in the plates, are accurately drilled and properly spaced to insure uniform distribution of heat on both surfaces. The maintenance of equal heat is essential in dry glue methods and this type of plate fully answers these requirements. This is in contrast with the old style plates used for low pressure in gluing with thermo-setting wet glues, which consisted of relatively thicker (2 to 4 in.) sections with unevenly distributed steam channels. The high tensile strength of the alloy steel plates permits the use of thinner plates, averaging $1\frac{1}{2}$ in., substantially increasing press capacity. The surfaces must be machined accurately so that their parallelism insures uniform pressure on the plywood, otherwise a serious variation of thickness (crushing) and uneven glue bonds might occur in the finished plywood. Step devices are provided to suspend the plates in the open press.

2 *Upper and Lower Platens.* The press head, or the upper platen, should be a one-piece heavy steel casting to insure a maximum deflection of 0.003 in. The deflection in the cold press is seldom serious since it is distributed over 30 in. of content, or a clamped bale, while in the hydraulic hot plate press, there

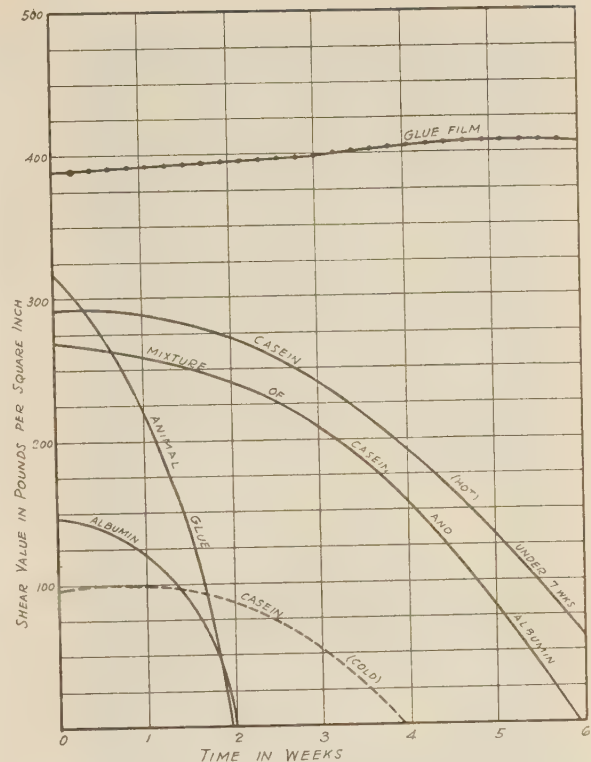


CHART 5 INFLUENCE OF MOLD AND FUNGI ON DIFFERENT PLYWOOD GLUES

(Dotted line, wet glue in cold press. Full lines, wet glue in hot press. Full line with dots, dry film glue in hot press.)

is usually but one panel between each pair of plates, or a content of less than 1 in., and the whole deflection may come in each panel. The lower platen, or head, should also be a one-piece casting and together with the plates should be well aligned and guided during the opening and closing of the press to insure against displacement.

3 *Pump System.* The modern hot plate press must be equipped with a satisfactory hydraulic pump system to insure rapid closing in not more than 30 sec and also to maintain accurate continuous pressure. The temperature of the plates is usually thermostatically controlled to maintain a constant heat. The pump system should be so designed that after reaching the maximum pressure it will ease off smoothly.

4 *Mechanical or Manual Loading.* While many of the smaller presses are manually operated, as to loading and unloading, the larger presses are equipped with automatic charging devices as illustrated in Fig. 7. In some instances the charging equipment is designed to operate similarly to the lumber lift. This permits the loading and unloading of the openings, or "day-lights," of the charging device at the level of the truck or table used.

5 *Cauls.* Aluminum cauls, usually $1\frac{1}{16}$ in. thick, are used to facilitate the loading and unloading of the assembled plywood. The aluminum caul is a good conductor of heat, requiring but a few seconds for attaining the temperature of the steam-heated platens, especially when under pressure. For this reason the aluminum caul should not be used to retard the penetration of heat, or to compensate for slow acting pump systems.

TECHNIQUE OF PROCESSING

The preparation of the face veneer, cross bands, and cores does



Fig. 1

Fig. 2

Fig. 3

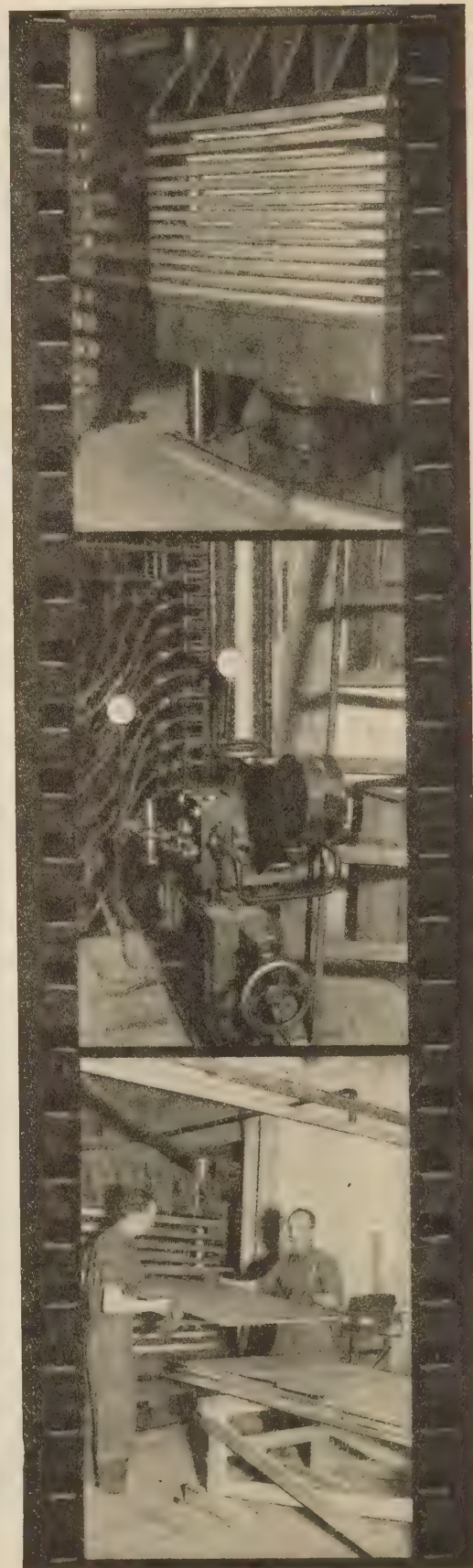


Fig. 4

Fig. 5

Fig. 6

not differ from regular methods employed for ordinary wet gluing, except as to the moisture content of cross bands and face veneers.

1 *Tapeless Face Jointing.* A great deal of time and attention has been devoted to discovering some means of eliminating the paper veneer tape used in splicing face veneers and cross bands. Attempts have been made to perfect a thin fibrous paper tape to be applied to the under side of face veneers, so that when the gluing operation is completed the surface of the plywood will require no sanding other than the ordinary polishing for finishing purposes.

As the plywood comes from the hot plate presses when glued with aluminum cauls, the surface has a very high sheen or polish and requires no sanding by the plywood manufacturer if the face veneers are free of tape. Some recent developments have been made in perfecting a tapeless veneer splicer as shown in Fig. 1. This machine has been designed along the lines of the ordinary veneer splicers. Prior to splicing the faces, the edges of the veneers are coated with a good grade of animal glue and allowed to dry. The glue is usually applied immediately after jointing and before the pressure is released in the jointer. The veneers are passed through the splicer and under heat units, which redissolve the animal glue and set it. The speed at which the stock can be jointed or welded depends on the number of spindles built in the machine. For example, a four-spindle machine will weld approximately 35 lineal feet of $1/16$ -in. veneer a minute.

The elimination of taped faces will greatly reduce the cost of plywood manufacturing, especially in the sanding departments. It also permits the manufacture of plywoods, utilizing narrow veneers, with absolutely waterproof joints, having no tape remaining under the joints to decrease the strength of the dry glue bond.

Development work is now being carried on to produce a veneer tape manufactured from dry glue for use on the standard paper tape veneer splicer.

2 *Dimensioning the Dry Glue Film.* There has been some question as to the proper method of cutting dry glue film to dimension sizes. This is clearly illustrated in Fig. 2. Usually the operator cuts the film on the table, as shown, to multiple dimensions that will recut to several smaller sizes. The recutting is completed on an ordinary veneer clipper. It is not practical to attempt to cut the film to final size in single sheets on a veneer clipper because of the extreme thinness of this film. The film is supplied in various widths up to 82 in. wide; therefore the waste can be held down to a minimum.

Captions for illustrations appearing on opposite page

FIG. 1 A FOUR SPINDLE TAPELESS VENEER SPLICER FOR EDGE UNITING VENEER WITHOUT THE USE OF THE CONVENTIONAL VENEER TAPE. THE CHAIN FEED PRINCIPLE IS SHOWN EMPLOYING STEAM OR ELECTRICALLY HEATED ROLLS FOR THE THERMO-SETTING ADHESIVE

FIG. 2 METHOD EMPLOYED IN CUTTING THE DRY GLUE FILM. THE CUTTING TABLE IS MARKED OFF IN INCHES TO ASSIST THE OPERATOR IN CUTTING THE FILM TO EXACT DIMENSION

FIG. 3 THE SIMPLE, CLEAN, AND QUICK METHOD OF ASSEMBLING THE VENEER, CORES, AND CROSS BANDS, PRIOR TO PRESSING, IS CLEARLY ILLUSTRATED

FIG. 4 THE ASSEMBLED PLYWOOD PLACED IN THE OPENINGS OF THE HYDRAULIC HOT PLATE PRESS JUST PRIOR TO THE FULL CLOSING OF THE PRESS

FIG. 5 CONTROL UNIT EMPLOYED ON A EUROPEAN HYDRAULIC HOT PLATE PRESS, AUTOMATICALLY REGULATING THE TEMPERATURE, SPECIFIC PRESSURE, AND TIME OF PRESSURE

FIG. 6 REMOVING THE COMPLETED PANELS FROM THE OPENINGS OF THE HOT PLATE PRESS

3 *Laying the Film.* The laying of the dry film is very simple and requires a minimum time, as illustrated in Fig. 3. Piecing of the film or lapping of the joints can be done to utilize the small cuttings that might otherwise accumulate.

4 *Loading the Press.* As mentioned before, in loading the press the stock is placed between aluminum cauls. Fig. 4 shows a press loaded and in the process of closing. The charging of the different openings of the press, as well as the closing time, should be done as quickly as possible. With modern pumps the specific pressure required can be secured in 30 sec, avoiding any pre-curing of the film by heat before pressure is effective. An automatic control, regulating the pressure, temperature, and time, is shown in Fig. 5.

5 *Unloading the Press.* The manual unloading operation is shown in Fig. 6. In this instance aluminum cauls were not used, due to the use of non-figured thick face veneers. Automatic loading and unloading devices are extensively used in Europe and are shown in Fig. 7. This equipment conserves press time and reduces the labor of the press crew. During the time of pressing, the moisture content of the veneer has been reduced to some extent. It is a common thought that immediately after the plywood is removed from the press, it begins to take on moisture. This is incorrect, as it will continue to give off moisture until the temperature of the plywood has fallen below 100 C. To hasten the manufacturing time plywood may be passed through a bath of water immediately after coming from the press and allowed to temper for several hours in bulk, after which it is placed on sticks and weighted for equalizing temperature and moisture content.

EFFECT OF CONTINUED HEAT WITHOUT PRESSURE

The problem of limited press output is certain to occur as the demand for dry glue film plywood increases. Two sheets of plywood can be placed in each press opening, provided suitable cauls are located *between* as well as *above* and *below* the plywood. Such a procedure is limited to plywood $1/8$ in. and thinner and will require only half as much additional time as a single sheet of plywood, increasing the press capacity 50 per cent.

Another method of conserving press time is that of placing plywood that has not been completely plasticized in the press in heat-controlled kilns immediately after removal from press. This has the effect of continuing the heat treatment to complete plasticization in the kiln, after the pressure element has completed its function.

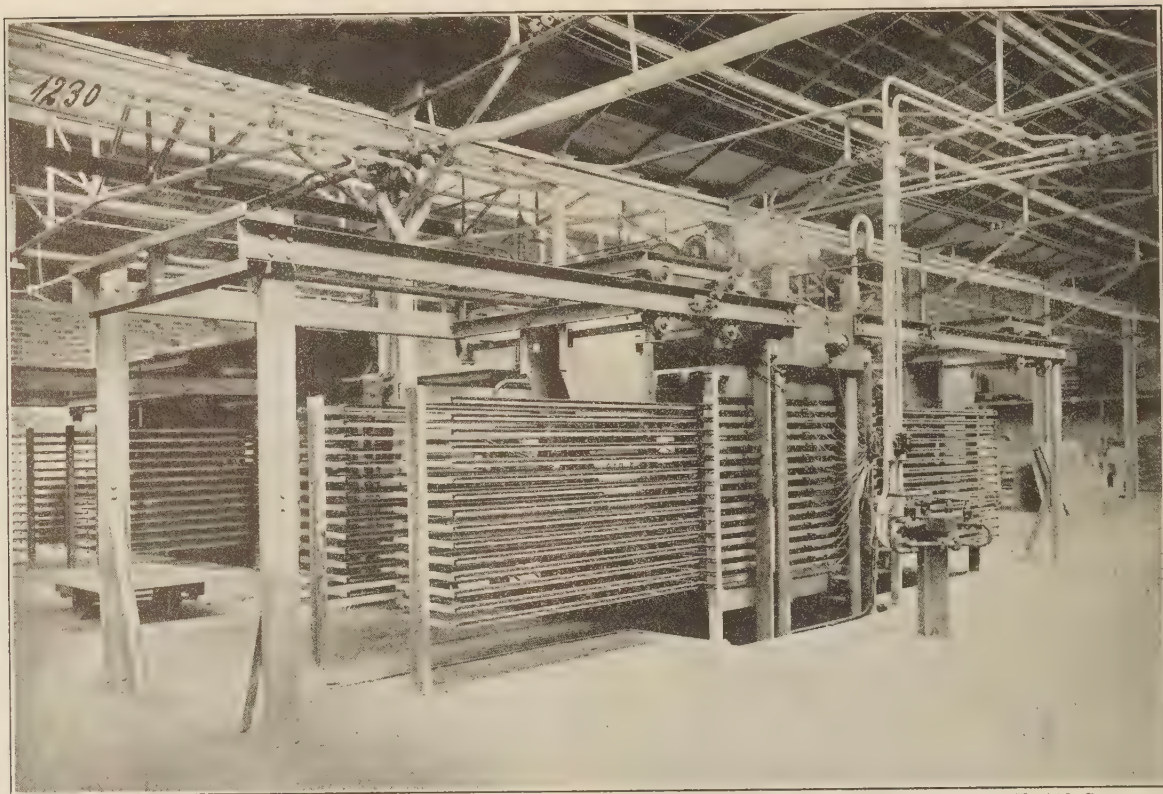
The results of a series of tests indicate that the pressing time can be reduced at least one-half without sacrificing bond strength. Table 5 shows the trends of such a procedure, with the press conditions in the left-hand side of the table and the kiln conditions directly across on the right-hand side.

ADVANTAGES OF DRY GLUE FILM

There are many advantages to be secured when laminating with dry glue film. The process is simple and quick. The assembling of the layers can be done in a suitable room near the press, as the time between assembling and pressing is not limited. Care can be exercised in assembling of the veneers and cores, while the haste and rush now so characteristic of the glue room operations is overcome.

The factor of time in gluing and conditioning plywood is reduced from days to a matter of hours. This time saving assists the manufacturer in meeting many urgent deliveries with utmost assurance of perfect material.

Dry glue film permits the gluing of *extremely thin, light-colored*, and porous veneers of all kinds without any staining effects. Because of this non-staining quality the beauty of the wood is



Courtesy, Becker & Van Hullen, Krefeld, Germany

FIG. 7 SHOWING LOADING AND UNLOADING DEVICES ON A HOT PLATE PRESS, CARRIED ON OVERHEAD CHANNEL RAILS

retained, finishing costs are lowered, and a rich, deep tone of artistic character is produced.

The bond effected with dry glue film resin is not only *water-resistant*, but is actually insoluble in water and chemically inert. Extensive tests have not only shown the glue line absolutely waterproof, but on redrying after immersion the bond always shows increased strength. Not only is the bond chemically inert but it is *resistant* and retardant to the attack of *mold*, *fungi*, and *bacteria*. Tests show that termites and wood vermin will not attack plywood laminated with a phenolic resin film when layers are $\frac{1}{8}$ in. or thinner.

Chart 5 shows the life of various wood adhesives when subjected to the attack of mold and fungi.² It should be mentioned that the time shown in weeks for full decomposition of the glues was partly absorbed by the building up of the mold culture. This time is shortened when subjecting the specimens to a culture of mold and fungi. For instance, in place of requiring approximately four weeks to decompose a casein glue line when applied in the cold method, the time is reduced to approximately ten days when subjected to a culture. It will also be observed that the hot plate press method of gluing with wet glues not only increases their water resistance but also improves their resistance to the mold attack. This shows that all of the wet adhesives are subject to full decomposition, while the bond made with the film resin is 100 per cent resistant to

these attacks. Other tests show no deterioration to the bond after being exposed to the attack of mold and fungi for two years.

The old theory that plywood must be made with a *balanced construction* has been disproved. It is now possible to produce 2-ply panels with lumber core and face veneer with substantial economy and showing no distortion. Many new forms of construction not heretofore possible can be developed when gluing, without introducing moisture into the veneer or lumber.

After gluing, plywoods can be placed in hot water or steamed without injury to the bond. This permits use of flat plywood construction in the forming of *bent* and *curved* products, and the resulting work is very satisfactory.

The dry glue film bond will not react, thus eliminating a *corrosive attack*.

It also has the quality of extreme *flexibility*. There is no crystallizing and cracking, and the bond cannot be destroyed by distortion.

The dry film is completely dissolved under pressure and heat and for the first time has effected a bond which is *stronger* than the contracting and expanding power of wood, when subjected to excessive moisture. This is illustrated in Fig. 8, showing a 3-ply flooring test, using $\frac{5}{16}$ -in. oak face and $\frac{5}{16}$ -in. chestnut core and back. The outer surface expanded in a one year's immersion test some 5 per cent, while the glue side of the oak was held to approximately original dimension by the dry glue film bond.

Dry glue film is very adaptable for the gluing of *crotch* and highly figured veneers in either a 5-ply construction or a 2-ply reinforced face construction. It insures these veneers against checking because the adhesive bond is stronger than the expansive power of the wood. For the same reason it also eliminates

² Since preparation of this article Naval Aircraft Specifications No. 39P13a, April 1, 1933, provide:

E-2c. The adhesive used shall be resistant to decomposition from mold, fungi, bacteria, and shall show a minimum average shear value of 250 lb per square inch when subjected to a culture of the above for a period of ten days.

the so-called hair-lining troubles which are so objectionable to all plywood and furniture manufacturers.

Another interesting feature is that dry glue film has made it possible to use the low-priced Western coniferous woods for core materials, and veneer over them with a thin face ($1/32$ in.) veneer without showing the effect of the underlying grain in the coarser woods. Absence of moisture in the gluing is the chief factor in making this possible.

There are many other advantages known and in the process of development, should space permit their discussion.

RECENT ADAPTATIONS OF PLYWOOD TO NEW PRODUCTS

The plywood industry has been eager to enter broader avenues of trade, but up to the present time the handicap of the standard wet glues has seriously retarded such expansion. The wide range of opportunities for these newer types of plywood are briefly suggested.

1 *Construction Trades.* To the building trade, dry glue film products offer a new material heretofore limited. The increased use of Ferroclad materials to meet fireproof requirements has demanded an adhesive which will not corrode the materials and will not crystallize and decompose under rapid change of temperature and humidity. The adaptation of ply-

wood to the building trade demands that the bond shall withstand all conditions of exposure, is not subject to vermin, termites, mold and fungi attack, is fully waterproof, and resistant to rapid change in temperature, both wet and dry. A few suggested uses are as follows:

Plywood flooring
Flush and panel doors
Veneer faced synthetic fiber boards
Prefabricated unit houses
Concrete forms
Paneling with built-in electrical heating units
Wall paneling.

2 *Automotive Industry.* The automobile industry is always searching for material of the greatest strength with the least weight. While plywood has been considered by designers in the past, the lack of waterproofness and resistance to decomposition by atmospheric elements, such as wet and dry decay, has retarded its adoption by the industry. The dry resin film has entirely overcome these difficulties and the designers are eager to specify plywood for the following items:

Floors, sides, and roofs of refrigerated and ordinary trucks
Roofs, floors, and interiors of buses
Roofs of closed passenger cars
Running boards and insulated floor boards
Battery separators and containers.

The plywood roof not only eliminates the deterioration now so common but supplies an unusual degree of rigidity.

The plywood battery separator and container offer a new and repetitive market to the plywood industry.

3 *Ship and Boat Building.* Due to the advent of the dry resin glue film the entire ship and boat building field is now open for plywood utilization. Waterproof plywood made possible

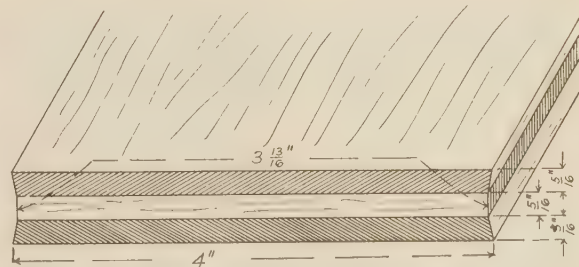


FIG. 8 SHOWING THAT THE WIDTHWISE SWELLING OF $1/16$ -IN., 3-PLY OAK PLYWOOD AFTER 1 YEAR'S SUBMERSION IS HELD BY THE DRY GLUE FILM BOND AGAINST THE CORE, BUT ASSUMES NORMAL EXPANSION AT THE OUTER SURFACES

the fabrication of canoes, racing hulls and outboard motor boats insuring greater strength and reduced weight. The new waterproof plywood insures indefinite durability under continuous immersion, and the bond is not affected by oil, acid, or salt water. Some of the watercraft applications are:

Canoes
Outboard motor boats and racing hulls
Ship bulkheads and partitions
Marine wall paneling
Ship furniture.

4 *Aircraft.* Innumerable tests in commercial and aircraft laboratories, both here and abroad, have conclusively established that the bond in phenolic resin plywood is far superior in strength and endurance to any type of plywood heretofore used.

The waterproofness of the bond, the absolute resistance to atmospheric elements, the tests that have proved the shear

TABLE 5 EFFECT ON PLYWOOD STRENGTH OF CONTINUED HEAT IN KILNS

(After removal from hot press)

Specific pressure in press: 285 lb per sq in.

No pressure in kilns

Shear tests: Wet or dry, in lb per sq in.

Wet tests after soaking in water at room temperature for 48 hr

Temperatures: Deg C, automatically maintained

Time: Hr and min

Pressing (before kilning)				Kilning (after removal from press)			
Time, H.—M.	Press temp., C	Shear dry	Shear wet	Time, H.—M.	Kiln temp., C	Shear dry	Shear wet
1/4 in., 3-ply, All Birch Plywood							
0—3	130	Nil	Nil	0—30	140	253	253
		Nil	Nil			253	264
		Nil	Nil			176	275
0—4	130	110	77	0—30	140	227	264
		116	77			264	341
		143	99			264	341
						286	301
		123	84	0—30	140	271	328
0—5	130	160	112			286	286
		165	118			286	275
		187	143			281	264
						284	275
0—6	130	206	176	0—30	140	220	294
		211	184			242	319
		242	184			330	319
						264	310
0—7	130	242	206	0—30	140	253	268
		253	209			308	297
		259	209			330	297
						297	287
		251	208				
3/16 in., 3-ply, All Birch Plywood							
0—10	110	187	94	0—30	140	429	462
		220	140			506	462
		264	Nil			519	308
						485	410
Same	Same	Same	Same	2—0	90	358	266
						358	279
						352	232
						356	292
Same	Same	Same	Same	17—0	90	341	365
						484	407
						462	462
						429	411
5/16 in., 3-ply, All Birch Plywood							
0—10	110	187	94	0—10*	130	534	341
		220	140			484	319
		264	Nil			418	341
						478	334
		224	78				

* Re-pressed and re-heated by returning to press, as in case of under-plasticized plywood, where kilns not available.

value of the bond to be the highest ever recorded, and the continuous increment of strength or frequent absorption of moisture all strengthen the hold of plywood in aircraft industry.

Plywood of unusual strength as thin as 3-ply, $\frac{1}{32}$ in., is now produced commercially for aircraft fabrication. This type of material now available to the industry permits the manufacture of aircraft at a reduced cost, with less weight, with increased strength, with longer life regardless of atmospheric conditions, and with a higher factor of safety. This will lead to greater demands for plywood and will mean the ultimate increase of the shear value of the glue bond in the present government and commercial specifications.

In addition to the major applications by industry, there are several outstanding combinations of dry glue film plywoods with synthetic sheet products which enter too many fields to permit such industrial classification.

5 *Asbestos Clad Plywood.* In the development of asbestos slate, manufactured under various trade names, phenolic resin plywood has again found many new applications.

Asbestos clad plywood, or plywood faced with asbestos slate, glued with dry glue film, has introduced many new possibilities for plywood for interior and exterior purposes. The slate can be had in various thicknesses from $\frac{1}{16}$ in. up, and can be nailed or riveted in a very satisfactory manner. As the slate is resistant to acids and alkalis, is non-porous, is incombustible, and has a smooth surface for paint or enamel, it may be used for either a face or a cross band. If used as a cross band, it can be faced with any type or thickness of fine veneers. With dry glue film unusually thin veneers can be applied to the slate without danger of staining the work. Tests show that the dry film bond is stronger than the slate. A few of its many adaptations might be listed as follows:

Wall paneling
(Interior or exterior)
Hospital interiors
Fireproof partitions
Greenhouse equipment
Lavatories and shower rooms
Laboratory equipment
Kneading boards
Steaming rooms

Telephone booths
Laundry equipment
Air-conditioning units
Electrical equipment
Elevator cabs
Railroad freight cars
Ice cream cabinets
Refrigerators.

Rubber Vulcanizing Directly on Plywood. The vulcanizing of rubber directly on plywood is a recent development which opens another field for the veneer and plywood industries. The rubber research laboratories have been eagerly searching for a suitable wood product on which rubber may be vulcanized. It was found that neither solid wood nor plywood glued with wet adhesives would answer the requirements of the vulcanizing process.

Successful vulcanizing of rubber to wood demands that the wood shall not have more than 2 per cent moisture content, and that it must withstand a heat from 350 to 380 F, under a specific pressure of 250 lb for a time of 20 to 30 min. It is immediately realized that neither solid wood nor wet glued plywood can meet such exacting demands. A dry glue film bond does not deteriorate under this heat, and since it permits the manufacture of plywood with not more than 2 per cent moisture content under 250 lb specific pressure, the new plywood answers fully all the requirements for vulcanizing rubber to wood. Some of the many uses for this type of material are as follows:

Desk tops
Rubber covered refrigerators
Table tops
Counter tops
Floor boards (auto)

Running boards (auto)
Toilet seats
Chair and stool seats
Caskets
Flooring and tile.

Other Plywood Products. Dry glue film plywood applications for other new products, discussion of which space does not permit, might be enumerated as follows:

Agricultural equipment
Brush backs
Athletic equipment
Artificial blackboards
Wood-metal desk tops
Flameproof plywood
2- and 3-ply shipping containers
Foundry pattern stock

Plywood milk racks
Archery bows
Golf shafts
Fret molding plywood
Tennis racket frames
Hockey sticks
Curved and bent plywood.

The phenolic resin bond of fret moldings from $\frac{1}{32}$ -in. and $\frac{3}{64}$ -in., 3-ply plywood has no injurious effect on the cutter heads or punches and dies. It is surprising to note the volume that can be made without renewing the cutting edges. The character of the phenolic resin glue line does not dull saws, knives, and cutter heads.

CONCLUSION

The development of dry glue film has introduced a number of distinct and definite advantages which the wet glues have not offered. The result is that new possibilities and applications for plywood are constantly being discovered and developed, and the horizon of the plywood industry is thereby greatly broadened.

NOTE: Various U. S. patents are applied for and pending on phenolic resin plywood, and prospective users should investigate carefully.

BIBLIOGRAPHY

- "Glues Used in Airplane Parts," Report No. 66. Forest Products Laboratory, Madison, Wisconsin, 1920.
"Modern Glues and Glue Testing," C. H. Teesdale, Periodical Publishing Co., Grand Rapids, Michigan, 1922.
"A Dry Glue Method of Laying Veneers," J. R. Truax, Veneers, Indianapolis, Indiana, vol. 24, no. 10, pp. 30-31, October, 1930.
"Gluing Wood in Aircraft Manufacture," J. R. Truax, Technical Bulletin No. 205, U. S. Department of Agriculture, 1930.
"Hydraulic Presses for Plywood," Harry G. Francis, A.S.M.E. Trans., WDI-53-21, September-December, 1931.
"Development of Wood Adhesives and Gluing Technique," J. R. Truax, A.S.M.E. Trans., WDI-54-4, February, 1932.
"The Dry Powder Glue Process," Veneers, pp. 13-14, Indianapolis, Indiana, March, 1932.
"Laminating With Phenolic Resins," E. H. Merritt, presented at Seventh National Meeting of the A.S.M.E. Wood Industries Division, Jamestown, N. Y., November, 1932.

FOREIGN

- "The Approach to Superior Plywood," L. M. Cohn-Wegner. Werkstattstechnik, vol. 22, no. 11 (June, 1928), Berlin.
"The Development of Plywood Manufacture" and what the practicing engineer must know about it. L. M. Cohn-Wegner. Zeitschrift für Wirtschaftliche Technik, November, 1929.
"Veneers and Plywood," 2 volumes. Knight, Wulpi, and L. M. Cohn-Wegner. The first volume a translation into German of the American publication and the second volume a complete description of the plywood industry in Germany. M. Krayn, Berlin, 1930.
"Wood Working Glues and Their Testing," with special reference to gluing wood with adhesive films. Otto Gerngross, Zeitschrift für Angewandte Chemie, vol. 44, p. 231, 1931, Berlin.
"Plywood, Its Production, Use and Properties." A. Mora, Timber and Plywood, 131-133 Middlesex St., London, 1932.

Discussion

CHARLES B. NORRIS.³ This is a valuable description of the use of phenolic sheet glue, particularly the technical data included in tables and charts. As Mr. E. H. Merritt has pointed

³ Mechanical Engineer, Haskelite Mfg. Corp., Grand Rapids, Mich. Mem. A.S.M.E.

out,⁴ the sheet glue process is only one of several processes of gluing made possible by the development of phenolic resins. Mr. Merritt favors a dry powder process. My company has developed a process of gluing with which the sheet glue could be used or, with the addition of some of Mr. Merritt's equipment, the dry powder could be used. However, we prefer using the phenolic resin in the form of a colloidal suspension in water.

In the process we have developed, the glue is spread upon the veneers by means of a glue roll of the usual design. Special rolls and scraper bars are necessary, and the condition of the air surrounding the rolls has to be controlled. The veneer passes di-

so that each panel has two heating elements adjacent to it, one on each side. The stack is moved into the press, pressure is applied, and the heating elements are energized. The pressing operation takes about 20 min. Fig. 11 shows one end of the press and the piling mechanism for placing the heating elements upon the stock. There is a similar unpiling device at the other end of the press. Fig. 12 shows the press-control apparatus, including an automatic valve for controlling the pressure and an automatic device for controlling the temperature. The apparatus shown makes panels 8 ft long and 6 ft wide. It has an output of 3000 sq ft of $\frac{3}{4}$ -in. panel per hour. The full production possibilities of this

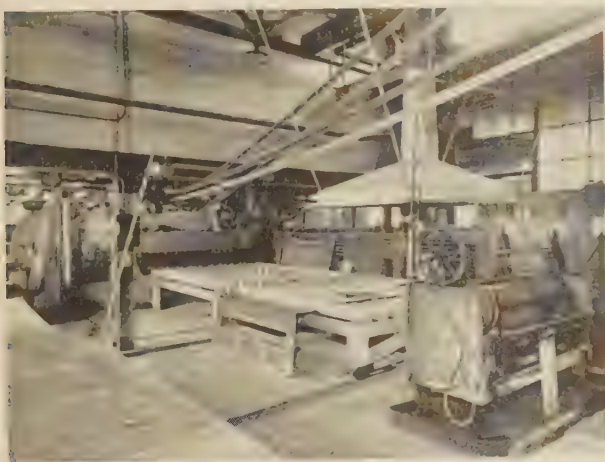


FIG. 9

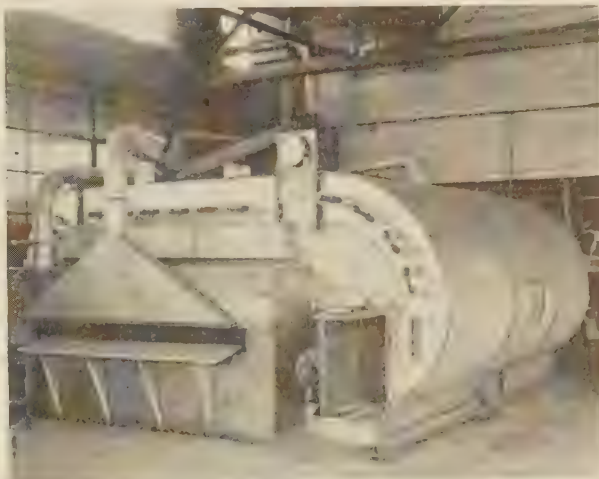


FIG. 10

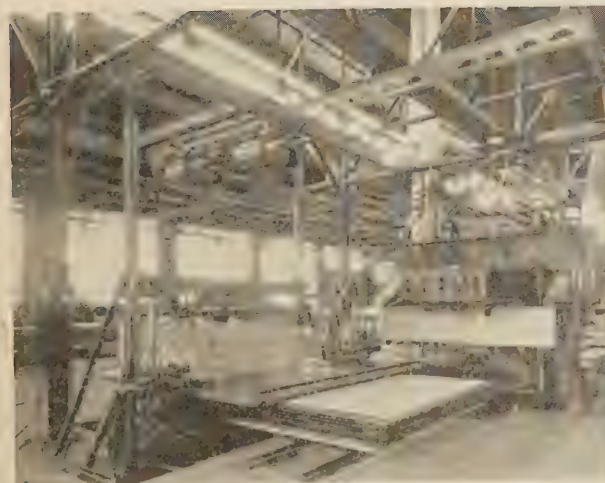


FIG. 11

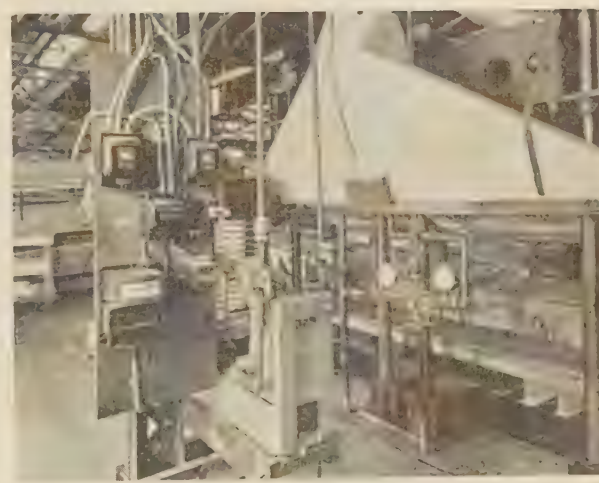


FIG. 12

rectly from the spreader into a simple surface drier which we have designed. High-velocity air is passed over the surfaces of the veneer in such a way that even thin veneers ($\frac{1}{8}$ in.) are not disturbed. Fig. 9 shows the glue spreader and the entrance end of the drier. Fig. 10 shows the exit end of the drier. After the veneers leave the drier they are ready for the gluing process.

The gluing process is similar to the usual cold gluing process in that a stack of panels is formed and moved into the press. Thin electric heating elements are piled alternately with the panels,

⁴"Laminating With Phenolic Resins," Trans. A.S.M.E., paper no. WDI-55-3 (June 30, 1933).

method of manufacturing panels are shown by plans of a larger machine, which we have completed. This larger machine makes panels 10 ft square at a rate of 22,000 sq ft per hr.

The author describes the ideal wood adhesive as "one which is of a uniform quality, which can be laid or spread in an even coating, which gives a perfect glue bond, and which can be applied economically." There are also other requirements which it should meet. There is almost an infinite number of possible chemical combinations of phenol and formaldehyde. In making a phenol formaldehyde glue it is possible to end up with any one of a great number of these compounds by slight changes in the

temperature-time relations of the process. It is very unlikely that the manufacturer of the glue will ever make two batches of glue that are chemically identical. Luckily the user of the glue is not interested in its chemical nature but in its physical properties. Uniform gluing results cannot be expected unless the physical properties of the glue are uniform. The user should be in a position to test these properties himself. The form in which he receives the dry glue film makes this almost impossible. We have developed simple physical tests which can be applied to the colloid glue to tell whether the glue is suitable for our purpose.

Regarding the uniformity of glue spread, in using a liquid glue we have at our command all the experience gained by the printing industry in spreading inks uniformly. We find that we can obtain very uniform spreads indeed. We also found that the dry glue film made by the author's company is not uniform in thickness. Fifty measurements taken around the edge of a piece 18 in. long and 5 in. wide show an average thickness of 0.00229 in., a maximum thickness of 0.0029 in., and a minimum thickness of 0.0020 in. This is a variation of 30 per cent above the average and 12 per cent below.

A further requirement of an ideal wood adhesive is that it should make as good a glue joint at the center of a thick panel as it does near the face. If a thick panel is placed between the plates of a hot plate press, the wood near to the plates is heated much more rapidly than the wood near the center of the panel. Therefore a glue line near the face of the panel is subjected to conditions different from those of a glue line near the center of the panel. The glue must be such that a good glue joint is obtained under both these conditions. The author does not give any data showing the properties of dry glue film joints made at different rates of heating.

Another requirement of an ideal wood adhesive is that it should give good results over quite a range of moisture content of the wood. A plywood panel should be glued up at a moisture content which is the mean moisture content the panel will obtain in use. For example, if a general purpose panel is to be made, it may be used indoors or outdoors. Indoors in winter its moisture content will probably drop to 4 or 5 per cent. Outdoors it may reach a value of 20 per cent. The panel should be made, therefore, at a moisture content of about 12 per cent in order that the shear stresses developed in the panel at the low and high moisture contents will not be great enough to cause failure of the wood. Chart 2 of the paper shows that the dry glue film is suitable for this purpose. In our process the water is dried out of the spread colloid so rapidly by the surface drier that the moisture content of the wood is not materially changed.

So far as we know there are only three reasons for the introduction of phenolic resin glues into the plywood industry: the greater strength of the glue joint, the greater water resistance of the glue joint, and the immunity of the glue to attack by fungi and bacteria. All other advantages claimed for the resin glues are obtainable with the older forms of glues. The author stresses the advantages of gluing with "dry" glues rather than "wet" glues, saying that the amount of water contained in glues cannot be kept uniform and that there is no possibility of regulating the influence of moisture upon the glued plies. We believe that these statements are an exaggeration of the facts. We have been controlling these factors in the use of blood-albumin glues for a number of years.

The warning that very excellent hot plate presses are necessary for making plywood is timely. However, we do not agree with

the reason given regarding the extreme thinness of the dry glue film.

An elementary discussion of the theory involved will show the reasons for the need of very excellent presses when any kind of glue is used. We can assume that the modulus of elasticity of wood is 80,000. If we assume also the variation in the press of 0.003 in. that the author allows, we find that the variation in pressure upon a plywood panel $\frac{1}{4}$ in. thick is 960 lb per sq in. That is, under normal gluing pressures certain parts of the plywood receive no pressure whatever. If it were not for the fact that wood becomes somewhat plastic when it is moist and hot, the steam platen method of gluing plywood could not be successful. It is a precarious method at best. The process we have developed has the advantage of the cold process method with regard to pressures. Under the same condition of 0.003 in. variation in the press, the variation in pressure is only 3 lb per sq in., figured by the method outlined.

The impression is gained from the paper that it is not practical to glue thick panels with the dry glue film if some of the glue lines are near the center of the panel. This is a real difficulty that is very often encountered with the use of phenolic resins. However, this difficulty can be overcome, and in fact is being overcome in our factory.

We are in perfect accord with the author that the phenolic resins make remarkable glues and that the dry glue film is a very good glue indeed. We think, however, that the use of the colloid overcomes some of the difficulties encountered in the use of the other forms of the resin and that our gluing method overcomes the difficulties inherent in the hot plate process.

A. J. NORTON.⁵ There are now three commercially developed methods of using phenolic resin glue lines. In addition to the film glue discussed by the author, there is the dry-powder method of spreading resins which was discussed by Mr. Merritt in the October meeting at Jamestown, and the method of spreading the synthetic resin in colloidal form as was brought out by Mr. Norris, of the Haskelite Company.

The colloidal method of spreading has proved satisfactory in large-scale production and lends itself to commercial operation very satisfactorily. The spreading equipment is slightly different from that already used, and hot plate presses, steam or electric, are the same as are used in any hot press gluing operation. The colloid lends itself to more widely diversified types of application, due to the ease of spreading low or high amounts of resin, and while it was not brought out at the meeting, we have since shown that the colloid works successfully over a lumber core under usual operating conditions. It was brought out at the Chicago meeting that the use of the colloid on sheet lumber might develop a panel core which would compete actively with the lumber core in construction work.

Dry resin and colloid are manufactured by General Plastics, Inc., and these products have sold under the trade name of Durez.

With the three methods of using phenolic resin glue line, and with the merits of such a glue line definitely established, there seems to be no doubt of a distinct and revolutionary change taking place in the lumber field.

⁵ General Plastics, Inc., North Tonawanda, N. Y.

NOTE: Statements and opinions advanced in papers are to be understood as individual expressions of their authors, and not those of the Society.

Noise Reduction in Cabin Airplanes

By PRESTON R. BASSETT¹ AND STEPHEN J. ZAND,² BROOKLYN, N. Y.

Any new form of transportation generally brings some new sort of nuisance to the persons using it. Air transportation, the newest and fastest form of travel, is no exception, and the chief deterrent to air travel is the noise to which the passengers are subjected. As it is impossible to discuss any physical phenomena without having measuring units and methods of securing them, a description of the decibel scale as well as a discussion of the commonly used noisemeter is given, including a description of a most inexpensive, simple, and yet very reliable tuning-fork method.

NOISE accompanies all forms of transportation. Over 90 per cent of the noise of a city is caused by transportation—trucks, trolley cars, trains, etc. In general, the amount of noise is proportional to the speed of transportation. The fact that the speed of transportation has been increasing so rapidly in recent years has brought about an increase in noise level in cities and in high-speed transportation to a point where the public has become very conscious of it. The traveling public remained uncomplaining and almost unaware of the noises of traveling until, with increased speed, these noises built up to what may be termed the discomfort level. When this discomfort level is reached, the traveling public then becomes acutely aware of it and tends to avoid such forms of transportation.

The airplane has been for some years the most rapid form of transportation, but only recently has it been making a bid for passengers. No attention has been paid to noise, however, until now. Pilots and early passengers took it for granted that the noise was just an unavoidable evil that went with flying and high speed. However, when air lines in this country started to go on schedules and carrying many passengers, who flew as a quick method of transportation rather than merely for a thrill, then the passengers began to complain. They not only complained, but many have decided that, except in emergencies, the discomfort of air transportation is not worth the speed, and therefore have

returned, whenever possible, to the use of more comfortable forms. The fact that air transportation is actually losing passengers because of discomfort is a challenge to the aviation industry. There are now very many people who are air-minded, but the majority cannot be converted to use air transportation until it is brought out of the discomfort level.

It is of course impossible totally to eliminate noise in any form of transportation. It is fortunate that there is no demand for complete elimination of noise. The demand is merely to keep the noise under the discomfort level. There is a very broad region of noise levels which can be termed as comfort level, and all that is necessary is that the general level within the airplane be kept in this region.

Lord Kelvin once said: "If you can measure that of which you speak, you know something of your subject, but if you cannot measure it, your knowledge is unsatisfactory." Only in recent years have means been found to measure noises quantitatively and qualitatively. A new unit of noise, the decibel, has come into common usage. Instruments for the measurement of noise levels in decibels have been developed rapidly to a stage where accurate measurements may be

made with portable apparatus.

The measure of the sensation of loudness is not easy to define. The difficulty may be circumvented in a way indicated by Weber's law: "The increase of stimulus to produce the minimum perceptible increase of sensation is proportional to the preexisting stimulus."³ That is, commencing with a certain sound intensity, the increase of intensity δE which produces a noticeable change of sensation δS may be measured. From Weber's law, Fechner derived the relation

$$\delta S = \frac{k\delta E}{E} \quad \text{or} \quad S = k \log E$$

where S is the magnitude of the sensation, E the intensity of the stimulus, and k a constant. While obviously it is not possible to measure S directly, there is no difficulty in determining the ratio $\delta E/E$ as a function of E . The simplest way of measuring this ratio is by means of electrical apparatus where the acoustical energy is transformed into electrical energy. The unit commonly used in this country for such measurement of loudness is the decibel,⁴ a unit which may be said to be, approximately, the smallest change in the level of sound which the normal ear can detect. More accurately, as seen from the Weber-Fechner relation, this unit may be defined as a ratio of intensities. Hence, if the intensities of two sounds are in a ratio of 10 to 1, they differ by 10 db; if the intensities are in a ratio of 10² to 1, i.e., 100 to 1, the sounds differ by 20 db; and so on. In general, therefore, the number of decibels measuring the difference between two sounds is ten times the Briggs logarithm of the intensity ratio, db = 10 log (I_1/I_2). It is obvious, therefore, that any decibel scale



P. R. BASSETT



S. J. ZAND

¹ Vice-President in Charge of Engineering, Sperry Gyroscope Company, Inc. Preston R. Bassett was graduated from Amherst College in 1913, with A.B. and M.A. degrees, and continued graduate work in engineering at Brooklyn Polytechnic Institute. He has been associated with the Sperry Gyroscope Company for 18 years, first as Research Engineer and since 1929 as Chief Engineer.

² Aeronautical Research Engineer, Sperry Gyroscope Company, Inc. Stephen J. Zand was graduated from the École Polytechnique Fédérale, Zurich, Switzerland, in 1920. He did post-graduate work at the École Supérieure d'Aéronautique in Paris, France. He came to America in 1925 and worked as airplane designer at the Ford Motor Company, as a research engineer in the Pioneer Instrument Company, and since April, 1932, he has been engaged in research work for the Sperry Gyroscope Company. In 1931, for his paper, "A Study of Instrument Boards and Airplane Structure" (*S.A.E. Journal*, October, 1931), he was awarded the Wright Brothers Gold Medal.

Contributed by the Aeronautic Division and presented at the Semi-Annual Meeting, Chicago, Ill., June 26 to July 1, 1933, of THE AMERICAN SOCIETY OF MECHANICAL ENGINEERS.

NOTE: Statements and opinions advanced in papers are to be understood as individual expressions of their authors, and not those of the Society.

³ Wood, "A Textbook of Sound," Macmillan, New York, N. Y.

⁴ See "The Decibel," by S. J. Zand, *Sperryscope*, vol. 6, no. 11; "The Decibel," by S. J. Zand, *Aeronautical Engineering*, Feb., 1933, vol. 8, no. 2, p. 19.

requires the more or less arbitrary adoption of some definite zero point from which the intensity or power ratio should be measured. Omitting this reference may cause misunderstandings.

The first scale used by the Noise Abatement Committee of New York City fixed the zero at 4.4×10^{-16} watts per sq cm. The scale we use has its zero at 1 millibar sound pressure, which, under normal atmospheric conditions, is approximately 24.4×10^{-16} watts per sq cm.

Recently, the Society of Acoustical Engineers of America has adopted a new zero equal to 1×10^{-16} watts per sq cm, or 0.207 mb of sound pressure.

Thus, 90 db above 1×10^{-16} watts is equivalent to 83 db above 4.4×10^{-16} watts and 76 db above 1 millibar. Throughout this article, the decibel-above-1-millibar scale is used.

While loudness appears to the ear to increase by simple arithmetical progression, the sound energy increases by logarithmic progression, rising from ten to ten billion (10^1 to 10^{10}), while loudness goes from ten to one hundred (10 to 100). This peculiar relation must be clearly understood, and hence we have gone into considerable detail to impress that decibels per se have no significance whatever and are only convenient symbols for expressing a ratio. The difference between 10 and 20 miles is the same as between 90 and 100 miles. But between sounds of 10 and 20 decibels above the threshold of hearing there is an intensity difference of 90, while the difference between sounds of 90 and 100 decibels is 9 billion units of energy. As a consequence of this relation, it is at once seen that doubling the intensity does not double the loudness, but merely increases the loudness by 3 db. Therefore, two sources, each producing 100 db, give a resultant noise of only 103 db instead of 200 db. Conversely, if an airplane cabin has a noise level of 100 db and we take steps to reduce the sound energy to one-half, we will have reduced the noise level to only 97 db, hardly a noticeable achievement. It is this discouraging fact that makes sound reduction so difficult.

While the measurement of acoustical energy by mechanical means is not impossible,⁵ it has been found highly impracticable, especially in measuring moving vehicles. This is due to the extremely small amount of energy which produces an auditory sensation. Thus, speech of a level of 60 db would appear to have a lot of energy, but measurements indicate that the average power of a speaker is between 25 and 50 microwatts or thereabouts. Thus, it would require 15 million persons speaking simultaneously to produce the equivalent of a single horsepower of acoustical energy. Obviously, then, the only method of measurement will be the electrical, by which the incoming sound wave produces a corresponding electrical variation. These are amplified in a known and always constant ratio by means of vacuum tubes, and the amplified output is a magnified but faithful reproduction of the acoustical disturbance which is measured.

The action of the noise meter, a simplified diagram of which is shown in Fig. 1, starts with a microphone, generally of the dy-



FIG. 1 SCHEMATIC DIAGRAM OF A NOISE METER

namic or condenser type, which picks up the sound wave and produces its electrical equivalent. The electrical impulse is then amplified, generally by means of a high-gain and high-grade resistance-coupled amplifier. (Great care must be exercised in order not to introduce distortion.) This magnified output is then rectified, finally actuating a meter causing the pointer or hand of the indicator to move along the meter scale to a point determined

by the intensity of the sound wave. The figure indicates that a noise meter is also supplied with an attenuator and a weighing network. The attenuator enables the observer to control the amplitude of the electrical wave by large steps, so that when a very loud sound is encountered which would drive the needle off the scale of the meter, a known amount of attenuation may be inserted, bringing the needle back into the range of the meter. The actual reading is then the sum of the attenuator setting and the meter reading. The weighing network is designed to render the noise meter more sensitive, and vice versa, so that the pitch of a tone will automatically affect the meter in the same way that it affects the ear. While this is only possible in rough approximation, owing to the complicated characteristics of the ear, it can be done with a reasonable amount of precision for all practical purposes.

In addition, a noisemeter may contain a series of band pass filters which may be thrown in and out of a circuit by means of a convenient selector switch or plug-in arrangement. The action of such filters is to suppress any wave the frequency or pitch of which does not lie in the particular frequency region passed by the filter. One filter passes waves of only very low pitch, having a frequency of, say, 64 cycles or less; a second passes frequencies from 64 to 128, etc. With six or eight such filters an "octave" analysis is possible—very valuable information which will generally facilitate the working out of proper acoustical treatments.

Naturally, noise meters and frequency analyzers are expensive and generally bulky and heavy. In order to use them it is necessary to have the vehicle to be tested at disposal for a certain amount of time. For a rough check, with skilled observers as close as ± 2 db, there is a very simple method which is based on the masking effect of one sound against another.⁶ The only tool necessary is a calibrated tuning fork and a watch. The observer strikes a tuning fork (256 or 512 cycles) with a constant force and brings the fork in front of his ear canal, moving the fork slightly to create a warble. At the same time, he observes the second hand of a watch (a stopwatch is preferable). He observes the time until the noise of the fork is masked by the noise to be measured. Suppose the fork held in such a position near the ear canal makes a noise of 90 db, and from the calibration of the fork it is known that it decays at the rate of 1.5 db per sec. Then if the fork remains audible only 20 sec, it will follow that the noise at this frequency is approximately $90 - (1.5 \times 20) = 60$ db. If measurements of this type are made, using a number of forks, a surprisingly good picture of intensity and frequency distribution can be gathered with the simplest instrumentation.

Returning now to the relationship of speed to acoustical comfort, we may now study it on a decibel scale. Fig. 2 has been prepared in a unique way to show both methods of determining noise levels; decibels as measured on the noise meter are plotted against masking time of a tuning fork. All readings on this chart were obtained by the authors on various tests and trips within the last year. The readings include every form of transportation from sailboat to open-cockpit airplane. Included are readings on both American and European subways, trains, and passenger airplanes. The grades of comfort are indicated approximately at the right of the chart.

Although the high readings on the chart are all airplanes, it is to be noted that the newer soundproofed airplanes have moved down into the region of subways and trolley cars as regards noise level.

To show more clearly the relation of sound level to speed, Fig. 3 presents several curves of different transportation units, plot-

⁵ Lord Rayleigh, "Theory of Sound," vol. 1, Macmillan, 1926.

⁶ V. O. Knudsen, "Architectural Acoustics; Method of Measuring Noise," p. 255.

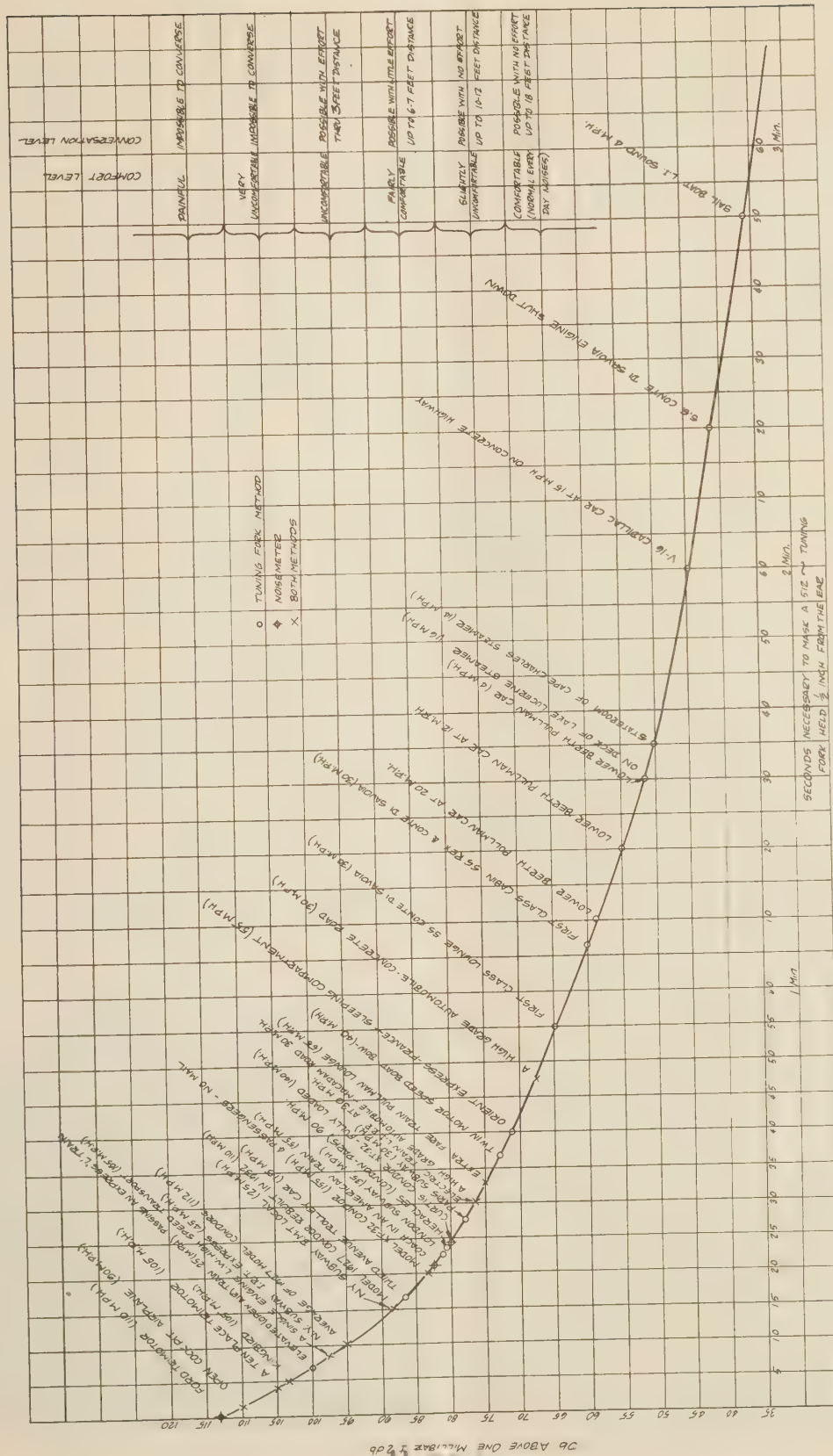


FIG. 2 NOISE LEVELS IN DIFFERENT MODES OF TRANSPORTATION

06 ABOVE ONE MILLION 1206

LIBRARY

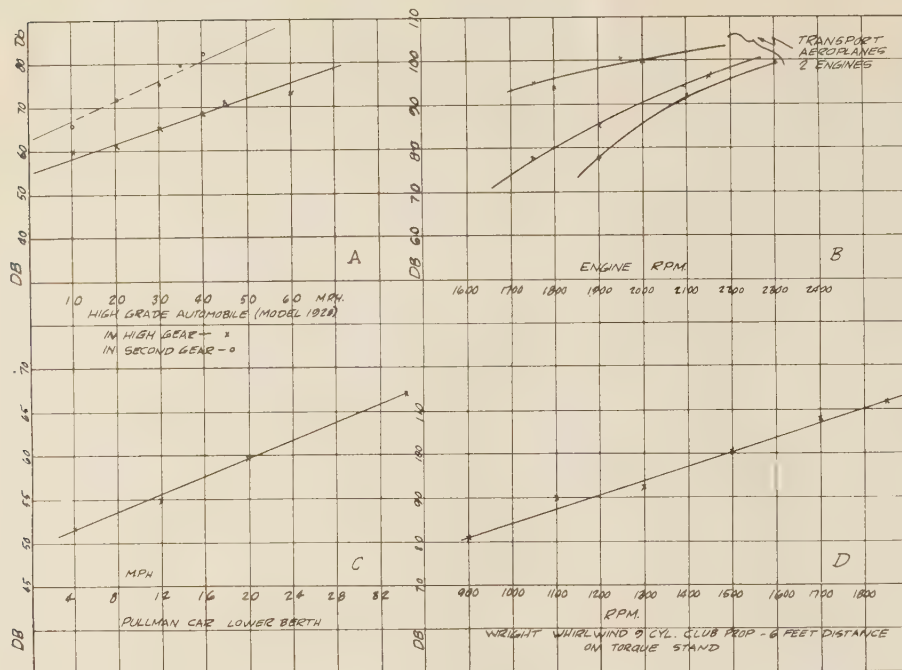


FIG. 3 DIAGRAM OF SPEED VERSUS NOISE

ting speed against decibels. A shows that the noise of an automobile increases approximately as a straight-line function of its speed. B gives the increase of noise level in three different types of transport airplanes with increased engine rpm. It is interesting to note the convergence of the airplane curves toward some point above 110 db. It is suspected that this is due to the propeller-tip speed, which increases in noise output rapidly as it approaches the velocity of sound, and produces so much noise at these high velocities as to completely mask the engine noises. Hence, all airplanes would have about the same maximum noise if they could be pushed to the point of having tip speeds of 1100 fps. Some military and racing ships reach this point, and, as is well known, they make a terrific and penetrating noise, measuring well over 110 db.

Chart C gives the increase of noise level in a Pullman car with increased speed. It is to be noticed that in this case the increased noise is not caused by the engine, but by local noises. It is apparent that the train has an advantage over an airplane in that the power plant or engine is so far removed from the passengers that its noise is attenuated to a harmless level in the passenger compartments. Furthermore, if soundproofing is still found desirable, additional weight is easily permissible for the purpose. In the airplane, there are, on the other hand, severe weight limitations.

Chart D gives the relationship of noise and engine speed of a standard Wright Whirlwind engine. When it is realized that one, two, or three of these noise-producing units must be placed in the close vicinity of the passengers, it is apparent that noise reduction in airplanes is a most difficult undertaking.

The following list covers the handicaps under which the acoustical engineer must work to reduce the noise in aircraft:

- (1) The airplane is the fastest vehicle, and hence inherently the noisiest
- (2) The acoustical disturbances are very near the travelers (engine, propeller, exhaust)
- (3) Frequency analyses show that the noise of an airplane is of a very complex character, containing sounds of

- both high and low frequency, with the low frequency predominant
- (4) Low-frequency noises are very difficult to deal with because most materials are much better barriers to high-pitch sound than to low-pitch
- (5) The power plant is attached directly to the structure which contains the cabin, which allows vibration from the engine and propeller to be transmitted by direct solid conduction into the cabin
- (6) On multiengine airplanes, the possibility of beats of low-pitch character and high intensity is very troublesome, with no direct remedy as yet in sight
- (7) Weight limitations are very severe, and it is a known fact that sound

insulation is a direct function of mass.⁷

In April, 1932, the Sperry Gyroscope Company started on the study of noise reduction in airplanes. Before any program of research could be established, it was necessary to determine what had already been done or written in this field, and then to determine for ourselves the sound levels in existing airplanes.

Available data were very few. The work of Dr. W. S. Tucker in England (A.M.I.E.E., January, 1928) and the Bureau of Standards (Research Paper No. 63, 1929) in this country were about the only valuable contributions that we found. The former showed the important part played by the propeller in noise production and the necessity of slow tip speeds. The latter showed the extreme difficulty of obtaining a good sound

⁷ Bureau of Standards Research Paper no. 63, 1929.

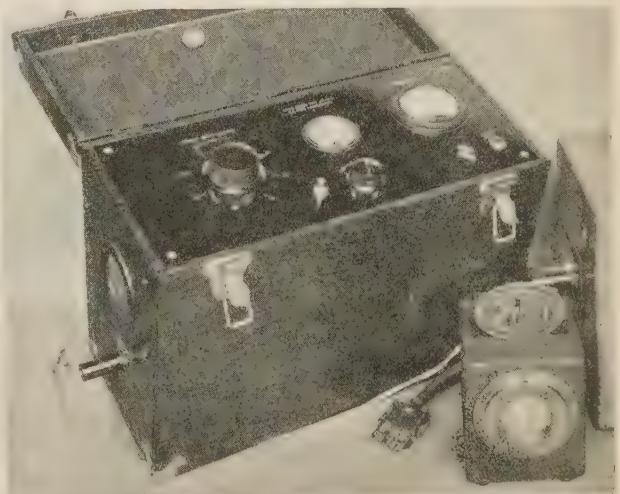


FIG. 4 NOISE METER REBUILT FOR AIRPLANE USE

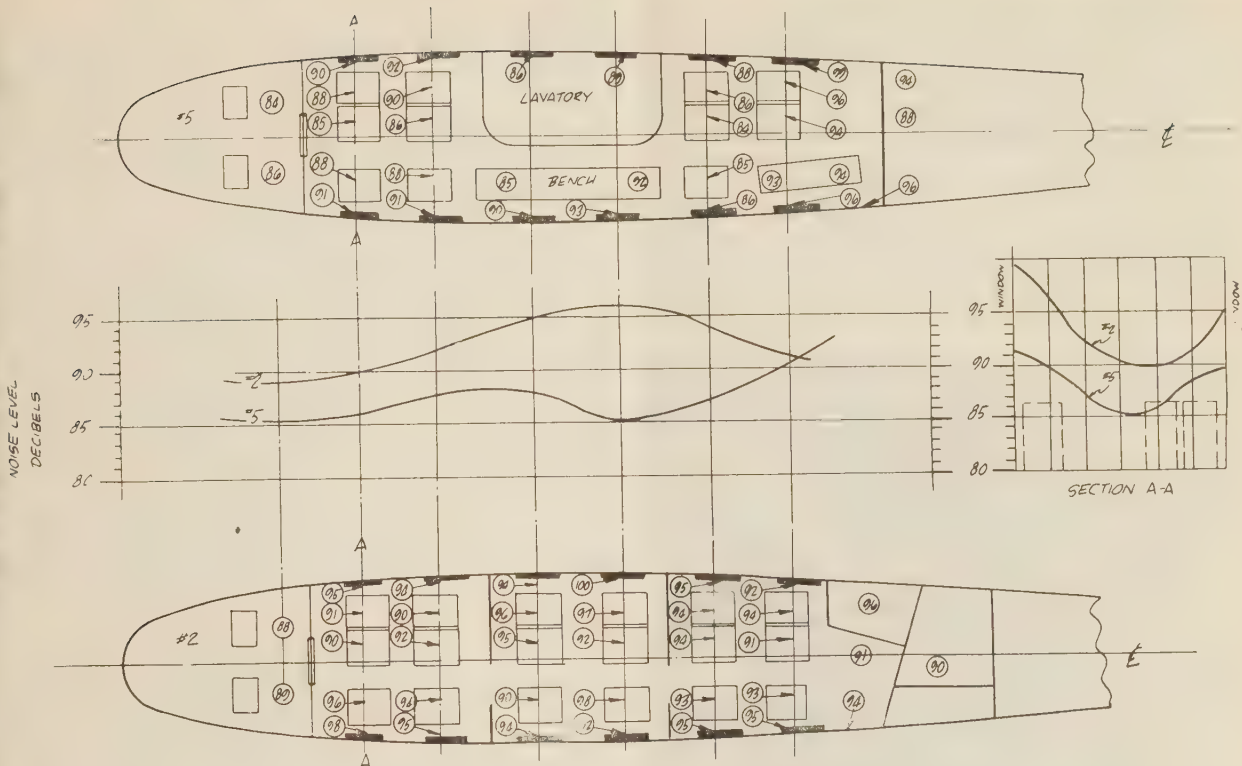


FIG. 5 NOISE DISTRIBUTION IN CONDOR NOS. 2 AND 5

insulator without excessive weight; in fact, it proved in a very disconcerting way that most sound insulators were only as good as they weigh.

The years 1930 and 1931, apparently on account of the depression, produced nothing in this field. So 1932 started from scratch. We first checked up a number of airplanes, paying particular attention to large transport planes. The tests were carried out either by the use of a noise meter (see Fig. 4), system Free, type 123, a commercial apparatus built by Dr. E. E. Free to our specifications for airplane use, or by the tuning-fork method. In many cases both methods were used to form a useful check. Generally, the tests were carried out at cruising speed, but in some cases at varying rpm, the latter check to establish relations of speed versus noise level. We took at least 20 to 40 readings in selected places along the cabin, the arithmetical mean serving as a basis of comparison of the noises of one airplane against the other.

As the research program was started in cooperation with Eastern Air Transport, Inc., we checked their ships first. This system owns a fleet of five Curtiss Condors, built about 1927 and 1928, which were scheduled for a complete overhaul that was to include acoustical treatment. Tests were made before and after this rebuilding. The Condor is an example of a relatively quiet ship. It probably was the quietest transport at the time it was put in service. The following summary of our tests will give a good idea of the noise levels encountered in this type of ship:

The E.A.T. Condor No. 2, an 18-passenger biplane, with Conqueror V-12 engine, geared three-blade metal propeller, speed about 110 mph. The exhaust of the inside bank of cylinders was piped on the near side of the nacelle. The average noise level (arithmetical mean of 31 readings) was 98.5 db; the highest was 102 db, near the fourth window from the front of the ship; the lowest was 88 db, in the pilot's cockpit.

The E.A.T. Condor No. 5, which was the same as No. 2, with the exception that here the exhaust was piped on the far side of the nacelle. The average noise level (arithmetical mean of 36 readings) was 94.5 db; the highest was 99 db, near the last window; the lowest was 86, in the pilot's cockpit.

The pitch in both ships was decidedly in the lower octaves, lower than 150 cycles, but a great variety of high-pitch noise was also present, coming from loose accessories such as ash trays, lamp shades, etc. Hissing sounds, about 2000 to 5000 cycles, came from the individual ventilators.

Before proceeding further with other tests, let us now analyze the two ships. Fig. 5 shows a longitudinal and a transverse curve of noise distribution.

It is at once apparent that one side of either ship is more quiet than the other. The reason is very simple. It is more quiet, as it should be, on the side where there are two seats in a row. The absorptive area is greater; hence this side is less noisy. The fact that No. 5 ship is generally quieter than No. 2 is due mainly to the exhaust manifold arrangement. In No. 5, the exhaust is farther away from the side of the ship and is concealed behind a large and heavy mass, the engine. Therefore the noise cannot reach the walls of the cabin as easily as on No. 2, where it is on the near side. Both ships show a decided drop in noise level in the pilot's cockpit, which is not at all what one would expect. Upon analysis, it is not extraordinary if one considers the fact that the cockpit of the Condor is far forward of the propeller and engine, the chief noise makers.

The Kingbird, with two radial direct-drive engines and a two-blade propeller, a six-place high-wing monoplane, speed about 115 mph. At the time of the tests, this particular ship had double windows. The highest reading was 100 db, in the pilot's cockpit and first right seat; the lowest, 94 db, rear left seat; the average, 99 db.

An interesting observation can be made here regarding the noise distribution. On this particular ship, the propellers and the engines are quite ahead of the cabin proper and rather near the cockpit. Consequently, the center of disturbance is ahead of the passengers and the noise decays about 6 db when measured in the rear of the airplane. Probably the most striking and important observation that was made on this airplane was on a retest of the same airplane after removing the double windows. With single windows, the average noise level was still 99 db. The double windows added weight, but were totally ineffective. At first this seems paradoxical, as it is known from the experience of architectural acoustics that double windows will materially quiet down a room where they are properly installed.

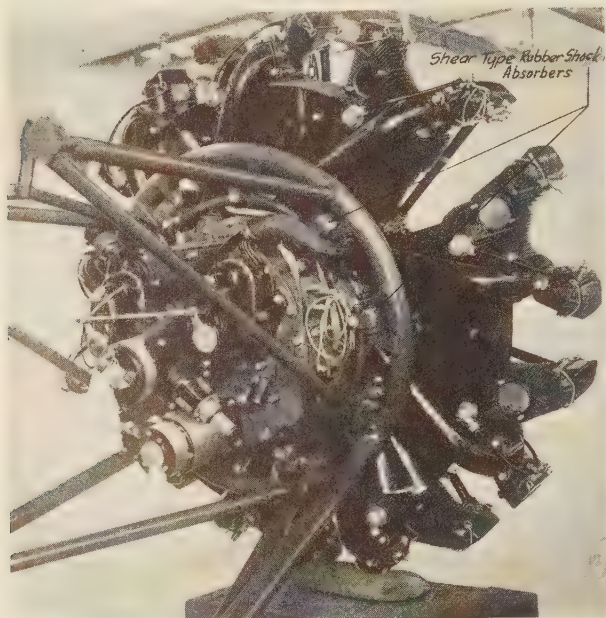


FIG. 6 SHEAR-TYPE SHOCK ABSORBERS AT THE ENGINE MOUNT

Let us now compare the two cases. In a building located on a busy thoroughfare, we have an outside noise level of about 65 db. The transmission loss of the masonry in a well-constructed building may be as high as 40 db, thus bringing the room without windows down to a noise level of 25 db. According to Sabine, a single window will have a transmission loss of about 30 db. So, if a single window is inserted in the wall of the room, more noise would be transmitted through it than through the wall, the room noise level would increase to 35 db, and the window would be properly blamed. If we install a double window of such characteristics that it will have a transmission loss of 40 db, then the wall and window will have a uniform opacity to sound and the room will show a remarkable improvement. Now, with the airplane, the case is reversed; the window is a better sound insulator than the thin cabin walls. The best cabin wall will have a transmission loss of about 25 db, so that no matter how opaque the windows are, the sound will come through the walls. Instead of using double glass for a local sound insulator (weighing as much as 3 lb per sq ft), if the same weight is spent for absorbing materials within the cabin, much better results will be obtained.

The result with double windows against single windows has been checked by the authors in the case of another airplane and fully confirmed our idea of the fallacy of this construction.

We tested next the Ford Tri-Motor. This airplane, no longer

in production, is an example of what complete neglect of acoustic considerations may produce. The highest reading was 118 db in the pilot's cockpit, the highest reading we have obtained in a passenger ship. The lowest was 104, near the rear. The average was 108.5. Prolonged exposure to this high level of sound can temporarily injure the sense of hearing. Ringing of the ears and physical discomfort persist for several hours after being subjected to this noise level. A long period of subjection to this level causes permanent hardness of hearing.

This airplane had no soundproofing whatsoever. This is especially true in the inside of the cabin, where not a piece of fabric or other fibrous material is introduced, and the noise reverberates constantly. Further, no attempt has been made on this airplane to prevent vibration from the engines reaching the passengers. Thus, noise is transmitted in the cabin by solid conduction. The propellers, being of the two-blade type, create a greater amount of noise than would a three-blade one. The center exhaust manifold runs under the floor of the airplane, where its pulses can be directly transmitted to the passenger compartment.

It has been further observed on another Ford Tri-Motor that the noise level was about the same as on the former. Further, the pitch is between 300 and 700 cycles, thus corresponding to the average pitch of human speech, and consequently no conversation is possible.

A different type of Tri-Motor airplane was also tested, and it was found that the noise level was around 100 db. This particular ship has its engine mounted by means of rubber shock absorbers. While no particular scientific attempt was made in soundproofing, the noise is less than in the Ford Tri-Motor, which is attributable to the discontinuity of surface between the engine and the fuselage. Owing to the very flexible engine mounts, the propellers precessed and created highly unpleasant beats, some of them lasting as long as 4 sec. A later type of the same airplane shows a certain improvement. The noise level was about 96 db and the pitch between 400 and 600 cycles, and in this airplane conversation was possible by shouting.

A very modern high-speed low-wing all-metal monoplane with a single-gear two-blade propeller was tested. This airplane was one of the first commercial high-speed airplanes in which an attempt was made to sound-insulate the ship scientifically. The highest noise level at a speed of 175 mph was about 96 db, the lowest was 86 db, and the noise distribution was unusually uniform. This ship at the original test had double windows. When these were removed, no appreciable decrease in noise level was experienced.

One of the authors was fortunate enough to fly from London to Paris in the new 44-passenger Handley-Paige Heracles. This is a four-engine biplane of a speed of about 90 mph, in which the cabin is divided into two compartments—one far ahead of the plane of the propellers and the other far behind. The space of the greatest acoustical disturbance is reserved for mail, for cargo, and the steward's compartment. This airplane uses four-blade wooden propellers, and was the quietest airplane flying up to 1933, as far as we know. The noise level was found to be around 78 db. Of course, when saying that it was the quietest airplane, we must make reservation that this type of airplane would be entirely unsuitable for American air transportation, where speeds of 90 mph are considered obsolete. The design of this ship is of great interest in showing how much may be accomplished by merely removing the passengers as far as possible from the plane of the engines and propellers.

A pair of wooden propellers were built and tested on the E.A.T. Condor No. 4. First, we tested it with the standard three-blade and then with the four-blade. The average noise with the three-blade propellers was 96 db, and with the four-blade 92.5 db, a

reduction which our calculations predicted.⁸ With the wooden propeller, we found that beats and momentary vibrations due to sudden changes of azimuth lasted but 2 to 3 sec, while with the metal propeller we could hear and feel them as long as 6 to 8 sec. This is again natural, if one considers the fact that the damping constant⁹ for wood is 0.022, while that for aluminum is 0.0034 and for steel 0.0023. Hence, any vibration will be damped out quicker in a wooden propeller than in a metal one.

Numerous other airplanes and special tests have been made by the authors during the past year, but the foregoing examples have all been selected to show certain factors of the problem and to make the following list of principles more easily understandable. From these tests, we can conclude certain basic features to be included in the design which will make an airplane inherently more quiet.

- (1) The engines should be mounted as far ahead of and as far away from the cabin as practical, consistent with good aerodynamic efficiency
- (2) Three- or four-blade slow-moving propellers are better acoustically than two-blade fast-moving propellers
- (3) Great care must be exercised to prevent the transmission of vibration to the cabin by solid conduction; thus, vibration control through the use of properly designed vibration insulators is imperative
- (4) Double windows are at present of no value in an airplane cabin
- (5) The cargo compartment should be located preferably in such a position as to form a barrier to the source of noise
- (6) Exhaust manifolds should be located at a point as far removed from the cabin as possible, and either wing or nacelle should be used as a sound shadow between exhaust and the cabin
- (7) The cabin should be as tight as possible, as small leaks will offset the value of elaborate acoustical treatment
- (8) Ventilating and heating systems should be made quiet by filtering out the noise before admitting the air to the cabin
- (9) The inside of the cabin should be covered with a material which will absorb as much noise as possible; the material should be particularly

⁸ Davis, in his paper on "Noise," *Jl. Royal Aero. Soc.*, vol. 36, no. 224, claims that a decrease of 100 fps in tip speed will give a reduction of 10 db of the noise generated by the propeller. The N.A.C.A. has worked out the relation $db_{prop} = 40 \text{ to } 60 (\log_{10} V_2/V_1)$, where V_1 and V_2 are the tip velocities.

⁹ See Kimball, "Vibration Prevention in Engineering," J. Wiley, p. 133; S. J. Zand, "Vibration of Instrument Boards and Airplane Structures," *S.A.E. Journal*, November, 1932.

effective in the absorption of the predominant frequency of that particular airplane

- (10) All accessories, such as lamp shades, ash trays, curtain rods, etc., should be fastened very securely to the structure to prevent acting as localized sound sources
- (11) Avoid the use of large unsupported panels of thin section, as they act as loud-speaker diaphragms
- (12) Blanket materials which will pack are not suitable and should be avoided.

While all of the foregoing points are self-evident, the last one needs amplification. Some sales people have products which are excellent when used under different conditions than on the airplane. Not knowing what vibration and constant changes of acceleration will do to this material, they convince the airplane manufacturer to use it.

Recently, in rebuilding one of Eastern Air Transport's "Condors" (1928 model), it was interesting to discover what time and vibration had done to the old sound-insulating mattress when the fabric was removed. We found that about 75 per cent of the blanket was pulverized and packed on the sides and bottom of the airplane, leaving whole areas without treatment. Therefore, only materials which will not pack should be used on airplane soundproofing work.

And so Condor No. 3 was rebuilt, and we made the cabin a tight shell, using a newly developed material called Onazote,¹⁰ an extremely light exploded and molded rubber compound (weight 4.75 lb per cu ft, impact strength 75 lb per sq in.). Further, we endeavored to improve the reverberation control by the use of certain fabrics and a fluffy backing of same. The ventilating system was also changed, and all doors were gasketed.

¹⁰ The inventor of this material is Mr. C. L. Marshall, Montclair, N. J. The material, while excellent in many respects, is not available commercially as yet.

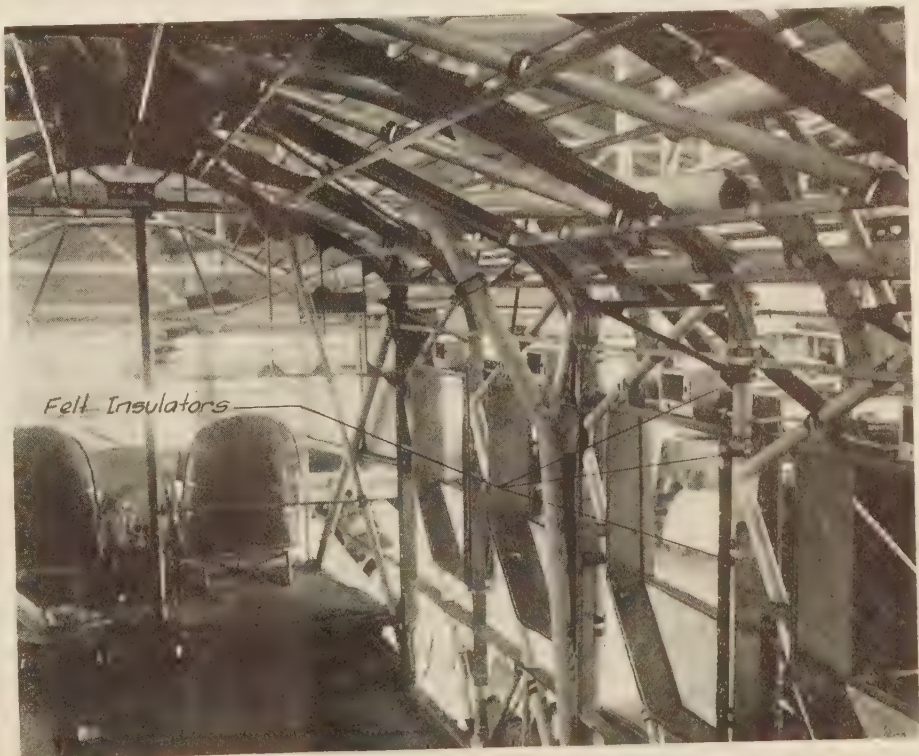


FIG. 7 VIEW OF THE CABIN BEFORE INTERIOR WAS PUT IN



FIG. 8 FINISHED CABIN

Being an old ship, it was impossible to change the structure, and naturally the results were far from perfect. Nevertheless, the noise level was brought down from 97 to 85 db in the front of the cabin, the center of the cabin showing an even greater improvement. This was the first ship in which it was possible to talk without much difficulty.

Since that time, other Condors have been rebuilt, using similar methods but different materials, with very gratifying results. On most of the ships it was possible to reduce the noise level to about 85 to 88 db.

When plans were made for the new Condors, Model XT-32, we were retained for the acoustical work at the beginning of the project. Thus, it was possible to incorporate in the basic design many features contributing to quietness. The location of the propeller was chosen so that its plane passes between the cockpit and the cabin proper, intersecting the radio compartment. This room is separated from the cabin by a bulkhead and fully gasketed door of generous dimensions. This bulkhead was treated with an acoustical material which would be particularly suited to absorb frequencies generated by the propeller. The engines were mounted on rubber shock absorbers of such characteristics

and so located as to give the power-plant assembly the lowest natural frequency far removed from the operating range. We used shear-type rubber shock absorbers, which give the maximum vibratory isolation with minimum weight (see Fig. 6). The whole cabin structure is insulated from the main structure by means of specially designed felt shock absorbers (see Fig. 7). The cabin was built of a panel made of a combination of two materials giving a transmission loss of about 25 db at 300 cycles, and weighing less than 0.4 lb per sq ft. The windows are floating, which was accomplished by the use of a radically different construction in mounting the pane to the frame. Further, we used a special non-shatterable glass which was made in accordance with our specifications. This glass is lighter, acoustically as efficient as any standard glass, and its vibration-damping coefficient is ten times higher than ordinary safety glass. The result is that these windows do not "sing."

The floor was not specially insulated because the baggage and mail compartment was located underneath it, and this has such considerable mass that it acts automatically as a sound barrier. The cabin framework was insulated from the main structure by means of a felt shock absorber (see Fig. 7).

The ventilating systems, both intake and exhaust, were provided with acoustical filters of such characteristics as to attenuate the predominant frequencies.

The reverberation control included such refinements as the making of the parcel rack of a blanket material which acts as an efficient sound absorber (see Fig. 8).

The exhaust manifolds, tuned to unison, were located under the lower wing, their clamps being insulated from the structure by asbestos gaskets.

Attention was paid to all details, and the result was a noise level of about 78 db at cruising speed of 145 to 150 mph with four passengers and no baggage. Fully loaded, the noise level dropped to about 76 db (at 150 mph), or no more than in the average railroad car (at 60 mph). Conversation is fully possible, and radio loud speakers installed in the cabin can be distinctly heard and enjoyed by the passengers.

For quick reference, all the ships tested have been listed in Table 1, which gives also certain basic features of these ships.

TABLE 1 DIFFERENT AIRPLANES COMPARED

		(Noise level above 1 mb)					Remarks
No.	Airplane	Power plant	Speed, mhp	Average noise level, db	Soundproofing material	Conversation level	
1	Condor No. 2	Conqueror 2-gear 3-blade propeller	110	98.5	Dry zero blanket	Possible with difficulty	Test before overhaul
2	Condor No. 2	Same	110	86.0	Seapack-plywood and Sperry soundproofing	Possible with normal voice up to 3 to 4 ft	After overhaul. The 86 db is with ventilators closed; when open, 92 db
3.	Condor No. 3	Same	110	96.5	Dry zero blanket	Possible with certain effort	Before overhaul
4	Condor No. 3	Same	110	85.0	Onazote and Sperry soundproofing	Possible with normal voice up to 3 to 4 ft	After overhaul; added weight 285 lb
5	Condor No. 5	Same	110	94.5	Dry zero blanket	Possible with certain effort	Test before overhaul
6	Kingbird	2 Wright J-6, direct 2-blade	105	99.0	Dry zero blanket	Possible with great difficulty	Test after overhaul
7	Kingbird	Same	105	100.0	Dry zero blanket	Possible with great difficulty	Test before overhaul
8	Condor No. 4	2 Conquerors, 3-blade geared propeller	112	95.0	Dry zero blanket	Possible with difficulty
9	Condor No. 4	2 Conquerors 4-blade wooden propeller	107	92.0	Dry zero blanket	Possible with difficulty	Decidedly different pitch: less vibration
10	Ford	Wasp 3 direct, 2-blade	112	110.0	None; no reverberation control	Impossible, not even shouting	Highly unpleasant, vibration excessive
11	Ford	Same	115	106.0	None; no reverberation control	Impossible, not even shouting	Highly unpleasant; vibration excessive
12	A tri-motor	3 radials, direct, 2-blade	105	100.0	Unknown; no reverberation control	Possible with great difficulty
13	A tri-motor	Same	110	98.5	Seapack; poor reverberation control	Possible with effort
14	A high-speed low-wing monoplane	Radial geared 2-blade propeller	165	88.0	Downy material; poor reverberation control	Possible with little effort	Spectrum of noise in the neighborhood of human speech; ventilating system noisy
15	A high-speed low-wing monoplane	Same	190	90.0	Same	Possible with some effort	With improved ventilating and cabin interior this airplane could be made about 10 db more quiet
16	Curtiss Condor XT-32	2 geared Cyclones, 3-blade propeller	150	76.0	Seapack, insulite, special cement, Sperry soundproofing	Possible in normal tones; with raised voice, full length of the cabin	The most quiet ship flying at 150 mph

Some Studies on the Flutter of Airfoils and Propellers

By W. HAROLD TAYLOR,¹ ANN ARBOR, MICH.

During the last few years there has been considerable interest in the study of vibration of airfoils and propellers, both in Europe and in this country, and most of the literature regarding it is of fairly recent date. A complete solution to the problem has not yet been attained, the complicated mathematics having proved too involved. Again, some of the factors are only now the subject of research. This paper deals with a few of the many interesting phases of the problem. Because of the complexity of the mathematical expressions for the airfoils in common use, a flat plate has been used. It has also been assumed that the angle of attack in the range to be covered is below the burble point and that the amplitude of the vibrations is considered small. The paper is divided into three main parts: (a) A theoretical development of the deflection curve of a cantilever flat bar of uniform cross-section, by air forces distributed according to an elliptic-load grading curve, to show the effect of the warping produced by such loading in the strain energy of the bar so loaded. (b) An approximate solution of the free torsional vibrations of a cantilever bar of thin rectangular cross-section. (c) An analysis of the problem of self-induced torsional vibrations which will apply for any airfoil.

1—INTRODUCTION AND STATEMENT OF PROBLEM

DURING the last few years considerable interest has been attached to a study of vibration of airfoils and airplane propellers. Several severe accidents occurring prior to 1925 led such investigators as Younger in the United States, Fraser and Cox in England, and Blenk and Liebers and Kussner in Germany to attempt solutions. A general solution has not yet been de-

rived; so far the mathematics has proved too involved. This contribution deals with a few of the many interesting phases of the problem.

The work of Younger gives an approximate solution of vibrations of two degrees of freedom as applied to propellers. The differential equations have been solved by means of graphical integrations. His solution, however, does not take into account the aerodynamic couples which exist on the airfoil.

Fraser investigated the torsional and bending vibrations of a

wing with spars, and also with various settings of ailerons or flaps. Since that time it has been shown by Younger that ailerons or flaps are not completely responsible for the vibration of airfoils. Cox investigated the torsional properties of the stripped airplane wing.

Liebers² calls attention to the recent propeller failures ascribable to vibration troubles. He attributes one of the main causes to the periodic changes in the loading curves due to interruptions and disturbances by such things as wings, other propellers, or disturbed inflow air. Again³ in another paper the same author states that the aerodynamic forces are of less importance for the bending vibrations of aircraft propellers than for the torsional vibrations. He mentions the great difference in frequency at which bending and torsional vibration exist and suggests that each can exist without involving the other. Blenk and Liebers⁴ in their papers show the equations set up for the torsion of the airfoil and give in more detail practically the same information as in the two papers by Liebers. Kussner calls attention to the vibration of wings from the point of view of the two-spar wing. He shows that the manner in which ailerons or flaps are attached determines the manner in which monoplane wings will vibrate.

It will be the endeavor of this paper to show (1) a theoretical development of the deflection curve of a cantilever flat bar of uniform cross-section by air forces distributed according to an elliptic load-grading curve and to show the effect of the warping produced by such loading in the expression for the strain energy of the bar so loaded; (2) to give an approximate solution of the torsional vibrations of such bar; (3) to show that induced torsional damping exists in an airfoil and to indicate the effect of self-induced torsional vibrations on the bending of the bar.

With respect to the first section of this paper, the method used is suggested by Liebers' papers, but the evaluation of the warping due to aerodynamic forces is original. The second point covered contains nothing new and is here inserted for comparison purposes. The third point covered is original and, to the best of the author's knowledge, has not appeared elsewhere.

Restrictions. The airfoil sections commonly used are of conventional type, such as Clark Y, N.A.C.A. M6, RAF 15, and Gottingen 387, or are modifications of these. A mathematical development of these sections is highly complicated; consequently a thin flat plate was chosen for investigation because of the known factors applying to such a plate. Further, we will investigate for vibrations of small amplitude only, and in order to keep the problem at or near some practical value, the aspect ratio of length of airfoil to chord has been chosen with 6 as its value.

2—NOTATIONS AND SYMBOLS

The axis system as specified for N.A.C.A. reports and the symbols employed by Timoshenko for the study of vibration have been used. The following notations have been employed:

² F. Liebers, "Zur Theorie der Luftschraubenschwingungen," *Zeitschrift für technische Physik*, vol. X, 1929, pp. 361-369.

³ F. Liebers, "Resonanzschwingungen von Luftschrauben," *Luftfahrtforschung*, May 16, 1930, pp. 137-152.

⁴ See Bibliography.

¹ Department of Aeronautical Engineering, University of Michigan. Mem. A.S.M.E. Mr. Taylor received the degrees of B.Sc. from McGill University in 1915 and Sc.D. from University of Michigan in 1933. He was chief designer of the Chisholm Moore division of the Columbus-McKinnon Chain Company. He was instructor in mathematics in the University of Buffalo, and was assistant to the director of the 1933 summer school at the University of Buffalo.

Contributed by the Aeronautic Division and presented at the Semi-Annual Meeting, Chicago, Ill., June 26 to July 1, 1933, of THE AMERICAN SOCIETY OF MECHANICAL ENGINEERS.

NOTE: Statements and opinions advanced in papers are to be understood as individual expressions of their authors, and not those of the Society.

- A = area of airfoil under consideration, sq ft
 a = constant
 $a_1, a_2, a_3, \dots, a_n$ = constant coefficients
 α = angle of incidence, radians
 $\Delta\alpha$ = small change in angle of incidence, radians
 α_0 = angle of incidence at root, radians
 α_1 = angle of incidence due to vibration, 2 radians
 α_2 = angle of warp at point $y = l$
 b = breadth of plate, in.
 b = constant coefficient
 b_1 = value of L_c at $y = 0$
 β = slope of lift curve for infinite aspect ratio = 2π
 C = torsional rigidity factor
 c = distance from the fixed end to point of application of load P , in.
 c = thickness of plate, in.
 c_1 = chord, ft
 C_D = coefficient of drag
 C_{Di} = coefficient of induced drag
 C_L = coefficient of lift
 γ = plan form ratio = $l/b = l/c_1$
 D = drag, lb per sq in. of span
 δ = induced drag factor = 0.096 for $R = 12$
 E = Young's modulus of elasticity, lb per sq in.
 f = frequency of vibration, cycles per sec
 G = modulus of rigidity in shear, lb per sq in.
 g = acceleration due to gravity = 386 in. per sec²
 I = moment of inertia of cross-section
 k = constant
 L_c = lift coefficient at point y
 \bar{L}_c = lift coefficient at point y at angle of incidence α
 ΔL_c = change of L_c accompanying change of incidence $\Delta\alpha$
 L = lift, lb per in. length of airfoil, in.
 M_t = torque or twisting moment, lb-in.
 $M_{t/2}$ = torque or twisting moment, about the position $c_1/2$, lb-in.
 m = slope of lift curve for aspect ratio being investigated; in this paper $R = 6$
 P = concentrated load, lb
 $p = 2\pi f$
 ρ = mass density of air, slugs per cu ft
 q = weight of bar per unit of length, lb per in.
 q_1 = intensity of distributed loading at point c on the bar, lb per in.
 R = aspect ratio
 r = distance from center of rotation to center of pressure, in.
 T = kinetic energy, lb-in.
 t = time, sec
 τ = coefficient of induced angular change for rectangular wings
 V = strain energy, lb-in.
 v = velocity, ft per sec
 v_0 = velocity at infinity parallel to x axis, ft per sec or in. per sec
 v_r = relative velocity, ft per sec
 ω = angular velocity, radians per sec

3—CONCEPT OF FORCES ACTING

Let us consider a flat bar $ABCD$, the center line of which lies in the y -axis of a right-handed system of axes. (See Fig. 1.) Its chord or width CD is c_1 . Our bar has an angle of attack of α_0 deg to a wind of velocity v . The lift developed is considered

to be quarter ellipse $EFGH$, with maximum lift at the built-in end and zero at the tip.

The center of pressure of any cross-section at angle of attack α_0 is represented by the line EF . Due to the lift developed, we can think of the airfoil bending to some position ABC_1D_1 , but the eccentricity of the load produces a torque which twists the airfoil to, say, ABC_2D_2 . Now there has been a change of angle of attack at the tip, reducing to zero at the root as indicated by the angle CJC_2 . This change increases the lift forces along the bar and deflects it to, say, ABC_3D_3 , where the torque so built up might be considered to have further twisted it. This process can be considered to continue until the bar finally takes a position of equilibrium of, say, ABC_4D_4 , where the angle CKC_4 will represent the total twist angle α_2 at the tip. Now of course our lift curve has also encountered some change of shape, such that on the straight bar it might be represented by EFG_1H . We must remember that the increment GG_1 is small because the angle CKC_4 is by hypothesis considered a small angle.

The lift at any point is given by

$$L = C_L A \frac{\rho v^2}{2}$$

Since the coefficient C_L contains all the variables for a given airfoil and velocity, we may deal with the coefficient, and in order to avoid confusion let us call C_L the lift coefficient at any point y .

Referring to Fig. 2, from analytic geometry we have:

$$L_c = b_1 \sqrt{1 - \left(\frac{y}{l}\right)^2} \dots \dots \dots [a]$$

Now let L_c receive a small increase ΔL_c such that for practical purposes the dotted figure may still be considered an ellipse. This small increase accompanies a change of angle of incidence $\Delta\alpha$, as explained in the opening paragraphs of this section. It is to be noted that at the built-in end the change of angle of incidence due to lift forces is zero and that the value of $\Delta\alpha$ will increase from zero at the built-in end to a maximum at the tip. The value of L_c will remain the same value at the built-in end. At the tip the value of ΔL_c must also be zero. So that

$$\Delta L_c = \frac{dC_L}{d\alpha} \cdot \Delta\alpha \dots \dots \dots [1]$$

The slope of the lift curve for angles of incidence below the burble⁵ point may theoretically be considered a constant of slope 2π ; nevertheless such value is not attained due to the aspect ratio being finite. Glauert⁶ gives the following coefficient as the correction of the slope of the lift curve for aspect ratio:

$$\frac{\beta}{1 + \frac{k\beta}{\pi R}}$$

Again, because, in the wind tunnel, viscosity affects the circulation about the airfoil, we cannot hope to attain this value. We may introduce a factor k to allow for that portion of the slope of the lift curve which may be attained, so that

⁵ The burble point occurs at that angle of incidence where the vortices in the wake of the airfoil have approached the trailing edge of the airfoil and are about to start rolling on the upper surface of the airfoil, or at that angle of attack where streamlined flow over the top of the airfoil ceases. See Ewald Poschl and Prandtl, "Physics of Solids and Fluids," Blackie, pp. 321-322.

⁶ "Airfoil and Airscrew Theory," H. Glauert, Cambridge Press.

$$m = \frac{k\beta}{1 + \frac{k\beta}{\pi R}}$$

would represent the slope of the attainable lift curve at the particular aspect ratio under consideration. In this expression k would have a value of from 0.85 to 0.90. Then

$$\bar{L}_c = L_c + \Delta L_c \dots \dots \dots [b]$$

$$= b_1 \sqrt{1 - \left(\frac{y}{l}\right)^2} + m \Delta \alpha$$

$$= m \alpha_0 \sqrt{1 - \left(\frac{y}{l}\right)^2} + m \Delta \alpha \dots \dots \dots [2]$$

4—TORQUE

The torque on the element with reference to the center of gravity of the rectangular section is given by

$$M_{i_{c/2}} = \bar{L}_c (0.5 - \text{c.p.}) c_1 \frac{\rho v^2}{2} c_1 dy \dots \dots \dots [c]$$

The distance from the leading edge to the center of pressure has been tabulated by various writers, and Eiffel's⁷ results for aspect ratio 6 have been used herein. Working with values below 10 deg incidence, an empirical⁸ equation has been found which fits the data with a very close approximation—in fact, well within the experimental error of the data—so that the equation

$$M_{i_{c/2}} = (0.23478 - 1.8055\alpha^2) c_1 \left[\left\{ m \alpha_0 \sqrt{1 - \left(\frac{y}{l}\right)^2} + m \Delta \alpha \right\} \frac{\rho v^2}{2} c_1 \right] dy \dots \dots \dots [4]$$

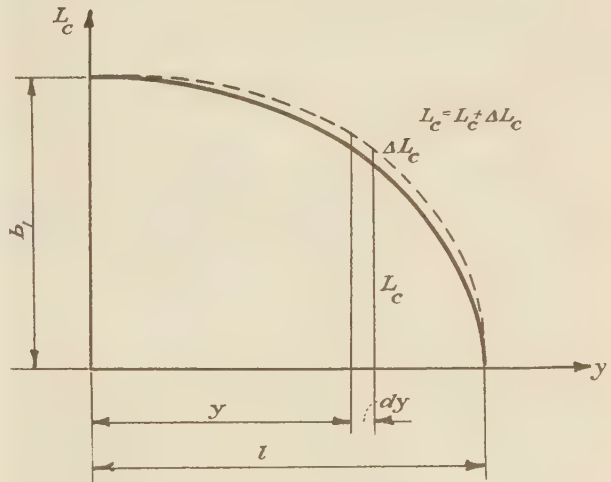


FIG. 2

It will be noticed that Equation [4] is of two parts; the first part may be interpreted as the torque producing static torque, while the second part containing $\Delta \alpha$ may be interpreted as the torque produced and maintained by warping.

As was noted previously, $\Delta \alpha$ is not constant, but varies along the length. As it is a function of y , it must satisfy the end conditions:

$$(\Delta \alpha)_{y=0} = 0 \quad \text{and} \quad (\Delta \alpha)_{y=l} = \text{maximum}$$

A suitable expression for $\Delta \alpha$ would be:

$$\Delta \alpha = \left(1 - \cos \frac{\pi y}{2l} \right) \alpha_2 \dots [5]$$

the end conditions being satisfied thereby.

The torque due to warp is then given by the expression:⁹

$$m(0.23478 - 1.8055\alpha^2) \left(1 - \cos \frac{\pi y}{2l} \right) \alpha_2 c_1^2 \frac{\rho v^2}{2} dy \dots \dots [d]$$

5—TRANSVERSE BENDING

In this place in our problem we propose to express the deflection of a cantilever bar, by a series; by using the energy method to evaluate the constants of such series and by the superposition theorem find the deflection curve for a bar loaded with a distributed load of the type of a quarter ellipse; then determine

⁹ Liebers, in his article, "Zur Theorie der Luftschraubenschwingungen," from *Zeitschrift für technische Physik*, vol. X, 1929, quotes Reissner for authority for the approximate use of a quadratic distribution of this factor. Whether a quadratic or $(1 - \cos \pi y/2l)$ expression is used makes very little difference, as the error introduced is extremely small and hence negligible.

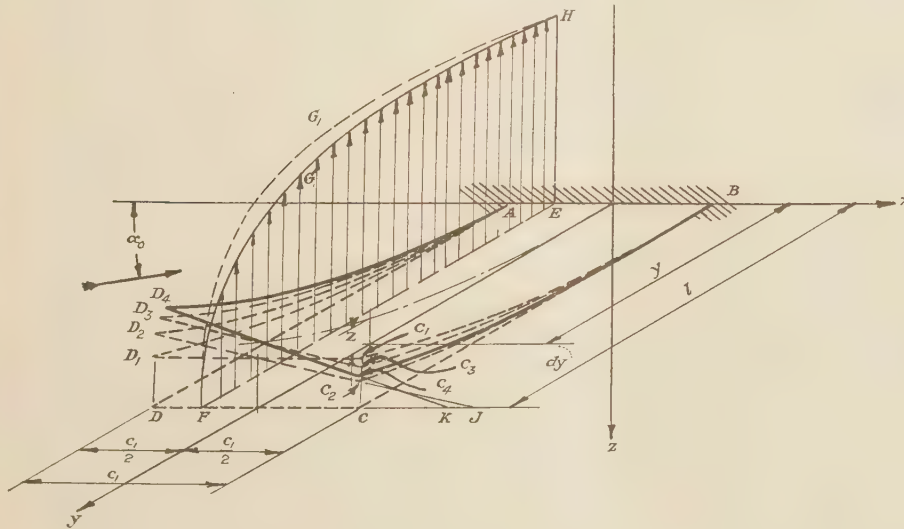


FIG. 1

tion of the center pressure referred to the mid-point of the chord is given by

$$(0.23478 - 1.8055\alpha^2) c_1 \dots \dots \dots [3]$$

where α is expressed in radians, or

$$(0.23478 - 0.00055\alpha^2) c_1 \dots \dots \dots [3a]$$

where α is expressed in degrees. The torque may then be written:

⁷ G. Eiffel, "Nouvelles Recherches sur la Resistance de l'air et L'Aviation," 1914.

⁸ See methods shown in Prof. T. R. Running's book, "Empirical Equations," John Wiley & Sons.

the strain energy of bending for such a deflection. (See Fig. 3.)

A suitable series to express the deflection of the bar is given by:

$$z = a_1 \left(1 - \cos \frac{\pi y}{2l}\right) + a_2 \left(1 - \cos \frac{2\pi y}{2l}\right) + a_3 \left(1 - \cos \frac{3\pi y}{2l}\right) + \dots + a_n \left(1 - \cos \frac{n\pi y}{2l}\right) + \dots [6]$$

Such series satisfies the end conditions, for when $y = 0, z = 0$, and $y = l, z$ has a finite value.

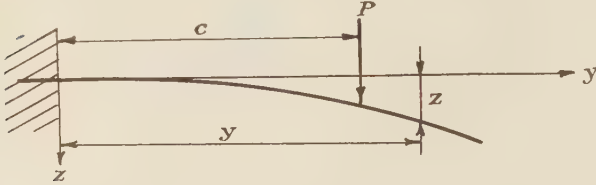


FIG. 3

Differentiating the series we get for the slope:

$$\frac{dz}{dy} = a_1 \frac{\pi}{2l} \sin \frac{\pi y}{2l} + a_2 \frac{2\pi}{2l} \sin \frac{2\pi y}{2l} + a_3 \frac{3\pi}{2l} \sin \frac{3\pi y}{2l} + \dots + a_n \frac{n\pi}{2l} \sin \frac{n\pi y}{2l} + \dots [7]$$

when $y = 0, \sin \frac{\pi y}{2l} = 0 \quad \sin \frac{n\pi y}{2l} = 0 \quad \therefore \frac{dz}{dy} = 0$. Hence the curve is horizontal at the fixed end, satisfying that condition.

In calculation of the coefficients a_1, a_2 , etc. of this series, we will use the energy method. The strain energy is given by

$$V = \frac{EI}{2} \int \left(\frac{d^2z}{dy^2}\right)^2 dy \dots [e]$$

and in substituting for d^2z/dy^2 the value

$$\frac{d^2z}{dy^2} = a_1 \frac{\pi^2}{4l^2} \cos \frac{\pi y}{2l} + a_2 \frac{2^2\pi^2}{4l^2} \cos \frac{2\pi y}{2l} + \dots + a_n \frac{n^2\pi^2}{4l^2} \cos \frac{n\pi y}{2l} + a_m \frac{m^2\pi^2}{4l^2} \cos \frac{m\pi y}{2l} + \dots [f]$$

We note that even-numbered terms must be dropped in order to satisfy the boundary condition at $y = l$, where the curvature is zero. Equation [e] involves the square of this derivative, which contains terms of two kinds in which n is an odd integer:

$$a_n^2 \frac{n^4\pi^4}{l^4} \cos^2 \frac{n\pi y}{2l} \quad \text{and} \quad 2a_n a_m \frac{n^2 m^2 \pi^4}{l^4} \cos \frac{n\pi y}{2l} \cos \frac{m\pi y}{2l}$$

By direct integration it may be shown that

$$\int_0^l \cos^2 \frac{n\pi y}{2l} dy = \frac{l}{2} \quad \text{and} \quad \int_0^l \cos \frac{n\pi y}{2l} \cos \frac{m\pi y}{2l} dy = 0$$

where $m \neq n$. Hence in integral [e] all terms containing products of coefficients such as $a_m a_n$ disappear and only terms with squares of these coefficients remain. Then

$$V = \frac{EI}{2} \frac{\pi^4}{16l^4} \cdot \frac{l}{2} (1^4 a_1^2 + 3^4 a_3^2 + \dots) = \frac{EI}{64} \frac{\pi^4}{l^3} \sum_{1,3,5} n^4 a_n^2 \dots [8]$$

We will consider one concentrated force and find the expression for the deflection curve.

For a single force P applied at a distance c from the built-in end, and considering now a slight change in one of the terms of the series, say, the n th term, with all the other terms remaining fixed, we get for the additional displacement of P :

$$da_n \left(1 - \cos \frac{n\pi c}{2l}\right)$$

The work done by the force P in moving through

$$da_n \left(1 - \cos \frac{n\pi c}{2l}\right)$$

is:

$$da_n \left(1 - \cos \frac{n\pi c}{2l}\right) P \dots [g]$$

The corresponding change of strain energy is

$$dV = \frac{\partial V}{\partial a_n} \cdot da_n = \frac{EI\pi^4}{64l^3} n^4 \cdot 2a_n \cdot da_n \dots [h]$$

Equating this to the work done [g]

$$\frac{EI\pi^4}{32l^3} n^4 a_n = \left(1 - \cos \frac{n\pi c}{2l}\right) P$$

from which

$$a_n = \frac{32Pl^3}{EI\pi^4} \cdot \frac{1}{n^4} \left(1 - \cos \frac{n\pi c}{2l}\right) \dots [9]$$

Then Equation [6] becomes¹⁰

$$z = \frac{32Pl^3}{EI\pi^4} \left[\frac{1}{1^4} \left(1 - \cos \frac{\pi c}{2l}\right) \left(1 - \cos \frac{\pi y}{2l}\right) + \frac{1}{3^4} \left(1 - \cos \frac{3\pi c}{2l}\right) \left(1 - \cos \frac{3\pi y}{2l}\right) + \dots \right] \frac{32Pl^3}{EI\pi^4} \sum_{1,3,5} \frac{1}{n^4} \left(1 - \cos \frac{n\pi c}{2l}\right) \left(1 - \cos \frac{n\pi y}{2l}\right) \dots [10]$$

Checking Equation [10] for the accuracy of solution, it may be shown that if we consider a cantilever with a single force concentrated at the outer extremity, the equation gives an accuracy within 1.2 per cent when the first term only of the series is used, while if three terms are used, the error will be less than $1/10$ of 1 per cent.

Having the solution for a concentrated load, we will now solve for the actual distributed load. From Equation [2] the lift on any element is given by

$$L_c \cdot \frac{\rho v^2}{2} c_1 dy$$

and substituting the value of \bar{L}_c , we get the intensity of load at any cross-section:

$$q_1 = \left[m\alpha_0 \sqrt{1 - \left(\frac{y}{l}\right)^2} + m\alpha_2 \left(1 - \cos \frac{\pi y}{2l}\right) \right] \frac{\rho v^2}{2} c_1 dy \dots [11]$$

From Equation [10], by substituting for P the value $q_1 dc$:

¹⁰ For similar development of these equations, see Timoshenko, "Strength of Materials," vol. II, Van Nostrand Pub. Co.

$$z = \frac{32l^3}{EI\pi^4} \frac{\rho v^2}{2} c_1 m \int_0^l \alpha_0 \sqrt{1 - \left(\frac{c}{l}\right)^2} \sum_{1,3,5}^{\infty} \frac{\left(1 - \cos \frac{n\pi c}{2l}\right) \left(1 - \cos \frac{n\pi y}{2l}\right)}{n^4} \cdot dc + \frac{32l^3}{EI\pi^4} \frac{\rho v^2}{2} c_1 m \alpha_2 \int_0^l \left(1 - \cos \frac{\pi c}{2l}\right) \sum_{1,3,5}^{\infty} \frac{\left(1 - \cos \frac{n\pi c}{2l}\right) \left(1 - \cos \frac{n\pi y}{2l}\right)}{n^4} \cdot dc \dots [12]$$

This equation has terms of two types:

$$\alpha_0 \sqrt{1 - \left(\frac{c}{l}\right)^2} \sum_{1,3,5}^{\infty} \frac{\left(1 - \cos \frac{n\pi c}{2l}\right) \left(1 - \cos \frac{n\pi y}{2l}\right)}{n^4} \dots [j]$$

and

$$\alpha_2 \left(1 - \cos \frac{\pi c}{2l}\right) \sum_{1,3,5}^{\infty} \frac{\left(1 - \cos \frac{n\pi c}{2l}\right) \left(1 - \cos \frac{n\pi y}{2l}\right)}{n^4} \dots [k]$$

Dealing with expression [j], choosing $n = 1, 3, 5$ in turn, evaluating the integral for each value of n , and then summing the integrals, will give the factor depending upon α_0 . In performing these operations, it will be readily seen that by substituting $c/l = \sin u$, $c = l \sin u$, and $dc = l \cos u \, du$, there will come terms of the form:

$$\begin{aligned} \int_0^{\frac{\pi}{2}} du &= \frac{\pi}{2} \\ \int_0^{\frac{\pi}{2}} \cos 2u \, du &= \left[\frac{1}{2} \sin 2u \right]_0^{\frac{\pi}{2}} = 0 \\ \int_0^{\frac{\pi}{2}} \cos \left(\frac{\pi}{2} \sin u \right) du &= \frac{\pi}{2} J_0 \left(\frac{\pi}{2} \right) \\ \int_0^{\frac{\pi}{2}} \cos 2u \cos \left(\frac{\pi}{2} \sin u \right) du &= \frac{\pi}{2} J_2 \left(\frac{\pi}{2} \right) \end{aligned}$$

The latter two of these are of course Bessels functions and readily evaluated.

Dealing now with the expression [k], this may be handled by direct integration after removal of the Σ sign and putting the expression in the form of a series, so that on reduction:

$$z = \frac{32l^3}{EI\pi^4} \frac{\rho v^2}{2} c_1 m \frac{l}{2} \left[\frac{(0.438\alpha_0 + 0.4535\alpha_2) \left(1 - \cos \frac{\pi y}{2l}\right)}{1^4} + \frac{(1.758\alpha_0 + 1.1512\alpha_2) \left(1 - \cos \frac{3\pi y}{2l}\right)}{3^4} + \frac{(1.472\alpha_0 + 0.4721\alpha_2) \left(1 - \cos \frac{5\pi y}{2l}\right)}{5^4} + \frac{(1.6217\alpha_0 + 0.8177\alpha_2) \left(1 - \cos \frac{7\pi y}{2l}\right)}{7^4} + \dots \right] \dots [13]$$

The factor 12 in the denominator is here introduced so that the load intensity may be expressed per inch of span for length being taken in inches, the chord c_1 in feet, while v is taken in feet per second. To this point there must be careful adherence. From Equation [13] the coefficients a_1, a_3 , etc. in Equation [6] may be evaluated, and on squaring these coefficients and substituting them in Equation [8], an expression for the strain energy becomes:

$$V = \frac{1}{36} \frac{l^3}{EI\pi^4} \frac{\rho^2 v^4}{4} m^2 \left[\frac{(0.438\alpha_0 + 0.4535\alpha_2)^2}{1^4} + \frac{(1.758\alpha_0 + 1.1512\alpha_2)^2}{3^4} + \frac{(1.472\alpha_0 + 0.4721\alpha_2)^2}{5^4} + \frac{(1.6217\alpha_0 + 0.8177\alpha_2)^2}{7^4} + \dots \right] \dots [14]$$

Since $\frac{M}{EI} = \frac{d^2 z}{dy^2}$, we have $M = EI \frac{d^2 z}{dy^2}$, and we have now found the values of a_1, a_3 , etc. in Equation [f], so that the stresses may be determined.

In the present problem the determination of the relative stress distribution was based on solving for the moment, statically. The foregoing series is given so that the problem of combined bending and torsion may be approached in a series form. Such series may possibly be combined with the series evaluations for vortex circulation about the airfoil.

From consideration of the bending moment for an elliptic load on a cantilever beam, it may be shown that the moment at the root is given by

$$M = m \frac{\rho v^2}{2} c_1 l^2 [0.333\alpha_0 + 0.269\alpha_2]$$

from which we conclude that when

$$\alpha_2 = \frac{0.333}{0.269} \alpha_0 = 1.24 \alpha_0 \dots \dots \dots [15]$$

there will be as much stress produced by twisting forces as is produced by bending forces.

In adjustable metal propellers which are relatively thin, it is quite evident that this effect will contribute greatly to the stresses carried. This effect may account for some of the numerous propeller failures noted by Liebers.

If a wing is rigid and if possible does not have any torsional vibration, then $\alpha_2 = 0$, and the remaining portion of Equation [14] will give an expression for the strain energy of a wing of constant moment of inertia.

6—VIBRATION OF PLATE AIRFOIL

(a) *Torsional Vibrations.* In this section it is proposed to calculate the frequency of free torsional vibrations of our cantilever plate airfoil, so that the frequency of resonance may be known. A suitable expression for the mode of vibration is of the form:

$$\varphi = \varphi_0 \left(1 - \cos \frac{\pi y}{2l}\right) \sin pt \dots \dots \dots [16]$$

We will use the energy method in this case, equating the maximum strain energy to the maximum kinetic energy, and solve for the frequency.

The strain energy is expressed by the equation:

$$V = \frac{C}{2} \int_0^l \left(\frac{d\varphi}{dy}\right)^2 dy$$

Differentiating Equation [16], squaring, and integrating, we have

$$V = \frac{C}{2} \varphi_0^2 \frac{\pi^2}{4l^2} \cdot \frac{l}{2} \sin^2 pt \dots \dots \dots [17]$$

Referring to Fig. 4, we note that if we reckon time from the mid-position of the vibration, V_{max} occurs when $\sin pt = 1$, or when $t = 1/4$ cycle.

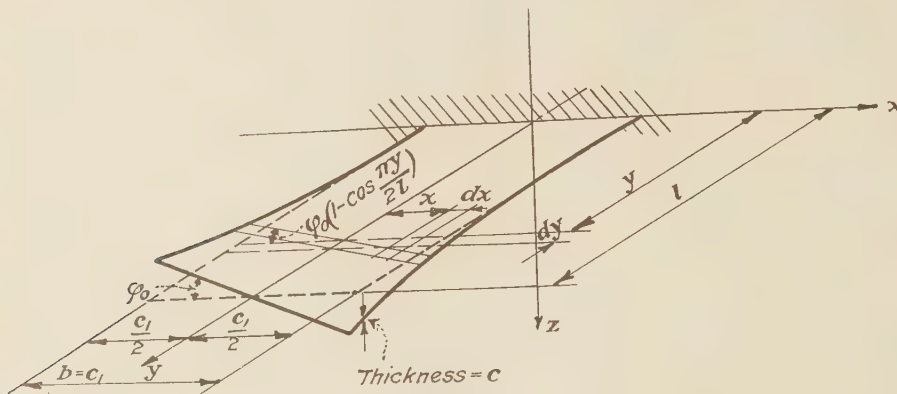


FIG. 4

So that

$$V_{max} = \frac{C}{2} \varphi_0^2 \frac{\pi^2}{8l} \quad [17a]$$

The kinetic energy is given by the equation

$$T = \frac{1}{2} \frac{g}{g} \int_{x=-b/2}^{x=b/2} \int_{y=0}^{y=l} (\dot{\varphi})^2 dy dx$$

which, by differentiating Equation [16] with respect to time, squaring, and integrating, reduces to

$$T = \frac{0.2267 \, q l \varphi_0^2 p^2 b^2 \cos^2 pt}{24g} \dots \dots [18]$$

T_{max} occurs at time $t = 0$, so that

$$T_{max} = \frac{0.2267 \, q l \varphi_0^2 p^2 b^2}{24g} \dots \dots \dots [18a]$$

Assuming no loss of energy, we equate the maximum strain energy and kinetic energy, and solving for p^2 we have:

$$p^2 = \frac{6gC\pi^2}{4 \times 0.2267 \, q l^2 b^2} \dots \dots \dots [19]$$

$$p = \frac{\pi}{2lb} \sqrt{\frac{6Cv}{0.2267q}}$$

$$f = \frac{p}{2\pi} = \frac{1}{4lb} \sqrt{\frac{6Cq}{0.2267q}} \dots \dots \dots [20]$$

We note that the frequency is independent of the angular amplitude.

From consideration of the rectangular cross-section of our plate, and noting that the width is long compared with the thickness, the torsional rigidity may be expressed in the form $C = G \cdot 1/3 \, bc^3$, where c represents the thickness of the plate.

Again we must note that a long rectangular prism, so constrained that one section does not distort when a torsional moment is applied, has the effect of shortening the bar by an amount equal to 0.425 times the half width.¹¹ If we apply a correction to the coefficient of torsional rigidity C , to offset this reduction of length, the frequency may be approximately expressed:

$$f = \frac{1}{4lb} \sqrt{\frac{Gbc^3}{3} \left(\frac{l}{l - 0.2125b} \right) \frac{g}{0.2267q}} \dots [21]$$

The ratio of length of plate to width of plate may be called the plan-form ratio, and we may denote such ratio by

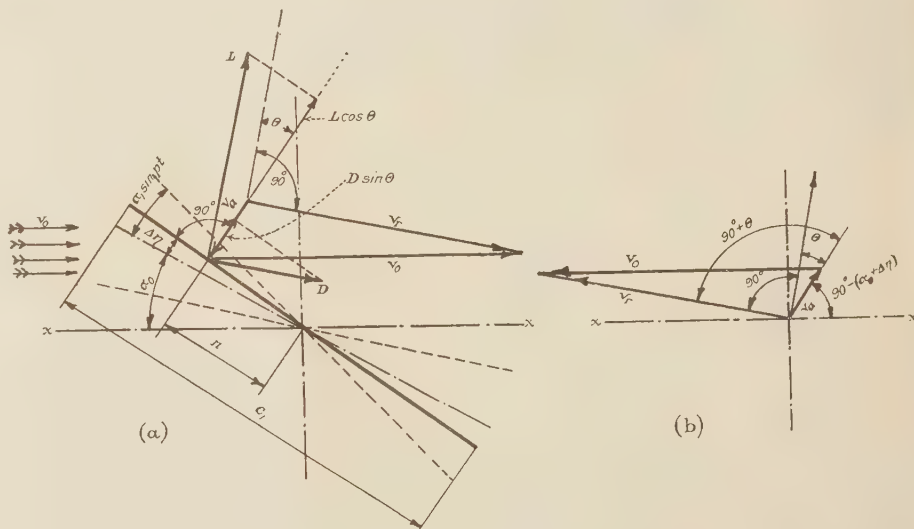


FIG. 5

$$\gamma = \frac{l}{b} = \frac{l^2}{\text{area of plate}} = \frac{l^2}{A}$$

Dealing with the expression $l/l - 0.2125b$, we may by substitution put this in the form $\gamma/\gamma - 0.2125$.

Again in Equation [21] we note in the denominator in front of the radical the factors lb , for which we may substitute l^2/γ , so that we may express this Equation [21] in the following form:

$$f = \frac{1}{4l^2} \sqrt{\frac{6}{0.2267} \cdot \frac{1}{3} \frac{qGbc^3}{q} \frac{\gamma^3}{(\gamma - 0.2125)}}$$

¹¹ S. Timoshenko, "On the Torsion of a Prism, One of the Cross-Sections of Which Remains Plane," *Proc. London Math. Soc.*, 1921, p. 389.

and substituting c_1 for b

$$f = \frac{1}{4l^2} \sqrt{\frac{6}{0.2267} \cdot \frac{1}{3} \frac{gGc_1c^3}{q} \frac{\gamma^3}{(\gamma - 0.2125)}} \dots [21a]$$

Thus, for example, a plate of these dimensions: $l = 18$ in., $b = c_1 = 3$ in., $c = 1/8$ in., $\gamma = 6$, $G = 11,650,000$ lb per sq in., $q = 0.10625$ lb per sq in. of span, $g = 386$ in. per sec². By direct substitution in Equation [21a] and solving, we obtain for the frequency 46.7 cycles per sec.

(b) *Induced Torsional Damping.* Mr. J. P. Den Hartog¹² has called attention to the self-induced vibrations of sleet-covered wires at various wind velocities. He notes that the relative wind is inclined at an angle to the axis of the shape considered to simulate a sleet-covered circular wire, and therefrom obtains a driving force to maintain vibrations in a vertical plane.

We will apply the method to another problem, but this time in erosion. Consider an airfoil to be loaded in such manner that the lift and drag forces may be considered as the only external forces acting, and allow these to act at the center of pressure of the airfoil. In general, the center of pressure and the axis of twist will not coincide, but will be at some distance apart. The relative wind due to the velocity of vibration will be inclined to the translatable flow, so that the relative wind on the upswing of the vibration will be different from the relative wind on the downswing. Because the lift and drag act normal and parallel to the relative wind at any instant, they will both have components normal to the airfoil. Designating the sum of these components as the driving force F_D , we get therefore an induced torsional damping as a result.

Consider an airfoil to be represented by a flat plate and let it be at an angle of incidence α , such that

$$\alpha = \alpha_0 + \alpha_1 \sin pt \dots [22]$$

as shown in Fig 5a. Let $\Delta\eta$ be a small change in the angle of incidence; assume the plate to be in torsional vibration about its mid-point and that such vibration is small and simple harmonic; let r be the distance from the center of twist to the center of pressure, and v_a be the tangential velocity of the center of pressure at any instant during vibration. If the angular velocity of the plate is ω , then the tangential velocity of the point P is given by ωr .

Combining the velocity v_a taken in proper sense to allow for the direction of representation of the translatable wind flow, we can obtain the relative wind velocity v_r . The lift and drag forces act normal and parallel to the relative velocity. The normal component of the lift will then be $L \cos \theta$, where θ ¹³ is the angle between the normal to the plate and the direction of the lift at the instant under consideration. Similarly $D \sin \theta$ will represent the drag component normal to the plate. The driving force F_D will then be the sum of these two components. It will be noted that the angle of attack θ of the airfoil is greater at mid-position on the downswing than at the same position on the upswing. Hence we may expect a greater value of F_D at that time, and since this increase of force opposes the motion, damping will result.

Plotting the driving force F_D against time for one cycle, we get a curve as in Fig. 6a, and plotting the angle of incidence against a time base we get a sinusoidal curve, Fig. 6b. Now plotting the product of the driving force and its moment arm r against the angle of incidence, we get a loop, Fig. 6c, which is a measure of the damping per cycle. This damping is small but positive.

¹² J. P. Den Hartog, "Transmission-Line Vibration Due to Sleet," A.I.E.E., June, 1932.

¹³ See Appendix for mathematical derivation of θ .

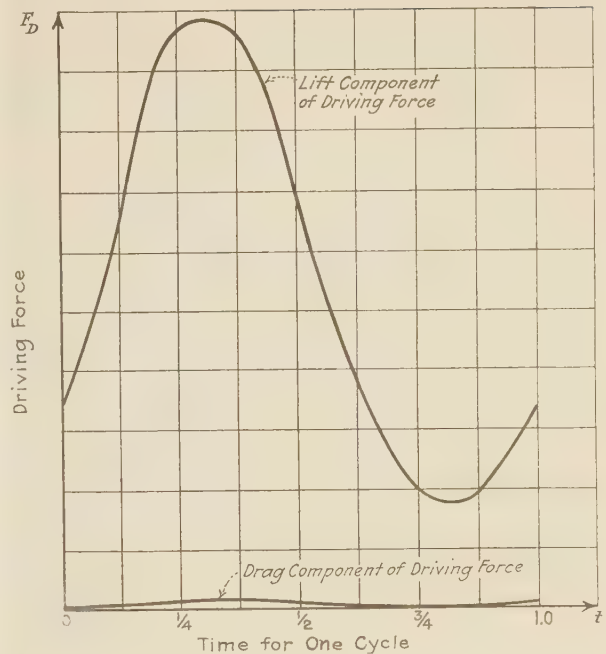


FIG. 6a

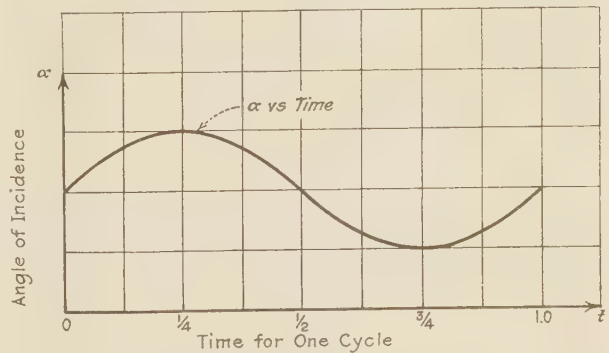


FIG. 6b

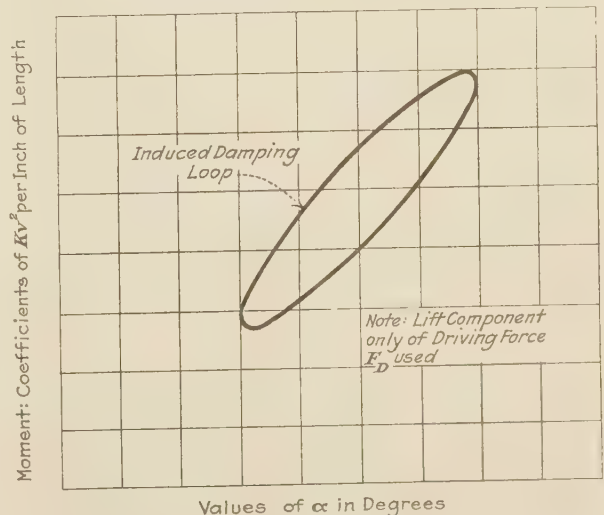


FIG. 6c

For self-induced torsional vibrations to exist there must be a moment acting on the airfoil greater than the damping moment. Such a moment may possibly be attributed to the impulsive moment connected with the shedding of the Karman-type vortices from the airfoil.

6—CONCLUSIONS AND SUMMARY

Self-induced torsional vibrations were observed at the natural frequency of the plate airfoil. The amplitude of the observed vibration being approximately 5 deg, there is little doubt that the forces producing such vibrations must appreciably exceed the damping as indicated in Fig. 6c.

If we denote the amplitude of the vibration as being a part of α_0 , we see the effect on the lateral bending as expressed in the equations for the stress distribution. From the expressions for the strain energy and moment we note that the vibration must play a major part in the energy and stresses in the airfoil.

Since a propeller is a rotating airfoil, it is probable that it also has a period of self-induced torsional vibration. Centrifugal force will have no effect on the torsional vibration so set up. This vibration is confirmed by the peculiar torsional fracture with which propellers frequently fail.

We cannot expect to remove these self-induced vibrations, but we should endeavor to keep the periods of other vibrations such as lateral vibration of a wing or fore-and-aft vibration of a propeller as far removed as possible from the self-induced vibration. In this manner we will remove the likelihood of resonance conditions being set up with damaging or critical results.

The method used in making observations in the wind tunnel has indicated that great studies may be made in the vibration measurements by such means.

Appendix

Referring to Fig. 5a, let xx be the line of reference, α_0 be the angle of incidence at the root, and $\alpha = \alpha_0 + \alpha_1 \sin pt$. Assume distribution of load over the chord, represent the center of pressure as c.p. and its distance from the axis of rotation by r , and consider the c.p. to be moving in the direction of α increasing.

For the sake of representing motion of the airfoil in true sense, let us refer again to Fig. 5b.

In the complex form $v_r = v_a + v$. Now

$$v_a = \omega r e^{(90 + \alpha_0 + \Delta\eta)i} \dots \dots \dots [A1]$$

$$= \omega r e^{90i} \cdot e^{\alpha_0 i} \cdot e^{\Delta\eta i} \dots \dots \dots [A2]$$

But $e^{zi} = 1 + \frac{zi}{1} - \frac{z^2}{2} - \frac{z^3}{6} \dots \dots$ and $e^{90i} = i$ and if z is small, we may approximate and write

$$v_a = \omega r i [1 + \Delta\eta i] e^{\alpha_0 i} \dots \dots \dots [A3]$$

Hence

$$v_r = \omega r i [1 + \Delta\eta i] e^{\alpha_0 i} + v_0 \dots \dots \dots [A4]$$

$$L = v_r \cdot i = -\omega r [1 + \Delta\eta i] e^{\alpha_0 i} + v_0 i \dots \dots \dots [A5]$$

Amplitude is

$$\frac{L}{v_a} = \frac{-\omega r [1 + \Delta\eta i] e^{\alpha_0 i} + v_0 i}{\omega r i [1 + \Delta\eta i] e^{\alpha_0 i}} \dots \dots \dots [A6]$$

since $1/1 + \Delta\eta i = 1 - \Delta\eta i$.

Then

$$\begin{aligned} \frac{L}{v_a} &= i + \frac{v_0}{\omega r} e^{-\alpha_0 i} [1 - \Delta\eta i] \\ &= i + \frac{v_0}{\omega r} e^{-\alpha_0 i} - \frac{v_0 \Delta\eta}{\omega r} e^{(90 - \alpha_0)i} \dots \dots \dots [A7] \end{aligned}$$

since

$$e^{90i} = i$$

Now take components as real and imaginary and remembering that

$$e^{ui} = \cos u + i \sin u$$

$$\begin{aligned} \frac{x}{0} &= \frac{z}{1 \times i} \\ \frac{v_0}{\omega r} \cos \alpha_0 &= -\frac{v_0}{\omega r} \sin \alpha_0 \times i \\ -\frac{v_0 \Delta\eta}{\omega r} \sin \alpha_0 &= -\frac{v_0 \Delta\eta}{\omega r} \cos \alpha_0 \times i \\ \tan \Theta &= \frac{1 - \frac{v_0}{\omega r} \sin \alpha_0 - \frac{v_0 \Delta\eta}{\omega r} \cos \alpha_0}{\frac{v_0}{\omega r} \cos \alpha_0 - \frac{v_0 \Delta\eta}{\omega r} \sin \alpha_0} \dots \dots \dots [A8] \end{aligned}$$

Dividing through by $v_0/\omega r$, we get

$$\tan \Theta = \frac{\omega r - \sin \alpha_0 - \Delta\eta \cos \alpha_0}{\cos \alpha_0 - \Delta\eta \sin \alpha_0} \dots \dots \dots [A8a]$$

Now consider the denominator

$$\frac{1}{\cos \alpha_0 - \Delta\eta \sin \alpha_0} = \frac{1}{\cos \alpha_0 (1 - \Delta\eta \frac{\sin \alpha_0}{\cos \alpha_0})} = \frac{1}{\cos \alpha_0} \cdot \left(1 + \Delta\eta \frac{\sin \alpha_0}{\cos \alpha_0}\right)$$

Substituting this last expression, expanding, and neglecting the 2d order of small quantities of $\Delta\eta$, we get

$$\begin{aligned} \tan \Theta &= \frac{\frac{\omega r}{v_0} - \sin \alpha_0 - \Delta\eta \cos \alpha_0 + \frac{\omega r}{v_0} \Delta\eta \tan \alpha_0 - \Delta\eta \sin \alpha_0 \tan \alpha_0}{\cos \alpha_0} \\ &= \frac{\omega r}{v_0} \sec \alpha_0 - \tan \alpha_0 - \Delta\eta \left(1 + \tan^2 \alpha_0 - \frac{\omega r}{v_0} \sec \alpha_0 \tan \alpha_0\right) \\ &= \frac{\omega r}{v_0} \sec \alpha_0 - \tan \alpha_0 - \Delta\eta \left(\sec^2 \alpha_0 - \frac{\omega r}{v_0} \sec \alpha_0 \tan \alpha_0\right) \dots \dots [A8b] \end{aligned}$$

Now in Equation [A8b] we substitute for

$$\begin{aligned} \omega &= \frac{d}{dt} (\alpha_0 + \alpha_1 \sin pt) = \alpha_1 p \cos pt, \Delta\eta = \alpha_1 \sin pt \\ r &= (0.23478 - 1.8055\alpha^2) c_l, p/2\pi = f \end{aligned}$$

for flat plate airfoil.

We can now solve for the value of Θ for any instant in one cycle. It will be noted for $\alpha_1 = 3$ in., $\alpha_0 = 4$ deg, $\alpha_1 = 1$ deg = 0.0175 radian, that Θ has a different value on the downswing than on the upswing. Computing the lift per inch of airfoil and resolving it normal to the chord gives the driving force due to the lift.

It is a well-known aerodynamic law that

$$CDi = \frac{CL^2(1 + \delta)}{\pi R} \dots \dots \dots [A9]$$

and that for $R = 12$

$$(CL)_{R=12} = 0.804$$

$$(CDi)_{R=12} = \frac{CL^2(1 + \delta)}{\pi \cdot 12} \dots \dots \dots [A9a]$$

and Glauert¹⁴ in his book on airfoil theory gives $\delta = 0.096$

$$D = (CDi)_{R=12} \cdot \alpha_1 \cdot 1 \frac{pv^2}{2} \dots \dots \dots [A10]$$

and hence its normal component may be found, so that the driving force due to the drag may be found, and hence the total driving force F may be determined at any instant.

BIBLIOGRAPHY

- "Schwingungen mehrfach gestutzter Stäbe mit Axialkräften," H. G. Kussner, D.V.L., Sept., 1928. Jahrbuch D.V.L., 1929, S. 335.
- "Schwingungen von Flugzeugflügeln," H. G. Kussner, D.V.L., Feb., 1929. Jahrbuch D.V.L., 1929, S. 313.
- "Gekoppelte Biege- Torsions- und Querruderschwingungen von freitragenden und halbseittragenden Flügeln," H. Blenk and Fritz Liebers. Jahrbuch D.V.L., 1929.
- "Gekoppelte Torsions-Biegeschwingungen von Tragflügeln," Blenk and Liebers, Z.F.M., 1925, S. 479 und Z.F.M., 1926, S. 286 (errata sheet for 1925 articles).
- Fraser, "An Investigation of Wing Flutter," Great Britain, R. & M., 1042 (1926).
- C. F. Greene, "An Introduction to the Problem of Wing Flutter," Trans. A.S.M.E., 1928.
- "Transmission-Line Vibration Due to Sleet," J. P. Den Hartog, A.I.E.E., June, 1932, Cleveland meeting.
- "Self-Induced Vibrations," J. G. Baker, A.S.M.E., June, 1932, Jan., 1933, Bigwin Inn meeting.
- "On Relaxation Oscillations," B. Van Der Pol, *Phil. Mag.*, vol. 2, 1926, p. 978.
- J. B. Younger, "Dynamics of Airplanes," and B. M. Woods, John Wiley & Sons.

¹⁴ H. Glauert, "Airfoil and Airscrew Theory," Cambridge University Press.

Characteristics of Large Hell Gate Direct-Fired Boiler Units

By W. E. CALDWELL,¹ NEW YORK, N. Y.

Among the outstanding features which characterize this boiler installation is a capacity of each of the two units in excess of 1,000,000 lb per hr. The direct-fired, slag-tapped furnace with a twin arrangement of sectional header boilers above a single furnace is an innovation. The building that houses the two boilers, bunkers, and all auxiliaries is 78.7 ft by 106.5 ft and is 162 ft high, or a building volume of 680 cu ft per 1000 lb steaming capacity per hour. The steam conditions of 275 lb per sq in. pressure and 725 F temperature are the same as those prevailing in the remainder of the plant. The circulation of each half of the boiler unit, with its accompanying proportion of water walls, is independent. The superheater, economizer, and air heater of each half of the unit are also independent. The air-inlet end of the air heaters and similarly the gas-discharge end of the air heaters are connected to a com-

mon plenum chamber to eliminate the fan auxiliaries as a source of boiler outage. By this arrangement the unit may develop about 75 per cent of maximum capacity with half of the fan equipment idle. Aside from innovations regarding the twin arrangement, the boiler and furnace are of conservative design. Heat-release rates, absorption rate per unit of surface, and gas velocities entering the tube bank are moderate. Large boiler drums were provided in order to confine water-level fluctuations within safe limits regardless of the rapidity or range of load changes. The visible range within the water glass accommodates a 13 per cent change in the volume of water contained in the boiler and water walls up to the normal water level. This is equivalent to 4.5 per cent of the hourly output at maximum capacity on the basis of solid water.



THIS boiler installation at Hell Gate Station was erected as a boiler-room extension on land which was limited in area by existing structures and a street boundary. This limitation in area necessitated a design which would utilize the site to the greatest advantage without exceeding the height limit imposed by the city building code. The quantity of steam necessary to satisfy the installed turbine capacity was greater than could be produced by the boiler-plant extension. This

consideration rendered necessary an installation capable of developing the maximum rational capacity in the available space in order to reduce the extent of revamping of the older boilers which otherwise would be necessary. As a railroad siding which enters the turbine-room basement passes across one side of the chosen site, it was necessary to arrange the design to accommodate this sidetrack below the boiler level.

Among the outstanding features which characterize this installation consisting of two units is a capacity of each unit in excess of 1,000,000 lb per hr. Direct-fired, slag-tapped furnaces

with a twin arrangement of sectional header boilers above the common furnace is somewhat of an innovation. The furnace is the largest so far installed, and this is the first application of sectional header boilers with the twin-setting or end-to-end arrangement.

The building is 78.7 ft by 106.5 ft and is 162 ft high, housing two units, and the ratio of building volume to boiler capacity is 680 cu ft per 1000 lb steaming capacity per hour. Correcting the building volume for the space devoted to railroad tracks and court entry, the ratio becomes 636 cu ft per 1000 lb per hr capacity.

With the limited space conditions, the flat-bottom slagging type of furnace became almost a necessity. In the absence of space for an ash hopper of the dry-bottom type, careful thought was given to the slagging furnace for the grades of coal and type of load to be encountered. Earlier problems with slagging furnaces at Sherman Creek Station had been experienced, and this pioneering work left little doubt as to the attractive possibilities of the system.

The four mills and their auxiliaries are directly below each furnace, while the forced- and induced-draft fans are immediately above the air heaters. The coal bunkers are below the fan platform, from which coal is fed by gravity through vertical chutes to the mill feeders. Each chute supplies one mill and is provided with a Richardson automatic scale ahead of the feeder, with remote indication at the control board. These scales facilitate accounting and control, as well as testing. There are two drag-conveyer feeders per mill located on the operating floor and accessible from the control board. The feeders are driven by direct-current motors from motor-generator sets with Ward Leonard speed control.

BOILERS

The steam conditions, 275 lb per sq in. pressure and 725 F temperature, are the same as those in the remainder of the plant.

With the end-to-end arrangement of boilers over the common furnace, access space was necessary between the headers, and a seal had to be provided between the furnace and this opening. This was accomplished by bringing the bottom slag-screen tubes under the bottom of the high-end headers and entering the op-

¹ Research Engineer, The United Electric Light and Power Company. Mem. A.S.M.E. Mr. Caldwell received his engineering education at Drexel Institute, Philadelphia, Pa. He joined the United company in 1913 as chemist and engineer of tests, successively serving in other capacities. He was identified with engineering design, operation, and testing of pulverized-fuel boilers installed in 1924 at Sherman Creek Station. These were the first pulverized-fuel boilers provided with water-wall furnaces, and a variety of combustion systems featured the installation. In the same installation the first commercial slagging furnace was introduced. Experience here also included work on the development and testing of flue-dust catchers. Mr. Caldwell also was identified with engineering design, testing, operation, and betterment work in Hell Gate Station, on both stoker and pulverized-fuel equipment.

Contributed by the Fuels and Power Divisions and presented at the Semi-Annual Meeting, Chicago, Ill., June 26 to July 1, 1933, of THE AMERICAN SOCIETY OF MECHANICAL ENGINEERS. Awarded the Melville Medal for 1933.

NOTE: Statements and opinions advanced in papers are to be understood as individual expressions of their authors, and not those of the Society.

posite side of the header by a wide-sweep return bend in the tube. This arrangement provides a water-cooled support for the protecting tile beneath the headers and also the baffle between header access space and furnace. The circulation of the two boilers is not interconnected, and each supplies its half of the furnace water walls, so that the circulation of each half of the units is entirely independent. The superheater, economizer, and air heater of each half of the unit are also independent, although the discharge end of the air heaters is connected to a com-

boiler and furnace are of conservative design. Heat-release rates, absorption rate per unit of surface, and gas velocities entering the tube bank are moderate. The water capacity of the boiler and economizer is rather large, and while the resulting accumulator effect renders the unit somewhat slow in response to changes of rating, it has a very desirable stabilizing influence with fluctuating loads. The 72-in. boiler drums are adequate to permit wide changes in rating without danger of carry-over from the drum. Large drum capacity is especially important with the moderate pressure and relatively high specific steam volumes prevailing, in order to accommodate the swelling contents of the boiler with wide increase in rating. This removes one of the possible limitations to flexibility and responsiveness, since water-level fluctuations are confined within safe limits regardless of the rapidity and range of load changes. With adequate drum capacity, the feed-control problem is simplified and the attention required by the operators is reduced to a minimum.

The visible range within the water glass accommodates a 13 per cent change in the volume of water contained in the boiler and water walls up to the normal water level. This is equivalent to 4.5 per cent of the hourly output at maximum capacity, on the basis of solid water.

The boilers are provided with three horizontal circulator tubes per section, arranged to minimize discharge friction and insuring an effective hydraulic head on all tubes. This lessens the likelihood of stagnant circulation, with the accompanying problems, and is of benefit from the standpoint of boiler maintenance and availability. The boiler drum is fitted with shutter-type baffles for moisture separation. Saturated steam is distributed to the superheater by means of a number of off-take tubes distributed along the length of the boiler drum and connected with the saturated-steam header on the superheater. This arrangement assures uniform steam distribution through the superheater, with a minimum of pressure drop. The economizer is of the conventional hairpin type, while the air heater is the standard tubular type, both being arranged for countercurrent flow.

BURNERS AND FURNACES

Each mill delivers to three cross-tube burners in a horizontal row, distributed across the furnace width, there being two rows at each end of the furnace, one above the other. This provides well-balanced furnace conditions with almost any combination of mills. Individual burners may be cut out by closing a valve in the top of the mill, which diverts the coal and primary air from that burner to the remaining outlets and burners. There is an oil burner just below each coal burner, for ignition purposes only. The Bailey water-cooled furnaces are, roughly, 41 ft long between burners, with a width of 34 ft and a mean height of 30 ft. The furnace volume is 40,770 cu ft, giving a heat liberation of about 35,000 Btu per cu ft, at 1,000,000 lb per hr evaporation.

The furnace bottom is provided with air cooling by forced circulation from a centrifugal compressor delivering air at about 1 lb pressure. Immediately below the slag bed is an impervious layer of crushed magnesite supported on a porous layer of chrome ore. The cooling air is distributed by transverse ducts in the layer of chrome ore, from which it is discharged into the furnace at the side walls above the slag bed. The quantity of air used for cooling is determined from the Bailey air-flow meters which form a part of the regular operating equipment.

The preheated-air temperature being moderate, permits normal operation without the use of tempering air and the attendant manipulation required where higher preheat is used. With a direct-fired system there are many adjustments which must be readily coordinated, and in the interest of reliability these were kept to the minimum.

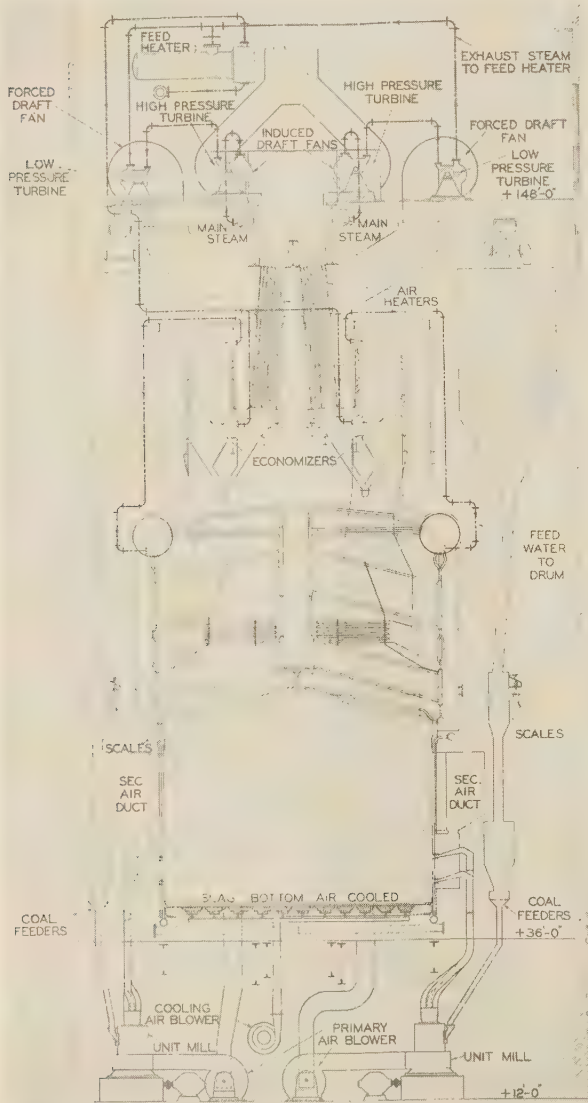


FIG. 1 CROSS-SECTION OF BOILER

mon plenum chamber. This common-plenum-chamber arrangement renders the installation more independent of induced-draft fan outage, since the unit may develop about 75 per cent capacity with half of the fan equipment idle. The same general practise is applied to the forced-draft connection to obtain the same benefits of diversity and availability. This combination was obtained by a slight inclination of the air preheaters and by the elimination of separating partitions.

Aside from innovations regarding the twin arrangement, the

FANS

There are four induced-draft fans per boiler unit and two forced-draft fans. The induced-draft fans are connected in pairs and driven through reduction gears by a high-pressure, high-speed turbine, the exhaust steam from which is used to operate the low-pressure turbine driving the forced-draft fan.

Local conditions of plant expansion constituted a factor in the selection of fan drives. With the existing conditions evaluated, the differences between various types of drives were small, and the turbine drives were chosen for convenience. The exhaust steam from the low-pressure turbines which drive the forced-draft fans is discharged through short con-

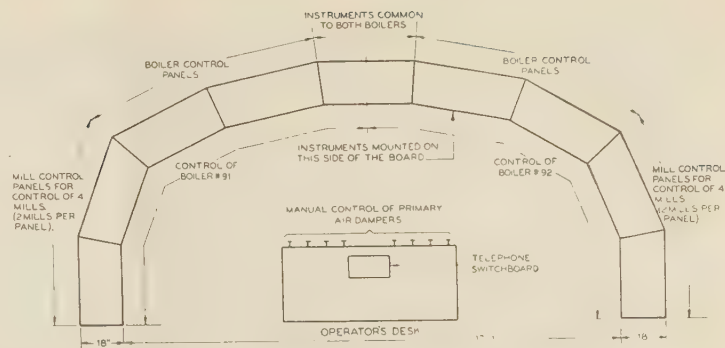


FIG. 5 DIAGRAMMATIC PLAN VIEW OF CONTROL BOARD FOR BOILERS 91 AND 92

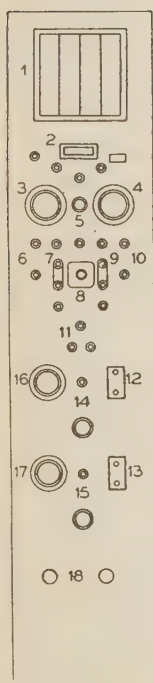


Fig. 3

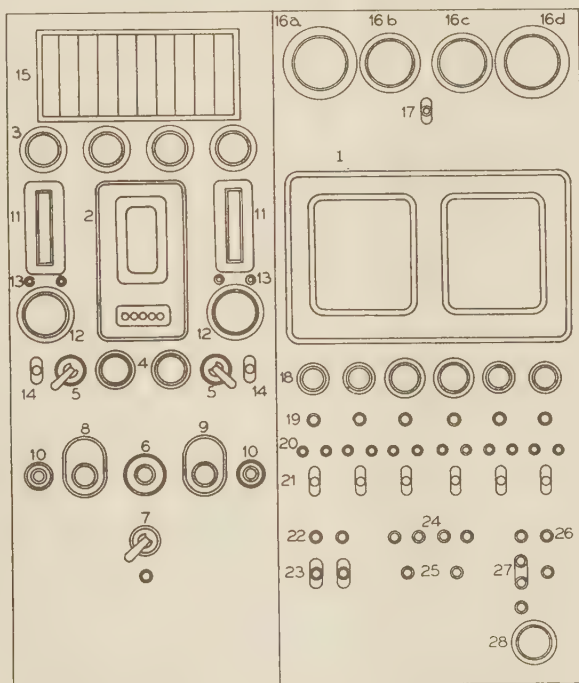


Fig. 2

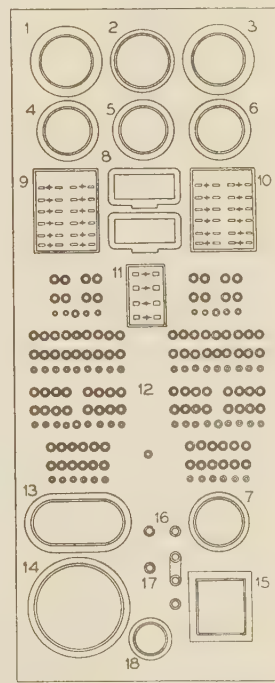


Fig. 4

FIGS. 2, 3, AND 4 CONTROL BOARDS FOR THE 90-ROW BOILERS, THE MILLS, AND THE INSTRUMENTS

[Fig. 2. Section of the Control Board Showing Control for Each Boiler. Legend: 1, Bailey steam-flow-air-flow meter. 2, Smoot control panel (individual boiler control). 3, air- and oil-line pressure gages. 4, control air-pressure gages. 5, transfer cocks (from manual to pressure control), two valves. 6, control wheel (manual control). 7, transfer valve (coal-feed safety device). 8, maximum-rating-limit valve. 9, minimum-rating-limit valve. 10, control air-wheel (manual control). 11, drum pressure-level indicator. 12, feedwater-valve position indicator. 13, supply valve, two valves. (Nos. 2 to 10 are in the Smoot control). 14, switch controlling feedwater valve. (There are two sets of 11, 12, 13, and 14 for each boiler.) 15, draft gages, 10 indicating lights for feedwater valve. 16, pressure gages: (a) drum pressure, west drum. (b) and (c) receiver pressure. (Pressure in receivers of two sets of points (boiler, economizer, air heater). 17, emergency trip switch for coal feeders, mills, and mill compound steam turbines driving forced- and induced-draft fans.) 18, tachometers (four for fan turbines), voltmeters (two for Ward Leonard coal-feeder control). 19, transfer switches (four for fan turbines, two for blowers. 20, regulator position indicating lights for use when changing from hand to automatic control (in connection coal feeders) from hand to automatic control. 21, push-pull switches for hand control of fan turbines and coal feeders (four for fan turbines, two for Ward Leonard coal-feeder control). 22, damper control, position-indicating light (damper between economizer and air heater). 23, damper control, switch. 24, lights indicating the functioning of an alarm for failure of Ward Leonard motor-generator sets (two sets for two boilers). 25, switches for controlling bell alarm for failure of Ward Leonard motor-generator sets (two sets for two boilers). 26, indicating lights. 27, switch. 28, ammeter. (Instruments 26, 27, and 28 are for control of furnace-bottom cooling blower.)

Fig. 3 Section of the Control Board Showing Control for Each of the Four Mills for Each Boiler. Legend: 1, air suction, pressure, and differential gages, four points (for mill blower and mill). 2, coal-scale counter. 3, mill-motor ammeter. 4, mill-blower-motor ammeter. 5, sequence cut-out switch and indicating lights. 6, mill-motor alarm-signal switch and indicating lights. 7, mill-motor control switch and indicating lights. 8, coal-calcating light (mill, blower, and feeder). 9, mill-blower-motor alarm-signal switch and indicating lights. 10, mill-blower-motor alarm-signal switch and indicating light. 11, coal-flow indicating lights. 12 and 13, mill-feeder-motor-control switches (two feeders per mill). 14 and 15, mill-feeder-motor rheostats (two feeders per mill). 16 and 17, mill-feeder-motor tachometers (two feeders per mill). 18, line switches for mill-feeder-motor power supply, from Ward Leonard generators (two feeders per mill).

Fig. 4 Section of the Control Board Showing Instruments Common to Both Boilers. Legend: 1, pressure gage, steam-line pressure. 2, Telechron clock. 3, pressure gage, feedwater-line pressure. 4, pressure gage, suction head on heater condensate pump. 5, load indicator, total station load. 6, pressure gage steam pressure in feedwater heater. 7, pressure gage, fuel-oil pressure. 8, temperature indicators, two indicators, one for low-temperature range and one for high-temperature range, on boilers 91 and 92. 9, switches for temperature indicators, boiler 91. 10, switches for temperature indicators, boiler 92. 11, high-temperature range, on boilers 91 and 92. 12, signal lights, signal sending and receiving stations to and from mills, mill blowers, and fans switches for temperature indicators, common to both boilers. 13, belt-coal-scale indicating counter, one for main belt conveyor serving both boilers. 14, water-flow-meter indicator. 15, water-flow-meter integrator. (Instruments 14 and 15 are for both boilers.) 16, indicating lights. 17, switch. 18, ammeter. (Instruments 16, 17, and 18 are for control of furnace-bottom cooling blower, a spare blower serving either of the two boilers.)]

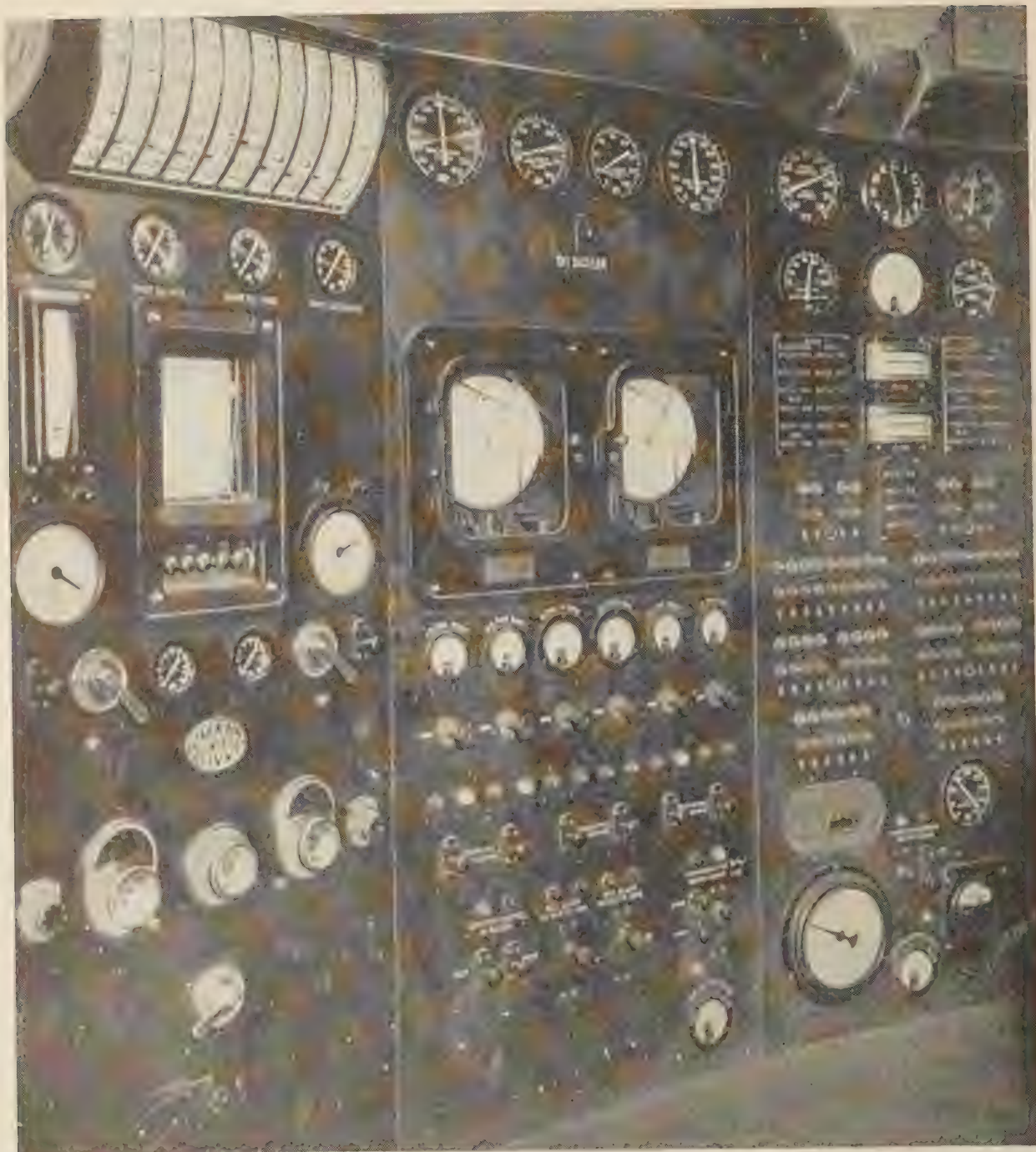


FIG. 6 PART OF BOILER CONTROL BOARD

necting piping to a closed heater in the feedwater supply to the boilers.

CONTROL

Control of this installation has been brought to a central location, with the necessary instruments and devices provided so that operation is greatly simplified. The control board is illustrated in Figs. 2 to 7, inclusive. Practically all adjustments for starting, stopping, and changing the output are made from this con-

trol station. Sequence interlock relay protection is provided to guard against flarebacks or explosions due to mechanism failures or mishandling.

The installation is fitted with the same type of control mechanism as that on the earlier boilers and is designed to operate in conjunction with the other apparatus. Control may be changed from automatic to hand, or vice versa, at will. The importance of the control board is more apparent when the operations that must be closely coordinated in starting are considered. Figs. 8

and 9 depict graphically the sequence of operations followed in starting the boiler from the cold condition and also the method followed after a normal shutdown over the midnight watch.

The intent of this method of starting from cold is to apply heat very gradually about the furnace, so that proper circulation may be established throughout in order to avoid excessive temperature stresses. With the direct-firing arrangement, this necessitates operating the mills for short intervals in rotation and is conveniently accomplished from the central control board. The boilers are started each morning on weekdays, at which time the furnace is hot from the previous day's operation and there has been very little loss of steam pressure. Under these conditions

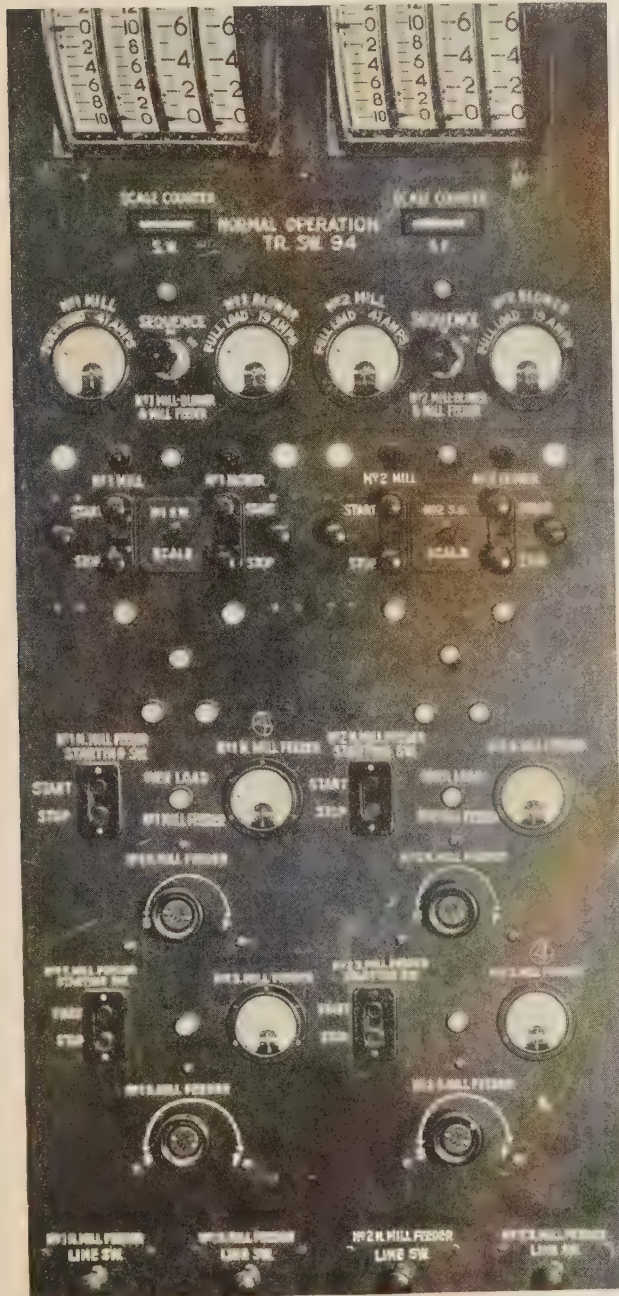


FIG. 7 ONE OF THE MILL CONTROL PANELS (2 MILLS)

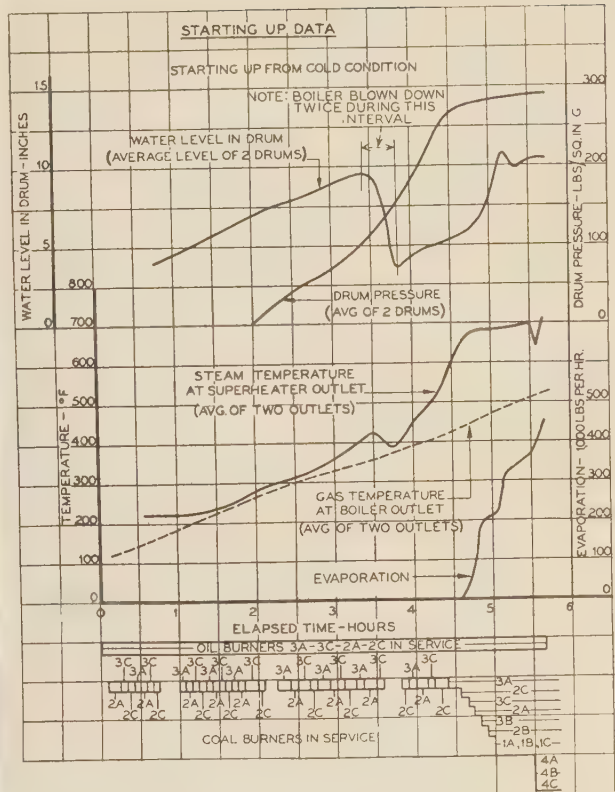


FIG. 8 STARTING UP FROM COLD CONDITION, BOILER 92
(During warming-up period, four corner burners, 2A, 3C, 2C, 3A, are operated alternately, one burner at a time.)

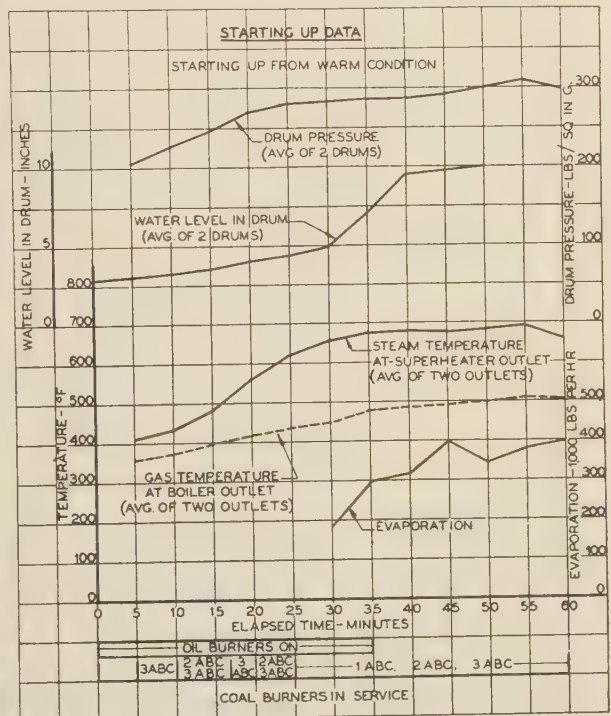


FIG. 9 STARTING UP FROM WARM CONDITION, BOILER 92

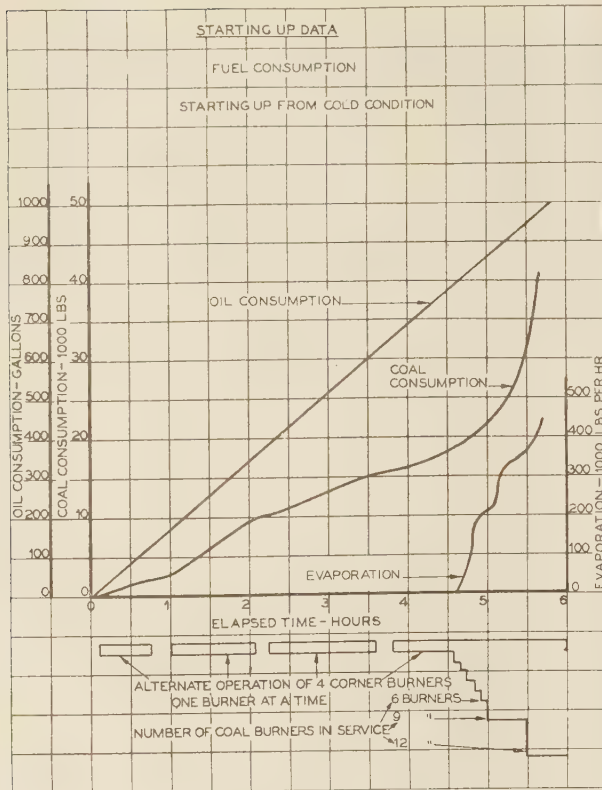


FIG. 10 FUEL CONSUMPTION, STARTING UP FROM COLD CONDITION, BOILER 92

the unit goes on the line within a few minutes after the first burner is lighted.

CAPACITY AND FLEXIBILITY

The maximum capacity of the installation is limited by the fans and pressure drop through the superheater. With the average grade of coal used, the mill capacity is near the limit when other limiting conditions are approached. The lower limit of output is established by the minimum practical capacity of one mill, together with secondary-air leakage through the burner dampers of the idle mills. The heat radiated by the hot slag

bottom provides strong ignition and minimizes the danger of flarebacks with one-mill operation or under unfavorable coal-feed conditions. The boiler has been operated for sustained periods at outputs as low as 200,000 lb per hr and as high as 1,080,000 lb per hr. Under test conditions these figures could be considerably bettered at both ends of the range by means well known to many operators. However, a more rational basis of rating for daily operation may be considered as from 300,000 lb per hr to 1,000,000 lb per hr.

RESPONSIVENESS

Tests were conducted under the supervision of the manufacturer's representatives to determine the rate of response of the mills for various changes in the feeder speed, together with the time effect on steam output from the boiler. These data are

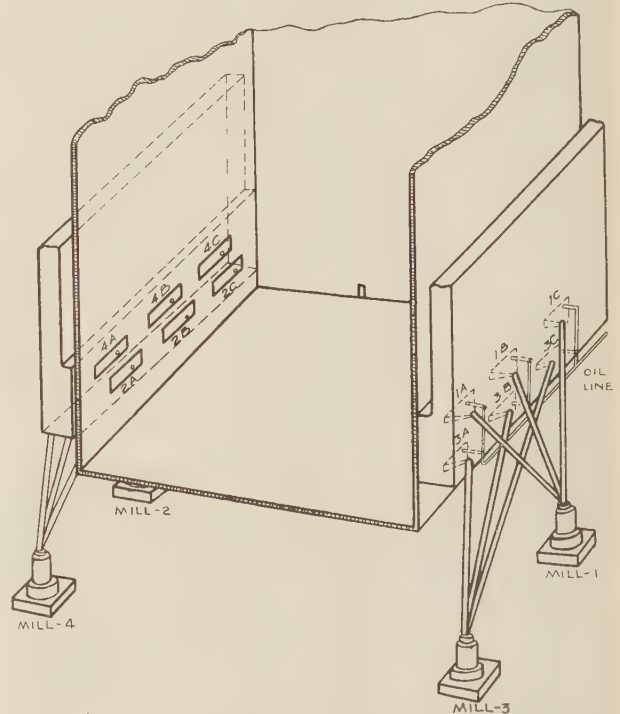


FIG. 11 ARRANGEMENT OF PIPING BETWEEN MILLS AND BURNERS

TABLE 1 TEST OF BOILER NO. 92, HELL GATE STATION—RESPONSIVENESS OF BOILER TO INCREASE IN LOAD

Before change in coal feed	After change in coal feed	Diff.	Increase in steam flow, per cent	Speed of coal-feeder motors, rpm			Increase in coal-feeder speed, per cent	Over-travel of coal feeders, per cent	Period of over-travel of coal feeders, min	Time lag, min ^b	Air supply ^c	Rate of change in steam flow, lb per hr per min		Change in steam pressure, lb per sq in.	Change in water level, in.
				Initial	Maximum during change	Final						Per boiler	Per mill		
600	725	125	20.8	637	832	832	31	0	0	3.25	FS	38,400	9,600	+ 5.3	+1.25
520	740	220	42.3	585	855	855	46	0	0	4.0	FC	55,000	13,750	+ 4.1	-2.25
530	810	280	52.8	587	959	959	63	0	0	4.5	FC	62,200	15,540	+ 6.0	-2.0
420	720	300	71.5	450	1005	806	79	25	3.0	4.75	FS	63,200	15,800	+ 3.3	-2.0
400	720	320	80.0	450	1200	800	78	50	3.0	4.25	FS	72,300	18,075	+ 8.7	-3.0
410	710	300	73.0	450	1400	800	78	75	3.0	3.75	FS	80,000	20,000	+ 5.5	+2.0
410	740	330	80.5	450	1500	800	78	87	3.0	4.5	FS	73,300	18,325	+12.5	-2.5
400	710	310	77.5	500	1250	925	85	35	2.5	2.75	FC	112,700	28,175	+ 0.5	-6.25
390	590	200	51.3	500	1250	800	60	56	1.5	2.25	FC	88,800	22,200	+ 7.0	+1.1
380	640	260	68.5	500	1350	800	60	69	1.5	3.25	FC	77,000	19,250	+ 5.0	-1.0
380 ^a	660	280	73.7	500	1300	850	70	53	1.5	2.75	FC	102,000	25,500	+ 3.0	+3.5
410 ^a	720	310	75.6	619	1341	1080	75	24	1.5	3.25	FC	95,400	23,850	+10.0	+3.25
350 ^a	700	350	100.0	620	1350	1240	100	9	1.5	2.5	FC	140,000	35,000	+11.5	-0.5

^a During these tests the speed of the coal feeders was increased in four steps, so as to approximate an automatic control; the period of the maximum over-travel was 1 min and that of the total over-travel 1.5 min. ^b Time lag represents the interval of time required for the stabilization of the steam flow after a change in the coal feed. ^c FS means the air supply follows the steam change; FC means the air supply follows the coal change.

NOTE: The actual tests for the last two runs indicated a temporary stabilization at a lower final speed of 850 rpm due to the accumulation of coal in the mills during the over-travel period, but since these runs were not sufficiently prolonged to establish the correct final speeds, the reported values for these final speeds were assumed to be in proportion to the increase in steam flow.

indicative only, since it was not convenient to carry out the tests with the precision of an evaporative test nor to entirely eliminate influences tending to affect the result of the observations.

Some of these tests are recorded in Tables 1 and 2 and are also shown in Figs. 12, 13, and 14. The tests covered both increase and decrease in output, with observations recorded on 15-sec intervals. The time lag between the coal-feeder change and the change in heat input to the furnace was determined by ascertaining the variation in CO_2 in the flue gas while maintaining a constant supply of primary and secondary air. The change in CO_2 at the boiler outlet commenced within 15 sec from the start of the change in coal feed, and the stabilized condition was reached in about 2 min. The beginning of the change in the steam flow commenced from 12 to 18 sec after the change in coal feed, and it reached the final value in from 2.5 to 4.5 min. The shortest lag was obtained by giving considerable overtravel to the coal feeders and by adjusting the secondary-air supply to follow the change in coal supply instead of following the steam flow. The most rapid increase in output was 350,000 lb per hr in a period of 2.5 min. The rate of the increase was 35,000 lb of steam per hour per mill per minute, or 140,000 lb of steam per hour per minute for the boiler. This increase in evaporation represents 100 per cent change if referred to the load at the beginning of the change, and 14 per cent change if referred to the maximum capacity.

Very little change is required in the primary-air control for the full range of mill capacity, and this may be accomplished with one or two adjustments for the complete range. It is probable that a simple automatic control could be provided which would independently maintain constant air flow through the mill for practically all conditions. This would lessen the probability of a mill plugging up and would simplify operation somewhat, but operating conditions thus far have not warranted this refinement.

SLAGGING

With the load conditions necessitating shutting down these boilers about eight hours daily on the midnight watch, a problem was introduced in slag removal. This was somewhat aggravated by the occasional delivery of coal having a high fusion ash and the necessity for running a rather high furnace draft to protect the upper seal in the furnace against the furnace-stack effect and consequent gas pressure. The high furnace draft greatly in-

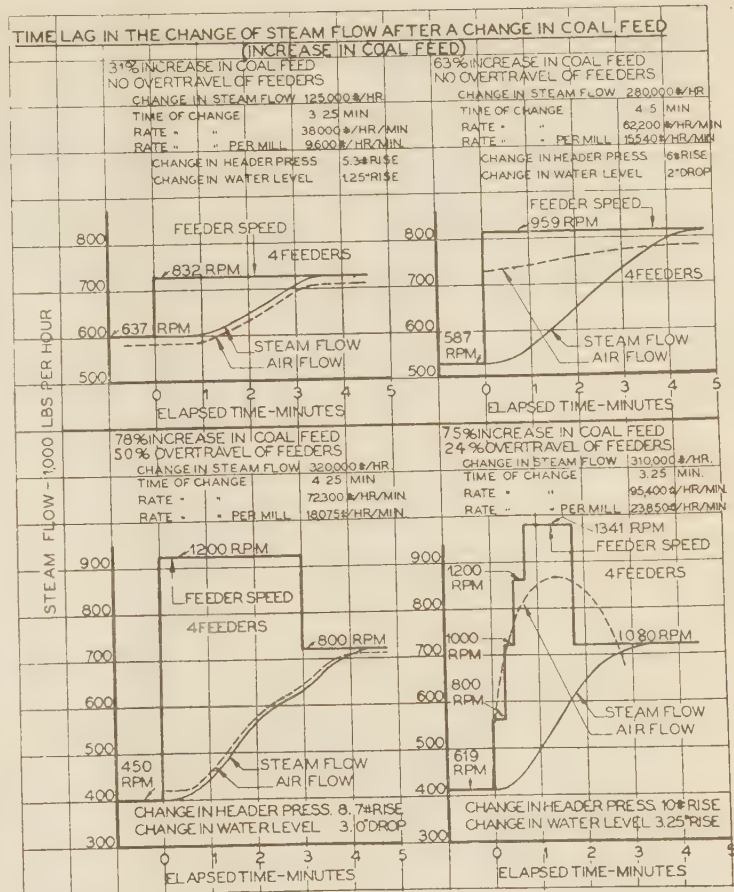


FIG. 12 TIME LAG IN THE CHANGE OF STEAM FLOW AFTER A CHANGE IN COAL FEED (INCREASE IN COAL FEED), BOILER 92

(Note: The Rate of Change, at top of diagram, should be 38,400, instead of 38,000.)

convenienced slag removal, due to the chilling effect of the air drawn against the slag stream at high velocity through the slag-tap opening. The chilling of the slag necessitated almost continuous use of bars and hooks to keep the slag flowing, at the expense of much physical labor.

The situation was improved somewhat by the substitution of water-cooled slag liners, to which the slag did not adhere so tenaciously. This rendered the labor of clearing the slag spout much easier, but still required, with normal grades of fuel, constant attendance to insure a continuous flow. Tests were made with fluxes, and some improvement in slag removal resulted.

TABLE 2 TEST OF BOILER NO. 92, HELL GATE STATION—RESPONSIVENESS OF BOILER TO DECREASE IN LOAD

Steam flow, 1000 lb per hr			De- crease in steam flow, per cent	Speed of coal— feeder motors, rpm			De- crease in coal- feeder speed, per cent	Under- travel of coal feeders, per cent	Period of under travel of coal feeders, min	Time lag, min ^b	Air supply ^c	Rate of change in steam flow, lb per hr per min		Change in steam pres- sure, lb per sq in.	Change in water level, in.	
Be- fore change in coal feed	After change in coal feed	Diff.		Initial	Min- imum during change	Final						Per boiler	Per mill			
750	540	210	28.0	855	587	587	31.0	0	4.75	FS	44,300	11,075	16,475	- 7.3	+1.0	
690	410	280	40.6	800	450	450	44.0	0	4.25	FS	65,900	16,475	11,875	- 3.0	-3.5	
680	490	190	28.0	925	500	700	24.0	29	2.0	4.0	FS	47,500	11,875	14,375	-14.0	-1.5
590	400	190	32.2	800	250	500	37.5	50	1.5	3.75	FS	50,800	12,700	15,000	- 6.7	-1.7
620	410	210	33.8	800	250	500	37.5	50	1.5	3.5	FS	60,000	15,000	14,375	- 5.8	-2.3
630	400	230	36.5	800	250	500	37.5	50	2.0	4.0	FS	57,500	14,375	16,100	- 6.2	-1.5
690	400	290	42.0	950	250	500	47.0	50	2.0	4.5	FS	64,400	16,100	19,350	+ 9.0	-2.0
690 ^a	400	290	42.0	850	606	606	29.0	0	3.75	LS	77,400	19,350		- 7.3	-0.5	

^a During this test the speed of the coal feeders was decreased in three steps, so as to approximate an automatic control. ^b Time lag represents the interval of time required for the stabilization of the steam flow after a change in the coal feed. ^c FS means the air supply follows the steam change; LS means the air supply leads the steam change.

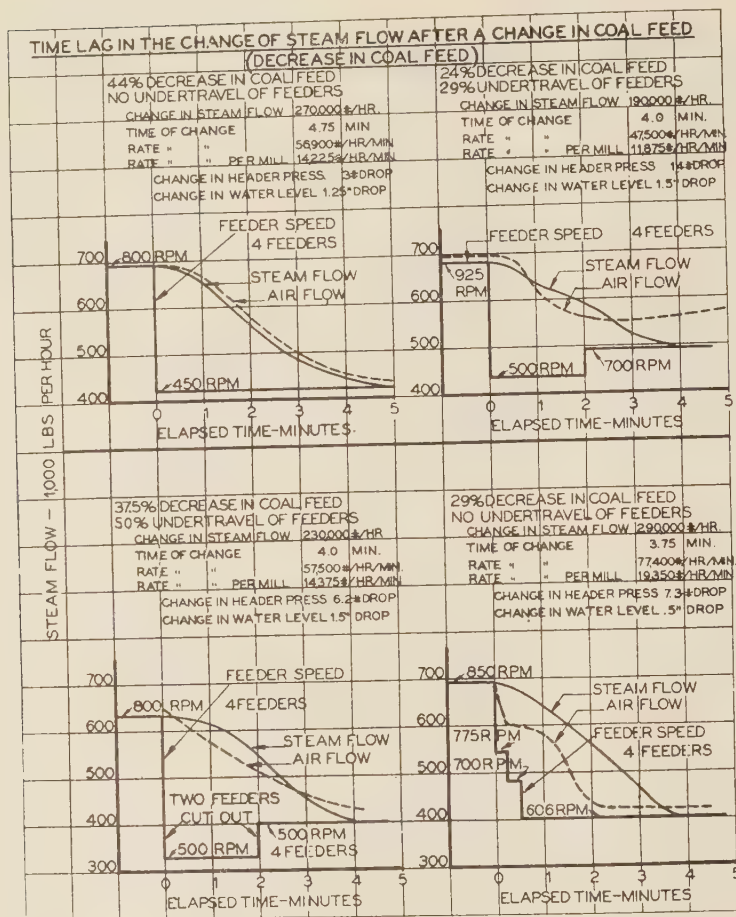


FIG. 13 TIME LAG IN THE CHANGE OF STEAM FLOW AFTER A CHANGE IN COAL FEED (DECREASE IN COAL FEED), BOILER 92

The fluxes, however, did not seem to combine chemically with the ash, but appeared to form an insulating scum on the surface which protected the underlying slag against the chilling effect of the inrush air. The method of introducing the fluxes was rather crude, but the benefit appeared to be physical rather than chemical. This also seemed to be borne out by the fact that fluxes which should be expected to have little effect in depressing the melting point appeared to have a pronounced influence in preventing chilling of the slag stream.

As a final corrective measure one slag opening and its receiving chamber were encased, and means were provided for inducing draft in this chamber during the slagging period. By inducing draft in this chamber greater than that existing in the furnace hot gases from the furnace are withdrawn with the slag instead of permitting cool air to exert a countercurrent effect on the slag stream during its passage. This resulted in a marked improvement in the slagging operation, eliminating the frequent use of hooks and shortening the time required for slag removal. With this improvement, slag which is fluid enough in the furnace to approach the opening may be readily withdrawn.

COOLING RATE

The boilers have a low radiation loss due to tight, well-insulated settings, with slag bottoms and tight-fitting uptake dampers. Observations made during a shutdown in winter with low

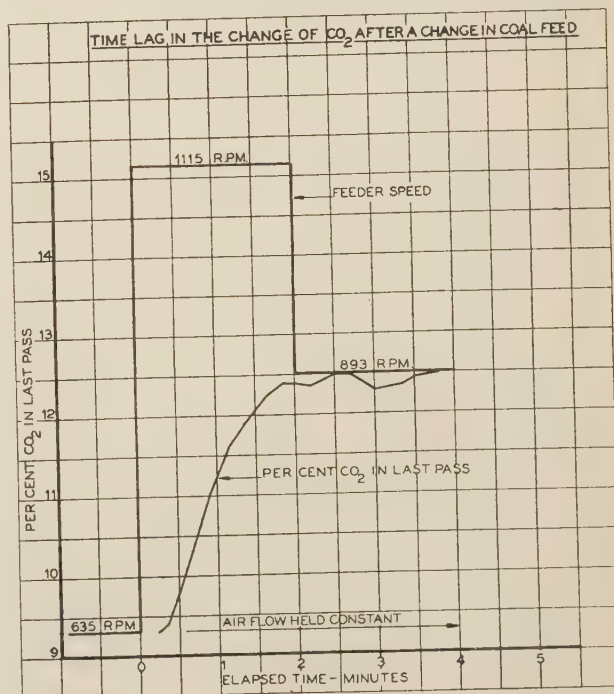
FIG. 14 TIME LAG IN THE CHANGE OF CO₂ AFTER A CHANGE IN COAL FEED, BOILER 92

ambient temperature conditions prevailing are reproduced in Fig. 15. The decline in pressure has been used as a measure of radiation, and while this is not a strictly accurate method, it is an indication of relative value for comparison purposes. The pressure in one of the boilers of the unit declined more rapidly than the other, due to the fact that damper leakage on that half was somewhat greater. Immediately after shutting down there was a slight delay in closing the dampers, after which, it may be observed, the pressure in the boiler increased due to the absorption of heat from the hot slag bottom.

After about six hours the rate of change in heat content of water in the boiler became nearly constant, and this may be regarded as a rough indication of the radiation rate. This rate of radiation is equivalent to about 0.2 per cent of the heat input at maximum capacity. This method of accounting presupposes water temperature throughout the boiler corresponding to the pressure and includes the water equivalent of the metal parts in contact with the boiler water. Undoubtedly, a large proportion of the heat loss is due to unavoidable infiltration and damper leakage, and it is probable that the hot slag bed acts as a heat accumulator in reducing the rate of pressure loss in the boilers. In any event, the characteristic is advantageous in this installation, since it simplifies the problem of starting the boiler daily after an overnight shutdown.

PRIMARY AIR

The primary-air fans are located on the inlet side of the mills with the mills operating under pressure. The primary-air supply to the fans is taken from the main air duct and protected against possible backflow by light unbalanced non-return dampers. In addition, the primary-air supply pipe is extended



vertically a substantial distance within the air duct, so that it does not communicate with any part of the plenum chamber adjacent to the burner openings into the furnace. As an additional precaution a balanced relay is provided to cut out the mills and other apparatus in the event the furnace pressure exceeds the air-duct pressure for an appreciable time interval.

TEST PROCEDURE

The tests were conducted by a staff of experienced engineers under the direction of the engineer of tests, with the cooperation of the manufacturer's representatives. Special care was exercised in preparations and arrangements for the evaporative tests to render the results accurate and reliable. Means of measurements of some of the quantities are indicated by illustrations and diagrams, and reference will be made only to some of the more important items.

COAL

The weight of coal was obtained from Richardson dump scales, with which each mill is provided. These scales are adjusted to deliver 400 lb at each dump, which rendered checking very convenient by the use of eight 50-lb test weights. Frequent checks were made on the balance of the scale during the test, and adjustment for impact was found unnecessary due to the uniform texture of the slack coal which was used. At the beginning of a run for a chosen rate of evaporation the exact time of a scale dump to each mill was noted and the reading of the counter was taken by individual observers. Thereafter, the counters were read hourly and so continued until the end of the run, when they were taken in the same manner as at the beginning.

The hopper and chute capacity between the scales and mills is about 5 tons per mill, or 20 tons per boiler. With the uniform grade of fuel used, there was little likelihood of appreciable error introduced by this intermediate storage due either to differences in composition or density. Variations in moisture and ash were small throughout the series of tests.

Samples of raw coal for moisture and Btu values were taken every hour, simultaneously. The moisture sample was collected in two 2-qt Mason jars, which were carefully sealed. One jar was delivered to the company laboratory and the other to the manufacturer. The Btu sample was collected in a large can equipped with a cover. At the end of each run the coal from the can was quartered, and a sample was taken again in two 2-qt Mason jars, one for the company laboratory and the other for the manufacturer. A sample of the pulverized coal at each burner was taken hourly. A graded traverse of the coal pipe was made with a sampling tube through which the coal sample was discharged into the pail. The tube was connected to the pail with a conical sleeve made of 10-oz canton flannel, selected for its ability to retain the finest coal. Pains were taken to make this apparatus leakproof against coal dust. At the conclusion of a run a careful sample was drawn from each of the three pails serving a single mill and was collected in two 2-qt Mason jars, sealed and labeled, one for the company and the other for the manufacturer. Thus the fineness samples for each run were contained in eight Mason jars.

FEEDWATER

Feedwater was measured by means of venturi tubes and manometers. Two tubes were used—one of 600,000 lb per hr capacity in the east section and the other of 400,000 lb per hr capacity

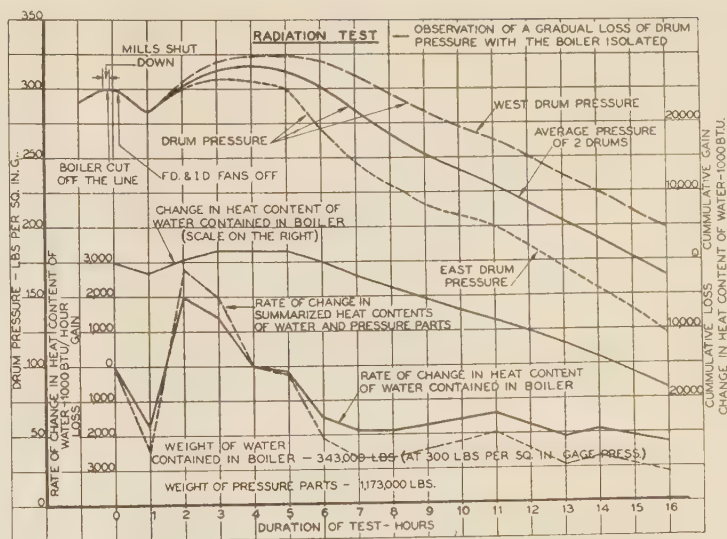


FIG. 15 RADIATION TEST, BOILER 91

in the west section. In order to maintain steady flow for accurate measurement with the venturi meters, boiler 92 was shut down and blanked off, so that the feedwater loop serving this boiler could be utilized in passing the feedwater to the west side section of boiler 91.

The manner in which the feedwater measurement in each section was taken care of was as follows: A venturi manometer in each section was placed at the boiler-drum floor level close to the station of the operator, who, by the manipulation of a chain-operated feed valve, maintained the reading of the manometer constant as long as the water in the nearby gage glass remained at the allowable level near the center of the gage glass. At the beginning of each run it was aimed to have the level in the gage glass in the middle, and the exact level was marked so that at the end of the run it could be properly reestablished. Drum pressures at termination of each run were maintained as close as possible to those existing at the start to obviate errors due to changes in heat quantities in the boiler contents. Both venturi tubes had been calibrated, together with the manometers, before the test, and they were found accurate within one-fourth of 1 per cent.

For readings beyond 800,000 lb per hr, at which the capacity of the venturi manometer on the west side was exceeded, a similar manometer was employed to read the differential on the steam nozzle serving the west side Bailey steam flowmeter. A similar arrangement was also used on the east side, but was supplemented by reading the regular venturi manometer in the feedwater lines. Both steam-flow venturi manometers were calibrated with the feedwater venturi meters. Temperature of the feedwater at entrance and exit of both heater and economizer were read with accurate chemical thermometers.

FLY ASH

In the measurement of fly ash, efforts were made to obtain accurate measurement of losses without necessitating an elaborate arrangement. At the boiler outlet of each section a suitable horizontal lane for sampling fly ash was chosen, as shown in Fig. 16. This lane contained equidistant holes, through each of which normally was inserted a movable tube drawing a sample of cinder-laden gas in three different positions, as illustrated in Fig. 17. Care was exercised in drawing this sample at the same velocity as that of the gas at the point of sampling. This velocity was determined at the beginning of the run with a pitot-tube

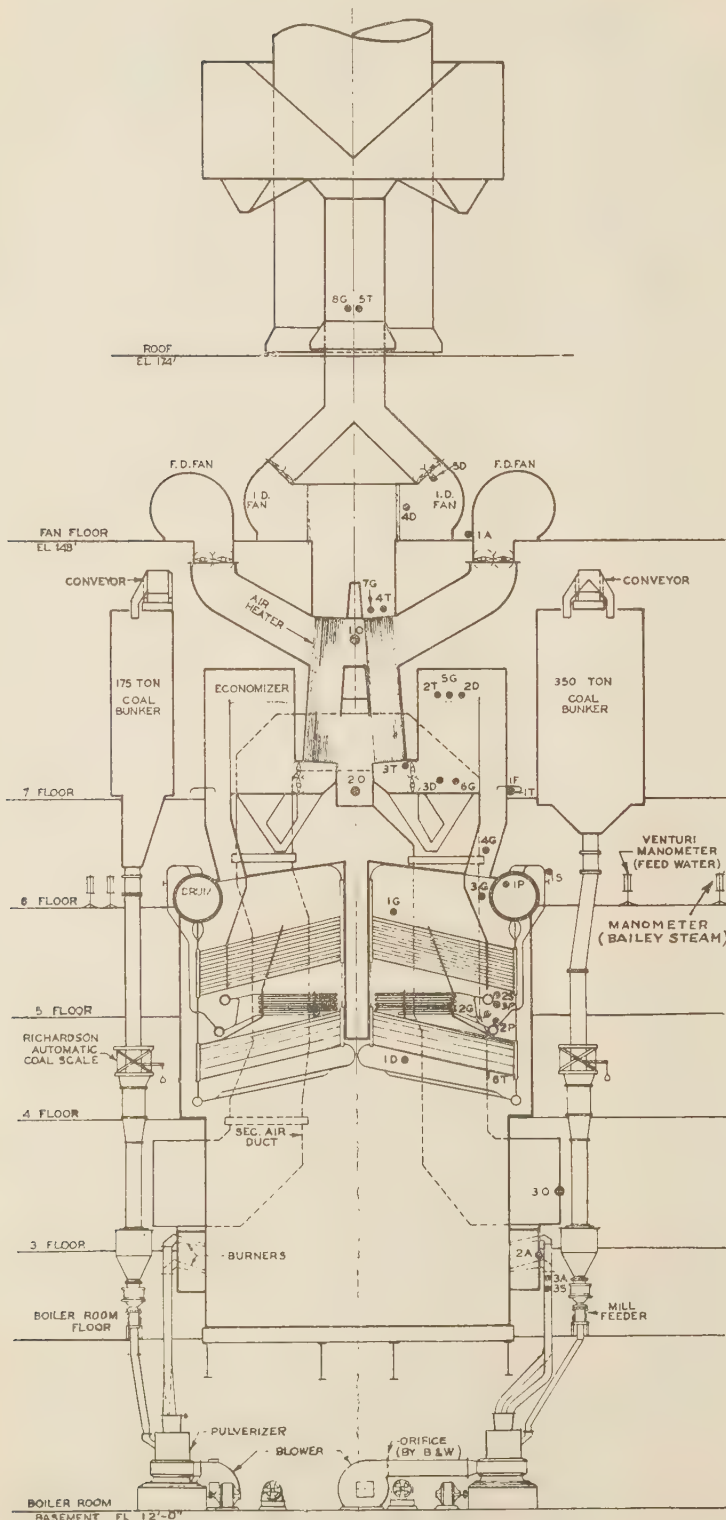


FIG. 16 SECTION THROUGH BOILER 91, LOOKING SOUTH

(For key to Fig. 16, see bottom of next column)

traverse and was checked occasionally during and at the end of the run. Temperatures of the gas at the points of sampling were measured with a thermocouple at the same time the pitot-tube traverse was made. For the values of velocity and temperature thus obtained a rate of gas sampling was read from a calibration curve for the individual orifices serving each sampling tube. This rate was determined by the pressure differential across the orifice and was maintained constant throughout the run as long as the gas velocity, temperature, and suction remained unchanged. Orifices were calibrated with commercial gas meters, which in turn were standardized with a standard gas meter provided by the gas company. In this calibration actual flue gas was employed. The gas sample was drawn by means of an air-actuated aspirator, as shown in Fig. 17.

This gas, on leaving the sampling tube, was filtered through a bag, contained in a carefully sealed Mason jar. The material of the bag was 10-oz canton flannel chosen from a selection of other weights as the most suitable for its ability to retain finest cinders without offering undue resistance to the gas flow. The bags were weighed before each run, the tare weight being subtracted from the gross weight of bags containing cinders at the end of the run, after a preliminary drying. The resulting net weight of cinders divided by the measured quantity of gas, corrected to standard

*Operating Connections:**Pressure (Air):*

- 10 Air-heater inlet, 1 point
- 20 Air-heater outlet, 1 point
- 30 Secondary-air duct, 1 point

(Note: The regular operating connections were used in obtaining test results.)

*Test Connections:**Thermocouple:*

- 1T Boiler outlet, 8 points
- 2T Economizer inlet, 3 points
- 3T Air-heater inlet, 3 points
- 4T Air-heater outlet, 3 points
- 5T After induced-draft fan, 3 points
- 6T Secondary-air duct, 2 points

Gas Sampling:

- 1G Top of first pass, 3 points
- 2G Bottom of second pass, 3 points
- 3G Top of last pass, 6 points
- 4G Boiler outlet, 6 points
- 5G Economizer inlet, 3 points
- 6G Economizer outlet, 3 points
- 7G Air-heater outlet, 3 points
- 8G After induced-draft fan, 3 points

Draft (Gas):

- 1D Furnace, 1 point
- 2D Economizer inlet, 1 point
- 3D Economizer outlet, 1 point
- 4D Induced-draft-fan inlet, 2 points
- 5D Induced-draft-fan outlet, 2 points

Pressure (Air):

- 1A Forced-Draft-fan outlet, 1 point
- 2A Secondary air at burner chamber, 3 points
- 3A Primary air and coal mixture at burners, 6 points

Temperature:

- 1S Calorimeter, 4 points
- 2S Superheater outlet, 2 points
- 3S Primary air and coal mixture, 6 points

Pressure (Steam):

- 1P Drum, 1 point
- 2P Superheater inlet, 1 point
- 3P Superheater outlet, 2 points

Fly Ash:

- 1F Boiler outlet, 8 points

(Note: Dampers were open during tests, although shown closed in the drawing. Test connections are symmetrical about the center line of the boiler, except for 5T and 8G. The number of points refers to one side of the boiler only.)

conditions, gave the density of cinders in the flue gas. Fineness tests and combustible determinations were made on the cinder samples that were obtained.

FLUE GAS

Owing to the great width of the boiler-outlet connections, six gas-sampling tubes were employed. To simplify the problem of gas analysis, an average sample was drawn from every three sampling positions of a given region and passed through a common bubbling bottle to an Orsat apparatus. Gas temperatures were measured chiefly with calibrated thermocouples. Gas temperatures in the furnace were obtained by the manufacturer's representative with an optical pyrometer.

STEAM

The quality of steam entering the superheater at each section was determined with four steam-jacketed calorimeters about equally spaced. The normal correction for this type of calorimeter is very small, and since tests indicated a blank correction of less than one-tenth of 1 per cent, no correction was applied to the observations. Temperatures of the superheated steam were read with accurate chemical thermometers. Steam pressures at the drum outlet and the superheater inlet and outlet in each section were read with the same calibrated gages connected to a common manifold which served all the pressure points.

GENERAL

During the tests observations were made covering the performance of all major auxiliaries as well as the feedwater heater.

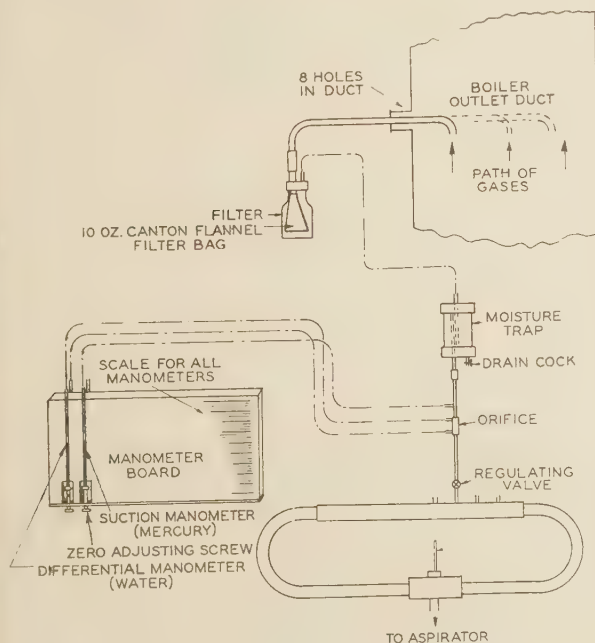


FIG. 17 FLY-ASH TEST LAYOUT

All gages were calibrated before and after the test, while the potentiometer used with the thermocouples was calibrated before the test. The tests here reported consisted of six runs, conducted in the following order:

Run No.	Rating, lb per hr	Duration, hr	Number of mills
1	402,700	10	3
2	542,100	8	4
3	689,800	10	4
3a	688,100	8	4
4	791,300	8	4
5	923,200	6	4
6	1,078,000 (max)	2	4

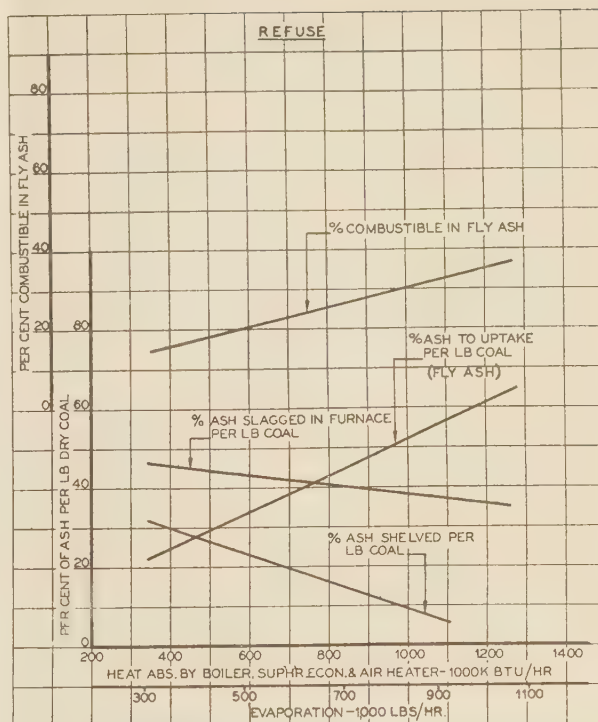


FIG. 18 REFUSE, BOILER 91

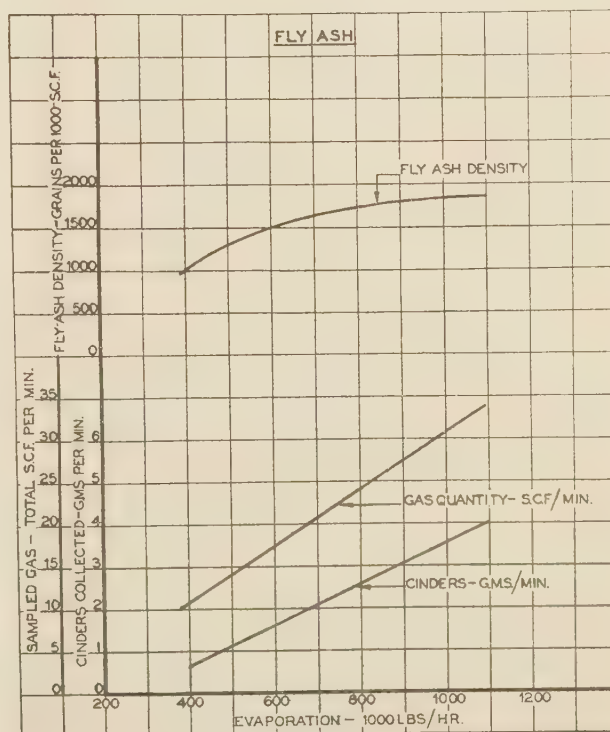


FIG. 19 FLY ASH, BOILER 91

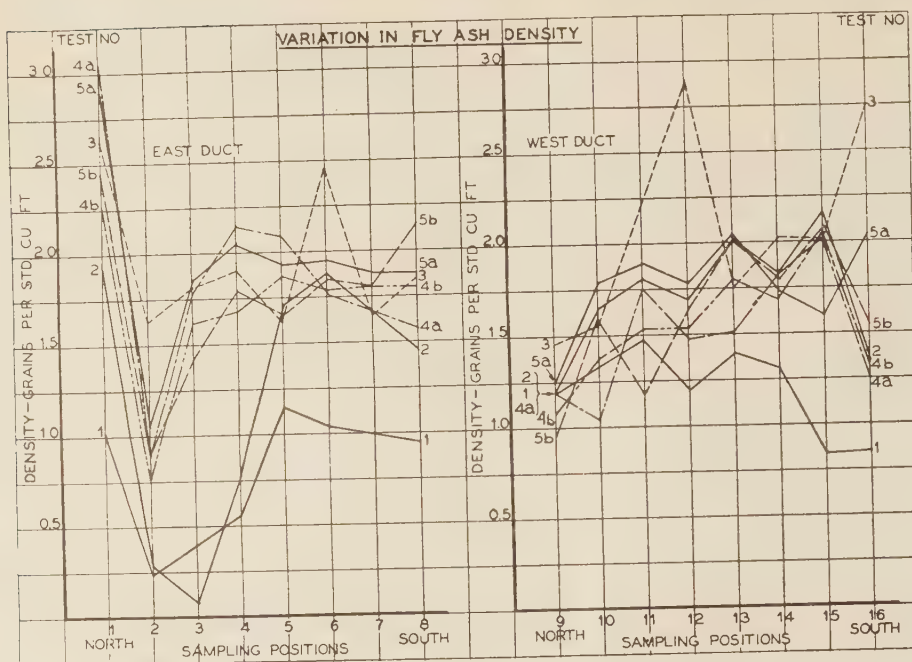


FIG. 20 VARIATION IN FLY-ASH DENSITY, BOILER 91

Prior to each test run the tubes of the boiler, economizer, and air heater were blown by means of soot blowers. Before starting any test, the boiler was operated at the chosen rating for several hours, and secondary air was adjusted to give approximately 15 per cent CO_2 about $\frac{1}{2}$ hr before actual testing commenced.

In the case of run No. 3, which was scheduled for 8 hr duration, it was observed that during the first two hours, evaporation was improving steadily. This observation led to the belief that for this higher rating than the previous ones the boiler needed longer time to reach stable conditions. As a result the original run was prolonged by two hours, and test No. 3a is therefore the official run.

Pulverizing characteristics and mill limitations at the time of the test made it necessary to employ only three mills during run No. 1. It was also these limitations that made operation at substantially lower rating somewhat uncertain. The maximum rating test was run in the evening, and to avoid an unnecessary hazard the manual control of the feedwater was dispensed with, recourse being made to the standard automatic water regulation.

The venturi manometers were read every 2 min. Excess air was reduced to maintain about 17 per cent CO_2 for the purpose of reducing the duty on the induced-draft fans. Smoke at the stack for this rating did not appear to be of a prohibitive density and differed very little from that observed during the preceding run.

The entire series of tests were conducted in close cooperation with representatives of the manufacturer. Aided by their assistants, they made supplementary observations on the primary-air supply to the mills, on the temperatures of the Bailey blocks on the furnace walls, and on the temperature of the furnace.

COMPUTATIONS

Results of the tests were calculated in accordance with the latest issue (January, 1930) of the Test Code for stationary steam-generating units, use being made of Table S-4-b for heat balance. To render the heating value of the coal more truly representative in the computations of the heat balance for each run and by agreement with the manufacturer's representatives, an average of the following three values was used:

- That determined by the manufacturer for his sample
- That determined by the United company for its sample
- That from the analysis by the United company of the manufacturer's sample.

This method of averaging was applied to the complete

coal analysis, both for the proximate and the ultimate.

Curves shown in Fig. 18 give, in a graphic form, the approximate relationship between the three components of the total ash

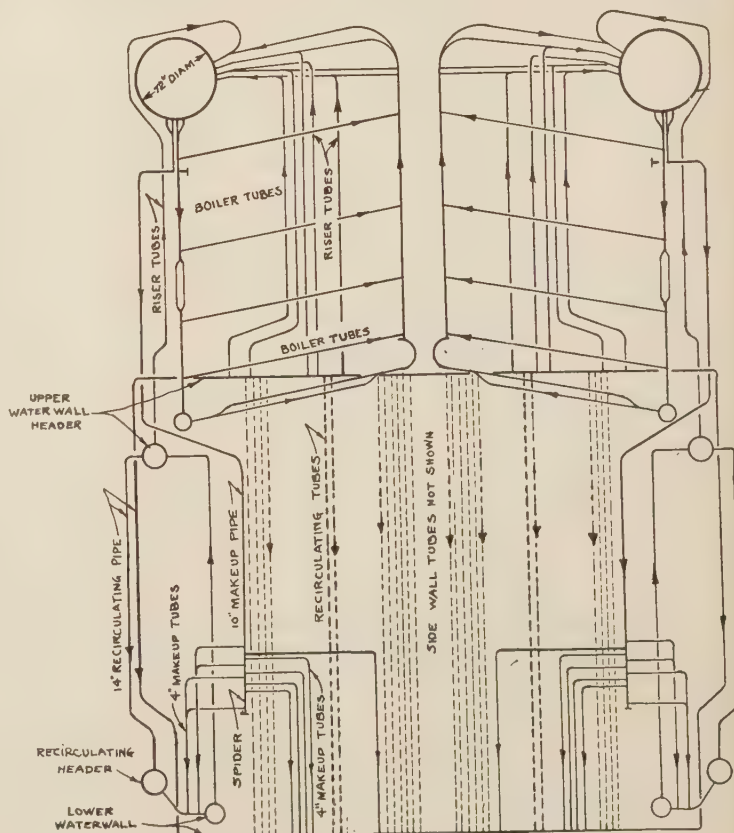


FIG. 21 RECIRCULATION DIAGRAM, BOILER 91

at various ratings. The "fly ash to uptake" component was determined at all ratings by measurements. The other two components were determined on the following basis: For the low rating, the "ash slagged in furnace" component was estimated 45 per cent, this figure being substantiated by the experience of the manufacturer, and the "ash shelved" component was determined by the difference; for the high rating, it was observed that the "ash shelved" component was zero, due to high gas

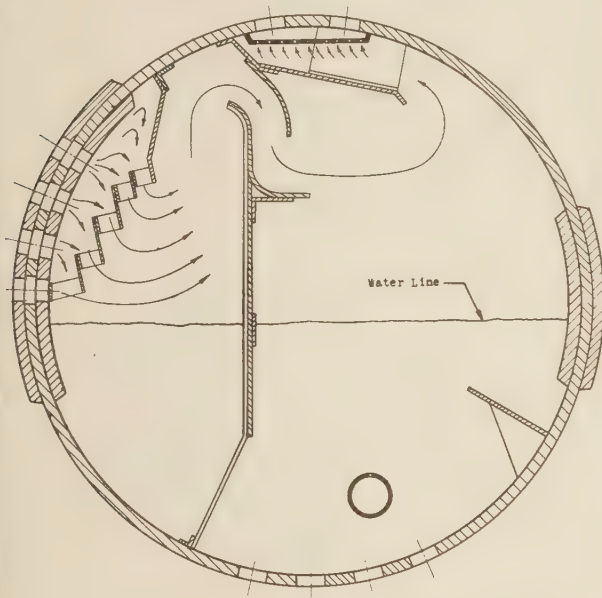


FIG. 22 CROSS-SECTION OF DRUM SHOWING SYSTEM OF BAFFLING
(Diameter of drum, 72 in.; thickness of wall, 17/s in.)

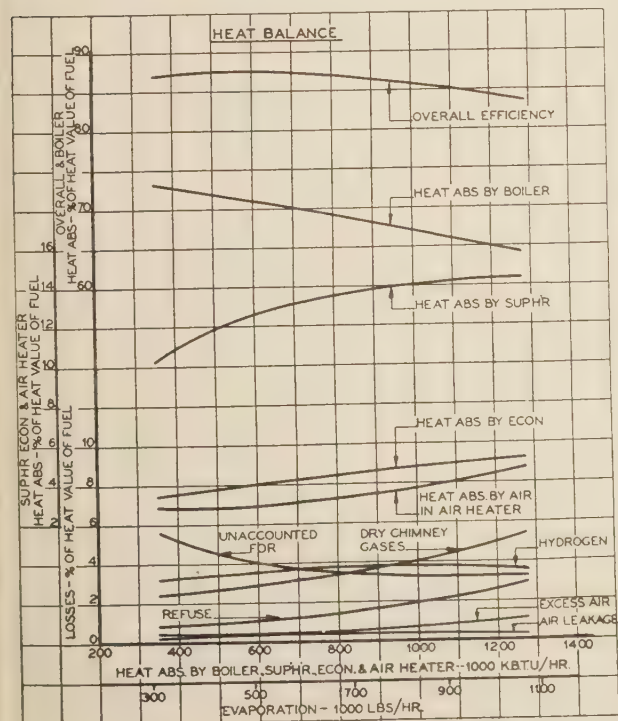


FIG. 23 HEAT BALANCE, BOILER 91

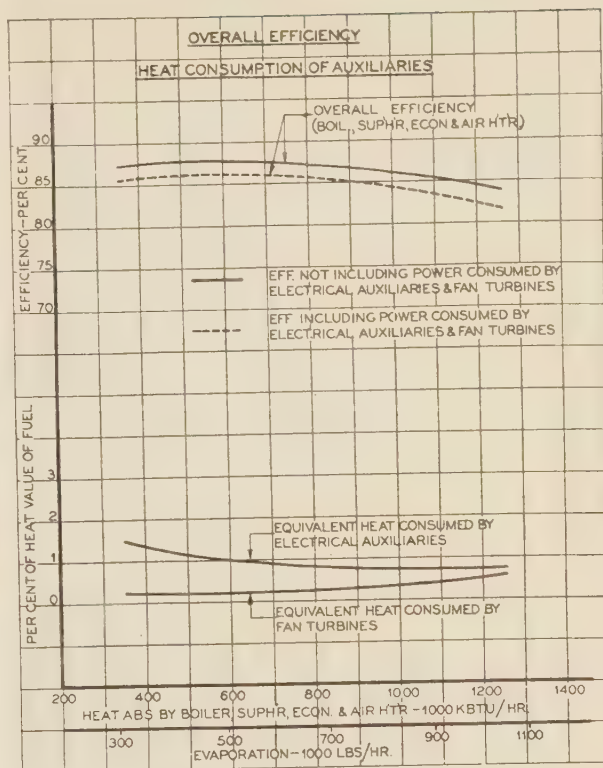


FIG. 24 OVERALL EFFICIENCY, HEAT CONSUMPTION OF AUXILIARIES
Boiler 91

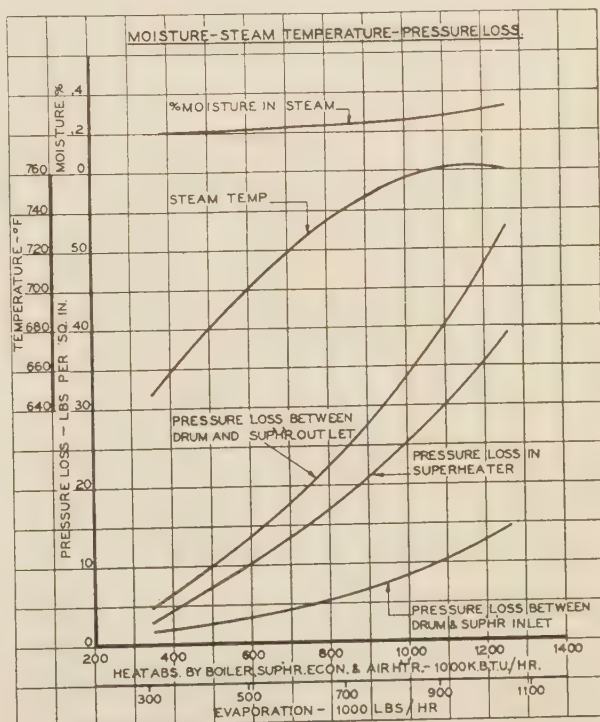


FIG. 25 MOISTURE, STEAM-TEMPERATURE, AND PRESSURE LOSS,
Boiler 91

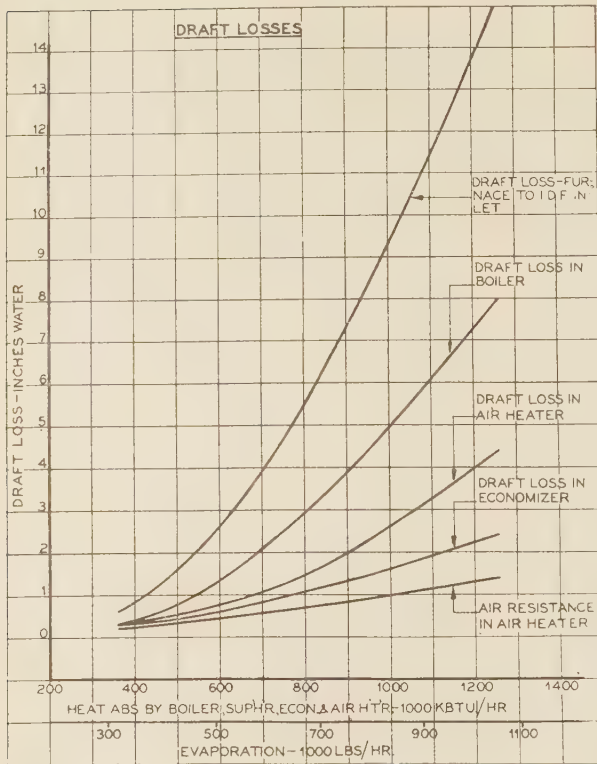


FIG. 26 DRAFT LOSSES, BOILER 91

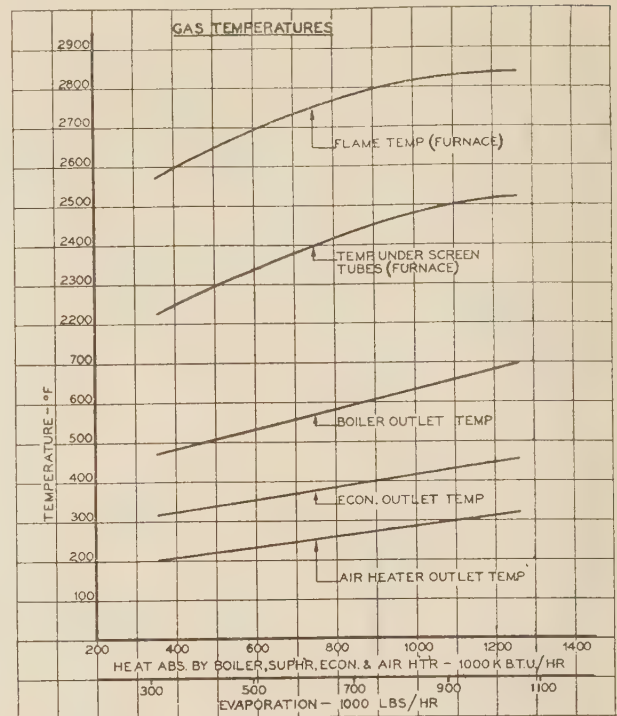


FIG. 27 GAS TEMPERATURES, BOILER 91

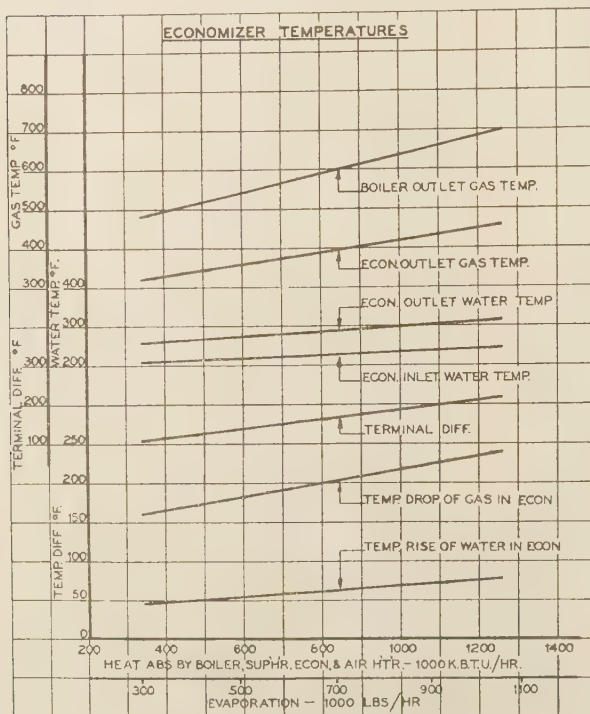


FIG. 28 ECONOMIZER TEMPERATURES, BOILER 91

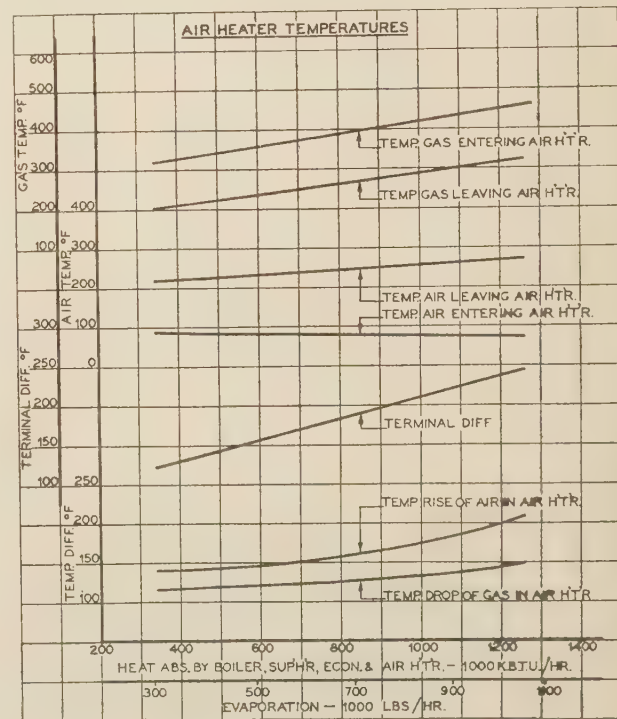


FIG. 29 AIR-HEATER TEMPERATURES, BOILER 91

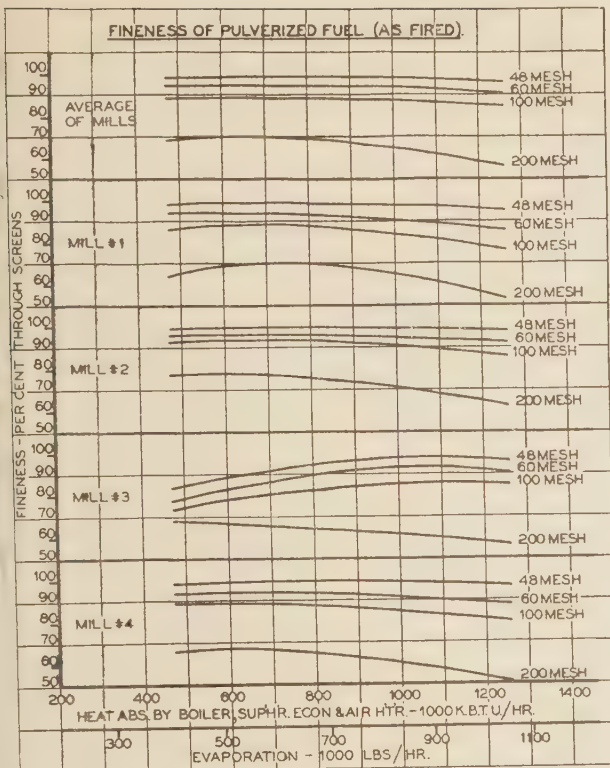


FIG. 30 FINENESS OF PULVERIZED FUEL (AS FIRED), BOILER 91

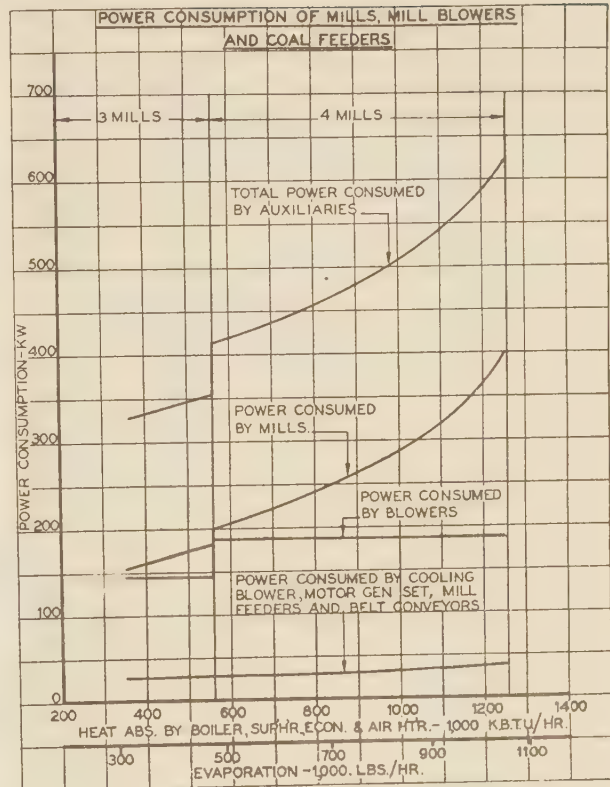


FIG. 31 POWER CONSUMPTION OF MILLS, MILL BLOWERS, AND COAL FEEDERS, BOILER 91 (TOTAL CONSUMPTION)

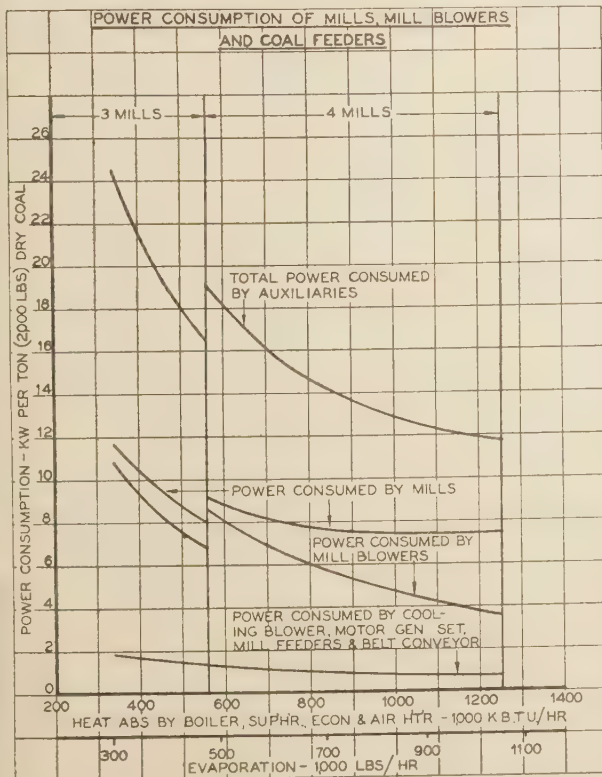


FIG. 32 POWER CONSUMPTION OF MILLS, MILL BLOWERS, AND COAL FEEDERS, BOILER 91 (CONSUMPTION PER TON)

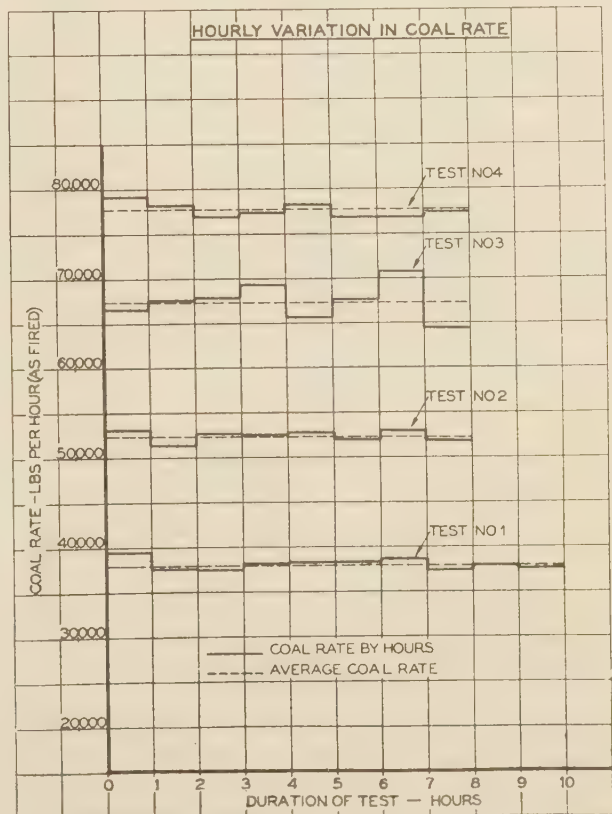


FIG. 33 HOURLY VARIATION IN COAL RATE, BOILER 91

velocity, and the "ash slagged in furnace" component was determined by the difference. Although the "ash shelved" component could not be accurately measured, its content of combustible was determined from the samples taken from various baffles. The content of combustible in the fly ash to uptake was determined by measurements, and the ash slagged in the furnace was assumed to contain practically no combustible.

Figs. 21 and 22 illustrate various features of this installation. The results of the test are given in a graphic form in a series of curves and also in Table 3.

The general data on the major boiler equipment are included in the Appendix.

The author gratefully acknowledges the assistance rendered by his associates and the manufacturer's representatives in the preparation of this paper.

Appendix

DATA ON THE MAJOR EQUIPMENT OF THE 90-ROW BOILERS, HELL GATE STATION

Number of boilers, two

Year of installation, 1930

Boiler: Babcock & Wilcox sectional, twin, cross-drum, water-tube type

Drums: Two drums (one for each half) 72 in. diam, 17/8 in. thick, 40 ft 9 in. long

Tubes: 58 sections of 18 tubes 4 in. o.d. No. 6 Bwg, 20 ft long in each half of the boiler

Heating surface: 53,926 sq ft

Water walls: Bailey blocks mounted on 4-in. o.d. No. 6 Bwg tubes, spaced on 6 in. centers; manufactured by Fuller Lehigh Company. (The Bailey blocks are of three types, the refrac-

TABLE 3 TEST OF BOILER NO. 91, HELL GATE STATION, THE UNITED ELECTRIC LIGHT AND POWER COMPANY

Item	1	2	3	4	5	6
1	Test No.	12-2	12-3	12-4	12-8	12-9
2	Date of test, 1931.	10	8	8	6	2
3	Duration of test, hr.					
	<i>Fuel, Proximate Analysis (Dry):</i>					
4	Volatile matter, per cent.	22.46	22.57	22.37	21.94	23.01
5	Fixed carbon, per cent.	70.17	71.28	72.37	71.62	71.33
6	Ash, per cent.	7.36	6.15	5.26	6.44	5.65
7	Moisture (as fired), per cent.	3.90	4.15	4.15	4.55	4.90
8	Heating value per lb (as fired), Btu.	14,012	14,200	14,350	14,055	14,130
9	Heating value per lb (dry), Btu.	14,581	14,814	14,967	14,734	14,855
10	Fusion temperature of ash, F.	2,405	2,425	2,435	2,428	2,445
	<i>Fuel, Ultimate Analysis (dry):</i>					
11	Carbon, per cent.	83.05	84.35	84.78	84.10	84.54
12	Hydrogen, per cent.	4.45	4.49	4.77	4.59	4.49
13	Oxygen, per cent.	3.36	3.29	3.60	3.15	3.57
14	Nitrogen, per cent.	1.08	1.17	1.16	1.16	1.21
15	Sulphur, per cent.	0.70	0.55	0.54	0.57	0.53
16	Ash, per cent.	7.36	6.15	5.26	6.44	5.65
	<i>Pulverized-Fuel, Proximate Analysis (Dry):</i>					
17	Volatile matter, per cent.	22.30	22.00	23.00	22.40	22.50
18	Fixed carbon, per cent.	71.76	72.38	71.44	72.05	71.97
19	Ash, per cent.	5.94	5.62	5.56	5.55	5.53
20	Sulphur, per cent.	0.58	0.60	0.55	0.55	0.60
21	Heating value per lb, Btu.	14,767	14,842	14,811	14,808	14,808
	<i>Fineness of Pulverized Fuel (as Fired):</i>					
22	Mill No. 1:					
	Through 48 mesh, per cent.	98.5	99.0	97.5	98.5	96.5
	Through 60 mesh, per cent.	93.5	95.0	92.5	91.0	90.0
	Through 100 mesh, per cent.	86.0	89.5	88.5	85.0	83.0
	Through 200 mesh, per cent.	63.0	70.5	74.0	59.0	63.0
23	Mill No. 2:					
	Through 48 mesh, per cent.	99.0	99.5	99.0	99.5	98.0
	Through 60 mesh, per cent.	96.0	96.0	95.0	96.0	91.5
	Through 100 mesh, per cent.	93.0	93.5	92.0	93.0	87.5
	Through 200 mesh, per cent.	77.0	78.0	74.0	76.0	65.0
24	Mill No. 3:					
	Through 48 mesh, per cent.	a	91.5	95.0	96.5	96.5
	Through 60 mesh, per cent.	a	85.0	89.5	91.5	91.0
	Through 100 mesh, per cent.	a	81.0	81.0	85.5	85.0
	Through 200 mesh, per cent.	a	66.0	63.5	60.5	63.5
25	Mill No. 4:					
	Through 48 mesh, per cent.	98.0	99.0	97.5	98.0	97.5
	Through 60 mesh, per cent.	93.5	94.5	93.0	91.0	89.5
	Through 100 mesh, per cent.	87.5	89.0	87.5	84.5	83.0
	Through 200 mesh, per cent.	64.5	69.0	66.0	61.0	58.0
	<i>Gas Analysis, Furnace:</i>					
26	CO ₂ , per cent.	15.6	15.9	15.8	15.8	17.9
27	O ₂ , per cent.	3.4	3.0	3.2	2.9	0.3
28	CO, per cent.	0.0	0.0	0.0	0.0	0.0
29	N ₂ , per cent.	81.0	81.1	81.0	81.3	81.8
	<i>Gas Analysis, Boiler Outlet:</i>					
30	CO ₂ , per cent.	15.2	15.0	15.1	15.1	14.9
31	O ₂ , per cent.	3.9	4.1	4.0	4.0	4.3
32	CO, per cent.	0.0	0.0	0.0	0.0	0.0
33	N ₂ , per cent.	80.9	80.9	80.9	80.9	81.0
	<i>Gas Analysis, Economizer Outlet:</i>					
34	CO ₂ , per cent.	14.9	14.8	14.8	14.7	14.5
35	O ₂ , per cent.	4.1	4.3	4.3	4.4	4.8
36	CO, per cent.	0.0	0.0	0.0	0.0	0.0
37	N ₂ , per cent.	81.0	80.9	80.9	80.9	80.7
	<i>Gas Analysis, Air-Heater Outlet:</i>					
38	CO ₂ , per cent.	14.4	14.2	14.3	14.2	14.2
39	O ₂ , per cent.	4.7	5.0	4.9	5.0	5.0
40	CO, per cent.	0.0	0.0	0.0	0.0	0.0
41	N ₂ , per cent.	80.9	80.8	80.8	80.8	81.1
	<i>Gas Analysis, Induced-Draft-Fan Outlet:</i>					
42	CO ₂ , per cent.	13.9	13.8	13.8	13.6	13.4
43	O ₂ , per cent.	5.1	5.3	5.3	5.6	5.8
44	CO, per cent.	0.0	0.0	0.0	0.0	0.0
45	N ₂ , per cent.	81.0	80.9	80.9	80.8	80.8

^a Not in operation.

TABLE 3 TEST OF BOILER NO. 91, HELL GATE STATION, THE UNITED ELECTRIC LIGHT AND POWER COMPANY—Continued

Item	Test No.	1	2	3	4	5	6
<i>Dry Gas per Pound of Fuel (Dry):</i>							
46	Furnace, lb.	13.40	13.47	13.43	13.34	13.43	10.86
47	Boiler outlet, lb.	13.74	14.10	13.95	13.86	14.17	11.71
48	Economizer outlet, lb.	14.10	14.32	14.30	14.29	14.57	12.10
49	Air-heater outlet, lb.	14.46	14.87	14.75	14.77	14.87	12.10
50	Theoretical, lb.	11.48	11.53	11.69	11.58	11.65	10.70
<i>Air Supplied per Pound of Fuel (Dry):</i>							
51	Furnace, lb.	12.89	12.84	12.93	12.83	12.91	10.41
52	Boiler outlet, lb.	13.23	13.57	13.45	13.35	13.65	11.26
53	Economizer outlet, lb.	13.59	13.79	13.80	13.78	14.05	11.65
54	Air-heater outlet, lb.	13.95	14.34	14.25	14.26	14.35	11.65
55	Air supplied by cooling blower, lb.	0.42	0.29	0.23	0.20	0.18	0.14
56	Moisture in air, lb per lb air.	0.0048	0.0063	0.0102	0.0073	0.0104	0.0177
<i>Pressures and Drafts:</i>							
57	Water pressure economizer inlet, lb per sq in. gage ^b	391.1	390.6	386.5	402.4	401.8	427.5
58	Water pressure economizer outlet, lb per sq in. gage ^b	387.4	384.2	375.5	387.0	380.5	399.0
59	Steam pressure boiler, lb per sq in. gage ^b	279.9	291.4	302.2	310.1	315.0	325.7
60	Steam pressure superheater inlet, lb per sq in. gage ^b	277.7	287.5	296.3	302.6	304.7	310.5
61	Steam pressure superheater outlet, lb per sq in. gage ^b	271.3	275.8	278.5	279.3	273.6	269.5
62	Pressure loss in economizer, lb per sq in.	3.7	6.4	11.0	15.4	21.3	28.5
63	Pressure loss in superheater, lb per sq in.	6.4	11.7	17.8	23.3	31.1	41.0
64	Pressure loss between drum and superheater outlet, lb per sq in.	8.6	15.6	23.7	30.8	41.4	56.2
65	Draft in furnace, in water	0.09	0.10	0.10	0.09	0.10	0.12
66	Draft at economizer inlet, in water	0.7	1.8	3.4	4.6	6.4	8.7
67	Draft at economizer outlet, in water	1.1	2.5	4.4	6.0	8.3	12.3
68	Draft at induced-draft-fan inlet, in water	1.5	3.3	6.0	8.3	11.6	12.3
69	Draft at induced-draft-fan outlet, in water	0.3	0.2	0.0	+0.1	0.0	+0.2
70	Draft loss, furnace to economizer inlet, in water	0.6	1.7	2.3	4.5	6.3	6.6
71	Draft loss, economizer inlet to economizer outlet, in water	0.4	0.7	1.0	1.4	1.9	2.0
72	Draft loss, economizer outlet to induced-draft-fan inlet, in water	0.4	0.8	1.6	2.3	3.3	3.6
73	Draft loss, furnace to induced-draft-fan inlet, in water	1.4	3.2	5.9	8.2	11.5	12.2
74	Draft loss, induced-draft-fan inlet to induced-draft-fan outlet, in water	1.2	3.1	6.0	8.4	11.6	12.5
75	Pressure at air-heater inlet, in water	3.0	4.58	5.94	7.30	8.40	8.60
76	Pressure at air-heater outlet, in water	2.74	4.14	5.11	6.40	7.30	7.20
77	Pressure loss in air heater, in water	0.26	0.44	0.83	0.90	1.10	1.40
<i>Pressure at burner (primary air), in water (3 burners per mill):</i>							
78	Mill No. 1, A.	1.40	1.30	1.92	1.80	2.00	2.50
	Mill No. 1, B.	1.10	1.00	1.46	1.40	1.40	1.50
	Mill No. 1, C.	1.30	1.20	1.77	1.60	2.00	2.60
79	Mill No. 2, A.	1.20	1.10	1.62	1.60	1.59	2.40
	Mill No. 2, B.	1.73	1.53	1.91	1.73	1.93	2.52
	Mill No. 2, C.	1.65	1.37	1.98	1.89	2.04	2.62
80	Mill No. 3, A.	1.65	1.30	1.67	1.60	1.60	2.10
	Mill No. 3, B.	1.10	1.10	1.62	1.50	1.60	2.10
	Mill No. 3, C.	1.13	1.20	1.59	1.40	1.60	2.10
81	Mill No. 4, A.	1.78	1.22	1.65	1.46	1.72	2.04
	Mill No. 4, B.	1.78	1.72	2.15	1.86	2.28	2.62
	Mill No. 4, C.	1.42	1.37	1.85	1.52	1.83	2.18
<i>Secondary air pressure at burner, in water:</i>							
82	East duct	1.92	2.54	2.68	3.31	2.76	2.93
83	West duct	2.00	2.50	2.80	2.90	2.90	2.79
<i>Temperatures:</i>							
84	Steam temperature at superheater outlet, F ^b	663.2	718.3	739.1	752.5	761.8	713.0
85	Moisture in steam, per cent ^b	0.20	0.23	0.27	0.23	0.28	0.47
86	Superheat, F ^b	250.2	303.9	323.9	337.0	348.1	300.6
87	Temperature of coal-and-air mixture at burners, F ^b	131	131	131	120	110	108
88	Temperature of air entering air heater, wet, F ^b	57	60	67	61	59	75
89	Temperature of air entering air heater, dry, F ^b	80	82	85	78	60	76
90	Temperature of air leaving air heater, F ^b	215	232	246	246	253	267
91	Temperature of furnace (optical pyrometer), F:						
	Furnace temperature, floor	2470	2408	2400	2460	2450	2655
	Furnace temperature, flame	2600	2741	2793	2580	2773	2873
	Furnace temperature, under first row of tubes ^b	2250	2372	2440	2450	2496	2500
92	Temperature of gases leaving boiler, F ^b	504	554	596	625	660	652
93	Temperature of gases leaving economizer, F ^b	334	366	396	412	436	448
94	Temperature of gases leaving air heater, F ^b	217	247	269	280	300	306
95	Temperature of feedwater entering boiler, F ^b	262.0	278.0	280.7	292.4	303.7	294.8
96	Temperature of feedwater entering economizer, F ^b	212.5	222.8	219.4	229.1	237.5	239.8
97	Temperature of fuel, F.	60	59	70	60	64	62
98	Temperature of air surrounding boiler, F.	115	115	115	115	115	115
99	Temperature of air surrounding economizer, F.	125	125	125	125	125	125
100	Temperature of air surrounding air heater, F.	125	125	125	125	125	125
<i>Primary-air temperature at burners, F (three burners per mill):</i>							
101	Mill No. 1, A.	125	121	133	118	113	105
	Mill No. 1, B.	126	120	131	118	113	105
	Mill No. 1, C.	125	121	132	118	113	106

^a Not in operation.^b Average reading for east and west boilers.

TABLE 3 TEST OF BOILER NO. 91, HELL GATE STATION, THE UNITED ELECTRIC LIGHT AND POWER COMPANY—Continued

Item	Test No.....	1	2	3	4	5	6
<i>Temperatures:—Continued</i>							
102	Mill No. 2, A.....	139	131	130	124	106	107
	Mill No. 2, B.....	142	133	133	126	111	108
	Mill No. 2, C.....	137	132	130	123	110	109
103	Mill No. 3, A.....	135 ^a	135	129	122	113	109
	Mill No. 3, B.....	136	136	128	119	112	110
	Mill No. 3, C.....	136	136	125	119	112	110
104	Mill No. 4, A.....	134	135	133	118	105	107
	Mill No. 4, B.....	136	135	133	117	106	108
	Mill No. 4, C.....	133	133	130	116	103	105
<i>Hourly Quantities:</i>							
105	Duration of test, hr (repetition of item 3).....	10	8	8	8	6	2
	Fuel per hour (as fired), lb:						
106	Mill No. 1.....	12,748	13,860	16,263	19,183	22,733	29,097
107	Mill No. 2.....	12,534	13,273	16,868	19,689	22,662	29,400
108	Mill No. 3.....	12,254 ^a	12,254	16,820	18,605	21,998	27,105
109	Mill No. 4.....	12,577	12,865	17,300	20,131	23,200	28,161
110	Total.....	37,859	52,252	67,251	77,608	90,593	113,763
	Fuel per hour (dry), lb:						
111	Mill No. 1.....	12,251	13,285	15,588	18,310	21,778	27,671
112	Mill No. 2.....	12,045	12,722	16,168	18,793	21,710	27,959
113	Mill No. 3.....	11,745 ^a	11,745	16,122	17,758	21,074	25,777
114	Mill No. 4.....	12,086	12,332	16,582	19,216	22,226	26,782
115	Total.....	36,382	50,084	64,460	74,077	86,788	108,189
116	Combustion space per lb coal per hr (dry), cu ft.....	1.123	0.815	0.634	0.550	0.47	0.377
117	Refuse per hour, lb.....	3,113	3,656	4,565	5,971	6,203	15,713
	Actual water per hour, lb:						
118	East boiler.....	202,600	264,900	341,000	400,500	455,200	515,000
119	West boiler.....	200,100	277,200	347,100	390,800	468,000	563,000
120	Total.....	402,700	542,100	688,100	791,300	923,200	1,078,000
<i>Unit Quantities:</i>							
	Heat absorbed by water in economizer, Btu per lb:						
121	East boiler.....	49.6	57.0	62.4	64.2	67.4	55.8
122	West boiler.....	50.6	54.8	62.6	65.0	67.9	56.0
	Heat absorbed by water and steam in boiler, Btu per lb:						
123	East boiler.....	970.0	952.9	950.7	939.9	927.7	935.2
124	West boiler.....	970.0	955.0	951.0	939.1	927.6	936.0
	Heat absorbed by steam in superheater, Btu per lb:						
125	East boiler.....	150.9	180.6	188.2	194.6	201.9	176.3
126	West boiler.....	145.2	174.2	188.8	195.9	199.5	175.7
127	Rate of heat absorption in economizer, kB per hr.....	20,174	30,290	43,006	51,114	62,457	60,265
128	Rate of heat absorption in boiler, kB per hr.....	390,619	517,149	654,281	743,430	856,406	1,008,236
129	Rate of heat absorption in superheater, kB per hr.....	60,140	96,129	129,708	154,495	185,271	189,714
130	Total rate of heat absorption by steam generating unit, kB per hr.....	470,933	643,568	826,995	949,039	1,104,134	1,258,215
	<i>Refuse:</i>						
131	Refuse, per cent of fuel (dry), per cent.....	8.56	7.30	7.08	8.06	7.15	14.53
132	Combustible in refuse, per cent.....	14.0	15.7	25.6	20.0	24.0	61.1
133	Carbon burned per lb fuel (dry), lb.....	0.8185	0.8320	0.8297	0.8249	0.8312	0.7566
	<i>Evaporation:</i>						
134	Rate of heat absorption per lb fuel (as fired), kB.....	12.44	12.32	12.30	12.23	12.19	11.06
135	Rate of heat absorption per lb fuel (dry), kB.....	12.94	12.85	12.83	12.81	12.72	11.63
136	Rate of heat absorption per sq ft of steam-generating unit surface per hr, kB.....	5.35	7.30	9.39	10.75	12.54	14.30
	<i>Efficiency:</i>						
137	Efficiency of steam generating unit, per cent.....	88.7	86.7	85.7	86.9	85.4	78.3
138	Efficiency of boiler and superheater, per cent.....	85.0	82.7	81.2	82.2	80.4	74.6
	<i>Heat Balance:</i>						
139	Heating value of fuel (dry) { Btu.....	14,581	14,814	14,967	14,734	14,899	14,855
	{ per cent.....	100	100	100	100	100	100
140	Heat absorbed by water in economizer { Btu.....	555	605	667	690	720	557
	{ per cent.....	3.8	4.1	4.5	4.7	4.8	3.7
141	Heat absorbed by water and steam in boiler { Btu.....	10,736	10,326	10,150	10,036	9,868	9,319
	{ per cent.....	73.6	69.6	67.7	68.0	66.3	62.8
142	Heat absorbed by steam in superheater { Btu.....	1,653	1,919	2,012	2,086	2,135	1,754
	{ per cent.....	11.3	13.0	13.5	14.2	14.3	11.8
143	Heat absorbed by steam-generating unit { Btu.....	12,944	12,850	12,829	12,812	12,723	11,630
	{ per cent.....	88.7	86.7	85.7	86.9	85.4	78.3
144	Heat loss due to combustible in refuse { Btu.....	175	168	266	237	251	1,296
	{ per cent.....	1.2	1.1	1.8	1.6	1.7	8.7
145	Heat loss due to incomplete combustion of carbon, { Btu.....	0.0	0.0	0.0	0.0	0.0	0.0
	{ per cent.....	0.0	0.0	0.0	0.0	0.0	0.0
146	Heat loss due to theoretical dry gases { Btu.....	376	456	516	560	670	591
	{ per cent.....	2.6	3.1	3.4	3.8	4.5	4.0
147	Heat loss due to moisture in coal, moisture accompanying theoretical air, and water from combustion of hydrogen, { Btu.....	495	515	548	538	537	548
	{ per cent.....	3.4	3.5	3.7	3.7	3.6	3.7

^a Not in operation.

TABLE 3 TEST OF BOILER NO. 91, HELL GATE STATION, THE UNITED ELECTRIC LIGHT AND POWER COMPANY—Continued

Item	Test No.	1	2	3	4	5	6
148	Heat loss due to excess air and accompanying moisture entering furnace { Btu..... per cent.....	64 0.4	74 0.5	79 0.5	87 0.6	105 0.7	9 0.1
149	Heat loss due to air and moisture leaking through boiler, economizer, and air-heater setting { Btu..... per cent.....	24 0.2	46 0.3	48 0.3	56 0.4	64 0.4	58 0.4
150	Heat loss due to unconsumed hydrogen and hydrocarbons, radiation, and unaccounted for { Btu..... per cent.....	502 3.5	705 4.8	681 4.6	444 3.0	549 3.7	723 4.8
<i>Economizer:</i>							
151	Heat available to economizer, Btu per lb fuel (dry).....	1030	1203	1368	1420	1554	1284
152	Efficiency of economizer, per cent.....	53.9	50.3	48.3	48.6	46.3	43.4
153	Coefficient of heat transfer, Btu per sq ft per deg F per hr	6.26	8.13	9.76	11.0	12.58	11.87
<i>Air Heater:</i>							
154	Heat available to air heater, Btu per lb fuel (dry).....	836	952	1051	1120	1294	1076
155	Heat absorbed by air heater, Btu per lb fuel (dry).....	408	457	501	516	602	487
156	Efficiency of air heater, per cent.....	48.8	48.0	47.6	46.1	46.5	45.3
157	Coefficient of heat transfer, Btu per sq ft per deg F per hr	1.92	2.54	3.22	3.45	4.10	4.26
<i>Fly-Ash Data:</i>							
158	Combustible in fly ash, per cent.....	17.50	22.50	29.96	27.95	33.13	66.68
159	Gas per lb coal, lb.....	13.61	14.17	14.06	13.62	14.16	11.68
160	Specific volume of gas, standard cu ft.....	12.56	12.57	12.69	12.69	12.79	12.71
161	Gas per lb coal, standard cu ft.....	170.94	178.12	178.42	172.84	181.11	148.45
162	Cinders per 1000 standard cu ft of gas, lb.....	0.1443	0.1934	0.2846	0.241	0.252	0.888
163	Cinders per lb coal, lb.....	0.0246	0.0344	0.0508	0.0415	0.0455	0.1318
164	Cinders per lb gas, lb.....	0.00181	0.00243	0.00361	0.00305	0.00321	0.01128
165	Heat loss due to fly ash, Btu per lb coal.....	60	110	220	170	220	1280
166	Fineness of fine dust:						
	Through 60 mesh, per cent.....	90.5	86.5	82.0	84.0	83.0	77.0
	Through 100 mesh, per cent.....	85.5	80.5	75.5	78.5	77.5	69.5
	Through 200 mesh, per cent.....	70.5	67.5	62.5	67.0	67.0	63.0
	Through 325 mesh, per cent.....	56.0	55.5	52.5	57.0	55.5	33.5
<i>Power Consumed by Pulverizers, Blowers, and Feeders (Electric Drive):</i>							
Power consumed by mills:							
167	Mill No. 1, kw.....	51.6	58.7	61.6	69.5	81.3	98.0
168	Mill No. 2, kw.....	59.8	59.0	63.7	66.5	82.0	98.0
169	Mill No. 3, kw.....	0.0	41.0	56.5	60.5	79.3	86.0
170	Mill No. 4, kw.....	57.6	56.3	66.2	74.0	92.7	102.0
171	Total for mills, kw.....	169.0	215.0	248.0	270.5	335.3	384.0
Power consumed by mill blowers:							
172	Mill No. 1, kw.....	47.2	44.8	44.0	46.0	45.3	48.0
173	Mill No. 2, kw.....	50.8	49.2	49.5	49.0	49.3	50.0
174	Mill No. 3, kw.....	0.0	46.5	47.0	45.5	45.3	42.0
175	Mill No. 4, kw.....	47.6	46.0	48.8	43.0	49.3	46.0
176	Total for mill blowers, kw.....	145.6	186.5	189.3	183.5	189.2	186.0
177	Power consumed by motor-generator set, mill feeder, belt conveyor, and bottom cooling blower, kw.....	28.5	28.4	29.4	31.0	35.9	38.8
178	Total power consumed by electrically driven auxiliaries, kw	342.9	429.9	467.0	485.0	560.4	608.8
179	Power consumed by electrically driven auxiliaries in terms of heat per lb of coal { Btu..... per cent heating value.....	163 1.2	148 1.0	125 0.9	113 0.8	111 0.8	97 0.7

NOTE: Typical water analysis: Suspended solids, 1000 ppm; dissolved solids, 1030 ppm; total solids, 2030 ppm; NaOH, 44 ppm; Na₂CO₃, 106 ppm; NaCl, 412 ppm.

tory-faced blocks, the rough bare-metal blocks, and the smooth bare-metal blocks. The refractory-faced blocks are used in the lower section of the furnace about 12 ft high, followed up first by rough bare-metal blocks for the height of 3 ft, and then by the smooth bare-metal blocks extending 15.5 ft to a point within 2 ft of the top. The top section of the Bailey blocks is 2 ft wide and is made of refractory-faced blocks. Smooth bare-metal blocks are used in the vicinity of burners.)

Heating surfaces: Two downtake walls, 1880 sq ft; two side-walls, 2380 sq ft; total for water walls, 4260 sq ft

Total heating surface for the boiler and water walls, 58,186 sq ft
Furnace: Width, 34 ft; depth (between burner sides), 41 ft; height, 30 ft; furnace volume, 40,770 cu ft

Superheater: Babcock & Wilcox return-bend type; two superheaters per twin boiler unit. (Each superheater consists of five loops of 2-in. o.d. No. 9 Bwg tubes, 107 elements.)

Heating surface: 5800 sq ft each superheater; total, 11,600 sq ft

Economizer: Babcock & Wilcox return-bend type; two economizers per twin boiler unit (one for each half). (Each economizer consists of 2-in. o.d. No. 6 Bwg tubes, 24 tubes high, 24 tubes wide, 30 ft long.)

Heating surface: 9200 sq ft each economizer; total, 18,400 sq ft
Air heater: Babcock & Wilcox straight tubular type; two air heaters per twin boiler unit (one for each half). (Each air heater consists of 28 staggered rows of vertical tubes, 2 1/2 in. o.d. No. 11 Bwg, 22 ft long, 75 tubes in each row.)

Heating surface: On air side, 30,238 sq ft each air heater; total, 60,476 sq ft. On gas side, 27,350 sq ft each air heater; total, 54,700 sq ft

Burners: Fuller Lehigh, cross-tube type; 12 burners per twin boiler, six in each downtake wall, three burners per mill; 12 Babcock & Wilcox mechanical oil burners for lighting torches

Mills: Fuller Lehigh type-B pressure-type mills; four mills per twin boiler; capacity of each mill, 10 short tons

Mill blowers: B. F. Sturtevant single-inlet, paddle-wheel type, 18 in. static pressure; one blower per mill

Fans: Forced-draft fans, two fans per twin boiler; each fan 150,000 cfm capacity at 11.5 in. static pressure. Induced-draft fans, four fans per twin boiler; each fan 125,000 cfm capacity at 17 in. static pressure. (Forced- and induced-draft fans for each boiler unit are driven by two cross-compound steam turbines. Each high-pressure element drives two induced-draft fans through a reduction gear and is rated 974 hp at 7500 rpm. Each low-pressure element drives one forced-draft fan through a reduction gear and is rated 393 hp at 6000 rpm.)

Water-storage capacity: Volumetric contents of the boiler: Two drums (up to the normal water level), 1039 cu ft; boiler tubes, headers and nipples, 3756 cu ft; water walls (including downtake and uptake headers and recirculating tubes), 1713 cu ft; total 6508 cu ft

Weight of water and pressure parts: Weight of water contained in the boiler, water walls, and drums up to the normal water level at 421.7 F (300 lb per sq in. gage), 343,000 lb. Weight of water contained in the drums at 421.7 F within the water column connections, 58,000 lb; within the visible range of gage glass, 45,000 lb. Weight of pressure parts (in contact with water and steam), 953,000 lb. Weight of Bailey blocks in the furnace, 220,000 lb. Weight of pressure parts in terms of the equivalent weight of water on the basis of the ratio of the specific heats of steel and water, 112,000 lb. (Note: Weights of water and pressure parts are approximate.)

Ratios: Furnace volume per sq ft of water-heating surface, 0.7 cu ft. Superheater surface per sq ft of water-heating surface, 0.2 sq ft. Economizer surface per sq ft of water-heating surface, 0.317 sq ft. Total water-heating surface (boiler and water walls) per sq ft of boiler-room floor area (for both boilers, including aisles), 14.8 sq ft. Building volume per 1000 lb evaporation at maximum capacity, 636 cu ft.

Discussion

H. J. KERR.² A full discussion of the paper would require more space than the paper itself, in which, like the installation described, little space has been wasted and much material to work with has been presented in a small volume. Although these units are the first twin B. & W. sectional-header boilers installed, we have in operation many single boilers of the same size and capacity as one of the halves of these twin units. The idea of the twin unit was not new, as units similar in principle but using Stirling boilers had been installed in several plants. In shape, these units are rectangular, with the mills and primary-air fans below the furnace and the economizers and air heaters above the boiler. They therefore permit maximum utilization of the building space. The design of these units is based on conservative values for heat release, gas velocities, and steam capacity.

Only a few of the main features of these units can be mentioned, such as the special slag-screen tubes, the large-diameter drums with shutter-type baffles, steam circulators, slag-tap furnaces with block-covered wall tubes, and pressure-type mills used for direct firing.

The general principle of the boiler slag-screen tubes used with these units was developed some years ago and has been used extensively since then. In this design of boiler unit they permit the placing of two boilers together over a single furnace, with an access space between the boilers that is definitely sealed from the furnace. At a million pounds of steam per hour, the heat-liberation rate per square foot of equivalent cold surface exposed to radiation from the furnace is approximately 300,000 Btu. With preheated air at approximately 250 F, the temperature of gases entering the first pass should be in the neighborhood of 2500 F, which is checked by the test data. The value of the boiler slag-screen tubes as a preventive of slag difficulties is therefore obvious, even when burning fuel having as high an ash-fusion temperature as that of the coal used at this station, approximately 2450 F. Without the boiler slag-screen tubes, a certain amount of slag trouble would be experienced. In other words, the boiler slag-screen permits of the maximum combustion rate in a single-stage furnace set by the limitation of slag on the boiler tubes. For capacities beyond those thus obtainable, it is necessary to use the two-stage furnace, with its furnace slag screen, such as those that have been installed by the State Line Generating Company and those that are now being installed by the Potomac Electric Power Company in Washington, D. C.

The large-diameter drums on this installation are of interest. By concentrating on the problem of moisture and carryover it has been possible to bring these down to such quantities as to be negligible. With the boilers described, operating at their comparatively low steam pressure, the moisture content is shown to be below $\frac{1}{2}$ of 1 per cent at the maximum rating. Further developments have permitted the reduction of this percentage, in later installations, to such a point that we now deal with two or three parts per million, and we are pressing the chemist as to his accuracy on one part per million. We have succeeded in obtaining steam containing less than 0.1 of 1 per cent of moisture at a rate of more than 16,000 lb of steam per foot length of 48-in.-diameter drum. Drum diameter will, in the future, no longer be set by the amount of moisture in the steam, but rather it will be decided by the amount of water storage required to handle the variation in load necessary for any particular installation. This requirement is well discussed in the paper, and the value of a large-diameter drum from the standpoint of water-level fluctuation is well covered. In the past there have been certain limitations in obtaining large-diameter drums. The development of

welding processes and of material of higher tensile strength is expected to extend this limitation in the future.

The paper calls attention to the three rows of horizontal circulating tubes on these boilers. In this connection it might be well to point out that the number of circulators depends upon certain factors, one of which is the steam pressure. With some other designs, it would not be necessary to have this number of circulators, and, as a matter of fact, boilers are being constructed, of higher capacity per section than the units described, that are fitted with only one circulator per section.

The slag-tap furnace and block-covered tubes have been thoroughly discussed. Furnaces of this construction are in successful operation in so many plants that little need be said about them. Attention, however, is called to the fact that they are in successful operation in this plant with coal containing ash of high fusion temperature and in boilers that are off the line each night. In fact, it might be mentioned in this connection that, as compared with normal central stations, the starting up and shutting down each day of these large units constitutes very severe service. The value of this type of furnace is also to be observed in the extreme range in capacity, nearly five to one, as mentioned in the paper. Its value as it affects the cubical contents of the station is of course obvious.

The direct-firing pulverizers used at this plant are of the pressure type and were among the first of this type to be installed. The pressure type of mill was adopted for this installation to simplify various factors, and since then has been generally accepted as a standard because of simplification of coal distribution and piping, use of fans handling air only, instead of exhausters handling abrasive coal dust, reduction in fan power due to higher fan efficiency, and ease of control.

The test data show a high carbon loss with the boiler operating at a capacity of 1,078,000 lb of steam per hour. This was due to the fact that, at this capacity, the steam unit was operating 34 per cent above that contemplated in the mill design, with the result that the fineness was decreased. Subsequent changes in some of the mills have shown that even this capacity is obtainable, with high fineness from the mills and low carbon loss.

The ball-bearing principle of pulverizing as used in these mills is ideally suited to the art of pulverizing coal. The correctness of this principle of grinding has been demonstrated in many and varied applications.

Relative to the variation in superheat temperature from 700 to 760 deg, with the rating changed from 500,000 to 1,000,000 lb of steam per hour, as shown by Fig. 25, this variation in superheat can be materially reduced by a variation from standard in the operation of the burners. This method of taking care of the natural drop in superheat that takes place with reduction in rating is being used extensively where superheaters are not fitted with desuperheaters. The author is requested to cover this point in his closure.

The success of these boiler units in developing their high capacity may suggest to some the question, "What is the limit in capacity?" Although present practise tends toward the use of high steam output per foot width of furnace in single boiler units, and we could today furnish a single unit having the same capacity as the twin units at Hell Gate, the capacity of single units can, presumably, always be doubled, as was done in this case. The possibilities in high-capacity boilers are therefore considerably in excess of any present or probable future requirements in the use of single boiler units to serve individual turbines. The capacity of the boiler units will be limited by the maximum burner capacity it is possible to install per foot of furnace width, by the volume and capacity of the furnace it is possible to construct under the boiler, the amount of steam it is possible to raise per section, the length, thickness, and diameter of the boiler

² Chief Engineer, Service Department, Babcock & Wilcox Company, New York, N. Y. Mem. A.S.M.E.

drum, the length of tubes, available draft, quality of feedwater, and solids in steam to the turbine.

M. K. DREWRY.³ Never have the design and the performance of large boiler units been reported so comprehensively as in this paper. It is a valuable contribution and deserves much study. Appropriate discussion is difficult because of the magnitude of the information afforded. A few of the most interesting points obtained from it were found as follows:

- 1 The 72-in. boiler drums emphasize the desirability of appreciable boiler-water storage.
- 2 Steam-turbine drives for fans were chosen for other reasons than their reliability, for the coal pulverizers are motor driven.
- 3 Direct firing does not afford direct response to coal-feed demands, for differences in coal storage in the mills cause 2 to 4 min lag in heat output.
- 4 Removing ash in the molten form under all conditions of plant operation is not readily accomplished.
- 5 Unusually low radiation loss of the boiler-unit equivalent to only 0.2 per cent of maximum output emphasizes one economy of large sizes.
- 6 The time of 5½ hr is prudently used to start the units from cold and get them to normal rating. Each of the four mills is started and stopped 10 times during the starting procedure, and 8000 lb of oil is used for reliable ignition.
- 7 A drop of 100 deg fahr in superheat temperature occurs as output lowers from 1100 kB to 400 kB.
- 8 The reported boiler-unit efficiencies appear conservatively low because of the 3.5 per cent to 4.8 per cent "radiation and unaccounted" figure.

The author is thanked for his painstaking and intelligent reporting of a vital subject.

J. J. GROB.⁴ This paper goes farther than the usual report of a boiler-performance test. The author gives an exceptionally broad and lucid explanation of the many-sided problems facing the designing engineer responsible for developing a huge block of steam-generating capacity from a limited available space. The various engineering factors discussed so clearly and the mass of test data covering the performance of the various elements of the boiler installation should be of immeasurable value to other engineers responsible for boiler-station design. A discussion of the various outstanding points of interest in this paper would require considerable space, and therefore it will be confined to a few of the many points of interest.

In the rapid development of higher pressures and capacities in power stations, a number of problems, heretofore little heard of, have been forced upon the operating engineers, and one of the most persistent of these is "carryover moisture" in the steam. Trouble from this carryover moisture manifests itself in a number of ways, among them being the plugging up of superheater elements with sediment carried over with the moisture and left in the superheater, fouling up of steam valves with the residue salts and phosphates, line gasket leaks, fouling up of turbine spindles and casings, and frequently sharp steam-temperature dips and moisture slugs passing through the turbines, resulting finally in reduced turbine capacities due to fouling, if not in serious blade troubles.

Some phases of this problem are controlled by the installation of purifiers or baffles in the steam drum, but the author raises an important point in his introduction of the factor of boiler-surge capacity.

³ Assistant Chief Engineer, Power Plants, Milwaukee Electric Railway & Light Co., Milwaukee, Wis. Mem. A.S.M.E.

⁴ Engineer of Tests, United Electric Light & Power Co., New York, N. Y. Mem. A.S.M.E.

In the old section of the boiler house at Hell Gate Station, nine of the stoker boilers have been revamped to carry a maximum rating of 250,000 lb per hr steam apiece. The 54-in. drums originally provided were standard practise at the time of installation and were not altered when the boilers were revamped. Tests to determine the speed of pick-up in these revamped boilers have indicated that the rate of pick-up is limited by the rapidity of water-level change. In these tests attempts were made to assist water-level control by hand control of the feedwater cut-off valves and with automatic regulators in operation. On boiler 62 a drop of rating from 230,000 lb per hr to 120,000 lb per hr rating was accomplished in 7 min. The gear-controlled feed valve was restricted at the start to three turns open.

In the first 4 min the water level dropped from the 5-in. level to the 1-in. level, and then rose rapidly, until at the end of 7 min it had risen to the 14-in. level, at which time the gear valve was further restricted. After stabilization of rating at 80,000 lb per hr, the water level was established at the 3-in. level and the gear valve was kept restricted to one turn open. The rating was then raised from 80,000 lb per hr to 153,000 lb per hr in a space of 7½ min. In the first 4 min the rating rose to 115,000 lb per hr and the water level rose to 15 in., a gain of 12 in. The level then dropped off, until at the end of the 7½-min period it had reached the 7-in. level.

In another such test on boiler No. 33, when the start was made without restriction of the gear-controlled feed valve, a reduction of rating from 254,000 lb per hr to 83,000 lb per hr was accomplished in a space of 7 min. In the first 4½ min the water level dropped from the 5-in. level to the 2-in. level. It then rose to the 10-in. level on the rebound while the boiler was banked. Starting with a banked rating of 54,000 lb per hr and the gear-controlled feed valve one turn open, the rating was raised, as shown in the curves of Figs. 34 and 35, to 250,000 lb per hr. In the first 1½ min the rating had reached the 94,000 lb per hr rate and the feed valve was closed tight. It was then opened slightly and closed at intervals during the rise in rating, until full capacity had been reached. The water-level surges, although dampened by this control, show a swing from the 7½-in. level up to the 13-in., and then down to the 6½-in., finally settling near the 6-in. level.

A study of these curves and log entries will yield interesting information and makes clear the reason for the prevailing water-level problems in many plants.

Many other such tests on the stoker boilers indicate that while the speed of pick-up can be increased sharply by overtraveling on air pressure, the violence of water-level change requires manual control of the feedwater to avoid troublesome carryover.

Carrying the thought a step farther, perhaps it should be asked whether limited drum capacities and rapid rating response are worth the price of carryover-moisture troubles. It is clear that the surge characteristics and limitations of a specific boiler design should be determined to assist in the control of "moisture carryover."

In this connection and because of the growing importance of water-carryover problems, further comments are desired as to whether future design trends should take into account this troublesome factor. This apparently was done in the case of the million-pound-capacity boiler under discussion by allowing ample surge capacity of the boiler drums.

The completeness of the performance data helps to visualize the growing importance of heat-balance checks at intervals. With complete heat-balance information showing changes in boiler losses, it should be possible to correct pulverization and combustion impairment, and thus realize the maximum performance possibilities of the equipment.

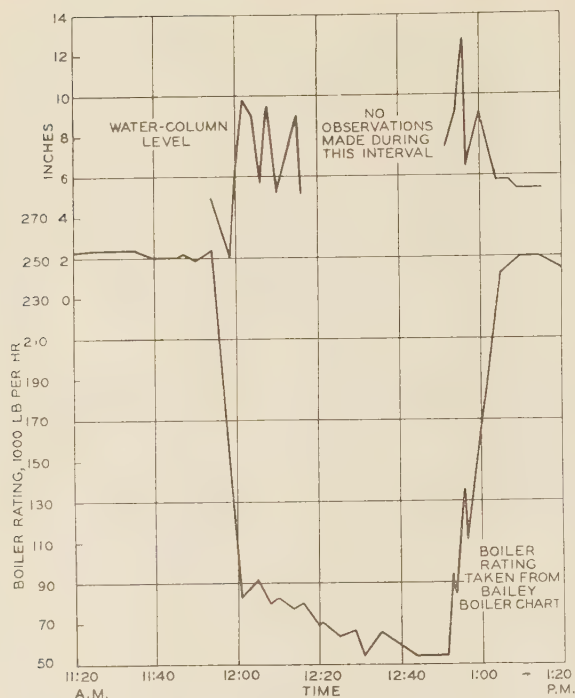


FIG. 34 SPECIAL TEST OF BOILER 33, HELL GATE STATION

(Log on boiler rating, boiler 33, tested Jan. 14, 1932: 11:54 a.m., start to drop; 11:57, no visible change in rating, boiler banked; 11:59 $\frac{1}{2}$, reached 90,000 lb per hr; 12:50 p.m., one turn on gear valve; 12:51 $\frac{1}{2}$, 54,000 lb per hr, end of banked period; 11:53, closed gear valve; 11:53 $\frac{1}{2}$, opened gear valve to one turn; 11:56, closed gear valve; 11:56 $\frac{1}{2}$, opened gear valve to one turn; 1:00 p.m., gear valve opened to 10 turns.)

GEORGE D. HETRICK.⁵ While the paper characterizes the two-unit boiler, fired with a common furnace and the single-unit capacity of 1,000,000 lb per hr, as the outstanding feature of the Hell Gate installation, it would seem that the engineering feat of producing 2,000,000 lb of steam per hour within a ground area of approximately 8400 sq ft, with a net ratio of building volume to boiler capacity of 636 cu ft per 1000 lb per hr capacity, is the outstanding accomplishment, when it is considered that with designs prevailing only three or four years ago this same capacity would occupy about 40,000 sq ft and require a building volume ratio of over 1700 cu ft. In the campaign for lower first costs, at least in the matter of space requirements, the Hell Gate installation is an excellent example of what can be accomplished.

An interesting feature is that these large boilers are shut down daily during night periods, demonstrating the operating flexibility of the units.

With two separate boilers served with one furnace, it would seem that difficulty would be encountered in maintaining a uniform temperature throughout the furnace and that physical conditions would tend toward a difference in superheat, feedwater, and air temperatures between the two units. The data presented make no reference to these conditions, so that it may be assumed that no appreciable difference in the performance of the dual installation is noticeable. However, with remote control it would be of interest to know how the action of each of the 12 burners is observed and adjusted to maintain uniform conditions. If one of the burners is not receiving its proper quota of fuel—a condition which occurs at times—how is the control operator notified of this condition?

It is not quite clear why relatively large drum capacity should

⁵ General Superintendent, Montaup Electric Company, Somerset, Mass. Mem. A.S.M.E.

in any way permit less vigilance on the part of the operators in the matter of attention to feedwater control. Certainly with a large drum, water-level fluctuation would be less noticeable, but the work to be done by the feed regulator is in no way lightened and water level is dependent on regulator performance.

Providing three circulator tubes per section is certainly a desirable arrangement, and should, as claimed, lessen the likelihood of stagnant circulation—a condition which has occurred in some high-pressure installations.

The information presented in the radiation test, Fig. 15, indicates the great value of the modern insulated furnace which makes possible quick starting of boilers after many hours of shutdown. The fact that these large boilers are in steaming service 30 min after lighting burners each morning after having been shut down during the night is a highly interesting operating condition, especially when we consider that the furnaces are of the slag-tap type. The slag probably remains in a molten state during the shutdown period and serves as a heat reservoir, which results in a much faster steaming schedule than would be the case with a water-cooling installation equipped with dry-ash hopper. It is of importance to observe that it takes less than five hours to put these boilers on the line from a cold condition.

The chilling of slag by air drawn through the slag-tap openings is information of value to the design engineer. The fact that it was necessary to install induced-draft equipment to reverse the air currents in the furnace adds not only to first cost but to operating costs also. This somewhat objectionable feature is of small consequence compared to the advantages of the slag-tap furnace, which include avoidance of slagging of ash on tubes, reduction to a large extent of the discharge of ash and dust from the

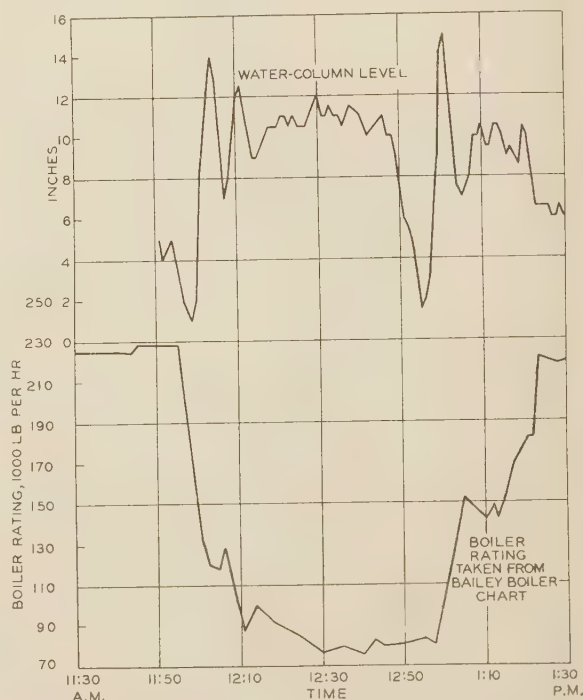


FIG. 35 SPECIAL TEST OF BOILER 62, HELL GATE STATION

(Log on boiler rating, boiler 62, tested Jan. 15, 1932: 11:30 a.m., rating at 225,000 lb per hr, east and west check valve open, three turns on gear valve, $3\frac{1}{2}$ in. H_2O on forced-draft duct, induced-draft-fan vane opening 98 per cent, induced-draft fan overloaded, overfire draft -0.1 ; 11:55 $\frac{1}{2}$, start to bring rating down; 12:03 p.m., gear valve closed to one turn open, fire in banked condition; 12:48, closed gear valve; 12:57 $\frac{1}{2}$, opened gear valve to one turn open; 1:15, opened gear valve to three turns; 1:17, rating at 168,000 lb per hr, induced-draft fan put in high speed; 1:21 p.m., Smoot forced-draft damper stuck closed, and then opened.)

furnace, and an increase in furnace volume on property of limited area.

H. M. CUSHING.⁶ In connection with the load pick-up tests shown in Figs. 12, 13, and 14, data on a pick-up test in Buffalo might be of interest. As is normal during light-load periods, two boilers rated at 560,000 lb per hr were feeding 65,000 lb per hr, each to an 80,000-kw turbine carrying a 10-megawatt load. The boiler operator was notified that a pick-up would be made, but the time was not given. The electrical operator, when ready to increase, set the bulletin boards to 60 mw, and proceeded to build up the load at a uniform rate to that point in 2 min, and held at that point. The boiler pressure dropped from 460 lb to 390 lb at the 4-min mark, and then came back to normal. A 12-in. rise in boiler-drum level resulted from this pick-up.

Babcock & Wilcox cross-drum boilers, 60 sections wide, 22 tubes high, 24-ft tubes, with a 60-in. drum, were used.

A. G. CHRISTIE.⁷ The paper is of timely interest, not only on account of the fact that the tests were made upon one of the largest-capacity boilers in the world, but particularly by reason of the great mass of valuable performance data contained in the tests. The twin setting of B. & W. boilers represents a new practise. Similar twin settings for 30,600 sq ft Stirling boilers were designed by McClellan and Junkersfeld, with whom the writer was then associated, for the Lake Shore Station of the Cleveland Electric Illuminating Company, and tests of these boilers were reported by John Wolff in a paper entitled, "Tests of Pulverized-Fuel-Fired Boilers at the Lake Shore Station, Cleveland." (A.S.M.E. Trans., Vol. 47, p. 1255, 1925.) The excellent performance of these boilers led to the use of similar twin boilers and furnaces at Avon Beach and Ashtabula Stations. Mr. Caldwell's boiler operates at a higher capacity than any of these Stirling boilers and appears to have a larger furnace.

The use of smaller boiler drums was advocated a few years ago, but experiences with the water-cooled furnaces at the Gould Street Station indicated the desirability of large water capacity in the boiler drums. When the India Basin Station at San Francisco was designed, the largest drums available (72 in. in diameter) were purchased. The use of this size of drum has since extended, and this size is employed in the Hell Gate boilers.

As Mr. Caldwell points out, these drums simplify control problems and decrease fluctuations of water level. He also refers to its accumulator effect, which may be of considerable value under certain conditions.

Many recent plants employing slag-bottom furnaces have provided water cooling for these bottoms. Mr. Caldwell uses air cooling, undoubtedly on account of the high fusing temperature of the ash, which, as shown in the data, exceeds 2400 F. This high fusing temperature undoubtedly adds to the difficulties experienced in tapping slag. Mr. Caldwell states that fluxes were tried to increase the fluidity of the slag. It would be interesting if he could add some further information on the chemical nature of the ash and the character of the fluxes that were tried. Many suggestions have been made regarding the use of fluxes, but specific data on the action of these are few.

Steam-turbine drives for both forced- and induced-draft fans represent a departure from the current practise of all-electric drive. Have the performances of small turbines been improved and first costs lowered to the point that these again are serious competitors of motors to drive power-plant auxiliaries?

The data upon the response of the boiler to increase in coal feed

⁶ Chief Engineer, Buffalo General Electric Company, Buffalo, N. Y. Mem. A.S.M.E.

⁷ Professor of Mechanical Engineering, Johns Hopkins University, Baltimore, Md. Mem. A.S.M.E.

indicate a rather slow action. This was undoubtedly measured with constant pressure at the superheater outlet throughout the test. One would at first infer that this boiler would not respond quickly to large fluctuations in load on the given turbine. If, however, the steam pressure is allowed to drop when the sudden increase in load occurs, the accumulator effect of the large drum will come into play, and this will permit a sudden increase in the flow of steam to carry the increased load. The contrary effect occurs if pressure is allowed to rise on sudden decrease of load. One can therefore expect such large boilers to meet load swings satisfactorily in actual service.

The test results are unusually complete. One is impressed by the large pressure drop through the superheater at high capacities, and also with the sizeable draft required of the induced-draft fans. However, an overall efficiency of 85 per cent and above was maintained for outputs up to over 900,000 lb per hour, which in itself is a remarkable performance. Fig. 24 indicates that the total equivalent heat required by the boiler auxiliaries remains substantially constant at all loads. The total power consumed by the powdered-coal equipment shows much lower figures than indicated by earlier tests.

The experience gained on these large boilers and their auxiliary equipment must have led to certain ideas on the part of the author in regard to future installations. In the light of this performance, what modifications would Mr. Caldwell recommend in a new plant to meet similar load conditions?

AUTHOR'S CLOSURE

In regard to the variation in superheat referred to by Mr. Kerr, it should be noted that the tests were conducted with approxi-

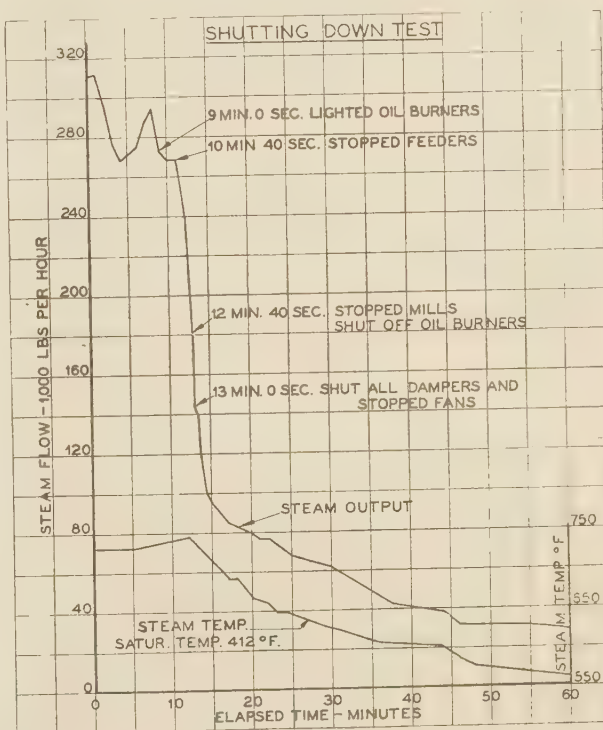


FIG. 36 SHUTTING-DOWN TEST ON BOILER 91

mately constant excess air. In normal operation the amount of excess air is reduced as the rating increases due to practical considerations, and the resulting superheat curve is consequently flatter than that reported in the test.

Mr. Drewry calls attention to some of the characteristics of the installation, and among other things mentions the lag in heat output associated with direct firing. Direct firing undoubtedly contributes somewhat to the time lag, but there are other factors which also have an influence. As an indication of the heat inertia of the installation, Fig. 36 is introduced from observations taken during a normal shutdown.

It may be observed that there is considerable lag in reduction of steam output even after the fuel supply to the furnace is interrupted. This indicates the extent of the lag which is independent of the combustion system. Where rapid response to changes in rating is desirable, the design should provide for less water-storage capacity and less heat-storage capacity in the furnace and boiler. On the other hand, a large water-storage capacity and large heat-storage capacity in many instances is a desirable characteristic, since the accumulator effect imparts a certain degree of stability to the steam pressure and steam flow with fluctuating loads. Opinion is divided on the degree of responsiveness which should be designed into steam-generating equipment, and as this consideration is dependent upon the nature of the system load and operating practise, there are many conditions where extremely rapid response is not so important.

Concerning Mr. Hettrick's reference to the distribution of work between the two boilers in the twin setting, it has been found that there is no noticeable difference in output with equalizing dampers wide open. In regard to the distribution of coal to the burners, this is controlled by a dividing arrangement for each mill which supplies its three burners. The coal from each mill divides fairly uniformly, and compensating adjustments are made at the secondary air dampers, based on observation of furnace conditions through openings provided for this purpose.

Regarding the question of large drum capacity, water-level fluctuations are less violent with fluctuating loads and afford the attendant more time to attend to his duties than would otherwise be the case.

Replying to Professor Christie's inquiry concerning the slag, the analysis herewith is typical of two of the coals which are used.

The fluxes used were fluorspar and soda ash, the latter appearing to be somewhat more effective. The choice of steam-driven fans was due largely to local conditions and space limitations which somewhat favored the use of steam turbines. Under

ASH ANALYSIS, PER CENT

	Pocahontas	Revloc
Loss on ignition.....	2.5	1.5
SiO ₂	49.8	33.8
Fe ₂ O ₃	16.8	24.7
Al ₂ O ₃	24.7	35.7
CaO.....	3.9	2.0
MgO.....	2.0	1.2
	99.7	98.9

ordinary conditions motor drives would be expected to show a substantial advantage, unless handicapped by a high-capacity demand charge.

Professor Christie's last question is rather broad, and the author will only attempt to generalize on the subject. In the absence of space or height limitations, it would seem that the heating surface should be somewhat more efficiently utilized than in the conventional type of boiler described in the paper; that is, the unit should be more nearly countercurrent than customary. Where conditions permit the use of a steaming economizer, this may be accomplished with much less boiler surface and with good operating and investment efficiency.

The use of the slag-bottom furnace in many cases appears warranted as a heat accumulator, aside from its benefits to combustion stability. Where very rapid changes in output are demanded, however, the unit should be designed with a minimum of water storage and heat storage to eliminate this source of lag. In the use of direct firing, minor modifications in the arrangement of mills and burners supply may be provided to approximate the characteristics of a bin and feeder system in order to eliminate the lag incidental to the use of direct firing. The superheater and its supporting arrangement is one of the major problems in boiler design, especially with the relatively high-steam temperatures which are now prevalent. Wherever possible, water-cooled supports should be provided, even though this introduces some circulating problems in the water circuit. With higher pressures and the average water supply, some form of steam washing or purification would probably be justified. Some provision for steam-temperature control is essential in order to maintain at all ratings the highest possible steam temperatures permitted by the turbine design.

The type of boiler equipment which might be selected for any condition could only be determined by a careful evaluation, and the foregoing comments merely indicate an opinion of what might be arrived at by such an evaluation under present conditions.

Utility of Variable-Displacement Oil-Pressure Pumps for Hot-Pressing in Plywood Operations

By ELEK K. BENEDEK,¹ MOUNT GILEAD, OHIO

Variable-displacement pumps or generators form the primary part of a complete hydraulic energy transformer, the secondary part of which is a hydraulic motor. Hydraulic transformers of fluid drives are becoming more and more useful for all kinds of modern production machinery, such as presses, machine tools, automotive engines, cranes, etc., because of certain advantages offered along the line of the modern power-transmission problems. The flow of chemical energy occurs in the form of a fuel and air compound, into an internal-combustion engine, where it will be transformed to thermal and partly mechanical energy. The mechanical energy flows further in periodic impulses to the crankshaft of the engine in the form of a mechanical direct-current energy, where through the flywheel of the shaft it will be somewhat smoothed out, so that in a mechanical-electrical energy transformer it will be transformed to direct-current or alternating-current energy. These currents finally reach the electromotor of the shop, which operates the drive shafts of mechanical or hydraulic energy transmission apparatus, transmission-belt shafts, gear transmissions of machine tools, electromotors of press pumps, etc.



IT IS often necessary to conduct the primary form of nature's energy, e.g., the heat energy of coal, through a series of energy forms or to transform it by a series of electrical and mechanical devices which are capable of utilizing it for ultimate requirements. The heat energy of the coal can be transformed to the elastic pressure energy of the steam, and this to electric energy. The electric energy thus generated may have to be transmitted to a remote place. It is then necessary to step

up its tension by transformers and distribute it over large territories, and again to transform the tension down to a voltage that may be utilized at the place of remote consumption. But this

is not the end of the cycle of the change of form of the energy. To make it useful, in a hydraulic press for example, it is further necessary to transform it back to pressure energy—this time to oil-pressure energy.

For manufacturing purposes and processes, a series of steps and a series of mechanical, electrical, or hydraulic devices are needed. With increasing production requirements and with increasing demand for economy, flexibility, and low maintenance cost, the trend of modern machine operations is toward hydraulic drives and devices. This is because of the infinite flexibility of speed and of load control and because of the smoothness of action, the simplicity, and the efficiency through fluid-pressure power-driven transmissions and oil-pressure systems. Where a train of transmission gears wears out, becomes noisy, vibrates excessively, and yields only a few steps of speed, the dream of inventors and engineers still goes back to a variable-speed fluid transmission drive. Where the toggles of a mechanical machine wear out and incapacitate the entire machine under the high-speed production of modern times and where a constant pull or a constant pressure has to be maintained indefinitely or continuously, as for instance in paper mills and plywood operations, irrespective of the variation of the strength and the structure of the individual work elements, fluid-pressure devices and methods have proved to be able to perform automatically and uniformly.

OPERATING CHARACTERISTICS OF POSITIVE-DISPLACEMENT VARIABLE-DELIVERY RADIAL-PISTON-TYPE PUMPS

The underlying theory of the commercially known variable-delivery rotary-piston-type pumps or oil-pressure generators will be best derived in connection with the accompanying Fig. 1. In these types of pumps a primary rotor 1 is positively or floatingly coupled to a secondary rotor 2 or 2' by means of a number of radially reciprocating pistons 3, which reciprocate in coating radial cylinder bores provided in the primary rotor 1. Fig. 1 shows the two fundamental types of hydraulic generators, in one of which the secondary rotor 2 is a ring and the cooperating pistons have a semi-crank motion in regard to this ring, whereas in the other type of pumps the secondary rotor 2' is a regular polygon and the cooperating radial pistons have a crankless pure harmonic motion relative to this polygon along the respective sides of the polygon. Under ordinary conditions, each rotor 1, 2, or 2' rotates about its own axis O_1 and O_2 , thereby causing the pistons and cylinders 3, which are actuated by the secondary rotors 2 or 2' in a specific manner, to make a suction stroke and a pressure stroke during each simultaneous revolution of the rotors. The entire assembly comprises members 1, 2 or 2', and 3. The horizontal plane containing the individual rotational axis O_1 or O_2 of the rotors 1 or 2 or 2' is characterized in Fig. 1 by its intersection line $N-N$ with the plane of the drawing of Fig. 1, and which represents the dead-center position of all the pistons. The dead-center position therefore is the intersection line of the plane

NOTE: Statements and opinions advanced in papers are to be understood as individual expressions of their authors, and not those of the Society.

¹ Consulting Engineer, Hydraulic Press Mfg. Co. During the World War, E. K. Benedek was an officer in the Austro-Hungarian army. In 1916, he was captured by the Russians and was kept in Siberian prison camps until 1920. Returning to Budapest, he obtained the degree of Mechanical and Electrical Engineer from the Royal Joseph Institute of Technology in 1922. He then came to the United States and went with the General Electric Company in West Lynn, doing research and development work. Since 1926 he has been engaged in the development of variable-delivery high-pressure pumps. In 1929, at the Royal Joseph Institute, he obtained the Doctor's degree of Technical Science. A great part of his experimental work was carried out with the Oilgear Company, in Milwaukee, Wis., as development engineer, for the purpose of diagnosing the performance of the oil-gear pumps. The Hydraulic Press Manufacturing Company, of Mount Gilead, Ohio, invited him to develop and build a line of his patented pumps.

Contributed by the Wood Industries Division and presented at the Semi-Annual Meeting, Chicago, Ill., June 26 to July 1, 1933, of THE AMERICAN SOCIETY OF MECHANICAL ENGINEERS.

of the rotational axis and the main meridian plane containing all the pistons. Therefore it will be observed that each piston, with its outer end attached to the secondary rotor 2 or 2' during 180 deg of one of its revolutions, relatively will approach the primary rotor radially, whereas during the subsequent 180 deg of one of its revolutions it will move away from it, or vice versa. Thus the distance of the rotational axis O_1 and O_2 will determine the eccentricity ρ of the pump, which, as will be set forth later on, may be varied from zero to the maximum value, toward each side of the stationary center O_1 , which is the center of the primary rotor 1 in this instance, and thereby the stroke of the pistons will be accu-

or in the function of time t :

$$x = \rho[1 - \cos \omega t] \dots \dots \dots [4]$$

It may be that a particular design does not constrain the motion of the outer end of a piston at the straight line s of rotor 2', but it guides along a circular path 2 of the rotor, in which case it can be easily proved that the fundamental equation of the piston displacement will be similar to that given by Equation [4], with the addition of a modifying factor, which will express that at time t the outer end of the piston will not be at the line s , but it will be in point C on the circular path 2 instead of in point B of the path s .

From the triangle $AB'C$ of Fig. 1, which is a rectangular triangle with its hypotenuse AB' , the distance $BC = e$, in which the piston path x of the two fundamental designs are differing, shown in Fig. 1. The difference is called the modifying factor e , for the circular-piston-path type of pumps, and it may be expressed as follows:

$$e = \frac{\rho^2 \sin^2 \omega t}{D} \dots \dots \dots [4a]$$

The particular means which engage the pistons with the secondary rotor 2 form the "tendon of Achilles" of each design, and the ways by which the tremendous hydraulic load of each piston is

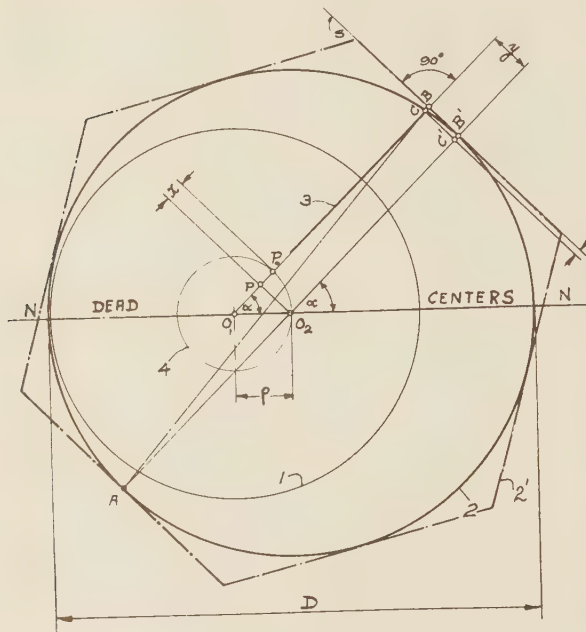


FIG. 1

ately controlled. When O_1 coincides with O_2 , the associated assembly will rotate bodily as a unit and no reciprocation of the pistons and cylinders will take place; hence the delivery will be zero, despite the full-speed rotation of the pump.

It is evident from Fig. 1 that as soon as the connection of piston 3 with its actuating rotor 2' is such that its outer end maintains a relative reciprocation on the side s of the regular polygon 2', the pumping movement of plunger 3 will be given. Path s is drawn tangentially to the secondary rotor 2 in point B and assuming that the operating eccentricity circle is 4 of the radius ρ , as shown in Fig. 1, and further assuming that the rotational angle of the piston 3 is measured from the line $N-N$ of all the dead centers, after a time period of t seconds, the angular speed ω will be:

$$\omega = \frac{\pi \times \text{rpm}}{30} \dots \dots \dots [1]$$

Piston 3 will cover an angle α , which will be given by the expression:

$$\alpha = \omega \cdot t \dots \dots \dots [2]$$

Assuming further an anti-clockwise rotation of the piston, after the dead-center position, the displacement x of the piston 3 will be given by the following expression:

$$x = \rho[1 - \cos \alpha] \dots \dots \dots [3]$$

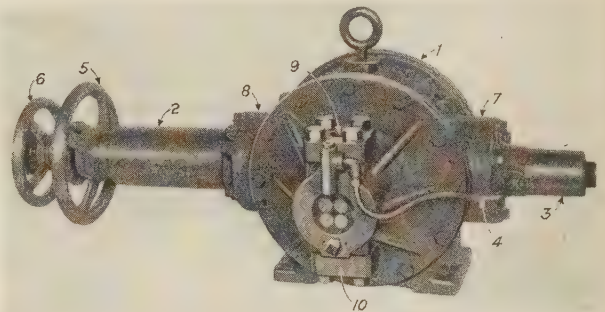


FIG. 2

transmitted to the secondary rotor or reaction member will determine the characteristics of each particular design.

Fig. 2 shows a pressure-control-equipped high-pressure pump of the author's design.

FLOW CHARACTERISTICS IN THE PUMP LINES

From the simple analysis expressed in Equation [4], it follows, as far as the atmospheric pressure is capable of accelerating the fluid behind a piston, that it will represent not only the displacement of a piston, but the motion of the fluid which is sucked in or expelled by the piston. Hence, the first and second derivations of the path in Equation [4], according to the time, will give the velocity and acceleration of the fluid following the pistons. Thus the velocity of a stream following a piston will be:

$$v = \frac{dx}{dt} \dots \dots \dots [5]$$

or

$$v = \rho \omega \sin \omega t \dots \dots \dots [6]$$

and the acceleration of a stream will be:

$$a = \frac{dv}{dt} \dots \dots \dots [7]$$

or

$$a = \rho \omega^2 \cos \omega t \dots \dots \dots [8]$$

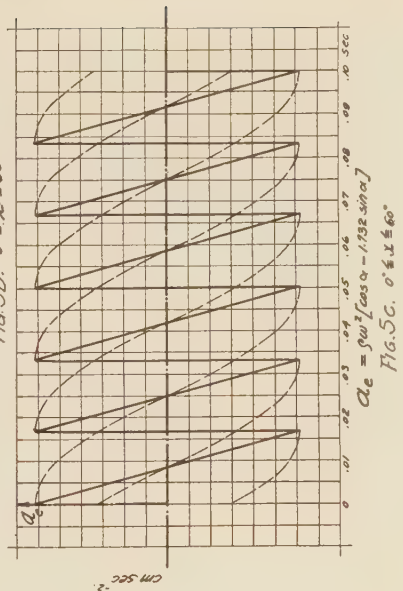
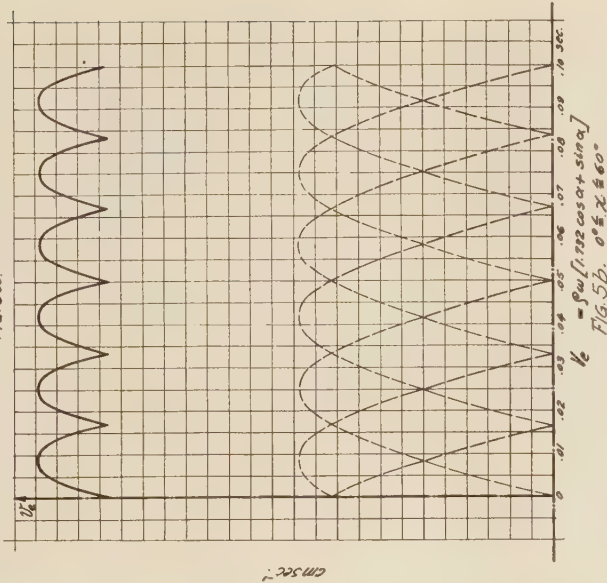
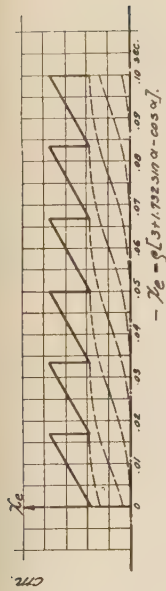


FIG. 5

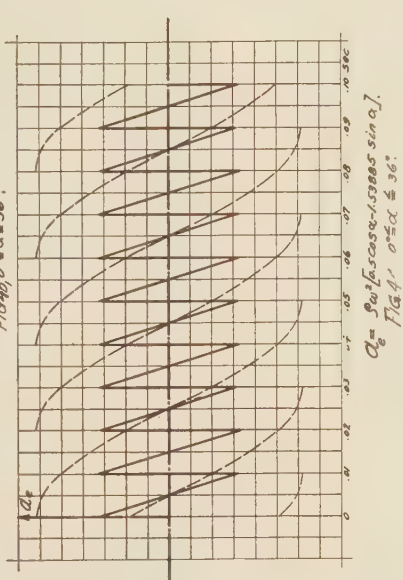
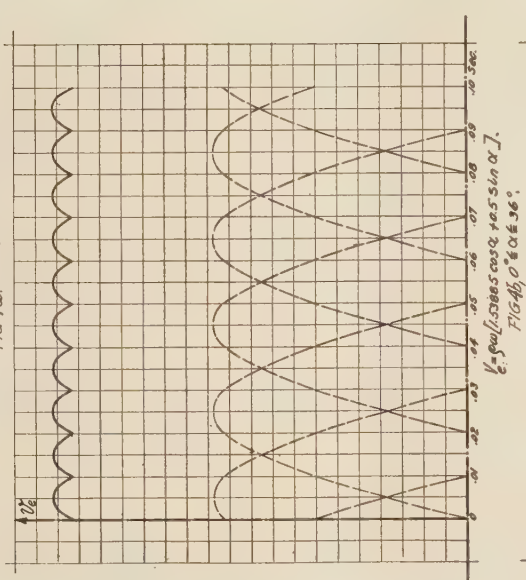
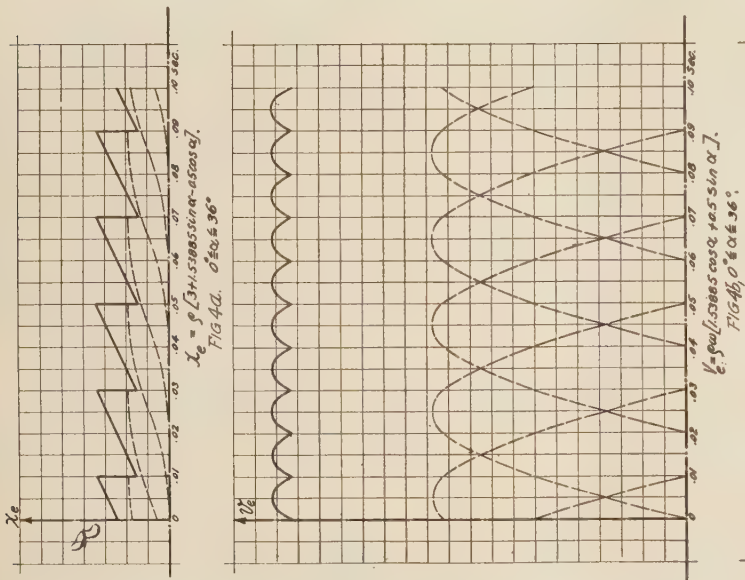


FIG. 4

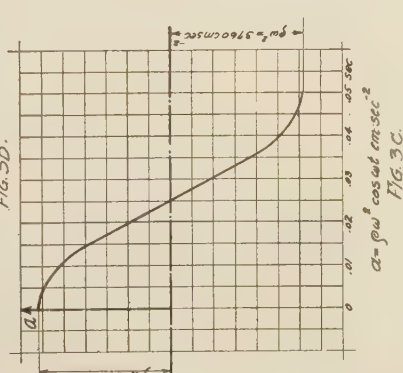
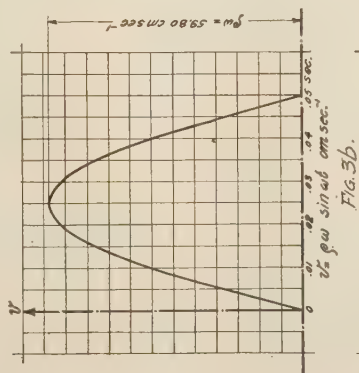
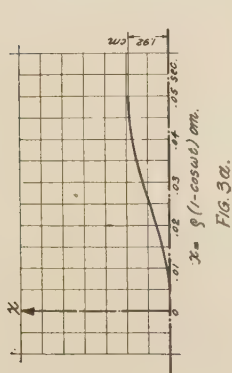
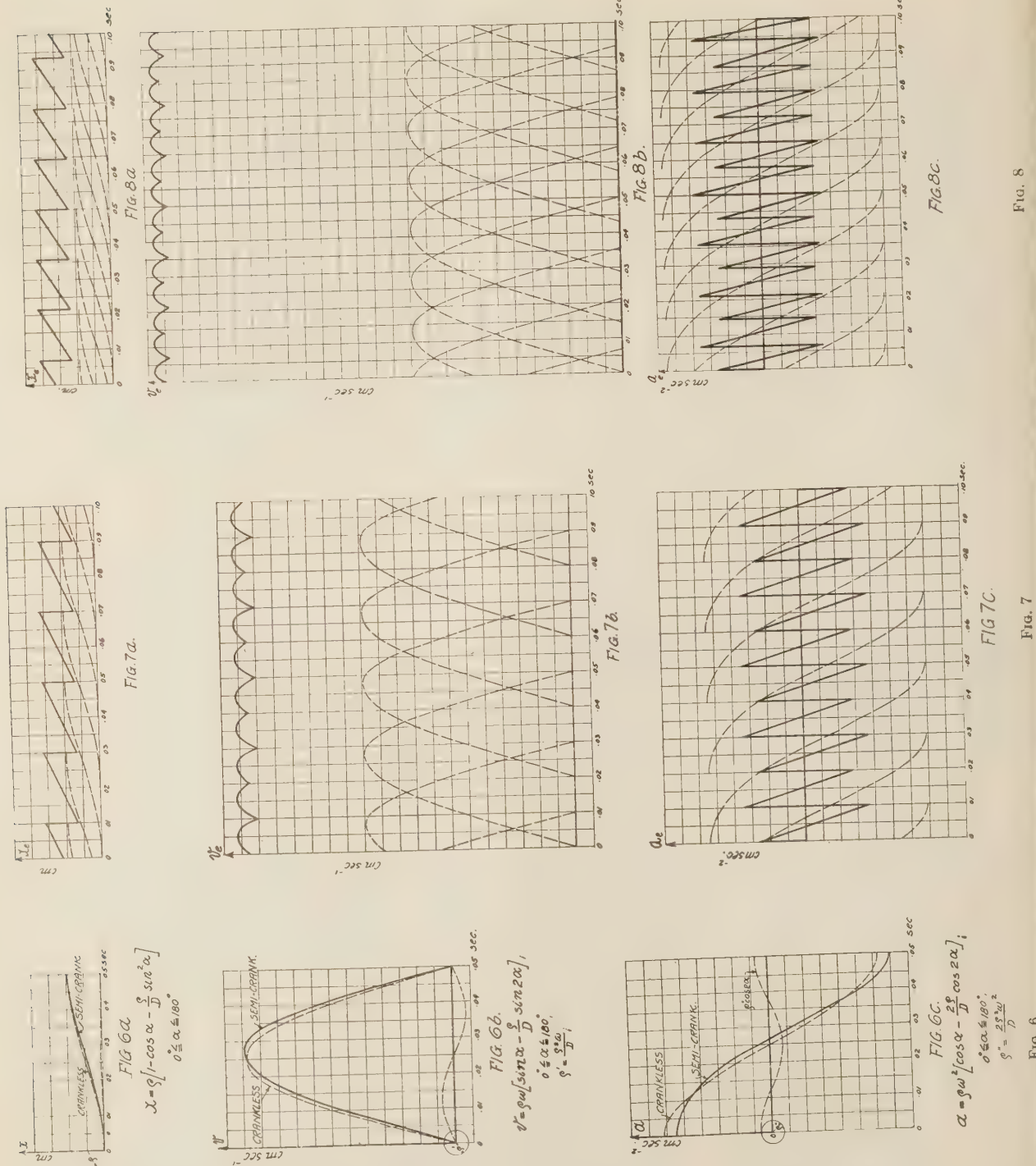


FIG. 3



The stream path, velocity, and acceleration Equations [4], [6], and [8] are represented in the time-flow diagrams Figs. 3a, 3b, and 3c.

In the case of a series of radial pistons and cylinders of 5- or 6-piston units, the diagrams are shown in Figs. 4a, 4b, 4c, and 5a, 5b, 5c, respectively. They give an interesting picture of the resultant flow conditions of a 5- or 6-cylinder unit of the type of pump in which the piston crossheads are guided on the line s.

They show that the displacement curves have critical sharp corners as well as the acceleration diagrams, whereas the velocity has small harmonic peaks; for instance, in the case of a five-plunger pump, ten small peaks, and in the case of a six-plunger pump, six large peaks. With similar deductions we would find that an odd number of pistons in a pump will give, during each revolution, a number of pulsations twice the number of pistons. The diagrams of Figs. 3, 4, and 5 are plotted for the duration

of one revolution, which in the present instance is one-tenth of a second, or for 600 rpm. These diagrams are given for the purpose of illustrating clearly that the delivery of multi-plunger pumps is externally smooth and that it gives a sufficiently high periodic fluctuation in the flow of the pressure fluid and energy which are required by the respective application.

Figs. 6a, 6b, 6c, 7a, 7b, 7c, and 8a, 8b, 8c are the parallel diagrams of resultant flow for the type of pumps represented in Fig. 1 by the secondary rotor 2, which carries the piston cross-heads on an actual arc instead of a straight line.

FLOW CHARACTERISTICS OF THE SEMI-CRANK-TYPE PUMPS

In Figs. 6a, 6b, and 6c, for the purpose of comparison, the effect of the modifying factor e , expressed in Equation [4a], is shown. From the figures of group 6 it is evident that the pure harmonic nature of the velocity of the suction or the discharge line of the crankless or semi-crank type rotary pumps is, practically speaking, the same in both types of pumps. The terms crankless and semi-crank are used for the two types. When the crosshead is compelled to slide on the straight line s in Fig. 1, it is evident that the crosshead will have no rocking movement in regard to the piston. In the second case, it has a rocking movement, and the piston itself forms the connecting rod.

The equation accompanying Fig. 4a is as follows:

$$x_e = \rho[3 + 1.538 \sin \alpha - 0.5 \cos \alpha] \dots \dots \dots [9]$$

and expresses the resultant displacement of the simultaneously sucking or delivering pistons in the function of the time in a five-piston pumping unit. Since the number of pistons is odd, it is evident that simultaneously there will be two or three pistons at the suction or at the delivery side of the pump, as shown in the figure. For instance, between the time 0.01 and 0.02 sec there are two stream waves, whereas between the interval 0.02 and 0.03 there are three stream waves or pistons. Consequently, for every 36-deg travel of the pump, there will be a two- or three-piston period in the resultant displacement expression. Equation [9] is the expression for the three-piston period as marked with the inequality equation:

$$0 \leq \alpha \leq 36 \dots \dots \dots [9a]$$

which means that after the dead-center position between zero and 36 deg, the first period is a three-piston period, as shown in Fig. 4a. The same is true of the equation of resultant velocity, which is as follows:

$$v_e = \rho\omega[1.538 \cos \alpha + 0.5 \sin \alpha] \dots \dots \dots [10]$$

which expression is valid for the interval of inequality [9a].

The resultant acceleration exerted by the atmospheric pressure in order to accelerate the suction fluid and keep it in contact with the bottom of the suction plungers will be expressed as follows:

$$a_e = \rho\omega^2[0.5 \cos \alpha - 1.538 \sin \alpha] \dots \dots \dots [11]$$

with the same region of validity as Equations [9] and [10].

In case of n pistons, the equations of resultant path, velocity, and acceleration were first developed by the author in 1929, in his doctor's dissertation on "The Analysis of Construction and Operation of Rotary Pumps, With Particular Regard to the Elimination of Destructive Phenomena in the Pumps."

In an n -piston pump, n being assumed to be an odd number, the maximum number m of the simultaneously sucking or delivering pistons will be

$$m = \frac{n+1}{2} \dots \dots \dots [12]$$

whereas the minimum number of such pistons will be:

$$n: 1 = \frac{n-1}{2} \dots \dots \dots [13]$$

The phase angle β of the individual pistons will be:

$$\beta = \left(\frac{360}{n} \right)^\circ \dots \dots \dots [14]$$

According to the analysis of the dissertation for the m and $m-1$ piston periods, the resultant displacement equations will be:

$$x_{em} = \rho \left[m - \cos \alpha \sum_{k=0}^{k=m-2} \cos k\beta + \sin \alpha \sum_{k=1}^{k=m-2} \sin k\beta \right] \dots [15]$$

and:

$$x_{e(m-1)} = \rho \left[(m-1) - \cos \alpha \sum_{k=0}^{k=m-2} \cos k\beta + \sin \alpha \sum_{k=1}^{k=m-2} \sin k\beta \right] \dots \dots [15a]$$

The velocity equations for the periods of m and $m-1$, respectively, of the resultant suction and delivery, will be:

$$v_{em} = \rho\omega \left[\cos \alpha \sum_{k=1}^{k=m-1} \sin k\beta + \sin \alpha \sum_{k=0}^{k=m-1} \cos k\beta \right] \dots [16]$$

$$v_{e(m-1)} = \rho\omega \left[\cos \alpha \sum_{k=1}^{k=m-2} \sin k\beta + \sin \alpha \sum_{k=1}^{k=m-2} \cos k\beta \right] [16a]$$

The resultant fluid acceleration in the suction pipe will be:

$$a_{em} = \rho\omega^2 \left[\cos \alpha \sum_{k=0}^{k=m-1} \cos k\beta - \sin \alpha \sum_{k=0}^{k=m-1} \sin k\beta \right] \dots [17]$$

$$a_{e(m-1)} = \rho\omega^2 \left[\cos \alpha \sum_{k=0}^{k=m-2} \cos k\beta - \sin \alpha \sum_{k=1}^{k=m-2} \sin k\beta \right] [17a]$$

Equation systems [15] to [17a] thus define the motion of the fluid for any piston number in a pump.² If m becomes even, then:

$$m = \frac{n}{2} \dots \dots \dots [18]$$

Thus the number of sucking and delivery pistons will be the same, and the foregoing equation system will be simplified and reduced to three fundamental equations, expressing the resultant path, velocity, and acceleration in the pipe lines of the pump or its associated circuit.

POWER REQUIREMENTS

In order to give another picture of other characteristics of the pump shown in Fig. 2, the pump was tested in regard to its mechanical and volumetric efficiencies with a General Electric wattmeter, to measure the input energy at various pressures. The results are shown in Fig. 9. The input kilowatts were measured at the clamps of the electromotor; therefore the efficiency of the driving motor was taken in consideration in

² It is assumed in these calculations that the pistons have a unit suction area and that the resultant passages have a unit section area also.

plotting these diagrams. In Fig. 9 η_v is the volumetric efficiency, η_m is the mechanical, and η_o is the overall efficiency of the pump.

Besides the full-stroke input-horsepower diagram and measurements, a time diagram was taken at various pressures, as indicated in Fig. 10, to determine the input horsepower at these pressures, when the pump is equipped with an automatic pressure control as shown in Fig. 2. In Fig. 10, in the time diagrams, section 1 of the curves represents the idle running of the pump, and peak 2 represents the time at which the pressure control unloads the pump against a spring pressure which tends to hold it at its maximum stroke. As the pressure approaches the set pressure of the control, say 2500 lb per sq in., the horsepower increases to peak point 2, then the control plunger against the spring pulls the pump to short stroke, and while the pressure is maintained at its constant value of 2500 lb per sq in., the input kilowatts drop down to line 3 in the figure. The difference

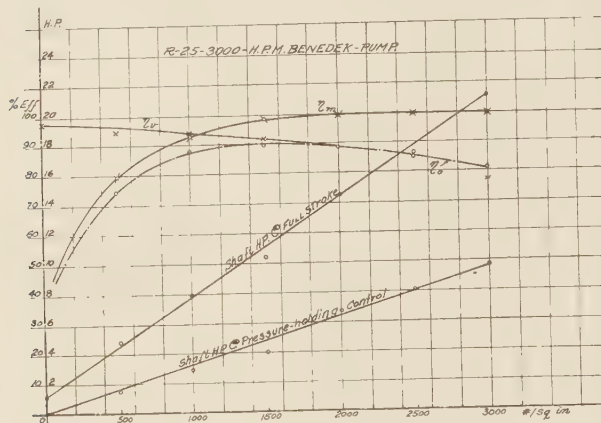


FIG. 9

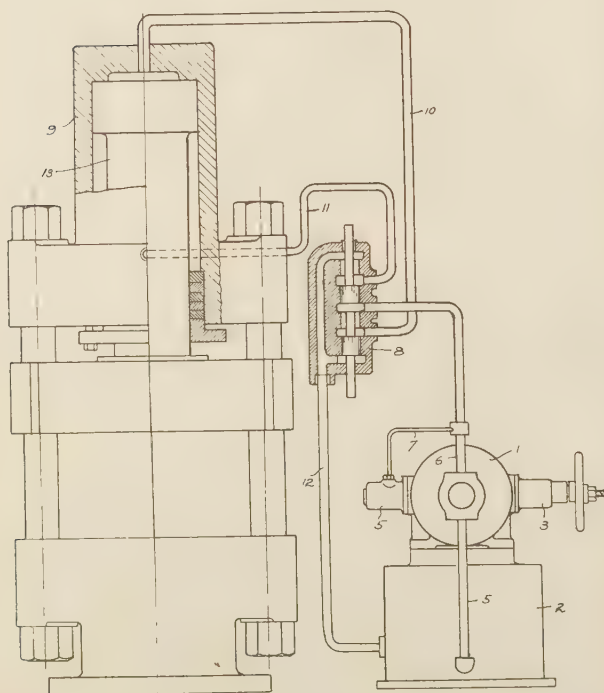


FIG. 11

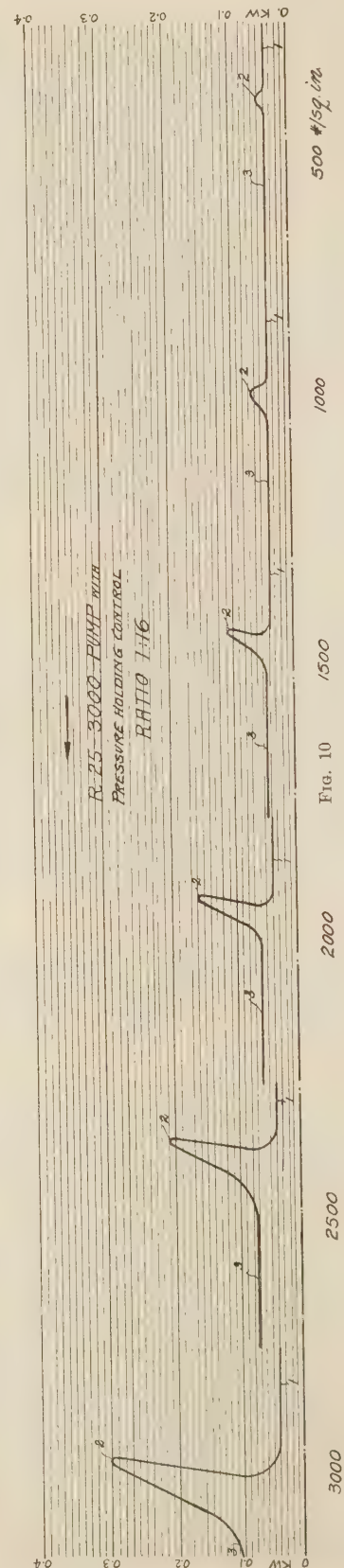


FIG. 10

between line sections 1 and 3 gives the kilowatts necessary to maintain the maximum pressure for an indefinite length of time.

The significance of the variable-delivery, positive displacement pumps is laid down in the diagrams of Fig. 10. Whereas in a constant-delivery pump a minimum of 17 hp would be necessary to maintain the 2500-lb pressure, in a control-equipped variable-delivery pump a peak of 8 hp is sufficient, although an average of 3 hp will hold the pressure indefinitely. Fig. 9 shows for comparative purposes the full-stroke horsepower and unloaded-pump horsepower.

PRESSURE MAINTENANCE

It must be remembered that in case of a constant-delivery pump, even if the fluid is bypassed prior to a maximum-peak pressure, the size of the electromotor must be as big as if the pump were to work at full pressure at all times. Hence, the economy of pressure-fluid energy for pressure-holding jobs, as is typical in plywood operations, is readily seen. Here, as is well known, the pressure must be kept at a constant value, during a critical length of time, which is necessary in order that the hot glue and plywood may take up a permanent shape and so that the glue will have time to penetrate into the intermolecular spaces of the wood and thus bind the layers permanently and elastically.

AUTOMATIC PRESSURE-HOLDING CONTROL

Fig. 2 shows the arrangement of a pressure-holding control of H-P-M radial-type high-pressure pump. Pump casing 1 is provided with diametrically opposite pads 7 and 8 for two control rods which connect directly to the stroke-adjusting member of the pump in the casing. On pads 7 and 8, there are a spring housing 2 and a cylinder 3. In spring housing 2 there is the control

spring pulling the control rod in a left-hand direction, thus putting the pump on maximum stroke to deliver in one direction only through pump main 9. Opposite to discharge main 9 is suction main 10. Handwheel 5 adjusts the tension of the spring, and thereby the force which resists any change of the pump stroke. Main 9 is, however, connected with unloading cylinder 3 through pipe 4, so that as soon as the main pressure reaches the maximum working pressure of the system, the piston in cylinder 3, which is a part of the right-hand control rod, pulls the control member of the pump toward the right and approaching the center position of the pump, when delivery becomes very small. As soon as an equilibrium between the spring force and the unloading pressure is reached, the pump will maintain the pressure against the spring force against any variation in temperature or slip; thus the main crosshead of the pump will float to the right and left to maintain that balance.

TYPICAL HOOK-UP

Finally, a schematical set-up of a pressure-control-equipped variable-delivery pump with a double-acting reciprocating ram might be introduced, as in Fig. 11. Pump 1 with control spring and housing 3 is mounted on a rigid reservoir 2, so that automatic unloading cylinder 5 will be in connection with pressure line 6 of the pump through control connection 7. A suction pipe 5 connects the suction main 4 and reservoir 2. A double-acting four-way valve 8 is interconnected between the pump, reservoir, and double-acting press cylinder 9 in a well-known manner so that line 10 will carry the pressure fluid and line 11 the suction fluid through the valve and pipe 12 back to the reservoir 2.

The simplicity of the press and the entire system, its dependability, and its ease of control place it among the mechanical devices that serve a large number of human needs.

Allowable Working Stresses Under Impact

By N. N. DAVIDENKOFF,¹ LENINGRAD, U.S.S.R.

This paper discusses the nature of failure under impact, and indicates how the factor of safety under these conditions is determined by the properties of the material employed.

THE proper factor of safety to employ in a given case is mainly dictated by two conditions: First, by the degree of reliability with which the stresses are calculated (data concerning the possible external loading, reliability of the fundamental theoretical assumptions, and correct representation of actual working conditions), and second, by the degree of certainty respecting the similarity of the mechanical properties of the material with those of the specimens used in the laboratory tests, (homogeneity of the material, sufficient similarity of working conditions of the material in service and under test). With respect to impact, however, both of these conditions are very complicated, as the calculation of the theoretical stresses can be made only in the simplest cases, and the conditions under which tests are made in the laboratory are usually those obtaining at static speeds, and very far from the conditions existing in actual service. Therefore, in order to determine the proper safe working stresses, it is necessary to study both sides of the question in detail.

1—METHODS OF CALCULATING STRESSES UNDER IMPACT

At the present time there are two ways of analyzing impact stresses: the theoretical, or, properly speaking, the dynamic, and the empirical, or static, with a correction made for dynamical conditions.

The first method gives an accurate solution of the problem only in exceptionally simple cases, such as elementary problems of longitudinal impact of bars with rounded ends,² impact of elastic spheres,³ impact of a sphere falling on an elastic beam,⁴ etc. This method is of but little practical importance. In the majority of cases other than those mentioned it is necessary to resort to approximate solutions, based upon the assumption of similarity of static and impact stresses and neglecting the time for propagation of the elastic wave (kinetic-energy method⁵). In longitudinal impact, this assumption is equivalent to the admission that at any given instant the whole bar is affected by a homogeneous state of stress. It is difficult to ascertain a priori the order of error, particularly because of the fact that the impact stresses are to a considerable degree affected by the local conditions of the impinging surfaces. These conditions for a given impact loading may vary, depending on details of the particular application (e.g., the state of the edges of a rail joint during

impact of a rolling wheel), and resulting in a different magnitude of stress. Therefore the reliability of the theoretical calculation of the stresses is very low.

The second method is applied in cases where series of impacts cause oscillation of the loading about a certain mean value corresponding to the static conditions. For instance, the loading exerted by wheels of a moving train on the rails or on a bridge truss, by the wheels of a truck on the highway pavement, etc. are of this kind. In such cases it is customary to judge the impact character of the loading by a dynamic coefficient greater than unity, expressing the ratio of the maximum impact load to the equivalent load under static conditions. The value of this coefficient can be determined in some cases in a purely empirical way, and our knowledge in this field is constantly increasing.⁶ However, in many cases we still have to be satisfied with arbitrary assumptions about the dynamic coefficients by employing merely general considerations.

In view of the uncertainty of calculation of the impact stresses and of the variety of solutions obtained, it is not possible to make any general statement concerning the allowable working stresses; therefore, in the following there will be considered only the case in which the impact stresses, calculated in one way or another, are checked experimentally and are consequently reliable.

As far as the actual methods of checking are concerned, difficulties arise because of the short duration of the impact (usually of the order of a few thousandths of a second) and of the wave character of the stress distribution. This checking will be treated in detail later.

2—DETERMINATION OF THE MECHANICAL PROPERTIES IN THE LABORATORY

In considering the mechanical properties of materials, the fundamental problem may be stated as follows: Is it permissible in calculating the allowable working stresses to use as a basis the yield point and the tensile strength of the material obtained under static conditions of loading?

The question has to be stated in this way for the reason that purely impact testing for rupture as usually carried out does not afford any means of determining directly the behavior of the metal during the impact. It is necessary to integrate the forces throughout the whole region of deformation, or to calculate the amount of the energy of deformation, which, however, cannot be used directly as characteristics for structures.⁷ Consequently there arises the following question: What relation exists between the dynamic and the static properties (mainly, the yield point and tensile strength), which of them is the larger, and how much? The answer can be given only with the help of scientific investigations which are of a complicated nature but are nevertheless available in large numbers.

In studying the influence of the variable speeds of static loading, we are enabled to predict the change of properties at impact speeds. Long ago it was noticed that in the plastic deformation of solid bodies internal friction increases with the speed, approaching the friction of viscous liquids; it is therefore natural to expect

¹ Professor of the Physico-Mechanical Institute in Leningrad; Head of the Mechanical Department of the Physico-Technical Institute in Leningrad.

² J. Sears, Proc. Cambridge Phil. Soc., vol. 21 (1908), p. 49.

³ A. Dinnik, Izv. Kieff Poly. Inst. (Trans. Poly. Inst. of Kieff), 1909, no. 4 (in Russian).

⁴ S. Timoshenko, *Zeit. f. Math. u. Phys.*, vol. 62 (1913), p. 198.

⁵ S. Timoshenko, "Strength of Materials," 1930, chap. 10, pp. 65-68.

Contributed by the Applied Mechanics Division and presented at the Annual Meeting, New York, N. Y., December 5 to 9, 1932, of THE AMERICAN SOCIETY OF MECHANICAL ENGINEERS.

NOTE: Statements and opinions advanced in papers are to be understood as individual expressions of their authors, and not those of the Society.

⁶ S. Timoshenko and B. Langer, "Stresses in Railroad Track," Trans. A.S.M.E., vol. 54 (1932), APM-54-26. See also works of the Russian Bridge-Testing Stations (HKBC), 1926.

⁷ N. Davidenkoff, "Factor of Safety in Dynamical Calculations," *Stroitel'naja Promishlennost* (Structural Industry), no. 11 (1924), p. 713 (in Russian).

an increase of resistance to plastic deformation with an increase of speed. On this property was based the further one of "relaxation" (at constant deformation) which was studied by Maxwell,⁸ and also one generally known as the creep of metal (at constant stress). The conception of Schmid and Polanyi⁹ gives perhaps the clearest physical idea regarding these properties. They propose to differentiate between "thermal" and "athermal" plasticity. It is assumed that in the process of plastic deformation the heat motion of the atoms (thermal plasticity) continuously reduces the strengthening caused by cold working (athermal plasticity); in the case of short-duration loading (high speed) or loading at low temperatures, the reduction of the strengthening is slackened, and it is necessary to supply more energy for the same deformation.¹⁰ The nearer the melting temperature of the metal is to the room temperature, the more evident is this influence of the speed because of the larger mobility of the atoms. Therefore, for example, lead is more susceptible to speed than iron.¹¹ Now, considering the speeds of impact, we have to expect this phenomenon to manifest itself to a still greater extent. Here, however, appear the experimental difficulties mentioned above.

One of the simplest, but at the same time one of the crudest methods of measuring the impact force during rupture of a specimen in the laboratory is to calculate the average strength of the specimen; for this purpose it is sufficient to divide the measured energy of deformation of the specimen by the total elongation of the latter. Comparing the stress-strain diagram obtained under dynamic loading with one obtained under static conditions, it is possible to obtain a preliminary idea regarding the influence of the speed. According to the experiments by Blount, Kirkaldy, and Sankey,¹² this influence for various steels at high impact speeds

(height of fall of the blow-imparting mass, or tup, 12 meters) was expressed by ratios ranging from 1.24 to 1.55, and from 1.23 to 1.37 according to experiments by Körber and Sack.¹³

The next difficult problem is the measuring of the elastic limit and the yield point for impact. This is easier to accomplish because of the fact that up to the appearance of the first permanent deformations the specimen obeys the laws of elasticity, and its deformations can be considered as a measure of the stresses. Of the various methods used for this purpose, only two employed by the author will be considered here.

During one investigation,¹⁴ the following arrangement shown in Fig. 1 was used. The specimen *A* was inserted in the two tups *C* and *D* of the Amsler testing machine in such a way that the lower tup *D* was suspended from the upper tup *C* not through the specimen, as is done in usual testing, but with the wires

E. When the projecting shoulders of the upper tup strike the fixed parts *F*, the wires break, the tup *C* rebounds, while *D* continues to move down until it causes an impact tension in the specimen, changing the speeds of the tups. These speeds were measured by means of diagrams made by both tups on a rotating cylinder. Knowing the weight of the tups, it was possible to calculate the amount of elastic energy expended by them on the specimen. The actual amount of the elastic energy accumulated in the specimen had to be larger than the amount of energy measured in this way, because of unavoidable losses. Knowing the amount of the potential energy, it was possible to calculate the stresses; and by observing the instant of appearance of the first Lüders lines on the surface of the specimen, the stress in the vicinity of the yield point could be determined.

Experiments made with a soft steel indicated that the dynamic limit of yielding exceeds the static in the ratio ranging from 1.23 to 1.42; this ratio can be only smaller than the actual one, according to the statement previously made.

Another series of experiments was performed by the author and K. Yurieff for the purpose of determining the relative

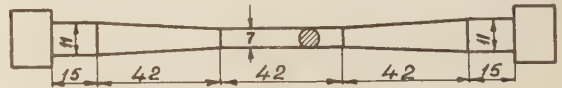


FIG. 2 TYPE OF SPECIMEN USED IN EXPERIMENTS OF DAVIDENKOFF AND YURIEFF

magnitude of the yield point with respect to the tensile strength of the material.¹⁵ The method of the Lüders lines was again used, but this time in the following manner: The specimen to be tested had the form and dimensions shown in Fig. 2, and its surface was polished. After its rupture in the Amsler machine, it was evident that the plastic deformation accompanied by the Lüders lines progressed on the conical portion to a certain section, usually easily noticeable by eye (especially if the sample had been previously covered with shellac). After having measured the area A_1 of this limiting section, in which, obviously, the stresses were at the dynamic yield point p_1 , it was possible to determine also the relative value of the latter from the conditions of equality of the maximum tensile force in all sections:

$$A_1 p_1 = A_0 p \quad \text{or} \quad \frac{p_1}{p} = \frac{A_0}{A_1} = \eta$$

where A_0 is the original area of the section in the cylindrical part and p is the tensile strength of the material. From static tests on similar specimens it was possible to determine the same ratio for low speeds and then to make a comparison.

Experiments performed on six different varieties of annealed carbon steel showed that the ratio η for impact loading is always larger than for static loading, the average of the two being 1.25, the ratio varying from 1.10 to 1.43.

Finally, A. Dinnik¹⁶ investigated the impact of steel spheres against a steel block with a plane polished surface; by observing the instant that the first permanent deformations appeared, and then employing the exact theory of H. Hertz, he calculated the corresponding stresses. By comparing these with the corresponding stresses in static loading, he found that the dynamic yield point exceeds the static in a ratio of at least 1.85.

The foregoing values, together with data from other series of investigations, are given in Table 1.

FIG. 1 DIAGRAM SHOWING ARRANGEMENT OF TUPS AND SPECIMENS IN THE AUTHOR'S EXPERIMENTS

⁸ Maxwell, *Encycl. Brit.*, 9th ed., vol. 7, p. 798.

⁹ E. Schmid, *Naturwissenschaften*, vol. 17, p. 301, 1929.

¹⁰ At very low speeds, lowering of strength must be expected, which actually was observed (Welter, 1927) for all metals with the exception of iron (Bottomley, 1879); for this latter, at low speeds, a special phenomenon appears, namely, aging, causing a new rise in strength.

¹¹ E. Siebel and A. Pomp, *Mitt. K.-W. Inst. für Eisenforschung*, vol. 10 (1928), p. 63.

¹² *Proc. Inst. M. E.*, 1910, p. 715.

¹³ F. Körber and B. Sack, *Mitt. K.-W. Inst. für Eisenforschung*, vol. 4 (1922), p. 11.

¹⁴ N. Davidenkoff, *Izv. St. Petersburg Poly. Inst. (Trans. Poly. Inst. of St. Petersburg)*, vol. 20 (1913), pp. 421-462, 547-580.

¹⁵ N. Davidenkoff and K. Yurieff, First communication of the NIATM, Zurich, 1930, p. 231.

¹⁶ A. Dinnik, *Izv. Kieff. Poly. Inst. (Trans. Poly. Inst. of Kieff)*, 1909 (in Russian).

TABLE 1 RATIOS OF RISE OF YIELDING LIMIT AT IMPACT

Authority	Year	Material	Ratio of rise	Remarks
B. Hopkinson ¹⁷	1905	Steel wire	1.68
		Copper wire	1.28
A. Dinnik ¹⁸	1909	Steel	1.85
N. Nemiloff ¹⁸	1910	Steel	1.90
N. Davidenkoff ¹⁴	1913	Steel	1.23-1.44
E. Meyer ¹⁹	1927	Iron	1.60
N. Davidenkoff and K. Jurieff ¹⁵	1927	Steel	1.10-1.43	Relative (not absolute) rise of yield point

All the experimental data show a considerable rise of the yield point at impact with the exception of those recently reported by Guest,²⁰ which are of opposite character. Guest measured and recorded the elastic deformation during longitudinal impact of two long iron bars (11 ft and 23 ft), and using this deformation, he checked the correctness of the methods employed in calculating the stresses. As the yielding limit, he assumed the stress at which the coefficient of recovery after the impact (relative height of rebound of the striking bar) started sharply to fall. This stress (31 kg per sq mm) but slightly exceeded (less than 1 per cent) the static value of the elastic limit.

It seems to be possible to reconcile these contradictions. In all experiments mentioned above, rather large deformations were used as criteria of passing beyond the yielding limit, such as the Lüders lines in the author's experiments or an apparent deformation changing the refraction of light (Dinnik); but Guest in his experiments with the most accurate measurements (± 0.0001 in.) discovered no change in the dimensions of the bar after passing beyond the yield point. Therefore it is possible to believe that the stress at which the first exceedingly small permanent deformation appears does not depend on the speed; but if the determination of the elastic limit or the yield point is connected with a definite value of the permanent deformation or with a definite degree of its external expression (Lüders lines), the difference from the data given in Table 1 is then apparent, because the short duration on the blow does not permit the deformation to sufficiently develop.

For the designer, the stresses beyond the yielding limit are dangerous only in connection with the above-mentioned external effects, and therefore the numerical results of Table 1 remain valid.

Finally, in measuring the strength of a material under impact it is necessary to use extremely elaborate experimental methods, which will permit determining fully the whole stress-strain diagram in impact. Many procedures have been proposed for this purpose, but none of them received has been employed in more than a single investigation. They all fall into one of two classes:

1 The curve of the motion of the tups that ruptures the specimen is recorded as a function of time, $s = f(t)$, and by differentiating this curve twice, the acceleration, d^2s/dt^2 , and consequently the strength of the specimen, is obtained. (See Plank,²¹ Elmendorf,²² Gett,²³ Homger,²⁴ Seehase,²⁵ Schwinning and Matthaes,²⁶ Körber and Storp,²⁷ and Yamada.²⁸) This

method has the disadvantage that considerable errors are unavoidable in the process of double graphical differentiation.

2 Elastic self-recording dynamometers are used: for example, in measuring the elongation of a steel bar (Moore,²⁹ Meyer³⁰); mutual compression of spherical lenses (Kirner,³¹ Davidenkoff³²); deformation of piezoquartz (Prince Galitzyn,³³ Kluge and Linckh³⁴). The difficulty in using dynamometer methods lies in the necessity of providing the elastic system of the dynamometer with a natural-vibration frequency several times smaller than the duration of that part of the investigation during which the change of the force must be correctly recorded. Apparently the use of piezoquartz gives the best results, although for recording the electric charge, which varies quickly, it is necessary to have an oscillograph of almost negligible inertia. This condition can be met only by using a cathode oscillograph.

Adopting this latter method, an experiment in measuring the impact resistance of specimens was carried out in the author's laboratory.³⁵ Fig. 3 is a schematic diagram showing the use of the oscillograph. The cathode beam was simultaneously affected by two fields giving transitory motion in two planes perpendicular to each other, namely, an electric field, obtaining its potential from the quartz crystals at *D*, and a magnetic field from special spools with large self-induction introduced automatically

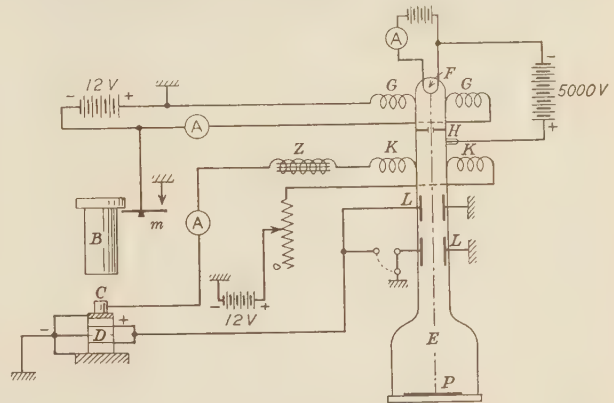


FIG. 3 DIAGRAM SHOWING USE OF CATHODE OSCILLOGRAPH FOR RECORDING IMPACT FORCES

- A = Ammeter
- B = Tup
- C = Specimen
- D = Piezoquartz (4 crystals)
- E = Cathode oscillograph (P, photographic film; H, diaphragm)
- F = Glowing wire
- G = Coil deflecting the cathode beam (— · — · —) from aperture in diaphragm H before impact (for protecting P)
- K = Coil connected with induction coil Z and introduced at the instant of impact, imposing on the cathode beam a transitory motion along the time axis
- L = Electrodes receiving potential from charge of the piezoquartz and moving beam along the axis of charges (forces). It is possible to work with one or with two pairs of plates
- M = Mechanical arrangement at tup B, grounding the coil G before B begins to fall and adjusting cathode beam in its normal position. Coil K is cut into circuit at the instant of beginning of impact, when connection with earth occurs through specimen C, tup B, and lever M

and simultaneously with the starting of the impact. The specimen receiving the impact from the falling tup, transmitted it to the quartz crystals on which it stood. The piezoelectric charge produced on the quartz transmitted itself to the plates of the oscillograph. The result was that the cathode beam pro-

²⁹ H. Moore, Proc. A.S.T.M., vol. 22 (1922), p. 124.

³⁰ E. Meyer, Forschungsarbeiten, V.D.I., no. 295, 1927.

³¹ J. Kirner, Ibid., no. 88, 1910.

³² Izv. Leningrad Poly. Inst., vol. 29 (1925), p. 53.

³³ Izv. Ross. Akad. Nauk (Proc. Russian Acad. Sciences), no. 11, 1915.

³⁴ J. Kluge and H. Linckh, Z.V.D.I., vol. 73 (1929), p. 1311.

³⁵ By the physicist W. J. Feoktistoff with assistance of Mr. Klausting.

¹⁷ B. Hopkinson, Proc. Roy. Soc., London, 1905, p. 498.

¹⁸ N. Nemiloff, The Engineer (Kieff), 1910, nos. 11 and 12 (in Russian).

¹⁹ E. Meyer, Forschungsarbeiten, V.D.I., no. 295, 1927.

²⁰ I. Guest, Proc. Inst. M. E., 1930, p. 1273.

²¹ R. Plank, Z.V.D.I., vol. 56 (1912), p. 17.

²² A. Elmendorf, J. Franklin Inst., 1916, p. 771.

²³ P. Breuil, Revue de Mecanique, 1909.

²⁴ Homger, Z.V.D.I., vol. 56 (1912), no. 37.

²⁵ H. Seehase, Forschungsarbeiten, V.D.I., no. 182, 1915.

²⁶ W. Schwinning and K. Matthaes, Deutscher Verbund für Materialprüfung der Technik, 1927, no. 78.

²⁷ F. Körber and H. Storp, Mitt. K.-W. Inst. für Eisenforschung, vol. 7 (1925), p. 81.

²⁸ R. Yamada, Science Reports, Tohoku University, vol. 17 (1928), p. 179.

jected a diagram on the photographic film, P , the ordinates of this diagram being proportional to the pressure on the quartz at each instant, while the abscissas represented the time to some (exponential) scale. Fig. 4 shows the diagrams obtained for brass and lead specimens. The results of these preliminary experiments showed the value of the method, and at present work is under way on the construction of more perfect apparatus for testing specimens in rupture.

In spite of the great variety of methods employed, the number of quantitative results obtained is very small, because most of the experiments were those in which the specimens were bent but not ruptured. All of them testify a general rise of the impact curve as compared with the static curve, this being more pronounced in

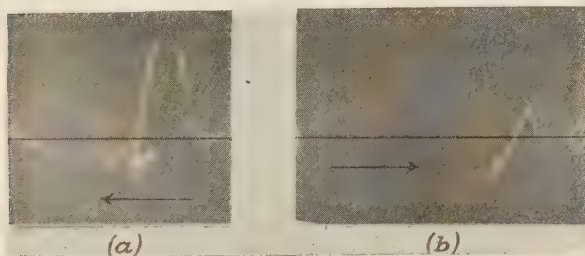


FIG. 4 IMPACT DIAGRAMS FOR BRASS (a) AND LEAD (b) SPECIMENS

the first half of the diagram than in the latter. Some of the ratios for metals are given in Table 2.

TABLE 2 RATIOS OF RISE OF STRENGTH OF MATERIAL UNDER IMPACT

Authority	Year	Material	Ratios of rise		Remarks
			Yield point	Strength	
Plank Meyer	1912	Steel	1.33	1.46	Initial speed of impact = 0
	1927	Iron	..	1.12	
		Steel	..	1.06	
Seehase	1915	Brass	..	1.01	Compression Stresses referred to equal deformations
		Copper	..	1.13	
		Steel	..	1.14	
		Copper	..	1.15	
		Brass	..	1.02	
		Iron	..	1.11	

The ratio of rise for strength is not so large as that for the yield point, but is large enough to be observed in all experiments (except perhaps those on brass).

The general and indisputable conclusion to be drawn from the foregoing data is as follows: The tensile strength of the material and especially the yield point are higher under impact than under static conditions; however, the amount of rise of the strength and yield point is difficult to state because of lack of agreement of the experimental data available at the present time.

3—SELECTION OF ALLOWABLE WORKING STRESSES

It is a question whether or not it is possible to base the determination of factors of safety upon the increased values of the yield point and strength under impact instead of using the static values. It seems to the author that the answer must be negative for the following reasons:

1 The static loading is imposed by a force (weight, pressure of water, etc.), while the impact is by a definite amount of kinetic energy and fundamentally different. Any local inhomogeneity of the material (blow holes, etc.), and the local weakening of any cross-section, leads to a decrease in strength of the specimen in the same ratio, while the work of deformation of such a bar decreases to a much greater extent because of the decrease in its total elongation.³⁶

2 In the case of repeating the same impact beyond the elastic

³⁶ See S. Timoshenko, "Strength of Materials," 1932, part 1, art. 64, problem no. 9.

limit (the author does not have in mind here the typical repeated loading encountered in problems of fatigue of metals), the permanent deformation received at the first impact may increase because of the increased duration of the activity of the same force, while under static load the permanent deformation does not depend on the number of applications of the force. This fact diminishes somewhat the favorable effect of the rise of strength occasioned by impact.

3 Incidentally, increases of the loading under impact, as compared with those determined by calculations, are more probable than under conditions of static action of the load, because of the larger number of factors which may influence the magnitude of the impact load.

All this can be considered as an argument for using the same allowable stresses in designing members of structures subjected to impact as are used in static calculations.

In making this statement, however, the question of reliability of the theoretical calculations used for the determination of stresses under impact has not been taken into account. Consequently the allowable working stresses have to be diminished by introducing an additional "coefficient of uncertainty," the magnitude of which depends on the degree of knowledge we have of actual impact loading.

4—IMPACT BRITTLENESS

The author has not as yet discussed the question of impact testing of notched specimens in bending. Would it now be possible for the designer to use the coefficients of "impact ductility" obtained from such tests as additional factors in determining the allowable stresses? In order to obtain a clear answer to this, it is necessary to treat the question of the physical significance of such tests in a somewhat more detailed way.

It is known that there are materials which, while giving quite satisfactory results in static and even in impact tests for rupture, fail with scarcely any expenditure of energy during notched-bar rupture tests. This involves an element of danger, because among the various members of structures working under impact conditions, there are very many in which abrupt changes in form occur, and these can cause the same effect as notches (holes, grooves, keyways, blowholes, etc.). Now, what is the reason for such brittleness and why does it not manifest itself in other types of test?

Before answering this question let us consider the conditions that differentiate the impact test of notched samples from the static test, namely, the notch and the high speed.

As shown by Ludwik,³⁷ during any plastic deformation the presence of a notch causes a special state of stress in the vicinity of the notch. In addition to the fundamental tensile stress caused by the external forces, there arise two other main tensile stresses representing the reaction of masses in the specimen not participating in the deformation but located in its vicinity. According to the hypothesis of maximum shear stress, the resistance to deformation is determined by the maximum difference of the principal stresses; therefore the presence of a special state of stress is accompanied to a certain extent by a rise of the stress diagram for the material at the base of the notch.

The speed, as was seen above, affects the stress-strain diagram of the tension in the same way—by further increasing the strength at a given deformation.

Referring to Fig. 5, let the curve AB represent the actual tensile stress (i.e., the stress as referred to the actual area of the cross-section and not to the original area, as it is usually assumed). The instant of rupture is determined by intersection of this curve with another curve CB , the ordinates of which represent the actual strength of the material in various states of cold working.

³⁷ P. Ludwik, *Zeit. für Metallkunde*, vol. 16 (1924), p. 207.

Unfortunately, we do not know the actual shape of this curve, and can only conjecture it, although recently Kuntze,³⁸ using results of tests, has determined a number of points thereon.

On the basis of certain known facts and by theoretical reasoning it is safe to assume that the location of the curve CB , which depends only on molecular attraction, is neither affected by speed nor by the special state of stress (and even if this should be the case, it would have but little effect as regards the rise of the curve). Then, due to notch action and speed, the curve AB will rise to the position $A'B'$, curve CB remaining fixed, and continue rising until at a certain critical instant point A of the curve reaches the point C . After this brittle rupture occurs, because the strength in shear will be greater than the strength in tension.

It is clear now how the simultaneous action of speed and notch will cause brittle rupture of a material which is entirely ductile when undergoing the usual tests. Soft steel (iron) behaves in this way as a result of improper heat treatment (coarse-grained, overburning³⁹), and chrome-nickel steel at a certain stage of annealing.⁴⁰

Variation in the conditions of the test (sharpness and depth of the notch, speed of the impact, temperature) will cause the same material to rupture sometimes as a brittle and sometimes as a ductile material. It is possible under given test conditions for two materials to prove equally ductile, while under more severe conditions one of them will experience brittle rupture and the other not. As a basis upon which to form an opinion regarding the tendency of a metal to brittle-rupture, it is necessary to carry out a series of tests in which one of the factors affecting the rupture is varied.

The most convenient procedure is to use the temperature of the test as the variable parameter. While temperature has not as yet been mentioned as a factor, nevertheless it is responsible for the location of the curve $A'B'$ (Fig. 5). According to Schmid and Polanyi⁹ the dependence of the stress-strain diagram on temperature is an established fact and appears to be the fundamental reason for introducing the term "thermal plasticity." It is to be expected that with a lowering of the temperature the curve $A'B'$ will rise, and for materials which at room temperature are characterized by a ductile rupture, brittleness will appear at some lower temperature. Indeed, testing at varying temperatures gives a curve of the form qualitatively shown in Fig. 6 and having a more or less sharply defined "critical temperature range"—which is steep for a steel of low carbon content and flatter for carbon and special steels.⁴¹

Fig. 7 shows the curves obtained in the author's laboratory⁴² for two specimens of the same boiler plate (carbon = 0.10 per cent): curve I was obtained after a standard heat treatment and curve II after an artificial overheating (two hours at 1200 C). It is seen that the overheating and the resulting coarse-grained structure displace the "critical range" toward the range of higher temperatures, in this case of room temperatures. The position of the critical range appears to be the best criterion for the tendency of the material to brittleness.

If the idea advanced concerning the effect of the notch is correct, then brittle rupture must occur also under conditions when one of the factors is excluded—for instance, speed or notch—and the third one, temperature, is simultaneously increased. Indeed the author succeeded in obtaining, for the same

boiler plate, brittle rupture of a cylindrical specimen (Fig. 8) on a pendulum testing machine. A similar exhibition of brittleness was observed by Sauerwald⁴³ in monocrystal iron, which ruptured without deformation under impact at 98 C. Schwinning and Matthes,²⁶ on the other hand, used a notched specimen and replaced the impact test by a static one, obtaining also a brittle rupture, of course with a corresponding decrease in temperature (of the order of 30 deg). Speed alone, however, is sufficient only in the case of materials exceptionally inclined to brittleness—for instance, phosphorus iron containing more than 0.25 per cent phosphorus undergoes brittle rupture in impact tests of cylindrical samples at room temperature. Such materials, according to the old terminology, are said to be brittle in impact, although the

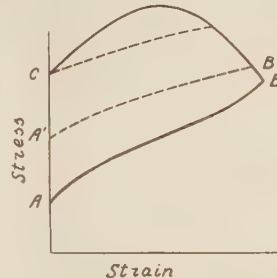


FIG. 5 SCHEMATIC STRESS-STRAIN DIAGRAM UNDER IMPACT

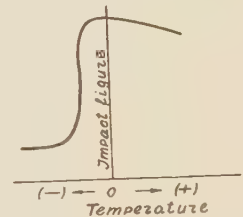


FIG. 6 RELATION UNDER IMPACT OF DUCTILITY TO TEMPERATURE

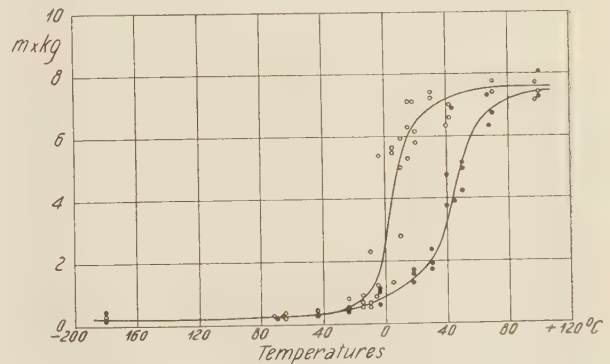


FIG. 7 CURVES SHOWING DUCTILITY OF STANDARD AND OVERHEATED BOILER PLATE UNDER IMPACT: RUPTURE OF NOTCHED SPECIMENS

brittleness is, as we see, rather a state than a property of the material.

Fortunately for practical work, not all materials exhibit impact brittleness at low temperatures (cold rupture). Up to date the latter has been observed practically only in the case of iron and its alloys (excluding such materials as zinc and bismuth, which are used very little in industry). It has not yet been found whether this is a general peculiarity of the given type of the crystal lattice-work of the material⁴⁴ or a property of a definite chemical element. Whatever it may be, neither copper, brass, nor aluminum and its alloys exhibit phenomena of cold rupture.⁴⁴ On the contrary, duralumin⁴⁵ shows at lower temperatures only increased ductility. Obviously, for these materials the lowering of the temperature (and the equivalent increase in speed) raises the yield point and generally the strength in a smaller degree than the increase of

³⁸ W. Kuntze, Sonderheft 20, deutsche Materialprüfungsanstalt, 1932.

³⁹ F. Körber and A. Pomp, Mitt. K.-W. Inst. für Eisenforschung, vol. 6 (1925), p. 33.

⁴⁰ N. Davidenkoff and Zaitzeff, Journal of Technical Physics, vol. 2, 1932, no. 5, p. 477 (in Russian).

⁴¹ F. Fettweis, Stahl u. Eisen, 1929, Heft 45.

⁴² By F. Witman.

⁴³ F. Sauerwald, B. Schmidt, and G. Kröner, Zeit. für Physik, vol. 67 (1931), p. 179.

⁴⁴ P. Schoenmaker, First communication, NIATM, 1930A, p. 243.

⁴⁵ W. Guldner, Zeit. für Metallkunde, vol. 22 (1930), pp. 240 and 412.

strength in rupture. This has been confirmed by static observations.⁴⁶

5—PRACTICAL SIGNIFICANCE OF IMPACT TESTS

From the foregoing considerations it is clear that the impact test of notched specimens, in spite of its necessity (at least for ferrous metals), does not afford results having any relation to the magnitude of the allowable stresses and should be used only for purposes of checking;⁴⁷ it may either reject the material, or approve it for use under stresses allowable with static loading.

The establishment of conditions for the rejection or approval of material requires careful preliminary study of the material and working conditions of the structure in which it is to be used. Only a few general considerations have been presented here.

Obviously, the matter must be decided by the position of the critical range of cold rupture. Therefore the impact test cannot be satisfied by any single factor (type of sample, speed, and

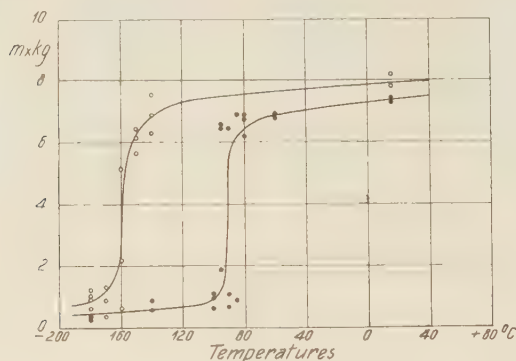


FIG. 8 CURVES SHOWING DUCTILITY OF STANDARD AND OVERHEATED BOILER PLATE UNDER IMPACT: RUPTURE OF SPECIMENS WITHOUT NOTCHES

temperature of test), or even by two of them, as proposed by Moser;⁴⁸ it must give the whole curve of the dependence, of the type indicated above, on the temperature. This of course introduces considerable complication into the impact test, and prohibits the employment of such tests in industry.

Perhaps in the future we shall learn how to determine in a reliable way the actual strength in rupture of a cold specimen and its yield point in impact at room temperature, raised by the influence of the notch; then, by introducing a definite ratio by which the first value exceeds the second one, we shall be enabled to ascertain the minimum tendency for brittle rupture. As long as this is not possible, as is generally admitted,⁴⁹ there is no other way in which to proceed but that indicated above: namely, determine the whole curve or at least a few of its most characteristic points.

In order to set standard conditions for the test, it is necessary to consider the dependence of the temperature of cold rupture on the form of the notch, determining the gradient of the stresses and, consequently, the degree of progress of the special state of stress. Obviously the most severe conditions of the test result from using that notch which causes for the same material the highest temperature of the critical range; therefore it is desirable to base the selection of the standard sample upon a comparison of the critical temperatures given by various notches. According to a proposal by the author, material is to be prepared in this way for standardizing of the impact test at the NATI⁵⁰ in Moscow.

⁴⁶ P. Goerens, R. Mailänder, Forschungsarbeiten, V.D.I., no. 295, p. 18.

⁴⁷ R. Greaves, First communication, NIATM, 1930A, p. 225.

⁴⁸ R. Moser, *Stahl u. Eisen*, vol. 43 (1923), p. 935.

⁴⁹ F. I. Werkstoffhandbuch, *Stahl u. Eisen*, 1927, D-1 (F. Fettweis).

⁵⁰ Institute for Scientific Research in Automobiles and Tractors.

Under such circumstances, we can be sure that worse conditions do not occur in actual service of the structure.

In stating the concrete requirement as to the position of the critical range, there appear to be no difficulties when the interval is sharply defined and does not exceed 20 to 40 deg C, as in the case of steel of low carbon content. In such cases it is sufficient to state that the beginning of the drop in impact ductility shall not be lower than 20 to 40 deg C (depending on the temperature conditions of the structure); the exact form of the notch will then appear as an assurance of a certain amount of ductility.

More doubt will exist in those cases where the critical range is not distinctly defined, having an amplitude of the order of 200–300 deg (chrome-nickel steel), the drop in ductility beginning at a temperature considerably higher than that of the room (80–100 °C). Here, obviously, it is not possible to exclude the structure from service in the range of initial brittleness. The question might easily arise: Is it not necessary to diminish the allowable stress in the ratio of the decrease of the impact ductility at the temperature of the structure in service as compared with the maximum value? Such a procedure, however, would not be correct. The experimental data available⁵¹ show that a decrease in the energy of deformation at a lowering of temperature occurs on account of the decrease in extension, and not on account of the strength of material, which remains approximately constant; therefore, in assuming equal allowable stresses there is no decrease in the factor of safety. Only the degree of ductility drops, and if this drop is not large (say, 10 per cent), then it is a matter of judgment of the designer whether such a drop is admissible or not. A necessary condition for its admissibility is the evidence given by the diagram of the test, that the drop in ductility occurs in a sufficiently slow manner and that complete brittleness occurs only at the lowest temperatures.

6—CONCLUSIONS

Summarizing the considerations already stated, we arrive at the following conclusions:

1 The yield point and tensile strength of a material under impact are always higher than those at low-speed tests, the yield point rising more rapidly than the strength.

2 The working conditions of the material under impact are less favorable than those under static action of a force.

3 As far as these two circumstances compensate each other, it is recommended that in calculations for impact the same allowable working stresses be used as for static conditions, employing the data obtained in static tests. (Neglecting, however, consideration of the reliability of the calculations.)

4 The impact test for notched specimens can be used only as a check test, approving the use of a material or rejecting it; in determining the allowable stresses to employ, however, the results of such tests are of no value.

Discussion

E. DILLON SMITH.⁵² There are certain data in the paper that seem to offer promise of revealing new truths about impact. The author's symposium is the expression of thought of the impact workers of European origin. The writer will try to bring out certain thoughts not mentioned by the author, as well as to present a critical review of some of the data and expressions in the paper.

Should not the conception of impact be based on the fundamental relation of force? This relation is:

⁵¹ W. Schwinning and K. Matthes, footnote 26; see also that the diagrams of the static tests are the more reliable ones.

⁵² Special Instructor, School of Technology, College of the City of New York, New York, N. Y.

$$F = M\alpha \dots \dots \dots [1]$$

In this, it would seem evident that the force is dependent upon the deceleration of the hammer (tup or bullet). An example of this idea may be given in the following manner. A common hammer is allowed to strike a steel beam. The hammer hits the beam with a velocity of 200 ft per sec, the hammer weighing 1.93 lb. Further, let us assume that the hammer will come to rest within 0.001 sec, which is not at all improbable, and in fact might come to rest in a much shorter time. The deceleration of the hammer may be a maximum at 200,000 ft per sec per sec. Substituting, in [1], we have $F = (1.93/32.2) 200,000 = 12,000$ lb.

If the assumption of a shorter time had been taken for the hammer to decelerate, it would be evident that this impact force is considerably greater than that just given. Further, place the force value computed by [1] upon this beam as a static load of 12,000 lb. Certainly we can conclude that the effects of the impact and the static forces are not the same.

The rapidity of the application of the force imparted by the hammer and the inertia of the beam will produce effects that will be varied. The result will be further qualified depending on the load being applied at a rate greater or less than the natural period of the specimen under observation.

Taking an average value from Table 1, we learn that a beam withstanding an impact loading (how determined, the author fails to mention) of 15,583 lb will not fail unless a static load of 10,000 lb is exceeded. Would not a moment's thought indicate that this condition is not valid for all cases, depending on the speed of the application of this 15,583 lb, the inertia, and the period of the beam?

Tables 1 and 2 also have been examined as to the agreement of the results secured by the different investigators. Although "the numerical results of Table 1 are valid," that is no indication that such numerical results are a correct measure of the specific phenomenon being studied. The results shown in this table are found to be homogeneous, or within highly significant agreement, although the author seems to question them. The commensurate data of Table 2 are also homogeneous; however, there is reason to believe that more data are needed to indicate that they are as significant as those data listed in Table 1.

Figs. 7 and 8 are to be questioned from the standpoint of general theory. Especially in Fig. 8, it seems illogical to connect the upper and lower sections of the dots with vertical lines, as is shown. One reason for this disagreement is based upon the writer's Fig. 9 for quartz piezoelectric crystals. (Although, for this case, tuned oscillatory circuits are one explanation; but, notwithstanding, there is a change due to temperature shift.) The ordinate has been translated to a function of impact loading. Another reason for the writer's disagreement to the treatment of data in this manner is that most generally reaction and growth curves follow some definite law. Fig. 7 follows a natural change by a law controlled by a mathematical logistic curve. But, in the case of Fig. 8, it would seem that there are two different and distinct changes in the state of the boiler plate—that there are two growth curves of the logistic type.

Referring to the two methods of determining impact forces, there are certain facts that should be mentioned about the schemes. Under class 1 the author mentions that considerable error is present when graphic means of double differentiation are resorted to for obtaining the acceleration curve from the space-time curve. The United States Bureau of Public Roads seems to have concluded differently.⁵³ But if this is not satisfactory enough, why not revert to a translation of the space-time curve

into a mathematical equation and then take the second derivative? At the same time it is possible to compute the error in any series or equation by which we wish to express the observed condition. The success of this method rests with one's ability to select the relation that most nearly fits the space-time curve plotted by the hammer.

As an example of this mathematical method, assume that the space-time curve is a straight line (which it is not—always being of second degree or higher, but its trend at certain sections can be shown linearly), and let us investigate the error

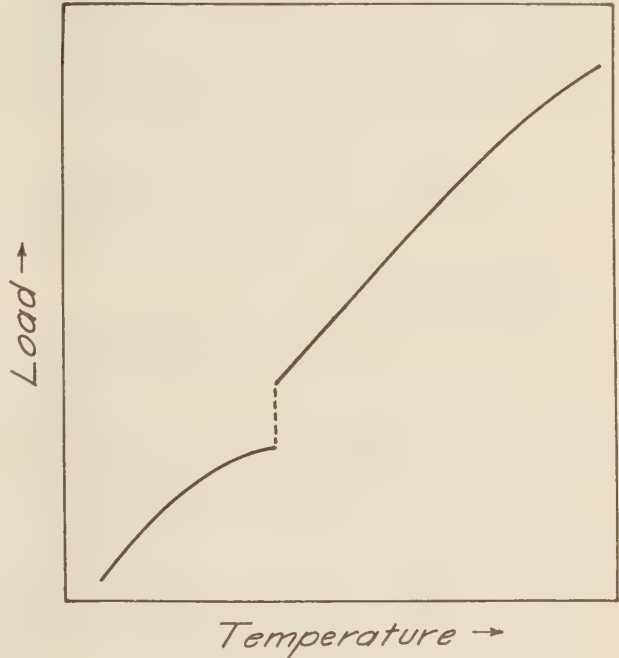


FIG. 9 EFFECT OF TEMPERATURE ON DAMPED OSCILLATIONS IN A QUARTZ PIEZOELECTRIC CRYSTAL

possible, based on the error of the operator in taking the comparator readings from the plotted curve.

The standard error of the straight line

$$f(x) \equiv y = a + bx \dots \dots \dots [2]$$

becomes

$$\sigma_f = \epsilon \left\{ [a_1^2] \left(\frac{\partial f}{\partial a} \right)^2 + [b_1^2] \left(\frac{\partial f}{\partial b} \right)^2 + 2[a_1 b_1] \left(\frac{\partial f}{\partial a} \frac{\partial f}{\partial b} \right) \right\}^{\frac{1}{2}} \dots [3]$$

The partial derivatives are

$$\frac{\partial f}{\partial a} = 1, \quad \frac{\partial f}{\partial b} = x$$

Now since we can take the origin at the middle of the range of the curve of x , $[a_1 b_1] = 0$. Substituting, we obtain the hyperbola

$$\sigma_f = \epsilon \left\{ [a_1^2] + [b_1^2] x^2 \right\}^{\frac{1}{2}} = \left\{ \sigma_a^2 + \sigma_b^2 x^2 \right\}^{\frac{1}{2}} \dots \dots [4]$$

Where

$$[a_1^2] = \frac{\Sigma x^2}{n \Sigma x^2} = \frac{1}{n} \dots \dots \dots [5]$$

$$[b_1^2] = \frac{n}{n \Sigma x^2} = \frac{1}{\Sigma x^2} = \frac{1}{n \sigma x^2} \dots \dots \dots [6]$$

⁵³ Smith, E. B., "Impact Tests of Road Materials, Symposium on Impact Testing of Materials," Proc. A.S.T.M., vol. 22, pp. 74-77 1922.

and where

$$\epsilon = \left(\frac{\sum (y - y')^2}{n - 1} \right)^{\frac{1}{2}} \dots \dots \dots [7]$$

for our specific case; y being the observed reading and y' the computed or mean value at that same value of x ; n is the total number of readings observed.

This can be shown graphically, as given in Fig. 10. Also, the results of a parabola, treated similarly, are shown in this same Fig. 10. In the case of the example cited, it is noticed that the error is the least at the point most concerned in our investigation, the point of maximum acceleration.

The difference or the tangential method of obtaining the results graphically seems to be as reliable as any mathematical method, and often better when only a few cases are to be studied; as the

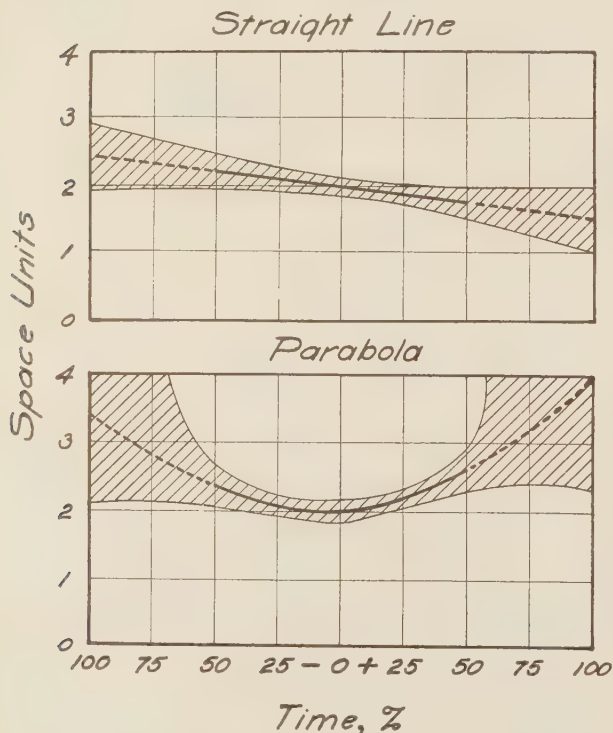


FIG. 10 THE STANDARD ERROR OF COMPARISONS AND EXTRAPOLATIONS OF THE STRAIGHT LINE AND PARABOLA FITTED TO THE SAME DATA

(Area shaded represents $f(x) \pm 2\sigma$, within which 95 per cent of the data will be distributed. Time is in terms of per cent of the observed or comparator readings. The dotted line is the extrapolation of the curves.)

evaluation of the constants in the mathematical equations is rather a long job. Since a certain fact has been mentioned about class 1, let us turn attention to class 2.

In the case of the self-recording dynamometer, the piezoelectric cell and the cathode-ray oscillograph device have been described. The writer does heartily agree that the author has a most excellent basic set-up for the measurement of impact directly, but he has not carried this idea far enough, nor does it seem that this device will be able to give data on impact when impact forces delivered by the hammer are above those forces at which the piezoelectric crystal will rupture. The rupture of the crystal will occur before the rupture of an iron or steel specimen. It is interesting to note that reference 34 in *Z.V.D.I.* uses this same idea for tool loads, but the loads are not severe enough to rupture

the crystal. Of course, below this point of rupture of the crystal possibly excellent data should be secured.

For quartz crystals we find that

$$de = kV \dots \dots \dots [8]$$

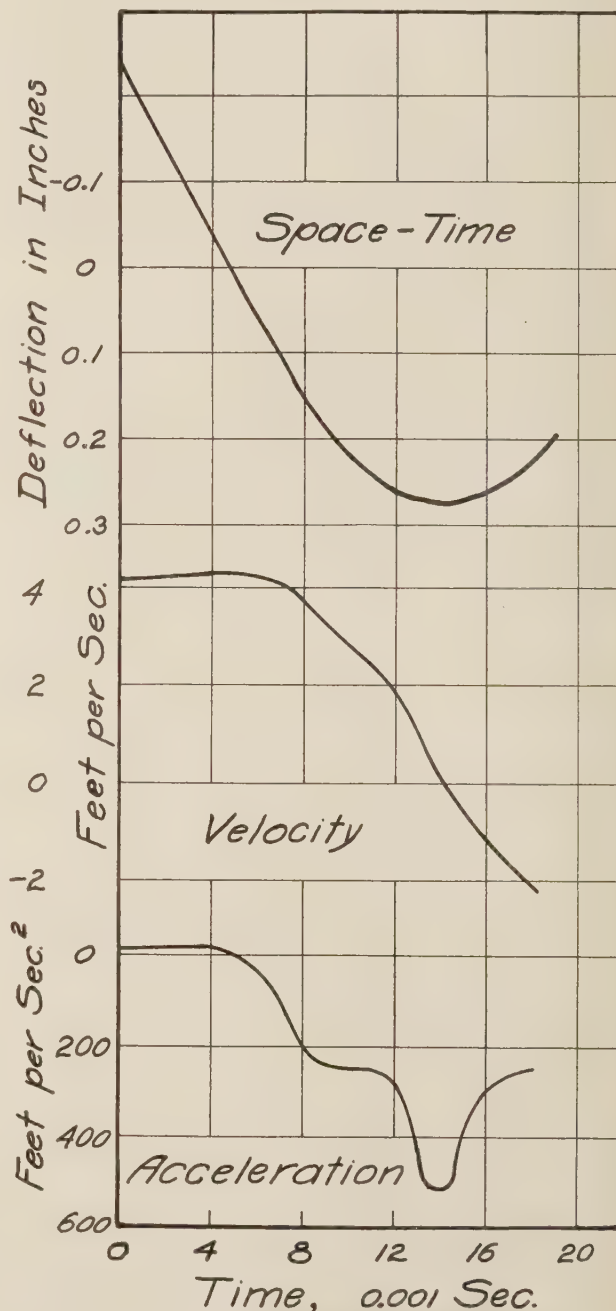


FIG. 11 SPACE-TIME AND DERIVED CURVES

where the differential of elongation varies as the change in the developed voltage upon its proper faces, being a maximum for the x or perpendicular cut. That being the case, the voltage developed by the external forces upon the crystal give a direct measure of the force applied. This has been shown in Fig. 4 as the ordinate. Incidentally, these photos are not those given by a

cathode-ray oscillograph; unless the beam is deflected in only one plane and recorded on a passing film, which is not customary.

It is noticed that these photos are not analyzed in this paper. Before they may be analyzed, calibration of the device is necessary. How does the author propose to calibrate his device? May the writer suggest that in reality the author has only one fundamental method—that of taking an autographic space-time curve of the hammer at the same time the oscillograph records the developed voltage from the crystal. But this is practicable only for impact forces less than the rupture point of the crystal.

It would seem that "an additional 'coefficient of uncertainty'" would not be required if the impact research is carried on under a proper scientific method and employing its best tools.

Perhaps it would be interesting to inspect a curve illustrating these things. Such a space-time and derived curves are shown in Fig. 11. A 34-lb hammer has fallen 3 in. on a $\frac{7}{8}$ -in. by $\frac{7}{8}$ -in. by 30-in. steel beam to record these data. It will be seen that the striking velocity of the hammer was 4.35 ft per sec with a maximum deceleration of 512 ft per sec per sec, with a deflection of a maximum of 0.270 in. Computation gives an impact force of 540 lb hitting the beam. In this particular case, a numerically equal static force would produce a deflection of approximately 20 per cent less.

R. V. SOUTHWELL.⁵⁴ Professor Timoshenko gave an account, with illustrative diagrams, of work conducted recently at the University of Oxford, England, by Mr. J. H. Lavery in collaboration with Prof. R. V. Southwell. This work was based upon two underlying ideas: First, that the stress distribution imposed by tests of the Izod and Charpy types is too complex to be estimated by theory, and involves an undesirably large amount of plastic distortion in regions not immediately adjacent to the surface of fracture; second, that machines which employ a rigid pendulum can transmit waves of stress away from the machine and to "earth," and energy so transmitted is included (incorrectly) in the estimated "work of fracture."

The first of these contentions is illustrated by Figs. 12a

⁵⁴ Professor of Engineering Science, Oxford University, Oxford, England.

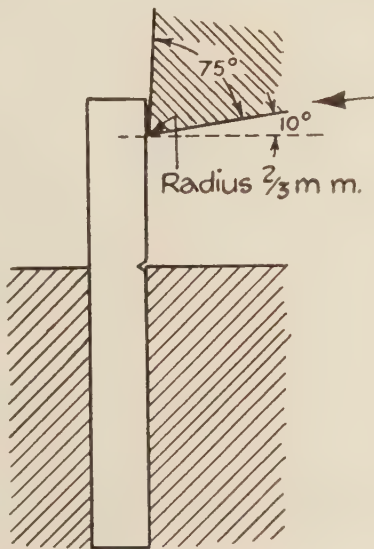


FIG. 12a

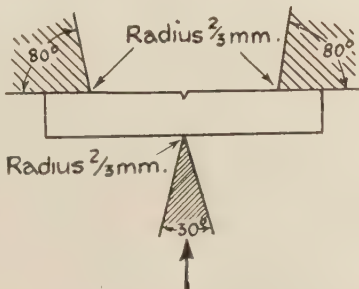


FIG. 12b

and b, and Fig. 13 shows the specimen and method of loading which has been adopted at Oxford. A hardened yoke transmits the blow of the hammer to the specimen, which accordingly is subjected to "four-point loading,"—i.e., to a uniform bending action (unaccompanied by shear) in the region adjoining the notched section. On account of the large bearing areas, there is little or no penetration, and no appreciable plastic distortion is involved,

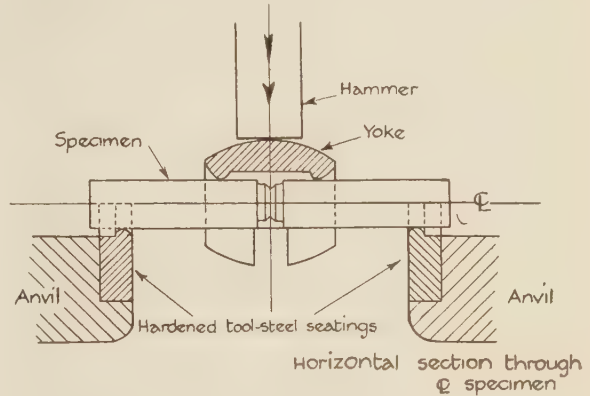


FIG. 13

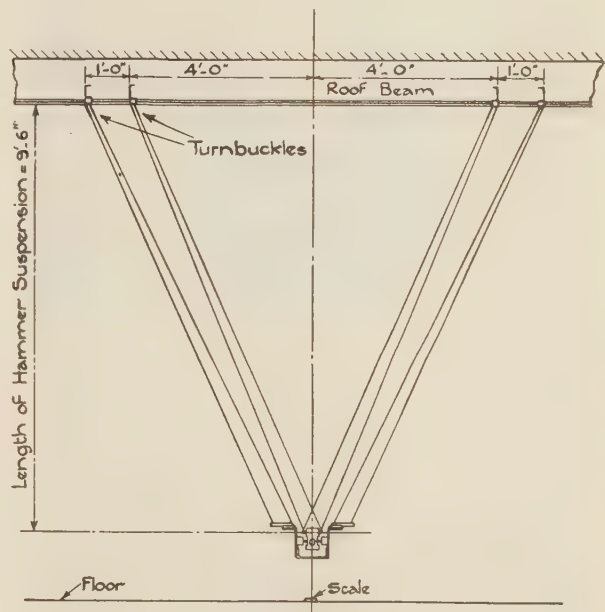


FIG. 14

except at the actual surface of separation. The specimen can be formed entirely in the lathe, since the "notch" is a concentric groove, and accordingly it is cheap to manufacture.

The objection made to machines of the rigid-pendulum type is obviated in the Oxford machine by suspending both "hammer" and "anvil" on flexible cords so that they can move without rotation. The blow occurs at the center of gravity of anvil, hammer, and specimen, and in a direction perpendicular to the cords; thus no energy can escape from the machine, and the energy involved in stress waves (which will be of the longitudinal type) is very small because the stresses are low. Figs. 14 and 15 illustrate the construction of the machine, and Fig. 16 is a photograph of the hammer, anvil, and specimen.

Comparative tests were made, using exactly the same shape of

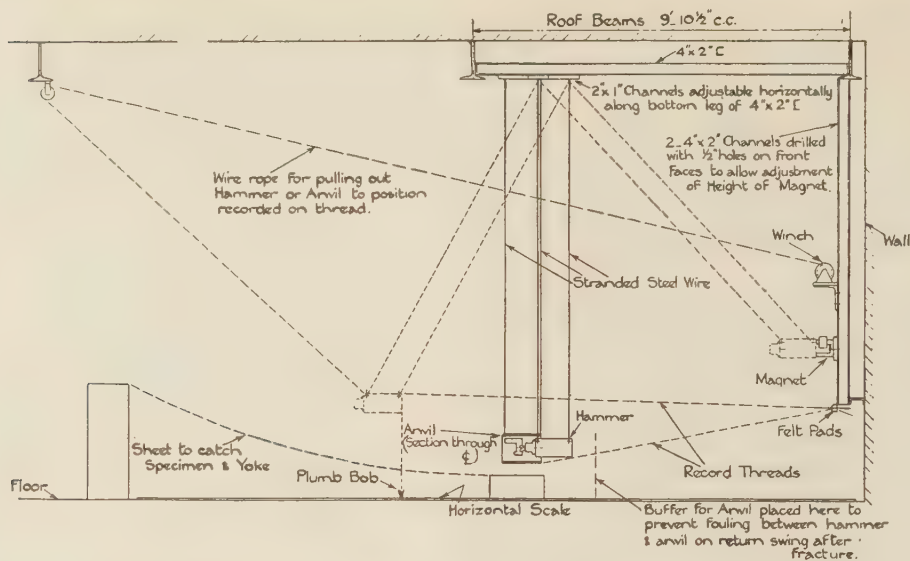


FIG. 15

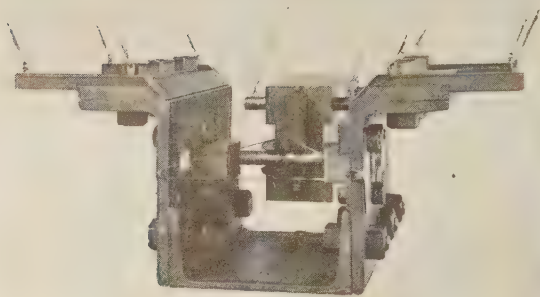


FIG. 16

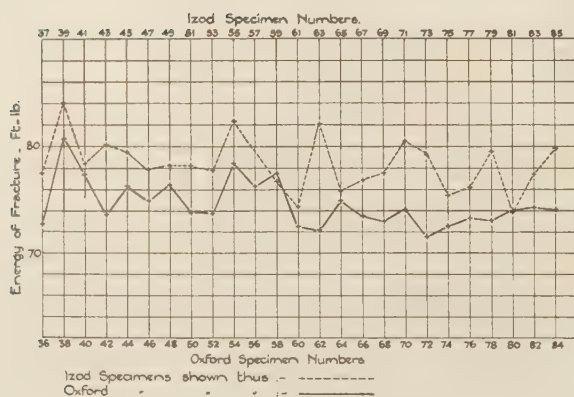


FIG. 17

specimen and method of loading, both in the Oxford machine and in a standard Izod machine suitably modified and provided with devices to permit specially exact measurement. Fig. 17 shows the results obtained with a nickel-chrome-molybdenum steel, in 50 tests made from material of a single batch, specimens being tested in the two machines alternately. The uniformity of the results is thought to be satisfactory, and a consistently lower

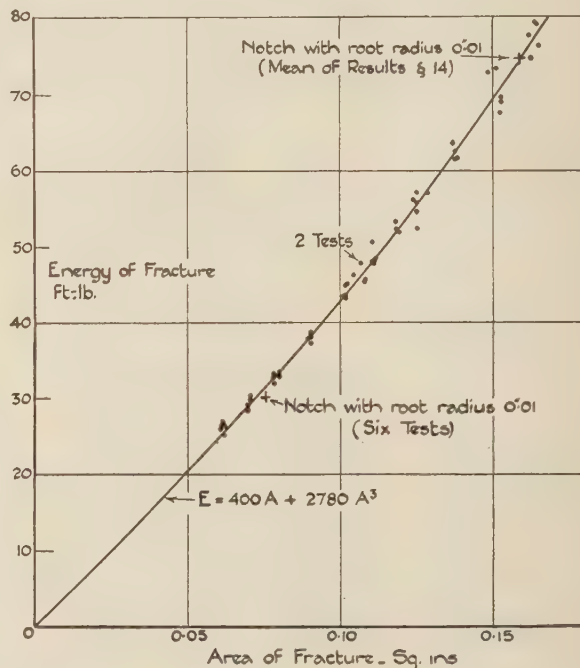


FIG. 18

figure for the work of fracture is obtained in the Oxford machine, as would be expected if the contention is correct that energy transmitted to earth has been wrongly included in the Izod figures.

Fig. 18 exhibits the results of 59 tests made on specimens having different areas under the notch, but otherwise identical. The work of fracture is closely proportional to the area of fracture. This result is explained by the concentration of plastic distortion within the material which immediately adjoins the fracture. It is thought that the slight rise of the curve (with increasing area) can be explained, and the results are evidently indicative of a satisfactory dimensional law.

These 59 tests relate to specimens made with as sharp a notch

as possible. On the same diagram are shown (by two crosses) results obtained from specimens made with a notch of 0.01 in. "root radius," but otherwise similar. It appears that the work of fracture is not sensitive to small variations in the "root radius," so that ordinary errors of workmanship will not have important consequences. This result is of course important from a practical standpoint.

MASON A. STONE.⁵⁵ In view of the difficulties in determining the stresses occurring under impact which the author discusses in section 1 of the paper, his conclusion in section 6, paragraph 1, which summarizes the figures in Table 1, are very comforting to designers who have to provide for impact. The paper is valuable not only for its content but for the bibliography of references to its subject contained in the footnotes—which the writer would have welcomed some five years ago when called upon to design a two-story outdoor switching station with the oil circuit breakers carried on the upper floor.

At this time the only discussion of a beam to carry a transverse impact load which he was able to find was in Merriman's "Mechanics of Materials" (page 335 of the 1906 edition). As the footnotes do not give many references to the subject matter of section 1, either to the dynamic or empirical method, and as the latter may turn out to be a very poor guess indeed, perhaps an outline of methods followed and results obtained in the design of a typical floor beam and girder of this switching station may be in order. It will serve to illustrate the practical advantages in the assumption of a high working stress in the design of beams under transverse loading and the dangers of trying to provide for impact by the addition of an arbitrary percentage to the static load.

The manufacturers of the circuit breakers advised us to provide for an impact load from the operation of the breakers under a short circuit equal to that which would result from the fall of twice the weight of the breaker (exclusive of the frame) through 2 in. This weight was 17,900 lb. Obviously, a blow of 6000 ft-lb on a floor system made up of beams of 20-ft span (necessitated by clearances) was not to be taken care of by this addition of "25 per cent for impact."

For a simple beam struck in the middle by a falling load P , Merriman derives the formula for the resulting maximum fiber stress T :

$$T = S + S(1 + 2\eta h/f)^{1/2}$$

where S = maximum fiber stress from static load

h = height through which load falls

f = deflection, caused by static load

η = the inertia coefficient.

The value of η for a beam with a concentrated impact load at the center is shown to be

$$\eta = \frac{1 + \frac{17}{35} W/P}{1 + \frac{5}{8} W/P}$$

in which W = weight of beam

P = weight of falling body.

These values are only valid for a simple beam struck at the middle, as they depend upon the form of the deflection curve and the velocity of the beam at the load after impact. The formulas are developed upon the assumption that the shape of the elastic curve is the same for impact as for static loading.

The breaker was carried upon a frame standing upon four legs, which were carried upon two floor beams 20 ft long. The length of the breaker was 13 ft 4 in. Besides the loading from the breaker, the floor beams were designed for the load from a floor panel 6 ft 4 in. wide of 4 1/2-in. concrete and a snow load of 25 lb per sq ft.

The value of η for a beam carrying two loads equidistant from the ends one-sixth the length of the beam was determined to be 0.69. After trying several sections, a Carnegie 14-in. 85-lb I-beam was finally decided upon.

The following fiber stresses were obtained: From the dead load of the breaker, 2130 lb per sq in.; from the dead load of beam, slab, and snow, 2600 lb per sq in.; from impact, 19,000 lb per sq in.; total combined stresses, 23,700 lb per sq in.

The impact stresses in this case amounted to four times those from the quiescent dead and live loads.

Inasmuch as these stresses occurred only for an instant, it was considered justifiable to adopt the practise generally followed in the case of stresses from wind load of adding 50 per cent to the allowable fiber stress of 16,000 lb per sq in.

The assumption of a high permissible fiber stress is desirable, because the usual expedient to deepening the beam to reduce stresses does not work out very well in the case of impact. A stiffer beam may result in higher fiber stresses. This was discovered many years ago when the experiment of deepening the rail section was followed by an increase in the number of broken rails in service. In designing beams for impact, therefore, flexibility rather than stiffness is desirable. This may be obtained by the use of cover plates so applied that the fiber stresses are approximately constant throughout the length of the beam, as a beam of uniform cross-section may have twice the stiffness of a beam of cross-section varied so that the fiber stress is constant throughout.

This may be illustrated by the design of the girders into which the floor beams framed. A 24-in. 110-lb Carnegie I-beam 23 ft 0 in. long was first tried, which gave a stress from impact alone of 25,200 lb per sq in. The girder finally decided upon was composed of a 18-in. 86-lb Carnegie I-beam and two 12-in. by 3/8-in. cover plates 11 ft 6 in. long and two 12-in. by 3/8-in. cover plates 5 ft 9 in. long.

This resulted in a dead and live load stress of 5360 lb per sq in. and 15,500 lb per sq in. from impact, or 20,860 lb per sq in. for the combined stresses. Of course the determination of η for such a built-up section with a variation in the moment of inertia is somewhat troublesome.

The explanation of the action of the boiler plates as shown in Figs. 7 and 8 was interesting. This phenomenon is well understood by boiler makers, as a plate which is being flanged goes through a temperature range, which is known to the smiths as a "blue heat" from the color of the oxide formed on the surface of the metal, at which the plate cannot be worked because of brittleness, although ductile above and below this range.

This may be of interest to the designers of power-plant piping if superheat temperatures continue to increase.

⁵⁵ 147 Cassidy Place, Staten Island, New York N. Y.

Stability of Thin-Walled Tubes Under Torsion¹

By L. H. DONNELL,² PASADENA, CALIF.

A THEORETICAL solution is developed for the torsion on a round thin-walled tube at which the walls become unstable and buckling occurs.

S = critical shear stress, assumed uniformly distributed

E, μ = Young's modulus and Poisson's ratio (0.3 for engineering metals)

l, t, d = length, wall thickness, and diameter of the tube

$$A = (1 - \mu^2) \frac{Sl^2}{Et^3}, \quad H = \sqrt{1 - \mu^2} \frac{l^2}{td}, \quad J = \frac{1}{\sqrt{1 - \mu^2}} \frac{l^2 t}{d^3}$$

The critical stress, for short and moderately long tubes, is given by the formulas:

$$A = 4.6 + \sqrt{7.8 + 1.67 H^{3/2}} \text{ (clamped edges)}$$

$$A = 2.8 + \sqrt{2.6 + 1.40 H^{3/2}} \text{ (hinged edges)}$$

It is assumed that end cross-sections of the tube remain circular and plane, that "clamped" edges are held perpendicular to these cross-sections, while "hinged" edges are free to change their angle with the cross-sections. It is found to be immaterial whether or not the ends of the tube are free to move as a whole. The buckling deformation is found to consist of a number of circumferential waves which spiral around the tube from one end to the other. For tubes of ordinary length-diameter ratios, with clamped edges, the number of waves n and their spiral angle near the middle of the tube θ are approximately $n = 2.6 J^{-1/4}$, $\theta = 1.5 \frac{d}{l} J^{1/4}$ rad. If $J > 8$, that is for long, slim tubes, n is

always 2, and the critical stress is nearly independent of the edge conditions and is given by the formula: $A = 0.77 (l/d) \sqrt{H}$, which is nearly the same as a formula found by E. Schwerin in 1924.

To check these theoretical results the author has made more than fifty experiments; in addition, the results of fifty or sixty more experiments have been published by the N.A.C.A. and others. All available tests give values for the failure stress somewhat lower than the values for critical stress predicted by

the foregoing formulas. The experimental values average about 0.75 of the theoretical, with a minimum about 0.60 of the theoretical. These relations hold consistently over an enormous range of sizes, proportions, and materials. The form of the buckling deflection, as measured by the number and angle of the waves, is found to check closely with that predicted by the theory. It is therefore reasonable to suppose that the discrepancy between the theoretical and experimental stress is due chiefly to initial eccentricities and other defects unavoidable in an actual tube, as well as to the fact that all tests were performed with "clamped" edges, while it is well known that a perfect clamped edge is impossible to attain. By multiplying the foregoing expressions for A by the factor 0.75 or 0.60, we can obtain expressions for the average and minimum resistance to buckling to be expected from an actual tube.

In developing the theory, the assumptions are made that the material obeys Hooke's law, that the tube is exactly cylindrical, that the thickness is small compared to the radius (as it must be if buckling is to occur before failure of any available material), and that the deflections are small compared to the thickness. With these assumptions, the differential equations of equilibrium are derived in the following form:

$$\frac{t^2}{12(1 - \mu^2)} \nabla^8 w + \frac{4}{d^2} \frac{\partial^4 w}{\partial x^4} + 2 \frac{S}{E} \nabla^4 \frac{\partial^2 w}{\partial x \partial s} = 0$$

$$\frac{d}{2} \nabla^4 v = -(2 + \mu) \frac{\partial^3 w}{\partial x^2 \partial s} - \frac{\partial^3 w}{\partial s^3}$$

$$\frac{d}{2} \nabla^4 u = -\mu \frac{\partial^3 w}{\partial x^3} + \frac{\partial^3 w}{\partial x \partial s^2}$$

where $\nabla^2 = \frac{\partial^2}{\partial x^2} + \frac{\partial^2}{\partial s^2}$, x and s are axial and circumferential

coordinates, and u , v , and w are axial, circumferential, and radial components of displacement, respectively. These equations are much simpler than those usually given, chiefly because many of the items commonly taken into consideration are of negligible importance for this and many other cases, as is shown in the complete paper.

The solution obtained is an exact solution of these equations of equilibrium and of complete boundary conditions, for the two extreme cases when the length-diameter ratio is zero and infinite and is a good approximation for intermediate cases.

¹ Abstract of paper presented at the Semi-Annual Meeting, Chicago, Ill., June 26 to July 1, 1933, of THE AMERICAN SOCIETY OF MECHANICAL ENGINEERS. The complete paper is published by the National Advisory Committee for Aeronautics as Report No. 479.

² In charge of Structures Laboratory, Guggenheim Aeronautical Laboratory, California Institute of Technology. Mem. A.S.M.E.

Influence of Lashing and Centrifugal Force on Turbine-Blade Stresses

By R. P. KROON,¹ SOUTH PHILADELPHIA, PA.

This paper gives a stress analysis for rotating segments of lashed blades under a given load. By using difference calculus, results were obtained, which apply to any blade out of any number of blades.



OWING to steam forces and to centrifugal force, the turbine blades are often highly stressed; moreover, they may be subject to vibration. In order to relieve these blades, it has become customary to connect them in groups with lashing wires, shrouding strips, or similar reinforcements. These constructions stiffen the blades, and also provide damping in case of vibration.

This paper is intended as a first attempt to investigate the behavior of such rotating groups of lashed blades.

The steam load and the centrifugal force on the blades may be assumed to be known, but the magnitude of the vibration stresses (which can be predominant) depends on the impulses and the damping and can be determined only by tests.

We will limit ourselves here by assuming definite forces, equal on all the blades of the group. It will be shown that the effect of these forces is not at all equal on the individual blades of the segment; the stresses vary in a characteristic oscillating manner.

The difference calculus,² which was developed to study groups of similar objects and which has proved to be extremely useful in dealing with civil-engineering problems such as bars on many supports, built-up beams, bridges, platforms on columns, etc., can also be successfully applied to the case of lashed blades.

Before going into detail analysis, it might be worth while to give a summarized physical description of the results obtained in this paper. For simplicity we have taken blades of constant cross-section connected with one lashing wire at the tip. Furthermore, we assumed the load and the wire to be in the same plane as the maximum axis of inertia of cross-section of the blades. Without any mathematics, it can immediately be seen that the load, which is equally divided over all the blades of the group, will not impose the same stresses on all the blades; the two end blades are only supported by the lashing wire on one side of the blades; all the other blades are supported on both sides.

¹ Experimental Engineer, Westinghouse Elec. & Mfg. Co. Jun. A.S.M.E. Mr. Kroon received his technical education at the Polytechnicum of Zürich, Switzerland, from which he was graduated in 1929. In 1931, he became connected with the Westinghouse company, went through the design school for mechanical engineers, and has since been in the experimental division of the South Philadelphia Works under Mr. Ormondroyd. Working mainly on problems in dynamics and stress analysis, he is studying the behavior of turbine blades theoretically and experimentally.

² See Bleich-Melan, "Die Gewöhnlichen und partiellen Differenzgleichungen der Baustatik," Springer, Berlin, 1927.

Contributed by the Applied Mechanics Division and presented at the Semi-Annual Meeting, Chicago, Ill., June 26 to July 1, 1933, of THE AMERICAN SOCIETY OF MECHANICAL ENGINEERS.

NOTE: Statements and opinions advanced in papers are to be understood as individual expressions of their authors, and not those of the Society.

Assume, for example, a very flexible lashing wire. Then the deflection of all the blades, and especially the angle of rotation at the tip, will be practically the same for all blades. Therefore the stresses in the wire will be the same in all the sections. This, however, means that the bending moment at the tip of the end blades is only half as great as the moment at the tip of all the other blades.

The opposite effect enters for an extremely thick wire. Here the angle of rotation at all the blade tips must necessarily be zero, the bending moments at the tips of all blades are equal, but the lashing wire is much more stressed just beside the end blades than in any other place.

Using difference calculus, it is possible to find the deflection and the bending moments for any blade out of a group of any number of blades of any dimensions.

Results for a segment of six blades under stationary lateral load are shown in Figs. 6, 7, and 18a. The bending moments are plotted as a function of a dimensionless quantity λ . In this way these curves obtain universal value for all the dimensions of blade and wire which we might wish to choose (for notation see list at end of paper). In order to find the value of any bending moment shown in these figures, it is necessary to multiply the numerical value, given on the ordinate axis, with $I_s E_b \varphi_0 / l$. As φ_0 is the angle of rotation which would exist at the blade tip for the same loading without lashing wire, $I_s E_b \varphi_0 / l$ can be looked upon as a "fundamental bending moment."

The maximum stress reduction which can be achieved by a single lashing wire is 33.3 per cent for uniformly distributed load and 50 per cent for a load concentrated at the tip.

The centrifugal force, apart from producing tensile stresses in the blades, plays an important role in reducing the bending stresses set up by the steam load as it tends to bend the blades back in their neutral position. A differential equation can be derived for the general case of blades with variable cross-section. Correction factors, taking into account the effect of the centrifugal force on single blades with various kinds of loading, may be found in Figs. 9, 10, and 11. They are given in function of k , which is a dimensionless parameter, proportional with the centrifugal force (see list of notations). The effect of the centrifugal force on bending stresses in long tapered low-pressure blades is enormous; it was found that a bending moment 1, applied at the tip of a 40-in. blade, produces a bending moment of only $1/30$ at the base.

The effect of centrifugal force on laterally loaded blades, lashed together in a segment, is shown in Figs. 12, 13, 14, and 18b. The maximum values of the bending moments in the group are given.

Another problem dealt with is the effect of the centrifugal force on the wire (no load on blades). The resulting forces and bending moments are shown in Figs. 15, 16, 17, and 18c. These values can again be slightly corrected by taking into account the centrifugal force acting on the blades.

The final picture of the stress distribution over a group of rotary blades under lateral load is obtained by superposition; a specific example is shown in Fig. 18d.

1—LASHING ON STATIONARY BLADES WITH LATERAL LOAD

As a first problem, let us investigate the influence of lashing on a group of stationary blades with steady load.

(a) *Segment of Three Blades; No Centrifugal Force.* As the most elementary interesting case take a group of three blades, equally loaded by lateral forces. At the point of intersection of blade and lashing wire we will assume all possible moments and forces (Figs. 1 and 2).

Using the notation listed at the end of this paper, we have for symmetry reasons:

$$\varphi_1 = \varphi_3, M_1 = M_3, M_1'' = M_3', M_2'' = M_2', \\ S_1 = S_3, T_1 = -T_3, T_2 = 0$$

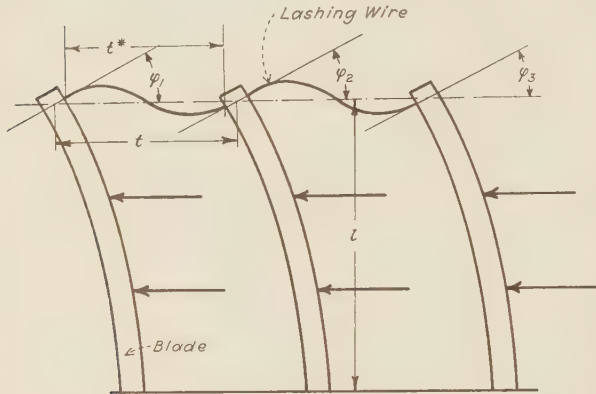


FIG. 1 THREE BLADES UNDER LATERAL LOAD

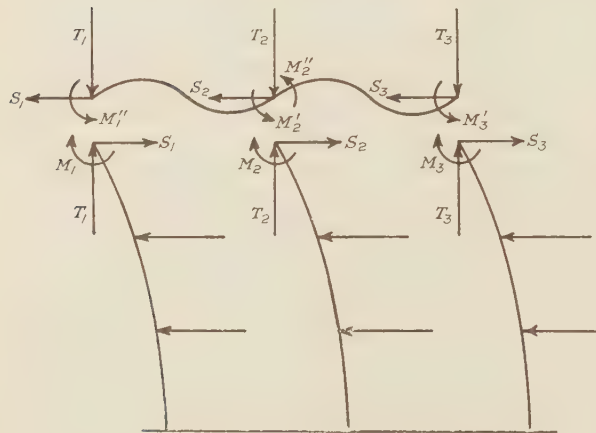


FIG. 2 REACTION FORCES ON LOADED SEGMENT

Furthermore, equilibrium conditions give:

$$M_1'' = M_1, M_3' = M_3, M_2' + M_2'' = M_2 \\ S_1 + S_2 + S_3 = 0 \quad -T_1 t^* = M_1 + (M_2/2)$$

This simplifies the picture of the reaction forces on the lashing wire to what is shown in Fig. 3.

The deformations can now be expressed as functions of the moments and forces. Tension, compression, and shear deformations are neglected. Using simple beam formulas,³ we have for the lashing wire:

$$\frac{-M_1 t^{*2}}{6 I_b E_b} + \frac{M_2 t^{*2}}{6 I_b E_b} = t \varphi_2 \dots \dots \dots [1]$$

$$\frac{-M_2 t^{*2}}{12 I_b E_b} + \frac{M_1 t^{*2}}{3 I_b E_b} = t \varphi_1 \dots \dots \dots [2]$$

³ See Timoshenko and Lessells, "Applied Elasticity," p. 74.

The angle of deflection which would exist at the blade tip for the same loading without a lashing wire will be designated as φ_0 . Then, for the lashed group:

$$(M_1 + S_1 l/2) \frac{l}{I_b E_b} = \varphi_0 - \varphi_1 \dots \dots \dots [3]$$

$$(M_2 - S_1 l) \frac{2}{I_b E_b} = \varphi_0 - \varphi_2 \dots \dots \dots [4]$$

As the elongation of the lashing wire may be neglected compared with the deformations caused by bending, the tip deflection of each blade has to be the same:

$$\frac{M_1}{2} + \frac{S_1 l}{3} = \frac{M_2}{2} - \frac{2 S_1 l}{3} \dots \dots \dots [5]$$

The Equations [1], [2], [3], [4], and [5] are sufficient to determine the quantities M_1 , M_2 , S_1 , φ_1 , and φ_2 .

Putting $\lambda = \frac{t^{*2} I_b E_b}{u I_s E_s}$, we find:

$$M_1 = \frac{6\lambda + 6}{\lambda^2 + 9\lambda + 6} \frac{I_b E_b \varphi_0}{l}; \quad M_2 = \frac{12\lambda + 6}{\lambda^2 + 9\lambda + 6} \frac{I_b E_b \varphi_0}{l}$$

$$S_1 l = \frac{3\lambda}{\lambda^2 + 9\lambda + 6} \frac{E_s I_s \varphi_0}{l}; \quad -S_2 l = \frac{6\lambda}{\lambda^2 + 9\lambda + 6} \frac{I_b E_b \varphi_0}{l}$$

$$\varphi_1 = \frac{\lambda(\lambda + 1/2)}{\lambda^2 + 9\lambda + 6} \varphi_0 \quad \varphi_2 = \frac{\lambda^2}{\lambda^2 + 9\lambda + 6} \varphi_0$$

The factor $I_b E_b \varphi_0 / l$ is a bending moment, depending on the distribution of the load and on the length of the blade only.

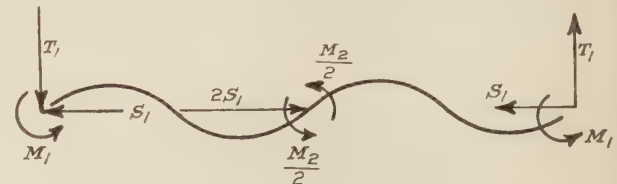


FIG. 3 GROUP OF THREE BLADES; REACTIONS ON LASHING

The λ is a dimensionless quantity, inherent with this problem. It takes into account the ratio of the flexibilities of blade and wire. By plotting the curves for moments, forces, tip angles, etc., as a function of λ , these curves obtain universal value for all the dimensions of blade and wire we might wish to choose. $\lambda = 0$ means a 100 per cent stiff wire; $\lambda = \infty$ represents an infinitely thin wire.

The stress distribution along the lashing wire does not depend on the way in which the blades are loaded (all quantities contain φ_0).

As Fig. 4 shows, the bending moment at the tip has for an infinitely stiff wire the same value for inner and outer blades; with a very thin wire the inner blade tip carries twice the stress of the outer ones. A 100 per cent stiff lashing wire gives at the outer blades a lashing-wire stress twice as high as at the inner blades. Decreasing the wire diameter within the practical range (up to $\lambda = 23.4$) increases the bending stress in the wire.

As can be seen from this simple example, there are for a group of three blades already 13 quantities involved—namely, two bending moments, two forces, and one angle at the tip of the middle blade, and one bending moment, two forces, and one angle at the tip of each end blade. By using conditions of symmetry and equilibrium, these 13 quantities could be reduced to 5, but still it is obvious that to analyze in this way a group of six or

more blades with 28 or more variables is a somewhat burdensome task.

It is for purpose of this kind that the difference calculus has proved to be very effective. In contrast to differential calculus it studies the changes of functions for finite constant increments of the variables. Applied to our case, it makes it possible to obtain stresses and deflections for any blade out of a group of any number of blades.

(b) *Any Number of Blades; No Centrifugal Force.* Suppose we have n blades and consider the i^{th} blade and its neighbors (Fig. 5). Again using simple beam formulas, we find for the deformation of the lashing wire between the i^{th} and the $(i+1)^{\text{th}}$ blade:

$$M_{i''} = \frac{2I_b E_b l}{t^{*2}} (2\varphi_i + \varphi_{i+1}) \dots \dots \dots [1']$$

Also, between the i^{th} and the $(i-1)^{\text{th}}$ blade:

$$M_{i'} = \frac{2I_b E_b l}{t^{*2}} (2\varphi_i + \varphi_{i-1}) \dots \dots \dots [2']$$

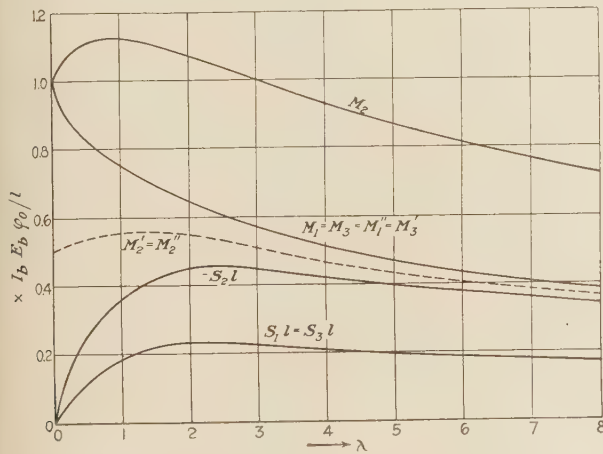


FIG. 4 BENDING MOMENTS AND SHEARING FORCES ON A SEGMENT OF THREE BLADES; LATERAL LOAD ONLY

The tip deflection of all blades is the same, and we can write:

$$\frac{S_i l^3}{3I_b E_b} + \frac{M_i l^2}{2I_b E_b} = C l \dots \dots \dots [5']$$

where C is a constant yet to be determined.

The tip angle of blade number i is then:

$$\varphi_i = \varphi_0 - \frac{M_i l}{I_b E_b} - \frac{S_i l^2}{2I_b E_b} = \varphi_0 - \frac{3}{2} C - \frac{M_i l}{4I_b E_b} \dots \dots [3']$$

For equilibrium of the connecting point of blade and wire we have the condition:

$$-M_{i'} - M_{i''} + M_i = 0 \dots \dots \dots [4']$$

This set of equations leads to:

$$\varphi_{i-1} + (4 + 2\lambda)\varphi_i + \varphi_{i+1} = \lambda(2\varphi_0 - 3C) \dots \dots [6]$$

where λ is again $\frac{t^{*2} I_b E_b}{4I_s E_s}$

Equation [6] establishes a relation between the values of the function φ at adjacent points with definite intervals; such a

relation is called a "difference equation." There are many types of these equations, and for some of these the solutions are known. Equation [6] is a "linear" difference equation, and the solution can be proved to be:

$$\varphi_i = A\beta^i + \frac{B}{\beta^i} + \frac{\lambda(2\varphi_0 - 3C)}{6 + 2\lambda} \dots \dots \dots [6']$$

where $\beta = -(\lambda + 2) + \sqrt{(\lambda + 2)^2 + 4\lambda + 3}$ = small negative number. A and B are constants which have yet to be found.

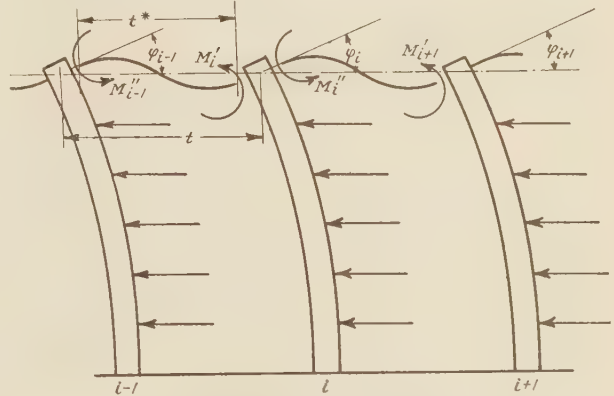


FIG. 5 THREE BLADES OF A LARGER GROUP

For symmetry reasons: $\varphi_i = \varphi_{n+1-i}$, so that [6'] becomes:

$$\varphi_i = A(\beta^i + \beta^{n+1-i}) + \frac{\lambda(2\varphi_0 - 3C)}{6 + 2\lambda}$$

The constants A and C are determined by the end condition

$$M_{i'} = 0 \therefore (2 + 2\lambda)\varphi_1 + \varphi_2 = \lambda(2\varphi_0 - 3C)$$

(compare [4'] and [6]), and by the condition of equilibrium for the wire:

$$\sum_{i=1}^{i=n} S_i = 0, \text{ which, in view of [5'] and [3'], can also be written:}$$

$$\sum_{i=1}^{i=n} (2C - \varphi_0 + \varphi_i) = 0$$

Thus, after neglecting high powers of β we finally arrive at the formulas:

Tip angle of deflection:

$$\varphi_i = \frac{\varphi_0}{D} \left(\beta^{i-1} + \beta^{n-i} + \frac{2 + 2\lambda + \beta}{3} \right)$$

Tip bending moment:

$$M_i = \frac{4I_b E_b \varphi_0}{Dl} \left(-\beta^{i-1} - \beta^{n-i} + \frac{2 + 2\lambda + \beta}{\lambda} \right)$$

Bending moment in wire left of blade:

$$M_{i'} = \frac{2I_b E_b \varphi_0}{\lambda D l} (2\beta^{i-1} + 2\beta^{n-i} + \beta^{i-2} + \beta^{n-i+1} + 2 + 2\lambda + \beta)$$

Bending moment in wire right of blade:

$$M_i'' = \frac{2I_b E_b \varphi_0}{\lambda D l} (2\beta^{i-1} + 2\beta^n - i + \beta^i + \beta^n - i - 1 + 2 + 2\lambda + \beta)$$

Lateral force on tip:

$$S_1 = \frac{6I_b E_b \varphi_0}{D l^2} \left(\beta^{i-1} + \beta^n - i - \frac{2}{n(1-\beta)} \right)$$

Bending moment at root:

$$M_i^* = M_0^* - \frac{2I_b E_b \varphi_0}{D l} \left(\beta^{i-1} + \beta^n - i + \frac{4 + 4\lambda + 2\beta}{\lambda} - \frac{6}{n(1-\beta)} \right)$$

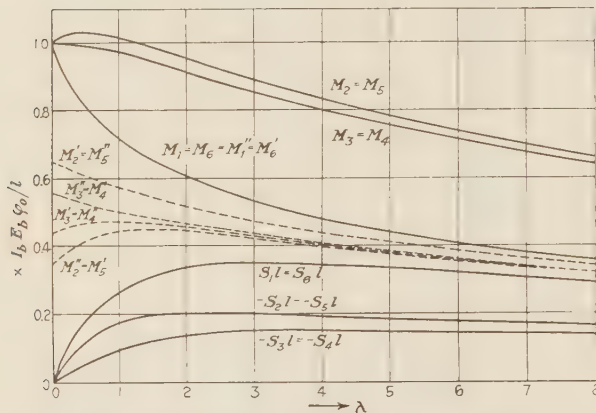


FIG. 6 BENDING MOMENTS AND FORCES ON A SEGMENT OF SIX BLADES; LATERAL LOAD ONLY

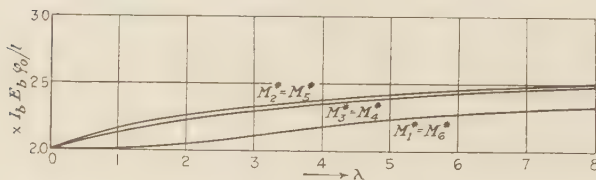


FIG. 7 ROOT BENDING MOMENTS FOR A GROUP OF SIX BLADES UNDER UNIFORMLY DISTRIBUTED LOAD

For notation see list at the end of this paper.

Calculations were made for a segment of six blades, and the results are shown in Figs. 6 and 7.

As may be concluded from the curves, the highest stress in the lashing wire is just beside the first and the last blade.

The second and the fifth blades have the greatest bending moment at the tip as well as at the root.

The weaker the lashing wire, the more variation between the values of the bending moments on the blades; the stronger the wire, the more difference between the values of the stresses in the wire sections. At the end blades the lashing wire and the blade tip carry the same bending moment. The bending stress at the root of the blade is for uniformly distributed load at least two times as high as the stress at the blade tip.

The maximum stress reduction which can be achieved by introducing a single lashing wire is 33.3 per cent for uniformly distributed load, and 50 per cent for a single force at each blade tip.

It was found that although the stresses in the individual blades vary a great deal, the deflections are almost identical for all the blades of the group. This suggested that under vibration the stress distribution around the lashing wire would be almost the same as under steady load.

E. Schwerin⁴ studied the vibration of single lashed blades. A comparison between his calculations and these shows that the stress distribution during vibration (first mode) can be simulated by steady load so closely that the difference is only about 1 per cent. This is of great value for experimental work (Table 1).

TABLE 1 COMPARISON BETWEEN THE STRESSES SET UP DURING VIBRATION AND THOSE PRODUCED BY STEADY LOAD (The table gives ratios between individual values and value for center blades $\lambda = 0.4$. n = total number of blades = 20. i = number of individual blade)

i	M vibrating	M steady	M' vibrating	M' steady	M'' vibrating	M'' steady
1	0.852	0.845	0	0	1.704	1.690
2	1.033	1.034	1.221	1.218	0.844	0.850
3	0.994	0.993	0.952	0.952	1.035	1.033
4	1.002	1.002	1.010	1.013	0.994	0.991
5	0.999	0.999	0.997	0.997	1.002	1.002
6-10	1	1	1	1	1	1

2—THE INFLUENCE OF CENTRIFUGAL FORCE ON BLADES WITH LATERAL LOAD

The centrifugal force reduces the deflection and the bending stress of radial beams with lateral load. Consider the case where a blade of variable cross-section but not "twisted" (the unbent axis of the blade being a radial line), is loaded by all kinds of bending forces, which are supposed to act in one of the principal planes of cross-section. When ξ is the variable distance from the tip, we may have bending moments M_ξ , lateral forces S_ξ , distributed load q_ξ , and centrifugal load p_ξ (per unit length). At a distance x from the tip, the variable moment of inertia will be called I_x and the deflection y_x (Fig. 8). The direction of the centrifugal force is taken parallel to the axis of the blade.

Assuming the simple beam theory to be correct, the bending moment at x will be:

$$I_x E_b \frac{d^2 y_x}{dx^2} = \int_{\xi=0}^{\xi=x} q_\xi (x-\xi) d\xi - \int_{\xi=0}^{\xi=x} p_\xi (y_\xi - y_x) d\xi + \sum_{\xi=0}^{\xi=x} \left\{ M_\xi + S_\xi (x-\xi) \right\}$$

Differentiating with respect to x , we get:

$$I_x E_b \frac{d^3 y_x}{dx^3} + E_b \frac{d^2 y_x}{dx^2} \frac{d I_x}{dx} = \int_{\xi=0}^{\xi=x} q_\xi d\xi + \frac{d y_x}{dx} \int_{\xi=0}^{\xi=x} p_\xi d\xi + \sum_{\xi=0}^{\xi=x} S_\xi$$

which is nothing else than the expression for the shearing force at x , consisting of a part

$$Q_x = \int_{\xi=0}^{\xi=x} q_\xi d\xi + \sum_{\xi=0}^{\xi=x} S_\xi$$

due to lateral load and a component

$$\frac{d y_x}{dx} P_x = \frac{d y_x}{dx} \int_{\xi=0}^{\xi=x} p_\xi d\xi$$

⁴ Zeitschrift für Technische Physik, no. 8, 1927.

from the centrifugal force. We write:

$$\frac{dM}{dx} = I_x E_b \frac{d^3 y_x}{dx^3} + E_b \frac{d^2 y_x}{dx^2} \frac{dI_x}{dx} = Q_x + P_x \frac{dy_x}{dx} \dots [7]$$

or putting $\frac{dy_x}{dx} = v$, this becomes:

$$\frac{dM}{dx} = Q_x + P_x v \dots [7a]$$

while

$$M = I_x E_b \frac{dv}{dx} \dots [7b]$$

Numerical and graphical methods exist for the solution of these simultaneous equations. As they are linear, it follows that the principle of superposition may be applied; during rotation the stresses (deflections) caused by several lateral forces can be found by considering each force alone and superimposing the obtained stresses (deflections).

Application to Constant Section Blades. In this case $I_x = I_b = \text{constant}$, and p_x will also be taken as a constant p . We will furthermore restrict ourselves to a uniformly distributed load q per unit length, a shearing force S , and a bending moment

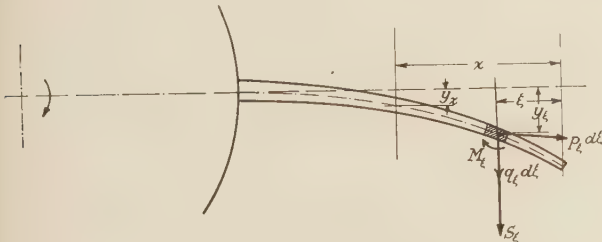


FIG. 8 INFLUENCE OF CENTRIFUGAL FORCE ON BLADE

M . S and M are acting at the blade tip. We have, then, for Equation [7]:

$$I_b E_b \frac{d^3 y_x}{dx^3} = qx + S + px \frac{dy_x}{dx} \dots [7']$$

or when we call $q + p \frac{dy_x}{dx} = u$:

$$\frac{I_b E_b}{p} \frac{d^3 u}{dx^3} = ux + S \dots [7'']$$

Defining $\frac{I_b E_b}{p} = a^3$ and introducing $\frac{x}{a} = z$, this reduces to

$$\frac{d^3 u}{dz^3} = uz + \frac{S}{a} \dots [8]$$

The exact solution of [8] leads to a cylinder function of the $1/3$ order, but by means of a power series the equation can be easily solved. This is carried out in the Appendix.

As a result, ratios between the bending stress (deflection) during rotation and the stress (deflection) when standing still have been established. Fig. 9 shows these ratios for a distributed load, Fig. 10 shows curves for a bending moment at the tip, and Fig. 11 gives curves for a shearing force at the tip.

The ratios are plotted as function of a dimensionless variable $k = \frac{pl^3}{I_b E_b}$ and are universal for all blade dimensions.

In practice, values of k up to 3 and higher are common, and

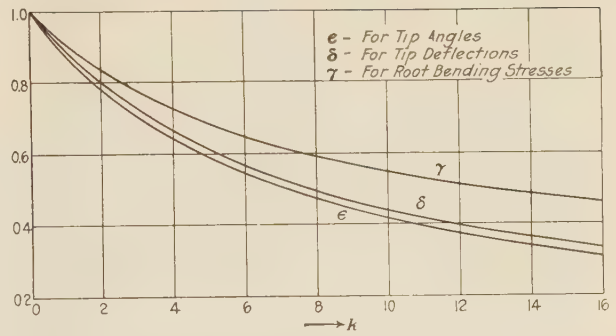


FIG. 9 CORRECTION FACTORS, TAKING INTO ACCOUNT THE EFFECT OF CENTRIFUGAL FORCE ON A BLADE WITH UNIFORMLY DISTRIBUTED LOAD

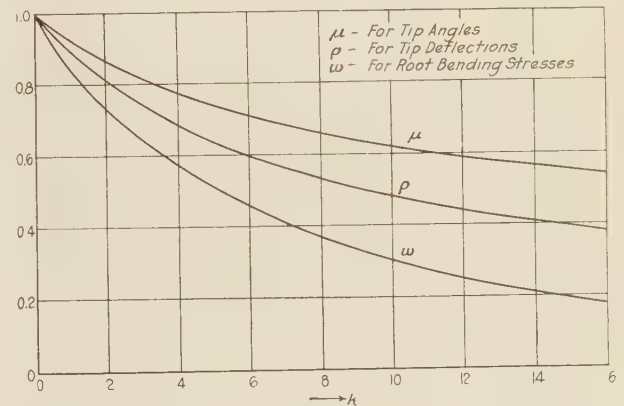


FIG. 10 CORRECTION FACTORS, TAKING INTO ACCOUNT THE EFFECT OF CENTRIFUGAL FORCE ON A BLADE WITH A BENDING MOMENT AT THE TIP

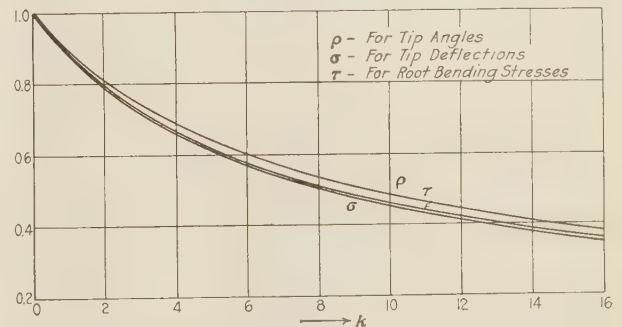


FIG. 11 CORRECTION FACTORS, TAKING INTO ACCOUNT THE EFFECT OF CENTRIFUGAL FORCE ON A BLADE WITH A LATERAL FORCE AT THE TIP

the reduction in bending stress may amount to 25 per cent or more for ordinary constant section blades.

3—LASHED BLADES UNDER BENDING LOAD; CENTRIFUGAL FORCE ON BLADES ONLY

Under Section 1 the influence of lashing on stationary blades was investigated, and under Section 2 we developed correction factors taking into account the effect of centrifugal force on blades with various kinds of leading. With these preliminaries, it is possible to compute stresses and deflections of centrifugally and laterally loaded lashed blades. Calculations were made for a

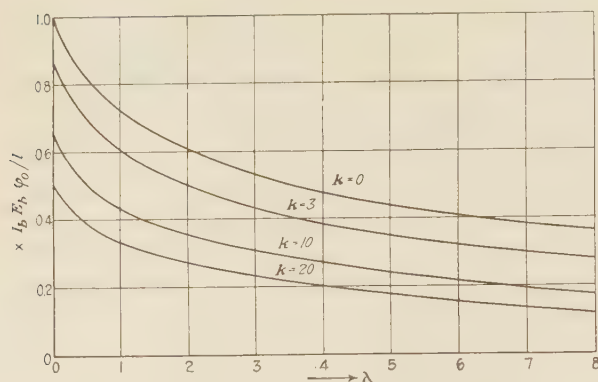


FIG. 12 GREATEST VALUE OF THE BENDING MOMENT IN THE LASHING WIRE FOR DIFFERENT VALUES OF THE CENTRIFUGAL FORCE (ACTING ON THE BLADE ONLY)

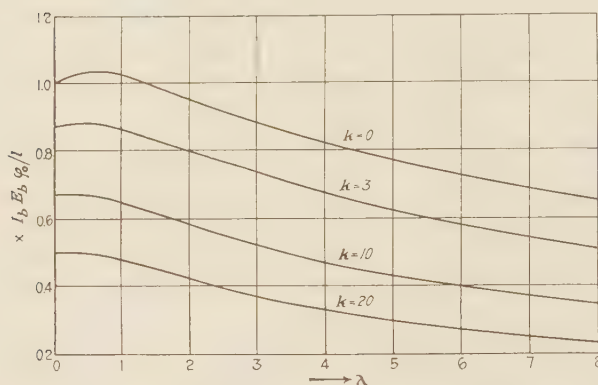


FIG. 13 MAXIMUM VALUE OF THE BENDING MOMENT AT THE BLADE TIP FOR SEVERAL VALUES OF THE CENTRIFUGAL FORCE (ACTING ON THE BLADES ONLY)

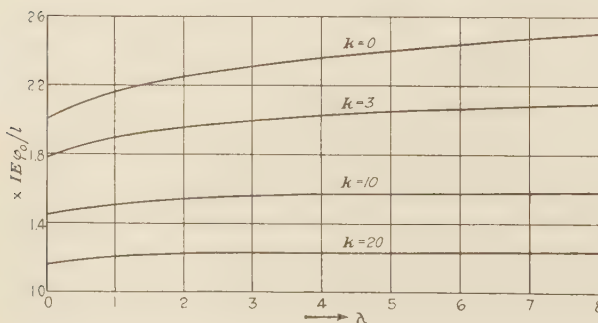


FIG. 14 GREATEST VALUE OF THE BENDING MOMENT AT THE ROOT FOR DIFFERENT VALUES OF THE CENTRIFUGAL FORCE (ACTING ON THE BLADE ONLY); UNIFORMLY DISTRIBUTED STEAM LOAD

segment of six blades, and the maximum bending moment in blades and wire was plotted as a function of the "ratio of flexibility" λ (Figs. 12, 13, and 14). This was done for different values of the factor k , which is directly proportional to the centrifugal force.

4—CENTRIFUGAL FORCE ACTING ON THE WIRE ONLY; THE BLADES ARE NOT LOADED

The case can again be worked out by difference calculus, and the results apply to any particular blade out of a segment of any number of blades. We have the difference equation:

$$\varphi_{i-1} + (4 + 2\lambda)\varphi_i + \varphi_{i+1} = 0$$

Observing boundary conditions and neglecting high powers of β leads to:

$$\varphi_i = \frac{-p^* t^{*4}}{24 I_s E_s t} \frac{(\beta^i - \beta^{n-i+1})}{1 + 2\beta}$$

$$M_i = \frac{p^* t^{*2} \lambda}{6(1 + 2\beta)} (\beta^i - \beta^{n-i+1}) \quad M_i^* = \frac{M_i}{2}$$

$$M_i' = \frac{p^* t^{*2}}{12} \left(1 - \frac{2\beta^i - 2\beta^{n+1-i} + \beta^{i-1} - \beta^{n+2-i}}{1 + 2\beta} \right)$$

$$M_i'' = \frac{p^* t^{*2}}{12} \left(-1 - \frac{2\beta^i - 2\beta^{n+1-i} + \beta^{i+1} - \beta^{n-i}}{1 + 2\beta} \right)$$

$$1 < i < n : T_i = p^* t^* \left(1 - \frac{\beta^{i-1} - \beta^{i+1} + \beta^{n-i} - \beta^{n+2-i}}{4(1 + 2\beta)} \right)$$

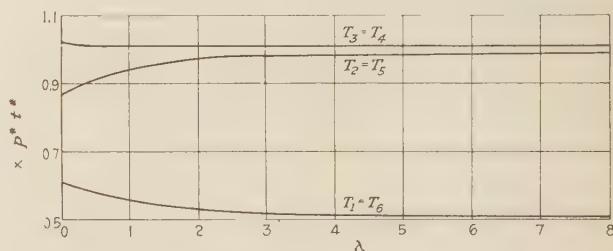


FIG. 15 PULL ON BLADES BY CENTRIFUGAL FORCE ON WIRE

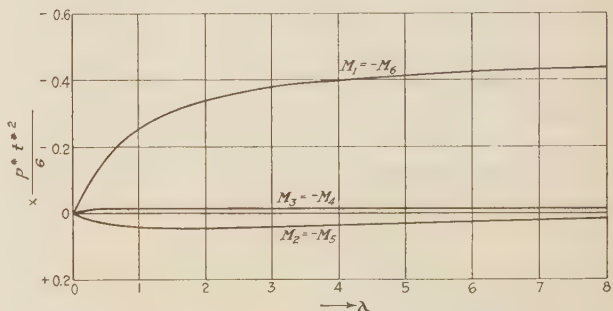


FIG. 16 BENDING MOMENTS ON BLADE TIPS DUE TO CENTRIFUGAL FORCE ON LASHING WIRE

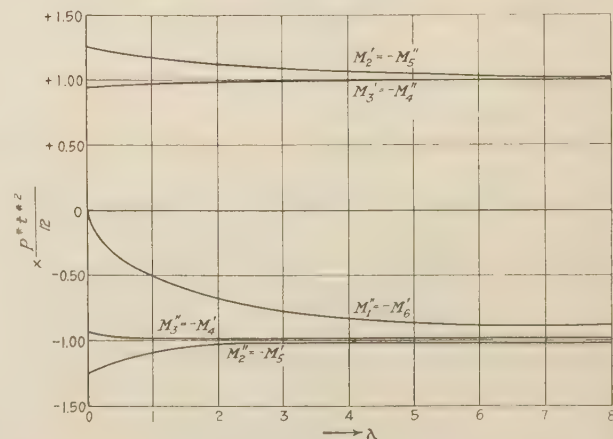


FIG. 17 BENDING MOMENTS IN LASHING WIRE DUE TO CENTRIFUGAL FORCE ON WIRE

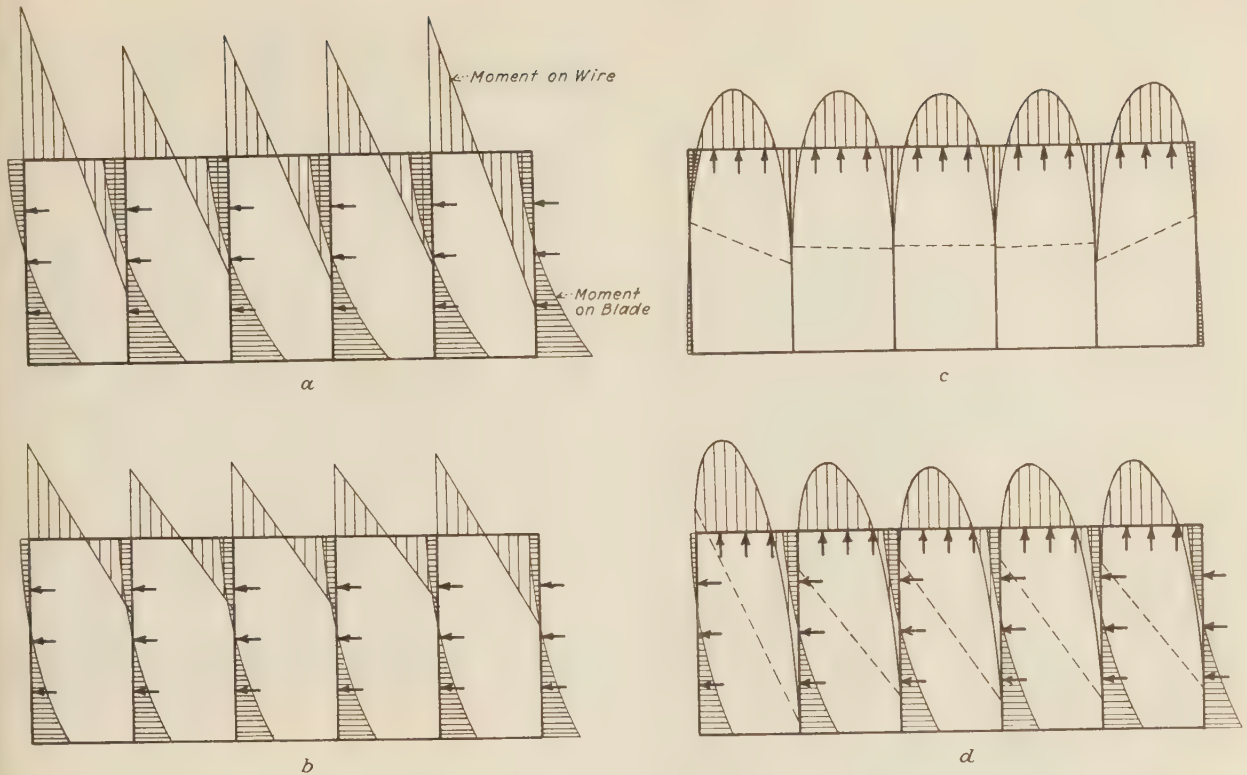


FIG. 18 BENDING MOMENTS FOR BLADES AND WIRE

(a, lateral load only; b, lateral load and centrifugal force on blades; c, centrifugal force on blades and wire; d, lateral load on blades, centrifugal force on blades and wire. Scale for moments on blades = 5 × scale for moments on wire.)

$$i = 1, i = n : T = p^* l^* \left(\frac{1}{2} + \frac{\beta^i + \beta^{i+1} - \beta^n - \beta^{n+1-i}}{4(1 + 2\beta)} \right)$$

These values are plotted again as a function of λ for a group of six blades (Figs. 15, 16, and 17). The bending stresses set up in the wire by centrifugal force are considerable for high speeds and large blade pitch.

5—CENTRIFUGAL FORCE ON LASHING WIRE AND BLADES; NO LATERAL LOAD ON BLADES

In Section 4 we gave results obtained for centrifugal force acting on the lashing wire only. It can be shown that the influence of centrifugal force on the blade can easily be taken into account by replacing λ by $\lambda^* = \frac{\lambda}{4\mu - \frac{3\rho^2}{\sigma}}$ where μ , ρ , and σ

are correcting factors shown in Figs. 10 and 11. The value of β in the expressions corresponds now also to λ^* and not to λ . With these modifications, the formulas developed in Section 4 may readily be used except for the bending moment M_1^* at the root, which is now:

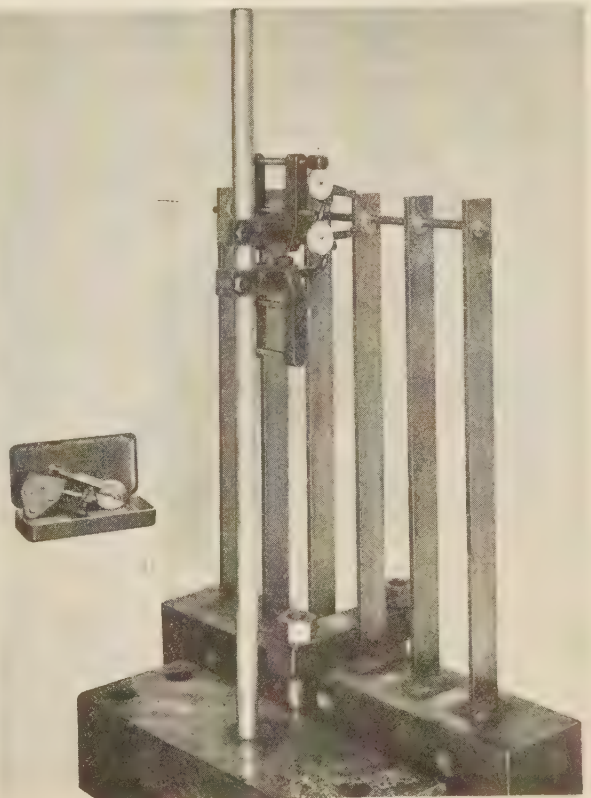
$$M_1^* = M_1 \left(-\omega + \frac{3}{2} \frac{\rho r}{\sigma} \right)$$

6—FINAL DISTRIBUTION

Actually, blades and lashing wire are subject to centrifugal forces and there is a steam load on the blade.

To give a complete picture of the distribution of the bending stresses, we have to superimpose the cases of Sections 3 and 5.

FIG. 19 MEASURING DEFLECTION AND TIP ANGLES
(Curvature instrument also shown.)



An example was worked out with the values:

$$\lambda = 1.84 \quad k = 10 \quad \frac{p^* l^2}{12} = 20 \text{ lb-in.} \quad \frac{IE\varphi_0}{l} = 50 \text{ lb-in.}$$

Fig. 18 illustrates the distribution of the bending moments along wire and blades for the following cases:

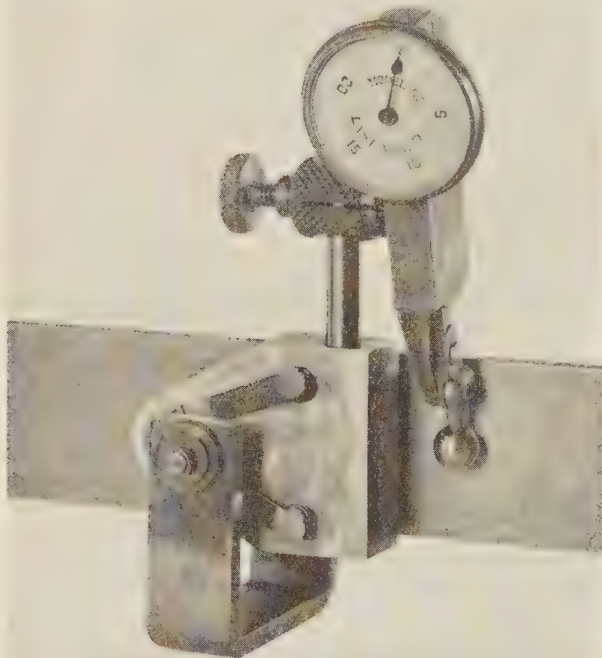


FIG. 20 CURVATURE INSTRUMENT ATTACHED TO TEST PIECE

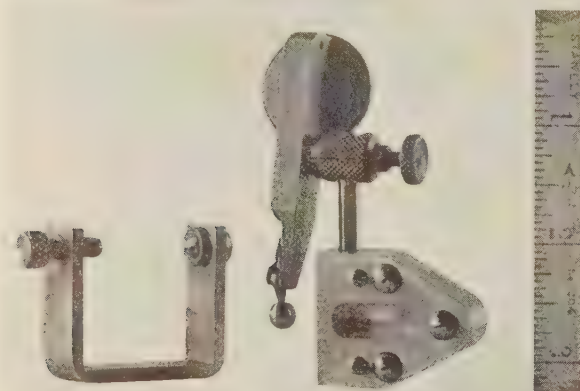


FIG. 21 CURVATURE INSTRUMENT WITH CLAMP

- (a) Blades under uniformly distributed load. No centrifugal force
- (b) Blades under lateral load. Centrifugal force on blades only
- (c) Centrifugal force on blades and wire. No lateral load
- (d) Actual case: a blade group under steam load and centrifugal force. This figure is obtained by a superposition of (b) and (c).

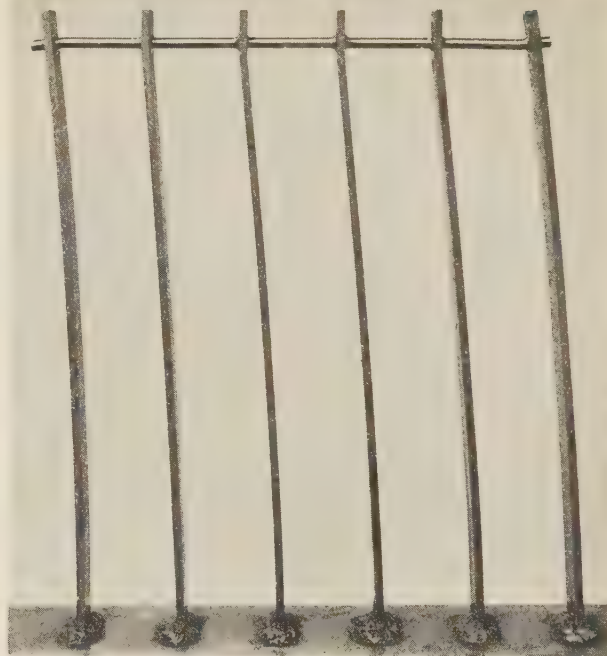


FIG. 22 MODEL OF BLADE SEGMENT WITH PERMANENT SET

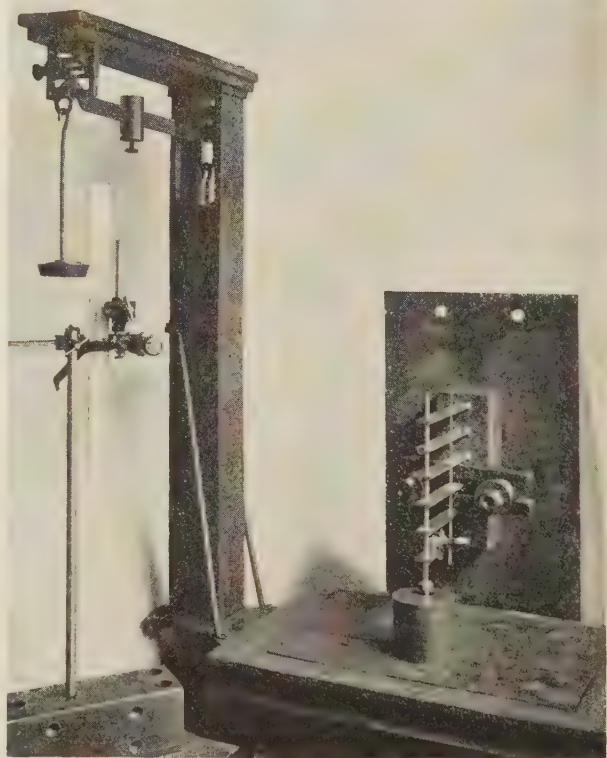


FIG. 23 MEASURING ANGLES OF DEFLECTION WITH TELESCOPE AND STRESSES WITH CURVATURE INSTRUMENT
(The load is read on the scale.)

MODEL TESTS

The necessity was felt to check these purely theoretical computations with model tests. A photograph of the set-up is shown in Fig. 19. There was used a group of steel strips welded on a massive block. Two sizes of lashing wire were tested. The load was applied by pulling the wire; this gives the same force at the tip of each blade (considering bending deformations only). The test data checked nicely with the theoretical values, the maximum discrepancy being 7 per cent for the stresses and 5 per cent for the deflection at the lashing wire.

On model tests of this size there is often no room for standard tensometers. A small simple instrument, based on measuring the change in curvature, has rendered very good services in our case and may be worth while to be described (Figs. 20 and 21). Three steel balls are fitted into a small triangular plate and pressed against the test specimen (in our case an ordinary steel strip). Rigidly connected to the plate is a dial indicator provided with a small ball which rests against the specimen. The indicator follows every change in curvature of the strip, and the readings on the dial are directly proportional to the bending stress.

Two conical points are used to fix the location of the instrument. For tests which require only a short time, the triangular plate can be pressed by hand against the test piece; otherwise a clamping arrangement, like the one shown in Figs. 20 and 21, can be used. The clamp must have a flexible part, as it may not have a stiffening effect on the specimen. For this purpose we used a small rubber gasket.

Fig. 22 shows a model where permanent set is produced by pulling in the direction of the lashing wire. It is interesting to note how the end blades deflect differently from the others. Yielding is (according to the theory) produced in the wire next to the end blades, but practically not next to the middle blades. The middle blades have yielded at the tip, where the end blades remain straight.

Fig. 23 shows a more elaborate set-up used to measure stresses and deflections in a blade segment. The block with the strips is clamped against a vertical plate, and the load is applied at the lashing wire by adjusting a screw, which varies the distance between the lashing wire and the platform of a scale. The load is read directly on the scale. The angles of deflection are measured by a telescopic arrangement, a small mirror being fixed on the blades.

ACKNOWLEDGMENT

The author wishes to thank Dr. S. Timoshenko, whose encouragement has been most helpful in carrying out this investigation.

Appendix

THE INFLUENCE OF CENTRIFUGAL FORCE ON SINGLE BLADES WITH UNIFORMLY DISTRIBUTED LOAD q , TIP MOMENT M , AND TIP FORCE S

In the text we derived for constant section blades:

$$\frac{d^2u}{dz^2} = uz + \frac{S}{a} \dots \dots \dots [8]$$

where $u = q + p \frac{dyz}{dx}$

We put:

$$u = \sum_{i=0}^{\infty} A_i z^{2i} + \sum_{k=0}^{\infty} B_k z^{2k+1} + \sum_{n=0}^{\infty} C_n z^{2n+3}$$

Equation [8] is satisfied when: $A_{i+1} = \frac{A_i}{(3i+2)(3i+3)}$

$$B_{k+1} = \frac{B_k}{(3k+3)(3k+4)}, \quad C_{n+1} = \frac{C_n}{(3n+4)(3n+5)}, \text{ where necessarily } C_0 = \frac{S}{2a}$$

Thus we find, observing boundary conditions:

$$u = A_0 \left\{ 1 + \frac{z^3}{2 \times 3} + \frac{z^6}{2 \times 3 \times 5 \times 6} + \frac{z^9}{2 \times 3 \times 5 \times 6 \times 8 \times 9} \dots \right\} + \frac{M}{a^2} \left\{ z + \frac{z^4}{3 \times 4} + \frac{z^7}{3 \times 4 \times 6 \times 7} + \frac{z^{10}}{3 \times 4 \times 6 \times 7 \times 9 \times 10} \dots \right\} + \frac{S}{2a} \left\{ z^2 + \frac{z^5}{4 \times 5} + \frac{z^8}{4 \times 5 \times 7 \times 8} + \frac{z^{11}}{4 \times 5 \times 7 \times 8 \times 10 \times 11} \dots \right\}$$

(1) Considering a uniformly distributed load q alone ($M = 0, S = 0$) At the blade root ($x = l$) the angle of rotation dyz/dx is zero, thus $u = q$ $= A_0 \left\{ 1 + \frac{k}{2 \times 3} + \frac{k^2}{2 \times 3 \times 5 \times 6} \dots \right\}$, where $k = \frac{l^3}{a^3} = \frac{\rho l^3}{I b E b} =$ directly proportional to the centrifugal force. This determines $A_0 = \frac{q}{1 + \frac{k}{2 \times 3} + \frac{k^2}{2 \times 3 \times 5 \times 6} \dots}$

$$\text{so that } u = \frac{q \left\{ 1 + \frac{z^3}{2 \times 3} + \frac{z^6}{2 \times 3 \times 5 \times 6} \dots \right\}}{1 + \frac{k}{2 \times 3} + \frac{k^2}{2 \times 3 \times 5 \times 6} \dots} = q + p \frac{dyz}{dx}$$

Expressions can now be derived for the deflection, the angle of rotation, and the bending moment at any point x . We are particularly interested in the maximum deflection y and angle dyz/dx (at the tip) and the maximum bending moment $I b E b (d^2yz/dx^2)$ (at the root). We find:

$$\text{Maximum deflection } y = \frac{ql^4}{8I b E b} \frac{\left(1 + \frac{4k}{3 \times 5 \times 7} + \frac{4k^2}{3 \times 5 \times 6 \times 8 \times 10} \dots \right)}{\left(1 + \frac{k}{2 \times 3} + \frac{k^2}{2 \times 3 \times 5 \times 6} \dots \right)} = \delta \frac{ql^4}{8I b E b}$$

$$\text{Maximum angle of rotation } y' = \frac{-ql^3}{6I b E b} \frac{\left(1 + \frac{k}{5 \times 6} + \frac{k^2}{5 \times 6 \times 8 \times 9} \dots \right)}{\left(1 + \frac{k}{2 \times 3} + \frac{k^2}{2 \times 3 \times 5 \times 6} \dots \right)} = -\epsilon \frac{ql^3}{6I b E b}$$

$$\text{Maximum bending moment } I b E b y'' = \frac{ql^2}{2} \frac{\left(1 + \frac{k}{2 \times 3 \times 5} + \frac{k^2}{3 \times 5 \times 6 \times 8} \dots \right)}{\left(1 + \frac{k}{2 \times 3} + \frac{k^2}{2 \times 3 \times 5 \times 6} \dots \right)} = \gamma \frac{ql^2}{2}$$

Noting that for stationary blades and the same load $\frac{ql^4}{8I b E b}$ is the maximum deflection y_0 , $-\frac{ql^3}{6I b E b}$ is the tip angle y'_0 , and $\frac{ql^2}{2}$ is the maximum bending moment $I b E b y''_0$, we can write:

$$y = \delta y_0, \quad y' = \epsilon y'_0, \quad I b E b y'' = \gamma I b E b y''_0$$

where δ, ϵ, γ are correction factors taking into account the effect of centrifugal force. These factors are functions of k only (Fig. 9).

(2) Considering a bending moment M (on the tip) alone. In a similar way as was done for uniformly distributed load, correction factors can be found which take into account the influence of the centrifugal force.

We may write:

For tip deflections: $y = \rho y_0$ (y_0 = without centrifugal force)
For tip angles: $y' = \mu y'_0$ (y'_0 = without centrifugal force)
For root bending moments: $I b E b y'' = \omega I b E b y''_0$ ($I b E b y''_0$ without centrifugal force)

$$\text{where } \rho = \frac{1 + \frac{k}{4 \times 5} + \frac{k^2}{4 \times 5 \times 7 \times 8} \dots}{1 + \frac{k}{2 \times 3} + \frac{k^2}{2 \times 3 \times 5 \times 6} \dots}$$

$$\mu = \frac{1 + \frac{k}{3 \times 4} + \frac{k^2}{3 \times 4 \times 6 \times 7} \dots}{1 + \frac{k}{2 \times 3} + \frac{k^2}{2 \times 3 \times 5 \times 6} \dots}$$

$$\omega = \frac{1}{1 + \frac{k}{2 \times 3} + \frac{k^2}{2 \times 3 \times 5 \times 6} \dots}$$

ρ, μ, ω are plotted as a function of k in Fig. 10.

(3) Considering the lateral force S on the tip alone.

Again we introduce correction factors for the centrifugal force:

Tip deflections: $y = \sigma y_0$
Tip angles: $y' = \rho y'_0$
Root bending moments: $I b E b y'' = \tau I b E b y''_0$

$$\text{where } \sigma = \frac{1 + \frac{k}{4 \times 6} + \frac{13k^2}{3 \times 4 \times 5 \times 6 \times 7 \times 8} \dots}{1 + \frac{k}{2 \times 3} + \frac{k^2}{2 \times 3 \times 5 \times 6} \dots}$$

$$\rho = \frac{1 + \frac{k}{4 \times 5} + \frac{k^2}{4 \times 5 \times 7 \times 8} \dots}{1 + \frac{k}{2 \times 3} + \frac{k^2}{2 \times 3 \times 5 \times 6} \dots}$$

$$\tau = \frac{1 + \frac{k}{4 \times 6} + \frac{k^2}{4 \times 5 \times 7 \times 9} \dots}{1 + \frac{k}{2 \times 3} + \frac{k^2}{2 \times 3 \times 5 \times 6} \dots}$$

Curves for σ , ρ , and τ are shown in Fig. 11.

LIST OF NOTATIONS

l	= length of blade (in.)
x	= variable distance from tip (in.)
t	= pitch on lashing wire diameter (in.)
t^*	= length of lashing wire between two blades (in.)
I_b	= minimum moment of inertia of blade (in. ⁴)
E_b	= modulus of elasticity of blade material (lb per sq in.)
I_s	= moment of inertia of lashing wire (in. ⁴)
E_s	= modulus of elasticity of lashing material (lb per sq in.)
λ	= $\frac{t^* I_b E_b}{t I_s E_s}$ = ratio of flexibility
β	= $-(\lambda + 2) + \sqrt{(\lambda + 2)^2 + 4\lambda + 3}$
n	= number of blades

D	= $\frac{2\lambda^2 + 26\lambda + 24}{3\lambda} + \frac{12 + \lambda}{3\lambda}\beta - \frac{6}{n(1 - \beta)}$
q	= distributed lateral load on blade (lb per in.)
p	= centrifugal load per unit length on blade (lb per in.)
p^*	= centrifugal load per unit length on wire (lb per in.)
$M(M_1, M_2, M_i)$	= bending moment (1st, 2d, i th blade) (lb-in.) on blade tip
$M', (M_1', M_2', M_i')$	= bending moment in lashing wire for a cross-section just to the left of the 1st, 2d, i th blade (lb-in.)
$M'' (M_1'', M_2'', M_i'')$	= bending moment in lashing wire for a cross-section just to the right of the 1st, 2d, i th blade (lb-in.)
$M^* (M_1^*, M_2^*, M_i^*)$	= bending moment at blade root (1st, 2d, i th blade) (lb-in.)
$S(S_1, S_2, S_i)$	= lateral shearing force at tip (lb)
$T(T_1, T_2, T_i)$	= vertical force on tip (lb)
$\varphi(\varphi_1, \varphi_2, \varphi_i)$	= angle of deflection at tip (radians)
y	= lateral deflection (in.)
φ_0	= angle of deflection at tip without lashing wire (= $\frac{ql^3}{6I_b E_b}$ for uniformly distributed load)
M_0^*	= bending moment at root without lashing wire (lb-in.)

$$a^2 = \frac{I_b E_b}{p} \quad z = \frac{x}{a} \quad k = \frac{l^3}{a^3} = \frac{pl^3}{I_b E_b}$$

The Effect of Openings in Pressure Vessels

By J. HALL TAYLOR,¹ CHICAGO, ILL., AND EVERETT O. WATERS,² NEW HAVEN, CONN.

Openings in pressure vessels, either reinforced or unreinforced, have presented to the engineering profession a difficult problem, and outside of a few isolated tests there appears to be little information available to the designing engineer. The authors set out in June, 1930, to establish by tests the stress relations existing about unreinforced holes, and in addition to determine the reinforcing effect of nozzles and other outlets of the type generally used for attachments to pressure vessels, and to make this information available to the engineering profession. Three commercial-sized pressure vessels were constructed, and readings were obtained on ten unreinforced openings and on

fourteen openings with nozzles attached. There are many local conditions that have a great effect on results. The tests as a whole indicate (1) the necessity of reinforcing all holes above a minimum diameter, because the stress concentration becomes much higher than that due to a hole in a stretched flat plate as the diameter increases; (2) the desirability of attaching the reinforcement as near the edge of the hole as practicable, on account of the local character of the stress concentration; (3) the danger of excessive stiffening when heavy, large-diameter reinforcing pads or saddles are used. A few numerical examples are given to illustrate the principles outlined.

IT IS common knowledge that, when metal is removed from the walls of pressure vessels in order to provide structural connections, passages for the flow of fluids, or access to the interior, an inevitable weakening results. If the hole is small—say, of the order of a rivet diameter in size—it has been standard practice either to neglect this effect altogether, if the hole is isolated, or if it is one of a series, as in a riveted seam, to take account of it by reducing the nominal strength of the vessel in proportion to the area of the metal removed, as measured on a critical cross-section. For larger openings, the practice has been to fasten a reinforcing pad to the vessel at the point where it is weakened, whose cross-sectional area, in the simplest cases, is made equal to that of the metal removed.³ For other cases, rules have been formulated and accepted with more or less unanimity by the trade, based partly on experience and partly on a simple, easily intelligible analysis of the supposed conditions of critical stress that exist in the neighborhood of the



E. O. WATERS



J. HALL TAYLOR

opening involved. The work of the Boiler Code Committee of The American Society of Mechanical Engineers, as represented by its publications and supplementary rulings on special questions, has undoubtedly crystallized the best thought in this field, and serves as an extremely reliable guide for designers and users of pressure vessels of all types.

Recently, however, designers of this type of equipment have felt the need of more accurate knowledge of the exact state of stress occurring in the neighborhood of openings, and have raised the question as to whether reinforcements, proportioned according to the best current practice and complying with all the rules, actually produce the effect that they are supposed to. Furthermore, new methods of making connections to pressure tanks, with new designs of nozzles, have involved the matter of reinforcement in a way that was perhaps not contemplated when the existing rules were adopted. Believing that a better understanding of this whole subject could best be gained by a thoroughgoing series of tests on full-scale apparatus, assembled as it would be in actual service, the authors undertook the program that will presently be outlined, and are pleased to present the results which they obtained, with their own conclusions deduced therefrom.

1—PURPOSE AND SCOPE OF TESTS; PROPOSED METHOD OF PROCEDURE

The purpose of the tests, in short, was to measure the stresses in pressure vessels in the neighborhood of openings, both reinforced and unreinforced. In order to cover as wide a range of conditions as practicable, three different vessels were used, of different shell and head thicknesses; holes were cut in both shell and head; five types of nozzles were used as reinforcement; and attachment of the latter was made both by riveting and welding. Thus it was possible to deal with the effect of the following variables, over the ranges indicated:

Variable	Range
Fluid pressure.....	Zero to 1200 lb per sq in.
Shell thickness.....	$\frac{3}{4}$, 1, $1\frac{1}{4}$ in.
Head thickness.....	$\frac{1}{8}$, $1\frac{1}{8}$, $1\frac{1}{2}$ in.
Diameter of opening cut.....	$\frac{6}{16}$, $\frac{6}{8}$, $\frac{7}{8}$, 8, $8\frac{1}{2}$, 9, $10\frac{1}{2}$, 11, 13 in.
Nominal size of reinforcing nozzle	3, 6, 8, 10 in.
Nozzle type.....	Sweep, straight neck, welding neck, thin-wall neck, welding nozzle
Nozzle attachment.....	Single row of rivets, double row of rivets, fillet weld, stud weld

The range of pressure was subject to the condition that, for any

¹ President of Taylor Forge and Pipe Works. Mem. A.S.M.E. J. Hall Taylor studied engineering at Lewis Institute, Chicago. In 1900, he organized the American Spiral Pipe Works. He later designed and developed various types of seamless forged-steel nozzles, manways, and welding necks for pressure vessels. In 1925 to 1927, his research work on stresses in forged-steel flanges led to the development of the Taylor-Waters formula for stresses in pipe flanges. He has devoted the last 33 years to handling the engineering and development work of his firm.

² Associate Professor of Mechanical Engineering, Yale University. Assoc-Mem. A.S.M.E. Everett O. Waters was graduated from Yale University in 1914 with the degree of M.E., since which time he has been teaching machine design and related subjects at that institution. During the war, he was engaged in the organization and maintenance of repair shops for ordnance material for the American Expeditionary Forces, being employed at first in the field and later in the office of the Chief Ordnance Officer. For the last eight years, he has collaborated with J. Hall Taylor in the investigation of the strength of pipe flanges and nozzles, in the course of which he developed formulas for the design of rings and flanges on a strength basis.

³ E.g., reinforcement of manholes, A.S.M.E. Boiler Construction Code, 1930 ed., par. P-260. (References throughout the paper are to the original 1930 edition of the Code.)

Contributed by the Applied Mechanics Division and presented at the Semi-Annual Meeting, Chicago, Ill., June 26 to July 1, 1933, of THE AMERICAN SOCIETY OF MECHANICAL ENGINEERS.

NOTE: Statements and opinions advanced in papers are to be understood as individual expressions of their authors, and not those of the Society.

given test, the elastic limit of the material in the region of the test should not be exceeded. In some instances, stress concentrations were encountered of such magnitude that the fluid pressure had to be limited to 300 lb per sq in.

It was proposed to determine stresses by means of strain-gage readings taken at definite stations on the outer surface of the shell and reinforcing nozzles, using a commercial gage reading elongations in ten-thousandths of an inch per inch over a 2-in. gage length. By taking readings along mutually perpendicular axes at each station, the direct stresses along these axes could be computed by the well-known relation for two-dimensional stress:

$$s_x = \frac{(\delta_x + \mu\delta_y)E}{1 - \mu^2}$$

$$s_y = \frac{(\delta_y + \mu\delta_x)E}{1 - \mu^2} \dots\dots\dots [1]$$

where E is the modulus of elasticity, δ_x and δ_y the unit elongations, μ is Poisson's ratio, and s_x and s_y are the unit stresses.

Taking the modulus $E = 29,500,000$ lb per sq in. and $\mu = 0.303$, these formulas reduce to

$$s_x = 32,480,000 \delta_x + 9,853,000 \delta_y$$

$$s_y = 32,480,000 \delta_y + 9,853,000 \delta_x \dots\dots\dots [1a]$$

It was realized that, when a nozzle or other reinforcement was fastened to an opening, the application of pressure would undoubtedly cause some relative displacement of reinforcing pad and pressure-vessel shell; accordingly, it was planned to take readings both on the exposed surface of the reinforcement and, through small drilled holes, on the surface of the shell that would be covered by the reinforcement. For readings at the latter stations, the strain gage was provided with extension legs which reduced its sensitivity, but nevertheless made it possible to get results of some quantitative value.

Obviously, it would be impossible to obtain a complete picture of the effects produced at an opening, unless the vessel were first tested without openings, then with unreinforced openings (closed off by pressure-sealed pads similar to a manhole cover), and finally with the openings reinforced by means of various nozzles. Plans were therefore made to test the solid shell, including the head, after which one hole was to be cut at a specified location, a loose patch applied from the inside, and readings taken in the neighborhood of the hole. Next, a nozzle would be attached to the hole, pressure again applied, and another series of readings taken. The process would then be repeated for a second, third, fourth, etc. hole and nozzle, until all the desired data had been secured for each pressure vessel. This method entailed much more labor than would have been required if all holes had been cut at one time and all nozzles attached at one time. But it had two decided advantages: it made it possible to detect mutual or reciprocal effects of adjacent holes on each other, and it left the way clear to a change in the size of an opening or the type of nozzle and means of attachment, as a result of experience with preceding openings and nozzles.

In carrying out a series of tests on a structure by the methods just outlined, there are unquestionably many difficulties that can be overcome only by compromise and there are sources of error for which the authors may be criticized. First, a manually applied strain gage, removed from each station and reapplied between each pair of successive readings, cannot be expected to "repeat" with absolute fidelity. Second, tanks of the size contemplated, built to commercial specifications, are apt to contain trapped stresses when first put in service, which are more or less

completely ironed out during repeated applications and removals of pressure. This seasoning action shows up on the strain gage as a mixture of elastic and plastic strain, and the readings will be somewhat discordant if interpreted solely on the basis of elasticity. However, in view of the great quantity of readings that had to be taken, the authors did not consider themselves justified in going to more refined methods of observation and analysis, but felt that the simple averaging of this mass of data would of itself reduce the observational errors to a minimum.

Some idea of the number of readings taken may be gathered from these figures:

Number of openings tested.....	10
Approximate number of stations per opening.....	25
Number of nozzles tested.....	14
Approximate number of stations per nozzle.....	15
Approximate number of readings per station.....	20
Approximate total number of readings.....	9200

This does not include tests on solid tanks, or tests run in the spring of 1933.

A further check on the accuracy and reliability of observations is given by the readings on the solid shells. For these tests, the relation between the observed strains and those computed from the theoretical stresses is shown in Fig. 6. The degree of agreement there shown may be taken as characteristic of the entire series.

Wherever riveted connections were used, a certain amount of slippage probably took place, in addition to the previously mentioned elastic displacement; with successive applications of pressure alternating with reductions to zero, this would affect the readings in the same way as elastic hysteresis, but would be more irregular. No attempt has been made to analyze this effect precisely; readings where it obviously occurred should simply be interpreted as having qualitative rather than quantitative value.

Finally, readings were taken on outside surfaces only. If membrane stresses are the only ones present, this indicates the true state of stress. But when bending is superimposed, the readings will indicate the sum or difference of the membrane and bending stresses and must be interpreted accordingly. In order to separate the stresses experimentally, it is necessary to get readings on both outer and inner surfaces. Under the circumstances, it was quite impossible to get direct readings on the inside of the tanks; indirect readings could have been obtained by straddling the strain gage across the tops of rigid pins secured to the outside of the tank at gage-length intervals, but the additional time and expense of this procedure were prohibitive. Possibly the authors may undertake an investigation of this sort at a future date, if the demand for more accurate data appears to warrant it.

2—DESCRIPTION OF APPARATUS TESTED

Tests were run during the years 1931 and 1932 and the spring of 1933, at the plant of the Taylor Forge and Pipe Works. Three cylindrical vessels were constructed, of the type shown in Fig. 1, each having a 2-to-1 ellipsoidal head at one end and a massive cover plate at the other end which could be unbolted and dropped down on to the inside of the shell when access was necessary for bucking up rivets, calk welding, etc. All shells were made of steel conforming to material specification 2 of the A.S.M.E. Boiler Code, and A.S.T.M. specification A-89-30 grade B for flange-quality steel for forge welding. The shells were hammer welded, formed and assembled, and end closure machined by the Taylor Forge and Pipe Works. Special attention was given to insure, as nearly as practicable, roundness of the shells. Heads were purchased from one of the principal sources of supply of spun heads, and were fusion welded to the shell. The major dimensions were as follows:

	No. 1	No. 2	No. 3
Shell diameter, inside, in.....	42	42	42
Overall length, approximate, ft.....	10	8	8
Shell thickness, in.....	$\frac{3}{4}$	1	$1\frac{1}{4}$
Head thickness, in.....	$\frac{7}{8}$	$1\frac{1}{8}$	$1\frac{3}{8}$
Max. allowable working pressure, lb per sq in. ^a	250	333	417

^a Based on 35,000 lb per sq in. ultimate strength of weld, and a factor of safety of 5. See Pars. P-180 and P-186, A.S.M.E. Boiler Code.

All boiler-making work in connection with the tests, such as riveting, laying-up nozzles, etc., was performed by the same man to eliminate inequalities of workmanship as far as possible. Where holes were cut in the shell by the oxygen process, the metal was removed by chipping for at least $\frac{1}{8}$ in. from the fused surface; the holes were then ground smooth and to the correct diameter.

The nozzles used for the tests were of regular commercial quality, Taylor Forge Seamless manufacture, with flanges and necks conforming to dimensions as specified in the maker's catalogs. In particular, the saddle flange thickness was kept to a tolerance of $\pm\frac{1}{32}$ in. and -0 in., so as to maintain the reinforcement value of the flange at its nominal amount, as covered by sec. 1, par. 260 of the A.S.M.E. Boiler Code. Special precautions were taken to insure high-grade workmanship in attaching nozzles. Laying-up was resorted to where necessary to insure close-fitting flanges; rivet holes were drilled and then reamed $\frac{1}{32}$ in. larger than rivet size; and after reaming, the nozzles were removed to allow complete removal of chips and burrs. True-tolerance hot-formed rivets were used; all rivets were hammer tested after driving, and unsound ones were cut out and replaced.

The Berry strain gage with 2-in. center-to-center points and dial indicator graduated in thousandths of an inch was used in all the tests. In taking readings, tenths of a division were estimated. Gage holes at each station were first marked with a standard 2-in. spacer punch, and then finished with two prick punches, the first having an angle slightly greater and the second one an angle slightly less than that of the strain-gage points; this was found by experience to be more satisfactory than drilling. In order to minimize the effects of trapped stresses and possible plastic strains, the net extensions for any given pressure application were always computed as the difference between the reading at that pressure and the next following zero pressure, the results for each station being then averaged and tabulated as strain (and stress) per 100 lb per sq in. applied fluid pressure. The following excerpt from one of the work sheets illustrates the procedure:

	0	100	0	300	0	500	0	700	0	800	0
Pressure, lb per sq in.....	165.1	166.0	165.3	167.2	165.2	169.7	165.1	170.0	165.1	172.0	165.1
z-reading, mils.....	0.7	...	2.0	...	4.6	...	4.9	...	6.9
Difference, mils.....
Strain, mils per in. per 100 lb per sq in. pressure.....	0.070	...	0.067	...	0.092	...	0.070	...	0.086
Average strain.....	0.077
y-reading, mils.....	138.1	138.9	138.6	139.1	138.2	139.2	138.1	139.7	138.3	140.0	138.3
Difference, mils.....	0.3	...	0.9	...	1.1	...	1.4	...	1.7
Strain, mils per in. per 100 lb per sq in. pressure.....	0.030	...	0.030	...	0.022	...	0.020	...	0.021
Average strain.....	0.025

From Equations [1a], $s_z = 2747$ lb per sq in., $s_y = 1571$ lb per sq in.

Two bourdon-type gages were mounted directly on the pressure vessel under test; one was used as a service gage and the other as

a master against which the service gage was checked at frequent intervals. On account of the small holes that were drilled through the saddle flanges of the nozzles in order to get strain-gage points on the surface of the shell plate underneath, there was for a time some trouble from loss of pressure due to leakage. This was obviated by applying a special packing between nozzle and shell, on the inside, which provided tightness without strength.

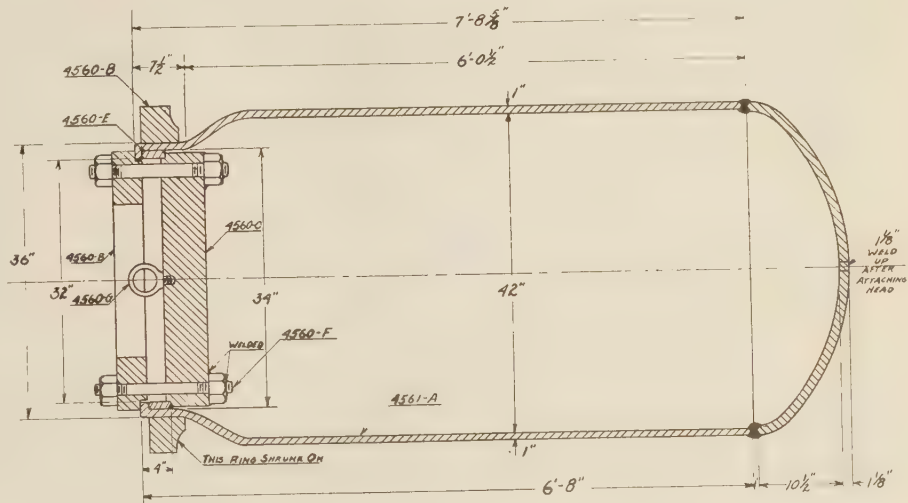


FIG. 1 TEST TANK, 42 IN. BY 1 IN., FOR STRAIN-GAGE TEST



FIG. 2 TANK NO. 1 AFTER NOZZLES HAD BEEN ATTACHED

Fig. 2 shows tank No. 1 as it appeared after all nozzles had been attached and the tests completed. Many of the gage stations may be seen, outlined in white circles and joined by white lines with their mating points. The small pipe tapped into the blind flange on the central nozzle is a bleeder for air trapped in the tank. The pressure gages were attached near the swaged end, and water was pumped in and drained out through a connec-

tion in the detachable head. Fig. 2 also indicates what may be called the standard arrangement of gaging stations at each open-

TABLE 1 SCHEDULE OF TESTS

Serial number	Tank	Hole Letter	Diam. in.	Letter	Type	Series	Size, in.	Nozzle Hole diam., in.	Rivet circle diam., in.	Rivet size, in.	No. of rivets
101 ^a	1									
102 ^b										
103		A	9				9	15	1	20
104				A	Sweep	30	6	9	15	1	20
105				B	Sweep	30	3	6 1/2	10 3/8	7/8	14
106		E	8							
107				E	Sweep	30	6	8	14 3/8	1 1/8	14
108		D	8							
109				D	Sweep	30	6	8	15	1	20
110		C	8							
111				C	Str. neck ^k	30	6	8	14 1/4	1	18
112				F	Welding neck ^k	30	6	8 1/2	Welded	Welded	Welded
113 ^k				G	Thin-wall wldg. neck ^k	Spl.	6(noml.)	8 1/8	Welded	Welded	Welded
114				F	Welding neck ⁱ	30	6	8 1/8	Welded	Welded	Welded
115 ^k				G	Thin-wall wldg. neck ^j	Spl.	6(noml.)	8 1/8	Welded	Welded	Welded
116 ^c	2									
201 ^d										
202 ^e										
203		A	8							
204				A	Str. neck	40	6	8	15 1/4	1 1/4	15
205		B	11							
206				B	Sweep	40	6	11	14 3/8	1 1/8	18
207		C	9							
208				C	Str. neck	40	8	9	18 1/8	1 1/8	18
209		D	11							
210				D	Dbl. riv.	40	10	11	16, 22 1/4	1 1/8	16, 16
211				E	Sweep	40	6	11	14 3/8	1 1/8 weld	18
212				F	Wldg. nozzle	Spl.	8	8	Welded	Welded	Welded
301 ^f	3									
302 ^g										
303		A	7							
304				A	Str. neck	60	6	7	15 1/4	1 1/4	18
305		B	13							
306				B	Dbl. riv.	60	10	13	22, 26 3/4	1 1/8	20, 20
307				C	Wldg. nozzle	Spl.	8	10 1/2	Welded	Welded	Welded
308				D	Wldg. neck	40	6	8	Welded	Welded	Welded

^a Head, from crown to junction with barrel, on two mutually perpendicular meridians. ^b Shell, at 23 in., 49 1/2 in., and 77 in. from junction with head, on an element of the cylinder, and at one additional point. ^c Tank with all nozzles attached subjected to 1000 lb per sq in. ^d Head, from crown to junction with shell, on two mutually perpendicular meridians. ^e Shell, at 19 in., 31 1/4 in., and 44 1/4 in. from junction with head, at locations of holes C, D, B. ^f Head from crown to point 9 in. beyond junction with shell, on two mutually perpendicular meridians. ^g Shell, at four random points. ^h Without reinforcing pad. ⁱ With reinforcing pad, 15 1/2 in. O.D., 9 1/2 in. I.D., 3/4 in. thick. ^j With reinforcing pad, 14 1/2 in. O.D., 8 1/2 in. I.D., 3/4 in. thick. ^k Special welding neck used in tests 113 and 115 had same dimensions as extra heavy pipe.

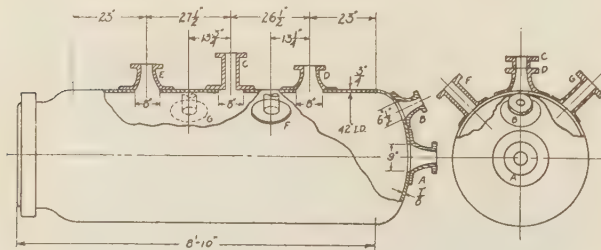


FIG. 3 TANK No. 1

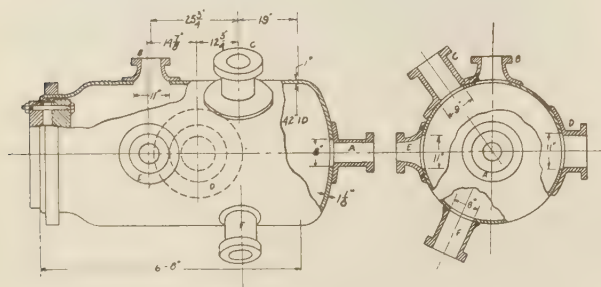


FIG. 4 TANK No. 2

ing: along two mutually perpendicular lines radiating from the center of the opening, one being an element of the cylindrical surface, and extending over the saddle flanges of the nozzles and up the necks as far as practicable. When openings without nozzles were tested, readings were on these same lines, which then extended to the edge of the hole and were supplemented by readings taken around the hole with gage points set as close to the edge as possible. In the case of the 3-in. offset nozzle on No. 1 head, the gage station lines were taken on a meridian of the head bisecting the nozzle and continuing for 7 in. along the shell, and

on an arc concentric with the tank and passing through the center of the nozzle hole.

3—RECORD OF TESTS

The tests may well be divided into three groups: (1) shell and head tests on the three tanks without holes; (2) strain measurements in the neighborhood of unreinforced holes; (3) strain measurements in the neighborhood of reinforced holes, including measurements on the reinforcing nozzles. This classification

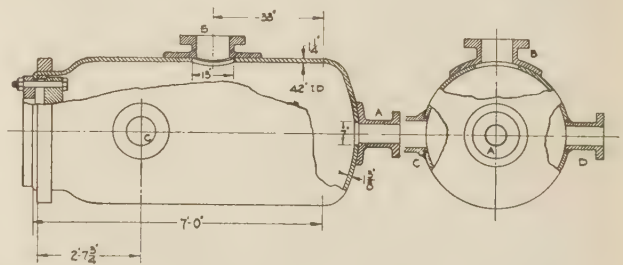


FIG. 5 TANK No. 3

will be followed in the discussion of the results, but for purposes of record it is perhaps better to present the material in chronological order for each tank, so that the reader may have a clear idea of the true sequence of events. Table 1 gives a list of the tests, together with general information as to the size of holes, size and type of nozzles, riveting, etc. The location of each test is shown in Figs. 3, 4, and 5.

(1) The results of tests 102, 202, and 302 may be compared directly with the theoretical elongations in a cylindrical shell, thus furnishing a check on the accuracy of the experimental work. Since this is quite important, Fig. 6 has been prepared, in which the observed strains have been plotted as points and the theoretical strains as oblique lines. The latter have been deduced from

the simple membrane analysis, using the inside diameter and taking the longitudinal stress as one-half the hoop stress; had the more precise method been used (Lamé's formula), the difference would have been of the order of 5 per cent for No. 3 tank and less for the other two. It will be noticed that the experimental values scatter rather widely when smaller than about 0.15 mil per inch, but above this figure they show good agreement with the theoretical lines. This may be taken as characteristic of the method of test employed; the authors do not believe that anything better can be obtained unless a more sensitive and accurate strain gage is used, and it is clamped rigidly to the member under test throughout the duration of the experiment.

Tests 101, 201, and 301 on the full heads are exhibited in Fig. 7, where the results are plotted as stresses per 100 lb per sq in. applied fluid pressure. The theoretical membrane stresses were figured from the standard formulas for such cases,⁴ wherein shear and bending are neglected, and the corrections for edge effects at the junction of head and shell were computed by Coates' step-by-step method,⁵ using zones divided into 5-deg intervals. The radial-stress correction gives the resultant stress on the outside of the vessel, and the hoop-stress correction gives the resultant stress at the middle surface, to which a second correction (due to the hoop bending moment) should be applied in order to obtain the resultant stress at the outside. Due to the small magnitude of this latter correction, it was not indicated in the figure.

Since the primary purpose of these tests was to determine the effect of holes rather than to check the membrane theory of thin shells, only one tank, No. 3, was explored beyond the edge of the head and along the shell. All three tests show tolerable agreement with the corrected theory, especially in view of the fact that the weld was reinforced, and the change in plate thickness and the position of the weld were both offset slightly from the geometrical junction of head and shell. However, one important discrepancy should be noted: from the crown to a point halfway

⁴ Timoshenko, "Strength of Materials," part II, p. 510. The radii of curvature to the inner surface were used in the calculations.

⁵ Coates, "The State of Stress in Full Heads of Pressure Vessels," Trans. A.S.M.E., 1930, paper APM-52-12, p. 117.

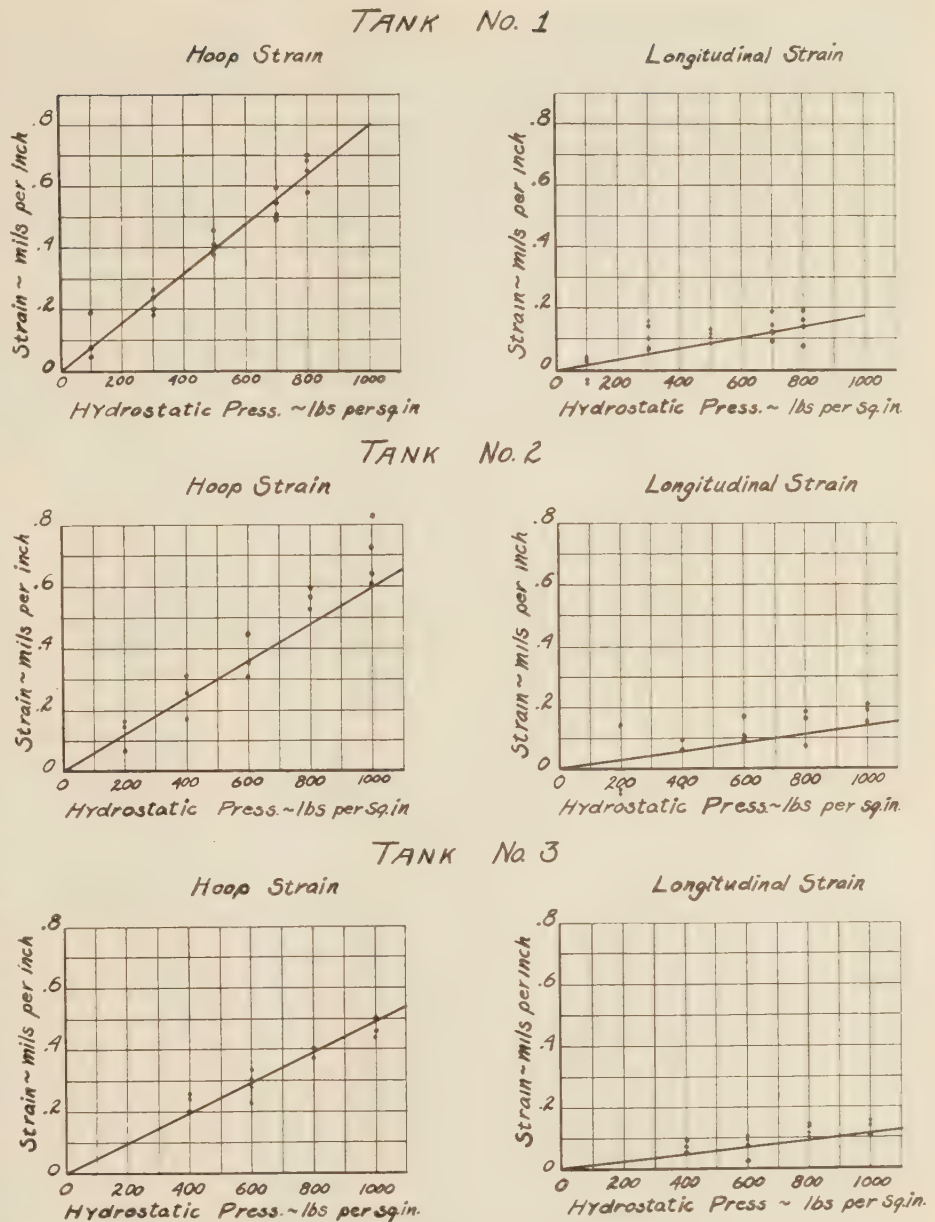


FIG. 6 OBSERVED AND THEORETICAL STRAINS IN TANK SHELLS

to the edge of the head, the observed stresses ran consistently higher than the computed values. The reasons for this are discussed in part 4 of the paper.

(2) The effect of an unreinforced hole in the center of an ellipsoidal head is shown strikingly in Fig. 8, where the results of tests 103, 203, and 303 are plotted. In this and succeeding figures, stresses are plotted as percentages of the theoretical hoop stress that would exist in the full head (or shell) at the point where the center of the hole is located. Solid and dotted fair curves are drawn to indicate the hoop and meridional stresses, respectively. For comparative purposes, the corresponding theoretical stress percentages in an infinite stretched flat plate have been plotted as dash and dot-dash lines. It will be seen at a glance that the actual conditions in the head, for the sizes of holes tested, are about the same as the flat-plate theory would predict,

as far as meridional stresses are concerned, but that for the hoop stresses they are far more severe, although it would be reasonable to assume that, as the size of the hole diminished in comparison with the major axis of the head, the experimental and theoretical values would tend to approach each other. As a matter of fact, the present tests show a trend toward lower percentage hoop stresses as the hole diameter is decreased from 9 in. to 7 in., i.e., from $21\frac{1}{2}$ to $16\frac{1}{2}$ per cent of the tank diameter. A rigorous theoretical analysis must include not only the change in membrane stress caused by the opening, but the bending stress due to the shear arising from the pressure of the loose patch, as well. A pipe attached to the head by a plain threaded connection, without reinforcement, would produce practically the same bending effect.

Unreinforced holes in the shells (tests 106, 108, 110, 205, 207, 209, and 305) give similar results; see Fig. 9, where the observed stress percentages are shown by circles and crosses with fair

curves drawn through them, while the theoretical percentages for an infinite stretched flat plate with a circular hole at the center are indicated by dash and dot-dash lines. The latter values were obtained by solving the Airy function for the particular case in which the normal stress on the x -axis at infinity equals twice the corresponding stress on the y -axis.⁶ The maximum permissible diameters of unreinforced holes are, respectively, 3.58, 4.14, and 4.64 in. for the three tanks,⁷ which are considerably less than the actual diameter of any hole tested, so that high stress concentrations are not surprising.

As would be expected, the stress at the edge of the hole, measured tangentially with respect to the latter, is greatest on the longitudinal axis. Moreover, in all cases except one, it is considerably greater than the corresponding flat-plate stress, and it oscillates about the 100 per cent line instead of approaching it as an asymptote. Test 106 shows an exceptionally high value, which may have been caused by a recess of tapered cross-section,

$\frac{1}{4}$ in. deep and 1 in. wide, that was chipped from the inside edge of the hole, due to a shop error. The stress in test 305 is also very high, possibly because of the large diameter of the hole.

On the circumferential axis through the holes, the observed stresses normal to this axis show the same general trend as the theoretical flat-plate stress, rising to a maximum a short distance away from the edge of the hole; but here again the actual values are far greater than the theoretical ones.

(3) We now come to the effect of reinforcements. Fig. 10 includes the results for the heads; Fig. 11, the holes in shells reinforced with sweep type, single-riveted nozzles; Fig. 12, the straight-neck, single- or double-riveted type of reinforcement; Figs. 13 and 14, the various welded reinforcements. Here again, as in Figs. 8 and 9, stresses are expressed as percentages. Table 2 gives the reinforcing values of these outlets, computed in accordance with the A.S.M.E. Boiler Code.

Test 104, when compared with test 103, shows a tolerable degree of reinforcement, with, however, a rather high radial stress due probably to concentrated bending of the head just beyond the nozzle. Test 204, on the other hand, shows comparatively poor reinforcement, although the computed value of

⁶ See Prescott, "Applied Elasticity," p. 347, et seq.

⁷ Based on par. P-193b, Equation [2], A.S.M.E. Boiler Code. The value of K has been assumed as (ultimate strength of longitudinal weld)/(nominal ultimate strength of shell plate), or 0.7.

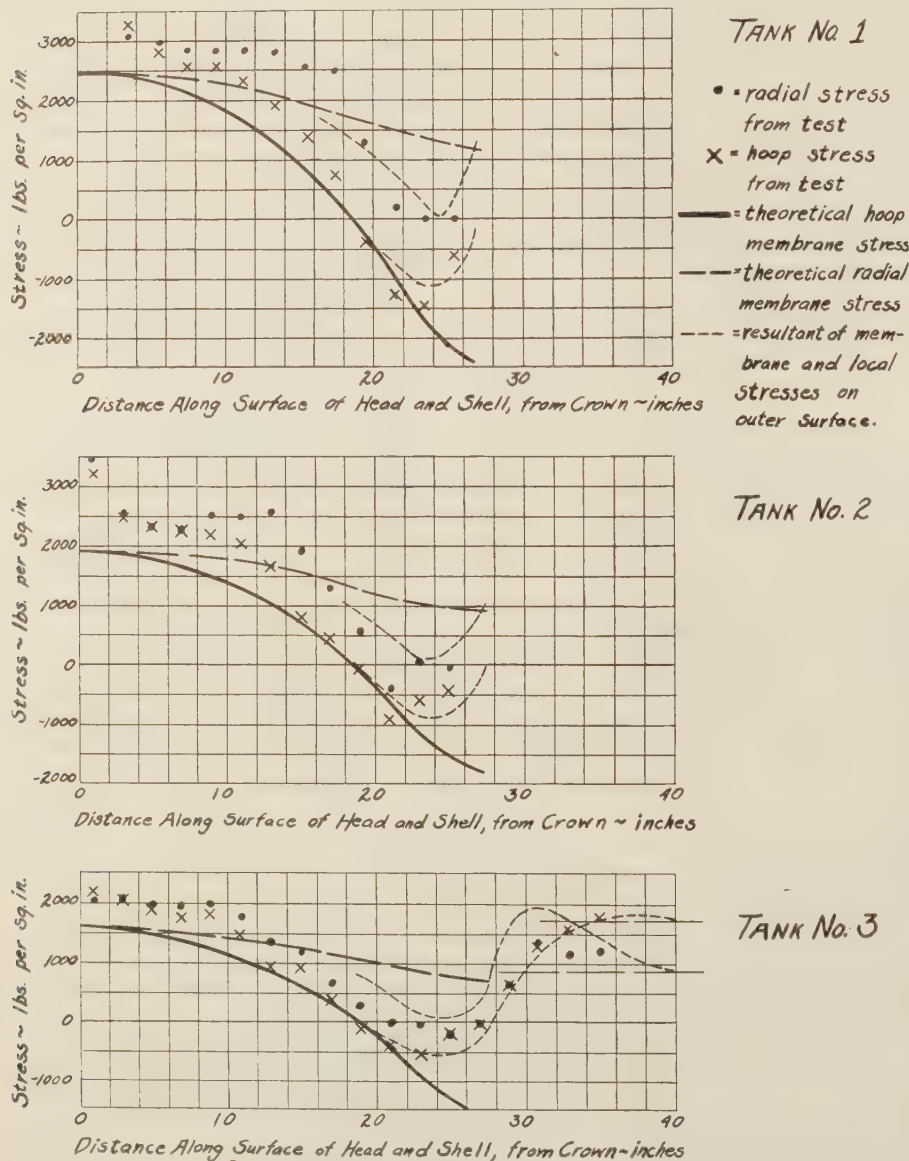


FIG. 7 STRESSES IN FULL HEADS

the nozzle (see Table 2) is entirely adequate. Because of these anomalous results, a nozzle of the same type (straight neck) was used in test 304. Here the results are fully as satisfactory as in test 104, showing that the form of the nozzle was not at fault. In all these tests, it should be added, gage readings on the nozzle flanges were low, indicating that the nozzles were capable of standing a much larger share of the load. It was therefore concluded that the high head stress in test 204 was due to riveting that was faulty, in spite of all efforts to make it of as high a grade as possible. This feature is discussed further in part 4.

strength of the rivets is only 89 per cent of that in test 109.

In Fig. 12 are given the results for straight-neck nozzles. In general, these are comparable with the sweep-type nozzle tests as far as the longitudinal axis is concerned; however, on the circumferential axis a sharp rise in the hoop stress, and in some cases in the longitudinal stress as well, is to be noted just outside the riveting. This is not so pronounced in test 111, where the rivet circle is only $3\frac{1}{8}$ in. from the edge of the hole, but in the other three tests it is unmistakable. The authors ascribe this phenomenon to the great, almost excessive, rigidity of the saddle

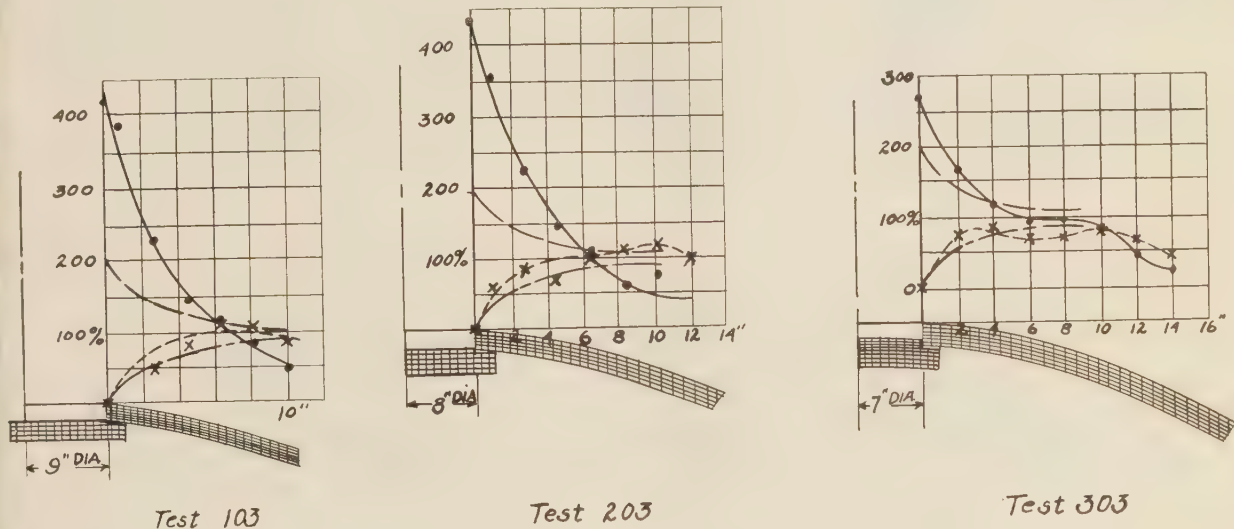


FIG. 8 EFFECT OF UNREINFORCED HOLES IN HEADS

A $6\frac{1}{2}$ -in. hole was cut in the head of tank No. 1, $17\frac{1}{4}$ in. from the crown, and reinforced with a 3-in. sweep-type nozzle, simply to get a qualitative picture of the stresses produced by an eccentrically located hole in the head (test 105). As would be expected, the radial stress is very high between the central and offset nozzles, whereas on the knuckle side both stresses are moderate, and, beyond the weld, approach the normal values of 100 and 50 per cent much as though no hole were present; compare with Fig. 7, tank No. 3. On a hoop passing through the center of the hole, there is an abrupt concentration of hoop stress just beyond the nozzle, which it is assumed is caused by bending due to eccentric rivet pull; beyond this point, both stresses fall rapidly to the low values that would naturally obtain in a full head at this radius—again compare with Fig. 7.

Fig. 11 shows the reinforcement that may be expected from sweep-type single-riveted nozzles applied to shell holes. It will be noticed that the high hoop stress at the edge of the hole on the longitudinal axis, in the unreinforced condition (Fig. 9), has been completely neutralized in all three tests; furthermore, the high longitudinal stress on the circumferential axis of the unreinforced hole has been satisfactorily reduced in test 109, although tests 107 and 206 leave something to be desired in this regard. On the other hand, the hoop stress on the circumferential axis, in all three tests, is too high. No doubt the eccentric rivet pull is largely responsible for this; also the fact that the saddle flange of the nozzle, which is the reinforcing agent, is completely symmetrical about its center, whereas the principal stresses to which it is subjected are individually symmetrical about the principal axes, but are unequal, so that it tends to distort into an elliptical shape. The somewhat poorer results for test 107, as compared with those for test 109, which was identical except for the riveting, may be attributed to that difference; in test 107, the theoretical shear

flanges against dishing that this type of nozzle exhibits, coupled with eccentric rivet pull, resulting in flexure of the shell plate just outside of the riveted area. Test 306, where the flange is very thick and the rivet circles are further removed from the edge of the hole, is the worst offender in this respect.

The final tests were made upon welded outlets, consisting of standard and special welding necks, a stud-welded sweep-type nozzle, and a standard welding nozzle. The earlier welding neck tests, Nos. 112 and 113, Fig. 13, show results not markedly different from those for the sweep-type riveted nozzles, i.e., good reinforcement on the longitudinal axis, but stresses above 100 per cent on the circumferential axis. The thin (special) neck, test 113, shows up very well in comparison with the standard neck, test 112—especially on the circumferential axis, where the greater stiffness of the standard neck introduces an undesirable bending moment.

When collars were applied to these two outlets, tests 114 and 115, the reinforcement on the longitudinal axis was increased unnecessarily, while the shell on the circumferential axis received a very heavy bending moment just beyond the outer weld. This might have been reduced somewhat if the joints had been annealed; however, experience with heavy saddles on previous tests leads one to expect a disadvantageous concentration of stress in any event, if the reinforcing collars are used.

None of these four welded connections was annealed to remove stresses set up in assembling. The effect of heat treatment is brought out in Fig. 14, test 308, where a standard neck was welded into the shell, with a slightly heavier fillet than was used in test 112. The results are eminently satisfactory, indicating that a well-proportioned neck, welded to the shell at a single point and then stress-relieved, gives all the reinforcement that is necessary.

The stud-welded nozzle, test 211, Fig. 14, is another example of

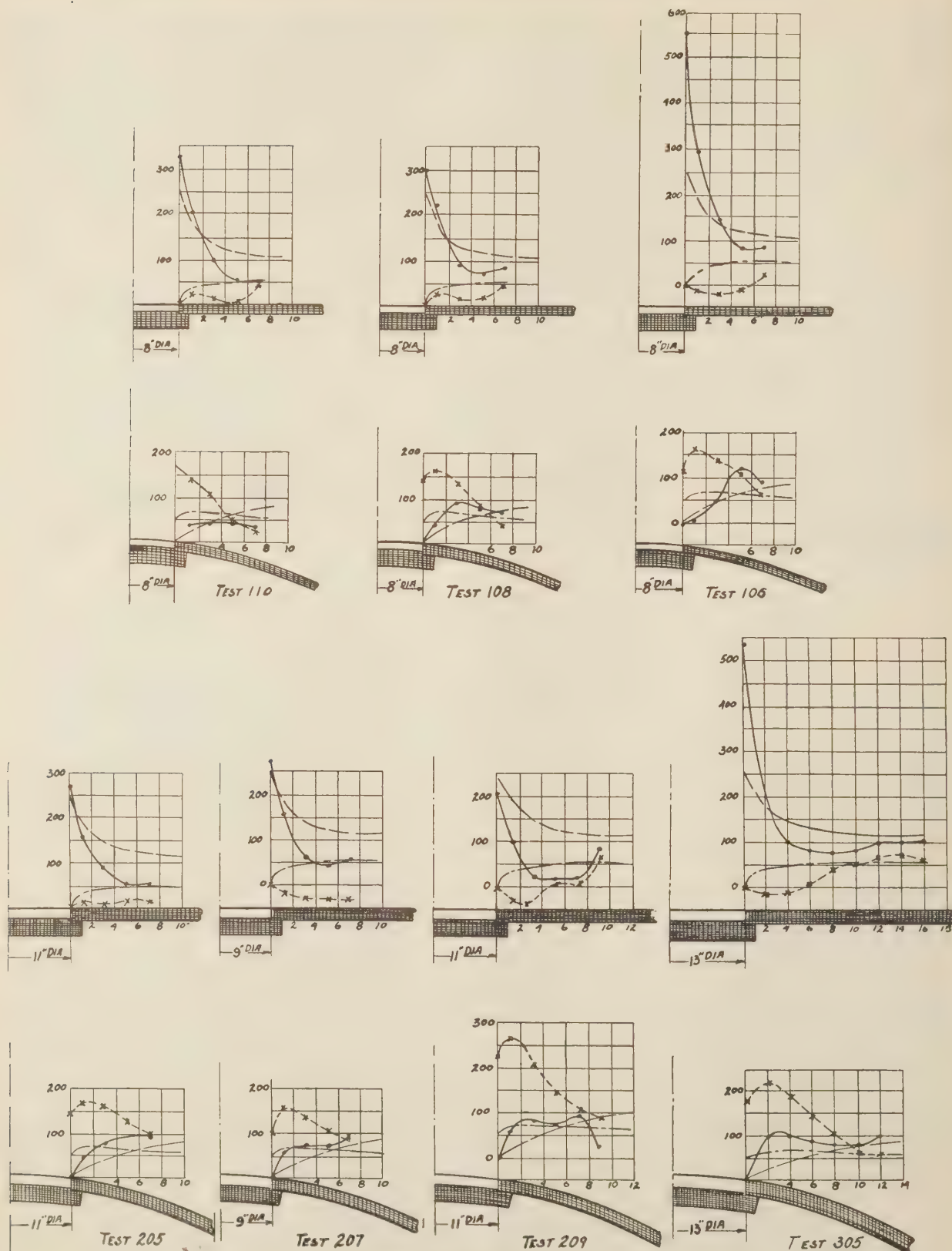


FIG. 9 EFFECT OF UNREINFORCED HOLES IN SHELLS

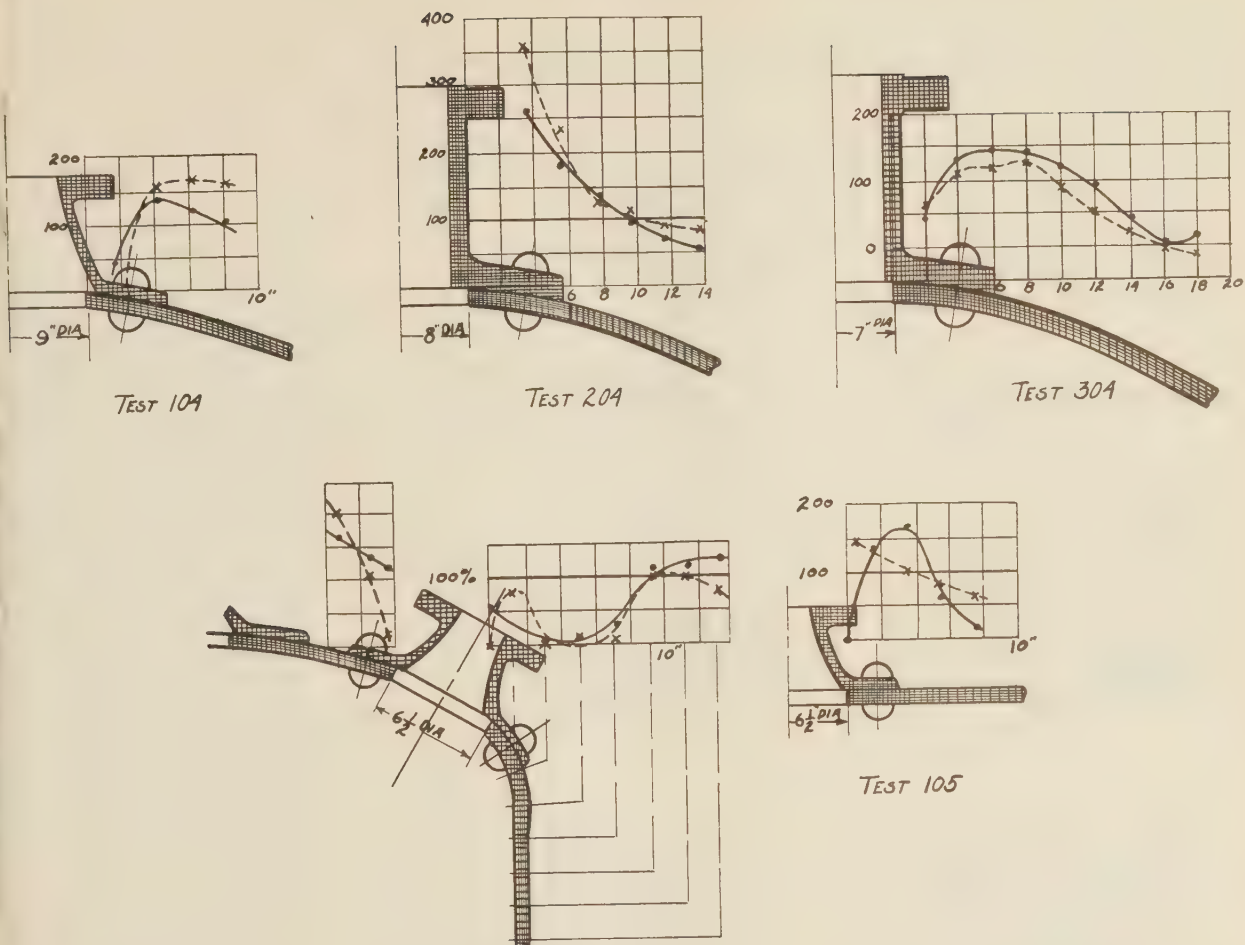


FIG. 10 REINFORCED HOLES IN HEADS

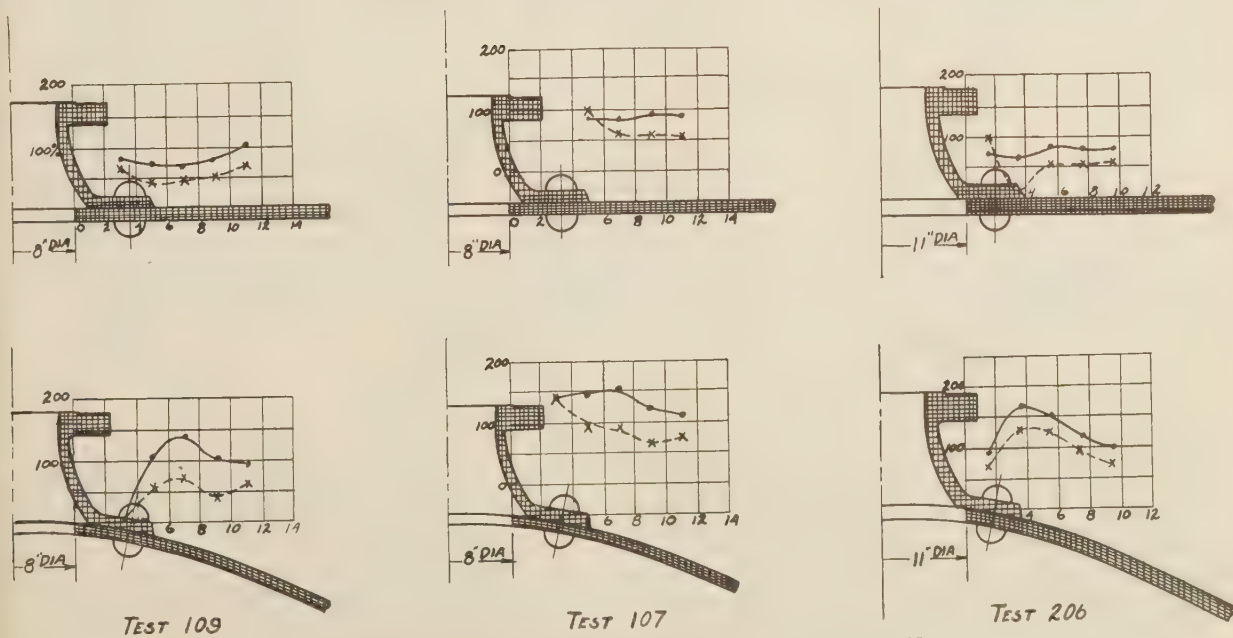


FIG. 11 REINFORCED HOLES IN SHELLS, SWEEP TYPE, SINGLE-RIVETED NOZZLES

adequate reinforcement on the longitudinal axis, coupled with objectionable bending effects on the circumferential axis. In this case, it is suggested that the difficulty might have been obviated by omitting the fillet weld around the outside of the saddle flange, and annealing.

The welding nozzle, tests 212 and 307, provides more reinforcement than the plain neck, and at the same time the area is con-

the most satisfactory type of design for pressure-vessel outlets that has been evolved to date, and when installed with proper care and workmanship, gives adequate reinforcement.

4—GENERAL CONCLUSIONS

(1) *Actual Stress in Full Ellipsoidal Heads.* It appears to be common practise in this country to base the thickness of ellipsoidal heads upon the simple membrane theory, neglecting bending. For example, the rule in the A.S.M.E. Boiler Code, P-195, is equivalent to specifying that the thickness of a 2-to-1 ellipsoidal head shall be computed by this theory, with the same factor of safety as for the shell. The authors wish to point out, however, that all such heads are subject to bending as well as direct tension. The impression seems to have gained ground that bending effects are important only at the knuckle, where the different rates of expansion of head and shell have to be equalized, whereas a close scrutiny of conditions reveals the fact that the displacement of the head under load must vary from point to point along each meridian, tending to make the ellipsoidal form approach a hemisphere and inducing bending moments that are far from negligible.

If we assume that the two principal stresses at any point in the head are given by the simple membrane theory, we can compute the corresponding strains from Equations [1]; then, by the theory of thin surfaces of revolution in which bending is considered,⁸ we obtain expressions for the components of displacement normal to the surface and parallel to the meridians, and by differentiation and substitution, the so-called "first" and "second" principal bending moments. At the crown, these latter reduce to the following simple value:

$$M = \frac{pt^2(k^2 - 1)}{6(1 - \mu)}$$

$$s' = \frac{6M}{t^2} = p \frac{k^2 - 1}{1 - \mu} \quad [2]$$

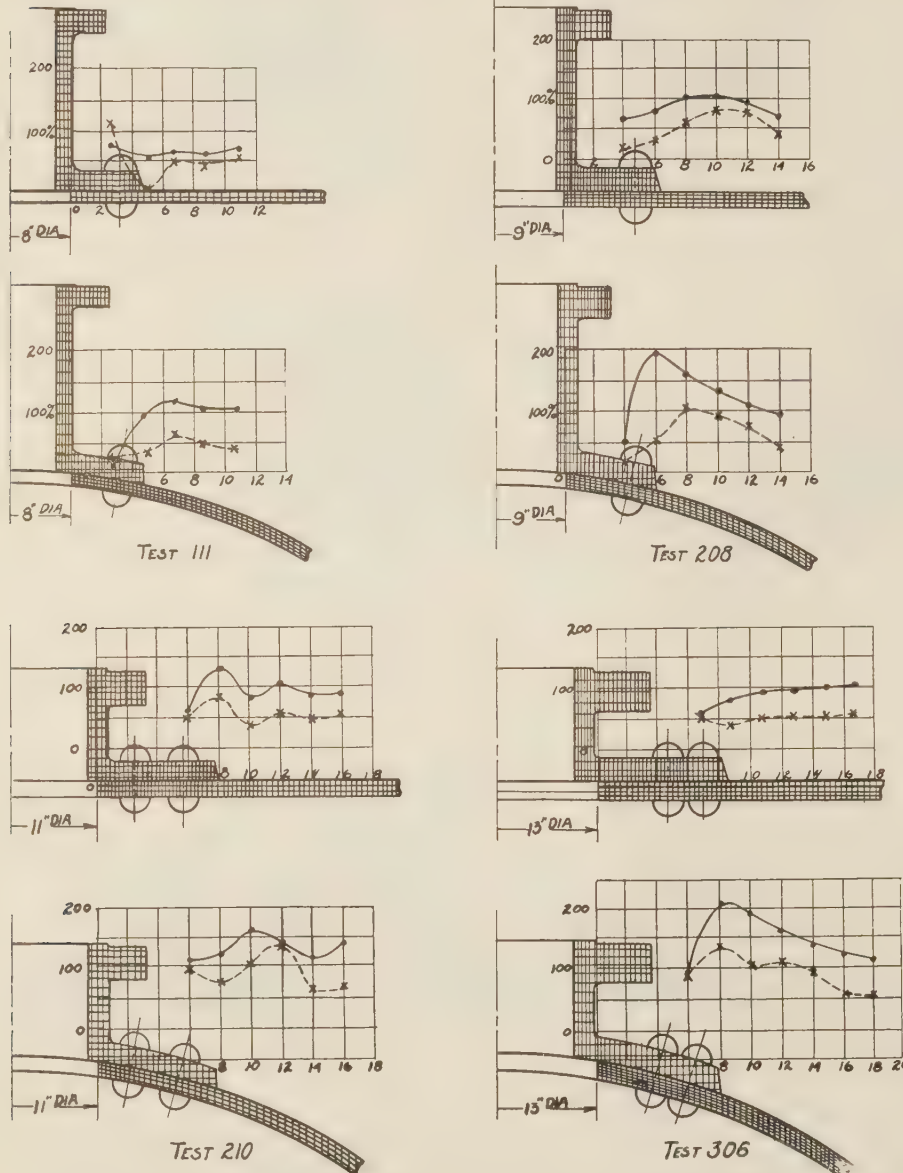


FIG. 12 REINFORCED HOLES IN SHELLS, STRAIGHT NECK, SINGLE AND DOUBLE RIVETED

centrated as nearly at one point as it is possible to get it. The two tests are structurally identical, except for the different thicknesses of shell plate and the extended inner lip on the nozzle in test 307. Both arrangements gave very satisfactory results on the longitudinal axis; and although the stress on the circumferential axis in test 212 did rise to about 180 per cent, there were no abrupt changes or narrow zones of high stress concentration, in contrast with riveted connections, such as test 208, or welded connections, such as test 114. This nozzle probably represents

where

M = moment acting on edge of element of unit length and breadth, tending to increase the convexity of the head, in-lb per in.

t = thickness of head, in.

p = fluid pressure required to produce the stresses in accordance with the simple membrane theory, lb per sq in.

⁸ Föppl, "Drang und Zwang," vol. 2, pp. 21-36; Pöschl, "Berechnung von Behältern," pp. 50-63.

k = ratio of major to minor axis

s' = stress in outermost fiber due to M , lb per sq in.

For a hemispherical head, $k = 1$ and $M = 0$; for a 2-to-1 ellipsoid, of steel, $M = 0.718 pl^2$ and

$$s' = \frac{6M}{t^2} = 4.31 p \dots \dots \dots [3]$$

$$= 431 \text{ lb per sq in. per}$$

100 lb per sq in. applied pressure.

There are two errors in the foregoing: The body has been assumed as a complete ellipsoid without edge loadings, and the strain energy of bending has been neglected. The first is unimportant, since it is well known that edge effects in a semi-ellipsoid are sensible only over a narrow zone and are imperceptible at the crown. The second would be serious in a thick head with large k , where conditions would approach those of a flat plate amenable to the Poisson analysis. In a 2-to-1 head, however, the bending energy is comparatively small. If we assume a strained configuration for the head identical with that which is given by the simple membrane theory, we can calculate the work done by the fluid pressure (using the value of p in the simple membrane formulas), the strain energy of direct extension, and the strain energy of bending. The authors have done this for the head of tank No. 1, using Coates' step-by-step method with 5-deg zones and finite differences of the displacements instead of differentials, and obtained 43.01×10^6 in-lb for the first, 43.05×10^6 in-lb for the second, and only 3.98×10^6 in-lb for the third, per lb per sq in. applied pressure. The close agreement between the first and second, which were obtained with a 12-in. slide rule, shows the efficacy of the step-by-step method; the small value of the third indicates that the specified configuration could be obtained by applying small supplementary corrective loadings (partly radial and partly meridional) to the elements of the head. A first approximation to the true state of stress could then be obtained by reducing or increasing the computed stress at any point by the ratio of the specified load to the corrected radial load at that point. But an examination of the equations of equilibrium shows that at the crown, where the shear is always zero, the corrective loading is zero; hence the first approximation gives, for the stress on the outer surface of the head at the crown:

$$\text{stress by membrane theory} + \text{stress by Equation [3]}$$

This is sufficient to account for the excess of observed over calculated stresses shown in Fig. 7, tanks Nos. 1 and 3. The trend of results for tank No. 2 is the same, with a single excessive result near the center, which may be a thermal stress caused by plugging the small central hole (see Fig. 1) with weld metal. The authors believe that these tests give clear evidence of the seriousness of bending in dished

heads and recommend that it be given due recognition by designers.

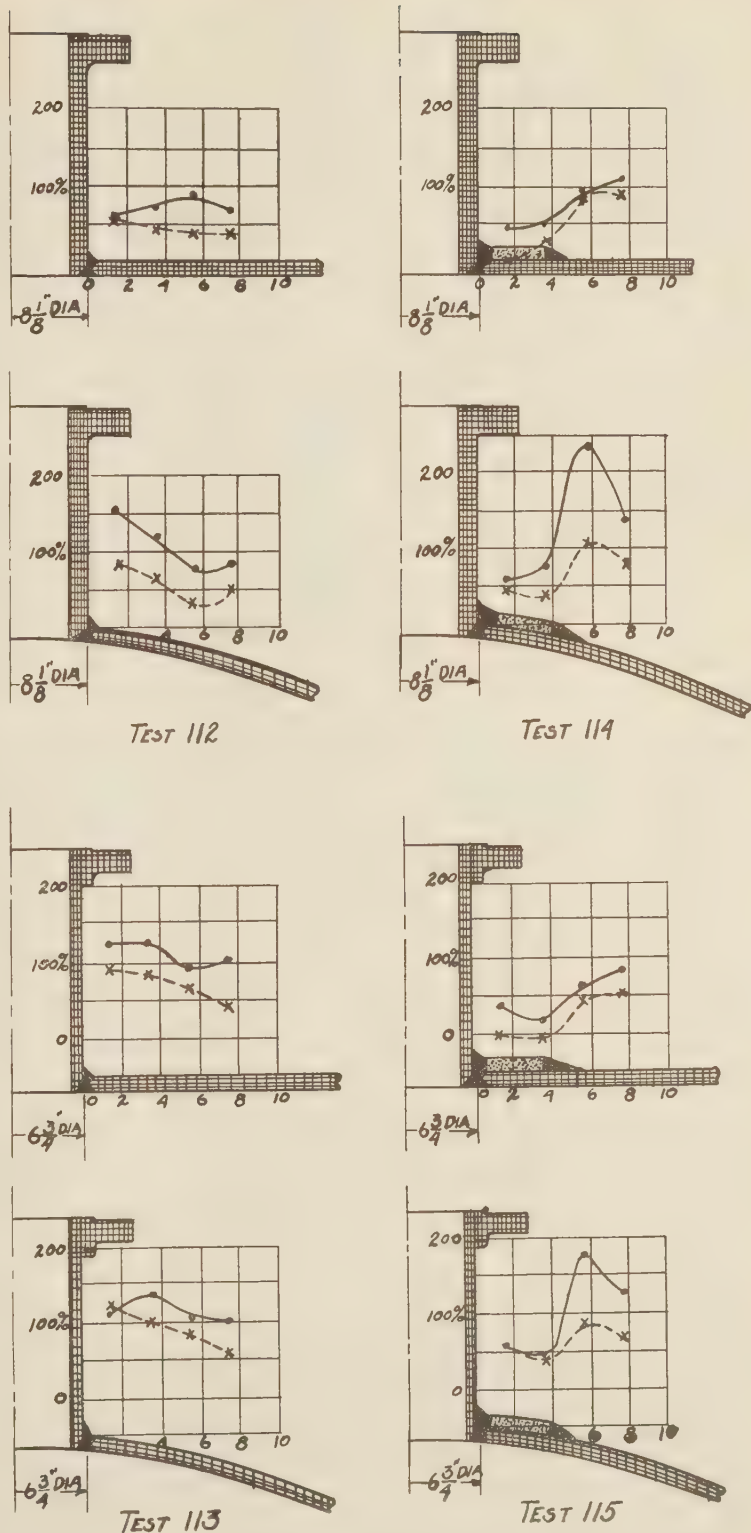


FIG. 13 REINFORCED HOLES IN SHELLS, WELDED NECKS

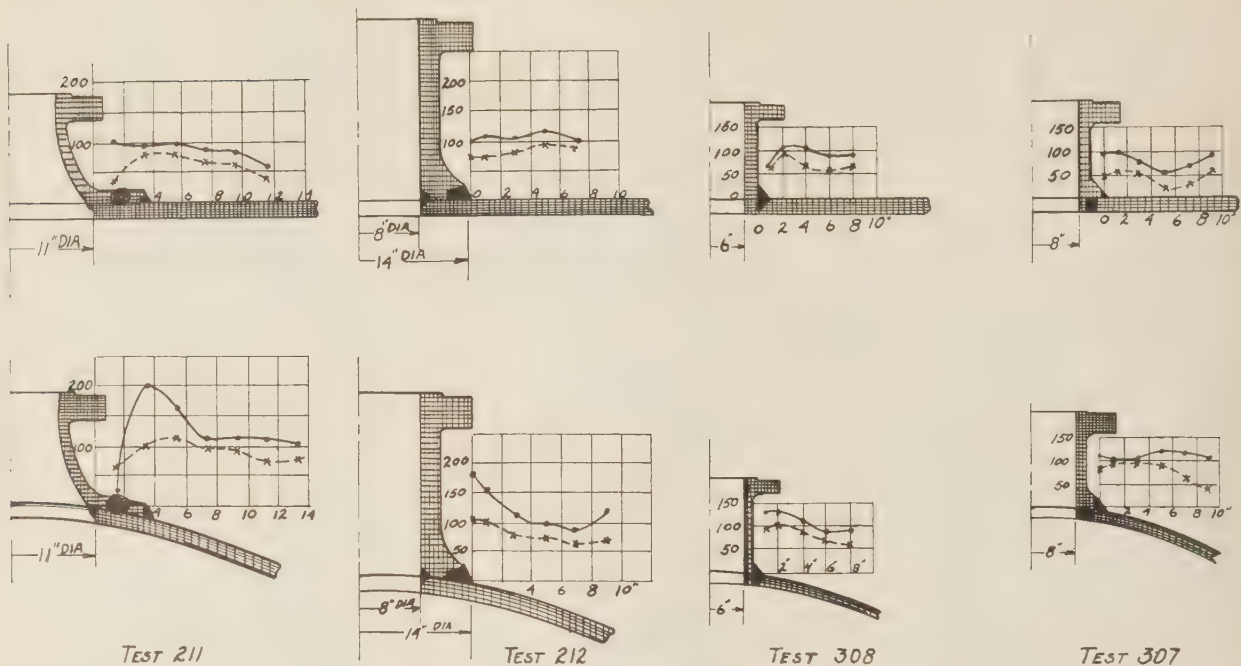


FIG. 14 REINFORCED HOLES IN SHELLS, WELDED NECKS, AND NOZZLES

(2) *Stresses Around Unreinforced Holes.* Figs. 8 and 9 show that the common two-dimensional formulas for stresses near a hole in a stretched plate give at best a poor representation of the actual conditions in a head or shell, of qualitative value only. The true state of stress in a head can be computed only from the equations for surfaces of revolution having flexural rigidity.⁹

TABLE 2 REINFORCEMENT VALUES OF NOZZLES

Tank and nozzle	Ratio of reinforcing metal to metal removed by hole	Ratio of actual to required rivet strength	
		Shear	Tension
1 A	0.892	1.066	2.22
1 B	0.827	0.907	2.28
1 C	2.435	1.293	2.11
1 D	1.146	1.44	2.22
1 E	1.093	1.23	1.968
1 F ^a	0.985
1 F ^b	2.19
1 G ^a	0.521
1 G ^b	1.997
2 A	2.06	1.132	1.753
2 B	0.747	0.865	1.90
2 C	2.47	1.11	1.333
2 D	1.596	1.233	1.503
2 E	1.08
2 F	1.97
3 A	1.866	1.454	1.678
3 B	1.557	1.087	1.212
3 C	0.91
3 D	1.063

^a Without collar. ^b With collar.

NOTE: Values in the table were computed in accordance with paragraphs P-180, P-193, P-195, P-260, P-261 and P-268, A.S.M.E. Boiler Code. Ultimate strengths were assumed as follows: 50,000 lb per sq in. for shells, heads, and nozzles in tension, 45,000 lb per sq in. for rivets in tension, and 44,000 lb per sq in. for rivets in shear. Weld metal was included in computing the areas of reinforcements. Efficiency of longitudinal weld in shells assumed as 0.7, equivalent to an ultimate strength for the weld of 35,000 lb per sq in. The weakening effect of rivet holes was not considered in computing the maximum allowable working pressure or the maximum permissible diameter of unreinforced opening. Had this been taken into account, the result would have been to reduce the working pressure, increase the maximum diameter of unreinforced opening, and increase the rivet strength ratios, in some of the entries in the table.

* See reference in footnote 8; also, for special solutions and approximate methods, the following: Geckeler, "Über die Festigkeit achsensymmetrischer Schalen," *Forsch. Ing.*, no. 276, 1926; Meissner, "Über Elastizität und Festigkeit dünner Schalen," and "Das Elastizitätsproblem für dünne Schalen," in *Phys. Zeit.*, vol. 14, 1913, p. 343; Reissner, "Spannungen in Kugelschalen," in *Müller-Breslau Festschrift*, 1912, pp. 181-193.

Unfortunately, these equations do not admit of exact solution except for a few simple cases of loading, with constant radii of curvature and special edge conditions. However, by means of Geckeler's approximation it is possible to get fairly easy solutions for spherical shapes with any desired edge conditions. The resulting shear stresses and angular displacements then take the form $e^{-c_1\psi} (c_2 \sin c_1\psi + c_3 \cos c_1\psi)$, where ψ is the angular distance from the edge of the hole, measured on a meridian; the corresponding linear displacements, direct stresses, and bending moments may then be computed directly by means of the exact formulas. It is recommended that this method be used for unreinforced central holes in heads, assuming a constant radius of curvature equal to the mean of the actual principal radii at the edge of the hole. It is also possible to obtain very accurate numerical results for individual problems by using difference equations over small intervals, instead of the more precise differential equations. Keller¹⁰ has given some interesting solutions, in which this method was employed, involving dished sheets with various edge conditions, with and without central holes, and with constant and variable thickness. It must be admitted that the amount of computation involved makes this last method a laborious one.

For holes in shells, the problem is complicated by the lack of symmetry. A suggested method of solution is to set the displacement equal to the regular displacement for a full cylindrical shell plus an exponential term with undetermined coefficients similar to that in the preceding paragraph, and solve by the minimum energy principle.

(3) *Characteristics of Good Reinforcement.* A survey of the data obtained by the authors in their tests points toward several principles of design which, when properly observed, result in good reinforcement of openings—i.e., reduction of the high stresses around unreinforced holes to values approximating 100 per cent of those which obtain in the full head or shell. Before

¹⁰ Z.V.D.I., vol. 56, pp. 1988-1993 and 2025-2028; *Forsch. Ing.*, no. 124, 1912, no. 195, 1917. See also "Berechnung gewölbten Boden," 1922 (Teubner).

discussing them, it should be well understood that a reinforcement is decidedly not the same as a connection or fastening, structurally speaking. A fastening must have strength, preferably equal to that of the parts it connects, but greater if so desired; a reinforcement needs not only strength but rigidity—and neither too much nor too little of the latter. For example, suppose two bars under tension are connected end to end by a tongue-and-groove joint in which a taper key is inserted; the key may be a loose fit, but the joint will hold if the key has sufficient area of cross-section. Now suppose that the joint is to be reinforced by cutting another slot and inserting a second key identical with the first. If this key (the “reinforcement”) is a loose fit, it will serve no useful purpose whatever, and on the other hand, if it is driven in too tight, it will relieve the first key of its share of the load and the joint will be no stronger than it was in the first place. Consequently, when rings and nozzles are attached by bolting or riveting, special effort must be made to see that the holes are completely filled; even then, it is not certain that the reinforcement will take its full share of the load—witness test No. 204 in comparison with 301, and 107 in comparison with 109.

In view of the foregoing, the authors would state that the actual connection between the reinforcing member and the pressure vessel should be as rigid as possible. Furthermore, the point of attachment should be as near the edge of the hole as practicable, to eliminate “dead metal” in the shell, and the reinforcing ring itself should be concentrated close to the edge of the hole, so as to distribute the stress more uniformly through it, and prevent the bending effects that are associated with broad, stiff rings attached to the shell at or near their outer edges.

In conclusion, a few numerical examples are given to illustrate the principles just outlined. They are based upon conditions in a thin flat plate with a hole at the center and uniform tension in all directions at infinity—admittedly not true of a curved shell or dished head, but approximate enough to serve for comparative purposes. In each example, the plate is assumed to have a thickness of 1 in., the radius of the hole is 5 in., and the stress at infinity is a tension of 11,000 lb per sq in. For simplicity, μ has been taken as 0.3. The following additional notation is used:

- s_r = radial stress in plate
- s_t = hoop stress in plate
- t = thickness of plate
- s = plate stress at infinity
- a = radius of hole
- u' = radial displacement of ring
- s_r' = radial stress in ring
- s_t' = hoop stress in ring
- t' = thickness of ring
- b' = outside radius of ring
- u = radial displacement of plate
- H = area of one section of ring
- $= (b' - a)t'$

Example 1. No reinforcement.

$$\begin{aligned}s_r &= s(1 - a^2/r^2) = 0 \text{ at edge of hole} \\ &= 8250 \text{ lb per sq in. 5 in. from edge of hole} \\ s_t &= s(1 + a^2/r^2) = 22,000 \text{ lb per sq in. at edge of hole} \\ &= 13,750 \text{ lb per sq in. 5 in. from edge of hole}\end{aligned}$$

This is the well-known result for a small hole in a plate, where the stress is doubled by the mere presence of the hole, regardless of size.

Example 2. 100 per cent nominal reinforcement, consisting of a ring of 5 sq in. (one section only), concentrated at the edge of the hole. The attachment of ring to plate is unyielding ($u = u'$ when $r = a$).

$$\begin{aligned}s_r &= s - \frac{sa^2}{r^2} \left[\frac{at - (1 - \mu)H}{at + (1 + \mu)H} \right] = 9570 \text{ lb per sq in. at edge of hole} \\ &= 10,650 \text{ lb per sq in. 5 in. out}\end{aligned}$$

$$\begin{aligned}s_t &= s + \frac{sa^2}{r^2} \left[\frac{at - (1 - \mu)H}{at + (1 + \mu)H} \right] = 12,430 \text{ lb per sq in. at edge of hole} \\ &= 11,350 \text{ lb per sq in. 5 in. out}\end{aligned}$$

$$s_t' = 9570 \text{ lb per sq in.}$$

Although the area of reinforcement equals the area removed by the hole, the ring is concentrated at one radius, and the attachment is unyielding, there is still an excess of 13 per cent in the hoop tension around the hole and a deficiency of 13 per cent in the full utilization of reinforcement.

Example 3. Same as example 2, but with a small amount of “slip” in the attachment ($u = 1.1u'$).

$$s_r = s - \frac{sa^2}{r^2} \left[\frac{1.1at - (1 - \mu)H}{1.1at + (1 + \mu)H} \right] = 9170 \text{ lb per sq in. at edge of hole}$$

$$s_t = s + \frac{sa^2}{r^2} \left[\frac{1.1at - (1 - \mu)H}{1.1at + (1 + \mu)H} \right] = 12,830 \text{ lb per sq in. at edge of hole}$$

The hoop tension is now $16\frac{1}{2}$ per cent in excess, and the utilization of reinforcement is correspondingly reduced.

Example 4. 200 per cent nominal reinforcement, consisting of a 10-sq-in. ring (one section only) concentrated at the edge of the hole, with unyielding attachment.

$$s_r = 12,200 \text{ lb per sq in. at edge of hole, 11,300 lb per sq in. 5 in. out}$$

$$s_t = 9800 \text{ lb per sq in. at edge of hole, 10,700 lb per sq in. 5 in. out}$$

$$s_t' = 6100 \text{ lb per sq in.}$$

Although the reinforcing metal has been doubled, conditions are no better than in example 2, the chief difference being an interchange in the values of hoop and radial stress; moreover, the reinforcement is only about 55 per cent utilized. Further reinforcement will only increase the radial stress and decrease the hoop stress, until in the limiting case the former equals 22,000 lb per sq in. and the latter equals zero. To secure actual 100 per cent reinforcement, the total cross-section of the ring must be 43 per cent greater than that of the hole, but in that case the strength of the ring is only 70 per cent utilized.

Example 5. 100 per cent nominal reinforcement consisting of a ring 1 in. thick, 5 in. inside radius, and 10 in. outside radius, attached rigidly to the plate at the edge of the hole.

$$\begin{aligned}s_r &= 6750 \text{ lb per sq in. at edge of hole, 9940 lb per sq in. 5 in. out} \\ s_t &= 15250 \text{ lb per sq in. at edge of hole, 12,060 lb per sq in. 5 in. out}\end{aligned}$$

$$\begin{aligned}s_r' &= -6750 \text{ lb per sq in. at edge of hole, 0 at outer edge of ring} \\ s_t' &= 11,240 \text{ lb per sq in. at edge of hole, 4480 lb per sq in. at outer edge}\end{aligned}$$

This shows the objectionable results accruing from poor distribution of the reinforcing metal; only the fibers near the edge of the hole are stressed the full amount, and the average utilization of the ring is less than 71 per cent; at the same time, the plate has a 39 per cent excess of stress at the hole edge.

Example 6. 100 per cent nominal reinforcement consisting of a ring of 5 sq in. area (one section only), rigidly attached to the plate, and concentrated on a circle of 7 in. radius.

$$\begin{aligned}s_r &= 0 \text{ at edge of hole, 3308 lb per sq in. out from edge of hole 2 in. —, 9855 lb per sq in. out from edge of hole 2 in. +,} \\ &10,440 \text{ lb per sq in. 5 in. out}\end{aligned}$$

$s_r = 13,486$ lb per sq in. at edge of hole, 10,178 lb per sq in. out from edge of hole 2 in. —, 12,145 lb per sq in. out from edge of hole 2 in. +, 11,560 lb per sq in. 5 in. out
 $s_t' = 9166$ lb per sq in.

Comparing with example 2, we find that the hoop stress in the plate, at the circle where the ring is attached, is slightly improved; but the metal around the edge of the hole, which is still carrying part of the load, even though from a very elementary and approximate point of view it is inside the ring and therefore "dead," is overstressed to the extent of 22½ per cent. Also, the ring is not as fully loaded as in example 2.

By making the ring 7.485 sq in. in area (one section), the radial and hoop stresses outside the ring are held exactly at 11,000 lb per sq in., and the annulus inside of the reinforcing ring is not overstressed; in this case, full reinforcement is secured by adding practically 50 per cent to the nominal area of reinforcing metal, but the stress in the reinforcing ring is only 7700 lb per sq in., representing 70 per cent utilization. This example shows the impossibility of getting full value out of both the reinforcement and the annulus of plate inside the circle where the reinforcement is attached, if this latter circle is but a small amount greater than the hole in the plate.

Appendix

The equations for a stretched flat plate of constant thickness having conditions symmetrical about a central axis are:

$$s_r = \frac{E}{1 - \mu^2} (\delta_r + \mu \delta_t) \quad s_t = \frac{E}{1 - \mu^2} (\delta_t + \mu \delta_r)$$

$$\delta_r = A - \frac{B}{r^2} \quad \delta_t = A + \frac{B}{r^2} \quad u = Ar + \frac{B}{r}$$

where r = distance of any point from the axis, and A, B are constants determined by the boundary conditions. Combining the stress and strain equations, we have

$$s_r = E \left[\frac{A}{1 - \mu} - \frac{B}{(1 + \mu)r^2} \right] \quad s_t = E \left[\frac{A}{1 - \mu} + \frac{B}{(1 + \mu)r^2} \right]$$

For an unreinforced plate, there are only two constants to be determined, requiring two boundary conditions. For example 1, these are: $s_r = s$ when $r = \infty$, $s_r = 0$ when $r = a$. Hence, from the equations for s_r , $A = \frac{(1 - \mu)s}{E}$, $B = \frac{(1 + \mu)a^2 s}{E}$. Substitution of these in the foregoing equations for s_r , s_t , and u , gives the stress and radial displacement at any point.

For a plate with a narrow reinforcing ring, examples 2, 3, and 4. — $s_r' = \frac{s_t'(b' - a)}{a}$, $u' = \frac{s_t'a}{E}$, the quantities for the ring being designated by primes. The boundary conditions are: $s_t = -s_r't'$ when $r = a$, $u = ku'$ when $r = a$, $s_r = s$ when $r = \infty$. Hence: $A = \frac{(1 - \mu)s}{E}$, $B = \frac{sa^2}{E} \left[\frac{(1 + \mu)kat - (1 - \mu^2)H}{kat + (1 + \mu)H} \right]$.

For a plate with a wide reinforcing ring, example 5, there are two systems of equations and four constants, A, B, A', B' . The four boundary conditions are: $s_r = s$ when $r = \infty$, $s_t = -s_r't'$ when $r = a$, $u = u'$ when $r = a$, and $s_r' = 0$ when $r = b'$. The radii for the plate and ring are assumed equal. Hence:

$$A = \frac{1 - \mu}{E} s \quad B = \frac{a^2 s}{E} \left[(1 + \mu) - \frac{2t'(b'^2 - a^2)}{tL} \right]$$

$$A' = \frac{2(1 - \mu)a^2 s}{(1 + \mu)EL} \quad B' = \frac{2a^2 b'^2 s}{EL}$$

$$\text{where} \quad L = \left(\frac{1 - \mu}{1 + \mu} - \frac{t'}{t} \right) a^2 + \left(1 + \frac{t'}{t} \right) b'^2$$

A plate with a reinforcing ring concentrated on a circle of radius c , larger than the radius of the hole, will have three systems of equations. Designating the quantities for the ring by primes, and those for the plate between radius a and radius c by double primes, the boundary conditions are: $s_r - s_r't + s_r't' = 0$ when $r = c$, $s_r'' = 0$ when $r = a$, $s_r = s$ when $r = \infty$, and $u = u' = u''$ when $r = c$. Also, as in example 2, $-s_r't' = \frac{s_t'H}{c}$ and $u' = \frac{s_t'c}{E}$.

Hence:

$$A = \frac{1 - \mu}{E} s$$

$$B = \frac{2c^2 s [(1 - \mu)c^2 + (1 + \mu)a^2]}{E \left\{ 2c^2 + [(1 - \mu^2)c^2 + (1 + \mu)^2 a^2] \frac{H}{ct} \right\}} - \frac{(1 - \mu)sc^2}{E}$$

$$A'' = \frac{2(1 - \mu)c^2 s}{E \left\{ 2c^2 + [(1 - \mu^2)c^2 + (1 + \mu)^2 a^2] \frac{H}{ct} \right\}}$$

$$B'' = \frac{2(1 + \mu)a^2 c^2 s}{E \left\{ 2c^2 + [(1 - \mu^2)c^2 + (1 + \mu)^2 a^2] \frac{H}{ct} \right\}}$$

Discussion

C. W. OBERT.¹¹ Professor Waters has very definitely outlined the objectives of the actual tests as made, but he has not undertaken to explain the reasons for the need of such experimental data. The writer will, accordingly, add some comments on this phase of the question.

The actual need for data along this line arose when the rules of the A.S.M.E. Boiler Construction Code were amplified in 1931 to provide for fusion-welded construction. It was then, and only then, that the outstanding difference between welded and riveted connections for attaching nozzles and other connections to shells or heads became apparent. The riveted attachment is capable of considerable slip or "give" before an overload will drive the plate metal thoroughly into contact with the rivets, and in the process of such slight deformation the structure usually resolves itself into somewhat stronger shape. Such is not the case with a welded attachment, however, as if the connection is strength-welded and the weld is thoroughly fused to the base metal, there is no "give" and the welded joint assumes the entire load from the outset; this is the reason for a number of failures that were not at first understood.

This characteristic of the welded joint has revealed many points of weakness in customary forms of attachments using flanges and fillet-welded connections; these weaknesses have been more apparent in nozzles, manhole frames, and the like where reinforcements are considered necessary. Probably the outstanding feature of this development was the revelation of the ineffectiveness of the ordinary nozzle-reinforcing pad as commonly attached by methods simulating a riveted connection. It soon became evident that welded attachments demanded a very different method of treatment if efficient transfer of stresses from shell to pad was desired, but there seemed to be no way of learning how to work this out unless an extensive series of tests was

¹¹ Consulting Engineer, Union Carbide and Carbon Research Laboratories, Long Island City, N. Y. Mem. A.S.M.E.

carried out to determine the actual effect of stressing various forms of riveted and welded attachments.

A few individual tests of certain forms of reinforcing construction were made by some concerns that had specific problems to handle, but the results from these were far from comprehensive. It was not until Mr. J. Hall Taylor, of the Taylor Forge and Pipe Works, volunteered to conduct a series of tests that there appeared to be any hope of securing these much-needed data. Mr. Taylor made comprehensive plans for this investigation. He retained Prof. E. O. Waters, assistant professor of mechanical engineering at Yale University, to consult and advise on the tests and to analyze the results. The work of testing was carried out in the testing laboratory at the Taylor plant in Chicago, with Mr. W. L. Bowler in charge of the testing crew. Mr. Taylor consulted frequently with the Boiler Code Committee in order to work out the most needed phases of the problem, and both Mr. Taylor and Mr. Bowler appeared from time to time before the Boiler Code Committee to present preliminary reports on the test results and to discuss the progress of the tests.

During the winter of 1931-1932, the Boiler Code Committee was confronted with some unusual problems in regard to the reinforcement of openings, and Mr. Taylor contributed freely of the data they had obtained from the tests up to that time. He also offered the committee the assistance of Mr. Bowler on several different occasions. It was largely on the basis of these test data that the new rules for reinforcement of openings were issued in 1932 in the form of revisions of pars. P-268 and U-59 of the code. These rules introduced a new and different method of computing the required reinforcement of any opening in a shell or head. They are adequate and comprehensive, and they have done much to enhance the value of the welding rules in the code. They are logical and cover all imaginable cases of nozzle construction. It is interesting to note that they constitute the first set of rules for this purpose that has appeared in any code in the world.

The experimental work reported in this paper has certainly had a profound effect on the design of nozzles and outlet connections for use on pressure vessels. Comparative data were produced that proved the theoretical estimates of the concentrations of stress at openings, and they were sufficiently quantitative to be definitely useful in studying the minimum requirements for safety. Without these data the recent revisions of pars. P-268 and U-59 could not have been made so complete and comprehensive. The Boiler Code Committee is therefore indebted to Mr. Taylor and is grateful to him for his cooperation. It is appreciative of his generosity in making this investigation possible, and recognizes the public-spirited attitude he has shown.

A. M. WAHL.¹² The authors are to be congratulated on having made a start toward a solution of such a difficult problem as that involving stress conditions near the openings of pressure vessels.

In connection with the use of a Berry strain gage, the writer believes that the use of an instrument for measuring curvature would also be of advantage. If both the strains and the changes in curvature on the outside of the tank wall are measured, then it is a simple matter to calculate, not only the stresses on the outside of the wall, but also those on the inside. It may possibly be that in certain cases the latter are greater.

In connection with these tests on the effect of holes in pressure vessels, some recent photoelastic work which has been done by the writer in collaboration with Mr. R. Beeuwkes may be of interest. This work had to do with finding stress concentration factors K (i.e., ratios of maximum stress to average stress in the minimum section) for bars of finite width with holes under tension and will be reported on in a future publication. A sketch of

the case considered is shown in Fig. 15. Here is also shown the stress-concentration factor K plotted against the ratio d/w = diameter of hole/width of plate. The small circles represent test results by the writer and Mr. Beeuwkes, using the photoelastic-fringe method and monochromatic light. The triangles represent photoelastic test results reported by Hennig,¹³ the black dots similar results reported by Coker,¹⁴ and the half-filled circles those of Preuss,¹⁵ who used extensometer methods. The dotted curve is based on mathematical calculations by Howland.¹⁶

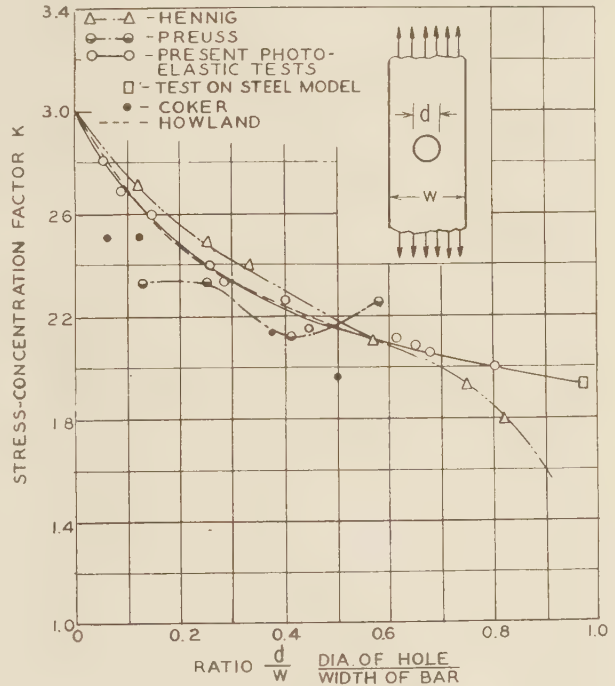


FIG. 15 STRESS-CONCENTRATION FACTOR VERSUS d/w FOR A FLAT BAR WITH A HOLE

The small square represents an extensometer test on a steel model having a hole with a diameter nearly equal to the bar width. It may be seen that the writer's test results agree well with the mathematical results of Howland and are in general higher than those of the earlier investigators, a fact which may be explained by the difference in the methods used. It is noteworthy that even for a bar with a hole of diameter 0.97 of the width the factor K is still nearly 2.

While the case represented in Fig. 15 is considerably different from that of a pressure vessel with an unreinforced opening, the results may possibly be of some interest in this connection.

C. G. WILLIAMS.¹⁷ No attempt will be made to give a true discussion of this paper, which without doubt is the best one ever presented on the subject, both as to means of performing the tests and of arriving at the formulas presented. The writer cannot hope to add to the facts presented in the paper, but he will give some facts regarding effects that have come to his notice as a foreman in railroad shops. He does not know why these things happen, but he does know that occasionally they do happen, and without resort to systematic tests, such as the authors

¹³ *Forschung*, vol. 4, no. 2.

¹⁴ *Proc. Lond. Phys. Soc.*, 1912-13, p. 95.

¹⁵ *Forschungsarbeiten*, no. 126, 1912, and no. 134, 1913.

¹⁶ *Phil. Trans. Royal Society, A*, 1929, p. 49.

¹⁷ Chief Engineer, Green Bay Barker Machine and Tool Works, Green Bay, Wis. Mem. A.S.M.E.

¹² Research Engineer, Westinghouse Research Laboratories, East Pittsburgh, Pa. Assoc.-Mem. A.S.M.E.

have carried on, he has tried to formulate a reason for their occurrence.

In this discussion five drawings will be given, Fig. 16 being the horizontal section of a steam dome as applied to the boiler of our oldest types of power and is made up of three parts. Fig. 17 is a view of the same dome when looking down upon it. Fig. 18 is a view of a two-piece dome as used some years ago on the largest power then in use. Fig. 19 is a view of the dome, formed from one piece of metal, that is used on modern locomotives of the largest types.

As the checks or cracks shown in Fig. 17 are those also encountered in steam dome tops as depicted in Fig. 18, no separate top view is given of this dome. In the case of Fig. 19, only one dome has shown signs of cracking, to the writer's knowledge, and this case was only a slight crack that might be termed a fatigue crack from breathing in the knuckle and one short crack at the opening, but on the opposite side of the dome, and which would therefore be similar to the cracks shown in Fig. 17.

An outline will also be given of the barrel and throat sheet of a locomotive boiler for a use that will be explained later and which was made necessary by a question asked at the meeting.

In Figs. 16, 18, and 19 are shown the usual location of breathing cracks, and in Fig. 17 is shown the extent to which they may spread. This figure also illustrates the manner in which they may join up with the cracks originating from the dome head opening as at *F* and *H*; there also is shown at *x* and *y* how some of the cracks extend from the dome-head opening that have no relation whatsoever to the breathing cracks.

In some cases these cracks have been chipped out and electric welded so successfully that they have been in service for at least three years and no failure has been recorded. Before the advent of electric welding, these checks or cracks had in some cases been chipped out and a copper strip dovetailed in place so that the locomotive could be continued in service. One such case was noted after 12 years' service in a switch engine.

In the case here presented, that part of the crack, Fig. 17, from *A* to *B* and from *C* to *D* is caused by breathing, but what actually causes the crack from *A* to *F* and from *D* to *H*? It must be remembered that the opening is covered with a circular, slightly crowned steel plate fully as thick as the metal in the dome head, in most cases $1\frac{1}{4}$ in. thick, machined around the outer edge for approximately $1\frac{1}{2}$ in. width to form a bearing seat. Generally this seat is grooved slightly to hold a copper-wire gasket. There is a ring machined around the opening in the dome head corresponding to that on the cover. This machined portion reduces the thickness of the metal approximately $\frac{1}{16}$ in. In this faced portion of the head is drilled a series of holes that are tapped with a tapered tap, 12 threads to the inch. In these holes are screwed the studs that retain the cover in place.

In some few cases where the dome heads have cracked from breathing only, the crack has been filled up with an electric weld to keep the locomotive in service, and up to date the writer does not know of one such welded dome head that has failed in service and of only one that has opened up new cracks. In this one head, apparently the new crack started at the edge of the opening, passed through a stud hole, and continued to a breathing crack nearly 1 in. from the weld. The new crack traveled around the end of the weld, but had no connection with it.

Though but one welded head has failed by cracking from the opening outward, several have failed from cracks in the knuckle and have been removed. In those cases where breathing cracks have extended into the opening or where breathing cracks and opening cracks have existed in the same head, that head has been removed and a new one put in place.

On one or two occasions a section of metal that would be bounded roughly by the lines *FAB* and *CDH*, Fig. 17, prolonged

until they meet, has been torn completely away. In other cases, the cracks have been detected, and the dome head has been replaced.

Though having no connection with the subject, the writer will mention that cracks have appeared in the throat sheet, Fig. 20, at points say *A* and *B*. These have been variously designated as tension cracks from internal strains, as embrittlement cracks, and as breathing cracks.

In Fig. 20, it will be noticed that the boiler is supported at the front end on the cylinder saddle; then on two belly braces (in some cases on old types of locomotives only one belly brace and in some cases with the largest types of power three or four belly braces); at the front end of the firebox is an expansion pad and at the rear of the firebox may be either a brace or another expansion pad.

The question was asked if cracks in the dome head were on the longitudinal axis more often than on the lateral axis. The answer is, in all locomotive boilers there is a tendency for the boiler to sag in the center, where supported by the belly braces, from the weight of the boiler shell and the enclosed water. This has been so pronounced in some cases that the bolts in the bottom of the braces have been sheared off and the plates forced off the ledge machined for their support. This might cause the belly of the boiler to assume the shape of the dotted lines, Fig. 20, and the back or top of the boiler to assume a similar contour. This it is believed would tend to cause a closing up of the cracks in the dome where they show on the lateral axis. However, they do appear fully as often on the lateral as on the longitudinal axis.

A suggestion was made that the older types of dome heads might be more prone to crack than would the new types of dome in use on modern heavy locomotives and illustrated by Fig. 19. The writer would say that he has seen one of these low one-piece domes crack in the knuckle and also has seen cracks from the opening outward, but in none of them were sections of the dome head completely surrounded by cracks, and in no case did breathing cracks and opening cracks tend to extend until they met.

It was also suggested that the stud holes might be a source of weakness, but the writer has seen the cracks open up between the studs as well as through the stud holes, as illustrated in Fig. 17.

In a paper (A.S.M.E. meeting, December 2 to 6, 1926) Frederick G. Straub, of the University of Illinois, on "Recent Instances of Embrittlement in Steam Boilers," gives a record of failures that had been shown to be the cause of cracks in throat plates (*A* and *B*, Fig. 20), but an examination of steam-dome cracks and checks has not shown any tendency toward embrittlement, although metallurgical examination of the steel in one cracked dome head did show a grain structure at the edge of the opening and extending outward toward the knuckle some 2 in. that indicated an overheating of the plate at some time during fabrication.

In the paper, "Fracture in Boiler Metal" (A.S.M.E. meeting, June, 1930), A. E. White and P. Schneidewind, of Ann Arbor, Mich., state: "Failure in mild carbon steel through tension seems to start in the relatively strong but brittle pearlite constituent." Again, referring to fatigue cracks: "Cracking does not proceed through the pearlite grains. The pearlite undoubtedly transmits the stresses to the next ferrite grain, which will then crack in the usual manner. When actual fracture occurs, the pearlite fails because it alone is bearing all the load." The writer has found the same condition to show in embrittlement cracking. It is believed that the cracks in the knuckle of the dome head are the result of fatigue produced by breathing, but this may be induced by the methods of fabrication of the head.

F. H. Moore, "Tests of the Resistance to Repeated Pressure of Forged, Riveted, and Welded Boiler Shells" (A.S.M.E. meeting,

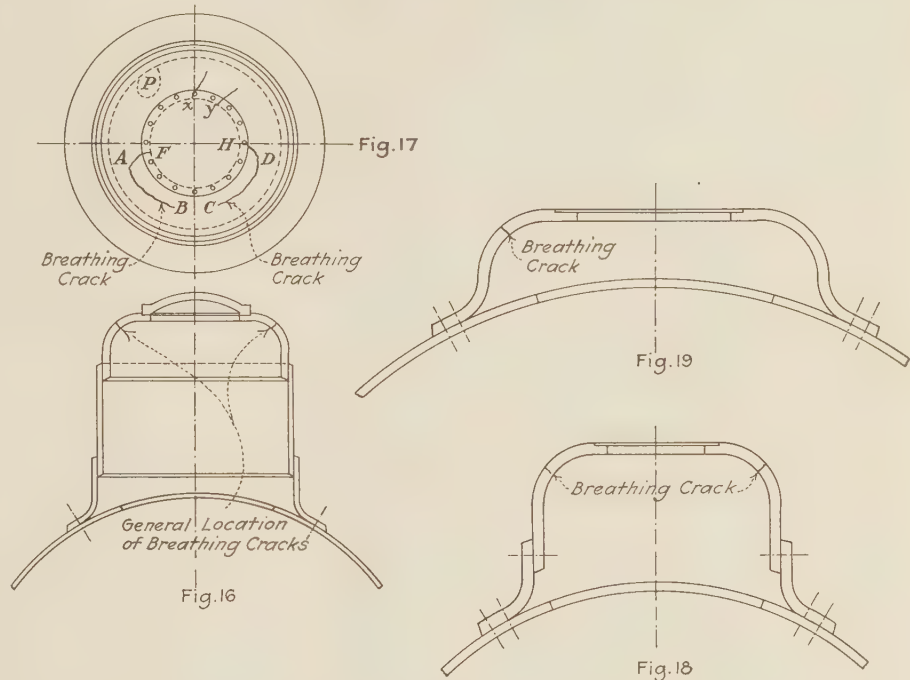
Detroit, June, 1930), referring to the test of a manganese-steel test drum, states: "The measurements of stress during this test showed no evidence of appreciable distortion of the drum, except in the immediate vicinity of the crack;" and again in referring to the fracture of a seamless forged test shell, states: "It was quite evident that this tapped hole acts as a region of stress concentration, where a spreading fatigue crack is likely to start." The crack in the manganese-steel drum started at the edge of a manhole opening. This was chipped out and welded, but no statement was made of the method of weld nor the nature of the weld except that: "After 143 additional cycles of pressure, the drum head split violently through the crack repaired by welding." This would infer that welding was a dangerous procedure. The writer has found welding with the acetylene torch to give the same results, while good electric welds have given the best of results.

An interesting study that might give some light on constructive analysis is the paper by W. M. Coates, Ann Arbor, Mich. (A.S.M.E. meeting, December, 1929), "The State of Stress in Full Heads of Pressure Vessels," wherein he shows that breathing effects are not only shown in the knuckle of the head, but also throughout the surface of an ellipsoidal head. The question would naturally arise, if this condition exists, whether it would not be possible that the cracks in the circumference of the opening in the heads of pressure vessels are the effects of fatigue from those very conditions imposed on the metal of the head and localized by some defect in the contour of the opening caused in fabrication, or perhaps by inclusions in the steel.

Formerly it was thought that this cracking was the result of internal strains, but for at least 14 years dome heads have been annealed after processing and still failures have resulted.

The question was asked if, as all steels are not homogeneous but contain dirt spots, blowholes, gas pockets, or various forms of inclusions, it could not be that these could have started the cracks referred to. The answer is that, in one case at least, an examination of the metal in the head, which was sawed in several pieces, showed that the metal traversed by the crack was homogeneous without inclusions of any type, but there was a spot, let us say at P, Fig. 17, that was full of dirt and other inclusions, but for some reason the crack, either the radial or the breathing, did not extend in that direction. It has seemed to the writer that in these types of usages of materials, such as in locomotive steam-dome heads, air-reservoir heads, hydraulic-tank heads

etc., checks start in the stiffest section of the metal because of resistance to flexion. Howe, "Metallography of Steel and Cast Iron," p. 296, states: "The path of deformation and rupture is governed first by the nature of the existing stresses and second by the properties of the material itself."



(Fig. 16 Three-Piece Locomotive Steam Dome. Fig. 17 Typical Cracks in a Steam Dome. Fig. 18 Two-Piece Dome. Fig. 19 Modern One-Piece Dome.)

FIGS. 16 TO 19 CRACKS OCCURRING IN STEAM DOME OF OLD-TIME AND OF MODERN LOCOMOTIVES

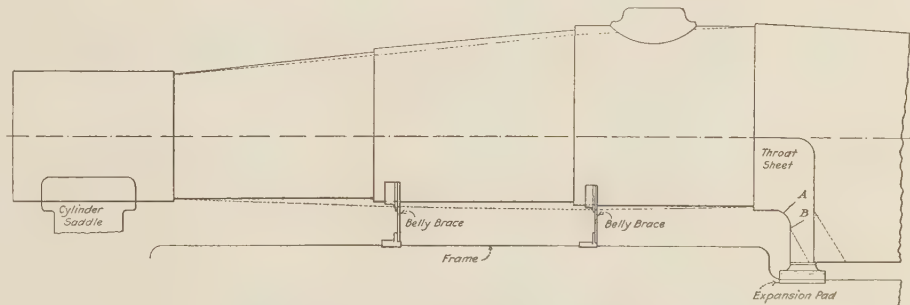


FIG. 20 THROAT SHEET FAILURE AND BOILER SAG

The writer does not know what causes these radial cracks from the opening in the head. It may be fiber stresses that are in excess of the tensile strength of the steel, as suggested by Mr. Waters, and it may be that the machining of the edge of the opening for the seat for the dome cap weakened the edge of the opening so that excessive fiber stresses were generated. However, this must be determined by test.

W. TRINKS.¹⁸ These experiences of Mr. Williams lead me to believe that, in addition to the stresses mentioned by Mr. Taylor and Professor Waters, other important stresses enter, which account for the failures described by Mr. Williams. Professor Waters has shown that in an unreinforced hole the stress at the

¹⁸ Professor of Mechanical Engineering, Carnegie Institute of Technology, Pittsburgh, Pa. Mem. A.S.M.E.

edge of the hole is very high. From theory it is known that in a flat circular disk the stress at the edge of the hole equals twice the average stress and that it drops off rather quickly as we go away from the edge of the hole toward the solid metal. Using Mr. Williams' sketch, the writer has indicated roughly how that stress would distribute itself near the edge of the hole. In addition to these stresses we have magnification of stress around the stud hole.

These studs seem to be dangerously close to the inner edge of the hole, and since around these stud holes we have a magnification factor of three, it appears that at the edge of the stud hole the stress may be even higher than it is at the edge of the center hole. In that way we would exceed the elastic limit.

With regard to exceeding the elastic limit, no harm is done as long as we deal with a fairly constant pressure in the pressure vessel. When the elastic limit is exceeded, in simple theory those parts which are more highly stressed can yield and can shift the stress to their neighbors which are not stressed so highly. Then if we have a material which does not flow-harden to any extent, no harm is done. We must never forget that the shrink links in flywheels always work at the elastic limit. All the rivets in bridges are continually stressed to the elastic limit, and yet we are not afraid to walk across the bridge on account of that fact.

Boiler tubes and other boiler parts are strained beyond the elastic limit due to heat expansion and contraction, and yet nothing untoward happens.

Matters are different if we use a material which does not possess sufficient deformability beyond the elastic limit or which by forming below the critical temperature has been stressed in such a way that its additional deformability is limited; in that case a crack may easily occur.

From the fact mentioned by Mr. Williams that the crack runs radially outward and then becomes peripheral or circumferential, the writer judges that there is an initial stress in the corner of the dome. The circumferential crack may be due to the residual stresses left over from the fabricating of the material. If the material is bent below the critical temperature, and is bent so as to get a permanent set, then and in that case the stress distribution in the bent plate is as indicated in the left-hand part of Fig. 22. The stress distribution then consists of approximately two rectangles. The instant the bending action stops, the material of the curved plate springs back to such an extent that no free moment is left. The back spring is elastic, with the result that the stress distribution in the plate after bending is as indicated at the right of Fig. 22. In other words, we have residual stresses.

Now, if we put the pressure on the vessel, we can readily exceed the elastic limit in the bent section, although our calculations apparently show that we are safely below the elastic limit. If the pressure in the vessel goes up and down, we may even have alternations of stress in places where we do not expect a change in direction of stress.

With regard to the fact mentioned by Mr. Williams that some of the domes broke while others did not break, it should be stated that steel is not a homogeneous material. It is full of phosphides, sulphides, oxides, and sand, not to mention small particles of refractory material which may have been torn loose from the lining of the ladle or the pouring nozzle. If a piece of foreign material happens to be at the region of very high stress, we have another very high concentration of stress, because the foreign particles are as a rule rather jagged, which means that the stress is magnified by more than three. This fact would easily explain the circumstance mentioned by Mr. Williams in his discussion that only a certain number of the steam domes let go, whereas others held and stood the tests very well.

GEORGE W. WATTS¹⁹ AND W. R. BURROWS.²⁰ The problem of reinforcement of vessel openings has been actively discussed for several years, but prior to this paper, no work of sufficiently general character to establish the problem on a sound basis has been published. Isolated measurements of strain have been available and also some theory, but much of the latter appears to have been developed from statical rather than from elastic considerations. Perhaps the necessities of construction that have produced the empirical rules for reinforcement have retarded rather than advanced a knowledge of this subject.

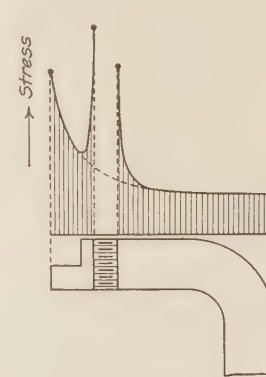


FIG. 21 STRESS MAGNIFICATION AT EDGE OF HOLE

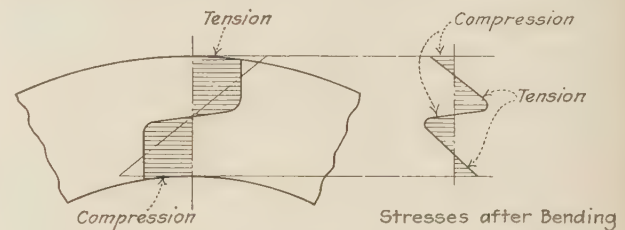


FIG. 22 INTERNAL STRESS REMAINING AFTER FORMING HAS PRODUCED PERMANENT SET

understanding of the underlying theory. The correction of the relationship between stress and strain for two-dimensional stress systems has not been over-looked. Important points that are emphasized are:

- 1 Rigidity as well as strength is required by reinforcement.
- 2 Reinforcing metal should be concentrated nearer the opening than is now customary.
- 3 The possibility of the use of excessive reinforcing metal exists.

These points do not seem to have received much previous attention, but confirm the writer's conclusions.

Perhaps an easy method of visualizing reinforcement is to consider an unstressed shell with a set of concentric circles drawn on its surface. When the shell is subjected to internal pressure, the circles become slightly elliptical, but this deformation is comparable with that in other parts of the shell not near points of localized stress. For purposes of this illustration, these deformed circles will be designated as normally strained circles. If it is an experimental possibility to remove the shell metal inside one of the circles and still subject the shell to internal pressure without reinforcing the shell metal around the hole, the circles will be strained beyond their normal deformation. Perfect reinforcement will maintain all the circles in their normally strained condition, but if any of these circles are strained either more or less than that designated as normal, the reinforcement is not perfect. Although this illustration neglects flexural strains, it is accurate enough to establish the importance of rigidity. No matter how large is the reinforcement or how strong is the reinforcing metal statically, it does not constitute perfect reinforcement unless the normal deformation of the circles is maintained.

¹⁹ Chief Engineer, Standard Oil Company (Indiana), Whiting, Ind. Assoc. Mem. A.S.M.E.

²⁰ Designing Engineer, Standard Oil Company (Indiana), Whiting, Ind. Jun. A.S.M.E.

The discussion of elastic analogs is of considerable interest, and while these analogs do not represent a perfect picture of vessel reinforcement, they are, as pointed out in the paper, "approximate enough to serve for comparative purposes." An investigation of these analogs has been in progress in the Engineering Department of the Standard Oil Company of Indiana since 1929. In 1930 stress and strain equations, similar to those given in the paper, were developed for the analogs shown in Figs. 23 and 24. The basis of calculation for the analog shown in Fig. 24 is that at the juncture of the plate and ring the total radial load per inch of circumference of the juncture is the same for both the plate and the ring, and uniformly distributed over the edge of each. Naturally this assumption becomes decreasingly accurate as the ratio of the ring and plate thicknesses increases. Stresses derived from the analog of Fig. 24 are plotted in Fig. 25. This chart shows that perfect reinforcement is attained at approximately the following conditions:

$$\frac{\text{External radius of ring}}{\text{Internal radius of ring}} = 1.35$$

$$\frac{\text{Thickness of ring}}{\text{Thickness of plate}} = 4.5$$

However, when the thickness of the ring is 4.5 times that of the plate, the validity of the assumed conditions of stress and strain at the juncture of the plate and ring appears extremely doubtful. Owing to the inaccuracy of these assumptions, the chart probably is of no great value, but it appears to indicate the advantage of massing the reinforcement nearer to the opening.

To eliminate to some extent the doubtful assumptions of the analog of Fig. 24, a more accurate elastic analog, shown in Fig. 26, has been studied. Here the component parts are the infinite flat plate, the conical fillet ring, and the flat ring. While the assumptions of this analog are by no means perfect, they are

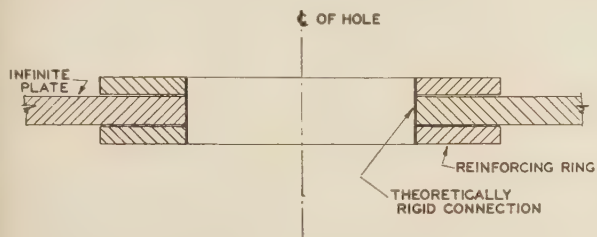


FIG. 23 TYPE ONE ANALOG

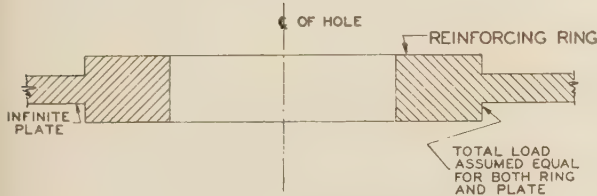


FIG. 24 TYPE TWO ANALOG

certainly more accurate than those for Fig. 24, as long as the angle remains reasonably small.

The conditions of equilibrium are that the radial and tangential stresses and displacements of each element must be equal at each of the two junctures. These conditions are eight in number, but immediately reduce to four, because the displacement equations for the three elements are identical and depend on the stresses.

The equations for the infinite flat plate and for the flat ring are drawn as before from the results of Lamé. It is not necessary to employ the Airy stress function for this special symmetrical case

of the infinite flat plate; Lamé's results with an infinite external radius suffice.

The equations for the fillet ring are obtained from Martin's solution of the conical disk (*Engineering*, London, Vol. 115, Jan., 1923, p. 1). The differential equation is of the hypergeometric form. Consequently, the solution is the hypergeometric series (A. R. Forsyth, "A Treatise on Differential Equations," Ed. 6, 1929, p. 210, and others). This series solution does not complicate the problem excessively, but adds to the tedium of the computations. Martin's results, required for this problem, are given in Table 3.

The important stresses are those at the juncture of the infinite flat plate and the fillet ring and at the edge of the hole. Of these

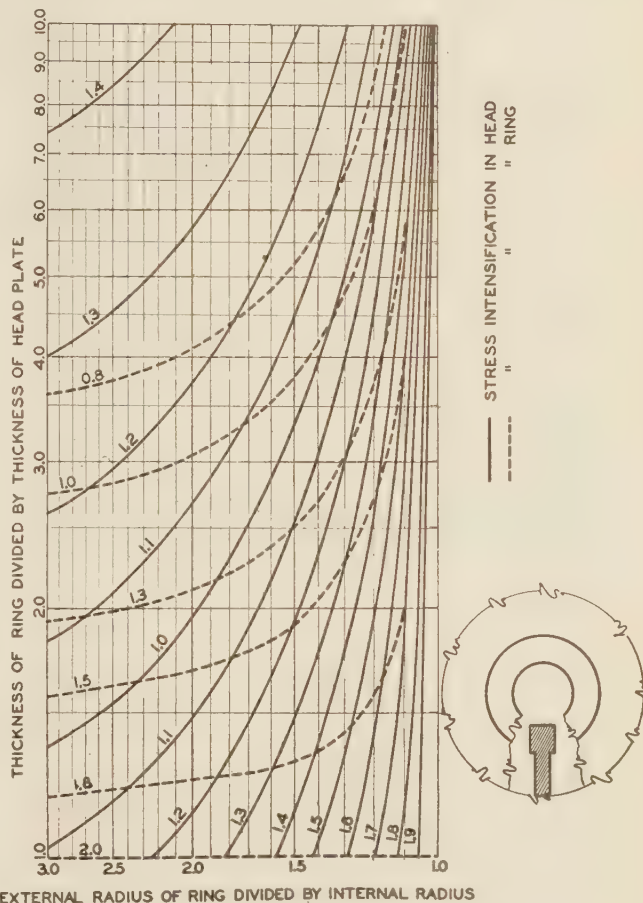


FIG. 25 STRESSES FOR TYPE TWO ANALOG

four stresses, it is sufficient to calculate the tangential stress at the edge of the hole, and the radial stress at the juncture of the infinite flat plate and the fillet ring. The remaining two stresses follow at once from the first two. To make the study more complete, the effect of internal pressure on the edge of the hole is introduced.

The notation necessary for a brief statement of the equations involved in the stress-and-strain solutions of the analog of Fig. 26 is as follows:

T = unit tangential stress at any radius

R = unit radial stress at any radius

$\tau = T/S$

$\rho = R/S$

a , b , and c = specific radii (used with the foregoing)

S = unit stress in flat plate at infinite distance from hole
 P = unit internal pressure
 U = radial displacement
 E = modulus of elasticity
 σ = Poisson's ratio
 a = radius of hole
 b = external radius of flat ring
 c = external radius of fillet ring

$+$ = tension
 $-$ = compression

For the determination of the two important stresses the necessary relations are:

For an infinite flat plate:

$$R = S + \frac{c^2}{r^2} (R_c - S)$$

$$T = S - \frac{c^2}{r^2} (R_c - S)$$

For a fillet ring:

$$R = Ap_1 - Bp_2$$

$$T = Aq_1 + Bq_2$$

For a flat ring:

$$R = \frac{Pa^2 + R_b b^2 - \frac{a^2 b^2}{r^2} (R_b + P)}{b^2 - a^2}$$

$$T = \frac{Pa^2 + R_b b^2 + \frac{a^2 b^2}{r^2} (R_b + P)}{b^2 - a^2}$$

For the three elements:

$$U = \frac{r}{E} (T - \sigma R)$$

To make the stresses equal at the junctures of the elements, four simultaneous equations are available:

$$Ap_{1c} - Bp_{2c} = R_c$$

$$Aq_{1c} + Bq_{2c} = 2S - R_c$$

$$Ap_{1b} - Bp_{2b} = R_b$$

$$Aq_{1b} + Bq_{2b} = \frac{2P + R_b(K^2 + 1)}{K^2 - 1}$$

Additional relationships are:

$$T_a = \frac{2R_b K^2 + P(K^2 + 1)}{K^2 - 1}$$

$$T_c = 2S - R_c$$

The method of solution is to express the various stresses, and the internal pressure, as ratios of the stress S at infinity. Then, by means of determinants, and six additional functions derived from Martin's four functions, the following stress expressions are obtained:

$$\tau_a = \frac{\left[(K^2 + 1) I - III \right] \frac{P}{S} + 2K^2 VI_b}{K^2 I - II}$$

$$\rho_c = \frac{K^2 IV - V - VI_c \frac{P}{S}}{K^2 I - II}$$

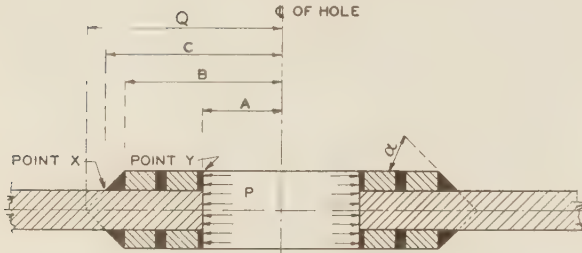
$$\tau_c = 2 - \rho_c$$

$$\rho_a = -\frac{P}{S}$$

The six extensions of Martin's functions are defined as follows:

$$I = q_{2b}(p_{1c} + q_{1c}) - q_{1b}(q_{2c} - p_{2c}) + \frac{III}{2}$$

$$II = q_{2b}(p_{1c} + q_{1c}) - q_{1b}(q_{2c} - p_{2c}) - \frac{III}{2}$$



NOTE:

CALCULATIONS ARE BASED ON INTEGRAL PLATE AND REINFORCING RING CONSTRUCTION. SKETCH SHOWS HEAVY WELDING APPROXIMATING THIS INTEGRAL CONSTRUCTION.

CALCULATIONS FOR 10" DIA HOLE IN PLATE 1" THICK

K	K_B	K_C	B	C	α	$\frac{T}{P}$	$\frac{R}{P}$	MAXIMUM STRESS RATIOS			
								$\frac{P}{S} = 0.00$	$\frac{P}{S} = 0.05$	$\frac{P}{S} = 0.10$	
								X	Y	X	Y
2.0	.90	.95	10	10.56	42°	2	1.056	1.02	1.34	1.01	1.40
1.6	.90	.95	8	8.44	48°	2	.644	1.10	1.42	1.12	1.49
1.2	.80	.90	6	6.75	34°	2	.275	1.34	1.60	1.39	1.69
2.0	.85	.95	10	11.18	40°	3	2.236	1.16	1.01	1.14	1.07
1.6	.85	.95	8	8.94	47°	3	1.388	1.06	1.09	1.04	1.17
1.4	.85	.95	7	7.82	51°	3	.964	1.03	1.18	1.07	1.27
1.2	.85	.95	6	6.71	55°	3	.542	1.21	1.35	1.27	1.45
1.35	.55	.90	6.75	11.05	22°	4.5	2.380	1.17	0.82	1.16	0.90

FIG. 26 TYPE THREE ANALOG

Q = radius of periphery of conical disk extended

α = angle of fillet

$K = b/a$

$K_b = b/Q$

$K_c = c/Q$

r = any radius

T_p = thickness of plate

T_r = thickness of flat ring

p_1, p_2, q_1, q_2 = Martin's stress functions for a conical disk

I, II, III, IV, V, VI = extensions of Martin's functions

A, B = constants of integration

TABLE 3 MARTIN'S FUNCTIONS

r/Q	p_1	p_2	q_1	q_2
1.00	∞	0.0000	∞	2.051
0.95	20.645	0.0555	8.890	2.140
0.90	10.620	0.1203	5.554	2.263
0.85	7.263	0.1995	4.276	2.421
0.80	5.563	0.2971	3.557	2.614
0.75	4.559	0.4161	3.111	2.835
0.70	3.860	0.5670	2.794	3.102
0.65	3.390	0.7523	2.556	3.419
0.60	3.021	0.9988	2.369	3.816
0.55	2.733	1.309	2.217	4.301
0.50	2.501	1.743	2.090	4.944
0.45	2.311	2.328	1.983	5.788
0.40	2.151	3.158	1.890	6.915
0.35	2.015	4.387	1.809	8.531
0.30	1.898	6.371	1.738	10.89
0.25	1.796	9.553	1.674	14.85
0.20	1.707	15.54	1.617	21.91
0.15	1.627	28.68	1.565	36.55
0.10	1.559	66.62	1.518	77.28
0.05	1.497	273.40	1.475	288.60
0.00	1.435	∞	1.435	∞

TABLE 4 EXTENSIONS OF MARTIN'S FUNCTIONS

K_c	K_b	T_r/T_p	I	II	III	IV	V	K_b & K_c	VI
0.95	0.95	1.000	89.3474	0.0000	89.3474	89.3474	89.3474	0.95	89.3474
0.95	0.90	2.000	80.9509	29.5700	51.3809	97.8441	90.2674	0.90	49.4024
0.95	0.85	3.000	83.6229	41.5590	42.0639	107.8689	93.0066	0.85	36.8736
0.95	0.80	4.000	90.1608	49.4190	40.7418	119.9767	96.6771	0.80	31.1969
0.95	0.75	5.000	99.0396	55.4541	43.5855	134.0772	100.7278	0.75	28.4385
0.95	0.70	6.000	110.5860	61.0010	49.5850	151.3747	105.4088	0.70	27.1158
0.95	0.65	7.000	124.9378	66.3666	58.5713	172.1404	110.7680	0.65	27.0266
0.95	0.60	8.000	143.5642	71.9706	71.5937	198.7307	116.9205	0.60	27.7886
0.90	0.90	1.000	49.4024	0.0000	49.4024	49.4024	49.4024	0.55	29.3134
0.90	0.80	2.000	51.3824	17.9321	33.4503	61.3491	51.4052	0.50	32.0156
0.90	0.75	2.500	55.6859	22.6888	32.9971	68.7050	53.2228	0.45	35.9850
0.90	0.70	3.000	61.6265	26.7436	34.8830	77.6731	55.4444	0.40	41.6855
0.90	0.65	3.500	69.2536	30.3907	38.8629	88.3978	58.0713	0.35	50.2521
0.90	0.60	4.000	79.2716	34.0162	45.2554	102.1095	61.1342	0.30	63.4840
0.90	0.55	4.500	91.8418	37.7862	54.0555	119.0323	64.7411	0.25	85.4324
0.90	0.50	5.000	109.0362	41.9359	67.1003	141.9330	69.0938	0.20	125.0571
0.90	0.45	5.500	131.9710	46.7613	85.2097	172.3049	74.5235	0.15	208.7021
0.80	0.80	1.000	31.1969	0.0000	31.1969	31.1969	31.1969	0.10	443.2174
0.80	0.65	1.750	39.9746	10.5440	29.4305	45.9143	33.2028	0.05	1670.5984
0.80	0.60	2.000	45.4216	13.2048	32.2168	53.1820	34.5469		
0.80	0.55	2.250	52.3587	15.8184	36.5403	62.1103	36.2303		
0.80	0.50	2.500	61.9377	18.5582	43.3815	74.1553	38.3423		
0.80	0.45	2.750	74.7779	21.6084	53.1714	90.1037	41.0475		
0.80	0.40	3.000	92.4705	24.9013	67.5692	111.9171	44.2015		
0.80	0.35	3.250	118.2894	28.9335	89.3560	143.6033	48.3784		
0.80	0.30	3.500	157.7910	32.7890	125.0020	191.9508	52.4389		
0.80	0.25	3.750	223.1116	40.5426	182.5690	271.7691	61.3301		
0.80	0.20	4.000	341.7525	50.3930	291.3595	416.6152	72.8477		
0.80	0.15	4.250	595.0413	64.3789	530.6624	725.7121	89.4583		
0.70	0.70	1.000	27.1158	0.0000	27.1158	27.1158	27.1158		
0.70	0.45	1.833	54.8353	12.1375	42.6978	62.2836	31.5806		
0.70	0.40	2.000	67.6874	14.7551	52.9322	77.4676	33.5865		
0.70	0.35	2.167	86.4786	17.8803	68.5983	99.4934	36.3281		
0.70	0.30	2.333	115.2603	20.8522	94.4081	133.0735	39.0099		
0.70	0.25	2.500	162.8865	26.6494	136.2370	188.4844	45.0594		
0.70	0.20	2.667	249.4205	33.9596	215.4608	289.0119	52.9458		
0.70	0.15	2.833	434.1976	44.2753	389.9223	503.5053	64.3761		
0.70	0.10	3.000	957.6145	63.1314	894.4831	1110.8615	85.7845		
0.70	0.05	3.166	3739.6038	93.6068	3645.9970	4338.6151	120.7142		

$$III = 2[p_{1b}(q_{2c} - p_{2c}) + p_{2b}(p_{1c} + q_{1c})]$$

$$IV = 2[p_{1c}(p_{2b} + q_{2b}) - p_{2c}(p_{1b} - q_{1b})]$$

$$V = 2[p_{1c}(q_{2b} - p_{2b}) + p_{2c}(p_{1b} + q_{1b})]$$

$$VI = 2(p_{1q_2} + p_{2q_1})$$

Some values of these functions are given in Table 3. Extensions of Martin's functions are given in Table 4.

In Fig. 27 and in the table of Fig. 26 a few results of calculations of stress in this analog are given. Slight irregularities in the curves of Fig. 27 are no doubt due to errors in the calculation of the ordinates. These computations are not checked at present, but it appears that they are, in general, accurate. An exhaustive study of the stress functions has not been made, but in so far as the computations are completed, they indicate:

- 1 Perfect reinforcement is not attained by this analog.
- 2 Excessively heavy reinforcement rings are required for the maximum elastic reinforcement.
- 3 Considerable reinforcement is provided by rather small rings.
- 4 A comparison of line 1 and line 6 of the table of Fig. 26 indicates a considerable advantage in massing the reinforcing metal nearer the hole.

It should be noticed that the values tabulated in Fig. 26 are for the same example discussed by the paper. Variations in the size of the hole and the thickness of the metal may have a considerable influence on the shape of the optimum reinforcement. These points have not been investigated. It should be noticed also that the fillet ring assumed for the analog of Fig. 26 is a part of a conical disk. It is possible to employ a fillet ring with curved fillets by using Stodola's solution (Prescott, "Applied Elasticity," 1924, p. 343). It may be possible to extend the methods described in this reference to determine a better profile for reinforcing rings.

If it is reasonable to draw conclusions about the reinforcement of openings in vessels from the elastic behavior of this analog, it might be said in conclusion that:

- 1 It does not appear practicable to attempt to reduce the elastic stresses below 130 per cent.
- 2 For large holes in thin plates, the reinforcement should be

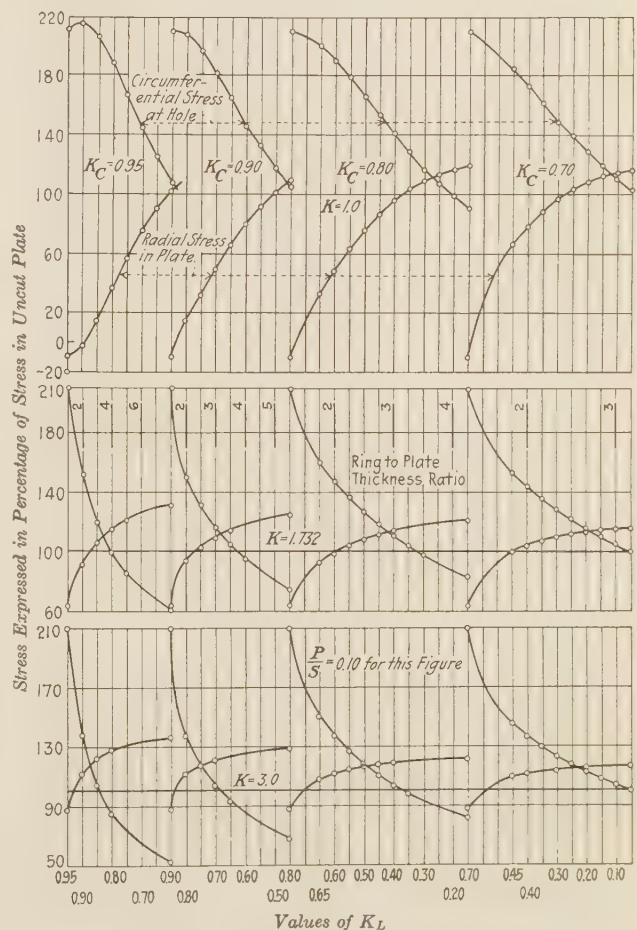


FIG. 27 STRESS FOR TYPE THREE ANALOG

massed nearer the hole; for small holes in heavy plates, the reinforcement should be extended further from the hole.

3 The conclusions of "2" may make practicable the design of integral nozzle and reinforcement units by reducing the external diameter of the reinforcement and giving a reasonable length to the welded butt joint. While these joints have the advantage that they can be X-rayed, they are very difficult to make by welding.

4 The fact that elastic stresses in excess of 100 per cent are indicated or observed does not mean that yielding before failure in a test to destruction will not sufficiently redistribute the stresses to cause ultimate failure in the uncut shell rather than at the hole.

Additional relationships that may prove helpful in further studies of this problem are:

$$\frac{\text{Thickness of ring}}{\text{Thickness of plate}} = \frac{1 - K_b}{1 - K_c}$$

$$\frac{\text{Area ring and fillet}}{\text{Area hole}} = \frac{(K_c - K_b)(KK_b + KK_c - 2K_b)}{2K_b(1 - K_c)}$$

T. McLEAN JASPER.²¹ The paper represents an attempt at analyzing stresses in openings which may be helpful in the work of design. Could the author state if the vessels before testing were completely strain relieved? Obviously, this could not be done with the riveted connections.

The writer has discovered that in making tests of this kind the strains cannot be interpreted in terms of stress without running a risk of very much overestimating them in certain spots and underestimating them in others. He has insisted in going to the yield value of the steel in the vessel. This of course involves distortion. Finally, we have been able to test each vessel to destruction, and this has confirmed our general test data. Incidentally, we have so tested 21 full-size vessels, and most of them with appropriately designed reinforcing, which allows us to readily state that the openings are as strong as the plain cylinder.

In testing designs, we have almost completely discarded the strain gage and substituted lime wash to indicate the zones of first yield in various parts of the design. This eliminates assumption with reference to interpreting the test results. This was first done in conjunction with strain-gage measurements in which the obvious assumptions were used to interpret stresses in terms of strains. We discovered that our calculated stresses from strain-gage readings below the yield point did not check with the yielding of the lime wash nor with the final failure of the vessels. We therefore in subsequent tests put more reliability on the lime-wash experiments, and finally abandoned the strain-gage measurements altogether as being misleading at crucial points. Most of our test vessels were also strain-relieved before the tests were performed.

AUTHORS' CLOSURE

At the time when the equipment was designed for these tests, and the first tests were run and preliminary reports worked up, the 1930 edition of the Boiler Code was in force. This edition was therefore used as a guide by the authors, and computations of maximum allowable working pressures, maximum permissible diameters of unreinforced holes, etc. were based upon the rules

set forth in this edition in its original form. As addenda sheets were issued from time to time, some of these rules have been modified. In particular, par. P-268 has undergone a major revision.

It would be interesting to compare the reinforcement values of the various nozzles on the basis of the new rules with those in force three years ago. This, however, is really a side issue. The point to be noted is the use in the new rules of an important principle—namely, the concentration of all reinforcement within a definitely limited area bordering the hole. This is in exact agreement with the authors' conclusions, and, in their belief, marks a notable step forward in the progress of safe pressure-vessel design. In this connection, the authors wish to express their deep appreciation of Mr. Obert's remarks and to state that it has been a pleasure to cooperate with the Boiler Code Committee in the solution of some of its problems.

Dr. Wahl's point regarding the measurement of curvature is well taken. There are undoubtedly marked differences between the tensions on the outer and inner skin of a vessel adjacent to the hole edge, but for a first study of the problem, it seemed to be hardly worth while to make any investigation beyond the outer skin. The authors admit that they have made little more than a start toward the solution of the problem, and in later investigations would probably consider measurements of curvature.

Professor Trinks has, we believe, pointed out the two most important causes of Mr. Williams' difficulties—namely, high stress concentrations around the steam-dome opening for the cover plate and loss of strength at the knuckle due to cold working. In addition, it is suggested that breathing at the knuckle could be minimized by better reinforcement of the main boiler shell at the point where the dome is attached to it. Possibly some of the designs to which Mr. Williams refers would not measure up to the requirements of par. P-268 (b) of the 1933 Boiler Code.

Messrs. Watts and Burrows have evidently been doing some searching analytical work along the same lines that the authors have pursued, and it is gratifying to learn that they have, quite independently, reached the same general conclusions. The elastic analogs have been worked out in great detail, and it is hoped that they will be studied by designers who wish to make a more than usually careful analysis of their reinforcements. Another analog worth investigating is the combination of an infinite flat plate with a hole at its center, joined to a tube of infinite length; in this case the equations for a beam resting on an elastic foundation, with specific moments and shears at one end and zero loading at the other end, would hold.

In reply to Dr. Jasper's inquiry, the authors would state that the nozzles which were acetylene-welded to the shell were stress-relieved locally. In the last two tests the nozzles were electric-welded and were subsequently stress-relieved by bringing the entire vessel to the proper temperature. The lime-wash treatment certainly gives a good indication of the commencement of plastic strain, but in the present tests the authors wished to determine local stress distributions for a large number of different set-ups with the same vessels, and therefore did not wish to subject the vessels to the repeated overloads that the lime-wash method would have entailed. As a matter of fact, the vessel in test 116 was lime-washed, but the locations of initial plastic yield evidenced by cracking of the wash did not conflict with what would have been predicted from the strain-gage readings or adduce any facts with regard to the state of stress in the vessel that were not already known.

²¹ Director of Research, A. O. Smith Corp., Milwaukee, Wis. Mem. A.S.M.E.

Graphostatics of Stress Functions

By H. M. WESTERGAARD,¹ URBANA, ILL.

Graphostatics is interpreted here in the broader sense, as statics in which geometry plays a part. A stress function defines stresses or forces by its values or derivatives. If a stress function associated with points of a horizontal plane is represented by elevations above this plane, a stress surface is obtained. The geometry of such surfaces has useful applications. Ordinarily, the stress functions are introduced through the differential equations of equilibrium, and thereafter one may derive the geometry of the stress surfaces. Instead, one may define the stress surfaces by some of their geometrical properties, and afterward derive the differential equations. This scheme offers

advantages in economy of thought, and is used here. The following stress functions are considered: (A) Two stress functions for transverse shears in slabs. (B) Prandtl's stress function for torsion. (C) Timoshenko's stress function for the bending of beams. (D) The deflection of an elastic slab as stress function for the moments, shears, and reactions. (E) Airy's function for a plane state of stresses in a slice. Discussions of the following subjects are added: (F) The analogy of slabs and slices. (G) Elastic weights for deformations of slices found as reactions in slabs. (H) Influence surfaces for moments and shears in slabs determined as Airy's surfaces for slices.

A—TWO STRESS FUNCTIONS FOR TRANSVERSE SHEARS IN SLABS



FIG. 1 shows a part of a horizontal slab. The slab need not be homogeneous and elastic. Within the region R , which is bounded by a single curve, there must be no vertical external forces, but there may be horizontal external forces. Points o , m , and n , and the curves C and C' drawn from m to n lie within the region. Let Q_{mn} and Q'_{mn} represent the sums of the vertical shears on the vertical sections along the curves C and C' . The rule is adopted that such

shears are taken positive upward when acting on the part on the left of the curve, the direction of the curve being indicated by the order of the letters in the double index. Equilibrium of the part of the slab between the two curves requires that $Q_{mn} = Q'_{mn}$. If C is replaced by some other curve from m to n within the region, the total vertical shear remains the same. Thus Q_{mn} depends only on the points m and n , and one may say that Q_{mn} is the total vertical shear transmitted between m and n . Similarly, Q_{om} is the total vertical shear between points o and m , and Q_{on} is the total vertical shear between points o and n .

The stress surface f is now constructed by the following rule: The elevation at point o is chosen as f_o . Then the elevation at any point m is defined as $f_m = f_o + Q_{om}$. By this rule the elevation at point n becomes $f_n = f_o + Q_{on}$. It follows that the rise of the surface from any point m to any point n becomes $f_n - f_m =$

$Q_{on} - Q_{om} = Q_{mn}$. With m and n close together, the vertical shear per unit of length of the section will be represented as the slope of the surface in the direction mn . A section following a contour line (curve of constant elevation) on the stress surface will be without vertical shears. The contour lines define "paths of travel of shear." If contour lines are drawn for equal small intervals of elevation, their density represents the intensity of shear. Areas of the type $\int xdf$, obtained in plane vertical sections through the stress surface, represent moments of the vertical shears. Thus the shaded area in Fig. 2 is equal to the sum of the moments of the vertical shears between A and B with respect to point O , and the resultant of these shears will be located as shown in Fig. 2.

The second function to be considered is defined as a function of deformations, but it becomes a stress function when the material is elastic, homogeneous, and isotropic. The usefulness of this stress function has been shown especially by A. Nadai.² It is required that there be no horizontal loads and reactions within

NOTATION

x, y, z = rectangular coordinates, z vertical
 ξ, η, ζ = displacements in the directions of x, y , and z

$\sigma_x, \sigma_y, \sigma_z, \tau_{xy}, \tau_{yz}, \tau_{zx}$ = normal stresses (positive as tension) and shearing stresses in the directions of x, y , and z

$\epsilon_x, \epsilon_y, \epsilon_z, \gamma_{xy}, \gamma_{yz}, \gamma_{zx}$ = strains and detrusions in the directions of x, y , and z

M_x, M_y, M_{xy} = bending moments and twisting moment in a slab in the directions of x and y , per unit of width of section

f, F, φ = stress function, identified with points of a horizontal plane; elevation of a point on the stress surface

E = modulus of elasticity in tension and compression when the material is elastic

μ = Poisson's ratio when the material is elastic

h = thickness of slab

$N = Eh^3/12(1 - \mu^2)$ = measure of stiffness of an elastic slab

Δ = operator defined by Equation [2].

¹ Professor of Theoretical and Applied Mechanics, University of Illinois. Harald Malcolm Westergaard was born on Oct. 9, 1888, in Copenhagen, Denmark. He received B.S. in Civil Engineering from the Royal Technical College, Copenhagen, in 1911; was engaged in the design of reinforced concrete in Copenhagen, Hamburg, and London in 1911 to 1914; studied in Göttingen in 1913, in Munich in 1914, and at the University of Illinois 1914 to 1916; received Ph.D. from the University of Illinois, 1916; Dr.-Ing., Munich, 1925; Dr. Techn. (honorary), Copenhagen, 1929; and D.Sc. (honorary), Lehigh, 1930; has been on the faculty of the University of Illinois since 1916; assistant professor, 1921; professor of theoretical and applied mechanics, 1927; was senior mathematician 1929-1930 and consulting engineer 1930-1932 in the U. S. Bureau of Reclamation, dealing with structural problems of Boulder Dam. He has written papers on structural mechanics and the theory of elasticity.

Contributed by the Applied Mechanics Division and presented at the Semi-Annual Meeting, Chicago, Ill., June 26 to July 1, 1933, of THE AMERICAN SOCIETY OF MECHANICAL ENGINEERS.

NOTE: Statements and opinions advanced in papers are to be understood as individual expressions of their authors, and not those of the Society.

² A. Nadai, "Die elastischen Platten," 1925, p. 21, Equations [36], and pp. 87 to 106. See also, H. M. Westergaard, "Computation of Stresses in Bridge Slabs Due to Wheel Loads," *Public Roads*, vol. 11, March, 1930, p. 1.

the region considered, but there may be vertical loads and reactions. The proportions of the slab and the distribution of the load must be such that the ordinary theory of slabs may be applied, which permits ignoring the influence of deformations due to vertical shears and the influence of stretching of the middle surface. The particular stress function may be written as

$$\varphi = -N\Delta\zeta \dots \dots \dots [1]$$

in which N is the measure of stiffness (see "Notation"), ζ is the deflection, and

$$\Delta = \frac{\partial^2}{\partial x^2} + \frac{\partial^2}{\partial y^2} \dots \dots \dots [2]$$

The vertical shears per unit of length in sections in the directions of $-y$ and x are found to be equal to the slopes $\partial\varphi/\partial x$ and

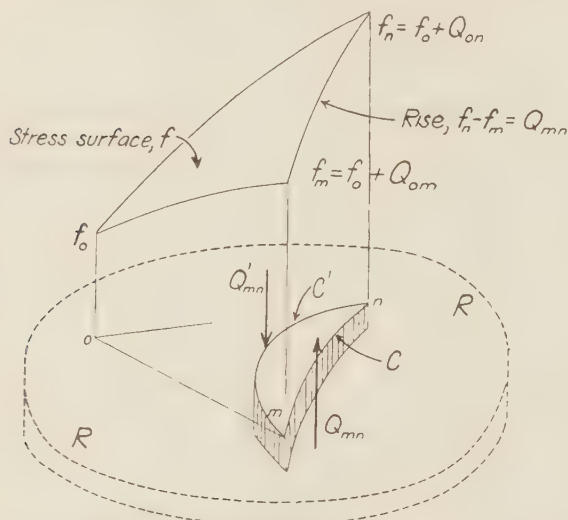


FIG. 1 STRESS SURFACE FOR TRANSVERSE SHEARS IN A SLAB IN A REGION WITHOUT VERTICAL LOADS

$\partial\varphi/\partial y$, respectively. It follows that the vertical shear per unit of length in any section will be equal to the slope of the surface in a direction making an angle of 90 deg with the section.

If the slab is elastic, homogeneous, and isotropic, and if there are neither vertical nor horizontal external forces within the region considered, then both f and φ may be used. A. Nadai³ introduced the function f in this case through its relation with φ , and he showed the geometrical significance of the two functions used jointly. It follows from the representation of the shears in the slab by slopes on the two stress surfaces that contour lines on the surface f will appear as lines of greatest fall on the surface φ , and vice versa. Also, the two surfaces will have the same maximum slope at any point of the slab. From these properties it follows that f and φ may be interpreted as the real part and the imaginary part of an analytic function of the complex variable $x + iy$, so that one may write

$$\psi(x + iy) = f(x, y) + i\varphi(x, y) \dots \dots \dots [3]$$

which gives $\Delta f = \Delta\varphi = 0$ and $\Delta^2\zeta = 0$.

The surfaces f and φ supply pictures of the structural action of slabs. The surface f serves the additional purpose of applications to the following two problems.

³ Loc. cit., pp. 89-106.

B—PRANDTL'S STRESS FUNCTION FOR TORSION

L. Prandtl⁴ showed in 1903 that the shearing stresses in the cross-section of a straight elastic member in torsion may be represented as slopes of a soap film which is extended over a hole in a plane plate; the hole having the shape of the cross-section of the member and the film being deflected by a slight excess pressure on one side. The film serves as a stress surface.

Prandtl's stress surface for torsion may be introduced in the following way: Consider a straight vertical solid member subject to torsion. The member need not be homogeneous or perfectly elastic. It is assumed only that if vertical normal stresses σ_z occur, they are independent of z . Consider a horizontal slice through the member. Let the thickness of the slice be one unit, this unit being assumed small. The slice may be interpreted as a slab without vertical loads, as dealt with in Fig. 1. The stress surface f applies again; it becomes the stress surface for torsion, defining both vertical and horizontal shearing stresses. Since the edge of the slice may be considered as a section in the slab, and since there are no vertical shears on this section, f will be constant at the edge. It is convenient to choose $f = 0$ at the edge. Then the stress surface defines a stress hill with its base at the elevation zero.

One may choose the directions of x and y after the stress hill has been obtained. When z is positive upward, the shearing stresses on the top of the slice in the directions of x and y become

$$\tau_{xz} = \frac{\partial f}{\partial y}, \quad \tau_{xy} = -\frac{\partial f}{\partial x} \dots \dots \dots [4]$$

By considering horizontal slices of this stress hill, Prandtl showed that the total twisting moment is twice the volume of the hill. It is profitable also to consider a vertical slice of the hill. By the principle shown in Fig. 2 the resultant of the horizontal

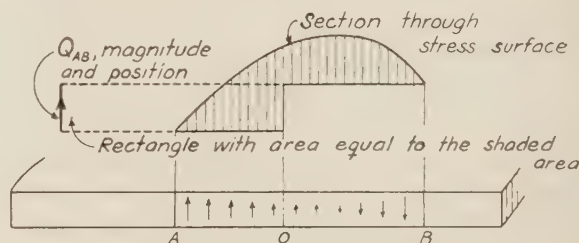


FIG. 2 RESULTANT Q_{AB} OF THE VERTICAL SHEARS IN A STRAIGHT SECTION FROM A TO B

(The shaded area is equal to the sum of the moments of the vertical shears with respect to 0.)

shear components perpendicular to the vertical slice at the base of this slice is a couple, equal to the volume of the slice. It follows that the resultant of all shear components acting in this direction on the whole cross-section of the member will be a couple equal to the volume of the stress hill, and this couple is one-half the total twisting moment. To illustrate: When the cross-section is a long rectangle, it follows that the shearing stresses parallel to the long edges account for one-half the twisting moment; the shearing stresses parallel to the short edges, which act mainly at the ends of the rectangle, account for the other half.

When the material is elastic, homogeneous, and isotropic, it is found that the stress function is governed by the equation, $-\Delta f =$ twice the modulus of elasticity in shear times the angle of twist per unit of length.⁵ Prandtl pointed out that this equa-

⁴ L. Prandtl, "Zur Torsion von prismatischen Stäben," *Physikalische Zeitschrift*, vol. 4, 1903, p. 758.

⁵ See, for example, A. and L. Föppl, "Drang und Zwang," vol. 2, second edition, 1928, p. 50; or, A. Nadai, "Plasticity" (Engineering Societies Monographs), 1931, p. 130.

tion is analogous to that governing the soap film. A. Nadai⁶ obtained the stress function f for the case in which the shearing stress has reached a constant yield point everywhere in the member. He represented the stress hill by a sand hill with constant slope, or the stress surface by a roof with a constant maximum slope. Furthermore, by assuming a shear-detorsion diagram consisting of a straight line up to the yield point and thereafter a horizontal line, he obtained for the intermediate stage a representation of f by a roof and a membrane: the constant maximum slope of the roof represents the yield point; the membrane is inflated from below and deflects to begin with like Prandtl's soap film, but later it will touch a greater and greater area of the roof.

The extension of the geometrical principles to apply to hollow members is simple: Prandtl pointed out that the stress function f must be constant at the edge of any hole in the cross-section; the stress hill has a plateau over each hole; and in computing the volume of the stress hill the parts under the plateaus are included. Prandtl also stated that in case of elastic action the vertical force per unit of area must be the same on the flat part representing the hole as on the soap film.⁷ As an example of the treatment of hollow sections, Fig. 3 shows the contour lines of Nadai's roof in case of a circular section with an eccentric circular hole. The elevation of the plateau is equal to the yield point times the shortest distance from the outer boundary to the edge of the hole.

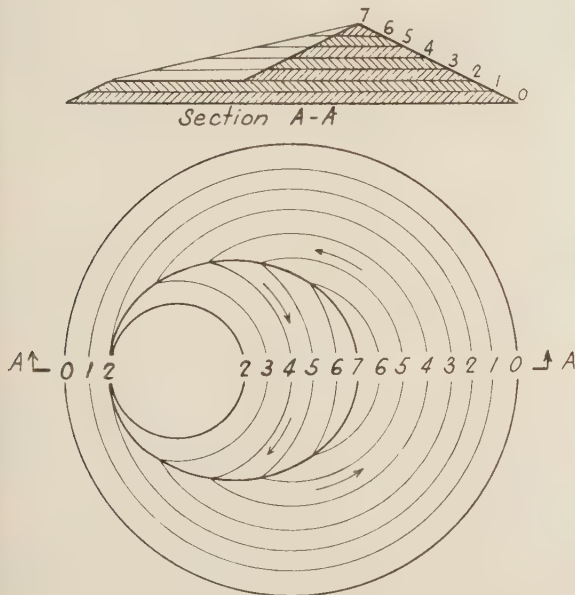


FIG. 3 EXAMPLE OF NADAI'S ROOF FOR PLASTIC TORSION
(Cylinder with eccentric hole.)

A ridge is formed by the intersection of two cones. This ridge appears in the horizontal projection as an ellipse with foci at the centers of the two circular boundaries.

C—TIMOSHENKO'S STRESS FUNCTION FOR THE BENDING OF BEAMS

Fig. 4 shows a vertical cantilever loaded at the top by the forces P and Q in the directions of y and x , and by a twisting couple T .

⁶ A. Nadai, "Der Beginn des Fließvorganges in einem tordierten Stab," *Zeitschrift für angewandte Mathematik und Mechanik*, vol. 3, 1923, p. 442; also his book, "Plasticity," 1931, pp. 132-143.

⁷ A proof is given by A. and L. Föppl, "Drang und Zwang," vol. 2, second edition, 1928, p. 82.

Saint-Venant⁸ showed in 1856 that when the material is elastic, homogeneous, and isotropic, a solution exists in which the vertical normal stresses on any cross-section are proportional to the distance from a neutral axis, as in the ordinary theory of beams, and in which the horizontal stresses on any vertical section are zero. The problem that remains, then, is to determine the shearing stresses on the cross-sections. Saint-Venant solved this problem in a number of cases. In 1921, S. Timoshenko⁹ introduced a

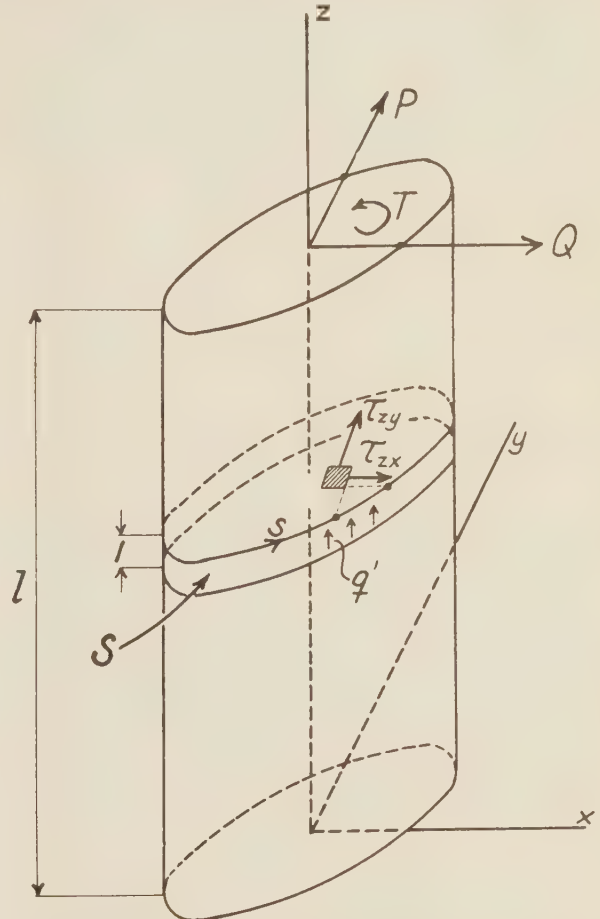


FIG. 4 VERTICAL CANTILEVER
(Shearing stresses to be determined by Timoshenko's stress function.)

stress function which is particularly suitable for determining the shearing stresses on the cross-sections. This stress function is represented by a non-uniformly loaded membrane with a plane boundary. A variant of this stress function can be represented by an unloaded or uniformly loaded membrane or soap film, the boundary of which is a space curve which can be determined in advance. This scheme was applied by P. A. Cushman in an experimental investigation presented in a doctoral thesis at the University of Michigan in 1932, under the direction of Professor Timoshenko. He used unloaded soap films stretched over holes, the edges of which had been distorted properly in advance.

Assume that $\sigma_x = \sigma_y = \tau_{xy} = 0$, as in Saint-Venant's theory. Assume furthermore that the fiber stresses σ_z have the same distribution on all cross-sections, so that one may write

⁸ See, for example, A. E. H. Love, "Mathematical Theory of Elasticity," third edition, 1920, chap. XV.

⁹ S. Timoshenko, "A Membrane Analogy to Flexure," London Mathematical Society, Proceedings, ser. 2, vol. 20, 1921, p. 398.

$$\sigma_z = (z - l) p(x, y) \dots \dots \dots [5]$$

In most applications p must be assumed to be a linear function of x and y , but if the fibers have different stiffness, as, for example, in reinforced concrete (not yet cracked), p may be a non-linear function of x and y . It follows, from the assumptions made, that τ_{xz} and τ_{xy} will be functions of x and y only. Now consider the horizontal slice S in Fig. 4. Its thickness is one unit, and this unit is assumed small. The slice may be interpreted as a slab which carries a vertical load equal to the difference between the stresses σ_z on the top and the bottom. This load is seen to be equal to p in Equation [5], per unit of area, positive upward. The slab is loaded additionally by the horizontal shears τ_{xz} and τ_{xy} on the top and bottom, and these stresses appear also as vertical shears in the slab. The resultant effects in the slab may be obtained by superposition of two actions. In action No. 1,

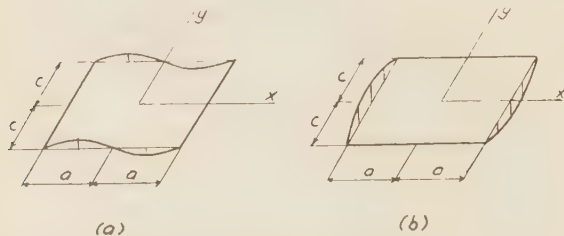


FIG. 5 BOUNDARIES OF TIMOSHENKO'S STRESS SURFACE FOR A RECTANGULAR CROSS-SECTION

the loads p are balanced by a set of shearing stresses τ' , which may include vertical shears q' , appearing as reactions at the edge of the slab. In action No. 2, vertical shears $q'' = -q'$ are applied at the edge of the slab, but the slab carries no vertical loads distributed over the area. Consequently, a stress surface f for shears in slabs, of the type shown in Fig. 1, will define the corresponding vertical and horizontal shears τ'' . In this application the function f becomes Timoshenko's stress function for bending. After obtaining a suitable set of stresses τ' for action No. 1, the values of f at the edge may be computed by the formula

$$f_{\text{edge}} = - \int_{\text{edge}} q' ds = \int_{\text{edge}} (\tau'_{xy} dx - \tau'_{xz} dy) \dots [6]$$

When f is known, the stresses in the combined action may be computed as

$$\tau_{xz} = \tau'_{xz} + \frac{\partial f}{\partial y}, \quad \tau_{xy} = \tau'_{xy} - \frac{\partial f}{\partial x} \dots \dots \dots [7]$$

Assume now that the material is elastic, homogeneous, and isotropic. Then p is a linear function of x and y . Timoshenko showed how in this case one may obtain $f = 0$ at the edge. The following scheme is also convenient: The stresses in action No. 1 are chosen so that they maintain not only equilibrium, but also geometrical continuity of the material. Then the stresses in action No. 2 must maintain equilibrium and geometrical continuity. Since the vertical normal stresses are zero in action No. 2, the stresses τ''_{xz} and τ''_{xy} must be governed by the equations for elastic torsion except the boundary conditions. That is,

$$\Delta f = -C \dots \dots \dots [8]$$

in which C is a constant. C will be zero for a particular value of the twisting couple T , possibly when $T = 0$. When $C = 0$, the surface f may be represented by an unloaded soap film, as in Cushman's investigation.

To obtain simple expressions for the stresses in action No. 1, let the neutral plane be taken as the xz -plane. In this case

$$p = \frac{Py}{I} \dots \dots \dots [9]$$

in which I is the moment of inertia of the cross-section with respect to the neutral axis. Then one finds by substitution in the proper equations that the requirements of equilibrium and geometrical continuity are satisfied by the following two solutions, in which a and c are arbitrary distances:

Solution (a):

$$\tau'_{xz} = 0, \quad \tau'_{xy} = \frac{P}{2I} \left[c^2 - y^2 + \frac{\mu}{1 + \mu} \left(x^2 - \frac{a^2}{3} \right) \right] \dots [10]$$

Solution (b):

$$\tau'_{xz} = - \frac{\mu P}{(1 + \mu)I} xy, \quad \tau'_{xy} = \frac{P}{2(1 + \mu)I} (c^2 - y^2) \dots [11]$$

As an illustration, consider the rectangular cross-section in Fig. 5. Equations [10] and [6] give

$$f_{y=\pm c} = \frac{\mu P}{6(1 + \mu)I} (x^3 - a^2 x), \quad f_{x=\pm a} = 0 \dots \dots [12]$$

while Equations [11] and [6] give

$$f_{y=\pm c} = 0, \quad f_{x=\pm a} = \mp \frac{\mu P a}{2(1 + \mu)I} (c^2 - y^2) \dots [13]$$

Fig. 5 shows the complete boundaries. Knowing the boundaries, one may visualize the soap film. With $T = 0$, the soap film is unloaded. In this particular problem the surfaces f may be determined easily by computation. For example, with the boundary in Fig. 5 (b), one finds

$$f = - \frac{12\mu P}{\pi^2(1 + \mu)c} \sum_{1,3,5,\dots}^n \frac{(-1)^{\frac{n-1}{2}}}{n^3} \frac{\sinh \frac{n\pi x}{2c} \cos \frac{n\pi y}{2c}}{\sinh \frac{n\pi a}{2c}} \dots [14]$$

which leads to convenient expressions for the stresses by Equations [7] and [11].

D—THE DEFLECTION OF AN ELASTIC SLAB AS STRESS FUNCTION FOR THE MOMENTS, SHEARS, AND REACTIONS

In case of a slab of elastic, homogeneous, and isotropic material,¹⁰ the bending moments, twisting moments, transverse shears, and the reactions can be expressed in terms of second and third derivatives of the deflections ζ , with the stiffness N (see "Notation") and Poisson's ratio μ entering in the formulas. The elastic surface ζ , therefore, is a stress surface.

The bending moments M_x and M_y and the twisting moment M_{xy} in the directions of x and y per unit of width of the section are expressed by the equations

$$M_x = -N \left(\frac{\partial^2 \zeta}{\partial x^2} + \mu \frac{\partial^2 \zeta}{\partial y^2} \right), \quad M_y = -N \left(\frac{\partial^2 \zeta}{\partial y^2} + \mu \frac{\partial^2 \zeta}{\partial x^2} \right) \dots \dots [15]$$

$$M_{xy} = -(1 - \mu)N \frac{\partial^2 \zeta}{\partial x \partial y} \dots \dots [16]$$

It was mentioned in section A that the transverse shears are derivatives of the function $-N \Delta \zeta$ (Equation [1]). The reaction at an edge parallel to the axis of x consists, in the general case, of shears V_y , bending moments M_y , and twisting moments M_{xy} .

¹⁰ See, for example, A. Nadai, "Die elastischen Platten," 1925, pp. 20, 21, and 36, or H. M. Westergaard, "Computation of Stresses in Bridge Slabs Due to Wheel Loads," *Public Roads*, vol. 11, March, 1930, p. 1.

Kelvin and Tait showed in 1867 that the twisting moments may be replaced by an equivalent set of vertical forces. One may imagine one beam bent by the couples M_{xy} and another beam bent into the same shape by vertical forces. With the twisting moments replaced by vertical forces, the total vertical reaction per unit of length becomes

$$R_y = V_y + \frac{\partial M_{xy}}{\partial x} = -N \left(\frac{\partial^3 \zeta}{\partial y^3} + (2 - \mu) \frac{\partial^3 \zeta}{\partial x^2 \partial y} \right) \quad [17]$$

In addition, two concentrated forces $\pm M_{xy}$ are found at the ends of the edge. Equation [17] may be applied at any point of the slab. At a distance from the edge, R_y represents an internal reaction.

The equilibrium of each element of the slab requires that

$$V_y = \frac{\partial M_y}{\partial y} + \frac{\partial M_{xy}}{\partial x} \quad [18]$$

which leads to the additional formula

$$R_y = \frac{\partial M_y}{\partial y} + 2 \frac{\partial M_{xy}}{\partial x} \quad [19]$$

This equation will be used in section G.

E—AIRY'S FUNCTION FOR A PLANE STATE OF STRESSES IN A SLICE

Consider a horizontal slice, one unit thick, this unit being chosen small. Assume that there are no horizontal shearing stresses on the top and bottom of the slice. Assume that the variations of the stresses as functions of the vertical coordinate

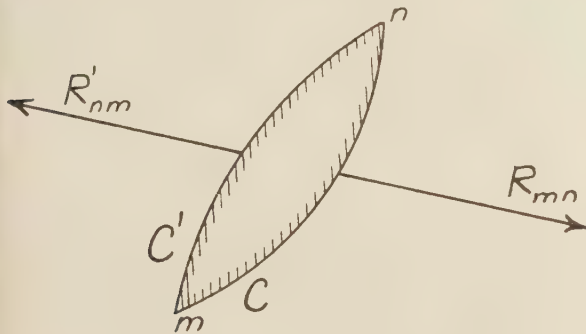


FIG. 6 RESULTANTS ON TWO SECTIONS IN A SLICE

z are so small within the slice that they may be ignored. Then the vertical shearing stresses will be zero, and the remaining stresses will be functions of the horizontal coordinates x and y only. In 1862, G. B. Airy¹¹ introduced a stress function F , in terms of which the horizontal stresses can be expressed as follows:

$$\sigma_x = \frac{\partial^2 F}{\partial y^2}, \quad \sigma_y = \frac{\partial^2 F}{\partial x^2}, \quad \tau_{xy} = -\frac{\partial^2 F}{\partial x \partial y} \quad [20]$$

Maxwell and later Klein and Wieghardt¹² extended this theory, and in doing so emphasized the geometrical features. The practical usefulness of Airy's function in solving problems has been

¹¹ G. B. Airy, "On the Strains in the Interior of Beams," British Association for the Advancement of Science, Report of Meeting, October, 1862, published 1863, pp. 82-86.

¹² F. Klein and K. Wieghardt, "Über Spannungsflächen und reziproke Diagramme, mit besonderer Berücksichtigung der Maxwell'schen Arbeiten," *Archiv der Mathematik und Physik*, series 3, vol. 8, 1905, pp. 1-10 and 95-119.

demonstrated by a number of authors; for example, A. and L. Föppl.¹³

Fig. 6 shows a part of the slice. The resultant R_{mn} of the stresses on the vertical section along the curve C from m to n must balance the resultant R'_{nm} of the stresses on the vertical section along the curve C' from n to m . In referring to such resultants, the rule is adopted that the order of the letters in the double index indicates the direction of the curve; then the stresses are considered to act on the part on the left of the curve. This rule applies in Fig. 6. If the curve C is replaced by another curve from m to n , the resultant R_{mn} remains the same. That is,

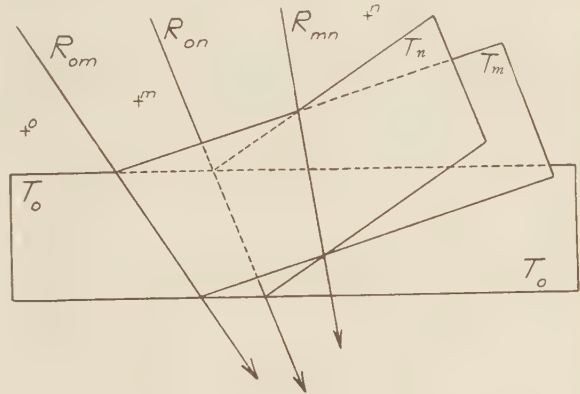


FIG. 7 PLANES ASSOCIATED WITH POINTS OF A SLICE

with a given state of stresses R_{mn} depends only on m and n , and one may say that a definite resultant R_{mn} is transmitted through the material between any two points m and n .

With each point m of the slice there is now associated a plane T_m . The elevation of T_m at any point p is denoted by T_{mp} . Fig. 7 shows three such planes, associated with the points o , m , and n . The planes are located as follows: T_o is chosen; then any other plane T_m is defined by the requirement that the intercept $T_{mp} - T_{op}$ at any point p shall be equal to the moment of the resultant R_{om} transmitted between o and m , this moment being positive in the counter-clockwise direction. The plane T_n is located by applying this rule to R_{on} . The moment of R_{mn} with respect to p is equal to the moment of R_{on} minus that of R_{om} ; therefore, it is found as $(T_{np} - T_{op}) - (T_{mp} - T_{op}) = T_{np} - T_{mp}$. That is, the moment of R_{mn} with respect to any point p is equal to the intercept at p from T_m to T_n . It follows that the intersection of T_m and T_n locates the resultant R_{mn} ; that the difference in slope of T_m and T_n in a direction perpendicular to R_{mn} is equal to R_{mn} ; and that if the resultant is a couple, the two planes are parallel, with the vertical intercept equal to the couple. It is seen, furthermore, that a plane vertical section through T -planes which are associated with a series of points may be interpreted as a string polygon. The polar distance is one unit. The forces are perpendicular to the plane vertical section and are components of the resultants which are transmitted between successive points of the series.

Let point n approach point m . Assume that there are no infinite stresses in a region surrounding and including m . When the distance mn becomes infinitesimal of the first order, then R_{mn} becomes infinitesimal at least of the first order, and the moment of this resultant with respect to n becomes infinitesimal at least of the second order. This moment is represented by the intercept $T_{nn} - T_{mn}$. It follows that the plane T_m is tangent to the surface T_{mm} at point m . All the T -planes are tangent to the surface $F = T_{mm}$.

¹³ A. and L. Föppl, "Drang und Zwang," vol. 1, second edition, 1924, chap. 4.

The function $F = T_{mm}$ can be shown to be same as Airy's function, which was introduced originally through Equations [20]. It is assumed that the second derivatives of F exist at point m . In Fig. 8 the intercept $T_{nA} - T_{mA}$ will be equal to the moment $\sigma_x dy \cdot 1$. Since the T -planes are tangent to the surface F , this intercept may be expressed as $d\left(\frac{\partial F}{\partial y}\right) = \frac{\partial^2 F}{\partial y^2} dy$. It follows that $\sigma_x = \frac{\partial^2 F}{\partial y^2}$ and, by analogy, $\sigma_y = \frac{\partial^2 F}{\partial x^2}$. Similarly, the intercept $T_{nB} - T_{mB}$ is equal to the moment $-\tau_{xy} dy \cdot 1$ and equal to $d\left(\frac{\partial F}{\partial x}\right) = \frac{\partial^2 F}{\partial x \partial y} dy$, which gives $\tau_{xy} = -\frac{\partial^2 F}{\partial x \partial y}$. It is noted that by this derivation of Equations [20] the surface F is obtained first, and the axes of x and y may be oriented afterward in any direction.

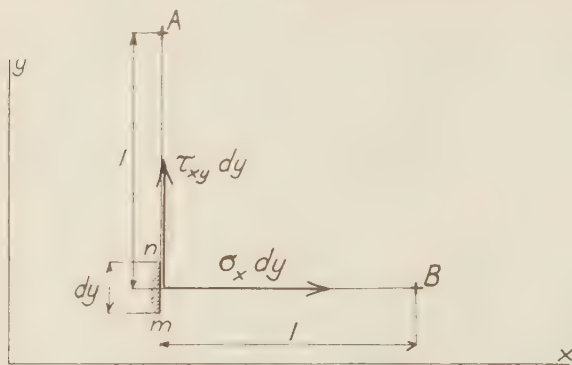


FIG. 8 STRESSES IN A SLICE

When the scale of the elevations is small, the normal stresses and shearing stresses in any direction are represented by curvatures and twists of Airy's surface.

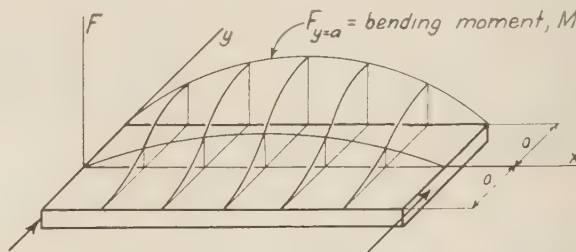
The relation $\sigma_y = \frac{\partial^2 F}{\partial x^2}$ shows that any plane vertical section through Airy's surface is a string curve, with polar distance 1, for the normal stresses on the corresponding section in the slice. The same is concluded by considering the string polygon formed by the intersection of a vertical plane with the T -planes for a series of closely spaced points.

It is noted that the derivation of Equations [20] presupposed the existence of the second derivatives of Airy's function. This assumption is not necessary in the derivation of Airy's surface from its tangential planes. A consideration of the tangential planes will show that if at no place within a region a finite force or couple is transmitted between two points which are an infinitesimal distance apart, then a smooth Airy's surface is obtained within this region, regardless of discontinuities of the material. A ridge on Airy's surface would indicate a concentrated force transmitted along the curve following the ridge. An Airy's surface with ridges defines a state of statically possible stresses; these stresses may be significant, for example, in applications of the equation of virtual work.

Klein and Wieghardt¹⁴ determined tangential planes of Airy's surface at the edge of the slice. If the loads and reactions on the edge of the slice are known completely between two points of the edge, then after choosing the tangential plane of Airy's surface at one point on this piece of edge the tangential plane at any other point of the piece of edge can be located definitely by means of the resultant transmitted between the two points. That is, the elevations and slopes of Airy's surface may be determined at all points of this piece of boundary.

¹⁴ Loc. cit.

As an example, Fig. 9 shows an Airy's surface for a beam. The xy -plane is chosen as tangential plane at one point of the unloaded edge, $y = -a$. Then the xy -plane will be tangential plane at all points of this edge. Sections through Airy's surface parallel to the yF -plane are string curves for the stresses σ_x . Each of the string curves has horizontal tangents at both ends, the tangent at the loaded edge, $y = a$, having an elevation equal to the bending moment in the particular section. The same results are found

FIG. 9 AIRY'S SURFACE FOR A BEAM WITH A DISTRIBUTED LOAD IN THE DIRECTION OF $-y$ AT THE EDGE $y = a$

by noting that the moment diagram is a string curve for the stresses σ_y on the loaded edge, and that at this edge $\tau_{xy} = 0$.

F—THE ANALOGY OF SLABS AND SLICES

In the deliberations which follow, the material of the slices and slabs is assumed to be elastic, homogeneous, and isotropic. The slices and slabs are still assumed horizontal.

Two types of slices must be considered: free slices and constrained slices. The free slice is without pressure on the top and bottom, so that $\sigma_z = 0$. The constrained slice requires that the top and bottom remain in their original planes, so that the vertical strain $\epsilon_z = 0$. In case of the free slice the strains ϵ_x and ϵ_y and the detrusion γ_{xy} in the directions of x and y are expressed as

$$\epsilon_x = \frac{1}{E} (\sigma_x - \mu \sigma_y), \quad \epsilon_y = \frac{1}{E} (\sigma_y - \mu \sigma_x) \dots \dots \dots [21]$$

$$\gamma_{xy} = \frac{2(1 + \mu)}{E} \tau_{xy} \dots \dots \dots [22]$$

It is easy to prove that these equations may be applied also to the constrained slice, provided only that E and μ be replaced by an apparent modulus of elasticity E' and an apparent Poisson's ratio μ' , defined as follows:

$$E' = \frac{E}{1 - \mu^2}, \quad \mu' = \frac{\mu}{1 - \mu} \dots \dots \dots [23]$$

For this reason it will be sufficient here to consider the free slice.

With Airy's function introduced in Equations [21] and [22] through Equations [20], one finds

$$\epsilon_x = \frac{1}{E} \left(\frac{\partial^2 F}{\partial y^2} - \mu \frac{\partial^2 F}{\partial x^2} \right), \quad \epsilon_y = \frac{1}{E} \left(\frac{\partial^2 F}{\partial x^2} - \mu \frac{\partial^2 F}{\partial y^2} \right) \dots [24]$$

$$\gamma_{xy} = -\frac{2(1 + \mu)}{E} \frac{\partial^2 F}{\partial x \partial y} \dots \dots \dots [25]$$

These equations may be compared with Equations [15] and [16] for the moments in a slab. It is seen that if one makes $N = 1/E$, $\mu_{slab} = -\mu_{slice}$ and $\zeta = F$ (F being represented to a small scale), then one obtains

$$\epsilon_x = -M_y, \quad \epsilon_y = -M_x, \quad \gamma_{xy} = 2M_{xy} \dots \dots \dots [26]$$

It is seen, furthermore, that the expression in terms of F for the

internal energy of the slice becomes identical to the expression in terms of ζ for the internal energy of the slab.

Assume that the edge of the slice is a single closed curve, and that the loads and reactions on the edge are known. Then one may establish definite elevations and slopes of Airy's surface at the boundary. Let the same boundary conditions be imposed on the elastic surface of the slab. The slab then is bent by distortions of the edge, but let it be unloaded otherwise. Airy's surface for the slice will be governed by Castiglione's principle of minimum of energy by variation of the stresses. The elastic surface of the slab will be governed by the principle of minimum of energy by variation of the shape of the slab. Since the two expressions for the energy have been made identical, it follows that the result $\zeta = F$ is obtained when the slab is unloaded. It was noted in connection with Equation [3] that in a region without loads the deflections of a slab satisfies the equation $\Delta^2 \zeta = 0$. One finds, therefore,

$$\Delta^2 F = 0 \dots \dots \dots [27]$$

These equations for ζ and F do not contain μ . Therefore, in determining Airy's surface for the slice as an elastic surface of a slab, any value of μ in the slab is permissible. Nor is it necessary in this application to specify N . These deliberations establish the analogy of slabs and slices.

Equation [27] may very well be derived by other methods; for example, by substituting from Equations [24] and [25] in the equation of compatibility¹⁸ for ϵ_x , ϵ_y , and γ_{xy} . The consideration of the energy is advantageous, however, because of its further application to the following general problem: Assume that the slice has a hole. Assume that there are no loads on the edge of the hole. With definite loads on the outer edge, one may establish definite elevations and slopes of Airy's surface at the outer boundary. At the edge of the hole Airy's surface will have a common tangential plane. The analogous slab, accordingly, may be equipped with a rigid flat portion covering the hole in the slice, this rigid part being attached firmly to the flexible part representing the solid part of the slice. It can be shown that the reactions of the flexible part of the slab on the rigid part covering the hole are independent of Poisson's ratio for the slab when N and the elastic surface are given. Then application of the principles of minimum of energy leads to the conclusion that the proper position of the rigid part of the slab is that which it will assume freely when no external forces are acting on it except the reactions exerted by the flexible part of the slab; and this position, which the rigid part assumes freely, is independent of the values of N and E and the values of Poisson's ratio for the slab and the slice. The position of the plane representing Airy's surface over the hole is defined by three constants, and this corresponds to the triple indeterminacy of a fixed arch.

The same reasoning may be applied if the slice is loaded on the edge of the hole, but has no loads on the outer edge. Definite elevations and slopes of Airy's surface can be established at the edge of the hole. At the outer boundary Airy's surface will have a single tangential plane, which may be represented by a rigid plane slab attached to the flexible slab. The proper position of the rigid slab is that which it will assume freely. This principle may be applied to a slice with any number of holes, provided that the load on each closed boundary balances itself.

A simple application is to a thick ring bounded by two concentric circles, and loaded by one constant pressure on the inner boundary and another constant pressure on the outer boundary. The rigid parts forming the extensions of the flexible slab will produce no vertical reactions. Therefore, the flexible slab will be

without transverse shears, and the otherwise possible term $C r^2 \log r$ in Airy's function (r = radius vector) will drop out. The remaining significant terms $A r^2 + B \log r$ lead readily to Lamé's formulas for the stresses in thick cylinders.¹⁸

K. Wieghardt¹⁷ utilized the analogy of slabs and slices in an experimental investigation published in 1908. By bending a brass plate, he obtained information concerning the concentration of stresses in a slice at reentrant corners. The slice was loaded by two equal and opposite forces. V. P. Jensen¹⁸ in an experimental investigation completed in 1931 applied the same principle with a more complex load. Cooperating with the United States Bureau of Reclamation, he investigated the nonlinear distribution of stresses in a vertical slice of Boulder Dam by bending a rubber slab. The edges of the active area of the slab were distorted by clamps which he had designed for this purpose. This study has been continued with the same equipment by engineers of the Bureau of Reclamation.

Like the soap-film analogy, the analogy of slabs and slices not only furnishes experimental procedures, but it supplies ways of thinking of one problem in terms of another, and ways of visualizing solutions.

As a further illustration, the beam in Fig. 9 is considered again. Assume that the load p on the edge $y = a$ is a linear function of x . Airy's surface is to be obtained as the elastic surface of a slab. If one wishes, one may take F positive downward in this case instead of upward as in Fig. 9; then the deflections of the slab are positive downward. It is convenient to choose $N = 1$ and $\mu = 0$ for the slab. The resultant deflections of the slab will be found by superposition of two actions. The deflections F_1 in action No. 1 are chosen so that Airy's function F_1 will represent the stresses in the beam according to the ordinary theory of flexure. That is, F_1 must satisfy the boundary conditions in Fig. 9 and must make the normal stresses on any cross-section proportional to y . One finds,

$$F_1 = \frac{M}{4} \left(2 + 3 \frac{y}{a} - \left(\frac{y}{a} \right)^3 \right) \dots \dots \dots [28]$$

To maintain these deflections, the slab requires a load distributed over the area. Lagrange's equation,¹⁹ $\Delta^2 \zeta = w/N$, defines the relation between the load w per unit of area and the deflection ζ in the general case. In the present case, noting that $p = -d^2 M/dx^2$, one finds the load

$$\Delta^2 F_1 = \frac{3py}{a^3} \dots \dots \dots [29]$$

In action No. 2 there is required an equal and opposite distributed load. Furthermore, the deflections and slopes must be zero at the edges $y = \pm a$. If the slab were divided into independent beams in the directions of y , these beams would obtain the deflections

$$F_2 = - \frac{p}{40a^3} y(y^2 - a^2)^2 \dots \dots \dots [30]$$

¹⁸ See for example, A. and L. Föppl, "Drang und Zwang," vol. 1, second edition, 1924, p. 313.

¹⁷ K. Wieghardt, "Ueber ein neues Verfahren, verwickelte Spannungsverteilungen in elastischen Körpern auf experimentellem Wege zu finden," *Mitteilungen über Forschungsarbeiten auf dem Gebiete des Ingenieurwesens*, Heft 49, 1908, pp. 15-30. See also, A. and L. Föppl, "Drang und Zwang," vol. 1, second edition, 1924, p. 248.

¹⁸ V. P. Jensen, "Experimental Determination of Non-linear Distribution of Stresses by the Slab Analogy, With Application to Hoover Dam," thesis for the degree of Master of Science, University of Illinois, 1931; also as Technical Memorandum, United States Bureau of Reclamation; not yet published.

¹⁹ A. Nadai, "Die elastischen Platten," 1925, p. 21. H. M. Westergaard, loc. cit.

¹⁸ A. and L. Föppl, "Drang und Zwang," vol. 1, second edition, 1924, p. 53; see also pp. 247-248.

This function satisfies Lagrange's equation for the slab. Consequently, Airy's function F_2 defines the supplementary stresses, which must be added to those obtained by the ordinary theory of flexure. For example, the supplementary normal stress in the direction of x becomes²⁰

$$\sigma''_x = \frac{p}{10} \left(3 \frac{y}{a} - 5 \left(\frac{y}{a} \right)^3 \right) \dots \dots \dots [31]$$

G—ELASTIC WEIGHTS FOR DEFORMATIONS OF SLICES FOUND AS REACTIONS IN SLABS

In the next application of the analogy of slabs and slices it is assumed again that $N = 1/E$ and $\mu_{\text{slab}} = -\mu_{\text{slice}}$ in the flexible part of the slab. Then Equation [26] will apply.

The relation $\epsilon_x = -M_y$ shows that the decrease of the distance between two points of the slice may be determined as the total bending moment in the slab on a straight section covering this distance, provided that the section is entirely within the flexible part of the slab.

With ξ and η denoting the displacements of the point x, y in the directions of x and y , one may write,

$$\epsilon_x = \frac{\partial \xi}{\partial x}, \quad \gamma_{xy} = \frac{\partial \xi}{\partial y} + \frac{\partial \eta}{\partial x} \dots \dots \dots [32]$$

By differentiating and subtracting, one finds²¹

$$\frac{\partial^2 \eta}{\partial x^2} = -\frac{\partial \epsilon_x}{\partial y} + \frac{\partial \gamma_{xy}}{\partial x} \dots \dots \dots [33]$$

which defines the curvatures of an originally straight line parallel to the axis of x . Knowing the curvatures, one may determine deflections or relative deflections of the points on the line, using any one of the methods by which deflections of beams are obtained from the elastic weights, $\pm M/EI$. The curvature is an elastic weight.

Equations [33], [26], and [19] give

$$\frac{\partial^2 \eta}{\partial x^2} = \frac{\partial M_y}{\partial y} + 2 \frac{\partial M_{xy}}{\partial x} = R_y \dots \dots \dots [34]$$

That is, the elastic weights for the bending of any straight line on the slice may be found as reactions on the corresponding section in the slab.

With the required change of sign of μ , Equation [17] leads to the following additional formula for the elastic weight:

$$\frac{\partial^2 \eta}{\partial x^2} = -\frac{1}{E} \left(\frac{\partial^3 F}{\partial y^3} + (2 + \mu) \frac{\partial^3 F}{\partial x^2 \partial y} \right) \dots \dots \dots [35]$$

As an example, consider once more the beam in Fig. 9. Assume again that the load p is a linear function of x . Then the deflection of the slab at any point is the sum of F_1 in Equation [28] and F_2 in Equation [30]. It is to be expected that F_1 , which represents the stresses according to the ordinary theory of flexure, will contribute elastic weights at the edges equal to M/EI , with $I = 2a^3/3$. That this expectation is correct is proved easily by substituting F_1 in Equation [35]. By substituting F_2 , one finds the supplementary reaction or elastic weight

$$\frac{\partial^2 \eta_2}{\partial x^2} = \frac{6p}{5Ea} \dots \dots \dots [36]$$

Then the supplementary deflection becomes

²⁰ Compare, for example, A. and L. Föppl, "Drang und Zwang," vol. 1, second edition, 1924, p. 261.

²¹ A. E. H. Love, "Mathematical Theory of Elasticity," third edition, 1920, p. 343.

$$\eta_2 = -\frac{6M}{5Ea} + c_1x + c_2 \dots \dots \dots [37]$$

in which c_1 and c_2 are integration constants. It may be noted that the conventional approximate computation of the supplementary deflection, by considering the energy due to the shearing stresses, gives nearly the same result; the approximate computation exaggerates the first term on the right side in Equation [37] in the ratio of $1 + \mu$.

H—INFLUENCE SURFACES FOR MOMENTS AND SHEARS IN SLABS DETERMINED AS AIRY'S SURFACES FOR SLICES

In the preceding applications of the analogy of slabs and slices, the slab served in the study of the slice. It is also possible to

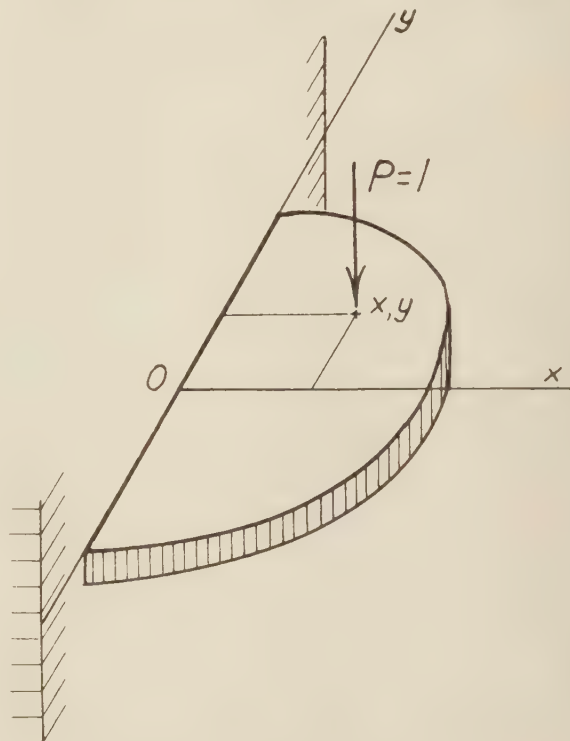


FIG. 10 LARGE SLAB CANTILEVERED FROM A RIGID WALL

let the slice serve the slab. For example, one might determine stresses in a slice by polarized light and interpret these stresses as curvatures and twists of a slab.

Müller-Breslau²² established the principle that any influence diagram representing an effect at one place due to a unit load at any point may be obtained as a deflection diagram. The application to slabs will be illustrated by the derivation of the influence surface for a bending moment in the slab in Fig. 10; namely, the bending moment M in the direction of x at 0. The slab is cantilevered from a rigid wall along the axis of y , and it is assumed to extend indefinitely far in the directions of x and $\pm y$.

Two actions are considered. In action A the slab carries the load $P = 1$ at the point x, y as in Fig. 10. This load produces the bending moments M' in the direction of x at the fixed edge, with $M' = M$ at 0. The surface representing M as a function of x and y is the desired influence surface. In action B the slab carries no vertical load, but the edge at the wall is distorted

²² H. Müller-Breslau, "Die graphische Statik der Baukonstruktionen," 1887-1908.

within the interval $-a < y < a$ by creating the slopes $\partial\zeta/\partial x = \alpha$. The resulting deflection at point x, y is denoted by ζ .

Now two applications are made of the equation of virtual work. In application No. 1 the loads, reactions, and stresses are defined by action A and the deformations by action B. With U_{AB} denoting the internal virtual work, the equation becomes

$$1 \cdot \zeta + \int_{-a}^a M' \alpha dy = U_{AB} \dots \dots \dots [38]$$

In application No. 2 the loads, reactions, and stresses are defined by action B and the deformations by action A. No external virtual work is done; therefore the internal virtual work U_{BA} becomes zero. Since $U_{AB} = U_{BA}$, one finds

$$- \int_{-a}^a M' \alpha dy = \zeta \dots \dots \dots [39]$$

Let a be chosen small, and adopt a function α , so that

$$\int_{-a}^a \alpha dy = -1 \dots \dots \dots [40]$$

The difficulty of large deflections is disposed of by adopting temporarily a small scale for vertical distances. Then Equation [39] becomes

$$M = \zeta \dots \dots \dots [41]$$

That is, the influence surface for M is the elastic surface ζ .

This elastic surface is obtained conveniently as an Airy's surface. With the slice loaded as in Fig. 11, one may choose the xy -plane as tangential plane of Airy's surface at points of the y -axis at which $y > a$. Then Airy's function will be zero at all points of the y -axis. In the interval $-a < y < a$, the slope of Airy's surface in the direction of x becomes $\alpha = -1/2a$. For $y < -a$, the xy -plane again becomes tangential plane. This Airy's surface satisfies the boundary conditions for the elastic surface ζ , which was defined by Equations [38] to [40].

Let $F' = F'(x, y)$ denote a possible Airy's function for a load $P = 1$ at 0 in the direction of $-y$. Then possible Airy's functions for the loads P_1 and P_2 may be written as

$$F_1 = -\frac{1}{2a} F'(x, y - a), \quad F_2 = \frac{1}{2a} F'(x, y + a) \dots [42]$$

respectively. With a small, by permitting $2a$ to be interpreted as dy , one finds for the two loads combined the possible Airy's function

$$F = F_1 + F_2 = \frac{\partial F'}{\partial y} \dots \dots \dots [43]$$

To this Airy's function it may be necessary to add a constant in order to make $\zeta = 0$ at the edge.

Airy's function F' , for the load $P = 1$ at 0 in the direction of $-y$, is expressed conveniently in terms of polar coordinates, as

$$F' = -\frac{1}{\pi} r \theta \cos \theta \dots \dots \dots [44]$$

Noting that

$$\frac{\partial}{\partial y} = \sin \theta \frac{\partial}{\partial r} + \cos \theta \frac{1}{r} \frac{\partial}{\partial \theta} \dots \dots \dots [45]$$

one finds²³

²³ The results in Equations [46] and [48] are stated in the paper in *Public Roads*, March, 1930, referred to in previous footnotes.

$$F = -\frac{1}{\pi} \cos^2 \theta = \zeta = M \dots \dots \dots [46]$$

no constant having to be added to F . Equation [46] defines the influence surface for the bending moment M .

The influence surface for the vertical shear V_x at 0 in Fig. 10 may be obtained in the same way. Instead of the forces in Fig.

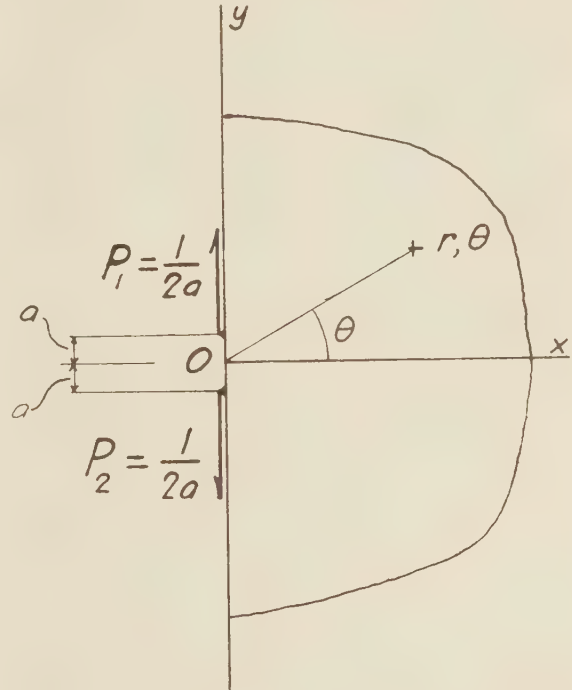


FIG. 11 SLICE CORRESPONDING TO THE SLAB IN FIG. 10

11, two couples $\pm 1/2a$ are applied at the same points. Airy's surface for a unit couple at the origin of the coordinates may be written as

$$F' = \frac{1}{2\pi} (\sin 2\theta + 2\theta) \dots \dots \dots [47]$$

Then one finds

$$V_x = \zeta = F = \frac{\partial F'}{\partial y} = \frac{2}{\pi r} \cos^2 \theta \dots \dots \dots [48]$$

which defines the influence surface for the shear.

CONCLUSIONS

Graphostatics is helpful in the theory of elasticity. It provides visualization and furnishes ways of thinking about problems and solving them. It extends the useful overlapping of the theory of elasticity, mechanics of materials, and structural mechanics.

Discussion

A. NADAI.²⁴ The highly instructive and similarly useful geometry of certain surfaces having a close relation to a number of important engineering problems of statics, of which some are known while several groups of these surfaces have just been newly introduced and described in the brief and clear study by

²⁴ Westinghouse Research Laboratories, East Pittsburgh, Pa. Mem. A.S.M.E.

Dr. Westergaard on graphostatics, deserves the full attention of engineers. Dr. Westergaard has in other of his extensive recent investigations shown how by these methods, if cleverly applied, the distributions of stress in difficult cases of loading of elastic bodies could be found—such as, for example, in a section of the Boulder Dam of the Colorado River.

The mathematical difficulties for finding the distribution of stress in the sections of such a dam, even if great simplifications as to the nature of the problem are assumed by reducing it to one of plane strain, arise from various reasons: the action of the weight of the material of the dam has to be combined with that by the lateral pressure increasing with the depth, the cross-sections of the dam being limited by curves that are not simple. The details exposed in Dr. Westergaard's paper deserve attention therefore, and perhaps also for their pedagogical influence, which they may exert in the future. The various stress surfaces extremely simplify the description of the corresponding problems and help greatly to visualize the states of stress and of elastic strain in more complicated cases.

It is perhaps of some interest in this connection to note the recent progress made in stress analysis by the more extended use of all kinds of mechanical model-testing methods by which various other methods were gradually replaced. Model testing based on the principles of mechanical similarity has been extensively applied in hydraulics, aerodynamics, photoelastic testing, etc. However, it may be based on certain analogies existing from a mathematical point of view between two or more apparently different problems of mechanics or physics. A number of interesting new examples where these second methods might prove useful have been pointed out by Dr. Westergaard. Instead of measuring stresses or strains in one particular case, one may convert the problem to another mathematically corresponding, similar or identical one and then observe another quantity, such as, for example, a deflection or the slope of a curved surface (membrane, plate), which lends itself to a simpler observation. From this point of view a model based on an analogy may be considered as a special integrating machine for finding the numerical solution of an actual problem, offered either by nature itself or designed by ingenuity of men. When comparing the various means which have been proposed for finding numerical values of certain important quantities, the engineer finally decides to let the analogy model do the tedious integrating (or differentiating) job for him.

Although some of the geometrical properties of Airy's stress surfaces have long ago attracted mathematicians such as Maxwell, Felix Klein, K. Wieghardt, and others, these properties in the hands of the engineer have perhaps not yet been applied so extensively as may become useful. The author of the paper himself has stated that since Wieghardt's work it is known that the lateral deflections $\xi(x,y)$ of a plate bent by a system of forces acting perpendicularly to the plane of the plate and distributed only along its edges satisfy the same differential equation (Equation [27] of the paper) as Airy's stress function $F(x,y)$ for a state of plane stress or strain in a flat slab subjected to forces acting along the edges of the slab and in the direction of its middle plane.

F. Klein and Wieghardt have suggested to substitute a bending test with a plate for the experimental determination of Airy's stress function for a flat slab, but the writer felt that the correspondence between the stresses in the two problems (plate and slab) was not a simple one. Also a double differentiation was required to find values of stresses. The writer of these lines was therefore particularly interested and pleased to see that Dr.

Westergaard has now established an analogy between the two problems with a complete correspondence between the quantities involved: to the bending moments M_x, M_y, M_{xy} of the bent plate correspond the unit strains $\epsilon_x, \epsilon_y, \gamma_{xy}$ of the slab, etc., and that he has utilized this method when computing the stresses in the Boulder Dam. It is perhaps worth while to note that Dr. Westergaard's suggestion to introduce the resultant of the transverse shearing forces of a slab as a new stress function Q expresses certain mathematical properties inherent to a number of similar problems in the theory of elasticity. If these resultant forces are Q_x , respectively, Q_y for sections $x = \text{const.}$, respectively, $y = \text{const.}$, and p_x , respectively, p_y are the shearing forces per unit of length, then

$$Q_x = \int p_x dy, \quad Q_y = - \int p_y dx$$

For p_x, p_y in many cases the equilibrium conditions being

$$\frac{\partial p_x}{\partial x} + \frac{\partial p_y}{\partial y} = 0$$

p_x, p_y can be found assuming

$$p_x = \frac{\partial \psi}{\partial y}, \quad p_y = - \frac{\partial \psi}{\partial x}$$

The stress function Q introduced above is identical with the function ψ . If p_x, p_y are interpreted as velocity components of a moving fluid in a plane, $\psi(x,y)$ is known as the stream function, and hence the stress function Q of a slab has quite an analogous meaning as the stream function ψ in the plane movement of a liquid.

The general bending and torsion problem of a bar can indeed be reduced for the shearing stress components τ_x and τ_y to two equations of the form:

$$\frac{\partial \tau_x}{\partial x} + \frac{\partial \tau_y}{\partial y} = \text{div } \tau = A y$$

$$\frac{\partial \tau_x}{\partial y} - \frac{\partial \tau_y}{\partial x} = \text{rot } \tau = Bx + C$$

where A, B, C are constants depending on the external load and twisting moment and the shearing stress indicated by the letter τ is the resultant vector of the components τ_x, τ_y .

Separating τ into two vector parts τ' and τ'' according to

$$\tau = \tau' + \tau''$$

it can be shown that the part τ' may be determined, for example, by assuming $\text{div } \tau' = 0$ and the other part τ'' by assuming that $\text{rot } \tau'' = 0$, or, in other words, by dividing the resultant stress field of the vector τ into a vector field for which the divergence is zero (hence a "stream function" ψ exists so that $\tau_x' = \frac{\partial \psi}{\partial y}$,

$\tau_y' = - \frac{\partial \psi}{\partial x}$) and into a remaining field for which the rotation (curl) vanishes (hence a "velocity potential" ϕ exists, so that

$\tau_x'' = \frac{\partial \phi}{\partial x}, \tau_y'' = \frac{\partial \phi}{\partial y}$). The function ψ is known as Prandtl's

stress function in the case of the torsion problem. It is hoped that the various suggestions contained in Dr. Westergaard's paper will stimulate the further application of these stress functions to practical engineering problems.

The Use of the Wind Tunnel in Connection With Aircraft-Design Problems

BY TH. VON KÁRMÁN¹ AND CLARK B. MILLIKAN,² PASADENA, CALIF.



T. VON KÁRMÁN



C. B. MILLIKAN

The paper is divided into two parts, the first of which deals with the general problem of extrapolating wind-tunnel results to full-scale free-flight conditions in connection with the initial prediction of overall performance characteristics of airplanes. Using the notation of Oswald, it is found that the three parameters about which the designer would like information from the wind tunnel are: the "airplane efficiency factor" giving the variation in parasite drag with lift coefficient, the "equivalent parasite area" giving essentially the minimum parasite drag, and the maximum lift coefficient. If the tests are made at Reynolds' numbers of the order of 1,500,000 or larger and on models of modern "clean" airplanes, the extrapolation of the first parameter to full scale is felt to be trustworthy

for gliding flight. The need for further data on the influence of the change to power-on flight is mentioned. For the second parameter the effect of the change in Reynolds' number involved in the extrapolation is shown to be important, and a method for carrying out the extrapolation is described. This method is based on the modern hydrodynamical theory of skin friction, and has already met with some success as developed and used at the Guggenheim Aeronautics Laboratory of the California Institute of Technology. In connection with the third parameter, it is shown that the influence of Reynolds' number and turbulence on the value of the maximum-lift coefficient is very large. The importance and confusion attending this phenomenon led some time ago to its intensive investigation at the laboratory. The more important results of an experimental and a theoretical approach to the problem are discussed. The experimental researches involved the testing of a 6-ft-span N.A.C.A. 2412 airfoil at a series of Reynolds' numbers and with various degrees of turbulence produced artificially in the wind tunnel through the introduction of grids or screens upstream from the model. The results furnish quantitative evi-

dence of the considerable dependence of $C_{L_{max}}$ on Reynolds' number and turbulence, and in particular demonstrate the fact that, even at fairly large Reynolds' numbers, the value of $C_{L_{max}}$ may be increased by as much as 30 per cent by introducing artificial turbulence into a normally very smooth wind-tunnel flow. The theoretical investigation involves an analysis of the boundary-layer flow around an N.A.C.A. 2412 airfoil, and is particularly concerned with the transition from the laminar to the turbulent regime and with the separation of the laminar boundary layer from the upper surface of the airfoil. The second part of the paper gives illustrations of the diverse nature of the special aircraft-design problems for which the wind tunnel may give valuable information. The examples discussed are all chosen from investigations initially undertaken at our laboratory at the request of aircraft manufacturers and at their expense. Many of the problems so begun developed an independent scientific interest, so that the tests were subsequently amplified by the staff to a degree not at all contemplated when the work was started. A series of six distinct types of investigations is included in the samples considered.

INTRODUCTION

IT IS ABOUT 25 years since systematic tests on stationary models in artificially created air streams were first used as an aid to the design and performance prediction of airplanes. Widely varying opinions as to the practical applicability of this type of measurement have been held by aeronautical engineers. The naive idea that the results of such measurements could be applied without corrections to full-scale conditions was very early

abandoned. The corrections due to the finite dimensions of the wind stream have been found comparatively easily by the application of aerodynamic theory. The establishment of model rules to take into account the effect of scale in size and velocity, i.e., Reynolds' number, has proved to be much more difficult. The opinion has been widely expressed that full information could be obtained only by carrying out the model tests at full-scale Reynolds' number. It is well known that the so-called variable-

¹ Director of Guggenheim Aeronautics Laboratory, California Institute of Technology. Mem. A.S.M.E. Dr.-Ing. von Kármán received his M.E. at Budapest in 1902 and Ph.D. at Göttingen in 1908; honorary degree of Doctor of Engineering, University of Berlin, 1929. He was Privat-Docent, Göttingen, 1910-1913; Professor of Mechanics and Aerodynamics, Director of the Aerodynamical Institute, University of Aachen, 1913; member of Gesellschaft der Wissenschaften zu Göttingen, 1925; foreign member of the Royal Academy of Sciences, Turin, 1928; Director of the Graduate School of Aeronautics, California Institute of Technology, 1928.

² Assistant Professor of Aeronautics, Daniel Guggenheim Graduate School of Aeronautics, California Institute of Technology. Assoc-

Mem. A.S.M.E. Professor Millikan was born in Chicago in 1903, and received his Ph.B. from Yale University in 1924 and Ph.D. in Physics and Mathematics from California Institute of Technology in 1928. He was a Teaching Fellow at the California Institute of Technology from 1924 to 1928, and since then has held his present position.

Contributed by the Aeronautic Division and presented at the Semi-Annual Meeting, Chicago, Ill., June 26 to July 1, 1933, of THE AMERICAN SOCIETY OF MECHANICAL ENGINEERS.

NOTE: Statements and opinions advanced in papers are to be understood as individual expressions of their authors, and not those of the Society.

density wind tunnels and the N.A.C.A. giant tunnel have been built for this purpose. Both of these types of wind tunnel have already made very valuable contributions to the development of experimental aerodynamics, but there are certain difficulties connected with each. The relatively small size of the models used in the variable-density tunnel makes the reproduction of small details rather difficult. Also, the initial cost of such wind tunnels is so large as to almost rule out their use by other than governmentally supported institutions. The latter remark applies *a fortiori* to the giant tunnel, and furthermore, the cost of models and of operations is very large. A further complication is introduced by the fact that measurements carried out at the same Reynolds number may lead to very different results if the internal structure of the artificial air streams (i.e., their state of turbulence) is different. In view of this situation, the authors believe that it is very important to analyze the conditions under which measurements in a medium-sized wind tunnel can be applied reliably to full-scale conditions. Obviously, it is necessary that the measurements be carried out at a Reynolds number above those producing critical changes in the flow and in a range where certain theoretical extrapolations connected with friction can be safely made. It is also desirable that the wind stream for the tests be as free from turbulence as possible, since it is very simple to introduce artificial turbulence, but extremely difficult to remove an already existing turbulence. The wind tunnel of the Guggenheim Aeronautics Laboratory of the California Institute of Technology has been built in such a way as

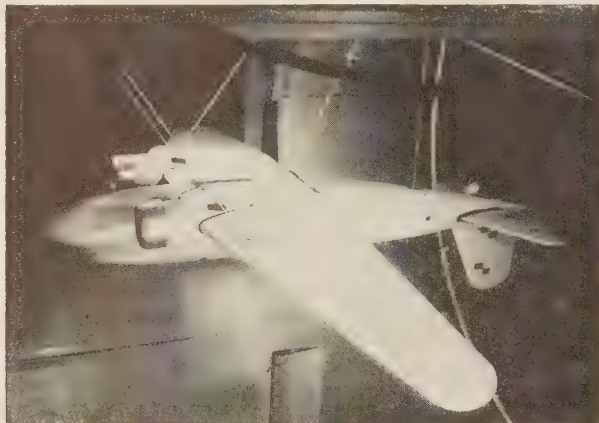


FIG. 1 MODEL SUSPENDED (INVERTED) IN THE GUGGENHEIM AERONAUTICS LABORATORY WIND TUNNEL READY FOR TESTS
(The model span is 7 $\frac{3}{4}$ ft.)

to satisfy these conditions as fully as possible. The first part of this paper is devoted to a discussion of the applicability of the measurements made in such a wind tunnel, with particular reference to performance predictions. The second part discusses a series of investigations collected in order to show the wide range in the type of design problems which can be attacked using this type of wind tunnel.

A detailed description of the wind tunnel has previously been published,³ so that only the chief characteristics will be repeated here. The diameter of the closed working section is 10 ft, and the wind speed for normal operation is 200 mph. The airplane models tested have, in general, spans of between 5 and 8 ft, so that the usual Reynolds number based on the wing chord lies

between 1,500,000 and 2,000,000. The suspension system has been very carefully designed to eliminate interference between the model and its supports to as large an extent as possible. A photograph of a typical model mounted in the wind tunnel and ready for testing is given in Fig. 1. All of the experimental data discussed in this paper were obtained in this wind tunnel. Unless otherwise specified, the notation employed is that defined by the N.A.C.A. as the standard American notation using absolute coefficients.

A considerable group of graduate students under the direct supervision of Drs. A. L. Klein and C. B. Millikan has carried out the wind-tunnel investigations discussed in this paper. In particular, acknowledgment should be made of the contributions of Messrs. W. B. Oswald, W. H. Bowen, N. B. Moore, and R. Mills. The design of the wind-tunnel balances, rigging, and all auxiliary apparatus has been done by Dr. Klein.

I—INITIAL PERFORMANCE PREDICTION

The modern methods of performance estimation which have recently been published here and abroad substitute for a graphical method of calculation an analytical one using certain definite design parameters of the airplane to which numerical values are assigned. The problem of the airplane designer is to determine these numerical values as accurately as possible. At our laboratory the most accurate, rapid, and satisfactory method of performance prediction has been found to be the analytical one developed by Oswald and presented in full in N.A.C.A. Technical Report No. 408.⁴ The design parameters used in this method are: the gross weight W , the design thrust horsepower thp_m , the wing area S , the effective span b , the equivalent parasite area f , and the maximum-lift coefficient $C_{L_{max}}$. Of these, the weight and wing area are known for any proposed design. The design thrust horsepower is the product of the design brake horsepower and the design propulsive efficiency. The first is given by the engine, and the second may now be very satisfactorily estimated for any normal engine and cowling arrangement as a result of the very beautiful and complete investigations carried out in its propeller research wind tunnel by the N.A.C.A. The effective span may be expressed by the relation $b_e^2 = e(kb)^2$, where e is the so-called airplane efficiency factor, b is the largest span of the airplane, and k is Munk's span factor; b is given, and k may readily be calculated from the geometry of the wing cellule. Hence, the three parameters for which the designer must obtain values are e , k , and $C_{L_{max}}$. In the remainder of this section the methods for estimating the full-scale values of these parameters which have been used at the laboratory are described.

1 EFFICIENCY FACTOR e

A polar of C_D versus C_L is plotted from the wind-tunnel measurements corrected for tare drag and wind-tunnel wall interference. The parasite-drag coefficient C_{D_p} is defined as

$$C_{D_p} = C_D - C_{D_i} = C_D - \frac{C_L^2}{\pi b_e^2 / S}$$

An induced-drag parabola (C_{D_i} versus C_L) is now plotted on the same sheet as the original polar, in such a manner that the difference in abscissas (C_{D_p}) between it and the original polar is as nearly constant as possible over the range of C_L 's included in the normal flying range below the stall. This is assumed to be the corrected induced-drag polar for the airplane in Oswald's sense; i.e., it is the curve corresponding to

³ C. B. Millikan and A. L. Klein, "Description and Calibration of 10-Foot Wind Tunnel at California Institute of Technology," presented at the Pacific Coast Aeronautics Meeting, Berkeley, Calif., June 9 to 10, 1932 (mimeographed).

⁴ W. B. Oswald, "General Formulas and Charts for the Calculation of Airplane Performance," N.A.C.A. Technical Report No. 408 (1932).

$$C_{Di} = \frac{C_L^2}{\pi b^2/S}$$

From this polar b^2S is determined, and, since S , b , and k are known, the value of e is easily deduced. This value of e is assumed to be the same as that for the full-sized airplane in free flight.

The assumptions which are made in this extrapolation are that the influences of the following changes in passing from model to full scale are unimportant:

- (a) Changes in shape especially in small details
- (b) Change in Reynolds' number
- (c) Change in character of air flow (turbulence)
- (d) Change from power off to power on.

The validity of (a) depends upon the accuracy of the model work, the size of the model, and the cleanness or complication of the external design of the airplane. All three of these points are interrelated. For a very complicated design with many wires, struts, fittings, and excrescences, it is almost impossible to duplicate the airplane accurately enough in any model much smaller than one to be tested in the N.A.C.A.'s full-scale wind tunnel. For modern high-speed designs, with cantilever or simply braced wings, retractable or completely faired landing gears, enclosed cockpits, etc., it is our belief that models of sufficient accuracy can fairly readily be constructed with spans of the order of 6 to 8 ft. With regard to (b), there is no evidence with which the authors are familiar to indicate that there is any important change with Reynolds' number in the variation of C_{Dp} with C_L , at least above Reynolds' numbers (based on wing chord) of the order of 1,000,000. The same state of affairs holds for (c) as for (b). With respect to (d), recent flight test researches, especially those carried out by the D.V.L. in Germany, indicate that in certain cases there is a very considerable change in e in passing from gliding to power-on flight. Hence predictions of e made in the manner here suggested are strictly valid only for gliding flight, but are believed to furnish valuable indications, at least for power-on flight. Experiments are now in hand at the Guggenheim Aeronautics Laboratory here, using small motors mounted in the wind-tunnel models and driving small propellers during the experiments, which it is hoped will give sufficient data to enable the extension of accurate predictions of e to the case of power-on flight.

2 EQUIVALENT PARASITE AREA f

Having determined the parasite-drag coefficient by the method of the last section, f for the full-scale airplane is most naively obtained from the formula (defining f):

$$f = C_{Dp}S \dots \dots \dots [1]$$

where S is the wing area of the full-size airplane. Such an extrapolation involves the same assumptions (a) to (d) as were discussed in the preceding section; (a) has already been considered; and any question as to (d) is eliminated if propulsive efficiencies are taken from the N.A.C.A.'s reports previously referred to, in which propulsive efficiencies are so defined as to take into account the effects of changes from power off to power on. With respect to (c), turbulence can exert an influence on C_{Dp} in two different ways: eddy resistance depends on the location of separation points, which may change with the turbulence conditions; skin friction is influenced by the transition between the laminar and turbulent régimes in the boundary layer. Both influences can be eliminated if the models tested are clean enough and the tests are carried out at such high Reynolds' numbers that critical points do not occur near the high-speed attitude of the plane and the boundary layer is turbulent over the major part of the

model surface. It appears that these conditions are satisfied for models of modern high-speed airplanes tested at Reynolds' numbers above 1,000,000 or 1,500,000. There remains (b), the effect of the change in Reynolds' number or the scale effect proper. For modern high-speed transport planes a considerable extrapolation is here necessary, even for tests carried out in the N.A.C.A.'s variable-density or full-scale wind tunnels, since for such planes at maximum speed the Reynolds number based on wing chord may reach values of the order of 20,000,000 to 30,000,000. The following method of making this extrapolation has recently been devised by the junior author and used with some success.

Parasite drag may be divided into two categories: eddy resistance or form drag, which is approximately independent of Reynolds' number (assuming that no critical points occur in the range considered), and skin friction. If the scale of the tests is sufficiently large, as previously indicated ($R \sim 1,000,000$ to 1,500,000), the boundary layer may be assumed to be turbulent over practically all of the model, so that the friction may be considered as purely turbulent skin friction. The theory of turbulent skin friction has been actively investigated in the last decade. It was for some time accepted that the coefficient of skin friction for smooth, flat surfaces was proportional to the $1/5$ power of the Reynolds number, so that it appeared at one time as if this "power law" represented a basic physical law.

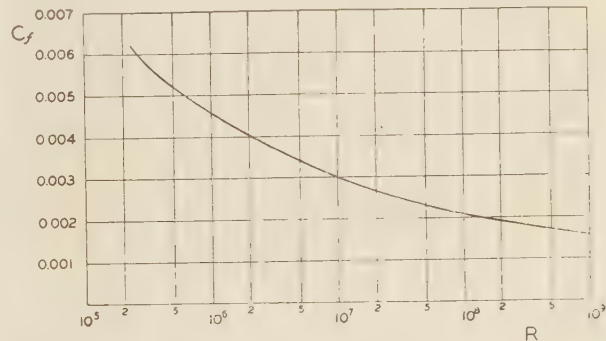


FIG. 2 COEFFICIENT OF SKIN FRICTION C_f AS FUNCTION OF THE REYNOLDS NUMBER R , FOR SMOOTH FLAT PLATES
(From Von Kármán's theory.)

This belief was subsequently proved to be false when further experimental data obtained at higher Reynolds' numbers than had previously been investigated showed that as R increased, the exponent decreased from $1/5$ to $1/6$, then to $1/7$, and so on. These discoveries left the basic theory of turbulent skin friction in a very troubled and unhappy state. Finally, the senior author, using reasoning based on considerations of dynamical similarity, was able to show that a general law could be formulated giving a logarithmic formula for the variation of the coefficient of skin friction with Reynolds' number.⁵ The earlier power laws were shown to be essentially interpolation formulas for this general law, which has since been verified experimentally up to the highest Reynolds' numbers yet attainable. According to this theory, the formula connecting the coefficient of the skin friction and Reynolds' number can be written⁶

$$\frac{0.242}{\sqrt{C_f}} = \log_{10} (RC_f)$$

⁵ Th. von Kármán, "Mechanische Ähnlichkeit und Turbulenz," *Göttingen Nachrichten* (Math.-Phys. Klasse), 1930; see also Proceedings of the Third International Congress for Applied Mechanics, Stockholm (1930), vol. I, p. 85.

⁶ Th. von Kármán, "Quelques Problèmes Actuels de L'Aérodynamique," *Journées Techniques Internationales de l'Aéronautique*, Paris, 1932.

The values of C_f and R are represented in Fig. 2. C_f is strictly the skin friction on a flat plate parallel to the flow and is defined as the average frictional force per unit "wetted area" on a flat plate of length l in the direction of flow divided by the dynamic pressure. R is defined in terms of the free-stream velocity and the length l .

In applying the results of this theory to the problem under consideration, two extreme cases are considered:

Case 1: Only the wing-profile drag is considered as turbulent skin friction; the remaining parasite drag is assumed to be form drag and as such is independent of Reynolds' number

Case 2: The entire parasite drag is assumed to be skin friction. The characteristic length l is taken as the mean wing chord.

Considering case 1, and letting $()_m$ correspond to model conditions and $()_f$ correspond to full scale, while C_{D_o} denotes wing-profile drag and R the Reynolds number, we have

$$\frac{C_{D_{of}}}{C_{D_{om}}} = \frac{C_f(R_f)}{C_f(R_m)} \dots \dots \dots [2]$$

where the length in R is taken as the mean wing chord, and C_f is read from Fig. 2. From the $C_{D_{of}}$ determined in this way, f_{wings} is calculated from Equation [1]. The equivalent parasite area for the remainder of the airplane is calculated in the same way, assuming the drag coefficient to be independent of R . The total f for full-scale conditions is then the sum of these two parasite areas. For case 2, the procedure is the same except that

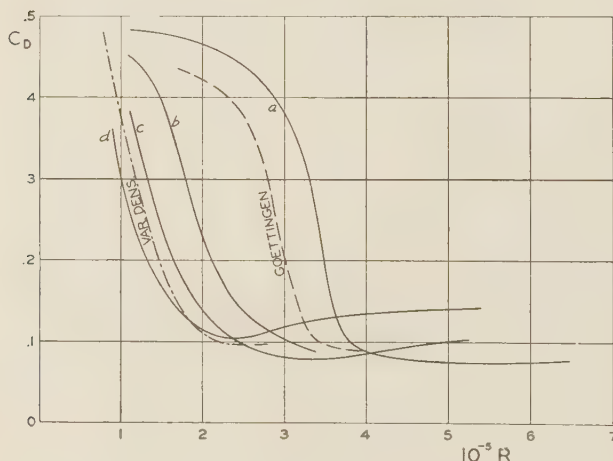


FIG. 3 SPHERE-DRAG COEFFICIENT C_D , VERSUS REYNOLDS' NUMBER R , FOR VARIOUS WIND STREAMS

(Curves a , b , c , and d refer to the wind tunnel of the Guggenheim Aeronautics Laboratory of the California Institute of Technology, with no grid and with grid 48 in., 20 1/2 in., and 10 1/2 in. upstream from the model, respectively. The curves for the N.A.C.A. variable-density and the Göttingen wind tunnels are also included.)

in Equation [2] the profile-drag coefficient is replaced by the total parasite-drag coefficient C_{D_p} , and there is no additional term with constant-drag coefficient. Case 1 should give too large a full-scale f and case 2 somewhat too small a value. The actual f should be between the two, its proximity to one or the other being estimated on the basis of the amount of form drag to be expected—i.e., on the cleanness of the airplane design. As an example, the following data are given, derived from tests on a model of an observation-type military monoplane with wire bracing, pylon above the wing, tripod landing gear with wheel fairings, and open cockpit. The maximum velocity V_m was cal-

culated from f , using the methods of Oswald's paper (loc.cit.):

Model results scaled up without Reynolds' number correction: $V_m = 180$ mph.

Wing-profile drag only corrected to full scale: $V_m = 186$ mph.

Total parasite drag considered as skin friction and corrected to full scale: $V_m = 205$ mph.

Flight tests on the actual airplane gave $V_m = 195$ mph—i.e., almost exactly half-way between the two extrapolations. This airplane was not especially clean in comparison with modern transport planes, the total parasite drag being about four times as large as the wing-profile drag. For some recent planes the total parasite drag is only about twice the wing-profile drag, and in such cases the two extrapolations would give results much less far apart, with the actual V_m lying nearer to the higher estimate because of the smaller percentage of form drag.

3 MAXIMUM LIFT COEFFICIENT $C_{L_{max}}$

In extrapolating wind-tunnel results for $C_{L_{max}}$ to full scale in order to estimate landing speeds, the same changes (a) to (d) previously discussed must again be considered. Item (d) may be neglected, since in practise the landings are almost always made with the motor idling, although there is evidence that in some cases of unfortunate placing of the propeller relative to the wing the presence of an idling or stopped propeller lowers $C_{L_{max}}$ to some extent. With regard to (a), investigations here at the Guggenheim Aeronautics Laboratory and elsewhere have shown that slight roughness or protuberances near the leading edge of a wing may lower its $C_{L_{max}}$ very appreciably. Hence the finish of this portion of the model should be as perfect as possible. At the aeronautics laboratory here this is accomplished by spraying the model with several coats of lacquer and rubbing down to a high polish. In some cases of rather protracted or interrupted tests this process has been repeated several times during the course of an investigation. By this means highly reproducible values of $C_{L_{max}}$ are attained which are thought to permit safe extrapolation to full scale, at least in so far as (a) is concerned. The effects of (b) and (c) (i.e., Reynolds' number and turbulence) are very large and have in the past been very confusing, as is evidenced by the large discrepancies between the values of $C_{L_{max}}$ reported by different wind tunnels for the same airfoil section. The confusion in this matter prompted Drs. Klein and Millikan to undertake an elaborate experimental investigation of the phenomenon in the spring of 1932, introducing turbulence artificially into the wind-tunnel stream by means of screens placed upstream from the model. Shortly afterward the present authors began work on a theoretical discussion of the problem, which turned out to be correspondingly elaborate. The complete results of both researches are appearing currently in technical journals. In the remaining paragraphs of this section a brief account of the most important results will be given.⁷ The experiments were carried out on a model of the N.A.C.A. 2412 section with rectangular plan form, aspect ratio 6, and span 6 ft. The model was furnished by the Boeing Airplane Company and was very accurately made of laminated wood finished to a high polish. For the results to be discussed here, turbulence was introduced into the wind stream by placing a grid of rods 1/8 in. in diameter, spaced 3/4 in. apart, at various distances upstream from the model. The rods were perpendicular to the wind stream and to the span of the model, and the grid was of such a size and so placed that the entire wing was in its "wind shadow" at all angles of attack. For each position of the grid, measurements were taken of the resistance of a sphere placed in the position normally occupied by the center

⁷ See also Th. von Kármán, "Quelques Problèmes Actuels de l'Aérodynamique," Journées Techniques Internationales de l'Aéronautique, Paris, 1932.

of the wing. Using the criterion suggested by Dryden and Kuethe,⁸ the values of the Reynolds number at which the sphere-drag coefficient had the value 0.3 furnished a measure for the degree of turbulence caused by the grid in the different positions. The sphere-drag curves obtained for three positions of the grid and with the grid removed are given in Fig. 3. The curve re-

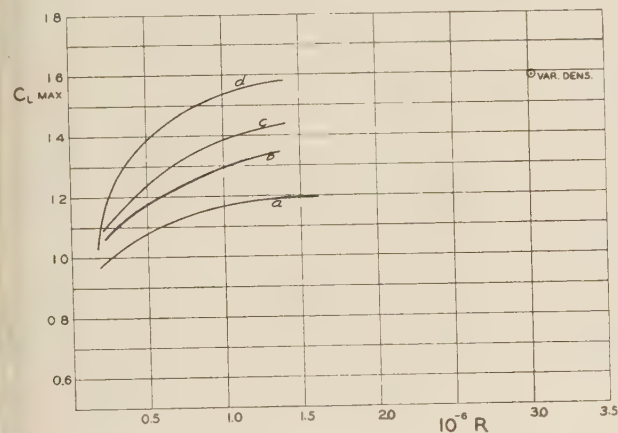


FIG. 4 C_{Lmax} VERSUS R FOR N.A.C.A. 2412 AIRFOIL (CHORD = 12 IN.)

(The curves *a*, *b*, *c*, and *d* refer to the same flow conditions as to the corresponding curves of Fig. 3. The value reported from the variable-density tunnel is indicated.)

ported for the N.A.C.A. variable-density tunnel is also included for comparison.⁹ It will be noticed that the degree of turbulence in the variable-density tunnel is apparently about midway between those obtained in the laboratory tunnel with the grid in the two positions nearest the model (*c* and *d*). The variable-density tunnel is chosen for the comparison, since one of the main purposes of the investigation was originally an attempt to explain the extremely large discrepancy between the values of C_{Lmax} for the 2412 wing reported from the variable-density tunnel and those obtained in our laboratory experiments.

For each of the configurations *a*, *b*, *c*, and *d*, polars were observed for the wing at a series of seven or eight Reynolds' numbers. Curves giving the result as regards C_{Lmax} are plotted in Fig. 4, together with a point giving the C_{Lmax} reported by the variable-density tunnel.¹⁰ A curve midway between *c* and *d* extrapolated to $R = 3,000,000$ would apparently come very close to the latter point. This result is entirely consistent with the sphere-drag curves of Fig. 3.

The conclusion to be drawn from these results is that both Reynolds' number and turbulence have very pronounced effects on C_{Lmax} . The variation with R is the more pleasant of the two, since it appears that at $R \sim 1,500,000$ the curves are rapidly approaching horizontal asymptotes, so that extrapolation to higher values of R should be possible with some measure of confidence. This seems to be especially true for the curve *a* corresponding to the clean tunnel or the normal operating state. The variation with turbulence at once raises the question as to the degree of turbulence to be expected in free flight. Experiments are under way to determine the critical Reynolds' number

of a sphere mounted on an airplane flown under various conditions. It is hoped that these tests will furnish data pertinent to this question.

The theoretical investigation mentioned was undertaken in the hope that the physical mechanism underlying the results just described might be elucidated. The experimental fact was known that, even in the case that the general flow outside of a boundary layer is turbulent, the boundary layer starting from the stagnation point has a laminar character. However, the degree of the outside turbulence has a large effect on the transition point between the laminar and turbulent state in the layer itself. It was therefore suspected that the large influence of external turbulence on C_{Lmax} might be connected with this phenomenon. In view of the complexity of the phenomena, it was not at all expected that theoretical curves duplicating those of Fig. 4 could be deduced, but it was hoped that results similar enough to the experimental ones might be predicted, so that the essential physical processes involved might be visualized. For this purpose an analysis of the laminar boundary layer about a two-dimensional airfoil with external pressure gradients was developed, of which the only element which need be discussed here is the following: Instead of using the distance along the solid surface from some origin as one of the variables of the problem, it was

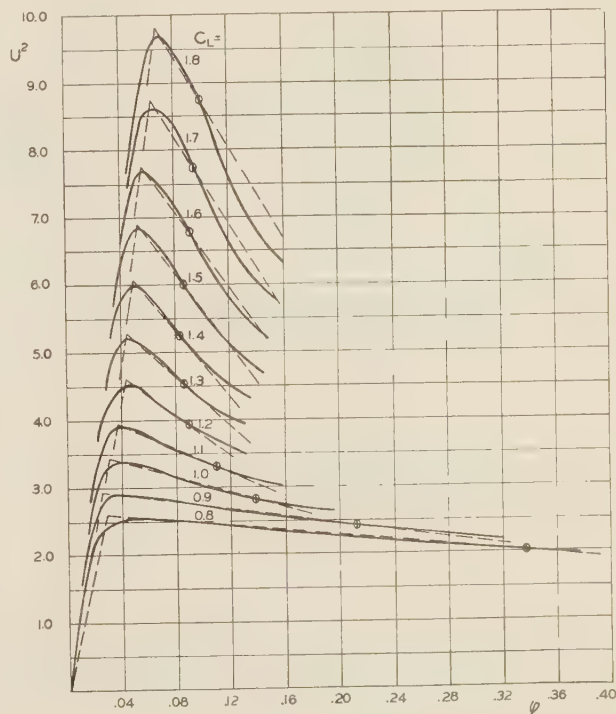


FIG. 5 COMPUTED VALUES OF U^2 VERSUS ϕ FOR N.A.C.A. 2412 AIRFOIL AT VARIOUS LIFT COEFFICIENTS

(The position of the separation point for each C_L is indicated by the oval crossing each curve. In order to make the figure clearer, the curves have not been extended to the origin. The dotted straight lines give the approximations to the theoretical curves which were used in the boundary-layer calculations.)

found convenient to use the value of the potential function ϕ associated with the external potential flow measured from the forward stagnation point as origin. The value of ϕ at any point is then merely of the line integral $\int U ds$ along the surface from the stagnation point to the point in question, where U is the ratio of the potential velocity outside of the boundary layer to the

⁸ H. L. Dryden and A. M. Kuethe, "Effect of Turbulence in Wind-Tunnel Measurements," N.A.C.A. Technical Report No. 342 (1930).

⁹ John Stack, "Tests in the Variable-Density Wind Tunnel to Investigate the Effects of Scale and Turbulence on Airfoil Characteristics," N.A.C.A. Technical Note No. 364 (1931).

¹⁰ E. N. Jacobs and K. E. Ward, "Tests of N.A.C.A. Airfoils in the Variable-Density Wind Tunnel, Series 24," N.A.C.A. Technical Note No. 404 (1932).

undisturbed flow velocity, and ds is an element of length along the airfoil surface, perpendicular to the span, divided by the airfoil chord.

The potential flow-velocity distribution over the upper surface of an N.A.C.A. 2412 airfoil from the stagnation point downstream was calculated by Theodorsen's method¹¹ for a series of values of C_L . The squares of the velocities so obtained are plotted against φ in Fig. 5. For simplicity in making the succeeding calculations, each of these curves was approximated by two intersecting straight lines, which are shown dotted in Fig. 5. The errors introduced by this approximation should be relatively unim-

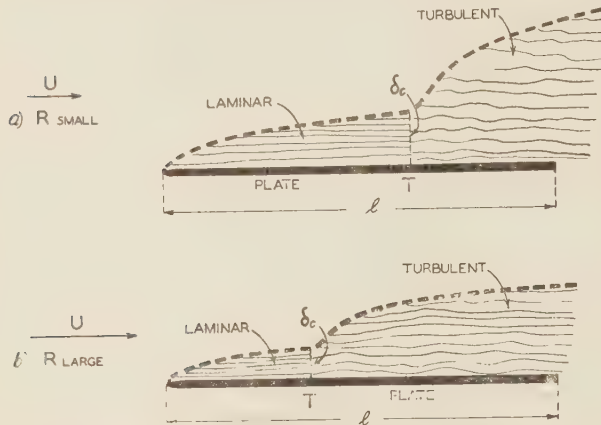


FIG. 6 SCHEMATIC DIAGRAM OF THE BOUNDARY LAYERS FOR FLOW ALONG A FLAT PLATE AT TWO REYNOLDS' NUMBERS ($R = U_1/\nu$) (The motion upstream of the transition point T as R increases is indicated.)

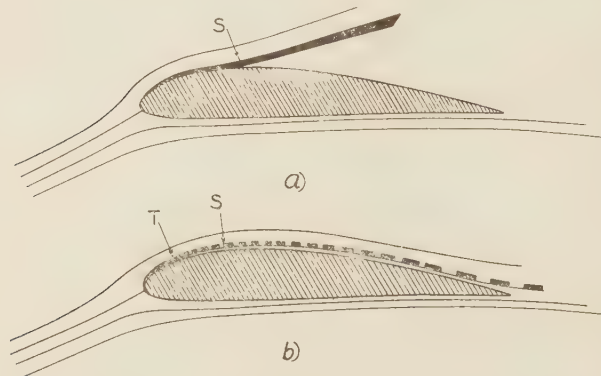


FIG. 7 DIAGRAM OF ALTERNATIVE FLOWS ABOUT AN AIRFOIL NEAR C_{Lmax}

(The boundary layer over the upper surface is indicated by the heavy line. In (a) the transition point would be downstream from the separation point S , and the flow separates from the airfoil. In (b) the transition point T is upstream from the calculated separation point S , the turbulent layer (dotted) clings to the surface, and the separation does not occur.)

portant in view of the nature of the problem. The separation points at which the flow breaks away from the airfoil surface were calculated for the boundary layer associated with each of the curves, and are indicated on the figure. The boundary-layer thickness at the separation point δ_s was determined for each of the curves, and a corresponding boundary-layer Reynolds' number R_{δ_s} was defined by

$$R_{\delta_s} = \frac{U_s \delta_s}{\nu} \quad [3]$$

¹¹ Theodore Theodorsen, "Theory of Wing Sections of Arbitrary Shape," N.A.C.A. Technical Report No. 411 (1932).

where U_s is the potential velocity just outside the boundary layer and at the separation point and ν is the coefficient of kinematic viscosity.

A result obtained both experimentally and theoretically for boundary layers along flat plates in a uniform flow was now extended to the boundary layers under consideration. This result is the following: If a boundary-layer Reynolds' number R_{δ} be associated as in Equation [3] with the laminar boundary-layer thickness δ , along a flat plate parallel to a uniform flow, then for any given degree of turbulence in the external flow there exists a definite critical value of R_{δ} , called R_{δ_c} , at which the laminar flow in the boundary layer becomes unstable. Hence, when R_{δ} (which increases continuously as one goes downstream from the leading edge) reaches the value of R_{δ_c} , a transition point occurs. Upstream from this transition point the flow in the boundary layer is laminar, while downstream the flow is turbulent (see Fig. 6).

The variation of δ with the external velocity U is such that, as U (or the basic Reynolds' number R referred to the length of the plate) increases, the transition point moves upstream for a given R_{δ_c} . The value of R_{δ_c} depends on the degree of turbu-

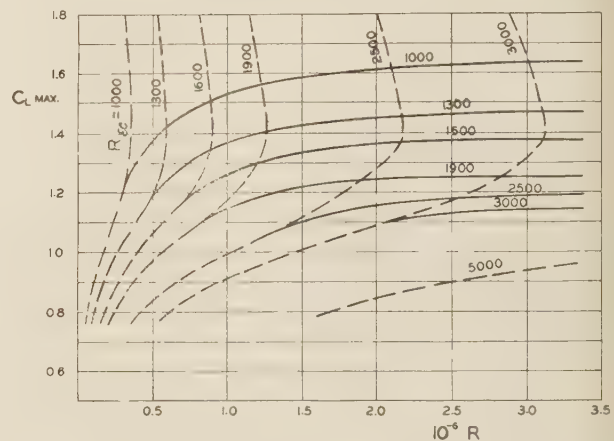


FIG. 8 THEORETICAL CURVES OF C_{Lmax} VERSUS R FOR VARIOUS VALUES OF R_{δ_c}

(Dotted curves represent calculated values. Solid curves represent rough extrapolations for the larger values of R , based upon reasoning given in the text.)

lence in the external flow in such a way that, as the turbulence increases, R_{δ_c} decreases. For flow along a flat plate the values of R_{δ_c} lie between about 10,000 for very smooth flows and about 1500 for very turbulent flows.

It was assumed that conditions are similar for the flow over an airfoil; i.e., for any external flow there exists an R_{δ_c} such that when the boundary-layer Reynolds' number R_{δ} reaches R_{δ_c} , a transition point occurs and the boundary layer changes from laminar to turbulent. The problem under consideration can be put in the following way: Under what conditions can a certain value of C_L be reached? Obviously, it depends on which of R_{δ} or R_{δ_c} is the larger. If $R_{\delta} < R_{\delta_c}$, then the flow will separate from the airfoil at the calculated separation point, the assumed potential flow cannot exist, and the corresponding assumed value of C_L cannot be reached. If, on the other hand, $R_{\delta} > R_{\delta_c}$, the transition point will be upstream from the calculated separation point, and the flow at the latter point will no longer be laminar, as was assumed, but will instead be turbulent.

From experiments on spheres and other bodies, it is known that a turbulent boundary layer clings to a surface and resists separation to a much greater extent than does a laminar layer.

Therefore, in the case that $R_{\delta_e} > R_{\delta_c}$, the boundary layer will cling to the upper surface of the airfoil, and the possibility is given that the lift coefficient in question will be attained. The alternatives are illustrated schematically in Fig. 7. Whether the value of C_L in question will actually be reached depends on the behavior of the turbulent layer after the transition. Since very little is known about the laws governing the separation of turbulent boundary layers, it was assumed for this investigation that such a separation never occurs. Under this assumption, $R_{\delta_e} = R_{\delta_c}$ is a limiting case such that the assumed C_L is just

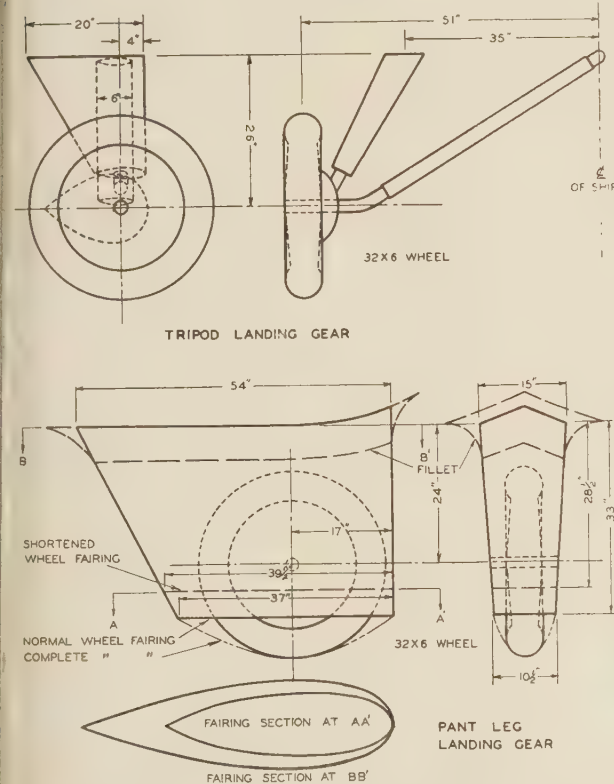


FIG. 9 TRIPOD AND "PANT LEG" LANDING GEARS OF NORTHROP ALPHA
(Dimensions correspond to full scale. Model one-sixth full scale.)

attained. If the basic flow Reynolds' number $R (= Ut/\nu$, where t = airfoil chord) is decreased, R_{δ_e} is decreased, separation occurs, and the assumed C_L is not attained. If R is increased, no separation occurs, and the assumed C_L is attained. Hence for every set of values of C_L and R_{δ_e} we get certain definite values of R such that the assumed C_L is just the $C_{L_{max}}$ which can be obtained. Hence for a given R_{δ_e} we may determine $C_{L_{max}}$ as a function of R . This has been done for a series of values of R_{δ_e} and the results are plotted as dotted curves in Fig. 8.

It will be observed that our assumption as to the lack of separation for turbulent boundary layers implies that unlimited values of $C_{L_{max}}$ are possible. This obviously represents an oversimplification, since somewhat analogous laws almost certainly govern the separation of turbulent and laminar boundary layers. Hence it is probable that those portions of the curves of Fig. 8 which are concave upward or have negative slopes are quite incorrect and should actually be replaced by branches similar to those drawn in solid lines.

If one compares the theoretical curves of Fig. 8 with the experimental ones of Fig. 4, one sees that for $C_{L_{max}} < 1.2$ to 1.4 the

general nature of the two families is very similar. For larger values of $C_{L_{max}}$ the theory gives very considerable effects of turbulence, but the shape of the theoretical curves is not satisfactory, for the reasons mentioned. The rather low values of R_{δ_e} are not at all surprising when the unstable nature of the velocity profiles near a separation point is remembered. In any case the investigation shows without doubt that the physical basis of the large effect of the turbulence on the maximum-lift coefficient has been correctly determined as resting upon a transition-point versus separation-point contest. It will be noted that this is the same type of explanation as was given many years ago by Prandtl in connection with the then mysterious sphere-drag phenomenon.

II—SPECIAL DESIGN PROBLEMS

In this second part of the paper there will be discussed a series of different types of aircraft-design problems which have arisen and have been investigated in the wind tunnel of the Guggenheim Aeronautics Laboratory of the California Institute of Technology. Many of the tests to be considered originated at the request of commercial firms, in which cases the costs were borne by the firms concerned and the results were to remain confidential for a definite length of time. In such cases the illustrative data here furnished are of necessity incomplete.¹² In several in-



FIG. 10 PHOTOGRAPH OF NORTHROP ALPHA WIND-TUNNEL MODEL
(With shortened "pant leg" landing gear.)

stances investigations begun in this manner developed a considerable scientific importance in the eyes of the laboratory staff, so that the tests were made much more extensive than had originally been contemplated, and arrangements were made for fairly early publication. The experiments discussed in Sections 2, 4, and 5 following belong in this latter category. The results to be presented here fall naturally into rather distinct groups, as indicated by the titles of the sections.

1 COMPARATIVE DRAG INVESTIGATIONS

The precision attained in ordinary drag measurements is limited essentially by the accuracy with which the tare drag can be determined. The precision of tare-drag measurements is considerably less than that for gross-drag observations, due chiefly to difficulties inherent to the tare-drag set-up and to unavoidable interference between the model and the supporting system. It is conservatively estimated that the tare drag is accurate to within about 5 per cent, which means that the minimum drag of airfoils may be determined with about the same accuracy, while the determination of the minimum drag of complete airplane models should be accurate to within 2 per cent or better.

¹² The authors wish to make particular acknowledgment of the courtesy of the Douglas, Boeing, and Northrop Aircraft Companies in permitting the inclusion of the results of such tests as are here discussed.

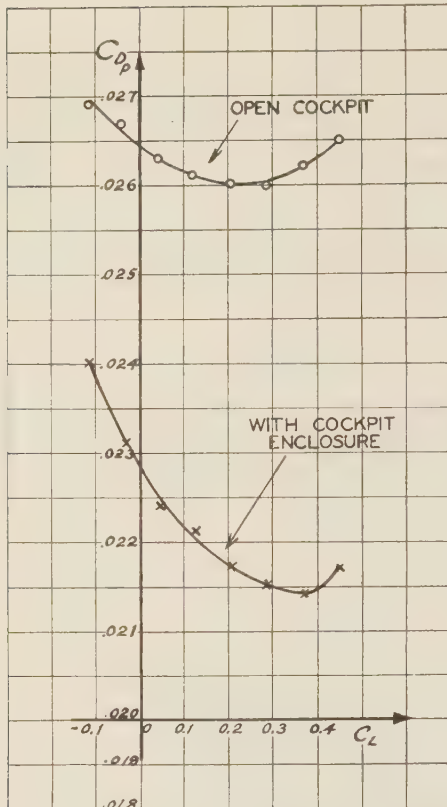


FIG. 11 PARASITE-DRAG COEFFICIENT VERSUS LIFT COEFFICIENT
(For complete airplane model with and without cockpit enclosure.)

However, if a given model is tested successively with various modifications, the tare drag remains the same for all the tests and the differences in drag between the various model configurations can be determined with much higher accuracy than the foregoing figure. A considerable number of investigations of this type have been made at our laboratory, some of which will be briefly described here.

(a) *Tripod and "Pant Leg" Landing Gears.* A series of measurements was completed in December, 1930, on a model of a Northrop Alpha airplane without engine, cowl, cockpit, or tail surfaces. A normal tripod landing gear and a "pant leg" gear with various modifications were attached. Dimensioned drawings of the landing gears are given in Fig. 9, and a picture of the wind-tunnel model with shortened pant-leg landing gear is given in Fig. 10. The model was tested in the high-speed attitude, the results being obtained at a wind speed of 210 mph. The drag of the model with no landing gear (corresponding to a completely retracted gear) was taken as a standard of comparison, and the percentages of this standard drag added by the various gears are given in Table 1.

Landing gear	Percentages of standard drag added by gear
Pant leg, completely faired	11.0
Pant leg, normal	15.1
Pant leg, shortened	20.0
Tripod	76.2

It will be noticed that the normal pant-leg gear has only one-fifth the drag of the tripod gear, and that the latter would be

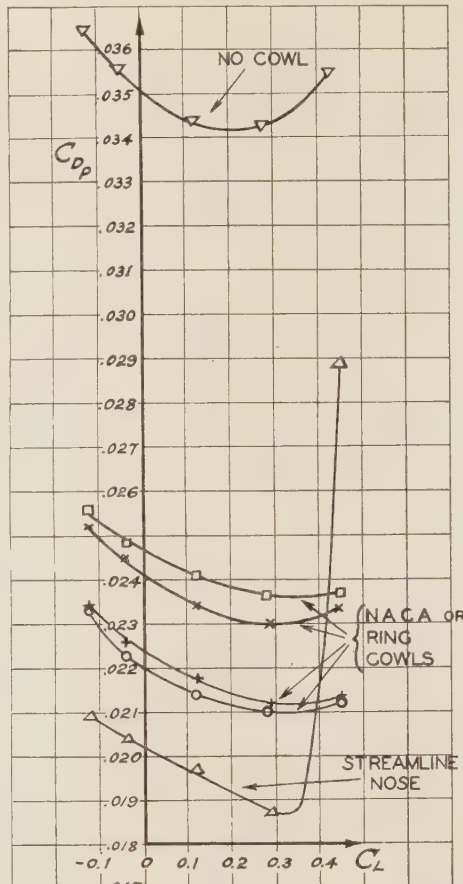


FIG. 12 PARASITE-DRAG COEFFICIENT VERSUS LIFT COEFFICIENT FOR COMPLETE AIRPLANE MODEL
(With various radial-engine cowling arrangements. The streamline nose replaced engine and cowl.)

estimated to furnish about 35 per cent of the gross minimum drag of the complete airplane in flying condition. The question as to whether the additional 7 per cent which could be saved by a completely retractable gear is worth the added weight and complication which such a gear entails is one for the designer himself to decide. It might be mentioned that removing the very small fillet which may be seen in Fig. 10 between wing and fuselage caused an increase of 20 per cent over the standard drag.

(b) *Cockpit Enclosures.* In connection with a recent series of tests made for the Boeing Airplane Company, the details of which are still confidential, a model of a very clean airplane was tested with a normal open cockpit with windshield and headrest, and the same model was then tested with a completely streamlined cockpit enclosure. The results given in Fig. 11 furnish a typical example of the very large effects to which such modifications may lead.

(c) *Engine Cowlings.* In connection with the aforementioned tests, the model,

which was furnished with a very accurate small-scale reproduction of a standard air-cooled engine, was investigated with a series of four ring- and N.A.C.A.-type cowls. The differences between some of the latter were so slight as to be difficult of detection

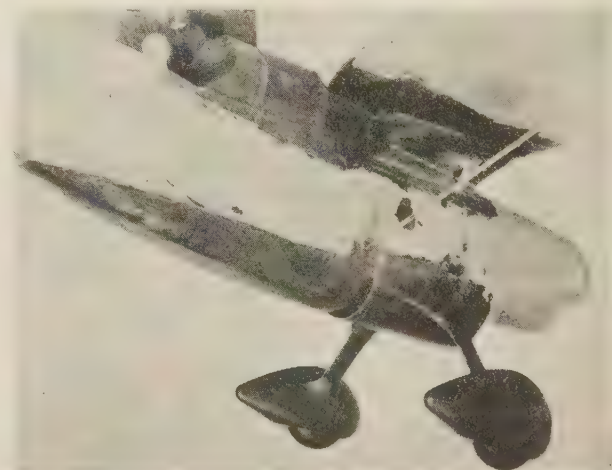


FIG. 13 PHOTOGRAPH OF OPTIMUM COWLING AND STREAMLINING
(For "belly" radiator of Douglas YO-31 airplane model.)

upon casual observation. The results given in Fig. 12 show the well-known reduction in drag due to the use of this type of cowl and also furnish evidence as to the possibility of choosing the optimum of a series of very similar configurations, in view of the accuracy indicated by the experimental points.

(d) *Radiator Cowling and Fairing.* In the course of an investigation on a model of a Douglas YO-31 observation plane, it was noticed that a rather large bump placed on the bottom of the fuselage some distance behind the normal "belly" radiator caused no increase in drag. An investigation into the influence of cowlings and fairings in connection with such a radiator was accordingly undertaken. The optimum configuration arrived at is shown in Fig. 13, and the comparative drag measurements showing the results with this configuration and with the standard radiator installation (a short tunnel and no fairing behind) are given in Fig. 14. The precision as indicated by the scatter of the experimental points is again interesting.

(e) *Wing-Engine Nacelles.* A model of a large airplane with two air-cooled wing engines was recently tested in our laboratory wind tunnel. The nacelles and engine cowlings were designed in accordance with the latest recommendations embodied in the exhaustive reports published on the subject by the N.A.C.A. In connection with the particular wing used, it appeared, however, that there were certain undesirable interference effects, especially in the cruising range and near the stall. In the attempt to improve the aerodynamic characteristics, a series of eight modified nacelle-

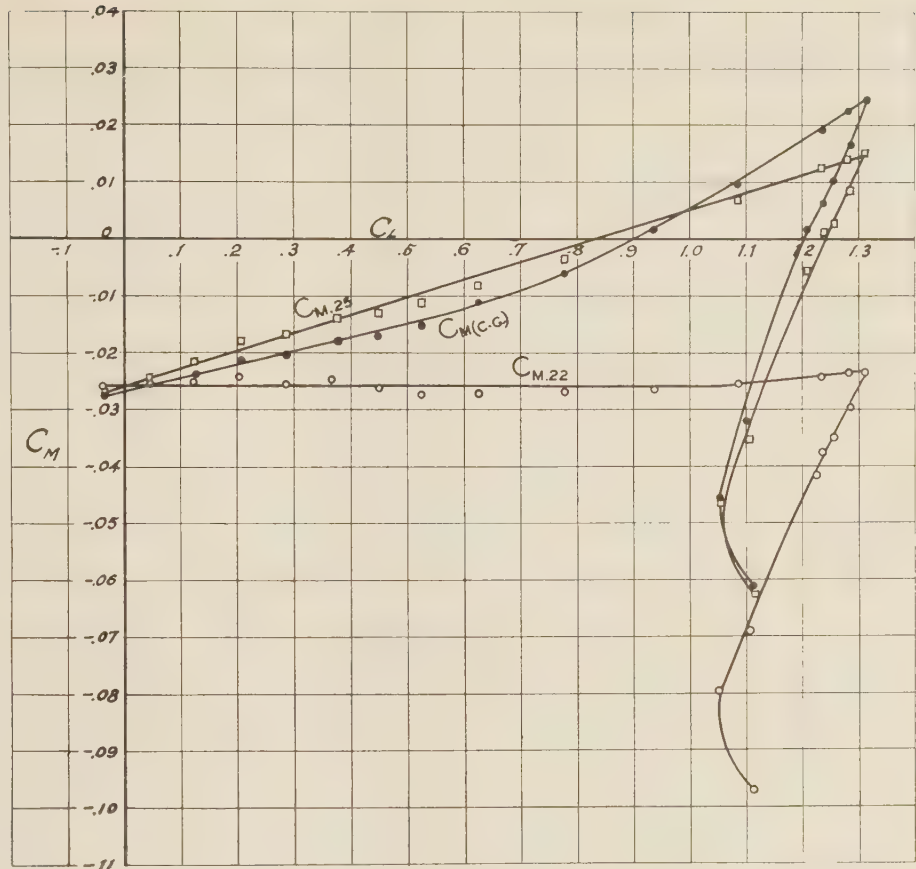


FIG. 15 STALLING-MOMENT COEFFICIENT VERSUS LIFT COEFFICIENT

(For transport airplane wing only. $C_{M,25}$ and $C_{M,22}$ give moments about the 25% and 22% points of the calculated mean aerodynamic chord, respectively. $C_{M,c.g.}$ gives moments about the assumed center-of-gravity position of the airplane.)

cowling arrangements and three wing-nacelle fillets was tested. The final or optimum configuration gave, with reference to the original nacelle and cowling as mounted on the model—

- a decrease in minimum parasite-drag coefficient of 0.0006, or 3 per cent of the gross minimum drag;
- a decrease of parasite-drag coefficient in the attitude for single-engined operation of 0.003, or about 10 per cent of the gross drag at this attitude;
- an increase in maximum-lift coefficient of 0.12.

The results of this particular investigation are particularly significant in that they indicate the great value of having one of the designers, who is working on the plane, present and cooperating during the tests. It is very difficult to see how so considerable an aerodynamic improvement, which was structurally and economically entirely feasible, could have been effected if this procedure had not been followed during the investigation.

2 INTERFERENCE PROBLEMS

In this field the most elaborate studies undertaken at our laboratory have been those connected with wing-fuselage interference and reported by A. L. Klein¹³ at an aeronautic meeting one year ago. The technique employed in this type of research involves the use of physicist's wax for making alterations to a model, the

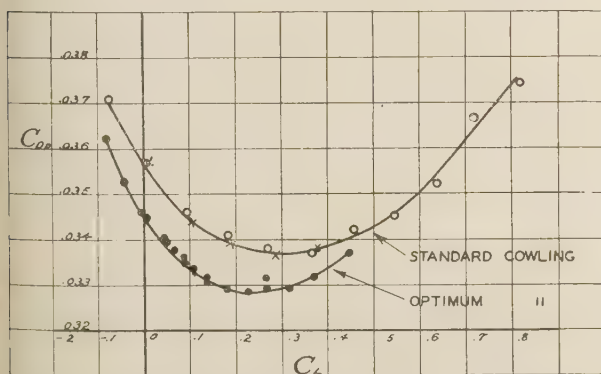


FIG. 14 PARASITE-DRAE COEFFICIENT VERSUS LIFT COEFFICIENT
(For the configuration of Fig. 13 and for the same model with standard radiator cowling.)

¹³ A. L. Klein, "The Effect of Fillets on Wing-Fuselage Interference," presented at Pacific Coast Aeronautics Meeting, June 9 and 10, 1932 (mimeographed).

measurement of lift, drag, and pitching moment on the wind-tunnel balances, and an investigation of the flow pattern behind the model by means of a large number of small pitot and static-pressure tubes connected to a multiple manometer. Since Klein's paper discusses the problem in detail, no further discussion will be attempted here, except the statement that the same technique has been successfully applied in investigating the interference between wings and nacelles, landing gears, protuberances, etc.

3 LONGITUDINAL STABILITY AND CONTROL

An interesting example of the contribution which the wind tunnel can make to the problem of static longitudinal stability occurred recently in the course of tests on a model of a large and very carefully designed transport monoplane. The wing had a rectangular center section and considerably tapered outer sections. The mean aerodynamic chord was estimated by the customary methods accepted by present-day designers, and the center-of-gravity location was determined relative to this mean aerodynamic chord so as to give the desired degree of stability. When the complete model was tested, the stability was found to be too small, and when the wing was tested alone, it appeared that the pitching moment coefficient was constant, not about the 25 per cent point of the mean aerodynamic chord, as was to be expected, but about the 22 per cent point. The pitching-moment curves for this wing are shown in Fig. 15. In this case also a designer of the airplane was present at the tests, and a new wing was promptly designed which had the effect of moving the center of gravity of the airplane 3 per cent forward. When the model was retested with this new wing, the stability was almost precisely that expected. In cases which involve more unorthodoxy than mere wing taper, the contribution which the wind tunnel can make is still more important.

In connection with the recent development of fixed stabilizers

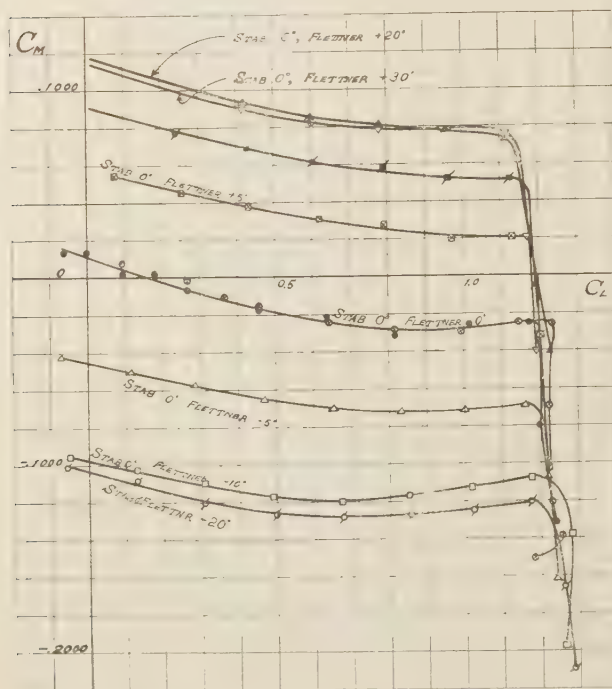


FIG. 16 STALLING-MOMENT COEFFICIENT VERSUS LIFT COEFFICIENT (For model of a complete transport plane with fixed stabilizer, various Flettner angles, and free elevator. The elevator was statically balanced and had ball-bearing hinges.)

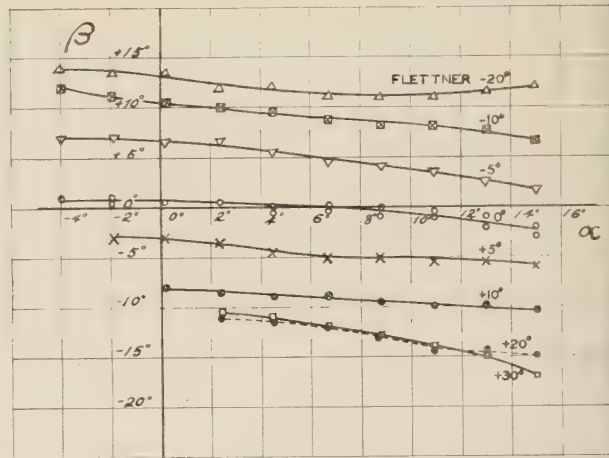


FIG. 17 ELEVATOR ANGLES β FOR VARIOUS FLETTNER SETTINGS [As a function of the angle of attack α (elevator free). The model was the same as for Fig. 16.]

in which trim is obtained by means of Flettner controls on the elevator, the problems of stabilizer setting, adequacy of elevator control, and effectiveness of the Flettner become extremely important. If the designer is to build the stabilizer as a rigid portion of the fuselage structure, he must know the correct stabilizer setting before building or even designing the plane. This question (at least for power-off flight) can very easily be answered in the wind tunnel, and several such investigations have been made at our laboratory. In order to obtain data with regard to adequacy of elevator control and Flettner effectiveness, the most straightforward procedure is to measure elevator-hinge moments as well as pitching moments for various elevator and Flettner angles. This, however, is a rather awkward and difficult matter on a complete airplane model. The alternative procedure here described has proved very satisfactory. The elevator is attached to the stabilizer by means of very small-size ball bearings which cause no disturbance of the surface of either portion of the tail. Arrangements are also made to clamp elevator and Flettner independently at any desired angle. Runs are first made with Flettner clamped neutral and elevator free, so as to determine the hands-off stability. Then with the model at a series of angles of attack, the Flettner is clamped at various angles and the free-elevator angle is observed. Finally, measurements of the pitching moment are made with the elevator clamped in its extreme positions, both with Flettner neutral and with Flettner setting such that the free elevator assumes its extreme position. These data are sufficient to tell whether or not the plane can be trimmed at any point in the flying range with no force on the elevator controls. A more extensive series of pitching-moment measurements may also be made with elevator free and Flettner clamped at a series of angles. A set of curves of the latter type for an airplane whose controls are ample but whose stability near the stall is not satisfactory are shown in Fig. 16, and a typical family of curves for free-elevator angle at a series of Flettner settings is given in Fig. 17.

4 HIGH-LIFT AND AERODYNAMIC BRAKING DEVICES

Several types of high-lift and drag-increasing, or aerodynamic braking, devices have been studied in our laboratory wind tunnel, but of these only one will be discussed here, since it appears at the present time to have considerable advantages over all the others. The bottom surface or split trailing-edge flap was first investigated, as far as the authors are aware, in 1921 in the wind tunnels at McCook Field and the Navy Yard. Unfortunately,

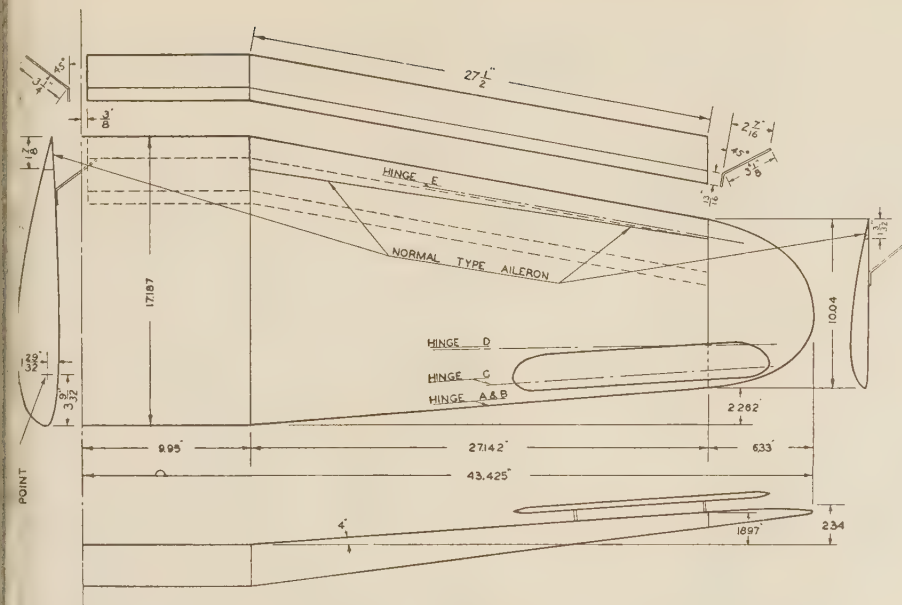


FIG. 18 TAPERED WING WITH BOTTOM SURFACE FLAP
(Dimensions are in inches and correspond to model scale.)

he reports on these tests have remained confidential and have never been published. A series of tests on a split trailing-edge flap was described by Bamber in 1929.¹⁴ More recently there has been considerable activity in connection with such devices, sponsored to a large extent by the Zap Corporation. Finally, systematic tests dealing with bottom-surface flaps have very recently been made at Göttingen, and an explanation for their effect has been given.¹⁵ In March, 1932, an investigation of an extremely simple type of bottom-surface flap was undertaken for the Northrop Corporation and furnished very interesting results, some of which are here discussed. A paper by Drs. Millikan and Klein describing the experiments and results in detail is appearing currently in one of the technical journals.

The wing used in the tests was a tapered wing whose center section was originally that of the N.A.C.A. 2415, while the tip was 409. Unfortunately, the wing, which was made of wood, warped considerably during the investigation, so that these sections were not accurate. The wing and flaps are shown in Fig. 18. The auxiliary airfoil there indicated will be discussed in the next section.) The flap was made of 0.039-in. galvanized iron sheet and was screwed to the bottom of the wing in three sections—one on the center section and one on each outer wing panel. The wing was tested

¹⁴ M. J. Bamber, "Wind-Tunnel Tests on an Airfoil Equipped With a Split Flap and Slot," N.A.C.A. Technical Note No. 324 (1929).

¹⁵ E. Gruschwitz and O. Schrenk, "On a Simple Method of Increasing the Lift of Wings," *Zeits. für Flugtechnik und Motorluftschiffahrt*, vol. 23, no. 20, p. 597 (Oct. 28, 1932).

without flaps, with flap on the center section only, with flaps on the outer wing panels only, and with flaps across both center section and outer wing panels. The results are given in Fig. 19. The curves for flaps and free-air ailerons are discussed in the next section. (It should be mentioned that the curves for the wing without flaps were taken near the end of the investigation, which extended over several months. Similar curves from runs near the beginning of the series of tests did not show the curious flat top at the stall and reached values of C_{Lmax} of 1.33. It is thought that warping of the model during the investigation caused a twist, so that in the later runs one side of the wing stalled before the other. Slight asymmetries in the flaps might easily counteract this effect, as was apparently the case.) The

increase in C_{Lmax} from about 1.3 to 2.04 effected by the complete flaps is the most striking feature of the curves. In this connection the effects of center-section and outer-wing flaps appear to be nearly additive. However, the decrease in the L/D ratio just below the stall from about 13 to about 6 is almost equally noteworthy, since it corresponds to a very considerable increase in the gliding angle for this condition. The increase in the diving moment is rather appalling, and at first sight seems almost to rule out the possibility of using the device practically. However, subsequent tests on a model of a low-wing airplane, with a wing similar to the foregoing, but complete with tail surfaces, eliminate this apparent difficulty. The pitching-moment coefficients for this airplane are shown in Fig. 20 for the configurations without flaps, with outer-wing

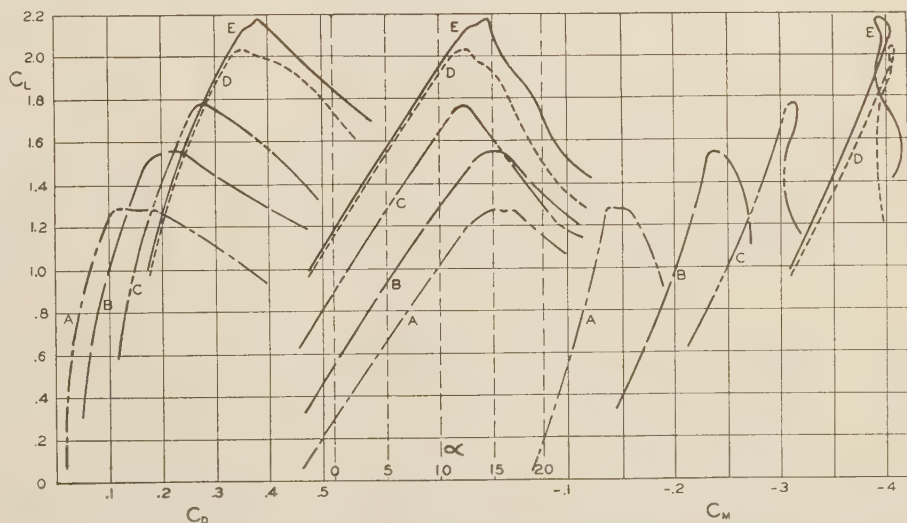


FIG. 19 C_D , α , C_M VERSUS C_L FOR THE WING OF FIG. 18

(Stalling-moment coefficients C_M are referred to an axis through the trunnion point indicated in Fig. 18. The curves refer to the following configurations: A, normal wing, no flaps; B, wing with center-section flap; C, wing with outer-wing flaps; D, wing with complete flaps; E, wing with complete flaps, and free-air ailerons in position A with neutral setting -10° from reference axis.)

flaps, and with complete flaps. It appears that the addition of the flaps increases the downwash at the tail so much that the large diving moment of Fig. 19 is entirely neutralized for the complete flaps. For the outer-wing flaps the downwash is not quite enough to completely neutralize the flap diving moments, but even in this case the net diving moment produced by lowering the flaps is not unmanageable. In this connection it might be remarked that the Northrop Gamma as built for Frank Hawks and the Ellsworth Antarctic Expedition was equipped with flaps

tion of the problem was undertaken by Klein and Millikan, the detailed results of which appear in the paper to which reference was made in the last section. A brief survey of the most important results is given here.

The two free-air ailerons employed are shown in Fig. 21, and the five locations investigated are indicated in this figure and in Fig. 18 by the hinge locations A-E. In Fig. 18 the aileron is shown in position C. The wing was also tested with the normal type ailerons indicated in Fig. 18. Rolling- and yawing-moment

coefficients will be denoted by C_r and C_y to avoid confusion, where C_r = rolling moment/ qSb , C_y = yawing moment/ qSb , q = dynamic pressure, S = wing area (not including that of free-air ailerons), b = wing span. Aileron angles refer to displacements from assumed neutral settings, plus angles corresponding to a lowering of the aileron trailing edge, and minus angles to a raising. The neutral settings are defined by the angle between the reference axes of the aileron and wing as indicated in Fig. 21. The same convention as to signs holds as in the foregoing. The aileron angles are given in pairs, the first figure corresponding to the right aileron and the second to the left. A positive rolling moment is one tending to lower the right wing, and a positive yawing moment is one tending to retard the right wing. It is assumed that if the right aileron is given a negative angle (trailing edge raised), the desirable characteristics are that both rolling and yawing moments are positive. Moments of the desired sign are plotted as full lines, while undesirable signs or reversals of control are plotted as dotted lines. Unfortunately, at the time of these experiments there were not sufficient wind-tunnel balances available to measure lift simultaneously with rolling moment, yawing moment, and side force. Hence the moment curves are plotted against angle of attack uncorrected for wind-tunnel interference (α_w), and an auxiliary curve of C_L versus α_w is included. This curve is taken from a run with the same wing configuration, but without free-air ailerons. The normal ailerons had a total area of 7.0 per cent of the normal wing area, while the free-air ailerons had 5.6 per cent of the normal wing area.

In Fig. 22 the moments are plotted for the normal ailerons. The yawing moments are unfavorable throughout, and the rolling moments fall off badly at the stall. The relatively small values of C_r at low lift coefficients are not surprising in view

of the size of the ailerons. Rolling moments for the free-air ailerons in positions E and D are plotted in Fig. 23. These results are not as accurate as the others presented, since a correction due to side force was not included. However, they show that for the trailing-edge position E, C_r falls off very badly just above the stall, and at D the magnitude of the rolling moments up to the stall is unsatisfactory. Position B gave results much inferior to A, and C was likewise not quite as satisfactory as A, so that only the latter will be discussed. In Fig. 24, rolling and yawing moments for position A without flaps are given, while in Fig. 25 are similar results for position A with outer-wing flaps. Several very striking features are apparent. C_r increases with C_L up to the stall. This is a very desirable characteristic, since it means that for a given rolling effect the tendency is for the aileron angles to be roughly the same for all angles of attack; i.e., if the control is adequate near the stall, it is not oversensitive at the high-

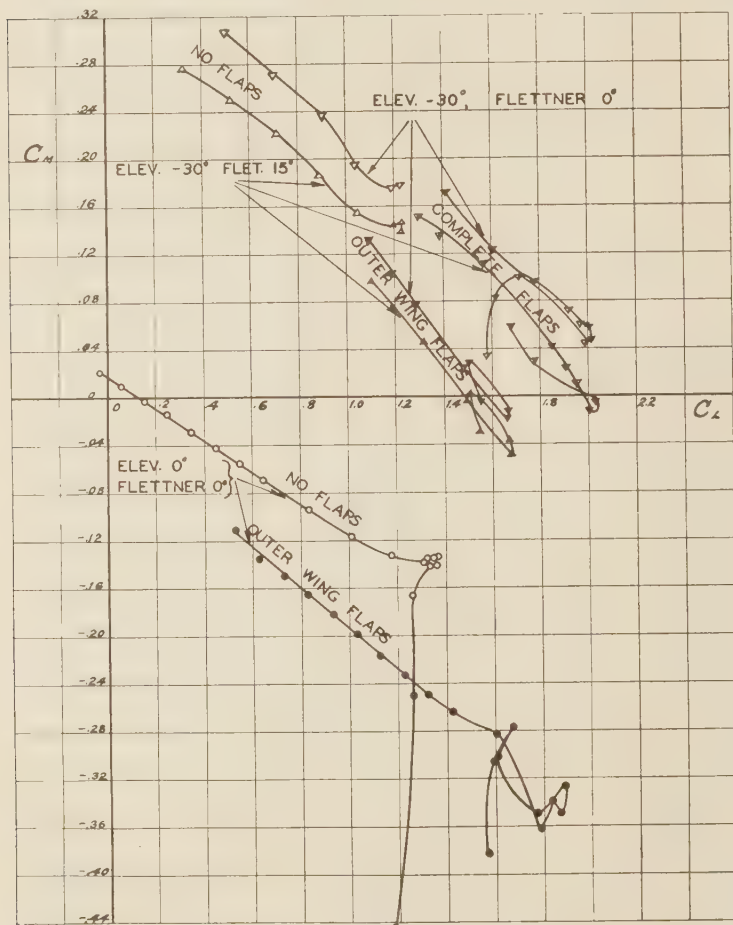


FIG. 20 STALLING-MOMENT COEFFICIENT VERSUS LIFT COEFFICIENT
(For a low-wing monoplane model with and without bottom surface flaps and with various elevator and Flettner angles. C_M is referred to the center of gravity of the airplane.)

on the outer wings only, and the lowering of the flaps in flight was accomplished with no difficulties by the pilot.

5 LATERAL-CONTROL DEVICES

At the time of the first tests on the bottom-surface flaps attempts were made to secure satisfactory lateral control with the flaps lowered, by various modifications to the normal aileron system. None of these met with success. When the flap mechanism of the Northrop Gamma was designed, there was not sufficient time to permit of wind-tunnel tests on a lateral-control system. Consequently, free-air ailerons were used which were designed in accordance with suggestions from Mr. Temple Joyce. These ailerons were mounted above the trailing edge of the wing. It appeared to the Junior author that these ailerons must lose much of their effectiveness at the stall and that a more suitable location should be possible. Accordingly, an extensive investiga-

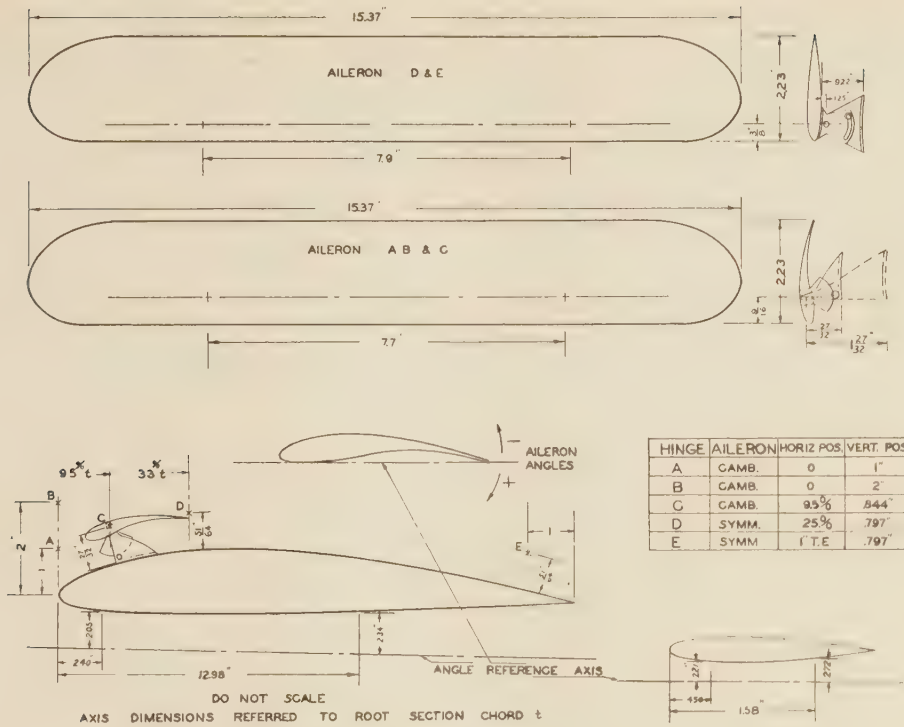


FIG. 21 FREE-AIR AILERON DIMENSIONS AND LOCATIONS
(As tested on the wing of Fig. 18. Dimensions are in inches and correspond to model scale.)

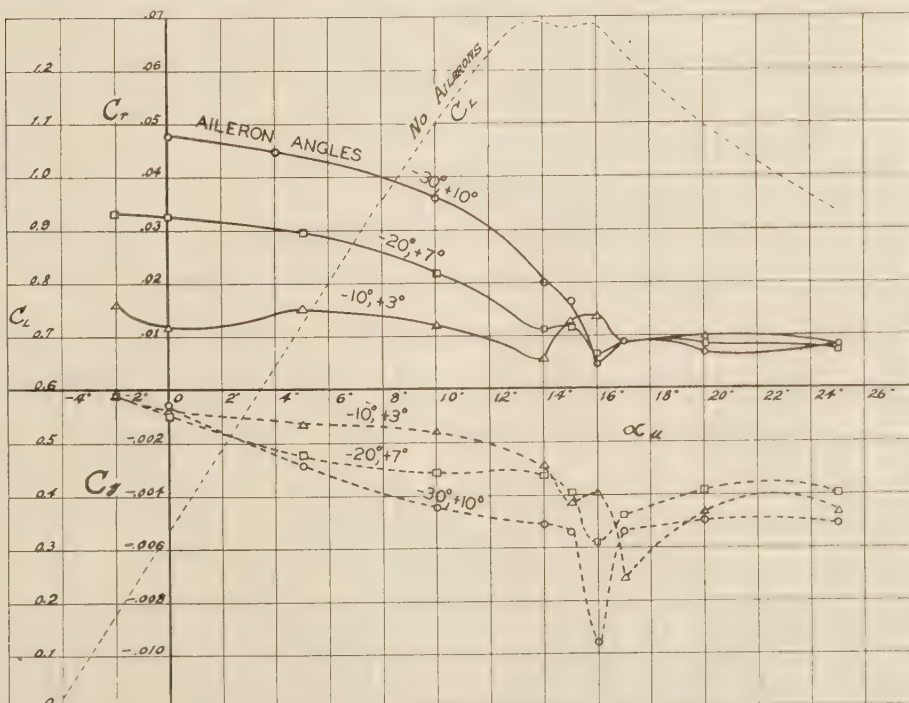


FIG. 22 ROLLING AND YAWING-MOMENT COEFFICIENTS FOR NORMAL AILERONS AT VARIOUS SETTINGS
(α_u is the angle of attack uncorrected for wind-tunnel wall interference. Desirable moments correspond to full lines, undesirable ones to dotted lines.)

speed attitude. The magnitude of C_r just below the stall is much larger than with the normal ailerons, and a considerable C_r still remains after the drop above the stall. In this connection it is believed that the oscillations of the curves above the stall are probably due to the lack of symmetry in the wing; i.e., for an accurate and symmetrical wing the curves would probably go approximately through the middle of the waves which appear in the figures. The yawing moments are in the correct sense, except for the cases in which one aileron is at $4\frac{1}{2}$ deg. This, as well as the negative values of C_r for -6 deg, $+4\frac{1}{2}$ deg at

flown in this state. It appears from the results that the most satisfactory linkage for the ailerons would probably be one giving only up travel (i.e., complete differential) and allowing maximum displacements from the neutral setting of about 45 deg. Such a free-aileron system can apparently be designed to give lateral control considerably better than that furnished by most present-day systems, and having the great advantage that its practical effectiveness is not decreased by the use of bottom surface flaps. It should be explicitly pointed out that flight tests on such a free-air aileron system have yet to be reported and

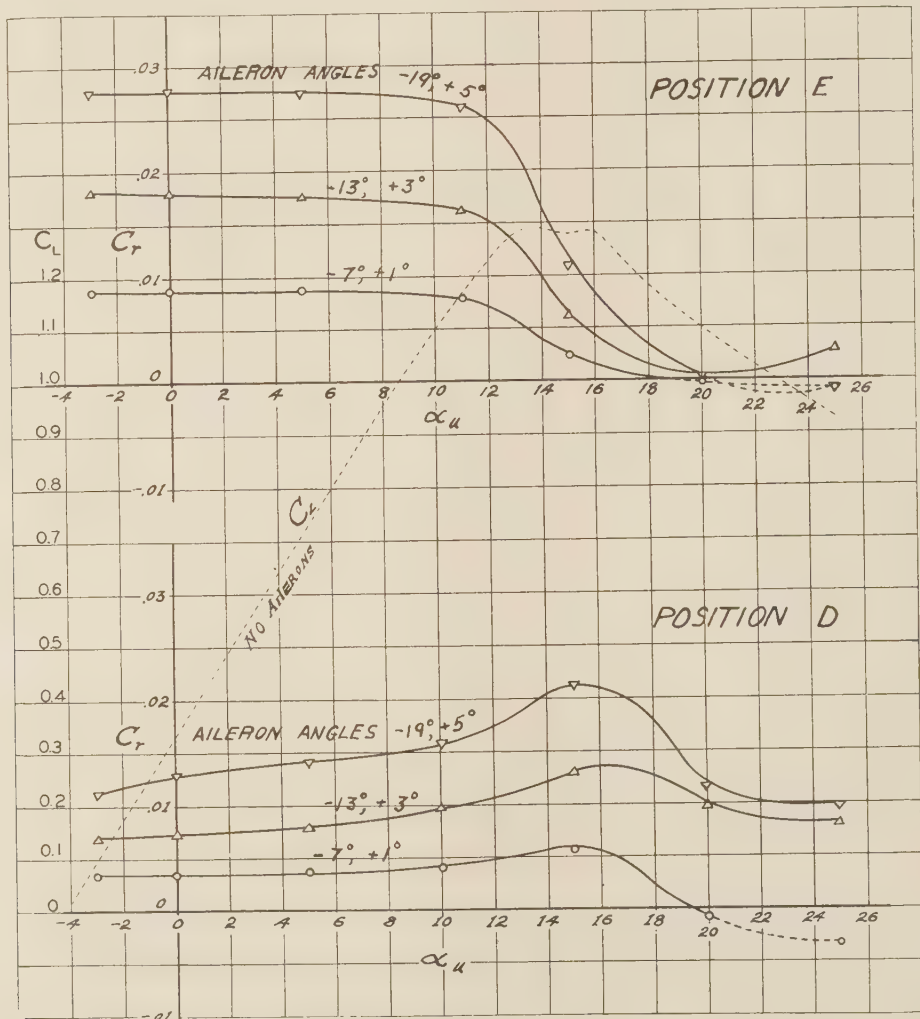


FIG. 23 ROLLING MOMENTS FOR SYMMETRICAL FREE-AIR AILERONS IN POSITIONS D AND E, AT VARIOUS AILERON ANGLES

[The neutral setting in both positions corresponded to aileron angles of $+1^\circ$ from the wing reference axis (cf. Fig. 21).]

large angles of attack, suggests that for the particular aileron-wing combination employed the optimum arrangement might be one with no down travel of the ailerons. The very large favorable yawing moments for large aileron deflections just below the stall are very satisfactory. The effect of the flaps, at the angles of attack above 5 deg at which they would normally be used, is to increase both rolling and yawing moments for large aileron deflections. The apparent decrease in effectiveness at small angles of attack when the flaps are lowered is probably of no practical importance, since an airplane would almost certainly never be

that the configuration is such that its effectiveness will almost certainly be much affected by minor changes. Hence great caution should be used in the initial attempts to apply the system to an actual airplane.

The effect of the ailerons in position A on C_L , C_D , α , and C_M is shown by the highest curves of Fig. 19. $C_{L_{max}}$ is increased nearly 10 per cent, attaining a value with ailerons and flaps of practically 2.2. The addition to the minimum drag coefficient of the wing only is somewhat less for position A than for any of the others. In the present tests this addition amounts to about

13 per cent of the minimum drag of the wing alone, but a large proportion of this is undoubtedly due to the very crude hinges which were necessary for the wind-tunnel model. The Northrop Gamma was equipped with free-air ailerons in position *E*, which causes more drag than position *A*, and the high performance obtained in flight tests indicates that the overall minimum drag is comparatively small.

6 PRESSURE-DISTRIBUTION MEASUREMENTS

One more field in which the wind tunnel can be of great service to the designer has been brought out by investigations such as those described. Whenever a new device is discovered such as the N.A.C.A. cowl, the bottom surface flap, the free-air aileron, etc., a serious problem arises when the designer attempts to apply it to an actual airplane. For if the device is radically

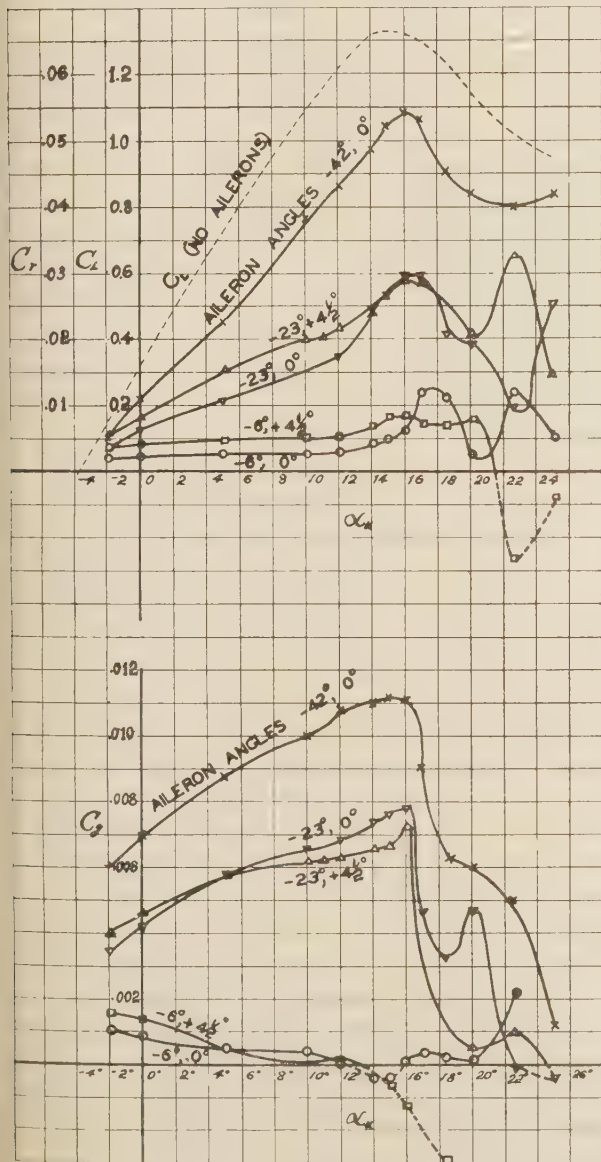


FIG. 24 ROLLING AND YAWING MOMENTS FOR CAMBERED FREE-AIR AILERONS

(In position *A* without trailing-edge flaps. The neutral setting corresponded to aileron angles of -15° from the wing-reference axis.)

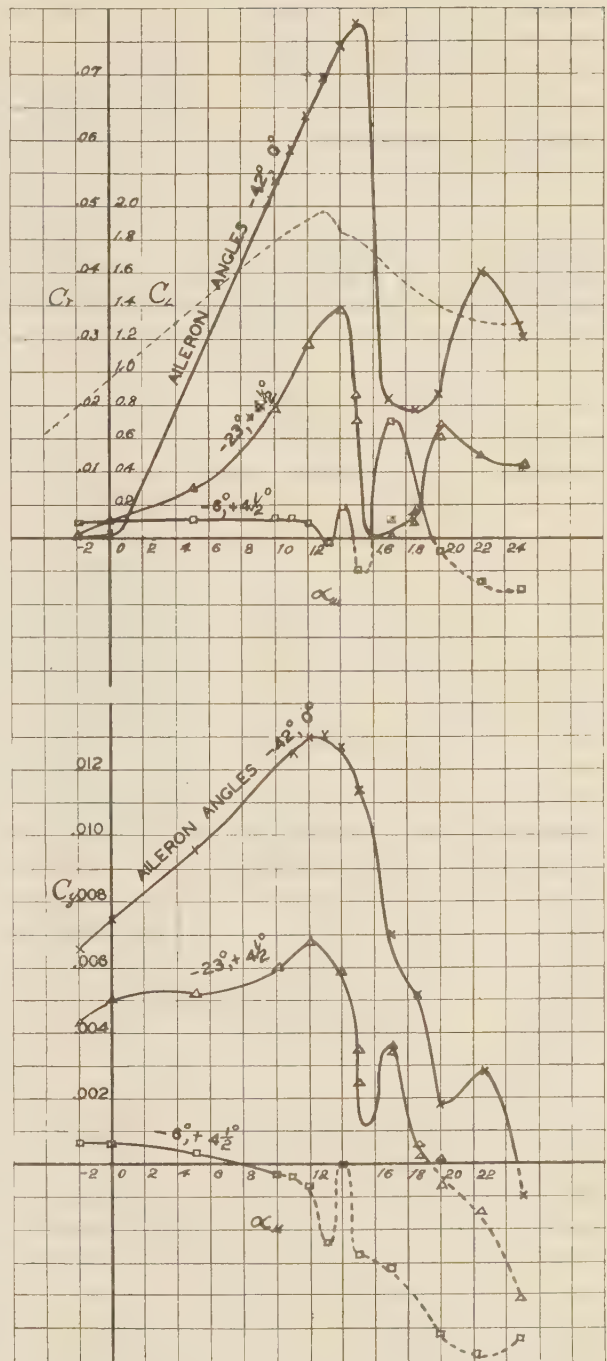


FIG. 25 ROLLING AND YAWING MOMENTS FOR THE CONFIGURATION OF FIG. 24

(But with bottom surface flaps attached to the outer wing panels.)

new, very few, if any, data exist as to the distribution of forces on which the designer can base his stress analysis. In such cases pressure-distribution measurements are almost essential to obtain the necessary information. Experiments of this nature using a multiple manometer have recently been made at our laboratory on the three devices mentioned and have furnished what are believed to be valuable data for the stress analyst. As long as

new devices are discovered, there will always remain an important field of this character.

CONCLUSION

In the first part of this paper a series of general investigations of a more or less scientific nature has been discussed. It possesses in addition to a theoretical interest, a possibility for rather general application to the practical phases of airplane design. In the second part a group of more specialized problems has been considered, all of which originated as investigations of special aspects of particular designs and at the request of airplane manufacturers. The attempt has been made to indicate the varied nature of the problems for which the wind tunnel may

be advantageously used, and the valuable results which may be achieved by close cooperation between the designer and the aerodynamicist conducting the tests have been mentioned. Finally, the way in which such detailed researches often lead to investigations of broad scope and general interest has been illustrated with examples.

[NOTE: Since the paper was presented, the results of the experimental investigation on the effects of turbulence on $C_{L_{max}}$ and of the free-flight measurements of atmospheric turbulence have been published in a paper by C. B. Millikan and A. L. Klein, "The Effect of Turbulence; An Investigation of Maximum Lift Coefficient and Turbulence in Wind Tunnels and in Flight," *Aircraft Engineering*, August, 1933, London.]

Performance of Two 101,000-Sq-Ft Surface Condensers

By J. N. LANDIS¹ AND S. A. TUCKER,² BROOKLYN, N. Y.

The results of tests of two 101,000-sq-ft single-pass condensers in the Hudson Avenue Station of the Brooklyn Edison Company are summarized, and the design features are briefly described. The steam-flow path of the Worthington condenser is through an effectively shallow tube bank of the folded-layer type, having deep inlet lanes to facilitate the passage of steam with minimum pressure drop. The entire tube bank is contained in a practically cylindrical shell. In the Ingersoll-Rand unit the generally heart-shaped shell maintains with a decreasing volume of steam an active flow over all tubes. Bypass lanes around the top sections of tubes allow part of the steam to reach

the lower tube banks without passing through the top section. The Worthington air cooler is placed internal to the shell as being the most convenient location and involving the least costly construction. The Ingersoll-Rand design uses an external air cooler to provide a more efficient design of flow areas. Reheating is provided for in the condensate circuits of both units, the Worthington using a contact-type reheating hotwell integral with the condenser and the Ingersoll-Rand having a 1600-sq-ft-surface closed reheater after the condensate pump, supplied with steam from one of the top bypass belts. Steam-flow control, air removal, and circulating systems are compared.

THIS paper presents a brief summary of the results of tests of two 101,000-sq-ft single-pass condensers in the Hudson Avenue Station of the Brooklyn Edison Company.

DESIGN COMPARISONS

Since these two condensers have been extensively described elsewhere,³ only a brief statement of their design features is given here.

The steam-flow path of the Worthington condenser, shown in Fig. 1, is through an effectively shallow tube bank of the folded layer type, having deep inlet lanes to facilitate the passage of steam with minimum pressure drop. The entire tube bank is contained in a practically cylindrical shell. In the Ingersoll-Rand unit, the generally heart-shaped shell maintains with a decreasing volume of steam an active flow over all tubes. Bypass lanes around the top sections of tubes allow part of the steam to reach the lower tube banks without passing through the top section.

The Worthington air cooler is placed internal to the shell as being the most convenient location and involving the least costly construction. The Ingersoll-Rand design uses an external air cooler to provide a more efficient design of flow areas.

Reheating is provided for in the condensate circuits of both



J. N. LANDIS



S. A. TUCKER

units, the Worthington using a contact-type reheating hotwell integral with the condenser and the Ingersoll-Rand having a 1600-sq-ft-surface closed reheater after the condensate pump, supplied with steam from one of the top bypass belts.

In the Worthington unit, a free longitudinal flow of steam is permitted by openings cut in the six tube support sheets wherever possible. Quite in contrast, the Ingersoll-Rand unit, as shown in Fig. 2, is divided into five separate longitudinal compartments by four closely fitted tube-supported sheets. Each of the three cold-end compartments is separately connected to its own section of the external air cooler, and the two warm-end compartments are connected in parallel to the remaining section of the air cooler with a throttle plate to limit the flow from the end compartment. Air removal is accomplished on the Worthington unit by a three-element two-stage steam jet, and on the Ingersoll-Rand unit by eight primary and three secondary jets.

Each condenser is served by two circulators, with separate water circuits from the inlet to the discharge tunnels. The Worthington unit, as shown in Fig. 3, has a conventional vertically divided water box, whereas the Ingersoll-Rand water box is divided into four horizontal sections, arranged for each circulator to supply two alternate sections. There are no valves in the main circulating-water system of either condenser.

ACCEPTANCE TESTS

The tests on these two condensers represent the culmination of several years' experience in performing tests on large power-plant equipment, including several condensers, by a group of test men organized principally for acceptance testing. The results are presented with the belief that they summarize the most comprehensive and carefully executed condenser tests publicly reported.

The tests were unusual in that they determined the "cleanliness ratio" of the condensing surface. The manner of making the cleanliness ratio measurements has already been discussed in detail before the A.S.M.E. by Messrs. Hardie and Cooper.⁴

⁴ "A Test Method for Determining the Quantitative Effect of Tube Fouling on Condenser Performance," by P. H. Hardie and W. S. Cooper. Trans. A.S.M.E., vol. 55 (1933), paper RP-55-3

¹ Mechanical Engineer, Brooklyn Edison Company, Inc. Assoc. Mem. A.S.M.E. Mr. Landis received the degree of B.S. in Mechanical Engineering in 1922 from the University of Michigan. He went with the Brooklyn Edison Company in 1923 as technical assistant to the mechanical engineer, and since that time has been intimately associated in various capacities with the design and construction of the Hudson Avenue Generating Station. He was appointed to his present position in 1932.

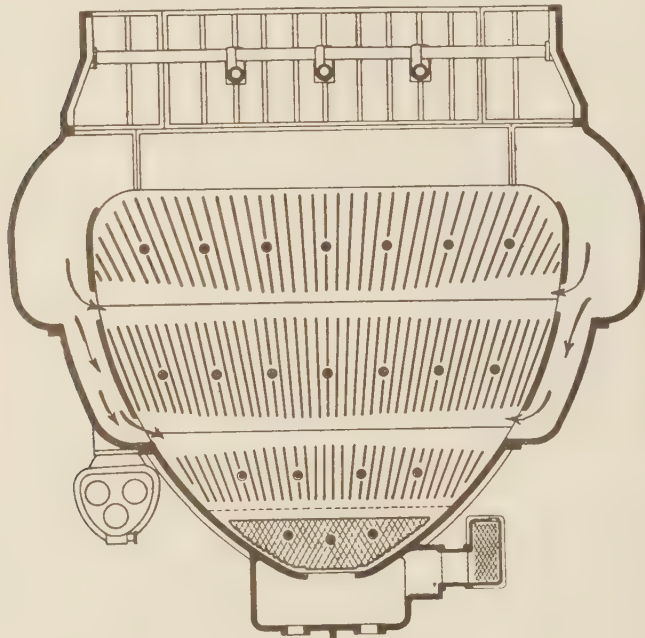
² Division Engineer, Plant Equipment Bureau, Brooklyn Edison Company, Inc. Mr. Tucker received his B.S. in Electrical Engineering in 1926 from Yale University. He was employed by the Brooklyn Edison Company, Inc., in 1926 as a cadet engineer, and since 1928 he has been a member of the Plant Equipment Bureau.

³ *Power Plant Engineering*, April 15, 1932, November, 1932; *Power*, May 31, 1932.

Presented at the Semi-Annual Meeting, Chicago, Ill., June 26 to July 1, 1933, of THE AMERICAN SOCIETY OF MECHANICAL ENGINEERS.

NOTE: Statements and opinions advanced in papers are to be understood as individual expressions of their authors, and not those of the Society.

In brief, the test consisted of determining the individual performance of 30 isolated tubes in various parts of the condensers, arranged in six groups of five tubes each, supplied with independently controlled circulating water. Each group of five tubes consisted of two new tubes and three existing used tubes representative of the condition of the condensing surface at the time of test. One new tube in each group was supplied with salt water, and the other, for purposes of a separate investigation, with fresh water. The ratio of the average thermal transmittance of the used tubes to the average transmittance of the salt-water new tubes was taken as the "cleanliness ratio" of the condenser. In their contracts these condenser manufacturers and all others made guarantees which were to be corrected downward from a 100 per cent clean transmittance guarantee in direct proportion to the cleanliness ratio obtaining at time of test.



Above - Ingersoll-Rand
Right - Worthington

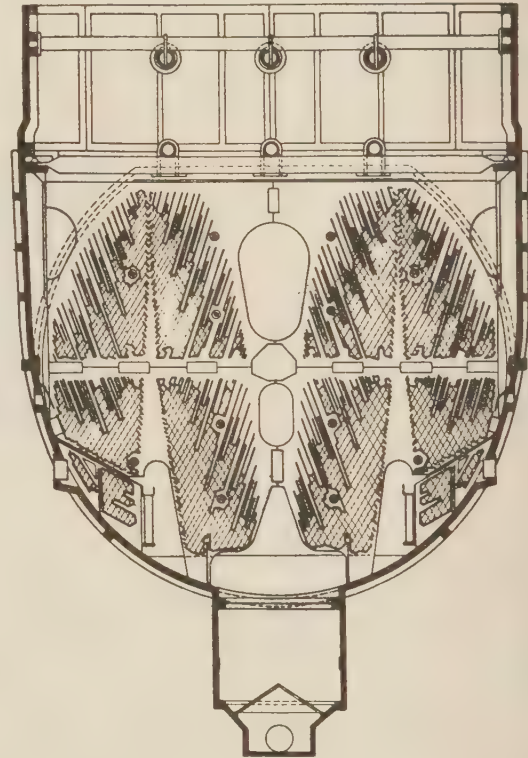


FIG. 1

Each of the two acceptance tests consisted of nine 1-hr runs, confined to a period of two days. These runs covered the normal operating range of the turbine for both high and low speeds of the circulating pumps. During the night preceding the start of test runs, each condenser was completely rubber-plugged to secure uniformity of tube condition, and thus the most representative cleanliness ratio as measured from the relatively few sampling tubes.

ACCEPTANCE-TEST PROCEDURE AND APPARATUS

Readings were taken at 5-min intervals of—

- 1 Inlet circulating-water temperature by two precision mercurial thermometers graduated to 0.1 deg F
- 2 Outlet circulating-water temperatures by six precision mercurial thermometers graduated to 0.1 deg F
- 3 Absolute pressure at the steam inlet by 11 specially constructed absolute-pressure gages connected to an equal

number of basket-type pressure tips distributed over the area of the turbine exhaust

- 4 Absolute pressure at (each compartment of) the hotwell by absolute-pressure gages identical with those used at the turbine exhaust
- 5 Condensate temperature leaving the hotwell (and the reheater) by precision mercurial thermometers.

The amount of steam condensed was determined by weighing the condensate in the station weighing tanks. Sufficient readings were taken of turbine-throttle and feedheating conditions to permit computing the heat content of the exhaust steam.

To ascertain the condenser-cleanliness factor during the period of test, six groups of isolated tubes were connected by a rubber hose to a separate supply of salt water measured at the outlet end by a calibrated bell-mouthed nozzle. One new tube in each

group was supplied with fresh water as a reference standard to indicate any tendency of the salt-water new tube to foul. The flow of water in each tube was held approximately the same as the average of all the condenser tubes. For measuring the temperature rise in each tube, mercurial thermometers were inserted through rubber stoppers directly into the water stream.

Air offtake temperatures were measured by mercurial thermometers inserted through rubber stoppers, and air leakage was determined from the standard equipment furnished by each manufacturer as part of the contract.

Pressure drops for each part of the circulating-water system and the total and suction heads on the pumps were determined by mercury U-tubes. The electrical input and speed of the circulator motors were also separately measured. The principal test data are given in Table 1.

Fig. 4 shows for the Worthington unit the absolute pressure and the calculated heat-transmittance coefficients obtained for

both high- and low-speed pump operation. Fig. 5 is a plot of the same results obtained on the Ingersoll-Rand unit.

A question may arise as to why the curves of both tests show different cleanliness ratios at low and high speed on the circulators. Fig. 6 shows the results of calorimeter measurements per-

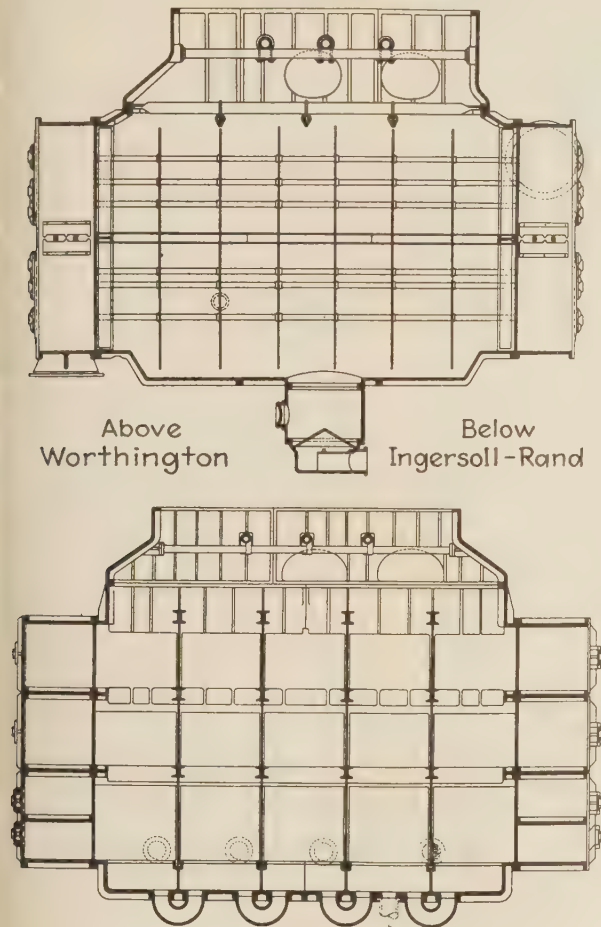
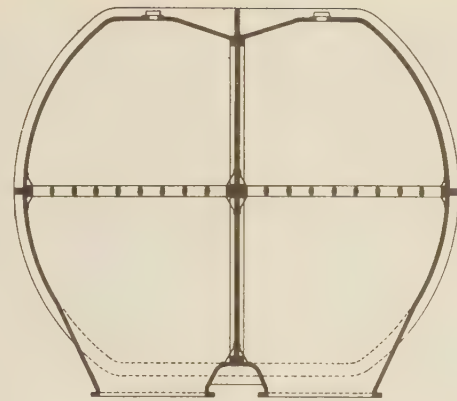
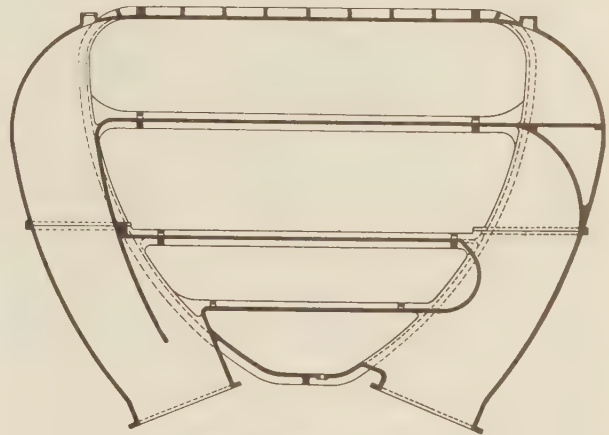


FIG. 2



WORTHINGTON



INGERSOLL-RAND

FIG. 3

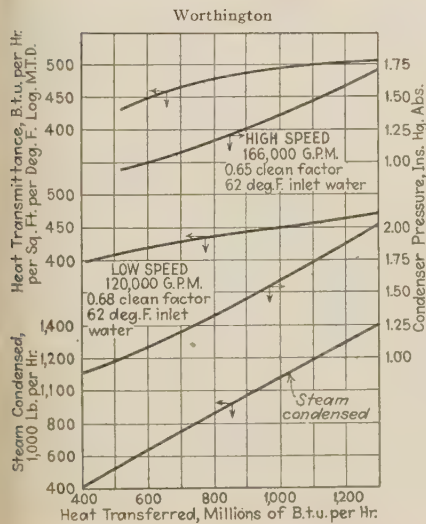


FIG. 4

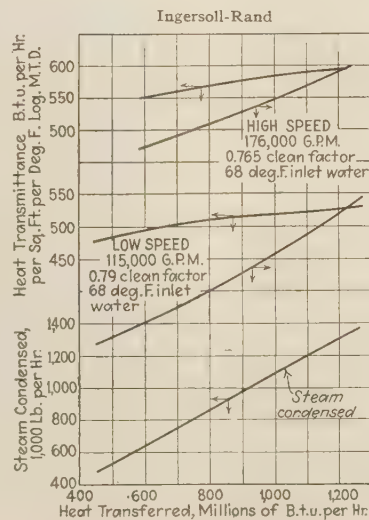


FIG. 5

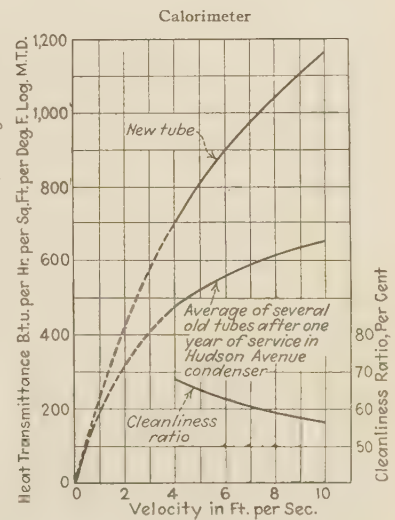


FIG. 6

TABLE 1 ACTUAL CONDENSER PERFORMANCE

TABLE 1. ACTUAL CONDENSER PERFORMANCE																	
Run No.	Date, 1932	Steam condensed, per hr	Heat transf. by cond., million Btu per hr	Abs. pressure condenser nozzle, in. Hg	Hotwell temp., ¹ deg F	Circu-water temp.		Circu-water flow, gpm	Condenser friction		Heat transmittance, Btu per hr per sq ft per deg F log m.t.d.		Clean- liness factor	Air moved, c.f.m.	Av. temp. air off-take, °F	Heat transmittance ⁵ Btu, per hr per sq ft per deg F log m.t.d.	Abs. pressure ⁶ at condenser nozzle, in. Hg
						Out, deg F	In, deg F		A ft ²	B ft ²	F log m.t.d.	Re- moved, c.f.m.					
Worthington Condenser, High Speed																	
1	6-13	732,100	684.0	1.09	81.7	71.6	63.3	167,800	.. ³	17.3	490	0.68	.. ⁴	76	459	1.08	
5	6-13	562,900	531.4	0.93	76.5	68.1	61.6	165,400	.. ³	17.7	455	0.68	4	73	437	0.95	
6	6-14	995,800	923.4	1.36	88.5	74.0	62.7	166,500	17.3	17.6	463	0.61	5	82	489	1.29	
9	6-14	1,389,700	1282.1	1.82	97.7	77.5	61.9	167,800	17.9	17.7	459	0.59	5	90	507	1.70	
10	6-14	731,300	682.1	1.09	81.7	69.9	61.4	163,800	17.9	17.9	432	0.59	6	79	483	1.05	
Worthington Condenser, Low Speed																	
2	6-13	721,600	675.3	1.20	84.2	74.1	62.7	120,500	.. ³	9.5	449	0.72	4	79	419	1.19	
3	6-13	432,600	416.4	0.89	75.6	68.9	61.7	118,300	.. ³	9.5	421	0.72	5	72	400	0.91	
4	6-13	568,700	536.4	1.01	79.5	71.0	61.9	119,500	.. ³	9.7	425	0.71	4	76	408	1.04	
7	6-14	992,600	920.9	1.57	92.8	78.4	62.9	121,200	9.6	9.7	422	0.64	5	87	442	1.49	
8	6-14	1,395,500	1286.2	2.13	102.9	83.1	61.6	121,900	9.7	9.6	428	0.62	5	96	472	2.01	
11	6-14	735,900	684.5	1.21	84.9	73.1	61.5	119,800	9.9	9.9	399	0.60	6	81	453	1.16	
Ingersoll-Rand Condenser, High Speed																	
5	6-27	643,000	601.7	1.10	82.1	74.3	67.3	176,400	15.6	14.7	553	0.78	4	78	542	1.13	
6	6-28	1,008,000	932.3	1.46	90.7	79.4	68.5	175,300	14.5	15.2	563	0.75	4	85	575	1.42	
9	6-28	1,350,300	1249.5	1.80	97.0	82.7	68.2	176,300	14.3	15.4	576	0.74	2	91	596	1.76	
10	6-28	768,600	714.1	1.22	85.3	75.9	67.6	175,100	14.3	15.3	551	0.74	2	81	575	1.21	
Ingersoll-Rand Condenser, Low Speed																	
3	6-27	487,200	463.2	1.08	81.3	75.5	67.3	115,500	7.1	6.8	493	0.82	4	80	479	1.11	
4	6-27	643,100	602.1	1.24	85.8	78.1	67.4	115,300	7.0	6.8	493	0.81	4	83	480	1.27	
7	6-28	1,012,000	935.3	1.75	96.5	85.4	68.6	113,600	7.0	6.8	501	0.77	2	92	513	1.69	
8	6-28	1,361,000	1256.9	2.26	105.2	90.5	68.1	114,500	6.8	6.8	513	0.76	2	99	531	2.20	
11	6-28	772,500	717.6	1.40	89.9	80.7	68.0	114,900	6.8	6.8	496	0.76	2	86	517	1.38	

¹ For Ingersoll-Rand temperature at reheater outlet. ² Feet of salt water. ³ Gage inoperative. ⁴ Air leak found after first half-hour. ⁵ Worthington corrected to: High speed, 166,000 gpm; 0.65 cleanliness factor; 62 F inlet temperature. Low speed, 120,000 gpm; 0.68 cleanliness factor; 62 F inlet temperature. Ingersoll-Rand corrected to: High speed, 176,000 gpm; 0.765 cleanliness factor; 68 F inlet temperature. Low speed, 115,000 gpm; 0.79 cleanliness factor; 68 F inlet temperature.

formed by the Ingersoll-Rand Company in 1929 on several used tubes taken from a Hudson Avenue condenser and on two sections of new tube. This test work illustrates that dirty tubes do not respond to increases of velocity as do clean tubes. This condition is explained by the fact that an increase of water velocity effects a reduction only in the resistance to heat flow of the water film, which is a much smaller proportion of the total resistance in the case of a dirty tube than in the case of a clean tube.

CONCLUSION

It is natural to expect this paper to make a final comparison of the performance of the two condensers. In order to do this it would be necessary to make corrections to the test results because of the unavoidable differences in test conditions relating to cleanliness, circulating-water quantity, and circulating-water temperature. The manufacturers' correction for cleanliness has been discussed, and the correction factors commonly used by condenser manufacturers for the effect of circulating-water velocity and temperature are available in the technical press.⁵ The authors might use these correction factors as a basis for a final comparison of the two condensers, but because they are of the nature of values accepted by the manufacturers for commercial purposes instead of being values derived from test from the specific condensers in question, it is considered better to confine this paper to the reporting of test facts and to leave to others the making of comparisons.

The test results are believed to show fairly the performance of two modern condensing units under as closely parallel conditions as it is practical to secure.

Both condensers have performed satisfactorily, and in their ability to hold materially better than the guaranteed full-load vacuum they have exceeded expectations by a comfortable margin.

ACKNOWLEDGMENT

The acceptance tests on both condensing units were performed

⁵ "Commercial Factors for Designing Surface Condensers," Power, September, 1932.

under the direction of Mr. P. H. Hardie, Test Engineer of the Brooklyn Edison Company's Research Bureau.

Discussion

PAUL BANCEL.⁶ The paper is an important contribution to the literature on surface condensers. A great deal of thought, time, and money lies behind the testing work of the Brooklyn Edison Company. The difficulties incident to testing a condensing plant of this great capacity can hardly be realized.

The design of the Ingersoll-Rand condenser follows the fundamental principles of all condensers built by the company, but in view of the special problems associated with the size of this unit, two sets of experiments employing models were made preliminary to construction.



FIG. 7 TYPICAL MODEL WATER-BOX TEST

⁶ Manager, Condenser Department, Ingersoll-Rand Company, New York, N. Y. Jun. A.S.M.E.

Tests were made to study the flow lines and areas in the water boxes, 28 model set-ups being photographed. The actual boxes were to be divided into four horizontal compartments, with side admission, and the model tests were made to determine the best flow paths for minimum turbulence when feeding the water from twin nozzles located at the bottom of the inlet box and discharging from two nozzles on opposite sides near the top of the outlet box. Photographs shown in Figs. 7 and 8 are typical. The model is a composite arrangement for both inlet and discharge to the first and third compartments served by these water nozzles.

Side admission to a water box divided into horizontal compartments at different heights improves the flow conditions at the entrance to the tubes, thus eliminating troubles from inlet-tube corrosion. The frothing effect of the water is greatly reduced because of the shallowness of each compartment and the relatively small difference in water pressure between the top and the bottom; furthermore, the horizontal flow tends to prevent pocketing and regions of air liberation and frothing. At the East River Station of the New York Edison Company, this design, combined with venting, in a water box divided into three horizontal compartments, has eliminated inlet-tube corrosion.

The second series of tests were more elaborate. Figs. 9A to 9E show model condensers which were built to study comparative pressure losses of different tube layouts. In each case the number of tubes per square foot of tube-sheet area is the same. Relatively large quantities of steam at high vacuum were passed through these small condensers, part of the steam being condensed and the remainder being rejected to a supplementary condenser. The total steam flow was several thousand pounds, so that the steam condensed, steam rejected, velocities, pressure drops, etc. were amply large

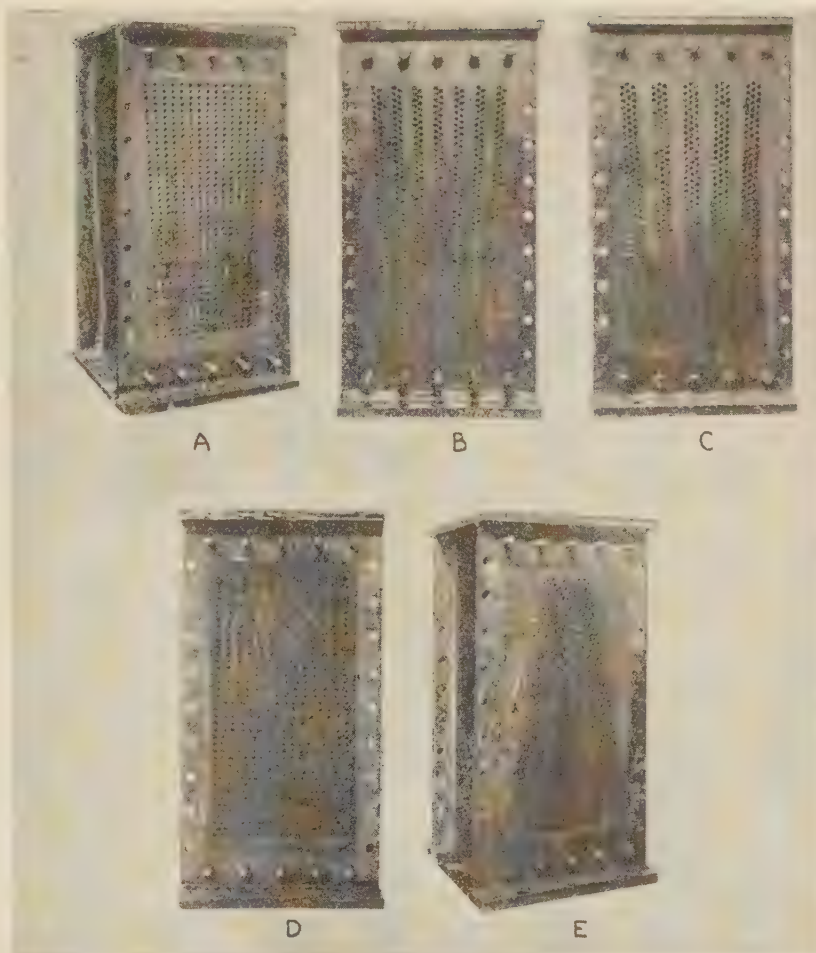


FIG. 9 MODEL CONDENSER-TUBE SHEETS AS USED FOR COMPARATIVE PRESSURE-DROP TESTS

for accurate measurement. In this way characteristic curves were obtained of the pressure loss with varying flows through the different tube banks. On the basis of these tests, the tube arrangement for the actual condenser was selected and the pressure drops calculated.

The actual pressure drops for the five longitudinal compartments during test 11 are given in Fig. 10 based on observations taken by the Brooklyn Edison Company's Research Bureau. The table gives the calculated loading per square foot in each compartment when the entire surface is satisfied. The relatively cold water in the first compartment results in a condensing capacity over twice that of the last compartment. The agreement of the measured drops with the calculated gradations is very close.

The average pressure loss is 0.104 in., as shown. On the warm end it is so small that it was difficult to measure. The pressure loss at the cold end is about 0.2 in., and this is evidence that the steam flow in this section was in accordance with the calculated condensing capacity.

The paper may give the impression that there is insufficient area between the turbine and the entrance to the tube bank of the Ingersoll-Rand condenser for easy or free deflection of flow toward the cold end. Figs. 10 and 11 and the following calculations show that any force to cause deflection of the steam between the time it leaves the turbine and enters the tube bank is



FIG. 8 TYPICAL MODEL WATER-BOX TEST

negligible. The writer appreciates that steam flows and pressure are far from uniform in a turbine-exhaust casing, but this does not alter the present line of reasoning.

As shown, one-half of the steam is condensed by the first two

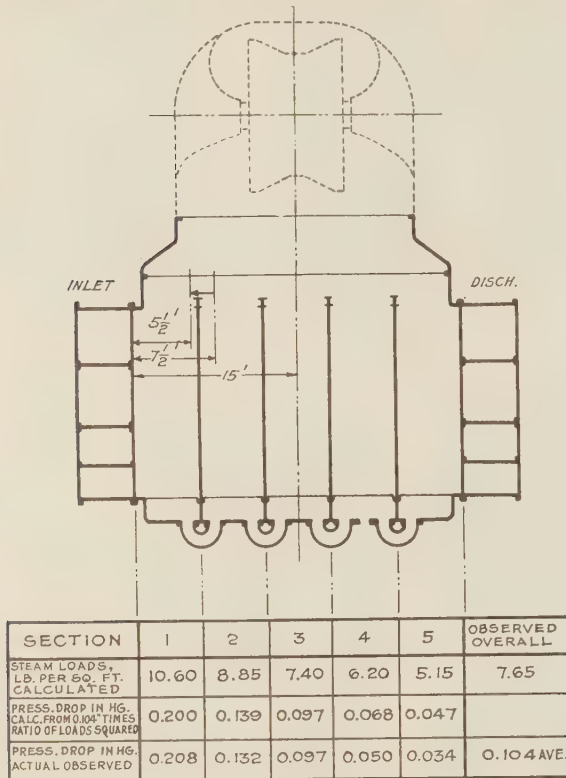


FIG. 10 DATA FROM ACCEPTANCE-TEST RUN OF INGERSOLL-RAND CONDENSER

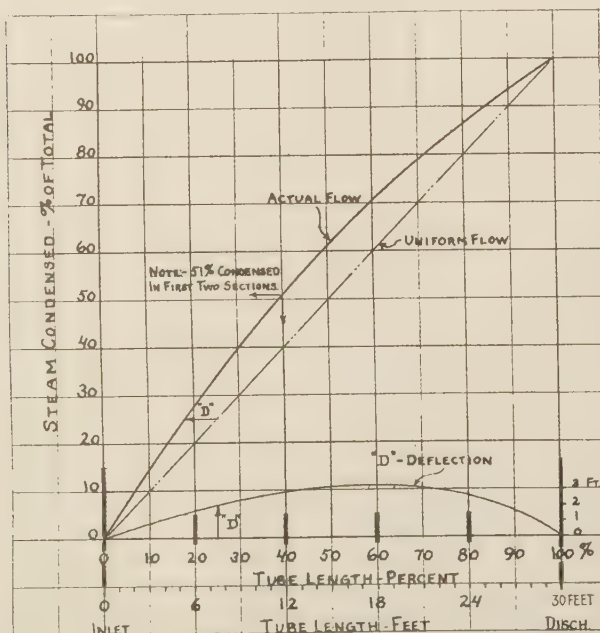


FIG. 11 LONGITUDINAL STEAM DISTRIBUTION, INGERSOLL-RAND CONDENSER

compartments; the center of flow of this half of the steam is shifted about 2 ft toward the cold end. Therefore, the horizontal component of the velocity diagram is 2 ft as against 20 to 10 ft vertical component, depending on whether the stream starts to bend near the top or near the bottom of the turbine casing. The horizontal component is therefore 10 to 20 per cent of the vertical. The average flow velocity is about 250 ft per sec at the turbine nozzle and considerably less (150 to 200 ft) at the condenser. It follows that the horizontal component may be as low as 15 to 25 ft per sec and not over 50 ft per sec. In other words, the required velocities and forces of deflection are exceedingly small. In contrast the forces required for penetration at one end as compared to the other are appreciable and can be readily measured in terms of pressure drop. It should be emphasized that the problems of steam deflection are entirely distinct and different from those of steam penetration.

C. F. HARWOOD.⁷ The method developed for determining the relative percentage of tube cleanliness in a surface condenser discloses the skill and accuracy displayed in obtaining the data reported in this paper. The performance of both condensers as

WORTHINGTON - FULL LINES INGERSOLL - DOTTED LINES FROM FIG 5.

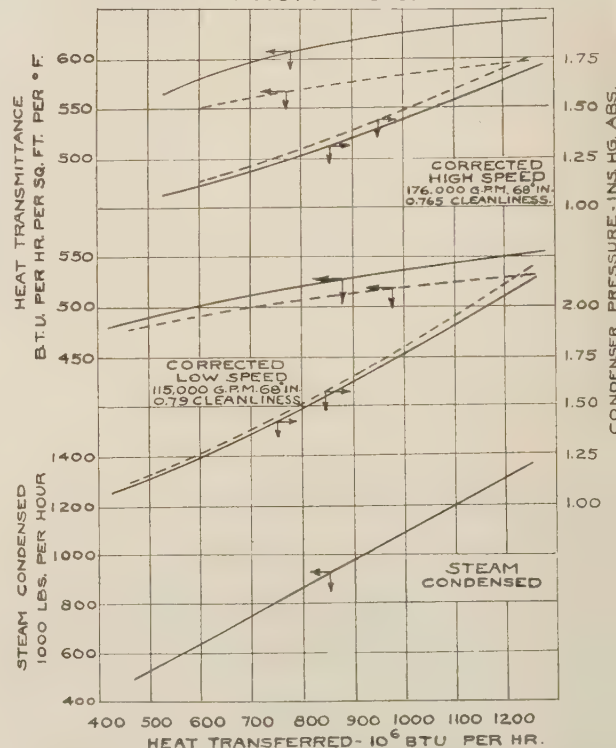


FIG. 12 CORRECTIONS OF CURVES SHOWN IN FIG. 5 OF PAPER

indicated by these tests is of a high order, especially so in view of the percentage of tube fouling present.

It is unfortunate that the tests on both units were not made under more nearly equal conditions of tube cleanliness and circulating-water temperature, so that a comparison of performance could be made without the necessity of applying any corrections for the differences in water temperature, quantity, and tube

⁷ Manager of Steam Power Plant Sales, Worthington Pump and Machinery Corp., Harrison, N. J.

cleanliness obtaining when the observations were taken, but unless such corrective factors are applied it is difficult to obtain a correct idea of the relative performance of the two condensers. A casual inspection of the data and curves indicates that the Worthington condenser is producing a lower absolute pressure with a lower temperature of circulating water and with dirtier tubes, and that the Ingersoll-Rand condenser is showing a higher coefficient of heat transfer with a higher temperature of circulating water and cleaner tubes, but the extent to which these differences in water temperature and tube cleanliness would affect comparative performances can only be made evident by the application of correction factors which will place both units on a common basis of tube cleanliness, circulating-water temperature, and quantity. The authors state that the application of such corrections has been left to others, and there are therefore submitted herewith curves for both condensers showing absolute pressures and coefficients of heat transfer based upon equal conditions of circulating-water temperature and quantity, and equal percentages of tube cleanliness.

These curves have been constructed in the following manner: The performance curves of the Ingersoll-Rand condenser, drawn in dotted lines, have been reproduced in Fig. 12 as shown by the authors in Fig. 5 of their paper. The performance curves of the Worthington condenser, shown in full lines, have been plotted from the "actual condenser test performance" data contained in the paper, with the necessary corrections applied to the observed circulating-water temperatures and quantities and percentage of tube cleanliness, so that these correspond to those of the Ingersoll condenser as indicated in Fig. 5 of the paper.

These corrections are made on the following bases: (a) Circulating-Water Temperature. By means of the temperature correction curve incorporated in the September, 1932, issue of *Power* and which is in common use by practically all condenser manufacturers today. (b) Circulating Water Velocity. In accord with ratio of square roots of velocities. (c) Tube Cleanliness. In ratio of observed percentages of cleanliness, as such cleanlinesses are stated in the paper.

Both condensers are therefore placed on a common basis of operating conditions, and their relative performance is more clearly indicated.

D. W. R. MORGAN.⁸ The main value of the paper is that it demonstrates the feasibility of equating actual performance with guarantees, and if properly applied, eliminates the argument between manufacturer and operator concerning the condition of the tube surface at the time of tests. Further, the data may be used by the operator in determining what factor to apply as regards excess surface and water, in order to maintain the desired vacuum under average operating conditions.

The authors state that both condensers have performed satisfactorily and maintain better than guaranteed full-load vacuum. Emphasis should be laid on the fact that this good performance is not evident if one simply accepts from casual examination the actual Btu transfer rates referred to in the paper. As an example, the maximum rate of the Worthington condenser is 507 Btu; the maximum rate for the Ingersoll-Rand is 596 Btu. Equating these values to the nominal guarantee basis, they become, respectively, 780 Btu for both condensers, assuming the average cleanliness specified.

However, it should be noted that although the Btu rates are good, they were obtained at the expense of high velocity, and therefore increasing the pumping cost. Based on information published in *Power*, the water velocities through the tubes are

8.3 fps at high-speed operation and 5.93 fps at low-speed for the Worthington condenser, and 8.88 fps at high-speed operation and 5.8 fps at low-speed for the Ingersoll-Rand condenser.

The tube-fouling conditions at this station may warrant and justify the high velocities used, as high velocity is conducive to maintenance of clean tubes under certain conditions of fouling.

The authors mention the fact that the two condensers described are radically different in design. This leads one to suggest that No. 6 unit, operating in the same station, should have been included in the comparison. Naturally, in expressing this thought the writer has a selfish motive in mind.

The performance of No. 6 unit was creditable, and when equated to the same basis indicates performance comparable with the condensers described by the authors. This condenser gave a Btu rate of 410 at high-speed operation, corresponding to 7.0 fps water velocity. Compared on the same basis as the Worthington and the Ingersoll-Rand, the rate becomes 594 to 630 Btu, depending upon whether a cleanliness factor of 65 per cent or 69 per cent is used.

Equating the velocities to a common basis would justify a rate of 780 Btu for No. 6 unit, at the equivalent velocity.

Results indicating the performance with larger quantities of air leakage would be of interest, because experience indicates that condenser performance is appreciably affected by increased leakage.

The writer has noted a reduction in the transfer rate of approximately 35 per cent on isolated tubes located in the so-called active part of the tube nest, merely by increasing the air leakage, all other conditions remaining the same. He mentions this fact because of its importance in comparing test results. It should be noted that in the case of the Ingersoll-Rand the leakage varies from a minimum of 2 to a maximum of 4 cu ft per min. The Worthington varies from 4 to 6 cu ft per min. The air leakage on the No. 6 unit varied from 4 to 16 cu ft per min.

The authors mention the fact that tests illustrate that dirty tubes do not respond to increased water velocity. This statement is verified by tests made under the writer's direction, and covering the period from 1917 to 1926. The slope of the curve with clean tubes closely approximates the established law, varying as 0.5 power, whereas, depending upon the nature of fouling, a dirty tube varies as 0.2 to 0.3 power.

Referring to Fig. 6, the writer would like to know if tests were made condensing or non-condensing.

The authors suggest the great need of advancing the knowledge of the subject of condensers, comparable to that of turbines. The writer thoroughly agrees with the conclusion. However, he wishes to point out that difficulties lie before us, and a greater amount of standardization must be accepted by the operator on such vital points as: (1) Relation of condenser to turbine exhaust—namely, set at right angles or parallel to the turbine shaft. (2) More thorough exploration of pressure at inlet of condenser and through the tube nest. (3) A uniform distribution of steam from the turbine exhaust.

JOHN F. GRACE.⁹ Were both condensers tested under more uniform cleanliness and water temperature and were they the product of one maker, discussion of factors of correction would not be so wide or so susceptible to the sales viewpoint, against which engineers have developed no satisfactory screening equipment.

The layout engineer senses that performance is influenced by simplicity of arrangement and connections. The builder of the heart-shaped condenser required a wider turbine supporting structure and more liberal space than the builder of the cylindrical

⁸ Westinghouse Elec. & Mfg. Co., South Philadelphia, Pa. Assoc. Mem. A.S.M.E.

⁹ Condenser Engineer, Worthington Pump and Machinery Corporation, Harrison, N. J., Mem. A.S.M.E.

condenser, who would have further improved performance if granted equal space. Figs. 1, 2, and 3 show both condensers to the same scale, and Fig. 1 shows the cylindrical condenser presenting the longer line of "front row" tubes.

The layout of the 160,000-kw units at Brooklyn is with condenser tubes parallel to turbine shafts and both 90 deg to crane rails. Lateral space is thus important to accessibility, operation, and performance. Seven such units can be comfortably housed in a turbine room of the dimensions at Hudson Avenue if heart-shaped condensers are installed, while eight can be as well housed if the cylindrical type is chosen. Space is thus a serious "performance" factor, and the cost of a building to house an additional 160,000-kw turbo-generator and auxiliaries is a not inconsiderable item when limits of output and of downtown real estate are approached.

PAUL DISERENS.¹⁰ The paper seems to be the first serious attempt to take into account the condition of surface cleanliness in reporting condenser tests, especially where units of large size are concerned. The thoroughness with which the authors have conducted their tests and the painstaking care which they have exercised in planning and completing their work should lend a high degree of credibility to the results which they publish.

Consideration of the cleanliness factor in appraising the performance of a condenser is extremely important, because without definite information as to the magnitude of this factor, no conclusive significance can be attached to any condenser test results. In stating their conclusion, the authors say they "doubt the soundness of the cleanliness correction for making accurate comparisons where large differences are involved," and "recent test work confirms the inaccuracy of a straight-line cleanliness correction."

It would seem that what the authors mean to say is that the correction factor applying to any selected group of sample tubes within a condenser cannot be taken with absolute assurance to represent the actual cleanliness factor of the entire condenser. No one would question the straight-line relationship of the cleanliness correction in so far as the selected groups of sample tubes is concerned except for any small change in steam distribution within the condenser which might accompany changes in heat transmittance at any given load. This, however, is a factor which need not be discussed at this time. What we are really interested in is an examination of the data reported by the authors to see how closely the factor reported for the selected groups of tubes represents the corresponding factor for the entire condenser. Various suggestions have been made to the Power Test Code Committee for securing the best possible average of the various sample tubes selected. Mr. Hodgkinson has suggested an average weighted to account for any variation in rate at which the various tubes may be working. The authors have preferred to use the arithmetical mean. If we refer back to the paper by Messrs. Hardie and Cooper presented in November, 1932, and recalculate the average as suggested by Mr.

¹⁰ Chief Consulting Engineer, Worthington Pump and Machinery Corp., New York, N. Y. Mem. A.S.M.E.

TABLE 2 WEIGHTED AVERAGE AS RECOMMENDED BY MR. HODGKINSON

Test No.	as reported	U
W-1.....	0.68	0.712
W-5.....	0.68	0.675
W-6.....	0.61	0.610
W-9.....	0.59	0.587
W-10.....	0.59	0.586
IR-5.....	0.78	0.789
IR-6.....	0.75	0.743
IR-9.....	0.74	0.742
IR-10.....	0.74	0.737

TABLE 3 PERFORMANCE OF TWO 101,000-SQ-FT SURFACE CONDENSERS

Test No.	Date, 1932	Sample tubes, average	Entire condenser, average	As reported	Corrected to average U for condenser	Water-inlet temperature	Water-inlet temperature factor for 70 F	Average heat-transfer coefficient, clean condenser, 70 F inlet temperature
W-5.....	6-13	463	455	0.68	0.685	61.6	0.937	708
W-6.....	6-14	448	463	0.61	0.597	62.7	0.947	819
W-9.....	6-14	436	459	0.59	0.577	61.9	0.940	846
W-10.....	6-14	419	432	0.59	0.568	61.4	0.935	813
IR-5.....	6-27	591	553	0.78	0.794	67.3	0.984	708
IR-6.....	6-28	581	563	0.75	0.758	68.5	0.992	749
IR-9.....	6-28	590	576	0.74	0.746	68.2	0.990	780
IR-10.....	6-28	571	551	0.74	0.749	67.6	0.986	746

Hodgkinson, we note a remarkably close agreement, as indicated in Table 2.

An examination of the data in the Hardie and Cooper paper does, however, throw some light on the possible explanation of the small discrepancy to which the authors call attention. It will be noted that for some of the tests reported, noticeably those on the Ingersoll units, the average heat-transfer coefficient for the dirty tubes in the selected sample groups does not coincide with the average coefficient for the entire condenser, the margin in some cases being of considerable proportions. In the case of the Worthington tests, the margin of difference is very

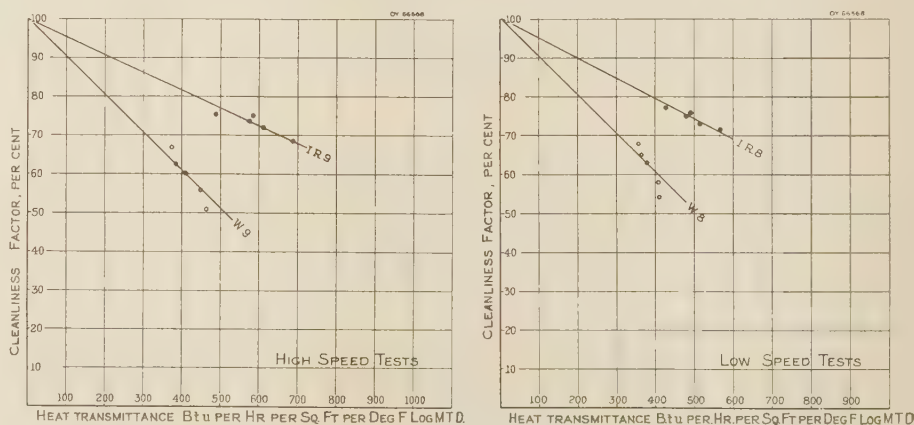


FIG. 13 RELATION BETWEEN CLEANLINESS FACTOR AND COEFFICIENT OF HEAT TRANSFER AS AFFECTED BY POSITION IN CONDENSER

much smaller, all of which is shown by columns 3 and 4 in Table 3.

It is apparent, therefore, that if we know the relationship between cleanliness factor and coefficient of heat transfer for a tube of given cleanliness, we can calculate from the factor actually measured on the selected groups of sample tubes the actual factor for the entire condenser in order to correct for the discrepancy noted. This relationship is discussed in the paper by Mr. Townsend Tinker at the A.S.M.E. meeting, Chicago, June, 1933,

and need not be enlarged upon here. It will be interesting to note, however, that experimental data reported by Messrs. Hardie and Cooper applying to the identical tests reported by the authors of this paper clearly show this relationship. Fig. 13 has been plotted from the data covering tests Nos. IR-9, W-9, IR-8, and W-8. Certain of the tests at lower capacity do not indicate this relationship quite so clearly, but we may assume that the decrease in cleanliness factor is directly proportional to the heat transmittance as indicated in Fig. 13, and this therefore gives us a basis for calculating the true cleanliness factor for the entire condenser based on the cleanliness factor as measured in the

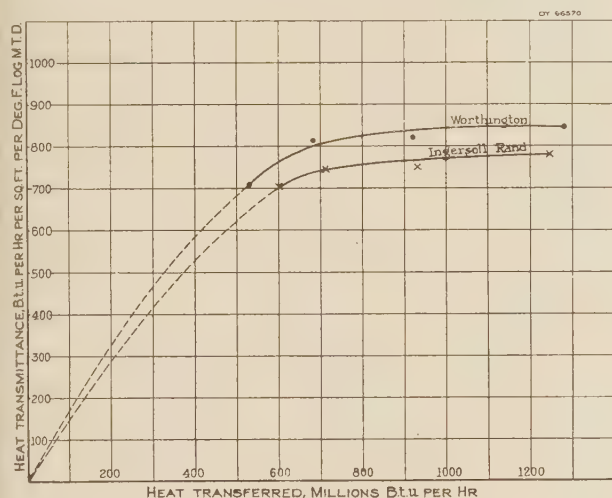


FIG. 14 COMPARISON OF PERFORMANCE, WORTHINGTON CORRECTED TO INGERSOLL-RAND CONDITIONS

selected groups of sample tubes. In Table 3, the factors as reported and corrected are in columns 5 and 6.

While the modification as calculated may seem small, it is nevertheless of sufficient magnitude to account largely for the discrepancy reported by the authors, all of which will be apparent upon referring to Fig. 14. It should be noted that test No. W-1 has been omitted, because during this test as reported by the authors air leakage was excessive.

It is hoped that the analysis of the authors' data which the writer has given will assist in enhancing the credibility of their methods for measuring cleanliness factor. Their experience in conducting tests of this character will be of great assistance to the committee now engaged in considering the possibility of including a condenser cleanliness factor in the Power Test Code.

C. L. WADDELL.¹¹ This paper states that the tests conducted by the Brooklyn Edison Company and reported in detail by Messrs. Hardie and Cooper determined the "cleanliness ratio" of the condensing surface. In reality, the tests only established the "cleanliness ratio" for the selected tubes. The tests do, however, give us all the necessary data to determine very accurately the true "cleanliness ratio" for the entire condensing surface by calculation. This correction has been covered by Mr. Diserens in his discussion.

The paper states that the condenser manufacturers made guarantees which were to be corrected downward from 100 per cent clean transmittance guarantee in direct proportion to the "cleanliness ratio" obtaining at the time of the test. Using the authors' definition of "cleanliness ratio," it would seem from

Mr. Diserens' discussion that this method of correcting guarantees for cleanliness might either be unfair to the buyer or the manufacturer of the condenser. If the average heat-transfer coefficient for the selected tubes is higher than for the entire condenser, the cleanliness ratio as determined by the tests would be unfair to the buyer of the condenser, because the tests would show better performance than was actually obtaining. If the average heat-transfer coefficient for the selected tubes is lower than for the entire condenser, it would be unfair to the manufacturer of the condenser, because the tests would show poorer performance than was actually obtaining. It is therefore necessary to correct the cleanliness ratio in the manner suggested by Mr. Diserens to obtain the true performance.

The graphs by Mr. Diserens show that all the actual test points on the dirty tubes are at fairly high heat transfer. He has assumed a straight-line variation between the average of these points and the point of 100 per cent cleanliness factor and zero heat-transfer coefficient. We must take into account that the correction is small where the location of the selected tubes is such that their average heat-transfer coefficient is close to that for the entire condenser. Therefore, it is not only permissible but logical to assume the straight-line relationship for these small corrections.

The Subcommittee on Condenser Tests of the Power Test Code Committee recommended tentatively in its report dated Sept. 24, 1932, the type of test for obtaining condenser cleanliness factor as covered by this paper. No mention was made in these recommendations as to the maximum allowable variation between average heat-transfer coefficient for the selected tubes and for the entire condenser. In the light of the data in this paper and the discussion upon it, it would appear advisable for the Power Test Code Committee to consider limiting this variation. It is suggested that the allowable variation be set at 5 per cent plus or minus, and when the variation exceeds this amount, that the test-tube locations be changed to bring the results within this limitation.

The curves for heat-transfer coefficient and absolute pressure shown in this paper do not show the actual test points and are not corrected for differences between average heat-transfer coefficient for the selected tubes and for the entire condenser. When the test points are plotted without this correction, they do not fall as nearly on the curve as they do with the correction as shown by Mr. Diserens' figure. This further substantiates the writer's belief that this correction is desirable in a proper interpretation of the test data.

It might be well to outline in detail the method for correcting the test data to obtain the true cleanliness factor for the entire condenser:

- Average the cleanliness factors for the selected dirty tubes.
- Average the heat-transfer coefficients for the selected dirty tubes and check to see whether this is within 5 per cent plus or minus of the heat-transfer coefficient for the entire condenser.
- Plot the average heat-transfer coefficient for the selected dirty tubes as abscissa against the average cleanliness factor for the selected dirty tubes as ordinates.
- Draw a straight line from this point to the point of 100 per cent cleanliness and zero heat-transfer coefficient.
- Read up from the average heat-transfer coefficient to this straight line to obtain the true cleanliness factor for the entire condenser.

AUTHORS' CLOSURE

Mr. Bancel's comments are in the nature of an addition to the paper and call for no comment by the authors.

¹¹ Test Engineer, Worthington Pump & Machy. Corp., Harrison, N. J.

The discussion offered by Mr. Harwood shows a computed curve of performance for the Worthington condenser corrected to the Ingersoll-Rand test conditions. The authors can neither substantiate nor repudiate the correctness of this computation by test fact. The corrections employed for water velocity and water temperature are generally accepted and are of relatively small importance to the comparison. The correction for tube cleanliness in direct proportion to the cleanliness factors reported is entirely in agreement with the correction factor relationship which forms a part of each contract, but which is subject to question.

The authors have in hand some additional data from a series of test runs made in connection with an entirely independent investigation of the accuracy of sampling possible with isolated test tubes. These runs were at lower water temperature and lower cleanliness ratio than either of the acceptance tests reported in the paper. Since the Ingersoll-Rand acceptance test was made at higher water temperature and higher cleanliness ratio than the Worthington test, a sort of interpolation of the Ingersoll-Rand performance is now possible.

This interpolation is limited in that the recent runs were made only in low circulating-pump speed and in that the two variable elements in the comparison—the water temperature and the cleanliness ratio—cannot be separated from each other without assuming that the manufacturer's correction for temperature holds for the performance of this Ingersoll-Rand condenser. Such an interpolation, when performed on the Ingersoll-Rand heat transmittance coefficient, shows that substantially no difference in performance would exist between the condensers were they both to be tested under the conditions existing at the time of the Worthington test.

In drawing a comparison between the Westinghouse No. 6 condenser at Hudson Avenue and the tests reported in this paper, Mr. Morgan is using commercial correction factors to an even greater extent than is required to compare the Worthington and Ingersoll-Rand units. The authors have stated in the paper that they have hesitated to use such correction factors not supported by their own test work on the specific condenser to which the correction is applied, and for this reason can make no further comment on Mr. Morgan's discussion.

Mr. Diserens, in his discussion, calls attention to the fact of position of isolated test tubes in the condenser affecting the cleanliness ratio even when assuming a specific condition of dirt

film common to all tubes. Tubes near the steam inlet having high heat-transfer rates are adversely affected by a given dirt film to a greater extent than those near the air offtake whose heat-transfer rate is relatively lower. Mr. Tinker's paper contains an analysis which can be applied to the explanation of this fact.

Our test work attempted to eliminate the necessity for a correction such as Mr. Diserens has suggested by an initial selection of test tubes such that the average heat transmittance of the isolated tubes would be as near as possible to the average of the entire condenser. The degree of success with which this has been accomplished is shown by the very small magnitude of Mr. Diserens' correction.

A refinement is necessary to the computation of the Ingersoll-Rand results in Table 3 before a true comparison is possible. Mr. Diserens' values for sample-tube averages are based on temperature differences between the circulating water in the tube and the estimated temperature of the steam surrounding the tube as presented in the Hardie and Cooper paper for comparison of isolated tube performance. For comparison of isolated tube performance with overall condenser transmittance, the authors prefer to use the temperature of steam at the condenser inlet. When transmittance coefficients are computed on this basis, the sample tube averages are found much closer to the average for the entire condenser.

Since the receipt of Mr. Diserens' discussion, the authors have plotted the results of the additional test work previously referred to in a manner similar to Fig. 13. This data would not justify the straight lines projected through to 100 per cent cleanliness factor at zero heat transmittance, as shown in Fig. 13.

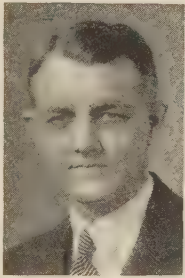
The authors take this opportunity to acknowledge the value of Mr. Diserens' analyses and will utilize additional data as they become available to establish by test fact the principles he has pointed out.

At the present time the authors do not have sufficient information to justify endorsing Mr. Waddell's proposed method for correcting test data. It does appear highly desirable, as he has pointed out, to select the isolated tube groups so that the average of the isolated-tube heat-transfer rates shall be as close as possible to the average for the entire condenser. As will be seen from the comparisons brought out in Mr. Diserens' discussion, these correction factors will be quite small when the average transmittance of the isolated tubes and that of the entire condenser are nearly alike.

Radiation From Luminous and Non-Luminous Natural-Gas Flames

By RALPH A. SHERMAN,¹ COLUMBUS, OHIO

From the data presented in the paper, these conclusions in regard to the transfer of heat from luminous and non-luminous gas flames are made: Luminous gas flames are now being obtained principally with slow-moving, stratified streams of air and gas, which, from the viewpoint only of efficient combustion, are much inferior to non-luminous flames. Combustion is extremely rapid in pre-mixed, non-luminous flames, which results in a high-temperature zone near the burners. Although natural-gas flames can be produced that have an emissivity approaching that of a black body and consequently a higher rate of heat transfer than a non-luminous flame, the total radiant-heat transfer from the flame and the wall, in those furnaces having walls hotter than the work being heated, will not be much greater for the same flame temperature than with a non-luminous flame. The advantage of a luminous flame in many heating processes lies not in a higher rate of heat transfer, but in a more uniform transfer over the entire furnace as a result of the slow combustion and slow heat liberation. The presence of free carbon probably has a beneficial effect in the reduction of oxidation and the scaling of steel.



RENEWED interest has recently been evidenced in the combustion and radiation characteristics of gas flames. This has come about from the greater availability of gas for industrial use through the wide spread of natural-gas pipe lines, the desire for increased efficiency in combustion, and the need in certain applications for better control of the oxidizing characteristics of the flame. Gas may be so burned as to produce either luminous or non-luminous flames,

and discussion has arisen as to the merits of the two types of flames, particularly in regard to the rate of heat transfer by radiation from the flame to the work in the furnace. Conflicting statements that have appeared in these discussions and in the technical press show that a clear understanding of the differences between the two types of flames is lacking. This paper presents a discussion of the knowledge of the chemistry and physics of combustion and heat transfer of gas flames and some new data on large-scale laboratory combustion experiments in the hope that some of the haze that now surrounds the subject may be dispelled.

¹ Fuel Engineer, Battelle Memorial Institute. Mem. A.S.M.E. R. A. Sherman is a graduate of the University of Iowa. For ten years he was in the fuel section of the U. S. Bureau of Mines at Pittsburgh. Since 1930 he has had charge at Battelle Institute of the research work on the combustion of fuels.

Presented at a meeting, Pittsburgh, Pa., February 17, 1933, of the Pittsburgh Section of THE AMERICAN SOCIETY OF MECHANICAL ENGINEERS, with the Iron and Steel Institute and the Engineers' Society of Western Pennsylvania.

NOTE: Statements and opinions advanced in papers are to be understood as individual expressions of their authors, and not those of the Society.

SOURCES OF FLAME RADIATION

There are two sources of radiation from flames: (1) the non-luminous gases, CO_2 and H_2O , and (2) the luminous carbon particles. The radiation from CO_2 and H_2O does not follow the "fourth-power of the temperature," or Stefan-Boltzmann law that applies to solids; these gases radiate in only certain bands of the spectrum, and although Schack(1)² made available formulas for the calculation of their radiation, their use is so complicated that they are best found from curves which have been published in English units by Hottel(2) and recently by Fishenden and Saunders.(3) The data of Schack on the radiation of water vapor have lately been superseded by the work of Schmidt;(4) these data have been presented in English by King.(5)

Luminous radiation—that is, the radiation from solid particles suspended in the flame—follows more nearly the laws of radiation from solids. A flame containing carbon particles is, however, partly transparent, and the radiation depends on the concentration of the particles in the flame. Wohlenberg(6) and Haslam and Hottel(7) have made attempts to derive formulas for the calculation of the radiation from powdered-coal flames, but for gas flames no method is yet available for the calculation, largely because the concentration of particles is unknown.

SOURCE OF LUMINOSITY

The luminosity of gas flames arises from the decomposition, also called pyrolysis or cracking, of the hydrocarbons of the gas. The unsaturated hydrocarbons, as ethylene, C_2H_4 , and acetylene, C_2H_2 , decompose most readily; saturated hydrocarbons, methane, CH_4 , ethane, C_2H_6 , propane, C_3H_8 , and butane, C_4H_{10} , decompose the more readily the higher their carbon content. Therefore, natural gas which contains 80 to 90 per cent of methane, CH_4 , is one of the most difficult of the industrial gases with which to obtain a luminous flame. Complete data on the rate of decomposition of methane at various temperatures are lacking; Trinks(8) has collected data from various original sources in a family of curves showing the rate at different temperatures.

The rates of oxidation of methane and ethane, even if mixed with only a part of the air necessary for complete combustion, are extremely rapid. The rates are so high relative to their rates of decomposition that, to obtain a luminous flame with these gases, it is necessary to heat natural gas to a high temperature before it is mixed with air. The possibility is evident that the cracking might be obtained by passing the gas through heated chambers, possibly with a catalyst, but the liberated carbon tends to deposit on the surfaces and stop the passages.

The method used, therefore, in luminous burners so far developed is to introduce the gas and air into the furnace in separate streams, with care in the design of the furnace to avoid mixing until the desired cracking has taken place. The gas is heated by convection and by radiation from the burning gas at the interface of the air and gas streams. Methane and ethane do absorb radiant heat, but data are lacking to calculate their rates of heat absorption.

Because the air and gas cannot be thoroughly mixed by tur-

² Numbers in parentheses apply to references at the end of the paper.

bulence and luminosity obtained, the mixing must occur principally by diffusion, and one manufacturer has applied the name diffusion burner to his luminous-flame burner.

CHARACTERISTICS OF LUMINOUS FLAMES

The ratio of air to gas for the maximum rate of flame propagation of natural gas is almost exactly the ratio for the theoretical air requirements. The perfect mixture of natural gas and air is therefore an explosive mixture, and the rate of burning is so rapid that it is practically a detonation. Because the heat is liberated

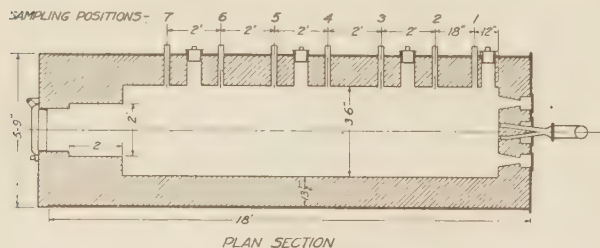


FIG. 1 PLAN SECTION OF EXPERIMENTAL FURNACE

in a small volume of flame, the heat loss is low, and high temperatures are developed very close to the burner when the gas and air are premixed.

Where stratification and slow mixing are used to obtain luminosity, the combustion is slow, the heat is released in a large volume of flame from which the heat loss is higher, and the maximum temperature developed may be considerably lower than with a premixed, non-luminous flame.

As previously mentioned, the concentration of carbon particles in a flame may not be readily determined and the radiation cannot be calculated. Nor is it possible to judge accurately the luminosity of a flame by visual observation. Some conception of the degree of blackness of a flame may be obtained by the ability to see the opposite wall or objects in the flame, but accurate information can be obtained only by actual measurement of radiation.

ACKNOWLEDGMENTS

This work has been carried on under the general direction of Clyde E. Williams, assistant director, Battelle Memorial Institute. Lionel F. Fairthorne, assistant fuel engineer, has been engaged in the conduct of all tests. H. W. Russell, physicist of the Institute, has assisted in many phases of the work.

EXPERIMENTAL STUDY

The work reported in this paper includes data on the progress of combustion and on the radiation from the flame when burning natural gas with premixed non-luminous flames and with luminous flames in a large-scale laboratory furnace.

APPARATUS AND METHODS

The Furnace and Burners. Fig. 1 shows a section of the furnace which consists of a horizontal, refractory-lined, steel shell whose seams and joints are welded or cemented to prevent the entrance of air. The inside diameter of the combustion chamber is 3 1/2 ft, and the length from front wall to stack is 14 ft. The drawing shows, at intervals along the furnace, holes through which gas samples are drawn and temperatures are measured. Four 6-in. square ports are provided through which radiation measurements are made.

Fig. 2 shows the details of the burners used in the tests. Fig. 2A is the burner for pulverized coal which is being used in an investigation, the results of which have been presented in part;(9)

comparative data on the radiation of pulverized-coal flames are included in this paper. Fig. 2B shows the premixed non-luminous flame burner, which was made similar to the pulverized-coal burner to obtain comparable flame shape. The inner cone was made larger to reduce the annular section so that the velocity of entrance of the gas-air mixture was above the velocity of flame propagation. The gas entered through 64 1/16-in. holes distributed radially in the 1 1/2-in. pipe at the elbow of the burner pipe. The entrance of the gas through the large number of small holes and the passage of the mixture through the venturi throat resulted in good mixing. Fig. 2C shows the luminous-flame burner which was purchased from the manufacturer. This type of burner is used with satisfaction in a number of types of industrial furnaces and has been seen by the author in satisfactory operation in "sheet and pair" and annealing furnaces. The solid lines

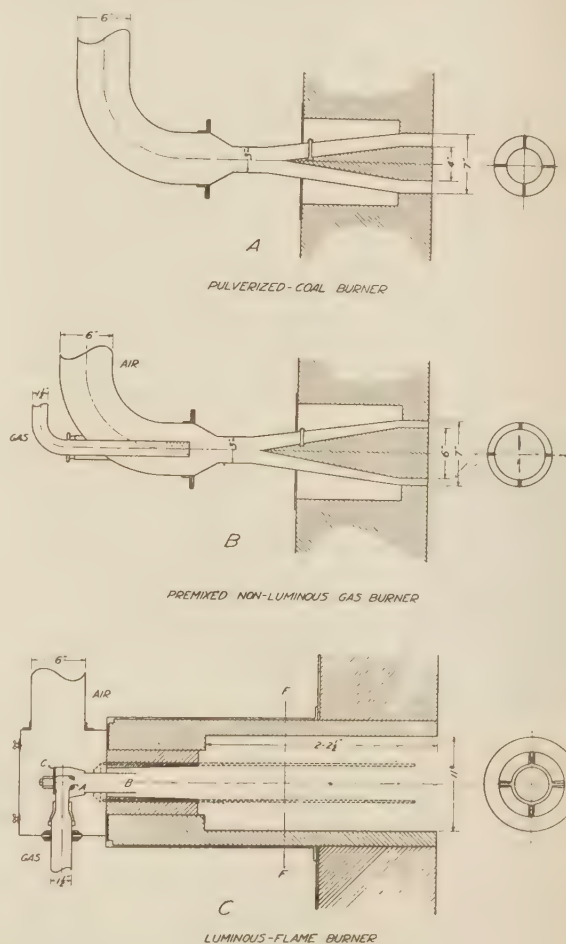


FIG. 2 STYLES OF BURNERS

show the burner as furnished; this was installed first with the line F-F at the face of the front wall and later with an 18-in. longer tunnel, as shown. The dotted lines show a 4-in. pipe which replaced the original refractory insert in one test.

In this burner the gas enters at A through a 1/2-in. orifice and passes into the refractory insert or 4-in. pipe through the 1 1/2-in. nipple B. A shutter C is provided which can be opened to permit air to be inspired with the gas. This was closed during all of these tests. Air can also enter the gas stream between the nipple B and the refractory insert. When the 4-in. pipe was used, an adjustable shutter was placed on nipple B to vary the

amount of air entering with the gas at this point. The air entered the burner box, and the principal part passed around the refractory insert or pipe and mixed with the gas in the tunnel or in the furnace.

Natural Gas. The natural gas used in these tests came from the Columbus mains; it was supplied to the laboratory at a pressure of 10 to 15 lb per sq in. and was reduced by a regulator before the meter used on the tests to 3 to 4 lb per sq in. The gas was measured by a dry displacement meter; the pressure was measured by a mercury column and the temperature by a thermocouple in the gas stream at the meter. All gas volumes were corrected to standard gas conditions, 30 in., 60 F. A thin-plate orifice meter in the gas line allowed easy adjustment of constant flow. The gas furnished during the period of the tests varied rather widely in its composition. Table 1 shows the composition of seven samples of gas.

These analyses were made in a Bureau of Mines type orsat in which the hydrocarbons are determined by slow combustion and can only be calculated as CH_4 and C_2H_6 . The gas supplied in Columbus may come from 3400 different wells in 14 producing sands, and a small amount of petroleum-refinery gas is also used. The gas from some of these wells is wet; that is, it contains considerable amounts of the higher hydrocarbons. As these could not be determined on the apparatus available, the analyses are to some extent in error.

TABLE 1 NATURAL GAS COMPOSITION

Test Date	3 7-14	5 7-20	8 9-2	9 9-15	10 9-22	12 10-4	13 10-12
CH_4	67.4	66.3	60.9	66.2	72.4	76.8	78.7
C_2H_6	17.2	16.8	25.4	21.7	16.1	12.4	9.7
CO_2	1.0	1.2	1.6	1.5	0.8	0.7	0.8
O_2	0.5	0.6	0.5	0.8	0.6	0.6	0.4
N_2	13.9	15.1	11.6	10.0	10.1	9.5	10.4

The variation in the composition is caused by the necessity of mixing of widely different gases and of the introduction of inerts, CO_2 and N_2 , to maintain the calorific value as close to 1000 Btu per cu ft as possible.

Air Supply. In all tests all the air was supplied at the burner through the 6-in. duct shown in the burner drawings. The weight of air supplied was determined from the pressure drop across an orifice in this duct.

Heating of Furnace. The furnace was heated by burning gas at the rate and with the air supply desired for about 4 hours to approach equilibrium conditions before taking data. The actual taking of data, which included the collection of two sets of samples of gas at six points in the furnace, the measurement of gas temperatures, and the measurement of the radiation from the flame at four points, required about 3 hours.

Sampling of Gases. Gas samples were withdrawn through water-cooled samplers and collected over mercury. The samples were analyzed in an orsat apparatus using mercury as the displacing fluid.

Samples were taken along the central axis of the furnace only. Although, because of stratification of gases, particularly with the luminous-flame burner, this did not give the average composition in any plane, it was thought that it did give a better record of the progress of combustion than would an average. The stratification in the furnace and the flow of gases were discussed more completely in the report on the pulverized-coal tests.(9)

Measurement of Temperatures. A Pt, Pt-Rh thermocouple supported in a water-cooled tube with $3\frac{1}{2}$ in. at the hot junction exposed to the gases was used for most of the temperature measurements. Comparative trials with a suction-type thermocouple showed that when the two couples were so placed as to read the temperatures at the same point simultaneously, the indications checked within 0.1 millivolt, 15 F, which was the

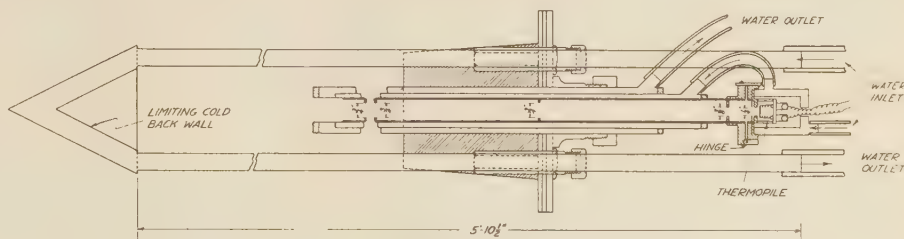


FIG. 3 APPARATUS FOR MEASUREMENT OF RADIATION

limit of graduation on the potentiometer used. The differences should not be great, because the temperature of the walls of the furnace was not greatly different from that of the gas. Such close agreement was not obtained when successive traverses of the furnace were made with the two thermocouples, particularly near the burner, where there was stratification. The lack of agreement was largely caused by the instantaneous variations in the temperatures.

Trials were also made in the luminous-flame tests of the two-color pyrometer principle so nicely worked out by Hottel,(10) but, as he predicted in a private communication to the author, the momentary variations in the flame made accurate readings of the temperatures with the optical pyrometer impossible.

It is freely admitted that the temperature measurements were the weakest part of this work, as they generally are of similar investigations. As it was not indicated that any other method would give enough greater accuracy to warrant the difficulties of use, the exposed thermocouple was principally used.

Measurement of Radiation. Fig. 3 shows the arrangement of the apparatus used for the measurement of the radiation from the flame; this was similar to that described by Koessler.(11) It consisted of a Moll thermopile mounted on the end of a water-cooled tube which contained four diaphragms to limit the angle of vision. Around the thermopile was a water jacket through which the water flowed in series with the tube; in this way the cold ends of the thermopile junctions and the surface of the tube that the thermopile "saw" were at the same temperature, and the output was zero independent of changes in room or water temperature.

A water-cooled copper cone served as a limiting cold screen to insure that the radiation falling on the surface of the thermopile was from the flame only. The cone shape was adopted to insure more nearly black conditions by decreasing the possibility of reflection from the surface. This limiting screen was adjustable to obtain any thickness of flame up to the diameter of the furnace.

The entire assembly was mounted in a plate and refractory block and could be changed from one to another of the four ports provided in the furnace.

Another plate and block were provided so that the thermopile and tube could be placed in it to obtain the radiation from the wall and flame or wall alone when the flame was cut off.

The water-jacket assembly for the thermopile was hinged so that it could be swung back from the end of the tube. The tube containing the diaphragms could then be removed and a thermocouple run into the furnace for the measurement of gas temperature.

The output of the thermopile was read on a semi-precision potentiometer with external reflecting galvanometer; this could be read to 1 microvolt.

The thermopile was calibrated with water jacket and water-cooled diaphragm tube as a unit. This eliminated the necessity

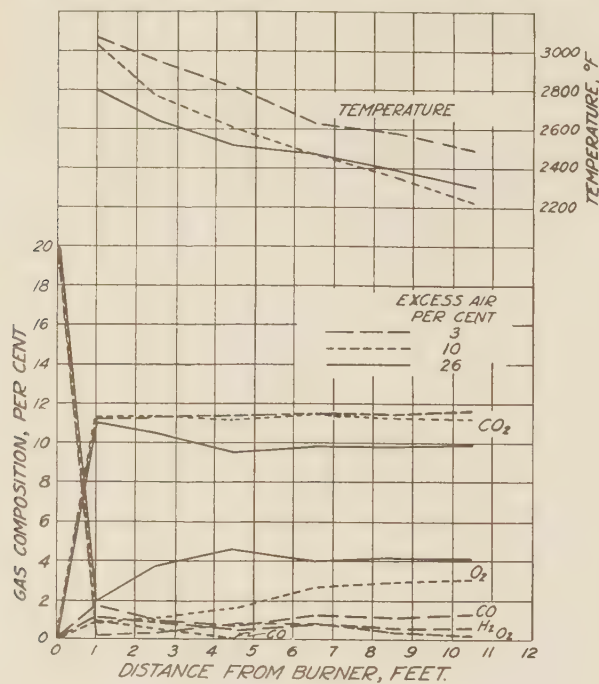


FIG. 4 TEMPERATURE AND COMPOSITION OF GASES, NON-LUMINOUS NATURAL-GAS FLAME

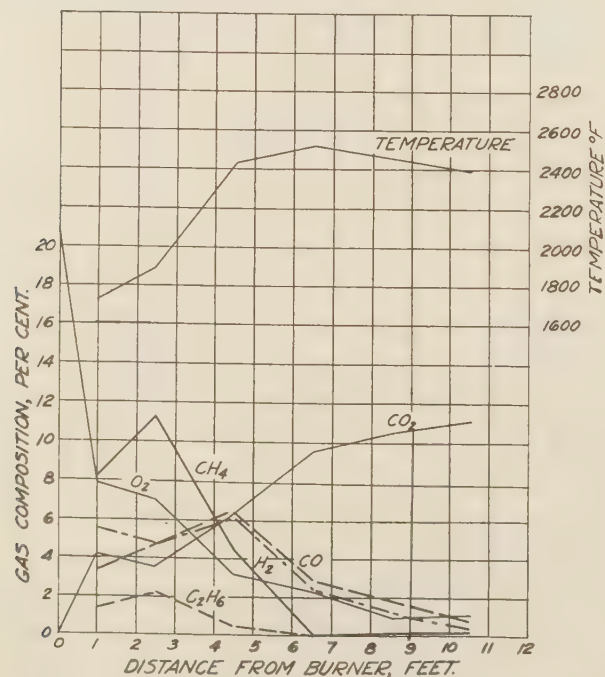


FIG. 5 TEMPERATURE AND COMPOSITION OF GASES, SEMI-LUMINOUS NATURAL-GAS FLAME

(Rate of heat input, 2,800,000 Btu per hr; nominal excess air, 0 per cent.)

of making any calculations for the correction for the angle of vision. A graphite cylinder heated in a gas furnace was used as a black-body source; a thermocouple on the inside back wall of the body measured its temperature. A straight-line calibration curve was obtained; the factor was 145 Btu per sq ft per hr per microvolt output.

The thermopile attained full output quickly, but had enough lag so that it ironed out small fluctuations in the flame radiation. Only with violent fluctuations in the flame temperature did the galvanometer swing so rapidly as to make accurate readings difficult.

DISCUSSION OF RESULTS

Process of Combustion. Fig. 4 shows the change in the temperature and composition of the furnace gas at varying distances from the burner when burning natural gas at a rate of approximately 2800 cu ft per hr with the non-luminous burner with different amounts of excess air. The percentages of excess air given in the figure are the nominal amounts. Because of the

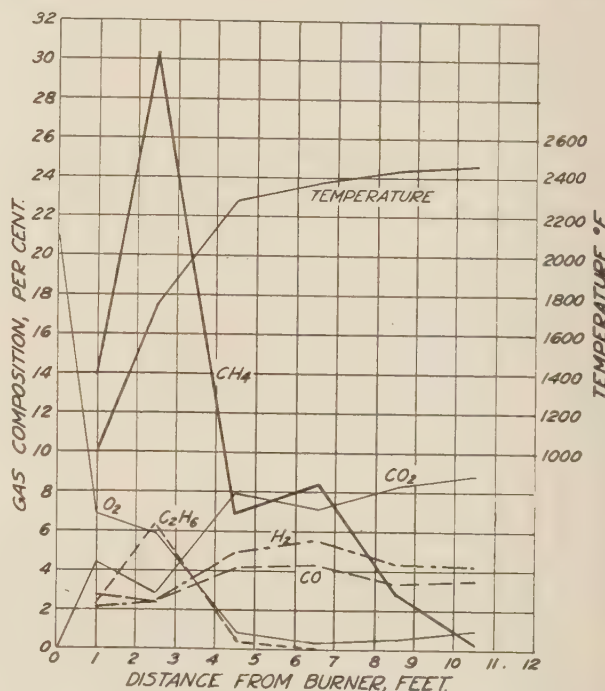


FIG. 6 TEMPERATURE AND COMPOSITION OF GASES, LUMINOUS NATURAL-GAS FLAME

(Rate of heat input, 2,840,000 Btu per hr; nominal excess air, 0 per cent.)

change in the composition of the gas, the actual excess air was somewhat different; for example, in the test marked 0 excess air, there was a deficiency of air, for CO and H₂ were present at the last point of sampling without enough O₂ to burn them.

The curves show the great rapidity of the combustion of the gas. At the first point of sampling, 1 ft from the burner, the CO₂ was at or above the maximum reached at the last position of sampling. That the CO₂ was higher at 1 and 2½ ft from the burner than later in the curve for 20 per cent excess air shows that even with this burner the mixture was not uniform.

With 10 per cent excess air some CO was found at 1 and 2½ ft from the burner, but it was completely burned at 4½ ft. With the nominal 0 per cent excess, both CO and H₂ were found at all positions of sampling.

The temperature curves also show the rapidity of combustion.

The temperatures were the highest, 2800 to 3070 F, at 1 ft from the burners, and then decreased regularly through the furnace.

Fig. 5 shows the temperature and composition of the gases in the furnace when burning natural gas in the burner shown in Fig. 2B with the short tunnel. Here the CO₂ content increased slowly, and CO, H₂, and CH₄ were found at all points of sampling; even ethane, C₂H₆, was found up to 4 1/2 ft from the burner. The content of H₂ was greatest at 4 1/2 ft, at which point the flame first became strongly luminous. The temperature of the gas was lowest near the burner, increased to a maximum at 6 1/2 ft, and then decreased. The maximum was 2500 F as compared with 3070 F for similar rate of heat input and excess air with the non-luminous burner.

The temperature and composition of the gases when using the long tunnel on this burner, as it is shown in Fig. 2C, were very similar to those just shown. Some combustion took place within the burner tunnel, so the CO₂ content and temperatures were somewhat higher in the first points of measurement, but the general trend was similar.

Fig. 6 shows the temperature and composition along the path of the gases when using the long pipe insert shown in Fig. 2C, with which mixing of the gas and air occurred only in the furnace. The CO₂ content increased slowly, large amounts of CH₄ and C₂H₆ were found in the early part of the flame, and about 4 per cent each of CO and H₂ remained at 10 1/2 ft from the burner. The temperature of the gases increased slowly and did not attain a maximum; heat was still being liberated faster than it was being lost from the flame.

Radiation From Flame. Table 2 shows the results of measurements of the radiation from the non-luminous gas flame which are typical of other results. At each position the radiation was measured at five flame depths. Q_F is the product of the thermopile calibration constant and the output E_F . The temperatures given in the table are averages of six measurements made at different points in the flame. Q_{BF} is the calculated radiation from a black body at the temperature of the flame to a body at absolute zero; the emission of the thermopile at room temperature is so small relative to that of the flame that the thermopile may be considered as at absolute zero. The term p_F is the ratio of the measured radiation to Q_{BF} .

TABLE 2 RESULTS OF RADIATION MEASUREMENT
(Non-Luminous Natural Gas Flame, Heat Input, 2,632,000 Btu/Hr
Excess Air, 0 Per Cent.)

Distance from burner, ft	L_F , depth of flame, in.	E_F , m.v.	Q_F , Btu per sq ft per hr	t_F , deg. F. avg.	Q_{BF} , Btu per sq ft per hr	p_F	K
0.5	10	0.056	8,120	2597	150,500	0.054	0.0055
	15	0.084	12,200			0.081	0.0058
	20	0.123	17,850			0.119	0.0065
	30	0.160	23,200			0.154	0.0055
	35	0.176	25,500			0.169	0.0053
3.5	10	0.064	9,280	2645	160,500	0.058	0.0060
	15	0.105	15,200			0.095	0.0067
	20	0.138	20,000			0.125	0.0067
	30	0.195	28,300			0.176	0.0065
	35	0.214	31,000			0.193	0.0053
7.5	10	0.078	11,300	2580	147,500	0.077	0.0081
	15	0.106	15,400			0.105	0.0074
	20	0.130	18,850			0.128	0.0069
	30	0.178	25,800			0.175	0.0062
	35	0.212	30,700			0.208	0.0067
11.5	10	0.060	8,700	2389	114,500	0.076	0.0078
	15	0.078	11,300			0.099	0.0071
	20	0.101	14,650			0.128	0.0069
	30	0.142	20,600			0.180	0.0071
	35	0.165	23,900			0.209	0.0067

The measurements at varying flame thickness were taken in the hope that data would be made available for the calculation of the radiation of a flame of any given thickness. The relation of the emission of a "gray" flame to the thickness is given by:

$$Q = Q_B(1 - e^{-KL}) \dots \dots \dots [1]$$

or:

$$\frac{Q}{Q_B} = p = 1 - e^{-KL} \dots \dots \dots [2]$$

where Q_B is the emission of a black body at the temperature of the flame, K is the absorption coefficient, L is the thickness, and p is the emissivity. However, as stated before, non-luminous flames are not "gray," but are strongly selective radiators. Therefore, the emission of a non-luminous flame even in infinite thickness will not have the emission of a black body at the same temperature.

The relation of the emission of a non-luminous flame to thickness is given by

$$Q = Q_M(1 - e^{-KL}) \dots \dots \dots [3]$$

where Q_M is the emission of the flame at infinite thickness. For any given temperature and concentration of CO₂ and H₂O, Q_M will have a definite relation to Q_B . Hence [3] may be written

$$Q = CQ_B(1 - e^{-KL}) \dots \dots \dots [4]$$

where $C = Q_M/Q_B$.

Having given the measured radiation at two thicknesses, we have two equations with two unknowns, K and C , but as there may be a zero correction in the distance L , it is better to consider three measurements at three thicknesses. From [3] it develops that

$$\frac{L_2 - L_1}{L_3 - L_2} = \frac{\log \frac{Q_M - Q_1}{Q_M - Q_3}}{\log \frac{Q_M - Q_2}{Q_M - Q_3}} \dots \dots \dots [5]$$

If L_1 , L_2 , and L_3 are so chosen that the ratio on the left-hand side of [5] is 1, then

$$Q_M = \frac{Q_3Q_1 - Q_2^2}{Q_1 + Q_3 - 2Q_2} \dots \dots \dots [6]$$

Equation [6] has been applied to a number of the measurements on the non-luminous flames, but the agreement was poor and some absurd results were obtained. Possible reasons for this are (1) lack of uniformity of temperature of the gas, (2) lack of uniformity of composition, or (3) inaccuracy of measurements.

The foregoing argument is based on the general assumption that non-luminous flames are truly selective radiators which have no emission except in narrow bands. If this were not true and other gases radiated over the entire spectrum or there were small amounts of carbon in the flame, even so little that it could not be visually detected, then an infinite thickness of the flame would radiate as a black body and K could be calculated from [1]. The last column of Table 2 gives the values of K so calculated for this set of readings. Although the constancy of K is by no means all that could be desired, it may be significant that the constancy is as good as it is.

With flames that should be truly "gray" and where, therefore, K can be validly computed by [1], as pulverized-coal and lumi-

TABLE 3 COMPARISON OF ABSORPTION COEFFICIENTS K , FOR VARIOUS FLAMES

(Heat Input, 2,600,000 to 3,000,000 Btu per Hr. Excess Air, 0 Per Cent Depth of Flame, 35 In.)

Distance from burner, ft	Pulverized Hocking coal		Non-luminous natural gas		Semi-luminous natural gas		Luminous natural gas	
	p_F	K	p_F	K	p_F	K	p_F	K
0.5	0.63	0.0249	0.17	0.0053	0.19	0.0060	0.72	0.0366
3.5	0.47	0.0159	0.19	0.0053	0.21	0.0067	0.44	0.0222
7.5	0.42	0.0136	0.21	0.0067	0.31	0.0106	0.69	0.0344
11.5	0.43	0.0141	0.21	0.0067	0.26	0.0085	0.68	0.0325

nous gas flames, the agreement of the calculated values of K for various flame thicknesses was not so good as for the non-luminous flames. This is explained by the known greater variation in the temperature and composition of the gas and in the concentration of solids across the flame.

Table 3 shows comparative values of pf and K for pulverized-fuel, non-luminous, semi-luminous, and luminous natural-gas flames. The greater the emissivity, the greater is the value of K . As K is the slope of the curve when the logarithm of the transmissivity, $1 - pf$, is plotted against depth of flame, the greater is K , the more rapidly does the emission of the flame increase with increase in the depth of the flame.

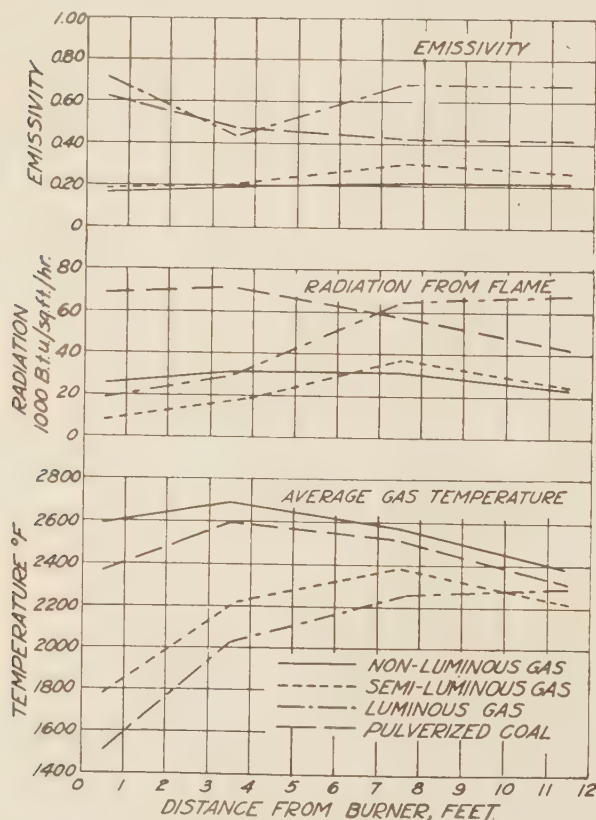


Fig. 7 TEMPERATURE, RADIATION, AND EMISSIVITY OF GAS AND COAL FLAMES

(Rate of heat input, 2,600,000 to 3,000,000 Btu per hr; nominal excess air, 0 per cent.)

Comparison of Calculated and Measured Radiation. Although it is apparently impossible to obtain data from these measured values of the radiation from non-luminous flames to permit the calculation of the radiation of any thickness of flame, the fact that the radiation from these flames is presumably due only to the CO_2 and H_2O in the flame permits comparison of the measured and calculated values according to the published data of Schack and Schmidt. Table 4 shows the comparative values for 15 measurements. The first position of measurement, 6 in. from the burner, was not included because of the uncertainty of the composition of the gas and the exact thickness of the flame.

By chance, two of the measured values agreed exactly with those calculated, and only one measured value was less than the calculated. The other 11 measured values were higher than those calculated by 2 to 21 per cent; the findings of other investigators have been similar. If Schack's values for the radiation of

TABLE 4 COMPARISON OF CALCULATED AND MEASURED RADIATION FROM NON-LUMINOUS NATURAL-GAS FLAMES

Test	Heat input, million Btu per hr	Excess air, per cent	Distance from burner, ft	Radiation, 1000 Btu per sq ft per hr			Per cent
				Calc.	Meas.	Diff.	
1	2.71	20	3.5	23.9	23.9	0.0	0.0
			7.5	22.5	23.8	+1.3	+5.8
			11.5	20.05	21.0	+0.95	+4.7
2	2.67	14	3.5	22.5	24.7	+2.2	+9.8
			7.5	21.0	24.1	+3.1	+14.7
			11.5	19.0	19.4	+0.4	+2.1
3	2.63	4.5	3.5	22.6	23.9	+1.3	+5.8
			7.5	25.4	30.7	+5.3	+20.9
			11.5	27.7	31.0	+3.3	+11.9
4	2.77	10	3.5	30.2	30.7	+0.5	+1.8
			7.5	28.3	29.0	+0.7	+2.5
			11.5	23.1	22.3	-0.8	-3.7
5	2.17	12	3.5	22.0	25.4	+3.4	+15.5
			7.5	19.9	23.2	+3.3	+16.6
			11.5	17.8	17.8	0.0	0.0

H_2O had been used, the discrepancies would have been greater; this shows that Schack's values for CO_2 radiation need careful experimental checking, and it is understood that this is being done.

The maximum deviation of the measured from the calculated radiation was 21 per cent and the average was 7 per cent. For this type of measurement this is considered excellent agreement and indicates that for non-luminous flames the radiation may be calculated with a probable error of not more than 10 or 15 per cent.

Comparison of Radiation From Various Flames. Fig. 7 shows graphically the temperature, radiation, and emissivity at varying distances from the burner with non-luminous, semi-luminous, and luminous natural-gas flames and pulverized Hocking coal at similar rates of heat input and excess air. The temperatures shown are the average of a number of readings across the flame, and are therefore lower than those taken on the axis of the furnace, as shown in the preceding figures.

The highest temperatures occurred with the non-luminous gas flame; the temperature curve of the pulverized-coal flame was lower, but similar in shape to that of the non-luminous gas flame. The temperature of the semi-luminous flame reached a maximum at 7.5 ft from the burner, and then decreased below that of the fully luminous flame, which increased at each point of measurement.

The highest radiation from the flame was found when burning pulverized coal; it was practically the same at the first two points of measurement, and then decreased as the solid carbon was burned from the flame.

The radiation from the non-luminous gas flame was practically constant over the length of the furnace. The decrease in the temperature was compensated by the increase in the actual thickness of the flame. The radiation from the flame called semi-luminous was greater than that from the non-luminous flame at only one point, although the flame was so luminous that one could not see the opposite wall, whereas the non-luminous flame was perfectly transparent.

The radiation from the luminous flame increased along the length of the furnace until at 11.5 ft from the burner it was practically as great as that from the pulverized-coal flame near the burner.

The emissivity (the ratio of the radiation from the flame to that of a black body at the same temperature) of the non-luminous flame was the lowest of those of the four flames; it was practically uniform at 0.17 to 0.21. The emissivity of the semi-luminous flame was not much higher, but that of the luminous flame was higher even than that of the pulverized-coal flame, except at the second position; this low value may have been a chance occurrence in this test. The emissivity attained, 0.70, shows that with a not much greater depth this flame would radiate practically as a black body.

PRACTICAL CONCLUSIONS

BURNER DESIGN

The purpose of this investigation was not to study burners, but the principles of combustion and radiation; therefore the study of the luminous-flame burner was not carried to any degree to develop a better burner. From the data presented on the progress of combustion, it is quite obvious that from this viewpoint either the semi-luminous or fully luminous burner was much inferior to the non-luminous burner. The ultimate capacity of the non-luminous burner with complete combustion of the gases had apparently not been approached, if at least 10 per cent excess air were supplied. With the luminous-flame burner the heat input would have had to have been decreased considerably to have attained complete combustion in the furnace.

On the assumption that the rate of combustion depends on the rate of diffusion between air and gas layers, Burke and Schumann(12) developed a theory for the prediction of flame length, and report excellent agreement with measured values.

It is apparent, therefore, that the non-luminous burner could have been much improved in regard to completeness of combustion with the proper changes in thickness of air and gas layer and with regard to the possibility of mixing. It is possible, although not probable, that this could be accomplished without decrease in the emissivity of the flame. The low temperature in the early part of the flame probably could be increased, and it and the radiation made more nearly uniform throughout the length of the furnace. Few data on the actual performance of commercial luminous-flame burners have been published; it would be desirable to have such data.

NET RATE OF HEAT TRANSFER

The data presented have shown that the radiation and emissivity of the fully luminous flame were much higher than those of the semi-luminous and non-luminous flames. If, however, the test furnace had been an industrial furnace which heated plates or bars of steel, or had been a glass furnace, the steel or glass would not have been shielded from the opposite wall by a water-cooled plate as was the thermopile with which these measurements were made. In addition to receiving heat from the gases, the work would have received heat from the refractory walls as well, which are heated nearly to the temperature of the gases and which have a high emissivity.

The heat which passes through the gases from the roof or walls to the work depends on the transmissivity of the gases to radiant heat; the transmissivity is equal to 1 minus the absorptivity, which is equal to the emissivity. Therefore the total net heat received by radiation by the work whose temperature is T_W and emissivity 1 from the flame whose temperature is T_F and emissivity is p_F and a parallel roof whose temperature is T_R and emissivity 1 may be calculated as follows, assuming for simplicity both the work and the roof as infinite parallel planes:

$$Q = \sigma p_F (T_F^4 - T_W^4) + \sigma (T_R^4 - T_W^4) (1 - p_F)$$

where σ is the constant of radiation. The first term represents the transfer from the flame to the work and the second the transfer from the roof to the work.

From this equation it can be seen that, although the rate of heat transfer from the flame to the work increases as the emissivity of the flame increases, the rate of heat transfer from the wall to the work decreases. Therefore, the total net rate of transfer from the flame and wall will not be greatly increased with an increase in emissivity of the flame, even if the temperature of the flame does not change. Table 5 gives some numerical calculations that may make this point clearer. Flame emissivities of 0.2 to 0.8 with a constant flame temperature of 3000 F

have been assumed. The temperature of the surface of the work has been assumed as 2000 F, and the temperature of the roof has been assumed to increase from 2600 to 2900 F as the emissivity of the flame is increased; the exact temperature increase assumed may not be valid, but the order of increase is correct.

TABLE 5 CALCULATED NET TRANSFER OF HEAT BY RADIATION WITH INCREASE IN EMISSIVITY OF FLAME

p_F	$T_F, ^\circ F$	$T_W, ^\circ F$	$T_R, ^\circ F$	$\frac{\sigma p_F}{(T_F^4 - T_W^4)}$	$\frac{\sigma(1 - p_F)}{(T_R^4 - T_W^4)}$	Q
0.2	3000	2000	2600	36,600	70,400	107,000
0.4	3000	2000	2700	73,200	65,400	138,600
0.6	3000	2000	2800	109,800	52,600	162,400
0.8	3000	2000	2900	146,400	31,300	177,700

The values show that as the emissivity is doubled, the net transfer is increased by only about 30 per cent, and when the emissivity is made four times as great, the radiation is increased by only about 70 per cent.

The calculations assume that the temperature of the flame remains constant as the emissivity is increased, but it has been shown that, other things being equal, the temperature will normally decrease; therefore the increase in the rate of heat transfer by radiation will be lower than that calculated.

Measurements were made of the radiation from the flame, flame and wall, and the wall only at 7.5 ft from the burner on similar tests, with luminous and non-luminous flames. The radiation from the flame was measured as usual; then the water-cooled background was removed and the radiation of the wall and flame was measured. The gas and air were then shut off, and readings of the radiation and temperature of the wall were taken at intervals of 1 min to extrapolate back to time of shut-off, as the temperature of the wall decreased rapidly at first. Table 6 presents the results.

TABLE 6 MEASURED AND CALCULATED RADIATION FROM WALL AND FLAME

	Non-luminous	Luminous
Measured radiation, Btu per sq ft per hr:		
Flame.....	27,700	64,600
Wall.....	103,800	88,450
Flame and wall.....	120,500	104,000
Emissivity of flame.....	0.19	0.69
Calculated radiation:		
Flame and wall = $27,700 + 103,800 (1 - 0.19) = 106,300$		
$64,600 + 88,450 (1 - 0.69) = 92,020$		
Difference of calculated and measured =		
$\frac{(120,500 - 106,300) 100}{120,500} = 12 \text{ per cent}$		
$\frac{(104,000 - 92,000) 100}{104,000} = 11 \text{ per cent}$		

At this position in this furnace, therefore, work on the hearth would have received heat by radiation at a greater rate when burning the gas with a non-luminous than with a luminous flame.

The transfer of heat by convection has been neglected in this consideration, but it is obvious that, because of the higher temperature of the gas, the higher velocity, and the possibility of impingement of a non-luminous flame directly on the work, or both, whereas the non-luminous flame must flow with less turbulence, the rate of heat transfer by convection should be higher with non-luminous than with luminous flame.

The problem of radiant-heat transfer in actual furnaces is somewhat more complex than the illustration, because the factors of the relative areas of the work and the walls, their angular relation, and their emissivities enter. However, it can safely be stated that in furnaces where the roof and walls are at a higher temperature than the work to be heated, the possibility of increasing the rate of heat transfer by increasing the luminosity of the flame is limited.

This important factor, the effect of the emissivity of the flame on the radiation from an opposite wall, is one apparently generally overlooked. It has, however, been very well covered by

Schack.(13) He believes that in furnaces, such as open-hearth steel furnaces, where the roof temperature is kept only about 50 F above the slag temperature, an increase in the emissivity of the flame may increase the rate of heat transfer by radiation. In furnaces, such as boiler furnaces, with water-cooled walls where no high-temperature solid radiating surfaces are found, the overall transfer of heat by radiation can be increased directly as the emissivity of the flame is increased.

EFFECT OF DISTANCE ON RADIATION EXCHANGE

The observation has been made that engineers frequently misapply the "inverse square of the distance" law which they loosely quote as saying that the radiation received per unit area of a surface varies inversely as the square of the distance from the source. They then conclude that this means that, if the flame can be placed near the work, the rate of heat transfer by radiation will be much greater than if it is farther away or is being received from the roof.

This law applies strictly, however, only to radiation from a point source. The actual effect of the distance between planes has been presented by Hottel.(14) He expresses the heat exchange as

$$Q = A \cdot F_A \cdot F_E \cdot \sigma(T_1^4 - T_2^4)$$

where A is the area, F_A is the angle factor including the effect of distance, and F_E is the emissivity factor. He presents a curve in which F_A for squares or disks connected by non-conducting but re-radiating walls is plotted against the ratio of the side or diameter to the distance between the planes. For values of the ratio above 1, the change in F_A is not rapid—not nearly so rapid as the inverse square law would show. For example, the following points have been taken from his curve:

Ratio.....	4	2	1
F_A	0.78	0.63	0.50
Ratio to 0.78.....	1	0.81	0.64
Ratio by inverse square law....	1	0.25	0.06

The wide departure of the true relation from the inverse square law is obvious.

ADVANTAGES OF LUMINOUS FLAMES

If luminous flames do not transfer heat at a greater rate than non-luminous flames, wherein do their advantages lie, or are they merely imaginary? The term "soaking heat" is a common one among practical furnace men, and there is some evidence of their belief that the heat of a luminous flame is more penetrating than that of a non-luminous flame.

The difference may probably best be explained by a practical example. A continuous furnace for heating steel for forging in which the steel moved countercurrent to the gas was operated with a non-luminous gas flame and with a highly luminous oil flame. With the oil flame the steel was withdrawn at just the right temperature for forging and was heated entirely through to a practically uniform temperature. With the non-luminous gas flame, although the steel was almost dripping when withdrawn, it did not forge well because only the surface was heated.

The difficulty here was not a difference in the overall transfer of the two flames, but the difference in the distribution of the transfer over the length of the furnace. At any point in the oil flame the rate of transfer was not so great as the maximum from the gas flame, but it was more uniform over the entire length of the flame. The heat was not transferred at a greater rate than it could penetrate the steel; therefore, as commonly expressed, it "soaked in"—that is, the temperature increased substantially uniformly through the piece. In the gas flame the rate of heat transfer was low until the zone of combustion was reached; here the sum of the rates of heat transfer by radiation from the flame

and walls and of the convection from the high-temperature gases was greater than the possible rate of heat penetration into the steel, and the outer surface was raised to the melting point while the inside was yet at too low a temperature for forging.

The proper heating of the steel might have been obtained with a non-luminous flame, if the heat input had been distributed among a number of burners along the furnace to maintain a uniform and not too high a rate of heat transfer.

CHEMICAL EFFECTS OF LUMINOSITY

As this paper is principally concerned with radiant-heat transfer, the problem of the chemical effect of the flames will only be briefly mentioned. This is of particular importance in the heating of steel which will oxidize and scale not only in atmospheres containing oxygen, but also in those containing no oxygen but CO_2 and H_2O . It is therefore necessary to maintain a reducing

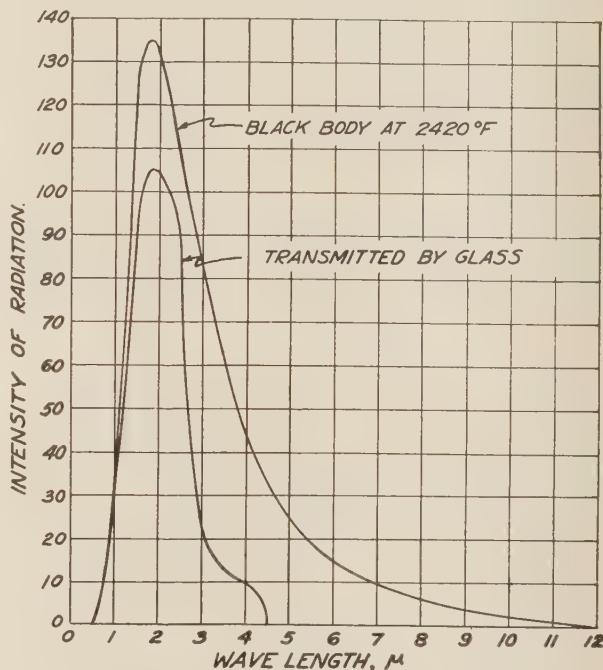


FIG. 8 COMPARISON OF RADIATION OF BLACK BODY AND TRANSMISSION OF GLASS, 2.11 MM THICK, AT 2420 F

atmosphere, a certain percentage of CO , to avoid the scaling of steel when burning gas with a non-luminous flame. This will usually result in an appreciable loss of heat in unburned gases.

In a luminous flame CO , H_2 , and perhaps methane will be present, but free oxygen also remains. However, there is free carbon present, and as this will deposit on the work, it probably reduces the oxidation of the steel. In some luminous-flame burners a raw-gas blanket is introduced over the work being heated. This will result in an increased consumption of gas, but this may be more than offset by the better quality of the product.

HEAT TRANSFER IN GLASS TANKS

In the melting and refining of glass it is highly desirable that the glass be heated as uniformly as possible from top to bottom of the tank. Convection from the gases can heat the top of the glass only, and this heat can be transferred to the bottom only by conduction and by convection currents set up in the glass. The conductivity of glass is comparatively low, and until the

glass is at high temperature, convection will be low because of its high viscosity; therefore, the rate of heating of the bottom may be low.

As glass is transparent to visible radiation, it is frequently assumed that it is transparent to the invisible thermal radiation also. Data are lacking on the transmission of glasses at high temperatures, but the transmission of a number of glasses at room temperature has been measured; these measurements show that even in thin layers practically all glasses are opaque to wave lengths beyond 3 to 4 μ .

Fig. 8 shows in the upper curve the intensity of black radiation at different wave lengths at 2420 F, and the lower curve shows the intensity of radiation transmitted by a piece of window glass 2.11 mm in thickness, assuming that the transmission of the glass at 2420 F is the same as at room temperatures at which the transmission was measured by Coblenz.⁽¹⁵⁾ The area under the curves is the total radiation over the entire band. Measurements of these areas by a planimeter show that the glass would transmit about 48 per cent of the energy entering it. As molten glass may not have the same transmission as cold glass and as the depth of glass baths is much greater than that of the example, the actual transmission would probably be much different from this value.

The relation of the absorption of radiant heat to the thickness is, as for gases, expressed by

$$Q = Q_0(1 - e^{-KL})$$

where Q is the amount absorbed and Q_0 the amount entering the thickness L . A consideration of this expression brings out an interesting fact. If the absorption coefficient K were 0 (that is, if the glass were perfectly transparent), then $Q = 0$, and with any depth of glass no radiant heat would be absorbed. All the radiant heat would pass to the bottom of the tank and would be transferred to the glass by conduction. On the other hand, if $K = \infty$, the glass is perfectly opaque; then any thickness would absorb all the heat, and none would reach the bottom of the bath. It is clear, therefore, that for a maximum absorption of radiant heat in a layer at same depth in a bath, there is a definite intermediate value for the absorption coefficient.

A complete understanding of the problem of heat transfer to molten glass cannot be had until data are obtained on its absorption of radiant heat. It is considered possible that the advantages reported in the current literature for the use of luminous flames lie not in an increased rate of heat transfer, but in a more uniform rate of heat transfer over the area of the bath. This would avoid the formation of localized areas of high-temperature and thinly fluid glass and other localized areas of low-temperature and viscous glass.

SUMMARY

From the data and analytical considerations presented, the following conclusions in regard to the transfer of heat from luminous and non-luminous gas flames can be made:

1 Luminous gas flames are now being obtained principally with slow-moving, stratified streams of air and gas, which, from the viewpoint only of efficient combustion, are much inferior to non-luminous flames.

2 Combustion is extremely rapid in premixed, non-luminous flames which results in a high-temperature zone near the burners, whereas combustion is spread out over a larger area in luminous flames which results in a lower maximum temperature. With proper burner design a more uniform temperature over the length of the furnace could probably be obtained with a luminous flame.

3 Although natural-gas flames can be produced that have an emissivity approaching that of a black body and consequently a

higher rate of heat transfer than a non-luminous flame, the total radiant-heat transfer from the flame and the wall, in those furnaces having walls hotter than the work being heated, will not be much greater for the same flame temperature than with a non-luminous flame. As the temperature and convection transfer are generally lower, the total rate of heat transfer will normally be lower with a luminous than with a non-luminous flame.

4 The advantage of a luminous flame in many heating processes lies not in a higher rate of heat transfer, but in a more uniform transfer over the entire furnace as a result of the slow combustion and slow heat liberation.

5 The presence of free carbon probably has a beneficial effect in the reduction of oxidation and the scaling of steel.

6 A complete analysis of the transfer of heat to molten glass is not possible because of lack of data on its absorption of radiant heat, but the conclusion is reached that any advantage of a luminous flame in glass melting lies in a more uniform distribution of heat transfer rather than an increased rate of transfer.

REFERENCES

- 1 Schack, A., *Zeit. für Tech. Physik*, vol. 5 (1924), p. 266.
- 2 Hottel, H. C., *Ind. & Eng. Chem.*, vol. 19 (1927), p. 888.
- 3 Fishenden, M., and Saunders, O. A., "The Calculation of Heat Transmission," H. M. Stationery Office, 1931.
- 4 Schmidt, E., *Forschungsarbeiten auf dem Gebiete des Ingenieurwesens*, vol. 3 (1932), p. 57.
- 5 King, W. J., *Mechanical Engineering*, vol. 54 (1932), p. 495.
- 6 Wohlenberg, W. J., and Morrow, D. G., *Trans. A.S.M.E.*, vol. 47 (1925), p. 127. Wohlenberg, W. J., and Lindseth, E. L., *Trans. A.S.M.E.*, vol. 48 (1926), p. 849. Wohlenberg, W. J., and Anthony, R. L., *Trans. A.S.M.E.*, vol. 51 (1929), no. FSP-51-36.
- 7 Haslam, R. T., and Hottel, H. C., *Trans. A.S.M.E.*, vol. 50 (1928), paper no. FSP-50-3.
- 8 Trinks, W., *Heat Treating & Forging*, vol. 18 (1932), p. 319.
- 9 Sherman, R. A., *Proceedings of the Third International Conference on Bituminous Coal* (1931), vol. 2, pp. 510-551.
- 10 Hottel, H. C., and Broughton, F. P., *Anal. Ed., Ind. and Eng. Chem.*, vol. 4 (1932), p. 166.
- 11 Koessler, P., *Archiv für Warmewirtschaft*, vol. 11 (1930), p. 229.
- 12 Burke, S. P., and Schumann, T. E. W., *Ind. & Eng. Chem.*, vol. 20 (1928), p. 998.
- 13 Schack, A., *Der Industrielle Wärmeübergang*, Verlag Stahleisen (1929), p. 303.
- 14 Hottel, H. C., *Mechanical Engineering*, vol. 52 (1930), pp. 699-704.
- 15 Coblenz, W. W., Emerson, W. B., and Long, M. B., *Bulletin of the Bureau of Standards*, vol. 14 (1918-19), p. 670.

Discussion

H. V. FLAGG.³ The paper shows evidence of careful planning, deep study, and patient experimental work. The contribution should be very helpful and valuable, and it is hoped that it may be followed up by further experimentation. The writer's observations and plant work do not lead to complete agreement with the conclusions reached in the paper, but it is believed that the differences can be accounted for by what are believed to be errors in the basic assumptions.

The writer would like to consider the subject as a comparison of the relative merits of luminous and non-luminous flames for metallurgical heating rather than as a discussion of the two types of flame from natural gas alone. Luminous flame can be developed from any of the commercial fuels in common use, so that the differences become merely those of degree, either in heat-transfer rates or in flue-gas compositions which affect the chemistry in the furnace. The assumption throughout the work that the net transfer of heat in a furnace is the sum of the heat transfer from the flame and that from the furnace wall, or at least the method of arriving at the same, is open to question. This is

³ Combustion Engineer, The American Rolling Mill Co., Middletown, Ohio.

certainly not right in the case of a sharp-working open-hearth furnace where, as is often the case, the furnace is so organized that the roof temperature is actually lower than the bath temperature. In such a furnace the heat transfer from the flame certainly plays the predominant part. The convection transfer is undoubtedly important, but cannot be the predominant influence, as is evidenced by repeated failure of tests to run an open-hearth furnace with a premixed natural-gas flame, which is practically non-luminous, and with a heat transfer that is predominantly convective. In a metallurgical heating furnace, it is necessary to secure the maximum heat transfer with the least possible difference between the temperature of the flame and the temperature desired in the work in order to obtain uniform heating.

This result can be obtained with non-luminous flame by making the heating time sufficiently long, but in many cases this requires a furnace size and space that is prohibitive. The use of a luminous flame in such furnaces makes it possible either to obtain better heating for given production or greater production for the same standard of heating, because of a higher heat transfer from the flame and the decidedly lessened influence of the transfer from the walls. The development of the luminous-flame burner has resulted from the need to secure from natural gas a flame with this resultant higher heat transfer which is so easily secured from producer gas or fuel oil. The old-time heater who burned natural gas prior to the time of the development of the premix burner knew how to get the luminous flame, but his control of furnace atmosphere and of fuel economy left much to be desired, since one vital element, that of combustion-air supply, was never completely under his control. The new luminous-flame burner is designed to produce the luminous flame from natural gas with all three essential factors—fuel input, air supply, and furnace pressure—under exact control. Evidently, the heat transfer in a furnace under luminous-flame conditions is very largely from the flame, the wall transfer being of minor importance. In this type of combustion, the most important function of the wall is to screen off heat losses so that flame temperature can be maintained. The old sheet heater maintains a heavy flame in his furnace, not only to establish the maximum possible heat transfer from the flame, but also to hold the wall temperature down so as to prevent radiation from the wall surfaces which might cause local overheating.

The author's reservation as to the use of the "inverse square of the distance" law is open to question. It is commonly accepted that the heat transfer to an open-hearth bath is predominantly radiation from the flame. Furthermore, it is axiomatic that the flame must "wipe the bath." A non-luminous flame will melt down a charge very rapidly, but as soon as the bath is under cover "it goes dead," which indicates that convection transfer is not the controlling factor. When a luminous flame "wipes the bath," the distance between the source of radiation and the work approaches zero, so that the distance factor is practically eliminated. It is probable that this law has much more importance in the range of very small distance than it has in the range considered in this paper, so that the importance of the effect of distance on radiation may be much greater than the author believes. The example of the forging furnace using non-luminous flame and the one using the luminous flame for the same work and the comparison of results obtained is a familiar one, but the author's solution is not borne out in practise. The writer has in mind two continuous annealing furnaces similar in size and construction. One of these is fired with a large number of natural-gas premix burners over its entire length and the other with fuel oil over its entire length. The output from the luminous-flame furnace is distinctly larger than that from the non-luminous furnace. One could cite other instances equally as convincing

which indicate that the solution offered of merely adding more burners would not have remedied the situation.

The question of efficiency of combustion is referred to in connection with improvements in burner design. In metallurgical heating, the aim is to secure maximum production and greatest yield at least overall cost. Fuel practise under these conditions may appear wasteful from the standpoint of efficiency of fuel utilization, but the waste may be justified from the results secured. In most steel-mill heating operations, luminous-flame combustion helps to meet these conditions, so that any experimental work which has as its aim the improvement of flame heat transfer is bound to have value.

F. B. JONES.⁴ The writer agrees that this subject in the past has been shrouded with some mystery and that many conflicting statements have appeared in the technical press as well as in discussions on this subject. There seems to be a great need for determining fundamental data regarding the subject of combustion.

The author states that the purpose of this investigation was to study the principles of combustion and radiation. It is regretted that he found it necessary to limit the investigation to this phase of the subject, as a much more valuable contribution could have been made had he been able to study not only different types of flames as produced by different types of burners, but also the effect of the furnace chamber on the various types of flames.

It seems that the two phases of this subject are very closely interrelated, and it would be most difficult to arrive at conclusions on the luminous and diffusion types of combustion if the data were limited only to one type of flame and one type of furnace chamber. With this thought in mind, the writer would seriously question whether sufficient data were available from this investigation to justify the author's conclusions 3 and 4.

The author uses the terms "luminous" and "diffusion" flames interchangeably. To the writer's mind there is a distinct difference. He can find no evidence in the author's data to show whether the flame that he produced with his burner and furnace was a luminous or a true diffusion flame. Taking into consideration the design of the burner that the author terms a "luminous" burner, and also the fact that the experimental furnace was a cylinder 3½ ft in diameter and about 14 ft long, the writer does not believe it is possible to produce a true diffusion flame with such a burner and with such a furnace chamber. Therefore, the flame the author used was a luminous flame of the delayed combustion and incomplete mixing type.

If we are to assume that true diffusion combustion is obtainable only when we have parallel streams of gas flowing in a suitable furnace chamber that permits parallel or streamline flow without turbulence, it would seem to be most difficult to produce a true diffusion flame with the furnace set-up used in this investigation.

A cylindrical type of furnace of a rather restricted diameter and length as used in this investigation, having a gas capacity of 2800 cu ft per hr, would tend to break up and distort parallel lines of flow if they were once set up by a suitable burner. In fact, the combustion of the gases that the author shows with his luminous flame indicates incomplete and delayed combustion even at the point of discharge of the furnace gases.

Fig. 6 shows that, even at a point 10 ft from the burner, about 4 per cent of CO and hydrogen existed in flame products; also, that the percentage of CO₂ was about 9 per cent, which is below that secured with his non-luminous natural-gas flame of 11.5 per cent at the same point in the furnace. The oxygen content at the same point in the furnace was about 1 per cent.

A rectangular type of furnace, much longer, would be more

⁴ Equitable Gas Company, Pittsburgh, Pa.

adaptable for studying various types of flames, because there would be less tendency to set up turbulence in the flame, and there would be ample length for the full development of the flame length. Of course, the cylindrical type of furnace would be satisfactory for studying a non-luminous flame.

It seems that this whole question of energy radiation from the combustion in various types of flames is still one on which much experimental and fundamental data are lacking. We are told by physicists that heat radiation is a phenomena involving energy waves in the ether, very similar to sound waves in the air. We are also told by men who have made studies of various wave lengths in the air that we have a wide variety of wave lengths possible in the ether. At one extreme we have very short cosmic rays, gradually getting longer through the X-rays, ultra-violet, visible rays, solar, heat, short radio, and finally the regular radio rays. It seems that we need data as to when and how the radiation waves from a flame are produced. Is the radiation produced at the moment of chemical union of the various contents of the gases such as carbon and hydrogen with oxygen, or are they produced continuously after combustion has taken place and after the resulting flue gases consisting of carbon monoxide and carbon dioxide and water vapor have been heated to a very high temperature? Possibly the total radiation is a combined effect of radiation sent out from the molecules of gas, both during the process of combustion and after they have been chemically united.

The writer's conception of the true diffusion flame is a flame in which microscopic or even ultra-microscopic particles of carbon are produced from the carbonaceous gases in the fuel and hang in suspension in the flame and set up energy radiations from the carbon particles as a result of the carbon particles being heated to a high temperature by the release of heat energy as a part of the fuel has been united with oxygen. He is of the opinion that the total radiation from the true diffusion flame is a result of the heat waves produced from the incandescent carbon particles, plus the heat waves sent out at the moment the chemical union of oxygen with either carbon or hydrogen is effected, plus the heat waves sent out from the resulting flue products which are still at a high temperature. If we could determine, for example, the total amount of energy that might be radiated from any flame from the instantaneous production of heat radiation due to the chemical union of oxygen and fuel—if it is true that such union produces heat radiation—and then determine the amount of energy that will be radiated from the resulting hot flue gases at various temperatures, then we would be in a position to predict the value of a true diffusion flame as a means of increasing the heat radiated to the work in the furnace.

If we had such data we would also be able to evaluate the efficiency or effectiveness of various diffusion burners in terms of the amount of energy they would release in radiant form from the incandescent carbon particles that they produce in the flame. Until we have such data we will continue to remain, so far as this question of applying luminous and diffusion combustion to industrial heating operations is concerned, in a process of engineering guessing as to the value of one type of flame or burner over another.

F. M. WASHBURN.⁵ A large number of those who have not made a study of heat transmission as a rule have in their minds several misconceptions; chief among these are the thought that no heat transfer by radiation takes place from a non-luminous flame, the thought that the heat transfer by radiation from a flame is directly proportional to the luminosity or brightness of the flame, and the thought that the "inverse square of the dis-

tance" law applies to radiant-heat transfer in a furnace. The author shows clearly that all of these conceptions are indeed more or less erroneous.

Schack, of course, developed some time ago the formulas for radiation from the CO₂ and H₂O vapor present in a non-luminous flame, but the magnitude of the quantities of heat transferred by such radiation is not generally realized by operators of industrial furnaces. The excellent agreement between the experimental data obtained by the author and the results calculated by means of the published formulas should serve to bring home the importance of the consideration of radiation from a non-luminous flame. It is only natural, since a strictly non-luminous flame is invisible, to consider that no great amount of radiation is taking place from it, but when it is remembered that by far the greater part of the radiation which transmits heat from a flame is outside of the visible spectrum and that at the highest temperatures met with in industrial furnaces the visible radiation is only a fraction of the total radiation, it is seen that it is possible for a flame to be practically invisible—that is, devoid of luminosity—and still radiate a considerable amount of heat. In a non-luminous flame the radiation comes principally from CO₂ and H₂O, which substances emit radiation in bands entirely outside of the visible spectrum, or in other words, such radiation is invisible.

Table 5 and the statement by the author that as the emissivity of a flame is doubled the net heat transfer is increased by only 30 per cent shows that the thought that the heat transfer by radiation is directly proportional to the luminosity of the flame is incorrect. However, from a standpoint of practical operation, an increase in the luminosity of a flame does mean an increase in heat transfer by radiation, and although the increase in heat transfer may not be directly proportional, nevertheless a considerable gain in heat transfer may be made by this means.

The application of the "inverse square of the distance" law for radiation, which holds for a point source only, where no reflecting walls are present, to the conditions existing in a furnace, is shown to be erroneous by the author. However, although this "inverse square of the distance" law cannot be applied in the case of a furnace, where radiation emanates from walls, roof, and flame, from a practical standpoint, when using a luminous flame, there is a distinct gain in heat transfer obtainable by keeping the flame close to the work.

In this case, while the gain in heat transfer would, as shown by the author, not be nearly as great as would be shown by application of the "inverse square of the distance" principle, when using a luminous flame, it is highly desirable, if not essential, to keep the flame close to the work. Another point which is not generally well understood, and which is clarified by the author, is the effect of a luminous flame in screening or shutting off the radiation from the walls and roof of a furnace. It is rather startling to find that as much or in some locations even more heat is transferred from a non-luminous flame as from a luminous flame, when the sum of radiation from flame and from roof and walls is considered. Since, as pointed out by the author, a non-luminous flame is certainly more efficient for the transfer of heat by convection, the total amount of heat transferred by a non-luminous flame would be considerably greater than by a luminous flame. However, although this greater transfer of heat, due to the sum of radiation and convection, may take place from a non-luminous flame in some parts of the furnace, it is still possible that when the greater area covered by the luminous flame with its nearly uniform heat transfer is considered, the total heat transferred to the work in the furnace may be greater when a luminous flame is used. There are, in addition, other factors which greatly influence the heat transfer. For example, a non-luminous, sharp, high-velocity flame is more efficient in melting down the charge in an open-hearth furnace, where heat transfer by convection can

⁵ Chief Chemist, International Harvester Co., Wisconsin Steel Works.

take place readily due to the penetration of the interstices of the charge by the hot gases, as well as taking advantage of radiation from flame and from roof and walls. However, after such a charge is melted down, and a liquid bath is formed, practical experience shows that heat transfer is facilitated by the use of a slow moving, highly luminous flame.

This latter effect is particularly well shown in the case of an open-hearth heat where the slag has risen up in a foam. Under these conditions, it is very difficult and frequently impossible to transfer enough heat to the bath with a non-luminous or weakly luminous flame, to flatten down the foam and to cause the reactions in the bath to proceed. If the flame is made highly luminous, enough heat can be transferred to the bath to reduce the foam and proceed with the heat with much less delay than in the former case.

Chief among the advantages of a luminous flame, the author lists "soaking heat." The explanation of "soaking heat" as applied to a continuous steel heating furnace is undoubtedly correct, and explains clearly the advantage of a luminous flame in this application. There is, however, another distinct advantage obtained by the use of a luminous flame, particularly in open-hearth furnaces, where the refractories are required to withstand an extremely high temperature, and that is that a luminous flame transfers a much greater portion of its heat by direct radiation to the work than a non-luminous flame, and makes this transfer with a lower flame temperature. When a non-luminous flame is used, a much greater portion of the heat transferred must take place by radiation from the walls and roof than when a luminous flame is used. Such a large transfer of heat by the walls and roof necessarily means heating these parts of the furnace to a higher temperature than when more heat is transferred direct from the flame. Having the refractories at a higher temperature necessarily means shorter life and a higher refractory cost. From a practical standpoint, this factor in favor of the luminous flame cannot be neglected.

C. GEORGE SEGELER.⁶ Not only Mr. Sherman but also other workers in the field of luminous or diffusion combustion have assumed that the air and gas layers introduced into a furnace absorb considerable heat prior to combustion at the interfaces. This point is open to some question, because the absorption of any considerable amount of heat, such as raising the absolute temperature of the gas from an incoming 520 F to, let us say, double that amount, or 1040 F, will be accompanied by an expansion in volume to double the initial volume. The same is true, of course, of the air volume, and under such conditions there would be expected a high degree of turbulence and an immediate destruction of anything remotely resembling air and gas layers. It seems to the writer that rather the contrary should be true; that in order to preserve luminous-flame conditions in the way they can be observed in diffusion-combustion operations, it is essential that a relatively small amount of heat be absorbed by the layers of air and gas. Consequently, combustion speed remains rather slow. Reference to Fig. 30 in the new American Gas Association book, "Combustion," would show that raising the temperature of natural gas to, say, 500 F would approximately triple its flame speed. Thus, from the admission end to the discharge end of a luminous-flame furnace one would expect combustion to be progressing at respectively increasingly rapid rates. Observation on these points, although superficial as yet, does not seem to indicate that any such procedure is taking place.

Since radiation is not a one-sided phenomenon, but in practise must represent the net result between the heat radiated from the hottest point and that re-radiated and reflected from other points, it is possible that other factors influencing the heat

transfer of a furnace also affect the net radiation from a flame. It has roughly been established that there is a relation between heat transfer, at any given temperature, and the pressure loss over a given length of heat travel. To be sure, such a relationship is only a rough measure, but it is of importance in this connection that the results obtained by the author strictly apply only to the furnace conditions which were set up by the physical limitations of the furnace in use. The relation of flue area to total heat input affected the heat transfer over the entire furnace. It affected in part the emissivity of the walls, although to only a small extent, as near as is known from the limited data of brick emissivities at high temperatures. This point is raised in connection with the attempt to draw practical conclusions from the material at hand. It is the thought of this writer that insufficient information is available from the tests performed to draw any definite conclusions on the rates of heat transfer which can be accomplished by various types of flame.

Recent investigation⁷ of forging practise comparing both diffusion flame and non-luminous types of heating indicates that the diffusion flame does permit higher rates of heating in general. At the same time this paper discusses the limitations of heating rates determined by the thickness of the stock, the physical nature of the steel, and other considerations, which of course should not be looked upon as limiting the theoretical nature of the flames. However, the fact remains that faster work has been reported regularly from the diffusion-flame operations, which is contrary to the conclusions drawn by the author. It is quite possible that this difference has been due in part to the difficult question of furnace layout and design, which in turn affects the rate of heat transfer. Mr. Sherman calls attention to some of these points in the discussion which he makes of the transmissivity and the absorptivity of flames in relation to the roof and walls. It is possible that further efforts along this line will bring to light why certain diffusion-flame operations were capable of being carried on more rapidly than with non-luminous flames.

These considerations might suggest reconsideration of the summary statements made by the author. For example, statement 1 has already been discussed.

In statement 2, the author indicates that the luminous flame would give a more uniform temperature. This statement is only partly true, as it overlooks the present practical methods for obtaining uniformity by using a multiplicity of burners properly located.

Statement 3 is subject to question based on the data collected and reported in the A.G.A. Industrial Service Letter on "Forging." The conclusions drawn therein are somewhat contrary to the theoretical considerations made by the author. It is quite possible, however, that additional data will eventually correlate these apparent discrepancies.

W. J. KING.⁸ This paper represents a valuable contribution to the data of combustion and radiation in gases. The practical significance of the results is enhanced by the large scale of the tests, the amount of data obtained, and the excellent experimental technique. With regard to the latter, there is just one question which occurs to the writer: Referring to Fig. 3, is it not possible that the water-cooled tube containing the thermopile at its right end may have become filled with gases, including about 11 per cent CO₂, which would absorb part of the radiation from the flame? Perhaps a very slow stream of dry air or nitrogen might have been passed into the tube to clear out these gases.

An examination of the data of Table 2 suggests that the

⁷ As published in the A.G.A. Industrial Service Letter No. 11 on "Forging."

⁸ Engineering General Department, General Electric Co., Schenectady, N. Y.

⁶ Engineer of Utilization, American Gas Association.

failure of Equation [6] and the significance of the constancy of K may be explained by the fact that the depth of the flame was not extended far enough to get beyond the almost linear increase of p_F with L . In other words, up to a depth of $L = 35$ in. the curve of p_F against L had not begun to bend over and approach the limiting value, i.e., the value of C in Equation [4]. On the flat portion of the curve beyond this bend, any variation of K would be revealed more plainly and the value of Q_M in Equation [6] could be calculated more accurately.

Perhaps a system of mirrors could be used with this apparatus to secure the effect of greater flame depth, by reflecting the heat rays back and forth across the flame several times, as was done by E. Schmidt in his measurements of the emissivity of water vapor.

No mention is made in the paper of the possible effect of radiation due to chemical reactions in the combustion process. This would not appear in the non-luminous flame, since combustion was complete within a very short distance from the burner, but if this effect has any significance in this type of combustion, it might have been revealed if more complete data were given for the luminous flames.

The conclusions drawn in the paper should not be applied too generally in practise, and the data should be used advisedly. For example, it is stated that, "In furnaces, such as boiler furnaces, with water-cooled walls where no high-temperature solid radiating surfaces are found, the overall transfer of heat by radiation can be increased directly as the emissivity of the flame is increased." This is true, as the author points out elsewhere, only when the temperature is maintained constant. In small boilers particularly, the flame temperature will decrease rapidly as the luminosity and emissivity are increased, and if the surrounding water-backed surfaces are not protected by refractory material, the temperature may be too low to support proper combustion. In such cases a non-luminous flame will give higher temperatures, better combustion, and higher rates of heat liberation in a given combustion space with smaller amounts of refractory.

And in connection with Fig. 7 it should be observed that the curves of gas temperature and radiation versus distance from the burner will be quite different when a charge of cold metal is being heated in the furnace. Due to the transfer of heat from the flame to the work, all of the curves would be rotated clockwise, so that the luminous flame would probably show the most uniform temperature and radiation.

It is to be hoped that the author will continue his investigations in this field. Similar data on combustion and radiation in oil flames would be welcomed by designers of combustion equipment.

J. D. KELLER.⁹ In the mass of glittering generalities talked and extravagant claims made with regard to luminous-flame burners, it is refreshing to listen to a paper dealing with actual facts. On a few small points, errors may be pointed out, with the understanding that they are not emphasized as detracting from the value of the paper. Thus, exception may be taken to the statement that, of the industrial gases, natural gas is the most difficult to crack. Coke-oven gas is much more difficult to crack than natural gas, while blue water gas cannot be cracked. The statement that mixing must be by diffusion is too broad—mixing can be effected *after* cracking by means of turbulence. Similarly, the conclusion that luminous flames transmit no more heat than non-luminous flames must be limited to present commercial burners which are "cracking" but not "mixing." With "cracking and mixing" burners much higher heat-transmission rates are attainable than with non-luminous flames.

⁹ Engineer with Prof. W. Trinks, Carnegie Institute of Technology, Pittsburgh, Pa.

It is possible that there are three sources of radiation from flames, instead of two as stated in the paper. Besides the radiation from solid particles and the continuing radiation from the non-luminous gaseous products of combustion after they have reached equilibrium, there may be additional radiation resulting from the act of combustion or chemical combination. The experiments of David on combustion in gas-engine cylinders seem to point to something of this sort. This possibility has already been alluded to by Mr. Jones in his discussion. It is to be noted, however, that the author measured *total* radiation from all sources; hence if radiation due to chemical action is present, its effect is included in the values found by the author.

It may be pointed out that there is one special case where a luminous flame is of outstanding advantage—namely, in heating large ingots for forging where the furnace interior is cooled down before a cold ingot is charged, and walls and ingot heat up together. In that case, the compensating radiation from the walls, as in Table 5 of the paper, is not present, and the heat transmission (for a given flame temperature) is almost directly proportional to the emissivity of the flame.

All of the author's tests were made with cold air. Much better results are obtainable if the air can be highly preheated (to 1800 F or over). As far as concerns luminosity of the flame, it is useless to preheat the air a small amount, such as 400 to 800 F, because this decreases the luminosity below that obtained with cold air. The same applies to preheating the gas, because methane does not dissociate appreciably below 1400 F, and must be heated to 1800 or 2000 F for really rapid cracking.

Exception must be taken to conclusion 6, that the advantage of the luminous flame in glass tanks lies in a more uniform distribution of heat transfer. The advantages which would accrue from deeper penetration of heat into the glass bath are almost self-evident. The reasons why the luminous flame should cause radiant heat to penetrate more deeply are by no means clear, but that it does so has been shown beyond doubt by tests made by the writer and by independent tests made by others. In fact, when standing underneath the tank and looking upward through the joints of the bottom blocks, one can easily observe that the glass at the bottom of a tank working with a luminous flame is decidedly hotter than in one with non-luminous flame.

The fact that the author tested only one type of luminous-flame burner may lead to claims that better results would have been obtained with other commercial luminous-flame burners. While tests of other burners would be very desirable, it seems improbable that such claims would be substantiated, since there is no essential difference in principle between the various luminous-flame burners now on the market. Since the present uncertain state of the art—illustrated by the rapidity with which some makers shift from one design to another, changing almost overnight—indicates that the ideal luminous-flame burner has not yet been attained, it may not be amiss to state the requirements which such a burner should fulfil:

- 1 It should produce a flame of high emissivity and high temperature. This requirement apparently would necessitate cracking first and, later, turbulent mixing. The latter is necessary not only for attaining high temperature, but also for avoiding too great an incomplete-combustion loss.

- 2 The gas and air should leave the burner with sufficient velocity to give direction to the flame.

- 3 The emissivity or luminosity should be regulable. Present luminous-flame burners often cause trouble when starting up from cold, because combustion with a luminous flame is then very slow indeed; the furnace smokes excessively and heats slowly. If the flame could be made non-luminous when starting up, and changed to luminous when the furnace comes up to temperature, operation would be much more satisfactory.

4 The luminosity should not change greatly with the degree of turndown; it should be nearly the same when gas is burned at one-third the rated capacity as when it is burned at full capacity.

5 The action of the burner should not interfere with the maintenance of a neutral or reducing gas blanket over the hearth.

6 The burner should be simple, not too bulky, and so designed as to avoid burning-off of metal parts, binding of sliding or turning parts, or clogging by carbon deposits.

7 Cracking gas should be kept out of contact with brickwork.

Additional requirements would no doubt have to be taken into account for special applications of the burner.

In the discussion, the penetration of radiant heat into the interior of steel pieces was mentioned as a possibility. The calculations of Dr. Northrup have shown, however, that heat radiation consisting of the usual wave lengths can penetrate into steel, as radiation, only to a depth of the order of 1/20,000 millimeter. Beyond this, heat penetration can, so far as at present known, take place only by conduction.

P. NICHOLLS.¹⁰ The paper will be very helpful to combustion engineers and operators in that it crystallizes one's ideas on the relative action of different types of gas flames. Although what the tests show and the author's deductions are in accordance with the general ideas one has had and which follow from first principles, yet this confirmation and illustration of their relative numerical values will enable operators to plan changes with more assurance.

Knowing the difficulties in obtaining true temperatures and radiation measurements, one would expect that much more work will be needed before assured values for the constants of the theoretical equations can be determined exactly, and it is rather remarkable that the agreements were as close as those cited in the paper. The definition of flame depth at a given location must have been somewhat arbitrary; the uncertainty of the outer edge of the flame and the effect of the depth of the cooling cone could be quite a large percentage of the nominal value. One would expect that a much larger flame would be needed and that allowance would have to be made for the variation of the temperature through the flame.

The paper makes no attempt to evaluate the effect of the loss of heat to the walls or to give the magnitude of this heat transfer, nor is there any assurance that it was similar in the various tests. When one compares the temperature curves of Fig. 7, it does not look logical that the curves for the semi-luminous and the luminous flames do not show more tendency to cross that of the non-luminous; one would expect that the loss of heat from the luminous flame previous to the 11-ft position would have been considerably greater than that from the other flames, and that in consequence its temperature would have been below those of the other two.

It is to be presumed that the gas-air ratio was the same for all the tests shown in Fig. 7. There is some omission in stating these ratios for all the tests, and there is uncertainty as to their values for Figs. 5 and 6.

There is need for a better understanding of the relative advantage of the type of flame as well as for the methods by which a desired type of flame may be obtained and controlled. As the author points out, all the advantages do not accrue to one type, and therefore a clear understanding of the principles involved is necessary in the interpretation of results obtained when experimenting with a given installation. The Bureau of Mines had planned to make such studies of the application of gas to brick kilns, in the investigations which it was conducting at Roseville, Ohio, in cooperation with the Ohio State University. A special

experimental kiln was built, and studies of the effect of burner placement and of the flame control were two of the main features to be investigated, but this work was stopped because of the lack of the relatively small additional funds required.

F. B. MCKUNE.¹¹ It is very evident from the paper that facts are now being obtained on these two flames, the luminous and the non-luminous. The writer does not wish to enter into any discussion on the merits and demerits of the non-luminous flame. So far as combustion is concerned, there is no stratified combustion so rapid and efficient as where you get turbulence. You will understand, of course, that these lighter gases lend themselves to turbulence more readily than the highly luminous flame.

We have been using for the last year straight by-product gas, and there are no reasons why we should not continue to do so. When our blast furnaces are in operation, we also mix blast-furnace gas with by-product gas and get good results.

One very important point in the use of the non-luminous flame is the balanced condition of the furnace. We balance our furnaces in such a manner that the flame will start out the holes in the doors, but return and go back through the furnace. If we did not do this, we would find cold spots in different parts of the furnace. Another advantage this has is that it does not matter what velocity you have coming out of the burner or the port; the flame immediately starts to slow up and distribute itself equally through the furnace. This balanced condition of the furnace is so important that the successful burning of the by-product gas depends on it.

The writer can very easily see that one could rash up a piece of steel much faster with a non-luminous than with a luminous flame. He believes from experience that, if you put two pieces of steel in different furnaces and use the two different flames and watch, if you did not rash up the non-luminous flame too fast, your heat transfer would be much faster than with the luminous flame. If you properly balanced your furnace, you would have an equal distribution of the heat from both flames.

At present we are running our soaking pits with straight by-product gas, with no complaints that this gas is inferior to any other gas.

Three fundamentals about which we are very careful are the velocity of gas, the direction of the gas, and the balanced condition of the furnace. Any success that we have had is entirely due to following the foregoing procedure rigidly.

The combustion is so complete in our furnaces that we have no record of any CO in the outgoing end of the furnaces.

W. J. WOHLBERG.¹² The paper merits a thorough study and contains information that should be of considerable value to the industry. It presents in a simple and clear-cut way the relations which are involved in radiation from gas flames. It shows also how the radiation characteristics of these flames compare with the radiation from a dust cloud in which the dust is pulverized coal. There is, no doubt, information in this paper which may be used to advantage by engineers engaged in the design of pulverized-coal furnaces for boilers as well as that which is contained relative to the operation of industrial furnaces in which gas may be used as a fuel.

From the engineer's point of view, the formulas set up to express the characteristics of the radiation are perhaps fundamental. From the point of view of the more exact scientist, they are of course empirical. The writer is referring in particular to the equations in which the specific radiation characteristics of

¹¹ Steel Company of Canada, Hamilton, Ontario.

¹² Professor of Mechanical Engineering, Sheffield Scientific School, Yale University, New Haven, Conn. Mem. A.S.M.E.

¹⁰ Supervising Fuel Engineer, U. S. Bureau of Mines, Pittsburgh Experiment Station, Pittsburgh, Pa.

the flame are really included in the factor K , which appears in the product KL as an exponent of e in Equations [1] to [4]. As these formulas are set up, K is really a function of the composition of the gases, of the concentration of the various constituents, and in the case of a dust cloud also of the concentration and mean size of the dust particles. For a given composition of the mixture, K may also vary with the temperature, because for a given temperature it will depend on the wave-length bands in which the radiation occurs. As the temperature of a gas of given composition is changed, the number and position of the bands in which an appreciable amount of radiation occurs may change. It is therefore not surprising that K varies by the amounts shown in Table 3 when the radiation is measured from different parts of the furnace for the same flame. Obviously, most of the factors which have been mentioned as influencing the specific radiation characteristics, and therefore K , may vary from station to station in the flame. Therefore it is something of a relief to find out that the factor K does not vary with position in the flame more than is indicated by the values shown for it in Table 3.

This information, although perhaps not obtained in an experiment conducted with the preciseness which would be characteristic of work done in a physical laboratory, nevertheless, because the data are taken on a mixture of gases rather than on the separate constituents, furnishes bench marks of a sort for comparison with a more fundamental type of information on radiation taken for the separate constituents each by itself, and which data are available from such work as Schmidt on the radiation from water vapor and the more recent data which have been furnished by Schack and also by Hottel and Guerri. The latter appeared in the recent book on heat transfer published under the auspices of the Heat Transfer Committee of the National Research Council. In this book appears also some information based on theoretical considerations of the radiation from luminous flames. It will be very interesting to see how Sherman's data on such flames check with this when the latter is applied to flames of the character on which Sherman has carried on his work. It still remains to be seen whether, by means of such information as is contained in Sherman's tables, simple expressions can be developed to represent the variations of K which would yield results, when applied to furnace conditions, close enough to the actual conditions so that the results could be applied practically.

From a practical point of view, some of the curves showing variations of temperature along the flame axis for the different types of fuel are particularly important. It appears to the writer as though the different distribution of energy which is indicated for the different types of fuel must be of considerable practical significance to the operator of industrial furnaces. It is also of considerable importance to the operator of boiler furnaces in that by means of such information, if this could be extended to the boiler furnace, might be found the zones of high and low heat absorption, and this might lead to information on how water-cooled surfaces should be distributed for best results.

AUTHOR'S CLOSURE

The complete and frank discussion that has resulted from the presentation of the paper is greatly appreciated. The interest shown proves that the work was timely.

Mr. Nicholls has called attention to the omission of the values for the air ratios on Fig. 7. These were stated in Table 3, but will be put on the published figures to avoid any confusion. He has also questioned the heat loss from the walls and raised the point as to whether they were the same for all tests. The resistance of the walls was the same for all tests, and the temperature attained by the walls was governed only by the rate of heat transfer from the flames. This was considered the only fair way to conduct the tests.

Mr. Nicholls questions why the temperature of the luminous flame was not much lower than that of the other flames. It was lower than that of the non-luminous flame at all points, but it was lower at the first two points, not because of its high emissivity (the absolute radiation was actually somewhat below that of the non-luminous flame), but because of the low rate of heat liberation.

Professor Wohlenberg has properly pointed out that this work is of the engineering type, and the accuracy can not be expected to be equal to that of physical laboratory work. He also has emphasized the many variable factors that enter into the absorption coefficient K , which explain its lack of constancy.

Mr. King has asked about the possibility of CO_2 and H_2O filling the diaphragm tube and absorbing radiation from the flame. This possibility was foreseen, as trouble was had from this source in the calibration of the unit. As the furnace was at all times under a pressure less than atmospheric, however, and as the joints of the thermopile case were not hermetically sealed, enough air flowed in to keep the tube free of absorbing gases. This was proved by taking a reading, opening the case to allow air to flow in freely, and closing the case; the second reading checked the first.

Mr. King and others have brought out the point that, if a furnace is cooled down by a cold charge, the rate of heat transfer will increase directly as emissivity. That is quite true, and review of the text will show that the author limited his conclusions as to the total radiant-heat transfer to furnaces with walls hotter than the work.

Mr. Flagg discusses this subject in the light of much experience with high-temperature heating problems and with all kinds of fuel. He points out the truth that efficiency is secondary to quality in most heating processes. He has questioned whether the inverse-square law may not hold more closely for small distances between planes. He will find, however, on consulting Hottel's curves, to which reference was made by the author, that the smaller the distance between the planes, the wider the departure from the inverse-square law.

Mr. Flagg speaks of the repeated failure of tests to run an open-hearth steel furnace with non-luminous flames. However, an outstanding example of success with this type of operation is that of Mr. McKune, of the Steel Company of Canada, whose remarks speak for themselves. Although it may be more difficult to operate an open-hearth furnace with a non-luminous flame, it is not impossible.

Mr. Flagg, Mr. Segeler, and others have insisted that the output of a furnace is frequently increased by the use of a luminous flame. They do not insist, however, that the output per unit of heat input is increased. The author admits that the output of product per square foot of hearth may well be increased with a luminous flame, but not because of a higher over-all rate of heat transfer. On the contrary, the output may be low with a non-luminous flame because of an excessive rate of heat transfer near the burners which would damage the product. To avoid such damage, the heat input must be reduced and the rate of transfer at distances from the burner is made very low. With the proper luminous flame the heat transfer may be made more uniform over the hearth area and the rate of transfer so adjusted as to raise the temperature substantially uniformly through the work. The increased efficiency in the use of the hearth area will obviously increase the hourly output of the furnace and may even increase the thermal efficiency.

Mr. Keller has properly corrected the author in the inexact statement that natural gas is the most difficult of the industrial gases to crack. He has also pointed out that luminous flames can be produced with mixing rather than with complete reliance on diffusion.

The statements in the paper in regard to the application to glass

tanks were primarily speculation, put in to promote discussion. There seems to be no reason in the light of our present theoretical knowledge why luminous flames should heat the bottom of a glass tank more readily than non-luminous flames. If, however, practise shows that luminous flames are more effective, then some parts of our present theories must be incorrect; they certainly are far from complete.

The author has no fault to find with Mr. Keller's statements of the requirements of luminous-flame burners.

Mr. Segeler questions whether the gases absorb heat before combustion at the interface, because he feels that this would promote turbulence. The gas must absorb heat before mixing with air or there will be no cracking. At any rate, in the combustion at the interface the gases absorb the liberated heat and increase in volume, so that a certain amount of turbulence is undoubtedly the result.

In discussion of the effect of temperature on the rate of combustion, Mr. Segeler refers to Fig. 30 of the American Gas Association book, "Combustion," where the relation between the maximum velocity of flame propagation V to the absolute temperature T is expressed as $V = BT^2$, where B is a constant. That refers, however, to premixed gases; when, and if, combustion occurs only when the gases diffuse together, the rate is governed by the rate of diffusion, which is slow relative to the rate of combustion. Taylor, in his "Treatise on Physical Chemistry," states that the diffusion coefficient for gases is proportional approximately to $T^{3/2}$. Burke and Schumann made some rough experiments on the effect of temperature on the length of "diffusion" flames, but arrived at no definite conclusion.

Mr. Segeler believes there is some doubt as to the application of the author's results because of the type of furnace. He states that there is a relation between pressure drop and heat transfer, which is true for convection, and that therefore the ratio of the flue area to the heat input affected the heat transfer. The connection between the pressure drop or flue area to the radiant-heat transfer would need further amplification by the discussor for a conception of its significance by the author.

Mr. Jones has questioned the relation of the furnace shape to the possible turbulence of the flame and has suggested a rectangular furnace. The author feels that the furnace was the proper shape to conform to the round burner.

Mr. Jones states that there is a distinct difference between luminous and diffusion flames, but in his extended discussion of diffusion, delayed combustion, and various types of energy waves he fails to make the distinction clear.

The inference is made that a luminous flame radiates only in the narrow visible band, below 0.7μ , as shown in Fig. 8, whereas a diffusion flame radiates over the entire band. This is obviously untrue. There can be no visible radiation without simultaneous infra-red radiation; cold light has not yet been discovered.

Actually what the author believes Mr. Jones meant to convey was (1) that luminous flames do not necessarily have high emissivities and (2) that diffusion flames and only diffusion flames have high emissivities. The first statement is entirely correct, as has been proved by the experimental data of this paper. The second statement, however, is incorrect. As Mr. Keller pointed out in his discussion, flames of high emissivity can be obtained with mixing, and such flames are highly desirable, as they can be given direction in the furnace. All flames, including those used in the present experiments, in which the gas and air are introduced in separate streams without later provision in the furnace for turbulence, must depend to a certain extent on diffusion for combustion. Diffusion is only the mechanism of mixing of gas and air and is a form of slow mixing and delayed combustion; it has nothing to do with radiant-heat transfer. A diffusion flame may be strongly luminous or semi-luminous; it may have a high or a low radiation and emissivity.

The merits of luminous flames are clearly enough defined and are great enough for certain applications to stand on the determined facts without an attempt to attribute to them properties they do not possess or to interject fine distinctions in terminology that are not supported by the facts. It is the earnest hope of the author that the statement of facts in this paper and the discussion will result in clarification of the subject.

Zap Flaps and Ailerons

By TEMPLE N. JOYCE,¹ DUNDALK, BALTIMORE, MD.

The early history of the Zap development is covered, including work done on the Flettner rotor plane in 1928. Because of phenomenal lift obtained by changes in flow around a cylinder, investigations were begun on improving existing airfoils. This led to preliminary work on flapped airfoils in the tunnel of New York University, and later its application to an Aristocrat cabin monoplane presented to the B/J Aircraft Corporation early in 1932. A chronological record of the reactions of the personnel of the B/J organization to the Zap development is set forth, particularly the questions regarding lift and drag coefficients, effect upon stability and balance, and the operating forces necessary to get the flaps down. The effectiveness of lateral control, particularly with regard to hinge moments and whether the rolling moments were obtained primarily through spoiler action or positive lift increases and the relative percentage of spoiler rolling moments to positive rolling moments, is also included. Comparative data of forces and lift and drag coefficients of several types of flaps are given, with a discussion of the relative practical results. There is a discussion of the practical flying problems in which engineers and pilots are interested, including the effect upon landing and take-off, reactions in a stall, and lateral control below minimum flying speed, as well as the anti-spinning characteristics which have been displayed in actual flight tests.

FOR THE last five or six years, the demand on the part of operators for increased high speed has forced designers practically to disregard the importance of the steadily increasing landing speeds of aircraft. During the same period there has been another influence that has allowed us to still further neglect this factor. It is the fact that modern engines are so reliable and forced landings occur so seldom that their importance has

been looked upon with more or less contempt. This was particularly true during the boom days when everybody was using a new engine and when landing speeds were thought of only in terms of getting into recognized airports. Three things have occurred since then, however, that have again brought to the front the importance of low landing speed: First, a very distinct realization that the public was afraid of aviation because of high stalling speeds and the frequent crack-ups with serious consequences. Second, the fact that increased high speeds could not be obtained without increasing still further high landing speeds unless some new aerodynamic development was brought into existence. Third, as speed ranges and wing loadings went up, takeoff run was increased and angle of climb decreased alarmingly.

The Zap development is a successful effort to reduce landing speeds without impairing high speed and thereby to bring about the best overall increase in the efficiency of an airplane with the least added complications. Experimental work on the Zap flap was stimulated by investigations on a Flettner rotor airplane by Mr. Edward F. Zaparka, through the support of the Chrysler Corporation. Because of high lift reactions obtained by the change in flow around a cylinder, the research drifted to a practical investigation of the problem of influencing the flow around an airfoil. The first work was done in a miniature tunnel and was supplemented by larger scale work in the New York University tunnel under the able consultation of Professor Klemin. Subsequently, the flap was installed on a commercial Aristocrat cabin airplane of 165 hp, and flight tests proved that the flap was very effective. These also showed that though lift increases were essential for slow-speed landings, almost equally important was the question of lateral control; Zap ailerons were the result.

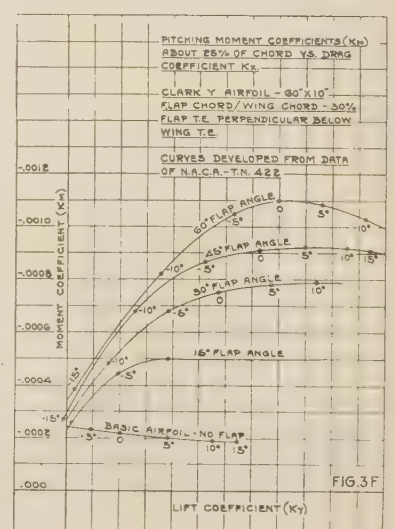
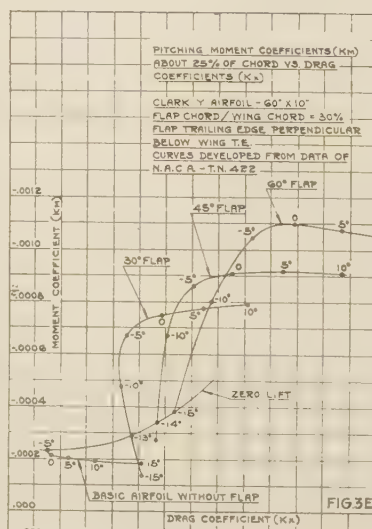
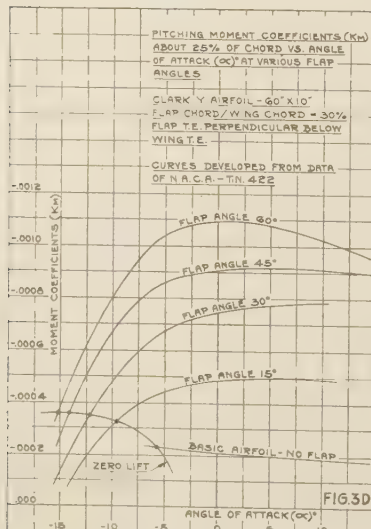
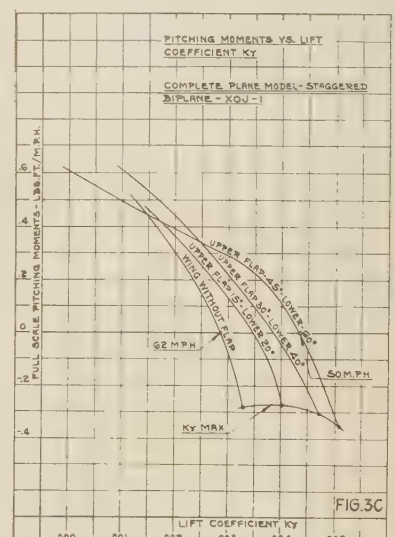
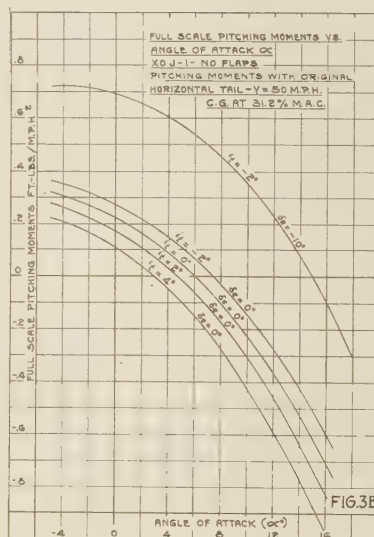
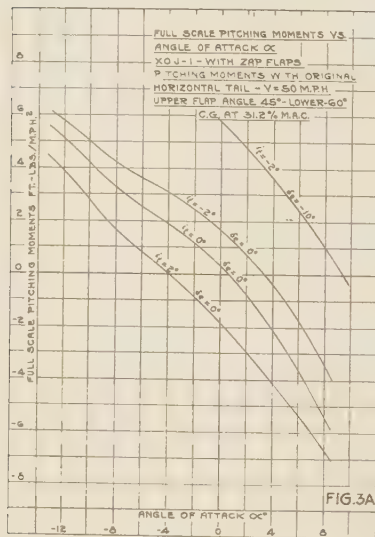
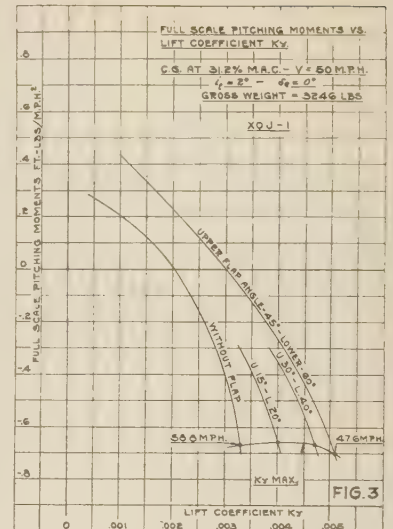
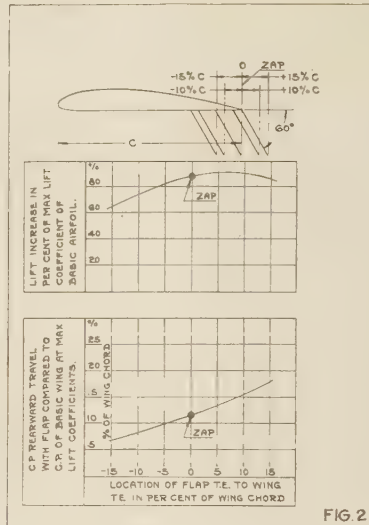
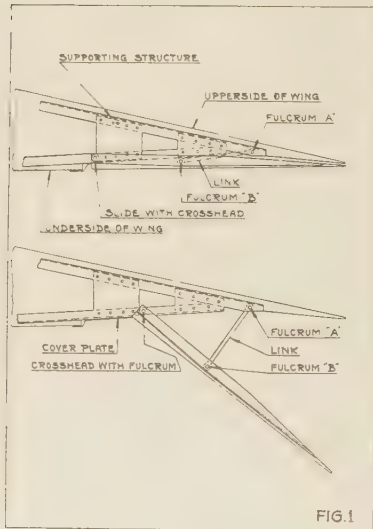
In the Spring of 1932, the Aristocrat with Zap flaps and ailerons was presented to the B/J Aircraft Corporation. The author will outline here chronologically the questions and answers that were made and the reactions that he had to the Zap development, because in so doing most of the questions that one would ask regarding Zap flaps and ailerons will be answered.

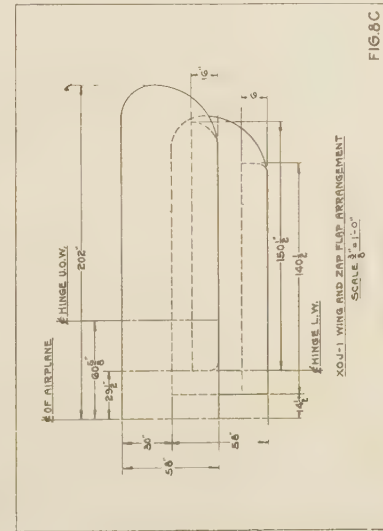
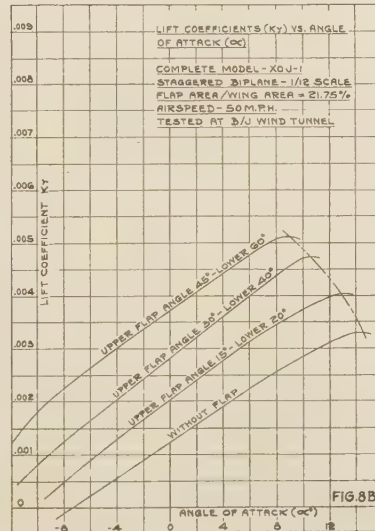
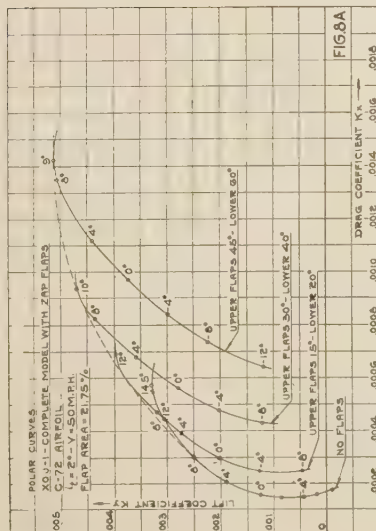
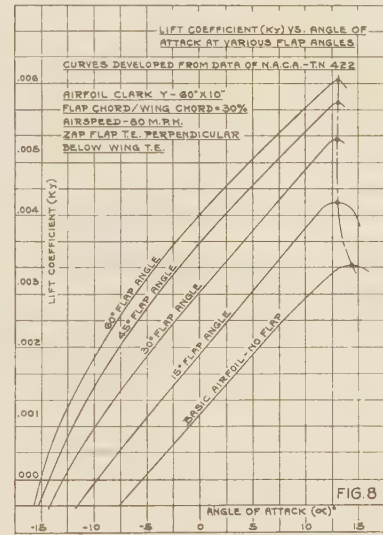
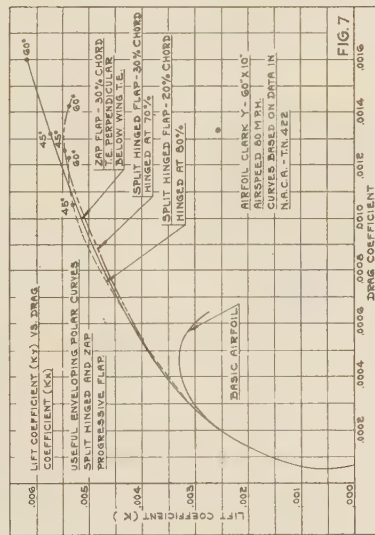
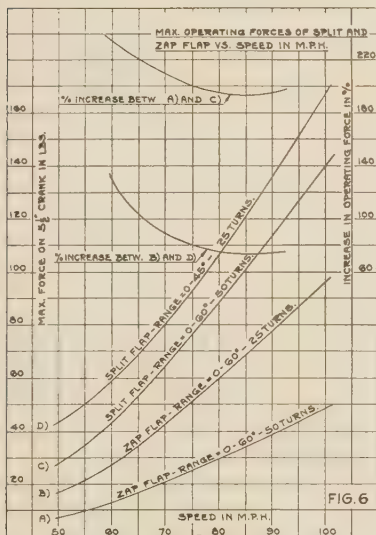
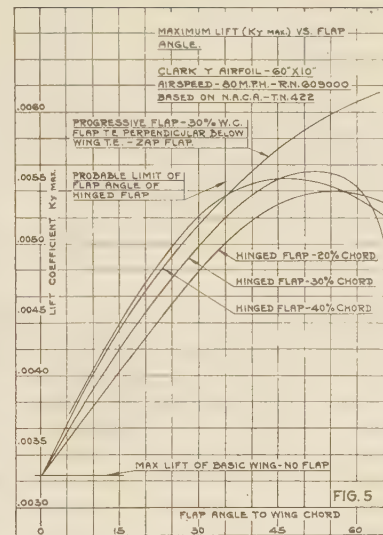
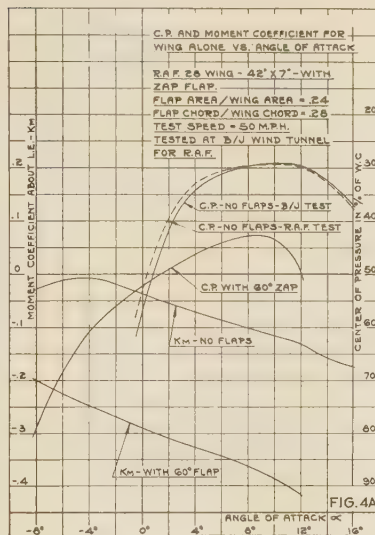
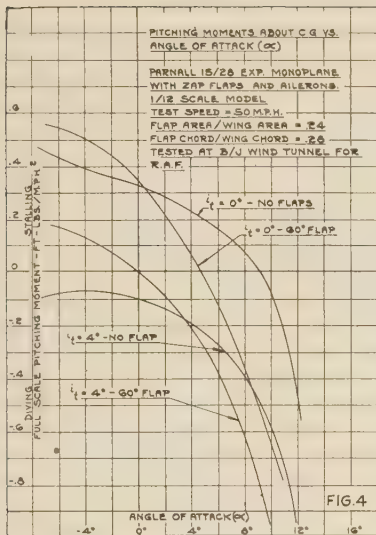
Our first impression at the B/J plant when we were told that a plane was to be sent down was that it was just another flap airplane and that it would be a waste of time to look it over, particularly because, to our best knowledge, lift coefficients of 0.0044 engineering units were the maximum that could be expected on a simple flap applied to a Clark-Y airfoil. When the airplane arrived at our field, it was observed that it had a split flap and that the ailerons were placed above the wing. This caused considerable apprehension, as it was felt that the ailerons in such a position would surely be blanketed when the plane was brought to a stall, and would not only be inadequate but dangerous. The author was quite reluctant to fly the machine at first, but finally did so, with the expectation of finding that the ailerons would be completely ineffective at 10 to 15 miles above the stalling speed of the airplane. Much to our surprise, they were found to be very effective down to and below the stall of the airplane with flaps up, and materially improved when the flaps were down. After a very short flight, the plane was brought down, with the conviction that it was a bad example of an airplane, but that the flaps and Zap ailerons almost made it a reasonable vehicle. The next step was to investigate the wind-tunnel data which had been carried out by New York University. The results shown in the data presented by Mr. Zaparka were extremely interesting,

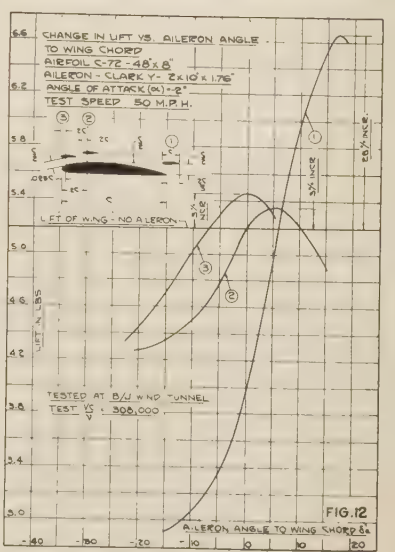
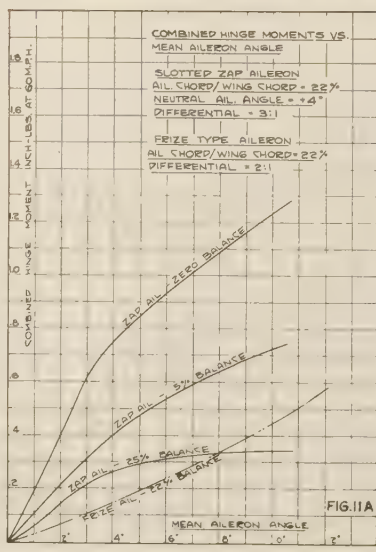
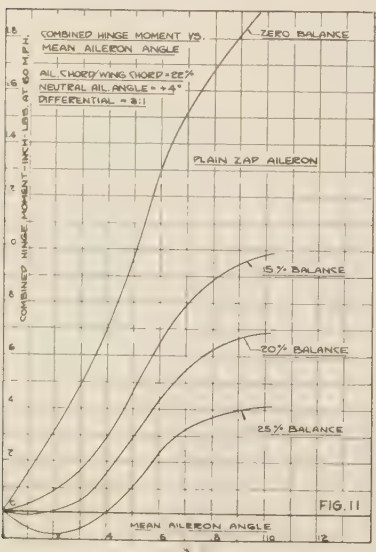
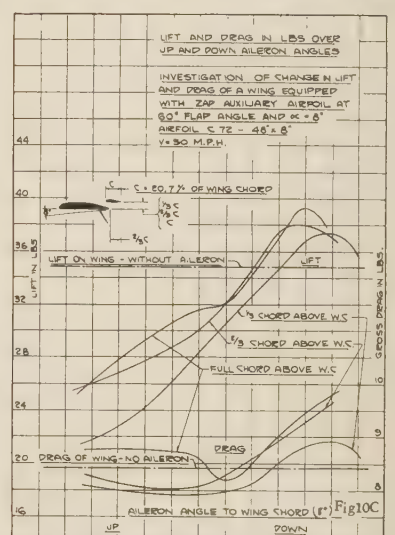
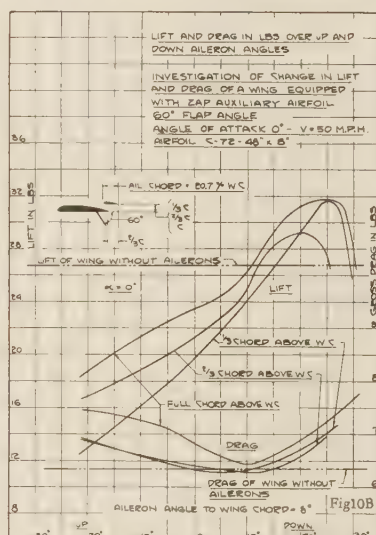
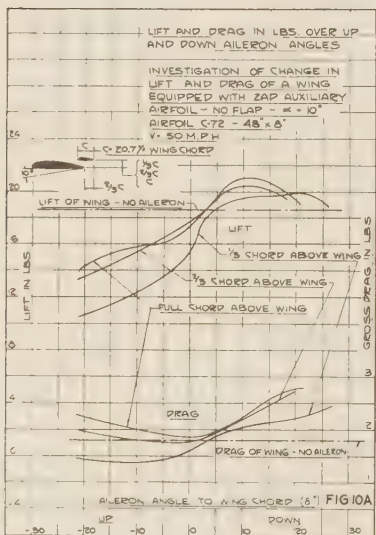
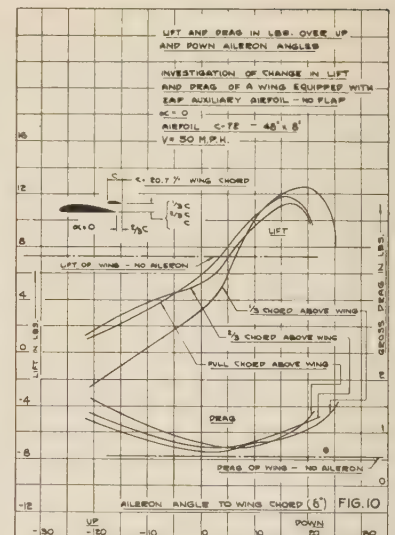
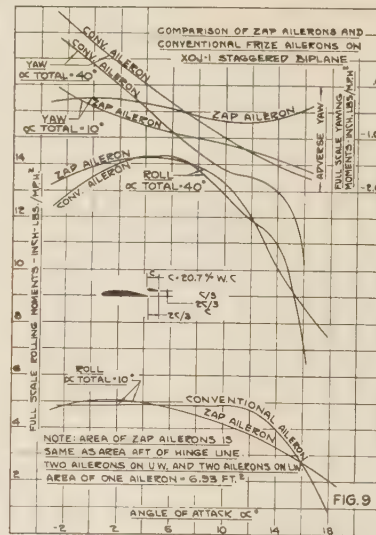
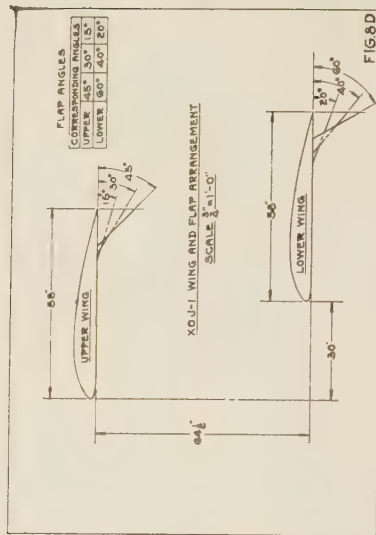
¹ President, B/J Aircraft Corporation. Temple N. Joyce was born in Baltimore, Md., on June 27, 1895. He was educated at Baltimore Polytechnic Institute and Lehigh University. He was sales engineer for Truscon Steel Company, of Baltimore, 1915-1916. Applied to Signal Corps for aviation training immediately after declaration of war and was ordered to active duty in May, 1917, receiving commission as first lieutenant and being ordered overseas in November, 1917. At Issoudun, France, was ordered to test department. Received promotion as captain in January, 1919, and last position held at Issoudun was that of assistant chief test pilot. From 1919 to 1925, represented Societe Morane Saulnier in United States and South America, contracting to the United States Army and Navy, Mexico, Argentina, Brazil, and Peru. Entered the employ of the Curtiss Company in 1925 and was Washington representative until 1927. Sales Manager for Chance-Vought Corporation in 1927 and 1928. Organized the Berliner-Joyce Aircraft Corporation in 1928-1929 with Henry Berliner, becoming vice-president in charge of sales. With the acquisition of Berliner-Joyce Aircraft Corporation by North American Aviation, Inc., in June, 1930, was made vice-president and general manager of the newly formed B/J Aircraft Corporation. On May 2, 1932, was elected president of the B/J Aircraft Corporation, and so served until early in 1933, when North American Aviation acquired, through General Motors Corporation, the General Aviation Manufacturing Corporation. In June, 1933, was made executive vice-president and general manager of the latter, supervising consolidation of operations of both companies.

Contributed by the Aeronautic Division and presented at the Semi-Annual Meeting, Chicago, Ill., June 26 to July 1, 1933, of THE AMERICAN SOCIETY OF MECHANICAL ENGINEERS.

NOTE: Statements and opinions advanced in papers are to be understood as individual expressions of their authors, and not those of the Society.







and the B/J company requested models from New York University, with the idea of checking them in its own tunnel. This was done, and the results of New York University as to lift and drag coefficients were substantiated.

The B/J company had always been interested in slots and flaps, and the Zap development fell into sympathetic hands. We had always felt that the success of slow flying, regardless of how it was obtained, whether with slots and flaps, boundary layer control, or any other means, was dependent upon adequate control at the reduced low speeds. When it was found that an adequate slow-speed lateral-control device was in existence and at the same time did not impair the utilization of the whole span of the wing to obtain maximum lift increases, our enthusiasm for the Zap combination of flap and ailerons was intensified. In previous designs of a simple flap, as stated before, it was known that the maximum lift coefficients did not exceed 0.0044, and when the split flap presented possibilities of 0.0065, an explanation of the theory became necessary. It might be of interest to theorize on what actually takes place in a split-flapped airfoil. With a normal wing, when the simple flap constitutes an actual break in the contour of the upper surface, the increase in lift is primarily due to change in camber, and there is no reaction due to increase of chord or change in flow over the top surfaces other than that which would normally be expected from increasing the camber. With a split-type flap, where the contour of the upper surface of the airfoil is preserved intact, the increase in lift can be divided into three possible heads: First, increase in camber of the bottom surface, which naturally stimulates the flow over the top surface; second, the preservation of the upper surface with the same chord and possibly an increase with certain types of flap movement; and, third, a change in flow over the upper surface brought about by the fact that the split trailing edge and undisturbed upper contour create a combination which causes a further increase in flow over the wing. In the illustrations, the flow reactions back of a simple flap versus the split flap will be seen, and also the effects of moving the trailing edge of the flap forward along the chord. Whether the additional increase in flow over the top of the wing referred to is due to the presence of an area of depression at the trailing edge of the wing caused by the split flap or whether it is due to the displacing of the reversal flow away from the trailing edge so that the bottom surface flow unites with the upper surface flow with less detrimental vortices, is a matter for the theoretical aerodynamicists to thrash out. It is a fact, however, that as the flap is moved forward so that the phenomenon, whatever it might be, is taken away from its influence at the trailing edge, there is an appreciable loss in maximum lift and is best when the trailing edge of the flap is approximately below the trailing edge of the wing, as is the case of the Zap arrangement. Some very interesting data on lift increase devices have been prepared and published by Mr. Richard M. Mock.

With this explanation, the next question was why the airplane did not require greater changes in the horizontal stabilizer to take care of flap up and flap down positions. In Fig. 2 is shown the change in center of pressure brought about by the use of this particular flap movement on an airfoil and the consequence of moving the trailing edge of the flap fore and aft. In an airplane with flaps, the center of pressure travel and effect of changes in angle of downwash must be taken into consideration, and in most cases with the Zap it has a favorable reaction. In Figs. 3, 3A, 3B, and 3C, pitching moments of a conventional naval biplane equipped with Zap flaps and ailerons are shown. Figs. 3D, 3E, and 3F give pitching-moment coefficients for an airfoil, while in Figs. 4 and 4A, the pitching moments of a conventional Zap-equipped monoplane are shown. The net result is that the balance and stability is undisturbed, and increases in tail area or abnormal stabilizer adjustments are not necessary.

The next point of interest, stimulated by the flights of the Aristocrat, was the extremely low operating forces necessary to move the flap down. With a simple flap of the type used on the Breguet observation airplanes in France as early as 1917, the forces necessary to get the flap down were excessive, so much so that the flap could only be deflected approximately 30 deg when usable operating forces and time to operate are taken into consideration. Even if it were deflected to greater angles, the lift coefficients would still be below that of the Zap. (Reference is made to the N.A.C.A. Technical Report No. 422, from which curves on Fig. 5 are interpolated.)

With the straight type of split flap, such as the Wright, where the leading edge of the flap is a fixed hinge, the operating forces are compelled to work against the full aerodynamic load. If the mechanism is of cantilever construction, the forces are prohibitive. If it is of a toggle arrangement, which would have to be some modification of the Zap toggle, without the beneficial effect of the sliding front edge, there again the forces are extremely high and particularly excessive at small angles of flap opening. These forces diminish after the flap has caused sufficient drag to slow the plane a great amount. (See Fig. 6, showing relative loads of Zaps versus straight flap for same angles.) The hypothetical airplane we used in arriving at these figures had a wing area of 309 sq ft, 48 ft 8 in. span, 83-in. chord, Clark-Y airfoil, gross weight of 4600 lb, wing loading of 14.8 lb, power

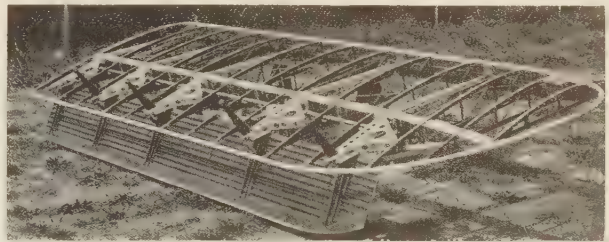


FIG. 13

loading of 10.8 lb, and maximum speed of 150 mph. The flap area for both the Zap and simple flap was 30 per cent of the total area and the flap chord 30 per cent of the wing chord. The total span of flap was 45 ft and total area of flap 93.8 sq ft. Two calculations of forces were made for the simple flap, one a maximum angle of 60 deg and the other a maximum angle of 45 deg. The mechanism for operating the simple flap was the most efficient in our opinion, and the geometry chosen seems to be the one requiring the smallest effort on the operating crank handle. The Zap-flap geometry and operating mechanism are approximately the same as those developed by the B/J company when Zaps were supplied to the XOJ-1 observation airplane for the Navy. A photograph of the XOJ mechanism is shown in Fig. 13, while Fig. 1 shows a schematic view of the Zap toggle mechanism.

When a comparison of lift coefficients is made, it is seen that even though it were practical, from an operating force standpoint, to get the straight hinged flap down to 60-deg angles, in order to obtain the benefit of large drag, the lift would be materially less than the Zap flap, and in fact less than its own 45-deg position. (See polar curves, Fig. 7.)

With the Zap type of toggle arrangement, wherein the leading edge of the flap slides back and the toggle is concealed in the wing in such a manner that one end of it is located close to the center of pressure of the flap and the other fastened to the structure at the top of the rib, it can be seen from Fig. 6 that the number of turns on the operating crank and the forces necessary are extremely low; in fact, with certain types of airfoils, permitting a

more favorable geometry of the flap linkage, it will be possible to have actual opening forces.

This phase of the Zap mechanism is extremely important when it is realized that light operating forces have two very important results: First, in that the weight of the operating mechanism can be considerably less, and second, even more important, the fact that in an emergency landing it enables the pilot to get the flap down quickly. In an existing monoplane which has recently been flown in the United States, a straight hinged flap is utilized in conjunction with Zap ailerons for lateral control, and the operating forces are so great as to require 45 turns to get the flap down to 45 deg with a lift increase of only 35 per cent. It can be seen in Figs. 7 and 8 that the maximum lift coefficients of the Zap flap at 60 deg is 0.00615, and also from Fig. 7 that the straight hinged flap has only a maximum lift of 0.00545. These curves were developed by interpolating the data in the N.A.C.A. Report No. 422, because this report did not test the best Zap flap position, but took two flaps on either side of its general location. It must be borne in mind, however, that the angular movement of the flap and the lift coefficients obtainable are intimately connected with the practical results that can be obtained and which of course depend upon the operating forces and the time required to get the flap into action at maximum lift. In Figs. 8A and 8B are shown the lift coefficients for a staggered biplane with the different flap settings on upper and lower wings necessitated by the stagger. Figs. 8C and 8D show wing and flap arrangement.

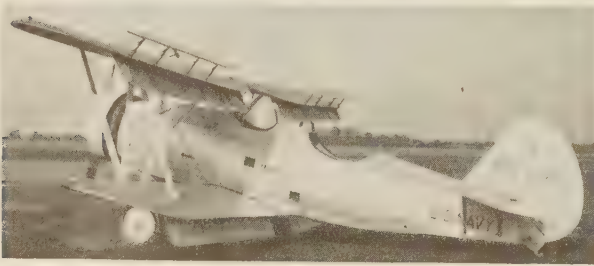


Fig. 14

During the explanation to the engineers of the B/J company and the Zap Corporation when the Aristocrat was first brought to our plant, the discussion of the phenomena surrounding Zap ailerons became quite intense. It had been noted that the ailerons were effective at or near the stall and greatly improved when the flaps were in operation. It was disclosed that the ailerons have a material effect upon the downwash of the wing, and in view of the fact that the flow over the top surfaces is increased by the presence of the split flap at the trailing edge, the ailerons are actually operating in a stimulated flow when the flap is down. These facts were substantiated later when it was found that the ailerons were at their best efficiency when relatively very close to the wing and diminished at a substantial rate when placed too far forward of the trailing edge and too far away in a vertical direction. The original rolling-moment curves presented by the Zap Corporation only represented meager researches as to the proper vertical and fore-and-aft position, aileron-airfoil section, aspect ratio, etc., but the data that were available indicated that the control at low speeds would be excellent. It will be noted in comparing the values of rolling and yawing moments of Fig. 9 that the plain Zap ailerons are approximately equal to the conventional ailerons of the same area. Subsequent tests and present research with modified slotted Zap ailerons show increased rolling moments with considerably lower hinge forces, which are now regarded as not only being equal to but in some instances are superior to conventional Frise types when acting in conjunction with unflapped or flapped airfoils.

The B/J company was very much interested in determining just how much rolling moment the Zap ailerons were capable of producing, how much of this was due to lift increase, and how much to spoiler in contrast with conventional ailerons. In order to determine this, our first tests consisted of an 8-in. by 48-in. airfoil on which a Zap aileron was superimposed throughout the span with the idea of determining the actual flow phenomena that took place when the ailerons were deflected through positive and negative angles. It was found that when the ailerons were suspended independently of the wing and were deflected through positive angles, there was a large increase in lift induced in the major airfoil as well as the lift created by the aileron itself due to its own airfoil action. On Figs. 10, 10A, 10B, and 10C are some of the results of these tests with the 8-in. by 48-in. airfoil showing the lift increases with positive angle and its spoiler action due to negative angles, as well as the drag increases or decreases. In these figures the drag of these auxiliary airfoils across the entire span for various angles of attack of the main airfoil is also shown. This increase in drag will be in the nature of approximately 1 per cent loss in speed of the airplane when the ailerons cover 50 per cent of the semi-span. In the application of the Zap ailerons to a conventional Navy biplane, shown in Fig. 14, where there was no particular attempt made to have a clean installation, the loss in speed was 1 per cent plus. There is additional research now being done on this type of aileron to absolutely determine the optimum fore-and-aft position and the best combinations of this with vertical location as well as the proper airfoil shape, the correct aspect ratio, the best shape of wing tip, and the proper relation of aileron chord to main airfoil chord. In Fig. 11 the hinge moments of a straight Zap aileron are shown, which indicates that for high-speed airplanes there will be excessive stick forces (but which are quite practical on slow planes of the private class). It is interesting to compare the hinge moments of the conventional unbalanced aileron, plain Zap, and slotted Zap ailerons in Figs. 11 and 11A. All Zap ailerons are quite sensitive to vertical and horizontal location, depending to some extent on the wing section, and their neutral setting is most important. The slot of the aileron is quite different from that which is used on a wing due to its proximity to the wing upper surface, and its form and setting must be carefully determined. In Fig. 12 is shown the effect of placing the aileron in several fore-and-aft positions on the forward part of the wing as compared to the best position ascertained so far by us.

It might be interesting to bring out the following facts to differentiate between the Zap ailerons and the conventional and floating types. Previous to the development of the Zap aileron, any attempt to use a trailing-edge flap was immediately handicapped by the fact that from one-half to two-thirds of the span was used for lateral control, thereby diminishing the available maximum lift increase. When evaluating their respective merits with any type of lateral control, there are two conditions of flight that must be considered: control above the stall and control below the stall. With the conventional aileron, if the plane is approaching a landing in a glide above the stall but very close to the maximum lift, and a wing is unavoidably dropped, when the aileron is moved to a positive angle with the idea of picking up the low wing, several conditions are to be observed. Any small deflection of the aileron is reflected in a change in the lift on the major airfoil. This is of distinct advantage, because small aileron surfaces can be made to produce a rather substantial rolling moment by influencing the flow over the major airfoil. The conventional aileron, however, is at a disadvantage in that a large movement of the aileron might create a resultant angle of attack that would be beyond the critical angle and cause the wing to stall and further accentuate the dropped-wing condition. Simultaneously with this, due to the unfavorable yawing moment,

the wing tends to rotate backward and still further decreases the lift with the possibility of entering a spin. Any further positive movement of the aileron only aggravates the stalled condition from a standpoint of flow over the major airfoil and at the same time induces further unfavorable yawing.

We will compare this with the floating aileron and later the Zap.

In the condition where the airplane is approaching the ground, close to the point of maximum lift, but with floating aileron, if the wing is inadvertently dropped a positive deflection of the floating aileron will create an increase in lift, but only an amount equal to the lift generated by an airfoil of that particular aileron area and section at that particular angle of attack. There would be no induced flow over the surface of the major wing. In designing such an aileron, this would have to be taken into consideration, and the aileron would have to be quite large so as to produce within itself a practical rolling moment at the reduced speed of flight brought about by the use of flaps or any other slow-speed device. The resultant aileron, by reason of its size, would then present very difficult structural features, as well as added weight and drag. This type of aileron naturally would have no bad effect of aggravating the stalled attitude of the dropped wing either when the airplane was coming in slightly above the stall or beyond and would have still further the advantage, by reason of the angle of its lift vector, of a favorable yawing moment that would tend to pull the low wing forward and increase its velocity and consequently its lift.

With the Zap aileron, the first reaction is that it is just another airfoil suspended above the wing, of which there have been numerous designs in the past. The original Curtis type was mounted at a considerable distance from either surface of the wing, and through its angular movements produced a workable rolling moment. These ailerons went out of existence because of the fact that they were inefficient. They induced no increase in lift over the major airfoil sections, and if they were large enough to produce a usable rolling moment, their drag, mechanism, and structural features were decidedly objectionable.

The Zap aileron, by reason of its proximity to the upper surface of the wing, naturally affects the flow over the top surface. Analyzing the several conditions, as was done in the case of the conventional floating ailerons, we find that if the airplane is being brought in close to the point of maximum lift and the wing is inadvertently dropped with a positive movement of the Zap

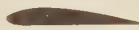









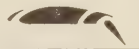

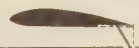
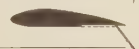
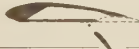
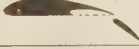
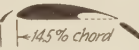
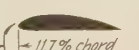
		Angle of lift increasing surface to basic airfoil	Flap chord in per cent of basic airfoil chord	Max. lift coefficient C_L max.	Speed range factor C_{Lmax} C_{Dmin}	L/D at max lift ②	Angle of attack of basic airfoil at max. lift	Per cent improvement in lift		Per cent improvement in speed-range factor		Reference, N.A.C.A. report
								Over plain airfoil ①	Over simple flap	Over plain airfoil ①	Over simple flap	
Plain basic airfoil ①				1.291	85.0	7.6	15°					T.R. 427
Simple flap		45°	30%	1.950	128.2	4.0	12°	51%		51%		T.R. 427
Slotted flap with cover plate		45°	30%	1.980	120.5	4.0	12°	53%	15%	42%	None	T.R. 427
Double slot and flap		45°	30%	2.442	117.5	4.0	16°	89%	25%	38%	None	T.R. 427
Fixed slot, cut in basic airfoil				1.772	73.8	5.3	24°	37%	None	None	None	T.R. 427
N.A.C.A. fixed auxiliary airfoil, ahead of basic airfoil ③		0°	14.5%	1.705	104.5	3.5 Approx.	24°	32%	None	23%	None	T.R. 428
N.A.C.A. optimum fixed slot ③				1.648	76.4		24°	27%	None	None	None	T.R. 400
Handley Page type automatic slot ③				1.632	114.2 ⑤ 129 ⑤		28°	26%	None	34.5% ⑤ 52% ⑤	None	T.R. 400
Front slot and simple flap		45°	30%	2.182	91.0	3.8	19°	69%	12%	7%	None	T.R. 427
Front slot and slotted flap		45°	30%	2.261	93.2	3.8	19°	75%	16%	10%	None	T.R. 427
Triple slot and flap		45°	30%	2.600	87.3	3.8	20°	101%	33%	3%	None	T.R. 427
Split flap, rotated down, no backward movement		50°	30%	2.16	138.5	4.3	14°	70%	10.7%	63%	8%	T.N. 422
Split flap, trailing edge moved vertically downward (Zap)		60°	30%	2.35	150.8	3.7 Approx.	13°	85%	20.5%	77%	17.5%	T.N. 428
Split flap, hinge point moved back to 90% of chord		54°	40%	2.222	142.2 ② 161 ⑤	3.8	13°	75%	14%	67% ③ 89% ⑤	11% ③ 126% ⑤	T.N. 422
Hall wing, front slot closed		48°	34%	2.08	138.8	3.6	13°	64%	6.7%	63%	8.1%	T.N. 417
Fowler wing, projected (area increased approx. 51% over basic airfoil) ③		40°	40%	2.422	156.3 ③ 203 ⑤	4.25	15°	90%	24.3%	83% ③ 140% ⑤	21.2% ③ 59% ⑤	T.N. 419
Fowler wing with N.A.C.A. 22 slot and round nose of basic airfoil		Slot -40° Flap +40°	Slot 14.5% Flap 40%	2.49	137 ③ 199 ⑤	3.76	21° to 25°	96%	28.1%	61% ③ 134% ⑤	7% ③ 55% ⑤	T.N. 459
N.A.C.A. 22 slot on plain wing with rounded nose		Slot -45°	Slot 14.5%	1.78	97.7 ④ 114.2 ⑤	4.8	30°	40%	None	15% ③ 35% ⑤	None	T.N. 459

FIG. 15

(This table was compiled by Richard M. Mock and was published in *Aviation*, May and July, 1933. The Reynolds number for all tests is 609,000, which corresponds to about one-third that for an ordinary small airplane at landing speed (T.R. 400). ① In comparing properties of modified sections with the plain basic section, the coefficients used in each case were obtained under similar test conditions. Drag coefficients were taken with slot closed (if movable) and with flap neutral. ② A low value of L/D at maximum lift indicates a steep glide angle and consequently a short landing. An L/D of 8 corresponds to a gliding angle of approximately 7 deg, and a value of 3.5 means about 16 deg (T.R. 428). ③ Based on total wing area; lift-increasing device extended and projected on original chord line. Actually this area is structural area necessary and forms the basis for the comparison with the simple flap. ④ With slot and flap retracted, the airfoil is not perfect, having a drag coefficient of 0.0182 compared with 0.0156 for the plain airfoil. ⑤ Based on contracted area.)

aileron, there is not only created a rolling moment by the increase in lift on the aileron acting as an airfoil section alone, but there is also an induced lift on the major airfoil, together with a yawing moment that is slightly less than the conventional aileron. (See Fig. 9.) At or below the minimum flying speed at which an unflapped airplane can fly, by reason of the fact that the Zap ailerons are used in conjunction with Zap flaps, the aileron is actually operating in an area of stimulated flow, and consequently produces favorable rolling moments at speeds far below the speed at which a conventional-wing airplane can be controlled with Frise or floating types. Even without the effect of stimulated flow due to the flap, the ailerons produce rolling moments comparable with conventional ailerons per unit of area. It must again be borne in mind that conventional ailerons cannot be used efficiently with flaps located across the entire span of the wing by reason of the fact that they would be blanketed by the flap. If they are used, the flap can only occupy the inner portion of the span. At the reduced flying speed accomplished with the aid of any slow-speed device which is below that of the minimum flying speed of an airplane without flaps, the conventional aileron is all the more ineffective by reason of the fact that it is operating in a reduced flow of air, whose velocity is equal to that of the plane and not the stimulated flow over the top surface, as is the case with the Zap type. This penalty also applies to floating ailerons, which, however, do have the overall advantage of permitting the utilization of the whole trailing edge for flap. Preliminary investigation indicates that Zap ailerons will also be quite interesting in any slot and flap application in the future.

At this point there might be given some of the practical reactions had in flying Zap-equipped airplanes. There is no doubt that reduced minimum speed, with adequate lateral control and good inherent stability, will materially lessen the fatal crashes in aviation. In the majority of instances, fatal crashes occur from flying too slowly or gliding into a forced landing immediately after motor failure. The loss in lift at a speed just below the minimum naturally causes the airplane to mush, with a consequent increase in the resultant angle of attack, which, when beyond the critical angle, results in a critical loss in lift and altitude. The reason for flying slowly is brought about by the fact that the pilot is forced to do so in order to get into a given airdrome over surrounding obstacles. Realizing that the modern airplane glides so flat and so fast, as is becoming more evident each day with the cleaning up of designs and increasing of wing loadings, and in attempting to consume the smallest possible amount of airdrome while in the glide, and also after leveling out, the pilot invariably brings the plane in as close to the point of maximum lift as he feels that he is capable of doing—and the better the pilot, the more likely he is to feel that he can play close around the stall point. If a sudden gust or if inattention on the part of the pilot inadvertently brings the flight attitude over the critical angle, a crash is likely to result, and the impact with the ground must be very close to the minimum flying speed of the ship, which, as assumed, is already very high. The pilot cannot put his nose down after coming in over an obstacle and pursue a steep angular path to the ground at a safer angle of attack because of the large pick-up in flying speed. This increase in speed would prolong the path of flight tangential to the ground, which almost invariably results in a high-speed two-point landing. With a Zap-equipped airplane, it is not necessary for the pilot to bring the airplane in close to the point of maximum lift, as far as excessive utilization of the airdrome is concerned. The Zap-equipped airplane, because of its high lift and drag, can be brought in along a flight path that is so steep as to permit only a small utilization of available airdrome distance. Even when the nose is put down at a 45- to 50-deg angle, the increase in speed is small, and when the airplane is leveled out, the drag

causes it to decelerate very rapidly and the high lift permits a slow minimum speed when it drops on the ground. It might be pointed out that the steep approach to the ground is a disadvantage from a standpoint of the technique required in landing. This would be admitted if it were not for the fact that the increased lift permits a speed along the flight path so materially reduced that from actual experience there have been no adverse comments by pilots. There have been instances of airplanes being equipped with airbrakes, but without the necessary increases in lift. The result has been that, as the airplane must be dived at the ground at a sharp angle and at an unreduced minimum speed, the rate of descent is so great as to be quite disconcerting. The reaction is caused by the necessary sharp flaring action close to the ground and the short time interval, aggravated by the high vertical velocity. With the modern airplane whose cleanness has gone so far beyond the airplane of several years ago, the addition of the drag imposed by a flap does nothing more than bring the gliding angle back to what we were accustomed to and eliminates the bad floating characteristics. If an airplane were infinitely dirty from a drag standpoint and had a high wing loading and flaps in addition, it would be conceivable that the airplane would have to be dived at the ground at a 50- to 60-deg angle, and the transition from this attitude to the 12- to 15-deg angle of attack for landing would quite complicate the technique of landing.

Here we come to the problem that is often advanced by the automatic-landing proponents. It is the author's opinion that flying will not reach popular enthusiasm sufficiently to warrant a large industry until the human element of flying has been reduced far beyond what it is today. The place where the greatest human judgment is necessary is in that transition which takes place when the airplane comes in at a given negative angle in a glide and must be leveled off with the angular attitude changing to 12 to 15 deg positive. It would be most desirable to build an airplane in which the pilot could wind a crank adjustment to a point where an indicator would designate "landing attitude," pull back his throttle, and let the airplane do the rest. There are certain things, however, which make this difficult at this time, and under certain commercial operating conditions, they will be difficult to meet in the future. This is qualified, however, by considering only existing practical high-lift devices. Rates of descent beyond 12 to 15 ft a second are going to be difficult to take care of except in a very awkward type of landing gear. A rate of descent of 12 ft a second at or near maximum lift can only be accomplished at the present time with a lightly loaded airplane of clean lines and with flaps or with slots and flaps. As the wing loading is increased, the velocity along any given flight path very adversely affects the rate of descent, and the total overall L/D of the airplane with retracted flaps must be very good in order not to have too steep an angular gliding attitude for the particular wing loading. With a lightly wing-loaded airplane, somewhere under 10 to 12 lb per sq ft, and a good L/D , it is perfectly possible today to build a private or sport-type airplane with Zap flaps that could be mushed into a landing without the necessity of the pilot redressing by touching the controls. When we get into the commercial transport field where high wing loadings are imperative from a standpoint of speed and pay-load efficiency, it will be essential that the pilot use quite an amount of judgment in approaching the ground and in the following leveling off for landing. This condition will continue, in my opinion, until such time as we are able to create much higher lift coefficients than are practical today.

In closing it might be added that as one becomes more experienced with flap airplanes, he arrives at the conclusion that the ability to raise and lower the flap quickly is almost as important as lateral control, particularly under forced-landing conditions.

In a number of practise forced landings, it has been found that it becomes necessary to alternately lower and raise the flaps to compensate for errors in judgment of gliding angle.

The importance of this can hardly be appreciated until one has attempted a forced landing under several varying wind conditions. For instance, when approaching a landing field under forced conditions, the flap is lowered and half way down in the glide it is discovered that the wind is blowing quite rapidly and the plane will not make the field, it is extremely desirable to be able to wind the flaps up very quickly, pick up speed, and extend the gliding angle until it is assured that the field can be made with safety.

By the time this decision has been reached, the airplane in most cases is at a very low altitude right over the edge of the field, and therefore the flap must be brought into action again very rapidly. It can be seen that a flap requiring a high operating force, necessitating too many turns of the handle, is quite impractical for anything other than landings on normal airdromes with full control of the engine and where there is ample time, and such a flap would be actually dangerous under forced-landing conditions.

Many engineers have asked about the spinning characteristics of Zap flaps, and in a recent controversy in one of the international aviation magazines a correspondent has claimed that the split flap should have very undesirable spinning characteristics. There are two things to offset this impression: First, the relation between drag and the slope of the lift curve is very favorable; and second, in the B/J company's XOJ biplane on which flaps were installed, it was absolutely impossible to spin the airplane either with power on or off, even when the center of gravity location was 4 per cent farther back than the plane was designed for. In a normal stall there is no particular tendency for the plane to rotate in either direction, and the nose merely drops forward until the plane has picked up speed.

In this connection it is interesting to compare the difference

between the acute stalling of a Zap-equipped airplane of 12 or 13 lb wing loading and that of an airplane of straight airfoil section with the same wing loading. When the latter type is acutely stalled, where the landing speed is around 55 to 60 mph, there is a resultant dive from which the pilot does not attempt to recover until the airplane has reached a speed of at least 70 to 80 mph. Because of the attitude of the plane in the downward plunge and the relatively horizontal attitude of the lift vector whose vertical component necessary to overcome the force of gravity is relatively small, the airplane must be allowed to traverse a considerable vertical distance in order that the lift vector may be acting efficiently in overcoming gravity. Any attempt to pull the plane out previous to this time is more or less injudicious, because the inertia of the plane at the speed of 70 to 80 mph is so great as to cause a mushing action, with a resultant angle of attack that might again put the airplane into a spin. Those who have seen the training that went on during the war in JN-4's realize exactly what this means, because time and again students have been seen to spin for several hundred feet, stop the rotation, enter a dive, and immediately go into a spin from the dive in the opposite direction. With a lightly loaded airplane, say of 5 to 6 lb per sq ft, which means a flying speed of approximately 40 mph, in a similar stall, the airplane can be pulled out of its dive at 20 to 30 mph less speed than under the first condition, simply because the inertia is reduced as the difference between the square of two velocities, and being so much less the airplane can be brought to a level flying attitude with a considerable reduction in vertical descent. Because a flapped airplane also flies at a reduced rate, the inertia forces are consequently less, and therefore a stall is less dangerous when close to the ground, as it acts similar to the light-wing-loaded type.

There is a mass of additional data of a specific nature that might have been included, and the author will be very glad to furnish this to those engineers who are further interested in the application of Zap flaps and ailerons to their particular designs.

A Thermal Study of Available Steam-Power-Plant Heat Cycles

BY G. A. HENDRICKSON¹ AND S. T. VESSELOWSKY,² DETROIT, MICH.

Turbine and plant heat rates obtainable in large modern power plants are compared over a wide range of the pressure-temperature-cycle realm. These results were estimated from heat balances based on typical expansion lines for 50,000-kw turbines, which size was deemed sufficiently representative to draw rather general conclusions regarding large units. Cost estimates are not included, but the results are given in a form readily adaptable to the needs of those making economic comparisons. To this end, plant heat rates are given for estimating the rate of use of fuel, and turbine heat rates with supplementary data for estimating the size, and hence the cost, of the various equipment in a plant. The difference between turbine

and plant heat rates allows for auxiliary power in proportion to the cycle requirements, and for miscellaneous losses sufficient to give the expected annual average value of the plant heat rates. While the computations are purposely fitted to a particular type of turbine and plant, the results apply approximately to most of the modern central stations. Comparisons of the thermal efficiencies of practical cycles with corresponding Carnot efficiencies are used to point out the best direction for future efforts. It is concluded that regenerative-feed-heating plants with the highest practicable initial temperature offer the greatest promise, both for immediate use and for future development.

DURING the last 10 years the efforts of steam-power engineers to lower plant heat rates has prompted an intensive study of the relative efficiencies of available power cycles, and this in turn has brought forth a number of valuable papers³ on both the thermal and economic factors of the problem. Early in this period The Detroit Edison Company, recognizing the need for an exchange of ideas on a national scale, sponsored the paper by C. F. Hirshfeld and F. O. Ellenwood on "High Pressure, Reheating, and Regenerating for Steam Power Plants."⁴ That paper and others published then and later embraced all of the pressure-temperature-cycle realm of interest at the time of their presentation. A recent extension of the field considered practicable for operation, coupled with the publication of enlarged steam-table data by the A.S.M.E., has warranted a more complete survey to guide an extension of practise.

¹ Engineer, The Detroit Edison Company. Assoc.-Mem. A.S.M.E. Mr. Hendrickson was graduated from the Oklahoma A. and M. College, Stillwater, in 1922 and entered the service of The Detroit Edison Company the same year. He spent four years in routine testing and operation in Delray Power House, and then entered the engineering division of the company to work on problems of thermodynamics in the generation and use of power.

² Engineer, The Detroit Edison Company. Mr. Vesselowsky was graduated from the University of St. Petersburg, Russia, in 1905 and from the Federal Polytechnical School, Zurich, Switzerland, in 1908. For eight years he was connected with the Russian General Electric Company in various capacities in the factory at Riga and in the central offices at St. Petersburg. From 1919 to 1924 he was superintendent of the power house of the Société Ottomane d'Electricité at Constantinople, Turkey. He came to America in 1924, and since 1925 has been engaged in the research department of The Detroit Edison Company, working on problems in mechanics and thermodynamics in power-plant practise.

³ See Bibliography, Appendix III.

⁴ A.S.M.E. Trans., 1923, pp. 663-711.

Contributed by the Power Division and presented at the Semi-Annual Meeting, Chicago, Ill., June 26 to July 1, 1933, of THE AMERICAN SOCIETY OF MECHANICAL ENGINEERS.

NOTE: Statements and opinions advanced in papers are to be understood as individual expressions of their authors, and not those of the Society.



G. A. HENDRICKSON



S. T. VESSELOWSKY

available steam-turbine cycles, which is reported in the present paper.

The purpose of this paper is to supply data for a quick, accurate comparison of the probable performances of projected plants over a wide range of the pressure-temperature-cycle realm, so that future projects may be developed along the most promising lines. Although ultimate comparisons necessarily include economic factors, such as fuel costs and capital investments, these factors vary greatly with location and with economic conditions; hence their final inclusion in the computed results is omitted from this paper. Thermal results, however, are presented in a form readily adaptable to the needs of those making economic comparisons. To this end two complete sets of heat rates are given—namely, plant heat rates for estimating the rate of use of fuel and turbine heat rates with supplementary data for estimating the size, and hence the cost, of the various equipment in a plant.

The field covered is not limited by established practise, but is extended to include cycles and steam conditions of possible interest for future development. The cycles studied include Rankine, regenerative-feedheating, reheating-regenerative-feedheating, and a cycle using regenerative preheat of the combustion air by bled steam.

Since the regenerative-feedheating cycle is of greater immediate importance than any other, it is studied in detail in one, two, three, and four feedheating stages. The reheating cycles studied include one-stage boiler-room reheat by combustion gases, one- and two-stage local reheat by live steam,

and one-stage local reheat by bled steam. These cycles are designated throughout by the following symbols:

- A_0 = Rankine
- A_1 = Regenerative feedheating in one stage
- A_2 = Regenerative feedheating in two stages
- A_3 = Regenerative feedheating in three stages
- A_4 = Regenerative feedheating in four stages
- A' = *Regenerative air preheat in four stages
- B = *Boiler-room reheat in one stage
- C = *Live-steam reheat in one stage
- D = *Live-steam reheat in two stages
- E = *One-stage regenerative reheat (by bled steam)

* NOTE: These five cycles have four regenerative-feedheating stages.

Fig. 9 gives a line diagram of all of these cycles.

The initial steam conditions covered include temperatures of 700 to 1000 F and pressures of 200 to 3500 lb per sq in. Not all cycles, however, are extended to this upper pressure limit. With each cycle and temperature the initial pressure is restricted to a value near that which gives the maximum permissible moisture content of the exhaust. A common exhaust pressure of 1.0 in. Hg abs is assumed for all cycles and steam conditions, and in addition all computations for the Rankine and regenerative-feed-

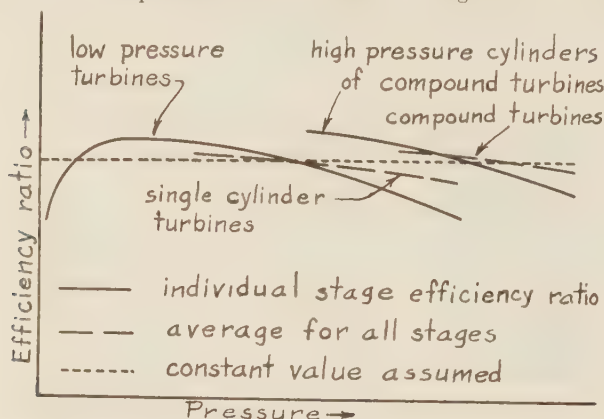


FIG. 1 EFFECT OF COMPOUNDING ON STAGE-EFFICIENCY RATIOS

heating cycles are repeated with 1.5 and 2.0 in. Hg. The expansion lines of Fig. 10 aid in visualizing the range of steam conditions covered. Feedwater temperatures of principal interest are those frequently designated as the "optimum"—that is, feedwater temperatures with which the most favorable heat rate is obtained.

The discussion is divided into four major sections. The first section, on basic data and methods, outlines the choice of assumptions and methods for their use in the final computations. The second section, on accuracy of the results, attempts to determine the errors in heat rates computed from the methods and data chosen. The third section, on the correlation of results, outlines the results presented and their interpretation in terms of actual turbines and plants. The fourth section, on general deductions, outlines the development of the heat cycle used in present conventional plants, points out the imperfections in fitting the basic cycle to its heat source, and shows how ideal conditions may be approached to the greatest possible degree.

Following these four sections, a few general conclusions are presented, and three appendixes are added for reference. Appendix I is an alphabetical list of all the nomenclature used; Appendix II is a collection of all the important formulas; and Appendix III is a bibliography of the principal papers covering studies of steam cycles in the last 10 years. Finally, the results of the computations are presented in graphical form.

BASIC DATA AND METHODS

Great care was necessary in choosing the basic data and

methods. The type of turbine expansion line used, the manner of accounting for the kinetic energy of the exhaust, and the miscellaneous assumptions allowing for pressure and temperature loss in various parts of the circuit determine the significance of the heat rates obtained in the final result. These items are discussed in detail in the following paragraphs to supply a basis for interpreting the computed results in terms of actual turbines and plants.

All computations are based on the 1930 A.S.M.E. "Steam Tables and Mollier Diagram," by J. H. Keenan. The work done by a pound of steam expanding between given pressure limits is determined from turbine expansion lines drawn on an enlarged version of this steam diagram with a constant dry-state individual-stage efficiency ratio⁶ evaluated in collaboration with two of the large turbine manufacturers to agree with the operating results obtainable from large modern turbines. This method is adopted in preference to the use of adiabatic expansion lines and engine-efficiency ratios, because a stage-efficiency ratio can be extrapolated into unexplored steam-chart regions with greater confidence than the more complex engine-efficiency ratio. The use of turbine expansion lines has the objection that only one particular type and size of turbine can be represented accurately in the results, whereas the use of ideal cycles and engine-efficiency ratios permits the adaptation of the results to any type and size of turbine by the insertion of a suitable engine-efficiency ratio. Since all modern turbines of interest to central-station operators have about the same efficiency under given conditions, this is not a serious objection to the turbine-expansion-line method.

Only a few expansion lines are drawn (see Fig. 10), and each is used for a number of cases with different cycles and different initial and final steam conditions. This requires a composite line representing, not the expansion characteristic for some given turbine, but an average condition for all possible turbines. Expansion lines for hypothetical turbines with an infinite number of stages and infinite exhaust area satisfy this need. Such lines are readily drawn by means of the relations given in Equations [1], [2], and [3], Appendix II.

Fig. 1 shows how the dry-state efficiency ratio e appearing in these equations varies in actual turbines. Gradually rising during expansion, it reaches a maximum and drops abruptly in the last few stages. As the initial pressure increases, the efficiency ratios of the higher pressure stages decrease, with a consequent decrease in the average stage-efficiency ratio as shown. Finally a point is reached where it is desirable to use compound turbines. The liberties in choice of wheel and shaft diameters and the number of stages afforded to the turbine designer by compounding permit an increase in the efficiency ratio of the upper stages and a discontinuity in the average as shown. With extremely high pressures, multi-expansion turbines would be used with further discontinuities in the average efficiency ratio. For simplicity in use, e is assumed constant at 0.845 throughout the dry-steam region. This value, when corrected for the effect of moisture in the wet-steam region, reproduces with fair accuracy the results obtainable from large modern turbines. The moisture correction used is 1 per cent for each 1 per cent of moisture present in a given stage. The resulting efficiency ratio is given in Equation [3]. The end-points of the expansion lines of Fig. 10, drawn from these data and Equations [2] and [3], are reproducible within 0.1 Btu per lb of steam.

These lines give the expected expansion end-points for hypothetical turbines having no exhaust loss—that is, for turbines

⁶ For accuracy in expression, the terms stage-efficiency ratio and engine-efficiency ratio are used in place of the more common stage efficiency and engine efficiency. It should be noted that these terms do not represent true efficiencies, but ratios of the actual efficiencies to the corresponding basic-cycle efficiencies.

with infinite exhaust area. In such a turbine the kinetic energy of the exhaust would be available for conversion into useful work at the efficiency obtaining in the lower stages. To determine the effective expansion end-point in an actual turbine, an exhaust-loss correction is necessary. Since the stage loss for this correction is already charged against the expansion efficiency, the correction desired is the actual exhaust loss multiplied by the efficiency ratio of the last stage. This relation is given in Equation [4].

Variation of the kinetic energy of the exhaust E in Equation [4] is so complicated that no complete, satisfactory representation of it is available. Moreover, it is necessary to make a more or less arbitrary disposal of some points on which practise is not uniform. For example, some manufacturers proportion nozzle and blade areas of their bleeding turbines for the actual conditions of operation, while others prefer to proportion all turbines for non-extraction operation, with a consequent reduction in development charges during manufacture. Unfortunately, a single set of computations cannot show the results for both of these practises. Since all of the turbines with which the authors have occasion to work are proportioned for non-extracting operation, allowances for exhaust loss are made on the basis that the kinetic energy of the exhaust at layout steam flow or maximum-efficiency load non-extracting is the same for all turbines considered. The exhaust loss chargeable depends then on the amount of steam extracted. An approximate solution for this dependence is given in Equation [5], Appendix II. At maximum-efficiency load non-extracting the value of the kinetic energy of the exhaust E in Equation [4] is assumed at 12.1 Btu per lb of steam exhausted. A 10 per cent allowance for hood losses makes the total exhaust loss $E_1 = 13.5$ Btu per lb. This exhaust-loss allowance and the expansion lines of Fig. 10 define completely the assumed turbine performance.

The computation of overall turbine-room results necessitates further assumptions involving the characteristics of accessory equipment. For example, the pressure and heat loss in extraction lines, the terminal temperature difference in feedheaters, and other losses must be determined before extraction-turbine performance can be computed.

Exact determination of the pressure loss in extraction lines for an actual installation is usually done as a trial-and-error computation. For hypothetical cases or projected installations, a direct computation is possible if the pressure loss is assumed on the basis that the plants in question may be designed to fit. Preliminary computations showed a 5 per cent pressure drop in extraction lines and fittings to be fairly representative of average conditions. This allowance provides for an extraction line length equivalent to 75 ft of straight pipe and four 90-deg bends and a steam velocity of 200 ft per sec.

The following assumptions covering the characteristics of feedheaters, condensers, reheaters, air preheaters, and throttle valves are estimated from practise without detailed investigation: 5 F terminal temperature difference in the feedwater heaters, 4 F undercooling of condensate⁶ in the main condenser, 10 per cent pressure reduction through the steam reheaters, 10 F terminal temperature difference in steam reheaters and bleed-steam air preheaters, and 4 per cent pressure reduction through the turbine throttle valve at full primary opening. Other pressure losses assumed are, for steam mains, 10 per cent, and for feedwater mains, 100 lb per sq in. It was further assumed on the advice of the turbine manufacturers that the most favorable locations of the individual feedheaters are obtained with that distribution in which equal amounts of steam are extracted to

each heater. These assumptions make possible the computation of expected operating data for turbines and their accessory apparatus.

Expected annual average plant heat rates are obtained from turbine heat rates by making proper allowances for auxiliary power consumption, loss to flue gas, cost of feedwater make-up, and miscellaneous plant losses.

In the allowances for auxiliaries, the power for boiler-feed pumps, for coal handling and firing auxiliaries, and for circulators was computed separately in proportion to the cycle requirements. Equations [6], [7], and [8] for these items assume 0.60 as the combined efficiency of each auxiliary and its drive. Miscellaneous losses such as station lighting, air compressing, and general service-water pumping are assumed constant at 0.005 kw per gross kw for all conditions. This value gives a total auxiliary power consumption of 5 per cent for a 400-lb regenerative-feedheating plant. Summing these, Equation [9], Appendix II, gives the total auxiliary power allowance.

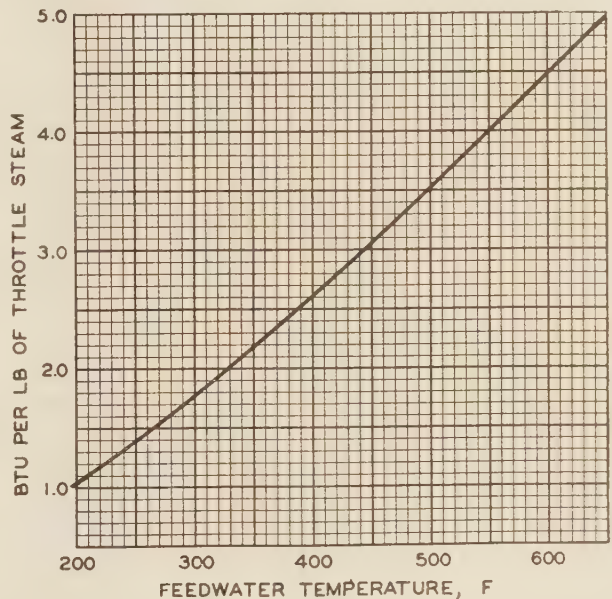


FIG. 2 REDUCTION OF USEFUL WORK BY ADDING EVAPORATORS

Loss to the flue gas is estimated on the assumption that a boiler with a maximum test efficiency of 0.88 may be designed for any plant considered.

The cost of feedwater make-up for the regenerative-feedheating cycles is computed from the change in steam rate by bleeding the steam required for an interstage evaporator located between the two highest pressure feedheating stages. This in turn is determined by the change in work given in Equation [10], Appendix II. Similar equations could be developed for the reheating cycles, but a considerable amount of computation is avoided by using a curve of the data computed in the treatment of the regenerative-feedheating cycle. In this curve given in Fig. 2, the cost of feedwater make-up is almost independent of initial steam conditions and depends principally on the feedwater temperature.

The foregoing allowances for auxiliary power and other losses give a basis for determining plant heat rates from turbine heat rate with continuous "test condition" performance under optimum conditions throughout the plant. To account for miscellaneous losses arising from sudden changes in load, operation off the maximum efficiency points, and other unpredictable causes,

⁶ Recent changes in condenser practise in the plants of The Detroit Edison Company indicate that less undercooling might have been assumed. This is a small item and has no appreciable effect on the results.

a plant operating heat rate ratio is introduced. It is assumed that the annual average plant heat rate will be 10 per cent greater than the computed optimum "test condition" plant heat rate. This factor is chosen to agree with plants in the experience of the authors.

These assumptions for auxiliary power, flue-gas loss, cost of feed-water make-up, and miscellaneous losses complete the data necessary for a final computation of complete plant performance.

ACCURACY OF RESULTS

It is proper to inquire into the accuracy of these data and assumptions as a means for computing the expected performances of actual turbines and plants on a comparable basis. The following discussion attempts to outline the faults of the more important items of basic data, and to determine their probable effect on the accuracy of the results.

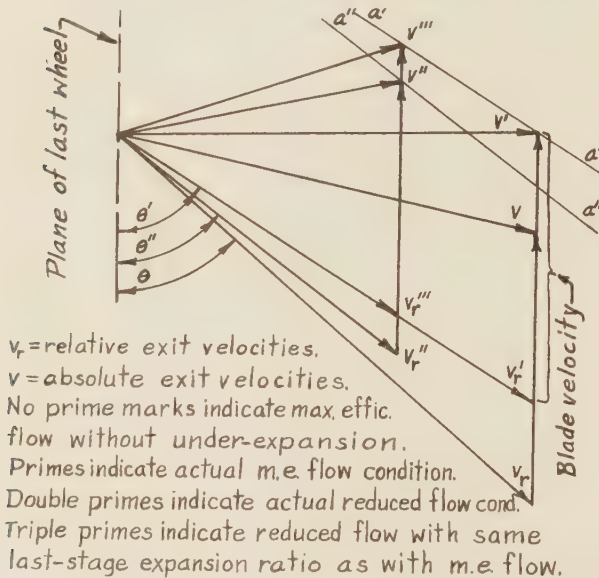


FIG. 3 VARIATION OF EXHAUST LOSS WITH CHANGE IN STEAM FLOW

The steam chart used is probably most important. Fortunately, the chart region of chief immediate interest, which includes steam temperatures up to 750 F at all pressures considered, is supported by sufficient data from the A.S.M.E. Steam Research Committee to insure its accuracy within the limits desired for this study.⁷ Comparison with European steam-research data indicates further that the chart is sufficiently accurate at all temperatures considered for pressures below 1000 or 1200 lb per sq in. Thus the region in which the steam chart accuracy is at all questionable is represented by pressures above 1000 or 1200 lb per sq in. when the temperature is above 750 F. The A.S.M.E. Steam Research Committee does not estimate the probable magnitude of the error in this area, and it is therefore impossible to give a reliable estimate of the error introduced from this source into the computed heat rates. It probably does not exceed 30 Btu per kw-hr, and tends to show a lowered heat rate in the computed results.

Another small error that enters into the results by way of the steam chart concerns not the accuracy of the chart itself, but the readability of its scale. The large-scale Mollier diagram used in the computations is readable to the nearest 0.1 Btu per lb of steam. Since the end-points of the expansion lines are accurate

within that limit, they determine the work done by a pound of steam expanding over a given pressure interval to the nearest 0.1 Btu. The corresponding error in heat rate is about ± 5 Btu per kw-hr.

The work indicated by the expansion lines depends on the dry-state-efficiency ratio used in their construction. Since this efficiency was determined from actual turbine data, it represents actual turbine performance very accurately for steam conditions in the immediate vicinity of these data (375 lb gage and 750 F). There naturally arises the question of how accurately this same dry-state-efficiency ratio portrays the operating characteristics of other turbines operating under different steam conditions. One manufacturer of large turbines states that the expected performance is predictable over the entire known field by this method with an error less than 1 per cent—that is, about ± 100 Btu per kw-hr.

This question is related very closely to the use of so-called compound and multi-cylinder turbines. The relation of the average dry-state-efficiency ratio of a single-cylinder turbine to that of a compound or multi-cylinder turbine has already been shown in Fig. 1. It is there indicated that compounding increases the efficiency. Since the fields of these two turbine types overlap, it is necessary to consider the effect of this point when comparing compound and single-cylinder turbines in the same steam chart region. Further it is evident from Fig. 1 that even with compound and multi-expansion turbines the stage efficiency may continue to drop with higher pressures. The effect of extreme pressures is not accurately predictable at this time, and it is possible that for pressures above the limits of present experience the error allowance previously stated would be insufficient.

The discussion of errors so far pertains wholly to those introduced in the determination of the end-points of the computed expansion lines. The location of the actual expansion end points is affected by the error of the exhaust loss charge as determined by Equation [5]. This formula assumes that the curve of exhaust loss plotted against exhaust flow F is a parabola. This would be true if the exhaust steam left the last wheel with a relative velocity v_r (Fig. 3) always at the angle θ with the plane of the wheel. Here θ is the exit angle of the last wheel blades. Actually, because of underexpansion in the last turbine stage, there is a deflection of the exhaust steam to a different angle θ' , and the relative discharge velocity becomes $v_{r'}$, with a corresponding absolute discharge velocity v' . The kinetic energy E_1 in Equation [5] corresponds to the absolute velocity v' in Fig. 3 for non-bleeding operation at the layout steam flow, and the equation assumes that the end of the vector representing absolute velocity moves along the line $a'a'$ parallel to v_r' when the exhaust flow changes with bleeding. Any variation in the exhaust flow, however, results in another expansion ratio for the last stage, and consequently a different exit angle θ'' . Thus when the turbine is bled, the relative velocity of the exhaust is $v_{r''}$ instead of $v_{r'}$ and the actual exhaust loss chargeable is determined by the corresponding absolute velocity v'' rather than v' accounted for in Equation [5]. Computations on an actual turbine indicate the magnitude of this error to be about ± 25 Btu per kw-hr in the cases with greatest bleeding. It is of course zero in the Rankine cycles.

The foregoing items constitute the most important errors in the non-reheating heat rates attributable to the nature of the available data and assumptions. A further possible error of ± 10 Btu per kw-hr is introduced by two graphical interpolations in reducing the results to presentable form.

An error that applies only to the reheating cycles enters through the determination of the optimum points for extraction when a reheat point intervenes between two extraction points.

⁷ See "Correlation of Steam-Research Data," by Dr. Harvey N. Davis, MECHANICAL ENGINEERING, vol. 51, p. 129.

Failure to ascertain the exact optimum point introduces a possible error estimated at 0 to +25 Btu per kwhr.

Another minor error arises in converting turbine heat rates into overall plant heat rates, as follows: Evaporators for make-up supply are assumed to be located between the two highest-pressure extraction stages in every case. In the lower pressure cycles this is necessary to keep the volume of make-up vapor low so that sufficient relieving capacity may be obtained with reasonably small surface. The same assumption is extended to all cases for simplicity in treatment. In consequence the make-up is heated from its supply temperature to its vaporization temperature in a single step, and the advantages of regenerative heating are lost. The magnitude of this loss is estimated at 0 to +25 Btu per kwhr, and depends principally on feedwater temperature. It affects all cycles except the Rankine and one-stage regenerative-feedheating.

All the errors discussed may be tabulated as follows:

Source of error	Magnitude, Btu/kwhr	Operates
Steam-chart inaccuracy.....	- 30*	Above 1000 lb and above 750 F
Steam-chart reading.....	± 5	In all results
Stage efficiency used.....	±100	With differences in initial pressure
Computation of exhaust loss.....	+ 25	In cycles employing extraction
Graphical computation.....	± 10	In all results
Optimum feed temperature with reheat.....	+ 25	In reheating cycles
Evaporator location.....	+ 25	In plant results with high feed temperatures, all cycles except Rankine and one-stage regen- erative-feedheating
Total.....	+190 to -145	

* NOTE: A negative error indicates that the computed heat rate is below the actual.

In most cases the error would be much less than the total given as the maximum.

CORRELATION OF RESULTS

In addition to the heat rates presented in this paper, a large amount of pertinent data was made available in the course of the computations. A complete presentation is not practicable, but a sufficient amount of this supplementary data is included for a ready redetermination of all the important items not directly exhibited.

Two complete sets of heat rates are given in Figs. 13 to 19, inclusive. Turbine and plant heat rates are presented side by side for each cycle considered. Of these the plant heat rate may be used for comparing the thermal economy of projected plants. However, since these data contain arbitrary allowances for auxiliary power and other losses, the turbine heat rates are much more definite, and should be used whenever they can be made to give the comparison desired.

Optimum feedwater temperatures for all cycles are given in Fig. 11. These data, together with the reheater data for cycle B in Fig. 18, permit the ready determination of steam rates, heat rates, heats rejected to the circulating water, and the volume of the steam exhausted. Equations [11] to [18], Appendix II, apply in these determinations, and may be followed by Equations [6] to [9] to obtain an itemized estimate of the auxiliary power required.

The expansion lines of Fig. 10, with the data and equations given, may be used for an approximate determination of the condenser steam rate, total steam extracted, steam extracted to each heater, and other minor items. These uses are not described in detail. Since the scale of Fig. 10 is quite small, any one with a considerable amount of such work to do could profitably construct expansion lines on a larger chart to suit his needs.

For plants operating on any of the cycles studied, these data permit a detailed analysis in a fraction of the time required for a complete computation.

Since, as previously stated, no single set of results can accurately represent the different types of turbines in general use, the assumptions made apply particularly to a throttle-governed 1200-rpm turbine of 30,000 kw or larger with straight impulse blading. It is necessary to consider this point when comparing two turbines of different type; and if the greatest possible accuracy is desired, a complete detailed computation may be necessary for each case. For example, in a comparison between a throttling turbine and a cut-out-governing turbine having a two-blade-row first-stage wheel, with the same initial steam conditions in each case, the respective actual expansion lines would show differences, not only at the end-points of the expansion, but at intermediate points as well. Further, because of differences in the heat rate versus load curves, the load-duration characteristic would affect the relation between turbine heat rate and plant heat rate differently in each case. Hence it is evident that errors not mentioned among those previously listed may influence the comparison when considering turbines with differing expansion characteristics.

Another instance, illustrating the discrepancy between calculations and the performance of actual turbines, is in the treatment of the exhaust loss at different back pressures. The exhaust loss for which any actual turbine should be designed would be determined at the point of economic balance between capital charges and the cost of fuel with different last-wheel and exhaust-hood sizes. Determination of exhaust loss for each case in this study on such a basis would be an almost endless task and would enhance the value of the results only slightly. Although the constant value assumed is believed to be quite satisfactory when comparing cases with the same back pressure, comparisons involving a change of back pressure may require special consideration if the greatest possible accuracy is desired.

These points are mentioned to illustrate that care must be exercised in applying these computed data to the performance of actual turbines and plants.

With one exception, the results presented are on a comparable basis for all cycles considered. Since any given boiler efficiency is harder to obtain when preheating the combustion air by bled steam, the assumption of a constant boiler efficiency for all cycles is slightly favorable to the cycle using preheat by bled steam as compared to a straight four-stage regenerative-feedheating cycle.

Some remarks on the allowances for auxiliary power may be helpful. Strictly, the plant results are applicable only to plants with completely motorized auxiliaries supplied with power directly from the main bus. Actually there is little difference between such a plant and one having a separate steam-driven auxiliary power supply, provided the auxiliary turbine exhausts to the same back pressure as the main turbine, and has its condensate heated in the main feedheating system or its equivalent. Further, the steam-driven emergency apparatus used in many places has a negligible effect on the plant heat rate. The results given, therefore, should apply approximately to most of our present-day conventional plants.

GENERAL DEDUCTIONS

Any survey of the efficiencies obtainable from different steam or cycle conditions undertakes to indicate those developments most promising for increasing the basic cycle efficiency. The problem may be approached from two distinct points of view. First and most important, any particular improvement should pay an economic return on the required investment. This phase of the question must be left for individual treatment. Second, but important also, each detail of improvement should be examined to determine the relation of its efficiency increase to that of another possible development which might be sub-

stituted. The remainder of this paper is occupied with a brief examination into the past development of power production, and attempts to point out other possible lines of development for the future. The shortcomings of present-day cycles are illustrated by comparison with ideal cycles, and an optimum cycle, subject to practical restrictions, is developed from these comparisons.

The atmospheric engine of Newcomen, which is generally ac-

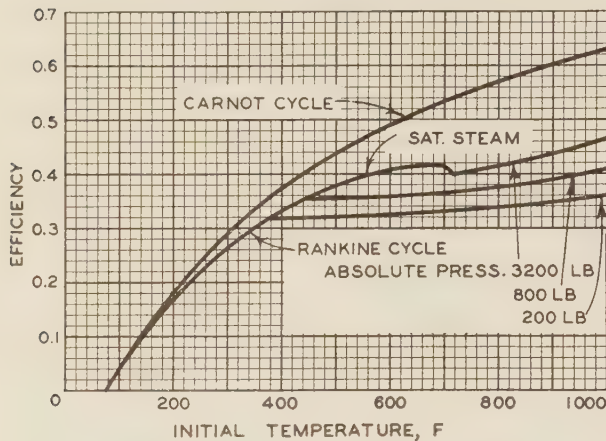


FIG. 4 COMPARISON OF CARNOT AND RANKINE CYCLE EFFICIENCIES

cepted as the first practical attempt to use steam for the production of power, operated on what may be called a full-admission Rankine cycle taking steam at atmospheric pressure and exhausting into a vacuum. Over a period of about 200 years following the advent of this engine there ensued a gradual improvement in the working steam-pressure range. At the close of the nineteenth century, triple-expansion engines were operating with pressures as high as 150 lb per sq in. A few quadruple-expansion engines used even higher pressures, but the large expansion ratio limited the range of initial pressures practicable with a displacement engine. Because of the fear of lubrication

alloy steels capable of withstanding yet higher temperatures, and then to increase the pressure to the economic limit. As indicated by the installation of several plants to operate at temperatures of 750 to 850 F, this seems to be the line of action favored by both European and American producers. The semi-experimental 1000-F unit at Delray is a further step in this direction.

This brief survey of the growth of power production outlines the present state of the art. A Rankine-cycle plant with the initial steam conditions of the Newcomen engine would have an efficiency of 8 to 10 per cent, which is more than doubled by the substitution of 400 lb per sq in., 700 F initial steam conditions into the same cycle. This improvement has paid handsomely on the added capital invested.

Theoretically this same line of development might be followed indefinitely, for it may be observed that as the superheat temperature is increased the limiting Carnot efficiency also is raised, and indefinite efficiency increments are therefore possible. Naturally this possibility should be pursued as far as it gives promise of paying an adequate economic return, but the comparison with alternate developments must not be neglected. Fig. 4 shows a comparison of Carnot efficiencies with those of the Rankine cycle at different temperatures. Carnot efficiency, being the limiting efficiency, indicates when any appreciable improvement over a given cycle is possible. Fig. 4 may thus be used to determine when changes from the Rankine cycle should be considered. A glance at the saturated-steam line shows that in the earlier years of steam-power production with low-pressure saturated steam, the basic cycle efficiency was very near the Carnot limit for the temperature employed. Higher pressures and temperatures widen the gap between actual and Carnot cycles. It is apparent that as the initial temperature is raised at constant initial pressure—that is, with increases in superheat—the resulting efficiency increase does not keep pace with the corresponding Carnot efficiency. This is no indictment against the use of superheat, for as previously mentioned it is purely an economic question. If a higher degree of superheat pays an adequate return, it should be used. The point it is meant to emphasize here is that the time has arrived when some attention

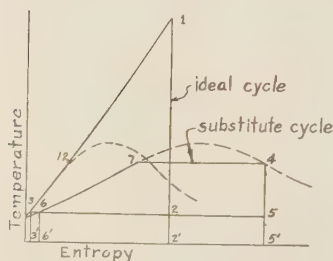


FIG. 5 TEMPERATURE-ENTROPY DIAGRAM OF IDEAL AND RANKINE CYCLES WITHOUT AIR PREHEAT

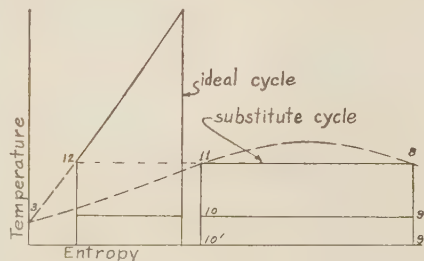


FIG. 6 TEMPERATURE-ENTROPY DIAGRAM OF IDEAL CYCLE AND SUBSTITUTE VAPOR CYCLE WITH AIR PREHEAT

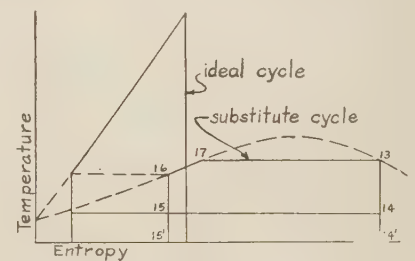


FIG. 7 TEMPERATURE-ENTROPY DIAGRAM OF IDEAL CYCLE AND SUBSTITUTE VAPOR CYCLE WITH LIMITED AIR-PREHEAT TEMPERATURES

troubles, superheat was not used; indeed, the value of increased temperatures was not fully realized until the very close of the period of supremacy of the reciprocating engine. The introduction of steam turbines made possible almost immediately the use of temperatures around 450 F, and opened the way to future pressure increases. Since the erosion of the lower-stage blades by moisture in the exhaust restricts the initial pressure practicable for turbines, even this higher temperature limited the pressure to around 150 lb per sq in. Subsequent use of steel castings in the high-pressure casing permitted temperatures around 700 F and pressures of 400 lb per sq in. Following the same line of development, the next step was to substitute

should be given to possible changes in the basic cycle itself, so that actual cycle efficiencies nearer the Carnot limit may be attained. Some progress has already been recorded in this direction, notably the general adoption of regenerative feedheating by extracted steam. Reheating and binary cycles, not yet generally accepted, may be mentioned. Each of these improvements tends to lessen the gap between actual cycle efficiencies and the Carnot limit, but still the difference is large.

Any attempt to improve this condition must consider the incongruities between the basic cycle used and its heat source and endeavor to eliminate them. Since a complete elimination of losses is not always possible under the restrictions of practise,

the following discussion is intended to outline the optimum basic cycle subject to operating requirements.

Energy for the production of power is obtained from the irreversible release of the chemical energy of the fuel by combustion. Point 1 on the temperature-entropy diagram of Fig. 5 represents the condition of the combustion products, and the cycle 1-2-3 would produce the greatest amount of work that it is possible to obtain from them on any continuous operating basis. Because of the very high temperature at the initial point, and the mechanical difficulty of the isothermal compression along line 2-3, the Rankine vapor cycle 4-5-6-7 is substituted in actual plants. The loss by this substitution is evident from a consideration of an intermediate Rankine vapor cycle 1-2-3 which is ideally suited to the heat source and which obviously has the same efficiency as the gas-cycle 1-2-3. As areas in this diagram represent energy, the areas 1-2'-3'-3 and 4-5'-6'-6-7 are the same; and each represents the energy available from the fuel. Then since the mean ordinate of 4-5'-6'-6-7 is much lower than that of 1-2'-3'-3, it follows immediately that the heat rejected 5-5'-6'-6 for cycle 4-5-6-7 is greater than 2-2'-3'-3 from cycles 1-2-3. This increased loss to the circulating water is the direct result of the decrease in top temperature at which the heat of combustion is added to the working medium.

In the conventional type of power plant three things are done to lower this loss which enters by the dissimilarity of the cycle and its heat source. The top temperature T_{7-4} is raised to the highest practicable limit, the addition of heat along the liquid line 6-7 is eliminated by the use of regenerative feedheating, and air preheaters are added to absorb the heat of combustion along line 3-12 formerly going into the liquid. The limiting condition for this cycle, i.e., the case with an infinite number of feedheating stages, is equivalent to the Carnot cycle 8-9-10-11, of Fig. 6. With stoker-fired plants it would be necessary to limit the air-preheat temperature to a value considerably below the initial vapor temperature. Regenerative feedheating also should stop at that temperature, and the best cycle then becomes 13-14-15-16-17 of Fig. 7.

Except for the omission of superheat, this is the ordinary regenerative-feedheating cycle of conventional plants. With the omission of superheat, however, the cycle has the practical disadvantage that the moisture content of the exhaust would be high enough to cause excessive erosion of the turbine blades. To overcome this difficulty, it is necessary to introduce some form of reheating; and, if no reduction in efficiency is permissible, the reheating must be regenerative. Consider the circuit of Fig. 8, which accomplishes this result. Saturated steam enters the turbine and expands to the limiting moisture content beyond which the turbine blades would suffer from erosion. The steam is then removed from the turbine, reheated by steam extracted from the next higher pressure stage, and returned for further expansion. When the limiting moisture content is again reached, the reheating process must be repeated, and so on to the exhaust. Steam is withdrawn at each of these reheat points for feedheating. With an infinite number of stages, this cycle also

becomes equivalent to the Carnot cycle of Fig. 6, and the exhaust steam is dry and saturated. Thus, if the reheaters of Fig. 8 or a substitute can be developed, the last barrier to practical application is removed, and the gap between basic-cycle efficiency and the Carnot limit shown in Fig. 4 is eliminated.

The discussion so far has considered only the use of steam as a working medium. Since the critical temperature of steam is considerably below the practicable operation limit of present materials, a working medium other than steam must be adopted

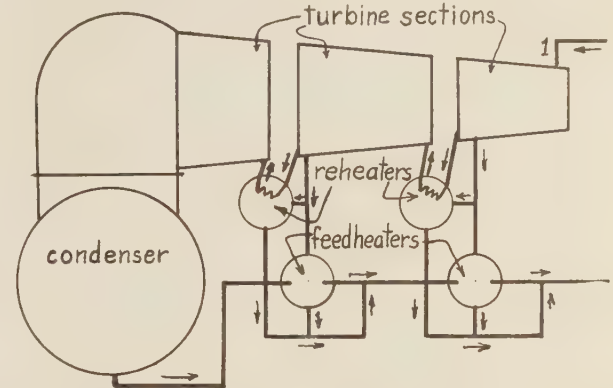


FIG. 8 CIRCUIT DIAGRAM OF PRACTICAL CYCLE WITH CARNOT EFFICIENCY LIMIT

to obtain the full benefits from the foregoing cycle. Further, because of the long expansion and the consequent great difference between specific volume at the head and tail ends of a single-expansion cycle, a binary expansion cycle might be necessary.

Development of plants to operate on the cycles of Figs. 6 and 7 with 1000 F top temperature would make possible the production of power at a coal pile to switchboard heat rate of about 9000 Btu per kw-hr estimated from the ideal cycle heat rate of 5400 Btu per kw-hr. Note that this heat rate is possible with processes that are all in present use. The only special features of this plant are an expanding medium other than steam and the unusual application of reheat. Since the heat source for reheat is extracted wet vapor instead of vapor at throttle pressure, the reheater may offer some difficulties in design. Excepting these characteristics, a plant designed to operate on the cycle suggested would be much like present conventional plants using local reheat, regenerative feedheating, and air preheat. It would have the highest efficiency obtainable with the irreversible combustion of coal and the irreversible transfer of the heat of combustion to a working medium, at a temperature that can be used with existing metals.

CONCLUSIONS

The principal value of this paper is in the possible use of the results for estimating purposes. For example, Table 1 summarizes the data for several pressure-temperature-cycle condi-

TABLE 1 COMPUTED AND ACTUAL HEAT RATES FOR SEVERAL IMPORTANT CYCLES
(Back Pressure in All Cases 1 In. Hg Abs)

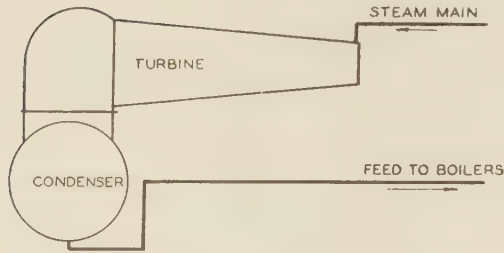
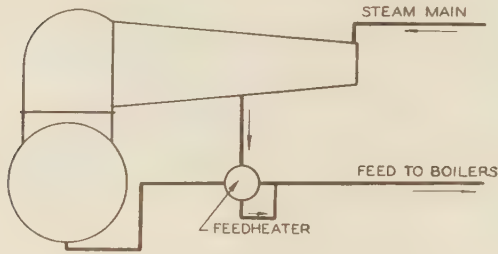
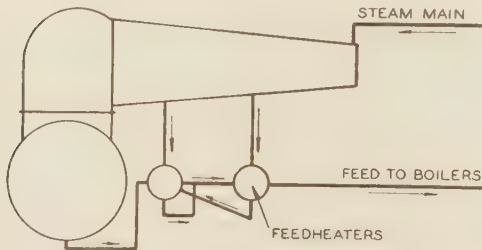
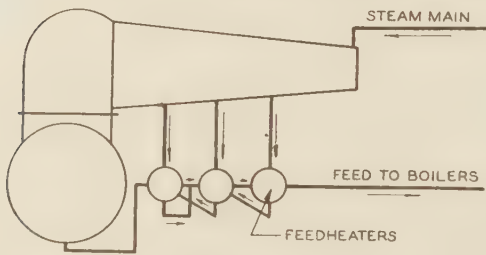
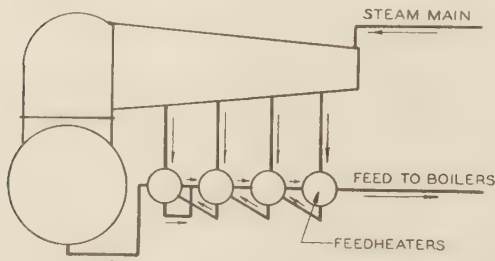
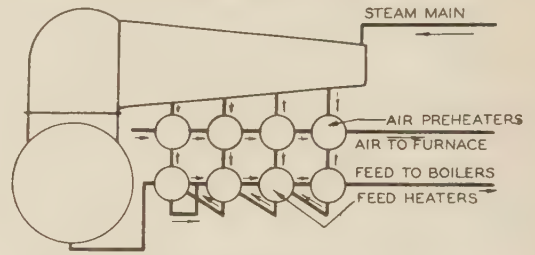
Throttle steam, deg F and lb per sq in. gage	Heat rates, Btu per kw-hr				Cycle description
	Plant	Computed Turbine	Condenser plant	Actual plant	
700 F—375 lb	14,150	10,720	7176	14,110 ^a	Regenerative (three-stage extraction)
700 F—400 lb	13,710	10,450	6876		Regenerative (three-stage extraction)
750 F—400 lb	13,260	10,070	6506		Regenerative with air preheated by steam bled from turbine (four-stage extraction)
750 F—650 lb	12,940	9,800	6236	^b	Reheating by live steam (one stage of reheating)
750 F—650 lb	12,900	9,800	6236		Reheating by steam bled from turbine (one stage of reheating)
1000 F—365 lb	12,780	9,650	6086		Regenerative (three-stage extraction)
750 F—600 lb	12,500	9,550	5986	12,560 ^c	Reheating by boiler gases (one stage of reheating)
750 F—1250 lb	11,830	8,910	5346	12,720 ^d	Reheating by boiler gases (one stage of reheating)

^a Trenton Channel, 12 month average.

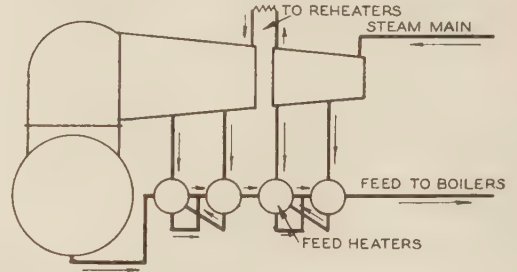
^b Crawford Avenue, units 5 and 6.

^c Columbia, published results before renozzling turbines for greater capacity.

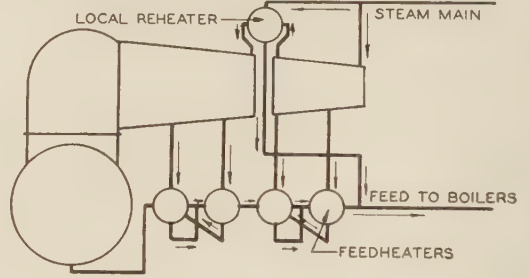
^d Gilbert, early operating results, which will undoubtedly be reduced.

CYCLES A_0 —RANKINECYCLE A_1 , REGENERATIVE—FEEDHEATING IN ONE STAGECYCLE A_2 , REGENERATIVE—FEEDHEATING IN TWO STAGESCYCLE A_3 , REGENERATIVE—FEEDHEATING IN THREE STAGESCYCLE A_4 , REGENERATIVE—FEEDHEATING IN FOUR STAGESCYCLE A' , REGENERATIVE—FEEDHEATING IN FOUR STAGES
WITH AIR PREHEAT BY BLED STEAM

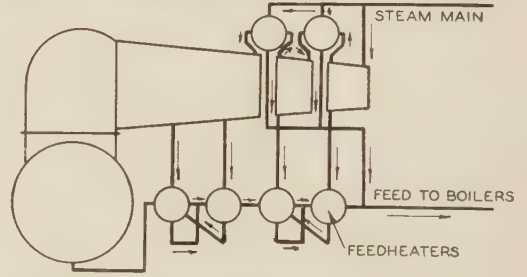
CYCLE B, BOILER ROOM REHEAT IN ONE STAGE



CYCLE C, LOCAL REHEAT BY LIVE STEAM IN ONE STAGE



CYCLE D, LOCAL REHEAT BY LIVE STEAM IN TWO STAGES



CYCLE E, LOCAL REHEAT BY BLED STEAM IN ONE STAGE

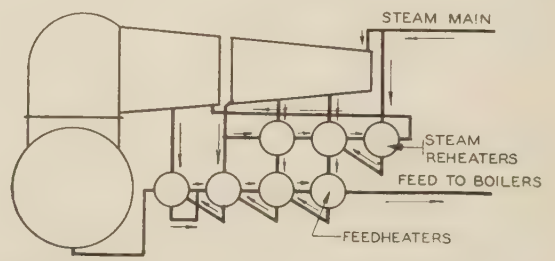


FIG. 9 LINE DIAGRAMS OF CYCLES STUDIED

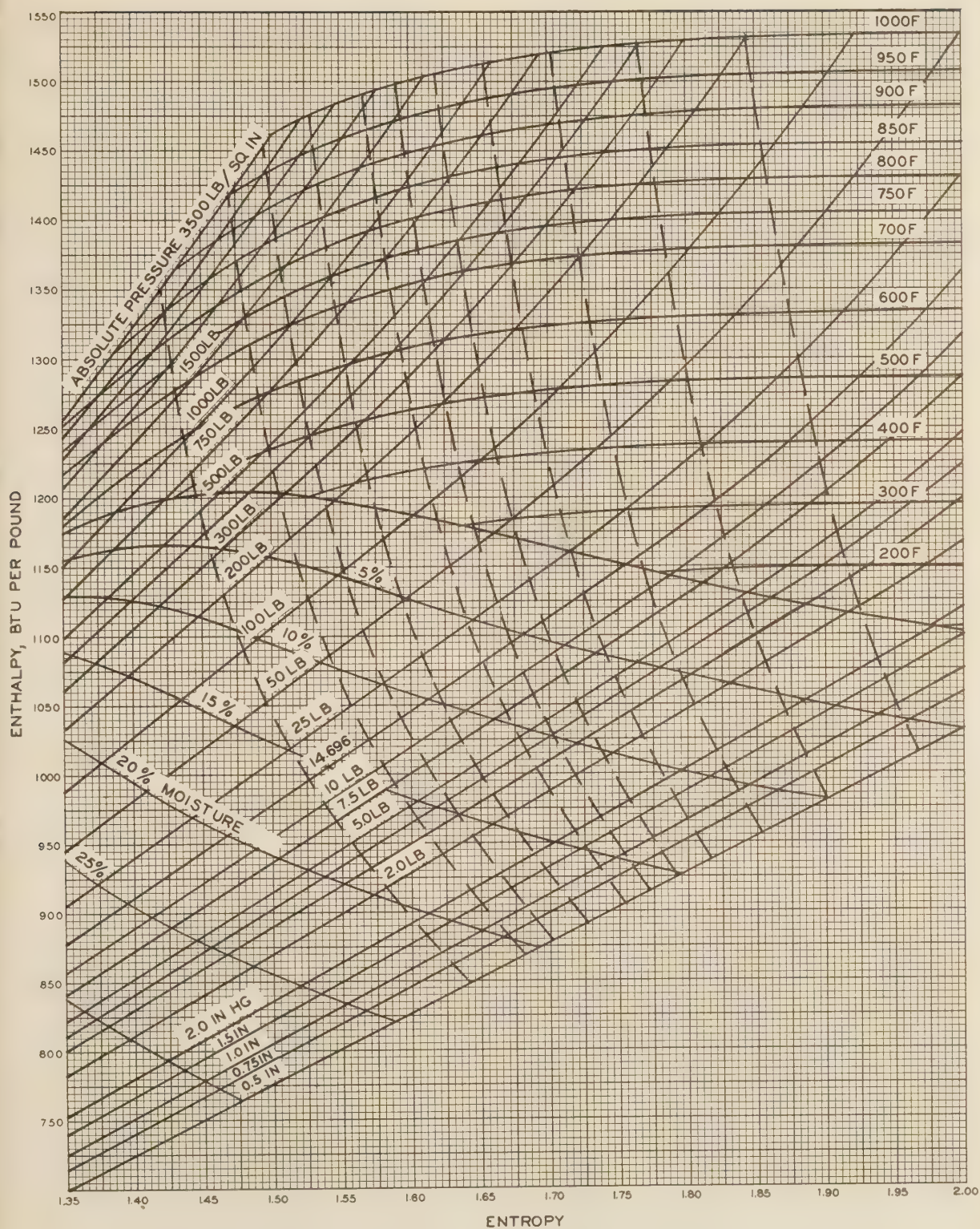


FIG. 10 MOLIER DIAGRAM WITH TURBINE EXPANSION LINES

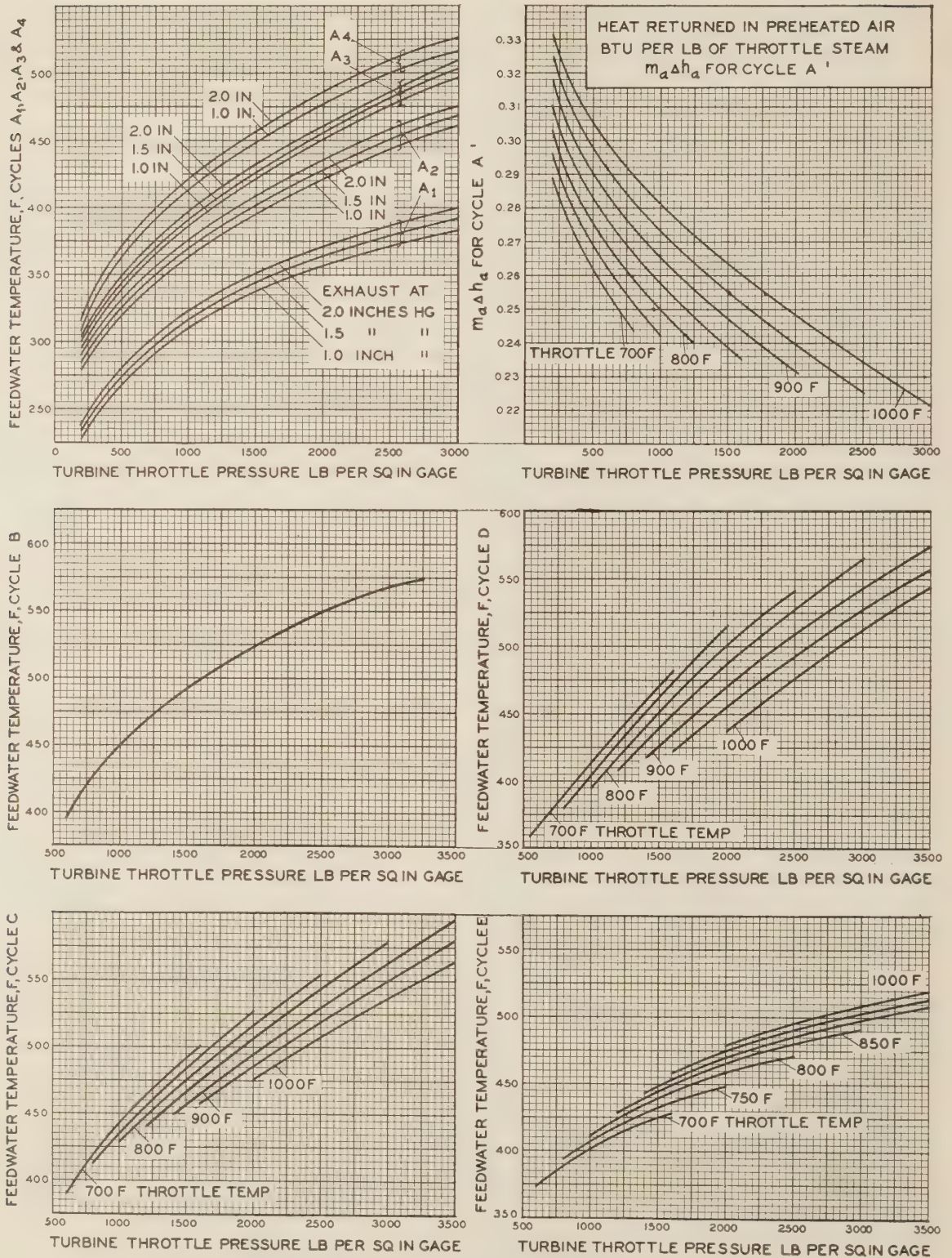


FIG. 11 OPTIMUM FEEDWATER TEMPERATURES AND HEAT RETURNED IN PREHEATED AIR

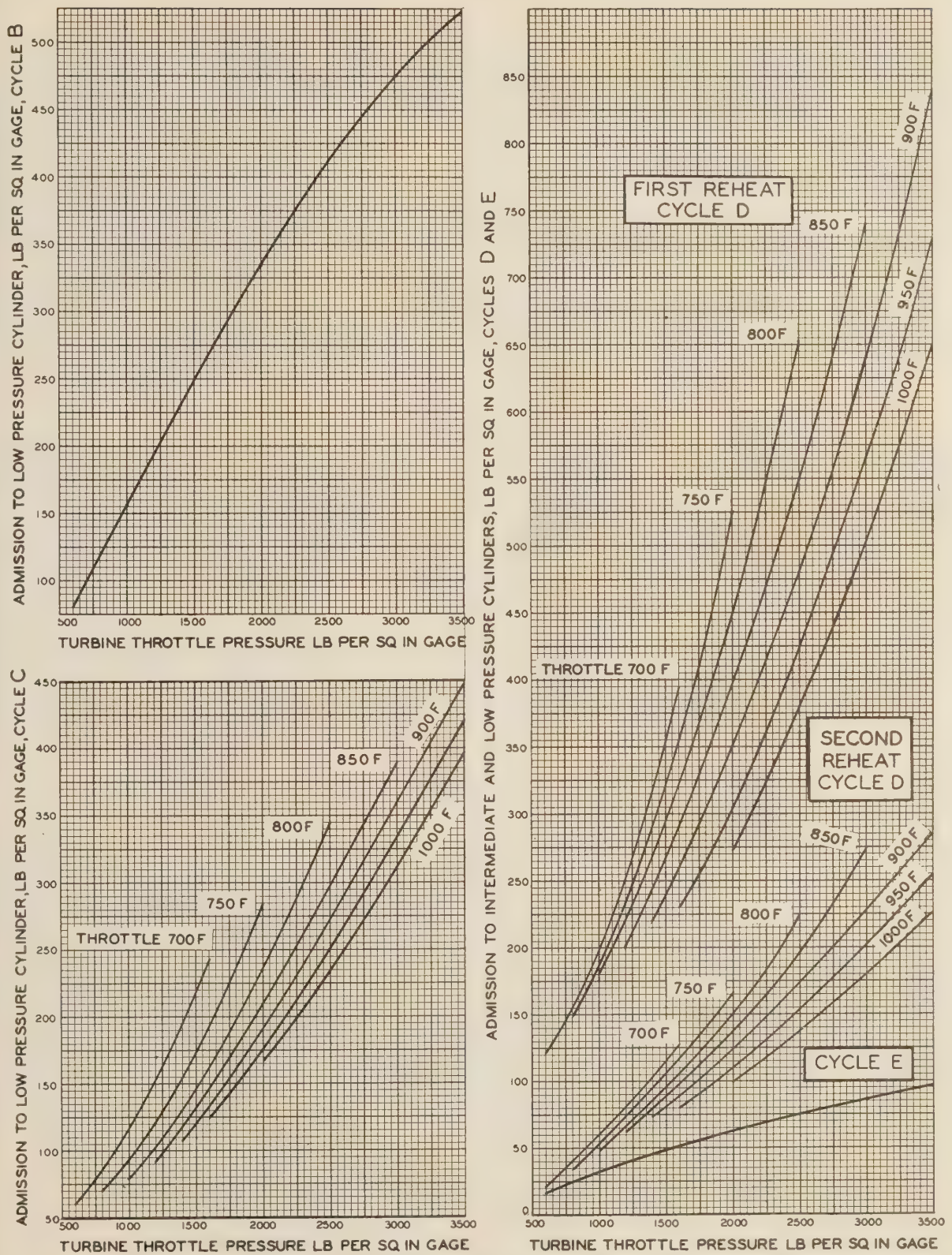
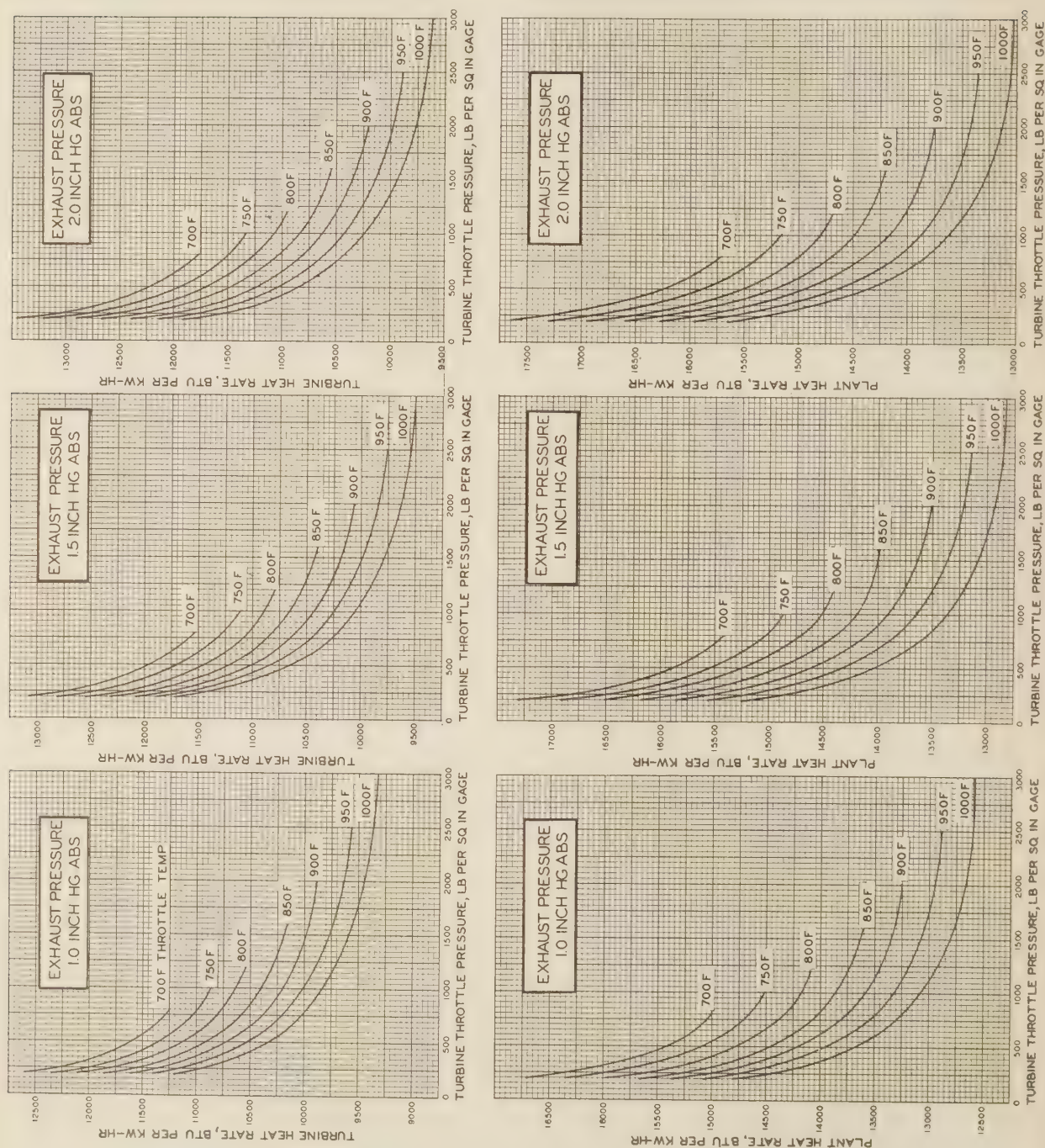
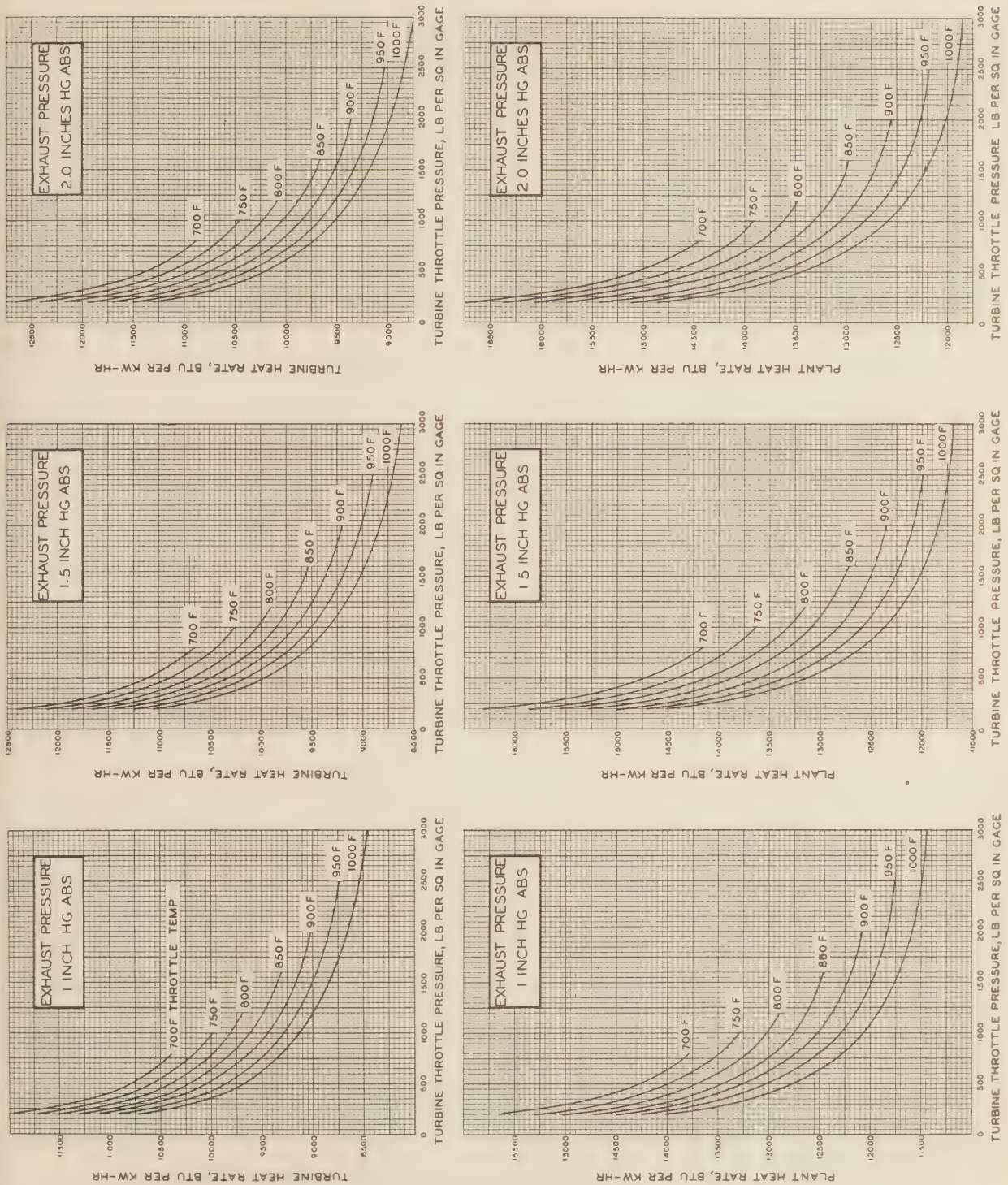


FIG. 12 OPTIMUM REHEAT PRESSURES

FIG. 13 TURBINE AND PLANT HEAT RATES, CYCLE A₀, RANKINE

FIG. 14 TURBINE AND PLANT HEAT RATES, CYCLE A₁, REGENERATIVE FEEDHEATING IN ONE STAGE

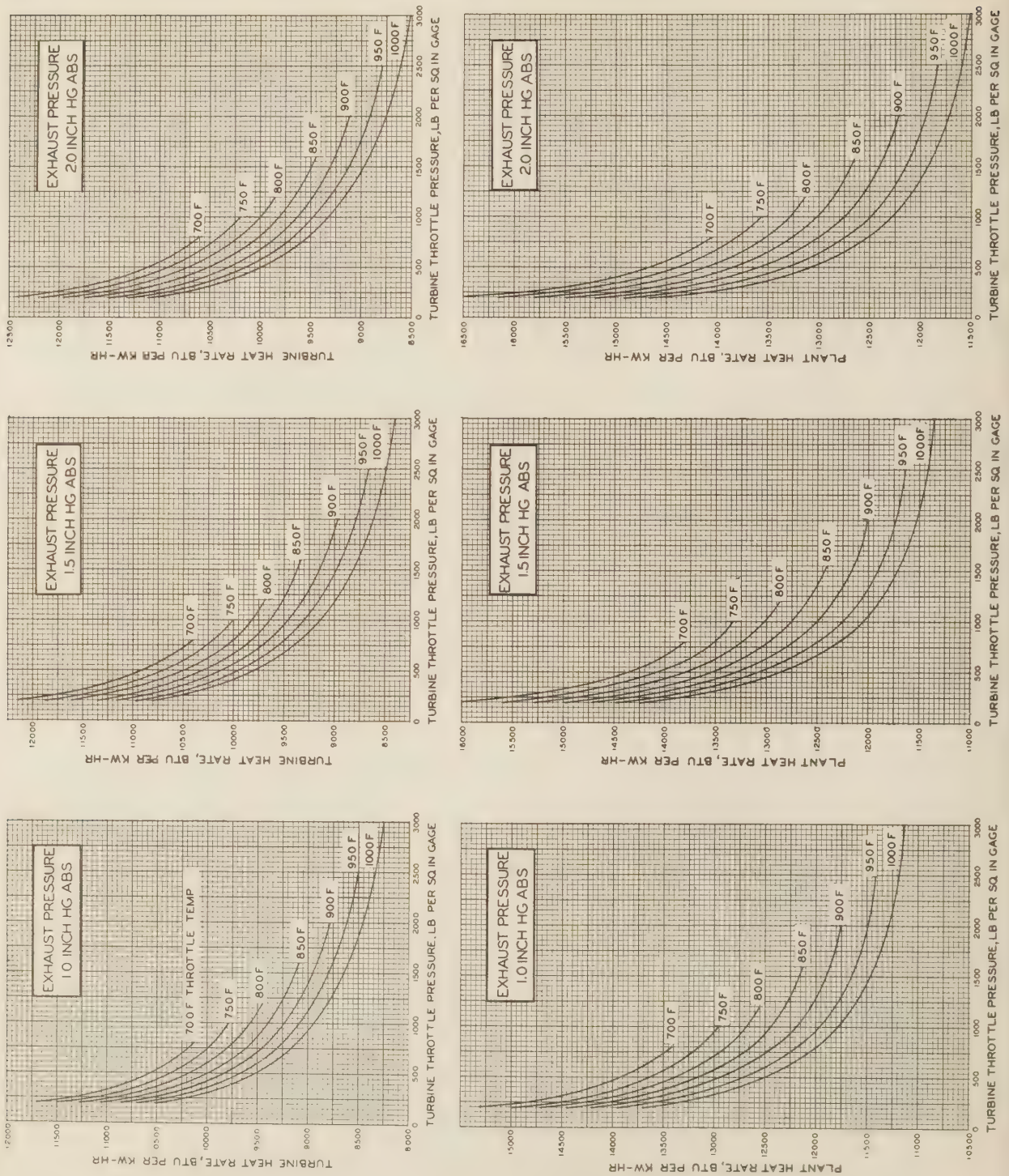
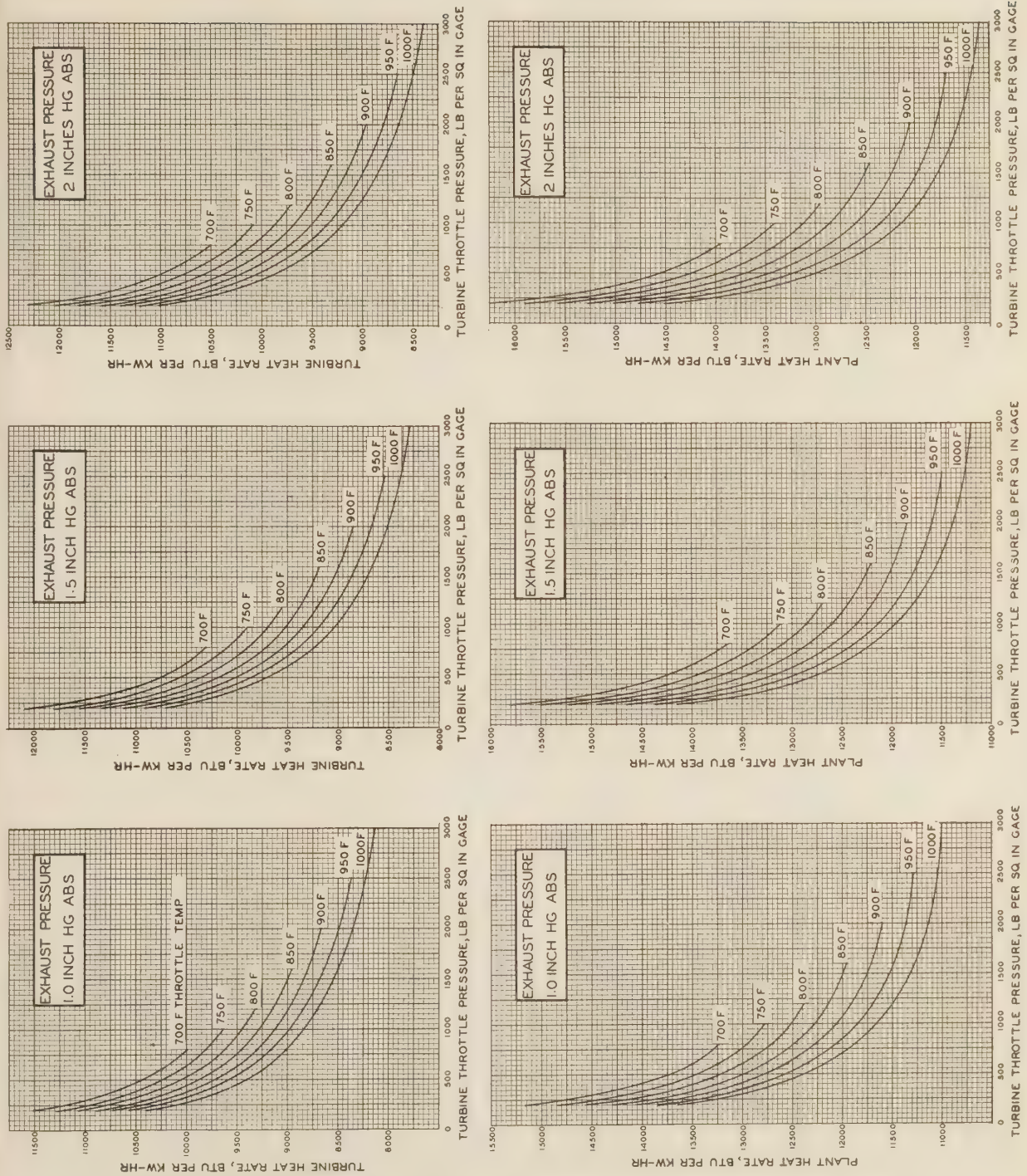


FIG. 15 TURBINE AND PLANT HEAT RATES, CYCLE A₂, REGENERATIVE FEEDHEATING IN TWO STAGES

FIG. 16 TURBINE AND PLANT HEAT RATES, CYCLE A₃, REGENERATIVE FEEDHEATING IN THREE STAGES

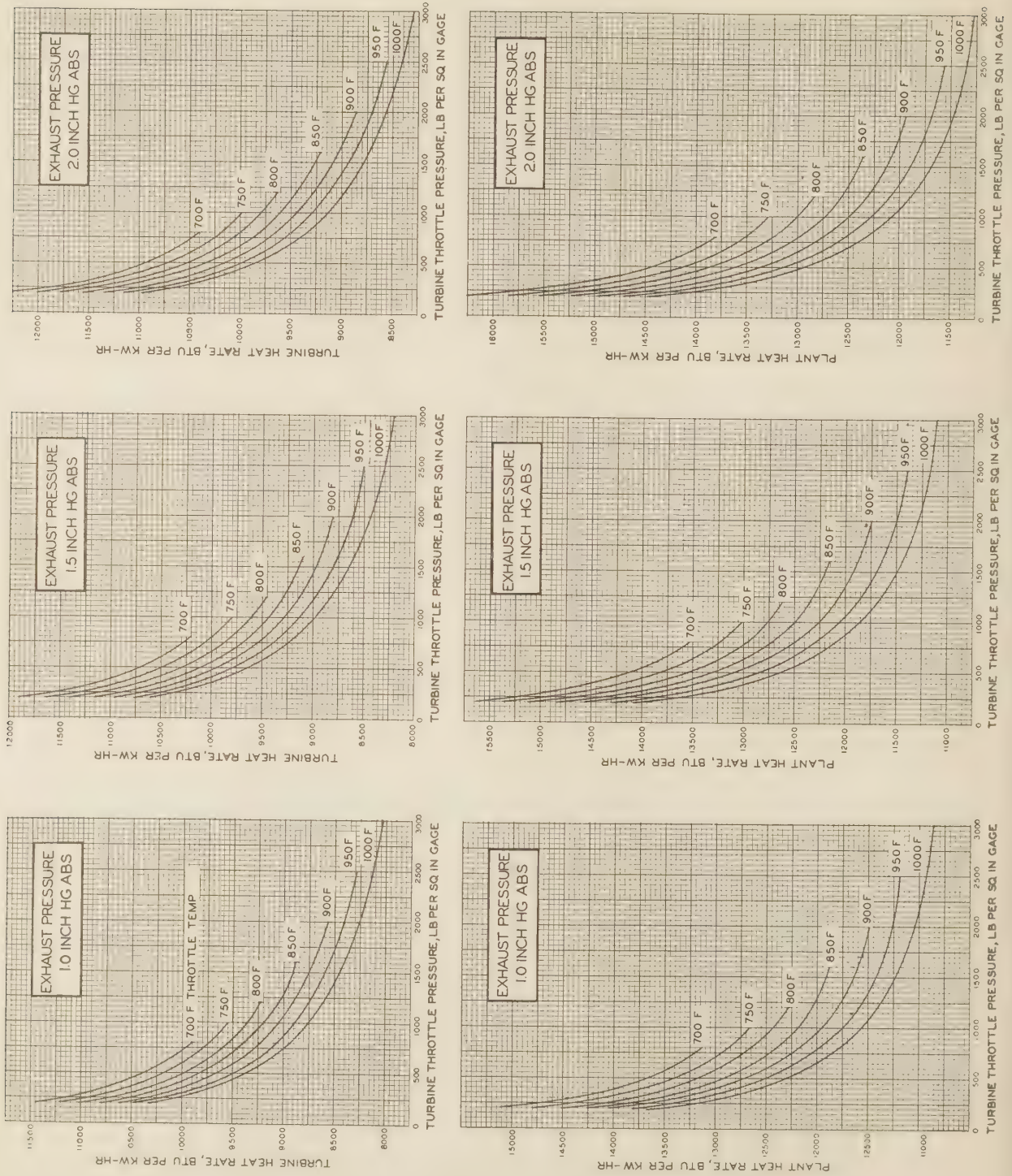


FIG. 17 TURBINE AND PLANT HEAT RATES, CYCLE A₄, REGENERATIVE FEEDHEATING IN FOUR STAGES

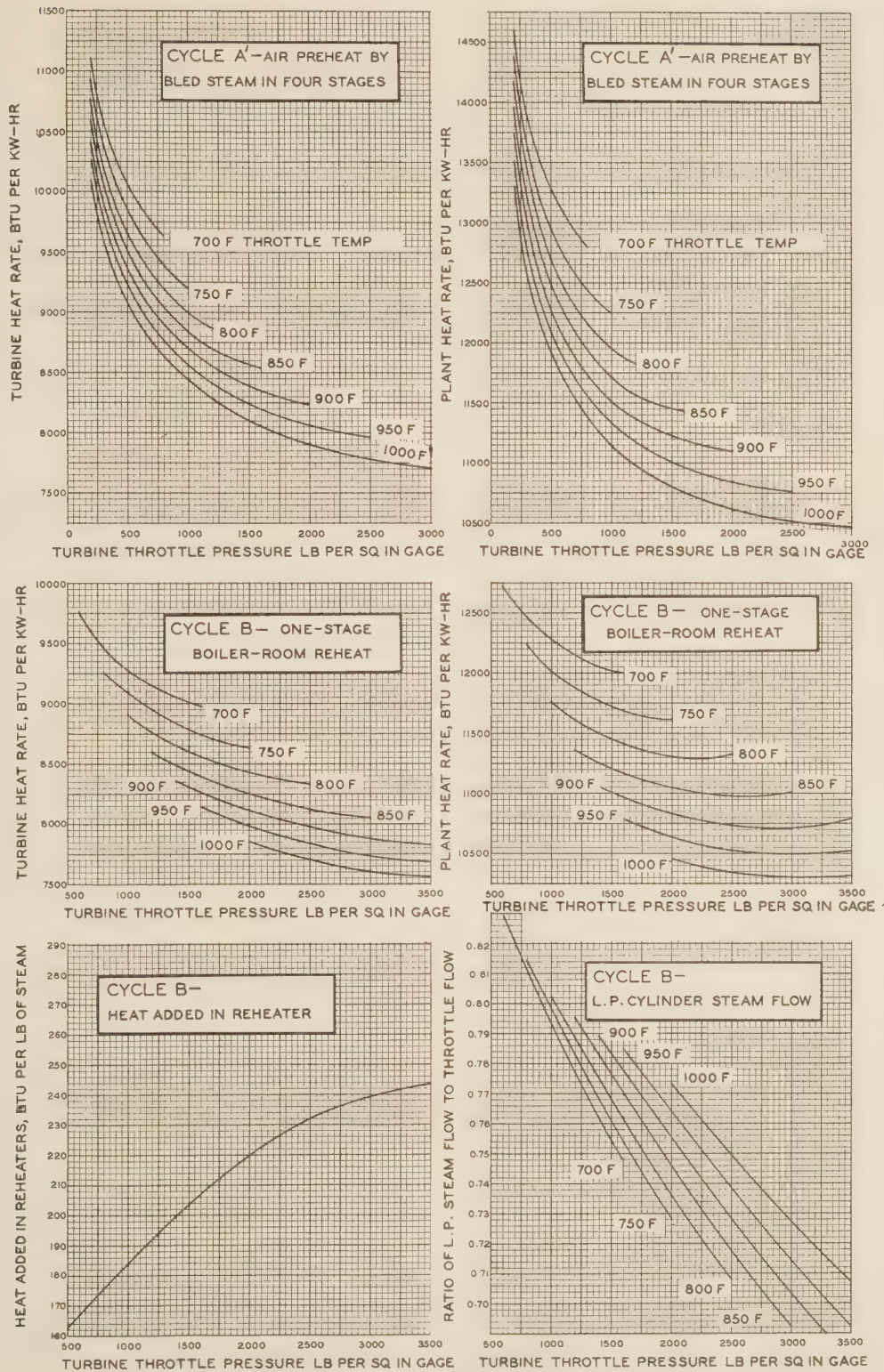


FIG. 18 TURBINE AND PLANT HEAT RATES, CYCLE A' AND B, WITH DATA ON CYCLE B REHEATER

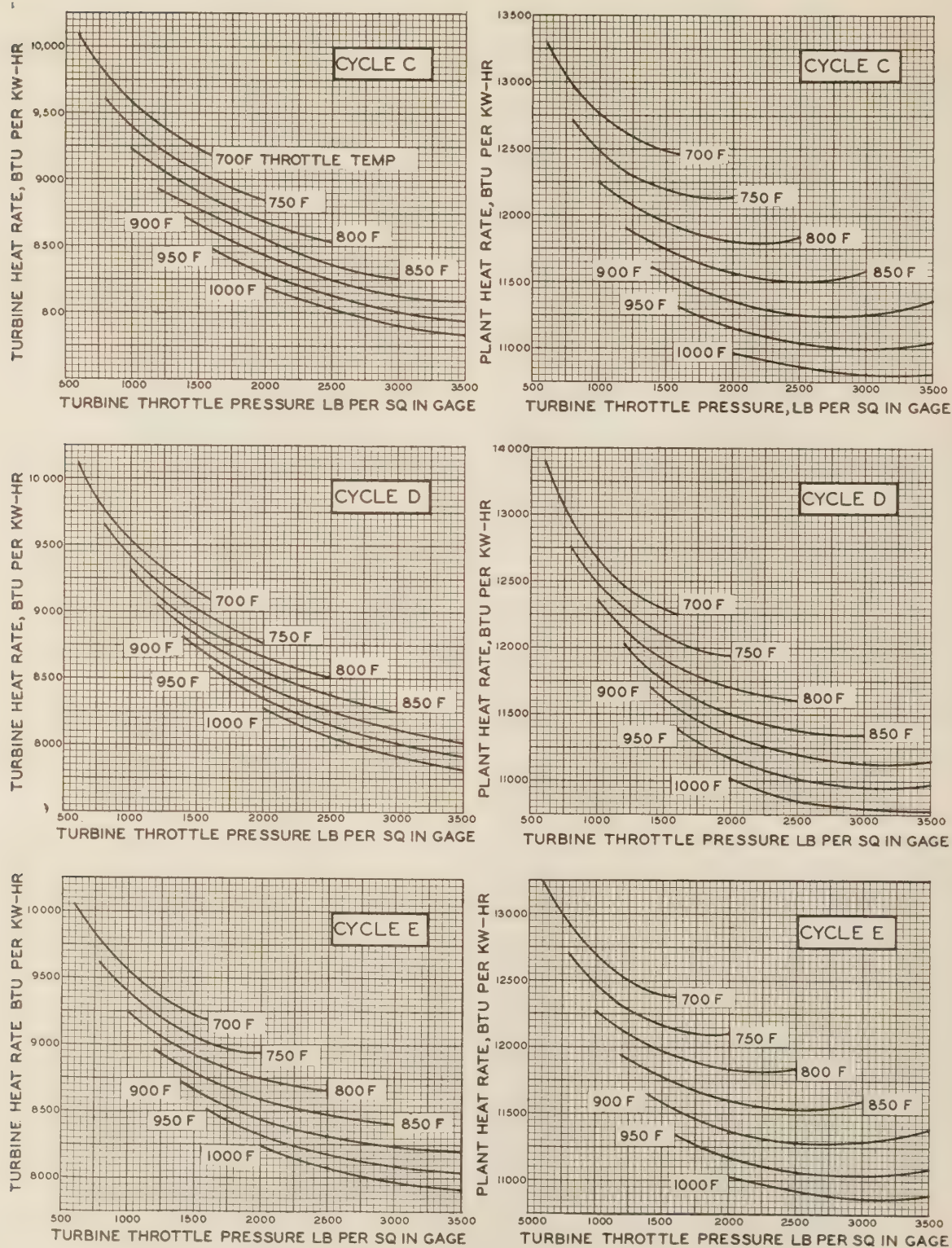


FIG. 19 TURBINE AND PLANT HEAT RATES, CYCLES C, D, AND E

tions, and compares them with actual-plant heat rates when available.

However, some general conclusions regarding the advantages of different steam and cycle conditions can be made. For the present, the simplicity and the high thermal efficiency of the regenerative-feedheating cycle make it the most promising for ordinary conditions. On the other hand, because of the tempting heat-rate margin of reheating plants, it is not unlikely that more of these will be built, especially when a high use factor is possible. In any case the best overall results are obtained when using the highest practicable initial temperature. The initial pressure would then be limited by the maximum permissible moisture content of the exhaust.

Among the cycles offering possibilities for future improvement the regenerative-feedheating cycle is again most promising. Without superheat, but with air preheat by the flue gas and feedheating by bled steam up to or near the initial temperature, it would give the most favorable cycle heat rate obtainable from any engine subject to practical initial temperature restrictions.

Its maximum development is contingent on three items: adoption of a working medium other than steam, removal of condensing liquid from the expanding medium, and the use of a binary expansion cycle. A comparison of the heat rate obtainable from present plants with the heat rate obtainable with this cycle suggests that its development should be given thoughtful consideration now.

This plant, however, does not represent the ultimate theoretical possibility in lowered heat rates. Although, if ever attained, such a plant might be the best practical plant, the goal of power-plant development should be a basic-cycle heat rate of 3412 Btu per kw-hr. Realization of this ideal heat rate requires two major changes in the heat cycle: First, the irreversible transfer of the heat of coal from the combustion gases to the vapor of the working medium at a lower temperature must be replaced by a reversible transfer; this would reduce the basic-cycle heat rate to about 4200 Btu per kw-hr. Second, the irreversible liberation of the chemical energy in fuel also must be replaced by a reversible process; this would give a basic-cycle heat rate of 3412 Btu per kw-hr. All processes would then be reversible, and the available energy of the fuel could be completely and continuously converted into mechanical work. Undoubtedly this last step would change the form of the plant completely, thereby introducing the possibility of many developments in the use of power which cannot even be pictured until the form of that ultimate plant becomes at least vaguely known. Admittedly such a plant is purely visionary, and discussion of it is probably of little immediate economic significance. Nevertheless, it is an enticing goal, which allows untold new uses of power. The report of progress during the next century may record some of these changes.

ACKNOWLEDGMENT

The authors wish to express their appreciation for the hearty cooperation of every one concerned with the preparation of this paper. We are particularly indebted to Mr. J. W. Parker for material help in the development of this paper, to Dr. C. F. Hirshfeld for timely suggestions and helpful criticism, to Mr. Sabin Crocker for his kindly supervision of the work; to Mr. J. L. Bannoff for material help with the calculations; to Dr. A. DeSmaele, former Research Fellow at Cornell University, for his help with the work in its initial stages; to Professor B. Weaver for help in editing the text; to Mr. G. B. Warren, of the General Electric Company, for suggestions and data on turbine performance; to the General Electric Company and the Westinghouse Company for data on steam tables and turbine per-

formance; and to The Detroit Edison Company for making this study possible.

Appendix I Nomenclature

The following list of nomenclature used in this paper is appended for convenience:

A	= Combustion air, lb per lb coal burned
D	= Density of feedwater at the temperature in the boiler feed pump, lb per cu ft
E	= Exhaust loss, Btu per lb of exhaust steam
E_1	= Exhaust loss at maximum efficiency load, non-extracting, Btu per lb of exhaust steam
E_c	= Exhaust loss chargeable at end-point of the computed expansion lines, Btu per lb of exhaust steam
E_t	= Energy developed into mechanical work by a turbine with extraction feedheating system but without evaporators, Btu per lb of throttle steam
E_p	= Energy developed into mechanical work by a turbine with extraction feedheaters and an evaporator, Btu per lb of throttle steam
e	= Individual-stage efficiency ratio, fraction
e_d	= Dry-state individual-stage efficiency ratio, fraction
F_1	= Steam flow to turbine throttle at maximum efficiency load, lb per hr
F_e	= Exhaust steam flow, lb per hr
g	= Acceleration of gravity, 32.16 ft per sec ²
h_a	= Enthalpy (total heat) of combustion air, Btu per lb. (The term enthalpy here denotes the quantity ordinarily named "total heat" or "heat content." It may be defined as $h = u + pv$, where u is the internal energy, p the pressure, and v the specific volume.)
h_e	= Enthalpy of exhaust steam, Btu per lb
h_{fe}	= Enthalpy of main condensate, Btu per lb
h_{fm}	= Enthalpy of make-up water supply, Btu per lb
h_m	= Enthalpy of make-up vapor leaving evaporator, Btu per lb
h_r	= Enthalpy of working steam entering one-stage reheater, Btu per lb
h_{r1}	= Enthalpy of working steam entering the first reheater in a two-stage reheat cycle, Btu per lb
h_{r2}	= Enthalpy of working steam entering the second reheater in a two-stage reheat cycle, Btu per lb
h_{R}	= Enthalpy of working steam leaving one-stage reheater, Btu per lb
h_{R1}	= Enthalpy of working steam leaving the first reheater in a two-stage reheating cycle, Btu per lb
h_{R2}	= Enthalpy of working steam leaving the second reheater in a two-stage reheating cycle, Btu per lb
h_t	= Enthalpy of steam entering turbine throttle, Btu per lb
h_{ft}	= Enthalpy of condensate drains from live-steam reheaters, Btu per lb
h_1	= Enthalpy of steam extracted to the highest pressure-stage feedheater, Btu per lb
h_2	= Enthalpy of steam extracted to the highest-but-one pressure-stage feedheater, Btu per lb
h_3	= Enthalpy of steam extracted to the highest-but-two pressure-stage feedheater, Btu per lb
h_4	= Enthalpy of steam extracted to the highest-but-three pressure-stage feedheater, Btu per lb
$h_{f1}, h_{f2}, h_{f3}, h_{f4}$	represent the enthalpy of the condensate drains from h_1, h_2, h_3 , and h_4 , respectively, Btu per lb
$h'_{f1}, h'_{f2}, h'_{f3}, h'_{f4}$	represent the enthalpy of water leaving the feedheaters, the temperatures being 5 F lower than those corresponding to h_{f1}, h_{f2}, h_{f3} , and h_{f4} , respectively
h_f	= Enthalpy of feedwater if different from h'_{f1} , Btu per lb
h_{fe}	= Latent heat at exhaust pressure, Btu per lb steam
$H_{A0}, H_{A1}, H_{A2}, H_{A3}, H_{A4}, H_{A'}, H_B, H_C, H_D, H_E$	are the heat rates with cycles $A_0, A_1, A_2, A_3, A_4, A', B, C, D$, and E , respectively, Btu per kw-hr chargeable to the turbine
$H'_{A0}, H'_{A1}, H'_{A2}, H'_{A3}, H'_{A4}, H'_{A'}, H'_B, H'_C, H'_D, H'_E$	are plant heat rates corresponding to the preceding turbine heat rates, Btu per kw-hr
H_e	= Heat to circulating water, Btu per kw-hr
J	= Mechanical equivalent of heat, 778.6 ft-lb per Btu
m	= Make-up water, lb per lb of total feedwater
m_a	= Combustion air, lb per lb steam generated
m_{et}	= Exhaust-steam flow for a turbine and feedheating system without evaporators, lb per lb steam supplied to the turbine
m_{ep}	= Exhaust-steam flow for a turbine and feedheating system with evaporators, lb per lb steam supplied to the turbine
m_R	= Ratio of low- to high-pressure throttle flow in a compound turbine
m_{R1}	= Ratio of intermediate- to high-pressure throttle flow for triple-expansion turbines
m_{R2}	= Ratio of low- to high-pressure throttle flow for triple-expansion turbines
m_r	= Steam supplied from mains to a one-stage local reheater, lb per lb steam supplied to the turbine throttle
m_{r1}	= Steam supplied from the mains to the first reheater of a two-stage local reheat cycle, lb per lb steam supplied to the turbine throttle
m_{r2}	= Steam supplied from mains to the second reheater of a two-stage reheat cycle, lb per lb of steam supplied to the turbine throttle
m_1	= Steam extracted to the highest pressure-stage heater, lb per lb of steam supplied to the turbine throttle
m_2	= Steam extracted to the second highest pressure-stage heater, lb per lb steam to the turbine
m_3	= Steam extracted to the third highest pressure-stage heater, lb per lb steam to the turbine
m_4	= Steam extracted to the lowest pressure-stage heater, lb per lb steam to the turbine
n	= Number of regenerative-feedheating stages
p_f	= Boiler-feed pump discharge pressure, lb per sq in.
p_i	= Steam pressure before first turbine stage nozzles, lb per sq in.
p_a	= Auxiliary power, ratio to total generated
P_b	= Power to boiler auxiliaries, ratio to total generated
P_c	= Power to circulators, ratio to total generated
P_p	= Power to boiler-feed pump, ratio to total generated
q	= Steam quality, fraction
q_e	= Steam quality at end-point of expansion lines, fraction

s	= Entropy of steam, Btu per lb per deg F
s_c	= Steam generated, lb per lb coal
T	= Absolute temperature, F
u	= Velocity of last turbine wheel blades measured on the pitch circle, ft per sec
v	= Absolute velocity of steam leaving last turbine wheel (see Fig. 3), ft per sec
v_r	= Relative velocity of steam leaving last turbine wheel (see Fig. 3), ft per sec
v_0	= Axial component of exhaust-steam velocity, ft per sec
v_1	= Exhaust-steam velocity at ME load ft per sec (assumed axial)
V_s	= Volume of steam leaving the last turbine wheel, cu ft per kw hr
v_s	= Specific volume of steam leaving the last turbine wheel, cu ft per lb of steam
W	= Turbine throttle steam rate, lb per kw hr
W_e	= Condenser-steam rate for any cycle, lb per kw hr
W_{A0}	= Turbine-steam rate for cycle A_0 , lb per kw hr
W_{A1}	= Turbine-steam rate for cycle A_1 , lb per kw hr
W_{A2}	= Turbine-steam rate for cycle A_2 , lb per kw hr
W_{A3}	= Turbine-steam rate for cycle A_3 , lb per kw hr
W_{A4}	= Turbine-steam rate for cycle A_4 , lb per kw hr
$W_{A'}$	= Turbine-steam rate for cycle A' , lb per kw hr
W_B	= Turbine-steam rate for cycle B , lb per kw hr
W_C	= Turbine-steam rate for cycle C , lb per kw hr
W_D	= Turbine-steam rate for cycle D , lb per kw hr
W_E	= Turbine-steam rate for cycle E , lb per kw hr

Other items of nomenclature are used only where locally explained.

Appendix II Formulas

The following is a listing of all formulas used:

- (1) Slope of expansion lines at any point on the enthalpy-entropy diagram:

$$\left(\frac{\partial h}{\partial s}\right)_e = -\frac{e}{1-e}T \dots \dots \dots [1]$$

- (2) Entropy increment for a finite interval on an expansion line (see "Reheat Factors," by E. L. Robinson, *Mechanical Engineering*, February, 1928, pp. 155-156):

$$\Delta s = \frac{1-e}{e} \frac{\Delta h}{\Delta T} \log_e \frac{T_1}{T_2} \dots \dots \dots [2]$$

- (3) Expansion efficiency in the wet-steam region:

$$e = q_{ed} \dots \dots \dots [3]$$

- (4) and (5) Exhaust loss chargeable at end-point of computed expansion lines:

$$E_c = 1.1 q_{ed} E, \text{ Btu per lb steam} \dots \dots \dots [4]$$

$$= q_{ed} \left\{ E_1 \left[\frac{F_e}{F_1} \right]^2 + \frac{1.1u^2}{2gJ} \left[1 - \frac{F_e}{F_1} \right]^2 \right\} \dots \dots \dots [5]$$

- (6) Power used by boiler-feed pumps

$$P_b = \frac{0.1851}{0.60} \frac{W}{D} \frac{W}{3412} \text{ kw per gross kw} \dots \dots \dots [6]$$

- (7) Power used by boiler auxiliaries:

$$P_b = 2.0 \times 10^{-6} \times H \text{ kw per gross kw} \dots \dots \dots [7]$$

- (8) Power used by circulators:

$$P_c = 1.343 \times 10^{-6} \times W_e(h_{e0} - h_{fa}) \text{ kw per gross kw} \dots \dots \dots [8]$$

- (9) Total auxiliary-power consumption:

$$P_a = P_p + P_b + P_c + 0.005 \text{ kw per gross kw} \dots \dots \dots [9]$$

- (10) Loss of useful work by addition of evaporators:

$$E_t - E_p = (m_{et} - m_{ep})(h_e - h_{fa}) + m(h_f - h_{fm}) \dots \dots \dots [10]$$

- (11) Steam rate for cycle A_n :

$$W_{An} = \frac{H_{An}}{(h_t - h'_{f1})_{An}} \text{ lb per kw hr} \dots \dots \dots [11]$$

- (12) Steam rate for cycle A' :

$$W_{A'} = \frac{H_{A'}}{(h_t - h'_{f1} - m_a \Delta h_a)_{A'}} \dots \dots \dots [12]$$

- (13) Steam rate for cycle B :

$$W_B = \frac{H_B}{(h_t - h'_{f1} + m_R(h_R - h_r))_B} \text{ lb per kw hr} \dots \dots \dots [13]$$

- (14) Steam rate for cycle C :

$$W_C = \frac{H_C}{(h_t - h_f)_C} \text{ lb per kw hr} \dots \dots \dots [14]$$

- (15) Steam rate for cycle D :

$$W_D = \frac{H_D}{(h_t - h_f)_D} \text{ lb per kw hr} \dots \dots \dots [15]$$

- (16) Steam rate for cycle E :

$$W_E = \frac{H_E}{(h_t - h_f)_E} \text{ lb per kw hr} \dots \dots \dots [16]$$

- (17) Heat rejected to the circulating water:

$$H_o = H - 3564 \text{ Btu per kw hr} \dots \dots \dots [17]$$

- (18) Volume of exhaust steam:

$$V_e = H_{ev} + h_{fe} \text{ cu ft per kw hr} \dots \dots \dots [18]$$

- (19) Total steam bled, cycle A_1 , with evaporators:

$$(1 - m_{ep})_{A1} = \frac{1}{h_1 - h_{fe} - (h_{f1} - h'_{f1})} [(1 + m)(h'_{f1} - h_{fe}) + m(h_m - h_{fm})] \dots [19]$$

- (20) Total steam bled, cycle A_2 , with evaporators:

$$(1 - m_{ep})_{A2} = \frac{1}{h_2 - h_{fe} - (h_{f2} - h'_{f2})} \frac{h_1 - h_2}{h_1 - h_{f1}} \times \left[\left\{ (1 + m)(h'_{f1} - h'_{f2}) + m[h_m - h_{fm} - (h_{f2} - h'_{f2})] \right\} \frac{h_2 - h_{f1}}{h_1 - h_{f1}} + h'_{f2} - h_{fe} - m \left\{ h_m - h_{fe} - (h_{f2} - h'_{f2}) \frac{h_1 - h_2}{h_1 - h_{f1}} \right\} \right] \dots [20]$$

- (21) Total steam bled, cycle A_3 , with evaporators:

$$(1 - m_{ep})_{A3} = \frac{1}{h_3 - h_{fe} - (h_{f3} - h'_{f3})} \frac{h_2 - h_3}{h_2 - h_{f2}} \times \left\{ \left[(1 + m)(h'_{f1} - h'_{f3}) + m(h_m - h_{fm}) \right] \frac{h_2 - h_{f1}}{h_1 - h_{f1}} \frac{h_3 - h_{f2}}{h_2 - h_{f2}} + \left[(1 + m)(h'_{f2} - h'_{f3}) - m(h_m - h_2 + h_{f3} - h'_{f3}) \right] \frac{h_3 - h_{f2}}{h_2 - h_{f2}} + h'_{f3} - h_{fe} - m \left[h_3 - h_{fe} - (h_{f3} - h'_{f3}) \frac{h_2 - h_3}{h_2 - h_{f2}} \right] \right\} \dots [21]$$

- (22) Total steam bled, cycle A_4 , with evaporators:

$$(1 - m_{ep})_{A4} = \frac{1}{h_4 - h_{fe} - (h_{f4} - h'_{f4})} \frac{h_3 - h_4}{h_3 - h_{f3}} \times \left\{ \left[(1 + m)(h'_{f1} - h'_{f4}) + m(h_m - h_{fm}) \right] \frac{h_3 - h_{f1}}{h_1 - h_{f1}} \frac{h_4 - h_{f3}}{h_3 - h_{f3}} + \left[(1 + m)(h'_{f2} - h'_{f4}) + m(h_2 - h_m) \right] \frac{h_4 - h_{f3}}{h_3 - h_{f3}} \frac{h_4 - h_{f3}}{h_3 - h_{f3}} + \left[(1 + m)(h'_{f3} - h'_{f4}) - m(h_4 - h_{f4} - h'_{f4}) \right] \frac{h_4 - h_{f3}}{h_3 - h_{f3}} + h'_{f4} - h_{fe} - m \left[h_4 - h_{fe} - (h_{f4} - h'_{f4}) \frac{h_3 - h_4}{h_3 - h_{f3}} \right] \right\} \dots [22]$$

- (23) Total steam bled, cycle A' with evaporators, computed from cycle A_1 :

$$(1 - m_{ep})_{A'} = (1 - m_{ep})_{A4} \frac{m_a \Delta h_a}{h'_{f1} - h_{fe} + m(h'_{f1} - h_{fm})} \dots [23]$$

- (24) Total steam bled, cycle B , without evaporators:

$$(1 - m_{et})_B = 1 - \frac{1}{h_4 - h_{fe} - (h_{f4} - h'_{f4})} \frac{h_3 - h_4}{h_3 - h_{f3}} \left[(h'_{f3} - h'_{f4}) \frac{h_4 - h_{f3}}{h_3 - h_{f3}} + h'_{f4} - h_{fa} \right] + \frac{h_r - h'_{f3} - (h_{f2} - h'_{f2})}{h_r - h_{f1}} + \frac{h'_{f2} - h'_{f3}}{h_1 - h_{f1}} \dots [24]$$

- (25) Total bled steam, cycle C , without evaporators:

$$(1 - m_{et})_C = 1 - \frac{(1 - A_1)(1 - B_1)(1 - C_1)}{1 - A_1 B_1} \dots [25]$$

- (26) Where:

$$A_1 = \left[\frac{h_R - h_r}{h_t - h'_{f1} + h_R - h_r} \right]_C = \left[\frac{m_r}{1 - (m_1 + m_2)} \right]_C \dots [26]$$

- (27):

$$B_1 = \frac{h'_{f2} - h'_{f3} + (h'_{f1} - h'_{f2}) \frac{h_r - h_{f1}}{h_1 - h_{f1}}}{h_r - h_{f2} - (h_{f2} - h'_{f2}) \frac{h_1 - h_r}{h_1 - h_{f1}}} = \left[\frac{m_1 + m_2}{1 - m_r} \right]_C \dots [27]$$

- (28):

$$C_1 = \frac{h'_{f4} - h_{fe} + (h'_{f3} - h'_{f4}) \frac{h_4 - h_3}{h_3 - h_{f3}}}{h_4 - h'_{f4} - (h_{f4} - h'_{f4}) \frac{h_3 - h_4}{h_3 - h_{f3}}} = \left[\frac{m_3 + m_4}{1 - m_r - (m_1 + m_2)} \right]_C \dots [28]$$

- (29) Total bled steam, cycle D , without evaporators:

$$(1 - m_{et})_D = m_{R2} \left[\frac{h_{R2} - h_{r1}}{h_t - h_{f1}} + \frac{(h'_{f1} - h'_{f2})(h_{r2} - h_{f1}) + (h'_{f2} - h'_{f3})(h_{r1} - h_{f1})}{(h_{r1} - h_{f1})(h_{r2} - h_{f2}) + (h_{f1} - h_{f2})(h_{r2} - h_{f1})} + \frac{(h'_{f3} - h'_{f4})(h_4 - h_{f3}) + (h'_{f4} - h_{fe})(h_2 - h_{f2})}{(h_2 - h_{f2})(h_4 - h_{fe}) - (h_{f4} - h'_{f4})(h_3 - h_4)} \right] + m_{R1} \left(\frac{h_{R1} - h_{r1}}{h_t - h_{f1}} \right) \dots [29]$$

- (30) Where:

$$m_{R1} = \frac{1}{D_2} \left[\frac{h_{R1} - h_{r1}}{h_t - h_{f1}} - \frac{h'_{f1} - h'_{f2}}{h_{r1} - h_{f1}} + \frac{(h'_{f1} - h'_{f2})(h_{r2} - h_{f1}) + (h'_{f2} - h'_{f3})(h_{r1} - h_{f1})}{(h_{r1} - h_{f1})(h_{r2} - h_{r2}) - (h_{f1} - h_{f2})(h_{r2} - h_{f1})} \right] \dots [30]$$

$$(31):$$

$$m_{R2} = \frac{1}{D_2} \left[\frac{h_{R1} - h_{R2}}{h_t - h_{f1}} - \frac{h_{R2} - h_{R3}}{h_t - h_{f1}} - \frac{(h'_{f1} - h'_{f2})(h_{R2} - h_{f2}) + (h'_{f2} - h'_{f3})(h_{R1} - h_{f1})}{(h_{R1} - h_{f1})(h_{R2} - h_{f2}) - (h'_{f1} - h'_{f2})(h_{R2} - h_{f1})} \right] \dots [31]$$

$$(32):$$

$$D_2 = \frac{h_t - h_{f1} + h_{R1} - h_{R2}}{h_t - h_{f1}} - \frac{h_{R1} - h_{R2}}{h_t - h_{f1}} - \left[\frac{h_{f1} - h'_{f2}}{h_{R1} - h_{f1}} + \frac{h_{f1} - h'_{f2}}{h_{R1} - h_{f1}} \times \frac{(h'_{f1} - h'_{f2})(h_{R2} - h_{f1}) + (h'_{f2} - h'_{f3})(h_{R1} - h_{f1})}{(h_{R1} - h_{f1})(h_{R2} - h_{f2}) - (h'_{f1} - h'_{f2})(h_{R2} - h_{f1})} \right] \times \left[\frac{h_t - h_{f1} + h_{R2} - h_{R3}}{h_t - h_{f1}} - \frac{h_{R2} - h_{R3}}{(h_{R2} - h_{f1})(h_{R2} - h_{f2}) - (h'_{f1} - h'_{f2})(h_{R2} - h_{f1})} + \frac{(h'_{f2} - h'_{f3})(h_{R1} - h_{f1})}{(h_{R2} - h_{f2}) - (h'_{f1} - h'_{f2})(h_{R2} - h_{f1})} \right] \dots [32]$$

(33) Total steam bled, cycle E , without evaporators:

$$(1 - m_{et})E = (A_3 + B_3 + C_3) \div D_3 \dots [33]$$

(34) Where:

$$A_3 = \frac{h'_{f1} - h'_{f2}}{h_1 - h_{f1}} \frac{h_2 - h_{f1}}{h_2 - h_{f2}} + \frac{h'_{f2} - h'_{f3}}{h_2 - h_{f2}} \dots [34]$$

(35):

$$B_3 = \frac{h'_{f3} - h'_{f4}}{h_3 - h_{f3}} + \frac{h'_{f4} - h_{f5}}{h_4 - h_{f3}} \frac{h_3 - h_{f3}}{h_3 - h_{f2}} \dots [35]$$

(36):

$$C_3 = \left[\frac{h_{R1} - h'_{f1}}{h_t - h_{f1}} \frac{h_1 - h_{f1}}{h_1 - h_{f2}} + \frac{h'_{f1} - h'_{f2}}{h_1 - h_{f1}} \right] \frac{h_2 - h_{f1}}{h_2 - h_{f2}} + \frac{h'_{f2} - h_3}{h_2 - h_{f2}} \dots [36]$$

(37):

$$D_3 = \frac{h_{f4} - h'_{f4}}{h_3 - h_{f2}} \frac{h_4 - h_3}{h_4 - h_{f2}} + \frac{h_4 - h_{f5}}{h_4 - h_{f2}} \frac{h_3 - h_{f3}}{h_3 - h_{f2}} \dots [37]$$

Formulas for the change in total steam bled with cycles A_1 , A_2 , A_3 , and A_4 follow readily from Equations [19], [20], [21], and [22], respectively, by rewriting each of these equations with $m = 0$ and subtracting. The resulting equations follow:

(38) Increase in bled steam by the addition of evaporators, cycle A_1 :

$$(m_{et} - m_{ep})A_1 = \frac{m}{h_1 - h_{fe} - (h_{f1} - h'_{f1})} \times \left[h'_{f1} - h_{fe} + h_m - h_{fm} \right] \dots [38]$$

(39) Increase in bled steam by the addition of evaporators, cycle A_2 :

$$(m_{et} - m_{ep})A_2 = \frac{m}{h_2 - h_{fe} - (h_{f2} - h'_{f2})} \times \left[\frac{h_1 - h_2}{h_1 - h_{f1}} \times \left[(h'_{f1} - h_{f2} + h_m - h_{fm}) \frac{h_2 - h_{f1}}{h_1 - h_{f1}} + h_m - h_{fe} - (h_{f2} - h'_{f2}) \frac{h_1 - h_2}{h_1 - h_{f1}} \right] \right] \dots [39]$$

(40) Increase in bled steam by the addition of evaporators, cycle A_3 :

$$(m_{et} - m_{ep})A_3 = \frac{m}{h_3 - h_{fe} - (h_{f3} - h'_{f3})} \times \left[\frac{h_2 - h_3}{h_2 - h_{f2}} \times \left[(h'_{f1} - h'_{f2} + h_m - h_{fm}) \frac{h_2 - h_{f1}}{h_1 - h_{f1}} \frac{h_3 - h_{f2}}{h_2 - h_{f2}} + (h'_{f2} - h'_{f3} + h_2 - h_m + h'_{f3} - h_{f3}) \frac{h_3 - h_{f2}}{h_2 - h_{f2}} + h_3 - h_{f2} - (h_{f3} - h'_{f3}) \frac{h_2 - h_3}{h_2 - h_{f2}} \right] \right] \dots [40]$$

(41) Increase in bled steam by the addition of evaporators, cycle A_4 :

$$(m_{et} - m_{ep})A_4 = \frac{m}{h_4 - h_{fe} - (h_{f4} - h'_{f4})} \times \left[\frac{h_3 - h_4}{h_3 - h_{f3}} \times \left[(h'_{f1} - h'_{f2} + h_m - h_{fm}) \frac{h_2 - h_{f1}}{h_1 - h_{f1}} \frac{h_3 - h_{f2}}{h_2 - h_{f2}} \frac{h_4 - h_{f3}}{h_3 - h_{f3}} + (h'_{f2} - h'_{f3} + h_2 - h_m) \frac{h_3 - h_{f2}}{h_2 - h_{f2}} \frac{h_4 - h_{f3}}{h_3 - h_{f3}} + (h'_{f3} - h'_{f4} + h_3 - h_m) \frac{h_4 - h_{f3}}{h_3 - h_{f3}} + h_4 - h_{fe} - (h_{f4} - h'_{f4}) \frac{h_3 - h_4}{h_3 - h_{f3}} \right] \right] \dots [41]$$

Appendix III Bibliography

The following is a chronological list of extensive papers appearing in the last ten years on steam cycles and related subjects:

- "High-Pressure Reheating and Regenerating for Steam Power Plants," by C. F. Hirschfeld and F. O. Ellenwood, Trans. A.S.M.E., 1923, pp. 663-711.
- "The Margins of Possible Improvement in Central-Station Steam Plant," by E. Robinson, Trans. A.S.M.E., 1923, pp. 644-662.
- "Economy Characteristics of Stage Feedwater Heating by Extraction," by E. H. Brown and M. K. Drewry, Trans. A.S.M.E., 1923, pp. 713-739.
- "Reheating in Central Stations," by W. J. Wohlenberg, Trans. A.S.M.E., 1923, pp. 741-765.
- Discussion of the four previous papers, Trans. A.S.M.E., 1923, pp. 766-823.
- "The Increase of Turbine Efficiency Due to Resuperheating in Steam

Turbines," by W. E. Blowney and G. B. Warren, Trans. A.S.M.E., 1924, pp. 563-593.

"A Review of Steam Turbine Development," by Hans Dahlstrand, Trans. A.S.M.E., 1925, pp. 283-310.

"Steam Bleeding and Turbine Performance," by C. D. Zimmerman, Trans. A.S.M.E., 1925, pp. 1041-1071.

"The Use and Economy of High-Pressure Steam Plants," by A. L. Melanby and W. Kerr, Proc. Inst. Mech. Engrs., 1927, pp. 53-98.

"The Economic Use of Increased Steam Pressure," by H. L. Guy, Proc. Inst. Mech. Engrs., 1927, pp. 99-128.

Discussion of the two previous papers, Proc. Inst. Mech. Engrs., 1927, pp. 129-213.

"Higher Steam Pressures and Their Application," by A. H. Law and J. P. Chittenden, J. Inst. Elec. Engrs., 1928, pp. 89-123.

"Modern Feedwater Circuits," by J. G. Weir, Proc. Inst. Mech. Engrs., 1929, pp. 5-40.

"Tendencies in Steam-Turbine Development," by H. L. Guy, Proc. Inst. Mech. Engrs., 1929, pp. 453-490.

"Some Considerations Affecting the Future Development of the Steam Cycle," by K. Bauman, Proc. Inst. Mech. Engrs., 1930, pp. 1305-1396.

"Simplified Method for the Calculation of Feedwater Heating and Reheating in the Design of Power Plants," by N. Hilgers, *Das Kraftwerk*, A.E.G., 1931, pp. 58-65.

"Steam-Turbine-Plant Practice in the United States," by Vern E. Alden and W. H. Balcke, Trans. A.S.M.E., 1933, vol. 55, no. 3, pp. 9-35.

"British Practice in Steam Turbine Design," by F. W. Gardner, Trans. A.S.M.E., 1933, vol. 55, no. 33, pp. 37-58.

Discussion

M. G. S. SWALLOW.⁸ While the contents of the paper and, in particular, the graphical presentation of the turbine and plant heat rates given in the Appendix for the various cycles considered are of considerable interest for purposes of comparison among themselves, there are certain points which need to be cleared up if these results are to be comparable with those obtained in plants which do not exactly conform to those considered in the paper. The curves giving the turbine heat rates would seem to be of more value than those giving the plant heat rates, as the latter from their very nature must be based on assumptions such as load factor, variation in turbine efficiency when the load is different from the economic rating, power consumption of auxiliaries, boiler-house efficiencies, etc., which factors vary considerably in different cases. It is not clear from the paper whether the alternator efficiency has been included in the turbine heat rate, and in order to enable the comparison of the authors' curves with other figures to be made, the alternator efficiency which has been used would be of interest.

In the section on the variations of the kinetic energy of the exhaust, the authors state that allowances for exhaust losses have been made on the basis that the turbine is designed for the optimum pressure distribution and the most economic exhaust area when operating without extraction. They then calculate the exhaust losses, taking into account the amount of steam extracted. While the reduction in turbine efficiency under the normal condition of extraction may not seriously be reduced by proportioning the blading for operation without extraction when the feed temperature is low and the amount of steam extracted therefore small, for plants with four-stage feed heating and a final temperature of 350 F the amount of steam passing to the condenser will be some 15 per cent less when operating extracting, and the resultant loss in efficiency due to a less favorable pressure distribution along the blading may well reach the value of 1 per cent. In the consideration of those cycles where additional steam is bled off for air preheaters, evaporators, or steam reheaters, this discrepancy obviously becomes greater. A comparison has been made between a 48,000-kw economic rating two-cylinder 1500-rpm turbine operating with steam at a pressure of 600 lb per sq in. gage and temperature of 800 F, exhausting to a vacuum of 1 in. Hg. abs, for which the design data were available, and the corresponding figures from the curves given in Fig. 17 of the paper. The turbine is of the impulse-reaction type having a single two-row impulse wheel with nozzle governing at the high-pressure end, the rest of the blading being of the reaction type.

⁸ Director, Richardsons, Westgarth & Co., Ltd., Hartlepool Engine Works, Hartlepool, England.

On a basis of four feedheaters with a final feed temperature of 356 F, the heat consumption at the economic rating with an alternator efficiency of 97.71 per cent would be 9630 Btu per kwhr. From Fig. 11 the optimum feedwater temperature would be 375 F, and the correction to be applied to the curves in Fig. 17 for the lower feed temperature of 356 F would be about 0.1 per cent. Fig. 17 gives the turbine heat rate as 9800 Btu per kwhr, which with the correction would give 9810 Btu per kwhr. This is about 1.85 per cent higher than that of the design of turbine on which the lower figure is based. If the alternator efficiency is not included in the curves given in the paper, this difference becomes about 4.15 per cent.

It is unfortunate that for only three out of eight examples given in Table 1 actual plant efficiencies are available for comparison with the computed rates. It would be interesting to know the actual turbine heat rates for those cycles and conditions which are based on existing stations.

In the consideration of cycle C with boiler-room reheat, the losses in the reheater and auxiliary pipe work must vary considerably with the relative position of turbine and boiler plant, and to some extent with the pressure at which reheating is carried out. Additional pressure losses are entailed in the provision of cut-off valves on the low-pressure cylinder to prevent the turbine from running away after the main steam valve is closed owing to the large volume of steam contained in the reheater and its pipe work. These factors have a considerable influence on the fraction of the theoretical reduction in heat consumption consequent upon an introduction of reheating which is actually obtained in practice, and the question must be carefully investigated with due regard to the local conditions prevailing before reheating can be adopted as an economic gain. In any case, as the authors point out, the load factor is of great importance in estimating the practical economy resulting from the use of reheating plant. The comparison of a number of cases of actual turbine heat rates with those computed from the results given in the paper for the relevant conditions would go far toward increasing confidence in the applicability of the turbine-heat-rate curves to actual practice.

AUTHORS' CLOSURE

Mr. Swallow's discussion brings out several points of interest that might have been more fully covered in the text.

Of these the alternator efficiency used certainly should have been stated clearly, and the authors offer an apology for this omission. The turbine heat rates given contain an allowance for an alternator efficiency of 96.5 per cent. In addition, losses in the turbine bearings, oil pumps, and other constant sources are accounted for. This is the origin of the figure of 3564 Btu per kwhr

in Equation [17]. At rated load the turbine wheels develop 3564 Btu of work for every kwhr of net alternator output, for all cycles considered. Of this amount 152 Btu per kwhr make up the 3.5 per cent generator loss and the constant losses in the turbine. These figures were fixed with particular regard to a 50,000-kw, 1200-rpm, single-cylinder turbine. If the study were being repeated now, an alternator efficiency of 97 per cent or slightly greater would be used.

It is very interesting to have the figure of 1 per cent as the probable decrease in turbine efficiency when 15 per cent of the total throttle steam is bled from the turbine. While a change of this magnitude is possible at some loads, computations by the authors using diagram efficiencies indicate that at maximum efficiency load considered in the paper the effect of bleeding is very much less, or about 0.1 per cent. Some exact data on this point, using actual instead of diagram efficiencies, are needed from the turbine manufacturers. Whatever may be the magnitude of this effect, it is not included in the tabulated errors.

The comparison with the data for a 48,000-kw, 1500-rpm, two-cylinder turbine at 600 lb and 800 F brings out in a most opportune way the point illustrated in Fig. 1 and discussed in the text in connection with the question of compounding (see section Accuracy of Results). At 600 lb and 800 F, either a single- or two-cylinder turbine might conceivably be used. The results given in the paper do not distinguish between these two turbines. It is expected by the authors that a two-cylinder turbine would be better than the data presented for this region, and a single-cylinder turbine would be poorer.

In this connection, and regarding also the tables of comparisons with actual plants in the concluding section of the text, many such comparisons have been made with about the same agreement as that cited by Mr. Swallow. When allowance is made for the difference between his 97.71 per cent alternator efficiency and the 96.5 per cent used in the paper, the turbine results are checked within 60 Btu per kwhr, or 0.6 per cent. The authors regret their inability to give more such comparisons which are authentic. Those given in the table are restricted to particularly interesting conditions for which reliable data have been published recently.

Prof. F. O. Ellenwood writes to condemn the use of the term "heat-cycles" in the title and at other points in the paper. It must be admitted that for exactness in terminology "heat-utilization cycles" would have been a better choice.

It is regretted that other communicated discussions arrived too late to be included in the final printing. A discussion by Dr. A. DeSmaele, in particular, contains many points of interest which could not be put into the space available.

The authors take this opportunity to thank all discussors for their interest in the paper.

Problems of Modern Pump and Turbine Design

By WILHELM SPANNHAKE,¹ NEWTON CENTER, MASS.

This is a general review of the present status of design principles which apply equally to centrifugal pumps and hydraulic turbines. The author first develops step by step the fundamental ideas underlying the theoretical behavior of a runner having an infinitely large number of thin blades which guide the fluid perfectly. The resemblance between the blading ordinarily used and the wing of an airplane has led to analysis on the basis that each blade acts as an airfoil. The author points out the many limitations of this theory and advocates a new beginning, taking as a starting point the theoretically perfect runner. By decreasing the number of blades first from infinity to a finite but very large number, he analyzes the forces and influences that are at work. Although he does not claim to have arrived at a final solution, he demonstrates the play of one effect upon another, and suggests that further experimentation should assist in making proper allowances for the uncertainties not subject to strict analysis and which become more and more important as the num-

ber of blades is reduced. The final section deals with the best conditions for the design of high-speed runners. The influence of the principal figures of layout upon which both efficiency and cavitation are dependent are discussed, and complete curves for efficiency and cavitation coefficient are given for three different specific speeds. This speed is defined by the same figure for pumps and turbines. He feels that both theories in spite of their defects can be used to advantage as experimental knowledge is progressively increased, and demonstrates that mathematics will throw light on a number of vital problems dealing particularly with efficiency and cavitation. He suggests for consideration a special type of profile, and expresses the hope that by combining the laboratory with theory, it will be possible to realize improvements in existing equipment, and finally to build up a strict method for pump and turbine design meeting properly and satisfactorily all of the requirements for high specific speed and small number of blades.



THE design of turbines and pumps has been developed extensively during the last 15 years. Possibly the progress in turbine design has had more recognition because the problems connected with the building of hydraulic turbines are more commonly appreciated. Pumps are usually of comparatively small capacity, and serve purposes which do not appeal so readily to the popular imagination, whereas the conditions for which turbines are designed are more exacting and vary

widely from one installation to another. In many cases special effort must be taken to fulfil the requirements of the particular installation, in order to adapt the design to the given specifications for head and discharge, together with the desire of the customer regarding speed. On the other hand, pumps are often manufactured for stock, as a design once developed may be readily adapted to meet special requirements.

It should be stated that to the present time both branches have progressed hand in hand, and are together benefiting by the

achievements of modern hydrodynamics. Although modern theoretical and experimental methods, or rather the ideas upon which these methods are based, are successfully used in the design of both high- and low-head machinery, it is in the low-head design that these are most important. Furthermore, it is true that practical ability backed by engineering judgment must still take the place of strict mathematical rules and formulas.

For this reason there are as yet many unsolved problems, but in the field of turbines in general these appear to be most critical for low-head machines operating at high specific speeds. It is the purpose of this paper to discuss these questions without claiming to give exact and final solutions, but attempting to point out the essence of the problems, and to show in which directions the answers may possibly be found.

In order to have a general background for this discussion, an understanding of the turbine principle is necessary.

1 THE TURBINE PRINCIPLE—FUNDAMENTAL EQUATIONS

Fig. 1 shows a sectional elevation of a vertical runner which could be used either as a turbine or as a pump—i.e., to transform energy of flowing water to mechanical energy or vice versa. The efficiency as one or the other depends primarily upon the shape of the blades, but in principle it is possible to use the same blading for either. It will be seen that there are guide vanes above and outside the runner, whereas in the throat below the runner no means of guiding the water is used.

The arrangement shown is quite usual for turbines, and for pumps it is used frequently. As far as an analysis of conditions is concerned, it makes no difference whether the flow, approaching or leaving, passes through a scroll case or an open flume, or any other type of passage. Fig. 1 shows, therefore, only the guide apparatus and the runner.

According to the theory of conservation of momentum, a torque will be produced in the shaft providing the runner changes the "moment of whirl" of the fluid. One of the fundamental principles of mechanics is that force of impact or reaction in pounds is equal to weight per second, which is equal to the dis-

¹ Visiting Professor of Hydraulics, Massachusetts Institute of Technology. Professor Spannhake was born in 1881 in Germany. He had nine years of high school (Humanistisches Gymnasium) at Cologne and Mannheim, and four years at the Technische Hochschule, Munich, graduating in 1904 with the degree of Diplom-Ingenieur. He was designing and chief engineer at the Vulcan-Werke, Hamburg and Stettin, until 1920; after that chief engineer of the turbine works of Fritz Neumeyer A.G., Munich (combined with Briegleb, Hansen & Co., Gotha). Since 1921 he has been Professor of Hydraulic Engineering at the Technische Hochschule, Karlsruhe, Baden, Germany, and from September to April of 1931-1932 and 1932-1933 visiting professor of hydraulics at the Massachusetts Institute of Technology.

Contributed by the Hydraulics Division and presented at the Annual Meeting, New York, N. Y., December 5 to 9, 1932, of THE AMERICAN SOCIETY OF MECHANICAL ENGINEERS.

NOTE: Statements and opinions advanced in papers are to be understood as individual expressions of their authors, and not those of the Society.

charge Q in cubic feet per second, times the weight per cubic foot γ , times the change in velocity, divided by the acceleration of gravity. It follows, therefore, that if the tangential component of velocity v_{tang} is substituted for velocity, and force may be multiplied by the radius to give torque in pounds perpendicular feet, this fundamental law may be expressed by the following equation:

$$T = \frac{W}{g} \left\{ (v_{\text{tang}} r)_2 - (v_{\text{tang}} r)_1 \right\} \dots \dots \dots [1]$$

The torque is therefore proportional to the amount of water flowing and to the change produced by the blading in the moment of the whirl, the subscripts 2 and 1 indicating the conditions after

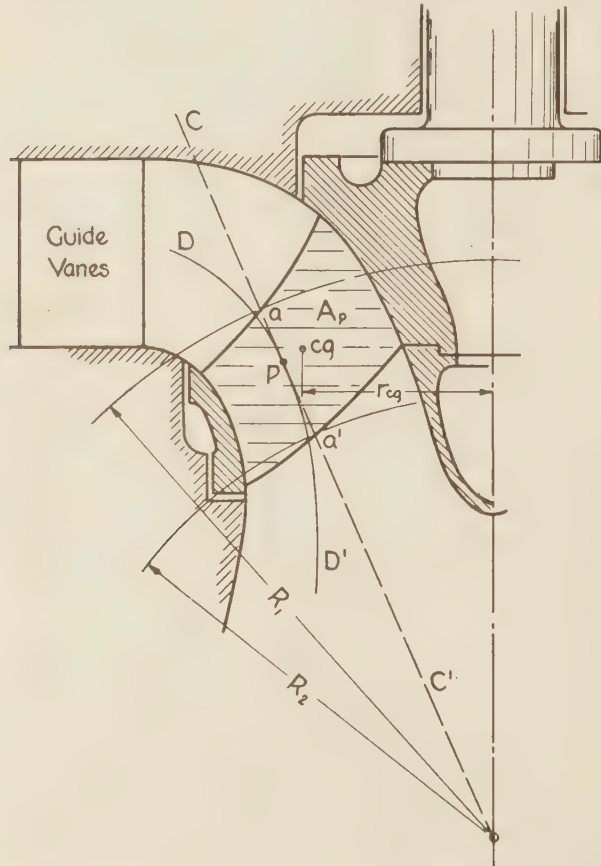


FIG. 1 SECTIONAL ELEVATION OF A HIGH-SPEED PUMP OR TURBINE

and before passing the runner, respectively. From this it follows that it is essential for a pump or turbine to produce in the whirl an alteration, which is termed the "deflecting effect."

It will be appreciated that to have torque it is not necessary that the runner should revolve, as a runner blocked in a stationary position would exert a twist in the shaft even though it acted on the water passing through it simply as a set of guide vanes. When the shaft does rotate, then mechanical work either has to be furnished from some outside source, such as a motor, or else has to be absorbed in driving some other machine, such as an electrical generator.

In order to be consistent in the use of signs, torque will be considered positive when the outside force acts in the direction that the runner is turning, since in the case of a pump the moment of whirl at exit then exceeds that at entrance, giving the right-

hand term of the foregoing formula a positive value. On the other hand, the torque for a turbine will be considered negative as the moment of whirl is reduced by the delivery of energy to the outside.

It should be mentioned in regard to the use of symbols that in order to avoid duplication it may be necessary to depart somewhat from the accepted standard both in America and abroad: v will be used for absolute velocity, thus avoiding the c , which is regularly used abroad, because to the American mind this letter is generally reserved to signify a constant. In order to make the formulas more graphic, the components are denoted by the subscripts tang for tangential, ax for axial, rad for radial, and peri for peripheral, etc., rather than to use arbitrary subscripts which are not easily remembered by the reader. Subscript 1 will denote the conditions at the beginning or entrance to the runner, 2 at the end or exit, and 0 the conditions for approaching flow in the case of a stationary blade.

The next step is to multiply both sides of Equation [1] by angular velocity ω and derive as equation for the power HP :

$$HP = \frac{T\omega}{550} = \frac{W\omega}{550g} \left\{ (v_{\text{tang}} r)_2 - (v_{\text{tang}} r)_1 \right\} \dots \dots [2]$$

In exchange for the work done per second, there must be in the case of a pump an increase in specific energy of the flow, but a corresponding decrease in the case of a turbine. The specific energy may be measured in terms of a manometer column of height H according to the definition $H = p/\gamma + h + v^2/2g$, which means that the energy per unit of weight is equal to the sum of the potential and kinetic energy, p being the pressure exerted in pounds per square foot, γ the density, or specific weight in pounds per cubic foot, h is the elevation of the point where the pressure is measured, and $v^2/2g$ the velocity head. If we designate the specific energy of the flow at entrance to the runner by H_1 and that leaving the runner by H_2 and assume for the present no losses, then the power, expressed by Equation [2], is also equal to:

$$HP = \frac{W}{550} (H_2 - H_1) \dots \dots \dots [3]$$

which simply states the familiar expression that power is equal to the weight of water falling or raised, times the head.

By combining [2] and [3], we get the familiar equation of the turbine theory for ideal conditions:

$$H_2 - H_1 = \frac{\omega}{g} \left\{ (v_{\text{tang}} r)_2 - (v_{\text{tang}} r)_1 \right\} \dots \dots \dots [4]$$

Now by taking ω into the parentheses and combining with r_2 and r_1 to give u_2 and u_1 , the velocities of the runner at entrance and exit, we have

$$H_2 - H_1 = (v_{\text{tang } 2} u_2 - v_{\text{tang } 1} u_1)/g \dots \dots \dots [5]$$

In the ideal turbine or pump, in which no losses occur, H_2 minus H_1 is equal to the total or gross head. Actually, account must be taken of the head losses. To do so makes [5] become:

$$H_2 - H_1 = (v_{\text{tang } 2} u_2 - v_{\text{tang } 1} u_1)/g - H_f \dots \dots \dots [6]$$

where H_f represents the losses expressed in terms of head.

Keeping in mind the convention in regard to signs, it follows that in the case of pumps ($H_2 - H_1$) is positive; that is to say, there is a positive increase in the energy of flow. In the case of turbines it is negative, as there is a decrease of energy which is transformed into mechanical energy delivered to the shaft. In the case of pumps the power supplied must always be greater than the power delivered to the water on account of the losses,

whereas in the case of turbines the conditions are reversed. To adopt a shorthand expression for that head which regardless of leakage losses, bearing losses, and disk friction corresponds to the torque absorbed or developed by the shaft and referred to in this paper as the net or effective head, we set $H_2 - H_1 + H_f = \Delta_1^2 H$. Making this substitution, we arrive at the equation

$$\Delta_1^2 H = (v_{\text{tang } 2} u_2 - v_{\text{tang } 1} u_1)/g \dots \dots \dots [7]$$

which is fundamental to the design of turbines and pumps.

2 DISCUSSION AND APPLICATION OF THE FUNDAMENTAL FORMULA

The values of v_{tang} in Equation [7] are to be considered as averages with respect to time and space existing in the free passages of the turbine or pump, before or after, or even between the blades. The initial whirl moment ($v_{\text{tang } r}$)₁ in a turbine is created by the discharge through the guide vanes, and is determined by their angles and opening, whereas the final whirl moment ($v_{\text{tang } r}$)₂ is governed essentially by the discharge, the angles of the blades, and also the cross-sectional area and speed of the runner at its outlet. Fluctuations in smooth flow are caused by the interference of the runner blades and the guide vanes, but these may be neglected, at least for the present, even though it has been shown that they can create vibration if conditions are proper.^{(1)*} These whirl moments vary also from place to place, because it is necessary to have a finite number of blades, and it is just for this reason that there are many difficulties in determining exactly the amount of deflecting effect exerted by any system of blading upon the flow.

In the development of the elementary theory, this difficulty was avoided by assuming the number of blades to be infinitely high and the blades themselves to be infinitesimally thin. Thus the fluid when passing through the system is guided exactly by the blade surfaces, and so the angles of relative discharge with respect to the blades may be taken as equal to the blade angles. In addition, a uniform exchange of energy is assumed for all layers or filaments of flow. This is equivalent to the assumption of a constant value of ($v_{\text{tang } r}$) in all passages where no blades or vanes, or other devices such as the scroll case, influence the flow, an assumption which is only true for ideal conditions.

Now in order to apply formula [7] in adopting a proper design, it is necessary to select from all possible values of whirl moment those which promise to be conducive to best efficiency. In the case of pumps there are, as a rule, no guiding devices such as vanes or scroll cases ahead of the runners, and therefore the initial whirl is generally taken as zero. In other words, the flow is assumed to approach the runner with purely axial or radial motion, or a combination of both.

From this it follows that $\Delta_1^2 H$ is equal to $\omega/g(v_{\text{tang } r})_2$.

On the other hand, turbines are usually designed to secure an axial discharge from the runner. Hence, in this case, the ($v_{\text{tang } r}$)₂ is equal to zero, and $\Delta_1^2 H$ is equal to $\omega/g(v_{\text{tang } r})_1$. The meaning of this is that, for both turbines and pumps as ordinarily designed, the difference in energy between outlet and entrance, which is proportional to the effective head, is dependent upon the value of the moment of whirl in the transitional passage between the runner and the guide apparatus, and also upon the angular velocity of the runner.

A given value of ($v_{\text{tang } r}$) may be made up of a large v_{tang} and a small r , or vice versa, and consequently different designs can be derived for definite specific speeds. To compare these ideas with American practise, let us rewrite formula [7] in the form $\Delta_1^2 H = \omega v_{\text{tang}}/g$, u and v_{tang} referring to the conditions at the

entrance of the turbine or the outlet of the pump. Introducing now a ratio $m = v_{\text{tang}}/u$, which is a characteristic of the velocity diagram, and by substituting mu for v_{tang} , we then have $\Delta_1^2 H = mu^2/g$.

Furthermore, in American practise it is common to use the coefficient ϕ , which is the ratio between the peripheral speed of the runner and spouting velocity corresponding to the head, which, neglecting losses for the present, may be expressed $\phi = u/\sqrt{2g\Delta_1^2 H}$.

Still assuming that there are no losses, $u = \phi\sqrt{2g\Delta_1^2 H}$. Squaring, we have $u^2 = \phi^2 2g\Delta_1^2 H$. Transposing, $\Delta_1^2 H = u^2/2g\phi^2$, which, as shown, is also equal to mu^2/g . By canceling

u^2 and g , m becomes equal to $\frac{1}{2\phi^2}$ and $\phi = \sqrt{\frac{1}{2m}}$. Both m and ϕ are characteristic of the velocity diagram, and their special significance will be shown later.

3 MODERN POINT OF VIEW REGARDING THE FUNDAMENTAL FORMULA

Modern high-speed runners must be designed with but a few blades which are not excessively long, as otherwise the high relative velocities would cause too high skin friction and the efficiency would be impaired. Therefore, it cannot be assumed that blades can be made to guide each filament of flow exactly, or that the values of $v_{\text{tang } r}$ can be computed exactly from the discharge, the speed, the cross-section, and the blade angles.

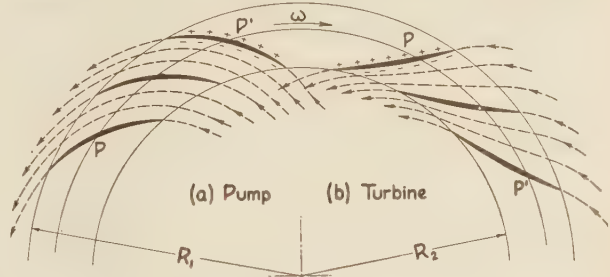


FIG. 2 CONE CC' OF FIG. 1 DEVELOPED
(Showing blade profiles and relative stream lines for a pump and turbine.)

In this connection it is very important to bear in mind that modern turbine blades operate with a considerable difference in pressure between their two surfaces. This difference may be termed the "blade differential pressure" and will be designated by Δp . To understand its significance, the expression for torque should be derived in another way. Fig. 2 is the development of a cone intersecting the blading along the line CC' . Two usual shapes for the blades are shown, the direction of rotation being the same for both. The circle PP' corresponds to the point P in Fig. 1, located in the horizontally cross-hatched area A , which is a circular projection of the blade against a radial plane. It is evident that the torque of the shaft is equal to the unbalanced force caused by the effect of Δp . As a first approximation let it be assumed that this is uniformly distributed, in which case the torque is equal to the projected area, A_p , in Fig. 1 times the unbalanced pressure Δp , times the radius r_{cg} , again multiplied by the number of blades z . This may be expressed by

$$T = \Delta p A r_{cg} z = \frac{W}{g} (v_{\text{tang } 2} r_2 - v_{\text{tang } 1} r_1) \dots \dots \dots [8]$$

all losses such as leakage, disk, and bearing friction being neglected.

It is possible by the use of this simple expression to compute the average blade pressure, although this is but an average with

* Numbers in parentheses refer to the Bibliography at the end of the paper.

no way of telling how it is distributed or divided between the push on one surface and the pull on the other. Two facts are obvious from Fig. 2:

(1) As the flow lines approach the leading edge of the blade, they are inclined away from the high-pressure side and bend toward the region of lower pressure. A corresponding effect is present at the trailing edge, and so it follows that the blades must be curved more than would be required to satisfy the average deflection as computed from application of the fundamental formula [7]. This fact, however, does not affect the validity of the elementary theory which assumes an infinite number of blades and perfect guiding of the stream.

(2) Along any concentric circle the pressure varies systematically from one side of one blade to the adjacent side of the next. Referring to the average pressure as computed from the elementary assumptions as zero, the pressure at one end of the distance separating two adjacent blades is minus and plus at the other, in much the same manner as indicated in Fig. 3.

This is all well illustrated by comparing Fig. 2, which shows the relative stream lines through the blade system, and emphasizes the fact that the average deflection is smaller than the curvature of the blades, with Fig. 3, which shows the corresponding pressure distribution with varying pressure from the leading surface of one blade to the trailing surface of the other. Also in Fig. 3 there is plotted the relative velocities w , which are greater in the regions where the pressure is lower and vice versa.

Figs. 2 and 3 represent the conditions on the average surface of revolution DD' along which lies the paths of the filaments of flow and to which the cone CC' is tangential. It has been as-

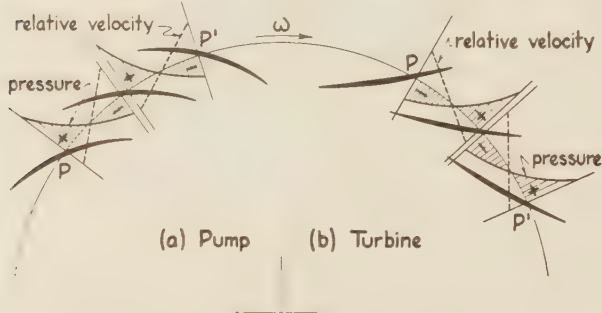


FIG. 3 PRESSURE AND RELATIVE VELOCITY DISTRIBUTION FOR BLADING SHOWN IN FIG. 2

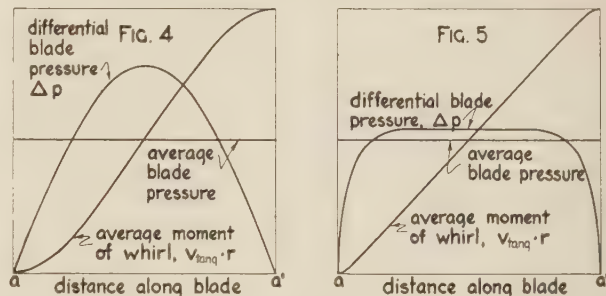
sumed that this surface of revolution can be replaced by the cone for the purpose of illustrating the conditions as existing in the flow. On every other such surface of revolution similar conditions exist, and so it is evident that the distribution of blade pressure is actually not uniform, as was assumed in Equation [8].

It is furthermore obvious that the pressure difference Δp at the leading and trailing edges must be zero, because such a difference can only exist when sustained by a material surface or body. Thus the blade pressure must drop to zero at the edges of the blades. In order to compensate for this reduction, below the average, the maximum values must naturally exceed the average. The actual distribution of blade pressure will be shown to depend upon how the flow exchanges its energy with mechanical energy during its passage between the blades. This exchange is determined by the rate of increase or decrease of moment of whirl ($v_{\text{tang}} r$), as shown by Equation [2], which is valid for intermediate partial distances between the outlet and inlet of the runner.

The value that has been taken for the moment of whirl ($v_{\text{tang}} r$) has been understood to be an average for all the filaments of flow in the space between two blades. It corresponds to the intensity and direction of the average relative flow which na-

turally is dependent upon the shape of the blades, especially the radius of curvature at any particular point along the contour. To illustrate this, in Figs. 4 and 5, two curves showing different types of variation in the average value of ($v_{\text{tang}} r$) and the corresponding distribution of blade pressure are plotted against the developed distance aa' of Fig. 1. Closer investigation shows that Δp is proportional to the slope of the curve representing ($v_{\text{tang}} r$). Although these diagrams are equally applicable for pumps or turbines, they do not intend to show the exact conditions for the shape of the blades illustrated in Figs. 2 and 3, but they do show how the distribution of Δp is affected by the rate of change of moment of whirl, which in turn is proportional to the rate of change of total energy H .

As before mentioned, even if the magnitude of Δp at each point of the blade is known, so far there is no way of determining how it is proportioned between surplus of pressure above the average on one side of the blades and deficiency below the average on the other. As a first approximation it could be assumed that it would be divided equally so that $\Delta p/2$ would represent both the surplus and the deficiency. Based on this assumption, and



FIGS. 4 AND 5 RELATIONSHIP BETWEEN CHANGE IN MOMENT OF WHIRL AND DISTRIBUTION OF DIFFERENTIAL BLADE PRESSURE

also allowing that there is a reasonably small deviation from uniform distribution of Δp over the entire projected area, it would be possible to design a blade of required properties with respect to the lowest pressure occurring in the blade system. It is this lowest pressure which is critical in determining under what conditions cavitation will take place. This idea will be discussed further in a later section. (See sections 7 and 9.)

4 ANALOGIES TO THE AIRFOIL THEORY

If we again consider the flow in that layer represented by aa' in Fig. 1, and as developed in Fig. 2, it is evident that each blade operates under conditions which are very similar to that of an airfoil or wing of an airplane. In fact, there is a strong resemblance between the cross-section of a blade and the shape of an airfoil. Furthermore, such a wing has a surplus of pressure on one side and a deficiency on the other, as indicated in Fig. 6. The side having the higher pressure is marked plus and the other minus. As a result of this distribution of pressure, there is produced an effect which in aeronautics is called "lift," but for blades it may better be considered as a thrust which is perpendicular to the direction of the approaching flow. The other component at right angles is called drag, or resistance to flow. In an ideal fluid the lift is the only reaction acting upon the wing or blade, but in a real fluid the drag component exists and must be taken into account.

On the high-pressure side of the profile the velocities are somewhat lower than on the low-pressure side. In Fig. 6 the stream lines have been drawn to indicate this fact by having the distance between each pair of lines so that there will be the same partial discharge. It will be seen furthermore that the stream

lines approaching and leaving are deflected in the direction indicated by the two arrows by the effect of the pressure gradient around the edges.

A most significant difference between the behavior of a single wing and the blades of a turbine or pump is that in the case of the latter we must deal with a series of profiles arranged in circular



FIG. 6 FLOW ALONG AN AIRFOIL PROFILE

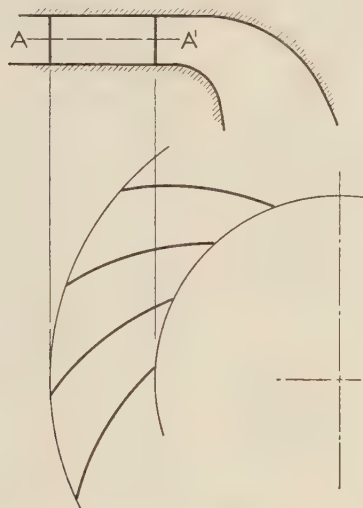


FIG. 7 RADIAL ARRANGEMENT OF BLADES

formation. It was seen in Figs. 1 and 2 that sections of the profiles cut by a layer of flow extend over circles of differing radius and the angle formed by an element of the cone, and the shaft may have any value from 90 deg to 0. It would be well to consider first the two extreme conditions:

(1) A radial arrangement of profiles is shown in Fig. 7. The surfaces of the blades are cylindrical, and the flow is bounded by two parallel planes normal to the shaft. For each plane parallel to the bounding surfaces, there are assumed to be the same conditions of flow, and furthermore, the flow is two-dimensional—i.e., it can be represented on a single plane. This arrangement is used for runners of high-pressure centrifugal pumps, and is useful for studying the influence of the number, shape, and angles of the blades upon the torque and head under different conditions of discharge and speed. (2) Such a series of blades may also be assumed to represent approximately the conditions of flow in any given layer, as in Figs. 1, 2, and 3.

(2) An axial arrangement of blades is shown in Fig. 8, similar to Fig. 7, except that it has been drawn for an axial blade arrangement. The result of developing a flow layer is a straight and infinitely long series of profiles parallel to each other. Such a series may likewise be used to study the influence of the previously mentioned details by considering that the flow in the thin layer represented by the cylindrical section, having a thickness of dr , is identical with a similar section AA' in Fig. 7. In the axial runner, each cylindrical section is different from the others in angles, pitch, and shape of the blades. It is therefore necessary to investigate whether or not, and under what conditions, the flow in one layer influences that in the neighboring layers.

Whatever the result of such investigation may be, we could determine the torque in the shaft and, in consequence, the effective head absorbed or created by the runner, if we could only know the magnitude and direction of the resulting force caused by the reaction against the deflection of flow working upon each individual circular section. If, furthermore, we could obtain information from experiments made with profiles under simplified conditions, we possibly would have a good foundation for a theory of few-bladed axial runners.

A great many experiments have already been made for the purpose of investigating the airfoil theory. Wings or vanes having special profiles have been held in a fixed position opposed to a uniformly approaching flow. For a thin layer near the central plane normal to the width of the body and parallel to the approaching flow, the action can be considered to take place in a single plane, and the lift L and drag D may be computed from the experiments. (4)

It is obvious that conditions for the radial arrangement are so different that the results of such experiments cannot be transferred directly without investigating very closely the corrections to be applied. An attempt to make this transfer may not be worth while; it may be better to experiment in the first place with a radial arrangement of blades, or else to apply special theoretical calculations. Certainly in the case of the axial as con-

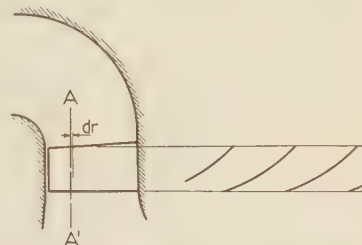


FIG. 8 AXIAL ARRANGEMENT OF BLADES

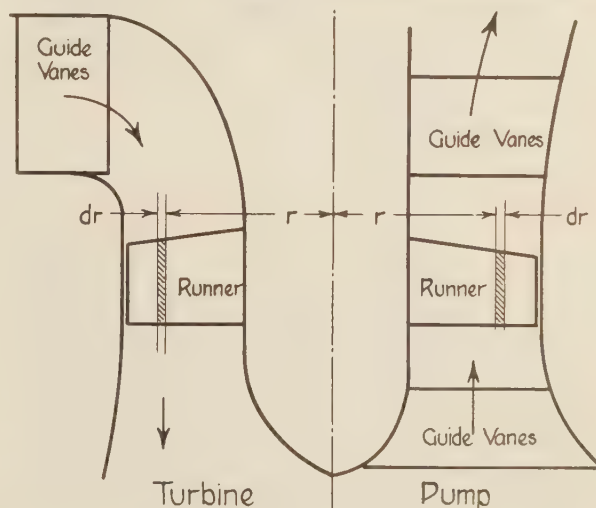


FIG. 9 CYLINDRICAL LAYERS OF RADIUS r AND THICKNESS dr USED IN ANALYSIS OF THEORY OF AXIAL RUNNERS

trasted with the radial runner, there is much more reason to apply directly, or with few corrections, experimental results and so get an approximation of the underlying theory. For this reason the next section gives a short outline of how such a theory may be applied.

5 APPLICATION OF THE AIRFOIL THEORY TO RUNNERS OF PROPELLER PUMPS AND TURBINES(5)

If we treat, as suggested in Fig. 8, the thin cylindrical layer of flow, see Fig. 9, having an average radius r and a thickness dr

which is so small that uniform conditions may be safely assumed to exist across this incremental distance, the development of this layer may be represented by Fig. 10 for a pump and by Fig. 11 for a turbine. These diagrams show the cross-sections of the blade profiles and the relative flow which can be assumed to take place in this cylindrical section. In both cases the inclination of the chord of the blades relative to the direction of motion is given by the angle θ , while the distance from a point on one blade to the corresponding point on the next is given by the pitch S . The width of the blade is defined by the distance l between two perpendiculars to the chord. The height of the blading is given by X .

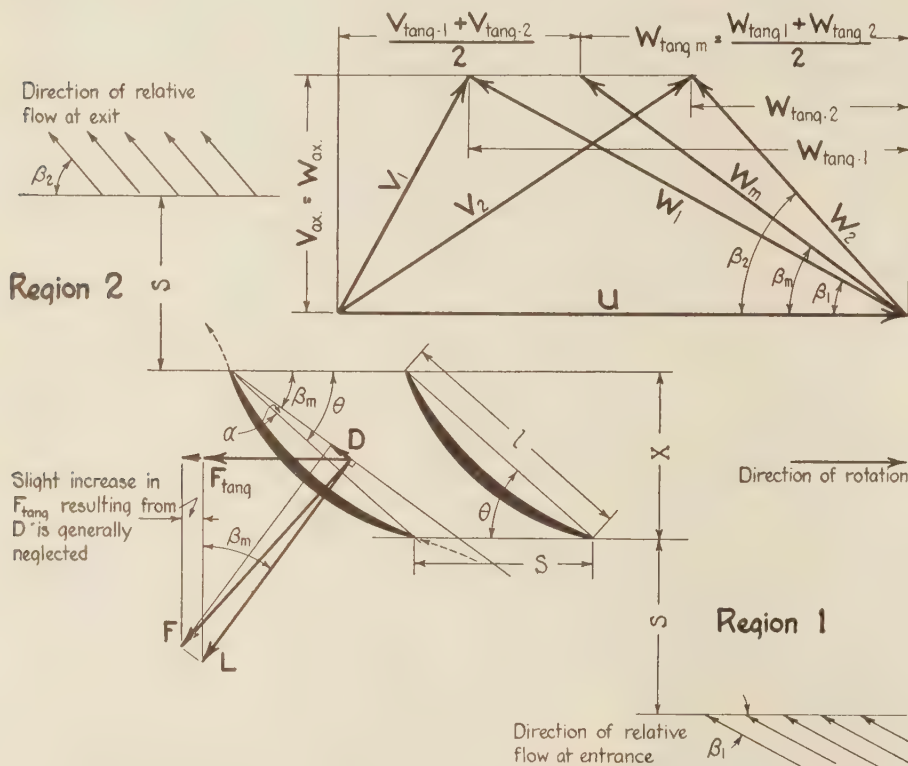


FIG. 10 BLADING AND VELOCITY DIAGRAM FOR AN AXIAL PUMP

The oncoming flow is assumed to be uniformly distributed and approaching at an angle β_1 , relative to the direction the blade is moving until it enters region 1 at a distance of approximately S from the tips of the blades. The discharge is likewise considered to be uniform after passing through region 2 of like width, and leaves at an angle of β_2 . These two angles correspond to those which would be required to satisfy the elementary theory. The effect exerted on the flow is therefore the same as would be exerted by a series of thin blades extending to include regions 1 and 2, and having an infinitesimally small pitch.

The tangential component of reaction between the flow and all the blades can in theory be computed from a knowledge of the forces acting on a single blade. These forces are determined experimentally and are usually stated in terms of the two components, lift and drag. Of course, when the same profile is mounted in a series, the conditions are altered, but for the ideal flow it may be shown theoretically that the lift is normal to the direction of the mean relative velocity w_m , which may be determined from the velocity diagrams as follows:

The axial components for all velocities w_1 , w_2 , v_1 , v_2 , w_m are all the same, since these are determined by the quantity of water

passing and the discharge area, assuming uniform distribution over the entire area. It is customary to consider the tangential component of the mean relative velocity equal to the mean between the tangential components for w_1 and w_2 —that is to say:

$$w_{\text{tang } m} = \frac{w_{\text{tang } 1} + w_{\text{tang } 2}}{2} \dots \dots \dots [9]$$

Thus w_m may be determined in both magnitude and direction. The lift is taken as being normal to the direction of the average relative velocity, while the drag is considered to be parallel to it. In this situation this average relative velocity takes the place of the approach velocity in experiments with a single profile,

(6) and so L acts in a direction perpendicular to it. It will be seen on Figs. 10 and 11 that β_m differs from θ by a small angle α . It is furthermore evident that if L and D are known, the resulting force F can be found, and from it the tangential component F_{tang} can be determined.

Experimental results give the desired values of L and D as functions of this angle α , which is defined as the difference between the direction of the approaching velocity and the chord of the profile and corresponds to the angle of attack. (7)

According to the airfoil theory, the lift and the drag are given by

$$L = \zeta_l A \gamma \frac{v_0^2}{2g} \dots [10]$$

$$D = \zeta_d A \gamma \frac{v_0^2}{2g} \dots [11]$$

where A is the area, which is equal to the length l times the distance b , between the parallel walls of the testing tunnel or

flume; v_0 is undisturbed velocity of approach, and ζ_l and ζ_d , the lift and drag coefficients, respectively, are determined experimentally as functions of α . There is one value of α for which the ratio of drag to lift is a minimum, and which will be seen to be desirable to approximate as far as possible in the selection of blade-design data.

In the case under consideration, the area is the product of ldr , and as w_m corresponds to v_0 , appropriate substitutions in the foregoing equations give

$$dL = \zeta_l l dr \gamma \frac{w_m^2}{2g} \dots \dots \dots [12]$$

$$dD = \zeta_d l dr \gamma \frac{w_m^2}{2g} \dots \dots \dots [13]$$

In order to make the formulas developed in the course of this reasoning the same for turbines and pumps, let us introduce the subscripts p for pressure side and s for suction side in place of 1 and 2 as used previously for entrance and exit.

To cover a general case rather than the conventional design, it will not be assumed that $(v_{\text{tang } r})$ is zero, because it is very pos-

sible that in the future it will be found desirable to have positive or even negative values of moment of whirl on the suction side of the runner, even though such practise might require a guide apparatus or similar device at the intake of a pump. It should be repeated that in present practise the $v_{tang\ p}$ of a pump is determined by the outlet conditions, and for a turbine by the guide vanes, whereas $v_{tang\ s}$ is governed by the inlet conditions of a pump and the outlet conditions of a turbine.

The effect of drag was shown by Figs. 10 and 11 to increase the tangential component in a pump and to reduce it in the case of a turbine. Now in order to avoid complication and because D is generally but 1 or 2 per cent of the lift, it is allowable to neglect it when computing this tangential component, but to take it into account when calculating the losses and the efficiency.

It will be seen from the geometrical construction that neglecting the slight effect of drag

$$dF_{tang} = \zeta_1 l dr \gamma \frac{w_m^2}{2g} \sin \beta_m \dots \dots \dots [14]$$

It is furthermore apparent from the velocity diagram of these same figures that

$$w_m^2 = v_{ax}^2 + \left(u - \frac{v_{tang\ s} + v_{tang\ p}}{2} \right)^2 \dots \dots \dots [15]$$

and

$$\sin \beta_m = v_{ax}/w_m \dots [16]$$

By substituting v_{ax}/w_m for $\sin \beta_m$ in [14], it follows

$$dF_{tang} = \zeta_1 l dr \gamma \frac{v_{ax}}{2g} w_m \dots \dots \dots [17]$$

Taking the square root of [15] and substituting it for w_m in [17],

$$dF_{tang} = \zeta_1 l dr \gamma \frac{v_{ax}}{2g} \sqrt{v_{ax}^2 + \left(u - \frac{v_{tang\ s} + v_{tang\ p}}{2} \right)^2} \dots [18]$$

Since force multiplied by velocity is power, which in turn is equal to the quantity of water in pounds times the effective head in feet, $F_{tang} u$ would equal the effective head $\Delta_1^2 H$ times W . W is equal to the density γ in pounds per cubic feet times Q in cubic feet per second, which is itself the product of the axial velocity v_{ax} and the discharge area $S dr$. Consequently there is built up

$$dF_{tang} u = v_{ax} S dr \gamma \Delta_1^2 H \dots \dots \dots [19]$$

But $\Delta_1^2 H$ being previously shown to be $u(v_{tang\ p} - v_{tang\ s})/g$, a substitution gives

$$dF_{tang} u = v_{ax} S dr \gamma u (v_{tang\ p} - v_{tang\ s})/g \dots \dots \dots [20]$$

Either side of this equation expresses the foot-pounds of work per second done or absorbed by the flow passing through the space between two adjacent blades. Now combining [18] and [20] and canceling v_{ax} outside the radical, as well as dr , γ , and g , we get

$$\frac{\zeta_1 l}{2} \sqrt{v_{ax}^2 + \left(u - \frac{v_{tang\ s} + v_{tang\ p}}{2} \right)^2} = S(v_{tang\ p} - v_{tang\ s})$$

which may be simplified to

$$\frac{\zeta_1 l}{2S} = \frac{v_{tang\ p} - v_{tang\ s}}{\sqrt{v_{ax}^2 + \left(u - \frac{v_{tang\ s} + v_{tang\ p}}{2} \right)^2}} \dots \dots \dots [21]$$

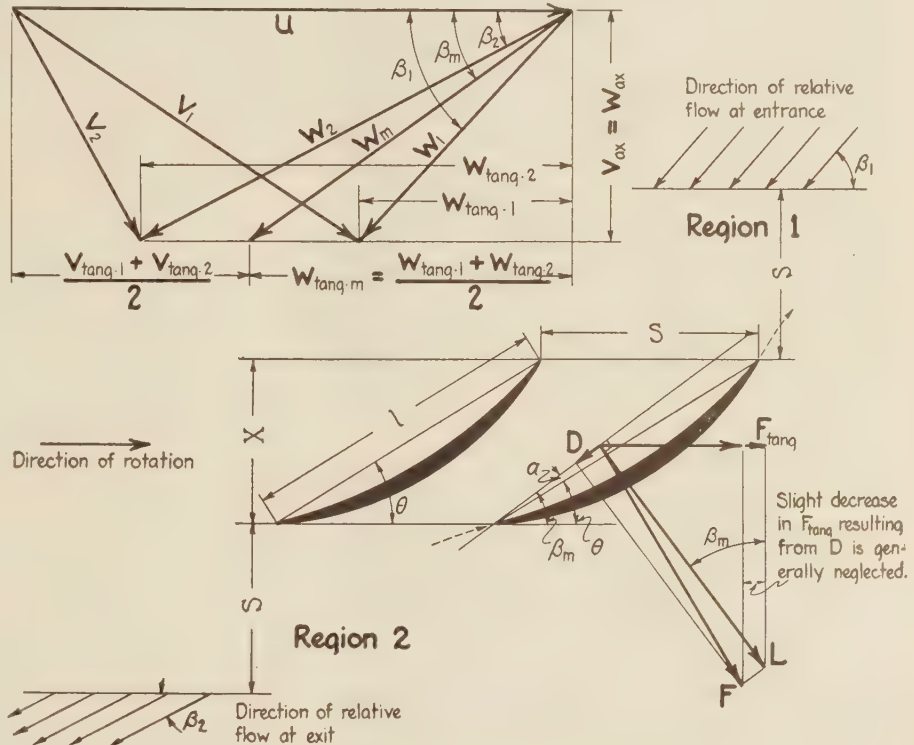


FIG. 11 BLADING AND VELOCITY DIAGRAM FOR AN AXIAL TURBINE

This equation has been written purposely in such a form that the four values which may be considered as known will be on the right-hand side, as these must be selected in advance. (Remarks concerning this selection will be contained in section 9.) It appears therefore that there are three unknowns, the combination of which must be constant.

Assume first that a profile, the properties of which are known, is chosen, and it would be advantageous to select first the value of ζ_1 that would give a minimum ratio ζ_d/ζ_1 , thus leaving but two variables. There are only a limited number of possible values for S , as $2\pi r/S = z$, which must be an integer, so l remains to be determined by trying various combinations until a convenient length of blade is found, and then

$$\theta = \beta_m + \alpha \dots \dots \dots [22]$$

all of the values are known which are necessary for the design of the profile for this circular section. The subsequent sections are analyzed in the same way. In so doing it is possible to change the shape and dimensions of the profile in the several successive sections, or else to hold to one profile and change only the dimensions to satisfy Equation [21]. Efficiency and strength of the blades, together with danger of cavitation, all have to be taken into account as governing the selection of these variables.

It is now necessary to look further to be assured against cavitation. It may prove necessary to revise the initial choice of ξ by altering α in spite of sacrifice in efficiency. This subject will be discussed more in detail in section 9.

6 CRITICISM OF THE AIRFOIL THEORY

In the preceding section there has been discussed the utilization of experimental results on one profile for the design of a turbine or pump. It should next be considered whether or not such results obtained from a single profile are applicable to a series of blades, particularly when arranged like the spokes of a wheel. A number of theoretical investigations have been made in which the fluid has been considered as ideal, but because of difficulties in the mathematics involved, such studies cannot take into account all the details such as curvature, thickness, etc., and especially the drag caused by friction. Consequently, the problem should be looked at from the material point of view in order to see what can be expected in practise.

It has been shown in Fig. 6 that when a profile is exposed to an approaching flow, there is a definite pressure distribution. In the beginning we were concerned simply with the distribution at the surface, because it is this alone that determines the lift and the drag. To look further and study the effect of mutual interference of several profiles upon each other, it is necessary to remember that the elements of pressure increase or decrease at the surface are radiating out into the flow. This influence does not extend very far as long as the deflecting effect is small, and in such cases the disturbances in the pressure field caused by each individual blade do not interfere.

However, there is another very marked effect which results from the narrowing of the passages between the blades. All of the velocities in the spaces between the blades are increased, with consequent general lowering of pressure. Thus the pressures that would otherwise be high are decreased, and the low pressures on the other side of the blade are still further reduced. The effect of this change upon the lift cannot be predicted without detailed study of the shape of the blade, but Fig. 12 shows what happens in a specific case where the wings of a biplane are exposed to an approaching flow with small angle of attack. The original pressure distribution for the two wings each taken separately is indicated by the solid pluses and minuses, while the influence of the combination of the two is denoted by the broken minuses, --. It will be seen that the net effect is that the lift of the upper wing is decreased, whereas for the lower it is increased. It has actually been found by experiments that the lower wing carries the greater part of the weight of the ship.

For higher angles of attack this effect is less marked as it becomes more and more obliterated by the increasing magnitude of the pressures set up by the wings themselves. It is furthermore evident that this influence is affected by the relative positions of the profiles themselves, which may be set farther apart or nearer together or shifted longitudinally with respect to each other. As a rule for all angles of attack, profiles arranged as shown in Fig. 12 have a total lift less than the sum of the lifts of the individual wings.

The principal difference between the wings of a biplane and the blades of a turbine or pump is that, on account of being arranged symmetrically about the axis, the tangential thrust and the drag for each must be the same. It is now a question as to whether the

forces acting upon a single blade of a series are greater or less than those working upon a single blade alone exposed to the same conditions of flow. The mathematical investigations previously mentioned(8) unfortunately cannot take into consideration all of the details which are so essential to this problem. Such studies are only carried out for a parallel series of blades, and the results so derived are valid for but one circular section of the actual runner. If there is built up a special runner composed of a number of parallel series, each of them satisfying the design conditions for the corresponding cylindrical section, then two problems must be encountered: The first is to determine the correct position of the established cylindrical sections with respect to each other to be sure that the pressure distribution along the several contours will correspond to each other and not cause cross-flow from one section to another. The second is to see whether after all this desired result is possible with the profiles that have been selected.

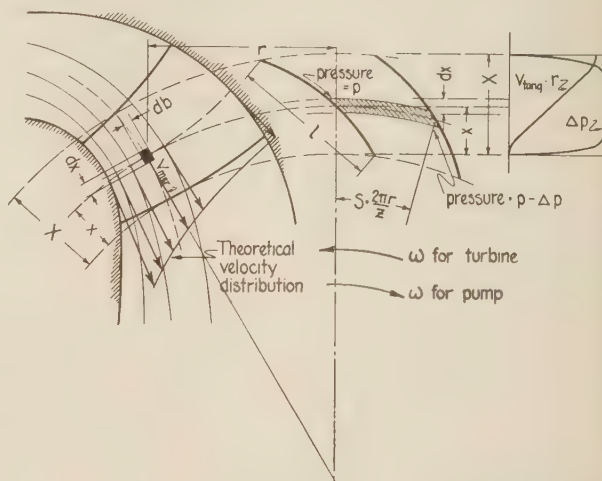


FIG. 13 THEORETICAL VELOCITY DISTRIBUTION AND DEVELOPED LAYER OF FLOW FOR A GENERAL TYPE OF RUNNER

Difficulties do not end here, for the mutual interference of a series of blades in parallel arrangement is certainly different from that of the same profiles in radial arrangement constantly changing in contour from one section to another throughout the distance from periphery to the hub.

It will thus be appreciated that there are many unknown factors in the direct application of airfoil theory and experimental knowledge to the design of turbines and pumps. Laboratory experience with such runners must certainly be called upon to check the results of the use of such a theory, and therefore it may be questioned whether or not the airfoil theory is, after all, the best one upon which to base our ideas.

In the following section there is given another point of view which is based more nearly upon the elementary theory discussed at the outset.

7 ANOTHER THEORY FOR RUNNER DESIGN

The fundamental assumption in the airfoil theory of design is that similar conditions exist for a single blade exposed to approaching flow as exist in the blading system of a runner. Another way of looking at the problem would be to begin with a consideration of a theoretically perfect system having an infinite number of thin blades, and then study the corrections that are necessary when the number of blades is reduced to a finite and finally to a very small number, while at the same time their thickness is correspondingly increased. The blades are initially

taken as geometrical surfaces, representing the relative flow at any point in the space occupied by the runner. As such a method of establishing a logical theory, susceptible to check by progressive experimentation, is valid for all types of runners, there has been selected for illustration the general type shown in Fig. 13.

The same conventions in regard to subscripts p and s will be observed as explained in section 5. It should be remembered that this is a discussion of a general case, and so $(v_{\text{tang}} r)_s$ is not assumed to equal zero.

The first step is to consider how free flow would pass through the annular spaces between the hub and the casing if there were no blading at all. The free flow may be considered to follow along meridians of surfaces of revolution, and the velocities

therefore are designated as v_{mer} . The theory of an ideal flow allows us to figure out the velocity distribution, taking into account the effect of centrifugal force caused by the curvature of the stream lines.⁽⁹⁾ Fig. 13 shows also the velocity distribution in one of the cross-sections of this annular passage. This velocity curve should next be corrected for the effect of skin friction and turbulence.⁸ So far this

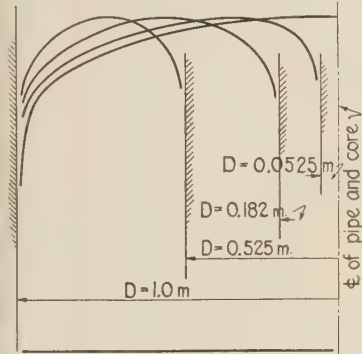


FIG. 14 ACTUAL VELOCITY DISTRIBUTION IN PIPE WITH CORES OF THREE DIFFERENT DIAMETERS

can be done only by comparison with experimental results in similar cases. The author has started systematic tests in his laboratory at Karlsruhe to study the velocities through annular passages in a region of turbulent flow. Fig. 14 shows such a diagram for four straight pipes having the same diameter, but three of them having cores of different diameters. These results can be applied to propeller turbines, and the axial flow bounded by the throat ring and hub, although theoretically uniform, should be corrected in the light of these experiments.

Fig. 15 shows a corresponding diagram of velocities actually measured in an annular passage used for centrifugal pumps. The velocities for an ideal fluid are plotted in dash lines to show the contrast with the actual in solid lines. The change of shape of the curves for different cross-sections depends upon whether the flow is being accelerated or retarded.

Such tests should be made to cover a sufficiently wide range of conditions, and a theory should be evolved which would enable us to predetermine the velocity distribution in actual installations. So far it is necessary to depend upon estimates and judgment.

It follows that if the velocity distribution is altered, then the stream lines would have to be revised so that there will always be the same partial discharge between each adjacent pair of lines.

Based upon knowledge of stream lines for free flow, the next step is to isolate a thin layer between two stream lines. The velocity v_{mer} along the distance X measuring the length of the layer along a meridian and beginning at the suction edge of the blading is now known.

In order to study the flow inside this layer of revolution, the tangent cone may be resorted to and developed by unrolling, as

⁸ The expression "turbulence" is considered here as the property which distinguishes a flow from "laminar" or "streamline flow." In a turbulent flow the individual fluid particles change from one stream line to another.

in the right-hand part of Fig. 13. Now the overall increase in $(v_{\text{tang}} r)$ is given from fundamental considerations, and $(v_{\text{tang}} r)_s$, whatever its value may be, corresponds to $x = 0$, while $(v_{\text{tang}} r)_p$ corresponds to $x = X$ and may be so plotted. In the meantime $v_{\text{tang}} r$ is a function of x , and the law by which one varies with respect to the other may be selected arbitrarily, but the consequences of such selection must be investigated.

Now if the number of blades is not infinitely high, but still very high, the variations in pressure and velocity along the circle between them will be correspondingly very small, and it is allowable to make a simple but reasonable assumption in this regard. This is that the pressure varies linearly over the distance between the blades and that the variation in velocities can still be neglected. Now the momentum theory can be applied to that incremental volume having the form of a prism extending between the front and back surfaces of two adjacent blades, in exactly the same way in which it was applied to the average flow at the outset of this discussion.

The cross-section as shown in Fig. 13 is the area $dx db$, and the length is S , or $2\pi r/z$.

By following the same reasoning as in the development of Equation [1], we get two expressions for the small part of the torque balanced by the reaction of the flow during its passage through that volume:

$$dT = \frac{d}{dx} (Fr) dx = \frac{dW}{g} \frac{d}{dx} (v_{\text{tang}} r) dx \dots \dots \dots [23]$$

$$= v_{\text{mer}} S db \frac{\gamma}{g} \frac{d}{dx} (v_{\text{tang}} r) dx$$

The transposition from one expression to another shows that $v_{\text{mer}} S db$, the incremental discharge, times the density γ is the incremental weight, the deflection of which corresponds to the incremental change in the tangential velocity $\frac{d}{dx} (v_{\text{tang}} r) dx$.

Likewise in the same manner that Equation [8] was developed

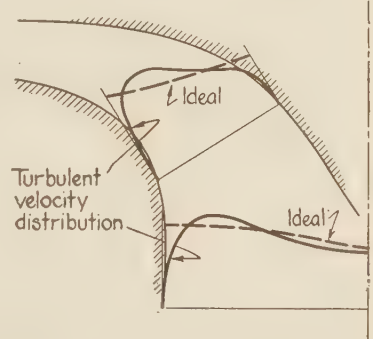


FIG. 15 COMPARISON OF THE IDEAL AND TURBULENT VELOCITY DISTRIBUTIONS IN THE ANNULAR PASSAGE OF A PUMP

$$dT = \pm db dx r \Delta_0^2 p \dots \dots \dots [24]$$

By combining [23] and [24], the result is:

$$\Delta_0^2 p = \pm \frac{2\pi v_{\text{mer}} \gamma}{z g} \frac{d}{dx} (v_{\text{tang}} r) \dots \dots \dots [25]$$

The term $\frac{d}{dx} (v_{\text{tang}} r)$ is a measure of the rate of increase of $(v_{\text{tang}} r)$ along x . If the relation between $v_{\text{tang}} r$ and x is plotted, then the slope of this curve gives $\frac{d}{dx} (v_{\text{tang}} r)$. It is necessary to keep in mind, as brought out in section 3, that Δp at the edges of the blades must be zero. When the number of blades is infinite, $S = 0$, and so Δp is indeterminate from this equation, but we are not interested in this case. When, on the other hand, the number of blades is finite, then Equation [25] shows that $\frac{d}{dx} (v_{\text{tang}} r)$ must be zero at the edges of the blades. Therefore,

whatever may be the relation between x and $(v_{\text{tang}} r)$, the curve must have a slope of zero at the end-points and consequently be S-shaped.

On the other hand, the average pressure between the blades can be computed by an equation which corresponds to Equation [7].

If we consider H , the specific energy which is increased by transfer to the flow from the blades, to be a function of x and designate by H_s the value at the suction side where $x = 0$ and by H_z the value at any intermediate point at distance x from the entrance, then we can write

$$H_z - H_s = \frac{\omega}{g} \{ (v_{\text{tang}} r)_z - (v_{\text{tang}} r)_s \} \dots \dots \dots [26]$$

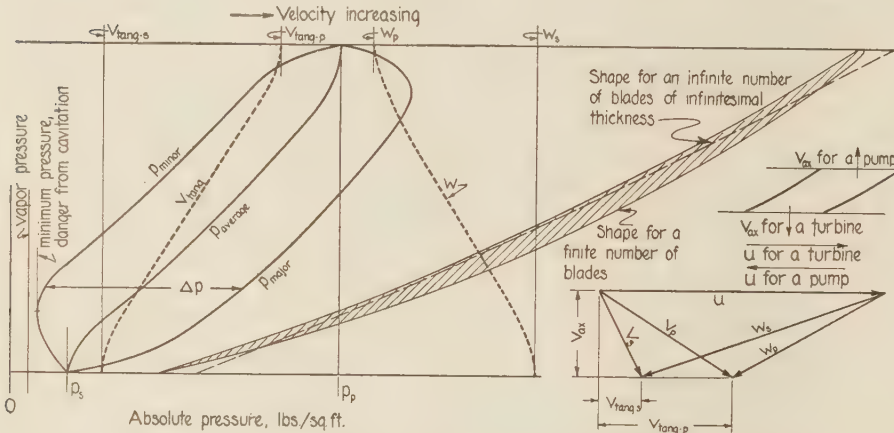


FIG. 16 RELATIVE VELOCITY, TANGENTIAL COMPONENT OF WHIRL, AND PRESSURES IN CYLINDRICAL SECTION OF AXIAL RUNNER PLOTTED AGAINST DISTANCE ALONG BLADE
(Together with profile that would be used for runner having a few blades compared with shape for infinite number of blades.)

But by definition

$$H = \frac{p}{\gamma} + h + \frac{v^2}{2g} \dots \dots \dots [27]$$

therefore

$$H_z - H_s = \frac{p_z - p_s}{\gamma} + h_z - h_s + \frac{v_z^2 - v_s^2}{2g} \dots \dots [28]$$

Combining Equations [26] and [28] and transposing, gives

$$\frac{p_z - p_s}{\gamma} = \frac{\omega}{g} \{ (v_{\text{tang}} r)_z - (v_{\text{tang}} r)_s \} - \frac{v_z^2 - v_s^2}{2g} - (h_z - h_s) \dots \dots \dots [29]$$

It now appears that if $(v_{\text{tang}} r)_z$ is a function of x , then the value corresponding to any value of x can be found. The moment of whirl $(v_{\text{tang}} r)$ is determined by the fundamental data. The r 's being fixed by the physical layout, both v_{tang} 's may be determined, and from them the v 's, since $v^2 = v_{\text{tang}}^2 + v_{\text{mer}}^2$. The h 's also are determined by the height above a datum plane, so that with p_s known, p_z may be computed for all values of x .

In the case of a large number of blades the pressure may be considered to vary uniformly along the arcs connecting the corresponding parts of two adjacent blades. In other words, one-half the pressure difference Δp is a drop below the average pressure and the other half an increase above it. Thus we are in a position to calculate the pressure on the low-pressure side of the blade, p_{min} , since

$$\frac{p_{\text{min}}}{\gamma} = \frac{p_z}{\gamma} - \frac{\Delta p}{2\gamma} \quad \text{or} \quad p_{\text{min}} = \frac{2p_z - \Delta p}{2} \dots \dots [30]$$

Substituting for $(p_z - p_s)/\gamma$ the expression given by Equation [29] and for $\Delta p/2\gamma$ the expression according to Equation [25],

$$\frac{p_{\text{min}}}{\gamma} = \frac{p_s}{\gamma} + \frac{\omega}{g} \{ (v_{\text{tang}} r)_z - (v_{\text{tang}} r)_s \} - \frac{v_z^2 - v_s^2}{2g} - (h_z - h_s) - \frac{S v_{\text{mer}}}{2rg} \frac{d}{dx} (v_{\text{tang}} r) \dots \dots \dots [31]$$

The foregoing may be worked out and the results presented graphically, but to illustrate the principles involved it is sufficient to show simply the case of an axial runner. Fig. 16 gives the plots of all the functions. In the general case it is necessary to consider the changes in r and u between the pressure and suction edges, and therefore the velocity diagrams which follow having a common line for u apply only to axial runners. This diagram applies for turbines as well as for pumps, simply by reversing the directions of flow and rotation as indicated and by properly shaping the leading and trailing edges. It is important to note in this connection that even with many blades it is possible and almost inevitable that the lowest pressure on some part of the blade will be below that of the suction pressure. The diagram indicates that it is this point that is critical in determining whether cavitation will take place or not.

If the number of blades is made progressively smaller, the assumptions introduced so far are no longer true and the method must be improved. Nevertheless, as far as we have gone, Equation [31] shows that the pressures depend to a large extent upon the rate of change in the moment of whirl produced by the blades themselves. If in this Equation [31] the values $(v_{\text{tang}} r)$ and $\frac{d}{dx} (v_{\text{tang}} r)$ are taken as average values, it is still valid even for comparatively few blades according to the momentum theory.

There is now before us the same problem that appeared in the case of the application of the airfoil theory. If the $(v_{\text{tang}} r)$ is fixed as a function of x in one layer, how is it to be determined upon for adjacent layers? It is evident that this cannot be done arbitrarily. The general law which must be followed is that in the entire blading system the equation

$$\frac{p}{\gamma} + h + \frac{w^2 - u^2}{2g} = \text{constant} \dots \dots \dots [32]$$

must be fulfilled. This equation, which was developed with particular reference to ideal flow, can also be applied to turbulent flow. The reason why this result is not secured at first is that the distribution of v_m is first fixed, and the choice of $(v_{\text{tang}} r)$ together with the fixed v_m determines the absolute velocities v and the relative velocities w . This restriction applies only for average values between the blades of multi-bladed runners. In the case of a few blades it is necessary not only to compare the average values of several layers, but also to compare the conditions varying along the parallels.

Again assumptions have to be introduced to simulate more

closely the actual conditions. For instance, it may be assumed that over the distance which separates two blades the relative velocity is varying in a straight-line relation, which means that the pressure is varying with some higher power. A further assumption is that the angle that the relative velocity makes with the tangential direction of a point on the runner varies together with the magnitude of this velocity.

To allow for these points which are not readily susceptible to analysis, simple and reasonable assumptions can be introduced as the result of experimentation carried out with special forms of blades arranged either in a series or singly, or perhaps more exact calculations. By such successive approximations a method can be developed, the final purpose of which is to establish a basis for the selection of the relation between $(v_{\text{tang}} r)$ and x , and to carry out a detailed determination of velocities and pressures between the blades as well as upon their surfaces.

It is necessary, for two reasons, to know the distribution of velocities and pressures. In the first place, Equation [32] must be satisfied, for if it is not, there will be secondary flows across the blades which will lead to additional complications arising from the need of considering their radial and axial components. In order to appreciate this more fully, it is desirable to consider the conditions existing for a straight series of parallel blades arranged between two parallel and plane bounding surfaces, as shown at the top of Fig. 17.

Suppose, first, that the blades are identical cylindrical surfaces, which means that they have the same profile in each layer parallel to the bounding planes, and suppose, furthermore, that the flow approaches this blading system uniformly in all of these parallel planes. This means that between the blades the flow also takes place in a plane, and the pressure along each straight line perpendicular to the planes is uniform. Consequently, there would be no reason why secondary flow across the blade should exist. The variations in v_{tang} , which here is analogous to the $v_{\text{tang}} r$ in the case of runners, are necessarily the same for all positions along this perpendicular.

Imagine, on the other hand, that the blades have different profiles, as shown in the lower portion of this Fig. 17. Then the distribution of pressure along the perpendicular obviously can no longer be uniform, since there would be a pressure gradient from one point to another. Consequently, a flow along the perpendicular is sure to take place. The variation of v_{tang} is no longer uniform across the blades, and is therefore analogous to the conditions which exist in a turbine or pump runner where the blades do not satisfy Equation [32] because of improperly selected distribution of $v_{\text{tang}} r$.

A second reason for knowing the pressure inside the blading system is because it is essential to know not only the lowest pressure, but its location. This is necessary in order to predict the maximum conditions of head or discharge with which it would be possible to operate the pump or turbine without danger of cavitation, as cavitation will take place when the minimum pressure approaches the vapor pressure of the water, as indicated in Fig. 16.

There now remains to be determined the shape which the blades take corresponding to a given distribution of $v_{\text{tang}} r$. For that purpose again consider a single layer and suppose the number of blades to be very high and the blades themselves to be very thin. Under these assumptions, the relative flow in the layer follows the curves which are identical to the intersection of the blades with the surfaces of revolution forming the layers; we can then write (see velocity diagram in Fig. 18).

$$v_{\text{tang}} = u - v_{\text{mer}} \cot \beta \dots \dots \dots [33]$$

from which there follows by simple transposition $\cot \beta =$

$(u - v_{\text{tang}})/v_{\text{mer}}$. The angle β is considered to be positive and always less than 90 deg.

The fraction on the right side is a known function of x , inasmuch as $v_{\text{tang}} r$ is known from the fundamental assumptions. Therefore, $\cot \beta$ and β itself become functions of x for this layer. From this relation the profile of the blade in this layer can be determined by some graphical method, and in the end the surface of the blade is represented by the intersection of the curves with all layers.

From this arises the main problem: If there are but a few blades, how must they be curved to force upon the flow the same average deflection as assumed by the choice of the relation between $v_{\text{tang}} r$ and x ? An offhand answer is that they must be curved *more* than determined by the foregoing calculation. That means that the blade angle must be exaggerated at the leading edge to compensate for the bending effect of pressure described in sections 3 and 4 and Figs. 2(a) and (b) and 6. At the trailing edge this exaggeration has also to be made to overcome the similar bending effect which would otherwise reduce the total deflecting effect of the blades. The amount of the correction which must be applied for comparatively few blades as compared with that for many, must as yet be estimated. In Fig. 16 a comparison is shown between the shape which would be adopted for infinitely

many thin blades and the one that would be used for a few blades of a definite thickness. The infinitesimally thin blade in this figure has been plotted to correspond with the variation of v_{tang} with x , as shown in this same figure.

8 ADAPTATION OF BOTH THEORIES TO ACQUIRING PROGRESSIVE EXPERIENCE AND KNOWLEDGE

Obviously it is prudent to check any theory of runner design by model test. If such tests do not give results in agreement with the theory, it is first hard to find out whether it is the theory as a whole or

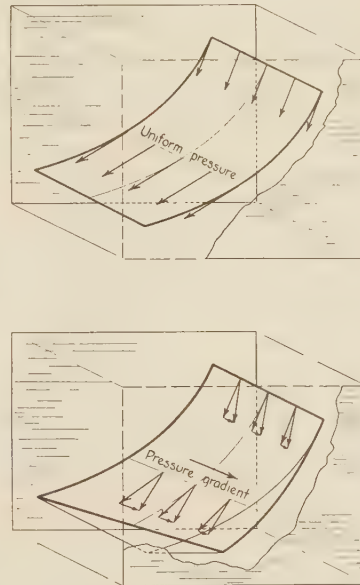


FIG. 17 CROSS-FLOW INDUCED BY PRESSURE GRADIENT ACROSS BLADE

only the details that are incorrect and then just which details these may be. On the other hand, if the results agree with the theory with respect to unit discharge, unit speed, and efficiency, we only know that the composite effect is satisfactory while the details may simply mutually compensate. Of course, a comprehensive test made with models, especially with prototypes, would lead to a more profound knowledge. For example, to measure the distribution of pressure on revolving blades would help very much to compare the theoretical with the actual conditions. With small models it is not easy to take such readings on the revolving runner. With prototype machines, for instance on large propeller runners, it should be much easier, because of the actual dimensions of the blades, hub, and shaft, to allow the arrangement of piezometer holes connected through the hub and hollow shaft by the means of small tubes coming out at the end of the shaft. Even then it would be decidedly difficult

to carry out, either with models or full-size machines, the complete system of tests which would be necessary to develop a reliable theory for turbine and pump design—that is, reliable in the sense that it could be adapted for all conditions and secure the highest efficiency and safety against cavitation.

It may not be expected that such a theory would result in still higher efficiency than those that have been obtained already, for example, 92 per cent in Europe at the Ryburg Schwörstadt plant on the Upper Rhine, but a more perfect theory would give assurance against mistakes, failures, and disappointments. It follows that because it is impossible to run a systematically arranged series of tests on turbines or turbine models, for the purpose of checking all the details underlying any theory, it is necessary to make detailed tests under simplified conditions. Undoubtedly a combination of both theories as previously described will prove the best foundation for runner design. Therefore, experimental devices, based on the ideas underlying both of these, will be needed. For example, the resulting forces exerted upon a series of profiles in parallel or even radial arrangement should be measured to determine the lift, the drag, and the velocity and pressure distribution under various angles of approach.⁴

Such tests should be made with profiles which are intended to be used for runner blading, and the difference of the effect upon the profiles when arranged in parallel or radial series should be determined; in this way the mutual interference can be studied. This is one of the two main problems in turbine design.

The other is to form a blade, having blade pressure distribution Δp as uniform as possible. The success of any effort in this line can be verified by taking readings of pressures along the blades.⁽¹⁰⁾

To analyze the results of tests of these two types, either the airfoil theory or the theory developed from infinitely many blades may be used, but in either case both must then be corrected and adapted to the conditions under which the profiles are used in the runners. This must be accomplished by actual tests themselves, for performance cannot be predicted in detail.

Other incidental problems, not so essential as those mentioned, but still important, should be studied in like manner. For example, one question is how the product $v_{\text{tang}} r$ generated by the guide vanes influences the distribution for free flow. In this case the guide vanes overhanging the curb ring cannot give the flow a constant moment of whirl if the distribution of velocity v_{mer} remains the same as for free flow. An alteration in the natural moment of whirl causes a pressure distribution which is not conducive to the same velocity distribution as for free flow. Hence the conclusion must be drawn that guide vanes overhanging the curb ring change the distribution from that for free flow, and therefore must be taken into account in the design of the runner. The effect can be studied mathematically, but the results should be checked by experiment made with guide vanes arranged only in circular or parallel series and with and without overhang. The velocity distribution in three dimensions should be observed for such flows.⁽¹¹⁾

If it is necessary to arrange the guide vanes overhanging the curb ring in order to reduce the over-all diameter of the distributor, then there are three questions. Is it necessary to deform the lower parts of the guide vanes in order to get constant $v_{\text{tang}} r$? Is it possible, or perhaps better, to allow some difference in $v_{\text{tang}} r$ and to adapt runner blades to that distribution?

⁴ A large number of tests have been made in Germany. The author, in his laboratory at Karlsruhe, has tests now under way in order to compare the effect of several profiles when arranged in parallel, with the effect of the same profiles when arranged as turbine runners. A close mathematical investigation is being made at the same time, and attention is called to a very interesting study, both mathematical and experimental, by Busmann.

Finally, is it worth while, after all, to worry about this discrepancy? Again, in this case, preliminary tests with parallel series of blades can be made to study the fundamental principles before the turbine as a whole has been designed and tested.

These examples show on the whole that the study of modern hydrodynamics offers a wide possibility of assisting in the search for a logical theory of turbine design, especially in the field of high specific speed. This does not require in every case tests of entire turbines or pumps, but often detailed problems can be studied by simplified set-ups, bringing out the essential points in a more distinct way than is possible even with complete tests.

Naturally, investigations using the remarkable methods that have been very successful in the development of airfoil theory should be employed in such experimental research work.

One thing is certain: If we want to operate our equipment safely, or to extend the development to even higher speeds, we cannot depend solely on the experience of yesterday. We must use all weapons of modern hydrodynamics in its experimental and mathematical branches, in order to solve these problems.

9 GENERAL DISCUSSION OF FUTURE TENDENCIES IN THE DESIGN OF HIGH-SPEED RUNNERS WITH REGARD TO EFFICIENCY AND CAVITATION

All of the foregoing paragraphs have dealt with the problem of how to develop a blading system providing the difference of the moment of whirl or ($v_{\text{tang}} r$) is given by its relation to the net or effective head. Taking a more general viewpoint, we have assumed that in the future there will be a demand to determine in advance and control the whirl moment at both pressure and suction side of the runner.

There is now to be considered what should be the selection for moments of whirl on the two sides of the runner to suit a given specific speed. Although the answer to this problem depends to some extent upon the details that have been discussed in the foregoing sections, it is well to emphasize some of the essential elements in the fundamental layout of the velocity diagram and their effect on specific speed.

(a) Mathematical Background.

As a starting point it is necessary to have before us a concrete conception of specific speed. By definition it is the number of revolutions for a homologous machine operating at 1 ft head and developing 1 hp⁶ and may be expressed

$$n_s = n \frac{HP^{1/2}}{H^{3/4}} \quad [34]$$

where n_s is the specific speed, n the number of revolutions per minute for the actual machine, HP is the horsepower, and H the head, which will be used as a shorthand expression for $H_p - H_s$.

Although this formula is very commonly used, its significance would be more appreciated if engineers would give consideration as to how it is derived. In an attempt to clear away any feeling that this expression is mysteriously evolved, let us imagine a given machine turning n revolutions per minute with horsepower HP and diameter D . The transfer to the specific con-

⁵ The cavitation test stand at the Massachusetts Institute of Technology, Cambridge, shows that it is possible to study special problems in turbine design under very much simplified conditions. The phenomenon of cavitation has been demonstrated in venturi-shaped passages having two flat faces and having different angles of flare.

⁶ These definitions might be given in dimensionless figures in order to be readily understood internationally, as then they are the same in metric or English units. In the author's book "Turbines and Pumps" (English translation in preparation) such definitions are given. In order to avoid complication in this paper, the terms and constants will be given only for English units.

ditions is made in two steps: First to unity head and then to unity horsepower. The changing values may be recorded in tabular form as follows:

	Head	Horse-power	Diameter	Rpm
Actual.....	H	HP	D	n
Reduce to 1 ft head.	unity	$HP \frac{1}{H^{3/2}}$	D	$n \frac{1}{H^{1/2}}$
Reduce to unit HP ..	unity	unity	$D \left(\frac{H^{3/2}}{HP} \right)^{1/2}$	$\frac{n}{H^{1/2}} \frac{HP^{1/2}}{H^{3/4}} = \frac{n HP^{1/2}}{H^{5/4}}$

In the first step the head is reduced to 1 ft, and so the horsepower is changed to $HP \times 1/H^{3/2}$ and the revolutions per minute to $n \times 1/H^{1/2}$. In the second step the horsepower is in turn reduced from $HP/H^{3/2}$ to unity or in the ratio $1/(HP/H^{3/2})$, so that the diameter must be altered by the square root of this ratio or $1/(HP/H^{3/2})^{1/2}$, while the number of revolutions must again be changed by the inverse of this latter ratio, since ϕ must be maintained the same. Therefore $n/H^{1/2}$ times $(HP^{1/2}/H^{3/4})$ equals $n HP^{1/2}/H^{5/4}$.

Not only does this demonstrate that the specific speed can easily be deduced without resorting to formula, but the method of deduction lays a good foundation for the following paragraphs through exercise of the principles of transfer of head.

Now by separating the expression in Equation [34] into two parts, and inserting D outside the radical and $1/D^2$ inside, the expression becomes

$$n_s = \frac{nD}{H_t^{1/2}} \sqrt{\frac{HP}{D^2 H_t^{3/2}}} \dots \dots \dots [35]$$

Keeping in mind that unit speed n_1 , or the speed of a homologous runner at 1 ft head and 1 ft in diameter, is

$$n_1 = \frac{nD}{H_t^{1/2}} \dots \dots \dots [36]$$

and that unit power HP_1 , or the power of a runner 1 ft in diameter operating at 1 ft head, is

$$HP_1 = \frac{HP}{D^2 H_t^{3/2}} \dots \dots \dots [37]$$

it will be seen that Equation [35] readily resolves itself into

$$n_s = n_1 HP_1^{1/2} \dots \dots \dots [38]$$

The following formulas apply equally well to pumps or turbines, the only difference being the question as to which head and power should be used, on account of the losses. The situation can be simplified by assuming for the present an efficiency of 100 per cent, so that $HP = WH/550 = Q \gamma H/550$.

Considering u as the tangential velocity of the runner at the periphery, in other words u_{peri} , it is recalled that a ratio commonly used in American practise is

$$\phi = \frac{u_{peri}}{\sqrt{2gH_t}} \dots \dots \dots [39]$$

For u_{peri} can be substituted $\pi nD/60$, so

$$\phi = \frac{\pi nD}{60\sqrt{2gH_t}} \text{ or } \frac{\pi}{60\sqrt{2g}} \frac{nD}{H_t^{1/2}} = 0.00652 n_1 \dots \dots [40]$$

Unit discharge Q_1 may be defined in a manner similar to HP_1 and n_1 as

$$Q_1 = \frac{Q}{D^2 H_t^{1/2}} \dots \dots \dots [41]$$

and if the efficiency is 100 per cent

$$HP_1 = \frac{Q_1 \gamma}{550} \dots \dots \dots [42]$$

and hence

$$n_s = n_1 Q_1^{1/2} \sqrt{\frac{\gamma}{550}} = 0.3368 n_1 Q_1^{1/2} \dots \dots \dots [43]$$

This equation is particularly important as forming the basis for the following, in which it will be demonstrated that specific speed can be reduced to terms of a few ratios that are characteristic of the type of velocity diagram and design of runner.

A given specific speed may be secured as the product of either a comparatively high unit speed and small unit discharge, or vice versa. High unit speed is conducive to high peripheral and relative velocities, and consequent high friction losses. On the other hand, high unit discharge leads to large losses in the draft tube. It appears from this that if two extremes are detrimental, then there should be some optimum value of their ratio, or perhaps more than one. The problem is now:

(1) Are those ratios n_1/Q_1 which are used at present really the best ones?

(2) Which ratios should be chosen to suit the higher specific speeds that will certainly be adopted in the future?

When seeking the answer for these questions, it must be remembered that a given specific speed can be obtained by various shapes of blades, which are distinguished from each other by various combinations of $(v_{tang} r)_p$ and $(v_{tang} r)_s$, even though these moments may have the same difference. This is not true in conventional practise as long as $(v_{tang} r)_s$ is considered to be zero, but in a general case this limitation no longer applies, and so a further question is:

(3) Which values of $(v_{tang} r)_p$ and $(v_{tang} r)_s$ are to be selected for a given specific speed?

Although the questions are pertinent to any type of machine, it is desirable to limit this paper to a consideration of purely axial runners.⁷

Although any concentric circular section may be used, because each layer has to be designed for the same moments of whirl as well as the same difference between them, let us consider as the one most convenient to treat simply the outer one—i.e., the one at the periphery of the runner.

Now because $r_p = r_s$ for axial runners, and since $u = r\omega$, the head may be expressed

$$H_p - H_s = H_t = \frac{u}{g} (v_{tang p} - v_{tang s}) \dots \dots \dots [44]$$

We now have use for two characteristic figures in the velocity diagram, one of which has been introduced before. These are m , the ratio of the difference in tangential velocities v_{tang} divided by the tangential velocity of the runner, or u , and s , the ratio of the tangential velocity at the suction side $v_{tang s}$ divided by this same u . As this discussion applies to the conditions in the outer layer, u will be given the subscript $peri$, to keep this fact in mind, but it should be understood that the other velocities appearing in the same equations with u_{peri} are the ones which correspond to the conditions at the periphery. Therefore

$$m = \frac{(v_{tang p} - v_{tang s})}{u_{peri}}; \quad s = \frac{v_{tang s}}{u_{peri}} \dots \dots \dots [45]$$

⁷ Professor Moody discussed the same problem in 1921, but without using the details of modern experience in aerodynamics and hydrodynamics. See Bibliography, section E, reference 5.

By substituting in Equation [44] the equivalent of ($v_{\text{tang } p} - v_{\text{tang } s}$)

$$H_t = \frac{m u_{\text{peri}}^2}{g} \dots \dots \dots [46]$$

or, because $u_{\text{peri}} = \pi n D / 60$

$$H_t = \frac{\pi^2 m n^2 D^2}{3600 g} \dots \dots \dots [47]$$

or by extracting the square root of both sides and combining and setting $n D / H_t^{1/2} = n_1$

$$\frac{n D}{H_t^{1/2}} = \frac{60 g^{1/2}}{\pi m^{1/2}} = \frac{108.4}{m^{1/2}} = n_1 \dots \dots \dots [48]$$

Another characteristic ratio in the design of a turbine or pump is the relation between the head corresponding to the axial velocity at the suction tip of the blades and the total head. This will be denoted by k

$$k = \frac{v_{\text{ax}}^2}{2gH_t} \quad \text{or} \quad v_{\text{ax}} = \sqrt{2gH_t k} \dots \dots \dots [49]$$

In case $v_{\text{tang } s}$ is zero, which means that s is also zero, k is then the per cent that the kinetic energy on the suction side of the runner bears to the total energy available. This figure is important with respect to efficiency and danger of cavitation for turbines, but for pumps it has significance only with regard to cavitation. The reason is that the suction line of a pump has accelerated flow, and as it is allowable to have the area before the runner small, a high figure of k can be used. On the other hand, the draft tube of a turbine has retarded flow, and although the passage may be enlarged very gradually, nevertheless the loss for the same value of k is greater.

Considering now that the flow may not be axial, the total kinetic energy expressed in per cent of the total head is

$$\frac{v_{\text{ax}}^2 + v_{\text{tang } s}^2}{2gH_t} = \frac{v_{\text{ax}}^2 + s^2 u_{\text{peri}}^2}{2gH_t} = k + \frac{s^2}{2m} = (2km + s^2)/2m \dots \dots \dots [50]$$

Now there appears still another characteristic ratio f , the net discharge area after deduction for the hub, divided by the area of the runner, $\pi D_h^2/4$. Then if D_h is the diameter of the hub, $f = \pi D^2/4 - \pi D_h^2/4$ divided by $\pi D^2/4$, which in turn equals $1 - (D_h/D)^2$, and so from Equation [49] it follows:

$$Q = \frac{\pi}{4} f D^2 \sqrt{2gH_t k} \dots \dots \dots [51]$$

from which comes the expression for unit discharge

$$Q_1 = \frac{Q}{D^2 H^{1/2}} = \frac{\pi}{4} f \sqrt{2gk} = 6.30 k^{1/2} f \dots \dots \dots [52]$$

Now as Equation [48] gives an expression for n_1 and Equation [51] defines Q_1 , these values can now be set in Equation [43] to give

$$\begin{aligned} n_1 &= 0.3368 n_1 Q_1^{1/2} = 0.3368 \frac{108.4}{m^{1/2}} \sqrt{6.30 f k^{1/2}} \\ &= 91.6 \frac{f^{1/2} k^{1/4}}{m^{1/2}} \dots \dots \dots [53] \end{aligned}$$

which is most important in showing the bearing which the factors f , k , and m have on the specific speed.

First consider f . Although increase in D_h decreases the unit discharge, a larger hub is ordinarily to be preferred because of the

difficulty in designing the blades near the hub if it is too small. Even though meeting these conditions by improving the design at this part of the blade is a means of securing higher unit discharge, and therefore more power in a given space, let us for the present consider f as fixed at representative average value of 0.75. In which case

$$n_s = 79.4 \frac{k^{1/4}}{m^{1/2}} \dots \dots \dots [54]$$

Combining the two facts expressed in Equation [45]

$$v_{\text{tang } p} + v_{\text{tang } s} = (m + 2s) u_{\text{peri}} \dots \dots \dots [55]$$

as will be appreciated by reference to Fig. 18. Then introducing

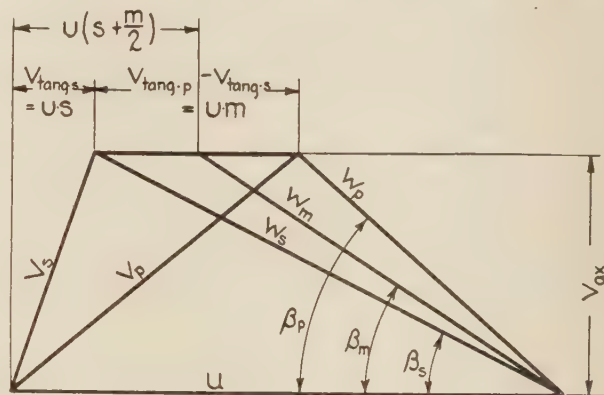


FIG. 18 GENERAL VELOCITY DIAGRAM FOR AN AXIAL RUNNER

mu for its equivalent in Equation [21] and making use of Equation [55], and removing the factor u from the parentheses, we have

$$\frac{z_1 l}{2S} = \frac{m u_{\text{peri}}}{\sqrt{v_{\text{ax}}^2 + u_{\text{peri}}^2 (1 - m/2 - s)^2}} \dots \dots \dots [56]$$

which after dividing by u may also be expressed as

$$\frac{z_1 l}{2S} = \frac{m}{\sqrt{(v_{\text{ax}}/u_{\text{peri}})^2 + (1 - m/2 - s)^2}} \dots \dots \dots [57]$$

Keeping now in mind that by definition $k = v_{\text{ax}}^2/2gH_t$, which transposed is $v_{\text{ax}} = k 2gH_t$, and also that $u^2 = gH_t/m$, the right-hand sides combined give

$$\frac{v_{\text{ax}}^2}{u_{\text{peri}}^2} = 2km \dots \dots \dots [58]$$

Substituting in [57], this leads to

$$\frac{z_1 l}{2S} = \frac{m}{\sqrt{2km + (1 - m/2 - s)^2}} \dots \dots \dots [59]$$

By transposing Equation [52]

$$k = \left(\frac{n_s}{79.4} \right)^4 m^2 \dots \dots \dots [60]$$

k may be replaced and [59] may now be rewritten

$$\frac{z_1 l}{2S} = \frac{m}{\sqrt{2(n_s/79.4)^4 m^3 + (1 - m/2 - s)^2}} \dots \dots \dots [61]$$

It is desirable to show graphically the meaning of these equations by a velocity diagram that is made dimensionless by simply dividing all vectors by u_{peri} as in Fig. 19. It will be seen that

$v_{tang\ s} - v_{tang\ s}$ of Fig. 18 become simply m . In the same way $v_{tang\ s}$ becomes s , while v_{ax} becomes v_{ax}/u_{peri} . By taking the square root of Equation [58], this is seen to be $(2km)^{1/2}$.

With s fixed, the locus of the left-hand end of the line m is a line perpendicular to the base line $u_{peri}/u_{peri} = \text{unity}$. The locus of the right-hand end depends upon the specific speed, since Equation [60] may be written $k = (n_s/79.4)^2 m^2$. Consequently, for a given specific speed, k is proportional to m^2 . Furthermore, as $v_{ax}/u_{peri} = (2km)^{1/2}$, it is in turn proportional to $m^{3/2}$, and so the lines of equal specific speed will have the form shown. It will be seen that this relation is independent of s , the significance of which will appear in the following section (b).

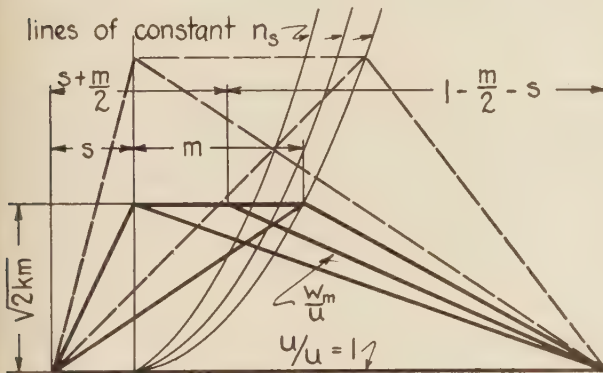


FIG. 19 DIMENSIONLESS VELOCITY DIAGRAM FOR AN AXIAL RUNNER
(Showing influence of s , m , and specific speed.)

Such a dimensionless velocity diagram is useful in showing what restrictions will be placed upon the actual diagram by a definite value of specific speed.

Equations [57], [59], and [61] also show that the three quantities determining the characteristics of the airfoil section to be selected for a blade depend also upon these ratios k , m , and s . It should be remembered that the constants used have been based upon an assumption of an average value of f , and so apply only when $f = 0.75$.

(b) Consideration of a Special Profile.

There is now the question of determining which values of m , s , and k should be selected in order to secure both high efficiency and assurance against cavitation. The method of solution is to develop and analyze equations expressed in terms of these ratios. As far as the lowest pressure, which controls cavitation, is concerned, the same treatment will apply to both turbines and pumps, but the expressions for efficiency will be seen to differ.

In the general formulas dealing with conditions conducive to cavitation, it is impossible to take into account all of the pertinent details, principally because the relations of these details to the whole have so far not definitely been determined. Furthermore, it has never been conclusively established that any one profile may be considered superior to all others with respect to cavitation. Therefore, it is necessary to consider in this discussion simply a profile which is known to have properties having a strong possibility of satisfying the requirements for good pressure distribution. It is possible that such a method of attack will not give very good efficiency for the first trial, but at least the results will be useful in showing the general relations and the underlying laws, and so serve as a foundation for further search for perfection.

The profile proposed for consideration has a crescent shape. It is formed as shown in Fig. 20 by the arcs of two eccentric circles, and may be defined by three principal dimensions: l , as

before, the length between two perpendiculars to the chord, but as we do not consider at first any rounding of the edges, l is actually the length of the chord itself; t , the thickness; and a , the altitude of a segment formed by the chord and a circle passing through the middle of t at the center of the blade. As a and l define the radius of curvature, the ratio a/l may be considered as a measure of the curvature of the blade, and in like manner the ratio t/l may be called the relative thickness.

The property of this profile which is particularly interesting is that if it is exposed to flow parallel to the chord, so-called "shockless approach," the lowest pressure will occur at the center of the blade, and the pressure distribution will be similar to that shown in Fig. 5, which was contrasted with Fig. 4 to demonstrate that the maximum value of Δp for a given average can be smaller if the distribution is even. The pressure along the blade is given for three examples in the lower part of Fig. 20. One of these is contrasted with the pressure distribution of an actual airfoil having the same total lift, and the superiority of the crescent in this respect is readily appreciated. This is particularly desirable, for if the reduction of pressure is not only unnecessarily great, but also occurs near the leading tip, then in large propeller turbines the conditions are aggravated by the fact that this point of lowest pressure is by the very size of the runner raised considerably above the center line and so is at a point where the static pressure is already low.

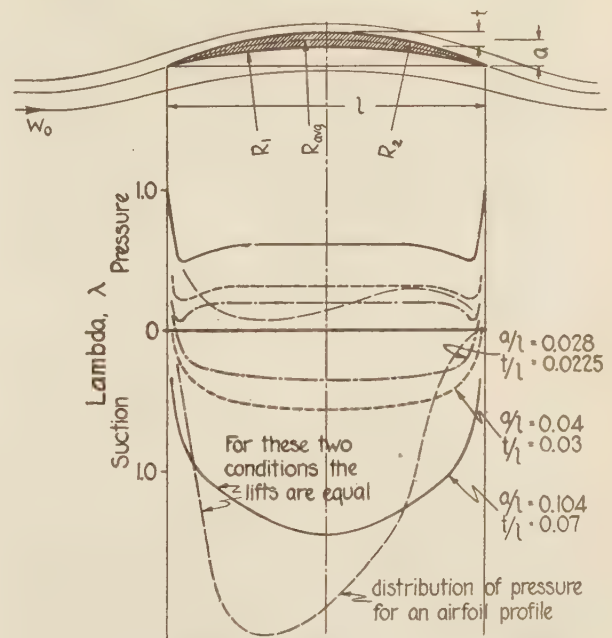


FIG. 20 CRESCENT-SHAPED PROFILE AND DIAGRAM OF PRESSURE DISTRIBUTION

Such a profile is readily adaptable to theoretical computation of pressure distribution, which has later been verified by experiment, and it has been found that the lift coefficient ζ_l in Equation [10] becomes $4\pi a/l$ for shockless approach. Substituting then in the expression $\zeta_l b \gamma v_0^2 / 2g$ and setting $b = 1$, we have for lift per unit of breadth

$$L = 4\pi a \gamma v_0^2 / 2g \dots \dots \dots [62]$$

It is very interesting to note that in this particular case the l 's cancel, and so the lift becomes independent of the length of the chord.

In Fig. 20 the pressures have been given in terms of λ , as is customary, as λ is useful in expressing the ratio between reduction or increase in pressure at various points and the pressure corresponding to the velocity of the approaching flow. For example, the pressure at the nose is always the stagnation pressure or exactly +1. The λ for any point located at a distance of x from the trailing edge will be termed λ_x . Furthermore, if the shape of this curve is the same regardless of the velocity of approach, that is to say if the pressure at any point can always be expressed as a constant times the velocity pressure of the approaching flow as long as the angle of attack is the same, then it follows that the ratio between λ_x and the lift coefficient ζ_l is constant and may be designated by μ .

$$\mu = \lambda_x / \zeta_l \dots \dots \dots [63]$$

The lowest value of λ , which may be denoted as λ_{\min} , occurs for this profile at the mid-point, and is of particular interest. Fig. 21 shows its value as computed for various degrees of curva-

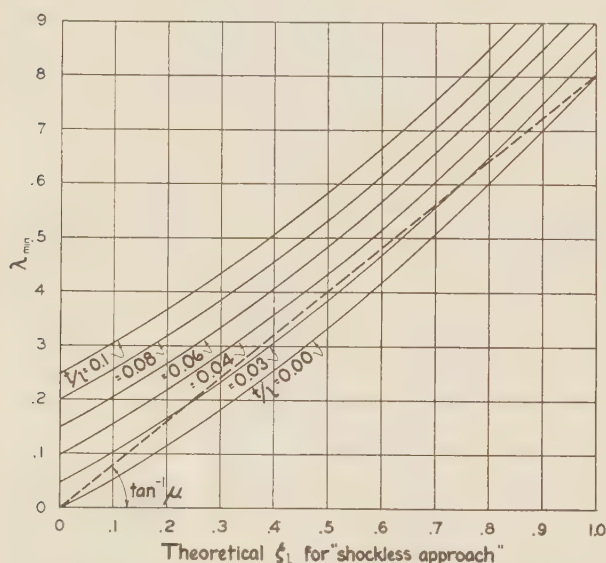


FIG. 21 LAMBDA AS A FUNCTION OF LIFT COEFFICIENT FOR SHOCKLESS APPROACH AND FOR VARIOUS THICKNESSES OF BLADE

ture and for various thicknesses of blade. It will be seen that λ_{\min} increases practically in proportion to ζ_l , and that it is also affected by increasing thickness of the blade. Leaving strength out of consideration for the present, it is apparent that the average relationship between λ_{\min} and ζ_l may be represented approximately by a straight line having a slope, which is the μ referred to above, of 0.8. Consequently, for this profile λ_{\min} becomes $3.2\pi a/l$, which multiplied by $\gamma w_m^2/2g$ gives the minimum pressure on the blade with respect to the surrounding pressure, w_m now corresponding to the approach velocity v_0 .

$$p_{\min} = \lambda_{\min} \frac{w_m^2}{2g} = \mu \zeta_l \frac{w_m^2}{2g} = 3.2\pi \frac{a\gamma}{l} \frac{w_m^2}{2g} \dots \dots [64]$$

(c) Effect of m , s , and k on Cavitation.

Having determined the properties of the special profile, it now remains to express the lowest pressure in terms of the ratios m , s , and k , for the assumed values for $\epsilon s l$ and μ . Only an outline of the mathematics will be given on account of the lack of space.

Inasmuch as λ , for any given point, multiplied by the square

of the mean relative velocity, gives the depression below the mean pressure p_m/γ , then

$$\frac{\lambda_x w_m^2}{2g} = \frac{p_m}{\gamma} - \frac{p_{\min}}{\gamma} \dots \dots \dots [65]$$

for p_m/γ may be written $p_s/\gamma + (w_s^2 - w_m^2)/2g - x$, x being as before the vertical height from the suction side of the runner to the point of lowest pressure.

It also is true that the pressure at the suction edge of the blades is equal to the barometric height H_b , minus the draft head, or lift, H_s , measured from the free water surface to the lower tip of the blade, again minus an expression which is equal to the efficiency of the draft tube ϵ_s times the velocity head at that point. Thus

$$\frac{p_s}{\gamma} = H_b - H_s - \epsilon_s \frac{v_{ax}^2 + v_{tang}^2}{2g} \dots \dots \dots [66]$$

and so by substitution and transposition, and because under the conditions where cavitation is just beginning, the lowest pressure is equal to the vapor pressure H_v , we get

$$H_b - H_v - H_s - x = \epsilon_s \frac{v_{ax}^2 + v_{tang}^2}{2g} - \frac{w_s^2 - w_m^2}{2g} + \frac{\lambda_x w_m^2}{2g} \dots \dots \dots [67]$$

This Equation [67] has been written so that the terms $H_p - H_v - H_s - x$, $H_s + x$ together being the draft head to the point of lowest pressure and commonly written just H_s , the point of reference usually being taken arbitrarily, stand on the left-hand side, so that when divided by $\Delta^p H$, commonly called just H , they will equal the familiar expression for Σ . Dividing the other side of the equation by the equivalent of $\Delta^p H$, which is equal to $m u_{peri}^2/g$, we have

$$\frac{H_b - H_v - H_s - x}{\Delta^p H} = \Sigma = \frac{\epsilon_s (v_{ax}^2 + v_{tang}^2) - (w_s^2 - w_m^2) + \lambda_x w_m^2}{2m u_{peri}^2} \dots \dots [68]$$

Because the losses that occur in a turbine or pump have not been taken into account, which means that $\Delta^p H$ has to be used instead of the total head H_t as is customary in determining Σ , and also because ideal conditions were assumed, such as sharp leading edges etc., it cannot be expected that the values that would be computed from Equation [68] and those which are later derived from it, would agree exactly with actual cavitation tests. Nevertheless, such formulas are useful in showing general relationships and the effects of variables upon Σ .

It is necessary to free Equation [68] from the terms v_{ax} , v_{tang} , w_s , w_m , and λ_x . $w_s^2 - w_m^2$ may first be eliminated by consideration of Fig. 18, whereby they may be reduced to the expression

$$w_s^2 - w_m^2 = \left[2(1-s) - \frac{m}{2} \right] \frac{m}{2} u_{peri}^2 \dots \dots [69]$$

By substituting $2km$ for v_{ax}^2/u_{peri}^2 and considering that v_{tang}^2/u_{peri}^2 is equal to s^2 , then

$$v_{ax}^2 + v_{tang}^2 = (2km + s^2) u_{peri}^2 \dots \dots \dots [70]$$

Referring to Equation [56], we find that ζ_l is equal to $\frac{2S}{l} m u_{peri}$

divided by an expression which is equivalent to w_m . It follows that

$$\lambda_z = \mu \zeta_1 = \frac{2\mu}{l/S} \frac{m u_{\text{peri}}}{w_m} \dots \dots \dots [71]$$

Now finally

$$w_m = u \sqrt{2km + (1 - m/2 - s)^2} \dots \dots \dots [72]$$

and so by these substitutions the basic formula is derived

$$\Sigma = \frac{m}{8} + \epsilon_s k + \frac{1}{2} \left(s + \frac{\epsilon_s s^2}{m} \right) + \frac{\mu}{l/S} \sqrt{2km + (1 - m/2 - s)^2} - \frac{1}{2} \dots \dots \dots [73]$$

It will be noted that there appear constants which must be considered as given: ϵ_s = efficiency of draft tube, which is not the same for pumps as for turbines; S = spacing between blades; l = the length of the blade; μ (as explained in preceding section) = the ratio between λ_z and ζ_1 , as well as the three ratios m , s , and k .

Σ has been computed for conditions which will be assumed for the sake of demonstrating the effect of the ratios m , s , and k , not only upon cavitation but upon efficiency as well (see following section (d)).

Three specific speeds have been selected, 125, 175, and 225. Inasmuch as it is well known from experience that with the higher specific speeds, it is necessary to incline toward narrower blades, two ratios of l/S have been taken for each speed. Because these are not the same for each, no final curves plotted as a function of specific speed will be shown for fear that they would give the impression that only one variable had been changed. These assumptions are:

Specific speed n_s	Wider blades l/S	Narrower blades l/S
125	1.0	0.5
175	0.9	0.45
225	0.8	0.4

Fig. 22 shows for $n_s = 175$ the values of Σ plotted against s for constant m and gives the picture for turbines and pumps with both wider and narrower blades. It should be noted that as Σ decreases with lower values of m , s does not change greatly. It is furthermore interesting to see that Σ continues to decrease with diminishing m , so that there is no optimum value of m as far as cavitation is concerned. The same was found to be true with both the higher and the lower specific speeds, and so it is impossible to show the effect of changing speed for best conditions of cavitation. The effect will be shown later when the best m for efficiency has been determined.

Comparison of the four panels shows plainly that narrower blades are conducive to cavitation and that conditions for pumps are more severe than for turbines.

(d) Influence of m , s , and k on Efficiency.

As previously mentioned, the question of efficiency for pumps and turbines must be treated separately. Therefore, distinct sets of equations will have to be developed to suit these two cases. In general, however, it may be said that the total losses consist of three parts: (1) the loss in the suction line or draft tube, (2) the loss in the runner itself, and (3) the loss in the diffuser, or in the scroll case and distributor. Inasmuch as head loss has previously been designated by H_f , these three components will be given appropriate subscripts, H_{fs} , H_{fr} , and H_{fp} , respectively.

In computing H_{fs} , the difference between pumps and turbines is based upon the fact that in the former the flow is accelerated,

whereas in the latter the kinetic energy must be converted into pressure. This process is more difficult and the loss is always greater.

For pumps, the loss at entrance under favorable conditions could not be expected to exceed that of the good nozzle, which is but a few per cent of the velocity head, $v_s^2/2g$. Thus H_{fs} may be expressed in terms of a constant c_s times the square of the axial and tangential components $c_s (v_{ax}^2 + v_{tang}^2)/2g$. For v_{tang}^2 may be written $u^2 s^2$, whereas for v_{ax}^2 may be written $2km u^2$, so

$$H_{fs} = c_s u_{\text{peri}}^2 (2km + s^2)/2g \dots \dots \dots [74]$$

In the case of turbines, it is only necessary to substitute in place of c_s in Equation [74] the expression $1 - \epsilon_s$, ϵ_s being draft-tube efficiency referred to in the section on cavitation. Thus

$$H_{fs} = (1 - \epsilon_s) u_{\text{peri}}^2 (2km + s^2)/2g \dots \dots \dots [75]$$

It may be a question whether ϵ_s may be assumed to be constant for all values of whirl at the outlet of the runner. This certainly would not be true for any tube selected at random, but experience has shown that at least for small values of s the draft

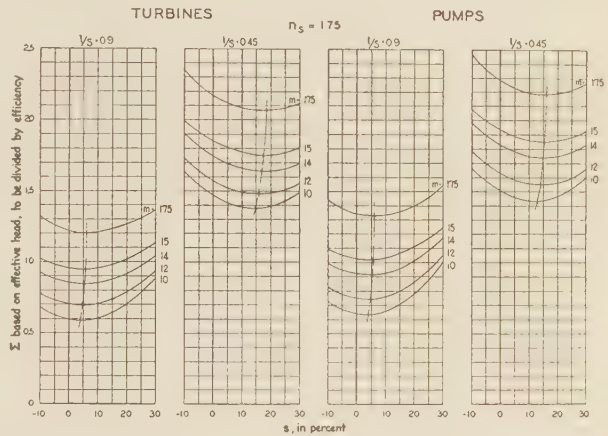


FIG. 22 VALUES OF Σ PLOTTED AGAINST s

tube efficiency can be the same as, or even a little better than, that for a straight axial flow. The author in his laboratory at Karlsruhe, Germany, has had experience with a special form of tube used with a Kaplan runner and investigated by Dr. Kriessam.(12) This tube had an extreme amount of flare, being much shorter and more spreading than those proposed by Moody, and was especially shaped to avoid the amount of excavation required for an elbow tube. The results compared very favorably with the straight conical tube that was selected out of a series of five as being the most suitable for this particular wheel. It showed better efficiency than the elbow tube, and in extreme cases of whirl it was even better than the straight conical tube.

On the basis of this experience it may be assumed that if the turbine is not too small, ϵ_s may be considered to be a constant and to have a value of 0.875.

Consider now the losses in the runner itself which are caused essentially by the work absorbed in overcoming the drag of the blade passing relative to the water with a velocity of w_m . The work lost in the incremental layer at the periphery is therefore dDw_m and must be supplied by the partial discharge passing through this incremental layer in the space between a single pair of blades. This discharge is therefore $v_{ax} \gamma S dr$, and the head loss is H_{fr} . Consequently,

$$dD w_m = \gamma v_{ax} S dr H_{fr} \dots \dots \dots [76]$$

Recalling Equation [13] for dD , which multiplied by w_m gives

$$dD w_m = \xi_d l dr \gamma w_m^3 / 2g = \gamma v_{ax} S dr H_{fr} \dots [77]$$

canceling γ and dr , and by setting w_m^3 equal $u^3 [2km + (1 - \frac{m}{2} - s)^2]^{3/2}$ and v_{ax} equal $u\sqrt{2km}$, then canceling u , H_{fr} may be expressed

$$H_{fr} = \frac{\xi_d l}{2g S} \frac{u_{peri}^2 [2km + (1 - m/2 - s)^2]^{3/2}}{\sqrt{2km}} \dots [78]$$

This applies for turbines or pumps, except that for pumps ξ_d must be assumed to be slightly higher than for turbines. Fair values may be considered approximately 0.015 and 0.010, respectively.

On the pressure side the losses again differ for a reason which corresponds with that given for the suction side, but reversed.

Recapitulating, formulas [74], [78], and [79] may be combined and divided by $\Delta_s^2 H$ on one side and by its equivalent $m u_{peri}^2 / g$ on the other side, and then written in the form

$$\frac{H_f}{\Delta_s^2 H} = \frac{c_s(2km + s^2)}{2m} + \frac{\xi_d l}{2m S} \frac{[2km + (1 - m/2 - s)^2]^{3/2}}{\sqrt{2km}} + \frac{1 - \epsilon_p}{2m} [2km + (s + m)^2] \dots [81]$$

In like manner Equations [75], [78], and [80] may be combined and written in the form

$$\frac{H_f}{\Delta_s^2 H} = \frac{(1 - \epsilon_s)(2km + s^2)}{2m} + \frac{\xi_d l}{2m S} \frac{[2km + (1 - m/2 - s)^2]^{3/2}}{\sqrt{2km}} + \frac{c_p}{2m} [2km + (s + m)^2] \dots [82]$$

These formulas give the losses in per cent of the head effectively used so that appropriate adjustment must be made to express these losses in per cent of the total head H_t . Remembering now that for a given specific speed, k may be replaced by $(n_s/79.4)^4 m^2$, and so given the n_s and l/S , the losses may be computed for various combinations of m and s . This has been done for three specific speeds using the same blade width l/S as in the previous section on cavitation.

The results for specific speed of 175 are presented in Fig. 23, which shows the losses for turbines and pumps having l/S of both 0.9 and 0.45. It will be noted that all of these curves have a minimum for some s , and that for a combination of m and s the best conditions, as far as efficiency is concerned, are found as illustrated by the minimum of the dotted curve passing through the minima of the individual curves. The same was done for specific speeds of 125 and 225, the results being shown in Table 1.

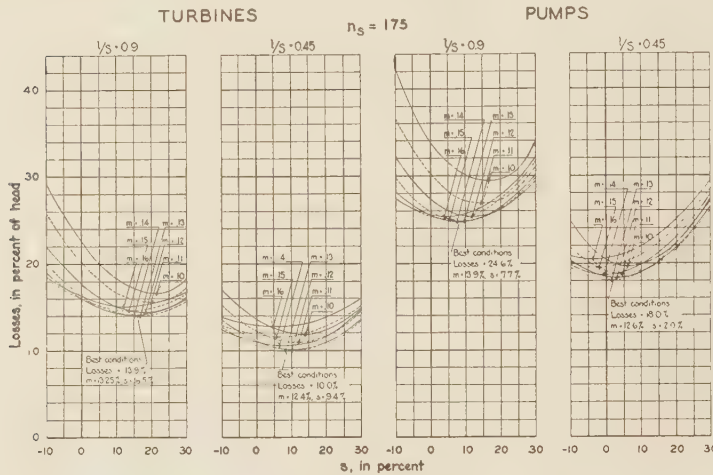


FIG. 23 LOSSES VERSUS s

The same design of water passages that are used for turbine draft tubes might be used for pumps except that commercially it would not be possible to sell them with the size of diffuser that would be required. There is less incentive in this direction in the case of higher head pumps with longer pipe lines because the high velocity of discharge may be used to save in the diameter of the pipe line. In such a case it is not fair to charge against the pump the entire loss corresponding to the high velocity of discharge, but for the purpose of this paper, which deals primarily with low-head design, it will be considered that the discharge line is short and that it would be desirable to reconvert as much kinetic energy as possible into head. Consequently, it will be assumed that the efficiency of the diffuser is 0.80.

From Fig. 18 it will be seen that the discharge velocity squared v_p^2 is equal to $v_{ax}^2 + (su_{peri} + mu_{peri})^2$. Multiplying the entire expression by u_{peri}^2 and dividing each term individually by the same, and then replacing by their equivalent in terms of s , m , and k , gives

$$H_{fp} = \frac{(1 - \epsilon_p)}{2g} u_{peri}^2 [2km + (s + m)^2] \dots [79]$$

For turbines the expression is similar except that in place of $1 - \epsilon_p$ a coefficient corresponding to that used for the suction line of pumps, c_p , must be used. Thus

$$H_{fp} = \frac{c_p}{2g} u_{peri}^2 [2km + (s + m)^2] \dots [80]$$

TABLE 1 VALUES FOR MINIMUM LOSSES (IN PERCENTAGES)

n_s	l/S	Turbines			Pumps		
		Losses	m	s	Losses	m	s
125	1.0	9.2	20.0	16.4	16.6	23.6	0.4
	0.5	6.8	17.5	13.5	12.8	21.0	4.6
175	0.9	13.9	13.2	16.5	24.6	13.9	7.7
	0.45	10.0	12.4	9.4	18.0	12.6	2.0
225	0.8	19.2	9.5	15.0	31.8	9.8	8.6
	0.4	14.2	8.5	10.0	23.5	8.7	4.5

It should be noted that for higher specific speeds there is a tendency for the losses to increase in spite of the beneficial effect of the narrower blades. The best value of m decreases with increase in n_s , whereas the whirl s is inclined to increase with pumps, but shows no marked tendency for turbines. Furthermore, it is interesting to see that for the lower specific speeds and narrower blades there is an advantage in having the flow approach the pump with a negative whirl.

It must be remembered that when the crescent profile was proposed it was not expected that good efficiency could be secured at the first trial, and so it should not be assumed from the table that the values for losses represent by any means the best that can be expected. This table is simply to show the general tendencies. Furthermore the curves do not represent the performance that any one runner will give, as it is necessary to alter the design to correspond with the changes in the velocity diagrams.

(e) General Discussion and Conclusions.

Returning now to Fig. 23, comparison between the four panels shows plainly that in general the losses in the case of a pump

are greater than those for a turbine. As explained before, this is largely because adequate diffusers cannot be provided at reasonable cost. It is also plain that in both turbines and pumps the narrower blades are more conducive to higher efficiency. This should now be contrasted with Fig. 22, which shows the values of Σ for these same conditions. In this respect wider blades are more advantageous, since the narrower blades are more conducive to cavitation. Consequently, it is necessary to strike a compromise sacrificing to some extent efficiency for the sake of better Σ .

In order to give a better idea how Figs. 22 and 23 may be coordinated, the corresponding values of losses and Σ have been listed for various combinations of m and s , the data being taken for the wider bladed turbines. Curves for constant m showing Σ plotted against losses are shown in Fig. 24. It will be seen from this diagram that if the designer could assign a comparative value between depth of excavation required to satisfy Σ and the capitalized value of loss in efficiency, it would be possible to arrive at the economical solution in the manner indicated, and so determine the proper m and s to suit the conditions. It would be necessary then to investigate for various ratios of l/s to be sure that all variables are properly balanced to give the best results.

Now that the results showing the proper combination of m and s are approximately known, it is interesting to see the effect of specific speed upon Σ . In preparing Fig. 25 the m that would probably be selected as a compromise between cavitation and efficiency has been bracketed by two values between which the most economical may be considered to lie. This was done for each specific speed, and examination of the diagram shows plainly that with higher speed the value of Σ increases very materially, a fact which adds greatly to the cost of setting. It is interesting to note that at the same time the design becomes more sensitive to having the proper component of whirl, and although the broader blades have their best value of s at approximately 5

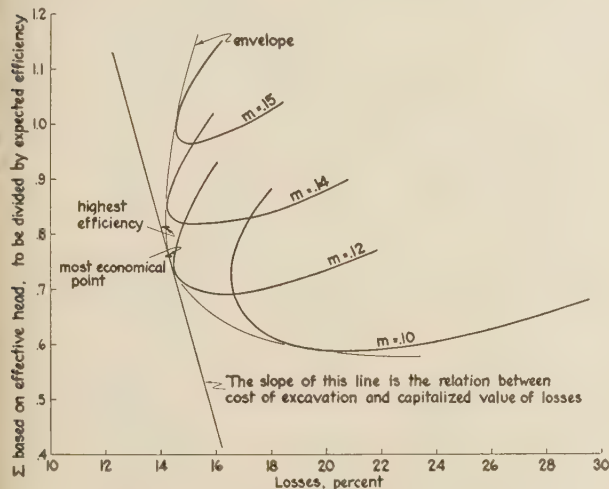


FIG. 24 COMPROMISE IN SELECTION OF m BETWEEN EFFICIENCY AND CAVITATION

per cent, the narrower blades require that the whirl should be increased.

In the interpretation of these curves it should be borne in mind that they have been worked out for one profile for which the ratio λ_{min} to lift coefficient ξ_l is 0.8. These calculations may be applied to another profile providing this ratio is substantially constant. Equation [73] shows that if μ can be made smaller, Σ will be affected favorably. Therefore, there is a distinct advantage in finding a profile which will have a very even distribu-

tion of pressure similar to that shown in Fig. 5. The foregoing suggests that the solution may be in finding a blade shape that will have a constant or nearly constant rate of change of whirl component.

Although these curves have been worked out for a special profile, it should be considered that as long as the distribution of pressure in terms of $V_0^2/2g$ is independent of the approach velocity itself, then there is a constant ratio μ between the pressure

TURBINES

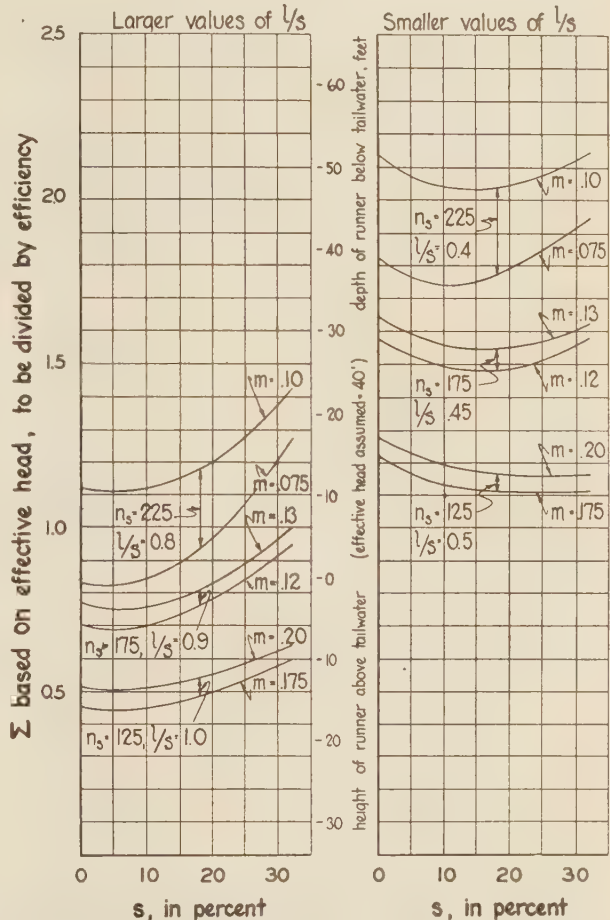


FIG. 25 EFFECT OF SPECIFIC SPEED ON CAVITATION

at any point and the lift coefficient. Consequently, as long as the angle of attack α is maintained by the alteration of the position of the blade to suit the changing angle β_m , then the method outlined is general and might apply to any profile.

As a further refinement, it must not be overlooked that the point of actual lowest pressure on a runner, particularly one with large dimensions, may not be identical with that corresponding to λ_{min} because pressure is decreased with increase in the distance x above the lower tip of the blade. Consequently, it may be necessary to determine the pressure of points slightly above the one where the lowest pressure would otherwise be expected.³

³ Investigations are at present under way at Karlsruhe to determine the effect of the shift of the point of lowest pressure with change of scale. This shift, the amount of which depends upon the characteristics of pressure distribution, is one of the principal uncertainties in transferring cavitation results from models to prototypes.

While making calculations for the results shown in Figs. 22 to 25, the effect of friction upon s was very impressive. It becomes evident that when friction is but a small part of the losses, there is little interest in increasing s , but when friction is high, it is better to sacrifice loss from increased kinetic energy at the suction side of the runner in order to reduce the relative velocity which affects the friction loss in proportion to the square. This opinion was expressed by the author in his lecture before the Hydraulic Power Committee of the National Electric Light Association, February, 1932, (13) although at that time quantitative results were not shown. The value of whirl in the draft tube was realized previously by Moody. (14)

From the fact that high friction tends toward high values of s , it may be deduced that the presence of high whirl when a unit is operating at point of best efficiency is an indication of high friction and possibly defective blade profile.

It would be interesting to continue these mathematical investigations to analyze the conditions in the inner layers of the turbine, but to do so is beyond the scope of this paper. It is hoped that the studies that have been made so far will prove useful in emphasizing the underlying principles that must be observed if successful design is to be secured by means other than by trial and error, an evolutionary process that is costly and time consuming.

In conclusion the author would like to leave the impression that the attractive advantages of higher specific speed, which open the possibility for hydro development in fields that otherwise would be closed, are going to create a demand for further achievement. It will be appreciated, however, that the prize is not easily won, for with higher speeds the design is exceedingly sensitive to having the proper conditions in every respect. To realize these advantages it is therefore very necessary that we should seek a better knowledge of the problem and solve one by one the many unknown factors that have been enumerated in this paper.

BIBLIOGRAPHY

Numbers in parentheses appearing in text refer to bibliography as follows:

	See reference below		See reference below
1	E-1	8	A
2	A-4,5,6,7,8	9	E-2
3	A-1,2,3,7,8,9	10	B-1
4	B	11	E-4
5	C	12	D-2
6	C, E-2	13	N.E.L.A. 222
7	B, C	14	E-5

Abbreviations: *Z.A.M.M.*, *Zeitschrift für angewandte Mathematik und Mechanik*, published by von Mises, Berlin. *Mittel. Institut, Mitteilungen aus dem Institut für Strömungsmaschinen der Technischen Hochschule Karlsruhe*. *V.D.I. Zeit.*, *Zeitschrift des Vereines deutscher Ingenieure*.

REFERENCES

- A Theoretical Studies of the Ideal Flow Through Series of Blades:
 - 1 Kutta: "Ueber ebene Zirkulationsströmungen nebst flugtechnischen Anwendungen" (Circulation of Flows in Planes and Their Application to Aeronautics, Sitzungsberichte der Bayerischen Akademie der Wissenschaften, Muenchen, 1911.
 - 2 Grammel: "Die hydrodynamischen Grundlagen des Fluges" (The Hydrodynamic Laws Which Govern Aeronautics), published by Vieweg, Braunschweig, 1918.
 - 3 Koenig: "Potentialströmungen durch Gitter" (Potential Flows Through Vanes), *Z.A.M.M.*, 1922.
 - 4 Spannake: "Anwendung der conformen Abbildung auf die Berechnung von Strömungen in Kreiselaedern" (Application of Conformal Transformation to the Investigation of Flows Through Runners), *Z.A.M.M.*, 1925. Ferner: "Eine strömungstechnische Aufgabe der Kreiselaerforschung und der Ansatz zu ihrer Lösung" (A Problem of Flow as Presented to the Research on Impellers and a Way to Its Solution), *Mittel. Institut*, published by Oldenbourg, Muenchen, 1930.

5 Spannake and Barth: "Potentialströmung durch ruhende oder bewegte Schaufelgitter mit beliebiger Schaufelform" (Potential Flows Through Stationary or Moving Systems of Vanes), *Z.A.M.M.*, 1929.

6 Busemann: "Das Foerderhoehenverhaeltnis radialer Kreisel-pumpen mit logar.-spiral. Schaufeln" (The Ratio of Lift of Radial Centrifugal Pumps With Logarithmic Spiral Vanes), *Z.A.M.M.*, 1928.

7 Weing: "Ueber die graphische Berechnung der Strömungsverhaeltnisse und der Leistungsaufnahme in einem gegebenen Turbinenrad" (The Graphical Computation of Flow Conditions of the Transmission of Energy to a Given Water Wheel), *Z.A.M.M.*, 1930.

8 Weinel: "Potentialströmungen in Kreiselaedern und Schaufelgittern" (Potential Flows in Impellers and Systems of Vanes), *Z.A.M.M.*, 1932.

9 Schilhansl: "Naecherungsweise Berechnung von Auftrieb und Druckverteilung in Fluegelgittern" (Approximate Computation of Uplift and Distribution of Pressure in Systems of Vanes), *Jahrbuch der Wissenschaft, Gesellschaft fuer Luftfahrt*, 1927.

B Experimental Studies With Profiles and Series of Blades:

1 Prandtl and Betz: "Ergebnisse der Aerodynamischen Versuchsanstalt zu Goettingen" (Results From the Aerodynamic Laboratory in Goettingen), 1st, 2d, and 3d editions, published by Oldenbourg, Muenchen.

2 Bauer: "Kraeftemessung am radialen Kreisgitter" (Measurement of Forces Acting on a Radial System of Vanes), *Mittel. Institut*, Vol. 1, 1930.

3 Holl: "Untersuchungen ueber Propellerprofile mit verminderter Kavitationsempfindlichkeit" (Investigations on Propeller Profile With Reduced Susceptibility to Cavitation), *Forschung auf dem Gebiete des Ingenieurwesens*, Berlin, 1932.

C Application of Airfoil Theory to Turbine and Pump Design:

1 Bausersfeld: "Die Grundlagen zur Berechnung schnelllaufender Kreiselaeder" (The Basic Considerations for the Design of High Speed Runners), *V.D.I. Zeit.*, 1922.

2 Schilhansl: "Fragen der neuen Turbinentheorie" (Problems of the New Theory of Turbines), *V.D.I. Zeit.*, 1925.

3 Pantell: "Tragflaechenauftrieb und Turbinentheorie" (Uplift on Vanes and the Theory of Turbines), *Deutsche Wasserwirtschaft*, 1926.

4 Numachi: "Aerofoil Theory of Propeller Turbines and Propeller Pumps With Special Reference to the Effects of Blade Interference Upon the Lift and the Cavitation." "On the Hydraulic Efficiency of Propeller Turbines and Propeller Pumps." "On Two-Stage Propeller Pumps." These three articles are reprinted in *The Technology Reports of the Tohoku Imperial University, Japan*.

5 Ackeret: "Maximum Permissible Suction Head on Water Turbines," *Schweizerische Bauzeitung*, Vol. 91, No. 11, 1928, and "Cavitation Phenomenon in Hydraulic Turbines," *Escher Wyss News*, publication No. 2. Both articles referred to in *Mechanical Engineering*, July, 1928.

6 Kaplan-Lechner: "Theorie und Bau von Turbinen-Schnell-laeufern" (Theory and Construction of High Speed Turbine Runners), published by Oldenbourg, Muenchen and Berlin.

D Experimental Studies With Turbines, Pumps, and Draft Tubes:

1. Busmann: "Arbeitsströmung einer Propellerturbine" (Effective Flows Through a Propeller Turbine), *V.D.I. Forschungsheft*, No. 349.

2 Krisam: "Untersuchung einer neuen Saugrohrform fuer Turbinen-Schnell-laeufer" (Investigation of a New Draft Tube Form for High-Speed Turbines), *Mittel. Institut*, Vol. 2, published by the *V.D.I. Zeit.*, Berlin, 1932.

3 Krisam: "Versuche und Rechnungen zum Kavitationsproblem der Kreiselpumpen" (Tests and Computations Regarding the Problem of Cavitation on Centrifugal Pumps), *Mittel. Institut*, special issue published by the Institut, 1931.

4 W. M. White: "American Hydraulic Turbine," *Mechanical Engineering*, April, 1930. See there the remarks about "Hydracone" and "Spreading Tube."

5 Davis and Spaulding: "Design of Setting and Cavitation Limit as Developed at the Holtwood Hydraulic Laboratory," *Elec. Eng.*, Vol. 51, No. 10, October, 1932.

E Miscellaneous and General:

1 Den Hartog: "Mechanical Vibrations in Penstocks of Hydraulic Turbine Installations," *A.S.M.E. Trans.*, Vol. 51, 1929, pp. 101-110.

2 Spannake: "Kreiselaeder als Pumpen und Turbinen" (Runners as Impellers and Propellers), Berlin, Springer, 1930 (English translation prepared).

3 Pfeider: "Kreispumpen" (Centrifugal Pumps), Berlin, Springer, 1932.

4 Krisam: "Die Messung von Geschwindigkeit und Druck in einer dreidimensionalen Stroemung" (The Measurement of Velocities and Pressures in a Three Dimensional Flow), *Zeitschrift fuer Flugtechnik und Motorluftschiffahrt*, 1932.

5 Lewis F. Moody and Frank H. Rogers: *Engineers and Engineering*, Vol. 42, No. 7, July, 1925, pp. 169-187.

6 Karpov: "Low-Head Hydroelectric Developments," American Institute of Electric Engineers, meeting October, 1932.

7 Spannhaake: "Cavitation and Its Influence on Turbine Design," National Electric Light Association, publication No. 222.

NOTE: This bibliography is necessarily incomplete, and drawn from sources nearest at hand. For a more complete list of references, see Engineering Index.

SYMBOLS

For convenience, the symbols used in this paper have been listed in alphabetical order.

A	= area, sq ft
A_p	= projected area, sq ft
a	= altitude of segment formed by chord and mean circle of crescent profile, ft
b	= breadth, ft
c	= coefficient of discharge applied to intake of pump and distributor of turbine
cg	= center of gravity
D	= drag, lb
D	= (also) diameter of runner, ft
D_h	= diameter of hub, ft
d	= sign of differential
F	= force, lb
f	= ratio $D^2 - D_h^2 / D^2$
g	= acceleration of gravity, 32.2 ft per sec ²
H	= specific energy per unit of weight, ft
H_f	= head lost through friction, etc., ft
H_{fs}	= head lost at suction, ft
H_{fr}	= head lost in runner, ft
H_{fp}	= head lost in diffuser or scroll case, ft
H_P	= horsepower, ft-lb per sec ÷ 550
H_t	= $H_2 - H_1$, total head, ft
Δh	= net or effective head, ft
h	= elevation of point of pressure measurement, feet above datum plane
k	= ratio between velocity head at suction side of runner and effective head
L	= lift, lb
l	= length of blade between two perpendiculars to the chord, ft
m	= ratio between change of tangential velocity and velocity of runner
n	= number of revolutions per minute
n_s	= specific speed, rpm
p	= pressure, lb per sq ft
Δp	= differential pressure, lb per sq ft
p_{min}	= minimum pressure, lb per sq ft
Q	= quantity of water, cfs
r	= radius, ft
r_{cg}	= radius center of gravity to center of shaft, ft
s	= spacing, or pitch of runner blades, ft
s	= ratio tangential velocity at suction to speed of runner
T	= torque, lb at 1 ft radius
t	= thickness of blade, ft
u	= tangential velocity of a point on the runner, ft per sec
v	= absolute velocity, ft per sec
v_0	= velocity of approach to fixed profile, ft per sec
W	= quantity of water, lb per sec
w	= relative velocity, ft per sec
X	= height of runner from suction to pressure side measured perpendicularly to direction of motion
x	= distance measured along X from suction side, ft
z	= number of blades
α	= angle of attack, deg
β	= angle formed by flow approaching or leaving the runner with reference to direction of motion, deg
γ	= density, or specific weight for water, 62.4 lb per cu ft
ϵ	= difference
ϵ	= efficiency, per cent
ξ_d	= drag coefficient
ξ_l	= lift coefficient
θ	= angle formed by chord of blade to direction of motion
λ	= ratio pressure at any point on the blade to velocity pressure corresponding to v_0
μ	= ratio λ / ξ_l
Σ	= cavitation coefficient
ϕ	= ratio of velocity of point on periphery of runner to spouting velocity corresponding to total head
ω	= angular velocity, cu ft per sec

Discussion

ARNOLD PFAU.⁹ Much was published shortly before the outbreak and after the stagnation caused by the World War about turbines of high specific speeds. Theories were advanced which, on practical application, failed to bring about the expected and desired results. Again results obtained in a rather empirical

manner were explained by theories of which one could not but gain the impression that the theory was made to fit the results, rather than to produce results.

The actual results obtained by Prof. Dr. V. Kaplan abroad and simultaneously to some extent by Forest Nagler in our country were gratifying and certainly most valuable for practical application, yet the writer personally was not satisfied to accept them without having at least in a simple, practical way an explanation of what is actually taking place in a propeller runner.

Prof. Dr. Hans Baudisch, of Vienna, published in 1914 his theory of the so-called suction-jet turbine, which appealed to the writer as having real merit. Unfortunately, a runner designed purely along his principles did not perform correctly, because it neglected other more practical factors, the effect of which was fundamental.

In Prof. Dr. Baudisch's axial-discharge suction-jet runner he attempted to compel the water to decelerate in its relative flow through the runner channels. These flared too much, because too short; the water could not decelerate as fast, with the result that it cut loose from the walls of the channels; or in other words, it did not keep the channels filled, so that the desired deceleration and subsequent suction effect did not materialize. The old relation:

$$W_2^2 - W_1^2 = C_p^2 < 0$$

defining the so-called reaction velocity, or reaction pressure

$$p_p = \frac{C_p^2 \gamma}{2g}$$

did not apply, because W_2 did not become smaller than W_1 . No negative pressure p_p was produced, so that neither speed nor discharge capacity came up to expectation.

In a propeller runner, and particularly in one of a projected blade area smaller than the full circle area, we cannot deal with actually existing runner channels, because the lower end of one blade does not overlap the upper end of the preceding blade. Consequently, we cannot speak of a relative discharge angle in the sense in which it would permit the use of our old customary velocity diagrams. It is here that a pictorial explanation assisted the writer in obtaining a clearer conception.

How does the water flow, and in what manner does it leave the propeller runner? At the time of his studies in 1916, there was no means of obtaining the stroboscopic pictures which are now available. The writer's studies convinced him, however, that the most vital process takes place "not within but below" a propeller runner. This at once pointed to the fundamental difficulties to be encountered in the use of a propeller turbine. It deals with negative pressures, which naturally are limited to the barometric value, whereas overpressure, in case of the reaction turbine, and atmospheric pressures, in case of the impulse wheel, never become negative, no matter how high the head may be.

Again using the old relation:

$$W_2^2 - W_1^2 = C_p^2, \text{ or } a p_p$$

we have:

$$\text{Reaction turbines: } W_2^2 - W_1^2 = C_p^2 > 0; p_p > 0$$

$$\text{Impulse wheel: } W_2^2 = W_1^2; C_p = 0; p_p = 0$$

$$\text{Propeller turbines: } W_2^2 - W_1^2 = C_p^2 < 0; p_p < 0$$

Taking the values of the coefficients of the diagram

$$W_2^2 = \frac{W_2}{\sqrt{2gH}}; \quad W_1^2 = \frac{W_1}{\sqrt{2gH}}, \text{ etc.}$$

⁹ Consulting Engineer, Milwaukee, Wis. Mem. A.S.M.E.

we find at once:

$$2gH(W_2^{*2} - W_1^{*2}) = 2gHC_p^{*2} \equiv b p_p^{*2} H$$

from which we conclude that in the case of the propeller (or the suction-jet turbine directly applicable to Professor Baudisch's theory) the value

$$\sigma p_p^{*2} H < 0$$

can attain, or even would exceed the barometric limit B .

This immediately points out the danger of failure of performance of a propeller turbine, when used to operate under a too high head or a too high elevation above sea level (B'), or by reason of design of a too great hydrodynamic suction effect p_p , aside from the effect of the draft tube.

It may be permitted to state that it was the realization of these effects which prevented the application of the propeller in cases where failure of satisfactory performance would have been certain.

In the writer's paper, entitled "Permissible Suction Head of High-Speed Propeller Runners," A.S.M.E. Trans., HYD-51-9, he has fully explained what in his opinion actually takes place

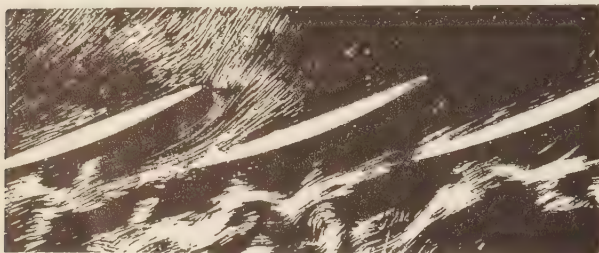


FIG. 26

underneath a propeller runner. Fig. 26 is a reproduction from the cover of the March-June, 1931, bulletin of Escher-Wyss & Co., Zurich, Switzerland, and plainly discloses the "hypothetical channel," with its contraction and subsequent expansion, resulting in a deceleration of the relative water velocity and of the "surface of discontinuity." The irregularity of this surface as evidenced is caused by the interference of the angle at the top of the propeller blades and the actual stream-flow lines of the approaching water, as also by the shape of the rear surface of the blade, and it clearly supports the necessity of adjusting also the runner blades in order to maintain a most favorable efficiency throughout, all as introduced by the design of Prof. Dr. V. Kaplan's adjustable-blade propeller.

The more nearly the stream-flow lines correspond with the angle and the more the rear surface of the blade conforms to the conditions of a correct diffuser, the more perfect will be the "hydrodynamic suction" effect p_p ; the smoother also will be the surface of discontinuity and the farther removed will be the danger of cavitation.

W. WATERS PAGON.¹⁰ The paper gives a clear and comprehensive discussion of the general principles of turbine and pump design and the problems awaiting solution in this field. The suggested use of higher specific speed as a result of better understanding of flow phenomena is interesting.

In aerodynamics there has been accumulated a vast amount of knowledge and data that should help greatly in the hydraulic field. The boundary layer, turbulence, form drag, viscous flows, and other general questions are coming to be understood

much better. The aerodynamic research worker has gone back to Osborne Reynolds' methods and followed new paths. The problem of similitude between model and prototype involves similarity of geometric flow as well as of body, and the character of flow has been found to vary systematically with Reynolds' number, but also with such factors as turbulence, roughness, eddy formation, etc. As the author's work continues, it is the writer's belief that he will come in time to consideration of the theory of discontinuous flow. The author's work in his laboratory at Karlsruhe has already produced valuable results.

The writer has found evidence of the effects of turbulence and what in aerodynamics is called "burble," and apparent evidence of radial flow which may be associated with the varying circulation along the blade which in airplanes causes "induced drag."

The writer hopes that this paper will stimulate research and experiment looking toward the elimination of cavitation and the improvement of efficiency.

R. E. B. SHARP.¹¹ The writer believes that this work will stand as a most important advance in rationalizing the design of turbine and pump runners of high specific speed and that it deserves careful study. A valuable feature is the consideration of both the practical and theoretical aspects. The writer would make the following comments:

As to sections 7 and 8, the writer agrees with the importance of establishing the best form of blade for a given layer or section through the runner, in order to set up as uniform a value of pressure distribution ΔP as possible, in this way establishing the correct form of the runner blade at this section.

Whether the correctness of these sections, as demonstrated by tested values of ΔP , obtained from stationary blades, can be thus established as holding true also for revolving blades, as in an actual runner, would appear to be somewhat open to question, although this method of analysis is undoubtedly of considerable value in view of the impossibility of determining this pressure distribution in an actual runner, as pointed out by the author.

The author states that, among other incidental problems, is the influence of the design and location of the guide vanes on the manner in which the whirl moment $v_{\text{tang}} r$ varies across the space between the runner periphery and the runner hub. The writer is of the opinion that the manner in which this whirl component is distributed is of great importance as affecting decidedly the design of the runner blades across this space, in order to deal properly with the true values of the whirl moment. Not only is it important to consider the design and location of the guide vanes actually to be used, as affecting the whirl component on the pressure side of the runner, but it is also equally important to know the characteristic of the draft tube to be used, as affecting the manner in which the whirl moments at the runner discharge vary across the radial blade space. Unless some definite information about the foregoing effects of the guide vane and draft tube are known, the highest runner efficiency possible cannot be obtained by knowing the proper blade shape at a given layer or section.

In section 9 (b), a crescent shape of blade, as illustrated in Fig. 20, undoubtedly has distinct advantages theoretically, in maintaining a low value of ΔP maximum. For the central portion of the blade, that is, between the periphery and the hub, this shape, for the reasons set forth by the author, might well be used as a guide. At the periphery, however, the blade shape is virtually straight, that is, a/l will be very small, and R_1 will approach a straight line. Here, if the low-pressure side of the blade is formed by a radius R_2 , either the thickness t will be unduly great (resulting in reduced lift) or else the blade at each end

¹⁰ Consulting Engineer, Baltimore, Md.

¹¹ Hydraulic Engineer, I. P. Morris Division, Baldwin-Southwark Corp., Philadelphia, Pa. Mem. A.S.M.E.

will be too thin for strength and construction. Therefore, for this portion of the blade a profile approaching the airfoil appears reasonable. Near the hub, on the other hand, the relatively great value of t/l demanded by strength considerations requires that the crescent shape be departed from, and that the maximum t be near the leading edge in order to give proper streamline shape to the trailing edge. This again results in a shape approaching the airfoil.

In Table 1 it is noted that there is no tendency for the discharge whirl ratio s to become less with reducing values of specific speed. In fact, the value of s is greatest for the lowest specific speed selected. It is the writer's experience with both propeller and Francis type runners that there is a marked reduction, for best efficiency, in this value of s with lower specific speeds, this value becoming zero at a specific speed of about 27, and below this value becoming negative. It is noted that for pumps in the author's table this tendency does exist.

Figs. 22, 23, and 25 are most interesting as forming a rational guide (for confirmation by actual tests) for the selection of the controlling factors in the design of higher specific speed runners, namely, m , which varies inversely with ϕ^2 , and s , the whirl factor at the runner discharge. These figures, however, are for one section or layer of the runner only, and the departure of the blade profile at other sections, from the crescent shape, might result in a materially different picture, for the entire runner, from the relations shown.

The author does not bring into his calculations the number of runner blades. This factor of course has a very decided effect on the efficiency secured. With a given value of l/s , the number of blades determines the axial depth of the profile and the rate of change from $v_{tang\ p}$ to $v_{tang\ s}$. Therefore an added factor dealing with the number of blades would add to the usefulness of these data.

J. D. SCOVILLE¹² AND HENRI DEGLON.¹³ The paper presents a number of interesting and useful formulas dealing with the design problems of pumps and turbines. The author has shown how the theory of Euler can be combined with the airfoil theory. The theory of Euler when properly used gives the correct entrance and discharge angles for a runner having an infinitely large number of blades of infinitesimal thickness. It does not give the proper shape of blade for the practical runner, which must have a few blades of considerable thickness. As the author states, the blades on the practical runner must have somewhat greater curvature than the theoretical runner. It is possible that by means of the two theories the correct angles and shapes may be found to give the maximum efficiency with the minimum danger of cavitation.

For a turbine, $H_1 - H_2$ in Equation [5] is the actual head working on the runner, from which must be subtracted the head lost in friction. In Equations [5] to [7] it is evident that it is the author's intention to introduce the friction, but they are not entirely clear. The friction factor in [6] should be the loss in the runner only and not H_f , which is the sum of H_{fs} , H_{fr} , and H_{fp} .

In combining this with the airfoil theory, the author states that it is customary to neglect the effect of drag in computing the component, since it is only 1 or 2 per cent of the lift. Is this justifiable? The tangential component of the drag is much larger than 1 or 2 per cent of the tangential component of the lift, and to neglect it may introduce an appreciable error. The error is large, especially at the periphery, where the blade angle is small.

The author states that in an ideal fluid the lift is the only reaction acting upon the wing or blade. All forces can be resolved

into components parallel and perpendicular to the chord of the wing. For the drag to be zero, the parallel components must balance. Can this be true?

The writer agrees that the knowledge as to the correct distribution of velocity within the runner is rather meager and that here is a field for considerable research. This lack of knowledge is a weak point in all turbine theories. How does the author arrive at the curve of theoretical velocity distribution shown on Fig. 13?

From formulas [25], [29], and [30] the author designs the blades on the assumption that there are an infinite number of infinitesimal thickness. He then shows in Fig. 16 that when the blades are few in number they must have more curvature than the theory would indicate. How does the author estimate the correction in curvature?

In Fig. 20 the author compares the pressure distribution of the crescent shape of blade with that of an actual airfoil having the same lift and states that the superiority of the crescent is readily appreciated. How do the lift-to-drag ratios of these two forms compare? What are lift coefficients of the two sections?

AUTHOR'S CLOSURE

(Written at Karlsruhe in December, 1933.)

In order to answer the different writers, the following remarks may be permitted:

Mr. Pfau's statement that "the more the rear surface of the blade conforms to the conditions of a perfect diffuser, the more perfect will be the hydrodynamic suction effect," does not, in the author's opinion, meet the real conditions of turbines. In each turbine, even in a propeller or Kaplan turbine, the relative flow between two adjacent blades is accelerated, and therefore may not be compared with a flow through a diffuser. Furthermore, the formation of surfaces of discontinuity should be carefully avoided, which undoubtedly is possible by providing shockless entrance and by proper shape of leading and trailing edges. The author's developments presume these conditions to be fulfilled, so that the lowest pressure is caused by the unavoidable deflecting effect, which is conducive to an unavoidable differential blade pressure.

Generally it must be realized that danger of cavitation also exists for turbines of low specific speeds when being used for high heads. These turbines simply have a smaller critical value of Σ .

Mr. Pagon mentions the theory of discontinuous flow. Unfortunately, the author is not quite sure what he really means. On the other hand, the author is quite aware that the ideal flow he pictures for carrying out his calculations is not exactly existing. But experience strengthens his opinion that the ideal flow is a very good background for fundamental considerations and that turbulence plays very often only the part of a factor of correction—and that the more, the higher is the Reynolds number.

The induced drag, so important for the theory of airplanes, comes into consideration with respect to turbines—provided an ideal flow is assumed—only when the flow through the gaps between the blades and the curb ring and the hub is discussed, or when conditions of partial load are to be studied, or when it is not possible to arrange the guide vanes for generating a uniform whirl moment.

Mr. Sharp's comments deal with a number of uncertainties that the author himself has pointed out. Especially he feels that the developments of the author, when carried out for the entire runner, not only for the outer layer, would result in a different picture. The author quite agrees, but unfortunately has had so far no time to develop the methods in question for

¹² Hydraulic Engineer, S. Morgan Smith Company, York, Pa.

¹³ Engineer, S. Morgan Smith Company, York, Pa.

a whole runner. In one of the next volumes of the transactions of his Institute at Karlsruhe (Mitteil. Institut) he expects to be able to do so.

In using well-known airfoil profiles great care must be taken to avoid local cavitation. Profiles advantageously applied to airfoil design often show comparatively thick forms of the leading edges, which, in the flow of a compressible medium, do not do any harm so long as the local surplus of velocity does not approach the velocity of sound, whereas in an incompressible fluid they very soon may create local cavitation. The author prefers forms of leading noses like hatchets with edges rounded only a little. (See reference E1.)

The number of blades is not determined by the author's calculations. Only the ratio l/s comes into consideration. In other words, the theory does not answer the question whether a fixed ratio l/s should be secured by a smaller number of longer blades or a greater number of shorter ones and which way is more favorable for high efficiency. The answer can be given so far only by experience, but the problem is essentially influenced by the conditions of the mechanical design.

Messrs. Scoville and Deglon do not agree with the author's formula [5]. In fact, however, this holds true. The term

$$(v_{\text{tang } 2} u_2 - v_{\text{tang } 1} u_1)/g$$

is equivalent to the work delivered by the shaft to the runner of a pump and, vice versa, by the runner to the shaft of a turbine. Therefore in case of a pump just this term must cover *all* losses except side friction of the runner, leakage, and mechanical losses, whereas in case of a turbine a gross head must be available to cover the above term and *all* losses except the aforementioned.

In case of turbines the terms

$$v_{\text{tang } 2} u_2 - v_{\text{tang } 1} u_1 \quad \text{and} \quad H_2 - H_1$$

become negative; so Equation [5] may be rewritten as:

$$H_1 - H_2 = (v_{\text{tang } 1} u_1 - v_{\text{tang } 2} u_2)/g + H_f$$

which is in accordance with the above.

Neglecting the drag in computing the tangential component is possibly more the author's own than a general custom. But if Messrs. Scoville and Deglon will calculate a very extreme case (for instance $m=0.15$, $s=0$, $k=0.45$), they will find that the effect of drag upon the tangential component is actually of the order of only a few per cent.

In an ideal flow there is no drag at all, which will be understood by recalling that drag is a component not parallel to the chord of the profile, but to the oncoming velocity in case of a single wing and to the mean velocity in case of a series of blades. It is in this way that it is introduced into the author's formulas.

The diagram of Fig. 13 gives only a plot of the whirl moment corresponding to the desired and assumed plot of the differential blade pressure. These two diagrams (plotted against distance x) are entirely conformable to those of Fig. 16. How to form the blades for securing those distributions is explained in connection with Fig. 16.

The distribution of velocity over the spacing between two adjacent blades can be computed theoretically so far only in a few cases by higher mathematical methods. Also the correction in curvature can be exactly determined only in a few simplified cases. The author, in Fig. 16, has estimated it by roughly comparing the effect of a single airfoil profile under similar conditions.

As to Fig. 20, it may be stated that with respect to drag the two profiles can be assumed to differ very little. A fair value of the ratio of drag to lift would be 0.015.

The author wishes to express his sincerest thanks to the A.S.M.E. for the highly appreciated opportunity of discussing vital problems of hydraulic design with American engineers. Also he thanks cordially the engineers for their interest in his paper.

Determination of Initial Stresses by Measuring the Deformations Around Drilled Holes

By JOSEF MATHAR,¹ AACHEN, GERMANY

Methods have been proposed for determining the inherent stresses in structural components by disturbing their stress equilibrium through some mechanical device and measuring the resulting deformations. This principle is the basis of the stress methods of E. Heyn and O. Bauer, the casting of stress grids for determining the tendency of various cast irons to develop stresses, and the drilling methods of G. Sachs. These methods have the disadvantages, however, that they can be successfully used only with specially shaped pieces (e.g., those with round or rectangular cross-sections), that every form of test piece requires another kind of injury and hence of calculation, and that the tested parts are rendered useless. In part, moreover, only mean stresses can be determined, which may differ greatly from the maximum stresses. The new test method, which seeks to eliminate these disadvantages, is likewise based on a disturbance of the equilibrium of forces, and is done by drilling a hole, which, however, is so small that the part can be used again. This method serves, among other things, for determining the inherent stresses in castings, welded parts, rolled structural shapes, and finished structures.

VARIOUS methods have been proposed for determining the initial stresses in structural members, by disturbing their stress equilibrium through some mechanical device and measuring the resulting deformations. This principle is the basis of the stress investigations of E. Heyn and O. Bauer,² the casting of stress grids for determining the tendency of various cast irons to develop stresses,³ and the drilling methods of G. Sachs.⁴ The methods used have the disadvantages, however, that they work only with specially shaped pieces (e.g., those with round or rectangular cross-sections), that every form of test piece requires a different kind of injury and hence of calculation, and that the tested parts are rendered useless. In part, moreover, only mean stresses can be determined, which may differ greatly from the maximum stresses.

The new test method, which seeks to eliminate these disadvantages, is likewise based on a disturbance of the equilibrium of forces, and is done by drilling a hole, which, however, is so small that the part can be used again. This method serves, among other things, for determining the initial stresses in cast-

ings, welded parts, rolled structural shapes, and finished structures.

In order to explain the fundamental principle, it is at first assumed that the part to be tested is very wide, and that it is subjected to a constant monaxial stress which is uniform throughout the thickness and has a known direction. A tensometer is then placed on this test piece in the direction of the stress. If a hole is now drilled between its foot points *a* and *b* (Fig. 1a), this hole will become an ellipse under the stresses and the distance between the points *a* and *b* will be changed—increased if the stress was tension, decreased if the stress was compression. If the relation between the change in this distance and the stress is determined by calculation or by a calibration test, then the stress in the test piece in the direction *ab* can be calculated from the change in the distance between *a* and *b*.

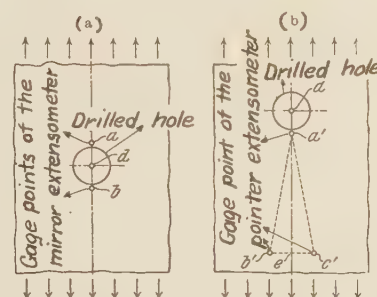


FIG. 1 POSITION OF TENSOMETER FOOT POINTS RELATIVE TO HOLE

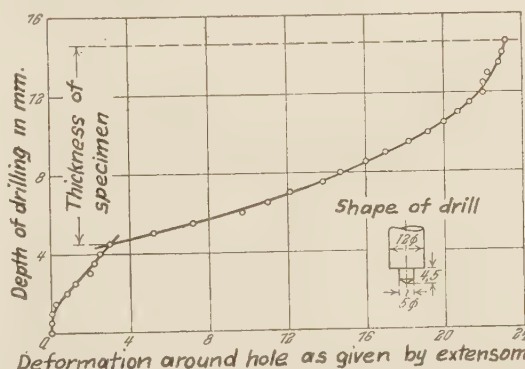


FIG. 2 TENSOMETER READINGS AT DIFFERENT DRILL DEPTHS

Fig. 2 shows, by way of example, how the distance between the points *a* and *b* is affected by the penetration of the drill into the material. The shape of the drill, which largely determines the form of this curve, was determined experimentally to give the smoothest possible operation. When the tip of the small drill penetrates the test piece, the change in the distance must be extremely small, since the resulting conical hole is small and far from the points. It is still small when the cylindrical part of the first drill penetrates. When the main drill begins to cut, the change in the distance suddenly increases, as shown by the break in the curve, but then increases more slowly until the exit of the

¹ Privat-dozent (assistant professor) at the Technical University in Aachen (Germany). Josef Mathar was graduated at the same institution; received the degree of Dr.-Ing. in 1924; was in charge of the structural department of the Aerodynamical Institute at Aachen under the directorship of Dr. Th. von Kármán. He published a series of papers on problems related to the theory of elasticity, strength of materials, and airplane structures. He died on July 25, 1933. Paper translated by Th. von Kármán.

² "Stahl und Eisen," vol. 31, 1911, pp. 760-765.

³ R. v. Steiger, Dissertation (Zurich, Gebr. Leemann, 1913); compare "Stahl und Eisen," vol. 33, 1913, pp. 1442-1443.

⁴ Z. Metallkunde, vol. 19, 1927, pp. 352-357.

Contributed by the Iron and Steel Division and presented at the Semi-Annual Meeting, Chicago, Ill., June 26 to July 1, 1933, of THE AMERICAN SOCIETY OF MECHANICAL ENGINEERS.

NOTE: Statements and opinions advanced in papers are to be understood as individual expressions of their authors, and not those of the Society.

main drill. In a thick piece, the change in the distance approaches a limiting value, since the stresses which are liberated through the removal of material by the drill at some distance below the surface have no appreciable effect on the deformation at the surface. From this fact it follows that it is not necessary to drill clear through thick pieces to determine the stresses. Tests show that the depth of the holes need be only 1.5 to 2 times their diameter.

In testing a piece in which the stress is known to be uniform with the depth, it is of course not absolutely necessary to plot the distance change against the depth of the hole. The total distance change at the end of the drilling is sufficient, although to be on the safe side it is always advisable to plot the whole curve.

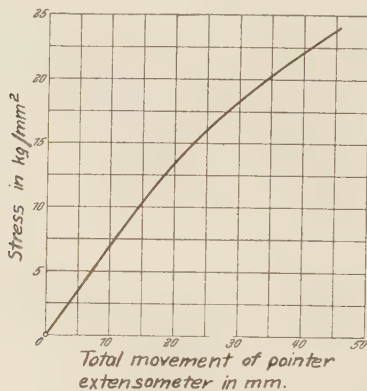


FIG. 3 CALIBRATION CURVE FOR A SOFT STEEL

The basic principle of the test method is the same whether the change in the distance between the points *a* and *b* (Fig. 1a) or between the points *a'* and *e* (Fig. 1b) is measured. In the latter case, if the point *e* were infinitely distant from *a'*, the distance change would be just half that between *a* and *b*. In practise, the point *e* need not be very far from *a'*, since most of the deformation is close to the hole. In the experimental arrangement this distance was 15 cm (5.91 in.).

If the test piece is subjected, not to a monaxial, but to a biaxial state of stress, then one measurement is not enough, and the deformation of the hole must be measured in three different directions in order to determine the magnitude and direction of the maximum and minimum principal stresses. If only one measuring instrument is available and it is known that the stress remains constant over a large area, three holes can be drilled in this area and measurements made on each at a different angle.

If the stress varies along the depth of the hole, as in bending or surface stresses, the shape of the curve (Fig. 2) gives qualitative indications regarding these changes. For very thick parts, as for instance large rolls, the process gives no indications as to the stresses in the center of the rolls, since only the stresses near the upper surface can be determined. However, it is often possible, when the surface stresses are known, to make qualitative estimates about the size and direction of the stresses inside of the rolls, by taking into consideration the fact that the sum of all stresses and moments must be equal to zero.

The diameter of the drill used in the test apparatus was 12 mm (0.472 in.). It might, of course, be larger or smaller. The upper limit is given by the requirement for the least possible weakening of the specimen, while the lower limit is determined by the accuracy and sensitivity of the measuring apparatus. For laboratory apparatus, the diameter could be reduced to 6 mm (0.236 in.). This is probably the limit, however, as with

smaller holes the magnification of the measuring instrument would have to be too large.

After the test, a rivet or plug can be inserted in the hole, according to whether the hole goes clear through or only part way. A tightly fitting rivet will reduce stress concentration during subsequent loading, since the pressure of the rivet head around the hole will partially prevent the deformations which would occur with an open hole. The strength of the structure or the utility of the part will seldom be affected by the slight weakening produced by the test. If the test is made on a girder, for example, a 12-mm hole would have little effect in comparison with the many larger holes required for assembling.

The calibration of the measuring device, i.e., the determination of the relation between the final elongation of the test distance and the stress, can be made once for all, for the principal materials. So long as the stresses are less than 40 per cent of the proportionality limit, they are proportional to the final elongations (see Fig. 3). For this range the calibration can also be made by calculation. Above this point it must be made by experiment. The fact that the stresses which can be calculated are so low is due to the high stress concentration at the edge of the hole.

The calibration of the measuring device by calculation is based on a report by Kirsch,⁵ who calculated the elongation of a hole in a member of infinite width in terms of the tensile stress, and on a report by Willheim and Leon,⁶ who extended this method approximately to members of finite width.

The experimental calibration can be made by mounting a broad flat plate with a 12-mm (0.472-in.) hole in a tensile machine. Then a tensometer, preferably the one used in the hole tests, is so mounted on the plate that its measuring points rest on the points *a* and *b* (Fig. 1a), or *a'* and *e* (Fig. 1b). The plate is then stressed and the resulting increase in the distance between *a* and *b*, or *a'* and *e*, is measured. From this must be subtracted the distance increase which would be obtained if the hole did not exist. The resulting calibration curve is valid only for plates of the width used in the test.

After calibration curves have been plotted for plates of different widths, the values for plates of infinite width can be extrapolated.

The calibration test can also be made like the subsequent investigation, excepting that the distance increase is measured in terms of a known stress. A flat plate is subjected to a known load, the measuring instrument is installed, and the hole is drilled. The increase in distance between *a* and *b*, or *a'* and *e*, is thus determined in terms of the depth of the hole, and from this the total increase corresponding to the stress. If this test is repeated for a series of different stresses, a series of curves is obtained from which the final calibration curve, i.e., the total distance changes in terms of the stresses, can be determined. If, for the material under investigation, the stress-strain line for tension differs from that for compression, the test must be made for each. The width of the plate is taken into consideration in the same way as in the calibration test previously described.

To measure the deformation, two instruments have been de-

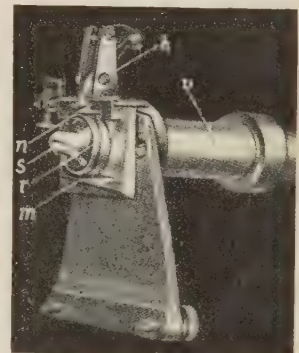


FIG. 4 DRILL MOUNTING WITH MIRROR EXTENSOMETER

⁵ Z.V.D.I., vol. 42, 1898, pp. 797-807.

⁶ Z. Mathematik und Physik, vol. 64, 1916, p. 233.

signed. The first is a mirror instrument which works in a manner similar to the Martens tensometer (Fig. 4). Since the installation of the telescope required with this apparatus is often difficult, an indicator has been developed, in which the change in the distance actuates a pointer through a mechanical magnification. This indicator does not span the hole like the reflecting instrument, but rests on the points a' , b' , c' of the test piece (Fig. 1b). The movable leg is at the edge of the hole, and the fixed legs are about 15 cm (5.9 in.) from the hole. Fig. 5 shows the whole test apparatus with this indicator q . The indicator has a magnification of about 1:3200 and is balanced in every position. It is clamped to the test plate by the arm u on the drilling machine z . The drillings are carried away by a sleeve t . The 0.3-hp drilling machine is driven by a flexible shaft and runs very smoothly. The drilling pressure is kept nearly uniform by the interposition of a spring. The depth drilled is measured by a Zeiss gage v . The drilling machine is clamped to the test plate by the frame f .

A great many tests have been made by these methods in many different fields. A number of these experiments are discussed in the following paragraphs. The methods used in making the tests are described, and the results which are of general interest are given.

ROLLING STRESSES IN STRUCTURAL STEEL

The standard profiles, especially the H-beams, are seldom free from initial stresses, as proved by many experiments. These stresses are in part due to the conditions during cooling from the hot rolling, but are chiefly due to the rolling itself. H-beams have been tested which showed tension in the web, while others showed compression. This is proof that the stresses are produced primarily during the rolling process, since if they were produced by the cooling process all beams should have compression stresses in the web, as this is the part which cools first.

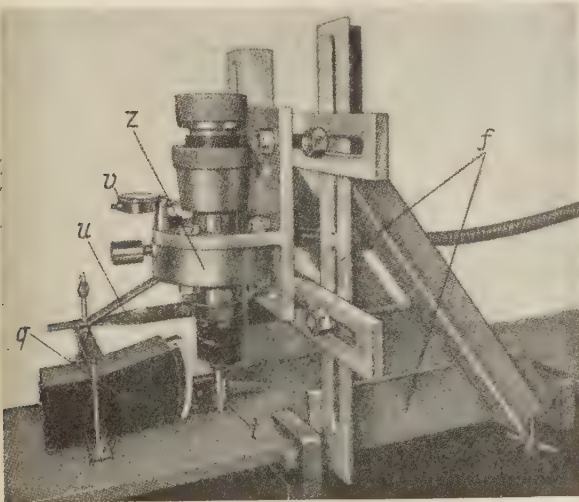


FIG. 5 TEST APPARATUS WITH POINTER EXTENSOMETER

As examples of tests of structural shapes, the experimental results for a relatively highly worked H-beam NP20, an I-beam NP20, and a channel beam NP26, all 6 m long (about 20 ft) have been selected. In the H-beam the initial stresses were determined over the whole length of the web (Fig. 6) and in both flanges at the points of maximum web stresses (Fig. 7). For every test point the full curve was plotted, showing the elonga-

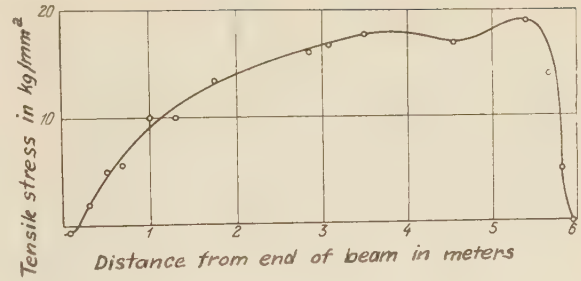


FIG. 6 DISTRIBUTION OF INITIAL STRESSES IN WEB OF H-BEAM

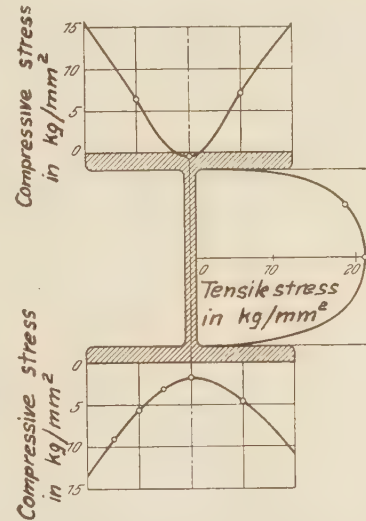


FIG. 7 DISTRIBUTION OF INITIAL STRESSES OVER CROSS-SECTION OF H-BEAM

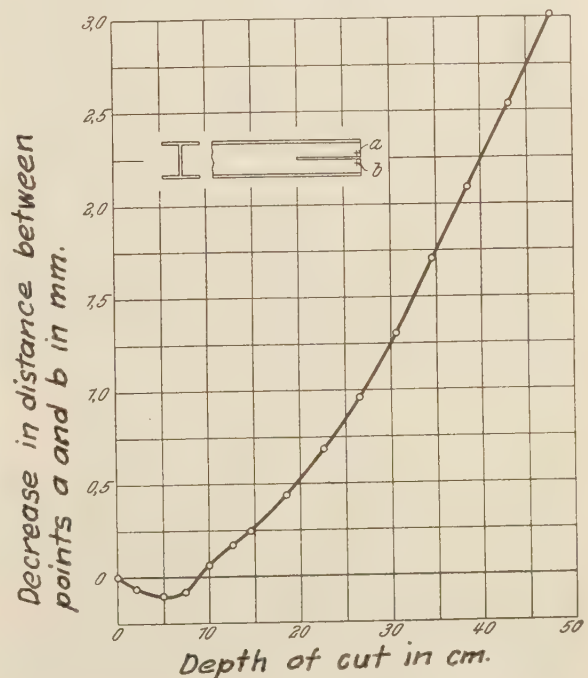


FIG. 8 EFFECT OF CUTTING SLOT IN WEB AT END OF H-BEAM

tion of the test length against the depth of the hole. All the places were drilled clear through, with the exception of the middle of the flange. The curves, almost without exception, resemble Fig. 2, from which it may be concluded that the stresses vary but little throughout the thickness. For this reason and from the fact that the stress in the girders must be chiefly monaxial, the calibration curve of this stress condition was taken as the basis for the stress determination. There were extremely high tensile stresses in the middle of the web of the beam in the direction of the length, amounting in the middle of the length to about 20 kg per sq mm. (28,400 lb per sq in.). At this stress, the pointer of the instrument was deflected about 36 mm (1.42

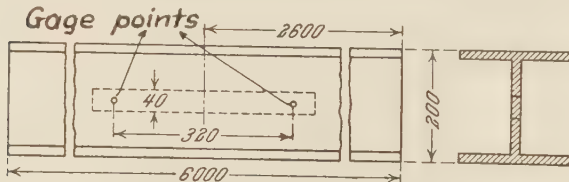


FIG. 9 LOCATION OF TEST STRIP IN WEB OF H-BEAM

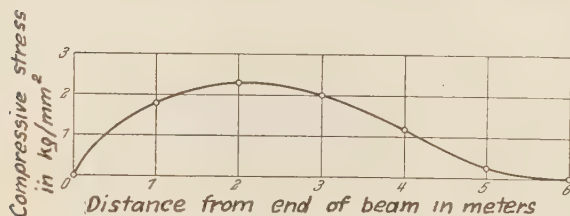


FIG. 10 DISTRIBUTION OF INITIAL STRESSES IN WEB OF I-BEAM

in.). The maximum stress was in the central part of the beam. At both ends, as was to be expected, the stresses dropped to zero. The flanges were stressed in compression, the stresses being small in the middle and increasing toward the edges. Analysis of the results showed that the sum of the moments of the stresses found for a cross-section was nearly zero.

To check the test results, the H-beam was sawed in the middle of the web at the right end for a distance of about 50 cm (about 20 in.). If there were tensile stresses in the web, as indicated by the test, the halves of the beam after sawing would approach each other. As shown by Fig. 8, the ends separated a little at first, but drew strongly together again after being sawed 5 cm (about 2 in.). After sawing 48 cm (about 19 in.), the separation of the ends had diminished about 3 mm (0.12 in.). A second test consisted in sawing out, at a distance of 2.6 m (8.53 ft) from the right-hand end of the H-beam, a strip 32 by 4 cm (about 12.6 by 1.57 in.), as shown in Fig. 9. If there were tensile stresses of about 20 kg per sq mm (28,400 lb per sq in.) at this place in the web, the sawed-out strip should have contracted about 0.29 mm (0.0114 in.), according to the formula

$$\text{Contraction} = \frac{\text{Stress}}{\text{Young's modulus}} \times \text{Test length}$$

The test showed a contraction of 0.27 mm (0.0107 in.). The results of the proposed method are thus confirmed.

The stresses were considerably smaller in the I-beams than in the H-beams (Fig. 10). The stresses were determined only in the middle of the web, the tests showing stresses of about 2 kg per sq mm (2845 lb per sq in.). In the channel the stresses were likewise determined for the middle of the web and in general were relatively small (Fig. 11). In the middle there was a sudden increase in stress, which was probably due to overstressing in handling.

STRESSES IN CASTINGS

In order to obtain, for various types of cast iron, the relation of the casting stresses to the wall-thickness ratios and the temperatures of casting, frames of the shape shown in Fig. 12 were cast. This frame shape was selected in order to obtain as nearly a monaxial stress system as possible. The wall thickness ratio was varied by changing the outer frame thickness from 10 to 60 mm (0.39 to 2.36 in.), while the inner cross had the same thickness in every experiment. Measurements were made chiefly at the points designated by *a*. The measurements taken in all four positions proved very consistent. As an illustration of a series of experiments, the relationship between the casting stresses in the center cross and the wall thickness of the outer frame, with constant casting temperature, is shown in Fig. 13. As can be seen from the curve, small tension stresses occur in the cross when the frame and cross-thickness are equal, but as the thickness of the frame wall is increased, the stresses in the cross become compressive, and of greater and greater magnitude.

STRESS DETERMINATION IN BRIDGES AND STRUCTURES

The total stresses in the elements of such structures are composed of:

- (1) Stresses produced by the weight of the structure
- (2) Stresses produced during the manufacturing process and therefore present before assembling
- (3) Stresses produced during the assembly by forcing members into place and by riveting, bolting, welding etc.

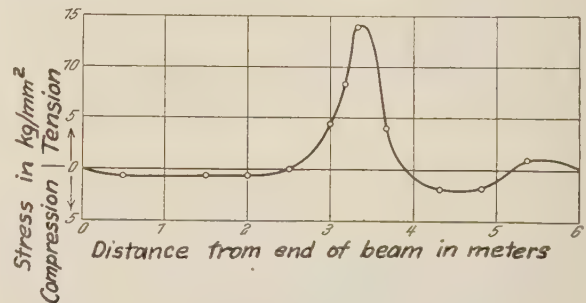


FIG. 11 DISTRIBUTION OF INITIAL STRESSES IN WEB OF CHANNEL

In structures designed for low stresses, the stresses produced by assembling and manufacturing will often be higher than those due to the weight of the structure. This is especially true in welded structures, where the calculated stresses can only be considered as rough approximations, as they are likely to differ from the actual stresses by a factor of 2 or 3. To obtain the three types of stresses separately by measurement is often a difficult task, possible only through repeated measurements upon the same structural member. In general, this separation is not required, since one wishes only to know how much the actual stresses differ from the calculated ones.

As an illustration of a measurement of this kind, where the "weight stresses" could easily be separated from the assembly stresses, the inspection of a large arch bridge (span length about 100 m, or 330 ft) may be mentioned. A diagram of the entire bridge and a sketch of the upper side of the arch are shown in Fig. 14. The calculated stress was about constant over the cross-section, and had a value of about 400 kg per sq cm (5700 lb per sq in.). This value was also found experimentally in the web. But in the top flange, which was composed of three riveted plates (1300 × 15 × 5000 mm, or 51.2 × 0.59 × 196.6 in.), seven measurements in the top plate showed almost zero stresses.

This contradiction was explained when the lowest plate, the one closest to the web, was tested; here there was a compression stress of about 850 kg per sq cm (12,100 lb per sq in.). The average stress in the whole plate therefore checked with the calculated one. The difference between the stress in the top and the bottom plate was due to the fact that, in assembling, one end of the plate had been riveted solid and then bent down by force to fit the web, already curved to the proper bridge curvature. This bending produced tension in the top plate and compression in the lower one, which in the present case happened to be equal to the "weight stresses." The final stress picture thus showed a zero stress in the top plate of the flange and double the value of the "weight stress" in the bottom one.

THE DETERMINATION OF WELDING STRESSES

While measurements with a single extensometer—that is, measurements in a single direction—were sufficient in the previous tests, it was necessary to use two instruments in this type of investigation, since the stresses were almost always in two directions (biaxial).

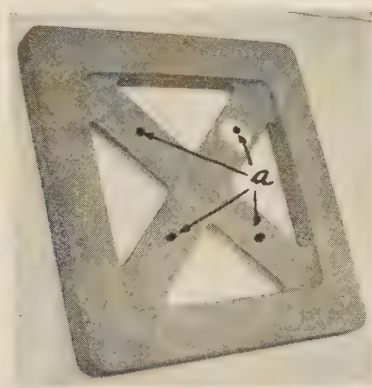


FIG. 12 CAST-IRON TEST FRAMES

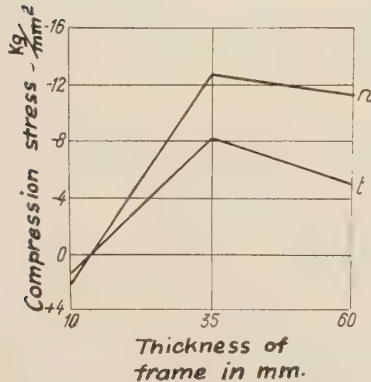


FIG. 13 EFFECT OF OUTER WALL THICKNESS ON CASTING STRESSES IN GRIDS

The experiments made on welded seams can be divided into two groups. The first group includes, besides determination of stresses in plates subjected to various types of local heating, a systematic study of electric- and gas-welded plates. The dimensions of the plates used were all the same, $600 \times 600 \times 15$ mm ($23.6 \times 23.6 \times 0.59$ in.). The second group includes studies of welds in various types of structural parts used in practise, as for instance welded high-pressure tanks, ship plates, steel railway ties, etc.

The great number of measurements taken led to the following conclusions:

- (1) That the general opinion that in electrically welded plates the seams have lower stresses than in gas-welded plates was not confirmed by experiment. In most cases electro-welds showed rather higher stresses
- (2) Stresses in the direction of the seam are high, both in electric and gas welds, and are almost always near the yield point

Location of test

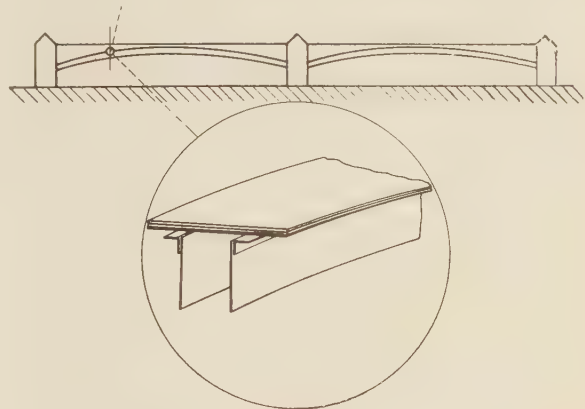


FIG. 14 DIAGRAM OF ARCH BRIDGE AND POINT WHERE TEST WAS MADE

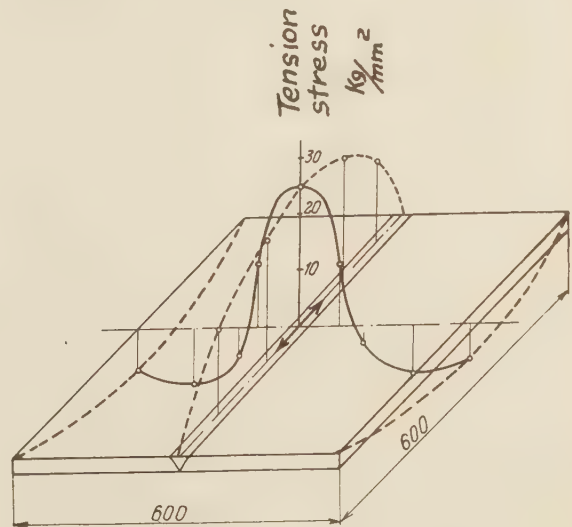


FIG. 15 DISTRIBUTION OF INTERNAL STRESS IN GAS-WELDED SEAM

- (3) In electric welds, the stresses extend over a narrower area around the seam than in gas welds, where the heated zone is a larger one
- (4) In most cases stresses parallel to the seam are higher than at right-angles to it
- (5) In electro-welds, the stresses are higher in continuous seams than in interrupted ones
- (6) No difference in stresses from using bare or covered electrodes was noticed.

A typical stress distribution of two gas-welded plates is shown in Fig. 15. The seam is under high tension stress. The stress drops to zero on both sides, and then changes to compression.

The sum of all moments and stresses is evidently equal to zero. With electrically welded plates, the center stress is usually somewhat higher. The stress rises quickly to its maximum value at the start and the end of the seam, and the zero-stress region lies closer to the seam than with gas welds.

In order to refute the widespread opinion about the dangers of initial stresses, it may be said that the initial stresses mentioned in the foregoing paragraphs (especially in the paragraph on the testing of welds) are not nearly as dangerous as might be thought without further examination. This is especially true for static loadings, because if the yield point is passed at the most highly stressed point, the metal starts to creep locally at this point, and the load then distributes itself more evenly over the cross-section. Under repeated overloadings, the stress distribution in the whole structure approaches more and more the stress distribution which would exist without initial stresses. However, this is only true if the material used is ductile. Hence, the most important requirement for weld material is a very high ductility. For repeated or variable loading, the presence of initial stresses is of no great importance, although the initial

stresses may well reduce the factor of safety. In cases of impact loading, the presence of initial stresses is extremely undesirable.

In conclusion, a remark may be made about an as yet undiscussed field of application of the apparatus. The method of investigation which has been described is not limited to purely metallurgical experimentation only. This method is applicable to the determination of stresses in concrete structures such as dams, or stresses in tunnel walls produced by the weight of mountains or landslides, or the stresses in deep shafts. The diameter of the drill should be selected with consideration for the non-homogeneity of the material, and should be very much larger than with steel, say about 6 to 10 cm (2.4 to 3.9 in.). It is obviously important that, in testing rocks, the same material be used for calibration as in the actual tests, and that it be oriented in the same way, as many rocks are not isotropic. This difficulty may be avoided by using a crown drill, which leaves a core of 6 to 9 cm (2.4 to 3.5 in.). This core is broken off later on and used in an ordinary rock-testing machine to obtain the calibration constants. No experiments of this sort have been carried out as yet, but plans have been made for them.

Report on Oil-Engine Power Cost for 1932¹

THIS report presents information on the production cost of oil-engine power plants. Production cost in the meaning of this report is defined to consist of fuel cost; lubrication cost; cost of attendance and superintendence; cost of supplies and miscellaneous; cost of engine and plant repairs.

The report includes information from 140 oil-engine generating plants, containing 377 engines, totaling 213,910.5 rated brake horsepower. The total *net* output for the 140 plants in this report amounted to 282,466,690 kilowatt-hours. The coverage of this report as compared to that of previous reports is shown by the following table:

Year of report.....	1929	1930	1931	1932
Number of plants...	36	94	119	140
Number of engines...	107	283	330	377
Total rated bhp.....	68,775	161,583	190,768	213,910.5
Total output, net kwhr.....	134,766,761	309,369,930	333,066,644	282,466,690

The engines listed in the report are full-Diesel, vertical type, direct-connected to generators, unless otherwise noted in Tables III, IV, and V. All Diesel plants listed are located in the United States.

Plant Numbers. The system used in former reports of designating plants by number has been retained. Numbers identifying plants previously reported correspond to the same plants in this report.

Period Covered. All but ten of the plants of this report submitted data for a period of exactly 12 months each. Of the ten exceptions, five submitted data for periods varying between 11 and 13 months. The other five submitted data for 5 months, 6 months, 6.7 months, 8 months, and 8.1 months, respectively.

Bases for Costs and Performances. Unit costs referred to in this report were calculated on the basis of net kilowatt-hours. The net kilowatt-hour output is found by subtracting the power used for plant auxiliaries and station lights from the total gross output of the plant.

Figures given for power output per gallon of fuel oil and of lubricating oil were calculated on the basis of the gross outputs of the individual units and plants.

Formulas defining running engine capacity factor, running plant capacity factor, annual plant load factor, and plant service factor are as follows:

Running engine capacity factor, per cent

$$= \frac{\text{Engine output in gross kwhr} \times 100}{\text{Kw rating} \times \text{number of hours operated}}$$

Running plant capacity factor, per cent

$$= \frac{\text{Plant output in gross kwhr} \times 100}{\text{Total rated kwhr of individual units}}$$

Annual plant load factor, per cent

$$= \frac{\text{Plant output in gross kwhr} \times 100}{\text{Peak load in kw} \times \text{number of hours in period}}$$

Plant service factor, per cent

$$= \frac{\text{Total rated kwhr of individual units} \times 100}{\text{Total installed kw} \times \text{number of hours in period}}$$

¹ Submitted by the Subcommittee on Oil Engine Power Cost, Oil and Gas Power Division, A.S.M.E., H. C. Major, Chairman, Committee of Public Utilities, Municipal Building, Rockville Center, L. I., N. Y.

Presented at the Sixth National Oil and Gas Power Meeting, Atlantic City, N. J., August 23-26, 1933, of THE AMERICAN SOCIETY OF MECHANICAL ENGINEERS.

The expression "rated kwhr" refers to the kilowatt rating of an engine-generator set multiplied by the number of hours operated. For example, if a unit having a rating of 200 kw was operated 4000 hours, the rated kwhr equals 800,000, no matter what the actual output may have been. Thus the denominator of the expression for "Running plant capacity factor" and likewise the numerator for the "Plant service factor" are arrived at by totaling the rated kilowatt-hours of all plant units. In this report, the kilowatt rating of an engine-generator set is considered equal to: Rated bhp \times 0.746 \times 0.9.

In the strict sense of its definition, the annual plant load factor cannot be correctly applied to data covering any period other than one year. However, the committee extended the application of this to plants operated 8760 hours plus or minus 2 per cent, using the actual number of hours in the denominator in each case.

The formula for "Plant service factor" requires further explanation for special cases. The expression is an index of the actual number of hours of operation as compared to the total number of hours installed for operation. Therefore, when some units have been installed for longer periods than have others in the same plant, account must be taken of the fact in the calculation. For example, assume that a plant is reported for a twelve-month period, during which time one unit rated at 200 kw, installed before the start of the period, was operated 5000 hours.

Six months after the start of the period, a unit rated at 300 kw was installed, and subsequently operated 2500 hours. The plant service factor in per cent is therefore:

$$\frac{200 \times 5000 + 300 \times 2500}{200 \times 8760 + 300 \times 4380} \times 100$$

Since the 300-kw unit was not installed during the entire 8760 hours, but only for 4380 hours, this adjustment must be made.

Fuel and Lubricating-Oil Data. The lubricating-oil economies of 110 plants generating 95 per cent or more of their outputs by means of full-Diesel units are shown graphically in Fig. 1, in which the kwhr output per gallon of lubricating oil is plotted against running plant capacity factor. (Eight of the full-Diesel plants did not report unit hours of operation, and running capacity factors could not be calculated for these.) Fuel-oil economies of the same 110 plants are shown graphically in Fig. 2, in which the gross kwhr output per gallon of fuel oil is likewise plotted against running plant capacity factor. The values plotted in Fig. 2 are corrected neither for the heat content of the fuel nor for altitude. The lubricating-oil and fuel-oil economies of 20 plants generating more than 5 per cent of their output by means of semi-Diesel units are shown in Figs. 3 and 4, respectively. (Two plants generating more than 5 per cent of their output by semi-Diesel units did not report unit hours of operation, and the running capacity factors could not be calculated for these.)

The type of the plant was judged to be that of the engines generating 95 per cent or more of the gross output. The following types of plants are illustrated in Figs. 1 to 4, inclusive:

- Diesel four-stroke cycle, air injection
- Diesel four-stroke cycle, mechanical injection
- Diesel two-stroke cycle, air injection
- Diesel two-stroke cycle, mechanical injection, separate scavenging

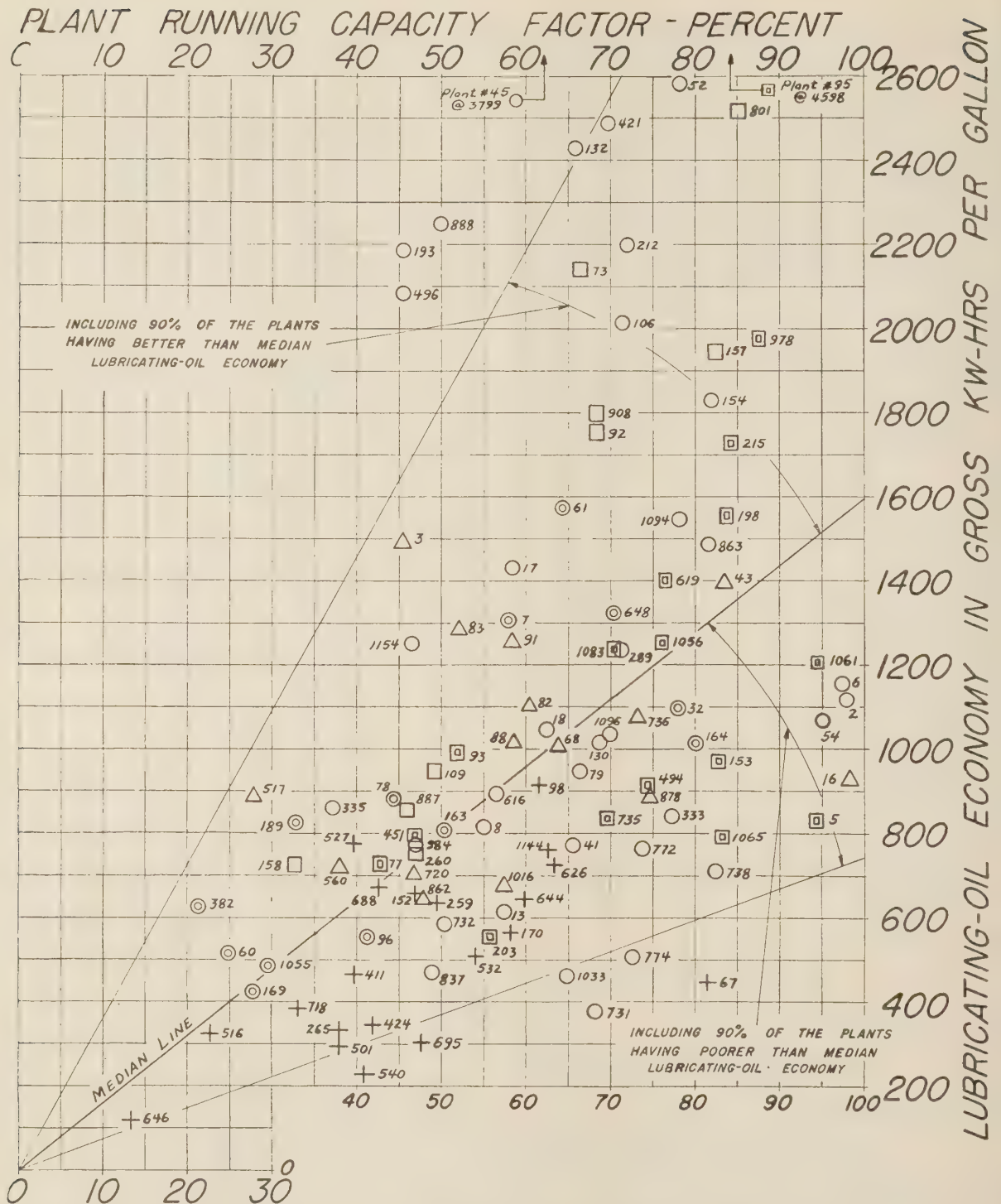


FIG. 1 LUBRICATING OIL ECONOMIES OF 110 FULL DIESEL PLANTS, NOT INCLUDING 8 FULL DIESEL PLANTS, RUNNING CAPACITY FACTORS FOR WHICH ARE NOT AVAILABLE
(For Key to Plant Symbols see Fig. 2.)

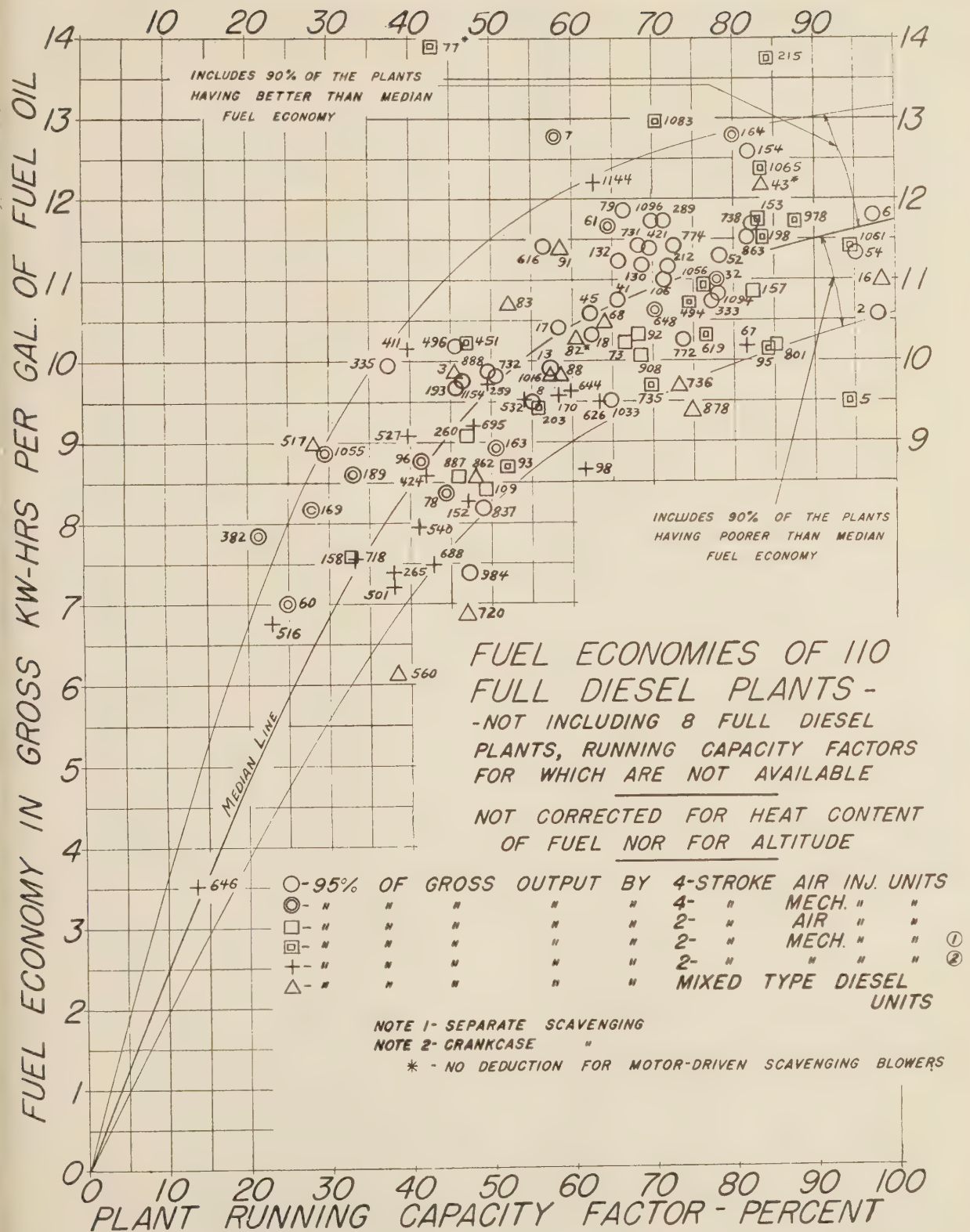
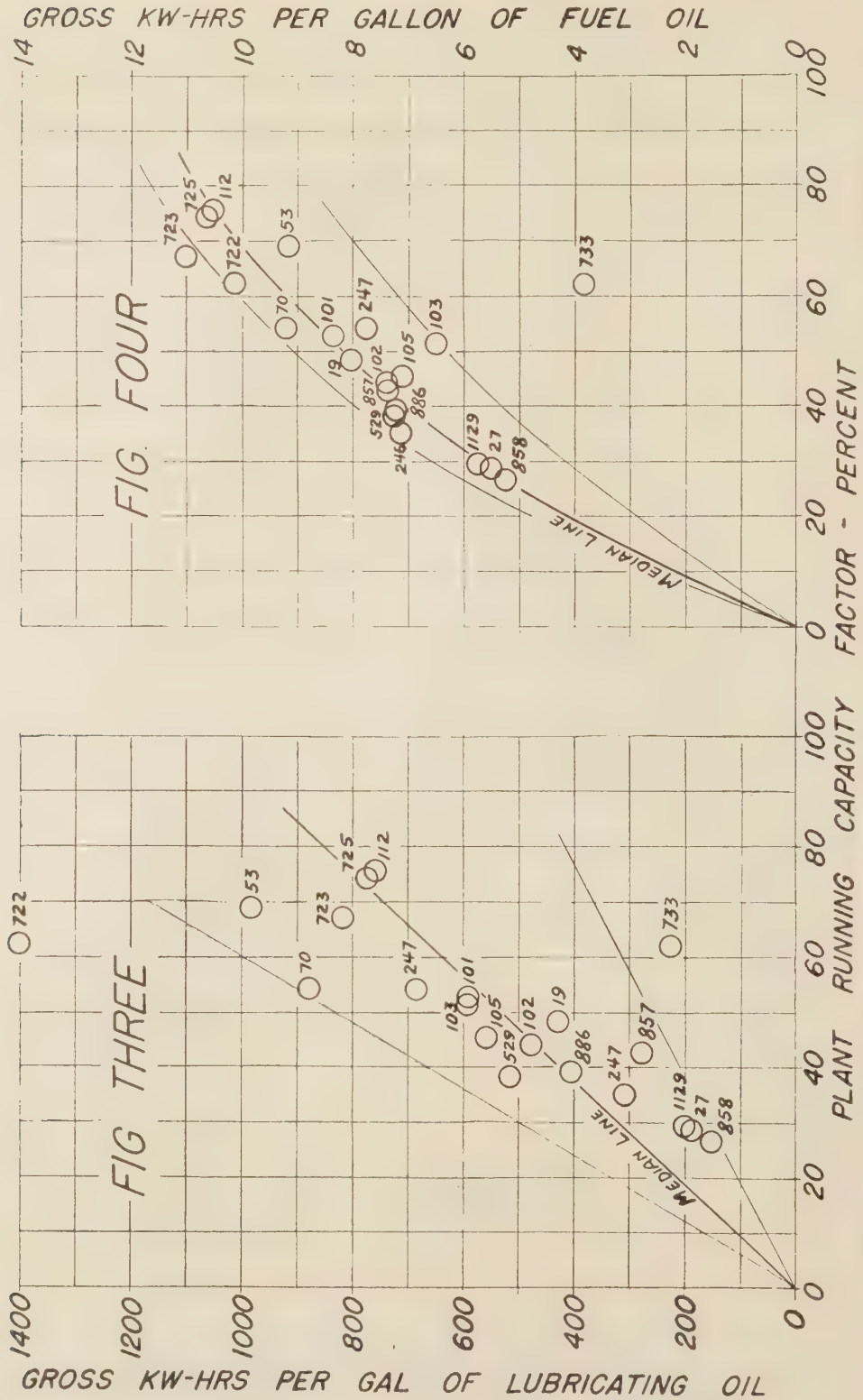


FIG. 2



FIGS. 3 AND 4 FUEL- AND LUBRICATING-OIL ECONOMIES OF 20 PLANTS GENERATING MORE THAN 5 PER CENT OF OUTPUT BY SEMI-DIESEL UNITS, NOT INCLUDING TWO SUCH PLANTS, RUNNING CAPACITY FACTORS FOR WHICH ARE NOT AVAILABLE

Diesel two-stroke cycle, mechanical injection, crankcase scavenging

Mixed-type full Diesel

Mixed Diesel and semi-Diesel

A median line was drawn on each chart, the number of points above the line being equal to the number below. High and low boundary lines were drawn to include all but 10 per cent of the plants on the high and low sides, respectively.

Unless it is otherwise noted in Table IV, plants received fuel oil in tank cars.

All fuel- and lubricating-oil costs include costs for the handling of oil from the cars to the tanks.

Cooling Water. The various water-cooling systems are indicated by the following symbols:

System A, raw water going to waste after one pass

System B, raw water recirculated after passing over cooling tower or spray pond

System C, soft water continuously recirculated, cooled by raw water going to waste after one pass through heat exchanger

System D, soft water continuously recirculated, cooled by raw water also recirculated after cooling by cooling tower or spray pond

System E, any of the foregoing systems with engine circulating water treated (added as a suffix).

Investment Costs. Due to the difficulty in obtaining reliable information on expenditures over past years and to the fact that such data may not reflect current costs, the committee decided to discontinue this feature of its investigations and did not solicit any information on this subject in this questionnaire for 1932.

Enforced Shutdowns. The term "enforced shutdown" is defined as any stoppage caused by actual or imminent engine trouble. The duration of an enforced shutdown is the time elapsing from the shutdown of the engine to the time at which the engine is again ready for service. A prearranged shutdown for maintenance work is not considered an enforced shutdown. There were some misunderstandings in regard to the committee's question calling for the number of hours expended on regular maintenance work. The uncertainty was, however, either corrected by correspondence with operators where sufficient time was available or a blank was left for the data. Regular maintenance time where listed is therefore the total time put in on regular maintenance work whether or not the units were actually needed during the time.

Peak Loads. The peak loads presented in the report are the highest average loads sustained for 15 minutes, unless otherwise stated in Table V.

Liner Wear. The committee realizes that liner wear is a complicated subject worthy of a separate investigation, and therefore decided not to continue a question on liner wear in the questionnaire for 1932. The committee has made recommendation to the Executive Committee of the Division that a separate investigation on this subject is advisable.

Repair Costs. All costs for repairs, whether to engines only or to all other plant equipment, listed in Table I, include the cost of materials delivered at the plant in question and the cost of any extra labor employed for the purpose of making these repairs. Unless otherwise noted, however, these costs do not include any charges for work done by regular attendants. Correspondingly, unless otherwise noted, the costs noted in Table I for attendance and superintendence have not been subject to deductions because of repair work done by the regular attendance crews. The committee has incorporated a new feature in the current report—

namely, the listing of major parts renewed during the period. This information is set forth in Table V.

Attendance and Superintendence. The committee has extended the range of reported data in connection with attendance by securing and reporting the number of shifts per year and the net kwhr produced per man-hour of attendance and superintendence. Attendance ratios for 103 full-time attended plants are shown graphically in Fig. 5, in which the net kwhr output per man-hour is plotted against plant service factor. (Twenty plants of the report were attended part-time; twelve plants did not report data required for calculating service factors; five plants did not report shift data necessary for the calculation of net output per man-hour. None of these plants are shown in Fig. 5.)

Supplies and Miscellaneous. Supplies in the meaning of this report are such items used in the power-generating plant which are consumed in the operating process—namely, such items as waste, packing, wipers, gage glasses, gaskets, bolts, screws, nails, dynamo and motor brushes, cans for containing rags and waste, transformer oil and hand oil cans. The term "miscellaneous" as used in this report refers to such items as expenditures for lighting, heating, and cleaning systems, fire-protection systems, janitor's supplies, ice water, meals and carfares, stationery, telephone and toilet service, care of streets, yards and sidings.

Type of Load. The terms used for type of load are defined as follows:

Complete Power.—The plant is run regularly alone when needed, without assistance from any base- or peak-load service

Base Load.—The plant is run at substantially full load whenever its capacity can be used, usually supplemented by a peak-load service. When full or nearly full capacity cannot be used, the plant is shut down

Peak Load.—The plant is run only when the load exceeds the capacity of the regular source of power

Standby.—The plant is run only when the regular source of power is interrupted.

For this investigation, the committee requested information also on the type of power supplemented by base load, peak load, and standby plants. Information obtained in accordance with this request is presented in Table I.

Total Production Costs. Total production costs for 135 plants reporting for one year each (plus or minus one month) are shown graphically on logarithmic coordinates in Fig. 6, in which total production cost in mills per net kwhr is plotted against specific output, or the output in net kwhr per year per kw of installed capacity.

Calculations. All original calculations and correspondence with operators were carried on by Messrs. Robert T. Brown and George V. Khrennikoff, who were employed to assist the committee.

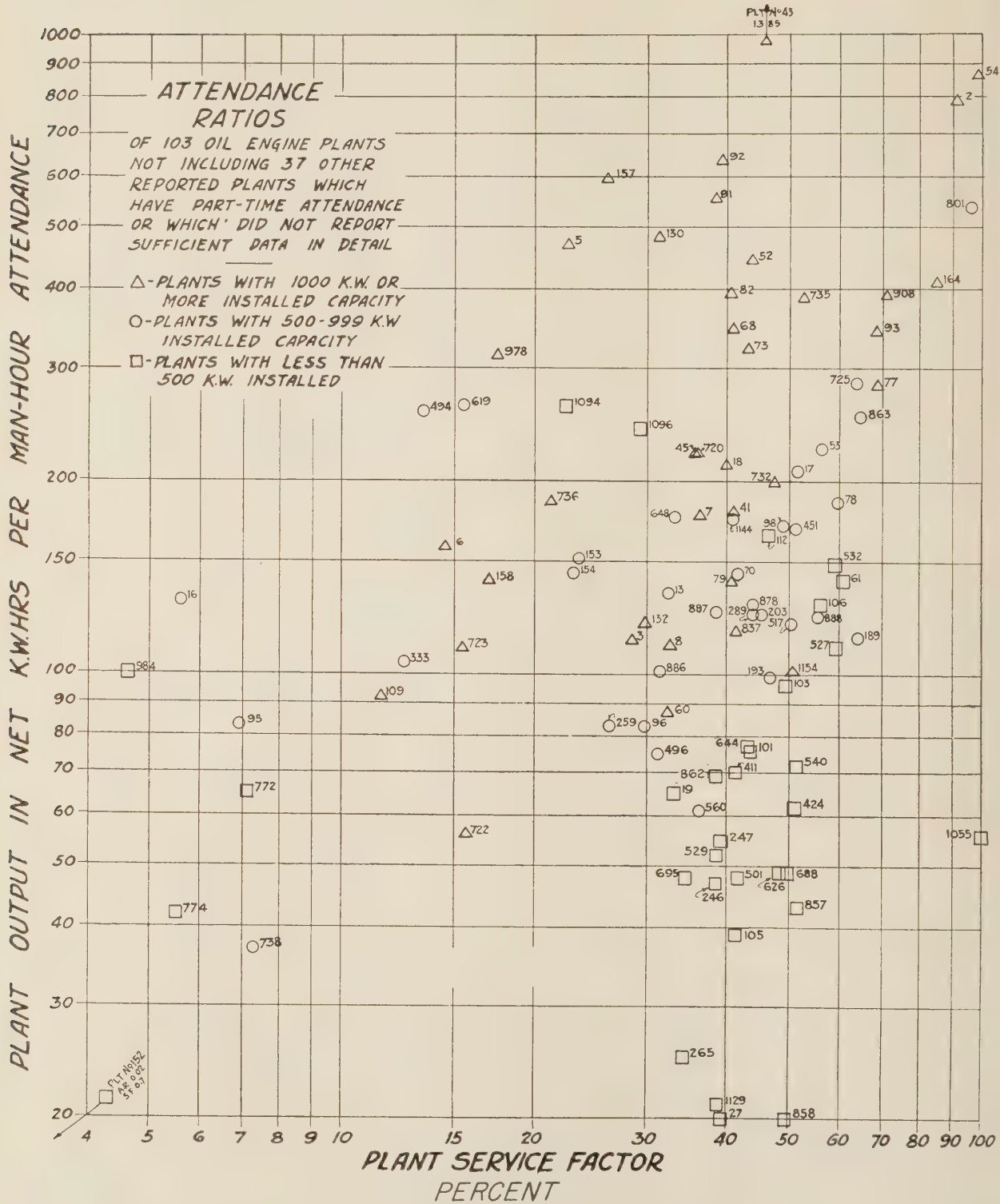
The committee wishes to acknowledge its appreciation of the splendid services of Franz Eder, who has been chairman of the committee since its organization, and to announce with regret his resignation as chairman. H. C. Major has been appointed to succeed Mr. Eder as chairman.

SUBCOMMITTEE ON OIL-ENGINE POWER COST

H. C. Major, Chairman
M. J. Reed, Secretary
C. H. Berry
F. J. Fischer
L. R. Ford
W. G. G. Godron

K. M. Irwin
E. J. Kates
H. C. Lenfest
A. B. Morgan
L. H. Morrison
Lee Schneitter

H. C. Thuerk



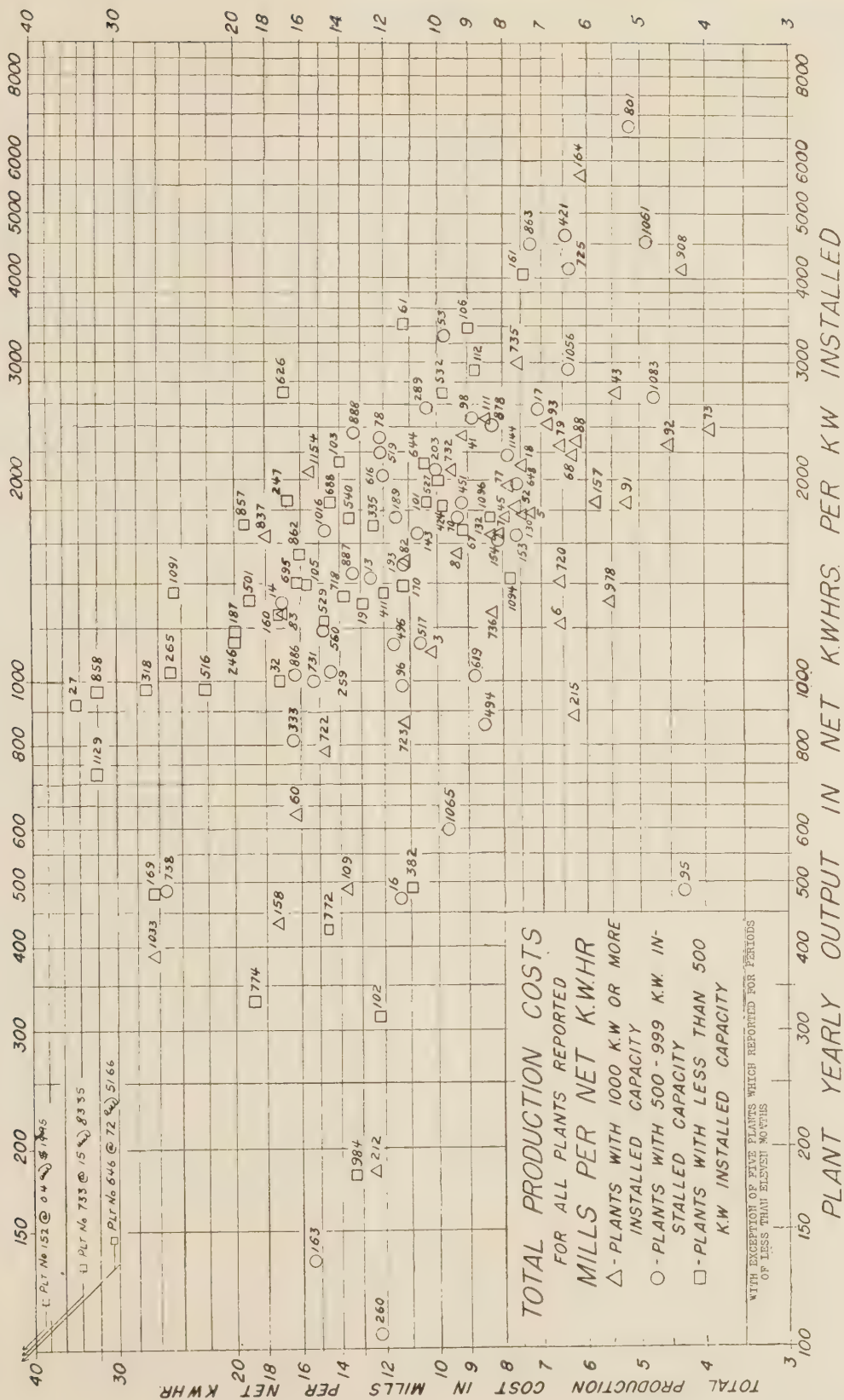


TABLE I - INFORMATION ON PRODUCTION COST (PAGE 1)

TABLE I - INFORMATION ON PRODUCTION COST (PAGE 1)																								
PLANT NUMBER	CHARACTER OF PLANT (SEE NOTES)	TYPE OF LOAD (SEE (C))	NUMBER OF ENGINES	TOTAL INSTALLED H. P.	TOTAL INSTALLED K. W. A.	TOTAL PLANT HOURS OPERATED IN REPORTED PERIOD	NUMBER OF MONTHS IN REPORTED PERIOD	TOTAL GROSS OUTPUT K. W. HRS.	TOTAL NET OUTPUT K. W. HRS.	PER CENT OF GROSS K. W. HRS. FOR PLANT PURPOSES	ANNUAL PLANT LOAD FACTOR (SEE TEXT)	RUNNING PLANT CAPACITY FACTOR (SEE TEXT)	PLANT SERVICE FACTOR (SEE TEXT)	AVERAGE COST OF FUEL OIL - CENTS PER GALLON	AVERAGE COST OF LUBRICATING OIL - CENTS PER GALLON	FUEL COST	LUBRICATING OIL COST	ATTENDANCE COST, IN- CLUDING SUPERINTENDANCE	COST OF SUPPLIES AND MISCELLANEOUS, INCLUDING WATER	COST OF ENGINE REPAIRS	COST OF ALL OTHER PLANT REPAIRS	COMBINED COST OF ALL REPAIRS, SUPPLIES, AND MISCELLANEOUS	TOTAL PRODUCTION COST	PLANT NUMBER
43	U	C	9	15640	14850	8784	12	32,116,114	28,374,009	11.6	87.1	83.3	46.0	3.48	37.7	3.23	0.51	0.86	0.30	0.56	0.14	1.00	5.40	43
82	U	C	7	8960	8102	8740	12	9,426,480	9,065,533	5.8	33.0	50.3	45.4	4.48	66.3	4.52	0.63	2.81	1.13	1.57	3.17	11.13	82	
88	U	C	6	7445	6380	6760	12	9,281,200	9,110,000	1.8	36.3	78.1	43.8	4.41	69.8	3.97	0.27	2.35	0.52	0.35	0.14	1.01	7.60	88
91	U	C	6	8250	4505	6784	12	6,942,100	6,490,080	6.8	46.6	58.4	38.4	3.12	41.8	2.93	0.36	1.57	0.14	0.12	0.05	0.31	5.17	91
73	U	C	6	4250	4252	6784	12	6,509,500	6,030,200	5.6	42.0	66.4	43.4	1.28	58.4	1.26	0.29	2.01	0.16	0.16	0.02	0.34	3.92	73
92	U	C	3	4900	4250	6784	12	7,757,200	7,451,947	3.9	44.2	68.2	39.3	2.04	47.9	2.05	0.28	1.34	0.26	0.54	0.03	0.83	4.50	92
45	U	C	3	4250	3625	6784	12	5,377,375	5,015,875	10.1	42.3	62.1	35.8	3.87	35.3	1.07	0.11	2.05	0.06	0.54	0.03	0.55	4.50	45
54	U	C	4	4200	3150	8859	84	18,507,500	15,107,500	2.1	---	95.1	98.7	1.38	30.0	1.24	0.29	1.02	0.54	0.53	1.07	3.62	54	
150	U	C	4	3600	3150	6784	12	4,556,800	4,281,230	6.0	44.7	68.6	31.3	4.02	62.9	3.83	0.66	1.65	0.47	0.68	0.19	1.24	7.48	150
157	U	C	2	3520	3000	7350	12	4,436,850	4,376,509	1.4	19.8	82.3	26.0	4.16	46.8	3.68	0.24	0.80	0.24	0.58	0.05	0.87	5.79	157
2	U	C	3	3450	3000	4300	81.5	6,901,260	6,839,511	0.7	---	97.8	91.2	2.33	27.2	2.22	0.24	1.03	0.10	1.11	0.08	1.29	4.78	2
104	U	C	4	3350	4000	6784	12	13,433,500	12,538,281	4.6	---	80.0	84.9	2.59	26.2	2.12	0.27	1.23	0.58	1.37	0.48	2.38	6.05	104
720	U	C	5	3125	2632	6784	12	2,384,995	2,351,585	2.7	31.6	45.4	28.5	3.17	42.0	3.37	0.73	2.09	0.37	0.35	0.01	0.61	10.19	720
77	U	C	1	3080	2500	6784	12	3,053,100	2,920,600	4.3	34.8	66.5	29.2	4.00	44.5	3.59	1.24	0.77	0.80	0.01	0.28	6.56	77	
109	U	C	3	2925	2450	6784	12	973,120	959,606	1.4	8.9	49.2	11.5	5.69	60.0	6.85	0.64	5.01	0.48	0.49	0.97	7.88	109	
732	U	C	3	2730	2625	6784	12	3,383,400	3,105,742	8.2	42.5	57.9	36.3	3.27	29.6	2.78	0.25	2.29	0.42	0.96	0.39	1.77	8.09	732
978	U	C	3	2520	2100	6784	12	3,550,500	3,497,537	1.5	27.5	45.4	28.5	3.17	42.0	3.37	0.73	2.09	0.37	0.35	0.01	0.61	10.19	978
908	U	C	2	2500	2100	6784	12	2,274,700	2,223,852	2.2	14.4	87.6	17.5	5.57	51.2	3.11	0.27	1.41	0.35	0.36	0.01	0.74	5.53	908
93	U	C	4	2480	2116	6858	12.1	4,325,200	4,058,720	6.2	34.9	52.0	68.5	3.09	36.9	3.78	0.42	1.81	0.10	0.67	0.05	0.62	4.29	93
111	U	C	4	2475	2120	6784	12	4,529,900	4,105,401	9.4	37.6	---	---	3.23	50.6	3.03	0.49	1.98	0.57	0.24	0.48	1.03	6.43	111
1149	U	C	3	2400	2025	6784	12	1,135,200	1,015,200	10.6	13.7	24.8	32.3	4.49	33.5	3.48	0.73	3.88	0.40	0.62	0.00	0.81	17.39	1149
60	U	C	4	2370	2010	6784	12	1,445,700	1,371,4804	5.1	10.9	67.2	15.4	4.31	57.1	4.13	0.74	3.71	0.78	1.79	2.55	11.13	60	
723	U	C	4	2370	2010	6784	12	1,445,700	1,371,4804	5.1	10.9	67.2	15.4	4.31	57.1	4.13	0.74	3.71	0.78	1.79	2.55	11.13	723	
41	U	C	3	2370	1800	6784	12	3,748,080	3,698,0904	1.3	35.6	65.5	41.0	4.10	46.9	3.88	0.62	4.08	0.23	0.26	0.08	0.57	9.10	41
79	U	C	5	2170	1888	6784	12	3,456,400	3,280,387	5.1	39.3	65.4	40.6	2.49	40.7	2.21	0.46	3.58	0.11	0.23	0.14	6.53	79	
6	U	C	3	2160	---	6784	12	2,721,770	2,597,100	4.8	21.5	94.4	22.6	3.54	51.4	3.90	0.65	1.51	0.53	0.86	1.39	7.25	6	
68	U	C	4	2040	1744	6784	12	1,751,200	1,720,413	1.8	11.7	87.4	14.5	3.94	50.9	3.40	0.46	1.64	0.86	0.40	0.62	0.81	6.54	68
83	U	C	3	2000	1735	6784	12	1,767,500	1,687,500	5.8	35.1	52.0	---	5.00	58.0	4.95	0.45	4.60	1.42	1.72	1.06	5.08	16.88	83
215	U	C	2	1960	1690	6784	12	1,195,000	1,163,3704	2.6	9.8	84.2	12.3	5.14	48.9	3.84	0.29	1.48	0.85	0.07	0.07	0.62	6.23	215
736	U	C	3	1925	1572	6784	12	1,785,500	1,637,155	7.3	---	73.2	21.2	2.74	64.2	3.04	0.64	1.87	0.35	1.91	0.46	2.72	8.27	736
637	U	C	4	1875	1605	6784	12	2,027,740	2,027,699	7.6	37.9	48.8	41.2	2.45	54.8	3.29	0.80	0.89	0.40	0.62	0.00	0.81	17.39	637
1023	U	C	4	1850	1300	6784	12	4,99,020	4,600,770	3.7	6.2	64.8	7.1	3.42	68.9	3.73	0.58	10.33	4.05	6.44	1.18	11.67	26.31	1023
158	U	C	1	1760	1500	3660	12	577,178	512,498	11.2	6.0	32.7	17.0	5.87	28.2	8.69	1.06	3.00	2.62	1.09	0.77	4.48	17.23	158
752	U	C	2	1750	1342	6784	12	217,800	217,1474	0.3	4.4	71.8	2.9	3.60	65.2	3.22	0.30	2.14	0.29	0.40	0.10	0.69	12.35	752
735	U	C	4	1705	1450	6784	12	884,690	896,2204	9.0	10.0	62.4	15.7	4.66	79.2	3.07	0.63	6.53	0.54	1.61	0.85	8.46	7.22	735
18	U	C	3	1650	---	6784	12	2,422,800	2,337,071	4.0	26.3	62.4	40.0	3.74	51.4	3.78	0.51	1.72	0.34	1.10	1.44	7.45	18	
88	U	C	4	1620	---	6784	12	2,529,724	2,497,042	1.3	41.2	58.6	---	2.31	47.3	2.39	0.47	2.85	0.36	0.10	0.0	0.46	6.22	88
1154	U	C	3	1560	---	6784	12	1,652,960	1,627,980	1.5	31.4	55.0	32.7	3.04	43.0	3.26	0.64	4.85	---	---	---	0.62	9.27	1154
132	U	C	3	1500	1120	6784	12	2,073,500	2,044,307	1.4	36.3	46.5	60.6	5.08	85.8	0.67	0.70	7.04	1.17	0.07	0.39	1.63	14.76	132
289	U	C	4	1465	1232	6784	12	2,589,380	2,559,0174	0.0	86.5	71.1	42.9	4.17	50.0	3.78	0.51	1.72	0.34	0.12	1.13	1.57	10.65	289
496	U	C	3	1450	1246	6784	12	1,207,025	1,101,985	8.7	21.1	45.5	51.1	4.02	64.0	4.32	0.34	4.48	0.52	0.51	0.42	1.45	11.69	496
70	U	C	3	1420	1190	6784	12	1,889,800	1,875,037	11.3	36.4	41.5	30.3	4.12	7.1	0.53	0.26	0.27	0.53	0.0	0.0	0.62	9.27	70
198	U	C	1	1400	1392	2791	6.7	2,155,580	2,089,899	4.8	---	54.3	56.7	3.63	50.3	3.31	0.34	0.42	0.56	0.12	0.06	0.23	4.70	198
165	U	C	3	1400	1311	6784	12	1,41,590	1,27,353	10.1	1.7	50.4	3.4	0.97	26.2	1.21	0.36	7.30	0.36	5.53	0.58	6.47	15.34	165
154	U	C	3	1400	---	6784	12	1,546,980	1,581,613	1.8	29.4	81.8	25.0	3.47	51.5	2.61	0.29	4.18	0.33	0.48	0.81	6.09	154	
888	U	C	3	1375	1200	6784	12	2,236,100	2,168,2504	3.0	31.0	49.8	55.4	4.02	75.5	4.21	0.35	5.19	1.43	1.36	0.76	2.54	14.29	888
537	U	C	3	1375	1250	6784	12	1,129,200	1,050,715	7.0	30.7	57.4	3.74	3.74	50.0	4.46	0.61	8.4	0.23	0.23	0.22	1.29	14.77	537
1016	U	C	3	1355	1112	6784	12	1,853,830	1,827,580	3.6	28.													

TABLE 1 - INFORMATION ON PRODUCTION COST (PAGE 2)

TABLE I - INFORMATION ON PRODUCTION COST (PAGE 2)																									
PLANT NUMBER	CHARACTER OF PLANT (See Notes)	TYPE OF LOAD (See Notes)	NUMBER OF ENGINES	TOTAL INSTALLED H. P.	TOTAL INSTALLED K. V. A.	TOTAL PLANT HOURS OPER- ATED IN REPORTED PERIOD	NUMBER OF MONTHS IN REPORTED PERIOD	TOTAL OILS OUTPUT - K. W. HRS.	TOTAL NET OUTPUT - K. W. HRS.	PER CENT OF OILS K. W. HRS. FOR PLANT PURPOSES	ANNUAL PLANT LOAD FACTOR (See Text)	ENGINE PLANT CAPACITY FACTOR (See Text)	PLANT SERVICE FACTOR (See Text)	AVERAGE COST OF FUEL OIL - CENTS PER GALLON	AVERAGE COST OF LUBRICAT- ING OIL - CENTS PER GALLON	COSTS PER NET K.W. HR. - MILLS									
																FUEL COST	LUBRICATING OIL COST	ATTENDANCE COST, IN- CLUDING SUPERINTENDANCE	COST OF SUPPLIES AND REPAIRS, INCLUDING WATER	COST OF ENGINE REPAIRS	COST OF ALL OTHER PLANT REPAIRS	COMBINED COST OF ALL REPAIRS, SUPPLIES, AND MISCELLANEOUS	TOTAL PRODUCTION COST		
365	M	C	1	900	774	---	12	369,160	363,000	4.5	8.7	83.3	8.6	5.51	49.9	5.22	0.66	1.65	1.82	1.04	1.25	4.11	9.64	1065	
366	M	C	1	900	776	8784	12	731,530	719,930	1.6	26.9	38.2	35.2	2.76	82.1	4.57	0.74	6.79	0.32	0.28	0.19	2.77	14.87	560	
280	M	C	1	900	758	319	12	90,700	63,389	30.1	1.7	47.0	3.6	3.39	75.0	5.34	1.42	5.26	0.32	0.18	0.19	0.18	12.20	260	
98	M	C	1	900	740	8784	12	1,097,580	1,500,880	6.1	48.5	61.5	46.9	3.74	40.6	4.59	0.47	3.04	0.41	0.33	0.09	0.80	8.90	96	
53	M	C	1	900	738	8784	12	2,037,980	1,975,860	0.4	44.2	39.7	36.2	2.36	38.6	2.90	0.41	0.21	0.41	0.72	0.02	4.22	9.74	53	
169	M	C	1	850	730	8784	12	1,052,120	998,200	5.1	41.4	32.8	34.1	2.76	64.3	5.36	0.82	5.66	0.34	1.12	0.46	11.52	169		
1056	M	C	1	840	700	4166	12	1,791,070	1,655,114	7.6	34.0	76.2	47.4	3.12	26.4	3.09	0.23	1.80	0.62	0.42	0.24	1.28	6.40	1056	
619	M	C	1	840	700	2186	12	886,300	575,200	2.2	12.2	76.5	15.5	3.53	50.0	3.51	0.37	1.96	1.06	1.55	0.32	2.33	8.77	619	
494	M	C	1	840	700	1884	12	495,200	492,220	2.6	11.5	74.5	13.4	3.61	48.6	3.38	0.54	1.88	0.67	0.60	0.22	2.69	8.49	494	
153	M	C	1	840	700	---	12	969,410	929,450	0.1	10.7	23.6	3.85	37.2	37.2	5.18	0.53	2.65	0.78	0.46	0.46	1.24	7.60	153	
731	M	C	1	825	750	8784	12	585,765	584,765	5.5	11.1	68.2	17.7	4.00	42.0	3.70	1.17	7.50	1.20	1.63	0.09	2.92	15.29	731	
648	M	C	1	800	666	6280	12	1,009,530	1,068,900	2.8	31.5	70.2	33.2	3.28	50.0	5.12	0.59	8.13	0.40	0.46	0.11	0.97	7.63	648	
151	M	C	1	800	681	8784	12	2,631,800	2,485,908	5.5	57.1	69.6	80.2	3.23	43.0	2.04	0.18	4.23	0	0	0	0	6.45	421	
312	M	C	1	740	680	8784	12	1,545,900	1,443,130	6.7	41.9	75.8	46.7	3.52	45.4	3.57	0.54	4.19	0.23	0.76	0.04	0.33	8.73	312	
532	M	C	1	720	600	8784	12	717,320	644,337	10.2	51.0	33.0	51.3	3.51	4.98	1.02	0.59	0.64	0.05	0.77	2.46	13.85	718		
532	M	C	1	720	600	8784	12	1,352,200	1,304,390	5.5	38.5	54.0	59.0	4.17	53.7	3.55	1.09	2.97	0.81	0.39	0.10	1.20	9.81	536	
170	M	C	1	720	600	8784	12	997,200	967,000	3.0	31.1	59.6	59.2	3.10	61.0	3.52	0.81	0.58	0.24	0.25	0.03	0.52	9.93	527	
170	M	C	1	720	600	2778	12	783,156	675,376	4.0	17.4	58.2	28.5	5.53	45.8	6.01	0.64	2.71	0.22	1.41	0.63	1.53	11.19	170	
19	M	C	1	720	600	8784	12	811,000	810,190	0.1	44.0	81.5	23.4	4.47	42.2	4.39	0.94	2.30	0.30	1.04	0.12	1.46	9.09	67	
411	M	C	1	680	580	8784	12	661,930	612,950	7.4	36.7	46.5	33.2	3.63	53.7	4.87	1.35	4.96	1.01	0.79	0.38	1.68	12.86	19	
109	M	C	1	680	490	8784	12	657,070	628,670	6.1	34.0	39.7	41.3	3.36	37.2	3.58	0.85	6.97	0.15	0.21	0.20	2.37	14.78	417	
109	M	C	1	680	490	8784	12	997,836	997,836	6.3	34.3	38.4	38.6	3.60	45.0	5.28	0.93	6.21	1.92	0.21	0.20	2.33	14.78	529	
106	M	C	1	600	---	---	12	1,409,410	1,358,285	3.6	31.5	71.4	55.8	3.77	53.0	5.27	0.27	3.07	0.74	1.33	0.27	2.37	8.98	107	
1094	M	C	1	600	513	2028	12	725,980	708,626	2.4	19.7	69.9	29.3	3.88	50.1	3.59	0.80	2.09	0.55	1.45	0.27	2.37	8.35	1096	
1094	M	C	1	600	513	2196	12	619,170	572,600	7.5	17.2	78.0	22.4	3.79	49.7	5.78	0.35	1.62	1.24	0.27	0.50	2.11	7.75	1094	
644	M	C	1	600	496	8784	12	915,400	848,016	7.2	40.4	59.5	43.1	4.04	58.5	4.53	0.98	4.02	0.75	0.04	0.06	0.85	10.38	644	
61	M	C	1	600	572	8784	12	1,365,900	1,360,330	0.2	37.9	64.5	60.7	4.63	60.3	3.97	0.38	5.76	0.04	1.02	0.03	1.09	11.20	61	
32	M	C	1	600	572	8784	12	414,600	402,800	2.9	10.5	77.9	15.0	4.45	65.1	5.09	0.31	10.95	0.17	0.28	0	0.46	27.11	32	
160	M	C	1	580	440	8784	12	890,340	842,314	5.4	40.5	51.4	49.7	3.94	39.9	6.42	0.71	6.13	0.50	1.00	0.25	1.75	14.01	103	
662	M	C	1	580	495	8784	12	644,280	609,820	5.4	31.2	47.9	58.6	3.14	45.9	3.87	0.78	6.99	0.47	1.71	0.48	2.66	15.97	882	
102	M	C	1	580	475	2262	12	139,210	122,220	12.2	9.9	44.2	9.2	2.51	45.2	2.58	1.08	7.04	0.29	0.10	0.11	0.85	18.18	102	
540	M	C	1	540	420	8784	12	1,068,200	633,751	8.2	28.2	40.8	51.3	3.36	41.7	4.46	1.91	6.82	0.69	0.19	0	0.88	13.47	540	
246	M	C	3	540	430	8784	12	431,636	412,636	4.4	30.7	35.1	38.5	6.17	54.9	9.05	1.86	8.60	0.28	1.10	0	0.58	19.95	246	
160	M	C	3	540	440	8784	12	435,340	423,414	3.0	29.2	47.6	34.6	4.59	22.5	5.13	0.77	9.03	0.62	0	---	3.08	17.15	160	
335	M	C	3	540	475	8784	12	723,900	670,782	7.3	44.5	52.8	45.1	2.44	42.6	3.12	0.78	4.40	0.33	0.88	0.08	2.09	10.42	101	
778	M	C	3	500	513	2196	12	183,680	142,730	7.1	6.2	73.7	7.1	3.72	45.7	3.90	0.64	4.90	4.18	0.57	0.46	5.18	14.62	778	
501	M	C	3	480	380	8668	11.9	441,408	421,162	4.6	33.4	37.9	41.7	4.71	54.5	6.85	1.94	3.97	0.40	1.24	0.39	1.83	39.10	501	
424	M	C	2	480	400	8784	12	602,508	566,935	2.6	35.1	41.8	50.9	3.00	45.0	5.56	1.34	4.37	0.34	0.14	0	0.48	9.77	424	
695	M	C	2	480	390	8784	12	435,340	423,414	3.0	29.2	47.6	34.6	4.59	22.5	5.13	0.77	9.03	0.62	0	---	3.08	17.15	695	
335	M	C	2	430	369	8784	12	802,130	490,130	2.4	36.9	37.1	53.4	3.11	60.0	3.20	0.71	7.15	1.26	0.03	0.03	1.32	12.38	335	
247	M	C	3	390	275	8784	12	487,960	465,760	0.5	24.7	54.2	39.2	4.55	55.0	5.88	0.81	9.78	0.07	0.12	0.56	0.24	16.65	247	
1129	M	C	4	380	341	8784	12	805,450	184,346	9.4	29.0	29.6	39.5	4.09	45.0	7.83	2.48	16.51	1.90	3.68	0.60	5.28	39.10	1129	
105	M	C	3	370	275	8784	12	410,220	346,440	16.5	35.9	45.5	41.2	2.35	47.6	3.92	1.01	8.32	0.40	1.78	0.24	2.39	15.64	105	
1091	M	C	2	350	300	8784	12	325,408	325,408	---	---	---	---	1.98	55.0	9.30	0.40	10.85	3.20	0.40	0.46	4.06	24.61	1091	
161	M	C	3	350	---	---	12	1,003,500	982,300	1.1	45.7	---	---	3.95	49.5	0.68	0.68	2.49	0.16	0.58	0	0.84	7.45	161	
152	M	C	3	350	---	---	12	6,600	88	98.7	0.3	47.0	0.7	3.90	54.7	0.35	0.08	18.68	5.97	0.69	0.69	4.88	19.95	152	
688	M	C	3	350	---	---	12	437,500	432,500	1.1	29.3	42.8	49.9	3.93	30.0	5.32	0.45	6.32	0.12	0.25	0.12	0.49	14.58	688	
187	M	C	2	356	281	9446	12.8	315,000	297,000	5.7	---	---	---	4.15	47.0	5.02	2.18	11.84	0.88	0.10	0.03	0.95	19.09	187	
774	M	C	2	346	270	1830	12	81,542	77,122	5.1	72.5	6.5	3.68	49.7	3.31	1.03	6.37	3.62	1.36	8.97	7.85	18.75	774		
897	M	C	1	338	---	8784	12	428,704	379,350	11.6	---	---	---</												

TABLE II - COMPARATIVE COSTS - 1929, 1930, 1931 AND 1932 REPORTS (PAGE 1)

TABLE LI - COMPARATIVE COSTS - 1929, 1930, 1931 AND 1932 REPORTS (PAGE 1)																		
PLANT NUMBER	YEAR	TOTAL INSTALLED B. H. P.	TOTAL NET OUTPUT K. W. HRS.	ANNUAL PLANT LOAD FACTOR	RUNNING PLANT CAPACITY FACTOR	PLANT SERVICE FACTOR	AVERAGE COST OF FUEL OIL CENTS PER GALLON	COSTS PER NET K.W. HR. - MILLS								TOTAL PRODUCTION COST	YEAR	PLANT NUMBER
								FUEL COST	LUBRICATING OIL COST	ATTENDANCE COST, IN- CLUDING SUPERINTENDANCE	COST OF SUPPLIES AND MISCELLANEOUS, INCLUD- ING WATER	COST OF ENGINE REPAIRS	COST OF ALL OTHER PLANT REPAIRS	TOTAL OF ALL SUPPLY, REPAIR, AND MISCELL- ANEOUS COSTS				
43	1929	11,540	22,591,027	----	69.9	----	4.25	3.82	0.69	0.60	----	----	----	1.04	6.15	1929	43	
	1930	11,540	26,221,176	46.1	70.4	57.8	4.37	3.95	0.53	0.94	0.21	0.67	0.05	0.93	6.35	1930		
	1931	11,540	29,849,848	52.5	73.2	65.7	3.78	3.51	0.47	0.70	0.28	0.63	0.29	1.20	5.68	1931		
	1932	15,640	28,374,009	57.1	83.3	46.0	3.48	3.23	0.31	0.86	0.30	0.56	0.14	1.00	5.40	1932		
46	1931	9,250	Operation Greatly Reduced in 1932 because of lack of Load; Records Incomplete														46	
82	1930	5,630	7,958,851	31.3	65.0	35.9	5.71	5.22	0.52	3.73	1.38	1.91	1.08	4.37	13.86	1930	82	
	1931	5,660	8,778,880	33.2	69.0	39.1	5.13	4.93	0.45	2.94	0.92	1.96	1.22	4.10	12.42	1931		
	1932	8,930	9,065,633	33.0	60.3	40.5	4.48	4.52	0.63	2.81	0.47	1.13	1.57	3.17	11.13	1932		
168	1931	8,500	Operation Greatly Reduced in 1932 because of lack of Load; Records Incomplete														168	
52	1929	3,330	5,722,032	31.1	65.3	45.2	5.58	5.38	0.55	3.83	0.88	0.74	0.40	2.02	11.78	1929	52	
	1930	4,580	7,257,703	33.5	75.2	45.4	5.70	5.30	0.38	2.83	0.74	0.56	0.48	1.75	10.29	1930		
	1931	4,580	8,317,102	33.7	78.6	40.4	4.83	4.46	0.30	2.55	0.63	0.49	0.38	1.50	8.81	1931		
	1932	7,445	9,116,000	36.3	78.1	43.8	4.41	3.97	0.27	2.35	0.52	0.35	0.14	1.01	7.60	1932		
91	1929	3,450	7,565,725	46.6	52.0	72.8	3.90	3.72	0.48	1.18	0.16	0.22	0.07	0.45	5.83	1929	91	
	1930	5,250	8,157,025	53.7	53.1	52.4	4.09	3.95	0.29	1.06	0.16	0.33	0.04	0.53	5.33	1930		
	1931	5,250	7,734,325	48.2	59.3	45.0	3.20	3.03	0.27	1.21	0.26	-----	-----	0.70	5.21	1931		
	1932	5,250	6,490,050	48.6	58.4	38.4	3.12	2.93	0.36	1.57	0.14	0.12	0.05	0.31	5.17	1932		
73	1930	5,000	8,016,000	37.9	64.0	44.4	1.30	1.34	0.31	2.62	0.01	0.10	0.01	0.12	4.39	1930	73	
	1931	5,000	8,341,500	41.9	66.3	45.1	0.95	0.93	0.26	1.63	0.13	0.22	0.05	0.40	3.52	1931		
	1932	5,000	3,030,200	42.0	66.4	43.4	1.22	1.26	0.29	2.01	0.16	0.16	0.02	0.34	3.00	1932		
92	1929	2,500	6,662,389	44.1	71.6	61.6	2.15	2.20	0.55	1.24	0.17	1.85	0.12	2.14	6.13	1929	92	
	1930	4,900	10,027,739	58.8	65.0	61.1	2.09	2.25	0.33	0.92	0.26	0.26	0.06	0.58	4.08	1930		
	1931	4,900	9,378,900	52.9	63.5	53.1	2.03	2.12	0.36	1.08	0.20	-----	-----	0.70	4.26	1931		
	1932	4,900	7,451,947	44.2	56.2	39.3	2.04	2.05	0.28	1.34	0.26	0.54	0.03	0.83	4.50	1932		
129	1931	4,750	Operation Greatly Reduced in 1932 because of lack of Load; Records Incomplete.														129	
45	1929	4,250	7,442,350	36.8	72.5	43.6	5.23	5.04	0.09	1.65	0.06	-----	-----	0.32	7.70	1929	45	
	1930	4,250	6,908,500	34.9	69.5	42.4	5.29	5.18	0.09	1.77	0.04	1.01	0.10	1.15	8.20	1930		
	1931	4,250	5,537,000	46.4	66.5	36.6	4.79	4.89	0.09	2.04	0.07	1.28	0.55	1.90	8.32	1931		
	1932	4,250	5,015,575	42.3	62.1	35.8	3.87	4.07	0.11	2.05	0.05	1.33	0.32	1.70	7.33	1932		
54	1930	4,200	22,910,000	94.0	99.9	98.9	2.53	2.16	0.55	1.18	1.16	-----	-----	1.97	5.85	1930	54	
	1931	4,200	22,518,000	92.6	95.6	98.8	1.03	0.91	0.36	1.19	0.38	-----	-----	1.75	4.21	1931		
	1932	4,200	15,187,500	-----	95.1	98.7	1.38	1.24	0.29	1.02	0.54	-----	-----	1.07	3.32	1932		
864	1931	4,000	Not Operated in 1932 -- Reduced Industrial Activity														864	
130	1930	3,000	4,484,700	41.8	54.1	50.7	4.72	4.59	0.89	1.36	0.77	0.32	0.17	1.76	8.50	1930	130	
	1931	2,600	4,188,750	42.4	67.0	31.4	4.19	3.93	0.56	1.55	0.71	1.90	0.18	2.85	8.92	1931		
	1932	3,000	4,281,230	44.7	68.6	31.3	4.02	3.83	0.56	1.65	0.47	0.58	0.19	1.34	7.48	1932		
2	1929	3,450	16,479,500	83.2	94.4	84.5	2.71	2.62	0.33	1.40	0.13	-----	-----	0.47	4.82	1929	2	
	1930	3,450	15,077,095	78.8	94.3	77.1	2.18	1.98	0.45	1.14	0.09	1.56	0.09	1.74	5.31	1930		
	1931	3,450	17,745,325	88.5	97.8	89.8	2.11	2.00	0.26	1.09	0.08	1.16	0.09	1.33	4.86	1931		
	1932	3,450	8,639,511	-----	97.8	91.2	2.33	2.22	0.24	1.03	0.10	1.11	0.08	1.29	4.78	1932		
164	1930	3,360	14,709,450	81.4	90.7	72.7	3.66	2.91	0.31	1.38	0.16	1.12	0.19	1.47	6.07	1930	164	
	1931	3,360	11,037,481	59.5	76.3	76.9	3.34	2.56	0.28	1.73	0.35	1.52	0.30	2.17	6.84	1931		
	1932	3,360	12,838,281	-----	80.0	84.9	2.59	2.12	0.27	1.28	0.55	1.37	0.46	2.38	6.05	1932		
3	1929	3,125	2,341,730	32.1	42.2	36.2	4.53	5.95	0.54	5.62	0.47	1.20	0.15	1.82	13.93	1929	3	
	1930	3,125	2,357,153	27.8	40.4	32.7	5.00	5.49	0.46	4.71	0.23	1.94	0.03	2.10	12.76	1930		
	1931	3,125	No Reply to Inquiries for 1931														1931	
	1932	3,125	2,321,395	31.6	45.4	28.5	4.60	4.78	0.27	4.54	0.25	0.35	0.01	0.61	10.19	1932		
720	1930	3,060	3,225,050	34.7	52.5	35.7	3.99	5.21	0.94	1.37	0.37	0.26	0.35	0.98	8.50	1930	720	
	1931	3,060	3,124,300	34.1	-----	-----	3.07	4.42	1.10	1.43	0.22	0.05	0.35	0.62	7.67	1931		
	1932	3,060	2,920,600	34.8	45.8	35.9	2.92	4.45	0.59	1.24	0.07	0.20	0.01	0.28	6.56	1932		
109	1930	1,800	885,399	-----	48.1	16.3	5.53	6.33	1.26	3.76	0.88	0.60	0.11	1.59	12.96	1930	109	
	1931	2,825	1,858,860	-----	54.1	30.3	5.60	6.29	1.25	2.32	0.27	0.40	0.00	1.07	10.93	1931		
	1932	2,825	959,606	8.9	49.2	11.5	5.69	6.85	0.64	5.01	0.24	0.75	0.10	1.09	13.59	1932		
7	1929	1,830	3,231,938	36.0	64.8	53.2	5.77	5.31	0.36	3.03	1.74	-----	-----	3.96	12.71	1929	7	
	1930	2,730	3,211,821	38.0	61.8	53.1	4.79	4.52	0.35	3.17	1.19	1.57	0.31	3.07	11.11	1930		
	1931	2,730	3,088,885	43.9	57.3	36.4	3.43	3.08	0.39	3.79	0.38	1.28	0.51	2.47	9.72	1931		
	1932	2,730	3,105,742	42.5	57.9	36.3	3.27	2.78	0.25	3.29	0.42	0.96	0.39	1.77	8.09	1932		
732	1930	2,520	4,848,480	37.4	59.7	61.1	3.65	3.73	0.91	1.61	-----	-----	-----	2.08	8.33	1930	732	
	1931	2,520	2,632,385	25.0	49.1	44.1	2.82	3.68	1.14	2.19	0.59	1.33	0.77	2.69	9.70	1931		
	1932	2,520	3,497,637	27.5	50.4	47.4	3.17	3.27	0.73	2.09	0.57	2.48	0.37	3.42	9.51	1932		
978	1931	2,520	2,247,295	-----	-----	-----	3.33	3.11	0.47	1.23	0.42	-----	-----	0.71	5.52	1931	978	
	1932	2,520	2,223,652	14.4	87.6	17.5	3.57	3.11	0.27	1.41	0.35	-----	-----	0.74	5.53	1932		

TABLE II - COMPARATIVE COSTS - 1929, 1930, 1931 AND 1932 REPORTS (PAGE 2)

TABLE II - COMPARATIVE COSTS - 1929, 1930, 1931 AND 1932 REPORTS (PAGE 2)																		
PLANT NUMBER	YEAR	TOTAL INSTALLED B.H.P.	TOTAL NET OUTPUT K.W. HRS.	ANNUAL PLANT LOAD FACTOR	RUNNING PLANT CAPACITY FACTOR	PLANT SERVICE FACTOR	AVERAGE COST OF FUEL OIL - CENTS PER GALLON	COSTS PER NET K.W. HR. - MILLS								TOTAL PRODUCTION COST	YEAR	PLANT NUMBER
								FUEL COST	LUBRICATING OIL COST	ATTENDANCE COST, IN- CLUDING SUPERINTENDANCE	COST OF SUPPLIES AND MISCELLANEOUS INCLUD- ING WATER	COST OF ENGINE REPAIRS	COST OF ALL OTHER PLANT REPAIRS	TOTAL OF ALL SUPPLY, REPAIR, AND MISCELL- ANEOUS COSTS				
93	1929	1,960	2,838,950	27.4	44.8	59.4	4.16	5.25	0.52	2.50	0.15	0.38	0.09	0.62	8.89	1929	93	
	1930	1,960	2,659,910	30.9	43.4	58.6	4.09	5.35	0.39	2.65	0.16	0.51	0.02	0.69	9.08	1930		
	1931	1,960	3,403,390	29.9	52.3	60.6	2.79	3.36	0.38	2.14	0.13	---	---	0.44	6.32	1931		
	1932	2,480	4,058,720	34.9	52.0	68.5	5.09	3.78	0.42	1.81	0.10	0.67	0.05	0.82	6.83	1932		
60	1930	2,400	1,658,900	24.1	37.0	35.7	4.62	5.54	0.94	4.81	---	---	---	3.24	14.53	1930	60	
	1931	2,400	No Reply to Inquiries for 1931	---	---	---	---	---	---	---	---	---	---	---	---	1931		
	1932	2,400	1,015,200	15.7	24.8	32.3	4.68	7.48	0.73	5.22	0.60	---	---	2.76	16.19	1932		
	1932	2,400	---	---	---	---	---	---	---	---	---	---	---	---	---	---		1932
723	1930	1,320	1,270,520	19.7	68.0	26.3	5.62	6.46	1.15	4.01	0.39	2.37	0.97	3.73	15.35	1930	723	
	1931	2,370	1,556,510	---	73.3	---	4.21	4.23	0.95	3.56	0.53	0.86	0.70	2.09	10.83	1931		
	1932	2,370	1,371,460	10.9	67.2	15.4	4.31	4.13	0.74	3.71	0.76	---	---	2.55	11.13	1932		
	1932	2,370	---	---	---	---	---	---	---	---	---	---	---	---	---	---		1932
41	1929	2,370	3,798,810	39.6	---	---	5.51	5.43	0.48	4.11	0.24	0.22	0.07	0.53	10.55	1929	41	
	1930	2,370	4,068,290	39.2	59.0	44.2	5.19	5.09	0.48	4.08	0.37	0.63	0.15	1.15	10.80	1930		
	1931	2,370	4,092,730	39.4	67.3	44.2	4.57	4.48	0.51	3.85	0.25	0.24	0.13	0.62	9.46	1931		
	1932	2,370	3,698,090	35.6	65.5	41.0	4.10	3.86	0.62	4.05	0.23	0.26	0.08	0.57	9.10	1932		
79	1930	2,170	3,184,025	42.6	67.3	38.8	3.33	3.12	0.46	4.13	0.08	0.49	0.31	0.88	8.59	1930	79	
	1931	2,170	3,204,390	38.6	66.8	39.6	2.62	2.38	0.30	3.51	0.15	0.20	0.13	0.46	6.45	1931		
	1932	2,170	3,280,357	39.3	66.4	40.6	2.49	2.21	0.45	3.53	0.11	0.23	0	0.34	6.53	1932		
	1932	2,170	---	---	---	---	---	---	---	---	---	---	---	---	---	---		1932
5	1929	2,160	319,120	3.7	---	---	4.15	5.45	1.77	11.61	3.56	---	---	17.99	36.82	1929	5	
	1930	2,160	1,013,269	8.1	---	---	4.04	4.86	1.25	5.66	1.14	---	---	8.17	19.84	1930		
	1931	2,160	1,789,653	10.0	---	---	3.33	3.86	0.80	2.15	0.79	---	---	2.18	8.99	1931		
	1932	2,160	2,597,100	21.5	94.4	22.6	3.54	3.90	0.65	1.81	0.53	---	---	1.39	7.25	1932		
80	1931	2,150	No Reply to Inquiries for 1932	---	---	---	---	---	---	---	---	---	---	---	---	---	80	
	1929	2,100	1,318,898	10.0	---	---	4.70	4.17	0.72	2.67	0.47	---	---	1.61	9.17	1929		6
	1930	2,100	1,576,234	18.8	---	---	4.51	3.93	0.57	2.07	0.40	---	---	2.03	8.60	1930		
	1931	2,100	1,612,957	11.8	---	---	4.12	3.53	0.62	1.89	0.31	---	---	1.13	7.17	1931		
68	1930	2,060	1,720,413	11.7	97.4	14.5	3.94	3.40	0.45	1.64	0.25	---	---	1.05	6.54	1930	68	
	1931	2,060	3,336,860	59.4	67.5	42.7	3.37	3.30	0.44	1.41	0.11	0.31	0.37	0.79	8.94	1931		
	1932	2,060	3,038,210	54.8	63.9	40.9	3.60	3.60	0.42	1.54	0.18	0.43	0.08	0.69	6.25	1932		
	1932	2,060	---	---	---	---	---	---	---	---	---	---	---	---	---	---		1932
728	1931	2,040	No Reply to Inquiries for 1932	---	---	---	---	---	---	---	---	---	---	---	---	---	728	
	1930	1,000	1,512,520	33.6	51.6	53.1	6.75	6.37	0.46	7.34	0.54	1.00	0	1.54	15.71	1930		83
	1931	1,000	1,720,560	33.5	54.4	55.8	6.00	5.71	0.31	6.46	0.81	1.05	0	1.86	14.34	1931		
	1932	2,000	1,687,500	35.1	52.0	---	5.00	4.95	0.45	6.40	1.48	1.72	1.08	5.08	16.88	1932		
215	1930 ^d	1,960	1,372,941	---	78.5	17.5	5.40	4.68	0.58	1.12	0.33	0.01	0.10	0.44	6.82	1930	215	
	1931	1,960	1,568,700	13.1	89.9	15.5	3.97	3.45	0.21	1.40	0.38	0.53	0.08	0.89	6.05	1931		
	1932	1,960	1,163,370	9.8	84.2	12.3	5.14	3.84	0.29	1.48	0.55	0.07	0	0.62	6.23	1932		
	837	1930	1,875	2,016,465	33.2	49.0	38.8	3.07	3.80	0.68	7.39	0.66	3.32	1.12	5.10	16.97	1930	837
1931		1,875	2,101,374	35.9	51.1	40.2	2.72	3.43	0.65	6.01	0.49	3.36	0.92	4.77	14.86	1931		
1932		1,875	2,057,699	37.9	48.9	41.2	2.49	3.29	0.80	5.89	0.48	6.63	0.90	6.01	17.99	1932		
997		1931	1,800	Part Time Operation in 1932; Records Incomplete	---	---	---	---	---	---	---	---	---	---	---	---	---	997
	1931	1,750	228,700	3.6	69.6	3.2	4.43	4.13	0.51	2.21	0.28	0.09	0	0.37	7.22	1931	212	
	1932	1,750	217,147	4.4	71.8	2.9	3.60	3.22	0.30	2.14	0.29	6.40	0	6.69	12.35	1932		
	1932	1,750	---	---	---	---	---	---	---	---	---	---	---	---	---	---		
722	1930	1,705	796,450	9.3	82.1	11.2	5.61	5.97	0.69	7.99	1.49	1.19	0.90	3.58	18.23	1930		722
	1931	1,705	826,340	10.1	72.8	13.2	4.26	4.63	0.56	8.48	1.03	0.14	0.44	1.61	15.28	1931		
	1932	1,705	896,220	10.0	62.4	15.7	4.68	5.07	0.63	6.53	0.94	---	---	2.55	14.78	1932		
	735	1931	1,680	2,760,680	20.7	77.8	37.2	3.33	4.03	0.49	1.43	0.09	0.52	0.36	0.97	6.92	1931	735
1932		1,680	3,390,240	36.8	69.7	52.5	3.64	4.01	0.81	0.89	0.22	1.11	0.50	1.83	7.54	1932		
18		1929	1,650	2,351,123	26.4	---	---	4.71	4.52	0.41	2.58	0.38	---	---	2.30	9.81	1929	18
		1930	1,650	2,406,890	27.2	---	---	4.49	4.51	0.61	2.08	0.21	---	---	4.80	12.00	1930	
	1931	1,650	2,406,609	26.0	---	---	3.94	3.93	0.58	1.98	0.41	---	---	2.24	8.73	1931		
	1932	1,650	2,327,071	26.3	62.4	40.0	3.74	3.78	0.51	1.72	0.34	---	---	1.44	7.45	1932		
8	1930	1,560	2,049,000	34.2	57.0	39.1	3.37	3.40	0.58	4.68	0.70	0.27	0	0.97	9.63	1930	8	
	1931	1,560	1,876,410	33.4	58.7	35.3	2.81	2.92	0.41	3.61	---	---	---	0.54	7.48	1931		
	1932	1,560	1,627,980	31.4	55.0	32.7	3.04	3.26	0.54	4.85	---	---	---	0.62	9.27	1932		
	10	1931	1,500	Intermittent Operation in 1932; Records Incomplete	---	---	---	---	---	---	---	---	---	---	---	---	---	10
1930		1,500	1,446,160	33.9	63.5	29.9	4.64	4.98	0.32	4.51	0.34	0	0	0.34	10.15	1930	132	
1931		1,500	1,655,300	38.5	69.1	31.3	3.63	3.68	0.26	4.30	0.34	0	0	0.34	8.58	1931		
1932		1,500	1,665,900	36.7	65.7	29.9	3.56	3.31	0.24	4.41	0.33	0.02	0	0.35	8.31	1932		
289	1931	1,465	2,523,740	38.4	71.3	42.7	4.15	3.67	0.51	4.71	0.32	---	---	1.44	10.33	1931	289	
	1932	1,465	2,528,017	36.5	71.1	43.9	4.17	3.78	0.43	4.60	0.32	0.12	1.13	1.67	10.38	1932		
	865	1931	1,450	Not Operated During 1932; - Reduced Industrial Activity	---	---	---	---	---	---	---	---	---	---	---	---	---	865
		1930	1,420	1,980,400	---	---	---	3.68	3.81	0.44	3.84	0.13	0.12	0.05	0.30	8.39	1930	
1931		1,420	1,668,725	41.7	62.0	39.4	2.83	3.25	0.46	3.48	0.32	0.85	0.38	1.55	8.74	1931		
1932		1,420	1,675,057	38.4	54.3	41.5	3.03	3.71	0.53	4.25	0.27	0.53	0	0.80	9.29	1932		
163	1930	1,400	5,125,835	60.4	71.4	82.1	2.44	2.13	0.21	1.12	0.29	---	---	3.44	6.90	1930	163	
	1931	1,400	3,793,300	43.6	76.3	63.7	1.92	1.75	0.16	1.60	0.21	---	---	2.16	6.67	1931		
	1932	1,400	127,335	1.7	50.4	3.4	0.97	1.21	0.36	7.30	0.56	5.53	0.58	6.47	15.34	1932		
	154	1930	1,400	1,571,594	26.8	---	---	4.48	3.79	0.32	3.95	0.35	---	---	0.71	8.77	1930	154
1931		1,400	1,608,939	29.3	---	---	3.59	2.94	0.22	4.22	0.44	---	---	1.58	8.96	1931		
1932		1,400	1,521,613	29.4	81.9	23.0	3.47	2.81	0.29	4.18	0.33	---	---	0.81	8.09	1932		

TABLE II - COMPARATIVE COSTS - 1929, 1930, 1931 AND 1932 REPORTS (PAGE 3)

TABLE 11 - COMPARATIVE COSTS - 1929, 1930, 1931 AND 1932 REPORTS (PAGE 3)																	
PLANT NUMBER	YEAR	TOTAL INSTALLED B.H.P.	TOTAL NET OUTPUT K.W. HRS.	ANNUAL PLANT LOAD FACTOR	RUNNING PLANT CAPACITY FACTOR	PLANT SERVICE FACTOR	AVERAGE COST OF FUEL OIL - CENTS PER GALLON	COSTS PER NET K.W. HR. - MILLS								YEAR	PLANT NUMBER
								FUEL COST	LUBRICATING OIL COST	ATTENDANCE COST, IN- CLUDING SUPERINTENDANCE	COST OF SUPPLIES AND MISCELLANEOUS, INCLUD- ING WATER	COST OF ENGINE REPAIRS	COST OF ALL OTHER PLANT REPAIRS	TOTAL OF ALL SUPPLY, REPAIR, AND MISCELLANEOUS COSTS	TOTAL PRODUCTION COST		
11	1931	1,350	Intermittent Operation in 1932; Records Incomplete														11
13	1929	1,225	1,169,971	33.8	55.9	34.1	6.00	7.44	0.57	4.74	1.00	0.89	0.77	2.66	15.41	1929	13
	1930	1,225	1,131,661	32.7	59.2	31.2	5.69	6.60	0.65	4.88	0.54	0.39	0.08	1.01	13.14	1930	
	1931	1,225	1,259,958	38.4	58.3	34.1	5.41	6.29	0.73	4.69	0.24	0.31	0.05	0.60	12.31	1931	
	1932	1,225	1,176,048	36.0	57.4	32.4	5.13	5.94	0.68	4.50	0.48	0.59	0.37	1.44	12.56	1932	
725	1930	1,310	1,976,000	----	----	----	4.40	4.39	0.84	2.58	0.38	0.46	0.20	1.04	8.85	1930	725
	1931	1,310	2,640,671	----	----	----	3.35	3.16	0.58	1.78	0.40	0.21	0.15	0.76	6.28	1931	
	1932	1,200	3,324,653	59.8	74.4	63.8	3.62	3.43	0.81	1.70	0.18	0.24	0.02	0.44	6.38	1932	
451	1931 ⁶	1,200	833,560	----	----	----	3.25	3.47	0.82	4.02	0.36	0.12	0.27	0.75	9.06	1931	451
	1932	1,200	1,481,990	41.0	46.9	51.0	3.43	3.83	0.52	3.50	0.21	0.11	0.98	1.30	9.15	1932	
333	1931	1,200	606,740	9.1	83.3	10.8	5.40	5.40	1.80	5.00	4.00	2.47	0	6.47	18.67	1931	333
	1932	1,200	650,831	5.2	77.2	12.5	5.50	5.36	0.70	6.66	2.86	0.75	0.02	3.63	16.36	1932	
17	1929	1,200	1,611,876	20.7	----	----	4.52	4.69	0.53	2.64	0.67	----	----	2.11	9.97	1929	17
	1930	1,200	2,148,910	27.5	----	----	4.45	4.23	0.50	2.06	0.36	----	----	1.96	8.75	1930	
	1931	1,200	2,207,300	27.2	----	----	3.97	3.83	0.40	1.82	0.42	----	----	1.89	7.94	1931	
	1932	1,200	2,064,882	24.1	58.3	51.4	3.71	3.67	0.38	1.66	0.38	----	----	1.36	7.07	1932	
94	1931	1,200	Not Operated in 1932, Territory Served by High Line														94
980	1931	1,200	No Reply to Inquiries for 1932														980
616	1930	1,150	1,553,500	37.2	----	----	5.10	4.83	0.85	4.81	----	----	----	0.39	10.88	1930	616
	1931	1,150	1,609,550	38.8	----	----	4.50	4.35	0.76	4.32	----	2.48	----	2.79	12.22	1931	
	1932	1,150	1,565,000	39.0	56.5	44.7	4.51	4.31	0.64	4.04	1.06	1.97	0	3.03	12.02	1932	
95	1929	1,120	1,675,810	26.0	48.0	57.8	3.23	3.76	0.32	3.60	0.32	0.36	0.15	0.83	8.51	1929	95
	1930	1,120	1,408,900	23.3	50.7	45.4	3.12	3.83	0.21	3.54	0.38	0.68	0.02	1.08	8.66	1930	
	1931	1,120	869,940	21.4	51.9	27.4	2.36	2.91	0.23	4.05	0.42	----	----	1.14	8.33	1931	
	1932	1,120	365,350	9.7	84.2	6.9	2.38	2.44	0.09	1.48	0.25	0.03	0	0.28	4.29	1932	
96	1929	1,100	1,133,027	17.0	49.1	37.7	3.61	4.30	0.99	3.87	0.54	4.39	0.19	5.12	14.28	1929	96
	1930	1,100	1,215,181	24.3	61.5	32.2	3.56	3.54	0.66	4.26	0.43	0.78	0.21	1.42	9.88	1930	
	1931	1,100	967,500	19.7	50.9	31.5	2.74	2.95	0.45	5.03	0.20	----	----	1.47	9.90	1931	
	1932	1,100	727,300	17.7	41.2	29.8	2.82	3.51	0.84	5.78	0.32	0.62	0.18	1.12	11.25	1932	
721	1931	1,060	Incomplete Data Furnished For 1932														
78	1928/30 ^f	1,060	4,867,305	----	55.5	88.7	5.08	4.92	0.82	2.79	0.08	0.61	0.13	0.82	9.55	1928/30	78
	1931	1,060	1,906,347	31.4	46.5	69.2	5.07	5.88	1.13	4.69	0.23	0.15	0.19	0.57	12.27	1931	
	1932 ⁵	1,060	1,507,615	----	44.4	59.8	5.15	6.23	0.38	4.50	0.49	----	----	1.00	12.11	1932	
801	1930	1,000	4,110,052	74.3	74.6	94.9	3.82	4.19	0.43	1.25	0.79	0.89	0.17	1.85	7.72	1930	801
	1931	1,000	4,616,205	78.0	84.9	95.8	3.31	3.28	0.30	1.04	1.20	0.28	0.02	1.50	6.12	1931	
	1932	1,000	4,524,387	78.7	85.2	96.2	3.20	3.36	0.27	1.04	1.14	0.30	0.06	0.50	5.17	1932	
738	1931	1,000	1,091,000	21.9	76.3	25.7	3.00	3.47	0.60	3.73	0.46	1.28	0.35	2.09	9.89	1931	738
	1932	1,000	324,600	6.7	82.3	7.3	1.87	1.74	0.59	8.10	1.64	11.29	1.98	14.91	25.34	1932	
1061	1930	980	1,405,473	----	96.7	49.4	4.32	3.22	0.56	0.68	0.10	----	----	0.55	5.01	1930	1061
	1931	980	1,974,459	33.4	81.4	43.7	3.98	3.59	0.56	0.92	0.18	0.63	0.10	0.91	5.98	1931	
	1932	980	2,974,884	50.1	94.5	56.4	3.25	2.95	0.36	0.61	0.14	0.59	0.25	0.98	4.90	1932	
863	1930	1,100	2,136,540	41.0	69.4	52.7	3.55	3.29	0.91	1.76	0.46	2.32	0.06	2.84	8.80	1930	863
	1931	975	2,780,400	59.3	82.7	60.3	3.50	3.13	0.66	1.98	0.19	0.55	0.06	0.80	6.57	1931	
	1932	975	2,950,500	62.6	81.6	64.5	4.01	3.57	0.46	1.60	0.59	0.85	0.19	1.63	7.26	1932	
49	1931	970	Data Not Received for 1932														
98	1929	1,000	1,677,817	----	63.2	----	5.57	7.31	1.05	3.05	0.45	1.68	0.21	2.34	13.75	1929	98
	1930	900	1,774,521	39.9	64.5	56.7	4.73	6.37	0.90	3.28	0.60	1.00	0.31	1.91	12.46	1930	
	1931	1,000	1,352,480	35.4	65.8	38.0	3.44	4.85	0.50	3.67	0.64	----	----	2.42	11.44	1931	
	1932	900	1,500,880	42.8	61.5	48.9	3.74	4.59	0.47	3.04	0.41	0.30	0.09	0.80	8.90	1932	
53	1930	900	2,300,000	50.4	70.6	63.7	3.26	3.68	0.73	2.12	0.43	1.76	0.05	2.24	8.77	1930	53
	1931	900	2,355,470	52.8	71.0	65.2	2.65	3.06	0.53	2.00	0.42	2.94	0.05	3.41	9.00	1931	
	1932	900	1,975,660	44.2	69.0	56.2	2.55	2.90	0.41	2.21	0.41	3.79	0.02	4.22	9.74	1932	
260	1931	900	38,740	1.5	50.6	3.0	5.00	11.17	0.65	6.24	4.44	0	0	4.44	22.50	1931	260
	1932	900	68,369	1.7	47.0	3.6	3.39	5.34	1.42	5.26	0	0.18	0	0.18	12.20	1932	
74	1931	885	Incomplete Data Furnished for 1932 Because of Reduced Force:														
189	1930	850	800,000	32.4	27.4	59.5	4.10	5.22	0.93	8.63	1.03	----	----	2.53	17.31	1930	189
	1931	850	951,426	38.4	31.5	64.0	3.68	4.40	0.36	5.99	0.78	----	----	2.44	13.19	1931	
	1932	850	998,200	41.4	32.8	64.1	2.76	3.38	0.82	5.86	0.34	----	----	1.46	11.52	1932	
1056	1930	840	2,122,057	46.5	92.5	50.2	4.10	4.13	0.56	1.61	0.15	----	----	0.37	6.67	1930	1056
	1931	840	1,906,182	41.5	76.2	55.0	3.84	3.70	0.51	1.56	0.50	0.66	0.28	1.44	7.21	1931	
	1932	840	1,555,114	34.0	76.2	47.4	3.12	3.09	0.23	1.80	0.62	0.42	0.24	1.28	6.40	1932	
619	1931	840	828,880	18.1	74.1	23.9	3.72	3.21	0.65	1.66	0.85	1.70	0	2.55	8.07	1931	619
	1932	840	575,200	12.2	76.5	15.5	3.53	3.51	0.37	1.96	1.06	1.55	0.32	2.93	8.77	1932	
494	1931	840	915,865	21.4	76.8	24.7	3.56	3.09	0.34	1.89	0.70	0.61	0.28	1.59	6.61	1931	494
	1932	840	482,220	11.3	74.5	13.4	3.51	3.38	0.54	1.88	0.87	0.60	1.22	2.69	8.49	1932	
153	1930	840	49,340	2.2	----	----	4.08	7.70	1.01	44.30	11.92	----	----	24.43	77.44	1930	153
	1931	840	557,470	12.1	----	----	3.41	3.46	0.61	4.71	0.90	----	----	1.83	10.61	1931	
	1932	840	929,460	19.7	82.7	23.6	3.55	3.18	0.53	2.65	0.78	----	----	1.24	7.60	1932	

TABLE II - COMPARATIVE COSTS - 1929, 1930, 1931 AND 1932 REPORTS (PAGE 5)

TABLE II - COMPARATIVE COSTS - 1929, 1930, 1931 AND 1932 REPORTS (PAGE 5)																		
PLANT NUMBER	YEAR	TOTAL INSTALLED B.H.P.	TOTAL NET OUTPUT K.W. HRS.	ANNUAL PLANT LOAD FACTOR	RUNNING PLANT CAPACITY FACTOR	PLANT SERVICE FACTOR	AVERAGE COST OF FUEL OIL - CENTS PER GALLON	COSTS PER NET K.W. HR. - MILLS								YEAR	PLANT NUMBER	
								FUEL COST	LUBRICATING OIL COST	ATTENDANCE COST, IN- CLUDING SUPERINTENDANCE	COST OF SUPPLIES AND MISCELLANEOUS, INCLUD- ING WATER	COST OF ENGINE REPAIRS	COST OF ALL OTHER PLANT REPAIRS	TOTAL OF ALL SUPPLY, REPAIR, AND MISCELL- ANEOUS COSTS	TOTAL PRODUCTION COST			
194	1931	400	No Reply to	Inquiries for	1932													194
247	1930	390	428,290	28.9	----	----	6.00	8.12	1.10	10.79	0.11	0	0	0.11	20.12	1930	247	
	1931	390	480,204	25.1	44.6	47.1	4.62	6.03	1.01	9.62	0.05	0.40	0.26	0.71	17.37	1931		
	1932	390	485,760	24.7	54.2	39.2	4.55	5.88	0.81	9.76	0.07	0.12	0.05	0.24	16.69	1932		
105	1929 ^d	370	272,138	----	51.7	----	3.20	5.97	3.69	14.60	1.76	6.59	0.90	9.25	33.51	1929	105	
	1930	370	372,330	33.4	56.5	35.7	3.14	4.77	1.09	11.00	0.97	0.44	-0.17	1.58	18.44	1930		
	1931	370	349,820	33.1	47.4	39.2	2.67	4.25	1.01	8.66	0.38	----	----	1.35	15.27	1931		
	1932	370	346,440	35.9	45.5	41.2	2.35	3.92	1.01	8.32	0.40	1.75	0.24	2.39	15.64	1932		
1091	1931	360	349,169	33.6	36.2	49.8	5.33	8.11	1.50	12.02	2.10	----	----	2.79	24.42	1931	1091	
	1932	360	326,408	----	----	----	1.98	9.30	0.40	10.85	3.20	0.40	0.46	4.06	24.61	1932		
161	1931	360	981,240	44.8	95.4	49.5	5.33	4.45	0.76	2.72	0.22	0.10	0	0.32	8.25	1931	161	
	1932	360	982,300	45.7	----	----	3.96	3.44	0.68	2.49	0.16	0.68	0	0.84	7.45	1932		
152	1930	360	25,948	2.2	----	----	5.35	6.55	0.69	81.00	12.28	----	----	22.28	110.52	1930	152	
	1931	360	52,080	4.2	----	----	4.75	5.47	0.79	32.57	4.80	----	----	12.21	51.04	1931		
	1932	360	88	0.3	47.0	0.7	3.90	\$0.35	\$0.06	\$12.66	\$5.97	----	----	\$6.88	\$19.95	1932		
688	1931	350	437,000	----	----	----	5.00	6.69	0.65	6.86	0.51	0.17	0.69	1.37	15.57	1931	688	
	1932	350	432,500	29.3	42.6	49.8	3.93	5.32	0.45	8.32	0.12	0.25	0.12	0.49	14.58	1932		
365	1931	345	Data Not Received for 1932														365	
774	1931	345	109,735	7.2	66.2	8.4	3.79	4.74	0.71	9.97	3.03	6.09	1.07	10.19	25.61	1931	774	
	1932	345	77,122	5.1	72.6	5.5	3.58	3.31	1.03	6.57	3.52	1.36	2.97	7.85	18.76	1932		
857	1930	330	307,163	44.3	----	----	3.39	5.91	2.06	11.50	1.75	1.22	0.84	3.81	23.28	1930	857	
	1931	330	No Reply to	Inquiries for	1931											1931		
	1932	330	379,380	----	42.8	51.3	2.80	4.30	1.57	6.92	1.82	3.97	0.84	6.63	19.42	1932		
265	1930	180	184,000	----	----	----	9.14	13.48	1.76	13.58	1.10	0.71	0	1.81	30.63	1930	265	
	1931	320	216,000	----	----	37.0	7.79	11.81	1.83	11.57	0.32	0.46	0.58	1.36	26.57	1931		
	1932	320	220,000	25.4	37.9	34.3	7.30	11.00	1.86	11.37	0.16	0.11	0.34	0.61	24.84	1932		
27	1930	315	190,375	30.1	----	----	4.93	9.00	2.42	12.68	0.77	----	----	6.68	30.78	1930	27	
	1931	315	208,890	30.8	----	----	4.06	7.72	1.52	10.58	0.95	----	----	7.29	27.16	1931		
	1932	315	194,105	32.0	28.8	39.4	3.63	7.12	3.05	11.06	0.92	----	----	13.05	34.28	1932		
382	1931 ^a	300	86,887	----	20.5	37.4	3.35	3.62	0.82	4.47	0.43	0	0	0.43	9.34	1931	382	
	1932	300	99,300	----	21.2	28.4	3.48	4.76	0.66	5.08	0.42	0	0	0.42	10.92	1932		
1129	1931	300	195,850	30.4	29.7	40.7	4.02	7.69	2.38	16.28	0.92	5.52	0.83	7.27	33.62	1931	1129	
	1932	360	184,346	29.0	29.6	38.9	4.09	7.83	2.48	16.51	1.00	3.68	0.60	5.28	32.10	1932		
858	1930	180	123,538	23.0	----	----	3.41	6.87	3.26	31.90	4.02	4.66	2.08	10.76	52.79	1930	858	
	1931	180	No Replies to	Inquiries for	1931											1931		
	1932	270	175,200	----	26.7	49.7	2.82	6.46	2.78	17.45	3.31	1.54	0.43	5.28	31.97	1932		
156	1931	270	Incomplete	Data Furnished for	1932													
1097	1931	270	No Reply to	Inquiries for	1932													
516	1931	240	185,000	----	----	----	4.30	7.21	1.37	13.12	0.38	0	0	0.38	22.08	1931	516	
	1932	240	156,800	18.3	22.8	49.9	4.12	6.23	1.01	14.54	0.26	0.15	0	0.41	22.19	1932		
169	1930	240	151,850	11.3	41.5	27.1	5.98	6.23	0.94	2.56	0.55	0.51	0	1.06	10.79	1930	169	
	1931	240	184,360	13.7	42.5	31.9	5.56	6.23	0.89	2.11	0.87	4.39	0	5.26	14.49	1931		
	1932	240	77,310	5.8	27.7	20.9	5.04	6.52	1.25	3.84	0.85	----	----	14.77	26.38	1932		
222	1931	180	Incomplete	Data Furnished for	1932													
733	1930	175	14,800	1.6	65.0	1.6	4.82	5.54	2.91	8.92	2.91	0	0	2.91	20.28	1930	733	
	1931	175	3,293	0.3	62.5	0.5	5.78	10.93	0.91	10.93	9.72	0	0	9.72	32.49	1931		
	1932	175	1,788	0.2	62.1	0.3	3.00	7.92	1.96	18.18	34.30	0.56	20.43	55.29	63.35	1932		
646	1930	120	15,893	3.8	13.7	7.0	7.00	12.65	3.15	147.25	11.26	0	0	11.26	174.31	1930	646	
	1931	120	21,035	5.3	16.1	20.4	7.00	16.70	2.57	16.97	3.28	0	0	3.28	39.52	1931		
	1932	120	5,832	1.6	13.4	7.6	5.37	18.82	5.70	27.14	0	0	0	0	51.66	1932		
201	1931	100	Reported "No Data" For 1932														201	
NOTES:																		
			a - 8 months															
			b - 8.1 "															
			c - 13 "															
			d - 10 "															
			e - 7.5 "															
			f - 36 "															
			g - 11 "															

NOTES:

- a - 8 months
 b - 8.1 "
 c - 13 "
 d - 10 "
 e - 7.5 "
 f - 36 "
 g - 11 "

TABLE III - INFORMATION COVERING LUBRICATING OIL (PAGE 1)

[illegible]

TABLE III - INFORMATION COVERING LUBRICATING OIL (PAGE 2)

PLANT NUMBER	ENGINE DESIGNATION	ENGINE CYCLE	INJECTION SYSTEM (See Note)	EXHAUST SYSTEM (See Note)	CRANK PISTON OR CROSS-HEAD?	CYLINDERS OPEN OR CLOSED TO CHAMBER?	RATED B.H.P.	EQUIVALENT K.W. - 60% GENERATING EFFICIENCY	NUMBER OF CYLINDERS	CYLINDER BORE - INCHES	STROKE - INCHES	RATED R.P.M.	GENERATOR RATING - K.W.A.	YEAR ENGINE STARTED TO WORK	ENGINE HOURS OPERATED IN REPORTED PERIOD	RATED HORSEPOWER HOURS IN REPORTED PERIOD	TOTAL GALLONS OF NEW LUBRICATING OIL USED	GALLONS OF NEW LUBRICATING OIL FOR CYLINDER LUBRICATION ONLY	GALLONS OF UNFIT LUBRICATING OIL DISCARDED	RATED H.P. HRS. PER GALLON OF NEW LUBRICATING OIL	ENGINE CAPACITY FACTOR (See Text)	ENGINE PLANT CAPACITY FACTOR (See Text)	GROSS OUTPUT - K.W. HRS.	GROSS K.W. HRS. PER GALLON OF NEW LUBRICATING OIL	LUBRICATING OIL TREATMENT (See Note)	AVERAGE COST OF LUBRICATING OIL - CENTS PER GALLON
978	12 M V P	0	0	0	0	0	840	564	6	16	20	257	700	1931	1,509	1,267,560	-----	-----	-----	-----	-----	-----	-----	-----	-----	-----
	Plant						2,580	1,692	6	16	20	257	700	1931	1,527	1,114,680	-----	-----	-----	-----	-----	-----	-----	-----	-----	-----
908	12 M V P	0	0	0	0	0	1,250	840	5	20.75	26	180	1,100	1925	6,152	7,690,000	-----	-----	-----	-----	-----	-----	-----	-----	-----	51.2
	Plant						2,500	1,680	5	20.75	26	180	1,100	1925	6,284	15,543,750	3,980	1,098	3,366	69.8	67.6	68.5	3,604,300	1,976	CC & S	-----
93	12 M V P	0	0	0	0	0	700	470	5	16	20	257	600	1928	5,680	3,976,000	-----	-----	-----	-----	-----	-----	-----	-----	-----	38.4
	Plant						700	470	5	16	20	257	600	1928	5,680	3,976,000	-----	-----	-----	48.0	-----	-----	-----	1,281,100	-----	-----
							560	376	4	16	20	257	400	1924	3,439	4,549,300	-----	-----	-----	51.3	-----	-----	-----	1,569,300	-----	CC
							520	348	4	16	20	257	400	1924	3,439	4,549,300	-----	-----	-----	51.3	-----	-----	-----	1,569,300	-----	CC
							520	348	4	16	20	257	400	1924	3,439	4,549,300	-----	-----	-----	51.3	-----	-----	-----	1,569,300	-----	CC
							520	348	4	16	20	257	400	1924	3,439	4,549,300	-----	-----	-----	51.3	-----	-----	-----	1,569,300	-----	CC
							520	348	4	16	20	257	400	1924	3,439	4,549,300	-----	-----	-----	51.3	-----	-----	-----	1,569,300	-----	CC
							520	348	4	16	20	257	400	1924	3,439	4,549,300	-----	-----	-----	51.3	-----	-----	-----	1,569,300	-----	CC
							520	348	4	16	20	257	400	1924	3,439	4,549,300	-----	-----	-----	51.3	-----	-----	-----	1,569,300	-----	CC
							520	348	4	16	20	257	400	1924	3,439	4,549,300	-----	-----	-----	51.3	-----	-----	-----	1,569,300	-----	CC
							520	348	4	16	20	257	400	1924	3,439	4,549,300	-----	-----	-----	51.3	-----	-----	-----	1,569,300	-----	CC
							520	348	4	16	20	257	400	1924	3,439	4,549,300	-----	-----	-----	51.3	-----	-----	-----	1,569,300	-----	CC
							520	348	4	16	20	257	400	1924	3,439	4,549,300	-----	-----	-----	51.3	-----	-----	-----	1,569,300	-----	CC
							520	348	4	16	20	257	400	1924	3,439	4,549,300	-----	-----	-----	51.3	-----	-----	-----	1,569,300	-----	CC
							520	348	4	16	20	257	400	1924	3,439	4,549,300	-----	-----	-----	51.3	-----	-----	-----	1,569,300	-----	CC
							520	348	4	16	20	257	400	1924	3,439	4,549,300	-----	-----	-----	51.3	-----	-----	-----	1,569,300	-----	CC
							520	348	4	16	20	257	400	1924	3,439	4,549,300	-----	-----	-----	51.3	-----	-----	-----	1,569,300	-----	CC
							520	348	4	16	20	257	400	1924	3,439	4,549,300	-----	-----	-----	51.3	-----	-----	-----	1,569,300	-----	CC
							520	348	4	16	20	257	400	1924	3,439	4,549,300	-----	-----	-----	51.3	-----	-----	-----	1,569,300	-----	CC
							520	348	4	16	20	257	400	1924	3,439	4,549,300	-----	-----	-----	51.3	-----	-----	-----	1,569,300	-----	CC
							520	348	4	16	20	257	400	1924	3,439	4,549,300	-----	-----	-----	51.3	-----	-----	-----	1,569,300	-----	CC
							520	348	4	16	20	257	400	1924	3,439	4,549,300	-----	-----	-----	51.3	-----	-----	-----	1,569,300	-----	CC
							520	348	4	16	20	257	400	1924	3,439	4,549,300	-----	-----	-----	51.3	-----	-----	-----	1,569,300	-----	CC
							520	348	4	16	20	257	400	1924	3,439	4,549,300	-----	-----	-----	51.3	-----	-----	-----	1,569,300	-----	CC
							520	348	4	16	20	257	400	1924	3,439	4,549,300	-----	-----	-----	51.3	-----	-----	-----	1,569,300	-----	CC
							520	348	4	16	20	257	400	1924	3,439	4,549,300	-----	-----	-----	51.3	-----	-----	-----	1,569,300	-----	CC
							520	348	4	16	20	257	400	1924	3,439	4,549,300	-----	-----	-----	51.3	-----	-----	-----	1,569,300	-----	CC
							520	348	4	16	20	257	400	1924	3,439	4,549,300	-----	-----	-----	51.3	-----	-----	-----	1,569,300	-----	CC
							520	348	4	16	20	257	400	1924	3,439	4,549,300	-----	-----	-----	51.3	-----	-----	-----	1,569,300	-----	CC
							520	348	4	16	20	257	400	1924	3,439	4,549,300	-----	-----	-----	51.3	-----	-----	-----	1,569,300	-----	CC
							520	348	4	16	20	257	400	1924	3,439	4,549,300	-----	-----	-----	51.3	-----	-----	-----	1,569,300	-----	CC
							520	348	4	16	20	257	400	1924	3,439	4,549,300	-----	-----	-----	51.3	-----	-----	-----	1,569,300	-----	CC
							520	348	4	16	20	257	400	1924	3,439	4,549,300	-----	-----	-----	51.3	-----	-----	-----	1,569,300	-----	CC
							520	348	4	16	20	257	400	1924	3,439	4,549,300	-----	-----	-----	51.3	-----	-----	-----	1,569,300	-----	CC
							520	348	4	16	20	257	400	1924	3,439	4,549,300	-----	-----	-----	51.3	-----	-----	-----	1,569,300	-----	CC
							520	348	4	16	20	257	400	1924	3,439	4,549,300	-----	-----	-----	51.3	-----	-----	-----	1,569,300	-----	CC
							520	348	4	16	20	257	400	1924	3,439	4,549,300	-----	-----	-----	51.3	-----	-----	-----	1,569,300	-----	CC
							520	348	4	16	20	257	400	1924	3,439	4,549,300	-----	-----	-----	51.3	-----	-----	-----	1,569,300	-----	CC
							520	348	4	16	20	257	400	1924	3,439	4,549,300	-----	-----	-----	51.3	-----	-----	-----	1,569,300	-----	CC
							520	348	4	16	20	257	400	1924	3,439	4,549,300	-----	-----	-----	51.3	-----	-----	-----	1,569,300	-----	CC
							520	348	4	16	20	257	400	1924	3,439	4,549,300	-----	-----	-----	51.3	-----	-----	-----	1,569,300	-----	CC
							520	348	4	16	20	257	400	1924	3,439	4,549,300	-----	-----	-----	51.3	-----	-----	-----	1,569,300	-----	CC
							520	348	4	16	20	257	400	1924	3,439	4,549,300	-----	-----	-----	51.3	-----	-----	-----	1,569,300	-----	CC
							520	348	4	16	20	257	400	1924	3,439	4,549,300	-----	-----	-----	51.3	-----	-----	-----	1,569,300	-----	CC
							520	348	4	16	20	257	400	1924	3,439	4,549,300	-----	-----	-----	51.3	-----	-----	-----	1,569,300	-----	CC
							520	348	4	16	20	257	400	1924	3,439	4,549,300	-----	-----	-----	51.3	-----	-----	-----	1,569,300	-----	CC
							520	348	4	16	20	257	400	1924	3,439	4,549,300	-----	-----	-----	51.3	-----	-----	-----	1,569,300	-----	CC
							520	348	4	16	20	257	400	1924	3,439	4,549,300	-----	-----	-----	51.3	-----	-----	-----	1,569,300	-----	CC
							520	348	4	16	20	257	400	1924	3,439	4,549,300	-----	-----	-----	51.3	-----	-----	-----	1,569,300	-----	CC
							520	348	4	16	20	257	400	1924	3,439	4,549,300	-----	-----	-----	51.3	-----	-----	-----	1,569,300	-----	CC
							520	348	4	16	20	257	400	1924	3,439	4,549,300	-----	-----	-----	51.3	-----	-----	-----	1,569,300	-----	CC
							520	348	4	16	20	257	400	1924	3,439	4,549,300	-----	-----	-----	51.3	-----	-----	-----	1,569,300	-----	CC
							520	348	4	16	20	257	400	1924	3,439	4,549,300	-----	-----	-----	51.3	-----	-----	-----	1,569,300	-----	CC
							520	348	4	16	20	257	400	1924	3,439	4,549,300	-----	-----	-----	51.3	-----	-----	-----	1,569,300	-----	CC
							520	348	4	16	20	257	400	1924	3,439	4,549,300	-----	-----	-----	51.3	-----	-----	-----	1,569,300	-----	CC
							520	348	4	16	20	257	400	1924	3,439	4,549,300	-----	-----	-----	51.3	-----	-----	-----	1,569,300	-----	CC
							520	348	4	16	20	257	400	1924	3,439	4,549,300	-----	-----	-----	51.3	-----	-----	-----	1,569,300	-----	CC
							520	348	4	16	20	257	400	1924	3,439	4,549,300	-----	-----	-----	51.3	-----	-----	-----	1,569,300	-----	CC
							520	348	4	16	20	257	400	1924	3,439	4,549,300	-----	-----	-----	51.3	-----	-----	-----	1,569,300	-----	CC
							520	348	4	16	20															

TABLE III - INFORMATION COVERING LUBRICATING OIL (PAGE 3)

[illegible]

TABLE III - INFORMATION COVERING LUBRICATING OIL (PAGE 4)

PLANT NUMBER	ENGINE DESIGNATION	ENGINE CYCLE	INJECTION SYSTEM (See Notes)	OVERHAUL SYSTEM (See Notes)	OPERATION OR CRASHDOWN	CRASHDOWN ON CLOSED TO CHAMBERS?	RATED B.H.P.	SECTORAL K.W. - 80% GENERATING EFFICIENCY	NUMBER OF CYLINDERS	CYLINDER BORE - INCHES	STROKE - INCHES	RATED R.P.M.	GENERATOR RATIO - K.V.A.	YEAR ENGINE STARTED TO WORK	ENGINE HOURS OPERATED IN REPORTED PERIOD	RATED RESERVE POWER IN REPORTED PERIOD	TOTAL GALLONS OF NEW LUBRICATING OIL USED	GALLONS OF NEW LUBRICATING OIL FOR CYLINDER LUBRICATION ONLY	GALLONS OF UNFIT LUBRICATING OIL DISCARDED	RATED H.P. HRS. PER GALLON OF NEW LUBRICATING OIL	ENGINE CAPACITY FACTOR (See Text)	ENGINE PLANT CAPACITY FACTOR (See Text)	CRASH OUTPUT - K.W. HRS.	GROSS K.W. HRS. PER GALLON OF NEW LUBRICATING OIL	LUBRICATING OIL TREATMENT (See Notes)	AVERAGE COST OF LUBRICATING OIL - CENTS PER GALLON
616	1 4 A	1 4 A	1 4 A	1 4 A	1 4 A	1 4 A	300	202	3	16.5	23	200	250	1923	4,588	1,976,400	750	0	1,835	70.4			652,010	865	CC	52.2
	1 4 A	1 4 A	1 4 A	1 4 A	1 4 A	1 4 A	100	67	4	14	17	257	75	1920	161	16,100	31	0	519	50.0			8,700	333		
	1 4 A	1 4 A	1 4 A	1 4 A	1 4 A	1 4 A	750	504	14	32	150	657	1925	4,186	3,117,000	1,133	0	2,750	50.1			1,049,600	926			
	1 4 A	1 4 A	1 4 A	1 4 A	1 4 A	1 4 A	1,150	775	17	24	226	938			4,509,500	1,914	0	2,355				1,711,510	884			
887	1 2 A	1 2 A	1 2 A	1 2 A	1 2 A	1 2 A	150	101	3	14	17	257	125	1922	24	3,600									BC	
	1 2 A	1 2 A	1 2 A	1 2 A	1 2 A	1 2 A	350	369	5	15	20	225	375	1930	8,495	3,736,920									BC	
	1 2 A	1 2 A	1 2 A	1 2 A	1 2 A	1 2 A	1,140	765	17	24	226	938			3,876,920	1,396								BC		
95	1 2 A	1 2 A	1 2 A	1 2 A	1 2 A	1 2 A	560	376	4	16	20	257	469	1929	370	207,200									BC	
	1 2 A	1 2 A	1 2 A	1 2 A	1 2 A	1 2 A	560	376	4	16	20	257	469	1929	370	468,160									BC	
	1 2 A	1 2 A	1 2 A	1 2 A	1 2 A	1 2 A	1,120	752	17	24	226	938			675,360	83								BC		
96	1 4 A	1 4 A	1 4 A	1 4 A	1 4 A	1 4 A	600	403	6	17	24	225	500	1925	849	509,400									BC	
	1 4 A	1 4 A	1 4 A	1 4 A	1 4 A	1 4 A	200	202	3	17	24	225	250	1923	7,476	2,242,800									BC	
	1 4 A	1 4 A	1 4 A	1 4 A	1 4 A	1 4 A	200	134	4	14	17	257	170	1921	584	116,800									BC	
	1 4 A	1 4 A	1 4 A	1 4 A	1 4 A	1 4 A	1,100	755	17	24	226	920			2,869,000	1,435									BC	
143	1 2 A	1 2 A	1 2 A	1 2 A	1 2 A	1 2 A	350	242	6	14	17	257	300	1928											BC	
	1 2 A	1 2 A	1 2 A	1 2 A	1 2 A	1 2 A	350	242	6	14	17	257	300	1928											BC	
	1 2 A	1 2 A	1 2 A	1 2 A	1 2 A	1 2 A	1,080	726	17	24	226	900				2,225									BC	
78	1 2 A	1 2 A	1 2 A	1 2 A	1 2 A	1 2 A	400	269	4	17	24	225	375	1928	3,936	1,574,400									BC	
	1 2 A	1 2 A	1 2 A	1 2 A	1 2 A	1 2 A	650	443	6	17	24	240	625	1930	5,385	3,554,100									BC	
	1 2 A	1 2 A	1 2 A	1 2 A	1 2 A	1 2 A	1,080	712	17	24	240	1,000			5,128,500	1,725								BC		
519	1 2 A	1 2 A	1 2 A	1 2 A	1 2 A	1 2 A	200	134	4	14	17	257	170	1925											BC	
	1 2 A	1 2 A	1 2 A	1 2 A	1 2 A	1 2 A	550	202	6	14	17	257	250	1925											BC	
	1 2 A	1 2 A	1 2 A	1 2 A	1 2 A	1 2 A	1,050	712	17	24	226	890				2,541									BC	
144	1 2 A	1 2 A	1 2 A	1 2 A	1 2 A	1 2 A	210	141	3	14	17	300	167	1931	4,532	1,035,720									BC	
	1 2 A	1 2 A	1 2 A	1 2 A	1 2 A	1 2 A	420	282	6	14	17	300	353	1931	3,240	1,350,800									BC	
	1 2 A	1 2 A	1 2 A	1 2 A	1 2 A	1 2 A	420	282	6	14	17	300	353	1931	3,276	1,375,920									BC	
	1 2 A	1 2 A	1 2 A	1 2 A	1 2 A	1 2 A	1,050	705	17	24	226	873			3,772,440	2,079								BC		
250	1 2 A	1 2 A	1 2 A	1 2 A	1 2 A	1 2 A	210	141	3	14	17	300	170	1931	6,177	1,297,170									BC	
	1 2 A	1 2 A	1 2 A	1 2 A	1 2 A	1 2 A	350	242	6	14	17	257	300	1926	1,767	636,120									BC	
	1 2 A	1 2 A	1 2 A	1 2 A	1 2 A	1 2 A	460	322	4	16	20	257	400	1926	968	474,240									BC	
	1 2 A	1 2 A	1 2 A	1 2 A	1 2 A	1 2 A	1,050	705	17	24	226	870			2,407,530	1,260									BC	
203	1 2 A	1 2 A	1 2 A	1 2 A	1 2 A	1 2 A	525	352	5	14	17	300	447	1931	3,898	2,046,450									BC	
	1 2 A	1 2 A	1 2 A	1 2 A	1 2 A	1 2 A	525	352	5	14	17	300	447	1931	4,064	2,135,600									BC	
	1 2 A	1 2 A	1 2 A	1 2 A	1 2 A	1 2 A	1,030	704	17	24	226	894			4,160,050	2,829									BC	
801	1 2 A	1 2 A	1 2 A	1 2 A	1 2 A	1 2 A	1,000	671	4	20.75	26	180	937	1927	8,451	8,451,000									BC	
738	1 4 A	1 4 A	1 4 A	1 4 A	1 4 A	1 4 A	1,000	671	6	22	32	150	900	1916	640	640,000									BC	
1061	1 2 A	1 2 A	1 2 A	1 2 A	1 2 A	1 2 A	980	658	7	16	20	257	975	1930	4,955	4,855,900									BC	
863	1 2 A	1 2 A	1 2 A	1 2 A	1 2 A	1 2 A	300	202	3	17	24	200	250	1925	8,601	1,980,300									BC	
	1 2 A	1 2 A	1 2 A	1 2 A	1 2 A	1 2 A	675	453	6	17	24	225	655	1927	5,260	3,550,500									BC	
	1 2 A	1 2 A	1 2 A	1 2 A	1 2 A	1 2 A	975	655	17	24	226	875			6,530,800	2,035									BC	
1065	1 2 A	1 2 A	1 2 A	1 2 A	1 2 A	1 2 A	900	605	6	16	20	257	774	1931	755	679,500									BC	
560	1 2 A	1 2 A	1 2 A	1 2 A	1 2 A	1 2 A	200	134	4	12.5	13.25	327	169	1924	4,927	985,400									BC	
	1 2 A	1 2 A	1 2 A	1 2 A	1 2 A	1 2 A	200	134	4	12.5	13.25	327	169	1924	4,927	985,400									BC	
	1 2 A	1 2 A	1 2 A	1 2 A	1 2 A	1 2 A	900	604	5	17	24	200	776	1924	1,814	907,000									BC	
260	1 2 A	1 2 A	1 2 A	1 2 A	1 2 A	1 2 A	900	605	6	14.75	21	257	750	1928	319	287,100									BC	
98	1 2 A	1 2 A	1 2 A	1 2 A	1 2 A	1 2 A	350	242	6	14	17	257	300	1926	4,043	1,455,480									BC	
	1 2 A	1 2 A	1 2 A	1 2 A	1 2 A	1 2 A	350	242	6	14	17	257	300	1929	4,006	1,442,160									BC	
	1 2 A	1 2 A	1 2 A	1 2 A	1 2 A	1 2 A	180	121	3	14	17	257	140	1926	5,366	969,480									BC	
	1 2 A	1 2 A	1 2 A	1 2 A	1 2 A	1 2 A	900	605	17	24	226	740			3,867,120	1,749									BC	
53	1 2 A	1 2 A	1 2 A	1 2 A	1 2 A	1 2 A	200	134	4	14	17	257	170	1923	1,959	391,800									BC	
	1 2 A	1 2 A	1 2 A	1 2 A	1 2 A	1 2 A	300	201	6	14	17	257	250	1923	2,544	763,200									BC	
	1 2 A	1 2 A	1 2 A	1 2 A	1 2 A	1 2 A	400	269	4	16.25	25	225	338	1925	8,221	3,288,400									BC	
	1 2 A	1 2 A	1 2 A	1 2 A	1 2 A	1 2 A	900	604	17	24	226	758			4,440,400	2,094									BC	
109	1 4 A	1 4 A	1 4 A	1 4 A	1 4 A	1 4 A	550	369	5	17	24	240	470	1929	8,643	4,755,650									BC	
	1 4 A	1 4 A	1 4 A	1 4 A	1 4 A	1 4 A	200	134	2	17	24	200	170	1922	141	28,200									BC	
	1 4 A	1 4 A	1 4 A	1 4 A	1 4 A	1 4 A	100	67	1	17	24	200	90	1915	0	0									BC	
	1 4 A	1 4 A	1 4 A	1 4 A	1 4 A	1 4 A	850	570	17	24	226	730			4,781,850	1,272									BC	
1056	1 2 A	1 2 A	1 2 A	1 2 A	1 2 A	1 2 A	840	564	6	16	20	257	700	1929	4,166	3,499,440									BC	
619	1 2 A	1 2 A	1 2 A	1 2 A	1 2 A	1 2 A	840	564	6	16	20	257	700	1929	1,363	1,144,920									BC	
494	1 2 A	1 2 A	1 2 A	1 2 A	1 2 A	1 2 A	840	564	6	16	20	257	700	1930	1,178	989,520									BC	
163	1 2 A	1 2 A	1 2 A	1 2 A	1 2 A	1 2 A	840	564	6	16	20	257	700	1929	2,078	1,745,520									BC	
731	1 4 A	1 4 A	1 4 A	1 4 A	1 4 A	1 4 A	625	554	4	23	32	164	750	1928	1,555	1,282,675									BC	
648	1 4 A	1 4 A	1 4 A	1																						

TABLE III - INFORMATION COVERING LUBRICATING OIL (PAGE 5)

TABLE III - INFORMATION COVERING LUBRICATING OIL (PAGE 5)																													
PLANT NUMBER	ENGINE DESIGNATION	ENGINE CODE	INJECTION SYSTEM (See Notes)	SCAVENING SYSTEM (See Notes)	TRIMMING PISTON OR CROSSHEAD?	CYLINDERS OPEN OR CLOSED TO CRANKCASE?	RATED B.P.P.	EXHAUSTING K.W. - 80% OPERATING EFFICIENCY	NUMBER OF CYLINDERS	CYLINDER BORE - INCHES	STROKE - INCHES	RATED R.P.M.	GENERATOR RATING - K.V.A.	YEAR ENGINE STARTED TO WORK	ENGINE HOURS OPERATED IN REPORTED PERIOD	RATED HORSEPOWER HOURS IN REPORTED PERIOD	TOTAL GALLONS OF NEW LUBRICATING OIL USED	GALLONS OF NEW LUBRICATING OIL FOR CYLINDER LUBRICATION ONLY	GALLONS OF DRIFT LUBRICATING OIL DISCARDED	RATED H.P. HRS. PER GALLON OF NEW LUBRICATING OIL	RUNNING ENGINE CAPACITY FACTOR (See Text)	RUNNING PLANT CAPACITY FACTOR (See Text)	GROSS OUTPUT - K.W. HRS.	GROSS K.W. HRS. PER GALLON OF NEW LUBRICATING OIL	LUBRICATING OIL TREATMENT (See Text)	AVERAGE COST OF LUBRICATING OIL - CENTS PER GALLON			
52	1 Plant	12 M	C	C			350	232	6	14	17	257	300	1930	5,404	1,945,440	-----	-----	0	-----	-----	-----	-----	-----	-----	-----			
	2 Plant	12 M	C	C			350	242	6	14	17	257	300	1930	5,000	1,800,000	-----	-----	0	-----	-----	-----	-----	-----	-----	-----			
	3 Plant	12 M	C	C			720	484	6	14	17	257	600	-----	-----	3,745,440	1,281	-----	0	2,924	-----	39.6	997,200	778	C & S	61.0			
170	1 Plant	12 M	C	C			350	242	6	14	17	257	300	1925	2,425	874,440	614	82	1,424	-----	-----	-----	-----	-----	-----	-----			
	2 Plant	12 M	C	C			350	242	6	14	17	257	300	1925	2,572	925,920	629	70	1,471	-----	-----	-----	-----	-----	-----	-----			
	3 Plant	12 M	C	C			720	484	6	14	17	257	600	-----	-----	1,800,360	1,243	152	1,447	-----	-----	56.2	703,156	566	F & S	45.6			
67	1 Plant	12 M	C	C			350	242	6	14	17	257	250	1925	2,122	765,920	816	62	936	81.5	-----	-----	-----	-----	-----	-----			
	2 Plant	12 M	C	C			350	242	6	14	17	257	250	1925	1,998	719,280	993	74	724	81.4	-----	-----	-----	-----	-----	-----			
	3 Plant	12 M	C	C			720	484	6	14	17	257	500	-----	-----	1,483,200	1,809	136	820	-----	-----	81.5	811,000	448	F & C	42.2			
19	1 Plant	12 M	C	C			1001	67	2	14	17	257	---	---	2,137	213,700	-----	-----	-----	-----	-----	-----	-----	-----	-----	-----			
	2 Plant	12 M	C	C			240	161	4	12.5	13.25	325	---	---	2,975	1,276,560	-----	-----	-----	-----	-----	-----	-----	-----	-----	-----			
	3 Plant	12 M	C	C			350	242	6	14	17	257	---	---	2,927	544,880	-----	-----	-----	-----	-----	-----	-----	-----	-----	-----			
	4 Plant	12 M	C	C			700	470	4	15.25	16	275	---	---	1,513	2,034,940	1,544	---	---	1,318	-----	46.5	661,930	429	CC & C	53.7			
411	1 Plant	12 M	C	C			2001	131	4	14	17	257	140	1914	40	8,000	-----	-----	-----	-----	-----	-----	-----	-----	-----	-----			
	2 Plant	12 M	C	C			120	81	4	14	17	257	90	1922	2,892	347,040	-----	-----	-----	-----	-----	-----	-----	-----	-----	-----			
	3 Plant	12 M	C	C			350	242	6	14	17	257	240	1930	5,867	2,112,120	1,406	75	1,755	-----	39.7	657,670	468	CC & C	37.2				
	4 Plant	12 M	C	C			680	457	6	14	17	257	470	-----	-----	2,467,160	1,406	-----	-----	-----	-----	-----	-----	-----	-----	-----			
529	1 Plant	12 M	C	C			1001	67	2	14	17	257	75	1922	1,062	106,200	85	0	1,249	-----	-----	-----	-----	-----	-----	-----			
	2 Plant	12 M	C	C			1001	67	2	14	17	257	75	1922	1,009	100,900	90	0	1,122	-----	-----	-----	-----	-----	-----	-----			
	3 Plant	12 M	C	C			300	201	6	10.5	12.5	360	250	1931	4,591	514,200	349	0	2,618	-----	-----	-----	-----	-----	-----	-----			
	4 Plant	12 M	C	C			620	416	6	10.5	12.5	360	490	-----	-----	2,098,600	1,050	0	2,000	-----	38.4	541,636	516	BC & F	45.0				
106	1 Plant	14 A	TF	O			600	403	6	17	26	200	---	1929	4,899	2,939,400	701	---	---	4,190	71.4	71.4	1,409,410	2,012	---	53.0			
109C	1 Plant	14 A	TF	O			600	403	6	16.25	23	225	513	1928	2,576	1,546,600	700	200	2,208	69.9	69.9	725,880	1,037	BC&S&C	50.1				
109A	1 Plant	14 A	TF	O			600	403	6	16.25	23	225	513	1928	1,969	1,181,400	400	80	2,954	78.0	78.0	619,170	1,546	BC&S&C	49.7				
644	1 Plant	12 M	C	C			240	161	4	14	17	257	196	1931	7,503	1,800,720	1,032	0	1,745	-----	-----	-----	-----	-----	-----				
	2 Plant	12 M	C	C			350	242	6	14	17	257	300	1931	1,308	2,070,680	386	0	1,220	-----	-----	-----	-----	-----	-----				
	3 Plant	12 M	C	C			600	403	6	14	17	257	496	-----	-----	4,771,600	1,418	0	1,602	-----	59.8	912,400	643	BC	56.6				
61	1 Plant	14 M	TF	O			300	202	3	17.75	22	225	275	1928	4,289	1,286,700	-----	-----	-----	68.7	-----	-----	578,100	-----	-----	-----			
	2 Plant	14 M	TF	O			300	202	3	17.75	22	225	275	1928	6,372	1,911,600	-----	-----	-----	62.5	-----	-----	804,400	-----	-----	-----			
	3 Plant	14 M	TF	O			600	403	6	17.75	22	225	550	-----	-----	5,198,300	880	35	3,635	-----	64.3	1,382,500	1,571	---	60.3				
32	1 Plant	14 M	TF	O			600P	404	5	17.75	22	234°	272	1928	1,321	792,600	378	60	2,097	77.9	77.9	414,600	1,096	C&F	65.1				
103	1 Plant	12 M	C	C			240	161	4	14	17	257	260	1927	3,753	900,720	-----	-----	-----	51.2	-----	-----	329,300	-----	-----	-----			
	2 Plant	12 M	C	C			2001	134	4	14	17	257	200	1920*	3,874	774,800	-----	-----	-----	57.6	-----	-----	299,300	-----	CC	-----			
	3 Plant	12 M	C	C			1501	101	3	14	17	257	125	1923	6,003	900,450	-----	-----	-----	46.6	-----	-----	281,940	-----	---	-----			
	4 Plant	12 M	C	C			590	396	6	14	17	257	525	-----	-----	2,878,970	1,505	---	1,712	-----	51.4	890,540	592	---	39.9				
862	1 Plant	12 M	C	C			751	60	2	12	15	300	60	1920	4	300	-----	-----	-----	-----	-----	-----	-----	-----	-----	-----			
	2 Plant	12 M	C	C			751	60	2	12	15	300	60	---	78	5,850	-----	-----	-----	-----	-----	-----	-----	-----	-----	-----			
	3 Plant	12 M	C	C			180	121	3	14	17	257	150	1925	3,708	606,360	-----	-----	-----	-----	-----	-----	-----	-----	-----	-----			
	4 Plant	12 M	C	C			588	394	3	16.5	24.5	180	225	1918*	5,159	1,831,082	633	378	2,103	-----	-----	-----	-----	-----	-----	-----			
	5 Plant	12 M	C	C			588	394	3	16.5	24.5	180	225	1918*	5,159	2,003,532	1,000	675	2,004	-----	47.9	644,280	644	CC & F	45.9				
102	1 Plant	12 M	C	C			240	161	4	14	17	257	200	1928	765	183,600	-----	-----	-----	41.3	-----	-----	50,800	-----	-----	-----			
	2 Plant	12 M	C	C			240	161	4	14	17	257	200	1928	915	219,600	-----	-----	-----	42.4	-----	-----	62,530	-----	CC	-----			
	3 Plant	12 M	C	C			1001	67	2	14	17	257	75	1922*	662	66,200	-----	-----	-----	58.3	-----	-----	25,880	-----	---	-----			
	4 Plant	12 M	C	C			580	589	6	14	17	257	475	-----	-----	469,400	292	---	1,607	-----	44.2	139,210	477	---	45.2				
540	1 Plant	12 M	C	C			350	242	6	14	17	257	300	1930	4,857	1,748,520	-----	-----	-----	38.6	-----	-----	453,400	-----	F	-----			
	2 Plant	12 M	C	C			180	121	3	14	17	257	120	1928	5,788	661,840	-----	-----	-----	47.0	-----	-----	214,900	-----	---	-----			
	3 Plant	12 M	C	C			540	353	6	14	17	257	420	-----	-----	2,430,360	2,902	-----	637	-----	40.9	668,300	230	---	41.7				
24c	1 Plant	12 M	C	C			1001	67	2	14	17	257	60	1918	2,320	232,000	-----	-----	0	-----	-----	-----	-----	-----	-----	-----			
	2 Plant	12 M	C	C			2001	134	4	14	17	257	170	1922	4,390	978,000	-----	-----	0	-----	-----	-----	-----	-----	-----	-----			
	3 Plant	12 M	C	C			540	362	6	14	17	257	820	1928	2,998	718,800	1,396	0	1,311	-----	35.1	451,636	309	C&W	54.9				
16c	1 Plant	12 M	C	C			120	81	2	14	17	257	90	1920	3,724	446,880	289	20	1,546	-----	-----	-----	-----	-----	-----	-----			
	2 Plant	12 M	C	C			180	121	3	14	17	257	150	1930	4,003	720,540	509	44	1,415	-----	-----	-----	-----	-----	-----	-----			
	3 Plant	12 M	C	C			240	161	4	14	17	257	200	1930	1,534	368,160	289	24	1,368	-----	-----	-----	-----	-----	-----	-----			
	4 Plant	12 M	C	C			540	363	6	14	17	257	440	-----	-----	1,555,560	1,067	88	1,439	-----	-----	-----	-----	-----	-----	-----			
101	1 Plant	12 M	C	C			240	161	4	14	17	257	200	1926	5,899	1,415,760	-----	-----	-----	85.1	-----	-----	523,700	-----	BC	-----			
	2 Plant	12 M	C	C			1501	101	3	14	17	257	150	1919	1,418	212,850	-----	-----	-----	41.9	-----	-----	69,460	-----	S&S	-----			
	3 Plant	12 M	C	C			1501	101	3	14	17	257	125	1923	2,782	414,300	1,222	---	---	---	50.5	-----	-----	160,740	-----	S&S	-----		
	4 Plant	12 M	C	C			540	363	6	14	17	257	475	-----	-----	2,042,910	1,222	---	---	---	52.8	723,900	592	---	42.6				
772	1 Plant	14 A	TF	D			250	168	4	13.75	17.5	275	250	1916	551	137,750	100	20	1,378	70.7	70.7	66,336	663	S&S	-----				
	2 Plant	14 A	TF	D			250	168	4	13.75	17.5	275	253	1916	690	172,600	100	28	1,725	75.3	75.3	87,214	872	---	-----				
	3 Plant	14 A	TF	D			500	336	6	14	17	257	513	-----	-----	310,260	200	45	1,551	-----	75.7	153,550	768	---	45.7				
501	1 Plant	12 M	C	C			120	81	2	14	17																		

TABLE III - INFORMATION COVERING LUBRICATING OIL (PAGE 6)																											
PLANT NUMBER	ENGINE DESIGNATION	ENGINE CYCLE	INJECTION SYSTEM (See Notes)	SAVING SYSTEM (See Notes)	TRUNK PISTON OR CROSSHEAD?	CYLINDERS OPEN OR CLOSED TO CHAMBERS?	RATED B.H.P.	EQUIVALENT K.W. - 80% OPERATING EFFICIENCY	NUMBER OF CYLINDERS	CYLINDER BORE - INCHES	STROKE - INCHES	RATED R.P.M.	GENERATOR RATING - K.V.A.	YEAR ENGINE STARTED TO WORK	ENGINE HOURS OPERATED IN REPORTED PERIOD	RATED HORSEPOWER HOURS IN REPORTED PERIOD	TOTAL GALLONS OF NEW LUBRICATING OIL USED	GALLONS OF NEW LUBRICATING OIL FOR CYLINDER LUBRICATION ONLY	GALLONS OF WHITE LUBRICATING OIL DISCARDED	RATED H.P. HRS PER GALLON OF NEW LUBRICATING OIL	RUNNING ENGINE CAPACITY FACTOR (See Text)	RUNNING PLANT CAPACITY FACTOR (See Text)	ON-GRASS OUTPUT - K.W. HRS.	ON-GRASS K.W. HRS. PER GALLON OF NEW LUBRICATING OIL	LUBRICATING OIL TREATMENT (See Notes)	AVERAGE COST OF LUBRICATING OIL IN CENTS PER GALLON	
695	1 3/4 2 1/2 Plant	1 3/4 2 1/2 Plant	1 3/4 2 1/2 Plant	1 3/4 2 1/2 Plant	1 3/4 2 1/2 Plant	1 3/4 2 1/2 Plant	185 165 180 480	111 111 111 303	3 3/4 3 3/4 3 3/4 3 3/4	12 12 12 14	15 15 15 16	360 360 360 257	150 150 150 390	1931 1931 1931 1931	2,689 2,482 409,530 423,680	433,785 409,530 623,680 1,566,995	----- ----- ----- 1,447	0 0 0 0	----- ----- ----- 945	----- ----- ----- -----	----- ----- ----- -----	----- ----- ----- -----	----- ----- ----- -----	----- ----- ----- -----	BC BC	22.5	
335	1 1/4 2 1/2 Plant	1 1/4 2 1/2 Plant	1 1/4 2 1/2 Plant	1 1/4 2 1/2 Plant	1 1/4 2 1/2 Plant	1 1/4 2 1/2 Plant	250 180 430	168 121 388	4 4 4	13.75 11.75 15	17.5 15 15	257 300 360	219 150 150	1924 1920 1920	6,288 2,472 2,472	1,572,000 444,960 2,016,960	439 144 583	65 35 98	3,582 2,090 2,460	34.9 44.8 -----	----- ----- 37.1	47.6 ----- -----	368,100 134,030 502,130	836 931 801	S ----- -----	60.0	
247	1 1/2 2 1/2 Plant	1 1/2 2 1/2 Plant	1 1/2 2 1/2 Plant	1 1/2 2 1/2 Plant	1 1/2 2 1/2 Plant	1 1/2 2 1/2 Plant	240 100 50 390	161 87 34 282	4 4 4 4	14 14 14 14	17 17 17 14	257 257 257 275	160 78 40 275	1928 1920 1915 1920	2,900 5,850 1,200 1,541,000	686,000 5,850 60,000 1,541,000	----- ----- ----- 712	0 0 0 0	----- ----- ----- 1,883	----- ----- ----- -----	----- ----- ----- 54.2	----- ----- ----- 487,960	----- ----- ----- 885	C C P -----	85.0		
1189	1 1/2 2 1/2 Plant	1 1/2 2 1/2 Plant	1 1/2 2 1/2 Plant	1 1/2 2 1/2 Plant	1 1/2 2 1/2 Plant	1 1/2 2 1/2 Plant	75 100 50 380	50 50 50 255	5 5 5 5	10.5 10.5 10.5 14	14 14 14 14	257 257 257 341	125 75 75 341	1926 1926 1923 1923	4,467 2,317 3,918 -----	870,060 278,040 31,800 1,023,785	----- ----- ----- 1,018	----- ----- ----- -----	----- ----- ----- 1,004	29.2 25.3 34.6 29.5	29.6 ----- ----- -----	245,000 57,920 107,300 410,220	----- ----- ----- 659	----- CC ----- -----	45.0		
106	1 1/2 2 1/2 Plant	1 1/2 2 1/2 Plant	1 1/2 2 1/2 Plant	1 1/2 2 1/2 Plant	1 1/2 2 1/2 Plant	1 1/2 2 1/2 Plant	150 120 100 370	101 67 249	3 3 3 3	14 14 14 14	17 17 17 17	257 257 257 275	125 75 75 275	1926 1926 1923 1923	4,467 2,317 3,918 -----	870,060 278,040 31,800 1,023,785	----- ----- ----- 734	----- ----- ----- -----	----- ----- ----- 1,825	54.3 30.9 40.9 -----	45.5 ----- ----- -----	245,000 57,920 107,300 410,220	----- ----- ----- 659	----- CC ----- -----	47.6		
1091	1 1/2 2 1/2 Plant	1 1/2 2 1/2 Plant	1 1/2 2 1/2 Plant	1 1/2 2 1/2 Plant	1 1/2 2 1/2 Plant	1 1/2 2 1/2 Plant	180 180 360	121 121 242	3 3 3	14 14 14	17 17 17	257 257 257	150 150 300	1930 1929 -----	----- ----- -----	----- ----- -----	----- ----- 237	----- ----- -----	----- ----- -----	----- ----- -----	----- ----- -----	----- ----- -----	----- ----- -----	----- ----- -----	----- ----- -----	55.0	
161	1 1/2 2 1/2 Plant	1 1/2 2 1/2 Plant	1 1/2 2 1/2 Plant	1 1/2 2 1/2 Plant	1 1/2 2 1/2 Plant	1 1/2 2 1/2 Plant	860	242	6	14	17	257	300	1929	-----	-----	1,346	95	-----	-----	-----	-----	1,003,500	7			

- n - With baffles
- o - Originally sold for 257 R.P.M.
- p - Supercharged to reproduce sea level conditions
- r - Date of original installation; installed in this plant in 1928
- s - Date of original installation; installed in this plant in 1930
- t.-- Second unit was discarded end of 11th month, and third unit started in its place
- u-- Started first day of 8 month period
- v - All units belt drive, D.C. generators
- w - Date of original installation; date of installation in this plant unknown

TABLE IV - INFORMATION COVERING FUEL OIL (PAGE 1)

PLANT NAME	ENGINE DESIGNATION	ENGINE CYCLE	IGNITION SYSTEM (SEE NOTES)	SAVERING SYSTEM (SEE NOTES)	RATED B. H. P.	EQUIVALENT L.W. - 50% GENERATING EFFICIENCY	NUMBER OF CYLINDERS	CYLINDER BORE - INCHES	STROKES - INCHES	RATED R.P.M.	GENERATOR RATING - K.V.A.	YEAR ENGINE STARTED TO WORK	ENGINE HOURS OPERATED IN REPORTED PERIOD	GRGAS OUTPUT - K.W. RES.	FUEL OIL USED - GALLONS	GROSS K.W. RES. PER GALLON OF FUEL OIL	RUNNING ENGINE CAPACITY FACTOR - (SEE TEXT)	RUNNING PLANT CAPACITY FACTOR (SEE TEXT)	NATURE OF FUEL OIL USED - (SEE NOTES)	AVERAGE COST OF FUEL OIL - CENTS PER GALLON	IS FUEL CENTRIFUGED	PLANT ALTITUDE - FEET ABOVE SEA LEVEL	PURPOSE FOR WHICH PLANT WATER HEAT IS UTILIZED (SEE NOTES)	PURPOSE FOR WHICH STEAM HEAT IS UTILIZED (SEE NOTES)	
43	14A	1	4	4	500	356	3	22	29.5	150	375	1915	295	67,792	7,100	9.55			24° A.P.I.; 0.7% S						
	4A	4	4	4	500	356	3	22	29.5	150	375	1915	295	67,792	7,100	9.55			19° A.P.I.; Asph. after 8 Hour @ 400° C-74.6%; Ash-0.22% ES - 0.7%; W - 0.1%	3.48	No	2,500	N	N	
52	14A	1	4	4	1,000	671	6	30.5	36	160	925	1915	284	68,472	7,106	9.62			28°-32° A.P.I.; 32° S.U. @ 100°F; S-0.27%; CC-0.06%; Trace Ash and ES & W; partly by Tank Truck						
	4A	4	4	4	1,000	671	6	30.5	36	160	925	1915	284	68,472	7,106	9.62									
	4A	4	4	4	820	340	4	18	24.5	200	500	1919	471	126,210	14,458	8.73									
	4A	4	4	4	3,750	2,517	6	30	42	124	1,920	1922	2,869	6,659,800	636,741	10.20									
	4A	4	4	4	3,750	2,517	6	30	42	124	1,920	1922	2,869	6,659,800	636,741	10.20									
	4A	4	4	4	4,100	2,753	6	30	42	124	1,920	1922	2,869	6,659,800	636,741	10.20									
	4A	4	4	4	15,640	10,499	6	30	42	124	1,920	1922	2,869	6,659,800	636,741	10.20									
53	14A	1	4	4	360	242	4	16.25	21	225	312	1921	3,941	288,440	28,433	10.14			28°-32° A.P.I.; 32° S.U. @ 100°F; S-0.27%; CC-0.06%; Trace Ash and ES & W; partly by Tank Truck						
	4A	4	4	4	750	504	4	17	27	180	740	1924	1,771	442,440	51,685	8.86									
	4A	4	4	4	1,150	772	6	17	27	180	1,000	1927	5,454	1,585,105	156,687	10.17									
	4A	4	4	4	1,150	772	6	17	27	180	1,000	1927	5,454	1,585,105	156,687	10.17									
	4A	4	4	4	1,500	1,007	8	17	27	180	1,350	1929	6,168	4,315,600	401,634	10.74									
	4A	4	4	4	3,500	2,217	10	19.5	27	240	3,120	1932	655	49,800	11,633	24.3									
	4A	4	4	4	8,960	6,017	10	19.5	27	240	3,120	1932	655	49,800	11,633	24.3									
54	14A	1	4	4	830	557	4	23	32	144	700	1928	5,507	1,374,500	122,953	11.17			25.6° A.P.I.; SU-43° @ 100° P, S-0.05% CC-0.05%, Ash-trace; ES & W-0.6%						
	4A	4	4	4	1,850	840	6	23	32	144	1,060	1928	4,569	3,074,600	271,051	11.34									
	4A	4	4	4	1,850	840	6	23	32	144	1,060	1928	4,569	3,074,600	271,051	11.34									
	4A	4	4	4	1,850	840	6	23	32	144	1,060	1928	4,569	3,074,600	271,051	11.34									
	4A	4	4	4	2,865	1,924	8	29	46	120	2,500	1935	20	22,700	1,970	11.62									
	4A	4	4	4	7,445	5,001	8	29	46	120	2,500	1935	20	22,700	1,970	11.62									
51	14A	1	4	4	600	403	6	17	24	225	500	1927	2,374	544,000	-----	-----			22° A.P.I.						
	4A	4	4	4	1,125	755	6	22	30	180	1,000	1927	4,365	1,778,500	-----	-----									
	4A	4	4	4	1,125	755	6	22	30	180	1,000	1927	4,365	1,778,500	-----	-----									
	4A	4	4	4	1,500	1,008	8	24	32	225	1,350	1930	5,120	2,387,000	-----	-----									
	4A	4	4	4	5,250	3,524	8	24	32	225	1,350	1930	5,120	2,387,000	-----	-----									
73	12A	1	2	4	1,250	840	5	20.75	26	180	1,063	1928	5,261	2,875,700	279,926	10.28			10°-14° A.P.I.						
	2A	2	2	4	1,250	840	5	20.75	26	180	1,063	1928	5,261	2,875,700	279,926	10.28									
	2A	2	2	4	1,250	840	5	20.75	26	180	1,063	1928	5,261	2,875,700	279,926	10.28									
	2A	2	2	4	1,250	840	5	20.75	26	180	1,063	1928	5,261	2,875,700	279,926	10.28									
	4A	4	4	4	5,000	3,360	5	20.75	26	180	1,063	1928	5,261	2,875,700	279,926	10.28									
92	12A	1	2	4	2,400	1,512	8	21	24	285	2,000	1930	5,170	5,295,000	-----	-----			22° A.P.I.						
	2A	2	2	4	1,250	840	5	20.75	26	180	1,125	1928	2,580	1,408,600	-----	-----									
	2A	2	2	4	1,250	840	5	20.75	26	180	1,125	1928	2,580	1,408,600	-----	-----									
	4A	4	4	4	4,900	3,242	8	20.75	26	180	4,250	1928	4,583	7,757,200	750,631	10.33									
45	14A	1	4	4	600	403	6	16.5	24	200	500	1923	1,081	186,900	19,166	9.85			21° A.P.I.; SU-55° @ 122° F S-1.47%; CC-7.74% Ash-0.06%; ES & W-2.5%						
	4A	4	4	4	600	403	6	16.5	24	200	500	1923	1,081	186,900	19,166	9.85			32°-36° A.P.I.; SU-43° @ 26° C; 75% S-0.5%; CC-0.05%; ES & W-trace All oil in tank wagons						
	4A	4	4	4	750	504	4	18	32	160	1,000	1926	4,446	2,780,425	261,160	10.65									
	4A	4	4	4	1,150	772	6	23	32	160	1,000	1926	4,446	2,780,425	261,160	10.65									
	4A	4	4	4	4,250	2,854	6	23	32	160	1,000	1926	4,446	2,780,425	261,160	10.65									
54	14A	1	4	4	600	403	6	17	25	200	450	-----	-----	-----	-----	-----			27.5° A.P.I.; SU-280° @ 60° F; S-0.75%; ES & W-2.0% (EST.) Crude oil thru pipe line from oil field						
	4A	4	4	4	600	403	6	17	25	200	450	-----	-----	-----	-----	-----									
	4A	4	4	4	600	403	6	17	25	200	450	-----	-----	-----	-----	-----									
	4A	4	4	4	600	403	6	17	25	200	450	-----	-----	-----	-----	-----									
	4A	4	4	4	600	403	6	17	25	200	450	-----	-----	-----	-----	-----									
	4A	4	4	4	4,800	2,821	6	17	25	200	3,150	-----	-----	-----	-----	-----									
130	14A	1	4	4	600	403	6	16.25	23	225	513	1924	4,720	1,509,700	113,696	11.52			16°-20° A.P.I. S - 0.6%						
	4A	4	4	4	600	403	6	16.25	23	225	513	1924	4,720	1,509,700	113,696	11.52									
	4A	4	4	4	1,800	906	6	20	34	300	1,082	1929	2,168	1,211,700	113,670	10.77									
	4A	4	4	4	1,800	906	6	20	34	300	1,082	1929	2,168	1,211,700	113,670	10.77									
	4A	4	4	4	3,600	1,812	6	20	34	300	2,164	-----	-----	-----	-----	-----									
157	12A	1	2	4	1,750	1,128	8	17	23	257	1,600	1930	2,063	2,000,000	182,880	10.94			24°-26° A.P.I. ES & W 0.25%						
	2A	2	2	4	1,750	1,128	8	17	23	257	1,600	1930	2,063	2,000,000	182,880	10.94									
	4A	4	4	4	5,920	3,520	8	17	23	257	5,000	-----	-----	-----	-----	-----									
2	14A	1	4	4	1,150	772	6	23	29.5	166.7	1,000	1928	3,743	2,827,090	287,307	10.37			27° A.P.I.; S.U.-40° @ 100° P S-0.5%; CC-2%; Ash-0.04%						
	4A	4	4	4	1,150	772	6	23	29.5	166.7	1,000	1928	3,743	2,827,090	287,307	10.37									
	4A	4	4	4	1,150	772	6	23	29.5	166.7	1,000	1928	3,743	2,827,090	287,307	10.37									
	4A	4	4	4	3,450	2,316	6	23	29.5	166.7	5,000	-----	-----	-----	-----	-----									
164	14A	1	4	4	840	564	6	19.5	24	214	1,000	1928	7,259	3,314,100	-----	-----			27° A.P.I.; SU 47.2° @ 100° P S-0.40%; Ash - 0.210%; ES & W; 1.965%; Thru Pipe Line from Refinery						
	4A	4	4	4	840	564	6	19.5	24	214	1,000	1928	7,259	3,314,100	-----	-----									
	4A	4	4	4	840	564	6	19.5	24	214	1,000	1928	7,259	3,314,100	-----	-----									
	4A	4	4	4	3,350	2,256	6	19.5	24	214	1,000	1928	7,259	3,314,100	-----	-----									
3	14A	1	4	4	400	269	6	14.5	18	277	344	1923	651	-----	-----	-----			28.5° A.P.I.; S-0.16% ES & W 0.04%						
	4A	4	4	4																					

[illegible]

TABLE IV - INFORMATION COVERING FUEL OIL (PAGE 3)

TABLE IX - INFORMATION COVERING FUEL OIL (SEE PAGE 3)																							
PLANT NUMBER	ENGINE DESIGNATION	ENGINE TYPE	ENGINE SPEED - R.P.M.	ENGINE HORSEPOWER (SEE NOTES)	SAVING SYSTEM (SEE NOTES)	RATED B. H. P.	EQUIVALENT I.H. - 50% GENERATING EFFICIENCY	NUMBER OF CYLINDERS	CYLINDER BORE - INCHES	STROKE - INCHES	RATED R.P.M.	GENERATOR RATING - K.V.A.	YEAR ENGINE STARTED TO WORK	ENGINE HOURS OPERATED IN REPORTED PERIOD	GROSS OUTPUT - K.W. RES.	FUEL OIL USED - GALLONS	GROSS K.W. RES. PER GALLON OF FUEL OIL	REPORTING ENGINE CAPACITY FACTOR - (SEE TEXT)	REPORTING PLANT CAPACITY FACTOR (SEE TEXT)	AVERAGE COST OF FUEL OIL - CENTS PER GALLON	IS FUEL CERTIFICATED?	PLANT ALTITUDE - FEET ABOVE SEA LEVEL	PURPOSE FOR WHICH ALLOCATED (SEE NOTES)
735	12 M	12 M	1800	564	6	16	20	257	700	1923	3,342	1,368,600	72.8	34°-36° A.P.I.									
	12 M	12 M	1800	564	6	16	20	257	700	1928	3,342	1,368,600	72.8	34°-36° A.P.I.									
	12 M	12 M	1800	564	6	16	20	257	700	1928	3,342	1,368,600	72.8	34°-36° A.P.I.									
18	12 M	12 M	1800	564	6	15.25	16	276	-----	1922	386	-----	-----	-----	-----	-----	-----	-----	-----	3.64	Ho	200	N
	12 M	12 M	1800	564	6	17	28	200	-----	1926	4,569	-----	-----	-----	-----	-----	-----	-----	-----	-----	-----	-----	
	12 M	12 M	1800	564	6	17	28	200	-----	1928	4,789	-----	-----	-----	-----	-----	-----	-----	-----	-----	-----	-----	
86	12 M	12 M	1800	564	6	15.25	24	200	240	1920	5,148	542,960	54.16	32°-36° A.P.I.; S - 0.35% Free Carbon-Trace Ash - 0.01%	54,160	10.43	57.4	-----	-----	3.74	---	---	N
	12 M	12 M	1800	564	6	15.25	24	200	240	1920	5,148	542,960	54.16	32°-36° A.P.I.; S - 0.35% Free Carbon-Trace Ash - 0.01%	54,160	10.43	57.4	-----	-----	-----	-----	-----	
	12 M	12 M	1800	564	6	15.25	24	200	240	1920	5,148	542,960	54.16	32°-36° A.P.I.; S - 0.35% Free Carbon-Trace Ash - 0.01%	54,160	10.43	57.4	-----	-----	-----	-----	-----	
	12 M	12 M	1800	564	6	15.25	24	200	240	1920	5,148	542,960	54.16	32°-36° A.P.I.; S - 0.35% Free Carbon-Trace Ash - 0.01%	54,160	10.43	57.4	-----	-----	-----	-----	-----	
8	12 M	12 M	1800	564	6	15.25	24	200	240	1920	5,148	542,960	54.16	32°-36° A.P.I.; S - 0.35% Free Carbon-Trace Ash - 0.01%	54,160	10.43	57.4	-----	-----	-----	-----	-----	
	12 M	12 M	1800	564	6	15.25	24	200	240	1920	5,148	542,960	54.16	32°-36° A.P.I.; S - 0.35% Free Carbon-Trace Ash - 0.01%	54,160	10.43	57.4	-----	-----	-----	-----	-----	
	12 M	12 M	1800	564	6	15.25	24	200	240	1920	5,148	542,960	54.16	32°-36° A.P.I.; S - 0.35% Free Carbon-Trace Ash - 0.01%	54,160	10.43	57.4	-----	-----	-----	-----	-----	
	12 M	12 M	1800	564	6	15.25	24	200	240	1920	5,148	542,960	54.16	32°-36° A.P.I.; S - 0.35% Free Carbon-Trace Ash - 0.01%	54,160	10.43	57.4	-----	-----	-----	-----	-----	
1154	12 M	12 M	1800	564	6	17.5	24.5	225	560	1931	4,494	1,042,900	176.145	28° A.P.I.	4,494	1,042,900	9.22	46.4	-----	3.04	Ho	1,160	EF
	12 M	12 M	1800	564	6	17.5	24.5	225	560	1931	4,494	1,042,900	176.145	28° A.P.I.	4,494	1,042,900	9.22	46.4	-----	-----	-----	-----	
	12 M	12 M	1800	564	6	17.5	24.5	225	560	1931	4,494	1,042,900	176.145	28° A.P.I.	4,494	1,042,900	9.22	46.4	-----	-----	-----	-----	
132	12 M	12 M	1800	564	6	17.5	24.5	225	560	1929	2,835	600,300	58.589	34° A.P.I.; S.U. 350° @ 100°F; S. by Volume less than 0.5% C.C.-Trace; Ash less than 1.0%	2,835	600,300	11.78	72.0	-----	5.04	Ho	1,450	F
	12 M	12 M	1800	564	6	17.5	24.5	225	560	1929	2,835	600,300	58.589	34° A.P.I.; S.U. 350° @ 100°F; S. by Volume less than 0.5% C.C.-Trace; Ash less than 1.0%	2,835	600,300	11.78	72.0	-----	-----	-----	-----	
	12 M	12 M	1800	564	6	17.5	24.5	225	560	1929	2,835	600,300	58.589	34° A.P.I.; S.U. 350° @ 100°F; S. by Volume less than 0.5% C.C.-Trace; Ash less than 1.0%	2,835	600,300	11.78	72.0	-----	-----	-----	-----	
	12 M	12 M	1800	564	6	17.5	24.5	225	560	1929	2,835	600,300	58.589	34° A.P.I.; S.U. 350° @ 100°F; S. by Volume less than 0.5% C.C.-Trace; Ash less than 1.0%	2,835	600,300	11.78	72.0	-----	-----	-----	-----	
289	12 M	12 M	1800	564	6	13.75	17.5	257	210	1920	5,158	602,130	52.374	28°-36° A.P.I. S.U. - 75° @ 100°F	5,158	602,130	11.49	68.6	-----	4.17	Ho	1,670	F
	12 M	12 M	1800	564	6	13.75	17.5	257	210	1920	5,158	602,130	52.374	28°-36° A.P.I. S.U. - 75° @ 100°F	5,158	602,130	11.49	68.6	-----	-----	-----	-----	
	12 M	12 M	1800	564	6	13.75	17.5	257	210	1920	5,158	602,130	52.374	28°-36° A.P.I. S.U. - 75° @ 100°F	5,158	602,130	11.49	68.6	-----	-----	-----	-----	
	12 M	12 M	1800	564	6	13.75	17.5	257	210	1920	5,158	602,130	52.374	28°-36° A.P.I. S.U. - 75° @ 100°F	5,158	602,130	11.49	68.6	-----	-----	-----	-----	
496	12 M	12 M	1800	564	6	16.5	24.5	200	240	1925	2,514	354,475	32.058	32°-36° A.P.I. S - Less than 0.5%	2,514	354,475	11.06	52.6	-----	4.02	Ho	1,200	-
	12 M	12 M	1800	564	6	16.5	24.5	200	240	1925	2,514	354,475	32.058	32°-36° A.P.I. S - Less than 0.5%	2,514	354,475	11.06	52.6	-----	-----	-----	-----	
	12 M	12 M	1800	564	6	16.5	24.5	200	240	1925	2,514	354,475	32.058	32°-36° A.P.I. S - Less than 0.5%	2,514	354,475	11.06	52.6	-----	-----	-----	-----	
	12 M	12 M	1800	564	6	16.5	24.5	200	240	1925	2,514	354,475	32.058	32°-36° A.P.I. S - Less than 0.5%	2,514	354,475	11.06	52.6	-----	-----	-----	-----	
70	12 M	12 M	1800	564	6	16	20	257	470	1928	4,357	894,133	-----	32°-36° A.P.I.	4,357	894,133	-----	54.6	-----	54.3	-----	-----	
	12 M	12 M	1800	564	6	16	20	257	470	1928	4,357	894,133	-----	32°-36° A.P.I.	4,357	894,133	-----	54.6	-----	54.3	-----	-----	
	12 M	12 M	1800	564	6	16	20	257	470	1928	4,357	894,133	-----	32°-36° A.P.I.	4,357	894,133	-----	54.6	-----	54.3	-----	-----	
108	12 M	12 M	1800	564	6	16	20	300	1,392	1932	2,791	2,105,680	190.523	31° A.P.I.; S.U. 69° @ 100°F; S-0.55% C.C.-0.05%; Ash Trace	2,791	2,105,680	11.82	83.6	-----	5.03	Ho	1,350	N
	12 M	12 M	1800	564	6	16	20	300	1,392	1932	2,791	2,105,680	190.523	31° A.P.I.; S.U. 69° @ 100°F; S-0.55% C.C.-0.05%; Ash Trace	2,791	2,105,680	11.82	83.6	-----	-----	-----	-----	
	12 M	12 M	1800	564	6	16	20	300	1,392	1932	2,791	2,105,680	190.523	31° A.P.I.; S.U. 69° @ 100°F; S-0.55% C.C.-0.05%; Ash Trace	2,791	2,105,680	11.82	83.6	-----	-----	-----	-----	
163	12 M	12 M	1800	564	6	17.75	22	225	343	1924	80	8,300	783	348 A.P.I.; S.U.-48° @ 100°F; S-0.55% Ash-0.0015%; S.S. & W.-Trace By Pipe Line From Refinery	80	8,300	10.88	81.4	-----	5.63	Ho	1,100	N
	12 M	12 M	1800	564	6	17.75	22	225	343	1924	80	8,300	783	348 A.P.I.; S.U.-48° @ 100°F; S-0.55% Ash-0.0015%; S.S. & W.-Trace By Pipe Line From Refinery	80	8,300	10.88	81.4	-----	-----	-----	-----	
	12 M	12 M	1800	564	6	17.75	22	225	343	1924	80	8,300	783	348 A.P.I.; S.U.-48° @ 100°F; S-0.55% Ash-0.0015%; S.S. & W.-Trace By Pipe Line From Refinery	80	8,300	10.88	81.4	-----	-----	-----	-----	
154	12 M	12 M	1800	564	6	17	24	200	-----	1927	2,121	-----	-----	-----	-----	-----	-----	-----	-----	-----	-----	-----	
	12 M	12 M	1800	564	6	17	24	200	-----	1926	1,586	-----	-----	-----	-----	-----	-----	-----	-----	-----	-----	-----	
	12 M	12 M	1800	564	6	17	24	200	-----	1925	2,277	-----	-----	-----	-----	-----	-----	-----	-----	-----	-----	-----	
888	12 M	12 M	1800	564	6	17	24	200	250	1925	874	46,620	-----	18.0° A.P.I.; C.C.-0.1% B.S. & W. 0.1% Delivered in Oil Tanker	874	46,620	-----	40.1	-----	5.47	---	---	N
	12 M	12 M	1800	564	6	17	24	200	250	1925	874	46,620	-----	18.0° A.P.I.; C.C.-0.1% B.S. & W. 0.1% Delivered in Oil Tanker	874	46,620	-----	40.1	-----	-----	-----	-----	
	12 M	12 M	1800	564	6	17	24	200	250	1925	874	46,620	-----	18.0° A.P.I.; C.C.-0.1% B.S. & W. 0.1% Delivered in Oil Tanker	874	46,620	-----	40.1	-----	-----	-----	-----	
	12 M	12 M	1800	564	6	17	24	200	250	1925	874	46,620	-----	18.0° A.P.I.; C.C.-0.1% B.S. & W. 0.1% Delivered in Oil Tanker	874	46,620	-----	40.1	-----	-----	-----	-----	
517	12 M	12 M	1800	564	6	17.5	26	225	625	1932	4,497	978,330	65.816	28°-36° A.P.I.; S.U.-70° @ 100°F; S-0.5%; C.C.-0.5%	4,497	978,330	9.21	25.6	-----	3.74	Ho	1,100	N
	12 M	12 M	1800	564	6	17.5	26	225	625	1932	4,497	978,330	65.816	28°-36° A.P.I.; S.U.-70° @ 100°F; S-0.5%; C.C.-0.5%	4,497	978,330	9.21	25.6	-----	-----	-----	-----	
	12 M	12 M	1800	564	6	17.5	26	225	625	1932	4,497	978,330	65.816	28°-36° A.P.I.; S.U.-70° @ 100°F; S-0.5%; C.C.-0.5%	4,497	978,330	9.21	25.6	-----	-----	-----	-----	
1018	12 M	12 M	1800	564	6	11.14	14	277	160	1924	2,020	201,100	-----	-----	-----	-----	-----	-----	-----	5.08	Ho	5,600	N
	12 M	12 M	1800	564	6	11.14	14	277	160	1924	2,020	201,100	-----	-----	-----	-----	-----	-----	-----	-----	-----	-----	
	12 M	12 M	1800	564	6	11.14	14	277	160	1924	2,020	201,100	-----	-----	-----	-----	-----	-----	-----	-----	-----	-----	
866	12 M	12 M	1800	564	6	14	17	257	85	1927	308	-----	-----	-----	-----	-----	-----	-----	-----	-----	-----	-----	
	12 M	12 M	1800	564	6	14	17	257	85	1927	308	-----	-----	-----	-----	-----	-----	-----	-----	-----	-----	-----	
	12 M	12 M	1800	564	6	14	17	257	85	1927	308	-----	-----	-----	-----	-----	-----	-----	-----	-----	-----	-----	
13	12 M	12 M	1800	564	6	13.5	19.5	257	219	1923	6,792	778,600	75.006	32°-36° A.P.I.; S.U.-41° @ 90°F; S-Less than 1%; C.C.-Less than 0.05%; Ash-Trace; B.S. & W. - Trace	6,792	778,600	10.38	62.2	-----	5.13	Ho	75	N
	12 M	12 M	1800	564	6	13.5	19.5	257	219	1923	6,792	778,600	75.006	32°-36° A.P.I.; S.U.-41° @ 90°F; S-Less than 1%; C.C.-Less than 0.05%; Ash-Trace; B.S. & W. - Trace	6,792	778,600	10.38	62.2	-----	-----	-----	-----	
	12 M	12 M	1800	564	6	13.5	19.5	257	219	1923	6,792	778,600	75.006	32°-36° A.P.I.; S.U.-41° @ 90°F; S-Less than 1%; C.C.-Less than 0.05%; Ash-Trace; B.S. & W. - Trace	6,792	778,600	10.38	62.2	-----	-----	-----	-----	
1083	12 M	12 M	1800	564	6	16	20	257	1,042	1931	3,944	2,182,827	168,274	27-30° A.P.I.; S-0.5%; B.S. & W. - 1									

TABLE IV - INFORMATION COVERING FUEL OIL (PAGE 4)

PLANT NUMBER	ENGINE DESIGNATION	ENGINE SIZE	ENGINE SPEED (SEE NOTES)	GENERATING CAPACITY (SEE NOTES)	RATED B. H. P.	SEV. MAX. E. W. - 60% GENERATING EFFICIENCY	NUMBER OF CYLINDERS	CYLINDER BORE - INCHES	STROKE - INCHES	RATED R. P. M.	GENERATOR RATING - K.V.A.	YEAR ENGINE STARTED TO WORK	ENGINE HOURS OPERATED IN REPORTED PERIOD	DESS OUTLET - I.W. HRS.	FUEL OIL USED - GALLONS	GROSS K.W. HRS. PER GALLON OF FUEL OIL	RUNNING ENGINE CAPACITY FACTOR - (SEE TEXT)	RUNNING PLANT CAPACITY FACTOR - (SEE TEXT)	NATURE OF FUEL OIL USED - (SEE NOTES)	AVERAGE COST OF FUEL OIL - CENTS PER GALLON	IS FUEL CENTRIFUGED?	PLANT IN USE - YES	PURPOSE FOR WHICH JACKET WATER HEAT IS UTILIZED (SEE NOTES)	PURPOSE FOR WHICH EXHAUST HEAT IS UTILIZED (SEE NOTES)
878	1 2 M F	560	276	4	14	20	257	470	1928	4,833	1,261,900	8,630	1,261,900	8,630	80.0	74.6	29.1° A.P.I. S-0.44%	2.71	No	2,163	N			
	2 2 M C	200	134	4	14	17	257	170	1919	83	170,800	83	170,800	83	80.0	74.6	29.1° A.P.I. S-0.44%	2.71	No	2,163	N			
	3 4 A	400	259	4	14	17	257	357	1924	4,382	1,261,900	4,382	1,261,900	4,382	80.0	74.6	29.1° A.P.I. S-0.44%	2.71	No	2,163	N			
	Plant	1,160	779					977																
103	1 4 A	675	453	5	18	25	225	625	1931	3,893	844,090	84,552	844,090	84,552	9.08	47.9	28°-30° A.P.I.	3.73	No	925	-			
	2 4 A	480	322	6	18	17	340	415	1932	4,431	600,900	66,669	600,900	66,669	9.28	42.7	28°-30° A.P.I.	3.73	No	925	-			
	Plant	1,155	775					1,040			1,453,990		1,453,990		9.57		28°-30° A.P.I.	3.73	No	925	-			
518	1 4 A	300	202	3	16.5	23	200	850	1923	4,588	668,010	53,792	668,010	53,792	12.12	70.4	20°-22° A.P.I. S-Less than 0.5%	6.51	No	20	M	F		
	2 4 A	750	504	4	23	32	150	657	1925	4,156	1,049,600	94,712	1,049,600	94,712	11.08	50.1	20°-22° A.P.I. S-Less than 0.5%	6.51	No	20	M	F		
	Plant	1,150	703					982			1,711,310		1,711,310		14.07		20°-22° A.P.I. S-Less than 0.5%	6.51	No	20	M	F		
807	1 2 M C	180	101	3	14	17	257	125	1922	84	288,300	84	288,300	84	8.59	45.0	22° A.P.I.	4.16	No	4,082	N			
	2 2 M C	440	295	4	15	20	225	375	1930	8,493	575,500	8,493	575,500	8,493	8.59	45.0	22° A.P.I.	4.16	No	4,082	N			
	3 4 A	350	242	5	17	24	225	438	1928	5,488	1,195,560	139,215	1,195,560	139,215	8.59	45.0	22° A.P.I.	4.16	No	4,082	N			
	Plant	1,140	765					938										22° A.P.I.	4.16	No	4,082	N		
98	1 2 M F	560	376	4	16	20	257	469	1929	370	113,300	469	1929	370	81.4	84.2	22° A.P.I.	2.38	No	746	N			
	2 2 M F	360	242	4	16	20	257	469	1929	370	113,300	469	1929	370	81.4	84.2	22° A.P.I.	2.38	No	746	N			
	Plant	1,120	752					938										22° A.P.I.	2.38	No	746	N		
98	1 4 A	600	403	5	17	24	225	500	1928	849	183,300	849	1928	849	53.6	41.2	26° A.P.I.	2.82	No	605	N			
	2 4 A	350	242	5	17	24	225	500	1928	849	183,300	849	1928	849	53.6	41.2	26° A.P.I.	2.82	No	605	N			
	3 2 M C	200	124	4	14	17	257	170	1921	584	35,600	584	1921	584	8.77	41.2	26° A.P.I.	2.82	No	605	N			
	Plant	1,100	759					920			792,400		792,400		9.70		26° A.P.I.	2.82	No	605	N			
143	1 2 M C	360	242	6	14	17	257	300	1928	-----	421,467	-----	421,467	-----	-----	-----	32°-36° A.P.I.	5.31	No	---	-			
	2 2 M C	360	242	6	14	17	257	300	1928	-----	421,467	-----	421,467	-----	-----	-----	32°-36° A.P.I.	5.31	No	---	-			
	3 2 M C	360	242	6	14	17	257	300	1928	-----	421,467	-----	421,467	-----	-----	-----	32°-36° A.P.I.	5.31	No	---	-			
	Plant	1,080	726					900			1,264,401		1,264,401		13.04		32°-36° A.P.I.	5.31	No	---	-			
78	1 4 A	400	269	4	17	24	225	375	1928	3,354	322,900	47,900	322,900	47,900	6.74	50.6	28°-32° A.P.I. S.U.-45° @ 100°	6.15	No	172	N			
	2 4 A	680	443	6	17	24	240	625	1930	5,385	1,205,597	134,677	1,205,597	134,677	8.95	50.6	28°-32° A.P.I. S.U.-45° @ 100°	6.15	No	172	N			
	Plant	1,060	712					1,000			1,628,497		1,628,497		18.27		28°-32° A.P.I. S.U.-45° @ 100°	6.15	No	172	N			
518	1 2 M C	300	134	4	14	17	257	170	1925	-----	-----	-----	-----	-----	-----	-----	32°-36° A.P.I.	5.42	No	500	N			
	2 2 M C	200	202	4	14	17	257	170	1925	-----	-----	-----	-----	-----	-----	-----	32°-36° A.P.I.	5.42	No	500	N			
	3 2 M F	560	376	4	16	20	257	470	1929	-----	-----	-----	-----	-----	-----	-----	32°-36° A.P.I.	5.42	No	500	N			
	Plant	1,060	712					890			1,657,470		1,657,470		13.12		32°-36° A.P.I.	5.42	No	500	N			
1144	1 2 M C	210	141	3	14	17	300	167	1931	4,932	370,800	32,240	370,800	32,240	11.49	53.3	28°-32° A.P.I. S.U.-45° @ 70°	6.28	No	672	N			
	2 2 M C	420	282	6	14	17	300	353	1931	3,240	607,000	48,800	607,000	48,800	12.43	56.4	28°-32° A.P.I. S.U.-45° @ 70°	6.28	No	672	N			
	3 2 M C	420	282	6	14	17	300	353	1931	3,240	607,000	48,800	607,000	48,800	12.43	56.4	28°-32° A.P.I. S.U.-45° @ 70°	6.28	No	672	N			
	Plant	1,050	705					873			1,566,000		1,566,000		12.90		28°-32° A.P.I. S.U.-45° @ 70°	6.28	No	672	N			
288	1 2 M C	210	141	3	14	17	300	170	1931	9,177	477,732	42,810	477,732	42,810	11.23	55.0	32°-34° A.P.I.	49.5	No	5,467	N			
	2 2 M C	360	242	6	14	17	300	170	1931	9,177	477,732	42,810	477,732	42,810	11.23	55.0	32°-34° A.P.I.	49.5	No	5,467	N			
	3 2 M C	480	322	4	18	20	257	400	1928	988	145,100	16,580	145,100	16,580	8.77	45.6	32°-34° A.P.I.	49.5	No	5,467	N			
	Plant	1,050	705					870			799,632		799,632		9.72		32°-34° A.P.I.	49.5	No	5,467	N			
208	1 2 M F	525	352	5	14	17	300	447	1931	3,898	814,800	78,080	814,800	78,080	10.44	59.4	32°-36° A.P.I.	55.7	No	---	N			
	2 2 M F	350	232	5	14	17	300	447	1931	3,898	814,800	78,080	814,800	78,080	10.44	59.4	32°-36° A.P.I.	55.7	No	---	N			
	Plant	1,050	704					894			1,562,600		1,562,600		16.54		32°-36° A.P.I.	55.7	No	---	N			
601	1 2 A F	1,000	671	4	20.75	28	180	937	1927	8,451	4,837,800	474,170	4,837,800	474,170	10.00	86.2	24°-26° A.P.I. S.U.-500° @ 100°	3.20	Yes	591	N			
758	1 4 A	1,000	671	6	22	32	150	900	1918	640	353,600	30,539	353,600	30,539	11.08	82.3	22°-26° A.P.I.	1.87	No	300	N			
1081	1 2 M F	980	658	7	16	20	257	975	1930	4,955	3,081,100	269,828	3,081,100	269,828	11.42	94.5	22°-26° A.P.I.	94.5	No	1200	N			
868	1 4 A	300	202	3	17	24	200	280	1928	8,601	995,700	91,667	995,700	91,667	10.86	74.6	24°-26° A.P.I. S.U.-275° @ 100°	81.6	No	932	L	B		
	2 4 A	675	453	6	17	24	225	625	1927	5,280	2,033,800	171,257	2,033,800	171,257	11.88	85.3	24°-26° A.P.I. S.U.-275° @ 100°	81.6	No	932	L	B		
	Plant	978	658					876			3,029,500		3,029,500		12.52		24°-26° A.P.I. S.U.-275° @ 100°	81.6	No	932	L	B		
1065	1 2 M F	900	605	6	16	20	257	774	1931	755	580,160	30,680	580,160	30,680	12.36	83.3	28°-30° A.P.I. S-0.5 to 0.75%	3.81	No	1,100	N			
	2 2 M F	800	534	4	16.5	13.25	327	169	1924	4,927	-----	-----	-----	-----	-----	-----	28°-30° A.P.I. S-0.5 to 0.75%	3.81	No	1,100	N			
	3 4 A	200	134	4	12.5	13.25	327	169	1924	4,919	-----	-----	-----	-----	-----	-----	28°-30° A.P.I. S-0.5 to 0.75%	3.81	No	1,100	N			
	Plant	900	604					776			1,814		1,814		11.94		28°-30° A.P.I. S-0.5 to 0.75%	3.81	No	1,100	N			
260	1 2 A F	900	605	6	14.75	21	257	780	1928	519	90,700	9,598	90,700	9,598	9.07	47.0	27° A.P.I. S.U.-5.5° @ 77°	2.76	No	---	N			
	2 2 A F	360	242	6	14	17	257	300	1928	4,043	589,300	-----	589,300	-----	60.2	-----	27° A.P.I. S.U.-5.5° @ 77°	2.76	No	---	N			
	3 2 M C	360	242	6	14	17	257	300	1928	4,043	589,300	-----	589,300	-----	60.2	-----	27° A.P.I. S.U.-5.5° @ 77°	2.76	No	---	N			
	Plant	900	605					740			1,597,500		1,597,500		8.68		27° A.P.I. S.U.-5.5° @ 77°	2.76	No	---	N			
53	1 2 M C	200	124	4	14	17	257	170	1923	1,959	197,150	-----	197,150	-----	71.2	-----	25°-30° A.P.I.	69.0	No	1,650	N			
	2 2 M C	300	201	6	14	17	257	250	1923	2,544	382,290	-----	382,290	-----	70.7	-----	25°-30° A.P.I.	69.0	No	1,650	N			
	3 4 A	400	269	4	16.25	23	225	358	1928	8,221	1,508,530	-----	1,508,530	-----	68.4	-----	25°-30° A.P.I.	69.0	No	1,650	N			
	Plant	900	604					758			2,057,980		2,057,980		9.18		25°-30° A.P.I.	69.0	No	1,650	N			
189	1 4 M	550	359	5	17	24	240	470	1929	8,643	1,041,080	-----	1,041,080	-----	32.6	-----	28°-30° A.P.I.	2.56	No	1,650	N			
	2 4 M	200	134	2	17	24	200	170	1922	161	11,040	-----	11,040	-----	58.4	-----	28°-30° A.P.I.	2.56						

TABLE IV - INFORMATION COVERING FUEL OIL (PAGE 5)

TABLE IV - INFORMATION COVERING FUEL OIL (PAGE 5)																				
PLANT NUMBER	ENGINE DESCRIPTION (ENGINE CYCLE) FUEL SYSTEM (SEE NOTES) EXHAUST SYSTEM (SEE NOTES)	RATED B. H. P.	EXHAUST K.W. - 60% GENERATING EFFICIENCY	NUMBER OF CYLINDERS	CYLINDER BORE - INCHES	STROKE - INCHES	RATED R.P.M.	GENERATOR RATING - K.V.A.	YEAR ENGINES STARTED TO RUN	ENGINES OPERATED IN REPORTED PERIOD	GROSS OUTPUT - K.W. NET.	FUEL OIL USED - GALLONS	GROSS K.W. NET. PER GALLON OF FUEL OIL	RUNNING ENGINE CAPACITY FACTOR - (SEE TEXT)	RUNNING PLANT CAPACITY FACTOR - (SEE TEXT)	MAKES OF FUEL OIL USED - (SEE NOTES)	AVERAGE COST OF FUEL OIL - CENTS PER GALLON	IS FUEL CENTRIFUGED?	PLANT ALTITUDE - FEET ABOVE SEA LEVEL	PURPOSE FOR WHICH ACCT WATER USED IN PLANT (SEE NOTES)
718	1 2 M 2 2 M Plant	360 360 720	242 242 484	6 6 14	14 14 17	17 17 17	257 257 257	300 300 600	1926 1926 1926	4,750 4,250 600	373,910 343,410 717,380	88,908 8.07	33.5 33.4	32-36° A.P.I.; S.U.-36° @ 100°F S-0.7%; C.C.-0.01%; Ash-0.001%; B.S.&W. Trace	3.61	No	1,200	N	M	
552	1 2 M 2 2 M Plant	360 360 720	242 242 484	6 6 14	14 14 17	17 17 17	257 257 257	300 300 600	1929 1929 1929	5,317 5,043 1,352,500	142,137 9.52	54.0	32°-36° A.P.I.	4.17	No	700	N	BF		
527	1 2 M 2 2 M Plant	360 360 720	242 242 484	6 6 14	14 14 17	17 17 17	257 257 257	300 300 600	1930 1930 1930	5,404 5,000 997,200	109,750 9.09	30.6	26° A.P.I.; S.U.-75° @ 100°F; S-less than 0.5%; C.C.-from Trace to 0.5%; Ash-trace B.S. & W. 0.5%	3.10	No	750	N	N		
170	1 2 M 2 2 M Plant	360 360 720	242 242 484	6 6 14	14 14 17	17 17 17	257 257 257	300 300 600	1929 1929 1929	2,429 2,572 703,158	73,484 9.58	58.2	29° A.P.I.; S.U.-38° @ 100°F; S-0.6% C.C.-0.04%; By Tank Truck	5.53	No	50	N	N		
67	1 2 M 2 2 M Plant	360 360 720	242 242 484	6 6 14	14 14 17	17 17 17	257 257 257	250 250 500	1925 1925 1925	2,122 1,998 500	418,240 392,760 811,000	40,401 39,151 78,552	10.35 10.03 10.19	81.5 81.4	25° A.P.I.; S.U.-52° @ 100° F S-0.005%; C.C. 0.037%	4.47	No	860	N	N
19	1 2 M 2 2 M Plant	100 ¹ 100 ¹ 700	67 67 470	2 2 14	14 14 17	17 17 17	257 257 257	100 100 700	1927 1927 1927	2,137 5,319 1,513	661,930 82,300 8.04	48.5	32°-34° A.P.I.	3.63	No	---	---	---		
411	1 2 M 2 2 M Plant	200 ¹ 120 680	134 81 487	4 2 6	14 14 17	17 17 17	257 257 257	140 240 470	1914 1926 1930	40 2,992 5,867	657,670 15,878 49,798	10.17	39.7	28°-30° A.P.I. - Warm weather 32°-36° A.P.I. - Cold weather	3.42	No	1,777	---	N	
529	1 2 M 2 2 M Plant	100 ¹ 100 ¹ 620	67 67 416	2 2 6	14 14 17	17 17 17	257 257 257	75 75 250	1922 1922 1931	1,062 1,009 4,591	4,031 4,022 541,836	7.28	38.4	32°-36° A.P.I. - Warm weather 32°-36° A.P.I. - Cold weather	3.60	No	700	B	B	
106	1 4 A	600	403	6	17	25	200	---	1929	4,899	1,409,410	128,358	10.99	71.4	28°-30° A.P.I.	3.77	---	---	---	
1096	1 4 A	600	403	6	16.25	23	225	513	1928	2,576	725,880	61,878	11.73	69.9	28°-30° A.P.I.	3.68	No	1,100	N	B
1094	1 4 A	600	403	6	16.25	23	225	513	1928	1,969	619,170	57,140	10.84	78.0	28°-30° A.P.I.	3.79	No	1,150	N	B
844	2 2 M 2 2 M Plant	240 360 600	161 242 403	4 6 14	14 14 17	17 17 17	257 257 257	196 300 496	1931 1931 1931	7,503 1,308 496	72,540 25,580 912,400	9.61	59.8	32°-36° A.P.I.; S-0.5%; B.S. & W. 0.5%	4.04	No	579	N	N	
61	1 4 M 2 4 M Plant	300 300 600	202 202 404	3 3 6	17.75 17.75 17.75	22 22 22	225 225 225	275 275 550	1928 1928 1928	4,289 4,372 1,382,500	78,100 804,400 118,484	11.66	64.3	30° A.P.I.; S-0.5%; C.C. 0.15% S.U.-40° @ 100°F; Ash-Trace B.S. & W. 0.5%	4.63	No	645	T	N	
32	1 4 M	600 ⁰	403	5	17.75	22	234 ¹	572	1928	1,321	414,600	37,677	11.00	77.9	36° A.P.I.; C.C. & Ash-Trace B.S. & W. - Trace	5.45	No	9,200 ⁰	BF	B
103	1 2 M 2 2 M Plant	240 200 ¹ 160 ¹	161 134 101	4 4 3	14 14 17	17 17 17	257 257 257	200 125 885	1927 1923 1923	3,753 5,874 6,003	309,300 299,300 281,940	6.60	51.2 57.5 46.5	34°-36° A.P.I.	3.94	No	3,100	N	F	
862	1 2 M 2 2 M Plant	78 ¹ 78 ¹ 588	50 50 394	3 3 16.5	12 15 24.5	300 300 180	1920 1920 1918 ¹	60 60 256	1920 1925 1918 ¹	4 7 5,159	644,280 75,138	8.58	47.9	33.1° A.P.I.; S-0.61% B.S. & W. Trace	3.14	No	221	N	N	
102	1 2 M 2 2 M Plant	240 240 580	161 161 389	4 4 14	14 14 17	17 17 17	257 257 257	200 ¹ 200 475	1928 1928 1922 ¹	765 915 662	50,800 52,530 25,880	7.40	41.3 42.4 58.3	24°-26° A.P.I.	2.31	No	565	N	F	
540	1 2 M 2 2 M Plant	360 180 540	242 121 363	6 3 14	14 14 17	17 17 17	257 257 257	300 180 450	1930 1928 1928	4,857 3,768 450	453,400 214,900 688,300	7.98	38.6 47.0	32°-36° A.P.I. S-0.85%	3.36	No	728	N	N	
246	1 2 M 2 2 M Plant	100 ¹ 200 ¹ 240	67 134 161	2 4 14	14 14 17	17 17 17	257 257 257	60 170 430	1918 1922 1929	2,380 4,890 2,985	431,636 60,477	7.14	35.1	36°-40° A.P.I.	6.17	No	5,000	B	N	
160	1 2 M 2 2 M Plant	120 120 240	81 121 161	3 3 14	14 14 17	17 17 17	257 257 257	90 150 200	1930 1930 1930	3,724 4,003 1,534	523,700 59,460 140,740	8.60	55.1 41.5 50.5	32°-36° A.P.I.	4.50	No	---	N	N	
101	1 2 M 2 2 M Plant	240 150 ¹ 540	161 101 385	4 3 14	14 14 17	17 17 17	257 257 257	200 180 475	1928 1929 1923	5,899 1,419 2,762	523,700 59,460 140,740	8.60	55.1 41.5 50.5	28°-30° A.P.I.	2.44	No	992	N	N	
772	1 4 A 1 4 A Plant	250 250 500	168 168 336	4 4 13.75	17.5 17.5 17.5	275 275 275	257 257 257	280 283 513	1916 1916 1916	851 960 513	66,336 87,214 183,860	10.06 10.42 10.25	71.7 75.3 75.7	28°-30° A.P.I.	3.72	No	1,100	N	N	
501	1 2 M 2 2 M Plant	180 240 480	81 161 323	2 4 14	14 14 17	17 17 17	257 257 257	90 200 380	1925 1925 1929	4,371 4,287 2,508	111,535 106,275 280,500	9.84 9.89 9.37	31.7 31.7 47.1	34°-36° A.P.I. and 37°-40° A.P.I.	4.71	No	1,106	N	N	
424	1 2 M 2 2 M Plant	240 240 480	161 161 322	4 4 14	14 14 17	17 17 17	257 257 257	800 800 400	1929 1929 1929	5,820 3,115 400	398,955 208,860 608,505	8.80 8.23 8.60	42.3 40.9 41.8	32°-36° A.P.I.	3.00	No	400	N	N	
695	1 2 M 2 2 M Plant	165 165 320	111 111 161	3 3 14	12 12 17	15 15 17	257 257 257	360 360 90	1921 1931 1931	2,629 2,482 4,364	359,100 134,030 436,340	9.66 10.96 9.22	34.9 44.8 47.6	32°-36° A.P.I.	4.59	No	300	N	D	
555	1 4 A 2 4 A Plant	250 180 430	168 121 289	4 4 11.75	17.5 15 15	275 300 300	257 257 257	219 150 369	1924 1920 1920	6,288 2,472 369	359,100 502,130 50,345	9.66 10.96 9.97	34.9 44.8 37.1	32°-36° A.P.I.; S-0.5%	3.11	No	867	N	B	

TABLE IV - INFORMATION COVERING FUEL OIL (PAGE 6)

PLANT NAME	ENGINE MANUFACTURER	ENGINE TYPE	RATED H. P.	ENGINE K.W. - 100% GENERATING EFFICIENCY	NUMBER OF CYLINDERS	CYLINDER BORE - INCHES	STROKE - INCHES	RATED R.P.M.	GENERATOR RATING - K.V.A.	YEAR ENGINE STARTED TO WORK	ENGINE HOURS OPERATED IN REPORTED PERIOD	LONGEST OUTPUT - K.W. HIG.	FUEL OIL USED - GALLONS	ENGINE K.W. HIG. PER GALLON OF FUEL OIL	ENGINE CAPACITY FACTOR - (SEE TEXT)	ENGINE PLANT CAPACITY (SEE NOTES)	NATURE OF FUEL OIL USED - (SEE NOTES)	AVERAGE COST OF FUEL OIL - CENTS PER GALLON	IS FUEL CENTRIFUGED?	PLANT ALTITUDE - FEET ABOVE SEA LEVEL	PURPOSE FOR WHICH JACKET WATER HEAT IS UTILIZED (SEE NOTES)	PURPOSE FOR WHICH EXHAUST HEAT IS UTILIZED (SEE NOTES)
247	12	M	240	161	4	14	17	257	160	1928	2,900	-----	-----	-----	-----	29° A.P.I.	-----	-----	-----	-----	-----	-----
1129	12	M	50 ¹	54	2	14	17	257	75	1920	5,850	-----	-----	-----	-----	34°-36° A.P.I. - Summer	-----	-----	-----	-----	-----	-----
	2	M	350	262	4	14	17	257	40	1916	1,800	-----	-----	-----	-----	36°-40° A.P.I. - Winter	-----	-----	-----	-----	-----	-----
	4	M	817 ²	50	2	10.5	14	257	72	-----	3,597	59,500	-----	-----	29.2	-----	-----	-----	-----	-----	-----	-----
	2	M	817 ²	50	2	10.5	14	257	72	-----	30	350	-----	-----	23.3	-----	-----	-----	-----	-----	-----	-----
	4	M	817 ²	64	2	11.32	16	257	72	-----	412	7,700	-----	-----	34.6	-----	-----	-----	-----	-----	-----	-----
	2	M	150	101	3	14	17	257	125	-----	4,792	149,900	-----	-----	29.5	-----	-----	-----	-----	-----	-----	-----
	2	M	380	255	-----	-----	-----	341	-----	-----	-----	203,450	35,299	5.76	29.6	-----	-----	-----	-----	-----	-----	-----
105	12	M	150 ³	101	3	14	17	257	125	1922	4,467	245,000	-----	-----	54.3	34°-36° A.P.I.	-----	-----	-----	-----	-----	-----
	2	M	120	81	14	17	257	75	1928	-----	2,317	57,990	-----	-----	30.9	-----	-----	-----	-----	-----	-----	-----
	2	M	100 ⁴	67	2	14	17	257	75	1923	3,918	107,300	-----	-----	40.9	-----	-----	-----	-----	-----	-----	-----
	2	M	370	249	-----	-----	-----	275	-----	-----	-----	407,300	57,713	7.11	45.5	-----	-----	-----	-----	-----	-----	-----
1091	12	M	180	121	3	14	17	257	150	1930	-----	-----	-----	-----	-----	38° A.P.I.	-----	-----	-----	-----	-----	-----
	2	M	180	121	3	14	17	257	150	1930	-----	-----	-----	-----	-----	-----	-----	-----	-----	-----	-----	-----
	2	M	360	242	-----	-----	-----	300	-----	-----	-----	-----	-----	-----	-----	-----	-----	-----	-----	-----	-----	-----
161	12	M	360	242	6	14	17	257	300	1929	-----	1,003,500	85,140	11.78	-----	30.6° A.P.I. S.U. 44° @ 100°P S-0.55% Ash & B.S. & W. 0.005% Trace	3.96	No	450	N	N	-----
152	12	M	260	242	6	14	17	257	-----	1925	58	6,600	798	8.27	47.0	-----	-----	-----	-----	-----	-----	-----
686	12	M	50 ¹	34	1	14	17	257	-----	1923	944	-----	-----	-----	-----	32°-36° A.P.I.	-----	-----	-----	-----	-----	-----
	2	M	120	81	2	14	17	257	-----	1926	6,068	-----	-----	-----	-----	-----	-----	-----	-----	-----	-----	-----
	2	M	350	235	-----	-----	-----	300	-----	-----	-----	437,500	58,480	7.48	42.6	-----	-----	-----	-----	-----	-----	-----
107	12	M	220	141	2	14	17	300	111	1931	-----	-----	-----	-----	-----	32°-36° A.P.I.	-----	-----	-----	-----	-----	-----
	2	M	350	235	-----	-----	-----	300	-----	1931	-----	-----	-----	-----	-----	-----	-----	-----	-----	-----	-----	-----
	2	M	350	235	-----	-----	-----	300	-----	-----	-----	313,000	35,875	8.77	-----	-----	-----	-----	-----	-----	-----	-----
774	12	M	165	111	4	11.75	15	277	135	1917	487	41,040	3,600	11.40	78.0	26°-30° A.P.I.	-----	-----	-----	-----	-----	-----
	2	M	180	121	4	11.75	15	300	135	1920	480	40,302	3,509	11.49	69.4	-----	-----	-----	-----	-----	-----	-----
	2	M	345 ⁴	232	-----	-----	-----	270	-----	-----	-----	81,342	7,109	11.44	72.6	-----	-----	-----	-----	-----	-----	-----
697	12	M	180	121	3	14	17	257	150	1929	5,571	321,200	-----	-----	47.6	S-1.0% (approx.)	-----	-----	-----	-----	-----	-----
	2	M	150 ¹	101	3	14	17	257	-----	1927	3,842	107,504	-----	-----	32.8	-----	-----	-----	-----	-----	-----	-----
	2	M	380	222	-----	-----	-----	300	-----	-----	-----	429,704	58,127	7.28	42.8	-----	-----	-----	-----	-----	-----	-----
1055	12	M	320	215	4	15	18.5	300	265	1932 ¹	5,672	235,385	26,367	8.86	29.6	28°-30° A.P.I.	-----	-----	-----	-----	-----	-----
285	12	M	60	40	1	14	17	257	48	1927	2,555	-----	-----	-----	-----	38° A.P.I.	-----	-----	-----	-----	-----	-----
	2	M	120	81	2	14	17	257	90	1927	3,718	-----	-----	-----	-----	-----	-----	-----	-----	-----	-----	-----
	2	M	140	94	2	14	17	300	111	1931	2,615	-----	-----	-----	-----	-----	-----	-----	-----	-----	-----	-----
	2	M	320	215	-----	-----	-----	249	-----	-----	-----	245,000	33,130	7.40	37.9	-----	-----	-----	-----	-----	-----	-----
27	12	M	75 ¹	50	2	12	15	300	-----	1926	6,173	-----	-----	-----	-----	-----	-----	-----	-----	-----	-----	-----
	2	M	240	161	4	12.5	13.25	335	-----	1928	2,611	-----	-----	-----	-----	-----	-----	-----	-----	-----	-----	-----
	2	M	315	211	-----	-----	-----	-----	-----	-----	-----	219,470	36,111	5.52	28.8	-----	-----	-----	-----	-----	-----	-----
282	12	M	150	101	4	9.5	14	300	140	1927	4,458	96,700	-----	-----	21.9	36°-40° A.P.I. S-1% Ash & C.C.-Trace; B.S. & W. Not over 1%	-----	-----	-----	-----	-----	-----
	2	M	150	101	4	9.5	14	300	140	1927	555	7,600	-----	-----	14.3	-----	-----	-----	-----	-----	-----	-----
	2	M	300	202	-----	-----	-----	-----	-----	-----	-----	106,300	13,543	7.85	21.2	-----	-----	-----	-----	-----	-----	-----
656	12	M	150 ¹	101	3	14	17	257	125	1929	4,144	112,800	-----	-----	27.0	S-1% (approx.)	-----	-----	-----	-----	-----	-----
	2	M	120	81	2	14	17	257	90	1929	4,640	86,300	-----	-----	26.2	-----	-----	-----	-----	-----	-----	-----
	2	M	270	182	-----	-----	-----	215	-----	-----	-----	211,100	40,136	5.26	26.7	-----	-----	-----	-----	-----	-----	-----
626	12	M	120	81	2	14	17	257	95	1930	4,066	216,000	-----	-----	66.0	28°-30° A.P.I.	-----	-----	-----	-----	-----	-----
	2	M	120	81	2	14	17	257	95	1930	4,458	219,300	-----	-----	60.8	-----	-----	-----	-----	-----	-----	-----
	2	M	240	182	-----	-----	-----	190	-----	-----	-----	435,300	45,610	8.50	65.4	-----	-----	-----	-----	-----	-----	-----
516	12	M	120	81	2	14	17	257	94	1926	4,380 ¹	-----	-----	-----	-----	29°-31° A.P.I.	-----	-----	-----	-----	-----	-----
	2	M	120	81	2	14	17	257	94	1930	4,380 ²	-----	-----	-----	-----	-----	-----	-----	-----	-----	-----	-----
	2	M	240	162	-----	-----	-----	188	-----	-----	-----	160,600	23,700	6.78	22.8	-----	-----	-----	-----	-----	-----	-----
160	12	M	240	161	6	10.75	13.75	327	200	1928	1,834	81,890	10,007	8.18	27.7	30-32° A.P.I. S.U.-45° @ 100°P; S-0.5% (Max.) Ash & B.S. & W.-Trace	5.04	No	20	B	N	-----
664	12	M	225	151	6	9.5	13.5	400	219	1928	405	28,800	3,900	7.38	47.1	Delivered in Tank Wagon	4.50	No	190	N	M	-----
718	12	M	22 ¹	17	1	10	15	325	-----	1918	-----	13,100	-----	-----	-----	-----	-----	-----	-----	-----	-----	-----
	2	M	27 ¹	21	1	12	18	300	-----	1924	-----	44,310	-----	-----	-----	-----	-----	-----	-----	-----	-----	-----
	2	M	50 ¹	24	1	14	17	257	-----	1920	-----	46,200	-----	-----	-----	-----	-----	-----	-----	-----	-----	-----
	2	M	100	67	2	12.5	13.25	327	-----	1922 ²	-----	40,820	-----	-----	-----	-----	-----	-----	-----	-----	-----	-----
	2	M	212 ²	145	-----	-----	-----	-----	-----	-----	-----	149,430	23,039	6.27	-----	-----	-----	-----	-----	-----	-----	-----
752	12	M	100	67	2	12.5	13.25	327	80	1922	21	951	272	3.50	67.4	-----	-----	-----	-----	-----	-----	-----
	2	M	75 ¹	50	2	12	15	300	60	1914	30	864	200	4.32	67.2	-----	-----	-----	-----	-----	-----	-----
	2	M	175	117	-----	-----	-----	120	-----	-----	-----	1,615	472	3.64	62.1	-----	-----	-----	-----	-----	-----	-----
144	12	M	120	81	2	14	17	257	90	1927	668	7,220	2,043	3.53	13.4	36°-40° A.P.I.	5.37	No	600	N	N	-----

NOTES: INJECTION SYSTEM

A - Air
M - Mechanical

SCAVENING SYSTEM (2 STROKE CYCLE ONLY)

C - Crank Case Compressor
P - Attached Pump or Blower
B - Independently Driven Blower

HEAT UTILIZATION

N - Not Utilized
B - To Heat Building
F - To Heat Fuel Oil
L - To Heat Lubricating Oil (Before Purification)
B - To Heat Boiler Feed Water
T - Thawing Ice Cans

NATURE OF FUEL

A.P.I. - American Petroleum Institute
S.U. - Seconds Saybolt Universal
S.F. - Seconds Saybolt Furol
S. - Sulphur
C.C. - Carbon by Conradson Method
B.S. - Bottom Sediment and Water
ASPH. - Asphaltic Residue

LETTERED NOTES:

a - Started Fifth Day of 5th Month
b - No Deductions Made for Motor Driven Scavenging Blower
c - Installed Twenty-first Day of 9th Month
d - Started Twenty-fifth Day of 12th Month
e - Horizontal Engine
f - Revised from Previously Reported Figure by Operator
g - Date of Original Installation; Started Here on First Day of Fourth Month
h - Estimated
i - Seal-Glass
j - Started Tenth Day of 8th Month
k - Started Before Beginning of Period
l - Started Twenty-ninth day of Second Month
m - Date of Original Installation; Started Here in 1924
n - Sold For 257 R.P.M.
o - Supercharged to Give Sea Level Intake
p - Date of Original Installation; Installed in This Plant in 1930
r - Date of Original Installation; Installed in This Plant in 1928
s - Second Unit Discarded Thirtieth Day of 11th Month; Third Unit Started on That Date
t - Started First Day of Fifth Month Period
u - All Belt Driven Direct - Current Generators
v - Date of Original Installation; Date Installed Here Unknown

TABLE V INFORMATION COVERING MAINTENANCE AND OPERATING LABOR (PAGE 1)

TABLE V INFORMATION COVERING MAINTENANCE AND OPERATING LABOR (PAGE 1)																												
PLANT NUMBER	ENGINE DESIGNATION	ENGINE CYCLE	INJECTION SYSTEM (SEE NOTES)	STARTING SYSTEM (SEE NOTES)	NUMBER OF CYLINDERS	RATED B. H. P.	EQUIVALENT S.F. - 60% OPERATING EFFICIENCY	YEAR ENGINE STARTED TO WORK	PEAK LOAD DURING REPORTED PERIOD - GROSS E.H.P.	B.M.S.P. AT RATED B. H. P. LBS. PER SQ. IN.	S.M.S.P. AT PEAK LOAD - 50% GENERATING EFFICIENCY	ENGINE CAPACITY FACTOR (SEE TEXT)	RUNNING PLANT CAPACITY FACTOR (SEE TEXT)	PISTON COOLING (SEE NOTES)	ARE AIR FILTERS USED?	TYPE COOLING SYSTEM (SEE TEXT)	COST OF REGULAR ENGINE MAINTENANCE - MATERIAL - EXTRA LABOR	COST OF REPAIRS PER ENGINE ACCIDENTS - TOTAL DOLLARS - MATERIAL - EXTRA LABOR	TOTAL ENGINE REPAIRS IN DOLLARS PER RATED S.H.P. PER YEAR	MAJOR ENGINE PARTS REPAIRED DURING REPORTED PERIOD	NUMBER OF ENFORCED ENGINE SHUTDOWNS DUE TO DEFECTS IN THE SHUTDOWNS - HOURS	TOTAL ENGINE MAINTENANCE TIME NOT INCLUDING EXPOSED SHUTDOWNS - HOURS	NUMBER OF SHIFTS IN PERIOD	NUMBER OF HOURS PER SHIFT	NUMBER OF ATTENDANTS PER SHIFT	OUTPUT PER MAN-HOUR - NET K.W. HRS.		
43	14	A	4	500	336	1915	300	78.4	70.0	88.9	W	No	W	W	No	106-311	0	0.48										
43	14	A	4	500	336	1916	300	78.4	70.0	71.8	W	No	W	W	No	303-881	0	0.58										
43	14	A	4	1,000	671	1922	740	73.9	81.5	65.2	W	No	W	W	No	520-234	0	0.73										
43	14	A	4	580	349	1919	400	74.0	84.8	76.7	W	No	W	W	No		0	0.38										
43	14	A	4	580	349	1920	400	74.0	84.8	76.7	W	No	W	W	No		0	0.38										
43	14	A	4	3,750	2,517	1928	2,800	67.2	74.5	101.4	W	Yes	W	W	Yes		8,512-5,506	1.60										
43	14	A	4	3,750	2,517	1929	2,800	67.2	74.5	88.0	W	Yes	W	W	Yes		920-652	0.38										
43	14	A	4	4,100	2,753	1934	2,800	73.5	74.8	75.8	W	Yes	W	W	Yes													
43	14	A	4	15,640	10,499		6,400																					
82	14	A	4	560	242	1921		72.7		64.6	A	No	W	W	No	20-323	0	0.95										
82	14	A	4	750	504	1923		67.3		50.7	A	No	W	W	No	182-597	0	1.04										
82	14	A	4	760	504	1924		67.3		49.6	A	No	W	W	No	170-525	0	1.08										
82	14	A	4	1,150	772	1927		68.1		50.1	A	No	W	W	No	361-548	0	0.75										
82	14	A	4	1,150	772	1927		68.1		60.1	A	No	W	W	No	957-2,181	0	2.71										
82	14	A	4	1,500	1,007	1929		67.3		69.4	A	No	W	W	No	479-2,234	0	1.81										
82	14	A	4	3,300	2,213	1932		67.6		54.3	A	No	W	W	No	171-556	0	0.13										
82	14	A	4	8,960	6,017		3,860																					
52	14	A	4	850	557	1928	880	75.3	79.4	70.4	W	No	W	W	No	120-606	0	0.88										
52	14	A	4	1,250	840	1928	880	75.7	79.4	80.1	W	No	W	W	No	87-754	0	0.87										
52	14	A	4	1,250	840	1928	880	75.7	79.8	90.3	W	No	W	W	No	101-338	0	0.75										
52	14	A	4	2,865	1,924	1933	1,880	74.5	79.4	59.0	W	Yes	W	W	Yes	49-590	0	0.51										
52	14	A	4	7,445	5,001		2,920																					
91	14	A	4	600	403	1927		64.6		56.9	A	Yes	W	W	No		0	0.88										
91	14	A	4	600	403	1927		64.6		61.8	A	Yes	W	W	No		0	0.88										
91	14	A	4	1,125	755	1928		72.3		54.1	A	Yes	W	W	No		0	0.88										
91	14	A	4	1,125	755	1928		72.3		56.1	A	Yes	W	W	No		0	0.88										
91	14	A	4	1,800	1,208	1930		72.9		62.6	A	Yes	W	W	No		0	0.88										
91	14	A	4	5,250	3,524		1,625																					
73	12	A	2	1,250	840	1928	880	62.8	70.7	65.1	W	Yes	W	W	No		0	0.88										
73	12	A	2	1,250	840	1928	880	62.8	70.0	66.6	W	Yes	W	W	No		0	0.88										
73	12	A	2	1,250	840	1928	880	62.5	64.0	66.1	W	Yes	W	W	No		0	0.88										
73	12	A	2	1,250	840	1926	880	62.5	63.2	69.8	W	Yes	W	W	No		0	0.88										
73	12	A	2	3,560			2,305																					
92	12	A	2	2,400	1,612	1930		63.5		64.5	W	Yes	W	W	No		0	0.88										
92	12	A	2	2,400	1,612	1930		63.5		64.5	W	Yes	W	W	No		0	0.88										
92	12	A	2	1,250	840	1928		62.5		74.4	W	Yes	W	W	No		0	0.88										
92	12	A	2	4,900	3,292		2,000																					
45	14	A	4	600	403	1923	350	77.2	67.0	45.4	A	No	W	W	No		0	0.88										
45	14	A	4	600	403	1923	350	77.2	67.0	47.6	A	No	W	W	No		0	0.88										
45	14	A	4	700	504	1923	400	75.1	84.0	54.0	A	No	W	W	No		0	0.88										
45	14	A	4	1,150	772	1926	800	76.1	78.9	64.3	A	No	W	W	No		0	0.88										
45	14	A	4	1,150	772	1926	800	76.1	78.9	64.2	A	No	W	W	No		0	0.88										
45	14	A	4	4,950	2,684		1,500																					
54	14	A	4	600	403			69.8			A	No	W	W	No		0	0.88										
54	14	A	4	600	403			69.8			A	No	W	W	No		0	0.88										
54	14	A	4	600	403	1926		69.8			A	No	W	W	No		0	0.88										
54	14	A	4	600	403			69.8			A	No	W	W	No		0	0.88										
54	14	A	4	600	403	1926		69.8			A	No	W	W	No		0	0.88										
54	14	A	4	600	403			69.8			A	No	W	W	No		0	0.88										
54	14	A	4	600	403			69.8			A	No	W	W	No		0	0.88										
54	14	A	4	4,200	2,821		2,875																					
150	14	A	4	600	403	1924	460	73.8	84.3	88.8	A	Yes	W	W	No	149-31	0	1.60										
150	14	A	4	600	403	1924	460	73.7	79.4	85.2	A	Yes	W	W	No	172-0	0	1.12										
150	14	A	4	1,000	506	1929	975	70.1	84.8	69.4	A	Yes	W	W	No	627-42	0	0.56										
150	14	A	4	1,200	806	1930	975	70.1	84.8	70.2	A	Yes	W	W	No	633-57	0	0.58										
150	14	A	4	3,600	2,418		1,160																					
167	12	A	2	1,760	1,182	1930	1,400	64.9	76.8	82.0	W	No	W	W	No	8,545-0	0	0.72										
167	12	A	2	1,760	1,182	1930	1,400	64.9	76.8	82.5	W	No	W	W	No		0	0.72										
167	12	A	2	2,320	2,364																							
2	14	A	4	1,150	772	1925	755	74.3	75.6	98.0	W	No	W	W	No		0	2.85										
2	14	A	4	1,150	772	1925	755	74.3	75.6	97.7	W	No	W	W	No		0	2.85										
2	14	A	4	2,450	2,316		2,355																					
164	14	A	4	840	564	1926	542	72.4	69.6	81.0	W	No	W	W	No		0	0.88										
164	14	A	4	840	564	1926	542	72.4	68.0	74.4	W	No	W	W	No		0	0.88										
164	14	A	4	840	564	1926	542	72.4	70.0	81.0	W	No	W	W	No		0	0.88										
164	14	A	4	840	564	1926	542	72.4	70.6	83.2	W	No	W	W	No		0	0.88										
164	14	A	4	3,360	2,256		2,075																					
3	14	A	4	400	289	1923	275	64.1	65.5		A	No	W	W	No		0	0										
3	14	A	4	800	537	1924	540	72.7	73.1		A	No	W	W	No		0	0										
3	14	A	4	800	537	1926	540	72.7	73.1		A	No	W	W	No		0	0										
3	14	A	4	1,126	765	1927	700	72.3	67.0		A	No	W	W	No		0	0										
3	14	A	4	3,125	2,098		860																					
720	12	A	2	840	564	1928	460	53.6	42.8	53.1	W	No	W	W	No	195-0	0	0.23										
720	12	A	2	840	564	1928																						

TABLE V—INFORMATION COVERING MAINTENANCE AND OPERATING LABOR (PAGE 2)

TABLE V-INFORMATION COVERING MAINTENANCE AND OPERATING LABOR (PAGE 2)																											
PLANT NUMBER	ENGINE DESIGNATION (SEE NOTES)	ENGINE SYSTEM (SEE NOTES)	SCAVENGING SYSTEM (SEE NOTES)	RATED B. H. P.	EQUIVALENT K.W. - 90% GENERATING EFFICIENCY	YEAR ENGINE STARTED TO WORK	PEAK LOAD DURING REPORT- ED PERIOD - GROSS K.W.	B.M.P. AT RATED B. H. P. - LBS. PER SQ. IN.	B.M.P. AT PEAK LOAD - LBS. PER SQ. IN.	90% GENERATING EFFICIENCY	RUNNING ENGINE CAPACITY FACTOR (SEE TEXT)	RUNNING PLANT CAPACITY FACTOR (SEE TEXT)	PISTON COOLING (SEE NOTES)	AIR FILTER USED (SEE TEXT)	TYPICAL COOLING SYSTEM (SEE TEXT)	COST OF REGULAR ENGINE UPKEEP - TOTAL DOLLARS MATERIAL - EXTRA LABOR	COST OF REPAIRS FOR ENGINE ACCIDENTS - TOTAL DOLLARS - MATERIAL - EXTRA LABOR	TOTAL ENGINE REPAIRS IN DOLLARS PER RATED B.H.P. PER YEAR	MAJOR ENGINE PARTS RENEWED DURING REPORTED PERIOD	NUMBER OF ENFORCED ENGINE STOPPAGE	SUBSTITUTION OF REPAIRS MADE - HOURS	TOTAL ENGINE MAINTENANCE TIME NOT INCLUDING RE- PAIRED STOPPAGE - HOURS	NUMBER OF SHIFTS IN PERIOD	NUMBER OF HOURS PER SHIFT	NUMBER OF ATTENDANTS PER SHIFT	OUTPUT PER MAN-HOUR - NET K.W. HRS.	
109	2825 Plant	2825	1963	675	453	1927	395	57.4	50.0	44.5	49.2	0	No	Yes	7.5	0.24	-----	-----	-----	103	200	366	8	1	92		
7	3500 Plant	3500	1925	235	225	1925	225	100.3	96.1	58.9	57.9	0	Yes	Yes	1968 - 1040	1.10	1-Head Wedges; Spray Valve Tips and Rods; Governor Bearings; Exhaust Valve Spring Valve Cage Studs	0	0	640 ⁵	0	0	366	8	1	177	
732	2520 Plant	2520	1925	250	168	1918	---	74.1	---	---	---	50.4	0	Yes	Yes	8091 - 0	3.45	-----	-----	-----	366	8	1	199			
978	2520 Plant	2520	1925	840	564	1931	---	53.6	---	---	---	27.6	0	Yes	Yes	-----	-----	-----	-----	-----	366	8	1	313			
908	1250 Plant	1250	1925	840	800	1925	800	62.5	59.8	69.8	68.5	0	No	Yes	5354-	0	2.14	1-Piston Head; 50 Piston Rings Top and Bottom Eccen. Straps	0	0	366	8	1	393			
93	2480 Plant	2480	1928	700	470	1928	---	53.6	---	51.3	52.0	0	Yes	Yes	-----	2723	1.10	Cylinder Heads And Gaskets	0	0	366	8	1	344			
111	2475 Plant	2475	1928	900	604	1928	600	72.6	72.1	---	---	---	0	No	Yes	1,604-	0	0.41	Packing/Gaskets; Air Compressor Valve Discs	0	0	366	8	2	234		
1149	1200 Plant	1200	1932	806	806	1932	---	57.5	---	---	---	---	0	Yes	Yes	-----	-----	-----	-----	-----	366	8	1	202			
60	800 Plant	800	1924	537	537	1924	550	60.3	61.6	24.0	24.8	0	No	Yes	-----	-----	-----	-----	-----	366	8	1	87				
723	300P Plant	300P	202	1925	190	1924	190	29.4	27.7	74.6	67.2	0	No	Yes	-----	-----	-----	-----	-----	0	0	54	10	2	110		
41	2370 Plant	2370	1925	520	348	1925	400	74.6	85.6	80.2	65.5	0	No	Yes	-----	968	0.41	Valve Seats, Heads & Stems; Air Comp. Valves; Valves and Piston Parts for Air Bottles	0	0	366	8	2	130			
79	2225 Plant	2225	1911	110	75.0	54.6	53.0	54.6	54.6	68.3	66.2	0	No	Yes	751-0	0	0.36	Piston Rings Piston Rings Piston Rings	0	0	366	8	2	140			
5	720 Plant	720	1926	484	484	1927	---	46.0	---	---	94.4	0	No	Yes	-----	-----	-----	-----	-----	0	0	366	8	1	470		
8	300P Plant	300P	202	1926	---	29.4	---	---	---	---	97.4	0	No	Yes	-----	-----	-----	-----	-----	0	0	366	8	1	158		
68	240 Plant	240	1925	120	35.3	26.3	54.4	54.6	54.6	68.3	66.2	0	No	Yes	-----	1303	0.63	Injection Pump; Cyl. Heads; Cyl. Heads; Scav. Pump Valves; Injection Pump & Nozzle Parts	0	0	366	8	1	346			
83	400 Plant	400	1927	269	1922	---	77.2	79.0	79.0	36.0	62.0	0	Yes	Yes	400-2,500	0	1.45	Piston Rings, Gaskets, Etc.	0	0	366	8	2	96			
215	980 Plant	980	1930	800 ⁵	53.6	65.2	84.5	53.6	65.2	83.7	84.2	0	Yes	Yes	83-0	0	0.04	-----	0	0	366	8	1	17			
735	1125 Plant	1125	1924	755	755	1924	---	67.3	---	62.6	75.2	0	Yes	Yes	1,779-303	0	1.85	-----	0	0	606	12	1	185			

TABLE V INFORMATION COVERING MAINTENANCE AND OPERATING LABOR (PAGE 4)

PLANT NUMBER	ENGINE DESIGNATION	ENGINE SIZE (SEE NOTES)	SAVENING SYSTEM (SEE NOTES)	NUMBER OF CYLINDERS	RATED B. H. P.	EQUIVALENT K.V. - 50% GENERATING EFFICIENCY	YEAR ENGINE STARTED TO WORK	PEAK LOAD DURING REPORT-ED PERIOD - GROSS K.W.	B.M.P.P. AT RATED B. H. P. - LBS. PER SQ. IN.	B.M.P.P. AT PEAK LOAD - 90% GENERATING EFFICIENCY	RUNNING ENGINE CAPACITY FACTOR (SEE TEXT)	RUNNING PLANT CAPACITY FACTOR (SEE TEXT)	PISTON COOLING (SEE NOTES)	ARE AIR FILTERS USED?	TYPE COOLING SYSTEM (SEE TEXT)	COST OF REGULAR ENGINE OILKEEP - TOTAL DOLLARS - MATERIAL - EXTRA LABOR	COST OF REPAIRS FOR ENGINE ACCIDENTS - TOTAL DOLLARS - MATERIAL - EXTRA LABOR	PLANT ENGINE REPAIRS IN DOLLARS PER YEAR B.M.P. PER YEAR	MAJOR ENGINE PARTS REPAIRED DURING REPORTED PERIOD	NUMBER OF ENFORCED ENGINE STOPPAGE - HOURS	TOTAL LUBRICATION OF ENFORCED ENGINE STOPPAGE - HOURS	TOTAL ENGINE MAINTENANCE TIME NOT INCLUDING ENGINE STOPPAGE - HOURS	NUMBER OF SHIFTS IN PERIOD	NUMBER OF HOURS PER SHIFT	NUMBER OF ATTENDANTS PER SHIFT	OUTPUT PER MAN-HOUR - NET K.W. HIG.
886	1 2 3 4 5 6 7 8 9 10 11 12 13 14 15 16 17 18 19 20 21 22 23 24 25 26 27 28 29 30 31 32 33 34 35 36 37 38 39 40 41 42 43 44 45 46 47 48 49 50 51 52 53 54 55 56 57 58 59 60 61 62 63 64 65 66 67 68 69 70 71 72 73 74 75 76 77 78 79 80 81 82 83 84 85 86 87 88 89 90 91 92 93 94 95 96 97 98 99 100 101 102 103 104 105 106 107 108 109 110 111 112 113 114 115 116 117 118 119 120 121 122 123 124 125 126 127 128 129 130 131 132 133 134 135 136 137 138 139 140 141 142 143 144 145 146 147 148 149 150 151 152 153 154 155 156 157 158 159 160 161 162 163 164 165 166 167 168 169 170 171 172 173 174 175 176 177 178 179 180 181 182 183 184 185 186 187 188 189 190 191 192 193 194 195 196 197 198 199 200 201 202 203 204 205 206 207 208 209 210 211 212 213 214 215 216 217 218 219 220 221 222 223 224 225 226 227 228 229 230 231 232 233 234 235 236 237 238 239 240 241 242 243 244 245 246 247 248 249 250 251 252 253 254 255 256 257 258 259 260 261 262 263 264 265 266 267 268 269 270 271 272 273 274 275 276 277 278 279 280 281 282 283 284 285 286 287 288 289 290 291 292 293 294 295 296 297 298 299 300 301 302 303 304 305 306 307 308 309 310 311 312 313 314 315 316 317 318 319 320 321 322 323 324 325 326 327 328 329 330 331 332 333 334 335 336 337 338 339 340 341 342 343 344 345 346 347 348 349 350 351 352 353 354 355 356 357 358 359 360 361 362 363 364 365 366 367 368 369 370 371 372 373 374 375 376 377 378 379 380 381 382 383 384 385 386 387 388 389 390 391 392 393 394 395 396 397 398 399 400 401 402 403 404 405 406 407 408 409 410 411 412 413 414 415 416 417 418 419 420 421 422 423 424 425 426 427 428 429 430 431 432 433 434 435 436 437 438 439 440 441 442 443 444 445 446 447 448 449 450 451 452 453 454 455 456 457 458 459 460 461 462 463 464 465 466 467 468 469 470 471 472 473 474 475 476 477 478 479 480 481 482 483 484 485 486 487 488 489 490 491 492 493 494 495 496 497 498 499 500 501 502 503 504 505 506 507 508 509 510 511 512 513 514 515 516 517 518 519 520 521 522 523 524 525 526 527 528 529 530 531 532 533 534 535 536 537 538 539 540 541 542 543 544 545 546 547 548 549 550 551 552 553 554 555 556 557 558 559 560 561 562 563 564 565 566 567 568 569 570 571 572 573 574 575 576 577 578 579 580 581 582 583 584 585 586 587 588 589 590 591 592 593 594 595 596 597 598 599 600 601 602 603 604 605 606 607 608 609 610 611 612 613 614 615 616 617 618 619 620 621 622 623 624 625 626 627 628 629 630 631 632 633 634 635 636 637 638 639 640 641 642 643 644 645 646 647 648 649 650 651 652 653 654 655 656 657 658 659 660 661 662 663 664 665 666 667 668 669 670 671 672 673 674 675 676 677 678 679 680 681 682 683 684 685 686 687 688 689 690 691 692 693 694 695 696 697 698 699 700 701 702 703 704 705 706 707 708 709 710 711 712 713 714 715 716 717 718 719 720 721 722 723 724 725 726 727 728 729 730 731 732 733 734 735 736 737 738 739 740 741 742 743 744 745 746 747 748 749 750 751 752 753 754 755 756 757 758 759 760 761 762 763 764 765 766 767 768 769 770 771 772 773 774 775 776 777 778 779 780 781 782 783 784 785 786 787 788 789 790 791 792 793 794 795 796 797 798 799 800 801 802 803 804 805 806 807 808 809 810 811 812 813 814 815 816 817 818 819 820 821 822 823 824 825 826 827 828 829 830 831 832 833 834 835 836 837 838 839 840 841 842 843 844 845 846 847 848 849 850 851 852 853 854 855 856 857 858 859 860 861 862 863 864 865 866 867 868 869 870 871 872 873 874 875 876 877 878 879 880 881 882 883 884 885 886 887 888 889 890 891 892 893 894 895 896 897 898 899 900 901 902 903 904 905 906 907 908 909 910 911 912 913 914 915 916 917 918 919 920 921 922 923 924 925 926 927 928 929 930 931 932 933 934 935 936 937 938 939 940 941 942 943 944 945 946 947 948 949 950 951 952 953 954 955 956 957 958 959 960 961 962 963 964 965 966 967 968 969 970 971 972 973 974 975 976 977 978 979 980 981 982 983 984 985 986 987 988 989 990 991 992 993 994 995 996 997 998 999 1000	1 2 3 4 5 6 7 8 9 10 11 12 13 14 15 16 17 18 19 20 21 22 23 24 25 26 27 28 29 30 31 32 33 34 35 36 37 38 39 40 41 42 43 44 45 46 47 48 49 50 51 52 53 54 55 56 57 58 59 60 61 62 63 64 65 66 67 68 69 70 71 72 73 74 75 76 77 78 79 80 81 82 83 84 85 86 87 88 89 90 91 92 93 94 95 96 97 98 99 100 101 102 103 104 105 106 107 108 109 110 111 112 113 114 115 116 117 118 119 120 121 122 123 124 125 126 127 128 129 130 131 132 133 134 135 136 137 138 139 140 141 142 143 144 145 146 147 148 149 150 151 152 153 154 155 156 157 158 159 160 161 162 163 164 165 166 167 168 169 170 171 172 173 174 175 176 177 178 179 180 181 182 183 184 185 186 187 188 189 190 191 192 193 194 195 196 197 198 199 200 201 202 203 204 205 206 207 208 209 210 211 212 213 214 215 216 217 218 219 220 221 222 223 224 225 226 227 228 229 230 231 232 233 234 235 236 237 238 239 240 241 242 243 244 245 246 247 248 249 250 251 252 253 254 255 256 257 258 259 260 261 262 263 264 265 266 267 268 269 270 271 272 273 274 275 276 277 278 279 280 281 282 283 284 285 286 287 288 289 290 291 292 293 294 295 296 297 298 299 300 301 302 303 304 305 306 307 308 309 310 311 312 313 314 315 316 317 318 319 320 321 322 323 324 325 326 327 328 329 330 331 332 333 334 335 336 337 338 339 340 341 342 343 344 345 346 347 348 349 350 351 352 353 354 355 356 357 358 359 360 361 362 363 364 365 366 367 368 369 370 371 372 373 374 375 376 377 378 379 380 381 382 383 384 385 386 387 388 389 390 391 392 393 394 395 396 397 398 399 400 401 402 403 404 405 406 407 408 409 410 411 412 413 414 415 416 417 418 419 420 421 422 423 424 425 426 427 428 429 430 431 432 433 434 435 436 437 438 439 440 441 442 443 444 445 446 447 448 449 450 451 452 453 454 455 456 457 458 459 460 461 462 463 464 465 466 467 468 469 470 471 472 473 474 475 476 477 478 479 480 481 482 483 484 485 486 487 488 489 490 491 492 493 494 495 496 497 498 499 500 501 502 503 504 505 506 507 508 509 510 511 512 513 514 515 516 517 518 519 520 521 522 523 524 525 526 527 528 529 530 531 532 533 534 535 536 537 538 539 540 541 542 543 544 545 546 547 548 549 550 551 552 553 554 555 556 557 558 559 560 561 562 563 564 565 566 567 568 569 570 571 572 573 574 575 576 577 578 579 580 581 582 583 584 585 586 587 588 589 590 591 592 593 594 595 596 597 598 599 600 601 602 603 604 605 606 607 608 609 610 611 612 613 614 615 616 617 618 619 620 621 622 623 624 625 626 627 628 629 630 631 632 633 634 635 636 637 638 639 640 641 642 643 644 645 646 647 648 649 650 651 652 653 654 655 656 657 658 659 660 661 662 663 664 665 666 667 668 669 670 671 672 673 674 675 676 677 678 679 680 681 682 683 684 685 686 687 688 689 690 691 692 693 694 695 696 697 698 699 700 701 702 703 704 705 706 707 708 709 710 711 712 713 714 715 716 717 718 719 720 721 722 723 724 725 726 727 728 729 730 731 732 733 734 735 736 737 738 739 740 741 742 743 744 745 746 747 748 749 750 751 752 753 754 755 756 757 758 759 760 761 762 763 764 765 766 767 768 769 770 771 772 773 774 775 776 777 778 779 780 781 782 783 784 785 786 787 788 789 790 791 792 793 794 795 796 797 798 799 800 801 802 803 804 805 806 807 808 809 810 811 812 813 814 815 816 817 818 819 820 821 822 823 824 825 826 827 828 829 830 831 832 833 834 835 836 837 838 839 840 841 842 843 844 845 846 847 848 849 850 851 852 853 854 855 856 857 858 859 860 861 862 863 864 865 866 867 868 869 870 871 872 873 874 875 876 877 878 879 880 881 882 883 884 885 886 887 888 889 890 891 892 893 894 895 896 897 898 899 900 901 902 903 904 905 906 907 908 909 910 911 912 913 914 915 916 917 918 919 920 921 922 923 924 925 926 927 928 929 930 931 932 933 934 935 936 937 938 939 940 941 942 943 944 945 946 947 948 949 950 951 952 953 954 955 956 957 958 959 960 961 962 963 964 965 966 967 968 969 970 971 972 973 974 975 976 977 978 979 980 981 982 983 984 985 986 987 988 989 990 991 992 993 994 995 996 997 998 999 1000	120 200 242 282 300 320 340 360 380 400 420 440 460 480 500 520 540 560 580 600 620 640 660 680 700 720 740 760 780 800 820 840 860 880 900 920 940 960 980 1000 1020 1040 1060 1080 1100 1120 1140 1160 1180 1200 1220 1240 1260 1280 1300 1320 1340 1360 1380 1400 1420 1440 1460 1480 1500 1520 1540 1560 1580 1600 1620 1640 1660 1680 1700 1720 1740 1760 1780 1800 1820 1840 1860 1880 1900 1920 1940 1960 1980 2000 2020 2040 2060 2080 2100 2120 2140 2160 2180 2200 2220 2240 2260 2280 2300 2320 2340 2360 2380 2400 2420 2440 2460 2480 2500 2520 2540 2560 2580 2600 2620 2640 2660 2680 2700 2720 2740 2760 2780 2800 2820 2840 2860 2880 2900 2920 2940 2960 2980 3000 3020 3040 3060 3080 3100 3120 3140 3160 3180 3200 3220 3240 3260 3280 3300 3320 3340 3360 3380 3400 3420 3440 3460 3480 3500 3520 3540 3560 3580 3600 3620 3640 3660 3680 3700 3720 3740 3760 3780 3800 3820 3840 3860 3880 3900 3920 3940 3960 3980 4000 4020 4040 4060 4080 4100 4120 4140 4160 4180 4200 4220 4240 4260 4280 4300 4320 4340 4360 4380 4400 4420 4440 4460 4480 4500 4520 4540 4560 4580 4600 4620 4640 4660 4680 4700 4720 4740 4760 4780 4800 4820 4840 4860 4880 4900 4920 4940 4960 4980 5000 5020 5040 5060 5080 5100 5120 5140 5160 5180 5200 5220 5240 5260 5280 5300 5320 5340 5360 5380 5400 5420 5440 5460 5480 5500 5520 5540 5560 5580 5600 5620 5640 5660 5680 5700 5720 5740 5760 5780 5800 5820 5840 5860 5880 5900 5920 5940 5960 5980 6000 6020 6040 6060 6080 6100 6120 6140 6160 6180 6200 6220 6240 6260 6280 6300 6320 6340 6360 6380 6400 6420 6440 6460 6480 6500 6520 6540 6560 6580 6600 6620 6640 6660 6680 6700 6720 6740 6760 6780 6800 6820 6840 6860 6880 6900 6920 6940 6960 6980 7000 7020 7040 7060 7080 7100 7120 7140 7160 7180 7200 7220 7240 7260 7280 7300 7320 7340 7360 7380 7400 7420 7440 7460 7480 7500 7520 7540 7560 7580 7600 7620 7640 7660 7680 7700 7720 7740 7760 7780 7800 7820 7840 7860 7880 7900 7920 7940 7960 7980 8000 8020 8040 8060 8080 8100 8120 8140 8160 8180 8200 8220 8240 8260 8280 8300 8320 8340 8360 8380 8400 8420 8440 8460 8480 8500 8520 8540 8560 8580 8600 8620 8640 8660 8680 8700 8720 8740 8760 8780 8800 8820 8840 8860 8880 8900 8920 8940 8960 8980 9000 9020 9040 9060 9080 9100 9120 9140 9160 9180 9200 9220 9240 9260 9280 9300 9320 9340 9360 9380 9400 9420 9440 9460 9480 9500 9520 9540 9560 9580 9600 9620 9640 9660 9680 9700 9720 9740 9760 9780 9800 9820 9840 9860 9880 9900 9920 9940 9960 9980 10000	81 134 242 282 300 320 340 360 380 400 420 440 460 480 500 520 540 560 580 600 620 640 660 680 700 720 740 760 780 800 820 840 860 880 900 920 940 960 980 1000 1020 1040 1060 1080 1100 1120 1140 1160 1180 1200 1220 1240 1260 1280 1300 1320 1340 1360 1380 1400 1420 1440 1460 1480 1500 1520 1540 1560 1580 1600 1620 1640 1660 1680 1700 1720 1740 1760 1780 1800 1820 1840 1860 1880 1900 1920 1940 1960 1980 2000 2020 2040 2060 2080 2100 2120 2140 2160 2180 2200 2220 2240 2260 2280 2300 2320 2340 2360 2380 2400 2420 2440 2460 2480 2500 2520 2540 2560 2580 2600 2620 2640 2660 2680 2700 2720 2740 2760 2780 2800 2820 2840 2860 2880 2900 2920 2940 2960 2980 3000 3020 3040 3060 3080 3100 3120 3140 3160 3180 3200 3220 3240 3260 3280 3300 3320 3340 3360 3380 3400 3420 3440 3460 3480 3500 3520 3540 3560 3580 3600 3620 3640 3660 3680 3700 3720 3740 3760 3780 3800 3820 3840 3860 3880 3900 3920 3940 3960 3980 4000 4020 4040 4060 4080 4100 4120 4140 4160 4180 4200 4220 4240 4260 4280 4300 4320 4340 4360 4380 4400 4420 4440 4460 4480 4500 4520 4540 4560 4580 4600 4620 4640 4660 4680 4700 4720 4740 4760 4780 4800 4820 4840 4860 4880 4900 4920 4940 4960 4980 5000 5020 5040 5060 5080 5100 5120 5140 5160 5180 5200 5220 5240 5260 5280 5300 5320 5340 5360 5380 5400 5420 5440 5460 5480 5500 5520 5540 5560 5580 5600 5620 5640 5660 5680 5700 5720 5740 5760 5780 5800 5820 5840 5860 5880 5900 5920 5940 5960 5980 6000 6020 6040 6060 6080 6100 6120 6140 6160 6180 6200 6220 6240 6260 6280 6300 6320 6340 6360 6380 6400 6420 6440 6460 6480 6500 6520 6540 6560 6580 6600 6620 6640 6660 6																						

TABLE V- INFORMATION COVERING MAINTENANCE AND OPERATING LABOR (PAGE 5)

TABLE V - INFORMATION COVERING MAINTENANCE AND OPERATING LABOR (PAGE 5)																												
PLANT NUMBER	ENGINE DESIGNATION	ENGINE TYPE	INJECTION SYSTEM (SEE NOTE 1)	STARTING SYSTEM (SEE NOTE 2)	NUMBER OF CYLINDERS	RATED B. H. P.	EQUIVALENT K.W. - 80% GENERATING EFFICIENCY	YEAR ENGINE STARTED TO WORK	PEAK LOAD DURING REPORTED PERIOD - GROSS K.W.	B.H.P. AT RATED B. H. P. - 80% GENERATING EFFICIENCY	B.H.P. AT PEAK LOAD - 90% GENERATING EFFICIENCY	RUNNING ENGINE CAPACITY FACTOR (SEE TEXT)	RUNNING PLANT CAPACITY FACTOR (SEE TEXT)	PISTON COOLING (SEE NOTES)	ARE AIR FILTERS USED?	TYPE COOLING SYSTEM (SEE TEXT)	COST OF REGULAR ENGINE OILKEEP - TOTAL DOLLARS - MATERIAL - EXTRA LABOR	COST OF REPAIRS FOR ENGINE ACCIDENTS - TOTAL DOLLARS - MATERIAL - EXTRA LABOR	TOTAL ENGINE REPAIRS IN DOLLARS PER YEAR B.H.P. PER YEAR	MAJOR ENGINE PARTS REPAIRED PERIOD	NUMBER OF ENFORCED ENGINE SHUTDOWNS - REPAIRS OF ENFORCED ENGINE SHUTDOWNS - REPAIRS	TOTAL ENGINE MAINTENANCE TIME NOT INCLUDING ENFORCED SHUTDOWNS - HOURS	NUMBER OF SHIFTS IN PERIOD	NUMBER OF HOURS PER SHIFT	NUMBER OF ATTENDANTS PER SHIFT	UNEMPLOYED PER MAN-HOUR - TEST & REPAIR		
8/3	1-1	1-1	1-1	1-1	1-1	300	372	1925	150	72.7	54.0	71.6	01.6	A	No	A	2,494--	0	2.56	Piston Rings Piston Rings	0	0	366	8	1			
1065	1-1	1-1	1-1	1-1	1-1	975	655	1927	400	72.7	64.2	83.2	01.6	A	No	D-E	300-77	0	0.42	None	0	0	366	8	1			
500	1-1	1-1	1-1	1-1	1-1	200	134	1924	100	72.7	54.0	71.6	01.6	A	No	A	102-22	0	1.40	4 New Pistons & Rings 1 New Piston & Rings Fuel Pump Plungers and Miscellaneous Shop Work	0	0	366	8	2			
260	1-1	1-1	1-1	1-1	1-1	900	605	1928	600	64.4	62.9	47.0	47.0	0	No	A	11-0	0	0.01	Gaskets	0	0	366	8	1	61		
98	1-1	1-1	1-1	1-1	1-1	350	242	1926	---	25.3	---	60.2	---	A	Yes	A	---	---	0.51	Bearings and Gaskets	---	---	366	8	1			
53	1-1	1-1	1-1	1-1	1-1	900	605	1926	425	35.3	---	59.8	61.5	A	Yes	D	---	---	---	Rebabbit Lower Half All M.B.s and Six Crank Bear- ings; All new Piston Rings; All Cyls. Debored; Piston Rings and Pins; Rebabbit Lower Half All M.B.s and All Crank Bearings Minor Parts	---	---	366	8	1	171		
170	1-1	1-1	1-1	1-1	1-1	400	269	1925	260	73.2	71.3	68.4	69.0	A	No	E-L	---	---	---	10 New Piston Rings None None	0	0	366	8	1	229		
1056	1-1	1-1	1-1	1-1	1-1	840	564	1929	600	53.6	57.0	76.2	76.2	0	Yes	D	---	---	1.35	Main Bearings	2	360	366	8	1			
610	1-1	1-1	1-1	1-1	1-1	840	564	1929	500	53.6	52.3	76.5	76.5	0	Yes	B-E	104-0	---	1.06	Crank Shaft Bearings as	0	0	366	6	1	262		
494	1-1	1-1	1-1	1-1	1-1	840	564	1920	500	52.6	47.5	74.5	74.5	0	Yes	D-E	200-09	0	0.34	Minor Parts	0	0	366	6	1	256		
153	1-1	1-1	1-1	1-1	1-1	840	564	1929	500	53.6	53.2	82.7	82.7	0	---	---	---	---	---	---	---	---	---	---	---	151		
721	1-1	1-1	1-1	1-1	1-1	825	554	1926	600	74.0	81.1	68.2	68.2	W	Yes	D	906-0	0	1.10	---	0	0	366	9	1	---		
648	1-1	1-1	1-1	1-1	1-1	400	269	1928	200	64.6	48.0	70.4	---	A	Yes	A	0	---	0	Piston and Liner	0	0	366	10	1	---		
421	1-1	1-1	1-1	1-1	1-1	800	537	1930	525	72.7	71.1	69.6	69.6	A	Yes	A	0	0	0	---	0	0	366	10	1	170		
112	1-1	1-1	1-1	1-1	1-1	200P	134	1925	100	25.4	20.6	77.1	---	A	No	D-E	93-0	0	0.13	Piston Rings and Head Gaskets	0	0	349	10	1	164		
718	1-1	1-1	1-1	1-1	1-1	360	242	1926	100	35.3	23.4	32.5	---	A	No	A	---	---	0.94	3- Crank Bearings; 2-M.B.s 18 Piston Rings 3- Crank Bearings; 1-Lub. Sump Pump; 18 Piston Rings	---	---	366	12	1	---		
522	1-1	1-1	1-1	1-1	1-1	360	242	1928	210	35.3	35.0	---	---	A	Yes	D-E	---	---	0.71	Piston Rings	0	0	366	8	1	149		
527	1-1	1-1	1-1	1-1	1-1	360	242	1930	210	35.3	35.0	---	---	A	Yes	D	94-0	0	0.23	2 Rings on each Piston re- placed by one-piece Double Seals	---	---	366	8	1	---		
170	1-1	1-1	1-1	1-1	1-1	360	242	1929	210	35.3	35.0	---	---	A	No	B-E	156-0	0	0.43	All New Rings	---	---	366	8	1	110		
67	1-1	1-1	1-1	1-1	1-1	360	242	1925	210	35.3	30.6	81.5	---	A	No	A	---	---	1.17	1-Sealed Piston & Cyl 1-Connecting Rod; 1-Cyl. Head	---	---	366	10	2	---		
19	1-1	1-1	1-1	1-1	1-1	200	134	1927	---	25.4	---	---	---	A	---	---	---	---	---	---	---	---	---	---	---	---		
411	1-1	1-1	1-1	1-1	1-1	200	134	1924	100	25.4	21.9	---	---	A	No	B-E	0	0	0	Gaskets	0	0	366	8	1	65		
529	1-1	1-1	1-1	1-1	1-1	200	134	1926	70	32.3	30.5	---	---	A	No	B-E	0	0	0.11	1- Inj. Valve	0	0	366	8	1	70		
106	1-1	1-1	1-1	1-1	1-1	200	134	1922	55	29.4	24.1	---	---	A	No	A	0	0	0	Minor Parts	---	---	348	10	1	52		
1086	1-1	1-1	1-1	1-1	1-1	200	134	1922	55	29.4	24.1	---	---	A	No	A	0	0	0.30	Inj; Nozzle Parts	---	---	348	10	1	---		
1094	1-1	1-1	1-1	1-1	1-1	200	134	1922	55	29.4	24.1	---	---	A	No	A	0	0	0.30	Inj; Nozzle Parts	---	---	348	10	1	---		
644	1-1	1-1	1-1	1-1	1-1	240	161	1921	156	35.3	34.2	---	---	A	No	D	100-60	680-200	1.72	Gor. Gears & Thrust Bear- ings; Failure due to lub- oil failure; Lub. System New changed	2	192	72	366	4	1	242	
61	1-1	1-1	1-1	1-1	1-1	200	134	1928	220	35.3	35.0	---	---	A	No	D	150-64	0	0.36	Minor Parts	0	0	366	3	1	261		
	1-1	1-1	1-1	1-1	1-1	240	161	1921	156	35.3	34.2	---	---	A	No	D	35-0	0	0.06	Gaskets	0	0	366	10	1	77		
	1-1	1-1	1-1	1-1	1-1	200	134	1928	220	35.3	35.0	---	---	A	No	D	475-218	522-193	2.31	Intermediate Cyl. Heads Intermediate Cyl. Heads (due to Scale and cold water)	2	1.5	366	9	1	140		

TABLE V - INFORMATION COVERING MAINTENANCE AND OPERATING LABOR (PAGE 6)

PLANT NUMBER	ENGINE DESIGNATION	ENGINE CYCLE	INJECTION SYSTEM (SEE NOTES)	SAVING SYSTEM (SEE NOTES)	NUMBER OF CYLINDERS	PLANT B. H. P.	EQUIVALENT K. W. - 90% GENERATING EFFICIENCY	YEAR ENGINE STARTED TO WORK	PEAK LOAD DURING REPORTED PERIOD - GROSS K. W.	B. H. P. AT RATED B. H. P. LESS PER SQ. IN.	B. H. P. AT PEAK LOAD 50% GENERATING EFFICIENCY	RUNNING ENGINE CAPACITY FACTOR (SEE TEXT)	RUNNING PLANT CAPACITY FACTOR (SEE TEXT)	PISTON COOLING (SEE NOTES)	AIR FILTERS USED?	TYPE COOLING SYSTEM (SEE TEXT)	COST OF REGULAR ENGINE UPKEEP - TOTAL DOLLARS - MATERIAL - EXTRA LABOR	COST OF REPAIRS FOR ENGINE ACCIDENTS - TOTAL DOLLARS - MATERIAL - EXTRA LABOR	TOTAL ENGINE REPAIRS IF DOLLARS PER RATED B.H.P. PER YEAR	MAJOR ENGINE PARTS REPAIRED DURING REPORTED PERIOD	NUMBER OF ENGINES IN SERVICE	TOTAL DURATION OF ENFORCED SHUTDOWNS - HOURS	TOTAL ENGINE MAINTENANCE HOURS - ENGINES	NUMBER OF SHUTS IN PERIOD	NUMBER OF HOURS PER SHIP	NUMBER OF ATTENDANTS PER SHIP	COST PER MAN-HOUR - PER A.M. HRS.
103	12 M C 4	2	150P	161	1927	450	74.6	83.3	77.9	77.9	A	No	A	No	A	No	30 - 10	41 - 36	0.20	3 - Intermediate Cyl. Heads; Small pinion of Fuel Distrib.	3	24	120	166	12	17	96
862	12 M C 4	2	150P	161	1927	450	74.6	83.3	77.9	77.9	A	No	A	No	A	No	30 - 10	41 - 36	0.20	3 - Intermediate Cyl. Heads; Small pinion of Fuel Distrib.	3	24	120	166	12	17	96
102	12 M C 4	2	150P	161	1927	450	74.6	83.3	77.9	77.9	A	No	A	No	A	No	30 - 10	41 - 36	0.20	3 - Intermediate Cyl. Heads; Small pinion of Fuel Distrib.	3	24	120	166	12	17	96
540	12 M C 4	2	150P	161	1927	450	74.6	83.3	77.9	77.9	A	No	A	No	A	No	30 - 10	41 - 36	0.20	3 - Intermediate Cyl. Heads; Small pinion of Fuel Distrib.	3	24	120	166	12	17	96
246	12 M C 4	2	150P	161	1927	450	74.6	83.3	77.9	77.9	A	No	A	No	A	No	30 - 10	41 - 36	0.20	3 - Intermediate Cyl. Heads; Small pinion of Fuel Distrib.	3	24	120	166	12	17	96
160	12 M C 4	2	150P	161	1927	450	74.6	83.3	77.9	77.9	A	No	A	No	A	No	30 - 10	41 - 36	0.20	3 - Intermediate Cyl. Heads; Small pinion of Fuel Distrib.	3	24	120	166	12	17	96
101	12 M C 4	2	150P	161	1927	450	74.6	83.3	77.9	77.9	A	No	A	No	A	No	30 - 10	41 - 36	0.20	3 - Intermediate Cyl. Heads; Small pinion of Fuel Distrib.	3	24	120	166	12	17	96
772	12 M C 4	2	150P	161	1927	450	74.6	83.3	77.9	77.9	A	No	A	No	A	No	30 - 10	41 - 36	0.20	3 - Intermediate Cyl. Heads; Small pinion of Fuel Distrib.	3	24	120	166	12	17	96
501	12 M C 4	2	150P	161	1927	450	74.6	83.3	77.9	77.9	A	No	A	No	A	No	30 - 10	41 - 36	0.20	3 - Intermediate Cyl. Heads; Small pinion of Fuel Distrib.	3	24	120	166	12	17	96
424	12 M C 4	2	150P	161	1927	450	74.6	83.3	77.9	77.9	A	No	A	No	A	No	30 - 10	41 - 36	0.20	3 - Intermediate Cyl. Heads; Small pinion of Fuel Distrib.	3	24	120	166	12	17	96
695	12 M C 4	2	150P	161	1927	450	74.6	83.3	77.9	77.9	A	No	A	No	A	No	30 - 10	41 - 36	0.20	3 - Intermediate Cyl. Heads; Small pinion of Fuel Distrib.	3	24	120	166	12	17	96
335	12 M C 4	2	150P	161	1927	450	74.6	83.3	77.9	77.9	A	No	A	No	A	No	30 - 10	41 - 36	0.20	3 - Intermediate Cyl. Heads; Small pinion of Fuel Distrib.	3	24	120	166	12	17	96
247	12 M C 4	2	150P	161	1927	450	74.6	83.3	77.9	77.9	A	No	A	No	A	No	30 - 10	41 - 36	0.20	3 - Intermediate Cyl. Heads; Small pinion of Fuel Distrib.	3	24	120	166	12	17	96
1129	12 M C 4	2	150P	161	1927	450	74.6	83.3	77.9	77.9	A	No	A	No	A	No	30 - 10	41 - 36	0.20	3 - Intermediate Cyl. Heads; Small pinion of Fuel Distrib.	3	24	120	166	12	17	96
106	12 M C 4	2	150P	161	1927	450	74.6	83.3	77.9	77.9	A	No	A	No	A	No	30 - 10	41 - 36	0.20	3 - Intermediate Cyl. Heads; Small pinion of Fuel Distrib.	3	24	120	166	12	17	96
201	12 M C 4	2	150P	161	1927	450	74.6	83.3	77.9	77.9	A	No	A	No	A	No	30 - 10	41 - 36	0.20	3 - Intermediate Cyl. Heads; Small pinion of Fuel Distrib.	3	24	120	166	12	17	96
161	12 M C 4	2	150P	161	1927	450	74.6	83.3	77.9	77.9	A	No	A	No	A	No	30 - 10	41 - 36	0.20	3 - Intermediate Cyl. Heads; Small pinion of Fuel Distrib.	3	24	120	166	12	17	96
152	12 M C 4	2	150P	161	1927	450	74.6	83.3	77.9	77.9	A	No	A	No	A	No	30 - 10	41 - 36	0.20	3 - Intermediate Cyl. Heads; Small pinion of Fuel Distrib.	3	24	120	166	12	17	96
688	12 M C 4	2	150P	161	1927	450	74.6	83.3	77.9	77.9	A	No	A	No	A	No	30 - 10	41 - 36	0.20	3 - Intermediate Cyl. Heads; Small pinion of Fuel Distrib.	3	24	120	166	12	17	96
187	12 M C 4	2	150P	161	1927	450	74.6	83.3	77.9	77.9	A	No	A	No	A	No	30 - 10	41 - 36	0.20	3 - Intermediate Cyl. Heads; Small pinion of Fuel Distrib.	3	24	120	166	12	17	96
774	12 M C 4	2	150P	161	1927	450	74.6	83.3	77.9	77.9	A	No	A	No	A	No	30 - 10	41 - 36	0.20	3 - Intermediate Cyl. Heads; Small pinion of Fuel Distrib.	3	24	120	166	12	17	96
857	12 M C 4	2	150P	161	1927	450	74.6	83.3	77.9	77.9	A	No	A	No	A	No	30 - 10	41 - 36	0.20	3 - Intermediate Cyl. Heads; Small pinion of Fuel Distrib.	3	24	120	166	12	17	96

TABLE 1 - INFORMATION COVERING MAINTENANCE AND OPERATING LABOR (PAGE 2)

TABLE 2 - INFORMATION COVERING MAINTENANCE AND OPERATING LABOR																														
PLANT NUMBER	ENGINE DESCRIPTION		ENGINE COOLING	EXHAUST SYSTEM (SEE NOTES)	MAINTENANCE PERIOD (SEE NOTES)	NUMBER OF CYCLES	RATED B. H. P.	EQUIVALENT I.H. - 100% GENERATING EFFICIENCY	YEAR ENGINE STARTED TO WORK	PEAK LOAD DURING REPORTED PERIOD - GROSS I.H.	B.M.E.P. AT RATED B. H. P. - LBS. PER SQ. IN.	B.M.E.P. AT PEAK LOAD - 100% GENERATING EFFICIENCY	RUNNING ENGINE CAPACITY FACTOR (SEE TEXT)	RUNNING PLANT CAPACITY FACTOR (SEE TEXT)	PISTON COOLING (SEE NOTES)	ARE AIR FILTERS USED?	TYPE COOLING SYSTEM	COST OF REGULAR ENGINE UPKEEP - TOTAL DOLLARS - MATERIAL - EXTRA LABOR	COST OF REPAIRS FOR ENGINE ACCIDENTS - TOTAL DOLLARS - MATERIAL - EXTRA LABOR	TOTAL ENGINE REPAIRS IN PERIOD - TOTAL DOLLARS PER RATED B.H.P. PER YEAR	MAJOR ENGINE PARTS REPAIRED DURING REPORTED PERIOD	NUMBER OF REPORTED ENGINE SHUTDOWNS	TOTAL DURATION OF REPORTED ENGINE SHUTDOWNS - HOURS	TOTAL ENGINE MAINTENANCE PERIOD - HOURS	NUMBER OF SHUTS IN PERIOD	NUMBER OF HOURS PER SHIFT	NUMBER OF ATTENDANTS PER SHIFT	OUTPUT PER MAN-HOUR - NET I.H. HRS.		
1055	1	4 M - 4	320	215	1928	190	64.6	57.1	29.6	29.6	A	Yes	D	0				0	0	0	None	0	0	0	153	8	1	56		
265	1	4 M - 4	60	40	1927	30	35.3	26.5	---	---	A	No	---	---				25 - 0	0	{0.08}	{Minor Parts Only}	0	0	---	---	---	---	---	---	
	2	2 M - 4	180	81	1927	65	35.3	28.3	---	---	A	No	---	---				---	0	---	---	0	0	---	---	---	---	---	---	
	Plant	320	215	---	110	---	---	---	---	---	---	---	---	37.9	---	---	---	---	---	---	---	---	---	---	---	---	---	---	---	
27	1	2 M - 2	75P	50	1926	---	29.1	---	---	---	A	---	---	---				---	---	---	---	---	---	---	---	---	---	---	---	
	2	2 M - 4	840	161	1926	---	45.0	---	---	---	A	---	---	---				---	---	---	---	---	---	---	---	---	---	---	---	
	Plant	315	211	---	78	---	---	---	---	---	---	---	---	---				---	---	---	---	---	---	---	---	---	---	---	---	
382	1	4 M - 4	150	101	1927	---	99.7	---	---	---	A	Yes	---	---				0	0	0	None	0	0	---	---	---	---	---	---	
	2	2 M - 4	150	101	1927	---	99.7	---	---	---	A	Yes	---	---				0	0	0	None	0	0	---	---	---	---	---	---	
	Plant	300	202	---	---	---	---	---	---	---	---	---	---	---				---	---	---	---	---	---	---	---	---	---	---	---	
558	1	2 M - 2	150P	101	1929	---	29.4	---	---	---	A	No	---	---				---	---	---	---	---	---	---	---	---	---	---	---	
	2	2 M - 2	120	81	1929	---	35.3	---	---	---	A	No	---	---				---	---	---	---	---	---	---	---	---	---	---	---	
	Plant	270	182	---	60P	---	---	---	---	---	---	---	---	---				---	---	---	---	---	---	---	---	---	---	---	---	
626	1	2 M - 2	120	81	1930	---	35.3	---	---	---	A	Yes	---	---				0	0	{0 - 100}	{0.42}	{Minor Parts}	0	0	---	---	---	---	---	---
	2	2 M - 2	120	81	1930	---	35.3	---	---	---	A	Yes	---	---				0	0	---	---	---	0	0	---	---	---	---	---	---
	Plant	240	162	---	---	---	---	---	---	---	---	---	---	---				---	---	---	---	---	---	---	---	---	---	---	---	---
510	1	2 M - 2	120	81	1926	80	35.3	21.8	---	---	A	No	---	---				18 - 6	0	{0.10}	{Gaskets}	0	0	11	---	---	---	---	---	
	2	2 M - 2	120	81	1930	80	35.3	21.8	---	---	A	No	---	---				---	0	---	---	0	0	0	---	---	---	---	---	---
	Plant	240	162	---	100	---	---	---	---	---	---	---	---	---				---	---	---	---	---	---	---	---	---	---	---	---	---
169	1	4 M - 6	240	161	1928	160P	77.6	77.2	27.7	27.7	A	Yes	B	---				---	---	---	Injection Nozzles Reconditioned At Factory, Piston Rings	8.5	64	215	8.5	1P	---	---		
984	1	4 A - 6	225	151	1928	200	77.6	102.8	47.1	47.1	A	Yes	D	0				0	0	0	---	0	0	0	42	6.5	1	100		
318	1	2 M - 1	25P	17	1918	10	29.8	17.5	---	---	A	No	---	---				---	---	---	---	---	---	---	---	---	---	---	---	---
	2	2 M - 1	57.5P	25	1924	18	29.1	21.0	---	---	A	No	---	---				---	---	---	---	---	---	---	---	---	---	---	---	---
	3	2 M - 1	50P	34	1920	35	29.4	30.3	---	---	A	No	---	---				---	---	---	---	---	---	---	---	---	---	---	---	---
	4	2 M - 2	100	67	1922	55	37.2	30.6	---	---	A	No	---	---				---	---	---	---	---	---	---	---	---	---	---	---	---
	Plant	212.6	143	---	---	---	---	---	---	---	---	---	---	---				---	---	---	---	---	---	---	---	---	---	---	---	---
733	1	2 M - 2	100	67	1922	63	37.2	35.0	67.4	67.4	A	No	---	---				---	---	---	---	---	---	---	---	---	---	---	---	---
	2	2 M - 2	75P	50	1914	54	29.1	31.4	57.2	57.2	A	No	---	---				---	---	---	---	---	---	---	---	---	---	---	---	---
	Plant	176	117	---	115	---	---	---	---	---	---	---	---	---				---	---	---	---	---	---	---	---	---	---	---	---	---
646	1	2 M - 2	120	81	1927	60	35.3	21.8	13.4	13.4	A	No	B-D-E	0				0	0	0	---	0	0	---	---	---	---	---	---	---

Notes:

Injection System
A - Air
M - Mechanical

Scavenging System (For 2-Stroke Cycle Only)
C - Crank Case Compression
P - Attached Pump or Blower
B - Independently Driven Blower

Piston Cooling
A - Air
O - Oil
W - Water

Lettered Notes

a- Installed Fifth Day of Fifth Month
b- Sixty Minute Peak
c- Installed Twenty-first Day of Ninth Month
d- Installed Twenty-fifth Day of Twelfth Month
e- Air Filtered for Air Compressor
f- Changed to B near End of Period
g- Includes Five Cylinder Heads Broken by Sabotage in 1929
h- Twenty-four Hour Peak
i- A, in Summer; C in winter
j- Replacement Due to Experiment With Steel Heads; Manufacturer Made No Charge For Replacement
k- Horizontal
l- High Maintenance Time Due to Experimenting with Main Bearings and Fuel Pump Construction and Also Due to Fulfillment of Acceptance Conditions
m- Rating Revised From Previous Report By Operator
n- Excessive Maintenance Time Due to Extensive Surveys Made Possible Because Units Were Not Needed
o- Date of Original Installation; Started In This Plant On First Day Of Fourth Month
p- Semi Diesel
q- Part Time
r- Includes Total Maintenance Labor
s- Not Including Several Shutdowns Due To Lightning Damage To Generators
t- Installed Tenth Day Of Sixth Month
u- Started Before Period Began
v- Started Twenty-ninth Day Of Second Month
y- Thirty Minute Peak
z- Date Of Original Installation; Installed In This Plant In 1924
aa- Operation Started Unit Without Water Circulating Through Oil Cooler
bb- Cylinders Scored Due To Cooling Water Failure. Four Weeks Required To Ship Parts
cc- Date Of Original Installation; Installed Here In 1930
dd- Date Of Original Installation; Installed Here In 1928
ee- Second Unit Discarded Thirtieth Day Of Eleventh Month; Third Unit Started On That Date
ff- Not I.H.
gg- Started First Day Of Fifth Month Period
hh- Estimated
ii- Supercharged to Produce Sea Level Conditions
jj- Date Of Original Installation; Date Installed Here Unknown

Power Supplies for Suction-Driven Gyroscopic Aircraft Instruments

By C. S. DRAPER¹ AND A. F. SPILHAUS,² CAMBRIDGE, MASS.

At the present time gyroscopic instruments constitute an essential part of the equipment in any well-equipped airplane. The "turn indicator," the "artificial horizon," and the "directional gyro" are three widely used gyroscopic aircraft instruments which have reached a very satisfactory state of development. However, in order that proper results may be attained in practice, it is necessary that some reliable and sufficient source of suction be provided. It is the object of this paper to present a study of the various devices used in operating the gyroscopic instruments.

AIR REQUIREMENTS FOR INSTRUMENTS

AS a preliminary to the problem of suction supply it is necessary to study the air-consumption requirements of the gyro instruments. Figs. 1, 2, and 3 indicate diagrammatically the gyro-wheel arrangements in the three instruments. In each case the wheel is supported on gimbals within a chamber which is closed except for an air entrance leading to a nozzle and a connection to the intake side of the source of suction. Air flowing through the nozzle into the evacuated chamber impinges on the wheel and produces the necessary driving torque.

Fig. 4 shows the experimentally determined relation between the pressure difference provided and the rotor speed for the three instruments. In a similar manner Fig. 5 indicates the variation of air consumption with pressure difference. Table 1 is a summary of the conditions for normal operation.

TABLE 1 NORMAL OPERATING CONDITIONS AT SEA LEVEL

Instrument	Pressure difference, inches of mercury	Rotor speed, rpm	Air consumption, cfm
Turn indicator.....	2 to 2.5	10,000	0.5
Artificial horizon.....	3.5 to 4	17,000	1.7
Directional gyro.....	3.5 to 4	12,000	1.0

Effect of Altitude. It is very interesting to note that for a constant pressure difference the curves indicate that the gyro wheel experiences an increase in speed with increasing altitude. A study of this phase of the problem has shown that the experi-

mental results check nicely with the predictions of theory.³ Physically this means that a considerable portion of the energy required to keep the gyro wheel in rotation is expended in the maintenance of eddies in the air around the wheel. The energy thus expended will decrease as the air density decreases.

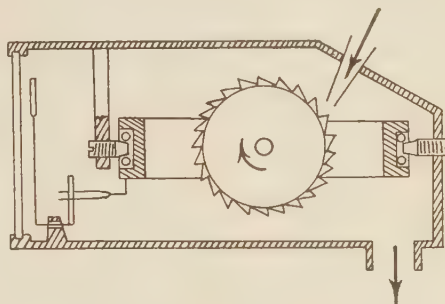


FIG. 1 TURN INDICATOR

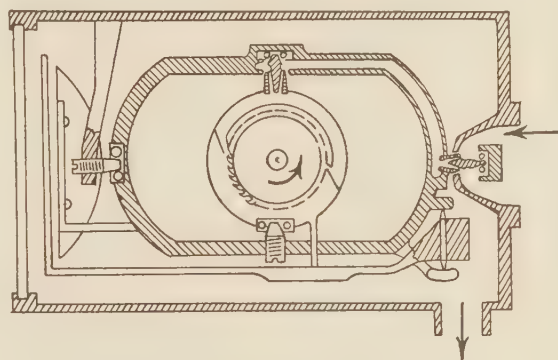


FIG. 2 ARTIFICIAL HORIZON

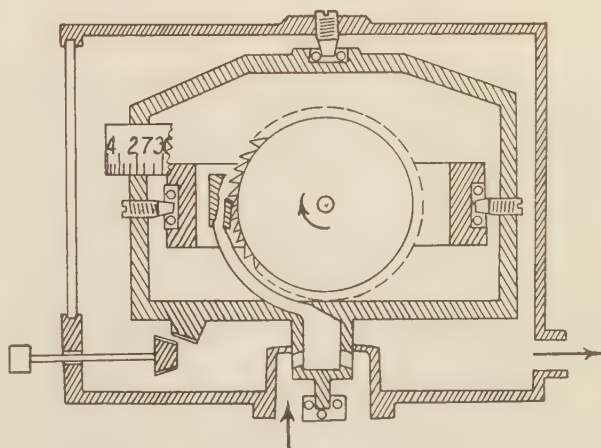


FIG. 3 DIRECTIONAL GYRO

¹ Member of Staff, Massachusetts Institute of Technology. Mr. Draper attended Missouri University in 1917, received the degree of A.B. from Stanford University and the degrees of S.B. and S.M. from the Massachusetts Institute of Technology. He is a commissioned officer in the Army Air Corps Reserve and holds a pilot's license from the Department of Commerce. Since 1928 he has been a member of the staff of the Massachusetts Institute of Technology engaged in internal-combustion-engine research and in charge of aircraft-instrument work at the Institute since 1930.

² Graduate Student, Massachusetts Institute of Technology. Mr. Spilhaus attended school in England and later the University of Cape Town, South Africa, where he received the degree of B.Sc. From the Massachusetts Institute of Technology he received the degree of S.M. in Aeronautical Engineering. Mr. Spilhaus' work on aircraft instruments was begun at M.I.T. and later continued for the Sperry Gyroscope Co. in Brooklyn, N. Y.

Contributed by the Aeronautic Division and presented at the Metropolitan Section Meeting, New York, N. Y., November 23, 1933, of THE AMERICAN SOCIETY OF MECHANICAL ENGINEERS.

NOTE: Statements and opinions advanced in papers are to be understood as individual expressions of their authors, and not those of the Society.

³ "Air Suction Methods in Driving of Gyroscopic Instruments for Aircraft." Thesis by A. F. Spilhaus, Mass. Inst. of Tech., 1933.

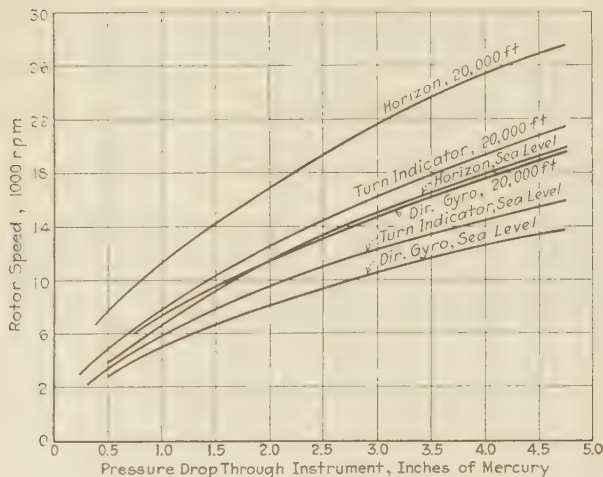


FIG. 4 ROTOR SPEED VS. PRESSURE DROP

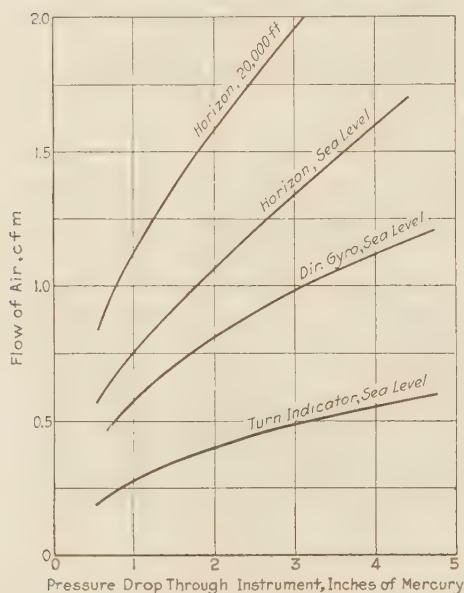


FIG. 5 FLOW OF AIR VS. PRESSURE DROP

Effect of Temperature. The three instruments are required to pass an operation test at minus 35 F. At sea level, the lowering of the temperature increases the density of the air and slows the wheels down slightly. However, as altitude is increased and the temperature decreased there is a net loss of density and therefore a small gain in rotor speed.

The only requirement that seems necessary, therefore, is to maintain a constant pressure difference for the instruments within ± 0.5 in. of mercury, because altitude and temperature changes do not have any marked detrimental effect. This conclusion applies to the air-driven wheel itself considered as free from the effects of bearing friction.

POWER SOURCES FOR OPERATING INSTRUMENTS

The source of power for gyro instruments, in order to be satisfactory, must have certain characteristics:

- (1) It must be reliable and of reasonable efficiency
- (2) It must handle the required air volume per unit time

at the proper pressure difference under all flying conditions near sea level

- (3) It must fulfil condition (2) at the ceiling of the airplane.

At present three types of suction supply are in common use for gyro instruments:

- (1) Venturi with air introduced at the throat section
 - (a) Single venturi for turn indicator
 - (b) Double venturi for horizon and directional gyro
- (2) Displacement air pump
 - (a) Propeller driven
 - (b) Mechanically driven
- (3) Engine carburetor pressure drop.

VENTURI

In the past, specially constructed venturis have been in almost universal use for operating gyro instruments. These venturis have the advantage of being simple, reliable, and inexpensive. On the other hand, they have certain disadvantages:

- (1) The suction supplied varies widely with flight conditions
- (2) The efficiency of the venturi as a power supply is exceedingly low
- (3) Ice formation renders the venturi inoperative.

As long as installations are confined to airplanes with cruising speeds of around 100 mph the advantages of a venturi installation somewhat outweigh the disadvantages.

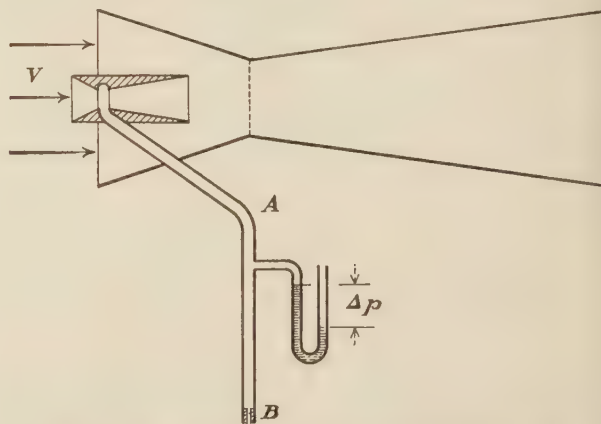


FIG. 6 ARRANGEMENT OF APPARATUS FOR VENTURI TESTS

However, for the modern high-speed airplane it becomes imperative that the problem be reconsidered. This section is devoted to a study of the performance of the venturi in this connection.

Suction Produced by Venturi. The essentials of the system used in the experimental work are indicated in Fig. 6.

In general, the pressure difference given by a venturi producing static suction, that is, with no flow through the line A, may be written.⁴

$$\Delta p = K(1/2\rho v^2) \dots \dots \dots [1]$$

where Δp = pressure difference

ρ = mass density

v = relative velocity of the venturi and the air stream

⁴ "The Theory of Pitot and Venturi Tubes," by Earle Buckingham. National Advisory Committee for Aeronautics, Technical Report No. 2.

$K = \text{constant}$ (except for second order effects)⁵

Variation of Suction With Flow. Experiments made by the writers, with venturis drawing air through orifices of different areas, have shown that for any particular orifice the suction is given by the relation:

$$\Delta p_1 = K_1(1/2\rho v^2) \dots\dots\dots [2]$$

Fig. 7 shows the variation of K_1 for a standard venturi as the effective orifice area is changed. The rapid decrease of K_1 as the orifice area is increased shows that the venturi is unsatisfactory for operating a load with other than a very small orifice area. In practise this means that a separate venturi is required for the horizon and the directional gyro. The turn indicator could be connected in with the directional gyro to even up the amount of air drawn in by each venturi (See Table 1).

Suction Affected by Airplane Speed. Equation [2] shows that the suction supplied by the venturi varies as the square of the relative air velocity v . This means that, if a venturi is to supply sufficient pressure difference at low airplane speeds, it will produce large suction values at high speeds. This may result in rapid deterioration of the gyroscopic instruments due to excessive rotor speeds. On the other hand, if the suction is adjusted

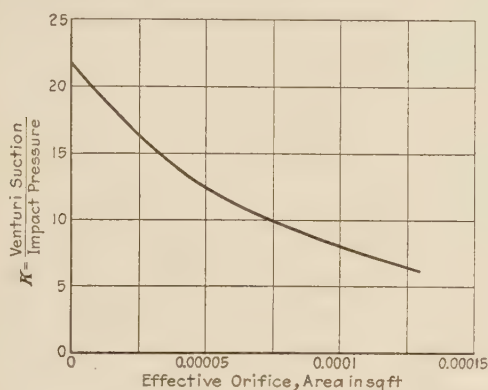


FIG. 7 VARIATION OF VENTURI CONSTANT WITH ORIFICE AREA FOR DOUBLE VENTURI
(From wind-tunnel tests at Mass. Inst. of Tech.)

to a proper value at high airplane speeds, at low speeds the instruments will not operate satisfactorily.

Fig. 8 shows the measured suction on a standard installation with the venturis mounted on the fuselage, in the slipstream, of an airplane with a cruising speed of 160 mph. It is evident that within the cruising range the suction supplied to the gyroscopic instruments was far too great. In such an installation some form of vacuum regulator certainly should be included in the system.

Suction Affected by Altitude. It is evident from Equation [2] that for the same air speed as indicated by a pitot-static meter, that is with $1/2\rho v^2$ constant, the pressure difference will be constant except for a second order variation with Reynold's number.⁶ This means that if a venturi installation gives sufficient suction at stalling speed near sea level, it will give the same value for stalling speed at any altitude. In general, the suction supplied at a given indicated air speed will be the same for all altitudes. In other words, the venturi and instrument combination will operate satisfactorily at the higher altitudes providing the speed, as indicated by the air-speed meter, remains

⁵ "The Altitude Effect on Air Speed Indicators," by M. D. Hersey, F. L. Hunt, and H. D. Eaton. National Advisory Committee for Aeronautics, Technical Report No. 110.

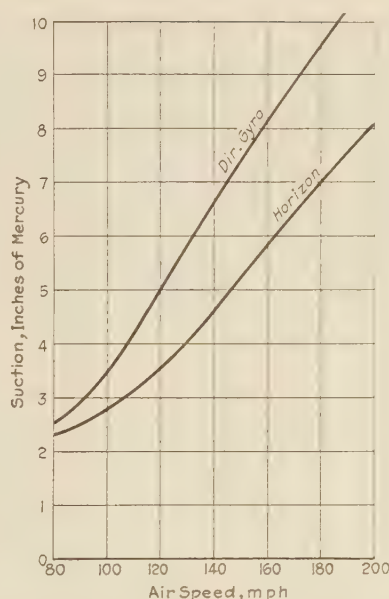


FIG. 8 VENTURI SUCTION AT HIGH SPEEDS
(Venturi mounted on side of fuselage and operating an instrument.)

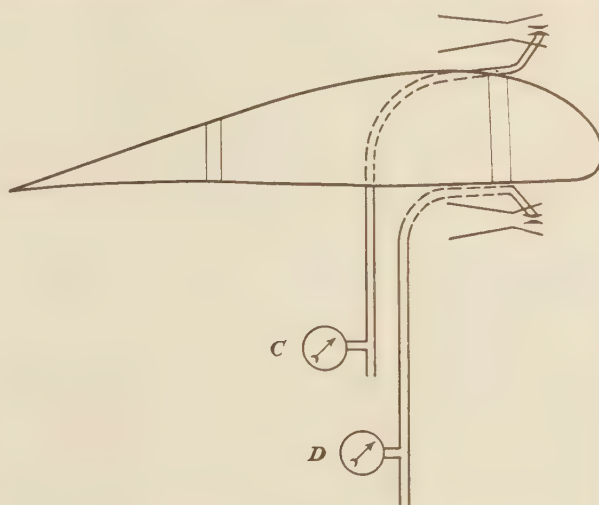


FIG. 9 ARRANGEMENT OF VENTURIS FOR FLIGHT TEST

above the speed at which the instruments cease to function at sea level.

Effect of Location and Flight Conditions on Venturi Suction. Possible positions of venturi.

- (1) On fuselage in slipstream
- (2) On strut in slipstream
- (3) Top of wing in slipstream
- (4) Under wing in slipstream
- (5) Above positions not in slipstream.

A series of flight tests were carried out by the writers with the cooperation of the Meteorological Department at the Massachusetts Institute of Technology. The purpose of these tests was to study the effect of various flight conditions on venturi operation. Two venturi positions were considered, one above the front wing spar and a second below the wing directly in line with the first. Both positions were well within the slipstream. Fig. 9

is a diagram of the experimental arrangement. A moving picture camera was used to record instantaneous readings of the pressure gages *C* and *D* in addition to data supplied by the other instrument equipment of the airplane. The information used in plotting the curves of Fig. 10 was obtained by examination of the moving-picture-film record. Apart from influences of air-speed as discussed above, the effect of maneuvers on venturi performance may be analyzed into two components, one due to the slipstream and a second due to the effective yaw of the venturi with respect to the relative air velocity.

Slipstream Effect. The slipstream effect will be considered first. In general, the pressure difference supplied by the venturi will be:

$$\Delta p' = K'1/2\rho v_e^2 \dots \dots \dots [3]$$

Where v_e is the effective velocity of the air past the venturi.

In practise v_e will be a function not only of slipstream velocity but also of local deviations of the air stream past parts of the airplane structure.

If the indicated velocity of the airplane is v the pressure differ-

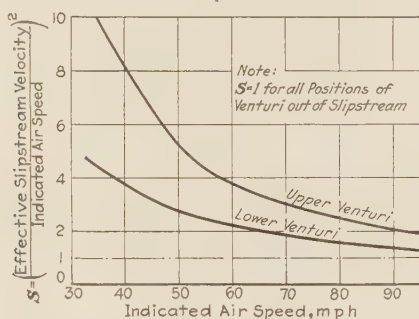


FIG. 10 SLIPSTREAM EFFECT ON VENTURI SUCTION
(Engine kept at constant throttle.)

ence furnished by a venturi without the slipstream and local effects would be:

$$\Delta p = K1/2\rho v^2 \dots \dots \dots [4]$$

The ratio between $\Delta p'$ and Δp may be taken as a measure of the influence of slipstream and position on venturi operation, that is:

$$\frac{\Delta p'}{\Delta p} = \frac{v_e^2}{v^2} = \frac{\Delta p'}{1/2K\rho v^2} = S \dots \dots \dots [5]$$

Fig. 10 is a plot of S against indicated air speed for the tests mentioned above and from this it is immediately apparent that the venturi mounted above the wing profile is much better than that mounted below the wing. This result is readily understandable since air passing above the wing will be accelerated to a greater extent than the air which flows under the wing. The plot also shows the great advantage of a venturi mounted within the slipstream, since a pressure ratio of from 5 to 10 is obtained for a low speed climb where suction is especially valuable.

Effect of Yaw. Data taken from the motion-picture record indicated that slipping or skidding of the airplane has a pronounced tendency to reduce the venturi suction. A series of tests on a venturi was carried out in the wind tunnel at the Massachusetts Institute of Technology. This work showed that the suction for practical purposes is independent of yaw up to an angle of forty degrees.

It was found impossible to explain the flight results on the basis of the wind-tunnel tests. The authors feel that this difficulty may be cleared up easily by further flight tests. It is ques-

tionable, however, if this part of the problem is of sufficient importance to warrant the effort.

VENTURI DRAG

There remains to be considered the power required for the operation of the gyroscopic instruments by means of venturis.

Wind-tunnel tests showed that venturi drag increases with the square of the relative air velocity. This, of course, leads to the usual cube-law increase of power consumption with speed. Fig. 11 shows the power required by the venturi equipment for driving various combinations of the gyroscopic instruments as the airplane velocity is varied. The data used in plotting these curves are based on the assumption of venturis mounted within the slipstream.

Efficiency. It can be shown for the case of a venturi drawing air through a fixed orifice, that efficiency, on a basis of the ratio of power output to power required, is substantially independent of air velocity under conditions of constant density. This efficiency as experimentally determined lies in the range of from 1 to 2 per cent.

The considerable amount of power absorbed by a venturi is a serious disadvantage, especially for use on high-speed, long-range airplanes. For this reason, venturi installations for instrument operation should be limited to airplanes cruising at 120 mph or less. More efficient equipment is available, but the relatively

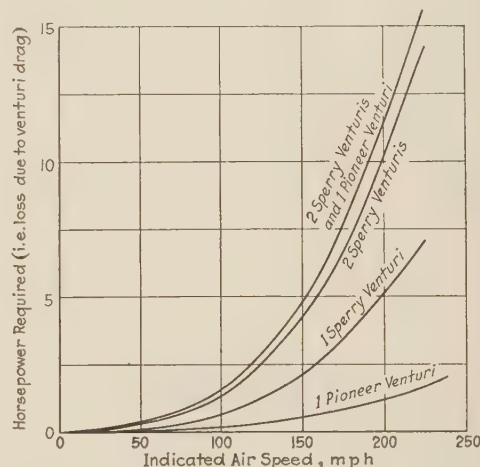


FIG. 11 HORSEPOWER REQUIRED VS. AIR SPEED

small power loss (less than 2 hp) makes the desirability of added complication questionable.

Ice Formation. During an extended series of flights carried out by the Meteorological Department at the Massachusetts Institute of Technology, it was found that under certain atmospheric conditions the venturi installation was rendered inoperative by ice formation. This problem is especially serious as it means that often the instruments will not be available when they are needed most.

It is possible to reduce the difficulties due to ice formation by mounting the venturis where they may receive heat from the engine exhaust. This may be accomplished by placing the venturis on the exhaust manifold itself or by allowing part of the hot gases to flow through the venturi throat. It was found in practise, however, that any simple arrangement for the use of exhaust heat did not prevent ice formation under severe conditions.

DISPLACEMENT PUMP

The problem of drawing air through a fixed orifice by means of

a displacement pump has been studied theoretically. The pressure difference maintained by a displacement pump across the orifice is given by the formula²

$$\Delta p = \frac{\gamma p}{2} \times \left(\frac{1}{1 + \frac{(a\alpha)^2 \gamma R T}{(nw)^2}} \right) \dots \dots \dots [6]$$

Where

- Δp = pressure difference across orifice
- p = atmospheric pressure
- $a\alpha$ = effective orifice area
- v = pump displacement per revolution
- n = revolutions per second
- T = temperature of atmosphere (absolute)
- R = gas constant for unit mass of gas
- γ = exponent of expansion process

This equation is valid for cases in which $(\Delta p)^2$ is small compared to p^2 .

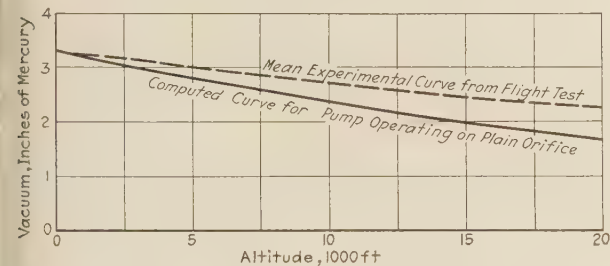


FIG. 12 RELATION BETWEEN VACUUM AND ALTITUDE FOR CONSTANT-SPEED, PROPELLER-DRIVEN, SINGLE-RECIPROCATING-VANE PUMP DRIVING DIRECTIONAL GYRO AND ARTIFICIAL HORIZON

Experiment showed that this equation represents very closely the actual behavior of a pump-orifice system. In practice it was found that with γ equal to unity a good check was obtained. Physically this means that the expansion process was almost isothermal. This is the result to be expected in the case of a well-cooled pump and exposed copper-tube connections.

Types of Pumps and Pump Drives. The various types of pumps can be listed as follows:

- (1) Piston pump
- (2) Multiple rotating vane eccentric
- (3) Single rotating vane
- (4) Single reciprocating vane
- (5) Gear
- (6) Roots blower

The different methods of driving the pumps are:

- (1) Propeller drive

- (2) Electric motor drive
- (3) Engine drive.

It is not the intention to discuss all the different types of pumps. Certain examples only will be considered below.

The pressure-altitude plot shown in Fig. 12 is a comparison of flight test results on a constant-speed, propeller-driven, single reciprocating vane pump with corresponding values calculated by formula [6]. In this case the pump was operating both an artificial horizon and a directional gyro. The theoretically predicted curve falls somewhat below the empirical points. This discrepancy has been shown to be due to a variation in effective orifice area of the instruments caused by the presence of the rotor.

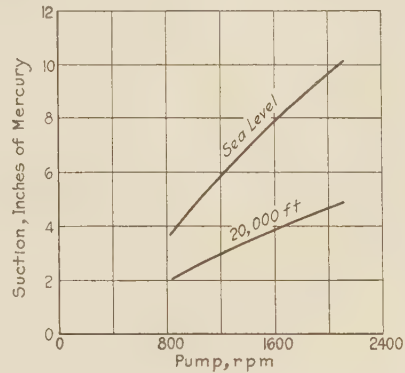


FIG. 14 RELATION BETWEEN PUMP SUCTION AND RPM FOR MULTIPLE-ROTATING-VANE ECCENTRIC PUMP (Sea level and 20,000 ft altitude.)

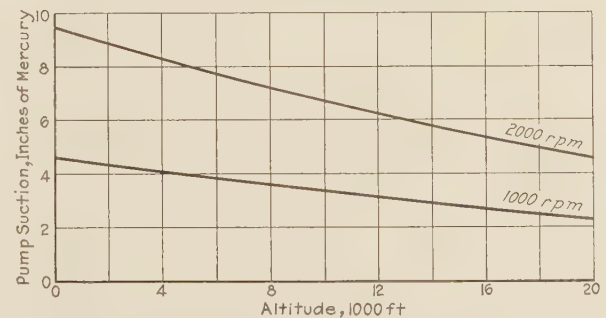


FIG. 15 RELATION BETWEEN PUMP SUCTION AND ALTITUDE FOR MULTIPLE-ROTATING-VANE ECCENTRIC PUMP FOR TWO ENGINE SPEEDS

(Pump operating on orifice equivalent to directional gyro and artificial horizon. Assumed volumetric efficiency = 70 per cent.)

If this effective orifice variation is taken into account,³ a much better check is obtained but in the interest of brevity the data are omitted here.

Fig. 13 shows a comparison between the drag of a venturi installation and the drag of a propeller-driven pump. These tests were carried out in the Massachusetts Institute of Technology wind tunnels. It was found that the blade element contributed little to the drag. The mounting and the pump housing caused the major portion of the resistance at all air speeds above 65 mph.

Fig. 14 is a plot of the relation between pump suction and rpm at sea level and 20,000 ft altitude for a multiple rotating vane eccentric pump. A pressure release valve was furnished with this pump to limit the pressure to 4 in. of mercury. Fig. 15 shows the relation between suction and altitude for two engine speeds, the pump operating on an orifice equivalent to the directional gyro and the artificial horizon.

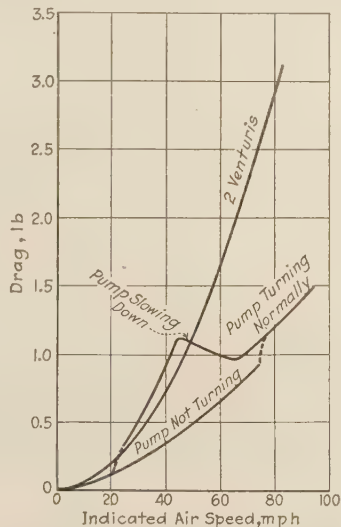


FIG. 13 COMPARATIVE DRAG CURVES FOR PROPELLER-DRIVEN, SINGLE-RECIPROCATING-VANE PUMP AND TWO VENTURIS

CARBURETOR DROP

One of the essential functions of an aircraft engine is that it must pump through itself the air required for combustion of the fuel. For any aircraft engine the total volume of air handled per unit time is very large compared to the quantity of air flowing through the gyroscopic instruments in the same time.

In general, for an engine with a brake thermal efficiency of 25 per cent, estimated on the basis of air consumption, and using a hydrocarbon fuel, the air requirement is about 1.8 cfm per hp. Thus the amount of air that an engine delivering 100 horsepower will draw through itself is about 180 cfm. The air flow through a complete set of gyroscopic instruments is about 3 cfm. These data show that the use of the carburetor drop for gyroscopic in-

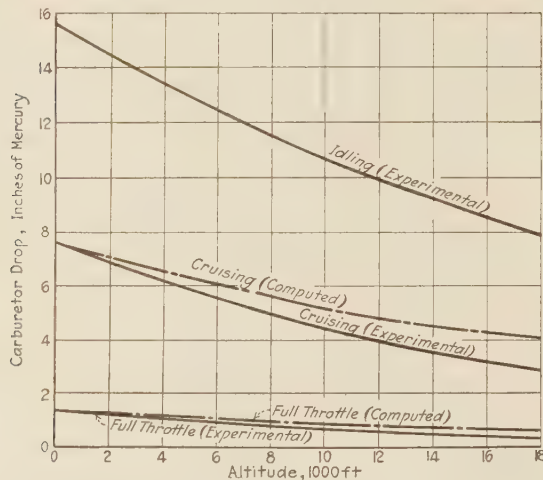


FIG. 16 CARBURETOR DROP VS. ALTITUDE AT VARIOUS THROTTLE POSITIONS

strument drive will affect the air flow by less than 2 per cent for a 100-hp output and consequently less than 0.5 per cent on a 400-hp output. In any case, the air entering the manifold through the instruments may be easily compensated for by use of the carburetor adjustment.

In the engine carburetor there is always a certain pressure drop through the choke and throttle assembly. A very desirable simplification would result if a satisfactory vacuum supply could be derived from this carburetor pressure drop.

In this discussion care has been taken to specifically consider pressure drop through the carburetor only. It is obvious that Diesel engines and engines using fuel injection with no air throttle are not available as sources of vacuum for instrument drive.

Fig. 16 indicates the results of a flight test made for the purpose of determining the variation of carburetor drop with throttle setting and altitude. Evidently the available vacuum is too low at full throttle and much too high with closed throttle for satis-

factory instrument operation. Under cruising conditions the pressure difference is somewhat higher than the normal value for the gyros.

The data outlined indicate that a connection to the intake system just above the throttle will serve as an excellent source of vacuum under cruising conditions. However, the high pressure-drop existing at closed throttle makes it imperative that some sort of pressure regulating valve be included in the system as a protection for the instruments. Such an installation is inexpensive and reliable but has the serious disadvantage of becoming inoperative as the engine reaches its maximum output. This feature would eliminate the scheme from consideration for airplanes which must make long flights at full throttle. However, under conditions which require full throttle operation for short periods only, the momentum of the gyro wheels will keep the instruments in operation during the low-vacuum intervals.

CONCLUSION

There remain to be considered briefly the relative merits of the three sources of suction for gyro-instrument operation.

In point of satisfactory operation over the entire range of flight conditions, a suitable displacement pump is undoubtedly superior to either the venturi or the carburetor drop arrangements. It seems reasonable, therefore, to expect that the final solution of the instrument drive problem will be some form of displacement pump.

From the standpoint of installation, the venturi, the propeller-driven pump, and the manifold vacuum-control valve present about equal advantages. The engine-driven pump may be difficult to install properly on an engine not specially fitted for the purpose.

Considering the matter of efficiency, the venturi is undoubtedly the least desirable of the three vacuum sources.

In the case of a manifold connection the useful work obtained in driving the gyroscope rotors does not reduce the output from the aircraft engine. Consequently the overall efficiency may be considered as infinitely great.

No data on the power requirements of engine-driven pumps were available so that no numerical estimate of efficiency for this system is given here. It seems certain, however, that the power absorbed by a displacement pump will be negligible compared to the output of the modern airplane engine.

ACKNOWLEDGMENTS

In conclusion the writers wish to express their appreciation of the many courtesies extended by the staff of the Department of Aeronautical Engineering at the Massachusetts Institute of Technology.

A number of the experimental results are published through courtesy of the Sperry Gyroscope Company. In particular, the writers wish to extend their thanks to Messrs. E. A. Sperry, Jr., and P. R. Bassett of that company, both of whom have shown helpful interest in the present work.

Stainless Steel in Aircraft Construction

By FREDRIC FLADER,¹ BUFFALO, N. Y.

The characteristics of a new material, commonly known as stainless steel, are considered, with facts and conclusions concerning its adaptability and suitability for use in aircraft construction. The type of steel discussed is called 18-8, by the proportions of chromium and nickel used. This material is selected because it is austenitic in character and is more readily procurable than some of its kindred alloys. The strength-to-weight ratios of 18-8 stainless steel are first considered in relation to comparable values from aluminum alloy, which is the most widely used metal in aircraft structures. This comparison is made using four criteria as representing the value of a material for structural uses. These criteria are (1) tensile strength, (2) the strength of columns, (3) the strength of members in bending, and (4) the deflection or stiffness characteristics. In this connection the finishes which are necessarily employed on aluminum alloy as corrosion preventives are charged against that material.

THE arrival of a new material in the construction of aircraft has been attended by considerable discussion regarding its merits as a structural material and its acceptability with respect to manufacturing costs. The characteristics of this material will be considered in this paper with the view of presenting such facts and conclusions as are available to permit an opinion to be formed as to its adaptability and suitability for use in aircraft construction. The discussion is a report of the development which has taken place up to this time and is only intended to represent a study of the art in its present condition. The material under consideration is the corrosion-resistant chrome-nickel alloy commonly known as stainless steel. There are many types of chrome and chrome-nickel irons and steels produced for a wide variety of purposes, many of the uses being of a highly technical and specialized nature. The particular grade chosen for aircraft work is known as 18-8, in reference to the proportions of the principal alloying constituents, chromium and nickel, used in its manufacture. This material is selected for the following reasons: It is the most common of the stainless steels, is most easily handled in its processing, and is therefore produced in larger tonnages and is available from a number of reliable sources of supply. It may be hard-rolled to a very high tensile strength. It is austenitic and non-magnetic, which properties make it a satisfactory material for use in and around pilot's cockpits because of its neutral effect on navigating and electrical

instruments. It is satisfactorily corrosion-resistant for aircraft work without painting. This quality is of particular value in flying-boat and seaplane hulls because of their continual contact with salt water.

An examination of the strength-weight ratios of 18-8 stainless steel will first be considered in relation to comparable values for other materials that are most widely used in aircraft structures at the present time. Four criteria are considered as representing the value of a material for structural uses. These criteria are (1) tensile strength, (2) the strength of columns, (3) the strength of members in bending, and (4) the deflection or stiffness characteristics. In this connection the weight of the finishes which are necessarily employed on aluminum alloy as corrosion preventives is charged against that material. It is considered that the use of paint on stainless steel is unnecessary except for external color requirements.

Fig. 1 shows a representative stress-strain curve taken from a specimen of hard-rolled 18-8 stainless-steel sheet material. Un-

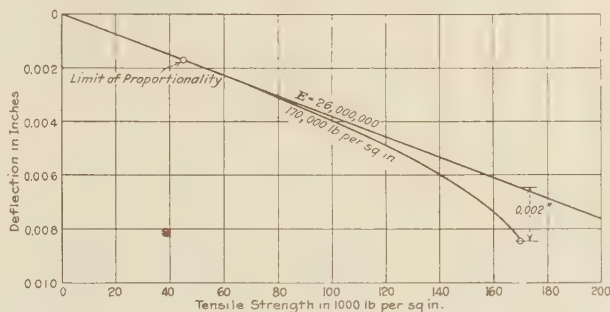


FIG. 1 REPRESENTATIVE STRESS-STRAIN CURVE OF HARD-ROLLED 18-8 STAINLESS-STEEL MATERIAL
(Ultimate tensile strength, 190,000 lb per sq in.)

like ordinary steel, this material does not have a definite yield point. The limit of proportionality is rather low, after which the material yields along a uniform curve of decreasing slope. In defining a yield point for a material of this character it is necessary to select a point at which the stress-strain curve has deviated a definite amount from the straight line of Hooke's law. The amount of this deflection is somewhat arbitrary, but not entirely so. An attempt is made to define a value for the yield point so that when structures are designed using this value, the design load will be sustained without a permanent set of any of the members of the structure. A definition of such a value is taken at that unit stress under which the test specimen shows an extension of 0.002 in. per inch in excess of that which will be computed from Young's modulus of elasticity and the formula:

$$\text{Unit stresses} = \text{Young's modulus} \times \text{Unit deformation}$$

From reliable test data a minimum yield point of 140,000 lb per sq in. is obtainable from 18-8 hard-rolled material. This value may be used in design work and is believed sufficiently conservative to take care of material variations and an allowance for discrepancies between test results and actual failing stresses in built-up structures.

Fig. 2 indicates the cost in weight due to paint. Curve 1 shows the relation between the weights of painted and unpainted aluminum-alloy surfaces. Some 25 to 30 per cent is added to

¹ Aeronautical Engineer, Curtiss Aeroplane and Motor Company, Inc. Fredric Flader received his education at Carnegie Institute of Technology, having the degree of B.S. in M.E. He was for five years with the Air Corps at McCook Field, on designing, stress analysis, and research, and was Air Corps representative at the Cox-Klemin plant during the design and construction of the A-1 ambulance airplane. He was designer for the Buhl Verville Aircraft Corporation, Detroit, Mich., producing the "Airster," designer for the Consolidated Aircraft Corporation and project engineer on the Consolidated Commodore flying boat; assistant chief engineer, Keystone Aircraft Corporation; design engineer at the Curtiss Aeroplane and Motor Corporation, at present working on stainless-steel construction research and other U. S. Navy projects.

Contributed by the Aeronautic Division and presented at the Semi-Annual Meeting, Chicago, Ill., June 26 to July 1, 1933, of THE AMERICAN SOCIETY OF MECHANICAL ENGINEERS.

NOTE: Statements and opinions advanced in papers are to be understood as individual expressions of their authors, and not those of the Society.

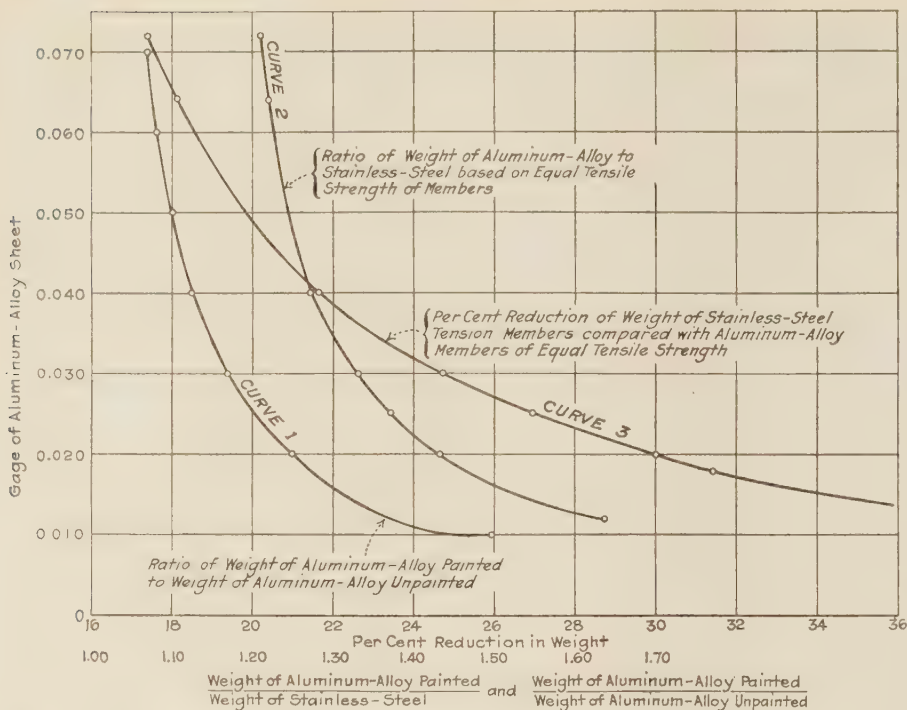


FIG. 2 COMPARISON OF TENSILE STRENGTH OF PAINTED ALUMINUM ALLOY WITH UNPAINTED STAINLESS STEEL

(Tensile strength of aluminum alloy, 55,000 lb per sq in.; tensile strength of stainless steel, 175,000 lb per sq in.)

the weight of the gages of sheet usually employed on skin-covered structures such as monocoque fuselages and tail surfaces. Curves 2 and 3 show the relationships between painted aluminum alloy and stainless steel. The foregoing data indicate clearly that a saving in weight is possible when using stainless steel in so far as tensile strength may be used as a criterion of structural efficiency.

In Table 1 are computed some values of the factor e defined by the formula given with the table.

This factor shows the relative strength of various sizes of aluminum-alloy tubes compared to stainless-steel members of the same weight when tested as columns. L/ρ values vary sufficiently to cover both the straight line and Euler ranges for the aluminum-alloy tubes. The variation of strength of stainless-steel columns is not clearly defined by either a straight line or a Euler relationship. The factor e indicates a definite advantage in the use of stainless steel in short columns up to an L/ρ of about 50. Above this value stainless steel is inferior to aluminum alloy.

This is simply because the weight ratio of stainless steel to aluminum alloy is 2.83, while the ratio of their moduli of elasticity, which is the governing factor in long columns, is only 2.48.

Two beam sections, one of aluminum alloy 1 ft long and one of stainless steel 20 in. long, were made and tested in compression. Both specimens were of similar design and were made to represent sections of a beam for the same airplane. The aluminum-alloy member weighed 0.57 lb per ft and sustained a unit stress of 40,500 lb per sq in. in compression. The stainless-steel section weighed 1.098 lb per ft and held a unit stress of 128,000 lb per sq in. The factor e (see Table 1) computed from these tests based on equal weight is 1.21, indicating approximately a 20 per cent advantage in favor of stainless steel, even though this specimen was the longer one.

Beam members of similar design to the compression specimens previously described but of longer lengths were made and tested in bending. The aluminum-alloy beam is an efficient design as evidenced by the development of 47,700 lb per sq in. stress in bending. Owing to a shear failure experienced in the stainless-steel beam test, no ultimate bending stress was obtained. The ratios of actual deflection to calculated deflections in the two beams were almost the same (about 0.90), which indicates that the same load would have been held by the stainless-steel beam that was sustained by the aluminum-alloy beam had not the shear failure occurred first. Data on the strength of stainless-

TABLE 1

Size aluminum-alloy tube	Area of tube	Weight per 100 in. length	Painted surface per 100 in. length	Weight per 100 in. painted tube	P/A aluminum alloy	P/A stainless steel	e
$1/4$	0.035	0.05113	0.51	1.09	0.568	152,000	1.360
1	0.049	0.1464	1.47	2.18	1.627		1.352
$1\frac{1}{4}$	0.065	0.293	2.93	3.27	3.165		1.320
2	0.095	0.5685	5.68	4.36	5.994		1.288
$1/4$	0.035	0.05113	0.51	1.09	0.568	76,000	1.070
1	0.049	0.1464	1.47	2.18	1.627		1.013
$1\frac{1}{4}$	0.065	0.293	2.93	3.27	3.165		0.973
2	0.095	0.5685	5.68	4.36	5.994		0.921

NOTES:

Weight of painted surfaces:

1 coat red oxide primer	0.007 lb per sq ft
2 coats navy gray enamel	0.040 lb per sq ft
1 coat aluminum bitumastic paint (inside)	0.025 lb per sq ft

Total

0.072 lb per sq ft

$$e = \frac{W_p}{W} \times \frac{P/A \text{ steel}}{P/A \text{ dural} \times 2.83}$$

W_p = weight of aluminum alloy painted

W = weight of aluminum alloy unpainted

2.83 = ratio weight of stainless steel to weight of aluminum alloy

Straight line $P/A = 48,000 - \frac{400}{\sqrt{c}} \times L/\rho$

$$\text{Euler } P/A = \frac{C\pi^2 E}{\left(\frac{L}{\rho}\right)^2}$$

steel beams in bending and in combined bending and compression are too meager to be of value in drawing any definite conclusions. Within the near future, however, a rather systematic series of tests along this line will be completed.

Data which have been obtained at the present point in the research program, while not fully conclusive, do indicate that a saving in structural weight of 10 to 15 per cent is possible when using stainless steel except in long columns. Owing to the slightly lower modulus of elasticity of stainless steel—26,000,000 as compared with 29,000,000 for other steels—structures made from stainless steel may be expected to deflect about 11 per cent more than equivalent members of chrome-molybdenum steel or aluminum alloy. Recent research has indicated that by special processing it will be possible to improve the modulus of elasticity and to raise the limit of proportionality of stainless steel. From information gained, it appears that the structural characteristics may be improved as more is learned about the material.

The remaining factor to be considered by the designing engineer is the matter of making joints and fastenings. Practically we are confined to riveting and bolting or welding. A riveted or bolted-up structure of stainless steel, aside from the cost of the rivets and bolts and their insertion, would be very expensive because of the difficulty in drilling holes. Acetylene welding and electric-arc welding are as a general rule not suited for use in fabricating joints which are strong and resistant to vibrations, because of their detrimental effects on the structure of the material. Electric-resistance welding of stainless steel is now an established and a reliable process.

A brief discussion of the physical characteristics of 18-8 stainless steel and the adaptation of electric spot welding to its peculiarities will be given. This alloy is normally austenitic, which means that the carbon content of the material is dissolved in the iron somewhat as salt may be in solution in water. The maintenance of this condition is necessary for the material to have its normal physical properties and to be resistant to fatigue and corrosive attack.

Microscopic examination of a sample of austenitic metal shows that its structure consists of rather uniform crystals of rectangular section and that they are bounded by sharp, well-defined lines. When the carbon in this metal is merely mixed with the iron and is not in solution, the alloy is said to be non-austenitic. In this condition the crystals are somewhat separated by rather blurred and indistinct lines wider than in the austenitic metal. The material between the crystals is supposed to be carbon which has separated from the iron. This change in the character of the material gives rise to the term "carbide precipitation," analogous to the crystallization of salt from a salt-water solution. Apparently this change from an austenitic to a non-austenitic material takes place when the metal is heated to a temperature between 950 F and 1550 F and is held at this temperature for a sufficient length of time.

At about 950 F the carbon is completely dissolved in the iron. Upon raising the temperature, carbon begins to precipitate. This precipitation takes place at an increasing rate until a temperature of 1200 F is reached. Above 1200 F the rate of carbide precipitation becomes less, until at 1550 F it stops entirely. If the temperature is carried on up above 1550 F, the carbon gradually goes back into solution and the alloy returns to its normally austenitic condition. If the metal, once more in its most desirable state, can be cooled sufficiently rapidly, it will pass through the critical temperature range just described without carbon leaving the solution again. This quality is of very great importance in selecting a method of welding the material.

Acetylene or arc welding, as all know, is a process of fusing two pieces of metal at the points where they are to be joined in such a way that the metal is melted and caused to flow together. During these processes a considerable mass of material is melted and cooled rather slowly. During this cooling an ideal condition is produced for carbide precipitation to take place. Electric spot welding is a more desirable method, since only sufficient

metal is melted to form the spot. Under ideal conditions a weld is made by pressing the two or more pieces of metal together and at the proper time allowing just sufficient current to pass between the electrodes to bring the metal to the fusing point. At this instant the pressure applied causes the fused metal to flow together, thus forming a homogeneous and firm bond between the plates. Because of the small amount of metal which has been melted and also because of the fact that the adjacent metal has not been heated, the molten spot cools very rapidly, so that the carbide precipitation does not have a chance to form.

To obtain welds of suitable quality and reliability for aircraft production it is necessary to make use of equipment somewhat more advanced in its development than the average power-driven spot welder used in commercial work. In spot welding there are three main variables:

- 1 Pressure of the electrodes on the work
- 2 The amount of current
- 3 The time of current application.

The pressure can be adjusted to the amount required by varying an electrode compression spring, which is ordinarily furnished with a machine. The current is easily adjusted by changing the setting of a control, which also comes with the welding machine. The timing control is more difficult and requires a special device. It is necessary to make resistance welds in as short a time as possible for several reasons:

- 1 High-speed production
- 2 Minimum oxidation or scaling
- 3 Prevention of carbide precipitation, distortion, and warping.

As previously explained, carbide precipitation, as well as distortion and warping, is held to a minimum when the heat is confined to the actual welding area, and this is possible only if the welding time is very short. If welded in a short enough time, it is theoretically possible to generate the necessary heat at the location of the weld, fuse the surfaces together, and allow the heat to be conducted rapidly away by the surrounding metal and electrodes after the weld has been completed without heating the outer surface of the sheets to an injurious temperature. It is not only necessary to complete the weld in a very short space of time, but it is also necessary to synchronize the make and break of the weld with points on the alternating cycle curve which pass through zero, or at the times when no current is flowing owing to a reversal of the cycle.

The reason for beginning and ending a welding operation at times of zero current flow is to avoid arcing when the electrodes are making or breaking a contact. The formation of an arc is a cause of oxidation and burning of a weld.

Each cycle of the sine wave representing a 60-cycle current takes a time of 0.0167 sec. If it is possible to weld in even cycles or half cycles, then the question of timing control is solved both as to accuracy of the duration of each weld and the fulfillment of the requirement of starting and stopping of a weld at exact instants when no current is flowing.

Actually with suitable equipment it is possible to make welds in one-half-cycle increments. Theoretically it is best to use this amount of time for all welding and vary the amount of current in direct ratio to the thickness of the parts being welded. Practically, however, a machine of normal capacity is not large enough to supply the needed current for welds on heavier gages, so that it is necessary to increase the time, using several cycles, so that the total amount of electrical energy dissipated at the weld is approximately the same as would be the case with the shorter welding time and more current.

The most satisfactory device for controlling the application of

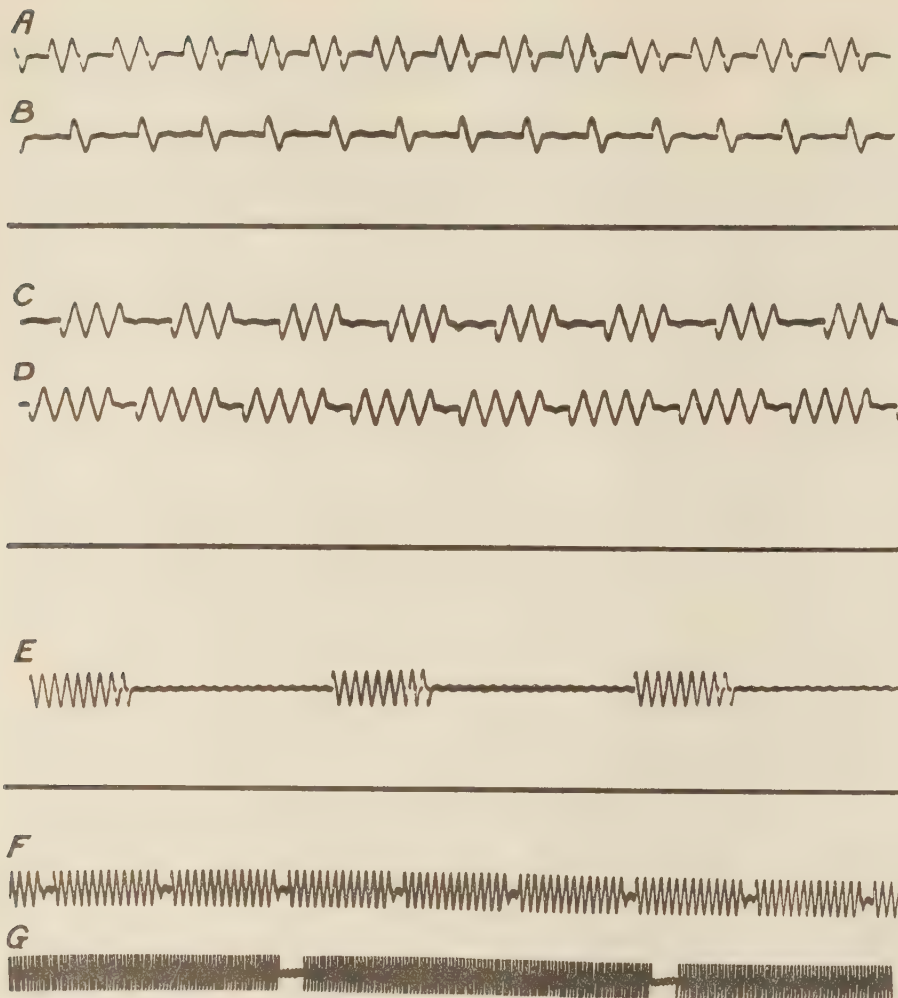


FIG. 3 WELDING PERIODS IN TERMS OF CYCLES OF CURRENT

(Oscillograms illustrating range of control to be obtained with G.-E. CR7503-B2 thyatron-tube control for resistance-welding machines. A, 2 cycles on, 1 cycle off; B, 1 cycle on, 2 cycles off; C, 3 cycles on, 2 cycles off; D, 4 cycles on, 1 cycle off; E, 9 cycles on, 19 cycles off; F, 13 cycles on, 2 cycles off; G, 97 cycles on, 7 cycles off.)

current to a weld at the proper instant, definitely measuring a predetermined time in even cycles of current, and stopping the weld at the proper time, is an electrical rectifier known as the thyatron contactor. The figures and microphotographs illustrate some of the results obtained with a device of this kind applied to a spot-welding machine as the time-control medium. Fig. 3 illustrates welding periods in terms of cycles of current. The symmetry and uniformity of these records show clearly the accuracy of control. Fig. 4 shows the results obtained by using long and short periods of dwell. The center spots were welded with 60 cycles or 1 sec time. A zone around these welds has been heated to the critical temperature at which carbide precipitates, so that these are not good welds. At the top of the photograph are three welds made with 12 cycles. These welds are more uniform in quality and appearance due to the more rapid heating and cooling periods. At the lower left side of the picture are four welds made in 1 cycle each. These welds are of excellent quality, without carbide precipitation or discoloration of the metal. Fig. 5 is a section of one of these welds magnified 500 diam. The excellence of the grain structure is noteworthy.

When using electric spot welding, the designer does not need to think in terms of rivet-shearing strength and bearing area.

He only needs to know the strength per spot for each gage of material. The strength of a spot varies in a fairly definite relation with the thickness of the thinnest of the material being welded. In stainless-steel sheet-metal construction equivalent to thin aluminum alloy such as wing and tail-surface covering material, the strength of a spot weld is about double that of the most efficient size rivet in aluminum alloy. This advantage gradually diminishes on the heavier gages in which the strengths of welds and rivets are comparable.

MANUFACTURING COSTS

It is not possible with available data to present any accurate figures to show the difference between the costs of aluminum-alloy and stainless-steel construction. However, it is possible to make some comparisons between the various processes involved so that a fairly definite conclusion may be drawn as to the relative merits of the two methods.

Normal forming and cutting operations are much more difficult and costly on stainless steel than on other commonly used materials. For this reason such operations are simplified and avoided as far as possible in designing stainless-steel aircraft parts. For the most part, shapes are made by a drawing process producing simple forms, but conforming to known principles

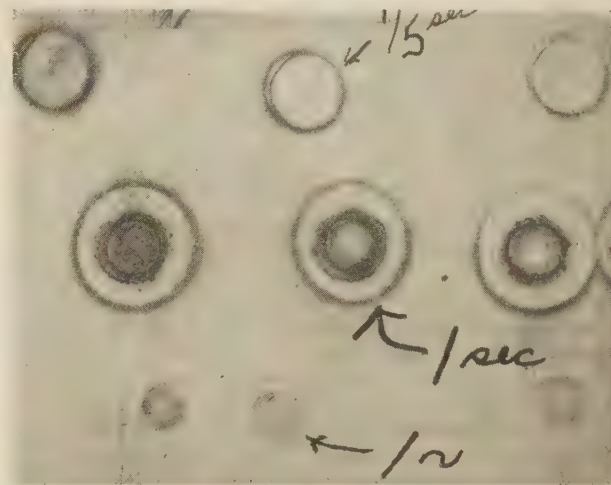


FIG. 4 WELDING RESULTS OBTAINED BY USING LONG AND SHORT PERIODS OF DWELL

TABLE 2 COMPARISON OF RIVETING AND SPOT-WELDING COSTS

Operation	Drilling (holes per minute one man)	Inserting and heading (rivets per minute two men)	Man-hr per rivet drilling, inserting, and heading	Cost per inch, cents	Spot welds per minute	Man-hr for four equivalent rivets	Cost of four spots, cents	Ratio of cost of rivets and cost of spots
Fastening bottom sheet on boat hull	0.915	1.07 ^a	0.0493	4.93	40	0.00166	0.166	29.7
Fastenings on truss type wing beam	0.958	0.64 ^b	0.0694	6.94	10	0.00694	0.664	10.5
Fastening skin on monocoque fuselage	0.850	1.33 ^c	0.0446	4.46	40	0.00166	0.166	26.8

^a $\frac{3}{16}$ rivets.^b Approximately 70 per cent are $\frac{3}{16}$ rivets and 30 per cent $\frac{1}{4}$ rivets.^c $\frac{1}{6}$ rivets.

for their structural efficiency.

Because of the high density of the material (the same as ordinary steels) it is necessary to use it in thin gages in order to build structures of comparable weights to wood and aluminum alloy.

A thin sheet inherently lacks stiffness normal to its own plane.

For this reason it is considered necessary in order to take full

advantage of this metal as a structural material to resort in general to the principle of using frequent stiffeners in such a manner as to keep the flat-sheet element widths down to low values, and further to make use of frequent supports along the lengths of the members to keep the column lengths down to low values.

Owing to this method of design with additional formers and stiffeners, it is believed that probably four times the number of spots will be used compared with rivets in aluminum-alloy construction. The cost of drilling, inserting, and heading operations on aluminum-alloy rivets has been compiled from actual time records for the three operations shown in Table 2. A comparison of the cost of spot welding is made based on the rate of speed in welding which has been obtained in work of a similar nature to that which employs the rivets.

This comparison indicates a great advantage in favor of spot welding considering only the present application of the method. The possibilities of spot welding may be more fully realized by considering what may be done using production methods. It is within the realm of possibility to produce 75 ft of linear welding per minute, making four spots per inch, which amounts to 3600 spots per minute. At such a speed it would of course be necessary to properly feed and guide the work through the machines. This is and will be accomplished to an increasing degree of efficiency by indexing and feeding devices operated in synchronism with the welding operation.

Figures compiled from the parts lists of a large airplane which has recently been produced in limited quantities show that 142,000 rivets were used in each airplane. This corresponds to a cost of \$6390 at $4\frac{1}{2}$ cents per rivet, including overhead. Assum-

ing that 568,000 spot welds would be used in this same machine in stainless steel, the cost of welding would be only \$471.44, taking the average of the figures given in Table 2. The saving per plane would be \$5918, or in this instance a total of \$147,950 on a production of 25 planes.

Stocking and handling costs of stainless-steel material are much less than these costs of aluminum alloy. In many cases it is necessary to store aluminum-alloy sheets between alternate pieces of oiled or waxed paper to avoid scratches when sheets are pulled from the racks. It is also necessary to take care to prevent abrasion and scratching of the metal while in process of fabrication, and the use of sharp marking tools is prohibited. This care of aluminum alloy is important because abrasion of the mill surface provides places for corrosion to set in, particularly on parts which are to be used near salt water. The same care is not required when using stainless steel, since this material is much harder and less susceptible to damage of this kind. Another important point is the difficulty of distinguishing between annealed and heat-treated aluminum alloy. One instance has recently been experienced of a very costly mistake in which improperly heat-treated rivets were in some way used in production. The visual differentiation between annealed and high-strength stainless steel is pronounced enough to avoid confusion, as annealed stock may be purchased with a dull pickled finish, whereas hard-rolled material is bright.

The physical properties of 18-8 steel are derived from cold working, and it does not respond to any sort of heat treatment except normalizing. Therefore this phase of manufacturing when using this metal is eliminated except for such normalizing as is considered to be necessary.

In the author's experience a very costly item in aluminum-alloy construction has been the rejections and reworking made necessary by wrongly drilled holes, elongated holes, and bad rivets. [The use of stainless steel and the spot-welding process obviates these difficulties to a large extent as no holes are required and a lesser degree of care is required in spacing the welds than is the case with rivets.

Next in importance to the saving effected by replacing the riveting process by welding is the practical elimination of the elaborate finishing operations on aluminum alloy and other steel construction. Anodizing at approximately 25 cents per square foot and sand blasting and painting at approximately 20 cents per square foot are

FIG. 5 SECTION OF ONE OF THE WELDS SHOWN IN FIG. 4 $\times 500$

almost entirely eliminated when using the stainless steel.

Summarizing the probable advantages of stainless-steel construction from the airplane manufacturer's viewpoint, the method should yield lighter structures for equal strength and should materially reduce construction costs. The outstanding factors in

costs are the use of electric resistance welding and the reduction of costly finishing processes. From the operation standpoint the foregoing considerations lead to greater operating economy through increased pay loads and reduced maintenance costs, particularly the item of continually renewing protective coatings.

Improving Airship Performance

By GARLAND FULTON,¹ WASHINGTON, D. C.

The economic advantages of the large airship as a long-distance carrier depend to a great extent upon its useful-load capacity, its speed and its cruising radius. Improvement in design or in auxiliary equipment, therefore, which will increase materially any or all of these three factors, is of prime importance.

This paper touches on the fundamentals underlying the carrying capacity of lighter-than-air craft and points out possible changes in construction, means of ballasting, power-plant equipment, and fuel characteristics whereby substantial economic and operating advantages may be effected in future designs.

LARGE airships are seeking recognition as long-distance, rather than short-distance, carriers and propose to operate principally on over-water routes. Any improvement in performance of useful load carried or of maximum speed attainable is certain to enhance the economic advantages of the airship.

Up to the present, airship development has not been benefited, as airplane development has, by the competitive effort involved in the construction of many units representing a variety of types. Airship development more closely parallels steamship history. Single units are costly and require time to design and build. But the increasing potentialities of airships as a medium of transport are gradually being unfolded through experience, and it is realized that the sizes and performance of our present airships will not adequately meet the requirements of the future. Technical progress is so rapid that a design is found to be inadequate almost before an airship can be built from it.

EFFECT OF SIZE AND WEIGHT ON SPEED AND LIFT

One direct method of improving airship performance would be to build larger airships, since with increase in size it would be possible to increase the speed and cruising range and otherwise to effect improvements that would be of great benefit. It is noteworthy and is a significant index of the strides that have been made and are being made in airship development that each of the six large airships built (and they are the only ones built in the whole world) in the last twelve years has, on completion, been found inadequate, principally on account of size.

For large rigid airships of conventional design, built to present-day standards as to strength criteria (which incidentally are more severe than in 1922 and correspondingly increase structural weights), the dead weight will amount to from 55 to 60 per cent of the gross lift when filled at sea level with helium. This leaves from 45 to 40 per cent as useful lift, which must include the crew and their effects, ballast, fuel, passengers, and mail, and such other loads as are to be carried. These percentages are unlikely to change very much through minor changes in materials and minor variations in types of structural members and their arrangement. If hydrogen were used instead of helium, these percentages would become about 48 to 53 per cent for dead weight and 52 to 47 per cent for useful lift.

¹ Commander, U. S. N., Construction Corps; Bureau of Aeronautics, Navy Dept., Washington, D. C.

Contributed by the Aeronautic Division and presented at the Annual Meeting, New York, N. Y., December 4 to 8, 1933, of THE AMERICAN SOCIETY OF MECHANICAL ENGINEERS.

NOTE: Statements and opinions advanced in papers are to be understood as individual expressions of their authors, and not those of the Society.

If the attempt is made to increase the speed of a large airship from the present maximum of from 80 to 85 statute miles per hour to, say, 100 mph, additional weight will be required not only in the power plant but in the general structure as well. Aerodynamic forces increase rapidly as maximum speed increases.

Attempts to gain increased speed without sacrifice in the ratio of useful to gross lift brings up anew the possibility of obtaining the added strength required for the higher speed by superposing some of the principles of a pressure airship upon the conventional type of rigid airship, commonly thought of as being a "pressureless" airship. The result would be a composite type of construction which might have a thin metal covering. This covering, if placed under tension by interior pressure, would be made to function in a definite manner as a strength member. Such a composite type of construction would probably show a weight advantage for large airships only, i.e., for airships with air displacements of more than 8,000,000 cu ft.

From questions that are frequently asked, it appears that there exist a great many misconceptions as to airship performance because of failure to understand the fundamental physical laws upon which the performance depends. There is generally much speculation about the altitude attainable by an airship, sometimes spoken of as the airship's "ceiling." An airship does not have a "ceiling" in the same sense that an airplane does. The altitude attainable by an airship varies with the loading, and the "ceiling" of a fully loaded airship is close to zero. It is customary to assign an arbitrary rating on lift that is about 95 per cent of the total lift under average conditions. This allows a margin for seasonal variations in lift, impurity of the lifting gas, and other variables, and at the same time allows the airship the possibility of attaining a flying altitude of about 1800 ft before her gas containers become 100 per cent full (pressure height).

The maximum static altitude an airship may attain is that point in the atmosphere where the air density bears the same ratio to the air density at sea level as the dead weight bears to the total lift of the airship at sea level. If the dead weight of an airship is 55 per cent of its total lift, it cannot rise statically beyond the point where the atmosphere is 55 per cent as dense as it is at sea level. This point happens to be around 16,000 ft. If the same airship should be filled with hydrogen (instead of helium) its dead weight might be only 50 per cent of the total lift and it could then rise higher, say, to 19,000 ft.

HELIUM VS. HYDROGEN

Any discussion of airship performance must include the effect of using helium instead of hydrogen. In practise, the use of helium instead of hydrogen to inflate an airship reduces the initial total lift by as much as from 10 to 15 per cent, and reduces the cruising range by perhaps from 30 to 40 per cent. This is a serious handicap to the helium airship and can be justified only by the absolute safety from fire hazard that is expected with helium. There is no hazard from the helium itself, of course, but so long as gasoline fuel is used, the existence of a fire hazard cannot be denied, although it is not very great and extra precautions are taken against it.

So far as is known, helium exists in large quantities only in the United States. At one time it was very expensive, but with improved processes and greater quantities of production, the price has been lowered remarkably, so that at present using helium involves questions of distribution and storage rather than of pro-

duction costs. It is expensive to transport helium, and steel containers for storing the gas under pressure are also expensive. But even considering these expenses and the additional one of occasionally repurifying the helium, it can be shown that the use of helium year in and year out is not more expensive than operation with hydrogen. Care is taken not to waste helium not so much because of the desire to preserve a valuable commodity as to avoid the difficulty of replenishing the supply at some remote point.

EQUILIBRIUM BETWEEN WEIGHT AND BUOYANCY

In flight, an airship takes care of minor and even substantial variations in equilibrium through the use of her elevators. It is desirable, however, especially where the lifting gas should be conserved, to enable the airship to maintain throughout the flight a reasonable balance between weight and buoyancy. The means adopted for this purpose in helium-filled American airships is an air-cooled condenser for recovering moisture from the engine exhaust. The use of this so-called "water-recovery apparatus" has involved many problems, notably those induced by the high temperature and corrosive nature of the exhaust products. Although the apparatus now in use functions, it is heavy and not sufficiently durable. If airship performance is to improve, some more satisfactory solution to the problem of maintaining equilibrium must be found. Airships are the only known agency that considers the exhaust products from an internal-combustion engine worth saving. Every other agency tries to get rid of them as promptly as possible.

The essential results of burning ordinary gasoline in an internal-combustion engine can be written as a word equation: Gasoline + air = carbon monoxide + carbon dioxide + water. The water will be approximately 1.4 times, and the carbon dioxide nearly 4.0 times, the weight of the original gasoline. This invites consideration of the possibility of accumulating weight in flight through capturing in some way and retaining a portion of the carbon dioxide, but practical means of doing it within permissible weight allowances have not yet been discovered.

Meanwhile, helium-filled airships continue to struggle with means for recovering water by condensing moisture from the exhaust. The results are influenced by composition of the fuel, by paucity of accurate data on thermodynamics of heat transfer under like conditions, and by mechanical and corrosion problems, as well as by the constant effort to reduce weight to a minimum and to avoid any unnecessary drag. Recovery of better than 115 per cent is frequently realized and an average of from 90 to 100 per cent is usually maintained.

The problem of insuring that the necessarily large quantity of ballast water does not freeze in winter is a serious one and the solution now employed of carrying alcohol as an anti-freeze agent entails extra weight.

As illustrating, perhaps by an extreme case, the handicap on airship performance imposed by water-recovery apparatus, consider the case of a 6,500,000-cu ft airship equipped for a maximum endurance flight of six days' duration in freezing temperatures. She will be forced to carry a weight of from 18 to 20 tons which could otherwise be devoted to useful fuel. This figure is made up as follows:

	Tons
Water-recovery apparatus proper.....	6.5
Bags and piping for recovered water.....	1.5
Anti-freeze materials.....	6.0
Increased fuel consumption, due to increased drag caused by apparatus.....	4.5
	18.5

This is a severe penalty and indicates the importance of finding

some other solution to the general problem of gaining weight during flight. Rain water can be easily captured if it is available. Water pick-up from the sea is another, and a very attractive, idea. The earliest water-recovery apparatus was a bucket thrown over the side. One of the most promising ideas is to place a quantity of cheap, readily available, hydrogen inside a mantle of helium and to valve out this hydrogen as the airship burns fuel and hence becomes lighter. A variation of this would be to burn some or all of the hydrogen instead of throwing it away. Still another solution, and a good one, is to use as fuel a gas having a density nearly that of air, so that burning fuel causes very little change in equilibrium. This type of fuel is now employed by the *Graf Zeppelin*. It is used there primarily because fuel gas having a high Btu value per pound is advantageous as a fuel and not especially because it avoids the necessity for valving out large quantities of lifting gas to maintain equilibrium as flight progresses.

Another attractive idea for accumulating weight during flight is to recover moisture from the air, instead of from exhaust gases, and to do this by means of some hygroscopic substance from which the moisture can later be extracted by the application of heat, so as to allow the complete cycle to be carried out on board the airship. Several substances are available for consideration, but as yet none has been found that offers a definite solution within a reasonable weight.

ENGINE AND POWER-PLANT IMPROVEMENTS

The most potent effect on the performance of future airships will come through improvements in engines, engine installations, and general power-plant arrangements. At present these items represent about 20 to 25 per cent of the dead weight of the airship. Existing power-plant weights on airships are abnormally high, this being the price paid for reliability and the result of a number of circumstances, many of which are in process of being improved or corrected.

Relatively scant attention has been paid to the development of engines, propellers, and other power-plant appliances suited to the special requirements of airships. This situation seems all the more peculiar when it is realized that an airship is really an excellent flying laboratory for the general study of engine and propeller performance. With the exception of high altitude and very high speed conditions, an airship is capable of providing all power-plant conditions that are essential to an airplane or an airship and to do this under conditions that permit almost complete accessibility for adjustments, minor repairs, taking measurements or readings, and so on. Given time and more airships in operation, we should accumulate a mass of precise data on power-plant performance, and with the analysis of these data there should be opened up avenues for improvements.

It is to be hoped that eventually there will become available engine units satisfactory as to type and of a size ample to fit the requirements of a particular airship design. Airship sizes have increased far more rapidly than have the sizes of engines suitable for airship purposes. As a result, airship designers have been forced to such expedients as gearing two engines to a single propeller or providing an excessively large number of power-plant units.

LOW SPECIFIC FUEL CONSUMPTION

But aside from the weight of the engines themselves, low specific fuel consumption is of great importance, since the fuel load is by far the largest single item comprised in useful load and even a fractional saving in specific fuel consumption mounts into a sizable figure for long voyages.

Considering the requirements of long cruising periods and the necessity for reversing the direction of propeller thrust, and also the desirability of securing thrust in vertical directions, an airship

power plant compares more nearly to that of a surface vessel than to the rather simple unidirection installations on airplanes.

There is no fundamental reason why air-cooled engines cannot be employed for airships, especially to give that extra boost in power necessary to attain the highest speeds. A combination of a small number of air-cooled engines with liquid-cooled engines which are used at nearly full power for normal cruising has a number of advantages. Their relatively high fuel consumption would be an argument against a complete outfit of air-cooled engines. Arrangements for reversing and tilting propellers with air-cooled engines would be somewhat cumbersome, but might be made. An arrangement for mounting air-cooled engines on retractable brackets has been seriously considered and could be made practical.

Despite very serious efforts and the expenditure of large sums of money, there is not in existence today a light-weight, compression-ignition, oil-burning engine that is really satisfactory for airship purposes, although there are several promising entries in the field. Such an engine is desired because of the decreased fire hazard which will result from using oil as fuel and the anticipated low specific fuel consumption. If a saving over gasoline of 25 per cent can be realized, it will amount to four or five tons for an average flight of 50 hours' duration.

Adequate water recovery from exhaust gas appears impracticable with Diesel fuels because of the somewhat low hydrogen content of the fuel and still more because of the large excess of air over the theoretical requirements for combustion. When Diesel fuels are actually in use, airships will probably have to find some new solution to the weight accumulation problem or else be content with a rather heavy, low-efficiency water-recovery apparatus that yields only from 40 to 60 per cent instead of from 90 to 100 per cent in recovered weight.

There has recently been much intensive work done in the development and application of hydrogenated gasolines or so-called "safety fuels" for airship purposes. The use of fuels of this class holds promise of great benefit to airships. Successful operation with safety fuels appears at the moment to be nearer realization than successful operation with Diesel fuels. The most promising of the "safety fuels" from an airship standpoint have a flash point of about 130 F and cannot be used with present carburetors. They must be injected by means of a pump. Tests made with such fuels in existing engines indicate that their use will entail no loss in power, but fuel consumption may increase by a few per cent. The use of such fuels would result in a considerable reduction in the fire hazard which is present when gasoline is used. Despite their hydrogen content, these "safety fuels" are not well adapted to water recovery, but it does appear that they are better adapted to water recovery than Diesel oils and that a recovery of from 60 to 80 per cent might be realized from them under optimum conditions.

The German solution to the airship fuel question is in many ways ideal, but it unquestionably entails some increased risk over the use of Diesel oils or safety gasolines. This solution is to carry at atmospheric pressure a quantity of hydrocarbon gas having a density approximately equal to that of air and to burn this gaseous fuel in ordinary engines through the employment of a special type carburetor or mixing chamber. A small quantity of benzol-gasoline is carried for use under certain conditions. The fuel gas serves neither as lifting gas nor as ballast and its consumption therefore does not involve much alteration in the airship's balance between buoyancy and weight. Furthermore, the Btu value per pound is high. The whole arrangement results in an important gain in cruising range for the fuel-gas airship. This increase may be as much as 40 per cent more than the range of an airship using helium as the lifting gas and gasoline as fuel.

For an airship carrying hydrogen in any form—for lifting purposes, or in ballonets as dischargeable "negative ballast"—the idea occurs, "Why not burn this hydrogen as fuel instead of merely exhausting it to the atmosphere?" A number of years ago before helium was available, serious efforts were devoted to using hydrogen as a fuel. A small Navy airship was equipped with hydrogen carburetors and made a successful flight from New York to Newfoundland, burning hydrogen and gasoline alternately. Recently, laboratory work by the National Advisory Committee for Aeronautics has shown that hydrogen can be burned with high thermal efficiency and without the risk of backfiring that handicapped some of the earlier work along similar lines. The thermal efficiency of an engine running part on hydrogen and part on oil is less at low loads than that of a pure Diesel engine, but at high loads the efficiency is greater. It is believed conservative to estimate that with a Diesel-engine-hydrogen-ballonet installation, and with water-recovery apparatus eliminated, a gain of from 15 to 20 per cent in range can be realized through burning the hydrogen in conjunction with the fuel oil instead of wasting the hydrogen by valving to the atmosphere. The question of what added risk is involved through burning the hydrogen would have to be judged on the basis of final arrangements for conducting the hydrogen to the engines.

A recent suggestion has been made that liquid hydrogen for fuel be carried in insulated spherical metal containers surrounded by helium. The hydrogen would be allowed to boil off as a vapor and be conducted to the engines. The mechanical features of the installation would not prove insurmountable or excessive as to weight, but questions of control of gas flow and safety as well as of the practical availability of liquid hydrogen, require investigation. The cruising range of such an airship would be nearly twice that of our present gasoline-burning airships. Water-recovery problems would be very much simplified.

FIRE HAZARDS

Lest it be considered that the question of fire hazard has been over-emphasized in this discussion, it should be pointed out that there is a fire hazard in any craft that carries gasoline, either in bulk or as fuel. The fire hazard in airships on account of gasoline is not considered to be any greater than that existing in airplanes or motor boats. The question of fire hazard from hydrogen and from fuel gas is another matter, but here again the actual risk, assuming that the hydrogen purity is always well above the explosive range, is considered to be far less than is popularly believed. Perfection of interior mechanical arrangements and prudent operation of the airship and all her appliances are the greatest factors in reducing and eliminating fire hazards from whatever source, and all airship installations are very carefully worked out to eliminate these hazards.

From the foregoing general and perhaps superficial discussion, it will be apparent that the performance of future airships is going to be very materially affected by the fuel adopted for use in their engines. There are several fuels which might be used—gasoline, "safety gasolines," Diesel oils, fuel gas, hydrogen gas, liquid hydrogen. Each fuel will have its own peculiar effects on interior arrangements and may even influence noticeably the method of operation of the airship. A designer must trace the influence of possible fuels through all of their ramifications, and his choice, as usual, will have to be a compromise. The final comparison of the weight efficiency and performance of various alternative power-plant combinations and arrangements should be made on the basis of their performance over a considerable number of hours—say not less than 50 hr—since this figure represents the average length of voyage for a modern airship.

The Application of the Hardy Cross Method of Moment Distribution

By H. A. WILLIAMS,¹ STANFORD UNIVERSITY P. O., CALIF.

This paper presents the basic principles of the Hardy Cross method of analyzing continuous frames by distributing fixed-end moments and illustrates the application of the method to various types of structures, including an elevator spar with supports on a line, the same spar with deflected supports, and an airplane fuselage truss with loads between panel points.



FOR years, structural engineers have been searching for a simple method of determining stresses in statically indeterminate structures. The Maxwell-Mohr, least-work, and slope-deflection methods have been employed to a large extent, but the laborious computations involved, together with the tendency for small errors to accumulate, have discouraged their use.

In May, 1930, Prof. Hardy Cross, of the University of Illinois, presented in the Proceedings of the American Society of Civil Engineers a paper entitled, "Analysis of Continuous Frames by Distributing Fixed End Moments."² The method proper was one of successive approximation involving only the simplest arithmetic and eliminating the use of simultaneous equations. The widespread discussion which followed would seem ample proof of the profession's interest in this method. Professor Cross purposely limited his paper to definitions and to a brief illustration and discussion of the application of the method to one type of frame. He also suggested other possible applications, many of which have been covered in subsequent discussion.

Due to the brevity of the original paper, it seems desirable that a more detailed presentation be made in which emphasis should be placed on the correlation between moment distribution and the physical action of a structure. The writer has attempted to accomplish this by simple illustrations, while explaining the basic principles.

Only a few practical applications to aeronautical problems have been given in this paper. But it is felt that familiarity with the basic principles should enable the airplane designer to apply the method to his special problems without difficulty.

The author is very much indebted to Prof. A. S. Niles for the

criticisms and suggestions that he has given. Numerous features of the paper have been instigated by him.

DEFINITIONS

In order to clarify the immediate discussion of the Hardy Cross method, the sign conventions and four terms will be defined as follows:

(1) *Fixed-end moment* is the moment which would exist at the ends of a loaded member if those ends were held rigidly against rotation. This is in accord with the ordinary usage for beams ending in heavy walls.³

(2) *Unbalanced moment* is numerically equal to the algebraic sum of all moments at a joint. The joint is balanced when the sum of the moments equals zero.

(3) *Stiffness* as herein used "is the moment at one end of a member (which is on unyielding supports at both ends) necessary to produce unit rotation of that end when the other end is fixed."⁴ For a straight beam of constant section, the stiffness is proportional to the moment of inertia divided by the span length—i.e., the usual $K = I/L$ used in the slope deflection method. Of course, the relative rather than the actual values of K can be used in computations.

(4) *Carry-over factors* result from the fact that if a beam simply supported at one end and fixed at the other is acted on by a bending moment at the simply supported end, a certain moment is induced at or "carried over" to the fixed end. The ratio of the moment at the fixed end to the bending moment at the simply supported end is called the "carry-over factor." It is $+1/2$ for straight beams of constant section.⁵

(5) The *sign conventions* used in this paper are as follows: A clockwise moment couple acting on the end of a member is positive; a counter-clockwise moment couple is negative. If, at a joint, the tangent to the elastic curve of a member rotates through a clockwise angle, the rotation is positive. Hence, a positive moment acting on the end of a member causes a positive rotation.⁶

BASIC PRINCIPLES

It will be recalled that, in the analysis of statically indeterminate structures, various temporary expedients are resorted to in order to obtain the moments and stresses in the members. Redundant members are assumed to be cut or a fixed or partially restrained joint is taken as hinged, and the resulting statically determinate structure is analyzed for this condition. Then certain external forces or moments are assumed to come into

¹ Department of Civil Engineering, Stanford University. Mr. Williams was graduated from Stanford University in 1925, and then entered the employ of the Standard Oil Company of California as draftsman and structural designer, where he remained until 1930. He then returned to Stanford as a graduate student and teaching assistant in civil engineering. Since 1931 he has been an instructor. Mr. Williams received his engineer's degree from Stanford, specializing in structural engineering.

² Since published, with all discussion, in Trans. Am.Soc.C.E., vol. 96, 1932, p. 1.

Contributed by the Aeronautic Division of THE AMERICAN SOCIETY OF MECHANICAL ENGINEERS and presented at the Pacific Coast Aeronautic Meeting, University of California, Berkeley, Calif., June 9-10, 1932.

NOTE: Statements and opinions advanced in papers are to be understood as individual expressions of their authors, and not those of the Society.

³ See Appendix B for fixed-end moments for beams with various types of loading.

⁴ Quoted from Hardy Cross paper. See Trans. Am.Soc.C.E., vol. 96, 1932, p. 2.

⁵ See footnote 10.

⁶ The sign conventions adopted here are the same as those used by Messrs. Wilson, Richart, and Weiss in "Statically Indeterminate Structures," Bulletin 108, University of Illinois, Engineering Experiment Station. They also are used by Sutherland and Bowman in their text, "Structural Theory." Note that these sign conventions bear no relation to the signs used in ordinary design, and hence are not the same as those used in the original paper by Hardy Cross. See Appendix A for more extensive definitions of sign conventions.

action and draw the cut member together or return the hinged joint to the restrained condition, and the same statically determinate structure is separately analyzed for the effects of the latter forces or moments. The principle of superposition⁷ is assumed to apply, and results of the separate analyses are added algebraically to determine the final stresses. The procedure involves the application to the structure of certain arbitrary restraining forces or moments. These forces or moments are later removed, leaving the frame acted on by the original loads. The arbitrary restraints can be removed and re-applied any number of times as long as in the end the true force system prevails.

Consider, for illustration, a simple beam uniformly loaded. By fixing or restraining the ends, which are normally free to rotate, we can prevent the beam from sagging as far as it ordinarily would when similarly loaded and resting on knife-edged supports. If we now release the restraint at one end only, further deflection will take place; and the subsequent removal of the restraint at the other end will allow the beam to sag to its final position. In this case only two steps are involved. However, by alternately releasing and fixing the ends, the beam could have been lowered to its final position in as many stages as was desired. Each stage would have resulted in certain changes in the end moments of the beam. By the principle of superposition, the effects of all of these separate changes could be added algebraically to determine the final moments. Obviously, this summation would be zero for the end moments of this particular structure.

ILLUSTRATION, SIMPLE BEAM OF ONE SPAN

Suppose, in order to make the foregoing example more specific, we follow through in detail the steps suggested, using Figs. 1 to 9 to help in visualizing the physical action which takes place.⁸

(1) Fig. 1: We have the simple beam AB resting on unyielding knife-edged supports. The uniformly distributed load has not yet been applied.

(2) Fig. 2: It is assumed that before the load is applied, the ends are fixed by casting a heavy imaginary wall around the beam at each end.

(3) Fig. 3: The load is assumed to be applied. By well-known methods,⁹ the end moments are found to be $-WL/12$ at A and $+WL/12$ at B as shown. By definition, these are "fixed-end moments."

(4) Fig. 4: The restraint at A is removed. As a result: (a) The moment of $-WL/12$ at A is entirely released. This effect is the same as though a new external moment of $+WL/12$ had been exerted at A . Hence, adding $+WL/12$ to the previous $-WL/12$ gives zero, the new moment at A . (b) It is obvious from the figure that the action of the external moment ($+WL/12$) at A caused additional strain or moment to be set up at B , the far end of the beam. This is the "carry-over" moment from A to B . It is equal to $+1/2 \times +WL/12 = +WL/24$.¹⁰ The net moment at B is now $+WL/8$, as would be expected.¹¹

⁷ The principle of superposition states that the total effect of a number of loads on a structure is the same as the sum of the effects of each load when separately applied. It is only approximately true for combined bending and compression.

⁸ Since we are concerned only with moments at this time, no shears or support reactions will be shown in Figs. 1 to 9.

⁹ That is, by theorem of three moments, moment areas, or slope deflection. Moments for fixed-ended beams of one span can also be found in any handbook.

¹⁰ The ratio $+1/2$ is the carry-over factor for a straight beam of constant section. See Appendix B for derivation.

¹¹ The foregoing moments for a beam fixed at one end and hinged at the other can be checked from any handbook.

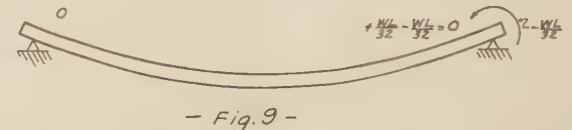
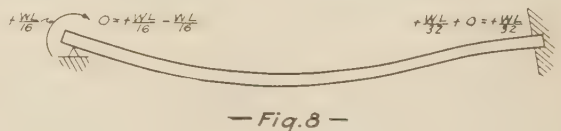
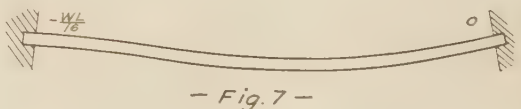
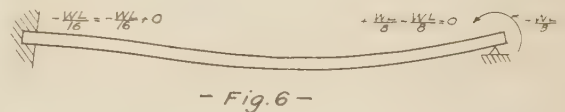
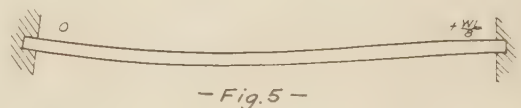
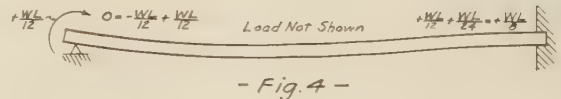
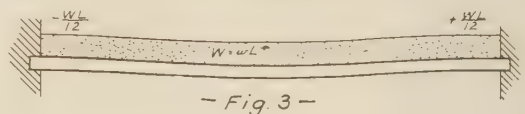
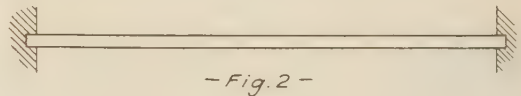
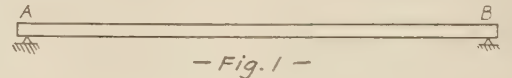
(5) Fig. 5: Joint A^{12} is assumed fixed in its new position.

(6) Fig. 6: Joint B is released; i.e., an external moment of $-WL/8$ is applied, thus canceling the previously existing moment of $+WL/8$. The beam sags still further and sets up a strain at the fixed end A . That is, a moment of $+1/2 \times -WL/8 = -WL/16$ is carried over to A and added to the existing moment, which is zero.

(7) Fig. 7: Joint B is again fixed.

(8) Fig. 8: Joint A is released, leaving zero moment at A and a carry-over moment of $+WL/32$ at B .

(9) Fig. 9: If we now decide arbitrarily to release B without



¹² In this paper, the term "joint" will be used not only to describe the point of intersection of the axes of two or more members as in a truss, but also to refer to the intersection of the axis of a beam and the center line of a support.

first fixing *A*, as was previously done, we can do so, and the beam reaches its final sag with zero moment at each end.

Inspection shows that each step brought us closer to the true condition for the loaded beam. Each time a moment was added due to a change in position of the beam, the added value was smaller than before, since the carry-over factor was $+1/2$. The principle of superposition was applied at each step in that the new moment was added to the existing moment before proceeding to the next step.

The foregoing example is of course extremely simple. Since the beam is of one span only and the ends are both hinged, it can be allowed to deflect to its final position at any time by simply releasing all restraining moments and allowing both end moments to become zero. However, this can be done only because both ends actually are hinged and we know that the final end moments must equal zero. In even a slightly more complicated structure, such as a continuous beam on three supports, the situation is different. Certain moments will exist at the interior ends of the spans when the structure reaches its final state of equilibrium. The magnitudes of these moments are unknown as a rule. Hence, the moment over the middle support resulting from releasing both end joints at once will not equal the actual final moment except by coincidence.

ILLUSTRATION, CONTINUOUS BEAM

Let us now follow through the analysis, in the same general manner as before, of the continuous beam shown in Fig. 10. The cross-section is constant throughout, and all spans are of equal length. The supports are assumed as unyielding. The only external force is the load *P* on the end of the overhang. Moments are designated in the usual fashion. M_{ab} is the moment in beam *AB* at end *A*; M_{ba} is the moment in beam *AB* at end *B*.

Assume that, before the load *P* is applied, all joints are fixed against rotation. This fixity can be thought of as being effected by casting a heavy wall around the beam at each support. Under these circumstances, the only immediate result of applying the load *P* is that a fixed-end moment ($M_{ao} = +1000$ ft-lb) is set up in the cantilever. All other moments equal zero. From this point, the procedure is as follows:

(1) Balance joint *A*: Suppose joint *A* is now released; i.e., the wall is assumed replaced by a knife-edged support. If $\Sigma M = M_{ao} + M_{ab} = 0$, the joint would be in equilibrium and no rotation would take place. However, $\Sigma M = +1000 + 0 = +1000$, which means that an unbalanced moment of $+1000$ exists at the joint for an instant after the wall is removed. While the joint was fixed, this moment was resisted by the wall. After release, it must obviously be resisted by an equal and opposite moment in the beam. Hence, the release and subsequent rotation of the joint causes no change in M_{ao} , but adds a -1000 to M_{ab} . This value is written as shown in Fig. 12. Joint *A* is now said to be balanced, since $\Sigma M = 0$.

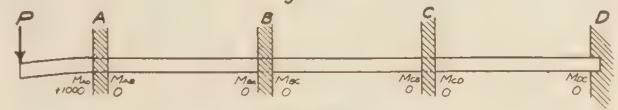
(2) Carry-over moment to joint *B*: The balancing of joint *A* actually amounted to applying a moment of -1000 to end *A* of beam *AB*. This -1000 deflected the center of the beam upward (Fig. 12) and also caused a moment to be "induced at" or "carried over" to M_{ba} , since joint *B* was fixed against rotation. This moment change at M_{ba} is equal to $+1/2 \times -1000 = -500$.

(3) Joint *A* is assumed fixed in its new position.

(4) Balance joint *B*: It will be noticed that this joint differs from any encountered so far in that its rotation affects and is affected by a beam on each side. The instant after joint *B* is released, the unbalanced moment is $M_{ba} + M_{bc} = -500$. In order that the moments on each side of the joint will be equal and opposite, the equilibrant of the unbalanced moment of



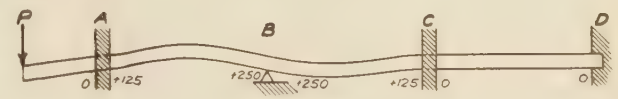
— Fig. 10 —



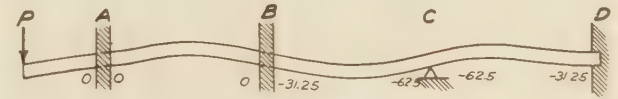
— Fig. 11 —



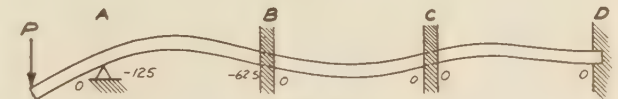
— Fig. 12 —



— Fig. 13 —



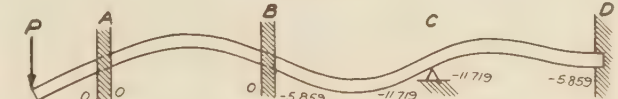
— Fig. 14 —



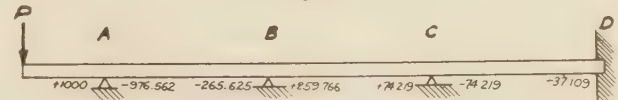
— Fig. 15 —



— Fig. 16 —



— Fig. 17 —



— Fig. 18 —

-500 must be distributed to each beam so that the equation $\Sigma M = 0$ is satisfied. That is, the joint rotates clockwise, relieving M_{ba} of some moment and adding an equal amount to M_{bc} .¹³ If M_{ba} is relieved by $+250$ and the same amount is added to M_{bc} :

$$M_{ba} = -500 + 250 = -250$$

¹³ This is true only when I/L is the same for the member on each side of the joint. Also, one-half is given to each member only when there are but two members coming into the joint. For further development and discussion of balancing moments at joints, see under heading, "Effect of Rigidity on Distribution of Moments at a Joint."

adjacent joints. The general method is one of assuming the structure to deflect to its natural loaded position through a series of steps. Each step is paralleled by a computation of the moments needed to balance the joints released and the resulting carry-over moments imposed on adjacent joints. The moment changes at each step are evaluated before proceeding to the next step. By the principle of superposition, the results of the various steps are added algebraically to determine the final moments. The accuracy of these final moments depends on the number of steps or cycles used in the computations.

The general physical action upon which the Hardy Cross method depends is aptly illustrated by a building frame as shown in Fig. 20. All joints of the frame are free to rotate if desired, but it is assumed that they are fixed as far as translation in any direction is concerned. Suppose a moment acts on joint 1 when all other joints are assumed as fixed against rotation as well as lateral movement. As a result, certain fixed-end moments are set up at 2, 3, 4, and 5 due to the carry over from joint 1. These carry-over moments will be unbalanced moments at the instant these joints are released. If all joints except 2 are now fixed, and joint 2 is released so that $\Sigma M_2 = 0$, this release will in turn cause a further spread of moment, not only to new joints, but also back to joint 1. The same effect will result from releasing joints 3, 4, and 5 in turn. It will be noticed that the releasing of joints 2, 3, 4, and 5 affects some joints in common (Fig. 21).

If joint 10 (Fig. 22) is now released, joints 2 and 3 are affected, as well as some new joints. Hence, it might be said that as the wave spreads out from the origin, it not only affects new joints in its path, but it also affects the joints in its wake. As it recedes from the point of origin, its intensity decreases until it "dies out." A new wave of less intensity now moves out from the origin, leaving still smaller moments in its wake. Successive waves grow smaller until their effect is practically negligible.

EFFECT OF RIGIDITY OF MEMBERS ON JOINT ROTATION

It has been stated under "Definitions" that the stiffness or rigidity of a straight beam of constant section is proportional to the moment of inertia divided by the span length. That is, the value of $K = I/L$ is an index of rigidity.

It will be recalled that the continuous beam used for illustration, was of constant section and that the spans were of equal length. Hence the value of K was the same for all members. Also, in balancing joint B (see item 4 under heading "Illustration, Continuous Beam") it was stated that the equation of equilibrium for the joint was satisfied by distributing a moment equal to minus one-half the unbalanced moment to the member on each side of the joint. However, it should be observed that this was true only because the beams on either side of joint B were equally stiff. Since $K_{ba} = K_{bc}$, the distribution was actually in the ratio of $\frac{K_{ba}}{K_{ba} + K_{bc}} M_u = \frac{K_{ba}}{2K_{ba}} M_u = \frac{1}{2} M_u$,

where M_u is the unbalanced moment. If $K_{ba} = 2$ and $K_{bc} = 3$, the amount distributed to M_{ba} and M_{bc} would be $\frac{2}{2+3} = \frac{2}{5}$ and $\frac{3}{2+3} = \frac{3}{5}$ respectively. That is, the distribution of the unbalanced moment to the members was in proportion to their relative rigidities.

The physical effect of relative rigidity can best be seen by following through the various steps illustrated in Figs. 23 to 28.

Fig. 23 shows a two-span continuous beam with a load P on one span, a knife-edged support at B , and fixed at ends A and C . The knife-edge is assumed to have no restraining effect on joint B so far as rotation is concerned. Suppose joint B is assumed fixed while the load P is being applied and is then released—the usual procedure in the Hardy Cross method. If, as in Fig.

24, beam BC is infinitely stiff compared to beam AB , obviously there will be no rotation at joint B when the fixity is removed and the moment M_{ba} will be the same as the original fixed-end

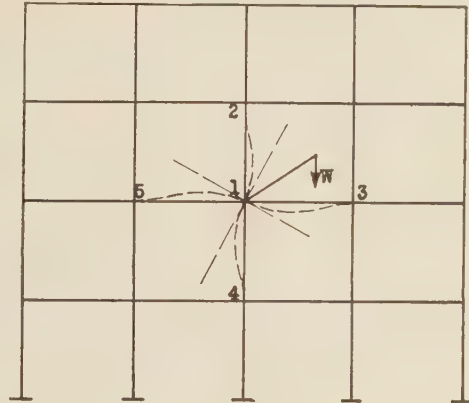


FIG. 20
(First stage, joint 1 rotates.)

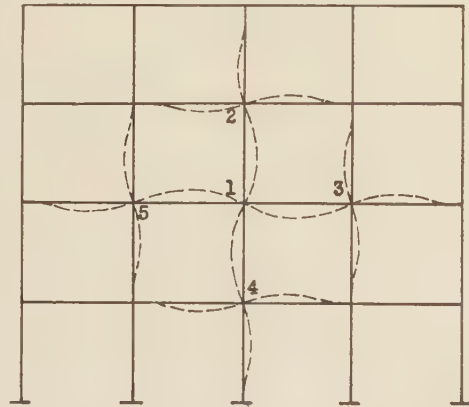


FIG. 21
(Second stage, joint 1 fixed, joints 2 to 5 rotate.)

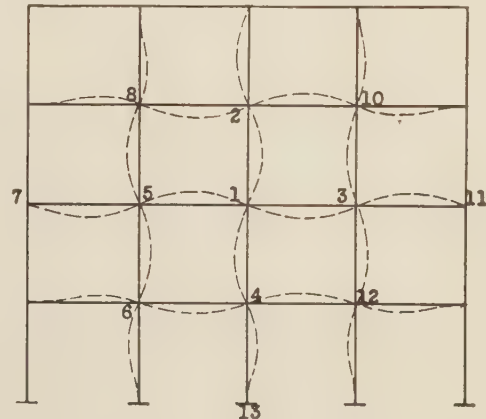
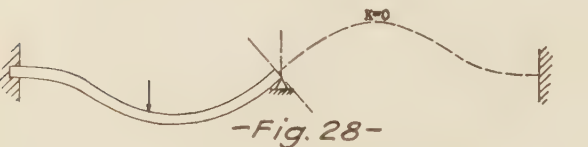
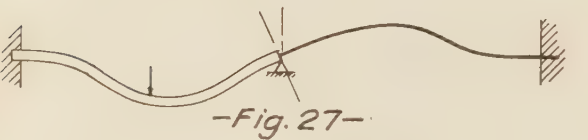
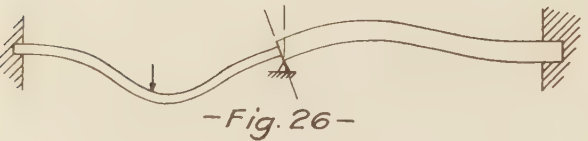
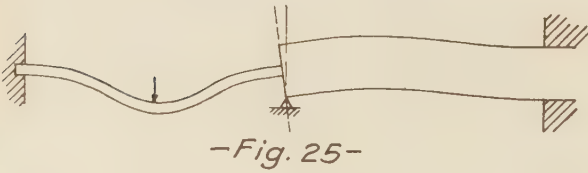
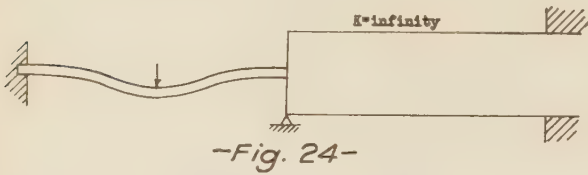
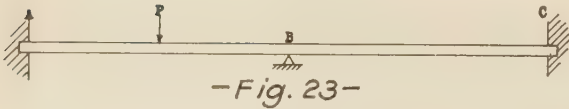


FIG. 22
(Third stage, joints 1 to 5 fixed, joints 6 to 12 rotate.)

moment. If, as in Fig. 25, beam BC is less rigid but still relatively stiff as compared to AB , some rotation of B will take place upon release and the resulting moment M_{ba} will be less



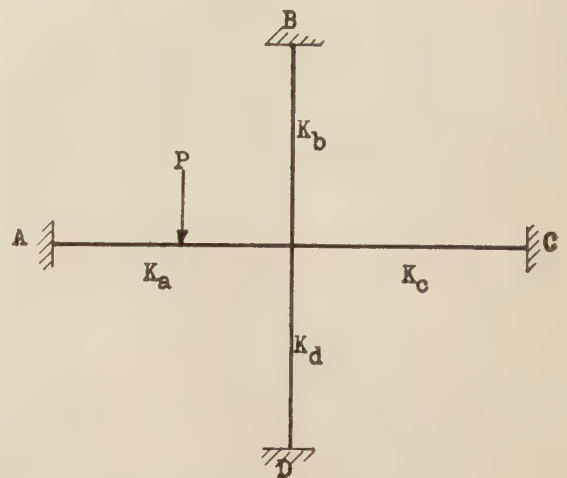
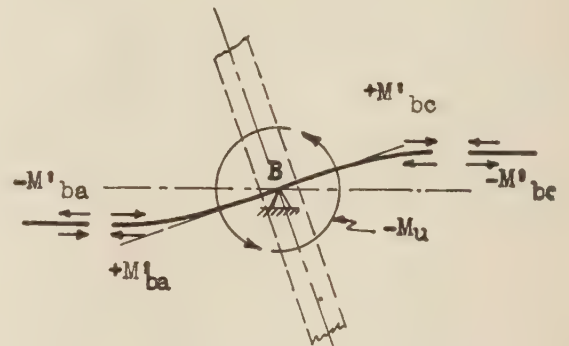
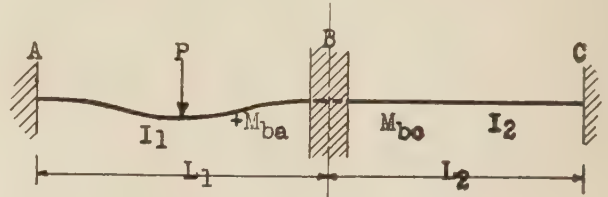
than the original fixed-end moment. Figs. 26 and 27 show the effect of further reduction in the stiffness of beam BC. If, as in Fig. 28, beam BC ceases to exist or is of infinitely small cross-section, joint B can rotate until $M_{ba} = 0$. Hence, it is seen that the rotation of a joint is largely dependent on the relative rigidities of the members common to the joint.

EFFECT OF RIGIDITY ON DISTRIBUTION OF MOMENTS AT A JOINT

Let us now take the same beam as was used in Fig. 23, designate the moment of inertia and span length as shown in Fig. 29, and apply the first step of the Hardy Cross method—fix joint B and apply the load P. As a result $M_{bc} = 0$; but M_{ba} is a fixed-end moment depending on the load and span length. This fixed-end moment is held in equilibrium by the clockwise couple exerted by the hypothetical wall at B. Let us call this $+M_u$. If the wall is suddenly replaced by the knife-edged support, the moment $+M_u$ is momentarily unbalanced until it is removed. Removing a moment is the same as applying an equal and opposite moment. Hence, it can be considered that the unbalanced moment $+M_u$ is removed by the application of an equal and opposite moment $-M_u$. This moment rotates the tangent to the elastic curve of the beam through the angle $\theta_{ba} = \theta_{bc}$ (Fig. 30) and causes corresponding changes in the beam moments. Let us call the moment changes due to the rotation M'_{ba} and M'_{bc} . From the moment area or elastic-weights method of determining moments:¹⁴ $\theta_{ba} = M'_{ba}L_1/4EI_1 = M'_{bc}L_2/4EI_2 = \theta_{bc}$, or, since

E is a constant, if both spans are of the same material, and if we let $I_1/L_1 = K_1$ and $I_2/L_2 = K_2$:

$$M'_{ba}/K_1 = M'_{bc}/K_2 \dots\dots\dots [1]$$



So as to have equilibrium at the joint after rotation (Fig. 31):

$$M'_{ba} + M'_{bc} = -M_u \dots\dots\dots [2]$$

Therefore, from Equations [1] and [2]:

$$M'_{ba} = -M_u \times K_1/(K_1 + K_2) = -M_u \times K_1/\Sigma K$$

$$M'_{bc} = -M_u \times K_2/(K_1 + K_2) = -M_u \times K_2/\Sigma K$$

¹⁴ See Appendix B.

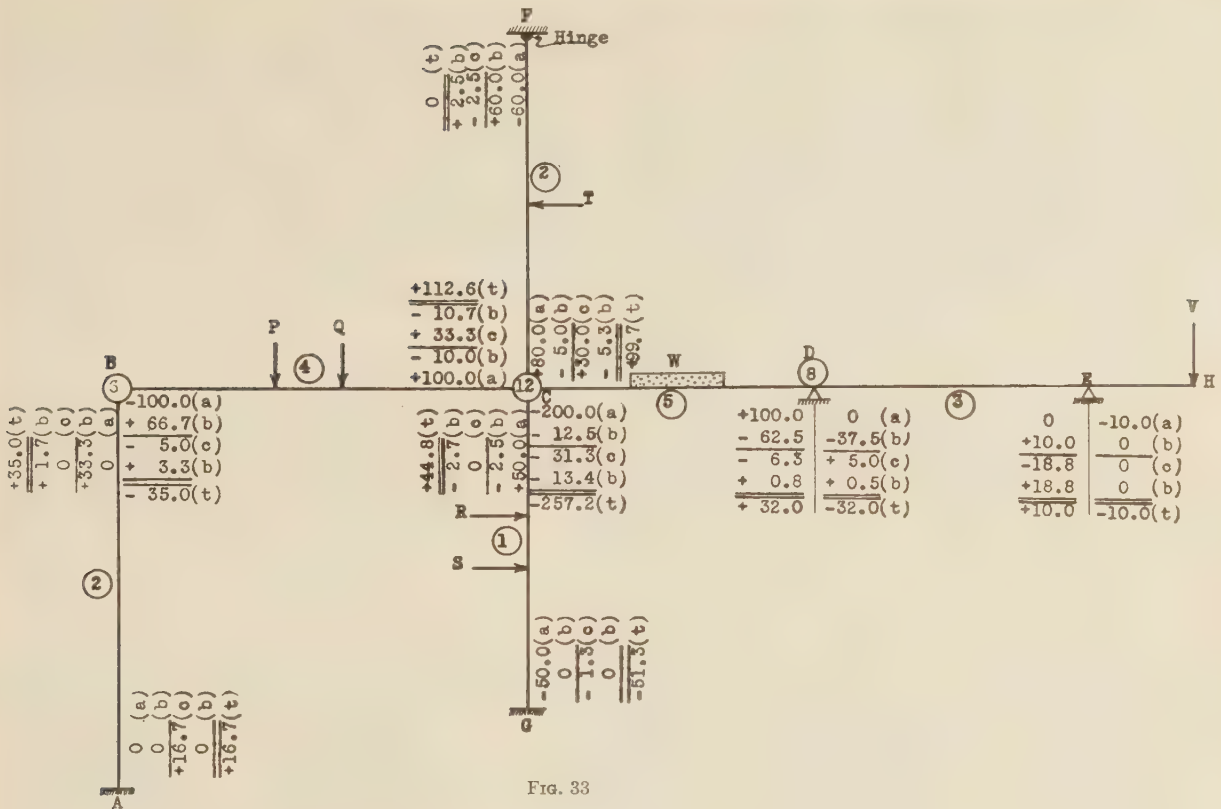


FIG. 33

Attention is again called to the fact that M'_{ba} and M'_{bc} are only the moments due to the rotation of joint B after the fixity is removed. The actual total moments in the two members are found by adding the moments M'_{ba} and M'_{bc} algebraically to the original fixed-end moments M_{ba} and M_{bc} , respectively.

In so many words, the foregoing equations tell us that when a joint is released, a moment equal and opposite to the unbalanced moment is distributed to the members common to the particular joint in proportion to their rigidities. If the unbalanced moment is positive, the moments distributed will be negative, and vice versa.

If there are more than two members common to the joint released (Fig. 32), the rule still holds. That is:

$$M'_{ba} = -M_u \times K_a / (K_a + K_b + K_c + K_d) = -M_u \times K_a / \Sigma K$$

APPLICATION OF HARDY CROSS METHOD TO AN ELEVATOR SPAR

Fig. 34 shows the vertical-load curve for an elevator spar.¹⁵ The spar will first be considered as a symmetrical continuous beam with five supports. A simplified attack will then be shown.

If a $1\frac{1}{4}$ -in. by 0.035-in. Dural tube is used, the moment of inertia is 0.02467 throughout, and the value of K will be the same for all spans except the overhangs, where it will be zero. Hence, a relative value of $K = 1$ is used.

All joints are assumed fixed against rotation, and the fixed-end moments are calculated.¹⁶

¹⁵ The author is indebted to Mr. Ben W. James, of Stanford University, for the numerical data used in this illustration.

¹⁶ The expressions for determining fixed-end moments can be derived by moment areas or slope deflection as shown in Appendix B. Values for various types of loadings are given in Fig. 41.

$$M_{Fao} = -M_{Fef} = 1.32 \times 5 \times 10/3 = 22$$

$$-M_{Fab} = +M_{Fed} = \frac{1.32(45)^2}{12} + \frac{0.96(45)^2}{2 \times 15} = 288$$

Similarly:

$$M_{Fba} = -M_{Fde} = 320$$

$$-M_{Fbc} = +M_{Fdc} = 450$$

$$M_{Feb} = -M_{Fed} = 482$$

These quantities are recorded as shown on Fig. 35, step (f). In accordance with the conventions given under "Definitions," clockwise-resisting moment couples are positive, counter-clockwise couples are negative. The subsequent procedure is as follows:

Joint A: The instant after this joint is released, the summation of moments around the joint is $+22 - 288 = -266$. To make the joint balance, a moment of $+266$ must be distributed to the two members in proportion to their rigidities (see heading, "Effect of Rigidity on Distribution of Moments at a Joint").

Hence, distribute to AO, $\frac{0}{0+1} \times +266 = 0$; to AB $\frac{1}{0+1} \times +266 = +266$. These quantities are recorded as shown (step b) and a line is drawn under each to indicate that the joint is now in balance, i.e., $\Sigma M_A = 0$. As stated before, this line does not indicate an addition.

Joint B: The instant after this joint is released, the unbalanced moment is $+320 - 450 = -130$. The subsequent rotation will be the same as if a $+130$ acted on the joint. Hence, distribute $1/(1+1) \times +130 = +65$ to BA and the same to BC.

Joint C: There is no unbalanced moment at this joint because of symmetry.

Joints *D* and *E*: Balance and record in the same way as for joints *B* and *A*, respectively. Note that the signs are reversed on this side.

All joints are now in balance. Since the balancing actually consisted in allowing one joint at a time to rotate while all others were fixed, the resulting carry-over moments must now be computed as indicated in step (c). As has been previously shown, the carry-over moment at one end of the member is the distributed moment just determined at the opposite end multiplied by $+1/2$.

The moments just carried over throw the joints out of balance again. These new moments must be distributed in the same way

cal action of the beam when *A* is released while *B* is assumed fixed. Now balance joint *B*. The unbalanced moment is $+320 + 133 = +453$. Therefore, distribute -453 as shown, $3/7$ to *BA* and $4/7$ to *BC*, and at once record the corresponding carry-over moment at *C*.

There will be no carry-over to *A*, since this joint was free to rotate. It will be noticed that the solution is completed, since *C* need not be released.

This procedure can be followed with more complicated structures even when symmetry and freely supported joints are not involved.

In most structures, there will be certain joints with a larger

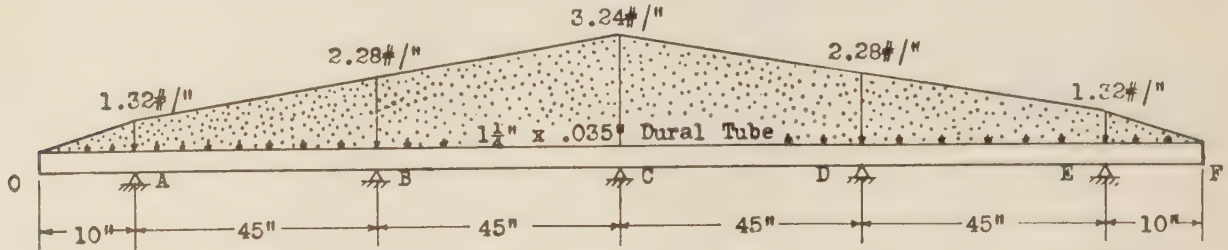


FIG. 34

K=0		K=1		K=1		K=1		K=1		K=0	
A		B		C		D		E			
+22	-288	+320	-450	+482	-482	+450	-320	+288	-22(f)		
0	+266	+65	+65	0	0	-65	-65	-266	0(b)		
0	+33	+133	0	+33	-33	0	-133	-33	0(c)		
0	-33	-66	-66	0	0	+66	+66	+33	0(b)		
0	-33	-17	0	-33	+33	0	+17	+33	0(c)		
0	+33	+8	+8	0	0	-8	-8	-33	0(b)		
0	+4	+17	0	+4	-4	0	-17	-4	0(c)		
0	-4	-8	-8	0	0	+8	+8	+4	0(b)		
+22	-22	+452	-451	+486	-486	+451	-452	+22	-22(t)		

FIG. 35

as the fixed-end moments. In Fig. 35, the computations are carried through four cycles, after which a double line is drawn and the algebraic totals are written.

Other quantities such as moments, shears, and reactions can be found now by the usual laws of statics.

SOLUTION SIMPLIFIED

The foregoing computations for the elevator spar can be greatly simplified. Because of symmetry, only one-half of the beam need be considered, as shown in Fig. 36. The center joint *C* can be assumed fixed, since we know it does not rotate on account of the symmetry of structure and loading. Joint *A* is freely supported and, once released, need not be fixed again. This necessitates the use of a value for K_{ab} equal to $3/4$, the true relative value. Hence, to simplify computations, K_{bc} is made equal to 4 and K_{ab} equal to 3^{17} .

Joint *A* is now balanced as before, and $+133$ is immediately carried over to joint *B*. This procedure is more nearly in accord with the physi-

cal action of the beam when *A* is released while *B* is assumed fixed. Where the unbalanced moment is quite small, it is a waste of effort to balance the joint carefully, only to have this balance entirely disrupted later by a large carry-over moment from adjacent joints. Hence, more rapid convergence will be obtained if the highly unbalanced joints are first balanced and the resulting carry-over moments are recorded before proceeding to the better balanced joints.¹⁸

¹⁸ This method was proposed by L. E. Grinter in discussion of the Hardy Cross paper. See Trans. Am.Soc.C.E., vol. 96, 1933, p. 11. It is suggested that this method should not be used until complete familiarity with the usual procedure is obtained.

K=0		K=3		K=4		Center Line	
A		B		C			
+22	-288	+320	-450	+482			
0	+266	+133					
		-1	-2	-1			
+22	-22	+452	-452	+481			

FIG. 36

¹⁷ It can be shown by slope deflection or moment areas that the moment needed to produce a given rotation at one end of a beam when the other end is free is three-fourths as great as if the other end is fixed.

APPLICATION TO ELEVATOR SPAR WITH DEFLECTED SUPPORTS

The elevator spar of Fig. 34 is attached to the stabilizer. Let us suppose that it has been determined from computations or from tests that the supports at *A*, *B*, *D*, and *E* are deflected by known amounts with respect to *C*. The moments in the spar can be found by moment distribution as before, once the revised fixed-end moments are determined.

It will be recalled that the first step in the Hardy Cross method is to assume all joints fixed and then apply the external loads. If this fixity is also assumed to take place before the joints are deflected, this deflection will set up fixed-end moments in any one span, as shown in Fig. 37.

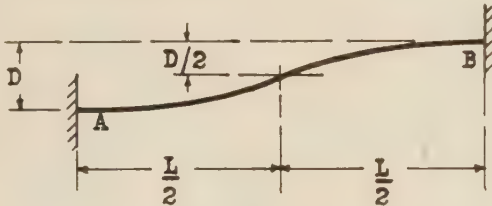


FIG. 37

K=0		K=3		K=4	
+22	-193	+415	-355	+577	
0	+171	+86			
		-63	-83		
<u>+22</u>	<u>-22</u>	<u>+438</u>	<u>-438</u>	<u>+535</u>	

FIG. 38

If the member *AB* is of constant cross-section, the point of contraflexure will be at the mid-point and each half can be treated as a cantilever beam with an end deflection of *D*/2.

Then:

$$\frac{D}{2} = \frac{PL^3}{3EI \times 8} = \frac{ML^2}{12EI} \quad (L = \text{total length of member})$$

or:

$$M = \frac{6EI}{L^2} D$$

Let us suppose it has been found that *A* deflects downward $\frac{1}{8}$ in. with respect to *B*, and *B* deflects the same with respect to *C*. The deflections of *E* and *D* are the same as *A* and *B*, respectively. For a $\frac{1}{4}$ -in. by 0.035-in. Dural tube, *I* = 0.02467 and *E* = 10,400,000. Then the foregoing formula gives the following fixed-end moments due to deflection of supports alone:

$$M_{aa} = 0$$

$$M_{ab} = \frac{6 \times 10,400,000 \times 0.02467 \times 0.125}{45 \times 45} = 95$$

and

$$M_{ba} = M_{bc} = M_{cb} = 95$$

The sign of this moment must be determined by inspection. If *A* deflects downward with respect to *B*, as in Fig. 37, obviously a positive clockwise moment at each end results. When these values are added algebraically to the fixed-end moments caused by the external loading (Fig. 35), the results are as shown in

Fig. 38, step (f). The succeeding steps in the solution are the same as for the example of Fig. 36.

PRACTICAL APPLICATION OF THE METHOD TO A CONTINUOUS FRAME

A more general use of the method will now be illustrated by determining the moments in the continuous frame shown in Fig. 33. This is the same frame that Professor Cross used in his original paper. As he stated at that time, the illustration is entirely academic and is selected only because "it involves all of the conditions that can occur in a frame which is made up of straight members and in which the joints are *not displaced*." In Fig. 33, the sign convention has been revised to agree with that defined at the beginning of this paper. Other minor changes from the original paper, suggested in the subsequent discussions, have been adopted where it was felt that the chance of error would be lessened. No attempt has been made to introduce short cuts in this solution. Joints *E* and *F* could obviously be treated like joint *A* in Fig. 36.

The relative $K = I/L$ value for each member is shown by the number in the circle near the middle of the span. The sum of the *K*'s for all members common to a joint is shown in the circle at the joint.

It is assumed that all joints are fixed, and then the loads *P*, *Q*, *R*, *S*, *T*, *W*, and *V* are applied as shown. The resulting fixed-end moments are then determined and are recorded, as shown in the figure, parallel to the member concerned and followed by the letter (*a*) for reference.

The unbalanced moment at all joints is first distributed, step (b). It will be noticed that the algebraic sum of the fixed-end moments at joint *C* is +30.0. This is the unbalanced moment the instant after the joint is released. The subsequent rotation will be the same as if a moment of -30.0 acts on the joint. The distribution will be 4/12 to *CB*, 2/12 to *CF*, 5/12 to *CD*, and 1/12 to *CG*, as shown. The subsequent procedure for this and other joints should be apparent in view of the previous illustrations.

Only two cycles are used in this example. Further cycles will improve some of these results, especially at joint *D*. The probable effect of further computation can always be ascertained by inspection of the last set of carry-over moments.

PRACTICAL APPLICATION OF HARDY CROSS METHOD TO DESIGN OF AIRPLANE FUSELAGE TRUSS

Fig. 39 shows the forward section of an airplane fuselage truss. Member 2U-4U has a concentrated load of 62 lb located 13 in. from one end, due to instruments. Members 3L-4L and 4L-5L are subjected to a uniform floor load in addition to concentrated loads between panel points due to passengers. Member 5L-6L has a concentrated baggage load of 310 lb located as shown.

The sizes, lengths, and axial loads determined in the usual way,

TABLE 1

Member	Size, in.	Length, in.	Axial Load, lb
2U-4U	$1\frac{1}{4} \times 0.035$	58	+3260
4U-5U	1×0.035	48	-2600
5U-6U	1×0.035	37	-3860
6U-7U	$1\frac{1}{8} \times 0.035$	50	-3865
2L-3L	1×0.035	39	-5340
3L-4L	$1\frac{1}{4} \times 0.035$	26	-6733
4L-5L	$1\frac{1}{4} \times 0.035$	36	-3700
5L-6L	1×0.035	51	-2650
6L-7L	1×0.035	51	-2065
2U-3U	$1\frac{1}{8} \times 0.035$	57	-2520
3L-4L	$1\frac{1}{8} \times 0.035$	58	-1475
4L-5L	$1\frac{1}{4} \times 0.049$	60	-4700
5L-6L	$1\frac{1}{4} \times 0.049$	54	-5216
6L-7L	1×0.035	65	-1200
7L-8L	$\frac{7}{8} \times 0.035$	60	-870
8L-9L	$\frac{7}{8} \times 0.035$	71	+550

assuming pin joints for each member, are shown in Table 1 (the axial loads are the critical values based on a combination of high angle of attack and three-point landing conditions).

Under present practise, a truss with this type of loading would be analyzed by assuming the members which have no side loads to act as struts with ends restrained in such a manner that the restraint coefficient $c = 2$ could be used. For the members subjected to side loads between joints, the Department of Commerce requires that the bending moments be properly taken into account, but does not specify how this should be done.

This paper proposes a method of attack for analyzing the effect of these intermediate loads which will give definite results even though it is not claimed that they will be perfectly accurate. It is believed to be an improvement over the present uncertainty and to constitute the first step toward obtaining a practical rational solution of the problem.

The most important errors in the method are due to the following factors:

(a) Bending moments due to joint deflection, resulting from changes in length of members, are neglected. (See discussion of Hardy Cross paper by Thompson and Cutler, Trans. Am. Soc. C.E., vol. 96, p. 108, for a method of obtaining these moments.)

(b) An axial compression load acting on the ends of a continuous beam causes a deflection in each span. These deflections in themselves result in additional moments at supports. These moments are neglected.¹⁹

(c) To get the allowable stress in compression members from Fig. 11 of Aeronautics Bulletin, No. 7-A, edition of Jan. 1, 1932, arbitrary assumptions are made regarding the location of points of inflection in selecting the value of L .

(d) To reduce labor, only a part of the truss is considered, and the end joints of this portion are assumed as fixed against rotation. This is a minor error.

The proposed procedure is made up of the following steps:

1 Compute the primary bending moments in all members due to loads between panel points by the Hardy Cross method. If desired, the secondary moments listed under (a) could be included in this computation, though that is not done in the illustrative example.

2 Determine maximum bending moment and unit stresses due to bending and axial load.

3 Determine effective slenderness ratio and compute margin of safety from Figs. 10 to 12 of Bulletin 7-A.

The determination of the maximum bending moment is likely to lead to some difficulties. The present practise of using a restraint coefficient of 2.0 in designing a fuselage member implies that the magnitudes and directions of the end moments are such that there is a point of inflection

¹⁹ Since this paper was written, Mr. Ben W. James, of Stanford University, has worked out a method of moment distribution modified to include the effect of axial loads upon the bending moments.

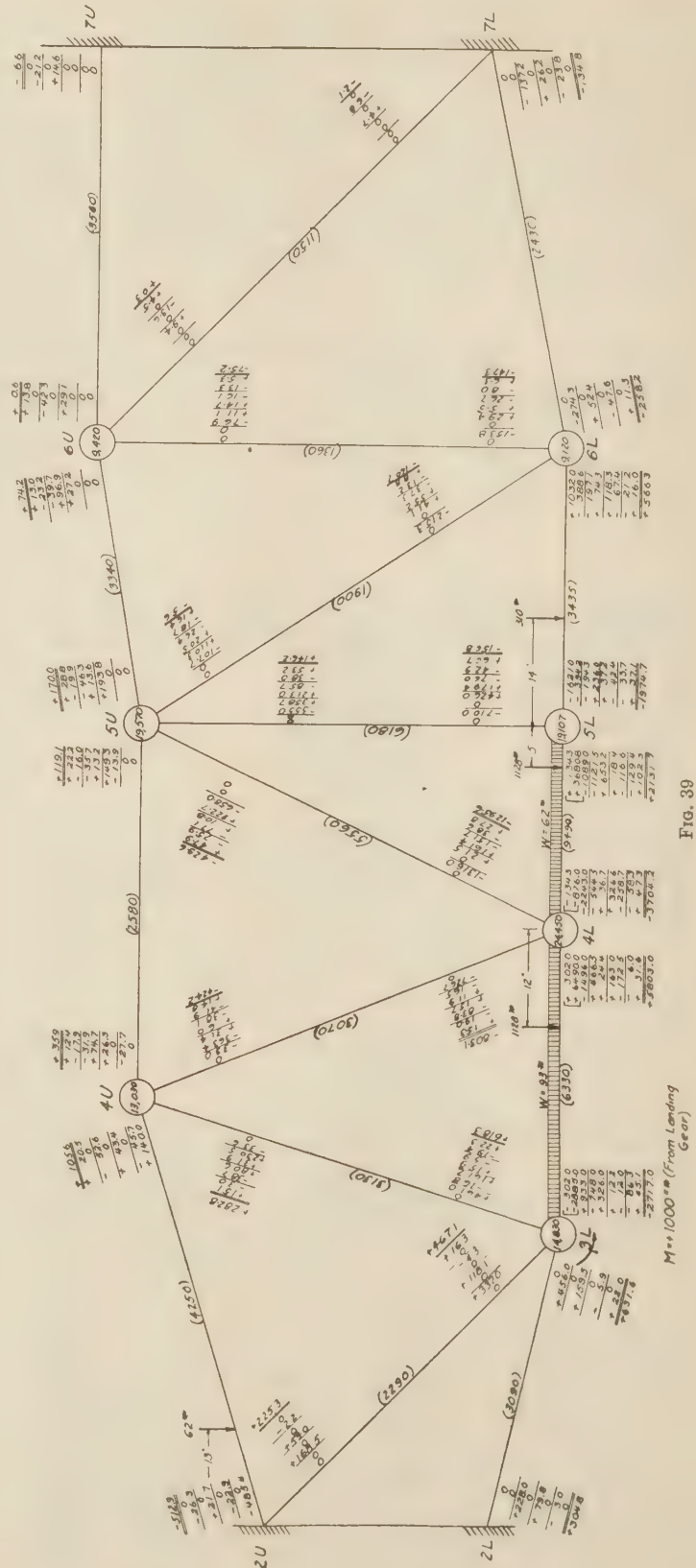
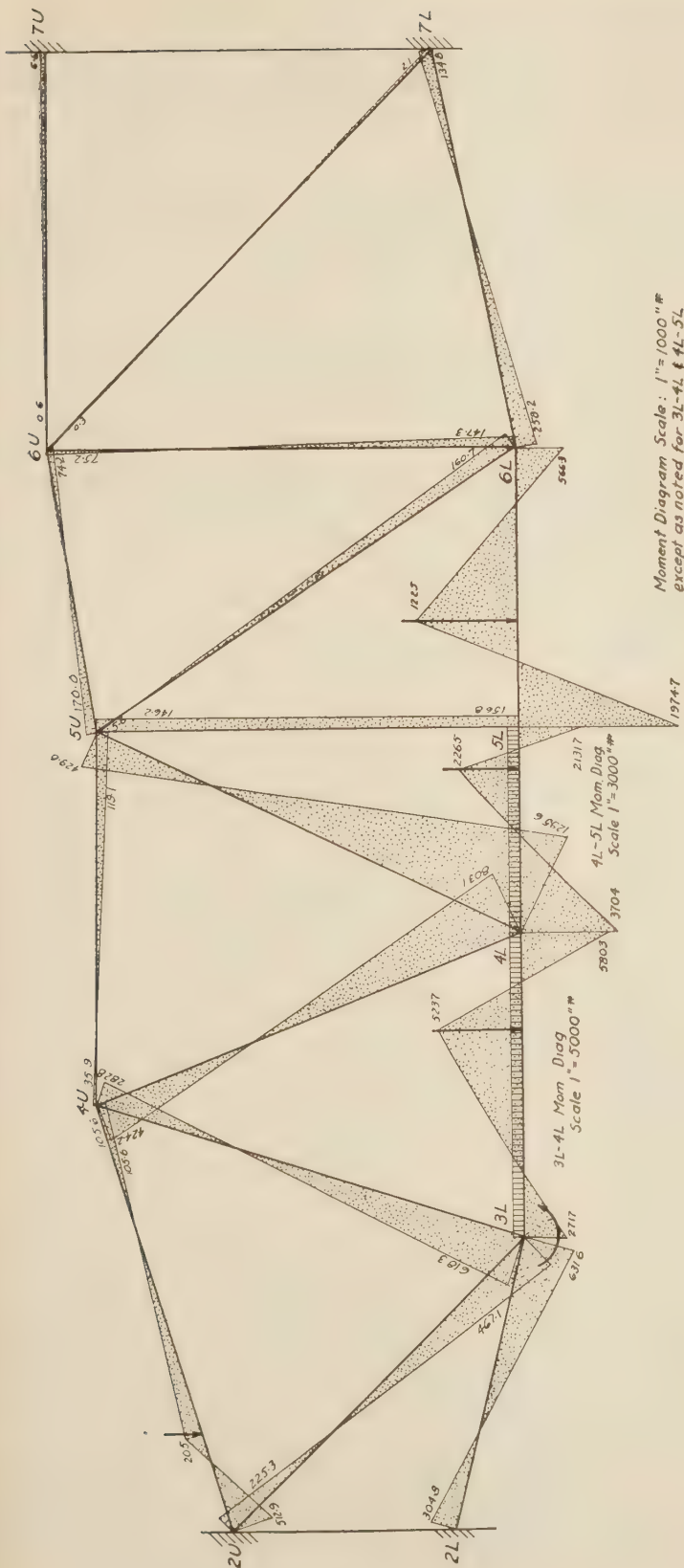


Fig. 39



Note: All moment diagrams drawn with ordinate on compression side of member

Fig. 40

distant not more than $0.7 L$ from the end of the member. As a result, if a member is designed on this basis with a small margin of safety for axial load only, the value of L/j will very likely be greater than π . If the moments at the ends of such a member were independent of the deflections of the member (as in a single span with cantilever ends as shown in Fig. 11:12 of "Airplane Structures" by Niles and Newell), the axial load would be greater than the critical and the member unable to carry it. A member of a fuselage truss, however, is more like one span of a continuous beam, such as is shown in Fig. 11:13 of "Airplane Structures." The end moments are very much influenced by the deflections in the member, and the critical load is not that which gives $L/j = \pi$, but a larger value that would be obtained by computations similar to those in article 11:7 of "Airplane Structures."

The rational method of computing the end moments would have to include computations of the effect of the secondary deflections between panel points to be made by some suitable modifications of the extended three-moment equation of chapter 11 of "Airplane Structures," but it has not yet been found possible to accomplish this. In the meantime, it is necessary to make certain assumptions.

For members in which the axial load is tension it seems conservative to neglect the effect of combined bending and axial load in producing secondary moment. The unit stress due to axial tension may be added to that due to the bending computed by applying the Hardy Cross method and the sum compared to the allowable unit tension.

If there is no side load on the member and the Hardy Cross computations indicate that there is no point of inflection in the member, it would seem unwise to use a member designed on the basis of $c = 2.0$, but the design should be based on $c = 1$ so that L/j would be less than π , and the formulas of chapter 11 of "Airplane Structures" could be used with some confidence to determine the maximum moment in the span.

If there is no side load and the Hardy Cross computations indicate a point of inflection, the same practise could be followed, but it seems unnecessarily conservative. Owing to the continuity of the structure, the end moments will increase faster than the external loads and the point of inflection will probably have only a small movement. If this were not the case, the failing loads for fuselages subjected to static test would have indicated the necessity of designing for $c = 1$ or less, instead of $c = 2$. The designer has two reasonable assumptions he might make. He might assume the point of inflection to be $0.7 L$ from the end with the larger moment or that it was, say, one-third of the

distance from the point of inflection indicated by the Hardy Cross computations and the end with the smaller moment. In either case, the distance from the assumed point of inflection to the end with the larger moment would probably give a value of L_i/j less than π . This segment of the beam could then be analyzed in the usual manner with the formulas of "Airplane Structures" and the margins of safety computed by the system recommended in Bulletin 7-A.

When there is a side load on the span, there are two similar choices. The first is to use a member of such size that L/j is less than π and compute the maximum moment from the formulas of "Airplane Structures." The other is to find the points of inflection indicated by the Hardy Cross computations of end moment and assume points of inflection a little further apart.

In all of these methods, the end moments are assumed to be those computed by the Hardy Cross method, neglecting the secondaries due to the combination of bending and axial load in each member of the structure. This is a serious error, but one that cannot be eliminated until a method of applying the extended three-moment equation to a structure like a fuselage side truss has been developed. When that has been done, and efforts to this end are being made, a more rational solution of the problem can be developed. Until then, the method proposed here may be taken as a preliminary step in this direction and should give very reasonable results.

The chief alternative is to assume that all members subjected to side load have pin ends and to compute the bending moments in them by the formulas of "Airplane Structures." The objections to that procedure would be:

1 No computation would be made of the bending moments imposed on adjacent members without side load due to the continuity of the structure.

2 Members which probably have no point of inflection would not be detected, and would be designed for $c = 2$ instead of $c = 1$.

3 The effect of the end moments in reducing the bending moments near the center of the member would be neglected. Though this would be conservative, it would often be unnecessarily so.

These objections are quite as weighty as those against the proposed method.

In Fig. 39, the fixed-end moments are computed for the dead loads between panel points, and the moments at the ends of all members are determined from these by the usual Hardy Cross method. The results of those computations are used to draw the moment diagrams (Fig. 40) in which the ordinates are shown on the compression side of the member. The margins of safety are found for several representative members as shown below.

Member 2U-4U is subjected to an axial tension of +3260 and a concentrated side load. The maximum moment is -513 at the left end.

Hence:

$$f_b = \frac{My}{I} = \frac{513}{0.03948} = 12,980 \text{ lb per sq in.}$$

$$f_c = \frac{P}{A} = \frac{3260}{0.1336} = 24,400$$

$$f_t = 37,380 \text{ lb per sq in. tensile stress}$$

Assuming allowable stress for combined bending and tension = 80,000 lb per sq in.,

$$\text{Margin of safety} = \frac{80,000}{37,380} - 1 = +1.15$$

Member 6U-7U is a tension member. Obviously, the moment

at the right end of the member is maximum. Hence the procedure is the same as for 2U-4U, and the margin of safety is +14.8.

Member 5U-5L is subjected to a compressive load of -5216 lb and end moments as shown in Fig. 40. These end moments are opposite in rotation, so there are no points of contraflexure in the member.

From "Airplane Structures," we find $L/j = 3.96$ for a $1\frac{1}{4}$ by 0.49 member. This value is too large, since it is greater than π . Moreover, there are no points of inflection, so that we are not justified in using a length of less than 54 in. It would seem most logical to redesign the member so that $L/j < \pi$, as suggested.²⁰

In practise it would be necessary to select a larger member and re-figure all end moments by the Hardy Cross method, since the larger strut would have a different stiffness factor.

Suppose we next try a $1\frac{1}{8}$ by 0.049 member, and assume for the purposes of this illustration that a redistribution of moments gives $M_1 = -165$ and $M_2 = -155$. (Transforming the signs to agree with those used in the formulas of "Airplane Structures.")

For these conditions, $L/j = 2.64$, and from case A of "Airplane Structures" it is found that the maximum moment of -645 in.-lb occurs at a point approximately 27 in. from the bottom end of the strut.

At this point:

$$\begin{aligned} M_{\max} &= M_1 \sec x/j \\ &= -165 \times 3.91 = 645 \\ f_b &= 645/0.0928 = 6,950 \\ f_c &= 5216/0.2426 = 21,500 \\ f_t &= 28,450 \\ f_b/f_t &= 6950/28,450 = 0.244 \\ L/r &= 97 \end{aligned}$$

Allowable stress from Fig. 11 of Bulletin 7-A = 37,000

Margin of safety = $37,000/28,450 - 1 = +0.30$, or +30 per cent

Member 4U-4L: This member is subjected to a compressive load and counter-clockwise moments at each end. The latter cause a point of inflection approximately 20 in. from 4U, as shown by Fig. 40, and it would seem reasonable to use $L_i = 38 \text{ in.} + 20 \text{ in.}/3 = 44.7 \text{ in.}$, or 45 in., say, measured from 4L. This is more conservative than using $0.7L$, since the latter would give $L_i = 40.6 \text{ in.}$

For $L_i = 45 \text{ in.}$, $L_i/j = 2.4$, and since this is greater than $\pi/2$:

$$M_{\max} = \frac{M_2}{\sin L_i/j} = \frac{805}{0.6754} = 1190 \text{ in.-lb}$$

and

$$\begin{aligned} f_b/f_t &= 0.753 \\ L_i/r &= 116.5 \end{aligned}$$

Allowable stress from Bulletin 7-A = 51,000

Margin of safety = +2.2 per cent

Member 4L-5L: This member is acted on by an axial compressive force, end moments of opposite rotation, a concentrated side load, and a uniformly distributed side load. For this member $L/j = 2.525$. Since this value is less than π , combined formulas from cases B and E of "Airplane Structures" may be used to compute the moments at several points and draw the moment diagram. Points on the moment curve are shown in Table 2, in which x is the distance from 4L.

Points of inflection occur at $x = 13.4$ and $x = 23.9$. The value of L_i is first assumed as 15 in. (estimated from the fact that $x =$

²⁰ A similar computation would also show the necessity of re-designing 3L-4L.

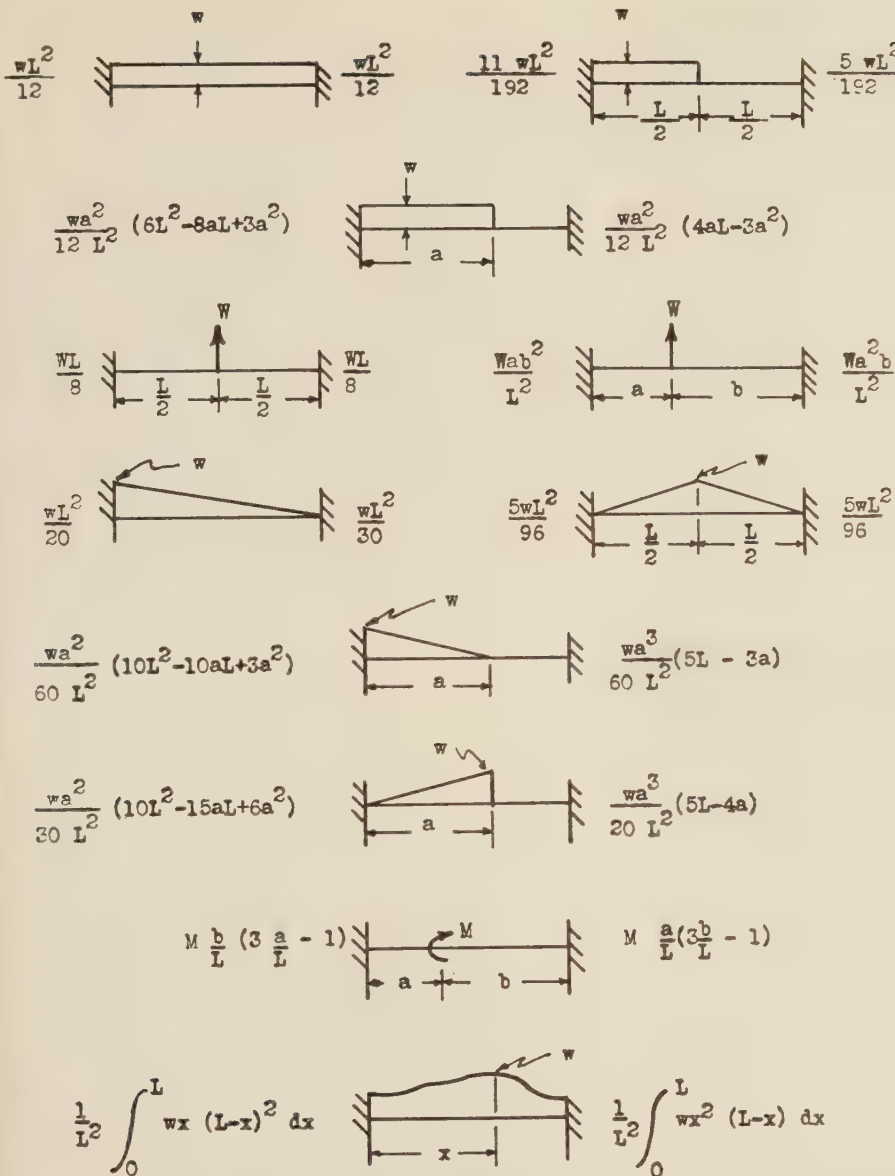


FIG. 41

TABLE 2 POINTS ON THE MOMENT CURVE

x	Moment
0	-3704 (end 4L)
5	-2795
10	-1106
15	+687
21	+2490 (concentrated side load)
23	+717
26	-2140 (end 5L)

13.4 to first point of inflection). The maximum moment for this case is -3704 at 4L. Using these values, it is found that the margin of safety is -39 per cent.

L_i is next assumed as 12 in., which is somewhat in excess of the distance between the two computed points of inflection. The maximum moment in this part of the span is +2490 under the concentrated side load. For these conditions the margin of safety is -25 per cent. Since these margins are negative, a heavier member should be used and new computations made throughout.

Member 5L-6L: This member is also a compression strut acted on by end moments of opposite rotations and a concentrated side load.

Since $L/j = 3.66$, which is greater than π , the method of attack used for member 4L-5L cannot be used. Owing to the continuity of the structure, it might be assumed that the points of inflection moved only one-third of the distance from their locations as indicated on Fig. 40, to the ends of the member. Then the central part of the member could be treated as a beam 25.6 in. long with a load of 310 lb located 8.25 in. from one end and with no end moments. For this beam L/j would be only 2.60, and the formulas of "Airplane Structures" could be used to determine the moment at the concentrated load. For this case we obtain $M_{\max} = 432$ in.-lb. Then

$$\begin{aligned} f_b &= 432/0.02474 = 17,500 \\ f_c &= 3700/0.10611 = 34,800 \\ f_t &= 52,300 \\ f_b/f_t &= 0.34 \\ r &= 0.341 \\ L_i/r &= 75 \\ F_t &= 51,000 \end{aligned}$$

$$\begin{aligned} \text{Margin of safety} &= -0.024, \\ &\text{or } -2.4 \text{ per cent} \end{aligned}$$

This is evidently less conservative than the method used for member 4L-5L, since that method would have involved the use of a member with L/j less than π . It is difficult to say which method gives results more nearly approaching the facts of the case. Since there are seldom many members with side loads applied to them directly, it would seem desirable to use

the more conservative method illustrated first.

It will be apparent that there is no necessity for using much accuracy in distributing moments by the Hardy Cross method, especially in the earlier trial designs. Even in the final design, the necessity of using more than three or four cycles is somewhat questionable.

The foregoing examples are intended as illustrations of the general method of attack. It is felt that this is a step in the right direction, and it is hoped that others will be sufficiently interested to develop it still further.

CONCLUSION

The Hardy Cross method of analyzing continuous frames by moment distribution has been received with widespread enthusiasm by structural engineers. It is hoped that some of this interest will spread to the aeronautical field. One aeronautical

engineer²¹ has pointed out in discussion of the Hardy Cross paper that the method is of particular value for making rapid comparative studies of continuous closed frames, for assisting in digesting test results, and for solving other complex problems encountered in airplane design.

This method is not claimed to be the most practical for analyzing every structure encountered in design, but it is felt that its

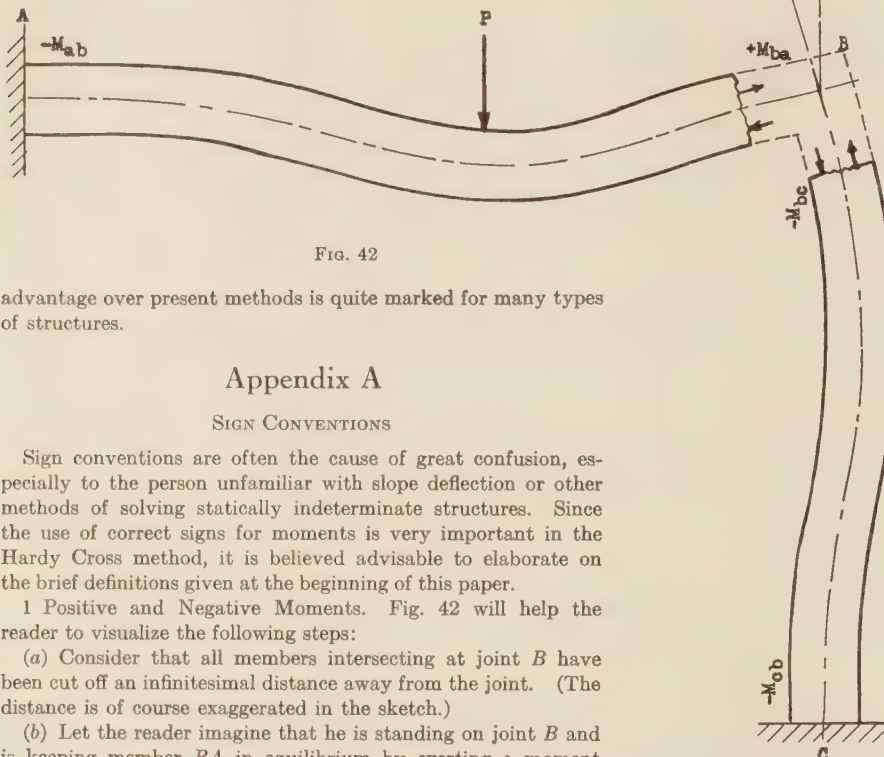


FIG. 42

advantage over present methods is quite marked for many types of structures.

Appendix A

SIGN CONVENTIONS

Sign conventions are often the cause of great confusion, especially to the person unfamiliar with slope deflection or other methods of solving statically indeterminate structures. Since the use of correct signs for moments is very important in the Hardy Cross method, it is believed advisable to elaborate on the brief definitions given at the beginning of this paper.

1 Positive and Negative Moments. Fig. 42 will help the reader to visualize the following steps:

(a) Consider that all members intersecting at joint *B* have been cut off an infinitesimal distance away from the joint. (The distance is of course exaggerated in the sketch.)

(b) Let the reader imagine that he is standing on joint *B* and is keeping member *BA* in equilibrium by exerting a moment couple on the end of the cut member. Obviously he must exert compression and tension on the opposite side. In this case, he must exert a clockwise moment couple on the end of *BA*. If he now turns toward joint *C*, he must exert a counter-clockwise moment couple on it. From the definition:

If he exerts a clockwise moment couple on the end of the member, the moment is positive.

If he exerts a counter-clockwise moment couple on the end of the member, the moment is negative.

Hence, the signs of the moments at *A*, *B*, and *C* are as shown in the sketch.

2 Joint Rotation. Joint rotation angles are not used in the moment-distribution method proper. However, the slope-deflection equations are used in the derivation of several formulas in this paper, so the sign convention for joint rotation is given to help the reader in following the steps of the derivations.

Referring to Fig. 42, when the load was applied to beam *BA*, the effect was to apply a counter-clockwise moment on the end of beam *BC*, which caused the tangent to the elastic curve of this beam to rotate counter-clockwise also. By definition, this rotation was negative.

The moment at *BA* is positive under these conditions, because it is resisting the load. If the load were removed, the beam would deflect upward and the positive moment *Mba* would rotate the

tangent to *BA* in a positive clockwise direction.

DISCUSSION OF SIGN CONVENTION

The sign convention which Professor Cross used in his paper was one with which structural engineers are ordinarily most familiar—i.e., a positive moment *ca* uses compression and a negative moment causes tension in the top fibers of a beam. For columns he suggested turning the drawing clockwise 90 deg and treating them as if they were beams.

The advantages of this system in the analysis of ordinary rectangular building frames are obvious. The disadvantages are more apparent when one tries to use it on a frame where members meet at various angles. The checking of a joint to see that the moments are in equilibrium is somewhat difficult, especially if there happen to be more than four members meeting at the particular joint. Care must also be used in determining the unbalanced moment at a joint where more than two members meet.

Hence, it has seemed to the author that the Wilson sign conventions²² adopted for this paper are in general more satisfactory

and less likely to lead to confusion, in that they automatically care for the sign of horizontal, vertical, and diagonal members. The checking of joints for equilibrium and the determination of unbalanced moments are facilitated, since the moments at a joint can be added algebraically. If the algebraic sum is zero, the joint is in equilibrium; if the sum is not zero, there is an unbalanced moment. A further although perhaps less important advantage of using the sign conventions selected for this paper is that multiplying by a carry-over factor of $+1/2$ instead of $-1/2$ allows less chance for error in computations.

In their text, "Statically Indeterminate Stresses," Parcel and Maney use sign conventions which are the reverse of those used by Messrs. Wilson, Richart, and Weiss. The choice between these two is largely a matter of personal preference.

It should be noticed that it is more satisfactory to transform both the Wilson and the Parcel and Maney sign conventions to the convention used by Hardy Cross before computing bending and shearing stresses. This transformation will be greatly facilitated if a rough sketch is made for each member showing the moments and forces acting on it.

Appendix B

FIXED-END MOMENTS, CARRY-OVER AND STIFFNESS FACTORS

Fixed-End Moment for Member Having Constant *I*: Fixed-end moment was defined at the beginning of this paper as the

²¹ See discussion by Elmer F. Bruhn, Trans. A.S.C.E., vol. 96, 1932, p. 22.

²² See footnote 6.

moment which would exist at the ends of a loaded member if those ends were held rigidly against rotation. These fixed-end moments for a beam of constant I can be found for different types of loadings in numerous texts or handbooks,²³ since they are also used in the slope-deflection equations. They can also be found quite readily by applying the three-moment equation and solving for the two unknown end moments or they can be determined by use of the M/EI diagram.

The latter method is applied to a uniformly loaded beam such as that shown in Fig. 3 as follows:

Area of the M/EI diagram for uniform loading is $WL^2/12EI$ (the area under a parabola of base L and maximum ordinate $WL/8EI$). Then the slope of the tangent to either end of the curved beam is numerically equal to the shear at the end when the span is loaded with the M/EI diagram. That is, $\theta_a = -\theta_b = WL^2/24EI$. To fix the ends in a horizontal position it is now necessary to apply a counter-clockwise moment at A and a clockwise moment at B , such that the ends will be rotated through an angle $-\theta_a = +\theta_b$. The M/EI diagram, when only the end moments act on the beam, will be a rectangle of height $M_a = M_b$ and length L . Hence,

$$\theta_a = \frac{-M_a L}{2} = \frac{WL^2}{24EI}$$

and

$$M_a = \frac{-WL}{12EI}$$

also

$$M_b = \frac{+WL}{12EI}$$

²³ References are "Structural Theory," by Sutherland and Bowman, p. 191, and "Stresses in Framed Structures," by Hool and Kinney, p. 485. (See also Fig. 41.)

The fixed-end moments can be worked out for other loadings in the same way.

Carry-Over Factor for Member Having Constant I : As previously stated under "Definitions," the carry-over factor for a beam fixed at A and simply supported at B is the ratio M_{ab}/M_{ba} and is equal to $+1/2$ for straight beams of constant section. This relation can be found from the three-moment equation, by use of the M/EI diagram or from the slope-deflection equations. By the latter method:

$$M_{ab} = 2EK(2\theta_a + \theta_b - 3R)$$

$$M_{ba} = 2EK(2\theta_b + \theta_a - 3R)$$

If the fixity is at end A , $\theta_a = 0$. $R = 0$, since there is no movement of supports. Whence $M_{ab}/M_{ba} = +1/2$.

Fixed-End Moments and Carry-Over Factors for Members Having Varying Moments of Inertia: A structure made up of members in which the moment of inertia varies from point to point along the span is quite complicated to analyze by any of the methods proposed so far. The Hardy Cross method can be advantageously applied to this type of frame, although considerable labor is involved in obtaining the required fixed-end moments, stiffness factors, and carry-over factors. In the general case, where the member not only has a changing cross-section, but also is unsymmetrical with respect to loading and form, it is necessary to find a fixed-end moment, stiffness factor, and carry-over factor to use with each end of the member, a total of six constants for the beam.

No attempt will be made in this paper to present the method of determining these constants. The reader is referred to a very able presentation offered in discussion of the Hardy Cross paper by A. W. Earl (Trans. Am.Soc.C.E., Vol. 96, 1933, p. 112). A somewhat different method was proposed by Prof. George E. Large in discussing the same paper (Trans. Am.Soc.C.E., Vol. 96, 1933, p. 101).

The Principles of Underfeed Combustion and the Effect of Preheated Air on Overfeed and Underfeed Fuel Beds¹

By P. NICHOLLS² AND M. G. EILERS,³ PITTSBURGH, PA.

This paper is based on investigations conducted at the Pittsburgh Experiment Station of the U. S. Bureau of Mines. It shows that in underfeed burning the factor of rate of ignition is much more important than it is in overfeed fuel beds and that it fixes limits to the outputs that can be obtained. It uses the principles determined from the experimental results to interpret the much more com-

plex action in fuel beds of commercial underfeed stokers. It also shows what effect preheated air has on overfeed and underfeed fuel beds and how this preheat is utilized. The results from burning a number of fuels on the underfeed principle, both without and with preheat, are given. The variables investigated were kind and size of fuel and rate and temperature of the air supplied.

THE purpose of this paper is to present the results of an investigation conducted at the Pittsburgh Experiment Station of the U. S. Bureau of Mines. It is one of a series of studies which have been made by the bureau on the burning of solid fuels to obtain measures of the actions which occur in fuel beds, in the burning of fuel and the clinking of its ash. When the investigation was started, it was intended to restrict it to a study of the effect of preheat; however, as preheated air is more commonly used with underfeed stokers, it was necessary to include underfeed burning in the investigation, and this then became its major feature.

Because the two types of tests were interlocked, it is not convenient to separate them entirely in this report; the study on the effect of preheat on overfeed fuel beds will be treated first, and the effect of preheat on underfeed fuel beds will be included with the report on underfeed combustion.



P. NICHOLLS



M. G. EILERS

and did not include the economy or desirability of preheat or even its effect on combustion above the fuel bed, except as far as the latter can be deduced from the composition and temperature of the gases leaving the fuel bed without and with the use of preheated air.

Although there have been numerous papers and reports on the effect of preheat on the over-all operation of furnaces and on economy, no record was found of any detailed studies of its effect on combustion. Reports have referred to the increased clinker formation caused by preheat, and

the limiting of preheat temperature because of clinker troubles or increase in the cost of upkeep of the stoker parts, but it can be understood that there would be little opportunity to measure the effect of preheat on combustion in the fuel bed.

The over-all effect of the preheat on a fuel bed is given by the change in the composition and temperature of the gases leaving the bed. It can be predicted that the rate of reaction in the bed will be increased and that, as a consequence, the rate of burning will be increased for the same rate of air supply. If a fuel bed is deep enough, the endothermic reaction of the conversion of CO₂ to CO occurs. If the formation of CO is increased by the preheat, then some of the sensible heat of the preheated air will be absorbed, and the increase in temperature of the gases leaving the fuel bed will be less than that which would be computed from the preheat added; of course, even supposing there were no increase in CO, the increase in temperature of the hot gases would be less than that of the preheat because of the increase in the specific heat of gases with temperature.

A further cause for the loss of some of the preheat will exist if the clinkers or ashes leave the system at a higher temperature than they would without preheat.

It was evident that the differences in the quantities to be measured would be small, so that all auxiliary conditions of test would have to be identical, while measurements must be accurate. Even with the closest regulation it is very difficult to get two burnings to give exactly the same result, particularly with fuels

EFFECT OF PREHEAT ON OVERFEED FUEL BEDS

The objects of the investigations were restricted to studies of the effect of preheated air on the combustion in the fuel bed,

¹ Published by permission of the Director, U. S. Bureau of Mines. (Not subject to copyright.)

² Supervising fuel engineer, Pittsburgh Experiment Station, U. S. Bureau of Mines. Percy Nicholls was graduated from Leeds University, England, and later was awarded National and Whitworth scholarships in engineering. His earlier association was in mechanical and electrical work with the Westinghouse, Western Electric, and General Electric companies, followed by positions as engineer of works for manufacturing concerns. He became interested in heat-transmission research and heat insulations and is the author of a number of papers on these subjects. In 1925 he joined the Bureau of Mines, and has presented papers on fuel utilization and allied subjects.

³ Associate fuel engineer, Pittsburgh Experiment Station, U. S. Bureau of Mines. Mark G. Eilers was graduated with the degree of Chemical Engineer from the University of Notre Dame in 1919, following which he entered the employ of the Rochester Gas and Electric Corporation at Rochester, N. Y. For three years he was engaged in laboratory work in connection with plant problems, and subsequently for a period of eight years acted in the capacity of assistant operating engineer supervising operation in the coal-carbonization plant for the same company. In 1930, Mr. Eilers joined the Fuels Section of the U. S. Bureau of Mines at Pittsburgh.

Presented at the Semi-Annual Meeting, Chicago, Ill., June 26 to July 1, 1933, of THE AMERICAN SOCIETY OF MECHANICAL ENGINEERS.

NOTE: Statements and opinions advanced in papers are to be understood as individual expressions of their authors, and not those of the Society.

which cake. Considerable experience had been obtained in the study of fuel beds in connection with the determination of the combustibilities of cokes;⁴ also, coke forms the main part of the bed, even when burning coal. It was therefore decided to follow the same method and, as a beginning, to use coke as a fuel, as the principles involved could be more easily determined and better illustrated by a fuel free of volatile matter.

Apparatus Used. Fig. 1 shows the set-up used. The furnace was of welded construction with refractory lining. The inside was 20 in. in diameter and 44 in. high from the grate bars. There were 26 1/2-in. pipe sampling holes at 1 1/2-in. intervals from the grate level, these being scattered round the circumference. The air was supplied by a fan capable of giving 9 in. of water

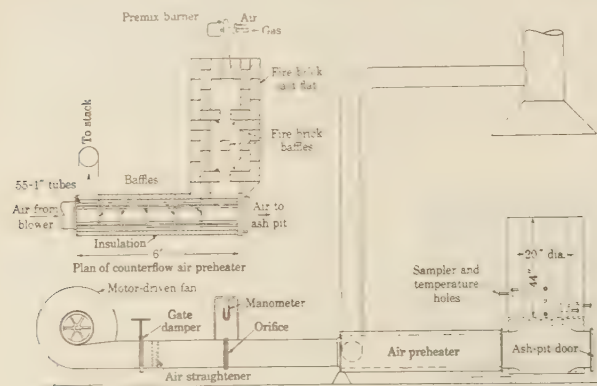


FIG. 1 APPARATUS USED IN THE TESTS

pressure; the air passed through a measuring orifice and the quantity could be closely regulated. The preheater was built specially for these tests, and was designed to give up to 1000 F preheat with the maximum estimated quantity of air. Two sizes of premix gas-burners were used; the gas was burned in a combustion chamber with checker-brick to avoid flame impingement on the preheater tubes. The temperature of the hot gases was controlled by the addition of air, so that it would be the minimum above the preheat temperature. The air leaving the preheater passed through a mixer before entering the ashpit. Its temperature was measured by a shielded thermocouple at a position of high velocity.

The bureau's standard water-cooled gas samplers were used for inserting into the bed through the various sampling holes. Fuel-bed temperatures were taken by optical pyrometer. All gas samples and temperature observations were taken at 1 in. distance from the vertical axis of the furnace. Other instruments and measurements were of standard type.

Test Procedure. Because the procedure was essentially the same as that used in the combustibility tests already referred to, it will not be described in detail. A very rigid specification was followed to insure duplication of conditions. It consisted in building up a fuel bed to a 24-in. depth, allowing it to come to equilibrium of burning, and then maintaining it at that depth during the period when measurements were taken.

Three complete sets of gas samples and other measurements were taken during one test, and the bed was frequently restored to its standard condition at fixed times. The samples were taken one at a time, starting at the top of the bed, so that the part below the sampling position was not disturbed previous to the taking of the sample.

⁴ Nicholls, Brewer, and Taylor, "Properties of Cokes Made From Pittsburgh Coals," Proc. A. G. A., 1926, pp. 1129-1143. Nicholls, P., "Study of Cokes From Various Types of Plants Using Pittsburgh Coal," Proc. A. G. A., 1928, pp. 1127-1136.

The coke used was made by the Philadelphia Coke Company in Koppers ovens, using a mixture of 80 per cent Powellton seam coal and 20 per cent Pocahontas coal. It was crushed and carefully screened to 1 to 1 1/2-in. square mesh. Its analyses and properties were:

Proximate analysis, per cent:	
Moisture.....	0.6
Volatile matter.....	0.7
Fixed carbon.....	91.3
Ash.....	7.4
Ultimate analysis, per cent:	
Hydrogen.....	0.5
Carbon.....	89.5
Nitrogen.....	0.9
Oxygen.....	1.0
Sulphur.....	0.7
Ash.....	7.4
Softening temperature, F	2730
Weight per cu ft of 1 to 1 1/2 in. size, lb.	31.8

Results of Tests. Four air temperatures were used, 80 (normal), 400, 600, and 800 F. Fig. 2 shows the values of the CO₂, CO, O₂, and N₂ in per cent by volume against the height of the fuel bed, and also the temperatures by optical pyrometer. Each point is the average of the nine sets of readings. A few gas-analysis values were rejected because they showed internal evidence of errors in the sampling or the analysis. The water vapor is not plotted; from the analysis of the coke its value would be 0.7 per cent by volume. It is also possible that some producer action of the water vapor in the air and from the coke had occurred; it was not considered worth while to include the extra precision and labor necessary to check these factors. The parts of the curves in the first 1 1/2 in. of the bed below the first sampling position are drawn arbitrarily. The largest variations between individual observations occurred with the first two sampling positions, because these are most affected by pieces of clin-

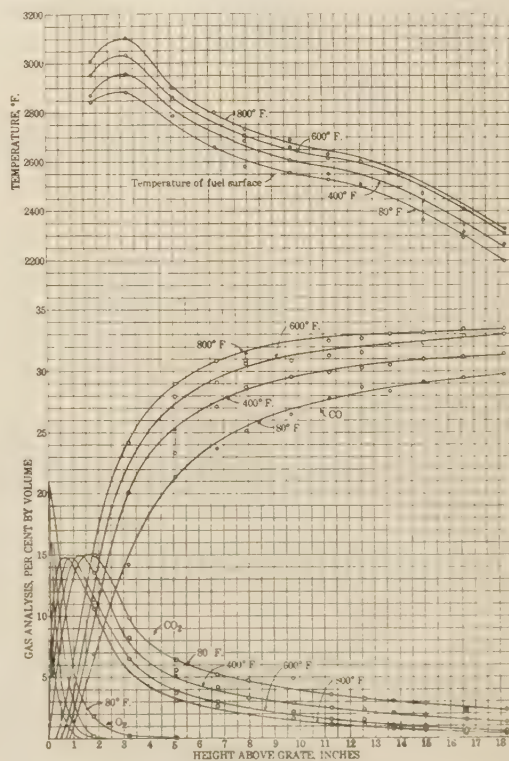


FIG. 2 EFFECT OF PREHEAT ON THE GAS ANALYSES AND FUEL-BED TEMPERATURES OF AN OVERFEED FUEL BED OF HIGH-TEMPERATURE COKE

ker, although the attempt was made to remove the clinker each time the bed was brought back to standard.

The figure shows that the preheat caused larger differences in the reaction in the lower part of the bed and that it increased the rate of reaction.

The temperature observations were, as usual, the weakest part of the measurements. At best, they are the temperature of the coke surface, and the optical pyrometer will show large variations over the small area which is seen through each hole; several readings were taken at each observation and the results averaged. The dip in the temperature curves at 12 in. height shows a drop in temperature which should not occur and is due to conduction to the walls or by convection of cooler gases from the walls.

The figure shows that the preheat is used partly in increasing the CO reaction and partly in raising the temperature. Comparing the values for 80 and 600 F at the 15 in. height, computations show that about 45 per cent of the preheat was used in the conversion of CO_2 to CO and 55 per cent in increasing the sensible heat. The curves of Fig. 2 are based on the test points; computations show that from the heat balances the 600 F curves should be closer to the 400 F curves.

Fig. 3 shows the total carbon and hydrogen content of the gases per pound of air; the rate of burning is proportional to the carbon content; the dotted line will be referred to later.

The results illustrate the principles of the effect of preheated air in a thick fuel bed. One could deduce the order of the effect on a 10-in.-deep fuel bed; for example, by taking the values at the 10 in. height. The actual values by gas analysis and by temperatures would be somewhat lower, however, because of the loss of heat by radiation from the top of the bed and by the quantity of heat required to raise the temperature of the incoming coke, assuming that it is fed in continuously at a rate equal to the rate of burning.

The values given in Figs. 2 and 3 are based on samples and temperatures taken at the center of the bed, and therefore depict the actions in a uniform bed free from holes or cracks or the effect of side walls. In service these factors are always present and reduce the average combustible in the gases below that which would be predicted for a given depth from Fig. 3; also, ash and clinker would always be present in service and would increase the apparent depth. One can, however, use Fig. 2 to predict with fair accuracy the relative rate of burning that will result from the maintenance of various depths of fuel bed.

Further Work With Preheat. The investigation could have been extended to obtain actual values with normal depths of fuel beds; there would be no object in doing this for cokes, but it could have been done for coals. Preheat is but little used with the overfeed type of fuel bed. Such tests with caking coals would necessitate introducing the factor of breaking up the fuel bed, and this operation is difficult to standardize, so that the accuracy of results is affected. If such tests had been made, it would probably have been of most practical value to have used fuels high in moisture. However, it was not considered worth while to extend this phase of the investigation, but rather to study the effect of preheat on the burning of bituminous coals on the underfeed principle.

UNDERFEED BURNING

Previous Work. The principles of overfeed or hand-fired burning are well understood, and there have been many investigations of them. The fundamental ones are those made at the Bureau of Mines by Mr. Kreisinger and his coworkers.⁶ Although other investigators have not studied the actions at

different heights in the fuel bed, yet all tests of domestic and other small types of furnaces yield over-all data on the principles of the burning of different fuels, but relatively rarely has the effect of secondary air, supplied purposely or by leakage, been eliminated. The investigation made by the bureau on the burning of coke⁶ extended the study of overfeed fuel beds to the effect of the size of free-burning fuels on characteristics of combustion. A similar investigation has been completed for anthracites.

No corresponding studies have been published of the principles of underfeed burning. There have been investigations of some details of the combustion with underfeed stokers, but these give little information on the action in the bed. Mr. Bert Houghton⁷ removed a section of fuel from a retort and by

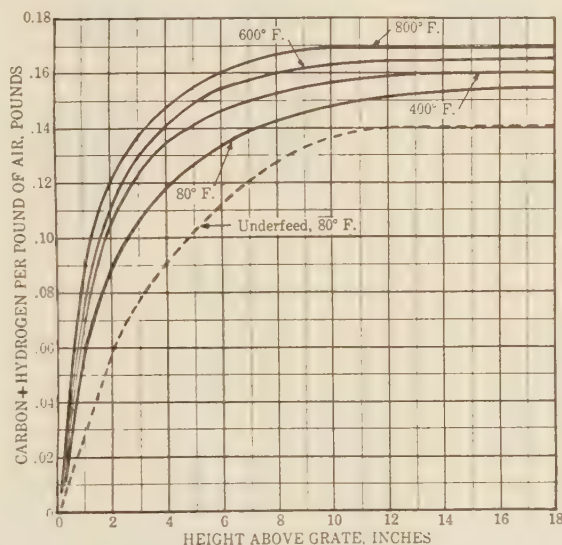


FIG. 3 OVERFEED-BURNING, HIGH-TEMPERATURE COKE. EFFECT OF PREHEAT ON TOTAL COMBUSTIBLE IN GASES

analyses of various sections determined how far the fuel had been consumed. The composition of the gases arising from the fuel bed at various locations has been studied by others. The progress of combustion on a chain-grate stoker was rather ingeniously examined recently by J. D. Maughan,⁸ who fed in a wire screen with the coal and, when it completely covered the grate, quickly withdrew it and quenched the fuel. Analyses of various sections through the bed showed the distribution of the fixed carbon and volatile remaining.

Types of Fuel Beds. Although the term "underfeed fuel bed" is used in this report, yet the same principle of combustion occurs in beds to which that term would not apply. The term "up-burning" is sometimes used, but that also is not comprehensive enough. It is therefore worth while to review various types of fuel beds and to connect them with the principles they include. The discussion which follows may be considered somewhat elementary, but at least it insures clarity of thought.

The type of a fuel bed is fixed by the absolute direction of flow of the fuel and its relative flow to the air; both fuel and air can be constrained to move in any direction desired. The ash will flow in the same direction as the fuel, independent of gravity, unless it becomes fluid, when gravity and the temperatures of the zones it flows into will influence its motion.

⁶ U. S. Bureau of Mines Report of Inv. 2980.

⁷ Houghton, "The Burning of Bituminous Coal on Large Underfeed Stokers," Int. Conf. on Bit. Coal, 1931, vol. 2, p. 282.

⁸ Grumell, E. S., *Jour. Inst. of Fuel*, vol. 5, Aug., 1932, p. 366.

⁵ U. S. Bureau of Mines Tech. Papers 137 and 139.

Fig. 4 shows six of the possible types. Type A, representing hand firing, is of the overfeed principle. Type B shows what we have termed the "unrestricted-ignition underfeed" principle. Type C evidently is the same as B in its combustion principles, but differs in the ash disposal; it is illustrated by the Hawley down-draft heating boiler. Type D, as representing a traveling-grate stoker, is of interest; the length U of the fuel bed is burning on the pure underfeed principle; the length O is burning on the

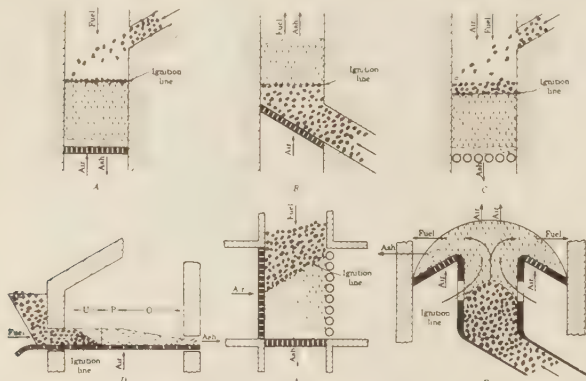


FIG. 4 DIAGRAMMATIC REPRESENTATION OF SIX TYPES OF FUEL BED

overfeed principle; and some unknown length P is in what we have termed the change-over state—that is, the burning is adjusting itself because of the cessation of the ignition action. Type E, as represented by the burning in a Molby heating boiler, has some of the underfeed principle at the upper part. Type F represents the pot-type stoker; the burning will be of the underfeed type with restricted ignition.

Pure Underfeed Burning. The term "unrestricted-ignition underfeed" burning implies that with a fixed rate of air supply there is no imposed restriction which limits the rate at which fresh fuel may be ignited; thus in type B of Fig. 4 the fuel is free to ignite and the level of the line of ignition will rise or fall as the rate at which the coal is pushed in is greater or less than the rate of ignition. In type D there is no imposed condition limiting the rate at which the fuel in the length U can ignite, and unrestricted-ignition underfeed burning results, but as soon as the line of ignition reaches the grate bars, the type of combustion changes.

The rate of ignition in type F is controlled, and it can only conform to the definition of unrestricted-ignition underfeed burning when the rate of coal feed is equal to or greater than the rate of ignition; in addition, the burning is not completed in the pot. The same arguments would apply presumably to all larger underfeed stokers, with the addition that the motion of the fuel may be much more complex.

Equilibrium Fuel Beds. The term "equilibrium fuel bed" is used in connection with the experimental work and requires a definition, although the term is self-explanatory. It is used to define a fuel bed which, for a constant rate of primary air, maintains the same character of combustion and thickness.

In the overfeed, type A, the bed will be in equilibrium when such a thickness is reached that the rate of burning is equal to the rate of fuel feed. In the underfeed, type B, the bed is in equilibrium when such a thickness is reached that the rate of burning is equal to the rate of ignition; if the rate of fuel feed in type A or the rate of ignition in type B is greater than the rate of burning, then the thickness of both beds will increase indefinitely.

Method of Test Discussion. Evidently it was desirable to attempt to determine some of the fundamental principles of

underfeed burning—that is, to study a fuel bed as represented by type B of Fig. 4. The use of a bed such as type F would correspond more nearly to practise, but it would be difficult, if not impossible, to separate the fuel characteristics from the conditions imposed by the particular design of pot used. It was preferable to have a furnace such as type B in which both the fuel and air would be fed from the bottom and a number of schemes were considered. One of the requirements was that the fuel should be fed uniformly over the area of the bed, which would be difficult to insure without considerable expense of construction. Finally, the same method was adopted as was used in a previous investigation on clinkering.⁹

The method consisted in starting with a deep bed of fuel and igniting it at the top. This gives a true underfeed burning and restricts the factors affecting the combustion to the fuel and the rate of air supply; for fundamental studies it has the further

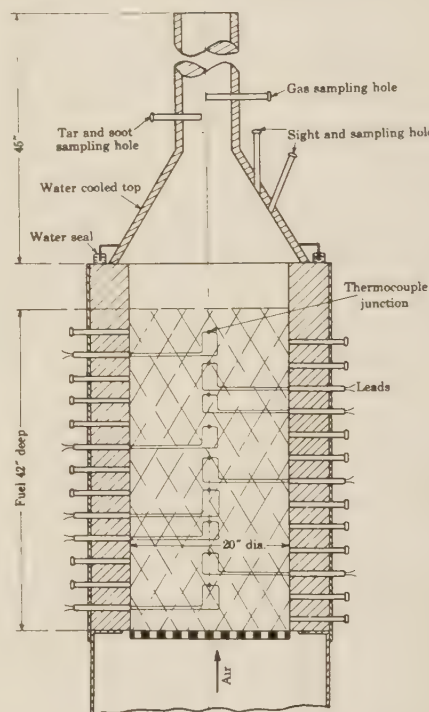


FIG. 5 DIAGRAM OF FUEL BED FOR UNDERFEED-BURNING TESTS

advantage that the fuel is stationary. It has the disadvantage, compared with forcing the coal in and keeping the burning zone at one position, that the cooling effect of the refractories is greater.

Successful operation when burning caking coals in underfeed stokers is dependent on the breaking up of the caked or coked fuel. This is a necessity in practise, yet it introduces a variable that is difficult to control. Although it was recognized that the caking would seriously affect the burning, it was nevertheless thought advisable to make the first series of tests without disturbing the fuel bed in any way; so doing gave truer measures of the fuel characteristics. Knowing these characteristics, the breaking-up factor could be superimposed in other tests.

Apparatus. The set-up was essentially the same as shown in Fig. 1 except that a water-cooled cone with chimney was used as a top cover to collect the gases so that average samples could

⁹ Nicholls and Selvig, "Clinker Formation as Related to the Fusibility of Coal Ash," U. S. Bur. of Mines Bull. 364, p. 50.

be obtained; this cover had a water seal for prevention of leakage and for ease of removal.

Fuel Bed and Observations. Fig. 5 shows how the fuel bed was arranged. The diameter of the pot was 20 in. and the depth of the fuel 42 in. All fuels were carefully screened to definite size limits, and the furnace was loaded by small increments. Nine thermocouples of No. 28 B.&S. chromel-alumel bare wire were laid in as shown; the junctions were on the center line and were placed in a 1 in. length of small porcelain tubing. The exact height of each junction was recorded by measuring from a crossbar over the top of the furnace. The wires from the junction were run down so that the heat would strike the junction first. The couple leads went to a cold junction and thence to a switching arrangement by which each could be connected to a portable potentiometer, or one or more connected to a recording potentiometer; usually only one at a time was connected to the recorder.

The fuel was ignited by means of a fixed weight of small-sized charcoal and petroleum coke, wetted with kerosene, which was spread over the top of the fuel. The cover was not put on until it was seen that there was even ignition all over the area.

The air rate was maintained constant at a fixed weight of dry air, the pressure drop through the orifice being changed during the test for any material change in the air temperature or barometric pressure. Gas sampling was started after the cover was put on; the samples were taken continuously over periods of 10 to 20 min, depending on the rate of burning.

The top couple was connected to the recorder first. When the ignition line reached the couple, its temperature would begin to rise, and the record obtained gave a good measure of the progress of the ignition. When the temperature reached 30 mv (1340 F), the couple was switched to the portable potentiometer, and the next lower couple was connected to the recorder.

The progress of combustion was also recorded by observations through the 26 sampling holes in the furnace, and the time when the top of the bed or the ignition reached each hole could be very closely fixed.

No samples were taken or temperatures measured in the bed itself during the regular tests, except that some special observations were made of the top of the bed through the sampling holes in the cone cover.

The tests with preheat were conducted in the same manner except for the preliminary period of bringing the whole of the fuel bed up to the temperature to be used. During this period the couple giving the temperature of the entering air and the couples placed at mid-height and at the top of the bed were put on the recorder to assist in avoiding excess heating of any part of the fuel.

The test was continued until the fuel was consumed, except for some tests of bituminous coals in which the caking caused very uneven burning. The furnace was allowed to cool, and then the residue was examined and measures were taken of the ash, the clinker, and their combustible content.

Data Obtained. All the main data were plotted against time as abscissa. Against height above the grate as ordinate were plotted the 30 mv position of the thermocouples in the bed and the level of ignition by observation; the slope of these lines gave the rate of ignition in inches per hour, and from the known weight per cubic foot of the fuel as placed in the furnace the rate of ignition in pounds per square foot per hour could be computed. The plot of the observed level of the top of the fuel bed on the same diagram gave the thickness of the ignited portion at any time.

The flue-gas analyses were also plotted against time; from those and the known rate of air supply, the rate of burning was plotted. The integral of the rate of burning gave a computed

value of fuel burned, which was checked against the known weight of the fuel fired, corrected for combustible in the residue and the fuel used for igniting the bed.

Underfeed Burning of High-Temperature Coke. Coke is not burned in underfeed stokers, although it is reported to have been tried in small domestic pot-type stokers; also it has been burned on chain grates, and, as shown in Fig. 4, underfeed burning occurs in a portion of the bed. In spite of this lack of application in service, high-temperature coke was used for the first, and also the most complete, set of tests of underfeed burning. Coke is the most convenient fuel to use when investigating prin-

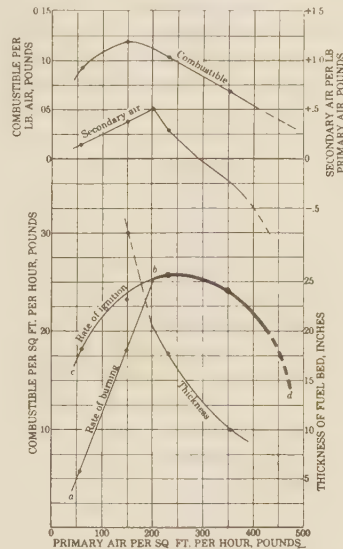


FIG. 6 UNDERFEED-BURNING, HIGH-TEMPERATURE COKE

ciples of burning, because it eliminates the uncertainty of size of pieces that is present when one has to break up a caked or coked fuel, because the bed does not have to be disturbed by poking, and because the cost of the tests is very much reduced in that the gas analyses can be made in a much shorter time and in a water Orsat.

The primary factors to be investigated were (1) rate of air supply, (2) size of coke pieces, (3) temperature of primary air—that is, preheat. A series of tests was therefore planned that would give enough data to permit of fairly complete plots being made; the first were made with normal air temperature.

The high-temperature coke used in these tests was made from No. 8 Pittsburgh seam by the Lowell Gas Light Company in horizontal through retorts; its properties have previously been reported.¹⁰ Those of interest are:

Ultimate analysis, per cent:	
Hydrogen.....	0.6
Carbon.....	88.8
Nitrogen.....	1.1
Oxygen.....	0.6
Sulphur.....	0.6
Ash.....	8.3
Ash softening temperature, F.....	2730
Weight per cu ft of 1 to 1½ in. size, lb.....	26.8
Pounds of fuel per pound of combustible, ratio.....	1.12

The rates of combustion will be expressed in terms of the available combustible in the fuel, as this eliminates the variations in the non-combustible.

Variables of Rate of Primary Air and Size of Coke Pieces.

¹⁰ Nicholls, Brewer, and Taylor, "Properties of Cokes Made From Pittsburgh Coal in Various Plants," Proc. A. G. A., 1926, pp. 1129-1143.

The sizes of coke adopted as standard were those between the square-mesh screen sizes of $\frac{1}{2}$ to 1, 1 to $1\frac{1}{2}$, $1\frac{1}{2}$ to 2, and 2 to $2\frac{1}{2}$, all in inches. The air rates were kept constant during each test.

To understand the meaning of the results it is better to consider first those for one size of coke. Fig. 6 shows plots of the data for coke of the $1\frac{1}{2}$ to 2 in. size. It will require a detailed explanation and some study to interpret their meaning; because the same method of presenting data is used for other results, they will be discussed at some length.

The abscissa is pounds of dry air per hour per square foot of grate surface. The left-hand ordinate scale is pounds of combustible (carbon + hydrogen) per hour per square foot of grate surface. The test points are shown, and the curves beyond the range of the points are dotted. The two main plots are the rate of ignition and the rate of burning of combustible. The light-line part *cb* of the ignition curve means that it is for ignition only; the heavy-line part *bd* means that it is part of both the ignition and the rate of burning curves. The rate of burning curve is thus *abd*.

Considering these two curves, they show that at 100-lb air rate the rate of ignition is about 21.5 lb per sq ft per hr, but that the rate of burning is only 12 lb; therefore the coke at the bottom of the burning zone is being ignited at a faster rate than the coke above it is burning (being gasified); consequently, the thickness of the burning zone is increasing continually. At an air rate of about 200 lb, the rate of burning is the same as the rate of ignition, so that the live-fuel bed will maintain a constant thickness. At air rates greater than 200 lb, the rate of burning could increase along a continuation of the line *ab*, but it cannot be greater than the rate at which the fuel is ignited, and consequently it does the best it can and follows the rate of ignition curve *bd*, which for this fuel increases a little at first, reaches a maximum at 250 lb of air, and then decreases with further increase of rate of air supply.

The ignition curve indicates that at high air rates the rate of ignition tends to approach zero; results given later will show that this occurred in some tests and it was impossible to maintain burning. Such occurrences are a common experience and are usually spoken of as blowing the fire out. This falling off of the ignition curve was, as might be expected, more in evidence with the high-temperature coke than any one of the other fuels tested. The causes for this action are two: First, the fuel is ignited by the heat radiated from the hot fuel above; very little of the heating of the fresh fuel will be by conduction; at the same time the surfaces of the fuel are being cooled by the air passing over them and this will tend to counteract the heating by radiation, and after some unknown rate which will vary with the fuel and its size, the counteracting effect will increase more rapidly than the increase in the radiation due to a higher rate of combustion. The second cause is that the fuel bed gets thinner as the air rate increases; after some undefined thickness is reached, the temperatures through the bed will decrease, and consequently the radiation will be less.

One curve in Fig. 6 shows the observed thickness of the live fuel bed. This thickness includes the clinker and unfused ash; the values given for this, and other curves which follow, were selected in the same manner from the plots of the observed values during the whole test. The full-line part of the curve covers the range in which the thickness is constant. One would expect that the observed thickness would increase with time because of the accumulation of clinker, but the increase was usually small compared with variation caused by the method of observation. For these equilibrium beds of constant thickness, a mean value was selected.

The dotted part of the curve covers the range in which the

thickness is increasing; the height of the bed when the ignition plane reached the grates is used for the thickness in this range.

The two upper curves of Fig. 6 show the pounds of combustible in the flue gas per pound of air supplied, and the pounds of secondary air required for perfect combustion per pound of primary air. The secondary-air curve shows that secondary air would be required up to a primary-air rate of 280 lb.

The foregoing results and the interpretations of them relate to the condition of unrestricted ignition. Commercial underfeed stokers have restricted ignition in the sense that the rate at which the stream of fresh fuel passes into the primary-air stream can be controlled. It is worth while at this stage to consider how the data of Fig. 6 can be applied to restricted burning. The following deductions refer to continuous operation with ability to restrict the rate of feed of the fuel.

(1) To obtain the maximum rate of burning possible with each rate of air supply, the rate of feed must follow the curve *abd*;

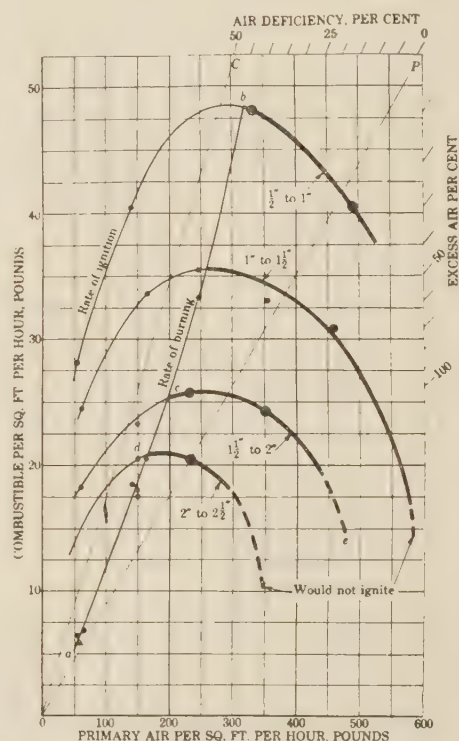


FIG. 7 UNDERFEED-BURNING, HIGH-TEMPERATURE COKE; RATE OF IGNITION AND RATE OF BURNING, WITH RATE OF PRIMARY AIR AND SIZE OF COKE AS VARIABLES

no manipulation other than changing the area of the plane of ignition can make the rate of burning continuously exceed the values fixed by this curve.

(2) The maximum rate of burning possible with this coke and this particular size is about 26 lb of combustible (or 29 lb of coke) per sq ft per hr, and no manipulation can increase it.

(3) The equilibrium thickness of the live-fuel bed for rates of air supply above 200 lb and for the corresponding rate of fuel feed fixed by the line *bd* will be those shown by the thickness curve of Fig. 6. The equilibrium thickness for air rates below 200 lb and for the corresponding rates of fuel feed fixed by the line *ba* cannot be predicted from these tests; they will not be as large as the values indicated by the dotted part of the thickness line, but they will continue to increase with decrease of the rate of air supply.

(4) An equilibrium fuel bed will result when operating at any point within the area enclosed by curve *abd*. An increase or decrease of the rate of feed, provided it does not cross the curve *abd*, will result in a gradual change to a new rate of burning and thickness of fuel bed corresponding to the new rate of feed.

(5) If any increase in rate of feed crosses the curve *abd*, the rate of burning will not increase beyond that fixed by the curve *abd*; if it crosses the portion *ab*, the thickness of the live-fuel bed will increase continuously; if it crosses the portion *bd*, the thickness of the live-fuel bed will not increase beyond that for

lb, the burning gradually decreased and finally the fire was extinguished. This showed that ignition could not be maintained.

With this fuel, the rates of burning that can be attained are very much affected by the size of the pieces. With the 2 to 2½ in. size, the maximum rate of burning possible was 21 lb, whereas with the ½ to 1 in. size it was 48 lb. This shows a fundamental difference between overfeed and underfeed burning principles; in a hand-fired furnace any size of coke can be burned continuously at any rate by keeping the fuel bed deep enough.

It must be remembered that the curves of Fig. 7 are for the conditions used in these tests and that the cooling by the side walls affects the results. It is not probable that it influences the rate of ignition materially, but it does lower the average rate of burning because of the poorer combustion at the sides. For an absolute value—that is, for a fuel bed of very large area—the rate-of-burning line *ab* would be swung somewhat to the left. However, it could never cross the line *OC*, which corresponds for this fuel to a dry-gas analysis containing only CO and N₂—that is, one with the maximum carbon content.

The curves for the pounds of secondary air required per pound of primary air are not shown, because this is fixed by the position of each rate of burning point on the plot. All points on the line *OP* have perfect combustion; those to the left of the line require secondary air, and those to the right have excess air. The scales on the top and sides permit of reading off the secondary-air requirement at any rate of burning.

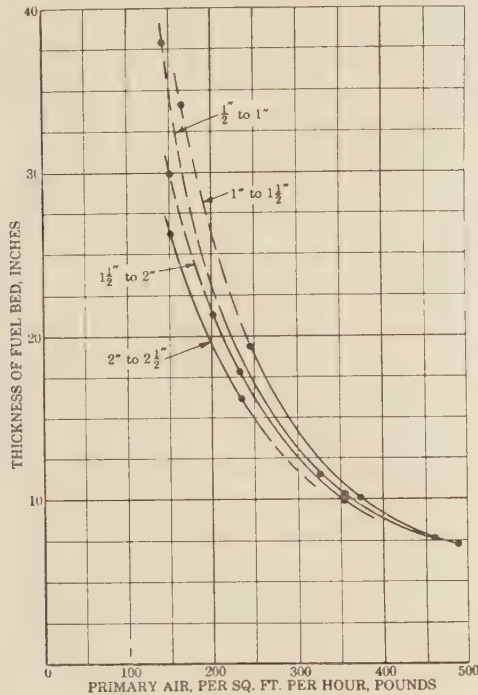


FIG. 8 UNDERFEED-BURNING, HIGH-TEMPERATURE COKE; THICKNESS OF FUEL BEDS, WITH RATE OF PRIMARY AIR AND SIZE OF COKE AS VARIABLES

bd, but the plane of ignition will gradually be raised by the un-ignited fuel below it.

Fig. 7 shows the rate-of-ignition and rate-of-burning curves for the four sizes of coke when using air at 80 F; to avoid crowding, the thickness of fuel-bed curves are shown in a separate plot, Fig. 8. The test points are shown, and it will be noted that fairly symmetrical curves can be drawn to fit the points.

It is of interest that the rate-of-burning curves previous to their intersection with their individual rate of ignition curves all fall on a common curve which bends upward slightly for the smaller sizes, as would be expected from previous investigations on the effect of size.

The figure shows that the rates of ignition increase rapidly with decrease in size, which is in agreement with common experience when starting a fire in one's home furnace. The relationship, based on the points of intersection of the ignition and burning curves, is of the order shown by Fig. 9.

If the air rates were carried high enough, the ignition curves may be expected to have a shape like that of the 2 to 2½ in. size. An attempt was made to burn this size at an air rate of 345 lb. There was difficulty in getting the fuel to start burning; by using larger quantities of igniting fuel and reducing the air rate, it was ignited, but when the air rate was increased to 345

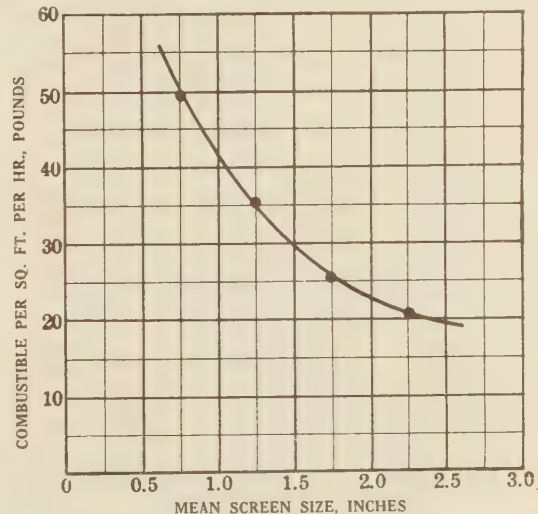


FIG. 9 UNDERFEED-BURNING, HIGH-TEMPERATURE COKE; RATE OF IGNITION AGAINST SIZE OF COKE

It is worth while to grasp fully the meaning of the type of chart represented by Fig. 7 because it is used for all results and because it is interesting and informative. Considering the curves for one size of coke—the 1½ to 2 in., for example—it has been shown that one can operate continuously anywhere within the area *adc*. Selecting, then, any point of operation—17.5 lb of combustible per hour and 200 lb of air, for example—this point fixes the rate of combustion and the deficiency or excess of air. This is true independently of whether the fuel bed is in a good or bad condition, but it does not show how complete the combustion was; for instance, the dry gas analysis for this example might be 20.9 CO₂, 0.8 CO, 0.0 O₂, 79.2 N₂, or it might be 12.3 CO₂, 7.8 CO, 3.5 O₂, 76.4 N₂. In the latter the oxygen is available, and whether the CO is burned will depend on the action in the combustion space. A fuel bed which gives the first

of the two analyses would be classed as being in a good condition because the loss of heat due to free combustible in the gases is reduced to a minimum; the second shows that there were holes in the bed or leakage at the sides. This is elementary and not novel; also, the same type of diagram could be used for overfeed burning.

It is also necessary to define the terms "primary air" and "secondary air." Primary air as used in this report means the air supplied below the bed. In the method of test employed, all the air passed through the plane of ignition and also through the whole of the live fuel, although even in these tests its distribution over the area of the bed was not uniform. In stokers the distribution of the air is more complex, and at moderate ratings the plane of ignition not as definite; however, if a stoker operates continuously with the same shape of bed, then the rate of ignition, however we may define or explain that action, must be equal to the rate of burning.

The secondary air in these tests is that which might be supplied and mixed with the gases over the fuel bed. In a stoker some of the air supplied below the fuel bed may not pass through any fuel, so that, correctly speaking, it is secondary air. It seems to be the usual custom to apply the term "secondary air" only to that which is purposely supplied over the fuel bed and to that which leaks through the setting.

If one assumes that in a stoker no air is supplied over the fuel

of burning could be obtained with each size by passing a smaller weight of air through the plane of ignition and supplying some more as secondary air in its meaning as defined above.

Fig. 8 shows the thickness of the fuel beds. It will be noticed that the curve for the $1\frac{1}{2}$ to 1 in. coke falls out of order. There are two factors which influence the thickness; one, the rate of ignition which tends to increase it, and the other, the rate of reaction which tends to decrease it with decrease in size. A previous investigation⁶ shows that the second factor increases very rapidly for decrease in size below 1 in.

Effect of Preheating the Air on the Underfeed Burning of High-Temperature Coke. The air temperatures used were 80, 200, 300, and 400 F. There was no necessity to test all sizes, because the characteristics will be similar; therefore only the 1 to $1\frac{1}{2}$ in. coke was used.

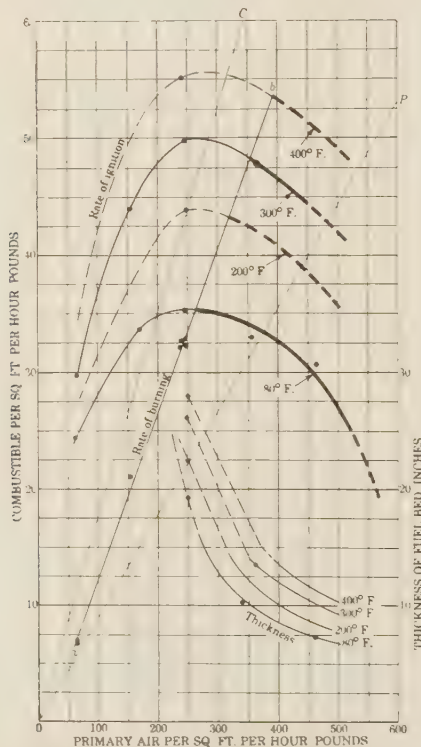


FIG. 10 UNDERFEED-BURNING HIGH-TEMPERATURE COKE, 1 TO $1\frac{1}{2}$ IN. SIZE, WITH RATE OF PRIMARY AIR AND ITS TEMPERATURE AS VARIABLES

and that it is desired to have 20 per cent excess air in the flue gases, then one is limited to operating along the 20-per cent excess-air line of Fig. 7. If all this air passes through the plane of ignition, the maximum rates of burning possible with each size is reduced to the value given by the intersection of each curve with the 20-per cent excess-air line. A higher maximum rate

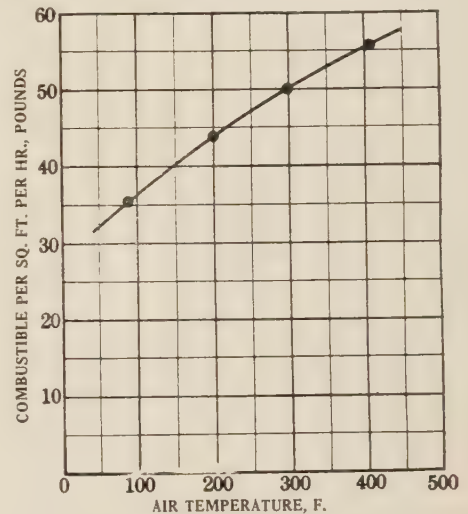


FIG. 11 UNDERFEED-BURNING, HIGH-TEMPERATURE COKE; RATE OF IGNITION AGAINST TEMPERATURE OF AIR

Fig. 10 shows the results; the lines OC and OP have the same meaning as in Fig. 7. The parts of the rate of combustion curves falling on the line ab are not materially affected by the preheat; because the same size of coke is used, ab has not an upward bend and is nearly a straight line to the origin.

The rates of ignition increase rapidly with increase of air temperature. Fig. 11 shows the maximum values plotted against air temperature; at some higher temperature the curve would turn upward very rapidly because at a certain temperature, probably between 1100 and 1200 F, the coke would ignite spontaneously.

Fig. 10 shows that preheat will have little effect on operation at rates of air supply below that at which the ignition curve meets the burning curve. Above the rate of air supply where the ignition curve for normal air temperature (80 F) meets the burning curve (265 lb of air), preheat permits of large increase in the rate of burning with a given rate of air supply, but of course with the necessity of increasing the secondary air.

The lower set of curves of Fig. 10 show the thicknesses of the live fuel beds, for which, however, there were not many test points. The full-line portion indicates that the burning is in equilibrium. The fact that for the same rate of air supply the thickness increases with increase in temperature of the air at first sight may seem an anomaly. The explanation is that the increase in the rate of burning that occurs with the preheat requires a thicker fuel bed for equilibrium burning; the increase

thus required is more than can be offset by the increase in the rate of reaction resulting from the preheat. Fig. 2 illustrates this, but to a different scale.

Underfeed Burning Tests of Low-Temperature Coke. Low-temperature coke is a good example of a truly non-caking fuel with relatively high volatile content. The coke used was a fairly dense and non-fragile type; its properties were as follows:

Proximate analysis, per cent:	
Moisture.....	3.4
Volatile matter.....	13.7
Fixed carbon.....	72.0
Ash.....	10.9
Ultimate analysis, per cent:	
Hydrogen.....	3.5
Carbon.....	73.4
Nitrogen.....	1.5
Oxygen.....	9.9
Sulphur.....	0.9
Ash.....	10.9
Softening temperature, F.....	2721
Weight per cu ft of 1 to 1½ in. screen size, lb.....	28.3
Pounds of coke per pound of combustible.....	1.25

The tests made were confined to the 1 to 1½ in. size. The main series were at increasing rates of air supply without preheat; these were followed by single tests at the same air rate but increasing preheat.

Fig. 12 shows the results plotted in the same manner as were those of the high-temperature coke. The line OP , as before, is that of perfect combustion for a fuel with the foregoing analysis. The line OC shows the maximum rate of combustion. The rate of ignition curves for 210 and 300 F air temperature are each based on one test point, but their general shapes will be somewhat as shown.

The plots do not differ in their general relationships from those of Fig. 10 for high-temperature coke, and the principles that would be deduced are the same. The slope of the rate-of-burning line *ab* is a little steeper than of Fig. 10; that is, the gases contain more combustible per pound of air; the main difference is that the rate-of-ignition curves are higher and do not fall off after they reach a maximum. The air rate was carried to 680 lb to see whether the ignition would not fall off, but it did not; to have gone higher would have meant blowing fuel out of the bed. The interpretation of this is that the fire with this low-temperature coke cannot be extinguished as it could with the high-temperature coke.

The increase of the rate of ignition by the same preheat was greater than that with the high-temperature coke. A test with an air temperature of 400 F was included, but the coke ignited spontaneously in the center of the bed. This does not mean that the average coke would ignite at this temperature, but that exothermic reactions occurred in some individual pieces.

For the same air rate the thickness of the fuel bed was increased by the preheat, as it was with the high-temperature coke.

Although this coke is easily ignited, yet the principle still holds that its rate of burning on the underfeed method did not exceed a certain maximum, which for this 1 to 1½ in. size, without preheat, is 49 lb of combustible per square foot per hour; for the high-temperature coke of the same size it was 35 lb.

Underfeed Burning With Anthracite. A complete set of tests have not as yet been made with anthracite, but three different kinds of anthracite were tested at one rate and without preheat to see if they would give their relative ignitibilities for use on another investigation. The size used was 1 to 1½ in. square-mesh screen and the rate of air supply 240 lb of primary

air per square foot per hour. A few of the results are given in Table 1.

TABLE 1 UNDERFEED BURNING, ANTHRACITES

Item	No. 1	No. 2	No. 3
Volatile matter, per cent.	3.2	3.8	8.2
Fixed carbon, per cent.	82.5	79.4	78.3
Ash, per cent.	11.0	13.2	12.3
Weight per cubic foot, lb.	53.0	51.2	46.3
Primary air, qz ft per hr, lb.	240	240	240
Rate of ignition, qz ft per hr, lb.	2.4	2.8	3.2
Rate of burning, qz ft per hr, lb.	27.4	27.8	37.0
Thickness of fuel bed, in.	15.0	15.7	10.5

Anthracites 1 and 2 both burned with equilibrium fuel beds because in each test the rate of burning is equal to the rate of ignition. The rate of burning of anthracite 3 was less than its rate of ignition, and therefore the air rate was too low to give equilibrium. Fig. 6 shows that the same size of high-temperature coke also burned in equilibrium at the air rate of 240 lb and that the ignition and burning rates were 26 lb, which is a little below that of anthracite 1.

This measure of ignitibility shows that No. 3 was 43 per cent more easily ignited than No. 1 or No. 2. These comparisons are

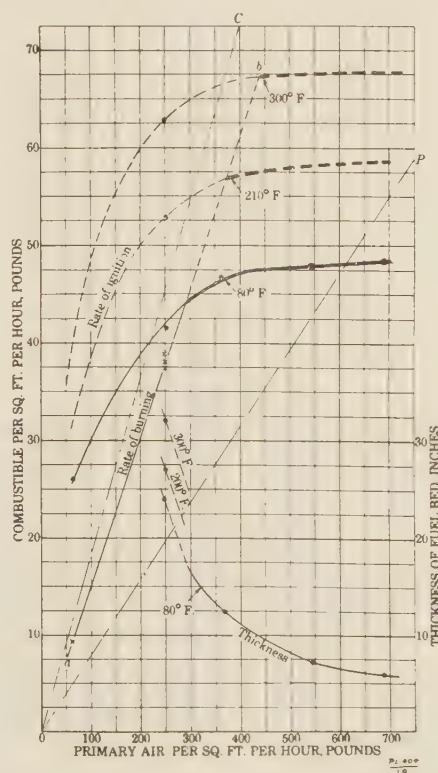


FIG. 12 UNDERFEED-BURNING, LOW-TEMPERATURE COKE; RESULTS FOR 1 TO 1½ IN. SIZE, WITHOUT AND WITH PREHEAT

on the weight of combustible basis; to the eye the coke would appear to ignite 1.6 times as fast as anthracite No. 1; that is, the plane of ignition of the coke travels faster because of the relative densities and ash contents of the two fuels.

Underfeed Burning With Bituminous Coals. It was realized that more difficulty would be experienced in obtaining reliable

data with coals which fuse and cake, but earlier tests⁹ had shown that they could be burned with equilibrium fuel beds by igniting the bed at the top, provided the air rate was high enough and the coal of uniform size.

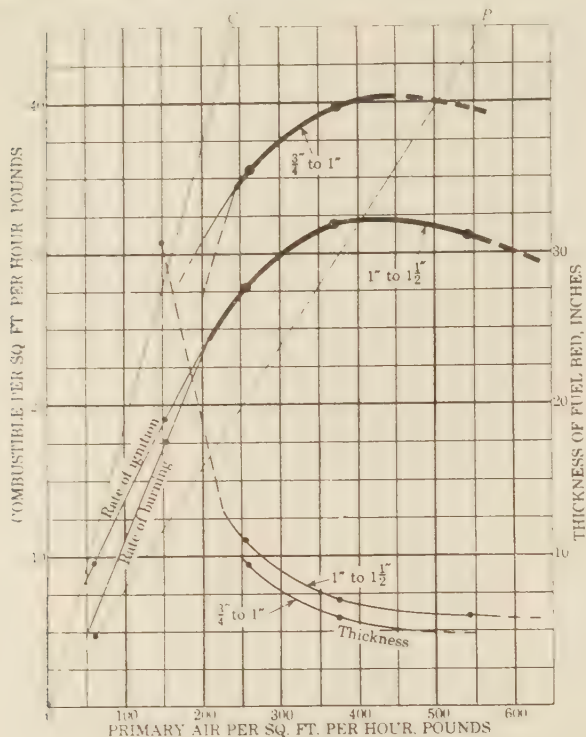


FIG. 13 UNDERFEED-BURNING ILLINOIS COAL, WITH RATE OF PRIMARY AIR AND SIZE AS VARIABLES

The troubles caused by uneven burning that were encountered in the individual tests will not be described, but they can be summarized as follows. When burning at low rates of air supply, the plane of ignition advanced downward at such a rate that the tar exuding from the coal was not consumed, and thus it would tend to close up the air spaces, or the surface of the coal pieces would not be burned away fast enough to make up for the swelling, and consequently the spaces were closed. Either of these actions is cumulative, because, as the spaces started closing, the air would divert from the center, and thus the quantity of air

TABLE 2 BITUMINOUS COALS USED IN UNDERFEED TESTS

Name, designation.....	Illinois Illinois County Bed.	Pittsburgh Pennsylvania Allegheny Pittsburgh	Splint Kentucky Harlan	Westmoreland Pennsylvania Westmoreland Pittsburgh
Proximate analysis, per cent:				
Moisture.....	6.5	1.7	3.1	1.3
Volatile matter.....	35.1	34.7	37.0	32.3
Fixed carbon.....	50.4	55.8	55.3	58.5
Ultimate analysis, per cent:				
Hydrogen.....	5.5	5.2	5.8	5.2
Carbon.....	68.8	77.2	77.5	77.5
Nitrogen.....	1.5	1.5	1.5	1.5
Oxygen.....	14.1	7.2	10.1	6.9
Sulphur.....	2.1	1.1	0.5	1.0
Ash.....	8.0	7.8	4.6	7.9
Caloric value, Btu....	12,340	13,780	13,800	13,850
Softening temperature, F.....	2203	2780	2510
Weight per cubic foot, 1 to 1 1/2 in. size, lb.	44	44	42	43
Pounds of fuel per pound of combustible	1.37	1.22	1.22	1.22

passing through the center would be reduced; this further reduced the rate of burning and allowed more closing of the spaces. As the air rate was maintained constant, that passing up the sides would be increased, or sometimes a hole or channel would develop along the sides which might be straight, but usually had a somewhat spiral form.

At some rate of air supply the bed burned uniformly and acted in the same manner as the cokes. Tests could not be made with the rates close enough together to determine the exact rate at which this change occurred, but it appeared to be comparatively sudden, as would be expected from the cumulative action referred to. A uniform burning can be interpreted to be such a rate of air supply over the surfaces that all volatile matter is burned as soon as it is evolved, or in which the rate of burning is greater than the rate of swelling.

Good data could be obtained in the tests in which the rate of air supply gave equilibrium burning, but in the tests below this

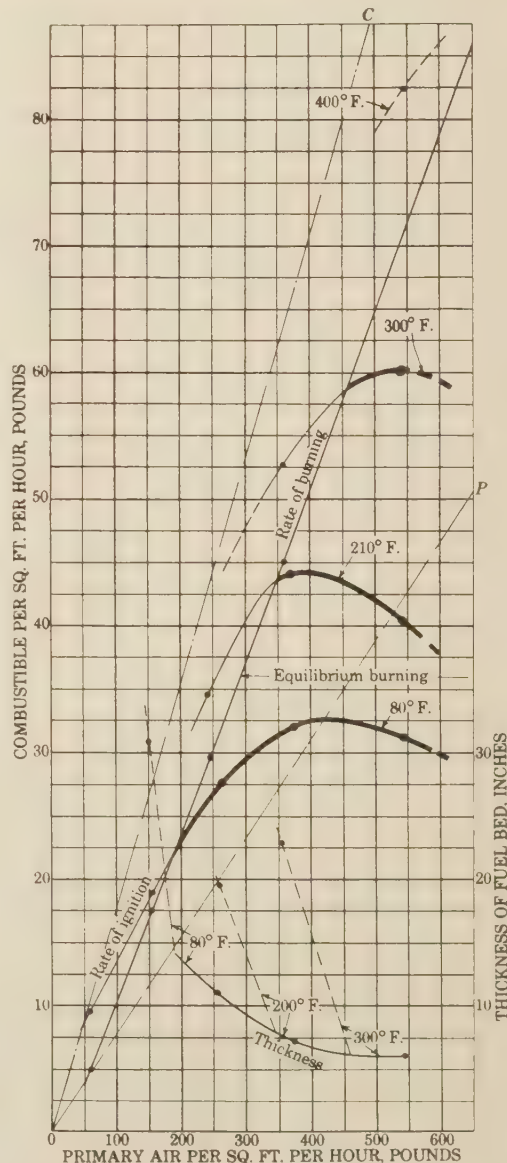


FIG. 14 UNDERFEED-BURNING ILLINOIS COAL, 1 TO 1 1/2 IN. SIZE, WITH RATE OF PRIMARY AIR AND TEMPERATURE OF AIR AS VARIABLES

rate there was no certainty as to the air rate to use for the ignition except that it should be lower than that of the known air supplied; also, the rate of burning obtained from the gas analysis was not that of the whole fuel bed.

All the coals were crushed and screened over square mesh to definite sizes; some of the sizes used were larger than would ever be employed in underfeed stokers, but it was desired to obtain data which could be compared with those of the cokes to facilitate generalization.

Table 2 lists the properties of the bituminous coals tested. When different sizes were used, the analyses differed somewhat, but not enough to affect comparisons of the results.

Underfeed Burning, Illinois Coal. The Illinois coal was tested last, but it is discussed first because its caking properties are lower than those of the Pittsburgh coal and the tests were more complete.

Fig. 13 shows the results with two sizes of coal without preheat. The heavy lines indicate the rates with which equilibrium burning occurred. The actual data for rates below equilibrium burning are given, but, as explained, these values are associated with the test furnace used and include the factor of the clogging of the bed by the caking.

The plot is exactly similar to Fig. 7 for high-temperature coke, and the same deductions as made for coke apply; namely: (1) decrease in size increases the rate of ignition; (2) decrease in size decreases the thickness of the fuel bed; (3) there is a maximum rate of burning which cannot be exceeded, which was 32 lb for the 1 to 1½ in. size, as compared with 35.5 lb for the high-temperature coke.

It would seem that the rate of ignition tends to decrease with very high air rates, similar to that which occurred with high-temperature coke but to a lesser degree.

Fig. 14 shows the results for the 1 to 1½ in. Illinois coal with various preheat temperatures. Again, the general plot is similar to Figs. 10 and 12, and the increases in the rate of ignition by the preheat are of the same order.

The light line designated as rate of burning has not exactly the same meaning as it had in the plots of the coke tests; rather it is the dividing line between non-equilibrium and equilibrium burning, as fixed by there being no clogging of the bed by caking. This means that the tar that is exuded from the pieces of coal is consumed as fast as exuded, or that the rate of burning at the surface counteracts the swelling. Thus the coal acts as a free-burning fuel, and the area of the figure which is designated as equilibrium burning could be called the free-burning area.

A test was attempted with 400 F air temperature; it will be seen that the point for the test falls to the left of the equilibrium line. The test started out well, but when the ignition line had fallen 20 in., almost suddenly the bed clogged up tight and no air could be forced through it with the pressure available. The rate of ignition given is approximate.

It is obvious that if the caked fuel had been broken up as quickly as it was formed, the light-line curves would have been swung to the left and the shapes of the curves would have been more similar to those for the cokes.

The dotted parts of curves for the thickness of the live-fuel bed indicate non-equilibrium burning; the thicknesses for equilibrium burning fall approximately on a common curve.

Underfeed Burning, Pittsburgh Coal. This being the first bituminous coal tested, attempts were made to improve the method and procedure. To obtain accurate data on the non-equilibrium burning, it was necessary that the air supplied should pass uniformly through the area of the bed instead of being diverted to the sides by the caking. Attempts were made to insure this by increasing the resistance of the bed at the sides by packing it with small-sized coal, so that the coal being

tested formed a core 16 in. in diameter with a ring of fine coal around it 2 in. thick; it was accomplished by using a sheet-iron cylinder 16-in. in diameter and 12 in. long, and gradually building up the bed.

This kept the center of the bed more open, but it did not entirely eliminate the clogging, and the small coal at the sides also burned out more rapidly or channels were formed. However, this method did increase the rate of ignition in the low-air-

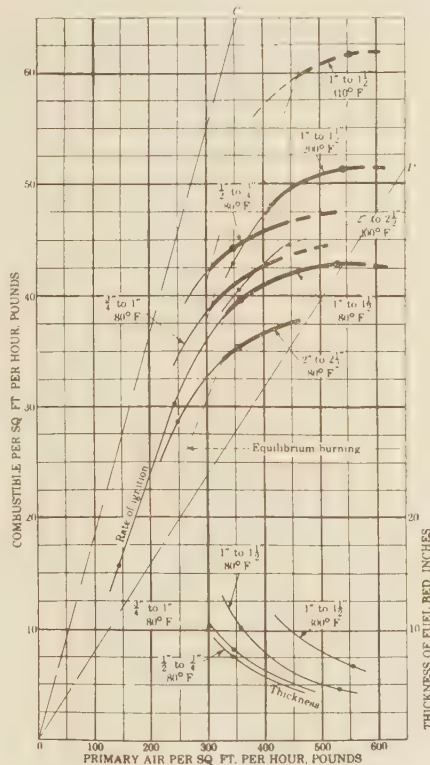


FIG. 15 UNDERFEED-BURNING PITTSBURGH COAL

rate, non-equilibrium area as much as 100 per cent. As would be expected, it made little difference in the equilibrium area but increased the ignition rate a little, both because of the effect of the small-sized coal and because, even with a non-caking fuel, there is always less resistance to air flow at the sides.

Numerous tests were made with the Pittsburgh coal, the majority with small fuel at the sides. Fig. 15 shows plots of most of the tests, both for different sizes of fuel and for different air temperatures. The order of the results is the same as for the Illinois coal; with the same-sized coal, 1 to 1½ in., the maximum rate of burning possible without preheat was higher, 43 to 32 lb; with 300 F air temperature, the maximum rate of burning was about the same, 61 lb. As before, the rate of ignition decreased with increase in size; the sizes were carried to the 2 to 2½ in. screen.

There is no common line fixing the area of equilibrium burning; those drawn in the plot can be considered only approximate. It is certain, however, that the line is further to the left for the smaller coals; this can be interpreted to mean that the openings between coal pieces can be kept clear more easily as the size of the coal decreases. Knowing that it occurs, an explanation can be given, but one's first guess would probably be the reverse.

There is no necessity to discuss the results of Fig. 15 in detail.

Underfeed Burning, Splint Coal. Splint coals differ from other bituminous coals in that they do not fuse when heated. On the other hand, they exude their volatile matter as a tarry substance, which will tend to fill the air spaces. It is not known whether splint coal is used on large underfeed stokers, but it has been used in domestic stokers. The coal was not specially obtained, but was tested because it was available and because it had distinctive properties.

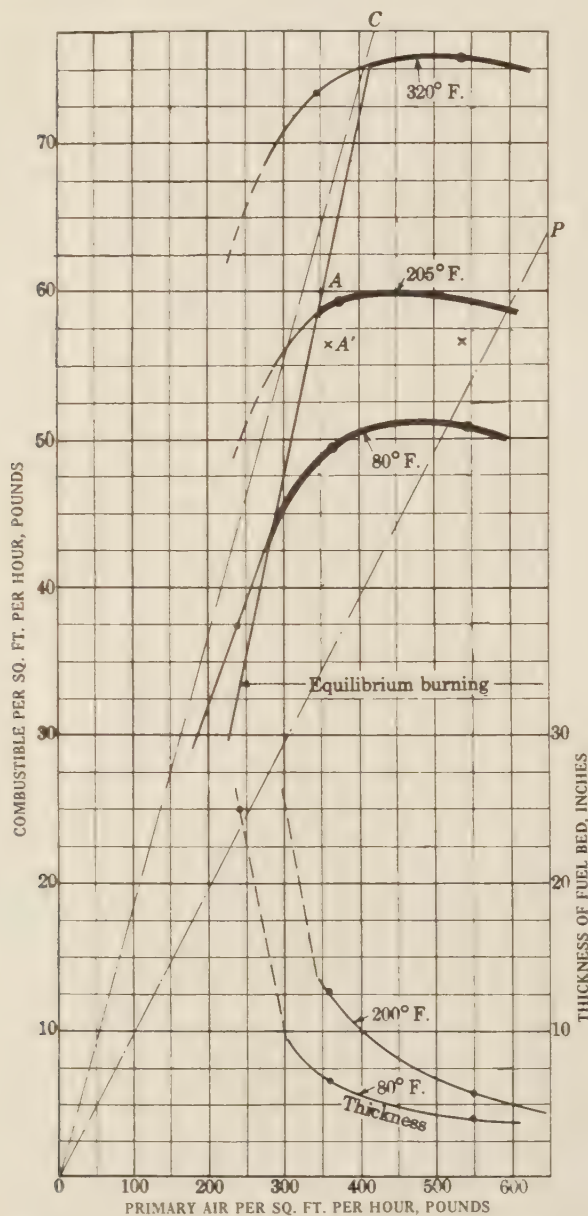


FIG. 16 UNDERFEED-BURNING SPLINT COAL, 1 TO 1½ IN. SIZE

All tests were with 1 to 1½ in. size, the temperature of the air being varied. Fig. 16 shows the result. All tests are for beds packed with small coal at the sides, except the two tests indicated by crosses. Thus tests A and A' are duplicates, except that the latter had no packing; their positions indicate the order of the difference obtained by the two methods.

The results show the same relationships as for the other fuels,

but the line fixing the equilibrium area is further to the left, thus giving a larger equilibrium area. The maximum rate of burning possible without preheat is decidedly greater than the rates for the other bituminous coals, being 51 lb as against 42.5 lb for the Pittsburgh. However, the increase in the rate of burning by the same preheat is about the same as for the Illinois and Pittsburgh coals.

At non-equilibrium rates this coal burned around the sides, leaving a solid pillar of coke in the center. It would seem that the tarry matter filled up the spaces and coked, but the whole coked mass did not tend to open up cracks as much as in the other two coals, and thus little if any air passed through the center mass.

A test on this coal was also tried at 412 F air temperature and a rate of 535 lb of air. It burned for a time and indicated a rate of ignition of about 100 lb; it then clogged up very rapidly, but not so quickly as did the Pittsburgh coal at 400 F. This clogging would be expected, because Fig. 16 shows that the point of operation used lies outside the equilibrium area.

Summary of Underfeed Tests. There is no necessity to make a detailed summary, nor at this time will this method of test as a means of determining the burning characteristics and of comparing fuels be discussed in full. There is one characteristic important in the operation of stokers which the method does not measure—namely, the ease of breaking up the caked or coked masses. It can be imagined that this quality is compounded of tensile strength and brittleness as measured by elasticity.

The results justify the method of attack used of thoroughly testing high-temperature coke first, as the clear view-point this gave of the relations between quantities, set a standard for interpreting results with fuels which were more difficult to test.

Because the fuels had been in dry storage, their moisture content was low. Some study of the effect of moisture on the rate of ignition is of interest.

REACTIONS IN AN UNDERFEED FUEL BED

It was desirable to have records of the reactions in fuel beds burning on the underfeed principle that would show the same data as does Fig. 2 for overfeed. These tests involved some difficulties because the zone of burning is moving, but complete data were obtained for the high-temperature coke and for the Illinois coal, the latter including tar and soot determinations.

The complete results are not given in this report; they present a good picture of what occurs in the bed and how the ignition progresses. The following are some of the conclusions one can deduce:

(1) In an underfeed bed heat is abstracted from the lower part of the burning zone to heat up the incoming fuel so that reactions all through the bed lag because of this abstraction of heat.

(2) In an overfeed bed the heat required by the incoming fuel is not abstracted until the reactions through the bed are completed; although the same quantity of heat is required as with the underfeed, and the temperature of the outgoing gases is lowered, yet this does not affect the reactions in the bed below.

(3) The fact that the fuel is being heated up and is of a larger size at the ignition end of an underfeed bed reduces the rate of reaction, or, in other words, lengthens the time required for the same total reaction more so than for the overfeed bed, where the rate of reaction is very slow, as is shown by Fig. 2.

(4) Consequently, for the same rate of air supply, and the same weight of combustible per pound of air carried by the exit gases—that is, the same rate of burning—the equilibrium depth of an underfeed bed will be greater than that of an overfeed.

To give an idea of the burning of the underfeed bed when using high-temperature coke, the dotted curve was added to Fig. 3; the rate of air supply in the underfeed tests was the same as that in the overfeed. The relative positions of the 80 F. curves illustrate the foregoing conclusions.

That the process of ignition hampers the burning in an underfeed bed was shown in a number of tests made at air rates for which the rate of burning was less than the rate of ignition, and the thickness of the live bed was continually increasing; in these tests the rate of burning was approximately constant when the plane of ignition reached the grate. When it reached the grate, and there was no more fuel to ignite, the rate of burning increased very rapidly, although the air rate was not changed. This increase with the cokes was sometimes more than 50 per cent; with the bituminous coals there was sometimes no increase, because at low rates the burning was not uniform over the area of the bed.

Evidences of this action should occur in stokers; when at low rates the coal feed has been too rapid, and it is stopped, then the boiler output may be expected to rise temporarily.

APPLICATION OF RESULTS TO UNDERFEED STOKERS

Some deductions on how the experimental burnings are related to the actions which occur in the fuel beds of underfeed stokers have been suggested in the previous part of this report. All the tests were made with unrestricted ignition, and it was shown that the burning which results is the maximum which can occur with each rate of air supply, and that with a given rate of air supply a restriction of the rate of feed below its corresponding rate of ignition will result in a thinner fuel bed and a rate of burning equal to the rate of feed, together with a reduced requirement for secondary air.

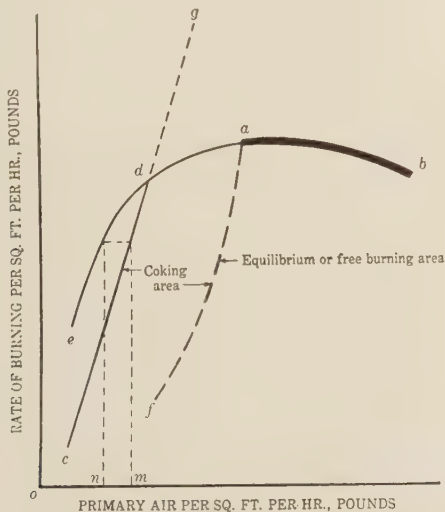


FIG. 17 DIAGRAM OF OPERATION

It also was shown that the main difference between overfeed and underfeed burning is that, with the former, the rate of burning can be increased indefinitely, provided the fuel is not blown out of the bed, but with the underfeed, there is a limitation to the rate fixed by the rate of ignition.

No attempt will be made to picture completely what goes on through the length of the fuel bed of a large underfeed stoker, because that would necessitate defining the paths of the various streams of incoming coal and the distribution of the air. Pres-

umably some coal may have a superimposed vertical motion, and undoubtedly even in the same stoker the actual paths will not be the same at all rates and with different coals. In addition, the distribution of the air flow through the coal will depend on the caking and on how the caked coal is broken up by the motion. However, one can draw some conclusions as to possibilities, especially for rates of burning near the limit of the ignition rate, because this is the range covered by these tests.

Considering Fig. 17, the line *ab* corresponds to the heavy lines of one of the figures for bituminous coal, and it gives the rate of burning with unrestricted ignition in a quiet (that is, unagitated) fuel bed; because a caking coal burns as a free-burning fuel along this line, presumably the burning would not be changed much if the bed were agitated. Considering still the unagitated bed, and assuming that one is operating at the feed and air rates of point *a*, if one began to restrict the rate of feed and to reduce it below the ordinate of point *a* and at the same time to reduce the air rate just enough to maintain the non-caking or free-

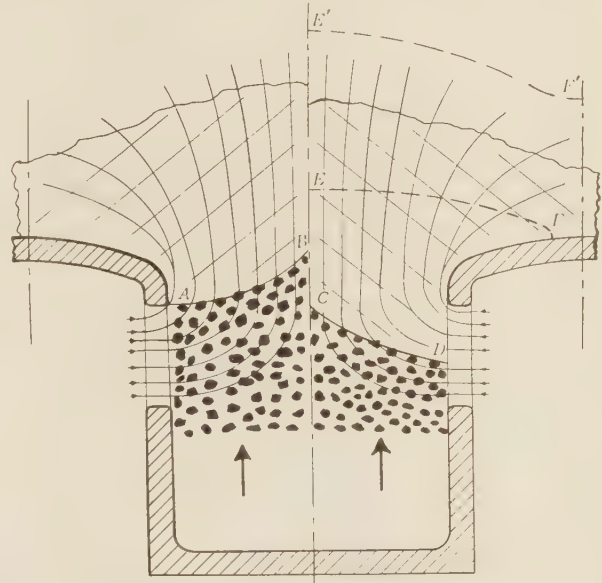


FIG. 18 AT HIGH-BURNING RATE

burning condition, then probably one would move along some curve *af*, although this suggestion is not based on experimental data. Therefore, with a non-agitated bed, operation anywhere in the area *fab* would be free burning.

Assuming that the bed were agitated enough to keep the fuel pieces free from each other, then the curves for unrestricted ignition would be similar to those for non-caking fuel, such as *cdb* and *edb*; it follows that with a restricted feed, operation with an equilibrium bed would be possible anywhere within the area *cdb*.

These deductions are based on the assumption that the air passes through the incoming coal and keeps it cool; if it did not, and if the coal were heated up and coked before it reached the air stream, then, unless this coke were broken up, the deductions for the non-agitated bed would not hold.

One has to use more imagination when trying to picture a cross-section of the fuel bed of an actual stoker, but one is on safer ground if the stoker is operating at the limit of its ignition rate—that is, on the line *db* of Fig. 17 for an agitated bed. Fig. 18 represents a section of a stoker operating at maximum rate, but on the assumption that the fuel is moving vertically.

Assume that the coal feed has brought the ignition plane to the position AB shown in the left-hand half; then the conditions of ignition are the same as those of these tests, and the same values should apply. The rate of air supply per square foot would be fixed by the area of the surface AB , and the rate of ignition by the ordinate of the point on db of Fig. 17 which corresponds to the air rate. If the coal feed were reduced for a time so that the ignition line fell to what would probably be the line CD of the right-hand half of Fig. 18, then the average air flow through the ignition plane would be reduced, although the total air was not changed, and the measure of the ignition rate would move along the line bd of Fig. 17; as it approached d , the rate of ignition, and consequently the rate of burning, would decrease. With a fixed rate of coal feed and air supply, it is probable that the plane of ignition would find some position along the height of the air slot which would produce equilibrium.

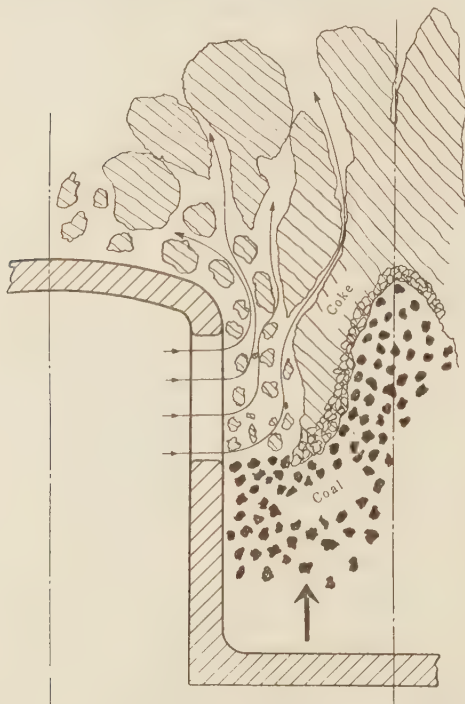


FIG. 19 PROBABLE NORMAL ACTION

As one tried to push the output by increasing the coal feed, it can be conceived that the line of ignition might be raised to EF with the top of the bed as shown dotted; because this increases the area of ignition, a corresponding increase in the maximum rate of burning would be possible.

It must be recognized that in all these illustrations there is no question about the ability to burn the coal; as long as one is operating, for an agitated bed, along the line db , the rate of burning for any rate of air supply could and would be limited only by the line dg if it were not that it is limited by the rate-of-ignition line db . It does not matter whether the stoker is a simple pot, which was the type used in these tests, or whether the fuel flows over the side, as is represented in Fig. 18; with continuous operation the height and shape will adjust themselves to give a rate of burning equal to the rate of ignition.

Although non-caking fuels are not burned in underfeed stokers, yet it is of interest to extend the argument of the last paragraph to what would occur at low ratings. If a non-caking fuel were

being burned under conditions represented by Fig. 18, and if the rate of air supply were less than that of point d of Fig. 17, under continuous operation the ignition plane would find some level like CD of Fig. 18 which would make the rate of ignition equal to the rate of burning. If in Fig. 17 the total quantity of air supplied is om , the quantity passing through the ignition plane would be on and that above the ignition plane nm .

In the foregoing discussion of the ignition in an agitated bed it was assumed that the caked or coked coal is well broken up by its movement. This will not occur with a good caking coal, and the motion will split the mass into relatively large pieces. The result will be that most of the coal will not come in contact with air until it has been coked and that most of the actual ignition will occur at the surfaces of the large coke pieces. Fig. 19 presents such a conception. Because of the large size of the pieces of coke, the equilibrium depth of the bed must be greater to allow enough area of the surface of the fuel for the reactions to occur. The fuel around the air slot will be consumed more rapidly, thus undermining the coke mass so that it may fall over.

At low rates of coal feed for which the point of operation would fall well below the line cd of Fig. 17, the rate of ignition would be large compared with the rate of burning. The ignition line would sink as low as it could, but it could not go below the air-stream line; however, the coal below the ignition line would be heated by radiation and conduction and would not be cooled by the air stream, and consequently it would coke and its volatile would rise into the air stream. Although the volatile would be ignited and burned, yet the remainder of the coal, or the coke, cannot be said to be ignited until it rises and its surface meets the air stream. If the conditions are as conceived in Fig. 19, there is no definite plane of ignition, but at low rates the actions will undoubtedly be somewhat as depicted. It would be under such conditions that the coking qualities of the coal and the agitation it gets would be of the most importance in determining the fuel bed that would result.

The following generalization on large stokers is probably warranted. The more usual mode of operation as represented by a humped fuel bed implies that the type of bed is an enlargement of that represented by Fig. 19, with possibly a small part as represented by Fig. 18. This will mean that a deep bed will be required to present a large enough surface area of coke for the ignition and burning actions. A type of bed as advocated by Mr. Houghton⁷ is premised on a design and on a method of operation which will distribute the plane of ignition over a larger area of the bed, so that more of the action will correspond to that represented by Fig. 18. This mode of operation should permit of more even distribution of the air, result in a thinner fuel bed, and the composition of the gases arising from the fuel bed should be more uniform; one would also expect that the bed can be better controlled to make the analyses of these gases conform more nearly to the average desired, and to require less mixing of the gases in the combustion space.

EFFECT OF FUEL SIZE IN UNDERFEED STOKERS

The effect of the size of the coal pieces on the burning in a stoker will depend on the rate of burning. When working at high ratings, as illustrated by Fig. 18, a decrease in size will permit of an increase of the maximum rating possible, of course neglecting limitations to the quantity of air that can be forced through the bed because of increase in resistance with decrease in size. When working at low ratings in which masses of coke are formed, the first effect will not come into play, and then it can be presumed that the effect of size will be that larger sizes will give a better chance for the air to penetrate into a mass when it is only partially fused together and is not fully coked; this will mean that the mass will be partly burned, and therefore more open and fragile.

EFFECT OF PREHEAT IN UNDERFEED STOKERS

The results of the use of preheat with underfeed stokers have been described in a number of papers by operators, and the subject has also been debated extensively. It is therefore worth while to attempt to interpret the results of these tests. The argument will be itemized.

(1) Neglecting the effect of ignition and considering only the effect of preheat on a fuel bed of a given depth, the tests show that the additional heat contained in the preheated air is utilized partly in increasing the rates of reaction in the fuel bed—that is, in increasing the rate of combustion for the same air rate—and partly in increasing the temperature of the gases leaving the fuel bed. The partition of the total heat into these two portions will depend on the depth of the bed, but approximately it can be said that 50 per cent goes to each action.

(2) As a result of item 1, there will usually be more CO in the gases, and more secondary air will be required.

(3) Presumably the higher temperature of the gases leaving the fuel bed will tend to cause better combustion in the combustion space, but as this increase is added to an already high temperature, it is questionable whether the benefits gained because of the increased temperature of the gases from the preheat will offset the disadvantage that there is more CO in the gases, and thus more secondary combustion action is required; moreover, the available higher temperature of the top of the fuel bed and the gases will be lowered because of the increased radiation to the water surfaces. Such questions could only be settled by tests, but the variations to be determined would usually be less than those of operation.

(4) It would thus appear that preheat will give only limited assistance to the combustion. This does not, of course, affect its value as a means of producing an increased over-all economy of the system.

(5) The tests showed that the outstanding effect of preheat on all fuels was that it increased the rate of ignition; for example, based on normal air temperature of 80 F, preheating the Illinois coal increased the maximum rate of ignition 35 per cent for 200 deg and 85 per cent for 300 deg. For Pittsburgh coal the increases were 19 per cent for 200 deg and 43 per cent for 300 deg.

(6) It would therefore appear that the most useful function of preheat is that it permits of a higher rating being obtained and that a moderate preheat will materially increase the range of output.

(7) No attempt has been made to suggest the position or shape of the ignition plane in the complex fuel beds of large stokers. Still confining our argument to high ratings, for which the ignition would correspond in principle to Fig. 18, it would seem that the quantity of preheat will influence the position of the plane of ignition and might to some extent be used to control it.

(8) Because preheat increases the rate of ignition, if the preheat used produces a rate of ignition greater than that required for the rate of burning, then it will in general tend to bring the burning nearer to the metal work of the stoker. Consequently, the burning of stoker parts with preheat may be directly due, not to the increase in temperature because of the added heat, but because the burning of the fuel is nearer to the metal. It would therefore appear that troubles might be lessened by reducing the preheat temperature if it is higher than that required to give the rate of ignition necessary for the rate of burning.

(9) In this investigation it was not possible to make a successful test with 400° F preheat, whereas higher temperatures have been used in service. This is no anomaly, because the method of test necessitated heating up the whole of the coal used and maintaining it at the full temperature for one hour or more. In service the coal will not be heated materially until it meets the air stream.

(10) It is difficult to suggest any advantages because of improvements in burning characteristics resulting from the use of preheat at low rates of burning as represented by Fig. 19. The coal will be more thoroughly coked, and the improvements must be found in the actions covered in items 1, 2, and 3.

It is recognized that the pictures suggested in the foregoing may not be in agreement with what occurs in a large stoker. A much larger proportion of the coal may be heated, lose its volatile, and be coked before it meets an air stream. The pictures may, however, help those who operate such stokers better to analyze what actually happens.

One could use the experimental data of this paper to deduce approximations of the thickness of fuel bed that would occur and the secondary air that would be required for various assumed conditions. However, such data can be reliably obtained only by experimentation with each type of stoker and of coal, and the usefulness of the data presented in this report is limited to presenting a picture which may help in explaining what has been found to happen or in suggesting the causes of troubles and possible methods for alleviating them.

IGNITION ON CHAIN-GRATE STOKERS

As pointed out in connection with Fig. 4, the length U (the ignition part) of the bed of a chain-grate stoker is burning on the underfeed principle; the ignition is by radiation. In the tests of this report the top of the bed was ignited by a layer consisting of 1½ lb of charcoal and 2 lb of petroleum coke, both wetted with kerosene; the fan was started as soon as the kerosene was alight and was at once brought up to the air rate to be used in the test. There may be a question as to whether this type of ignition is the same as that by radiation, but there can be little difference except in the rate at which the temperature of the top surface will rise; this will also vary in furnaces, both with type and with rate of operation.

The time required for the ignition plane to travel down the first 4 in. or more would correspond to the similar action on the chain-grate stoker; compounding this rate with the speed of the grate gives the slope of the ignition plane.

The test data on this phase have not been analyzed completely; in general, they show that the rates of ignition for the upper part of the bed are of the same order as those given by the curves; the rate of air supply, the size of fuel, and the preheat affected the rates of ignition in the same manner, but not to the same degree. The effect of the caking of the coal at low rates of air supply is of interest; caking does not affect the rate of ignition for about the first 4 in. of depth, but below that the bed apparently cakes enough to lower materially the rate of travel of the plane of ignition. This phase may be investigated further by using shallower beds, corresponding to those used on chain-grate stokers.

PERSONNEL AND ACKNOWLEDGMENTS

This investigation was conducted under the authorization of Mr. O. P. Hood, chief engineer, Mechanical Division, U. S. Bureau of Mines. Mr. D. T. Rosenthal, junior fuel engineer, assisted in the investigation from its beginning. Acknowledgments are given to the Philadelphia Coke Company, which supplied the coke used for the overfeed tests, and to Eavenson, Alford & Hicks, Pittsburgh, Pa., which supplied the splint coal.

Discussion

BERT HOUGHTON.¹¹ This paper is worthy of careful consideration because it presents a study of the fundamental re-

¹¹ Operating Superintendent, Brooklyn Edison Company, Brooklyn, N. Y. Mem. A.S.M.E.

actions which take place within the fuel bed, and while the investigations were made on a small experimental furnace, the authors have been able to set up certain basic principles and to apply them in their conclusions to large underfeed-stoker operation.

The processes that take place within the fuel bed of a large underfeed stoker are of considerable importance to the stoker operator, and while again the authors had made a majority of their runs using high-temperature and low-temperature coke in graded sizes (and in this respect the results are not comparable with stoker operation), the principles of combustion which they were able to investigate in their small closely controlled furnace have no doubt a certain relation to plant practice.

In the underfeed tests the curves showing the variation of the rates of ignition and burning with air flow are significant. The fact that the rate of ignition reaches a definite maximum with any given fuel and primary air temperature indicates that there are definite limitations on the coal-burning capacity of any underfeed stoker which depend on the individual design. The marked increase in ignition rate with increased preheat temperature would, at first glance, appear to offer a very valuable method of increasing the burning capacity of a stoker, but, as the authors point out, other factors work to limit the usefulness of preheated air. Our experience with stokers using preheated air has been that the plane of ignition of the coal is much closer to the metal parts of the stoker, which explains the excessive burning of stoker castings found with stokers using preheated air. Furthermore, we have experienced excessive secondary combustion resulting from the high CO content of the gases leaving the fuel bed.

In discussing the principles of operation of large underfeed stokers, it cannot be too strongly emphasized that an ideal fuel bed is one which is relatively thin, homogeneous, and porous. In such a case the air distribution is even and combustion practically complete in the furnace itself. As the authors point out, a greater effective plane of ignition is obtained. It is of course obvious that the ideal fuel bed is one in which the burning rate is uniform over the entire area. This condition, we have found, is most nearly attained by the use of a thin fuel bed and a high furnace draft. High draft improves air distribution through the fuel bed, and also assists in the dissipation of heat, with a consequent elimination of excessive temperatures. Lower fuel-bed temperatures will reduce volatilization of the ash, slagging, and furnace-wall maintenance.

Our experiments on underfeed stokers burning bituminous coal have not been as detailed as those that the authors were able to carry out on their small stoker, but it is indeed interesting that some of the principles that we have made use of in stoker operation are confirmed by the authors in their work. They are to be commended for their contribution.

E. G. BAILEY.¹² This paper lies closer to the fundamental principles of burning fuel in solid form on grates than any that has yet been published, to the writer's knowledge. Had such work been done earlier in the history of fuel burning, there is no question that a great deal would have been gained toward more efficient and more nearly smokeless combustion years ago than has been the case.

Even though this paper comes rather late in the experience of some of us in burning fuel on grates and stokers, it is still very opportune for those who have this problem in hand in assisting to define the limitations, especially with respect to rates of combustion that can be expected from different methods of feeding solid fuels to grates.

This is the kind of research work which I think the U. S. Bureau of Mines should do, and I understand from Mr. Nicholls that much more data have been collected than are presented in this paper. It is to be hoped that all of this research can be made available.

AUTHORS' CLOSURE

Although the subject matter of the paper is relatively simple, yet it requires rather close study to follow the arguments; consequently much detailed discussion was not expected because of the short time the paper has been available. It is hoped that this attempt to formulate principles will be supplemented by those who are associated with stoker design and operation; no data are available at present on the motion of the streams of coal in the fuel bed, or their dependence on the properties of the coal.

There is, however, room for considerable more work of the type reported in the paper; in particular, studies are required to determine whether this method of testing could be used to measure the relative burning characteristics of coals closely alike, and whether these measures could be used to predict their characteristics or peculiarities when used in stokers.

¹² Vice-President, Babcock & Wilcox Co., New York, N. Y. Mem. A.S.M.E.

The Economic Significance of Replacement Cycles in Demand

By THOMAS M. McNIECE,¹ NEW YORK, N. Y.

For many generations, the even flow of trade among peoples has been interrupted by recurring depressions. Abnormally high levels of commerce have always preceded the serious declines. It is neither logical nor sufficient to explain a disastrous decline in business by stating that the levels before the decline were too high and characterized by excessive inflation. What produced these latter conditions?

This study is concerned not only with the periods of enforced retrenchment but also with those eras of high business levels which invariably precede them. The effort has been made to discover and isolate the underlying causes of these recurring fluctuations. By underlying causes is meant the initial influences, invisible and undetermined at the time, which set in motion the multitude of powerful and obvious forces which are almost instantly transformed into potent sources of further change. The only consistent or normal characteristic of business trends is constant change.

It cannot be seriously doubted that the various indexes of business and the paths described by them are but the composite results of many components. Why, therefore, is it not logical to investigate the movements of general business by analyzing the fluctuations of its principal components?

EXCESSIVE fluctuations in a power circuit can only be traced to their source and eliminated by determining the characteristics of each important component of the load. What are the dominating units in the many divisions of trade and production?

The final objective of all productive enterprise of every kind is the satisfaction of individualistic requirements which in integrated form we know as "consumer demand." There is no kind of so-called "producer goods" which is not made solely as part of the process of supplying the wants of individuals. The cost of all such production is normally and eventually borne by the ultimate consumer as part of the cost he pays for goods used by him.

¹ Industrial and marketing analyst, New York, N. Y. Mr. McNiece was graduated from Case School of Applied Science in 1907, and was awarded his E.E. degree in 1911. After some years' experience in production of pumps, plumbing supplies, and sanitary enameled ware, he entered the employ of National Carbon Company, Inc., at Cleveland, Ohio. He was successively in charge of electrical research, production activities at Cleveland, and finally of plant and cost accounting for all factories of National Carbon Company. Later he assumed charge of the plant-accounting control division of Union Carbide and Carbon Corporation in New York City. Some years later he became manager of the sales record and research division of the National Carbon Company, coordinating the activities of market research, sales and distribution accounting, and budgetary control. This was followed by a period devoted to security analysis. He is the author of articles appearing in various commercial and technical publications and has presented papers before a number of trade associations and professional societies.

Contributed by the Management Division and presented at the Semi-Annual Meeting, Chicago, Ill., June 26 to 30, 1933, of THE AMERICAN SOCIETY OF MECHANICAL ENGINEERS.

NOTE: Statements and opinions advanced in papers are to be understood as individual expressions of their authors, and not those of the Society.

Depreciation and obsolescence charges bring this about. Even that portion of such costs as may be at times charged off in some form of liquidation losses is borne by the consumer. All taxes direct or indirect are finally paid by this same individual. These elements embrace all costs and are all paid out of individual income. There is no other source. Since the cost of all producer goods is finally paid by the ultimate consumer, such cost is but part of the total he pays. It is difficult to conceive of the part assuming greater importance than the whole.

Inasmuch as the individual pays all costs and since the ultimate objective of all productive and commercial effort is the satisfaction of individual wants, we may gain a good idea of the relative importance of basic activities by determining the purpose for which consumers' major expenditures are made. Analysis of existing data upon this subject indicates that when weighted for the various groups within the different income classes in the United States approximately 70 per cent of all individual income is expended for the three essentials, food, clothing, and shelter. If to this large percentage we add the expenditures for automobiles in this country, the total will be close to 75 per cent of consumer income. The Ministry of Labour estimates that, in Great Britain, 88 per cent of wage earners' income is expended for food, clothing, and shelter. We therefore find that in the United States three-quarters of individual income which pays for everything is expended for these four important requirements. This leaves but 25 per cent for the great variety of other expenditures and savings. It should be obvious at once that the combined influence of these four non-duplicating elements must govern to a great extent the movements of all business.

What do we find when we analyze the trends of these four industries? These facts stand out:

- (1) No two of these industries follow the same path
- (2) No one of them describes with fidelity the trend of aggregate business as pictured by the various accepted indexes
- (3) When the four are combined on a weighted basis, the composite trend reproduces with significant fidelity the trend of aggregate business.

In a sense this latter condition is the pivotal point of this study. Considering the great importance and differing characteristics of these industries, a logical and mathematical conclusion may be drawn. Briefly it is that consumer demand, dominated by these four outstanding requirements, sets the pace for all industry. There are at least two analogous developments of scientific acceptance and use that are well known and afford a basis for this reasoning. One is the analysis of sound waves into their simple components and the other is the similar resolution of electric voltage and current wave forms into their various component waves.

In these two divisions of scientific endeavor it is accepted without question that the shape of a composite wave is due to the shape and relative importance of the individual components. Likewise, it follows that the contour of the aggregate business trend is due to the weighted contours of its components. It may be reasoned directly therefrom that if definite causes can be discovered for the varying and dissimilar performance of the

predominant industries, causes for the variations in the composite trend will have been determined. This study undertakes to develop these explanations.

Business normally pursues a wave-like course with the passage of time. Used in its correct sense, the term "cyclical" may be applied to this progression. This is true of all industries. The use of the term "cyclical" does not imply waves of equal length but merely wave-like fluctuations that may or may not be equal in length or duration. While all industries are subject to cyclical fluctuations, some of them also manifest certain periodic tendencies, that is, they tend to follow a rhythmic variation in which the wave lengths or time intervals are approximately equal. Due to certain fundamental characteristics inherent in them, the maintenance of periodic fluctuation is more constant in some industries than in others. As will be described later in this study, the reason suggested for the periodic characteristic of some industries is what we have termed the "replacement cycle." This is a phenomenon of demand that tends to reassert itself at intervals following some prior distortion in demand of sufficient magnitude to cause an appreciable disturbance.

It is a fact set forth in the statistical history of the industries themselves that all of the four major industries analyzed in this study were simultaneously depressed in the period of 1920 and 1921 and did not again reach this condition of common agreement in downward trend until 1929 and 1930. These years mark the last two major depressions. Intervening, were the milder depression of 1924 and the even milder one of 1927. At these times only part of these four industries were at abnormally low levels. In similar manner we find that the periods of extraordinary prosperity are marked by a general agreement in timing of the higher levels of the component industries. The conclusions suggested in no way minimize the importance of credit and other monetary questions affecting these situations. Increasing volume of business begets increased volume of credit, and declining volume of business forces liquidation commensurate with the severity of decline. We must explain this fluctuation in demand. In the replacement cycle, we have both a cause for, and an explanation of a variation in demand that is not induced by a prior change in income levels but which will actually precede such a change in income, either upward or downward.

It should be clearly stated that in the prosecution of this study the first step was the accumulation of available, pertinent facts and the second was the interpretation of these facts. Out of this sequence were developed the conclusions set forth in this paper. The investigation was begun with no preconceived notions and with no predetermined conclusions to which the evidence was to be fitted.

The question may arise in the minds of many that a study omitting such important industries as iron and steel and the railroads, for example, must be inconclusive. The answer to this does not depreciate the importance of these industries but rather defines their sequence in these economic movements. Important as they are, they still owe their very existence to the requirements of individuals. Of first rank in the sequence of movements are those industries which produce commodities actually used and consumed by individuals. The backbone of the iron and steel industries is the demand from the railroad, automotive, and building industries. The very life-blood of the railroads is the traffic flow engendered by the movement and consumption of goods in other industries. Neither the iron and steel business nor the railroads can show any improvement in their business levels without prior improvement in the industries which they serve. The iron and steel business may be accepted as a barometer of trade conditions, but the fact remains it is an averaging point for changes that precede it.

If it can be ultimately shown that the repeated economic disturbances are largely the result of unobserved changes in individual demand induced by some prior major disturbance and that these initial, causative changes are due to thoroughly natural buying programs on the part of the great mass of the people, some of the bitterness should be eliminated from our consideration of constructive measures. Real remedies may then find expression in cooperative rather than antagonistic views and actions.

METHOD OF APPROACH

The data utilized in this study are largely in index form. For this purpose the indexes of productive activity computed by the Federal Reserve Board for the food, textile, and building industries were used. The actual output of motor cars was used for the automotive industry. The first, second, and fourth are purely quantitative while the third, embracing contracts awarded, involves the element of value. This latter index is more commonly used.

One modification, however, of the existing data was made for significant reasons. The period chosen as unity or 100 per cent for the Federal Reserve Board data embraces the interval from 1923 to 1925, inclusive. Both the Federal Reserve Board and the Department of Commerce use this period as a basis for measuring trends. It is undoubtedly the longest period adopted as standard in this country for such extensive series of data as published by these two organizations. This interval or shorter ones are entirely satisfactory for tracing the paths of individual industries but are not long enough to measure accurately their relative importance with respect to each other. As an example of this, it may be said that the years 1923 to 1925, inclusive, were in an era of abnormally high building activity and to accept this level as normal for building involves an error when the concurrent levels of other industries are to be compared with it. It is also a fact that, if a composite wave length such as that of aggregate business is to be broken up into its components, the more rapidly fluctuating industries should be related in correct proportion to the longer wave taken as standard. For these reasons, the data previously mentioned were converted from the 3-year base of 1923 to 1925 to the 10-year base of 1920 to 1929. This has the technical advantage of setting up as standard a full span of years between major depressions.

This conception of the statistical problem suggests that the various statistical agencies, both private and public as they exist in this country, might do well to agree upon a common standard of sufficient length to provide adequate accuracy for all purposes, rather than to base their data upon such widely varying times and periods. This would greatly facilitate the comparative use of such data.

In the indexes used in this analysis, the 10-year average for each of the twelve months of the year is used as 100 per cent and all points on the trends represent the activity for the corresponding months expressed as a percentage of the 10-year average for that month. Seasonal movements are thus eliminated or thoroughly minimized. Other and more extended methods involving a much greater expenditure of time would result only in refinements that would not affect the conclusions drawn. The various charts computed in this manner, therefore, show both secular trends and non-seasonal deviations therefrom. It is these non-seasonal deviations that become so highly significant in this work.

FACTS DEVELOPED

The outstanding characteristics of the trends shown by this data will be briefly summarized for each industry and will be illustrated in each case by charts.

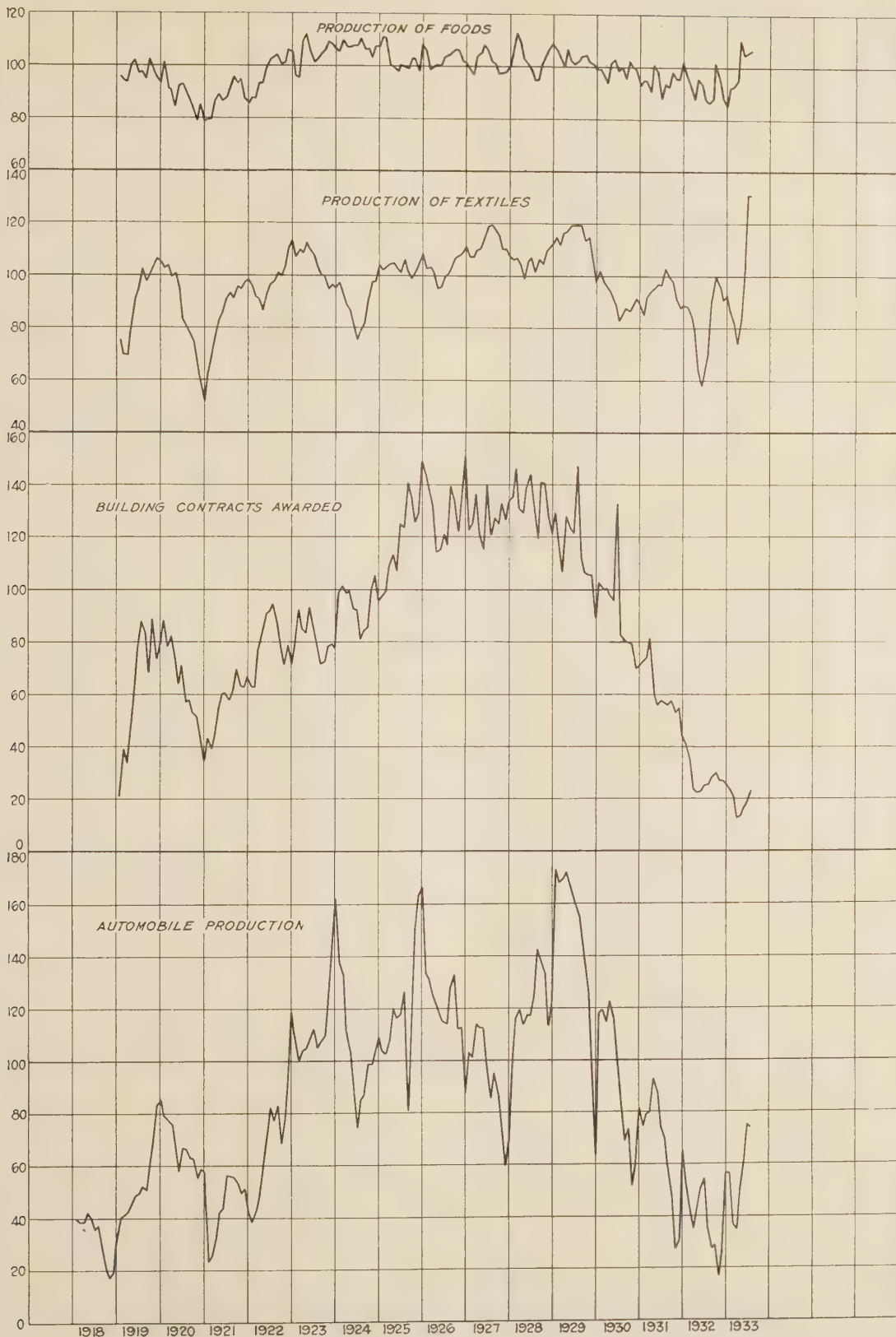


FIG. 1 PRODUCTION INDEXES FOR FOODS, TEXTILES, BUILDING CONSTRUCTION, AND AUTOMOBILES

Food Production. The trends in food production are shown by the first chart in Fig. 1. Food production maintains a sharp reversal in production from time to time but these fluctuations are irregular in timing and deviate but little from an average trend. This is to be expected as man must eat to live and his capacity and requirements are very uniform. The secular trend in this industry should properly show a slight upward inclination to the right. It does not do so chiefly because it has not been adjusted for the gradual decline in recent years in the consumption of meats and grains and coincident increase in the use of fruits and vegetables. During times of economic stress there is always a reduction in the demand for the less essential foods and at the same time a decline in the amount of food thrown away. This naturally results in a slight decline in food production of some types.

Textile Production. By far the predominant class of textiles is clothing. The second chart in Fig. 1 indicates the progress of this industry. This trend is very striking. The secular increase is definitely shown but the graph is chiefly significant for two other reasons. First, deviation from the average trend is much wider than that for foods and second, the variations are sharply periodic. It will be noticed that there are clearly depressed levels of varying intensity every other year. The low areas are in the even- and the high levels in the odd-numbered years. While the effect of the present depression has been to lower the level of operations, the sharp periodicity has continued to the present time. In other words, the peculiar periodicity has not been destroyed by the present economic crisis up to this time. While this index of production levels is based largely on spindle activity, the same oscillating trends are shown in number of people employed and wages paid. These are completely independent data that cover the whole industry.

Building Construction. The third major activity of man is the provision of shelter for his family and his various pursuits. Building construction constitutes by far the greatest single class of man's fixed assets which he himself produces. The third chart in Fig. 1 portrays the activity in this industry. This picture is characterized by an extremely irregular month-to-month movement, a rapid increase in trend up to 1926 followed by an even more rapid decline beginning early in 1928 and by a wide divergence from the average.

The irregular movements from month to month are to be expected from the highly individualistic and widely scattered nature of the business. The rapid increase in trend up to 1926 calls for further explanation which will be given later. The wide divergence from average is also a subject for later discussion but it may be said that conditions of the industry make possible extreme activity at times to be followed by extensive recessions. Due to long structural life and the ability to "double-up" in the use of shelter, deferment of additional construction may continue long after any real surplus of housing has disappeared.

Residences should be considered solely as consumer goods for purpose of this analysis. Residential construction is such an important part of the total building program that the trend of the whole industry normally assumes that of the residential component. The importance of the residential division may be illustrated by the data in Table 1. These data show the importance of each class of construction regularly included in the statistics gathered by the F. W. Dodge Corporation. The proportions shown are based on totals of each class for the five-year period from 1925 to 1929, inclusive.

These figures show that residential construction is virtually as large as the next three largest classes combined but this does not express the full measure of importance. The F. W. Dodge statistics on residential construction do not include the projects valued at less than five thousand dollars each.

TABLE 1 RELATIVE BUILDING CONSTRUCTION VALUES IN 37 STATES

Class	Per cent of total value
Residential.....	40.9
Public works and utilities.....	18.9
Commercial.....	14.6
Industrial.....	9.9
Educational.....	6.3
Social and recreational.....	3.6
Hospital and institutional.....	2.3
Religious and memorial.....	2.2
Public.....	1.3
Total.....	100.0

If these were included the ratio of residential to total construction, conservatively stated, would be at least 55 to 60 per cent. The great importance of individual requirements in this tremendous industry is very significant. Incidentally, the extreme futility of attempting to initiate recovery by an increase in public-building construction should be indicated by the very small value of this class in a period of great activity in such work.

The great irregularity in the trend of building construction during the relatively short period covered makes it difficult to draw definite conclusions regarding any trend toward periodicity. Standard Statistics Company, utilizing available sources of data, has compiled a statement covering probable annual building construction based on contracts awarded in millions of square feet. These data are shown by them in adjusted series from 1900 to 1930, inclusive. From this source the data shown in Table 2 were derived.

There is obviously a strong tendency toward a 3-year periodicity measured in annual terms only. This is apparent in years intervening both between successive peaks and successive valleys. In each case where the interval between peaks was 4 or 6 years instead of 3 years there was an interrupting influence in the form of a business depression. These may be defined as the depressions of 1907, 1914, 1921, and 1924. The present depression is having the same effect and the extension of decline has been carried through the year 1932, making the longest decline in building construction since the turn of the century.

Irrespective of cause, the effect of such depressions would be to retard construction and to interfere with any influences that might otherwise be at work.

TABLE 2 PERIODS OF FLUCTUATION IN BUILDING CONSTRUCTION

High volume	Intervening difference, years	Low volume	Intervening difference, years	Decline, per cent	Years of decline ^a
1905 ^b	..	1908	..	18.6	3
1909	4	1911	3	17.0	2
1912	3	1914	3	14.4	2
1916	4	1917	3	16.8	1
1919	3	1921	4	31.0	2
1925	6	1927	6	9.6	2
1928	3

^a Annual basis only.

^b Construction volume in 1906 was only 0.8 of one per cent less than that of 1905. If 1906 had chanced to be larger than 1905, the intervening difference first shown between high points would have been three years instead of four, and under "years of decline" the first figure would have been two years instead of three years.

There is another peculiar manifestation in these figures which calls for examination. Reference was made earlier to the rapidly rising trend in construction levels up to 1926 followed by the sharp decline beginning early in 1928 as shown by the third chart in Fig. 1. The data developed by Standard Statistics offer a means for further analysis. This series was smoothed by calculating a 3-year running average and plotting the averages at the middle year. The results of this are displayed in Fig. 2. The normal shown in this chart was calculated by Standard Statistics from the data as compiled by them. This chart shows two very striking and sustained peaks centering, respectively, in 1906 and 1926, that is, just 20 years apart. The peaks are so

evident that no real question as to their existence can be raised. The behavior of this trend and the interpretation to be made later suggest that the computed normal may be somewhat high, especially in the later years. This thought is also supported by the fact that the building normal as calculated is increasing materially faster than population in this 30-year interval. While population was increasing by 65 per cent, the calculated normal for building construction increased 130 per cent. A relative increase in building construction is to be expected but the difference in this case seems too great. This has some significance in view of later interpretation.

The trend of building construction shown in this analysis seems to be composed, since 1900, of two major waves some 20 years apart superimposed on the top of which are ripples of a predominating length of 3 years. The immediate effect of depressions is to cause some deviation from this interval. It should be understood that this three-year period is assumed to be approximate in view of the fact that monthly data throughout this interval are not available.

Automobile Production. With the development of our present mode of living and with the prevailing distribution of population and trade, individual transportation by motor car has become a necessity for many people. The automobile is one of the most widely distributed articles of high unit value and is predominantly utilized in the transportation requirements of the individual. As far as this country is concerned, the automotive industry is one of man's most important economic activities.

Automobile production by years as reported by the National Automobile Chamber of Commerce is recorded in Table 3.

In the foregoing table the combined production of cars and trucks is shown in order to indicate the full activity of the industry. In general, the declines in a number of the years indicated would have been numerically greater if passenger cars only were listed. The passenger car is by a wide margin the predominating factor in the industry.

While annual production is shown in Table 3, the fourth chart in Fig. 1 shows the trend of the industry by months from 1918 to 1932, inclusive. The terrific non-seasonal fluctuations in this important industry are apparent at a glance. Table 3 shows that the first decline in annual output in this industry was encountered in 1918. Since then declines have occurred at intervals of 3 years or in 1921, 1924, 1927, and 1930. The continued decline in 1931 and 1932 is the first time such a decline has exceeded one calendar year. The significance of these three-year fluctuations will be discussed later.

TABLE 3 PASSENGER CAR AND TRUCK PRODUCTION IN THE UNITED STATES

Year	Number	Year	Number	Year	Number
1900	4,192	1911	210,000	1922	2,544,176
1901	7,000	1912	378,000	1923	4,034,012
1902	9,000	1913	485,000	1924	3,602,540 ^a
1903	11,235	1914	569,054	1925	4,265,830
1904	22,830	1915	969,930	1926	4,300,934
1905	25,000	1916	1,617,708	1927	3,401,326 ^a
1906	34,000	1917	1,873,949	1928	4,358,748
1907	44,000	1918	1,170,686 ^a	1929	5,358,414
1908	65,000	1919	1,933,595	1930	3,354,870 ^a
1909	130,986	1920	2,227,349	1931	2,390,000 ^a
1910	187,000	1921	1,616,119 ^a	1932	1,369,000 ^a

^a Years of decline from prior years.

Composite Trend of Four Industries. The foregoing summaries of the progress of individual industries are confined to a recital of facts determined in the manner described. Surely there can be no serious question raised regarding these facts. In order to emphasize the dissimilar trends of these industries, the four prior charts have been combined in one. In this combined chart each of the four trends has been slightly smoothed by three-month-running averages. The comparison is shown in Fig. 3.

It is apparent at once that no two of these industries are following the same path and that no one of them agrees with the fluctuating trend of aggregate business as commonly pictured. It is also obvious that in 1920 and 1921 all of them were simultaneously depressed and that this did not again occur until 1929 and 1930. It is apparent also that there have been partial agreements in downward trends as well as complete and partial agreements in upward trends in the interval covered.

It should be beyond logical question that during any period of common agreement in trend, either upward or downward, there will exist an extraordinarily strong stimulus to strengthen and extend the movement due to the increased interaction of the industries upon each other and the consequent influence on purchasing power. In other words, full phase agreement upward tends to create a condition of extraordinary prosperity while the same agreement downward will promote abnormal decline. This interaction which tends to be self-generating when under way and accumulative in its total effects may be compared to the phenomenon of "resonance" in electric circuits and in acoustics.

It seems logical to suggest in view of the picture shown in Fig. 3 that if the prime origin of these economic movements resides in general problems of money and credit, the stimulating and depressing effects on the four industries should be more nearly simultaneous throughout the period. That this is not so is shown by the widely divergent peaks and valleys except at certain intervals. It appears equally logical to suggest under

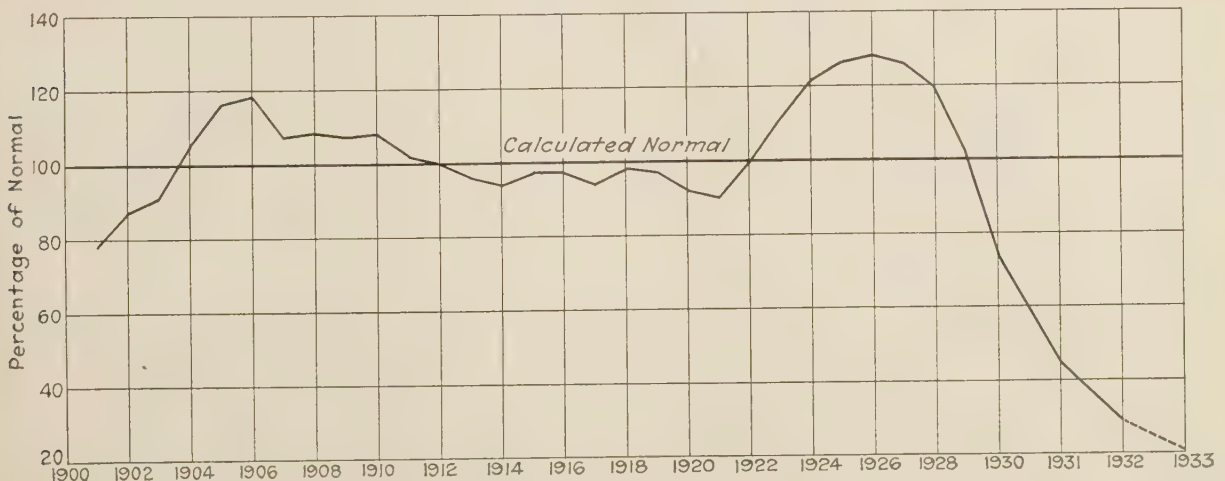


FIG. 2 LONG-TERM TREND OF BUILDING CONSTRUCTION

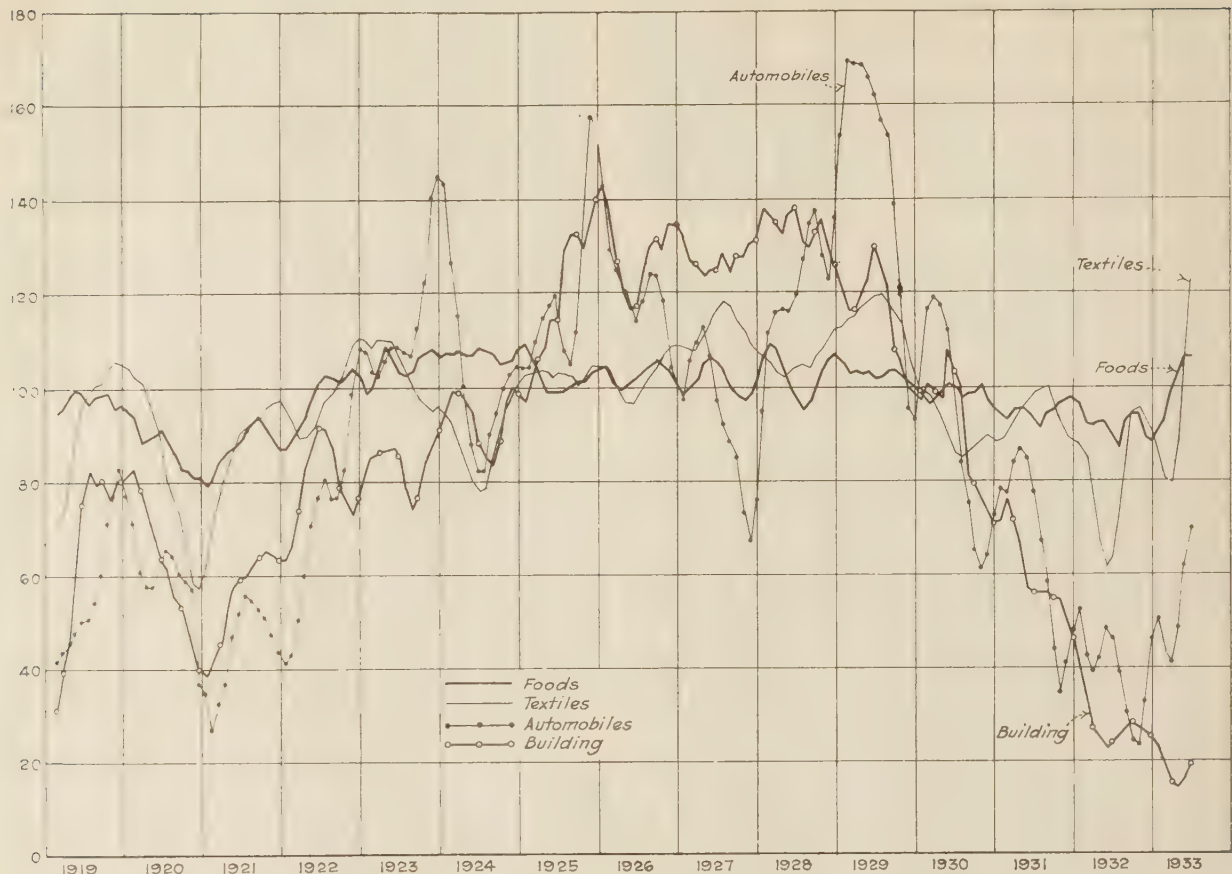


FIG. 3 COMPARATIVE TRENDS OF FOODS, TEXTILES, BUILDING, AUTOMOBILES

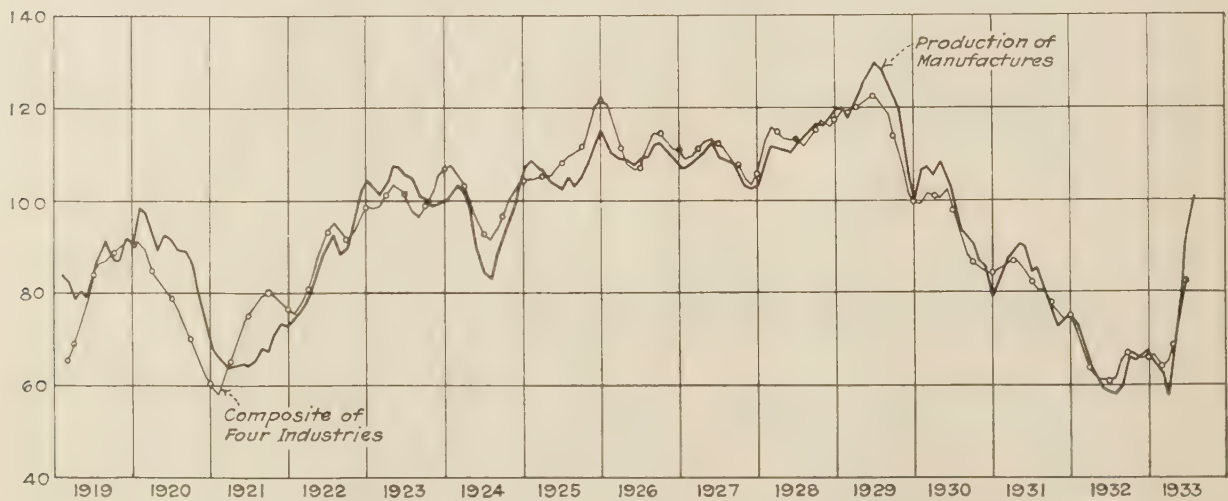


FIG. 4 COMPARISON OF COMPOSITE TREND OF FOUR PRIOR INDUSTRIES AND PRODUCTION OF MANUFACTURES

this conception of trade movements that the individualistic behavior of these industries may be due to other causes and, that the money and credit structure does not suffer and finally fail until a sufficient number of the all-important industries come into phase. Thus the stimulus gained from simultaneous upward trends engenders an extraordinary demand for credit which creates a heavy burden of debt, the orderly liquidation of which demands a continuance of trade at existing levels. The sudden recession in trade which always follows extreme heights begins, of necessity, at a high debt level. The satisfaction of these debts results in a liquidation that becomes for a period increasingly severe and under this strain the credit structure may crack.

With these thoughts in mind it is in order to determine the result of combining the trends of the four industries. When this is done upon a weighted basis, approximating the proportions which the four components assume in the family budget, the composite trend shown in Fig. 4 results. For the purpose of comparison, the trend in "Production of Manufactures" as determined by the Federal Reserve Board is plotted to the same scale and base. This is a volumetric index and embraces a sampling of all the basic industries of the country included in the census of manufactures. In addition to three of the four industries embraced in this study it covers such industries as iron and steel, non-ferrous metals, chemicals and oils, rubber, leather, paper, ceramics, railroad equipment, and others.

The close agreement between these two graphs, with such radically different components is obvious and of great significance. This accord is not due to preponderant weighting assigned to the four consumer industries in the Federal Reserve Board index. The latter index includes no component from building construction. This was assigned a weighting of 25 in the index of consumer industries, leaving a combined weighting of 75 for the remaining three industries. These same three components in the Federal Reserve Board index have an aggregate weight slightly under 31. It should therefore be clear that the agreement shown is not due to coincidence in weighting. If the Federal Reserve Board index was thus heavily weighted with these consumer industries it would be tacit admission of their outstanding importance.

This agreement between these two widely differing indexes has been previously mentioned as the pivotal point in this study. It is of great scientific significance. The principles involved in the analysis and synthesis of harmonic and inharmonic wave forms have been widely accepted and used in the scientific world for years. As mentioned earlier in this paper, a striking analogy exists in the treatment of composite wave forms of electric voltage and current, and of sound. A sound wave is normally composed of a certain fundamental wave length upon which are superimposed a number of waves of higher frequency or shorter lengths. If this longer wave length is a multiple of all the shorter wave lengths included in the tone, the shorter waves are said to be harmonics of the longer and the result is a musical tone. If these shorter wave lengths are not exactly divisible into the longer, the relationship is inharmonic and the result is noise. The latter condition governs the aggregate business curve, a fact which is not inappropriate as this wave has certainly produced its full quota of noise. If these relationships were strictly harmonic their onset would be predictable with greater accuracy and the disturbance would assuredly be of even greater severity.

Whether these relationships are harmonic or inharmonic, one fact of scientific acceptance stands out and this is that the outline or contour of the composite wave form is definitely due to the shape and relative importance of its components. A corollary of this is that those influences which are responsible

for the differing fluctuations of the components are inherently responsible for the movements or shape of the compound form.

A clearer conception of the result of combining two periodic and symmetrical waves may be gained from Fig. 5. In this case the wave indicated by the heavy line is the resultant of the two waves of 2- and 3-year periodicities which are shown in full and dotted light lines, respectively. If undistorted by external causes this wave would be repeated every six years.

The problem then remains to discover the motivating influences that result in the widely differing paths of the four dominant industries.

Before proceeding further with this analysis, it will be well to develop briefly the relationship between production and demand. There is much misunderstanding and disagreement about these two divisions of economic endeavor. The statistics of the De-

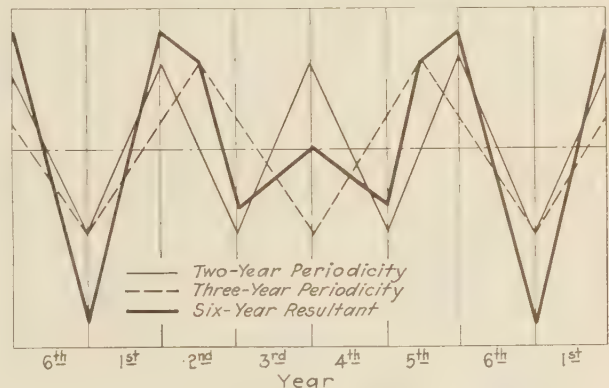


FIG. 5 COMBINATION OF PERIODIC WAVES

partment of Commerce and of the Federal Reserve Board jointly include much valuable data on inventories and production. Unfortunately, there is relatively little information on sales or demand. Reference has just previously been made to the index of production of manufactures computed by the Federal Reserve Board and which is plotted in Fig. 4. The Department of Commerce calculates an index of stocks or inventories of manufactured goods. The industries sampled in this case include the same comprehensive list of basic industries as those used in the production index. These indexes may then, for the moment, be considered as comparable. Notwithstanding the lack of sales data, the existence of these two measures affords a thoroughly convenient means of securing the sales trend.

The accuracy and significance of the following formula are obvious: $\text{Inventory}_1 + \text{Production} - \text{Inventory}_2 = \text{Shipments or Sales}$, where "Inventory₁" and "Inventory₂" are respectively the inventories at the beginning and the end of the month and "Production" is the goods added to inventories during the month. It only remains therefore, to apply these existing indexes to this formula month by month to determine the sales trend during the same interval. This has been done and the results are shown in Fig. 6. The vertical scale on this chart is double that used on the prior charts in order to magnify any existing difference between production and sales. It will be noted at once that production and sales are virtually inseparable in their irregular march over the peaks and through the valleys. This extremely close agreement in two highly fluctuating trends month by month through this interval of years would be utterly impossible if either of the indexes of production and stocks was seriously in error and it may be safely concluded, therefore, that the two are comparable as tentatively assumed. The secular trends of production and inventories are identical, which indi-

cates a uniformity in inventory control measured in terms of annual turnover. It is not the size of a plant which determines its output, but the load that is placed upon it.

In view of this convincing relationship, what becomes of the need for a master planning control to balance production and demand? When all the mists are blown away, does it not come clearly to mind that one of the principal objectives of management these many years has been such a balance attained by planning, scheduling, and inventory control? Stock rooms are not made with rubber shelves and if they were the bankers

search, we wish to inquire more closely into the characteristics of demand.

CHARACTERISTICS OF DEMAND

The term "demand" as used in this discussion is comprised of two components—desire, supplemented by the ability to pay—which together are translated into dynamic action or purchase. Such demand, based on the nature and use of the goods purchased, may be divided into producer and consumer classifications. All demand, both producer and consumer, may be di-

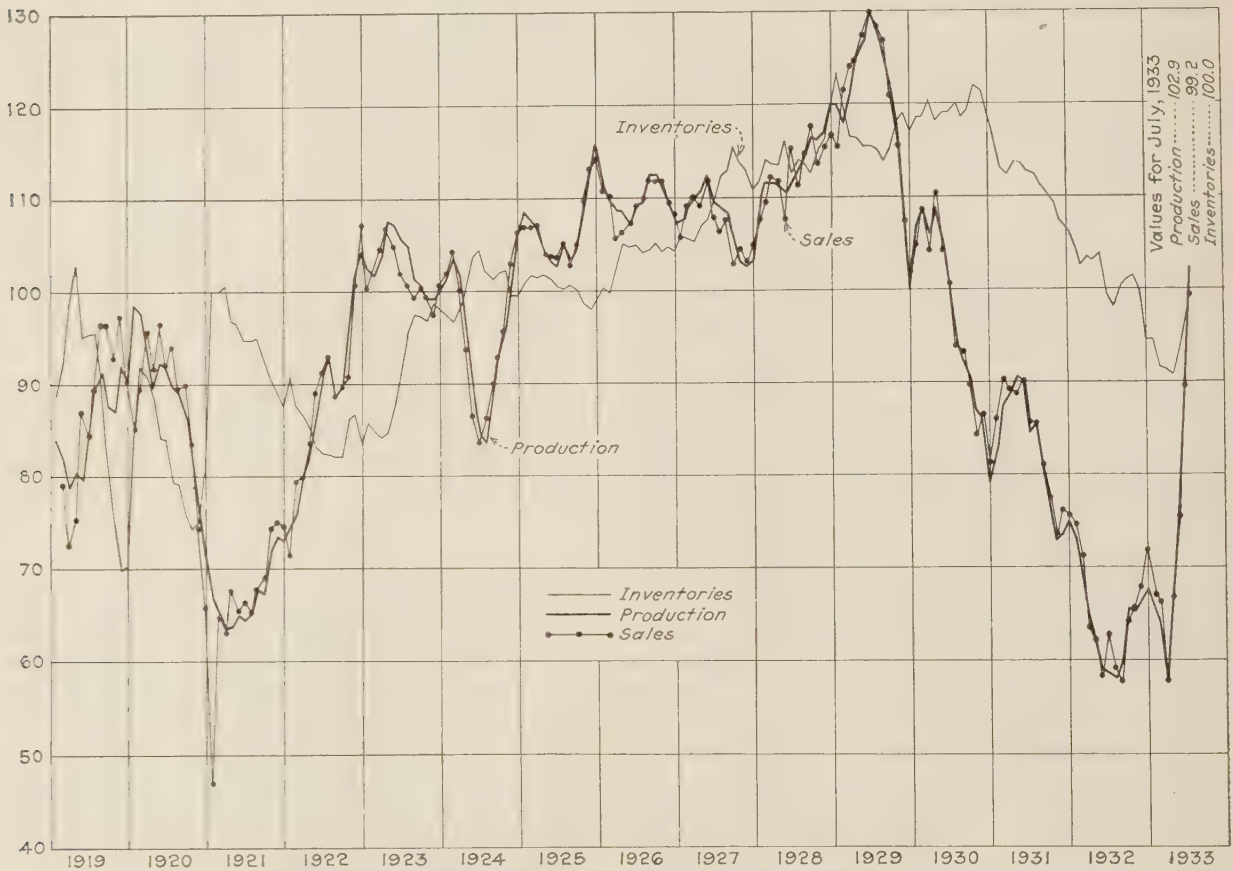


FIG. 6 COMPARISON OF PRODUCTION, INVENTORIES, AND SALES OF MANUFACTURED GOODS

would soon limit their elasticity. To suggest that production and demand in the broad economic sense are in balance in the great world of manufactures is not to say that some individual component never gets out of step. The ever-working laws of chance will usually smooth out such irregularities through compensating variations.

One important interpretation to be made from Fig. 6 is that the agreement between production and demand is so close that the two are almost interchangeable. This means that the production indexes used in describing the trends of the four consumer industries are essentially equivalent to those of demand. This close agreement may also be taken as a measure of ability and practise on the part of an industry in following closely the pace set by its customer industries. This is an important consideration in the classification of industries to be mentioned later. With this picture of agreement between production and demand, we may revert to the problem of determining the causes for the highly individualistic behavior of the four industries. In this

vided into two classes: namely, new or first-time and replacement. It will be advisable to define each.

New or first-time demand emanates from those industries and individuals who come into the market for the first time for the commodities in question.

Replacement demand, for the purpose of this discussion, is composed of those purchases which replace similar commodities which have been worn out, discarded, or transferred to other users.

It will be obvious upon a moment's consideration that these two basic classes of demand may have widely varying importance in different industries. For example, the demand for clothing is overwhelmingly that of replacement; the demand for automobiles is rapidly reaching this condition; while the demand for electric refrigerators is preponderately first-time demand.

We have previously classified commodities into producer and consumer merchandise. Before proceeding further with the study of demand, still another classification of commodities

should be made. All commodities may be divided into two groups, perishable and durable. In the use of these terms in this discussion, perishable commodities are considered to be those whose useful life is less than one year, while durable commodities are those which will last over one year. It is apparent that both producers' and consumers' goods are divisible into these two classes. We therefore find that demand, itself, is composed of producer and consumer requirements both of which embrace perishable and durable goods for which the demand is either first-time or replacement. The significance of this classification is that activity in demand and production follows the same principles in both consumer and producer industries and that these principles may prove to have great economic significance.

The demand for short-lived goods is in some respects the simplest we encounter. This is especially true with regard to perishable staples. Growing style influence and consciousness are transferring more and more goods from the staple to the style class with increasing difficulties in properly balancing supply and demand. This is also having no small part in the increasing flood of small orders. The trend of such demand, plotted against time as a base, instead of showing a relatively stable performance will rise rapidly from zero to some indefinite height and then decline more or less symmetrically to zero and before this time it usually will be supplanted by another style which repeats the cycle.

The demand for durable goods in continuing use presents a totally different picture although such goods are in part subject to style influences.

The natural growth trend for such goods is shown in Fig. 7.

With the passage of time the total sales of a durable commodity in continuing use will normally follow the trend illustrated by graph A. Total sales after replacement begins is made up of two components, first-time sales to new buyers and replacement sales to former buyers. The total sales trend will set the pace for replacement sales at the expiration of the average life of the commodity before replacement. Therefore if the total sales curve be reproduced at a later interval equal to the average life before replacement, the trend of replacement sales will be indicated. This is shown by graph B. Original sales to new buyers are obviously the difference between total sales and replacement sales. This difference is shown by graph C. This graph is particularly interesting because it shows the turning point and maximum value of original sales.

As the life of any business is extended, its replacement sales will normally become of greater importance. The increasing percentage of replacement sales to total sales is shown by graph D.

THE REPLACEMENT CYCLE

It is obvious that with the passage of the years, a tremendous proportion of merchandise has attained a use that is preponderantly replacement. In other words, the replacement market and any outstanding characteristics which it may assume will have great economic significance. There is a characteristic of the replacement market which may prove to be of first importance in our study of economic conditions. It is a phenomenon of demand.

It may be assumed for the moment that the trend of demand for a durable commodity in broad general use for a long period of years will be reasonably uniform from year to year if not influenced by shortage of supply or lack of income at any particular time. Since this discussion applies to a durable commodity in long-continued use, it will follow that the replacement demand is an important share of the total market. Suppose now some transient event takes place of such nature and importance that the supply or demand is seriously impaired; for example, our entrance into the World War. This immediately created

chaos in the automobile industry and reduced the output and demand for passenger cars in 1918 over 45 per cent below that of 1917; the first actual decline in any year within the history of the business. Such an interruption means that a large number of original as well as replacement sales will be deferred until a

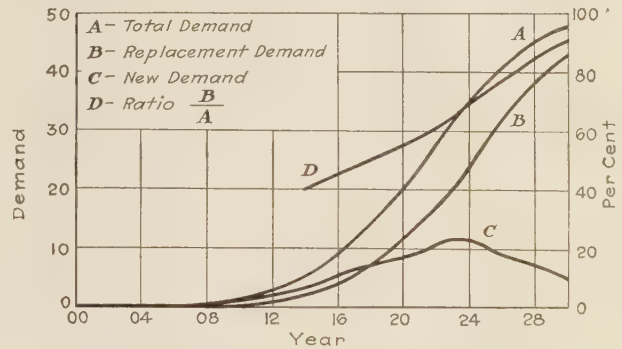


FIG. 7 NATURAL GROWTH TRENDS OF INDUSTRY

later time. However, this commodity under discussion is a durable commodity whose useful life in the hands of its original purchaser will be fairly definite because of wear and tear or obsolescence in style or design.

The serious decline in sales during the period of interruption, no matter what the cause, means that at a later time equal to

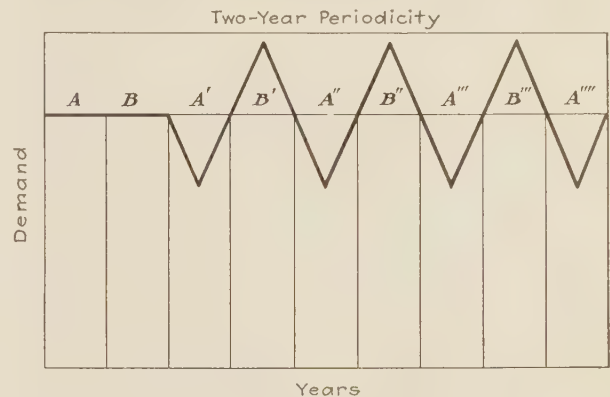


FIG. 8 ORIGIN OF REPLACEMENT CYCLE

the prevailing life of the commodity before replacement, another decline will be induced. This follows because the number of units of the commodity to be replaced during the subsequent period will be less than normal by the amount of the enforced decline in the prior period, but this decline is only a deferment, not an elimination. When normal conditions return, the usual replacement for that period will occur on schedule but to that quantity will be added the deferred buying from the prior period which will carry the total demand above the prior uniform trend. Thus a decline in demand is followed by a resurgence which carries the total above any prior levels and a period of depressed demand is followed by one of super-normal magnitude. The commodity, however, still possesses the same useful life which means that replacement which is an important share of the total demand will in subsequent years tend to follow the same surging pattern. This is illustrated diagrammatically in Fig. 8 in which the life of the commodity before replacement is assumed to be two years. In this illustration sales made in the year A are normally due for replacement in the year A' and sales made in

the year B are likewise due for replacement in the year B' . This progression of demand will carry forward into the years A'', B'', A''', B''' , etc. as shown.

Thus the decline in total sales in any one period becomes in effect a decline in replacement sales in a subsequent period. But no material decline in replacement, when replacement is a large share of the total, can occur without inducing a simultaneous decrease of some magnitude in first-time sales for that period. This is true because a disturbance of this nature will result in declining demand for the commodity itself as well as for raw materials thereby causing unemployment in contributory industries as well as in the one directly affected. The effect thus begins to spread in all directions. The total decline in demand will then be the sum of the two. The translation of these declines

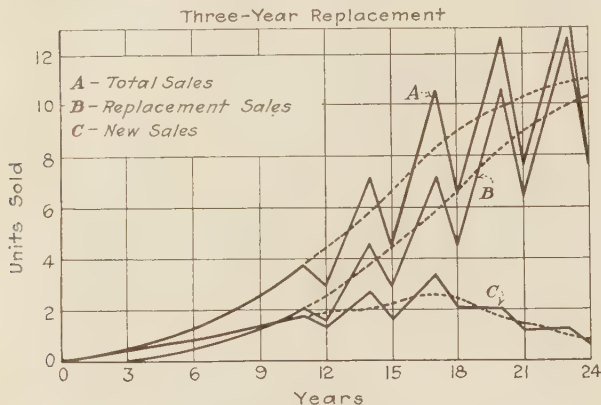


FIG. 9 PROGRESSION OF REPLACEMENT CYCLE

from period to period in both types of demand is illustrated, diagrammatically only, in Fig. 9.

This phenomenon or characteristic of demand for durable goods may be termed the "Replacement Cycle."

Conditions Necessary for Formation of the Replacement Cycle.

From the foregoing considerations it may be said that the conditions necessary to produce recurring declines in demand for any durable commodity are:

- (1) Any external or internal event that will cause a serious break in the continuity of demand
- (2) The commodity and its use must be of such nature that purchase may be deferred for a reasonable length of time
- (3) The existence of any factors such as wear and tear, style changes, or similar conditions which result in an average life before replacement that is fairly definite and greater, for example, than one year when the year is the unit used for the measurement of time
- (4) The absence of an unusual new or original demand that would counterbalance the loss in replacement sales resulting from the prior period of decline.

In the third condition just previously outlined, the existence of a "fairly definite" life of the commodity before replacement is imposed. This term needs further explanation. It means that the replacement buying habits of purchasers must be sufficiently uniform to produce a certain degree of concentration in the life of the commodity before replacement. Thus if ten men each bought a suit of clothes at the same time and if the first one replaced at the end of one year, the second at the end of two years, and so on uniformly until the tenth man replaced at the end of the tenth year, the replacement cycle would not exist. However, if five or six of the ten replaced at the end

of the second year or if three replaced during each of the second and third years, there would be a concentration of buying that would satisfy this condition for the replacement cycle. These latter figures are illustrative only. It is necessary only that there be some predominant or typical time at which a higher proportion of replacements is made.

Replacement of commodities bought at any particular time will usually conform to this requirement because they tend to follow the general trend of the normal "frequency distribution" or "probability curve" with the area of highest concentration around the average life before replacement. This will be illustrated later when the replacement cycle in the automobile industry is discussed.

A thought that will naturally arise is that, by an averaging process, such oscillations should soon die out through a series of constantly diminishing fluctuations. This attenuation most assuredly would occur if no other influences were at work. The operation of the cycle would also ultimately cease with the disappearance from the market of those whose buying was first affected by the external event that produced the distortion. As previously mentioned, however, no real disturbance of the replacement market, when this demand is an important part of the total, can occur without disturbing the buying program of original buyers about to come into the market. Thus some additional purchasers are affected at each recurrence. Furthermore, each time there is a major coincidence of these trends, as in the present depression, a new impetus of wide amplitude is provided and the train of surges is renewed with additional vigor. In addition, war as a disturbing factor comes into the picture with sufficient frequency to leave a new heritage of such trouble in its wake. War has this unique effect in participating countries: It unduly stimulates certain industries while greatly depressing others. No other random event possesses the power to do this on a large scale. Thus, the very onset of war gives birth to the major fluctuations which result in the ensuing replacement cycle.

What is the real significance of this replacement cycle in its operations? It provides both a cause for and an explanation of a variation in demand that is not induced by a variation in income or loss in buying power. It is inherent in demand, itself, and initially independent of buying power. When such a decline in replacement demand is due, it will begin without any prior change in income levels for the reason that the existing replacement market is satisfied for the time. During a period of market disturbance, the only replacement demand that is subject to deferment is that which is due for replacement during that period. Other replacement demand is not affected at the time and will reassert itself on schedule after normal conditions return. To this will be added the deferred demand as it gradually comes into the market. From this time forward, as far as the individual is concerned, replacement goes on normally until the next disturbance. The subsequent decline induced by the operation of the replacement cycle does not arise through the conscious act of any group of individuals. Rather is each one pursuing his normal replacement schedule. What does happen is that integrated replacement demand is no longer uniform from time to time because more of us are now making some important purchase at one time than at another. These surges due to the replacement cycle are similar to those caused by seasonal changes but occur at longer intervals and last for longer periods.

We are then brought face to face with the conclusion that those industries producing durable goods in sustained demand may sooner or later be subjected to the influence of an oscillating or surging demand induced primarily by the operation of the replacement cycle following some prior major disturbance. Furthermore, the time interval between these surges will vary

among different industries according to the prevailing life of their commodities before replacement.

It is not suggested that the full amplitude of variation above and below normal is directly measured by the volume involved in the replacement cycle. On the contrary, a relatively small proportion of the whole change may be traced directly to this cycle. Business is in such a state of sensitive balance that relatively minor changes will put in motion the involved forces that will cause the movement to feed upon itself and grow with accumulative effect. In other words, changes induced by the operation of the replacement cycle may be compared with the loosening of the first stone that causes the avalanche.

To the scientist and the engineer this latter thought may again suggest the similarity between the generation of the replacement cycle with its accumulative spread in all directions and the origin of resonance in a power circuit. In this latter case, the source of what ultimately becomes of serious consequence may reside in some minute, periodic change in voltage that builds up with astonishing rapidity and effect when conditions are favorable to it. Likewise, destructive vibration may be progressively set up in a mechanical structure or prime mover by sources originally so minute as to avoid detection providing physical conditions are favorable to the propagation of this influence.

Because of the sensitive balance in industry and commerce, a deviation of ten per cent above or below usual levels means the difference between prosperity and depression. A fractional amount of this disturbance may then be sufficient to start the self-propagating movements on their way. The terms "vicious circle" and "destructive spiral" have been frequently used to describe the business condition wherein a relatively small change induces further change of accumulative intensity. In truth, it seems that the instruments we have set up to detect these disastrous changes lack the sensitivity to catch the early movements which later become so obvious. When once released, the expansive power of these small self-generative movements is enormous.

INFLUENCE OF THE REPLACEMENT CYCLE ON VARIOUS INDUSTRIES

How do the characteristics of the four industries conform to the conditions necessary for the formation of the replacement cycle? If the periodic tendencies, where they do exist, coincide in duration with the usual life of the commodity before replacement, the indication is very strong that this phenomenon may furnish the origin of such fluctuations at repeated intervals. In discussing this question as it applies to the several industries, it will be well to consider the automobile industry first as the records are simpler and more complete.

The Automobile Industry. From the beginning of this industry to 1918, the output did not show a decline from one year to the next. In the depression years during this interval there was a retardation in the rate of increase but never a reduction in output. This retardation should be considered as an effect, not a cause. In 1918 there was a decline in output and sale of over 800,000 passenger cars or about 45 per cent of the 1917 output. This was unquestionably due to war conditions which reacted on the passenger-car industry with peculiar force. Following this first and large reduction, a major decline reappeared every third year—namely, in 1921, 1924, 1927, and 1930—and in no intervening years. This seemed too often and too regular to be a coincidence and the question arose as to what induced it. From a consideration of this question it seemed obvious that, if the output of passenger cars in 1918 was 800,000 less than that of 1917, the replacement of 1918 sales should be 800,000 cars fewer than replacement of 1917 sales, and this decline would occur in the normal replacement period for 1918 sales. If the successive

reductions were the result of enforced fluctuations in replacement, it seemed logical to conclude that the average new-car buyer kept his car about three years before trading for a new one. The conclusion seemed logical, the three-year period seemed to be in accord with common practise, but there were no available records to answer the question.

Finally, one of the large motor-car companies after a check of its records furnished the following information regarding the length of time new-car buyers retain their cars: For one, two, three, four, and five years the percentages are, respectively, 9.9, 38.6, 29.8, 13.6, and 7.7.

This accounts for 99.6 per cent of the new-car buyers and the weighted average time is approximately 2.75 years. The actual average computed in months might vary slightly from this figure and a more extensive search might modify the results to some extent. The data, supplemented by common experience, are sufficiently representative to support the conclusion previously reached, that the typical new-car buyer replaces his car about every third year. It should be realized that the new-car replacement demand does not come from those who drive old ones to the scrap heap but from those who trade used cars on new purchases. The Ford Motor Company was out of production several months in 1927 and this naturally increased the severity of decline in that year. It will be noted, however, that the depth reached in the latter part of 1927 merely marked the end of a drastic decline that began at a high level early in 1926. This downward surge was far greater and started much earlier than that induced by the closing of the Ford plant in 1927.

It must be clearly stated that the operation of the replacement cycle does not account for the full depth of the decline. On the contrary it may directly produce a relatively small part of it. The calculated reduction in replacement sales in 1921 due to the original decline in 1918 was 62 per cent of the actual total decline; very much more than necessary to start the downward trend. The corresponding ratio for 1924 was 18 per cent and for 1927 and 1930, 16 per cent. These percentages are still sufficiently large to start the self-generating surges which develop accumulative energy as they progress. As suggested previously, this action is closely analogous to that of resonance in an electric circuit where enormous surges may be initially started by very minute oscillations when conditions are favorable.

While the new-car buyer exchanges his car on the average every third year, the average useful life of the car according to the National Automobile Chamber of Commerce is seven years. There is, then, an average life of four years in a car after it has left its original owner. This margin provides a relatively long period during which the original purchaser may defer replacement if the incentive to do so is sufficiently strong. This is exactly what is happening during the current depression and is responsible for the long-continued decline in the industry. When replacement is actively resumed, the period during which such deferred demand will be satisfied will undoubtedly make the recovery period longer than those in the recent past. Thus, there is in these conditions the opportunity to force the automobile cycle out of its prior periodicity, but unless buying habits are definitely changed the former surge will be resumed after renewed demand is satisfied. The present decline will induce a later one. The greater the possibility of deferment of replacement demand, the greater is the possibility of such demand temporarily departing from its natural fluctuations. Thus the automobile and building industries are now forced out of their strides while the clothing industry which is much closer to the level of necessity and the product of which is subject to much shorter life, is maintaining its rhythm although at definitely lower levels.

It seems apparent from the foregoing discussion that logical

causes for the recurring three-year cycle in automobile output have been determined. We therefore have in this case, a serious recurring condition in our economic life that for the most part is the direct result of the interruption of the natural flow of trade by the great war. It is a fact, however, that surges similar to this but of much smaller magnitude would ultimately have been introduced into the automotive industry as an effect of the recurring depressions such as have visited us long before the origin of the automobile. What originally were merely periods of retarded growth would have become net declines as the demand stabilized in accordance with the trends shown in Fig. 7. Effect and cause then become hopelessly intermingled. Certainly it seems reasonable to suppose that similar movements having their origin in the replacement cycle in other important industries may induce serious distortions in all trade when they occur simultaneously.

Food. It is evident that food and its use will not conform to the conditions outlined for the formation of the replacement cycle. The existence of this phenomenon should therefore not be expected and it is not found. The trend is the most stable of the four examined and such minor fluctuations as do occur are quite irregular. Strictly speaking, there is a distinct periodicity in replenishment of food supplies. This is manifested in any locality by the well-defined "rush hours" in retail grocery stores. This is of technical interest only inasmuch as we are measuring such frequency of replacement in terms of months or years. In this sense, reflection will suggest that characteristic or predominant frequency of buying may apply to most commodities.

Textiles. In this industry we find wider divergence from the average and a very definite two-year periodicity. What characteristic of this industry should result in such pronounced two-year variations? The industry is divided into three main groups, namely, cotton, wool, and silk. Each of these, as measured by textile fiber consumption, is found to display in varying degree the same two-year fluctuations. The industry as a whole produces a countless variety of products and yet as is usual in such cases a few lines predominate. Wearing apparel is of overwhelming importance and of this class, durable garments are of greatest value. It is to be expected therefore that they may impress their characteristics on the industry.

How often on the average do most people replace their durable garments? Unfortunately, there is a serious lack of data upon this important question. The following facts, however, are known:

- (a) A critical study of the levels of production and inventory shows that the sales of textiles as a whole decline every other year. While data are not available for evidence, it is known that the sales of certain large textile companies show decided reductions every other year in agreement with the timing shown by the second curve in Fig. 1.
- (b) One statistical organization specializing in the textile industry announced that for a period of years between 1920 and 1930, examination had disclosed that on the average each man bought one-half a suit of clothes per year. This obviously is equal to a suit every two years. According to this same agency the foregoing average was reduced to 0.38 of a suit per year in the current depression.
- (c) A large manufacturer of women's coats has stated that the records over an extended period positively show that women's coats are replaced on the average every two years.
- (d) One commercial survey in a small city showed an average purchase of one suit approximately every two years by the men of the family.
- (e) Detailed investigations on cost of living in workmen's families, made by the National Industrial Conference Board,

have resulted in the provision for replacement of women's coats and dresses every two years while two-thirds of a suit per year for the men is provided in the budget. This average would tend to be lower in rural areas and higher among the greater incomes in the urban areas.

These fragmentary bits of information taken in connection with the characteristics of the replacement cycle and the unmistakable trend of the textile industry warrant the conclusion that the replacement cycle is probably the source of the repeated oscillations in this industry. Final proof of the truth or falsity of this position can be secured by a comprehensive survey of buying habits and of sales in the industry.

Building Construction. It has been shown that the trend in building construction is featured by short-term fluctuations, approximating three years in length, superimposed on longer variations indicated in one 30-year span to be about 20 years apart. Are these fluctuations manifestations of the replacement cycle? It is obvious that any short period of three years can have no direct relationship with the life of buildings before replacement. It is not so certain that this can be said of the 20-year span. Studies by various real-estate and building agencies and decisions of the Treasury Department for tax purposes seem to fix upon a typical structural life of 40 to 50 years. Any building, however, is obsolete long before it has reached this age. This is caused by changes in design and equipment and by migration of commercial, industrial, and residential centers.

The National Building Owners' and Managers' Association, in a comprehensive study of operating income and expenses on a large list of identical buildings in a number of cities, found that income from rentals takes a sharp drop after twenty or twenty-one years of life. This is undoubtedly significant. There can be no doubt that after twenty years of life a building is no longer of first rank. Early tenants of commercial buildings have in most cases moved to more modern quarters and have been replaced by others yielding lower rentals. Residential property for the most part will have been replaced with more modern quarters long before its structural life has ended. It seems entirely possible that the 40- to 45-year life of the building corresponds to the seven-year life of the automobile and the 20-year period in the life of the structure to the three-year period in the life of the automobile.

A most interesting confirmation of the long- and short-term movements in real estate activity is described by Lewis A. Maverick in the *Journal of Land and Public Utility Economics* for May, 1932, in an article entitled "Cycles in Real Estate Activity." Mr. Maverick studied three measures of real-estate activity for the period from 1853 to 1929. Official county records were utilized in this analysis which included the number of lots added by subdivisions, the number of deeds recorded, and the value of property transferred. When these long series were statistically smoothed, he found throughout the interval a series of long fluctuations of fifteen to twenty years between centers and, superimposed on the top of this trend, a series of short-term movements predominantly three years in length. These movements had no relation whatever to increases in population and have absolutely nothing in common with building construction data. The last two peaks were coincident with those shown in Fig. 2. Similar long-term movements in residential construction have occurred in Greater London where, between 1871 and 1916, such construction progressed in two great waves just twenty years apart.

The short-term surges in construction are of much interest. They not only appear definitely in building construction but are also typical of many of the fluctuations in general business throughout the life of the nation. Prior to the advent of the

automobile, building construction was certainly the most highly variable industry of large magnitude. From the standpoint of economic value and extent of fluctuation combined, it is probably of the greatest importance today. Is the three-year period in construction activity the cause or the effect of similar movements in other branches of business? If a logical reason can be found for these oscillations in construction, it may indicate their causative influence.

This industry is widely scattered and highly individualistic. It is not subject to the control afforded in manufacturing by proper scheduling of production to meet the requirements of inventory and sales. There can be no reasonable doubt but what there are recurring times when we are overbuilt, but why should the three-year periods appear with such consistency? An immense amount of credit is needed to finance this industry. The unit value of the transactions is large and the percentage of credit required is high. These credit requirements are undoubtedly larger than those needed for any other single industry.

While the long-term investor ultimately supplies much of this credit, a large part of the actual construction is usually carried on by loans subject to relatively rapid turnover. Time will not permit an extended discussion of these conditions but it may be said that much residential construction money may at intervals be turned over two or three times a year by those who make a business of supplying such funds. Mortgage loans are commonly extended for periods of one, three, five, and ten years. Examination of data pertaining to such credit indicates that the weighted average duration of all such loans may fall between three and four years and probably nearer the former. Data have not yet been found from which such an average can be accurately computed. The fact remains, however, that except for those mortgages going into the hands of permanent investors and remaining there, the turnover of such loans would no doubt be somewhat less than once every four years. There is undoubtedly a definite typical length of such loans.

Under these conditions, it seems entirely possible that the principle of the replacement cycle applies to the extension and release of credit in construction. Capital available for financing construction is not unlimited. As the volume of construction increases in an era of prosperous times, more and more capital is involved until credit so extended reaches abnormal heights. This naturally means that during such a rise less and less capital is available for this purpose. The end of such an upward movement is usually featured by a surplus of available facilities and a greater inability to dispose of the mortgages created through this activity. This naturally results in a retardation of building and construction then begins to recede from its high levels. The capital tied up in these enterprises, however, will be released only as mortgages are sold or payments are due under existing contracts. It follows directly, therefore, that after a building peak, the maximum funds released from prior contracts will be attained at that time representing the maturity of the greatest amount of funds loaned. Such a time would be determined by the weighted average of maturity dates on the credit extended. Thus it will be seen that if there is no other influence to distort the flow of funds, such flow will tend to follow a surging path with the interval between waves represented by the average duration of loans. It seems entirely probable that the three-year fluctuation in construction is induced by this behavior. It is not to be supposed that this periodicity would remain fixed under all circumstances. The conditions imposed by the credit instruments themselves will usually prevent a quicker repayment of the loans than that specified, but there is nothing to compel the reloading of such funds as soon as they are repaid. This means that if three years be assumed as the average duration of a loan, this interval between surges will not be materially

decreased but it may be increased if conditions are not favorable for reinvestment of construction funds in the industry.

A continuous production and consumption of food is essential to life itself and therefore is not subject to serious interruptions. The long life of buildings is supplemented by the ability of people to "double-up" under stress and this means an enormous and sustained capacity to retard normal construction. These are the fundamental reasons why building construction is subject to much wider fluctuations than food production. The fact that the nominal three-year cycle does not maintain itself during times of economic storms is therefore to be expected. Conditions at such times are not favorable to extension of credit. It will be recalled that mention was previously made of the fact that the only deviation from the three-year oscillation between 1900 and 1930 was when depression periods intervened.

If this conception of the ebb and flow of credit is correct, it is of tremendous importance and is worthy of much study. The conclusions and the questions arising in this analysis in no way minimize the importance assigned to credit control by many investigators. Rather do they supplement these convictions by breaking the problem up into its component parts and suggesting their real sequence. The reasoning behind these conclusions is sound. The proof of the average duration of loans has yet to be derived.

CLASSIFICATION OF INDUSTRIES

From the consideration of the differing characteristics exhibited by the various industries is derived a basic classification of all industries:

First, there is that class that displays the greatest stability of all yielding only slightly to the influence of major depressions. It is typified by staple foods and tobacco.

Second, comes that group which yields sharply to general business conditions and whose path follows that of aggregate business. The duration of depressions in these industries will be shorter or longer than that of general business depending on the ability to defer purchase. Examples of such products are shoes and food luxuries.

Third, there is that group which, due to conditions inherent in them and their use, yield to the influence of the replacement cycle and develop characteristic periodicities of their own. Examples of this class are automobiles and textiles.

Fourth, comes a group which, subject to their own inherent conditions only, might fall into any of three prior groups but which are so thoroughly dominated by the industries they serve that they follow the production levels of those industries. Examples of this class are the production of cans as strongly influenced by the food-canning industries, and machine tools whose activity is predominantly controlled by the automotive industry. It is in this class that most of the so-called producer industries will be found.

With this conception of the nature of fluctuating demand upon business, it becomes clear that the so-called producer industries take their tempo in last analysis from the demands placed upon them by the production of consumer goods. It may then be suggested that all industries fall into one or more of four basic groups with a pilot industry or pacemaker leading each group. This intricate interlacing of industries, with each group following its own path, ultimately weaves the pattern of aggregate business. This pattern is only relatively fixed and may be distorted by the extraordinary reaction of industries upon each other when their trends are simultaneously upward or downward or when they are all confronted by some major random event such as a declaration of war between major countries.

This ability to "follow-the-leader" may be definitely inferred from the extreme fidelity with which production follows demand as previously described and shown in Fig. 6.

This idea of the ebb and flow of industrial and commercial activity in various channels defined by a few dominant industries should be of value to any organization in charting its own course. Its position on its normal growth curve as illustrated in Fig. 7 should be determined. The relative importance of its principal customers by industries can be evaluated from the sales records. The probability and degree of fluctuation in demand from each customer can be approximated by working from the foregoing classification of industries. Such a picture should be of great aid in facilitating proper control of production schedules, inventories, advertising, sales effort, and capital investment.

INCREASING DEPTHS OF MAJOR ECONOMIC DEPRESSIONS

It is almost axiomatic to say that those industries which have carried us down into these depressions are the ones which must finally lift us out of them. The discussion of industry trends and of the replacement cycle has conveyed a picture of widely differing characteristics in these dominant industries. The capacity of any industry to carry us into the depths of decline and to bring us out of them is dependent on two things: first, the economic weight or importance of the industry in meeting human requirements, and second, the degree of fluctuation characteristic of it between good and bad times. Thus if this capacity be considered as a product of these two factors, it becomes in reality an energy component in these movements and may be termed economic momentum. The great food industry with the heaviest weighting of all is of little importance in recurring economic surges because its amplitude of fluctuation is so small. Building construction, on the other hand, is of lesser weight but vastly more important in promoting economic surges because of its extremely wide fluctuations. The conception should then be held of a vast array of industries, each of its own proportionate importance in our budgets, but each subject to a varying degree of oscillation through the years. This variation in amplitude will be in proportion to our ability to eliminate, defer, and expand purchases with the needs and desires of the day.

The replacement cycle is set forth in this analysis as the continuing cause of these recurring surges in certain industries. If this be true, the initial distortion that first gave impetus to the replacement cycle must still be isolated. It is quite characteristic to assign the reason for each recurring economic storm to some special condition predominating at the time. But a succession of these surging movements of trade has run through organized society for many generations. Why is it not logical to suppose that there may be some factors common to all these generations that have produced these serious results?

The replacement cycle is a phenomenon of demand, and demand has existed through all generations since barter began. Food, clothing, and shelter have been the dominating requirements of man through all this time and will continue to be as long as he exists. The combination of these three basic necessities in a weighted total matches the timing of the business fluctuations very closely but with generally diminished amplitude. This latter point is of economic interest and importance. Observation of the long-time trends of business shows clearly that the major depressions are growing deeper. As the standard of living rises, a larger and larger percentage of the family budget is expended for more articles that are farther removed from the levels of bare subsistence and minimum demand. More and more people are employed in the industries that make these products, and more of the profits of all business are derived from them. With this increase in the standard of living the per capita

purchases of durable goods are increasing. The longer the useful life of a durable commodity, the longer can deferment of replacement occur. The replacement of a rug can be postponed longer than replacement of a suit of clothes. We find statistically what judgment tells us should be so, namely, that those industries producing luxuries and the longer-lived durable goods are the ones which suffer the greatest decline in times of economic stress. Since these industries are gradually comprising an increasing share of our activities, it follows directly that our retrenchment capacity is increasing. This means that as the standard of living rises we are naturally subject to greater hazards of unemployment and deeper depressions. As the standard of living rises, the elasticity of demand increases. A wider distribution of income would tend to raise the standard of living but by the same token to increase the depths of major depressions when they do come. It is not the amount of money spent but the rate of spending which governs uniformity in trend.

INITIAL DISTURBANCES IN ECONOMIC TRENDS

The question still remains as to what was the first disturbing influence that destroyed the even flow of goods between producer and consumer and what events have happened to renew these impulses.

Among the transient events of both natural and human origin that may exert seriously disturbing effects on industry and trade are famine, pestilence, flood, drought, earthquake, tornado, revolution, war, an occasional excess or short yield of crops, and various other happenings. Most of them are usually quite localized and would be incapable of producing wide-spread unfavorable effects. Of all the isolated and random events of importance, war seems to predominate. It has accompanied man through history and is probably the most potent force for producing the original impact of which the replacement cycle is but the continuing echo. This thought does not exclude the possible effect of important random events. The behavior of the business graph rather suggests the existence of quite regular or periodic forces of varying frequency and amplitude upon which are occasionally superimposed certain irregular and transient forces of varying importance.

The conjunction of downward trends in a number of important industries may precipitate a general depression of such severity that it will break up for a time the natural periodicity of some industries. The onset of a major war might have the same effect, the result of which would be to start a new succession of surges of increased amplitude. Thus each new disturbance is the progenitor of more to follow.

CORRECTIVE MEASURES

Granting the validity of these thoughts regarding the replacement cycle, what can be done about it? It is not within the scope of this paper to present a treatise on all phases of these economic oscillations. Nevertheless, some reference to corrective treatment is impelled by the nature of the suggestions regarding causation. Corrective measures may be considered as of two types—preventive and remedial. It seems logical to say that neither of these can attain maximum effectiveness until substantial knowledge of the actual causes can be acquired.

When Elmer Sperry studied the application of the gyroscope to the stabilization of ships, he realized the difficulties in the way of counteracting the roll of a ship when it was once fully developed. The energy required is too great. He noticed that the roll of the ship was essentially periodic but was not directly in unison with the pounding of the individual waves. He reasoned that it was the accumulative resultant of a series of wave impacts modified by the design of the ship. From this conception, he concluded that if he could make the apparatus sufficiently

sensitive to detect and counteract the individual wave components before their energy accumulated, the idea might be feasible. The application was developed in this manner.

In the same way, under this conception of economic surges, preventive measures applied to a massive roll of the whole business structure must lack the compensating energy required. On the other hand, the application of counteracting forces properly timed to neutralize the oscillations in the individual industries before they attain real momentum might prove effective. It should be remembered that these surges are initially due to the fact that more of us are buying certain important goods at one time than at another and that this numerical and economic inequality should be adjusted by shifting the buying periods of part of the people. Thus demand should be stabilized by damping the surges of the replacement cycle in their incipient stages. The same type of consideration should be applied to the short-term fluctuations in building construction. This would possibly involve elements of control similar to those applied to production and inventories in manufacturing.

Those industries whose operation and control are more highly centralized may offer a more favorable opportunity for co-ordinated action than those which are highly individualistic. The way might have to be cleared legally for joint action on price and supply so timed as to retard buying at the peaks and accelerate it in the valleys. Such methods, if effective at all, might have to be applied in degree through several cycles before sufficient leveling resulted. It may be suggested that our luxury taxes are usually imposed and removed at just the time to accentuate the surges in the industries to which they apply and that these same industries are among the ones which naturally are subjected to the greatest fluctuations. Stability of tax receipts requires stability in source.

Centralized control of a highly individualized and widely scattered enterprise like building construction is scarcely feasible. Even the smallest of manufacturing plants cannot operate successfully without balancing of inventories, production, and sales. In the tremendous building industry there is nothing to compare with the records and methods so necessary in manufacturing. Decentralized control through a running record of available facilities modified by building permits, completion, occupancy, vacancy, and demolition notices might prove to be of advantage providing necessary control of credit can be maintained. Speaking generally, the more speculative classes of building construction are subject to the widest fluctuation.

Timely control of this speculative credit would be essential.

While any remedial treatment to be undertaken is intimately involved with preventive measures, separate consideration must nevertheless be given to the former. These recurring declines in trade are always featured by serious contraction in prices, volume of trade, employment, and, finally, in enforced liquidation throughout the business structure. If there is a break in demand when demand and output are at abnormally high levels, the increase in inventories will tend to be very rapid. This will very quickly force a break in prices which in turn will accelerate the decline and the vicious movement is under way. Stability of demand is a prerequisite of stability in prices. When prices are at abnormal heights they are increasingly sensitive to changes in demand. Up to a certain point increases in demand at such times are extremely likely to induce further extraordinary growth because such times are eras of high wages and profits. Earnings at high price levels are ordinarily greater than at low levels. This most naturally drives the security markets in the same direction. Thus, the ability supplemented by the desire to buy before another price increase tends to elevate all factors of trade with the resulting periods of inflation so common to these movements. In due time the turn will come, invisible at first but rapidly approaching the stage where all the upward momentum is reversed with disastrous effect.

No real perspective of the price trend and its importance can be gained without reference to the long-term movement of prices which is shown in Fig. 10.

Mechanical analogies will suggest the extreme instability of the towering price structures existing in the three peaks. The cause of the three enormous peaks is obvious from the chart. As against the level in 1926 which is taken as 100 per cent, the average for the 135-year period is 76.9. The long-term trends following the three high peaks are certainly significant. The facts that only 18 years out of 135 were featured by prices at or above 1926 levels and that these were solely induced by war should point to the futility of price stabilization at 1926 levels as a sound means of recovery. Due to the effect of the extraordinary price levels on the average, only 52 years in the period shown were above the average while 83 were below. In 38 years prices have been lower than the average of 1932.

The source of recovery is an increase in demand. An increase in prices would be a powerful stimulus to this end but it seems dangerous to build recovery on a foundation of 1926 prices. How can a sound increase in demand be stimulated? To be

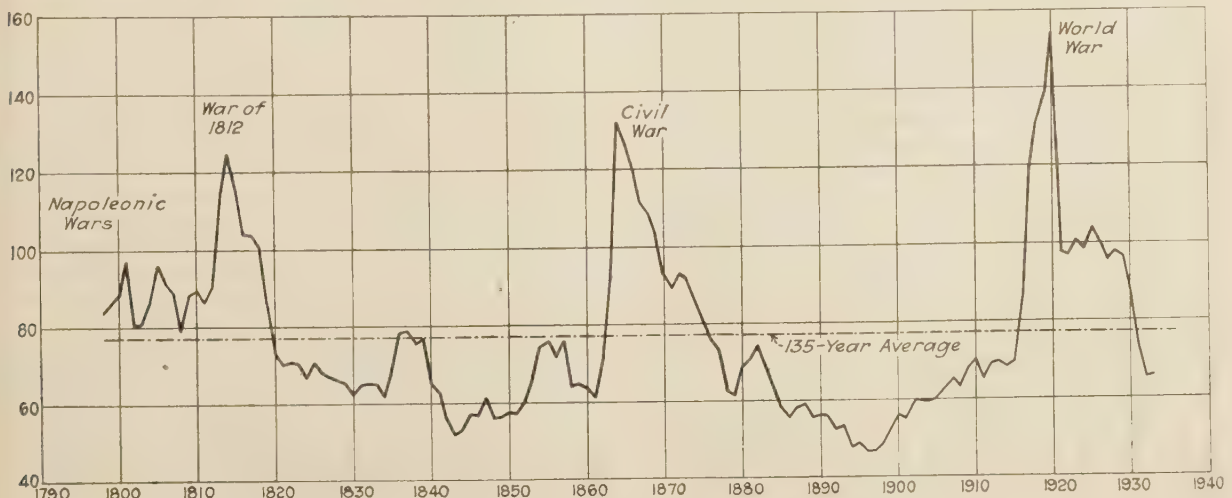


FIG. 10 LONG-TERM PRICE TREND

effective, such effort should be directed toward a revival of those basic industries whose economic momentum has dragged us down. As an engineering conception this thought is sound.

The two pacemaking industries which have had the maximum depressing effect are residential building and automobile activities. The reconstruction energy latent in the deferred demand for automobile replacement is enormous. A similar need in residential building is not so obvious and yet it exists if we grant the validity of our living standards for a generation past. The present period of depressed activity in residential building has been longer and deeper than that which resulted from the World War when a large shortage of housing developed. Nevertheless, the actual net increase in population is greater than it was during this war period. The acute shortage in housing during the former period and the apparent surplus at the present time were influenced by the totally different income conditions in the two periods.

Wages were high during the war period. For nearly two years after the close of the war there was a great revival in trade due to the satisfaction of demand deferred so seriously during the war. These conditions magnified the demand for housing during and immediately following the period of curtailment. During the present contraction of residential construction, income conditions are reversed from those of the war period. The result is that the real need based on families to be housed is obscured by the necessity of "doubling-up" in existing facilities. When the regenerative forces break loose in this industry, activity will develop with rapidity and certainty.

Many conceive the reduction in demand to be due to loss of buying power on the part of the unemployed and that as a corollary, there can be no recovery until the unemployed are put to work. This thought is hopeless from the viewpoint of recovery. The unemployed will not go back to work until the dollar begins to work. In other words, a revival of demand must arise before payrolls will be increased. A critical study of the concurrent inventory, production, and sales trends shown in Fig. 6, especially during the period 1920 to 1922, will illustrate the significance of this statement.

What is the source of increasing demand? The country possesses the buying power necessary for recovery. If this were not true, there would have been no recovery from prior major crises. The difficulty is that this buying power is dormant. The initial source of recovery lies not with the unemployed but with the vast majority who are still at work but who are spending nothing except for bare necessities. In this course they are impelled by fear of the future and of the mysterious nature of these tempests that sweep over us in the midst of plenty. The enormous flow of money from bank deposits into hoarding should convince the most sceptical of the existence of a large amount of latent buying power which is very wide spread. When it is considered that these hoarded funds are but a fraction of such static buying power, the evidence seems overwhelming.

When desire overcomes fear and when necessity of replacement outweighs further deferment, demand will increase and the idle will begin to work. Each increase in healthy demand will beget its own share of increased credit and regenerative reconstruction will be under way. Stimulants applied to this process should be designed to move the idle funds of those who have them (their number and economic power are enormous) and this movement must start the wheels in those industries of maximum effectiveness in promoting recovery.

To increase the public debt, already at dangerous levels, by inducing an increase in spending for public buildings and public works is not to provide a real leverage for recovery. As shown in Table 1, the value of these two classes of construction in a period of abnormally high levels for each is less

than half that of residential construction and would be less than a third if the latter figures could be properly adjusted. One of the keystones of recovery will be the extension of credit for residential building to those who are waiting to build and who can supply their own reasonable share of funds. Such credit is dynamic in results as compared with purely static effect afforded by credit relief. Any retardation of this credit is a block to recovery. There may be a real shortage of homes when there are still visible vacancies.

It must be realized that economic momentum is derived ultimately from demand and that the motivating force behind this demand is supplied by the great mass of the people. The predominant characteristics of this demand will be imparted not by the rich nor yet by the poor but by the great median group representing the common or average man. After all the business graph may be considered as measuring the ebb and flow of human energy. The driving power behind this movement comes from the great intermediate group. The vicious circle must be broken at this point.

Remedial measures, to be effective, must reach this class of people and stimulation must be applied to those predominant industries which serve it and have contributed principally to the decline. Fear that has grown to panic proportions is retarding recovery. There is no more insidious fear than that of the unknown. One of the greatest needs of the times is the determination of real causation. Let the veil of mystery be torn from these crises and much of the unreasoning fear will vanish with it. And yet how little interest is really displayed in actual causation is indicated by the relatively small amount of intensive work upon the subject.

CONCLUSION

This conception of the formation of economic trends explains why we enter periods of recurring expansion and inflation and why the ensuing periods of depression creep upon us almost without accepted warning. Each of the important industries is moving along in what may be described as its natural path when merely by the passage of time, their concurrent movements may come into phase with the result that their mutual interaction stimulates or reduces volume at a rapid rate. The greater the number of industries in phase, the greater is the regenerative influence prevailing among them. The higher the abnormal price level the lower is the stability of the structure.

The higher the amount of credit outstanding, the more sensitive is the situation to any decline in demand. High demand at high price levels multiplies debt. Orderly satisfaction of this debt demands a continuance of trade at levels not materially lower than those at which the debt was contracted. Any decline in demand accelerates the liquidation of this debt with disastrous consequences in a falling market. It is the initial decline in demand which precipitates the downward trend. The high debt level and strained credit conditions lower the resistance of the business system to the inroads of the germ in the disguise of the replacement cycle. This same cycle in its upward trend induces the stimulation that leads to the inflated condition. Thus the changes in credit are initially effects which are almost instantly transformed into causes far more potent than those of primary origin.

The origin of demand preceded that of credit. Credit originated as the result of demand and is the device used to bridge the gap between purchase and payment which are out of phase. This sequence in relationship has not changed. The replacement cycle is possible under conditions of pure barter, but its potential power is drastically increased as the volume of outstanding credit is enlarged.

Whether or not the theory of the replacement cycle as set.

forth in this study is ultimately proved or disproved, the facts covering the importance of the industries analyzed can scarcely be refuted and the differing fluctuations described are written into the very history of these industries. The close fidelity with which the weighted total of these components matches the trend of aggregate business cannot be seriously denied. The point, that explanation of the individualistic behavior of these industries will provide the reason for the ultimate trend of composite industry, is scientifically sound. This question then comes to mind: *If the replacement cycle does not furnish the proper explanation of the differing oscillations of these industries, what is the explanation?* The answer to this question is of tremendous economic importance. Some one should go to work upon it. This conception of underlying causes should carry an appeal to those whose training and experience have made them familiar with the real significance of harmonic and inharmonic forces.

The composite trend manifested by the four consumer industries bears very significant relationship to the movement of interest rates which is a barometer of credit conditions. It accords closely with the fluctuations in rate of deposit in savings

banks. It bears a striking similarity to the changing trends in individual bank debits when allowance is made for the growth of speculative activity beginning about 1925. Its variations are in close timing with those of car-loadings throughout the period.

These thoughts are not offered as the result of finished work. On the contrary, the field to be surveyed has scarcely been entered. The possibilities of further exploration are enormous. It does seem that the work done and conclusions derived are sufficiently logical to warrant earnest thought upon the points raised. If and when it can be found that these economic catastrophies are not the effect of mismanagement by any one group of society, but are rather the integrated results of the thoroughly natural actions of the great mass of consumers, a forward step toward solution will have been taken. With due consideration of all the technical factors involved in this study, one seems to be drawn to the conclusion again and again that the devastating peace-time catastrophies which we call economic depressions may be, after all, the repercussions of the deadly conflicts of the past.

Elements of Milling, Part 2

BY O. W. BOSTON¹ AND C. E. KRAUS,² ANN ARBOR, MICH.

The results are given of a series of experiments in which a single-point tool corresponding to a single tooth of a milling cutter was used in removing metal in a dynamometer of a pendulum type. The values of energy as a function of variable feed, depth, width, and front- and side-rake angles of the cutter were determined when cutting three steels and a brass, in both groove and land cutting. It is found that all data obtained follow the general equation for energy in which $E = Cwf^2d^2$. It is shown that invariably groove cutting requires greater energy than land cutting. It also is shown that greater values of front rake on the cutter reduce the energy required to remove a chip, while the value of side rake for a given value of front rake exerts no appreciable influence on energy values. The results of some 24,000 commercial tests made by students at the Ohio State University in cooperation with the Cincinnati Milling Machine Company are presented and analyzed. The results are shown to agree substantially with those obtained with the single-point tool and that the foregoing energy equation holds for all types of milling, such as slabbing, groove cutting, half-side milling, and facing.

THE object of this paper is to extend the tests reported on in the previous paper, "Elements of Milling,"³ presented before the Society in December, 1931.

In that paper, the variables studied, as they affect energy, were feed per tooth, depth of cut, width of cut, cutting up versus cutting down, and cutting fluids. Those tests were run on a number of ferrous and non-ferrous metals, including Bakelite and wood fiber. All cuts were made to form a groove in the work. The tool shape was constant, being end-cutting and having a 15-deg rake with no side rake.

This paper contains the results of experiments with cutters having variable back-rake angles, or hook, and side-rake angles,

¹ Professor, College of Engineering, University of Michigan. Mem. A.S.M.E. O. W. Boston was graduated from the University of Michigan, Engineering College, in 1913, received a master's degree in 1917, and the degree of mechanical engineer in 1926. After graduation he was engaged at the university as instructor in engineering mechanics and mechanical engineering for four years. In October, 1917, he was commissioned in the U. S. Navy and assigned to duty in the Bureau of Ordnance on design and manufacture of submarine mines used in the North Sea Blockade. From 1919 to 1921 he was engaged in industrial engineering work for the Cleveland Tractor Co., in Cleveland, as assistant to the vice-president and works manager. In the fall of 1921, he returned to the University of Michigan, where he is now professor of shop practice and director of the department of engineering shop. He is author of many papers dealing with the subject of metal cutting and is serving on several committees dealing with cutting fluids, and standardization and nomenclature of small tools and machine-tool elements.

² Assistant to Professor Boston, University of Michigan. Jun. A.S.M.E. Mr. Kraus received his bachelor of science degree in mechanical engineering from the University of Michigan in June, 1932. He is now continuing work on his master's degree at the University, and is an instructor in the department of engineering shop.

³ Trans. A.S.M.E., vol. 54, 1932, paper No. RP-54-4.

Contributed by the Special Research Committee on the Cutting of Metals and presented at the Semi-Annual Meeting, Chicago, Ill., June 26 to July 1, 1933, of THE AMERICAN SOCIETY OF MECHANICAL ENGINEERS.

NOTE: Statements and opinions advanced in papers are to be understood as individual expressions of their authors, and not those of the Society.

or helix. Tests with each cutter were made when cutting in a groove and when cutting the top from a land which had been prepared previously. Several types of metals were included, all cutting being done with one cutting fluid—namely, an emulsion consisting of 1 part soluble oil to 50 parts water, No. 3.

Power data also are presented from a series of experiments on steel and cast iron, in which various types of commercial milling cutters were used as obtained by cooperative research by students at Ohio State University for the Cincinnati Milling Machine Company. The results have been recomputed to a basis similar to that used by the authors, for the purpose of direct comparison.

CUTTERS AND EQUIPMENT

The machine used in these tests was the same as used and described previously in "Elements of Milling." This machine is of the pendulum type, such as an impact testing machine, and uses a single-tooth cutter. The cutters in all cases were adjusted to have a radius of 1.75 in., and all had end- and side-clearance angles of 4 deg. Nine series of cutters were used, divided into two groups. The first group, consisting of five cutters with 0-deg helix angles and with rake angles of 0, 10, 15, 20, and 25 deg, were designed to study the influence of variable rake. The second group had rake angles of 15 deg and helix angles of 10, 20, 30, and 40 deg, which, together with a 0-deg helix cutter having 15-deg rake angle, were used to study the influence of variable helix angles.

High-speed-steel blades $\frac{3}{8}$ in. wide by $\frac{3}{4}$ in. deep were used. They first were ground all over on a surface grinder, after which the various cutting angles were accurately ground on the same machine. All cutters were 0.300 in. wide. As this width decreased slightly from subsequent grindings, the data were corrected for original width on the assumption that the energy varies directly as the width. This assumption had been proved previously.

MATERIALS AND CUTTING FLUIDS USED

The first material tested was a free-cutting leaded brass and was selected because it was believed that more accurate data could be obtained using a metal which would not cause rapid dulling of the cutter. Three other steels then were tested: S.A.E. 1020, S.A.E. 1112, and S.A.E. 3250. These metals have been described previously and are listed in Table 1, together with their chemical compositions, heat treatments, and hardness values.

The cutting fluid used consisted of 1 part soluble oil in 50 parts water, and is listed and described as cutting fluid No. 3 in the previous paper.

EXPERIMENTAL METHOD AND SCOPE OF TEST

As in the previous paper, all cuts were made with work locked in position as the chip was removed. Tests in all cases were made both cutting up (that is, with the work fed against the cutter) and cutting down (that is, with the work fed with the cutter). All of the cuts were taken both in a groove and on a land to determine the relation between the two types of cuts.

Each test value indicated is the average of from 10 to 30 cuts, and the data presented represent a total of some 6000 or 7000 cuts. Great care was taken to keep the cutter in the sharp condition. By sharp is meant the edge produced by the surface grinder with the final slight burr removed by a hand hone.

TABLE 1 MATERIALS USED IN THE MILLING TESTS

Bar number	Material	Chemical analysis	Heat treatment	Hardness		
				Brinell	Rockwell B	Sclero-scope
BF	Leaded screw-stock brass	62% Cu, 34% Zn, 3% Pb	Extruded and cold-drawn	70	66.0	..
EF	S.A.E. 1020 steel	0.22 C, 0.52 Mn, 0.011 P, 0.026 Si	Annealed	131	65.0	..
MF	S.A.E. 1112 steel	0.09-0.13 C, 0.7-0.9 Mn, 0.08-0.40 P, 0.085-0.12 S	Cold-drawn	217	89.5	..
A-7	S.A.E. 3250 steel	Commercial	Normalize 1650 F, anneal 1475 F	207	92.5	30

TABLE 2

(Energy values in foot-pounds per chip when milling a free-cutting brass, bar BF, up and down, in a groove, and on a land for various combinations of feed and depth of cut with several different shaped cutters. The width of each cutter was 0.300 in., and an emulsion consisting of 1 part soluble oil to 50 parts water was used as a cutting fluid)

Tool angles	Feed in inches	Depth in inches	Cutting in groove		Cutting on land	
			Up	Down	Up	Down
0-deg helix, 0-deg rake	0.020	0.010	0.74	0.68	0.74	0.70
		0.025	1.76	1.68	1.66	1.57
		0.050	3.48	3.23	3.10	2.88
	0.100	0.010	6.80	6.29	5.81	5.62
		0.030	4.08	3.73	3.55	3.23
		0.040	9.69	9.11	8.18	7.83
0-deg helix, 10-deg rake	0.020	0.010	11.99	11.38	9.88	9.57
		0.025	0.66	0.59	0.57	0.50
		0.050	1.62	1.39	1.40	1.26
	0.100	0.025	3.14	2.73	2.80	2.50
		0.100	6.12	5.54	5.52	5.02
		0.040	3.45	3.12	3.14	2.84
0-deg helix, 20-deg rake	0.020	0.010	8.87	3.97	7.60	7.15
		0.030	11.53	10.29	9.88	9.14
		0.040	0.68	0.62	0.57	0.52
	0.100	0.025	1.55	1.43	1.32	1.19
		0.050	2.88	2.62	2.50	2.25
		0.100	5.32	4.97	4.73	4.27
0-deg helix, 25-deg rake	0.020	0.010	3.03	2.75	2.77	2.47
		0.030	7.50	6.95	6.59	5.97
		0.040	9.81	8.90	8.66	7.66
	0.100	0.010	0.66	0.60	0.65	0.53
		0.025	1.47	1.34	1.42	1.31
		0.050	2.78	2.47	2.52	2.24
0-deg helix, 15-deg rake	0.020	0.010	5.11	4.76	4.64	4.22
		0.030	2.95	2.65	2.74	2.46
		0.040	7.22	6.72	6.43	5.78
	0.100	0.010	9.31	8.61	8.26	7.36
		0.025	0.64	0.56	0.60	0.53
		0.050	1.56	1.33	1.38	1.24
10-deg helix, 15-deg rake	0.020	0.010	3.03	2.64	2.63	2.33
		0.030	5.88	5.04	4.94	4.50
		0.040	3.20	2.76	2.83	2.56
	0.100	0.010	8.27	7.18	7.00	6.30
		0.030	10.41	9.15	8.85	8.10
		0.040	0.80	0.56	0.67	0.61
20-deg helix, 15-deg rake	0.020	0.010	1.69	1.50	1.55	1.46
		0.025	3.20	2.85	3.14	2.87
		0.050	6.26	5.53	6.03	5.57
	0.100	0.010	3.55	3.08	3.48	3.25
		0.030	8.88	7.82	8.58	7.76
		0.040	11.40	10.00	11.13	9.94
30-deg helix, 15-deg rake	0.020	0.010	0.74	0.65	0.73	0.65
		0.025	1.72	1.54	1.66	1.48
		0.050	3.33	2.92	3.24	2.81
	0.100	0.010	6.20	5.51	5.93	5.35
		0.030	3.44	3.06	3.41	3.07
		0.040	8.85	7.85	8.30	7.65
40-deg helix, 15-deg rake	0.020	0.010	11.10	10.01	10.90	9.85
		0.025	0.72	0.61	0.69	0.62
		0.050	1.73	1.51	1.56	1.49
	0.100	0.010	3.45	2.96	3.15	2.74
		0.030	6.85	5.90	5.70	5.18
		0.040	3.90	3.41	3.23	2.95

The values presented, therefore, are somewhat lower than could be expected from the average cutter condition. The authors have found that consistent results can be obtained in no other way, as the degree of cutter wear is almost impossible to measure and has such a decided effect upon the energy values when milling.

RESULTS OF TESTS

The experimental data for the four metals tested are presented separately below.

Tests on Free-Cutting Brass (Bar BF). The experimental data for the leaded free-cutting brass are listed in Table 2. Similar tables have been made up for each of the other materials, but

are not shown. As in the first paper, these values are plotted on log-log paper to determine the milling-energy formulas for each tool and method of cut.

Lines have been drawn through the energy data plotted on log-log paper in Fig. 1. One set of lines is for constant feed by variable depth, while the other set is for constant depth but variable feed. Lines also are shown for milling up and milling down on a land in each case. From these lines, an equation for energy in foot-pounds per chip, as a function of the depth of cut and feed, is determined. The tangent of the angle between the line and the horizontal represents the exponent of the variable involved.

Formulas for a variety of shapes of tools and methods of cutting are listed for brass in Table 3, together with the values of

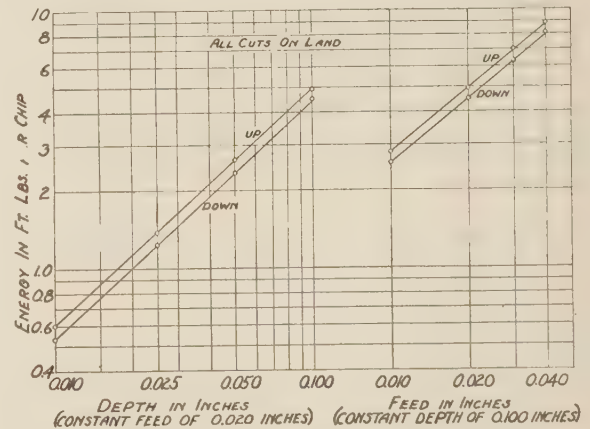


FIG. 1 ENERGY REQUIRED TO MILL A FREE-CUTTING BRASS USING A SOLUBLE OIL CONSISTING OF 1 PART OIL TO 50 PARTS WATER

(One series of cuts was made with a constant feed of 0.020 in. as the depth was varied, while the second was made with a constant depth of 0.100 in., while the feed was varied. The cutter was of an end-cutting type having a 15-deg rake angle and no helix. The following formula was obtained: $E = C_{up} F^{0.32} D^{0.84}$ in which $C_{(up\ milling)} = 3750$, and $C_{(down\ milling)} = 3392$.)

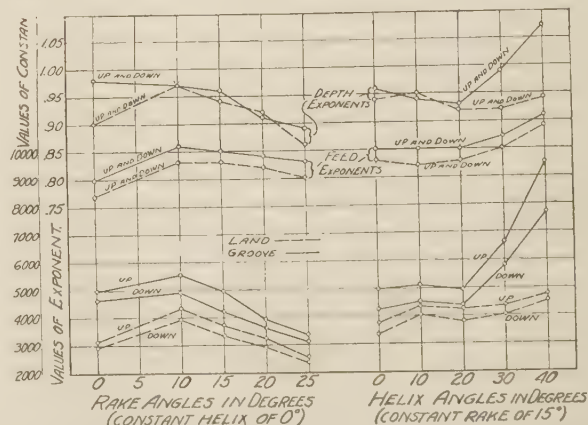


FIG. 2 EFFECT OF VARIOUS RAKE AND HELIX ANGLES OF THE CUTTER ON THE EXPONENTS OF FEED AND DEPTH AND THE CONSTANT OF THE MILLING-ENERGY EQUATION WHEN MILLING FREE-CUTTING BRASS, BAR BF

(Data taken from Table 3.)

TABLE 3 RESULTS OF TESTS WHEN MILLING FREE-CUTTING BRASS

(An emulsion of 1 part soluble oil to 50 parts water, cutting fluid No. 3, was used. The width of the cutter was 0.300 in.)

Helix angle, deg	Tool angles, deg	Method of cutting	Formulas, energy E , in foot-pounds per chip		Values of C		Horsepower per cu. in. per min formulas		Horsepower per cu. ^a in. per min	
			Groove	Land	Groove	Land	Groove	Land	Groove	Land
0	0	{ Up Down	$Cwf^{0.8}d^{0.98}$	$Cwf^{0.77}d^{0.9}$	4970 4670	3124 2984	C C	C C	0.3960 0.3750	0.3442 0.3285
0	10	{ Up Down	$Cwf^{0.88}d^{0.97}$	$Cwf^{0.83}d^{0.97}$	5575 4905	4360 3942	C C	C C	0.3452 0.3040	0.3100 0.2800
0	15	{ Up Down	$Cwf^{0.86}d^{0.98}$	$Cwf^{0.82}d^{0.94}$	4975 4260	3750 3392	C C	C C	0.3290 0.2820	0.2855 0.2580
0	20	{ Up Down	$Cwf^{0.84}d^{0.91}$	$Cwf^{0.82}d^{0.92}$	3905 3630	3240 2925	C C	C C	0.3040 0.2825	0.2700 0.2440
0	25	{ Up Down	$Cwf^{0.83}d^{0.88}$	$Cwf^{0.80}d^{0.86}$	3380 3115	2580 2365	C C	C C	0.2888 0.2660	0.2713 0.2484
10	15	{ Up Down	$Cwf^{0.83}d^{0.94}$	$Cwf^{0.82}d^{0.93}$	5120 4540	4340 4090	C C	C C	0.3465 0.3078	0.3380 0.3182
20	15	{ Up Down	$Cwf^{0.82}d^{0.93}$	$Cwf^{0.82}d^{0.92}$	4915 4385	4240 3800	C C	C C	0.3490 0.3110	0.3380 0.3030
30	15	{ Up Down	$Cwf^{0.87}d^{0.99}$	$Cwf^{0.85}d^{0.92}$	6690 5800	4355 4060	C C	C C	0.3775 0.3275	0.3162 0.2950
40	15	{ Up Down	$Cwf^{0.81}d^{1.07}$	$Cwf^{0.89}d^{0.94}$	9540 8720	4785 4515	$Cd^{0.07}$ C	C C	0.3722 0.3400	0.2760 0.2609

^a 0.010 in. feed, 0.100 in. depth, and 0.300 in. width.

the constants, the formulas for horsepower per cubic inch of metal removed per minute, and the computed horsepower per cubic inch per minute value for a specific cut 0.100 in. deep, 0.010 in. feed per tooth, and 0.300 in. wide. The last values are included in the table in order to furnish a basis of comparison between the different conditions. It is impossible directly to compare constants or exponents from the equations with energy and horsepower values computed therefrom, because of the several variables involved in the formulas.

It will be noticed from Table 3 that no difference in the formula was found for up and down milling with a single cutter, except in the value of the constant. Changing the tool angles, however, does change the exponents of the feed and depth of cut.

Better to indicate the effect of different angles on the exponents and constants, Fig. 2 has been prepared. In the upper left part of Fig. 2 are shown the depth and feed exponents for both up and down milling for variable rake angles with a constant helix angle of 0 deg. The effect on these exponents when the helix angle is varied is shown on the right, the front rake angle being constant at 15 deg. In the lower portion of Fig. 2 are shown plotted the constants obtained to show the effect of varying the angles.

A study of these curves indicates several interesting characteristics. Except for a few values, all exponents and constants are lower for land cutting than for groove cutting. This, of course, would be expected of the constants, inasmuch as in groove cutting it is necessary to free the chip along the sides of the groove as well as on the bottom. Also, in general the difference is greater for the larger helix angles, due probably to friction on the side of the cut because of the end thrust or drag. The general tendency of the exponents is to drop with increasing rake angles above 10 to 12 deg, and to rise with increasing helix angles above 20 deg. This effect is more noticeable with the depth exponents than with the feed exponents, but is not great in any case, except for the 30- and 40-deg helix angle with groove cuts which, undoubtedly, is caused by side friction. The same effect also is noticed in the values of the constants.

To compare the actual energy and horsepower values as affected by a change in rake and helix angles for the various cuts, Fig. 3 is shown. The difference between up and down milling is very noticeable. Increasing the rake angle is found to decrease energy values, first rapidly up to about 20 deg, and then more slowly. This probably would continue to an optimum angle, such as that formed by the built-up edge on the tool. It probably would be less pronounced for longer chips where the built-up edge would be more effective. The effect of a helix angle for this material appears to be quite favorable, but is consistently upward for groove cutting.

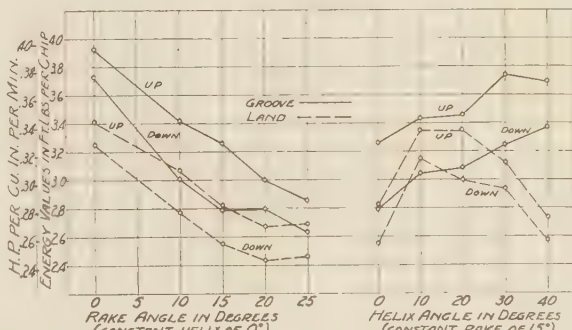


FIG. 3 EFFECT OF VARIOUS RAKE AND HELIX ANGLES OF THE CUTTER ON THE POWER AND ENERGY VALUES WHEN MILLING FREE-CUTTING BRASS

(Cuts were taken up and down both in a groove and on a land as indicated. Data taken from Tables 2 and 3.)

Tests on S.A.E. 1020 Steel (Bar EF). The complete series of tests as presented for the free-cutting brass were duplicated on the S.A.E. 1020 steel. Table 4 summarizes the formulas and the values in horsepower per cubic inch per minute. It is apparent that for most cuts in steel, a different formula is found for up and down cutting. This differs from the results of the tests on brass.

Again, to compare exponents and constants as a function of tool angles, Fig. 4 has been prepared. This figure is for steel, as Fig. 2 is for brass. The effect on the exponents of variable rake angles appears slight, but greater, with a less definite tendency indicated, when the helix angle is varied. The depth exponent appears to drop off with the greatest rake angle. The constant varies over a wide range as the rake angle is changed, being reduced considerably as the rake angle is increased from 0 to 25 deg. The constant of the equation appears to be little influenced by the value of helix angle up to and including 30 deg, but increases sharply for groove cutting when the helix angle is 40 deg. Again, it should be pointed out that a direct comparison of either the exponents or constants with rake angles cannot be made, inasmuch as both the exponents and constants of the equations vary.

The net effect on energy values in foot-pounds per chip and on the values of horsepower per cubic inch of metal removed per minute is shown for variable rake angles and variable helix angles in Fig. 5. The energy values for the 0-deg rake tool are more than 100 per cent greater than those for the 25-deg rake tool. The effect of the helix angle, however, appears to be negligible, except as affected by side friction in groove cutting.

TABLE 4 RESULTS OF TESTS WHEN MILLING S.A.E. 1020 STEEL, BAR EF
(An emulsion of 1 part soluble oil to 50 parts water, cutting fluid No. 3, was used. The width of the cutter was 0.300 in.)

Tool angles, deg	Helix	Rake	Method of cutting	Formulas, energy E , in foot-pounds per chip		Values of C		Horsepower per cu. in. per min formulas		Horsepower per cu. in. per min	
				Groove	Land	Groove	Land	Groove	Land	Groove	Land
0	0	{	Up	$C_{up} f^{0.77} d^{0.57}$	$C_{lf} f^{0.66} d^{0.91}$	15000	9040	$33000 f^{0.22} d^{0.13}$	C	1.77	1.678
			Down	$C_{lf} f^{0.70} d^{0.92}$		17080	8680	C	$33000 f^{0.22} d^{0.09}$	1.638	1.617
0	10	{	Up	$C_{up} f^{0.76} d^{0.92}$	$C_{lf} f^{0.70} d^{0.89}$	10860	7300	$33000 f^{0.21} d^{0.08}$	C	1.253	1.132
			Down	$C_{lf} f^{0.70} d^{0.93}$	8670	7350	C	$33000 f^{0.20} d^{0.11}$	1.000	1.041
0	15	{	Up	$C_{up} f^{0.74} d^{0.89}$	$C_{lf} f^{0.71} d^{0.88}$	8250	6340	$33000 f^{0.20} d^{0.11}$	C	1.070	0.940
			Down	$C_{lf} f^{0.74} d^{0.91}$	$C_{lf} f^{0.71} d^{0.91}$	7250	5340	$33000 f^{0.20} d^{0.09}$	C	0.898	0.757
0	20	{	Up	$C_{up} f^{0.74} d^{0.91}$	$C_{lf} f^{0.71} d^{0.92}$	7380	5600	$33000 f^{0.20} d^{0.08}$	C	0.910	0.778
			Down			7280	4870	$33000 f^{0.20} d^{0.08}$	C	0.798	0.677
0	25	{	Up	$C_{up} f^{0.76} d^{0.87}$	$C_{lf} f^{0.71} d^{0.88}$	6450	4570	$33000 f^{0.24} d^{0.13}$	C	0.798	0.727
			Down			5450	4130	$33000 f^{0.24} d^{0.13}$	C	0.677	0.657
10	15	{	Up	$C_{up} f^{0.78} d^{0.90}$	$C_{lf} f^{0.74} d^{0.93}$	10360	8330	$33000 f^{0.22} d^{0.10}$	C	1.091	0.990
			Down	$C_{lf} f^{0.79} d^{0.96}$		10490	7060	$33000 f^{0.21} d^{0.06}$	0.940	0.838
20	15	{	Up	$C_{up} f^{0.76} d^{0.87}$	$C_{lf} f^{0.72} d^{0.93}$	9770	5750	$33000 f^{0.24} d^{0.13}$	C	1.201	0.940
			Down	$C_{lf} f^{0.76} d^{0.96}$	$C_{lf} f^{0.73} d^{0.94}$	10000	6430	$33000 f^{0.24} d^{0.06}$	C	1.030	0.778
30	15	{	Up	$C_{up} f^{0.70} d^{0.87}$	$C_{lf} f^{0.67} d^{0.84}$	7520	4970	$33000 f^{0.20} d^{0.13}$	C	1.233	1.000
			Down	$C_{lf} f^{0.72} d^{0.98}$	$C_{lf} f^{0.69} d^{0.98}$	10310	4350	$33000 f^{0.25} d^{0.02}$	C	1.192	0.758
40	15	{	Up	$C_{up} f^{0.79} d^{1.04}$	$C_{lf} f^{0.69} d^{0.85}$	20200	5270	$33000 f^{0.21}$	C	1.465	0.940
			Down	$C_{lf} f^{0.79} d^{1.07}$	$C_{lf} f^{0.69} d^{0.91}$	19900	5450	$C_{d0.04}$	C	1.344	0.849

^a 0.010 in. feed, 0.100 in. depth, 0.300 in. width.

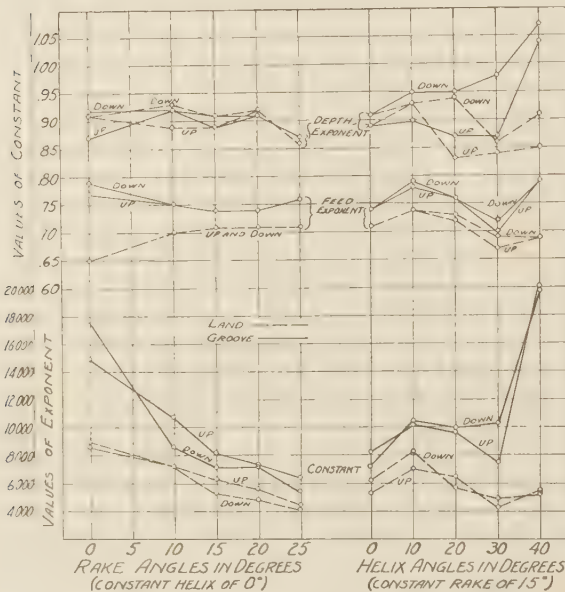


FIG. 4 EFFECT OF VARIOUS RAKE AND HELIX ANGLES ON THE EXPONENTS OF FEED AND DEPTH AND THE CONSTANT IN THE MILLING-ENERGY EQUATION WHEN MILLING S.A.E. 1020 STEEL, BAR EF (Milling cuts were made up and down on a land and in a groove as indicated. Data taken from Table 4.)

Tests on S.A.E. 1112 Steel (Bar MF). The results of the milling tests on this steel are summarized in Table 5, in which are given the formulas obtained, the constants for the formulas, and the horsepower per cubic inch cut per minute for a specific cut for both groove and land cutting, as well as for up and down cutting. Fig. 6, similar to Figs. 2 and 4, shows the exponents and constants for the free-cutting steel as a function of the tool angles. It is seen that the values of the constants are reduced appreciably with an increase in rake angle up to 10 deg, but only

slightly for greater values of rake angle. There does not appear to be a great difference in general characteristics between the curves for land and groove cutting. When the constants are plotted over the helix angles, however, there is shown to be a general and gradual increase in value, although a minimum value is reached in nearly all cases for the helix angle of 10 deg. The values of the depth exponent appear to be little affected by an increase in rake angle until an angle of 20 to 25 deg is reached, when there is a slight falling off in the curves. The feed exponent, on the other hand, seems to increase rather generally for rake angles above 10 deg. The depth exponent appears to be influenced but slightly for helix angles up to and including 30 deg, while the feed exponent seems to be increased uniformly for angles above 10 deg, for which minimum values occur.

A comparison of energy values in foot-pounds per chip and horsepower per cubic inch of metal removed per minute, as indicated, are expressed as a function of the variable rake angle and

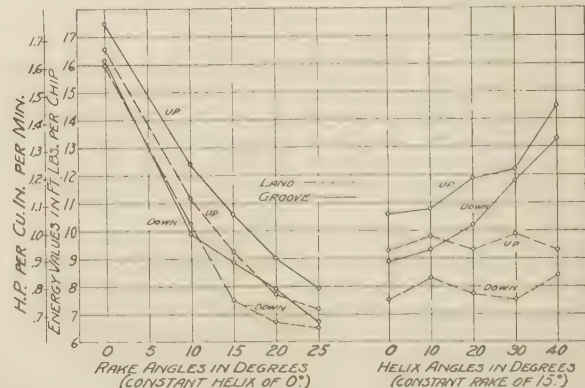


FIG. 5 EFFECT OF VARIOUS RAKE AND HELIX ANGLES OF THE CUTTER ON THE POWER AND ENERGY VALUES WHEN MILLING S.A.E. 1020 STEEL, BAR EF (Cuts were taken up and down both in a groove and on a land as indicated. Data taken from Table 4.)

TABLE 5 RESULTS OF TESTS WHEN MILLING S.A.E. 1112 STEEL, BAR MF
(An emulsion of 1 part soluble oil to 50 parts water, cutting fluid No. 3, was used. The width of the cutter was 0.300 in.)

Tool angles, deg	Helix	Rake	Method of cutting	Formulas, energy E , in foot-pounds per chip		Values of constant		Horsepower per cu in. per min, formulas		Hp per cu in. per min Groove	Hp per cu in. per min Land
				Groove	Land	Groove	Land	Groove	Land		
-0	0	0	Up	$C_{wf} f^{0.74} d^{0.80}$	$C_{lf} f^{0.73} d^{0.86}$	10180	8350	C	$33000 f^{0.27} d^{0.14}$	1.293	1.212
			Down	$C_{wf} f^{0.74} d^{0.80}$	$C_{lf} f^{0.69} d^{0.86}$	8440	5670	$33000 f^{0.26} d^{0.10}$	C	1.071	0.99
0	10	10	Up	$C_{wf} f^{0.71} d^{0.88}$	$C_{lf} f^{0.70} d^{0.90}$	6360	6050	C	$33000 f^{0.30} d^{0.10}$	0.959	0.93
			Down	$C_{wf} f^{0.71} d^{0.88}$	$C_{lf} f^{0.69} d^{0.83}$	5270	4440	$33000 f^{0.29} d^{0.12}$	C	0.798	0.778
0	15	15	Up	$C_{wf} f^{0.77} d^{0.86}$	$C_{lf} f^{0.74} d^{0.90}$	7550	6560	C	$33000 f^{0.24} d^{0.10}$	0.930	0.848
			Down	$C_{wf} f^{0.76} d^{0.86}$	$C_{lf} f^{0.71} d^{0.86}$	5710	4570	$33000 f^{0.26} d^{0.15}$	C	0.768	0.725
0	20	20	Up	$C_{wf} f^{0.79} d^{0.83}$	$C_{lf} f^{0.74} d^{0.87}$	6450	4920	C	$33000 f^{0.23} d^{0.11}$	0.755	0.73
			Down	$C_{wf} f^{0.76} d^{0.86}$	$C_{lf} f^{0.69} d^{0.87}$	5360	3910	$33000 f^{0.24} d^{0.14}$	C	0.677	0.664
0	25	25	Up	$C_{wf} f^{0.80} d^{0.82}$	$C_{lf} f^{0.76} d^{0.84}$	6250	5080	C	$33000 f^{0.26} d^{0.16}$	0.718	0.705
			Down	$C_{wf} f^{0.80} d^{0.82}$	$C_{lf} f^{0.70} d^{0.84}$	5710	3710	$33000 f^{0.20} d^{0.18}$	C	0.657	0.643
10	15	15	Up	$C_{wf} f^{0.74} d^{0.86}$	$C_{lf} f^{0.72} d^{0.82}$	6340	4960	C	$33000 f^{0.26} d^{0.16}$	0.899	0.828
			Down	$C_{wf} f^{0.76} d^{0.86}$	$C_{lf} f^{0.69} d^{0.82}$	5940	3810	$33000 f^{0.24} d^{0.16}$	C	0.768	0.726
20	15	15	Up	$C_{wf} f^{0.81} d^{0.86}$	$C_{lf} f^{0.74} d^{0.90}$	9100	7740	$33000 f^{0.19} d^{0.14}$	C	0.910	0.815
			Down	$C_{lf} f^{0.70} d^{0.86}$	8180	4370	$33000 f^{0.20} d^{0.16}$	0.819	0.74
30	15	15	Up	$C_{wf} f^{0.76} d^{0.87}$	$C_{lf} f^{0.76} d^{0.82}$	8800	6470	C	$33000 f^{0.24} d^{0.17}$	0.960	0.877
			Down	$C_{wf} f^{0.76} d^{0.87}$	$C_{lf} f^{0.73} d^{0.82}$	7770	4930	$33000 f^{0.21} d^{0.18}$	C	0.839	0.77
40	15	15	Up	$C_{wf} f^{0.82} d^{0.86}$	$C_{lf} f^{0.76} d^{0.88}$	12780	7170	C	$33000 f^{0.24} d^{0.12}$	1.051	0.87
			Down	$C_{wf} f^{0.82} d^{0.86}$	$C_{lf} f^{0.76} d^{0.88}$	12100	6520	$33000 f^{0.18} d^{0.06}$	C	0.940	0.788

variable helix angle in Fig. 7 for both groove and land cutting. The curves for groove cutting are higher than the corresponding curves for land cutting. Also, the curves for down cutting are uniformly lower than those for up cutting. The energy or power values are seen to be maximum for 0-deg rake angle, and to fall off uniformly, as the rake angle is increased, to almost a minimum for a rake angle of 25 deg. It appears that for greater values of rake angle there would be no further appreciable reduction in energy values. The energy values as a function of the helix angle are shown to be practically constant when cutting on the land, indicating that the helix angle does not lead to efficiency from a power point of view. When cutting in a groove, the energy values for both up and down cutting increase for

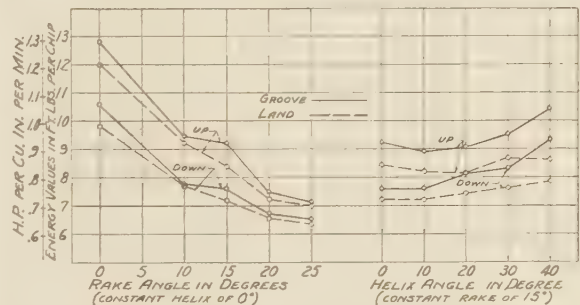


FIG. 7 EFFECT OF VARIOUS RAKE AND HELIX ANGLES OF THE CUTTER ON THE POWER AND ENERGY VALUES WHEN MILLING S.A.E. 1112 STEEL, BAR MF

(Cuts were taken up and down both in a groove and on a land as indicated. Data taken from Table 5.)

values of helix angle above 20 deg, due undoubtedly to the drag of the chip on one side of the groove.

Tests on S.A.E. 3250 Steel (Bar A-7). The results of the experiments in milling S.A.E. 3250 steel are shown in Table 6, in which are given the formulas for energy per chip, the values of the constants for the energy equation, and formulas for horsepower per cubic inch per minute, together with specific values of horsepower per cubic inch of metal removed per minute when milling up and down in a groove and on a land. An analysis of the constants and exponents of the formulas as influenced by variable rake or variable helix angles is shown in Fig. 8.

The depth exponent appears to be nearly constant over a wide range of rake angles and also over a wide range of helix angles. For the largest rake and helix angles, however, the exponent for groove milling is high. The feed exponent seems to fall off uniformly and appreciably as the rake angle is increased, but remains practically constant over the whole range of helix angles used. This holds for both up and down milling on a land or in a groove. The constants of the formula fall off quite uniformly

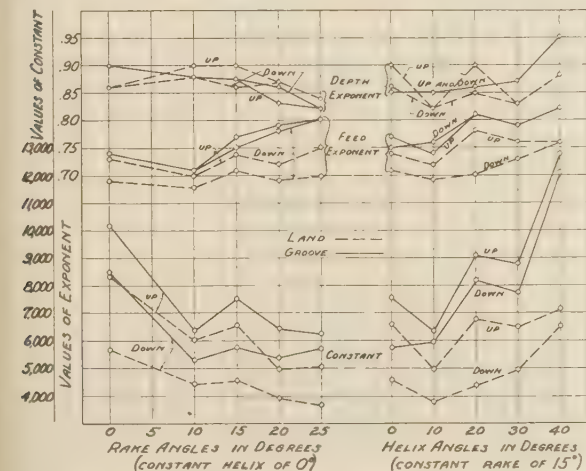


FIG. 6 EFFECT OF VARIOUS RAKE AND HELIX ANGLES ON THE EXPONENTS OF DEPTH AND FEED AND THE CONSTANT IN THE MILLING-ENERGY EQUATION WHEN MILLING S.A.E. 1112 STEEL, BAR MF (Cuts were made up and down on a land and in a groove as indicated. Data taken from Table 5.)

TABLE 6 RESULTS OF TESTS WHEN MILLING S.A.E. 3250 STEEL, BAR A-7

(An emulsion of 1 part soluble oil to 50 parts water, cutting fluid No. 3, was used. The width of the cutter was 0.300 in.)

Tool angles, deg	Helix	Rake	Method of cutting	Formulas, energy E , in foot-pounds per chip		Values of constant		Horsepower per cu. in. per min, formulas		Horsepower per cu. in. per min	
				Groove	Land	Groove	Land	Groove	Land	Groove	Land
0	0		Up	$C_{10}f^{0.77}d^{0.87}$	$C_{10}f^{0.85}d^{0.86}$	11400	13360	$\frac{33000}{C}f^{0.25}d^{0.13}$	$\frac{33000}{C}f^{0.18}d^{0.15}$	1.343	1.313
			Down	$C_{10}f^{0.77}d^{0.96}$	$C_{10}f^{0.84}d^{0.86}$	14880	13630	$\frac{33000}{C}f^{0.25}d^{0.06}$	$\frac{33000}{C}f^{0.18}d^{0.16}$	1.455	1.212
0	10		Up	$C_{10}f^{0.76}d^{0.91}$	$C_{10}f^{0.78}d^{0.90}$	10750	10500	$\frac{33000}{C}f^{0.26}d^{0.09}$	$\frac{33000}{C}f^{0.22}d^{0.10}$	1.263	1.11
			Down	$C_{10}f^{0.74}d^{0.92}$	$C_{10}f^{0.76}d^{0.88}$	9720	8860	$\frac{33000}{C}f^{0.26}d^{0.08}$	$\frac{33000}{C}f^{0.24}d^{0.12}$	1.172	1.07
0	15		Up	$C_{10}f^{0.71}d^{0.87}$	$C_{10}f^{0.73}d^{0.87}$	6780	6880	$\frac{33000}{C}f^{0.29}d^{0.13}$	$\frac{33000}{C}f^{0.27}d^{0.13}$	1.05	0.939
			Down	$C_{10}f^{0.68}d^{0.86}$	$C_{10}f^{0.67}d^{0.89}$	7040	5280	$\frac{33000}{C}f^{0.32}d^{0.06}$	$\frac{33000}{C}f^{0.33}d^{0.11}$	1.041	0.99
0	20		Up	$C_{10}f^{0.76}d^{0.88}$	$C_{10}f^{0.76}d^{0.88}$	9880	8480	$\frac{33000}{C}f^{0.26}d^{0.12}$	$\frac{33000}{C}f^{0.26}d^{0.12}$	1.242	1.07
			Down	$C_{10}f^{0.72}d^{0.86}$	$C_{10}f^{0.76}d^{0.90}$	8000	9530	$\frac{33000}{C}f^{0.28}d^{0.14}$	$\frac{33000}{C}f^{0.24}d^{0.10}$	1.212	1.11
0	25		Up	$C_{10}f^{0.75}d^{0.88}$	$C_{10}f^{0.76}d^{0.93}$	10000	10670	$\frac{33000}{C}f^{0.29}d^{0.14}$	$\frac{33000}{C}f^{0.24}d^{0.07}$	1.516	1.15
			Down	$C_{10}f^{0.74}d^{0.96}$	$C_{10}f^{0.78}d^{0.93}$	18450	12250	$\frac{33000}{C}f^{0.26}d^{0.02}$	$\frac{33000}{C}f^{0.24}d^{0.07}$	1.940	1.212

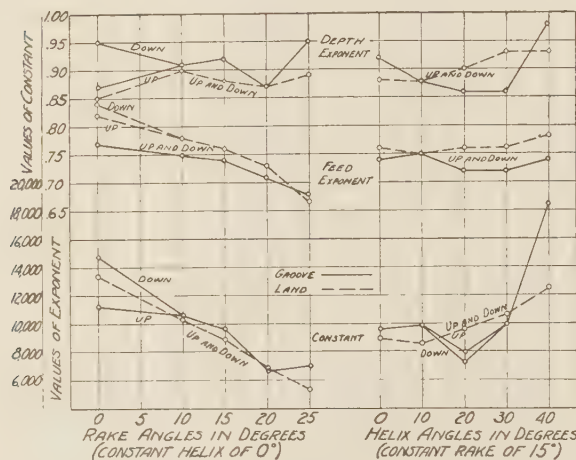


FIG. 8 EFFECT OF VARIOUS RAKE AND HELIX ANGLES ON THE EXPONENTS OF FEED AND DEPTH AND THE CONSTANT IN THE MILLING ENERGY EQUATION WHEN MILLING S.A.E. 3250 STEEL, BAR A-7 (Milling cuts were made up and down and on a land and in a groove as indicated. Data taken from Table 6.)

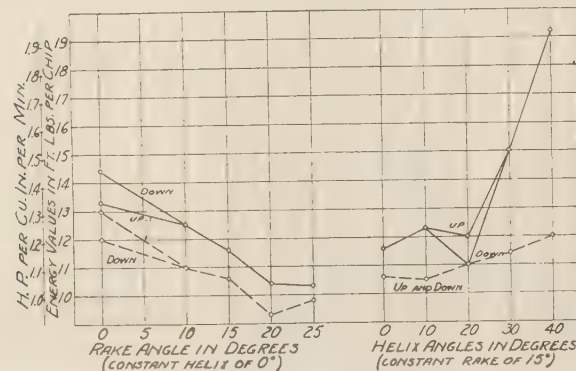


FIG. 9 EFFECT OF VARIOUS RAKE AND HELIX ANGLES OF THE CUTTER ON THE POWER AND ENERGY VALUES WHEN MILLING S.A.E. 3250 STEEL, BAR A-7

(Cuts were taken up and down both in a groove and on a land as indicated. Data taken from Table 6.)

for all cutting conditions as the rake angle is increased from 0 to 25 deg. The constant slightly increases, however, for up and down land milling for helix angles above 10 deg. For groove milling, the constant appears to be quite erratic, particularly

for helix angles of 20 and 40 deg; otherwise they are unaffected by the helix angle.

The energy and power values appear to fall off for both up and down milling, as well as land and groove milling, as the rake angle is increased, as shown in Fig. 9. In up and down milling on a land, the energy values for the 0- and 10-deg. helix angles are the same, but they become greater as the helix angle is increased above 10 deg. The energy values for groove milling both up and down, as a function of helix angles, are extremely out of order for helix angles above 20 deg, as shown by the unusual lines of the curve. Again it is noticed that the power values for groove cutting are consistently above those for land cutting as would be expected.

DISCUSSION OF SINGLE-POINT-CUTTER DATA

In beginning the discussion, the authors wish to point out and make clear a fact which has been found repeatedly: if the material is changed, the constants and exponents in the formulas, as well as the energy values, are changed. Also, if the cutter is changed, the constants, exponents, and energy values are changed.

With this in mind, the object of this particular study in the Elements of Milling has been to compare various tool angles, various sizes, and methods of cut on only enough metals to be reasonably sure that the conclusions reached will hold in general for most metals.

After a complete series of tests was run on the free-cutting brass and formulas were determined, it was discovered that the formula for the 0-deg helix, 15-deg rake tool did not check the corresponding formula given in the first report. The two equations were as follows:

From the first paper:

$$E = C_{10}f^{0.76}d^{0.96}$$

From the second test:

$$E = C_{10}f^{0.85}d^{0.96}$$

A certain experimental error, of course, was to be expected. A difference in the feed exponent from 0.76 to 0.85, however, hardly could be considered as an experimental error. Also, the energy values and constants varied somewhat. Repeated checks confirmed the accuracy of the second series as represented by the second formula. The cutters used were the same brand of high-speed steel, and equal care was taken in each case in the grinding. Further check tests were run on the piece of stock used in the first paper. These tests were found to give a feed exponent of 0.77, comparing favorably with 0.76 of the first

paper. Obviously, the material used in the experiments for this second paper had some different physical characteristics from the specimens used in the first paper, showing that the material at different parts of the same bar was not uniform.

Recently, a series of comparative tests was run on cold-drawn brass rod about $7/16$ in. in diameter, which showed machining differences in different lengths depending upon which end of the billet was machined. Differences in grain size, in heat treatment, or small differences in composition all affect the values obtained. It is surprising, however, to note the uniformity obtained in the value of the exponents of feed and depth in the energy equation when cutting different types of steels as explained below. It previously has been found that, in determining equations for torque and thrust in drilling steel under a wide variety of cutting conditions and covering many types of steels, the same equations have been developed repeatedly.

In order to arrive at the general tendencies introduced by the variables of the cutters and methods of cutting steel, the results in the three steels tested have been correlated. Of the three steels tested, S.A.E. 1112 steel gives energy values slightly below the average for steel, S.A.E. 1020 gives energy values presumably fairly average for steel in general, while S.A.E. 3250 gives power values slightly above the average steel. Steels S.A.E. 1020 and S.A.E. 1112 give lower values of energy when cutting down than when cutting up, while S.A.E. 3250 shows very little difference in energy values for these two types of cuts. By averaging all of the data for these three steels, it is believed a general picture of the effect of angles, methods of cutting, etc. is obtained for an average steel. This picture may be compared with that for each individual steel.

Variation of Constant in Energy Equation. The average values of the constants in the energy formula for the three steels are shown plotted over the rake angle or hook in Fig. 10. The constants for cutting down are considerably lower in all cases, except that for 0-deg rake, than when cutting up. The constant

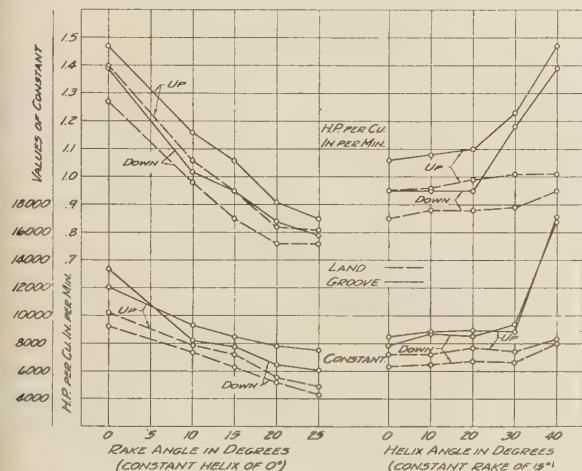


FIG. 10 AVERAGE VALUES OF THE CONSTANTS IN THE ENERGY FORMULA FOR THE THREE STEELS S.A.E. 1112, 1020, AND 3250, FOR UP AND DOWN MILLING AND FOR LAND AND GROOVE CUTTING, PLOTTED OVER THE RAKE ANGLE AND HELIX ANGLE IN DEGREES AS THE VARIABLES

(The horsepower-per-cubic-inch-per-minute values as averaged for the three steels also are shown. The cut was 0.300 in. wide, 0.100 in. deep, and the feed per cut was 0.010 in.)

on an average for the 25-deg rake angle is about 55 per cent of that for the 0-deg rake angle. There is a tendency, however, for the constant curves to become horizontal for the greater values of rake, which agrees in general with similar experiments

conducted with an end-cutting planer tool in which the back rake was varied. It also is seen that the constants for land cutting are considerably lower than the corresponding values for groove cutting.

The constants when plotted over side rake or helix angles in Fig. 10 are seen to remain practically the same, with perhaps a slight increase, for all side-rake angles up to and including 30 deg. There is a marked increase in the value of the constant for the 40-deg side-rake angle, due presumably to excessive metallic distortion of the chip. This same condition was found when studying side-rake angles on end-cutting planer tools. The constants are higher for groove cutting due undoubtedly to increased friction.

Variation of Horsepower per Cubic Inch per Minute. Average values of horsepower per cubic inch per minute when taking a

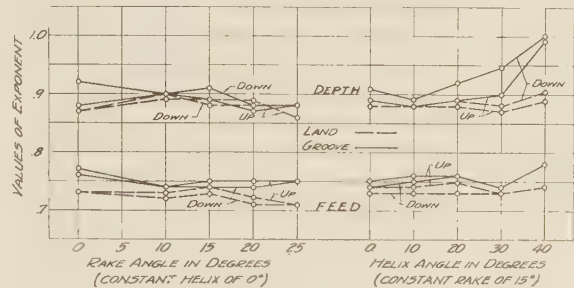


FIG. 11 AVERAGE VALUES OF THE EXPONENTS OF FEED AND DEPTH FOR THE FORMULAS OF THE THREE STEELS ARE SHOWN PLOTTED OVER THE RAKE ANGLE AND HELIX ANGLE AS VARIABLES

cut 0.300 in. wide, 0.100 in. deep, with a feed per cut 0.010 in., when using a tool 0.300 in. wide with various values of side rake and helix, are shown in Fig. 10. The power per cubic inch per minute is seen to fall off in almost direct proportion to the increase in rake up to and including 20 deg. There appears to be little increased efficiency due to a further increase of the rake angle to 25 deg. The curve for groove cutting up is well above that for land cutting up; also, that for groove cutting down is above that for land cutting down. However, the curves of horsepower per cubic inch per minute for groove cutting down and land cutting up show about the same values. The values of horsepower per cubic inch per minute, as an average, show but a slight increase for the 15-deg rake tool when the helix angle is increased from 0 to 20 deg. For higher helix angles, however, when cutting in a groove, the power increases rapidly due to side friction, but for land cutting the same tendency as indicated for lower helix angles is maintained.

Variation of Exponents of Depth and Feed. With the average of the exponents for feed and depth plotted over the variable rake or helix angle in Fig. 11, it is seen that the exponent for depth when cutting down averages higher than when cutting up; also, that the exponent of the feed when cutting down averages lower than when cutting up. Except for high depth exponents for high helix angles in groove milling, all exponents are practically constant, with the following slight but consistent tendencies:

- 1 The depth exponents fall off slightly with high rake angles, and rise slightly for high helix angles when milling in a groove. But when the milling is done on a land, they are practically constant.

- 2 The feed exponents remain practically constant as the rake angle increases, although a slight decrease is apparent for land cutting. The feed exponents remain practically constant as the helix increases, except for extreme values of helix in groove cutting where the exponent is high.

COMMENTS ON FINISH PRODUCED

No great difference in finish for a given type of cut was noticed due to changing tool angles. The nature of the tests excluded any possibility of studying cutter life. An investigation of finish, cutter life, and pressures is planned on apparatus already set up.

The difference in finish on up and down milling, however, was quite apparent. The finish on up milling was, in general, smooth and shiny or glassy in appearance. Very often it showed distinct feed marks and scratches which were sometimes quite deep. The chips had a tendency to cling to the cutting edge, and, if left on, would be dragged under the cutter on the next cut, marring the surface. On down cutting, the finish was smooth but duller with a satin-like appearance. Feed marks were usually not visible, but on some materials the surface produced was rougher. Chips had little tendency to cling to the tool and did no harm, as they would be knocked off at the start of the cut, whereas the finish is made at the end of the cut.

Chatter marks were more common when cutting up than when cutting down. As far as chatter and finish were concerned it was usually possible when milling down to increase the feed considerably over that when milling up.

Shape of Chip. Chips taken by the two different methods often showed distinct characteristics. When down milling the screw-stock steel S.A.E. 1112, for example, very tightly rolled chips were produced. On up milling, the chips were straight or flat. These characteristics were observed for all variable back-rake-angle tools, but when the tools of increasing helix angle were used the chip forms approached each other, the down-milled chips becoming less tightly rolled and the up-milled chips tending to curl. Chips from the 30- and 40-deg helix-angle cutters were almost identical for both methods of cutting.

When down milling the chromium-nickel steel S.A.E. 3250, the chips were flat, whereas tightly rolled chips were obtained on up milling. Again these differences disappeared with the higher helix-angle tools.

In general, it may be said that the down-milled chips are rolled more tightly than the up-milled chips, the exceptions occurring, in most cases, with those metals that show little or no difference in energy values for the two methods.

Built-Up edge. Undoubtedly, chip form is influenced by the built-up edge. In general, a better developed built-up edge forms on milling down. It seems reasonable to expect that a large, well-developed edge will coil the chip, while a small poorly developed edge might allow a flatter chip to be formed. This is borne out by observing the chips. In the case of the S.A.E. 3250 steel, a well-developed edge was formed, the chip was flat in down milling, but was coiled in up milling. This action was contrary to that generally observed. In fact, exceptionally large edges were noticed for this steel, and the surface left by down milling was rougher than usual, due to the roughening effect of the built-up edge.

Because of this roughening effect of the built-up edge, it is possible to detect from the chip the history of its formation. The under face of the chips is highly burnished for a distance, depending upon the metal, up to $1/16$ in., which corresponds to $1/8$ to $3/16$ in. actual length of cut. Then the surface loses its luster and reaches a maximum degree of roughness in an added $1/16$ in. of length. Well-developed edges are often found with depths of cut of 0.025 in. or less, corresponding to about $1/4$ in. length of cut with the 3.5 in. in diameter cutter, but as a rule somewhat longer length of cut is necessary for the fully developed edge. After being built up, further increase in depth of cut does not change it materially. Also, less length of cut to form this edge is required for down milling than for up milling, the amount of this difference depending upon the metal and appar-

ently influenced by tool angles, especially back rake. This difference usually decreases as the back-rake angle increases.

The burnished length on the chip generally increases somewhat as the back rake is increased, but some of this increase may be due to less compacting of the metal in the chip. That is, the chips are longer for the same size of cut. The edge is usually thicker for the low back-rake angles, but does not seem to require much, if any, greater length of cut for its formation. Changing the side rake or helix angle does not seem to change the formation of built-up edge to any extent, but does affect the rolling of the chip.

A more detailed and scientific study of the important factor of built-up edge has not been undertaken because of the nature of the tests. The authors expect to do this in the course of tests for the next paper of this series when a standard milling machine will be used and cuts will be taken as the work is fed.

ANALYSIS OF SOME MILLING DATA OBTAINED UNDER COMMERCIAL CONDITIONS

In 1929, a thesis, "Milling Cutter Efficiency" (Experiment Station Project No. 85), was presented at the Ohio State University by four men, Otto W. Winter, Charles E. Beard, Howard W. Allison, and Robert J. Duerler. The work, involving an expenditure of several thousand dollars, was sponsored by the Cincinnati Milling Machine Company. A total of about 24,000 cuts were run.

In discussing "Elements of Milling,"⁴ Mr. Winter⁵ suggested that a comparison of these data with those given in his report might be of distinct value.

In the Ohio State experiments, standard coarse-tooth high-speed-steel cutters were used having spiral and under-cut teeth. A wide range of feeds and depths of cut were covered. The materials cut consisted of cast iron and S.A.E. 3125 to 3140 steels. Power data were presented as calibrated net horsepower at the cutter for specified cuts, feeds, cutters, and material. All cuts were taken in the conventional manner—that is, up cutting. An emulsion consisting of 1 part Sunoco soluble oil to 20 parts water was used on the steel, but the cast iron was cut dry.

Because the data were taken with standard cutters on a standard milling machine and because such a wealth of data is available covering a range of feeds, depths of cut, and widths that were not possible with a small pendulum tester, the authors believed that much could be learned and many questions answered by recomputing these data and comparing the results with those of the paper.

Apparatus. The apparatus used in the Ohio State experiments consisted of a no. 2M Cincinnati plain miller of the latest (1929) inclosed, 7.5-hp-motor type, equipped with a wattmeter for registering gross power developed.

By means of a prony brake mounted on the spindle of the machine, efficiency curves of the motor and machine were determined for every speed and load variation. Power absorbed in the feed mechanism was neglected. This introduced a small variable error. Standard cutters of the shell-end, half-side, slotting, and slabbing types were used.

Procedure. The procedure of the tests was to take four cuts, from which the average power value was determined. If the data varied widely, additional cuts were taken. The dimensions of the cut, that is, the width and depth, were determined from the size and type of the cutter used, as indicated in Table 8. The feeds varied from $1/2$ to 20 in. per min.

As stated in the thesis, "Probably the greatest cause of power requirement variation, and certainly one that caused us much trouble, was the condition of the cutting edge. Throughout the

⁴ Trans. A.S.M.E., vol. 54, 1932, paper no. RP-54-4.

⁵ Cincinnati Milling Machine Company, Detroit, Mich.

course of the tests, we endeavored to run each of the four cuts, constituting a test, at varying periods of the life of the cutter between sharpenings." It follows that the data presented are not for the sharp condition, but rather for an average or partially dull condition of the tool.

Data. The data were presented as a series of curves, as illustrated in Fig. 13, for specified widths and depths of cut giving net horsepower (at the cutter) values plotted over feeds in inches per minute. A separate set of curves was presented for each combination of cutter and material.

In the following analysis by the authors, by depth of cut is meant the distance of metal cut measured in the plane of rotation of the cutter, and width of cut the distance measured on a line parallel to the axis of the cutter, and has nothing to do with the shape of the work or the position of the cut. This is a logical procedure and enables direct comparison of all data including that of the authors. It is usual to think of these dimensions as being reversed in a face-milling type of cut, and consequently the meaning of the designations d for depth and w for width, as shown in Fig. 12, should be kept in mind.

In Fig. 12 are shown five different types of cutters, each taking its typical cut. The principal object of this illustration is to indicate what is meant in each case by depth of cut d and the width of cut w . In the case of the plain milling cutters at A,

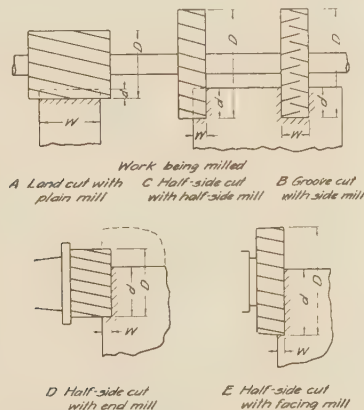
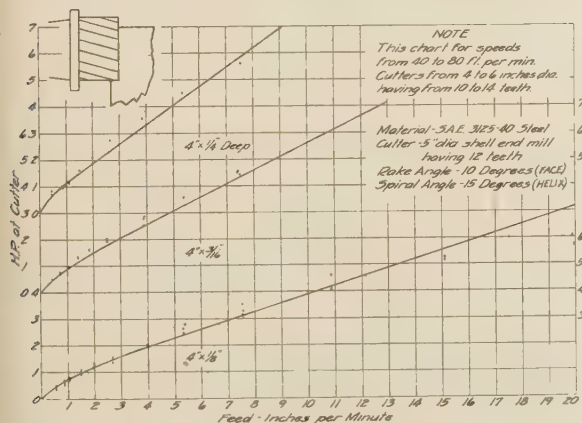


FIG. 12 ILLUSTRATIONS OF VARIOUS TYPES OF CUTS SHOWING A LAND CUT BEING MADE BY A PLAIN MILL, A GROOVE CUT BY A SIDE MILL, AND A HALF-SIDE CUT BY A HALF-SIDE, SHELL-END AND FACING MILL



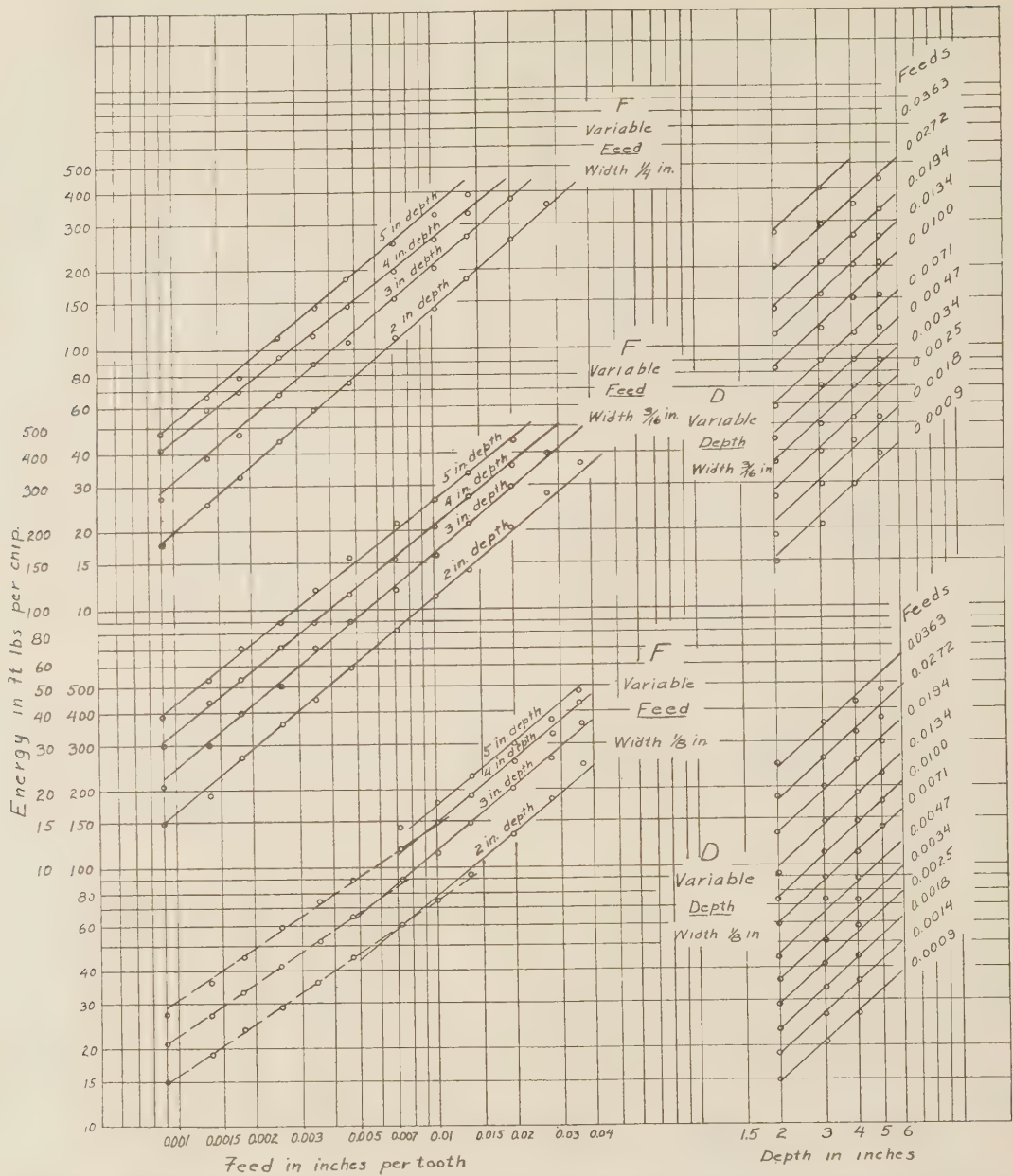


FIG. 14 VALUES OF ENERGY AS COMPUTED FROM THE OHIO STATE EXPERIMENTS FOR THE SHELL-END MILL HAVING 12 TEETH, 10-DEG RAKE, AND 15-DEG HELIX, SHOWN IN FIG. 13

(Cutting S.A.E. 3125–3140 steels and plotted on log-log paper for various combinations of feed, depth of cut, and width of cut. An emulsion of 1 part soluble oil to 20 parts water was used. Energy values from Table 7. The general formula was obtained in which $E = 14,600 w^{0.82} d^{0.90}$.)

angle and 15-deg spiral or helix angle. It operated at 46 rpm, corresponding to a peripheral cutting speed of 60 ft per min.

The data cover tests on S.A.E. 3125, 3130, 3135, and 3140 steels as shown plotted in Fig. 13. For recomputing, however, an average of the values was used.

The number of chips removed per minute is the rpm times the number of teeth in the cutter and equals 46×12 , or 552, in this case. The feed in inches per tooth is found by dividing the feed in inches per minute by the number of chips removed per minute. The horsepower is equal to the energy in foot-pounds per chip times the number of chips removed per minute divided by 33,000. In this case, E (the energy per chip) = 60 times hp.

Table 7 shows the feed in inches per minute and inches per tooth for 12 different feeds, and the horsepower and energy values for 4 depths and 3 widths of cut and for all feeds for this combination of cutter and material.

Discussion of Ohio State Data. Data for the shell-end mill cutting S.A.E. 3125–3140 steels, as taken from Table 7, are shown plotted in Fig. 14. Three widths of cut, $1/8$, $3/16$, and $1/4$ in., were run, and the data are grouped accordingly into three groups. Four depths of cut of 2, 3, 4, and 5 in. were taken for each of 12 feeds, ranging from $1/2$ to 20 in. per min. These feeds correspond to 0.00091 to 0.0363 in. per tooth. In Fig. 14 the three sets of curves at the left, indicated by F , show energy values in foot-

pounds plotted over feed per tooth as abscissas. In the upper two cuts, for the $\frac{3}{16}$ and $\frac{1}{4}$ in. widths, the points are seen to lie very consistently on straight lines. In the lower set for the $\frac{1}{8}$ in. width, however, the points appear to lie on a line slightly concave for the lighter feeds. The solid lines in this set at the right have the same slope as those of the two upper groups, while the dotted lines represent the energy data for these light feeds.

The average slope of the solid lines is 0.833, while that for the dotted lines is 0.68. The slopes of the 4- and 5-in.-depth curves of the $\frac{3}{16}$ -in.-wide cuts and the 4-in.-depth curves of the $\frac{1}{4}$ -in. cuts are slightly lower than the average. For these lines, it will be noticed that the energy values are relatively higher for the lighter feeds. This may indicate the influence of a dull cutter. The slope of the 2-in.-depth curve of the $\frac{1}{4}$ -in.-width cuts is higher and the energy values are also somewhat lower, compared with the other data, toward the lighter feed end of the curve, which may indicate that the cutter was a little sharper than average.

It is known that the energy per chip varies very nearly as the first power of the width of cut, other conditions remaining the same. However, the relatively high values of the points on the dotted lines probably are not due to dulling, as they are too consistent, but may be due to the radius of the cutter teeth nose, which would have much more effect on this narrow cut, especially at smaller feeds.

The data for the two widths of $\frac{1}{8}$ and $\frac{3}{16}$ in. have been re-plotted over the various depths of cut, resulting in the two sets of curves at the right in Fig. 14, labeled *D*. Apparently, a

change in the slope of the variable-feed lines for the $\frac{1}{8}$ -in.-width cuts has had little effect on the variable-depth curves. The average slope for both sets is 0.903.

From the slopes of the variable-feed and variable-depth curves, a general milling-energy formula for this material and cutter can be written as

$$E = 14,600 wf^{0.83}d^{0.90}$$

in which E is in foot-pounds per chip, f the feed per tooth in inches, d the depth of cut in inches, and w the width of cut in inches, as illustrated in Figs. 12 and 13.

From Fig. 14 several interesting and valuable facts are noted. A formula of the type $E = Cwf^x d^y$ is found to hold, even when the depth of cut equals the diameter of the cutter. As is mentioned farther on under "Mathematical Analysis," for this latter condition there is no difference in cutting action between up and down milling. The curves verify the fact that the dulling of a cutter not only increases the energy values, but reduces the slope of the curves. The reduced slope and high values indicated by the curves for the smaller feeds of the narrow $\frac{1}{8}$ -in.-wide cuts may involve the effect of nose radius.

Fig. 15 shows graphically on log-log paper the energy data for an alternate tooth slotting cutter 6 in. in diameter and 1 in. wide. It has 24 teeth, having 10-deg rake and 15-deg alternate helix. S.A.E. 3125-3140 steels were used, and six depths, namely, $\frac{1}{8}$, $\frac{1}{4}$, $\frac{3}{8}$, $\frac{1}{2}$, 1, and $1\frac{1}{2}$ in. were run, each with 12 feeds varying from 0.000488 to 0.0195 in. per tooth. Two sets of curves are shown. Those labeled *F* at the left are for variable feed and

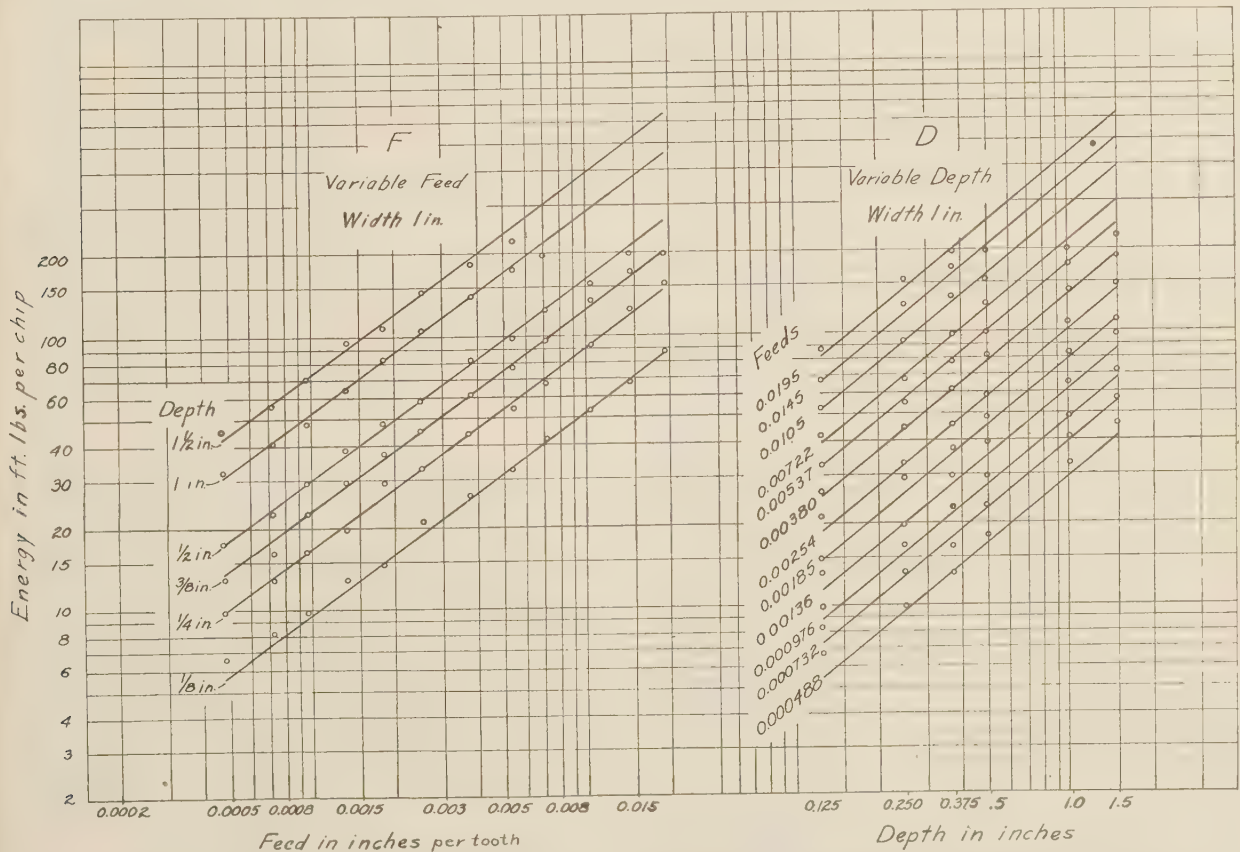


FIG. 15 VALUES OF ENERGY AS COMPUTED FROM THE OHIO STATE EXPERIMENTS FOR ALTERNATE-TOOTH SLOTTING CUTTERS 6 IN. IN DIAMETER, 1 IN. WIDE, HAVING 24 TEETH, EACH HAVING A RAKE ANGLE OF 10 DEG AND A SPIRAL ANGLE OF 15 DEG (Cutting S.A.E. 3125-3140 steels and plotted on log-log paper for various combinations of feed, depth, and width of cut. An emulsion of 1 part soluble oil to 20 parts water was used. The formula developed from these data is $E = 8800 wf^{0.78}d^{0.83}$.)

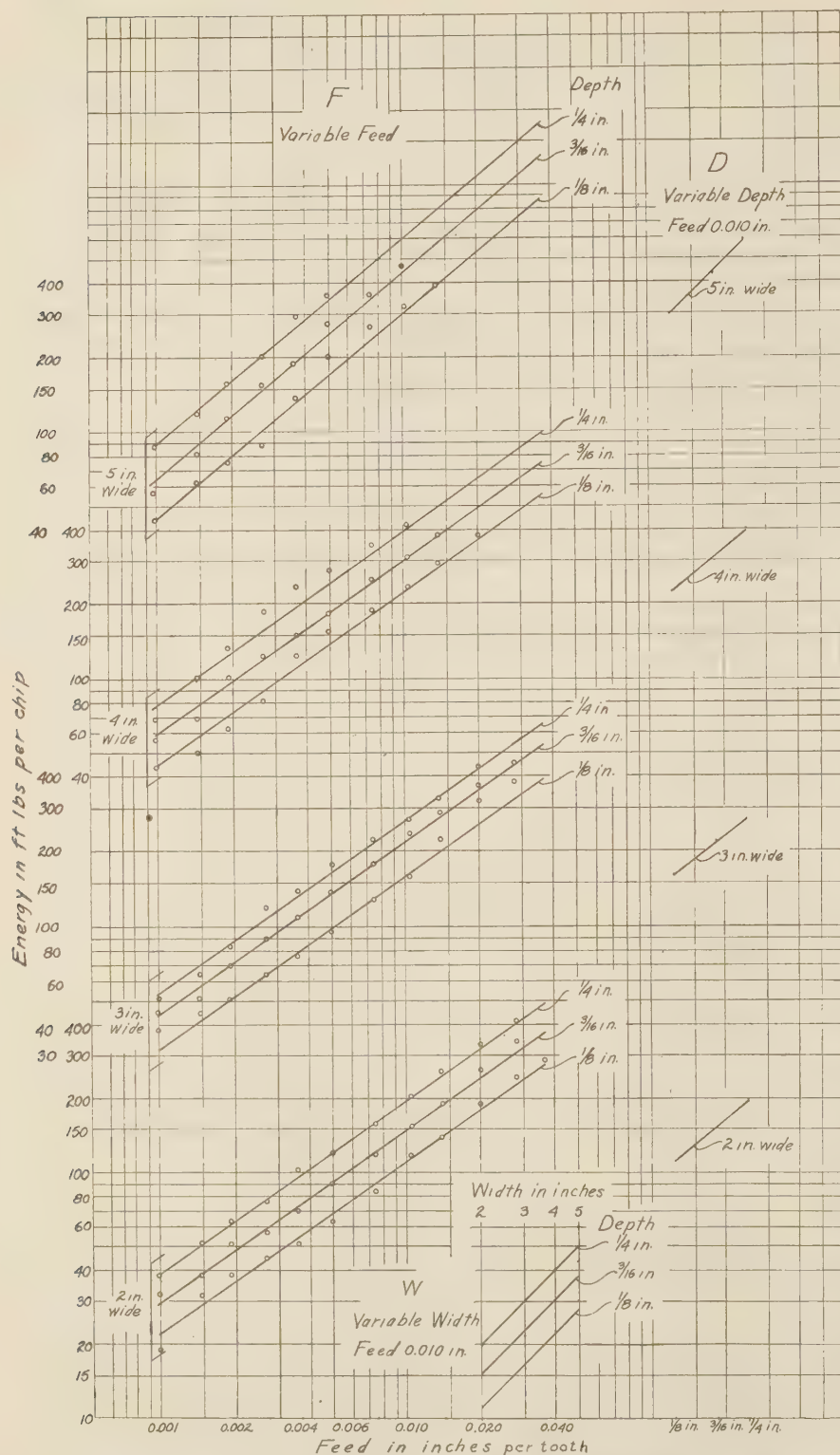


FIG. 16 VALUES OF ENERGY AS COMPUTED FROM THE OHIO STATE EXPERIMENTS FOR THE SPIRAL SLAB MILL 4 IN. IN DIAMETER, 6 IN. WIDE, HAVING 10 TEETH, WITH A RAKE ANGLE OF 10 DEG AND A SPIRAL ANGLE OF 25 DEG

(Cutting S.A.E. 3125-3140 steels and plotted on log-log paper for various combinations of feed, depth, and width of cut. The 1-to-20 emulsion was used. The general formula obtained is $E = 8000 wf^{0.72}d^{0.81}$.)

constant depth, with the energy values plotted over the feed, and those labeled *D* at the right are for variable depth and constant feed, with the energy values plotted over the values of depth.

The data are exceptionally consistent, and, due to the comparatively large number of depths run, the slope of the variable-depth lines is well defined. The slopes of the two sets have been measured and result in the equation for energy values per chip for this cutter and material, as follows:

$$E = 8800 wf^{0.74}d^{0.83}$$

It was assumed that the length of each tooth was equal to the width of the slot, inasmuch as definite information was lacking. This is not correct, however, so the constant given is slightly lower than is actually true.

The energy values for a spiral slab mill when milling the S.A.E. 3125-3140 steels are shown plotted in Fig. 16. The cutter was 4 in. in diameter, 6 in. wide, and had 10 teeth, with 10-deg rake and 25-deg helix. Four widths of cut of 2, 3, 4, and 5 in. were run for each of three depths of 1/8, 3/16, and 1/4 in. The 12 feeds used ranged from 0.000953 to 0.0381 in. per tooth. Four sets of variable-feed curves, labeled *F* at the left in Fig. 16, result from the recomputation. Of these, three sets, namely, the curves for widths of 2, 3, and 4 in., have approximately the same slope of 0.72, while the set for the 5 in. width is somewhat steeper with a slope of 0.81. Variable-depth curves are not shown because of insufficient number of depths run and general inconsistency of the data. To estimate what this exponent would be, points have been taken from the straight lines and plotted, resulting in curves *D*. The average slope of these lines is 0.81, which probably is not exact.

These same points have been plotted over variable-width values in an attempt to check the assumption that energy values vary directly as width. These curves are shown at *W*, but the data are too inconsistent to draw definite conclusions. The resultant straight lines shown have a slope of 1.0, which would be expected for this range of widths.

The milling-energy formula for this cutter and material is then

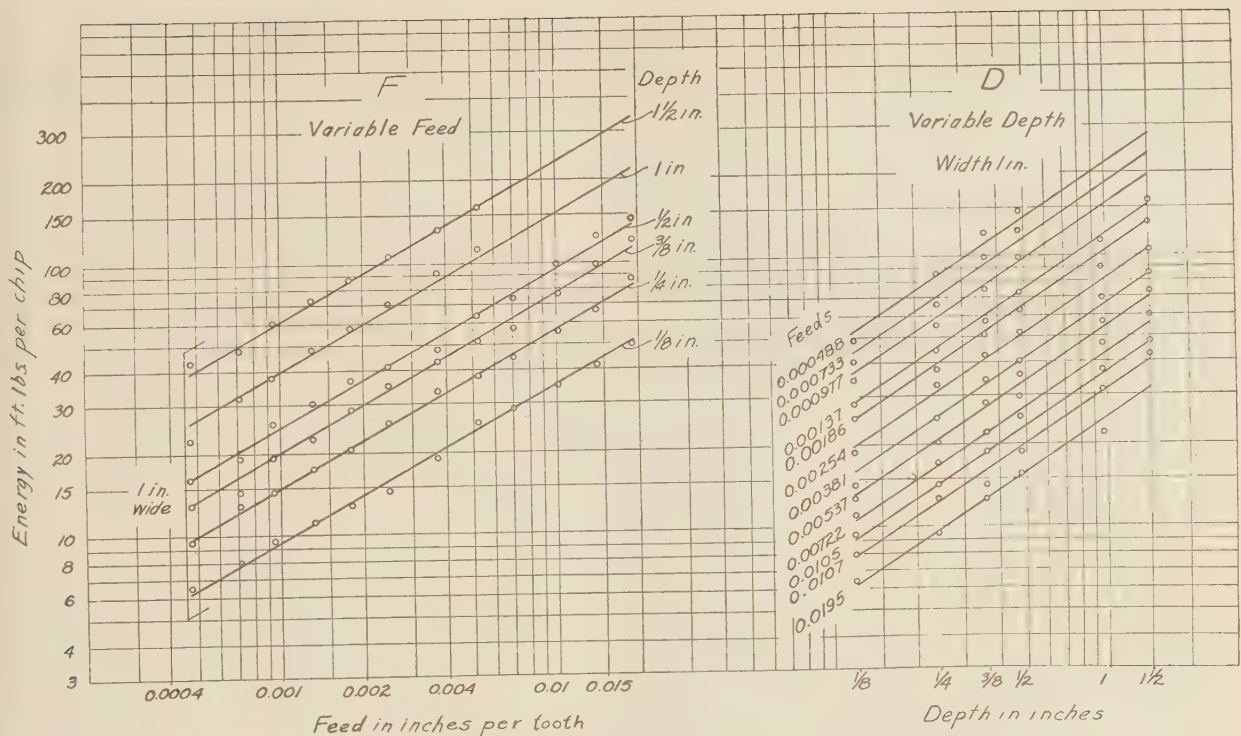


FIG. 17 VALUES OF ENERGY AS COMPUTED FROM THE OHIO STATE EXPERIMENTS FOR THE ALTERNATE-TOOTH SLOTTING CUTTER DESCRIBED IN FIG. 15

(Cutting cast iron dry, as summarized in Table 8. The energy equation is $E = 2000 wf^{0.56}d^{0.66}$.)

$$E = Cwf^{0.72}d^{0.81}$$

in which $C = 8000$.

Recomputed values of the Ohio State Experiments are given for the alternate-tooth slotting cutter cutting cast iron dry. The values are shown graphically in Fig. 17, with the energy values for a constant width of 1 in., for various depths from $1/8$ to $1 1/2$ in., plotted over the feed in inches per tooth. A series of parallel lines are obtained, the slopes of which all equal 0.56. When the energy values for constant feed are plotted over depth of cut in inches, again a series of practically parallel straight lines are obtained the slopes of which are 0.66. This gives an energy equation as developed from these series of lines of

$$E = 2000 wf^{0.56}d^{0.66}$$

Recomputed values of energy in foot-pounds per chip for the half-side mill cutting cast iron are shown plotted over the feed in inches per tooth in Fig. 18. Four sets of curves are shown, for widths of cut of $1/8$, $3/16$, $1/4$, and $5/8$ in. These data are seen to be more erratic than any other presented. For each width of cut, four lines indicate the general tendencies of energy fluctuations over feed per tooth, for four depths of cut of $1/2$, 1, $1 1/2$, and 2 in. While there are numerous inconsistencies, the general tendency of the lines is to slope from the horizontal at an angle whose tangent is 0.71. The results were quite inconsistent for accurate determination of the slope of the variable depth lines for constant feed, although a slope of 0.91 had been obtained as representing an average. This gives the general energy equation in foot-pounds per chip as

$$E = 5300 wf^{0.71}d^{0.91}$$

It is believed that, in the case of half-side milling in which only one cutter is mounted on the arbor, an end thrust is imposed on

the spindle bearing which gives rise to frictional forces which materially influence the power developed by the motor. This influence is not accounted for in the calibration.

Graphs similar to those shown in Figs. 14 to 18, inclusive, were prepared for the half-side mill cutting S.A.E. 3125-3140 steels, and for the shell-end mill, slabbing mill, and a face mill when cutting cast iron dry. For brevity, however, only Figs. 14 to 18 are presented here. Data for all of these curves are summarized in Table 8.

In milling the S.A.E. 3125-3140 steels with the 1-to-20 emulsion with the shell-end mill, alternate-tooth slotting mill, slabbing mill, and half-side mill, various formulas and constants were obtained as summarized in Table 8. It is seen, for instance, that the energy in foot-pounds per chip formulas for slotting and slabbing are practically identical with the coefficients of feed and depth and also the constants of the slotting mill only slightly higher than those for slabbing. The rake angle of the two cutters is 10 deg, while the helix angle is 15 deg for the slotting mill and 25 deg for the slabbing mill. The results confirm those of the authors' experiments that a difference in helix angle causes very slight, if any, differences in the equations. The energy equation for the half-side mill cutting steel has exponents only slightly higher than the corresponding ones in the slotting and slabbing mill equations. It might be expected that this equation would be between those for slotting and slabbing, inasmuch as it represents only one-half side of the slotting. This is not borne out, however, and, the constant itself being considerably higher than the constants for the slotting and slabbing mills, would indicate greater friction on the spindle bearings due to end thrust. There appears to be considerable difference between the equations for the shell-end mill and the half-side mill. This, from analysis, would not be expected, inasmuch as they have the same rake and helix angles. The constant for the

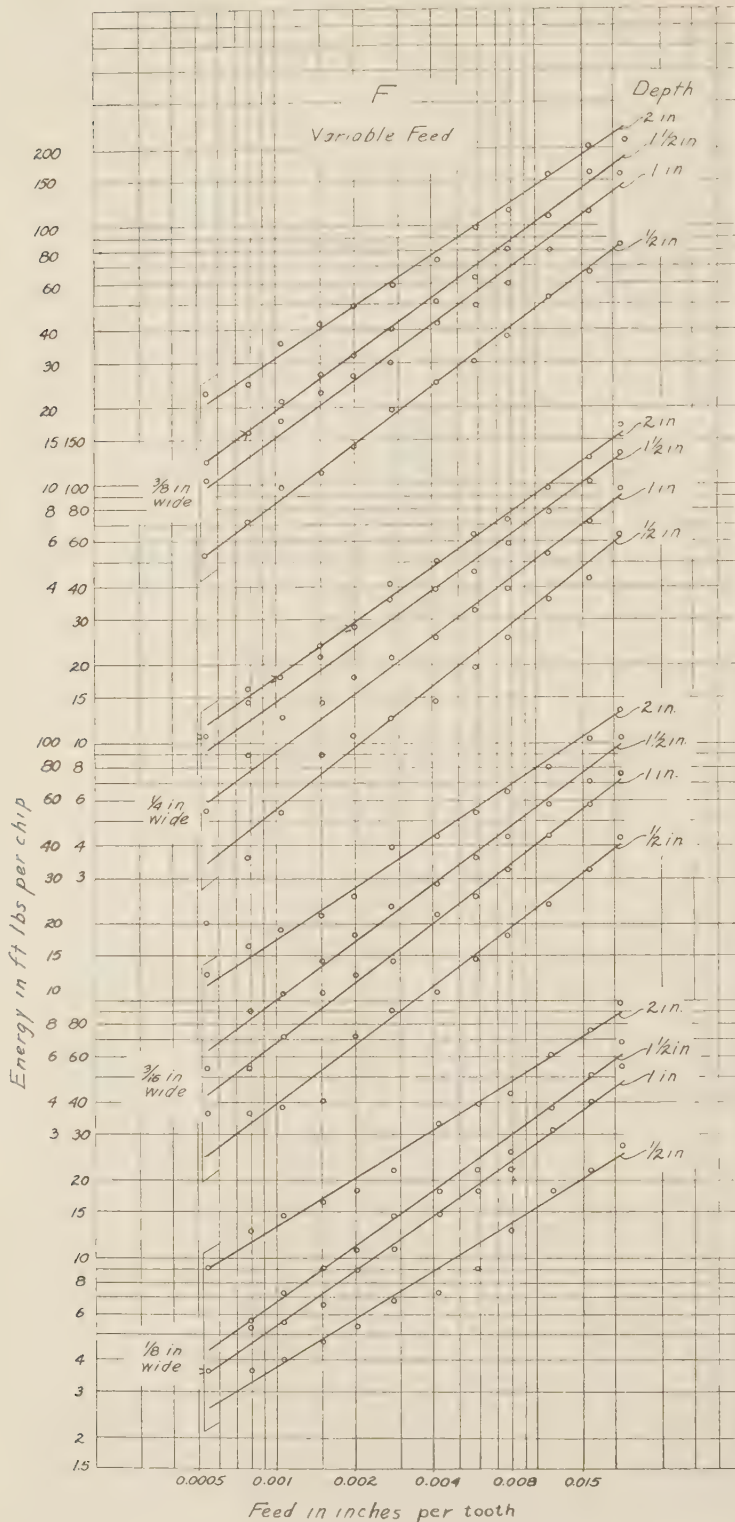


FIG. 18 VALUES OF ENERGY AS COMPUTED FROM THE OHIO STATE EXPERIMENTS FOR THE HALF-SIDE MILL 6-IN. IN DIAMETER, HAVING 24 TEETH WITH 10-DEG RAKE AND 15-DEG HELIX

(Cutting cast iron dry, under the conditions summarized in Table 8. The general equation developed is $E = 5300u^{0.71}d^{0.81}$.)

shell-end mill formula is greatest of all cutters, due presumably to greater end thrust on the spindle, inasmuch as the depth of cut ranges from 2 to 5 in., whereas that for the half-side mill is from $\frac{1}{2}$ to 2 in.

At the extreme right in Table 8 are shown values of horsepower per cubic inch per minute for each of the various cutters when taking 0.010 in. feed per tooth and a depth of 1 in. The slabbing mill is most efficient, while the half-side mill is least efficient.

An analysis of the equations resulting from the use of different cutters when machining cast iron, as given at the bottom of Table 8, shows the effect of the same tendencies as when milling steel, as previously discussed. The horsepower per cubic inch per minute is least when using the slotting and slabbing cutters and greatest when using the face mill. That for the face mill is slightly greater than that for the side mill, due again presumably to the additional thrust because of the great depth of cut, 4 to 8 in.

From the data shown in Table 8, it is obvious that a half-side type of cut does not give values midway between that for the slabbing mill and the slotting mill, presumably due to the influence of friction on the spindle due to end thrust. This might be true where the half-side cuts are made by straddle milling, in which no thrust is put on the spindle.

A MATHEMATICAL ANALYSIS OF CUTTING FORMULAS

In concluding this paper, the authors wish to present a mathematical analysis of milling-energy formulas. These formulas have all been of the form

$$E = Cwf^x d^y$$

where, in most cases, the value of the constant C was different for up and down milling, and often the values of the exponents x and y also were different.

When d , the depth of cut in inches, equals one-half the cutter diameter, the greatest difference between up and down cutting is obtained, but as it increases beyond one-half of the diameter, the two methods of cutting approach each other. When d is equal to the cutter diameter, the two methods are identical, and it is obvious that, for this case, the energy values E for a specific chip size will be the same for up and down milling. This condition occurs commonly in face-milling operations where the width of the cut, corresponding to the depth of cut in these investigations, is often the full width or diameter of the cutter.

Let subscript u denote up milling and subscript d denote down milling. Also, let d , the depth of cut in inches, equal D , the cutter diameter in inches, which is a constant. For this condition, then

$$E_u = C_u w f^x u D^y u$$

$$E_d = C_d w f^x d D^y d$$

TABLE 8

(A summary of the results of the Ohio State Experiments, together with the recomputed data based on feed and depth of cut)

Material and cutting fluid	Cutter Kind	Diam and width	No. of teeth	Tool angles		Speed— Rpm Min	Range of test data			Energy per chip formulas	Value of constants	Horsepower per cu in. per min formulas	Horsepower per cu in. per min ^a
				Rake deg	Helix deg		Width	Feed	Depth				
S.A.E. 3125-3140 steels; 20-to-1 Sunoco emulsion	Shell-end mill	5" d	12	10	15	46	60	1/8 to 1/4	0.00091 to 0.0363	2-5	$Cwf^{0.83}d^{0.90}$	14600	$\frac{C}{33000 f^{0.17} d^{0.10}}$ 0.99
	Slotting ^b mill, alternate tooth	6" d 1" w	24	10	15	43	68	1 to 1 1/2	0.000488 to 0.0195	1 1/2	$Cwf^{0.74}d^{0.83}$	8800	$\frac{C}{33000 f^{0.26} d^{0.17}}$ 0.885
	Slabbing mill	4" d 6" w	10	10	25	53	55	2-5	0.000953 to 0.0381	1/8 to 1/4	$Cwf^{0.72}d^{0.81}$	8000	$\frac{C}{33000 f^{0.28} d^{0.19}}$ 0.877
	Half-side mill	6" d	24	10	15	38	60	1/8 to 1/8	0.00055 to 0.0218	1/2 to 2	$Cwf^{0.75}d^{0.85}$	10700	$\frac{C}{33000 f^{0.25} d^{0.15}}$ 1.05
	Shell-end mill ^c	5" d	12	10	15	46	60	1/8 to 3/8	0.00091 to 0.0364	3-5	$Cwf^{0.60}d^{0.90}$	3100	$\frac{C}{33000 f^{0.40} d^{0.10}}$ 0.592
Cast iron, dry	Slotting ^d mill, alternate tooth	6" d 1" w	24	10	15	43	68	1 to 1 1/2	0.000488 to 0.0195	1 1/2	$Cwf^{0.56}d^{0.66}$	2000	$\frac{C}{33000 f^{0.44} d^{0.34}}$ 0.460
	Slabbing mill	4" d 6" w	10	10	25	62	65	2-6	0.000807 to 0.0322	1/8 to 1/8	$Cwf^{0.51}d^{0.67}$	1600	$\frac{C}{33000 f^{0.49} d^{0.33}}$ 0.465
	Half-side mill	6" d	24	10	15	38	60	1/8 to 3/8	0.00055 to 0.0218	1/2 to 2	$Cwf^{0.71}d^{0.91}$	5300	$\frac{C}{33000 f^{0.29} d^{0.09}}$ 0.610
	Face mill (inserted blade)	8" d	14	15	7	29	60	1/8 to 1/4	0.00125 to 0.050	4-8	$Cwf^{0.52}d^{0.90}$	2300	$\frac{C}{33000 f^{0.48} d^{0.10}}$ 0.635

^a 0.010-in. feed, 1.00-in. depth. ^b Two other slotting mills, 1/4 and 1/2-in. wide, were tested. ^c A 2-in.-diameter shell-end mill was tested also; the data were inconsistent. ^d A 1/2-in.-wide slotting cutter also was tested.

But, $E_u = E_d$. Then, by transposing and eliminating w , the equations become

$$\frac{C_u D^{y_u}}{C_d D^{y_d}} f^{x_u} = f^{x_d}$$

For convenience in this analysis, let

$$\frac{C_u D^{y_u}}{C_d D^{y_d}} = K$$

Then

$$K f^{x_u} = f^{x_d}$$

By taking logarithms,

$$\log K + x_u \log f = x_d \log f$$

or

$$x_d - x_u = \frac{\log K}{\log f}$$

Since f is always less than 1, $\log f$ is always negative.

This becomes a very illuminating equation, showing that the difference between the feed exponents for up and down milling is a function of the log of K . The farther the value of K is from 1, the greater will be the difference between these exponents. If K equals 1, then $\log K$ equals zero, and the two exponents must be equal. For this case

$$C_u D^{y_u} = C_d D^{y_d}$$

If the values of C are not the same, which in general is true, then the depth exponents y_u and y_d cannot be equal.

Similarly, when K does not equal 1, x_u is greater than x_d if $C_u D^{y_u}$ is greater than $C_d D^{y_d}$. And conversely, x_u is less than x_d , if $C_u D^{y_u}$ is less than $C_d D^{y_d}$.

The equation also points out that the difference between the feed exponents in the up and down milling equations is not constant, but is a function of the log of the feed. If the difference varies, the exponents also must vary and the variable feed lines cannot be absolutely straight lines on log-log paper. This effect will be very small when K is nearly unity.

Examination of the experimental data will reveal many cases which do not check this theoretical analysis. The reason is

obvious from the foregoing analysis. An equation of the form $E = Cwf^x d^y$, while accurate enough for all practical purposes, is not strictly correct. The exponents themselves are a function of the variables f and d involved.

CONCLUSIONS

There are numerous final conclusions drawn from the single-point cutter data and the Ohio State Experimental data which may be summarized briefly as follows:

Single-Point Cutter (when milling the free-cutting brass):

1 All exponents of feed and depth and constants in the energy equations are lower for land than for groove cutting, due presumably to greater friction in groove cutting or because the chip is cut at each side, as well as along the periphery when groove cutting, as shown in Fig. 2.

2 The exponents of the feed and depth are found to be the same for up and down milling for groove cutting and also different but the same for land cutting.

3 Constants in the energy equation are lower for down milling for the same type of cut.

4 Increasing the rake angle materially decreases the energy value E , as shown in Fig. 3.

5 Increasing the helix angle has no consistent influence on the exponents, constants, or energy until high values are obtained which produce excessive friction.

(When milling S.A.E. 1020 steel):

6 The conclusions given for free-cutting brass hold in general.

7 It is found that the exponents of feed and depth are slightly different when cutting up than when cutting down, as indicated in Fig. 4.

8 The drop in energy due to higher values of rake angle is very appreciable, as indicated in Fig. 5. This falling off of energy with increased rake angle appears to become much less rapid when the rake angle is 25 deg. The value of E for the 0-deg rake angle is over 100 per cent more than that for the 25-deg rake.

(When milling S.A.E. 1112 steel):

9 The results obtained, as shown in Figs. 6 and 7, confirm those for the S.A.E. 1020 steel. The percentage drop in energy due to rake angle is less pronounced.

(When milling S.A.E. 3250 steel):

10 There appears to be little or no difference in values of exponents, constants, or energy values when milling up or down. For this steel it appears that the values of the feed and depth exponents are somewhat higher for land cutting than for groove cutting, as indicated in Fig. 8.

11 The energy values decrease uniformly with increase in rake angles up to 20 deg, but show that the energy for groove milling is greater than for land milling shown in Fig. 9.

(By comparing the results obtained from the three steels discussed):

12 It is seen that the S.A.E. 1112 steel gives energy values slightly below the average for the three steels, the S.A.E. 1020 steel gives values about equal to the average of the three, while the S.A.E. 3250 gives values slightly above the average steel.

13 Steels S.A.E. 1020 and S.A.E. 1112 give lower values of energy when cutting down than when cutting up, while S.A.E. 3250 shows very little difference in energy values for these two types of cuts.

14 The constants for cutting down for all steels averaged as shown in Fig. 10 are considerably lower than when cutting up in all cases except that for the 0-deg rake. The average constant for the 25-deg rake angle is about 55 per cent of that for the 0-deg rake angle. There is a tendency for the constant curves to become horizontal for the greater values of rake.

15 The constants for land cutting are considerably lower than the corresponding values for groove cutting.

16 The constants, when plotted over the side rake or helix angles in Fig. 10, are seen to remain practically constant.

17 The average horsepower per cubic inch per minute values for all steels are shown in Fig. 10 to fall off uniformly with an increase in rake angle until a 20-deg rake angle is reached, after which there is little additional reduction in power values for an increase in rake angle.

18 The power values remain practically constant for various values of helix angle when the rake angle is constant. For groove cutting, the energy increases perceptibly for helix angles above 20 deg, due presumably to increased friction.

19 Energy values for groove cutting are shown to be higher than those for land cutting, due presumably to the types of cut.

20 It is shown in Fig. 11 that the values of the exponents of feed and depth remain practically constant for all values of rake and helix. Variations are introduced for high values of helix angle in groove cutting, however.

The Ohio State Data:

21 After reworking all of the Ohio State experimental data and plotting energy values on a basis of feed per tooth and depth of cut as variables, the conclusion is reached that energy equations of the form $E = Cwf^x d^y$ hold for all combinations of feed and depth, even for values of depth of cut up and equal to the diameter of the cutter.

22 It also is shown that this formula holds alike for plain mills, half-side mills, side mills when groove cutting, shell-end mills, and face mills. It must be remembered, however, that the depth of cut in these cases is measured in the plane of the diameter of the cutter, while the width is measured axially, as shown in Fig. 12. Half-side cuts, as shown at *C*, *D*, and *E* in Fig. 12, do not give equation values midway between slabbing cuts as shown at *A* and groove cutting as shown at *B*, as might be expected from an analysis. This is due, undoubtedly, to the unbalanced effect of a single cutter. This condition would, it is believed, be rectified if half-side cuts were taken with two opposed cutters so as to eliminate the end thrust on the spindle.

General Conclusions:

23 It has been found from all experiments with the single-

point cutter, as well as from the commercial type of cutter of various classes, that all milling-energy data can be expressed by the equation $E = Cwf^x d^y$.

24 It is shown that the net power values of commercial milling, when reduced to energy in foot-pounds per chip as a function of feed and depth of cut, agree very closely with corresponding values obtained from the single-tooth cutter in the pendulum-type machine. It is believed that for research purposes, the values obtained with the pendulum-type machine are more accurate than those obtained with the commercial machine, particularly where net motor horsepower, as measured by a wattmeter, is used.

25 It is shown that the different materials respond differently to the same change in front-rake angle of the tool, as far as energy is concerned. One metal may be removed much more efficiently with a high rake angle than with a low rake angle, while another may be removed with only slightly greater efficiency. This also has been shown previously in Fig. 26 of a paper, "Research in the Elements of Metal Cutting."⁶

26 Different exponents and constants are obtained in the energy equation for the same tool when cutting different materials. Each material seems to give rise to its own characteristic constants and exponents. Small changes in structure or composition of a metal also will produce these changes.

ACKNOWLEDGMENTS

The authors wish to express their appreciation to Mr. Carl Oxford, of the National Twist Drill and Tool Company, Detroit, Mich., for the use of the pendulum-type dynamometer used in these tests.

Messrs. Harold McLean and William Gilbert assisted in running the tests, while Messrs. Gilbert, Louis Veenstra, and Maurice Bates assisted in drawing the curves and preparing the drawings.

Grateful acknowledgment also is made to the Cincinnati Milling Machine Company and to Ohio State University for furnishing a copy of a report of their cooperative investigation of milling which the authors have herein analyzed and compared with the results of their own investigation.

Discussion

HANS ERNST.⁷ The investigation described in this paper is an excellent extension of the field covered by "Elements of Milling, Part 1." It is gratifying to see that this investigation has covered the effect of helix angle on both land and groove cutting; also the effect of front rake in both cases.

Many interesting points are brought out in the tables and charts that accompany the paper. Chief among these is the very marked decrease in the energy per chip as the rake angle is increased. This is particularly true in the case of S.A.E. 1020, the large reduction in this case being probably due to the ductile nature of this material.

A peculiar feature of the test on free-cutting brass is the considerable increase in energy value per chip between 0- and 10-deg helix angle when cutting on a land. It is difficult to account for this, as one would normally expect a gradual reduction between 0 and 10 deg, just as has been found from 10 to 40 deg. The increase in energy with increase in helix angle when milling in a groove is of course readily explained by the increased opposition to free flow of the chip by interference with the size of the groove.

It is hard to account for the slight rise in the energy value per chip which was found in some cases when the rake angle

⁶ Trans. A.S.M.E., vol. 48, 1926, pp. 749-848.

⁷ Research Engineer, Cincinnati Milling Co., Cincinnati, Ohio. Mem. A.S.M.E.

(when cutting on a land) was increased from 20 deg to 25 deg. In the case of S.A.E. 3250, one might reason that with this tough material the vertical component of the chip pressure against the nose of the cutting tool was sufficiently great to deflect it downward against the work surface, thus possibly causing an additional drag thereon, but this argument appears to fall to the ground in the case of the free-cutting brass where a similar increase in power is noted, yet where the chip pressure must be very much lower.

The somewhat erratic changes in the values of the feed and depth exponents (particularly the latter) is likewise difficult to explain. It is possible that this may be due to chance differences in the smoothness of the lip surface of the cutting teeth, when changing from one rake angle to another. In our own work, we have found that the condition of lip surface has a tremendous influence on the formation of the built-up edge. In fact, I have recently found in the case of a special cemented carbide that no built-up edge whatever was produced under the same conditions that, with other cutting materials, would produce a very substantial built-up edge. Obviously, as the formation of the built-up edge is usually a function of the instantaneous chip thickness, it would seem that very slight differences in the character of the lip surface of the tool would have a marked effect upon the value of the depth exponent.

It is interesting, and important, to note the general cor-

respondence between the results obtained in the Ohio State experiments and those obtained with the single-point tool, though here again the perplexing variations in the values of the feed and depth exponents show how dependent all the energy values are upon the particular mechanism of chip formation existing in the case of each test.

In commenting on the finish produced on up and down milling it is mentioned that, in cutting up, "the chip has a tendency to cling to the cutting edge, and, if left on, would be dragged under the cutter on the next cut, marring the surface." From our experience we believe that such a condition depends largely on the material, feed per tooth, and cutting fluid used and can scarcely be considered as a condition inherent in up cutting. In commercial milling, the finish with down cutting is usually worse than with up cutting on ductile materials such as the low-carbon steels, but may be better in the case of high-carbon steels or cast iron.

In commercial milling we have found that the chips in down milling are usually flatter than in up milling, which is contrary to the results reported in the paper. Here again, the action of the built-up edge on chips produced under commercial conditions may be responsible for the difference.

The authors should be commended for their painstaking work in the conducting of these tests and their analysis of the results obtained.

The Study of Calcium-Sulphate Scale Prevention at Higher Steam Pressures¹

By FREDERICK G. STRAUB,² URBANA, ILL.

The results of previous tests run by the author indicated that there was a possibility of using soda ash for treatment of boilers operating even as high as at 1000 lb steam pressure. However, these tests were run in steel bombs without the generation of steam and were equilibrium tests. In actual operation the results might be different. Consequently, a small one-tube boiler was built for test purposes. The boiler was constructed so that heat could be furnished to the heating tube at a constant rate and as high as 100,000 Btu per sq ft per hr. The boiler was operated so that the concentration of chemicals in the boiler would be independent of the steaming rate. At the same time scale could be formed, removed, or prevented from forming on the heating tube. The thickness of the scale formed could be measured and the scale analyzed. The temperature increase of the tube wall due to the scale could also be measured. This boiler has been operated at steam pressures between 160 and 2700 lb. The results obtained are given in the paper.

IN 1930, research was started in the Chemical Engineering Division of the University of Illinois in cooperation with the Utilities Research Commission, Inc., of Chicago, in regard to the cause of calcium scale in steam boilers and the methods to be used for the prevention of this difficulty. This work was to start at 150 lb steam pressure and extend to the critical pressure. Since very few data were available in regard to the solubility of calcium in the presence of positive and negative ions and since such data were deemed essential to the postulation of any fundamental theory of scale formation, the preliminary work involved the determination of the solubility of calcium salts at the desired temperatures. Part of the data collected has been published.^{3,4,5,6}

¹ Part of research being conducted in the Chemical Engineering Division of the Engineering Experiment Station, University of Illinois, and financed by the Utilities Research Commission, Inc., of Chicago. Released by permission of Dean M. S. Ketchum, Director of the Engineering Experiment Station.

² Special Research Assistant Professor in Chemical Engineering, University of Illinois. Mr. Straub was graduated from the University of Illinois in 1920. After leaving the university, he was associated with Mellon Institute, Pittsburgh, Pa.; Semet Solvay, Syracuse, N. Y.; and Guggenheim Brothers Research Laboratories, New York, N. Y. He holds the degrees of Master of Science and Metallurgical Engineer from Pennsylvania State College. He has been conducting special research for the Utilities Research Commission, Inc., on boiler-feedwater treatment for the last eight and one-half years at the University of Illinois. This has included work on determining the causes and methods of prevention of embrittlement in steam boilers and a study of the methods of preventing scale in high-pressure boilers.

³ "Solubility of Calcium Salts in Boiler Water," Frederick G. Straub, *Trans. A.S.M.E.* vol. 54 (1932), paper FSP-54-17, p. 221.

⁴ "Solubility Studies of Boiler Water," Frederick G. Straub, *Combustion*, April, 1932.

⁵ "Solubility of Calcium Sulphate and Calcium Carbonate at Temperatures Between 182 and 316 Deg C," Frederick G. Straub, *Ind. & Eng. Chem.*, vol. 24, p. 914, August, 1932.

⁶ "The Behavior of Calcium Salts at Boiler Temperatures," Frederick G. Straub, *Ind. & Eng. Chem.*, October, 1932.

Contributed by the Power Division and presented at the Semi-Annual Meeting, Chicago, Ill., June 26 to July 1, 1933, of THE AMERICAN SOCIETY OF MECHANICAL ENGINEERS.

In the paper presented before The American Society of Mechanical Engineers in December, 1931,³ the author called attention to the fact that interpretation of boiler-water conditions in terms of the solubility data must be done conservatively. These data were equilibrium data, and it was possible that such conditions were not reached in all parts of the boiler. At the same time, it was realized that these tests were run without steam generation, and direct comparison with a steaming boiler would not be justified. Attention was also called to the possibility of the rate of steam generation at the heating surface having more influence on the rate of scale formation than the relative solubility of the calcium.

These data already reported indicated the solid and liquid phases which would be desirable for high-pressure boiler operation. However, they were solubility measurements made under conditions approaching equilibrium in the absence of steam generation. Consequently, for the reasons already indicated, the direct application of these data to boiler operation without correlating them with data from a steaming boiler would be likely to give undesirable results. In order to obtain this correlation, a small one-tube steaming boiler was built. The boiler may be operated with a heat transfer up to 100,000 Btu per sq ft per hr through the heating tube. The concentration of the boiler water is independent of the rate of steam generation, and tests may be run up to the critical temperature. Scale may be formed on the heating tube. This scale is analyzed, and the conditions under which the scale is formed, removed, or prevented may all be studied. Consequently, the boiler has been called a "scaling boiler."

DESCRIPTION OF THE SCALING BOILER

The scaling boiler is a one-tube water-tube boiler (shown in Fig. 1). The tube *A* is heated by means of No. 14 chromel *A* resistance wire wound around the tube, with a layer of alundum cement about 1/16 in. thick separating the wire from the tube. Fig. 2 shows the heating tube after the resistance wire is wound and before the top layer of cement is applied. The current input at the tube is measured by means of a kilowatt-hour meter, the energy input being between 2 and 3.5 kw. The drum is insulated with 85 per cent magnesia and heated by means of resistance wire. The amount of heat added to the drum is just enough to compensate for radiation. In this way the heat added at the tube is practically all utilized to generate steam. The steam generated is taken off from the top of the drum by means of a pipe *B*, which connects to the bottom of the water column. A pipe *C* surrounds the steam pipe, and a small amount of water is introduced into this pipe. This acts as a condenser, condensing the steam on the inside and boiling the water on the outside which is at atmospheric pressure. The steam formed is condensed by means of glass condensers *D*, and the condensed steam returns to the jacket surrounding the steam pipe. The amount of steam being condensed in the main steam line is adjusted so that it just balances the steam being generated in the heating tube. This maintains a constant pressure in the boiler.

By returning the condensed steam to the boiler there is no

NOTE: Statements and opinions advanced in papers are to be understood as individual expressions of their authors, and not those of the Society

change in concentration of chemicals in the boiler water, and the chemical concentration, in the absence of chemical reaction, remains constant and independent of the rate of steam generation.

The water level is observed by means of a gage column *E*. The water is introduced into the boiler by means of a plunger-type pump *F*. The pump has two plungers, and may be so arranged that one plunger pumps water into the boiler while the other pumps it out. In this manner a constant feed may be maintained

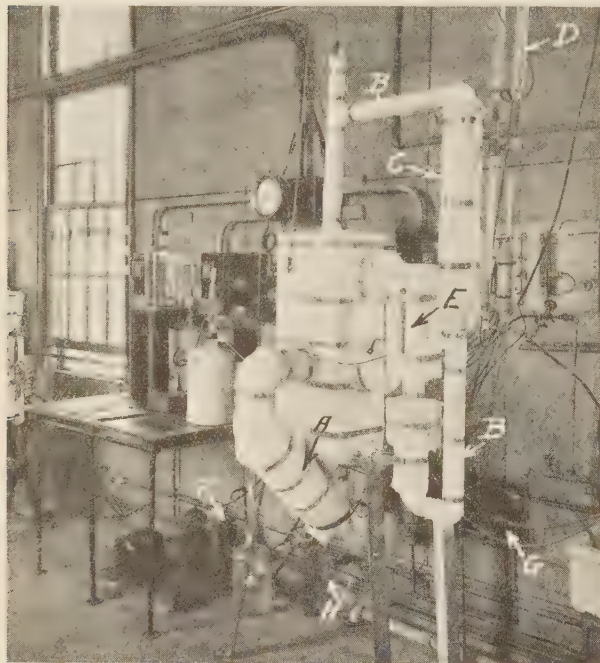


FIG. 1 SCALING BOILER USED IN TESTS

without changing the volume in the boiler, and thus hold any desired concentration of chemicals in the boiler at any desired period.

The heating tube is made of seamless steel tubing with screw flange unions on each end, so that the tube may be easily removed. An iron-constantan thermocouple is inserted in holes drilled in the outer portion of the tube near the center of the heated area. In this manner a record of the temperature of the outer area of the tube may be obtained. Another thermocouple is inserted in a well which gives the temperature of the steam and water as they leave the heating tube and enter the drum. A continuous record is made of these two temperatures by means of a multiple-point recording potentiometer. A second thermocouple introduced in the well is connected to a controlling potentiometer which regulates the heat input at the heating tube and maintains a constant temperature in the boiler.

The temperature of the heating wire is over 2000 F when the rate of heat transfer is high.

The rates of heat transfer through the heating tube may be varied between 30,000 and 100,000 Btu per sq ft per hr. The heating tube is $\frac{15}{16}$ in. inside diameter and $\frac{1}{16}$ in. outside diameter, and has an effective heating length of 5 in., thus giving a heating area of 0.102 sq ft.

The volume of the boiler to the bottom of the gage glass is 1.3 gal, and it holds 11 lb of water at room temperature. The volume to the top of the gage glass is 2.0 gal. The rate of steam generation is about 10 lb per hr at 150 lb pressure.

OPERATION OF BOILER

The boiler has been operated under two different conditions: First, with continuous feed and blowdown, and second, with intermittent feed and blowdown. When operated according to the first condition, the boiler was cleaned out and the desired solid salt was added; a new tube which had been acid-cleaned was put in place, and the boiler was filled with distilled water. The current was then turned on, and the boiler was heated to the desired temperature. When the boiler was up to temperature, sufficient water was put in the condensing unit to hold the temperature constant. A continuous record was kept of the water temperature and of the temperature of the outside of the heating tube. When the boiler had operated for sufficient time to have a record of the temperature difference between the temperature of the outside of the heating tube T_2 and the water temperature on the inside T_1 for distilled water, the feed pump was started. Distilled water containing the desired concentration of calcium sulphate was then added to the boiler by means of the motor-driven feed pump. The stroke of the feed and discharge plungers was so adjusted that the water being pumped out of the boiler was equal to that being admitted (about 1.5 lb per hr), and in this manner the water level in the boiler remained constant. As scale formed in the heating tube, the temperature difference ($T_2 - T_1$) became larger. At regular intervals samples of the blowdown water were analyzed.

When the boiler had operated for the desired period of time, the current was shut off, the blowdown valve *G* was opened, and the entire contents of the boiler blown out within a few minutes. The tube was then removed for examination. By rapid removal of the boiler water the solid phase on the tube did not have time

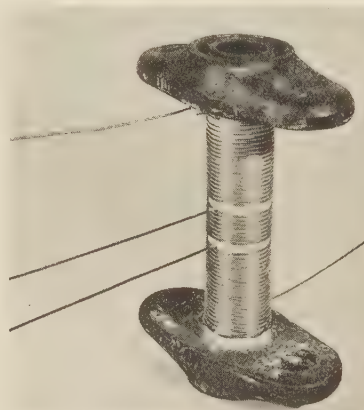


FIG. 2 HEATING TUBE

to change its composition. The flange unions were removed and the tube split longitudinally into two pieces, thus exposing the scale for examination.

When the feed was intermittent, the desired solid phase, either calcium sulphate or carbonate or both, was added to the boiler before putting the tube in place. When the tube was assembled, distilled water containing the desired liquid phase was introduced, and the boiler was heated to the desired temperature. Records were kept of $T_2 - T_1$ as in the other tests. Samples of the liquid in the boiler were collected in a steel bomb by sampling into the sealed bomb from the valve *H*. When the bomb had cooled, it was disconnected, and the contents were removed and analyzed.

From time to time the blowoff valve was opened, and the level of the water dropped to the bottom of the gage glass. The valve was closed, the feed pump was started (the discharge plunger was disconnected), and sufficient water was added to bring the level

to the top of the gage glass. The composition of the water that was added varied according to the various tests. At the completion of these tests, the boiler was shut down, as in the previously reported tests.

Records were kept in all tests of the heat input into the heating or scaling tube in kilowatt-hours, the rate of heat input in kw per hr, the temperature difference $T_2 - T_1$, the amounts of water being added to and removed from the boiler, the composition of the various solutions, the thickness of the scale produced, and its chemical composition.

METHODS OF ANALYSES

Analyses were made on the various solutions for hydroxide, carbonate, sulphate, and chloride. The hydroxide content was determined by pipetting 50 cc of the solution into a 200-cc Erlenmeyer flask to which 10 cc of a 10 per cent solution of BaCl_2 in CO_2 free water had already been added. The flask was stoppered, let stand 15 min, and then titrated with N/50 HCl solution to the phenolphthalein end point.

The carbonate was determined by evolving the carbon dioxide from an acidified solution and absorbing it in a standard solution of barium hydroxide. About 400 cc of the solution was put in a 500 cc Erlenmeyer flask previously swept clean with carbon dioxide-free air. A stream of carbon dioxide-free air was passed through the solution, through a reflux condenser fitted to the Erlenmeyer flask, through granulated zinc, and finally through a Meyers sulphur bulb containing 0.02 N barium hydroxide. The solution was then acidified and heated to boiling, and the air was bubbled through for 20 min. After sufficient air had been passed through, the barium hydroxide was washed into a 200-cc Erlenmeyer flask and titrated with 0.02 N HCl to the phenolphthalein end-point. The difference between the amount of HCl needed to titrate a similar volume of barium-hydroxide solution before absorbing the carbon dioxide, and that after absorption, gave a measure of the carbon dioxide. The sodium carbonate in the solution was calculated from the amount of carbon dioxide evolved.

The sulphate was determined by precipitation as barium sulphate and weighing the filtered and ignited precipitate.

The chloride was determined by titration with silver nitrate and using sodium chromate as an indicator.

OUTLINE OF TESTS RUN

Tests have been run to answer the following questions:

- 1 What is the relationship between solubility of the calcium sulphate and the rate of scale formation?
- 2 What factors influence the rate of calcium-sulphate scale formation?
- 3 What factors influence the prevention of calcium-sulphate scale?

RELATION OF SOLUBILITY OF CALCIUM SULPHATE TO RATE OF SCALE FORMATION

Hall,⁷ concluded that calcium sulphate decreasing in solubility with increase in temperature became less soluble at the heating surface and formed crystals of scale on the heating surface. Calcium carbonate did not form scale according to his theory, since it would become more soluble at higher temperatures and thus precipitate out as sludge. Partridge⁸ conducted research at the University of Michigan along lines similar to those that Hall had followed and concluded

⁷ Hall, R. E., Carnegie Institute of Technology, Bulletin 24 (1927).

⁸ Partridge, E. P., Department of Engineering Research, University of Michigan, Bulletin 15 (1930).

that the rate of scale formation was proportional to the slope of the solubility curve. He also predicted that the solubility of calcium carbonate decreased with increase in temperature. Thus, calcium sulphate decreasing in solubility rather rapidly would form scale rapidly, while calcium carbonate decreasing in solubility very slowly would form scale very slowly.

Figs. 3 and 4 show the solubility of calcium sulphate and calcium carbonate as determined in the author's solubility tests. Table 1 gives the rate of decrease of solubility of calcium in parts per million per deg F, for both calcium sulphate and calcium carbonate.

In order to establish the relationship between solubility and rate of scale formation, the boiler was run with a constant rate of heat input at the heating tube, and a solution of calcium sulphate was added to the boiler continuously. Table 2 gives the

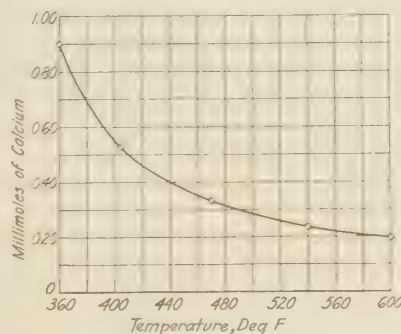


FIG. 3 SOLUBILITY OF CALCIUM; SOLID PHASE ADDED, CALCIUM SULPHATE
(Millimoles $\times 40$ = ppm of calcium.)

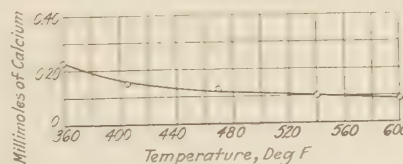


FIG. 4 SOLUBILITY OF CALCIUM; SOLID PHASE ADDED, CALCIUM CARBONATE
(Millimoles $\times 40$ = ppm of calcium.)

results of tests run under these conditions at 150-, 250-, and 500-lb pressure. The tests at 1000-, 1500-, 2000-, and 2700-lb pressure, also given in Table 2, were run with a solid phase of calcium

TABLE 1 RATES OF DECREASE OF SOLUBILITY OF CALCIUM IN CaSO_4 AND CaCO_3 WITH INCREASE IN TEMPERATURE

Temperature, deg F	Steam pressure, lb per sq in. gage	Rate of decrease of solubility of calcium in ppm of calcium per deg F temperature increase	
		CaSO_4	CaCO_3
360	150	0.55	0.10
405	250	0.22	0.05
470	500	0.07	0.02
540	1000	0.05	0.01
600	1500	0.03	0.005

TABLE 2 RATE OF CALCIUM-SULPHATE SCALE FORMATION

Test no.	Pressure, lb per sq in. gage	Rate of heat transfer at heating tube, Btu per sq ft per hr	Total kw-hr input to heating tube	Thickness of scale, in.	Rate of scale formation in. per kw-hr $\times 10^{-4}$	Rate of scale formation, in. per million lb steam per sq ft	Solubility of calcium in boiler water, ppm
2	150	80,000	425	0.022	0.52	1.45	26
7	250	75,000	356	0.018	0.51	1.35	18
6	500	76,000	398	0.018	0.49	1.20	9
33	1000	70,000	445	0.009	0.50	0.44	5
27	1500	83,000	347	0.008	0.23	0.42	4
36	2000	83,000	224	0.004	0.178	0.26	3
28	2000	83,000	411	0.004	0.10	0.149	3
37	2000	83,000	1416	0.008	0.056	0.082	3
34	2700	83,000	296	0.005	0.17	0.147	2

sulphate in the boiler at the start, and the feed of distilled water was intermittent.

The increase in temperature difference ($T_2 - T_1$) between that at the start and after various periods of operation is plotted against the total kilowatt-hour input at the heating tube in Fig. 5 for 250-, 500-, and 1000-lb pressure. The rate of temperature increase is proportional to the heat input at the heating tube, and almost identical at 250- and 500-lb pressure. The rate of scale formation per kilowatt-hour is also almost identical for 250- and 500-lb pressure. These results would indicate that the scale forms at the same rate at pressures between 150- and 500-lb per sq. in. It is also evident that the rate of scale formation per pound of steam generated is almost the same at 150-, 250-, and 500-lb pressure.

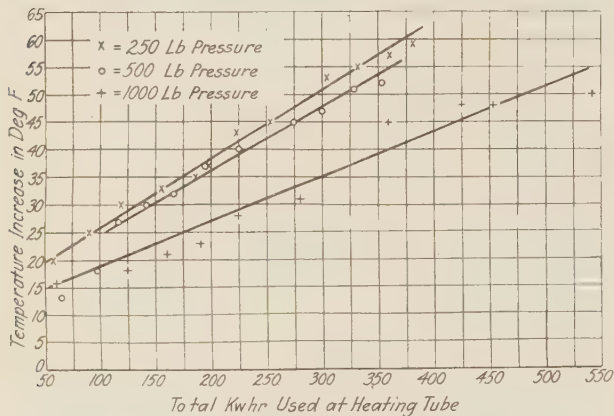


FIG. 5 TEMPERATURE INCREASE OF HEATING TUBE DUE TO SCALE FORMATION AT 250, 500, AND 1000-LB PRESSURE

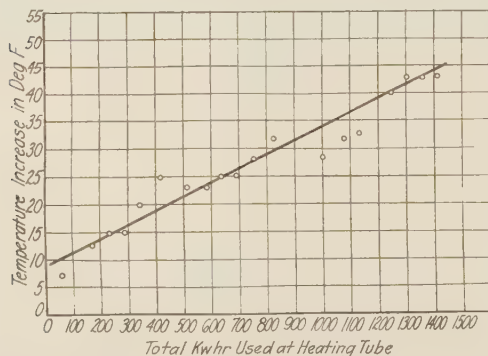


FIG. 6 TEMPERATURE INCREASE OF HEATING TUBE DUE TO SCALE FORMATION AT 2000-LB PRESSURE

Thus, in the test run at 150-lb pressure, a feedwater containing 250 parts per million of calcium sulphate was fed at the rate of 1.45 lb per hr. The solubility of calcium in the boiler water immediately dropped to an average of 36 parts per million, which agrees with the solubility data obtained from the bomb tests. The excess calcium was thrown out of solution in the boiler proper as fast as it was being added. The rate of scale formation was 0.000052 in. per kw/hr. At 500 lb pressure a feedwater containing 200 parts per million of calcium sulphate was added at a rate of 1.56 lb per hr. The solubility of calcium in the boiler water dropped to 9 parts per million, again showing that the excess calcium was thrown out of solution in the boiler. However, the rate of scale formation was almost the same as that obtained at the lower temperatures.

At 1000-lb pressure the rate of scale formation is much slower

than at 500-lb pressure. The rate of temperature increase is proportional to the kilowatt-hour input, thus indicating that scale has been forming throughout the test at a fairly constant rate.

At 2000-lb pressure the rate of scale formation becomes still slower. Three tests were run at this pressure, as reported in Table 2. In test No. 36, with 224 kw/hr used at the heating tube, a scale 0.004 in. in thickness formed, while in test No. 26, with 411 kw/hr used at the heating tube, a scale 0.004 in. in thickness was also formed. A third test was run in which 1416 kw/hr was furnished to the heating tube, and a scale of 0.008 in. was formed. The rate of temperature increase for this test (No. 37) is shown in Fig. 6. These results indicate that at this higher pressure a thin scale forms at the beginning of the test and that the rate of increase in thickness is very slow. Thus, with an input of 224 kw/hr, 0.004 in. of scale was formed, and with 1416 kw/hr, only 0.008 in. The rate of increase in thickness of scale per kw/hr, if calculated according to the amount of additional scale formed, would be only 0.033×10^{-4} in. per kw/hr at 2000-lb pressure, which is 6.3 per cent of the rate of 150-lb pressure, or 6.7 per cent of the rate at 500-lb pressure. If calculated according to the total scale



FIG. 7 TUBE SECTIONED TO SHOW SCALE

formed in run No. 37, it would be 0.056×10^{-4} in. per kw/hr, or 10.7 per cent of the rate at 150 lb pressure.

WHAT FACTORS INFLUENCE THE RATE OF CALCIUM-SULPHATE SCALE FORMATION?

The data obtained in the tests reported in Table 2 should serve to answer this question. As already stated, the scale forms from a saturated solution and is independent within reasonable limits of the rate at which the excess of calcium sulphate is being added. Thus, at 150-lb pressure the calcium sulphate was being added at the rate of 0.22 lb per hr in excess of the solubility, while at 500-lb pressure it was being added at the rate of 0.34 lb per hr in

excess; at 1000, 1500-, 2000-, and 2700-lb pressure a large excess of solid phase was in the boiler from the start.

Fig. 7 shows one of the tubes after sectioning, and illustrates very clearly the manner in which the scale is laid down. The scale is of even thickness for the entire length of the heated area, and then it suddenly stops. This shows that the scale forms on the surface being heated and but very little forms on the unheated surface. This would indicate that the scale is forming from a saturated solution, and the rate is apparently dependent upon the amount of steam being generated at the heating surface and the amount of calcium in solution.

Examination of the crystal form of the scale formed at 1000 lb pressure and lower showed defined crystals at the extreme ends of the scaled section where the rate of formation was slowest. However, at the center of the tube the crystal growth was so dense that the crystals were poorly defined. The definite crystals obtained indicate that the scale is forming by crystallization from a saturated solution and not by precipitation from a supersaturated solution.

At pressures above 1000 lb the scale was no longer white and crystalline. It became very dense and black and the crystalline appearance was not evident. Analyses made on these scales (Table 3) showed that up to 1000 lb pressure the scale was practically pure calcium sulphate. Above this pressure the sulphate content of the scale became lower. This would indicate that the stable solid phase at the lower temperature was calcium sulphate (CaSO_4) without any water of hydration, while at the higher temperature it was a complex salt being made up of CaO and CaSO_4 in varying proportions. The solid in the boiler water at the higher temperatures was also analyzed. The sludge was found to be calcium sulphate. This indicated that the scale forming at the heating surface at pressures above 1000 or 1500 lb pressure was changing in composition. At the higher temperature the calcium sulphate is likely to be unstable, forming a complex salt of calcium oxide and calcium sulphate, and the sulphate trioxide released undoubtedly reacts with the iron present. If this is true, one would not expect the scale to be crystalline in form or to deposit at a definite rate. This is apparently what is taking place at the higher temperatures.

PREVENTION OF CALCIUM-SULPHATE SCALE

The results obtained in the bomb tests indicated that much lower concentrations of sodium carbonate in the liquid phase were necessary to prevent calcium-sulphate scale than had been previously assumed to be necessary. Thus, a few years ago it was assumed that sodium carbonate could not be used above 250-lb pressure, since the amounts necessary to prevent sulphate scale would give such high alkalinities that the embrittlement ratios could not be maintained. However, the results of the solubility tests indicated that at 1000-lb pressure a sodium-carbonate concentration of 85 parts per million would prevent sulphate scale even with the sodium sulphate above 150 grains per gallon. The data were obtained in bombs which were not generating steam; consequently the partial pressure of the CO_2 in the steam space was high and the undecomposed sodium carbonate would be high. Thus it was realized that tests must be run under actual steaming conditions in order to be in position to make this statement with any assurance of its being applicable to power-plant operation.

Tests were run in the scaling boiler in which a scale of calcium sulphate was formed on the tube with an excess of calcium sulphate in the boiler as a solid phase. After sufficient scale had formed, a solution of sodium hydroxide, sodium sulphate, and sodium carbonate was fed to the boiler. The boiler water was analyzed for sodium hydroxide, sodium carbonate, sodium sulphate, and calcium. The results of these tests are given in Tables 4 and 5.

TABLE 3 CHEMICAL ANALYSES OF SCALE FORMED WHEN CaSO_4 WAS PRESENT IN THE BOILER WATER

Test No.	Pressure, lb per sq in. gage	% Ca	% SO_4	% FeO and insoluble	% unaccounted for	% total
2	150	29.0	72.3	...	1.3	101.3
6	250	29.0	69.0	1.5	0.5	99.5
7	500	27.0	70.0	2.0	1.0	99.0
33	1000	29.8	68.1	3.5	1.4	101.4
27	1500	28.4	66.6	3.5	1.5	98.5
26	2000	29.9	59.5	6.2	4.4	95.6
34	2700	28.1	41.0	8.6	22.3	77.7
34S ¹	2700	28.0	69.2	3.7	0.9	100.9

¹ Sludge removed from boiler.

TABLE 4 RUN NO. 12, 500-LB STEAM PRESSURE (470 F)
(50 grams CaSO_4 added to boiler at start; filled with distilled water; intermittent feed and blowdown)

Sample no.	Time duration between feeding sample and blowdown sample, hr	NaOH, ppm		Na ₂ SO ₄ , ppm		Na ₂ CO ₃ , ppm		Ca, ppm
		Feed	Boiler	Feed	Boiler	Feed	Boiler	
2	0.0	180	...	1550	...	100
3	0.25	...	44	...	384	...	23	13
4	2.5	...	44	...	450	...	11	7
5	0.0	180	...	1550	...	100
6	0.5	...	100	...	830	...	20	9
7	3.5	...	105	...	830	...	12	9
8	15.5	...	105	...	810	...	8	7
9	0.0	180	...	1550	...	100
10	5.0	...	125	...	1080	...	13	8
11	8.0	1040	...	10	7
12	23.0	...	122	...	1080	...	10	6
13	0.0	190	...	1550	...	1000
14	2.0	...	166	...	1650	...	34	6
15	6.0	...	201	...	1660	...	17	6
16	11.0	...	227	...	1680	...	25	7
17	0.0	190	...	1550	...	1000
18	12.0	...	256	...	2180	...	31	6
19	16.5	...	275	...	2140	...	28	6
20	0.0	190	...	1550	...	1000
21	3.0	...	246	...	2410	...	28	6
22	19.0	...	280	...	2370	...	26	6
23	0.0	190	...	1550	...	5000
24	7.0	...	503	...	3760	...	238	2
25	22.5	...	580	...	4530	...	45	3
26	29.5	...	590	...	4200	...	25	2
27	0.0	190	...	1550	...	5000
28	20.0	...	850	...	4520	...	644	2
29	37.0	...	1040	...	4130	...	248	1
30	49.0	...	1080	...	4940	...	109	1

TABLE 5 RUN NO. 13, 1000-LB STEAM PRESSURE (540 F)
(50 grams CaSO_4 added to boiler at start; filled with distilled water intermittent feed and blowdown)

Sample no.	Time duration between feed and taking sample, hr	NaOH, ppm		Na ₂ SO ₄ , ppm		Na ₂ CO ₃ , ppm		Ca, ppm
		Feed	Boiler	Feed	Boiler	Feed	Boiler	
3	0.0	0	...	0	...	0
4	90.0	...	15	...	12	...	3.8	11
4	112.0	...	18	...	14	...	7.8	11
5	134.0	...	20	...	11	...	5.5	11
7	0.0	197	...	1550	...	100
7	6.5	...	160	...	270	...	20.0	3
8	22.0	...	240	...	238	...	14.0	2
9	0.0	197	...	1550	...	100
9	8.0	...	254	...	483	...	27.0	4
10	24.0	...	304	...	583	...	23.0	2
11	0.0	197	...	1550	...	100
11	8.0	...	308	...	845	...	21.0	3
12	0.0	296	...	1550	...	1000
12	13.0	...	425	31.0	...
13	0.0	296	...	1550	...	1000
13	7.5	...	390	...	1615	...	28.0	5
14	0.0	296	...	1550	...	1000
14	15.0	...	485	...	1675	...	31.0	4
15	0.0	425	...	1550	...	5000
15	6.0	...	1020	...	2560	...	187.0	3
16	21.0	...	1200	...	3140	...	47.0	3
17	0.0	425	...	1550	...	5000
17	24.0	...	1840	...	4110	...	138.0	0

In run No. 12 at 500 lb pressure (Table 4), the sodium carbonate in the boiler was reduced to as low as 25 parts per million, even with a feed containing 1000 parts per million of sodium carbonate, within three hours after the addition of the feed, and at the same time the sodium sulphate was 1600 parts per million. When a feed of 5000 parts per million of sodium carbonate was added, the soda ash did not reduce so fast. However, calcula-

tion showed that at this point practically all the calcium sulphate had been converted to sodium sulphate and calcium carbonate.

In run No. 13 at 1000-lb pressure (Table 5) the sodium-carbonate content in the boiler was reduced to practically the same figure as at 500 lb pressure.

These results indicate that it is possible to maintain sufficient sodium carbonate at 1000-lb pressure to prevent calcium-sulphate scale even when the sodium-sulphate content is over 100 grains per gallon.

At the completion of these runs, the tubes, when examined, showed that the scale was on the tube in two distinct layers. The top layer was a thin black scale, which could be readily removed from the other layer. It was magnetic and appeared to contain appreciable quantities of magnetic iron oxide. The lower scale next to the tube was a hard white crystalline scale similar to the regular calcium-sulphate scale. The scale appeared as though it was starting to loosen up and rot off. Analyses of the two distinct layers of scale in the two tubes gave the following results:

RESULTS OF ANALYSES OF BOILER SCALES IN PER CENT COMPOSITION

Scale no.	12	12	13	13
Location	Lower	Top	Lower	Top
Ca	24.5	28.9	27.1	31.0
SO ₄	63.3	16.5	64.4	11.9
CO ₃	4.4	40.5	6.8	47.3
Fe ₂ O ₃	2.0	15.2	1.2	5.1
Undetermined	5.8	0.0	0.5	4.7

These results show that calcium-sulphate scale was formed first, and the sodium carbonate reacted with the top portion of this scale to change it to calcium carbonate, which protected the lower portion of calcium sulphate from further attack. This would indicate that the removal of calcium-sulphate scale by means of soda-ash treatment would be rather slow. However, a study of the increase of $T_2 - T_1$ during these two runs showed that as soon as the sodium-carbonate content became greater than 25 parts per million in both runs, the temperature difference remained constant, indicating that calcium-sulphate scale was no longer forming. This would indicate that a concentration of 25 parts per million ($1\frac{1}{2}$ grains) of sodium carbonate in the boiler even at 1000-lb pressure will prevent calcium-sulphate scale formation even when the sodium-sulphate content is greater than 3000 parts per million (175 grains).

In order to determine the limiting value of sodium carbonate more definitely, a study was made of the reaction starting with

calcium carbonate in the boiler and adding sodium sulphate and hydroxide to the boiler water.

Table 6 gives the results of a test conducted at 540 F (1000-lb pressure), in which calcium carbonate was added to the boiler and a solution containing sodium hydroxide and sodium sulphate was used as feedwater. The sodium-carbonate content of the boiler water increased to between 20 and 30 parts per million and appeared to stay there. The sodium-hydroxide content remained at between 400 and 500 parts per million. The sodium-sulphate content was maintained around 4000 parts per million (230 grains per gallon). The sludge remaining in the boiler at the completion of this test had 37.5 per cent carbonate or 62 per cent calcium carbonate, thus showing that calcium carbonate as a solid phase was stable in the presence of sodium sulphate when the sodium sulphate was over 4000 parts per million and the sodium carbonate not over 30 parts per million.

The reactions involved in these studies are as follows:



If calcium sulphate is the solid phase at the beginning of the tests as in run No. 13 (Table 5) and sodium carbonate is added, the sodium carbonate will react to form sodium sulphate and calcium carbonate. However, the reaction is reversible, and if the sodium carbonate becomes less than the amount required to force the reaction to the right, the reaction will proceed to the left. Thus, if calcium carbonate is used as a solid phase as in run No. 16 (Table 6) and sodium sulphate is added, sodium carbonate and calcium sulphate will be formed. The sodium carbonate will tend to react according to reaction (2).

The results given in Tables 5 and 6 indicate that the amount of soda ash required to prevent the formation of calcium sulphate is about 25 parts per million, and this amount should be effective with the sodium sulphate as high as 3000 parts per million.

It was desirable to check still further the amount of carbonate necessary to prevent calcium-sulphate formation as a stable phase in the boiler. The procedure followed was to add calcium carbonate and calcium sulphate to the boiler and then fill with a solution containing definite amounts of NaOH, NaCl, Na_2CO_3 , and Na_2SO_4 . If the carbonate content was too low, the sulphate would precipitate and lower the sulphate content of the solution. Thus, if samples removed from the boiler showed no loss of sulphate, calcium sulphate was not forming and the carbonate content present would be sufficient to prevent calcium-sulphate formation. The chloride present, since it does not enter into any reaction, would serve as a measure of concentration if any took place. Thus, if the $\text{Na}_2\text{SO}_4/\text{NaCl}$ ratio of the water in the boiler was the same as that of the water being added, no calcium sulphate was forming, while if this decreased, calcium sulphate was forming. The test was run first with intermittent feed, only feeding sufficient water to make up for that removed for the analyses, and second, with a continuous feed. The results of the test run at 1000- and 2000-lb pressure are given in Tables 7 and 8; the results of the 1000-lb test are also shown in Fig. 8. Fig. 8 shows that at 1000-lb pressure (540 F), with intermittent feed, the sodium-sulphate-sodium-chloride ratio decreased rapidly and the Na_2CO_3 content remained about 10 parts per million Na_2CO_3 . When the continuous feed was started feeding at the rate of 1 lb per hr with a solution having 50 parts per million Na_2CO_3 present, the $\text{Na}_2\text{SO}_4/\text{NaCl}$ ratio increased to a value equal to that of the solution being added. The Na_2CO_3 content increased to around 25 parts per million. The $\text{Na}_2\text{SO}_4/\text{NaCl}$ ratio of the feedwater was then raised, and that in the boiler also increased to the same figure, and the Na_2CO_3 content remained around 25 parts per million. The sodium-carbonate content of

TABLE 6 RUN NO. 16, 1000-LB STEAM PRESSURE (540 F)
(50 grams CaCO_3 added to boiler at start; intermittent feed and blowdown)

Sample No.	Time duration between feed and taking sample, hr	NaOH, ppm—Feed	NaOH, ppm—Boiler	Na ₂ SO ₄ , ppm—Feed	Na ₂ SO ₄ , ppm—Boiler	Na ₂ CO ₃ , ppm—Feed	Na ₂ CO ₃ , ppm—Boiler	Ca, ppm
1	0	180	...	1550	...	11	...	0
	18	...	330	...	1330	...	21	0
	0	180	...	1550	...	11	...	0
2	6	...	288	...	1420	...	27	0
3	23	...	352	...	1370	...	18	0
4	30	...	384	...	1340	...	16	0
5	47	...	427	...	1280	...	17	0
	0	180	...	3040	...	18	...	0
6	7	...	352	...	1980	...	17	0
7	24	...	380	...	1980	...	23	4
8	47	...	445	...	1970	...	18	4
	0	180	...	6150	...	18	...	0
9	24	...	400	...	3680	...	21	4
10	48	...	456	...	3750	...	19	4
11	72	...	493	...	3880	...	26	4
	0	194	...	3630	...	10	...	0
12	24	...	436	...	4000	...	21	4
13	48	...	485	...	4120	...	13	4
	0	194	...	3630	...	10	...	0
14	24	...	420	...	4110	...	26	4
15	52	...	468	...	4300	...	26	4
	0	194	...	3630	...	10	...	0
16	21	...	410	...	4150	...	27	4
17	45	...	460	...	4370	...	29	4
	0	194	...	3630	...	10	...	0
18	24	...	405	...	4340	...	18	4

the feedwater was lowered to 25 parts per million, and the $\text{Na}_2\text{SO}_4/\text{NaCl}$ ratio started to decrease. The sodium-carbonate content was then lowered to 15 parts per million, and the Na_2CO_3 in the boiler dropped to around 15 parts per million, and the $\text{Na}_2\text{SO}_4/\text{NaCl}$ ratio of the boiler water continued to decrease.

These results indicate that the Na_2CO_3 content necessary to prevent the formation of calcium sulphate as a stable phase in the boiler at 1000-lb pressure is about 25 parts per million and independent of the sulphate content (at least in the range tested).

Similar tests were run at 2000-lb pressure. The results are given in Table 8. When the intermittent feed was used, the $\text{Na}_2\text{SO}_4/\text{NaCl}$ ratio decreased in value very rapidly and the Na_2CO_3 content remained about 20 parts per million. When the continuous feed was used and the sodium carbonate was above 40 parts per million Na_2CO_3 in the feedwater, the $\text{Na}_2\text{SO}_4/\text{NaCl}$ ratio remained almost constant and indicated that the calcium sulphate was not forming. The Na_2CO_3 in the boiler water increased to about 30 parts per million. When the Na_2CO_3 content in the feedwater was raised to 100 parts per million, the $\text{Na}_2\text{SO}_4/\text{NaCl}$ ratio increased and the Na_2CO_3 content also increased, indicating that the CaSO_4 in the boiler was being converted to CaCO_3 . This indicated that if the Na_2CO_3 content is above 30 parts per million, CaSO_4 will not form as a stable phase at 2000-lb pressure.

The results of the tests conducted in the scaling boiler check very closely the results obtained in the bomb tests. These results obtained in the boiler test were secured by running the tests under three different conditions. Thus, by adding CaSO_4 to the boiler and then feeding Na_2CO_3 , NaOH , and Na_2SO_4 , it was found that the amount of sodium carbonate necessary to prevent CaSO_4 formation as a stable phase was around 25 parts per million at 1000-lb pressure. When CaCO_3 was used as a solid and the equilibrium approached from the opposite side, it was found that about 25 parts per million of Na_2CO_3 was also necessary at 1000-lb pressure. When CaSO_4 and CaCO_3 were both present and a continuous feed of Na_2CO_3 , NaOH , Na_2SO_4 , and NaCl was used, it was found that 25 parts per million of Na_2CO_3 was also the critical concentration at 1000-lb pressure. From these results it appears evident that if a concentration of sodium carbonate greater than 30 parts per million is maintained in the boiler water at all times, calcium-sulphate scale should be prevented even at pressures as high as 2000-lb pressure.

Since obtaining these data, tests have been started in several large power plants to see if these figures will apply to actual operation. In three plants the sodium carbonate is being maintained over 50 parts per million as a factor of safety. One plant has operated at 450-lb pressure for more than six months with scale-free tubes. The boiler concentrations at this plant are as follows:

	Concentration in parts per million		
Na_2SO_4	1276	1675	1327
NaOH	275	377	269
Na_2CO_3	50	65	45
Total alkalinity.....	415	565	403
Ratio: $\text{Na}_2\text{SO}_4/\text{Total alkalinity}$...	3.08	2.96	3.30

The sodium-carbonate concentration was obtained by the evolution method previously described. It has been noted that when the titration figures for carbonate show below 150 parts

TABLE 7 TEST RUN AT 1000-LB STEAM PRESSURE (540 F)
(CaCO_3 and CaSO_4 added to boiler at start)

Feed	Total kw input to heating tube	Composition of feedwater, ppm				Composition of boiler water, ppm				Ratio $\text{Na}_2\text{SO}_4/\text{NaCl}$	
		NaCl	Na_2SO_4	NaOH	Na_2CO_3	NaCl	Na_2SO_4	NaOH	Na_2CO_3	Feed	Boiler
Intermittent	61	62	495	51	12	62	222	138	11	8.0	3.6
"	125	62	495	51	12	62	183	165	11	8.0	2.9
"	223	62	495	51	12	62	110	173	12	8.0	1.8
"	411	62	495	51	12	62	62	173	10	8.0	1.0
Continuous	431	62	495	0	56	62	194	139	17	8.0	3.1
"	495	62	495	0	56	63	380	100	21	8.0	6.0
"	537	62	495	0	56	62	430	77	26	8.0	6.9
"	550	62	495	0	56	63	372	75	22	8.0	5.9
"	620	62	495	0	56	62	483	62	31	8.0	7.8
"	659	62	495	0	56	63	542	16	74	8.0	8.6
"	676	62	495	0	56	62	485	77	21	8.0	7.0
"	725	62	495	0	56	62	435	64	20	8.0	7.8
"	742	62	990	0	56	62	695	73	22	16.0	11.2
"	790	62	990	0	56	63	920	73	25	16.0	14.8
"	850	62	990	0	56	63	865	42	24	16.0	14.0
"	910	62	990	0	56	62	1010	53	20	16.0	16.3
"	971	62	990	0	56	62	950	48	21	16.0	15.3
"	982	62	990	0	56	63	990	32	23	16.0	16.0
"	1028	62	990	0	25	62	1020	67	19	16.0	16.5
"	1103	62	990	0	25	62	960	67	23	16.0	15.5
"	1150	62	990	0	25	62	840	62	15	16.0	13.5
"	1164	62	990	0	25	63	900	64	14	16.0	14.3
"	1207	62	990	0	15	62	860	59	15	16.0	13.8
"	1273	62	990	0	15	74	1020	69	15	16.0	13.8
"	1337	62	990	0	15	84	1020	40	14	16.0	12.2

TABLE 8 TEST RUN AT 2000-LB STEAM PRESSURE (640 F)
(CaCO_3 and CaSO_4 added to boiler at start)

Feed	Total kw input to heating tube	Composition of feedwater, ppm				Composition of boiler water, ppm				Ratio $\text{Na}_2\text{SO}_4/\text{NaCl}$	
		NaCl	Na_2SO_4	NaOH	Na_2CO_3	NaCl	Na_2SO_4	NaOH	Na_2CO_3	Feed	Boiler
Intermittent	42	62	495	51	9
"	104	62	218	51	9	77	218	294	15	8.0	2.8
"	122	62	182	51	9	78	182	288	19	8.0	2.3
"	168	62	179	51	9	71	179	277	20	8.0	2.5
"	296	62	158	51	9	71	158	284	23	8.0	2.2
Continuous	112	62	990	0	45	62	940	56	23	16.0	15.2
"	180	62	990	0	45	63	910	37	30	16.0	14.7
"	237	62	990	0	45	63	900	38	28	16.0	14.3
"	275	62	990	0	45	63	1020	42	27	16.0	16.2
"	301	62	990	0	65	63	1010	40	32	16.0	16.0
"	344	62	990	0	65	63	910	43	24	16.0	14.6
"	365	62	990	0	65	63	960	37	33	16.0	15.3
"	402	62	990	0	1.00	63	975	45	36	16.0	15.5
"	462	62	990	0	1.00	62	1055	80	37	16.0	17.0
"	505	62	990	0	1.00	62	1010	65	40	16.0	16.3

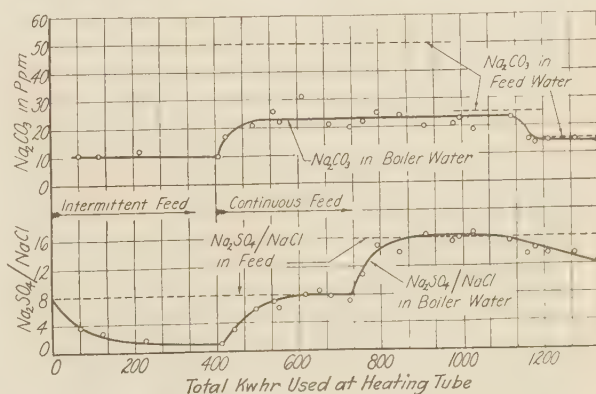


FIG. 8 Na_2CO_3 CONTENT AND $\text{Na}_2\text{SO}_4/\text{NaCl}$ RATIO FOR 1000-LB STEAM PRESSURE FOR INTERMITTENT AND CONTINUOUS FEED

per million for sodium carbonate, the actual sodium carbonate is much lower.⁹ Thus, if analyses of boiler waters by the regular A.P.H.A. method show the carbonate content below this figure, it would be advisable to determine the actual sodium carbonate by the more accurate evolution method.

⁹ "Determination of Alkalinity in Boiler Waters," Frederick G. Straub, *Ind. & Eng. Chem., Analytical Edition*, vol. 4, 290 (1932).

These results show that it will be possible in many higher pressure power plants to condition the boiler with soda-ash treatment. Thus, an external softener using lime and soda ash should, under efficient operating conditions, give an effluent which could be used as a feedwater for higher pressure boilers. It should be realized that sodium carbonate decomposes in the boiler water rather rapidly,¹⁰ and the introduction of a small amount of sodium carbonate continuously would prevent calcium-sulphate scale, whereas the intermittent feeding of larger quantities would not be effective.

CONCLUSIONS

(1) The rate of formation of calcium-sulphate scale is almost constant at 150-, 250-, and 500-lb pressure. At 1000-lb pressure the scale forms about one-third as fast as it does at 150-lb pressure (for a constant rate of heat transfer), while at 2000 lb it only forms about one-tenth as fast as at 150-lb pressure.

(2) The rate of formation of calcium-sulphate scale appears to be independent of the amount of calcium sulphate entering the boiler or the amount of sludge (within reasonable limits) in the boiler.

(3) The presence of more than 30 parts per million (17 grains per gallon) of sodium carbonate in the boiler water will prevent the formation of calcium-sulphate scale at pressures up to 2000 lb.

(4) The carbonate necessary to prevent sulphate scale is independent of the sulphate concentration within the limits of concentrations carried in the average high-pressure boiler.

Discussion

CYRUS WM. RICE.¹¹ Practise has definitely proved that organic matter, silicates, caustics, sulphates, pressures, ratings, and the degree of impurity concentrations in feedwater supplies influence both the rapidity and the characteristics of scale deposits in boilers.

Rarely is it possible in practise to find any two water and operating conditions alike. Under the circumstances no constant, chart, rule, treatment, or result of any experimental work has any definite practical value if cognizance is not taken of these facts.

Again, conclusions drawn from work which fails to include the mentioned influences only confuse the rank and file of those operators who are responsible for results in the majority of steam-boiler plants today. I may be wrong in my conclusions regarding this particular study but the brief does not show a complete analysis of the water used for the experimental work nor that of the boiler concentrates. It is due to the fact that past experimental work has almost totally failed in this respect that made me mention this necessity if the results obtained through any kind of study are to find practical value.

In view of the limited facts given in Professor Straub's paper, I would like to know whether there was no treatment applied where the statement is made "that calcium sulphate forms at a constant rate at 150-, 250-, and 500-lb pressure, practically independent of the rate at which the calcium sulphate is being added to the boiler." If this is the case, the effect is different under actual operating conditions, as SO_4 scale deposits within the boiler in proportion to the SO_4 content in the feedwater. In other words, the amount of SO_4 in the feedwater has a direct bearing on the amount of this which goes on deposit.

The direct effect the rate of heat transfer has on scale formations, as it is indicated in this study, is well borne out in practise by comparing the analyses of samples of scale taken from fire-exposed surfaces with those from surfaces away from the fire. A typical example of this is as follows:

Tube Scale, West Virginia Plant				
	Top	Middle	Bottom	
Silica (SiO_2)	2.60%	11.19%	7.30%	Steam pressure, 350 lb.; industrial load, 125 per cent rating; high SO_4 water and make-up evaporation largely in fire-exposed tubes and first pass
Iron oxide (Fe_2O_3)	1.30%	7.20%	3.20%	
Calcium sulphate (CaSO_4)	0.11%	12.35%	14.20%	

Tube Scale, Connecticut Plant				
	Front Row	First Upper	Steam Drum	
Silica	13.69	15.09	13.12	Industrial load; steam pressure, 115 lb.; condensate return, 65 %; per cent rating, normal
Iron oxide	6.85	9.08	3.55	
Calcium sulphate	5.40	1.29	1.42	

Such comparisons furnished early facts for showing whether the sulphate scales were evaporated or precipitated products.

The conclusions reached in the second paragraph of this study are interesting, especially in view of the fact that the rate of heat transfer at each of the mentioned pressures was the same, and I also assume there was no difference in the SO_4 feed. Under the circumstances, if the deposits at 2000-lb pressure are 10 per cent of these at 500, and it has been definitely shown in earlier experiments that the solubility of the sulphates decrease with increasing pressures, what became of the additional sulphates? Were these precipitated under the higher pressure? Did these go over with the steam? And was there a chemical balance to show just what became of the SO_4 introduced to the boiler?

In regard to the third paragraph of the summary, it is interesting to know that such a small amount (30 ppm) of sodium carbonate was sufficient to prevent SO_4 deposits. In this connection, was the sodium carbonate here calculated or was it determined by direct analysis? In the practise of treating in the field it is not so much the amount of remaining CO_2 that is to be considered in the conditioning as it is the amount of alkalinity needed to protect the boilers and equipment receiving steam against corrosion. This is the important matter to consider in the conditioning of high-pressure boiler operations because of the low, almost negligible, amount of solids contained in the feed in use for such operations and the tendency these waters have in causing corrosion.

We are directing treatments for some few of the very high-pressure plants, and we find it absolutely necessary to maintain a pH reading in excess of 10.5. This, because of the exceptional feedwater, is the most important consideration in the conditioning of concentrates for high-pressure boilers.

J. K. RUMMEL.¹² It is a real pleasure to have this opportunity to compliment Professor Straub on the very interesting work he has been doing in connection with the use of sodium carbonate for the prevention of calcium-sulphate scale.

His conclusion, to the effect that the necessary carbonate concentration of the boiler water is considerably less than has been shown by the physical-chemical theory agrees substantially with our own less exhaustive researches. We differ slightly in the quantitative results, but considering the differences in method and equipment, this is to be expected. Also, with some few exceptions, his general idea has been confirmed by our boiler-water and scale analyses.

¹⁰ "Decomposition of Dilute Sodium-Carbonate Solutions," Frederick G. Straub and R. F. Larson, *Ind. & Eng. Chem.*, vol. 24, 1416 (1932).

¹¹ President, Cyrus Wm. Rice & Co., Inc., Pittsburgh, Pa. Mem. A.S.M.E.

¹² Babcock & Wilcox Company, Barberton, Ohio.

When we come to the practical application of the use of sodium carbonate as the principal treating agent for the prevention of boiler scale or calcium-sulphate scale in particular, there are a number of things which must be considered, and, as has been true in the past, it is advisable to study each case separately. For example, in the case of a boiler fed with a high percentage make-up, it usually develops that there is sufficient carbonate in the feedwater to maintain a suitable carbonate concentration in the boiler water and the prevention of calcium-sulphate scale is not difficult or expensive. In a great many other cases the percentage of make-up is low and the feedwater is nearly all de-aerated condensate. With this type of feedwater it may be difficult to maintain the desired carbonate concentration without exceeding the limits of total boiler-water solids and per cent blowdown, which for the higher pressure operation are usually fixed at some low values. One may, of course, recarbonate the boiler water in an external treating system, but this procedure is likely to be expensive. Therefore, a careful analysis of the conditions at these plants will be especially helpful in choosing the method of treatment.

Unfortunately, calcium sulphate is not the only consideration in the prevention of troublesome boiler scale. For example, silica, the silicates and sometimes calcium carbonate are often more difficult to control than calcium sulphate, and in some stations we are still looking for a practical remedy. It is therefore hoped that this good work of Professor Straub will be continued, so that we may eventually arrive at the most practical methods of dealing with all scale problems and at the same time be able to control the boiler-water concentrations within limits which will inhibit other troubles due to water conditions. It seems extremely doubtful if any specific chemical will be found to cope with all boiler-water-treating problems, and in this connection any new information dealing with the limitations of the chemicals now available should be of considerable interest.

In conclusion, I wish to say that I have no reason to object to the use of sodium carbonate for the prevention of boiler scale, and my remarks are offered only with the idea of calling attention to some of the difficulties of its application.

ARTHUR J. HERSCHMANN,¹³ The fact that high-pressure boilers can be operated without difficulty from scale is proved by the performance of a number of Loeffler boilers in years of service. We remove all dirt which collects in the vaporizer, although it does no harm within that drum, which could accumulate much sludge without detriment.

It is conceded that these forced steam circulation boilers are free from scale and corrosion of internal surfaces. With the shut-down of the boilers for examination and external cleaning, specimens of condensate were withdrawn from radiant and convection superheaters. Tested in the laboratory, these showed absolute purity. This will appeal to practical engineers as a common-sense substantiation of the statement heretofore received with much surprise that no dirt reaches the tube elements of the Loeffler boilers, which stay clean and do not corrode.

W. C. SCHROEDER¹⁴ AND EVERETT P. PARTRIDGE,¹⁴ The paper presents interesting and valuable data. The author is to be commended for his ingenuity in experimentation at high pressures and for the care exercised in checking by these scaling tests the conclusions previously deduced from solubility studies.

With regard to the first conclusion stated at the end of the paper, the writers feel that some caution should be exercised in the interpretation of the apparent rates of scale formation in

Table 2. In the tests at pressures of 150, 250, and 500 lb per sq in. gage where relatively high and nearly identical rates of scale formation were measured, the boiler water must always have tended toward at least a slight degree of supersaturation as a result of the continuous feed of a calcium-sulphate solution which, at the moment of its introduction into the boiler, would have been approximately 100 per cent supersaturated in test 2 at 150 lb and approximately 550 per cent supersaturated in test 6 at 500-lb pressure.

In these tests where the feed solution continuously introduced more calcium sulphate than could remain in solution at the boiler temperature, most of this excess probably separated as loose crystals of calcium sulphate in the body of the boiler water. However, there would always be a tendency for this excess dissolved calcium sulphate to deposit from solution on any crystals of calcium sulphate already present in the boiler, whether as loose sludge or as scale on the heating tube. The growth of the crystalline scale on the heating tube would then depend to some extent on the difference between the amount of calcium sulphate in the entering feed, and the amount which could exist in solution at the boiler temperature. This difference was much greater in the test at 500 lb than in the test at 150 lb, with the test at 250 lb presumably intermediate, although the concentration of the calcium sulphate in the feed for this latter test is not mentioned in the paper. It seems possible to the writers that this fact may account for the nearly equal rates of scale formation in the tests at 150, 250, and 500 lb.

In the tests at the higher pressures the situation was quite different. Here the supply of dissolved calcium sulphate for the formation of scale could come only from solid calcium sulphate introduced into the boiler at the start of each test. The deposition of solid calcium sulphate as scale on the hot tube necessarily depended upon the solution of an equal amount of calcium sulphate from the sludge. Instead of tending toward supersaturation as in the tests at lower pressures, the boiler waters in the higher-pressure tests must actually have tended toward undersaturation, since only in this way could calcium sulphate be dissolved from the sludge.

From the preceding discussion it is evident that the rates of scale formation recorded in Table 2 represent not only the effect of increasing temperature and pressure in themselves, but also the effect of a widely differing potential for the process of scale growth. It is scarcely surprising that the rates show no proportionality to the slope of the equilibrium-solubility curve of anhydrite. Such proportionality would be expected only if other variables were held constant.

Although no general relation between boiler temperature and rate of scale formation should be drawn from the data of Table 2, the individual tests, when considered in the light of the conditions during each test, are of the greatest value because they extend our information concerning scale formation to higher rates of heat transfer and higher boiler temperatures and pressures than have hitherto been investigated.

In the treatment of the rate of scale formation in the paper the wording allows some confusion as to whether, at a constant rate of heat transfer, the rate of scale formation is dependent on the solubility of calcium sulphate in the solution, or on the rate of change of solubility with temperature, that is, the slope of the solubility curve. It is the slope of the solubility curve which has been used as a criterion of rate of scale formation. One reason for lack of proportionality between solubility slope and rate of scale formation in the present tests has already been discussed. Other factors, such as the effect of increase in temperature upon the density, viscosity, and amount of vaporization at constant heat input, with their resultant influence on circulation in the scaling boiler and the temperature drop from the hot surface to

¹³ Agent, Vitkovice Steel Works, New York, N. Y. Mem. A.S.M.E.

¹⁴ U. S. Bureau of Mines, Nonmetallic Minerals Experiment Station, Rutgers University, New Brunswick, N. J.

the solution, would also have to be considered in any rigorous test of the effect of solubility slope.

If the data given in Table 2 for the solubility of calcium as calcium sulphate in boiler water are compared with the data previously published by Professor Straub for the solubility of calcium as calcium sulphate in the studies with the solubility bombs, a rather marked difference is apparent. In both cases only calcium sulphate is supposed to be present in solution. At 360 F the data are in exact agreement, but at higher temperatures they diverge quite markedly until at 600 F the value in Table 2 is only one-third of the value from the solubility tests. It would be very interesting to know the reason for this divergence.

From Tables 4 and 5 the conclusion has been reached that a concentration of 25 ppm of sodium carbonate in the boiler at 1000 lb pressure will prevent calcium-sulphate scale formation even when the sodium-sulphate content is greater than 3000 ppm. Actually, in these two tables there is only one sample which contained 25 ppm of sodium carbonate or less and over 2000 ppm of sodium sulphate. It is stated, however, that as soon as the sodium-carbonate content became greater than 25 ppm in both runs, the temperature difference remained constant, indicating that calcium-sulphate scale was no longer forming. A log of the values for the temperature differences for these two runs would have made an interesting addition to the paper.

The data given in Table 6 were obtained by charging the boiler with calcium carbonate and then pumping in a feed containing sodium carbonate, hydroxide, and sulphate. At the end of the run the sludge contained 62 per cent calcium carbonate. Presumably most of the remaining 38 per cent was calcium sulphate, which would indicate that during some part of this run calcium sulphate was the stable phase, since it was actually formed from the calcium carbonate. In other words, during this run an equilibrium existed between calcium carbonate and calcium sulphate, the actual position of the equilibrium depending mainly on the concentrations of sulphate and carbonate in the boiler water. It is certainly impossible to conclude from this run that calcium carbonate was the stable phase at all times. If this were true no conversion should have occurred to calcium sulphate.

In the runs considered in Tables 7 and 8, with the exception of one sample the sodium carbonate ran from 10 to 40 ppm and the sulphate ran to slightly above 1000 ppm. These data are very valuable in predicting how much sodium carbonate is necessary to prevent calcium-sulphate scale up to this concentration of sodium sulphate but they cannot be used to state directly how much sodium carbonate will be necessary if the sodium-sulphate concentration is increased above this value of 1000 ppm.

It should be noted especially for runs 12 and 13 in Tables 4 and 5, which are intended to show the removal of calcium-sulphate scale, or at least the stoppage of its formation by the presence of certain concentrations of sodium carbonate, that no calcium sulphate was introduced with the feed. At the start, solid calcium sulphate was introduced into the bottom of the boiler, a scale was formed, and then a feed containing only sodium carbonate, hydroxide, and sulphate was added. As previously noted, this would tend toward undersaturation of the boiler water with respect to calcium sulphate. In actual boiler operation the calcium sulphate ordinarily comes in with the feed, and often in high enough concentration to tend toward supersaturation of the boiler water with respect to calcium sulphate at the temperature of operation. To make the scaling tests in the experimental boiler comparable with operating conditions this same procedure should be followed. This would make the process of scale formation independent of the rate of solution of calcium sulphate, and remove possibilities of undersaturation.

Professor Straub's results are significant from a practical viewpoint because they offer the possibility that sodium carbonate

may be used as a conditioning chemical at high as well as low boiler pressures. Too much emphasis cannot be placed, however, on the fact that such operation can be successful only when supervised by a competent chemist with a knowledge of solubility equilibria.

J. D. YODER.¹⁵ That the chemical reactions at the higher boiler pressures of the most common scale-forming substances should be so similar to the reactions at the lower pressures as established by Professor Straub should be assuring to engineers designing high-pressure boiler plants, particularly for industrial plants where the make-up water is generally high. When high-pressure boilers were first used in central stations they were fed with distilled water. There was some uncertainty on the part of engineers as to the practicability of the high-pressure boiler, where large quantities of make-up were required. The evidence submitted indicates that it might be somewhat easier to protect boilers at 500- or 2000-lb pressure from calcium-sulphate scale than at lower pressures.

No reference is made to the greater need of preventing even thin coatings of scale because of the higher temperature of the water, and therefore greater likelihood of burning tubes. He also takes no account of other substances which are scale-forming, such as magnesia and silica. By proper treatment with lime and soda ash the magnesia offers no trouble from scale. For some cause (the explanation of which may never have been given) there appears a greater tendency for formation of silicate scales at the higher boiler pressures. This tendency is more pronounced with lower sodium carbonate alkalinities, assuming that sodium carbonate alone is depended upon for the prevention of scale. In confirmation of Professor Straub's findings I have not observed the tendency for the formation of calcium-sulphate scale at the higher pressures, even though the relationship of the sodium carbonate to sodium sulphate was not increased beyond that required for lower pressures.

However, I advocate that for the higher boiler pressures the lime and soda treatment should be supplemented with phosphate. I have had the opportunity to compare the condition of boilers at a large number of plants where water has been treated with lime and soda ash and supplementary phosphate, with results obtained by lime and soda ash alone and I find that where the phosphate is properly fed the boilers have a greater freedom from scale than where lime and soda ash alone were fed. The scale most likely formed in high-pressure boilers in the absence of the phosphate treatment is largely a mixture of calcium silicate and carbonate. Supplementary phosphate treatment has, within my experience, been uniformly successful in preventing this calcium-silicate-carbonate scale.

The feeding of phosphate has the further advantage that scale can be prevented with a lower excess of sodium alkalinity. Various illustrations might be given but I have particularly in mind one paper mill which has been operating for three years at 600-lb pressure with a large percentage of make-up which is treated with a hot-process lime and soda softener supplemented with phosphate, directly to the boiler. This plant endeavors to operate with approximately 5 grains per gallon trisodium phosphate (50 ppm PO_4) and an alkalinity of sodium carbonate plus sodium hydrate of 5 to 10 grains per gallon. This treatment has given the boilers substantially perfect protection from scale.

The custom at this plant is to open the boiler annually for inspection. After the third annual inspection no scale was found in the boiler even though it is not customary to wash out the boilers between the annual inspections. During this time no tubes have been lost, nor have they shown any indications of blisters due to scale. The boiler conditions are better than

¹⁵ Cochrane Corporation, Philadelphia, Pa.

could have been expected by the feeding of lime and soda ash alone.

The advantage of holding the excess sodium alkalinity in boiler water as low as possible are well known, both with respect to giving the boilers less tendency to prime and also to provide greater assurance against embrittlement. In addition to this (as the prior work of Straub has shown) the phosphate radical of itself is of value in preventing embrittlement of boiler plate.

It is correct, as Professor Straub has pointed out, that the feeding of phosphate adds to the cost of chemical treatment but the greater assurance given to prevent formation of scale and embrittlement as shown by experience, well justifies its cost for the higher boiler pressures. For the lower boiler pressures the cost of the phosphate treatment does not seem justified.

AUTHOR'S CLOSURE

The various questions which have been raised by those discussing this paper show that they are very much interested in the subject and have read the paper in detail.

However, quite a few of their questions were anticipated by the author, and additional data have been gathered to answer these and other questions. It would take too much space to answer them in detail here. Since presenting this paper, a bulletin of the Engineering Experiment Station, University of Illinois (No. 261) entitled "The Cause and Prevention of Calcium Sulphate Scale in Steam Boilers" has been published, and in it has been published the additional data. Consequently, I believe that answers to practically all of the questions which have been raised may be found in this bulletin.

Some Design Aspects of the Rigid Airship

By DR. KARL ARNSTEIN,¹ AKRON, OHIO

This paper reviews earlier airship design and present-day trends in the light of modern design practise as exemplified in the construction of large size airships such as the "Akron" and "Macon."

It is pointed out by the author that a saving in specific deadweight has always accompanied increases in airship size, except in those cases where specifications have been markedly altered or where the designer has deliberately sacrificed a weight advantage for an expected improvement in performance.

The design of bulkheads and main frames is discussed with regard to the restraint of gas cells and the distribution of planar loads. The influence of the number of corridors in strengthening the main frames against torsion and in assisting in the support of the intermediate frames is also discussed.

There have been but few developments in the engine field during the past few years but it does appear that in the matter of power-plant location the "inboard" installations will have the advantage over "outboard" installations for the faster long-range airships now projected for commercial service.

In discussing means of maintaining the ship's equilibrium under varying conditions the author touches on disposal of ballast and aerodynamic lift to compensate for localized loss of gas, water recovery from the exhaust to replace the weight of the fuel consumed in a ship using liquid fuel, some advantages and disadvantages of gaseous fuels, and general design problems involved in guarding against uncontrolled descent.

IN A PAPER presented to this Society in 1927 and published in the 1928 Transactions,² the possible development of large rigid airships was generally discussed, based on an extrapolation from the known performance data on the medium-size airship *Los Angeles*. It was suggested in this earlier paper that the ideas advanced should be reviewed after the actual construction of a large-size airship. In line with this suggestion, it is proposed

- (1) To revise the data on specific deadweights
- (2) To offer additional information on the subject of rigid mainframes and bulkheads
- (3) To discuss the functions of multiple corridors
- (4) To give a comparison of inside and outside power plants, and

- (5) To point out the general design problems in connection with loss of gas and forced uncontrolled descent.

REVISION OF DATA ON SPECIFIC DEADWEIGHTS

In 1928, when the original paper was presented, the largest airship in existence was the *Los Angeles*. Her volume, at a nominal inflation of 95 per cent, was about 2,500,000 cu ft. The experience and weight data associated with the design of this airship were important factors in the preparation of the curves presented in that paper.

In the intervening five years the world has witnessed the construction of five large rigid airships, all of them appreciably larger than the *Los Angeles*, and two of them more than twice as large. During this period the viewpoint on some of the basic design assumptions has changed appreciably. This appears to be an opportune time to review the earlier assumptions and to adjust the conclusions to be derived therefrom.

The earlier paper presented a graph³ showing the decrease in the unit weight for the entire deadweight of an airship as the volume was increased. While the basic trend of this curve is still correct, there have been changes in design requirements during the intervening years which have rendered the absolute values obsolete. As a specific case a designer extrapolating from past experience might have concluded that a 5,000,000-cu ft airship could be built for from 135,000 to 140,000 lb, and yet the construction of the British *R-100* and *R-101* airships showed that even their expected deadweight of 90 tons could not be met.

The original data should be revised in the light of modern experience and the newer design specifications. The nature and magnitude of the revisions may be determined from a consideration of the assumptions used in formulating the original graphs.

Our original prediction assumed that a light-weight, low-fuel-consumption, reversible engine, built along the lines of American airplane engines, would become available for airships and that as larger airships were built these engines would become available in larger power units, thereby decreasing the unit weight per horsepower. This prediction has not yet come true. The *Graf Zeppelin* and the *Macon* are both equipped with Maybach 560-hp engines weighing about 4.5 lb per hp.

Progress is being made in the design of such light-weight American engines for airship use, and the engine situation may improve in the future. There is, however, considerable pressure for the use of the so-called "safe fuels" in airship engines, and it is possible that airship Diesel engines may become available before suitable safety-fuel engines can be developed. The Diesel engines will have a high-unit weight, possibly higher than that of the present Maybach gasoline engines, so that it seems advisable to predict future development on the basis of heavier engines. A large portion of the overweight in the British-built *R-101* can be attributed to the use of Diesel engines weighing 8 lb per hp.

For simplicity in the original calculations a common airspeed of 70 knots was used for all sizes. In actual practise there has been a gradual increase in speed from the *Los Angeles* to the *Macon*, which, incidentally, is the fastest airship ever built. The original predictions, therefore, are subject to correction for the increased speeds which have been realized in practise.

³ See Fig. 13 of original paper.

¹ Vice-President in charge of engineering, Goodyear-Zeppelin Corporation. Mem. A.S.M.E. Dr. Arnstein was born in Prague, Czechoslovakia, and received his education at the University of Prague, and the Institute of Technology, serving for two years as a member of the faculty of the latter. From 1914 to 1924 he was with the engineering staff of the Luftschiffbau Zeppelin Co., Friedrichshafen, Germany, in which capacity he designed about 70 military and commercial airships, including the *Los Angeles*. He came to this country in 1924 as technical director of aircraft construction of the Goodyear Tire and Rubber Company. In 1925 he assumed his present position. He designed the *Akron* and the *Macon* and the great airship dock at Akron.

² A.S.M.E. Transactions, 1927-1928, paper no. AER-50-4.

Contributed by the Aeronautic Division and presented at the Annual Meeting, New York, N. Y., December 4 to 8, 1933, of THE AMERICAN SOCIETY OF MECHANICAL ENGINEERS.

Speed has a double influence upon the weight of the airship. In the first place the installed power-plant weight varies with the cube of the maximum speed to be obtained. A ship like the *Macon*, designed for a top speed of 72.5 knots, could be expected to carry 12 per cent more power-plant weight than a ship of the same size designed for only 70 knots. (Actually, with attained speeds of 74 to 75 knots, the *Macon* power plant would have been justified in being 20 per cent overweight by the old 70-knot standard.) The second influence of speed is noticed in the weights of the hull and the empennage. The beam strength of the hull, with the exception of the bow section, can generally be taken to vary with the square of the maximum speed. The fins and rudder structure must also be increased in strength and weight in accordance with the increase in the square of the design velocity.

The higher flight speeds also require additional outer cover support in the panels and along the fin and control surfaces. The accidental ripping of the fin covering on both the *Graf Zeppelin* and the *R-101* during squalls encountered on trans-atlantic flights has resulted in the use of more rigid outer cover supports in ships built since that time.

The practise of deriving strength calculations for the hull of an airship on the assumption of a hypothetical bow force, representing the action of a gust on an airship as it was flown at full speed into a zone of cross-wind, was not adopted until after the *Shenandoah* disaster. There had been no incentive for serious consideration of this case in the design of the *Los Angeles* and other early German airships since much reliance was placed upon the experience factor; that is, the knowledge of what strengths had proved adequate in the wide range of operation conditions actually experienced in the past. C. P. Burgess⁴ subsequently analyzed a series of airships in the light of this hypothetical gust theory and from his knowledge of the structural strength built into the various airships concluded that the maximum gusts they could withstand with safety at full speed were 17, 20.6, and 56 fps for the *Shenandoah*, *Los Angeles*, and *Akron*, respectively.

There is a strong possibility that commercial ships of the future will be designed to a similar type of bow-force specification. In some respects this would correspond to the practise in naval architecture where surface vessels are designed to resist the action of a hypothetical wave. It appears that a correction for this item must be introduced if the original data are to be used for predictions of the weights of future commercial airships.

Our opinion regarding interior arrangements for the crew has changed considerably. The allowances made for the quartering of the crew had been admittedly low, being based on the wartime practise of letting the crew sleep in hammocks or bunks arranged along the gangways with little wall or floor space. In both the *Los Angeles* and the *Graf Zeppelin* the quarters appear meager compared to the light, ventilated staterooms for the crew of the *Macon*. Improved standards of living and the maintenance of high crew morale during long flights suggest that the crew be given accommodations superior to those of wartime ships, but probably not necessarily as ample as those carried by the *Macon*.

In utilizing these predicted weight curves one must keep in mind the fact that they apply only to the basic operating weights. Commercial equipment like the staterooms of the *Los Angeles* and the commodious passenger accommodations in the *Graf Zeppelin* must be charged against the commercial payload. In the same manner the weights built into the *Akron* and *Macon* for military equipment, such as gun emplacements, inside airplane compartments, airplane landing trapezes, etc., all belong in the military load and not in the basic deadweight. They

should not be used in arriving at prediction curves for a range of sizes.

It is evident, therefore, that a fair comparison will involve two sets of changes; one adjusting the basic unit-weight curve of the original prediction to the present standards of strength, comfort, and reliability, and the other a correction of the reported deadweights by the removal of those portions of the reported weight which are attributable to the useful load and their reduction to the basic design values. The weight statements for the last six rigid airships to be built have been analyzed and adjusted in conformance with the preceding discussion, the final comparative unit weight values being presented in Table 1.

TABLE 1 COMPARATIVE UNIT WEIGHTS
(Lb per 1000 cu ft of air volume)

Airship	Adjusted prediction	Actual weights	
		Reported value	Basic value
<i>Los Angeles</i>	30.9	32.1	30.9
<i>Graf Zeppelin</i>	28.6	32.1	30.5
<i>R-100</i>	28.3	38.1	34.7
<i>R-101</i>	28.0	46.9	42.0
<i>Akron</i>	27.1	32.8	29.8
<i>Macon</i>	27.1	31.8	28.6

The adjusted prediction values in the first column have been obtained from the original values presented in the 1928 paper by the addition of reasonable weight allowances for those items which have been discussed as representing new standards or specifications in the airship industry. These revised unit weights represent the values which are now considered necessary if airships are to be built according to modern standards. For this reason they may be compared with the corresponding returned weights of airship structures and the "theoretical" overweights determined.

The column headed "reported value" has been obtained by dividing the reported deadweight of each airship by its estimated air volume. The values for the deadweights used here are those published by the designers in recognized aeronautical journals or released by governmental agencies during the course of investigations. The "basic value" figures have been obtained by making appropriate allowances for items generally included in the reported weight but more properly attributable to the useful load.

The difference between the reported and basic values for the *Los Angeles* and the *Graf Zeppelin* is due to the removal of the weights for passenger accommodations. The correction of the data for the British airships has been complicated by the absence of published detailed weight statements. The reported deadweight of *R-100* has been reduced by 17,700 lb. This is a combined correction making allowances for her passenger accommodations and the use of light-weight engines. A total of 26,000 lb was subtracted from the deadweight of *R-101* to correct for passenger accommodations and for excessively heavy engines.

The *Akron* and *Macon* values are entitled to a correction of about 22,000 lb of directly removable weight. Something like two-thirds of this weight is in water-recovery apparatus (not carried by the other ships in the table of comparison), the remainder being made up of such miscellaneous items as airplane compartment, accessibility features, machine-gun stands, the elaborate control stand in the lower fin, and an unusual amount of handling equipment.

The first and third columns of Table 1 may be used for comparisons, but there is one other correction which should be applied to the *Graf Zeppelin*, *Akron*, and *Macon* weights in order to make the comparison fair and complete. This is the allowance for deliberate "overweight" built in by the designers with the knowledge that it would be more than paid back by the improved performance and the reduction of the fuel load needed to ac-

⁴ Journal, American Society of Naval Engineers, August, 1931.

comply any given mission. The combined weight of the lifting-gas cells and fuel-gas ballonets in the *Graf Zeppelin* is considerably greater than the weight of the lifting-gas and liquid-fuel tankage for a conventional airship of the same type. The efficiency of the fuel-gas system, however, more than offsets the increased dead-weight allowance. If the *Graf Zeppelin* were to be converted to straight liquid-fuel operation the modified unit weight would be in excellent agreement with the adjusted prediction in Table 1.

The inside power-plant arrangement of the *Akron* and *Macon* will be discussed later in this paper. From the weight standpoint it can be shown that an outside power-plant installation would require the expenditure of at least 10,000 lb more fuel to attain the same maximum cruising range as the *Macon*. The specification of this airship stated that it was to be used "primarily for scouting at sea" where long range is a necessity. The comparative or basic value for the *Macon* may, therefore, be lowered by about 1.3 units, thus bringing it into agreement with the adjusted prediction.

In preparing this plot, these three ships have been left in their

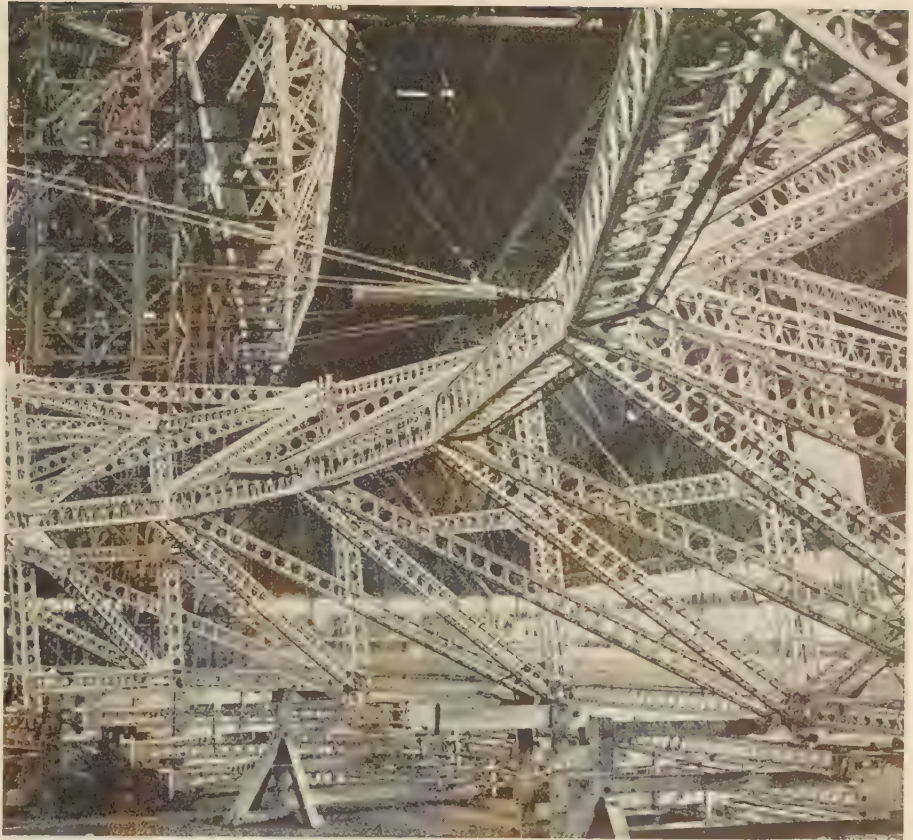


FIG. 1 RESILIENCY DEVICES (AEROL STRUT) MOUNTED IN AIRSHIP STRUCTURE

comparative positions in the "basic" table. Actually, in these cases, the designers were able to build airships with the unit weights in the "predicted" table if they so desired, but they chose the alternative of building heavier ships because they expected that the improved performance of the heavier designs would more than compensate for the apparent waste of weight.

RIGID MAIN FRAMES AND BULKHEADS

The earlier paper described main frames consisting of a series of diamond-shaped trusses, the ends of which were connected by a system of taut bracing, as typical for "medium-size class" airships, and discussed the type of built-up rigid ring frame which it was planned to adopt for "large-size class" airships.

The paper also mentioned the possible use of a loose flexible network as a bulkhead in connection with these built-up frames, leaving the carrying of load entirely to the rigid ring. The rigid ring frames of the *Akron* and *Macon* were designed to carry the specified loads without the assistance of the bulkheads, but the original alternative plan of using loose bulkheads between adjacent gas cells was abandoned in the early stages of design development as soon as it became apparent that it would not permit a desirable degree of static stability with the original type of construction. In other words, it was feared that the gas cells would surge excessively under conditions of pitch unless some more rigid method of holding the cell ends in place was adopted.

The expedient of using a netting which was installed under sufficient initial tension to give the desired control of the gas-surfing tendency was to be preferred and, in addition, the netting installed in this manner stiffened the main frame in a way similar

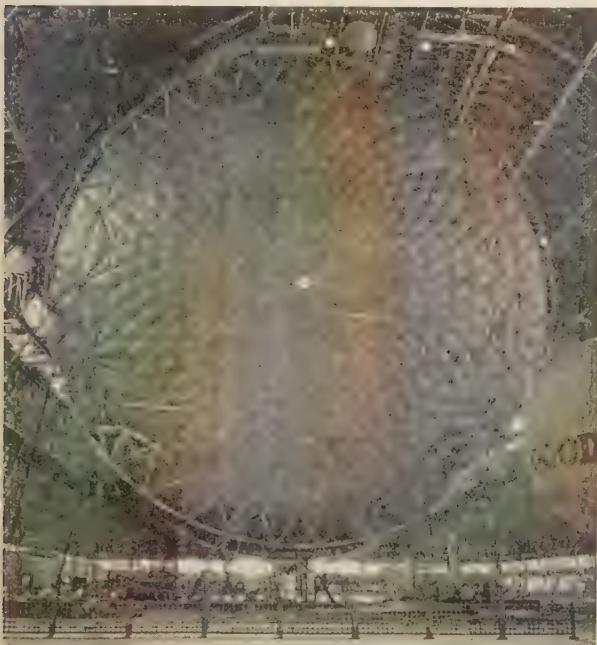


FIG. 2 RIGID RING FRAME AND NETTING

to the wire bracing which had been used in smaller ships like the *Los Angeles*. The new type of initially taut netting was attached to the majority of the main frames through the medium of resiliency devices. (See Fig. 1.) These devices could be set so that the netting would have an initial tension sufficient to give a reasonable control of the surging tendencies during normal flight. Under more severe conditions, and particularly with a deflated cell, the resiliency devices would elongate, allowing a

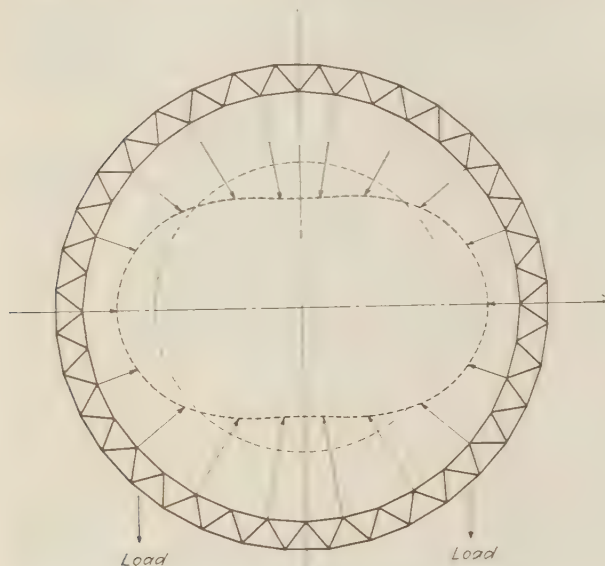


FIG. 3 TYPICAL PARTICIPATION OF BULKHEAD IN THE TRANSMISSION OF LOAD

change in the effective length of the netting and permitting it to assume a better shape for the transmission of the bulkhead load to the longitudinals. This combination of built-up ring frames, netting, and resiliency devices was successfully incorporated for the first time in the *Akron* and *Macon* class. (See Fig. 2.)

While the deflated cell condition is perhaps the most severe which the design of the frame and wiring must meet, it must also be suitable for the transmission of the concentrated loads to be experienced particularly in ground handling. In this respect, the built-up main frame has the advantage that a locally applied load is distributed over a large sector of the frame, and, therefore, affects a large portion of the netting. A frame consisting of consecutive diamond trusses is not so well adapted for the ready distribution of concentrated loads and the brunt of them must be borne by the wires connected to the particular joint under load. It appears that inherently rigid ring frames offer better distribution of concentrated loads.

The resiliency devices can be readily adjusted with sufficient initial tension so that they will not start to elongate under the radial component of any external concentrated load which is likely to occur. Where the external loads are expected to be very high, as is the case with the frames to which the ground-handling gear is attached, it may be desirable to eliminate the devices entirely. This step has already been made on some of the frames in the *Akron* design and the combination of built-up frames and wiring alone has been found to be practicable.

The resiliency devices are automatic units, the functioning of which is particularly important in the case of a deflated cell. Since this emergency seldom arises and since the units add to the initial cost, maintenance, and deadweight, there is some thought that they might be dispensed with altogether or their function

discharged by some simpler automatic extension device, or even by devices which could be operated by the crew at the time of the emergency.

The load-distributing effect of a bulkhead of the netting type can be best demonstrated from wire stress measurement made in connection with frame-loading tests. Fig. 3 shows the typical participation of a bulkhead of the netting type in the transmission of planar loads. The dotted inner circle shows the initial tension uniformly distributed over the ring. Vertical loads increased the tensions in the vertical plane and decreased those in the horizontal plane. The amount of load carried by the bulkhead can be varied at will by adjustment of the wire lengths. It can be reduced by equalizing the tensions, or it can be increased by shortening the wires in the vertical plane and lengthening the wires in the horizontal plane.

The installation of a radial or cord-type bulkhead in a rigid ring frame is also a possibility. Comparative tests with the netting and the radial type of wiring are being conducted. Both types may have merits. The netting probably will allow somewhat better elasticity under side pressure and will dis-

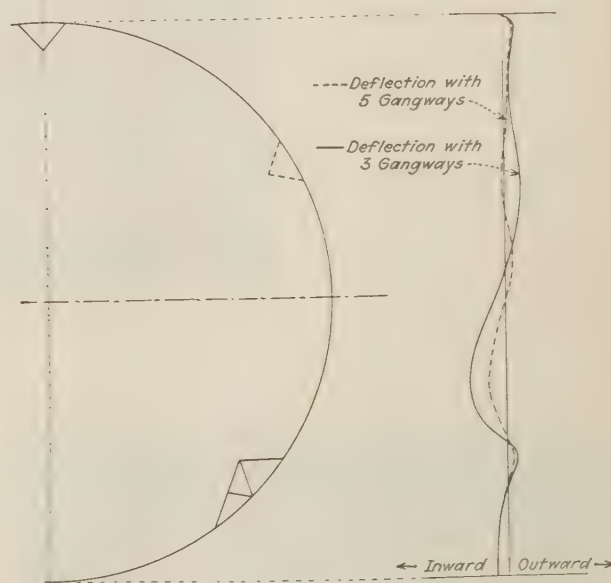


FIG. 4 TYPICAL RADIAL DEFLECTION OF INTERMEDIATE FRAME AGAINST CHORD BETWEEN MAIN FRAMES UNDER GAS PRESSURE AT ABOUT 90 PER CENT INFLATION
(Ordinates of deflection shown greatly exaggerated.)

tribute loads over a larger area of the frame; the radial type because of lesser flexibility, however, may relieve the ring frame of a somewhat larger portion of the load in the plane of the frame.

Another, and older, solution of the problem is the use of an axial tension element which is connected to the wiring of each bulkhead and thus removes a large share of bulkhead load due to difference of pressure in adjacent cells. More recently a central beam has been substituted for this tension element. This type of structure complicates the gas-cell installation, but is not appreciably heavier since the weight for the axial element may be partly compensated for by reduced weight requirements in the bulkhead wiring and the main-frame girders. The axial element may be designed to offer assistance in the attachment and installation of the additional ballonets which are required for fuel-gas and hydrogen-ballast airships.

MULTIPLE CORRIDORS

The earlier paper discussed two main-load-carrying lower corridors located 45 deg from the vertical axis, as well as the use of a gas-valve inspection corridor on the top of the ship. It is evident that the two side corridors apply the loads to the structure in a very efficient way, since the weights are brought close to the shear-transmitting equatorial part of the structure and there is a minimum of distortion in the frames.

The multiple-corridor arrangement permits the whole airship structure to be observed, inspected, and repaired in flight in a manner heretofore impossible. The two load-carrying corridors also provide more space for the installation of fuel and ballast.

The three-corridor arrangement costs some weight and gas space, but it offers the advantage of a structural support to the intermediate frames and main frames. The intermediate frame must change its contour under the buoyant forces and finds support from the three keels, thus also benefiting the longitudinals indirectly. The main frames have, among other load conditions, to take care of a twisting load in case of side pressure on a bulkhead. Again, the three corridors relieve the main frames of a part of this torsion.

The displacement of the joints of the intermediate frames in their own planes under the influence of the buoyant forces has been the subject of very extensive research by actual full-size measurement. Ingenious apparatus was devised by which an observer stationed on the dock floor could, by looking through a powerful telescope, actually read the relative displacements of intermediate joints against an optical chord line between main

frames. Readings were obtainable to an accuracy of a millimeter, either while the ship was on its assembly towers or while it was floating free in the dock. An optical system of scales, lenses, and mirrors was so worked out that the accuracy of the observations did not depend on the exact location of the telescopes. This expedient made it practical to follow these measurements on hundreds of joints for several weeks. Fig. 4 shows the character of displacement of the joints of a typical intermediate frame under the effect of the forces from the buoyant gas at 90 per cent inflation. The plot reveals the predominance of expansive forces in the upper quadrant and a contractive



FIG. 6 "MACON" TYPE OF OUTBOARD DRIVE

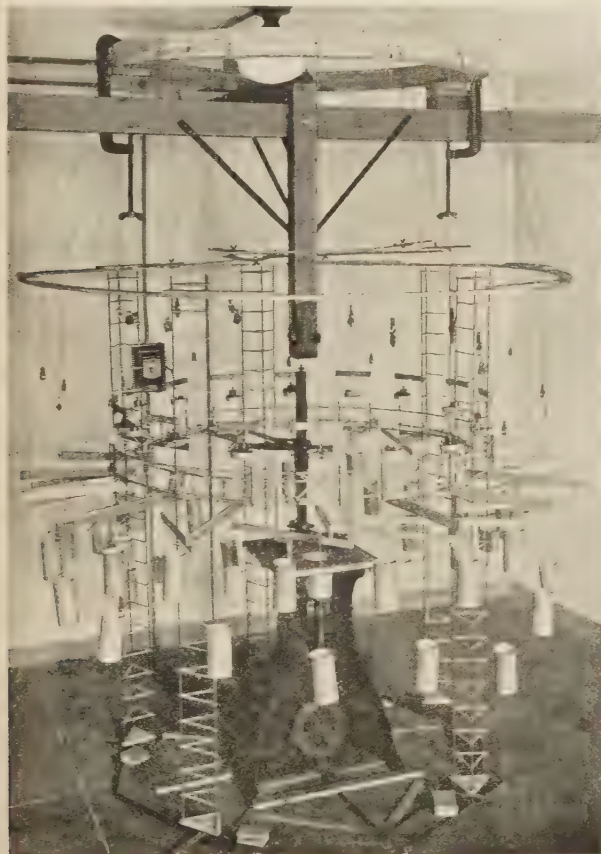


FIG. 5 MAIN FRAME MODEL TEST (CASE SCHOOL OF APPLIED SCIENCE)

flattening out of the arcs between the lateral gangways and the equator. From this actually observed behavior in the presence of three gangways, the probable type of distortion that can be expected if two additional corridors were installed, has been approximated in the same figure by dotted lines.

In order to study the effect of the side gas pressure transmitted through a bulkhead adjacent to an empty cell upon the twist of the main frame, a series of interesting experiments was carried out in cooperation with Professor Plummer of Case School of Applied Science, Cleveland, Ohio. Students, there, have built a model of a trussed main frame of celluloid tubes as girders and brass wires for bracing elements, as shown in Fig. 5. This model was designed to obey, as nearly as was possible, the laws governing elastic similitude. These laws are that homologous forces, applied to the model and to the full-size prototype, produce geometrically similar deformations, when all model forces are reduced in magnitude according to a definite scale. Suitable selection of materials and load conditions permits of the study of elastic deformations greatly in excess of those occurring in full-size service, and thus renders them amenable to much more accurate measurement. This ring model was subjected to twisting loads, the twist of all sections being measured in several experiments with restraint offered by five or three gangways respectively. These investigations are being continued and are throwing considerable light on the extent to which the multiple corridors stiffen the main frame against torsion.

COMPARISON OF INSIDE AND OUTSIDE POWER PLANTS

The merits of inboard and outboard power plants can be impartially compared only when the same required design speed is taken into consideration. The attainment of a specified air speed with outboard plants requires the expenditure of more

power than would be necessary with an inboard installation for ships of the same size and other similar characteristics.

It is interesting to compare the merits of the outboard installations of some previous ships with the inboard installation of the *Macon* (see Fig. 6), using the propulsive coefficient K as a measure of merit. The propulsive coefficient K can be expressed as being in direct proportion with the third power of the speed and the two-thirds power of the volume, and in inverse proportion with the required horsepower:

$$K = \frac{\rho v^3 \times \text{vol}^{2/3}}{550 \text{ hp}} \dots \dots \dots [1]$$

K can also be defined as twice the propulsive efficiency divided by the ship's drag coefficient. It is a measure of the efficiency of the drive and the aerodynamic qualities of the ship, combined. Table 2 shows the improvement of the propulsive coefficient of the *Macon* over that of previous ships:

TABLE 2

	Shenandoah	L-49	Los Angeles	Macon
Air volume, cu ft.....	2,300,000	2,062,000	2,800,000	7,401,000
Speed, knots.....	53	52	63.5	72.5
Horsepower.....	1500	1200	2000	4480
Power-plant weight, lb.....	14,849	12,000	20,800	50,412
Unit weight lb per hp.....	9.9	10	10.4	11.3
K	36.14	39.52	53.00	66.38

It is interesting to consider hypothetical versions of these earlier ships having the nominal volume of the *Macon* (6,500,000 cu ft) and her guaranteed top speed of 72.5 knots. The power required for the propulsion of such ships may be roughly estimated from a consideration of the ratio of the cubes of the actual and hypothetical air speeds and the ratio of the increase in volume to the two-thirds power. Values of these ratios, or "power multipliers," are given in Table 3.

It should be remembered, however, that the propulsive coefficients will not remain constant over this range between the actual and the hypothetical ships, but will improve slightly with increasing size and speed. This "scale effect" influence is also listed in Table 3. The probable horsepower needed to attain the desired performance in these hypothetical ships has been computed with the help of these "power multipliers" and the "scale effect" adjustment.

TABLE 3

	Shenandoah	L-49	Los Angeles	Macon
Ratio of cubes of speeds.....	2.560	2.710	1.488	1.000
Ratio of two-thirds powers of volumes.....	2.150	2.314	1.886	1.000
Allowance for scale effect, per cent.....	13.5	15	10
Original horsepower (as built)...	1500	1200	2000	4480
Hypothetical horsepower.....	7274	6543	5102	4480
Hypothetical power-plant weight, lb.....	72,013	65,430	53,061	50,412

The figures of Table 3 assume that ships of the size and speed of the *Macon* were built under the status of the art existing at the time of construction of the original ships. The contention may be made that the art of outboard-power-plant design has improved in the intervening years, and this is undoubtedly true, but one must remember that the *Macon* inboard power plant has by no means exhausted the design potentialities of this type and much further improvement is still possible. In any event the figures of Table 3 strongly indicate that the inside arrangement may possess advantages for high-speed airships.

As previously stated, more power is required to attain a given air speed with outboard than with inboard plants, but the unit weight (pounds per horsepower) for an outboard plant is generally less than that for an inboard installation. The total power required depends not only on the drag of the ship but also on that of the power plant itself, so that the importance of the drag

varies with the speed to be attained. The greater the speed required, the more important the drag due to power plant becomes. In other words, the greater the relative drag area contributed by any power-plant arrangement, the sooner the weight increase necessary for a further increase in speed assumes impenedimental proportions. Under certain circumstances there is a speed at which the weights of the two competitive arrangements would be the same. At higher speeds the weight advantage would pass from the one to the other. The speed for which the total

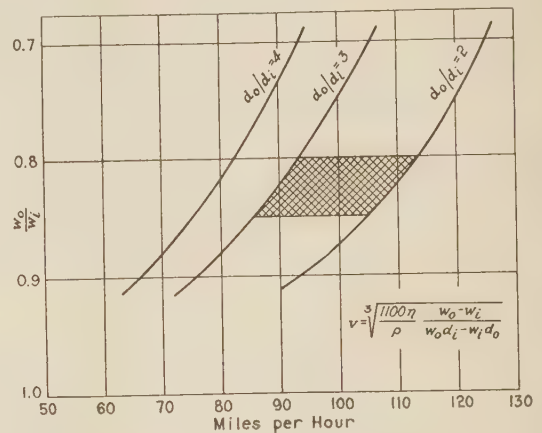


FIG. 7 TOP SPEED IN MILES PER HOUR AT WHICH THE TOTAL WEIGHT OF INSIDE AND OUTSIDE POWER PLANTS BECOMES THE SAME (7,500,000-cu ft commercial airship.)

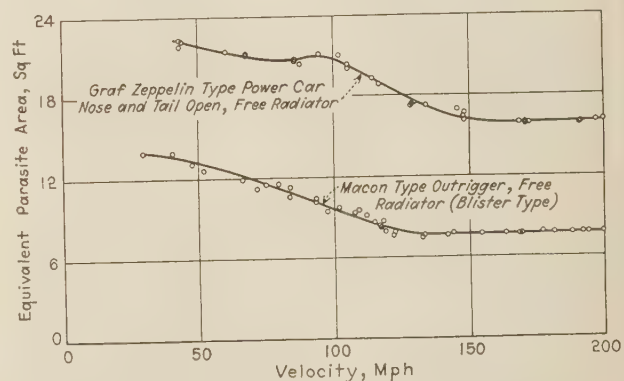


FIG. 8 DRAG COMPARISON, INBOARD VS. OUTBOARD DRIVE (Guggenheim Laboratory, California Institute of Technology, Report No. 116, model scale 1:5.)

weights would be alike can be calculated if the drag area of the power plant can be expressed in terms of horsepower accommodated. Assuming, for instance, direct proportionality between the two, the "equivalent weight" speed may be expressed as

$$v = \sqrt[3]{\frac{1100 \eta (w_o - w_i)}{\rho (w_o d_i - w_i d_o)}} \dots \dots \dots [2]$$

where

η = the propulsive efficiency (assumed the same in both cases)

w_o = specific weight, lb per hp, for outboard plants

w_i = specific weight for inboard power plants

d_o = specific drag area, sq ft per hp, for outboard power plants

d_i = specific drag area for inboard plants

If w_o were equal to w_i , the inboard power plant with its smaller drag area would have the advantage at all speeds. Since, how-

ever, outboard power plants are lighter than inboard, they have the deadweight advantage for low speed. As they have more drag area per horsepower, however, they lose out on the higher speeds where more horsepower is required.

Assuming practical numerical values for w_0 equal to 0.7, 0.8, and 0.9 times the value of $w_i : d_0$, as two, three, and four times as great as d_i (ratios which are not out of order), and taking a reasonable value for η , then the "equivalent weight" speeds will be those shown in Fig. 7 where the shaded area represents the range of contemporary projects. A clue as to the relative drag areas of inboard and outboard power plants is given in Fig. 8, which presents the results of tests⁶ made on models of outriggers similar to those employed on the *Macon* and power cars like those of the *Los Angeles* and *Graf Zeppelin*.

The center region of the shaded field (see Fig. 8) indicates that with a design speed of about 100 mph, the net weights of the power plants, inboard and outboard, are on a par. Of course, other things being equal, the low-drag ship having the engines within the hull will always hold an advantage in the way of fuel consumption, over the other, regardless of the length of the flight.

The fuel consumption at cruising speeds is an even more important criterion. In fact, an actual advantage may be gained from the inboard plants on an airship of present or contemplated sizes at speeds considerably below 100 mph. For any given speed, the hourly fuel consumption is proportional to the drag at that speed. Therefore, even if the higher drag airship has less initial deadweight it will eventually have consumed enough fuel to outweigh the difference in power-plant weights. If the time required for this to happen is well within the flight duration scheduled for the service for which the airship is intended, there remains no question as to the advantage of the inside power plant from the weight standpoint; even though it may be heavier, it may start its flight with a much lower fuel load, offsetting the deadweight penalty.

Under the same assumptions as introduced before, the number of hours which the airship with inboard power plants must fly to overcome its handicap of deadweight can be expressed approximately by

$$h = \frac{w_i - w_0}{F_0 - F_i} \quad [3]$$

where w_i and w_0 represent the total weights of the power plants of the ships with inside and outside plants, respectively, and F_i and F_0 their respective hourly fuel consumptions at the same speed. Since the total weights are functions of the power and unit weights and the hourly fuel consumption are functions of power and unit drags, it is possible to arrive at the following expression for the "equalizing time:"

$$h = \frac{1}{f} \frac{\frac{w_i}{Z_m - d_i} - \frac{w_0}{Z_m - d_0}}{\frac{1}{Z_c - d_0} - \frac{1}{Z_c - d_i}} \quad [4]$$

where

$$\begin{aligned} f &= \text{specific fuel consumption, lb per hp-hr} \\ Z_m &= \frac{1100}{\rho v_m^3} \\ v_m &= \text{top speed} \\ Z_c &= \frac{1100}{\rho v_c^3} \\ v_c &= \text{the cruising speed} \end{aligned}$$

⁶ Made at Daniel Guggenheim Aeronautical Laboratory, California Institute of Technology, Pasadena, Calif., under the supervision of Dr. Th. von Kármán and Dr. C. B. Millikan.

The other symbols are the same as those used in Equation [2]. Fig. 9 has been prepared from Equation [4] by substituting a set of reasonable values as before and assuming top speeds of 80, 90, and 100 mph and cruising speeds of nine-tenths of the top speeds (73 per cent power). Again narrowing the field to the more definite limits of contemporary projects, it is seen that a weight advantage is realized after flying for 30 to 35 hr with a ship having a top speed of about 90 mph. It is evident that on commercial airships of the future the inside arrangement will either be worth its weight from the start or will pay for itself on flights of less than 50 hr. Transatlantic flight schedules will probably average more than 50 hr so that in such a service the inside arrangement would be justified.

In this discussion, the greatest emphasis has been placed on weight, since that is a primary consideration. Next in importance is the possibility of exerting a vertical force, positive or negative lift, with propellers in tilted position. In this respect the inboard

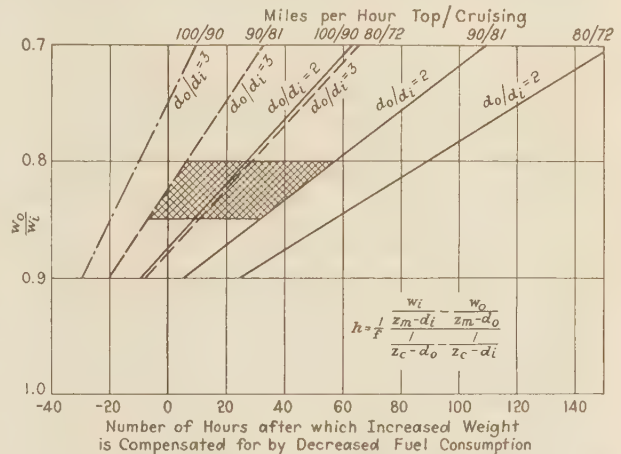


FIG. 9 HOURS IN WHICH INBOARD DRIVE COMPENSATES FOR COMPARATIVE OVERWEIGHT

(7,500,000-cu ft commercial airship, cruising speed = $0.9 \times$ maximum speed.)

drive has a positive advantage. Another important consideration is propeller efficiency and gear losses. For the individual power-plant arrangement equipped with reversing and swiveling gear, there is probably no decided difference in efficiency between outside and inside power plants. In the case of the multiple in-line arrangement, similar to the one used on the *Macon*, some efficiency has admittedly been sacrificed for the benefit of a very practical installation. Among the other points for discussion may be mentioned the comfort of the mechanics, ease of inspection and repair, fireproofness, etc., but most of these items either have a relatively small effect or offset each other in these two types. In the final analysis, the criterion must be combined weight of the power plant and fuel load for the accomplishment of the given service.

The discussion of this controversial subject has been confined to the accepted types of airship power-plant installations as they are now being built. In the future, we may see airships driven by power eggs suspended outside the hull and perhaps utilizing air-cooled engines. At the present time there is considerable reluctance on the part of airship operators to accept any proposal of remote control for airship engines. It may be that this is an old prejudice which could be modified in the light of existing reliability records. Consideration of such units merely involves the use of the appropriate unit weight, drag, and fuel consumption figures in the comparative formulas.

DESIGN PROBLEMS IN CONNECTION WITH LOSS OF GAS AND FORCED UNCONTROLLABLE DESCENT

In his paper,⁶ delivered at the A.S.M.E. Annual Meeting in December, 1933, Commander Garland Fulton has pointed out the importance of maintaining equilibrium during flight while fuel is being consumed. His discussion covers the three possibilities, (a) of valving gas (hydrogen), (b) regaining ballast either by recovery from exhaust gases or by picking it up from the sea or taking it out of the air, and (c) by burning gaseous fuel of about the density of air.

The method selected for maintaining equilibrium during flight has also a bearing on the general design arrangement with regard to the ability of the ship to maintain its equilibrium after loss of buoyant gas.

A reasonable solution of the problem is to so dimension the largest gas cell that the loss of its lift may be offset by disposal of the available ballast or may be carried by the aerodynamic lift of the ship. The combination of these two means of maintaining altitude is naturally permissible although the designer must keep in mind the fact that as the ship approaches its landing, the air speed, and hence the aerodynamic lift, may frequently become very small and for this reason the ship must be reasonably close to buoyancy equilibrium at this time.

The choice of the proper amount of trim ballast is intimately connected with the question of what quantity of disposable load is always available. The answer may depend largely upon the type of airship and the service in which it is to be used. A helium inflated, gasoline-engined ship, like the *Macon*, when on a long-range scouting expedition, would carry liquid loads of more than 100,000 lb. As the fuel is burned, the exhaust gases are cooled in the water-recovery equipment and an equivalent weight of water is recovered. The airship remains in weight equilibrium since the sum of the fuel and water is always equal to the total liquid load, the liquid load being mostly fuel at the start of the flight and mostly water at the end of the flight. It is evident that in airships of this type the captain has an abundance of liquid ballast at his disposal and that fairly large gas cells are permissible.

Another type of airship is the fuel-gas ship, exemplified by the *Graf Zeppelin*. This airship operates on a gaseous fuel having a density very near that of air so that the consumption of the fuel does not seriously interfere with the equilibrium of the airship and no water-recovery equipment is required. On the other hand, the lack of effective weight in the fuel renders it practically useless as ballast in the emergency of a deflated gas cell. Ballast must be provided for this contingency and some of it is usually carried in the form of liquid fuel which may be burned in the ship's engines as a reserve fuel, the gaseous fuel being used for all normal operations. It is naturally desirable to keep this liquid ballast (in the form of a fuel reserve) as small as possible since it cannot be fully counted upon as useful load. The smaller quantity of ballast available has necessitated greater subdivision of buoyancy in this design.

The two most recent airship disasters may be analyzed as due to unchecked descent, the descent being perhaps due in one case to a loss of gas and in the other to vertical currents associated with storm conditions. Means of checking such descents are at the captain's command in the form of disposable ballast and

powerful aerodynamic control. These two remedies have always been available in the past and to a larger degree than before in recent American designs, but it may be expedient to supply them in even greater quantity or power on future airships.

But there is something just as fundamental as the availability of the remedies: It is the necessity that each remedy be applied at the proper time and in the proper degree to assure recovery and prevent serious consequences. There must be reliable methods of informing the captain of the exact position, motion, and condition of his craft in space. He must be enabled to know why the ship is in downward motion the instant such a motion starts, in order that he may take the proper corrective steps in time.

For this purpose concentration of efforts toward perfection of flight instruments is recommended. The most important of these instruments are an absolute altimeter (reading height above the ground), a dynamic-lift indicator, a gust indicator, and an angle-of-attack indicator. While instruments can never replace human judgment, they can and will present the exact facts of the crisis to the captain in such a manner that he can make a clear-cut decision. Improvement upon the existing instruments of this group and the introduction of new instruments of this type will go a long way toward making airship operations under a conservative operating policy a safe and reliable service.

Discussion

G. V. WHITTLE.⁷ Some of the broader aspects of the design of rigid airships are excellently presented by Dr. Arnstein. It is an illuminating and worth-while procedure to pause occasionally and compare progress already made with that previously anticipated as has been done in this paper. The statistical comparisons given clearly illustrate the great progress in design and the substantial improvement in performance of airships which have been realized in the past decade. There appears to be ample justification for the expectation that the advance in the art of designing, building, and operating airships will be as great in the next decade as it was in the last.

Airship progress has been greatly hampered by non-availability of suitable airship engines. It seems that five or six reliable engine units are a sufficient number for a rigid airship and the present outlook favors units having a power rating of at least 1000 hp. The performance of an airship such as the *Macon* would be greatly improved if this airship were equipped with six engines having a total power rating equal to the eight engines with which it is now equipped. The weight to be gained by the elimination of two engine rooms and the improvement possible in specific engine weight with a modern engine are only part of the gain, as the reduction in crew with attendant savings in facilities and consumables for the crew would also contribute an appreciable share. The drag of the airship and hence the fuel consumption would also be reduced by the elimination of the two power units. It is hoped that sufficient encouragement will be forthcoming to foster development in this country of suitable high-powered engines for airship use so that this laggard in the path of airship progress may catch up with the procession.

⁷ Lieutenant-Commander (Construction Corps), U. S. Navy. Inspector of Naval Aircraft, Goodyear-Zeppelin Corp., Akron, Ohio.

⁶ A.S.M.E. Transactions, May, 1934, paper no. AER-56-8.

Some Observations on Spins

By J. M. GWINN, JR.,¹ BUFFALO, N. Y.

Spins may be divided into two classes, controlled and uncontrolled. In the controlled spin there is immediate response to control, while in the uncontrolled spin the response occurs some time later or even not at all after the controls have been moved. The problem is to avoid the accidental controlled or uncontrolled spins and to make the uncontrolled spin controllable. The author has made many observations of uncontrolled spins. The flights were carried on over a period of three years and show to a limited extent the independent effect of wing loading, center-of-gravity position, tail-surface plan form, tail-surface airfoil section, control-surface throw, and wing airfoil. The author indicates a number of conclusions from these observations, the first one of which is that wing loading is one of the major factors in uncontrolled spins.

IT IS now more or less generally recognized that there are two kinds of spin, controlled and uncontrolled. The difference is that in the controlled spin there is immediate response to control, whereas in the uncontrolled spin the response occurs some time later or even not at all after the controls have been moved. By definition, a controlled spin is not dangerous, aside from the loss of altitude if near the ground. Few modern airplanes spin accidentally from the normal maneuvers which are permissible close to the ground. In consequence the controlled spin is no longer as dangerous as it used to be. The problem is, however, still twofold: (1) to avoid the accidental controlled or uncontrolled spin and (2) to make the uncontrolled spin controllable.

The following discussion is mainly concerned with uncontrolled spins. The observations have all been on the one type of airplane shown in Fig. 1, most of them with the same engine, but all with air-cooled engines of similar external physical dimensions. The flights in which these observations were made were carried on over a period of three years and show to a certain limited extent the independent effect of wing loading, center-of-gravity position, tail-surface plan form, tail-surface airfoil section, control-surface throw, and wing airfoil.

EFFECT OF WING LOADING AND BALANCE

Table 1 gives some of the results in terms of the number of turns required for recovery with full opposite rudder for the various combinations of wing loading and balance tested. We were fortunate in being able to vary these items more or less independently. Conditions "A" to "E," inclusive, were obtained in one airplane with the same engine. Condition "F" was obtained in the same airplane with a heavier engine and the wings

¹ Project Engineer, Consolidated Aircraft Corporation. Mr. Gwinn was graduated from Tulane University in 1917 with the degree of B.E. During the World War he served as pursuit pilot with the 27th Aero Squadron, and has at present a private pilot's license. From 1920 to 1923 he was connected with the Gallaudet Aircraft Corporation in metal-airplane construction. Since 1923 Mr. Gwinn has been associated with the Consolidated Aircraft Corporation. He also holds the position of chief engineer with Fleet Aircraft, Inc., and Fleet Aircraft of Canada.

Contributed by the Aeronautic Division and presented at the Sixth National Aeronautic Meeting, Buffalo, N. Y., June 6 to 8, 1932, of THE AMERICAN SOCIETY OF MECHANICAL ENGINEERS.

NOTE: Statements and opinions advanced in papers are to be understood as individual expressions of their authors, and not those of the Society.

moved forward to produce about the same balance as in the original airplane. Conditions "G" and "H" were tested in the same airplane with a heavier engine but with the wings in the original position. Inasmuch as all of these airplanes had identical wing cellules, tail surfaces, and fuselages, and the noses in all cases had quite similar air-cooled engines, it is felt that the differences observed are due entirely to the differences in weight and balance and not to fuselage nose. Elevator position at beginning of recovery made little difference, recovery being slightly faster with up-elevator. All spins excepting "A" were of the uncontrolled type.

TABLE 1

Air-plane	Test	Wing loading	C.G. position on M.A.C.	Number of turns for recovery	Remarks
1	A	7.0	0.250	1/4	Rear cockpit empty
1	B	7.0	0.333	1	Front cockpit empty
1	C	8.5	0.328	1 3/4	Two men
1	D	9.4	0.315	2 1/4	Extra gas on c.g. and baggage slightly forward of c.g.
1	E	9.4	0.370	3	Extra gas on c.g. and baggage aft of rear cockpit
2	F	10.3	0.340	6	Extra gas on c.g., two men
3	G	8.6	0.228	1	Front cockpit empty
3	H	10.2	0.249	3	Extra gas on c.g., two men

These results are plotted in Fig. 2, and two curves for center-of-gravity positions of 25 and 33 per cent have been drawn on the plot. Apparently the position of the center of gravity has a more or less constant effect, while increasing wing loading has a greatly increasing effect, on recovery. As shown later, the variation in distribution in the tests was negligible.

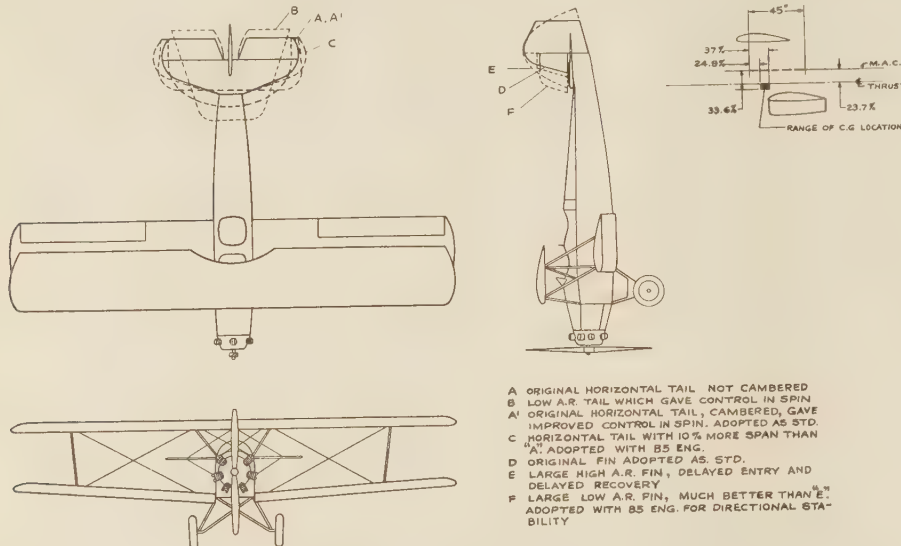
EFFECT OF VARYING FIN AREA

A great many tests were run to show the effect of changes in fin area, the aspect ratio of the fin, rudder area and throw, and fin airfoil (see Fig. 1). The first change made was the complete removal of the cover from the original small fin. This hastened entry into a spin and greatly hastened recovery. This did not seem reasonable, it being thought at that time that an increase of fin area should check spinning. The increase in fin area was assumed to provide additional damping which, in turn, would slow down the spin. Larger fins were therefore tried and the larger the fin the harder it was to produce a spin and the longer it took to recover once a spin was produced. This was quite discouraging. In varying aspect ratio of the fin it was found that a low-aspect-ratio fin produced more directional stability at high angles of yaw than a high-aspect-ratio fin of the same area, but no appreciable difference was noticed in a spin. Restricting the rudder throw made a spin more difficult to achieve and recovery more difficult. The effect of reducing the rudder throw was identical with the effect of increasing fin area. Due to poor rigging in one test, the rudder throw was greater in one direction than in the other. This made it easy to spin in the direction of the greater throw but difficult to come out, and vice versa. It being assumed that the fin was completely stalled in a spin and that delaying the stalling point of the fin would aid in recovery, a very thick fin was built but the results were negative. This was due probably to the fact that when completely stalled the camber has very little effect on C_n . This checks with the negative results obtained with changed aspect ratio. It is conceivable, however, that delaying the stalling of the fin might prevent some airplanes from spinning.

We finally arrived at an explanation for the fact that after a spin was accomplished the larger fin did not seem to provide damping. In contemplating the probable effect of a fin 20 feet square, one immediately saw that the airplane would rotate around the fin.² This led to the idea that increasing fin area moves the point of rotation of the spin aft. Since the effective-

tation was further aft. When the rudder was reversed, the fin area was increased by a lesser amount, due to the reduced throw, and the increase was of little benefit on account of the greatly reduced lever arm. It is conceivable that, if the rudder were reversed slowly, the center of rotation could be moved slowly aft and that the airplane would not recover at all. In other words, recovery should be executed with as sudden an application of opposite rudder as possible so that the increase of fin area can dampen out the spin before the center of rotation has moved aft.

Nearly all airplanes are known to spin differently to the right and left and this difference usually has been ascribed to gyroscopic forces from the propeller or to lack of symmetry in rigging of the wing cellule. The fin is usually offset to line up with the race rotation of the propeller at cruising speed. The fin will therefore stall sooner in spinning in one direction than in the other. This of course produces a lack of symmetry in spin. Offsetting the fin zero-lift line by camber reverses the direction in which the fin stalls later. The proper combination



A ORIGINAL HORIZONTAL TAIL, NOT CAMBERED
B LOW A.R. TAIL WHICH GAVE CONTROL IN SPIN
A' ORIGINAL HORIZONTAL TAIL, CAMBERED, GAVE IMPROVED CONTROL IN SPIN, ADOPTED AS STD.
C HORIZONTAL TAIL WITH 10% MORE SPAN THAN A' ADOPTED WITH B5 ENG.
D ORIGINAL FIN ADOPTED AS STD.
E LARGE HIGH A.R. FIN, DELAYED ENTRY AND DELAYED RECOVERY
F LARGE LOW A.R. FIN, MUCH BETTER THAN E' ADOPTED WITH B5 ENG. FOR DIRECTIONAL STABILITY

FIG. 1 FLEET MODEL 1 AIRPLANE USED IN SPIN TESTS

(Engines used in tests—Warner Scarab, Kinner K5 and B5, Challenger, wings 5 in. forward, Continental.)

ness of the fin in damping is proportional to the fin area and the cube of its distance from the center of rotation, any increase in the fin area,³ accompanied by moving the point of rotation aft, is likely to be of negative benefit. Prior to the occurrence of this idea it had been noted on one occasion that the center of rotation with a large fin seemed to be further aft, but it had been passed by. With this new idea in mind, the observation was recollected, and it was felt strongly that a theory of attacking the fin area problem was at hand. The test with the reduced rudder throw indicated merely that the fin effect of the rudder in a spin was greater with reduced rudder throw and therefore the center of ro-

of offset and camber should therefore produce a fin which stalls at the same angle to both the right and left. This was tried and found to work and we were able to produce airplanes with very

² This however is an exaggeration inasmuch as the center of rotation could not move aft of the center of gravity unless the airplane spun with the tail lower than the nose.

The airplane will tend to rotate about that axis about which damping moments are a minimum. This tendency to rotate about the axis having minimum damping is usually opposed by other factors, namely, lift moments and centrifugal forces, but with an absurdly large fin these other forces would become negligible.

³ It is to be noted that blanketing of the vertical tail surfaces by the horizontal tail surfaces has not been mentioned. The reason for this omission was twofold, (a) the blanketing effect was thought to be so well known as not to merit additional discussion, and (b) we observed actual changes in spin characteristics with changes in vertical fin area above the stabilizer, and noted differences of the same kind and amount with similar changes in the fin area below the stabilizer (in one test a false bottom was added to the fuselage gradually increasing its depth from the rear cockpit to the tail post). It was felt, in consequence of this, that blanketing was not the whole story.

It has been suggested that the improvement due to low-aspect-ratio, horizontal tail surfaces might have been due to less blanketing. This can hardly be so as the reduction in aspect ratio was obtained by a large increase in chord and a small decrease in span, the elevator hinge line not being moved. Considering the relative position of this surface to the fin and rudder and the probable angle of airflow, +60 deg in side view and about 45 deg in rear view, it is apparent that the blanketing was, if anything, increased by the low aspect ratio of the stabilizer.

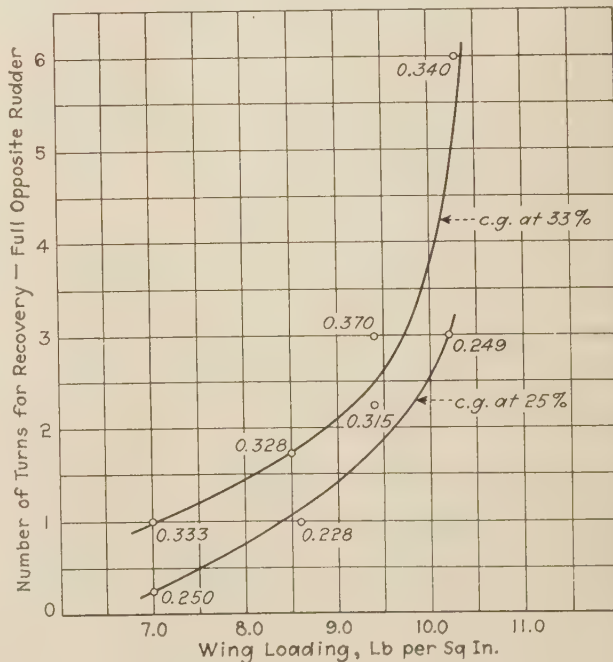


FIG. 2 NUMBER OF TURNS FOR RECOVERY VS. WING LOADING AT VARIOUS CENTERS-OF-GRAVITY LOCATIONS
(Figures by points indicate center-of-gravity locations on M.A.C.)

nearly identical right and left spins and right and left snap rolls. In passing it might be stated that prior to this, in one test, the airplane recovered from a prolonged spin in $1\frac{1}{2}$ turns to the left and $2\frac{1}{4}$ turns to the right. Putting the fin on the center line changed this to $2\frac{1}{2}$ turns to the left and $2\frac{1}{4}$ to the right. There was no gain, it must be admitted, as it was purely at the expense of the left-hand spin. On the other hand, it demonstrated that the lack of symmetry was due to the fin.

EFFECT OF VARYING HORIZONTAL TAIL SURFACES

Another series of tests was run with variations in horizontal tail surfaces. At the very beginning of these tests it was recognized that the fundamental problem in the uncontrolled spin is the stalling of the stabilizer, this being the principal difference between a controlled and an uncontrolled spin. There are several methods of delaying the stall of the stabilizer: (1) to lower the aspect ratio, (2) to use a high lift section, (3) to use slots on the stabilizer, (4) to use no fixed stabilizer, but to have a large elevator hinged somewhat aft of the leading edge so that when the elevator is up in a flat spin the angle of attack of this surface is not sufficiently high to stall it. Fig. 3c shows the probable flow with this latter type of tail; Figs. 3a and 3b show the flow with conventional stabilizer and highly cambered stabilizer, respectively. We first tried a great reduction in aspect ratio of the horizontal tail surfaces, with immediate beneficial results. The resulting tail was so horrible to look at, however, that we did not feel that it was the proper solution; so we resorted to camber on the top of the stabilizer. The results thus produced were not so good as with the low aspect ratio, but this solution was more adaptable to our purpose, and we immediately adopted the highly cambered stabilizer, which we have since used on all small two-seater planes.

It seems that the stalling of the stabilizer is the crux of the question and should be the point of attack of the problem. This made little difference in the old days, because we had thin wings which stalled sooner and low-aspect-ratio horizontal tails which stalled later. Therefore, the wing stalled so much sooner than the stabilizer that the airplane was not capable of being brought up to an angle of attack high enough to stall the stabilizer. Some of the tales heard of the old thin-wing airplanes getting into spins of a different nature were undoubtedly uncontrolled spins obtained through some uncommon means such as a bump in the air.

Experiments with changed elevator throw were conducted, the only noticeable effect being reduction in stick reversal with increased elevator throw. This is due to the fact that, with the increased throw, the elevator trails more nearly at its free trailing angle and therefore the force on it is less. At angles of attack of the stabilizer below the stall, the normal trailing angle of the elevator is approximately one-half of the angle of attack of the stabilizer. At a 20-deg stabilizer angle of attack this is 10 deg up.

If the total up-elevator motion is 30 deg, this is one-third the total up-elevator motion, and the stick therefore seeks a new neutral not sufficiently aft of true neutral for the pilot to notice. At angles of attack in which the stabilizer is truly stalled, the elevator probably trails free at the angle of attack of the stabilizer. In other words, at a 30-deg angle of attack of the stabilizer the elevator tends to trail up 30 deg and the stick comes all the way back. Thus, when the stabilizer stalls there is a sudden movement of the stick aft. An airplane of another make was tested in the course of the experiments and, although it was found to have a spin quite similar to our airplane, the stick reversal force was much lower. The elevator throw was measured and found to be 40 deg up compared to 29 deg on our ship. We felt that this explained the difference in stick reversal.

EFFECT OF AIRFOIL SECTION

Four wing-airfoil sections were tried. Our normal airfoil, a Clark Y-15, had no rigid leading-edge cover to maintain the airfoil at the nose. Our first experiment was therefore to use a duralumin leading-edge cover. The pilots reported a "wicked" spin; one of much faster entry. They all pulled out of this spin as quickly as possible and we did not deem it advisable at that time to make a long spin. This was undoubtedly due to the greater autorotative couple resulting from the greater forward slope of the resultant force on the outer tip.

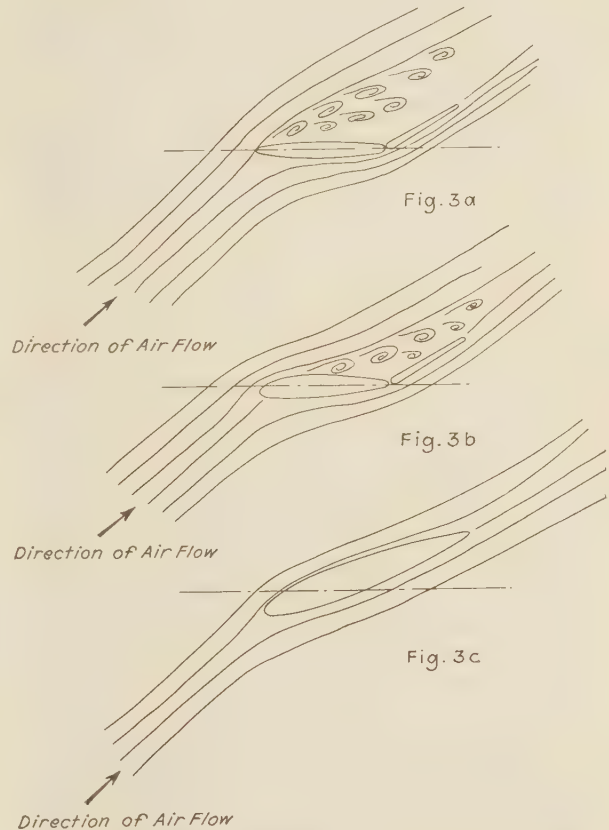


FIG. 3 AIR FLOW ON HORIZONTAL TAIL SURFACES IN A SPIN

The next change in airfoil section was the trial of a Göttingen 398 airfoil. The spins were absolutely the same as those found with the Clark-Y. It is to be noted that the 398 wing had no rigid leading-edge cover.

The third change in airfoil section came about by accident. We were making tests at one time with a 2000-ft ceiling in which we climbed up into the clouds to about 4000 ft and spun down through the clouds, recovering when we came out of them. It has been forgotten just what variation we were trying at the time, but we were greatly gratified to discover that the ship recovered much more rapidly than before. We were about to congratulate ourselves on some great discovery in the way of tail-surface change, when we noticed that there was ice on the airplane. We did not know whether this ice had produced the effect, so we broke it off and repeated the test, gathering ice on our climb, and had the same rapid recovery. We first assumed that the ice had greatly increased the drag on the interplane brace wires, so we made a flight with the streamline tierods flat to the wind. No great difference was noticed. We then put a piece of

wood on the leading edge to imitate the ice. We were not attempting to sharpen the leading edge, however. On the airplane we were using there was a very sharp break in the contour where the fabric left the leading edge. We felt that probably the ice ahead of the leading edge faired out the sharp break and produced probably a smoother lift curve, so our wooden strip was made with the intention of fairing out this curve. This did not help as much as the ice, but it did help, and we adopted a modified leading edge on some of our later airplanes. This idea was mentioned to Mr. Diehl, of the Bureau of Aeronautics, who in turn conveyed it to another aircraft manufacturer. This manufacturer put a triangular strip of wood on the leading edge of his airplane and greatly improved its spinning characteristics. The National Advisory Committee for Aeronautics took the matter up and ran some wind-tunnel tests. Their report⁴ shows that sharpening of the leading edge to all intents and purposes makes a thin wing out of a thick wing. Naturally then, the spin would be changed to the spin of a thin wing. The maximum lift, however, was reduced 26 per cent. It is not felt that using airfoils with reduced maximum lift is the proper line of attack. So much for observation.

MATHEMATICAL ANALYSIS

Equations [9], [10], and [11] of Appendix 1 give a starting point for qualitatively examining the effects of various changes in the airplane on a spin.

Equilibrium of Pitching Moments. The most striking thing about these equations is the term $\sin^2 \theta_x \cos \theta_x$ in Equation [9]. This term varies from 0 at $\theta_x = 0$ to a maximum of 0.385 at $\theta_x = 54.8$ deg and back to 0 again at $\theta_x = 90$ deg. This indicates that as far as the balance of flattening couples against pitching couples is concerned, the airplane may be in equilibrium in a spin in two positions for every center-of-gravity location excepting that center-of-gravity location which gives $\theta_x = 54.8$ deg. Equation [9] shows that if the center of gravity is moved aft (s is decreased), the required decrease in the right side of the equation will probably decrease ω and, except for the effect of the change of ω and the requirements of θ_x in regard to autorotation, $\sin^2 \theta_x \cos \theta_x$, will change θ_x away from 54.8 deg.

Equilibrium in a spin depends of course not only on the equilibrium of Equations [9] and [10], but also on the presence of an autorotative force on the wing sufficient to overcome the moments in Equation [11] plus the damping moments of the fuselage and vertical fin areas. For this reason θ_x is not controlled so much by the value of s as it is by the requirements for autorotative couples.

Effect of Wing Loading. From a consideration of lift coefficients an increase in W will normally increase the sinking speed and ω provided no change in s or any of the radii of gyration accompanies the change in W .

Effect of Vertical Location of Center of Gravity. If the center of gravity is raised, t becomes smaller by an amount equal to the rise in the c. of g. $\times \sin \phi$. This, in turn, must reduce the right-hand side of Equation [10] which means a reduction in either ω , θ_y , or θ_x . A decrease in either ω or θ_x might be sufficient to make an uncontrolled spin controllable, the amount of the effect depending mainly on the value of ϕ which in turn is determined by the amount of skid in the spin. If ϕ is negative, i.e., there is inward slip, raising the c.g. would have the opposite effect.

Effect of Longitudinal Distribution of Mass. Increased longitudinal distribution which increases p_x and p_y , directly increases the right-hand side of Equation [9]. This requires either an increase in s (c.p. must move aft, requiring increase in θ_x as the center of gravity is assumed fixed), a decrease in ω , or a change in θ_x away from 54.8 deg. If the effect is on θ_x , note that the

spin may become either more flat or less flat. The right-hand side of Equation [10] tends to decrease very slightly with increased longitudinal distribution, inasmuch as increased longitudinal distribution increases p_y more than p_x (p_x assumed greater than p_y). It should be noted in passing that most spin experiments, in which it has been assumed that the addition of useful load aft of the center of gravity increased the longitudinal distribution actually do not have increased longitudinal distribution. That is p_y and p_x do not increase. In Appendix 2 it is shown that the radius of gyration of a mass with additional weight is less than the original radius of gyration unless the weight is added at a distance from the center of gravity slightly greater than the original radius of gyration. It has been shown⁵ that p_y and p_x vary on military airplanes between 4.4 and 5.14 and 5.8 and 7.91, respectively. The useful load usually added to an airplane aft of the center of gravity is not on the average as far back as these radii of gyration. As useful load was added,⁶ therefore, to move the center of gravity aft, no increase in longitudinal distribution really occurred, and in consequence, no effect should have been expected. The amount that p_y and p_x can be increased by adding loads in the nose and tail of the fuselage is probably not great enough to profoundly affect either Equation [9] or [10]. For instance, one test was made⁶ with 555 lb in the nose and 450 lb in the tail, increasing I_y and I_z 800 slug-feet squared. The approximate average lever arm of these added weights was

$$\sqrt{\frac{800 \times 32.2}{450 + 555}} = 5.06 \text{ ft.}$$

Before this load was added, p_y and p_x were probably not less than 5.06. Therefore, no real increase in distribution accompanied the addition of these loads.

Effect of Lateral Distribution of Mass. A change in distribution of weight along the lateral axis changes p_x and p_z . An increase in lateral distribution increases p_x more than p_z (p_z assumed greater than p_x). This affects Equation [9] by decreasing both $(p_z^2 - p_x^2)$ and $(p_y^2 - p_x^2)$. To maintain equilibrium, s must decrease (c.p. goes forward, requiring a decrease of θ_x), ω must increase or θ_x must change toward 54.8 deg. The right side of Equation [10] tends to increase with increased lateral distribution, requiring either an increase in t or a decrease in ω , θ_y , or θ_x . An examination of Equation [11] shows that any change, which increases M_y , decreases M_x , or decreases θ_x , will decrease the damping moment D . Reducing this damping couple would either speed up the spin or at least require more additional damping for recovery. M_y is probably more affected by lateral distribution which increases p_x without changing p_y . The effect of this on Equation [10] is either greatly to increase t and therefore M_y or to produce changes in ω , θ_x , or θ_y to prevent t from increasing so much. The effect of lateral distribution on Equation [9] probably being small due to compensating changes in the other variables, the increase in M_y is probably not accompanied by an increase in M_x , and therefore a reduction in damping moment is probable with increased lateral distribution.

TABLE 2

Airplane	c.g.	ω	θ_x	θ_y
1	0.19	3.1	20°	?
1	0.389	2.5	50°	?
2	0.17	3.1	55°	?
2	0.385	2.1	30°	?

The gross weights and values of θ_y and θ'_y in the tests⁶ being unknown, it is not possible to apply these formulas⁶ with any degree of accuracy. The main point to be seen is that the existence of two possible positions of spin for every center of gravity location accounts for the possibility of the two airplanes⁶

⁵ "Moments of Inertia of Several Airplanes," N.A.C.A. Technical Note No. 375.

⁶ "Airplane Tail-Spins Analyzed," by Harry A. Sutton, S.A.E. Journal, November, 1930.

⁴ "Characteristics of Two Sharp-Nosed Airfoils Having Reduced Spinning Tendencies." N.A.C.A.

behaving so differently as the center of gravity moved aft. The data on these two airplanes is given in Table 2.

A series of spins was made⁷ in which weight, center-of-gravity location, and distribution were varied as independently as possible. Added weight on center of gravity without changing moments of inertia or balance finally produced a flat (uncontrolled) spin. This is to be expected from a standpoint of increased wing loading alone. However, as the weight increases without increasing the moment of inertia, p^2 , p_v^2 , and p_x^2 vary inversely as the weight. Therefore in Equation [9], with s constant, increasing weight decreases p_x , p_v , and p_z , requiring an increase in ω or a change in θ_z toward 54.8 deg, probably both. The tests with varying c.g. position (40 per cent to 26 per cent) all showed uncontrolled spins, thereby checking Equation [9], which indicates that, as long as the wing will furnish autorotative couples, equilibrium can be reached in a spin over a wide range of center-of-gravity positions. In this series of tests decalage and washout of considerable amount were found to eliminate the uncontrolled spin. This is a difficult case to try to explain. The first effect one would expect from a washout would be to increase the forward inclination of the resultant force on the outer wing tip with a lesser effect on the inner tip. This should speed up rotation which was found to be the case.⁷ This being so and the c.g. being constant, Equation [9] indicates that θ_z must change away from 54.8 deg to compensate for the increase in ω . Apparently θ_z moved away from 54.8 deg by decreasing to such an angle that the horizontal tail was no longer stalled. On some other airplane, especially if it already spun at θ_z greater than 54.8 deg, the change in θ_z due to adding washout might be to increase θ_z which would be of no help.

It is stated⁷ also that as much as 80 per cent increase in horizontal tail area hastened recovery but did not eliminate the uncontrolled spin. So far as Equation [9] is concerned, increasing the horizontal tail area is mainly an increase in s (combined c.p. of stalled wing and tail moves aft with larger tail). Increasing s should ordinarily decrease θ_z and increase ω , and such a change in θ_z would usually mean a hastening of the return of control in recovery from a spin. (All that is necessary to regain control is a reduction of θ_z sufficient to eliminate the stalling of the horizontal tail.) However, the increase in ω should delay reduction in θ_z , so one can really take his choice. For instance, in the case of airplane No. 2 with the c.g. aft,⁶ θ_z was 30 deg (see Table 2) and recovery was difficult. It was not stated⁶ however whether the difficulty was due to high stick forces to be overcome by the pilot or merely to the longer time required to regain control.

Our own observations on the negligible benefit of increased fin area also have been checked.⁷

Causes of Autorotation. Airplane designers have been censured at different times for not using the wind tunnel to determine the cure of the spin trouble. On the other hand, the airplane designer can justify himself for not so doing by pointing out that, for example, although the wind tunnel proclaimed that monoplanes would not flat-spin, nevertheless they do. It seems to me that this false conclusion was due to the conditions under which airfoils are tested in spinning being so far from the conditions in a spin. Nearly all tests in spinning of airfoils and the criteria for autorotation derived from them are made with the spin axis a rigid body capable of taking bending moment and shear. Equations⁸ for the forces on an airfoil spinning around a fixed axis have been applied to the problem, and some of these equations are for forces which tend to bend the spinning axis. However, the spinning axis of an airplane cannot take bending mo-

ments except those that are absorbed by the flattening couple due to inertia. Therefore, when an airplane spins it must spin about such an axis that the bending moments in the axis are equal to the flattening couples due to inertia. Furthermore, there can be no shear in the spinning axis, that is, the resultant air force must be exactly equal to and opposed to the resultant force due to the weight and centrifugal force. If the equations are written for the spinning tendency of an airplane around an axis in which there is no bending moment, it will be found that the only cause of autorotation is the variation along the span of the slope σ of the resultant force, i.e., variation in chord component. The variation along the span of the amount of the resultant force merely shifts the axis of rotation along the span.

This is discussed mathematically in Appendix 3. Equation [11] of Appendix 1 is really a statement of the autorotative couples with σ assumed constant and shows that when the center of rotation is in the position normally obtained in an airplane spin this so-called autorotative couple with σ constant is usually negative. In other words, it tends to dampen rotation.

The reason that high-lift airfoils spin more viciously than the thin airfoils is that σ varies farthest from 0 just prior to the stall and is greater as the lift before stall increases. Fig. 17 of Knight's report⁸ shows this difference.

The shape of the normal force curve of the airfoil does have an effect on the spin in another indirect manner. If the normal force becomes much smaller at high angles of attack, as it does for instance on a biplane without stagger, the sinking speed and therefore the rotational speed in a spin will increase at high angles of attack. This will in turn possibly produce flatter or more uncontrolled spins. The pilot's observation that increasing stagger makes spins more controlled is therefore strictly in accord with theory—not the theory that the shape of the normal force curve determines autorotative couples, but with the theory that the shape of the normal force curve determines sinking speed.

There is an item that may have some effect on a pilot's observations which, as far as is known, has not been discussed. This is the effect of altitude on a spin. Since sinking speed, and therefore rotational speed, increase with increasing wing load and with decreasing density, spins at high altitudes will be faster, and in consequence possibly less controlled, than spins at low altitudes, all other conditions being equal. It is conceivable then that a spin might be entered at 10,000 ft from which recovery could not be made at that altitude but, as the altitude decreased and denser air was encountered, the spin would slow down, producing changes in attitude, which finally would permit recovery.

CONCLUSIONS

It is difficult to draw conclusions from the limited observations given, but apparently the following are indicated:

- 1 Wing loading is one of the major factors in uncontrolled spins.
- 2 The stalling of the horizontal tail surfaces is the distinguishing factor in uncontrolled spins.
- 3 For speedy recovery from uncontrolled spins the largest possible controlled variability in vertical fin areas is desired. This means a large rudder of high angular throw and a small fin. Unfortunately this combination also hastens entry into a spin.
- 4 If sufficient fin area, in connection with a small rudder, to prevent entry into a spin is provided, recovery from any spin produced by accidental circumstances would probably be impossible.
- 5 Center-of-gravity location is a secondary factor, being of more importance with lighter wing loadings.
- 6 An autorotative couple is necessary both for starting a spin and for its continuance, there being damping couples due not only to vertical fin areas but also to the lift force.
- 7 The shape of the normal force-coefficient curve of the cellule

⁷ "Spinning Experiments," by Paul E. Hovgard, *S.A.E. Journal*, November, 1930.

⁸ "Wind Tunnel Tests on Autorotation and the Flat Spin," by Montgomery Knight. N.A.C.A. Report No. 273.

is not a major factor in producing an autorotative couple, because of the tendency of the spin axis to shift and thereby eliminate the couple thus set up.

8 The major source of autorotative couples is the variation in slope of the resultant air force relative to the normal to the wing chord at varying angles of attack. Since this variation is greater on high-lift airfoils than on low-lift airfoils, the former have greater autorotative couples at higher mean angles of attack.

9 The shape of the normal force-coefficient curve has a secondary effect on spinning in that, if the normal force coefficient decreases at higher angles of attack, the sinking speed and therefore rotational speed in a spin increase.

10 It is possible to recover from a spin at low altitude from which it might be impossible to recover at high altitude.

11 There are two possible positions of equilibrium in a spin for every center-of-gravity position and either of these spins may be obtained if the wing will furnish the required autorotative couples in the two positions.

12 With accurate observations on the spin of a given airplane, mathematics may indicate the most promising changes in the airplane to favorably alter the spinning characteristics.

13 The effects of center-of-gravity location and longitudinal distribution that have been noted in most spinning experiments have been primarily due to increased wing loading, the change in center-of-gravity position usually being accomplished by additional load aft. The change in radius of gyration due to these added weights has usually been negligible in that the moment of inertia has not increased faster than the weight.

Appendix 1

PART 1—DERIVATION OF EQUATIONS FOR THE COUPLES DUE TO INERTIA TENDING TO CHANGE THE POSITION OF AN AIRPLANE IN A SPIN (SEE FIG. 4)

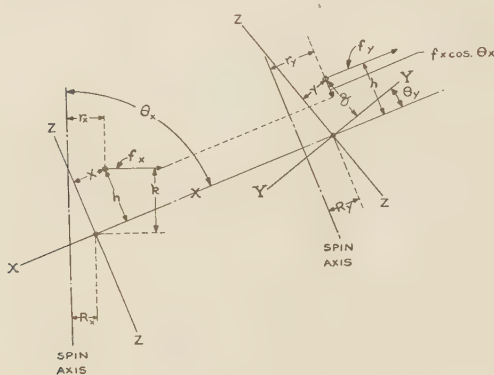


FIG. 4 INERTIA OF FORCES IN A SPIN

Let θ_x = angle between spin axis and X-X axis
 θ_y = angle of bank viewed parallel with X-X axis
 x, y, z , be coordinates of any particle referred to X-X, Y-Y, and Z-Z axes.

dm = small particle in airplane

$$\int dm = M = \text{mass of airplane} = \frac{W}{g}$$

R_x = distance of c.g. from spin axis in side view

R_y = distance of c.g. from spin axis in rear view

r = true radius of particle $dm = \sqrt{r_x^2 + r_y^2}$

ω = angular velocity of rotation of airplane about spin axis

f = centrifugal force on $dm = \omega^2 r dm$

$$f_x = \text{component of } f \text{ parallel to } r_x = \frac{fr_x}{r} = \omega^2 r_x dm$$

$$f_y = \text{component of } f \text{ parallel to } r_y = \frac{fr_y}{r} = \omega^2 r_y dm$$

Moment arm of f_x around origin (c.g.) in side view = k

Moment arm of f_y around origin (c.g.) in rear view = h

$$h = y \sin \theta_y + z \cos \theta_y$$

$$k = x \cos \theta_x + h \sin \theta_x = x \cos \theta_x + y \sin \theta_x \sin \theta_y + z \sin \theta_x \cos \theta_y \dots \dots \dots [1]$$

$$r_y = R_y + y \cos \theta_y - z \sin \theta_y$$

$$r_x = R_x + x \sin \theta_x - h \cos \theta_x$$

$$r_z = R_z + x \sin \theta_x - y \cos \theta_x \sin \theta_y - z \cos \theta_x \cos \theta_y \dots [2]$$

Let dM_x = moment of f_x about origin in side view

$$dM_x = f_x k = \omega^2 dm r_x k \dots \dots \dots [3]$$

since the origin is the c.g. of the airplane

$$\int x dm, \int y dm, \text{ and } \int z dm, \text{ all} = 0$$

Assuming that axes X-X, Y-Y, and Z-Z are the principal axes of inertia (the error is very small)

$$\int xy dm, \int xz dm, \text{ and } \int yz dm, \text{ all} = 0$$

Substituting values [1] and [2] of k and r_x in [3] and integrating gives

$$M_x = \omega^2 \sin \theta_x \cos \theta_x \left[\int x^2 dm - \sin^2 \theta_y \int y^2 dm - \cos^2 \theta_y \int z^2 dm \right] \dots \dots \dots [4]$$

$$I_x = \int (y^2 + z^2) dm = \int y^2 dm + \int z^2 dm$$

$$I_y = \int x^2 dm + \int z^2 dm$$

$$I_z = \int y^2 dm + \int x^2 dm$$

Solving

$$\int x^2 dm = \frac{I_x + I_y - I_z}{2}$$

$$\int y^2 dm = \frac{I_x + I_z - I_y}{2}$$

$$\int z^2 dm = \frac{I_x + I_y - I_z}{2}$$

Substituting the above in [4] we get

$$M_x = \omega^2 \sin \theta_x \cos \theta_x \left[(I_x - I_z) \cos^2 \theta_y + (I_y - I_z) \sin^2 \theta_y \right] \dots [5]$$

Similarly

$$dM_y = f_y h + f_x \cos \theta_x (y \cos \theta_y - z \sin \theta_y)$$

This integrates to

$$M_y = \omega^2 \sin \theta_y \cos \theta_y (I_x - I_y) \sin^2 \theta_x \dots \dots \dots [6]$$

M_y is the couple due to inertia tending to flatten the spin laterally. It is opposed by the moment between the weight of the airplane and the lateral shift in c.p. of lift on the entire airplane together with other moments due to vertical distribution of fin area. Mathematics is at present unable to cope with either of these factors. M_x is opposed mainly by the couple between the weight of the airplane and the center of lift.

PART 2—APPROXIMATE STATEMENT OF THE AIR FORCES IN A SPIN OPPOSING THE FORCES DUE TO WEIGHT AND INERTIA (SEE FIG. 5)

When a wing is stalled the air force is very nearly normal to the wing regardless of angle of attack. We may assume, therefore,

with little error, that both the air force and the opposing resultant of W , and centrifugal force F_z are normal to the X - X axis.

$$\tan \theta_x = \frac{W}{F_z}$$

$$F_z = \frac{W}{g} \omega^2 R_z$$

$$\tan \theta_x = \frac{Wg}{W\omega^2 R_z}$$

$$R_z = \frac{g}{\omega^2 \tan \theta_x} \dots \dots \dots [7]$$

The resultant air forces are not perpendicular to the Y - Y axis however due to the cross wind forces on the side of the fuselage.

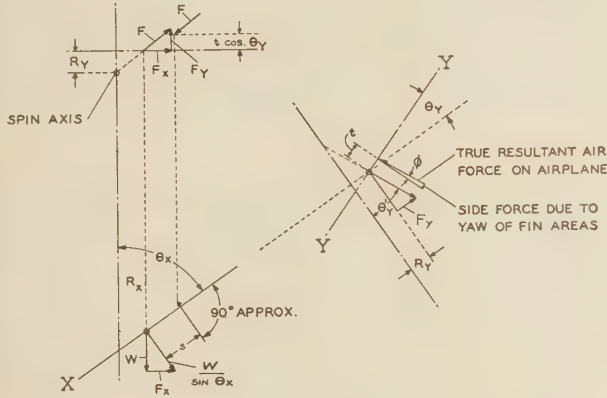


FIG. 5 BALANCE OF FORCES IN A SPIN

age, landing gear, and vertical tail surfaces. This variation in angle from the perpendicular to the axis Y - Y will be called ϕ and $\theta_y + \phi = \theta'_y$

$$\tan \theta'_y = \frac{F_y \sin \theta_x}{W}$$

$$F_y = \frac{W}{g} \omega^2 R_y$$

$$\tan \theta'_y = \frac{W\omega^2 R_y \sin \theta_x}{gW}$$

$$R_y = \frac{g \tan \theta'_y}{\omega^2 \sin \theta_x} \dots \dots \dots [8]$$

Referring to Fig. 4, the couple opposing M_x is $\frac{Ws}{\sin \theta_x}$

s = longitudinal distance from c.g. to c.p. of all lift forces

Equating to [5]

$$\frac{Ws}{\sin \theta_x} = M_x = \omega^2 \sin \theta_x \cos \theta_x [(I_x - I_z) \cos^2 \theta_y + (I_y - I_z) \sin^2 \theta_y]$$

$$s = \frac{M_x \sin \theta_x}{W}$$

$$s = \omega^2 \sin^2 \theta_x \cos \theta_x \left[\frac{I_x - I_z}{W} \cos^2 \theta_y + \frac{I_y - I_z}{W} \sin^2 \theta_y \right]$$

$$s = \frac{\omega^2}{g} \sin^2 \theta_x \cos \theta_x [(p_x^2 - p_z^2) \cos^2 \theta_y + (p_y^2 - p_z^2) \sin^2 \theta_y] \dots \dots \dots [9]$$

Similarly the couple opposing M_y is $\frac{Wt \cos \phi}{\sin \theta_x \cos \theta'_y}$

t = lateral distance from c.g. to c.p. of all lift forces measured parallel to lateral axis

Equating to [6]

$$\frac{Wt \cos \phi}{\sin \theta_x \cos \theta'_y} = M_y = \omega^2 \sin \theta_y \cos \theta_y \sin^2 \theta_x (I_x - I_y)$$

$$t = \frac{M_y \sin \theta_x \cos \theta'_y}{W \cos \phi}$$

$$t = \frac{\omega^2 \sin \theta_y \cos \theta_y \cos \theta'_y \sin^2 \theta_x}{g \cos \phi} (p_x^2 - p_y^2) \dots \dots \dots [10]$$

Taking moments about the c.g. in the plan view there is an unbalanced moment D tending to stop rotation.

$$D = F_y (s \sin \theta_x - t \sin \theta_y \cos \theta_x) - F_z t \cos \theta_y$$

which reduces to

$$D = M_x \sin \theta_x \tan \theta'_y - M_y \frac{\cos \theta'_y \cos \theta_x \cos \theta_y}{\cos \phi} (1 + \tan \theta'_y \tan \theta_y) \dots \dots \dots [11]$$

where M_x and M_y are the moments given by Equations [5] and [6].

Appendix 2

CHANGE IN RADIUS OF GYRATION OF A BODY DUE TO ADDED WEIGHT (SEE FIG. 6)

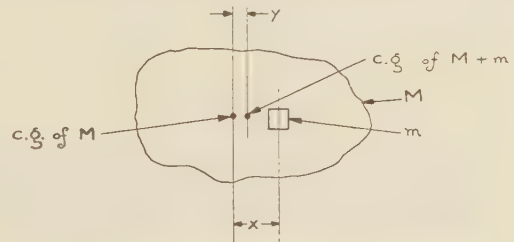


FIG. 6 EFFECT OF ADDED WEIGHT ON INERTIA

Let M = original mass

I = moment of inertia of M

p = radius of gyration of M

$m = KM$ = added mass at distance x from original c.g.

Assume moment of inertia of m about its own c.g. is negligible

I' = moment of inertia of $M + m$

q = radius of gyration of $M + m$

$$y = \frac{mx}{M + m} = \frac{Kx}{1 + K}$$

$$I' = I + My^2 + m(x - y)^2$$

$$(M + m)q^2 = Mp^2 + \frac{MK^2x^2}{(1 + K)^2} + \frac{mx^2}{(1 + K)^2}$$

$$M(1 + K)q^2 = Mp^2 + \frac{MK^2x^2}{(1 + K)^2} + \frac{KMx^2}{(1 + K)^2}$$

$$q^2 = \frac{p^2 + \frac{Kx^2}{1 + K}}{1 + K}$$

Letting $q = p$ and solving for x

$$x = p \sqrt{1 + K}$$

When $x < p \sqrt{1 + K}$ the new radius of gyration is less than the old.

Appendix 3

THE EFFECT ON A SPIN OF THE INABILITY OF THE SPIN AXIS TO TAKE BENDING MOMENT (SEE FIG. 7)

Fig. 6 and Equations [12] and [13] below are lifted bodily from the appendix of Knight's report⁸ with slight changes, however, in the symbols to agree with those used in Appendixes 1 and 2 of this paper.

$$C_a = \frac{1}{S^2} \int_{-S/2}^{+S/2} C_{ky} \sec^2 \delta dy \dots \dots \dots [12]$$

$$C_b = \frac{1}{S^2} \int_{-S/2}^{+S/2} C_{vy} \sec^2 \delta dy \dots \dots \dots [13]$$

Where

C_a = coefficient of autorotation
 C_b = coefficient of bending in spin axis
 S = span of airplane

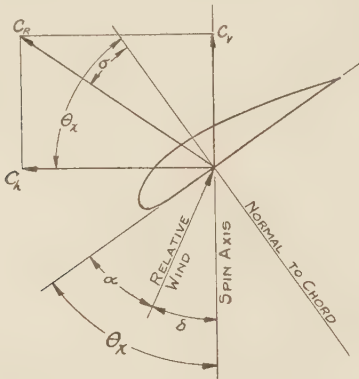


FIG. 7 WING ELEMENT IN AUTOROTATION

If the spin axis cannot take bending, Equation [13] becomes $C_b = 0$. This is accomplished physically by the spin axis shifting off the center of the wing an amount e so that [13] becomes

$$C_b = \frac{1}{S^2} \int_{-S/2-e}^{+S/2-e} C_{vy} \sec^2 \delta dy = 0$$

But $C_b = C_e \cot (\theta_x - \sigma)$

Therefore if σ is constant, Equation [12] becomes

$$C_a = \cot (\theta_x - \sigma) \frac{1}{S^2} \int_{-S/2-e}^{+S/2-e} C_{ky} \sec^2 \delta dy$$

$$C_a = C_b \cot (\theta_x - \sigma)$$

Therefore, when $C_b = 0$ (the spin axis takes no bending) C_a differs from 0 only if σ is not constant. Therefore C_a does not exist by virtue of the shape of the resultant force-coefficient curve of the airfoil. It follows then that variation in σ is the major source of autorotation, not variation of C_R .

Discussion

ALEXANDER KLEMIN.⁹ I think the following points are worthy of consideration.

It is quite clear that moving the c.g. forward diminished the number of turns for recovery. Is this due to greater diving beyond the stall? If so, it may be supposed that the stabilizer setting remained the same when the c.g. was changed.

In discussing the effect of wing loading, would it be proper to point out that the increase in wing loading at a given angle of incidence increases the vertical velocity and hence the centrifugal

force? From this it follows that at same $\lambda = \frac{\Omega R}{V}$.

The Ω increases, while R diminishes, so that heavier loading means a faster, tighter spin and hence greater difficulty of recovery.

In varying the fin aspect ratio, might not both fin and rudder have been blanketed by the stabilizer, so that the increasing aspect ratio did not help?

In discussing the "Effect of Varying Fin Area" the author states that "the airplane would rotate around the fin." The writer does not follow the argument here. Perhaps this thought could be expanded farther.

AUTHOR'S CLOSURE

Spins were made with stabilizer in all settings with apparently very little change.

Usually the spins were made with stabilizer set for cruising.

The effect of wing loading is discussed early in the paper under that heading and also indirectly in conclusion 9.

Blanketing of tail has been covered in footnote 3. With constant fin area, the directional stability at small angles of yaw was the same regardless of fin-aspect ratio but with low fin-aspect ratios this stability was maintained to higher angles of yaw, there being a distinct feeling of stall of the fin when the directional stability became negative. This was long before anything like a spin was approached.

⁹ Professor of Aeronautical Engineering, New York University, New York, N. Y. Mem. A.S.M.E.

Burning Characteristics of Pulverized Coals and the Radiation From Their Flames

By RALPH A. SHERMAN,¹ COLUMBUS, OHIO

This paper deals with a laboratory investigation of Hocking, Pocahontas, Illinois No. 6, and Pittsburgh No. 8 coals to determine the relation of the rate of burning of pulverized fuels and of the radiation from their flames, to the type of coal and the fineness of pulverization. The principal conclusions drawn from the results of this investigation are: That fineness of grinding becomes increasingly important as the combustion space is restricted; that the type of coal influences the rate of combustion; that increased furnace temperature increases the rate of combustion; and that, although the temperature and total radiation of the flame are affected by fineness of grinding, excess air, and rate of firing, the emissivity of the flame at any position is affected to a marked degree only by the type of coal.

FOR some time, the Battelle Memorial Institute has conducted an experimental investigation of the combustion of pulverized fuels in a large-scale laboratory apparatus. The object of this investigation was to determine the relation of the rate of burning of pulverized fuels and of the radiation from their flames to the type of fuel and the fineness of pulverization.

A previous paper² discussed the work of other investigators, described in detail the apparatus and the methods of testing, and presented data on the progress of combustion and the amount of carbon remaining unburned at various points in the flame when burning Ohio No. 6 or Hocking and Pocahontas No. 3 coals and some semi-cokes made from Hocking coal. The conclusions presented in that paper were:

1 The primary product that appears in the combustion of fuel in pulverized form is CO_2 . With ratios of air to coal equal to or greater than required, CO appeared only in small amounts in the initial carbonization of the coal. CO found in industrial furnaces burning pulverized fuel is undoubtedly formed in the stream of coal and primary air which is generally much less than the amount required for complete combustion; the CO once formed may persist for a considerable distance of flame travel because of slow mixing with secondary air.

2 With Hocking coal at 8.5 or 10.5 ft from the burner, the unburned carbon loss did not decrease with increase of excess air above 20 per cent.

3 No one numerical value that fully expresses the fineness of pulverized fuel with significance in regard to its combustion characteristics was found. The specific surface did not

appear to have greater general significance than the percentage passing 200-mesh. For equal percentages passing 200-mesh the amount retained on 100-mesh was markedly significant. Pulverized-fuel-equipment manufacturers would undoubtedly do well to develop equipment that would deliver a uniformly sized product rather than one of extreme fineness.

4 The rates of combustion and percentages of unburned carbon varied greatly with the type of fuel. The loss in unburned carbon was greater for Pocahontas than Hocking coal at equal percentages through 200-mesh and other conditions equal, although the "superfines" and specific surface were much greater for the Pocahontas coal. A wide enough range of fuels has not yet been covered to develop a relation between the burning characteristics and other known properties of the fuels.

5 Semi-cokes having contents of volatile matter as low as 12.8 per cent burned satisfactorily as pulverized fuel, although their carbon loss was higher for similar conditions than that of the coal from which they were made.

6 Pulverized fuels were burned in the test furnace at rates of heat liberation equal to those of industrial furnaces. The unburned carbon losses after only 10.5 ft of flame travel and with a burning time of approximately 0.3 sec were equal to those attained with longer flame travel in industrial furnaces. This was attained with a simple burner which admitted all the air with the coal and with no attempt at turbulence. If this principle were extended to burners of high capacity, it would not work as well, inasmuch as conditions would not be as favorable for ignition of the fuel, because the volume of the cone of fuel would increase so much more rapidly than the surface. Division of the coal and air among a large number of small burners would offer certain mechanical difficulties, as (1) the uniform distribution of coal and air among a number of burners, particularly in a direct-fired unit, (2) the increased power consumption for blowing air through small ducts with the coal, and (3) the increased difficulties in the use of preheated air.

SCOPE OF PAPER

The present paper includes further work that has been done on the Hocking and Pocahontas coals and on Illinois No. 6 and Pittsburgh No. 8 coals. Data are presented on the following four relationships:

- 1 Excess air to combustion of Hocking and Pocahontas coals.
- 2 Fineness of grinding to combustion of the four coals.
- 3 Rate of firing and furnace temperature to completeness of combustion.
- 4 Radiation and emissivity of flames to excess air, fineness and rate of firing for the four coals.

APPARATUS AND METHODS

The testing apparatus included a drier, conical ball mill, air classifier, storage and weighing bins, screw feeder, fan, burner, furnace and equipment for sampling gases and solids and for the measurement of temperature of the gases and their radiation. As the apparatus and methods, except for the radiation work, were described in detail in the previous paper, they will not be repeated.

¹ Fuel Engineer, Battelle Memorial Institute, Columbus, Ohio. Mem. A.S.M.E. Mr. Sherman is a graduate of the University of Iowa. For ten years he was associated with the U. S. Bureau of Mines, Fuel Section, at Pittsburgh. Since 1930 he has been with the Battelle Memorial Institute in his present capacity and is in charge of the research work on the combustion of fuels.

² R. A. Sherman, Proc. Third Int. Conf. on Bituminous Coal, 1931, vol. II, p. 510.

Contributed by the Fuels Division and presented at the Annual Meeting, New York, N. Y., December 4 to 8, 1933, of THE AMERICAN SOCIETY OF MECHANICAL ENGINEERS.

NOTE: Statements and opinions advanced in papers are to be understood as individual expressions of their authors, and not those of the Society.

For convenient reference, however, Fig. 1 shows details of the furnace and burner. The furnace was tightly sealed and all the air used for combustion was supplied through the burner with the coal. The purpose was to study the combustion in a stream of coal and air of uniform mixture and samples were taken on the center line of the furnace as the closest approximation to the desired ideal. The apparatus and methods for the determination of the radiation from the flame are described later.

CHARACTERISTICS OF COALS

Table 1 gives the source, proximate and ultimate analyses, calorific value, softening temperature of ash and true specific gravity of the coals burned. The analyses are on the basis of

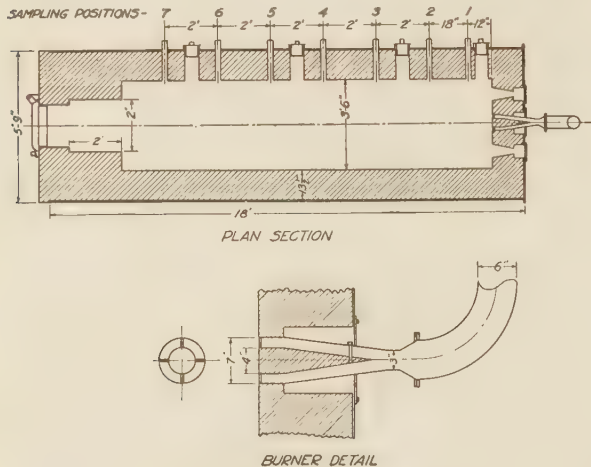


FIG. 1 DETAILS OF FURNACE AND BURNER

typical moisture as fired. The Illinois coal was furnished by the Union Collieries Co., through the courtesy of E. H. Tenney, chief engineer of power plants, Union Electric Light & Power Co., St. Louis, Mo.

Table 2 gives typical size characteristics of the pulverized coals as determined by screen tests and by microscopic counting. The pulverizing equipment, ball mill and classifier, gave a lower percentage of coarse particles, +30 or 50-mesh sieve, than is frequently obtained in industrial practise. Thus, with 75 per cent or more passing the 200-mesh sieve, not over 0.2 per cent remained on the 50-mesh sieve. The importance of the elimination of the coarse sizes was shown by data given in the earlier paper.

TABLE 1 CHARACTERISTICS OF COALS

Coal	Ohio No. 6 Hocking	Pocahontas No. 3	Illinois No. 6	Pittsburgh No. 8
Source	Ohio	West Virginia	Illinois	Ohio
State	Athens	Mercer	Jackson	Belmont
County	Lick Run	Louisville	Kathleen	Blaine
Mine				
Composition, as fired				
Proximate				
Moisture	2.3	0.4	1.1	0.5
Volatile matter	35.4	17.2	33.6	40.0
Fixed Carbon	52.3	76.6	50.4	50.2
Ash	10.0	5.8	14.9	9.3
	100.0	100.0	100.0	100.0
Ultimate				
Carbon	71.8	85.0	66.7	72.3
Hydrogen	5.1	4.4	4.6	5.0
Oxygen	10.3	2.2	11.0	7.4
Nitrogen	1.3	2.0	1.5	1.2
Sulphur	1.5	0.6	1.3	4.8
Ash	10.0	5.8	14.9	9.3
	100.0	100.0	100.0	100.0
Calorific value, Btu per lb	12,420	14,790	11,770	13,200
Softening temp. of ash, F	2,590	2,630	2,250	1,985
True specific gravity	1.42	1.33	1.46	1.40

TABLE 2 SIZE CHARACTERISTICS OF COAL

U.S.S. sieve no. Size opening, mm	Cumulative oversize, per cent				—200, per cent	Mean diam., mm	Total surface, cm ² /gm	Surface in —200-mesh coal, per cent
	30	50	100	200				
0.590	0.297	0.149	0.074					
<i>Hocking</i>								
0.2	2.0	19.8	56.6	43.4	0.053	790	79.1	
0.0	0.2	7.8	44.2	55.8	0.035	1215	88.2	
0.0	0.0	0.6	24.6	75.4	0.032	1325	93.4	
0.0	0.0	0.4	19.8	80.2	0.028	1514	95.4	
<i>Pocahontas</i>								
0.6	9.0	31.4	61.6	38.4	0.039	1155	85.6	
0.0	0.2	9.2	39.2	60.8	0.025	1800	92.6	
0.0	0.0	1.0	21.0	79.0	0.012	3615	97.7	
0.0	0.0	0.6	9.0	91.0	0.010	4685	99.3	
<i>Illinois</i>								
0.2	2.0	23.0	60.6	39.4	0.059	695	75.6	
0.0	0.6	10.2	48.8	51.2	0.044	930	83.6	
0.0	0.2	7.4	44.2	55.8	0.041	1005	85.9	
0.0	0.2	1.2	24.0	76.0	0.033	1245	92.1	
0.0	0.0	0.4	15.0	85.0	0.027	1535	96.7	
<i>Pittsburgh No. 8</i>								
0.2	1.8	19.0	57.8	42.2	0.055	765	77.3	
0.0	0.8	10.6	48.2	51.8	0.048	900	82.9	
0.0	0.2	4.6	35.0	65.0	0.037	1175	90.0	
0.0	0.0	0.2	14.8	85.2	0.022	1925	97.2	

The size characteristics of the three high-volatile coals were similar but the Pocahontas coal was marked, not only by the greater fineness shown by the smaller average diameter or greater specific surface, but also by the larger percentage of the coarse sizes.

DISCUSSION OF COMBUSTION DATA

Excess Air and Unburned Carbon. Fig. 2 shows the relation of the percentage of carbon remaining unburned at 8.5 and

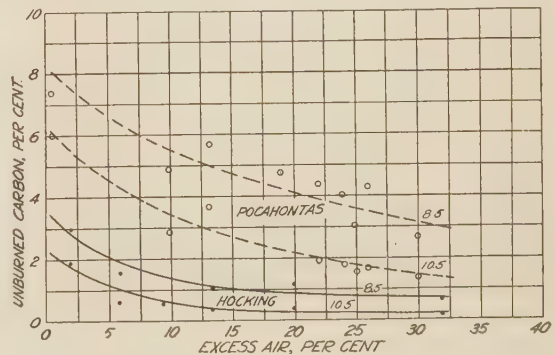


FIG. 2 RELATION OF UNBURNED CARBON TO EXCESS AIR, HOCKING AND POCAHONTAS COALS
(Through 200-mesh, 80 per cent; rate of heat input 2,650,000–2,800,000 Btu per hr. Figures on curves are distances from burner in ft.)

10.5 ft from the burners to the percentage of excess air when burning Hocking and Pocahontas coals; the data for the Hocking coal are set forth in Fig. 17 of the previous report. The unburned carbon continued to decrease up to 30 per cent excess air with the Pocahontas coal, whereas the curves for the Hocking coal were practically flat beyond 20 per cent.

Fineness of Grinding and Unburned Carbon. Figs. 3 to 6 show the relation of the percentage of carbon unburned at various points in the flame to the percentage of the coal passing the 200-mesh sieve for the four coals when burned at similar rates of heat input and with 20 per cent excess air. The percentage through 200-mesh is used as a basis for plotting for, as stated above in conclusion 3 from the previous paper, no better basis has been found. The data for the Hocking coal

are based on coal of the fineness characteristics given in Table 2. The unburned carbon for coal of 70 per cent or more through 200-mesh sieve is, therefore, less than that shown in Fig. 15 of the first paper.

The curves show the great importance of fineness of pulverization as the combustion space is restricted. An exception, however, was the Pocahontas coal at 4.5 ft from the burner where increased fineness apparently did not decrease the amount of unburned carbon.

Although they do not break sharply, the curves for 10.5 ft from the burner tend to become flat and indicate approximately the limit beyond which increased fineness results in

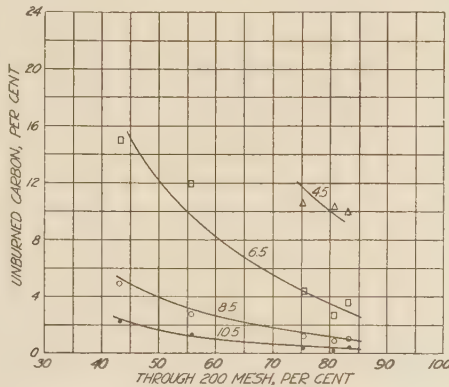


FIG. 3 RELATION OF UNBURNED CARBON TO FINENESS OF HOCKING COAL

(Excess air 20 per cent; rate of heat input 2,650,000 Btu per hr. Figures on curves are distances from burner in ft.)

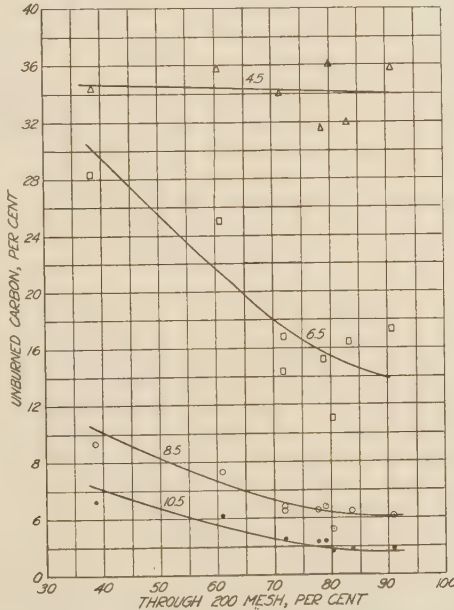


FIG. 4 RELATION OF UNBURNED CARBON TO FINENESS OF POCAHONTAS COAL

(Excess air 20 per cent; rate of heat input 2,780,000 Btu per hr. Figures on curves are distances from burner in ft.)

little decrease in unburned carbon. These limits are approximately 70 per cent for Hocking, 85 per cent for Pocahontas, 75 per cent for Illinois, and 65 per cent for Pittsburgh coal. Obviously, for a particular installation the optimum fineness of

pulverization must be determined by an economic balance between the decrease in the loss in unburned carbon and the increased power for finer pulverization. No power-consumption data were taken in this investigation.

Relation of Type of Coal to Unburned Carbon. Figs. 3 to 6

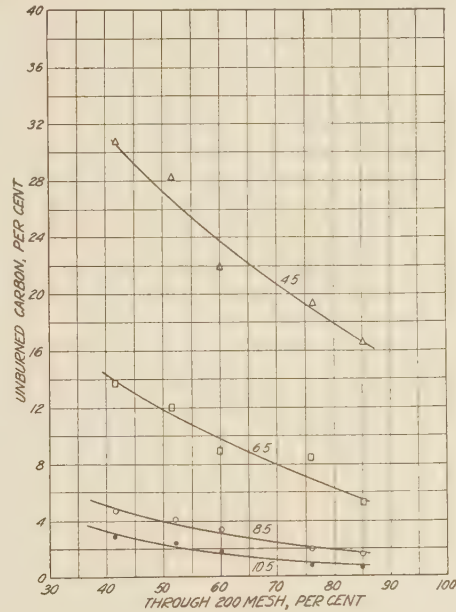


FIG. 5 RELATION OF UNBURNED CARBON TO FINENESS OF ILLINOIS COAL

(Excess air 20 per cent; rate of heat input 2,650,000 Btu per hr. Figures on curves are distances from burner in ft.)

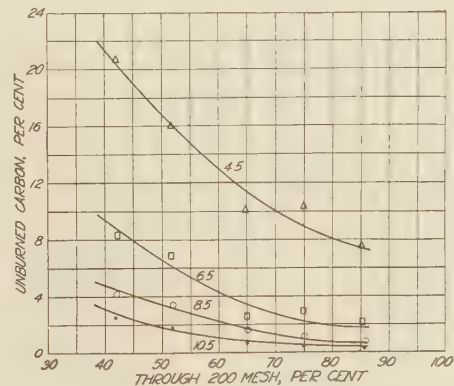


FIG. 6 RELATION OF UNBURNED CARBON TO FINENESS OF PITTSBURGH NO. 8 COAL

(Excess air 20 per cent; rate of heat input 2,700,000 Btu per hr. Figures on curves are distances from burner in ft.)

also indicate the relative rates of combustion of the four coals but Fig. 7, in which the unburned carbon and temperature are plotted against the burning time, shows the relation more clearly. The times were calculated from the velocity readings taken with a water-cooled pitot tube on the center line of the furnace. Although only approximate, they afford better comparisons than distance only.

The curves for the Hocking and Pittsburgh coals are practically coincident. They burned much more rapidly than the other two coals and Pocahontas coal burned much the slowest of the four. The temperature curves show similarly the differ-

ence in the rates of burning. The temperature at the first position was lowest for the Pocahontas coal and it increased most slowly. The greatest difference in the final temperature was about 100 F. It was highest for the Pocahontas coal and lowest for the Illinois coal.

That Pocahontas and other coals of similarly low content of volatile matter burn more slowly in pulverized form than coals of higher volatile content is well known. An obvious explanation is the fact that, because less carbon is distilled in gaseous hydrocarbons, more must be burned as solid carbon which burns less rapidly than the gas.

However, these data show that the rate of burning is not directly proportional to the content of volatile matter. The Illinois coal burned more slowly than the Hocking coal, although their volatile contents were practically the same on the moisture- and ash-free basis. Pittsburgh coal burned only slightly more rapidly than Hocking coal, although their volatile contents on the moisture- and ash-free basis were 44 and 40 per cent, respectively.

The ash content, oxygen content, quality of volatile matter, and probably other factors undoubtedly control the rate of burning as well as volatile matter content and many coals would have to be investigated before even an approximate relation were found between the rates of burning and the composition of the coals. Godbert³ found that a reactivity index was closely related to the burning time. It is also considered possible that the ignition temperature of the coal may be an important factor if it were determined under conditions of actual suspension of the coal in an air stream. The initial rate of combustion is so rapid that a small gain in time by earlier ignition would make a great difference in the rate of combustion as measured from the time of entrance of the coal into the furnace.

Relation of Rate of Combustion to Furnace Temperature. Griffin, Adams, and Smith⁴ in a series of small-scale experiments on the

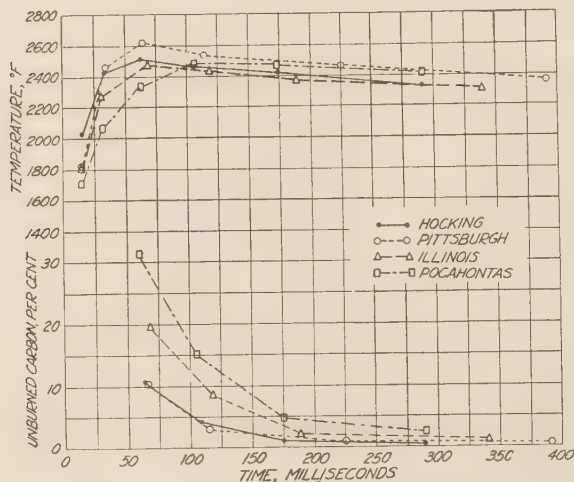


FIG. 7 COMPARISON OF RATE OF BURNING OF FOUR COALS
(Rate of heat input 2,650,000–2,710,000 Btu per hr, excess air 20 per cent; through 200-mesh, 75 to 79 per cent.)

burning of individual particles of fuel found, among other results, that the burning time increased with increase of temperature.

An explanation of this surprising result has been proposed

³ A. L. Godbert, *Fuel*, vol. 9, 1930, p. 57.

⁴ H. K. Griffin, J. R. Adams, and D. F. Smith, *Ind. Eng. Chem.*, vol. 21, 1929, p. 808.

by Burke and Schumann⁵ as due to the fact that the mass of oxygen per unit volume of the film surrounding the particle decreases with increase of temperature.

The possible change in the temperature of the large-scale

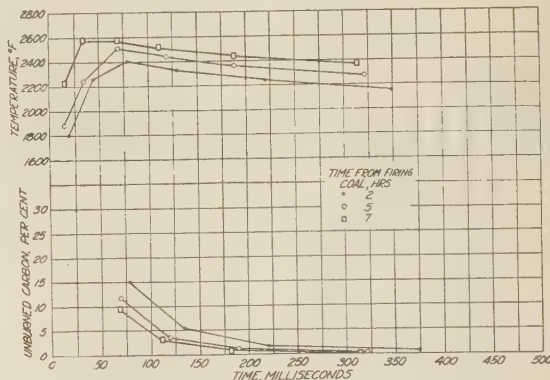


FIG. 8 RELATION OF RATE OF BURNING TO FURNACE TEMPERATURE, HOCKING COAL
(Excess air 18 per cent; through 200-mesh, 82 per cent; rate of heat input 2,660,000 Btu per hr.)

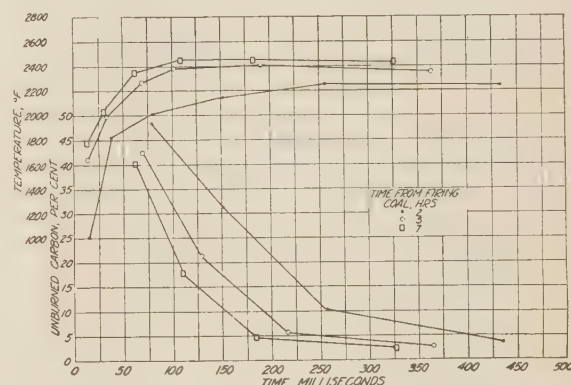


FIG. 9 RELATION OF RATE OF BURNING TO FURNACE TEMPERATURE, POCAHONTAS COAL
(Excess air 20 per cent; through 200-mesh, 78 per cent; rate of heat input 2,800,000 Btu per hr.)

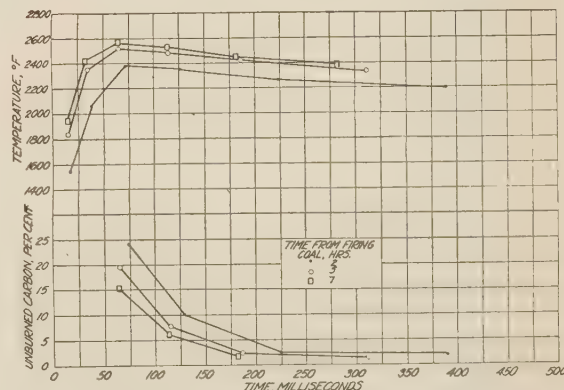


FIG. 10 RELATION OF RATE OF BURNING TO FURNACE TEMPERATURE, ILLINOIS COAL
(Excess air 20 per cent; through 200-mesh, 78 per cent; rate of heat input 2,650,000 Btu per hr.)

⁵ S. P. Burke and T. E. W. Schumann, *Ind. Eng. Chem.*, vol. 23, 1931, p. 406.

furnace was not large. It could be obtained in two ways: (1) by taking data at varying intervals from initial lighting of the furnace and (2) by change in the rate of firing.

Figs. 8, 9, and 10 show, respectively, for Hocking, Pocahontas, and Illinois coals, the relation of the unburned carbon to the burning time with varying furnace temperature. The different temperatures were obtained by taking observations at 2, 5, and 7 hours after lighting the furnace. The increase in the maximum temperature with increase in time from lighting the furnace was about 200 F with each coal. As the temperature of the gases increased, their velocity increased and the time in the furnace decreased.

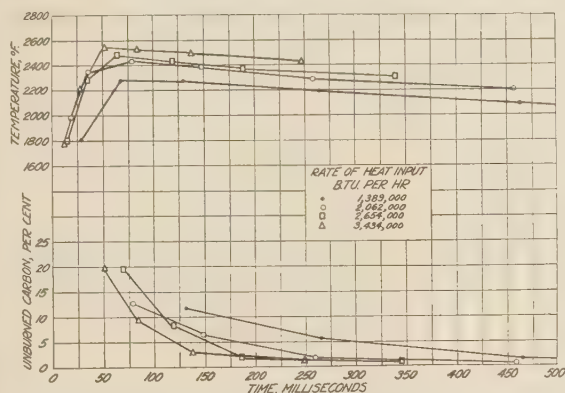


FIG. 11 RELATION OF RATE OF BURNING TO RATE OF HEAT INPUT, ILLINOIS COAL
(Excess air 20 per cent; through 200-mesh, 80 per cent.)

The actual difference in unburned carbon with difference in time was greatest for the Pocahontas coal. The difference decreased with increasing distance from the burner. The general similarity of the slope of the three curves for each coal again suggests that the principal difference may have been in the time of ignition of the coal. As the furnace became hotter near the burner, the ignition occurred earlier and this again increased the temperature in the front part of the furnace.

Fig. 11 shows the effect of temperature on the rate of burning of Illinois coal when the change in temperature was effected by change in the rate of heat input. The amount of unburned carbon at each position increased with increase in the rate of firing, but, as the velocity also increased, these curves show that the burning time to a given percentage of unburned carbon decreased with increase in the rate of firing.

These results show that in this furnace, and by analogy, undoubtedly, in large boiler furnaces, the burning time decreased with increase in furnace temperature rather than increased as indicated by the small-scale experiments to which reference was made. It will be seen, however, that the greatest difference was, in general, in the early part of the flame and the slope of the curves for the latter part of the travel was so similar that the principal difference may have been the time of ignition of the coal. As the walls of the furnace near the burner became

hotter with increase in time or increase in rate of firing, the ignition occurred earlier.

A similar change in the temperature of a boiler or other furnace would have a similar effect on the rate of ignition; therefore, the desirability of maintenance of a hot zone near the burner is obvious. However, it cannot be concluded that water-cooled boiler-furnace walls will, in general, decrease markedly the overall rate of combustion. In large furnaces the flames are so thick that, as shown later in this paper, they become practically black and the cold wall does not so greatly affect the temperature at the burner as it did in the experimental furnace. In small furnaces, such as those of Scotch Marine or domestic boilers, the temperature of the walls has an important effect on the temperature in the flame and, therefore, on the combustion process.

RADIATION FROM PULVERIZED COAL FLAMES

The percentage of the heat liberated in a furnace that is transferred to the heat-receiving surface by radiation is an important factor in the design of boilers, oil stills, and similar equipment, as it determines the desirable relation of the radiation and convection surfaces. Broido,⁶ Orrok⁷ and DeBaufre⁸ have considered empirical formulas, and Wohlenberg⁹ and co-workers, and Haslam and Hottel¹⁰ have proposed formulas of more fundamental basis for the calculation of the fraction of the total heat liberated in the furnace that is radiated to the tubes in a boiler or other furnace. Experimental determinations of the radiation from the flame have been lacking. Koessler¹¹ has published the results of the determination of the radiation in several types of furnaces.

Apparatus and methods were developed to measure the radiation from the flames in the experimental furnace in the hope that the results could be interpreted for other furnace conditions and that they would serve to determine the validity of the formulas that have been set up.

APPARATUS AND METHOD

Fig. 12 shows the arrangement of the apparatus used for the measurement of the radiation from the flame, which was similar

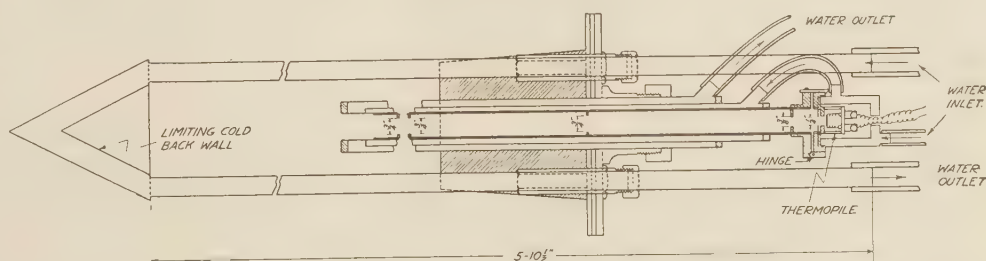


FIG. 12 APPARATUS FOR MEASUREMENT OF RADIATION

to that used by Koessler.¹¹ It consisted of a Moll thermopile mounted on the end of a water-cooled tube which contained four diaphragms to limit the angle of vision. Around the thermopile was a water jacket through which the water flowed in series with the tube; in this way the cold ends of the thermopile junctions and the surface of the tube that the thermopile "saw" were at the

⁶ B. N. Broido, A.S.M.E. Trans., vol. 47, 1925, p. 1123.

⁷ Geo. A. Orrok, Ibid., vol. 47, 1925, p. 1148.

⁸ W. L. DeBaufre, Ibid., vol. 53, 1931, p. 253.

⁹ W. J. Wohlenberg and D. G. Morrow, A.S.M.E. Trans., vol. 47, 1925, p. 127; W. J. Wohlenberg and E. L. Lindseth, A.S.M.E. Trans., vol. 48, 1926, p. 849; W. J. Wohlenberg and R. L. Anthony, A.S.M.E. Trans., vol. 51, 1929, p. 235.

¹⁰ R. T. Haslam and H. C. Hottel, A.S.M.E. Trans., vol. 50, 1928, p. 443.

¹¹ P. Koessler, Archiv für Wärmewirtschaft, vol. 11, 1930, p. 229.

same temperature and the output was zero independent of changes in room or water temperature.

A water-cooled copper cone served as a limiting cold screen to insure that the radiation falling on the surface of the thermopile was from the flame only. The cone shape was adopted to obtain more nearly black conditions by decreasing the possibility of reflection from the surface. This limiting screen was adjustable to obtain variable thicknesses of flame.

The entire assembly was mounted in a plate and refractory block and could be changed from one to another of the four ports provided in the furnace.

The water-jacket assembly for the thermopile was hinged so that it could be swung back from the end of the tube. The tube containing the diaphragms could then be removed and a thermocouple run into the furnace for the measurement of gas temperature.

The output of the thermopile was read on a semi-precision potentiometer with external reflecting galvanometer; this could be read to one microvolt.

The thermopile was calibrated with water jacket and water-cooled diaphragm tube as a unit. This eliminated the necessity of making any calculations for the correction for the angle of vision. A graphite cylinder heated in a gas furnace was used as a black-body source; a thermocouple on the inside back wall of the body measured its temperature. A straight-line calibration curve was obtained; the factor was 145 Btu per sq ft per hr per microvolt output.

The thermopile attained full output quickly, but had enough lag that it ironed out small fluctuations in the flame radiation. Only with violet fluctuations in the flame temperature did the galvanometer swing so rapidly as to make accurate readings difficult.

ACCURACY OF RESULTS

The greatest weakness of this work, as it is with most similar work, was the measurement of the temperature. The exposed thermocouple was subject to gain or loss of heat by radiation, but shielded velocity thermocouples, although tried, were found, as to be expected, impossible to use with pulverized-coal flames because of the accumulation of ash on the wire and in the shielding tube. Because the temperature differences in

this furnace were not great and as it was not indicated that any other method would give enough greater accuracy to warrant the difficulties of use, the exposed thermocouple was used.

The radiation from non-luminous flames consists only of the radiation from CO_2 and H_2O . The radiation of these gases has been calculated and determined by Schack¹² and Schmidt¹³ therefore, a comparison of the measured and calculated radiation from non-luminous flames allows some estimation of the order of accuracy of the measurements.

Table 3¹⁴ shows a comparison of the calculated and measured radiation from non-luminous natural gas flames in the experimental furnace.

TABLE 3 COMPARISON OF CALCULATED AND MEASURED RADIATION FROM NON-LUMINOUS NATURAL GAS FLAMES

Test	Heat input million, Btu per hr	Excess air, per cent	Distance from burner, ft	Radiation —1000 Btu per sq ft per hr—				Per cent
				Calo.	Measd.	Diff.		
1	2.71	20	3.5	23.9	23.9	0.0		0.0
			7.5	22.5	23.8	1.3		5.8
			11.5	20.05	21.0	0.95		4.7
2	2.67	14	3.5	22.5	24.7	2.2		9.8
			7.5	21.0	24.1	3.1		14.7
			11.5	19.0	19.4	0.4		2.1
3	2.63	4.5	3.5	22.6	23.9	1.3		5.8
			7.5	25.4	30.7	5.3		20.9
			11.5	27.7	31.0	3.3		11.9
4	2.77	10	3.5	30.2	30.7	0.5		1.8
			7.5	28.3	29.0	0.7		2.5
			11.5	23.1	22.3	0.8		3.7
5	2.17	12	3.5	22.0	25.4	3.4		15.5
			7.5	19.9	23.2	3.3		16.6
			11.5	17.8	17.8	0.0		0.0

By chance, two of the measured values agreed exactly with those calculated and only one measured value was less than the calculated. The other measured values were 2 to 21 per cent higher than those calculated. The findings of other investigators have been similar. The average difference was 7 per cent. For this type of measurement this is considered excellent agreement. If we assume that the calculated values are correct, the probable error in the measurements should be not more than 10 or 15 per cent.

¹² A. Schack, *Zeit für Tech. Physik*, vol. 5, 1924, p. 266.

¹³ E. Schmidt, *Forschungsarbeiten auf der Gebiete des Ingenieurwesen*, vol. 3, 1932, p. 57.

¹⁴ R. A. Sherman, *A.S.M.E. Trans.*, vol. 56, 1934, p. 177.

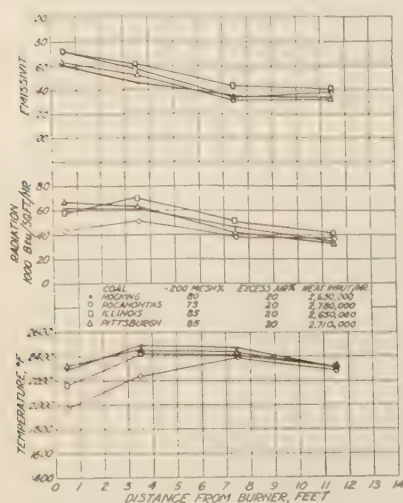


FIG. 13 COMPARATIVE TEMPERATURE, RADIATION, AND EMISSIVITY OF HOCKING, POCAHONTAS, ILLINOIS, AND PITTSBURGH COAL FLAMES

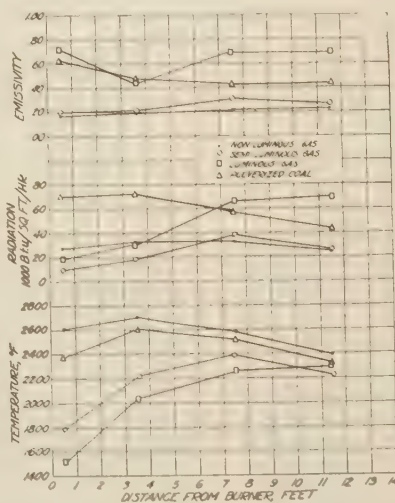


FIG. 14 TEMPERATURE, RADIATION, AND EMISSIVITY OF GAS AND HOCKING COAL FLAMES

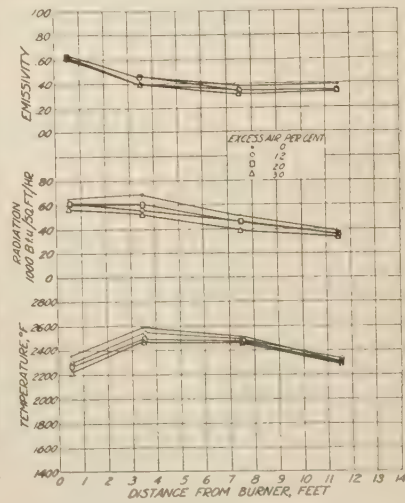


FIG. 15 TEMPERATURE, RADIATION, AND EMISSIVITY OF HOCKING COAL FLAMES WITH VARYING EXCESS-AIR PERCENTAGES (Through 200-mesh, 80 per cent; rate of heat input 2,650,000 Btu per hr.)

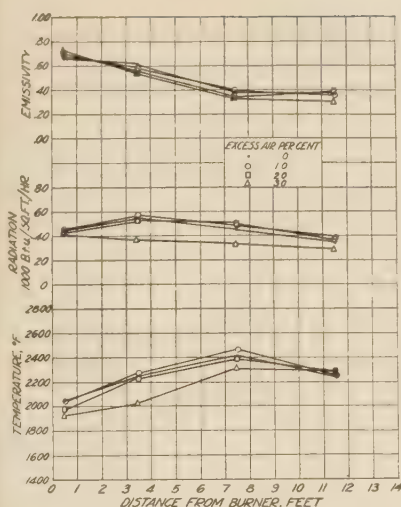


FIG. 16 TEMPERATURE, RADIATION, AND EMISSIVITY OF POCAHONTAS COAL FLAMES WITH VARYING EXCESS-AIR PERCENTAGES (Through 200-mesh, 73 per cent; rate of heat input 2,780,000 Btu per hr.)

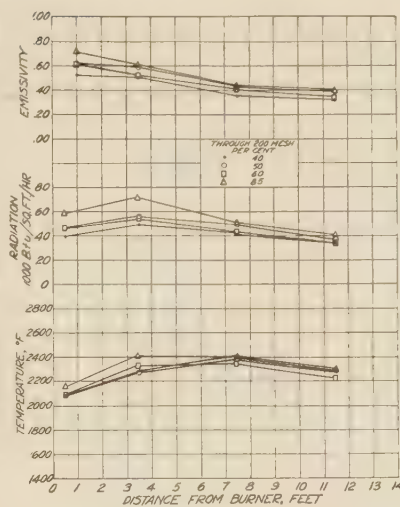


FIG. 17 TEMPERATURE, RADIATION, AND EMISSIVITY OF ILLINOIS COAL FLAMES, VARYING PERCENTAGES THROUGH 200-MESH (Excess air 20 per cent; rate of heat input 2,650,000 Btu per hr.)

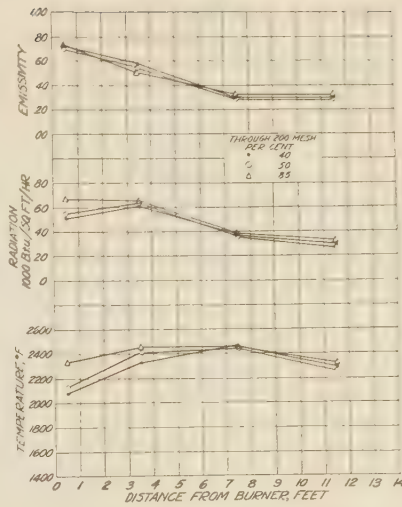


FIG. 18 TEMPERATURE, RADIATION, AND EMISSIVITY OF PITTSBURGH COAL FLAMES, VARYING PERCENTAGES THROUGH 200-MESH (Excess air 20 per cent; rate of heat input 2,700,000 Btu per hr.)

DISCUSSION OF DATA

The data on the radiation from the flames are presented in a series of curves. In each figure the temperature of the gases, the radiation from the flame, and the emissivity are plotted in the lower, middle, and upper parts, respectively, against distance from the burner. The temperatures given are the averages of a number of readings across the flame and are, therefore, mostly lower than those shown in the previous figures which were taken only on the axis of the furnace.

The radiation is that calculated from the thermopile output, when 34 or 35 in. of flame were included between the water-cooled back plate and the end of the water-cooled diaphragm tube, and the calibration constant of the thermopile. The emissivity is the ratio of the measured radiation to that of a black body at the temperature of the flame.

Relation of Radiation to Type of Coal. Fig. 13 shows the radiation data for the four coals at similar rates of heat input, fineness, and excess air. The curves show that the radiation from the flame does not reach its maximum in the zone of maximum temperature. For example, the maximum temperature with the Pocahontas coal was found at 7.5 ft from the burner, but the maximum radiation measured was at 3.5 ft from the burner.

The slow-burning Pocahontas coal had the lowest temperature and radiation of the four coals, except at 11.5 ft from the burner where both the temperature and radiation were not greatly different for the four coals.

The emissivities of the fast-burning Hocking and Pittsburgh coal flames were lower than those of the other two coals at the first two positions of measurement. The emissivity of the Illinois coal flame was the highest of the four at all positions. However, the maximum difference in emissivities at any position was only 0.10 to 0.15, or about 30 per cent, and the trend for all coals was the same. The emissivity decreased with increasing distance from the burner as the carbon burned out.

Fig. 14 shows a comparison of the temperature, radiation, and emissivity of pulverized Hocking coal, and non-luminous and semi- and fully luminous natural gas flames at similar rates of heat input and excess air. The luminous natural gas flames were obtained by injection of the gas and air in separate streams

so that mixing was delayed and the hydrocarbons were cracked to give free carbon. The temperature curves of the pulverized-coal and non-luminous gas flames were similar, but the temperature of the luminous gas flames was low near the burner because of slow combustion.

The radiation and emissivity curves show that, although the non-luminous and semi-luminous natural gas flames had much lower radiation and emissivity than the pulverized-coal flames, yet by a design of burner to give proper cracking natural gas can be made to give flames which have as high radiation and emissivity as pulverized coal.

Radiation and Excess Air. Figs. 15 and 16 show the temperature, radiation, and emissivity of Hocking and Pocahontas coal flames with varying excess air. The temperature and radiation both increase as the excess of air decreases, as expected, except that the temperature and radiation were somewhat higher with 10 per cent than with no excess air when burning Pocahontas coal.

No great differences in emissivity with differences in excess air were found and the curves are somewhat intermingled but the emissivities decreased slightly with increase in excess air.

Radiation and Size of Coal. Figs. 17 and 18 show the relation of the radiation to the fineness of grinding for the Illinois and Pittsburgh coals, respectively. Although the temperature and radiation did not increase uniformly with increasing percentages through 200-mesh with either coal, they were greatest with the finest coal. When burning Illinois coal the change in radiation with size of coal was greater than when burning Pittsburgh coal and the emissivity of the Illinois coal flames was 30 to 40 per cent greater with 85 per cent than with 40 per cent through 200-mesh, whereas the emissivity changed only slightly with the size of the Pittsburgh coal.

Radiation and Rate of Heat Input. Figs. 19, 20, and 21 show the relation of the radiation to the rate of heat input for Hocking, Pocahontas, and Illinois coals, respectively. The temperatures increased with the rate of firing and the radiation increased in about the same proportion. Consequently, the emissivity at any position varied within small limits and not in any definite relation to the rate of firing. As shown in Fig. 13 at one rate of firing, the radiation and emissivity of the Illinois coal flames were

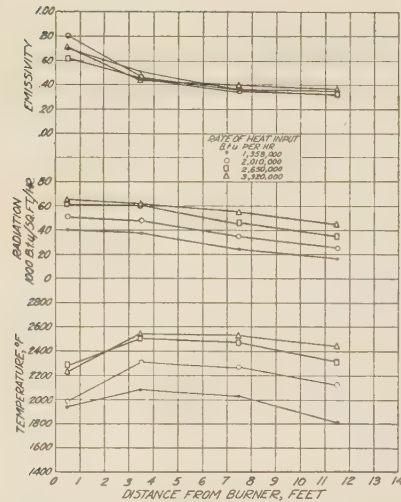


FIG. 19 TEMPERATURE, RADIATION, AND EMISSIVITY OF HOCKING COAL FLAMES, VARYING RATE OF HEAT INPUT (Excess air 20 per cent; through 200-mesh, 80 per cent.)

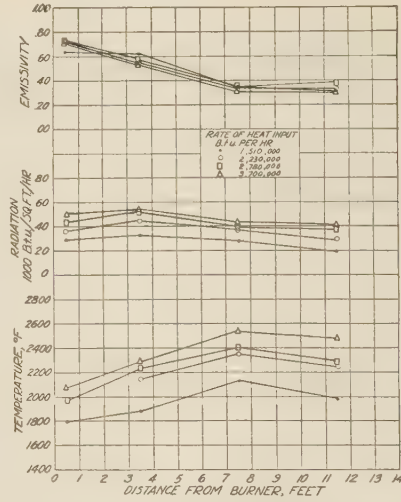


FIG. 20 TEMPERATURE, RADIATION, AND EMISSIVITY OF POCAHONTAS COAL FLAMES, VARYING RATE OF HEAT INPUT (Excess air 20 per cent; through 200-mesh, 70 to 76 per cent.)

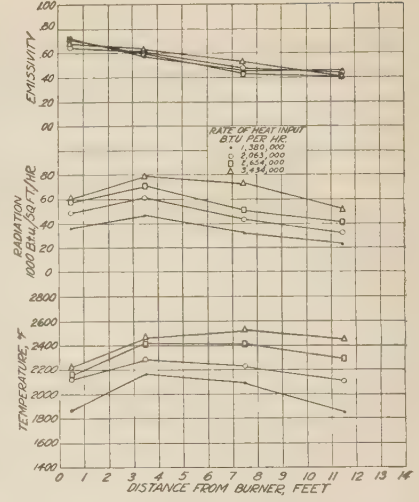


FIG. 21 TEMPERATURE, RADIATION, AND EMISSIVITY OF ILLINOIS COAL FLAMES, VARYING RATE OF HEAT INPUT (Excess air 20 per cent; through 200-mesh, 77 to 85 per cent.)

higher than those of the other two coals at corresponding rates of heat input.

Variation of Radiation With Depth of Flame. As boiler and other furnaces may have flame depths up to 20 ft, it is desirable, if the data obtained in the test furnace are to be of practical value, to be able to calculate the radiation of flames of greater depth. The general expression for the relation of the radiation to the thickness of the flame is:

$$Q = Q_B (1 - e^{-KL}) \dots \dots \dots [1]$$

where Q is the radiation from the flame, Q_B is the radiation of a black body at the temperature of the flame, e is the base of natural logarithms, K is the absorption coefficient, and L the depth of the flame. As $\frac{Q}{Q_B} = p_F$, the emissivity of the flame, then

$$p_F = 1 - e^{-KL} \dots \dots \dots [2]$$

As the radiation from these flames is that from CO_2 , H_2O , and solid carbon and ash particles, the absorption coefficient

depends on the partial pressure of the CO_2 and H_2O and on the concentration of the solids in the flame. As neither these nor the temperature of the gas are uniform across the flame at any position, it would not be expected that absorption coefficients, K , calculated from the radiation of various depths of flame, would be constant.

Table 4 shows the emissivity p_F and absorption coefficient K calculated for the four coals burned under similar conditions for five flame thicknesses at each of the four points of measurement. The flame thickness was measured in inches for the calculation of K . As expected, K is not constant but the constancy increases with increasing distance from the burner as conditions become more uniform across the flame and, in general, the constancy increases with increase in flame thickness.

TABLE 5 CALCULATED EMISSIVITY OF PULVERIZED ILLINOIS COAL FLAME

Distance from burner, ft	K	Depth of flame, in.				
		35	60	120	180	240
0.5	0.036	0.72	0.88	0.99	1.00	1.00
3.5	0.026	0.60	0.79	0.96	0.99	1.00
7.5	0.016	0.44	0.62	0.85	0.94	0.98
11.5	0.015	0.41	0.59	0.83	0.93	0.97

TABLE 4 COMPARATIVE EMISSIVITIES AND ABSORPTION COEFFICIENTS FOR PULVERIZED-COAL FLAMES

Coal	Hocking				Pocahontas				Illinois				Pittsburgh			
Heat input, Btu per hr	2,680,000				2,780,000				2,650,000				2,710,000			
Excess air, per cent	20				20				20				20			
Fineness, per cent—200-mesh coal	79.6				73.2				85				85.2			
Distance from burner, ft	Depth flame, in.		Depth flame, in.		Depth flame, in.		Depth flame, in.		Depth flame, in.		Depth flame, in.		Depth flame, in.			
	<i>pF</i>	<i>K</i>	<i>pF</i>	<i>K</i>	<i>pF</i>	<i>K</i>	<i>pF</i>	<i>K</i>	<i>pF</i>	<i>K</i>	<i>pF</i>	<i>K</i>	<i>pF</i>	<i>K</i>		
0.5	10	0.184	0.0203	10	0.254	0.0293	10	0.172	0.0189	10	0.138	0.0147	10	0.138	0.0147	
	16	0.248	0.0177	16	0.336	0.0256	15	0.283	0.0221	15	0.211	0.0159	15	0.211	0.0159	
	22	0.374	0.0212	22	0.508	0.0323	20	0.390	0.0247	20	0.193	0.0166	20	0.193	0.0166	
	28	0.586	0.0316	28	0.680	0.0408	30	0.680	0.0380	30	0.586	0.0295	30	0.586	0.0295	
3.5	34	0.619	0.0283	34	0.721	0.0376	35	0.718	0.0362	35	0.635	0.0288	35	0.635	0.0288	
	10	0.149	0.0161	10	0.246	0.0283	10	0.168	0.0182	10	0.132	0.0143	10	0.132	0.0143	
	16	0.246	0.0175	16	0.366	0.0283	15	0.260	0.0200	15	0.199	0.0147	15	0.199	0.0147	
	22	0.348	0.0193	22	0.470	0.0344	20	0.370	0.0232	20	0.341	0.0209	20	0.341	0.0209	
7.5	28	0.404	0.0187	28	0.530	0.0266	30	0.548	0.0265	30	0.518	0.0244	30	0.518	0.0244	
	34	0.458	0.0180	34	0.568	0.0219	35	0.601	0.0263	35	0.504	0.0200	35	0.504	0.0200	
	10	0.159	0.0173	10	0.157	0.0173	10	0.156	0.0170	10	0.137	0.0147	10	0.137	0.0147	
	16	0.219	0.0147	16	0.214	0.0150	15	0.223	0.0168	15	0.182	0.0136	15	0.182	0.0136	
11.5	22	0.270	0.0145	22	0.253	0.0134	20	0.279	0.0164	20	0.220	0.0124	20	0.220	0.0124	
	28	0.312	0.0134	28	0.312	0.0136	30	0.382	0.0159	30	0.284	0.0111	30	0.284	0.0111	
	34	0.353	0.0129	34	0.336	0.0120	35	0.435	0.0164	35	0.318	0.0108	35	0.318	0.0108	
	10	0.147	0.0159	10	0.246	0.0284	10	0.153	0.0165	10	0.088	0.0092	10	0.088	0.0092	
	16	0.203	0.0143	16	0.285	0.0209	15	0.209	0.0157	15	0.133	0.0095	15	0.133	0.0095	
	22	0.243	0.0129	22	0.323	0.0177	20	0.260	0.0150	20	0.185	0.0104	20	0.185	0.0104	
	28	0.290	0.0131	28	0.359	0.0159	30	0.353	0.0145	30	0.259	0.0094	30	0.259	0.0094	
	34	0.335	0.0120	34	0.380	0.0141	35	0.406	0.0150	35	0.320	0.0111	35	0.320	0.0111	

To be strictly correct, the emissivity at increasing flame depths cannot be calculated from values of K so determined. Flames, containing the amounts of CO_2 and H_2O that these would, probably reach their maximum radiation in the wave-length bands of these gases at less depth than the maximum would be reached for the solid particles. Therefore, the solid and gaseous radiation should be separated, but it was not considered that the accuracy of the data would warrant the complications.

Table 5 gives the calculated emissivities for Illinois coal for increasing flame thicknesses using K calculated for the maximum depth of measurement from Table 4. For a flame thickness of 10 ft the flame at 0.5 or 3.5 ft from the burner would be practically black and emissivity almost 1, and at 7.5 and 11.5 ft the emissivities would be over 0.8. At a flame thickness of 20 ft the flame would be practically black at all distances from the burner.

Although the amount of carbon was small at 11.5 ft from the burner, less than 2 per cent, most of the ash was still suspended in the gas and this, with the CO_2 and H_2O , gave a high emissivity to the flame.

These data indicate that for flames such as these in large furnaces, 15 ft or more of uniform flame, the emissivities can be taken as 0.9 to 1.0 for the calculation of radiation.

An outstanding conclusion from these measurements is that, because of the variations in temperature, radiation, and emissivity along the length of the flame, the problem of the development of a fundamental expression for even the over-all transfer of a flame is tremendously difficult and that the problem of estimating the transfer in different parts of a furnace is even more difficult. The latter problem is frequently of more importance than the first because the proper distribution of cooling surface in a furnace would necessitate a knowledge of the temperature and radiation characteristics in various parts of the flame.

The data on the emissivity of the flame for various depths should be helpful in calculations but in addition to the emissivity the temperature of radiation is required. What this should be in a furnace where the temperature rises to a maximum and then falls is not easily determined.

The value of the present results is considered to be principally: (1) That it has been shown that, of the factors investigated, the type of coal had the most effect on the radiation and emissivity and that the size of coal, excess air, and rate of heat input were of decreasing importance, and (2) that the measured values with their accompanying data furnish a test for the validity of fundamental or empirical formulas that may be proposed. The test of such formulas by these data is left to their sponsors.

SUMMARY

The experimental investigation of the burning characteristics of four coals in pulverized form has shown:

- 1 That the rate of decrease of unburned carbon with increase of excess air was not the same for different coals. The unburned carbon continued to decrease up to 30 per cent excess air with Pocahontas coal, whereas the curves for Hocking coal were practically flat beyond 20 per cent excess air
- 2 That the fineness of grinding becomes increasingly important as the combustion space is restricted and that the optimum limits of fineness, without regard to power consumption in these experiments, differed with the type of coal
- 3 That, as shown by the above conclusions, the type of coal markedly influences the rate of combustion. Although the low-volatile Pocahontas coal, 18 per cent on moisture- and ash-free basis, was the slowest burning of the four coals, Illinois coal, volatile content 40 per cent,

burned more slowly, and Pittsburgh coal, volatile content 44 per cent, burned only slightly more rapidly than Hocking coal whose volatile content was 40 per cent

- 4 That increased furnace temperature increased the apparent rate of combustion of the coals
- 5 That, as the difference in the rate of combustion with different coals and furnace temperatures was particularly marked in the early part of the combustion, the ignition temperature of the coal and the temperature in the ignition zone are indicated as important factors in the over-all combustion process. The need is evident for a method for the determination of the ignition temperature or relative ease of ignition of pulverized coal when actually suspended in air.

The determination of the radiation from the pulverized-coal flame has shown:

- 1 That, although the temperature and total radiation of the flame were affected by the fineness of grinding, excess air, and rate of firing, the emissivity of the flame at any position was affected to a marked degree only by the type of coal. The maximum differences in emissivities at any position were only 0.10 to 0.15 or about 30 per cent
- 2 That the radiation from the suspended carbon and ash particles is an important part of the total radiation for the emissivity of non-luminous gas flame in this furnace was about 0.2, whereas those of the pulverized-coal flames were 0.7 to 0.3, decreasing as the carbon burned from the flame
- 3 That a gas flame could be made so luminous, by inducing cracking of the hydrocarbons, that its emissivity could be made greater than that of a pulverized-coal flame
- 4 That the absorption coefficient of the flame as calculated from the measurement of the radiation of different thickness of flame was not constant because of variable conditions in the flame, but was more constant the greater the thickness and the greater the distance from the burner
- 5 That by calculation from the absorption coefficients at the maximum depth of measurement, the emissivities of Illinois coal flames in thickness of 15 to 20 ft would be 0.9 to 1.0
- 6 That the variations in temperature, radiation, and emissivity along the flame render the problem of developing fundamental expressions for radiant heat transfer in different parts of a furnace, or even for an entire furnace, extremely difficult
- 7 That these data furnish a test for the validity of fundamental or empirical formulas for radiant heat transfer.

Discussion

R. M. HARDGROVE.¹⁶ We appreciate Mr. Sherman's having made available the data presented in this paper. It will be of real value and use provided it is not interpreted too broadly as it was obtained on a very specific arrangement of equipment. The type of burner used is probably inferior to any other being offered on the market today and far better and more representative results would have been obtained if a good turbulent burner had been used.

The unburned carbon loss is relatively consistent with the actual losses in commercial installations. Fig. 2 shows that 20

¹⁶ Research Engineer, Fuller Lehigh Co., New York, N. Y. Mem. A.S.M.E.

per cent excess air is ample for Hocking Coal, while 25 per cent would be better for Pocahontas Coal.

The effect of fineness of the coal on unburned carbon, as shown on Figs. 3, 4, 5, and 6, indicates that the unburned carbon reaches an approximate minimum at the following fineness:

- 77 per cent-200 for Pocahontas coal corresponding to 3 per cent unburned carbon
- 60 per cent-200 for Pittsburgh coal corresponding to 1 per cent unburned carbon
- 60 per cent-200 for Hocking coal corresponding to 1 per cent unburned carbon
- 70 per cent-200 for Illinois coal corresponding to 1.3 per cent unburned carbon

The first three are consistent with actual installations, but Illinois coal usually gives a lower carbon loss with coarser coal than either Pittsburgh or Hocking coals.

One furnace in the Chicago district, with which we are familiar, burning Illinois coal averages a loss in combustible in the flue dust of approximately 0.2 per cent. This furnace has vertical burners and slag tap furnaces. Other units having horizontal burners and water cooled hopper bottoms average about 0.4 per cent loss in flue dust.

In an attempt to find a reason for this inconsistency, it was noted that this Illinois coal, which usually carries 11 to 15 per cent moisture as fired, was dried to a moisture of 1.1 per cent. In modern direct fired installations, enough hot air would be used to remove the excess surface moisture only, leaving about six per cent inherent moisture plus one per cent surface moisture in the coal.

Whether the absence of this moisture can account for the unusual behavior of this coal or whether it was overheated during drying or in storage is difficult to say, but we would suggest that tests on this coal be repeated using freshly mined coal dried only enough to remove the surface moisture in excess of one per cent. It is noted from the analyses in Table 1 that all of the coals contain appreciably less moisture than would usually be present and even lower than if dried in the usual manner for either bin operation or direct fired systems.

The liberations of approximately 20,000 Btu per cu ft are all relatively low. With a good burner approximately complete combustion should be obtained with liberations $3\frac{1}{2}$ times as great in a furnace this size.

The effect of furnace temperature on reducing unburned carbon is well illustrated in Figs. 8, 9, and 10, where at the same liberation the highest furnace temperature produces the lowest carbon loss. The temperatures were mostly above 2200 F

which rather contradicts the theory that temperatures of 1600 F are needed for ignition and temperatures above this retard combustion.

The relative radiation of the different coals is of interest and further data of this sort is greatly needed.

It is to be hoped that the author will be able to continue this work with additional fuels over a wide range of liberations and using burners and moistures more analogous to present day practise.

AUTHOR'S CLOSURE

The comments by Mr. Hardgrove in which he compares the laboratory results with actual boiler-furnace performance are very helpful. He has done well to warn against too broad an interpretation of these results as they were obtained on an experimental furnace.

Although the suggestion, that the low moisture content of the Illinois coal affected the results, may have merit, the author does not believe that these results are particularly questionable. It should be understood that the values for the unburned carbon are not the heat loss in unburned carbon but the percentage of the total carbon in the gas that appears as unburned carbon. They must be multiplied, therefore, by the percentage of carbon in the coal which reduces the values somewhat. This calculation would not bring the results down to the low figures of 0.4 and 0.2 per cent that Mr. Hardgrove quotes but it must be remembered that there may be considerable difference among Illinois coals. Tenney¹⁶ has presented results on coal from the same mines which allow of a more accurate comparison. With 53 per cent through 200-mesh he reports 13.2 per cent combustible in the flue dust when 3 to 4 sec were available for combustion. In the author's test, with 56 per cent through 200-mesh the average combustible in the dust was also 13.2 per cent at the last point of sampling when only 0.4 sec was available for combustion. Values for other finenesses are of the same order.

Although it would be valuable to extend the work to other burners analogous to commercial types the data would be of no more value for comparison of the burning characteristics of the fuel than with this simple one. Furthermore, this burner, although simple, has been shown to give as good results as the much more complicated varieties.

The work should go on to a wider variety of coals but its continuation is doubtful without support from the groups to which it is of particular benefit, namely, the equipment manufacturers, coal users, and coal producers.

¹⁶ E. H. Tenney, "Pulverization and Boiler Performance." A.S.M.E. Trans., vol. 54, 1932, paper no. FSP-54-7, p. 55.

Supersaturated Steam

By JOHN I. YELLOTT, JR.,¹ ROCHESTER, N. Y.

Supersaturation, or the failure of steam to condense when the saturated condition is reached in an expansion, has long been a matter of interest to engineers. This paper presents the account of an investigation of this phenomenon in which the principal objectives were the location of the Wilson line, which indicates the condition at which condensation actually occurs, and the measurement of the size of the drops which are formed when flowing steam condenses. Examination of the flow of low pressure steam through an illuminated nozzle fitted with a glass top revealed that the condensation process could be observed and that the pressure of the steam at the condensation point could be measured with the aid of a search tube. It was found that in a simple convergent-divergent nozzle condensation did not occur until the

steam had reached the condition approximately represented by the 3.5 per cent moisture line on the Mollier chart. The droplets which formed at that condition were extremely minute, their radii being of the order of magnitude of 6.2×10^{-8} cm, and there was no evidence of growth during their passage through the nozzle. Additional experiments with nozzles of other designs led to the discovery that under certain conditions condensation could take place when the steam had reached the 2 per cent moisture condition, and that the droplets so formed grew rapidly from about 10.0×10^{-8} cm to about 6.0×10^{-6} cm in radius. It was concluded that supersaturation invariably occurred in the condensation of flowing steam, and that the superheated steam formula should be used to estimate the flow of saturated steam through nozzles.

AN ACCURATE knowledge of the weight of steam which may be expected to flow through a given nozzle area under varying conditions is essential in the design of steam turbines and other equipment. The flow of superheated steam can be estimated with a high degree of accuracy by the use of the Saint-Venant formula. Applying the usual formula to the flow of saturated or wet steam, however, with the assumption that condensation begins as soon as the saturation condition is passed in an expansion, results in a theoretical flow which may be smaller than the actual. This excess, at first attributed to experimental error, has been so conclusively demonstrated by the work of able experimenters that the correctness of the conventional theory of condensation is questionable.

The theory of supersaturation was proposed to explain the phenomena involved in the flow of saturated or wet steam. It was suggested that steam in a rapid expansion from a dry or slightly superheated condition might not begin to condense when the saturated condition was reached, but might continue to expand as in the superheated region, thus becoming supersaturated. Such a theory explains the excess flow encountered in the expansion of saturated steam through nozzles.

Flow of a fluid through a nozzle depends upon the product of its density and velocity at any given cross-section. The conventional theory of condensation requires that steam begins to condense when the saturated condition is passed in an expansion. The condensed portion of the steam gives up its latent heat, causing a decrease in the density of the surrounding medium. If the condensation should fail to occur, the latent heat would be retained with the result that, for a given expansion, the density of

supersaturated steam would be greater than that of wet steam. The velocity of the supersaturated steam would be less than that of the wet steam because the isentropic heat drop is less for a supersaturated than for an equilibrium expansion. The product of the velocity and the density, however, is greater for the supersaturated than for the wet steam and hence the weight flowing through a given area is greater.

The actual mechanism of condensation in flowing steam, which is by no means clearly understood, involves the formation of water droplets. The nature of formation and the size of these droplets is of great importance in determining their behavior, particularly in respect to the erosion of the low pressure blades in steam turbines.

Need for further data on supersaturation in actual steam flow and the lack of information on condensation nuclei and drop size led to a two-year study in the laboratories of the Johns Hopkins University of the flow through nozzles of relatively low-pressure steam. The original object of this research was to investigate the condensation of steam in an effort to learn how and when it occurs and to discover the conditions under which supersaturation actually exists. It was desired to locate by experimental means the Wilson line which, on the Mollier chart, represents the condition at which condensation actually occurs in expanding steam at the termination of the supersaturated state.

In considering methods of attack, it appeared that Mellanby and Kerr (25)² had exhausted the possibilities of the weighed-flow analysis. The optical method used by Stodola (29) to study flow in nozzles and by Thomas (31) to examine moisture in steam did not appear to have been utilized to the fullest possible extent, and the possibility that drop sizes might be measured by optical means made this method more attractive. It was believed that, if the condensation point could be seen, the pressure at that point could be measured with a search tube and thus some positive knowledge of condensation conditions would be obtained. From this the supersaturation could be determined.

2 HISTORICAL

Supersaturation has been studied by many investigators. Aitken (1) concluded that all condensation occurred on dust particles as nuclei and he devised a dust counter which utilized this principle.

² Numbers in parenthesis refer to the bibliography, Appendix 3, at the end of this paper.

¹ Instructor in Mechanical Engineering at the University of Rochester, Rochester, N. Y. Jun. Mem. A.S.M.E. Mr. Yellott received the degree of Bachelor of Engineering in 1931 from Johns Hopkins University after which he returned to the University for two years graduate work under Prof. A. G. Christie. This work consisted primarily of advanced thermodynamics under Prof. J. C. Smallwood and of power engineering under Prof. Christie. The research described in this paper was the basis of the author's thesis for the degree of Master of Mechanical Engineering received from the University in 1933 and was carried out under the direction of Prof. Christie at the Hopkins Laboratories.

Contributed by the Power Division and presented at the Annual Meeting, New York, N. Y., December 4 to 8, 1933, of THE AMERICAN SOCIETY OF MECHANICAL ENGINEERS.

NOTE: Statements and opinions advanced in papers are to be understood as individual expressions of their authors, and not those of the Society.

Von Helmholtz (18) called attention to the supersaturation of steam issuing from an orifice into the open air. Observing that electrification of the jet greatly increased the number of droplets, he came to the conclusion that ions usually served as nuclei for condensation. The extension of Lord Kelvin's formula for the equilibrium pressure over curved surfaces is due to von Helmholtz.

G. T. R. Wilson (34-37), whose name is given to the line on the Mollier chart which marks the limit of supersaturation, investigated the nature of this phenomenon. By expanding in a glass chamber a sample of air or other gas saturated with moisture, he was able to measure the pressure at which condensation began. From this he deduced the supersaturation ratio by dividing the pressure at which condensation started by the saturation pressure corresponding to the temperature of the supersaturated steam. At -16°C , Wilson found a supersaturation ratio of 7.9, corresponding to a drop radius of 6.4×10^{-8} cm.

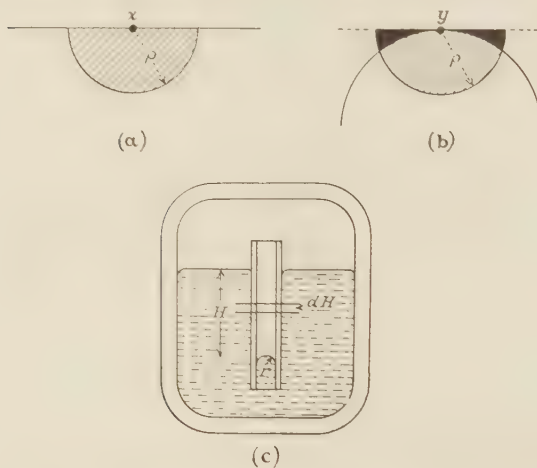


FIG. 1 VAPOR PRESSURE ABOVE PLANE AND CURVED SURFACES

J. J. Thomson (33) studied with great care the effect of ionization upon supersaturation and developed the theory underlying condensation upon ions. In general, his findings support those of Wilson.

Carl Barus (4-8) likewise obtained results which substantiated Wilson's. He was particularly interested in the problem of supersaturation as applied to meteorological phenomena.

C. F. Powell (27), at Wilson's suggestion, investigated with improved apparatus the supersaturation of saturated air at four temperatures. His results will be discussed later.

A. Stodola (29), by his work with illuminated glass nozzles, found positive evidence of the existence of supersaturation in actual nozzle flow. With characteristic thoroughness he repeated the work of earlier experimenters and then developed the method of attack which is used in this investigation. He has reported one measurement made in this manner in his book, "Steam and Gas Turbines" which contains a complete presentation of the theory of supersaturation.

Mellanby and Kerr (25) weighed and analyzed the flow of saturated steam through nozzles and concluded that, to account for their experimental results, supersaturation must exist.

Using the weighed flow method, Kearton (22) studied the flow of mercury vapor through nozzles and showed that supersaturation occurred during that process. The limitations of this method prevented him from placing a definite value upon the supersaturation to be expected with mercury.

Supersaturation has also been studied from purely theoretical considerations. Maxwell (24), discussing the Thomson iso-

thermal, first suggested the possibility of a supersaturated state for steam.

Sir William Thomson, Lord Kelvin (32) gave a theoretical foundation to supersaturation when he derived the relation between the vapor pressures above a curved and a plane liquid surface. His equation is the basis of all supersaturation calculations.

H. L. Callendar (9-11), studying the so-called missing quantity in reciprocating steam engines, concluded that supersaturation could account for at least a portion of that quantity. He discussed supersaturation at length in several publications and in his book, "The Properties of Steam."

H. M. Martin (23) brought the subject of supersaturation to the attention of engineers by his paper, "A New Theory of the Steam Turbine." He assumed that condensation always results in droplets of the same size. On this basis he applied Callendar's value of the droplet radius to the von Helmholtz equation making allowance for the variation of surface tension with temperature and estimated the supersaturation ratio which might be expected at any temperature. From these data, using the Callendar equations of state, he calculated the properties of steam for the conditions under which condensation should occur. His results, plotted on the Mollier chart, form the line to which he gave Wilson's name.

Goodenough (16) presented a thorough discussion of the theory of supersaturation and its effects and then, doubting the validity of the theory, proceeded to show that the same effect of increasing the flow over the calculated value could be produced by the presence in the steam of small water particles. His article is of particular interest for its exposition of the effect of water droplets upon velocity coefficients of nozzles.

3 THEORY OF SUPERSATURATION

Supersaturation is based upon the fact that the vapor pressure of a liquid at a given temperature is greater above a curved than above a plane surface. This can be understood by referring to Fig. 1 where (a) shows a molecule, x , on a plane liquid surface, which is attracted by all of the molecules of the liquid within the hemisphere of radius ρ , the distance over which the molecular attraction may be assumed to act, and (b) shows a molecule, y , on a curved surface, which is attracted by fewer molecules than x because those molecules in the solid area are no longer present. At the same temperature, then, molecule y will be tied less securely to the surface than will x , and conversely a greater pressure in the surrounding atmosphere will be required to force y to remain on the surface. In other words, the vapor pressure in case (b) is greater than that in (a). Thus a water droplet, if sufficiently small, will evaporate if placed in an atmosphere of saturated steam. If, however, the vapor is supersaturated or at a pressure greater than that corresponding to the temperature, equilibrium can exist between the vapor and the droplet when the pressure of the vapor is equal to the vapor pressure of the droplet. The conditions necessary for equilibrium between vapor and droplets were investigated by Lord Kelvin (32) and a formula to express these conditions was derived by von Helmholtz (18).

Lord Kelvin's equation evaluates the change in vapor pressure of a liquid caused by a change in the curvature of its surface. Fig. 1(c) shows the assumed conditions. A capillary tube of radius r is inserted into a liquid of which γ is the surface tension in lb per ft. The whole is enclosed in a vessel so that only the liquid and its vapor, both at temperature T , are present. If the liquid does not wet the tube, it will be depressed due to capillary action to a level below that of the plane surface of the remaining liquid in the vessel. The surface of the liquid in the tube may be assumed to be a hemisphere of radius r . The distance of the meniscus below the level of the liquid is H , and P and p are the

pressures in the liquid and the vapor, respectively, at the meniscus,

$$\pi r^2 P = \pi r^2 p + 2\pi r \gamma \dots [1]$$

Rearranging and eliminating πr ,

$$P - p = \frac{2\gamma}{r} \dots [1a]$$

When the concavity is downward r is assumed to be positive. Due to the difference in elevation, H , the pressure of the vapor, p , at the curved surface in the tube must be greater than that at the plane surface. The vapor, however, must be in equilibrium with both the curved and the plane surfaces; otherwise perpetual motion would result. Therefore, denoting by P_o and p_o the pressure in the liquid and in the vapor, respectively, at the plane surface,

$$P_o = p_o \dots [2]$$

If v is the specific volume of the vapor, the difference in pressure due to the difference in elevation will be

$$p - p_o = \frac{H}{v} \dots [3]$$

Likewise, if V is the specific volume of the liquid, the difference in the liquid pressures will be

$$P - P_o = \frac{H}{V} \dots [4]$$

We wish now to solve for $p - p_o$, the change in vapor pressure caused by the curvature of the surface. Combining [3] and [4] and eliminating H ,

$$(p - p_o) = (P - P_o) \frac{V}{v} \dots [5]$$

Inverting [3] and [4] and subtracting,

$$\frac{(v - V)}{H} = \frac{1}{p - p_o} - \frac{1}{P - P_o} \dots [6]$$

and recalling from [2] that $P_o = p_o$,

$$\frac{v - V}{H} = \frac{P - P_o - p + p_o}{(p - p_o)(P - P_o)} = \frac{P - p}{(p - p_o)(P - P_o)} \dots [6a]$$

Since $(P - P_o) = \frac{H}{V}$,

$$\frac{v - V}{V} = \frac{P - p}{p - p_o} \dots [7]$$

Substituting [1a] in [7], we have the desired relation:

$$p - p_o = \frac{2V\gamma}{r(v - V)} \dots [8]$$

Thus, for equilibrium to exist, the pressure of a vapor containing drops of radius r must exceed the vapor pressure of the drops by $\frac{2V\gamma}{r(v - V)}$, which may be very large if r is sufficiently small.

The equation first derived by von Helmholtz expresses the same relation in more convenient form. Referring again to Fig. 1(c) and Equation [2], we may define the pressure of the vapor at the plane surface, p_o , as the saturation pressure at temperature T , p_s . Rearranging Equation [1a] and subtracting p_s from each side of the equation, we have,

$$p - p_s + \frac{2\gamma}{r} = P - p_s = P - P_o \dots [9]$$

since $p_s = p_o$ by definition and $p_o = P_o$.

Equation [9] can now be written:

$$\frac{2\gamma}{r} + \int_{p_s}^p dp = \int_{P_o}^P dP \dots [9a]$$

Consider an elementary section, dH , on Fig. 1(c). The increase of the liquid pressure $dP = \frac{dH}{V} = D dH$, where D , the density of the liquid, equals $\frac{1}{V}$. The increase of the pressure of the vapor,

$dp = \frac{dH}{v} = d dH$, where d is the density of the vapor. Thus $dP = D dH$, and $dp = d dH$, so $dP = \frac{D}{d} dp$. Substituting in [9], we have:

$$\frac{2\gamma}{r} = \int_{p_s}^p \frac{D}{d} dp - \int_{p_s}^p dp = \int_{p_s}^p \left(\frac{D}{d} - 1 \right) dp \dots [10]$$

In general, d is very small compared to D , and $\frac{D}{d}$ is so large compared to 1 that without serious error we may omit the product $1 \times dp$. Likewise, over a small range, D may be taken as a constant, so we have:

$$\frac{2\gamma}{r} = D \int_{p_s}^p \frac{dp}{d} \dots [11]$$

Assuming that the perfect gas relationships are applicable to this case,

$$pv = RT \text{ and } \frac{1}{d} = v = \frac{RT}{p}$$

Equation [11] can now be rewritten and integrated:

$$\frac{2\gamma}{r} = RTD \int_{p_s}^p \frac{dp}{p} = RTD \log_e \left(\frac{p}{p_s} \right) \dots [12]$$

which we may express as:

$$\log_e \left(\frac{p}{p_s} \right) = \frac{2\gamma}{RTDr} = \log_e S \dots [13]$$

where p denotes the pressure in equilibrium with the drop of radius r at temperature T , and p_s is the saturation pressure at that temperature. This is the fundamental supersaturation equation of von Helmholtz.

The ratio $\frac{p}{p_s}$, denoted by the symbol S , is known as the supersaturation ratio. Equation [13] gives the relation which must exist between the actual pressure and the saturation pressure at the existing temperature if a drop of radius r is to be in equilibrium with the vapor about it. If this ratio is lowered, the droplet will evaporate. If it is raised, the droplet will grow.

It will be seen from Equation [13] that the logarithm of the supersaturation ratio varies directly with the surface tension and inversely with the absolute temperature and the radius of the drops. Surface tension decreases with increasing temperature and finally vanishes at the critical condition. Thus there can be no supersaturation at the critical condition. Conversely, surface tension increases with decreasing temperature and the supersaturation ratio for a given size of drop increases as the temperature is lowered.

Equation [13] also indicates the need for a nucleus upon which condensation can occur. If r is made very small, S must be very

large and finally, in the limiting case, when $r = 0$, $S = \infty$. Thus in order for a pure vapor to condense, there must be some nucleus of finite radius.

The search for such a nucleus motivated early workers in this field. Aitken at first concluded that dust particles always served as nuclei, but he rejected this conclusion upon finding that condensation occurred with filtered, dust-free vapor. Von Helmholtz believed that ions were the nuclei upon which condensation took place.

G. T. R. Wilson found three distinct types of nuclei. Working with air saturated with moisture, he found that a small expansion caused condensation upon the relatively large particles of dust which were present in the air. With dust-free air he discovered that at a higher expansion ratio condensation occurred upon ions. Wilson's "cloud chamber," well known to physicists, is based on this feature of the phenomenon. He was able to trace the path of ionizing rays by causing them to pass through an illuminated chamber and photographing their tracks, which are droplets of water condensed upon the ions formed by the ray.

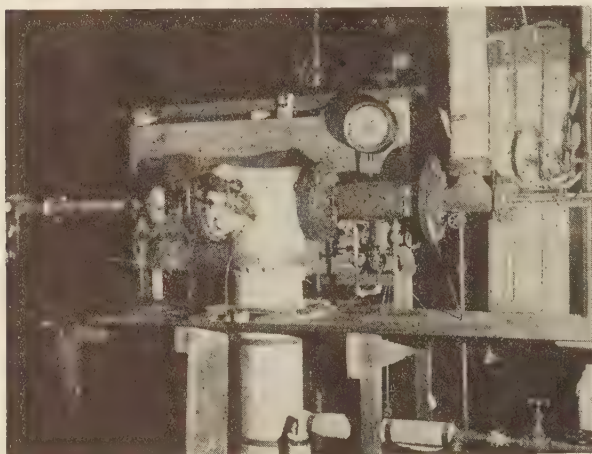


FIG. 2 APPARATUS USED IN INVESTIGATION

With air freed both of dust and of ions, Wilson found that a sufficiently high ratio of expansion would invariably cause a heavy condensation in the form of innumerable very small droplets. The nuclei responsible for this ultimate condensation, investigated at great length by Barus (6-8), were seemingly inexhaustible, and appeared to form an essential part of the water vapor, for they could not be removed by any process. The conclusion reached by both Barus and Wilson was that these nuclei are associated or agglomerated molecules.

Callendar (9-12), assuming that the time interval in the flow of steam through nozzles is too small to allow condensation to occur, used Wilson's value of 7.9 for the supersaturation ratio at 300 C, abs, in the von Helmholtz equation, and obtained 5.0×10^{-8} cm as the radius of the droplets formed when condensation takes place. The Wilson line, in his opinion, approximately coincided with the 3 per cent moisture line on the Mollier chart. Martin's original Wilson line lay between the 3 and 4 per cent moisture lines.

Powell's calculations resulted in a droplet radius of 6.4×10^{-8} cm, and his version of the Wilson line falls along the 2 per cent moisture line.

While the existence of supersaturation has been demonstrated by the work of the authorities mentioned above, a supersaturation limit, or Wilson line, based on theory alone is not acceptable. There are so many uncertain variables in the von Helmholtz equation and so many assumptions in its derivation that the

validity of results based upon it is open to question. An experimental investigation of the condensation conditions is therefore necessary to determine the actual supersaturation limit, and the following sections record such an investigation.

4 DESCRIPTION OF THE APPARATUS

The apparatus, Fig. 2, was designed to provide a nozzle with a transparent side through which the expanding steam could be observed with the aid of an intense beam of light passing axially through the nozzle. Observation at right angles to the illuminating beam was essential because, in this way otherwise invisible details could be seen as in the ultra-microscope. Referring to Fig. 3, steam entered through the main valve *A* and passed through a 2-in. line into the superheater, *B*, consisting of a 6-in.

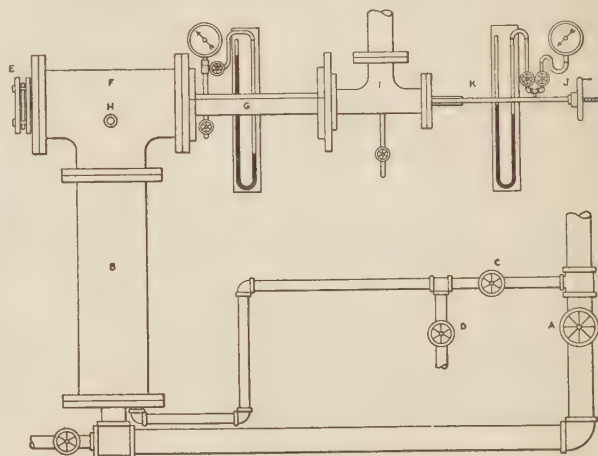


FIG. 3 DIAGRAM OF APPARATUS

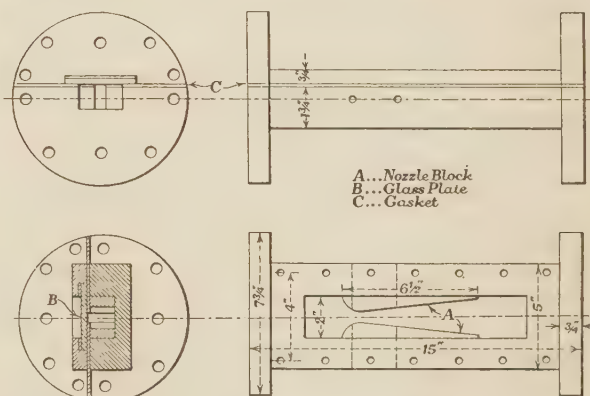


FIG. 4 DETAILS OF NOZZLE DESIGN

steel pipe within which was placed a copper coil supplied with high-pressure steam through valve *C*. Evaporation of the entrained moisture in the entering steam was the principal function of the superheater, but it could also be used as a de-superheater by closing valve *C* and the drain valve, and opening valve *D*, admitting to the coil cold water which was discharged to the sewer.

Steam passed from *B* into the tee, *F*, which had at one end a glass port, *E*, and at the other the nozzle assembly, *G*, shown in detail in Fig. 4. In the side of *F* (Fig. 3) was inserted a standard thermometer well which was provided with a mercury-in-glass thermometer to determine the temperature of the incoming steam.

The nozzle, rectangular in cross-section, was formed by two polished brass blocks bolted to the sides of a cast-iron channel. The glass plate which constituted the top of the nozzle was clamped tightly to the channel, with rubber gaskets above and below to prevent leakage. Fig. 5 shows the dimensions of the several nozzles used in the experiments.

The inlet pressure was measured by a Bourdon gage or a mercury manometer. The pressure connection, a $\frac{1}{32}$ -in. hole, was located at the center of the bottom of the channel, 1 in. above the throat of the nozzle. The steam from the nozzle passed through a second tee into a 2-in. line leading to a condenser in which a vacuum of 25 in. of mercury could be obtained. Valves in the discharge line permitted the back pressure to be raised to any desired value.

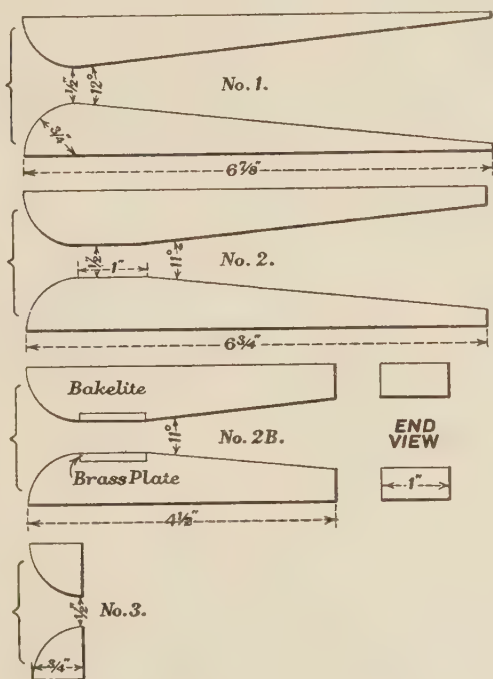


FIG. 5 DIMENSIONS OF NOZZLE BLOCKS

The static pressure of the steam at any point along the axis of the nozzle could be measured with the aid of a brass search tube, of 0.125 in. inside diameter and 0.189 in. outside diameter. The steam pressure was transmitted through six holes, $\frac{1}{32}$ -in. in diameter, in the form of a piezometer ring, located about 14 in. from the end of the tube. The search tube was soldered to a larger tube which passed through a stuffing box and was connected by means of flexible rubber tubing to a Bourdon gage and a mercury manometer. A hand-wheel and screw permitted the search tube to be moved along the axis of the nozzle, and the location of the pressure measuring holes could be found by a scale on the frame. To prevent vibration, the steam end of the search tube was held in place by a guide at the high pressure end of the channel. The back pressure was measured by a mercury manometer connected to a $\frac{1}{32}$ -in. hole in the bottom of the channel beyond the nozzle mouth.

Illumination was provided by a carbon arc, the light from which was concentrated by a pair of lenses and introduced through the port *E* (Fig. 3) along the axis of the nozzle. Usually a screen was used to keep the light from hitting the bottom of the nozzle, and a blue filter could be interposed between the arc and the nozzle if needed. When full illumination was desired, the search tube

was removed and in its place was installed a glass port through which the light from a second arc entered. This light could be focussed with a concave mirror into a sharp beam to study one portion of the nozzle or into a broad ray to illuminate it completely.

The pressure gages, calibrated frequently during the course of the work, could be read to within 0.5 lb per sq in. The probable error in the absolute pressure measurements thus varied between 0.84 per cent for low pressures and 0.35 per cent for high pressures. The mercury manometers were made of glass tubing 0.25 in. in diameter, mounted on varnished wood. The scales were made of portions of graph paper fastened to the wood and varnished to minimize the effect of humidity. The height of the columns could be read with an accuracy of 0.05 in., the probable error varying from 0.5 to 0.1 per cent. Correction was made for the water which condensed in the tubes by allowing 13.6 in. of water per in. of mercury. The barometric readings, obtained in an adjacent laboratory located about 10 ft above the apparatus, were not corrected for this difference in elevation, nor for the

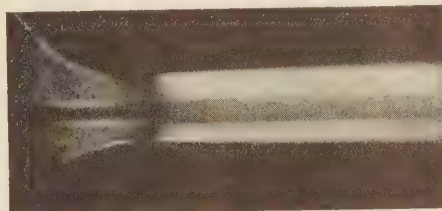


Fig. 6(a)

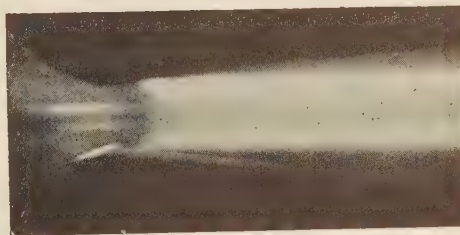


Fig. 6(b)

FIG. 6 FLOW THROUGH NOZZLE NO. 1

[a (upper)—Illumination confined to plane of search tube. b (lower)—Search tube in place. Entire cross-section illuminated. Initial conditions: 30 lb per sq in. gage, 300 F, 16 lb per sq in. abs back pressure.]

changes in room temperature, for such variations are of a small order of magnitude and have no significant effect.

The thermometer was tested and found to be correct within 0.5 F. It could be read to within 0.5 F by means of a magnifying lens attached to it. The maximum probable error in the temperature measurements was thus 1.0 F in 300 or 0.33 per cent.

5 METHOD OF MEASURING THE SUPERSATURATION RATIO

Supersaturation cannot be measured directly but must be calculated from an observed condensation pressure. Attempts to measure the temperature of supersaturated steam will fail because such steam will condense on any surface and a thermometer placed in such an atmosphere will immediately become covered with a thin film of moisture. The temperature of saturated steam at the existing pressure will thus be obtained.

When the apparatus was put into operation it was found that the intense light from the arc enabled the condensation point to be observed. The entering steam, superheated by throttling from the boiler pressure, was quite transparent and the occasional drops of entrained moisture were easily seen. When condensa-

conditions, and $n = 1.3$ is the index of isentropic expansion for superheated steam,

$$p_1 v_1^n = p v^n \dots \dots \dots [14]$$

$$p_1 v_1 = R T_1 \dots \dots \dots [14a]$$

$$p v = R T \dots \dots \dots [14a]$$

$$\frac{p_1 v_1}{T_1} = \frac{p v}{T} \dots \dots \dots [15]$$

where p , v , and T are the conditions of the supersaturated steam at the condensation point. Combining [14] and [15], we have the well-known isentropic relationship:

$$T = \frac{T_1}{\left(\frac{p_1}{p}\right)^{\frac{n-1}{n}}} \dots \dots \dots [16]$$

If T_1 , p_1 , and p are known, the temperature at the condensation point can be calculated from [16], and the pressure p_s corresponding to that temperature can be found from the steam tables. Substituting for n , [16] reduces to:

$$T = \frac{T_1}{\left(\frac{p_1}{p}\right)^{0.231}} \dots \dots \dots [17]$$

A sample calculation follows:

Initial pressure = 64.7 lb per sq in. abs

Initial temperature = 303.0 F 762.6 abs

Observed condensation pressure = 34.2 lb per sq in. abs

Then

$$\left(\frac{p_1}{p}\right) = 1.901, \text{ and } \left(\frac{p_1}{p}\right)^{0.231} = 1.159$$

$$T = \frac{T_1}{1.159} = \frac{762.6}{1.159} = 658.0 \text{ F abs}$$

and

$$t = (658.0 - 459.6) = 198.4 \text{ F}$$

From Keenan's steam tables, the pressure p_s corresponding to 198.4 F is 11.15 lb per sq in. abs so that the supersaturation ratio

$$S = \frac{34.2}{11.15} = 3.05$$

When the supersaturation ratio has been calculated for a given observation, it becomes possible to apply the von Helmholtz Equation [13], to estimate the radius of the droplets formed when condensation occurs. Thus:

$$\log_e 3.05 = \frac{2\gamma}{r R D T} = 1.1151 \dots \dots \dots [18]$$

D = density of water at temperature $t = 60.1$ lb per cu ft at 198.4 F

R = gas constant for superheated steam = 86 (approx.)

T = absolute temperature, F = 658.0

γ = surface tension of water at 198.4 F = 4.13×10^{-3} lb per ft (see Fig. 10).

Then, for $S = 3.05$

$$r = \frac{2 \times 4.13 \times 10^{-3}}{1.1151 \times 658.0 \times 60.1 \times 86} = 2.11 \times 10^{-9} \text{ ft} = 6.4 \times 10^{-8} \text{ cm}$$

The value thus obtained for the effective radius of the drops formed in condensation is in close agreement with those found by Wilson and Powell.

6 THE EXPERIMENTAL WORK

After it had been found that the condensation pressure could be measured with reasonable accuracy, the first feature to be investigated was the variation of that pressure with varying

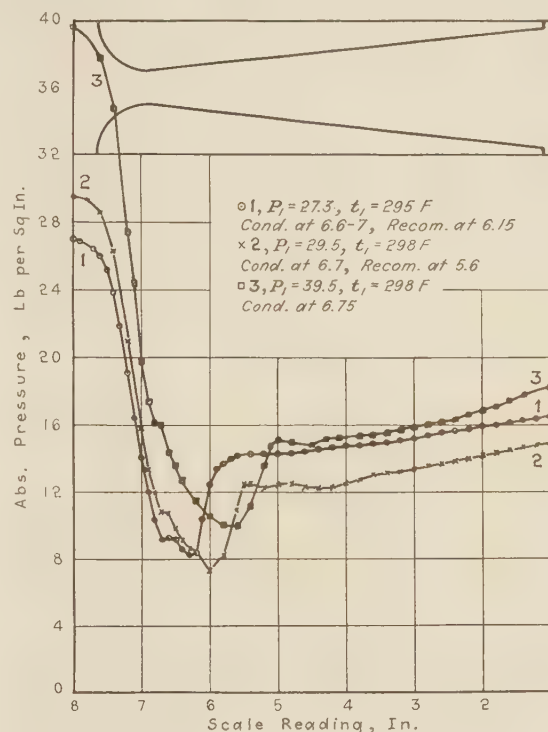


FIG. 8(a)

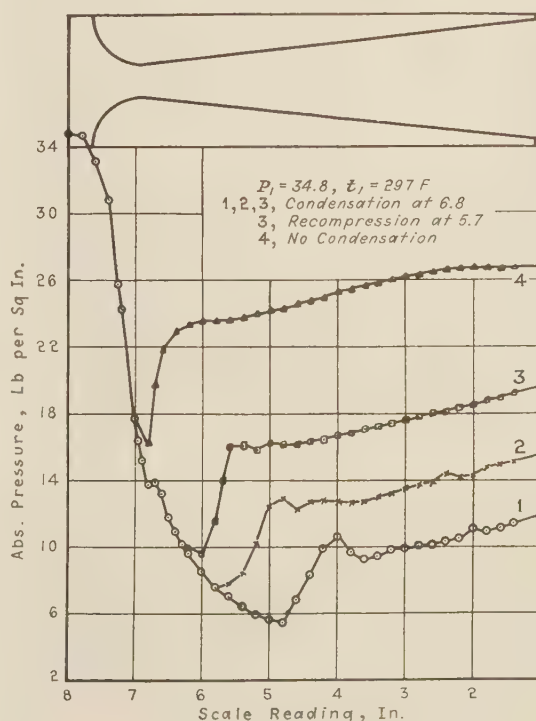


FIG. 8(b)

initial conditions. Using a simple convergent-divergent nozzle form, No. 1 in Fig. 5, a series of measurements was made in the manner outlined in Section 4. Inlet pressures varied from 11.0 to 75.0 lb per sq in. abs, the range in which turbine condition curves usually cross the saturation line on the Mollier chart. Above the latter pressure the incoming steam was too wet for satisfactory observation, and it was undesirable to subject the glass plate to unnecessary stress.

Figs. 8(a) and 8(b) show typical results of the observations with absolute pressures plotted against position along the nozzle axis. In these curves it will be seen that, at the point where condensation occurs, there is an abrupt halt in the fall of pressure. After the condensation point is passed the expansion continues as before. This unexpected feature was at first dismissed as an error in the manometer reading but it was repeated with such consistency that it must be accepted as an actual occurrence. A similar irregularity in the pressure-expansion curve was noticed by Prof. C. A. Robb in his work on recompression in nozzles, carried out at the Johns Hopkins University in 1931-32, but not yet published. The phenomenon was attributed by him to roughness in the nozzle wall, but this is improbable because the irregularity always coincides with the condensation point, and does not remain at the same spot in the nozzle when the pressure conditions are varied. It is probably due to the fact that the rapid increase in the specific volume of the steam, caused by the liberation of the latent heat of the condensed moisture, is not compensated by the increase in velocity and so must result in an increase in pressure, or in sustained pressure with increasing nozzle areas.

The pressure-distance curves, Figs. 8(a) and 8(b) show that the steam invariably over-expands and then recompresses to the back pressure. When in recompression the steam reached the pressure at which condensation originally occurred, a dark spot appeared in the nozzle, as in Fig. 13(a), to be followed once more by the familiar blue of the scattered light if the pressure again fell below the condensation value. The cause for such dark spots was the absence of droplets in the dark region. This disappearance of the droplets when the steam pressure was raised above the condensation value is evidence in favor of the supersaturation theory, which contends that droplets of a given size can exist only when the actual pressure of the surrounding vapor exceeds by a certain amount the saturation pressure of the liquid for the existing temperature. When this excess is not present the droplets should evaporate, and they apparently do so.

The test shown in Fig. 8(b) was performed to study the effect of variations in the back pressure, the inlet pressure remaining fixed at 34.8 lb per sq in. abs. In curves Nos. 1, 2, and 3, in which the back pressure was below 20.0 lb per sq in. abs, condensation occurred at the same point in the nozzle and at the same pressure, 13.9 lb per sq in. abs. The abrupt halt in the fall of pressure at the condensation point is evident. In curve No. 3, the recompression reached the condensation pressure and the droplets re-evaporated. In curve No. 4, the back pressure was so high that the condensation pressure was not reached and no condensation was seen.

The pressure along a vertical section through the nozzle did not appear to be constant. This was noticeable when different

sections of the nozzle were illuminated by the use of a narrow slit through which the light entered the nozzle. The center of the nozzle seemed to be at a higher pressure than the outer portions so that condensation could exist in the outer sections of the steam while the central part might be transparent and hence devoid of condensation. This was a source of error which had to be guarded against because, if the entire cross-section of the steam were illuminated, the condensation might appear to be continuous, whereas in reality, the central portion at which the pressure was being measured might be quite free from condensation. In order to be sure that condensation was actually occurring at the point where the search tube was measuring the pressure, a slit was used to confine the light to the vicinity of the search tube. Fig. 6(a) shows the illumination confined to the search tube section, with the search tube and the pressure holes clearly visible. Fig. 6(b) shows the effect of illuminating the entire cross-section of the nozzle, with the search tube almost hidden by the mist.

With nozzle No. 1, condensation appeared as a blue mist, and the blue color was maintained throughout the length of the nozzle, which indicates that there was no growth of the droplets during their passage. If growth had occurred, the blue light would have changed in color toward the red, and the intensity of the scattered light would have increased.

TABLE 1 SUMMARY OF RESULTS OF TESTS ON NOZZLE NO. 1

Point	Test no.	p_1 abs	t_1	Cond. pres.	t_2	S	$r \times 10^5$, cm
A	50-1	64.7	303	34	198.4	3.05	6.69
B	45-2	59.7	297	31	190.4	3.29	6.39
C	40-2	54.8	292	29	188.4	3.22	6.57
D	35-2	49.7	307	22	176.4	3.17	6.86
E	30-2	44.7	303	18.7	164.4	3.56	6.58
F	25-4	39.7	302	16.1	158.4	3.54	6.46
G	20-2	34.7	309	11.5	135.4	4.49	5.90
H	15-2	29.7	286	11.0	144.4	3.69	6.63
I	12.5-1	27.3	295	9.4	128.4	4.31	6.19
J	11-1	25.9	295	8.75	126.4	4.34	6.24
K	5-3	20.0	289	6.3	113.4	4.54	6.25
L	2.7-1	17.5	295	5.3	112.6	3.89	6.97
M	0-1	14.4	270	4.4	94.4	5.51	5.87
N	0-3	12.8	285	3.3	84.4	5.64	5.95
O	0-2	11.3	283	2.9	82.4	6.30	6.17
S	Stodola	71	Sat.	38.2	303	3.1

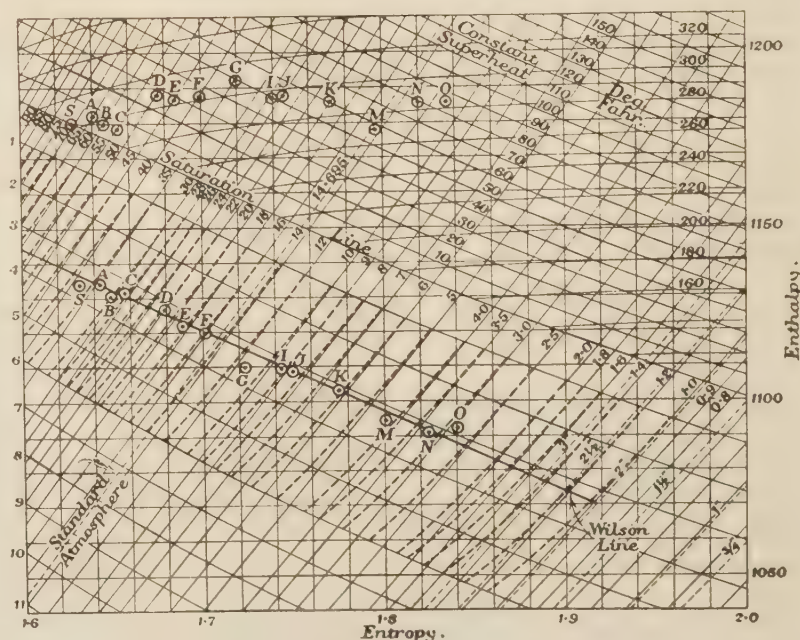


FIG. 9 WILSON LINE
(From tests made on nozzle No. 1.)

The data from the tests on nozzle No. 1 are tabulated in Table 1, which also contains the results of the calculations of the supersaturation ratio and the droplet radius for each condition. On Fig. 9, a revised Keenan Mollier chart, the condensation points found with nozzle No. 1 are located in the manner described in Section 4. The condensation points lie between the 3 and 4 per

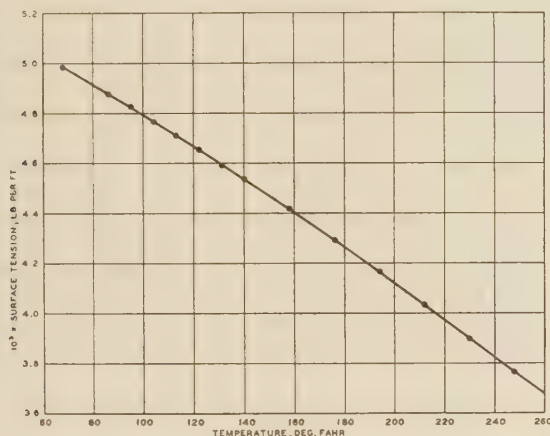


FIG. 10 VARIATION OF SURFACE TENSION OF WATER WITH TEMPERATURE
(Data from International Critical Tables.)

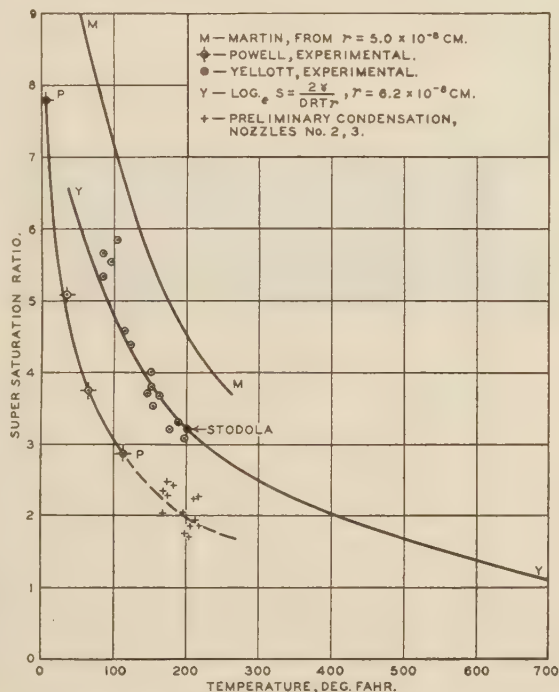


FIG. 11 DETERMINATION OF SUPERSATURATION RATIO AT THE WILSON LINE

cent moisture lines, and the line which is faired through them will be referred to as the Wilson line. Point S at the high pressure end of the Wilson line is the point found by Stodola.

It may be objected that there is a possibility of condensation occurring in droplets too small to be seen. This is improbable, because particles of any finite size, including molecules, scatter light to a noticeable extent. The scattering of light by steam

molecules was studied to establish this point and it was found by another experiment that a beam of concentrated arc light could be plainly seen in an atmosphere of superheated steam, just as a searchlight beam can be seen in the sky at night. The scattered light was dark blue in color, and, although faint, was bright enough to be visible against a black background. Whenever a drop of water crossed the beam, the light scattered by it stood out with great intensity. From this experiment, as well as from the work of many physicists (50) it may be concluded that any droplets resulting from condensation will be visible.

In Fig. 11 the supersaturation ratios at various temperatures are plotted against those temperatures. A mean value of the drop radius in Table 1, calculated by the von Helmholtz equation, is about 6.2×10^{-8} cm, which agrees with the values of Wilson, Powell, and Stodola. If this value is substituted in Equation [13], we have:

$$\log_e S = \frac{2\gamma}{D \times 86 \times T \times \frac{6.2 \times 10^{-8}}{2.54 \times 12}} = 1.15 \frac{\gamma}{D \times T} \times 10^7$$

Taking the proper values of γ , the surface tension, from Fig. 10, and of D , the water density, from Keenan's steam tables, and solving for S at various temperatures, curve (Y) in Fig. 11 is obtained. This curve is a fair representation of the experimental points, since as many lie above the curve as below it, and a reasonable number lie directly on it. Curve (P) presents data obtained by Powell in his experiments, and curve (M) values derived by Martin from his substitution of Callendar's value of r in the von Helmholtz equation. The results of the present

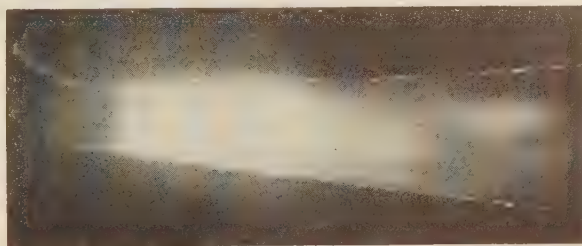


Fig. 12(a)

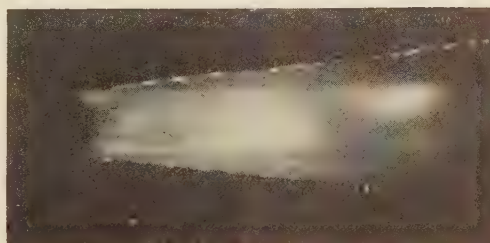


Fig. 12(b)

FIG. 12 FLOW THROUGH NOZZLE NO. 1

[a (upper)—Photographed through a Nicol prism, showing photoelastic effect. Initial conditions: 41 lb per sq in. gage, 290 F, 18 lb per sq in. abs back pressure. b (lower)—Prism turned slightly to show strain lines near throat. Conditions same as in case (a).]

investigation lie between those of Martin and Powell. The Wilson line, plotted in Fig. 9, also lies between their versions of the line and is closer to that of Martin.

A drop radius of 6.2×10^{-8} cm, while only approximate, is of a reasonable order of magnitude. The nature of the light scattered by the droplets is evidence in favor of a very small droplet size. (The optics of small particles is presented briefly in Appendix 1.) The intensity of the scattered light is sym-

metrical, resembling that shown in (a), Fig. 20. The light scattered at 90 deg to the incident light is completely plane polarized. The color of the scattered light is sky-blue. These three facts definitely associate the droplets with Rayleigh's theoretical infinitely small dielectric spheres.

Scattered light of this character can come only from particles whose radius is many times smaller than the wave-length of the light which falls upon them. It can only be estimated how much smaller they are than that wave-length, but the character of the scattered light suggests that the wave-length is from 100 to 1000 times as great as the radius of the drops. Assuming 6.0×10^{-5} cm as an average value of the wave-length of arc light, the optical evidence indicates that the radius is in the neighborhood of 6.0×10^{-8} cm, which is in good agreement with the value of

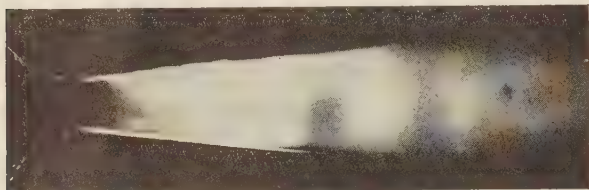


Fig. 13(a)

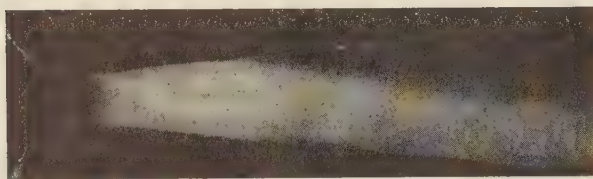


Fig. 13(b)

FIG. 13 FLOW THROUGH NOZZLE NO. 1

[a (upper)—Completely illuminated; dark bands indicate recompression above condensation pressure with evaporation of droplets. Initial conditions: 20 lb per sq in. gage, 287 F, 15 lb per sq in. abs back pressure. b (lower)—Photographed after pressure raised to 35 lb per sq in. gage, 23 lb per sq in. abs back pressure. Steam flow breaks away from one side of nozzle and continues down the other.]

the radius as calculated from the von Helmholtz equation. A reasonable figure for the radius of the droplets formed by the condensation of steam in a rapid expansion is therefore 6.2×10^{-8} cm or 2.03×10^{-9} ft.

The polarization of the scattered light gives rise to another interesting phenomenon. Since the glass plate which forms the top of the nozzle is under strain, stresses result, and the glass becomes doubly refractive, assuming photoelastic properties. Thus if the scattered light is observed through a Nicol prism, brilliant colors are visible, corresponding to the stresses in the glass. Figs. 12(a) and 12(b) were taken through a large Nicol prism, and, although the colors cannot be distinguished, dark lines can be seen which represent strains in the glass. These strain lines are probably caused by standing waves in the steam.

Several interesting features of steam flow were discovered with nozzle No. 1. Recompression and the breaking away of the jet from the nozzle walls, predicted by Stodola (29, p. 93), were seen and photographed. In Fig. 13(a) the steam breaks away from both sides of the nozzle during recompression, and then reexpands to fill the nozzle, while a second recompression is evidenced by a second dark band. In Fig. 13(b) the steam breaks away from the sides, but instead of returning to both walls, it continues down one side. This condition was very unstable, the jet alternating rapidly from one side of the nozzle to the other.

The observation of liquid water in steam was fully discussed by Thomas (31) and his work is substantiated by this investi-

gation. It is possible to see drops of water in flowing steam and the absence of moisture can be detected by the transparency of the steam. The light scattered by the steam molecules is so faint that it can be seen only against a perfectly black background; hence dry steam appears transparent. The moisture entrained in the entering steam appears as relatively large drops, a few hundredths of an inch in diameter. As the steam is accelerated through the nozzle, however, the large drops are broken up into much smaller droplets in the manner explained by Soderberg (28). This feature was not fully investigated in the present research and Soderberg's paper suggests an interesting problem which could be attacked profitably with the methods used in this work.

Summarizing the results so far presented, it is very improbable that any condensation will occur in the expansion of steam through a convergent-divergent nozzle of the type used in these tests until the steam has reached the condition approximately represented by the region between the 3 and 4 per cent moisture lines on the Mollier chart. When this region is reached, condensation apparently takes place on a vast number of tiny nuclei. The radius of the drops thus formed appears to be about 6.2×10^{-8} cm. When the steam in recompression again reaches

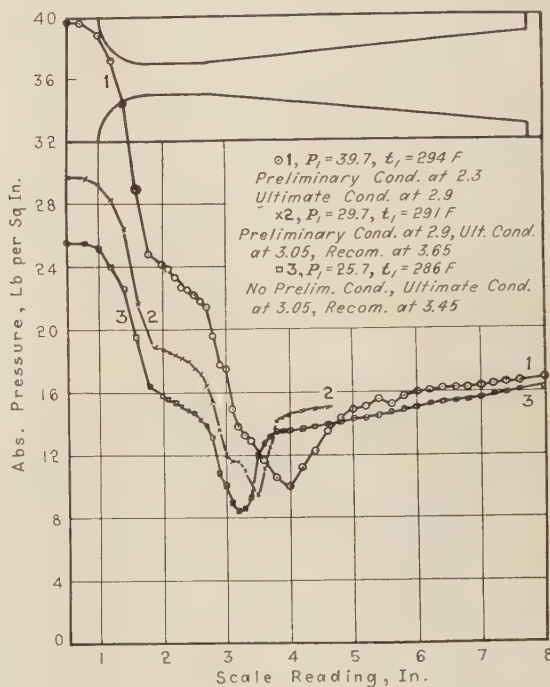


FIG. 14

the pressure at which condensation occurred, most, if not all, of the droplets seem to reevaporate, appearing again if the pressure once more falls below the condensation value. Only blue light, completely plane polarized when observed at right angles to the incident light, was to be seen in the nozzle. It is highly probable therefore that there is no growth of the droplets as they pass through the nozzle.

The effect of supersaturation upon the flow of steam has been treated in detail by Stodola (29), Goodenough (16), and others. It may be concluded that supersaturation always occurs in the expansion of saturated steam, and for that reason the formula for superheated steam should be used to calculate the flow of saturated or slightly wet steam through nozzles. The actual effect of supersaturation in turbine operation is small, but, as

has been pointed out previously, there is a certain loss of availability caused by the increase of entropy which accompanies condensation and the establishment of thermal equilibrium. This loss may amount to as much as 4 per cent of the isentropic enthalpy drop from the saturation line to the Wilson line.

Prof. J. H. Keenan of the Stevens Institute of Technology suggested that nozzle No. 1 be replaced by another designed to give a less rapid expansion in the region where supersaturation occurs. The nozzle chosen for this purpose, No. 2 in Fig. 5, had a rounded inlet identical to that of No. 1, but a 1.0 in. straight section was interposed between the convergent and the divergent portions. As shown in Fig. 14, this design produced the desired effect, for there was a rapid expansion through the rounded section, followed by a relatively slow drop in pressure through the straight throat. Additional expansion and recompression took place in the diverging portion.

The condensation which occurred in nozzle No. 2 differed radically in appearance from that encountered with No. 1. Observations of the flow through nozzle No. 1 showed that there was a distinct and relatively sharp curved line, concave toward the high-pressure end, which marked the beginning of condensation. A line of demarcation was thus provided between the transparent superheated steam and the misty wet steam. With nozzle No. 2 the condensation curve again appeared and the

condensation which began as a trace of bluish haze and rapidly became more dense as the ultimate-condensation curve was approached. Fig. 15 shows a photograph of the flow in nozzle No. 2 obtained by focussing the light from the arc at the low-pressure end into a sharp beam. The preliminary condensation

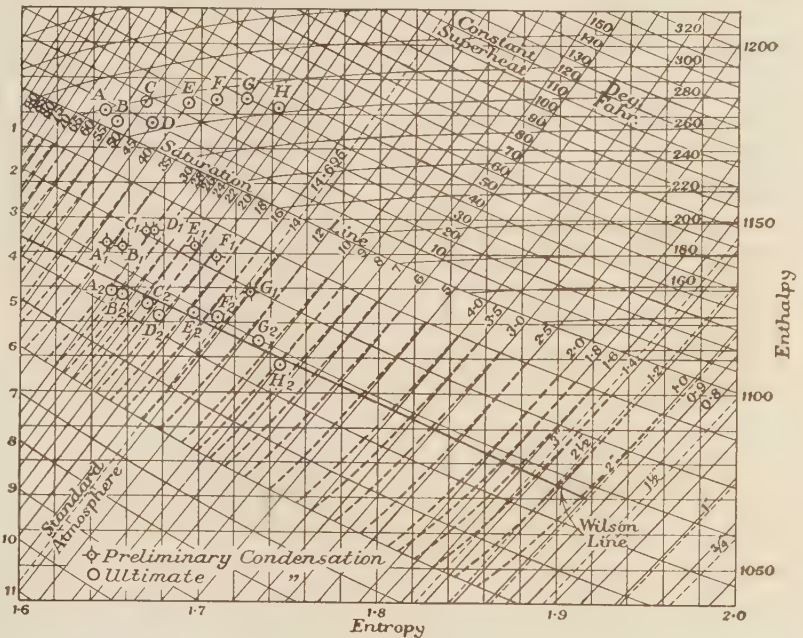


FIG. 16 PRELIMINARY AND ULTIMATE CONDENSATION FROM TESTS ON NOZZLE NO. 2

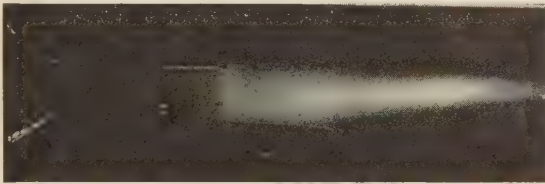


FIG. 15 FLOW THROUGH NOZZLE NO. 2

(Illuminated from low-pressure end by sharply focussed beam. Preliminary condensation can be seen before curved line denoting ultimate condensation. Initial conditions: 28 lb per sq in. gage, 288 F, 15 lb per sq in. abs back pressure.)

pressures measured at that curve for varying initial conditions were found to lie on the Wilson line shown on Fig. 9. The term "ultimate condensation" will be applied to that which occurs at the Wilson line to distinguish it from the "preliminary condensation" which is about to be discussed.

The concave curve in nozzle No. 2 was preceded by a slight

TABLE 2 SUMMARY OF RESULTS OF TESTS ON NOZZLE NO. 2

Point	Test no.	p_i abs	t_i	Cond. pres.	t_2	S	$r \times 10^4$, cm
<i>Preliminary Condensation</i>							
A ₁	45-1	59.8	298	37.0	218.0	2.24	8.75
B ₁	40-1	54.8	292	34.0	214.0	2.23	8.86
C ₁	35-1	49.8	297	31.0	219.0	1.86	11.28
D ₁	30-1	44.8	285	29.0	213.0	1.94	10.67
E ₁	25-1	39.8	295	23.0	204.0	1.84	11.98
F ₁	20-1	34.6	293	19.5	199.0	1.74	13.28
G ₁	15-1	29.8	291	14.0	170.4	2.32	9.52
<i>Ultimate Condensation</i>							
A ₂	45-1	59.8	298	30.0	183.4	3.54	6.17
B ₂	40-1	54.8	292	27.9	175.0	4.11	5.93
C ₂	35-1	49.8	297	23.5	183.4	2.94	7.15
D ₂	30-1	44.8	285	21.0	164.4	3.99	5.89
E ₂	25-1	39.8	295	17.5	164.4	3.33	6.78
F ₂	20-1	34.8	293	15.0	159.4	3.21	7.11
G ₂	15-1	29.8	291	9.0	98.4	9.88	...

can be seen and the curved line which denotes ultimate condensation is also visible, although slightly different in shape from that in Fig. 6.

In order to study this preliminary condensation, of which no trace had been found in nozzle No. 1, a series of tests was made as before with inlet pressures ranging from 10.0 to 45.0 lb per sq in. gage. Fig. 14 shows typical pressure-distance curves, while Table 2 includes the data and the results of the calculations of supersaturation ratios and droplet radii.

Fig. 16 shows the data plotted on the revised Mollier chart from which it is evident that while ultimate condensation occurs approximately at the Wilson line, preliminary condensation appears to take place at points scattered about the 2 per cent moisture line. Because of the nebulous character of the earliest traces of the preliminary condensation, it is difficult to measure the exact pressure at which it begins. This difficulty accounts for the wide variations in the droplet radii recorded in Table 2 as well as for the scattering of the points in Fig. 16.

As the droplets formed by preliminary condensation approached the line of ultimate condensation, the light scattered by the droplets changed rapidly in color from the initial blue through green and yellow to red. The red light was immediately lost in the more intense blue light scattered by the myriad of droplets formed at the curve of ultimate condensation. When the blue color disappeared because of recompression of the steam above the ultimate condensation pressure, the red again became visible. Analysis of these facts indicates that the preliminary droplets probably begin as very minute particles, about 10.0×10^{-8} cm in radius, but grow with extreme rapidity until they approach the size of red light waves, about 6.0×10^{-5} cm. Further growth is apparently halted by the crossing of the ultimate condensation curve, for the nuclei which come into ac-

tion in vast numbers at that line seem to acquire all of the available moisture. Coalescence of these drops is probably prevented by the high velocity at which they are traveling. Soderberg (28) presents curves which indicate that with steam velocities above 1200 fps the maximum drop size cannot exceed 2.5×10^{-5} cm if the specific volume of the steam is below 50.0 cu ft per lb. While this limit is certainly of the correct order of magnitude, it is perhaps too low because the drops which caused the red light in nozzle No. 2 were undoubtedly as large as red light waves, although the steam velocity was approximately 1600 fps and the specific volume about 20.0 cu ft per lb.

The nature of the light scattered by the preliminary droplets differed from that scattered by the smaller ultimate droplets. The intensity was much greater in the direction from which the

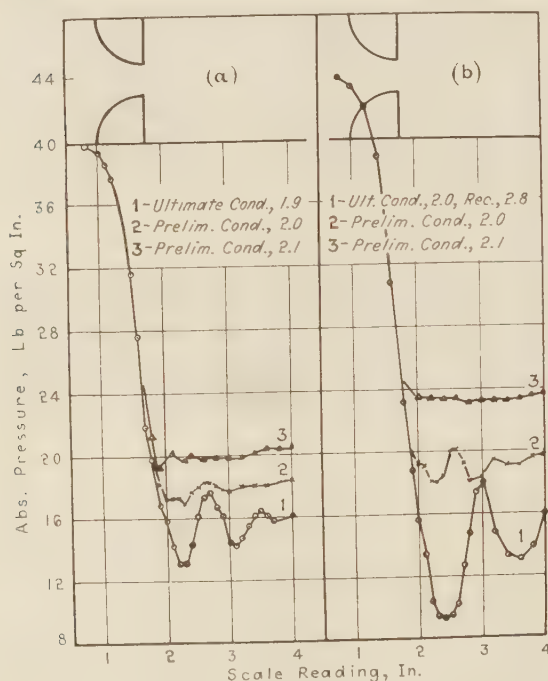


FIG. 17 RESULTS OF TWO TYPICAL TESTS ON NOZZLE NO. 3

light came and the polarization was not complete. Moreover, the colors other than blue were not visible unless the angle of observation was less than 90 deg to the incident light. It is therefore probable that the colors were produced by a complex interaction of scattering, refraction, and interference, and it is impossible to place an accurate limit on the size of the drops. The fact that the red light was partially polarized, however, indicates that 6.0×10^{-5} cm, or 2.3×10^{-5} in., is a reasonable value for the radius of the largest drops observed in nozzle No. 2.

The existence of preliminary condensation raised some interesting questions. Stodola found no traces of such condensation nor did the theoretical investigators consider the possibility of its existence. Up to the present time it has been assumed that supersaturation, if it existed at all, would continue until the Wilson line was reached, at which point condensation would occur and equilibrium would be reestablished. Dust or other foreign particles in the steam would cause the type of condensation mentioned above, but particles large enough to act as nuclei would also scatter light with visible intensity before any condensation occurs. No such particles were seen in any of the tests.

It was hoped that preliminary condensation could be proved to

occur upon ions, in which case the conventional theory would be vindicated. Condensation earlier than the ultimate was found by Wilson (34), Thomson (33), and Barus (7, 8) when electrified nuclei were present. In order to study the possible electrification of the droplets, nozzle No. 2 was replaced by No. 2B (Fig. 5), made of bakelite with brass plates set into the straight sections to act as electrodes. When the steam was flowing and condensation was occurring as in Fig. 15, a potential of 110 volts, dc, was connected across the electrodes. There was no apparent change in the character of the condensation, nor did reversing the polarity of the electrodes have any visible effect. If the drops were electrified, it would be supposed that the positive drops would be attracted to the negative electrode, and vice versa. There was, however, no evidence of attraction or repulsion. This test was by no means conclusive because the voltage was not high enough to produce a very vigorous attraction and the high velocity of the water particles might have obscured any effect which existed.

It was decided to apply another test. If preliminary condensation occurred on ions, increasing the number of ions should increase the density of the mist which indicated condensation. A similar experiment had been performed successfully by Wilson and Thomson. The most prolific source of ions which could be obtained was the spark from an induction coil. An insulated wire was led into the nozzle and so arranged that the spark could jump from the wire to the electrodes or to the bottom of the nozzle. When the coil was in operation a strong spark resulted but there was no visible effect upon the condensation. This is directly opposed to the evidence of von Helmholtz (19) who found that electrification of a steam jet increased the condensation. The duration of the spark from an induction coil, about 10^{-6} sec, is probably so short that any effect which occurred might not be visible because of the high velocity of the steam. The experiments to discover whether the droplets are electrified must therefore be regarded as inconclusive and it is hoped that more work can be done on this phase of the subject.

To develop a theory which will explain both the preliminary and the ultimate condensation, the tests on nozzle No. 2 must be analyzed. A very significant feature is that with an initial pressure of 10.0 lb per sq in. gage and a back pressure of 1.0 lb per sq in. gage, represented by point H in Fig. 16, no preliminary condensation was seen. When the inlet pressure was raised to 15.0 lb per sq in. gage, point G, preliminary condensation was visible. The only apparent difference between these two conditions was that the velocity of the steam at the condensation point was higher in the first case, about 1700 fps, when no pre-

TABLE 3 SUMMARY OF TESTS ON NOZZLE NO. 3

Point	Test no.	p , abs	t	Cond. pres.	t_2	S	$r \times 10^6$, cm
<i>Preliminary Condensation</i>							
A _{1,2}	5-1,2	20.1	284	9.55	166	1.75	14.5
B _{1,2}	10-1,2	24.5	289	11.65	168	2.84	11.3
C ₁	13-1	29.5	294	12.5	158	2.77	8.17
C ₂	13-3	29.5	290	14.4	173	2.27	9.77
D ₁	20-1	34.6	294	19.6	201	1.70	13.8
D ₂	20-2	34.6	297	17.0	176	2.47	8.76
E ₁	25-2	39.7	298	19.7	184	3.01	7.93
F ₁	30-3	34.7	303	19.5	184	2.40	8.79
G ₁	35-3	49.7	307	25.5	198	2.04	10.5
H ₁	40-3	54.7	307	30.7	218	1.86	11.3
<i>Intermediate Condensation</i>							
E ₂	25-2	39.7	298	18.0	170	3.01	7.89
F ₂	30-2	44.7	303	19.5	172	3.10	7.04
G ₂	35-2	49.7	303	22.0	172	3.49	6.88
H ₂	40-2	54.7	305	28.0	195	2.69	7.57
<i>Ultimate Condensation</i>							
A ₃	5-3	20.1	287	6.0	104	5.60	5.59
B ₃	10-3	24.5	290	7.5	114	5.26	5.65
C ₃	13-3	28.9	297	9.5	139	3.38	7.03
D ₃	20-3	34.9	299	13.0	144	4.07	6.17
E ₃	25-1	39.7	303	16.4	162	3.30	6.88
F ₃	30-1	44.7	306	18.0	169	3.08	7.16
G ₃	35-1	49.7	300	22.5	172	3.60	6.22
H ₃	40-1	54.7	305	25.0	171	3.92	5.86

liminary condensation occurred, than in the second, about 1500 fps.

The factor controlling the type of condensation to be expected under various conditions may be a function of the rate of change of pressure with time. Tests carried out on nozzle No. 3 (Fig. 5), a simple rounded orifice, lend support to this theory. A series of tests was made with this nozzle using inlet pressures up to 40.0 lb per sq in. gage and the back pressure was varied in each test. Typical results are presented in Fig. 17 and the data are tabulated in Table 3.

It was found that the nature of the condensation in the jet varied with changes in the back pressure. If the steam expanded to a pressure below that of ultimate condensation, for the given initial conditions, the jet appeared as in Fig. 18(a). There was no preliminary condensation and the concave ultimate condensation curve of nozzle No. 1 was again visible. In such expansions there was no color other than the blue and the general nature of the condensation was similar to that found in nozzle No. 1. The jet expanded freely, bending first toward one side of the channel and then toward the other. The wavy outlines of the jet corresponded to the oscillations in the pressure-length curves of Fig. 17. When the inlet pressure was raised to 40.0 lb per sq in. gage, the steam expanded to fill the entire channel, Fig. 18(b) and the dark bands due to recompression above the ultimate condensation pressure were quite distinct. Fig. 19 shows the data obtained from these tests plotted on the revised Mollier chart.

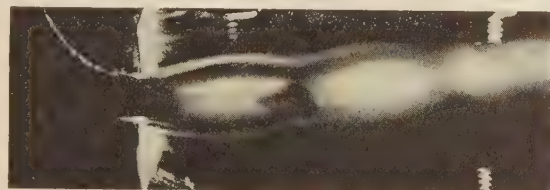


Fig. 18(a)

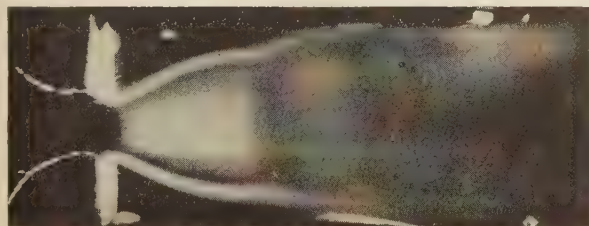


Fig. 18(b)

FIG. 18 FLOW THROUGH NOZZLE NO. 3

[a (upper)—Initial Conditions: 25 lb per sq in. gage, 300 F, 16 lb per sq in. abs back pressure. b (lower)—Photographed after pressure raised to 40 lb per sq in. gage. Jet expands to fill entire channel. Dark bands caused by recompression above ultimate condensation pressure.]

When the back pressure was raised until the ultimate condensation pressure was not quite reached during the expansion, the appearance of the jet changed completely. The well-defined wavy outlines disappeared and the initial blue changed to a whitish blue, indicative of larger droplets. This condensation

was apparently an intermediate type, being neither preliminary nor ultimate, but resembling each in some particulars. The pressures at which this intermediate condensation took place were slightly above the pressures at the Wilson line.

When the back pressure was raised to a still higher value, preliminary condensation occurred. The condensation first appeared as a bluish mist but the scattered light changed rapidly,

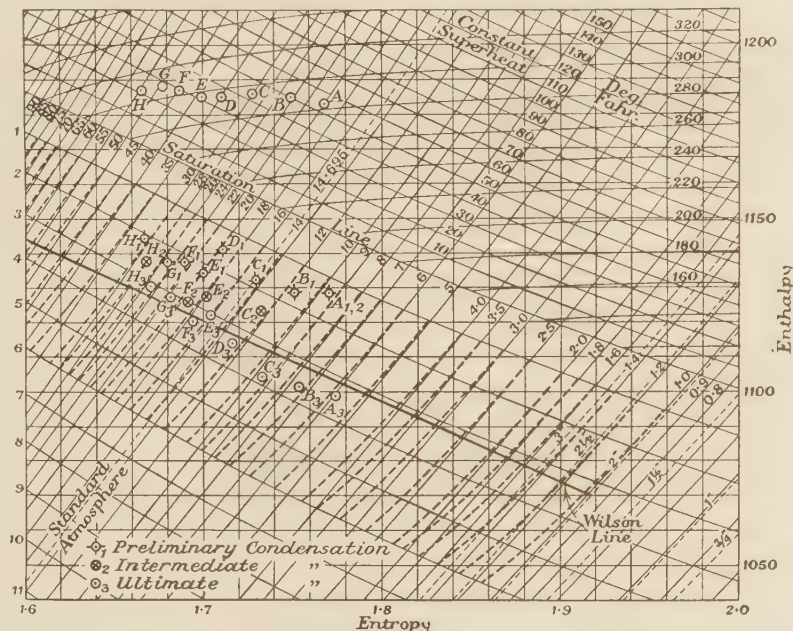


FIG. 19 PRELIMINARY, INTERMEDIATE, AND ULTIMATE CONDENSATION FROM TESTS ON NOZZLE NO. 3

through green and yellow to red. The red light was still partially polarized, indicating that the droplets were of the same order of magnitude as the wave length of red light.

The supersaturation ratio calculated for the conditions of preliminary condensation varies from 2.24 for the highest inlet pressures to 1.74 for the lowest. The droplet radius at the beginning of preliminary condensation ranges from 9.52 to 13.3×10^{-8} cm. The wide variations of droplet radius shown in Table 3 are probably due to the difficulty in determining the exact pressure at which preliminary condensation occurred. When the values of the supersaturation ratio at preliminary condensation are plotted against temperature as in Fig. 11, it is found that they lie well below the curve for the ratio at ultimate condensation, but that Powell's curve, if extended, will pass through the group. It is also evident from Figs. 16 and 19 that the preliminary condensation points are located near the 2 per cent moisture line, along which fell Powell's version of the Wilson line (27A). It seems quite probable that the condensation observed by Powell was a form of preliminary, rather than of ultimate, condensation.

The type of condensation which occurred in nozzle No. 3 for any given inlet conditions could be varied among the three types mentioned above by varying the back pressure. The nature of the condensation was apparently a function of the velocity of the steam and of the duration of the condensation process. If the expansion was rapid and continuous to the ultimate condensation condition, no preliminary condensation occurred, and at the Wilson line a vast number of tiny droplets was formed which did not appear to increase in size with further expansion. If, on the other hand, the expansion was slow or

the back pressure too high, some preliminary condensation occurred at a pressure higher than that at the ultimate condensation condition. The drops thus formed were larger than those formed at the Wilson line, and they continued to grow as they passed through the nozzle. Growth was apparently halted when the drops reached the order of magnitude of red light waves.

7 RESULTS AND CONCLUSIONS

The primary object of this investigation was to check the location of the limit of supersaturation, which, on the Mollier chart, is known as the Wilson Line. The secondary object was to determine the size of the water droplets formed by condensation from the supersaturated state, as their size may have some bearing on the erosion of the low-pressure blades in steam turbines.

The Wilson line was located by measuring the pressures at which condensation occurred in an illuminated nozzle. A series of such measurements, covering the range of 10.0 to 75.0 lb per sq in. abs in which turbine condition curves cross the saturation line, resulted in a number of points, through which the Wilson line was drawn. This will provide working data for turbine designers.

The Wilson line lies between the 3 and 4 per cent moisture lines on the Keenan Mollier chart, slightly higher than the original Wilson line of H. M. Martin. Callendar concluded from data on the Lusitania turbines that the Wilson line approximately coincided with the 3 per cent moisture line, and this investigation indicates that he was nearly correct in this assumption.

The radius of the droplets which are formed when condensation occurs at the Wilson line is approximately 6.2×10^{-8} cm, a value determined by the von Helmholtz equation and substantiated by the blue color and complete plane polarization of the light scattered by the droplets.

The theory of supersaturation is verified for rapid expansions through simple convergent-divergent nozzle forms, for not only do the droplets appear at the pressures theoretically predicted, but also they disappear under recompression conditions in a manner which can only be explained by the supersaturation theory.

It was found that the behavior of steam in the illuminated nozzle could be seen clearly and the phenomena of shock, recompression, and the breaking away of the jet from the nozzle walls were observed and photographed.

A second series of experiments on modified nozzles revealed that under certain circumstances condensation could occur before the Wilson line is reached in an expansion. The upper limit of this preliminary condensation region is close to the 2 per cent moisture line on the Mollier chart. Due to the difficulty in distinguishing the first traces of preliminary condensation, the experimental points obtained in the study of this type are too widely scattered to permit definite conclusions to be drawn. Evidence indicated that the velocity of the steam in the condensation region is the controlling factor. The tests for electrification of the droplets, although inconclusive, indicate that electrical methods for removing moisture from the low pressure sections of steam turbines are not likely to succeed.

With nozzle No. 1, the evidence is reasonably conclusive that there is no growth of the droplets during their passage through the nozzle. Growth of the droplets would cause the nature of the scattered light to undergo drastic changes which could easily be observed. The color, intensity, and polarization of the scattered light remain constant throughout the length of the nozzle, however, and there could have been no appreciable change in the size of the droplets.

With nozzles Nos. 2 and 3 it was found that the drops which are formed in preliminary condensation grow very rapidly from their original radius of about 10.0×10^{-8} cm to a magnitude comparable to the wave-length of red light, about 6.0×10^{-6} cm in radius. If, however, the preliminary condensation is followed by ultimate condensation, the first droplets cease to grow when the latter occurs, probably because all of the available moisture is acquired by the vast number of nuclei which become effective at the Wilson line. It may be concluded that no additional nuclei beyond those present in the dry steam are needed to effect complete condensation.

As yet no explanation can be given for the existence of this preliminary condensation. It was found to occur only when the expansion in the supersaturated region was slow or interrupted. This suggests that long parallel sections of converging nozzles in the low pressure stages of steam turbines may encourage preliminary condensation and the subsequent formation of droplets large enough to cause erosion of the blades upon which they are discharged.

Appendix 1 contains a brief presentation of the optics of small particles, and the construction of the revised Keenan Mollier chart is described in Appendix 2. A bibliography of the leading articles on supersaturation and related subjects will be found in Appendix 3.

ACKNOWLEDGMENTS

This research was carried on by the author at the Johns Hopkins University during two years of graduate study in mechanical engineering, under the direction of Prof. A. G. Christie, who rendered invaluable assistance in the experimental work and in the preparation of this paper. The author wishes to acknowledge his indebtedness for the helpful contributions of President J. S. Ames of that University, of Drs. A. H. Pfund, R. W. Wood, and R. B. Barnes of the Physics Department, and of Associate Professor J. C. Smallwood of the Mechanical Engineering Department. Prof. J. H. Keenan of the Stevens Institute of Technology offered many valuable suggestions, and his interest is greatly appreciated.

Appendix 1

THE OPTICS OF SMALL PARTICLES

FOR the purpose of optical study, small particles must be divided into two classes, those smaller than and those larger than the wave-length of light. Particles whose diameter is less than the wave-length of the light which falls upon them give rise to the phenomenon of scattering, which will be considered in detail since the droplets encountered in this work seem to be of that order of magnitude. Larger particles can be studied by means of the light reflected or refracted by them.

The scattering of light by small particles was studied by Lord Rayleigh (34, 35, 36), who developed the following formula for the intensity of the light scattered by dielectric spheres, the radius of which is many times smaller than the wave-length of the light which falls upon them. If I is the intensity of the scattered light,

$$I = k \frac{r^6}{\lambda^4} (1 + \cos^2 \beta) \dots \dots \dots [18]$$

where k = a constant

r = radius of the spheres

λ = wave-length of the incident light

β = angle between the line of observation and the incident light

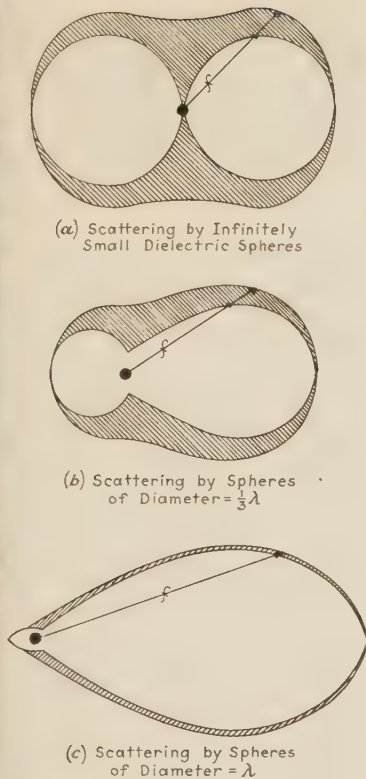


FIG. 20 GRAPHICAL REPRESENTATION OF LIGHT SCATTERED BY SPHERES
(Sizes ranging from infinitely small to a diameter equal to the wave-length of the incident light.)

tered light varies inversely as the fourth power of the wave-length, so for a given particle size the short wave-lengths will be scattered much more vigorously than the long and the scattered light will be blue in color. This blue color is the characteristic by which light scattered by very small particles can be identified.

There is no lower limit in size below which particles will not scatter light. Any particle of finite radius will scatter light to some degree, and the scattering can usually be observed if the proper care is taken. Strutt (58) has studied the scattering of light by the molecules of many gases. He found that the scattered light when examined spectroscopically was the same as the incident light except that the longer wave-lengths had been removed.

Mie (50), Shoulejkin (57), and Blumer (41-44) have studied the scattering of light by particles of all sizes. The work of Shoulejkin is of particular interest here because he has calculated the intensity of the light scattered by small dielectric spheres, in which class water droplets must be considered. He has represented graphically in polar coordinates the intensity of the light scattered by spheres ranging in size from infinitely small to equal to the wave-length of the incident light. In (a), (b), and (c), Fig. 20, the total length of any vector, as f , represents the total intensity of the light scattered along that vector, the incident light coming from the left. The portion of the vector between the inner and the outer curves represents the fraction of the light which is polarized. For infinitely small spheres, the scattering, following the Rayleigh formula, is symmetrical, and the polarization is complete at an angle of 90 deg to the incident light, as in (a).

In the radiation from particles whose diameter is about $1/3$

This formula gives a symmetrical distribution of the scattered light, with the intensity twice as great in the direction from which the light comes as in a direction normal to it.

The light which is scattered at right angles to the incident light is completely plane polarized, and can be extinguished if the incident light is properly polarized. This polarization is the distinguishing feature of scattered light.

It will be seen from Equation [18] that, at a given angle of observation, the intensity of the scattered light varies with the sixth power of the radius of the sphere. Thus a small increase in the radius will cause a large increase in the intensity. Likewise, the intensity of the scat-

tered light, as in (b), the polarization is nowhere complete and its maximum is shifted from 90 deg to the higher angles. The intensity is no longer symmetrical but is noticeably greater in the direction from which the light comes.

With particles of diameter equal to the wave-length, as in (c), the asymmetry is still greater, and the intensity is far greater in the direction of the incident light than in the opposite direction. The scattered light is only slightly polarized.

According to Shoulejkin, the nature of the scattered light does not change until the dimensions of the particles have become so great that one can just begin to study their behavior by applying the laws of interference, refraction, and reflection of light. Such particles are of microscopic dimensions and can be measured by various methods, an excellent discussion of which is given by Whytlaw-Gray and Patterson (60).

Appendix 2

A METHOD OF COMPUTING THE PROPERTIES OF SUPERSATURATED STEAM

IT has been found that, in the region near saturation, the isentropic expansion of superheated steam can be expressed with a high degree of accuracy by the equation:

$$p_1 v_1^{1.3} = p_2 v_2^{1.3} \dots \dots \dots [19]$$

where subscripts 1 and 2 denote the initial and final conditions, respectively.

Since supersaturated steam expands in the same manner as superheated, it may be assumed that the same law is applicable to both. If, therefore, a given superheated condition is assumed,

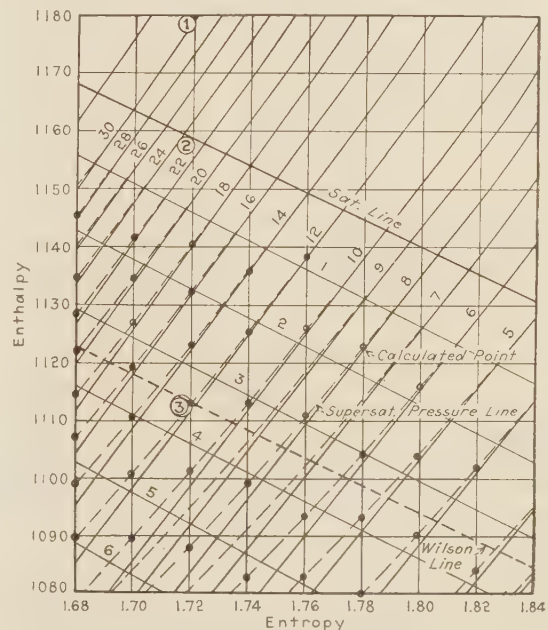


FIG. 21 LARGE-SCALE REPRODUCTION OF PORTION OF REVISED KEENAN CHART

it is possible to calculate the specific volume of superheated or supersaturated steam at the same entropy and at any desired lower pressure, from the equation:

$$v_2 = v_1 \left(\frac{p_1}{p_2} \right)^{0.77} \dots \dots \dots [20]$$

Since the work done in an adiabatic isentropic expansion is equal to the change in enthalpy,

$$h_2 = h_1 - \left(\frac{144}{778} \right) \left(\frac{1.3}{1.3 - 1} \right) (p_1 v_1 - p_2 v_2) \dots [21]$$

where p_1 and p_2 are in lb per sq in., and v_1 and v_2 are in cu ft per lb. Since h_1 , p_1 , v_1 , and p_2 are known, and v_2 can be calculated from Equation [20], it is possible to compute h_2 for any desired lower pressure.

Over a small range we may apply the perfect gas relationship

$$\frac{p_1 v_1}{T_1} = \frac{p_2 v_2}{T_2}$$

to calculate T_2 and consequently h_2 . Thus all of the properties of supersaturated steam can be obtained for any desired pressure.

In order to plot the revised Keenan chart used in Fig. 9, it was necessary to have at least five entropy-enthalpy values for each pressure line. Accordingly, eighteen points were chosen for entropies between 1.60 and 1.94. By calculating the isentropic enthalpy drop from each initial point to successively lower pressures, the required points were obtained. Fig. 21, a large scale reproduction of a small portion of the revised chart, shows the method of drawing the supersaturated pressure lines.

The accuracy with which this method can be applied is illustrated by the following sample calculation, in which the calculated values should agree with those given in the steam tables.

Initial conditions: Point 1, Fig. 21:

$$\begin{aligned} p_1 &= 30.0 \text{ lb per sq in. abs} \\ s_1 &= 1.7201 \\ v_1 &= 14.392 \text{ cu ft per lb} \\ h_1 &= 1178.9 \text{ Btu per lb} \\ t_1 &= 280 \text{ F} \end{aligned}$$

Assume an isentropic expansion to 23.0 lb per sq in., saturated, point 2, Fig. 21:

$$s_2 = 1.7204$$

Then

$$v_2 = 14.392 \left(\frac{30}{23} \right)^{0.77} = 17.65 \text{ cu ft per lb}$$

Keenan's value for 23 lb (saturated) = 17.63 cu ft per lb

$$\begin{aligned} h_2 &= 1178.9 - 0.804 (30.0 \times 14.392 - 23 \times 17.65) \\ &= 1178.9 - 20.58 = 1158.32 \text{ Btu per lb} \end{aligned}$$

Keenan's value for 23 lb (saturated) = 1158.6 Btu per lb

$$T_2 = (280 + 459.6) \frac{23 \times 17.65}{30 \times 14.392} = 695.6$$

$$t_2 = 236.0 \text{ F}$$

Keenan's value = 235.49 F

For the entropy value $S = 1.7201$, condensation will occur at approximately 12.0 lb per sq in. abs. The following example will serve to illustrate the loss due to supersaturation:

$$\begin{aligned} \text{Let } p_3 &= 12.0 \text{ lb per sq in. abs, point 3, Fig. 21} \\ s_3 &= 1.7201 \end{aligned}$$

$$\text{Then } v_3 = 14.392 \left(\frac{30}{12} \right)^{0.77} = 29.14 \text{ cu ft per lb}$$

$$\begin{aligned} \text{and } h_3 &= 1178.9 - 0.804 (30.0 \times 14.392 - 12 \times 29.14) \\ h_3 &= 1113.0 \text{ Btu per lb} \end{aligned}$$

From the Keenan steam tables and Mollier chart, for 12.0 lb per sq in. abs, wet steam, entropy of 1.7201,

$$h = 1111.39 \text{ Btu per lb}$$

The loss in enthalpy caused by supersaturation

$$\Delta h = (1113.0 - 1111.39) = 1.61 \text{ Btu per lb}$$

Since the enthalpy drop from the saturation line to the 12 lb pressure line along the entropy line, with s of 1.7201, is

$$H = (1158.6 - 1111.4) = 47.2 \text{ Btu per lb}$$

The loss due to supersaturation in this case is

$$\frac{1.61}{47.2} = 3.41 \text{ per cent of the isentropic enthalpy drop from the saturation line to the 12 lb wet-steam line.}$$

Appendix 3

BIBLIOGRAPHY ON SUPERSATURATION

THE numbers appearing in parentheses in the text after proper names refer to the following:

- 1 John Aitken, *Proc. Roy. Soc., Edin.*, vol. 11, p. 14, 1880.
- 2 John Aitken, *Trans. Roy. Soc., Edin.*, vol. 16, p. 14, 1888.
- 3 John Aitken, *Trans. Roy. Soc., Edin.*, vol. 35, p. 14, 1881.
- 4 Carl Barus, *Phil. Mag.*, vol. 35, p. 315, 1893.
- 5 Carl Barus, *Phil. Mag.*, vol. 38, p. 19, 1894.
- 6 Carl Barus, *Am. Meteor. Jour.*, vol. 9, p. 488, 1893.
- 7 Carl Barus, *Am. Meteor. Jour.*, vol. 10, p. 12, 1893.
- 8 Carl Barus, *Carnegie Inst. of Wash.*, Pub. No. 62.
- 9 H. L. Callendar, "The Properties of Steam," London, 1920.
- 10 H. L. Callendar, *Proc. Inst. Civ. Eng.*, vol. 131, p. 1, 1897-8.
- 11 H. L. Callendar, *Proc. Inst. Mech. Eng.*, vol. 53, 1915.
- 12 H. L. Callendar, *Encycl. Brit.*, 11th Ed., "Vapours," "Condensation."
- 13 H. L. Callendar, *Proc. Roy. Soc.*, vol. 67A, p. 266, 1900.
- 14 H. L. Callendar, *Proc. Roy. Soc.*, vol. 80A, p. 466, 1908.
- 15 Sir James Ewing, "Thermodynamics," Cambridge, 1920.
- 16 C. A. Goodenough, *Power*, vol. 66, p. 466, 1927.
- 17 H. L. Green, *Phil. Mag.*, vol. 4, p. 1046, 1927.
- 18 R. von Helmholtz, *Annalen der Phys.*, vol. 27, p. 509, 1886.
- 19 R. von Helmholtz, *Annalen der Phys.*, vol. 32, p. 1, 1888.
- 20 Henderson, *Proc. Inst. Mech. Eng.*, Feb. 1913.
- 21 Hirn and Cazin, *Comptes Rendus*, p. 1144, 1866.
- 22 Kearton, *Proc. Inst. Mech. Eng.*, p. 993, 1929.
- 23 J. H. Keenan, "Steam Tables and Mollier Diagram," 1931.
- 24 H. M. Martin, *Engineering*, vol. 106, p. 1, 1918.
- 25 J. C. Maxwell, "Theory of Heat," 4th Ed., 291.
- 26 Mellanby and Kerr, *Proc. Inst. Mech. Eng.*, p. 85, 1922.
- 27 Owens and Hughes, *Phil. Mag.*, vol. 15, p. 746, 1908.
- 28 C. F. Powell, *Proc. Roy. Soc.*, vol. 114A, p. 553, 1928.
- 29 C. F. Powell, *Engineering*, vol. 127, p. 711, 1927.
- 30 C. R. Soderberg, A.S.M.E. Semi-Ann. Meeting, July, 1933, "The Moisture Problem in Steam Turbines."
- 31 A. Stodola, "Steam and Gas Turbines," New York, 1927.
- 32 C. C. Thomas, "Observation of Water in Steam." Presented A.S.M.E. Ann. Meeting, 1932.
- 33 Sir W. Thomson, Lord Kelvin, *Proc. Roy. Soc., Edin.*, vol. 7, p. 63, 1870.
- 34 J. J. Thomson, "Conduction of Elec. Through Gases," 1921.
- 35 G. T. R. Wilson, *Trans. Roy. Soc.*, vol. 189A, p. 265, 1897.
- 36 G. T. R. Wilson, *Proc. Roy. Soc.*, vol. 85A, p. 285.
- 37 G. T. R. Wilson, *Proc. Roy. Soc.*, vol. 87A, p. 277.
- 38 G. T. R. Wilson, *Proc. Roy. Soc.*, vol. 104A, p. 192.
- 38 Niels Bohr, *Phil. Trans.*, vol. 209A, p. 281.
- 39 N. E. Dorsey, *Sc. Papers Bur. Stand.*, vol. 21, No. 541. (This paper contains a complete bibliography of the subject.)
- 40 International Critical Tables, vol. 4, p. 447.
- 41 H. Blumer, *Zeit. für Phys.*, vol. 32, p. 119.
- 42 H. Blumer, *Zeit. für Phys.*, vol. 38, p. 304.
- 43 H. Blumer, *Zeit. für Phys.*, vol. 38, p. 920.
- 44 H. Blumer, *Zeit. für Phys.*, vol. 39, p. 195.
- 45 Cabannes, *Annales de Phys.*, vol. 19, p. 1.
- 46 Ehrenhaft, *Annalen der Physik*, vol. 56, p. 81.
- 47 Kimball, "College Physics."
- 48 J. Kunz, *Phil. Mag.*, vol. 39, p. 416.
- 49 Maxwell-Garnett, *Phil. Trans.*, vol. 203A, p. 385.
- 50 G. Mie, *Annalen der Physik*, vol. 25, p. 377.
- 51 Muller-Pouillet, "Lehrbuch der Phys.," Optik, p. 882.
- 52 Patterson and Whytlow-Gray, *Proc. Roy. Soc.*, vol. 112A, p. 302.
- 53 Porter and Paris, *Engineering*, vol. 28, p. 610.

- 54 Rayleigh, *Phil. Mag.*, vol. 4-41, p. 107.
- 55 Rayleigh, *Phil. Mag.*, vol. 35, p. 373.
- 56 Rayleigh, *Proc. Roy. Soc.*, vol. 97A, p. 435.
- 57 Shoulejkin, *Phil. Mag.*, vol. 48, p. 307.
- 58 R. J. Strutt, *Proc. Roy. Soc.*, vol. 94A, p. 453.
- 59 G. F. A. Stutz, *Jour. Franklin Inst.*, 1930.
- 60 Whytlow-Gray and Patterson, "Smoke," London, 1932.
- 61 R. W. Wood, "Physical Optics," p. 624.

Discussion

A. G. CHRISTIE.³ Mr. Yellott's paper forms a real contribution to our knowledge of the properties of steam. Much has been written upon supersaturation but this unstable state is so difficult to determine by ordinary instruments which measure temperature and pressure that all the material previously published has been in the form of deductions based on certain theories. Mr. Yellott's optical methods enabled him not only to observe the steam conditions in his nozzles but also to measure the droplet sizes and the pressures at which these formed. Greater reliance therefore can be placed upon these observations than upon any previous data.

It is a matter of regret that colored photographs of the actual jets could not be secured, particularly when polarized light was used. These would provide still more convincing evidence of the nature of the phenomena and the changes that actually take place in the flow of steam.

While Mr. Yellott's results have great value, many new problems arose in the course of his work. Another graduate student, J. T. Rettaliata, is continuing this research in an endeavor to determine whether roughness of the nozzle wall surface is the cause of the abrupt halt in pressure drop at the moment condensation starts from the supersaturated steam. This step in the pressure drop curves was noted by both Prof. Robb and Mr. Yellott.

An attempt will also be made to investigate the pressures at which condensation starts with varying nozzle shapes. Mr. Yellott found no preliminary condensation with nozzle No. 1 while with nozzle No. 2 preliminary condensation was usually present. We believe that a nozzle can be built between these two limiting sizes in which the condensation would be either ultimate or preliminary depending upon the pressure conditions. When this nozzle is developed and tested, its performance should give some clue to the determination of the conditions under which either form of condensation may be expected.

We also propose to try some actual turbine nozzles and to study both the supersaturation effects, the loss of contact of jets with walls, and the recompression in the issuing jet by means of light rays of definite wave-length.

It is undoubtedly a fact that this supersaturation phenomenon has an effect upon the expansion of steam in turbines at the saturation line and possibly even throughout the whole section of the turbine below saturation. In an earlier paper by Mr. Colburn and myself we suggested that supersaturation at the last blade row of the turbine may be an influencing factor in blade erosion. The influence of supersaturation on turbine performance with saturated or wet steam is another problem that has not yet been fully analyzed.

The paper before us will direct attention to these problems and as a result of further studies it is hoped that improvements in turbine performance may be effected.

J. GERSHBERG.⁴ The writer would like to know if the author made experiments with a mixture of air and steam to bring out

what influence, if any, air may have on supersaturation of steam.

This question is prompted by a rather peculiar phenomenon observed in a recent test of heat transfer in experimental condenser tubes. Two test tubes were placed side by side in the lower portion of the first pass of a two-pass condenser. One of these tubes was new and clean and the other old and dirty. The new tube was supplied with fresh water and the old one with salt water drawn from the house-service line. It was found that for a constant load on the turbine the water in the new tube was giving up instead of absorbing heat at the lowest water velocity employed in the test, this effect becoming progressively less as the water velocity was increased. However, the adjacent old test tube displayed a normal behavior, i.e., absorption of

TABLE 4

Inlet water temp, F, condenser	46.3
Inlet water temp, F, new test tube	58.5
Inlet water temp, F, old test tube	55.6
Outlet water temp, F, new test tube	53.3
Outlet water temp, F, old test tube	59.0
Condenser hot-well temp, F	68.0
Abs pressure at turbine exhaust, in. Hg	1.13
Abs pressure at hot well, in. Hg	1.02
Air leakage, cu ft per min	7

heat from the steam. Table 4 gives some of the test data at a water velocity of 2 ft per sec.

It is to be noted that the two test tubes were located in proximity of the bank of tubes intended for cooling the air on its way to the air offtake.

Attempts were made to explain this phenomenon as due to partial pressures. However, computations do not seem to support this contention. They show that on the basis of partial pressures the lowest temperature of the fluid enveloping the new tube may be about 65 F which is close to 68 F in the hot well. The exterior fluid would be thus about 12 F hotter than the water at the outlet of the tube when, logically, it should be somewhat cooler. Also it was thought that, perhaps, a local cooling to this fluid was brought about by the 46.3 F inlet temperature of the main circulating water. Or is it possible that, notwithstanding the presence of water drops, a local supersaturation of vapor took place because of a comparatively richer mixture of air in that part of the condenser?

J. H. KEENAN.⁵ Supersaturation is a phenomenon which yields up its secrets only to the most persistent and intelligent observers. Mr. Yellott is one of these. He has presented data on supersaturation in an expanding stream that are more comprehensive and more illuminating than anything previously published.

It is well to recall that there are two classifications of supersaturated or undercooled steam. Supersaturated steam of the first class is any steam entirely free from water, but at a temperature lower than the steam table saturation temperature corresponding to its pressure. Supersaturated steam of the second class is steam in thermal equilibrium with small drops of water. This second kind of supersaturation, despite the presence of water drops, is undercooled relative to the saturation temperature given for its pressure in the steam table, because the steam table saturation temperature is correct only for an equilibrium mixture of steam with infinitely large drops of water. The first kind of supersaturated steam involves no liquid and its behavior is much like that of superheated steam. In fact, the best available method of determining its properties consists of extrapolating the constant temperature lines and other characteristics of superheated steam across the saturation line.

Mr. Yellott's photographs and the corresponding pressure curves show that supersaturation of the first kind exists in

³ Prof. of Mechanical Engineering, Johns Hopkins University, Baltimore, Md. Mem. A.S.M.E.

⁴ Chief Testing Engr., United Electric Light and Power Co., New York, N. Y. Mem. A.S.M.E.

⁵ Assistant Prof. of Mechanical Engineering, Stevens Institute of Technology, Hoboken, N. J. Assoc-Mem. A.S.M.E.

nozzle No. 1 down to a certain point at which two things occur: First, a dense fog of fine water particles is formed, not gradually but with great suddenness, and second, a step occurs in the pressure curve. It is reasonable to suppose that the steam carrying the fog is supersaturated in the second sense, but its degree of supersaturation depends upon the size of the fog particles.

The phenomenon of sudden condensation at a given section of the nozzle can be analyzed by means of the equations of continuity, energy, and momentum for a steadily flowing stream. Let p_0 and t_0 represent the pressure and temperature immediately before the nozzle where the velocity is negligible, and let sub-

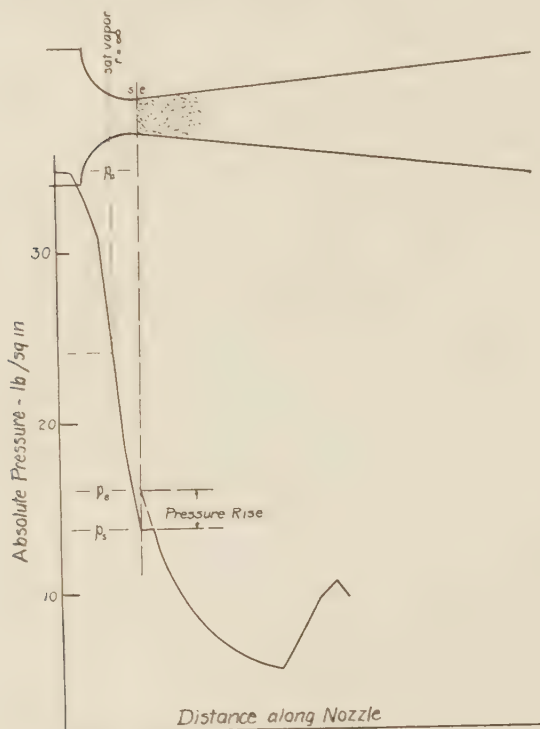


FIG. 22 SAMPLE PRESSURE DISTRIBUTION CURVE
(The crossing of the normal saturation line and the condensation point are shown.)

scripts s and e designate properties of the steam at sections that are, respectively, immediately above and immediately below the condensation point, Fig. 22. Then the three equations may be written:

$$\text{Continuity, } V_s/v_s = V_e/v_e, \text{ since } a_s = a_e \dots \dots \dots [22]$$

$$\text{Energy, } h_s + V_s^2/2g = h_e + V_e^2/2g \dots \dots \dots [23]$$

$$\text{Momentum, } wV_s/g + p_s a = wV_e/g + p_e a \dots \dots \dots [24]$$

where V = stream velocity
 v = specific volume
 a = stream cross-section area
 p = stream pressure
 w = weight rate of flow
 h = enthalpy

As expansion proceeds from p_0 , t_0 to p_s the steam is at first superheated but it becomes undercooled steam of the first kind once it has crossed the steam table saturation line. However, the change in name is not justified by any change in the characteristics of the expansion, because undercooled steam of the first kind has all the characteristics of superheated steam.

Its name is changed only because a change in characteristics indicated by the steam table failed to materialize. Consequently, the velocity of the steam at p_s and its properties may be found by extending down to p_s the characteristics of the expansion from p_0 , t_0 to the steam table saturation line. Investigation shows that within the range covered by Mr. Yellott's tests isentropic expansion in the superheat region follows the polytropic

$$pv^{1.316} = \text{constant}$$

to a high degree of approximation. This relationship, combined with the properties of the steam approaching the nozzle and the measured pressure p_s , yields h_s , v_s , and V_s . Equations [22], [23], and [24] then become relationships between the four unknowns p_e , h_e , v_e , and V_e .

If we assume for the moment that the fog particles at e are infinitely large, that is, more than 1×10^{-6} in. in diameter, the ordinary table of the properties of saturated liquid and saturated vapor yields a fourth relationship between the four unknowns and offers the possibility of solution by a "cut and try" process. In a representative case for which p_0 and t_0 were 34 lb per sq in. and 297 F and p_s was 13.7 lb per sq in. (Fig. 22) the solution indicated a pressure at e 3.8 lb per sq in. higher than the pressure at s . In other words, to fulfil the requirements of the continuity, energy, and momentum equations, the pressure must rise suddenly when a sudden return to equilibrium occurs from the supersaturated state.

The step in the pressure curve at p_s serves to confirm this result. If a sudden pressure rise existed at this point, a search tube with a sampling hole of finite size would round off the discontinuity. Furthermore, since it is unlikely that all of the drops form at precisely the same instant, some additional flattening of the peak might be expected. However, an approximation to the pressure rise corresponding to instantaneous condensation may be found from the measured pressures by extending the trend of the curve following condensation back to the section at which condensation starts and measuring the difference between the extrapolated value and the measured value at that point. In the following paragraphs the pressure difference found in this fashion will be referred to as the measured pressure rise.

In the case under discussion the calculated pressure rise was roughly twice the measured rise, but the discrepancy might be explained by the small size of the drops. It seemed likely that if a solution of the analysis could be carried out for different drop sizes, each, of course, involving a different steam table relating p , h , and v for mixtures of that drop size with the correspondingly saturated steam, the drop size for which the calculated pressure rise agreed with the measured pressure rise would be, at least approximately, the size of the fog particles formed at s .

Consequently relationships between p_s , h_s , and v_s were found for equilibrium mixtures of vapor and water drops of different sizes. For this purpose the Kelvin-Helmholtz equation for the supersaturation ratio, the Stodola equation for capillary energy of the drops and the polytropic exponent 1.316 for steam at temperatures above the corresponding equilibrium temperature were employed.

The condensation pressure rise for a number of different drop sizes was then computed and plotted in Fig. 23. It should be noted that the drop size corresponding to zero pressure rise upon condensation is the size given by Mr. Yellott. That is, Mr. Yellott calculated the drop size starting from the assumption that condensation begins as soon as the expanding steam crosses the saturated vapor line corresponding to the size of the drop formed. In this he was following the precedent set by authoritative earlier investigators. That condensation does not begin, however, as soon as the expanding steam crosses the saturated

vapor line corresponding to the size of the drops about to be formed is indicated by Mr. Yellott's own experimental results as follows:

(a) His photographs of nozzle No. 1 do not indicate a gradual increase in the number of water particles starting from a trace at the saturation point and increasing in numbers to a thick fog further on. On the contrary, a thick fog is formed suddenly as the steam crosses a definite section. It is true that traces of liquid appear in nozzle No. 2 before the thick fog is formed, but even here the major condensation occurs suddenly

(b) The step in the curve of pressure through the nozzle is an indication of a discontinuity in the sequence of state changes through the nozzle. Had condensation occurred at the proper saturation line no more discontinuity would have been observed than would be calculated from the ordinary steam table for isentropic expansion into the moisture region.

The measured pressure rise for an initial pressure of 34 lb per sq in. was about 1.8 lb per sq in. which, according to Fig. 23,

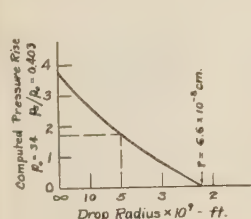


FIG. 23 PRESSURE RISE FOR SUDDEN CONDENSATION FROM SUPERSATURATED STEAM, PLOTTED AGAINST RADIUS OF DROPS FORMED

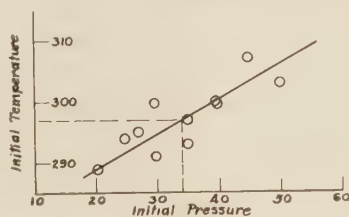


FIG. 24 INITIAL TEMPERATURE OF THE EXPANDING STEAM

corresponds to a drop radius of about 5×10^{-9} ft which is about two and one-half times the radius, or about fifteen times the volume, calculated by Mr. Yellott.

Whether this same size drop was formed in all of the tests on nozzle No. 1 could be learned by comparing calculated pressure rise with measured pressure rise in each instance.

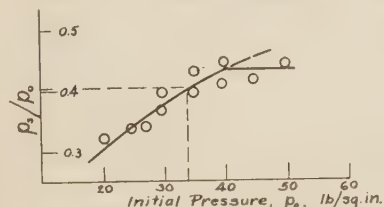


FIG. 25 CONDENSATION PRESSURES FOR VARIOUS INITIAL PRESSURES (Circles are measured pressures.)

In both instances the test values, shown as circles, departed little from the curve assumed. Two tests were omitted from the analysis, though they conflict in no way with its results, because their initial temperatures were out of line with those of the other tests.

The measured pressure-rise values are shown as circles in Fig. 26. They were obtained before the analytical values were computed in order to avoid, as far as possible, the influence of personal prejudice.

The condensation pressures, p_s , plotted in Fig. 25 show a consistent trend for initial pressures between 20 and 40 lb per sq in. Two tests at higher pressures failed to follow that trend. It seemed best to extrapolate the trend to obtain condensation pressures for computation purposes until it was found that there was no corresponding solution for an initial pressure of 50 lb per sq in. It became evident that the requirements of continuity,

energy, and momentum cannot be satisfied for this drop size and for the extrapolated condensation pressure. But solutions were found at the higher pressure when values of p_s were chosen from the solid line of Fig. 25 which follows the measured values. These solutions give the solid line of Fig. 26.

The agreement between the circles and the solid curve of Fig. 26 is evidence of the validity of the analysis. The discontinuity in the trend of the condensation pressure data proves, quite unexpectedly, to be further evidence in its favor.

It appears, then, that the expansion of steam in a nozzle into the region below the normal saturation line involves complete supersaturation until a vapor state is reached which would exist in stable equilibrium with droplets of about 2×10^{-9} ft radius (6.5×10^{-8} cm), but which is undercooled compared with steam in equilibrium with any larger size drops. From this state some of the steam suddenly condenses to form a fog of droplets 5×10^{-9} ft radius and releases energy sufficient to bring the surrounding vapor into substantial equilibrium with these relatively large drops. This process is essentially irreversible as indicated by the suddenness with which it occurs, but gradual condensation to drops of 2×10^{-9} ft radius would have been reversible except for friction between vapor and droplets. Irreversibility does not mean that the drops cannot be reevaporated upon compression of the vapor carrying them. It means only that some "hysteresis" effect must accompany such reevaporation. Thus, a vapor which expands to a state undercooled relative

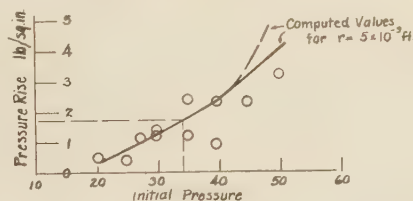


FIG. 26 MEASURED PRESSURE RISE COMPARED WITH CALCULATED PRESSURE RISE FOR FORMATION OF DROPS 5×10^{-9} FT RADIUS (Circles are values obtained from test curves. The solid line is calculated using values from the solid line of Fig. 25. The broken line is based on the broken line of Fig. 24 for which solution became impossible between 45 and 50 lb per sq in. initial pressure.)

to the size of drop subsequently formed must be compressed after condensation to a temperature markedly higher than that at which condensation occurred before all drops are evaporated again.

The discontinuity in the course of the pressure which characterizes the condensation point is doubtless evidence of further irreversibility. In fact it is not very different in nature from the shock effects occurring in the diverging portions of nozzles discharging against a back pressure higher than the throat pressure. It results in a kinetic energy loss in excess of the amount usually calculated for supersaturation by assuming that condensation proceeds, however irreversibly, at constant pressure. Table 5 compares the kinetic energy in a stream which expands from 34 lb per sq in. 297 F to various pressures for

(a) isentropic expansion in equilibrium with infinitely large drops for all pressures below the normal saturation line

(b) isentropic expansion without moisture ($pv^{1.316} = \text{constant}$), and

(c) isentropic expansion without moisture to a pressure below the final pressure followed by sudden compression to the final pressure simultaneous with the formation of infinitely large drops.

The difference between (a) and (b) is what has hitherto been called the supersaturation loss. The difference between (a) and

(c) is a somewhat larger value by virtue of the shock effect and is doubtless more nearly correct for this case. The differences between the losses calculated by the two methods are rather small and somewhat irregular, perhaps from slight steam table irregularities. They indicate, however, that the shock effect increases the loss by about $1\frac{1}{4}$ per cent of the kinetic energy if condensation forms as very large drops. Computations have not been made for drops 5×10^{-9} ft in radius but it is likely that they would show an additional loss of about $\frac{5}{8}$ per cent instead of $1\frac{1}{4}$ per cent.

It is of some importance to know whether condensation occurs in the steam stream of a turbine in the constant pressure fashion or in the shock fashion. In general it may be said that condensation will occur where the pressure of the steam is falling since once a stream reaches a given pressure without condensation no continuance at that pressure will result in condensation (except on cold walls), particularly if the temperature of the

and which require large friction forces as their speeds are alternately increased and decreased down through the turbine.

F. W. GARDNER.⁸ Mr. Yellott's results seem to give a very satisfactory confirmation of the work of others who have carried out research in the same field, and the existence of supersaturation in a simple nozzle seems now to be well established. Our difficulty in actual turbine work is that we have never been able to obtain any satisfactory evidence that it occurs in turbine blades, or at all events, that it has any appreciable effect on the turbine performance.

It is questionable whether the drop size, as deduced from the saturation experiments, has an important influence on the problem of blade erosion. The drops that produce erosion on the exhaust end blades of an actual turbine are probably of a much greater order of magnitude and result from the accumulation of water on the preceding blade surfaces. The size of drop that can persist under these conditions is discussed by Soderberg, and in an ordinary turbine is probably of the order of a hundredth of a centimeter in diameter, as compared to the figure of 6×10^{-6} centimeters given by Mr. Yellott.

In connection with the effect of ionization on condensation, Sir Charles Parsons and Mr. Dowson carried out some experiments a few years ago. Following some preliminary experiments in which a high-tension discharge was observed to produce a marked effect on the steam cloud issuing from an open ended nozzle, an apparatus was developed for ionizing the steam supply to a small turbine driving a dynamo. In this experiment voltages up to 100,000 were employed and tests were made to see if any difference in consumption, speed, or output could be detected. These experiments, however, gave a negative result, and the performance of the unit appeared to be quite unaffected by the introduction of the high-tension discharge.

AUTHOR'S CLOSURE

The new problems mentioned by Professor Christie have been the subject of further research carried on by Mr. Rettaliata at the Johns Hopkins University and by the author at the University of Rochester. It is hoped that the results of this work may be presented at a subsequent meeting of the Society, and that colored motion pictures will be available to illustrate the optical features.

In response to Mr. Gershberg's question, the presence of air in steam cannot be detected by this method, for the air is quite as transparent as the steam. It is probable that the phenomena which he noted are due in some manner to the low temperature of the main cooling water rather than to supersaturation.

The author wishes to express his gratitude to Professor Keenan for his excellent analysis, which not only gives encouraging support to the accuracy of the experimental results, but also provides a new theoretical method of attack upon the condensation problem. The only amendment to his method which the author can suggest is a slight modification of the Stodola equation for the capillary energy of droplets. Introduction of an improved equation for surface-tension results in values slightly greater than those calculated from Stodola's equation.

The experimental work which the author has been conducting with improved apparatus during the past year at the University of Rochester may supply the answer to some of the questions raised by Professor Keenan. A number of interesting and perhaps significant facts have been observed, and an attempt is being made to deduce the general laws which control the condensation of flowing steam.

TABLE 5 KINETIC ENERGIES AND SUPERSATURATION LOSSES FOR EXPANSION FROM 34 LB PER SQ IN. AND 297 F

Final pressure, lb per sq in.	(Condensation on infinitely large drops)			Loss in kinetic energy		Shock condensation	
	a	b	c	Const. p	Shock	a-b	a-c
	Equilibrium with large drops	Supersaturation constant p	Supersaturation shock condensation	Condensation	Condensation		
				Btu/lb	%	Btu/lb	%
6.89	114.4	108.4	106.6	6.0	5.25	7.8	6.8
12.63	73.7	72.0	71.2	1.7	2.3	2.5	3.4
17.51	50.9	50.2	49.6	0.7	1.3	1.3	2.6

stream is rising because of friction. A stream which is falling in pressure along its direction of motion is generally constrained by walls or by dynamic limitations to a certain sequence of cross-section areas and under such conditions the equation of continuity will doubtless be valid when applied to the two sides of the condensation section. Consequently, it is logical to assume that this shock type of condensation is the important type to the turbine designer and it will justify further study.

Mr. Yellott should be strongly urged to investigate further these supersaturation and moisture region phenomena about which much has been said and little has been known. It is of great importance to find out what happens in stages succeeding the initial condensation stage. Does supersaturation persist in each succeeding nozzle, or does the presence of the original fog inhibit it? On the answer to this question hinges our further understanding of moisture region phenomena in the steam turbine. Various authorities on steam turbine design have agreed that the loss due to moisture and supersaturation combined, affects the efficiency of a turbine stage slightly more than 1 per cent for each per cent of moisture present. One authority⁶ has attributed practically all of this effect to supersaturation. Others⁷ show that the entire moisture region loss might be readily accounted for by friction between steam and water particles.

Would it not be possible to feed the glass walled nozzle with steam from a turbine stage? A suitable moisture content might be found by tapping the proper stage of a multistage turbine. Large water drops swept from metal surfaces could be largely eliminated by a centrifugal separator leaving only the fine fog within the stream. Then, photographs and pressure tube explorations might tell something of how condensation progresses in these later stages, whether continuously or by shock effects. Something might be learned concerning the relative distribution of water between the minute fog particles, which probably result in but small friction loss between steam and particle, and the relatively enormous drops which are swept from surfaces

⁶ H. M. Martin, *Engineering*, vol. 106, p. 1, 1918.

⁷ G. A. Goodenough, *Power*, vol. 66, p. 466, 1927.

⁸ C. A. Parsons and Co., Ltd., Heaton Works, Newcastle-on-Tyne, England.

Locomotive Counterbalancing

By LAWFORD H. FRY,¹ PITTSBURGH, PA.

The paper offers a method for computing and analyzing the counterbalance system of a locomotive. As a result of a straightforward simple series of computations, a clear and exact picture is obtained, showing the resultant forces set up by the rotating and reciprocating parts and the counterbalance in any given locomotive. A method is also provided for determining the proper counterbalance to meet any given conditions. The problems involved are of importance to the designer of modern locomotives of large size. The day has passed when it is satisfactory to provide static balance only for the rotating engine parts of a locomotive. Many locomotives now in service, which are balanced for static conditions only, have the main pair of wheels out of balance dynamically by as much as

400 lb. At "diameter speed," that is, at as many miles per hour as the driving wheels have inches of diameter, this lack of balance is sufficient to increase and decrease the axle load by over 20,000 lb during each revolution of the wheels. Up to the present there has been no adequate study of the effect of unbalanced horizontal forces on the locomotive. The proposed method of analysis offers a simple but accurate basis for such study. It seems probable that with proper cross-balancing a very large proportion of the mass of the reciprocating parts can be left unbalanced. In the case of the locomotive examined, over 80 per cent of the mass of the reciprocating parts is unbalanced and the locomotive is reported to ride very satisfactorily.



IN MODERN locomotive designing, the proper counterbalancing of the rotating and reciprocating parts deserves close attention. Methods used up to a few years ago are inexact and allow high unbalanced inertia forces, with destructive effect on the track. In Europe the civil engineers of the railroads require all possible protection for the permanent way, and as a result correct balancing of locomotives has been common practise. In recent years some locomotive engineers in this country have adopted methods of cross-balancing which have reduced the unbalanced inertia forces and have thus cut down the dynamic augment of wheel loads produced by these forces. However, the great majority of locomotives designed ten years or more ago are balanced for static conditions only. In these locomotives the main axle load on the track may be increased and decreased by 20,000 lb or more during each revolution. Little argument should be needed to show the desirability of avoiding the large and unnecessary stresses thus imposed on the track.

Acceptance of this unnecessary dynamic augment in the axle load cannot be excused on the grounds of simplification of design. The great reduction in track stresses secured by elimination of unnecessary dynamic augment requires only that the counterbalance be set a few degrees off the center line of the crank. The necessary increase in weight of the counterbalance is small.

¹ Railway Engineer, Edgewater Steel Company, Mem. A.S.M.E. Mr. Fry was born in Richmond, Province of Quebec, Canada, of English parents and came to the United States at an early age. After schooling in this country and England he studied engineering at the City and Guilds Institute in London and the Hannoversche Technische Hochschule. He started work in the erecting shop of the Baldwin Locomotive Works and was later engineer of tests there. Later he became technical representative of the Baldwin Locomotive Works in London and Paris, returning to this country to become Metallurgical Engineer of the Standard Steel Works Company. Since 1930 he has been associated with the Edgewater Steel Company. He is the author of "A Study of the Locomotive Boiler" and of many articles and papers dealing with locomotive and metallurgical subjects.

Contributed by the Railroad Division and presented at the Annual Meeting, New York, N. Y., December 5 to 9, 1933, of THE AMERICAN SOCIETY OF MECHANICAL ENGINEERS.

NOTE: Statements and opinions advanced in papers are to be understood as individual expressions of their authors, and not those of the Society.

Some refinements are necessary in weighing the wheels to see that they are correctly balanced. These, however, should present no real difficulty with adequate mechanical engineering talent and proper shop management.

It is occasionally argued that it is unnecessary to consider cross-balancing for certain types of locomotives, because the wheel centers are too small to take all of the balance desired. This excuse is not valid. It is shown later that even with less than complete balance a shift of the center of gravity of the balance by about 7 degrees may reduce the dynamic augment on the main axle by over 10,000 lb. The possibility of this reduction should not be neglected.

It is not easy to see why American civil and mechanical railway engineers have neglected for so long the proper balancing of locomotives. Probably one reason for this neglect has been the lack of a simple method for analyzing the inertia forces and presenting the facts. The present paper attempts to fill this gap. It offers a complete and accurate method for analyzing the inertia effects of the rotating parts of a locomotive engine. The method serves a double purpose. In the first place, it shows exactly what unbalanced inertia forces are developed by a given locomotive. In the second place, it enables a designer to arrange the counterbalance of a locomotive so as to secure the best possible results for any given conditions.

The paper describes in detail all of the computations to be carried out and keeps the mathematics down to the inescapable minimum. The final results are presented in simple form so that they may be readily understood by executives too busy to unravel the usual intricacies of cross-balancing.

It is believed that general use of this method will accelerate the progress in improved balancing that has begun in the last few years. The present interest in the reduction of track stresses by proper balancing is directly traceable to the track stress measurements begun in 1913 by Prof. A. N. Talbot for the American Railway Engineering Association. Mr. C. T. Ripley, of the Atchison, Topeka & Santa Fe Railway, cooperated with Professor Talbot in this work and was much impressed by advantages to be gained by designing locomotives to reduce track stresses. Improved distribution of weight and elimination of flangeless tires were tried and found to be efficacious. Professor Talbot's tests also showed that large unnecessary stresses were due to imperfect balancing of locomotives. In 1924, Mr. Ripley arranged for the cross-balancing of a large Santa Fe type locomotive, and the author worked with Mr. Ripley on the preliminary computations of the balance for this engine. In 1926,

Mr. Ripley reported to the American Railway Association, Mechanical Division, that the experimental locomotive gave a satisfactory reduction in track stresses. On this foundation a considerable amount of improvement in locomotive balancing has been built. In 1930, the Committee on Locomotive Construction reported to the American Railway Association, Mechanical Division, a proposed method for dynamic or cross-balancing, and in 1932 the committee's method was adopted by the Association as recommended practise.

The present paper starts with the American Railway Association's method of computation and modifies and extends this. In addition, a method is provided for a complete analysis of the inertia forces of an existing locomotive. Special attention is called to the method of presenting the results of this analysis. Although entirely accurate, the results are presented in very simple form.

In each pair of wheels all of the inertia forces of the rotating parts and of the counterbalances are combined so that they are completely represented by two equivalent weights in each wheel. These weights act in the plane of rotation of the center of gravity of the counterbalance. In this plane one equivalent weight acts along the wheel diameter through the crankpin and the other perpendicular to this diameter. When this pair of representative equivalent weights is set down for each wheel, as shown in Fig. 2, the exact conditions of balance of the locomotive can be seen very readily. The equivalent weight acting along the crank diameter represents, in each wheel, the overbalance or underbalance acting to balance or to reinforce the inertia forces of the reciprocating parts. The equivalent weight acting at right angles to the crank is a parasitic effect due to incomplete cross-balancing. The resultant of the two equivalent weights at right angles to each other, shown by broken lines in Fig. 2, determines the maximum value of the dynamic augment. If the parasitic effect is large enough to produce an undesirably large increase in the dynamic augment, it can be reduced by cross-balancing.

With this as introduction, the method proposed by the author will be considered in more detail. The method is illustrated by using it to analyze the inertia forces set up by the rotating parts of an existing 4-8-4 type of locomotive. This engine, which has been in satisfactory service for about six years, has the main pair of driving wheels partly cross-balanced. The locomotive is of the 4-8-4 type, with dimensions as follows:

Cylinders, diameter, in.....	30
Cylinders, stroke, in.....	30
Driving wheel, diameter, in.....	73
Weight on first pair of drivers, lb.....	66,500
Weight on second pair of drivers (main axle), lb.....	70,500
Weight on third pair of drivers, lb.....	66,500
Weight on fourth pair of drivers, lb.....	66,500
Total weight on drivers, lb.....	270,000
Total weight of locomotive, lb.....	420,000

When the original design of the locomotive was under consideration, it was stipulated that at diameter speed, that is, at 73 mph, the combined static and dynamic rail load of any axle should not exceed 75,000 lb.

This is a highly intelligent method of setting the limits to be worked to in counterbalancing. After each static axle load has been established, the difference between this static load and the permissible maximum of 75,000 lb is the maximum allowable dynamic augment permitted for the axle in question. From this can be computed the amount of overbalance which may be put into each wheel to balance the reciprocating parts.

The locomotive under consideration had the main wheels partially cross-balanced. The analysis which follows shows that the final results in this pair of wheels differed somewhat from that aimed at. The deviation is due to two causes. In the first place, the eccentric cranks were assumed to be concentrated at the

crankpin, while the present more accurate analysis takes into account the fact that the center of gravity of the eccentric cranks does not fall on the main crank radius. In the second place, the position of the counterbalance to give correct cross-balance for the rotating parts was determined, and the overbalance for the reciprocating parts was then added without changing the position of the counterbalance.

The difference between the result aimed at and that obtained is not large, but is sufficient to show that any counterbalance scheme should be accurately analyzed before the locomotive design is accepted as satisfactory.

All computations necessary for an accurate analysis of the system of rotating parts are described in detail in the Appendix. A step-by-step method is used, so that those who carry out such computations infrequently may be able to follow the reasoning involved.

Before considering the application of the method to the example, a word of explanation of the term "equivalent weight" is in order. This term has been introduced to simplify the mathematics and to avoid the necessity for introducing the speed of the locomotive. Instead of calculating with "masses" or with "centrifugal forces," the "equivalent weights" are used. The inertia effect of each rotating mass is represented by its equivalent weight. Equivalent weight is defined as the weight of that mass which, rotating at crank radius about the axis of the axle, produces the same centrifugal force as the mass represented. The equivalent weight is assumed to act radially through the center of gravity of the mass it replaces.

If their positions, directions, and magnitudes are taken into account, the various equivalent weights can be resolved and combined just as though they were forces. They of course represent forces which are proportional to their magnitudes and to the square of the speed of rotation of the wheel. To speak mathematically, they are vector quantities.

We now consider the processes by which, in each pair of wheels, the inertia effects of all rotating parts, including the counterbalances, are resolved into and represented by two pairs of equivalent weights. One pair acts in each wheel in the plane of rotation of the center of gravity of the counterbalance. In each of the counterbalance planes, one equivalent weight of the pair acts along the diameter through the crankpin, with the other weight of the pair acting at right angles to this diameter.

The main pair of wheels is taken as an example. Weights and positions of the rotating masses are assumed to be as given in the Appendix. Steps in the analysis are illustrated in Fig. 1. First, by the method of section 1 of the Appendix, all rotating parts in one wheel, except eccentric cranks and counterbalance, are replaced by a single equivalent weight of 2490 lb acting in a plane 71.3 in. from the central plane of the counterbalance in the opposite wheel. (See Fig. 1a.) The distance between the central counterbalance planes is 62 in. This resultant equivalent weight of 2490 lb must be resolved into two components, one in each counterbalance plane, as described in section 2 of the Appendix. When this is done for both wheels of the pair, each wheel has an equivalent weight of 2870 lb acting along the crank radius and an equivalent weight of 380 lb at right angles to the crank, as shown in Fig. 1b. The inertia effect of the eccentric cranks must now be similarly resolved into two equivalent weights in each counterbalance plane. The method of computation is described in section 3 of the Appendix. The result is shown in Fig. 1c, together with the component equivalent weights already found for the other rotating parts. In the left main wheel the inertia effect of the eccentric cranks is represented by two equivalent weights. One weight, of 156 lb, acts along the main crank radius. The other, of 17 lb, acts along the radius 90 deg ahead of the crank. In the right wheel the components for the eccentric

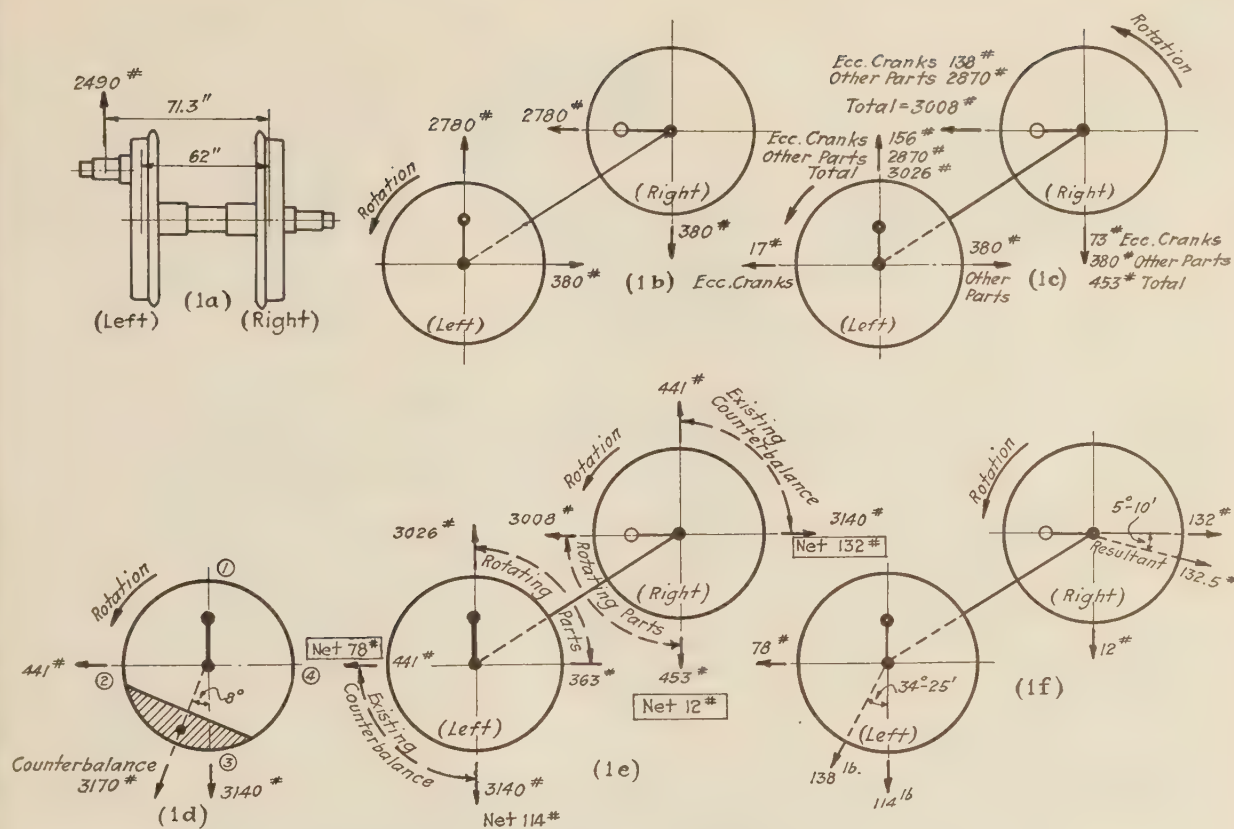


FIG. 1 ANALYSIS OF INERTIA EFFECTS IN MAIN WHEELS

(1a, equivalent weight representing all rotating parts in left main wheel except eccentric cranks and counterbalance. 1b, equivalent weight in counterbalance planes representing all rotating parts except eccentric cranks and counterbalances. 1c, equivalent weight representing eccentric cranks and all other rotating parts except counterbalances. 1d, equivalent weight and position of existing counterbalance and component equivalent weight representing counterbalance. 1e, component equivalent weights representing all rotating parts including counterbalances. 1f, component and resultant equivalent weights in counterbalance planes of main wheels representing combined effect of all rotating parts including counterbalances.)

cranks are 138 lb along the crank radius and 73 lb at 90 deg ahead of the crank. Owing to the position of the eccentric cranks, their effect is not symmetrical in the two wheels of the pair.²

Combining the components of eccentric cranks and other rotating parts, the result is set down as in Fig. 1c, and to this the inertia effect of the counterbalance as determined later is added. The locomotive under analysis had in each main wheel a counterbalance with an equivalent weight of 3170 lb, with its center of gravity set in each wheel 8 deg behind the crank diameter. (See Fig. 1d.) This can be resolved into two components at right angles to each other, as shown in Fig. 1e. The detailed method for this resolution of the counterbalance effect into two component equivalent weights is given in section 7 of the Appendix. These components are an equivalent weight of 3140 lb along the crank diameter opposite the main pin and another equivalent weight of 441 lb 90 deg behind the first.

It is now only a matter of simple subtraction to arrive at the final result of Fig. 1f. The unbalanced inertia effect of all rotating parts including eccentric cranks and counterbalance in the left counterbalance plane is represented by an equivalent weight of 114 lb along the crank diameter opposite the main pin and 78 lb at 90 deg back of this. In the right-hand counterbalance plane the unbalanced inertia effects are represented by an equivalent weight of 132 lb opposite the right-hand crankpin and

by another equivalent weight of 12 lb acting 90 deg back of this.

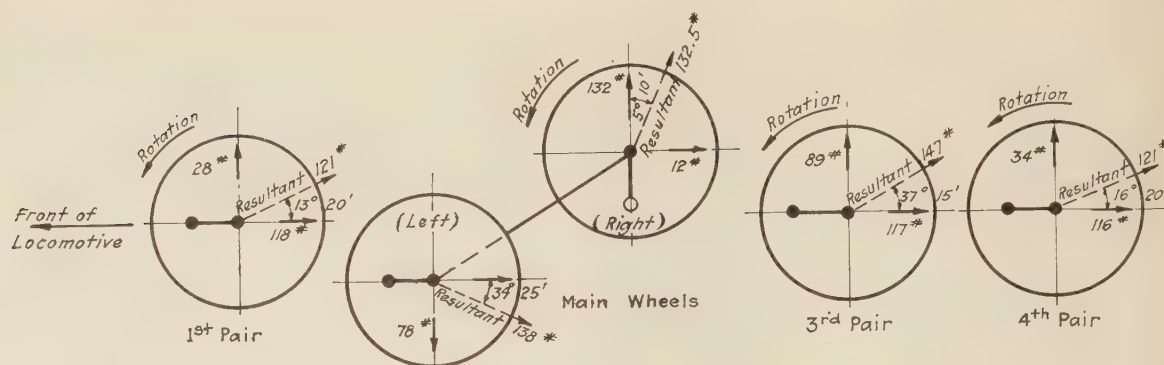
Fig. 1f gives a complete representation of the unbalanced inertia forces in the main wheels. All rotating parts, including eccentric cranks and counterbalances, are covered. In each counterbalance plane there are two component equivalent weights at right angles to each other. These can be combined into a single resultant as shown.

The main pair of wheels being disposed of, the other coupled wheels must be dealt with in the same way. It is convenient to use a blank form similar to Fig. 1 for setting down the various steps in the calculation, omitting details which pertain only to the main wheels. Details of the computations are not given here, but the final results for the four pairs of main and coupled wheels are shown in Fig. 2. Except in the case of the main pair of wheels, the right- and left-hand wheels on each axle have the same equivalent weights, and therefore only one wheel of each pair is shown. The lack of symmetry in the main wheels is due, as explained above, to the position of the eccentric cranks.

It is important to use a form similar to that of Fig. 2 for showing the results obtained, as this gives complete information regarding the unbalanced inertia forces in the simplest possible form. The information thus given puts the locomotive designer in a position to give critical consideration to the balance system which has been applied or which is proposed for application.

The balancing of the locomotive under consideration will now be reviewed. Two points are of major importance: the dynamic augment and the amount of balance provided for the reciprocating parts.

² The author is indebted to Mr. C. H. Bilty, mechanical engineer, Chicago, St. Paul & Pacific Railroad Company, for calling attention to the desirability of considering the eccentric cranks separately from the other revolving parts on the crankpin.



Line		1st Pair	Main Wheels		3rd Pair	4th Pair	
			Left	Right			
1	Resultant Equivalent Weight Producing Dynamic Augment	Lb	Lb	Lb	Lb	Lb	
		121	138	132.5	147	116	
2	Dynamic Augment at Diameter Speed	Per Wheel	5800	6630	7050	5800	
3		Per Axle	8200	6570	9950	8200	
4	Static Axle Load	66,500	70,500		66,500	66,500	
5	Maximum Combined Static and Dynamic Axle Load at Diameter Speed	74,700	77,070		76,450	74,700	Total Overbalance
6	Equivalent Weight Opposing Reciprocating Parts	118	114	132	117	116	465* Left 483* Right

FIG. 2 COMPONENT AND RESULTANT EQUIVALENT WEIGHTS REPRESENTING UNBALANCED INERTIA FORCES

The force producing dynamic augment in each wheel is proportional to the resultant equivalent weight shown for that wheel in Fig. 2. This force is computed from the resultant equivalent weight by the usual formula for centrifugal force:

$$F = 0.0000284 WRn^2$$

where

F = force in pounds

W = equivalent weight in pounds

R = crank radius in inches

n = revolutions per minute.

At diameter speed—that is, at a speed of as many miles per hour as the driving wheels have inches of diameter—the wheels make 336 revolutions per minute. At this speed the centrifugal force is:

$$F = 3.2 RW$$

For the locomotive under consideration, which has a crank radius of 15 in., this equation takes the form

$$F = 48 W$$

That is, the maximum dynamic augment in each wheel is 48 times the resultant equivalent weight in that wheel. Values corresponding to this are shown in line 2 of the tabulation in Fig. 2 for all of the wheels. The values here are the maximum values of the force which alternately increases and decreases the wheel load on the rail during each revolution. The maximum increase, or maximum dynamic augment, occurs in that position of the wheel in which the resultant equivalent weight is directed vertically downward. It is evident that the maximum values for right- and left-hand wheels on one axle do not occur at the same time. Consequently, the maximum increase in axle load is not the sum

of the maximum increases in the two wheels. Section 5 of the Appendix gives a method for determining the maximum axle load and the corresponding position of the wheels when the resultant equivalent weights in the two wheels are different and are set at any angle. If the resultant equivalent weights are the same in both wheels of a pair and act at 90 deg apart, the maximum axle load occurs when the resultants in both wheels are directed downward at an angle of 45 deg from the vertical. The maximum dynamic augment for the axle is then 1.414 times the maximum for each wheel. In the locomotive under consideration, this is the case for all of the coupled wheels except the main pair.

In the main pair of wheels, the planes through the resultant weights and the axis of the axle stand at an angle of 119 deg 15 min, and the resultants have the values of 138 lb in the left and 132.5 lb in the right wheel. By applying the method of section 5 of the Appendix, it is found that the equivalent weight producing the maximum axle load is 137 lb. This does not differ greatly from the individual resultants in the wheels.

It should be noted that the relation between maximum axle load and maximum wheel load depends on the angle between the wheel resultants. The extreme cases are, (1) with zero angle between the resultants the increase in axle load is twice the wheel load, and (2) with 180 deg between the resultants the increase in axle load is zero.

If the angle between the resultants is large, so that the increase in axle load is small, it will probably be desirable to consider the increase in wheel load as the limiting factor rather than the increase in axle load. The axle load measures the influence of the locomotive on a track unit such as a bridge, while the wheel load determines the influence on an individual rail.

Returning to a consideration of Fig. 2: Line 3 shows the maximum dynamic augment per axle at diameter speed and line 4 shows the static axle load. Line 5, the sum of the two preceding lines, gives the maximum combined static and dynamic axle load at diameter speed. As mentioned above, it was intended when designing the locomotive that this combined axle load should not exceed 75,000 lb. This limit is observed in the front- and back-wheel pairs, but is slightly exceeded in the main and third pairs of wheels. If an analysis had been made in this form before the locomotive had been built, it would have been a simple matter to determine the weight and position of counterbalances which would keep to the desired axle load.

The general method is described in section 6 of the Appendix. In the main axle, the maximum dynamic augment permissible is 75,000 - 70,500 = 4500 lb. This corresponds to an equivalent weight of 94 lb on the axle. If the resultants in the wheels are equal and act at 90 deg apart, the value of each will be 66.3 lb.* Assume then that each of the main wheels is to be balanced so that the resultant producing dynamic augment in the wheel is 66 lb. It is desirable to eliminate any parasitic effect and to have the full weight of this resultant acting opposite the crankpin so as to be available for balance of the reciprocating parts.

In the left main wheel, the rotating parts are represented as shown in Fig. 3a by equivalent weights of 3026 lb along the crank diameter and 363 lb acting 90 deg back of this. To produce the desired balance, the components of the counterbalance must be 363 lb opposing the same weight at right angles to the crank, and

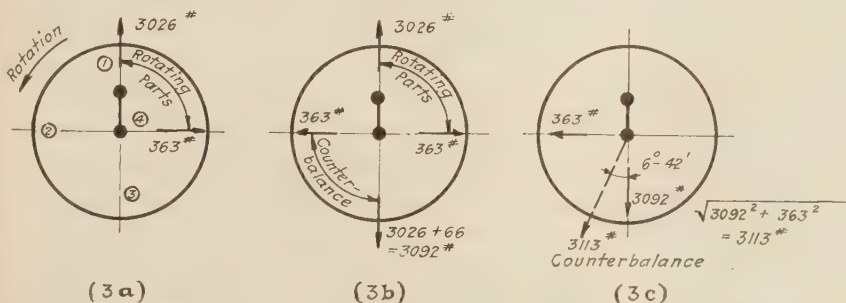


FIG. 3 DETERMINATION OF COUNTERBALANCE TO GIVE COMPLETE CROSS-BALANCE AND DESIRED OVERBALANCE OF 66 LB

(3a, equivalent weights representing rotating parts to be balanced in left main wheel. 3b, component equivalent weights representing rotating parts and desired counterbalance. 3c, components and resultant equivalent weight giving counterbalance desired.)

3026 + 66 = 3092 lb opposite the pin, as shown in Fig. 3b. These components, when combined as in Fig. 3c, show that the counterbalance itself must have an equivalent weight of 3113 lb, with its center of gravity set 6 deg 42 min back of the crank diameter. Comparing this with the counterbalance as applied, it is seen that by reducing the equivalent weight from 3140 lb to

* $66.3 \times 1.414 = 94$.

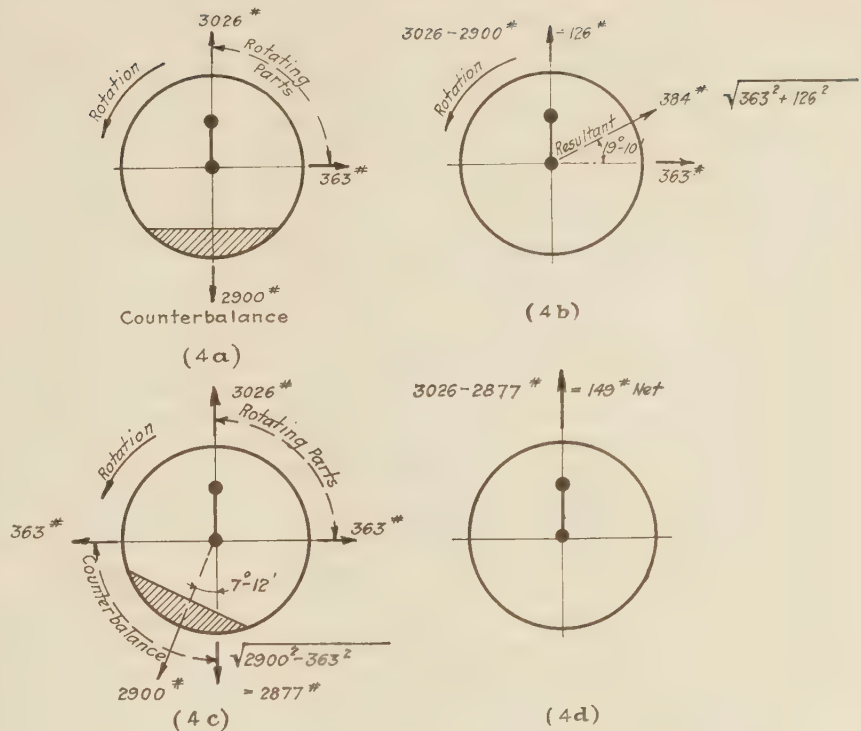


FIG. 4 INCORRECT AND CORRECT POSITIONS FOR INSUFFICIENT COUNTERBALANCE

(4a, component equivalent weights with insufficient counterbalance placed opposite crankpin. 4b, component and resultant equivalent weights representing unbalanced inertia forces of arrangement 4c. 4c, position of insufficient counterbalance to give least possible unbalanced inertia force. 4d, net equivalent weight representing unbalanced inertia force resulting from arrangement 4c.)

3113 lb and changing the angle from 8 deg to 6 deg 42 min, the unbalanced resultant equivalent weight is reduced from 138 to 66 lb, with a reduction of 3350 lb in the dynamic augment of the wheel at diameter speed.

This illustration shows that when the present method is used to resolve the inertia effects into two equivalent weights in each wheel, it is a simple matter to determine the balance required to meet any desired conditions.

By applying the same method to the right-hand main wheel, it is found that for complete balance, except for an overbalance of 66 lb opposite the pin, the counterbalance must have an equivalent weight of 3107 lb set 8 deg 23 min off the diameter. The difference between the counterbalance found for the right- and left-hand main wheels is not large. It is desirable for practical reasons of manufacture to make both wheels the same. A satisfactory balance can be obtained by giving the actual counterbalance in both wheels an equivalent weight of 3110 lb set at an angle of 7 deg 30

min off the diameter. This weight and angle are obtained by averaging the values found as above for the right- and left-hand wheels. With this counterbalance the left wheel will have an overbalance of 56 lb and a resultant of 71 lb, while the right wheel will have an overbalance of 74 lb and a resultant of 87 lb. The left wheel is slightly underbalanced and the right wheel slightly overbalanced, but the difference is not serious.

In addition to the main pair of wheels, it will be seen from Fig. 2 that the third pair also exceeds the proposed limit of 75,000 lb for combined static and dynamic load. The dynamic augment exceeds the estimated figure by 1450 lb, because the wheels were not cross-balanced. Cross-balancing would have involved changing the equivalent weight of the counterbalance from 1130 to 1133 lb and moving its center of gravity 4 deg 30 min away from the crank diameter. This would eliminate the parasitic effect of 89 lb, leaving the overbalance the same, 117 lb, and reducing the resultant producing dynamic augment from 147 to 117 lb. This reduction of 20 per cent in the dynamic augment is well worth considering if the locomotive is being built to a closely restricted weight.

In the fourth pair of wheels, the desired overbalance opposite the crankpin is 116 lb. The parasitic effect which could be eliminated by cross-balancing is 34 lb. These produce a resultant of 121 lb. Cross-balancing by eliminating the parasitic 34 lb would reduce the equivalent weight, producing dynamic augment from 121 to 116 lb—that is, by only 4.1 per cent. The reduction is hardly enough to be worth while.

As a general rule, it may be noted that unless the parasitic effect to be eliminated by cross-balancing amounts to more than 30 per cent of the overbalance the reduction in the resultant produced by cross-balancing will not be more than 4.5 per cent, and therefore hardly justifies the additional complication.

Before leaving the balance of rotating parts, consideration must be given to the desirability of cross-balancing when the wheel centers are too small to allow the full amount of balance to be applied. Assume that in a main wheel the component equivalent weights representing the rotating parts are as found for the left main wheel of the locomotive already examined—that is, 3026 lb along the crank radius and 363 lb at right angles to this. Assume also that the wheel design limits the equivalent weight of the counterbalance to 2900 lb. If this is put exactly opposite the pin, as in Fig. 4a, it is obvious that the unbalanced components will be as in Fig. 4b, 126 lb along the crank and 363 lb at 90 deg, giving an unbalanced component of 384 lb, producing dynamic augment. This can be reduced materially by shifting the equivalent weight of 2900 lb 7 deg 12 min off the crank diameter. As shown in Fig. 4c, this gives components of 2877 lb opposite the pin and 363 lb at right angles to this. The position is chosen so that the component at right angles to the crank diameter is just equal and opposite to the component of the rotating parts acting at right angles to the crank. The simple calculation required to determine the other component is obvious from Fig. 4c. The components being 363 and 2877 lb, the tangent of the angle at which the counterbalance must be set is $363/2877 = 0.1265$, which is the tangent of 7 deg 12 min. Combination of the four components in Fig. 4c shows that the net unbalanced equivalent weight is 149 lb, as in Fig. 4d, instead of 384 lb when the counterbalance was directly opposite the pin, as in Fig. 4a. This large reduction in the unbalanced force producing dynamic augment makes cross-balancing well worth while, even though full balancing is not possible.

Consideration must now be given to the overbalance provided for the reciprocating parts. Fig. 2 shows that the overbalance amounts to 465 lb on the left-hand and 483 lb on the right-hand side. The locomotive under consideration had reciprocating parts weighing 2241 lb on each side of the engine. Approximately 80 per cent of the weight of the reciprocating parts is unbalanced. This is very much more than the 50 per cent set up by the American Railway Association as recommended practise. In spite of this, the locomotive rides satisfactorily.

The fact is that the A.R.A. practise needs further consideration. In the first place, there is no logical reason for specifying the overbalance as a percentage of the weight of the reciprocating parts.

The proper course is to consider the unbalanced weight in comparison with the total weight of the locomotive. The unbalanced portion of the reciprocating parts tends to shake the locomotive. This shaking is resisted by the inertia of the locomotive as a whole. Consequently, the stability of the locomotive is determined by the relation of the mass of the whole locomotive to the mass of the unbalanced parts. This principle was stated by George R. Henderson over twenty-five years ago, but has not received the recognition it deserved.

Henderson suggested that one-four hundredth of the weight of the locomotive might remain unbalanced on each side. That would be 2.50 lb unbalanced per 1000 lb of locomotive weight. The 4-8-4 type locomotive analyzed has 4.2 lb unbalanced per 1000 lb. Other locomotives analyzed in the same way show unbalanced weights of 5.4 lb per 1000 for a 2-8-4 type and 3.8 lb per 1000 for a 4-6-4 type. All are reported to ride satisfactorily.

The conclusion to be drawn is that if the rotating parts are properly balanced, it is only necessary to balance a comparatively small portion of the reciprocating parts.

Further study of results obtained in practise is desirable, but if the reports of such results are to have any value they must be based on an accurate analysis of the balance similar to that which has been described.

To complete this examination of the inertia forces it is necessary to take into account the fact that the inertia forces of the reciprocating parts act in the vertical plane through the center of the main rod, while the inertia force of the overbalance acts in the central plane of the counterbalance. This difference in plane can usually be neglected. Its effect is to tend to turn the locomotive about a vertical axis. This tendency will have no perceptible effect on a long modern locomotive. In adjusting the overbalance to offset the inertia forces of the reciprocating parts, it is only necessary to consider the longitudinal forces. The couple about the vertical axis due to the difference between the planes of action can be neglected. Cross-balance is therefore not necessary for the overbalance for the reciprocating parts.

In conclusion, the author repeats what he has said before in addressing the Society. It is important for railroad engineers to adopt an accurate method for analyzing the balance of a locomotive. It is also highly important that the results which are obtained by the analysis be stated in a simple manner free from involved mathematics. If this is done, the advantages of proper balancing methods will be self-evident and improvements will follow.

Appendix

Locomotive Counterbalancing

SCHEDULE OF DATA AND COMPUTATIONS FOR DETERMINING THE PROPER COUNTERBALANCE FOR LOCOMOTIVE DRIVING WHEELS

THE principles of the method and the results to be obtained are discussed in the body of the paper. This schedule is drawn up to present the detailed methods of computation to be followed in order to secure the results desired.

Values corresponding to an actual locomotive are inserted for each item, and the schedule is arranged so that if it is rewritten with blank spaces for the values, it can be used as a work sheet for computing any other example.

The notes at the end of each section define any special terms used and provide any necessary discussion of the methods.

The data as to weights and dimensions called for by the schedule must of course be obtained from the design of the locomotive.

SECTION 1—TO FIND THE EQUIVALENT WEIGHT AND PLANE OF ACTION OF THE ROTATING PARTS IN EACH WHEEL

The schedule given here is drawn to cover the main pair of driving wheels. It should be applied successively to each of the other pairs of drivers, dropping out the items which do not apply. This section of the schedule is illustrated by Figs. 5 and 6.

1. E = distance in inches between central planes of right- and left-hand counterbalances.....62 in.
2. W_1 = equivalent weight in pounds of crankpin hub, together with part of pin encircled by hub⁴.....500 lb
3. A = distance in inches between centers of gravity of right- and left-hand crankpin hubs.....71 in.
4. M_1 = moment of crankpin hub parts about center plane of opposite counterbalance
 $M_1 = W_1 \times (A + E)/2 = 33,200$ in-lb

5. W_2 = equivalent weight in pounds of side rod carried on crankpin,⁴ together with weight of part of crankpin encircled by side-rod bearing.....550 lb
6. B = distance in inches between center planes of side rods.....77 in.
7. M_2 = moment of side-rod parts about center plane of opposite balance
 $M_2 = W_2 \times (B + E)/2 = 38,200$ in-lb

8. W_3 = equivalent weight in pounds of back end of main rod,⁴ together with weight of part of crankpin encircled by main-rod bearing.....1440 lb
9. C = distance in inches between center planes of main rods.....85 in.
10. M_3 = moment of main-rod parts about center plane of opposite counterbalance
 $M_3 = W_3 \times (C + E)/2 = 106,000$ in-lb

11. W_t = sum of all rotating equivalent weights, except those for eccentric cranks
 W_t = items (2 + 5 + 8)
 $= W_1 + W_2 + W_3 = 2490$ lb

12. M_t = sum of all moments of rotating parts, except eccentric cranks, about center plane of opposite counterbalance
 M_t = items (4 + 7 + 10)
 $= M_1 + M_2 + M_3 = 177,400$ in-lb

13. F = distance in inches between center of gravity of all rotating parts, except eccentric cranks, and center plane of opposite counterbalance
 F = item 12/item 11
 $= M_t / W_t = 71.3$ in.

Notes on Section 1:

Item 2. To find the equivalent weight of the crankpin hub, together with the part of the pin encircled by the hub, it is necessary to find the actual weight of these parts and their center of gravity. The weight to be taken into account is that of the cross-hatched area in Fig. 6 which lies outside the circumference of the axle hub. Then if:

- W = actual weight of these parts in pounds
 R_1 = distance in inches of their center of gravity from longitudinal axis of axle
 R = radius of rotation of crankpin in inches
 W_1 = equivalent weight of these parts

$$W_1 = W \times R_1 / R$$

"Equivalent weight" of any part rotating about the longitudinal center line of the axle is defined as the weight of that mass which rotating at the crank radius would produce the same inertia force as the actual mass under consideration. The above example shows how the equivalent weight is found when its actual weight and the radius of rotation of its center of gravity are known.

Item 5. The equivalent weight of the side rod carried on the

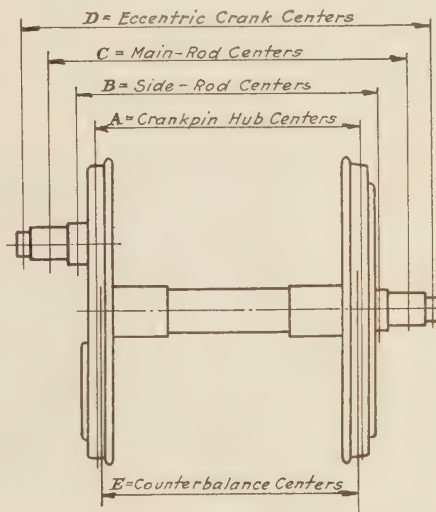


FIG. 5 DATA FOR COMPUTATION OF EFFECT OF ROTATING PARTS

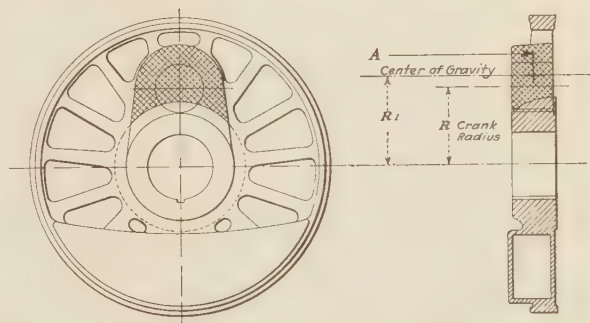


FIG. 6 PORTION OF CRANKPIN HUB SHOWN CROSS-HATCHED TO BE TAKEN INTO ACCOUNT AS ITEM 2, SECTION 1, APPENDIX

crankpin is the actual weight supported by the pin. For the front and back drivers this is the weight of one end of one side rod. For the main and intermediate drivers it is the weight of one end of each of two rods. As the center of gravity of the side-rod end rotates with the same radius as the center of the crankpin, the equivalent weight of these parts is the same as their actual weight.

Item 8. The equivalent weight of the back end of the main rod to be used in this item can be taken as approximately six-tenths of the total weight of the main rod. If strict accuracy is required, the weight to be used can be found from the equation:

$$W_{m2} = W_m \times k^2 / l^2$$

where

- W_m = total weight of main rod in pounds
 l = length of rod in inches between wristpin and main-pin centers

⁴ See Notes on Section 1.

k = radius of gyration in inches of the main rod about the wristpin center

W_{m2} = weight of main rod to be considered as rotating at the crankpin.

The radius of gyration k can be found by suspending the main rod to swing as a pendulum about the wristpin center. Then if

14. W_1 = component of left-hand rotating parts acting in center plane of left counterbalance

$$W_1 = W_i \times F/E = 2870 \text{ lb}$$

15. W_r = component of left-hand rotating parts acting in center plane of right counterbalance

$$W_r = W_1 - W_i = 380 \text{ lb}$$

SECTION 3—TO DETERMINE THE INERTIA EFFECT OF THE ECCENTRIC CRANKS

Fig. 7* shows the relative positions of the eccentric cranks. The center of gravity of each crank does not lie on the main crank radius. The crank cannot, therefore, be accurately represented by a single equivalent weight acting along the main crank radius. Each crank must be represented by two equivalent weights acting, one along the crank radius, the other along a radius 90 deg ahead of this. This is illustrated by the isometric diagram in Fig. 8. In this, each eccentric crank is represented by two equivalent weights in the plane of rotation of the center of gravity of the eccentric crank. These four equivalent weights must be replaced by four others, two acting in each counterbalance plane. These are computed as follows:

16. W_e = actual weight in pounds of one eccentric crank, together with weight of part of crank pin encircled by eccentric crank... 172 lb

17. b = length in inches of intercept of center of gravity of eccentric crank on crank radius (see Fig. 7). 10.4 in.

18. a = length in inches of intercept of center of gravity of eccentric crank on radius 90 deg ahead of crank. 3.15 in.

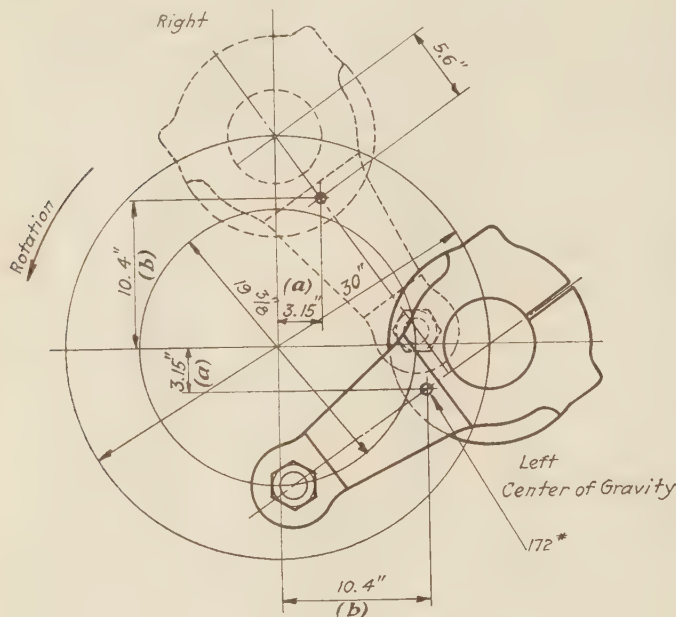


FIG. 7 POSITION OF ECCENTRIC CRANKS

x_0 = distance in inches of the center of gravity of the rod from the wristpin center, and

t = time of one swing in seconds

$$k^2 = 3.26 t^2 x_0$$

If the radius of gyration k cannot be found experimentally, and if the main rod is of normal design, a reasonably close approximation can be obtained by assuming a value of 0.6 for k^2/l^2 . The equivalent weight of the back end of the main rod is then six-tenths of the total weight.

$$W_{m2} = 0.6 \times W_m$$

SECTION 2—TO RESOLVE THE EQUIVALENT WEIGHT OF THE ROTATING PARTS ON ONE SIDE OF A PAIR OF WHEELS INTO TWO COMPONENTS, ONE IN THE WHEEL CARRYING THE ROTATING PARTS AND THE OTHER IN THE OPPOSITE WHEEL OF THE PAIR

This section is illustrated by Fig. 1 (a) and (b). Items which were taken from section 1 are given the same number here.

11. W_i = total equivalent weight of rotating parts (section 1), 2490 lb

13. F = distance in inches from center of gravity of rotating parts to center plane of opposite counterbalance (section 1) 71.3 in.

1. E = distance between center planes of counterbalances (section 1) 62.0 in.

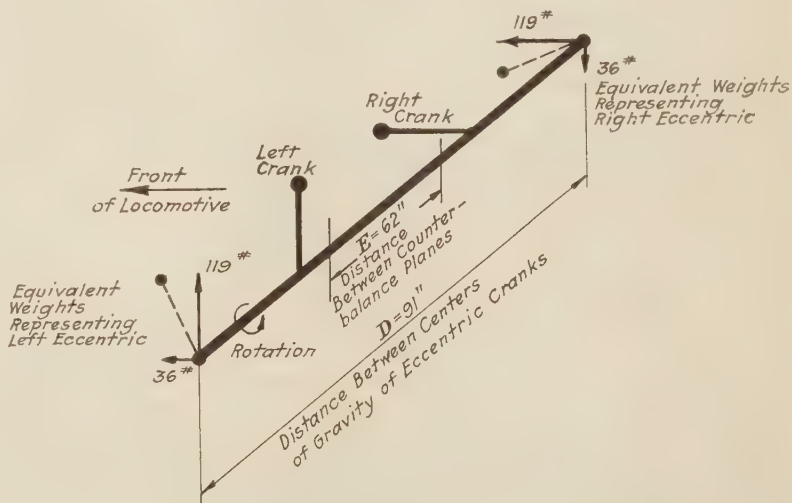


FIG. 8 ISOMETRIC DIAGRAM ILLUSTRATING REPLACEMENT OF EACH ECCENTRIC CRANK BY TWO EQUIVALENT WEIGHTS ACTING IN THE PLANE OF ROTATION OF THE CRANK

19. D = distance in inches between centers of gravity of eccentric cranks (Fig. 8) 91 in.

1. E = distance in inches between the center planes of counterbalances. 62 in.

R = crank radius in inches. 15 in.

From these data are computed the component equivalent

* The cranks are shown trailing. In Fig. 8 and the text, however, they are assumed to be leading the crank pins.

weights which, acting in the planes' left- and right-hand counter-balances, represent completely the inertia effects of the eccentric cranks.

In Left-Hand Counterbalance Plane:

20. L_{eb} = component equivalent weight acting along crank radius
$$= \frac{W}{2RE} [b(D + E) + a(D - E)] = 156 \text{ lb}$$
21. L_{ea} = component equivalent weight acting along radius 90 deg ahead of crank
$$= \frac{W}{2RE} [a(D + E) - b(D - E)] = 17 \text{ lb}$$

In Right-Hand Counterbalance Plane:

22. R_{eb} = component equivalent weight acting along crank radius

$$= \frac{W}{2RE} [b(D + E) - a(D - E)] = 138 \text{ lb}$$
23. R_{ea} = component equivalent weight acting along radius 90 deg ahead of crank

$$= \frac{W}{2RE} [a(D + E) + b(D - E)] = 73 \text{ lb}$$

Note: The equivalent weights are not the same in the two counterbalance planes, although the resultant is the same in both planes. The reason for the lack of symmetry can be seen in Fig. 8. In the horizontal plane through the main axle the 36-lb component of the left eccentric and the 119-lb component of the right eccentric both act in the forward direction. In the vertical plane, on the other hand, the 119-lb component of the left eccentric acts upward, while the 36-lb component of the right eccentric acts downward.

SECTION 4—TO COMBINE INERTIA EFFECT OF ECCENTRIC CRANKS AND OTHER ROTATING PARTS

In sections 2 and 3 the inertia effect of the other rotating parts and of the eccentric cranks have been resolved into equivalent weights acting in the center planes of the two counterbalances. The net effect of all the rotating parts is found by adding the values found in the two preceding sections. The operation is illustrated by Fig. 9. The quarters of each wheel are numbered for convenience of reference.

*In Left-Hand Counterbalance Plane,
Diameter Through Left Crankpin:*

- | | | |
|-----|--|---------|
| 14. | W_1 = equivalent weight representing other rotating parts at quarter (1) | 2870 lb |
| 20. | L_{eb} = equivalent weight representing eccentric cranks at quarter (1) | 156 lb |
| 24. | W_1' = net equivalent weight at quarter (1) | 3026 lb |

Diameter Perpendicular to Left Crank:

- | | | |
|-----|--|--------|
| 15. | W_r = equivalent weight representing other rotating parts at quarter (4) | 380 lb |
| 21. | L_{ea} = equivalent weight representing eccentric cranks at quarter (2) | 17 lb |
| 25. | W_4' = net equivalent weight at quarter (4) | 363 lb |

In Right-Hand Counterbalance Plane, Diameter Through Right Crankpin:

- | | | | |
|-----|----------|--|---------|
| 14. | W_1 | = equivalent weight representing other rotating parts at quarter (2) | 2870 lb |
| 22. | R_{eb} | = equivalent weight representing eccentric cranks at quarter (2) | 138 lb |
| 26. | W'' | = net equivalent weight at quarter (2) | 3008 lb |

Diameter Perpendicular to Right Crank:

- | | | |
|-----|--|--------|
| 15. | W_r = equivalent weight representing other rotating parts at quarter (3) | 380 lb |
| 23. | R_{ea} = equivalent weight representing eccentric cranks at quarter (3) | 73 lb |
| 27. | W_s'' = net equivalent weight at quarter (3) | 453 lb |

Fig. 9 illustrates these operations. The figures are the same as in Fig. 1 (c). Items 24, 25, 26, and 27 give the four equivalent weights which, acting two in each counterbalance plane, completely represent the inertia effect of all rotating parts,

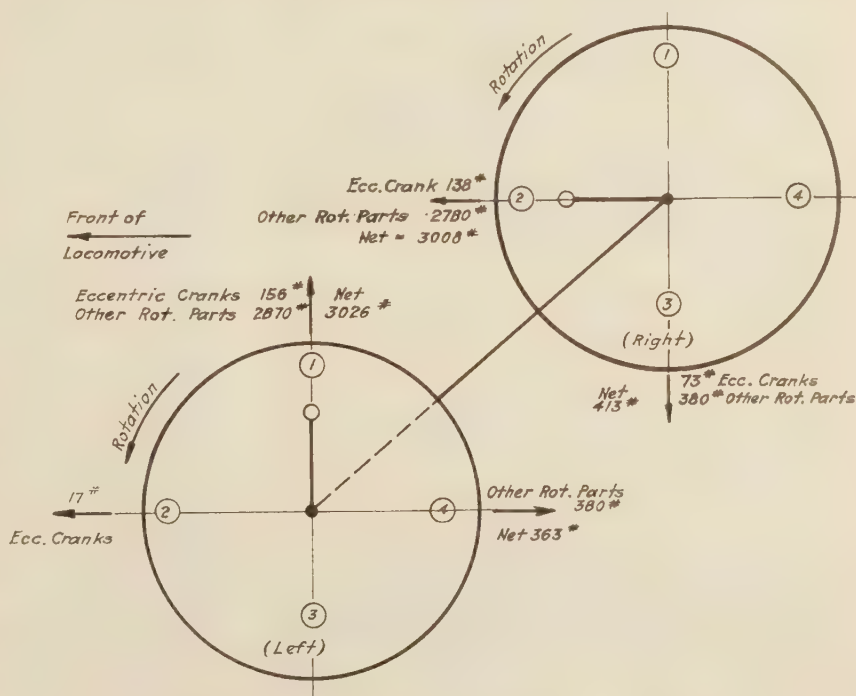


FIG. 9 EQUIVALENT WEIGHTS ACTING IN CENTER PLANES OF COUNTERBALANCES REPRESENTING ECCENTRIC CRANKS AND OTHER ROTATING PARTS

including the eccentric cranks. Having these, it is a simple matter to complete the analysis of the wheels by adding the effect of the counterbalance as in Fig. 1 (*f*). The net equivalent weights representing counterbalances and all rotating parts are shown in Fig. 1 (*g*). Details of the operation are given in section 7.

SECTION 5—TO FIND THE POSITION AND VALUE OF THE MAXIMUM DYNAMIC AXLE LOAD WHEN THE RESULTANT EQUIVALENT WEIGHTS PRODUCING DYNAMIC AUGMENT IN THE WHEELS ARE NOT THE SAME

This section is illustrated by Fig. 10.

28. W_l = resultant equivalent weight in pounds producing dynamic augment in left-hand wheel..... 138 lb
 29. W_r = resultant equivalent weight in pounds producing dynamic augment in right-hand wheel..... 132.5 lb
 30. Z = angle in degrees between planes in which the above equivalent weights act..... 119 deg 15 min

In the position of maximum axle dynamic augment, assume

31. X = angle in degrees between direction of left-hand resultant and the vertical
 then $Z - X$ = angle in degrees between the direction of right-hand resultant and the vertical

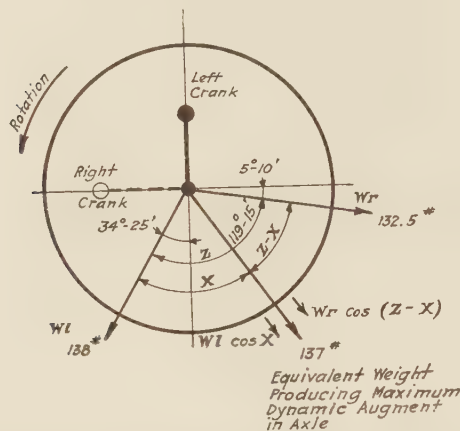


FIG. 10 COMPUTATION OF MAXIMUM DYNAMIC AUGMENT IN AXLE
 (When equivalent weight producing maximum dynamic augment in wheels have values W_l and W_r and stand at an angle of Z from each other.)

It follows that

$W_l \cos X$ = vertical component contributed by left-hand resultant

$W_r \cos (Z - X)$ = vertical component contributed by right-hand resultant

Then $W_l \cos X + W_r \cos (Z - X)$ is the total equivalent weight producing the maximum dynamic augment in the axle.

This has its maximum value when

$$\tan X = \frac{\sin Z}{W_l/W_r + \cos Z}$$

With the values given above for W_l , W_r , and Z , the value of X is found to be 57 deg 40 min. Then the total equivalent weight producing the maximum dynamic augment in the axle:

$$\begin{aligned} W_l \cos X + W_r \cos (Z - X) &= 138 \times 0.535 + 132.5 \times 0.476 \\ &= 74 + 63 \\ &= 137 \text{ lb} \end{aligned}$$

SECTION 6—DETERMINATION OF EQUIVALENT WEIGHT AND POSITION OF COUNTERBALANCE TO BALANCE EXACTLY THE ROTATING PARTS AND PROVIDE A GIVEN OVERBALANCE FOR THE RECIPROCATING PARTS

This section is illustrated by Fig. 3. A blank diagram similar to Fig. 3 should be used, and the values should be filled in as described. In the following description the diagram is assumed

to represent the left-hand wheel of the pair and the quarters are numbered 1, 2, 3, and 4, quarter No. 1 being that of the left-hand crankpin.

24. W_1' = component of rotating parts acting in plane of left counterbalance at quarter (1); see section 4. .3026 lb
 25. W_4' = component of rotating parts acting in plane of left-hand counterbalance at quarter (4); see section 4363 lb
 32. W_0 = equivalent weight of overbalance to be added to oppose the reciprocating parts.....66 lb
 The value to be given this item may be chosen arbitrarily. The better plan is to determine it to hold the dynamic augment to a definite limiting value.
 33. W_{c3} = component of counterbalance to act in quarter (3), opposite the crankpin:
 Item 29 = Item 24 + Item 32 = 3092 lb
 34. W_{c2} = component of counterbalance to act in quarter (2):

$$W_{c2} = W_r' = 363 \text{ lb}$$

35. W_c = resultant equivalent weight of counterbalance to produce the components shown in quarters 3 and 4 in Fig. 8 (a):

$$W_c = \sqrt{W_{c3}^2 + W_{c2}^2} = 3113 \text{ lb}$$

36. α = angle which radius through center of gravity of counterbalance makes with the diameter through quarters 1 and 3:

$$\begin{aligned} \tan \alpha &= W_{c2}/W_{c3} = 363/3092 \\ &= 0.1275 \\ \alpha &= 6 \text{ deg } 42 \text{ min} \end{aligned}$$

The equivalent weight and position of the counterbalance thus determined are shown in Fig. 3 (c).

Note: In designing the actual counterbalance to have this equivalent weight proper allowance must be made for the equivalent weight of the spokes and rim adjacent to the crankpin hub which occupy the space corresponding to the space covered by the counterbalance in the opposite quarter of the wheel.

The counterbalance determined by Items 35 and 36 will exactly cross-balance the reciprocating parts, and the only unbalanced mass producing dynamic augment will be the overbalance of equivalent weight W_0 acting in quarter (3) directly opposite the crankpin.

It may be noted that it is important to cross-balance when the value of W_r , the component due to the rotating parts of the opposite wheel, is large compared with W_0 , the overbalance.

If W_r does not exceed one-quarter of W_0 , it is unnecessary to cross-balance. If $W_r = 0.25 W_0$, a counterbalance of equivalent weight $W_{c4} = W_l - W_0$ can be placed directly opposite the pin at quarter (3) and the dynamic augment will not exceed that of the cross-balanced wheel by more than 3 per cent. This is practically negligible.

SECTION 7—ANALYSIS OF A GIVEN COUNTERBALANCE TO DETERMINE THE OVERBALANCE AND DYNAMIC AUGMENT

This section is illustrated by Fig. 1 (d) and (e).

37. W_c = equivalent weight of counterbalance in pounds3170 lb
 38. β = angle made by radius through center of gravity of counterbalance with diameter through quarters (3) and (1) Fig. 1 (c).....8 deg
 39. W_{c3} = component of counterbalance acting at quarter (3)
 $W_{c3} = \cos \beta \times W_c = 3140 \text{ lb}$
 40. W_{c2} = component of counterbalance acting at quarter (2)
 $W_{c2} = \sin \beta \times W_c = 441 \text{ lb}$

Discussion

A. I. LIPETZ.⁵ I quite agree with the author that "it is not easy to see why American civil and mechanical railway engineers have neglected for so long the proper balancing of locomotives," especially in view of the fact that "in Europe correct balancing of locomotives has been common practise." This situation has been always a puzzle to me, because at least one American engineer contributed a great deal to the question of counterbalancing in the early days of locomotive construction. Thomas Rogers, founder of the Rogers Locomotive Works, patented as early as 1837 the application of counterbalance opposite the crank with sufficient weight to counterbalance the crank and connecting rods, thus introducing counterbalancing of revolving parts.

Up to 1845 it was customary to balance only revolving weights, and the balancing of reciprocating weights was not recognized until later, when some European engineers started investigations of the problem of balancing. The disturbances caused by the unbalanced inertia forces first became apparent when Nollau⁶ in Germany made tests with a locomotive suspended by chains from a roof, although previously to that W. Fernihough in England, in October, 1845, suggested and apparently tried⁷ the use of weights for counterbalancing main rods, pistons, and other reciprocating parts.

Le Chatelier in France, in 1848, made tests similar to Nollau's and enunciated a very complete theory of balancing which is now known as cross-balancing. He published his theory in 1849,⁸ and shortly afterward his theory was further developed by various investigators, mostly French.⁹ Later the correct method of cross-balancing was popularized for the English-reading public by Daniel Kinnear Clark in his classic work book "Railway Machinery,"¹⁰ published simultaneously in Glasgow, Edinburgh, London, and New York.

Since then, all textbooks appearing in French,¹⁰ German,¹¹ Russian,¹² Hungarian,¹³ Japanese,¹⁴ and other languages made use of the Le Chatelier-Clark method as the only correct way of balancing locomotives. Locomotive builders all over the world, except the United States, adopted this method of counterbalancing. Some American books¹⁵ also expounded the cross-balancing theory, although they did not recommend it for practical use, and in England Professor Dalby, in his well-known book, "The Balancing of Engines," developed very con-

venient graphical methods of cross-balancing. Incidentally the tables given in his book are almost identical with the schedule given in the Appendix to Mr. Fry's paper.¹⁶

I have been looking for a long time for an explanation of the fact that cross-balancing of locomotives was not common practise in the United States. On the basis of the theory that nothing in engineering, like in nature, can exist for a long period of time without a justifiable reason, I tried to reach some explanation in my discussion of Dr. R. Eksergian's paper "The Balancing and Dynamic Rail Pressure."¹⁷ To a great extent such a condition was probably due to the attitude of the American Railway Association, Mechanical Division, which followed for many years certain rules of what is called "static balancing" and did not recommend cross-balancing until 1931.¹⁸ Locomotive builders nevertheless, were applying the cross-balancing method to locomotives, when specified, as it is evidenced by applying the correct method in locomotives built for use abroad, like France in 1908, Russia during the war, and Japan after the war, and some isolated cases for different experimental locomotives, in the United States since 1905.

Cases are known when American railroads recently converted statically balanced high-speed passenger locomotives into cross-balanced. That the question of cross-balancing is attracting attention now more than before is probably due to the increase in speed of our present-day locomotives, both passenger and freight, the limitations of weight, and the necessity of refinements. I should therefore say that Mr. Fry's paper is very timely, notwithstanding the fact that a long time has elapsed since the correct method of balancing was made known to the world by Le Chatelier.

In my opinion, of all the questions of locomotive engineering, counterbalancing is probably the only complete, well-founded, and clear-cut exposition of a theory which permits the establishing of indisputable formulas and laws. Even in its general algebraic form it is very simple and does not call for "simplifications." The whole theory of counterbalancing can be represented by the following five formulas:

$$W_{cs} = \Sigma W \frac{D+E}{2E} + k W_{rc} \frac{C+E}{2E} \dots\dots\dots [1]$$

$$W_{c2} = W_{cs} - \Sigma W - k W_{rc} \dots\dots\dots [2]$$

$$W_o = \sqrt{W_{cs}^2 + W_{c2}^2} \dots\dots\dots [3]$$

$$\tan \alpha = \frac{W_{c2}}{W_{cs}} \dots\dots\dots [4]$$

$$K = \Sigma k \dots\dots\dots [5]$$

The designations are mostly those used by the author. Symbol Σ stands for the sum of products given by him in Appendix; W are the various weights W_1, W_2, W_3, W_4 of revolving parts, and D stands for the corresponding distances A, B, C, D of the Appendix. Coefficient k is the percentage of balancing of reciprocating weights in the particular wheel, K is the total percentage of balancing of reciprocating weights of the locomotive. W_{rc} is the value of these weights on one side. Other symbols are the same as used by Mr. Fry.

The author is actually following these formulas. Although he asserts that the analysis which he made is stated in a simple, non-mathematical manner, it is hardly so. Arithmetic is also part of mathematics, and the author's arithmetic in the Appendix

¹⁶ "The Balancing of Engines," by W. E. Dalby, London, 1907, p. 82.

¹⁷ A.S.M.E. Trans., 1929, paper no. RR-51-5.

¹⁸ Proc. Am. Ry. Assn., Division V, Mechanical, 1930, pp. 805-828, and 1931, p. 99.

⁵ Consulting Engineer, American Locomotive Co., Schenectady, N. Y., and Non-Resident Professor of Locomotive Engineering, Purdue University, Lafayette, Ind. Mem. A.S.M.E.

⁶ *Journal des Chemins de Fer Allemands*, October, 1848.

⁷ Report of the Gage Commissioners, 1846.

⁸ *Etudes sur la Stabilité des Machines Locomotives en Mouvement*, by Le Chatelier, Paris, 1849. (This and references 6 and 7 are quoted from "Railway Machinery," D. K. Clark, 1855, p. 166.)

⁹ *Voie, Matériel Roulant et Exploitation Technique des Chemins de Fer*, by M. Ch. Couche, Paris, 1873, vol. 2, p. 389.

¹⁰ *Ibid.*, p. 411, and the subsequent French literature on locomotives; for instance, "La Machine Locomotive," by E. Sauvage, Paris, 1918, pp. 211-212.

¹¹ *Die Gesetze des Lokomotivbaues*, by F. Redtenbacher, Mannheim, 1855, pp. 132-134, and subsequent German literature on Locomotives, for instance, *Kurzes Lehrbuch des Dampflokotivbaues*, by F. Meineke, Berlin, 1931, pp. 108-109.

¹² "Parovozy" (Steam Locomotives), by Romanoff, St. Petersburg, 1903.

¹³ "Lokomotivok," by Dr. Szűbó Gusztáv, Kapus László, Budapest, 1919, pp. 114-119.

¹⁴ "Locomotive Engineering," by Mori and Matsuno, vol. 2, pp. 275-277; published by the Okura Book Co., Inc., Tokyo, Nitronbashi, 1926, eighth edition. Also *Locomotive Designers' Handbook* Nos. 232-2, 232-3, issued and printed by Rolling Stock Section, Department of Mechanical Engineering, Japanese Government Railways, 1931.

¹⁵ "Locomotive Operation," by G. R. Henderson, published by *Railway Age*, Chicago, 1904, pp. 70-72.

is actually carrying out a numerical example by using the foregoing formulas, at least in so far as the revolving weights are concerned. As regards the reciprocating weights, there is a slight difference; namely, in the example worked out by the author, the excess balance is added to the large component of the rotating balance (Appendix 1, section 6, item 33), while in the cross-balancing method that part of the reciprocating weights which is to be balanced in this particular wheel would be added to the part of the revolving weights W_3 which is balanced in the plane of the main rod (Appendix, section 1, item 8), thus requiring no additional calculation.

The difference between the results of these two procedures is this: In the ordinary method the percentage of balancing of the fore-and-aft vibrations is different from that of the nosing vibrations of the locomotive; or, in other words, the balancing of the forces is different from the balancing of the couples due to forces of inertia of reciprocating parts, whereas by the cross-balancing method forces and couples are balanced to the same degree, and the meaning of the term "percentage of balancing" assumes definiteness which is lacking in the ordinary method. So, for instance, the author states that the weight of the balanced reciprocating parts is 465 lb on the left-hand and 483 lb on the right-hand side, an average of 474 lb, which in reference to the total reciprocating weights on one side (2241 lb) may seem to amount to 21.1 per cent, but the actual percentage of balancing the couples will be, using the author's designations, represented by:

$$\frac{474}{2241} \times \frac{2E}{C+E} = 21.1 \times \frac{124}{147} = 17.8 \text{ per cent}$$

or less than the percentage of balancing the reciprocating forces (21.1 per cent). It is true that while the difference between these two figures may seem large, these figures do not represent the actual conditions, because the unbalanced, not the balanced, forces and couples are what actually matters, and they are 78.9 per cent in the case of forces and 82.2 per cent in the case of couples.

Thus the difference between the two methods is slight. But there is no real balancing of forces, unless the moments (couples) are balanced too. Moreover, the percentage of balancing has no real meaning, if the couples are neglected. The writer is, therefore, of the opinion that cross-balancing is also preferable with respect to reciprocating weights.

As to the dynamic augment, it is immaterial which method is followed, as long as the excess balance in the wheel is the same. If there should be a slight numerical difference, it would be due to the fact that the smaller figure might be an approximate one while the other is the correct one.

It is interesting to note that the author, in section 3 of the Appendix, resorted to a rather involved algebraic method in determining the components of inertia forces of the eccentric crank. Everybody who can master these formulas (items 20 to 23) will be able to follow the formulas of the cross-balancing method in a general way, and need not be shown a numerical example in the belief that he is avoiding mathematics. It is further interesting to note that in this particular point a simplification is possible when, as the case normally is, the right and left main wheels are made from one pattern. In this case the author recommends to consider the averages of the components acting along the crank radius and at 90 deg to it. But from items 20 to 23, using Fig. 9, it can be seen that

$$\frac{L_{ab} + R_{ab}}{2} = \frac{Wb}{R} \frac{D+E}{2E}$$

$$\frac{R_{ea} - L_{ea}}{2} = \frac{Wb}{R} \frac{D-E}{2E} = \frac{L_{ab} + R_{ab}}{2} - \frac{Wb}{R}$$

In other words, we may consider the equivalent weight of the eccentric crank (Wb/R ; see Fig. 7) as a revolving weight attached to the crankpin in the plane of the eccentric crank, and need not be bothered with intercept a or any eccentric crank calculations.

By the way, I wish to mention that the Russian Decapods built in 1916-1917 in this country had counterbalances figured by the cross-balancing method with taking into account the equivalent weights of the eccentric crank (and also half-weights of the eccentric rod), and averaging the counterbalances and angles of the right and left wheels resulting from calculations in accordance with the author's suggestions.¹⁹

I agree with the author that the revolving parts should be completely balanced, so that no parasitic forces should take place. It is very essential that the revolving weights should be balanced completely, because otherwise the balance of the reciprocating weights is unfavorably affected. As the balances for both revolving and reciprocating weights are combined into one balance in the wheel, the action of the counterbalance for balancing the reciprocating weights does not start if and until the complete balancing of the revolving weights takes place. Consequently, if there is a deficiency in the balances of the revolving weights, the balancing of the reciprocating weights is impaired.

This is borne out by some of the author's numerical examples and because of that I do not understand the author's attempt to introduce simplifications in the balancing of revolving weights. I have in mind his statement "that unless the parasitic effect to be eliminated by cross-balancing amounts to more than 30 per cent of the overbalance, cross-balancing hardly justifies the additional complication." The writer cannot agree with this statement, as it should be remembered that no real simplification will be achieved by neglecting the small component and the angle of the balance. The calculation has to be made anyway, in view of the differences in planes, and in order to determine the major component; and the increase in the amount of work involved in the calculation by figuring the other component and the proper angle, as well as in preparing the pattern of the counterbalance, of the proper size and direction, is so insignificant that it is hardly possible to consider it a complication. I could never appreciate the "simplification" of saving a calculator several hours of work in a design of a locomotive, the building of which requires tens of thousands of man-hours, especially as very often only one calculation is made for a great number of duplicate locomotives.

I think cross-balancing should be made on all coupled wheels, irrespective of the ratio of the components or of the angle, and this for the sake of correct balancing of the reciprocating weights.

Another point I wish to touch upon is the distribution of the excess balance between coupled wheels. The author's example proves that very little is gained by placing an excess balance in the main wheel. The main axle is usually the one with the heaviest load. In addition, there is a piston-thrust component increasing the load on the main wheel during the forward movement of the locomotive, which the author did not take into consideration. At long cut-offs and low speeds this component amounts to a considerable force, sometimes 12,000 to 15,000 lb per wheel. At high speeds, when the counterbalancing effect gets into play, this component is much smaller—probably not over several thousand pounds, due to the shorter cut-off used at the higher speed. Nevertheless, this should not be neglected in considering the maximum permissible load. In view of this, as suggested by me in my discussion of Dr. Eksergian's paper, it would be just as well to leave the main wheel without any excess balance, and have it properly cross-balanced for revolving weights only. The balance for the reciprocating weights could be distributed among the coupled axles.

¹⁹ A. I. Lipetz, "Russian Decapod Locomotives Built in the United States" (in Russian), New York, 1920, pp. 148-149.

Summarizing my remarks, I should say that I am in favor of applying the correct cross-balancing method for all revolving weights (both for main and coupled axles), as well as for balancing reciprocating weights, and for omitting the overbalance for reciprocating weights on the main wheels.

S. S. RIEGEL.²⁰ The author has long been known as one of the pioneers in improving locomotive counterbalancing and has done much very valuable work on the subject. I am in accord with all of his points and recommendations.

As this subject was placed before the A.R.A. Locomotive Construction Committee, of which I am a member, Mr. Fry brought the present information to our attention early in the year, as he contemplated, if possible, reading it there, so that our committee had opportunity then to benefit by his constructive criticism, and a supplementary recommendation was made by the Locomotive Counterbalancing Committee in June, 1932, and is now a matter of record there.

In view of this fact it may not be amiss to review this part of our supplementary report as it, to a considerable extent, fits as a discussion of Mr. Fry's recommendations now advanced. I believe it will be as interesting here as it was there. In substance this is, namely:

In the modern superpower locomotives with large firebox overhang and weight, it seems permissible to regard considerations of nosing and swaying as less important when judging effects of the reciprocating balance on the smoothness of operation or riding qualities. This leaves only the fore-and-aft oscillations whose magnitude is in direct proportion to the total mass of the locomotive and the force causing the oscillation, which in turn is a function of the mass of the unbalanced reciprocating parts and its frequency of vibration.

The design of a locomotive modifies according to individual designers of separate railroads and builders, and is influenced by changes in transportation developments and demands. In some regions the traffic demands require high tractive effort with low total weight, concentrated on drivers and large reciprocating parts, while in others, even on the same road, a unit of equal or lower tractive force capable of higher sustained horsepower is needed.

The recent trend in locomotive building is toward the latter type; so that when we compare this with the older lighter units, on the basis of ratio of percentage of reciprocating weight balanced, we obtain from the modern locomotive a higher figure for pounds of total weight per pound of unbalanced reciprocating weight and have smoother operating units, or what may be more logical we can balance a lower percentage of the reciprocating weight and thus by increasing the unbalanced portion, retain the figure for pounds of total weight per pound of unbalanced reciprocating weight, and the newer locomotive will be as smooth in operation and cause lower track stresses. This will compensate in some measure for the increased weight per driver of the modern high-speed superpower locomotive.

The real question to determine in all this is: Which is to be permitted to suffer more, the rail and track structures or the locomotive? For, certainly if the recurring load is lifted from the track, it must be borne by the boxes, frames, and other parts of the running gear of the locomotive, whether considered as a percentage of the reciprocating weight, the ratio of the unbalanced weight to the total weight, or something else. A series of tests might be made with instruments to record the track stresses and the vibrations of the locomotive, to definitely determine the magnitude of these forces and movements and thereby increase the total sum of human knowledge. It is doubtful, however,

if a compromise could be made even then that would be perfectly satisfactory to both bridge and right-of-way interests and to those operating and caring for the locomotive.

There appears to be, however, one aid left which has long been recognized but not given the utmost consideration it deserves; namely, the lightening of reciprocating parts by use of higher strength alloy steels and non-ferrous metals. Lately many metallurgical advances have been made that were eagerly taken up by other industries. Perhaps our present steels of 60,000 to 80,000 lb per sq in. tensile strength should be replaced by those of 100,000 to 120,000 lb tensile strength, effecting saving of 30 to 40 per cent in weight with advantageous results.

It is believed that by the use of such alloy steels for main rods, crossheads, pistons and piston rods, and possibly aluminum-alloy crosshead shoes and piston bull rings, the unbalanced reciprocating weight can be reduced several hundred pounds per side. When we realized that any addition or reduction in the reciprocating weight increases or decreases the force on the driving boxes by 45 to 55 times its amount, at diameter speed, or by 64 to 78 times the force tending to shake the whole locomotive, it can be appreciated that even slight reductions of weight of these parts is worth while. Equally, then, some of this reduction can apply to reduce the reciprocating balance, which also is multiplied by the greater figure above stated to include both sides, and this also may be amplified by as much as 20 for the bridge stresses when the recurring load synchronizes with the natural frequency of the bridge span.

Considering the second, it seems, as may be expected from its simplified nature, that several refinements to the method outlined in the A.R.A. Committee Report of 1930 have been suggested. One, the weight to be added to the main wheel for part of the reciprocating balance should be added to the main revolving balance, designated W_c in the report, before it is combined with the weight added to offset the cross-effect of the overhanging parts. This point is well taken, as the reciprocating balance should naturally be placed directly opposite the crank-pin and not at an angle with it as previously obtained. By doing this, the main-wheel balance can be reduced in weight and a new slightly less angle for the balance be obtained. This refinement is to be recommended.

If desired to introduce further refinements, another suggestion is to cross-balance the intermediate driver, as an appreciable reduction of rail blow from this driver can in some cases be effected thereby. This is consistent, and while not stated, it was implied in the report and can also consistently be definitely recommended.

It is most important especially that greater exactness and care be observed in securing the weights we need in the balances and to see that like weights are applied in opposite wheels, as carelessness in allowing dissimilar weights to be placed in opposite wheels will have very disturbing effects, since we are now operating at much higher speeds.

A. H. FETTERS.²¹ I notice that the author uses the A.R.A. method as a basis. I have been practising this method verbatim for several years with satisfactory results. I have ridden many engines before and after having been cross-counterbalanced at the main wheel, and I find that the riding qualities of a locomotive are not always a safe guide to a perfect balance, especially if the main axle happens to be under or near the virtual center of the locomotive, as in this case the vertical component due to overbalance or underbalance does not exert its effect in teetering the engine, and therefore the effect is not felt in the cab. I have ridden a 4-8-2 with a cross-overbalance of 300 lb, and while the dynamic augment was 26,000 lb, it did not show up in the cab.

²⁰ Mechanical Engineer, Delaware, Lackawanna & Western Railroad Co., Scranton, Pa.

²¹ General Mechanical Engineer, Union Pacific System, Omaha, Neb.

Had any other axle on this locomotive been off-balance to that or less extent it would have shown up in the cab as a very rough-riding engine. Again, I have found many other physical things that caused rough riding that it is difficult to determine by trial if the counterbalance or some other factor is responsible for rough riding. I have put some engines in ideal counterbalance, and they would ride smooth one trip and very rough the next, due to stuck wedges, fouled equalizers, slack between engine and tender, and similar causes. We can depend, however, on proper calculations and applications of the cross-counterbalance to the main drivers to reduce dynamic augment, thereby reducing damage to track and wear of machinery of the locomotive.

In view of the gradually increasing speeds of locomotives in freight service the last few years, the subject of cross-counterbalancing main wheels becomes of still greater importance than formerly, and the mechanical organization of any road which overlooks this fact and fails to take advantage of this very obvious improvement is remiss in its duties.

D. J. SHEEHAN.²² Since the subject of cross-counterbalance of locomotives became a subject of common discussion about four years ago, there have been many queer ideas advanced concerning counterbalance in general. To the busy mechanical engineer on the average railroad, who accepted the discussion of out-of-plane forces and dynamic balance as the work of the theorist and the master mind of locomotive design, it was merely another method of counterbalance. It was probably all right and would give results as satisfactory as the method that he had been using for the past fifteen or twenty years. But he was not having a lot of trouble with counterbalance considered from the standpoint of the old static balance method, and it was much easier to handle. Some day when he had time he would study this new method at least so that he could talk about it.

One day this mechanical engineer had a report that one of his passenger engines was riding rough and jumping up and down. He rode this engine and confirmed the report. When the counterbalance was checked by the old method of static balance, the figures indicated that 65 per cent of the weight of the reciprocating parts were balanced, the balance equally distributed among all the wheels. However, an additional weight equal to 175 lb at crankpin radius was applied. The subsequent reports indicated that the engine rode considerably better, but still vibrated up and down.

Imagine the astonishment, when the counterbalance was properly checked, with due consideration to the forces acting outside of the plane of the balance at their proper moment arms, and the results indicated that the balance in the main wheel still lacked approximately 100 lb at crankpin radius to balance the out-of-plane revolving forces.

Needless to say, when this engine was finally returned to service, properly counterbalanced for the forces acting in various planes outside the balance, both in the near and in the far wheel, the reports indicated that the locomotive rode like a "Pullman."

This little story, while possibly a little exaggerated, indicates the urgent need for a simple method of consideration of the subject of cross-counterbalance of locomotives. The engineer who spends a little time studying this subject soon discovers that primarily it contains only the simple fundamentals of mechanics, but he has thus far been somewhat frightened by complicated discussions and intricate mathematical analysis of the subject. Several unfamiliar terms such as out-of-plane forces, dynamic balance, dynamic augment, rail load, track load, and others were not to be found in his vocabulary of common usage.

²² Mechanical Assistant to the President, Chicago and Eastern Illinois Ry. Co., Chicago, Ill.

This subject is most important, and a simple method of analysis will greatly assist the busy railroad mechanical man to grasp the true significance.

JOHN A. PILCHER.²³ The paper outlines the principles involved in counterbalancing steam locomotives. The author has gone into a refinement of the counterbalance that is often very much neglected. The counterbalancing of a locomotive is entirely a compromise as between the horizontal and vertical forces. He has outlined the subject in a very intelligible way, showing the significance and importance of cross-balancing.

Reference is made to what are called "parasitic forces." These are forces introduced by improper location of the counterbalance. In other words, the component of the counterbalancing forces may be in a direction which is not available for balancing the reciprocating forces, but which would tend to increase the dynamic augment. In this connection it is significant to realize that in the case of non-cross-balanced engines the entire force of overbalance is not available for balancing the reciprocating weights.

The author points out the fact that by properly placing the counterbalance—that is, by shifting it the proper amount from the position directly opposite the crankpin—its effectiveness can be materially increased without increasing the weight of the counterbalance itself. This may be particularly valuable in counterbalancing engines in which the room in the main wheel is so limited as to make it impossible to secure as much balance as is desired. The importance of the cross-balancing is continually increasing on modern locomotives having heavy rotating parts and wide cylinder spacing, thus placing the plane of the rotating and reciprocating parts a very considerable distance outside of the plane of the counterbalance.

A. GIESL-GIESLINGEN.²⁴ It might be interesting to note that the author's figures for the weight of the unbalanced reciprocating masses compared with the weight of the locomotive correspond exactly to those for the 2-8-4 type passenger locomotive of the Austrian Federal Railways²⁵ where said unbalanced reciprocating masses are 1/231 of the engine weight exclusive of the tender. The writer is glad to acknowledge from his experience that this and similar relations proved entirely satisfactory. He would like to add some information which he found to be a good guide in quantitatively answering the questions connected with counterbalancing of locomotives.

One of the primary questions is: How great a dynamic augment may be permitted as a result of balancing the reciprocating masses (or, generally speaking, as a result of any free centrifugal force influencing the wheel pressure)? Many European railroads limit this dynamic augment, for the maximum operating speed, to 15 per cent of the static wheel load. This is a very conservative figure; it is often being exceeded in other countries on perfectly satisfactory locomotives. Two distinctly different considerations enter here: First, the limit imposed by the track structure and, second, the fluctuations of the wheel pressure that may be consistent with safe riding. Some light is thrown on the former by results obtained on a test track supported by helical springs, installed by Dr. Wirth of the Austrian Federal Railways in 1928.²⁶ Under the above-mentioned 2-8-4 type locomotive, having an axle load of 40,000 lb on the drivers, the maximum depression of the rails was 0.146 in. at very low speeds where

²³ Mechanical Engineer, Norfolk & Western Ry. Co., Roanoke, Va. Mem. A.S.M.E.

²⁴ Mechanical Engineer, New York, N. Y.

²⁵ See *Railway Mechanical Engineer*, May, 1930.

²⁶ See the Journal of the Austrian Society of Engineers and Architects, "Zeitschrift des Oesterr. Ingenieur- & Architekten-Vereines," 1930, p. 353.

the dynamic augment is zero. A dynamic augment of 12 per cent of the static load depressed the rail only 3 per cent more, corresponding to one-quarter of the theoretical excess load. This may be explained by the short time available for the process of depressing the rail in the neighborhood of the diameter speed—namely, about 1/10 of a second—yet it is remarkable that this effect was noticed with so stiff a track structure. Thus we may conclude that even with our highly stressed rails, a dynamic augment of 15 to 20 per cent of the static wheel load will impose upon the rail only a fractional additional stress. Similar results will probably be apparent from the otheograph records of the General Electric Company.

The other factor—namely, the fluctuations of wheel pressures as related to safe riding—is illustrated by the fact that a dynamic augment of 30 per cent will set up a theoretical fluctuation of the wheel pressure between the limits of 70 per cent and 130 per cent of the static load, but for the same reasons as just explained the actual fluctuations are much smaller. Therefore, much higher figures on certain locomotives have not led to apparent inconveniences, although they may be objectionable, especially when it is considered that locomotives often exceed regular speed limits.

As a result of experience and comparative studies, the writer submits the following recommendations for smooth and safe riding, leaving a good margin for occasional excess speeds:

Recommended for the maximum speed at which the locomotive is expected to operate regularly (80 to 100 per cent of the diameter speed for conventional engines, 115 to 125 per cent of the diameter speed for special high speed designs).

(1) Maximum dynamic augment $A = 25$ to 30 per cent of the static wheel load W for the wheel in question, but $(A + W) = 115$ to 120 per cent of the maximum static wheel load as permitted by the track structure; whichever of the two figures for the dynamic augment A thus obtained may be lower.

(2) Maximum weight of unbalanced reciprocating masses: 1/400 to 1/300 of the combined weights of the engine with 50 per cent loaded tender.

The latter condition limits the oscillating movement of the locomotive, resulting from the unbalanced reciprocating masses, to theoretically around $1/8$ in., but this amount is further reduced by frictional influences. The stiff connection between engine and tender makes it allowable to regard both as a unit. It appears that, if the reciprocating masses are light enough to fall within the foregoing limits, no counterbalancing of any part of them would be required for fairly smooth riding.

These recommendations are open to discussion. Cross-counterbalanced locomotives corresponding to them will be found satisfactory.

AUTHOR'S CLOSURE

It is gratifying to find that Mr. Lipetz has no fault to find with the general principles of the paper. The references that he gives to earlier work on the subject are interesting and valuable. The author had no intention of claiming any originality for the principles advocated. In fact, thirty years ago his first approach to cross-balancing was guided by von Borries' account of the subject.

The author appreciates the comments by Messrs. Riegel, Fetters, Sheehan, and Pilcher.

Mr. Giesl's remarks are not entirely clear and do not seem to be applicable to American practise. The suggestion that a dynamic augment of 15 to 20 per cent of the static load will impose on the rail only a fractional additional stress is not supported by Professor Talbot's experiments. The results of these as reported to the A.R.A. by Mr. Ripley show that as the locomotive speeds were increased, there was a very considerable increase in rail stress due to dynamic augment.

The two recommendations made by Mr. Giesl as to permissible dynamic augment and unbalanced reciprocating mass beg the whole question. He recommends that the dynamic augment should not exceed 25 to 30 per cent of the static wheel load. Surely the maximum combined dynamic and static wheel load should be determined by the civil engineer after due consideration of the particular track structures involved. When a limit has been set, the mechanical engineer will probably be interested in obtaining the maximum possible static load and consequently will aim at the minimum possible dynamic augment. Whether the dynamic augment is 10 per cent or 50 per cent of the static load is in itself immaterial. The important thing is that the combined loads shall not exceed the limiting value proper for the permanent way.

Mr. Giesl also suggests that the mass of the unbalanced reciprocating parts should not exceed 1/300 to 1/400 of the masses of the locomotive and of the half-loaded tender. The paper shows that locomotives with very much greater unbalanced masses are running satisfactorily in this country. The author feels that further study of this question should be carried out before any attempt is made to set up definite limits for the unbalanced reciprocating mass.

Slags From Slag-Tap Furnaces and Their Properties¹

By P. NICHOLLS² AND W. T. REID,³ PITTSBURGH, PA.

INTRODUCTION

THE work here reported may be considered the Third Progress Report presented for the A.S.M.E. Special Research Committee on Removal of Ash as Molten Slag From Powdered-Coal Furnaces. The second report⁴ outlined the objectives of the investigation and discussed the phases into which the problem could be divided; it also reported the experimental data rather fully.

This report presents the information available to date in a form that will be most useful to those concerned with the operation of slag-tap furnaces, but omits much information of general and technical interest. Although the investigation is nominally associated with slag-tap furnaces, yet from the standpoint of the Bureau it has the much broader purpose of obtaining data on the properties of coal ash and coal-ash slags, the coal ash being one of the fundamentals in the utilization of fuels.

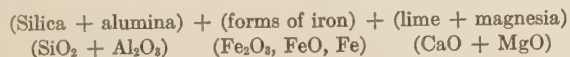
This report is divided into three main sections. The first discusses the properties of slags with relation to their chemical composition—a necessary groundwork for what follows. The second presents the data obtained through the cooperation of most of the stations operating slag-tap boilers on a wide range of fuels; this record should be valuable. The third reports a limited study of factors connected with the return of the fly ash to the furnace; the space given to it is out of proportion to the relative time spent on this phase.

RELATION BETWEEN FLOW TEMPERATURE AND CHEMICAL COMPOSITION OF SLAGS

This section deals with the relation between the composition of coal-ash slags and their fluidities as far as they pertain to slag-tap furnaces. In the second report the term "flow temperature"⁵ was introduced and was defined as that temperature at which a slag had such a fluidity that it would flow freely when tapping.

Unfortunately, the subject is complex, because of the number of components in coal ash, but it is the foundation for the interpretation of results and for predicting the properties of a slag. The underlying science and language are those of the ceramist, but this investigation has been carried out from the viewpoint of the combustion engineer, and an endeavor has been made to include only information required by him. This section discusses the information required by the plant engineer.

Coal-ash slags consist essentially of:



¹ Published by permission of the Director, U. S. Bureau of Mines. (Not subject to copyright.)

² Supervising fuel engineer, U. S. Bureau of Mines, Pittsburgh Experiment Station.

³ Junior fuel engineer, U. S. Bureau of Mines, Pittsburgh Experiment Station.

⁴ Nicholls, P., and Reid, W. T., "Fluxing of Ashes and Slags as Related to the Slagging-Type Furnace," A.S.M.E. Trans., vol. 54, 1932, paper RP-54-9, pp. 167-190.

⁵ Degrees Fahrenheit are used throughout this report.

Presented at the Annual Meeting, New York, N. Y., December 4 to 8, 1933, of THE AMERICAN SOCIETY OF MECHANICAL ENGINEERS.

together with oxides of other elements, usually in small quantities and varying little in total quantity. If the former can be grouped as shown, they can be treated as three constituents. The second report showed that in slags the ratio of SiO_2 to Al_2O_3 usually lies between 1.8 and 2 and that variations within these limits had little effect on the flow temperature; therefore they can be considered as one constituent. It also showed that the fluxing effect of MgO in small quantities differed little from that of CaO ; as the percentage of MgO is small, $\text{CaO} + \text{MgO}$ can be considered one constituent. The last report did not consider the effect of variations in the state of oxidation of iron; all the melts were made in air on the assumption that the iron would oxidize so as to give equilibrium with air. That this was true to the order of accuracy required was proved by the ability to duplicate results; therefore, the iron also was considered a single constituent. This ability to melt in air and work on a three-component basis was of great advantage and was a method of attack absolutely necessary if advance was to be made with any speed.

The second report (see Fig. 7) showed the relation of the flow temperature to the chemical composition on this basis and expressed the iron as equivalent Fe_2O_3 . Since that report was written, more determinations have been made in air, and a revised figure based on about 250 tests has been derived, but it does not differ materially from the old Fig. 7. This revised figure is not included, because analyses of the samples received from the stations show that the iron in the slags is much more reduced than were the slags melted in air; however, this new figure is the basis from which the effect of the forms of iron is derived.

The second report did not attempt to predict the effect of reduction of iron (that is, conversion of Fe_2O_3 to FeO and Fe), because no data were available. It is evident that if the investigation were to be thorough, each of the compositions represented by the 250 points should be tested with the iron in various proportions of Fe_2O_3 , FeO , and Fe , which again makes a three-component system for each point and for which many tests would be required—evidently an impossibility at this time. However, when the slags were reduced by subjecting them to a reducing atmosphere, it was found that, with few exceptions, the ratio of FeO to Fe was high and somewhat constant for the same degree of reduction; therefore, the first approach would be to consider them as one—for example, the equivalent FeO . This left one variable for each composition—namely, the ratio of the iron in the Fe_2O_3 to the total iron, or the ratio of the Fe_2O_3 to the total iron expressed as Fe_2O_3 .

Determination of the flow temperatures of slags with varying degrees of reduction required the development of new methods and apparatus; a full description of these is not included in this report. Briefly, they consisted of two new small furnaces. One was a platinum-resistance furnace similar in principle to that shown in Fig. 2 of the second report except that it was enclosed in a metal casing so that an atmosphere of nitrogen could be maintained around the slag contained in the crucible; thus slags previously reduced could be prevented from oxidizing. The other furnace was gas-fired. Various reducing atmospheres of the required temperature could be obtained by some combina-

tion of natural gas, air, and oxygen; this furnace was used for reducing the slags and for determining the resulting flow temperature.

The process of determining the flow temperature with the iron in a series of reduced states is more complicated and requires much more time than does a determination in air; in addition, each determination requires at least one chemical analysis. The determinations made have therefore been limited in number, but so scattered over the field of compositions represented by slags from slag-tap furnaces that the order of the effect over the whole field could be interpolated with fair probable accuracy.

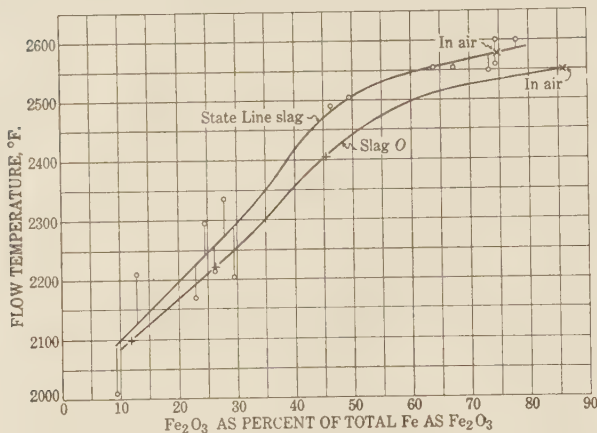


FIG. 1 EFFECT OF CHANGE IN FORMS OF IRON ON THE FLOW TEMPERATURES OF TWO SLAGS

Fig. 1 illustrates the type of results obtained and gives curves for two slags of different compositions. The flow temperature is plotted against the "ferric percentage," that is, the actual ferric iron (Fe_2O_3) in the slag, found by an analysis for the forms of iron, expressed as per cent of total iron in the slag calculated to Fe_2O_3 . This is given by

$$\text{Ferric percentage} = \frac{\text{Fe}_2\text{O}_3}{\text{Fe}_2\text{O}_3 + 1.11 \text{ FeO} + 1.43 \text{ Fe}} \times 100$$

where the values on the right-hand side are the percentages of Fe_2O_3 , FeO, and Fe found by analysis of the slag.

The two slags shown are State Line—the complete analysis of which is given in column D of Table 1—and a synthetic slag designated as slag O, one of those made to cover the field. Their essential compositions were:

	$\text{SiO}_2\text{-Al}_2\text{O}_3$ ratio	Equivalent Fe_2O_3 , per cent	$\text{CaO} + \text{MgO}$, per cent
State Line.....	2.51	37.5	8.4
Slag O.....	1.85	40.0	10.0

The test points are given; as the State Line slag was used in the original experimentation, a large number of tests were made. It was impossible, however, to make the same number for all

the other slags. As may be seen, some of the test points fall as much as 80 deg off the mean curve; the possible reasons for this will not be discussed, but the agreement of the two mean curves shows that the values for the part of the field covered by these compositions are probably reliable.

The curves show that the ferric percentages in air were 75 and 85 per cent, respectively; with decreasing ferric iron, the drop in flow temperature was not rapid down to 50 per cent, but below 50 per cent the flow temperature decreased 10 deg for each per cent drop of ferric percentage. For the State Line slag with a ferric percentage of 10, the flow temperature is 480 deg below that in air.

The forms of the curves for ferric percentages above the air values is of no interest, because slags will not be subjected to oxidizing conditions greater than that of air. What will be the relationship below 10 per cent ferric iron cannot be predicted definitely, because the conditions of testing did not give complete reduction. As the Fe_2O_3 becomes very small, the free iron has been found to increase; one would expect that the flow temperature would not be the same as it would have been if the metallic iron had remained low. It is also probable that for the same ferric percentage the flow temperature would increase with increase of metallic iron. There are few data on this phase of the subject. However, it is probable that the ratio of Fe to FeO may vary for ferric percentages below 10; the atmosphere required to reduce the slag to extreme limits may result in deposition of carbon on the slag, with corresponding uncertainty on the equilibrium between the Fe and FeO. In the extreme, all the Fe_2O_3 may disappear and another series of conditions arise in which there will be FeO and Fe in varying proportions. The slags from slag-tap furnaces have not indicated rapid increase of metallic iron with low Fe_2O_3 , but rather with increase in the total iron content of the slag. It has been shown, however, that if fly ash containing combustible is introduced into the furnace in large quantities, there may possibly be no Fe_2O_3 and a large proportion of Fe.

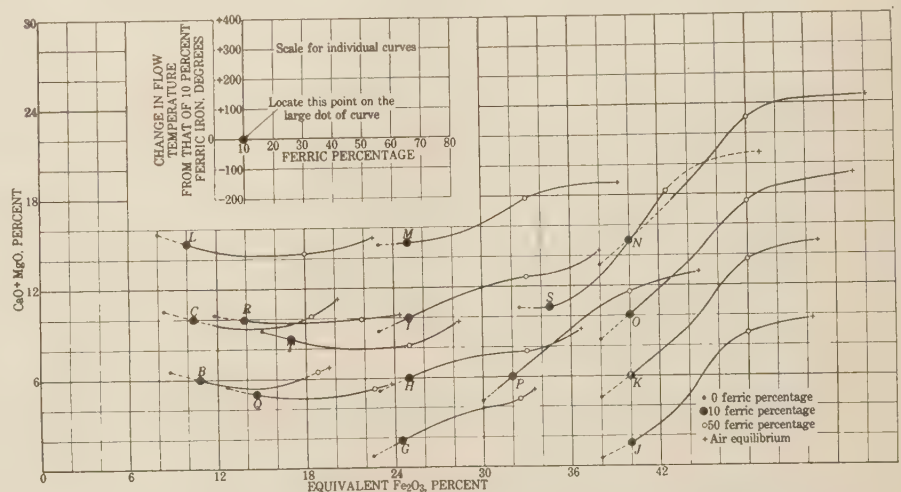


FIG. 2 EFFECT OF CHANGE IN FERRIC PERCENTAGE ON FLOW TEMPERATURE OF COAL-ASH SLAGS

Determinations similar to that of slag O for flow temperatures with various states of reduction of the iron were made for slags having other percentages of iron and lime. The desired compositions were obtained by mixing coal ashes of known composition in the correct proportions and by adding other constituents for small adjustments. Instead of giving individual figures for each slag, all have been plotted on one sheet so that their rela-

tion to the composition can be seen. A silica-alumina ratio of 1.85 was used in the synthetic slags.

Fig. 2 shows this plot. The compositions of the slags tested are indicated by the heavy dots; these dots are thus points related to the main axes. For example, on the basis used for eliminating the small quantities of alkalis and other constituents, slag C had a composition of equivalent $\text{Fe}_2\text{O}_3 = 10.4$; $\text{CaO} + \text{MgO} = 10$; $\text{SiO}_2 + \text{Al}_2\text{O}_3 = 79.6$.

The curves showing the effect on the flow temperature of the forms of the iron are drawn through the points representing the compositions and are so placed that the points on the curves which represent a ferric percentage of 10 are on the points of composition—that is, the big dots. The reason for this is made clear in the discussion of Fig. 3.

On the upper part of Fig. 2 a skeleton scale is given for the individual curves. In using this scale with any one of the curves, the intersection of its axes would be placed on the large dots of the curve, and the difference between the flow temperature for the ferric percentage of 10 and any other percentage can be read off; therefore, if the flow temperature at 10 per cent is known, that for any other ferric percentage can be found. It is not necessary to actually superimpose this scale, because the divisions are the same as those for the main plot of composition, and it is easy to find the required temperature difference.

If the composition of the slag being considered does not lie on or near one of the large dots, then it is necessary to interpolate, or to sketch in a curve the shape of which must be judged from those of the compositions surrounding it on the assumption that the shapes of the curves change gradually with change in composition; the relative shapes of the curves given show that such an assumption is reasonable.

However, a plant engineer would not usually want an exact value for the flow temperature, because he cannot predict the exact composition of the slag from day to day and still less the degree of reduction of the iron in it; rather, he will be interested in the general effect.

The relations between the curves and the composition of the slags need not be described; these can be best understood by studying Fig. 2. On each curve three other points are indicated; the points corresponding to the equilibrium which resulted by melting in air are indicated by crosses, the clear circles are the points of a ferric percentage of 50, and the small dots at the extreme left of the curves are the points of a ferric percentage of 0. As previously stated, the shapes of the curves between 10 and 0 were not determined; they are shown as prolongations of the known curves except for point T.

The outstanding principles can be summarized as follows:

1 With slags containing an equivalent Fe_2O_3 of 10 per cent, the minimum flow temperature occurs at a ferric percentage of about 30.

2 As the iron content of the slag increases above 10 per cent

Fe_2O_3 , the ferric percentage for minimum flow temperature decreases and reaches 10, with slags containing, probably, about 20 per cent equivalent Fe_2O_3 .

3 As the iron content of the slag increases beyond 20 per cent, the decrease in flow temperature for a given decrease in ferric percentage becomes greater.

4 With the same iron content and increasing lime (up to 16 per cent), the influence of the state of the iron on the flow temperature becomes less when the iron content is low (10 per cent) and is not affected if it is high (40 per cent)

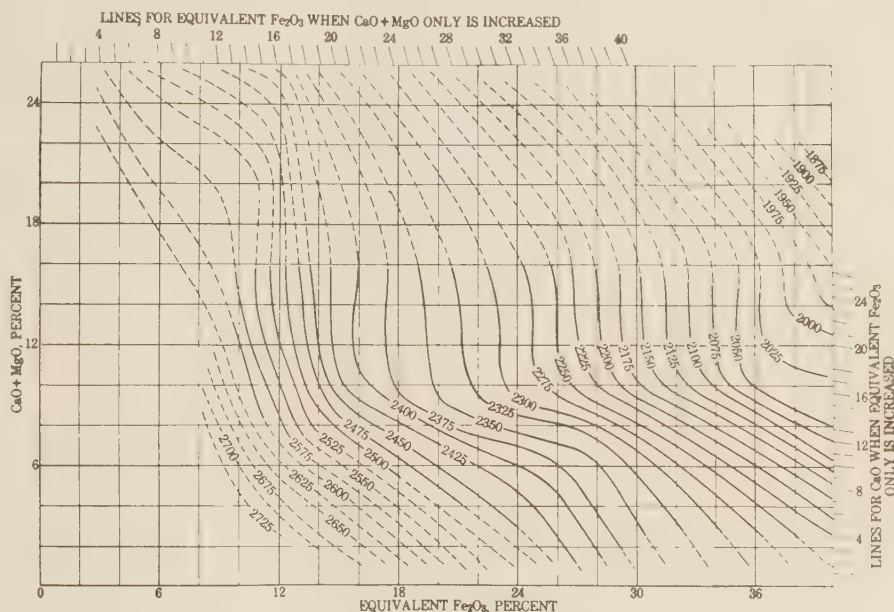


Fig. 3 covered by the full-line curves. Also the silica-alumina ratio usually lies within the limits of the figure, and the alkalis are usually not greater than 3 per cent. The following general rules can be used as a guide for unusual slags:

1 Variations of the silica-alumina ratio make little difference in the flow temperature within the field of 30 per cent Fe_2O_3 and 10 per cent $\text{CaO} + \text{MgO}$. As the quantity of these fluxes increases, an increase in the silica-alumina ratio will lower the flow temperature.

2 An increase in alkalis above 3 per cent will make little difference in the flow temperature if the $\text{CaO} + \text{MgO}$ is below 18 per cent; their effect can be approximated by adding $\frac{1}{2}$ (per cent alkalis — 3) to the $\text{CaO} + \text{MgO}$. The effect of alkalis in lowering the flow temperature increases materially with increase in lime above 18 per cent.

The information given in this section should be sufficient for present requirements in connection with slag-tap furnaces. It is probably as reliable as the furnace operator's knowledge of the composition of the slag and of operating conditions affecting it.

Only such information as will be useful in plant operation has been presented in this section of the report. It does not include discussion of factors which may have a bearing on the reliability of values, but which were not determined experimentally, and can rarely be defined or controlled in the furnace. Two such factors are the time that slags must be subjected to a given set of conditions in order that they may reach a constant state and the series of events through which they pass.

EFFECT OF FERRIC PERCENTAGES ON EFFECTIVENESS OF FLUXES

In the second report the tests of the fluxing effect of a number of materials on coal-ash slags were carried out in air; the iron in the slag was allowed to assume that state of oxidation (ferric percentage) that gave equilibrium with air, and the values for the lowering of the flow temperature which resulted were determined. The question is: Will that same lowering of temperature occur with other values for the ferric percentage?

Figs. 2 and 3 give a complete answer for the use of either iron or lime as fluxes *providing* the ferric percentage both before and after adding the flux is known. If limestone is used as a flux and if, for example, before fluxing the ferric percentage of the slag is 10, then there is the possibility that the limestone might oxidize the iron and the ferric percentage be raised to 30, in which event the fluxing might be less effective than it would have been if the ferric percentage had remained at 10. Tests have shown that, with some slags, oxidation did occur when limestone was added, even though there was an attempt to prevent it.

How much the reducing atmosphere at the surface of the bed of a furnace might retard the oxidizing effect or whether it could reduce the iron back to its original state of oxidation is not known, but this investigation has indicated that when the ash has once formed a slag, the reduction of the iron in the body of the slag by the action of gases at the surface is slow.

Such actions add complications which cannot be avoided. It is suggested, however, that Fig. 3 be used and that the possibility of oxidation be allowed for by adding to the decrease in flow temperature desired the following number of degrees:

Equivalent Fe_2O_3 content of slag before fluxing, per cent.	10	20	30	40
Addition, deg fahr.....	0	25	50	75

The procedure for finding the required quantity of limestone is the same as that described in the second report, Fig. 7, and will not be repeated.

The only other fluxes that might possibly be used are fluorspar, salt cake, or soda ash. No additional data are available, and it is suggested that the information given in the last report

for the lowering of temperature produced by these fluxes be used.

Adding fluxes as a regular procedure has not been found necessary; when they are added occasionally, only a general idea of the quantity required is necessary.

SAMPLES FROM STATIONS

The request for cooperation in obtaining samples was sent in June, 1932, to 16 stations operating slag-tap furnaces; four were not in a position to comply. The only stations not asked were Bremono, Hell Gate, South Amboy, and State Line; samples of slag had been received from these stations previously, and although these samples did not comply with all the conditions desired, yet the additional trouble and expense were not warranted.

The request specified small samples of coal, slag, and fly ash which were true average samples of the same period of operation—24 hr if possible. It also suggested methods, but recognized that conditions and facilities would not be alike. The temperature of the slag at the time of tapping, operating records during the test period, and details of furnace and burners were also requested.

Most of the stations sampled the coal at the feeders; in addition, some sent samples of the pulverized coal. The usual method of sampling the slag was to take grabs from the stream every few minutes during the tapping and to immediately quench the ladle. Some stations could not sample the fly ash. With one exception, those that did used a sampling pipe facing the gas stream and the exhaust and dust-bag method for collecting the dust; the position of sampling differed, but apparently no station attempted to traverse the stream. The stations reduced the total material collected to 2 to 4 qt for shipment.

The materials received by the Bureau were treated by its standard method and reduced to smaller samples ground to the requisite sieve size. The standard determinations made were:

- Coal: Proximate analysis and sieve sizes of pulverized coal
- Coal ash: Chemical analysis; A.S.T.M. cone fusion values; flow temperature in the air furnace
- Slag: Chemical analysis including forms of iron; A.S.T.M. cone fusion values; flow temperature in the air furnace; flow temperature in the nitrogen furnace; determination of forms of iron after the test in the nitrogen furnace to check for change
- Fly ash: Combustible and sulphur; chemical analysis of the ash, including forms of iron; A.S.T.M. cone fusion values; flow temperature in the air furnace.

These data, with the descriptive information received from the stations, make a formidable mass of information. Table 1 gives the minimum necessary. The data from the stations are only essential facts; the test data include all the standard determinations except the flow temperatures in the air furnace.

The stations are arranged in the order of increasing temperatures at which the slag as received would flow. This value is the flow temperature as determined in the nitrogen furnace, item 35, Table 1.

A study of this table is simplified by listing the items on which the table may throw some light. The following are outstanding:

- 1 Knowing the properties of the coal ash, is it possible to predict those of the slag, and how much will they differ?
- 2 Is there any outstanding difference in the slags caused by the furnaces or burners?
- 3 Is there any relation between the rate of burning and the type of slag produced?

The constructional data of the furnaces included (item 4) are limited to the horizontal cross-section in the direction of the

travel of the flame and at right angles to it. The burners are described (items 5 and 6) by type and whether they project the flame horizontally or on to the bed.

The rating at which the test was run is expressed (items 9 and 10) in pounds of fuel burned per hour and the heat release in Btu per square foot of horizontal area; it was thought that this one-figure value is more nearly related to the deposition of ash, although a number of other factors are undoubtedly related to it—an obvious one, the position of the burners, whether in one or two rows. At some stations the rate of burning was not constant; if it were maintained constant for several hours before tapping, that value was used for the heat release.

The fuels burned (item 11) included one lignite, eight bituminous coals, four semi-bituminous coals, and one petroleum coke. The ash contents of the coals ranged from 12.4 to 5.2 per cent, and 1 per cent for the petroleum coke.

Eight stations sampled the fly ash from the gas stream, and one (R) sent a grab from deposits. The combustible in the fly ash (item 17) ran from 1.5 to 27 per cent for the samples collected from the gas streams; that for the petroleum coke was 56 per cent because of the small amount of ash in the gas stream.

The analyses of the ash (items 18 to 27) present a good cross-section of the variations in coals the ash of which is fusible enough so that the coal can be used in a slag-tap furnace; the only type missing is that of coals from the Pacific Coast, which have shown peculiarities compared with other coals.⁶ The bases adopted for showing the analyses are:

(a) The coal ashes are shown with 0.0 per cent SO_3 (item 26). It is so given because the quantity of sulphur found by analysis is dependent on the temperature and time of ashing and has little meaning.

(b) The analyses of the slags are for the samples as received.

(c) The analyses for the fly ashes are on the combustible-free basis.

(d) The forms of iron are given for the slags and fly ashes. In addition, the total equivalent iron expressed as Fe_2O_3 (item 23) is given so that the total iron in the coal ash, slag, and fly ash can be compared.

(e) Item 29 is the actual Fe_2O_3 divided by the total equivalent Fe_2O_3 , in per cent; it is the value previously defined as "ferrie percentage."

(f) Although the analyses of the coal ash, slag, and fly ash are each shown on the most informative basis, yet in an attempt to compare them strictly or to apply them to diagrams such as Fig. 3 they must be reduced to the same basis of $\text{SiO}_2 + \text{Al}_2\text{O}_3 + \text{equivalent Fe}_2\text{O}_3 + \text{CaO} + \text{MgO} = 100$.

As the stations are arranged in increasing order of the flow temperatures (Table 1), the fluxing constituents in the ashes decrease from station A to R. In the coal ash of A, the Fe_2O_3 was 41 per cent and the $(\text{CaO} + \text{MgO})$ 9.3; in R, they were 9.1 and 1.8, respectively. The other main fluxing constituent, the alkalis (item 27), varied little.

COMPARISON OF ANALYSES OF COAL ASH, SLAG, AND FLY ASH

In spite of the care in sampling taken by the stations, the analyses show that the samples of slag and fly ash do not correspond to those of the coal. If they did and if the comparisons are made with the analyses reduced to the same basis, then the percentages for each component (SiO_2 , for example) should be such that the percentage for the coal ash would lie between those of the slag and the fly ash. If the samples corresponded exactly and if C, S, and F were the percentages of any one component of the coal, slag, and fly ash, respectively, then

$$\frac{C - F}{S - F}$$

should have the same value (W) for all the components, and W would be the pounds of slag per pound of coal ash. Not only does the value of W differ for the various constituents, but no set of three samples fulfils even the first general condition.

This is a good illustration of the difficulty of obtaining true samples. In all probability the greatest error is in the sampling of the fly ash. Even when the sample is collected by suction and a dust bag, the collecting pipe is placed in one small area of the gas stream, and ash is also deposited before it reaches the point of collection.

There may also be errors in the slag, although one would expect the tapping operation to mix portions from different parts of the bed. In addition, many stations followed the request that the test be made after burning the same coal for several days. Yet if the composition of the slag is not the same over the area of the bed, then the composition of that tapped will vary with the temperature of the furnace during the run preceding the tapping. In spite of such possibilities, the slag samples should be fairly representative, as was indicated by the test at station Q. This test was run continuously for three days and gave six sets of samples for periods of approximately 12 hr each; because of the space required, the individual tests are not given in Table 1; the values in column Q are averages, but the analyses are closely similar, as is shown by the following values for the slag:

Test	1	2	3	4	5	6
SiO_2	51.0	50.8	50.9	50.0	50.8	50.8
Al_2O_3	29.4	29.4	29.5	28.5	29.5	29.1
Fe_2O_3	13.1	13.9	14.6	14.2	14.5	12.4
CaO	4.8	4.6	4.4	4.6	4.4	4.3

It was unfortunate that the fly ash at this station could not be sampled.

The three analyses most nearly correspond at station H, which used lignite as the fuel. The weight W of the slag expressed as a percentage of the ash in the coal, as computed from the components, would be: On the SiO_2 basis, 27; Fe_2O_3 basis, 38; CaO basis, 34; MgO basis, 37. The Al_2O_3 was nearly the same in all three samples and cannot be used. The 37 per cent seems a reasonable figure.

Except for this one station, the percentage of slag cannot be deduced from the analyses. Two stations did, however, obtain values for this factor, and the values should be reliable because they are based on the weight of the slag tapped and great care was taken by both stations. The summary of the reports is:

Station.....	Q	R
Duration of test, days.....	3	7
Coal burned, tons.....	1029	3302
Slag as per cent of ash in coal.....	45.0	16.6

The test at R did not correspond with the sampling test, nor was exactly the same coal used. That at Q corresponded with the sampling period. The method of tapping at Q was very convenient for the storage and handling of the slag; when removed from the storage tank, it was placed on cars and allowed to dry until the weight became constant.

The slags of these two stations had the highest flow temperatures. Station A, with the lowest, sent no fly ash; the analyses of B do not line up well, but if the values for the Fe_2O_3 are taken as correct, the slag computes to 89 per cent of the ash in the coal, which, though high, is in the right direction for a very low-fusion ash.

Selective Action in Combustion Chamber. One would expect that particles of ash that fuse easily would have a greater chance of being deposited on the bed and that consequently the slag would contain a greater proportion of the fluxes and would have a lower flow temperature than the ash of the coal; as a result, the fly ash would contain less fluxes. This presumption is confirmed by the analyses, but the selective action was not as large as earlier samples indicated.

⁶ "Analyses of Washington Coals," U. S. Bureau of Mines Technical Paper 491, p. 100.

TABLE 1 DATA OF

Item	A			B			C ^b		
	Quindaro, Kansas City, Kan.			Powerton, Pekin, Ill.			Deepwater, Penn's Grove, N. J.		
1 Station.....							No. 2		
2 Location.....							17 × 34.5		
3 Boiler number.....	17.8 × 21.5			19 × 36			4, cross-tube		
4 Furnace, depth by width, ft.....	4, cross-tube			4, cross-tube			Horizontal		
5 Burner, number and type.....	Inclined			Horizontal			Refractory		
6 Inclination of burners.....	Water cooled			Water cooled					
7 Type of bottom.....							Not special		
8 Duration of test, hr.....	12			3					
9 Coal per hour, lb.....	12,220			43,700					
10 Heat release, per sq ft per hr, Btu.....	389,000			714,000					
11 Coal: Rank.....	Bituminous			Bituminous			Semi-bituminous		
12 Seam.....	Cherokee			No. 5			Miller, B		
13 Mine or location.....	Pittsburg, Kan.			Springfield, Ill.			Waterman, Pa.		
	Coal	Slag	F. A. ^d	Coal	Slag	F. A.	Coal	Slag	F. A.
14 Sample No.....	343	342	None	326	325	327	8.3	205	None
15 Ash in coal, per cent.....	12.4	11.7	3.4
16 Sulphur in coal, per cent.....	4.1	1.5
17 Combustible in fly ash, per cent.....
Analysis of ash, per cent:									
18 SiO ₂	31.4	27.2	...	39.8	42.1	49.5	34.5	38.1	...
19 Al ₂ O ₃	16.1	12.0	...	15.1	13.9	14.8	28.2	22.2	...
20 Fe ₂ O ₃	41.0	32.9	2.7	16.8	35.2	9.0	...
21 FeO.....	25.9	3.4	...	22.6	...
22 Fe.....	2.7	0.0	...	5.5	...
23 (Total Fe as Fe ₂ O ₃ for reference).....	...	47.9	35.4	20.4	...	42.0	...
24 CaO.....	8.4	15.2	...	8.4	9.6	8.6	1.9	1.4	...
25 MgO.....	0.9	1.4	...	0.8	1.2	1.0	0.2	0.1	...
26 SO ₂	0.0	2.4	...	0.0	0.7	3.2	...	0.1	...
27 Na ₂ O + K ₂ O, by difference.....	2.2	3.0	1.2	2.7	...	0.9	...
28 Ratio SiO ₂ to Al ₂ O ₃	1.95	2.26	...	2.64	3.01	3.34	1.22	1.72	...
29 Fe ₂ O ₃ to total Fe as Fe ₂ O ₃ , per cent.....	7.6	82.0	...	21.0	...
Ash fusions, F:									
A.S.T.M. standard cone:									
30 Initial temperature.....	2010	1905	...	1880	1910	1910	...	2260	...
31 Softening temperature.....	2120	1970	...	1935	1945	1980	...	2320	...
32 Fluid temperature.....	2380	2180	...	2190	2240	2470	...	2590	...
Electric furnace, in N ₂ :									
33 Sticky temperature.....	...	1945	1980	1985	...
34 Penetration temperature.....	...	1975	2025	2315	...
35 Flow temperature.....	2095
36 Ease of tapping.....	...	Freely	Freely	Freely	...
37 Slag temperature, F.....

^a Presence of sulphide iron interfered with determination of forms of iron. ^b Sample collected in 1931. ^c Analysis of coal made by station. ^d F.A. =

TABLE 1 DATA OF SAMPLES

Item	J			K			L		
	Huntley, No. 2, Buffalo, N. Y.			Edgewater, Sheboygan, Wis.			Bremo, Bremo Bluff, Va.		
1 Station.....									
2 Location.....	Nos. 2 and 3			21 × 23					
3 Boiler number.....	19.8 × 35			Cross tube			6, intertube		
4 Furnace, depth by width, ft.....	6, cross tube			Vertical			Horizontal		
5 Burner, number and type.....				Air cooled					
6 Inclination of burners.....									
7 Type of bottom.....							Not special		
8 Duration of test, hr.....	10 (test No. 9)			7					
9 Coal per hour, lb.....	40,000			20,000					
10 Heat release, per sq ft per hr, Btu.....	750,000			545,000					
11 Coal: Rank.....	Bituminous			Bituminous			Semi-bituminous		
12 Seam.....	Pittsburgh			No. 5			Sewell, Va.		
13 Mine or location.....	South of Pgh., Pa.			Kenwar, Ky.			Crichton mine		
	Coal	Slag	F. A.	Coal	Slag	F. A.	Coal	Slag	F. A.
14 Sample No.....	411	410	412	357	356	358	288	289	...
15 Ash in coal, per cent.....	11.3	6.4
16 Sulphur in coal, per cent.....	1.9	0.5
17 Combustible in fly ash, per cent.....	12.0	27.6
Analysis of ash, per cent:									
18 SiO ₂	48.1	49.3	48.5	44.8	45.7	42.5	48.1	46.9	...
19 Al ₂ O ₃	24.5	24.2	22.6	27.2	26.0	29.6	28.0	26.7	...
20 Fe ₂ O ₃	17.5	5.3	12.4	16.4	3.9	9.3	15.8	2.0	...
21 FeO.....	...	15.1	6.5	...	7.2	2.5	...	18.3	...
22 Fe.....	...	0.2	0.0	...	0.4	0.0
23 (Total Fe as Fe ₂ O ₃ for reference).....	...	20.2	19.6	...	12.5	12.1	...	22.3	...
24 CaO.....	7.2	5.5	6.9	4.3	5.7	5.1	4.1	2.8	...
25 MgO.....	1.0	0.9	0.7	1.8	7.3	2.3	1.2	1.2	...
26 SO ₂	0.0	0.0	1.2	0.0	0.1	1.4	0.0
27 Na ₂ O + K ₂ O by difference.....	1.7	1.5	1.2	5.5	3.7	4.4	2.8	2.1	...
28 Ratio SiO ₂ to Al ₂ O ₃	1.97	2.04	2.14	1.65	1.76	1.53	1.72	1.76	...
29 Fe ₂ O ₃ to total Fe as Fe ₂ O ₃ , per cent.....	...	26.0	64.0	...	31.0	77.0	...	9.0	...
Ash fusions, F:									
A.S.T.M. standard cone:									
30 Initial temperature.....	2070	1955	2120	2155	2085	2215	2180	2035	...
31 Softening temperature.....	2180	2175	2200	2310	2175	2305	2325	2260	...
32 Fluid temperature.....	2550	2315	2385	2530	2630	2625	2540	2535	...
Electric furnace, in N ₂ :									
33 Sticky temperature.....	...	1875	1880
34 Penetration temperature.....	...	2130	2065	2420 ^e	...
35 Flow temperature.....	...	2365	2435
36 Ease of tapping.....	...	Freely	Freely
37 Slag temperature, F.....	2700	2500	...

^e Estimated from Figs. 2 and 3.

SAMPLES FROM STATIONS

D			E			F			G			H			I		
State Line, Chicago, Ill. No. 5			Horseshoe Lake Oklahoma City, Okla. No. 9			Michigan City, Michigan City, Ind. No. 3			Toronto, Toronto, Ohio No. 7			Valmont, Denver, Colo. 19.5 × 23.7			Philo, Philo, Ohio No. 3-4		
4, cross-tube Inclined Refractory			16.5 × 23.5 2, Calumet Vertical Coke cans			20 × 26.5 4, cross-tube Inclined Refractory			22 × 23 4, intertube Horizontal Refractory			Cross tube Vertical Refractory			20.5 × 25 4, intertube Inclined Air cooled		
Not special			24 14,500			60 26,000 (est.)			20 19,100			24 26,000 (est.)			25 25,700		
Retainings Nos. 5 and 6 Kewanee, Ill.			430,000 Bituminous McAlester Mixture; Okla.			740,000 Petroleum coke Oil refinery E. Chicago, Ill.			494,000 Bituminous Pittsburgh, No. 8 Richland, Ohio			540,000 Lignite Grant mine Firestone, Colo.			605,000 Bituminous Middle Kittanning, No. 6 Mixture; Ohio		
Coal	Slag	F. A.	Coal	Slag	F. A.	Coal	Slag	F. A.	Coal	Slag	F. A.	Coal	Slag	F. A.	Coal	Slag	F. A.
229	227	None	389	388	390	405	404	406	360	359	361	382	381	383	422	421	None
...	11.7	1.0	10.3	5.9	12.1
...	2.3	3.5	0.6	2.6
...	4.4	5.6	5.6	2.1
41.1	38.6	...	39.4	42.1	39.0	12.4	35.8	5.4	44.8	42.2	42.6	39.6	47.5	36.5	42.2	39.8	...
17.9	15.4	...	23.2	22.5	22.6	4.4	16.8	3.7	21.4	22.7	22.6	19.1	18.8	19.5	26.5	23.7	...
30.9	11.7	...	23.5	2.2	16.6	11.2	0.7	9.2	28.3	4.0	21.6	9.8	1.4	6.9	24.6	7.6	...
...	19.3	15.6	5.0	...	6.5	1.7	...	23.8	5.5	...	8.5	1.3	...	21.0	...
...	3.1	1.3	0.0	...	1.5	0.0	...	1.1	0.0	...	0.8	0.0	...	1.1	...
...	37.5	21.4	22.5	...	10.0	11.1	...	32.0	27.7	...	11.9	8.3	...	32.5	...
6.4	7.6	...	9.0	11.2	9.1	68.6	35.3	49.5	3.3	4.2	3.6	20.7	16.7	22.2	4.1	4.3	...
1.9	0.8	...	2.3	2.6	2.6	3.4	3.6	2.2	0.7	0.8	0.9	5.7	3.2	7.0	0.8	0.8	...
0.0	0.2	...	0.0	0.3	1.9	0.0	0.1	25.3	0.0	0.3	1.9	0.0	0.3	2.3	0.0	0.1	...
3.6	3.3	...	2.6	2.2	3.2	3.0	1.5	0.9	1.3	5.1	2.8	4.3	1.7	1.6	...
2.42	2.51	...	1.69	1.87	1.72	2.82	2.13	1.47	2.09	1.82	1.88	2.08	2.52	1.88	1.59	1.68	...
...	31.0	10.0	73.0	...	7.0	83.0	...	12.0	78.0	...	12.0	84.0	...	23.0	...
...	1920	...	2050	2120	2105	2640	2265	2570	1880	1880	2015	2015	2085	2085	2065	1950	...
...	2090	...	2110	2195	2160	2645	2360	2580	2080	2015	2135	2060	2150	2130	2225	2100	...
...	2080	...	2450	2410	2450	2655	2430	2605	2325	2195	2500	2205	2470	2450	2500	2500	...
...	1880	1955	...
...	2075	2245	2230	2180	2010	2120	...
...	2305	2345	2365	2370	2380	2390	...
...	Freely	Freely	Slow and sticky	Very freely	Freely	Early freely	...
...	2300	2700	2310 to 2420	2737 to 2803	...

fly ash.

FROM STATIONS (Continued)

M			N			O			P			Q			R		
South Amboy, South Amboy, N. J.			No. 4 17 × 34.5 4, cross tube Inclined Coke			Deepwater Penn's Grove, N. J. No. 5 17 × 34.5 6, Lopulco Horizontal Coke			No. 6 17 × 34.5 4, cross tube Coke			Springdale, Springdale, Pa. No. 13 20 × 24.4 8, opposed Horizontal Air cooled			Glen Lyn, Glen Lyn, Va. No. 11 23 × 30 4, intertube Horizontal Air cooled		
Not special			12 22,200			12 24,000			12 26,400			72 28,600			24 35,200, avg.		
Semi-bituminous Pocahontas West Va.			757,000			825,000			905,000			769,000			604,000-final		
Mixture of Pocahontas and Beckley seams West Virginia			Semi-bituminous Mixture of Pocahontas and Beckley seams West Virginia			Semi-bituminous Mixture of Pocahontas and Beckley seams West Virginia			Semi-bituminous Mixture of Pocahontas and Beckley seams West Virginia			Bituminous Freepoint Logans Ferry, Pa.			Semibituminous No. 3, Pocahontas Kilpea mine		
Coal	Slag	F. A.	Coal	Slag	F. A.	Coal	Slag	F. A.	Coal	Slag	F. A.	Coal	Slag	F. A.	Coal	Slag	F. A.
287	286	None	336	334	335	340	338	339	322	321	324	Average of 6 tests			363	362	365
...	6.1	6.0	6.5	12.15	5.2
...	0.6	0.6	0.6	1.15	0.6
...	13.9	6.3	27.1	41.1
43.0	48.2	...	47.1	49.4	47.8	45.4	49.0	47.8	48.3	49.8	49.0	50.8	50.8	...	53.1	54.3	53.9
24.6	25.0	...	29.0	26.4	30.6	29.2	27.7	30.2	27.8	27.6	30.2	30.6	29.2	...	33.8	30.5	28.6
16.9	1.0	...	11.8	4.4	8.8	12.5	3.1	8.2	13.2	1.4	7.8	11.0	0.3	...	9.1	0.3	4.2
...	11.9	7.3	2.0	...	7.7	2.3	...	8.5	3.0	...	12.0	8.0	5.4
...	1.8	0.3	0.0	...	0.4	0.0	...	0.3	0.0	...	0.3	0.1	0.0
...	16.8	12.9	11.0	...	12.2	10.8	...	11.2	11.1	...	14.1	9.3	10.2
6.0	6.6	...	7.1	8.4	4.5	8.7	8.2	4.8	6.2	8.7	4.3	5.0	4.5	...	1.0	2.8	2.7
1.9	2.0	...	1.7	1.7	1.6	1.7	1.7	1.6	2.3	1.9	1.6	0.6	0.7	...	0.8	1.2	1.0
0.0	0.0	...	0.0	0.3	2.4	0.0	0.4	2.4	0.0	0.2	1.4	0.0	0.3	...	0.0	0.1	1.5
2.0	3.5	...	3.3	1.8	2.3	2.5	1.8	2.7	2.2	1.6	2.7	2.0	1.9	...	2.2	2.7	2.7
1.75	1.93	...	1.63	1.78	1.56	1.56	1.77	1.58	1.74	1.80	1.63	1.66	1.74	...	1.57	1.78	1.88
...	6.0	34.0	80.0	...	25.0	76.0	...	12.0	71.0	...	2.1	3.2	41.0
2110	2075	...	2240	2270	2245	2280	2280	2285	2235	2310	2180	2400	2170	...	2725	2350	2385
2225	2170	...	2335	2335	2380	2340	2320	2405	2305	2365	2415	2490	2300	...	2795	2530	2530
2520	2520	...	2640	2635	2750	2640	2635	2665	2585	2520	2645	2680	2675	...	2850	2815	2766
...	1805	1910	1870	1960	2170	...
...	2140	2110	2070	2180	2325	...
...	2445	2505	2565	2555	2685	+2730	...
...	Viscous	Viscous	Viscous	Viscous	Freely	Viscous	...
...	2615 to 2910	2795 avg.	2678 to 2896	2710 to 2780	2800 to 2950	...

TABLE 2 COMPARISONS OF SELECTIVE ACTION AND METALLIC IRON IN THE SLAGS

1 Station.....	A	B	C	D	E	F	G	H	I	J	K	L	M	N	O	P	Q	R	Avg.
2 Equivalent Fe_2O_3 as per cent of Fe_2O_3 in coal ash.....	117	108	119	121	91	(89)	113	123	132	116	76	141	99	109	98	85	128	102	111
3 CaO as per cent of CaO in coal ash.....	181	114	74	119	124	(52)	127	81	105	76	133	(68)	(100)	118	94	140	90	(280)	113
4 Metallic Fe as per cent of total Fe.....	...	11	19	12	9	21	5	8	5	2	5	...	15	3	5	4	3	2	8

Table 2 shows the iron and lime in the slag as percentages of those in the coal ash; the values in brackets are not included in the averages because they are not representative; at station F, where petroleum coke was burned, the slag would be expected to be contaminated with the lining of the bed or with slag remaining from the burning of coal. Four slags showed a decrease in iron and five a decrease in lime, but none of them showed a decrease in both.

The alkalis in the slag were invariably lower than in the coal ash, probably because some of the alkali was volatilized; most sets of samples show alkalis to be missing.

The average increase in iron was 11 per cent and of lime 13 per cent; although these increases are not large, yet they aid in lowering the flow temperature of the slags. The relative increases of the fluxes in the various slags cannot be explained with any certainty; the action is probably quite complicated.

Another selective action is important, namely—the increase of the silica as expressed by the silica-alumina ratio, item 29 of Table 1. The increase of silica in the slag is very definite and was noted for all the coals except G; this one exception cannot be explained. Neglecting F and G, the average increase in the silica-alumina ratio was about 10 per cent.

Ferric-Iron Percentage. Fig. 2 shows that the flow temperature is very dependent on the reduction of the iron, particularly as the total iron in the slag increases. Item 29, Table 1, gives the ferric percentage; for the slags, it ranged from 2.1 for Q to 34 for N. There is no apparent connection between the ferric percentage and the chemical composition, nor with the rates of heat release per square foot of item 10. Thus both N and R burned semi-bituminous coals, and the rate of heat release per square foot was the same, but N had a ferric percentage of 34 and R of 3.2; the heat release per cubic foot is not given, but they are also about the same for these two stations.

The factors that fix the degree of reduction of the iron in the slag cannot be named definitely. The iron in the coal ash is largely a sulphide. Are the particles reduced to the ferrous state in the flame before they reach the bed or are they reduced after reaching the bed? The evidence points to the latter supposition.

Item 29, Table 1, shows that the ferric percentages of the fly ashes were all high, averaging about 75. They were usually above those of the corresponding slags when in equilibrium with air, as shown by the following:

Station.....	B	E	F	G	H	J	K	N	O	P	R
Ferric percentage.....	82	73	83	78	84	64	77	80	76	71	41
Increase or decrease above air value....	11	-3	..	12	-2	0	20	26	22	16	-13

Although some oxidation may occur, it is not likely that the particles were highly reduced while in the flame and oxidized as they cooled, because the time would be short and they were in contact with the furnace gases. It is more likely that the time did not permit the average particles to be fully reduced before they reached the bed. What actually happens when a particle falls on the bed is conjecture, but by watching them one can see that a large number at least are not immediately absorbed.

That there is often a kind of scum on the bed has been noticed when attempts were made to take temperatures with an optical instrument. During the tapping of a furnace at station G, particles coming off the top of the slag were noticed, and a ladleful was caught without slag. This ash was analyzed and gave SiO_2 36 per cent; Al_2O_3 , 23 per cent; total Fe as Fe_2O_3 , 24 per cent;

CaO , 4.7 per cent; MgO , 0.7 per cent; sulphur, 5.4 per cent. Because of the sulphur the forms of iron could not be determined, but about half of the iron must have been sulphide. This analysis proves little, but shows that all the particles of sulphide are not fully oxidized when they reach the bed.

Station J sent samples collected during a special series of tests in which the rates of burning were varied, but only two sets have been analyzed to date. The results do not confirm the supposition that the ferric percentage decreases with rating; instead, they show the reverse as follows: Test 7, with 15,000 lb coal per hour, ferric percentage, 17.5; test 9, with 40,000 lb coal per hour, ferric percentage, 26.0. Thus the rate of burning is not the sole criterion. The appendix gives further data.

As stated, the general effect of the ferric percentage on the flow temperature can be judged from Fig. 2. With low iron the curves show that the minimum flow temperature does not occur with the smallest ferric percentage; one would infer, therefore, that when the iron is low it should not be reduced too much. This point was checked by tests on the slag of R, which had the highest flow temperature. On the basis called for in the title of Fig. 2, the slag had 9.5 per cent Fe_2O_3 and 4.1 ($\text{CaO} + \text{MgO}$); the point for this composition lies near point B of Fig. 2. The slag as received had a ferric percentage of 3.2, and the flow temperature was higher than the limit fixed for the furnace, but was above 2730 F. The slag was oxidized at a low rate with the temperature maintained at 2720 F; its fluidity increased and finally attained that fixed as a standard. An analysis of the slag in this state gave a ferric percentage of 14. However, it is quite possible that the station could not obtain this higher ferric percentage without a reduction in the furnace temperature, so that more would be lost than gained.

With high iron the effect of the ferric percentage on the flow temperature is great enough so that differences in ease of tapping may be explained by it. Thus the slag received from D had a ferric percentage of 21, but the station sent analyses of slag samples taken at other times for which the ferric percentages ranged from 3.5 to 34; this would mean a difference of about 250 deg in the flow temperature, which could make considerable difference in the tapping.

Metallic Iron in the Slags. Item 22, Table 1, shows the percentages of metallic iron in the slags; this ranged from 5.5 to 0.1 and tended to be lower as the total iron decreased. Item 4, Table 2, shows the metallic iron expressed as a percentage of the total iron; this also tended to decrease as the total iron decreased. The high value of M was probably connected with the trouble that was being experienced at the time the sample was taken. No evidence can be offered as to how closely the metallic iron is held in the slag and whether it can agglomerate or sink.

It will be noticed that in no instance was any metallic iron found in the fly ash.

Sulphur. Except for A, the sulphur in the slags was low, and in all but two slags it was below 0.12 per cent. Slag A contained sulphide iron, and the coal ash was very high in iron, which shows that before the sulphur was oxidized particles of iron sulphide were buried in what must have been a very fluid slag.

ASH FUSION DATA

Items 30, 31, and 32, Table 1, give the A.S.T.M. standard cone-fusion values. The chief interest in them is how much in-

formation they can convey and how far they indicate the nature of the slag.

There is need for further investigation on the relation between the cone values and the properties of slags measured by other methods; the data developed in this investigation will permit such studies. The discrepancies between the nature of the slag as obtained by the methods used in this investigation and the cone values require study; some partial studies were made and more are proposed. One factor is very prominent—namely, that the ash of a coal has not been melted previously, whereas the ground slag has.

The peculiarities will not be discussed here, but one outstanding example is the coal ash of R. The values obtained by the standard procedure appeared so out of line that they were investigated. It was found that if the ash was first melted in air, ground, and then tested, the values were more logical. The comparison is:

	Initial	Softening	Fluid
Natural coal ash.....	2725	2795	2850
After fusion.....	2458	2654	2936

Fig. 4 was plotted to show the relation between the fluid temperatures as given by item 32, Table 1, and the flow temperatures of the slags corrected on the assumption that they all had a ferric percentage of 10 instead of the actual ferric percentages given by item 29. The cone fluid temperatures of both the slag and the coal are plotted.

The dotted line is the best mean of the points shown as crosses, which indicate the cone fluid temperatures of the slag; eight of the points lie reasonably close to the line, but others are not near. The dotted line is also a fair average for the circles, which indicate the coal ashes, but this is more a matter of chance, because the points that depart from it are not the same as for the slags.

The plot shows that the cone fluid temperature may predict fairly the flow temperature of the slag, but that it may be much in error. If the dotted line is taken as the probable value of the flow temperature of the slag, then the flow temperature for a ferric percentage of 10 will be:

$$\text{Flow temperature} = 1.2 (\text{cone fluid temperature} - 470)$$

As stated, this formula should give the probable value, but the flow temperature computed may be much in error.

It would be very convenient if the values given by the A.S.T.M. standard cone test could be used to predict the flow temperature; it would be more convenient still if cone determinations of the ash of the coal could be made and be used to predict the probable flow temperature of the slag if the coal were burned in a slag-tap furnace.

As stated previously, such a possibility is based on a more thorough knowledge of the meaning of the values given by the cone test and how they are to be interpreted. This test is standardized and is not expensive; also such data are required for other applications. A chemical analysis of the ash, however, would probably be required in conjunction with the cone value; also correction would have to be made to the ferric percentage, either actual or assumed, of the slag in the bed.

Actual Fusibilities of the Slags. Items 33, 34, and 35, Table 1, show the fusibilities determined for the slags as received, the determinations being made in an atmosphere of nitrogen to prevent the forms of iron changing during the test.

The "sticky temperature" is that at which a particle of slag under slight contact pressure first adheres to an adjacent particle. It is of no interest in the present discussion.

The actual flow temperatures ranged from 1975 F for A to +2730 F for R, for which the probable value is about 2780 F. Item 35 shows that A and B are in a low class by themselves and

Q and R in a high class, the others spreading over a range of 2300 to 2550 F.

The penetration temperature is that at which the slag has that state of fluidity that a platinum rod of 0.050 in. in diameter can be pushed through it with a force of about 6 oz; it corresponds to a condition that would be described as soft. Item 34 shows that the values for the penetration temperature did not vary as much as did the flow temperature. The interest in the penetration temperature is whether the temperature "interval" be-

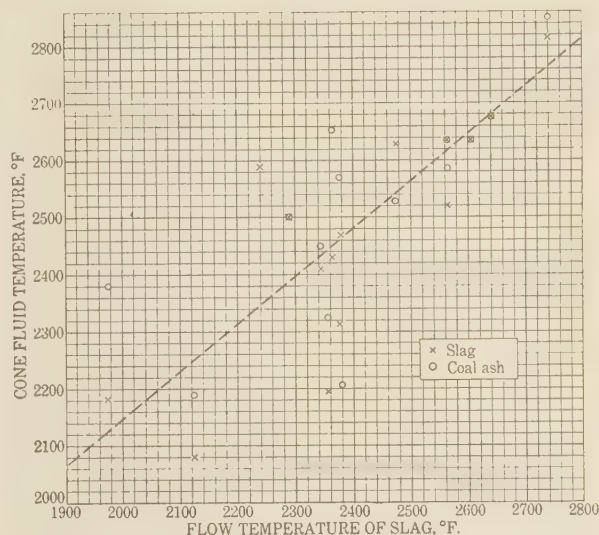


FIG. 4 PLOT OF THE A.S.T.M. CONE FLUID TEMPERATURES (For the slag from the furnace and for the ash of the coal against the flow temperature of the slags as received.)

tween it and the flow temperature is an indication of the rate of change of the fluidity at the tapping temperature; this rate of change both below and above the flow temperature is highly important to the operator. If in all slags the fluidity increased regularly between the penetration and flow temperatures, then one in which the interval was large would give more leeway in tapping than if it were small.

In general, the fluidity of slags with large intervals did not change uniformly and the rate of change was not proportional to the interval. The following peculiarities of a few of the slags are given:

Slag A had an interval of only 30 deg, and therefore became fluid very rapidly

Slag E was nearly fluid 70 deg below the flow temperature, and then changed very slowly

Slag F did not increase rapidly in fluidity until within 25 deg of its flow temperature and was excessively fluid at 15 deg above

Slag K was nearly fluid 130 deg below its flow temperature, and then changed very slowly

Slags N to R changed in fluidity very slowly; slag R would flow slowly at 2720 deg.

Item 37 gives the station reports on the ease of tapping. These independent observations may not be based on the same conditions, as the reactions of the observers would depend on the facilities for the operation. Station R reported that the flow was very free for the first 10 min, and then became sluggish.

Item 37 gives some reports on the temperature of the slag when tapping. All those reported by the stations were made by an optical instrument. The measurement is difficult to make, and optical instruments are not always reliable.

The Bureau investigators made the measurements at G and R. Particular pains were taken at R, and shields and supports were installed. The optical pyrometer was calibrated especially for the test, and in addition a platinum-rhodium thermocouple was immersed in the slag. The values obtained were:

Start of tap, optical, F.....	2770
At 10 min, optical, F.....	2740
At 10 min, thermocouple on surface, F.....	2705
At 10 min, thermocouple 1½ in. below, F.....	2625
At 1 hr, optical, F.....	2705

A similar attempt was made at station G, but excessive steam from the water spray prevented good readings from being obtained.

RETURNING FLY ASH TO THE SLAG BED

Disposal of the fly ash is one of the problems of power plants. When slag-tap furnaces are used, the idea of returning the ash to the furnace and absorbing it in the slag appears attractive. How many stations have attempted this practice is not known, but it has been followed at the Hell Gate Station, New York, with at least enough success to continue it. A recent letter from Mr. J. J. Grob, engineer of tests, says: "We have continued to return our fly ash to the furnace and have always utilized the dry fly ash from the hoppers to facilitate its injection into the furnace by feeders. It appears that most of the fly ash finds its way to the floor, but a large percentage of this settled fly ash does not melt, some of it becoming mechanically entrained in the slag which deposits in the combustion process or else lying on top of the slag mass in the form of a dust which is moved around by the draft currents. In some of our experiments we injected fluorspar, which helped the slag removal, and we also tried soda ash, which appeared to be even better than the fluorspar. We do not, however, use any fluxes as a regular proposition, since later developments improved the conditions of slag removal."

At the request of the committee the Bureau undertook a study of this phase. The analysis of the problem was that it can be divided as follows:

- 1 Handling the fly ash until it is delivered to the furnace.
- 2 Injecting it into the furnace.
- 3 Depositing it on the bed and preventing it from being carried out of the furnace.
- 4 Absorbing it in the slag.
- 5 Effect on the fluidity of the slag and its tapping.

Item 1 is a plant problem and will not be discussed.

The methods of injecting the fly ash and the success in depositing and retaining it on the bed depend on certain requirements which will be discussed. If the compositions and relative quantities of fly ash and slag are known, the resulting fluidity can be predicted from data already obtained. Evidently, the absorption of the fly ash by the slag must first be studied.

The problem of absorption in the slag appeared to fall into two fields—one in which the composition of the fly ash was such that it would melt and have the fluidity for tapping at the temperature of the slag bed and one in which it would not melt. It was also evident that the size of the lumps of fly ash might bear on the problem in so far as such lumps might project above the bed and be subjected to the hot gases or might be immersed below the surface and thus be at a lower temperature; also the size of the lump materially affects the area of fly ash in contact with the slag.

An attempt was made to gain some information in a small gas furnace with a pot 10 in. in diameter, but the high velocity of the gas swirled the compressed lumps of ash about, and the ash was carried away instead of being melted. Therefore, the remaining

studies were made in the large experimental furnace shown in Fig. 17 of the second report; the slag bed was 28 in. by 32 in. The technique of its use is described in the same report.

The test was run continuously day and night for 10 days. The first step was to form a bed of molten slag, for which that from Toronto (column G, Table 1) was used. The temperature of the slag surface was maintained at 2600 to 2650 F. The atmosphere was reducing, as shown by the percentage of Fe_2O_3 in the slag at progressive times:

Hours from start.....	0	22	168
Per cent Fe_2O_3	4.0	4.6	1.1

The average velocity of the gases as measured was 9 ft per sec ½ in. above the slag surface.

TABLE 3 PROPERTIES OF FLY ASHES USED IN TESTS

Ash.....	No. 1	No. 2	No. 3
From.....	Trenton Channel	Hell Gate	Hell Gate
Sample No.....	526	245	241
Combustible, per cent.....	5.8	17.0	58.0
Ash analysis, per cent:			
SiO ₂	51.6	50.2	53.0
Al ₂ O ₃	32.7	28.8	23.8
Fe ₂ O ₃	6.6
FeO.....	1.9
Fe.....	0.1
Total Fe as Fe ₂ O ₃	9.1	13.6	13.9
CaO.....	2.1	4.0	3.9
MgO.....	0.9	2.3	2.0
SO ₃	0.4	1.0
Alkalis.....	..	0.7	2.4
A.S.T.M. cone, F:			
Initial.....	2516	2150	2030
Softening.....	2619	2300	2290
Fluid.....	2804	2690	2580
Flow temperature.....	..	+2700	..

Fly ashes that were available were used; Table 3 gives their properties. No. 1 is quite refractory. Nos. 2 and 3 are closely similar, except for their combustible content; both also contained sodium and potassium salts, presumably from being wetted with sea water. These ashes had relatively high flow temperatures compared with the slag and were used to accentuate the factors involved.

The next step was to place lumps of the fly ash or other mixtures on top of the slag, watch what happened to them on a time basis, remove the lumps at various stages and examine them when cold, and perhaps analyze portions. The objectives of the experiment were developed for the main part as the tests proceeded. The results of the tests are summarized because the effects of the factors are interlocked; few experimental data are given.

SUMMARY OF RESULTS

Hell Gate reported that it was injecting the ash in a dry state; such a procedure did not seem logical, and it would be expected that a large part would be carried out of the furnace. This proved to be so, even with the relatively low velocities of the test furnace and in which the ash did not drop any distance. The logical method seemed to be to wet the ash, and a number of tests were made to determine the effect of wetting. However, wetting cannot be considered independent of the size of the lumps.

A dry ball or block was one that had been molded while wet and dried; it was fairly solid and would break into small pieces rather than dust. The relations between wetness and designation were, approximately, as follows:

Water, per cent of ash.....	10	20	30	45	55
Designation.....	Damp	Wet	Very wet	Plastic	Sludge

Under the condition of test in which the lumps were placed on the bed instead of being dropped from a height, wetting or even molding and drying eliminated dust. A dry ball retained its shape after it was placed in the furnace. After the lump had been placed on the bed, it did not flatten materially with moisture up

to 30 per cent; with larger amounts the balls tended to flatten out, and with 45 per cent and higher the round shape could not be maintained. A dry ball remained quiescent, and its exposed surface fused quickly; the height of its projection from the bed remained the same for a long time. With the ash wetted, "spluttering" occurred; that is, the exposed surface erupted and threw out showers of small pieces which increased in size with a wetness up to about 30 per cent. The result was that the exposed part of the ball decreased in height in a few minutes, and the small pieces were distributed over an area of about 6 in. radius; the surface of the ball did not fuse until the eruption ceased. For balls over 1 in., the percentage of the ball that was erupted appeared to decrease with increase in the size of the ball; with larger balls the action was slower; and with very large pieces the percentage of spluttering was small.

The maximum spluttering occurred with about 30 per cent moisture, although the difference between 10 and 30 was not great. As the material became so wet that the ball spread over a larger area and the layer became thinner, the spluttering decreased and pieces fell back on the lump. A $\frac{3}{8}$ -in. layer of sludge spread over 2 sq ft of the surface did not splutter, but heaved because of steam generated below it, and was split up into small floating pieces.

Examination of the residue of the balls removed after one or more hours showed another action attributable to the moisture, because there were fissures in the unmelted portions into which black slag had flowed. The number and size of these were greater with increase in moisture; this admittance of the slag will aid absorption.

Effect of Combustible in the Fly Ash. Before making the tests it was recognized that the presence of combustible in the fly ash would have some effect. First, it could reduce the Fe_2O_3 in the ash to FeO or Fe ; second, it could act as a mechanical separator between the particles of ash and prevent them from fusing together. Both these suppositions were found to be correct.

That a certain amount of the carbon is consumed in reducing the Fe_2O_3 to FeO or to Fe and that the excess carbon remains mixed with the ash are shown by the following: Balls of ash No. 1 were made up, each weighing 2 lb; the carbon was in the form of 60-mesh soft coke, and the carbon content of the balls was 5.8, 10.0, 23.5, and 46.0 per cent. These were dried, placed on the slag, watched, removed at the end of 2 hr, examined, and parts taken for analysis.

TABLE 4 EFFECT OF CARBON IN FLY ASH^a

Carbon per cent	Portion of ball	Analysis, per cent—				Metallic Fe as per cent of total Fe	Weight of piece removed, lb
		Combustible by ignition	Fe_2O_3	FeO	Fe		
5.8....	Center	3.6	0.1	2.9	3.9	62.0	0.46
	Surface	0.6	0.0	7.8	0.3	5.0	
10.0....	Center	7.0	0.1	3.1	3.5	60.0	0.36
	Surface	22.4	0.1	3.2	2.5	57.0	
23.5....	Center	46.2	0.0	2.9	1.3	37.0	0.57
	Surface	6.7	0.0	7.7	0.7	10.0	

^a Ash analyzed: Fe_2O_3 , 6.6 per cent; FeO , 1.7 per cent; Fe , 0.1 per cent; metallic Fe, 1.6 per cent of total Fe.

There was a distinct difference in the material at the centers of the lumps removed. With low carbon, the ash was well sintered together; as the carbon increased, it was looser and more friable. Table 4 gives the summary of the measurements. With all percentages of carbon the Fe_2O_3 in the original ash had all been reduced to FeO and Fe . Theoretically, each per cent of Fe_2O_3 requires 0.075 per cent of carbon to reduce it to FeO and 0.225 to reduce it to Fe . The carbon which the table shows to have disappeared at the center is well within the order of accuracy.

The surfaces for the 5.8 and 46.0 per cent samples were the tops of the balls; these surfaces were exposed to the furnace gases and

were not in contact with the slag. The table shows that most of the carbon at these surfaces had disappeared and that the percentages of metallic iron were much lower than those at the centers; these actions can be attributed to oxidizing by the furnace gases.

The deductions from these data are:

1 Carbon in the center of a lump of fly ash reduces a large portion of the iron to the metallic state, and only a small quantity of carbon is consumed in this action.

2 The remainder of the carbon is available for reducing the iron in the slag bed, as evidenced by the vigorous boiling around the sides of even a dry ball after it is inserted in the slag.

3 It is probable that most of the excess carbon released by the melting of a ball will rise to the surface and be oxidized.

4 Whether the addition of a large proportion of fly ash to the bed will cause trouble due to metallic iron is not known, but at least it will tend to lower the fluidity of the bed.

5 The carbon is partly burned out at the surface of the ash exposed to the furnace gases.

The presence of combustible is therefore another reason for spreading the added ash over the bed in a thin layer. This was further proved by tests on ashes Nos. 2 and 3, both having high combustible and containing sodium; the burning of the carbon could be seen. With 50 per cent water a thin sheet burned over the whole surface, and all visible signs of the ash were gone in 50 min. Even with a large lump having the same moisture, the ash tended to spread over the surface. Although the ash disappeared in both instances, yet that portion of the bed required much longer time to reach normal fluidity by feel.

All the many trials with balls containing combustible showed that it acted as an infusible diluent and thus prevented the ash fusing together and that this effect increased with increase of the carbon. However, all these three ashes were not free flowing at the temperature of the furnace; the Appendix gives tests which show the retarding effect of carbon on fly ashes, the flow temperatures of which are near the temperature of the slag bed.

Effect of Fluxes on Fly Ash. As ash No. 1 was quite refractory, it was logical to try the effect of adding fluxes to the ash. A flux in sufficient quantity was known to be effective because exactly the same thing was done in the tests in this same furnace, as given in the second report.

Hydrated lime and crushed limestone were added to give 10 per cent CaO in the mixture; the moisture was varied according to the type of lump inserted. Both appeared to increase the spluttering, and both reduced the time for absorption. This reduction amounted to 1 hr when judged by appearance and $3\frac{1}{2}$ hr when judged by the bed attaining uniformity by feel. The time required for the bed to reach a uniform feel was greater as the lump was larger, because that portion of it which was deeper in the slag would be at a lower temperature. Fluorspar also acted as expected and in a shorter time than did the lime.

The most important effect was that finally the portion of the bed to which the ash had been added acquired the same fluidity as the rest of the bed, whereas without the flux it was stiffened.

Effect of Common Salt. As stated, ashes Nos. 2 and 3 contained sodium and potassium chlorides, presumably because they had been soaked with sea water. It was thought that these salts might help in the melting, although it had been shown that at furnace temperatures chlorides volatilize before they can be absorbed by the slag. Tests were made with these ashes and also No. 1, to which NaCl had been added. This appeared to make the boiling more vigorous and because of the luminous flames gave the impression that it helped the carbon to burn.

There was nothing definite enough to show that the presence of the chlorides was an assured benefit.

General Conclusions on Absorption of Fly Ash. The samples

received from the stations showed that the fly ashes contained less flux and consequently were more refractory than the slag. As a consequence, any station that returned the fly ash to the furnace would be raising the average flow temperature and would have to increase the minimum rating at which it could tap with the same facility.

The studies reported deal with local actions on rate of absorption and the stiffening of the surrounding slag. This is all-important in a furnace, because floating lumps interfere with the flow of slag through the relatively small tap hole. Furthermore, when lumps are distributed over the whole bed, they may form large islands of solid slag, either stationary or floating; as long as they are stationary they will not interfere with tapping; on the other hand, if such large masses are melted during a period of operation at high rating, they will give a slag which will cause trouble in tapping if the temperature should fall.

At each station the best distribution of the fly ash would be a problem related to the relative properties of the slag and ash and to the quantity of ash it was desired to return. Whether distribution is considered from a local or general standpoint, it would seem that the ash should be distributed uniformly both on an area and a time basis and that an added layer should be thin. It would also seem necessary to wet the ash to prevent it from being carried out as dust. Whether wetting be slight to form small balls or pellets or whether the ash be made semi-fluid so that it can be distributed as a stream is a question of cost and convenience. The tests showed that the semi-fluid state was preferable, although small balls should be satisfactory if the ash is not refractory relative to the furnace temperature.

Assuming an extreme case of a coal with 10 per cent ash, with 40 per cent of the total ash of the coal returned to the furnace as fly ash, and with 50 per cent moisture, the water used per pound of coal would be 0.02 lb; with 400 F stack temperature of the gases, the loss per pound of coal would be about 22 Btu; this would be offset if the fly ash contained about 6 per cent combustible which burned.

The data from the stations showed that the greater part of the iron in the fly ashes was Fe_2O_3 ; that is, the ferric percentage was high. Fig. 2 shows that the effect of a high ferric percentage will depend on the total iron in the ash, but it will always be necessary for the iron in the fly ash to be reduced if it is not to raise the flow temperature of the slag bed. It is therefore very fortunate if the combustible insures this reduction, but only a small quantity of carbon is required. The samples from the stations show that if the fly ash comes from a collecting system, the combustible will usually be low; ash No. 1, Table 3, is an example of such an ash and had 6.8 per cent. The few samples of ash from hoppers that have been received were high in combustible, and presumably this will usually be so.

Actual tests in which large quantities of fly ash are added would be required to determine whether the excess carbon would result in high metallic iron and whether it would accumulate at the bottom.

It would, however, seem desirable to give the carbon an opportunity to oxidize on the surface by depositing the fly ash in a thin layer and not to sink it in the bed by adding the fly ash as large lumps.

ACKNOWLEDGMENTS

This investigation has been carried out under the authorization of O. P. Hood, chief engineer, mechanical division. M. E. Bessemer, junior fuel engineer, assisted in the experimental work throughout the investigation. The many chemical analyses required were made in the chemical section by W. H. Frederic under the direction of W. A. Selvig.

Acknowledgment is made to the support given to the investiga-

tion by the members of the committee and its chairman, K. M. Irwin. Both the committee and the Bureau express their appreciation for the very willing cooperation of the managements and engineers of the stations in making the special tests; considerable extra work would be necessary.

Appendix

SOME of the data obtained since the report was written is added to increase the completeness of the sections on samples from stations and returning fly ash to the slag bed.

SAMPLES FROM HUNTLEY No. 2, STATION J

Station J collected samples during a series of tests for other purposes in which the coal fired varied from 9600 to 40,000 lb per hr. The slag sample was collected in a box submerged in the water below the outlet from the slag-discharge pump. The fly ash was from that deposited in the third pass.

Five of the eight sets of samples were examined. The data for the highest rate are shown in Table 1; the full data for all five are not given because the analyses show inconsistencies which indicate that the samples are not true averages. The following values are of interest:

Coal, lb per hr.....	12,100	15,000	16,500	20,500	40,000
Slag, ferric percentage..	16.9	18.3	10.5	10.6	26.2
Fly ash					
Ferric percentage.....	72.1	70.6	75.2	74.0	63.1
Combustible, per cent.....	24.9	15.1	36.3	17.8	12.0

They indicate that the slag was more reduced at medium rates. That it was least reduced at the highest rate seems illogical, but reasons for it could be that the reducing area of the flame was further from the burner or that particles deposited were covered before they were fully reduced. The fly ash at the highest rate contained the least carbon and the ash was most reduced; the latter would seem logical, but both would depend on the effect of the gas velocity as fixing what is deposited in the pass. Closely controlled tests would be required before making safe generalizations and the effect of rate may not be independent of the equipment.

RETURNING FLY ASH TO THE SLAG BED

A further set of tests was made using fly ashes with lower flow temperatures than those on which the conclusions in the paper were based. The same slag was used for the bed—that from Toronto, Station G. That station also collected, by the dust-bag method, a supply of fly ash which by analysis contained 6.2 per cent combustible and its ash 28.8 total equivalent Fe_2O_3 and 3.9 (CaO + MgO). To form an ash free of carbon, the slag used in the bed was ground to 60 mesh.

These two ashes were made into balls weighing about 2 lb dry and from 4 to 5 in. in diameter; definite proportions of carbon and water were used as in the previous tests.

The actions when the balls were placed on the bed were much the same as with the higher fusion ashes with the exception that there were less eruptions and spluttering. The balls of ground slag did not have the binding quantity of the fly ash and tended to disintegrate; this and the larger size of the particles affected the results.

Table 5 gives the principal data on the effect of carbon and corresponds to Table 4 for the higher-fusion ashes. All these trials were made with balls molded moist and partly air-dried when placed in the furnace. The effect of carbon in delaying absorption is illustrated by the slag taking 0.3 hr, the fly ash with 6.2 per cent carbon 1.5 hr, and with 15 per cent carbon 4.2 hr.

The analyses must be considered relative to the time elapsing before the lumps were removed. Evidently the center of the slag

balls did not have the time or temperature necessary fully to reduce the iron. The centers of the balls of fly ash show high metallic iron which is largely oxidized when exposed at the surface; with the 50 per cent carbon and the 1.5 hr in the furnace, 51 per cent of the total iron was metallic, and 11 per cent of the metallic iron was in the form of pellets over 60 mesh. The shapes of these pellets showed that they were trickling through the particles of unfused ash; it is improbable that they would ever have been exposed at the surface so that they could oxidize, but would have ultimately sunk in the bed.

TABLE 5 EFFECT OF CARBON IN FLY ASH

Kind	Ash used— Carbon, per cent	Time to absorb or when re- moved, hr	Part analyzed— Portion	State	Analysis, per cent				Metallic Fe as per cent of total Fe
					Carbon	Ferrous FeO ₂	Ferrous FeO	Fe	
Slag	0	0.3
Slag	10	0.6
Slag	10	0.23	Center	Sintered	7.3	0.6	29.8	0.8	3
Slag	10	0.23	Surface	Slag	0	4.8	22.9	1.8	8
Slag	25	0.26	Center	Dust	19.2	3.5	26.9	0.4	2
Slag	25	0.26	Surface	Slag	0.1	2.4	24.3	2.4	10
Slag	50	0.27	Center	Dust	39.5	2.3	26.7	0.7	3 ^a
Ash	6.2	1.5
Ash	6.2	0.5	Center	Sintered	3.5	0.6	20.8	6.2	27
Ash	6.2	0.5	Surface	Slag	0.4	1.4	24.9	2.0	9
Ash	15	4.2
Ash	50	1.5	Center	Dust	39.9	0.8	14.1	12.1	51 ^b
Ash	50	1.5	Surface	Slag	0.1	2.8	23.4	1.9	9

^a Some iron pellets over 60 mesh.

^b 5.5 per cent pellets over 60 mesh.

Tests with varying proportions of water to cause the slag to spread when placed on the bed confirmed that to a large extent the effect of the carbon was counteracted; with 50 per cent carbon a layer $1\frac{1}{2}$ in. thick was absorbed in one hour but another, probably $2\frac{1}{2}$ in. thick in places, was not completely absorbed in 5 hr.

These results confirm the conclusion in the paper and show that even with low-fusion ashes carbon delays absorption and forms metallic iron, some of which may ultimately reach the bottom of the bed.

Discussion

E. G. BAILEY.⁷ The authors have presented a very complete report on a research subject of great interest to the "Fuels Division" of the Society. At the present time there are in operation about 80 large boiler furnaces from which the slag is removed in the molten form in a satisfactory manner.

A paper entitled "The Slag-Tap Furnace and Its Effect Upon the Selection of Coal for Burning in Pulverized Form," by E. G. Bailey and R. M. Hardgrove and presented at the Third International Conference on Bituminous Coal showed that 75 per cent of all coal used by public utilities and 87.5 per cent of all coal available had a fusion temperature of less than 2500 F, and could be successfully handled in slag-tap furnaces. The combination of pulverized fuel with molten ash removal is adaptable to a wider range of fuels for high capacity and efficiency than any other method of combustion. The characteristics of fuels which limit their application to other forms of combustion, such as volatile, coking properties, low fusion temperature of ash, etc., can be ignored and the purchase of fuel is greatly simplified as it becomes a matter of buying coal on a Btu price basis for slag-tap furnaces.

This method, however, has one limitation, viz., high fusion temperature of the coal ash at continued low rates of combustion. A better understanding of the properties of slags, which is provided by these "Progress Reports" on the research conducted

⁷ Vice-Pres., Babcock and Wilcox Co., New York, N. Y. Mem. A.S.M.E.

by the Bureau of Mines for the A.S.M.E. Special Research Committee, will be of great help to operators. As in the case of any new development the increase of knowledge through research and operating experience will extend and improve the usefulness of as important a process as the collection and removal of ash from coal-fired furnaces.

The effect of oxidation of iron in the slag on its flow temperature is reported very completely in this paper. The minimum flow temperature as shown in Fig. 2 occurs with 30 per cent of the iron in the ferric state for the slags low in iron, decreasing to 10 per cent or less for the slags higher in iron. The slags actually received had a maximum of 31 per cent of the iron in the ferric state with the average much lower than this. It would not seem therefore that changes in the path of the flame over the slag surface or in the amount of excess air used would be expected to lower the flow temperature appreciably, although detailed study of individual cases may be fruitful in the light of this information.

In general, a minimum excess air and a flame closely in contact with the slag should give a minimum amount of ferric iron. Both of these furnace conditions tend to raise the temperature of the slag pool which makes the slag flow easier. Furnaces D, H, and K have vertical burners impinging directly on the slag and in spite of this fact two of these slags show a high relative amount of ferric iron. A possible explanation of this may be that the secondary turbulence produced by this impingement of the flame on the floor may burn the coke on the surface of the slag before it can reduce the ferric iron. The slags from these three furnaces are all reported as tapping freely. It is believed that these burners directed vertically downward against the slag pool could be placed even closer than the present distance of about 16 ft, thereby securing even better results. This would extend the range of satisfactory operation and reduce the cost of the furnace through higher rates of heat liberation.

The discussion of melting fly ash in the slag bed is of interest as it provides a simple means of disposing of this dust.

A. L. BAKER.⁸ The work done by this Committee, so well presented in the paper by Messrs. Nicholls and Reid makes a valuable contribution in this field.

The extensive use of the locally famous "Kincaid" coal in the central stations of the Chicago District together with the rapid increase in number of slag-tap furnaces in use has been the cause of an unusual amount of interest in that rather neglected by-product of the steam central station, the slag ash. Research activities have been widespread in delving into the nature of the slag, both in molten and solid form, and its behavior under various conditions. This coal is unusual in that the percentage of ash is high, the sulphur content is high, and the slag is difficult to handle in the furnace or on boiler tubes due to a quality best described as "toughness."

Table 6 contains analyses of this coal from four mines in the Kincaid district.

Table 7 contains analyses of Kincaid coal slag in three forms as obtained from a slag-tap furnace and supplements data given in Table 1 of the Report for furnace D.

Table 8 contains analyses of Kincaid coal fly ash as obtained from gas samples and not shown in Table 1 of the Report.

Experience with this coal and slag in this district confirms the Report in that generally the flow temperature decreases with increase in reduction of the iron in the slag. However, a comparison of the total iron in the Michigan City and State Line analyses of slag from the slag tap furnaces indicates that for the same ferric percentage the flow temperature decreases with increase in total iron. Free flowing slag is an unusual thing at Michigan

⁸ Engineer, Sargent and Lundy, Inc., Chicago, Ill. Assoc.-Mem. A.S.M.E.

TABLE 6 FUEL ANALYSIS

Mine source			Analysis (as received)						
No.	Name	Location	Grade	No. of samples	Moisture	Ash	Sulphur	Btu	
7	Hawthorne	Kincaid, Ill.	Segs.	10	13.20	14.90	4.51	10,044	
8	Hawthorne	Humphrey, Ill.	Segs.	10	13.18	14.89	4.03	10,036	
9	Hawthorne	Calloway, Ill.	Segs.	8	13.80	13.89	3.81	10,127	
58	Taylorville	Taylorville, Ill.	Segs.	11	14.22	12.76	3.89	10,207	
				Averages	13.60	14.11	4.06	10,104	

TABLE 7 SLAG ANALYSIS

(Kincaid Coal)

Date	Sample no.	Metallic Iron, Fe	FeO	Fe ₂ O ₃	Total Fe	F	Mn	SiO ₂	Al ₂ O ₃	CaO	MgO	TiO ₂	S as S	S as S	S as S	True sp gr
8/6-7/30	GS-1	2.90	31.70	0.98	28.22	0.07	0.08	36.00	17.88	8.00	0.64	0.80	none	none	none	3.32
9/24/30	GS-2	3.93	25.65	11.03	31.58	0.07	0.10	34.60	16.31	6.00	0.28	0.57	none	none	none	3.32
10/3/30																
10/4-30/30	GS-3		28.09	3.20	24.08	0.025	none	37.40	19.65	6.40	1.44	0.55	0.21	none	0.36	3.23
10/23-27/30	GS-4	2.90	28.81	5.96	29.45	0.07	0.05	35.88	17.07	7.80	0.06	0.76	none	none	none	..
7/25/30	ACS-1	2.24	24.91	4.73	24.08	0.14	0.02	39.04	18.80	6.00	1.00	0.80	none	none	trace	3.20
8/6/30	CS-2	2.24	24.49	5.50	25.13	0.07	0.09	36.00	19.04	9.00	0.80	0.80	0.01	tr	0.34	..
8/7/30	CS-3	2.57	24.36	9.60	28.22	0.07	0.08	26.48	18.00	6.18	1.53	0.72	none	none	none	..
10/3/30	CS-4	3.37	24.18	5.63	26.10	0.07	0.07	38.60	18.77	6.40	0.28	0.55	none	none	none	..
8/6/30	ACS-2	none	none	none	..
Average		2.88	26.02	5.83	27.11	Ferric per cent = 15										
Michigan City 5/8/31		2.24	23.15	5.14	23.85	0.10	0.04	36.01	24.02	6.30	1.44	0.56	0.14	0.07	0.11	

Indiana Coal—Ferric per cent = 15 GS—Granulated slag CS—Sampled while running blocks ACS—Samples from annealed blocks

TABLE 8 ANALYSIS OF COTTRELL FLUE DUST

(CHICAGO DISTRICT ELECTRIC GENERATING CORPORATION, RESEARCH DEPARTMENT)

Sample no. (A)	Date	FeO	Fe ₂ O ₃	Calcd total Fe	SiO ₂	Al ₂ O ₃	CaO	MgO	TiO ₂	S as SO ₃	Free C	CO ₂	Sp gr	Loss on ignition
5	10/14-18/30	3.31	17.30	14.66	45.40	23.70	6.80	(B)	0.76	0.87	0.80	0.70	(B)	1.00
6	10/19-20/30	2.57	21.48	17.02	45.72	19.94	6.00	(B)	0.74	1.00	0.59	1.00	(B)	1.30
7	10/23-24/30	3.72	17.80	15.34	46.36	20.53	6.40	(B)	0.85	0.97	0.98	1.20	(B)	1.40
9	..	3.16	15.68	13.44	45.10	21.34	6.85	0.92	0.71	2.28	(B)	(B)	(B)	0.90
10	2/20/31	2.88	16.96	14.10	44.80	21.05	6.10	1.07	0.76	2.39	(B)	(B)	(B)	1.80
47	6/7/33	3.30	13.80	12.21	44.84	19.14	6.08	1.40	0.09	2.64	1.02	0	2.56	1.64
49	9/3-7/33	4.80	12.15	12.28	45.20	19.43	5.80	1.43	0.28	2.47	0.95	0	2.50	1.59
Michigan City 4/8/31		2.87	12.00	10.64	42.60	31.90	3.84	1.44	1.20	0.96	2.60

(A)—certified. (B)—no data.

City where the slag has a total iron content of about 23 per cent whereas the slag at State Line with the iron content averaging 27 per cent usually flows freely and sometimes dangerously so. The ferric percentage is about 15 for both these analyses. Another way of stating this point would be, that the total percentage of iron in coal ash is an important factor in determining the flow characteristics of the slag, other conditions being comparable, the flow temperature decreasing with the increase in total iron content.

From numerous experiments conducted over a period of years the flow temperatures of slag from slag-tap furnaces in this District may be stated as follows:

Kincaid coal; measurements by optical pyrometer at slag spout	
Extreme lowest flow temperature measured.....	2200 F
Average "low slag" temperature.....	2350 F
Average "high slag" temperature.....	2475 F
Maximum measured temperature.....	2750 F

At the lowest temperature the slag is of chewing gum consistency and very difficult to keep running. At the highest measured temperature the slag is very thin and runs like water. Care must be taken to keep the flow to reasonably small proportions when the slag is at high temperature as the slag stream will penetrate extremely small crevices and is highly corrosive. A slag gate of heavy cast iron, not cooled, has been cut out completely by a hot slag in a matter of a few minutes. Where the gate is water cooled the slag forms a protecting coating of frozen slag on the surface and erosion is prevented.

Our experience confirms the point made in the Report that there is a "selective action" in the furnace resulting in the fly ash being less fusible than the slag from the same coal; the total iron in the fly ash being about 50 per cent of that in the slag.

The statement of percentage of sulphur in the slag being below 0.1 per cent is confirmed also.

Although no quantitative experiments are available locally, it would seem that reduction of the iron in the slag increased with rate of burning. This may be explained by the fact that the increase in the ratio of FeO to total iron may be caused by the increased temperature or by a reduction in the excess air available. For a given excess air condition, the reduction of iron (expressed by the formula $\text{Fe}_2\text{O}_3 > 2\text{FeO} + \frac{1}{2}\text{O}_2$) is determined by the temperature because Fe_2O_3 is less stable at high temperatures and FeO more stable.

Comparison of Tables 6 and 7 illustrates the point made that the reduction of iron in the fly ash is much less than in the slag. In the fly ash most of the iron is present as Fe_2O_3 whereas in the slag most of the iron is present as FeO.

A very interesting and important experience in the burning of storage coal from under water storage illustrates the effect of small quantities of silica sand on flow temperatures.

Recently it was necessary to reclaim and burn practically an entire storage pile of which about half was under water. Some of this coal was burned in two slag-tap furnaces. As the percentage of under-water storage coal increased difficulties were experienced with the slag in tapping due to accumulation of sand in the molten bed. After struggling with the slag in an endeavor to maintain the boiler on the line it finally became necessary to shut the boiler down and mine out the slag bed by hand, an extremely difficult operation. Cone tests were made for the fusion points of the coal slag and of the coal-and-sand-mixture slag in accordance with the standards of the American Ceramic Society. The "end point" of the coal slag was at 2489 F and of the coal-and-sand slag, 2430 F. In spite of this apparently lower fusion

point for the coal-and-sand mixture the viscosity of the sandy mixture was so great it was impossible to tap.

A series of experiments have been made on returning fly ash to a slag-tap furnace, in the dry state as collected. No difficulty was experienced in introducing the ash into the furnace. Some recirculation of the fly ash was observed but it appeared to be a small percentage of the whole. The bulk of the ash lay at the bottom of the inlet opening in the furnace wall in the form of a large cone. The total ash introduced at one time in the furnace represented a twenty-four hour accumulation in the dust collector hopper. This amount of ash appeared partly melted after six hours and at the end of twenty-four hours was practically completely melted. The experiment was continued for a period of a week when trouble with the collector forced us to discontinue. From these tests it would appear desirable to spread the ash, as suggested in the report and to use a "pug mill" for introducing it into the furnace, the addition of water in the mill aiding in the spreading by mechanical action and formation of steam bubbles. Observation of the tapping operation indicated that the average flow temperature of the entire slag bed had increased materially due to the fly ash, though cone tests on the fusion point of the ash as compared with the slag indicated that their "end points" were within 50 F of each other, the fly ash having the higher.

There is little advantage to be gained by introducing the fly ash into the furnace and melting it to slag unless the slag is of value commercially. There is, of course, a loss of sensible heat in melting the ash, and disposal of the fly ash is not much more difficult when wetted and sluiced than disposal of the granulated slag itself. Under present operating conditions the combustible in the ash is under one per cent and will not offset the loss incurred in melting.

Disposal of the molten slag after leaving the furnace has been a problem attended with mechanical difficulties and considerable danger. Slag in itself is rather easily handled. It is granulated well with little trouble and is not at all sensitive to water quantities or velocities or angle of impact, etc. It is only when the molten iron itself taps with the slag but as a distinctly separate stream that the difficulties begin. Danger of explosion is great. If the stream of molten iron strikes even a small quantity of water in the spout there might be a dangerous explosion. This fact is recognized in the steel industry and great care is taken to keep the slag "monkey" and ladles dry before tapping in slag which may contain iron. The cause lies in the relative insulation value of the pure slag and the iron. The heat transfer rate of the molten iron is probably about 250 or more times that of the slag and therein lies the explanation.

The method adopted for disintegrating the molten slag when the slag-tap type furnaces first came into vogue was to use a break-up jet of water impinging directly on the slag stream at the furnace spout. There was usually an impact plate to assist in this process and a proper sluice-box system of alloy iron to carry the product away to the sluice trench.

In an effort to reduce the cost and difficulties of this system and to produce a coarser slag for commercial purposes, in this district a "granulator" has been used which permits the molten slag to flow into a cylindrical chamber of water with comparatively little agitation. The bottom of the granulator is fitted with an orifice to limit the flow of water and permit the outflow for the granulated slag. These granulators are successful and simple but still offer some hazard in that control of the slag flow must be manual and explosions may occur in the spout or granulator chamber during periods of heavy flow, "hot" slag or flows of pure molten iron.

A new method of tapping has been proposed to eliminate entirely the personal hazard and the attendant, and to make the entire method of tapping automatic. This is the "continuous-

tap" system, in which a suitable tap hole of fairly generous dimension is located in the bottom of the furnace floor and in a location to give good flow from all parts of the floor. It should be located in a hot area in relation to the burner flow lines. Slag drops through this hole as formed, through a refractory-lined flue and into a large tank of still water. This tank serves as both storage and disintegrator tank. Make-up water is added as needed to maintain temperature, preferably by thermostat control. The tank is emptied into the sluice system about once a day. The main difficulty with this method is to keep the floor hole open during periods of operation at low rating. This may be solved by drawing furnace gases through the hole or by separate heat source maintaining the slag hole at molten temperature. The method itself is attractive from many angles, but there will be some few details of operation to work out and contributions from all on this subject are welcome.

J. D. DONOVAN.⁹ We have installed in our Quindaro generating station two slag-tap furnaces, No. 17 boiler having been placed in operation in April of 1931 and No. 18 boiler having been placed in operation in June of this year. These steam-generating units operate at 450 lb per sq in. and a total temperature of 700 F, and have a normal rating of 150,000 lb of steam per hour with a four-hour rating of 180,000 lb of steam per hour. Both of these units are Babcock & Wilcox Stirling type and are complete with economizer, superheater, and air preheater. The furnaces of both of these units are water-cooled Bailey Block type with water-cooled bottom.

The bottom of boiler No. 17 is composed of 2½-in. tubes and the floor is built up with two courses of fire brick underneath the tubes resting on a steel plate bottom. The space between the tubes is packed with "KN" to within about four feet of the uptake wall, the balance of the distance being packed with magnesite and liquid "U." There is then another steel floor plate, on top of which is a course of pure magnesite. The furnace floor in No. 18 boiler is composed of 3¼ in. tubes which are swaged to 2½ in. at the rear end to permit passage through the rear water-wall tubes to the rear floor-tube header. The tubes in this floor are covered with Bailey Blocks the same as are applied to the side walls of the furnace and the underneath surface is insulated in the same manner as the side walls. Joints between the Bailey Blocks are filled with Krome Patch to give initial sealing only. Both furnaces are fired with Fuller-Lehigh pulverized-coal equipment, each boiler being equipped with four cross-tube burners.

The fuel used in this station is Southern Kansas screenings having an average received heat value of 11,500 Btu with a normal ash content of 15 per cent. This fuel contains an average of 3.75 per cent sulphur and produces an ash that fuses at a very low temperature.

Inasmuch as our No. 17 boiler was the first unit of this type in this territory using this particular fuel we encountered several difficulties in commencing our operation of this unit, most of which can be attributed directly to the high sulphur content of the ash. Our first trouble was the cutting of the cast-iron slag-spout liners. These liners were entirely satisfactory until the boiler had been on the line for several days and a sufficient quantity of sulphide had accumulated to appear during the tapping process. When this condition was reached and the tapping operation was going on, the sulphide would commence to flow immediately following the last output of slag and in just a very few minutes of time the stream would cut the spout liners in two. We first attempted to correct this condition by placing a water-cooling pipe on top of the cast-iron liner and covering it with a mixture of 50 per cent fire clay and 50 per cent powdered coal.

⁹ Manager of Production and Distribution, Board of Public Utilities, Kansas City, Kansas.

This method would protect the liner for 8 or 10 tappings before the mixture would have to be replaced. This method of protecting liners was finally abandoned when the Babcock & Wilcox Company supplied us with water-cooled liners which is simply a water-jacketed spout liner that has its temperature controlled by a stream of water from the sluicing system.

This iron sulphide created another difficulty just inside of the slag-spout openings and between the outer wall and the first floor tubes. During tapping operations when the tap had proceeded far enough to permit the sulphide to commence to flow, we found that a puddling condition was occurring just inside the door liner and that the sulphide would cascade over the last floor tube and puddle its way deep into the magnesite composing the floor thus floating it away. This condition was remedied by water cooling similar to the manner undertaken to correct the difficulty with spout liners, that is, a $\frac{3}{4}$ -in. pipe was run through the furnace jacket and into the furnace floor, water being fed in on one side of the spout, passing through a $\frac{3}{4}$ -in. pipe just inside of the door and being extracted on the other side of the spout, this pipe serving to cool the floor space between the last floor tube and the wall of the furnace.

After these difficulties had been corrected we commenced to encounter other difficulties with the fineness of the ash produced in our hydrojet ash-sluicing system, it being about the consistency of granulated sugar and when mixed with sluicing water taken from the Missouri River (which, by the way, carries a rather large amount of material in suspension) compacted in the ash-storage tank to such an extent that we were unable to get it out without rodding and the use of considerable other labor in removing it and loading into cars. Experimentation indicated that this fineness was due to nozzle arrangement in the disintegrating chambers immediately below the slag spout. This chamber was originally installed with a series of nozzles forming practically a sheet of water under high velocity, the slag stream running onto this sheet and being reduced in size about equivalent to granulated sugar. This fineness of ash was remedied by the installation of a small water chamber in the disintegrating box directly under the slag spout with a four-inch opening at the bottom, this chamber being kept full of water at all times from the sluicing system and the slag stream running directly into the solid body of water. This arrangement had the effect of increasing the size of ash to about the size of a grain of wheat which is sufficiently large to eliminate the packing trouble which was encountered in the ash-storage hopper.

However, in making this change we encountered another difficulty which proved quite serious and which resulted in one of the operators receiving some rather severe burns. This latter trouble came again as a result of the iron sulphide in the furnace. When the stream of sulphide spilled into the bowl in the disintegrating chamber full of water it, of course, chilled immediately on the outside of the stream but the center remained hot and soft. Very shortly after the sulphide stream commenced to come we had explosions in the disintegrating box which threw water, slag, ash, and every other thing that it contained all over the boiler room and incidentally all over the operator. In correcting this condition we resorted to the installation of a water-cooled baffle so located that the slag stream, before it came in contact with the water, would meet it and fan the stream into a wide sheet before entering the water in the disintegrating bowl. This made it possible to chill the entire slag stream uniformly and has practically eliminated the explosions. We still have minor explosions when the slag stream slows down due to obstruction but as long as it is maintained at sufficient flow to strike the baffle plate and fan into a sheet before meeting the water we have no difficulty. Our former experiences in this connection led us to provide our operators with asbestos coats and helmets and we in-

sist that they be worn at all times during the tapping operations.

The sulphur content of the ash in this furnace gave us further annoyance due to the fumes that were liberated from the ash-sluicing system in the vicinity of the ash-sluicing pumps. These fumes became so obnoxious when sulphide was flowing from the furnace that it was practically impossible to stay in the boiler room. Also the reaction on all exposed copper tubing and other equipment was very detrimental to the good appearance of the equipment. In remedying this situation we were forced to vent the ash-sluicing system with an external stack.

All of the foregoing troubles while somewhat minor in nature as viewed from our present experiences, nevertheless seemed quite serious as they were encountered and overcome. Generally speaking, however, the operation of these water-cooled slag-tap furnaces has been entirely satisfactory in our station and the availability of these units has been extremely high, none of the troubles and experiences to which I have referred ever having necessitated an outage of the units.

T. G. ESTEP¹⁰ AND H. L. BUNKER, JR.¹¹ For the past year the discussers have been making a study, both experimentally and analytically, of the relationship between coal-ash analyses and their softening temperatures. In all, over 300 analyses have been studied and many different systems of coordinates have been

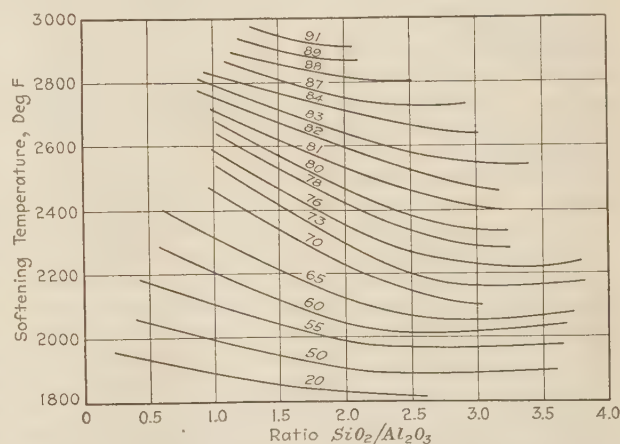


FIG. 5 RELATIONSHIP BETWEEN SOFTENING TEMPERATURE AND $\text{SiO}_2/\text{Al}_2\text{O}_3$ FOR VARIOUS SUMS OF $\text{SiO}_2 + \text{Al}_2\text{O}_3$
(The number above the curve indicates in each case the percentage of $\text{SiO}_2 + \text{Al}_2\text{O}_3$ in the slag.)

tried in plotting the data in an attempt to establish a graphical relationship by which it would be possible to predict ash-softening temperatures from their analyses.

One of the trial plots, Fig. 5, is submitted herewith because it is believed that it will be of interest to the general subject of "Slags and Their Properties." In this plot the ratio $\text{SiO}_2/\text{Al}_2\text{O}_3$ is the abscissa and softening temperature is the ordinate. On this system of coordinates are plotted lines of a constant sum SiO_2 plus Al_2O_3 . An exactly similar set of curves would obtain if lines of a constant sum Fe_2O_3 plus CaO were used since $\text{SiO}_2 + \text{Al}_2\text{O}_3$ varies inversely as $\text{Fe}_2\text{O}_3 + \text{CaO}$ in most coal ashes.

The plot shown, however, can be used in exactly the same manner as that shown in Fig. 3 of the authors' paper and covers a much wider range. The authors' plot is for a $\text{SiO}_2/\text{Al}_2\text{O}_3$ ratio of from 1.7 to 2.0 whereas the discussers' plot takes this ratio from 0.5 to 3.5. Of the 300 coals studied, only 25 per cent fall

¹⁰ Professor, Mechanical Engineering, Carnegie Institute of Technology, Pittsburgh, Pa. Mem. A.S.M.E.

¹¹ Research Fellow, Carnegie Institute of Technology, Pittsburgh, Pa. Jun. Mem. A.S.M.E.

within the limits of the authors' plot and, as a matter of fact, only two-thirds of the slags given in the paper fall within this limit. If the data given in Table 1 of the authors' paper are applied to the discussers' plot it is found that, within the A.S.T.M. limits, the softening temperature of 13 out of 15 coal ashes, 12 out of 17 slags and 8 out of 10 fly-ash analyses can be predicted. In a previous paper the authors gave a relationship between softening temperature and flow temperature which may be used in transferring from one to the other.

The authors' data in Table 1 show a very interesting point. In all cases except two the $\text{SiO}_2/\text{Al}_2\text{O}_3$ ratio for the slag is greater than that of the coal ash, indicating a gain in SiO_2 or a loss of Al_2O_3 . This may be explained by the fact that the eutectic of the system $\text{SiO}_2\text{-Al}_2\text{O}_3$ occurs at about 95 per cent SiO_2 and 5 per cent Al_2O_3 . In a boiler furnace when the ash particle becomes liquid in suspension and falls to the slag bed it may carry nearly all of the SiO_2 with it and the Al_2O_3 , being of a higher melting point, may drop on the slag bed and remain as a scum or leave in the fly ash. The scum in one case was sampled and analyzed and the result does not bear out the above reasoning, but unfortunately this one case is one of the two cases where the $\text{SiO}_2/\text{Al}_2\text{O}_3$ ratio did not increase in the slag and is not conclusive. In 6 cases out of 11 given in Table 1 the Al_2O_3 was higher in the fly ash than in the original coal ash. While this is a bare majority for the suggestion that some of the excess Al_2O_3 leaves in the fly ash, one hesitates to draw this conclusion when the difficulties of securing a satisfactory sample of fly ash are taken into consideration. Do the authors have any explanation of the change in this ratio?

There has always been some question as to whether or not chemical equilibrium between the ash components is reached in the standard A.S.T.M. method of determining ash fusion temperatures and, if equilibrium is not reached, what effect it has on the fusion temperature. The slag in the bottom of a slag-tap furnace has plenty of time to come to chemical equilibrium and, when the change in the composition of the slag from that of the original ash is taken into consideration, there seems to be little change in the softening temperatures between the slag and the ash. Perhaps it is unwise for us to draw conclusions from a study of only 15 fuels but the results would seem to indicate that no serious consideration need be given the question of chemical equilibrium in the usual method of softening-temperature determinations.

A. W. GAUGER.¹² The paper is very interesting and contains a wealth of valuable data.

While it is recognized that some empirical measure of fluidity which could be rapidly applied was necessary it is almost certain that using the "flow temperature" as determined by the "feel" is not the most satisfactory measure of relative viscosity which could be devised. In this connection it should be noted that the authors do not mention the factor of time and its influence on the flow temperature.

Littleton and Lillie at the Corning Glass Works have shown that the viscosity of glasses varies with time. That is to say, a glass which has been fired at a particular temperature and then cooled, will not, when reheated to some temperature high enough to permit viscous flow, assume its true viscosity for the temperature in question at once. On the contrary its viscosity varies exponentially with time and only after many hours does it become asymptotic to some fixed value. This phenomenon occurs whether the temperature of measurement is approached from a lower or a higher temperature, but it is of interest to note that the approach to equilibrium is much more rapid if the temperature of measurement is approached from above rather than from

below. This observation suggests that, in measuring slag or glass viscosities, it would be desirable to heat the slag to a higher temperature than that at which the measurement is to be made, and then to cool it to that temperature.

Because the authors made their measurements with the temperature rising, their reported flow temperatures have the advantage of being maximal, for in view of the foregoing considerations it will be seen that had they maintained their slags at the observed flow temperature for several hours they would almost surely have noted a decrease in viscosity even by the "feel" method since these changes in viscosity with time are quite large.

The treatment of Al_2O_3 and SiO_2 as one component is probably adequate for the small composition range of these two variables but in view of the results obtained by McCaffery and his co-workers in their investigation of the viscosity of blast-furnace slags, it does not seem that the treatment of CaO and MgO as one component is justified. McCaffery clearly showed that, if SiO_2 and Al_2O_3 are kept constant and successive increments of MgO are substituted for CaO , the viscosity of the slag first decreases, passes through a minimum, and then increases.

The utilization of the "ferric percentage" as a measure of the state of oxidation of the iron could, perhaps, be improved upon if all the iron in the sample were taken as 100 per cent and Fe_2O_3 , FeO , and Fe then plotted on triaxial coordinates. This being done, iso-flow temperature lines could be drawn over the field of composition to show the influence of the change in relative amounts of these three variables upon the flow temperature of the slag in question.

The statement that any station which returned fly ash to the furnace would be raising the softening temperature seems to be rather too inclusive. In this connection attention is called to a paper by Moody and Langan in the October, 1933, issue of *Combustion* in which these authors point out that the finest sizes of ash from Pennsylvania coals are very refractory whereas the finest sizes of ash from West Virginia coals have rather low softening temperature. This suggests that whether the return of fly ash to the furnace raised or lowered the flow temperature would depend rather largely upon the nature of the coal being burned.

J. J. GROB.¹³ This paper by Messrs. Nicholls and Reid is of considerable importance dealing as it does with the properties of slags from slag-tap furnaces and yielding information of great value to those interested in using the furnace as a means for disposal of fly ash from dust catchers, economizer and air-heater hoppers, and other settling chambers.

It has been difficult to get rid of dry fly ash. Because of its extreme fineness special precautions have to be taken in transporting it to avoid its loss in transit. While some commercial uses may be developed in the future, at present it cannot be given away as it is unsuitable even for ordinary fill purposes.

This problem has vexed designers and operators of power plants and in some cases has influenced the selection of fuel-burning equipment.

At Hell Gate, the retention of a substantial part of the ash in molten form in a slag-bottom furnace and the possibilities in the further disposal of captured fly ash by injection into this furnace for absorption in the slag bed is a factor of considerable interest to us.

Our early experience with slag tapping indicated that the amount of ash retained in the furnace in molten form approximated 40 to 50 per cent and the fluidity of the slag mass was sensitive to such factors as furnace temperature or CO_2 , fusion

¹² Director, Mineral Industries Research, School of Mineral Industries, The Pennsylvania State College, State College, Pa.

¹³ Engineer of Tests, The United Electric Light and Power Co., New York, N. Y. Mem. A.S.M.E.

temperature of the coal ash, fluxes such as fluorspar, soda ash, etc. Certain mechanical difficulties were encountered with tapping due to the chilling effect of air infiltration during the tapping periods. This difficulty was entirely overcome by sealing the tapping port with a boxed enclosure and during the tapping period placing this enclosure under a suction sufficient to absorb all leakage air and also to draw a little gas out of the furnace through the slag port.

This procedure has rendered the use of fluxes unnecessary with coals under 2500 F fusion temperature and it is possible to tap freely at moderate boiler ratings and with normal CO₂.

However the injection of captured fly ash into the furnace was only partially successful. Analysis showed that the unslagged fly ash was appreciably higher in fusion temperature than either the original coal ash or the slag itself. Injection of the dry fly ash into the furnace through a feeder caused the material to pile up near the cool walls and the process of absorption was slow. Attempts to distribute the material over the surface of the slag bed permitted a substantial percentage of the material to be picked up by the gases and recirculated through the boiler.

Some of the dust deposited would become absorbed and some would move around on top of the slag mass. This process did not appear to affect the fluidity of the slag mass enough to retard tapping.

The authors raise some new points in their paper which may result in elimination of recirculation of the fly ash and more complete absorption of it in the slag mass. I refer particularly to the suggestion that wet fly ash or lumps molded while the fly ash is still wet would prevent the recirculation of fly ash by the gases while injecting the ash into the furnace. These points are all the more important because of the growing interest in wet-type fly-ash catchers making it convenient to dispose of the wet partially dewatered fly ash. In this connection I would like to ask the authors if any harmful effects are likely to be experienced with furnace-wall refractories from the gases liberated if salt water is used as a binder for the fly ash?

We attempted recently to try out the effect of moistening fly ash with salt water before injection into the furnace and the lumps held together until reaching the slag bed where they gradually flattened out. The lumps were injected 24 hours before tapping. While there was some evidence during tapping of the existence within the pool of lumps less fluid than the main body of the slag no difficulty was experienced with tapping. I believe the indications are favorable enough to justify working out the mechanical problem of injecting the fly ash to the furnace in lumps or moistened form.

Samples Nos. 2 and 3 referred to in Table 3 of the authors' paper were caught in wet cinder catchers at Hell Gate utilizing salt water. Sample No. 2 comes within the range of normal combustible content which reaches 20 per cent at high ratings and falls below 8 per cent at moderate ratings.

The high carbon of No. 3 sample reflects the influence of coarse pulverization caused by an impaired mill classifier.

Regarding the comparison of slag-tap furnaces and dry-bottom pulverized-fuel furnaces, we are using both types at Hell Gate and my belief is that the slag-tap type of furnace possesses many advantages over the dry bottom type. It eliminates the troubles experienced in removing the ash from the bottom manually causing a boiler outage and frequently the ash may be glazed over requiring air hammers to chisel it out. It lessens the burden on a cinder catcher since the slag bottom generally retains about 40 to 50 per cent of the ash while on a dry bottom usually not more than 10 per cent of the ash is deposited. The choice of fuels which can be used successfully is widened. The furnace may be operated at more efficient temperatures since the furnace CO₂ does not need to be kept low in order to avoid slagging the

pit. Opportunity is afforded for disposal of captured fly ash by injection into the furnace since the coarser, broken up slag is more readily disposed of than light dry fly ash, much of it approaching a fineness of five or ten microns. The presence of a high-temperature pool of slag at the bottom of a furnace exercises a stabilizing combustion influence.

The conclusions drawn by the authors as to the effects of carbon, moisture, floating islands, etc., on the process of slagging are all of great interest and Mr. Nicholls and Mr. Reid certainly deserve a great deal of credit for their logical, careful, and valuable presentation.

O. HOWARD.¹⁴ The information brought out in the paper regarding the relationship between composition and liquid temperatures is very interesting and should be valuable to the operator who has a choice of coals, otherwise equally desirable but differing in ash composition, and also valuable to the designer confronted with the problem of whether or not to use a slag-tap furnace.

As to the operator's problems, it is our belief that most of the difficulties are encountered, not with the slag itself but rather with the effects of the slag on the floor and walls. Iron may be reduced to the metallic state and penetrate the floor thereby starting slag leaks. Iron sulfide has the same tendency also. Alternate contraction and expansion of the slag bed caused by taking the boiler out of service may push the furnace walls out of position. We have experienced all these difficulties.

The degree of reduction of iron from the ferric to the ferrous state, as well as the total amount of iron present, are shown to influence greatly the fusing temperature of the slag but it is not apparent just how the operator can exercise much control over either, after the fuel has been chosen.

P. L. LUGRIN.¹⁵ The authors have compiled and developed data which warrant the attention of all interested in this subject.

As no fluxes are used and the fly ash is not recovered at Glen Lyn, no discussion of the paper will be made by the writer, but as the condition at Glen Lyn is rather unique in that probably the highest fusion temperature is contained in the ash from the coal consumed, a general outline in the form of actual operating conditions and experiences of a "wet"-bottom pulverized-fuel boiler is herewith substituted.

Analyses of the coals used at the Glen Lyn steam plant of the Appalachian Electric Power Co. vary greatly, and coal from 30 different mines, principally from the Pocahontas field, has been consistently burned without any specific selection or regard for mixtures as supplied to the bunker serving this unit. The fusion temperature of the ash ranges between 2100 and 3050 F. Temperatures measured with an optical pyrometer show a range of from 2800 to 3050 F at the slag-bed surface, depending on load conditions. Approximately 17 per cent of the total ash in the coal is recoverable in the form of slag, and tapping is performed once daily, or every other day when load conditions and coals judged to be suitable are available, for from 30 to 60 min, or a length of time sufficient to maintain a satisfactory slag-bed level. This is important, as the temperature gradient of the bed determines the minimum depth to which the slag should be drawn in order to protect the bottom.

Naturally, due to furnace-temperature limits, high-fusion ash forms a viscous slag. The temperature gradient in the slag bed retards the slag flow, the slag being drawn off the surface; and when it is realized that the furnace bottom is rectangular and the

* ¹⁴ Assistant Superintendent of Generation, Oklahoma Gas and Electric Company, Oklahoma City, Okla. Mem. A.S.M.E.

¹⁵ Plant Superintendent, Appalachian Electric Power Co., Glen Lyn, Va. Mem. A.S.M.E.

"wet" slag is in the form of a circular or elliptical pool within this rectangle, and that there is therefore but a few inches of head of "wet" slag above the stiff slag level at the tap door, the slag must be fluid in order to flow at all. When the furnace is first tapped, by cutting through the rim of the pool basin, the flow is rapid, and drops to the ejector in a column about 3 in. in diameter for from 10 to 20 min, after which the flow gradually retards and the column of slag narrows to 1 to 1½ in. in diameter. One reason for this lessening of flow is the reduction in head of the fluid slag, and another is the gradual stiffening of the bed due to the temperature gradient. Fly ash or dust accumulates on the surface at times, but is readily floated off with the "wet" slag. It is noticed that when dust flows the slag spout is more readily kept clean during tapping.

The solution of the problem of continuous operation of this unit for protracted periods was the prevention of the formation of friable slag from building up under the burner ports and choking the burners, with ultimate coal ignition in the burner boxes. This was solved by cutting in poke-holes under the bottom rows of burners, and directly above the normal slag level between each water-wall tube across the front of the furnace.

It is of interest to know that this unit is in continuous operation for six-month periods and is then removed from service for the purpose of inspection, washing, and repairs to the boiler. The slag bottom is never disturbed during these shut-down periods except for the removal of loose friable surface slag, mostly droppings from the boiler tubes and walls.

While foreign to the subject, the importance of coal grindability cannot be too highly stressed, as tapping is comparatively simple when pulverization of coal is within the correct percentages of fineness.

AUTHORS' CLOSURE

The discussions and citations of experiences submitted by the engineers and operators have greatly added to the value and usefulness of the paper. It will be noted that in the main the discussions are from stations using coals with ash fusions at the extremes, and it can be assumed that the experiences of those burning coal with ash of medium fusion are more normal and freer from troubles. These discussions do not call for much comment from the authors.

Thanks are due to Mr. Baker for the data he has added. The discrepancy between the fusibility of the coal-ash slag and the coal ash and sand slag as indicated by the cone test and by experience while tapping may be due to the sand's not being fully melted in the furnace, whereas the fine grinding for the cone test may have overcome this. It is suggested that the nature of the coal may have been changed, and that the combustion was affected so that the temperature of the slag bed was lower. Table 1 shows that Michigan City (Station F) was using petroleum coke at the time the samples were collected and that they report the tap as being slow and sticky, whereas our data show that the flow temperature was 2345 F and that the slag became very thin above that temperature. The temperature of the bed was not measured and the assumption was that it was low in spite of the high rate of burning reported.

Mr Baker's Table 8 gives analyses of fly ash caught by precipitators. Accounting for the missing Al_2O_3 is of some interest—theoretically at least. Although Tables 7 and 8 may not be for corresponding samples, it will be seen that as they stand the $\text{SiO}_2:\text{Al}_2\text{O}_3$ ratio is no greater in the fly ash than in the slag. It might be worth while to attempt to catch and to analyze dust which passes the precipitator to determine whether its Al_2O_3 content is higher than that of the ash caught.

Several of the discussors have referred to troubles because of iron sulphide and metallic iron in the bed. This is a phase that has not been included in our investigation; are the pyrites in the coal to be blamed for both, or is some of the metallic iron reduced from the non-pyritic iron in the coal ash?

Replying to Mr. Grob, it is probable that the greater part of the alkalis present in sea water used will be volatilized, although several types of tests made on fuels containing salt have shown that some is retained in the slag. If these alkalis are deposited on the refractories, they would cause slagging, but the high temperature of the surface of the wall would not encourage the deposition of the alkalis. In other investigations by the Bureau, it was shown that clinker from boiler tubes has high alkalis near the tube—on which they could condense—but normal alkalis at the outer surface of the clinker. One would expect that the first evidence of appreciable amounts of salts would be that they would tend to cause the slag on the tubes to fall off, although this might not occur if the salts were present in the gases continuously.

Referring to the comments on the first part of the paper, it should be recognized that this investigation has not attempted to attain that full knowledge of the properties of slags from coal ash which has been done by others for fields of more limited chemical composition associated with other industries. It was thought preferable to cover the whole field broadly rather than to concentrate on a small portion, or to aim at great exactitudes. In addition, exact data are not required in the burning of fuels because the conditions to which the ash is subjected cannot be closely defined, are variable, and the composition of the ash itself varies in the same coal. In spite of this, much has not been done which should be done in the future.

The recent work¹⁶ by Professor Estep and Mr. Bunker in assembling existing data on cone softening temperatures and analyzing the relationship between temperature and ash composition was much needed. However, it cannot be assumed that these same relationships hold for the cone-fluid or the flow temperatures; the effect of small changes on composition is often greater at low fluidity than it is at the high fluidity of the flow point. The second report gives some data on the effect in air equilibrium of the $\text{SiO}_2:\text{Al}_2\text{O}_3$ ratio for values above 1.7; a variation of the ratio from 0.88 to 2 in a low-iron slag showed little change in the flow temperature but more work is needed.

Less Al_2O_3 in the slag than in the fly ash was noted in our work on clinkering. The assumption has been that the ash particles high in alumina are more refractory, lighter, and possibly smaller; however, usually alumina is missing even when the fly ash is included, so the explanation may not be complete.

Professor Gauger will find answers to some of his remarks in the second report. The effect of time and rising and falling temperatures were investigated; both affect the flow temperature and to different extents in different slags. The method adopted probably most nearly corresponds to the practise in slag-tap furnaces in which, for slags with flow temperatures near the furnace temperature, it is customary to increase the load previous to tapping. McCaffery and others worked on slags with low iron and very high lime and their results with MgO do not apply to coal ash. The data given in Table 1 support the statement that the flow temperature of the fly ash will be higher than that of the slag; one possible exception might be for a fuel very high in alkalis which were carried out with the fly ash.

¹⁶ T. G. Estep, et al., "The Effect of Mixing Coals on the Ash-Fusion Temperature of the Mixture." Coop. Bull. 62, Carnegie Institute of Technology and Mining and Metallurgical Advisory Boards, 1934.

Number of Active Coils in Helical Springs

By R. F. VOGT,¹ MILWAUKEE, WIS.

Due to the torsional displacement between cross-sections of the helical spring bar or wire in the so-called dead or inactive coils on each end of the spring, the total deflection of the spring is greater than that which corresponds to the deflection of the free coils. The exact amount of the spring deflection corresponding to the influence of the "inactive" coils can be calculated for known loading conditions of the spring and can be closely estimated for all springs subjected to conventional spring-practise loads. The deflections of the end coils are calculated in terms of the deflection of active coils. A test to determine the actual number of active coils is suggested and examples are given.



THE predetermination of the correct number of active coils in helical springs is, in many applications, very important. Centrifugal spring-loaded regulators, controlling the speed of prime movers, spring-loaded indicators, and many other apparatus require helical springs of which the correct number of active coils is essential.

If, in the use of the conventional helical-spring deflection equation

$$f = \frac{64 \cdot n \cdot r^3 \cdot P}{d^4 \cdot G}$$

f = deflection

r = mean radius of coil

d = diameter of wire

P = load

G = modulus of elasticity in torsion

n = number of active coils

an error is made in determining the correct value of n , the factor G is usually adjusted to offset the original error. The factors f , r , d , and P are always fixed in value and can easily be measured and checked.

In such cases it is erroneously assumed that G is a variable amount for different helical springs, the variation ranging from below 10,000,000 to 12,000,000.

The fact, however, is that the modulus of elasticity in torsion G is proportional to the modulus of elasticity in tension E and is characteristic for each material and constant within the elastic range:

$$G = \frac{E}{2(1 + \mu)}$$

¹ Assistant Chief Consulting Engineer, Allis-Chalmers Mfg. Co. Mem. A.S.M.E. Robert F. Vogt was born in Geneva, Switzerland, and had his primary and secondary schooling at Romanshorn, Canton School at St. Gall, and Swiss Polytechnicum at Zurich, Switzerland. His professional career began in the United States in 1903. He has been connected with the Allis-Chalmers Mfg. Co. as mechanical engineer since 1907.

Contributed by the Special Research Committee on Mechanical Springs and presented at the Mechanical Springs Session of the Annual Meeting, New York, N. Y., Dec. 5 to 9, 1932, of THE AMERICAN SOCIETY OF MECHANICAL ENGINEERS.

NOTE: Statements and opinions advanced in papers are to be understood as individual expressions of their authors, and not those of the Society.

where μ is Poisson's ratio. According to Hütte, 26th edition, for spring steel

$$E = 30,000,000 \text{ lb per sq in.}$$

$$\mu = 0.275$$

$$m = 1/\mu = 3.63$$

$$G = 0.392E = 11,700,000 \text{ lb per sq in.}$$

Any discrepancy between these given values and experimental values is due to an error in counting the number of active coils in the helical spring under consideration.

It is the purpose of this paper to show how the correct number of active coils can be determined both by analysis and experiment.

The number of active coils as used in the deflection formula for helical springs does not always equal the total number of coils or the number of free coils. Particularly, in most commercial helical compression springs we find that the number of active coils must be more than the number of free coils, if we assume $G = 11,700,000 \approx 12,000,000$ as correct and applicable to helical springs.

Tests of regulator tension springs, of which each end coil was held at two diametrically opposite points, checked closely with $G = 2/5 \cdot E$ when the number of active coils was counted from the middle of the two supporting points on one end of the spring to the corresponding point on the other end, i.e., when the number of active coils was taken as the number of free coils plus $1/2$ coil.

ROD UNDER TWIST

Let us consider, as shown in Fig. 1, a rod of the length L twisted by applying a force P perpendicular to a rigid arm of length r , which is perpendicular to the rod. The deflection of the point of application of the force P in the direction of P is expressed by the formula:



FIG. 1

$$f = r \cdot \omega = \frac{32 \cdot r^2 \cdot L \cdot P}{\pi \cdot d^4 \cdot G} \dots \dots \dots [1]$$

in which ω is the angle of twist in radians.

HELICAL SPRING WITH RIGID ARMS AT COIL ENDS

If the rod referred to for Equation [1] is coiled into the shape of a helical spring on which the rigid arms extend from the ends of the coil to the center line of the coil and are perpendicular to the coil center line, the force P acting on the arms at the center line of the coil in the direction thereof produces a deflection f of

$$f = r \cdot \omega = \frac{32 \cdot r^2 \cdot \frac{2 \cdot r \cdot \pi \cdot n}{\cos \alpha} \cdot P \cdot \cos \alpha}{\pi \cdot d^4 \cdot G}$$

$$f = \frac{64 \cdot n \cdot r^3 \cdot P}{d^4 \cdot G} \dots \dots \dots [2]$$

α = pitch angle

n = number of coils

In this case all coils are active, i.e., subjected to the twist of the full torque moment $P \cdot r$ and no coils or part of coils are inactive. The number of coils n is also the number of active coils.

COMMERCIAL SPRINGS

Commercial springs are not equipped with rigid arms at the ends. Many tension springs have loop ends, as shown in Fig. 2, which add a negligible amount of bending deflection to the torsional deflection given in Equation [2]. In such springs all coils between the base of the loops are active coils. The detailed discussion of this type of spring will be omitted in this paper.

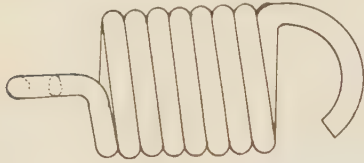


FIG. 2

In helical springs where the full length of the bar is within the cylindrical part of the spring, as is the case of commercial helical compression springs and also of many kinds of expansion springs, the active coils extend beyond the free coils. The free coils include the coils of the spring which are not connected with brackets or yokes through which the spring load is applied and do not make contact with the end coils. The active coils include all coils contributing to the deflection of the spring. The angle of twist of the bar changes from maximum in the free coil to zero in the end coils. The angle of twist within the end coils adds a certain amount to the total deflection of the spring, which can be determined in many cases with complete accuracy and in all other cases with sufficient accuracy to satisfy fully the practical applications.

HELICAL SPRINGS WITH DIFFERENT TYPES OF LOADING

In order to illustrate the deflection of the end coils in helical springs, various ways of spring loading will be analyzed:

1 The Two-Point Loading.

To an open-wound helical spring the load is applied by means of yokes reaching on each end diametrically from one side of the coil to the other (see Fig. 3). The load P is applied at the middle of the yoke by means of a pivot, so that each end of the yoke transmits the same pull $P/2$ on the spring.

As is shown in developing Equation [2], the effect of the pitch angle α is such that it may be correctly assumed that the end coil is in a plane perpendicular to the center line of the coil and that the forces are perpendicular to the plane of the coil.

Referring to Fig. 3, the load $P/2$ at A has no part on the deformation of the end coil between the points A and B . The load $P/2$ at B produces a moment of $P/2 \cdot 2 \cdot r = P \cdot r$ at point A which is balanced by the same moment $P \cdot r$ acting on the other side of the spring. All cross-sections of the spring bar between A and B' are under the influence of this moment $P \cdot r$.

If the end coil between A and B would be absolutely rigid, the cross-section at A would remain in the same position relative to the end coil as it had before loading took place. But the end

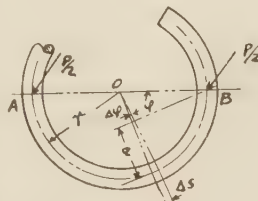
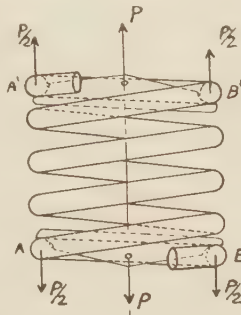


FIG. 3

coil is as flexible as the free coils located between A and B' and the bar between A and B will twist in accordance with the respective moment acting on the bar at its cross-sections. This moment is no longer constant and equals $P \cdot r$ for all cross-sections from A to B , but decreases gradually from the maximum of $P/2 \cdot 2 \cdot r = P \cdot r$ at A to $P/2 \cdot 0 = 0$ at B . Between A and B the acting moment is $M = P/2 \cdot (r - r \cos \varphi) = \frac{P \cdot r}{2} (1 - \cos \varphi)$

for the cross-section designated by angle φ . The total angle of twist of cross-section at A , due to the torsional resilience in the end coil from A to B and the moment $P \cdot r$ acting at A , is $\omega = \frac{16 \cdot P \cdot r^2}{d^4 \cdot G}$, and the center O of the coil, which we imagine

rigidly connected with cross-section at A , moves in reference to its original position O' , when the spring is not loaded, an amount of $f' = r \cdot \omega = \frac{16 \cdot P \cdot r^3}{d^4 \cdot G}$ (see Appendix 1). O' may be regarded

as the center of the end coil in its new position. O may be taken as the original location of the center. The distance between O and O' then equals f' , which is also the deflection of the end coil

$f' = \frac{16 \cdot P \cdot r^3}{d^4 \cdot G}$. This corresponds to the deflection of $1/4$ coil

which is subjected to the moment $P \cdot r$. The same, of course, occurs at the end $A'B'$, so that the total deflection of the helical spring amounts to

$$f = 2f' + f'' = 2 \frac{16 \cdot P \cdot r^3}{d^4 \cdot G} + \frac{64 \cdot n' \cdot r^3 \cdot P}{d^4 \cdot G}$$

$$f = \frac{64(n' + \frac{1}{2}) \cdot r^3 \cdot P}{d^4 \cdot G} = \frac{8(n' + \frac{1}{2}) \cdot D^3 \cdot P}{d^4 \cdot G}$$

n' = number of free coils (between A and A')

n = number of active coils

$D = 2r$ = mean diameter of coil.

In Fig. 3:

$$n' = 3\frac{1}{2}$$

$$n = n' + \frac{1}{2} = 4$$

ANALYSIS AT THREE-POINT LOADING

Proceeding in the same manner for three-point loading, shown in Fig. 4, where three equal forces $P/3$ are placed 120 deg apart on the end coil, it is found that the deflection, due to twist in the end coils amounts to

$$f' = \frac{64 \cdot \frac{1}{3} \cdot r^3 \cdot P}{d^4 \cdot G}$$

and the total spring deflection is

$$f = 2f' + f'' = \frac{64(n + \frac{2}{3}) \cdot r^3 \cdot P}{d^4 \cdot G}$$

In these analyses the effect of bending and shear have been omitted in favor of simplicity. The error made thereby is so small as to be of no practical consequence.

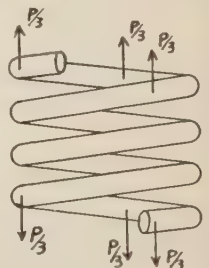


FIG. 4

CONCLUSIONS OF ANALYSES FOR DESIGN

Most commercial spring-loading conditions will conform to the two-point loading and the equivalent deflection of the two ends of a helical spring in terms of the deflection of a free coil will approximate 0.5.

The general expression for the deflection of helical springs which are not provided with rigid arms or loops at the ends and to which the load is applied in the common manner then takes a convenient form readily available to designers:

$$f = \frac{64 \cdot P \cdot r^3 \cdot (n' + 0.5)}{d^4 \cdot G} = \frac{8 \cdot P \cdot D^3 \cdot (n' + 0.5)}{d^4 \cdot G} \dots [3]$$

For compression springs the forces are applied in the opposite direction; the deflection is also in the reversed direction, but the calculations and results are otherwise the same. The design and application of a commercial helical compression spring are such that the load condition ranges between the two cases given. The first condition is the more common.

The foregoing calculations are based on full-bar cross-section in the end coil. This assumption applies to most commercial compression springs, for that part of the coil which must be considered in the calculation. The basic design of the spring is shown in Fig. 5.

The ends of such a spring are closed, $3/4$ of the end coil is tapered from full cross-section to $1/4$ thickness at the end, the pitch changes at contact point B from p to d . Full cross-section of bar is maintained from B to A , suggesting a load division of $P/2$ at A and $P/2$ at B . The variation is usually not far from this load division and comes within the range of the three-point loading of $3 \times P/3$, in which extreme case the difference would only correspond to $1/3 - 1/4 = 1/12$ coil for each end correction.

We must bear in mind that the resultant of these forces is in the center line of the coil. If it were to fall outside the center line, the spring would bend out sidewise, which, in most compression-spring applications, does not occur to any appreciable extent. Within the range of free coils, i.e., from B to B' (see Fig. 5), the bar is subjected to a shear force equal to $P/2$ and a torque equal to $P \cdot r$. The effect of shear upon the deflection is small and can be neglected. In a well-applied compression spring the torque $P \cdot r$ is uniformly the same all along the bar, P acting in line of the center line of the coil.

Due to the fact that the length of contact between the end coils increases slightly during increase in deflection, thereby effecting a slight decrease in active coils, the assumption of the $2 \times P/2$ load division is more justified, as the error in allowing for slightly less active coils than would correspond to an actual, possibly different load distribution, is compensated by the tendency for a slight decrease in active coils during compression. It is therefore logical and practically correct to choose the $2 \times P/2$ load division.

EXPERIMENTAL VERIFICATION OF ANALYSES

A large number of tests substantiate the mathematical analysis and the general application of the results. To illustrate, the following test records are presented. Errors in the dimensions of bar diameter, coil diameter, and deflection, on account of their large amount, are relatively small. The examples, therefore, are of especially high value as proofs of the analyses.

The following springs were made by the Railway Steel Spring Company for the Allis-Chalmers Manufacturing Company:

		I	II
Bar diameter (average), in....	d	1.839	1.122
Coil diameter (average), in....	D	7.53	4.140
Free length.....	f	$19\frac{1}{3}$	$19\frac{1}{3}$
Free coils.....	n'	6.075	$11\frac{1}{2}$
Active coils.....	$n = n' + 1/2$	6.575	12
Total number of coils from tip to tip of bar (taper)...		$8\frac{1}{2}$	$14\frac{1}{4}$
Load, lb.....	P	4580	4600
Deflection.....	f	0.760	1.660
Modulus.....	$G = \frac{8 \cdot n \cdot D^3 \cdot P}{f \cdot d^4}$	11,800,000	11,850,000

The springs were tested with a testing machine of 5000-lb capacity. The dimensions were carefully taken with micrometers and averaged from many measurements taken of diameters perpendicular to each other along the full length of the springs. The free coils were carefully determined and fixed by inserting spacers at the contact points with respective end coils.

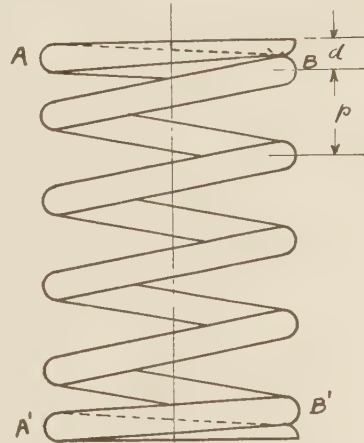


Fig. 5

The theoretical number of active coils n and the modulus of elasticity in torsion G may easily be determined by testing for deflection two compression springs made of the same material of equal bar and coil diameter, but with a different number of free coils, as follows:

	Spring 1		Spring 2
Coil diameter.....	D	=	D
Bar diameter.....	d	=	d
Number of free coils.....	n'	=	n''
Load.....	P	=	P
Deflection.....	f_1	=	f_2
Number of active coils.....	$n_1 = n' + x$	=	$n_2 = n'' + x$
Modulus of elasticity in torsion.....	G	=	G

Since both springs are alike except for number of free coils, the modulus of elasticity in torsion is the same for both springs as well as the effect of the end coils under the same load.

We find

$$G = \frac{8(n' + x) \cdot D^3 \cdot P}{f_1 \cdot d^4} = \frac{8(n'' + x) \cdot D^3 \cdot P}{f_2 \cdot d^4}$$

$$\frac{n' + x}{f_1} = \frac{n'' + x}{f_2} \quad \text{or} \quad x = \frac{n' \cdot f_2 - n'' \cdot f_1}{f_1 - f_2} \dots [4]$$

and

$$G = \frac{8(n' + x) \cdot D^3 \cdot P}{f_1 \cdot d^4} \dots [5]$$

If there should be any variation between the two springs in d , D , or P , then f_1 or f_2 must be corrected to correspond to values for d , D , and P adopted for the foregoing calculation. It will be found that x approximates the value of $1/2$ very closely and that G approximates 11,700,000 for any size and kind of steel spring bar.

Appendix 1

IN order to find the total angle of twist of cross-section at A under the influence of $P \cdot r$, the half-circle between A and B is divided into differential lengths $\Delta(s) = r \cdot \Delta\phi$. The moment

acting on any cross-section of the arc AB is $M = P/2 \cdot a = P/2 \cdot r \cdot (1 - \cos \phi)$. (See Fig. 3.) The twist angle ω between two cross-sections separated by the distance $\Delta(s)$ amounts to $\frac{32 \cdot M \cdot \Delta(s)}{\pi \cdot d^4 \cdot G} = \Delta\omega$. The total twist angle—that is, twist angle of cross-section at A in reference to cross-section at B —equals the sum of the angles of twist for all sections $\Delta(s)$ located between point A and point B . It is

$$\omega = \int_0^\pi \Delta\omega = \int_0^\pi \frac{32 \cdot \frac{P}{2} \cdot r \cdot (1 - \cos \phi) \cdot r \cdot \Delta\phi}{\pi \cdot d^4 \cdot G}$$

$$\omega = \frac{16 \cdot r^2 \cdot P}{\pi \cdot d^4 \cdot G} \cdot \int_0^\pi \Delta\phi (1 - \cos \phi) = \frac{16 \cdot r^2 \cdot P}{d^4 \cdot G}$$

If we assume the center O of the arc AB rigidly connected to the cross-section at A , it will move with the cross-section A the amount of $r \cdot \omega = \frac{16 \cdot r^3 \cdot P}{d^4 \cdot G}$, which distance corresponds to the deflection of the center O of arc AB from its original position under the influence of load $P/2$ at point B .

For the three-point loading of the end coil, we find the deflection of the center of the arc of the end coil, proceeding the same as in the case of the two-point loading, as follows:

$$f' = \frac{32 \cdot \frac{P}{3} \cdot r^3}{\pi \cdot d^4 \cdot G} \left[\int_0^{\frac{4\pi}{3}} \Delta\phi (1 - \cos \phi) + \int_0^{\frac{2\pi}{3}} \Delta\phi (1 - \cos \phi) \right]$$

$$= \frac{32 \cdot \frac{P}{3} \cdot r^3}{\pi \cdot d^4 \cdot G} \left[\left(\frac{4\pi}{3} - \sin \frac{4\pi}{3} \right) + \left(\frac{2\pi}{3} - \sin \frac{2\pi}{3} \right) \right]$$

$$= \frac{32 \cdot \frac{1}{3} \cdot r^3 \cdot 2\pi}{\pi \cdot d^4 \cdot G} = \frac{64 \cdot \frac{1}{3} \cdot r^3 \cdot P}{d^4 \cdot G}$$

Appendix 2

CASE WHEN $\phi < \alpha$

IN calculating deflections of a portion of a circular ring out of its plane by forces perpendicular to the plane of the ring, the known solution of Saint-Venant can be used.² If an incomplete circular ring is fixed at A and loaded by force P at B (Fig. 6),

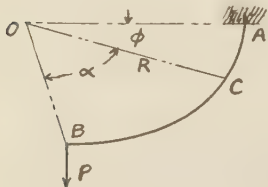


FIG. 6

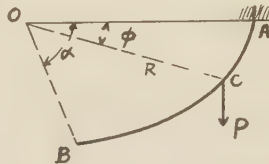


FIG. 7

then according to Saint-Venant's solution the deflection at any point C , defined by an angle ϕ , is given by the following equation:

² The Saint-Venant solution can be found in Love's "Mathematical Theory of Elasticity," pp. 456-457, or in "Strength of Materials," vol. 2, p. 469, by S. Timoshenko. This manner of solution was suggested by R. L. Peek.

$$V = \frac{PR^3}{C} \left[\phi - \sin \phi - \sin \alpha (1 - \cos \phi) \right]$$

$$+ \frac{PR^3}{2} \left(\frac{1}{EI} + \frac{1}{C} \right) \cdot \left[\phi \cos (\alpha - \phi) - \sin \phi \cos \alpha \right] \dots [a]$$

in which C is the torsional rigidity and EI the flexural rigidity. This equation is satisfactory for any value of ϕ between 0 and α .

TWO-POINT LOADING

If there are two forces $P/2$ acting at A and B , the deflection at B is readily obtained from the direct application of Equation [a], substituting in it $P/2$ for P , $\alpha = \phi = \pi$, $I = \frac{d \cdot \pi}{64}$, and $C = G \cdot \frac{d \cdot \pi}{32}$. Then the deflection of point B is:

$$V = \frac{30.4 \cdot P \cdot R^3}{G \cdot d^4}$$

Point O deflects

$$f = \frac{V}{2} = \frac{15.2 \cdot P \cdot R^3}{G \cdot d^4}$$

or

$$f \approx \frac{64 \cdot \frac{1}{4} \cdot P \cdot R^3}{G \cdot d^4}$$

in which form the equation shows that the deflection of an end coil is equal to the deflection of one-quarter of a free coil.

CASE WHEN $\phi > \alpha$

If ϕ is larger than α , the necessary deflection can be obtained by using Saint-Venant's equation in conjunction with the reciprocity theorem.³ From this theorem it follows that the load P applied at C (Fig. 7) produces at B the same deflection as the deflection at C produced by the load at B . Since Equation [a] gives the deflection at any point C in Fig. 6, we can get at once the deflection at any point B for the loading shown in Fig. 7.

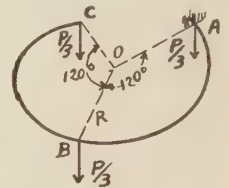


FIG. 8

THREE-POINT LOADING

Take now, as an example, the case of three loads $P/3$ put at points A , B , and C , 120 deg apart (Fig. 8). Point A is considered as fixed. The deflection of the point B consists of the two parts: (1) Deflection produced by the load $P/3$ at B and (2) deflection produced at B by the load $P/3$ at C . The first part is obtained by substituting into Equation [a] $P/3$ for P and $2\pi/3$ for the angles α and ϕ .

This gives: $V_{B \text{ due to } B} = 7.50 \frac{PR^3}{Gd^4}$ (assuming $E = \frac{5}{2} G$).

The second part is obtained from the same equation by putting $4\pi/3$ for α and $2\pi/3$ for ϕ . This gives: $V_{B \text{ due to } C} = 6.70 \frac{PR^3}{Gd^4}$.

Hence the total deflection of the point B is:

$$V_B = 14.20 \frac{PR^3}{Gd^4}$$

In calculating the deflection of the point C , we again have two parts: (1) Deflection at C produced by the load at C is obtained

³ Method proposed by Prof. S. Timoshenko.

by substituting $P/3$ for P and $\alpha = \phi = 4\pi/3$ into Equation [a], which gives $V_{C \text{ due to } C} = 33.10 \frac{PR^3}{Gd^4}$ and (2) deflection at C produced by the load at B . This is equal to deflection at B when the load is at C and is obtained from Equation [a] by substituting in it $P/3$ for P and taking $\alpha = 4\pi/3$ and $\phi = 2\pi/3$, which gives:

$$V_{C \text{ due to } B} = V_{B \text{ due to } C} = 6.70 \frac{PR^3}{Gd^4}$$

Then the total deflection at C is:

$$V_C = 39.80 \frac{PR^3}{Gd^4}$$

Having the deflections at B and C , the displacement of the center O is:

$$V_o = \frac{V_B + V_C}{3} = 18.0 \frac{PR^3}{Gd^4}$$

It will be seen that the method described can be used for any number of concentrated forces. It can be easily extended also to the case of distributed loads.

Appendix 3

THE Saint-Venant solution may be used directly to determine the total deflections of helical springs under various load conditions. The most simple case of its application for helical springs is a spring with the two-point loading as shown in Fig. 3, and Fig. 9.

For this analysis the spring is assumed to consist of two equal

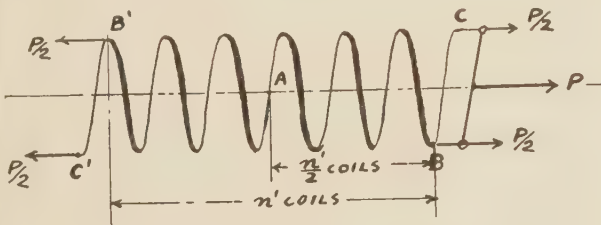


Fig. 9

parts, equally loaded, which meet at the center cross-section A of the spring bar. (See Fig. 9.) Point A is now considered the fixed point of two circular arcs. The center angles of these arcs are equal, $\alpha = (n'/2) 2\pi + \pi = (n' + 1)\pi$, $2n'$ being the number of coils between B and B' .

If ϕ is the pitch angle of the spring, the actual length of arc AC is $L = r \cdot \pi (n' + 1)$ and the

loads on the arc perpendicular to the plane of the arc would be $P/2 \cos \phi$. But as shown by developing Equation [2], the product $\frac{r \cdot \pi (n' + 1)}{\cos \phi} \cdot \frac{P}{2} \cdot \cos \phi$ eliminates $\cos \phi$.

Therefore, it may be assumed that $\cos \phi = 1$ without interfering with end results. This means that it may be assumed that arc ABC is $r \cdot \pi (n' + 1)$ in length, located in a plane perpendicular to the spring center line and loaded by the forces $P/2$ which are

parallel to this center line, i.e., perpendicular to the plane. The component $P/2 \cdot \sin \alpha$ is negligible, as it does not contribute directly to the deflection considered and has very little influence on the diameter of the coil.

The problem of finding the total spring deflection may, therefore, be illustrated by Fig. 10.

$$\alpha = \frac{n'}{2} \cdot 2 \cdot \pi + \pi = \pi \cdot (n' + 1)$$

$$\theta = \frac{n'}{2} \cdot 2 \cdot \pi = \pi \cdot n'$$

The deflection f_H of point H representing the center of the bracket BC is the mean of the deflection at B and C . The deflection f_B of point B is composed of the deflection f_B' of point B due to the load $P/2$ at B and f_B'' due to the load $P/2$ at C , and the deflection f_C of point C is composed of the deflection f_C' of point C due to the load $P/2$ at C and f_C'' due to the load $P/2$ at B .

The total deflection

$$f_H = \frac{f_B + f_C}{2} = \frac{f_B' + f_B'' + f_C' + f_C''}{2}$$

$f_B'' = f_C''$ according to the theorem of reciprocity, so that

$$f_H = f_B'' + \frac{f_B' + f_C'}{2}$$

The total deflection of the spring is $f = 2f_H$

$$f = 2f_B'' + f_B' + f_C'$$

The deflections f_B'' , f_B' , and f_C' can be determined by equation

$$V = \frac{W \cdot a^3}{C} \left[(\theta - \sin \theta) - \sin \alpha (1 - \cos \theta) \right] + \frac{1}{2} W \cdot a^3 \left(\frac{1}{C} + \frac{1}{A} \right) \left[\theta \cos (\alpha - \theta) - \sin \theta \cos \alpha \right]$$

in which

$$V = f_B'' \text{ or } f_B' \text{ or } f_C'$$

$$W = P/2$$

$$a = r$$

$$A = \frac{E \cdot d^4 \cdot \pi}{64}$$

$$C = \frac{G \cdot d^4 \cdot \pi}{32}$$

$$E = \frac{5}{2} \cdot G$$

The resulting total deflection of the spring is

$$f = \frac{64 \cdot P \cdot r^3 \cdot \left(n' + \frac{30.4}{64} \right)}{G \cdot d^4} \approx \frac{64 \cdot (n' + \frac{1}{2}) \cdot r^3 \cdot P}{G \cdot d^4} \dots [6]$$

To this result a correction must be added to compensate for the influence of the pitch angle and the deflection due to pure shear.

Saint-Venant's equation⁴ for the deflection of a helical spring with rigid end levers is:

$$\delta h = l r^2 \left(\frac{\sin^2 \alpha}{B} + \frac{\cos^2 \alpha}{C} \right) R \dots \dots \dots [7]$$

⁴ Love, "Mathematical Theory of Elasticity," p. 422; S. Timoshenko, "Strength of Materials," part 1, p. 289.

$$\begin{aligned}
 R &= \text{spring load} \\
 \delta h &= \text{deflection} \\
 l &= \text{length of spring bar} \\
 r &= \text{radius of coil} \\
 \alpha &= \text{pitch angle} \\
 B &= EI = \frac{E \cdot d^4 \cdot \pi}{64} \\
 C &= GI_p = \frac{G \cdot d^4 \cdot \pi}{32}
 \end{aligned}$$

If we transform this equation in terms used in Equation [2], we find

$$f = \frac{64 \cdot n \cdot r^3 \cdot P}{G \cdot d^4} \left(\frac{4}{5} \frac{\sin^2 \alpha}{\cos \alpha} + \cos \alpha \right) \dots \dots [8]$$

In the deflection Equations [2], [3], [5], [a], [6], [7], and [8], it is assumed that the spring bar or rod is thin in comparison with the radius of the curvature, i.e., $D/d \approx \infty$. The error caused by this assumption, when the equations are applied to commercial helical springs where $D/d = 3$ or more is very small and for all practical purposes negligible.

Equation [8] is given to show the influence of the pitch angle. Other influences which affect the accuracy, and are not considered in this equation are caused by preventing the free ends of the spring from turning freely about the axis of the spring during compression or expansion and the pure shear deflection. The complications affected by properly considering all these facts are too great, and the change in end results too minute to warrant the application of these highly refined methods of calculation in practical engineering work.

As far as the deflection effect of the end coil is concerned, it is, for all practical purposes, sufficient to consider its torsional deflection only in the manner shown in Appendix 1. This is especially justified when we realize that the mathematically more complicated method employed in Saint-Venant's solution is also not absolutely accurate because the effects of such items as pure shear deflection, coil pitch angle, spring index D/d , weight, and end conditions of the helical springs are neglected. Another factor, which demonstrates the fallacy of striving for accuracy to the extreme in calculating the deflection of the end coils, is the unavoidable variation in cross-section shape and size, coil diameter, and pitch angle in commercial springs. Equations $f = \frac{64 \cdot n \cdot r^3 \cdot P}{G \cdot d^4}$ and $f = \frac{64 \cdot (n' + \frac{1}{2}) \cdot r^3 \cdot P}{G \cdot d^4}$, respectively, can be regarded as being accurate for all practical purposes.

Discussion

T. McLEAN JASPER.⁵ The paper by Mr. Vogt on helical springs is exceedingly interesting. I am wondering if the values of E , G , and l/m are as constant for spring steel in general as is assumed in the paper. My reasons for asking this go back to some tests made in 1924 which were published in the Transactions of the American Society for Testing Materials of that year and some work presented in the *Philosophical Magazine* for October, 1923, which indicate that the state of the steel as well as the temperature at which the tests were made influences the values of the so-called elastic constants somewhat.

The only way that this should be determined for spring application is to make several tests on identically shaped springs made of different steels.

I am not familiar with the values of G to be assumed for steel when formed into helical springs and when using different steels,

and therefore the values presented in this paper may be an appropriate average for steel springs to be used at ordinary temperatures only.

W. M. AUSTIN.⁶ The writer has had to apply helical compression springs, both large and small, to quite a variety of machinery and has often observed the influence of the end turns. Particularly, he has observed that the average spring designed to be made like the author's Fig. 6, except having a length relative to diameter several times longer than Fig. 6, will usually buckle badly when fully loaded.

Small springs often have their ends malformed. The spring maker winds enough wire on his mandrel to make two or more springs, and then cuts them apart. He then presses the end of the spring against the flat side of a rapidly turning dry grinding wheel. The heat generated makes the end turn red hot at some point about $\frac{3}{8}$ to $\frac{1}{2}$ turn from the end of the wire. The wire bends at this red-hot place and the end of the wire moves back against the next turn. He then dips the spring in water in an attempt to restore the temper to the heated part, and finishes the grinding.

The end turn, instead of tapering uniformly in thickness for $\frac{3}{4}$ of a turn to $\frac{1}{4}$ the diameter of the wire at the end, tapers for $\frac{1}{4}$ turn to a thickness about $\frac{1}{2}$ diameter of the wire, then increases in thickness for another $\frac{1}{4}$ turn to $\frac{3}{4}$ diameter of the wire, then tapers another $\frac{1}{4}$ turn to $\frac{1}{4}$ diameter of wire at the end. This last taper may lie against the next turn for most of its length.

The writer has often had to show the machine assembler (not a spring maker) how to cut off part of the end turn and regrind so that the spring will not buckle in service. Even if the spring were made according to the drawing as usually made, the center of gravity of the load would not be in the extended axis of the spring. If the spring is not more than three times as long as its diameter, the buckling is usually not very noticeable.

The writer prefers to make the end turn so that the end of the wire does not touch the next turn until the spring is compressed solid, and instead of making the ground end exactly perpendicular to the axis of the spring, to make it a helicoid of small pitch relative to the pitch of the spring. If this is done, the end of the wire will take its proper share of the load without bending beyond the plane of the part, $\frac{3}{4}$ of a turn away, where the tapering of the wire began.

Most springs are never completely unloaded in service, many of them never more than $\frac{1}{2}$ unloaded. In cases like this the minimum load brings the end of the spring into a plane perpendicular to the axis. It is probable that the center of gravity of the load is not in the axis of the spring, at the time of minimum load, but as the load increases the center of gravity of the load approaches nearer and nearer to the axis, and when maximum load is attained the ideal condition exists with the center of gravity of the load in the axis of the spring.

It is then seen that the flat-ended compression spring and its modifications is at best only a compromise, more or less successful, so to load the spring that at no time during the compressing or releasing of the spring will any part of it be stressed beyond its safe load.

In tension springs provided with hooks bent up out of the end turn and having the same diameter as the main body of the spring, the hooks have to stand the same bending moment as the torsional moment in the body of the spring. This means that the tension stress on the inside of the hook is about twice the shearing stress on the inside of the body of the spring because, for

⁵ Director of Research, A. O. Smith Corporation, Milwaukee, Wis. Mem. A.S.M.E.

⁶ Engineer, Westinghouse Elec. & Mfg. Co., East Pittsburgh, Pa. Mem. A.S.M.E.

round wire, the section modulus for torsion is $\pi d^3/16$ and for bending is $\pi d^3/32$, so if S_T be the maximum tension stress in the hooks and S_s be the maximum shearing stress in the coils, then

$$\frac{\pi d^3}{32} S_T = \frac{\pi d^3}{16} S_s, \text{ or } S_T = 2 S_s$$

Thus, with the additional fact that the wire is often damaged by making the hooks, accounts for the observed fact that tension springs, if they break, always break where the hook connects to the body of the spring. There is a way to reduce the excessive stress in the hooks. It is to make the end turn a spiral and bend up the hook from the inner end of the spiral, making the mean diameter of the hook about one-half the mean diameter of the main body of the spring.

The author's tests on the two large springs would be much more valuable if the springs had been loaded to near their maximum safe loads instead of limiting the stress as calculated by the old formula to 34,400 for the small spring and 14,100 for the large one. In any event, I believe they should have both been loaded so as to produce the same stress.

It is quite generally known that Hooke's law gives only the first term of a rapidly converging series, so that Young's modulus E and the shearing modulus G both have higher values when determined by stress-strain measurements using low stresses than

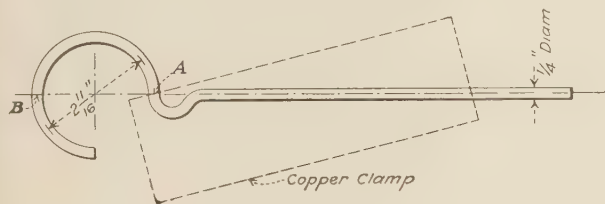


Fig. 11

they do when using stresses near but below the elastic limit.

The author's deflection $r \cdot \omega = \frac{16 \cdot r^3 \cdot P}{d^4 \cdot G}$ due to the torsion in the end turn is the deflection due to torsion of the point B, Fig. 3, and not the deflection of the pivot hole in the bar connecting points A and B. This would make the deflection of the pivot hold only $\frac{8 \cdot r^3 \cdot P}{d^4 \cdot G}$. In the author's analysis no account is taken of the deflection at B due to the bending of the end turn by the load $P/2$ at B. This would produce a deflection about as large as that due to torsion.

In order to get experimental data on the deflection of the end turn, the writer had a piece of $1/4$ -in. pretempered spring steel wire bent into $3/4$ of a turn of $2^{11/16}$ mean diameter, as shown in Fig. 11.

It was loaded at B with a 70-lb weight and the deflection at B was 0.29 in. If we let $G = 11,400,000$, the deflection per turn of the main body of the spring is 0.488, when loaded to 140 lb. The deflection at B is then seen to be 0.595 of the deflection of one turn, and the deflection at the center of the bar connecting A and B would be 29.7 per cent of the deflection of one turn, and for both ends the deflection due to the end turns is $59^{1/2}$ per cent of one turn.

J. P. MAHANEY.⁷ At the beginning of his paper the author shows that the value of G should be nearer 12,000,000 than 10,000,000. This is true provided Poisson's ratio is taken as 0.30 to 0.335 rather than 0.365. In some instances attempts have

been made to prove G equal to the lower value by substituting test data in the conventional spring formulas, but, since it is generally admitted that these formulas are approximate for "closely coiled" springs, such computations are not adequate proof.

The author states that the bar in the free coils is subjected to a shear force of $P/2$. This is incorrect. The total load on the spring is P ; consequently, the single bar must transmit this total load from one end of the coil to the other and the shear in the bar will be P instead of $P/2$.

Since present conventional spring formulas can be proved inaccurate, it does not follow that illogical corrections are acceptable. Adding one-half a coil to the number of free coils admits that a portion of the seated end coils deflect, which is beyond comprehension. It is true that torsional deformation extends beyond the free into a portion of the seated coils, for if this were not true, the first free coil at each end would not contribute its full share of deflection. To infer that there is axial deflection derived from the seated coils is a process of creating one error to compensate for another.

As the paper shows for balanced loading the load P on a compression spring may be resolved into two components of $P/2$ each acting 180 deg apart. If the spring in Fig. 3 is loaded in compression, $P/2$ at B will produce torsional stress at A, and $P/2$ at A increases this stress to the final value within the spring. The stress in the seated coil must build up to the proper value at A in order that the active end coils may be completely effective in contributing deflection. The stress within the seated coil A-B produces deflection indirectly but its contribution to the total should not be counted twice. The author's mathematical deduction clearly shows that the torque available in A-B is sufficient to produce deflection equivalent to one-quarter of an active coil provided it were free to move, which is of course impossible.

R. L. PEEK, JR.⁸ How accurately the solutions given for two- and three-point loading apply to helical springs compressed between parallel plane surfaces requires further analysis. Following the treatment given in Love's "Mathematical Theory of Elasticity," pp. 456-457, I have evaluated the force required to keep the extreme end of the inactive turn in contact with the point A (Fig. 3), a condition that must be satisfied under compression of this sort. I find this force trivial in comparison with the reaction at A under two-point loading, and this consideration therefore does not affect the validity of applying the result for two-point loading to compression between parallel plane surfaces. On the other hand, in such compression the change in pitch angle of the active coils will cause their axis to be no longer normal to the parallel plane surfaces applying load and their deformation will not be that corresponding to a purely axial thrust. Whether this effect will appreciably change the result, I have not ascertained.

A. M. WAHL.⁹ The exact solution of the additional deflection produced by the end turns of a helical compression spring is undoubtedly a very complicated problem, since it depends on the exact shape of the end turns and on the distribution of load thereon. The author has simplified the problem by assuming the end turns to have the full bar cross-section throughout their length. In addition he assumes various distributions of load on the end turns, finally choosing that which seems to agree best with test results.

Since, in most practical cases, the deflection due to the end

⁸ Bell Telephone Laboratories, New York, N. Y.

⁹ Westinghouse Research Laboratories, East Pittsburgh, Pa. Assoc.-Mem. A.S.M.E.

⁷ Assistant Professor, Industrial Engineering, Virginia Polytechnic Institute, Blacksburg, Va. Jun. A.S.M.E.

turns is but a relatively small part of the total deflection of the spring, a considerable error in estimating the effect of the end turns could be made without introducing much relative error in the total deflection of the spring. For this reason a rough approximation, such as the author has introduced, might be of value in practical work, provided it has been confirmed by a number of accurate tests.

The question of the effect of the end coils is closely bound up with that of the modulus of rigidity of the material. For years some spring manufacturers have used modulus values of 10.5×10^6 or 10×10^6 lb per sq in., as the author points out. It is well known that these values do not agree with modulus values obtained by means of torsion tests on ordinary spring steels. It has been the writer's opinion that these modulus values have been used largely to compensate for inaccuracy in estimating the effect of the end turns and possibly for errors in the spring dimensions.

To illustrate this point, some tests made on different springs at the Westinghouse Research Laboratories will be mentioned. The method used was to measure deflections between prick-punch marks on diametrically opposite points of the coil in the body of a helical spring and is described in a previous publication.¹⁰ The coil diameter and wire diameter were carefully measured at several points on each coil and the results averaged. By measuring deflections in the body of the spring, the effect of the end turns was eliminated. The values of "effective" modulus G could then be found from the known formula

$$G = \frac{8nD^3P}{fd^4}$$

Three springs from one manufacturer, having indexes of about ten, when tested in this manner, yielded the following values for the modulus:

Spring No.....	1	2	3
$G \times 10^{-6}$ lb per sq in.....	11.45	11.46	11.50

Three springs having indexes of about 6.5 from another manufacturer gave the following values:

Spring No.....	A	B	C
$G \times 10^{-6}$ lb per sq in.....	11.19	11.12	11.30

These values are all definitely higher than the value of 10 or 10.5×10^6 as assumed by some spring manufacturers.

It should be noted that this method of determining the modulus assumes that the effect of the spring curvature is small, i.e., that the spring acts like a straight bar subjected to a torsion moment Pr . This of course becomes more nearly true for springs of large index. As far as spring deflections are concerned, this assumption is born out by previous tests by the writer,¹⁰ wherein it was found that the ordinary deflection formula for helical round-wire springs was correct within 3 per cent for springs having indexes varying from 2.7 to 9.5. In other words, a fourfold increase in curvature of a spring having a given wire diameter did not seem to have an appreciable effect on the modulus. The same thing is known to be true of curved bars in bending; i.e., in general, a curved bar in bending may be computed within a few per cent accuracy as far as deflections are concerned by using the fundamental methods applied to straight bars, although this is not true when stress calculations are made. The effect of curvature on deflection was also found to be small in the case of helical springs of circular wire by O. Göhner,¹¹ who used more exact methods of calculation involving the theory of elasticity. The effect of curvature may be checked up experimentally by

¹⁰ A. M. Wahl, "Further Research on Helical Springs of Round and Square Wire," Trans. A.S.M.E., 1930, paper APM-52-18, p. 217.

¹¹ O. Göhner, "Die Berechnung zylindrischer Schraubenfedern," Z.V.D.I., March 12, 1932.

using the following method suggested by R. E. Peterson, of the Westinghouse Company. A heat-treated round bar of spring material is first tested in torsion, thus determining the technical value of the modulus G . This bar would then be wound into a spring, and heat treated, after which deflections would be measured in the body of the spring between prick-punch marks, so that the "effective" value of G could be found by use of the ordinary spring-deflection formula. The two values of G thus found should be nearly the same if the effect of curvature is small.

The writer would like to suggest that in determining the number of coils to add to the free coils to find the active coils, it is necessary to know the "effective" value of G accurately; in other words, a small error in G would produce a big error in the number of added turns. For example, in the case of the author's spring II, if G is assumed 11.85×10^6 , then from

$$G = \frac{8nD^3P}{fd^4}$$

it is found that $n = 12$, whence the added coils become $12 - 11\frac{1}{2} = \frac{1}{2}$. But suppose $G = 11.5 \times 10^6$ instead of 11.85×10^6 (a variation not at all unreasonable). Then we would find $n = 11.65$, from which the added coils would be found to be $11.65 - 11.5 = 0.15$, a value which differs greatly from $\frac{1}{2}$ as found by the author. This example shows the necessity for an accurate knowledge of the "effective" value of G . This could be determined, as mentioned previously, by measurements between prick-punch marks in the body of the spring, after which the average dimensions of the spring would be accurately measured. In this connection, the writer has found it to be extremely difficult to obtain accurately the average wire diameter of a spring, without cutting it up after the test, since, due to coiling, the wire section becomes slightly oval.

The method of determining the number of active coils, as proposed by the author, consisting of using two springs similar in every respect except in number of turns, would no doubt give an approximation which would be useful in practical work. For purposes of checking the theory, however, it would be necessary to find the average dimensions of each spring accurately. This would involve more labor than would the testing of one spring, as suggested above. Furthermore, there is a possibility that the modulus would vary some between the two springs, and this again would involve an additional error. For these reasons it is the writer's opinion that tests on one spring would be preferable in order to confirm the theory.

The value of Poisson's ratio $1/m = 0.363$ reported in the paper seems rather high for steel. Using $G = 11.7 \times 10^6$, $E = 30 \times 10^6$, this would give $1/m = E/2G - 1 = 0.283$. Taking $1/m = 0.3$ (a value commonly used for steel) and $E = 30 \times 10^6$, this would give $G = 11.53 \times 10^6$, which is not far from the values obtained in the writer's tests mentioned above.

AUTHOR'S CLOSURE

Answering Mr. McLean Jasper's discussion in regard to the constancy of the modulus of elasticity E and Poisson's ratio m for spring steel at various temperatures, we may, according to Hütte, for all practical purposes assume E and m and therefore G constant at temperatures between 0 F and 400 F.

Examples of springs applied at high temperatures are springs in steam indicators and on valves for internal-combustion engines and steam engines. As far as the author knows, the steam-indicator springs which are used for high-temperature steams and gases as well as for cold air have been accepted as accurate for practical purposes without using any correction factors for the various temperatures to which they are exposed.

The author, however, mainly considered springs used in at-

mospheric temperatures where accuracy in deflection values are essential.

Mr. Austin calls attention to irregularities in the shape of commercial compression springs especially in small sizes. However, he errs in his conclusion that the deflection $r \cdot \omega = \frac{16 \cdot r^3 \cdot P}{d^4 \cdot G}$ is the deflection of point *B* (see Fig. 3). This deflection is derived from the product $r \cdot \omega$ which (as is clearly explained in the paper and in Appendix 1) is nothing else than the deflection of the original end-coil center *O*, which, as well as that of the pivot hole between points *A* and *B*, is at a distance *r* from the center of the bar cross-section subjected to torsion.

Mr. Austin's claim that the bending effect of load $P/2$ on the deflection of point *O* would be as large as that of torsion only is unfounded as may be seen from the Saint-Venant solution (see Appendixes 2 and 3) which includes the bending effect of load $P/2$ at *B* and shows that the deflection of point *O* is even somewhat less than that given by the author for torsion only.

In Mr. Austin's experiment shown in Fig. 11 the deflection of point *B* is claimed to have been 0.29 in. for a load of 70 lb at *B*; but according to Saint-Venant's solution this deflection should have been 0.231 in. for $G = 11.4 \times 10^6$ or 0.225 in. for $G = 11.7 \times 10^6$.

Mr. Austin would have found more accurate and reliable results had he arranged his experiment according to Fig. 12. This arrangement consists of a helically and closely coiled spring-steel wire of one and a fraction of a turn. The coil diameter is about 20 or more times the diameter of the wire which latter should be about $1/4$ in. The wire and coil diameter and the deflection should be large enough to make unavoidable errors negligible in reference to the deflection. In Fig. 12 *BAB'* is

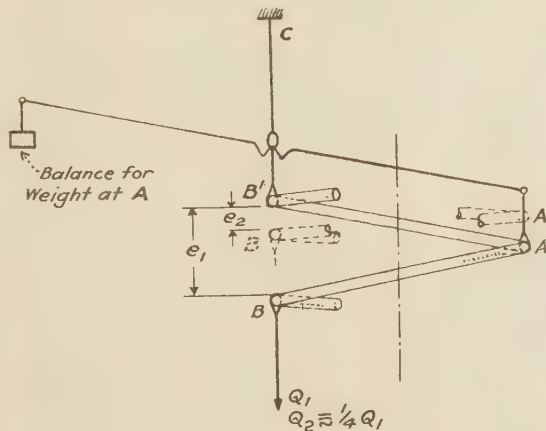


FIG. 12

exactly one full coil and $BA = AB'$ and each is one-half coil. In order to eliminate errors due to initial tension or deflection, the deflection $e_1 - e_2$ for the load $Q_1 - Q_2$ is determined. The deflection of a point *B* in reference to point *A* is $f = \frac{1 - e_2}{2}$

for the load $Q_1 - Q_2$ at *B*. In order that the stress in the wire is within the elastic limit of the spring steel Q_1 must be less than $15,000 \frac{d^3}{D} \left(1 - \frac{d}{D}\right)$ lb where *d* and *D* are given in inches. The

sum of the differential deflections in the two half coils *BA* and *AB'* is alike and opposite in direction. For this reason the wire cross-section at *A* does not turn and therefore does not cause a change in the true deflection of *B* in reference to point *A*.

In Mr. Austin's test, however, the cross-section at *A*, Fig. 11,

will turn and thereby increase the deflection of *B*, an amount corresponding to the torsional twist in the wire within the copper clamp near point *A*. This clamped portion of the wire cannot be held securely enough by the comparatively soft copper clamp to prevent twisting of the wire and consequently the turning of the wire cross-section at *A*. This torsional displacement of cross-section *A* of course increases the actual deflection due to the twist in half coil *BA* which stamps a test made according to Mr. Austin's arrangement, shown in Fig. 11, as unreliable.

The author has made a number of experiments according to Fig. 12 in which he found the deflections to check very closely with the Saint-Venant results.

J. P. Mahaney mentions that the pure shearing force in the free coils due to the load *P* must be equal to *P* which is quite correct. However, according to the explanation given by the author in answer to A. M. Wahl's discussion, the shearing force *P* is divided into halves. One-half balances an excess of the sum of the torsional shearing-force components parallel to the axis of the spring and acting in a direction opposite to *P*, while the other half adds a pure shear deflection to the torsional deflection as given by the conventional deflection equation $f = \frac{8 \cdot n \cdot D^3 \cdot P}{d^4 \cdot G}$.

Mr. Mahaney, after admitting that torsional deformation extends beyond the free coils into a portion of the seated coils, elaborates considerably on his conception that since the end coils in a compression spring are not free to move they cannot contribute to the deflection of the spring. The deformation of the end coil, Mr. Mahaney claims, makes it possible for the first free coil to contribute its full share of deflection. If this statement were true, the conventional spring-deflection Equation [2] as developed in the paper under the heading "Helical Spring With Rigid Arms at Coil Ends" would be faulty, as the first free coils in this case do not have the benefit of torsional deformation in end coils and therefore would not contribute their full share of deflection. Obviously, such a contention is against sound reasoning as the development of the deflection Equation [2] includes the contribution of the full share of deflection of all coils.

The fact that the end coils are held so that they can move only axially and parallel to their plane does not prevent the bar of the end coils from twisting due to the torque applied. Thus the axial deflection of the spring is increased proportionally to this twist and corresponds to one-fourth of an additional free coil per spring end beyond the deflection of a spring with rigid arms at free coil ends.

The author fully agrees with R. L. Peek, Jr., that in cases of compressing helical springs between parallel plane surfaces, the deformation of the spring as a whole and in particular of the end coil, will be different from the deformation as calculated in accordance with assumptions made in the analyses in the paper. This difference will vary with the different shapes of the spring ends as furnished in commercial helical compression springs.

However, when we consider the error range due to (a) using the conventional spring-deflection equation instead of the Saint-Venant equation given in Appendix 3, (b) unavoidable variations in spring-bar and coil diameters of commercial springs which appear in the equation in the fourth and third power, respectively, (c) change in pitch angle and coil diameter during compression, (d) uncertainty as to spring end loading conditions, (e) neglecting the influence of the spring index D/d , and (f) uncertainty as to the actual value of the modulus of elasticity *E* or *G*, respectively, the variation of the actual deflection of the end coil from the one calculated, and given as being equal to the deflection of $1/4$ coil due to maximum torque, is so small in comparison to other discrepancies that its disregard is fully justified. This is very apparent when we realize that a 5 per cent error in determining the end-coil deflection results in an error of less than

0.5 per cent in reference to the total deflection of a spring with five active coils.

An objection-free determination of the actual deflection of the end coil of a commercial helical compression spring with an accuracy within such a small error range would be very difficult.

Referring to A. M. Wahl's discussion, the values of E , G , and m were taken from the latest edition of Hütte, 1931, first volume, p. 689, where the following data for spring steels is given:

$$\begin{array}{ll} E = 2,100,000 \text{ kg per sq cm or} & E = 30,000,000 \text{ lb per sq in.} \\ G = 822,000 \text{ kg per sq cm} & G = 11,700,000 \text{ lb per sq in.} \\ G/E = 0.392 & m = 3.63, \text{ from } G = E/2(1 + 1/m) \end{array}$$

These data have always corresponded with spring tests made under the consideration of the proper number of active coils (regardless of small or large number of active coils), as given in the author's paper, and were therefore accepted by the author as being dependable. Hütte is considered one of the outstanding sources of reliable engineering information.

Mr. Wahl questions the accuracy of determining the value of G by testing two springs as suggested by the author, and in his example assumes $G = 11.5 \times 10^6$ instead of 11.85×10^6 , in which case Mr. Wahl calculates the effect of the end coils to be that of 0.15 free coils instead of 0.5 as demonstrated in this paper. Mr. Wahl's analysis is, on this point, incorrect and deceiving.

In the author's example, G is determined from actual values of $n' = 11.5$, $d = 1.122$, $D = 4.14$, $f = 1.66$, and $P = 4600$ and (in conformity with the theory developed in the paper) $n = n' + 1/2$.

If, in the example, the value of G had been different, say 11.5×10^6 , then the deflection f would have been 1.715 in. instead of 1.66 in. as it actually showed in the test, and $n = 12$ and not 11.65. The number of effective coils is fixed by the spring design and does not depend on the value of G .

The value of G cannot vary much for commercial spring steel. The skeptical engineer, however, can determine its value and concurrently the actual effect of the end coils, with satisfactory accuracy, by the method of testing two springs of equal dimensions but with greatly differing numbers of coils, as suggested by the author in the last part of his paper.

Mr. Wahl, in referring to the influence of the spring index on spring deflection, mentions that the conventional spring-deflection equation for helical round-wire springs is correct within 3 per cent for springs having indexes varying from 2.7 to 9.5.

The author determines the effect of the spring index on the spring deflection definitely by adding the direct shear deflection to the torsional deflection of the helical spring. The deflection

of direct or pure shear for the spring is $f'' = \gamma L = \frac{\tau}{G} L = \frac{P \cdot L}{F_s \cdot G'}$

where $L = 2R\pi n$, $F_s = \frac{d^2 \cdot \pi}{4 \cdot 1.2}$ (for circular cross-sections from

Hütte), P = spring load, or $f'' = \frac{9.6 \cdot P \cdot R \cdot n}{G \cdot d^2}$. About half

of this deflection is already included in the conventional spring equation, as in helical springs under load P about one-half the shear load P is balanced by the total sum of torsional shearing-

stress components parallel to the spring axis, as explained by Dr.-Ing. A. Röver in *Z.V.D.I.*, Nov. 20, 1913, p. 1907.

By using the conventional spring-deflection equation, it is assumed that a curved bar has the same torsional deflection as a straight bar of the same length. The stress distribution in the cross-sections of the straight and curved bars is, however, slightly different and causes a small difference in deflection, amounting to one-half the deflection due to pure shear. The deflection of the curved bar is less than that of the straight bar, when the pure shear deflection is considered for both.

The total deflection of the helical spring under load P is:

$$f = \frac{64 \cdot n \cdot R^3 \cdot P}{G \cdot d^4} + \frac{4.8 \cdot P \cdot R \cdot n}{G \cdot d^2}$$

or

$$f = \frac{P \cdot R \cdot n}{G \cdot d^2} \left(\frac{64 \cdot R^2}{d^2} + 4.8 \right)$$

or

$$f = \frac{P \cdot D \cdot n}{G \cdot d^2} \left(8 \frac{D^2}{d^2} + 2.4 \right)$$

γ = shear angle in radians

τ = shearing stress

R = mean radius of coil

D = mean diameter of coil

d = diameter of spring wire or bar

n = number of active coils

P = spring load

G = torsional modulus of elasticity

f = total spring deflection

L = effective length of wire or bar

f'' = deflection due to pure shear.

Applying the extended deflection equation in conjunction with accurate spring tests will result in finding more uniform values for G .

Plotting the shear deflection, in per cent of torsional spring deflection, against the spring index D/d we find the curve given in Fig. 13.

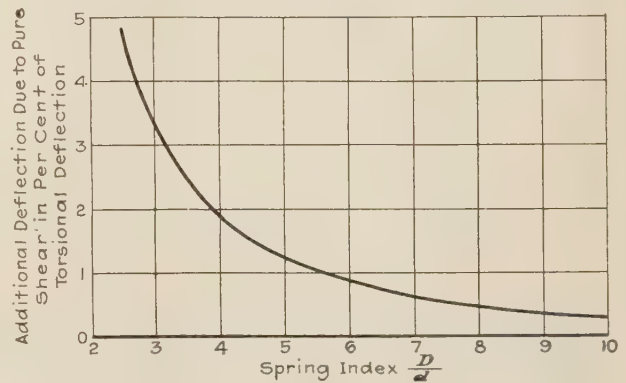


FIG. 13 ADDITIONAL SHEAR DEFLECTION IN HELICAL SPRING

Depositories for A.S.M.E. Transactions in the United States

BOUND copies of the complete Transactions of The American Society of Mechanical Engineers will be found in the libraries in the United States and other countries which are listed on the following pages.

Alabama

Auburn.....Engineering Library, Alabama Poly. Inst.
Birmingham.....Public Library

Arkansas

Fayetteville.....Engineering Library, Arkansas University

California

Berkeley.....Library, University of California
Long Beach.....Public Library
Los Angeles.....Public Library
University of Southern California
Oakland.....Oakland City Library
Teachers' Professional Library
Pasadena.....Library, California Institute of Technology
Santa Clara.....Library, University of Santa Clara
San Diego.....Public Library
San Francisco.....Public Library (Civic Center)
Engineers Club of San Francisco
Mechanics Institute
Stanford Univ....Library, Stanford University

Colorado

Boulder.....Library, University of Colorado
Denver.....Public Library
Fort Collins.....Colorado State Agricultural College

Connecticut

Bridgeport.....Public Library
Hartford.....Public Library
New Haven.....Public Library and Yale University
Waterbury.....Silas Bronson Library

Delaware

Newark.....University of Delaware
Wilmington.....Wilmington Free Institute

District of Columbia

Washington.....Scientific Library, U. S. Patent Office
Library of Congress
Bureau of Standards Library
George Washington University
Catholic University

Florida

Gainesville.....University of Florida
Jacksonville.....Free Public Library
Miami.....Public Library
Tampa.....Public Library

Georgia

Atlanta.....Carnegie Public Library
Georgia School of Technology
Savannah.....Public Library

Idaho

Moscow.....University of Idaho

Illinois

Chicago.....John Crerar Library
Western Society of Engineers
Library, Armour Institute of Technology
Public Library of Chicago
Moline.....Public Library
Urbana.....University of Illinois

Indiana

Evansville.....Public Library
Fort Wayne.....Public Library
Indianapolis.....Public Library and Indiana State Library
Notre Dame.....Library, University of Notre Dame
Terre Haute.....Rose Polytechnic Institute
West Lafayette...Library, Purdue University

Iowa

Ames.....Iowa State College
Des Moines.....Public Library
Iowa City.....State University of Iowa

Kansas

Kansas City.....Public Library, Huron Park
Lawrence.....Library, University of Kansas
Manhattan.....Kansas State Agricultural College
Wichita.....Wichita City Library

Kentucky

Lexington.....University of Kentucky
Louisville.....Speed Scientific School
University of Louisville

Louisiana

Baton Rouge....Louisiana State University
New Orleans....Howard Memorial Library
Louisiana Engineering Society
Public Library

Maine

Orono.....University of Maine

Maryland

Annapolis.....United States Naval Academy
Baltimore.....Johns Hopkins University
Engineers Club of Baltimore
Public Library

Massachusetts

Boston.....Northeastern University
Boston Public Library
Cambridge.....Harvard University (Engineering Library)
Massachusetts Institute of Technology
Fall River.....Public Library
Lowell.....Lowell Textile Institute
Lynn.....Free Public Library
New Bedford....Free Public Library
Springfield....Springfield City Library
Tufts College....Tufts College
Worcester.....Worcester Polytechnic Institute
Free Public Library

Michigan

Ann Arbor.....University of Michigan
Detroit.....Public Library
Cass Technical High School
Highland Park Public Library
University of Detroit
East Lansing....Michigan State College
Flint.....Public Library
Grand Rapids...Public Library
Houghton.....Michigan College of Mining & Technology
Jackson.....Public Library

Minnesota

Duluth.....Public Library
Minneapolis....University of Minnesota
Minneapolis Public Library (Engineering
and Circulating Libraries)
St. Paul.....James Jerome Hill Reference Library

Mississippi

State College....Mississippi State College

Missouri

Columbia.....University of Missouri
Kansas City.....Public Library
Rolla.....Missouri School of Mines and Metallurgy
St. Louis.....Engineers Club of St. Louis
Public Library
Washington University
Mercantile Library

Montana

Bozeman.....Montana State College

TRANSACTIONS OF THE AMERICAN SOCIETY OF MECHANICAL ENGINEERS

Nebraska

Lincoln.....University of Nebraska
Omaha.....Public Library

Nevada

Reno.....University of Nevada Library

New Hampshire

Durham.....University of New Hampshire

New Jersey

Bayonne.....Free Public Library
Camden.....Free Public Library
Elizabeth.....Free Public Library
Hoboken.....Stevens Institute of Technology
Jersey City.....Free Public Library
Newark.....Newark College of Engineering
Newark.....Free Public Library
New Brunswick...Rutgers University
Paterson.....Free Public Library
Princeton.....Princeton University
Trenton.....Free Public Library

New York

Albany.....New York State Library
Brooklyn.....Polytechnic Institute
Brooklyn.....Pratt Institute
Brooklyn.....Brooklyn Public Library
Buffalo.....The Grosvenor Library
Buffalo.....Engineering Society of Buffalo
Buffalo.....Buffalo Public Library
Ithaca.....Cornell University
Jamaica, L. I....Queens Borough Public Library
New York.....Engineering Societies Library
New York.....Public Library
New York.....College of the City of New York
New York.....Cooper Union
New York.....Columbia University
New York.....New York Museum of Science and Industry
New York.....New York University Library
Potsdam.....Clarkson College of Technology
Rochester.....Rochester Engineering Society
Schenectady.....Union College
Syracuse.....Syracuse University
Syracuse.....Public Library
Troy.....Rensselaer Polytechnic Institute
Utica.....Public Library
Yonkers.....Public Library

North Carolina

Chapel Hill.....University of North Carolina (Engineering Library)
Raleigh.....North Carolina State College

North Dakota

Fargo.....North Dakota State Agricultural College
Grand Forks....University of North Dakota

Ohio

Ada.....Ohio Northern University
Akron.....Public Library
Akron.....University of Akron
Canton.....Public Library
Cincinnati.....University of Cincinnati
Cincinnati.....Public Library
Cincinnati.....Engineers Club of Cincinnati
Cleveland.....Public Library
Cleveland.....Case School of Applied Science
Cleveland.....Cleveland Engineering Society
Columbus.....State of Ohio Library
Columbus.....Public Library
Columbus.....Ohio State University
Dayton.....Engineers Club of Dayton
Toledo.....Public Library
Toledo.....University of Toledo
Youngstown.....Public Library

Oklahoma

Norman.....Oklahoma University
Oklahoma City...Public Library
Stillwater.....Oklahoma Agricultural and Mechanical College
Tulsa.....Public Library

Oregon

Corvallis.....Oregon State Agricultural College
Portland.....Portland Library Association

Pennsylvania

Allentown.....Free Library
Bethlehem.....Lehigh University
Easton.....Public Library
Easton.....Lafayette College
Erie.....Public Library
Lewisburg.....Bucknell University
Philadelphia.....Engineers Club
Philadelphia.....Drexel Institute
Philadelphia.....University of Pennsylvania
Philadelphia.....Franklin Institute
Pittsburgh.....University of Pittsburgh
Pittsburgh.....Engineers' Society of Western Pennsylvania
Pittsburgh.....Carnegie Institute of Technology
Pittsburgh.....Carnegie Library (Schenley Park)
Pittsburgh.....Carnegie Free Library of Allegheny
Reading.....Public Library
Scranton.....Public Library
State College...Pennsylvania State College
Swarthmore.....Swarthmore College
Villanova.....Villanova College
Wilkes-Barre....Public Library

Rhode Island

Kingston.....Rhode Island State College
Providence.....Brown University
Providence.....Providence Engineering Society
Providence.....Public Library

South Carolina

Clemson College..Library, Clemson College

Tennessee

Kingsport.....Public Library
Knoxville.....University of Tennessee
Memphis.....Goodwin Institute
Nashville.....Vanderbilt University

Texas

Austin.....University of Texas
College Station..Agricultural & Mechanical College of Texas
Dallas.....Public Library
El Paso.....Public Library
Forth Worth.....Carnegie Public Library
Houston.....Rice Institute
Houston.....Public Library
Lubbock.....Texas Technological College (School of Engineering)
San Antonio.....Carnegie Library

Utah

Salt Lake City...University of Utah
Salt Lake City...Public Library

Vermont

Burlington.....University of Vermont

Virginia

Blacksburg.....Virginia Polytechnic Institute
Charlottesville...University of Virginia
Norfolk.....Public Library
Richmond.....Virginia State Library

Washington

Pullman.....State College of Washington
Seattle.....Public Library
Seattle.....Engineers Club
Seattle.....University of Washington
Spokane.....Public Library
Tacoma.....Public Library

West Virginia

Morgantown....West Virginia University

Wisconsin

Madison.....Library, University of Wisconsin
Milwaukee.....Public Library
Milwaukee.....Board of Industrial Education, Vocational School Library
Milwaukee.....Marquette University

Wyoming

Laramie.....Wyoming University

Depositories for A.S.M.E. Transactions

Outside the United States

Argentina

Buenos Aires.....Biblioteca de la Sociedad Cientifica

Australia

Adelaide.....Public Library of Adelaide
Melbourne.....Public Library of Victoria
Perth.....University of Western Australia Library
Sydney.....Public Library, N. S. W., Sydney

Brazil

Rio de Janeiro...Bibliotheca da Escola Polytechnica
Bibliotheca Nacional
Sao Paulo.....Bibliotheca da Escola Polytechnica

Canada

Montreal.....McGill University
Engineering Institute of Canada
Toronto.....University of Toronto, Library

Chile

Santiago.....Universidad de Chile, Facultad de Ciencias
Fisicas y Matematicas (Engrg. School)

Cuba

Havana.....Cuban Society of Engineers

Czechoslovakia

Prague.....Masarykova Akademie Prace
Society of Czechoslovak Engineers

Danzig Free City.....Bibliothek der Technischen Hochschule

Denmark

Copenhagen.....The Royal Technical College

England

Birmingham.....Birmingham Public Libraries
Bristol.....University of Bristol
Cambridge.....University of Cambridge
Leeds.....University of Leeds
Liverpool.....Public Library of Liverpool
Liverpool Engineering Society
London.....City & Guild Engineering College
Institution of Automobile Engineers
Institution of Mechanical Engineers
Institution of Civil Engineers
Institution of Electrical Engineers
The Junior Institution of Engineers
The Royal Aeronautical Society
Manchester.....Manchester Public Libraries (Reference
Library)
Oxford.....University of Oxford
Newcastle-upon-
Tyne.....The North East Coast Institution of
Engineers and Shipbuilders
Sheffield.....Sheffield Public Libraries

Wales

Cardiff.....Cardiff Public Library

France

Lyons.....University of Lyons
Paris.....École Nationale des Arts et Metiers
École Nationale Supérieure de L'Aeronau-
tique
École Centrale des Arts et Manufactures de
Paris
Société des Ingénieurs Civils de France

Germany

Berlin.....Verein deutscher Ingenieure
Bibliothek der Technischen Hochschule
Breslau.....Bibliothek der Technischen Hochschule
Cologne (Köln)...Universitäts- und Stadtbibliothek
Dresden.....Bibliothek der Technischen Hochschule
Düsseldorf.....Bücherei des Vereines deutscher Eisen-
hüttenleute
Frankfort.....Technische Zentralbibliothek

Germany (continued)

Hamburg.....Bibliothek der Technischen Staatslehran-
stalten
Hanover.....Bibliothek der Technischen Hochschule
Karlsruhe.....Bibliothek der Technischen Hochschule
Leipsic.....Stadtbibliothek
Munich.....Bibliothek der Technischen Hochschule
Bibliothek des Deutschen Museums
Stuttgart.....Bibliothek der Technischen Hochschule

Hawaii

Honolulu.....University of Hawaii Library

Holland

Amsterdam.....Koninklijke Akademie von Wetenschappen
Delft.....Bibliotheek der Technische Hoogeschool
The Hague.....Koninklijk Instituut van Ingenieurs
Rotterdam.....Nationaal Technisch Scheepvaartkundig
Instituut

India

Bangalore.....Mysore Engineers Association
Calcutta.....Bengal Engineering College
Poona.....Poona College of Engineering
Rangoon.....University of Rangoon

Ireland

Belfast.....Queen's University of Belfast

Italy

Milan.....Biblioteca della R. Scuola d'Ingegneria
Comitato Autonomo per l'Esame della
Invenzioni
Naples.....Biblioteca della R. Scuola d'Ingegneria
Rome.....Biblioteca della R. Scuola d'Ingegneria
Consiglio Nazionale delle Ricerche presso il
Ministero della Educazione Nazionale
Turin.....Biblioteca della R. Scuola d'Ingegneria

Japan

Kobe.....Kobe Technical College
Tokyo.....Imperial University Library
The Society of Mechanical Engineers
Yokohama.....Library of Yokohama

Mexico

Mexico City.....Asociacion de Ingenieros y Arquitectos de
Mexico
Library of the Escuela de Ingenieros
Mecanicos y Electricistas

Norway

Oslo.....Den Polytekniske Forening

Poland

Warsaw.....Biblioteka Publiczna

Porto Rico

Mayaguez.....University of Porto Rico

Portugal

Lisbon.....Institute Superior Technico

Roumania

Bucharest.....Scola Polytechnica din Bucharest

Scotland

Glasgow.....Royal Technical College
Mitchell Library

South Africa

Cape Town.....University of Cape Town
Johannesburg....South African Institute of Engineers

Sweden

Stockholm.....Kungl. Tekniska Hogskolan
Svenska Teknologforeninger
Gothenburg.....Chalmers Tekniska Institut

TRANSACTIONS OF THE AMERICAN SOCIETY OF MECHANICAL ENGINEERS

Switzerland

Zurich.....Eidgenossische Technische Hochschule

Turkey

Istanbul.....Robert College

U.S.S.R.

Kharkov.....Supreme Economic Council of Ukraine
Leningrad.....Leningrad Polytechnic Institute
Moscow.....Supreme Council of National Economy
Tomsk.....Tomsk Polytechnic Institute

The Thermal Performance of the Detroit Turbine Using Steam at 1000 F

By W. A. CARTER,¹ DETROIT, MICH., AND F. O. ELLENWOOD,² ITHACA, N. Y.

This paper gives the results of a large number of tests made to ascertain the thermal performance of a 10,000-kw turbine-generator designed for steam at 1000 F. The thermal efficiency was found to be 31.8 per cent and the engine efficiency 76 per cent for the complete unit. A companion paper, entitled "High-Temperature Steam Experience at Detroit" (A.S.M.E. Trans., 1934, FSP-56-9), by P. W. Thompson and R. M. Van Duzer, Jr., deals with the generation and utilization of the steam at this temperature, with special reference to the materials employed.

THE advantages of using high-temperature steam at the throttle of a turbine, as compared with low-temperature steam of the same pressure, used without reheating, are:

(a) more energy is available for transformation into work for any specified exhaust pressure; (b) a larger portion of this available energy can be utilized; and (c) less erosion of the turbine blades in the low-pressure stages is produced. These advantages are of sufficient importance in the operation of large central stations to justify the expenditure of large sums of money to ascertain new facts concerning the use of high-temperature steam. Even though steam temperatures above 1000 F have been used previously in certain static apparatus, the problems encountered in designing turbine parts to sustain high temperatures are much more difficult, because small clearances between the high-speed rotor and the stationary elements must be maintained in spite of the tendency of the materials to grow and become seriously distorted when heated to a tem-

perature nearly 1000 degrees above that prevailing when the machine is cold.

The main results obtained from the analysis of the tests of the Detroit unit may be briefly expressed as follows:

(a) The energy consumption of the complete unit (turbine-generator and three heaters) was 10,730 Btu per kw-hr, for a load of 10,000 kw, a throttle pressure of 390 lb per sq in. abs, a throttle temperature of 1000 F and an exhaust pressure of 1 in. Hg abs. This means a thermal efficiency of 31.8 per cent, and an engine efficiency of 76 per cent for the complete unit.

(b) A load of 10,000 kw with steam at 1000 F was not large enough to give the highest thermal efficiency of this unit.

(c) Increasing the steam temperature from 700 to 1000 F reduced the energy consumption of this unit 920 Btu per kw-hr or 7.9 per cent.

(d) The radiation and convection losses from the turbine and heaters with steam at 1000 F were relatively small, namely, 0.6 per cent of the available energy for a load of 10,000 kw.

(e) The loss due to the leakage of sealing steam was relatively large, namely, 4.4 per cent of the available energy for full-load conditions. This is probably not an inherent characteristic of large turbines designed for steam at 1000 F.

(f) The results of these tests become attractive when viewed from the future possibilities of steam at 1000 F used in large units with a far smaller percentage of loss due to the sealing steam, since the complete elimination of this loss (not an inconceivable attainment in a unit of 50,000 kw or larger) would mean an energy consumption of about 9900 Btu per kw-hr of net generator output for the same steam pressures as used in these tests. For a pressure of 1200 lb per sq in., and no reheating, one may reasonably expect that a very large unit (say 75,000 kw or more) would require an energy consumption of about 8600 Btu per kw-hr.

(g) The foregoing conclusions refer only to thermal efficiencies. The authors are not overlooking the difficulties of design and of material that have arisen in the building of the present small machine. Neither are they failing to recognize the opinions expressed on behalf of the turbine manufacturers that such a large machine as that described in (f) can be built, are implicit rather than explicit. The authors in this paper have made some suggestions as to modifications of design, and inasmuch as they are neither designers nor builders of turbines, they do not wish to expand these. But they take occasion, nevertheless, to say that in their opinion the difficulties of building such a large machine for steam having a temperature of 1000 F are not insuperable.

(h) The "nominal" over-all coefficients of heat transfer in the feedwater heaters that received highly superheated steam in these tests may seem to be high relative to those generally obtained when saturated steam is used. These, however, are merely "nominal" values based upon "nominal" mean temperature differences rather than upon the real ones; and the water velocities involved in each case should also be carefully considered. The temperatures of the feedwater leaving the heaters, as indicated by the "nominal" temperature differences which are based upon the saturated temperatures of the entering steam, approached closely the values applying to the ideal unit herein

¹ Technical Engineer of Power Plants, The Detroit Edison Company. Associate-Member A.S.M.E. Mr. Carter graduated from Cornell University, with the degree of M.E., in 1913. He was an engineer in the Research Department of The Detroit Edison Company from his graduation until 1926, and from then to date he has been Technical Engineer of Power Plants. He has been co-author of papers dealing with pipe covering and with boiler furnace refractories, which have been presented before A.S.M.E. He is a member of the Power Test Codes Committee No. 19 on Instruments and Apparatus, and of the Research Committee on Boiler Furnace Refractories.

² Professor of Heat-Power Engineering, College of Engineering, Cornell University. Member A.S.M.E. Professor Ellenwood graduated from Stanford University in 1904 with the degree of A.B. in Mechanical Engineering and in 1922 he received the degree of M.E. During the first four years after he graduated he worked for C. C. Moore & Co. of San Francisco, the Tonopah (Nev.) R.R. Co., and the American Smelting & Refining Co. From 1908 to 1911 he was an instructor in Mechanical Engineering at Stanford University, and from 1911 to 1916 he was Assistant Professor of Heat-Power Engineering at Cornell University. Since 1916 he has been Professor of Heat-Power Engineering at Cornell. He is author of "Steam Charts," and a joint-author with W. N. Barnard and C. F. Hirschfeld in the three parts of "Elements of Heat-Power Engineering." He was co-author with C. F. Hirschfeld of a paper entitled "High Pressure, Reheating, and Regenerating for Steam Power Plants," A.S.M.E. Trans., vol. 45, 1923, and in 1927 presented another paper before the A.S.M.E. entitled, "Efficiencies of Otto and Diesel Engines," A.S.M.E. Trans., vol. 49-50, 1927-1928.

Contributed by the Power Division and presented at the Annual Meeting, New York, N. Y., December 4 to 8, 1933, of THE AMERICAN SOCIETY OF MECHANICAL ENGINEERS.

NOTE: Statements and opinions advanced in papers are to be understood as individual expressions of their authors, and not those of the Society.

TABLE 1 SUMMARY OF TEST AT 1000 F

<i>Net Load, kw</i>				
At generator terminals.....	10,068	8,034	5,986	4,042
<i>Temperature, F</i>				
Of steam entering throttle.....	1,003	1,006	1,004	1,005
Of sealing steam entering regulator..	445	448	450	452
Of feedwater leaving 9th-stage heater	337	322	304	282
<i>Absolute Pressure, lb per sq in.</i>				
Of steam entering throttle.....	392	390	393	387
Of sealing steam entering regulator..	391	405	415	420
Of steam at 9th-stage bleeder nozzle..	128	103	78	55
Of steam at 14th-stage bleeder nozzle	40.5	32.5	24.3	17.4
Of steam at 17th-stage bleeder nozzle	10.5	8.4	6.3	4.5
Of steam entering condenser.....	0.50	0.49	0.46	0.52
<i>Steam Rate, lb per kw hr</i>				
To throttle.....	8.388	8.403	8.519	8.965
To sealing-steam regulator.....	0.541	0.530	0.523	0.559
<i>Generator Efficiency, per cent</i>				
Including bearings, ventilation, and excitation (furnished by B.T.-H.Co.)	95.58	95.07	94.11	91.90
<i>Energy Consumption Rate, Btu per kw hr</i>				
Of complete unit (turbine-generator and heaters).....	10,731	10,890	11,186	11,995
Of turbine and heaters.....	10,257	10,353	10,527	11,023
<i>Thermal Efficiency, per cent</i>				
Of complete unit.....	31.81	31.34	30.51	28.45
Of turbine and heaters.....	33.28	32.97	32.42	30.96
Of corresponding ideal unit.....	41.86	42.00	42.28	41.59
<i>Engine Efficiency, per cent</i>				
Of complete unit.....	75.99	74.62	72.16	68.41
Of turbine and heaters.....	79.50	78.49	76.68	74.44

used. On the other hand, the true terminal temperature differences of the heaters were much larger than the "nominal" as they were based upon the actual temperature of the highly superheated steam entering the heaters.

The most important data pertaining to the tests with steam at 1000 F and the results obtained from them are summarized in Table 1. Attention is called to the two items for the steam rate as given in this table. The sum of these two steam rates is purposely omitted, as such a result would be of little significance, since the energy supplied with each pound of throttle steam was much greater than that supplied per pound of sealing steam.

DESCRIPTION OF THE UNIT

The unit tested consists of a horizontal tandem-compound turbine, a 12,500-kva generator, and three regenerative feedwater heaters. The turbine was designed for a steam pressure of 380 lb per sq in. abs at the throttle, an exhaust pressure of 1 in. Hg abs, and a steam temperature of 1000 F at the throttle.

It operates at 3600 rpm and is of the impulse type with nine stages in the high-pressure cylinder and eleven in the low. The generator operates at 4800 volts and 60 cycles. A cross-section of the turbine is shown in Fig. 1. The pitch diameters of the blading in the first, second, ninth, tenth, and twentieth stage wheels are approximately 32.5, 23, 23.5, 32, and 50 in., respectively. The oil pump, exciters, and generator ventilating fans are driven by the turbine. The output of the generator, therefore, as given under the heading "Load" in the test data represents the net output of the unit, except for the negligibly small (0.1 per cent) amount of energy expended to operate the hotwell pump and the heater-drains pump. The feedwater heaters are of the horizontal four-pass type with heating surfaces as given in Table 6. The drains from the heaters are handled as shown by the diagrammatic sketch in Fig. 2. The exhaust steam from the turbine is delivered to an 8000-sq ft, two-pass condenser, which is slightly undersized for this service, as it was originally intended for another installation.

The turbine speed is regulated by a flyball-type governor driven directly from the turbine shaft, and the governing is accomplished by means of five control valves that are operated by a camshaft moved by an oil servo-motor controlled by the governor.

The high-pressure shaft packing constitutes an important part of the turbine because leakage of the high-temperature steam might cause serious heating of the shaft and bearing in addition to the loss of energy due to the leakage. The axial length of the high-pressure packing is greater than the assembly of the first nine wheels, as may be seen in Fig. 1. This extended form of the packing permits the shaft to be kept reasonably cool by the sealing steam leaking through the packing, and thus the main bearing is not endangered by the high steam temperature at the throttle. The steam leaving the first-stage wheel has a temperature of about 930 F and is kept from passing through the packing glands by using saturated steam of slightly higher pressure as sealing steam. When the sealing-steam regulator is set to give a pressure at entrance to the high-pressure packing of 0.5 lb per sq in. above that in the first-stage shell, the leakage of saturated steam past the inner packing and into this shell amounts to about 10 per cent of the total sealing steam, or about 0.6 per cent of the total flow to the turbine for a load of 10,000 kw. Part of the sealing steam from the intermediate high-pressure packing passes on to the outer

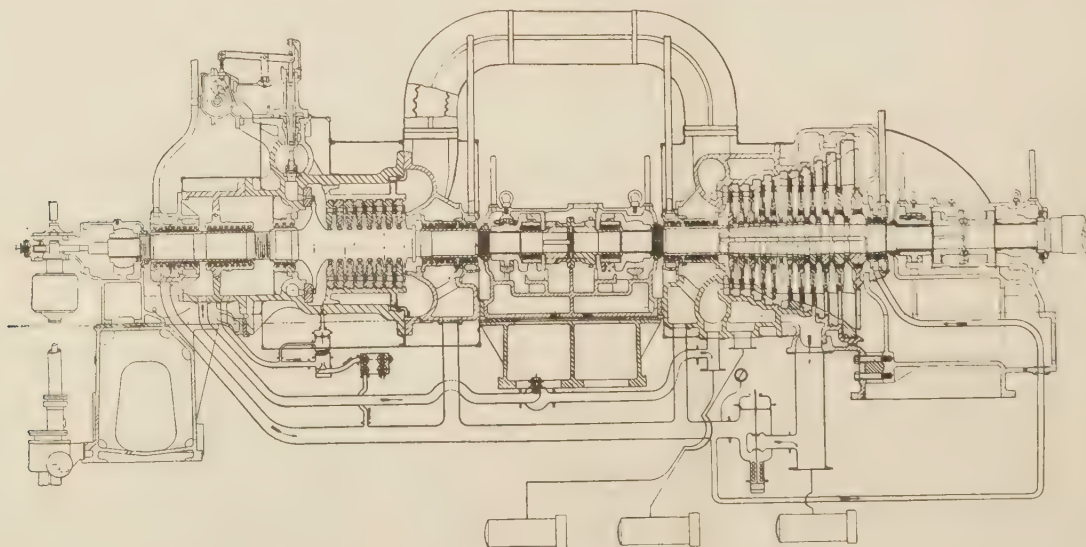


FIG. 1 SECTIONAL VIEW OF THE 1000-F TURBINE

packing and the remainder goes to the ninth-stage heater. Part of the leakage through the outer packing seals the shaft packing on the exhaust end of the turbine and the remainder passes through a pressure regulator on its way to the seventeenth-stage heater. The connecting lines between the turbine, heaters, pumps, and seals are shown in Fig. 2. The atmospheric vents, marked A in the diagram, discharge very small amounts of vapor, and thus serve to give constant evidence to the operator that all seals are being properly maintained. No water seals are used on any of the shaft packings. The packing is of the saw-tooth type, as shown in Fig. 3, and is arranged in the form of individual rings, each of which is composed of four sectors. The sectors are held in place by leaf springs, which are intended to provide sufficient flexibility to prevent damage to the packing from small shaft deflections that are likely to occur during starting.

The high-pressure cylinder has an inner and an outer casing, as shown in Fig. 1. The inner casing holds the eight interstage diaphragms and is made in two halves with axial flanged joints. The outer casing supports the inner one, fitting it snugly at the end nearer the throttle, and has only circumferential joints at its two ends. This construction eliminates the junctions of axial and circumferential joints used in the conventional design turbine cylinders with split casings, which might be difficult to maintain in a tight condition with steam at such a high temperature.

The materials used in the construction of the turbine are fully discussed in the accompanying paper on "High-Temperature Steam Experience at Detroit," by P. W. Thompson and R. M. Van Duzer, Jr. (A.S.M.E. Trans., 1934, FSP-56-9).

The turbine and generator were made by The British Thomson-Houston Company, Ltd., of Rugby, England, and the heaters

operation, some wear was undoubtedly caused by starting the unit eight times before the final tests were made.

TEST PROCEDURE

Forty runs were made on this unit under various conditions, such as load, temperature of steam at the throttle, temperature of sealing steam, and exhaust pressure. Only twenty-four runs are tabulated in this paper as they are the ones for which the operating conditions were the nearest to those for which the unit was designed.

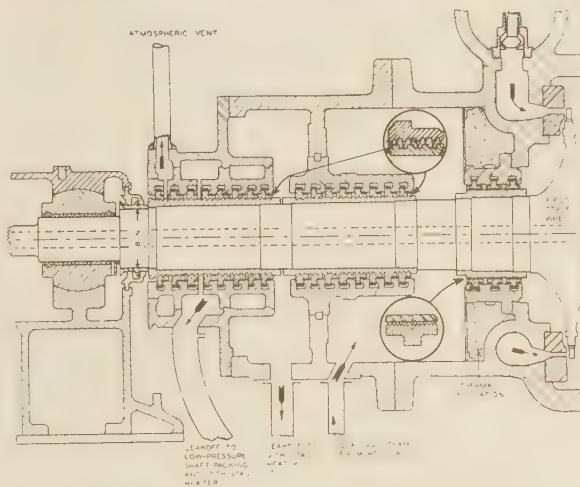


FIG. 3 SECTIONAL VIEW OF HIGH-PRESSURE SHAFT PACKING

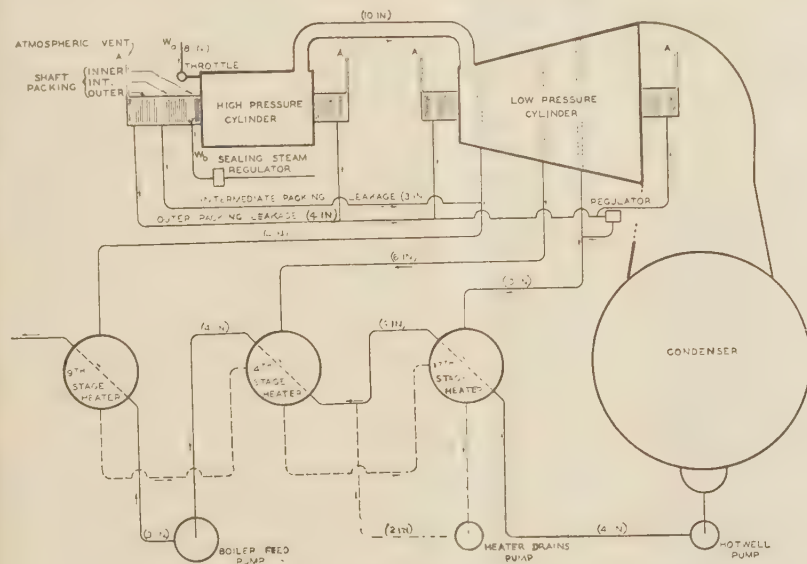


FIG. 2 DIAGRAM OF TURBINE AND HEATER CONNECTIONS

were made by The Griscom-Russell Company, of New York City. The unit was installed in Delray Power House No. 3, of The Detroit Edison Company in 1930. Before the tests were made the unit had been operated under load for more than 4700 hours, of which 1500 had been with steam at 1000 F. This operation involved a large number of separate runs, which caused noticeable wear of the high-pressure packing glands during the starting periods. Although the glands were refitted after this

The loads on the unit were nominally 10,000, 8000, 6000, and 4000 kw. The pressure of the steam at the turbine throttle was maintained at approximately 390 lb per sq in. abs by manual operation of a throttling valve at the superheater outlet. This throttle pressure was about 3 per cent above that for which the turbine was designed. The temperature of the steam at the turbine throttle was maintained at 1000 F during the principal runs and at 900, 800, and 700 F on the supplementary runs. The steam supplied to the throttle was station steam of approximately 700 F that had been further superheated in an oil-fired superheater.

During most of the runs saturated steam at a pressure slightly above that in the first-stage shell of the turbine was used to seal the high-pressure shaft packing. In the earlier runs this differential pressure was about 1.5 lb per sq in. and was gradually reduced to 0.5 as the runs progressed. Certain runs were repeated in order to study the effect of using seal-

ing steam at a temperature of 700 F.

The exhaust pressure during some of the runs was undesirably high as they were made in the summer time with warm condensing water and no attempt was made to regulate the exhaust pressure to some constant value. While the runs in the winter time were being made, the exhaust pressure was regulated to approximately 1 in. Hg abs for all loads by admitting air to the vacuum pump suction. During all runs the

power factor was maintained at the design value of 80 per cent.

Each run was of such duration that approximately 40,000 kw-hr were generated. This insured uniform accuracy in weighing condensate and measuring electrical output in all runs. The frequency of making instrument observations was adjusted on the runs of various lengths so that there would be approximately the same number of observations on each run. Portable telephones were used to synchronize the essential observations. The personnel consisted of eleven men.

The pressures of the steam at various locations were measured with different types of instruments. Those of the steam at the throttle, at the sealing steam inlet, and at the higher pressure bleeder nozzles were measured with Bourdon spring pressure gages. The pressure at the low-pressure bleeder nozzle was obtained by means of a mercury manometer. The exhaust pressure was measured by two barometer-type mercury columns connected to tapped openings in opposite sides of the distance piece between the turbine exhaust opening and the condenser. These two openings were in a vertical plane approximately 2 ft beyond the last-stage wheel. Atmospheric pressure was measured by a mercury barometer.

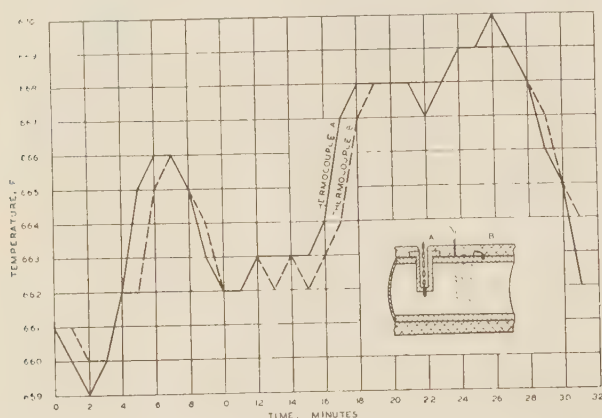


FIG. 4 COMPARISON OF THERMOCOUPLE READINGS RESULTING FROM TWO DIFFERENT METHODS OF INSTALLATION

Method of Measuring Temperatures. The temperatures of the steam entering the throttle and of the sealing steam were measured by means of a potentiometer-type thermocouple system. Iron-constantan thermocouples were peened into the outside surfaces of the pipe, which were well insulated. The wires of the thermocouples were electrically insulated from the pipe and were wrapped around the pipe before being led out through the pipe covering. The high accuracy of this method of measuring the temperature of steam flowing in a well-insulated pipe results from the very small temperature gradient from the flowing steam to the outside surface of the pipe. This temperature head is small, as there is a very small amount of heat conducted through the liberal thickness of pipe covering. The relative accuracy of this method of measuring the temperature of steam compared with that of using a thermocouple welded into the bottom of a thermometer well is indicated by the curves in Fig. 4. This comparison, which is one of several made by the Research Department of The Detroit Edison Company, is at a somewhat lower temperature than the maximum temperature of 1000 F encountered with this turbine, but these curves show that this method of measuring the temperature of steam in a well-insulated pipe is reliable.

All other temperature measurements except one were made with etched-stem thermometers. The exception was that of the steam entering the ninth-stage heater which was measured

with a thermocouple inserted in a thermometer well because of insufficient room to insert an etched-stem thermometer.

Steam Consumption Measurements. Measurement of the steam consumption was complicated because the amount of condensate from the hotwell, the sealing steam, the bled steam, the leak-off steam, and leak-off sealing water had to be made separately. The water for sealing the shaft glands of the pumps and the relief valves on the condenser and heaters was condensate from this unit.

During the tests with steam at 1000 F, the condensate from the hotwell, instead of being pumped directly to the low-pressure heater, as shown in Fig. 2, was delivered by two pumps in series to open weighing tanks. From these tanks it flowed by gravity to an open dump tank, through a deaerator, through a surface-type cooler and to the suction of the hotwell pump shown in Fig. 2. Thus it started through the feedwater heaters at substantially the same temperature that it had at the hotwell outlet. The weighing tanks were provided with leakproof dump valves and with large certified calibration weights which could be applied at will by means of hydraulic jacks.

The rates of flow of sealing steam to the high-pressure shaft packing and of the leak-off from this packing to the low-pressure shaft packing and heaters were measured by means of flow nozzles and differential manometers. Mercury under water was usually used in these manometers, but in order to increase the differential indicated by the manometers in some cases acetylene tetrabromide was substituted for the mercury. Its specific gravity is 22.1 per cent of that of mercury at 32 F.

The steam bled from the turbine for heating the feedwater was supplemented in two of the heaters by leak-off sealing steam from the shaft packings, as shown in Fig. 3. The condensate produced in the heaters was cascaded successively from the highest pressure heater to the lowest pressure one. From the latter it was pumped into the feedwater circuit beyond the outlet of the lowest pressure heater. The quantity of steam bled from each extraction nozzle was calculated from the energy balance of the three heaters. The known data entering into this energy-balance were, (1) the rate of flow of feedwater through the low-pressure heater, (2) the rate of sealing steam leak-off from the high-pressure shaft packing to the heaters, (3) the pressure of the steam entering each heater, and (4) the temperatures of the heater drains entering the water circuit beyond the low-pressure heater, of the feedwater entering and leaving each heater, and of the steam entering each heater.

The small amount of sealing steam escaping from each of the four shaft-packing atmospheric vents was measured once during the tests by collecting the steam in a pipe leading to a small condenser. The weight of the condensate formed during a definite period determined the rate of flow, which was assumed constant for all runs.

The steam leak-off from the throttle valve and the control valves was condensed and, being unmeasured, was admitted to the suction of the pump that delivered the hotwell condensate to the weighing tanks.

All of the water used for sealing the relief valves on the heaters, as well as on the turbine exhaust, and for sealing the shaft glands on the pumps was condensate extracted from various points in the water circuit of the unit. In some cases the water had not yet reached the weighing tanks before it was withdrawn to be used for sealing purposes, while in the other cases it had been through the weighing tanks before being diverted from the main water circuit. In the former cases the leak-off was collected in tanks and was periodically siphoned into the suction of the pump that delivered the hotwell condensate to the weighing tanks. In the latter cases the leak-off was measured in open tanks and was then discarded; but its magnitude was not

sufficient to affect the heater performance whether it passed through the heaters or not. Although the leak-off in the latter cases was small, it was applied as a correction to the weighed water to determine the amount of feedwater entering the low-pressure feedwater heater.

The piping system for this unit was thoroughly isolated from the rest of the plant at all connecting points, by means of double valves with open drips between them.

Tests for leakage of condensing water into the steam space of the condenser, and of cooling water into the weighed condensate as it passed through the cooler, which were continually made by the electrical conductivity method, showed that there was no leakage of water that was detectable. A careful test of the entire circuit through which condensate from both sources of steam passed was made and it showed that no steam or condensate escaped measurement. The errors in determining the entire steam flow very probably did not exceed plus or minus 1 per cent.

Generator Output. The generator output was measured by means of instrument transformers and an integrating wattmeter which had a low multiplier, namely, 100.

Radiation and Convection Losses. During one run with steam at 1000 F and a load of 10,000 kw, sufficient data were taken to calculate the heat transmission from the unit by radiation and convection. These data included, (1) the area or surfaces of the turbine, of the feedwater heaters, of the steam extraction lines, and of the water piping between heaters, (2) the temperatures of these surfaces, (3) the ambient air temperature, and (4) the temperatures of other bodies that absorbed radiation from the unit. The only parts of the unit that were not well insulated were the bonnets of the turbine control valves and the pumps.

Calibration of Instruments. All the instruments used in these tests were carefully selected for their appropriateness and reliability. They were calibrated with care both before and after the tests. Some of them were occasionally given additional checks between runs.

Alternate Test Procedure in Supplementary Runs. In the supplementary runs, during which the temperature of the steam at the throttle was 900, 800, or 700 F, all measurements were made as in the runs with steam at 1000 F, except that the hotwell condensate was not weighed, but was pumped directly to the feedwater heaters as during normal operation. A carefully calibrated integrating venturi meter on the discharge side of the high-pressure heater measured the hotwell condensate plus that from the heater-drains.

The probable errors in determining the entire steam flow in these supplementary runs were not more than plus or minus 1.5 per cent.

ENGINE EFFICIENCY AND THE IDEAL UNIT

The thermal performances of turbines and turbine generators may be expressed in terms of their thermal efficiencies, engine efficiencies, and rates of energy consumption per unit of mechanical or electrical energy delivered by the unit. Each of these forms of expression is useful, and the one of most value depends upon the purpose for which the performance data are desired. With a turbine that uses steam of higher temperature or higher pressure than is usual, however, the engine efficiency becomes of the greatest interest because this term expresses more satisfactorily than any other one the degree of perfection attained by such a turbine. The engine efficiency of any unit is defined as the ratio of the thermal efficiency of the actual unit to that of the corresponding ideal unit. The word "unit" in this definition may be taken to mean the turbine and its regenerative feedwater heaters, or the turbine generator and heaters.

All real turbines have the following imperfections: throttling at admission, leakage at the high-pressure and low-pressure packings, leakage between stages, nozzle and blade losses, rotational losses, exit velocity loss, bearing friction, and heat transmission from all external parts of the machine to its surroundings. The ideal turbine has none of these losses because it is defined as a machine that can utilize all of the available energy of the steam for any specified throttle condition, exhaust pressure, and any given number of feedwater heaters extracting steam at the same pressures as those used in the actual turbine.

When a turbine bleeds steam to heat feedwater the combination of the turbine and its heaters constitutes a regenerative unit, and the corresponding ideal unit may include an infinite number of heaters or the same number of heaters as are employed in the actual case. The choice of which ideal regenerative unit to select as a standard on which to base the engine efficiency of the actual unit depends chiefly upon the purpose for which the results are needed. For those cases, however, in which a specific turbine has been operated and tested with a finite number of heaters in use, there is one important advantage in comparing its performance with that of an ideal unit having the same number of heaters as the actual. With this procedure the effect of the number of heaters in use on the engine efficiency is eliminated; and the engine efficiency of the turbine and heaters will, therefore, be less than 100 per cent simply because of the imperfections in the turbine and heaters.

The actual heaters have certain losses such as those due to throttling of the steam in its passage from the turbine to the heaters, heat transfer from the outside of the heater to the surroundings, and a terminal temperature difference. These heater losses are not large, but nevertheless they tend to make the engine efficiency of the regenerative unit somewhat less than that of the same unit operated on the Rankine cycle. However, the efficiency of the ideal regenerative unit with a finite number of heaters is generally sufficiently higher than that of the Rankine to make the thermal efficiency of the actual regenerative unit far superior to that obtained without regenerative feedwater heating. In this connection, attention is called to the bare possibility of having a higher engine efficiency with the regenerative unit than with the same turbine operating on the Rankine cycle, because it is possible, at full load or overload, to have the blades in the last stage of a turbine too small to handle efficiently the total throttle flow, and thus the last-stage leaving loss may become sufficiently large to counteract the effect of the heater losses in the regenerative unit.

Ordinarily a turbine has but one supply of steam, that is, the amount coming through the throttle valve, but in this high-temperature unit the turbine has two sources of supply. The chief one is that of the throttle, and the secondary one is the steam supplied to the regulator to seal the high-pressure packing glands from which some of the sealing steam passes to the first-stage shell and thus through the remainder of the turbine. This secondary supply is used because steam of a lower temperature than the throttle steam is more satisfactory as sealing steam. This secondary supply of steam complicates to a considerable extent the calculation of the efficiency of the corresponding ideal unit, which is considered to fulfil the following conditions:

(1) The steam supplied to the ideal unit corresponds with that of the actual unit as to the quantity and condition at each of the two points where steam is admitted.

(2) All steam admitted to the ideal unit is assumed to have no throttling, leakage, fluid friction, turbulence, or heat transfer in its passage through the turbine. Any steam admitted, in addition to that at the throttle, is considered as mixed at con-

TABLE 3 TEST DATA OF THE 10,000-KW HIGH-TEMPERATURE UNIT
(Based on actual condition of steam at the throttle and the turbine-exhaust pressure)

Run No.	Duration of run, hr	Load, kw	Throttle steam		Condition at entrance to regulator	Sealing steam		Quantity, lb per hr		Temp. of feedwater		Enthalpy, Btu per lb		Energy consumption of unit, Btu per kw-hr	Thermal efficiency, per cent	Efficiency of regenerative unit, per cent	Engine efficiency, per cent	Generator efficiency, per cent	Engine efficiency, per cent
			Pressure, lb per sq in.	Temp., F	Flow, lb per hr	Pressure, lb per sq in.	Temp., F	To 17th-stage heater and low-pressure steam	To 9th-stage heater and high-pressure steam	Exhaust pressure, in. Hg	9th-stage heater, F	Steam entering regulator, Btu per lb	Saturating liquid, Btu per lb						
1	3.997	10068	392	1003	84448	391	445	540	696	4090	118	5444	1.012	337	1206	308	31.81	41.86	75.99
2	4.999	8034	390	1006	67512	405	448	634	564	2970	88	4256	0.997	322	1206	292	31.34	42.00	75.99
3	6.722	5986	393	1004	50996	415	450	527	465	2074	64	3130	0.938	304	1206	273	30.51	42.28	75.99
4	9.995	4042	387	1005	36237	420	452	525	350	1346	38	2259	1.059	282	1206	261	28.45	41.59	68.41
5	3.999	10063	389	700	106691	395	452	384	977	4301	118	5780	0.975	342	1211	313	29.05	39.96	73.32
6	4.992	8045	388	703	85088	414	456	436	707	2828	88	4256	0.957	327	1211	297	29.05	39.90	72.81
7	6.667	6036	389	701	64587	425	459	442	576	1374	93	2116	0.995	310	1211	278	28.32	39.68	71.37
8	10.004	4038	390	703	44602	428	459	530	437	1311	38	2259	1.059	282	1211	266	26.79	39.78	67.35
9	4.000	9960	389	1003	86030	396	445	1119	593	3218	118	4978	1.818	340	1205	311	31.12	39.98	77.84
10	5.000	8020	389	1003	67512	405	448	1171	482	2347	88	4088	1.631	326	1204	296	30.66	40.50	75.70
11	7.000	5963	390	1003	52183	410	447	1096	394	1622	64	3176	1.428	306	1204	276	29.78	40.86	72.88
12	10.000	3991	390	1002	36182	408	447	753	287	1020	38	2098	1.201	283	1204	252	28.26	41.22	68.56
13	4.019	9953	379	905	92858	395	439	1054	615	3158	118	4945	1.874	343	1204	314	30.27	39.12	77.38
14	4.985	8024	380	900	75815	404	445	1213	511	2215	88	4027	1.709	328	1204	299	29.56	39.29	75.24
15	6.713	5971	392	902	56844	407	445	1057	403	1558	64	3082	1.474	308	1204	277	28.75	39.93	72.00
16	10.061	3988	390	902	39034	416	448	791	310	966	38	2105	1.232	284	1204	253	27.41	40.43	67.80
17	4.017	9958	381	800	99610	397	443	1426	686	2855	118	5085	1.727	343	1204	314	29.68	38.56	76.97
18	4.986	8014	380	800	80707	403	446	1202	558	2017	88	3865	1.507	327	1204	297	28.75	39.29	75.24
19	6.700	5982	390	801	60197	408	447	1046	436	1480	64	3026	1.285	309	1204	279	28.15	39.82	71.73
20	10.085	3978	388	801	41551	414	448	774	338	937	38	2087	1.099	285	1204	254	26.94	39.97	67.40
21	4.000	10000	386	698	109406	399	445	1639	761	3052	118	5570	1.854	345	1204	317	28.62	37.72	75.87
22	4.999	8009	388	698	87281	411	447	1307	570	2203	88	4081	1.592	329	1204	300	28.34	38.34	73.92
23	6.670	6009	388	697	66082	417	448	973	560	1574	64	3093	1.318	310	1204	280	27.62	38.76	71.26
24	10.001	4011	387	699	45307	423	451	712	341	1038	38	2129	1.095	286	1204	256	26.26	39.34	66.75

Unregulated Exhaust Pressure

h_i = enthalpy of the sealing steam at entrance to the regulator, Btu per lb

$h_1 = \frac{(w_a h_a + w_i h_i)}{w_i}$ = enthalpy of steam entering the corresponding ideal unit at state 1, Btu per lb

p_a and p_b = steam pressures at entrance to the throttle and to the sealing-steam regulator, respectively, lb per sq in. abs

p_2, p_3, p_4 , and p_5 = steam pressures at the 9th-, 14th-, and 17th-stage bleeder nozzles, and at entrance to the condenser, respectively, lb per sq in. abs

h_2, h_3, h_4 , and h_5 = enthalpies of the steam after isentropic expansion from state 1 to p_2, p_3, p_4 , and p_5 , respectively, Btu per lb

h_6, h_7, h_8 , and h_9 = enthalpies of saturated liquid corresponding to p_5, p_4, p_3 , and p_2 , respectively, Btu per lb

h_f = enthalpy of saturated liquid corresponding to actual feedwater temperature leaving the 9th-stage heater, Btu per lb

L = load on the generator, kw

s_1 = entropy of the steam at pressure p_a after mixing the steam from the throttle with that from the sealing-steam regulator

$m_2 = \frac{h_9 - h_8}{h_2 - h_8}$ = fraction of w_1 bled at state 2 in the ideal unit

$m_3 = \frac{(h_8 - h_7)(1 - m_2)}{h_3 - h_7}$ = fraction of w_1 bled at state 3 in the ideal unit

$m_4 = \frac{(h_7 - h_6)(1 - m_2 - m_3)}{h_4 - h_6}$ = fraction of w_1 bled at state 4 in the ideal unit

$Wk_i = h_1 - h_5 - m_2(h_2 - h_3) - m_3(h_3 - h_4) - m_4(h_4 - h_5)$ = the mechanical energy available from the flow of 1 lb of steam through the ideal regenerative unit, assuming this steam to enter the unit at state 1, Btu per lb of total flow

$h_1 - h_9$ = net energy supplied the ideal unit with each pound of steam combined from both sources, Btu per lb of total flow

$e_i = \frac{Wk_i}{h_1 - h_9}$ = efficiency of the ideal unit

$E_c = \frac{w_i(h_1 - h_f)}{L}$
 $= \frac{w_a(h_a - h_f) + w_i(h_i - h_f)}{L}$
 = energy consumption rate of

the actual unit, Btu per kw hr

$$e_a = \frac{3413}{E_c} = \text{thermal efficiency of the actual unit}$$

$$\frac{e_a}{e_i} = \text{engine efficiency of the complete unit (turbine-generator and heaters)}$$

$$e_g = \text{efficiency of the generator, including bearings, ventilation, and excitation}$$

The generator efficiencies, as given in Tables 1 and 3, were supplied by the builder. The engine efficiency of the turbine and heaters is found by dividing the engine efficiency of the complete unit by the generator efficiency.

Sample calculations for the ideal and actual units in Run No. 1 (see Tables 1 and 2) are as follows:

$$\begin{aligned} h_1 &= \frac{w_a h_a + w_b h_b}{w_1 \text{ or } (w_a + w_b)} = \frac{84,448 \times 1529 + 5444 \times 1206}{1509 \text{ Btu per lb}} \\ m_2 &= \frac{h_2 - h_3}{h_2 - h_3} = \frac{317 - 237}{1355 - 237} = 7.16 \text{ per cent} \\ m_3 &= \frac{(h_3 - h_7)(1 - m_2)}{h_3 - h_7} = \frac{(237 - 163)(0.9284)}{1238 - 163} \\ &= 6.37 \text{ per cent} \\ m_4 &= \frac{(h_7 - h_6)(1 - m_2 - m_3)}{h_4 - h_6} = \frac{(163 - 48)(0.8647)}{1126 - 48} \\ &= 9.22 \text{ per cent} \\ Wk_i &= h_1 - h_5 - m_2(h_2 - h_3) - m_3(h_3 - h_4) - m_4(h_4 - h_5) \\ &= 1509 - 945 - (0.0716)(1355 - 945) - (0.0637)(1238 - 945) - (0.0922)(1126 - 945) \\ &= 499 \text{ Btu per lb} \\ e_i &= \frac{Wk_i}{h_1 - h_9} = \frac{499}{1509 - 317} = 41.86 \text{ per cent} \\ E_c &= \frac{w_1(h_1 - h_f)}{L} = \frac{89,892(1509 - 308)}{10,068} = 10,730 \text{ Btu per kw hr} \\ &\quad \text{kw hr} = \text{energy consumption rate of the actual unit} \\ e_a &= \frac{3413}{E_c} = \frac{3413}{10,730} = 31.81 \text{ per cent} = \text{actual thermal efficiency of the complete unit} \\ \frac{e_a}{e_i} &= \frac{31.81}{41.86} = 75.99 \text{ per cent} = \text{engine efficiency of the complete unit} \\ \frac{(e_a)}{(e_i)} \times \frac{(1)}{(e_a)} &= \frac{0.7599}{0.9558} = 79.50 \text{ per cent} = \text{engine efficiency of the turbine and heaters alone.} \end{aligned}$$

ENERGY CONSUMPTION RATE

It may be noted that throughout this paper the term "energy consumption rate" (energy rate) of the unit is used instead of the more common one "heat consumption rate" (heat rate). The former term is preferred because it is a more accurate expression for any steam turbine, although the term "heat rate" is entirely appropriate for a steam station. The reason for this distinction becomes apparent after careful consideration is given to the facts in the matter, regardless of what may have been heretofore commonly used. Steam passes through a turbine under steady flow conditions, and this steam cannot, therefore, continuously operate a turbine by merely having heat supplied to the fluid. Instead, the fluid must be constantly supplied with the more expensive mechanical energy delivered by suitable pumps before the absorption of heat takes place in a steam-generating unit. These two forms of energy supplied to the fluid are simply and accurately taken care of, in the equations previously given, by means of the enthalpies

of the fluid at entrance to, and exit from the unit. In this connection, particular attention is called to the term h_f because this is the enthalpy of saturated liquid corresponding to the feedwater temperature leaving the ninth-stage heater, and not the enthalpy of the feedwater corresponding to its actual state leaving this heater. The actual pressure of the feedwater leaving this heater is several hundred pounds higher than the saturation pressure corresponding to the feedwater temperature, merely because the feed pump is conveniently connected between the ninth- and fourteenth-stage heaters, as shown in Fig. 2. The three heaters and their pumps form part of the complete unit, but the feed pump is not included and thus the energy credited to the unit by the feedwater leaving the ninth-stage heater is determined by its temperature rather than by its temperature and pressure.

TEST DATA

In addition to the summary, given in Table 1, the principal test data are presented in Tables 2 and 3 for which the notation and methods of calculation have been given in the preceding section. The values given in Table 2 are needed to calculate the efficiency of the ideal turbine and three heaters under various conditions. In this table the pressures, temperatures, and rates of flow were obtained from observed values for the actual unit. The enthalpies and entropies corresponding to the test data and the methods of calculation previously given were taken from Keenan's Steam Tables. In both Tables 2 and 3, the data for the first eight runs were obtained with the exhaust pressure held as near to 1.0 in. Hg as could be obtained by regulating the air leakage into the suction line of the vacuum pump, since they were made when cold condensing water was available. The remainder of the runs, 9 to 24, inclusive, were made during warm weather when an exhaust pressure of 1 in. could not be obtained under full load conditions. For all of these runs, whether with regulated or unregulated exhaust pressures, the engine efficiencies given in Table 3 have been based on the ideal unit having the same conditions as those prevailing during the test; hence this table gives the actual engine efficiencies obtained with various exhaust pressures and throttle temperatures. From this table one may observe that the highest value of the engine efficiency of the turbine and heaters for steam at 1000 F and an exhaust pressure of 1.01 in. Hg abs was 79.5 per cent, as shown for Run No. 1. On the other hand, in Run No. 9, when the exhaust pressure was 1.82 in. Hg abs and the throttle temperature the same as in Run No. 1, the engine efficiency was 81.5 per cent. This is in keeping with the general characteristics of turbines, since the lower exhaust pressure involves a larger loss of available energy due to the greater losses due to moisture and to exit velocities from the wheels in the low-pressure region. The thermal efficiency in Run No. 1, however, is greater than that in Run No. 9, because the available energy is so much greater with the lower exhaust pressure.

To show the relation between the throttle temperature and the rate of energy consumption of the unit, the data must be reduced to a comparable basis, as shown in Table 3A. The correction factors in this table were obtained from the builder of the turbine; and these corrections are seen to be almost negligible, except in certain runs where the exhaust pressure was much above the nominal value. Since the corrections due to variation in the exhaust pressure were appreciable for some runs, the manufacturer's values of this correction were checked by actual test and found to be correct. After obtaining the corrected energy consumption, as given in Table 3A, the results were plotted as shown in Fig. 6, in which the triangles represent data for Runs 1 to 8, inclusive, and the circles for Runs 9 to 24, inclusive. Even

TABLE 3A TEST DATA OF THE 10,000-KW HIGH-TEMPERATURE UNIT
(Corrected to throttle pressure of 390 lb per sq in. abs, exhaust pressure of 1 in. Hg abs, and nominal throttle temperatures as tabulated)

(Corrected to throttle pressure of 390 lb per sq in. abs, exhaust pressure of 1 in. Hg abs, and nominal exhaust temperature of 1000° F)												
Run No.	Load, kw L	Temp. of steam at throttle, F		Actual pressure— At throttle, lb per sq in. abs		Actual pressure— At exhaust, lb per sq in. Hg abs		Correction factors		Throttle flow— lb per hr		Enthalpy, Btu per lb Saturated liquid corrected to nominal conditions Btu per kw-hr E_c'
		Nominal t_a	Actual t_a	At p_a	At p_b	For throttle temp. c_t	For throttle pressure c_p	For exhaust pressure c_p	Total ($c_t \times c_p$)	Actual w_a	Corrected to nominal conditions ($c \times w_a$) w_a'	
Regulated Exhaust Pressure of Approximately 1 in. Hg abs												
1	10068	1000	1003	392	1.012	1.0001	1.0006	0.9999	1.0006	84448	84500	10720
2	8034	1000	1006	390	0.997	1.0022	1.0001	1.0001	1.0024	67512	67670	10890
3	5986	1000	1004	393	0.938	1.0035	1.0036	1.0036	1.0049	50996	51250	11230
4	4042	1000	1005	387	1.059	1.0021	0.9995	0.9963	0.9979	36237	36160	11940
5	10063	700	700	389	0.975	1.0000	0.9999	1.0006	1.0005	106691	106740	11650
6	8045	700	703	388	0.957	1.0018	0.9998	1.0019	1.0035	85088	85390	11770
7	6036	700	701	389	0.995	1.0022	0.9999	1.0001	1.0002	64587	64600	12050
8	4038	700	703	390	0.986	1.0018	1.0000	1.0010	1.0028	44602	44730	12760
Unregulated Exhaust Pressure												
9	9960	1000	1003	389	1.818	1.0020	0.9999	0.9727	0.9745	86030	83840	10690
10	8020	1000	1003	389	1.631	1.0020	0.9999	0.9743	0.9762	69394	67740	10860
11	5963	1000	1003	390	1.428	1.0020	1.0002	0.9792	0.9813	52188	51210	11230
12	3991	1000	1002	390	1.201	1.0010	1.0001	0.9878	0.9889	36182	35780	11920
13	9953	900	905	379	1.874	1.0033	0.9978	0.9710	0.9721	92858	90270	10940
14	8024	900	900	380	1.709	1.0000	0.9978	0.9716	0.9695	75815	73500	11190
15	5971	900	902	392	1.474	1.0014	1.0004	0.9771	0.9789	56844	56040	11620
16	3988	900	902	390	1.232	1.0014	1.0001	0.9860	0.9875	39034	38530	12280
17	9958	800	800	381	1.727	1.0000	0.9980	0.9756	0.9736	90610	86980	11210
18	8014	800	800	389	1.507	1.0000	0.9786	0.9766	0.9748	80107	78980	11490
19	5982	800	801	390	1.245	1.0009	0.9870	0.9878	0.9878	60197	59470	11790
20	3978	800	801	388	1.099	1.0009	0.9997	0.9938	0.9944	41551	41320	12600
21	10000	700	698	386	1.854	0.9988	0.9993	0.9715	0.9715	109406	106090	11590
22	8009	700	698	388	1.562	0.9984	0.9998	0.9766	0.9748	87291	85090	11770
23	6009	700	697	388	1.318	0.9983	0.9997	0.9826	0.9826	66082	64800	12150
24	4011	700	699	387	1.095	0.9999	0.9994	0.9940	0.9933	45307	45000	12910

though the two sets of runs were made several months apart, as shown by Table 2, the results agree extremely well for the steam at 1000 F; this is largely due to the high degree of accuracy obtained by weighing all of the water from the condenser. For the supplementary runs with steam at 900, 800, and 700 F the results are also seen to be in satisfactory agreement, even though the condensate from the hotwell and heaters was measured by a venturi meter. The largest deviation from the curve is seen to be 1.1 per cent, for the small load of 4000 kw and a steam temperature of 700 F. These curves show that for all loads from 4000 to 10,000 kw, the energy consumption rate of the unit was decreased about 7 per cent by changing the throttle steam temperature from 700 to 1000 F.

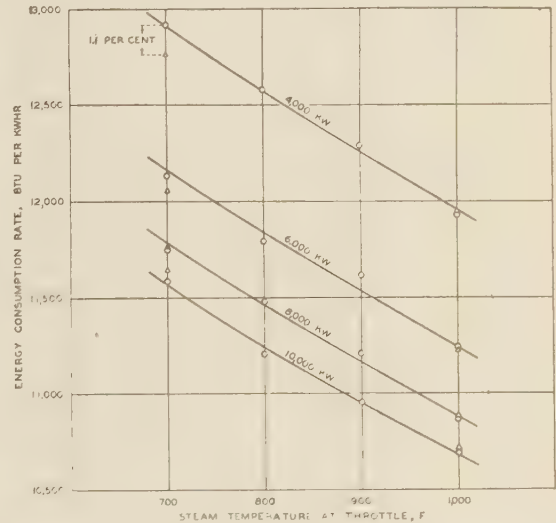


FIG. 6 ENERGY CONSUMPTION RATE OF TURBINE-GENERATOR AND THREE HEATERS

(Throttle pressure, 390 lb per sq in. abs; exhaust pressure, 1.0 in. Hg abs; and saturated sealing steam at throttle pressure.)

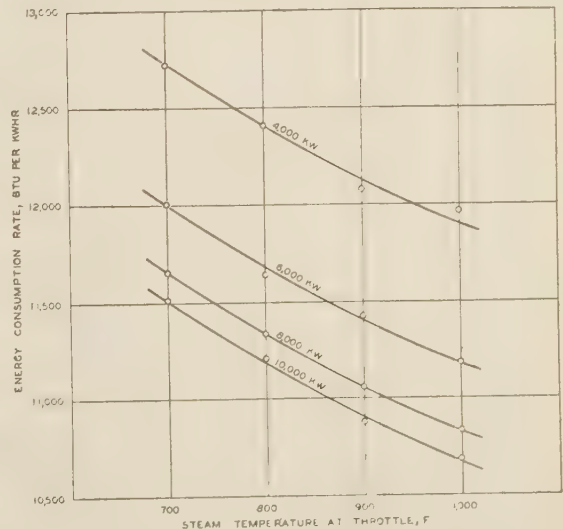


FIG. 7 ENERGY CONSUMPTION RATE OF TURBINE-GENERATOR AND THREE HEATERS

(Throttle pressure, 390 lb per sq in. abs; exhaust pressure, 1.0 in. Hg abs; and 700-F sealing steam at throttle pressure.)

The additional curves given in Fig. 7 show approximately the same slope as those in Fig. 6. Each curve in Fig. 7, however, is slightly below its corresponding one of Fig. 6, because those in Fig. 7 represent the results obtained by using superheated sealing steam ($t = 700$ F) instead of saturated. The difference in the energy consumption rate, however, is not large especially at high loads, as may be seen from the curves in Fig. 8; but these results clearly indicate that there is a slight thermal gain by using the superheated sealing steam. Such a result is to be expected because a portion of the sealing steam leaks into the first-stage shell and there mixes with steam of much higher temperature. The tests made with the super-

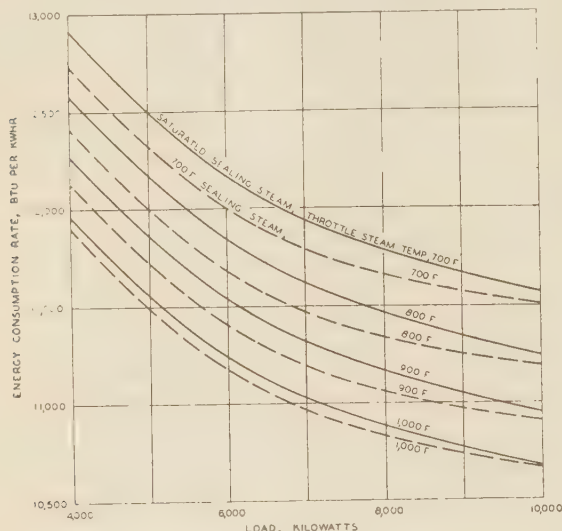


FIG. 8 ENERGY CONSUMPTION RATE OF TURBINE-GENERATOR AND THREE HEATERS

(Throttle pressure, 390 lb per sq. in. abs; exhaust pressure, 1.0 in. Hg abs. Derived from Figs. 6 and 7)

heated sealing steam are considered merely as supplementary ones, since the turbine was designed to use saturated sealing steam; hence the tabular data on which Fig. 7 is based have been omitted.

The engine efficiencies, as represented by the curves in Fig. 9, are plotted directly from Table 3 for Runs 1 to 8 with the regulated exhaust pressure.

These curves show that with steam at 700 F the turbine would reach its maximum engine efficiency with a load only slightly above 10,000 kw, but that with steam at 1000 F its maximum engine efficiency would be attained with an appreciably higher load—probably 13,000 or 14,000 kw.

The losses due to radiation and convection from the turbine and heaters are given in Table 4 for a load of 10,000 kw. This table shows that radiation accounted for about 65 per cent of the total amount of heat transferred from the unit. This proportion decreased slightly for lower loads until it became 62 per cent with a load of 4000 kw and steam at 1000 F. For this load the total loss by heat transmission was calculated to be 192,600 Btu per hr. In no case was this form of loss a serious one, because the unit was well insulated. The complete data for the observed temperatures and surfaces and the necessary calculations involved in the determination of these losses would require about 40 times as much space as that given in Table 4 and could not, therefore, be easily given in this paper.

ENERGY BALANCE OF THE TURBINE

An energy balance of a turbine is always of interest and

TABLE 4 RADIATION AND CONVECTION LOSSES FROM TURBINE AND HEATERS WITH STEAM AT 1000 F AND LOAD OF 10,000 KW

	Radiation, Btu per hr	Convection, Btu per hr	Total, Btu per hr
High-pressure cylinder and cross-over....	51,500	40,700	92,200
Low-pressure cylinder.....	14,500	6,100	20,600
9th-stage bleeder line.....	2,700	2,800	5,500
14th-stage bleeder line.....	21,500	7,200	28,700
17th-stage bleeder line.....	17,300	7,800	25,100
9th-stage heater.....	5,400	1,600	7,000
14th-stage heater.....	3,600	1,000	4,600
17th-stage heater.....	2,000	700	2,700
Condensate line from 17th- to 14th-stage heaters, lines and pump for heater drains.....	4,700	1,700	6,400
Condensate line from 14th- to 9th-stage heaters including pump.....	9,000	4,000	13,000
Drain line from 14th- to 17th-stage heaters.....	4,500	2,000	6,500
Drain line from 9th- to 14th-stage heaters.....	7,000	3,000	10,000
Line from sealing steam pressure regulating valve to shaft packing.....	1,600	1,000	2,600
Total losses.....	145,300	79,600	224,900

value, because it shows at a glance the distribution of the net amount of energy supplied to the turbine. Such a balance has been prepared for Run No. 1, since this was the one for the largest load carried, and is for steam at 1000 F. The results given in Table 5 show that one-third of the energy supplied to the turbine was delivered by the turbine shaft, and two-thirds

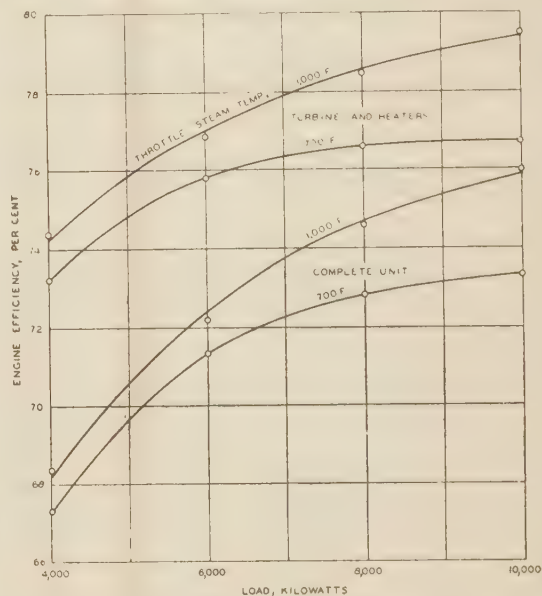


FIG. 9 ENGINE EFFICIENCY OF TURBINE-GENERATOR AND THREE HEATERS AND OF TURBINE AND HEATERS ALONE

(Throttle pressure, regulated to approximately 390 lb per sq. in. abs; exhaust pressure, regulated to approximately 1.0 in. Hg abs and saturated sealing steam at throttle pressure.)

were absorbed by the condensing water, the radiation and convection losses being extremely small. After the energy absorbed by the condenser per pound of total flow is found, it then becomes possible, by the aid of the other data, to determine the state of the steam leaving the turbine. To make this calculation, the amount of steam passing to the condenser must be found in terms of the total flow to the turbine.

The weighed water from the hotwell was 71,280 lb per hr for Run No. 1; the condensate from the heater drains, as determined by an energy balance of the heaters, was 18,430 lb per hr; and the amount of steam escaping from the atmospheric vents of the shaft packing glands was 185 lb per hr. Since the condenser received only 71,280 lb of steam out of a total flow to the turbine of 89,892 lb, the amount of energy absorbed from each pound of steam entering the condenser is found, by the aid of

Table 5, to have been $\frac{(89,892)}{71,280} (798.5) = 1007$ Btu. Then, since

the condensate in the hotwell had a temperature of 78 F its enthalpy was 46 Btu per lb, and the steam entering the condenser must have had a total amount of energy of $1007 + 46$ or 1053 Btu per lb. This total energy is made up of the enthalpy of the steam entering the condenser plus its velocity energy. Neglecting the velocity energy, temporarily, the enthalpy of the exhaust steam would then be 1053; and for the known exhaust pressure the corresponding moisture would be 4.0 per cent and the specific volume, 622 cu ft per lb, which may be used as a trial value to find the velocity. Since the area of the exhaust opening was 34.76 sq ft and the rate of flow to the condenser was 71,280 lb per hr, or 19.8 lb per sec, the exit velocity would be $19.8 \times 622/34.76 = 354$ ft per sec, or 21,240 ft per min. Such a result means that the velocity energy of the steam leaving the turbine would be 2.5 Btu per lb; and since the total energy of this steam has already been found to be 1053, its enthalpy would be $1053 - 2.5 = 1050.5$ Btu per lb. The corresponding value of the

TABLE 5 ENERGY BALANCE OF TURBINE FOR GENERATOR LOAD OF 10,068 KW AND STEAM TEMPERATURE OF 1000 F

Energy distribution	Btu per lb of total flow to turbine	Per cent
Energy delivered by turbine shaft.....	400.0	33.3
From Table 3,		
$\left[\frac{3413 \times \text{Load}}{(\text{Gen. eff.}) \times (w_a + w_b)} = \frac{3413 \times 10,068}{0.9558 \times 89,892} \right]$		
Energy lost by radiation and convection.....	2.5	0.2
From Table 4,		
$\left[\frac{\text{Loss}}{\text{Total flow}} = \frac{224,900}{89,892} \right]$		
Energy absorbed by condenser (to balance).....	798.5	66.5
Energy supplied turbine.....	1201.0	100.0
From Table 3,		
$\left[\frac{w_a h_a + w_b h_b}{w_a + w_b} - h_f = 1509 - 308 \right]$		

moisture then becomes 4.2 per cent; and the specific volume remains so close to the temporary value previously found that additional calculations of the velocity and moisture are not necessary.

Contrasted with this moisture of 4.2 per cent in the exhaust of the actual turbine, the steam from the corresponding ideal turbine would have 14.3 per cent moisture, as shown by state 5 in Fig. 5. This difference is due to the turbulence, which is created by the steam in passing through the actual turbine, and which could be reduced to some extent by decreasing the exit velocity from each wheel. In other words, a larger number of stages or an increase in the diameters of the wheels would undoubtedly increase the efficiency of the unit. On the other hand, more or larger wheels mean a higher first cost because the turbine is made of expensive metals, and an economic balance of these opposing factors must be considered, even in an experimental machine such as this one.

LOSS DUE TO THE SEALING STEAM

The unusual arrangement of handling the sealing steam used for the high-pressure packing may possibly cause a difference of opinion as to the most logical method of calculating the loss of available mechanical energy produced by the leakage through the packing. Since about 90 per cent of the sealing steam is finally delivered to the seventeenth-stage heater, the question arises as to whether this heater pressure or the condenser pressure is the proper one on which the throttling loss of this part of the sealing steam should be based. If the condenser pressure be chosen as the proper one, the loss of available mechanical energy caused by using the saturated sealing steam at full load and throttle steam at 1000 F amounts to 4.4 per cent of

the total available energy; but if the seventeenth-stage heater pressure be chosen as the proper base, the loss is only 2.3 per cent. The authors consider the 4.4 per cent to be the more logical value for reasons that will now be given.

If there were no feedwater heaters used, the condenser pressure would clearly be the one to which all the steam supplied the turbine would be expected to expand before leaving the turbine. With a regenerative feedwater heating system, all the heat delivered to the heaters is supposed to come from steam that has delivered some mechanical energy to the turbine blades before extraction, and thus an extremely high thermal efficiency is obtained from such steam because the bled steam rejects no energy to the condenser. The larger the proportion of throttle steam that may be extracted from the turbine for use in the heaters, the higher will be the thermal efficiency of a regenerative unit. On the other hand, when the leak-off from the sealing steam is delivered to heat the regenerative feedwater heaters, the amount of steam that may be bled from the turbine is thereby reduced and thus the advantages of the regenerative system are taken away from a certain amount of throttle steam that must now pass entirely through the turbine to the condenser. Since that part of the sealing steam that passes to the heaters delivers no work to the turbine blades, the result is not thermodynamically equivalent to that which would be obtained with the same feedwater temperature derived entirely from bled steam. Consequently the loss of available mechanical energy, due to the portion of the sealing steam that flows from the packing to the heaters, is calculated as if this steam had been throttled to condenser pressure. About 10 per cent of the sealing steam leaked through the inner shaft packing to the first-stage shell, and for this portion the loss of available energy is simply that due to the throttling caused by passing through the regulator and the inner packing.

HEATER PERFORMANCE

The three four-pass feedwater heaters which received steam bled from the turbine form part of the complete unit, and the data relating to the performance of these heaters, for runs 1 to 8, inclusive are given in Table 6. Possibly the most interesting information obtainable from the table is that pertaining to the terminal temperature differences and the rates of heat transfer in the heaters. The terminal temperature difference of a feedwater heater is commonly taken as the temperature of saturated steam corresponding to the pressure of the steam entering the heater minus the temperature of the feedwater leaving the heater; and this difference is called the "nominal" one in this table. The enormous differences between the actual and "nominal" values of the terminal temperature difference when highly superheated steam is used are clearly shown.

The last column of Table 6 shows the "nominal" over-all coefficients of heat transfer for the three heaters for various conditions of operation. It should be noted that when highly superheated steam is bled to a heater having high water velocity, the "nominal" coefficient is surprisingly high, as, for example, in the ninth-stage heater in Run No. 1. In this case the steam entering the heater was superheated 374 F (717-343), and by the usual method of calculation, the logarithmic mean temperature difference is only 28.4 F, whereas the actual mean temperature difference would be much greater. No general method of calculating the real mean temperature difference where superheated steam and latent heat are both involved has been developed, so far as the authors know, and thus the "nominal" values only are given. Regardless of what may appear from these "nominal" values, highly superheated steam probably does not increase the real coefficient of heat transfer, but does increase very much the difficulties of determining the actual mean

TABLE 6 FEEDWATER-HEATER PERFORMANCE DATA

Run No.	Turbine-generator load, kw	Actual steam temp. at throttle, t_a , F	Turbine stage heater con- tion	Steam from extraction nozzles and shaft packing				Feedwater				Terminal temperature difference, $(t_a' - t_a)$, deg F	Mean specific heat of water heater, Btu per lb per deg F	Heat absorbed by water heater, 1000 Btu per hr	Nominal diff. in temp. on the saturated steam, $t_a' - t_a$, F	Average velocity of water through tubes, ft per sec	Nominal overall coefficient of heat transfer based on saturated steam, Btu per sq ft per deg F
				Flow, lb per hr	Pressure of steam at entrance to heater, p_e , sq in. abs	Temp. of steam at entrance to heater, t_e , F	Temp. of saturated steam corresponding to p_e , t_{e_s} , F	Flow, lb per hr	Temp. at entrance to heater, t_a , F	Temp. at outlet of heater, t_a' , F	Temp. of line heater, t_a'' , F						
1	10068	1003	9	284	6219	122.6	717.0	88680	264.7	336.7	72.0	380.3	1.030	6651	28.4	7.83	824
			14	303	5424	39.7	536.8	89680	191.7	260.0	69.2	275.9	1.009	6242	27.2	6.24	760
			17	463	6756	10.2	362.8	71281	78.3	130.9	112.6	171.9	0.996	7994	31.4	3.16	550
2	8034	1006	9	284	4655	97.9	692.7	71595	253.5	321.8	68.3	370.9	1.027	5022	24.4	6.21	725
			14	303	4226	31.9	519.6	71592	182.0	249.6	67.6	270.0	1.007	4874	23.6	4.99	682
			17	463	5134	8.2	352.3	57580	75.4	181.4	106.0	170.9	0.997	6085	24.8	2.53	530
3	5986	1004	9	284	3378	72.8	662.2	53971	239.1	303.7	64.6	358.5	1.020	3556	18.2	4.66	688
			14	303	3085	24.0	501.2	53971	169.6	235.2	65.6	266.0	1.005	3553	20.1	3.73	584
			17	463	3600	6.2	333.7	44008	72.3	169.6	97.3	164.1	0.995	4261	22.1	1.94	416
4	4042	1005	9	284	2083	52.4	632.6	38392	223.9	282.3	58.4	350.3	1.016	2408	16.4	3.29	489
			14	303	2086	17.0	482.2	38392	155.7	218.3	62.6	263.9	1.002	2408	15.4	2.66	516
			17	463	2266	4.3	308.1	31957	71.1	155.7	84.6	152.4	0.990	2693	..	1.41	..
5	10063	700	9	284	9189	135.0	495.8	112271	267.1	342.2	75.1	153.6	1.031	8693	32.1	9.86	954
			14	303	6998	43.5	329.2	112271	197.6	263.3	63.7	65.9	1.011	7457	31.1	7.82	791
			17	463	9258	11.6	200.3	86826	78.4	156.4	118.0	3.9	0.997	10215	34.3	3.86	643
6	8045	703	9	284	6795	106.6	471.7	88985	256.0	327.4	64.8	144.3	1.029	6538	26.2	7.71	878
			14	303	5483	35.0	312.9	88985	187.5	252.3	61.8	60.6	1.008	5812	27.8	6.20	690
			17	463	6873	9.3	189.8	69834	77.2	186.5	109.3	3.3	0.997	7610	31.0	3.10	530
7	6036	701	9	284	4758	80.6	442.8	67317	242.4	301.5	67.1	133.3	1.022	4616	21.3	5.81	763
			14	303	4016	29.1	293.8	67317	175.9	238.9	63.0	54.9	1.005	4562	21.4	5.67	638
			17	463	4749	7.2	178.0	53794	77.0	175.4	98.4	2.6	0.996	5272	26.9	2.38	423
8	4038	703	9	284	2929	56.0	412.4	46626	225.9	286.6	60.7	125.8	1.017	2878	16.6	3.99	610
			14	303	2566	18.1	274.9	46626	160.9	219.4	58.5	53.5	1.002	2733	20.0	3.19	451
			17	463	2956	4.9	165.3	38175	73.7	160.2	86.3	5.1	0.996	3289	18.9	1.68	376

temperature difference and also the actual coefficient.

ACKNOWLEDGMENTS

The authors desire to thank C. F. Hirshfeld, J. W. Parker, P. W. Thompson, and R. M. Van Duzer, Jr., for their helpful suggestions and criticisms. Special credit is given to E. L. Liedel and his corps of assistants for the extreme care exercised in conducting the tests, to W. F. Kinney for calculating a large portion of the results and for drawing the curves, and to A. W. Thorson for his drawings and help in making the calculations.

FUTURE POSSIBILITIES AND PROBABILITIES

After examining the test data obtained from an experimental machine, such as this 1000-F steam turbine, engineers naturally desire to interpret such results in terms of the future possibilities and probabilities. However, in attempting to predict how good a performance may be expected from a large turbine using steam at 1000 F and considering the probability of such a turbine being built in the immediate future, one must consider a number of factors that are necessarily somewhat indeterminate at the present time. Thus one cannot be certain how successful future designers may be in reducing or eliminating the loss due to the leakage of steam past the high-pressure shaft packing; but with a large turbine, say 75,000 kw or more, the possibility of making the high-pressure cylinder of the double-flow type seems attractive, as such a scheme would eliminate this loss entirely. Furthermore, the elimination of the high-pressure packing glands would counteract the extra length of turbine shaft required by the double-flow type, and thus the distance between the bearings of the high-pressure cylinder would not be materially different from that required in a single-flow type with long shaft-packing glands.

The energy consumption rate of a very large turbine as determined by that of a relatively small one, such as a 10,000-kw machine, is also a matter about which there is certain to be a difference of opinion, because such comparisons are so often based on experimental data relating to turbines having many basic differences other than their sizes. The estimate made by the authors has already been given in the early part of the paper as about 9900 Btu per kw-hr for 50,000-kw units when operating with steam at 1000 F, 390 lb per sq in. abs, and 1 in. Hg abs exhaust pressure. For a 100,000-kw unit this rate might be brought down to 9600 or better; and for 1200 lb per sq in., without reheating, one might expect close to 8600 Btu per kw-hr. This would mean that the moisture in the last stage has reached or exceeded the allowable limit set by many turbine engineers, for it would be about 12 per cent. If reheating were employed with the high-pressure and 1000-F throttle steam, the energy consumption rate of the unit might then be brought down to about 8400 Btu per kw-hr.

The estimates previously given are further strengthened by the evidence furnished by several turbine builders in this country, who estimate that a 10,000-kw unit with three regenerative feed-

water heaters and designed for throttle steam at 700 F should have an energy consumption rate of about 10,860 Btu per kw-hr, when the throttle pressure is 390 lb per sq in. abs and the exhaust pressure is 1 in. Hg abs. By referring to Figs. 6 or 7, it may be seen that such a result is nearly 6 per cent better than that obtained from the Detroit turbine when operated with steam at 700 F. This difference is probably due in a large measure to the large shaft-packing leakage and possibly to a large interstage leakage. Consequently, if a 10,000-kw unit can be built for steam at 1000 F and operated without serious leakage, the slope of the curves in Figs. 6 and 7 show that such a unit would have an energy consumption rate of about $(1.00 - 0.07) \times 10,860$ or 10,100 Btu per kw-hr. Then for large units and high-pressure steam this rate may possibly be brought down to the figures previously given.

The cost of materials suitable for use with steam at 1000 F will probably be materially reduced in the future, if one may judge from similar developments of various other metals. As the development progresses and the production is increased, the costs of these materials are almost certain to be greatly reduced. Then the progress in the use of high-temperature steam will probably be greatly accelerated.

Discussion

W. E. CALDWELL.³ The performance and reliability of the unit appears to be good and undoubtedly very liberal clearances may have been employed for the sake of reliability. The high pressure shaft packing leakage of practically all machines and the attendant heat waste appears to be an unpreventable evil. This is further complicated in certain types of machines requiring balance pistons to compensate thrust. In the Detroit machine the cooling of the high pressure packing has been elaborately provided for but it appears that more shaft length has been devoted to this feature than is warranted by the present state of the art. Perhaps it is the small size of the machine which makes the contrast so pronounced and possibly no greater shaft length would be required even for a much larger unit. Essentially, the major difference between this turbine and ordinary turbines is the shaft packing at the high temperature end and admission valve arrangement. The sectional view shown in Fig. 3 does not clearly indicate whether the sealing strips are steel inserts or rolled sections, or whether they were machined from heavier material.

It appears that separate sleeves carrying the packing strips are on the shaft and it would be interesting to know what considerations dictated the general design of the shaft packing. In other words, if shaft sleeves could be eliminated a slight reduction in packing diameter and consequent leakage would result. The Ljungstrom type of packing which consists of very thin strips secured into grooves in the shaft and casing is becoming increasingly popular and appears to have much to commend it where conditions will permit its use.

It would appear that a hydraulic gland seal might have been more advantageous for the final atmospheric seal in permitting a reduction in length between bearing centers and for its more effective cooling. The supply of saturated steam adjacent to the gland of the first stage shell may have advantages even for consideration on conventional turbines, since it would simplify the usual means of disposing of high pressure packing leakage, and it would make available superheated steam for more important use in the turbine. In one machine with which the writer has had experience, the substitution of saturated steam for superheated steam on gland seals, improved starting and operating conditions materially by reducing temperature strains and dis-

tortion of the shaft and the gland box casing. It would be interesting to know the type of construction of the shaft and high pressure end of the machine, that is if the shaft is hollow and provided with ventilation opening, and are the disks separately attached or part of the shaft forging.

In referring to Fig. 9, the efficiencies of the installation are given for 700 and 1000 F. Inasmuch as the turbine was designed for 1000 F, its best performance should be expected under these conditions and it would be interesting to know how the curve would compare for two similar machines, one designed for 700 F and the other for 1000 F. In other words, how much of the difference between the two curves is represented by impaired blade performance due to reduction in velocity ratios and how much is due to increase in hydraulic losses from the low pressure unit?

The method of measuring steam temperature is simple and practical and sufficiently accurate for work of this kind. The comparative tests shown graphically in the paper reveal such small differences that this method of temperature measurement should become increasingly popular.

The bleeding of highly superheated steam for heating feed-water invites some speculation as to how far this practice might profitably be carried. It would be interesting if the authors could indicate the economic limit of temperature above which the steam is more efficiently used in the turbine than in the heater.

A. G. CHRISTIE.⁴ The authors of this paper deserve the hearty commendations of all power engineers for their skill and energy in carrying out and analyzing the series of tests that form the subject of this paper. The problems involved in the determination of the heat distribution called for a high degree of technical ability. Engineers have awaited the publication of test data on this 1000 deg. turbine with keen interest.

Both thermal and engine efficiencies are high for this size of turbine. The authors point out that the maximum capacity of the unit, 10,000 kw, was not sufficient to produce the highest thermal efficiency. In view of the leakage of sealing steam of 4.4 per cent and of the probable increased diaphragm leakages in the turbine due to increased clearances, one may infer that even better performance than shown by these tests could be secured if leakages were reduced to normal quantities.

The influence of this high temperature on overall station performance may be estimated by assuming an average load of 8000 kw, 6 per cent for auxiliaries, and 84 per cent boiler plant efficiency, which results in a station rate of 13,770 Btu per kw-hr output. This is an exceptional performance for this size of plant.

Little information has been published previously on radiation losses from bleeder lines, heaters, drain, and condensate lines. The figures given by the authors show that these losses vary among the different items of equipment but average about 5 Btu per lb of steam bled at the three heaters.

The high pressure packing on this unit seems unduly complicated as it involves the use of two qualities of steam in the turbine, the 1000 deg. steam at the throttle and a lower degree of superheat in the gland. Fig. 8 shows a slight improvement by using 700 deg. instead of saturated steam in the glands. One may therefore conclude that a simpler gland, designed to permit the steam at full superheat from the first stage to leak outward as in standard turbines and with the same leak-offs to stage heaters as on the present turbine, would result in a shorter, more rugged, and less complicated turbine. The bearing could be kept cool by a water gland through which condensate is circulated and which would prevent any steam from escaping into the

³ Research Engr., United Elec. Light & Power Co., New York, N. Y. Mem. A.S.M.E.

⁴ Prof. M.E., Johns Hopkins University, Baltimore, Md. Mem. A.S.M.E.

turbine room. From Fig. 8 one may conclude that this would show a slight improvement in efficiency over the present machine. Since a shorter shaft would permit lower clearances in the shaft packings and diaphragms, this design would lead to still further improvements in performance.

The heat transfer rates with superheat in the bleeder heater deserve some comment. About ten years ago the writer was not allowed to install bleeder heaters without desuperheating the bled steam because the heater manufacturers would not guarantee performance with superheat in a heater. They claimed that the heat transfer rate with this hot dry steam would be very poor. This idea was exploded when tests by Sprague at Pittsburg were published. Since then there has been no hesitation about using superheat in bleeder heaters. The heat transfer rates in the Detroit tests indicate that heat flows at rapid rates even with the dry superheated steam. The authors' predictions of future units are intriguing. Their suggestion of a double flow unit for the high pressure section has its possibilities but this would also lead to double flow low pressure units, resulting in a long unit. Possibly improved high pressure packing designs may eliminate the need of a double flow high pressure unit.

They estimate a heat rate of 8600 Btu per kw-hr for the turbine-generator unit of 100,000 kw with 1200 lb per sq in. abs steam pressure, 1000 F and no reheating. If one allows 6 per cent for auxiliaries and 86 per cent boiler efficiency, the station heat rate would be 10,600 Btu per kw-hr which is an excellent performance. If one stage of steam reheat were used at the cross-over between high and low pressure cylinders, this would result in a station performance of 10,400 Btu per kw-hr which, with 13,600 Btu per lb coal, represents a coal consumption of only 0.766 lb per kw-hr. This performance practically equals that of a Diesel engine and approaches the results published for the mercury-steam stations. Quite evidently high steam temperatures offer possibilities of still further improvements in steam station performance.

M. K. DREWRY.⁵ This paper, and its companion⁶ by P. W. Thompson and R. M. Van Duzer, contain a wealth of information for which many in the power industry are undoubtedly very grateful. Advancing into the 1000 F temperature field was certainly more difficult than was the elevating of steam pressure from 600 to 1200 lb per sq in. The Detroit company has aptly pioneered into a region requiring exercise of greater-than-ordinary skill.

A. M. GREENE, JR.⁷ Those in the profession who are connected with power-plant machinery, as builders, operators, or teachers, owe a special debt of gratitude to the authors of this paper for the clear statement of the problem and for the original data which they have supplied. I feel that we are indebted also to The Detroit Edison Company for their willingness to enter into this new field of high temperature for the purpose of improving their own cost of production and at the same time giving to all of us quantitative knowledge of the value of these high temperatures. It takes broad vision of the future to authorize an expenditure of money for investigations into regions beyond which we have not gone in commercial practise, and I for one wish to express my appreciation of what the company and the authors have done for us all in extending their investigations.

In looking over the energy balance of the turbine I note that 4.2 per cent of moisture was present in the exhaust in place

of 14.3 per cent on the isentropic line from the initial-point. Of course this difference is due to the so-called reheating factor which occurs in all of the stages of the turbine, and I drew upon the Mollier chart of Keenan the line passing through the various qualities and pressures given for the extraction steam in the various stages of the feedwater heaters. Since this steam is largely in the superheated region the curve of initial condition in two particular stages can be drawn from the data, and in this way the thermal efficiency of the various stages might be worked out.

The curve as drawn is not continuous but has a reverse curvature near the point corresponding to the seventeenth stage. I think this is due to the fact that these conditions at the ninth and seventeenth stages are occasioned by mixtures of sealing steam and turbine steam; whereas, the conditions in the condenser and the heater using steam from the fourteenth stage are really steam-turbine conditions. The employment of so much sealing steam prevents one from determining from the data furnished in the paper the exact conditions within the turbine casing.

The curves extending into the region of 1000 F steam, included in the paper, are of much interest and value to the teacher of heat engineering as they give actual plotted points and indicate the gains in efficiency or the reductions in energy consumption to be expected with increases in superheat.

P. H. HARDIE.⁸ The writer wishes to congratulate the authors on the presentation of such valuable experimental data. The Detroit Edison Company is noted for its pioneering work and this latest research into the region of high temperature steam is especially noteworthy.

Ample discussion of the improvement obtained by increasing the steam temperature will undoubtedly be given by turbine and power plant designers. There are, however, many other points of interest in this paper.

The computation of the engine efficiency of a regenerative unit based on an ideal unit having a finite number of heaters will probably be new to many engineers, although this method has been advocated by Professor Ellenwood for some time. This paper offers an excellent way of illustrating its usefulness, and should serve to encourage its use.

The authors should be commended for using the more correct term "energy consumption rate" instead of "heat consumption rate" or "heat rate."

No doubt the authors have a good reason for reporting efficiencies, energy consumption rates (Table 1) and loads to one one-hundredth of one per cent, and exhaust pressures to one one-thousandth of an inch. In view of the accuracy, however, with which the measurements were made this would seem to be a departure from accepted practise.

It would be interesting to know why the heater condensate was computed instead of weighed, since to have weighed it would not have required extra weighing equipment or test personnel. This could have been accomplished by combining the heater condensate with the condenser condensate and the total weighed. Such a procedure would have required only a minor piping change, and would have given a steam consumption, exclusive of incidental drips and atmospheric leakage, with an error less than ± 0.2 per cent instead of ± 1 per cent as reported. This would have necessitated passing all the condensate through the seventeenth-stage heater, but the correction for the change in the condensate circuit is very small and easily computed. This procedure was used successfully by the Brooklyn Edison Company several years ago when first making ac-

⁵ Asst. Chief Engineer of Power Plants, Milwaukee Elec. Ry. & Light Co., Milwaukee, Wis. Mem. A.S.M.E.

⁶ A.S.M.E. Trans., 1934, paper FSP-56-9.

⁷ Dean, School of Engineering, Princeton University, Princeton, N. J. Mem. A.S.M.E.

⁸ Test Engineer, Research Bureau, Brooklyn Edison Co., Brooklyn, N. Y.

ceptance tests on the regenerative cycle. For the tests on the last four units installed in the Hudson Avenue Station closed volumetric tanks were provided to measure the hot heater condensate. These tanks discharged into the same dump tank as the condenser condensate, where the two mixed before being pumped through the low pressure heater.

Very little is said in the paper about the measurement of the electrical output. Since this is one of the two most important measurements more elaboration on the electrical measurements would be interesting. Were panel board type meters or rotating standards used?

FRANCIS HODGKINSON.⁹ This paper is of interest because it describes the performance of a steam turbine operating commercially at the highest temperature yet recorded except for gas-driven superchargers in connection with internal-combustion engines. However, temperatures of this order or higher with extremes of reheating to approach an isothermal expansion were attempted with a steam turbine by Ferranti some thirty years ago. The attempt failed because suitable materials were not available. For example, Ferranti constructed his cylinder of cast iron.

It must be recognized that the physical dimensions of the machine described by the authors are small, that difficulties because of temperature increase with the size of structure and I would question the wisdom of adopting 1000 F for 1800 rpm machines of 50,000-kw to 100,000-kw capacity, concerning which the authors make some prognostications. Furthermore, considerably better heat consumption rates are to be secured than the speculation of the authors for larger machines by means of lower total temperature, say 850 F, but by employing much higher pressure and reheating. It is not clear that any material increased capital cost need be incurred by such a method.

Concerning the feedwater heaters, the authors remark that no general method of calculating performance, when both superheated steam and its heat of evaporation are involved, has been accepted. In this they present a problem. Inasmuch as extraction feedwater heaters will be supplied as a rule in modern practise with superheated steam, a method of determining their actual performance is desired.

In Table 6, the authors express a terminal temperature difference for the whole heater based in one column on the temperature of saturation of the steam and in another on the actual temperature of the admitted superheated steam. They base the heat transfer rate on the saturation temperature of the steam when actually highly superheated steam is introduced into the heater. All three of these expressions seem meaningless.

The designer of heaters for this service must regard them as comprising two separate elements, in which the functions are entirely different. In the first element, the steam is condensing and therefore remains at constant temperature; in the second element, the steam falls in temperature from that of the admitted superheated steam to that of saturation.

At some point in the steam path, the steam becomes saturated, at which point it is reasonable to expect there would be a low terminal temperature difference, certainly not exceeding 10 F. With knowledge of the quantity and temperature of ingoing feed and an assumption for the terminal difference at saturation of the steam, the lower-temperature portion of the heater may be proportioned and the quantity of extracted steam readily calculated. There then remains some further heating of feed due to the heat in the superheat of that quantity of steam, for which additional surface must be provided.

⁹ Consulting Mechanical Engineer, Westinghouse Elec. & Mfg. Co., Philadelphia, Pa. Mem. A.S.M.E.

If a temperature difference of 10 F is assumed at the saturation point of the steam, it is found from Table 6 that the mean hyperbolic logarithmic temperature difference for run No. 1 is as follows:

	In condensing the steam, F	In absorbing the superheat, F
9th-stage heater	33.2	101.6
14th-stage heater	32.3	80.1
17th-stage heater	43.2	57.1

The verification of the predictions of the designer and the true heat transfer rates cannot be calculated without knowledge of the temperature difference at the point where the steam becomes saturated and the amount of heating surface above and below this point.

In a given case, it might be possible to explore the steam space of the heater and determine, approximately at least, the point at which the steam becomes saturated, but it would be well nigh impossible to measure the feedwater temperature at this point.

It would seem, therefore, that designers' predictions as to respective mean temperature differences and heat transfer rates cannot be verified and that verification can only be made of quantity of feed and of extracted steam, and entering and leaving temperature, and that any tabulations of terminal temperature difference, mean temperature difference, and heat transfer rates following a test of this character are meaningless.

H. E. KEELER.¹⁰ After reading this paper, "The Thermal Performance of the Detroit Turbine Using Steam at 1000 F," by W. A. Carter and F. O. Ellenwood, the writer is of the belief that the first and most important part of any discussion will be to congratulate the authors most heartily on the very excellent character of their paper.

It is rather reassuring to know that the conclusions drawn are based on so many tests and that they are so consistent among themselves. Also the fact that the entire unit had seen a good many hours service previous to and during the long period of testing is a point of much importance. The hazard of publishing premature and incomplete data has been entirely avoided here.

It is evident that, apart from the main problem of converting as much of the available energy in the steam into electrical energy as is possible, a vast amount of data is available on the behavior of metals under continued high temperatures and fairly high pressures; also that a great amount of data is available on heat-transfer under conditions of steam temperature which, at the present time, are rather unusual. Creep-stress and the growth of metals have been carefully studied and, as a result, there is undoubtedly available a wealth of valuable data.

The test results are particularly timely right now because they can be studied simultaneously with the latest economy achievements of the mercury-steam cycle.

Past history shows that most developments at some time will show a sudden and distinct advance in some particular direction and every one will then focus his attention along the same general line of endeavor, whereas it would have been much better had there been many independent lines of attack progressing simultaneously.

With the fact staring the power engineer in the face that he is now much nearer the "end of the trail," with respect to conversion of heat into electrical energy, than he has ever been before and that he is now awaiting further metallurgical developments to permit him to use higher and higher pressures and temperatures it makes us all turn attention more than ever to the possi-

¹⁰ Professor of Mechanical Engineering, University of Michigan, Ann Arbor, Mich. Mem. A.S.M.E.

bilities of converting the potential chemical energy of a fuel more efficiently and directly into electrical energy.

Is it not time to consistently devote time and effort to a search for more efficient energy conversion methods on a scale at least moderately comparable to the present expenditure of both of these along the lines of improvement of the existing and possible power-plant cycles?

At present our only fairly efficient, large-scale method of converting the potential chemical energy of a fuel into electrical energy is by the following route:

- 1 Convert the chemical potential energy of a fuel into heat by the process of combustion
- 2 Transfer this heat to a suitable elastic working substance which can undergo a pressure-volume change
- 3 Allow this elastic working substance to undergo a pressure-volume change in a heat-utilizer and produce mechanical work such as the rotation of a shaft
- 4 Convert this mechanical work available from a rotating shaft into electrical energy by driving an electric generator.

In scanning these items it is seen that if the pressure feature of Item 3 could be eliminated, we could go with available materials to very much higher temperatures than we do at present.

In view of all this would it not be desirable to focus the attention of mechanical and chemical engineers, chemists, and physicists to a much greater degree, on the specific problem of finding a new method for the conversion of the potential chemical energy of a fuel into electrical energy, than has been done to date and to provide funds for supporting this line of research on a scale comparable to the development of existing steam and mercury-steam cycles?

Reference to Item 2 brings attention to the steam-generating equipment which we must recognize as a very efficient assemblage of heat-transfer apparatus but unfortunately a great destroyer of available energy. This element also could be conceivably eliminated by more direct and efficient energy conversion methods.

W. S. MONROE.¹¹ This paper is very interesting as it represents the only test data obtained at such high steam temperatures, and the experience gained in the operation of this unit will be of great value for future design of larger units to operate at these high steam temperatures.

Before discussing the technical side of the paper, a few words about the nomenclature used may be in order. It is common practise among power plant engineers to speak about adiabatic expansion as representing the theoretical maximum energy which could be obtained, but when it is called "isentropic" expansion, the average engineer is just a little bit baffled and wonders if this means something different, and is happy after a while to find that it is just another name for his old friend "adiabatic expansion." He is also familiar with the term "heat content of steam and feed water," and hesitates for a moment when confronted with the term "enthalpy" until he finds that in this case it really means heat content. Finally, his old acquaintance "the heat rate" has been called "energy consumption rate," all of which causes a slight confusion for the practical engineer as he wonders about the necessity of these new words in this particular case.

The most interesting part of the paper is that which deals with the method used for gland sealing as it was found necessary to use saturated steam for this purpose. We agree with the authors' statement that in a larger turbine the amount of sealing

steam could be reduced considerably below the 6.5 per cent determined for this turbine in relation to throttle steam.

It is stated in the paper that the thermal performance of turbines and turbo-generators may be expressed in thermal efficiency, heat rates, and engine efficiencies. Of these, the heat rate and overall thermal efficiency of the turbine and heaters are determined directly from the test data as it requires only the determination of total heat supplied to the turbine, minus credit for the heat returned in the condensate from the last heater, and the total kw load generated. These figures represent the overall performance of the turbo-generator with heaters, and can therefore not be used for direct comparison with any other machine, even if the pressure and temperature were the same, as the heater arrangement might differ. As stated in the paper, the engine efficiency is the only term which expresses the perfection of the engine (turbo-generator).

The actual heat rate has been compared to a theoretical cycle which assumes no thermal difference in the heaters, no pressure drop in extraction piping and return of heater drains directly without cascading to the next heater, as in the actual installation. This method charges the turbo-generator with all of these losses, and the engine efficiency calculated on that basis is therefore not an indicator of the efficiency of the machine alone. A simpler way of doing this, and one which is commonly used, is to determine the theoretical work which could have been done by the turbine with the actual throttle flow and actual extraction quantities. This is obtained by multiplying the adiabatic heat drop between the throttle and the different extraction points by the amount of steam which flows through each section of the turbine. This method is more universal, as it also applies in cases where steam is extracted for other purposes than for feed heating. The engine efficiency is then obtained as the ratio between the actual kw hrs produced expressed in heat units divided by the theoretical work, which could have been done with adiabatic expansion, as explained above.

Regardless of which of these methods is used for the determination of engine efficiency, the effect of gland leakage on engine efficiency becomes a separate problem due to the fact that the gland steam is admitted separately and has a different heat content than the throttle steam. In this particular case, (Run No. 1), it amounts to 6.5 per cent of the throttle steam, and is therefore of considerable importance. It would seem that the simplest way of including this steam in determining the engine efficiency would be to charge all of it to the throttle steam; but instead of using the actual amount of sealing steam, use an equivalent amount corrected for the difference in heat content of the two steam supplies. For test Run No. 1, the factor representing the difference in heat content would be

$$\frac{1206 - 48}{1529 - 48} =$$

0.78. On this basis the engine would be charged with $5444 \times 0.78 = 4250$ lb per hr (sealing loss), added to the throttle flow. By deducting the amount of extraction at each bleed point, the theoretical flow through different sections of the turbine can be determined from this figure. If the actual blade efficiency of the turbine is desired, the gland steam would have to be divided into different parts, and each part considered in connection with the turbine section where it flows. The report does not give all extraction quantities separated from gland leaks, so we have not been able to compare the two methods.

In calculating the ideal cycle, the paper assumes that all sealing steam mixes with the throttle steam, and the performance given in Table 2 has been based on the mixture. This does not seem to be justified as the temperature of the mixture will be 968 F, while the actual turbine was working on 1003 F. The adiabatic drop between throttle conditions and the condenser is $1529 - 951 = 578$ Btu per lb (Run No. 1), while the adiabatic

¹¹ Pres., Sargent & Lundy, Inc., Chicago, Ill. Mem. A.S.M.E.

drop from the assumed mixture condition is $1509 - 945 = 564$ Btu. The actual turbine, therefore, was working on an adiabatic heat differential of 578 Btu, while the theoretical cycle used in determining engine efficiency has been based on 564, or a difference of 2.4 per cent. This makes the efficiency of the ideal cycle, as shown in Table 2, lower than if based on the actual throttle temperature. The assumption of mixing the gland sealing steam with the throttle steam is questionable, particularly as only $\frac{1}{10}$ of the sealing steam enters the turbine at this pressure.

The difference mentioned above is slightly offset by basing the ideal cycle on heater performance without terminal difference and friction loss in extraction piping.

Under the discussion of the test data it is mentioned that the engine efficiency at 1.8 in. Hg absolute condenser pressure is 81.5 per cent, and with a condenser pressure of 1 in. it was 79.5 per cent, or 2 per cent difference. This difference is attributed to velocity loss from the wheels in the low pressure region. We are inclined to think that this difference is more a difference in test figures as the paper shows later that the entire leaving loss is 2.5 Btu, or only 0.5 per cent of the adiabatic drop.

It is stated that the test results of 10,730 Btu per kw-hr is used as a basis of estimating the performance of a 100,000-kw turbine operating at 1200 lb per sq in. and 1000 F with reheat, and for which 8400 Btu per kw-hr is indicated. This estimated figure is not really derived from the test figures—as shown in the paper which is calculated on basis of present day knowledge of turbine Rankine efficiency for larger machines and steam tables. The spread between heat rates at 390 lb per sq in. and 1000 F, for a 10,000-kw turbine, and 1200 lb, 1000 F, for a 100,000-kw turbine, in the above case, approximates 22 per cent.

We agree that the calculated figure of 8400 Btu per kw-hr is substantially correct. It may be of interest in this connection to mention that tests on a 105,000-kw turbine operating at 600 lb per sq in. and 725 F throttle temperature and 750 F reheat, gave a heat rate of 9400 Btu per kw-hr, which, when corrected to 1200 lb per sq in. and 1000 F approximates 8200 Btu per kw-hr, or 13 per cent correction from test basis.

In closing this discussion of the thermal performance we want to emphasize the valuable contribution made in design, operation, and test of this turbine, as it points out some of the mechanical difficulties which have been encountered. The adoption of higher pressures and temperatures is not today retarded by lack of information as to expected efficiencies, but mainly by uncertainty as to mechanical complications, operating trouble and outage of equipment, coupled with higher equipment cost.

S. A. Moss.¹² The figure of 1000 F with which the authors of the paper have been working, of course, represents quite an achievement. However, turbines are being successfully operated at even higher temperatures. It is true that these turbines are very small, and that the development is very minor as compared with that which the authors describe. Nevertheless, this development does show what can be accomplished in the way of securing materials to withstand high temperatures and gives evidence that temperatures such as those used by the authors will perhaps be commonplace in the coming years.

The turbines alluded to are those used on superchargers for airplanes, and are driven by the airplane engine exhaust gases. These are in moderate use on airplanes, and have also been operated quite extensively during ground tests. The temperature of the exhaust gases entering the turbine nozzles has been 1400 to 1500 F. The turbine buckets are, of course, bright red. They are often operated without a casing, and present a very

interesting sight in a dimly lighted room. The wheels have a pitch diameter of about 9 in. and operate at speeds of from between 20,000 and 30,000 rpm.

A number of alloys have been found suitable for use in these buckets. These alloys have not only to withstand stress at high temperature, but also to withstand the corrosive effect of Tetra-Ethyl Lead, so that they are more expensive than alloys suitable for the work of the authors.

During research tests on this apparatus, a line of 8 in. pipe was used, about 30 ft long. This pipe was, of course, a glowing red throughout its length. The pressures which have been used are much lower than those used by the authors of the paper. However, with proper thickness of pipe material and with proper tensile strengths at the temperatures involved, pressure would not create an appreciable problem. The lengths of pipe were turned up at the ends to give a slight flange on which a metal to metal joint was made. Very heavy separate steel flanges, with a proper number of bolts, were used to keep the two pipe ends together according to the well known Van Stone system. Several different materials have been used for these pipes and all have been found suitable.

No long-time tests have been made in any of this work to show the effects of creep. However, this work does give some idea of the many possibilities ahead of us in the use of high temperatures.

F. H. ROSENCRANTS.^{13,14} First of all, the writer wishes to commend the Detroit Edison Company and its engineers for the tremendous stride which their efforts represent toward the attainment of simplicity of design, construction and operation in our future steam plants. The results thus far attained point the way to the development of plants operating on the simple straight-through cycle having an efficiency equal to and perhaps ultimately exceeding that now attained by the more complex and expensive high pressure reheat installations.

The unostentatious manner in which they have undertaken the work and the absence of any mystery associated with it since the beginning, gives a dignity to the undertaking which inspires admiration for those responsible and a confidence in the results attained.

The authors conclude from their experiments that though a 1000 F plant is at the present time physically practical, it is not to be recommended at the moment on account of the high cost of the materials essential to its construction. Plants at the moment operating at 860 F are pretty well established in this country without the use of expensive materials. With the two limits, namely 860 F established by practise and 1000 F at the upper limit which is stated to be physically practical but not economically sound, the question arises as to what is immediately practical without running into excessive cost. Certainly it is something above 860 F.

With modern facilities for flash welding together alloy tubes and steel tubes having widely different physical characteristics, superheaters may be constructed at moderate cost for an outlet steam temperature of considerably above 900 F. Furthermore, alloy steels suitable for superheater headers and piping at temperatures something above 900 F are available at moderate increases in price above steel tubing. Assuming that the turbine builders are willing to accept 900 F or perhaps a little more for large size units, there appears to be no obstacle at the present

¹³ International Combustion Engrg. Co., New York, N. Y. Mem. A.S.M.E.

¹⁴ This discussion applies jointly to this paper and the companion paper, "High Temperature Steam Experience at Detroit," by P. W. Thompson and R. M. Van Duzer, Jr., A.S.M.E. Trans., 1934, paper FSP-56-9.

¹² M.E., Thomson Research Lab., General Electric Co., W. Lynn, Mass. Mem. A.S.M.E.

moment in the way of construction for at least 900 F at the turbine throttle.

It appears to be the consensus of opinion, however, that 900 F to 1000 F is getting beyond the limit for satisfactory flange joints. Welded joints are an essential requirement. Considering the extensive use of welded joints at the new steam plant of the General Electric Company, at the new extension to the Kearny plant of the Public Service Electric and Gas Company, New Jersey, and the examples of electric welding referred to by the authors, it would seem that the art of electric welding as applied to piping promises to keep pace with requirements.

A temperature of 900 F will permit an operating throttle pressure of around 800 lb per sq in. without running into excessive moisture at the turbine exhaust. Assuming 800 lb throttle pressure, the boiler design pressure would have to be approximately 900 lb. The boiler drums for such a pressure, assuming 70,000 lb steel, may be made by the electric fusion welding process. Prior to the adoption of 70,000 lb steel, such a pressure, particularly in a bent tube type of boiler, would have required forged drums, at a considerable increase in cost above what is now possible.

It appears that we are all set for the 900-F steam plant based on present-day developments. The rate and extent to which we may progress from this point continues to be a matter of materials and cost of construction.

AUTHORS' CLOSURE

The authors appreciate the commendation accorded by the discussers, because special effort has been made during all the work to secure reliable information and present it accurately, both as to data and form of expression.

Mr. Caldwell mentions the possibility of securing better results by means of a water seal on the low-pressure end of the turbine instead of using the steam seal; this point seems well taken,

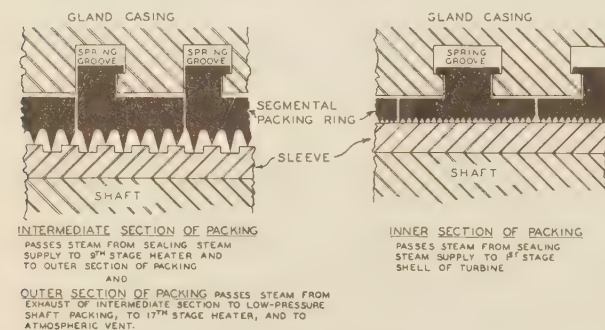


FIG. 10 HIGH-PRESSURE PACKING—TYPES OF PACKING RINGS USED IN DIFFERENT SECTIONS

as far as the authors are aware, and undoubtedly the hydraulic form of seal would be satisfactory.

As the details of the high-pressure shaft packing are not shown clearly in Fig. 3, Mr. Caldwell's misunderstanding of the construction is not surprising. Figs. 10 and 11 are introduced to show some details of the three sections of this packing. The packing rings consist of internally serrated segments fitted into T- or L-shaped grooves in the packing casings. A leaf spring holds each segment in position toward the shaft sleeve and against the shoulders of the groove. Although the use of the sleeves requires larger bores for the packing rings, and therefore increases the leakage, their use is desirable as they provide renewable surfaces on the shaft that can be replaced if damaged by packing abrasion. The clearances between the packing rings and the sleeves varied from 0.007 to 0.009 in. when the measurements

were taken with the turbine at room temperature. These clearances were somewhat larger when the unit was at operating temperature.

It may be possible that some other type of packing might provide an adequate shaft seal for the high-pressure end of the unit at a lesser expenditure of sealing steam.

The question raised by Mr. Caldwell regarding the economic limit of steam temperature above which bleeding should not

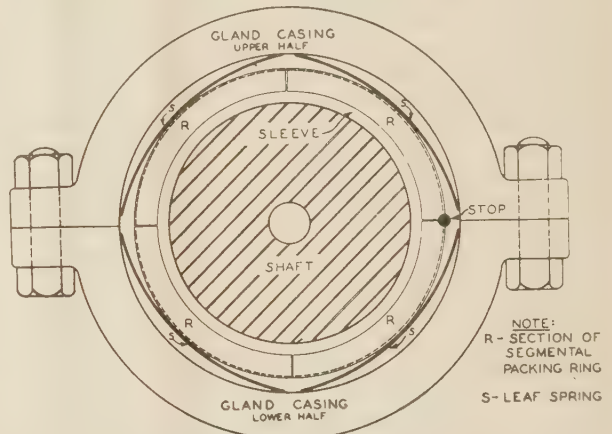


FIG. 11 SECTION THROUGH HIGH-PRESSURE SHAFT PACKING, SHOWING ARRANGEMENT OF SPRINGS HOLDING SEGMENTAL PACKING RINGS IN POSITION

occur is an interesting one and involves so many factors that it cannot be treated appropriately in this discussion.

Professor Christie's suggestion of a short, less-complicated gland design, wherein high-temperature steam would leak outward from the first stage and the shaft would be cooled by a water seal, seems to be a satisfactory arrangement, providing severe stresses are not induced in the shaft or casing.

Any curve drawn through points representing the steam condition in the extraction heaters is misleading and, as mentioned by Professor Greene, does not represent the true steam condition in the turbine casing, because high-pressure shaft packing leak-off steam enters the 9th- and 17th-stage extraction lines and affects the enthalpy of the steam mixture entering these heaters, thus producing such an incongruous curve. A reasonable steam condition line has been obtained by plotting data taken at the turbine casing and shows no reverse curvature.

It is especially gratifying to note that Mr. Hardie approves of the authors' method of calculation of the engine efficiency of the regenerative unit and the use of the term "energy consumption" in place of the less-accurate one, "heat consumption," when dealing with any kind of steam engine.

The efficiencies, the energy consumption rates, and the loads were reported to one one-hundredth of one per cent as a result of using calculating machines in making the computations from the original data which were not rounded off. These results undoubtedly should be rounded off to the nearest one-tenth of a per cent when considering them as actual values, but should be used as reported when checking the calculations.

The authors agree that it would have been better to have reported the exhaust pressures in one one-hundredths of an inch. The mercury column was capable of being read to one one-thousandth of an inch and the corrections applied for calibration error, temperature variations, and meniscus height were to the same fineness. But the uncertainty of the pressure at the mercury-column pipe connection at the turbine exhaust being representative of the average exhaust pressure does not warrant reporting

the exhaust pressure closer than one one-hundredth of an inch.

It would have been much more convenient to have weighed the condensate from the heater-drains along with that from the condenser hotwell than to have calculated it from the energy balance of the heaters, as was actually done. Such a scheme was considered but was not adopted, as it would have required making a correction to the performance of the unit due to a greater amount of water flowing through the low-pressure heater and a greater amount of steam extracted by this heater than was contemplated when the performance of the unit was predicted. Although this correction would not be large, it seemed undesirable to introduce such a requirement.

In answer to Mr. Hardie's final question, it should be stated that the electrical output was measured by a combination of instrument transformers and a switchboard-type kilowatt-hour meter which had a special register gear train that gave an unusually low multiplier of 100. The instrument transformers were calibrated previous to the tests and the kilowatt-hour meter was checked against a rotating standard frequently during the tests.

Mr. Hodgkinson points out that the difficulties of using high-temperature steam may be expected to increase when attempting to build units of large capacity—say 100,000 kw; his opinion is undoubtedly based on extensive experience, and is therefore of great value when considering the design of such units. Whether the thermal economy and capital costs of plants of the future will support the continued use of reheating systems or will be conducive to the development of materials suitable for steam of sufficiently high temperature to avoid reheating, is a big question that cannot be fully answered, probably by any one, at the present time.

Mr. Hodgkinson's comments regarding the feedwater heaters are largely approved by the authors. However, Table 6 contains information pertaining to actual terminal temperature differences, which is not "meaningless," but of considerable importance when considering the use of highly superheated steam in feedwater heaters. In such cases the actual terminal temperature difference is far greater than that obtained by the usual method of calculation. Furthermore, the values given in Table 6 under the heading of "Nominal Overall Coefficient of Heat Transfer" may possibly prove to be of considerable value, because they serve to call the attention of engineers to an unsolved problem in such cases. The word "nominal" is not fully expressive of the conditions involved; but it serves, in lieu of a better one, as a sort of red flag to warn the engineer that he is here confronted with a difficult problem because the real mean temperature difference in such a heater is not easily obtained.

The comments of Professor Keeler are very stimulating; but the authors prefer not to offer, at least during the present depression, any suggestions as to how we may successfully convert the potential chemical energy of a fuel directly into electrical energy and thereby justify scrapping all our steam power plants.

Mr. Monroe questions the "necessity" of using some of the nomenclature employed in the paper. Such matters are generally decided on the basis of preference rather than necessity, and in the present case the authors used the terms that they considered most suitable, because they believe that a greater degree of exactness is expressed by them. Thus, for example, the term "isentropic" is preferred to its equivalent, "reversible adiabatic," because the latter is too long and the word adiabatic by itself is incomplete. The word adiabatic alone simply means no heat transfer, and does not by itself convey any meaning as to whether the process is turbulent or not. Thus the expansion of a fluid through an insulated throttling device of any kind would be an adiabatic, but the large amount of turbulence produced would cause the entropy to increase; hence such an adiabatic

would not be an isentropic, or a constant-entropy process. On the other hand, the flow of steam through a nozzle, or any other device, would be an isentropic if the flow took place without any turbulence and without any heat transfer.

The term "enthalpy" has been used rather frequently during the past few years by many authors in place of "heat content" or "total heat" because both of the latter terms are likely to convey a misconception due to a former use of the terms in a slightly different sense and also due to the basic significance of the words. As now used, the term "enthalpy," "heat content," or "total heat" of a fluid means the sum of its internal energy plus the product of its pressure and volume. The authors consider the term "enthalpy" far from perfect; but it certainly has the merit of creating no misconception and that much can never be said for "total heat" or "heat content." Let us hope that we may eventually obtain for this important energy term a word that is more suitable than any of the three now in use.

In the original paper the word "unit" is defined to include the

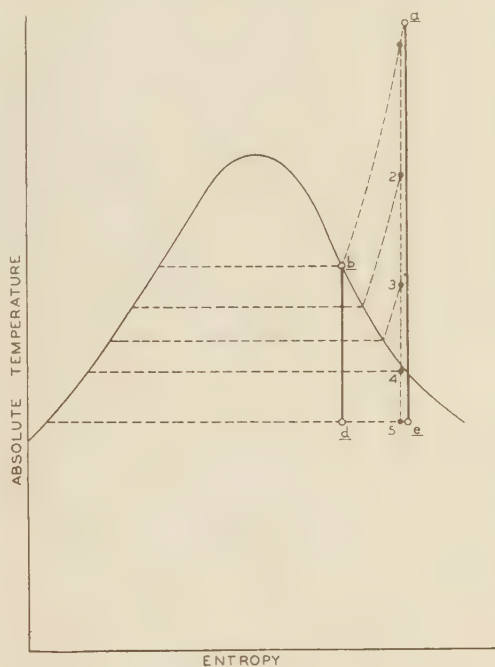


FIG. 12

turbine, generator, and heaters; hence the method used to determine the engine efficiency of such a unit is believed by the authors to be the correct one. The method of determining the engine efficiency of the turbine-generator, as suggested by Mr. Monroe, is not without merit; but the losses of available energy that occur between the heaters and turbine cannot be separated into parts some of which are charged to the turbine and others to the heaters. The regenerative unit is a combination of turbine and heaters that are operated together and also tested together; hence the authors believe that such a unit should be compared with a corresponding ideal, as defined in the paper. Furthermore, this method of testing such a unit requires only the additional measurement of the pressure at each of the bleeding points of the turbine, whereas the method suggested by Mr. Monroe requires the additional and troublesome measurement of the actual quantity of steam bled at each extraction point.

Possibly the authors should have mentioned in the original paper that they considered very carefully three different methods of making the calculations of the ideal cycle corresponding to

this turbine, which has two different sources of steam supplied to it. The method chosen, however, is relatively simple and gives results that differ from a more complicated one by about 0.5 per cent, a difference that is within the limits of error in the test data. One should note that any true calculation of the ideal cycle corresponding to this turbine must consider the available energy from both sources of steam, that are far different both as to quality and quantity. Just because the ideal turbine has no leakage, one should not ignore the energy available from the actual amount of sealing steam supplied to the actual unit.

For example, consider the state of the throttle steam supplied for Run No. 1, to be represented by a in Fig. 12, and that of the sealing steam by state b . Then, for this run having $w_a = 84,448$ and $w_b = 5444$ lb per hr, the total available energy (ignoring all bleeding to simplify the example) becomes

$$\begin{aligned} w_a (h_a - h_e) + w_b (h_b - h_d) \\ &= w_a (1529 - 951) + w_b (1206 - 800) \\ &= 84,448(578) + 5444(406) \\ &= 48,800,000 + 2,210,000 = 51,010,000 \text{ Btu per hr} \end{aligned}$$

Hence the real available energy (neglecting bleeding) from the two amounts of steam used by the turbine, becomes $51,010,000 \div (84,448 + 5444) = 567$ Btu per lb. This result is only 0.5 per cent greater than 564, which is the value of $h_1 - h_2$, where subscript 1 represents the state of the *mixture*, as calculated in the paper. In other words, the throttle-mixture method used in the paper involves an error of only 0.5 per cent instead of 2.4 per cent as given in Mr. Monroe's discussion. He apparently failed to consider any of the low-temperature steam used for sealing in his calculation of the ideal cycle, and naturally he obtains a cycle efficiency that is too high for comparison with this turbine that is supplied with two kinds of steam.

Regarding the two per cent higher engine efficiency obtained when a condenser pressure of 1.8 in. Hg abs was used instead of 1 in. Hg, the authors still believe, as stated in the original paper, that this difference is mainly due to the losses caused by the extra moisture and exit velocities resulting from the lower exhaust pressure. Naturally, a small part of the difference may be due to the test data, but additional check runs have confirmed the original figures.

The comments of Dr. Moss regarding the use of gas-turbine buckets at a bright-red temperature are very interesting, and possibly indicate what may some day be attained with large steam turbines.

Mr. Moulthrop¹⁵ has mentioned a number of interesting points that must always be considered in connection with high-pressure and high-temperature steam. His extensive experience in such matters makes his comments especially significant.

The authors note with much interest that Mr. Rosencrants believes the use of higher steam temperatures is rapidly becoming more feasible because suitable materials and good welded joints can now be made at a reasonable cost.

The comments of Mr. Soderberg¹⁵ are valuable to power-plant engineers who may be considering the installation of equipment to use higher steam temperatures than those now commonly employed. While it is true that high pressures are conducive to carry-over of impurities from the boilers, the authors are hopeful that boiler design will advance to such a state that by the time the turbine designer produces a turbine using steam of 1200 lb per sq in. and 1000 F, the scale formation on turbine-blades due to carry-over will no longer be a problem.

¹⁵ This discussion appears with the companion paper, "High-Temperature Steam Experience at Detroit," by P. W. Thompson and R. M. Van Duzer, Jr., A.S.M.E. Trans., 1934, paper FSP-56-9.

High-Temperature Steam Experience at Detroit

By P. W. THOMPSON¹ AND R. M. VAN DUZER, JR.,² DETROIT, MICH.

This paper is concerned with presenting the experience of The Detroit Edison Company with the various materials used in the construction of an 1100-F superheater and piping system in operation over 23,000 hr, for 21,169 of which the temperature was between 1000 and 1100 F; also a 10,000-kw, 1000-F turbine installation in operation 11,231 hr, for 7832 of which the temperature was 1000 F. A description of both installations, the reasons for the choice of materials used, and an account of the operating experience are included. The thermal performance of the turbine is dealt with in an accompanying paper (A.S.M.E. Trans., 1934, FSP-56-8) by W. A. Carter and F. O. Ellenwood.

EXPERIENCE gained from equipment operating with steam temperatures as high as 1100 F in one of the power plants of The Detroit Edison Company, since the fore part of 1929, leads the authors to believe that the design of steam-generating plants using temperatures in the neighborhood of 1000 F is entirely feasible provided users are prepared to specify the high-priced materials that experience so far dictates. A small oil-fired superheater, delivering steam at 1100 F to a piping system has been in operation at the Trenton Channel plant since March, 1929. The information obtained in the operation of this equipment served as a basis of design for the separately fired superheater, piping, and 10,000-kw turbine generator which was placed in operation with steam at 1000 F in the latter part of 1931 at Delray Power House No. 3.

The principal trouble with the two installations has been encountered at Trenton Channel and has been caused by the leakage at flanged pipe joints. The use of better bolting material and changes in flange design have materially improved conditions. Replacement of a cracked desuperheater casting was necessary in the Trenton Channel set-up and a new turbine throttle valve

of improved design has been installed to correct recurring leakage at the bonnet flange at Delray. With these exceptions no troubles of a serious nature have been experienced.

Examinations of the austenitic 18 per cent chrome, 8 per cent nickel alloy which was used in the construction of the Trenton Channel superheater and piping system, show that this material has deteriorated in service due, probably, to precipitation of chromium carbides along the grain boundaries. There is, however, no evidence thus far of inter-crystalline corrosion and no such serious reduction in physical properties such as would lead to rejection of this material for steam service in the range of temperatures from 1000 to 1100 F. Tests of other steels belonging to the low alloy class have disclosed no marked change in their properties. Since the time these two experiments were undertaken much more information concerning the behavior of alloy steels has become available. This, together with advances in the art of manufacture, has made the selection of stable alloys for this class of equipment a simple matter for the designer.

Operation with high-temperature steam has presented no problems of an unusual nature. The equipment, particularly the turbine, has been given close attention because of its experimental nature. The turbine at the present time, however, is receiving only the same care as other equipment in the Delray Power House.

This paper is primarily concerned with a discussion of the reasons for the selection of the materials that were used, results of metallurgical examination, operating features, and troubles that have been experienced and remedies applied. More detailed descriptions of the installations and design assumptions have already appeared in magazine articles (1), (2), (3), (4), (5), (6).³ Information regarding the thermal performance of the turbine has been presented in an accompanying paper (A.S.M.E. Trans., 1934, FSP-56-8) by Carter and Ellenwood.

PURPOSE OF EXPERIMENT

The choice of the unusually high temperatures for these experiments was made in order to determine what effects would be produced on alloys then available for power plant equipment. The experiments were undertaken as steps designed to eliminate one of the factors now limiting increase in efficiency of the simple regenerative turbine cycle by allowing initial pressures, higher than those now in use (1).

It was decided to divide the experiment into two parts at the time a decision was made in 1927 to proceed with the design and installation of a 1000 F turbine. The first part consisted of a separately fired superheater and piping system designed to operate at 1000 F and later with steam at 1100 F to give preliminary data regarding the effect of the high superheat on tubes, piping, pipe fittings, and particularly, pipe joints. The second step consisted of the installation of a 10,000-kw turbine-generator together with piping and superheating equipment designed for operation with steam at 1000 F.

Information gained from the first installation at Trenton Channel proved invaluable in the design and selection of materials especially for the piping system of the Delray apparatus.

³ Numbers in parentheses refer to similar numbered items in the Bibliography given at the end of the paper.

¹ Chief Engineer of Power Plants, The Detroit Edison Company. Mem. A.S.M.E. Mr. Thompson was graduated in 1910 from Cornell University with the degree of M.E., and for the two years following was an instructor in heat-power engineering at Cornell. In 1913 he was employed on designing and research engineering by the McIntosh & Seymour Corporation, Auburn, N. Y. Since 1913 he has been connected with The Detroit Edison Company, with the exception of two years' service in the U. S. Army as Major, in charge of inspection of all army ordnance material manufactured in the Cleveland district. Following the armistice he was appointed a member of the Cleveland District Army Ordnance Claims Board. Mr. Thompson has been a frequent contributor to technical literature. He is a member of the A.S.M.E. Critical Pressure Steam Boiler Research Committee.

² Engineer, Production Department, The Detroit Edison Company. Mr. Van Duzer received the degree of B.S. in Mechanical Engineering from the University of Michigan in 1927. Following graduation he spent two years at the Marysville Power House of The Detroit Edison Company and was then assigned to the staff of the Chief Engineer of Power Plants. One of his assignments has been the supervision of the experimental work involved in the two high-temperature installations at the Trenton Channel and Delray Power Houses.

Contributed by the Power Division and presented at the Annual Meeting, New York, N. Y., December 4 to 8, 1933, of THE AMERICAN SOCIETY OF MECHANICAL ENGINEERS.

NOTE: Statements and opinions advanced in papers are to be understood as individual expressions of their authors, and not those of the Society.

No provisions were made in either group to utilize steam at a pressure higher than 400 lb per sq in. It was believed that the high temperature without adding the possible complication of high pressure would provide the information most desired. Consequently, in both experiments, steam at station pressure was utilized.

DESCRIPTION OF EQUIPMENT

The Trenton Channel equipment consists of an oil-fired superheater supplied with steam at 400 lb per sq in. and 700 F from the station header. Approximately 65 ft of 5½-in. O.D. ⅜-in. wall tubing conducts the high-temperature steam to a desuperheater where the temperature is reduced before passing to one of the house-service turbines. The superheater is of the radiant type,

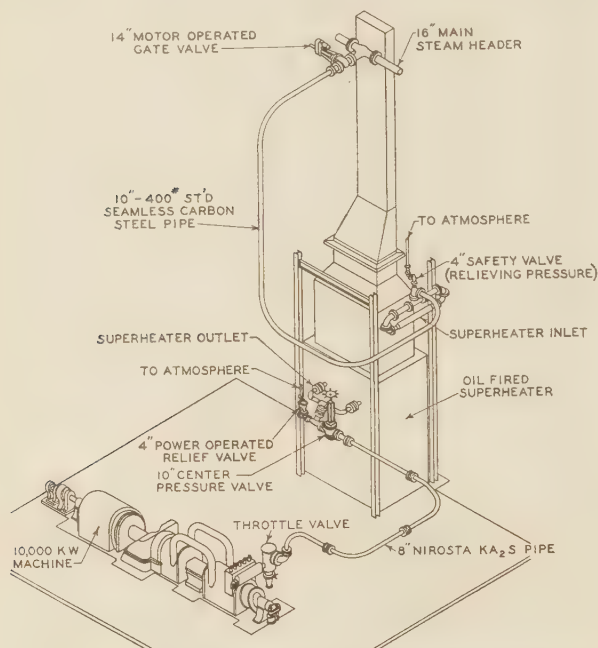


FIG. 1 ISOMETRIC VIEW OF HIGH-TEMPERATURE INSTALLATION

containing 153 sq ft of refractory covered heating surface, and is capable of adding 400 deg of superheat to 6000 lb of steam per hour from an initial temperature of 700 F. The tubes which comprise the rear and side walls of the unit are covered with refractory blocks cemented to welded-on-lugs on the tubes to prevent direct exposure to the radiant heat.

The high-temperature piping system included a valve, eight flanged pipe joints, and a desuperheater. The pipe ends were provided with Van Stone, Sarlun laps, the faces of which were provided with a serrated finish for obtaining experience with gasketed as well as seal-welded joints. All joints in the piping system as well as the superheater inlet and outlet joints were constructed in accordance with the 600-lb American Standard for Steel Flanges. The original line has been somewhat changed by the addition of experimental joints of heavier construction.

The Delray installation consists of an oil-fired superheater, interconnecting high-temperature piping, a 10,000-kw British Thomson-Houston turbine-generator, condensing equipment, and auxiliary pumps and heaters, together with the piping necessary to connect the turbine flow circuit into the existing plant systems (5), (6). An isometric view of the installation is shown in Fig. 1. The equipment occupies a space provided for a future boiler and is compactly arranged.

The superheater contains 3957 sq ft of surface arranged in three sections; a top convection section, a middle semi-convection-radiant portion, and a lower radiant section which encloses the combustion chamber on the two sides and bottom. The tubes in the lower section were provided with the same type of refractory covering as used in the Trenton Channel superheater. The unit was designed to superheat 90,000 lb of steam per hr from 700 to 1100 F at a pressure of 455 lb per sq in., although the ordinary operating pressure does not exceed 400 lb.

The interconnecting pipe line (2), consists of the superheater outlet fittings, a 10-in. center-pressure type stop valve, two reducing fittings, and 43 ft of 8½-in. O.D. ⅝-in. wall tubing. A power-operated safety valve was also added at the outlet. Several different types of joint construction are used in the twelve joints which are in the line. Five of these joints are made with full-strength butt welds and reinforced with bolted flanges; the remaining seven are bolted joints. The throttle valve joint is a modified tongue and groove, 1350-lb American Standard. The joint between the reducing ell and the tubing, is of the raised-face type in accordance with the 1350-lb American Standard. The tubing-reducer joint near the superheater is a modified 900-lb American Standard. The joints on either side of the valve are made up with hairpin spring washers to provide flexibility inasmuch as the valve flanges are made to the 600-lb American Standard. The sixth and seventh bolted joints are at the small tee where the safety valve is located, and are both in accordance with the 900-lb American Standard.

The turbine is a two-cylinder, single-shaft, 3600-rpm, straight-impulse type unit containing nine stages in the high-pressure cylinder and eleven stages in the low-pressure portion. It was designed for steam at 365 lb per sq in. gage at 1000 F, exhausting to 1 in. Hg absolute. Steam is extracted at the ninth, fourteenth, and seventeenth stages for feedwater heating. Except for the double-casing construction, and the external supply of saturated steam which is supplied to the high-pressure shaft packing to cool the shaft and bearing, the general design of the turbine differs little from impulse turbines manufactured in this country. A cross-section of the turbine unit is shown in Fig. 2. The generator which is rated at 10,000 kw at 0.8 power factor and 4800 volts is equipped with two direct-connected exciters and a closed ventilation system, and is of standard design. The condensing equipment and auxiliaries are identical with those used for the 4000-kw dc auxiliary turbine-generators in the power house.

MATERIAL SELECTIONS

At the time the Trenton Channel equipment was being designed in 1927, the austenitic 18 per cent chrome, 8 per cent nickel alloy was being offered as the ideal material for equipment operating at elevated temperatures. Various investigators in this country and abroad had established its high physical properties and resistance to creep at temperatures in the range from 1000 to 1100 F. The principal objections to its use were the high cost and difficulties of fabricating in either the cast or wrought form.

Inasmuch as this alloy possessed such desirable properties and was recommended by the builder of the superheater, it was selected for part of the radiant section of the superheater, the piping, and the valve and fittings. The superheater was fabricated with low-carbon steel tubing in the section where the steam temperature does not exceed 800 F while the remainder contained the so-called 18-8 tubing then known as Enduro S188 and now designated as Nirosta KA2. The typical analysis of this steel as given by the maker was C 0.16 (maximum), Cr 17-20, Ni 7-10, and Si 0.50 (minimum), all in per cent by weight. Subsequent analysis of a removed tube showed a carbon content

of 0.05 per cent, which places this material in the low-carbon or KA2S class.

This same material was selected for the high-temperature piping system because of its desirable properties and the fact that it could be obtained in a 5-in. pipe size. This 5 $\frac{1}{2}$ -in. O.D. $\frac{3}{8}$ -in. wall tubing was made by The Babcock & Wilcox Company to the same analysis as given above. Later determinations show a carbon variation from 0.06 to 0.09 per cent. The loose companion flanges, valve, and desuperheater castings were made from Rezistal 2C, a material similar to KA2 but having a maximum carbon content of 0.25 per cent and a silicon addition of 2.0 to 2.5 per cent. The bolted joints were made up with Seminole Hard, a chrome-tungsten-vanadium steel, heat-treated to give a yield point in the neighborhood of 200,000 lb per sq in. This alloy was selected as the result of creep tests conducted at the University of Michigan on a similar steel. The typical composition of this steel is given in Table 1. It possesses a resistance to creep of about 7000 lb per sq in. at 1000 F, based on an extension of one per cent per 100,000 hr, and is fairly stable at the operating temperature. Various other bolting steels have not proved as satisfactory. Numerous gasket materials have been used, the most successful being plain $\frac{1}{32}$ -in. sheet monel.

After the Trenton Channel equipment had been placed in service and before final decisions had been made regarding the

TABLE 1 PRINCIPAL PROPERTIES OF IMPORTANT ALLOYS USED IN TRENTON CHANNEL AND DELRAY INSTALLATIONS IN THE "AS RECEIVED" CONDITION

Alloy No.	Tensile strength, lb per sq in.	Yield point, lb per sq in.	Physical Properties		Remarks
			Elongation, % in 2 in.	Reduction of area, %	
1	85,000	25,000	40	40	Nirosta KA2
2	91,600	...	53 in 8 in.	59	KA2S
3	90,000	35,000	40	40	KA2B
4	68,000	...	4 in 1 $\frac{1}{8}$ in.	8	Rezistal 2C
5	137,000	118,000	25 in 1 in.	33	Used in turbine construction
6	78,000	45,000	25	40	$\frac{1}{2}$ % Mo
7	140,000	122,000	16	50	4-6% Cr-1% W
8	110,000	76,000	32	65	14% Cr
9	Hecla ATV1
10	67,000	40,000	31	45	Era 131
11	225,000	210,000	11	33	Seminole Hard

Alloy No.	Chemical Analyses							
	C	Cr	Ni	Mo	W	Mn	Si	P and S
1	{ 0.16 max.	17.0-20.0	8-10	0.50	0.25-0.75	0.025 max.
2	{ 0.06	17.6	9.2	0.53	0.57	0.02
3	{ 0.10-0.20	17.0-19.5	8.0-10.0	0.65	2.0-2.5	0.025
4	{ 0.23	17.5	9.0	1.8	0.03
5	{ 0.31	0.35	3.10	0.34	..	0.72	0.32	0.06
6	{ 0.25	0.50	..	0.75	0.36	0.035
7	{ 0.39	5.20	1.10	0.46	0.25	0.015
8	{ 0.25	14.28	0.28	0.52	0.34	0.015
9	{ 0.47	11.84	36.32	0.24	0.23	0.01
10	{ 0.17	0.24	..	0.84	..	0.71	0.24	..
11 ^a	{ 0.45-0.50	1.20-1.45	1.75-2.25	0.35	..	0.05

^a V—0.20 to 0.25.

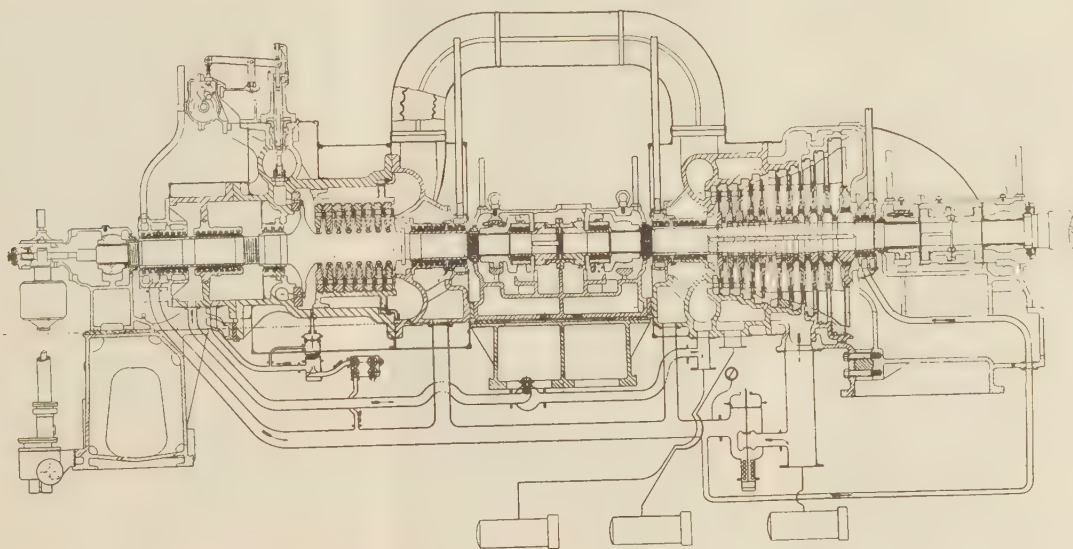


FIG. 2 CROSS-SECTION THROUGH 10,000-KW, 1000-F TURBINE AT DELRAY

materials for the Delray superheater and piping, reports were received from various sources, including steel makers in England and users in the oil industry, of failures that had been experienced with the 18-8 alloy. These failures had occurred in parts subjected to corrosive mediums and were due to intercrystalline corrosion which was believed to have been the result of precipitation of chromium carbides at the grain boundaries.

In view of these unfavorable reports, the performance of this material was carefully studied. A piece of the tubing from the Trenton Channel pipe line was removed and examined. Changes to the extent predicted were not found, as only slight carbide segregation and a 5 per cent loss in impact value at room temperature was in evidence. The physical properties after this period of service were so good that this alloy was used for the hotter sections of the Delray superheater and the piping between the superheater and the turbine. Care was taken to specify, where possible, the low-carbon KA2S material containing less

than 0.07 per cent carbon, in order to minimize any carbide formation.

The low-carbon KA2S alloy was used in making the 8 $\frac{5}{8}$ -in. O.D. $\frac{1}{2}$ -in. wall tubing and KA2B, which is KA2 plus 2-2.5 per cent Si, was used in the middle and lower portions of the superheater. This latter composition was recommended by the builder as being approximately ten times as resistant to sulphur corrosion from fuel oil as either KA2 or KA2S and was therefore given preference over the lower carbon alloy.

Several different classes of so-called low alloy steels were installed in both installations in an attempt to learn as much as possible regarding the behavior of various alloys under the action of the high-temperature steam and at the same time find materials other than the expensive austenitic group. Aside from the saving in material cost involved in using these cheaper alloys, they were more readily fabricated into sound castings and tubing. This was illustrated by the delay and expense involved in

the drawing and fabrication of the Delray superheater tubes and the pouring of the outlet fittings. It was impossible for the maker to draw and bend tubes long enough for the lower section of the superheater from the KA2B material. This section was finally completed by flash welding shorter tubes together. It was also necessary to recast the outlet fittings before sound ones were obtained.

Among these alloys that were placed in service were three castings made from 4-6 per cent Cr, 1 per cent W; one casting of 0.5 per cent Mo; a 5½-in. O.D. length of 4-6 per cent Cr, 1 per cent W tubing; a valve body of Era 131, an English alloy (see Table 1); and medium- and high-carbon calorized steel; together with the nickel-chromium-molybdenum steel adopted by the turbine builder for all parts of the turbine subjected to high-temperature steam.

The 4-6 per cent Cr, 1 per cent W alloy which was developed to withstand the high-temperature corrosive service in the oil industry offered possibilities due to its creep resistance of 1 per cent in 100,000 hr at a stress of 6000 lb per sq in., and its corrosion resistance properties. The 0.5 per cent Mo and Era 131 steels were recommended by English investigators as possessing good creep resistance properties. The nickel-chromium-molybdenum steel used for the turbine and throttle valve was selected as the result of investigations conducted by Thos. Firth and Sons, Ltd. at the request of The British Thomson-Houston Company, Ltd.

Typical analyses of all of the steels that have been discussed are given in Table 1.

Some idea of the creep resistance of these various materials can be gained from the values of stress required to produce a 1 per cent creep in 100,000 hr as given in Table 2.

TABLE 2 CREEP PROPERTIES

Part	Material	Temperature	Stress	Investigator
Tubing and castings	KA2	1000	15,000	Norton
Tubing	KA2S	1000	12,500	White and Clark
Tubing and castings	4-6 Cr, 1 W	1000	6,350	White and Clark
Casting	Era 131	1100	5,200	White and Clark
Bolts	Seminole Hard	1000	7,000	White and Clark
Casting	Ni, Cr, Mo	1000	5,900	White and Clark
	0.5 Mo	1000	7,200	White and Clark
	0.43 C	1100	1,500	Norton
Casting	0.42 C	1000	3,500	Norton
	0.20 C	1000	3,200	Norton

A few tubes of medium- and high-carbon calorized steel were installed in the Trenton Channel superheater to determine the degree of protection secured with aluminum coating. After the first installation of this material, tubes of 0.35 C steel, coated with aluminum, were installed in the middle section of the Delray superheater, together with a like number of tubes coated with 18-8 and 12-14 per cent Cr stainless steel applied with a Schoop metal spray gun.

Bolts used for the joints in the cooler sections of the Delray superheater interconnecting piping were made from SAE 3140, while the remainder of the joints were made up with 18-8 bolting. Seminole Hard material was used for the joints in the piping system and metal gaskets were used for all the unwelded joints. Flanges for the welded joints in the pipe line were SAE 3240, a low-chrome-nickel steel.

The selection of materials for the turbine was left entirely in the hands of the turbine builder. They, working with the Brown-Firth Laboratories, selected as the result of time-yield tests (7) the nickel-chromium-molybdenum alloy, the analysis of which is given in Table 1, for the turbine throttle valve, the high-pressure shaft packing casing, the inner and outer high-pressure cylinders, and the forged rotor. The time-yield test on this steel at 1000 F showed less than a 0.5 per cent extension during the first 24 hr. at a stress of 5600 lb per sq in., and no

further extension during the next 24 hr. A maximum design stress of 5000 lb per sq in. accordingly was used in the turbine design. The original interstage diaphragms were cast from the same material but due to the imperfect castings obtained, these were replaced with built-up diaphragms made from a 0.40 per cent carbon steel before operation with steam at 1000 F. The turbine nozzle partitions and wheel blading, with the exception of the first-stage buckets, were made from a 0.25 per cent C, 14 per cent Cr, stainless steel. Hecla ATV1 containing 0.47 per cent C, 11.8 per cent Cr, and 36.3 per cent Ni was used for the first-stage blading. All of the shaft packing was made from forged phosphor bronze except the three-ring section near the first stage wheel which was stainless steel. The interstage packing was later changed to a stainless steel at the time the original diaphragms were replaced. Nothing unusual in the way of materials was used in the low-pressure element.

With the exception of several parts, the careful attention that was given to the selection of the materials described, has resulted so far in trouble-free operation. The results of examinations which have been made and changes which were found necessary are discussed more in detail in the following sections of the paper.

METALLURGICAL EXAMINATIONS

Results of both physical and microscopic examinations made on various materials from the two installations have shown evidence of slight changes. In no case, however, have these changes, loss in strength, or tendency toward embrittlement, progressed to such an extent that any consideration has been given to replacement of parts. It is entirely possible that the changes which have been observed will progress at a much slower rate than has occurred during the initial period of operation.

Six different classes of alloy materials have been examined after varying lengths of service. These include wrought KA2 and KA2S and cast Rezistal; medium and high-carbon calorized steel; cast 4-6 per cent Cr, 1 per cent W; nitralloy; cast nickel-chromium-molybdenum used in the turbine; and Seminole Hard, together with several bolting materials.

Three different sections of 18-8 material have been removed from the Trenton Channel installation. The first of these was a section of the 18-8, 5½-in., ¾-in. wall tubing removed in 1930; the second was a similar piece removed in 1932; while the third section was a 2-in., ¼-in. wall superheater tube removed in May, 1933. These parts were in service at various steam temperatures as shown in Table 3.

TABLE 3 SERVICE PERIODS OF 18-8 ALLOY TUBING SAMPLES

Part No.	1	2	3
Date of removal	1930	1932	1933
Steam temperature	Hours in service		
Below 900 F	246	360	360
900 F	916	1,471	1,471
1000 F	1,732	3,254	4,068
1050 F	337	438	438
1100 F	3,177	10,012	15,159
Total	6,408	15,535	21,496

The physical properties of these specimens are given in Table 4. Included, also, are the properties of the material in the "as received" condition which, unfortunately, were not obtained from specimens cropped from the identical tubes tested, prior to final fabrication. They were taken, however, from identical sections and are considered representative of the material before service.

Microscopic examination of the samples show evidence of carbide segregation at the crystal boundaries. A typical photomicrograph of each sample is shown in Fig. 3. These give some idea of the extent to which this segregation has taken

place. Each successive sample has shown a widening of the grain boundaries, although in no sample thus far examined has there been evidence of inter-crystalline corrosion.

In an attempt to express quantitatively the extent to which the deterioration has taken place, the method used by Aborn

TABLE 4 PROPERTIES OF 18-8 ALLOY AFTER DIFFERENT SERVICE PERIODS

Specimens	Physical Properties			
	1	2	3	4 ^c
Tensile strength, lb per sq in.	95,100 ^a	91,600 ^a	113,000 ^b	91,600 ^a
Elongation, per cent	35	37	38.5	53
Reduction of area, per cent	36	54	57	59
Hardness, Brinell No.	148	152	202	143
Reduction in Izod impact value, per cent:				
At room temperature	5	17.5	68	0
At 1000 F.	19	11	12	0
Chemical Analyses				
C	0.06-0.07	0.09	0.05	0.05
Cr		17.4	17.4	
Ni		8.6	8.2	

^a 21-in. pipe coupons, 8-in. gage length.

^b 1/4-in. A.S.T.M. standard tensile specimen, 43/64-in. gage length.

^c "As received" condition.

and Rutherford was followed (8). This method consists of measuring the change in electrical conductivity caused by boiling

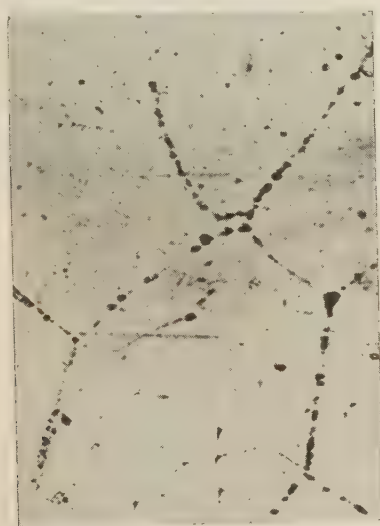
have not been of sufficient magnitude to cause any concern. It is improbable that failure, should it occur, will ever take place without warning, as evidenced by the good corrosion resistant properties exhibited by the third sample. Development of special 18-8 alloys (9) to inhibit chromium-carbide segregation should make this material even more suitable for high-temperature steam use.

Examination of an unused flange, a valve body, and a desuperheater, all made from cast Rezistal, showed that these castings contained inclusions and blow holes. The valve was removed after 6899 hr of service, for 5937 of which the tempera-

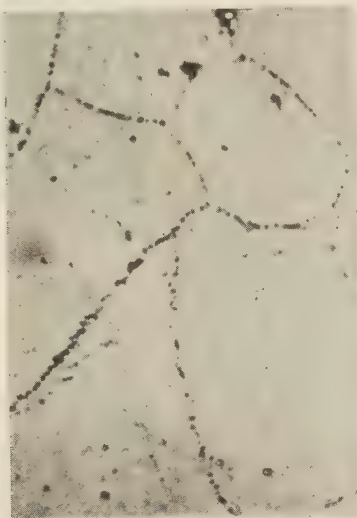
TABLE 5 PHYSICAL PROPERTIES OF REZISTAL 2C CASTINGS

	Valve	Desuperheater	Flange
Tensile strength, lb per sq in.	67,400	21,800	68,300
Elongation, per cent in 1 3/8 in.	7	0	4
Reduction of area, per cent	3	0	8
Izod impact value, ft-lb	27	7	11
Chromium, per cent by weight	18.7	15.9	17.5
Nickel	10.8	7.2	9.0
Silicon	1.2	1.25	1.6
Carbon	0.22	0.23	0.23

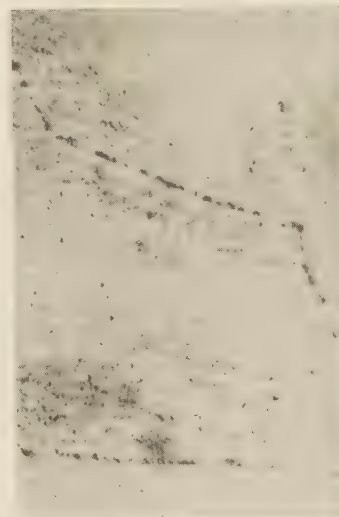
tures were between 1000 and 1100 F. The desuperheater was removed after 6408 hr of operation, for 5246 of which the temperature was above 1000 F, because of cracks caused by a



SPECIMEN 1
Removed in 1930, after 6408 hr service.
Murakami's etch $\times 1800$



SPECIMEN 2
Removed in 1932, after 15,535 hr service.
Murakami's etch $\times 1800$



SPECIMEN 3
Removed in 1933, after 21,496 hr service.
Murakami's etch $\times 1800$

FIG. 3 PHOTOMICROGRAPHS SHOWING CHROMIUM CARBIDE PRECIPITATION AT THE GRAIN BOUNDARIES OF 18-8

the specimen in a modified Strauss solution. Materials which are subject to inter-crystalline corrosion show a great increase in conductivity after being heated in the solution. The tubing samples were boiled for 48 hr, after which the first showed a 60 per cent increase in conductivity, the second showed a 260 per cent increase, while the third sample and the material in the "as received" condition showed no change. It is probable that the corrosion-resistant properties have been restored in accordance with test data presented by Bain, Aborn, and Rutherford (9). This rather favorable result, as compared with troubles encountered elsewhere, is due, no doubt, to the absence of an actively corrosive fluid and partly to the fact that the operating temperature is slightly below the range in which carbide segregation is most pronounced (1200 to 1300 F).

The physical properties would indicate that the material is slowly becoming embrittled as evidenced by the increase in hardness and drop in impact value. These changes, however,

combination of thermal stresses and the poor metal. No comparison or conclusions regarding the suitability of this alloy can be made due to the evident unsatisfactory condition of these parts as received. The physical properties and chemical analyses are given in Table 5.

Of the two installations of calorized carbon steel, the first at Trenton Channel has been cut up and examined. The second, which consists of five tube elements in the intermediate section of the Delray superheater has not been removed for examination.

The Trenton Channel material, consisting of surface-treated 0.13 C tubing, 0.25 C castings, and 0.40 C forged headers, comprised a small superheating unit connected in series at the outlet of the original unit. The heating surface was composed of eight elements extended into the combustion chamber and directly exposed to flame impingement at their lower ends. This unit was removed after 3821 hr of service, for 3305 of which the temperature was above 1000 F, due to the excessive growth of

the forged return bends at the lower ends of the furnace tubes. These tubes were subjected to surface temperatures as high as 1600 F and to combined stresses, due to internal pressure and heat flow, as high as 3000 lb per sq in. Approximately 10 per cent of the calorized coating on the furnace tubes had disappeared and the remaining 90 per cent was quite brittle. The inside of the tubes was coated with magnetic oxide 0.04 to 0.08 in. in thickness, and measurements showed creep rates as high as 2 per cent per 1000 hr. The tubing and headers outside the setting were in good condition; measurements indicated no growth; the coating was apparently in a similar condition as when installed; there was little evidence of magnetic oxide formation; and, the physical properties had changed only slightly.

The surface of the calorized and sprayed Delray tubes is apparently in good condition except in several spots where a coarse granular appearance indicates a brittle condition. The tubes now have become coated with a $\frac{1}{16}$ -in. layer of slag which protects the coating from attack. The development now being made to produce a more ductile aluminum coating and its application to low alloys possessing good creep properties offers possibilities for the adoption of this class of material for high-temperature equipment.

Information regarding 4-6 per cent Cr, 1 per cent W material received from several sources was to the effect that this steel had a tendency to embrittle when subjected to prolonged heating at temperatures ranging from 1000 to 1100 F. Inasmuch as several parts made from this alloy were in service at Delray and Trenton Channel, a valve of this composition was removed from the outlet of the Trenton Channel superheater for examination. The valve was of 600-lb American Standard construction and had been in service for a total of 12,995 hr, for 10,818 of which the temperature was 1100 F.

The test results showed that apparently the material in the valve body did not undergo embrittlement and that the long service at the high temperatures tended to increase the toughness and ductility. This statement cannot be made more definite as none of the valve material, before being subjected to service, was available. Comparison was made between supposedly similar samples supplied by the same vendor. Little reliance can be placed on the results of the tensile tests from the valve body, shown in Table 6, due to the presence of inclusions throughout the casting which made it impossible to obtain a sound test specimen.

TABLE 6 PHYSICAL PROPERTIES OF 4-6 PER CENT Cr, 1 PER CENT W VALVE BODY

	Material in "as received" condition	Material from valve body
Tensile strength, lb per sq in.	139,800	94,200 ^a
Yield point, lb per sq in.	121,700	45,900
Elongation in 2 in., per cent	16	7
Reduction of area, per cent	50	18
Izod impact value, ft-lb	7	6
Room temperature	24	36
1000 F	278	200
Hardness, Brinell No.		

^a Contained small flaw, 5 per cent of cross-section.

The increased impact strength at 1000 F, the decreased hardness, and reduced tensile strength of the valve material tend, however, to indicate an increase in toughness and ductility. The apparent change from martensitic to sorbitic microstructure is in agreement with the changes in physical properties. The valve material contained a somewhat greater amount of chromium and tungsten carbides than the material in the "as received" condition. In no sections of the valve casting examined were grain boundaries outlined with carbides. This fact, together with the impact values obtained, indicates that noticeable

embrittlement did not occur. The condition of the metal and the original low impact value, however, were considered unsatisfactory.

Experience with nitralloy would indicate that it is unsuitable for high-temperature valve trim. Continued service has resulted in scale formation and pitting of the surface of the trim of two valves installed in the Trenton Channel line. The trim in the first valve, removed after 6408 hr of service, for 5246 of which the temperature was above 1000 F, had a non-uniform case covered with a thin scale and had a maximum Vickers Brinell No. of 700. Examination of the nitralloy rings from the chromium-tungsten valve showed a condition of which Fig. 4 is typical. A coating of scale approximately 0.010 in. in thickness

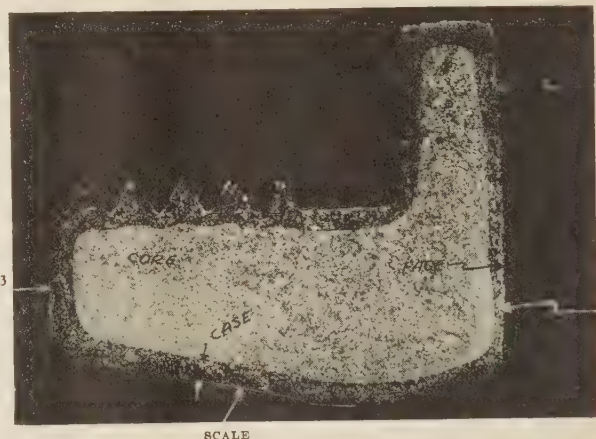


FIG. 4 MACROGRAPH OF NITRIDED SEAT RING AFTER 12,995 HR SERVICE

Designation	Depth of case, in.	Vickers Brinell hardness No.
1	0.012	470
2	0.028	560
3	0.036	550
Core	...	200

Etchant: 3 per cent nital—Magnification: 5×

covered the contact faces of the rings. This does not show in the illustration. The surface hardness values had dropped from 1000 Vickers Brinell No. to those shown under Fig. 4. These rings were fabricated in 1930 and had received a 24-hr treatment, six hours at 1000 F and the balance at 970 F. This material is supposedly stainless at steam temperatures in the 700 F region, but examination of these samples would indicate that it cannot withstand the attack of dissociated steam at the higher temperatures.

Results presented by Bailey and Roberts in a paper (10) before the Institution of Mechanical Engineers on the embrittling effect undergone by some nickel-molybdenum steels when subjected to stress at high temperatures, led to an investigation of the material used in the high-temperature section of the turbine. This material definitely fell within the range of nickel and molybdenum content which Bailey stated was susceptible to embrittlement. Material for the investigation was taken from the original ninth-stage cast diaphragm. This piece had been in service for 656 hr at temperatures not exceeding 250 F and, therefore, was considered representative of the nickel-chromium-molybdenum turbine parts before service.

The result of tests conducted similar to those by Bailey, except at 1000 F, indicated that the turbine material is not subject to the sort of embrittlement that he encountered on wrought steels of nearly the same composition, stressed as high as 20,000 lb per sq in. at 842 F. The results of the impact values obtained on the notched $\frac{1}{2}$ -in. round specimens in an Izod machine

are given in Table 7. All of the samples showed an increase in impact value rather than a decrease.

TABLE 7 RESULTS OF EMBRITTLING TREATMENT ON CAST Ni-Cr-Mo TURBINE MATERIAL

Embrittling treatment	Impact value at room temperature, ft-lb	Change in impact value resulting from treatment, per cent	Impact value at 1000 F, ft-lb
1 None	53	0	34
2 Heated at 1000 F for 200 hr	59	+11	34
3 Heated at 1000 F for 200 hr at 12,000 lb per sq in. notched prior to treatment	56	+6	41
4 Same as 3, except notched after treatment	60	+13	40

Small specimens suitable for hardness readings and microscopic examination were removed from the turbine throttle valve after 3809 hr of service, for 1450 of which the temperature was 1000 F, and compared with the diaphragm material. The little difference found was not pronounced and may have been caused by difference in the heat treatment of the original castings.

Various bolting materials have been tried with different degrees of success. The material which has given the best results is a properly heat treated A.S.S.T. No. 5 chisel steel, having the composition given for steel No. 1 in Table 8. This alloy

TABLE 8 CHEMICAL ANALYSES OF BOLTING MATERIAL

Steel No.	Trade name	C	Cr	Ni	W	Mn	Si	Mo	V	P and S max.
1	Seminole Hard	0.45-0.50	1.25	..	2.0	0.25	0.05
2	Rezilast, 2C	0.05	19.5	9.9	..	0.70	2.3	0.01
3	Supertemp	0.36	0.52	..	0.94	0.90	0.03
4	1722	0.45	1.40	..	0.77	0.50	0.71	..	0.28	..
5	D-1	0.08	1.17	..	0.97	0.25	0.28
6	SAE 3140	0.35-0.45	0.45-0.75	1.0-1.5	..	0.5-0.8	0.05
7	Vibrac	0.48	1.28	2.59	..	0.62	0.15	0.59	..	0.02

possesses good creep resistance properties and a high tensile value at room temperature. Bolts made from this steel are given an oil quench from 1650 F and drawn at about 1100 F to give a Brinell hardness No. of from 400 to 440. Threads are cut after heat treatment to prevent the formation of cooling cracks at the thread roots. Trouble experienced with quenching cracks has been eliminated by removing the decarbonized mill surface, prior to heat treatment. This steel is not entirely stable after prolonged service as is evidenced by a drop in impact value, hardness, and tensile strength. The results of examination of four bolts, two of which were removed after 6408 hr of service, for 4278 of which the temperature was between 1000 and 1100 F, and two of which were removed after 10,575 hr, for 7832 of which the temperature was 1000 F, are shown in Table 9. Less joint maintenance has been experienced with this bolting due to its high elastic and plastic properties, notwithstanding its change in properties after service.

Steel No. 2, although possessing good resistance to creep, was found to be subject to severe embrittlement and did not possess sufficient elastic strength to withstand the thermal stresses encountered in the warming and cooling of a steam line. One set of bolts made from Steel No. 3 required tightening once during 10,893 hr of service and showed a drop in impact value of approximately 50 per cent. Steels 4, 5, and 6, in the condition used, have required frequent tightening to compensate for creep. Bolts made from steel No. 7 were supplied with the turbine. Their behavior has been satisfactory except in the throttle valve bonnet joint where the stresses were too high. It is believed that with the new valve now installed this condition has been corrected.

PIPE-JOINT EXPERIENCE

Troubles encountered with bolted pipe joints have been many

and varied. In the authors' opinion, it is doubtful whether, with present materials, bolted joints can be designed to give the same trouble-free operation at temperatures of 1000 to 1100 F that has been experienced with present designs at 700 to 750 F. From experience gained, however, with the original joints at Trenton Channel, it has been possible to construct two joints that have now been in service for over 16,000 hr at steam temperatures above 1000 F without attention. Full-strength welded joints appear to be the answer to the high-temperature jointing problem, although there is much to be learned regarding the behavior of weld metal under stress at high temperature and the weldability of desirable high-temperature alloys.

It was rather fortunate, in one respect, that the original joints at Trenton Channel were not made heavier than the 600-lb American Standard as troubles were soon encountered which led to improvements in design. Some of the difficulties probably would not have been anticipated in the turbine installation at Delray had these joints been made more substantial. This original design led to the use of various joints which fall roughly into five classes.

Two types of stress, aside from stress due to internal pressure and bending moment imposed by change in position of a line, appear to cause most of the difficulty in high-temperature bolted joints. These are thermal stress caused by the temperature differential between the inside and outside of the joint and differences in coefficient of expansion of the joint materials, and creep stress caused by the plastic condition. In order to eliminate the thermal stresses, so-called temperature compensated joints were tried. These consisted of joints using 18-8 bolts and having spacers between the flange and nut of a material similar to Invar. The bolt and spacer lengths were so selected that any tendency to pick up or lose load was compensated for by the difference in coefficient of expansion. These joints failed due to the rather high stresses selected and failure to consider the plastic phase at the operating temperature.

TABLE 9 PHYSICAL PROPERTIES OF SEMINOLE HARD BOLTING MATERIAL

	Group in service 6408 hr (4278 hr at 1000 to 1100 F)		Group in service 10,575 hr (7832 hr at 1000 F)	
	Before	After	Before	After
Tensile strength, lb per sq in.	214,000	213,000	225,000	163,000
Yield point, lb per sq in.	204,000	202,000	210,000
Elongation in 2 in., per cent	11	12	11	14.4
Reduction in area, per cent	36	37.5	33	42.5
Hardness, Brinell No.	457	400	462	338
Izod impact value, ft-lb	12.5	8.5

The second class of joints used were similar to the original joints with materially increased flange and bolt dimensions. Two 5-in. joints in the Trenton Channel line, made up with the bolt stress limited to 10,000 lb per sq in., have been in service over 16,000 hr. These are Van Stone type with serrated facing, KA2 flanges, steel No. 1 bolting material, and $1/32$ -in. plain monel gaskets. The 900-lb flanges in one joint were increased to $3/8$ -in. while the 1350-lb flanges in the second joint were made $4/8$ -in. in thickness. All the bolted joints in the Delray line, with the exception of those on either side of the superheater outlet valve, were made to either the 900- or the 1350-lb American Standard. Leaks which occurred in two 8-in., 1350-lb joints after 6795 hr of service were due to plastic deformation of the gasket faces rather than to dishing of the flanges or creep of the bolts.

Full-strength mechanically reinforced welded joints are in service in both installations. The mechanical reinforcement, consisting of collars over three Trenton Channel joints and backing up flanges on the Delray joints was added to prevent

pulling apart should the 18-8 weld metal ever disintegrate due to inter-crystalline corrosion at the fusion zone. Additional time is needed to determine definitely whether such precaution is or is not necessary in 18-8 welds. It would appear from examination of the fusion zone of welding on the 18-8 tube removed from the Trenton Channel superheater, that the region affected by welding does not undergo any more rapid change than the parent metal, at least, when under no stress. This particular welding was used to fasten lugs to hold the tube protecting tiles. These joints have given no trouble.

Another class of joint in service, embracing the Sargol and Sarlun, is seal-welded. The original Trenton Channel joints were provided with Sarlun-welding lips, two of which were welded after trouble was experienced maintaining a tight-gasketed joint. During 17,236 hr of service it has been necessary twice to repair cracks which developed in each joint as a result of bolt elongation. The modified Sargol-type joints, used in the interconnecting and outlet piping of the Delray superheater, where the steam temperature varies from 850 to 1000 F, have given no trouble.

The high stresses encountered in the Trenton Channel joints and a desire to obtain satisfactory joints for the 600-lb flanges of the valve at the superheater outlet led to the design of the hairpin-type spring joint. The first of these joints installed at Trenton Channel consisted of springs, of hairpin shape, placed between the flange and one nut on each bolt. The springs were designed to maintain a unit gasket pressure of ten times the steam service pressure during the warming and cooling of the joint by compensating for the unequal expansion between flanges and bolts. The bolts were stressed to approximately 10,000 lb per sq in. and the outer end of the spring was stressed to about 17,000 lb per sq in. The joint was remade after 1532 hr service and has since remained tight for nearly 15,000 hr. The temperature at the highly stressed outer portion of the spring does not exceed 600 F with 1100 F steam in the line. The two Delray joints which were designed with a maximum spring stress of 62,000 lb per sq in. leak when being placed in service due to water accumulation. They tighten up, however, when this water is evaporated. This design is not recommended because of the spring weight and cost. Its use was desirable in our case to prevent over stressing the valve flanges which were ordered to the 600-lb American Standard before sufficient experience was obtained at Trenton Channel with this standard.

CREEP

Troubles due to growth or creep of parts, with the exception of the difficulties encountered with the 600-lb pipe joints, have been confined almost wholly to the turbine throttle valve. Excessive growth of the lower ends of the calorized superheater tubes at Trenton Channel caused their removal before failure occurred. Creep of other parts has been measured but in no case where changes have been observed is the creep occurring at an alarming rate.

The throttle-valve trouble has been caused by dishing of the bonnet-joint flanges, with the result that it has been impossible to maintain a tight joint. The body itself also has exhibited changes amounting to creep rates as high as 3.5 per cent per 100,000 hr based on measurements made during the last 6083 hr of operation. This growth caused slight binding of the main disk on one occasion.

Measurements of parts of the turbine, other than initial readings, have not been obtained except in the case of the valve chest where a special measuring device was provided by the makers to determine the overall change in length. The changes measured have been insignificant. The last reading obtained at this location showed a slight decrease which would indicate

warping. It is probable that excessive changes have not occurred in the turbine. The running characteristics have not changed and leaks have not been experienced at any of the bolted joints on the high-pressure cylinder.

The periodic measurements that have been made of the tubes in the Delray superheater are of rather doubtful value. Two types of readings are being taken from stainless-steel measuring points; diameters with micrometers and length measurements with a special 20-in. micrometer trammel. The close grouping of the tubes has made it impossible to obtain diameters other than at the top of the middle section where tube temperatures are in the neighborhood of 900 to 925 F. Where the length readings were taken, sag of the tubes caused by the resistance offered to expansion by the cast walls of the setting caused erratic measurements of no value as far as creep information is concerned. Changes in diameter of three of the 0.30 to 0.40 C, 2 $\frac{1}{2}$ -in. O.D., $\frac{7}{16}$ -in. wall, steel tubes and three KA2B, 2-in. O.D., 0.203-in. wall, alloy tubes observed during the last measuring period of 5005 hr indicates that the steel tubes are growing at an average creep rate of 4.4 per cent per 100,000 hr while the alloy tubes are growing at a corresponding rate of 5.3 per cent. The calculated design stress for the steel tubes was 2000 lb per sq in. and for the alloy tubes, 4300 lb per sq in. Measurements of the headers and fittings in the alloy sections have not been made since the equipment was placed in operation.

Changes of importance have not been observed at the point of maximum design stress of 6200 lb per sq in. in the 8-in. Delray pipe line or in any of the fittings in this system. Measurement of a section of 5 $\frac{1}{2}$ -in. O.D. chrome-tungsten tubing in the Trenton Channel line showed no change after 7465 service hours. The measurements made on the original 18-8 Trenton Channel piping have not been of sufficient accuracy to indicate the small changes that have probably occurred under the low design stress of 3200 lb per sq in. Dishing of the bonnet flanges of the 600-lb chrome-tungsten valve, removed from the Trenton Channel piping system after 12,995 hr, amounted to approximately 0.014 in. on the body flange and 0.011 in. on the bonnet flange. The contact faces of the main body flanges dished 0.004 in. on one end and 0.007 in. on the other.

It has been found in certain instances where diametrical measurements have been taken that it is desirable to take more than one dimension in the same plane. Part of the change which occurs may be due to relief of internal stresses not removed during fabrication causing the part to distort or to assume an out-of-roundness in no way connected with creep. This fact should be kept in mind as well in the measurement of parts subject to bending stresses since changes may occur in the plane of the bending moment which are not shown because of improper location of the measuring points. Welded stainless-steel measuring points, have been used for all measurements to prevent scale formation from influencing the accuracy of subsequent readings.

Observations have indicated that higher design stresses could have been selected for certain parts of both installations. The original design was based on a combined stress which would keep the creep rate of the order of one per cent in 100,000 hr. This was probably too conservative as in certain parts of the installation, such as piping, creep tends to relieve high bending stresses, thereby dropping the combined working stresses. The so-called elastic stresses cannot, however, be entirely disregarded as it is necessary during start-up periods to consider the magnitude of forces set up at anchor points and at flanges.

OPERATING EXPERIENCE

No unusual precautions have been found necessary in the operation of either the Trenton Channel or Delray installations. The turbine has received more than ordinary attention due pri-

marily to the experimental nature of the unit rather than from any hazard connected with the use of steam at 1000 F. Major troubles have not occurred with either the turbine or the superheater. Experience with the Trenton Channel superheater and piping system has had to do more with pipe joint troubles already mentioned in some detail. The following remarks regarding operation, therefore, are confined to the Delray apparatus.

Operating a turbine with steam at 1000 F is little different from operating with lower superheat. The present starting cycle used in placing the installation in operation consists in starting with steam at 700 to 750 F and applying 30 per cent load to the turbine before the temperature is increased. The same procedure, in the reverse order, is followed in taking the unit out of service. It is believed that the use of higher-temperature steam would tend to complicate the starting cycle because of large temperature differences which would exist in the turbine. It is the authors' opinion that units which in the future may be built for operation at 1000 F should be provided with either a low-temperature source of starting steam or a desuperheater in the turbine lead to prevent the occurrence of severe high thermal stresses during the starting period.

A clearance indicator mounted at the front end of the high-pressure cylinder showing the movement of the rotor relative to the casing has been used as a guide in determining a safe rate for changing load or steam temperature. The forged rotor, a smaller metal mass than the casing and in more intimate contact with the steam, is more responsive to temperature changes. Its movement is watched, therefore, to prevent going below a safe minimum axial clearance of 0.010 to 0.015 in. on the leading edge of the fifth wheel. No maximum rates of load or temperature change have been determined, but load has been applied at the rate of 1000 kw per min from 30 per cent to full load without producing vibration or a clearance change exceeding 0.045 in. Normally load is changed at a rate of 1000 kw per 3 to 4 min and temperature is changed at a rate of 100 F per hr. This last rate is an arbitrary one and might be exceeded without difficulty. Attention should be given to this detail of running clearance in any turbine designed to operate at high temperature or under rapidly fluctuating load conditions.

During the initial period of operation the steam temperature was increased in increments of 25 to 50 F above 900 F, allowing the unit to operate approximately one week at each temperature until 1000 F was reached. During this period of operation growth of the throttle-valve packing sleeve occurred causing the stem to bind. The original semi-steel bushing was replaced with one having a nitrided surface and no trouble has since been encountered. Similar bushings in the five control valves also were renewed with nitrided parts as a precaution.

Recurring leakage of the throttle-valve bonnet joint led to the installation of a new and heavier valve casting.

Upon examination of the high-pressure cylinder interstage packing after 3809 hr service, evidence was found of more than normal wear, presumably caused by the binding of the packing segments against the retaining pin which resulted in rubbing during starting. The outer high-pressure shaft packing which had been examined on previous occasions indicated a similar condition. Recent examination of the outer packing after being refitted and subjected to 7422 hr additional service still shows wear, but not to the extent previously found. All of the packing is of the saw-tooth type made in rings of four segments each. The rings are loosely fitted into tee-slots and held in proper relation to the shaft by flat leaf springs which allow the packing segments to move outward in case of shaft deflection.

Maintenance figures for the turbine are not in line with other turbines operating at lower temperatures because of the experi-

mental nature of the unit. It has been inspected at frequent intervals and has received more attention in general than normally would be thought necessary. With the exception of the throttle valve and bushing replacements, no maintenance costs of an extraordinary nature chargeable to the high-temperature steam have been incurred.

Expense contingent to the maintenance of the superheater has been principally for replacing the small tube-protecting tiles in the lower radiant section. The excellent results obtained with these tiles cemented to the straight tubes in the Trenton Channel unit led to their use for protection of the curved radiant tubes in the Delray superheater. Trouble developed at the start in maintaining these tiles in place because of insufficient clearance between the ends of the blocks and relative movement between adjacent tubes which tended to push them out of place. Insistence on the part of the manufacturer that operation should not be continued at outlet steam temperatures above 900 F when any radiant tubes were unprotected led to a change in the method of insulating the back of the tubes. Tie bars, holding the tubes in groups of twelve, were added to reduce the relative movement of adjacent tubes and the tile shape was altered slightly to provide greater clearance between tiles. These changes have materially improved the service continuity of the refractory lining. At the present time, should a tile drop out of place during operation, the temperature is not lowered and the tube is allowed to remain bare until the next shut-down.

TABLE 10 SERVICE RECORD OF THE TRENTON CHANNEL AND DELRAY INSTALLATIONS

Service Hours—Trenton Channel Installation					
Mar. 4, 1929, to Sept. 1, 1933					
Steam temperature					Hours
Below 900 F					360
900 F					1,471
1000 F					4,420
1050 F					438
1100 F					16,311
Total hours in service					23,000
Load Duration—Delray Installation					
Oct. 1, 1930, to Sept. 1, 1933					
Load, per cent	Hours in service				
	700 F	800 F	850 F	900 F	950 F 1000 F
20	40	6	2	3	3
40	191	123	28	106	41 3,545
60	327	170	60	438	377 1,959
80	404	139	480	211	85 582
100	62	38	19	37	12 1,743
Hours in service at 1000 F—7,832					
Total hours in service—11,231					

Water collecting in the U-shaped tubes forming the furnace bottom has complicated the starting process somewhat. The procedure is to admit no steam to the superheater until after the fire has been started and temperatures of about 300 F are indicated on the tube thermocouples located at the bottom of three arbitrarily selected tubes. The power-operated relief valve at the outlet is then opened to provide a sufficient circulation of steam to carry out any remaining water. Conditions are then satisfactory for admitting steam to the turbine for starting.

Up to September, 1933, the Trenton Channel installation has been operated for a total of 23,000 hr and the Delray equipment has been operated for 11,231 hr. The hours of operation at various temperatures are shown in detail in Table 10.

CONCLUDING COMMENT

In summing up the experience recorded to date with the two high-temperature installations, the information that has been gained on various types of construction and the results of metallurgical examinations would indicate that the use of steam equipment at temperatures as high as 1000 F is entirely feasible. It is safe to say that a plant could now be built to operate on steam at 1000 F and that reliable service could be expected.

Although the authors may have appeared to stress the shortcomings and difficulties, it is not their intention to convey the idea that these are of a serious nature or in excess of the general run of troubles to be expected with any equipment of an entirely new and untried design.

It is not the purpose of this paper to present the economics of such a choice of steam conditions. In the authors' opinion it is doubtful whether such a selection could be justified if high-temperature resisting materials now available were used. Further metallurgical research may produce such materials at a much lower cost which will in the future give economic justification to the use of steam at 1000 F.

BIBLIOGRAPHY

Numbers in parenthesis in the text refer to the following:

- 1 J. W. Parker, "1000-Degree Turbine for Delray No. 3," *Power*, May 28, 1929.
- 2 J. H. Walker, "Piping for 1000-Degree Steam," *Heating, Piping, and Air Conditioning*, April, 1931.
- 3 R. M. Van Duzer, Jr., "Steam at 1000 Degrees Fahrenheit," *Electrical Times*, June 18, 1931.
- 4 A. S. McCutchan, "Designing High-Temperature Piping," *Heating, Piping, and Air Conditioning*, October, 1931, and November, 1931.
- 5 P. W. Thompson, "High-Temperature Experiment Making Progress," *Electrical World*, October 24, 1931.
- 6 R. M. Van Duzer, Jr., "Detroit Edison Has Completed Its High-Temperature Installation," *Power*, October 27, 1931.
- 7 Dr. W. H. Hatfield, "Permanence of Dimensions Under Stress at Elevated Temperatures," *The Engineer*, October 10, 1930.
- 8 J. J. B. Rutherford and R. H. Aborn, "Quantitative Method for Estimation of Intercrystalline Corrosion in Austenitic Stainless Steels," *Trans. A.I.M.E. (Iron and Steel Division)*, February, 1932, pp. 293-301.
- 9 E. C. Bain, R. H. Aborn, and J. J. B. Rutherford, "The Nature and Prevention of Intergranular Corrosion in Austenitic Stainless Steels," *Trans. of A.S.S.T.*, vol. 21, no. 6, June, 1933, pp. 481-509.
- 10 R. W. Bailey and A. M. Roberts, "Testing of Materials for Service in High-Temperature Steam Plants," *Proceedings of Inst. of Mech. Engrs.*, vol. 122, 1932, pp. 209-284.

Discussion⁴

ROGER STUART BROWN.⁵ Time, I am sure, will show that this forward step by the engineers and management of the Detroit Edison Company in building a steam plant for 200 degrees higher temperatures than heretofore in use is a milestone of progress. It required a great deal more courage to launch this project in 1929 and 1931 than it would at present, because in the last two years there has been more development and investigation of high-temperature metals and their properties than in the last 2000 years. Messrs. Thompson and Van Duzer deserve specific credit for the clear and fair way they have recorded the specifications and the results of service of the various materials. Inasmuch as they point out that the commercial success depends upon the availability of less expensive materials than those now in service, it may be of interest to outline the development of one of the less expensive materials tried.

Calorized steel has been mentioned as tried out in a small way at both Trenton Channel and Delray. Calorizing is a process of alloying the surface of steel with aluminum. When exposed to an oxidizing atmosphere the aluminum oxide formed on the surface makes a gas tight film protecting the underlying steel from scaling. Due to dissociation of the steam with evolution of nascent oxygen at high temperatures this prevention of oxidation has been found to be as necessary inside the tube as

outside. Unfortunately up to the time of these installations it was found impossible to make this surface alloy anything but brittle. A start had been made in this direction at the time of the Delray installation. When applied to a tube subject to high enough internal pressure to cause creep at high temperatures the older calorizing surface alloy was cracked when the tube expanded by creep. This was particularly evident in the Trenton installation because contrary to our desires it was necessary to have the calorized tubing in an exposed radiant position, causing very much higher temperatures than the mild steel could

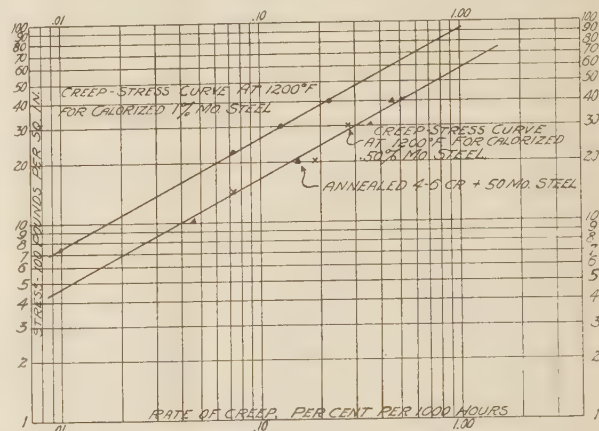


FIG. 5 RATE OF CREEP—STRESS CURVES AT 1200 F
[Calorized 1.0 and 0.50 per cent molybdenum steels and annealed 4-6 Cr + 0.50 Mo steel.]

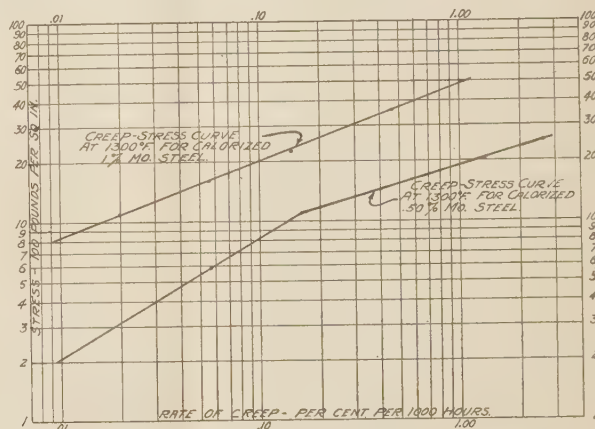


FIG. 6 RATE OF CREEP—STRESS CURVES AT 1300 F
(Calorized 1.0 and 0.50 per cent molybdenum steels.)

carry without excessive creep. In the later Delray installation the reduced tube wall temperature, because of the convection bank position, has caused much less creep and the calorizing that year was a little more ductile with the result that the surface is well preserved.

At the present time, however, the difficulty has been remedied from two angles. The introduction of 0.50 or 1.00 per cent molybdenum carbon steel has made possible startling reduction in creep for a given stress. For instance, Dr. Clark of the University of Michigan reports in a private communication that mild steel stressed to 2000 lb per sq in. at 1300 F will creep 5 per cent in the first 120 hr and thereafter at about 98 per cent per 1000 hr. Under the same load and temperature a 1 per cent molybdenum carbon steel after the first initial creep in 72 hours settles

⁴See also "The Thermal Performance of the Detroit Turbine Using Steam at 1000 F," by Carter and Ellenwood, *A.S.M.E. Trans.*, 1934, FSP-56-8, discussion by F. H. Rosencrans.

⁵Sales Engineer, The Calorizing Company, Pittsburgh, Pa. Assoc-Mem. A.S.M.E.

down to a straight line creep at the rate of 0.1 per cent per 1000 hr equivalent to 5 per cent in 50,000 hr compared to 5 per cent in 120 hr for mild steel. The same creep 0.1 per cent per 1000 hr under 2000 lb per sq in. is obtained on 0.50 per cent molybdenum steel at 1200 F. Yet the calorized 0.50 per cent molybdenum is only about 3 times the cost of plain mild steel. The 1 per cent molybdenum steel calorized will be about 3.5 times the cost of plain mild steel. This is about $\frac{1}{2}$ the price of the chrome-nickel stainless steel largely used in the Detroit installations. The above price ratios are based on calorizing straight 30-ft lengths. It is not so favorable when calorizing "loops."

For about 18 months there has been in production a calorizing treatment called "heavy duty," producing a tough adherent alloy up to 0.030 in. thick on heavy wall tubes. This will not chip and when hot will stretch as far as any bulge a prudent operator would continue to allow in operation. This is in use in over 30 vapor-phase oil-cracking units delivering 1080-F vapor, and in others with oil at 700 to 1000 lb per sq in. and 1050 F.

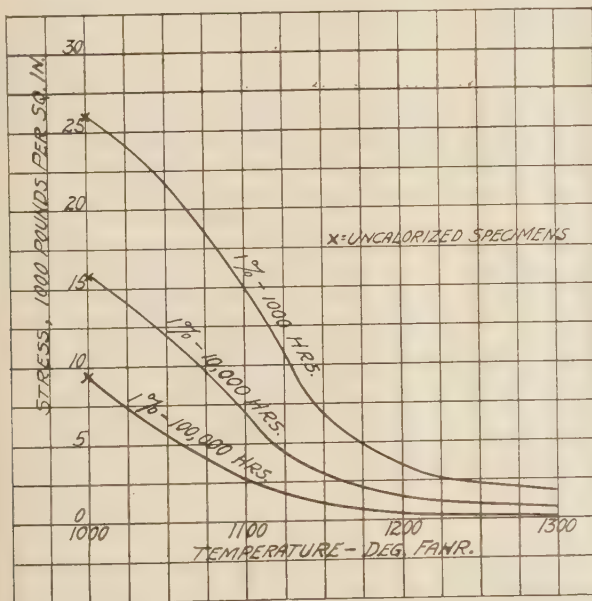


FIG. 7 CREEP CHARACTERISTICS OF CALORIZED 0.50 PER CENT MOLYBDENUM STEEL (1000 to 1300 F, incl.)

It has been used successfully also in radiant reheaters for steam at 850 F. The latest and largest cracking still in the world, with 32,000 barrels throughput daily, is provided at its hottest points with tubes $5\frac{1}{2}$ -in. O.D. \times $\frac{3}{4}$ -in. wall \times 42 ft long of heavy-duty calorized 0.50 per cent molybdenum-carbon steel. This single furnace just referred to is built for a release of approximately 340,000,000 Btu per hr.

Heavy-duty calorizing has approximately the oxidation resistance of 18-8 KA2 and superior resistance to hydrogen sulphide at 1200 F. It has in addition a property which should be investigated further, namely, erosion resistance. So far this has only been tested against mechanical erosion of turbo- and cutting-head tube-cleaners, which may be passed through a heavy-duty calorized tube 100 times at only 3 feet per minute with only a few thousandths of an inch wear. This should be tried for steam nozzles and perhaps for turbine blades—applied on molybdenum steel.

Figs. 5, 6, and 7 show the creep characteristics of certain calorized steels.

H. DAHLSTRAND.⁶ Designers of high-temperature equipment heretofore have depended upon information obtained from laboratory experiments for the selection of suitable materials. In steam turbine design, with the maximum temperatures so far adopted, this method has proved quite satisfactory. However, if higher temperatures are to be adopted in future installations, experiments with actual installations of complete power plant equipment, like those conducted at Detroit, are most desirable as this method will prove whether higher temperatures will be both practical and economical. From the practical standpoint, therefore, this paper by Messrs. Thompson and Van Duzer on the results of this experiment are most valuable as real facts are made available to the designers.

The paper explains in detail the characteristics of all materials exposed to high temperatures and their use in the various parts of the equipment. In addition to this information it would seem desirable that the working stresses in the various parts should be given in order to analyze completely the results of the experiment. The stresses are, of course, of variable magnitude in certain parts but it should be possible to give information based on maximum and minimum stresses which would still further illuminate the information given.

It would not seem to be necessary to use a high grade and expensive alloy steel for valve-body castings and other fittings. Ordinarily these parts can be designed for very low stresses and the use of a fully annealed material of a lower grade alloy steel undoubtedly would have proved satisfactory. It is realized that in the selection of material for this high temperature corrosion must be taken into consideration but on parts not rubbing or sliding against each other the corrosion does not seem to penetrate any appreciable depth. The first corrosive covering apparently acts as a protection as shown by experience with carbon-steel castings exposed to a temperature of 850 F for long periods without showing any signs of corrosion.

The Hecla ATVI steel, a high nickel-chromium austenitic steel for blading, is from previous experience a suitable material for high temperature. A similar steel with 20 per cent nickel and 8 per cent chrome (Cyclops No. 17 metal) has been used for blading, for both high temperatures and high stresses, because of its strength at high temperature, high-fatigue strength, and non-corrosive qualities. This steel has been used for a long period of time at a temperature of 850 F and undoubtedly will be suitable for still higher temperatures.

The experience with the 18-8 alloy used in the tubes of superheaters and in the piping is interesting. Previous experience with this alloy indicates that deterioration in the form of carbide segregations was experienced. This segregation would seem to depend to a large extent on the stress in the material when at high temperature. From experiment it has been found that some segregation will occur even at as low a temperature as 700 F. Judging by the lowering of the impact value reported in the paper it is possible that this segregation has proceeded farther than the micro-photograph indicates.

Whether a more readily obtainable and, at the same time, satisfactory material could have been used for this tubing is difficult to say. High grade carbon steel tubing used for steam piping up to 1200 lb per sq in. and 850 F is satisfactory. For this same condition we have adopted a chrome-molybdenum steel for piping because it was necessary to design the piping so as to be as flexible as possible and with this chrome-molybdenum steel instead of carbon steel the thickness of the walls could be materially reduced. The analysis of this material is given in the following tabulation:

⁶ Engineer-in-Charge, Steam Turbine Dept., Allis-Chalmers Mfg. Co., Milwaukee, Wis. Mem. A.S.M.E.

C.....	0.20 to 0.35
Cr.....	0.60 to 0.80
Mn.....	0.90 to 1.10
Mo.....	0.20 to 0.30
Si.....	0.24 max.
P.....	0.045 max.
S.....	0.045 max.

This material is not subject to carbide segregation, has a structure that will remain stable and at the same time the required physical properties. It is less expensive and can be welded readily.

Nitralloy steel is not non-corrosive and therefore the experience with this material as reported could be expected. For temperatures up to 850 F nitralloy seems to be entirely suitable for valve seats, valve stems, and bushings acting as guides. Apparently the surface maintains its hardness up to this temperature, which is a highly desirable quality for parts rubbing against each other. No corrosion at this temperature has been noticed. There are various methods used in the nitrating process and it has been found that the method used has certain influences on corrosion and if electrolytic action is present the corrosion will be further accelerated. For the high temperature used in the experiment a valve seat and valve made from some alloy steel, that would permit welding a light ring of stellite material for the seats and then grinding to the required shape, would undoubtedly have proved satisfactory. Materials used for high-temperature service should, where possible, be fully annealed as experience has shown that heat-treated material will gradually be annealed and, therefore, a design based on the heat-treated characteristics may not be perfectly safe.

Various materials have been tried for the bolts and the report indicates that Seminole Hard steel was the only material that was satisfactory. This material with its extreme hardness is difficult to machine and besides, as is evident from the report, the high stresses obtained before use dropped considerably after a certain length of service. It seems, therefore, that a more desirable material could have been selected; with a slightly lower creep characteristic, similar chemical analysis, and physical properties which would allow for ready manufacture. Such a material would be less liable to change its physical properties and its higher ductility would render it a safer material to use. We are now using a chrome-tungsten steel with the following analysis for certain bolting:

C.....	0.15 to 0.25
Cr	4.50 to 6.50
Mn.....	0.40 to 0.60
W.....	0.75 to 1.0
Si.....	0.50 max.
P.....	0.045 max.
S.....	0.045 max.

The physical properties of this steel are:

Tensile strength, lb per sq in.....	125,000 min.
Yield point, lb per sq in.....	105,000 min.
Elongation in 2 in., per cent.....	18 min.
Reduction of area, per cent.....	45 min.
Brinell hardness No	255

This material is being used for temperatures of 850 F and above. It would be interesting to find out definitely what maximum temperature with a certain stress this material will stand. SAE-3140 bolt material has been found satisfactory up to 850 F and has been in use for several years without requiring any replacement.

The authors conclude that, due to the expensive materials necessary, the economies of 1000 F are questionable. While this view may be correct from the standpoint of this experiment there are certain factors that should be thoroughly analyzed before any definite conclusion is made.

First, materials now quite costly will be, if used to any extent, greatly reduce in price.

Second, certain expensive materials used in experiments may be replaced by less expensive material when full knowledge of their behavior at high temperature is available.

Third, with only a very moderate lowering of the temperature, say to 950 F, we may be able to use materials that are standardized and available at comparatively low cost. With a temperature of 950 F the construction of the complete power plant would be considerably less because of the elimination of the reheating equipment now considered necessary when using 1200 lb per sq in. pressure and 850 F.

The efficiency of the steam turbine and auxiliary apparatus enter into this analysis. There are certain considerations that will determine both the selection of proper materials and the efficiency. The design should be such that little or no distortion will take place in any of the structures and that the expansion will be uniform in all directions in order to maintain the correct relative positions of all parts. The successful solution of all the above factors will determine whether the high temperature power plant is economically sound from the standpoint of efficiency.

M. D. ENGLE.⁷ The Detroit Edison Co. has been the only one to pioneer in the field of higher steam temperatures sufficiently far in advance of common practise to permit a substantial increase in steam temperature in a short time. In the past, temperatures have been raised fifty degrees at a time, but the Detroit Edison Co. has lead the way to an increase of from two hundred to three hundred degrees in one jump.

The principal advantage of the installation is not that it will immediately permit others to build stations using temperatures of around 1100 F but that it will permit others to proceed with 900- to 1000-F steam temperatures with confidence and assurance that they are not undertaking something that will result in failure or insurmountable operating difficulties.

The authors' frank discussion of the difficulties encountered and the means taken for their correction is a substantial contribution to the art of steam power generation.

It is to be hoped that the Detroit Edison Co. will continue operating these installations at temperatures around 1100 F because only commercial operation over a longer period of years will determine the life of such equipment and the maintenance to be expected.

As mentioned by the authors, the fact that equipment designed for 1100 F operates satisfactorily, does not necessarily prove that such a design is economically justified. It does indicate, however, that steam temperatures higher than customarily employed are probably justified. The one big difficulty is that the higher the temperature employed, the greater the need for steam-temperature control. If we are honest with ourselves we must admit that we have not satisfactorily solved the problem of controlling steam temperatures even in the more moderate ranges. We cannot satisfactorily control steam temperatures with varying load nor with varying cleanliness of the boiler and superheater surfaces.

In using the word "satisfactorily," the writer has in mind the broader sense. We can, of course, design and build for constant superheat, but the cost and operating complications of the designs developed make them far from satisfactory.

As has been described, the Detroit Edison Co. used a separate, oil-fired superheater which was the best design for their purpose but it is far from satisfactory for most installations and is much too expensive.

Undoubtedly the problem can be solved if the boiler and superheater manufacturers will bestir themselves and forget some of their inhibitions. They can develop a design that will give the

⁷ Assistant to Superintendent of Station Engineering Department, Edison Electric Co. of Boston, Mass. Mem. A.S.M.E.

advantages of a separately fired superheater and at nearly as low a cost and as simple as the unsatisfactory type of interdeck superheater commonly employed.

We have discussed this need for a superheater design that is really flexible in operation many times during the past decade. A superheater that will not maintain a constant temperature with varying load on the boiler and varying conditions of commercial cleanliness is just as absurd as a boiler which must allow the pressure to vary for these same reasons.

The advantages to the manufacturer who develops a satisfactory superheater would seem obvious. A pioneer has now made the need for satisfactory designs so clear that it can no longer be ignored. The Detroit Edison Company has in reality issued a challenge and we all hope that it will be answered by economical superheater designs suitable for the purpose.

V. F. ESTCOURT.⁸ The authors are to be congratulated on the comprehensive picture presented by their paper on a subject that is of paramount importance to the central-station industry.

We realize that the question of flexibility of operation must necessarily be one of the last subjects to be investigated. We note, however, that reference is made to the fact that the normal rate of load change is 1000 kw per 3 to 4 min and that load has been applied at the rate of 1000 kw per min. In plants where standby operation is essential during certain seasons of the year, rates of load change in the neighborhood of 1000 kw per sec from 10 per cent capacity to full load are not uncommon during interruptions to hydroelectric service. Such rates of load change have been handled in plants operating at 750 F without any difficulty and we would like to ask the authors if their present experience with the 1000 F unit has indicated that there would be any inherent reason why a turbine operating at this temperature could not be subjected to the same sort of load-change rates. Even in stations where standby operation is not a routine problem, there are occasions when the turbine is called upon to go through sudden load changes and it is to be hoped that further actual test data will be available in the future which will indicate just what the limitations are in this respect. Consideration should be given to both sudden increase and sudden loss of load.

D. S. JACOBUS.^{9,10} The Detroit Edison Company has pioneered in many improvements in power plant construction, an instance being in the use of large boiler units in which development the writer cooperated in making tests which were reported¹¹ at the Annual Meeting of the A.S.M.E. in 1911. The present development in the use of superheated steam at temperatures higher than so far employed is another example of its enterprise.

It is perhaps known to few that boilers installed at the Delray Station before I cooperated in making the tests of the large boilers located there, superheated the steam to such a high temperature when they were first started up that the station piping glowed in the dark. These were relatively small Stirling boilers with middle pass superheaters of a design no longer used. As the story was told to me, the builders of the boilers were asked to supply superheaters for giving the maximum amount of superheat obtainable, and those supplying the steam turbines were asked to design the turbines to handle the maximum amount of superheat the boilers would give. Because of the extreme condition

which resulted the superheaters were promptly changed to bring down the superheat to a more reasonable figure. The instance is cited to show the progressive attitude of the Detroit Edison Company and its willingness to explore new fields.

H. J. KERR.¹² When engineers departed from 650 F steam temperature, and metal temperature of 800 F, they entered a field where trouble was to be expected through oxidation, creep, and instability of material. The ordinary methods of quick testing were no longer to be depended upon and, in their place, it was necessary to develop and substitute tests of long duration. Progress, therefore, has been both costly and slow. For this reason, more than any other perhaps, we owe to the authors and their company our appreciation for the paper which has been presented, as it contains a wealth of information only to be obtained by long and costly tests.

Four important questions affecting power generation with steam at 1000 F are considered: Operation, troubles, materials, and costs.

Operation of a power plant of 1000 F is shown to require no special attention in so far as the superheater is concerned and with the turbine, little more than some extra attention to controlling the speed of temperature changes. This may well be considered an accomplishment.

The small troubles which have developed are those for which simple remedies were available. The superheater wall tube bricks gave some trouble in the beginning, due to more water and motion than expected. Simply stiffening the tubes, increasing the clearance for the bricks, and improving the method of handling the condensation water have practically eliminated these problems.

Evidently wise decisions were made in the selection of materials, and for this reason the paper merits careful study. I would like to emphasize certain facts in this connection. In the case of the Trenton Channel installation, the requirement was 1100 F outlet steam temperature. All tubes were exposed to the furnace and the high temperature was limited to these tubes and to the pipe line. In reading the paper, it is necessary to keep in mind not only the steam temperature, but also the actual metal temperatures at various locations in the system. Thus, the tubes at the high-temperature end were obviously at approximately 1200 F, whereas the piping operates at a temperature not above 1100 F.

For the tubes, the selection of KA2 steel seems to have been a wise one. While the metallurgical examination of this material after 21,000 hr shows some carbide precipitation, this has, apparently, reached an equilibrium condition and may be improved in further service. Many other cases of even longer life at higher stress and higher temperature have given confirmatory evidence of the value of this material. It is doubtful if any superior material is available today for continuous service at 1200 F actual temperature, either from the standpoint of oxidation resistance or creep. Superior stability of the material has, however, been obtained by supplying a stabilizing heat-treatment, which has been developed in the laboratories of The Babcock and Wilcox Tube Company. Tubes now supplied for such service would be so heat treated that the amount of carbide precipitation which would take place in service would be of no moment.

For the steam line itself, operating at a temperature of 1100 F, there might be some question of the selection of KA2 material as this temperature is approaching that where a cheaper material might be substituted. When both oxidation and creep are considered, however, reasonable conservatism would certainly lead to the choice of this type of alloy steel. In addition to its

⁸ Efficiency Engineer, Pacific Gas and Electric Co., San Francisco, Cal. Mem. A.S.M.E.

⁹ Advisory Engineer, Babcock & Wilcox Co., New York, N. Y. Mem. A.S.M.E.

¹⁰ This discussion applies also to "The Thermal Performance of the Detroit Turbine Using Steam at 1000 F," by Carter and Ellenwood, A.S.M.E. Trans., 1934, FSP-56-8.

¹¹ "Tests on Large Boilers at the Detroit Edison Company," by D. S. Jacobus, A.S.M.E. Trans., 1911, vol. 33, paper no. 1328.

¹² Research Department, Babcock and Wilcox Co., New York, N. Y. Mem. A.S.M.E.

corrosion resistance and creep value, this material has the advantage of being readily weldable by either the resistance method or electric arc methods, and without complicated subsequent heat treatment for these service conditions.

As to the castings for such pipe lines, it should be noted that since this installation was made there has been much advance in this field, and the present-day tonnage of KA2 castings gives evidence of the fact that their manufacture is on a definite commercial scale. Castings of this material are now being made of sections which would be, to say the least, difficult with ordinary steel.

In the case of the Delray superheater, certain conditions were fixed by the general conditions at the plant, such as:

- A pressure drop of the order of 20 lb
- A draft loss not to exceed $1/2$ -in. water column
- Entering steam temperature of 700 F
- An efficiency requirement fixed by a temperature differential between the entering steam and the leaving gas of 100 F.

These conditions restricted the maximum velocity of the steam through the tubes and the rate of heat input permissible throughout the unit. As stated by the authors, the design was on the basis of a final steam temperature of 1100 F.

This requirement of 1100 F final steam temperature, naturally, affected the choice of material. While the authors state that the unit was designed for this temperature, the paper refers throughout to 1000 F as the operating temperature at the turbine throttle, and in consequence the reader might possibly be led astray on this point.

With 1100 F outlet steam temperature, tube temperatures of the order of 1200 F had to be faced. Therefore, the choice of tube material was, at that time and would be today, practically limited to material of the KA2 type. Corrosion from combustion gases of high-sulphur fuel apparently is not serious at this temperature and below, whereas above 1200 F the writer has found in experiments with mercury boiler tubes that intensive corrosion effects developed.

In this connection, Table 2 in the paper is apt to be misleading. The table gives a list of materials and their creep values at 1000 F. I believe it would be clearer if this table were made up to show the creep values and oxidation resistance of the various steels at the temperatures at which they were to be operated, and at which they have actually operated during this service period.

The next material to be decided upon was the superheater outlet headers and piping. Here again 1100 F conditions were to be met. Sufficient knowledge was not available on either oxidation in the presence of steam or the creep values of lower alloy steels to warrant the chance of failure of this experiment and KA2 material was decided upon. Facing the same problem today, notwithstanding the efforts which have been expended on new alloys, the decision would undoubtedly be the same for this temperature.

While the installation has not been operated at the maximum temperature given, experience with this material in many installations throughout the country, has shown that it has given satisfactory service for long periods of operation. Its one objection is cost.

In the latter part of the paper reference is made to creep rates of coated carbon steel and KA2 tubes. Evidently, due to a typographical error the KA2 tube size is given as $2\frac{1}{4}$ -in. instead of 2-in. O.D. Aside from this, the statement made indicates that the creep rate of carbon steel at 2000 lb per sq in. stress and for KA2 steel at 4300 lb stress is approximately 5 per cent per 100,000 hr at temperatures from 900 to 925 F. This is hard to understand, as plain carbon steel pressure vessels of considerable size are in operation over long periods of time with stresses of

around 6000 lb per sq in. and have shown practically no creep. Again, we examined lately a number of KA2 tubes of 4-in. diameter which have been in service in an oil still for 35,000 hr at temperatures between 1000 and 1100 F and a pressure stress of approximately 4800 lb per sq in., and no appreciable creep could be detected. Material from these tubes was tested by Professor F. H. Norton and within the limits of experimental error the same value of creep was obtained as for the new KA2 material.

Dealing now with the concluding comment of the authors, this seems to be a depression statement. I do not know the efficiency possibilities of the cycle proposed but if this cycle shows a real gain, it would be well to consider carefully its commercial application today, having in mind that while this installation in all its details was being developed, metallurgists have been engaged in attempting to bring down the cost of accomplishing the results desired. Consider what would be required today, in the way of a superheater and piping to deliver 1000 F steam at the turbine throttle. Assuming a 25 F temperature loss in the steam line, which should be on the extreme side, we would need at the superheater outlet a temperature of 1025 degrees.

For the steam line we need a material which will withstand oxidation and have a reasonable creep resistance value at 1025 F. We need castings to withstand the same condition. Such material is available, not theoretically, but practically. Many tons of it have been furnished the oil industry and it has been in service at such temperatures for more than two years. I refer to 4-6 per cent chrome, 0.5 per cent molybdenum steel. With a temperature of 1000 F, a stress of approximately 7200 lb, the creep rate would be approximately 1 per cent in 100,000 hr. Its oxidation resistance at even higher temperatures has been found to be excellent in the oil industry. Its cost is reasonable.

Next we have the problem of the superheater itself. The Babcock & Wilcox Company has manufactured superheaters, made entirely of plain carbon steel, to give a final steam temperature of 850 F with a metal temperature of about 950 F and they are in successful operation. Therefore, to meet the condition of 1025 F final steam temperature, we need only sufficient surface to add 175 F, or approximately 100 Btu, to the steam in order to accomplish the result. At the outlet end of the superheater it will be necessary to operate the tubes with a metal temperature up to 1125 F. Assuming that we need the expensive KA2 material for the final 100 F of the superheater, to impart 60 Btu, surely it is not a very serious cost item to face. This leaves a zone of from 950 to 1025 F metal temperature for which the same material could be used as for the pipe line, namely, 4-6 per cent chrome, 0.5 per cent molybdenum steel. Other materials of even a cheaper type might be used with less margin of safety.

H. F. MOORE.¹³ The paper by Messrs. Thompson and Van Duzer is an interesting and valuable study of the behavior of various heat-resisting alloys under certain high-temperature conditions in service. The writer of this discussion is not in a position to discuss the details of this paper critically, because he has not had experience with power plant operation. However, this paper, taken in connection with the various laboratory studies of creep of metals at high temperature that have been published before this society and elsewhere, does seem to the writer to present an excellent example of the place and significance of service tests and laboratory tests.

When a new material, or a new process, is proposed there are frequently many who demand an immediate "full-size" test under service conditions. Such a test, if conducted at once, is usually very expensive, and can cover only a very few of the variables of service. Such a service test, undertaken before laboratory tests

¹³ Research Professor of Engineering Materials, University of Illinois, Urbana, Illinois. Mem. A.S.M.E.

and theoretical investigations, is very apt to yield very few significant results for the expenditure of time and money.

If, on the other hand, small-scale laboratory tests and theoretical investigations are undertaken first, it is usually possible to determine with a fair degree of accuracy what variables are most important and along what lines a service test can be made to show the best results. It is rarely that laboratory tests or theoretical investigations alone solve an engineering problem, but the supplementary service test or the record of service experiments can be made far more fruitful if laboratory tests have shown the most promising lines of investigation and the most promising test methods, than is the case if an elaborate and expensive service test is the first step toward solution of the problem.

The writer believes that this method of laboratory tests followed by service tests, as soon as clear indications of significant factors are obtained, is finely illustrated by the course of investigation of the effect of high temperature on the strength of metals. The present paper is a useful supplement to laboratory tests for creep and of metallographic structure. Future tests, both full-size service tests and laboratory tests, can be made more effectively because of the correlated evidence of these tests of Thompson and Van Duzer and the laboratory tests which have been reported by others. This paper adds greatly to the sense of security with which the engineer can design high-temperature apparatus. Coming as it does after considerable laboratory study of the behavior of metals at high temperature very little energy was wasted in unprofitable lines of investigation.

C. R. SODERBERG.^{14,15} One of the most important avenues of approach to the problem of improving the efficiency of power generation is to raise the inlet temperature. The benefits that can be brought about by this step are so great and so generally appreciated as to require no further comments. At the same time, it is also the most difficult of attainment. The importance of the step taken by the Detroit Edison Company in exploring this possibility cannot be over-estimated, and they are to be commended for making the results available in the excellent form of the present papers.

It would be unfair to criticize the present experiment at Detroit on the ground that the installation does not give remarkably high efficiency, because the original premises of the experiment did not include this requirement. There are certain points in this connection, however, which cannot be evaded if the results of the experiment are to be interpreted fairly.

In the present instance, it would appear that a certain sacrifice in turbine efficiency has been made, in order to insure reliability. This is undoubtedly necessary, but the incentive of the higher temperature is lessened materially, if it must be accompanied by a marked reduction in turbine efficiency.

The principal incentive for going to higher inlet temperatures is undoubtedly the possibility of raising the inlet pressure without the complication of reheat. The limit in pressure, for 1000 F inlet temperature is about 1200 lb per sq in. The mechanical difficulties of the undertaking would be greatly increased if the pressure were raised to this value, and it is not unreasonable to raise the question whether the outcome of the experiment might not have been changed had it been conducted at 1200 lb per sq in.

There are at the present time in the United States a number of turbines of various capacities operating on an inlet temperature of 850 F. The principal items of trouble are related to the

phenomenon of scale deposits on the blading due to impurities carried over by the steam. Turbine developments in the way of materials and processes have gradually made the consequences of such deposits less serious to the turbines, but the real seat of the trouble has not yet been removed. This problem must be solved by the boiler designers and there is no exaggeration in the statement that the progresses toward higher pressures depends entirely on the successful solution of this problem. It is of equal importance for the progress toward higher temperatures, because higher temperatures are of interest only as a means of utilizing the higher pressures more economically. Barring the scaling problem, however, the 850 F turbine may now be regarded as entirely practical.

Certain projects have been carried out in Europe, utilizing temperatures of 932 F (500 C) and 2000 lb per sq in. with one stage of reheating for turbine units of about 50,000 kw. The boilers in these installations are of the Löffler type and it appears that the scaling problem is not serious. Turbine troubles have been encountered, but these seem to have been overcome. This appears to come pretty close to the temperature of the Detroit project, but the step between 932 and 1000 F is in reality very large.

In planning for the future, there is a question whether it would not be advisable to approach the maximum practical temperature in small steps. It is entirely possible that 1000 F, when applied in conjunction with high pressures and large units, will be found too high. It is certain to give trouble if applied at present to large 1800 rpm units.

Regardless of what the ultimate temperature will be, the Detroit experiment will remain a milestone of real importance, and the results given in these papers are certain to affect power plant development in a fundamental manner.

A. E. WHITE.¹⁶ This paper sets forth in an exceptionally clear manner the experience of The Detroit Edison Company with metals in high-temperature power-plant service. Until recently, practically all of the metals used in power plants were either wrought iron, wrought steel, cast iron, and cast plain carbon steel. Within recent years cast plain carbon steel has taken the place of cast iron and wrought steel has taken the place of wrought iron. Of course metals other than these have been used for various parts such as in valve trim and in other special places. Likewise, cast iron still finds a use in certain parts of units entering into boiler construction such as in grates, and in certain sections of stokers.

Beyond question, there is no need to find special metals suitable for high-temperature service when operating temperatures are held to 850 F. With temperatures much above 850 F, however, ordinary plain carbon steels are not suitable as they do not possess sufficient strength over long periods of time.

This condition was recognized at the time the 1100 F superheater was built so that various types of alloy steels were used in its construction and in the piping system connected with it. The writer, who was in close touch with this installation, did not unduly fear trouble because of metal failure nor did he anticipate that there would be considerable difficulty in maintaining the flanged pipe joints free from leakage. This latter trouble was encountered but he is pleased to note that by changes in flange design and the use of better bolting material the leakages have been materially reduced. He feels, however, that the best way to eliminate this trouble would be by resorting to welded construction.

At the time this construction was started there was a general feeling on the part of many persons that the only suitable material

¹⁴ Manager, Turbine Apparatus Division, Westinghouse Elec. and Mfg. Co., Philadelphia, Pa. Mem. A.S.M.E.

¹⁵ This discussion applies also to "The Thermal Performance of the Detroit Turbine Using Steam at 1000 F," by Carter and Ellenwood, A.S.M.E. Trans., 1934, FSP-56-8.

¹⁶ Professor, Metallurgical Engineering, Director, Department of Engineering Research, University of Michigan, Ann Arbor, Mich. Mem. A.S.M.E.

for high-temperature properties was material of the austenitic type. Many scientists held that all steels, even alloy steels, of the pearlitic type would show high-temperature properties not greatly dissimilar from those found in plain carbon steels. The writer was among the few who felt in those days that various types of low-alloyed steels would be found to have good high-temperature properties. It is interesting to note in this paper that a number of low-alloyed steels were used and that in consequence a performance record with regard to them is available. These steels, of course, have an advantage over the austenitic type of steels in that their cost is considerably less. This is an important feature which must be given consideration in commercial installations.

It is not contended either by the writer or, I am sure, by the authors of this paper that all of the available low-alloyed steels have been tried. In fact, it is questionable if many of them have even yet been developed. The act is now in that stage in which literally hundreds of low-alloyed steels are receiving consideration and it will only be after several years of experiment that we can expect to arrive at the few most suitable compositions. What the power plants will pass through in the next few years in this respect is analogous to what the automobile manufacturers passed through a few years ago in the matter of the selection of proper materials for the various parts in an automobile. The selection of suitable materials is by no means a simple matter, for wherein one material has decided advantages in one way, another material has advantages in another. For instance, the experience with the use of KA2B is a case in point. This is an alloy of the austenitic type with between 2 and 2.5 per cent silicon which was added ostensibly to increase resistance to oxidation. The addition of this larger amount of silicon made the alloy extremely difficult to fabricate into long tubes. The result was that only short sections for the most part were available and the desired length had to be secured by welding.

Attention is directed to the reduction of the Izod impact value on some samples of 18-8 alloy after different service periods. It is interesting to note that the drop in impact is not as great at 1000 F as it was when the tests were made at room temperature. This is a matter worthy of receiving our consideration because without an appreciation of this fact, we may be apt to condemn a material as being too brittle on the basis of tests at room temperature when it has undergone little change in brittleness at the operating temperature. It is hoped that the authors are correct in assuming any failure that may take place in an 18-8 alloy will not occur without warning. We have too little operating experience, as yet, to make any definite statement with respect to this matter. We do know that failures of 18-8 have taken place in oil refineries without warning. Of course, the conditions may be different as the operating temperatures are higher and as other conditions of operation are different.

Castings have been, and still are, potential sources of trouble in pipe line installations. The metal is not always, if ever, as sound as wrought material, and in no case has it had the benefit of mechanical work. Whether or not one of these conditions accounted for the low impact values in the desuperheater metal and in the flange metal given in Table 5 is a question. It is presumed that such was the case. Also it is reasonable to suppose that the low tensile strength in the desuperheater metal was due to unsoundness.

For a number of parts it is highly desirable to have a surface which will resist oxidation. Calorizing has possibilities in this connection and it is interesting to note that we may look for a more ductile aluminum coating.

The paper is most interesting in that it shows quite clearly that nitrided surfaces in the presence of superheated steam undergo a deterioration. We all regret the necessity of making

this observation because we would all like to see good performance from nitrided surfaces.

The data with regard to the bolt stock is most interesting. It is quite conclusive that tungsten is more valuable than chromium especially at the temperatures in question in maintaining proper high-temperature strength. This is true at 1100 F, although it is felt that at temperatures of 1000 F the lower tungsten alloy would be found quite suitable.

In conclusion, the writer wishes to compliment the authors on the very full analysis which has been made of the various metals used in this installation. Though considerable judgment can be formed with regard to the service which may be expected from various metals as a result of a knowledge resulting from physical tests, it is only through the acid test of experience that the feasibility of various metals and alloys for high-temperature service can be fully determined.

I. E. MOULTROP.^{17,18} The engineering world was somewhat startled a few years ago by the announcement that the Detroit Edison Company was prepared to investigate the use of steam at temperatures up to at least 1000 F and had actually ordered a 10,000 kw turbine-generator and superheater for this purpose.

This was the most interesting information received by the central-station industry since the Boston Edison Company announced its decision to test the use of steam at 1200 lb per sq in. pressure and 700 F. At the time this decision was made 700 F was about the highest temperature any manufacturer was willing to meet. The desire to obtain a better thermal efficiency has been one of the aims of power-plant engineers for years and at the time the Boston Edison Company made its announcement the more practical ways of obtaining this end were through the use of higher pressure or higher temperature, or both.

The step to 1200 lb per sq in. seemed revolutionary at first but a little careful reflection indicated that it was a sound step and after all not as revolutionary as it appeared. However, there is a definite financial limit to the use of elevated pressures, namely, that point beyond which the increased carrying charges amount to more than the gain in efficiency. In other words, while thermal efficiency might be improved, dollar efficiency would be less. Pressures of 1200 to 1400 lb per sq in. seem to be about as high as can be utilized economically at the present time.

The use of much higher temperatures would seem to be the next step toward improved efficiency but it is one that involves more problems and more risks, and calls for considerable courage.

The use of steam at higher pressures and temperatures is really a question of economics with a diminishing return. There is also the humanitarian aspect as affected by accident hazard. We know that it is not difficult to obtain metals of the proper characteristics to withstand pressures of almost any amount but when the element of temperature is added we find that in order to obtain materials of the proper characteristics we have to enter the field of alloys. My experience has been that alloys are usually expensive and that they often become unstable after having been in use a certain length of time. The element of creep is added also; a consideration which may change the picture completely.

The operating experience at Detroit as related in these papers is very interesting. The authors state that operating at these higher temperatures is little different from operating at normal pressures and temperatures. It appears in the progress of the

¹⁷ Chief Engineer of Company and Supt. of Construction Bureau, The Edison Electric Illuminating Company of Boston, Boston, Mass. Mem. A.S.M.E.

¹⁸ This discussion applies also to "The Thermal Performance of the Detroit Turbine Using Steam at 1000 F," by Carter and Ellenwood, A.S.M.E. Trans., 1934, FSP-56-8.

paper, however, that extreme caution was exercised and that great care was considered necessary in bringing the steam up to the high temperature in the superheater, as well as in starting up the turbine and bringing it up to temperature. This, of course, was to be expected.

The fact that such precautions are necessary in changing load on this apparatus indicates that a unit of this type is better adapted to base-load, continuous-operation conditions than to operation under varying conditions. This point should be taken into consideration in deciding the question of whether one should accept extremely high temperature in designing for central-station use.

There are at least four other elements which should be given careful consideration in arriving at a decision as to the adoption of higher temperatures: capital cost, use factor, maintenance, and accident hazard.

The experience of the electric-power industry in the past several years should have taught us that anything that affects the capital cost or limits the use factor should be studiously avoided. Any increase in the cost of equipment becomes a liability which never can be escaped. In the writer's opinion it is better to muddle along with equipment of a somewhat lower thermal efficiency, if by so doing we can avoid much increase in capital charges.

In the matter of maintenance, it is not always true that high maintenance charges are entirely unjustified. If by incurring higher maintenance charges the over-all efficiency can be improved, the higher cost of maintenance may be entirely justified. The mere fact that maintenance charges per month are beyond our habitual expectation does not necessarily mean that they are not justified.

Accident hazard should be given due consideration in the design of any type of station and the choice of any material which tends to increase the accident hazard should be avoided. If the success of any equipment depends upon materials, the life of which cannot be readily predicted or of which the condition cannot be observed, or if there is likelihood that the material may become weakened in use to such an extent as to cause rupture of the material, its use should be avoided.

These papers are very instructive and the facts brought out by them are of great value to the profession but the conclusion at which the writer arrives from their perusal is that we need to know a great deal more about available alloys, their properties, and dependability before we advance very far beyond our present standards in the design and use of high temperatures for central-station practise.

It is interesting to note that the Detroit Edison Company thought it advisable to buy a turbine of English manufacture while the superheater, piping, etc., were domestic products. This is a little surprising when one considers that the superheater and piping connections to the turbine get the greatest punishment from high temperature. To be sure, the turbine throttle valve and nozzles also get this same punishment, but the bulk of the turbine is subjected to somewhat lower temperatures.

There is no question but what the British Thomson-Houston Company builds a very fine machine, and their designing engineers are second to none in the world. Some of us feel, however, that the American turbine builders are equally as capable and it is to be hoped that in the near future we can have an American-built machine installed under similar conditions.

In connection with this endeavor for improved thermal efficiency, it should be borne in mind that thermal efficiency is only one of the problems facing the power-plant engineer. Carrying charges on the complete plant is one of the most important items and, with a low load factor, could become the most important item over a period of years on the average plant.

I am inclined to believe that the most successful operating company of the near future will be the one which does not necessarily have a record-making generating plant from the standpoint of thermal efficiency but which has the lowest overhead. In other words, a company may be successful in paying reasonable dividends to its stockholders while operating a power plant which is far from the top as far as thermal efficiency is concerned.

Power-plant engineers the world over owe a debt of gratitude to the Detroit Edison Company and its engineers for making this interesting experiment and for telling the world so frankly and in much detail about their experiences and the results to date. They should be commended especially for their frankness in summing up the results of their work.

AUTHORS' CLOSURE

The authors appreciate the scope as well as the number of discussions that have been presented. The subject is one upon which comments are necessarily quite general; therefore, the authors will attempt to answer specific questions only.

Mr. Dahlstrand has inquired regarding the working stresses in the various parts—a question which is especially pertinent to a paper of this nature. Unfortunately, the stresses encountered in the high-pressure cylinder of the turbine are not available other than in a statement by the makers that no design stresses over 5000 lb per sq in. were used for the parts fabricated from the nickel-chromium-molybdenum alloy. Working stresses for the essential parts of the superheater, based on a leaving steam temperature of 1100 F, are given in Table 11. The allowable stresses used in the design were two-thirds of the stress required to produce creep at the rate of one per cent in 100,000 hr. All the values given in Table 11 are below these allowable stresses, the highest actual stress being 7400 lb per sq in. for the middle-section outlet header. In Table 12 are given the design stresses for flanged joints and tubing in the Trenton Channel and Delray piping systems. The flange and bolt stresses were calculated at room temperature with full pressure in the line without considering the effect of bending moment. Actual working stresses for these joints are not given due to the uncertainty of assumptions, such as the effect of creep and expansion, that are necessary in their calculation. They are much less, however, than the calculated values, because of the effect of rapid initial creep and rearrangement of the gasket faces. A calculation of the tubing stresses was made on the assumption that the material behaves elastically at 1000 to 1100 F. This method does not give the correct working stress as the material is approaching the plastic state at the operating temperature. It does, however, give an indication of the magnitude of the stress and one that is greater than the actual.

We quite agree with Mr. Dahlstrand that it should not be necessary to use high-grade and expensive alloy steel for fittings and valve-body castings. In the Delray installation, all fittings and valves were made from low alloy steels with the exception of the superheater outlet fittings. These were furnished by The Babcock & Wilcox Company from cast 18 chromium, 8 nickel steel because the superheater specification named an outlet steam temperature of 1100 F.

We have more or less anticipated Mr. Dahlstrand's suggestion regarding the use of Stellite for valve seat and disk material. Stellite No. 1, deposited with an oxyacetylene torch, has been used for the past several years in repairing valves in sizes up to three inches with very good results for both 400-lb saturated and 400-lb, 725-F steam service. In view of the excellent results obtained with this material, a 5-in. gate valve was installed at the outlet of the Trenton Channel superheater. One side was trimmed with Stellite No. 1, having a Brinell hardness of 512,

TABLE 11 CALCULATED STRESSES FOR PARTS OF THE DELRAY SUPERHEATER

Part	Material	Operating temperature, F	Stress, ^a lb per sq in.		Remarks
			Allowable	Actual	
2-in. O.D., 8-gage tubes	Steel	850	6750	5900	Located in upper section
1-in. O.D., 10-gage tubes	KA2B	1000	9000	3700	Radiant tubes in middle section
2-in. O.D., 6-gage tubes	KA2B	1033	7800	4300	Located in middle section
2 1/2-in. O.D., 7/16-in. wall tubes ^b	0.30-0.40 C steel	1033	...	2000	Located in middle section
11-in. O.D., 5/8-in. header	KA2	1100	7800	7400	Middle-section outlet header
2-in. O.D., 1/4-in. wall tubes	KA2B	1100	7800	3300	Located in bottom section
14 1/2-in. O.D., 1 3/8-in. header	KA2	1100	5400	5200	Outlet header
10-in. outlet flange, modified, 600-lb Am. Std. Sarlun type	KA2	1100	5400	5170	Flange 4 in. thick with 1 3/8-in. bolts. Stress based on unit gasket pressure of 4 X S.S.P. with pressure acting

^a Stress with 1100 F exit steam, from calculations supplied by The Babcock & Wilcox Company; allowable stress is two-thirds of stress required to produce creep at the rate of one per cent per 100,000 hr.

^b Supplied by the Superheater Company; sprayed and calorized tubes.

TABLE 12 CALCULATED STRESSES FOR HIGH-TEMPERATURE FLANGED PIPE JOINTS AND PIPING

Description	Material	Operating temperature, F	Stress ^a —Unit gasket pressure 1 X S.S.P. with pressure acting, lb per sq in.		Stress, ^a as made up, lb per sq in.		Remarks
			Flange	Bolts	Flange	Bolts	
5-in. flange, 600-lb Am. Std., Sarlun type	Rezistal 2C	1100	3500	6000	29,000	48,000	Original joints at Trenton Channel
5-in. flange, modified 900-lb Am. Std.	KA2	1100	1700	2200	7,900	10,000	Trenton Channel; flange, 3 3/8 in.; bolts, 1 1/2 in.
5-in. flange, modified 1350-lb Am. Std.	KA2	1100	1300	1600	8,100	10,000	Trenton Channel; flange, 4 1/8 in.; bolts, 1 3/4 in.
10-in. flange, 600-lb Am. Std., Sarlun type with hairpin springs	Era 131	1000	3900	3900	11,500	11,500	Delray, spring stress—62,000 lb per sq in.; bolts, 1 3/8 in.
8-in. flange, 900-lb Am. Std.	SAE 3240	1000	6,700	6,000	Delray; backing-up flanges for full-strength pipe weld
8-in. flange, 1350-lb Am. Std., Sarlun type	SAE 3240	1000	3400	3000	46,700	40,500	Delray
8 1/2-in. O.D., 5/8-in. wall tubing	KA2S	1000	Delray; max. stress, 6200 lb per sq in., includes bursting stress and bending stress due to expansion calculated at 1000 F and assuming material in elastic condition
5 1/2-in. O.D., 3/8-in. wall tubing	KA2	1100	Trenton Channel; max. stress, 3200 lb per sq in., calculated at 1100 F See, also, above note

^a Stress calculated by The Detroit Edison Company at room temperature, with full working pressure, using Waters-Taylor formula. Bending moment neglected.

and the other side was trimmed with the No. 6 grade, having a Brinell hardness of 402. The valve was examined after approximately 6000 hr of service at 1100 F. The body seat rings, likewise faced with Stellite, were in the same condition as when installed, while the trim on both sides of the disk had small hairline cracks. It is possible that a ring thicker than 1/8 in. might have prevented the formation of these cracks. Good results have been obtained, so far, at 1000 F with "Platnam" metal, a trim material developed by Hopkinsons, Ltd.

It was not the authors' intention to imply that Seminole Hard was the only satisfactory bolting material, as seems to have been inferred by Mr. Dahlstrand. In the two installations, and particularly at Trenton Channel, its use has resulted in the least maintenance. We are inclined, therefore, from this experience, to consider it the most satisfactory material for the purpose. The higher cost of Seminole Hard bolts as compared with bolts made of steels having lower physical properties is more than offset by the decrease in joint maintenance. On the other hand, the chrome-tungsten material mentioned by Mr. Dahlstrand would undoubtedly be a suitable bolting steel for high-temperature service, judging from our own experience with this alloy in the cast state for both fittings and valve bodies. Its use should be considered the next time such an installation is made.

In regard to the question of flexibility of operation raised by

Mr. Estcourt, the authors know of no inherent reason why a unit designed for 1000 F and for rapidly fluctuating load cannot be operated successfully. Experience with the Delray unit would indicate that the question is one of providing sufficient axial wheel clearance to compensate for the more rapid expansion movement of the rotor during sudden load change.

The creep values and oxidation resistance of the various materials at their operating temperature would be a desirable addition to Table 2, as mentioned by Mr. Kerr. These data were not obtained because of the extensive testing work which would have been required.

The authors are likewise at a loss, as is Mr. Kerr, to understand the high rate of creep observed on the KA2B tubes and on the coated carbon-steel tubes in the middle section of the Delray superheater. It is possible that the values given may decrease appreciably with the passage of time.

In connection with the creep stress of 7000 lb per sq in. given for Seminole Hard in Table 2, this value is an average one for this material. Coffin and Swisher¹⁹ have reported values from 6500 to 10,500 lb per sq in. on a similar steel tested at 1022 F.

¹⁹ Coffin, T. H., and Swisher, F. P., "Flow of Steel at Elevated Temperatures," A.S.M.E. Trans., vol. 54, 1932, paper APM-54-6.

Leaving-Velocity and Exhaust Loss in Steam Turbines

By ERNEST L. ROBINSON,¹ SCHENECTADY, N. Y.

This paper gives an exposition of the various items which go to make up the leaving velocity and exhaust loss of a steam turbine. The importance of this loss and the rapidity with which it increases at high loads cause it to be a determining influence in fixing the economic rating of a machine. The several elements necessary for an analysis are each evaluated in a fairly direct, although sometimes approximate, manner. More detailed and precise estimates might be made but are beyond the intent of this paper.

The loss in question occurs in the exhaust hood between the last wheel exit and the exhaust flange to the condenser. It is made up both of kinetic energy loss and of pressure loss through the hood and each effect varies with load and with location around the wheel annulus. Moisture is allowed for; supersaturation neglected.

The total loss may be expressed in Btu per pound flow to condenser or as a per cent of adiabatic heat drop or

preferably as a per cent of total energy theoretically available for conversion to switchboard power.

With a particular exhaust operating at fixed steam conditions, the leaving velocity and exhaust loss increases roughly as the square of the load (parabolic rule).

With a particular exhaust passing a fixed flow, increasing the total available energy in the higher stages of the turbine by improved steam conditions correspondingly reduces the percentage loss in the exhaust (hyperbolic rule).

With a fixed percentage loss in a particular exhaust the power may be increased by improved steam conditions as the $3/2$ -power of the total available energy by increasing the flow to the condenser.

Base-load operation justifies more liberal exhaust areas than peak-load service but in the ultimate the heat-rate-load curve is the characteristic which is of most importance to the operator and second only to the reliability of performance.

THE most important single loss in a condensing steam turbine is the "leaving loss," "exhaust loss," or "leaving-velocity loss" as it is variously called. There is a very general understanding of the magnitude and importance of this loss. But there is no set standard as to the items properly included under the heading nor as to the manner in which the loss is to be evaluated for comparative purposes.

The importance of this loss and the rapidity with which it increases at high loads cause it to be a determining influence in fixing the economic rating of a machine (see Fig. 1).

HYDRAULIC ANALOGY

The leaving velocity and exhaust loss from a steam turbine may be likened to the tailrace loss of a water wheel. If the tailrace runs downhill, there is a corresponding loss of head—the wheel setting should have been lower. If the tailrace runs level there is the loss of velocity head only, which may be small if the cross-sectional area is generous. If the tailrace runs smoothly uphill into quiet water, the leaving velocity is recovered because the wheel operates under a gross static head greater than its net head by the velocity head converted in its tailrace.

¹ Turbine Engineering Department, General Electric Co. Mem. A.S.M.E. Mr. Robinson was graduated from the St. Lawrence University in 1911 and from the Harvard Graduate School of Applied Science in 1914 (M.C.E.). For three years he was engaged in construction work and the design of steel and reinforced-concrete structures in New York and in water-power engineering in New England. During the war he served in the Oise-Aisne offensive as first Lieutenant with the 302nd Engineers, U. S. A., and later as Captain and Adjutant of the 2nd Engineer Training Regiment. For the past fifteen years he has been employed by the General Electric Company in its Turbine Engineering Department.

Contributed by the Power Division and presented at the Annual Meeting, New York, N. Y., December 4 to 8, 1933, of THE AMERICAN SOCIETY OF MECHANICAL ENGINEERS.

NOTE: Statements and opinions advanced in papers are to be understood as individual expressions of their authors, and not those of the Society.

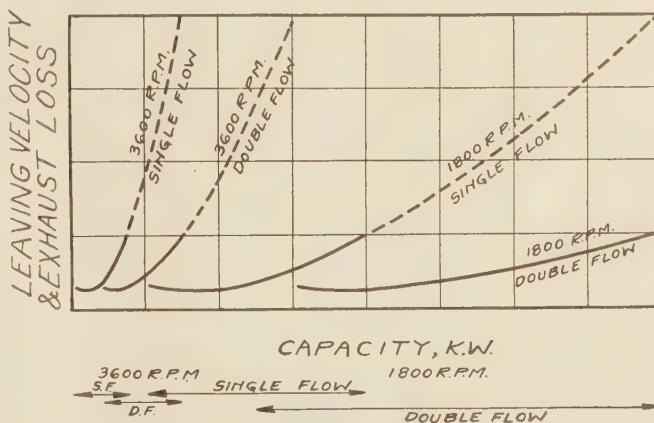


FIG. 1 RANGES OF ECONOMIC RATING

(Structural considerations limit the maximum annulus area at any speed to slightly less than in inverse proportion to the square of the speed. Thus a single exhaust of limiting size at 3600 rpm may be expected to handle not quite one-quarter as much capacity as a single exhaust at 1800 rpm.)

In the water wheel one deals with low velocities but a heavy fluid. With steam one deals with an exceedingly rarefied fluid but with velocities which are correspondingly high and with a kinetic energy content which varies with the square of the velocity.

MANUFACTURER'S VIEWPOINT

It is the intention of this article to discuss the more important items contributing to the leaving-velocity and exhaust loss of the steam turbine from the manufacturer's point of view. Typical curves will be given for a 35,000-kw turbine by way of illustration, but there is no intention of going into the finesse of design or of giving detailed formulas or test data. For reasons which will appear, it does not seem desirable to standardize any calculations or to recommend any set expressions or formulas. This does not mean that suitable comparisons among designs should not be

made. The idea is that each comparison should be made on its own merits.

RÉSUMÉ OF ITEMS

The several items of the leaving velocity and exhaust loss may be listed as follows; this list being intended to cover all losses

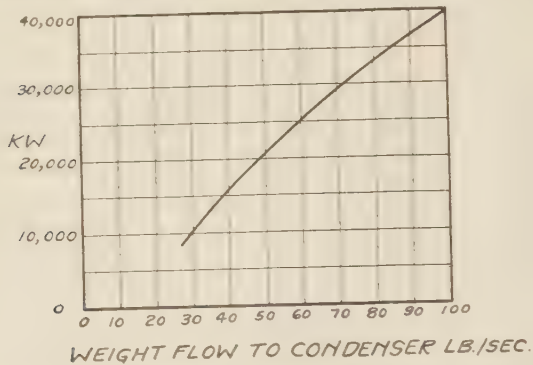


FIG. 2 CONDENSER FLOW
(35,000-kw extraction-feed-heating turbine operating at 250 lb per sq in. gage, 700 F, and 1 in. Hg.)

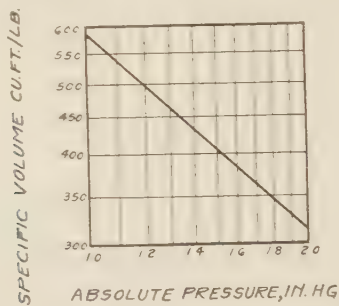


FIG. 3 SPECIFIC VOLUME OF STEAM APPROACHING 1 IN. HG ABS PRESSURE AND 10 PER CENT MOISTURE
(35,000-kw turbine.)

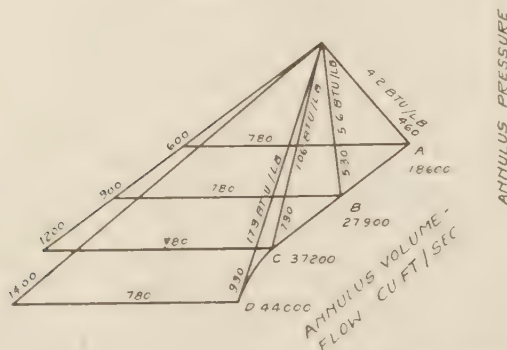


FIG. 4 VELOCITY DIAGRAMS A, B, C, AND D FOR STEAM EMERGING FROM LAST BUCKET OF A 35,000-KW TURBINE

(Figures are velocities in ft per sec except for the heat equivalents in Btu per lb of the kinetic energy of absolute exhaust velocity. Each diagram represents a particular annulus volume flow, as indicated. The volume may be made up of a larger weight of denser steam or a smaller weight of more rarefied steam. See Fig. 5.)

existing in the exhaust hood between the exit from the wheel annulus and the exhaust flange:

- (1) Normal velocity loss
- (2) Loss due to tangential component, or whirl loss
- (3) Eddy losses, associated with non-uniformity of flow
- (4) Pressure drop through the hood itself.

In evaluating these items it is necessary to consider the following:

- (5) Moisture content of the steam
- (6) Possibility of supersaturated expansion.

We shall rule out from this discussion:

- (7) Consideration of radial velocity in an axial-flow annulus
- (8) Eddy loss associated with edge thickness of buckets.

This last is properly chargeable to the nozzle and bucket efficiency and the stream is supposed to have healed into a cylindrical jet on emerging from the wheel annulus. This latter ruling is, of course, arbitrary. The N.E.L.A. Prime Movers Committee Report on Turbines, No. 234, July, 1932, recommended correcting for bucket-edge thickness, thus in effect charging the bucket-edge loss to the exhaust loss rather than to the bucket. Suffice it to say that in any case it should not be charged twice and the manner used should be clear in any particular case.

TYPICAL CURVES

Fig. 2 is the load-flow curve for a 35,000-kw turbine operating at 250 lb per sq in. gage pressure, 700 F temperature, and 1 in. Hg abs back pressure with two stages of extraction for feedwater heating.

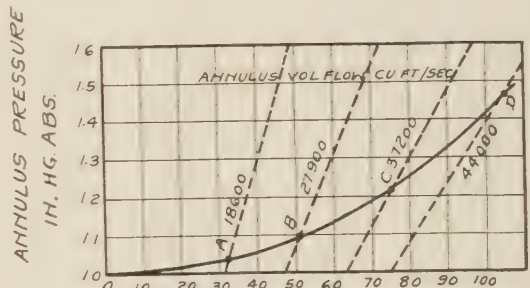


FIG. 5 RELATION BETWEEN ANNULUS PRESSURE AND WEIGHT FLOW FOR 1 IN. HG ABS PRESSURE AT THE FLANGE FOR A 35,000-KW TURBINE

(The dotted lines A, B, C, and D for constant annulus volume flows correspond to the velocity diagrams in Fig. 4 and show the relation between annulus pressure and weight flow for varying exhaust flange pressures.)

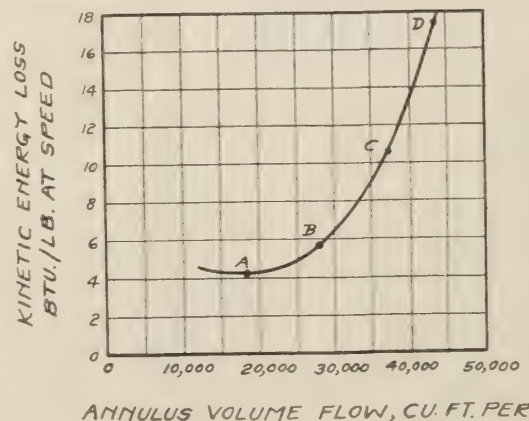


FIG. 6 KINETIC-ENERGY LOSS IN THAT FRACTION OF THE STEAM WHICH CROSSES THE ANNULUS OF A 35,000-KW TURBINE AT SPEED
(The moisture moves at very low speed. For 1 in. Hg abs pressure at the exhaust flange and the exhaust-hood drop shown in Fig. 5, the points A, B, C, and D correspond to the actual kinetic energy leaving loss and also to the several diagrams in Fig. 4.)

Fig. 3 gives the pressure-volume line for the exhaust of this turbine for an average moisture content. The variation from this line does not exceed approximately 1 per cent and is neglected.

Fig. 4 is a series of velocity diagrams characteristic of the last bucket exit in which we are interested only in the absolute exit velocity through the wheel annulus.

By way of identifying the conditions of operation to which these diagrams apply, it should be noted that each represents a definite volume flow, and Fig. 5 gives the corresponding lines for various weight flows and absolute pressures at the annulus. The heavy line shows, for a pressure of 1 inch Hg abs at the exhaust flange, what the annulus pressure will be at the several weight flows corresponding to the different loads of Fig. 2.

By associating each annulus pressure with a corresponding velocity diagram, it is possible to plot Fig. 6 showing the kinetic energy of the exhaust steam in Btu per lb of steam at speed.

It is necessary to bear in mind that the annulus pressure is not uniform and Fig. 7 shows how it varies around the circumference for two flows approximating full load and half load, in each case for a pressure at the exhaust flange of 1 inch Hg abs.

The kinetic-energy content in Btu per lb of steam at speed around the annulus is shown by Fig. 8 for the same two flows as

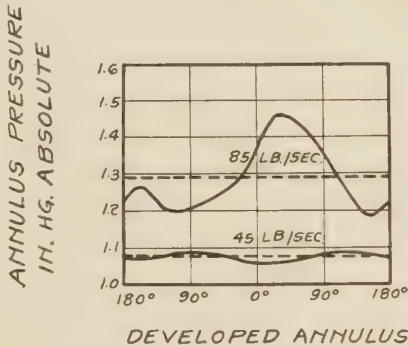


FIG. 7 VARIATION OF ANNULUS PRESSURE AROUND THE PITCH CIRCLE OF THE ANNULUS OF A 35,000-KW TURBINE FOR TWO SPECIAL WEIGHT FLOWS, 85 LB PER SEC AND 45 LB PER SEC

(The irregularity is due to the quarter turn of the hood and its internal bracing. Lack of symmetry is due to the tangential component in the exhaust velocity.)

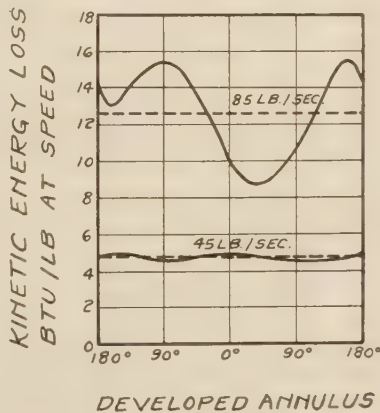


FIG. 8 VARIATION OF KINETIC-ENERGY LOSS PER POUND OF STEAM AT SPEED AROUND THE PITCH CIRCLE OF THE ANNULUS OF A 35,000-KW TURBINE FOR THE SPECIAL WEIGHT FLOWS, 85 LB PER SEC AND 45 LB PER SEC

(The weight flow is practically uniform around the annulus. The volume flow varies in inverse relation to the pressure and consequently the velocity and kinetic energy vary as shown.)

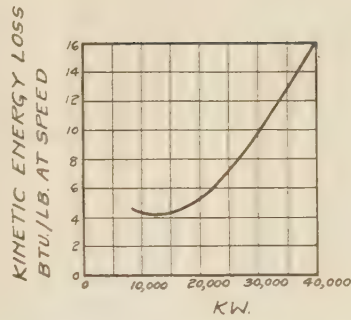


FIG. 9 TOTAL INTEGRATED KINETIC-ENERGY LOSS PER LB OF STEAM AT SPEED IN THE ANNULUS OF A 35,000-KW TURBINE

(This is the average for the entire annulus area and applies to the dry portion of the steam only since the moisture moves at very low velocity.)

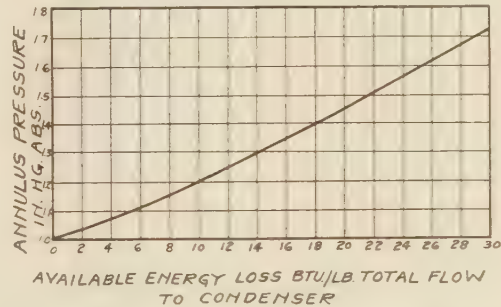


FIG. 10 AVAILABLE ENERGY LOSS DUE TO PRESSURE DROP THROUGH THE EXHAUST HOOD FROM THE WHEEL ANNULUS OF A 35,000-KW TURBINE TO THE EXHAUST FLANGE

(If the wheel annulus could exhaust directly at 1 in. Hg abs pressure, the adiabatic energy available ahead of the last wheel exit would be increased by the amount shown.)

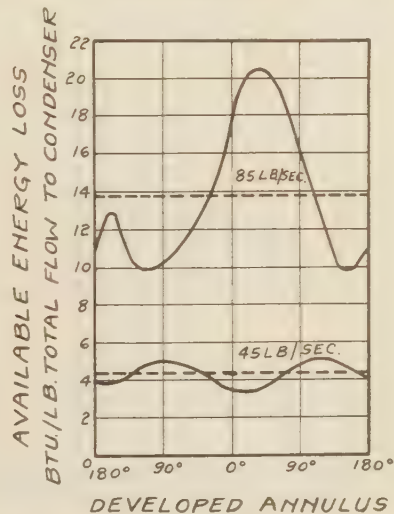


FIG. 11 VARIATION AROUND THE ANNULUS OF AVAILABLE ENERGY LOSS DUE TO PRESSURE DROP THROUGH THE EXHAUST HOOD OF A 35,000-KW TURBINE FOR TWO WEIGHT FLOWS, 85 LB PER SEC AND 45 LB PER SEC

(This variation is due to the variation of pressure shown in Fig. 7.)

Fig. 7. We arrive finally at Fig. 9 which shows the kinetic-energy loss plotted against the various loads in kw.

Returning to the résumé of items, the method of arriving at Fig. 9 has taken care of (1) normal velocity, (2) tangential component, and (3) non-uniformity of flow. It remains to

evaluate the loss of available energy due to pressure drop through the exhaust hood itself.

Fig. 10 shows the relation to be nearly linear so that Fig. 11, which illustrates the distribution around the annulus, is not absolutely essential for a satisfactory preparation of Fig. 12 which shows the available energy loss plotted against the various loads in kw.

ABSOLUTE VALUE OF LOSSES INSIDE EXHAUST HOOD

When it comes to expressing the total effect it is necessary to take account of the quantities involved. The kinetic-energy loss, Fig. 9, affects only the steam at speed, and since in this case 10 per cent of the condenser flow is in the form of moisture moving at low velocity, this is to be applied to 90 per cent of the con-

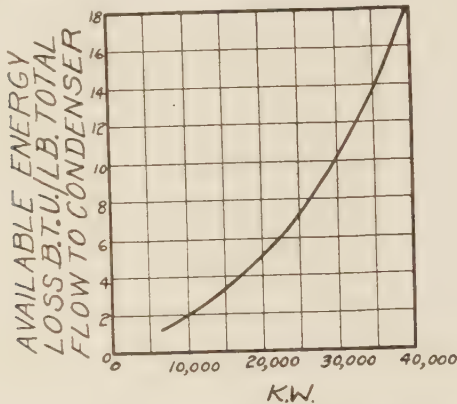


FIG. 12 TOTAL INTEGRATED AVAILABLE ENERGY LOSS DUE TO PRESSURE DROP THROUGH THE EXHAUST HOOD OF A 35,000-KW TURBINE

(This is the average for the entire annulus and applies to the total weight flow.)

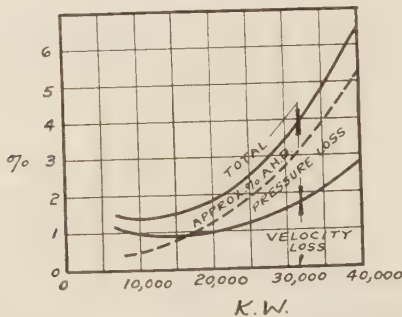


FIG. 13 TOTAL LEAVING VELOCITY AND EXHAUST LOSS OF A 35,000-KW TURBINE EXPRESSED AS A PERCENTAGE OF TOTAL THEORETICALLY AVAILABLE ENERGY IN ALL STEAM, BOTH TO CONDENSER AND TO EXTRACTION HEATERS

(The lower full line curve shows the subdivision between true velocity loss and pressure loss as they actually occur. The dotted line shows the approximate leaving velocity and exhaust loss based on computed normal annulus velocity, assuming exhaust flange pressure at the annulus and expressed as a per cent of the adiabatic heat drop in the turbine.)

denser flow. It should not be necessary to explain the difference in velocity between the moisture and the steam, further than to refer to the article "Supersaturation—The Flow of Wet Steam," by the late Prof. G. A. Goodenough,² describing steam-flow tests conducted at the General Electric Works by Prof. J. H. Keenan. The available-energy loss is expressed per pound total flow. Bearing in mind these relations, reference to Figs. 2, 9, and 12 leads to Fig. 13, the total leaving velocity and exhaust-loss curve for this turbine. For simplicity an average over-all "engine"

efficiency of 75 per cent has been assumed, whereas more accurate estimates use true efficiency curves, or true integrated available energy.

The total loss might be divided up in another way by defining the net exhaust-hood loss as the extra loss occasioned by having the specified exhaust or condenser pressure occur at the hood flange instead of at the wheel annulus. This viewpoint has a certain merit in setting up a standard for comparison of no pressure drop through the hood. The net hood loss viewed this way is less than the actual loss due to the pressure because the pressure drop reduces the kinetic-energy loss at the annulus. In order to divide the total loss in this way it is necessary to compute the leaving velocity loss at the annulus with the specified exhaust pressure occurring at that location. The balance between this and the total may be thought of as the net amount due to the presence of the exhaust hood. This is not the same as the approximate computation suggested below, because true performance (as nearly as can be estimated) under the supposed conditions is computed. The result especially depends on both the relation between the size of annulus and the hood and the load, and the method of computation employed for estimating what would happen under the assumed conditions. Thus a heavily loaded annulus discharging into a liberal hood will suffer very little additional loss because of pressure drop through the hood as compared with free discharge without any hood. On

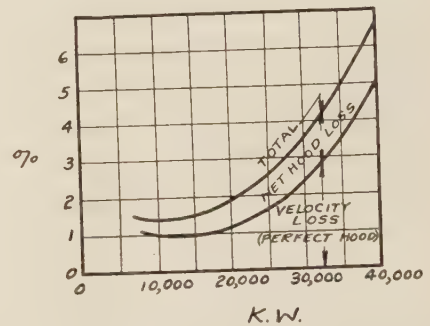


FIG. 14 TOTAL LEAVING-VELOCITY AND EXHAUST LOSS OF A 35,000-KW TURBINE, EXPRESSED AS A PERCENTAGE OF TOTAL THEORETICALLY AVAILABLE ENERGY IN ALL STEAM, DIVIDED SO AS TO SHOW THE NET LOSS CHARGEABLE TO THE PRESSURE DROP THROUGH THE HOOD

(In this case the velocity loss is that which would occur with exhaust pressure at the wheel itself.)

the other hand, a liberal sized or lightly loaded annulus discharging into a more restricted hood may easily have a net loss chargeable to the presence of the hood equal to the velocity loss with no hood present thus doubling the theoretical leaving loss.

It can be seen by reference to Fig. 14 that the net loss chargeable to the presence of the hood is really much less than would be inferred by looking at Fig. 13. The example here given has a rather high net hood loss.

APPROXIMATE ESTIMATES

For comparative purposes the dotted line in Fig. 13 has been prepared in a very simple manner by multiplying the weight flow to the condenser by the specific volume at the exhaust flange and dividing by the annulus area. This gives an average annulus velocity which has been converted to a kinetic energy heat content in Btu per lb and divided by the adiabatic heat drop, without regard to extraction. This curve may be compared with the more accurate estimate which is given in full lines. The apparent inconsistency of using exhaust flange volume as if present at

² *Power*, Sept. 27 and Oct. 4, 1927.

the annulus goes part way to compensate for the neglect of pressure drop through the hood with its corresponding loss of available energy.

SUPERSATURATION

In dealing with the results so far set down no account has been taken of any effects which may be caused by supersaturated expansion, that is, by expansion of the steam without condensation to a momentarily cooler, denser condition. In considering Fig. 13 as representing absolute values, this reservation has to be kept in mind in addition to the minor inaccuracies purposely assumed for simplicity.

It has been noted in comparing Fig. 14 with Fig. 13 that the true loss through the exhaust hood is accompanied by a reduction of velocity loss in the denser medium at the annulus. The two effects are, to a certain extent, compensating.

Similarly supersaturation, if present, results both in a reduction of energy made available for conversion and in a reduction of the leaving-velocity loss. With the amount of moisture present there is not likely to be any high degree of supersaturation in this particular case. However, in a different case with, say only 2 or 3 per cent of moisture theoretically present, supersaturated expansion should be allowed for.

COMPARISON OF TURBINES

While it is legitimate to express the leaving velocity and exhaust loss in a variety of ways, it is always well to bear in mind the significance of the type of expression used. For instance, the difference between the approximate calculation dotted in Fig. 13 and the more exact one in full lines may be quite different for another design. There are a number of turbines in sizes over 50,000 kw in which, under favorable load conditions, the hoods are diffusing and produce a lower pressure at the annulus than exists at the exhaust flange.

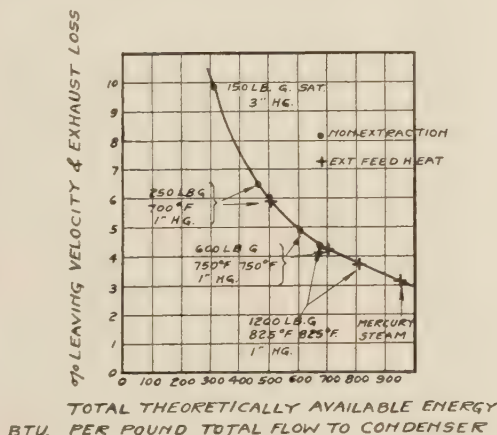


FIG. 15 PER CENT LEAVING-VELOCITY AND EXHAUST LOSS WITH VARIOUS STEAM CYCLES, IN EACH CASE WITH 30-BTU LOSS PER LB TOTAL FLOW TO CONDENSER

(If the same turbine exhaust is used for the same kw capacity while substituting modern steam conditions for lower pressures and older cycles, the percentage leaving loss will be greatly reduced and the exhaust will appear wastefully generous in size for the better steam conditions.)

Correct values of the loss may be expressed in terms of heat equivalent in Btu per lb flow to the condenser, or as a per cent of the adiabatic heat drop, or as a per cent of the total theoretical energy available within the flowing steam between throttle inlet and the several extraction and exhaust flanges, for conversion to switchboard power.

Thus it is correct to speak of a loss of 30 Btu per lb flow to the condenser. But such a statement is not very significant. If the adiabatic heat drop is 500 Btu, the loss may be said to be 6 per cent of the adiabatic heat drop. But there is still an uncertainty as to the effect on the power generated since the 6 per cent loss applies only to the steam going all the way through the turbine. If $\frac{5}{6}$ of the power generated comes from steam which goes all the way through the turbine, then the true loss

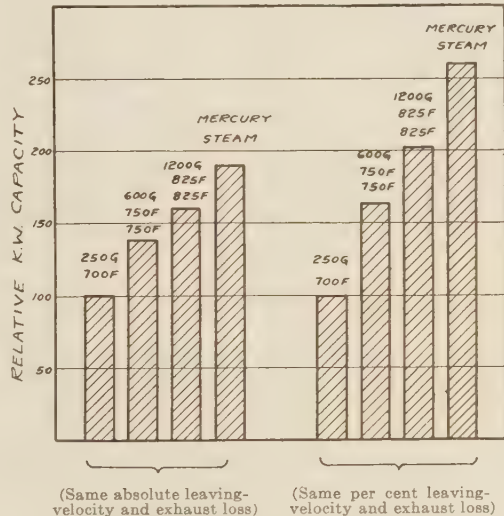


FIG. 16 APPROXIMATE INCREASE IN KW CAPACITY MADE AVAILABLE BY MODERN CYCLES WITH SAME TURBINE EXHAUST

is 5 per cent of the theoretically available power which, for the reasons discussed, fails to appear on the switchboard.

EFFECT OF MODERN STEAM CYCLES

For instance, take the same loss of 30 Btu per pound flow to the condenser (see Fig. 15). Such a loss amounts to 10 per cent of the adiabatic heat drop of an ancient low pressure turbine with 300 Btu available energy while it is only 5 per cent of the adiabatic heat drop of a modern high pressure resuperheating turbine with 600 Btu available. Similarly a full use of stage extraction for feed heating so increases the power generated from a particular exhaust that the importance of a fixed leaving-velocity and exhaust loss may be decreased as much as 20 per cent in this manner; an effect which is not shown at all by expressing the loss in terms of adiabatic heat drop, which does not change with extraction.

The use of the mercury turbine in conjunction with the steam turbine still further reduces the percentage importance of a fixed size loss.

In other words, modern cycles warrant the use of much higher absolute losses per pound of steam exhausted to condenser, because much less steam is being exhausted per kw hour generated.

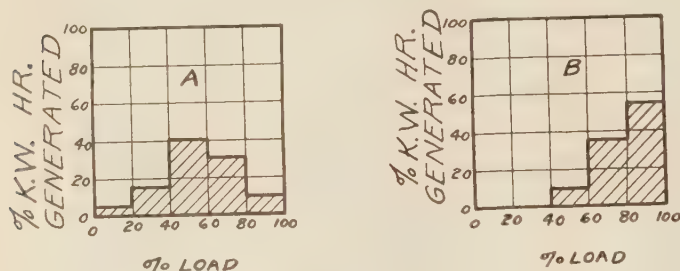
INCREASED CAPACITY

Fig. 16 is the counterpart of Fig. 15 showing how the capacity obtainable from the steam entering a given exhaust may be increased by the use of modern cycles. The relative capacities for constant percentage loss are based on the approximate relation that, for a given cycle, the absolute value of the leaving-velocity and exhaust loss increases as the square of the flow. This leads directly to the conclusion that relative capacity for a

constant percentage loss increases as the $3/2$ -power of the total energy theoretically available.

CONDITIONS OF OPERATION

The type of service and conditions of operation also are very important in evaluating the amount of leaving velocity and exhaust loss that is acceptable. This is because of the rapid change at high loads. Thus a base load machine which is to run most of the time at its maximum rated capacity requires a more



INTEGRATED LOSS 2.2% IN INTEGRATED LOSS 3.3%

FIG. 17 TYPICAL ANNUAL-LOAD CURVES

(Since the leaving-velocity and exhaust loss increases roughly in a parabolic manner with the load, a base load station such as *B* will experience a greater integrated loss than a station like *A* which shares light loads. Turbines for base load service warrant more liberal exhaust areas.)

liberal exhaust with smaller absolute loss than a machine designed for a broad range of service and the expectation of running at maximum capacity only a short part of the year.

Roughly speaking, the higher the annual capacity factor the lower should be the fixed loss in the exhaust but this is just another way of saying the more you run a machine the more efficient it should be. For careful comparison actual load requirements should be analyzed. For instance, Fig. 17 illustrates two types of service, the total energy generated being the same in each case, but Station *A* is taking the swings and does the bulk of its operation at half and three-quarters load while Station *B* is on base-load service and operates mostly around three-quarters to full load. If these two stations were each equipped with a single turbine of the type represented by Fig. 13, the integrated loss due to hood effects in Station *B* would be 50 per cent more than in Station *A*, the difference amounting to approximately 1 per cent of fuel requirements. From this it may be inferred that with medium coal prices a purchaser could afford to pay some 10 per cent more in the case of Station *B* for a turbine with more liberal exhaust and a different load curve from that which would be suitable for Station *A*.

This brings attention directly to the load curve as being considered a most important feature by operators in the selection of a turbine. It is second only to reliability of operation and with turbines as dependable as they have been of late years, attention (perhaps too often) is likely to be concentrated entirely on the load curve. Together with throttle loss at light loads, which dwindles out at full load, the leaving-velocity and exhaust loss, which increases from very little at light loads, is one of the most effective tools the turbine designer has at his disposal in producing the type of machine suited to the operating conditions.

Discussion

W. E. CALDWELL.* The paper presents a comprehensive method of calculating the exit loss in a condensing turbine. How-

* Efficiency Engineer, The New York Edison Co., New York, N. Y. Mem. A.S.M.E.,

ever, this method is somewhat difficult to apply and if a simpler method could be devised for comparing turbines it would be helpful in evaluation procedure. It would be interesting if the author could indicate the probable error which might be introduced in comparing the exhaust end of a variety of turbines on the basis referred to in the N.E.L.A. Prime Movers Committee Report No. 234 on Turbines.

The author speaks of load curves and conditions for which a turbine is chosen but these conditions are so subject to change that it is difficult to predict conditions far in advance. In case of doubt as to the future it may be wise to lean in the direction of capital savings at the expense of economy. Until quite recently growth of load throughout the country was rapid and new units were installed at fairly frequent intervals. Each succeeding installation carried design improvements rendered possible by the advance in the art. With new units of superior economy added to the system, the capacity factor of the earlier machines dropped and they are operated only at peak loads. For example, on one system new machines purchased some years ago were operated at 58 per cent capacity factor for about 6 years and after this period the use of these machines diminished almost annually until it finally reached a capacity factor in the neighborhood of 5 per cent in about 20 years. Experiences of this kind cannot be safely taken as a basis for purchase of new machines since it presupposes a continuation of load growth such as we have had in the past.

In the absence of continued load growth, the capacity factor and use factor of the more recent machines will increase materially above that which might be anticipated from earlier experience. Under such conditions machines evaluated for a relatively low capacity and use factor may ultimately become base-load units of the system. This is a situation which cannot always be foreseen and should not be lost sight of in the purchase of new units, especially as it influences exhaust areas.

Another important consideration in the choice of exhaust areas in the turbine is the cost of steam-generating capacity to meet full-load requirements. With a lower exit loss less steam-generating capacity is required and this should be carefully considered in evaluating turbine performance. Whether the value of the additional boiler-plant capacity required by a less efficient turbine is taken on a pro-rata base or increment cost base is largely a matter of judgment, but it is an important consideration if the highest economy in the use of capital is to be achieved.

Summarizing, the influences to be considered in the design of the turbine-exhaust end are the capacity factor, cost of boiler and condenser capacity, cost of steam, and quality, quantity and temperature-duration curves of circulating water available. The design is influenced also by the relation of the system demand period to the circulating water temperature, and if the period of maximum demand of the system coincides with the period of minimum circulating water temperatures, the conditions are favorable for a design with relatively low exit loss.

The paper clearly brings out the influence of higher initial steam conditions and other improvements in reducing the percentage exit loss, nevertheless there is often potential capacity available which might have been purchased at an attractive price. In latitudes favored with an abundance of cold condensing water during the period of maximum demand, it is probable that there are cases where available capacity might have been purchased in the last wheel and condenser well below the unit cost of the plant.

As the art advances progress in improving efficiencies will diminish as the more attractive possibilities have been exhausted

and we may find it profitable in the future to resort to more liberally designed exhaust areas in steam turbines, as well as more liberal condensers and auxiliaries. With each successive installation closer cooperation is developed between the engineers of the manufacturers and those of the power producers and it is through the mutual understanding of the common problems involved that the greatest progress may be made in achieving a well-balanced design in the ultimate plant.

A. G. CHRISTIE.⁴ As the author states in his opening paragraph, the combined leaving-velocity and exhaust loss constitute the most important single loss in condensing steam turbines. These losses have attracted the serious attention of the plant-designing and operating engineers only in the last few years.

Leaving losses were considered a few years ago by the Prime Movers Committee of N.E.L.A. Data on various turbines were collected and referred to the writer for analysis. In many cases arbitrary assumptions had to be made regarding the amount of steam to exhaust and other items. Certain of these such as the allowance for blade-outlet thickness on the last set of blades are, as pointed out by Mr. Robinson, open to question. Manufacturers at that time were somewhat reluctant to discuss leaving losses. There appeared to be no standard or other method of expressing leaving losses. The writer therefore proposed as a tentative measure the expression of leaving loss as the equivalent of the absolute velocity from the last row of blades assuming axial flow and found by assuming the exhaust pressure and volume at the blade annulus instead of at the exhaust nozzle. In other words the losses in the exhaust hood were not considered. The Prime Movers Committee then considered the question of a standard method of expressing leaving loss. However, differences of opinion developed and a suggestion was made that a leading authority on turbine design be asked to discuss this whole subject in a paper before A.S.M.E. Mr. Robinson's concise and enlightening paper is the result of this suggestion. A careful analysis of its contents will aid plant designers and operators to give intelligent consideration of these losses and to their influence on plant economy.

Mr. Robinson shows very clearly that the leaving-velocity loss and the pressure loss in the hood are interdependent and both should be considered. The method of indicating leaving loss used in the N.E.L.A. report does not give all the facts.

In Fig. 13 Mr. Robinson shows that the total leaving-velocity and exhaust-hood loss at 28,000 kw, the most efficient load on the 35,000-kw turbine under consideration, exceeds the loss calculated by the N.E.L.A. method by 0.6 per cent but he also points out that this may not be true for turbines with diffuser exhausts. Few of the turbines in the N.E.L.A. report have diffuser exhaust hoods so that the computed losses are probably not as large as the sum of the true leaving loss and hood loss. However, it is apparent that the computed figures published by the writer in the N.E.L.A. report can only be used with reservations.

Leaving loss depends upon the length of the last row of turbine blades and the quantity of steam flowing to the condenser. Hence the amount of this loss when the maximum length of blades is used, depends upon the output rating of a given casing as fully discussed in the writer's paper before the World Power Conference a few years ago.

Losses through the hood will also be dependent upon the output of a given casing but as Mr. Robinson states these will also depend upon exhaust outlet design. Certain exhaust hoods exert a diffuser effect so that the leaving velocity of the steam is partly converted into pressure head to overcome hood losses.

The question arises as to whether it would be desirable and economic to incorporate diffuser designs in the exhaust hoods of all turbines. Some savings would result from such an ideal design.

Regarding supersaturation, Mr. Robinson indicates that this only needs consideration when moisture contents of 2 to 3 per cent occur at exhaust. Generally the moisture content ranges from 8 to 11 per cent. Can any supersaturation exist at the last row of blades under these conditions? The late Professor Callendar and H. M. Martin, both of England, have advanced the opinion that supersaturation will persist even to exhaust. R. Colburn and the writer concluded two years ago that supersaturation might exist at high moisture contents for there appear to be indications that this was a contributing factor in blade erosion from moisture. But the question is by no means settled.

One of the Power Test Code Committees should consider a standard definition for the combined leaving and hood loss. Mr. Robinson indicates the different ways in which the loss can be expressed but has not given any method preference over the others. It is highly desirable that the expression of this loss be standardized so that all engineers can refer to it in the same terms.

A further comment may be made. These losses are fixed by the original design of the turbine and are inherent in its construction. They cannot be increased or decreased for given operating conditions by any efforts of the station operators. It is therefore incumbent upon the plant designer to give the fullest consideration to the economics of these losses in the initial selection of the turbine equipment. Mr. Robinson points out certain factors such as the character of load, etc., which influence the economic effect of leaving losses.

There are differences of opinion in regard to the allowance for leaving losses in determining the true end-point of the condition curve. In some cases, the whole of the leaving loss has been deducted from the total heat to exhaust to find the end-point of the condition curve. Others estimate the probable stage efficiency of the last stage and only deduct from the heat to exhaust, the product of this stage efficiency and the leaving losses. Obviously the latter method gives the higher end-point. Can Mr. Robinson indicate which method more nearly approaches the true end-point?

This paper will prove valuable to designing and operating engineers as it discusses a hitherto little understood subject in a clear and comprehensive manner.

SABIN CROCKER.⁵ Mr. Robinson's paper presents valuable information on turbine-exhaust loss as seen by a turbine designer. As such, the presentation of these data is an excellent and timely work. The writer would like to present the turbine user's view of these data as they may be applied to turbines in power plants.

As power-plant heat rates have been improved through the development of more efficient equipment and the adoption of more favorable heat-utilization cycles, it has become necessary for engineers charged with the design and operation of power plants to go progressively to greater refinements in order to continue an improvement of thermal efficiency within the economic limitations of the case. Consequently in order to obtain further improvements at the present time it is necessary to consider comparatively small differences and quantities, such, for instance, as are involved in the return of low-grade heat through the turbine feedheating circuit, in changes in condensing equipment to obtain better vacuum, or other changes which may affect the exhaust loss in different ways.

⁴ Professor of Mechanical Engineering, Johns Hopkins University, Baltimore, Md. Mem. A.S.M.E.

⁵ Engineer, Engrg. Div., Detroit Edison Co., Detroit, Mich. Mem. A.S.M.E.

Operating companies make many such studies in which the exhaust loss becomes an important item. Under present practice it is necessary to obtain specific data from the manufacturer for each case considered. This results in great expense to both parties, loss of time in correspondence, and a restriction in the number of comparisons that can be made in a given study. In consequence, while the manufacturer usually shows a willingness to cooperate in such matters, the results are not always satisfactory.

The present paper is a notable beginning toward clearing up these difficulties in that it enumerates all the items involved in the exhaust loss of a steam turbine. A detailed statement of the turbine-user's need for data of this type should likewise help the situation. Briefly, he should be able to determine the exhaust loss on his turbines for any possible operating condition. In this regard Figs. 4 and 7 from which can be determined the magnitude of the loss for a given turbine are of particular interest. It would seem that such information should be made available to a turbine owner in either of two different ways: (a) on request furnish him curves similar to Figs. 4 and 7 applying to his particular turbine and (b) make available to him the methods for computing such curves from the basic data for his type and size of turbine. Such material is indispensable to the turbine operator for an intelligent solution to his problems in power-plant design. Apparently Fig. 4 can readily be used for any desired operating condition but it appears that Fig. 7 would have to be given for a series of different condenser pressures and exhaust flows before it would be of much use to a plant designer. This would entail a large amount of detailed work on the part of the manufacturer, which it would seem he could eliminate by making more generalized computation methods available to the turbine user.

The writer is quite aware that many variables are involved in computing exhaust losses, and that turbine manufacturers and their designers prefer to pass out information piecemeal rather than to give an operating company's engineers sufficient information about a given turbine for them to compute the necessary correction factors for that turbine themselves. Nevertheless, it would seem that the author could well afford to give the user's requirements further consideration in closing an otherwise commendable paper.

C. C. FRANCK.⁶ In discussing the actual loss due to the pressure drop through the exhaust load, the author places considerable stress on the size of the cylinder-exhaust area, without a great deal of concern for the flow area of the last row of blades.

For a turbine of equal exhaust dimensions to that presented by the author, the loss resulting directly from the increase in exhaust pressure caused by crowding the exhaust hood, constitutes only a small part of the actual loss in heat converted into work.

By virtue of the consideration of $\frac{\sum u^2}{\Delta i_s}$ for not only the last row, but for the last three stages, which are affected by the change in vacuum, it may be pointed out that the reduction in adiabatic heat available, Δi_s , results in an increase in the operating efficiency of the group and partially offsets the reduction in available heat. Another important point to be considered is the so-called "explosion loss" or loss occurring when the volumetric flow through the last row of blading is of such magnitude that a portion of the expansion actually occurs outside of the last-row-blade passage. This results in an uncontrolled expansion which destroys a greater part of the energy liberated.

For example, assume that Δi_s for the last three stages at full

⁶ Turbine Apparatus Div., Engrg. Dept., Westinghouse Elec. and Mfg. Co., South Philadelphia Works, Philadelphia, Pa. Jun. A.S.M.E.

capacity including reheat, is 160 Btu/lb at 29 in. vacuum of which 105 Btu/lb can be converted into useful work. Then by virtue of limited exhaust dimensions the pressure at the exit of the last row of blades is reduced 0.5 in. vacuum to 28.5 in. Then the reduction in available energy will be (from Fig. 10) 21.6 Btu/lb and the resulting Δi_s will be 139.4 Btu/lb at 28.5-in. vacuum of which 100 Btu/lb can be converted into useful work.

Consequently from this consideration the actual reduction in heat to work will be 5.0 Btu/lb, not corrected for moisture losses which, for such small changes, could be neglected.

Carrying this example to a conclusion by adding the effect of moisture, we see on the i - s diagram that the average moisture for the expansion to 29-in. vacuum is 9.25 per cent while the average moisture for the expansion to 28.5-in. vacuum is 9.0 per cent. Assuming no moisture removal and applying a correction

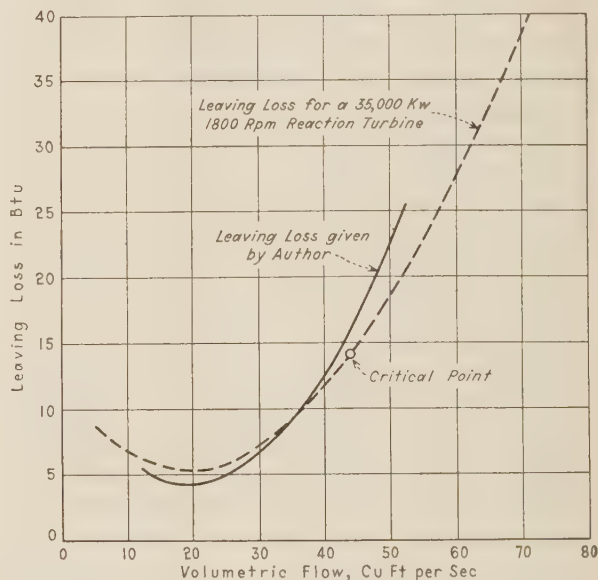


FIG. 18 TYPICAL LEAVING LOSS CURVE (35,000 kw, 1800 rpm.)

of 1 per cent loss in efficiency for 1 per cent average moisture content to the heat converted into work for the two expansions, we see that the heat converted to work for the 29-in. expansion is 95.3 Btu/lb and 90.5 for the 28.5-in. expansion. Hence the reduction in heat to work is 4.8 Btu/lb resulting from a reduction in available energy of 21.6 Btu/lb.

This points out that even with great care exercised in the design of the low-pressure exhaust load, a restricted last-row blade annulus may tend greatly to reduce the expected gain.

Another point of importance to be considered at this time is the possibility of correlating the design of the turbine and condenser in order to produce an approximately constant volumetric flow through the exhaust end for the normal range of operating loads. This could be obtained by controlling the condenser circulating water to produce the desired vacuum with changes in steam flow. In this manner the design consideration of the turbine with regards to exhaust dimensions could be simplified.

With such a system of variable vacuum the discussion on reduction in available work would have to be continued with lower flows. With such conditions of reduced volumetric flow, i.e., half load flow at 29 in. vacuum, the effect of explosion is entirely eliminated and the actual operating vacuum could be increased to 29.25 or 29.5 in. and at the same time the extra

available energy converted into work at approximately the same efficiency as in the case of the 29-in. expansion.

In regard to the question of designating leaving losses it appears that the most rational method of evaluating them would be to consider the loss in kw. By the use of kw an absolute loss is immediately determined and its magnitude is left without question.

Another point which should be considered is the method of carrying peak loads. Some installations carry peak loads with the bleeder heaters cut out of service and this condition lends itself to separate consideration by virtue of the added flow passed through an already crowded exhaust.

Fig. 18 shows a typical "leaving-loss" curve for a reaction machine of 35,000 kw.

H. G. HIEBELER.⁷ We are pleased to see such a thorough definition and explanation of a subject which has caused much comment by power engineers within the past few years.

We feel that it is a function of the turbine designers to define what should be understood by such losses and to show their relative magnitude.

From a strictly operating viewpoint, once the selection of a machine has been made, these losses are beyond control except to a limited degree by the plant men. In southern stations, such as the Deepwater (Houston) plant, the high circulating-water temperatures which prevail throughout most of the year limit the vacuum obtainable. In the north, however, with colder water conditions, particularly in the winter time, absolute pressures between 0.50 to 0.75 in. Hg abs may prevail for several weeks in extreme cases. In some instances, due to the pressure from operating departments together with the natural conservatism of designers, condensers are purchased for summer conditions. With such installations undoubtedly the magnitude of these leaving velocities and exhaust losses is very great. From the operating viewpoint, attention should be called therefore to the fact that many units are unable to use such high vacua effectively or that there is a limit beyond which it is not economical to go. This would suggest reduced speeds of the circulating pumps, resulting in a saving in auxiliary power. Further, on some types of condensers, refrigeration losses of the condensate are increased under high vacuum conditions.

The author's paper considers the performance of the unit assuming a constant back pressure of 1 in. Hg abs at the flange. We believe it would be of interest to call attention to the variation in the performance of modern condensers with variations in load and with variations in circulating-water temperatures, such as occur from season to season. The following will illustrate the typical performance of a condensing unit for a 35,000-kw machine under the conditions prevailing at Houston:

Temperature of inlet circ. water	Steam condensed, lb per hr— 360,000 315,000 235,000 170,000			
	Back pressure, in. Hg abs—			
50 deg F	0.86	0.78	0.64	0.59
65 deg F	1.30	1.20	1.02	0.94
80 deg F	2.00	1.85	1.60	1.44
95 deg F	3.04	2.82	2.48	2.21

In the tabulation above, the flows which correspond to maximum load (40,000 kw), full load (35,000 kw), three-fourths and half load happen to correspond very closely to the flows assumed by the author. This tabulation will show a variation of approximately 25 per cent in the specific volume of the steam to the condenser between half load and maximum load for the same water conditions and a change of approximately 300 per cent for the same load between summer and winter conditions. This of course neglects the consideration of moisture.

⁷ Assistant Superintendent of Power, Houston Lighting and Power Co., Houston, Tex. Mem. A.S.M.E.

The use of these factors would considerably alter the author's Fig. 13 and also call attention to the necessity of using weighted averages over the entire year in connection with the author's Fig. 17, showing typical annual load curves, in order to compute the total annual losses from this source.

P. H. KNOWLTON.⁸ This paper is an excellent presentation of the calculation of the total exhaust loss from a turbine. It appears worth while to supplement this work by a statement as to the background of the method and the reasons for believing that such calculations are adequate.

In the first place, for any particular turbine the characteristics of the last stage wheel and buckets are, of course, known to the designer. The calculations necessary for Fig. 4 are fairly simple, involving the aforesaid characteristics together with the laws of flow for wet steam as they are understood.

Fig. 7, however, requires something more than well-known rules. The flow of steam through the ordinary downward exhaust type of hood is rather complicated and resource must be had to tests to determine the characteristics of various types. Two ways of testing are open, namely, by means of models or by testing hoods on actual turbines in operation. In either case, the test consists of measurements of the annulus static pressure together with the steam flow through the last stage wheel.

Of the two means, the model tests are easier and more instructive. We are able to make models from $1/6$ to $1/12$ size or smaller, depending upon the size of the actual hood in question. We test these models using air as the flowing fluid, and are able to observe very closely the flow characteristics. This can, of course, be done in advance of the construction of the full-sized hood in the factory.

Any model tests should be checked if possible on the actual full-sized apparatus and we have been able to check in this case by making annulus pressure measurements in actual turbines operating in some of the power stations in the country. The agreement between model and full-sized hood is very good and justifies the model tests.

The curve marked "total loss" in Figs. 13 and 14 can be checked as to shape by still another means which is open to us. A turbine can be operated under test conditions so that the weight flow through the last stage buckets is at a constant rate. Then the turbine condenser pressure can be varied by bleeding air to the condenser, or by other means, and the variation of turbine output can be measured. This variation of output is really a difference between the change in available energy due to the change in exhaust pressure and the change in exhaust loss occasioned by the change in exhaust volume flow. The change in available energy is readily calculated from the steam chart, leaving a change in exhaust loss determined. Whenever possible, therefore, we obtain these variable vacuum curves at constant flow, as valuable aids and checks on our calculation methods. It is not always possible, since turbines of moderate and large capacities must be tested, if tested at all, in the operator's power station and operating conditions or other factors may make extended tests impracticable.

It is evident from the foregoing that means of testing have been developed and are used for checking and substantiating the methods of exhaust loss calculation as presented by Mr. Robinson.

H. V. RASMUSSEN.⁹ The author has written a very interesting paper which is of vital interest to the turbine designer, as the

⁸ Turbine Engineering Department, General Electric Co., Schenectady, N. Y. Jun. A.S.M.E.

⁹ Westinghouse Electric and Manufacturing Co., South Philadelphia Works, Philadelphia, Pa. Mem. A.S.M.E.

dimensioning of the last spindle row and the turbine-exhaust casing has a deciding influence on both the turbine performance and the manufacturing cost.

If a turbine element in the high-pressure end of a turbine is not very efficient, up to one-half the losses may be recovered in the rest of the turbine due to reduced moisture and increased heat drop, but losses in the exhaust end of a turbine are irretrievably lost to useful work. Any improvement obtainable in the exhaust end will have a direct bearing on the over-all performance of the turbine.

While the performance of a turbine is improved by a large last-row annulus with a correspondingly low kinetic leaving loss, the manufacturing cost of a turbine goes up rapidly with the increase of the dimensions of the last row. Also, blade and spindle stresses place a definite limitation on the physical dimensions involved. A proper compromise between these various factors must, therefore, be established in practical turbine design.

The present tendency toward large single-cylinder turbines makes it necessary to employ high peripheral blade speed in the last row, with a resulting high steam speed and a large kinetic leaving loss. The place for improvement, consequently, is in the exhaust casing which should be designed to offer the smallest possible resistance to flow from the last-row annulus to the exhaust opening.

It would be interesting to know how the author arrived at the annulus pressure drop shown on Figs. 5 and 7, and also how it was established that some exhaust casings are actually diffusing. Measurements on actual turbines are very difficult to obtain as they involve measurements of static pressure in the high velocity jet. Some attempts were made to measure the pressure drop in an exhaust casing of a large Westinghouse turbine by tapping the cylinder casing at various points in the cover and base. No conclusive results were obtained from this investigation as it was obvious that a velocity head created by the steam impinging against the measuring hole obscured the results and, at the very best, these measurements would only record the pressure existing at the periphery of the casing. They could not disclose the pressure distribution in the middle of the casing. Measurements with pressure-measuring tubes, such as the Fechheimer tube, were given up as impracticable, as the moisture in the steam would partly fill the passages and cause incorrect readings.

Another approach to this problem is to conduct tests with small-scale models. A number of exhaust model experiments for various exhaust-cylinder designs were run by the Westinghouse Company. Wooden models of the exhaust casing were made to $\frac{1}{8}$ of full size and air was blown through the models. A rotating blade row, mounted on a disk and driven by a motor, represented the last spindle row. Pressure measurements were taken with a Fechheimer tube at a number of points around the blade annulus and the velocity distribution over the exhaust opening was recorded with a Prandtl impact tube.

These experiments disclosed a number of interesting facts. First of all, it was found that steam is distributed most unevenly throughout the casing and the exhaust opening. The steam clings to the generator side of the exhaust casing and also crowds this side of the exhaust opening, while the part of the exhaust opening that is nearest to the turbine is hardly filled. If a part of the exhaust opening is located under the bladed part of the cylinder, the pressure drop through the casing will increase considerably.

The tests also showed that ribs and steam deflectors in an exhaust cylinder might improve the distribution of the steam over the exhaust end, but generally accomplishes this at a cost of an increased pressure drop from the last row to the exhaust opening. The older exhaust-cylinder design with a number of separate passages from the last row to the exhaust opening had thus a

considerably larger pressure drop through the casing than the bare exhaust cylinder. However it was found possible to design a deflector that was shaped as part of a rotative body and that reduced the pressure drop as it diminished the concentration of flow at the condenser side of the exhaust opening.

The pressure measurements around the periphery showed a somewhat similar distribution to that shown on Fig. 7 of the author's paper.

RONALD B. SMITH.¹⁰ Low-pressure end losses consist of friction due to wall resistance and curvature losses in the exhaust hood, and eddy friction resulting from the attempt to convert kinetic energy at the blade annulus to potential energy at the condenser flange. Physically these losses are an evaluation of the well-known relation

$$AR = (i_2 - i_1) - A \int_1^2 v dp \dots \dots \dots [1]$$

in which R is the total low-pressure end loss, i the enthalpy of the steam, A the Joule conversion factor, with the subscripts 1 and 2 referring to conditions at the exhaust annulus and the exhaust flange, respectively. In the design of the exhaust we are faced with four characteristic solutions of the relation expressed by Equation [1]. First, there may be complete reconversion of the kinetic energy at the exhaust annulus into potential energy. In this case we have an isentropic change in which

$$A \int_1^2 \frac{cdc}{g} = -A \int_1^2 v dp = -(i_2 - i_1)$$

and the low-pressure end losses AR become zero. This interchange of energy is contrived through a completely reversible process and while it represents the ideal in achievement it is, in the light of our present knowledge of the physical laws, quite beyond the realm of possibility.

The next possible solution to Equation [1] lies in the reconversion of a portion of the kinetic energy of discharge by a diffuser-shaped exhaust chamber. It is represented physically by the boundary condition $p_2 > p_1$ and by $(i_2 - i_1) > A \int v dp$. Practically, this solution is the aim of all good designs since the total low-pressure end losses become less than the leaving-velocity loss at the blade annulus. Unfortunately, mechanical restrictions, imposed largely by the purchaser, have prevented many exhaust-end designs of this type in the United States, although in Europe the practise is used frequently to advantage.

A solution almost akin to the one just described lies in a partial reconversion into pressure which is subsequently lost through wall friction in the exhaust chamber. In this case $p_1 = p_2$, and the low-pressure end loss is equal to the kinetic energy of the fluid from the last-blade annulus. This assumption was widely used in turbine design up to the past few years but increasing demands for economy have necessitated a solution more in keeping with the actual condition. This solution usually consists not only in a complete loss of the kinetic energy of discharge but in an additional pressure drop as well ($p_2 < p_1$). In this case the $A \int_1^2 v dp$ is negative. This is the condition to which the author devotes himself, and while far from the ideal it is at present the most common. The real problem in this design lies in the determination of the pressure drop. Since measurements on actual machines are practically impossible, models are usually prepared. However, the requirements of similarity are not wholly satisfied in the model due to the extreme velocity and pressure conditions that exist in the usual exhaust end.

¹⁰ Experimental Engrg. Dept., Westinghouse Elec. and Mfg. Co., South Philadelphia Works, Philadelphia, Pa. Jun. A.S.M.E.

As the author has already pointed out an expression for the low-pressure losses in per cent of the adiabatic enthalpy change means little unless one is familiar with the type of cycle. A term more closely representing the efficiency of the low-pressure end design proper would be the ratio of the average kinetic energy at the exhaust flange to the total frictional loss.

$$\eta_{exh} = \frac{A \frac{c_2^2}{2g}}{AR_c} \dots \dots \dots [2]$$

Equation [2] is a measure of the designer's skill, and for the perfect diffuser has a value of

$$\eta_{exh} = 100 \text{ per cent.}$$

In the 35,000-kw machine described by the author the net annulus area appears to be 31 sq ft. Assuming that the exhaust-flange area is about $31/0.4 = 78$ sq ft, the average kinetic energy at the exhaust is 6.7 Btu at full load. Then the efficiency of the exhaust end proper is $\eta_{exh} \cong 26.5$ per cent. The corresponding loss based on the adiabatic enthalpy change is about 4.9 per cent. These two factors would appear to define fully the conditions at the low-pressure end. The exhaust efficiency represented by Equation [2] is a measure of the relative merit of the exhaust hood, and to the designer it represents the internal efficiency of the low-pressure end. The conventional leaving loss on the other hand shown in Figs. 13 and 14, represents the low-pressure frictional losses in respect to the total available energy; it determines whether efforts to improve the exhaust end efficiency η_{exh} are justified from the standpoint of economy.

C. R. SODERBERG.¹¹ Turbine designers will welcome this paper on a subject which has always represented an important question in the art. Very little of the material as presented can be regarded as controversial, and the writer will limit himself to a brief discussion of a few points.

The leaving loss is undoubtedly one of the most important single items in condensing turbines, particularly because it can be influenced to a considerable extent by modifications in design, specifically by the size of the exhaust annulus. A similar investigation was made sometime ago by Prof. A. G. Christie and presented at the 2nd World Power Conference in 1930.¹² This investigation, as well as the one covered by the present paper, neglects another loss item which is of the same significance and which must be considered in connection with the leaving loss. This is the loss caused by the moisture in the low-pressure end of condensing turbines. Very little reliable information exists as to the magnitude of the latter loss, but some of the results obtained recently by the Westinghouse Company indicate that it is often greater than the leaving loss. In particular, it is increased rapidly with the peripheral speed. If the leaving loss is reduced by an increase in blade annulus, this reduction is accompanied by an increase of the moisture loss which may, in certain cases, more than offset the reduction of leaving loss. With this fact in mind, it is impossible to arrive at an economical size of exhaust annulus without injecting the moisture loss. Supersaturation, on the other hand, can generally be disregarded, at least for the moisture contents now common in condensing turbines.

The author has properly emphasized the importance of including in the leaving loss the losses in the exhaust hood. The

benefit of a generously dimensioned exhaust annulus may be lost unless the hood is properly proportioned and dimensioned.

It would be of great interest to know by what means the pressure distribution shown by Fig. 7 was obtained. We have made attempts at similar measurements and have been forced to conclude that it is exceedingly difficult to get the pressure readings inside the exhaust of an actual turbine. Fig. 7 indicates a degree of precision which I know is very difficult to reach.

AUTHOR'S CLOSURE

In concluding this discussion, it seems necessary first to set down the distinction between the leaving-velocity and exhaust loss on the one hand and the vacuum corrections applicable to the turbine-performance curve on the other hand. This paper has confined itself entirely to the former which is supposed to occur in the exhaust hood between annulus and exhaust flange. In preparing the vacuum corrections showing the variation of turbine performance with changing back pressure at the exhaust flange, it is necessary to take account of all other contributing or interrelated effects, whether or not they are parts of the loss in question. It is, of course, true that in many cases the vacuum corrections consist almost entirely of leaving-velocity and exhaust loss but the distinction is very real. Operators generally are interested in the vacuum correction. The leaving loss, as such, has always seemed to us a matter of interest particularly to the designer. It is one of the most important elements influencing turbine performance.

Mr. Caldwell is inclined to doubt the continuance of load growth. It is true that there has been a five-year cessation in this matter but it is also true that in many areas with favorable rate structures the per capita consumption of electricity is several times what it is in some of our largest metropolitan centers. In our opinion, any system that has the courage to look ahead 15 or 20 years may expect a load growth to two or three times its present size. While the annual percentage increments may fall off, it is likely that the actual kw increments may increase. Certainly the use of electricity is going to increase whether the present systems furnish the power or whether it is to be supplied in some other manner.

Professor Christie raises the question as to the desirability of incorporating diffuser exhaust hoods in all turbines and this matter is also touched upon by Mr. Smith. This question is largely an economic one and it is not easy to answer it briefly. However, this much may be said: that such diffusing hoods as are now in existence have that property as a by-product of other features of design and were not so made for that reason alone. The design is usually expensive and justified only under special conditions.

The author's remarks on supersaturation were based on the findings of the General Electric Company as set forth by Professor Goodenough in his published report in 1927. It must be admitted that the true condition is still a matter of argument but undoubtedly more specific analyses will be available in the future. Probably we should not have said it could be "neglected." When a manufacturer bases his promises on well-established past performance, it is impossible for him to neglect anything. But, on the other hand, the more specific his analysis, the greater are his opportunities to improve design.

Professor Christie also asks about the true end-point of the condition curve. It seems to the author that that is given by the exhaust heat and the exhaust pressure and that it is the only point definitely known except that fixed by the initial conditions. Given the initial conditions, known performance gives the end point. All intermediate points must be estimated by design technique and the better they are filled in, the better may they be used for improving design. For instance, to get back to the wheel exit, it is necessary to divide the exhaust heat between

¹¹ Manager, Turbine Apparatus Division, Westinghouse Elec. and Mfg. Co., South Philadelphia Works, Philadelphia, Pa. Mem. A.S.M.E.

¹² "Economic Considerations in the Application of Modern Steam Turbines to Power Generators" by A. G. Christie. Second World Power Conference, 1930.

pressure-volume energy, temperature energy, velocity energy, and if there is supersaturation, it may be necessary to include surface-tension energy. As a short cut from the true end-point to the wheel exit, one might draw a horizontal line to the left to annulus pressure and thence down the pressure line so as to deduct the velocity energy fraction of the leaving loss. That would locate what might be called the "chart condition" of the steam at the wheel exit, which would be useful to give the moisture content. This is to be distinguished from what would be the end-point of the machine if it had zero-leaving loss. The important point in this matter is to base predictions upon exactly the same conventions used in analyzing performance.

Mr. Crocker has pointed out how necessary it is for an operator to have all the essential information about his machine. Certainly the manufacturer intends to furnish all such information and if it has not been done in the past, that must have been due to a misunderstanding of the needs in the particular case.

Mr. Franck has called particular attention to a number of items and rightly expresses his concern about the flow area of the last row of blades. That is usually the most important feature of all, and, if the author did not show proper concern about it, that was because of its general recognition. Mr. Franck's remarks about the effects on the preceding stages help to bring out the distinction which is necessary between the total net effect on turbine performance of a change of vacuum, and the leaving-

velocity and exhaust loss by itself. Although the distinction might be thought of as only a matter of definition, it is none the less important.

Mr. Hiebeler points out the important effects of varying cooling-water conditions on the vacuum and consequently on the magnitude of the leaving losses. The diagrams in the paper have been based on 1 in. Hg abs back pressure. There is a certain back pressure below which better vacuum fails to yield any more power. Refrigeration, in itself, is detrimental. In deciding how much water to pump it is necessary for an operator to balance his pump requirements and refrigeration losses against the additional power shown by his vacuum corrections.

Mr. Knowlton's discussion anticipates the questions raised by Messrs. Rasmussen and Soderberg about the pressure measurements in exhaust hoods as shown in Figs. 5 and 7 and it does not seem necessary for the author to add anything further on that subject.

Mr. Soderberg also mentions the importance of proper consideration of moisture losses and here again it may help in clarifying the situation to point out that moisture effects have been considered in the paper only in so far as they affect the leaving-velocity and exhaust loss itself. Changing degrees of moisture in preceding stages affect the turbine performance and have to be considered in predicting vacuum corrections but such effects are not a part of the leaving loss even though in part due to it.

Performance of Cutting Fluids When Sawing Various Metals¹

BY O. W. BOSTON² AND C. E. KRAUS,³ ANN ARBOR, MICH.

This paper presents the results of a series of tests conducted on a Peerless high-speed, 9-inch-capacity hacksaw. Two types of tests were run: The first to determine the influence of four typical cutting fluids on the wear of the teeth of tungsten-steel hacksaw blades, the second to determine the influence of eleven cutting fluids on high-speed-steel blades when sawing each of eight different metals.

The time required to saw through a 1½-inch-square section of each metal was obtained and used to indicate the performance of the cutting fluid. In these tests high-speed-steel hacksaw blades were used, inasmuch as they retained the initial degree of sharpness without visible

change throughout the test. The comparative tests were run at constant speed and constant feeding pressures.

It is shown that a mineral-lard oil causes the tungsten-steel blades to wear fastest. Plain mineral oil produces the next fastest degree of wear, followed in order by an emulsion and a sulphurized mineral oil. The sulphurized mineral oil permitted the least degree of dulling on the saw blades and, at the same time, kept the sawing time to a time below that for any of the other cutting fluids. Cutting fluids produced a rather wide variation in cutting time when cutting steels, but gave more uniform values when cutting aluminum, malleable cast iron, cast iron, and brass.

THE MATERIALS TESTED

The materials selected for this series of tests consisted of eight ferrous and non-ferrous metals representing types commonly used. The various bars with their physical and chemical char-

TABLE 1 THE EIGHT METALS USED IN THE HACKSAW TESTS

No.	Bars Section (in.)	Material	Heat treatment	Analyses						Hardness Numbers Rockwell (100 Kg 1/16-in. ball)	Brin- ell	Physical Properties—		
				Al	Cu	Impurities						Yield point (lb per sq in.)	Ultimate strength (lb per sq in.)	Elongation (per cent in 2 in.)
AF	1½ × 2	Aluminum alloy S.A.E. 33	Chillcast	91.0	8.0	1.0				37.5	70
BF	1¾ × 1¾	Leaded free-cut- ting brass	Extruded and drawn	Cu 61.75 C	35.0	Pb 3.21 Ni 0.04 Mn 0.478	Fe			66.0	100	34,700	51,800	43.5
CF	1¾ × 4	Cast iron	Cast	3.44	2.62	0.986	0.478			83.5	179
DF	1¾ × 4	Malleable cast iron	<div style="display: inline-block; vertical-align: middle;"> 40¼ hr to 1550 F 48 hr at 1550- 1625 F 64½ hr to cool to 1200 F Annealed </div>	C	Si	P	Mn	S		71.0	137
				2.46	1.00	0.163	0.26	0.071	(Analysis of hard iron)					
KF	2 × 6	S.A.E. 3150 steel	Annealed	C	Ni	Cr	P	Mn	S	86.0	196	66,140	114,200	26.0
EF	1¾ × 4	S.A.E. 1020 steel	Annealed	0.50 C	1.16	0.62	0.022 P	0.68 Mn	0.023 S	65.0	131
FF	1¾ × 4	S.A.E. 1035 steel	Annealed	0.22 C			0.011 P	0.52 Mn	0.026 S	75.0	156
MF	1½ × 1½	S.A.E. 1112 steel	Cold drawn	0.38 C	0.18		0.017 P	0.53 Mn	0.031 S	89.5	217
				0.09-0.13		0.08-0.40		0.7-0.9	0.085-0.120					

presented to show the characteristics of the cutting fluids when used with each material. The wear on high-speed-steel and tungsten-steel hacksaw blades has been observed as indicated by the increase in time to cut a given cross-sectional area of a free-cutting steel, S.A.E. 1112, with three typical cutting fluids.

¹ Progress Report No. 5 of the A.S.M.E. Special Research Committee on the Cutting of Metals, Subcommittee on Cutting Fluids, of which C. J. Oxford⁴ is Chairman.

² Professor, College of Engineering, University of Michigan. Mem. A.S.M.E. Prof. Boston was graduated from the University of Michigan, Engineering College, in 1913, received a master's degree in 1917, and the degree of mechanical engineer in 1926. After graduation he was engaged at the university as instructor in engineering mechanics and mechanical engineering for four years. In October, 1917, he was commissioned in the U. S. Navy and assigned to duty in the Bureau of Ordnance on design and manufacture of submarine mines used in the North Sea Blockade. From 1919 to 1921 he was engaged in industrial engineering work for the Cleveland Tractor Co., in Cleveland, as assistant to the vice-president and works manager. In the fall of 1921, he returned to the University of Michigan, where he is now professor of shop practise and director of the department of engineering shop. He is author of many papers

acteristics are shown in Table 1. In the hacksaw tests, all bars were machined to a section 1½ inches square from the original size of the castings, forgings, or cold-finished bars listed in this table.

dealing with the subject of metal cutting and is serving on several committees dealing with cutting fluids, and standardization and nomenclature of small tools and machine-tool elements.

³ Assistant to Professor Boston, University of Michigan. Jun. A.S.M.E. Mr. Kraus received his bachelor of science degree in mechanical engineering from the University of Michigan in June, 1932. He is now continuing work on his master's degree at the University, and is an instructor in the department of engineering shop.

⁴ Chief Engineer, National Twist Drill and Tool Company, Detroit, Mich. Assoc. A.S.M.E.

Contributed by the Special Research Committee on the Cutting of Metals and presented at the Annual Meeting, New York, N. Y., December 4 to 8, 1933, of THE AMERICAN SOCIETY OF MECHANICAL ENGINEERS.

NOTE: Statements and opinions advanced in papers are to be understood as individual expressions of their authors, and not those of the Society.

TABLE 2 PROPERTIES OF CUTTING FLUIDS USED^a

No.	Composition	Base of mineral oil	Per cent compounding by analysis	Viscosity at 60 deg F		A.P.I. gravity at 60 deg F	d specific gravity	Temperature, deg F— Flash Pour Fire	N. P. A. color	Specific heat ^c			Thermal conductivity ^d		
				100	130	210				100	210	430	100	210	430
1	Dry cutting.....
2	1 1/2 per cent by weight of borax in water.....
3	1 part soluble oil in 50 parts water.....
4	1 part soluble oil in 10 parts water.....
5	No. 1 lard oil.....
6	Light mineral oil.....	Mixed
7	Heavy mineral oil.....	Mixed
8	10 per cent No. 1 lard oil in mineral oil.....	Paraffin
9	5 per cent oleic acid in mineral oil.....	Paraffin
10	Sulphurized mineral oil.....	Asphaltic
11	Sulphurized lard oil blended with 5 parts mineral oil....	Mixed

^a From "Performance of Cutting Fluids," by O. W. Boston and C. J. Oxford, A.S.M.E. Trans., vol. 53, 1931.^b F.F.A. is free fatty acids.^c Specific heat C_p computed from formula $C_p = (t + 670)(2.10 - d)/2030$, in which t = temperature of fluid in deg F, and d = specific gravity of oil at 60 F.^d Thermal conductivity k computed from formula $k = (0.813/t)(1 - 0.0003(t - 32))$, in which t = temperature of fluid in deg F; k is in units of Btu per hr per sq ft per in. per deg F.^e American Petroleum Institute.^f National Petroleum Association.

THE CUTTING FLUIDS

Eleven different cutting fluids were selected as representing the various classes found in general commercial use. They are listed in Table 2, together with their various properties. These cutting fluids have been used in previous tests on planing,⁵ drilling,^{5,6} and milling.⁷

THE TESTING EQUIPMENT

A Peerless power hacksaw was used in the tests. It was a standard high-speed machine with a capacity of 9 by 9 in. and a 6-in. stroke. A 1 1/2-hp motor mounted on the machine drove through a short belt to the tight and loose pulley. The saw made 120 strokes per minute. The saw blades used were of high-speed steel (Starrett Company No. 852) 17 in. long, 1 in. wide, and 0.065 in. thick. They had six teeth per inch with the set of the teeth one right, one left, two straight, etc., and cut a kerf 0.082 in. wide. A new hacksaw blade was used for each cutting fluid.

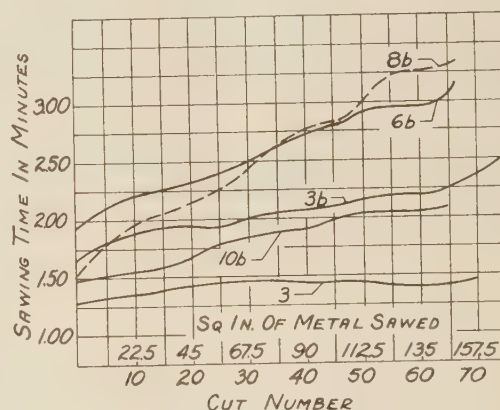


FIG. 1 WEAR ON HACKSAW BLADE

(The wear on a power hacksaw blade when cutting 1 1/2-in.-square sections of S.A.E. 1112 steel on the 9 X 9 in. Peerless hacksaw operating at 120 strokes per min with a feed pressure of 119 lb. For curve 3, a high-speed-steel saw blade, 6 teeth per in., was used with cutting fluid No. 3. For curves 3b, 6b, 8b, and 10b, a tungsten-steel blade was used: 12 in. long, 3/4 in. high, 0.049 in. gage, with 14 teeth per in., set right, left, straight, etc.)

The feed-pressure lever of the machine, which controlled the tension in the feed spring, was fixed in the twelfth notch from the bottom of the total of 23 notches in the ratchet. This setting was not changed during the course of the tests. The feeding pressure between the saw and work was measured carefully and was found to be 119 lb, equivalent to 13.2 lb per tooth for six teeth per inch. These feed pressures are maximum values, that is, the values for that point when the feeding finger has just caught another notch on the ratchet. The time required to saw a slice approximately 1/8-in. thick from the end of the various 1 1/2-in.-square bars was found for each cutting fluid by means of a stopwatch.

THE HACKSAW TESTS

Dulling Tests. The wear is indicated by the increase in sawing time per section in minutes as plotted in Fig. 1 over the serial number of the section cut and the total sq-in. area of metal cut. The results of some wear tests on tungsten- and high-speed-

⁵ O. W. Boston and C. J. Oxford, "The Performance of Cutting Fluids," A.S.M.E. Trans., vol. 54, 1932, paper MSP-54-2; Subcommittee on Cutting Fluids, Report No. 3.

⁶ O. W. Boston and C. J. Oxford, "The Performance of Cutting Fluids When Drilling Various Metals," A.S.M.E. Trans., 1933, vol. 55, paper RP-55-1; Subcommittee on Cutting Fluids, Report No. 4.

⁷ O. W. Boston and C. E. Kraus, "The Elements of Milling," A.S.M.E. Trans., 1932, vol. 54, paper RP-54-4.

steel hacksaw blades when cutting bar MF, S.A.E. 1112 steel, are given in Fig. 1 for each of four cutting fluids: the 50 to 1 emulsion, No. 3; the straight mineral oil, No. 6; the mineral-lard oil, No. 8; and the sulphurized mineral oil, No. 10. Curve 3 was first obtained using a high-speed-steel blade having six teeth per inch with a No. 3 cutting fluid. The sawing time of the high-speed-steel blade was found to increase uniformly from about 1.3 to 1.4 minutes in the first thirty cuts, during which time it sawed through $67\frac{1}{2}$ sq. in. of metal. From this point to the sixty-fifth cut, when the test was stopped, there was no appreciable change in cutting time. The blade was examined after the tests and showed no visible signs of dullness.

To reduce the time of the wear tests, ordinary tungsten-steel blades as described in Fig. 1 were used. Curve 3b, giving the time for each cut plotted over the number of the cut, was obtained with the tungsten-steel blade with cutting fluid No. 3. This shows a marked increase in sawing time up to the fifteenth cut, and a more gradual and non-uniform increase to the sixty-fifth cut, after which the time increased rapidly for each successive cut. The teeth at the end of the test were worn down about one-fifth of their height so that very appreciable flats were visible. The width of the set of the saw was reduced by wear from 0.067 in. when new to 0.064 in., or 0.003 in. One tooth was broken out from the leading end of the saw blade. It is interesting to note the difference in sawing time between curves 3 and 3b, due probably to the difference in tooth pressure.

Curve 6b, Fig. 1, shows the sawing time per cut when a straight mineral oil, No. 6, was used with the tungsten-steel blade. The time of the initial cut was greater than that when cutting fluid No. 3 was used. The cutting time increased more rapidly than when cutting fluid No. 3 was used. The blade was badly worn

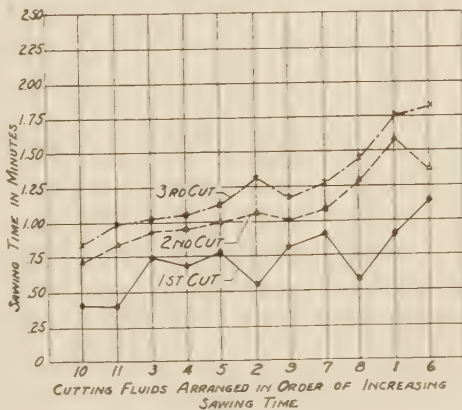


FIG. 2 SAWING TIME FOR FREE-CUTTING BRASS

(The time to saw off a $1\frac{1}{2}$ -in.-square section of free-cutting brass, bar BF, with various cutting fluids on a 9×9 in. Peerless hacksaw operating at 120 strokes per min and a feed pressure of 119 lb. A high-speed-steel hacksaw blade was used: 17 in. long, 1 in. high, 0.065 in. wide, 0.082 in. kerf, with the set of the teeth, right, left, two straight, etc. The time per cut for each of the first three series of cuts is shown. One blade was used with each cutting fluid for cutting one section each of seven different metals.)

at the end of the test, with nearly one-third of the height of the teeth worn off, and three teeth broken out from the leading end. The teeth were worn off on the side from 0.073 in. thick when new to 0.068 in., or a total of 0.005 in.

Curve 8b, giving the cutting time per cut when a mineral-lard oil, No. 8, was used, shows the greatest rate of dulling. The time of the cut at the start was low, but the sawing time per cut more than doubled in the sixty-five cuts taken, increasing from 1.5 minutes for the first cut to 3.3 minutes for the last cut. The blade showed somewhat more end wear than that used with cutting fluid No. 6 and had six teeth broken out, four from the

leading end and two from the following end. The side wear was 0.005 in. which reduced the set from 0.068 in. when new to 0.063 in.

The sawing time when using the sulphurized mineral oil No. 10, curve 10b, increases slowly up to the twentieth cut, after which it increases more rapidly. At the end of the test, however, very little end wear was apparent and no teeth were broken. The side wear was from 0.064 in. to 0.057 in., or a total of 0.007 in. It is probable that the blade would have cut several times as much metal.

From the curves of Fig. 1, it is apparent that a cutting fluid has an appreciable effect upon the dulling of hacksaw blades and it follows that the cutting fluid that gives a low sawing time when the blade is sharp is not necessarily satisfactory as the saw wears. It so happens that the saws requiring the greatest time

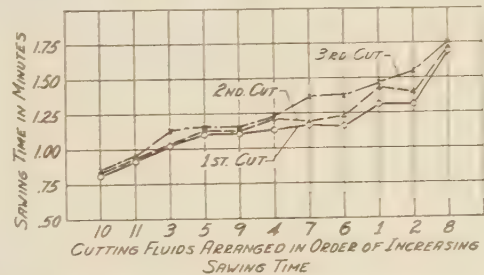


FIG. 3 SAWING TIME FOR CAST IRON

(The time required to saw through a $1\frac{1}{2}$ -in.-square section of gray cast iron bar CF, with various cutting fluids under conditions similar to those outlined in Fig. 2.)

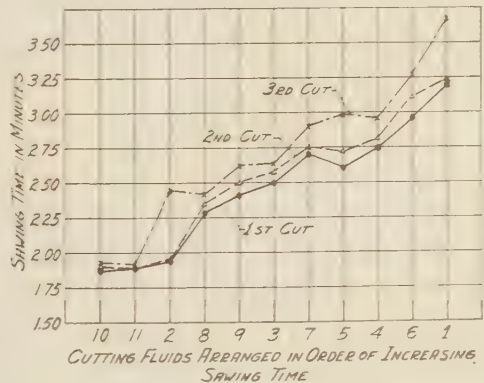


FIG. 4 SAWING TIME FOR S.A.E. 3150 STEEL

(The time required to saw through a $1\frac{1}{2}$ -in.-square section of S.A.E. 3150 steel, bar KF, with various cutting fluids under conditions similar to those outlined in Fig. 2.)

for the last cut were in the most worn condition. The sulphurized mineral oil No. 10 not only materially prolonged the life of the saw blades, but kept the cutting time for each cut below that of the other three cutting fluids used.

Tests to Compare Cutting Fluids. In order to obtain results which would permit a direct comparison of the various cutting fluids, the following procedure in running the comparative sawing tests was used. With a new high-speed-steel saw blade and a given cutting fluid, a single cut through a section $1\frac{1}{2}$ -in. square was taken on all test bars, one after the other, and the cutting times recorded. A second series of cuts was then taken on the bars in the reverse order, and a third series in the same order as the first. The actual time for each cut of all three series for each cutting fluid is shown plotted over the cutting-fluid numbers in order of increasing sawing time for free-cutting, cold-finished

TABLE 3 CUTTING TIMES FOR EIGHT METALS AND ELEVEN CUTTING FLUIDS

Bar No.	Material (1½ × 1½-in. section)	Cutting fluid numbers										Total time	Percentage	
		1	6	7	4	2	5	9	3	8	11			10
		Cutting time in minutes ^a												
AF	Aluminum alloy.....	0.64	0.60	0.56	0.54	0.56	0.57	0.46	0.47	0.48	0.38	0.40	5.67	19.6
DF	Malleable cast iron.....	1.12	1.02	0.97	1.06	1.16	1.03	0.87	0.94	0.86	0.72	0.68	10.43	36
BF	Free-cutting brass.....	1.40	1.45	1.11	0.90	1.00	1.00	1.03	0.90	1.25	0.85	0.67	11.56	39.9
CF	Cast iron.....	1.41	1.25	1.25	1.18	1.42	1.13	1.13	1.08	1.38	0.94	0.83	13.00	44.9
MF	S.A.E. 1112 steel.....	1.54	1.66	1.56	1.51	1.51	1.38	1.30	1.24	1.18	1.02	1.05	15.01	51.8
FF	S.A.E. 1035 steel.....	2.55	2.34	2.09	2.19	2.12	2.02	2.00	1.88	1.72	1.40	1.41	21.72	75
KF	S.A.E. 3150 steel.....	3.40	3.10	2.79	2.85	2.15	2.77	2.51	2.59	2.32	1.89	1.87	28.19	97.3
EF	S.A.E. 1020 steel.....	3.55	3.25	2.92	2.90	3.00	2.50	2.57	2.55	2.38	1.71	1.65	28.98	100
Total time.....		15.61	14.67	13.26	13.13	12.98	12.40	11.87	11.60	11.57	8.91	8.56
Percentage.....		100	94	85	84.2	83.2	79.5	76	74.4	74.1	57.1	54.9

^a Lengths of time tabulated are the averages of the first three cuts taken in each series as shown in Figs. 2, 3, and 4.

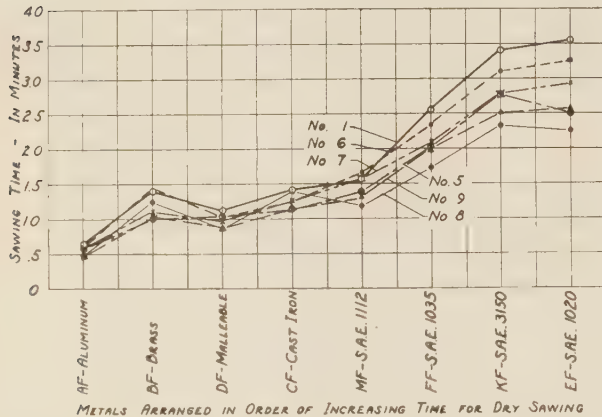


FIG. 5 POWER HACKSAW CUTTING TESTS

(The time required to cut off a 1½-in.-square section of eight different metals is shown, when cutting with various fluids on a Peerless high-speed standard-type hacksaw having a 9 × 9 in. capacity and operating at 120 strokes per min with a feed pressure of about 119 lb. A No. 852 Starrett high-speed-steel saw blade was used: 17 in. long, 1 in. wide, and 0.065 in. thick, 0.082 in. kerf, with six teeth per in., set right, left, two straight, etc. The experimental values are the average of the first three cuts of each material. The cutting fluids used were as follows:

- 1—Dry cutting
- 2—Water containing 1½ per cent borax
- 3—1 part soluble oil to 50 parts water
- 4—1 part soluble oil to 10 parts water
- 10—Sulphurized mineral oil
- 11—Sulphurized lard-mineral oil.)

brass in Fig. 2, cast iron in Fig. 3, and S.A.E. 3150 steel in Fig. 4.

It was found that the time for each cut of the first series of cuts on most metals was lower than the corresponding time per cut in the second and third series. For example, in Fig. 2 are shown the lengths of time per cut for the first series of cuts as well as the second and third series. The individual times of the first series are below those of the second and third series of cuts and the curve itself is not similar to the other two. Close agreement between the points of the first, second, and third series of cuts for each oil is shown in Fig. 3 for gray cast iron and in Fig. 4 for chromium-nickel steel. The corresponding curves for aluminum, malleable cast iron, and S.A.E. 1035 steel are in very close agreement. The curves representing the first series of cuts in S.A.E. 1112 steel and S.A.E. 1020 steel are about ten per cent below those representing the second and third series which, for each steel, are about equal.

There appears to be a progressive increase in sawing time as the blades are used, though visibly they showed no dulling, even after all tests were completed. The fact that the lines representing the second and third series of tests do not coincide more nearly may be due to progressive wear on the saw blade while making the cuts. One blade was used for each different cutting fluid, and there may have been some slight difference between one blade and another. This is not particularly apparent from the results of the second and third series of cuts in Fig. 2, nor do inconsistencies in Fig. 2 appear to be duplicated in Figs. 3 and 4 or for the other metals cut. It is of interest to note that the

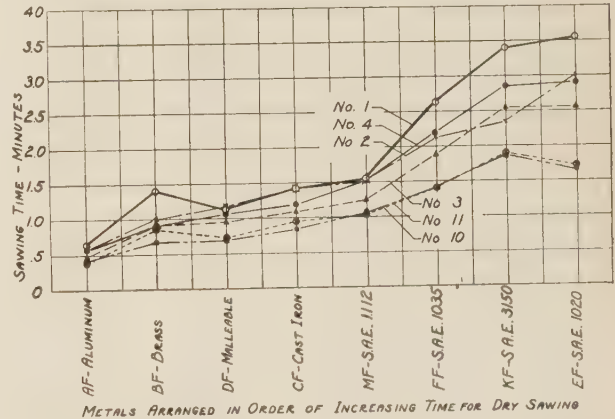


FIG. 6 POWER HACKSAW CUTTING TESTS (CONTINUED)

(The time required to cut through a 1½-in.-square section of each of eight different metals is given when cutting with additional cutting fluids, under conditions otherwise the same as outlined in Fig. 5. The cutting fluids used were as follows:

- 1—Dry cutting
- 5—No. 2 lard oil
- 6—Light mineral oil
- 7—Heavy mineral oil
- 8—Light mineral oil containing 10 per cent lard oil
- 9—Light mineral oil containing 5 per cent oleic acid.)

first series of cuts vary to the greatest extent from the average of the three series in every case.

The averages of the cutting times for the first three cuts for each metal and cutting fluid are tabulated in Table 3.

DISCUSSION OF COMPARATIVE TESTS

The metals are arranged in the vertical column of Table 3 in the order of increasing average time required to saw off a 1½-in.-square section. The order holds for all of the cutting fluids, although one of the time values is out of order for several cutting fluids, particularly for the free-cutting brass. The cutting fluids are arranged horizontally from left to right in order of increasing time.

The total time to cut one section of each metal with each cutting fluid is shown in the vertical column at the right. With 28.98 minutes total for S.A.E. 1020 steel representing 100 per cent, the proportional cutting time in per cent is shown for each metal. Aluminum is seen to cut in the least time of 5.67 minutes or 19.6 per cent of the time required to cut the S.A.E. 1020 steel.

The total cutting time for each cutting fluid on all metals is summarized at the bottom of the table. These values, also, are expressed in per cent with the maximum time of 15.61 minutes for dry cutting, No. 1, representing 100 per cent. Cutting fluid No. 10, sulphurized mineral oil, is shown to reduce the cutting time of all metals to 8.56 minutes or 54.9 per cent of that for dry cutting. It is seen that the sulphurized oils, Nos. 10 and 11, give the lowest average cutting-time values for all metals as a whole, with the mineral-lard oil, No. 8, next. The two straight mineral oils, Nos. 6 and 7, give the highest values next to dry

cutting. The water, No. 2, and the emulsions, Nos. 3 and 4, are seen to give rather intermediate values.

The average of the first three cuts for each cutting fluid and material is shown plotted in Figs. 5 and 6. In Fig. 5, the heavy line represents the length of time for cutting the various metals dry, cutting fluid No. 1. Corresponding times for the water compounds, cutting fluids Nos. 2, 3, and 4, together with the sulphurized oils, Nos. 10 and 11, also are shown. In Fig. 6, the curve for dry cutting is duplicated and curves are added representing the results obtained with the oils Nos. 5, 6, 7, 8, and 9. From Fig. 5 it is evident that dry cutting requires the greatest cutting time for all metals, with the possible exception of malleable cast iron and gray cast iron. The sulphurized oils, Nos. 10 and 11, produced the lowest cutting time, the values being almost identical except when cutting brass and cast iron, in which case, oil No. 10 produced slightly lower cutting times. In Fig. 6 it is seen that the oils do not produce a wide variation in cutting time, even when compared with dry cutting. It would appear from these two figures that the sulphurized mineral oil, No. 10, may, in the long run, be the cheapest cutting fluid to

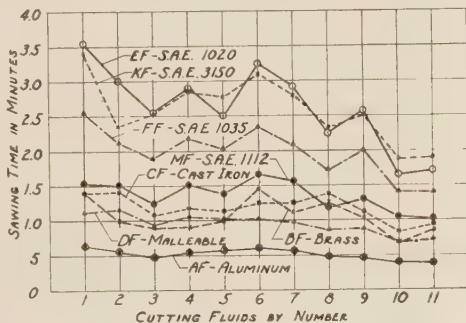


FIG. 7 INFLUENCE OF CUTTING FLUIDS ON EIGHT DIFFERENT METALS

(The influence of cutting fluids in cutting through a $1\frac{1}{2}$ -in.-square section of each of eight metals with a 9×9 in.-capacity Peerless power hacksaw, as outlined in Figs. 5 and 6.)

use in sawing, inasmuch as the lowest cutting time is obtained for all metals and the life of the saw is greatest.

Final summary curves representing the time required to cut eight materials with each cutting fluid are shown in Fig. 7. This emphasizes the influence of the various oils on the cutting time when cutting the various metals and shows the relatively small effect of cutting fluids when sawing aluminum and brass.

CONCLUSIONS

The conclusions reached in this paper are based on fixed conditions. These are: a specific saw blade operating with a constant total feeding pressure of 119 lb and with a constant cutting speed of 120 strokes per minute for the 6-in. length of stroke. The changing of any of these three variables would, it is believed, influence the results obtained. Conclusions may be summarized briefly as follows:

From the Dulling Tests.

(1) It is apparent that cutting fluids appreciably affect the rate of dulling of hacksaw blades.

(2) A cutting fluid giving a short sawing time with a sharp saw blade does not necessarily continue to give relatively short times after the blade has become dull. In other words, even though the initial cutting time per section is less than that for some other cutting fluids, the cutting time for a later cut, after the saw blade has become dull, may be higher.

(3) Of the cutting fluids tested, the least wear was obtained with sulphurized mineral oil, No. 10, while the greatest wear was found with the mineral-lard oil, No. 8. The emulsion, No. 3, produced faster cutting and a slower rate of wear than the light mineral oil.

(4) The wear, as indicated by the increase in time to saw through a $1\frac{1}{2}$ -in.-square section of S.A.E. 1112 steel, amounted to 8 per cent for the high-speed-steel saw blade with 6 teeth per in. and 41 per cent for the tungsten-steel blade with 14 teeth per in. while cutting sixty-five sections. The high-speed-steel blade showed no visible indications of wear other than polished tooth points at the end of each test.

(5) The tungsten-steel saws, requiring the greatest time for the sixty-fifth cut, were in the most worn condition.

From the Comparison Tests.

(6) Of the three series of tests made on all metals with the eleven cutting fluids, the first one gave the lowest length of time for each cut and varied most from the average of the three; that is, the times obtained from the second and third series of tests were nearly equal.

(7) The results of the three series of tests gave the greatest variation when sawing leaded brass and free-cutting steel, while those for the other metals were very close.

(8) A progressive increase in sawing time was noted for the three series of cuts: the first giving the smallest, the second slightly greater, and the third the greatest. The high-speed-steel saw blades showed no visible signs of wear at the conclusion of the test.

(9) It is apparent from these tests that considerable time in sawing a metal may be saved by using the most suitable cutting fluid.

(10) The effect of the cutting fluids varied with the metal sawed. The greatest variation in cutting time for the various cutting fluids was obtained when cutting the steels. The cutting time varied but little for the various cutting fluids when sawing aluminum, malleable cast iron, cast iron, and brass.

(11) Of the cutting fluids tested, the sulphurized mineral oil, No. 10, was found to be the best; it gave the least sawing time and also the least wear on the saw blade.

(12) Hack-sawing tests using cutting fluids are being continued to determine the influence of variation in cutting speed, variation in feeding pressure, and variation in the number of teeth in the saw blade.

ACKNOWLEDGMENT

This work has been conducted for the A.S.M.E. Special Research Committee on Cutting of Metal as a project of the Department of Engineering Research, University of Michigan. The authors wish to acknowledge the cooperation of Messrs. Maurice Bates, Vasily Prianihnikoff, and Louis Veenstra, who assisted in carrying out the work.

High-Temperature Tensile, Creep and Fatigue of Cast and Wrought High- and Low-Carbon, 18 Cr 8 Ni Steel From Split Heats

Progress Report of the A.S.M.E.-A.S.T.M., Joint Research Committee on Effect of Temperature on the Properties of Metals

By H. C. CROSS,¹ COLUMBUS, OHIO

Under the sponsorship of the Joint Committee, a comparison was made, chiefly at temperatures ranging from 1000 to 1200 F, of the resistance to short-time loading, to prolonged loading (creep) and to repeated stress (fatigue) of 18 per cent Cr, 9.5 per cent Ni, 0.5 per cent Mn, 0.6 per cent Si steels of 0.067 and 0.125 per cent C. Both carbon contents were studied in wrought and cast conditions and no "stabilizing" elements were used. Split induction-furnace heats were poured into ingots for rolling and into castings. Material of known melting history and of identical composition was thus available in both the fine-grained (rolled) and the coarse-grained (cast) states. Both cast and wrought materials were quenched from 2000 F.

The author describes in some detail the tests performed in comparing the characteristics of these steels under varied treatment and reports the results obtained together with certain conclusions which may be drawn.

INTRODUCTION

SINCE its formation in 1924, the A.S.M.E.-A.S.T.M. Joint Research Committee on Effect of Temperature on the Properties of Metals has carried on a program of determination and correlation of the fundamental properties of metals at low and high temperatures. The results of several laboratory studies on carbon and low-alloy steels have previously been reported.² More recently attention has been directed also to the austenitic stainless and heat-resisting steels of the 18 per cent Cr, 8 per cent Ni type, not only because of the intrinsic importance of that type but also, and especially, to reveal the possibilities and limitations for drawing generalized conclusions as to high-temperature behavior that will be valid both for pearlitic and for austenitic steels. A progress report on impact, magnetic permeability, and metallographic structural stability of rolled 18-8

steels of 0.06 per cent and 0.085 per cent carbon content obtained as regular commercial materials, was made in 1932.³ Further work on other problems, using these materials, and carried on cooperatively in several laboratories of committee and sub-committee members, is still in progress.

This work and other accumulated information brought up certain problems requiring clarification, as follows:

(1) Data so far available indicate that, for some carbon steels at least, high-temperature design based on creep, i.e., on allowable deformation within the life of the material, will not result in a fatigue failure, the endurance limits at high temperatures being at much higher stresses than those for creep at say a rate of 1 per cent in 10,000 hr. Does the same thing hold for an austenitic steel?

(2) Although there have been some indications to the contrary, considerable evidence has accumulated that in pearlitic steels, and especially at the upper range of temperatures, a relatively coarse structure, and a coarse cast structure in particular, is more resistant to creep than a finer-grained, rolled structure. The generalization is often made therefore that castings are superior to rolled material for high-temperature service. Does this generalization necessarily hold for austenitic material? Obviously it would be preferable to compare cast and rolled materials from the same melt.

(3) Embrittlement of 18-8 steel in the temperature range 1000 to 1400 F, usually ascribed to carbide precipitation and chromium depletion at the grain boundaries, is a major problem in the utilization of the steel for high-temperature service. An analogous problem, often discussed in connection with embrittlement but not necessarily having exactly the same cause or remedy, is the loss of corrosion resistance in aqueous corrosive media after sojourn in this temperature range. There has been great activity in the application of "stabilizing" elements for prevention of embrittlement and propensity to corrosion. The carbon content of 18-8 is found to be of extreme importance, material of the order of 0.02 per cent carbon, i.e., below the limit of solubility, being immune to deterioration, while, other conditions being equal, increasing the carbon above the solubility limit brings increased propensity toward deterioration. Hence, low-carbon 18-8 steel with carbon definitely below 0.07 per cent is classified separately from high-carbon material of say 0.10 to 0.15 per cent C.

Nevertheless, in either class, in the absence of stabilizers, and as long as the carbon is above the solubility limit, carbide precipitation does occur and the difference is one of

¹ Member of research staff, Battelle Memorial Institute. Upon graduation from high school Mr. Cross entered the Metallurgical Division of the Bureau of Standards. While so employed he attended George Washington University, being graduated in 1927 with the degree of B.S. in Chemical Engineering. In December, 1929, he joined the research staff of the Battelle Memorial Institute. In his work at both the Bureau of Standards and the Institute, Mr. Cross has concentrated on the investigation of the properties of metal at elevated temperatures.

² See reports, Joint Research Committee on Effect of Temperature on the Properties of Metals, Proc. A.S.T.M., 1925 to 1933, inclusive.

Contributed by the A.S.T.M.-A.S.M.E. Joint Research Committee on Effect of Temperature on the Properties of Metals and presented at the Annual Meeting, New York, N. Y., December 4 to 8, 1933, of THE AMERICAN SOCIETY OF MECHANICAL ENGINEERS.

NOTE: Statements and opinions advanced in papers are to be understood as individual expressions of their authors, and not those of the Society.

³ Report, Joint Research Committee on Effect of Temperature on the Properties of Metals, Proc. A.S.T.M., vol. 32, pt. 1, pp. 148-192.

degree only. In prior work of the joint committee,⁴ on 18-8 of 0.06 per cent and 0.085 per cent C (designated as K9c and K9d, respectively), both steels were found to behave "practically the same" as to change in impact properties at room temperature after 1000 hours without stress at 800 to 1400 F, and also as to carbide precipitation and agglomeration. What happens at such temperatures after long periods under stress?

Inasmuch as there is evidence that the creep resistance of 18-8 is higher with higher carbon, the relative deterioration in impact of high- and low-carbon grades made in the same way is an important problem

(4) It is known that changes in magnetic permeability occur during long heating of 18-8. No direct correlation of these changes with impact deterioration has yet been found, but added information would be of interest.

These problems called for the preparation, in the same way and from the same "pedigreed" raw materials, of heats of low and high-carbon content, the splitting of each heat into cast and rolled products, and the study of the four materials as to high-temperature fatigue and creep resistance, with attention to impact, structural stability, and magnetic properties of the materials after having been stressed for long periods in the critical embrittlement range. As the study was conducted from the fundamental point of view, relating to the 18-8 base itself, no "stabilizing" element was added.

ALLOCATION OF WORK AND ACKNOWLEDGMENTS

The program was too extensive to be handled speedily by division of the work among cooperating laboratories of the firms with which the committee and subcommittee members are connected; so funds provided by the National Electric Light Association, Engineering Foundation, National Research Council, American Petroleum Institute, and the Alloy Casting Manufacturers' Association were applied toward the cost of casting the steels which was undertaken by the Babcock and Wilcox Company, their rolling by the Carpenter Steel Company, of studies of fatigue at the University of Illinois (by N. J. Alleman under the direction of Prof. H. F. Moore), and of creep, impact, etc., at Battelle Memorial Institute (by H. C. Cross and F. B. Dahle with the advice of H. W. Russell and H. W. Gillett). The funds supplied did not cover the actual expenditures for the work done by Babcock and Wilcox Company, Carpenter Steel Co., University of Illinois, or Battelle Memorial Institute, and material financial aid was thus given the Committee by these groups. Help was also given by the Union Carbide and Carbon Research Laboratories, the International Nickel Company, and the Superheater Company in machining test materials. Short-time high-temperature tests were conducted by the Babcock and Wilcox Company and metallographic examination of some specimens was made by the Crucible Steel Company, Illinois Steel Company, and Union Carbide and Carbon Research Laboratories.

All the work was planned and carried out under the advice and general supervision of C. E. MacQuigg, Chairman of the Subcommittee on Technical Projects.

MATERIALS

Melting. The Committee designation for this series of materials was "K19." The steels were melted in ganister-lined high-frequency furnaces using a frequency of 960 cycles. To produce

⁴H. C. T. Han, Reports of Subcommittee G, "Cooperative Study of Charpy Notched Bar Tests of 18 Per Cent Cr 8 Per Cent Ni Stainless Steels," Proc. A.S.T.M., vol. 32, pt. 1, 1932, pp. 156-166.

L. Jordan, "Structural Stability of 18 Per Cent Cr 8 Per Cent Ni Stainless Steels at Elevated Temperatures in the Absence of Stress," Proc. A.S.T.M., vol. 32, pt. 1, 1932, pp. 170-192.

the desired amount of test material, about 4500 lb was required per heat. The largest furnace available had a capacity of 3000 lb; so the charge was divided between the 3000-lb furnace and a 1500-lb furnace, both parts of the heat melted and poured into one ladle for mixing. Approximately a third of each charge was scrap of similar composition to the material to be produced. The logs of these melts, as supplied by the Babcock and Wilcox Company are as recorded in Tables 1 and 2.

TABLE 1 HEAT B-1230—MAY 13, 1932—K19H (HIGH CARBON)

	Melt in lb	
	Large furnace	Small furnace
Armco sheet.....	640	320
Armco billet.....	640	320
65% ferro chromium 6 % carbon.....	30	15
65% ferro chromium 0.06% carbon.....	555	275
Nickel.....	185	95
Ferro manganese, low carbon.....	19	9.5
Ferro silicon.....	7	3.5
"KA2" scrap.....	960	400
Total.....	3,036	1,438
Deoxidizers added:		
Calcium silicide fines.....	4 lb	2 lb
Aluminum (block).....	4 oz	4 oz
Aluminum (pills).....	4 oz	none

LOG OF LARGE HEAT

6:50—Power on
8:05—All melted, skimmed and slag added made up of 1/3 lime, 2/3 ganister plus calcium silicide fines
8:20—Power off to melt 1500 lb heat
9:15—Power on
9:35—Last one pound of calcium silicide plus 4 oz aluminum pills plus 9 lb ferro silicon added
9:43—4 oz aluminum block added
9:45—Ferro manganese added
9:47—Power off, temperature 3025 F

LOG OF SMALL HEAT

8:20—Power on
9:15—Power off
Temperature 3015 F
Calcium silicide and aluminum added as in big heat
9:59—Small heat and big heat poured into ladle
Temperature 2940 F
10:03—10 in. fluted ingot poured; temperature 2690 F
8 in. fluted ingot poured; temperature 2675 F
10:05—Balance of melt returned to 3000 lb furnace and reheated
10:15—Temperature at pouring of No. 2 casting, 2860 F
10:30—Temperature at pouring of No. 11 casting, 2750 F
1 1/4 in. swank nozzle used; molds smoked.

TABLE 2 HEAT B-1234—MAY 13, 1932—K19L (LOW CARBON)

	Melt in lb	
	Large furnace	Small furnace
Armco sheet.....	620	320
Armco billets.....	600	300
"KA2s" hot rolled tubes.....	500	200
65% ferro chromium 0.06% carbon.....	500	200
Nickel.....	580	290
Ferro manganese, low carbon.....	185	95
Ferro silicon.....	19	9.5
	8	3.5
Total.....	3012	1418
Deoxidizers added:		
Calcium silicide fines.....	4 lb	2 lb
Aluminum (block).....	4 oz	4 oz
Aluminum (pills).....	4 oz	none

LOG OF LARGE HEAT

2:20—Power on
3:25—All melted, skimmed, slag added made up of 1/3 lime, 2/3 ganister plus calcium silicide fines
3:30—Power off to melt 1500 lb heat
4:30—Power on
4:40—Ferro silicon and remainder of calcium silicide added
4:42—Aluminum pills added
4:48—Temperature 3030 F
4:50—Ferro manganese added and poured into ladle; temperature 2950 F

LOG OF SMALL HEAT

3:30—Power on
4:30—Power off
4:50—Power on for short period and poured at same time as from big furnace
5:00—Both heats poured into ladle at 2950 F
5:06—10 in. fluted ingot poured; temperature 2775 F
5:06—8 in. fluted ingot poured; temperature 2715 F
5:22—Temperature No. 2 casting, 2890 F
5:35—Temperature No. 11 casting, 2650 F
1 1/4 in. swank nozzle used; molds smoked.

Rolling of Wrought Material. The metal for the rolled bars was cast into 10-in. and 8-in. fluted ingots weighing, respectively,

about 1000 and 490 lb. The ingots were rolled by the Carpenter Steel Company into one-inch rounds and shipped to Battelle as mill lengths of 9 to 11 ft marked to show carbon content and ingot size. A total of 2340 lb of rolled material was supplied.

Casting and X-Ray Inspection of Cast Material. The sand castings were poured after the ingots. Casting temperatures are given in the furnace logs. The molds were baked sand and poured tilted at 5 deg, gate-end down. The pattern shown in Fig. 1 was chosen to give proper feeding and to provide bars long enough for fatigue testing. It was agreed upon after considerable discussion by the committee as to the most practical form for the purpose in hand.

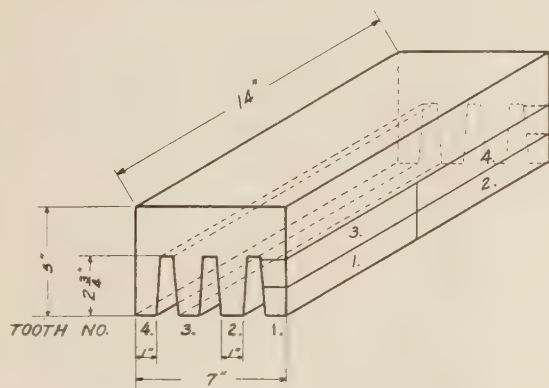


FIG. 1 KEEL-BLOCK PATTERN USED FOR PREPARATION OF THE CAST MATERIAL

The "teeth" or "keels" were deep enough to allow cutting two bars about 1 in. \times 1 in. \times 14 in. from each. Due to greater magnetic permeability of the upper part of the teeth in the case of the low-carbon cast material and the desire to have all material used as nearly alike as possible, only the lower 1 in. of the teeth from the low-carbon castings was used in the tests herein reported.

The teeth were cut off, marked for identification, and each tooth used was X-rayed for defects by Babcock and Wilcox, and tracings from the films were supplied to Battelle. All the low-carbon cast material used or examined was entirely sound. A few of the high-carbon teeth had slight defects from blowholes, apparently from mold gases or trapped air. The bars were machined at Battelle, in accordance with the X-ray indications, so as to give the maximum number of test bars but to exclude the slightest apparent defect from the test section of every bar. No visible imperfections were found on machining that had not already been revealed by the X-rays.

Heat Treatment. The previous lot of 18-8 (K9) used by the committee had been studied as rolled, air quenched (normalized) from 1950 F, and water quenched from 2100 F. The Subcommittee on Technical Projects first planned to study the present lots (K19) air quenched from 2000 F, and some rolled material was so treated at Battelle and a few creep tests made on it, when the subcommittee decided that water-quenching from 2000 F would be preferable and more representative of present practice; so all further creep work and all the fatigue work was done on material water-quenched from 2000 F. This same treatment was applied to both cast and rolled materials, of both high and low carbon.

All bars were heat treated in 14-in. lengths. The cast bars were split to 1 in. \times 1 in. \times 14 in. before heat treatment. One dummy bar of 18-8 with three thermocouples inserted in holes reaching to the center of the bar and located at the middle and half an inch from each end, and a dozen of the regular bars were placed together on the hearth of a gas furnace with the dummy in the center of the row. The bars were not piled upon one another. The furnace was preheated to 1600 F before charging the bars, and the temperature raised over a period of about 45 minutes until all thermocouples in the dummy bar reached 2000 F. The bars were then immediately water quenched. The few air-quenched bars tested were similarly treated save for air cooling instead of water quenching.

Analysis and Room-Temperature Properties. Chemical analyses as supplied by the Babcock and Wilcox Company are shown in Table 3.

TABLE 3 CHEMICAL COMPOSITION OF K19 18-8 STEEL

Element	Low-carbon heat K19L	High-carbon heat K19H
Carbon.....	0.067	0.125
Manganese.....	0.50	0.47
Silicon.....	0.65	0.58
Chromium.....	18.21	18.50
Nickel.....	9.56	9.67
Nitrogen ^a	0.056	0.035

^a Average of analyses by Union Carbide and Carbon Research Laboratories and Battelle Memorial Institute. These nitrogen analyses were in agreement to 0.001 per cent.

It will be noted that the nickel contents are above the 8 per cent of the type composition "18-8." The nickel contents of the K9 steels of the previous committee work were 8.50 and 9.15 per cent. The nitrogen content of K19L appears to be somewhat above that normally found in 18-8.

The room-temperature properties for the materials as water quenched from 2000 F, averaged from several closely agreeing tests, are shown in Table 4.

TABLE 4

Material	Yield strength, lb per sq in.	Tensile strength, lb per sq in.	Elongation, % in 2 in.	Reduction of area, %	Izod impact, ft-lb	Brinell
K19HRW: High-carbon, rolled	41,000	91,000	60 1/2	71	107	162
K19LRW: Low-carbon, rolled.	36,500	85,000	61 1/2	70 1/2	105	157
K19HCW: High-carbon, cast..	31,200	64,500	59	a	93	132
K19LCW: Low-carbon, cast..	28,000	64,500	66	a	92	137

^a Contour too irregular for accurate measurement because of large grain size.

The properties of the rolled material air quenched from 2000 F are shown in Table 4A.

TABLE 4A

Material	Yield strength, lb per sq in.	Tensile strength, lb per sq in.	Elongation, %	Reduction of area, %	Brinell
K19HRA: High-carbon, rolled.....	35,500	88,500	62	70 1/2	153
K19LRA: Low-carbon, rolled.....	33,500	85,000	61 1/2	72	150

SURVEYS FOR UNIFORMITY

Hardness. For determining the Brinell hardness two parallel flat surfaces were machined on the bars and five Brinell impressions made, three on one side and two on the other. Two readings at an angle of 90 deg to each other were made of the diameter of each impression. In the case of the cast bars the grain size was so large that in many cases irregularly shaped impressions were obtained. It was necessary in these cases to make a tracing of a magnified projection of the indentation and then measure its area and compute the mean diameter of the indentation. The maximum variation noted for the impressions on any one rolled bar was three points Brinell.

The range of hardness of the bars is given in Table 5.

All bars, both cast and rolled, used for creep tests were first

TABLE 5

		Hardness Range
K19HRW:	High-carbon, rolled, water quenched.....	155 to 165
K19LRW:	Low-carbon, rolled, water quenched.....	151 to 159
K19HCW:	High-carbon, cast, water quenched.....	128 to 134
K19LCW:	Low-carbon, cast, water quenched.....	134 to 140
K19HRA:	High-carbon, rolled, air quenched.....	153 to 154
K19LRA:	Low-carbon, rolled, air quenched.....	149 to 151

tested for magnetic permeability in 14-in. lengths, turned to 0.81 in. diameter, before machining into creep bars. The specimens were placed at the center of a carefully wound solenoid 30 in. long and 1.5 in. in mean diameter. A test coil of 500 turns inside this solenoid is connected with a ballistic galvanometer which gives a deflection of about 2 cm for a change in induction of 1 gauss. An auxiliary mutual inductance carrying the magnetizing current was adjusted to balance out the effect of changes in the magnetizing field. On reversing the current a galvanometer deflection proportional to the ferritic induction was obtained. The field was known and uniform to about 1 per cent. The value of $\mu - 1$ (permeability minus one) should be accurate to about ± 10 per cent. Tests were made at $H = 50$, $H = 100$, $H = 150$, and $H = 200$.

TABLE 6 MAGNETIC PERMEABILITY OF 18-8 BARS WATER QUENCHED FROM 1925 F

Material	Bar number	Carbon %	Magnetic Permeability—		
			Battelle	Westinghouse	
			$H = 50$	$H = 200$	$H = 202$
K19HR	30	0.125	1.0031	1.0026	1.0029
K19HR	40	0.125	1.0035	1.0030	1.0029
K19LR	82	0.067	1.0034	1.0030

Data for 50, 100, 150, and 200 gauss on any one rolled specimen agreed within 5 in the fourth decimal place. The values found ranged as follows:

K19HRW:	High-carbon, rolled, water quenched from 2000 F.....	1.0027 to 1.0037
K19LRW:	Low-carbon, rolled, water quenched from 2000 F.....	1.0027 to 1.0040
K19HRA:	High-carbon, rolled, air quenched from 2000 F.....	all 1.0031 (at $H = 50$ only)
K19LRA:	Low-carbon, rolled, air quenched from 2000 F.....	1.0031 to 1.0034 (at $H = 50$ only)

Since the values obtained on the rolled K19 steels of the present investigation were lower than those on the K9 steels of the previous investigation (which gave at $H = 200$ for 0.06 per cent C, air quenched from 1950 F, 1.027, and for 0.085 per cent C, 1.043), a check on the method was made by sending three bars to the Westinghouse Electric & Manufacturing Company. These comparisons were made before the heat treatment to be used in the investigation had been decided upon, and bars water quenched from 1925 F were used for the comparison. This comparison gave the results shown in Table 6, above, indicating that the test method was satisfactory.

Higher values were found for cast bars, and the variation was larger.

The upper halves of the teeth were slightly higher in permeability than the lower halves in the case of the high-carbon heat, but even the upper halves were not of as high permeability as the committee's previous K9 materials. The low-carbon castings, however, ran from 1.015 to 1.204 instead of the 1.003 or 1.004 of the rolled bars and the 1.004 to 1.022 of the cast high-carbon, and the upper part of the teeth was of distinctly higher permeability than the lower

part. The feeder block had still higher permeability. The difference was so marked that it was decided to utilize in general for the present series of tests only the lower part of the low-carbon teeth. Table 7 gives more complete data on the cast bars.

Macrostructure of the Cast Material. In the hope of determining the cause of these differences in permeability, sections were cut from the right and left ends of the four teeth of the high-carbon casting No. 7, part of which was known from the X-ray examination to be waste because of the blowholes shown in teeth 7-3 and 7-4. These sections were ground and macroetched and are shown in Fig. 2.

An area containing large grains is noted near the top and on the same side of the left-end sections of teeth Nos. 1, 2, and 3. The same is true for the right-end sections of teeth Nos. 1, 2, and 3, but surprisingly the large grain areas are on the opposite side of the tooth. Tooth No. 4, which on the left end has fine grains on all of both sides of the tooth, on the right end has large grains on almost all of both sides of the tooth. Apparently the grain size at the right end of the teeth is just the opposite of the corresponding locations at the left end.

The casting was gated at the right end, and the macrostructure shows the larger grains in the sections cut near the right end of the teeth.

Fig. 3 (slightly enlarged) shows the macrostructure of bars of $13/16$ in. in diameter cut from the upper and lower halves of teeth of the low-carbon cast 18-8. These bars were intended to be used for preparation of creep-test specimens, and no significant differences are shown between bars from the upper and lower halves of the teeth except the orientation of the grains. There is not such a large variation in grain size as appears in Fig. 2. Nevertheless, in view of the wide variation in permeability the upper halves were not used.

While some variation in behavior might be expected from specimens of such large and somewhat variable grain size, the large grain size was welcomed as tending to accentuate the factor of difference in grain size between rolled and cast material, one of the chief points to be investigated. Moreover, massive castings of irregular section, cooling from the melt at rates similar to the cooling rates of these teeth, would have similar grain size

TABLE 7 BRINELL HARDNESS AND MAGNETIC PERMEABILITY FOR CAST BARS USED IN THE CREEP AND FATIGUE TESTS

Material ^a	Specimen number	Location in tooth	Brinell hardness number	Magnetic Permeability—		
				$H = 50$	$H = 100$	$H = 200$
K19LCW ^b	583-1, 2	Lower half	136	1.0201	1.0201	1.0196
K19LCW	583-3, 4	Upper half	138	1.2040	1.1910	1.1810
K19LCW	583-1, 2	Lower half	140	1.0172	1.0173	1.0168
K19LCW	1382-3, 4	Upper half	137	1.1220	1.1160	1.1810
K19LCW	1382-1, 2	Lower half	136	1.0167	1.0169	1.0164
K19LCW	1383-3, 4	Upper half	135	1.1260	1.1170	1.1100
K19LCW	1383-1, 2	Lower half	135	1.0582	1.0552	1.0565
K19LCW	484-1, 2	Upper half	136	1.1080	1.1007	1.0954
K19LCW	484-3, 4	Upper half	134	1.1681	1.1525	1.1418
K19LCW	485	Feeder block	134	1.0042	1.0044	1.0045
K19HCW ^c	12-1-1, 2	Lower half	134	1.0047	1.0050	1.0052
K19HCW	12-1-3, 4	Upper half	132	1.0037	1.0039	1.0040
K19HCW	12-2-1, 2	Lower half	130	1.0079	1.0089	1.0087
K19HCW	12-2-3, 4	Upper half	133	1.0042	1.0039	1.0040
K19HCW	12-3-1, 2	Lower half	133	1.0099	1.0099	1.0100
K19HCW	12-3-3, 4	Upper half	133	1.0042	1.0042	1.0044
K19HCW	12-4-1, 2	Lower half	134	1.0058	1.0060	1.0061
K19HCW	12-4-3, 4	Upper half	134	1.022	1.022	1.022
K19HCW	3-3-3, 4	Upper half	132	1.015	1.015	1.014
K19HCW	F3-1'	Upper half	128	1.019	1.020	1.019
K19HCW	F3-2'	Upper half				1.018

^a All water quenched from 2000 F.

^b K19LCW material: low-carbon (0.067 per cent).

^c K19HCW material: high-carbon (0.125 per cent).

and similar junctions between families of grains.

Initial Microstructure. The microstructure of the four lots, K19HRW, K19LRW, K19HCW, and K19LCW, as water quenched from 2000 F is shown in Figs. 4, 5, 6, and 7. These original structures appear fully austenitic and free from carbide at grain boundaries.

TABLE 8 TEST DATA OF FATIGUE TESTS AT ELEVATED TEMPERATURES ON METAL K19

Material	Metal, approximate designation and carbon content, %	Rolled or cast ^a	Speed of testing machine, rpm	Temp., F	Stress (reversed) flexure), lb per sq in.	Cycles for fracture	Remarks
K19LRW	B—0.067	Rolled	2500	Room	54,000	26,000	Load above yield point
					49,000	22,000	Retest
					47,300	50,000	Retest
					44,000	115,000	
					41,000	443,000	
					40,000	164,036,200	Did not fracture
K19LRW	B—0.067	Rolled	2500	800	39,000	10,952,000	Did not fracture
					43,000	10,200	
					38,600	11,090,300	Did not fracture
					38,000	22,500	
					34,200	28,000	
					34,000	26,000	
K19LRW	B—0.067	Rolled	2500	1000	31,700	27,405,700	Did not fracture
					38,000	5,000	
					35,000	112,000	
					33,300	271,700	
					32,000	290,000	
K19LRW	B—0.067	Rolled	2500	1200	31,300	53,050,400	Did not fracture
					37,300	15,000	
					32,000	30,100	
					30,800	60,000	
					30,000	1,549,000	Retest
					30,000	5,808,000	Did not fracture
					29,500	42,000,000	Did not fracture
K19LRW	B—0.067	Rolled	200	1200	27,000	22,226,500	Did not fracture
					35,000	103,000	
					34,000	25,000	
					33,000	13,000	
					32,000	162,000	
					31,000	8,000,000	
K19LCW	S—0.067	Cast	2500	Room	29,000	1,415,000	Did not fracture
					42,800	32,000	
					38,300	60,000	
					36,300	1,293,700	
K19LCW	S—0.067	Cast	2500	1200	32,700	42,653,700	Did not fail
					28,200	5,000	
					27,100	11,000	
					24,000	25,600	
					21,000	305,000	
					20,000	15,000	Flaw
					19,000	23,104,100	Did not fracture
K19HRW	G—0.125	Rolled	2500	Room	18,000	109,726,700	Did not fracture
					50,000	25,000	Retest
					47,000	75,000	
					43,000	220,000	
					42,000	25,648,000	Did not fracture
					42,000	109,602,200	
K19HRW	G—0.125	Rolled	2500	800	41,000	21,262,800	Did not fracture
					40,800	39,300	
					38,700	155,000	
					37,000	22,149,900	Did not fracture
K19HRW	G—0.125	Rolled	2500	1000	36,000	31,794,000	Did not fracture
					41,000	2,000	Stress above yield point
					39,000	112,200	
					38,200	55,400	
					37,500	9,883,700	Did not fracture
K19HRW	G—0.125	Rolled	2500	1200	37,000	11,669,700	Did not fracture
					40,100	4,500	Accidental preliminary overstress
					35,000	29,000	
					34,000	30,000	
					33,000	127,000	
					32,000	24,193,400	Did not fracture
K19HRW	G—0.125	Rolled	200	1200	31,000	10,687,200	Did not fracture
					39,000	40,000	
					38,400	42,000	
					37,200	10,109,100	Did not fracture
K19HCW	F—0.125	Cast	2500	Room	35,000	10,089,900	Did not fracture
					45,000	50,000 ^b	
					39,000	2,000,000	
					38,000	2,518,000 ^b	
					36,000	20,000,000 ^b	
					33,500	204,619,900 ^b	Did not fracture
K19HCW	F—0.125	Cast	2500	1200	32,500	24,421,000	Did not fracture
					33,000	29,000	
					29,000	73,000 ^b	
					26,000	8,500,000	
					25,000	< 50,000	Flaw
					25,000	13,855,000 ^b	
K19HCW	F—0.125	Cast	2500	1200	24,000	189,000 ^b	
					23,500	10,275,500	Ball bearing broken
					22,000	152,578,900	Did not fracture
					21,000	102,730,800 ^b	Did not fracture

^a The castings were in the form of keel blocks about 14 in. × 7 in. × 5 in. with 4 longitudinal keels, or teeth, on the bottom. From each of these teeth were obtained test coupons about 14 in. × 2.5 in. × 1 in., and from each coupon were supplied 2 specimen blanks about 14 in. × 1 in. square.

^b Specimen from upper part of tooth as cast.

TABLE 9 RESULTS OF FATIGUE TESTS AT ELEVATED TEMPERATURES ON METAL K19

		(Endurance limits under reversed flexure)								Endurance Ratio ^a	
		Endurance Limit, Lb Per Sq In.				Endurance Ratio ^a					
Material	Metal	Room temp., 2500 rpm	800 F, 2500 rpm	1000 F, 2500 rpm	1200 F, 200 rpm	Room temp., 2500 rpm	1000 F, 2500 rpm	1200 F, 2500 rpm	1200 F, 200 rpm		
K19LRW	B—0.067% C—rolled	40,000	32,000	32,000	30,000	47	54	64	64		
K19LCW	S—0.067% C—cast	36,000	20,000	56	..	54	..		
K19HRW	G—0.125% C—rolled	42,000	37,000	38,000	37,000	46	57	66	76		
K19HCW	F—0.125% C—cast	35,000	23,000	54	..	57	..		

^a No short-time tensile tests made at 800 F.

The grain size in the cast material is very large, as was shown in the macrographs in Figs. 2 and 3, so that in the photomicrographs of the cast material in Figs. 6 and 7 only a small section of the grain boundaries of one or several grains is shown.

Fatigue Tests. The specimens were heat treated at Battelle by water quenching from 2000 F as described above and shipped to Professor Moore at the University of Illinois. The testing machine used, the testing procedure, and the means of controlling and measuring temperature of specimens were the same as those described in detail in the former report⁵ on fatigue test of structural steel at elevated temperatures.

Table 8 gives the test data of the fatigue tests on K19 metal, Table 9 gives a summary of the endurance limits determined, and Figs. 8 and 9 give the S-N diagrams for the various metals tested.

The cast metal required a larger number of cycles of stress to determine endurance limit than did the rolled metal.

Comparing the behavior of metal K19 with the behavior of

terial and at 1200 F for cast are also in the normal range, though on the high side of the normal range. Those for rolled material at 1200 F and 2500 rpm, averaging 65, are distinctly high, and the single value at 1200 F for 200 rpm is exceedingly high. Where tests were made both at 2500 and 200 rpm on the rolled materials, the results at the slower speed were no lower, and in one case markedly higher, than at the higher speed.

The endurance limits, together with the short-time tensile and creep data and the range of impact values after creep test, to be presented below, are plotted in Figs. 10 to 13. The general relations of tensile, fatigue, and creep values are quite similar to

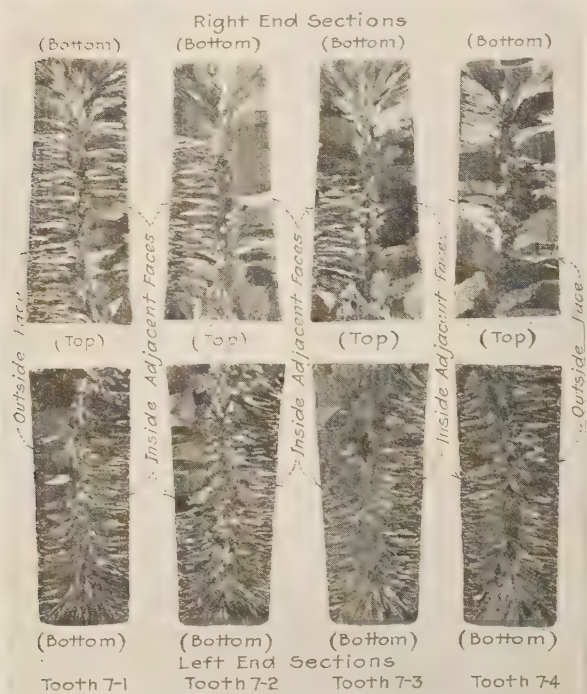


FIG. 2 MACROSTRUCTURES OF SECTIONS

(Taken $1\frac{1}{16}$ in. from right and left ends of the four teeth from casting No. 7, high-carbon K19HC. Etched by heating one hour at 160 F in a solution of 38 per cent hydrochloric acid, 12 per cent sulphuric acid, and 50 per cent water.)

the 0.17 per cent carbon steel K1, previously reported,⁵ it may be noted that at the highest test temperature, 1200 F, the fatigue fracture was decidedly better marked than in the case of the structural steel. With the soft structural steel it was sometimes difficult to tell whether the final failure was by spreading crack or by slow flow. While there were some evidences of flow in metal K19, they were not nearly so pronounced.

The room-temperature endurance ratios of the rolled material are normal for ferrous materials; those for the cast material are fairly high and of special interest in view of the large grain size.

The endurance ratios at 1000 F for both cast and rolled ma-

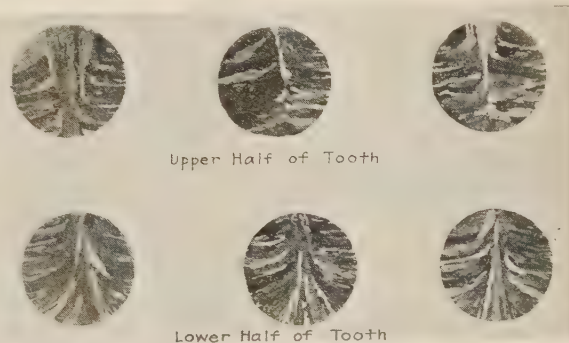


FIG. 3 MACROSTRUCTURES OF BARS $1\frac{1}{16}$ IN. IN DIAMETER
(Taken at center of 14 in. lengths of teeth of cast, low-carbon 18-8 Steel, K19LC.)

those previously found for a plain low-carbon steel.⁵ The comment made in respect to that steel (K1), "the curves indicate that a design based upon allowable deformation within the life of the material in service will not result in a fatigue failure," may be repeated as applying equally to these (K19) steels.

Short-Time High-Temperature Tests. The tests cited were made in the laboratories of the Babcock and Wilcox Company through the courtesy of H. J. Kerr and J. B. Romer.

All material subjected to the tensile tests was water quenched from 2000 F. No air-quenched specimens were tested.

The Babcock and Wilcox tests were made with equipment and by methods conforming to the requirements of the Joint High

TABLE 10 ELONGATION AND REDUCTION OF AREA; SHORT-TIME, HIGH-TEMPERATURE TESTS

	900 F		1000 F		1200 F	
	Elonga- tion, %	Reduc- tion of area, %	Elonga- tion, %	Reduc- tion of area, %	Elonga- tion, %	Reduc- tion of area, %
Low C, rolled, 2000 F, water	45	66 $\frac{1}{2}$	45	67 $\frac{1}{2}$	36 $\frac{1}{2}$	46
Low C, cast, 2000 F, water	47 $\frac{1}{2}$	65 $\frac{1}{2}$	44	59 $\frac{1}{2}$	39	55
High C, rolled, 2000 F, water	47 $\frac{1}{2}$	64	50	66	34 $\frac{1}{2}$	40
High C, cast, 2000 F, water	50	57 $\frac{1}{2}$	38	40	37	50 $\frac{1}{2}$

Temperature Committee's Code (Section 15 of A.S.T.M. Tentative Methods of Tension Testing of Metallic Materials, E8-32T).

Stress-strain diagrams, made with a head speed of less than 0.05 in. per minute, up to the time of removal of the extensometers, are shown in Figs. 14 to 16. The extensometers were mounted on the grips outside the gap-wound heating furnace.

⁵ Proc. A.S.T.M., vol. 31, pt. 1, 1931, p. 114; and vol. 32, pt. 1, 1932, pp. 153-155.

The tensile strengths are plotted in Figs. 10 to 13 while the yield strengths may be taken from Figs. 14 to 16. The elongation and reduction of area in the short-time high-temperature tensile tests are shown in Fig. 17 and recorded in Table 10.

No lack of ductility was shown at 900, 1000, or 1200 F, save perhaps in the high-carbon cast material at 1000 F, where the ductility was down to the relatively low figures of 38 per cent elongation and 40 per cent reduction of area. At 1200 F, however, both the elongation and the reduction of area were of the same order as in the wrought and the low-carbon specimens. No tensile tests are available as yet at 1100 F.

It will be noted subsequently, under the discussion of creep, that at 1100 and 1200 F, several specimens of cast high-carbon broke in the creep tests at loads above 10,000 lb per sq in., after having elongated only about $\frac{1}{2}$ of 1 per cent. A specimen at 1000 F, loaded at about 26,500 lb per sq in., broke in the test, but only after it had attained $9\frac{1}{4}$ per cent elongation, which could scarcely be called a very brittle behavior. The fracture under prolonged loading at 1100 to 1200 F at around $\frac{1}{2}$ per cent elongation does indicate tension-brittleness, but no sign of this is shown in the 1200 F tensile test.

CREEP TESTS

Equipment and Methods of Test. The creep-test equipment used in this work at Battelle Memorial Institute was in general similar to the equipment in use at the Crane Company laboratories, the details of which were described by Kanter and Spring.⁶

Gap-wound furnaces similar to those of Kanter and Spring were used. Fig. 18 shows the temperature calibration bar and the test specimen used for the creep tests herein reported.

Five thermocouples were located in the specimen during calibration of each furnace for temperature uniformity. The locations of these thermocouples are shown in Fig. 18. During the actual tests only thermocouples Nos. 1 and 5 were used. Thermocouple No. 1 is the control thermocouple and is connected to an automatic temperature controller. Thermocouple No. 5 is connected to an automatic temperature recorder and gives a continuous record of the specimen temperature.

Preliminary temperature explorations of furnaces as previously



FIG. 4 B38-9: ROLLED, LOW-CARBON K19, WATER QUENCHED FROM 2000 F



FIG. 5 G27-9: ROLLED, HIGH-CARBON K19, WATER QUENCHED FROM 2000 F

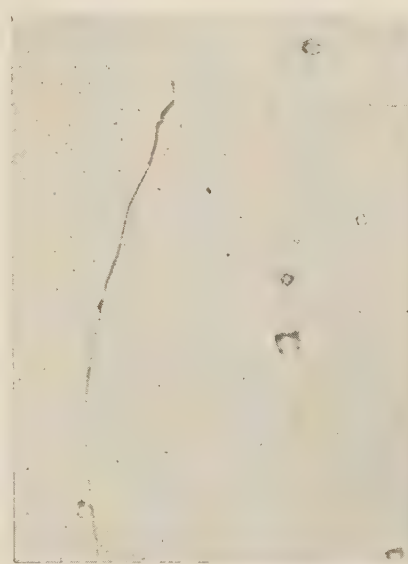


FIG. 6 3S2-2: CAST, LOW-CARBON K19, WATER QUENCHED FROM 2000 F



FIG. 7 11-1-1: CAST, HIGH-CARBON K19, WATER QUENCHED FROM 2000 F

(Magnification of etched specimens in Figs. 4, 5, 6, and 7—500 X. Etchant—two parts HCl, one part HNO₃, and one part acetic acid in three parts glycerin.)

constructed for use on pearlitic steels showed too large temperature gradients in the reduced section of the test specimens when used on 18-8 with its lower thermal conductivity. To improve and reduce the temperature gradient, some new furnaces were wound and lined with silver sheet 0.020 in. thick. A separate calibration was made for each furnace and temperature, using an 18-8 calibration bar. The following temperature variations were found between thermocouples Nos. 2, 3, and 4, whose locations are shown in Fig. 18. At 800 F the minimum variation along the gage length in different furnaces was 1 F and the maximum 4 F, at 1000 F the minimum was 2 F and maximum 3 F, and at 1200 F the minimum was 0 F and the maximum 6 F. The temperature at the center of the specimen was main-

⁶ J. J. Kanter and L. W. Spring, "Long-Time or Flow Tests of Carbon Steels at Various Temperatures With Particular Reference to Stresses Below the Proportional Limit," Proc. A.S.T.M., vol. 28, pt. 2, 1928, p. 80.

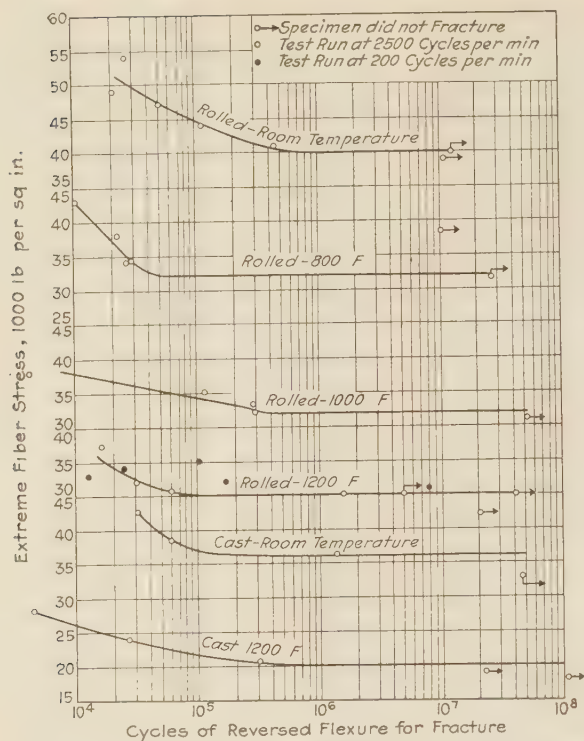


FIG. 8 S-N DIAGRAMS FOR 0.067 PER CENT CARBON, NICKEL-CHROMIUM STEEL

tained during the tests within a total variation of ± 1 F.

In some furnaces the differences between the center (No. 3), control (No. 1), and recorder (No. 5) thermocouples were as low as 2 F, and in others the difference was as high as 8 F. During the actual tests the temperature at thermocouple No. 1 was regulated to give the desired temperature over the gage length of the test specimen.

The room in which the creep apparatus is located is provided with thermostatic control. During the tests herein recorded the room temperature at the time of making readings was held constant within 7 F.

For measurement of elongation two platinum strips were used, one fastened on the shoulder at each end of the gage length of the test specimen as shown in Fig. 18. The strip fastened to the upper shoulder had its edges folded over to form a slot into which is fitted the strip fastened to the lower shoulder. The fit was loose enough so that movement of the strips relative to each other was not restricted. The strip fastened to the lower shoulder had a raised portion down the center, so that it would be in focus with the folded-over edges of the strip fastened to the upper shoulder when viewed through the telescope micrometer.

A series of very fine cross marks was ruled on the folded edges of the upper strip and on the center raised portion of the lower strip. Changes in length of the test specimen were measured by determining the changing distance between some two picked cross marks on the two strips. Those cross marks in best focus were used. If the rate of elongation was so rapid that the distance between the cross marks exceeded the range of the micrometer, conversion to another closer set of cross marks was made and the subsequent elongations added. This set-up was required because of the large extension of 18-8 in the early stages.

The telescope micrometer was fitted with a filar micrometer and mounted on a graduated screw. Calibration showed the smallest division on the filar eyepiece to read to 0.000048 in.,

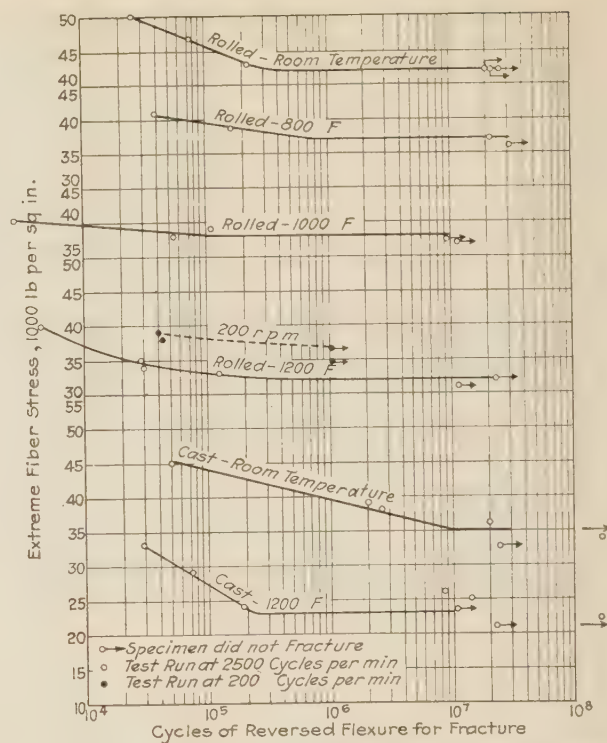


FIG. 9 S-N DIAGRAMS FOR 0.125 PER CENT CARBON, NICKEL-CHROMIUM STEEL

which on a 2.3-in. gage length gave readings to about 0.00002 in. per inch, or 0.002 per cent.

Readings of the elongation of each specimen were made daily by two observers. Time-deformation curves were plotted from the data of each observer, and the time-deformation curves shown in this report represent averages of the curves of the two observers. Either observer's data led to the same results, but two observers were a necessary precaution in case of illness or absence of one.

Axiality of Loading. No direct measurements were made during the tests to determine axiality of loading, although extreme care was exercised in setting up the tests to insure it as far as possible. All units were, of course, provided with ball and socket joints.

In some previous creep work one test unit was modified so as to permit attachment to the test specimen and reading of two sets of platinum strips spaced 180 deg apart. Since the completion of this research on 18-8 steel, all Battelle creep apparatus has been modified to permit readings of deformation on opposite sides of the test specimen. The earlier work and the results obtained in regular use since the equipment was modified show that in the early stages of the test period, in some instances, there were slight differences in the rate of elongation on the two sides. However, after a brief initial period, the rates of elongation became practically the same and the time-deformation curves parallel. For this reason it is felt that in the tests herein reported satisfactory axiality of loading was obtained.

Various precautions taken for accuracy in creep work at Battelle are described in more detail by Gillett and Cross.⁷ Although this creep work for the Joint Committee was practically

⁷ H. W. Gillett and H. C. Cross, "Obtaining Reliable Values for Creep of Metals at High Temperature," *Metals and Alloys*, vol. 4, July, 1933, pp. 91-98.

completed before the promulgation of the tentative creep "code,"⁸ it is believed that the requirements of the code have been met or exceeded. The creep tests were carried well beyond 1000 hr, as against the 500 hr specified by the code for determinations to be reported in terms of 1 per cent in 10,000 hr, in all cases, save where the deformation was so great as to make this unnecessary, or unless, as in the case of some of the high-carbon cast specimens, fracture occurred before that. A single run at 1400 F was carried only to 665 hr.

The Subcommittee on Technical Projects instructed the investigators to determine the stresses for a final creep rate of 1 per cent in 10,000 hr and to concentrate on temperatures of 1000 and 1200 F, and on the use of water-quenched material. Some tests were carried out at lower final rates of deformation, but no

⁸ Tentative Method of Test for Long-Time (Creep) High-Temperature Tension Tests of Metallic Materials, Proc. A.S.T.M., pt. 1, 1933, p. 1004, E22-33T.

attempt was made to carry the work to a complete determination of stresses for a final rate of 1 per cent in 100,000 hr. A few tests were made at 1100 F and a very few on air-quenched rolled material.

The initial program did not include testing the low-carbon cast material, though it was hoped to include this ultimately. The preliminary data on the high-carbon cast, however, made it appear important to include the low-carbon cast. Time and funds were not available for as complete a study of the low-carbon cast as of the other materials.

DETAILED RESULTS OF CREEP TESTS

Since the first heat treatment specified was air quenching from 2000 F, the first of the creep tests were made at 1000 and 1200 F on air quenched rolled bars. All later tests were made on water quenched bars. The time-deformation curves for the air-quenched material tested at 1000 and 1200 F are shown in Figs. 19 and 20.

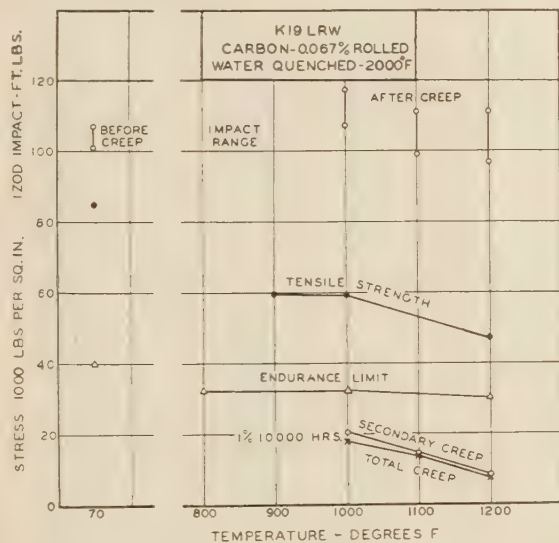


FIG. 10 COMPARISON OF IMPACT, TENSILE, ENDURANCE, AND CREEP DATA FOR ROLLED, LOW-CARBON K19 STEEL

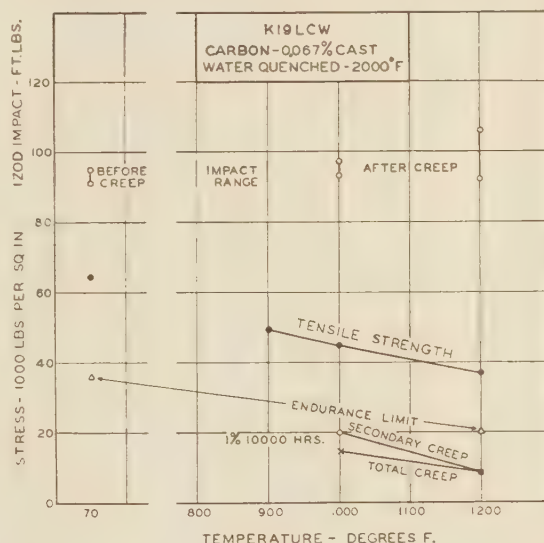


FIG. 11 COMPARISON OF IMPACT, TENSILE, ENDURANCE, AND CREEP DATA FOR CAST, LOW-CARBON K19 STEEL

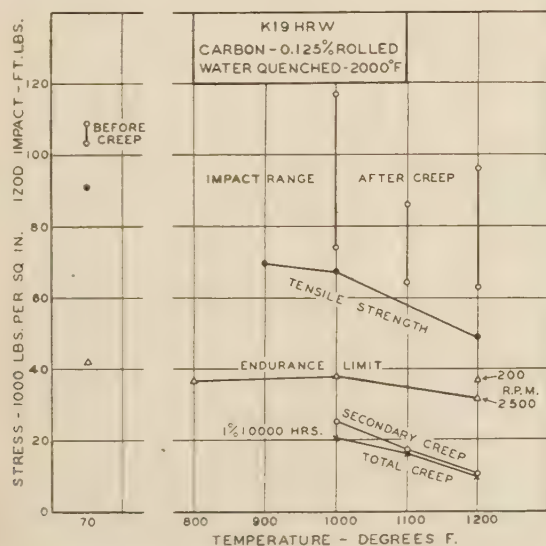


FIG. 12 COMPARISON OF IMPACT, TENSILE, ENDURANCE, AND CREEP DATA FOR ROLLED, HIGH-CARBON K19 STEEL

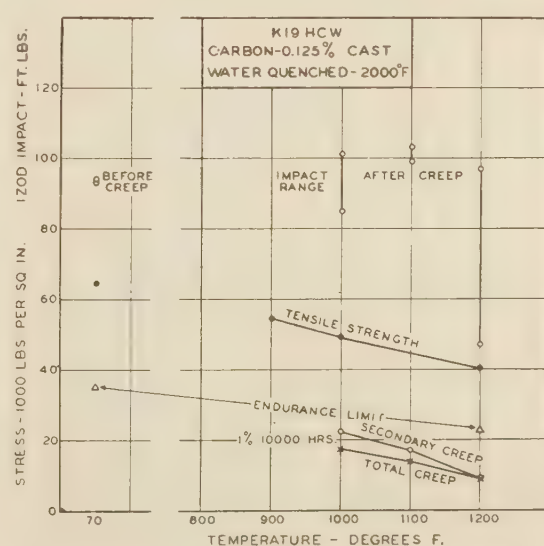


FIG. 13 COMPARISON OF IMPACT, TENSILE, ENDURANCE, AND CREEP DATA FOR CAST, HIGH-CARBON K19 STEEL

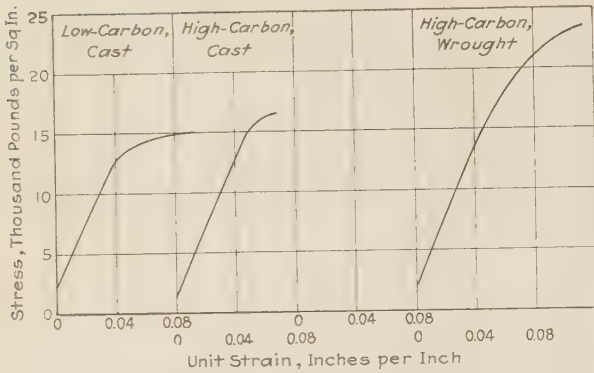


FIG. 14 STRESS-STRAIN DIAGRAMS FOR K19 STEEL AT 900 F

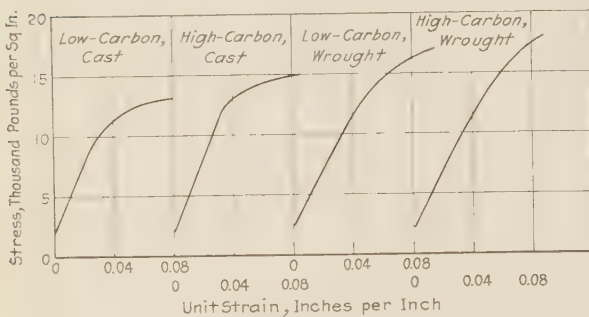


FIG. 16 STRESS-STRAIN DIAGRAMS FOR K19 STEEL AT 1200 F

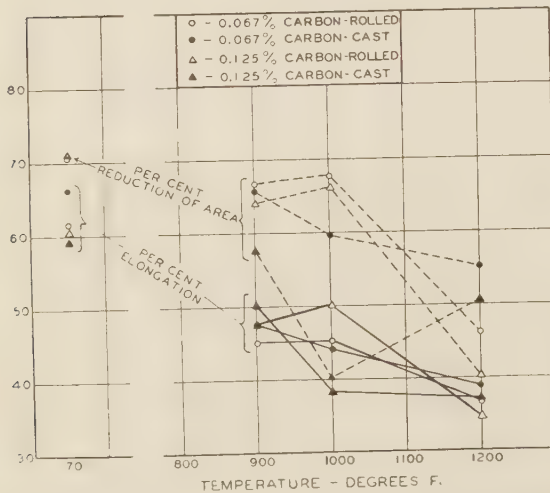


FIG. 17 ELONGATION AND REDUCTION OF AREA IN SHORT-TIME TENSILE TESTS OF K19 STEEL AT VARIOUS TEMPERATURES

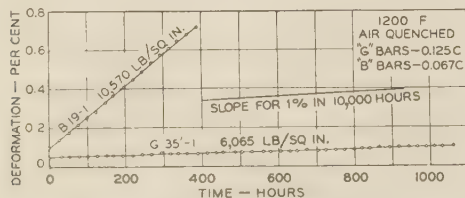


FIG. 20 TIME-DEFORMATION CURVES AT 1200 F FOR ROLLED, AIR-QUENCHED, HIGH- AND LOW-CARBON BARS (K19HRA AND K19LRA)

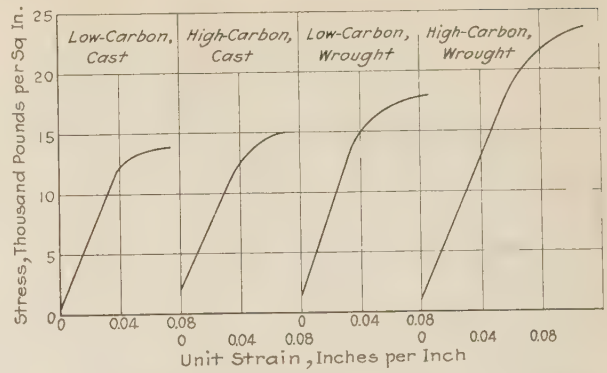


FIG. 15 STRESS-STRAIN DIAGRAMS FOR K19 STEEL AT 1000 F

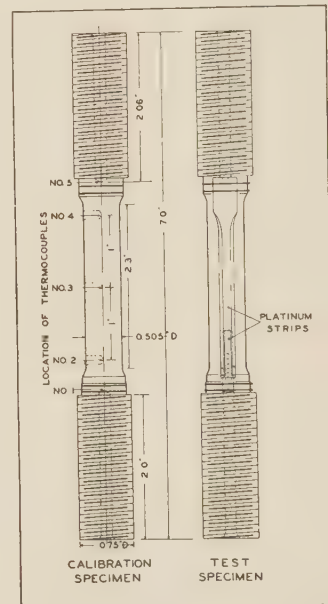
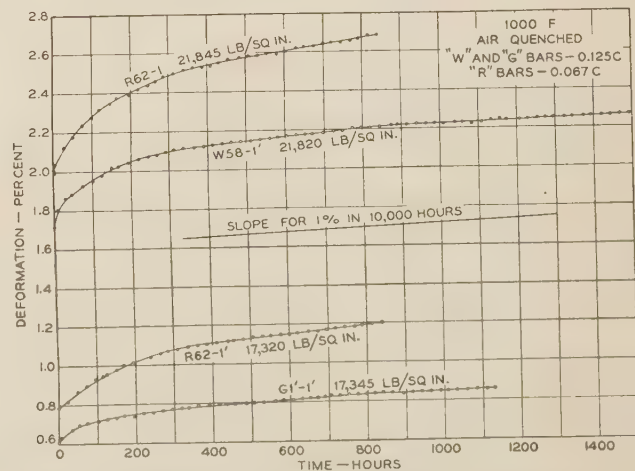
FIG. 18 CALIBRATION AND TEST SPECIMENS USED IN THE CREEP TESTS
(Note platinum strips used for measuring elongation.)

FIG. 19 TIME-DEFORMATION CURVES AT 1000 F FOR ROLLED, AIR-QUENCHED, HIGH- AND LOW-CARBON BARS (K19HRA AND K19LRA)

TABLE 11A CREEP TEST DATA FOR LOW-CARBON "18-S" STEEL (K19L)

Material and heat treatment	Specimen number	Temp. of creep test, deg F	Duration of test, hr	Load lb per sq in.	Initial elongation, %	Secondary elongation, % per hr, first 500 hr	Elongation, % per hr, after 500 hr	Final elongation, %	Remarks
<i>Low-Carbon, Rolled</i>									
K19LRA	R62-1'	1000	842	17,320	0.786	0.000234	1.2	Air quenched
K19LRA	R62-1	1000	842	21,845	2.01	0.000336	2.69	Air quenched
K19LRW	B21'-4	1000	1,061	15,040	0.174	0.000027	0.267	Water quenched
K19LRW	B21'-2	1000	1,108	17,325	0.26	0.000124	0.000058	0.467	Water quenched
K19LRW	B38-2'	1000	1,553	19,625	0.589	0.000109 ^a	1.007	Water quenched
K19LRW	B21'-3	1000	1,293	21,815	1.284	0.00015	1.841	Water quenched
K19LRW	B38-1'	1100	1,201	12,835	0.054	0.000048 ^b	0.170	Water quenched
K19LRW	B38-3	1100	768	17,325	0.110	0.000083	1.001	Water quenched
K19LRA	B19-1	1200	390	10,570	0.097	0.00165	0.717	Water quenched
K19LRW	B21-3	1200	1,252	6,100	0.054	0.000042	0.212	Water quenched
K19LRW	B38-2	1200	1,655	8,345	0.133	0.000122 ^c	3.344	Water quenched
K19LRW	48	1200	1,346	10,600	0.03	0.000265 ^d	0.623	Water quenched
K19LRW	B21-1'	1200	240	12,820	0.092	0.00558 ^e	1.614	Water quenched
<i>Low-Carbon, Cast</i>									
K19LCW	13S3-2	1000	1,276	12,800	0.145	0.000915 ^f	0.195	Water quenched
K19LCW	13S2-1	1000	1,132	15,115	1.19	0.000335 ^g	1.384	Water quenched
K19LCW	5S3-2	1000	1,612	17,325	3.263	0.000016	3.512	Water quenched
K19LCW	5S3-1	1200	1,300	5,000	0.057	< 0.00001 ^h	0.075	Water quenched
K19LCW	13S2-2	1200	1,300	7,000	0.095	< 0.00001 ^h	0.156	Water quenched
K19LCW	13S3-1	1200	964	9,500	0.104	0.000186 ⁱ	0.334	Water quenched

^a From 1000 to 1500 hr.^b From 700 to 1175 hr.^c From 1100 to 1650 hr.^d From 800 to 1350 hr.^e From 50 to 240 hr.^f From 500 to 1275 hr.^g From 700 to 1130 hr.^h From 1000 to 1300 hr.ⁱ From 500 to 950 hr.

TABLE 11B IMPACT AND MAGNETIC PERMEABILITY DATA AFTER CREEP TEST FOR LOW-CARBON "18-S" STEEL (K19L)

Material and heat treatment	Specimen number	Temp. of creep test, deg F	Duration of test, hr	Load, lb per sq in.	Final elongation in creep test, %	Izod impact resistance, ft-lb	After Creep Test—Magnetic permeability				Remarks
							H = 50	H = 100	H = 150	H = 200	
<i>Low-Carbon, Rolled</i>											
K19LRW	B38-9	None	107-107-101-103	1.0032	1.0032	1.0032	1.0032	Water quenched
K19LRA	R62-1'	1000	842	17,320	1.2	109-112	1.019	1.019	1.018	1.018	Air quenched
K19LRA	R62-1	1000	842	21,845	2.69	119-117	Air quenched
K19LRW	B21'-4	1000	1,061	15,040	0.267	114-116	Water quenched
K19LRW	B21'-2	1000	1,108	17,325	0.467	116-117	Water quenched
K19LRW	B38-2'	1000	1,553	19,625	1.007	107-109	1.0368	1.0324	1.0283	1.0263	Water quenched
K19LRW	B21'-3	1000	1,293	21,815	1.841	110-113	1.024	1.023	1.023	1.021	Water quenched
K19LRW	B38-1'	1100	1,201	12,835	0.170	111-109	1.117	1.166	1.160	1.140	Water quenched
K19LRW	B38-3	1100	768	17,325	1.001	99-100	1.112	1.175	1.166	1.149	Water quenched
K19LRA	B19-1	1200	390	10,570	0.717	114-113	Water quenched
K19LRW	B21-3	1200	1,252	6,100	0.212	111-108	Water quenched
K19LRW	B38-2	1200	1,655	8,345	0.594	99-99	1.1165	1.1010	1.0825	1.0691	Water quenched
K19LRW	48	1200	1,346	10,600	0.623	98-97	1.190	1.170	1.140	1.120	Water quenched
K19LRW	B21-1'	1200	240	12,820	1.614	98-103	1.202	1.222	1.197	1.170	Water quenched
<i>Low-Carbon, Cast</i>											
K19LCW	3S2-2	None	91-91-95	Water quenched
K19LCW	13S3-2	1000	1,276	12,800	0.198	93-93	1.021	1.022	1.024	1.024	Water quenched
K19LCW	13S2-1	1000	1,132	15,115	1.384	94-95	1.018	1.019	1.019	1.018	Water quenched
K19LCW	5S3-2	1000	1,612	17,325	3.512	95-97	1.0216	1.0245	1.026	1.018	Water quenched
K19LCW	5S3-1	1200	1,300	5,000	0.075	105-100	1.135	1.157	1.183	1.184	Water quenched
K19LCW	13S2-2	1200	1,300	7,000	0.156	106-101	1.127	1.147	1.167	1.159	Water quenched
K19LCW	13S3-1	1200	964	9,500	0.334	98-92	1.113	1.131	1.158	1.148	Water quenched

The details of all the creep tests on both air- and water-quenched rolled materials of both low- and high-carbon contents and the quenched cast material of both low- and high-carbon content are shown in Tables 11 and 12.

The time-deformation curves for the quenched cast and rolled materials of low-carbon content are shown in Figs. 21, 23, 25, 27, and 30; those for high-carbon are shown in Figs. 22, 24, 26, 28, 29, and 31.

In Fig. 32 the rates of secondary elongation produced by the various stresses are plotted against the stresses. These rates of secondary elongation were scaled from the latter portion of the time-deformation curves after a fairly uniform rate had been attained. It is of interest to note that in all but a very few instances the test had to progress at least 500 hr, and in many instances not until after a considerably longer test period, before a fairly uniform rate was attained. The data plotted in Fig. 32 do not take into consideration the initial elongation or subsequent elongation taking place during the first portion of the test period. In some instances where strain-hardening effects were noted there was considerable elongation during the first 500 hr before a uniform rate of elongation was approached.

Therefore, in Figs. 33 and 34 are shown data for the total deformations calculated to result from the various stresses in 10,000 hr. These values were obtained by extrapolating the time-deformation curves at the same rate of elongation as existed over the latter part of the test period, as indicated in Tables 11 and 12.

This method gives a lower stress value than that producing a secondary elongation rate of 1 per cent in 10,000 hr, since the values depend not only on the rate of elongation at the end of the test but also on the magnitude of the initial elongation and the strain-hardening effects.

Rather large initial elongations resulted upon application of the loads in the tests at 1000 F.

DISCUSSION OF THE CREEP TEST DATA

When tested at 1000 F in the air-quenched condition, the high-carbon rolled material showed both a lower initial elongation and a lower rate of secondary elongation than the low-carbon rolled material.

In the water-quenched condition at test temperatures of 1000, 1100, and 1200 F the high-carbon rolled material was again superior to the low-carbon material in regard to initial elongation, rate of elongation, and total deformation. These relations are clearly shown in Figs. 32, 33, and 34, and by the data shown in Tables 11, 12, and 13. Norton⁹ also shows, in his Figs. 55 and 56, superior creep resistance for high-carbon 18-S as compared with low-carbon 18-8. Comparison of the test data also shows that both the low-carbon and high-carbon rolled materials have

⁹ F. H. Norton, "Creep of Steels at High Temperatures," McGraw Hill Book Company, 1930.

H. D. Newell (quoting recent work of Norton), "Alloy Steel Tubes for Refinery Service," *Refiner and Natural Gasoline Manufacturer*, vol. 12, 1933, pp. 122-131.

TABLE 12A CREEP TEST DATA FOR HIGH-CARBON "18-8" STEEL (K19H)

Material and heat treatment	Specimen number	Temp. of creep test, deg F	Duration of test, hr	Load, lb per sq. in.	Initial elongation %	Secondary % per hr in first 500 hr	Elongation % per hr after 500 hr	Final elongation in creep test, %	Remarks
<i>High-Carbon, Rolled</i>									
K19HRA	G1-1'	1000	1,132	17,345	0.61	0.000124	0.000065 ^a	0.86	Air quenched
K19HRA	W58-1'	1000	1,535	21,820	1.72	0.000078 ^b	2.275	Air quenched
K19HRW	G30-2	1000	1,125	17,440	0.391	0.000017 ^c	0.496	Water quenched
K19HRW	G30-3	1000	1,703	22,315	0.417	0.000056 ^d	0.788	Water quenched
K19HRW	G30-8	1000	1,518	23,000	1.121	0.000073 ^e	1.648	Water quenched
K19HRW	G30-7	1000	1,758	24,065	1.25	0.000086 ^d	1.947	Water quenched
K19HRW	G27-1	1000	1,318	28,570	2.399	0.0002	3.157	Water quenched
K19HRW	G30-9	1100	1,529	17,280	0.266	0.000102 ^e	0.552	Water quenched
K19HRW	G27-1'	1100	1,000	19,570	0.216	0.000467	0.802	Water quenched
K19HRA	G35'-1	1200	1,078	6,065	0.048	0.000049	0.000034	0.107	Air quenched
K19HRW	G30-7	1200	1,493	8,320	0.025	0.000032	0.179	Water quenched
K19HRW	G30'-8	1200	1,518	9,500	0.004	0.000042 ^e	0.170	Water quenched
K19HRW	G30'-9	1200	1,822	10,585	0.006	0.000104 ^e	0.366	Water quenched
K19HRW	G30-6	1200	1,078	12,810	0.043	0.00054	0.818	Water quenched
K19HRW	G27-3'	1400	665	1,600	0.017	0.000015	0.031	Water quenched
<i>High-Carbon, Cast</i>									
K19HCW	12-1-3 ^m	1000	1,230	19,645	3.28	0.000024 ^h	3.437	Water quenched
K19HCW	12-4-4 ^m	1000	1,226	20,750	4.99	0.00004	5.315	Water quenched
K19HCW	12-2-1	1000	1,506	21,840	5.356	0.00005 ⁱ	5.662	Water quenched
K19HCW	12-1-1	1000	445	26,425	8.69	0.001	9.244 ^k	Water quenched
K19HCW	12-2-2	1100	1,139	15,080	0.316	0.000025 ^f	0.408 ^g	Water quenched
K19HCW	12-4-3 ^m	1100	475	17,385	0.181	0.00012	0.000035 ^f	0.189	Water quenched
K19HCW	12-1-4 ^m	1200	1,318	8,333	0.076	0.00016	0.399	Water quenched
K19HCW	12-3-2	1200	865	9,500	0.185	0.00033	0.55 ^k	Water quenched
K19HCW	12-3-1	1200	796	10,565	0.105	0.000319	0.00033	0.561 ^k	Water quenched
K19HCW	12-3-3 ^m	1200	652	11,485	0.052	0.000465	0.655 ^k	Water quenched
K19HCW	12-1-2	1200	259	12,845	0.354	0.00098	Water quenched

^a From 800 to 1130 hr.
^f From 500 to 1000 hr.
^k Broke.

^b From 800 to 1390 hr.
^g From 1200 to 1800 hr.
^l From 1000 to 1300 hr.

^c From 500 to 1100 hr.
^h From 600 to 1200 hr.
^m Specimen taken from upper half of tooth.

^d From 1000 to 1700 hr.
ⁱ From 800 to 1175 hr.

^e From 1000 to 1500 hr.
^j From 1200 to 1500 hr.

TABLE 12B IMPACT AND MAGNETIC PERMEABILITY DATA AFTER CREEP TEST FOR HIGH-CARBON "18-8" STEEL (K19H)

Material and heat treatment	Specimen number	Temp. of creep test, deg F	Duration of test, hr	Load, lb per sq in.	Final elongation in creep test, %	After Creep Test				Remarks	
						Izod impact resistance, ft-lb	Magnetic permeability				
						H = 50	H = 100	H = 150	H = 200		
High-Carbon, Rolled											
K19HRW	G27-9	None	108-103-109-108	1.0032	1.0032	1.0032	1.0032	Water quenched
K19HRA	G1-1'	1000	1,132	17,345	0.86	112-115	Air quenched
K19HRA	W58-1'	1000	1,535	21,820	2.275	112-110	1.026	1.028	1.026	1.025	Air quenched
K19HRW	G30-2	1000	1,125	17,440	0.496	117-117	1.032	1.031	1.029	1.028	Water quenched
K19HRW	G30-3	1000	1,703	22,315	0.788	110-107	1.032	1.031	1.029	1.0162	Water quenched
K19HRW	G30-8	1000	1,518	23,000	1.648	106-108	1.0202	1.0205	1.0197	Water quenched
K19HRW	G30-7	1000	1,758	24,065	1.947	96-93	Water quenched
K19HRW	G27-1	1000	1,318	28,570	3.157	74-77	1.0360	1.0338	1.0316	1.0306	Water quenched
K19HRW	G30-9	1100	1,529	17,280	0.552	86-85	1.0879	1.1688	1.1750	1.155	Water quenched
K19HRW	G27-1'	1100	1,000	19,570	0.802	64-69	1.1610	1.2740	1.2570	1.2280	Water quenched
K19HRA	G35'-1	1200	1,078	6,065	0.107	105-106	1.94	2.29	2.10	1.92	Air quenched
K19HRW	G30-7	1200	1,493	8,320	0.179	96-95	Water quenched
K19HRW	G30'-8	1200	1,518	9,500	0.170	91-88	1.298	1.358	1.315	1.265	Water quenched
K19HRW	G30'-9	1200	1,822	10,585	0.366	84-86	Water quenched
K19HRW	G30-6	1200	1,078	12,810	0.818	74-63	Water quenched
K19HRW	G27-3'	1400	665	1,600	0.031	92-93	Water quenched
High-Carbon, Cast											
						94-93-93					
K19HCW	11-1-1	None	100-100	1.0157	1.0152	1.0139	1.0135	Water quenched
K19HCW	12-1-3 ^b	1000	1,230	19,645	3.437	Water quenched
K19HCW	12-4-4 ^b	1000	1,226	20,750	5.315	Water quenched
K19HCW	12-2-1	1000	1,506	21,840	5.662	90-85	Water quenched
K19HCW	12-1-1	1000	445	26,425	9.244 ^a	101 ^c	Water quenched
K19HCW	12-2-2	1100	1,139	15,080	0.397 ^a	99 ^a	Water quenched
K19HCW	12-4-3 ^b	1100	475	17,385	0.408 ^a	103 ^a	Water quenched
K19HCW	12-1-4 ^b	1200	1,318	8,333	0.189	61-58	1.1202	1.1482	1.1324	1.1115	Water quenched
K19HCW	12-3-2	1200	865	9,500	0.399	97-69	Water quenched
K19HCW	12-3-1	1200	796	10,565	0.55 ^a	Water quenched
K19HCW	12-3-3 ^b	1200	652	11,485	0.561 ^a	84 ^a	Water quenched
K19HCW	12-1-2	1200	259	12,845	0.655 ^a	88 ^a	1.051	1.073	1.071	1.064	Water quenched

^a Broke.

^b Specimen taken from upper half of tooth.

TABLE 13 SUMMARY OF CREEP TEST DATA

(Stresses to produce secondary rate of elongation and total elongation of 1 per cent in 10,000 hours)

Material	Carbon content, %	Rolled or cast	Heat treatment	Temp. of test, deg F	Stress, lb per sq. in. to produce secondary rate of elongation of 1% in 10,000 hr	Stress, lb per sq. in. to produce total deformation of 1% in 10,000 hr
K19LRA	0.067	Rolled	Air quenched from 2000 F	1000	< 17,320	< 17,320
K19HRA	0.125	Rolled	Air quenched from 2000 F	1000	> 21,820	< 17,350
K19LRW	0.067	Rolled	Water quenched from 2000 F	1000	20,000	17,500
K19HRW	0.125	Rolled	Water quenched from 2000 F	1000	25,000	20,200
K19LRW	0.067	Rolled	Water quenched from 2000 F	1100	14,000	13,600
K19LRW	0.125	Rolled	Water quenched from 2000 F	1100	17,300	< 17,300
K19LRW	0.067	Rolled	Water quenched from 2000 F	1200	8,200	7,100
K19LRW	0.125	Rolled	Water quenched from 2000 F	1200	10,500	10,000
K19HRW	0.067	Rolled	Water quenched from 2000 F	1000	> 17,325	14,500
K19HRW	0.125	Rolled	Water quenched from 2000 F	1000	22,500	< 19,645
K19HCW	0.067	Cast	Water quenched from 2000 F	1000	17,000 ^a
K19HCW	0.125	Cast	Water quenched from 2000 F	1100	8,500	8,500
K19HCW	0.067	Cast	Water quenched from 2000 F	1200	9,300	9,000
K19HCW	0.125	Cast	Water quenched from 2000 F	1200

^a Both tests at 1100°F fractured before a total deformation of 1 per cent was attained.

greater creep resistance in the water-quenched than in the air-quenched condition. This fact is very clearly indicated in Figs. 32, 33, and 34, and in Table 13.

At the lower loads used at the higher test temperatures smaller initial elongations resulted than in the tests at 1000 F, and this fact along with decided diminution of strain-hardening effects accounts for the smaller differences between the stress producing a rate of elongation of 1 per cent in 10,000 hr and that producing a total deformation of 1 per cent in 10,000 hr. Fig. 35 shows the initial deformations of the cast and rolled materials at 1000 F and the high-carbon cast and rolled material at 1200 F. The results for the low-carbon material at the low loads used at 1200 F were irregular; they are shown only in Table 11 and not in Fig. 35.

It is of interest to note that in tests at 1000 F a large increase in initial elongation over that at 17,000 lb per sq in. resulted when bars were loaded at about 22,000 lb per sq in. for the quenched low-carbon material, over that at 22,000 lb per sq in. when bars were loaded at

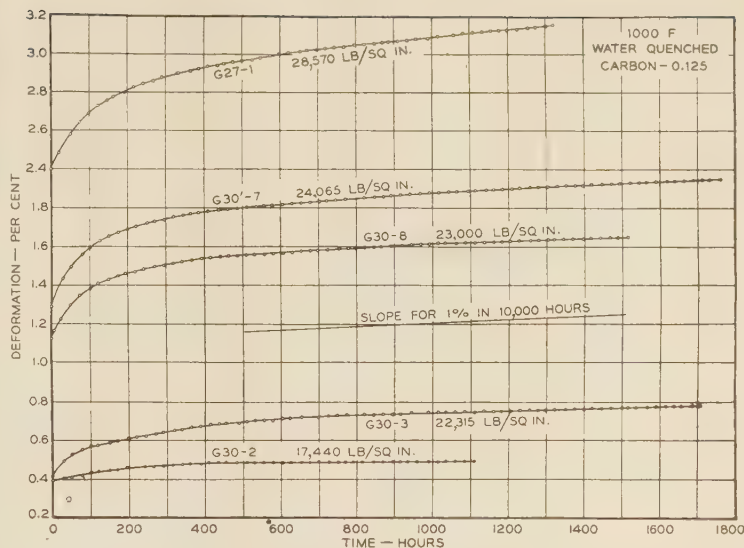


FIG. 22 TIME-DEFORMATION CURVES AT 1000 F FOR ROLLED, WATER-QUENCHED, HIGH-CARBON 18-8 STEEL (K19HRW)

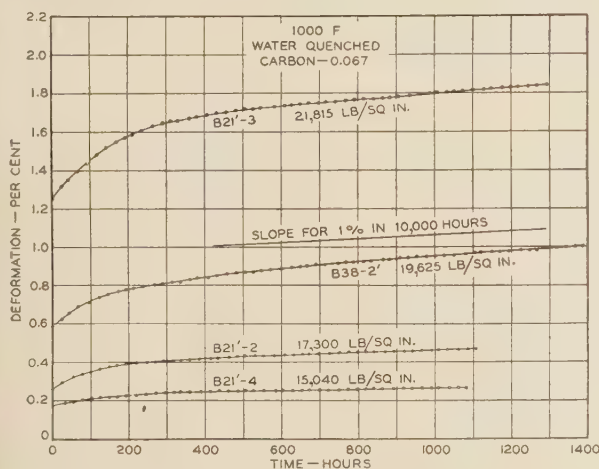


FIG. 21 TIME-DEFORMATION CURVES AT 1000 F FOR ROLLED, WATER-QUENCHED, LOW-CARBON 18-8 STEEL (K19LRW)

about 23,000 lb per sq in. for the quenched high-carbon material. This is important to note, for as shown in Tables 11 and 12 and Figs. 19, 21, 22, 27, and 28, although the subsequent rates of secondary elongation are not large at these higher loads, such large initial deformations are of prime importance in designs based on a fairly small permissible over-all deformation.

In several of the tests on the rolled materials the initial deformations were higher or lower than expected, but the secondary rates of elongation were in the proper order after the test period progressed a sufficient length of time. That is, erratic behavior was more common in the earlier than in the later stages of creep. This, combined with the fact that the specimens did not "settle down" to a fairly uniform rate of creep short of 500 hr or more, indicates that some of the "accelerated" methods of testing alleged to be competent to characterize creep resistance would be inadequate and inapplicable on this type of material.

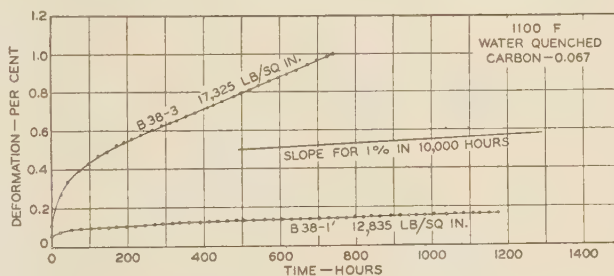


FIG. 23 TIME-DEFORMATION CURVES AT 1100 F FOR ROLLED, WATER-QUENCHED, LOW-CARBON 18-8 STEEL (K19LRW)

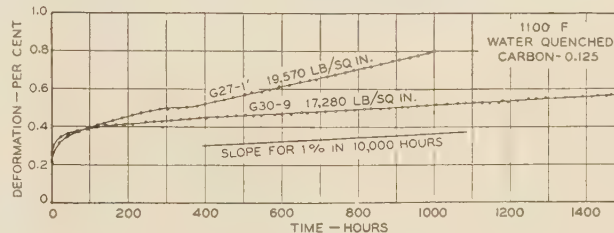


FIG. 24 TIME-DEFORMATION CURVES AT 1100 F FOR ROLLED, WATER-QUENCHED, HIGH-CARBON 18-8 STEEL (K19HRW)

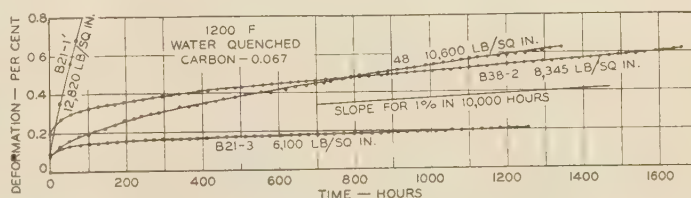


FIG. 25 TIME-DEFORMATION CURVES AT 1200 F FOR ROLLED, WATER-QUENCHED, LOW-CARBON 18-8 STEEL (K19LRW)

No creep tests were made on cast bars as air quenched. All cast bars tested were water quenched from 2000 F.

As shown in the various time-deformation curves and in Figs. 32, 33, and 34, the high-carbon cast material shows superior

creep resistance to the low-carbon cast material. It is realized that the data on the low-carbon cast material are limited, but the curves in Fig. 32 show considerably lower stresses for comparable rates of creep for the low- than for the high-carbon cast material.

Due to the fact that considerably lower loads were used in the tests at 1000 F on the low-carbon cast material, thus causing the initial elongations to be smaller, comparisons with the high carbon cast material on the basis of total creep are difficult.

Although the loads used for the two materials do not overlap, the data in Figs. 33 and 34 indicate superiority in regard to total creep for the high-carbon cast material when tested at 1000 F.

There seems little difference between the low- and high-carbon cast material tested at 1200 F when compared on the basis of total elongation.

Comparison of Results With Norton's Published Data. Comparison of the creep results of this investigation may be made with the published data of Norton⁹ for low-carbon rolled 18-8. The data are plotted in Fig. 36.

Very close agreement is shown at 1000 and 1200 F. Slight divergence at 1100 F is probably due to the fact that fewer specimens were tested at Battelle at 1100 F than at the other two temperatures. Detailed data on creep of high-carbon rolled or of cast 18-8, close enough in carbon content for accurate comparison, seem to be lacking.

COMPARISON OF ROLLED AND CAST MATERIAL IN CREEP TEST

It was found by Kanter and Spring¹⁰ that, in the case of plain 0.20 per cent carbon steel and a 2 per cent nickel, 0.87 per cent chromium, 0.41 per cent carbon steel tested at 1000 F, the creep resistance was greater in cast material of large grain size than with forged material of smaller grain size. These data, coupled with a previous indication leading to a similar conclusion for an 18-8 alloy containing 0.15 per cent carbon tested at 1180 F in the work of French, Kahlbaum, and Peterson,¹¹ have sometimes been taken to imply that cast material would uniformly show su-

¹⁰ J. J. Kanter and L. W. Spring, "Some Long-Time Tension Tests of Steels at Elevated Temperatures," Proc. A.S.T.M., vol. 30, pt. 1, 1930, p. 110.

¹¹ H. J. French, W. Kahlbaum, and A. A. Peterson, "Flow Characteristics of Special Fe-Ni-Cr Alloys and Some Steels at Elevated Temperatures," Bureau of Standards Journal of Research, vol. 5, no. 1, July, 1930, p. 182.

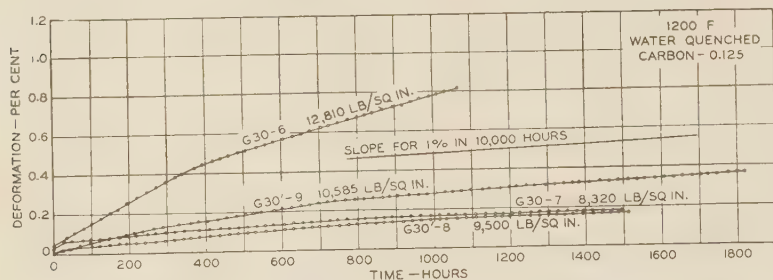


FIG. 26 TIME-DEFORMATION CURVES AT 1200 F FOR ROLLED, WATER-QUENCHED, HIGH-CARBON 18-8 STEEL (K19HRW)

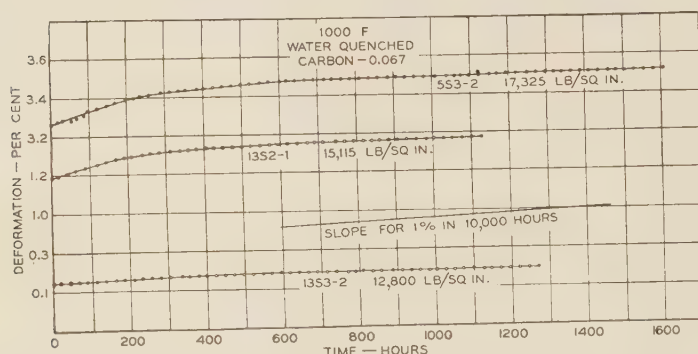


FIG. 27 TIME-DEFORMATION CURVES AT 1000 F FOR CAST, WATER-QUENCHED, LOW-CARBON 18-8 STEEL (K19LCW)

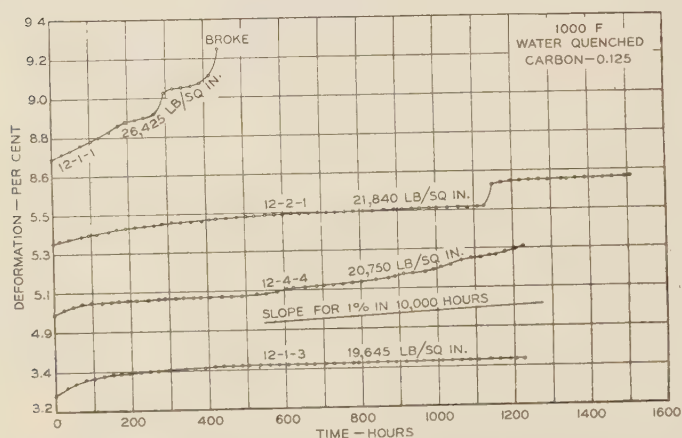


FIG. 28 TIME-DEFORMATION CURVES AT 1000 F FOR CAST, WATER-QUENCHED, HIGH-CARBON 18-8 STEEL (K19HCW)
(Jog in curve for specimen 12-2-1 due to jar from breaking of high-carbon cast bar in adjacent creep unit.)

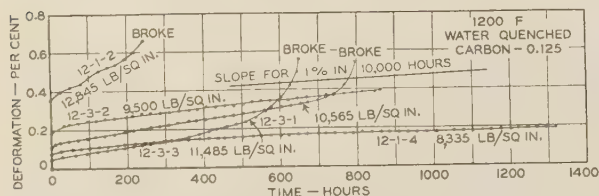


FIG. 31 TIME-DEFORMATION CURVES AT 1200 F FOR CAST, WATER-QUENCHED, HIGH-CARBON 18-8 STEEL (K19HCW)

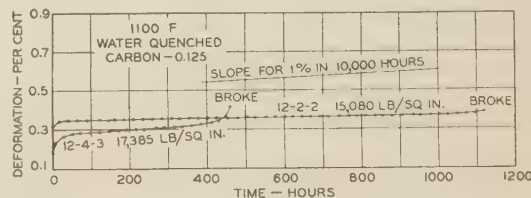


FIG. 29 TIME-DEFORMATION CURVES AT 1100 F FOR CAST, WATER-QUENCHED, HIGH-CARBON 18-8 STEEL (K19HCW)

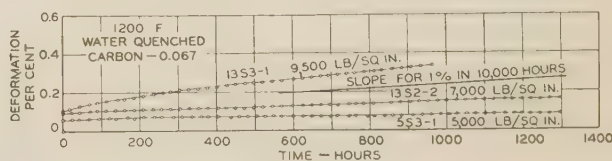


FIG. 30 TIME-DEFORMATION CURVES AT 1200 F FOR CAST, WATER-QUENCHED, LOW-CARBON 18-8 STEEL (K19LCW)

perior creep resistance to rolled material of the same analysis and treatment. On the other hand the work of Bailey and Roberts¹² indicated the opposite to be the case, though the cast and rolled steels compared were of somewhat different compositions. It has been pointed out^{10,13} that superiority of cast material is usually met only when the temperature exceeds or at least approaches the recrystallization temperature, in this case upward of 1500 F, nor need ferritic and austenitic materials show the same relations.

Pilling and Worthington¹⁴ remark that in short-time tests on Fe-Cr-Ni alloys cast and rolled materials behave approximately the same above 1200 F.

Tapsell¹⁵ comments that in general cast carbon steel between 400 and 500 C (750 and 930 F) is no better and perhaps worse in creep than rolled annealed or air-quenched material.

The tests on K19 steel indicate general superiority in creep resistance for rolled high-carbon material over the cast. Compared on the basis of rate of elongation, as shown in Fig. 32, the high-carbon cast material, except at low stresses at 1000 F, elongates at a more rapid rate than the high-carbon rolled material.

The limited data available show little difference between the low-carbon cast and rolled material when compared on the basis of rate of elongation. However, when the cast and rolled materials are compared on the basis of the total deformation in 10,000 hr, the superiority of the rolled material is quite evident in that the curves are at higher stresses than for the cast material, except for the low-carbon material tested at 1200 F. (See Figs. 33 and 34.)

This superiority found on the basis of total elongation is due in part to lower or equal rates of creep of the rolled material as compared with the cast material and also to the considerably lower initial elongation upon application of the load in the tests. Fig. 35 clearly shows the smaller initial elongations of the rolled material as compared with the cast material. This is in accordance with the room-temperature tensile and yield strengths. Since the cast bars deform more when the load is applied, they might, therefore, be considered much closer to the deformation beyond which fracture occurs in a relatively short time.

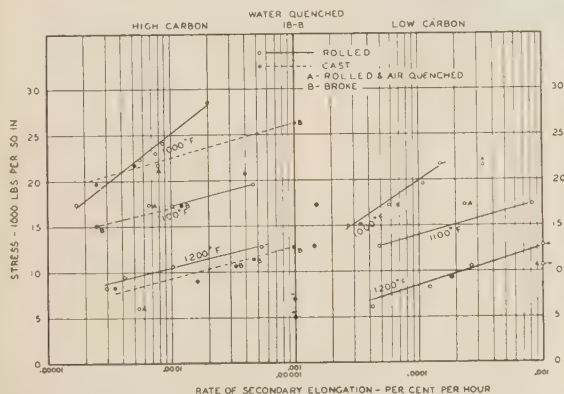


FIG. 32 EFFECT OF STRESS ON RATE OF SECONDARY ELONGATION FOR CAST AND ROLLED, LOW- AND HIGH-CARBON 18-8 STEEL (K19)

¹² R. W. Bailey and A. M. Roberts, "Testing of Materials for Service in High-Temperature Steam Plant," *Engineering*, vol. 133, 1932, pp. 261-265, 295-298.

¹³ W. Rosenhain and C. H. M. Jenkins, "Some Alloys for Use at High Temperatures, Ni-Cr Alloys, Part I," *Journal Iron and Steel Inst.*, vol. 121, 1930, p. 121.

¹⁴ N. B. Pilling and R. Worthington, "The Effect of Temperature on Some Properties of Fe-Cr-Ni Alloys," A.S.T.M.-A.S.M.E. Symposium on Effect of Temperature on Metals, 1931, p. 508.

¹⁵ H. J. Tapsell, "Creep of Metals," 1931, p. 215.

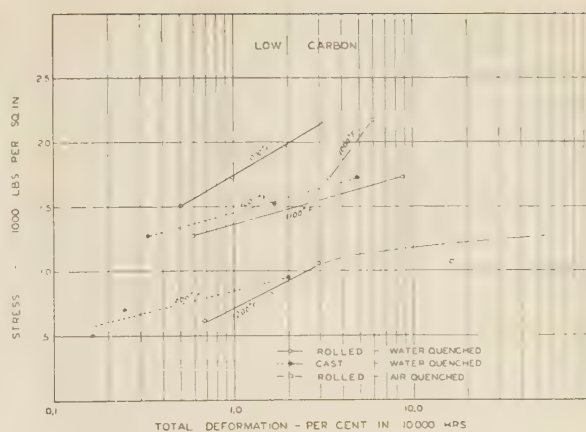


FIG. 33 EFFECT OF STRESS ON TOTAL DEFORMATION IN 10,000 HR FOR ROLLED AND CAST, LOW-CARBON 18-8 STEEL (K19LR AND K19LC)

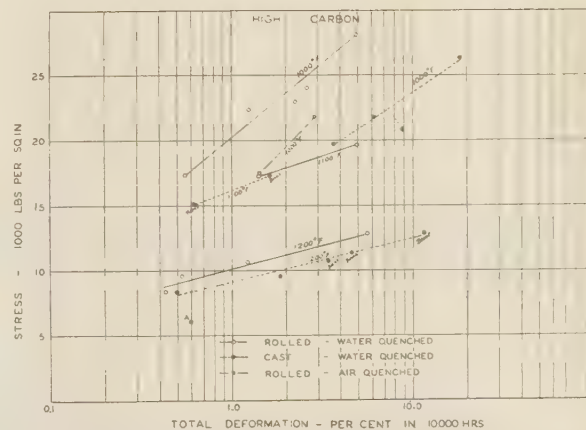


FIG. 34 EFFECT OF STRESS ON TOTAL DEFORMATION IN 10,000 HR FOR ROLLED AND CAST, HIGH-CARBON 18-8 STEEL (K19HR AND K19HC)

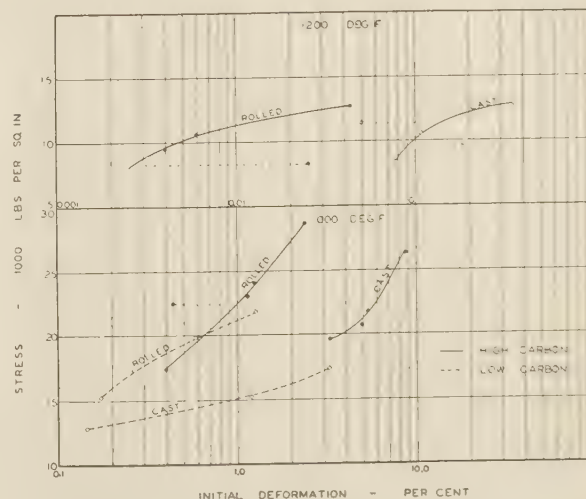


FIG. 35 EFFECT OF STRESS ON INITIAL DEFORMATION FOR ROLLED AND CAST, LOW- AND HIGH-CARBON 18-8 STEEL (K19)

EARLY FRACTURE OF HIGH-CARBON CAST SPECIMENS

No bars of the rolled materials or of the low-carbon cast material fractured during the creep tests. Several of the high-carbon cast bars, however, broke in creep tests at 1100 and 1200 F at lower elongations than the high-carbon rolled bars showed without fracture. The high-carbon cast material often acted in a decidedly brittle manner at these temperatures.

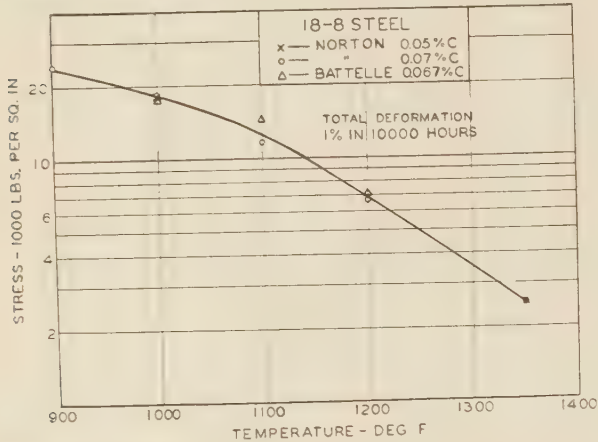


FIG. 36 COMPARISON OF CREEP DATA ON LOW-CARBON 18-8 STEEL OBTAINED BY NORTON AND BATTELLE MEMORIAL INSTITUTE

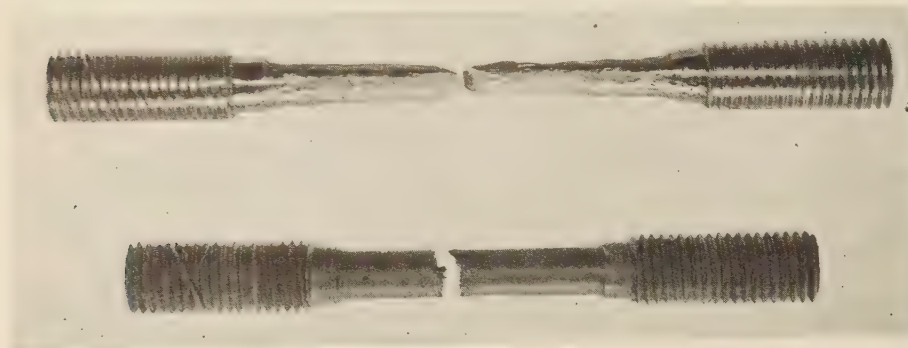


FIG. 37 BROKEN TEST BARS OF CAST, HIGH-CARBON 18-8 STEEL (K19HCW)

(The upper bar was broken at room temperature in a short-time test, and the lower bar (12-2-2, Fig. 29) broke in 1139 hours at 1100 F loaded to 15,080 lb per sq in. Impact for lower bar (12-2-2)—93 ft-lb as heat treated, and 99 ft-lb after creep test.)

To illustrate this, Fig. 37 shows a cast bar broken in a short-time test at room temperature and the creep-test specimen 12-2-2 loaded to 15,080 lb per sq in. at 1100 F which broke after 1139 hours. At room temperature this material had 59 per cent elongation and short-time tensile tests at 1000 and 1200 F indicated a probable elongation at 1100 F of 35 to 40 per cent yet the brittle appearance of the fracture of the bar tested in creep at 1100 F is evident. As can be seen, surface cracks and parting have occurred near the fracture.

These findings make interpretation of the creep results on the high-carbon cast bars entirely misleading, if merely the rates of secondary creep are considered. The data in Fig. 32 show the creep rates for the high-carbon cast material tested at 1100 and 1200 F to be only a little greater than for rolled bars, yet as shown in Fig. 32 and Table 12 some of the bars broke with but small deformation.

These findings suggest that in cases where design is based on a definite extension life, lower loads should be used for high-carbon cast bars in order that their initial deformation plus sec-

ondary creep would be no greater than the lower initial deformation and possible greater total secondary creep in the rolled bars at a somewhat higher load. Even then the data in the case of the high-carbon cast material suggest the use of a higher factor of safety for cast than for rolled 18-8, since in many tests the rolled bars deformed greater total amounts without fracture than did even the low-carbon cast bars. It should be recognized that the cast bars used had a structure of rather exaggerated coarseness and that the results of these tests are not necessarily applicable to castings of smaller cross-section, which would freeze more quickly and have smaller grain size. Nor is it to be concluded necessarily that at temperatures above 1200 F and closer to or above the recrystallization temperature the rolled material would be superior.

MAGNETIC AND MECHANICAL PROPERTIES OF THE MATERIALS AFTER CREEP TEST

Magnetic Permeability. For determining the magnetic permeability after creep test the threads and shoulders of the test specimens were removed by turning to the diameter of the reduced section.

Exposure to the combination of temperature and stress in the creep tests caused an increase in magnetic permeability for all materials. The values for those bars tested are shown in Tables 11B and 12B. The higher the test temperature, the greater was the increase in magnetic permeability. At 1000 and 1100 F the change was small and there was little difference between the low-carbon and high-carbon rolled bars, but at 1200 F the increase was considerable, and the high-carbon rolled bars showed the greater increase.

For the cast bars greater increases in magnetic permeability were noted for the bars tested at 1200 F than for the bars tested at 1000 F, but no definite difference was noted between the low- and high-carbon cast bars.

There does not seem to be any direct relation between the magnetic permeability and the time at temperature, the stress applied, or the resulting elongation.

Impact. For purposes of comparison, the Izod notched

impact resistance of the materials in the heat-treated condition was obtained. The test specimen used had the diameter and notch of the standard round Izod specimen.¹⁶ The end gripped in the anvil of the impact machine had to be shorter than standard, but comparative tests gave the same results on 18-8 specimens with the long and short grips. All Izod tests herein reported, whether on material after creep or not, were made on short-grip specimens, so that all are exactly comparable. This specimen was chosen instead of the Charpy specimen used on the work on K9, since it was the only standard specimen that could be obtained from the reduced section of the creep-test specimen after test and thus provide material for determining in duplicate the degree of embrittlement or loss of ductility in impact as affected by the time at temperature, stress, and elongation in the creep test.

Tables 11B and 12B show the values for impact resistance as heat treated. Both the low-carbon and high-carbon rolled materials show high impact values of 105 and 107 ft-lb, respectively,

¹⁶ National Metals Handbook, A.S.S.T., 1933, p. 447.

TABLE 14 SUMMARY OF THE IMPACT TEST DATA SHOWING COMPARISON WITH EARLIER TESTS ON K9c AND K9d STEELS

Material	Carbon content, %	Rolled or cast	Heat treatment	Charpy Impact Resistance, Ft-Lb				
				As heat treated	1000 hr at 1000 F, no stress	1000 hr at 1100 F, no stress ^a	1000 hr at 1200 F, no stress	1000 hr at 1400 F, no stress
K9c	0.06	Rolled	Water quenched from 2100 F	87	79	70	61	40
K9d	0.085	Rolled	Water quenched from 2100 F	83	83	70	56	41
K9c	0.06	Rolled	Air quenched from 1950 F	82	74	63	56	49
K9d	0.085	Rolled	Air quenched from 1950 F	77	78	64	53	39
				Izod Impact Resistance, Ft-Lb				
				As heat treated	(Hr under stress), 1000 F	(Hr under stress), 1100 F	(Hr under stress), 1200 F	(Hr under stress), 1400 F
K19LRW	0.067	Rolled	Water quenched from 2000 F	101-107	(1060-1550) 107-117	(770-1200) 99-111	(240-1650) (1078) 63-74
K19HRW	0.125	Rolled	Water quenched from 2000 F	103-109	(1120-1760) 74-117	(1000-1500) 64-86	(1500) 88-96 (1820) 85 (390)	(665) 93
K19LRA	0.067	Rolled	Air quenched from 2000 F	(842) 109-119	113-114 (1080)
K19HRA	0.125	Rolled	Air quenched from 2000 F	(1130-1500) 110-115	105-106 (960-1300)
K19LCW	0.067	Cast	Water quenched from 2000 F	91-95	(1130-1600) 93-97	92-106 (800-1300)
K19HCW	0.125	Cast	Water quenched from 2000 F	93-94	(440-1500) 85-101	(475-1140) 99-103 ^b	58-97 (270-650-800) 47-88 ^b

^a Values by interpolation.^b Tests on unbroken end of bars that broke in the creep tests.

while the cast materials show values of 92 and 93 ft-lb.

After creep test the two round Izod impact-test specimens were machined from the reduced section of each creep-test specimen. After taking a disk 0.3 in. thick from the center of the reduced section to provide material for metallographic examination, the impact specimens were taken so that the notches were located in the gage length at a distance of about 1/4 in. from the end of the reduced section. It was very surprising, in view of the results on K9, to find upon making the impact tests on these materials after creep test that in most cases very little change in impact resistance had occurred, and many engineers would consider that even in the worst cases no really serious lack of toughness was shown.¹⁷ For comparison some of the impact data on these K19 steels and on the K9 steels previously studied by the Committee³ are collected in Table 14, where the change in impact values within the series of Charpy tests on K9 steel and the absence of change in impact values within the series of Izod tests on K19 steel is clearly shown.¹⁸

It can be definitely stated that neither the rolled nor the cast low-carbon water-quenched K19L showed the slightest sign of room-temperature impact embrittlement after the creep test, all values being within experimental error of the initial values. The rolled high-carbon K19H, water-quenched, drops in individual bars from an initial 107 ft-lb to 63 or 64 after 1000 hr at 1100 F or 1078 hr at 1200 F, but longer time (1529 hours) at 1100 F brings it up to 86 ft-lb, 1500 to 1800 hr at 1200 F increases it to 85 to 96 ft-lb, and after 665 hr at 1400 F, the value is 93. It cannot be certainly stated whether the material definitely passes through a minimum range of impact values and then improves with longer times and higher temperatures, or whether the loss in impact varies in individual bars. However, it is very plain that the K19HR does not act like the K9 materials in showing a consistent drop in impact in both water and air-quenched conditions, for in the few tests made on air-quenched K19HR it showed no drop of impact at all after creep. Since K19HC, the high-carbon cast material, showed the notably brittle

behavior of breaking with only slight elongation in creep test, it would be expected that impact bars cut from the unbroken end of a bar that had fractured would show impact embrittlement. To the contrary, the impact bars from the unbroken ends of K19HC that broke in creep at 1100 F gave slightly higher impact values than the original 93 ft-lb on the material before creep. After creep at 1200 F the other ends of fractured bars, which may have been damaged by incipient cracks of the type that caused the tensile fracture in creep rather than having true impact embrittlement, ran from 47 to 88 ft-lb, while ends of bars that did not fracture ran from 58 to 97, the latter value being higher than the original. It is, therefore, possible for even this apparently tension-brittle high-carbon cast material to emerge from 865 hr at 1200 F under creep without being consistently impact-brittle.

With the thought that the highest test temperature of 1200 F might not be high enough to embrittle seriously these two particular heats, a creep test was run 665 hr at 1400 F on a high-carbon rolled specimen for the special purpose of detecting embrittlement. A value of 93 ft-lb was obtained after the creep test, a reduction of 14 ft-lb from the original value as heat treated but still very tough and comparable to specimens tested after creep at 1000 and 1200 F.

These data are in sharp contrast to the general idea that the range from 1100 to 1400 F is one of marked deterioration for all unstabilized 18-8 of carbon content over the solubility limit.

There were two differences between the tests on K9 and K19 steels besides differences in melting practise. In the tests reported⁴ the K9 steel was heated 1000 hr without stress. The K19 steel in the creep tests herein reported was heated under various stresses for periods mostly between 750 and 1750 hr (also 665 hr at 1400 F). It has been reported by Crocker¹⁹ and Newell⁹ that 18-8 steel, even without stabilizing additions like titanium, molybdenum, and tungsten, may emerge from long periods of active service without embrittlement.

Payson²⁰ reports an 18-8 alloy with 0.08 per cent carbon, 0.8 per cent tungsten as perfectly resistant, yet others using the same composition do not find it resistant, which is another instance

¹⁷ Bain, Rutherford, and Aborn (The Book of Stainless Steels, p. 346) point out that a 50 per cent drop "still leaves the metal in a highly ductile condition." Newell (p. 357) also points out that a 50 per cent drop leaves toughness "which is still ample to withstand any shock likely to be met."

¹⁸ Duff (The Book of Stainless Steels, p. 487) states that low-carbon 18-8 drops from an initial 75 ft-lb (Charpy) to 45 ft-lb after 3000 hr above 1000 F after which it is constant.

¹⁹ Sabin Crocker. Discussion. A.S.T.M.-A.S.M.E. Symposium on Effect of Temperature on the Properties of Metals, 1931, p. 63.

²⁰ P. Payson. "Prevention of Intergranular Corrosion in Corrosion-Resistant Chromium Nickel Steels." Trans. A.I.M.E. (Iron and Steel Division), vol. 100, 1932, p. 306; discussion, p. 332.



FIG. 38 B21'-3: ROLLED, LOW-CARBON K19, WATER QUENCHED FROM 2000 F AND TESTED AT 1000 F, 1293 HR AT 21,815 LB PER SQ IN.

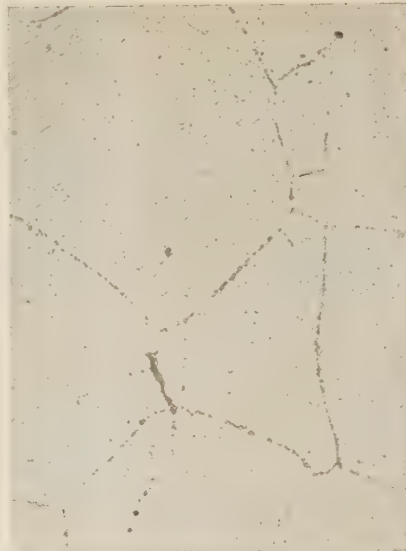


FIG. 39 48: ROLLED, LOW-CARBON K19, WATER QUENCHED FROM 2000 F AND TESTED AT 1200 F, 1346 HR AT 10,600 LB PER SQ IN.

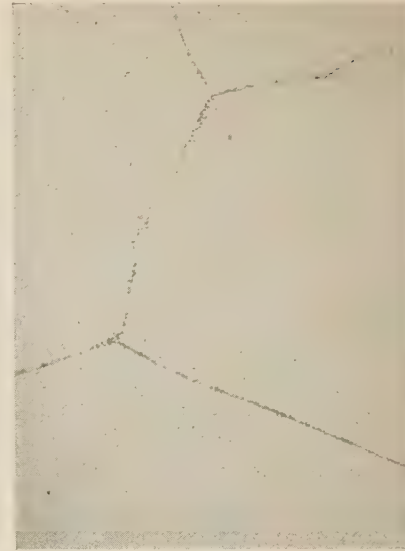


FIG. 40 13S2-2: CAST, LOW CARBON K19, WATER QUENCHED FROM 2000 F AND TESTED AT 1200 F, 1300 HR AT 7000 LB PER SQ IN.

(Magnification of etched specimens in Figs. 38, 39, and 40—500X. Etchant—two parts HCl, one part HNO₃, and one part acetic acid in three parts of glycerin.)

where a given lot of material is resistant while it seems that it should not be.

There is indication that stress hastens the progress of the alloy toward equilibrium, so that the changes that are taking place are accelerated. This tendency has been noted by Krivobok²¹ and Tucker and Sinclair²² and has been appraised as probable by Bain, Aborn, and Rutherford.²³

The acceleration of the changes, especially carbide precipitation, by stress might be expected to produce more instead of less embrittlement. But Bain, Aborn, and Rutherford show that a restoration period follows the period of susceptibility to intergranular embrittlement as determined in the Strauss corrosion test, and their Fig. 3 shows for an 0.08 per cent carbon 18-8 steel at 1200 F without load-increasing susceptibility up to about 100 hr but a recovery thereafter, so that at 1670 hr the original zero susceptibility of the quenched material was restored.

The period of 1670 hr is in the region of the times to which the K19 steels were subjected to stress at 1200 F; hence it is possible that the K19 creep specimens may have passed through a period of susceptibility and then recovered.

However, it is not certain that susceptibility to intergranular corrosion implies embrittlement as shown by impact tests, or vice versa. Tindula²⁴ and Krivobok²¹ do not find susceptibility to intergranular corrosion and impact embrittlement necessarily to go hand in hand. Bain, Aborn, and Rutherford²⁵ say specifically, "The loss of ductility and intergranular sensitization both accompany carbide precipitation but have otherwise no fundamental inter-relation."

²¹ V. Krivobok, unpublished report presented at the 1932 Metallurgical Advisory Board Meeting, Carnegie Institute of Technology.

²² W. A. Tucker and S. E. Sinclair, "Creep and Structural Stability of Nickel-Chromium-Iron Alloys at 1600 F (870 C)," *Bureau of Standards Journal of Research*, vol. 10, 1933, p. 851, Research Paper No. 572.

²³ E. C. Bain, R. H. Aborn, and J. J. B. Rutherford, "Prevention of Intergranular Corrosion in Austenitic Stainless Steels," *A.S.S.T.*, vol. 21, 1933, p. 481.

²⁴ Roy W. Tindula, "The Impact Properties of Austenitic Cr-Ni Steels," Thesis No. 22452, College of Engineering, Carnegie Institute of Technology.

²⁵ The Book of Stainless Steels, *A.S.S.T.*, 1933, p. 346.

It was proposed in the test program herein reported to make corrosion tests on pieces taken from the reduced section of the creep-test specimens after test. With the uncertainty regarding relation between corrosion and impact resistance, it was decided first to run a few tests on samples taken from bars of steels K9c and K9d, whose impact resistance had been previously reported. Six samples were selected for the test. Three samples were of steel K9c (0.06 per cent C) and three of steel K9d (0.085 per cent C). All three of each steel were water quenched, one being tested as quenched and the other two after 1000 hr at 1200 and 1400 F subsequent to quenching.

They were boiled for six hr in a solution containing 10 per cent by weight of c.p. sulphuric acid (anhydrous) and 10 per cent by weight of copper sulphate (anhydrous). After boiling for six hr the specimens were removed and washed and weighed to determine loss in weight.

The results obtained in one six-hour run and shown in Table 15, indicate that the samples tested as quenched had been attacked very little. It is shown that specimens Nos. 10 and 28 after the 1000-hr draw at 1200 F, as expected, had lost considerable weight in the six-hr corrosion test, the greatest loss occurring in the high-carbon specimen. But specimens Nos. 11 and 29 after the 1000-hr draw at 1400 F, which treatment produced the lowest impact resistance, were attacked very little and are comparable to specimens Nos. 7 and 25 tested as quenched.

These data, therefore, suggest the possibility that the proposed H₂SO₄-CuSO₄ corrosion tests may not indicate relative embrittlement of this 18-8 steel with regard to the resistance of the material to impact, and suggest that the specimens taken from the creep-test specimens after prolonged creep tests be reserved until more is known of the value of these proposed corrosion tests.

Schmidt and Jungwirth²⁶ record impact tests on a 19 per cent Cr, 7.8 per cent Ni alloy containing only 0.02 per cent carbon, a composition free from susceptibility to corrosion according to

²⁶ M. Schmidt and O. Jungwirth, "Warmsprödigkeit Austenitischer Stähle," *Archiv für das Eisenhüttenwesen*, June, 1933, p. 559 to 562.

others, which showed a loss of some 50 per cent of the impact strength of the quenched material after heating 400 hr at 1560 F. They also show a drop in tensile strength of 10 per cent after heating two hr at 1100 F and an increase of 20 per cent after five hr at 1300 F, and conclude that either a very small amount of carbon above the accepted solubility limit may induce marked precipitation-hardening effects or else that some other constituent, as an oxide, also exerts precipitation-hardening effects.

If it be assumed that embrittlement and recovery may occur on heating under load in some such manner as do susceptibility and recovery from it, and that the K19 creep specimens when subjected to the impact test had recovered but, that had they been tested for impact at an earlier stage in the creep tests they would have been found brittle, it is worthy of note that the creep curves do not show any changes of direction to indicate at what times embrittlement or recovery take place.

E. C. Smith²⁷ stated that induction-furnace material of the same analysis as arc-furnace material (18 Cr, 8 Ni) may show very much slower embrittlement. Although the chemical compositions as shown by ordinary analyses may be exactly the same, induction and arc-furnace alloys act differently under working and recrystallization temperatures by a large margin, and all through the plant are handled as different materials.

Without tests at much earlier stages (shorter times) in creep, it cannot be said whether K19 embrittled at first and recovered by the time the creep bars were removed or whether this induction-furnace material had not yet begun to be embrittled.

Some members of the committee have remarked that much of the work on susceptibility to corrosion embrittlement has been done on thin stock, sheet, and strip, and that perhaps there is a surface action which would make these

²⁷ E. C. Smith, Republic Steel Corporation, private communication.

TABLE 15 CORROSION TEST

Specimen number	Carbon content per cent	Heat treatment ^a	Surface area sq in.	Original weight, g	Final weight, g	Loss in weight, resistance g	Impact resistance ft-lb
K9c (7)	< 0.07	WQ	0.7380	6.1241	6.1239	0.0002	87
K9c (10)	< 0.07	WQ and D (1200 F)	0.7424	6.1771	6.1727	0.0044	60
K9c (11)	< 0.07	WQ and D (1400 F)	0.7434	6.1993	6.1989	0.0004	40
K9c (25)	0.08 to 0.12	WQ	0.7421	6.1839	6.1838	0.0001	84
K9c (28)	0.08 to 0.12	WQ and D (1200 F)	0.7411	6.1969	6.1737	0.0232	55
K9c (29)	0.08 to 0.12	WQ and D (1400 F)	0.7416	6.1984	6.1981	0.0003	40

^a WQ indicates water quench; D indicates draw for 1000 hours.

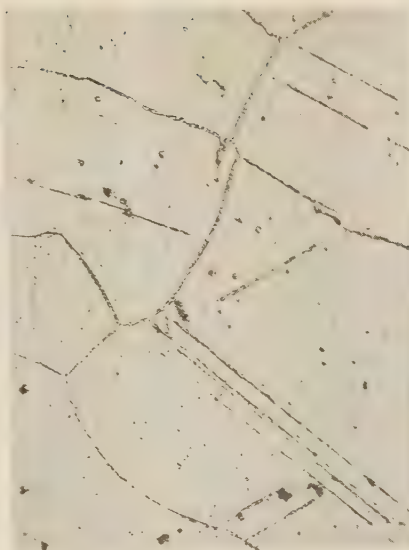


FIG. 41 G35-1: ROLLED, HIGH-CARBON K19, AIR QUENCHED FROM 2000 F AND TESTED AT 1200 F, 1078 HR AT 6065 LB PER SQ IN.



FIG. 42 G27-1: ROLLED, HIGH-CARBON K19, WATER QUENCHED FROM 2000 F AND TESTED AT 1000 F, 1342 HR AT 28,570 LB PER SQ IN.



FIG. 43 G27-1': ROLLED, HIGH-CARBON K19, WATER QUENCHED FROM 2000 F AND TESTED AT 1100 F, 1024 HR AT 19,570 LB PER SQ IN.

(Magnification of etched specimens in Figs. 41, 42, 43, and 44—500X. Etchant—two parts HCl, one part HNO₃, and one part acetic acid in three parts glycerin.)



FIG. 44 12-3-1: CAST, HIGH-CARBON K19, WATER QUENCHED FROM 2000 F AND TESTED AT 1200 F, 796 HR AT 10,565 LB PER SQ IN.

specimens embrittle faster than more massive specimens, or that the worst material was lost in machining the notch. Though this argument would hardly apply to the $\frac{5}{8}$ -in.-square specimens of K9 in the previous committee investigation, plans were made

to roll the K19 materials into thin stock and study its susceptibility in cooperating laboratories. This work has not yet progressed far enough to yield any information.

METALLOGRAPHIC EXAMINATION AFTER CREEP AND FATIGUE TESTS

Disks 0.3 in. thick were cut from the center of the gage length of the creep test specimens after

test. The first specimens were examined on a transverse section, but later specimens were examined on a longitudinal section.

Figs. 4, 5, 6, and 7 have shown the structures of the low- and high-carbon rolled and the high-carbon cast materials as heat treated by water quenching from 2000 F.

Figs. 38, 39, and 40 show photomicrographs of some of the water quenched low-carbon cast and rolled specimens after creep test. Fig. 38 shows specimen B21'-3 tested at 1000 F for 1293 hr, while Fig. 39 shows specimen 48 tested at 1200 F for 1346 hr. Both show precipitation of carbides in the grain boundaries, with the greater amount in the specimen tested at



FIG. 45 G30'-8: ROLLED, HIGH-CARBON 18-8 (K19), TESTED AT 1200 F, 1518 HR AT 9500 LB PER SQ IN.
(Magnification—1000 \times ; Murakami etch; photomicrograph by Payson.)

1200 F. There are indications that some precipitation has occurred within the grains in specimen 48 tested at 1200 F. Fig. 40 shows cast specimen 13S2-2 tested at 1200 F for 1300 hr. The grain size in the cast material is very large, as was shown in the macrographs in Figs. 2 and 3; so in Fig. 40 it was only possible to show the junction of several grains. It may be seen that there is considerable carbide precipitation in the grain boundaries of this cast specimen.

Figs. 41, 42, 43, and 44 show photomicrographs of some of both air-quenched and water-quenched high-carbon cast and rolled specimens after creep test. Fig. 41 shows specimen G35'-1 (air quenched) tested at 1200 F for 1078 hr. Heavy carbide precipitation has taken place in the grain boundaries and also very noticeable precipitation along twin lines within the grains. Figs. 42 and 43 show specimens G27-1 and G27-1' after test at 1000 F for 1342 hr and at 1100 F, for 1024 hr, respectively. Both show carbide precipitation, with the greater amount in specimen G27-1' tested at 1100 F. Fig. 44 shows specimen 12-3-1 (cast) tested at 1200 F for 796 hr. As in the case of the low-carbon cast specimen 13S2-2, a representative section shows the junction of several grains and considerable carbide precipitation in the grain boundaries.

There appears to be little if any difference in the amount of precipitation between the low- and the high-carbon material, whether as cast or rolled. A greater amount of precipitation appeared to take place in those specimens tested at the higher test temperatures of 1100 and 1200 F than in those tested at 1000 F.

In order to examine the hypothesis that stress may accelerate carbide precipitation, through the courtesy of C. L. Kinney,

John A. Mathews, and C. E. MacQuigg, selected specimens of the 1200 F series of fatigue bars were examined by Mr. Han of the Illinois Steel Company, and selected specimens from the creep tests were examined by Mr. Han, Mr. Payson of the Crucible Steel Company, and Mr. Vilella of the Union Carbide and Carbon Research Laboratories.

Messrs. Han, Payson, and Vilella were asked to note any difference in the amount or nature of the carbide separation from that which, from their experience in the examination of the materials of the compositions in question, they would expect to find after heating without load for the times and temperatures to which the K19 specimens had been subjected. Mr. Han was asked to note especially any difference between the periphery and the center of the fatigue bars, since the periphery of the reversed bending fatigue bar is subjected to the maximum stress, whereas the stress decreases to zero at the center of the bar.

The conclusions previously stated were verified by the findings of Mr. Payson of the Crucible Steel Company, who examined some of the creep-test specimens after test. Figs. 45 and 46 show photomicrographs made by Mr. Payson which indicate that the precipitation in the high-carbon cast and rolled specimens was of a similar nature to that previously noted. Mr. Payson stated that he was unable to detect any influence on the



FIG. 46 G30'-8: ROLLED, HIGH-CARBON 18-8 (K19), TESTED AT 1200 F, 1518 HR AT 9500 LB PER SQ IN.

(Outer edge of sample showing strain lines. Magnification—200 \times . Etchant—50 per cent HCl in alcohol; photomicrograph by Payson.)

manner or amount of precipitation due to the stressing of the creep-test specimens during the long test period at the high temperatures.

Mr. Vilella of the Union Carbide and Carbon Research Laboratories also examined some of the creep-test specimens. He found greater precipitation in the specimens tested at the higher temperature of 1200 F, irrespective of their carbon content, duration of test period, or load applied. He found no evidence of acceleration of precipitation due to stress. Specimens tested at 1200 F showed considerable intragranular precipitation, while in specimens tested at 1000 F no intragranular precipitation was detected.

Mr. Han of the Illinois Steel Company, after his examination of the fatigue specimens, concluded as follows:

- (1) Carbide precipitation in the K19 steels under this investigation is the same as that found in the average commercial stock of the same chemical composition.

- (2) Time and carbon content are directly controlling factors of the amount of carbide precipitation, and time is the more important factor of the two.
- (3) Under zero stress most carbides segregate in the grain-boundary regions in the wrought material, while they are concentrated mostly in the original location of ferrite areas in the castings.
- (4) For wrought steel there is no measurable difference in the amount of carbide precipitation between maximum repeated-stressed and zero-stressed zones in fatigue specimens tested at 1200 F. There is a definite difference in the distribution in the two extreme areas. Cold-

working, in terms of maximum repeated stress, causes uniform precipitation of very fine carbide particles along the slip bands, while in the absence of stress the natural tendency is for the carbides to segregate to the grain-boundary regions in relatively larger particle size. This difference is smaller in lower-carbon and shorter-duration samples than in the higher-carbon and longer-duration ones. Slower rate of stress alternation seems to induce greater difference in distribution between the stressed and unstressed regions.

- (5) Not much slip is developed in the limited number of cast samples examined.

Laws of Elastic Behavior in Metals

Summary Report on Experimental Program at Union College by A.S.M.E. Special Research Committee on Mechanical Springs

By M. F. SAYRE,¹ SCHENECTADY, N. Y.

To aid in rational spring design and in other problems of design where resilience or deflection are important matters, a general picture may be advisedly drawn of various phases of elastic behavior in metals, which deviates widely from the simple explanation given by Hooke's law. For rough computation these deviations need not be considered, but where loads are high enough so that an accurate knowledge either of stresses or of deflections is required, or where an accurate theoretical knowledge is desired, they cannot be ignored. The statement given below, which in places is necessarily more or less theoretical, summarizes this picture. It emphasizes particularly those various factors which have been brought out in the work carried on at Union College for the past few years under the auspices of the A.S.M.E. Special Research Committee on Mechanical Springs.² Accompanying tables give numerical values of these various effects for a range of different metals.

SINCE it was first enunciated by Robert Hooke in 1678, Hooke's law has served as a basic principle underlying mechanical design. Everything considered, this law is surprisingly well obeyed by our principal materials of construction. In cases, however, where high precision is needed or where very high stresses are used, as in many cases in spring design, the deviations from this rule become of importance. Backed by the A.S.M.E. Special Research Committee on Mechanical Springs, studies of these deviations and of other items, have been carried on for several years at Union College. The details of this investigation, particularly in regard to behavior in tension, compression, and bending, have been reported in several papers presented in the past.

The present paper is intended as a final report. Details of the studies of torsional behavior are included in the appendix while the body of the paper summarizes the results of the investigation and correlates them with information obtained elsewhere.

¹ Associate Professor of Applied Mechanics, Union College. Mem. A.S.M.E. Professor Sayre was graduated from Columbia University with the degrees of E.M. and A.M. Seven years of engineering experience were followed by twenty years at Union College, the latter portion diversified by research and consulting work carried on for the General Electric Company and for other concerns.

² "Elastic and Inelastic Behavior in Spring Materials," by M. F. Sayre, A.S.M.E. Trans., vol. 52, 1930, paper no. APM-52-9.

"Elastic Behavior of Spring Materials," by M. F. Sayre, Proc. A.S.T.M., vol. 30, part II, p. 546.

"Elastic and Inelastic Behavior in Spring Materials (Continued)," by M. F. Sayre, A.S.M.E. Trans., vol. 53, 1931, paper, no. APM-53-8.

"Elastic After-Effect in Metals," by M. F. Sayre, Journal of Rheology, vol. 3, 1932, p. 206.

"Thermal Effects in Elastic and Plastic Deformation," by M. F. Sayre, Proc. A.S.T.M., vol. 32, part III, p. 584.

Contributed by the A.S.M.E. Special Research Committee on Mechanical Springs and presented at the Annual Meeting, New York, N. Y., December 4 to 8, 1933, of THE AMERICAN SOCIETY OF MECHANICAL ENGINEERS.

NOTE: Statements and opinions advanced in papers are to be understood as individual expressions of their authors, and not those of the Society.

HYDROSTATIC PRESSURES

Under pressure acting from all directions simultaneously, or so-called hydrostatic compression, a body loses in volume at a decreasing rate with increasing pressure. It has been shown by Bridgman and others that the volume modulus of elasticity, K , may as a first approximation be expressed in the general form $K = K_0 = C_0/S$. Values of K also are affected by temperature, the stiffness decreasing with increasing temperature. As with a gas, the sudden or adiabatic application of pressure results in a slight increase of temperature, decreases in temperature being caused by sudden reductions of pressure, or by their equivalent, the application of hydrostatic tension. These changes in temperature naturally cause corresponding

TABLE 1 THERMAL CREEP IN TENSION
(Approximate value of coefficients for various materials)

Material	Density, ρ	Specific heat, s	Coefficient of linear expansion, $\alpha \times 10^{-6}$	Modulus of elasticity, E , lb per sq in. $\times 10^{-6}$	Coefficient of thermal expansion, m , $\times 10^{-4}$	$k_1 \times 10^{-6}$	k_2
Magnesium	1.74	0.24	25.8	6.25	9.4	29.80	0.00480
Aluminum	2.70	0.21	23.1	10	5.3	19.64	0.00454
Steel	7.88	0.102	11.7	30	3.27	7.02	0.00246
Nickel	8.9	0.102	13.2	30	2.6	7.02	0.00278
Copper	8.93	0.091	16.8	17.8	3.59	10.00	0.00299
Tungsten	19.3	0.034	4.44	55	0.87	3.27	0.00080
Platinum	21.37	0.030	8.99	23.5	0.73	6.77	0.00143

Change in temperature under elastic tensile strain = $k_1 S$.
Adiabatic value of $E = (1 + k_2) \times$ isothermal value.
Thermal creep = $k_2 \times$ adiabatic elastic elongation, approximately. (For exact equations, see "Thermal Effects in Elastic and Plastic Deformation," by M. F. Sayre, Proc. A.S.T.M., vol. 32, part II, p. 584.)

NOTE 1: Values of α and m are given per deg C. Different experimenters, working with different lots of material supposedly of the same general composition, have obtained widely varying values of m . Great reliability is therefore not claimed for values of m in Tables 1, 2, and 3.

NOTE 2: $k_1 = \frac{C\alpha T}{\rho s J}$, $k_2 = \frac{C\alpha^2 E T}{\rho s J}$, where $J = 4.185 \times 10^7$, and $C =$ conversion factor from dynes per sq cm to lb per sq in. = 6.894×10^8 .

secondary changes in volume and so affect the apparent change in size under loading. The adiabatic volume modulus of elasticity is, therefore, slightly larger than the isothermal modulus.

SHEARING STRESSES

(1) No change, or almost no change, of volume occurs under shearing stresses, and the adiabatic and isothermal moduli are essentially the same.

(2) Very precise studies carried on by John Chatillon and Sons, which will presently be reported in detail, indicate that the modulus of elasticity in torsion does not vary consistently with increasing stress in torsion.

(3) The torsional or shearing modulus varies with temperature, stiffness decreasing with increasing temperature.

(4) Overloadings beyond the elastic limit in torsion, whether on straight wire or on coiled springs, materially decrease the modulus of elasticity under future moderate loads.

(5) In very precise torsional-pendulum measurements at Union College, for small amplitudes of oscillation corresponding to torsional stresses below 1000 to 1500 lb per sq in. erratic variations in stiffness of from 1 to 10 per cent were found. For larger amplitudes consistent results were obtained. Further investigation of the causes for these erratic variations is needed. (For details of these tests, see the Appendix to this paper.)

(6) By varying the weight of the bob of the torsional pendulum, the torsional modulus, G , was determined for the same torsional ranges but in wire under a wide range of tensile stress, from small values up to almost the elastic limit of the wire. As the tension increased, values of G decreased as figured on the basis of the original unloaded dimensions of the wire. Most of this variation disappeared when G was refigured on the basis of the actual length and diameter of wire under load.

DIRECT TENSILE OR COMPRESSIVE STRESSES

From a theoretical point of view, uni-directional tension is a composite of hydrostatic tension and of shearing stresses, and behavior under tension represents a composite of the behaviors

TABLE 2 HYDROSTATIC COMPRESSION OR TENSION^a

Material	Modulus K , 30 C	Temperature coef. of mod., per deg C	$k_1 \times 10^{-4}$	k_2
Aluminum, hard drawn and annealed	10,320,000—3.9 S	0.00095	58.9	0.0140
Cast	10,250,000—5.5 S	0.00055
Copper, commercial	18,810,000—10.1 S	0.00021	30.0	0.0095
drawn rod	18,890,000—10.2 S	0.00024
Same, annealed	19,140,000—10.1 S	0.00045
Pure "best select"	23,470,000—12.0 S	0.00026	21.0	0.0058
Iron Armco, annealed	26,240,000—15.0 S	0.00012	21.0	0.0073
Nickel 99%, drawn and annealed	26,050,000—14.7 S	0.00028
Forged, drawn and annealed				

^a Computed on the basis of data by Prof. P. W. Bridgman, Proc. Am. Acad. Arts and Sciences, vol. 58, p. 166; vol. 59, p. 109, 1923.

TABLE 3 SHEARING MODULUS

Material	Shearing Modulus G at 20 C (10 ⁹ lb per sq in.)	Temp. Coef. of Shearing modulus (Col. 2), m	(3)	(4)
Aluminum	3.73	0.00058	0.00062	
Duralumin	3.93	0.00057	0.00062	
17 SRT alloy	3.82	
Monel annealed,	9.67	0.00036	0.00038	
Hard drawn	9.84	0.00040	0.00042	
Brass,	5.02	0.00046	0.00049	
As drawn	5.05	
Relief annealed	5.13	
Phosphor bronze	6.3	0.00045	0.00048	
Nickel	11.2	
Coin silver	4.24	0.00052	0.00056	
Nickel silver, as received	6.24	0.00041	0.00044	
Tempered at 475 C	6.93	0.00033	0.00036	
Tempered at 650 C	6.39	0.00035	0.00038	
Drill rod steel	11.2	0.00022	0.00023	
Oil tempered steel	11.3	0.00032	0.00033	
0.67% C steel, heat treated,				
0.080 in. diam.	10.95	
0.046 in. diam.	11.15	
0.0281 in. diam.	11.25	
Hard drawn steel wire	11.4	
Music wire	11.3	11.4	0.00038	0.00040
Chrome vanadium steel	11.4 to 12.6	0.00028	0.00029	
Chrome molybdenum steel	11.7	0.00043	0.00044	
Stainless steel	12.3 to 12.6	0.00026 to 0.00038	0.00027 to 0.00039	
18% Cr 8% Ni steel wire	10.9	

Column

1 Obtained in Union College investigation. For detailed description of materials see previous reports in A.S.M.E. Transactions.

2 See Report No. 358, Nat. Adv. Comm. for Aeronautics. "Temperature Coefficient of the Modulus of Rigidity of Aircraft Instrument Diaphragm and Spring Materials," by W. G. Brombacher and E. R. Melton.

3 Modulus as based on original size.

4 Modulus corrected to refer to actual size after temperature change.

as already described. The relation between the three moduli for a homogeneous³ isotropic material is given by the equation:

$$E = \frac{9GK}{G + 3K}$$

³ This equation, as well as the various equations connecting Poisson's ratio with E , G , and K , must be used with some care when dealing with metals, particularly when cold rolled or drawn. Due to the presence of preferred orientation of crystals, the material may not, properly speaking, be homogeneous or isotropic. Much more complex equations may be needed.

(1) Young's modulus of elasticity, E , varies with stress as given by the equation:

$$E = E_0 \pm C_2 S$$

+ being used for compression, and — for tension.

(2) E varies with temperature, decreasing with increasing temperature.

(3) The adiabatic value of E is greater than the isothermal value, but this difference is a smaller percentage than under hydrostatic compression since smaller changes in volume occur.

(4) In work done by D. K. Froman at the Ryerson Physical Laboratory in Chicago, variations in values of E under very small tensile loads were found. His results harmonize with the erratic values of G found for low torsional stresses in the Union College investigation. No explanation of these peculiar variations has as yet been given and further work is needed.

(5) As noted in earlier reports, over-stress beyond the elastic limit in tension usually but not always results in decreased values of E under future moderate stresses.

BENDING STRESSES

Bending stresses represent a composite of tensile and compressive stresses, usually with shear added.

(1) In bending, the increase in E with stress on the compression side of the beam counterbalances the corresponding decrease in E on the tension side, so that the over-all stiffness of the beam is virtually unaffected and may be computed on the basis

TABLE 4 MODULUS OF ELASTICITY IN TENSION^a

Specimen	Material ^d	Diam., in.	Modulus
Corrected to 20 C (68 F)			
Measurements Made Using Deadweight Loading, 52 Ft Gage Length			
481	0.67% C heat-treated steel wire	0.0281	30,010,000—6.6 S
479	0.67% C heat-treated steel wire	0.0465	30,170,000—6.5 S
532	Hard drawn spring wire	0.043	28,800,000—6.8 S
534	Music wire	0.025	29,920,000—4.8 S
533	Music wire	0.045	29,770,000—4.5 S
493	Spring temper brass wire, as drawn	0.040	14,300,000—4.6 S
485	Relief annealed ^b	0.040	15,500,000—4.6 S—0.0001 S ²
501	Relief annealed ^b	15,300,000—5.0 S—0.0001 S ²
494	Phosphor bronze wire	0.040	15,580,000—5.4 S
499	Nickel wire ^c	0.050	About 33,400,000
500	Redrawn to ^c	0.0458	About 32,300,000
497	Hard copper wire	0.051	19,120,000—6.0 S
483	17SRT aluminum alloy wire	0.065	10,290,000—10.9 S
495	17SRT aluminum alloy wire	0.065	10,280,000—6.2 S
Measurements Made Using Amsler Machine			
111	0.68% C heat-treated steel wire	1/8 × 1/2 in.	29,750,000—7.7 S
112	0.68% C heat-treated steel wire	1/8 × 1/2 in.	30,150,000—6.3 S
113	0.68% C heat-treated steel wire	1/8 × 1/2 in.	29,540,000—8.3 S
530	3 1/2% Nickel Steel	Diam., 1/2 in.	29,190,000—4.3 S
538	3 1/2% Nickel Steel	Diam., 1/2 in.	28,950,000—10.9 S
476	3 1/2% Nickel Steel	Diam., 1/2 in.	28,950,000—10.9 S
306	Spring tempered phosphor bronze	1/8 × 1/2 in.	14,700,000—10.8 S
	1% C heat-treated steel	Diam., 0.327 in.	29,040,000—5.0 S
	Heat-treated silicon steel	Diam., 0.328 in.	29,120,000—6.7 S

^a Union College investigation.

^b The spring temper brass wire, relief annealed, was exceptional in that both samples gave stress-modulus of elasticity relationships which called for an equation involving S^2 .

^c The results with the nickel wires were affected by the initial "curl" in the wire, and are given as approximate values, for information only.

^d For detailed description of materials, see previous reports in the A.S.M.E. Transactions.

TABLE 5 MODULI OF ELASTICITY

Material	E 10 ⁹	G 10 ⁹	G/E	$\nu = \frac{E}{2G} - 1$
0.67% C heat-treated steel wire	30.01	11.25	0.375	0.334
0.67% C heat-treated steel wire	30.17	11.15	0.371	0.351
Hard drawn spring wire	28.8	11.4	0.396	0.285
Music wire	29.92	11.35	0.379	0.319
	29.77	11.25	0.378	0.321
Brass wire, as drawn	14.3	5.05	0.353	0.415
Relief annealed	15.4	5.18	0.336	0.486
Phosphor bronze	15.58	6.3	0.404	0.236
Nickel	33.4	11.2	0.335	0.491
17SRT aluminum alloy	10.28	3.82	0.372	0.345

NOTE: The last column gives the values of ν = Poisson's ratio as computed from the values of E and G given in previous columns. See text for discussion of validity of these values.

of Hooke's law. True stresses on the compression side are somewhat greater, 1 to 4 per cent, and on the tension side somewhat less than on the basis of Hooke's law.

(2) Due to the difference between adiabatic and isothermal moduli, any case of sudden bending will be followed by a period of thermal creep. Heat transfer in metal is so rapid that except in thick beams this period is very short. For a rectangular cross-section one-half of the creep will occur within the first $3b^2$ seconds, where b is the side in inches. In shafting revolving at a moderate speed, or in small diameter high speed shafting, an appreciable amount of hysteresis loss may result from the thermal cycles through which this phenomenon causes the shaft to pass.

(3) The temperature effect upon stiffness is the same in the case of bending as in the case of direct tensile or compressive stress.

(4) As with direct tensile or compressive stresses, overstress in bending may result in decreased values of E under future moderate stresses.

(5) The compression side of a beam tends to widen laterally as it shortens longitudinally, while the reverse effect occurs on the tension side. As a result, the beam tends to warp, or curve, in the lateral direction. This is called the anti-clastic effect. In thin flat strips, as used in spiral springs, the development of this lateral curvature is obviously impossible. Prevention of the anti-clastic curvature produces as a secondary effect a fictitious stiffness in the strip as a whole, so that the apparent modulus of elasticity in bending may range up to 10 per cent higher than the measured value of E in tension for the same strip. In the limiting case, the stiffness will go up in the ratio of $(1 - \rho^2)$ to 1, where ρ is the value of Poisson's ratio.

EXPLANATION OF TABLES

Table 1 gives values necessary for the computation of the differences between the adiabatic and isothermal moduli of elasticity, and also of the thermal creep in tension, for several typical materials. The column headings in this table are self-explanatory except the last two headed k_1 and k_2 . The change in temperature resulting from rapid application of elastic tensile or compressive strain, in deg C, equals the stress change S , in lb per sq in., multiplied by the constant k_1 . Tensile strain causes a decrease and compressive strain an increase in temperature. The modulus of elasticity for rapid loading, or "adiabatic modulus," is greater than the value for slow or isothermal loading in the ratio $(1 + k_2)$ to 1.

In Table 2 the columns k_1 and k_2 give corresponding values for hydrostatic compression or tension. The column headed K gives the volume modulus of the material as of a temperature 30 C in terms of the stress. For hard drawn aluminum, for example, the modulus of elasticity under low stress is 10,320,000 lb per sq in., and this value increases at the rate of 3.9 for each lb per sq in. of applied pressure in compression. As noted in the table, these figures have been computed on the basis of data published by Dr. P. W. Bridgman. The terms are necessarily approximate only and equations involving higher powers of S would probably be needed to give the exact values. No experimental work has been possible, but for theoretical reasons, rate of decrease of the volume modulus under tensile stress should be the same as the rate of increase under compressive stress, giving, for example, for aluminum under 100,000 lb per sq in. hydrostatic tension, a modulus of 9,930,000.

Table 3 gives values of the shearing modulus G and of its temperature coefficient. As stated in the paper, the adiabatic and isothermal values of this modulus are essentially alike and this modulus also changes little with stress. Experimental results given by Keulegan and Houseman in the Bureau of

Standards *Journal of Research* for March, 1933, indicate that for any given material the temperature coefficients of Young's modulus and of the shearing modulus are essentially alike, so that the temperature coefficients for special spring materials in shear may also be used in tension, compression, and bending.

Table 4 gives values of Young's modulus as a function of applied stress as determined in the Union College investigation. For details of this investigation see previous reports in the A.S.M.E. Transactions. It will be noted that the rate of change with stress given here is essentially of the same order of magnitude as the rate of change of volume modulus with stress as determined by Bridgman. In this work every effort was made to eliminate or correct for the effect of plastic or pseudo-elastic creep and it is believed that these equations approximate to representing the true elastic behavior of the material. Due to the experimental difficulties involved in the measurement of Young's modulus under compressive stress, all work here was necessarily confined to tensile loading.

Table 5 gives comparisons of values of E and G as taken from Tables 3 and 4, and also values of Poisson's ratio as computed from E and G on the basis of the usual formula. A further discussion of this table is given in the Appendix. Caution should be exercised in using these values of Poisson's ratio. The formula $\rho = (E/2G) - 1$ is based on the assumption that the material has uniform properties in all directions. For cold-drawn wire particularly, it seems probable that, due to the preferred orientation of the crystals in the wire, the modulus of elasticity is different in different directions and that the formula for Poisson's ratio, therefore, is not valid in this instance.

Appendix

TESTS OF TORSIONAL BEHAVIOR

Three methods of testing the shearing, or rather the torsional behavior, of a wire are readily available. It may be tested directly by applying a known torque to a straight length of the wire, and measuring the resulting angular twist. As an alternative, two indirect methods may be used, either making the wire up in the form of a helical spring to be tested in extension or compression, or using the wire as the support rod for a torsional pendulum.

The first method gives more obvious and more convincing results, but it has the disadvantage, where high precision is desired, that it is difficult to measure either the applied torque or the angle of twist without being affected by friction. The torsional pendulum method permits of very rapid and accurate measurements, but it has the disadvantage that due to the weight of the bob of the pendulum, the wire is necessarily under a combination of torsional and tensile stresses, rather than under torsional stress alone, and the second practical objection is that it is a much less obvious method than to take measurements under direct torque. The third method avoids the first part of this last objection, but introduces the difficulty that the measurements made represent, not the behavior of the wire, but the behavior of the completed spring, as affected by any imperfections in the spring formulas used, or by any changes in the material resulting from the method of manufacture.

As the most advantageous method, it was decided to obtain the properties of the wires themselves by use of the torsional pendulum method, using a modification of the long wire set-up which was used in investigations in tension as described in the previous report; and then to make up these same lengths of wire into springs, to be tested by the third method, in order that the differences might be noted. This would give comparative data also, which would permit a direct comparison between values of

moduli of elasticity and hysteresis losses in tension and in torsion.

The modulus of elasticity in shear of the wire used to support the bob of a torsional pendulum is given by the equation:

$$G = \frac{8\pi LI}{gr^4 p^2}$$

where L = length of wire I = mass moment of inertia of bob
 r = radius of wire p = period in seconds

The pendulum bob was made up of a holder carrying a variable number of steel disks as weights, each 8.725 in. in diameter and slightly less than $1/2$ in. thick. It was so designed as to be accurately centered under the wire, and to offer the minimum possible resistance to rotation from air friction. The wire had an effective length of about 626 in. The same general set-up was used as for the tension test, the wires being suspended inside a 3-in. pipe which itself passed through the length of a 5-ft-diameter vertical tank filled with water. In this way the wires were held at a controlled temperature and were also protected from any side drafts. The weights were turned through a known angle so as to put the wire in torsion and then released and allowed to rotate freely. The period of the pendulum ranged from 15 to 250 sec, depending on the wire and on the weight of the bob. By using a stop-watch and timing over an interval of fifteen to thirty minutes, this period could be measured with a high degree of accuracy.

At the same time, the internal hysteresis in the wire was determined by measurements of the rate of decrease of amplitude of the vibrations. To do this, a small mirror adjustable in position was placed at the upper end of the bob, and by use of a telescope pointed at the mirror, readings on the reflected image of a scale fifty inches from the wire were taken at the end of each swing usually over a period of ten swings. The scale could be read with ease to a precision of 0.0002 radian of arc, and as the amplitude of vibration ranged from one-sixteenth of a revolution to as high as three to five full revolutions each side of the mean-position, the probable accuracy of measurement of the decrement ratio as obtained by dividing the decrease in amplitude in radians per vibration by the amplitude in radians, was relatively high. This decrement ratio incidentally is numerically equivalent to the logarithmic decrement as usually given. The results are of course still affected by air friction and by the errors in reading resulting from lateral oscillations of the bob, which it was almost impossible to prevent completely.

Tables 6 and 7 (not printed) give typical values of time of oscillation and decrement readings, and also of computed values of G and the decrement ratio for four different bob weights and for various amplitudes. Regarding these results the following statements may be made:

(1) Consistent values of G are found for amplitudes of vibration corresponding to torsional stress values greater than 1000 to 1500 lb per sq in.

(2) These consistent values of G become lower as the bob weight, and so the tensile stress on the wire, increases if figured on the basis of the unloaded dimensions of the wire. If, however, the true dimensions of the wire under load are used, the value of G is essentially constant.

(3) For low amplitude of vibration, the values of G are widely erratic, in some cases increasing, in other cases decreasing, as the stress range decreases. These variations are far greater than any experimental errors in the work itself. The wires were freely suspended, and air friction at these speeds was negligible, so that it is difficult to associate these variations except with deviations in elastic behavior within the wire itself. The variations are in general more pronounced for the smaller wires than for the larger ones, and so may be a surface effect. They do not seem to be in

any way connected with the amount of internal friction, which is measured by the decrement ratio. These large variations in G for any given material occur both with moderate and with large tensile loads, but no regular law of variation can be observed.

(4) The relation between Poisson's ratio and the moduli of elasticity in tension and shear for a homogeneous isotropic material is given by the equation:

$$G = \frac{E}{2(1 + \rho)} \text{ or } \rho = \frac{E}{2G} - 1$$

where ρ = Poisson's ratio.

Table 5 shows the values of G/E and of ρ as computed for various materials on the basis of this experimental work. It will be noticed that especially for those materials whose strength is due to cold drawing, there is a tendency for the computed value of ρ to approach 0.5. (Phosphor bronze seems to be an exception.) For theoretical reasons, it is difficult to accept these high values as being correct. A more probable alternative explanation is that these wires are not isotropic with respect to G , and that consequently the preceding equation must be used with caution.

Average values of logarithmic decrement as obtained for the various wires tested are as follows:

Material	Logarithmic Decrement
Duralumin (17 SRT alloy)	0.0014
Brass, as drawn	0.0052
Brass, relief annealed	0.0034
Phosphor bronze	0.0016
Nickel	0.0030
0.67% C Steel, heat treated	
0.080 in. diameter	0.0030
0.046 in. diameter	0.0012
0.0281 in. diameter	0.0027
Music wire	0.0040
18% Cr 8% Ni steel wire	0.0033

These values are given for information only and must be used with caution. They represent results obtained on one batch of wire only in each case. Further, in most cases for any given wire there is a considerable variation in logarithmic decrement in torsion, depending upon the amplitude of vibration and upon the tensile load which was simultaneously present.

Only a limited number of tests were made on coiled springs made up from this wire. In general the values of modulus of elasticity as computed from tests on the coiled springs were similar to the values as obtained by the torsion pendulum method. The hysteresis and creep in the coiled springs, which were tested as coiled (not subsequently heat-treated) was, however, great enough to prevent any great accuracy in this determination. To obtain exact values it will be necessary to give the spring some form of mild heat-treatment, as is usually done with springs for any form of measuring instrument. Experimental work was discontinued before it was possible to do this.

Overloading the springs in each case caused a sharp decrease in the value of the modulus, accompanied by an increase in hysteresis. This decrease in modulus was a real effect and not simply a pseudo-effect caused by the change in dimensions of the spring.

A number of measurements have been made of the deformations occurring in the half loop or whole loops bent up at the end of the tension springs, and these deformations have been compared with the deformations per coil in the spring proper under the same loads. The results suggest that a half coil turned up to form a loop should be treated as equivalent to an increase in effective length of spring of 0.10 of a full coil, and that a full coil turned up part way to form a loop, with load still centrally applied with respect to the spring, is equivalent to 0.50 of a full coil.

Plastic Behavior in the Light of Creep and Elastic Recovery Phenomena

By M. F. SAYRE,¹ SCHENECTADY, N. Y.

This paper briefly describes various phases of creep and elastic recovery in metals and offers a new theory of the mechanism by which these phenomena may be brought about. This explanation may also, in some measure, apply to the larger problem of plastic flow in metals in general.

No clear-cut differentiation seems to exist between the creep effects which occur below the elastic limit and the larger plastic yield occurring at higher stresses. One apparently merges gradually into the other.

The amount of creep and hysteresis seems to be definitely related to the temperature of the metal and to its state of internal stress. Any satisfactory theory of the mechanism of plastic flow must explain these facts and must also account for the elastic recovery effects, the time lag in initial creep, and the presence of continuity in metal even after slippage has extended from one crystal into a second differently oriented crystal.

The author suggests several hypotheses to explain these and his explanation seems to agree reasonably well with the facts observed from accurate measurements made at Union College, as well as with observations made by others. Various theoretical reasons also support these hypotheses.

THE phenomenon of creep in metals has been under intensive engineering study for the past ten years. In the main, however, attention has been directed to creep at high temperatures, and the existence of creep and elastic recovery in the same metals at room temperature has been in a measure ignored. In many cases the assumption seems to have been tacitly made that the two were of such widely different character that lessons from one were of no benefit in the study of the other phenomenon. As a result, in papers on high temperature creep, almost no attention has been paid to the large mass of material on room temperature creep gathered particularly in England, France, and Germany over the past fifty years.

The study of elastic behavior in spring metals carried on at Union College over the past six years under the sponsorship of the A.S.M.E. Special Research Committee on Mechanical Springs has necessarily involved a large number of measurements of creep and elastic recovery as well. In fact, the sensitivity of the measurements of elastic elongation in this work (sensitivity, one part in ten million; probable precision, one part in one to two million) was such that attention to the pseudo-elastic components of elongation could not well be avoided. Even in very high-strength steel and at low stresses, the work had to be done very carefully in order to isolate the true elastic strain from the

accompanying creep on loading and from the accompanying elastic, or pseudo-elastic recovery on unloading.

Evidence slowly accumulated indicating that no dividing line could be drawn between permanent creep, the so-called elastic creep, and recovery. One merged gradually into the other in such a way as to indicate that the two, except for the thermal component of the elastic creep, later described, were one and the same in nature. Evidence based on the peculiar characteristics of elastic recovery, easily measurable at room temperature, would appear to be valid for high-temperature creep. Any explanation of one would cover the other and would also in some measure apply to the larger problem of plastic flow in metals in general. The following statement of room-temperature behavior in a metal under loads within the so-called elastic limit must be read with that fact in mind.

APPARENT RESULTS OF THE LOADING-UNLOADING CYCLE

Application of a cycle of loading and unloading to a bar seems to result in the following events:

(1) On application of load, a wave of elastic strain moves through the bar with the velocity of sound. It is accompanied by a slight rise or fall of temperature, due to the adiabatic compression or extension, respectively, of the material.

(2) The resulting temperature gradient within the bar and between the bar and the surrounding atmosphere equalizes itself by conduction of heat, with resulting thermal creep.

(3) At isolated points along the bar, along crystal planes which are weak or unfavorably oriented, or subjected to internal stress, slip has meanwhile been occurring. Under light loads this initial slip does not pass beyond the bounds of an individual crystal. Minute changes in length of the bar result from these slippages.

(4) Under heavier loads these slip zones now begin in some cases to extend into adjoining crystals. Due to differences in orientation of slip planes this will necessarily be accompanied by a certain amount of fragmentation within the crystals and of flow among the boundary atoms. The resulting gradual creep may continue, but at a decreasing rate, over hours and even days.

(5) On removal of loading, the elastic changes, (1) and (2), reverse themselves. As a result of the thermal effect, a hysteresis loop will be formed. Even purely elastic changes are therefore accompanied by energy loss.

(6) Following the removal of loading, a gradual pseudo-elastic recovery occurs which will bring the piece back part way to its original length. This period of recovery, like the period of creep on initial loading, may last for many days.

(7) It has been stated by two or three experimenters that after sufficiently rapid loading and unloading the bar may exhibit an apparent memory of past events, first creeping slightly longer after being unloaded and then reversing itself and creeping in the opposite direction. This was not noticed in the Union College experiments but the conditions of the tests were not particularly favorable for its observation.

SUGGESTED THEORY OF PLASTIC FLOW

No clear-cut differentiation seems to exist between the creep effects which occur below the so-called elastic limit and the larger

¹ Associate Professor of Applied Mechanics, Union College. Mem. A.S.M.E. Professor Sayre was graduated from Columbia University with the degrees of E.M. and A.M. Seven years of engineering experience were followed by twenty years at Union College, the latter portion diversified by research and consulting work carried on for the General Electric Company and for other concerns.

Contributed by the A.S.M.E. Special Research Committee on Mechanical Springs and presented at the Annual Meeting, New York, N. Y., December 4 to 8, 1933, of THE AMERICAN SOCIETY OF MECHANICAL ENGINEERS.

NOTE: Statements and opinions advanced in papers are to be understood as individual expressions of their authors, and not those of the Society.

plastic yield occurring at higher stresses. One apparently merges gradually into the other.

In general the amount of creep and hysteresis seems to be definitely related (a) to the temperature of the metal, rise in temperature increasing creep, and (b) to its state of internal stress. Very mild heat treatments may greatly decrease hysteresis, while over-loads beyond the elastic limit greatly increase it.

Any satisfactory theory of the mechanism of plastic flow must explain these facts and must also account for (c) the elastic-recovery effects, (d) the time lag in initial creep, and (e) the presence of continuity in metal even after slippage has extended from one crystal into a second differently oriented crystal.

To explain these, the following hypotheses are suggested:

(1) Time delay may be explained as follows: The atoms in any material at temperatures above zero deg absolute are vibrating about equilibrium positions in the crystal net-work. Along any limited section of a crystal plane the resistance to shear is a function of the relative configuration of the individual atoms at any particular moment, and so will vary from moment to moment as the relative atomic positions change. Along that minute area, therefore, resistance to shear is not a constant but may be best expressed as a probability function ranging above and below some one most probable value. For any stress intensities below this most probable value, failure will be postponed until such an instant as this varying resistance to shear drops below the applied stress intensity. The probable time delay before this event will be controlled by this same probability function.

(2) Initial slippage usually occurs along only a minute fraction of the area of a weak crystal plane within an individual crystal, under the conditions explained above.

(3) This slip next extends across the area of the crystal, resulting in a development of zones of compressed and of correspondingly rarified atoms within the crystal on each side of the plane. Slippage may never extend beyond the limits of this crystal. In this case, on unloading, the stress within the crystal tends to force the atoms back to their original position and pseudo-elastic recovery occurs.

(4) The nature of metal structure is such that slippage extending across several adjacent crystals is impossible unless (a) the adjacent atoms are identically oriented, i.e., constitute essentially a single crystal, (b) the forces are so great as to compel actual rupture within the crystal, leaving a void, or (c) actual flow and readjustment of atomic position along grain boundaries, akin to diffusion, accompanies the slippage.

Along these boundary zones atoms are vibrating about equilibrium positions, but with somewhat greater freedom of movement due to the broken up crystalline structure. As already described, very high stress concentrations will be present along the edges of an individual crystal in which slip has already occurred.

Atoms in any compressed zone will be under strong tendency to migrate one by one into the adjacent less compressed area. The resistance offered by adjacent atoms to this movement will again be a function of their configuration and will fluctuate widely as this configuration changes due to the random vibrations of the atoms. Here, again, this opposing pressure will fluctuate according to the laws of probability, ranging above and below some one most probable value. The time delay for any individual atom may be small, but any finite movement hinges upon the successive migration of a large number of atoms, and so may be delayed for a considerable period. Rise in temperature will accelerate the vibration of the atoms and so modify the probability function toward more rapid flow, and also toward flow under lower stresses.

(5) In the case of the harder metals the vibration of the atoms will be so constrained by the crystal net-work that there will be a certain threshold pressure below which diffusion or plastic flow

cannot occur. In the case of a substance lacking crystalline structure, as tar, the crystalline net-work does not exist, the vibrations are less limited and the threshold pressure may be zero. In this case, flow may occur under infinitely small stresses, although according to the theory of probability the moments during which favorable configuration will occur will be so infrequent that diffusion or flow will be very slow.

(6) Creep, therefore, probably occurs in successive stages; first a slip within an individual crystal, then a gradual flow along the boundary lines followed by slip in the adjacent crystal, and so on.

(7) Slip not extending beyond the limit of an individual crystal is still more or less reversible in character. Forces exist within the crystal itself, which will tend, upon removal of external force, to drive it back to its original configuration. These restoring forces are resisted by the bond which reestablishes itself across the slip plane the moment the initial period of movement had ceased. There is, therefore, a back lash between the force at which, on initially applying the load, the first slip occurs and the force value at which, upon removing the load, the return movement occurs. The amount of creep after the initial loading is, therefore, likely to be greater than the amount of elastic recovery, thereby leaving some permanent set. Future repetitions of loading and unloading, however, tend to place the material in a cyclical state.

(8) In some cases elastic recovery may occur after slippage has extended into adjacent crystals, since even here large stresses exist tending toward recovery of shape. This return movement would probably take place in two or more successive stages and a larger time lag would be noticed.

(9) "Memory" within the crystal is less easy to explain. It is possible that the trapped stresses present within an individual crystal, resulting from slip within that crystal, may have been on the verge of breaking through into an adjacent crystal during the loaded stage. On unloading, these trapped stresses would be decreased in magnitude but a sufficient residual may have been present to complete a break-through which was almost ready to occur during the loaded stages. In this way, a slight forward creep would occur, to be immediately followed by a return creep as the various slip planes work back to their virgin positions. This would be most likely to occur if the load had been left on just long enough to initiate an active period of creep and if, thereafter, the load had been very rapidly removed and measurements taken.

(10) "Crackless plasticity," as defined by H. F. Moore, would be present in those cases where slip bands had not passed beyond their original crystal, and to a lesser degree beyond that stage.

(11) Permanent set would result (a) from slippage within individual crystals if the bond developed in the slip plane after the initial slip was sufficiently great to prevent reverse movement. In this case, subjecting the bar to cycles of equal positive and negative loading would remove the permanent set. (b) It would result from any slippage which had extended through several crystals, to such a distance that the resulting residual stresses in material are not sufficient to compel complete recovery. (c) It would result, obviously, also from any succession of slip planes which had worked their way across the entire width of the specimen. In this case no elastic recovery would occur.

(12) In many cases these phenomena would be complicated by the presence of twinning, which would aid in producing permanent changes of shape.

(13) In metals at higher temperatures, or in metals like zinc at room temperature, the process would be complicated by the occurrence of recrystallization. The mechanical phases of this process would occur by a mechanism following the same general

laws as those described for diffusion or flow of atoms. The same probability function would govern the time required for any rearrangement of an individual atom.

(14) Plastic flow would occur following these same rules. It would differ from the phenomenon of creep only in that the successive operations would be carried further and would occur more rapidly.

CONCLUSION

The above explanation is presented as a hypothesis only. It seems to agree reasonably well with the facts as observed in thousands of accurate measurements made at Union College, and with observations made by others as far as they have been described. Various theoretical reasons, which there has not been space to give in this article, also support the hypothesis. It is, therefore, presented here for criticism or modification.

Discussion

R. W. CARSON.² Behavior of cold-worked phosphor bronze is explained reasonably well by Prof. Sayre's hypothesis. For example, a bend-test specimen with a tensile strength of 120,000 and an elastic limit of 40,000 to 50,000 lb per sq in. shows no permanent strain under bending loads giving a maximum fiber stress of 15,000 lb per sq in. At lower stresses sensitive measurements on heat-treated specimens reveal no permanent deformations even after a steady load applied for ten days. When higher stresses are used, increasing amounts of permanent deformation are found. According to the views of the author, the stress of 15,000 lb per sq in. corresponds to the lowest load causing slip to advance across the crystal boundary.

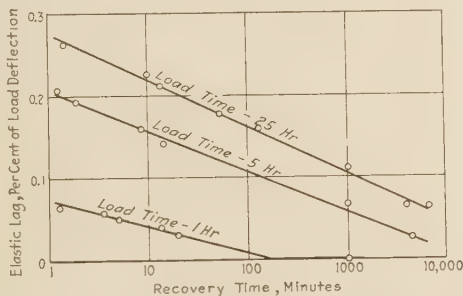


FIG. 1 EFFECT OF TIME UNDER LOAD ON ELASTIC RECOVERY OF A SPRING RIBBON LOADED IN BENDING

(5 per cent tin phosphor-bronze, 0.115 in. wide, 0.016 in. thick, 90 per cent cold reduction in area. Maximum fiber stress, 11,000 lb per sq in.)

Tests on this cold worked phosphor bronze, however, at less than 15,000 lb per sq in. show that the elastic recovery rate is much slower than the rate of creep under load. In an investigation³ of the inelastic properties of a series of copper-base alloys this characteristic was found to be common to all materials examined.

² Assistant Editor, Product Engineering, McGraw-Hill Publishing Co., New York, N. Y. Jun. A.S.M.E.

³ R. W. Carson, "Better Instrument Springs," *Electrical Engineering*, vol. 53, Feb., 1934, pp. 282-286.

As shown in the curve, Fig. 1, a bending load giving a maximum fiber stress of 11,000 lb per sq in. applied for one hour produced creep which subsequently recovered in approximately two hours. For the same load imposed for five hours, the recovery time would have been complete in 170 hours; and the curve for a 25-hour load indicates complete recovery in 1000 hours. These data plotted to logarithmic coordinates in Fig. 2 show that the ratio between creep time under load and time for complete recovery increases rapidly as the load time increases. Can the hypothesis advanced by Prof. Sayre account for this condition?

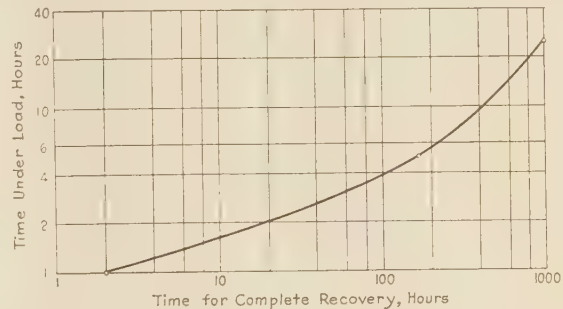


FIG. 2 RELATION BETWEEN RECOVERY TIME AND TIME UNDER LOAD FOR THE TESTS SHOWN IN FIG. 1

Although this hypothesis has been confined to the effects of applied strain, the same mechanism will also apply to other effects such as aging or the relief of internal stresses with passage of time, and the process of age-hardening. Likewise, it should also account for the aging of permanent magnets, and the "season cracking" of hard brass. Crystalline behavior will undoubtedly be the same for internal stresses as for applied stresses. For this reason, the hypothesis has much wider application than for stressed members alone, and confirmation or modification should therefore be available from many other sources.

Since higher temperatures and longer periods under load intensify elastic creep and recovery, the load conditions in high-temperature creep tests are favorable for producing large elastic lag effects. Further confirmation of Prof. Sayre's explanation should come from investigators of high temperature creep.

AUTHOR'S CLOSURE

Mr. Carson is correct, I believe, in his statement that this same hypothesis may be applied to such problems as the relief of internal stresses with passage of time, and the process of age hardening. Experimental confirmation or modification of the theory from these sources should therefore be available.

The difference between the rate of creep and rate of elastic recovery mentioned by Mr. Carson is, I believe, due to the difference between the forces acting in the two cases. During the recovery period the only forces acting are those due to the internal stresses which have been set up in the material as a result of the previous creep and these internal stresses will be, in general, much smaller than the direct stresses available during application of the load. This would naturally result in a slower rate for the recovery than for the initial creep.

Depositories for A.S.M.E. Transactions in the United States

BOUND copies of the complete Transactions of The American Society of Mechanical Engineers will be found in the libraries in the United States and other countries which are listed on the following pages.

Alabama

Auburn.....Engineering Library, Alabama Poly. Inst.
Birmingham.....Public Library

Arkansas

Fayetteville.....Engineering Library, Arkansas University

California

Berkeley.....Library, University of California
Long Beach.....Public Library
Los Angeles.....Public Library
Oakland.....University of Southern California
Oakland City Library
Teachers' Professional Library
Pasadena.....Library, California Institute of Technology
Santa Clara.....Library, University of Santa Clara
San Diego.....Public Library
San Francisco.....Public Library (Civic Center)
Engineers Club of San Francisco
Mechanics Institute
Stanford Univ....Library, Stanford University

Colorado

Boulder.....Library, University of Colorado
Denver.....Public Library
Fort Collins.....Colorado State Agricultural College

Connecticut

Bridgeport.....Public Library
Hartford.....Public Library
New Haven.....Public Library and Yale University
Waterbury.....Silas Bronson Library

Delaware

Newark.....University of Delaware
Wilmington.....Wilmington Free Institute

District of Columbia

Washington.....Scientific Library, U. S. Patent Office
Library of Congress
Bureau of Standards Library
George Washington University
Catholic University

Florida

Gainesville.....University of Florida
Jacksonville.....Free Public Library
Miami.....Public Library
Tampa.....Public Library

Georgia

Atlanta.....Carnegie Public Library
Georgia School of Technology
Savannah.....Public Library

Idaho

Moscow.....University of Idaho

Illinois

Chicago.....John Crerar Library
Western Society of Engineers
Library, Armour Institute of Technology
Public Library of Chicago
Moline.....Public Library
Urbana.....University of Illinois

Indiana

Evansville.....Public Library
Fort Wayne.....Public Library
Indianapolis.....Public Library and Indiana State Library
Notre Dame.....Library, University of Notre Dame
Terre Haute.....Rose Polytechnic Institute
West Lafayette...Library, Purdue University

Iowa

Ames.....Iowa State College
Des Moines.....Public Library
Iowa City.....State University of Iowa

Kansas

Kansas City.....Public Library, Huron Park
Lawrence.....Library, University of Kansas
Manhattan.....Kansas State Agricultural College
Wichita.....Wichita City Library

Kentucky

Lexington.....University of Kentucky
Louisville.....Speed Scientific School
University of Louisville

Louisiana

Baton Rouge.....Louisiana State University
New Orleans.....Howard Memorial Library
Louisiana Engineering Society
Public Library

Maine

Orono.....University of Maine

Maryland

Annapolis.....United States Naval Academy
Baltimore.....Johns Hopkins University
Engineers Club of Baltimore
Public Library

Massachusetts

Boston.....Northeastern University
Boston Public Library
Cambridge.....Harvard University (Engineering Library)
Massachusetts Institute of Technology
Fall River.....Public Library
Lowell.....Lowell Textile Institute
Lynn.....Free Public Library
New Bedford.....Free Public Library
Springfield.....Springfield City Library
Tufts College.....Tufts College
Worcester.....Worcester Polytechnic Institute
Free Public Library

Michigan

Ann Arbor.....University of Michigan
Detroit.....Public Library
Cass Technical High School
Highland Park Public Library
University of Detroit
East Lansing....Michigan State College
Flint.....Public Library
Grand Rapids...Public Library
Houghton.....Michigan College of Mining & Technology
Jackson.....Public Library

Minnesota

Duluth.....Public Library
Minneapolis.....University of Minnesota
Minneapolis Public Library (Engineering
and Circulating Libraries)
St. Paul.....James Jerome Hill Reference Library

Mississippi

State College....Mississippi State College

Missouri

Columbia.....University of Missouri
Kansas City.....Public Library
Rolla.....Missouri School of Mines and Metallurgy
St. Louis.....Engineers Club of St. Louis
Public Library
Washington University
Mercantile Library

Montana

Bozeman.....Montana State College

TRANSACTIONS OF THE AMERICAN SOCIETY OF MECHANICAL ENGINEERS

Nebraska

Lincoln.....University of Nebraska
Omaha.....Public Library

Nevada

Reno.....University of Nevada Library

New Hampshire

Durham.....University of New Hampshire

New Jersey

Bayonne.....Free Public Library
Camden.....Free Public Library
Elizabeth.....Free Public Library
Hoboken.....Stevens Institute of Technology
Jersey City.....Free Public Library
Newark.....Newark College of Engineering
Free Public Library
New Brunswick.....Rutgers University
Paterson.....Free Public Library
Princeton.....Princeton University
Trenton.....Free Public Library

New York

Albany.....New York State Library
Brooklyn.....Polytechnic Institute
Pratt Institute
Brooklyn Public Library
Buffalo.....The Grosvenor Library
Engineering Society of Buffalo
Buffalo Public Library
Ithaca.....Cornell University
Jamaica, L. I.....Queens Borough Public Library
New York.....Engineering Societies Library
Public Library
College of the City of New York
Cooper Union
Columbia University
New York Museum of Science and Industry
New York University Library
Potsdam.....Clarkson College of Technology
Rochester.....Rochester Engineering Society
Schenectady.....Union College
Syracuse.....Syracuse University
Public Library
Troy.....Rensselaer Polytechnic Institute
Utica.....Public Library
Yonkers.....Public Library

North Carolina

Chapel Hill.....University of North Carolina (Engineering Library)
Raleigh.....North Carolina State College

North Dakota

Fargo.....North Dakota State Agricultural College
Grand Forks.....University of North Dakota

Ohio

Ada.....Ohio Northern University
Akron.....Public Library
University of Akron
Canton.....Public Library
Cincinnati.....University of Cincinnati
Public Library
Engineers Club of Cincinnati
Cleveland.....Public Library
Case School of Applied Science
Cleveland Engineering Society
Columbus.....State of Ohio Library
Public Library
Ohio State University
Dayton.....Engineers Club of Dayton
Toledo.....Public Library
University of Toledo
Youngstown.....Public Library

Oklahoma

Norman.....Oklahoma University
Oklahoma City.....Public Library
Stillwater.....Oklahoma Agricultural and Mechanical College
Tulsa.....Public Library

Oregon

Corvallis.....Oregon State Agricultural College
Portland.....Portland Library Association

Pennsylvania

Allentown.....Free Library
Bethlehem.....Lehigh University
Easton.....Public Library
Lafayette College
Erie.....Public Library
Lewisburg.....Bucknell University
Philadelphia.....Engineers Club
Drexel Institute
University of Pennsylvania
Franklin Institute
Pittsburgh.....University of Pittsburgh
Engineers' Society of Western Pennsylvania
Carnegie Institute of Technology
Carnegie Library (Schenley Park)
Carnegie Free Library of Allegheny
Reading.....Public Library
Scranton.....Public Library
State College.....Pennsylvania State College
Swarthmore.....Swarthmore College
Villanova.....Villanova College
Wilkes-Barre.....Public Library

Rhode Island

Kingston.....Rhode Island State College
Providence.....Brown University
Providence Engineering Society
Public Library

South Carolina

Clemson College..Library, Clemson College

Tennessee

Kingsport.....Public Library
Knoxville.....University of Tennessee
Memphis.....Goodwin Institute
Nashville.....Vanderbilt University

Texas

Austin.....University of Texas
College Station..Agricultural & Mechanical College of Texas
Dallas.....Public Library
El Paso.....Public Library
Forth Worth.....Carnegie Public Library
Houston.....Rice Institute
Public Library
Lubbock.....Texas Technological College (School of Engineering)
San Antonio.....Carnegie Library

Utah

Salt Lake City..University of Utah
Public Library

Vermont

Burlington.....University of Vermont

Virginia

Blacksburg.....Virginia Polytechnic Institute
Charlottesville.....University of Virginia
Norfolk.....Public Library
Richmond.....Virginia State Library

Washington

Pullman.....State College of Washington
Seattle.....Public Library
Engineers Club
University of Washington
Spokane.....Public Library
Tacoma.....Public Library

West Virginia

Morgantown.....West Virginia University

Wisconsin

Madison.....Library, University of Wisconsin
Milwaukee.....Public Library
Board of Industrial Education, Vocational School Library
Marquette University

Wyoming

Laramie.....Wyoming University

Progress in Applied Mechanics

IN VIEW of the wide field covered by the term "Applied Mechanics," the work of the Division, so far as the review of papers and the preparation of progress reports is concerned, has been divided among several subcommittees. It is intended that each subcommittee shall act as a central clearing house of information in work relating to its particular field.

The subcommittees at present organized are:

- Elasticity
- Strength of Materials
- Plasticity
- Dynamics (including vibration)
- Mechanics of Liquids and Gases
- Heat and Thermodynamics.

Other subcommittees on mechanical measurements, kinematics and mechanism, and structural statics may be added as conditions warrant.

GENERAL

Of general interest is the appearance in April, 1933, of a new semi-monthly periodical, entitled *Zentralblatt für Mechanik* (Springer, Berlin). In this publication all papers appearing anywhere in the world on the broad subject of Applied Mechanics are discussed in abstracts of about ten lines. The enterprise has a truly international character.

The National Research Council in Italy has established a special institute for the assistance of research workers in problems requiring advanced mathematical analysis.

ELASTICITY¹

The review of new publications on the theory of elasticity may begin with consideration of the book by N. Muschelišvili published by the Russian Academy of Science (1).² The book represents a series of lectures on the theory of elasticity given at the Seismological Institute and at the Institute of Mathematics and Mechanics of the University of St. Petersburg. The chapter on two-dimensional problems is especially interesting and complete. The author develops a new method of solution of such problems (2) and applies it to the study of stress concentration due to the presence of holes of various shapes and inclusions. The case of an elliptical hole is treated in great detail and in a simpler way than has been done before. Of especial interest to engineers are the chapters on torsion and bending of prismatical bars in which the case of a bar consisting of two different materials is discussed in connection with stress analysis in reinforced-concrete structures (3, 4, 5).

Several interesting papers on two-dimensional problems have appeared this year. Among these is the paper by R. C. J. Howland and A. C. Stevenson (6) which discusses stress distribution around a circular hole in a rectangular strip subjected to bending; the paper by H. M. Westergaard (7) giving a geometrical interpretation of the stress function of the two-dimensional problem; and the paper by Ernest Melan (8) giving a rigorous solution of the problem on stresses produced by a concentrated

force applied at an internal point in the middle plane of a plate.

Further development in experimental methods of solving two-dimensional problems of elasticity has taken place during the last year. In photoelastic work the use of bakelite for a transparent material together with the "fringe method" is now accepted by the majority of experimenters. An interesting study of a bakelite model was made by A. M. Wahl (9), in which the stress concentration at a circular hole, measured photoelastically, is compared with the theoretical calculations of R. C. J. Howland and with extensometer measurements made on a steel model. A complete study of mechanical and optical properties of bakelite was made by E. E. Weibel (10). He used bakelite models in studying stress concentration at reentrant corners. In determining the sum of the two principal stresses, the membrane analogy, suggested by J. P. DenHartog, was successfully used. C. B. Biezeno and J. J. Koch (11) have developed a new method of solving two-dimensional problems by using an electrical analogy. The stress distribution is obtained from the potential distribution in a plate, along the boundary of which the potential is varying in a prescribed manner. Strain measurements in a tunnel wall were made by N. N. Davidenkoff (12, 13). For this purpose, special telemeters were constructed in which the strain was determined from the change of pitch of a stretched vibrating string. Very interesting experiments on models subjected to the action of large centrifugal forces have been made by N. N. Davidenkoff (14). From a consideration of similarity, it is found that in order to have the same stresses in a model as in an actual structure, the body forces must be inversely proportional to the scale of the model. The centrifugal forces were used by Davidenkoff to magnify the body forces in the required proportion.

Considerable work has been done during the past year on the theory of plates and thin shells. In the paper by H. Reissner (15), a rigorous solution of the problem of bending a cylindrical shell submitted to the action of hydrostatic pressure is given, and in the papers by S. Woinowsky-Krieger (16, 17, 18), several problems on the bending of plates are discussed.

Stability problems were discussed by several authors. E. Trefftz (19) developed the general theory of elastic stability based on the consideration of strain energy of the elastic system and applied this theory to the case of lateral buckling of beams. The same theory has been applied by T. E. Schunck (20) in studying various cases of stability of a cylindrical shell. A numerical application of the theory to the study of stability of a thin-walled gas container has been made. G. I. Taylor (21) solved the problem of the buckling of a compressed plate with clamped edges. L. H. Donnell (22) gave the solution of the problem of the buckling of a thin cylindrical shell under torsion and made a large number of experiments dealing with various cases of instability of thin-walled constructions. S. Timoshenko (23) investigated the problem of the buckling of the web of a plate girder. D. H. Young (24) discussed the rational design of solid and built-up steel columns.

Residual stresses due to cold working in thin brass tubes have been experimentally studied by N. N. Davidenkoff (25). Stresses in large forgings due to non-uniform cooling were experimentally studied by G. Kirchberg (26). J. Mathar (27) developed a special apparatus for studying residual stresses. The stress is obtained from the small distortions of a drilled circular hole.

REFERENCES

- 1 N. Muschelišvili: "Some Fundamental Problems in the Mathematical Theory of Elasticity." Published by Académie des Sciences (Akademiya Nauk), Leningrad, 1933. (In Russian.)

¹ Compiled by Dr. S. Timoshenko.

² Numbers in parentheses refer to similarly numbered references given at the end of the report.

Presented at the session of the Applied Mechanics Division, Tuesday afternoon, December 5, 1933, during the Annual Meeting, New York, N. Y., December 4 to 8, 1933, of THE AMERICAN SOCIETY OF MECHANICAL ENGINEERS.

Personnel of the Executive Committee of the Applied Mechanics Division for 1933: J. M. Lessells, Chairman; F. M. Lewis, Secretary; J. A. Goff, E. O. Waters, C. R. Soderberg.

- 2 N. Muschelišvili: "Praktische Lösung der fundamentalen Randwertaufgaben der Elastizitätstheorie in der Ebene für einige Berandungsformen." *Zeit. für angewandte Mathematik und Mechanik*, vol. 13, 1933, p. 264.
- 3 N. Muschelišvili: "Sur le problème de torsion des poutres élastiques composées." *Comptes Rendus Académie des Sciences*, Paris, vol. 194, 1932, p. 1435.
- 4 N. Muschelišvili: *Bul. Académie des Sciences (Akademiya Nauk)*, Leningrad, 1932, p. 907. (In Russian.)
- 5 A. Ruchadze et I. Vekua: "Sur la torsion d'un cylindre armé d'une tige." *Bull. Académie des Sciences (Akademiya Nauk)*, Leningrad, 1933, p. 373. (In Russian.)
- 6 R. C. J. Howland and A. C. Stevenson: "Bi-Harmonic Analysis in a Perforated Strip." *Phil. Trans. Royal Soc. London*, vol. 232, ser. A, 1933, p. 155.
- 7 H. M. Westergaard: "Graphostatics of Stress Functions." *A.S.M.E. Trans.*, vol. 56, no. 3, Mar., 1934, p. 141.
- 8 Ernest Melan: "Der Spannungszustand der durch eine Einzelkraft im Inneren beanspruchten Halbscheibe." *Zeit. für angewandte Mathematik und Mechanik*, vol. 12, 1932, p. 343.
- 9 A. M. Wahl and R. Beeuwkes: "Stress-Concentration Factors for Tension Bars With Holes and Notches." *A.S.M.E. Trans.*, APM-56-11.
- 10 E. E. Weibel: "Studies in Photoelastic Stress Determinations." *A.S.M.E. Trans.*, APM-56-13.
- 11 C. B. Biezeno and J. J. Koch: "Über einige Beispiele zur elektrischen Spannungsbestimmung." *Ingenieur-Archiv*, vol. 4, 1933, p. 384.
- 12 N. N. Davidenkoff: "Spannungsmessungen in Stollen aus kleidungen mittels Saitenteleostometern." *Zeit. für Technische Physik*, Leningrad, vol. 3, 1933, p. 431. (In Russian.)
- 13 D. D. Golowatschew, N. N. Davidenkoff, M. W. Jakutowitsch: "Bestimmung der Elastischen Reaction vom Felzboden mit Hilfe der Saitenmethode." *Zeit. für Technische Physik*, Leningrad, vol. 3, 1933, p. 406. (In Russian.)
- 14 N. N. Davidenkoff: "Neue Methode zur Anwendung von Modellen bei Stabilitätsuntersuchung des Bodens." *Zeit. für Technische Physik*, Leningrad, vol. 3, 1933, p. 131. (In Russian.)
- 15 H. Reissner: "Formänderungen und Spannungen einer dünnwandigen, an den Rändern frei aufliegenden, beliebig belasteten Zylinderschale." *Zeit. für angewandte Mathematik und Mechanik*, vol. 13, 1933, p. 133.
- 16 S. Woinowsky-Krieger: "Über die Biegung dünner rechteckiger Platten durch Kreislasten." *Ingenieur-Archiv*, vol. 3, 1932, p. 236.
- 17 S. Woinowsky-Krieger: "Der Spannung in dicken elastischen Platten." *Ingenieur-Archiv*, vol. 4, 1933, p. 203.
- 18 S. Woinowsky-Krieger: "Berechnung der ringsum frei aufliegenden fleischseitigen Dreiecksplatte." *Ingenieur-Archiv*, vol. 4, 1933, p. 254.
- 19 E. Trefftz: "Zur Theorie der Stabilität des elastischen Gleichgewichtes." *Zeit. für angewandte Mathematik und Mechanik*, vol. 13, 1933, p. 160.
- 20 T. E. Schunck: "Zur Knickfestigkeit schwach gekrümmter Zylindrischer Schalen." *Ingenieur-Archiv*, vol. 4, 1933, p. 394.
- 21 G. I. Taylor: "The Buckling Load for a Rectangular Plate With Four Clamped Edges." *Zeit. für angewandte Mathematik und Mechanik*, vol. 13, 1933, p. 147.
- 22 L. H. Donnell: "Stability of Thin-Walled Tubes Under Torsion." *Abstract, A.S.M.E. Trans.*, Mar., 1934, p. 108.
- 23 S. Timoshenko: "Stability of the Web of Plate Girders." Paper presented before Chicago joint meeting of Applied Mechanics Div., A.S.M.E., and Structural Div., A.S.C.E.
- 24 D. H. Young: "Rational Design of Steel Columns." Paper presented before Chicago joint meeting of Applied Mechanics Div., A.S.M.E., and Structural Div., A.S.C.E.
- 25 N. N. Davidenkoff: *Zeit. für Metallkunde*, vol. 24, 1932, p. 25.
- 26 G. Kirchberg: "Eigenspannungen in grossen schmiedestücken." *Zeit. V.D.I.*, vol. 77, 1933, p. 732.
- 27 J. Mathar: "Ermittlung von Eigenspannungen durch Messung von Bohrloch-Verformungen." *Archiv für das Eisenhüttenwesen*, vol. 6, no. 7, Jan., 1933, pp. 277-281.

STRENGTH OF MATERIALS³

Interest in the application of recent advances in the mechanics of materials was strikingly evidenced at the Symposium on Working Stresses held at the 1932 Annual Meeting of the A.S.M.E. Papers dealt with the creep of metals at elevated temperatures, buckling failure, impact, and fatigue, and included general discussions on theories of failure and working stresses.

³ Compiled by R. E. Peterson.

Important advances made in the technology of cast iron were presented at a Symposium on Cast Iron held in Chicago in June, 1933, under the joint auspices of the American Society for Testing Materials and the American Foundrymen's Association. A better appreciation of the proper application of cast iron as an engineering material has resulted from these papers and discussions.

In connection with corrosion fatigue, emphasis is being placed on the development of practical methods of surface protection. Nitriding has been shown to be effective (28). Surface cold working (29) has been found to increase the corrosion endurance limit of unnotched specimens by as much as 50 per cent. By cold working holes and grooves, the corrosion-fatigue fracture was shifted to the full section, where the area moment of inertia was 1.33 to 1.96 times as great.

With regard to impact testing, a torsion machine (30) for testing hard steels, such as are used in taps, drills, etc., has been developed, and should be of interest to investigators of impact phenomena.

Further research at the National Physical Laboratory, Teddington, England, on the fatigue strength of heat-treated leaf springs (31) has demonstrated the deleterious effect of surface decarburization and has also indicated means of prevention.

The important problem of the fatigue strength of clamped members and press-fit constructions (32) (shafts with gears, wheels, pulleys, collars, rotors, etc.) has been investigated for a number of conditions. Whereas, normally, the presence of a hub may reduce the fatigue strength of a shaft by as much as 50 per cent, means were developed (such as grooving the hub face and cold working the shaft surface) whereby the full strength of the shaft could be attained.

Under further tests, rail steels (33) have shown characteristics similar to those previously evidenced in connection with a consideration of transverse fissures. A process which controls the cooling of rails so as to take into account the properties shown in these tests has been developed (34).

A desire for tests on machine elements and construction members as actually produced is evidenced by fatigue tests of bolts (35) and tests of welded members.

28 R. Mailänder: "Über die Dauerfestigkeit von nitrierten Proben." *Zeit. V.D.I.*, Mar. 11, 1933.

29 A. Thum and H. Ochs: "Die Bekämpfung der Korrosionsermüdung." *Stahl und Eisen*, Sept. 17, 1932.

30 G. V. Luerrson and O. V. Greene: "The Torsion Impact Test." *A.S.T.M. Annual Meeting*, Chicago, 1933.

31 G. A. Hankins and M. L. Becker: "The Fatigue Resistance of Spring Steels." *Engineering* (London), Jan. 29, 1932.

32 A. Thum and F. Wunderlich: "Der Einfluss von Einspann- und Kraftangriffsstellen auf die Dauerhaltbarkeit der Konstruktionen." *Zeit. V.D.I.*, Aug. 5, 1933.

33 G. W. Quick: "Tensile Properties of Rail Steels at Elevated Temperatures." *Jour. Research*, U. S. Bur. Standards, Feb., 1932.

34 C. P. O. F., and N. P. Sandberg: "Effect of Controlled Cooling and Temperature Equalization on Internal Fissures in Rails." *Metals and Alloys*, April, 1932.

35 K. Schraivogel: "Dauerbiegeversuche mit Schraubenbolzen." *Stahl und Eisen*, Dec. 1, 1932.

PLASTICITY⁴

A few of the numerous reports of investigations which have been published during the past year may be mentioned briefly here on account of their particular interest. In a short paper L. Prandtl (36) has extended certain ideas he expressed some years ago in connection with the phenomena of elastic hysteresis, to the case of the rupture of a brittle material. He utilizes certain thoughts advanced by A. A. Griffith (37) in his fundamental study on the rupture conditions of amorphous materials. It will be recalled that to explain the comparatively low tensile strength

⁴ Compiled by A. Nadai.

of brittle amorphous materials, Griffith assumed that these materials are weakened by numerous small cracks or flaws. According to Prandtl, a mechanical model of a brittle material may be conceived as consisting of a great number of small parallel slabs partially separated by longitudinal cracks and oriented at random in space. He computes the stress required to separate the small slabs. By attributing to his model a further property, namely, that of starting to flow when it starts to break, he can account also for a finite time in which the completion of a fracture would occur. How far these ideas may be reconciled with those advanced by Zwicky (38) and other physicists, according to which small cracks are not sufficient to explain the discrepancy between molecular and technical strength, cannot be said. Schlechtweg (39) and Orowan (40), on the other hand, believe that discontinuous movements have an essential part in the plastic phenomena of the polycrystalline materials. H. Jeffreys (41) (Cambridge, England) derives the equations for an elastico-viscous solid known as Maxwell's solid in an extremely concise form. He suggests, as the writer of these lines repeatedly did, that the total strains should be separated into two parts: (a) the elastic part assumed as usually linearly related to stress; and (b) a plastic part. For the latter the law of viscous flow is assumed, i.e., that a given stress produces a given rate of strain. These equations may be modified to include also a finite plastic strength and they may become important some day as the possible base of a practical theory of the slow creep of the metals at high temperatures for which engineers are searching.

More recent attempts of the theory (H. Jeffreys, H. Hencky) concentrate on efforts to replace the constant time of relaxation in the equations by an expression dependent on the state of stress. A coincidence worthy, perhaps, of being mentioned, is that considerable experimental evidence which has been gathered, particularly by P. G. McVetty in years of testing the high-temperature properties of metals, speaks in favor of some of the hypothetically assumed properties of the elastico-viscous solid. The Working Stress Symposium, which was held at the 1932 Annual Meeting of the A.S.M.E. reflected in papers by Timoshenko, Soderberg, Moser, Peterson, McCullough, and others the present state of knowledge and of needs of engineers in this particular field.

36 L. Prandtl: *Zeit. für angewandte Mathematik und Mechanik*, vol. 13, no. 2, April, 1933, p. 129.

37 A. A. Griffith: *Phil. Trans. Royal Soc. London*, vol. 221, ser. A, 1921, p. 163.

38 F. Zwicky: "The Problem of the Solid State of Matter." *Mechanical Engineering*, vol. 55, July, 1933, p. 427.

39 Schlechtweg: *Physikalische Zeit.*, vol. 34, 1933, p. 404.

40 Orowan: *Zeit. für Physik*, vol. 79, no. 9, 1932.

41 H. Jeffreys: *Proc. Royal Soc.*, vol. 138, ser. A, 1933, p. 283.

DYNAMICS AND KINEMATICS⁵

Vibration. Of general interest is a new book by A. L. Kimball (42) which treats the elements of the vibration problem from the viewpoint of the turbine engineer. K. Hohenemser, in a pamphlet of the series "Ergebnisse der Mathematik und ihrer Grenzgebiete" (43), gives a valuable and comprehensive review of the various mathematical methods which have been devised for the solution of vibration problems.

J. P. DenHartog has devised a closer approximation for the forced vibration of a non-linear elastic system (44).

The problem of transmission line vibration has been treated by Maass (45), Schmitt and Behrens (46), and others.

Lehr (47) reviews and contributes to our present knowledge of valve-spring surge.

Kinematics and Mechanism. In this country but little attention has been given to the development of applied kinematics and

this branch of science has not as yet been represented in the activities of the Applied Mechanics Division. Abroad, kinematics has been intensively developed over a period of years, particularly by Continental writers. It should be pointed out that many of these developments are of interest to the engineer.

During the past two years R. Beyer has developed vector-diagram methods for the study of gear trains (48) and plane mechanism (49). The same author is also working on the development of space kinematics (50, 51).

K. Rauh has discussed the subject of coupler curve or link mechanism (52).

F. E. Myard (53) develops a general theory of the transmission problem between two axes in space.

Many other papers in this field have appeared abroad but space limitations allow the citation of only a few of them (54-57).

42 A. L. Kimball: "Vibration Prevention in Engineering." John Wiley & Sons, New York, 1932.

43 K. Hohenemser: "Die Methoden zur angenaherten Lösung von Eigenwertproblemen in der Elastokinetik." Springer, Berlin.

44 J. P. DenHartog: "Amplitudes of Non-Harmonic Vibrations." *Jour. Franklin Inst.*, Oct., 1933.

45 H. Maass: "Mechanische Schwingungen von Hochspannungsfreileitungen." *Phys. Zeit.*, vol. 34, 1933, p. 389.

46 H. Schmitt and P. Behrens: "Theoretische und experimentelle Untersuchungen über Seilschwingungen." *Elektrotechnische Zeit.*, no. 25, 1933.

47 E. Lehr: "Schwingungen in Ventildfedern." *Zeit. V.D.I.*, vol. 77, pp. 457-462.

48 R. Beyer: "Geschwindigkeitspläne von Differentialwerken." *Maschinen-Konstrukteur (Betriebstechnik)*, vol. 65, 1932, pp. 79-81.

49 R. Beyer: "Drehzahlvektorenplane ebener Getriebe." *Zeit. für Instrumentenkunde*, vol. 53, no. 4, 1933, pp. 164-167.

50 R. Beyer: "Neue Wege zur zeichnerische Behandlung der Raumlichen Mechanik." *Zeit. für Angewandte Mathematik und Mechanik*, vol. 13, no. 1, 1933, pp. 17-31.

51 R. Beyer: "Bemerkungen zur Anwendung des Satzes von Corioli." *Zeit. für Angewandte Mathematik und Mechanik*, vol. 12, no. 6, 1932, pp. 381-382.

52 K. Rauh and W. Knyrim: "Die Grösse der Genauigkeit der von Koppelkurven ableitbaren Stillstände." *Zeit. V.D.I.*, vol. 77, no. 8, 1933, pp. 196-198; and K. Rauh and P. Edler: "Verstellbare Koppelkurventriebe für die Hubbewegung mit einem Stillstand." *Zeit. V.D.I.*, vol. 77, no. 18, 1933, pp. 478-480.

53 F. E. Myard: "Théorie générale des joints de transmission de rotation à couple d'emboîtement." *Génie Civil*, vol. 102, 1933, pp. 345-348.

54 M. Tolle: "Beschleunigungsermittlung der sphärischen Bewegung mit Hilfe der darstellenden Geometrie" ("Determination of the Acceleration of Spherical Motions by the Aid of Descriptive Geometry"). *Zeit. für angewandte Mathematik und Mechanik*, vol. 12, no. 6, Dec., 1932, p. 382.

55 K. Kuba: "Anwendung des Verschiebungsplanes auf Schraubengetriebe" ("Application of the Displacement Diagram to Screw Mechanisms"). *Zeit. des Oesterreichischen Ingenieur und Architekten Vereins*, vol. 84, no. 41-42, Oct. 21, 1932, pp. 216-219.

56 K. A. Flocke: "Geschwindigkeitsermittlung beim Römertriebe und ähnlichen Getrieben" ("Determination of the Velocities in the Römer-Gear Link-Mechanism and of Similar Mechanisms"). *Zeit. für angewandte Mathematik und Mechanik*, vol. 13, no. 3, June, 1933, pp. 241-242.

57 H. E. Merritt: "The Analysis of Planetary Gear Trains." *Machinery (London)*, vol. 41, no. 1061, Feb. 9, 1933, pp. 545-548.

FLUID MECHANICS⁶

A considerable amount of work has been done in the field of fluid mechanics during the past year.

Potential Flow. Some examples of technical interest in two-dimensional flow between curved walls have been calculated by Miyadzu (58). The potential theory of the wake behind a circular cylinder was treated by Weinstein (59). Weinig (60) gave methods for the computation of velocity distribution along streamline bodies with sharp and rounded noses. Theodorsen and Garrick (61) worked out a method based on conformal representation suitable for practical computation of pressure

⁵ Compiled by F. M. Lewis and A. E. R. deJonge.

⁶ Compiled by Th. von Kármán and N. B. Moore.

distributions on airfoils with given aspect ratios. Betz (62) developed methods of finding forces and moments acting on bodies in potential flow by use of the singularities of the potential function. Hamel (63) studied the case of a rectilinear vortex moving around a corner. Golubev (64) and Durand (65) studied the question of the stability of vortex rows.

Laminar Flow in Viscous Fluids. The analytical theory of laminar motion of viscous fluids has been extended, especially by some British authors. Southwell and Squire (66) and Piercy and Winny (67) investigated and extended Oseen's approximate method for solution of the hydrodynamic equations. Thom (68) calculated and photographed the flow past circular cylinders for comparatively small Reynold's numbers.

Turbulence and Turbulent Flow in Pipes. Several experimental and theoretical contributions have been made to the fundamental problem of turbulent flow. Two summary papers should first be mentioned. Tollmien (69) reported on "The Present State of the Turbulence Problem" at the Berkeley Aeronautics meeting of the A.S.M.E.; Prandtl (70) reviewed experimental research done at Göttingen and showed that tests on skin friction in smooth and in rough pipes check very well with formulas given by von Kármán in 1930. Fage (71) also reviewed existing theories of turbulence and compared these with direct observations of the velocity fluctuations by means of an optical method.

The statistical theory of turbulence has been treated by Burgers (72), Noether (73), and Tollmien (74). New equations for the theory of turbulent flow with parallel mean motion were proposed by Mattioli (75).

The problem of "free turbulence" in the theory of wakes and of jets has been treated by Tollmien (76) and Kuethe (77). The corresponding problem of jets for laminar flow has been calculated by Schlichting (78). Ruden (79) investigated the propagation of turbulence in a free jet.

Ziegler (80) and Mock and Dryden (81) improved apparatus and methods for recording turbulent velocity fluctuations; Wattendorf and Kuethe (82) applied this technique to the determination of the turbulence in free air for the first time by means of a hot-wire apparatus mounted on an airplane and on an airship, and von Kármán (83) reported at the Washington meeting of the American Physical Society on investigations by Wattendorf (84) on the distribution of velocity fluctuations over the cross-sections of straight and of curved channels. Van der Hegge Zynen (85) made measurements of the velocity distribution in the boundary layer over a grating surface, and Reichardt (86) made fluctuation measurements in a straight channel. Kröber (87) investigated, theoretically and experimentally, flow through vane systems, such as used in wind tunnels, with the object of reducing energy losses in curved flow. The stability of laminar flow in the so-called Couette case and in the case of flow between rotating cylinders has been treated theoretically by Schlichting (88). Stability of flow in a curved pipe has been considered by Miyagi (89). Nikuradse (90) made some experimental investigations on the transition phenomena between laminar and turbulent flow in a boundary layer, and gave also a detailed report (91) on his measurements on flow in pipes with rough walls. Fette (92) worked on the flow in straight and curved channels in the Göttingen rotating laboratory. Nukiyama (93) made photographic investigations of the flow of water through tubes, and Spalding (94) extended Nippert's work on loss of flow in curved channels. Gibson (95) studied the breakdown of streamline motion at the higher critical velocity in pipes of circular cross-section. Viscous flow through pipes with cores was reported on by Piercy, Hooper, and Winny (96).

Ship Resistance and Waves. The present state of the problem of skin friction is sketched in the report (97) of the Hamburg conference dealing with hydrodynamic problems of ship pro-

pulsion. The work contains contributions of Eisner, von Kármán, Kempf, and Schoenherr, with discussions by several authors. Schoenherr (98) in addition checked the von Kármán formula for skin friction with experiments and gave new contributions to the problem of the transition between laminar and turbulent boundary layers.

The theory of wave resistance has been summarized by Have-lock (99). Wagner (100) gave an account of his previous investigations on wave resistance with special reference to high-speed boats. Burgers (101) studied the excitation of waves in a canal. At the Hamburg conference (97), interesting contributions to the problem of ship waves and resistance were given by Hogner, Weinblum, Wigley, and Barrillon.

Cavitation. Important contributions of Ackeret, Föttinger, Walchner, Martyrer, Lerbs, Weinig, Schmidt, Mueller, Flügel, Schroter, Gutsche, and Springorum are contained in the report (97) of the Hamburg conference. They deal with the causes of cavitation and corrosion, with the forces acting on hydrofoils under cavitation conditions, and with the influence of cavitation on propellers. These papers give an excellent summary of the present knowledge of the subject.

*Aerodynamics.*⁷ Schrenk (102) made further measurements on the effect of boundary layer suction on the lift of an airfoil. The influence of turbulence on maximum lift has been investigated by Millikan and Klein (103) and also by Randisi (104). The effect of turbulence on the drag of airship models was studied by Hilda Lyon (105); important boundary layer flow measurements on a model of the Akron were made by Freeman (106). Lock and Johansen (107) did work on the drag of pairs of streamline bodies. Turbulence was found by Dryden (108) to have an influence on the characteristics of cup anemometers.

Compressible Flow. G. I. Taylor and Maccoll (109) solved the equations of compressible flow around a cone and checked their calculations by measurements of air pressures on cones moving with supersonic velocities. A comparison of their calculations with the less accurate but more general ones of von Kármán and Moore show fairly good agreement for small cones. Contributions to the study of two-dimensional compressible flow have been made by Braun (110) and Poggi (111). Aerodynamical properties of airfoils moving with supersonic velocities have been measured by Busemann and Walchner (112). Riabouchinsky (113) gave an interesting hydraulic analogy for compressible flow.

58 O. Miyadzu: Proc. Imperial Acad. Japan, Tokyo, vol. 8, pp. 352-353.

59 A. Weinstein: Rendiconti, Atti. R. Accademia dei Lincei, Rome, vol. VI, no. 17, pp. 83-87.

60 F. Weinig: Zeit. für angewandte Mathematik und Mechanik, vol. 13, no. 3, June, 1933, pp. 224-235.

61 T. Theodorsen and I. Garrick: Nat. Advis. Comm. Aero., Rept. no. 452.

62 A. Betz: Ingenieur-Archiv, vol. 3, 1932, no. 5, pp. 454-462.

63 G. Hamel: Zeit. für angewandte Mathematik und Mechanik, vol. 13, no. 2, April, 1933, pp. 98-101.

64 V. Golubev: Bull. Académie des Sciences (Akademiya Nauk), Leningrad, vol. VII, no. 8, pp. 1103-1108. (In Russian.)

65 G. Durand: Comptes Rendus Académie des Sciences, vol. 196, pp. 383-385.

66 R. V. Southwell and H. B. Squire: Phil. Trans. Royal Soc. London, vol. 232, ser. A, pp. 27-64.

67 N. A. V. Piercy and H. F. Winny: Proc. Royal Soc., vol. 140, pp. 543-561.

68 A. Thom: Proc. Royal Soc., vol. 141, pp. 651-658.

69 W. Tollmien: Trans. A.S.M.E., vol. 55, 1933, APM-55-4.

70 L. Prandtl: Zeit. V.D.I., 1933, pp. 105-114.

71 A. Fage: Jour. Royal Aeronautical Soc., vol. 37, pp. 573-600.

72 J. M. Burgers: Proc. Koninklijke Akademie van Wetenschappen, Amsterdam, vol. 36, nos. 3, 4, 5.

⁷ Concerning this subject, a few papers of special interest from the point of view of fluid mechanics are mentioned. Papers on aerodynamics in general are considered by the Aeronautic Division.

- 73 F. Noether: *Zeit. für angewandte Mathematik und Mechanik*, vol. 13, no. 2, April, 1933, pp. 115-120.
- 74 W. Tollmien: *Physics*, vol. 4, no. 8, pp. 289-290.
- 75 G. D. Mattioli: *Comptes Rendus Académie des Sciences*, vol. 196, pp. 1282-1284; *Rendiconti, Atti. R. Accademie dei Lincei*, Rome, vol. VI, no. 17, pp. 217-223 and 293-299.
- 76 W. Tollmien: *Ingenieur-Archiv*, vol. 4, 1933, pp. 1-15.
- 77 A. M. Kuethe: Paper to be published shortly.
- 78 H. Schlichting: *Zeit. für angewandte Mathematik und Mechanik*, vol. 13, no. 4, Aug., 1933, pp. 260-263.
- 79 P. Ruden: *Naturwissenschaften*, vol. 21, pp. 375-378.
- 80 M. Ziegler: *Proc. Koninklijke Akademie van Wetenschappen*, Amsterdam, vol. 35, no. 3, pp. 419-426.
- 81 W. C. Mock and H. C. Dryden: *Nat. Advis. Comm. Aero.*, Rept. no. 448.
- 82 F. L. Wattendorf and A. M. Kuethe: *Physics*, vol. 5, no. 6, June, 1934, pp. 153-164. cf. (103).
- 83 Th. von Kármán: Paper to be published shortly.
- 84 F. L. Wattendorf: *Preprinted Papers, 1934 A.S.M.E. Aeronautic-Hydraulic Meeting*, Berkeley, Cal.
- 85 Van der Hegge Zynen: *Proc. Koninklijke Akademie van Wetenschappen*, Amsterdam, vol. 34, part 2.
- 86 H. Reichardt: *Zeit. für angewandte Mathematik und Mechanik*, vol. 13, no. 3, June, 1933, pp. 177-180.
- 87 G. Kröber: *Ingenieur-Archiv*, vol. 3, no. 5, pp. 516-541; translation, *Nat. Advis. Comm. Aero.*, Tech. Mem. 722.
- 88 H. Schlichting: *Annalen der Physik*, vol. 14, no. 8, pp. 905-936.
- 89 O. Miyagi: *Proc. Imperial Acad. Japan*, Tokyo, vol. 8, pp. 352-353.
- 90 J. Nikuradse: *Zeit. für angewandte Mathematik und Mechanik*, vol. 13, no. 3, June, 1933, pp. 174-176.
- 91 J. Nikuradse: *Forschungsheft, beilage zu Forschung auf dem Gebiete des Ingenieurwesens*, no. 361.
- 92 H. Fette: *Zeit. für Technische Physik*, vol. 14, no. 7, pp. 257-266.
- 93 D. Nukiyama: *Aeronautical Research Inst., Tokyo Imperial Univ.*, Rept. no. 90, pp. 233-290.
- 94 W. Spalding: *Zeit. V.D.I.*, vol. 77, 1933, pp. 143-148.
- 95 A. H. Gibson: *Philosophical Mag. and Jour. Science*, vol. 15, pp. 637-647.
- 96 N. A. V. Piercy, M. S. Hooper, and H. F. Winny: *Philosophical Mag. and Jour. Science*, vol. 15, pp. 647-676.
- 97 "Hydromechanische Probleme des Schiffsantriebs," herausgegeben von Kempf and Foerster, Hamburg.
- 98 K. E. Schoenherr: Paper read before Soc. Naval Arch. and Mar. Engrs., Nov., 1932.
- 99 T. H. Havelock: *Proc. Royal Soc.*, vol. 138, pp. 339-348.
- 100 H. Wagner: *Jahrbuch der Schiffbautechnische Gesellschaft*, vol. 34, pp. 205-227.
- 101 J. M. Burgers: *Zeit. für angewandte Mathematik und Mechanik*, vol. 13, no. 2, Apr., 1933, pp. 67-71.
- 102 O. Schrenk: *Zeit. für angewandte Mathematik und Mechanik*, vol. 13, no. 3, June, 1933, pp. 180-182.
- 103 C. B. Millikan and A. L. Klein: *Aircraft Engrg.*, Aug., 1933.
- 104 B. Randisi: *L'Aerotecnica*, vol. XIII, no. 7, pp. 3-25.
- 105 Hilda Lyon: *Aeronautical Research Comm.*, Great Britain, Tech. Rept. no. 1511.
- 106 H. B. Freeman: *Nat. Advis. Comm. Aero.*, Repts. nos. 430 and 432.
- 107 Lock and Johansen: *Aeronautical Research Comm.*, Great Britain, Tech. Rept., no. 1452.
- 108 H. C. Dryden: Paper presented at Washington meeting of Am. Phys. Soc., April, 1933.
- 109 G. I. Taylor and J. W. Maccoll: *Proc. Royal Soc.*, vol. 139, pp. 278-311.
- 110 G. Braun: *Annalen der Physik*, vol. 15, 1932, pp. 645-676.
- 111 L. Pogg: *L'Aerotecnica*, vol. XII, pp. 1579-1593.
- 112 A. Busemann and O. Walchner: *Forschung auf dem Gebiete des Ingenieurwesens*, vol. 4, no. 2, Mar.-Apr., 1933, pp. 87-92.
- 113 D. Riabouchinsky: *Comptes Rendus Académie des Sciences*, vol. 195, pp. 998-999.

THERMODYNAMICS⁸

The pressure-temperature relation for saturated steam has been the subject of careful investigation both in this country and in England during the past year. Osborne, Stimson, Flock, and Ginnings (114) at the United States Bureau of Standards, employing the so-called static method in which simultaneous readings of pressure and temperature of a saturated mixture in a

closed bomb are made, have obtained new and accurate data which they present in the form of a table giving values of pressure and its derivative with respect to temperature (in various units namely: standard atmospheres, centibars, kilograms per square centimeter and pounds per square inch) for the range 100 C to 374 C. They estimate their results to be reliable to ± 0.03 per cent. Egerton and G. S. Callendar (115), in England, have investigated the range, 170 C to 374 C, by a dynamic method in which simultaneous readings of pressure and temperature are taken under conditions of steady flow and at a point in the apparatus where the steam is known to be saturated. Particular attention was paid to the removal of air. The accuracy of their final results has been estimated by Jakob (116) to be at least ± 0.07 per cent. Keyes and Smith (117), at the Massachusetts Institute of Technology, report an independent redetermination of the pressure-temperature relation for use in connection with extrapolation of their specific-volume data to the saturation curve. Their method was of the static type. Jakob and Fritz (118) have published a comparison of the results of these three investigations with the previously accepted data of Holborn, Henning, and Baumann in which they show that all are in excellent agreement.

The work of Keyes and Smith (117) on specific volumes has been mentioned. Their latest measurements were carried out in a new nirosta steel bomb and cover the range of isometrics from 2 to 150 cu cm per g, extending to pressures as high as 350 atm. and to temperatures as high as 460 C. Together with earlier data (119), these new measurements give a rather complete picture of the p - v - t relation for compressed liquid and superheated steam. The isometrics for 2, 3, and 4 cc per g lie above the critical point in the region where water may be regarded either as liquid or as superheated vapor. In order to remove the uncertainty due to adhesion of water to the surface of the container in the measurement of large specific volumes by their present method, the authors propose to try an indirect, thermodynamic method which they briefly described. Keenan (120) has reported the recent data of Havlicek at the Masaryk Academy of Work which include more than seven hundred direct measurements of the enthalpy of compressed water and superheated steam extending from atmospheric pressure to 5600 lb per sq in. and from 70 F to 1030 F. Havlicek paid particular attention to the region above 374 C, but was unable to verify the contention of the late Professor Callendar that a considerable latent heat should be found there. Keenan calls attention to the significant progress that has been made since 1922 toward agreement on basic data for the formulation of steam tables.

The progress in steam research noted in the preceding paragraphs has its most immediate application to those problems in power generation arising from the use of water as a heat medium. In another field, that of combustion, the thermodynamic properties of water also play an important rôle. Thus, the specific heat of water vapor at high temperatures demands investigation on account of the wide discrepancy between the formerly accepted values of Pier, Bjerrum, Siegel, and others and the values deduced from theoretical equations based on spectroscopic data. Efforts are being made to bring these data into accord by applying various corrections.

R. Planck (121) has made an important contribution to the study of viscosity and its relation to other thermodynamic properties. For an ideal gas, he finds that the viscosity is a function of temperature only. For an actual gas, the viscosity can be satisfactorily represented as the product of the ideal gas viscosity and a factor depending on volume only. For water, the Mathias rule seems to apply, namely: The arithmetical mean of the reciprocal viscosities of saturated liquid and saturated vapor varies linearly with the temperature. On the thermal conduc-

⁸ Compiled by J. A. Goff.

tivity of water, new measurements have been reported by Schmidt and Sellschopp (122) which extend to 270 C and show an approximately parabolic variation with temperature which gives a maximum value at about 130 C. H. Eck (123) has published a review of existing data on the thermodynamic properties of mercury that ought to be of value to engineers interested in the mercury-steam power-generation cycle. The author gives a table listing the usual properties of saturated liquid and vapor from 0.0010 kg per sq cm (119.5 C) to 50 kg per sq cm (690.9 C). Formulas are given for extrapolation into the superheat region.

Finally, there should be mentioned an excellent article by E. Schmidt (124) summarizing the present state of knowledge in the field of heat transfer. American workers have been especially active in this field because of its fundamental importance to the problems of industrial and engineering chemistry.

114 N. S. Osborne, H. F. Stimson, E. F. Fiock, and D. C. Gin-

nings: A.S.M.E. Trans., vol. 55, 1933, RP-55-4; *Jour. Research*, U. S. Bur. Standards, vol. 10, 1933, pp. 155-188.

115 A. Egerton and G. S. Callendar: *Phil. Trans. Royal Soc. London*, vol. 231, ser. A, 1932.

116 M. Jakob: *Zeit. V.D.I.*, vol. 77, 1933, p. 820.

117 F. G. Keyes and L. B. Smith: *Mechanical Engineering*, vol. 55, 1933, p. 114.

118 M. Jakob and W. Fritz: *Forschung auf dem Gebiete des Ingenieurwesens*, vol. 4, no. 3, May-June, 1933, p. 153.

119 F. G. Keyes and L. B. Smith: *Mechanical Engineering*, vol. 53, 1931, p. 134.

120 J. H. Keenan: *Mechanical Engineering*, vol. 55, 1933, p. 172.

121 R. Planck: *Forschung auf dem Gebiete des Ingenieurwesens*, vol. 4, no. 1, Jan.-Feb., 1933, pp. 1-7.

122 E. Schmidt and W. Sellschopp: *Forschung auf dem Gebiete des Ingenieurwesens*, vol. 3, no. 6, Nov.-Dec., 1932, pp. 277-286.

123 H. Eck: *Forschung auf dem Gebiete des Ingenieurwesens*, vol. 4, no. 1, Jan.-Feb., 1933, pp. 21-25.

124 E. Schmidt: *Zeit. V.D.I.*, vol. 76, 1932, p. 1025.

Some New Experiments on Buckling of Thin-Wall Construction¹

By F. J. BRIDGET,² C. C. JEROME,³ AND A. B. VOSELLER,⁴ PASADENA, CALIF.

The first section of this paper describes a series of tests of the strength of thin-walled cylinders under a combination of torsion and axial compression or tension. Curves are obtained showing the strength of each of the several types of cylinders tested, under all possible combinations of these loads. All the curves obtained seem to have the same general form and the results suggest the possibility of finding a simple law by means of which a designer could determine the buckling strength of a structure under any combination of shear and normal stress, if he knows its strength under pure shear and under pure compressive stress.

The second section describes tests made to investigate the independence of different possible types of buckling of a structure. A set of L-section struts, identical except for the widths of the sides, were tested in compression. With small widths the struts buckle as Euler columns but with the wider widths buckling of the sides, as plates hinged on three edges, occurs first. Great care was taken to eliminate the effect of initial eccentricities. The results check the well-known theories for these two types of buckling and indicate that, for practical purposes, the two types can be considered independently of each other. The results also illustrate how enormously the strength-weight ratio of thin wall construction may be affected by details of design.

I—STRENGTH TESTS ON THIN-WALLED CYLINDERS

THE stresses produced by the loads in the skin of monocoque construction are usually combinations of compression or tension in one direction, with shear in the same and perpendicular directions. Much theoretical and experimental information is available to the designer on the behavior of thin sheets under compression or tension alone, or under shear alone, but nothing seems to be known about their behavior under combinations of these stresses.

The general nature of the behavior of thin sheet construction under such combination loadings can be predicted by some very

simple reasoning. Let σ and τ be the normal and shear stresses produced in the wall, and σ_0 and τ_0 the values of these stresses when failure occurs under pure axial compression or tension, and under pure torsion, respectively. Then by plotting σ/σ_0 against τ/τ_0 a curve is obtained, passing through the points 0-1 and 1-0, and showing how failure occurs under all possible combinations of these two types of stresses. This curve obviously must be symmetrical about the σ/σ_0 axis, as a change in the sign of the shear (for a symmetrical structure) can make no difference. Hence the curve must be perpendicular to the σ/σ_0 axis where it crosses it, as it is certainly continuous at this point. On the other hand the curve will not be symmetrical about the τ/τ_0 axis, but must cross it at some angle as shown in Fig. 1(a),

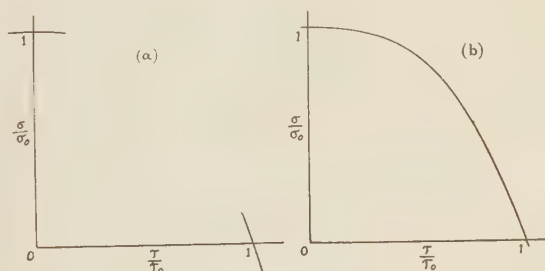


FIG. 1 SHAPE OF $\frac{\sigma}{\sigma_0} - \frac{\tau}{\tau_0}$ CURVE SUGGESTED BY ELEMENTARY REASONING

as compression will obviously decrease and tension increase the shear which the structure can take before buckling. This immediately suggests some kind of parabolic or power relation as in Fig. 1(b), with an equation:

$$1 - \sigma/\sigma_0 = (\tau/\tau_0)^n \dots \dots \dots [1]$$

where n is greater than 1. Of course n should be an even number to satisfy the condition of symmetry about the σ/σ_0 axis, but this relation can be used as an empirical formula with any value greater than 1 for n , provided τ/τ_0 is always considered positive.

¹ The tests described in this paper were made at the Guggenheim Aeronautical Laboratory of the California Institute of Technology. The authors have been assigned to the Institute by the Navy Department for graduate work in aeronautics, and this work represents part of the requirements for the Master's Degree. The first section is by Lieutenant Bridget and the second by Lieutenants Jerome and Vosseller. The authors wish to thank Dr. Th. von Kármán, director of the Guggenheim Laboratory of the Institute, for the opportunity for making these researches. The researches were suggested by and carried out under the direction of Dr. L. H. Donnell. Acknowledgment is also due to L. Secretan, who cooperated in the first research, also to Dr. A. L. Klein and E. E. Sechler (all of the staff of the Institute) for numerous helpful suggestions.

² Lieutenant, U. S. Navy. F. J. Bridget was graduated from U. S. Naval Academy in 1921 and served seven years on sea duty in the fleet with gunnery duties. He completed flight training in 1929 at Pensacola, Florida, served in a fighting squadron attached to the U. S. S. *Lexington* in 1929 and 1930, and on inspection duty of naval aircraft in 1931. He attended Post Graduate School, U. S. Naval Academy in 1932, and upon completion was assigned to duty at the California Institute of Technology for postgraduate work in Aeronautical Engineering.

³ First Lieutenant, U. S. Marine Corps. C. C. Jerome was graduated from U. S. Naval Academy in 1922 and was with various Marine Infantry units from 1922 to 1924. He served on aviation duty with the Marine Aviation in United States, China, Phillipines, Guam, and Nicaragua, from 1924 to 1932. He was assigned to duty at the California Institute of Technology for postgraduate work in Aeronautical Engineering in 1933.

⁴ Lieutenant, U. S. Navy. A. B. Vosseller was graduated from U. S. Naval Academy in 1924 and served in various ships of the fleet and on the staffs of Commander Battleships and Commander Destroyers, Battle Force, until assignment to aviation duty in 1930. Upon completion of flight training he served in the fighting squadron attached to the U. S. S. *Lexington*. He attended Post Graduate School U. S. Naval Academy in 1932, and upon completion was assigned to duty at the California Institute of Technology for postgraduate work in Aeronautical Engineering.

Contributed by the Applied Mechanics Division and presented at the Annual Meeting, New York, N. Y., December 4 to 8, 1933, of THE AMERICAN SOCIETY OF MECHANICAL ENGINEERS.

NOTE: Statements and opinions advanced in papers are to be understood as individual expressions of their authors, and not those of the Society.

This reasoning is perfectly general, applying to the stability of any type of symmetrical structure.

To get some experimental information on this subject, several series of similar thin-walled cylinders have been tested to failure under various combinations of torsion and axial compression or tension. In the most complete of these series (Series G), about forty cylinders made as nearly identical as possible, were tested. Fig. 2 shows for this series, the experimental values obtained for σ/σ_0 and τ/τ_0 plotted against each other. It obviously makes no difference whether σ , τ , σ_0 , τ_0 are defined as above, or if σ and τ are taken to mean the total axial load and torsional moment and σ_0 and τ_0 the values of these loads when failure occurs under pure axial compression or tension and under pure torsion, respectively. It seemed to make no difference in what order the loads were applied; that is, whether a fixed amount of torsion was applied first and the axial load increased until failure occurred, or vice versa.

The full line in Fig. 2 is a cubic parabola, which is the curve given by Equation 1 when n equals 3. This curve seems to fit

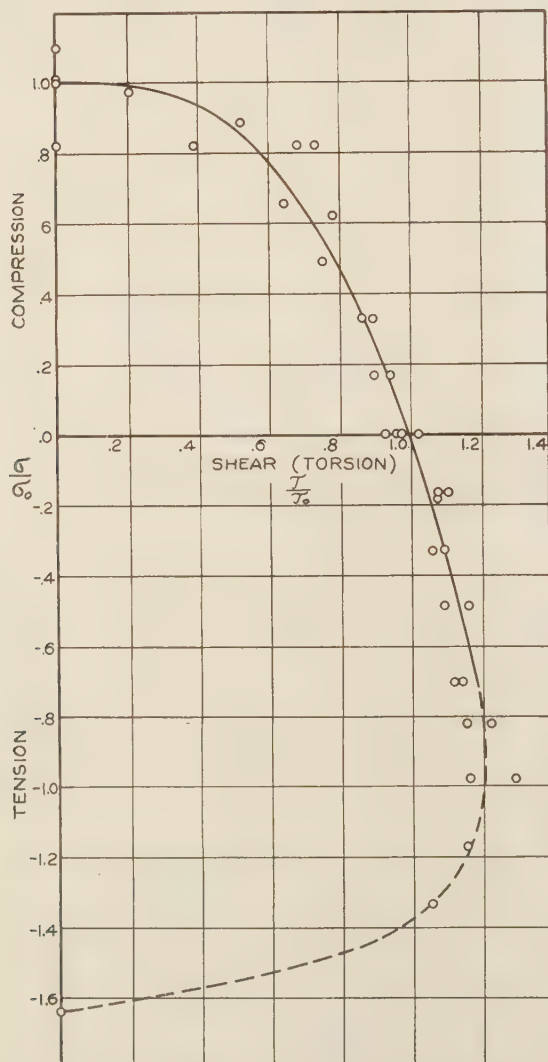


FIG. 2 BUCKLING OF CYLINDERS UNDER COMBINED TORSION AND COMPRESSION OR TENSION

(Experimental $\frac{\sigma}{\sigma_0} - \frac{\tau}{\tau_0}$ curve for "G"-type cylinders.)

the points reasonably well. More definite information as to the nature of the relation given by these experiments is obtained by plotting $1 - \sigma/\sigma_0$ against τ/τ_0 on double logarithmic paper, as has been done in Fig. 3 for Series G. It will be seen that the experimental points lie close to a straight line, which proves the validity of Equation 1 as an empirical formula for this case.

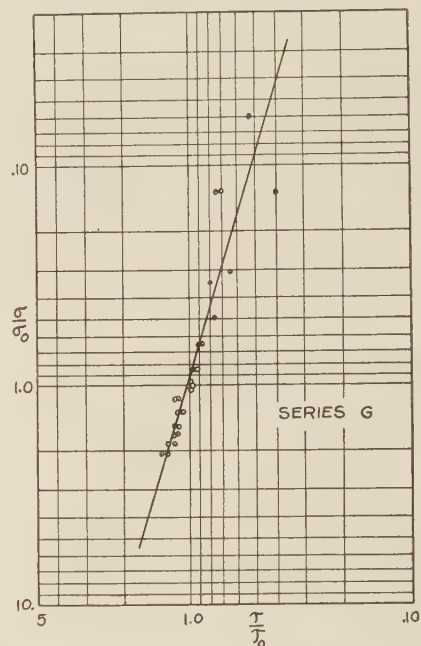


FIG. 3 CURVE IN FIG. 2 PLOTTED ON LOGARITHMIC COORDINATES

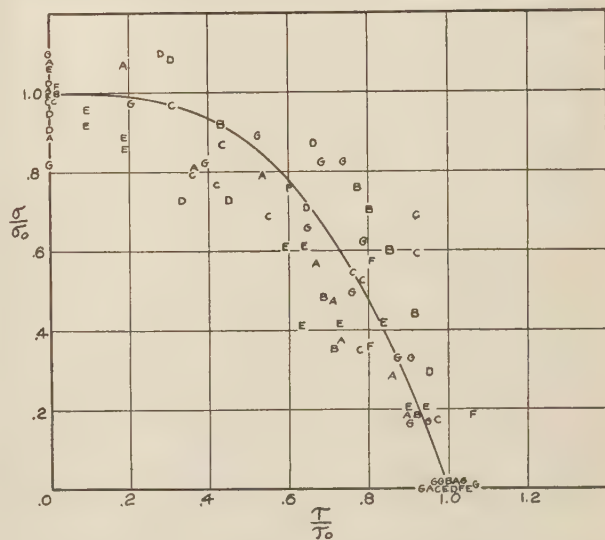


FIG. 4 BUCKLING OF CYLINDERS UNDER COMBINED TORSION AND COMPRESSION OR TENSION

(Experimental $\frac{\sigma}{\sigma_0} - \frac{\tau}{\tau_0}$ results for all series of cylinders tested.)

The slope of this straight line gives the value of n which, when substituted in Equation 1 will give the best empirical relation to fit these experiments. A determination of this slope by eye or the method of least squares gives a value of about 3.3 for n .

The lower portion of the curve in Fig. 2, shown dotted, obviously represents stress combinations for which some portion

of the cylinder has reached the elastic limit. The lowest point on the curve represents a pure tension test. Most practical applications do not fall within this region and no particular study has been made of this portion of the curve. Designers will realize, of course, that the relation given by Equation 1 can hold only when the principal stresses as given by elementary mechanics are within the elastic limit, or, according to the maximum shear theory, when the algebraic difference between these principal stresses is less than the elastic limit stress.

Six other less complete series of tests have been made, each series on a radically different type of cylinder. These tests were made with torsion and axial compression only, and with a much smaller number of cylinders. The results are shown in Fig. 4. Fig. 5(a to f) shows the results plotted on double logarithmic paper for series A to F, inclusive. These results are similar to those from the group of tests described above. The value of n appears to be different for each type of cylinder, the values obtained ranging from about 1.0 to 4.25 and apparently indicating that n is a function of the dimensions or material of the cylinder. Some of the sets of results, when plotted on logarithmic paper, do not seem to give a straight line, apparently indicating that Equation 1 is not exactly suitable as an empirical relation for these cases. However, the number of points is so few and the unavoidable experimental scatter so great, that nothing definite can be said on any of these questions. The results do indicate, however, that the general empirical relation given by Equation 1 covers all these tests and hence probably all thin-walled cylinders, and possibly all thin-walled structures of any kind, sufficiently well for practical purposes. If n is taken as 3 as was done in plotting the solid curve in Fig. 4, the deviation between the empirical law and the experimental results is not large compared to the general scatter of the points for any of the types of cylinders tested. It therefore seems safe to say that designers can use the relation given by Equation 1 with n equal to 3 for designing cylinders, with considerable confidence until better information is available.

Obviously this is only a small part of the research which should be done in this connection. It is planned to continue this work at the California Institute of Technology and it is hoped that this paper will stimulate other research organizations to enter this field. Some tests have already been started here on long square tubes under axial load and torsion. These give approximately the condition of flat hinged-edge panels under normal and shear stresses. The initial results are similar to those previously described. As already stated, there has been little investigation in this field up to the present time and it is felt that further work will result in information of great value to designers of stressed skin structures.

All of the tests were made on small-scale models of steel and brass "shim stock." They were made by a technique and tested on special testing machines developed by Dr. L. H. Donnell. These have been described by him in a previous paper⁵ and the Fig. numbers mentioned in the following paragraph refer to Dr. Donnell's paper.

⁵ N.A.C.A. Report No. 479.

He indicates that the results from such small-scale tests compare quite favorably with tests on a larger scale but it is necessary to use great care in selecting stock and in making the specimens, in order to reduce experimental scatter to a minimum. In spite of this care it is impossible to avoid considerable scatter, especially when the load is mainly compression. Much of this is due probably to the fact that it is impossible to obtain such thin stock entirely without initial waviness.

The thickness of the sheet was measured in the thickness tester shown in Fig. 14(a).⁵ The modulus of elasticity, E , was obtained with the special testing machine and tensometer shown in Fig. 15(a).⁵ The proportional limit stress σ_p was found at the same time, for purposes of record. The sheets were rolled around rods of the proper diameter to give them the correct cur-

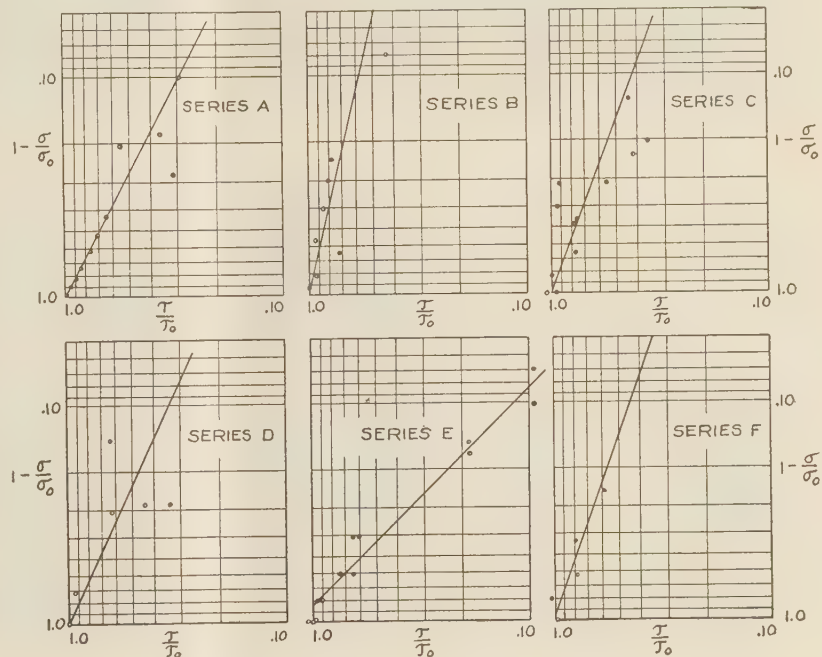


FIG. 5 RESULTS SHOWN IN FIG. 4 PLOTTED AS INDIVIDUAL SERIES ON LOGARITHMIC COORDINATES

vature. They were then wrapped around a wooden roll, of the diameter of the finished cylinder, which had previously been oiled to permit removal of the cylinder after soldering. The sheet was held against the roll with a metal strap, while a special clamp was used to prevent the edges from warping under the heat of soldering. The edges were soldered with about $1/8$ -in. overlap. It has been found that buckling waves seem to form across the joints as freely as elsewhere, so the effect of the double thickness at the joint is probably very small. After removal, the cylinders were soldered at each end to rings which fitted inside them, and the cylinder and ring were soldered to heavy base plates with which they were mounted in the testing machine. The shortening of the effective length of the cylinders due to the rings is allowed for in the following table. The cylinders

TABLE 1 PROPERTIES OF CYLINDERS IN SERIES TESTED

Series	Mat.	Length	Diam.	Thick.	$E \times 10^{-6}$	$\sigma_p \times 10^{-3}$	n
A	steel	5.315	1.88	0.00204	31.4	57.7	1.992
B	brass	5.315	1.88	0.0032	16.5	27.0	4.25
C	steel	5.315	3.75	0.00295	30.6	48.6	2.625
D	steel	11.315	1.88	0.00204	27.06	53.3	2.156
E	steel	5.315	1.88	0.00295	30.6	48.6	1.0
F	steel	1.32	3.75	0.00204	31.4	57.7	2.781
G	steel	5.315	1.88	0.00395	29.6	36.0	3.33

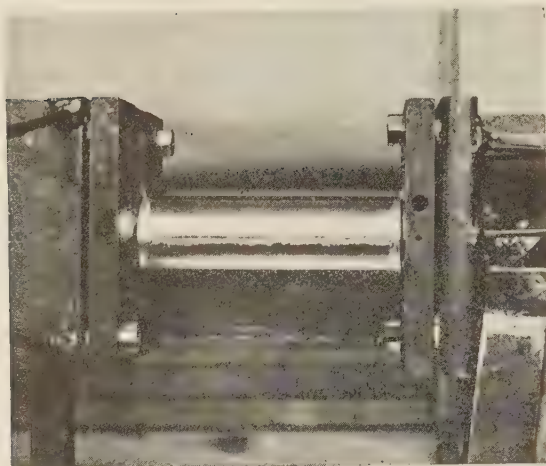


FIG. 6 TYPICAL SPECIMEN, "G" SERIES

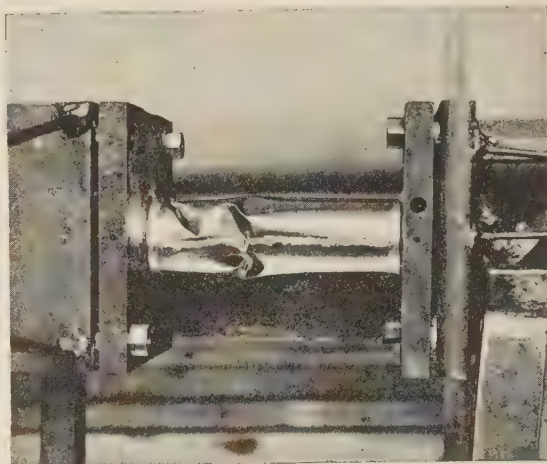


FIG. 7 COMPRESSION-TORSION BUCKLING, "A" SERIES

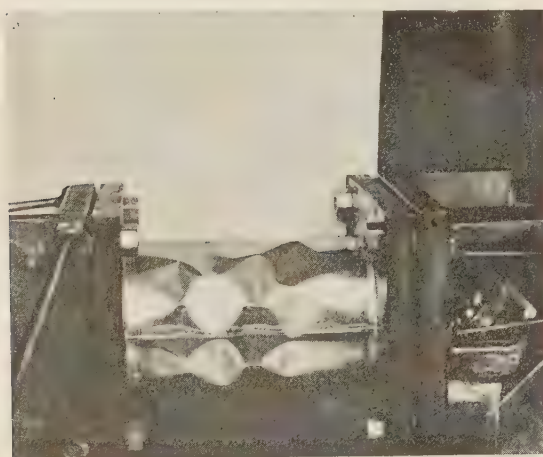


FIG. 8 AXIAL COMPRESSION BUCKLING, "C" SERIES

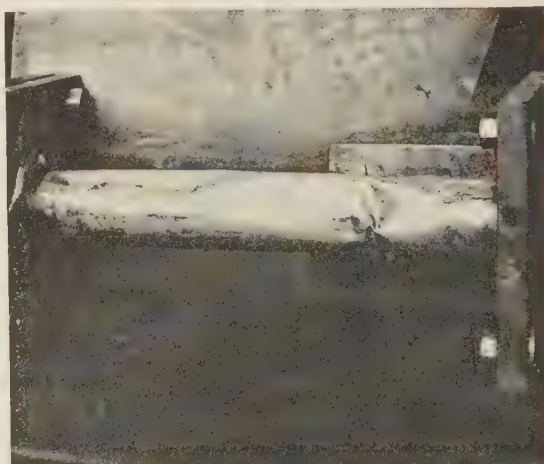


FIG. 9 COMPRESSION-TORSION BUCKLING, "D" SERIES



FIG. 10 COMPRESSION-TORSION BUCKLING, "F" SERIES

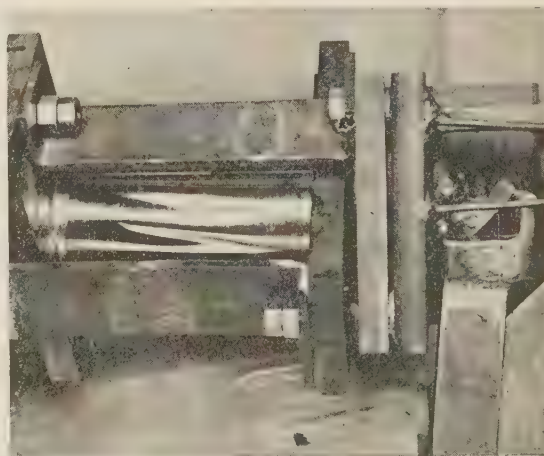


FIG. 11 TENSION-TORSION BUCKLING, "G" SERIES



FIG. 12 "G"-SERIES CYLINDERS AFTER TEST

were tested in the special testing machine shown in Fig. 6(a).⁵ This testing machine is capable of testing specimens in any combination of torsion, bending, and axial compression or tension.

Figs. 6 to 10, inclusive, of the present paper show typical failures under combined compression and torsion, while Fig. 11 shows a typical failure under combined tension and torsion with the

shapes and sizes. They are, however, usually made up of sheet material, formed into a great variety of shapes. They are, accordingly, subject to local wrinkling or buckling of the sheet under load.⁶ Stiffeners of such shapes are ordinarily constructed and installed in lengths which are large in comparison to the cross-section, so that the sections are also liable to failure as long slen-

TABLE 2 EXPERIMENTAL RESULTS USED IN PLOTTING CURVES

	Series A													
σ lb	0	20	40	60	80	100	120	170	172	230	192	218	231	...
τ lb in.	55	52	49	47	40	39	36	30	20	10	0	0	0	...
	Series B													
σ lb	20	45	90	110	120	150	175	190	230	250
τ lb in.	70	64	50	64	48	60	56	54	30	0
	Series C													
σ lb	0	0	50	100	150	155	170	200	200	220	230	250	279	287
τ lb in.	217	240	226	178	180	174	210	210	126	96	70	100	72	0
	Series D													
σ lb	0	40	97	100	100	120	125	130	140	150	151
τ lb in.	36	34	23	12	16	24	0	0	0	11	10
	Series E													
σ lb	0	0	100	100	200	200	200	300	300	420	430	455	470	490
τ lb in.	106	110	96	100	68	78	90	64	68	20	20	10	10	0
	Series F													
σ lb	0	25	50	75	100	132
τ lb in.	160	170	128	130	96	0
	Series G ¹													
σ lb	-980	-800	-800	-700	-600	-600	-500	-500	-400	-400	-300	-300	-200	-200
τ lb in.	0	166	200	220	248	224	220	234	215	218	222	210	204	210
σ lb	-100	-100	0	0	0	0	100	100	200	200	300	380	400	500
τ lb in.	206	216	178	196	186	184	172	180	166	174	144	150	124	0
σ lb	500	500	540	595	613	610	660
τ lb in.	132	140	100	40	0	0	0

¹ Minus values for σ indicate tension.

tension cage attached. Fig. 12 shows the cylinders of Series G after testing. Table 1 shows the properties of the cylinders in each of the series tested. The values given for n are the slopes of the straight lines in the logarithmic plots, Figs. 3 and 5(a to f) previously discussed.

Table 2 shows the ultimate axial loads σ , and torsion moments τ , for each of the cylinders tested. The values used for σ_0 and τ_0 , in plotting Figs. 2 to 5, were the averages of the values of σ and τ found in the pure compression and pure torsion tests. The values chosen for σ_0 and τ_0 have considerable influence on the value found for n and it is probable that part of the variation in the values of n , found for different types of cylinders, is due to the inaccuracy of these values. In conducting this type of research it is important to make numerous pure compression and pure torsion tests (especially pure compression, because the scatter is much worse here than for torsion), in order to get a good average value for σ_0 and τ_0 . In future research it is planned to make even more of such tests than have been made.

II—INVESTIGATION OF INDEPENDENCE OF DIFFERENT TYPES OF BUCKLING IN L-SECTION STRUTS

The stiffener shapes used in monocoque, or for that matter any other kind of aeronautical construction, are of many different

der columns, that is as so-called "Euler columns." The stiffener thus has the possibility of buckling in two entirely different manners: (1) as a Euler column, or (2) from local instability of the sheet of which it is composed. The question then arises as to whether these different types of buckling can be considered entirely independently of each other or if there is a transition stage between them in which a combination buckling can take place at a lower loading than for either alone. It was to find an answer to this question, both for this case and for other cases of structures which can buckle in two or more independent ways, that this investigation was undertaken.

The tests were made with struts of equal-leg "L" section, identical except for the widths of the sides. When the widths are small compared to the length such struts buckle as Euler columns, but for wide widths buckling of the sides occurs first.

The greatest importance is attached to an accurate knowledge of the end fixity for column buckling and of the edge fixity for sheet buckling. This type of specimen allowed all these conditions to be determined accurately. A column of this shape may be considered to be made up of two flat plates hinged along their

⁶ This type of buckling was considered by G. W. Trayer and H. W. March in N.A.C.A. Technical Report 382.

common edges with the other edges free, since they can obviously buckle in such a way that the angle between the sides at the corner will remain the same, and thus there will be no moments at these edges.⁷ To obtain definite end conditions for the flat plate buckling, each side of the angle section was chamfered along its complete width at the ends to an angle of 60 degrees (see Fig. 13) insuring hinged edge conditions. The end blocks for supporting the specimen each had two 120 degree "V" grooves cut on one surface, the grooves intersecting at an angle of 90

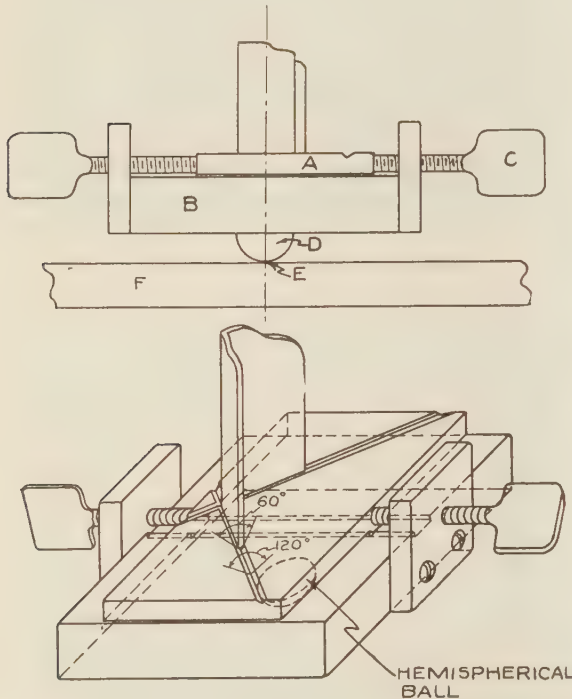


FIG. 13 END BLOCKS SHOWING SEAT GROOVE AND ADJUSTMENTS

degrees, to receive the ends of the specimens. In order to obtain definite end conditions for Euler buckling, a $\frac{5}{8}$ -in. hardened-steel ball was inserted in these end blocks, making the struts "ball ended" columns, hinged, in effect, about the center of the balls. The struts were thus free to buckle in any direction but of course actually buckled about the axis of minimum moment of inertia of the section (perpendicular to the axis of symmetry).

As stated above, for small widths the struts buckle as Euler columns. The theory for this type of buckling is well known. It was developed by considering the bending of a column under compression as a whole and consequently does not take into account the possibility of plate buckling nor stresses above the yield point of the material. The equation expressing Euler's theory for hinged end columns is⁸

$$\sigma_c = \pi^2 E \left(\frac{r}{l} \right)^2$$

where σ_c = critical buckling stress
 E = modulus of elasticity of the material
 l = length of column
 r = radius of gyration of the cross-section of column.

⁷ L. H. Donnell, "The Problem of Elastic Stability," A.S.M.E. Trans., (1933), AER-55-19a.

⁸ J. E. Boyd, "Strength of Materials," McGraw-Hill Book Co., p. 236.

This theory has been checked very closely by von Kármán⁹ who originated the general method of varying end conditions to counteract initial crookedness which was used in these experiments.

For wide widths the sides buckle as flat plates. This type of failure has been neglected to a certain extent by engineers, as it is of more or less infrequent occurrence in general construction, where the plates used are usually thick in comparison to length and width. The stability of rectangular thin flat sheets under compression has been analyzed by Bryan for plates hinged on all four sides and by Timoshenko¹⁰ for other cases. The general expression for the uniformly distributed stress on the ends which will cause buckling of the plate is⁷

$$\sigma_c = k E \left(\frac{t}{w} \right)^2$$

where

t = thickness of the plate

w = width of the plate

k = a constant, depending upon the ratio of the length to the width and upon the edge conditions.

Values of k for use with the above formula can be obtained from Fig. 7 of reference 7. In our case, sheets hinged on three

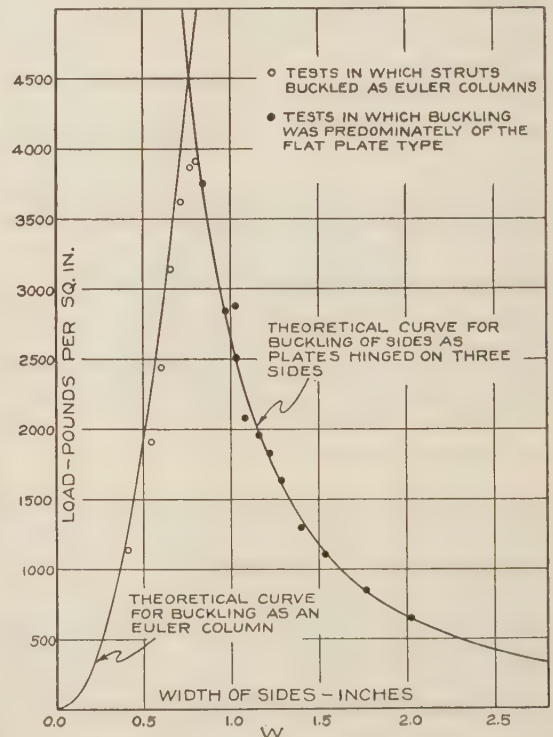


FIG. 14 THEORETICAL EULER AND PLATE BUCKLING CURVES COMPARED TO EXPERIMENTAL RESULTS

and free on the fourth, k , for the proportions used in the tests is practically independent of the length-width ratio and equals 0.4.

If all dimensions except the width are fixed, these two theories, for Euler and flat plate buckling give two relations between σ_c and the width. These relations have been plotted in Fig. 14. It will be seen that the two curves form an inverted "V." Ob-

⁹ Th. von Kármán, "Mitteilungen über Forschungsarbeiten," Verein deutscher Ingenieure, Berlin, 1909.

¹⁰ S. Timoshenko, "Strength of Materials," John Wiley & Sons, New York, part II, p. 604.

viously for widths up to the intersection of the two curves, the strut should theoretically fail as a Euler column, while for wider widths the strut should fail by buckling of the sides. The weight-strength ratio is, of course, proportional to σ_c and this figure shows that the maximum weight-strength ratio for this case is obtained for a width of 0.77 in. while for widths above or below this the ratio drops off greatly.

Nineteen satisfactory specimens were finally obtained, identical except for width, and all as free from initial eccentricities as is believed possible without an expenditure greatly out of proportion to the benefits to be obtained by the added refinement.

General experience is that in any buckling experiments it is impossible to make specimens sufficiently accurate to eliminate eccentricities entirely, and accordingly special precautions were taken to provide a means of eliminating initial eccentricities for Euler buckling. This was done by providing an adjustment in the end blocks whereby the ball could be moved relative to the axis about which buckling takes place. The horizontal relation between the center of the ball and the specimen could be varied along the axis of the greatest moment of inertia of the specimen so that the effect of initial eccentricities could be removed (see "Method of Testing" of this section for a more complete description of the apparatus). In this way very sharp buckling

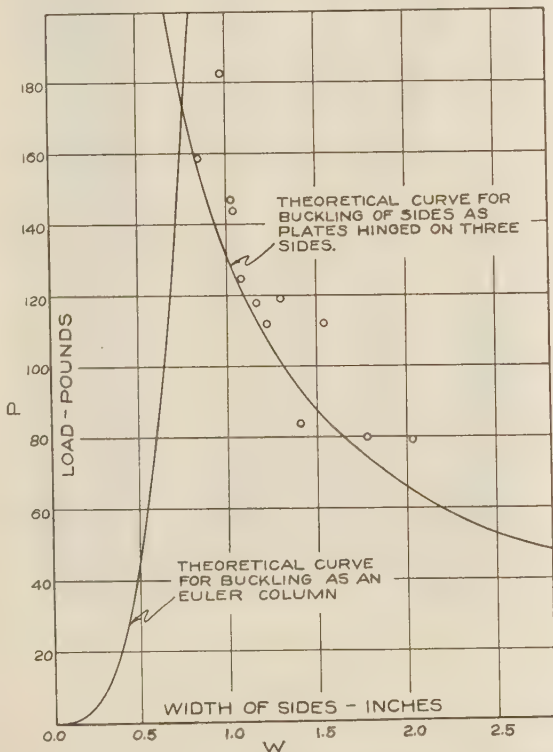


FIG. 15] CRITICAL LOADS AT WHICH PLATE BUCKLING OCCURRED IN TESTS

was obtained for Euler columns, as will be seen from Fig. 14. With these methods of construction the conditions of fixity then became known: For each plate-hinged at one side and at both ends; for the specimen as a Euler column-hinged at both ends. The specimens were made of such proportions that the buckling stresses were always far below the yield point of the material thereby eliminating any question of the failure of the material.

The effect of initial eccentricities upon the flat plate buckling was compensated for by use of a method developed by South-

well.¹¹ This is a mathematical method of finding the probable buckling strength, which a structure would have if it had no initial eccentricities, from measurements of small deflections. It is based upon the fact that in this region the load deflection curve approximates a rectangular hyperbola having the axis of zero deflection as one asymptote and the theoretical load deflection curve for no initial eccentricities as the other asymptote. (See "Method of Testing" of this section for a more complete description of the manner of use of this method.)

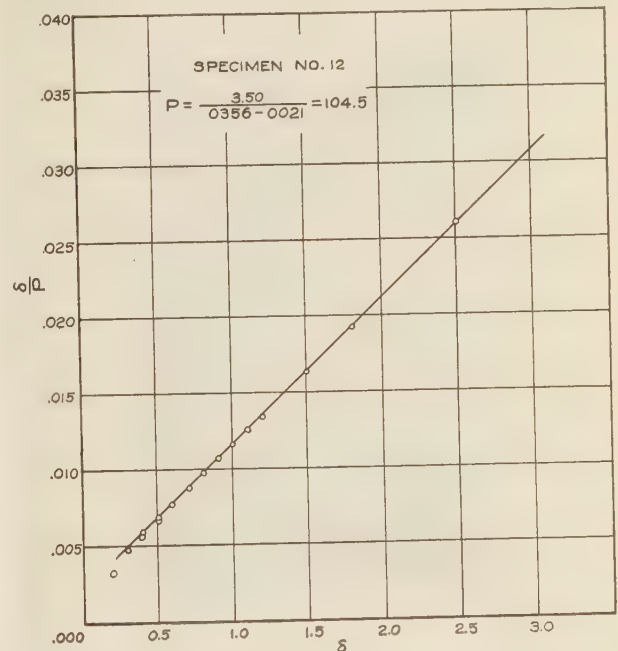


FIG. 16 STRAIGHT LINE OBTAINED FROM δ/P - δ RELATIONSHIP

Plates supported on three sides and free on the fourth buckle in one half wave in the lengthwise direction. In our case this amounted to a twisting of the middle portion of the strut about a longitudinal axis which was readily measured by the use of long light metal pointers attached to the sides of the specimen.

Fig. 15 shows the critical loads for the cases in which plate buckling occurred as recorded from the tests without the use of Southwell's method. It will be seen that the experimental scatter was quite large and most of the points are above the theoretical curve. Several reasons can be advanced for this. In these cases, when the ultimate buckling strength was obtained, the deflections were very large. The theory is based on the assumption of very small deflections and it is possible that a theory of large deflections would show greater values. But a more probable explanation of this discrepancy is that when the deflections became large it was no longer possible to keep the stress distribution uniform along the width of the sides.

By concentrating the stress at or near the corner of the angle of the specimen, the load can be carried far above the theoretical load for uniform stress distribution, due to the fact that the hinged edge is very much more stable than the free edge. By using Southwell's method based on deflection readings taken when the deflections were still small, experimental results are obtained which can justly be compared to the theory based on

¹¹ R. V. Southwell, "On the Analysis of Experimental Observations in Problems of Elastic Stability," Proc. Roy. Soc., A, vol. 135, 1932.

no initial curvatures and uniform stress distribution. The ultimate buckling loads without the use of Southwell's method were not critical and were largely a matter of judgment, it being possible to run the load up almost indefinitely if the end blocks were adjusted purposely to shift the stress toward the corners of the angle. Fig. 14 shows the critical buckling load of the specimens computed by Southwell's method from the last set of data referred to above. The scatter is greatly diminished and all points fall on or very close to the theoretical curve. The authors place great deal more confidence in this method of obtaining the

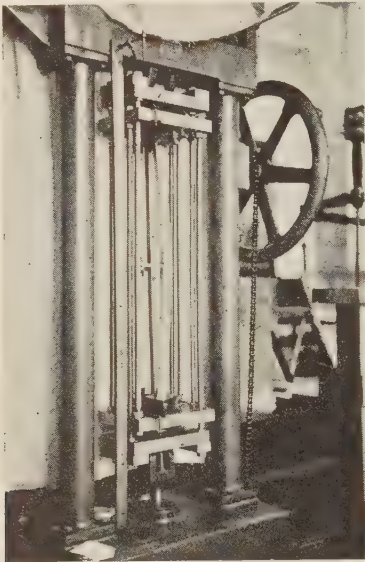


FIG. 17 TYPICAL STRUT IN TESTING MACHINE, SHOWING EULER TYPE FAILURE

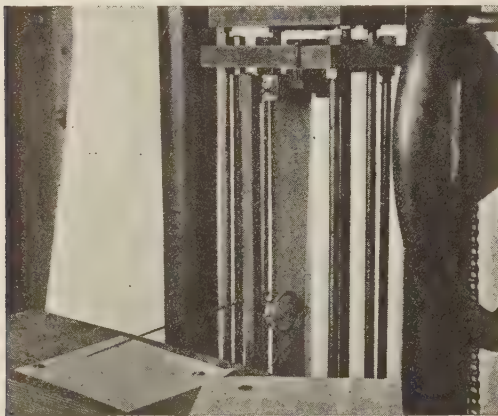


FIG. 18 VIEW OF SPECIMEN IN MACHINE, SHOWING CARRIAGE AND SCALES FOR READING LATERAL DEFLECTIONS

critical buckling stress than in relying simply on judgment, where it is probable that no two persons would agree exactly.

It is believed that the discrepancies occurring between the theoretical curve and the points obtained experimentally are well within the limits of experimental accuracy and that the results obtained therefore check the theory for Euler and flat plate buckling under the existing conditions.

It would appear from Fig. 14 that a very small fillet may exist in the experimental points near the apex of the inverted "V"

of the theoretical curves. The authors believe, however, that the apparent fillet may be merely a coincidence due to the experimental scatter and the difficulty of overcoming initial eccentricity, and hence obtaining a clear-cut type of failure in this region. It is believed to be established that any relation which does exist between Euler and flat plate buckling has a very small effect and exists only in the immediate vicinity of the intersection of the two theoretical curves for the two types of buckling.

It is felt that the results of this test establish the optimum dimensions for such a shape and that the engineer can design with confidence to the stress indicated by the intersection of the two curves provided a reasonable factor of safety is included.

METHOD OF TESTING

The tests were made on a Riehle Brothers testing machine of 3000 pounds load capacity. The machine was of the tension type, converted for compression tests by means of the cage shown

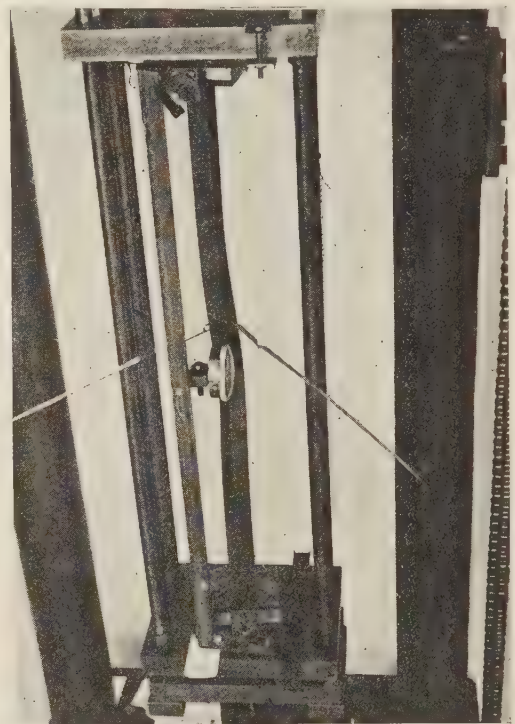


FIG. 19 GENERAL VIEW OF APPARATUS SHOWING ONE TYPE OF FLAT PLATE BUCKLING

in the accompanying photographs of the apparatus, Figs. 17, 18, and 19.

The specimens tested were all 22 in. in length and the width of the sides varied from 0.405 in. to 2.025 in. They were made of 24SRT aluminum alloy of 0.025 in. thickness, as this material and gage is being used to a large extent by the aircraft industry on the West Coast. The width of the side was taken as the overall width minus half the thickness of the sheet.

These specimens were made in an ordinary hand brake. It was necessary to adjust the brake for each width of specimen to get a bend of exactly 90 deg and a uniform radius at the corner. This radius was made as small as the material would stand, about $\frac{1}{16}$ in. The narrower specimens were liable to come out with considerable initial curvature, due to deflection of the brake, the peening of the material along the sheared edges, etc. It

was found possible to eliminate most of this by properly padding the brake with strips of paper.

Tests by the Bureau of Standards for the National Advisory Committee for Aeronautics on duralumin sheet¹² show a marked difference in the stress-strain curve taken normal or parallel to the direction of rolling. The authors felt that due to the shape of the sheet found in commercial practise, most long angle shapes would be made with the angle parallel to the direction of rolling, and consequently the specimens were made in this manner.

Specially constructed end blocks, identical for both ends of specimen, definitely established the desired end conditions. A sketch of the end block is shown in Fig. 13. The block *A* was machined on the upper side with 120 degree "V" grooves which made an angle of exactly 90 deg with each other. These grooves received the ends of the specimens which had been filed to an angle of 60 deg. In filing the ends great care was taken not to file away any of the center line.

A key and keyway between *A* and *B* allowed a movement of *A*, and hence the end of the specimen, relative to *E*, the point of application of the load. This movement could be made under load by means of the wing nuts *C*. The motion between *A* and *B* was such that *E* always moved along the axis of symmetry of the specimen. This insured an equal stress distribution on each leg and left the specimen free to buckle as a Euler column about the axis of least moment of inertia, which is perpendicular to the axis of symmetry.

To detect Euler failure of the specimen, an Ames dial gage was used, with counterbalancing spring removed. A small metal strip was attached to the gage point, which made point contact with the back of the angle at the middle of the length of the specimen. The gage was also mounted with the slide making point contact at the inside of the angle and results were the same as for the previous position. Both methods of attachment are shown in the accompanying photographs of the apparatus. The authors feel that in either position some slight rigidity was given to the specimen but that the results were not sufficiently in error to warrant setting up an optical system for this measurement.

To detect flat plate buckling, thin metal strips about ten inches long were attached to the free edges with paper clips as shown in Figs. 18 and 19. These pointers magnified the movement of the free edges.

For each test, the end blocks were set so that the axis of the least moment of inertia of the specimen was in a vertical plane with the point of contact of the ball, *D*, and the base plates of the cage. The specimen and end blocks were then mounted in the testing machine, a light load applied, and the measuring devices, Ames gage and pointers, were put in place. Both measuring devices were read as small increments of load were applied. Due to initial eccentricities or curvatures, it was found that the Ames gage would show a deflection of the column at comparatively low loads. By adjusting the wing nuts, *C*, so as to remove the apparent eccentricity a greater load could be applied without obtaining a deflection. This was repeated until finally the column would not stand a greater load without buckling. The loads at which Euler buckling occurred were for the most part very critical as the dial gage remained perfectly steady and then for one pound increase in load would show a very large deflection. The pointers, indicating plate buckling, remained practically steady during the test of a specimen which failed as a Euler column.

Where wider widths were used and flat plate buckling occurred before Euler buckling, the actual measured results were not so

significant, as there was no definite point at which this buckling occurred, due to initial eccentricities. Ranges were found for each specimen where, with the proper end adjustment, there was

TABLE 3 TYPICAL DATA TAKEN FOR DETERMINATION OF CRITICAL LOAD BY SOUTHWELL'S METHOD

	Load <i>P</i>	Deflection δ	δ/P
Specimen No. 17	67	0	
	70	0.2	0.00286
	72	0.5	0.00695
	74	0.7	0.0094
	76	1.0	0.01315
	78	1.3	0.0167
	80	1.8	0.0225
	82	2.4	0.0293
Specimen No. 12	84	3.0	0.0357
	0	0	0
	62	0.2	0.00323
	64	0.3	0.0047
	66	0.3	0.00455
	68	0.4	0.00588
	70	0.4	0.00571
	72	0.4	0.00555
Specimen No. 11	74	0.5	0.00675
	76	0.5	0.00658
	78	0.6	0.0077
	80	0.7	0.00875
	82	0.8	0.00975
	84	0.9	0.01072
	86	1.0	0.01165
	88	1.1	0.0125
Specimen No. 1	90	1.2	0.01335
	92	1.5	0.0163
	94	1.8	0.0192
	96	2.5	0.0261
	98	6.5	0.0664
	80	0	0
	85	0	0
	95	0.5	0.00577
	100	1.0	0.0100
Specimen No. 1	105	2.0	0.01905
	110	5.0	0.0455
	111	6.0	0.0541
	112	8.5	0.0758
	90	0.1	0.00111
	95	0.12	0.001264
	100	0.13	0.0013
	105	0.14	0.001333
Specimen No. 1	110	0.17	0.001545
	115	0.22	0.001913
	118	0.25	0.00212
	64.5	0.2	0.0031
	74	0.6	0.00812
	83	1.0	0.0121
	90	1.4	0.0157
	95.5	1.8	0.0189
Specimen No. 1	100.5	2.2	0.022
	104.3	2.6	0.0249
	108.5	3.0	0.0277
	111.5	3.4	0.0305
	113.7	3.8	0.0334

no Euler deflection, but where the edges showed considerable deflection with increase in load. These deflections were measured by the pointers and were used to compute the critical load by Southwell's method.

TABLE 4 VALUES OF LOAD, WIDTH, AND σ_c FOR EACH SPECIMEN

Specimen No.	Load, <i>P</i>	Width	σ_c
1	147.3	1.0255	2875
2	102	0.6475	3145
3	65	2.0255	641
4	148	0.767	3860
5	73	0.6000	2435
6	52	0.545	1907
7	130	0.7175	3620
8	159	0.8455	3760
9	138.1	0.9735	2840
10	129.5	1.0355	2500
11	113.2	1.1595	1955
12	104.5	1.2855	1625
13	83.8	1.5385	1090
14	23	0.4050	1135
15	112	1.0825	2075
16	111.6	1.2215	1828
17	89.5	1.4005	1280
18	75	1.7705	847
19	156	0.8041	3880

The use of this method consisted first of tabulating the deflections, δ , against the loads, *P*, which caused them, and from this tabulation obtaining δ/P . Then δ was plotted against

¹² E. E. Lundquist, "The Compressive Strength of Duralumin Columns of Equal Angle Section," N.A.C.A. Technical Note 413, 1932.

δ/P on ordinary cross-section paper and the slope of a straight line faired through the points so obtained was measured. Southwell proves that this slope is equal to the critical load at which buckling would theoretically take place if there were no initial curvatures or eccentricities. Table 3 gives the values for δ and P obtained for five typical runs. For specimen No. 9 the method was applied with two sets of deflections, one covering a range of loadings from 60 to 120 pounds and the other from 120 to 136 pounds; the resulting P from each was very nearly the same. Fig. 16 shows the method of plotting these values for specimen No. 12, which was typical for all of them. Table 4 shows the load, width, and σ_c for each specimen.

Discussion

A. V. KARPOV.¹³ The advantages of monocoque aeroplane constructions created a considerable demand for data that could be directly applied in the design. The stability of such structures, as a whole, and of the individual members are the limiting factors that are of particular interest to designers. Recently a considerable amount of experimental work was done and data collected, which can be and is applied to solve a number of pressing design problems in connection with such structures.

So far as the development of theories underlying such designs are concerned, a very opportunistic point of view is generally taken.

If the developed theory does not directly contradict the results of tests, it is considered satisfactory. Stating it frankly, none of the stability theories developed in connection with monocoque designs is satisfactory and these theories can be considered as rough approximations only.

The paper is a valuable addition to the available experimental data but so far as the theory is concerned no addition is made to our present and very insufficient knowledge.

It would seem that the main efforts should be directed toward development of a more satisfactory theory. That, in all probability, could be done by developing a line of attack that is radically different from the ones used in the past.

The development of such a theory would make possible a better correlation of data of the numerous tests and provide a more scientific basis for future designs.

E. E. LUNDQUIST.¹⁴ The authors are to be congratulated upon their paper and the timely contribution to the knowledge of the strength of thin-metal structures. However, there is one point raised in the paper that ought to be amplified somewhat.

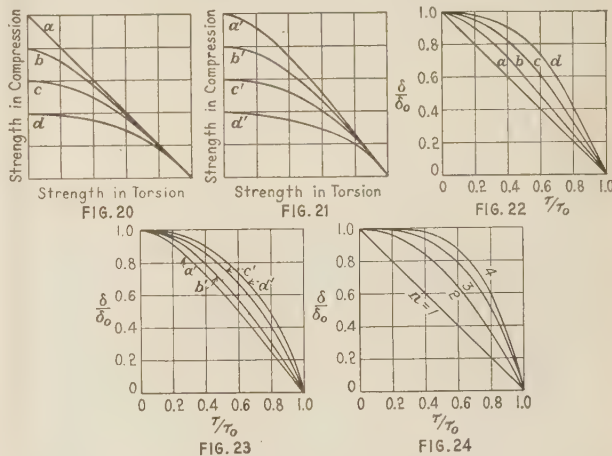
Toward the close of section I the authors make the following statements: "The values chosen for σ_0 and τ_0 have considerable influence on the value found for n , and it is probable that part of the variation in the values of n , found for different types of cylinders, is due to the inaccuracy of these values. In making this type of research it is important to make numerous pure compression and pure torsion tests (especially pure compression, because the scatter is much worse here than for torsion), in order to get a good average value for σ_0 and τ_0 ."

From this quotation it will be noted that n probably varies with the imperfections of the cylinders as these imperfections affect σ_0 and τ_0 as well as σ and τ . It therefore seems desirable to discuss the probable effects of imperfections upon the value of n .

In the course of an extensive series of tests on thin-walled cylinders made by the National Advisory Committee for Aeronautics at Langley Field, Virginia, it was found that the acci-

dental imperfections that occur in the cylinders do not affect greatly the strength in torsion, τ_0 . This fact has also been confirmed by tests made at the California Institute of Technology and elsewhere.^{15,16}

In these same tests at Langley Field it was found that the imperfections caused a very wide scattering of the strength in compression, σ_0 . This fact was also confirmed by tests made at the California Institute of Technology, the University of Illinois, and abroad.¹⁷



For the purpose of discussion let us assume that it is possible to construct and test perfect cylinders of identical dimensions. For these cylinders let us plot as abscissa the strength in torsion and as ordinate the strength in compression. Suppose, further, that it is found that the strength in combined compression and torsion is given by curve *a* in Fig. 20. Actually, it might be found that the true curve would be more like *a'* in Fig. 21, but for the purpose of discussion it is immaterial which curve is assumed.

Now, suppose that it is possible to control the imperfections. For a given degree of imperfection it is not likely that the new experimental curve would depart greatly from curve *a* near the torsion axis, but it is likely that the new curve will depart greatly from curve *a* near the compression axis. For a given degree of imperfection, we might, therefore, find the strength to be given by curve *b*, *c*, or *d*. Thus, such a Fig. as 20 or 21 shows clearly how imperfections affect the strength of cylinders in combined compression and torsion.

Now, plotting σ/σ_0 against τ/τ_0 , for the curves of Figs. 20 and 21 (the method used by the authors of the paper), Figs. 22 and 23 are obtained. It will be noted from reference to Figs. 22 and 23 that curves *a*, *b*, *c*, and *d* are reversed in order as compared to the corresponding curves in Figs. 20 and 21. If the authors' Equation [1] is presented in curve form with different values of n , Fig. 24 is obtained. In this figure it will be noted that the curves for the higher values of n correspond to the curves in the preceding figures for the imperfect cylinders. Thus, when a particular value of n is recommended for use with Equation [1] the corresponding value of σ_0 should be given. The value of 3 for n is probably a good average value for cylinders with the usual imperfections. However, with n equal to 3, σ_0 should not exceed the values obtained by the authors for the various radius-thickness ratios tested.

¹⁵ E. E. Lundquist, "Strength Tests on Thin-Walled Duralumin Cylinders in Torsion," N.A.C.A., 1932, T.N. No. 427.

¹⁶ L. H. Donnell, "Stability of Thin-Walled Tubes Under Torsion," N.A.C.A., 1933, T.R. No. 479.

¹⁷ E. E. Lundquist, "Strength Tests of Thin-Walled Duralumin Cylinders in Compression," N.A.C.A., 1933, T.R. No. 473.

¹³ Designing Engineer, Aluminum Company of America, Pittsburgh, Pa.

¹⁴ Junior Civil Engineer, Langley Field, Va.

Influence of Rate of Shear on Shearing Strength of Lead

By JAMES JAMIESON,¹ ANN ARBOR, MICH.

For many years the relationship between the velocity of deformation and the resulting stress has been occupying the attention of several investigators. In general, the tests have been made under uniform tensile- or compressive-stress conditions. It was with the object of investigating this relationship when under pure shear conditions that the work outlined in this paper was undertaken. Except for a few isolated cases, there are no results available with which comparisons may be made, but it appears from the tests made that the influence of the rate of deformation upon the ultimate strength is considerable. The results indicate that in all likelihood the same relationship that has been found to exist for conditions of direct stress will hold for conditions of pure shear. That is, the equation proposed by Ludwik, $\sigma = \sigma_1 + C \log (v/v_1)$, for the case of pure tension has been found to prove satisfactory for pure shear. Only one metal (lead) has been tested, but the results so found may be taken as representative of those materials with a low melting point. Further, in all probability the behavior of steels, when subjected to constant rates of shear and when maintained at some relatively high temperature, will lead to similar results.

THE influence of the velocity of deformation upon the strengths of materials has long been recognized, and a considerable amount of work has already been carried out in this field of investigation. One of the first to study this influence was P. Ludwik,² who, in 1909, suggested a mathematical formula to represent the relationship between the stress and the corresponding velocity of deformation. The equation which he then proposed, or later modifications of it,³ is accepted today as the most suitable mathematical expression available and is applicable over large ranges of speed; i.e., not only is it suitable to those tests where the velocity of deformation is appreciable, but it is also applied to creep testing where the rate of deformation is very low.

Ludwik carried out a series of tensile tests upon tin wires under various rates of deformation. These rates ranged from 5×10^{-2} per cent per second to 0.0485 per cent per second. From

consideration of the results of these tests he finally arrived at a suitable expression, of which the present-day interpretation is given as follows:

$$\sigma = \sigma_1 + C \log \frac{v}{v_1}$$

It should be noted that in this expression σ is the stress and v the corresponding rate of deformation, while σ_1 and v_1 and C are material constants.

Other investigators have also verified or shown independently that this expression represents the condition of stress at various rates of flow. In a paper published in 1930, R. W. Bailey⁴ adopted a logarithmic equation, similar to the foregoing equation, to express the relationship between stress and rate of creep. In a recent paper, H. Deutler⁵ also shows that this relationship holds for speeds very much greater than the ordinary speed of a slow tensile test. The rates of deformation investigated by Deutler varied from 0.001 per cent per second up to 1000 per cent per second.

Investigators have generally confined their research to narrower limits of speed variation, with the result that many of them adopt another mathematical expression in the treatment of their results. E. Siebel and A. Pomp⁶ tested steel, copper, and lead in compression over velocities of ratio 1:50, the greatest velocity being 1.25 per cent per second. The equation which they adopted is:

$$\sigma = \sigma_1 + C v^n$$

where σ is the stress, v the rate of deformation, and σ_1 , C , and n are material constants. This expression was first proposed by Ludwik, but later was rejected as unsuitable. He found that it is applicable only over a comparatively small range of speed.

From the results quoted here and from many others dealing with this problem, the general conclusion can be reached that the resistance to flow increases with the velocity of deformation. This increase, however, is insignificant in so far as materials such as mild steel are concerned when tests are made at room temperature and with velocities not of the order associated with impact. Should the temperature be increased or should the metal under consideration have a low melting point, then the same changes in speed of deformation may be accompanied by considerable changes in the acting stress. Except for the usual long-time creep tests, scarcely any investigations have been made to determine how the resistance to flow of steel varies with the rate of deformation when the rate is considerable and when the steel is maintained at some elevated temperature.

Since the temperature of recrystallization of lead is comparatively low, the results obtained from lead at ordinary temperature conditions may be taken as analogous to those obtained from

¹ Graduate student, Department of Engineering Mechanics, University of Michigan. Mr. Jamieson was graduated from the University of Glasgow, Scotland, in 1931, with the degree of B.Sc. in Mechanical Engineering.

² P. Ludwik, "Ueber den Einfluss der Deformationsgeschwindigkeit mit besonderer Berücksichtigung der Nachwirkungserscheinungen," *Phys. Zeitschr.*, 10, 1909, p. 411.

³ C. R. Soderberg, "Working Stresses," A.S.M.E. Trans., vol. 55, 1933, paper APM-55-16, p. 131.

Presented at the Semi-Annual Meeting of the American Society of Civil Engineers and THE AMERICAN SOCIETY OF MECHANICAL ENGINEERS, Chicago, Ill., June 26 to July 1, 1933, at a joint session of the A.S.C.E. Structural Division and A.S.M.E. Applied Mechanics Division. (This paper is part of a dissertation presented for the degree of Doctor of Philosophy in the University of Michigan. The experimental program was conducted in the Applied Mechanics Laboratory under the supervision of Prof. S. Timoshenko.)

NOTE: Statements and opinions advanced in papers are to be understood as individual expressions of their authors, and not those of the societies.

⁴ R. W. Bailey, "Thick-Walled Tubes and Cylinders Under High Pressure and Temperature," *Engineering*, vol. 129, 1930, p. 772.

⁵ H. Deutler, "Experimentelle Untersuchungen über die Abhängigkeit der Zugspannungen von der Verformungsgeschwindigkeit," *Phys. Zeitschr.*, vol. 33, 1932, p. 347.

⁶ E. Siebel and A. Pomp, "Einfluss der Formänderungsgeschwindigkeit auf den Verlauf der Fließkurve von Metallen," *Mitteilungen K.-W. Inst.*, vol. 10, 1928, p. 63.

materials with higher temperatures of recrystallization and when tested at elevated temperatures. It was with this analogy in mind that the investigation recorded herein was undertaken, and it is to be hoped that in the near future similar tests will be made upon steels at high temperatures.

It should be noticed also that as yet all tests have been made in tension or compression and that the behavior of metals subjected to a pure shearing action and deformed at some constant rate has



FIG. 1 GENERAL ARRANGEMENT FOR THE TESTING OF LEAD AT VARIOUS RATES OF DEFORMATION

been neglected. Further, since modern theories are in agreement that strengths of materials are intimately connected with the condition of shearing stresses in the metal, it has been thought reasonable to depart from the usual testing methods and to examine the relationship between strength and rate of deformation when materials are subjected to conditions of pure shear.

TESTING EQUIPMENT

The apparatus used in making this series of tests is a simple one and is illustrated in the photograph, Fig. 1, and in the line diagram, Fig. 2. It is an arrangement whereby tubular specimens of lead are sheared to destruction at various rates of deformation.

In the case of high-speed tests the necessary force is supplied by an 8-hp gasoline engine which carries two heavy flywheels and which runs at speeds up to 300 rpm. The specimen under test is fixed rigidly to one of the flywheels and rotates freely with it. At a specific speed, which is determined by use of a stroboscope, a clutch is thrown in, and this immediately brings one end of the specimen to rest. The inertia of the flywheels is such as to shear the specimen without any noticeable decrease in speed of the moving parts. The torque required for this shearing action is transmitted through the clutch to a dynamometer, which registers it through the medium of an Ames dial. A motion-picture camera is used to record the readings on the dial, and it is thus possible to investigate the effect of comparatively rapid rates of shear.

A more thorough explanation of the mechanism can be obtained from Fig. 2. Here grip *A* is fixed to the flywheel and is held in position by two keys and restrained so as to move only laterally. Tubular specimen *C* is gripped firmly in grips *A* and *B* such that *ACBD* forms one continuous member. *E* is the movable member of the clutch (*DE*), and while this can move laterally on the shaft, all rotation is eliminated by keys. The dynamometer *G* registers the applied load, and one end is fixed rigidly to the frame of the apparatus.

The specimen used is tubular, with an effective gage length of $\frac{1}{4}$ in. A fully dimensioned sketch of the test piece is given in

Fig. 3. It is held in position at each end by central pins and by four setscrews, each firmly holding a steel segment machined to fit the outside diameter of the tube.

In order to obtain much slower rates of deformation, use was made of the common type of torsion machine. This had two constant speeds, and, accordingly, the equipment described was used in cooperation with this machine.

The total range of speed over which tests were made was from 0.0312 rpm to 225 rpm, or 0.0135 radian per inch per second to 95 radians per inch per second—a ratio of 1:7000.

RESULTS

It is needless to enter into details with respect to the testing procedure, since the entire test is straightforward. It will be sufficient to add, however, that many tests were made, and all results were checked and rechecked several times.

Further, all the specimens were brought to a uniform condition by heating them in boiling water for a period of eight hours.

The calculation of the stresses is based upon the assumption that the stress is constant over the thickness of the tubular specimen. This is a reasonable assumption to make when the thickness of the tube wall is considered (0.055 in.). If *s* is the shear stress, *r* the mean radius of the tube, and *t* the thickness, then,

$$2\pi r^2 t s = T$$

where *T* is the torque which is measured by the dynamometer.

The results obtained from these tests are shown graphically in Fig. 4. It is at once apparent that variation in the rate of shear has an effect upon the strength of the material. The stresses found at the higher speeds at first appear somewhat confused. The curves, however, are of the same general shape, and upon further examination it will be seen that increasing speeds result in an increase in the strength of the metal. There is only one exception and that is the curve corresponding to a speed of 178 rpm (75.4 radians per inch per second). There is no explanation to account for this divergence, but, as will be

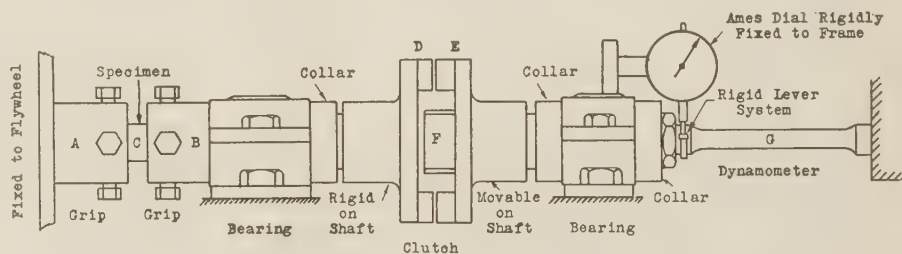


FIG. 2 APPARATUS USED FOR TESTING LEAD AT VARIOUS RATES OF SHEAR STRAIN

shown, this error is not so great as it might at first appear.

It is interesting to note the shape of the curves representing the two lowest speeds. In both cases it would appear that lead has some definite upper yield point. This point is characteristic of steels and has been found by many investigators, but as far as the author is aware, no one has recorded this peak for non-ferrous metals. Further, after this peak has been reached, the stress decreases continuously, first rapidly and then very slowly. This phenomenon of flow of lead at a constant speed at a constant

or decreasing stress has been observed by Siebel and Pomp. It may be explained by the fact that the temperature of recrystallization of lead is low and recrystallization occurs during the process of testing. To obtain recrystallization, a certain time must elapse, and naturally, therefore, this effect is more noticeable at low rates of deformation. This latter portion of the curve denotes, therefore, that the strain-hardening effect brought about by the deformation is compensated by the phenomenon of recrystallization. The curves given in Fig. 4 may be taken as fundamentally characteristic of the behavior of metals at comparatively high temperatures, although not necessarily above the temperature of recrystallization.

It should be noted also that the peak in the case of the higher rate of flow is displaced to the right and is not so sharply defined. From these two tests, therefore, it would seem that this upper yield point is most apparent at comparatively low rates of shear, while at high speeds, and with the equipment used, it cannot be detected at all. When tests at much lower speeds are carried out, it will be interesting

the lowest speed v_1 and the corresponding stress σ_1 at some particular value of deformation ($7\frac{1}{2}$ radians per inch), this equation takes the form:

$$\sigma = 1310 + 390 \log \frac{v}{0.0135}$$

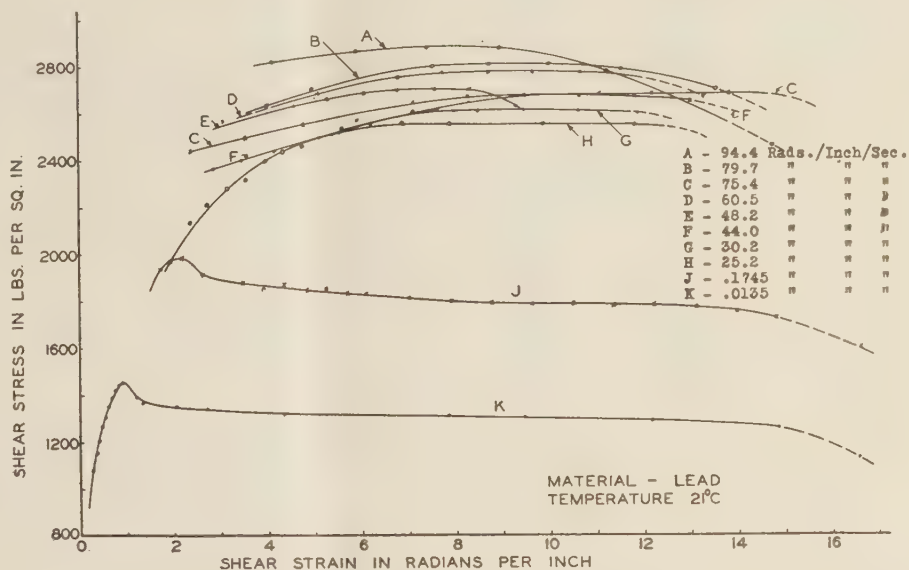


FIG. 4 CURVES SHOWING RELATIONSHIP BETWEEN STRESS AND STRAIN AT DIFFERENT RATES OF SHEAR STRAIN

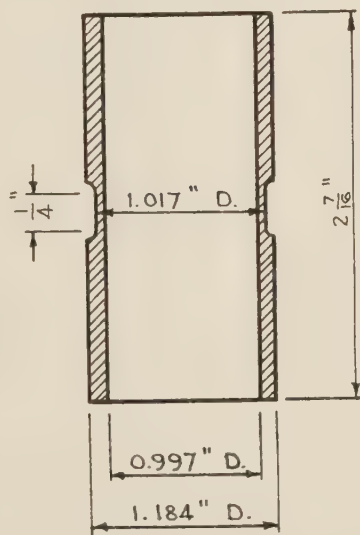


FIG. 3 CROSS-SECTION OF LEAD SPECIMEN

to note if this yield point becomes more pronounced or not.

In an endeavor to find a mathematical expression to represent the stresses found at various rates of shear, use has been made of the equation proposed by Ludwik:

$$\sigma = \sigma_1 + C \log \frac{v}{v_1}$$

This equation has been found to give results substantially in agreement with those found experimentally. By considering

By substituting values for v , the corresponding stress values σ are found. These results, tabulated against the experimental values, will be found in Table 1. From the small percentage errors listed there, there is no doubt that this expression is suitably adapted to the curves found by experiment. Similar calculations have been made at sections made in ordinates 6 and 11 radians per inch, and the corresponding results are shown in Tables 2 and 3, respectively. The agreement at the higher speeds is remarkable in view of the apparent irregularity the curves assume.

TABLE 1				
$(\sigma = 1310 + 390 \log (v/0.0135))$ when $\phi = 7\frac{1}{2}$ radians per inch)				
Velocity of shear	Calculated value of shear stress	Shear stress by experiment	Variation between σ and σ_E per cent	
rad./in./sec	lb/sq in.	lb/sq in.		
0.0135	1310	1310	0	
0.1745	1744	1798	3.0	
25.2	2588	2556	-1.2	
30.2	2615	2606	-0.4	
44.0	2680	2618	-2.4	
48.2	2700	2700	0	
60.5	2732	2763	1.1	
75.4	2772	2650	-4.5	
79.7	2783	2800	0.6	
94.4	2810	2875	2.3	
Average.....			-0.1	

The small variations in the stress values at high speeds illustrate that a change in velocity does not affect the resultant stress to any appreciable extent. It is for this reason that the curves at the higher rates of shear, although hardly symmetrical, give results in close agreement with those found by use of the aforementioned equation.

That a change in velocity at high speeds has comparatively little effect, is illustrated more clearly in Fig. 5, which is a graphical representation of the foregoing equation. The rate of the increase in strength at very low velocities of the order of 1 radian

TABLE 2

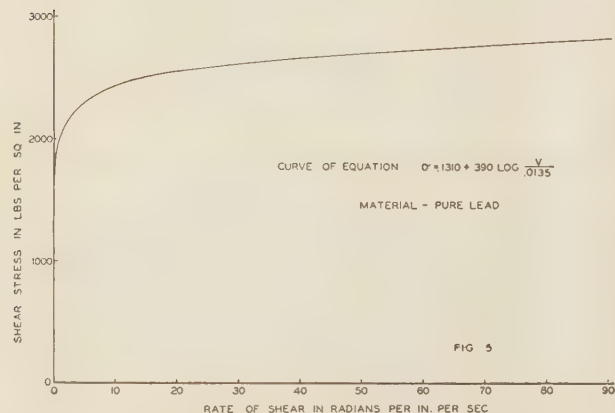
 $(\sigma = 1318 + 390 \log (v/0.0135) \text{ when } \phi = 6 \text{ radians per inch})$

Velocity of shear v rad./in./sec	Calculated value of shear stress σ lb./sq in.	Shear stress by experiment σE lb./sq in.	Variation between σ and σE per cent
0.0135	1318	1318	0
0.1745	1752	1820	3.7
25.2	2596	2540	-2.2
30.2	2623	2550	-2.9
44.0	2688	2550	-5.0
48.2	2708	2680	-1.0
60.5	2740	2725	-0.5
75.4	2780	2600	-6.9
79.7	2790	2750	-1.4
94.4	2818	2860	1.4
Average.....			-1.3

TABLE 3

 $(\sigma = 1295 + 390 \log (v/0.0135) \text{ when } \phi = 11 \text{ radians per inch})$

Velocity of shear v rad./in./sec	Calculated value of shear stress σ lb./sq in.	Shear stress by experiment σE lb./sq in.	Variation between σ and σE per cent
0.0135	1295	1295	0
0.1745	1729	1780	2.9
25.2	2573	2550	-1.0
30.2	2600	2610	0.4
44.0	2665	2680	0.6
48.2	2685
60.5	2717	2770	2.0
75.4	2757	2688	-2.5
79.7	2767	2795	1.1
94.4	2795	2790	-0.2
Average.....			0.3

FIG. 5 CURVE SHOWING RELATIONSHIP BETWEEN SHEAR STRESS AND RATE OF SHEAR ($\phi = 7\frac{1}{2}$ RADIAN PER INCH)

per inch per second is very great. At the higher velocities, say about 50 radians per inch per second, the slope of the curve is comparatively little, and accordingly variations in strength are decidedly less noticeable.

In view of the irregular shapes which the curves adopt at low values of deformation or degrees of twist, it can hardly be expected that this mathematical relationship will hold at all points. From consideration of these curves (Fig. 4) it may be said that, for the tests already made, Ludwik's general law is valid only over some specific range of deformation. From the results already quoted, however, there seems little doubt that this expression agrees closely with the stress values over an appreciable range of speed and of deformation. This degree of deformation can be taken to cover approximately all values between 5 and 12 radians per inch.

Although these results cannot be regarded as conclusive until a wider range of speed is covered, it may be said with every confidence that there exists a definite relationship between the shear strength of a metal and the rate of shear which it undergoes. There is every indication also that this relationship is similar to that already recognized as existing between tensile stress and the rate of deformation.

Discussion

H. HENCKY.⁷ The author shows experimentally that the form of the law of flow is the same for uniaxial stress as it is for pure shear. The flow of metals being quite independent of the comparatively very small volume changes, this result could be expected theoretically. However, on account of the probability that the plastic material becomes an isotropic, the experiments of the author are of considerable interest and should be exploited theoretically as much as possible.

It is to be regretted that the author did not try also the formula of Mr. Soderberg, which does not lead to obvious absurd results for small strain velocities. Perhaps the coincidence of experiment and formula would not be so striking in that case, but this coincidence has not such great value if the first part of the curve is uncertain.

As pointed out by the writer, the neglect of the elastic effects in relaxing materials is objectionable, especially in the region of small strains.

With this elastic effect taken into account, the curves A-H would have to be analyzed in a slightly different manner from the curves J and K.

P. G. McVETTY.⁸ In this study of the relation between stress and velocity of deformation, the author has made a valuable contribution to the knowledge of the subject. The use of a low melting material such as lead to simulate the action of steel at a relatively high temperature greatly facilitates the study of fundamental laws. Also, the conduct of tests in pure shear instead of tension gives results which are directly applicable to many practical problems.

The suggestion of the author that similar results may be expected in tests of steels at high temperature may require some qualification. The creep of metals at elevated temperatures usually represents an extremely small velocity of deformation, and no satisfactory proof that the same laws are applicable to low and high speeds has yet been presented. The fundamental investigations of Ludwik and of Cassebaum were not generally known in this country prior to the translation of Dr. Nadai's book⁹ in 1931. In referring to these investigations, Dr. Nadai was careful to avoid the use of the proposed relation between stress and velocity for very small velocities of flow. This is necessary because $\log v = -\infty$ when $v = 0$.

The minimum velocity of 0.0135 radian per inch per second is very rapid compared with creep rates of 10^{-9} to 10^{-6} per hour. While it is very interesting to have further verification of the conclusions of Ludwik, Cassebaum, and Deutler, especially when applied to shear, it does not necessarily follow that the same law will be applicable to creep of metals at elevated temperatures.

Various modifications of the Ludwik relation have been proposed, but none is entirely satisfactory. Soderberg¹⁰ suggests that (v/v_1) in the formula be changed to $(1 + v/v_1)$ to give a more rational interpretation at small creep rates. Dr. Nadai⁹ suggests for quite small velocities near zero, a linear relation between stress and creep rate, and for larger velocities the logarithmic relation. This would bring creep phenomena at low velocities within the laws of viscous flow.

The writer has tried many of the possible relations in studying creep-test data and in attempting to predict flow rates for low

⁷ Associate Professor of Mechanics, Massachusetts Institute of Technology, Cambridge, Mass. Mem. A.S.M.E.

⁸ Research Laboratories, Westinghouse Elec. & Mfg. Co., East Pittsburgh, Pa. Mem. A.S.M.E.

⁹ A. Nadai, "Plasticity," McGraw-Hill Book Company, New York, N. Y.

¹⁰ C. R. Soderberg, "Working Stresses." (See footnote 3.)

stresses. Promising results have been obtained, but a completely satisfactory substitute for the proposed relation is not available. Until these relations have been applied to data for many different kinds of material, it seems desirable to recommend caution in any extrapolation into the field of very low deformation velocities.

AUTHOR'S CLOSURE

Dr. Hencky has suggested that the results should be treated from the theoretical viewpoint as much as possible. The author is in complete agreement with Dr. Hencky on this point, but is confident that more tests should be made, and especially at low

rates of shear, in order to facilitate this work. He did not neglect the formula proposed by Mr. Soderberg, but found that his equation would require some modification before it could be used satisfactorily over a large range of rates of shear.

The author also thanks Mr. McVetty for the points he has raised and the references given. There is little doubt that insufficient data are at present available to enable one to predict stresses for different rates of flow, and especially so when referring to rates of deformation of very small magnitude. It is to be hoped that in the near future more extensive investigations will be made and that the results will provide a more satisfactory basis for calculation.

Wind Pressure on Buildings¹

By PROF. DR.-ING. O. FLACHSBART,² HANOVER, GERMANY

THE existing specifications for calculating wind pressure usually assume that the pressure normal to a plane surface is $W = w_0 A \sin^2 \alpha$, where α is the angle between the velocity of wind, which can be taken horizontal, and the surface, and w_0 is taken from 100 kg to 150 kg per sq m. Experiments show that such specifications are not satisfactory, since they do not take proper account of the actual conditions. For instance, in the case of hangars and roofs the action of suction forces usually remains without explanation. The aforementioned specifications are based on the old Newton theory which assumes that the wind pressure can be considered as the result of bombardment of particles. From this it follows that only the sides facing the wind are submitted to wind pressure and that wind action can consist only in some increase of pressure. Suction forces on the basis of this theory are impossible.

Expressions for wind force and wind pressure, as used in aerodynamics now, are $W = c_w \frac{\rho v^2}{2} \cdot A$ and $p_i = z_i \frac{\rho v^2}{2}$, where ρ is the air density—it is sufficiently accurate to take $\rho = 1/8$ (kg-sec²/m⁴); p_i is the wind pressure in kg/m²; while c_w and z_i are two numerical factors which are not constant but functions of stream condition; c_w is the coefficient of wind force, and z_i the coefficient of wind pressure. The investigation of wind forces consists in the determination of the functions c_w and z_i (problem of aerodynamics) and the determination of wind velocity (problem of aerology). An analytical solution of these problems does not exist at present. The solution of the same problems can be made by taking measurements on existing buildings, but this is a laborious and difficult method. A more feasible method of attack is the solution of the aerodynamical problem in a wind tunnel of an aerodynamical laboratory. This can be done by using models of buildings and by investigation of wind properties in natural conditions. The results of such investigations can be utilized in practical calculations of wind pressure only under the assumption that the results obtained on models can be applied in the case of actual buildings. The investigations show that the results obtained with models can be applied with sufficient accuracy in the case of such structures as houses, industrial buildings, and bridge trusses. In the case of structures without sharp edges, such as chimneys of circular cross-sections and cylindrical gas and liquid tanks, the problem

is more complicated, but in these cases also the model tests give important information. The usefulness of aerodynamical model tests is now generally recognized. There are numerous results from aerodynamical laboratories, which can be used for various shapes of buildings for calculating the numerical factors c_w and z_i . It is questionable whether sufficient knowledge regarding the properties of actual wind is available to apply the model tests in developing practical specifications.

It must be agreed that there are not many satisfactory aerological data. Since 1925 careful observations of weather stations have been made in Central Europe. On the basis of these, together with other reliable knowledge of aerology, the following statements regarding the wind problem can be made which will be of interest for structural engineers: The maximum velocity of 45 m/s was established by some reliable experiments which are applicable to Middle Europe conditions. Wind of 35 m/s happens often. Except in the lower strata, of 10 to 20 meters thick at the earth's surface, a uniform wind of constant velocity can be assumed with an accuracy sufficient for practical purposes. It is recommended to make calculations with velocity 40 m/s. This velocity should be reduced for the lower sheet of air in one or several steps, to the velocity 35 m/s (for windy regions 45 m/s and 40 m/s, respectively). There is the opinion that at the sea coasts the wind may have higher velocities. But this is not supported by aerological observations, and it is not recommended to introduce, for such cases, higher velocity requirements. In the case of very high structures which can be brought in oscillations by fluctuation of wind velocity it is necessary to increase the wind-pressure requirement. The new investigation showed that the dynamical effect of wind pressure is taken care of with sufficient accuracy by increasing the statical wind pressure by 20 to 30 per cent. Assuming wind velocity 40 m/s, i.e., $\rho v^2/2 = 100$ kg/m², it seems satisfactory to assume for slender structures such as chimneys, radio towers, and lighthouses, the wind velocity 45 m/s, i.e., $\rho v^2/2 = 125$ kg/m². Assuming these velocities, the wind pressures on structures can be calculated without difficulty on the basis of model experiments. In the paper several examples are discussed: Buildings with rectangular bases and with various shapes of roofing, open halls, bridge trusses, towers, chimneys, and gas containers. The experiments indicate in all cases the importance of suction forces. Cases of such forces acting on a roof and on cylindrical containers are discussed in the paper. Finally the author discusses the specifications for wind pressure and indicates rational ways of modifying such specifications so as to take into account actual conditions.

¹ Abstract of paper presented at the Semi-Annual Meeting, Chicago, Ill., June 26 to July 1, 1933, of THE AMERICAN SOCIETY OF MECHANICAL ENGINEERS.

² Technische Hochschule.

Design and Calculation of Steam-Turbine Disk Wheels

By I. MALKIN,¹ PHILADELPHIA, PA.

A simple procedure for calculation of steam-turbine disk wheels together with a discussion of some questions concerning their elastic resistance in various conditions is offered in the following article. New solutions of the problem of rotating disks are developed and their application in disk design is shown by practical examples. The resulting method in designing turbine disks is represented by a general scheme with a standard table.

INTRODUCTION

THE calculation of steam-turbine disk wheels often forms an actual problem of great importance in steam-turbine design, although many methods for the solution of the problem of rotating disks are known and used. To be of practical use in design and development, a satisfactory solution of the problems involved is expected to yield simple procedures and practical standards and to reduce the present cumbersome methods of stress calculation to a minimum of mathematical work. To develop new solutions of this kind is the main purpose of the present contribution.

By introducing certain new profile curves into the analytical form of the problem of rotating disks, formulas for the stresses are obtained, which are much simpler than those yielded by any other analytical solution of the problem. These curves are suggested by certain conditions of integrability of linear differential equations and are designated by the author as "exponential profiles." Due to the mathematical properties of the new formulas they easily admit of a simple and complete numerical representation by means of a "standard table," which when once calculated can be used in disk computations for any special given conditions. Such a table is presented in this paper for disks of the "first exponential profile." This will be followed in a later article by a similar table for the still more important "second exponential profile." Examples of disks of the new profiles with the corresponding stress distributions are given in Figs. 3 to 6.

Taking into consideration the varied wheel proportions resulting from modern blade dimensions, an additional investigation was necessary. This consisted of a revision of the mathematical fundamentals of disk design and a check of their validity under the new conditions. The approximate theory of rotating disks, developed by Stodola and used in this paper as in all calculations in disk design throughout the technical literature,

¹ Westinghouse Electric & Manufacturing Company, Dr. Malkin was the winner of the prize medal of the Technische Hochschule Berlin-Charlottenburg. His theoretical studies with Professor Dr. Max Planck and Professor Dr. R. von Mises at the University of Berlin were preceded by four years of practical work in mechanical engineering with industrial companies. Dr. Malkin was connected with the AEG-Turbinenfabrik, Berlin, in charge of research work in elasticity, especially in disk vibrations, and with the Institute of Applied Mathematics and Mechanics of Dr. R. von Mises at the University of Berlin. Since January, 1932, he has been connected with the Westinghouse Company, South Philadelphia Works.

Contributed by the Applied Mechanics Division and presented at the Annual Meeting, New York, N. Y., December 4 to 8, 1933, of THE AMERICAN SOCIETY OF MECHANICAL ENGINEERS.

NOTE: Statements and opinions advanced in papers are to be understood as individual expressions of their authors, and not those of the Society.

is based upon the results obtained from the exact methods of the mathematical theory of elasticity. These results are examined in Appendix No. 1.

The stresses in a turbine disk are usually calculated for overspeed conditions. A natural question arising in design is that concerning the stresses in the disk due to the fit pressure when the wheel is at rest; the design having been calculated originally for overspeed conditions. This particular problem admits of a simple general solution, as will be shown, by reducing the conditions to those of a disk of constant thickness at rest, the behavior of which is known. In this way we easily find that the profile curve has practically no influence on the stress distribution under static conditions; the tangential as well as the radial stresses at the bore being about 60 and 40 per cent, respectively, of the tangential stress at the bore in overspeed conditions. This result was checked on a system of disks of the "first exponential profile" and graphically represented by the curves in Fig. 8. These curves show the change in the radial and the tangential stresses at the bore corresponding to variations in the ratio of the disk thickness at the bore to that at the rim, under static conditions.

The discussion treating with the stress distribution in a disk at rest is completed by some general remarks concerning the problem of the stress variation with varying speed. This is in the interest of a better understanding of the elastic behavior of the disk under various conditions occurring in practical service.

The last section of this contribution deals with the influence of a hub relief, such as shown in Fig. 9, upon the stress distribution in the disk. The solution of this additional problem is graphically represented in Figs. 9 to 14 and may be expressed briefly as follows. In overspeed conditions no change of any practical importance is caused by a hub relief. Under static conditions, the stresses within the disk are smaller than in a disk without hub relief. Immediately at the bore the stresses undergo a certain modification, too, but the strength, as defined by Mohr's theory, is not affected.

THE FIRST EXPONENTIAL PROFILE

Consider the differential equation of rotating disks in the form [37],²

$$\frac{d^2u}{dr^2} + \left(\frac{1}{y} \frac{dy}{dr} + \frac{1}{r} \right) \frac{du}{dr} + \left(\frac{\nu}{y} \frac{dy}{dr} - \frac{1}{r} \right) \frac{u}{r} + \frac{\mu\omega^2(1-\nu^2)}{E} r = 0,$$

wherein E is Young's modulus of elasticity; ν , Poisson's ratio; ω , the angular velocity of the rotating disk given by the formula $30\omega = \pi n$, n being the number of revolutions per minute; μ , the specific mass of the disk material; r , the radius; $2y$, the thickness of the disk; and u the radial displacement. The coefficients of the differential equation, namely

$$\frac{\mu\omega^2(1-\nu^2)}{E} r = P; \quad \left(\frac{\nu}{y} \frac{dy}{dr} - \frac{1}{r} \right) \frac{1}{r} = P_0;$$

$$\frac{1}{y} \frac{dy}{dr} + \frac{1}{r} = P_1; \quad 1 = P_2,$$

² See Appendix No. 2.

being free of the function u , which is to be determined, a new profile $y = f(r)$ shall be introduced in using the following procedure suggested by elementary methods of integration of linear differential equations.³

By integrating the differential equation, term by term, according to the rules of partial integration we obtain

$$\int P dr + \int (P_0 - P_1 + P_2'') u dr + (P_1 - P_2') u + P_2 u' = 0$$

where $P_1' = dP_1/dr$, and so on. Hence the order of Equation [37] is lowered if $P_0 - P_1' + P_2'' = 0$, or

$$\frac{d}{dr} \left(\frac{1}{y} \frac{dy}{dr} \right) = \frac{\nu}{r} \left(\frac{1}{y} \frac{dy}{dr} \right)$$

This is a differential equation for the profile function y . Its solution is

$$y = \alpha e^{-\beta r^{1+\nu}} \dots \dots \dots [1]$$

where α and $-\beta$ are the two constants of integration. Only positive values of the constant β will be considered in studying the first exponential profile, for reasons which will be indicated.

For the profile [1] the original differential Equation [37] assumes the form

$$P_2 u' + (P_1 - P_2') u + \int P dr = 0$$

or

$$\frac{du}{dr} + \frac{1 - (1 + \nu)\beta r^{1+\nu}}{r} u + \frac{\mu \omega^2 (1 - \nu^2)}{2E} r^2 = C,$$

C being an arbitrary constant of integration.

In considering the reduced equation

$$\frac{du}{dr} + \frac{1 - (1 + \nu)\beta r^{1+\nu}}{r} u - C = 0$$

and putting temporarily $C = 0$ we find one of the two integrals of the reduced Equation [37]. This first integral is easily found to be

$$D \frac{e^{-\beta r^{1+\nu}}}{r} \dots \dots \dots [2]$$

D being again a constant of integration.

The particular integral corresponding to the term with ω^2 in original Equation [37] can now be determined by variation of the constant D occurring in the last integral. If ν is assumed to be equal to $1/3$, the particular integral appears in a finite form, namely

$$\frac{\mu \omega^2}{3E} r^3 \left[\frac{1}{\beta r^{4/3}} + \frac{2}{(\beta r^{4/3})^2} + \frac{2}{(\beta r^{4/3})^3} \right] \dots \dots \dots [3]$$

In using Equations [36]⁴ we find the corresponding expressions for the stresses. The last integral corresponding to the constant C , omitted before, can be determined as follows.⁵

Consider the homogeneous differential equation

$$r^2 \frac{d^2 \sigma_r}{dr^2} + r \left(3 + r \frac{1}{y} \frac{dy}{dr} \right) \frac{d\sigma_r}{dr} + \left[(2 + \nu) r \frac{1}{y} \frac{dy}{dr} + r^2 \frac{d}{dr} \left(\frac{1}{y} \frac{dy}{dr} \right) \right] \sigma_r = 0 \dots \dots \dots [4]$$

³ A. Forsyth, "Differential Equations," German edition, Braunschweig, 1912, p. 101.

⁴ See Appendix No. 2.

⁵ A. R. Forsyth, "Differential Equations," German edition, Braunschweig, 1912, p. 573.⁶

corresponding to the differential Equation [42], for the stress σ_r .⁶ We may restrict ourselves to the consideration of the homogeneous equation, because the particular integral corresponding to ω^2 is determined by [3].

By introducing our new profile [1] into Equation [4] and in using $z = \beta r^{4/3}$ as a new independent variable, we have, because of

$$r \frac{d}{dr} = \frac{4}{3} z \frac{d}{dz}, \quad r^2 \frac{d^2}{dr^2} = \frac{16}{9} \left(z^2 \frac{d^2}{dz^2} + \frac{1}{4} z \frac{d}{dz} \right),$$

the differential equation

$$z^2 \frac{d^2 \sigma_r}{dz^2} + \frac{1}{4} z (10 - 4z) \frac{d\sigma_r}{dz} - 2z \sigma_r = 0 \dots \dots \dots [5]$$

instead of Equation [4].

By following the method indicated by theory,⁶ we find that the last integral can be represented by an infinite series of the form

$$a_0 + a_1 z + a_2 z^2 + a_3 z^3 + \dots + a_n z^n + \dots \dots \dots [6]$$

Furthermore it is known from the teachings of the theory of functions of a complex variable, that the domain of convergency of this series is determined by that point (singular point) nearest to $z = 0$, for which the coefficient of $d^2 \sigma_r / dz^2$ in [5] vanishes. This coefficient being z^2 , the radius of convergency will be equal to ∞ ; the Series [6] will converge for any finite value of $z = \beta r^{4/3}$. Indeed, by introducing Series [6] into Equation [5] we find

$$\frac{a_n}{a_{n-1}} = \frac{1}{n} \frac{n+1}{n+3/2} \dots \dots \dots [7]$$

This shows that our Series [6] converges faster than that for the exponential function e^z , the ratio a_n/a_{n-1} in the latter case being equal to

$$\frac{a_n}{a_{n-1}} = \frac{1}{n}$$

As the series for e^z converges in the entire complex plane, our Series [6] converges even faster. From [7] we obtain by introducing $n = 1, 2, 3, 4, \dots$,

$$a_1 = \frac{4}{5} \frac{1}{1!}; \quad a_2 = \frac{4 \cdot 6}{5 \cdot 7} \frac{1}{2!}; \quad a_3 = \frac{4 \cdot 6 \cdot 8}{5 \cdot 7 \cdot 9} \frac{1}{3!};$$

$$a_4 = \frac{4 \cdot 6 \cdot 8 \cdot 10}{5 \cdot 7 \cdot 9 \cdot 11} \frac{1}{4!} \dots \dots$$

where

$$n! = 1 \cdot 2 \cdot 3 \cdot 4 \cdot \dots \cdot n$$

Correspondingly, the third integral for σ_r appears in the form

$$\varphi_2(z) = 1 + \frac{4}{5} \frac{z}{1!} + \frac{4 \cdot 6}{5 \cdot 7} \frac{z^2}{2!} + \frac{4 \cdot 6 \cdot 8}{5 \cdot 7 \cdot 9} \frac{z^3}{3!} + \frac{4 \cdot 6 \cdot 8 \cdot 10}{5 \cdot 7 \cdot 9 \cdot 11} \frac{z^4}{4!} + \dots \dots \dots [8]$$

In substituting this series into Equation [35] we find the expression

$$\frac{4 \cdot 6 \dots 2n(2n+2)}{5 \cdot 7 \dots (2n+3)} \left[1 - \frac{2}{3} \frac{n}{n+1} \right] \frac{z^n}{n!}$$

as the general term of the series representing the third integral for σ_r , which is, accordingly, given by

⁶ See Appendix No. 2.

$$\psi_2(z) = 1 + \frac{4}{5} \frac{2}{3} \frac{z}{1!} + \frac{4 \cdot 6}{5 \cdot 7} \frac{5}{9} \frac{z^2}{2!} + \frac{4 \cdot 6 \cdot 8}{5 \cdot 7 \cdot 9} \frac{1}{2} \frac{z^3}{3!} + \frac{4 \cdot 6 \cdot 8 \cdot 10}{5 \cdot 7 \cdot 9 \cdot 11} \frac{7}{15} \frac{z^4}{4!} + \dots [9]$$

By introducing the Integrals [2] and [3] for the displacement u in Equations [36] we find the corresponding integrals for the stresses σ_r and σ_t , and in using those integrals as well as expressions [8] and [9] we obtain the complete solution in the form

$$\sigma_r = Ar^2 f(z) + K\varphi_1(z) + L\varphi_2(z) \dots [10]$$

$$\sigma_t = Ar^2 g(z) + K\psi_1(z) + L\psi_2(z) \dots [11]$$

where K and L are arbitrary constants to be determined from the boundary conditions, while A is given by

$$A = \frac{1}{12} \mu \omega^2,$$

μ being the mass density and ω the angular velocity, and

$$f(z) = \frac{9}{z} + \frac{6}{z^2} - \frac{6}{z^3} \quad g(z) = \frac{7}{z} + \frac{10}{z^2} + \frac{6}{z^3}$$

$$\varphi_1(z) = e^z \frac{2z-1}{z^{3/2}} \quad \psi_1(z) = e^z \frac{2/3z+1}{z^{3/2}}$$

the profile curve being given by formula [1].

The functions $f(z)$, $g(z)$, $\varphi_1(z)$, $\varphi_2(z)$, $\psi_1(z)$, $\psi_2(z)$ can be calculated once for all and put together into a "standard table" to be used in practical design. Such a "standard table" is given in the next section and is followed by a detailed example of disk calculations.

GENERAL PROCEDURE IN DESIGNING DISKS OF THE FIRST EXPONENTIAL PROFILE

The results of the foregoing section can be summarized as follows: For a disk of the profile

$$y = \alpha e^{-\beta r^{4/3}}$$

the radial stress σ_r and the tangential stress σ_t can be represented by the formulas

$$\sigma_r = Ar^2 f(z) + K\varphi_1(z) + L\varphi_2(z); \quad \sigma_t = Ar^2 g(z) + K\psi_1(z) + L\psi_2(z) \dots [12]$$

where

$$z = \beta r^{4/3} \dots [13]$$

$$\beta = \frac{2.303}{a^{4/3} - r_0^{4/3}} \log_{10} \left(\frac{h_0}{h_a} \right) \dots [14]$$

h_0 and h_a being the boundary values of y , while

$$A = \frac{1}{12} \mu \omega^2$$

where μ = mass density and ω = angular velocity, K and L being constants determined by two conditions concerning the boundary stresses (see operation 4). The functions $f(z)$, $g(z)$, $\varphi_1(z)$, $\varphi_2(z)$, $\psi_1(z)$, $\psi_2(z)$ finally follow from the "standard table."

The general procedure will consist of the following operations (see Fig. 1):

(1) From the values of r_0 , a and h_a , which usually are given in practical design, and h_0 , which has to be assumed and varied, the constant β is to be calculated according to [14].

(2) With the constant β the values of z at the bore and at

the rim are to be calculated from [13], i.e., $z_0 = \beta r_0^{4/3}$, $z_a = \beta a^{4/3}$.

(3) For these two values of z the corresponding values of the functions $f(z)$, $g(z)$, $\varphi_1(z)$, $\varphi_2(z)$, $\psi_1(z)$, $\psi_2(z)$ are to be taken from the "standard table" and introduced into formulas [12].

(4) From the two boundary conditions, $\sigma_r = 0$ (or $\sigma_r = -p_0$, where p_0 is a comparatively small amount; see example in the following section) at the bore ($r = r_0$), and $\sigma_r = \sigma_{ra}$, where σ_{ra} is a given amount following from the centrifugal forces of the blading for $r = a$, Equations [12] yield the corresponding values of the constants K and L .

(5) With these values of the constants K and L the stresses σ_r and σ_t can be calculated easily for any point z by using Equations [12] and the "standard table."

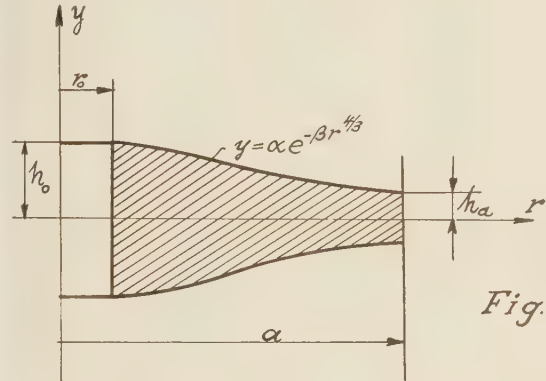


Fig. 1

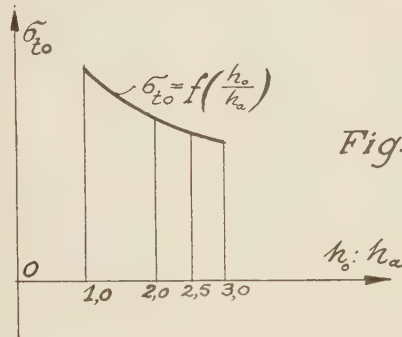


Fig. 2

FIGS. 1 AND 2

Further practical rules are given in the next section which covers a detailed example of disk design.

Finally it should be noted that, for practical purposes, it is of some advantage to introduce $r^2 = z^{3/2} \beta^{-3/2}$ into the terms $Ar^2 f(z)$ and $Ar^2 g(z)$ in Equations [12]. These terms then appear in the form $A\beta^{-3/2} F(z)$ and $A\beta^{-3/2} G(z)$, respectively, where F and G are functions of z only. The stresses, [12], then are independent of r , being functions of z , of β determined by [14], and of the constants K and L (boundary conditions).

PRACTICAL EXAMPLE OF DISK DESIGN—FIRST EXPONENTIAL PROFILE

We present now, following the general scheme given in the last section, a practical example of disk design which involves solving a problem characterized by the following data:

A disk is to be calculated for $r_0 = 6.75$ in., $a = 18.75$ in., the width at the rim, determined by the dimensions of the blading, being $b = 2h_a = 4$ in., while the working speed is $n = 3600$ rpm and the pull exerted by the centrifugal forces of the blading at 20 per cent overspeed is $\sigma_r = 13,000$ lb per sq in. for $r = a$.

STANDARD TABLE FOR DISKS OF THE FIRST EXPONENTIAL PROFILE

z	$f(z)$	$g(z)$	$\varphi_1(z)$	$\psi_1(z)$	$\varphi_2(z)$	$\psi_2(z)$
0	—	—	—	—	1.0000	1.0000
0.01	—593910.0000	6100700.0000	—989.8500	1016.7878	1.0080	1.0054
0.02	—728550.0000	775350.0000	—346.2690	365.5067	1.0161	1.0107
0.03	—215255.5555	223566.6666	—186.4090	202.2745	1.0243	1.0162
0.04	—89775.0000	100235.0000	—119.6920	133.5710	1.0326	1.0216
0.05	—45420.0000	52140.0000	—84.6203	97.1567	1.0409	1.0271
0.06	—25961.1111	30671.1111	—63.5790	75.1387	1.0493	1.0327
0.07	—16139.6426	19647.5199	—49.8007	60.6103	1.0577	1.0383
0.08	—10668.7500	13368.7500	—40.2156	50.4292	1.0662	1.0439
0.09	—7389.7119	9542.7982	—33.2304	42.9563	1.0748	1.0496
0.10	—5310.0000	7070.0000	—27.9587	37.2783	1.0835	1.0550
0.11	—3930.2012	5497.9696	—23.8659	32.8409	1.0923	1.0610
0.12	—2980.5555	4225.0000	—20.6139	29.2935	1.1011	1.0668
0.13	—2306.7290	3376.5495	—17.9790	26.4017	1.1100	1.0727
0.14	—1816.1832	2746.7961	—15.8100	24.0079	1.1190	1.0785
0.15	—1451.1135	2268.8915	—13.9991	21.9987	1.1280	1.0845
0.16	—1174.2186	1899.2186	—12.4686	20.2920	1.1372	1.0904
0.17	—960.6935	1608.4434	—11.1609	18.8269	1.1464	1.0964
0.18	—793.6180	1376.3327	—10.0334	17.5584	1.1557	1.1025
0.19	—661.1848	1188.6070	—9.0529	16.4544	1.1651	1.1086
0.20	—555.0000	1035.0000	—8.1935	15.4765	1.1745	1.1147
0.21	—469.1427	907.9636	—7.4356	14.6142	1.1841	1.1209
0.22	—398.6078	801.9126	—6.7623	13.8467	1.1937	1.1271
0.23	—340.5840	712.6055	—6.1617	13.1603	1.2034	1.1334
0.24	—292.3549	636.7936	—5.6221	12.5417	1.2132	1.1397
0.25	—252.0000	572.0000	—5.1361	11.9843	1.2231	1.1461
0.26	—218.0009	516.2246	—4.6958	11.4787	1.2331	1.1525
0.27	—189.4683	468.2058	—4.2949	11.0175	1.2431	1.1589
0.28	—164.6505	425.8751	—3.9294	10.5975	1.2533	1.1655
0.29	—143.6336	389.0549	—3.5941	10.2120	1.2635	1.1720
0.30	—125.5551	356.6661	—3.2861	9.8580	1.2738	1.1786
0.31	—109.9346	328.0398	—3.0017	9.5318	1.2842	1.1852
0.32	—96.3863	302.6362	—2.7388	9.2305	1.2947	1.1920
0.33	—84.5894	279.9977	—2.4947	8.9517	1.3053	1.1987
0.34	—74.1617	259.6280	—2.2677	8.6931	1.3160	1.2055
0.35	—65.2436	241.5737	—2.0560	8.4524	1.3268	1.2123
0.36	—57.3038	225.2043	—1.8580	8.2283	1.3376	1.2192
0.37	—50.3008	210.4173	—1.6725	8.0194	1.3485	1.2262
0.38	—44.1100	197.0166	—1.4982	7.8238	1.3596	1.2332
0.39	—38.6229	184.8422	—1.3341	7.6408	1.3708	1.2403
0.40	—33.7500	173.7500	—1.1794	7.4694	1.3820	1.2474
0.41	—29.4099	163.6137	—1.0331	7.3084	1.3933	1.2545
0.42	—25.5424	154.3402	—0.8946	7.1572	1.4048	1.2617
0.43	—22.0848	145.8272	—0.7633	7.0147	1.4163	1.2690
0.44	—18.9890	137.9965	—0.6384	6.8806	1.4280	1.2763
0.45	—16.2139	130.7818	—0.5195	6.7539	1.4397	1.2837
0.46	—13.7213	124.1178	—0.4062	6.6343	1.4516	1.2911
0.47	—11.4797	117.9529	—0.2979	6.5214	1.4635	1.2986
0.48	—9.4616	112.2390	—0.1944	6.4147	1.4756	1.3061
0.49	—7.6420	106.9335	—0.0952	6.3136	1.4877	1.3137
0.50	—6.0000	102.0000	—0.0000	6.2177	1.5000	1.3214
0.51	—4.5162	97.4031	+ 0.0915	6.1299	1.5124	1.3291
0.52	—3.1745	93.1146	0.1794	6.0407	1.5249	1.3368
0.53	—1.9606	89.1087	0.2642	5.9588	1.5374	1.3447
0.54	—0.8611	85.3600	0.3459	5.8812	1.5502	1.3526
0.55	+ 0.1353	81.8481	0.4249	5.8074	1.5630	1.3605
0.56	1.0388	78.5528	0.5013	5.7371	1.5759	1.3685
0.57	1.8582	75.4575	0.5753	5.6703	1.5889	1.3766
0.58	2.6016	72.5473	0.6469	5.6068	1.6021	1.3847
0.59	3.2765	69.8056	0.7165	5.5464	1.6153	1.3929
0.60	3.8888	67.2225	0.7841	5.4888	1.6287	1.4011
0.61	4.4419	64.7836	0.8499	5.4339	1.6422	1.4094
0.62	4.9496	62.4800	0.9139	5.3817	1.6559	1.4178
0.63	5.4074	60.2517	0.9763	5.3319	1.6696	1.4262
0.64	5.8228	58.2398	1.0371	5.2845	1.6834	1.4347
0.65	6.1994	56.2857	1.0966	5.2392	1.6974	1.4433
0.66	6.5407	54.4327	1.1547	5.1961	1.7115	1.4519
0.67	6.8496	52.6740	1.2116	5.1550	1.7258	1.4606
0.68	7.1292	51.0019	1.2673	5.1159	1.7401	1.4693
0.69	7.3836	49.4088	1.3218	5.0786	1.7546	1.4781
0.70	7.6094	47.9007	1.3754	5.0430	1.7692	1.4870
0.75	8.4445	41.3331	1.6297	4.8890	1.8442	1.5325
0.80	8.9062	36.0938	1.8662	4.7691	1.9225	1.5797
0.85	9.1227	31.8461	2.0899	4.6774	2.0044	1.6287
0.90	9.1769	28.3539	2.3045	4.6092	2.0899	1.6797
0.95	9.1237	25.4468	2.5133	4.5518	2.1792	1.7326
1.00	9.0000	23.0000	2.7183	4.5005	2.2727	1.7876
1.05	8.8306	20.9200	2.9216	4.4515	2.3701	1.8447
1.10	8.6326	19.1359	3.1248	4.4135	2.4722	1.9042
1.15	8.4178	17.5937	3.3292	4.3762	2.5787	1.9659
1.20	8.1944	16.2499	3.5360	4.3402	2.6902	2.0301
1.25	7.9680	15.0720	3.7462	4.3057	2.8065	2.0969
1.30	7.7424	14.0327	3.9608	4.2720	2.9283	2.1663
1.35	7.5202	13.1108	4.1807	4.2392	3.0555	2.2385
1.40	7.3032	12.2888	4.4065	4.2079	3.1885	2.3135
1.45	7.0926	11.5520	4.6390	4.1781	3.3275	2.3917
1.50	6.8889	10.8890	4.8791	4.1491	3.4729	2.4729
1.55	6.6926	10.2896	5.1272	4.1204	3.6250	2.5575
1.60	6.5039	9.7461	5.3841	4.0920	3.7839	2.6454
1.70	6.1490	8.7993	5.9270	4.0385	4.1238	2.8323
1.80	5.8231	8.0042	6.5132	4.0000	4.4955	3.0318
1.90	5.5241	7.3291	7.1481	3.9657	4.9021	3.2546
2.00	5.2500	6.7500	7.8373	3.9342	5.3468	3.4922
2.10	4.9983	6.2488	8.5869	3.9052	5.8355	3.7500
2.20	4.7671	5.8113	9.4036	3.8783	6.3688	4.0300
2.30	4.5541	5.4269	10.2941	3.8531	6.9511	4.3350
2.40	4.3576	5.0867	11.2663	3.8288	7.5889	4.6650
2.50	4.1760	4.7840	12.3271	3.8054	8.2882	5.0240

In using our "first exponential profile" [1] we find, according to operation 1 of the scheme, given in the last section,

$$\beta = \frac{2.303}{18.75^{4/3} - 6.75^{4/3}} \log_{10} \left(\frac{2h_0}{4} \right) = 0.062 \log_{10} \left(\frac{2h_0}{4} \right)$$

By varying the ratio $2h_0/4$ within the limits 2 and 3, respectively, we obtain the corresponding values of β and, according to operation 2 of the scheme, those of $z_0 = \beta r_0^{4/3}$, $z_a = \beta a^{4/3}$ from the following table:

TABLE 1

$2h_0/4.0$	β	z_0	z_a
2.0	0.0187	0.238	0.930
2.5	0.0247	0.315	1.230
3.0	0.0296	0.378	1.475

Now we introduce the boundary conditions according to operations 3 and 4 of the scheme. We first require that, at the overspeed $n_0 = 1.2 \times 3600 = 4320$ rpm, the pressure between the shaft and the disk should disappear, that is, the radial stress σ_r must be equal to zero at the bore ($r = r_0$) for $n_0 = 4320$ rpm, while at the rim ($r = a$) the disk is affected by a radial stress $\sigma_r = 13,000$ lb per sq in., as indicated above. The stresses are given by formulas [12], wherein the constant A is

$$A = \frac{1}{12} \mu \omega_0^2 = \frac{1}{12} \times 7.33 \times 10^{-4} \left(4320 \times \frac{\pi}{30} \right)^2 = 12.5$$

From the boundary conditions

$$\sigma_{r0} = 12.5 \times 6.75^2 f(z_0) + K \varphi_1(z_0) + L \varphi_2(z_0) = 0$$

for $r = r_0 = 6.75$ in.

$$\sigma_{ra} = 12.5 \times 18.75^2 f(z_a) + K \varphi_1(z_a) + L \varphi_2(z_a) = 13,000$$

for $r = a = 18.75$ in.

we find

$$K = \frac{\Phi_K}{\Phi} \quad L = \frac{\Phi_L}{\Phi}$$

where

$$\Phi = \begin{vmatrix} \varphi_1(z_0) & \varphi_2(z_0) \\ \varphi_1(z_a) & \varphi_2(z_a) \end{vmatrix} = \varphi_1(z_0) \times \varphi_2(z_a) - \varphi_1(z_a) \times \varphi_2(z_0)$$

$$\Phi_K = \begin{vmatrix} Z_0 & \varphi_2(z_0) \\ Z_a & \varphi_2(z_a) \end{vmatrix} = Z_0 \times \varphi_2(z_a) - Z_a \times \varphi_2(z_0)$$

$$\Phi_L = \begin{vmatrix} \varphi_1(z_0) & Z_0 \\ \varphi_1(z_a) & Z_a \end{vmatrix} = \varphi_1(z_0) \times Z_a - \varphi_1(z_a) \times Z_0$$

and

$$Z_0 = -569f(z_0) \quad Z_a = 13,000 - 4395f(z_a)$$

In using our "standard table" we find by interpolation the values which are tabulated in Table 2. (See page 589.)

Correspondingly we will have from our Formula [12], the following approximate values:

TABLE 3

No.	$2h_0/4.0$	σ_{10} (lb/in. ²)
1	2.0	59,000
2	2.5	52,500
3	3.0	49,500

As a result of our preliminary calculations, we obtain the curve shown in Fig. 2, representing the tangential stress σ_{t0} at the bore as a function of the ratio $h_0/h_a = 2h_0/4.0$ for given constant values of $\sigma_r = 0$ at the bore ($r = r_0$) and $\sigma_r = 13,000$ lb per sq in. at the rim ($r = a$), re-

TABLE 2

z_0	$f(z_0)$	Z_0	$\varphi_1(z_0)$	$\varphi_2(z_0)$	z_a	$f(z_a)$	Z_a	$\varphi_1(z_a)$	$\varphi_2(z_a)$	$g(z_0)$	$\psi_1(z_0)$	$\psi_2(z_0)$
0.238	-300	171,000	-5.75	1.22	0.930	9.15	-27,200	2.43	2.15	650	12.65	1.14
0.315	-108	61,500	-2.85	1.30	1.230	8.05	-22,400	3.65	2.77	323	9.35	1.19
0.378	-46	25,900	-1.55	1.36	1.475	7.00	-17,800	4.75	3.40	200	7.85	1.24

spectively. For $2h_0/4.0 = 1$ the ordinate is calculated from the known formulas for the disk of constant thickness inasmuch as the use of those for our exponential profile requires, in this special case, a complicated passage to the limit $\beta \rightarrow 0$.

Even by the approximate result represented by Fig. 2 the conclusion is justified, that the rate of the decrease in the amount of the tangential stress at the bore is getting smaller and smaller with the increase in the value of the ratio h_0/h_a . This result can be assumed to be of general character although it is obtained here for a special case.

From the diagram Fig. 2 we have now to decide upon the value of $h_0/h_a = 2h_0/4.0$ on the basis of the maximum admissible value of σ_{t0} . The question of the maximum admissible working stress at the bore in overspeed conditions will not be discussed here generally. For our example we consider $\sigma_{t0} = 52,500$ lb per sq in. as a permissible amount for the tangential stress at the bore for 20 per cent overspeed, corresponding to the value $h_0/h_a = 2.5$. Then we will have

$$\beta = 0.0247$$

from Table 1, giving a profile curve represented by

$$y = \alpha e^{-\beta z} \quad z = 0.0247r^{4/3} \quad 0.315 \leq z \leq 1.230$$

according to the same table. The constant α is given by

$$\alpha = y_{r=a} e^{1.230} = \frac{1}{2} \times 4e^{1.230} = 6.842$$

Now we use again our "standard table" of the first exponential profile and obtain the following table:

TABLE 4

z	y (in.)	r (in.)	$f(z)$	$g(z)$	$\varphi_1(z)$	$\psi_1(z)$	$\varphi_2(z)$	$\psi_2(z)$
0.30	5.07	6.50	-125.555	356.666	-3.286	9.858	1.274	1.179
0.60	3.76	10.94	3.889	67.223	0.784	5.489	1.629	1.401
0.90	2.78	14.83	9.177	28.354	2.305	4.609	2.090	1.680
1.10	2.28	17.21	8.633	19.136	3.125	4.514	2.472	1.904
1.25	1.96	18.94	7.968	15.072	3.746	4.579	2.807	2.097

Instead of the given limiting radii $r_0 = 6.75$ in. and $\alpha = 18.75$ in., we introduced in this table boundary values of r approximately equal to r_0 and a , respectively, which in our "standard table" correspond to tabulated values of z and its functions $f(z)$, $g(z)$, $\varphi_1(z)$, $\varphi_2(z)$, $\psi_1(z)$, $\psi_2(z)$. The reasons for this procedure are as follows.

In using interpolations as indicated above, we multiply by large numbers the errors introduced by these interpolations in the course of our calculations. Considerable inaccuracy can be caused hereby in the results. It is much better, therefore, to proceed in the way shown in our Table 4, namely, to use numbers tabulated in the "standard table" without interpolations. Naturally, some deviations will be caused by the fact that, in the special example treated, the boundary conditions actually refer to $z_0 = 0.315$ and $z_a = 1.230$, according to the Tables 1 and 2, and not to $z_0 = 0.30$ and $z_a = 1.25$, according to Table 4. But these deviations will be smaller generally than the errors produced by interpolations. And, besides, these deviations due to inaccuracy in fulfilling the boundary conditions are of negligible order, because in practical cases those boundary values cannot be stated very accurately anyway.

In using Table 4, with the approximate values of z_0 and z_a as given by the first and the last lines of that table, respectively, we find that

$$r_0 = 6.50 \text{ in.}$$

$$a = 18.94 \text{ in.}$$

Correspondingly, with $\sigma_{r0} = -500$ lb per sq in. for $r = r_0$ at the overspeed, $Z_0 = -500 + 12.5 \times 6.50^2 \times 125.56 = 65,900$ instead of $Z_0 = 61,500$ in Table 2; $Z_a = 13,000 - 12.5 \times 18.94^2 \times 7.968 = -22,750$ instead of $Z_a = -22,400$

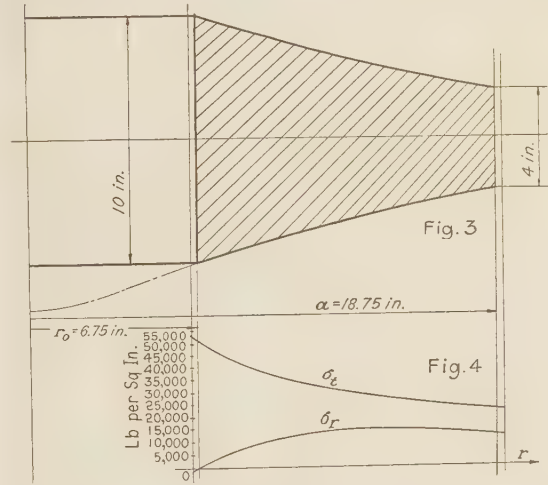
in Table 2. Therefore

$$\Phi = \begin{vmatrix} -3.286 & 1.2738 \\ 3.746 & 2.8065 \end{vmatrix} = -13.99$$

$$\Phi_K = \begin{vmatrix} 65,900 & 1.2738 \\ -22,750 & 2.8065 \end{vmatrix} = 213,900; K = -15,280$$

$$\Phi_L = \begin{vmatrix} -3.286 & 65,900 \\ 3.746 & -22,750 \end{vmatrix} = -172,000; L = 12,300$$

With these values of K and L we obtain from Table 4 the following



FIGS. 3 AND 4

stress distribution in using the stress Formulas [12], according to operation 5 of the scheme given in the last section:

TABLE 5

r (in.)	y (in.)	σ_r (lb/in. ²)	σ_t (lb/in. ²)
6.50	5.07	-500	52,400
10.94	3.76	13,850	34,200
14.83	2.78	15,700	28,200
17.21	2.28	14,600	25,200
18.94	1.96	13,000	23,400

The profile curve as given by the first two columns of this table is represented by Fig. 3. The stress distribution according to the third and the fourth columns of Table 5 is shown in Fig. 4.

According to the general conclusions drawn in Appendix No. 1 the maximum tangential stress at the bore will be about 5 per cent larger than the average amount given in our Table 5. The maximum stress, therefore, in our example will be about 55,000 lb per sq in.

As to the profile curve, it does not differ appreciably from a straight line. This, obviously, will be still more nearly the case for disks with a ratio $h_0/h_a < 2.5$, the radial dimensions being of the same order as in the example treated.

THE SECOND EXPONENTIAL PROFILE

If the foregoing method of developing the first exponential profile be applied to Equation [41],⁷ a new solution is obtained

⁷ See Appendix No. 2.

characterized by a profile curve for which

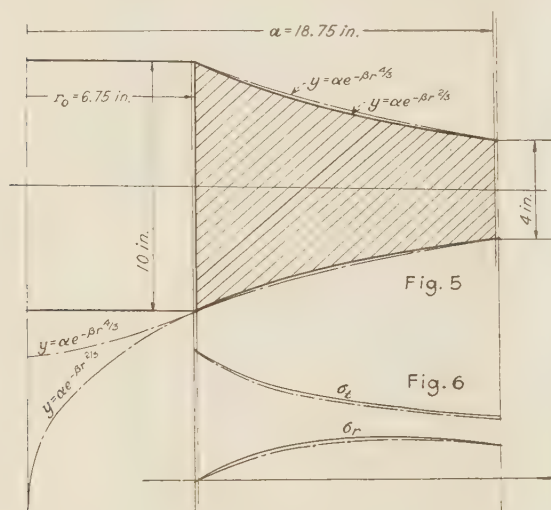
$$y = \alpha e^{-z} \quad z = \beta r^{2/3} \quad (\beta \leq 0) \dots \dots [15]$$

and which may be designated as the "second exponential profile." The stresses are, with $\nu = 1/3$, given by the expressions

$$\sigma_r = \frac{3A}{z^3} + B \frac{e^z}{z^3} (-6 + 6z - 3z^2) + \frac{\mu\omega^2}{12\beta^3} (60 + 45z + 18z^2) \dots \dots [16]$$

$$\sigma = -\frac{A}{z^3} (3 + 2z) + B \frac{e^z}{z^3} (6 - 2z - z^2) + \frac{\mu\omega^2}{12\beta^3} (60 + 35z + 12z^2) \dots \dots [17]$$

where A and B are the two arbitrary constants of integration, while β is determined by the ratio h_0/h_a ; h_0 and h_a being again



FIGS. 5 AND 6

the values of y at the bore ($r = r_0$) and at the rim ($r = a$), respectively.

This solution is remarkable for the fact that both of the stresses as well as the profile are given by finite expressions; as to the exponential function e^z , occurring in those expressions, it is tabulated very extensively. Therefore the formulas of the "second exponential profile" can be used for steep profile curves as well; that is, for curves characterized by large values of β . This is of some practical advantage for calculation of the disk part connecting the wheel with the rim. For such a part β has a large negative value, in either of both profiles, and the formulas of the "first exponential profile" cannot be used, because in the vicinity of such β values the series occurring in the stress expressions converge very slowly. Formulas [16] and [17] are, of course, free of such objections. This explains why positive values of $(-\beta)$ were not considered in our Formulas [1], [10], and [11]. It must be remarked, however, that the stress formulas are the less accurate, the steeper the profile curve becomes.

By tabulating the functions

$$f(z) = 60 + 45z + 18z^2;$$

$$\varphi_1(z) = \frac{3}{z^3}; \quad \varphi_2(z) = \frac{e^z}{z^3} (-6 + 6z - 3z^2)$$

$$g(z) = 60 + 35z + 12z^2; \quad \psi_1(z) = -\frac{3 + 2z}{z^3};$$

$$\psi_2(z) = \frac{e^z}{z^3} (6 - 2z - z^2)$$

all calculations can be accomplished in the manner outlined for the "first exponential profile."

COMPARISON OF THE TWO PROFILES

It is, of course, of practical interest to compare the two exponential profiles. Suppose

$$y_{II} = \alpha_{II} e^{-\beta_{II} r^{2/3}} \quad \text{and} \quad y_{II} = \alpha_{II} e^{-\beta_{II} r^{2/3}}$$

are the profile curves joining the point $r = r_0$, $y = y_0$ with the point $r = a$, $y = y_a$. Then we will have

$$\alpha_{II} e^{-\beta_{II} r_0^{2/3}} = \alpha_{II} e^{-\beta_{II} a^{2/3}} \quad \text{and} \quad \alpha_{II} e^{-\beta_{II} a^{2/3}} = \alpha_{II} e^{-\beta_{II} a^{2/3}}$$

From these two equations we find

$$y_{II}/y_I = e^{\beta_I(a^{2/3} - r^{2/3})} (r_0^{2/3} - r^{2/3})$$

This equation shows that y_{II} is always smaller than y_I , provided that at the boundaries ($r = r_0$ and $r = a$) y_I and y_{II} are, respectively, equal to each other. The profile curve y_I has a horizontal, and the profile curve y_{II} a vertical tangent at the point $r = 0$ (see Fig. 5).

PRACTICAL EXAMPLE OF DISK DESIGN—SECOND EXPONENTIAL PROFILE

As an example we treat here the same problem, as in the last section, in using our "second exponential profile." The procedure is essentially the same as indicated in the scheme given above for the "first exponential profile" and we find, for $h_0/h_a = 2.5$,

$$\beta = \frac{2.303}{18.75^{2/3} - 6.75^{2/3}} \log_{10} 2.5 = 0.263$$

We introduce the values $z_0 = 0.93$; $z_a = 1.86$ into our further calculations, according to the practical rules given in the last section. By substituting

$$\sigma_r = -250 \text{ lb per sq in. for } z = z_0 = 0.93$$

$$\sigma_r = 13,200 \text{ lb per sq in. for } z = z_a = 1.86$$

we find from Equations [16] and [17]

$$A = 53,200 \quad \text{and} \quad B = 29,400$$

With these values of the constants A and B and with that of β the following table is obtained by using some intermediate values of z :

TABLE 6

z	σ_r (lb/in. ²)	σ_t (lb/in. ²)	r (in.)	y (in.)
0.93	-250	53,000	6.65	5.07
1.00	4,650	47,400	7.42	4.75
1.25	13,700	36,300	10.37	3.68
1.50	17,000	30,800	13.60	2.87
1.75	14,800	26,600	17.15	2.23
1.86	13,200	24,500	18.85	2.00

The profile and the stress distribution according to this table are shown in Figs. 5 and 6, respectively. For a comparison with the results obtained above for the "first exponential profile" (see the first example) the profile curve and the stress distribution, represented by Figs. 3 and 4, respectively, are shown dotted in Figs. 5 and 6.

A "standard table" for the "second exponential profile" will be available later.

STRESSES DUE TO FIT PRESSURE—ELASTIC RESISTANCE WITH VARYING SPEED

The boundary conditions for the problem of stresses (p_r , p_t) in a disk due to fit pressure in resting conditions are⁸

$$p_t - p_r = \sigma_{t0} \text{ for } r = r_0 \text{ and } p_r = 0 \text{ for } r = a$$

where σ_{t0} is the tangential stress at the bore for $\omega = \omega_0$ (overspeed). With these boundary conditions the problem is to be confined to special profiles. It is, however, possible to draw general conclusions from the following consideration.

For a disk of constant thickness the general solution for stresses due to fit pressure under static conditions is given by the formulas⁹

$$p_r = -\frac{C_1}{r^2} + C_2; \quad p_t = \frac{C_1}{r^2} + C_2$$

($C_1 = \text{const.}$ and $C_2 = \text{const.}$)

By introducing the boundary conditions given above, we find

$$p_r = \frac{1}{2} \sigma_{t0} \left(\frac{r_0}{a} \right)^2 \left[1 - \left(\frac{a}{r} \right)^2 \right]; \quad p_t = \frac{1}{2} \sigma_{t0} \left(\frac{r_0}{a} \right)^2 \left[1 + \left(\frac{a}{r} \right)^2 \right] \dots [18]$$

where $2r_0$ and $2a$ are the bore and the rim diameter, respectively. The stress distribution given by [18] is shown graphically in Fig. 7. The formulas [18] together with Fig. 7 admit of a simple interpretation. As soon as the ratio a/r_0 exceeds a certain value, say $a/r_0 \geq 3$, the stress distribution according to the curves p_r and p_t in Fig. 7 does not vary essentially with varying a . The maximum values of p_r and p_t always take place at the bore, and these maximum values are always about 40 to 60 per cent respectively of the maximum tangential stress σ_{t0} at the bore under overspeed conditions. In other words, only the parts of the disk in the vicinity of the bore are essentially carrying the fit loading under static conditions, an increase of the outer radius a being of little influence on the functions [18].¹⁰

This result can be easily generalized for disks of other profiles. We have only to realize that the disk of constant thickness investigated above can be subdivided into several separate rings; the larger the diameter of any of them, the less its influence on the stress distribution of the whole disk under static conditions, as shown above, and the less, consequently, the stress variations in the disk due to the reduced thickness of that ring as compared with the original thickness of the parallel sided disk. This means that the statement developed above for disks of constant thickness is qualitatively and, with a certain approximation, also quantitatively true for disks of any profile.

This general result shall be checked now in calculating, for a special disk, the stresses p_r and p_t due to fit pressure under static conditions. The question may be treated on a somewhat more general basis by considering the disk as rotating with varying speeds. This is useful for a better understanding of the elastic behavior of the disk in various conditions of the actual service.

Having the general solution for rotating disks in the form

$$\sigma_r = A\omega^2 h_1(r) + Lf_1(r) + Mg_1(r)$$

$$\sigma_t = A\omega^2 h_2(r) + Lf_2(r) + Mg_2(r)$$

where A is a certain constant determined by the profile, while

⁸ See Appendix No. 2.

⁹ A. Stodola, "Steam Turbines," sec. 76, Eq. 22, with $\omega = 0$ and $A = 0$.

¹⁰ Cf. A. Föppl, Festigkeitslehre, Sect. 56 ("Dickwandige Roehren").

L and M are arbitrary constants of integration and $f_1(r)$, $f_2(r)$, $g_1(r)$, $g_2(r)$, $h_1(r)$, $h_2(r)$ are the integral functions for the profile considered, the boundary conditions are to be stated from which the constants L and M should follow as functions of the speed ω .

Designate by $p_r(\omega)$ and $p_t(\omega)$ the disk stresses as functions of ω . They usually are calculated for the overspeed $\omega = \omega_0$ and appear then as functions of r , so that, with our former designations,

$$p_r(\omega_0) = \sigma_r \quad \text{and} \quad p_t(\omega_0) = \sigma_t$$

The boundary conditions for σ_r and σ_t are, as we know,

$$\left. \begin{aligned} \sigma_r &= 0 \text{ for } r = r_0 \\ \sigma_r &= \sigma_a \text{ for } r = a \end{aligned} \right\} \text{at the overspeed } \omega = \omega_0$$

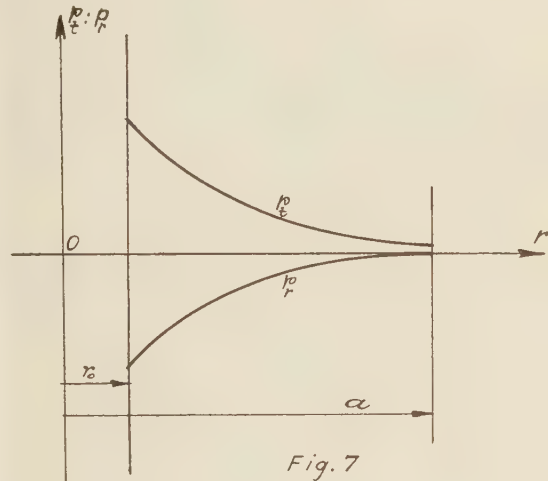


Fig. 7

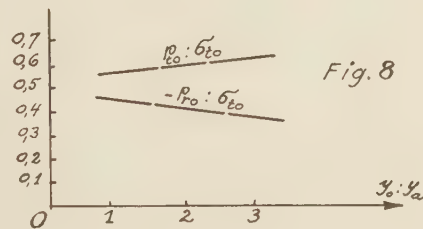


Fig. 8

FIGS. 7 AND 8

where r_0 and a are the radii of the bore and the rim respectively, while σ_a designates the radial tension at the rim exerted by the centrifugal forces of the blading at the overspeed. These boundary conditions for σ_r result in a corresponding value of σ_t at the bore, equal to σ_{t0} , and from the values of σ_{r0} and σ_{t0} at the bore, for $\omega = \omega_0$, the boundary conditions [43] and [44] for $p_r = p_r(\omega = 0)$ and $p_t = p_t(\omega = 0)$ under static conditions are obtained, as shown in Appendix No. 2. Now, by using the same manner of reasoning we find the condition

$$p_t(\omega) - p_r(\omega) - \frac{1}{4} (1 - \nu) \mu \omega^2 r_0^2 = K \quad (\text{for } r = r_0)$$

where K is a constant independent of the speed ω , to be true for any speed ω . This condition can be written, with close approximation, in the form¹¹

$$p_t(\omega) - p_r(\omega) = \text{const.} = \sigma_{t0} \quad (\text{for } r = r_0) \dots [19]$$

¹¹ See Appendix No. 2.

where σ_{t0} is the tangential stress at the bore ($r = r_0$) for $\omega = \omega_0$ (overspeed). At the outer boundary, $r = a$, we will have

$$p_r(\omega)(r=a) = \sigma_a \frac{\omega^2}{\omega_0^2} \quad (\text{for } r=a) \dots \dots \dots [20]$$

where σ_a is the value indicated above. The boundary conditions [19] and [20] are to be introduced into

$$\left. \begin{aligned} p_r(\omega) &= A\omega^2 h_1(r) + Lf_1(r) + Mg_1(r) \\ p_t(\omega) &= A\omega^2 h_2(r) + Lf_2(r) + Mg_2(r) \end{aligned} \right\} \dots \dots \dots [21]$$

from which we obtain

$$\left. \begin{aligned} \sigma_{t0} &= A\omega^2 [h_2(r_0) - h_1(r_0)] + L[f_2(r_0) - f_1(r_0)] \\ &\quad + M[g_2(r_0) - g_1(r_0)] \\ \sigma_a \frac{\omega^2}{\omega_0^2} &= A\omega^2 h_1(a) + Lf_1(a) + Mg_1(a) \end{aligned} \right\} \dots [22]$$

These are two equations for the two constants L and M . These constants of integration, therefore, appear as functions of the speed ω and in consequence the problem of stress distribution in terms of the speed is solved.

For the disk of constant thickness, for instance, we have

$$\begin{aligned} A &= -\frac{1}{8}\mu; \quad h_1(r) = (3 + \nu)r^2; \quad h_2(r) = (1 + 3\nu)r^2; \\ &\quad f_1(r) = f_2(r) = 1; \\ g_1(r) &= -\frac{1}{r^2}; \quad g_2(r) = \frac{1}{r^2} \end{aligned}$$

Correspondingly, the equations¹² for L and M are

$$\begin{aligned} \sigma_{t0} &= \frac{1}{2}(1 - \nu)\mu\omega^2 r_0^2 + \frac{2}{r_0^2}M = \sim \frac{2}{r_0^2}M \\ \sigma_a \frac{\omega^2}{\omega_0^2} &= -\frac{3 + \nu}{8}\mu\omega^2 a^2 + L - \frac{M}{a^2} \end{aligned}$$

and the constants of integration are

$$M = \frac{1}{2}r_0^2\sigma_{t0}; \quad L = \sigma_a \frac{\omega^2}{\omega_0^2} + \frac{3 + \nu}{8}\mu\omega^2 a^2 + \frac{1}{2}\left(\frac{r_0}{a}\right)^2\sigma_{t0}$$

So we finally have for the disk of constant thickness

$$\begin{aligned} p_r(\omega) &= \frac{3 + \nu}{8}\mu\omega^2(a^2 - r^2) + \frac{1}{2}r_0^2\left(\frac{1}{a^2} - \frac{1}{r^2}\right)\sigma_{t0} + \sigma_a \frac{\omega^2}{\omega_0^2} \\ p_t(\omega) &= \frac{1}{8}\mu\omega^2[(3 + \nu)a^2 - (1 + 3\nu)r^2] \\ &\quad + \frac{1}{2}r_0^2\sigma_{t0}\left(\frac{1}{a^2} + \frac{1}{r^2}\right) + \sigma_a \frac{\omega^2}{\omega_0^2} \end{aligned}$$

representing the stresses for any speed between $\omega = 0$ and $\omega = \omega_0$, provided that σ_{t0} and σ_a are the tangential stress at the bore and the radial stress at the rim, respectively, at the overspeed. If $\omega = 0$ is substituted, the solution as developed above applies to stresses due to fit pressure under static conditions.

Referring to the general Equations [21] for $p_r(\omega)$ and $p_t(\omega)$ and Equations [22] for the constants L and M as functions of the speed ω for any profile, it is easily seen that both stresses always can be represented in the form

$$F_1(r) + \omega^2 F_2(r)$$

where $F_1(r)$ and $F_2(r)$ are certain functions of r . In other words, the stresses vary proportionally to ω^2 , the proportionality factor being a function of r .

¹² See Appendix No. 2.

If we substitute $\omega = 0$ in the general Equations [22] and calculate the corresponding values of L and M , the following expressions for the stresses due to fit pressure under static conditions are obtained from [21]:

$$\left. \begin{aligned} p_r(0) &= \frac{\sigma_{t0}[g_1(a)f_1(r) - f_1(a)g_1(r)]}{g_1(a)[f_2(r_0) - f_1(r_0)] - f_1(a)[g_2(r_0) - g_1(r_0)]} \\ p_t(0) &= \frac{\sigma_{t0}[g_1(a)f_2(r) - f_1(a)g_2(r)]}{g_1(a)[f_2(r_0) - f_1(r_0)] - f_1(a)[g_2(r_0) - g_1(r_0)]} \end{aligned} \right\} \dots \dots [23]$$

According to the general statement developed above these stresses must reach amounts of about

$$p_{r0}(0) = \sim -0.40\sigma_{t0} \quad p_{t0}(0) = \sim 0.60\sigma_{t0}$$

respectively, at the bore, for any profile, if $a \geq 3r_0$. By substituting $r = r_0$ into [23] we find

$$\left. \begin{aligned} p_{r0}(0) &= \frac{\sigma_{t0}[g_1(a)f_1(r_0) - f_1(a)g_1(r_0)]}{g_1(a)[f_2(r_0) - f_1(r_0)] - f_1(a)[g_2(r_0) - g_1(r_0)]} \\ p_{t0}(0) &= \frac{\sigma_{t0}[g_1(a)f_2(r_0) - f_1(a)g_2(r_0)]}{g_1(a)[f_2(r_0) - f_1(r_0)] - f_1(a)[g_2(r_0) - g_1(r_0)]} \end{aligned} \right\} \dots \dots [24]$$

These formulas shall be applied to our "first exponential profile"

$$y = \alpha e^{-\beta r^{4/3}}$$

for a special example. Consider a disk with $a = 21$ in., $r_0 = 7$ in., while the ratio y_0/y_a may vary between 1 and 3. For $y_0/y_a = 1$ the formulas for disks of constant thickness are to be used. Generally we will have

$$\beta = \frac{2.303}{a^{4/3} - r_0^{4/3}} \log_{10} \left(\frac{y_0}{y_a} \right)$$

With the given values of a and r_0 we find the values of z_0 and z_a according to the formulas

$$z_0 = \beta r_0^{4/3} \quad z_a = \beta a^{4/3}$$

and then, by using the "standard table," with the symbols φ_1 , φ_2 , ψ_1 , and ψ_2 , occurring in that table, the corresponding values of f_1 , f_2 , g_1 , and g_2 are obtained as follows:

TABLE 7

y_0/y_a	z	$f_1 = \varphi_1$	$f_2 = \psi_1$	$g_1 = \varphi_2$	$g_2 = \psi_2$
2.0	$\begin{cases} z_0 = 0.208 \\ z_a = 0.902 \end{cases}$	$\begin{cases} -7.5 \\ 2.3 \end{cases}$	$\begin{cases} 14.6 \\ 4.6 \end{cases}$	$\begin{cases} 1.19 \\ 2.10 \end{cases}$	$\begin{cases} 1.12 \\ 1.69 \end{cases}$
3.0	$\begin{cases} z_0 = 0.330 \\ z_a = 1.430 \end{cases}$	$\begin{cases} -2.5 \\ 4.5 \end{cases}$	$\begin{cases} 9.0 \\ 4.8 \end{cases}$	$\begin{cases} 1.31 \\ 3.28 \end{cases}$	$\begin{cases} 1.20 \\ 2.36 \end{cases}$

By substituting these values in Formulas [24] we find the ratios $p_{r0}(0)/\sigma_{t0}$ and $p_{t0}(0)/\sigma_{t0}$ for the exponential profile with $y_0/y_a = 2$ and $y_0/y_a = 3$, respectively. For the disk of constant thickness the aforementioned ratios are to be found from the Formulas [18]. The results obtained in this way are set forth in the following table:

TABLE 8

y_0/y_a	$p_{r0}(0)/\sigma_{t0}$	$p_{t0}(0)/\sigma_{t0}$
1	-0.444	0.556
2	-0.397	0.603
3	-0.369	0.631

These results are graphically represented in Fig. 8. From these it is evident that, even for $r_0/a = 1/3$, the stresses due to fit pressure under static conditions do not depend essentially on the form of the disk; which is in full accordance with the statement developed above. The quantitative agreement with the result yielded by the general consideration is very satisfactory.

An important result is expressed, furthermore, by Equation [19] in its original physical meaning. The strength of an elastic

body is characterized, according to the well-known theory of Otto Mohr, by the difference of the largest and the smallest of the three principal stresses. The axial stress σ_z , i.e., the principal stress along the axial direction, being approximately equal to zero, the difference at the bore will be always equal to $p_t - p_r$, because at the bore $p_{r0}(\omega) \leq 0$ and $p_{t0}(\omega) > 0$. According to Equation [19] this difference in stress values at the bore is always the same at any speed. Therefore, we have, with close approximation, the general result, that the strength of the disk at the bore is always the same at any speed ω within the limits $0 \leq \omega \leq \omega_0$.

DISK WITH HUB RELIEF

An instructive example for application of the results developed in the last section will be obtained by studying stress conditions in disks with hub relief as shown in Fig. 9.

First consider a disk designed without hub relief (Fig. 10). The corresponding stresses may be represented by Fig. 11, the boundary conditions being given, for $\omega = \omega_0$, by the relations

$$\left. \begin{aligned} \sigma_r &= \sigma_{r0} \text{ for } r = r_0 \\ \sigma_t &= \sigma_a \text{ for } r = a \end{aligned} \right\} \dots \dots \dots [25]$$

where σ_a is the tension due to the centrifugal forces of the blading. Of course, the stress curves in Fig. 11 are also completely determined, if the conditions [25] are replaced by

$$\left. \begin{aligned} \sigma_r &= \sigma_a \text{ for } r = a \\ \sigma_t &= \sigma_{ta} \text{ for } r = a \end{aligned} \right\} \dots \dots \dots [26]$$

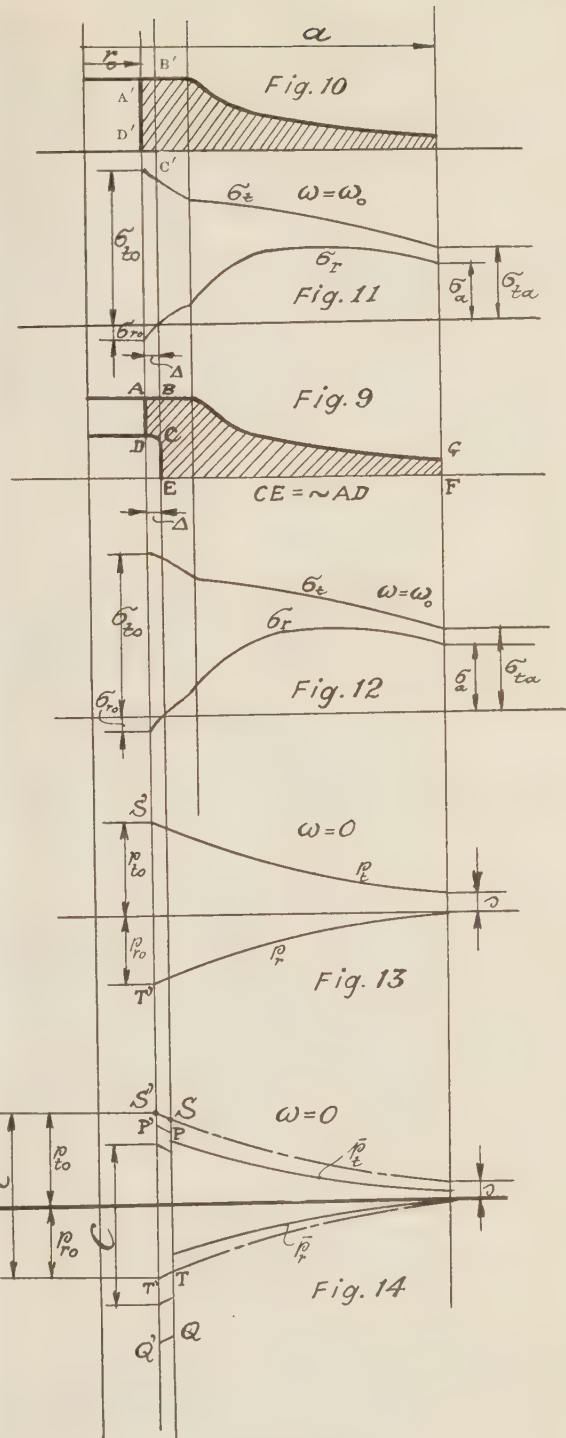
In other words, the stress curves are completely determined if two conditions are to be fulfilled corresponding to the two constants of integration occurring in the general expressions for the stresses.

Now consider the same disk with a hub relief according to Fig. 9. We require again the conditions covered by Equations [26] to be fulfilled. As these two relations determine the stress curves, we will have the same stress diagram (see Fig. 12) in the new conditions, as in Fig. 11, as long as the disk profile is the same, i.e., from $r = a$ to $r = r_0 + \Delta$, where $r_0 + \Delta$ is the radius corresponding to the point where σ_r vanishes in Fig. 11. This restriction (the vanishing of σ_r for $r = r_0 + \Delta$) will be removed below.

As to the stresses in the disk, or rather ring, represented by the section $ABCD$, it is easy to see that the radial stress is equal to zero at the outer edge BC . Indeed, the radial stress being zero at the edge BE of the disk $BGFE$, the equilibrium requires that the same be the case along BC in the disk $ABCD$. The tangential stress along BC in the same small disk is determined, as well known, by the condition that the tangential elongation ϵ_t at the cylindrical section BC must be the same for both disks. This elongation being given by the formula

$$\epsilon_t = \frac{\sigma_t - \nu \sigma_r}{E} \dots \dots \dots [27]$$

the stress σ_t must be the same on both sides of BC , since σ_r is the same on both sides. In other words, neither σ_r nor σ_t can jump at the outer edge BC of the disk $ABCD$. So both of the boundary values of σ_r and σ_t are known at the outer edge BC of the small disk, and the stresses are completely determined, therefore, for the part between $r = r_0$ and $r = r_0 + \Delta$ according to previous statements. Furthermore, these boundary values being the same in Fig. 9 (for the ring $ABCD$) and Fig. 10 (for the ring $A'B'C'D'$) the stresses within the part between $r = r_0$ and $r = r_0 + \Delta$ must be the same in both cases. Therefore



FIGS. 9 TO 14

the stress distribution for Fig. 12 is identical with that for Fig. 11.

This result is developed on the basis that $\sigma_r = 0$ for $r = r_0 + \Delta$ in Fig. 11, i.e., that the depth of the hub relief is equal to the distance Δ at the end of which σ_r vanishes in the disk without hub relief. If $\sigma_r = \delta$ for $r = r_0 + \Delta$ in Fig. 11, where δ is a small amount, positive or negative, then σ_r jumps in Fig. 12, and we will have

$$\sigma_r = \delta \frac{BE}{BC} \dots \dots \dots [28]$$

to the left of BC . The corresponding value of σ_t follows from the jump $\theta\sigma_t$ of σ_t according to our Equation [27]:

$$\theta\sigma_t = \nu\delta \frac{BE}{BC} \dots \dots \dots [29]$$

As δ is a small amount anyway, the stresses do not jump essentially at the section BC and the whole consideration above is practically not affected at all. This means that under rotating conditions no change in stress distribution is caused by the hub relief.

Now consider both disks, with and that without hub relief, under static conditions. The stress distribution in the latter is represented by Fig. 13 in accordance with our previous considerations, and we know, that

$$p_{t0} - p_{r0} = \sigma_{t0} - \sigma_{r0} \quad (\text{for } r = r_0)$$

or approximately

$$p_{t0} - p_{r0} = \sigma_{t0} \quad (\text{for } r = r_0)$$

σ_{r0} being of negligible amount. The stress distribution in the disk with hub relief under static conditions is again determined by the boundary conditions given above. These are that at the outer edge we must have

$$p_r = 0 \quad (\text{for } r = a)$$

while at the bore ($r = r_0$) the difference of both stresses p_t and p_r must be the same at any speed ω . Therefore, under static conditions, this difference must be, with reference to Fig. 12

$$p_{t0} - p_{r0} = \sigma_{t0} - \sigma_{r0} \cong \sigma_{t0} \quad (\text{for } r = r_0)$$

and the question is, to determine, in an approximate way, the stress distribution satisfying the last two boundary conditions in the disk shown in Fig. 9. Starting with the outer edge $r = a$ in Fig. 14 we state, that for the disk part $BEFG$ (Fig. 9) the stress distribution is completely determined if we assume a certain value of p_t for $r = a$, p_r being equal to zero at that point. Assuming p_t to be of the same amount s as in Fig. 13 at the outer edge $r = a$, we find, of course, the same stress curves p_r and p_t in Fig. 14, as in Fig. 13, for $r_0 + \Delta \leq r \leq a$. At the point $r = r_0 + \Delta$ the stresses σ_r and σ_t jump, according to Equations [28] and [29], from the points S and T to the points P and Q , respectively. Since

$$SP = \nu \times TQ$$

according to [28] and [29], we will have

$$P'Q' > S'T' = p_{t0} - p_{r0} \dots \dots \dots [30]$$

This shall be proved as follows.

For $r_0 + \Delta \geq r \geq r_0$ the profile represents a disk of constant thickness in both Fig. 9 and Fig. 10. Therefore the general expressions for the stresses in both of them, for static conditions, are represented by the relations

$$p_t(0) = b_1 + \frac{b}{r^2} \quad p_r(0) = b_1 - \frac{b}{r^2}$$

From these formulas we find, for static conditions

$$p_t(0) - p_r(0) = \frac{2b}{r^2}$$

For $r = r_0$ this difference must be equal to $S'T'$ in the case of Fig. 10 and to $P'Q'$ in the case of Fig. 9; so we have

$$S'T' = p_{t0}(0) - p_{r0}(0) = \frac{2b}{r_0^2}$$

and

$$P'Q' = \frac{2c}{r_0^2}$$

where c is an arbitrary constant of the same kind as b . Therefore, for $r = r_0 + \Delta$

$$ST = \frac{2b}{(r_0 + \Delta)^2}$$

or

$$\frac{ST}{S'T'} = \frac{r_0^2}{(r_0 + \Delta)^2}; \quad \frac{PQ}{P'Q'} = \frac{r_0^2}{(r_0 + \Delta)^2}; \quad \frac{ST}{S'T'} = \frac{PQ}{P'Q'} \dots [31]$$

Now we have

$$TQ > PS \quad \text{therefore} \quad PQ > ST$$

and, according to [31]

$$P'Q' > S'T'$$

which is nothing other than Equation [30].

We have found, therefore, that if, for $r_0 + \Delta \leq r \leq a$, the stresses p_t and p_r in Fig. 14 are the same as in Fig. 13, the difference of the stress values p_{t0} and p_{r0} at the bore, represented by $P'Q'$, will be larger than the same difference under rotating conditions as represented in Fig. 12. This being impossible, our assumption, according to which the stress curves are the same for $r_0 + \Delta \leq r \leq a$ in both disks with and without hub relief in resting conditions, must be altered. In other words, for $r = a$ the tangential stress must be less than s in Fig. 13. We then obtain stress curves \bar{p}_t and \bar{p}_r , determined by both boundary conditions for $r = a$. It is easily seen that the curves \bar{p}_t and \bar{p}_r qualitatively correspond to each other physically. If the radial stress, which is compression, is diminishing from p_r to \bar{p}_r (Fig. 14), the tangential stress, which is tension, must diminish from p_t to \bar{p}_t . At a certain definite decrease of both stress functions the state will be reached at which the previously mentioned stress difference at the bore will assume the required value, independent of the speed ω . This means that by using a disk with hub relief, the stresses are the same under rotating conditions, as in a disk without hub relief, and they are smaller, throughout the disk except the hub, under static conditions, while at the bore they remain within permissible limits determined by the relation $p_{t0} - p_{r0} = \text{const.}$ at any speed ω .

Appendix No. 1

THE PROBLEM OF ROTATING DISKS IN THE MATHEMATICAL THEORY OF ELASTICITY

The rigorous mathematical basis for the design of steam-turbine disk wheels consists in a solution of the following problem with boundary conditions.

Consider the state of strain and stress in an isotropic elastic body of revolution rotating about its axis $z-z$ with the angular velocity ω . The displacement will be symmetrical about the same axis. The components of the displacement being u in the radial and w in the axial direction, the conditions of elastic equilibrium are expressed by the differential equations¹³

¹³ A. E. H. Love, "Mathematical Theory of Elasticity," 4th ed., Cambridge, 1927, p. 146, and p. 104.

$$\left. \begin{aligned} \frac{E(1-\nu)}{(1+\nu)(1-2\nu)} \frac{\partial}{\partial r} \left(\frac{\partial u}{\partial r} + \frac{u}{r} + \frac{\partial w}{\partial z} \right) \\ + \frac{E}{2(1+\nu)} \frac{\partial}{\partial z} \left(\frac{\partial u}{\partial z} - \frac{\partial w}{\partial r} \right) = -\mu\omega^2 r \\ \frac{E(1-\nu)}{(1+\nu)(1-2\nu)} \frac{\partial}{\partial z} \left(\frac{\partial u}{\partial r} + \frac{u}{r} + \frac{\partial w}{\partial z} \right) \\ - \frac{E}{2(1+\nu)} \frac{\partial}{\partial r} \left(\frac{\partial u}{\partial z} - \frac{\partial w}{\partial r} \right) \\ - \frac{E}{2(1+\nu)} \frac{1}{r} \left(\frac{\partial u}{\partial z} - \frac{\partial w}{\partial r} \right) = 0 \end{aligned} \right\} [32]$$

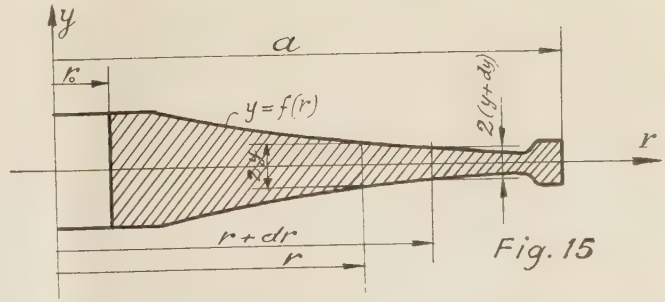


Fig. 15

The boundary conditions express the fact that the lateral surfaces of the disk, represented by the equation $y = f(r)$, where $f(r)$ is a known function of r , are free of stresses, while the edges $r = r_0$ and $r = a$ (Fig. 15) can be affected by given forces. In special problems the inner boundary surface can vanish (disk without bore). The stresses in the rotating disk are to be determined.

In the form [32] the problem has been solved for a few special forms of the meridian curve (profile) only, particularly for the cylinder¹⁴ and for the ellipsoid¹⁶ under certain boundary conditions.¹⁶

It is of practical interest and importance for comparison with the procedure used in technical applications as reproduced below to know the results yielded by the methods of the theory of elasticity. Therefore a concise report concerning the solutions just mentioned shall be given.

We designate by σ_r , σ_t , and σ_z the normal stresses along the radius r , the tangent, t , to the circle of the radius r , and the direction, z , of the axis of rotation, respectively. As to the shear stresses, the components τ_{rt} and τ_{zt} vanish by reasons of symmetry about the axis, while $\tau_{rz} \neq 0$ generally.

Consider now the stress distribution determined by the equations

$$\left. \begin{aligned} \sigma_r &= \frac{1}{8} \mu\omega^2 (3+\nu)(a^2 - r^2) + \frac{1}{6} \mu\omega^2 \nu \frac{1+\nu}{1-\nu} (l^2 - 3z^2) \\ \sigma_t &= \frac{1}{8} \mu\omega^2 [(3+\nu)a^2 - (1+3\nu)r^2] \\ &\quad + \frac{1}{6} \mu\omega^2 \nu \frac{1+\nu}{1-\nu} (l^2 - 3z^2) \\ \sigma_z &= 0 \end{aligned} \right\} [33]$$

$\tau_{rz} = \tau_{rt} = \tau_{tz} = 0$

This stress distribution is produced by a certain elastic displacement satisfying Equations [32].¹⁷ The solution [33], if applied to the case of a cylindrical disk without bore, fulfils the boundary conditions at the plane surfaces $z = \pm l$. Indeed, the stress component σ_z and the shear stresses vanishing identically, they vanish also at the surfaces $z = \pm l$. But at the cylindrical surface $r = a$ both the radial stress σ_r and the tangential stress σ_t follow a special law of distribution along the axial

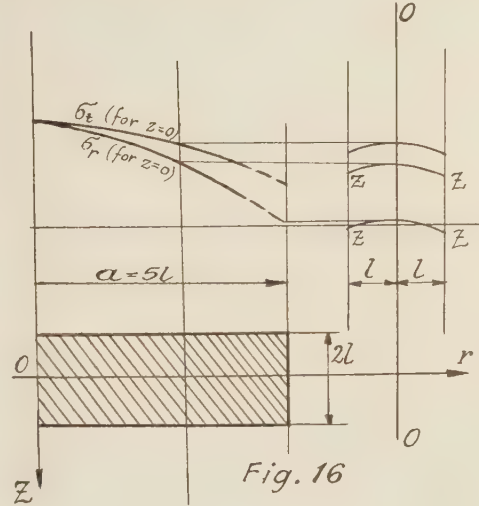


Fig. 16

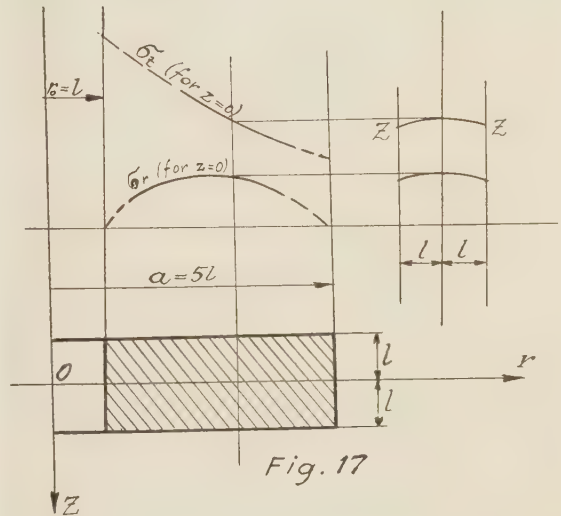


Fig. 17

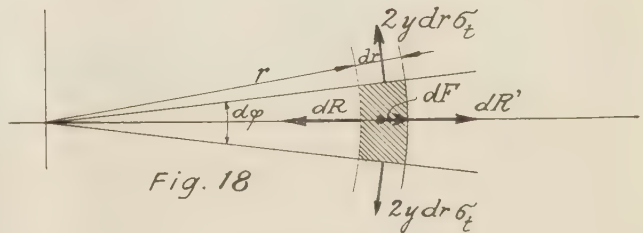


Fig. 18

Figs. 15 to 18

¹⁴ A. E. H. Love, loc. cit.; and F. Purser, Trans. Royal Irish Acad., vol. 32, 1902.

¹⁵ C. Chree, Royal Soc. Proc., London, vol. 58, 1895; treated the general ellipsoid.

¹⁶ See also Zeitschr. f. Ang. Math. u. Mech., vol. 3, 1923, p. 319.

¹⁷ A. E. H. Love, loc. cit., Eq. [70] and [71], and p. 56.

direction z , as shown by Equation [33]. According to this law the average amount of σ_r along that direction vanishes for $r = a$. The additive correction of Equation [33], necessary to produce boundary stresses $\sigma_r = 0$ for $r = a$, is discussed in the article of Purser, previously mentioned. This correction is of importance only for calculation of stresses in the vicinity of $r = a$. For parts which are not too near to the edge, the stress state of the disk is represented by Equation [33] with sufficient accuracy according to the well-known principle of de Saint Venant,¹⁸ provided that the thickness $2l$ is small compared with the diameter $2a$. The axial distribution of the stresses at the edge $r = a$ is here of little interest. That at the inner edge in disks with central bore is much more important. For such disks the solution [33] is to be replaced by the following formulas:

$$\left. \begin{aligned} \sigma_r &= \frac{1}{8} \mu \omega^2 (3 + \nu) \left(a^2 + b^2 - r^2 - \frac{a^2 b^2}{r^2} \right) \\ &\quad + \frac{1}{6} \mu \omega^2 \nu \frac{1 + \nu}{1 - \nu} (l^2 - 3z^2) \\ \sigma_t &= \frac{1}{8} \mu \omega^2 \left[(3 + \nu) \left(a^2 + b^2 + \frac{a^2 b^2}{r^2} \right) - (1 + 3\nu) r^2 \right] \\ &\quad + \frac{1}{6} \mu \omega^2 \nu \frac{1 + \nu}{1 - \nu} (l^2 - 3z^2) \end{aligned} \right\} \quad [34]^{19}$$

wherein b is the radius of the bore, and

$$\sigma_z = 0 \quad \tau_{rz} = \tau_{rt} = \tau_{tz} = 0 \dots \dots \dots [34a]$$

According to the solutions [33] and [34] the stress variation along the axial direction, z , is of an almost vanishing amount, if l , equal to a half the thickness of the disk, does not exceed a certain limit as compared with the outer radius of the disk.

Take, for instance, a solid cylindrical disk for which $a = 5l$. Suppose, this ratio justifies the application of the principle of de Saint Venant. In Fig. 16 the curves σ_r and σ_t show the stress distribution, according to Equations [33], for the middle plane, ($z = 0$), of the disk. The stress variation along the axial direction z is represented by the parabolical curves $Z-Z$, analytically expressed by the formula $\Delta\sigma = Cz^2$, C being a constant and $-l \leq z \leq l$. The amount of this stress variation is about 2.5 per cent of the maximum stress at the axis $r = 0$.

The lower parts of the curves in Fig. 16 are dotted, because in the vicinity of $r = a$ they do not represent the actual stress conditions, as explained above.

Fig. 17 shows the stress distribution according to Equations [34], in an analogous way, for the same disk as in Fig. 16, but having a bore, the radius of which is equal to l . The maximum stress appears again in the vicinity of the inner edge of the disk; but it is almost twice as large as in the case of the solid disk of Fig. 16. The stress variability along the axial direction is the same as before, or about 1.5 per cent of the maximum stress in the varied conditions.

The stress distribution in an ellipsoid according to the exact solution cited above is discussed in detail by Stodola.²⁰ We do not reproduce the complicated formulas for the stresses; only the general results shall be mentioned.

For a solid disk of elliptical meridian curve having a diameter $2a$ and a maximum thickness $2c$ at the axis, Stodola finds a stress variability along the axis ($r = 0$) as represented by the following table:

TABLE 9

c/a	$1/8$	$1/4$	$1/2$
$\Delta\sigma/\sigma$ (%)	5	13	45

¹⁸ A. E. H. Love, loc. cit., p. 132.

¹⁹ A. E. H. Love, *ibid.*, p. 148.

²⁰ A. Stodola, "Steam Turbines," New York, 1927, vol. II, sec. 184. See also his article in *Zeit. V.D.I.*, 1907, p. 1259.

where σ designates the tangential or radial stress for $r = 0$, $z = 0$, while $\Delta\sigma = \sigma(r=0, z=0) - \sigma(r=0, z=l)$.

It is interesting to observe, that the stress variability along the axis is of a larger amount for the elliptical disk than for the cylindrical one. This result is quite natural, if the uniform mass distribution along the axial direction in the case of a cylindrical disk, causing a uniform distribution of the centrifugal forces along the same direction, is taken into account. But even for a disk of elliptical profile, having a maximum thickness equal to $1/4$ of the diameter, the absolute value of the excess of the stress amount over the average stress along the axis remains within the limits of about 7 per cent of the maximum stress.

A remarkable detail is characterized by appearance of normal stresses σ_z in the axial direction. These stresses σ_z represent compression in the disk parts of larger, and tension in those of smaller thickness. They reach the amount of only a few per cent of the maximum normal stress.

From analogy with the cylindrical disk we may conclude, that, if the elliptical disk is provided with a bore, the non-uniformity in the stress distribution along the axial direction at the bore, as defined by the expression $(\sigma_{tmax} - \sigma_{tmin})/1/2(\sigma_{tmax} + \sigma_{tmin})$, will be about a half of the amount indicated by the last table, so that the absolute value of the excess over the average stress along the axial direction remains within limits of about $3 1/2$ per cent of the maximum stress for $c/a = 1/4$.

In summarizing we arrive at the following conclusion with certain approximation, special regard having been given to the increased proportions in modern disk design: By increasing the thickness of the disk from $1/8$ to $1/4$ of the diameter the absolute value of the excess of the stress values over the average stress along the axial direction increases in disks with bore from the order of about 1 per cent to that of about 4 per cent of the maximum stress, while the axial stresses σ_z still remain within negligible limits.

The rigorous treatment of the problem of rotating disks in general form, i.e., for given meridian curves, by using methods of mathematical physics, would be, at the present stage, in certain branches of the mathematical analysis, at least exceedingly complicated.²¹ A very valuable new method of analyzing plates and disks²² is invented by G. D. Birkhoff;²³ in its further development this method may acquire practical importance for disk design. As far as technical requirements are concerned the approximate method, introduced by Stodola,²⁴ is very satisfactory. His procedure is based upon the fundamental conclusion drawn from the exact solutions as previously reported. The non-uniformity of the stress distribution along the axial direction in rotating disks can be neglected within certain limits determined approximately by Table 9 and emphasized in the foregoing conclusion. This basis of strength calculations in disk design does not lose its validity in the new conditions characterized by increased disk proportions.

Appendix No. 2

DIFFERENTIAL EQUATIONS IN APPROXIMATE FORM OF ROTATING DISKS

Since the variability of the stresses σ_r and σ_t along the axial direction is, to all practical purposes, of negligible amount, they

²¹ See St. Bergmann, *Mathem. Ann.*, vol. 98, 1927, p. 248. A detailed report is given by I. Malkin, *Zeit. f. Ang. Math. u. Mech.*, vol. 10, 1930, p. 182.

²² The mathematical analogy between circular plates under bending and rotating disks is established by L. Foepl, *Zeit. f. Ang. Math. u. Mech.*, 1922.

²³ *Phil. Mag.*, vol. 43, 1922, p. 953; also C. A. Garabedian, *Amer. Math. Soc. Trans.*, vol. 25, 1923, p. 343.

²⁴ Stodola, "Steam Turbines," sec. 74.

use to be considered as functions of r only. With this simplification, Stodola obtains from the conditions of equilibrium [see Fig. 18] the equation²⁴

$$dR' - dR - dT d\varphi + dF = 0$$

where

$$dR' - dR = d(ry\sigma_r)d\varphi; \quad dT = y\sigma_t dr; \quad dF = \mu\omega^2 r^2 y d\varphi dr$$

so that the differential equation of equilibrium in approximate form can be written as follows:

$$\frac{d(ry\sigma_r)}{dr} - y\sigma_t + \mu\omega^2 r^2 y = 0 \dots\dots\dots [35]$$

In elastic conditions the stresses follow from the radial displacement u according to the relations

$$\sigma_r = \frac{E}{1-\nu^2} \left(\frac{du}{dr} + \nu \frac{u}{r} \right); \quad \sigma_t = \frac{E}{1-\nu^2} \left(\nu \frac{du}{dr} + \frac{u}{r} \right) \dots [36]$$

and by introducing [36] into [35] the equation

$$\frac{d^2 u}{dr^2} + \left(\frac{1}{y} \frac{dy}{dr} + \frac{1}{r} \right) \frac{du}{dr} + \left(\nu \frac{dy}{dr} - \frac{1}{r} \right) \frac{u}{r} + \frac{\mu\omega^2 (1-\nu^2)}{E} r = 0 \dots\dots [37]$$

is obtained. The elimination of u from Equations [36] yields the condition

$$\frac{d\sigma_t}{dr} - \nu \frac{d\sigma_r}{dr} = (1+\nu) \frac{\sigma_r - \sigma_t}{r} \dots\dots\dots [38]$$

of compatibility of both stresses.

In assuming a certain curve, $y = f(r)$, as the meridian curve (profile) of the disk a differential equation for u is obtained from Equation [37]. If the solution of this differential equation is known, the stresses can be determined by Equations [36] in connection with the boundary conditions. Should the stresses, as following from these calculations, exceed permissible limits, the assumed profile must be modified and the calculations repeated until satisfactory results are obtained.

Sometimes another equivalent procedure is used in solving the systems [35] and [38] of differential equations. A certain kind of stress function S is introduced by the formula²⁵

$$T_r = \frac{S}{r}; \quad T_t = \frac{dS}{dr} + \mu\omega^2 y r^2 \dots\dots\dots [39]$$

where

$$T_r = y\sigma_r; \quad T_t = y\sigma_t \dots\dots\dots [40]$$

By using these expressions Equation [35] is satisfied identically, while Equation [38] requires

$$\frac{d^2 S}{dr^2} + \left(\frac{1}{r} - \frac{1}{y} \frac{dy}{dr} \right) \frac{dS}{dr} + \left(\nu \frac{dy}{dr} - \frac{1}{r} \right) \frac{S}{r} + (3 + \nu) \mu\omega^2 y r = 0 \dots\dots [41]$$

an equation which does not differ much from Equation [37] for the displacement u .

Still another analytical expression for our problem can be obtained by eliminating σ_r or σ_t from Equations [35] and [38]. By eliminating σ_t , Stodola finds the following differential equation for σ_r :²⁶

$$\frac{d^2 \sigma_r}{dr^2} + \left(\frac{3}{r} + \frac{1}{y} \frac{dy}{dr} \right) \frac{d\sigma_r}{dr} + \left[\frac{2+\nu}{y} \frac{dy}{dr} + r \frac{d}{dr} \left(\frac{1}{y} \frac{dy}{dr} \right) \right] \frac{\sigma_r}{r} + (3+\nu)\mu\omega^2 = 0 \dots\dots [42]$$

The differential equations reproduced here are used in preceding sections for developing new solutions of the problem of rotating disks. Furthermore, in using Equations [36], the boundary conditions for the problem of stresses due to fit pressure in the disk under static conditions can be obtained as follows.

Designate by

d the bore diameter of the disk

D the diameter of the shaft

both under undeformed static conditions, and by

u_0 the radial displacement of the disk

u_0' the radial displacement of the shaft

both for $r = r_0$ and for any speed ω between 0 and the over-speed ω_0 . With these designations we obviously must have

$$d + 2u_0 = D + 2u_0'$$

provided that, at any speed $\omega \leq \omega_0$, there is a certain pressure between the disk and the shaft. The "shrink fit" is correspondingly given by

$$\Delta = \frac{1}{2}(D - d) = u_0 - u_0'$$

The displacements u_0 and u_0' are according to Equations [36]

$$u_0 = \frac{\sigma_t - \nu\sigma_r}{E} r_0; \quad u_0' = \frac{\sigma_t' - \nu\sigma_r'}{E} r_0$$

where σ_t and σ_r are the tangential and the radial stresses, respectively, for $r = r_0$ at the speed ω , in the disk, while σ_t' and σ_r' = σ_r are the corresponding stresses in the shaft for $r = r_0$. The shrink fit is, therefore,

$$\Delta = u_0 - u_0' = (\sigma_t - \sigma_t') \frac{r_0}{E}$$

In using the well-known formulas for a disk of constant thickness²⁷ without bore we will have

$$\sigma_t' - \sigma_r' = \sigma_t' - \sigma_r = \frac{1}{4} (1 - \nu) \mu \omega^2 r_0^2$$

Correspondingly

$$\Delta = \left[\sigma_t - \sigma_r - \frac{1}{4} (1 - \nu) \mu \omega^2 r_0^2 \right] \frac{r_0}{E}$$

Now, by introducing

$$\left. \begin{array}{l} \sigma_t = \sigma_{t0} \\ \sigma_r = \sigma_{r0} \end{array} \right\} \text{for } \omega = \omega_0 \quad \left. \begin{array}{l} \sigma_t = p_t \\ \sigma_r = p_r \end{array} \right\} \text{for } \omega = 0$$

we obtain

$$p_t - p_r = \sigma_{t0} - \sigma_{r0} - \frac{1}{4} (1 - \nu) \mu \omega_0^2 r_0^2 \quad (\text{for } r = r_0)$$

Herein σ_{r0} is equal or approximately equal to zero. As to the quantity $\frac{1}{4}(1-\nu)\mu\omega_0^2 r_0^2$, it is a small value which may be neglected in the last equation. Indeed, with reference to the example treated in the preceding section we have

$$\frac{1}{4} (1 - \nu) \mu \omega_0^2 r_0^2 = \frac{1}{6} \times 7.33 \times 10^{-4} \left(4320 \times \frac{\pi}{30} \right)^2 \times 6.75^2 = 1125 \text{ lb per sq in.}$$

²⁵ A. Foepl, "Technische Mechanik," vol. V, 1922, p. 87.

²⁶ A. Stodola, loc. cit., sec. 181b.

²⁷ See Stodola, *ibid.*, sec. 76.

or about 2 per cent of $\sigma_{10} = 52,400$ lb per sq in. So the boundary condition in question can be written as follows

$$p_i - p_r = \sigma_{10} \quad \text{for } r = r_0 \dots \dots \dots [43]$$

This is the inner boundary condition for the stresses p_i and p_r due to fit pressure under static conditions. The other boundary condition expresses the vanishing of p_r at the outer disk edge $r = a$:

$$p_r = 0 \quad \text{for } r = a \dots \dots \dots [44]$$

The boundary condition [43] is here obtained in a way somewhat different from that used by Stodola²⁸ in order to show the limits of accuracy of this condition.

Discussion

J. L. MAULBETSCH.²⁹ It can be shown that the two profiles given by the author belong to a series of profiles of the type

$$y = y_0 e^{-\beta r^\gamma}$$

where

$$\gamma = \frac{1}{a}, \frac{2}{a} \text{ or } \frac{4}{a}$$

and

$a = \text{any positive integer}$

i.e.,

$$\gamma = 4, 2, 1, \frac{1}{2}, \frac{4}{3}, \frac{2}{3}, \frac{1}{3}, \frac{1}{4}, \frac{4}{5}, \frac{2}{5}, \frac{1}{5} \dots$$

and that any profile of this series will allow a similar solution to the one presented by the author.

The solution for any value of γ consists of two infinite series and of an expression containing a few terms only. For $\gamma = \frac{4}{3}$ and $\gamma = \frac{2}{3}$, this last expression has three terms. In general, for any value of γ , the number of terms p is:

$$p = \frac{3 \pm 1}{\gamma}$$

We see that if γ becomes smaller, p will increase, i.e., we have more terms and the calculations are somewhat longer. However a study of the general solution shows that the series have a better convergence for small values of γ therefore fewer terms in the series need to be considered.

The method used by the author is practical only if tables for the values of the series are calculated beforehand. Such tables are given in this paper for the case $\gamma = \frac{4}{3}$, and the author also proposes to have tables calculated for his second case where $\gamma = \frac{2}{3}$. Since the calculations are rather long, it might be advisable to determine first which profile is better adapted for practical purposes.

Due to the more rapid convergence of the series for small values of γ , a larger range for the variable $z = \beta r^\gamma$ may be taken, therefore disk profiles differing more from the conical shape can be approximated with $\gamma = \frac{1}{4}$ or $\frac{1}{5}$ for instance, than with $\gamma = \frac{4}{3}$ or $\frac{2}{3}$. It seems then, that tables for a value of γ smaller than $\frac{2}{3}$ would offer more advantages to the designer of turbine disk wheels than the second profile proposed by the author.

A résumé of the general solution will be given here: the differential equation³⁰

$$\frac{d^2 u}{dr^2} + \left(\frac{1}{y} \frac{dy}{dr} + \frac{1}{r} \right) \frac{du}{dr} + \left(\frac{\nu}{y} \frac{dy}{dr} - \frac{1}{r} \right) \frac{u}{r} + \frac{\mu \omega^2 (1 - \nu^2)}{E} r = 0 \dots [45]$$

is not homogeneous. It is reduced to the following homogeneous equation³¹ which can be solved with series:

$$z^2 \frac{d^2 \sigma_r}{dz^2} + (m - z) z \frac{d\sigma_r}{dz} - n z \sigma_r = 0 \dots \dots \dots [46]$$

where

$$m = \frac{\gamma + 2}{\gamma} \quad z = \beta r^\gamma$$

and

$$n = \frac{1 + \nu + \gamma}{\gamma}$$

if we assume

$$y = y_0 e^{-\beta r^\gamma} \dots \dots \dots [47]$$

and limit γ to the values

$$\gamma = \frac{1}{a}, \frac{2}{a} \text{ or } \frac{4}{a} \quad (a = \text{positive integer}) [48]$$

This limiting condition for γ is due to the fact that we want to obtain a particular solution of Equation [45] so that a homogeneous equation may be obtained.

The particular solution is of the type

$$u = \sum_{i=1}^p M_i r^{\mu_i} \dots \dots \dots [49]$$

where

$$p = \frac{3 \pm 1}{\gamma}$$

$$\mu_i = 3 - i\gamma \quad (\text{for } i = 1 \text{ to } p - 1)$$

and

$$\mu_p = \pm 1$$

M_i is a function of γ and β .

The condition [48] for γ is obtained through the analysis by making the assumption [47] and [49].

C. R. SODERBERG.³² Dr. Malkin's contribution to the disk problem is a very real one and I feel certain that it will find its place among the classics of the subject.

It is of importance to the designer to have available a method of stress calculation which is sufficiently rapid to permit evaluation of the stresses for many combinations in a short time and yet of sufficient accuracy to make the results reliable. During the period of its use, we have had ample opportunity to demonstrate the great merits of the new method.

Concerning the problem of design limits, it seems that the following questions must be discussed: (a) tangential stress at the inner bore at overspeed; (b) permanence of the shrink fit on the shaft at the normal speed, and (c) normal pressure on the shaft at standstill. These aspects of the failure problem must be weighed in the order mentioned. The importance of the last item is difficult to evaluate. Failure in the ordinary sense of the word does not occur under normal pressure until its intensity materially exceeds the yield strength. This state is

²⁸ See Stodola, *ibid.*, sec. 81d.

²⁹ University of Michigan, Ann Arbor, Mich.

³⁰ Author's Equation [37].

³¹ Author's Equation [5].

³² Westinghouse Research Laboratories, East Pittsburgh, Pa. Mem. A.S.M.E.

seldom reached, but the pressures are usually so high that the designer does not feel he can ignore them.

AUTHOR'S CLOSURE

Mr. Maulbetsch's generalization of my solution involves two infinite series in each of the two stress expressions. In recommending $\gamma = 1/4$ he introduces two further expressions with

$$p = \frac{3 \pm 1}{1/4} = 12 \pm 4$$

terms in each. These two expressions, however, may be worse than any of the proposed infinite series, because there is no indication as to the rapidity of their convergence. The solutions, thus represented by six infinite series, cannot compete with the exponential profiles, the first of which involves only two infinite series, while the second entails the use of simple finite expressions. The more rapid convergence in the case of smaller values of γ in the first four of Mr. Maulbetsch's six series would not appear to be a factor of great weight.

There is, furthermore, another factor which is not to be overlooked in connection with the question of convergence. If γ becomes smaller, the independent variable z becomes larger, especially in the vicinity of the rim (see Tables 4 and 6). In using $\gamma = 1/4$ we easily find, for the disk analyzed in Figs. 3 to 6, that

$$z_a = \beta a^{1/4} = 2.303 \times \log_{10} 2.5 \times \frac{18.75^{1/4}}{18.75^{1/4} - 6.75^{1/4}} = 4.06$$

as compared with $z_a = 1.25$ and $z_a = 1.86$, respectively, in the above examples. The increase in z_a caused by decrease of γ is a factor of opposite effect to that of more rapid convergence.

The necessity of calculating tables cannot be considered as a disadvantage of the author's method, because such tables are necessary in any analytical solution, and it is contended by the writer that, for two reasons, the method of solution as set forth is simpler than any other analytical solution so far developed for the problem. First, it is much more convenient to calculate the tables in question by using simple finite expressions, or solutions with only two infinite series, than by dealing with six infinite series, as in the case of conical disks, or even with finite expressions of considerable complicity such as encountered in the case of hyperbolic disks. The other important advantage is the fact that the writer's method of solution is based upon the principle of similarity which, in the case considered, assumes the following form: If the profile curve is given by an expression $y = f(r, \beta)$, where β is the essential constant parameter characterizing the individual disk, the solution will be obtained generally in terms of two varying essential quantities, r and β . In using f. i. tables calculated for conical disks we have to multiply all values, for any special disk, by a constant varying with that disk. The calculations are, in other words, two-dimensional. In the case of the exponential profiles set forth by the writer the solution is given essentially in terms of a certain combination of the variable r and the parameter β , namely in terms of $z = \beta r^{1/4}$ and $z = \beta r^{1/2}$, respectively. The main calculations, consequently, include only one variable. These are the two advantages which are of practical value in tabulating the solutions and in using the tables for design purposes.

As to the question of technical adaptability of the writer's method of solution, our attention is called to Fig. 19 in conjunction with the following remarks.

The problem of practical disk design is not a problem merely of avoiding the conical profile. It is rather a problem of profile variation between two limiting profile curves, the conical and the hyperbolic. Fig. 19 is a typical example of the practical possi-

bilities of choice offered to the disk designer by the two exponential profiles. They not only represent definite special solutions, but practically fill the range between the two limiting solutions, inasmuch as, if completed by the latter, they approximate, with sufficient accuracy, any intermediate solution as well. Practical experience shows that a slight variation of the profile curve between the two fixed limiting points at the bore and the rim is of a practically negligible influence on the boundary stresses. After having used, for a certain time, the new method

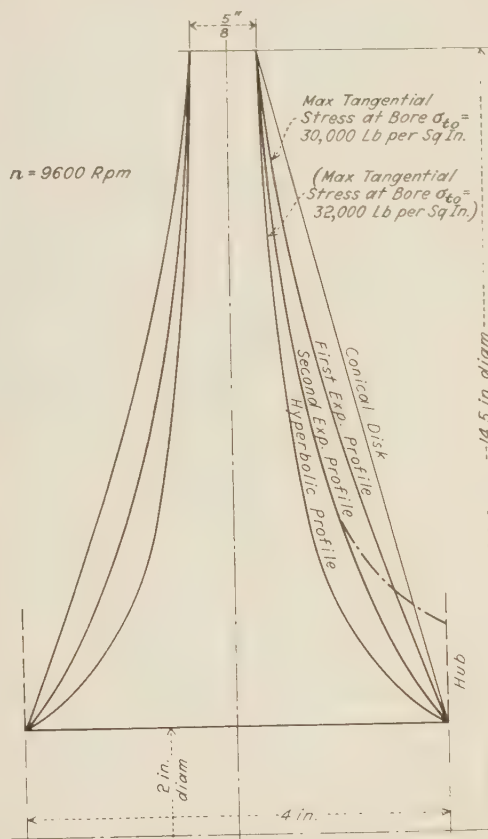


FIG. 19 TYPICAL EXAMPLES OF CHOICE OFFERED BY THE TWO EXPONENTIAL PROFILES

represented by the two exponential profiles the practical designer will, therefore, be able to modify more or less freely the theoretical profile curves, if this is advisable from the standpoint of weight reduction or required by the necessity of avoiding possible dangerous vibrations. The profiles $y = \alpha e^{-z}$, $z = \beta r^\gamma$, with $\gamma = 1/4$ or $\gamma = 1/2$, being of sharper curvature at the bore than the second exponential profile and, consequently, situated in the vicinity of the hyperbolic profile, appear quite unnecessary in this connection because they do not throw any further light on the problem of stress distribution and there would be no justification for the tedious calculations involved.

This is a case of special practical interest. Inasmuch as the hyperbolic disk is regarded as a limiting profile characterized by smaller weight but for the most part not adapted to technical-design purposes because of the sharp curvature in the vicinity of the bore, considerable modification of the profile curve is necessary, thereby reducing the degree of accuracy of the stress calculations. Fig. 19 shows that, by using the second exponential profile, the designer practically obtains the "modified" hyperbolic disk without being forced to abandon the basis of a reliable

stress analysis. This consideration once more demonstrates the technical importance of the second exponential profile. It leads to the conclusion that, while the hyperbolic disk represents a *theoretical* limiting profile with regard to the important question of uniformity of the stress distribution, the second exponential profile very often will represent the corresponding *actual* limiting curve. This applies especially to the case of smaller bore diameters (see Fig. 19) where the exponential profiles differ considerably from each other. But even in the case of large bore diameters (see Figs. 3 to 6), the second exponential profile can be considered at least as a good guide with respect to the question of a satisfactory stress distribution at the bore.

There will be perhaps another occasion later to discuss the problem of axial disk vibrations in connection with the problem of profile choice.

In summarizing so far, the following characteristic features of the new solutions should be emphasized: (a) simple mathematical representation, (b) compliance with the principle of similarity, (c) practical use in profile-curve variation within the limits represented by the conical profile and the hyperbolic disk, (d) reliable representation of the "actual" hyperbolic disk, and (e) tendency toward uniformity of stress distribution at the bore. These features make the new solutions well adapted for purposes of practical disk design.

Referring to the problem of design limits as stated by C. R. Soderberg, certain indications concerning the distribution of the

tangential stresses along the bore and their maximum amount at the middle plane (inner bore) of the disk have been given already in Appendix No. 1. If this maximum stress exceeds a certain limit, deformation processes of plastic character may be caused with the result that gradual changes will take place in the shrink fit. This is a question of entirely different nature and beyond the scope of this contribution.

The problem of normal pressure on the shaft under static conditions admits of a simple solution. We have seen (Fig. 8) that the normal pressure p_r between disk and shaft under these conditions is from 40 to 45 per cent of the tangential stress, σ_{t0} , at the bore in overspeed conditions. The principal stresses in the shaft under uniform compression are, according to the solution of a well-known special case of the elastic problem.³³ $\sigma_z = 0$ in the axial direction and $\sigma_x = \sigma_y = -p_r$ in any two directions in the cross-section of the shaft. If the problem of failure of the shaft under this uniform compression is judged from the standpoint of Mohr's theory, we would have to consider the characteristic amount of $\frac{1}{2}(\sigma_x - \sigma_z) = \frac{1}{2}(\sigma_y - \sigma_z)$ or, absolutely, $\frac{1}{2}p_r$, as compared with the amount of $\frac{1}{2}\sigma_{t0}$ in the case of the disk. In other words, according to Mohr's theory, the shaft would be in twice as favorable a condition as the disk, provided the corresponding cases of failure are comparable with each other.³⁴

³³ Loc. cit., A. E. H. Love, p. 144.

³⁴ "Festigkeitsversuche," by Th. von Kármán, *Zeit. V.D.I.*, 1911.

A Membrane Analogy Supplementing Photoelasticity

By J. G. McGIVERN¹ AND H. L. SUPPER,¹ CAMBRIDGE, MASS.

This paper describes a new method of finding the sum of the principal stresses in a two-dimensional model by means of ordinate measurements on a stretched rubber membrane as suggested by J. P. Den Hartog. The method is applied in detail to a simple phenolite tension member with a central circular hole and is found to be easy of operation and to yield results of good accuracy.

WHILE the analytical theory of elasticity has wide applications in the solution of engineering problems, it becomes very complicated and laborious when employed for investigating bodies other than those having the very simplest of geometrical shapes. It is because of this limitation of the mathematical theory that so much attention has been centered on photoelasticity as a method for determining the difference in value between the two principal stresses at any point in a body of uniform thickness subjected to a system of loading in its own plane. Since this difference is equal to twice the shear stress, this analysis becomes very useful when the object to be investigated is ductile and fails according to the maximum-shear theory. Many of our machine parts, however, are hard and brittle and fail according to conditions predicted by the maximum-normal-stress theory. Therefore, paralleling the development of photoelasticity there have been attempts to supplement its results by other methods, making it possible to obtain the sum of the principal stresses and hence from the two the individual principal stresses. The methods proposed have not been sufficiently accurate or simple in their execution to warrant their widespread adoption by engineers. In this contribution the authors apply a new procedure employing a membrane,² that they believe is both simple and accurate. This paper will consider those essentials of photoelasticity necessary for a proper explanation, give a general description of the membrane analogy and its technique and, finally, show its application to a typical problem.

ESSENTIALS OF PHOTOELASTICITY

The principle of photoelasticity was discovered by Sir David Brewster in 1816. He found that, when plane polarized light is passed through a transparent plate under stress, the polarized ray is broken up into two plane rays which vibrate in planes at right angles to each other and suffer retardation such that they are out of phase with each other by an amount proportional to the difference between the principal stresses. This phase difference

causes interference effects so that if a stressed specimen is viewed with white light a pattern of color bands results, or if a monochromatic light source is used the result is a pattern of alternating black and white fringes. Since the optical law governing this behavior is dependent only on the elastic and optical constants of the material, its thickness, and the value of the difference of the principal stresses, and not on geometrical shape, it is possible to determine the stress difference value from either the color or the black fringe pattern. The calibration of the constants is done by taking a simple tension specimen and measuring the loads corresponding to the various color values or by using a simple beam subjected to a constant known bending moment. In the latter case the stress is calibrated for various points in the beam and then divided by the fringe order to give the stress-difference value for each fringe. This value will of course vary with the material used and its thickness. For the tests described in this paper the most sensitive material existing, phenolite,³ was used with a calibration of 264.3 lb per sq in. per fringe.

In addition it is possible by pure optical methods to obtain the directions of the principal stresses as well as the value of their difference. This was discovered by Clerk Maxwell when he conceived the idea of using two polarizers having their axes at right angles and located on different sides of the specimen. By keeping the axes at right angles and revolving them together it is possible to obtain a series of black lines called isoclinics. Each one of these isoclinics has the property of being the locus of all points having the directions of their principal stresses the same as those of the setting of the axes of the polarizers. This follows since those rays which vibrate in the plane of the axes of the first polarizer cannot pass through the second polarizer, called the analyzer, as they have no component parallel to its axis and therefore appear black.

Since the maximum shear stress is equal to one half the difference between the values of the two principal stresses and acts on a plane 45 degrees from the plane of the maximum stress, it is possible by pure optical means to determine both the magnitude and direction of the maximum shear stress.

As stated previously, it is sometimes necessary for the engineer to know the values of the principal stresses P and Q individually. Knowing the value of $(P - Q)$ from photoelasticity, the usual procedure is to find the value of $(P + Q)$ by some other method and then to determine the values of the individual stresses P and Q separately.

VARIOUS METHODS FOR OBTAINING P AND Q SEPARATELY

In 1914 Coker proposed a procedure which was originally suggested by Mesnager and consists of determining the sum of the principal stresses, $(P + Q)$, by measuring the lateral contraction. By means of this measurement, together with a knowledge of Poisson's ratio and Young's modulus, the value of $(P + Q)$ can be determined at any point. This method has one serious disadvantage, however. This is that the deformations to be measured are so small that in practice reliable results are very improbable.

³ Developed by Z. Tuzi, see "A New Material for the Study of Photo-Elasticity," Scientific Papers of the Inst. of Phys. and Chem. Research, Tokyo, vol. 7, Oct., 1927; also Proc. Third Intern. Congress for Appl. Mech., Stockholm, 1930, vol. 2, p. 176.

¹ Graduate students at the Harvard Engineering School, Cambridge, Mass. Mr. McGivern was graduated from Northeastern University with the degree of B.M.E. in 1928 and served as an instructor there for the three following years. In 1931 he received the degree of Ed.M. from Boston University and in 1932 an M.S. from Harvard University. Mr. Supper was graduated from Ecole Speciale des Travaux in 1931 and was Stillman Fellow at Harvard University, 1931-32. He is now a member of the French Army.

² J. P. Den Hartog, *Zeitschrift für angewandte Mathematik und Mechanik*, 1931, p. 156.

Contributed by the Applied Mechanics Division and presented at the Annual Meeting, New York, N. Y., December 4 to 8, 1933, of THE AMERICAN SOCIETY OF MECHANICAL ENGINEERS.

NOTE: Statements and opinions advanced in papers are to be understood as individual expressions of their authors, and not those of the Society.

A method of graphical and numerical integration based on the equations of Mesnager was developed by Filon.⁴ The calculations are started at a boundary where P and Q are known and then continued along a stress trajectory, which is a line having the principal stress cross as tangent and normal at each point. The stress trajectories can be obtained graphically from the isoclinics but the whole procedure is very long and tedious as well as quite inaccurate in certain regions of the object.

A third method originated by Favre⁵ is a purely optical one. It requires the use of an interferometer and consists of breaking up the original plane-polarized ray into two parts, one passing through the stressed specimen and the other dodging around it.

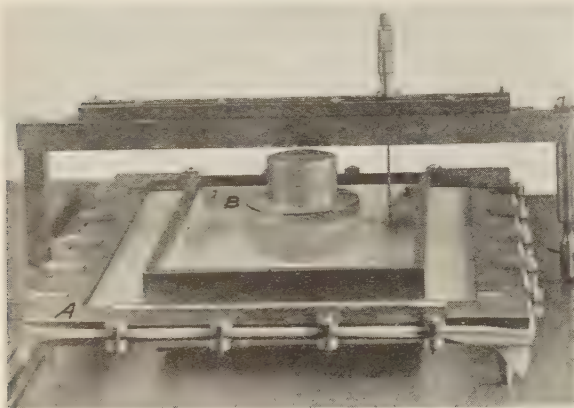


FIG. 1 ORDINATE-MEASURING APPARATUS

If the plane of the polarized light at a certain point of the specimen is parallel to its principal stress direction, the retardation of that ray is proportional either to P or to Q . Thus the two principal stresses are determined independently by comparing their retardation with respect to the unaffected ray. The directions of P and Q for each point, however, must be determined first by the ordinary isoclinic method so that the angle of the polarizer can be set for finding the retardations of P or Q for a particular point. This method is not of great practical importance, as it requires very sensitive precision apparatus, a large amount of time and a very high degree of technical skill for its operation.

The membrane method which is the subject of this paper requires a moderate amount of rather simple apparatus, gives results with less work than any of the three foregoing methods¹ of procedure and, in addition, is inherently more accurate.

GENERAL DESCRIPTION OF MEMBRANE ANALOGY AND APPARATUS

Due to the fact that at the unloaded boundaries of the specimen one of the principal stresses disappears, it is possible from a photoelastic photograph to evaluate $(P + Q)$ along all free boundaries since $(P - Q)$ equals $(P + Q)$. Now it so happens that the equation of the small ordinates of a membrane stressed with a constant tension and having the same pressure on both sides is the same as the equation defining the distribution of $(P + Q)$. This common equation is known as the differential equation of Laplace and is written for the two cases as follows:

For the ordinate z of the membrane⁶

$$\frac{\partial^2 z}{\partial x^2} + \frac{\partial^2 z}{\partial y^2} = 0 \dots\dots\dots [1]$$

For the distribution of $(P + Q)$ ⁶

$$\frac{\partial^2 (P + Q)}{\partial x^2} + \frac{\partial^2 (P + Q)}{\partial y^2} = 0 \dots\dots\dots [2]$$

In order to have a complete similarity it is only necessary to satisfy the same boundary conditions. Since the boundary values of $(P + Q)$ can be obtained from photoelasticity, we have only to make the *boundary* ordinates of the membrane proportional to the $(P + Q)$ values in order to have complete similarity between the $(P + Q)$ values and the z values of the membrane in the *interior* of the specimen.

Some care has to be exercised in evaluating the sign of $(P + Q)$ at the boundary. If the signs at the boundaries are not applied correctly, serious errors can be made. This point will be discussed in detail in the next section.

The requirement of a membrane as it is assumed in the derivation of Equation [1] is that the stress in tension is always constant



FIG. 2 FRINGE PHOTOGRAPH OF $(P - Q)$ PATTERN

and independent of any change in shape. This condition would be satisfied fully by using a soap film where the tension is a function only of the capillary constant of the film. Some investigators have succeeded in making soap films that have lasted for several hours but they require great care both in their making and their use. For this reason a rubber membrane was employed. With moderate care and protection from direct sunlight it will last for more than a month. If we select the scale of our boundary ordinates in such a manner that the tangent of the largest slope of the membrane will be one-fifth, the error introduced by a change in tension due to the change in shape is less than 2 per cent. In the derivation of Equation [1] it is assumed also that the angle of slope is sufficiently small that its tangent can be considered as

⁴ "On the Graphical Determination of Stress from Photo-Elastic Observation," by L. Filon, *Engineering*, Oct., 1923.

⁵ "Sur une nouvelle méthode optique de détermination des tensions intérieures," by H. Favre, Publications du Laboratoire de Photo-élasticité de L'Ecole Polytechnique Fédéral de Zürich, 1929.

⁶ For development see "Mathematical Theory of Elasticity," by A. E. H. Love.

equal to its sine. The error due to this assumption also is on the order of 2 per cent and occurs in the soap film as well.

The stated condition that the rubber membrane must be stressed with equal tension was fulfilled by ruling it into one-half inch squares and stretching it until the original small squares became one inch on each side. This was accomplished by fastening clamps, one inch wide, alternately around the edge of the rubber and fastening these clamps with strings to a large frame so that the membrane could be stretched until the original half-inch space between the clamps became one inch. The center portion of the rubber was then clamped between two permanent frames especially made for that purpose. These frames are marked A in Fig. 1. The boundary ordinates of the rubber membrane, as prescribed by the photoelastic test, are forced on it by a lower and an upper frame indicated by B in Fig. 1 and carrying celluloid inserts filed to the proper contours.

The ordinate-measuring apparatus consists of a base plate, an overhead beam the support at one end of which slides on the base plate, and a drop micrometer arranged to slide along the beam. By means of scales on both the base and the beam it is possible to locate definitely any point (x, y) on the model and measure its height z . Fig. 1 shows the complete apparatus set up and ready for use.

APPLICATION TO A DEFINITE CASE

The specimen selected for applying the new technique consisted of a simple phenolite tension member with a circular hole equal to one-half of its width centrally located in it. The fringe photograph for this model is shown in Fig. 2. On account of spherical aberration, it is of importance that a network of squares be ruled on the original specimen and that this be photographed together with the ($P-Q$) pattern. Fig. 3 represents the

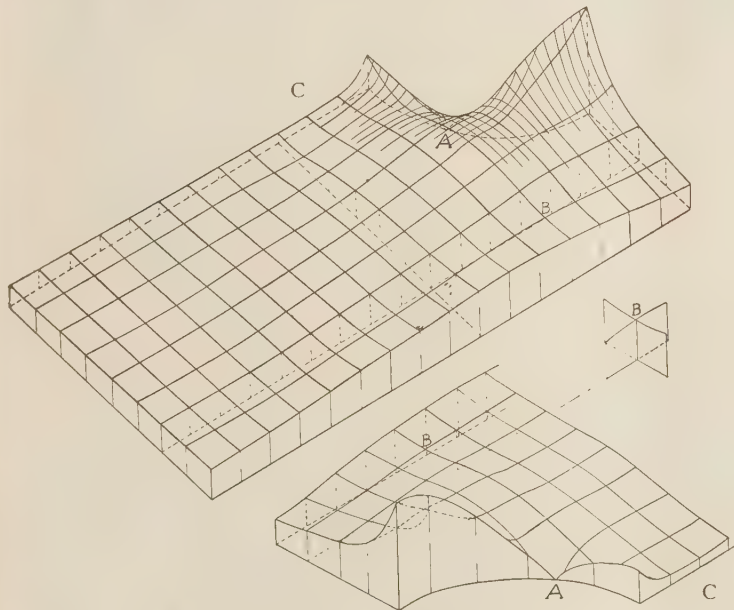


FIG. 3 ($P - Q$) STRESS SURFACE

($P - Q$) stress surface for one-quarter of the model. The photograph, Fig. 2, can be considered to be a civil engineer's contour map of the surface shown in Fig. 3.

Since the P stress was taken as the longitudinal stress at a distance far removed from the hole, it is seen that the maximum P

stress is tensile and is equal to approximately three times the average applied stress. This maximum is located at the surface of the hole on the horizontal center line and is shown as point 4 in Fig. 4. The maximum Q stress is approximately equal to the

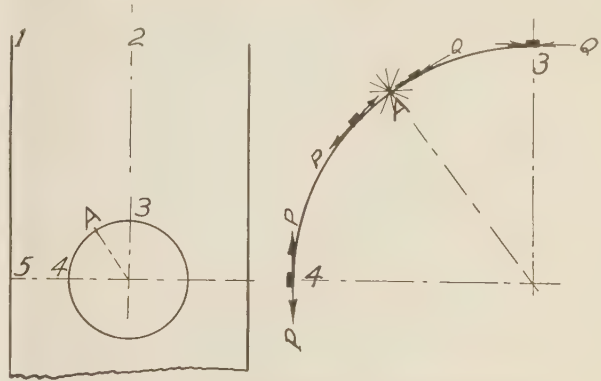


FIG. 4 DIRECTION PROPERTIES OF INNER BOUNDARY

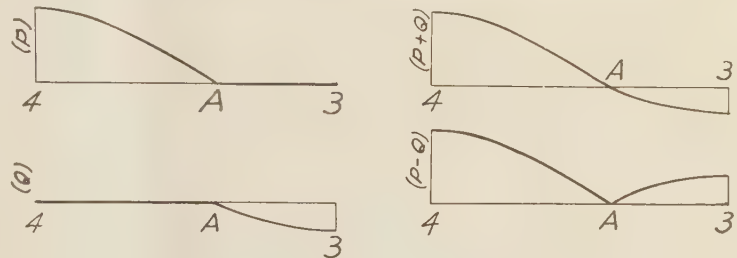


FIG. 5 STRESS DISTRIBUTION ALONG INNER BOUNDARY

average applied stress, is compressive, and is located at point 3 in Fig. 4. We know it to be compressive because in Fig. 3 ($P - Q$) is positive and P is equal to zero. An investigation of P and Q around the hole presents some interesting features, as can be explained by referring to Fig. 4.

Along the lines 1-5, 5-4, and 2-3 in Fig. 4, the direction of the P stress is vertical and has a positive value except at point 3 where it is zero. The Q stress remains horizontal in direction along these same lines and is equal to zero at the points 1, 5, and 4. Considering the contour of the hole, it is seen that at point 4 the P stress has a definite value and the Q stress equals zero, while for point 3 the reverse is true. Along the circular contour of the hole the stress cross is tangential and normal so that in moving from point 3 to point 4 the cross turns through 90 degrees and, if nothing particular happens, the P stress which is vertical at 4 would become nearly horizontal near point 3 which is inconsistent.

In order to avoid this it is necessary to reverse the meaning of P and Q at some point between 3 and 4. This naturally can happen only at a point where both these stresses become zero. This very important point is denoted by the letter A in Fig. 4, while Fig. 5 illustrates the relation

still more plainly. The directional properties of this singular point of zero stress, A, located approximately at 36 degrees from the vertical centerline will be best understood when we refer to the isoclinic and stress trajectory diagrams shown in Figs. 9 and 10.

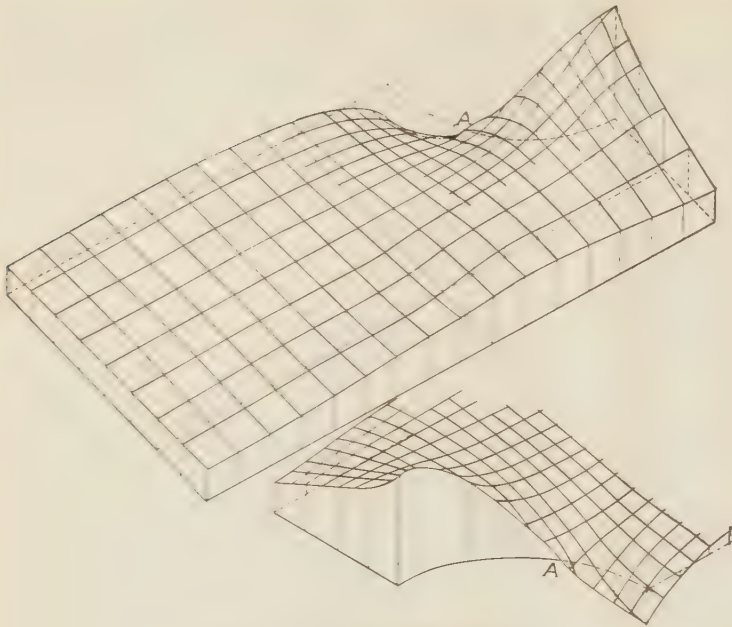
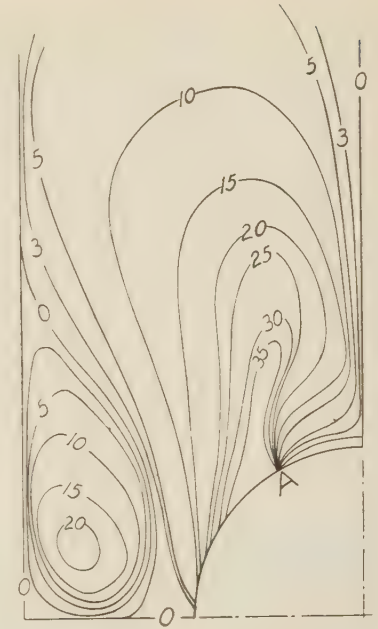
FIG. 6 $(P + Q)$ STRESS SURFACE

FIG. 9 ISOCLINIC LINES

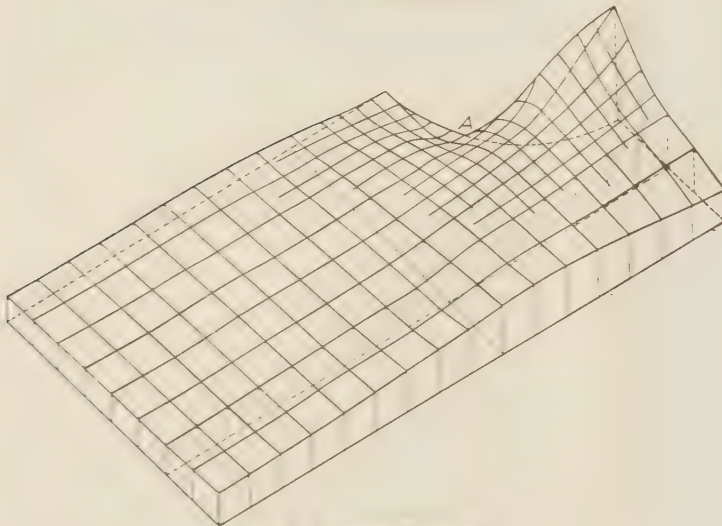
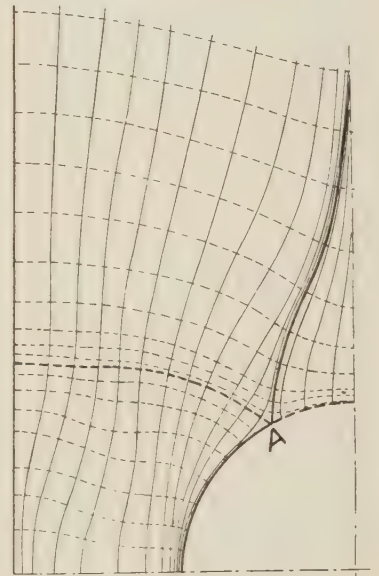
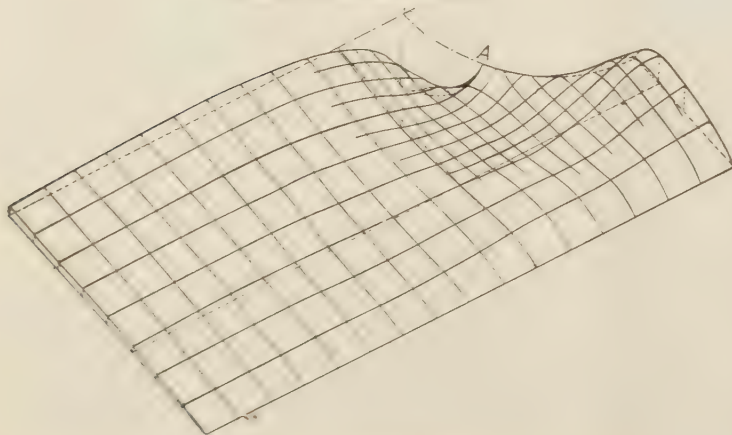
FIG. 7 P STRESS SURFACE

FIG. 10 STRESS TRAJECTORIES

FIG. 8 Q STRESS SURFACE

Now we can proceed to the finding of the $(P + Q)$ values along the boundaries from the known values of $(P - Q)$ in Fig. 3. Along the outside boundaries $Q = 0$ and therefore $(P + Q) = (P - Q)$ without further difficulty. The same is true at point 4 of the circular inner boundary or, for that matter, at any point between 4 and A. However, at point 3 we have a different situation. Here $P = 0$ and Fig. 3 shows that $(P - Q)$ is positive so that Q must be negative. Consequently $(P + Q)$ is also negative and equal in numerical value to $(P - Q)$. This reversal of sign between $(P + Q)$ and $(P - Q)$ holds for the whole boundary between points 3 and A. This is further illustrated in

Fig. 5. The value and the sign of the boundaries having been settled on, it is an easy matter to lay them out, attach them to their respective frames, and by means of the set-up shown in Fig. 1 force them on the rubber membrane. The ordinates measured on the membrane surface thus formed are shown in Fig. 6.

The resulting $(P + Q)$ surface of Fig. 6 on first sight does not appear very different from the $(P - Q)$ surface of Fig. 3 with the exception of the change in sign at the boundary from A to 3 . There are, however, two regions lettered B and C on Fig. 3 which do not appear in Fig. 6. Point B indicates a "saddle point" in the $(P - Q)$ surface. If we proceed in a longitudinal direction through this point, we go through a maximum $(P - Q)$ value while if we travel transversely through it a minimum $(P - Q)$ value is passed. This point B is of importance in interpreting the fringe order and is easily recognized on the fringe photograph of Fig. 2. Point C indicates a bowl in the surface and a minimum value of $(P - Q)$ is obtained irrespective of the direction one passes through it. This point is also easily recognized in Fig. 3. It is interesting to note that it would be impossible for any $(P + Q)$ surface to contain a bowl or a hill top since its differential equation requires that the sum of the two principal curvatures through a point must always be equal to zero. It is this characteristic that makes it possible to distinguish between a $(P + Q)$ and a $(P - Q)$ stress surface at first sight.

Having cataloged the values of $(P - Q)$ and $(P + Q)$ it is an easy matter to solve for P and Q separately. The P stress surface and the Q stress surface are represented in the Figs. 7 and 8 respectively. The P stress surface does not vary appreciably from either the $(P - Q)$ or the $(P + Q)$ surfaces except in the region from point A to point 3 near the edge of the hole. This similarity is due to the small values of Q except in the region indicated. Since the Q stress is so small, its ordinate scale in Fig. 8 was taken double that of Fig. 7. The P stress diagram makes it possible to apply a static check on the analysis in as much as the area under the curve at the center section between 4 and 5 in Fig. 4

should equal the area under the curve at a considerable distance from the hole, between 1 and 2 in Fig. 4.

Fig. 9 shows the isoclinic lines which were determined by the usual method. These lines show the significance of the singular point A by the fact that all the isoclinics pass through it. From these isoclinics the stress trajectories shown in Fig. 10 were drawn. There are two "singular trajectories," one represented by a heavy full line which shows the change in the direction of the P stress at A and the other represented by a heavy dotted line representing the change in the direction of the Q stress at A .

The behavior in the immediate neighborhood of A naturally is not affected by the width of the plate. Since an analytical solution is available for an infinitely wide plate, it is possible to solve for the angle that the principal stress makes with the radius. The tangent of twice this angle was reduced to a linear function of both the angular displacement from the singular point and the ratio of the radii of the point in question to the radius of the hole. This made it possible to show the detail in the region of point A in Fig. 10. The trajectories as given in Fig. 10 differ appreciably from those published by Coker on page 968 of the December, 1920, issue of the *General Electric Review*.

Discussion

ROBERT VICTOR BAUD.⁷ By solving the stress-field problem by means of the membrane analogy the edge stresses from photoelastic tests are required as a basis. For known reasons these stresses are most likely the least accurate and consequently all results for points inside become inaccurate to the same extent. Furthermore the problem must be such that for the complete contour both principal stresses are determinable, either photoelastically or on the basis of theoretical considerations. This restricts the field of application of the membrane-analogy method as discussed in this paper to a limited number of special cases.

⁷ Mechanics Division, Research Laboratories, Westinghouse Electric & Manufacturing Co., East Pittsburgh, Pa.

Oil-Film Whirl—A Non-Whirling Bearing

By BURT L. NEWKIRK¹ AND LLOYD P. GROBEL,² SCHENECTADY, N. Y.

The shafts of turbines, generators and other high-speed machines run in journal bearings on films of oil so that there is no metal-to-metal contact between the journal and the bearing. Although the bore of the bearing is only a few thousandths of an inch larger than the diameter of the journal the oil film supports the rapidly rotating journal and holds it steadily in a very definite position within the bearing clearance.

The position which the journal takes within the bearing clearance depends on the viscosity of the oil, the load on the journal, the speed of rotation, and the dimensions of journal and bearing. For example, if the rotation speed is only a few rpm the journal runs near the bottom of its clearance. At higher speeds the journal runs so that its closest approach to the bearing is at some point on the side opposite to that which it climbed at starting. For

very high speeds the same journal runs nearly centered in the bearing clearance.

Observation and experience teach that in general the oil film forms a very steady support for the journal and that it even exerts a dashpot action opposing outside disturbances that would cause the shaft to vibrate. This remarkable stability, however, has been found to be subject to a notable exception. When a shaft runs at twice its critical speed or at any higher speed the equilibrium between the load and the lift of the oil film becomes unstable, the journal moves in a minute spiral of increasing radius, and the whole shaft picks up a whirling motion. The whirl has the natural frequency of the shaft and the motion is one of resonance.

This paper deals with a laboratory study of oil-film whirl phenomenon and describes a means for combatting it.

THE phenomenon of what has been termed shaft whipping due to oil action in journal bearings³ is a whirling or vibration which develops when a rotor on journal bearings runs at approximately twice the critical speed of the shaft or at any higher speed. The whirl or vibration occurs at the resonant frequency which, in cycles per minute, is equal to the revolutions per minute at the critical speed. Thus the shaft builds up a resonant vibration or whirl when running at a number of revolutions per minute equal to, or greater than twice the resonant frequency. The stimulus which builds up and maintains the vibration lies in the oil film in the bearings. This was proved by shutting off the oil supply. As the oil ran out of the bearing the whirling ceased and it built up again when the oil supply was restored.

It was found that rotors did not develop this whirl when run on friction damped spring bearings and that increasing the unit loading of the bearing prevented the whirl up to speeds somewhat above twice the critical speed. An obvious means to escape the difficulty in commercial design is to make the rotor of such stiffness that the critical speed is more than half of the running speed.

The phenomenon has since been observed in commercial machines and all three of the expedients above mentioned have been used successfully at one time or another to combat it. With higher journal peripheral speeds the action of the oil film seemed

to be less easily suppressed by increased unit loading or by spring-supported bearings.

Some time ago this study was taken up again with a new apparatus built for study of this phenomenon as it develops with higher journal speeds. The highest speed of the previous investigation was that of a 1 $\frac{7}{8}$ -in. journal at 5000 rpm. In the

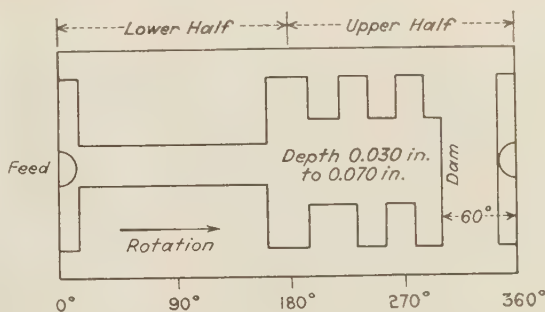


FIG. 1

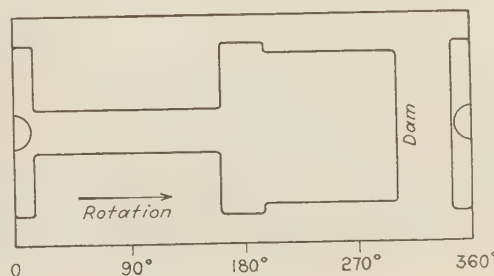


FIG. 2

new apparatus a 2-in. journal was run at more than 30,000 rpm, giving a journal peripheral speed of 16,000 fpm.

An object of the study was to develop if possible a system of grooves in the bearing that would control the behavior of the oil film so as to prevent development of the whirling phenomenon. Figs. 1 and 2 show developed bearing surfaces with systems of grooves that proved most satisfactory. Oil enters at the horizontal joint on the downgoing side of the journal. Some of the

¹ Research Laboratory, General Electric Company. Mem. A.S.M.E. Dr. Newkirk was graduated from the University of Minnesota in the classical course. After some graduate work there in physics and mathematics he studied at the Universities of Munich and Göttingen, Germany, and later became associate professor of mathematics and mechanics in the College of Engineering of the University of Minnesota. He entered the Research Laboratory of the General Electric Company in 1920.

² Research Laboratory, General Electric Company. Mr. Grobel was graduated from the University of Minnesota in 1924 with the degree of B.S. in Mechanical Engineering. Since graduation he has been with the General Electric Company, from 1925 to the present time in their Research Laboratory.

³ "Shaft Whipping Due to Oil Action in Journal Bearings," by B. L. Newkirk and H. D. Taylor, *General Electric Review*, Aug., 1925, p. 559.

Contributed by the Applied Mechanics Division and presented at the Annual Meeting, New York, N. Y., December 4 to 8, 1933, of THE AMERICAN SOCIETY OF MECHANICAL ENGINEERS.

NOTE: Statements and opinions advanced in papers are to be understood as individual expressions of their authors, and not those of the Society.

oil is pumped by action of the shaft through the central peripheral groove to the dam at the end of the groove where considerable hydrodynamic pressure builds up, especially if the peripheral speed of the journal is high. The upper half of the bearing fills up with oil and the axial grooves in the upper half of the bearing (Fig. 1) distribute the pressure. If the load on the bearing is sufficient to insure downward pressure under all circumstances the lands in the upper half may be omitted (Fig. 2). Thus the bearing is kept full of oil so that air is not drawn in at any point and a considerable downward pressure is exerted on the journal by the oil in the upper half of the bearing. The downward load on the journal due to the oil pressure developed in the upper half of the bearing is not sufficient to account for the nonwhirling characteristic of our bearing by the increased loading of the journal alone. In other words a bearing of conventional design with external loading on the shaft equal to the load produced by the oil pressure in the upper half of the new bearing will still whirl.

The weights of the rotors used in most of these tests imposed a load on the bearing of negligible amount. The whirling char-

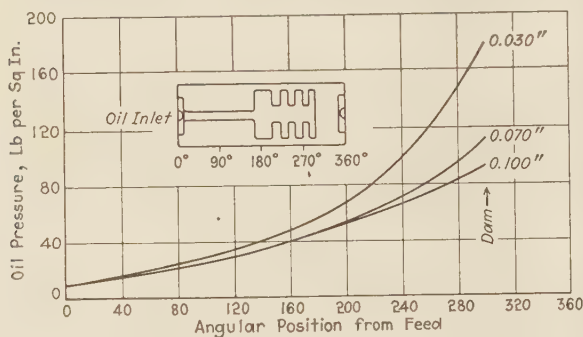


FIG. 3 OIL PRESSURE IN CIRCUMFERENTIAL GROOVE FOR VARIOUS DEPTHS OF GROOVE

(Bearing, 2 in. \times 2 1/8 in.; clearance, 2.75 parts per thousand; peripheral velocity of journal, 15,700 ft (4785 m) per min. Groove system in bearing surface developed is indicated in insert.)

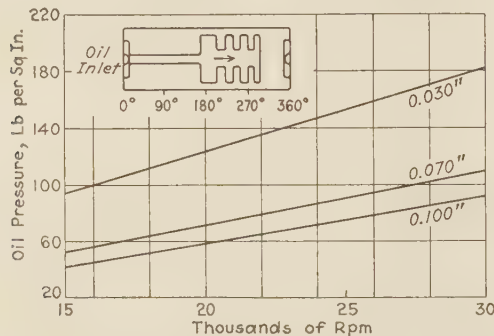


FIG. 4 PRESSURE AT DAM VERSUS RPM FOR VARIOUS DEPTHS OF GROOVE

(Bearing, 2 in. \times 2 1/8 in.; clearance 2.75 parts per thousand. Groove system in bearing surface developed is indicated in insert.)

acteristic is therefore avoided in bearings of this design with a shaft substantially without external loading, and with a peripheral journal speed of 16,000 fpm. Some hydrodynamic pressure develops in the lower groove so that the oil pressure increases continuously from the point of entrance of the oil to the dam. This groove in the lower half serves also to reduce the lifting power of the oil film in the lower half of the bearing by dividing the bearing surface into two sections and doubling the total effective end-leakage area besides shortening the leakage path.

The bearing has been called "non-whirling." This does not

imply resistance to vibration stimuli but simply that the stimulus to whirling does not develop because of the action of the oil film. In fact an exception must be made even to this narrowed claim, inasmuch as rotors with very heavy and relatively long overhangs mounted on bearings of this design do develop the whirl at a somewhat increased speed. This exceptional case will be discussed later.

Fig. 3 shows the development of hydrodynamic pressure along the peripheral groove as a function of the angular distance from the point of entrance of the oil. Fig. 4 shows the variation in pressure developed at the dam as a function of journal speed.

The oil is supplied to the bearing with a pressure of five or ten pounds per square inch to cause it to enter in sufficient quantity. There is no passage provided for oil exit, consequently end leakage carries away all the oil that passes through the bearing. It is essential that the bearing run full of oil. The amount that must be supplied depends, therefore, on end leakage which in turn depends on bearing diameter, clearance, pressure developed by the pumping action of the journal, and viscosity of the oil.

The bearing functions well throughout a range of clearance. Excessively small clearances result in overheating at high speeds as would be the case with any bearing. A clearance of 2.5 parts per thousand proved satisfactory for the two-inch journal up to the highest speed at which tests were usually run; 30,000 rpm, corresponding to 15,700 fpm. For journals of larger diameter and especially at the much lower journal peripheral speeds in commercial operation the commonly used clearances of 1.25 to

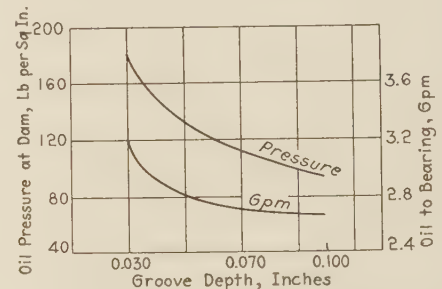


FIG. 5 OIL PRESSURE AND GPM OF OIL TO BEARING VERSUS GROOVE DEPTH

(Shaft running at 30,000 rpm. Bearing 2 in. \times 2 1/8 in. Clearance 2.75 parts per thousand.)

1.50 parts per thousand are presumably satisfactory. Larger clearances result in an excessive amount of oil passing through the bearing. This oil is pumped up to considerable pressure within the bearing and then discharged with correspondingly increased power consumption. Fig. 5 shows the amount of oil supplied, together with the pressure developed at the dam in tests of the 2-in. journal at 30,000 rpm with a 5.5-mil diametral clearance.

The grooves must be of ample capacity to carry oil enough to supply the end leakage and cause the bearings to run full. The circumferential grooves should have a cross-section from 2 to 4 or more times the product of radial clearance and journal circumference. In the lower half the peripheral groove is narrow and deep. In the upper half operation has been satisfactory with depths from 20 mils to 70 mils. Depths of from 30 to 40 mils are satisfactory at the higher speeds. If the lands are omitted in the upper half and a very wide groove used, the groove depth need not be decreased because of the greater width.

Figs. 1 and 2 do not show the grooves at the ends of the bearings that are required to carry away the end leakage oil. Conventional means for this purpose are satisfactory but more than the ordinary bearing end-leakage oil must be taken care of.

Some measurements of the power loss in the bearing were made. With a 2-in. diameter journal and a bearing $2\frac{5}{8}$ in. long, having a clearance of 2.75 parts per thousand and using oil of 155 sec Saybolt viscosity (27 centipoises) at 40 C, the following values of power consumption in the bearing were observed.

Rpm	Oil feed, deg C	Kw loss	Oil, gpm
15,000	35	2.3	...
20,000	35	3.9	...
25,000	35	6.2	...
30,000	35	9.6	...
20,000	50	3.1	1.5
25,000	50	5.4	2.1
30,000	50	8.7	3.2
20,000	60	2.9	...
25,000	60	5.1	...
30,000	60	8.3	...

THE EXPERIMENTAL APPARATUS

The apparatus developed for this study has some points of interest. A fundamental requirement was that the peripheral speed of the journal should be at least as high as that of a 12-in. journal at 3600 rpm. It was necessary also that the mounting be so rigid that resonant vibration would not develop in any of its parts at speeds within the range to be studied. One shaft, No. 1, had its critical speed above the range to be studied and another shaft, No. 2, had its critical speed considerably less than half the maximum speed to be studied. Most of the work was done with these two rotors. At a later date No. 2 was modified by adding a bell-shaped mass to the overhanging end and a third rotor was made with a long, heavy overhang.

The journal diameters were 2 in. (51 mm) and a speed of 30,000 rpm gave a journal peripheral speed of 15,700 ft (4785 m) per minute. The journal lengths were $2\frac{5}{8}$ in. (66 mm) for rotors Nos. 1 and 2, and 6 in. for No. 3. A 25-hp, 3600-rpm, d-c motor shunt wound, with a 10 to 1 spur-gear train was used for driving and the speed was controlled by varying the armature voltage. Shafts Nos. 1 and 2 are shown in Fig. 6. The longer one has a critical speed at 8500 rpm, and no other critical speed below 30,000 rpm. Both shafts have assemblies of punchings near the 2-in. bearing. These were used with a pair of electromagnets to load the shafts. Loads up to 400 lb (180 kg) could be applied. At the flanged end of each shaft a small plain journal bearing ($\frac{7}{8}$ in. \times $1\frac{1}{2}$ in.) and a ball bearing were used interchangeably. The coupling with the driving shaft was accomplished by lacing a light linen cord through holes in the two adjacent flanges on the driving spindle and the driven shaft, respectively.

The bearing standards were made of steel plates $2\frac{3}{8}$ in. thick and the main standard was approximately 14 in. wide. The standards were set on a heavy steel plate which was solidly grouted in on a concrete base on the concrete floor of the laboratory.

The apparatus was housed to confine the oil. No effort was made, however, to confine the oil within the bearing housings. Oil was supplied by a gear pump. A cooling coil and a heating coil were used to control the temperature of oil entering the bearing. Fig. 7 shows the apparatus with the longer shaft in place and the upper part of the housing removed.

To observe accurately the behavior of the journal under the action of the oil film the short shaft, No. 1, was provided with a stiff projection, the end of which was observed with a microscope while the shaft was running. Movements of the journal were amplified by the shaft extension 1.7 times at the pointer tip. To increase the refinement of observation the tips of the points were provided with recesses into which $\frac{1}{16}$ in.

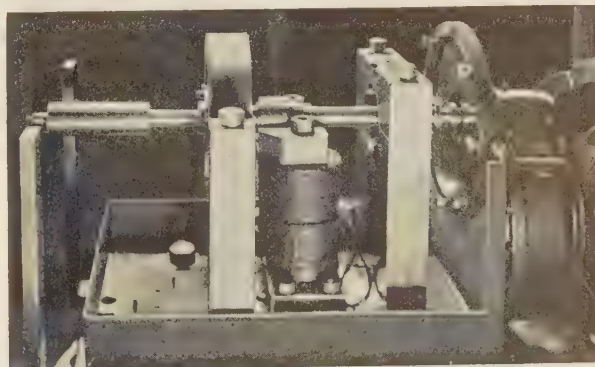


FIG. 7 APPARATUS FOR HIGH-SPEED BEARING TESTS

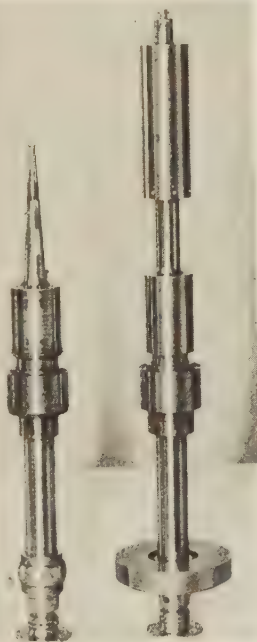


FIG. 6 SHAFTS FOR HIGH-SPEED BEARING TESTS

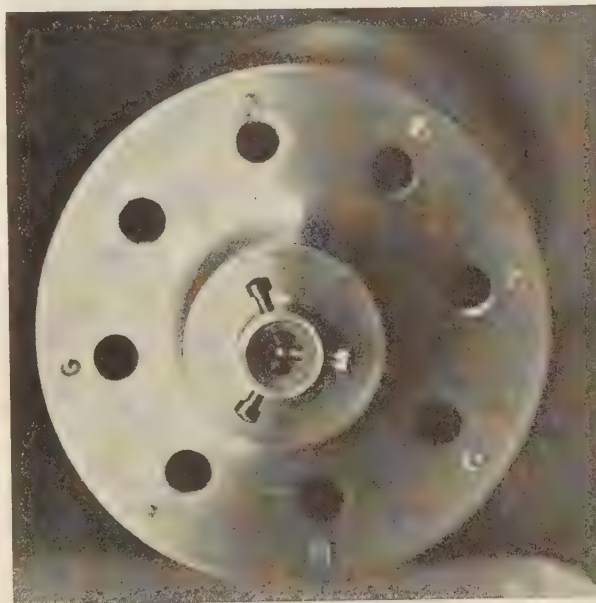


FIG. 8 SHAFT FOR HIGH-SPEED BEARING TESTS
(Enlarged view of $\frac{1}{16}$ -in. ball holder.)

(1.6 mm) steel balls were set and centered with small screws. Fig. 8 shows this considerably magnified. These balls acted as convex mirrors of small radius to give a virtual image of the crater of a small direct-current arc lamp placed about 10 ft (3 m) away. This image was only about one-ten-thousandth inch (0.0025 mm) in diameter. Since the diameter of the ball is small compared with the distance from the light source the position of the virtual image relative to the ball center changes very little

with small movements of the ball and the observed movements of the image represent with great fidelity the movements of the shaft tip and of the journal in the bearing.

A combined microscope and camera was used to observe and record the motion of the pointers. The magnification on the photographic film was 18 diameters. Applied to movements of the journal when the shorter shaft was used the power would be 30 diameters. One division of the scale which shows in some of the photographs represents 1.8 mils (0.045 mm) at the ball and 1 mil (0.025 mm) at the journal.

When the shaft is whirling or vibrating the image of the light source moves and leaves a track on the photographic film. On account of the retention of the image by the eye a track of light is observed visually also through the microscope. The arrangement of shutters is such that the image may be focused and cen-

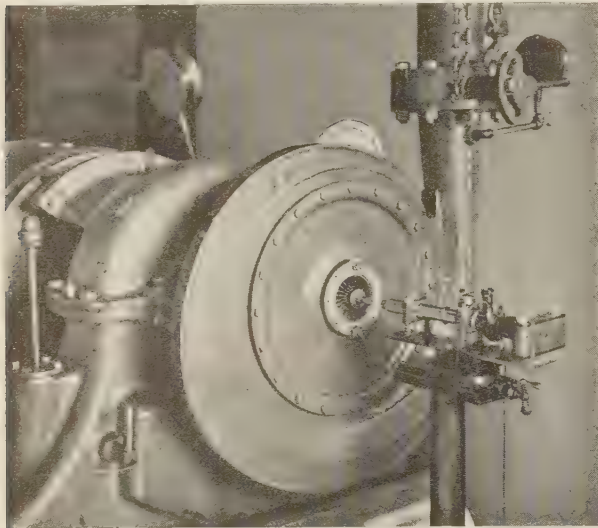


FIG. 9 CAMERA-MICROSCOPE SET-UP FOR OBSERVING AND PHOTOGRAPHING COMPRESSOR-IMPELLER-SHAFT VIBRATION

tered in the field visually and photographed immediately by operating two shutters. Fig. 9 shows the microscope and camera set up before a small compressor. The microscope was set with its axis in line with the shaft axis and the beam of light from the arc lamp made a small angle with this axis.

The shortest exposure obtainable with the shutter was $\frac{1}{60}$ sec. This corresponds to a complete revolution of the shaft at 3600 rpm. At 30,000 rpm the shaft makes 500 revolutions in a second. Shorter exposures corresponding to less than a revolution at the highest speed were obtained by using a revolving disk $11\frac{3}{4}$ in. in diameter with a notch of definite length in its periphery. The disk was so placed and rotated that it cut off the light beam except when the beam was passing through the notch. The shutter was then set for an exposure shorter than the period of one revolution of the disk. In this way the image recorded on

the film represented the movement of the pointer while the notch in the disk permitted the beam of light to pass.

With this equipment the behavior of both shafts in many bearings was observed and photographed. It is understood of course that shaft No. 2 would not behave as a rigid body when whirling or vibrating at a frequency near 8500 per minute (its natural frequency) or higher, and consequently would not indicate movement of the journal in its bearing while running at these high speeds. However, the ball at the end of shaft No. 2 gives a sensitive indication of the whirling movement of the rotor when it occurs. Numerous photographs show movement at the tip of shaft No. 2 of less than one scale division total displacement (1 division = 1.8 mils at the ball) at speeds up to 30,000 rpm, with no load on the shaft except its own small weight. Fig. 10 shows an example of these photographs made with shaft No. 2. With bearings of ordinary design this rotor breaks into violent whirling at speeds over 17,000 rpm. The numbers in Fig. 10 represent the following conditions:

Exposure number	Shaft speed, rpm	Magnetic load, lb
3 $\frac{1}{2}$	15,000	0
4	20,000	0
4 $\frac{1}{2}$	25,000	0
5	30,000	0
5 $\frac{1}{2}$	20,000	400
6	25,000	400
6 $\frac{1}{2}$	30,000	400
7	(Shows bearing clearance)	

No. 7 was made by taking six separate exposures with shaft stationary and the journal pulled by hand against the bearing in different directions. This gives a chart of the bearing clearance. Exposures Nos. 3 $\frac{1}{2}$ to 6 $\frac{1}{2}$, inclusive, all show images less than one-scale division in diameter and indicate very steady running of the rotor.

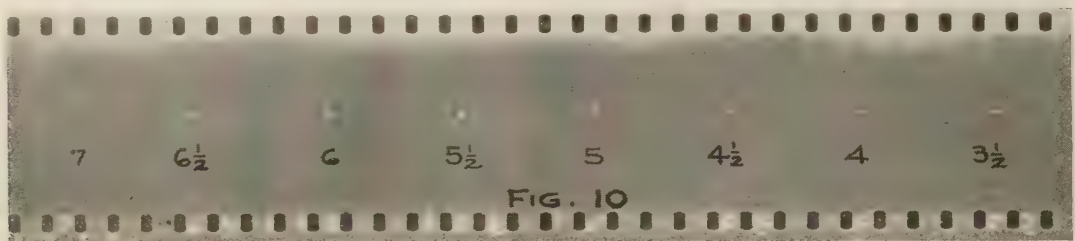
Photographs of the vibrations and whirls are difficult to reproduce and discussion in detail of their features is not necessary for present purposes. Most runs were made with bearings of unusual proportions or grooves. With a conventional overshot bearing the stiff shaft, No. 1, ran true and in the center of its clearance up to 13,000 rpm with no load.

With the non-whirling bearings the journal ran at a lower position in the bearing clearance at speeds above 15,000 rpm than it did at lower speeds.

HEAVILY OVERHUNG ROTORS

A subsequent study was made to throw more light on the nature of the oil-film whirl, especially its early stages when a rotor running in equilibrium begins to build up the whirl. Experience with two rotors having relatively long and heavy overhangs deserves mention because of its bearing on both design and theory.

A bell-shaped part was shrunk on shaft No. 2. This mass was so designed that the center of gravity of the overhanging end of the shaft was at the $\frac{1}{16}$ -in. ball which serves to reflect the image of the arc. The motion of the image, therefore, indicated the motion of the center of gravity of the mass. Fig. 11 shows a com-



bination microscope and motion-picture camera in position for observation and shaft No. 2 with its bell-shaped attachment.

The critical speed of this rotor was 2030 rpm. The load at the main bearing was 59 lb. The distance from the center of gravity of the overhanging end to the bearing center was 1.2 times the distance between bearing centers. This was run in a bearing of conventional overshot design $1\frac{3}{8}$ in. long with a clearance of 3 parts per thousand and with the oil mentioned previously. It ran somewhat unsteadily from 4000 rpm up to 4500 rpm. It began to whirl at 4500 rpm. The whirl built up slowly around the equilibrium position of the center of gravity of the overhung mass, in the natural frequency of the rotor. The rate of increase in the energy of whirling was approximately 0.005 watt in the early stages of development when the amplitude of movement was only two or three mils.

It was found that this rotor whirled feebly at speeds above 5000 rpm with bearings of the non-whirling design, the instability increasing very gradually with increasing speed. For further study of this matter a third shaft was made with a 6-in.-long bearing and a greater overhang. This is shown in Fig. 12.

This rotor had a critical speed of 1025 rpm. The load at the main bearing was 115 lb and the overhang, measured from the center of the bearing to the center of gravity of the overhung mass was 1.3 times the distance between bearing centers. It whirled at 2600 rpm in a conventional bearing and with non-whirling bearings the whirling developed at 3000 rpm. The behavior was similar to that of the rotor with bell-shaped overhang in that the whirling built up gradually about the equilibrium position. In this case the overhang was greater, compared to the distance between bearings, and the overhung mass was much heavier, thereby giving a lower critical speed.

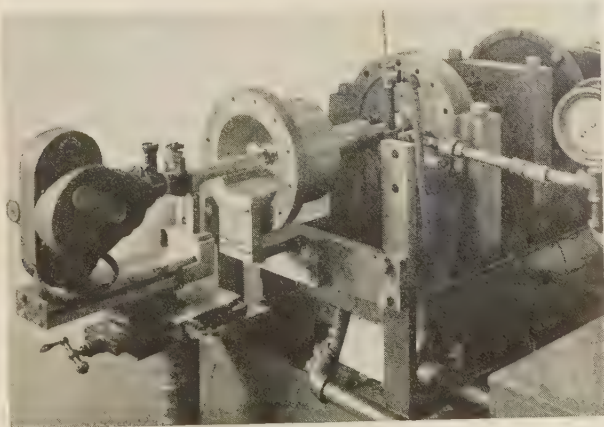


FIG. 11 PHOTOGRAPHIC MICRO-MOTION-PICTURE APPARATUS SET-UP TO OBSERVE SHAFT VIBRATIONS

It appears that rotors with relatively long, heavy overhangs show a very positive development of the oil-film whirl which is somewhat reduced but not obviated by the bearing design described above. From the point of view of theory it appears also that rotors having the same critical speed are not necessarily equivalent in their whirling tendencies since rotors in the same

critical speed range but having their mass between the bearings do not whirl with these non-whirling bearings.

THEORIES OF WHIRLING DUE TO OIL-FILM ACTION

The phenomena of shaft vibration or whirling due to oil-film action have been discussed recently on the basis of hydrodynamic theory.

Stodola⁴ discovered indications in theory that "critical speeds" may result from behavior of the oil film. The matter was ampli-

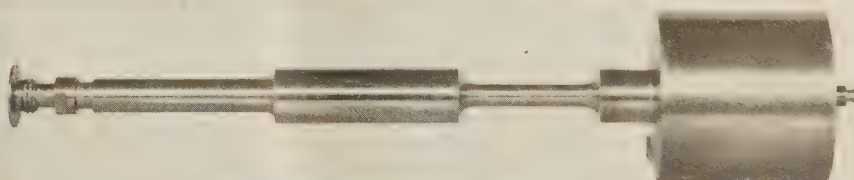


FIG. 12 SHAFT No. 3 FOR HIGH-SPEED BEARING TESTS WITH 42-LB WEIGHT SHRUNK ON

fied and an experimental study was made by Charles Hummel,⁵ a pupil of Stodola's.

David Robertson of the University of Bristol has published a valuable paper on the phenomena of whirling.⁶

The Stodola theory expressly excluded any effect of shaft elasticity. The shaft of Hummel's experimental apparatus was short and very stiff and operation was undoubtedly well below the critical speed.

The theory is based on the equations for the half bearing. The conclusion is reached that below a certain speed limit of shaft rotation the journal is supported by the oil film in stable equilibrium. When the shaft is running at any speed below that at which equilibrium becomes unstable, resonant vibration should build up due to the quasi-elastic behavior of the oil film if a periodic disturbance acts with the appropriate frequency. At two definite speeds the appropriate frequency is equal to the rotation frequency and consequently unbalance of the rotor acts to build up resonant vibration. Such speeds are therefore critical speeds due to oil film behavior. When the speed is increased above the critical value the vibration amplitude decreases.

According to the theory, the position of equilibrium of the journal in the bearing approaches the bearing center as speed increases, and the equilibrium becomes unstable if the distance between bearing center and journal center becomes less than about two-thirds of the radial bearing clearance. Hummel reports that his shaft did not run smoothly above the calculated limit of stability of the oil film.

The speed at which theoretical instability sets in depends on unit load, bearing clearance, peripheral speed of the journal, and oil viscosity. For our experimental shafts of very small weight, Nos. 1 and 2, the calculated limit of stable running is only a few revolutions per minute. Even when the bearing was loaded by the attraction of the electromagnets acting on the punchings which were mounted on the shaft (a non-massive load) the journal ran nearly central in the bearing at the higher speeds. Consequently our experiments have been made in a field where theory

⁴ "Kritische Wellenstörung Infolge der Nachgiebigkeit des Oel-polders im Lager," by A. Stodola, *Schweizerische Bauzeitung*, vol. 85, p. 265.

⁵ "Kritische Drehzahlen als Folge der Nachgiebigkeit des Schmiermittels im Lager," by Charles Hummel, *Forschungsarbeiten*, V.D.I. Heft 287, 1926.

⁶ "Whirling of a Journal in a Sleeve Bearing," by David Robertson, *The London, Edinburgh, and Dublin Philosophical Magazine and Journal of Science*, ser. 7, vol. XV, Jan., 1933, p. 113.

indicates instability. The earlier studies were made with heavier shafts but in those cases also the speeds at which whirling developed were well above the limits of stable operation indicated by the Stodola theory.

Stodola points out⁴ also that the theory of a full circular bearing indicates that whirling would build up if the conditions of clearance, load, speed, and oil viscosity are such that the journal center approaches the bearing center. This does not explain our oil-film whirl, however, since our journals run steadily at definite locations near the bearing center up to the speeds at which resonant whirling starts.

It is interesting to note that in both of the theories cited, instability is indicated when, as in the case of light unit loading, the equilibrium position of the journal approaches the bearing center. We have found that with heavy unit loading, which causes the journal to run in a lower position in the bearing, the lowest speed at which whirling develops may be considerably more than twice the critical speed of the shaft. In other words, heavy unit loading which acts against development of the oil-film whirl appears also in bearing theory as a factor making for stability.

The oil-film critical speeds of the Stodola theory are apparently not related to our oil-film whirl since our whirl occurs only with an elastic shaft, the frequency is determined by the shaft rather than the oil film, and for other obvious reasons. The instability of the oil film indicated by theory may however have a bearing on the matter inasmuch as the conditions for theoretical instability are satisfied when the oil-film whirl builds up.

Dr. Robertson's discussion is based on the theory of the full bearing. It is assumed that the journal is rotating about its own axis and whirling about the center line of the bearing. His theory explains the whirling of a vertical rigid rotor at a whirl frequency equal to half the running speed.

The conclusions regarding the horizontal rotor throw light on the force which maintains the whirl after it has developed to such an extent that the journal whirls substantially about the center line of the bearing. With horizontal (loaded) journal bearings, the whirl starts very gradually about the equilibrium position of the journal and in the natural frequency of the rotor. Dr. Robertson's theory does not account for the early stages of the whirl. After the whirl has built up to a large magnitude so that the journal whirls about the bearing center, the stimulus is represented, qualitatively at least, by the force F_{np} of Dr. Robertson's equation 4.25.

Dr. Robertson's theory does not account for the start of the oil-film whirl when a shaft is restrained from whirling while it is brought up to a speed more than twice critical speed and then released.

ORIGIN AND DEVELOPMENT OF THE WHIRL

Since the whirl is a resonant movement having the frequency of the rotor, the elastic properties of the rotor must be a major factor from the beginning. The whirl must start with a disturbance of the rotor and build up by energy fed back by the oil film. The action in detail must be as follows:

The beginning must be a disturbance of the rotor causing it to vibrate in its natural frequencies. Disturbances are caused by building tremors, neighboring machines running out of balance and by the unbalance of the rotor itself. It is not necessary to assume that such disturbances have the frequency of natural vibration of the rotor. Any shock or distortion sets up tremors in the natural frequencies of the distorted body.

Any plane vibration of the rotor in its natural frequency is quickly converted into a whirl of the same frequency by the action of the oil film. This occurs as follows:

The vibrating rotor causes corresponding movements of the journal. Movements of the journal change the bearing reaction

of the oil film. When the journal is displaced from its equilibrium position and moving, the resultant of load and bearing reaction is not zero and undoubtedly it is not directed exactly toward the equilibrium position of the journal. Consequently the journal does not return to its equilibrium position, and a plane vibration of the rotor is thus converted into a journal whirl in the natural frequency of the rotor.

When the journal is whirling in a minute spiral about its equilibrium position, the resultant of load and oil-film reaction undoubtedly has at any instant a component tangential to the direction of motion. When such a component is in the direction of motion the whirl builds up and the journal center spirals outward. When the tangential component is in the opposite direction the journal spirals inward and the whirl dies out. Such a tangential component must vary from point to point of the path of the journal whirl and it may change sign in the course of one whirl. However, if the integrated effect of the tangential components of the bearing reaction adds energy to the whirling motion of the rotor, the whirl of the journal builds up. This whirl in turn, since it has the shaft frequency, builds up the whirl of the shaft. We have therefore a sensitive feed-back system whenever the integrated effect mentioned above is in the right sense.

It appears that this integrated effect increases the energy of the whirling motion provided the speed of rotation is, in general, twice or more than twice the whirling speed, otherwise such integrated effect is in the opposite sense. This condition may be expressed in the following form:

$$\int f_t ds > 0 \quad \text{when } \omega > \omega_c$$

Where f_t represents the tangential component of the resultant force acting on the journal, ω represents the speed of rotation of the shaft, ω_c represents the whirling speed, and a represents some number, approximately equal to 2 in the cases studied and covered in this paper.

Since the incipient vibration of the rotor mass is of very small amplitude, and since an elastic shaft intervenes between the mass and the journal, the first movements of the journal out of its equilibrium position must be very minute but even these minute displacements arouse the component of the restoring force of the oil film that builds up the whirling.

While the journal whirls very near its equilibrium position in the early stages of the development, the whirl of the rotor mass may later build up to large amplitude so that the reaction at the bearing due to the centrifugal tendency of the whirling mass exceeds that due to the weight of the rotor. In this stage the tangential component of the oil film reaction is considerable since it supplies all the energy consumed in the whirl, which involves energy-consuming deformations of the entire structure.

For shaft speeds only slightly above twice the shaft critical speed the oil film stimulus is small and variable in sense, becoming larger and more positive at higher speeds. With a heavy-unit bearing loading the whirl does not build up unless the shaft speed is considerably higher than twice the critical speed of the shaft. In a speed range slightly above twice the critical speed of the shaft the whirl sometimes builds up somewhat and then dies out.

It is well known that critical speeds, that is, speeds at which resonant vibrations of rotating shafts develop, are affected by elasticity of the bearing supports, such elasticity reducing the shaft critical speeds. We have made tests to determine whether or not such elasticity of bearing supports affects the whirling of the shaft due to oil film action. It appears, as would be expected, that such whirling starts at reduced speeds corresponding to the reduced critical speeds and that the frequency of the whirl is that of the reduced critical speed.

Finally, further tests showed that the feed-back effect is greater when the overhanging mass is relatively heavy and the overhang great.

These remarks apply to all of the rotors used in our laboratory study and to larger machines in the field. Critical speeds have ranged from 600 rpm to 8500 rpm. Bearing pressures have ranged from 1 lb per sq in. to over 200, and speeds have been run up to 30,000 rpm, and 16,000 fpm. Shaft diameters have varied from one inch to twelve inches; bearing supports have been very rigid and again intentionally flexible. Bearing clearances have varied widely. Throughout this entire range of conditions a feed-back characteristic of the oil film has developed in general when the shaft speed has exceeded twice the speed of its whirling in the natural frequency.

Studies based on hydrodynamic theory have not yet accounted for the early stage of the oil-film whirl. An explanation is needed of the energy input from the oil film to a minute whirling motion of the journal about its equilibrium position, when the rotation speed is approximately twice the whirling speed or greater.

Another shaft-whirling phenomenon was reported⁷ a few years ago. This is maintained by a different feed-back mechanism, namely, internal friction of the rotor, due to working of shrunk-on members. In such cases the whirl undoubtedly originates from shaft vibration. After the whirl is started the restoring force, due to shaft elasticity and cramping action of the shrunk-on member, has a tangential component which is in the direction of whirl if the speed of rotation exceeds the critical speed of the shaft. The whirl builds up, therefore, until the energy consumed in working of non-rotating parts of the structure and in increased bearing friction equals the energy fed back to the whirl by working at the fits on the rotor.

The expression "shaft whirling due to action of the oil film" is cumbersome and unsatisfactory in other respects. The expression "shaft whipping" is unsatisfactory also since the word "whip" is frequently and properly used to designate motion of an overhung shaft. The name "oil-film whirl" seemed more appropriate. If this is acceptable the whirling described in the 1924 paper⁷ and called "shaft whipping" might be called the "cramped shaft whirl."

ACKNOWLEDGMENT

The experimental work has required good technique in balancing the rotors and great accuracy in adjusting the steel ball reflector, etc. In this work our assistant Mr. F. B. Quinlan has shown remarkable skill and enthusiasm.

Discussion

R. P. KROON.⁸ It has been brought out that the downward load on the journal due to the oil pressure developed in the upper half of the new bearing is not sufficient to account for the non-whirling characteristic. If this is the case, would the authors be able to tell what particular change in the oil flow affects the tendency of the journal to whirl. It seems to be a fact that quite a few bearings in the field have been made "non-whirling" by our service department simply by scraping away part of the bearing area. A hydrodynamic theory, if adequate, would probably explain quite a few practical points in the behavior of the whirl which, until now, appear mysterious.

In this respect the article,⁶ "Whirling of a Journal in a Sleeve Bearing," by Dr. Robertson which is mentioned in the paper is interesting. Dr. Robertson has attempted to attack the prob-

lem by a straightforward theoretical analysis but fails to come to conclusions which explain the physical facts. He is able to find, for speeds exceeding twice the critical speed, a force on the journal normal to the eccentricity, in other words pushing the journal around, but states that the oil force along the eccentricity is zero when there is no radial movement of the journal center. This is obviously not in line with what experience has shown about any horizontal non-whirling bearing. After equating the elastic force of the flexible rotor to the oil-whirl driving force, Dr. Robertson states that as the shaft speed is raised above twice its critical value, the eccentricity should decrease, and, at a certain limiting speed, the whirl should disappear. This is not what happens in the actual case, where the relations between the oil-whirl driving force and the damping are apparently such that the eccentricity usually increases with increasing speed. It seems, therefore, that a theoretical solution still has to be developed.

DAVID ROBERTSON.⁹ The authors are to be congratulated on finding a form of bearing which in most cases eliminates whirling at high speeds caused by the action of the oil in the bearings. It would add to the interest of their paper if they would reveal the process by which they arrived at the design shown. Were they guided by some sort of theory or did they merely make a lucky shot in a series of trials?

They have certainly set some new problems to those who deal with the theory of lubrication because the ordinary statement of that theory will not account for the building up of the pressure all round a groove of constant depth, and will find some difficulty in explaining the stability which the new bearing gives.

The two outer portions of this bearing completely surround the journal. Without allowing for the end leakage which, however, is a very important factor with this bearing, we should have a maximum pressure in these rims at about 135 deg and a minimum at about 225 deg. It is probable that these rims receive their oil by endwise flow from the groove between 180 deg and 300 deg and that the pressure inside the groove is sufficient to prevent the ingress of air to that low-pressure region from the ends of the bearing.

Endwise flow evidently plays a very important part in the action of these bearings and it is doubtful whether any satisfactory quantitative theory can be built up for them.

The force and couple transmitted by the shaft to each bearing must be balanced by the oil forces on the journal. Since the directions of the latter forces, and of the couple which they produce, have some definite relation to the distribution of the journal eccentricity along its length, both in direction and amount, a steady whirl must correspond to some journal position in which this relation is stably satisfied.

Working on these lines, the writer has studied several cases in which forces only, and no couples, act on the journals, and has made model experiments which give a general confirmation of the theoretical results arrived at. A paper on the subject is now in preparation but as it will not be ready for publication for some time a summary of the results may be given here.

With very little or no lubrication, the friction between the journal and the bearing drives the journal center backward, and can maintain, and even start, a backward whirl which runs just below the critical speed, provided the shaft speed exceeds a certain limit which is only a fraction of the whirl speed.

The whirl speed remains practically constant at all shaft speeds above that which corresponds to that of the journal when rolling around inside the bearing without slipping.

⁷ "Shaft Whipping," by B. L. Newkirk, *G. E. Review*, Mar., 1924, p. 169.

⁸ Experimental Division, Westinghouse Electric and Manufacturing Company, South Philadelphia, Pa. Jun. A.S.M.E.

⁹ Professor, Electrical Engineering Dept., Merchant Venturers' Technical College, Faculty of Engineering, University of Bristol, England.

With lower shaft speeds, the whirl speed adjusts itself to the rolling condition and, at a particular speed, it suddenly stops.

As expected from the theory, the backward whirl ceases as soon as the bearings are filled with oil and cannot be restarted until most of the oil has run out. There was, however, one notable exception to this statement.

With the model running vertically, hung from a ball bearing at its upper end and the bottom of the $1/4$ -in. shaft in a $5/8$ -in. diameter bearing immersed in a pool of oil, the journal would not stay in the central position but would whirl forward in the manner already described from theory⁶ by Dr. Robertson and mentioned by the authors. This whirl was a very slow one, probably because the ball bearing offered a lot of resistance to that kind of motion and the oil forces would be quite small with such abnormal bearing clearance.

But to our surprise, a stable high-speed backward whirl could be started by plucking the shaft and occasionally it would arise spontaneously. Most unexpectedly, it was found to run at precisely the same speed as it did when the bearing was dry, thus indicating that the angle of friction was the same in both cases.

It still remains a puzzle how the forward or the backward whirl can be equally well maintained by the same bearing under the same conditions with no change whatsoever beyond the mere starting of the backward whirl. The one whirl requires a forward component and the other a backward component of the force acting on the journal center.

In connection with this work, the writer has been making a fresh study of Newkirk and Taylor's paper on shaft whirling³ with the object of finding the cause of the whirling at high shaft speeds.

He has come to the conclusion that the oil has two distinct actions, the first depending on the force exerted on the journal when it is eccentric but substantially parallel to the bearing, and the second arising from the couple tending to tilt the journal when it does not lie in that direction.

In the paper already mentioned, it is shown that the first action of the oil completely explains the "oil resonance whirl" found by Newkirk and Taylor when the shaft runs just a little faster than twice its critical speed. It accounts for the whirl running at the critical speed and for its disappearance when the shaft runs too fast.

The authors seem uncertain about the way in which this theory explains how the whirl restarts after the shaft has been steadied at the center of the bearing. Since the central position is unstable, the least error in centering the journal or the slightest tremor from some external source is sufficient to start the journal on its outward journey.

The second action of the oil probably accounts for the whirling at shaft speeds above the limit at which the first action ceases to be effective but the theory is still only in a nebulous state.

When the journal moves away from its unstable central position, its two ends may move in opposite directions so that the journal assumes a tilted position and performs a conical whirl. Newkirk and Taylor observed this sort of motion in the bearing when it was free to move.

The tilting of the journal throws the rotor out of balance but the unbalance rotates with the journal whirl, not with the shaft. Consequently, the rotor whirl it induces must also go at the same speed as the journal whirl. We may easily suppose that the minimum speed, at which the oil-pressure forces are sufficient to produce enough tilt, is often above that at which the first oil-induced whirl dies away.

The eccentricity of the center of gravity of rotor which can be produced by tilting the journal within the limits set by the bearing clearance is much greater than that clearance. Hence the second oil-induced whirl⁷ may have a larger amplitude than the

first and the amplitude may be expected to grow as the shaft speed increases for this causes the oil forces to increase.

Further, the journal of a horizontal rotor is already tilted by the deflection due to gravity and may, therefore, be expected to give the second oil-induced whirl at a lower speed than when it is vertical.

All these conclusions agree with Newkirk and Taylor's experimental results and may also have some bearing on the present authors' experience with rotors having a heavy overhang.

C. RICHARD SODERBERG.¹⁰ The phenomenon referred to as oil-film whirl appears to belong to an extensive group of vibration phenomena, which may be called self-excited motions. It was covered by a separate paper¹¹ contributed by the Applied Mechanics Division, A.S.M.E., sometime ago and has proved to be of real practical significance in high-speed machinery. All that is needed is a vibrating system with "negative damping forces," that is, reaction forces which act in the direction of motion. During a few years, we have encountered several obscure vibration phenomena which, upon closer examination, appeared to belong to this class. The most representative group is governor hunting phenomena.

In those instances when we have run into the oil-film whirl, we have succeeded in eliminating it by modifications of the oil flow to the bearing. Some years ago, we used to have a "round-hole" type of bearing in our turbo-generator test arrangement. They very frequently gave rise to oil-film whirl, which at one time presented a very baffling problem. It was eventually overcome by side relief of the bearings. Our standard bearing with a pronounced side relief and only 90- to 120-deg active supporting arc has given rise to this problem in only a few rare cases which have been taken care of by detail modifications of the same nature.

The paper presents a welcome addition to this obscure subject and the authors are to be congratulated on their very complete results.

M. STONE.¹² The paper covers a very interesting and original research into a bearing problem that has had many expositions during the past ten years or so. The authors' experiments, leading to a practical method of reducing the whirling in bearings, form the type of investigation that is all too infrequent.

As to the theories of shaft vibration as affected by bearing oil films, there is much that remains controversial however. As a result of Stodola's and Hummel's work mentioned in the paper, this discussor undertook an investigation of such phenomena on large power machines. Very sensitive electromagnetic instruments, measuring the position of the shaft in its bearings to an accuracy of 10^{-5} in. were mounted on the 9 in. \times 18 in. bearings of a 10,000-kw, 900-rpm synchronous condenser. In this way the motion of the shaft in the hydrodynamic-force field was obtained accurately. At the same time, pedestal vibrations were measured with a Geiger vibrograph. Tests were run at various speeds from zero to 900 rpm and for perfect and poor mechanical balance. The results were briefly: (1) No relation between shaft motion and pedestal motion. The latter showed a resonance condition, for example, where none was revealed in the former. (2) Motions of shaft in the bearing were so large (0.003 in.) that corresponding critical speeds should be very low, where-

¹⁰ Manager, Turbine Apparatus Division, Westinghouse Electric and Manufacturing Co., S. Philadelphia Works, Philadelphia, Pa. Mem. A.S.M.E.

¹¹ "Self-Induced Vibrations," by J. G. Baker, A.S.M.E. Trans., 1933, paper APM-55-2.

¹² Mechanical Engineer, Westinghouse Electric and Manufacturing Company, East Pittsburgh, Pa.

as the actual pedestal critical speeds were practically as calculated, not including the apparently very great flexibility in the film itself. This work will be published later.

In Robertson's paper, referred to by the authors, assumptions are made that far from represent the actual hydrodynamic conditions in bearings, such as, for example, that the equilibrium position of a shaft in a horizontal bearing is when the two centerlines are on the same level, etc. Admittedly, an accurate analysis of these phenomena is very complex—but there is much to be discarded and much more to be carefully scrutinized in the already published works on the question.

AUTHORS' CLOSURE

In response to Mr. Kroon's request for our views of the mechanism of oil-film behavior in our bearing we can only repeat the suggestions made in the paper that reduction of lifting power due to the central groove in the bottom, and downward pressure, increasing with increasing speed, due to oil pressure in the top seem to make for stability. A satisfying answer to this question must wait until the hydrodynamic equations are set up for this case and adequately discussed.

It was stated in the 1925 paper that increased unit loading, accomplished by removing some part of the bearing area raised the speed at which whirling would develop. This might well prove a valuable help in cases of trouble in the field.

Dr. Robertson inquires about the process by which we arrived

at the design shown. In the view that bearings of conventional design run with considerable air in the clearance in the upper half we thought a dashpot effect might develop if the upper half could be kept full of oil. The first forms of our bearing were designed to accomplish this. A reduction in the whirling tendency was noted and further modifications were made to perfect the performance of the bearing. Later a careful study was made with this bearing and with conventional bearings of the amplitude of critical speed whirling and of the rate at which vibrations die out. It did not show any marked advantage for our bearing in dashpot or damping action.

While the developments of Dr. Robertson's theory are interesting and suggestive the conclusions must be accepted with reservation because the theory of the full circular bearing which Dr. Robertson has taken as his basis leads to conclusions known to be considerably at variances with observed behavior of journals and oil films in bearings.

The backward whirl has been observed in our work. A shaft may whirl at its resonant frequency in either direction if an appropriate tangential stimulus is present. Oil-film action and Coulomb friction act in opposite directions and either may maintain a whirl.

Mr. Soderberg reports that side relief of the bearings has proved effective in overcoming whirling tendencies. We have found this helpful but not so effective (for example in the case of light, high-speed shafts) as the bearing now proposed.

Stress Concentration Produced by Holes and Notches

By A. M. WAHL¹ AND R. BEEUWKES, JR.,² EAST PITTSBURGH, PA.

The problem of stress-concentration effects, produced by holes and notches in bars under tension is, of interest to machine designers. The present paper describes photoelastic tests and strain measurements to determine these effects more accurately than has been done heretofore, a more accurate extrapolation method being employed in connection with fringe photographs. Stress-concentration factors thus determined were, in general, higher than those obtained by previous investigators. In cases where mathematical calculations were available, the tests checked these. Empirical equations for use in calculation are also given.

BECAUSE of the importance in machine design of tension members having holes, notches, or other discontinuities, the problem of the stress-concentration effects produced by them is of practical interest. This is especially true where fatigue

conditions are involved, since as is well known in such cases the endurance strength is markedly lowered by such "stress raisers" even though the material be quite ductile. The problem has therefore been receiving considerable attention in recent years.³

Such fundamental cases as those represented in Fig. 1 are of importance in connection with fatigue tests on grooved specimens or specimens having holes. A review of the literature, however,

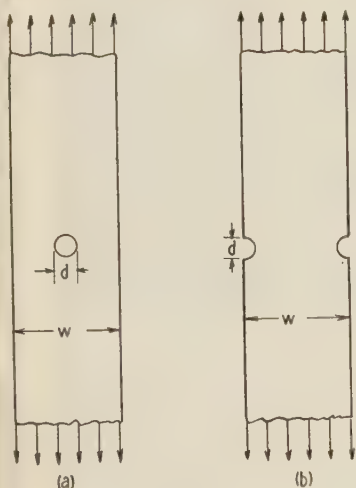


FIG. 1 BARS UNDER TENSION

¹ Westinghouse Research Laboratories, East Pittsburgh, Pa. Mem. A.S.M.E. Dr. Wahl received his education at Grinnell College and Iowa State College, being graduated from the mechanical engineering course of the latter in 1925. He then entered the employ of the Westinghouse Electric & Manufacturing Company as a graduate student. In 1927 he received his M.S. and in 1932 his Ph.D. degrees from the University of Pittsburgh. Since 1926 he has been engaged at the Research Laboratories of the Company on problems of applied mechanics, particularly in the field of stress analysis. He was the recipient of the 1929 A.S.M.E. Junior Award.

² Westinghouse Research Laboratories, East Pittsburgh, Mr. Beeuwkes was graduated from the University of Washington in electrical engineering in 1930 and then took the mechanical design school course of the Westinghouse Electric & Manufacturing Company. He has since been working on questions of applied mechanics and the creep of metals in the Research Laboratories.

³ "Stress-Concentration Phenomena in Fatigue of Metals," by R. E. Peterson, A.S.M.E. Trans., 1933, APM-55-19.

"Die Kerbe," by F. Laszlo, *Zeit. V.D.I.*, June 16, 1928, p. 851.

"Die Kerbwirkung," by A. Wewerka, *Maschinenbau*, vol. 8, p. 33.

Contributed by the Applied Mechanics Division and presented at the Annual Meeting, New York, N. Y., December 4 to 8, 1933, of THE AMERICAN SOCIETY OF MECHANICAL ENGINEERS.

failed to reveal accurate data on theoretical stress concentration factors for the complete range of variation of the ratio of the diameter, d , of the hole or notch to the width, w , of the bar, or d/w . An analytical solution for the case shown in Fig. 1(a) for values of the ratio d/w less than 0.5 was obtained by Howland⁴ but no accurate experiments were cited to confirm the results of the calculations. A very rough agreement was obtained with some tests made by Coker⁵ who also tested both cases of Fig. 1

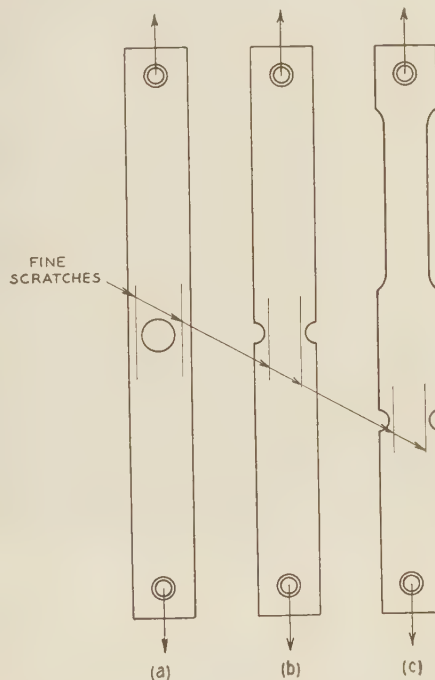


FIG. 2 SHAPES OF SPECIMEN TESTED

using celluloid specimens. However, as Coker himself states, at the edge of the hole or notch where the maximum stress occurs the accuracy of his tests was not great. This was due to the fact

⁴ "On the Stresses in the Neighborhood of a Circular Hole in a Strip Under Tension," by R. C. J. Howland, *Phil. Trans. Royal Soc. of London*, A 229 (1929), p. 49.

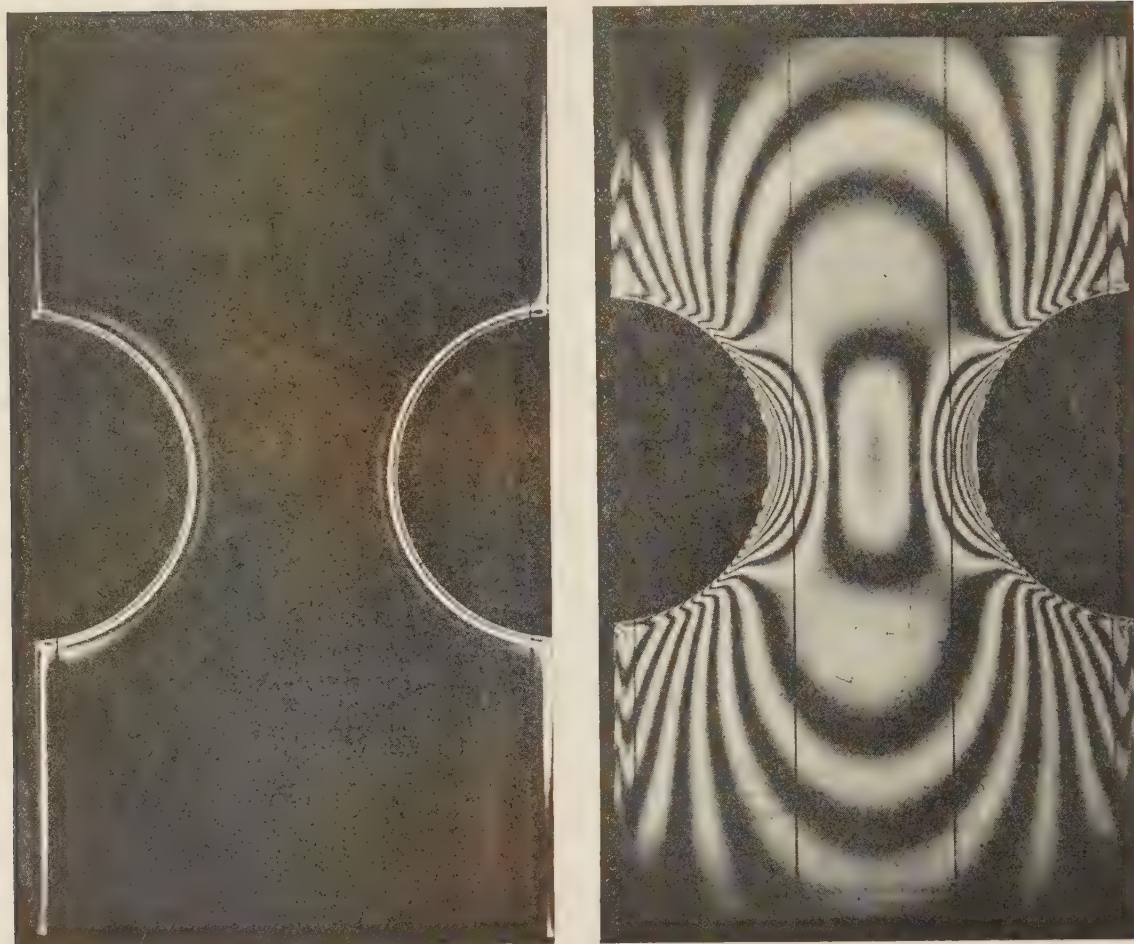
⁵ "The Effects of Holes and Semi-Circular Notches on the Distribution of Stress in Tension Members," by E. G. Coker, *Proc. Phys. Soc.*, 1912-1913, p. 95.

"Photoelastic and Strain Measurements of the Effects of Circular Holes on the Distribution of Stress in Tension Members," by E. G. Coker, K. C. Chakko, and Y. Satake, *Proc. Instn. of Engrs. and Shipbuilders in Scotland*, 1919-1920, p. 34.

"Stress Distributions in Notched Beams and Their Application," by E. G. Coker and G. P. Coleman, *Trans. Instn. Naval Arch.*, 72 (1930), p. 141.

"Stress Concentrations Due to Notches and Like Discontinuities," by E. G. Coker and P. Heymans, *Annual Rept. Brit. Assn. Advancement of Science*, 1921, p. 291.

NOTE: Statements and opinions advanced in papers are to be understood as individual expressions of their authors, and not those of the Society.



(a) Before Loading

(b) After Loading

FIG. 3 SPECIMEN WITH HIGH EDGE STRESS

that the compensation method was used to determine the stress, a method that is particularly difficult to use at a localized point of stress concentration. Coker's results, nevertheless, were valuable as a first attack on the problem.

Tests using an extensometer were also made a long time ago by Preuss.⁶ These are again not as accurate as might be desired because of the finite gage length required and because of the lack of sensitivity in extensometers of short gage length. These tests, however, do represent an excellent pioneering attack on the problem of photoelastic stress determination.

More recently, since the present investigation was started, the case represented by Fig. 1(a) was studied photoelastically by A. Hennig⁷ using specimens made of optical glass. The results he obtained agree quite well with those obtained herein for values of d/w less than about 0.7.

Because of the lack of accurate data on stress-concentration factors for these cases it was decided to make some additional photoelastic tests and strain measurements. The fringe method,

as developed by Tuzi,⁸ Mesmer,⁹ Frocht,¹⁰ Solakian and Karelitz,¹¹ and Baud¹² was applied. Tests were made on bakelite specimens of the shape shown in Figs. 1 and 2 to cover the complete range from $d/w = 0$ to $d/w = 1$. In addition some tests were made on a large steel specimen having a hole with a diameter almost equal to the width and of a size large enough so that accurate strain measurements could be made with Huggenberger extensometers.

TEST SPECIMENS

The types of test specimens used are shown in Fig. 2. It will

⁸ Z. Tuzi, Inst. Phys. and Chem. Research, Tokyo, vol. 8, p. 247, and vol. 12, p. 21. See also footnote 10, discussion to Dr. Frocht's papers.

⁹ "Vergleichende Spannungsoptische Untersuchungen und Fließ Versuche unter Konzentriertem Druck," by G. Mesmer, *Zeit. für Technische Mechanik und Thermodynamik*, V.D.I., vol. 1, nos. 2 and 3, Berlin, 1930.

¹⁰ "Recent Advances in Photoelasticity," by M. M. Frocht, A.S.M.E. Trans., 1931, APM-53-11.

"Kinematography in Photoelasticity," by M. M. Frocht, A.S.M.E. Trans., 1932, APM-54-9.

¹¹ "Photoelastic Study of Shearing Stresses in Keys and Keyways," by A. G. Solakian and G. B. Karelitz, A.S.M.E. Trans., 1932, APM-54-10.

¹² R. V. Baud, *Jour. Optical Soc. Am.*, vol. 21, 1931, p. 119.

⁶ E. Preuss, *Forschungsarbeiten (Mitteilungen über Forschungsarbeiten)*, V.D.I., no. 126, 1912, and no. 134, 1913.

⁷ "Polarisationsoptische Spannungsuntersuchungen am gelochten Zugstab und am Nietloch," by A. Hennig, *Forschung auf dem Gebiete Ingenieurwissenschaften*, V.D.I., vol. 4, no. 2, p. 53.

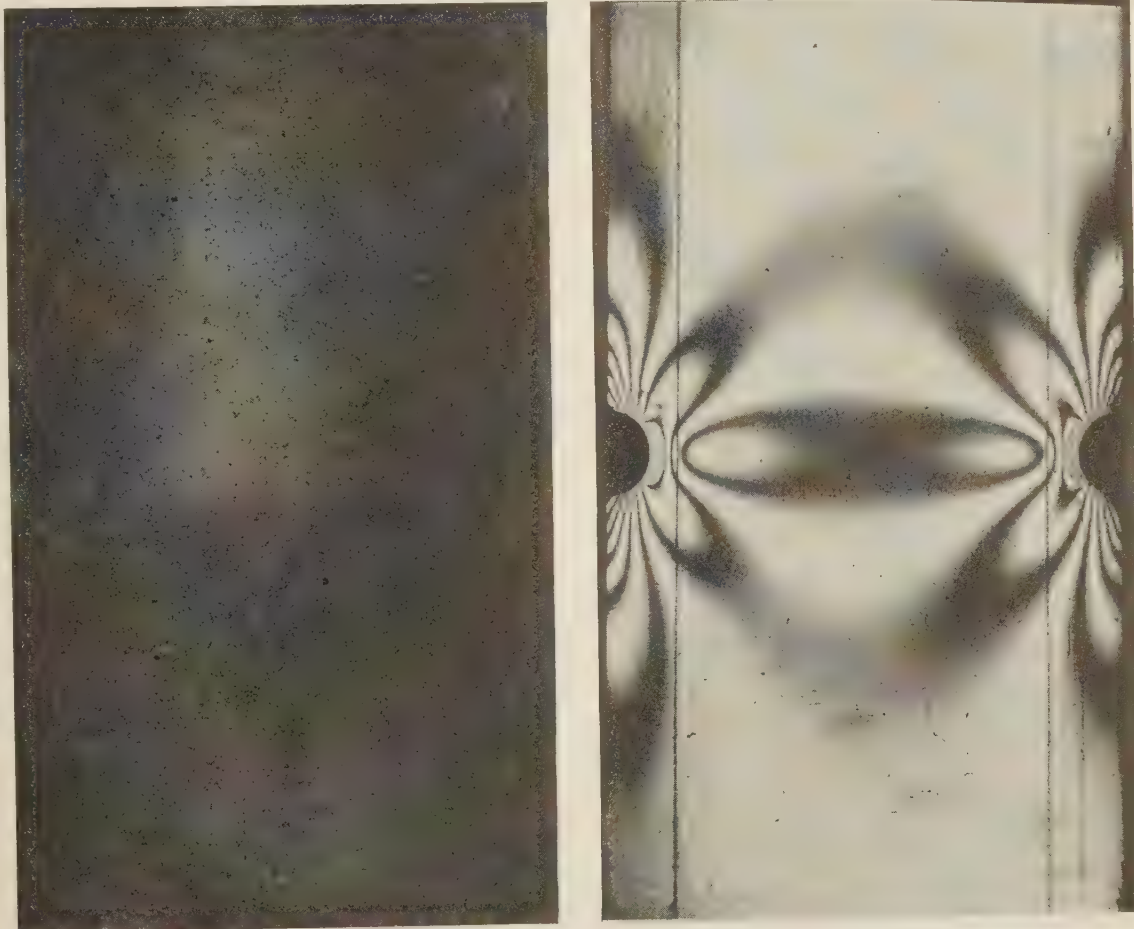
be noted that in each case the test piece was designed so that the stress was substantially uniform along a considerable portion of the specimen. By plotting the loads on the specimen against fringe order in the uniformly stressed portion, a calibration curve could be obtained thus permitting the determination of the stress per fringe for the material. In some cases a calibration bar in bending, such as employed by other investigators, was used but the results obtained in this manner were practically the same as those obtained by using the aforementioned method which was easier to apply in this case and which in our opinion was fully as accurate. The specimen shown in Fig. 2(c) permits the calibration to be made at a higher stress in the straight portion without producing an excessive stress in the minimum section at the notch.

On each of the test specimens fine scratches were made parallel to the axis of the specimen and in close proximity to the hole or notch. The purpose of these scratches was to permit the exact determination of the true edge of the hole or notch on the photograph. This was done by measuring the distance from the scratch to the edge of the hole or notch on the actual specimen using a microscope or a comparator. Then, knowing this distance and the actual magnification, the location of the true edge could be accurately determined on the photograph. It was necessary to know this location accurately since in most cases the stress gradient near the edge was fairly steep and in consequence a slight error in the location of the edge would make a relatively

great difference in the magnitude of the measured stress. In all cases, as will be discussed later, it was found necessary to extrapolate the stress difference curve to the true edge, which in each case was found to be slightly inside the apparent edge as shown by the photographs. (See Figs. 6 to 8.)

The test specimens were prepared from specimens of bakelite annealed by a process similar to that used by Mesmer,⁹ Frocht,¹⁰ and Solakian and Karelitz.¹¹ It was necessary to select certain of the best pieces of bakelite for use in preparing specimens, since it was found that some of the samples retained residual stresses of considerable magnitude even after repeated annealing. This is in agreement with results obtained by Tuzi⁸ and indicates that it is of importance to get material suitable for annealing in order to obtain satisfactory results, particularly when high accuracy is desired.

The test specimens were prepared by first annealing them and then machining them to size, care being taken to see that the final machining cuts were very light so as to introduce as little residual stress near the edge as possible. Precautions were taken also to carry out the photoelastic tests as soon as possible after completion of the machining operation since it was found that in a short time, the specimens would develop an edge stress which makes the determination of the maximum stress very difficult, if not impossible. This is illustrated by Fig. 3 which shows two photographs of a specimen, in the loaded and unloaded condition, and having the edge effect in both. The edge effect was produced by



(a) Before Loading

(b) After Loading

FIG. 4 SPECIMEN WITH PRACTICALLY NO EDGE STRESS

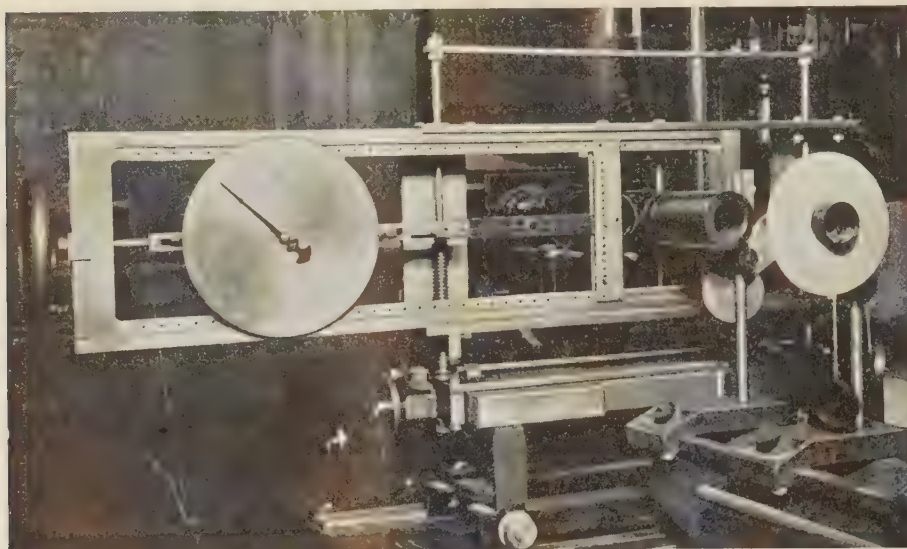


FIG. 5 SPECIMEN IN LOADING FRAME OF PHOTOELASTIC APPARATUS



FIG. 6 BAR WITH SMALL NOTCH



FIG. 7 BAR WITH MEDIUM-SIZED NOTCH

rather heavy machining cuts and by allowing the specimen to stand a few days before testing. It may be readily seen that a sudden discontinuity in the stress near the edge such as exists in this particular specimen would make an accurate extrapolation of the stress curve to the true edge almost impossible.

Fig. 4 shows two pictures of a specimen machined and tested with these precautions in mind. It may be seen that by careful attention to these details such edge effects may be practically eliminated. The scratches mentioned previously are plainly visible both in these two pictures and the two shown in Fig. 3.

PROCEDURE IN MAKING TESTS AND DETERMINING RESULTS

In carrying out the tests monochromatic light was employed, a mercury vapor lamp with an appropriate filter being used. The specimens were stressed at 3000 to 3500 lb per sq in. in the most highly stressed portions. This is approximately the proportional limit for the material. Photographs were then taken of the fringes. A view of one of the specimens mounted in the photoelastic apparatus is shown in Fig. 5. Typical photographs of various specimens tested are shown on Figs. 6, 7, and 8. At the time of making the photographic exposures, a calibration curve to find the stress per fringe was taken by loading the specimen and observing the fringe order of a uniformly stressed portion of the specimen as mentioned previously. This curve in all cases was found to be practically a straight line.

In working up the results the mean stress at the minimum



FIG. 8 BAR WITH LARGE HOLE

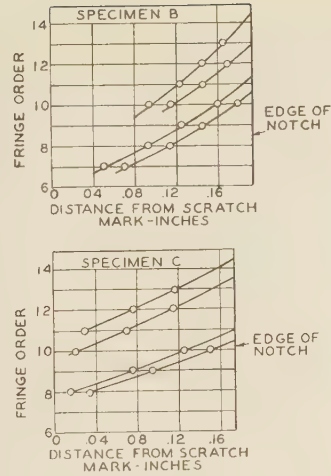


FIG. 9 CURVES OF FRINGE ORDER VS. DISTANCE FROM SCRATCH MARKS

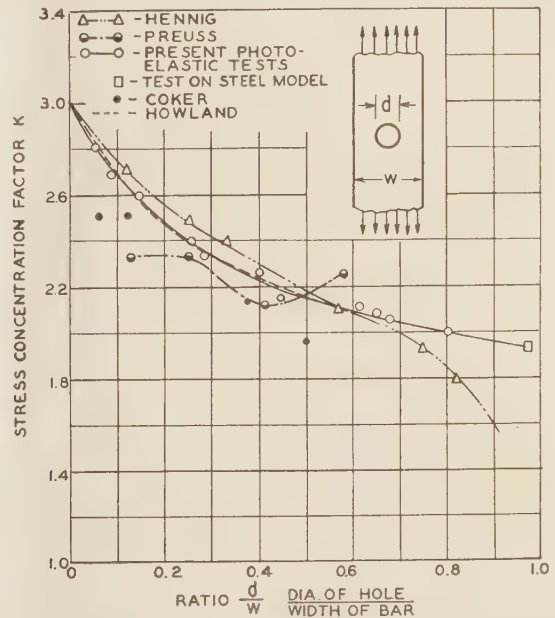


FIG. 10 STRESS CONCENTRATION FACTOR VS. d/w FOR FLAT BAR WITH HOLE

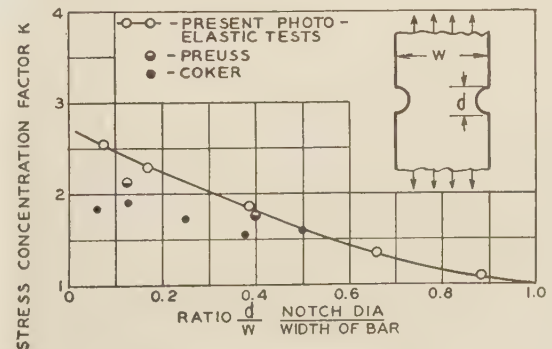


FIG. 11 STRESS CONCENTRATION FACTOR VS. d/w FOR FLAT BAR WITH NOTCH

section was determined from the known load and the dimensions of the test piece. The maximum stress was determined by plotting the fringe order against the distance from one of the scratch marks at the minimum section and extrapolating this curve to the true edge. Two typical curves showing these extrapolations are given in Fig. 9. In many cases, as for example in the case of Fig. 6, it was necessary to use a microscope since the fringes were very fine and close together. It was always found that one side of the specimen was stressed slightly higher than the other due to small eccentricities of loading, etc. To eliminate this effect in working up the results an average value for the two opposite sides was taken.

RESULTS OF TESTS

For the case of the test specimens with holes, the test points obtained in this manner are shown by the small circles in Fig. 10

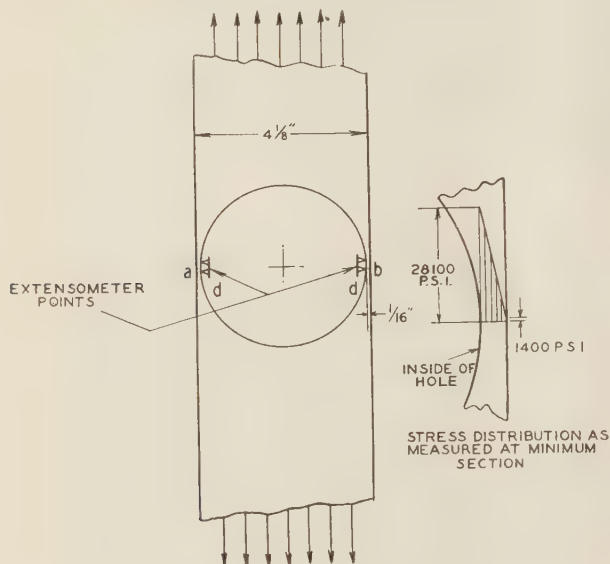


FIG. 12 BAR WITH LARGE HOLE

where the stress concentration factor, or ratio of maximum stress at the minimum section to the mean stress at this section, is plotted against the ratio d/w . The full line represents the mean of the test values. For comparison the calculated results obtained by Howland⁴ are shown by the dotted curve, the experimental results of Hennig⁷ by the dot and dash curve and small triangles, those of Preuss⁶ by the half-filled circles, and those calculated from tests made by Coker⁵ by the heavy dots. It will be seen that the present test results closely check the mathematical results of Howland for values of the ratio d/w less than 0.5. This is a confirmation of the relative accuracy of the method. They also check the experimental results of Hennig for values d/w less than about 0.7. The values calculated from the experimental results by Coker are, in general, considerably below the present results. This is due probably to the fact that he used the compensation method which is very difficult to apply right at the edge of a specimen and which tends to give an average value of stress near a localized point of stress concentration rather than the peak value. For this reason it would be expected that the test results thus obtained should be lower than the true values as is, indeed, the case. The fact that extensometer measurements require a definite gage length, and are not as accurate for small gage lengths, probably accounts for the discrepancy between the results of Preuss and the present results.

The single point in Fig. 10 for a value of $d/w = 0.97$ represents a test on a steel model which will be described and discussed more fully later.

A similar curve for the case of a notched bar is shown in Fig. 11, the half-filled circles and heavy dots representing values calculated from tests by Preuss⁶ and Coker.⁵ Again it may be seen that for reasons mentioned previously, the present test curve for the most part lies considerably above the points obtained by Coker or Preuss. It will be noted that this curve tends to intersect the zero value of d/w at some distance below the value 3, namely 2.75. A value between 2 and 3 would be expected from theoretical considerations. It also approaches unity for ratios d/w near to 1, which also would be expected.

The following empirical equations for the stress concentration factor K give results agreeing approximately with the test results: For a bar with a hole, under tension:

$$K = 3 - 3.13d/w + 3.76(d/w)^2 - 1.71(d/w)^3 \dots [1]$$

For a bar with a notch, under tension:

$$K = 2.75 - 2.75d/w + 0.32(d/w)^2 + 0.68(d/w)^3 \dots [2]$$

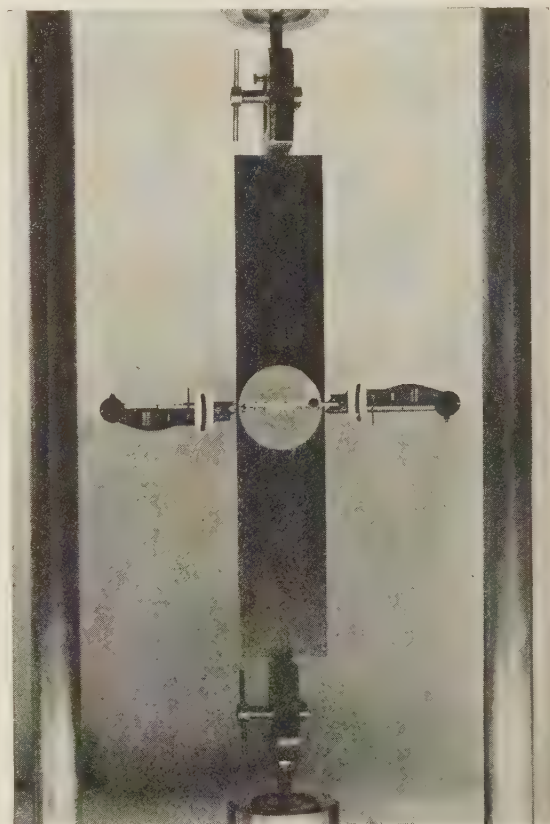


FIG. 13 TEST ON STEEL MODEL

In all cases d/w is the ratio of the hole or notch diameter to the width of the bar.

TESTS ON STEEL BAR WITH LARGE HOLE

In the case of a bar having a large hole with a diameter almost equal to its width, such as shown in Fig. 12, it would naturally be thought that very little stress concentration would exist. For example, the curve shown by Hennig⁷ is drawn so as to approach unity for $d/w = 1$. To check this and at the same time to avoid

the difficulty of making optical tests on such a specimen, it was decided to make measurements on a steel model as shown on Fig. 13, using an extensometer with a gage length of 0.3 in. and a hole of 4-in. diameter in a 4 1/8-in. wide plate ($d/w = 0.97$). It was found possible to place the extensometer points on the inside of the hole as indicated in Fig. 12, which shows the relative size of the hole as compared to the gage length. Since it is known that for such a thin section the stress distribution must be linear, the stress concentration factor may be found by dividing the stress readings on the inside of the hole by the average value between the stress obtained on the outside (see Fig. 13) and that obtained on the inside (see Fig. 12). The stress on the inside was found to be 28,100 lb per sq in. and that on the outside only 1400 lb per sq in., giving $K = 1.91$ for a load of 450 lb. As a check, the mean stress across the minimum section could be found from the known loads. The maximum stress measured on the inside at points, d , divided by this mean stress then gives the stress-concentration factor. The two methods gave results agreeing within 1 per cent, the average value of K being 1.92. In order to eliminate inaccuracies due to a slight eccentricity of loading average values on opposite sides of the specimen were used. This value of K is roughly in agreement with results obtained by Coker and Filon,¹³ who mention that the stress on the outside of the bar seems to approach zero as d/w approaches unity, which would correspond to $K = 2$.

Curves between load and stress on the inside of the hole (points d , Fig. 12) were found to be linear. The corresponding curves for points a and b were found to be roughly linear, although the exact shape of the curve at these points was very hard to determine because of the very small stresses involved. Measurements of the distance between points a and b (Fig. 12) indicate that these points approach each other during loading, the relation between load and deflection being again roughly linear. It may be seen that during loading the inward movement of these points is such as to increase the stresses on the outside (at points a and b), thereby reducing the stress concentration factor K below that which would be obtained for very small deformations, such as are assumed in elastic theory. It is possible that this is the reason for the value of K being 1.92, as obtained, rather than a higher value. In case the hole diameter so closely approaches the width of the bar that the minimum section becomes an infinitely thin filament, then for any finite deformation, this filament may move inward sufficiently to allow of a uniform stress distribution, thus giving $K = 1$. For infinitely small deformations relative to the thickness of this filament, however, K may still be equal to 2.

The tests nevertheless indicate that, for a value of $d/w = 0.97$, $K = 1.92$ with stresses on the order of those possible in engineering materials such as steel. They also indicate that the curve does not drop down to unity as fast as would appear from the curve given by Hennig (see Fig. 10).

CONCLUSIONS

The present tests on bars with holes agree closely with the mathematical results obtained by Howland. This agreement also suggests that the photoelastic method described, if precautions to avoid undesirable edge effects are taken, offers an accurate means to determine stress concentration factors for various machine parts.

The results indicate that for large holes having a diameter nearly equal to the width of the bar the stress concentration factor is not far from 2 in cases where the lateral displacements of the minimum section of the bar are small compared to the thickness of this section.

The results obtained on bars with semi-circular notches indicate in general higher stress-concentration factors than those obtained by using the results obtained by previous investigators. This is to be expected, considering the difficulty of using the photoelastic compensation method right at the edge of a specimen or of applying extensometers with short gage lengths. The fact that the compensation method tends to give an average value near a localized point of stress concentration, rather than the peak value, also tends to explain this difference.

Empirical equations are given for calculating the stress-concentration factors both for tension bars with holes and for bars with semi-circular notches.

ACKNOWLEDGMENT

The authors are indebted to R. E. Peterson, at whose suggestion the investigation was made, and to Drs. Nadai and Timoshenko for valuable advice and suggestions.

Discussion

O. J. HORGER.¹⁴ The authors have presented the stress-concentration factors over a complete range in a satisfactory manner. The test procedure is accepted as giving accurate results which explain the deviation from previous data and in this respect the authors should be commended.

While these concentration factors are of importance to the design engineer the presentation of this data is only the beginning of a study which should be pursued. Design problems often involve two stress-concentration factors, one due to shape and the other due to material. The present tendency toward reduced weights and costs of machine parts requires accurate knowledge of the factor of safety and demands consideration of these two factors separately. "Dauerfestigkeit und Konstruktion," in 1932, by Dr. A. Thum and W. Buchmann discusses this phase and give some data.

The extrapolation method employed is a worthy step in photoelastic analysis. After reading a preliminary report of this paper extrapolation was followed in an experiment made by the writer. Contrary to the findings of the authors the true edge was not always found inside the apparent edge. In one case the distance from the scratch to the edge on the model was 0.115 cm while the apparent edge measured 0.253 cm and in the same photograph directly opposite, the true position on the model measured 0.482 cm against 0.443 cm on the photograph. Measurements were made with a comparator.

M. M. FROCHT.¹⁵ The paper by Messrs. Wahl and Beeuwkes may, for the purpose of discussion, be divided into two parts: one part dealing with a reexamination of factors of stress concentration for two important engineering cases, and the other part dealing with suggestions for the determination of vague boundaries and the more accurate evaluation of boundary fringe-orders.

The writer has had difficulties in determining the true boundary similar to those experienced by the authors but he has found it possible to eliminate these difficulties and to obtain stress patterns in which the true boundary is clearly visible. Such a stress pattern is shown in Fig. 14. In order to determine the accuracy with which the boundary can be shown, two scratches were drawn on the model. One of these scratches was very fine and was subsequently determined to be in an interval of no more than 0.0025 in. from the edge, the other scratch was

¹⁴ Ann Arbor, Mich.

¹⁵ Photoelastic Laboratory, Dept. of Mechanics, Carnegie Institute of Technology, Pittsburgh, Pa.

¹³ "Photoelasticity," by Coker and Filon, Cambridge Univ. Press, 1931, p. 436.

considerably larger starting at 0.004 in. from the edge and having a width of about 0.006 in. These dimensions were determined very carefully when the edge of the model was machined after the photographs were taken. The larger of the two scratches is clearly visible in Fig. 14. The finer scratch can also be seen and is located between the white arrow-heads to the left of the model. Fig. 15 shows a stress pattern against a white back-

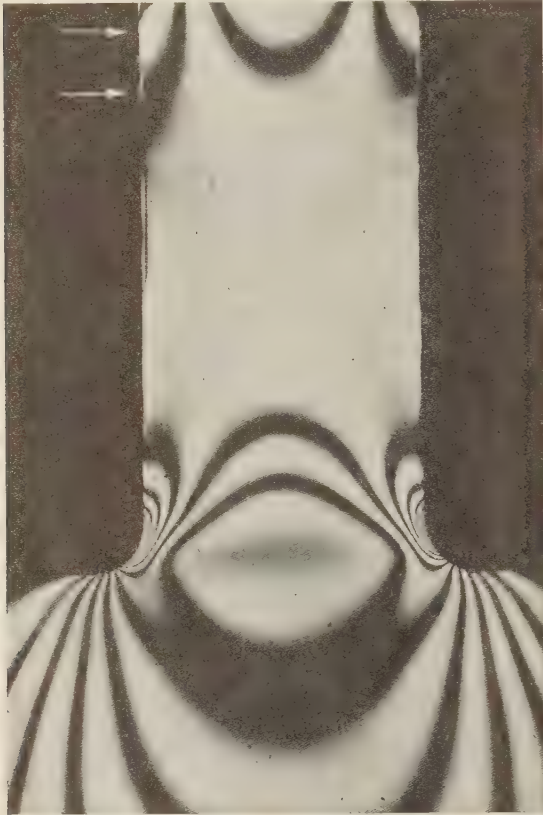


FIG. 14 BAKELITE MODEL IN COMPRESSION
(Showing true boundary against a black background. Arrow-heads point to fine scratch on the edge of model.)

ground instead of the conventional black background, from which it can be seen that this procedure adds to the clearness of the boundary. Inspection of the left edge reveals clearly the presence of even the fine scratch engraved on the boundary.

The writer prefers to take all the necessary precautions to obtain stress patterns in which the boundaries can clearly be seen rather than to determine these from engraved lines as suggested by the authors.

The determination of boundaries from engraved lines and of boundary fringe-orders from extrapolation is in reality a much more difficult procedure than would seem to be the case on first thought. In the first place, the distance between scratches changes with the load so that for accurate determination of the scale of magnification these measurements should be carried out after the load is applied and just before photographing the pattern. Also, extrapolation is not a unique and definite procedure, so that the results would probably vary with the investigator. The procedure of extrapolation may introduce errors as great or greater than the ones it is trying to correct. However, if it is desired to determine the boundary-fringe value by extrapolation it is suggested that, in tension members with holes or fillets, a circle concentric with the hole be inscribed rather than two

straight lines. There is a twofold advantage to the use of the circle over the straight line scratches: it calls for only one measurement and it gives greater accuracy.

With respect to the results proper, the writer computed the stress concentration factor, for a ratio $\frac{d}{w} = \frac{1}{5}$, of a bakelite specimen 0.625 in. \times 0.188 in. thick with a $\frac{1}{8}$ in. hole, and the average of two values for two different loads was 2.52, against 2.51 given by the authors' formula. The agreement between the authors' curve and that of Howland lends additional strength to the reliability of the results.

The writer observes with interest that the authors determined the fringe value from a pure tension rather than from a pure bending test. This agrees with the procedure adopted in our more recent work. Experience has shown that it is simpler to determine the fringe value from a tension or compression strip, and that the results are also more consistent. There is a special merit to it if the model in which the stresses are studied, as is the case in this instance, can be utilized as its own calibration piece.

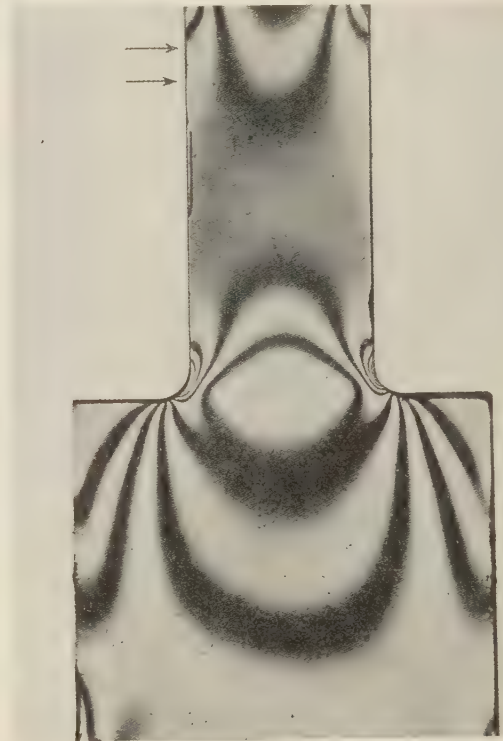


FIG. 15 BAKELITE MODEL IN COMPRESSION
(Showing true boundary against a white background. Arrow-heads point to fine scratch on the edge of model.)

In connection with the question of fringe-value determination, the writer wishes to make two suggestions—first, that this value can be determined with great accuracy in a tension or compression member by means of a good photometer, such as the photo-electric-cell type, thereby removing eye-strain and the subjective element of the observer; and, second, that fringe value be defined as the change in maximum shear stress necessary to cause a change from black to the next black or white to the next white, at any given point in a model of the given material 1 in. thick. At present the fringe value is associated not only with the material, but also with the thickness of the model. To obtain the fringe value for any particular model, it would only be necessary

to divide the fringe value for that material by the thickness of the model. This would simplify matters considerably and permit of easy comparison of relative optical sensitivities of different materials.

AUTHORS' CLOSURE

Dr. Frocht suggests that, by taking necessary precautions, the boundary of the test specimen may be made clearly visible on the photograph and that it is preferable to determine the true edge from such a photograph rather than by means of the extrapolation procedure used by the authors. In addition, as evidence of cases where the boundary is defined with sufficient clearness, he submits the photographs of Figs. 14 and 15. After examining these photographs, however, the authors do not feel that the edges were defined with greater clearness near the fillets than was the case in most of the tests made by them; it is also their opinion that the use of the extrapolation method would increase the accuracy of the determination of the peak stresses in the fillets of the models shown on Figs. 14 and 15.

In connection with the use of the extrapolation procedure, Dr. Frocht mentions that the distance between the engraved lines on the specimen would change when the load is applied, and this would involve an error in determining the scale of magnification. However, it can be shown that this error is negligible for such stresses as are practicable with bakelite. For example, in most of the specimens used by the authors, the scratches employed to determine the magnification ratio were about 1 in. apart while the contraction due to the applied stress amounted to about 0.001 in. as computed from the known values of stress and elastic constants. This would correspond to an error of 0.1 per cent, a negligible value. Even if the stresses used were doubled, the percentage error would still be only 0.2 per cent. Since the distance between the scratch and the edge is measured in the unstressed condition, there is a further error in locating the boundary on the extrapolation curves, due to the contraction of the stressed material between the scratch and the boundary. The error in fringe order due to this cause may also be shown to be of negligible importance. Calculating the contraction from the known stresses and multiplying by the magnification ratio, the amount of error in locating the boundary on the extrapolation curves is obtained. From this, by reference to actual test curves, the error in fringe order may be found. Several tests were checked by the authors and in no case was the error due to this cause over 0.2 per cent. Hence, it may be concluded that errors

in the extrapolation procedure due to lateral contraction of the stressed material are negligible, at least for engineering purposes.

It is true, as Dr. Frocht says, that extrapolation is not a definite and unique procedure, and that there will be some variation with different investigators. The authors have found, however, that such variations are relatively small, particularly when compared to the possible errors resulting when the peak fringe values are determined merely by inspection. This checks with the experience of Dr. Weibel¹⁶ of the University of Michigan who found that much more consistent results could be obtained by the use of the extrapolation method than had been possible without it. For these reasons, the authors believe that a considerable improvement in the accuracy of stress concentration determination is made possible by the use of this method.

With regard to the use of circular lines engraved on the specimen, as suggested by Dr. Frocht, the authors believe this would be of advantage in the case of fillets in tension or bending where the peak stress is at an unknown location along the fillet. In the cases tested by the authors, where the peak stress is always at the minimum section, the use of a straight line proved to be very satisfactory. It should be noted that it is rather difficult to make a fine circular scratch concentric with the fillet or hole, unless a special tool is used, while it is very easy to inscribe a straight line. The authors found that, for best results, an extremely fine scratch was desirable since if a coarse one were used a further error in estimating the center of the black line on the photographs was introduced.

With regard to Mr. Horger's statement that design problems involve two stress concentration factors, one due to shape and the other due to material, it may be of interest to note that in certain cases, particularly as regards large specimens of high strength alloy steels, there appears to be some tendency for the fatigue stress concentration factors to approach those found by photoelastic or mathematical methods.¹⁷ In such cases, then, these two stress-concentration factors mentioned by Mr. Horger may be considered as identical. The photoelastic test values, in these instances, would then give information of direct value to designers. The authors agree, however, that considerable additional work is desirable on these and similar questions.

¹⁶ E. E. Weibel, "Studies in Photoelastic Stress Determination," A.S.M.E. Trans., vol. 56, 1934, paper APM-56-13.

¹⁷ Note especially the discussion by Mr. R. E. Peterson of Dr. Weibel's paper, A.S.M.E. Trans., vol. 56, 1934, APM-56-13.



Bending of Circular Plates With Large Deflection

By STEWART WAY,¹ EAST PITTSBURGH, PA.

In the design of thin plates bent by lateral loading, formulas based on the Kirchhoff theory which neglects stretching and shearing in the middle surface are quite satisfactory, providing the deflections are small compared to the thickness. If deflections are of the same order as the thickness, the Kirchhoff theory may yield results which are considerably in error and therefore a more rigorous theory which takes account of deformations in the middle surface should be applied. The fundamental equations for the more exact theory are known,² and approximate solutions³ have been developed for the case of a circular plate.

This paper gives the general solution of the fundamental equations for the case of a circular plate bent to a figure of revolution. Particular solutions are found which satisfy one of the two boundary conditions, and stresses and deflections are calculated from these solutions. By interpolation, the stresses and deflections are then found for plates satisfying both boundary conditions. The deflections are compared with experimental results and with the approximate formulas. It is found that these deflections agree closely with the experimental results and also with those obtained by the approximate methods of A. Nadai and S. Timoshenko, as shown in Figs. 8 and 10.

FUNDAMENTAL EQUATIONS

1 NOMENCLATURE

CONSIDER an initially flat circular plate of uniform thickness and let

- a = radius
- h = thickness
- p = load intensity, assumed uniform
- $\sigma_r, \sigma_r', \sigma_r''$ = radial stresses
- $\sigma_t, \sigma_t', \sigma_t''$ = circumferential stresses
- z = distance from middle surface, downward direction positive
- r = distance from axis of symmetry to a point in the plate before deflection
- w = vertical displacement of points of the middle surface relative to the center of the middle surface
- $\varphi = dw/dr$
- E = Young's modulus
- μ = Poisson's ratio

¹ Research Laboratories, Westinghouse Electric & Manufacturing Co., East Pittsburgh, Pa.

² Due to von Kármán, Enzyk. d. Math. Wiss., vol. 4, art. 27. See also A. Nadai, "Die Elastische Platten," Springer, Berlin, 1925, p. 284.

³ Solutions such as that by A. Nadai and discussed in this paper.

Contributed by the Applied Mechanics Division and presented at the Annual Meeting, New York, N. Y., December 4 to 8, 1933, of THE AMERICAN SOCIETY OF MECHANICAL ENGINEERS. This paper was prepared by the author as a thesis for a Doctor's degree at the University of Michigan.

NOTE: Statements and opinions advanced in papers are to be understood as individual expressions of their authors, and not those of the Society.

- $D = Eh^3/12(1 - \mu^2)$ = flexural rigidity of the plate
- m_r, m_t = radial and circumferential bending moments per unit of length
- ρ = radial displacement of points in the middle surface

Displacements and stresses are assumed to be functions of r only; that is, they have radial symmetry.

Loads and deflections will be taken as positive when downward and moments as positive when they tend to make the plate concave upward.

2 EXPRESSIONS FOR STRESSES AND MOMENTS IN TERMS OF DISPLACEMENTS

Three assumptions are made as follows:

- (1) The material is homogeneous, isotropic, and obeys Hooke's law
- (2) The curvature of a meridian may be replaced by d^2w/dr^2
- (3) Straight lines initially normal to the middle surface remain straight and normal to that surface after bending.

It follows from the third assumption that if the radial and vertical displacements of every point in the middle surface are known the displacements of all points of the plate can be found.

The radial extension in the middle surface is

$$e_r' = \frac{d\rho}{dr} + \frac{\varphi^2}{2} \dots \dots \dots [1a]$$

and the circumferential extension is

$$e_t' = \frac{\rho}{r} \dots \dots \dots [1b]$$

At a distance z from the middle surface there are the additional extensions due to bending

$$e_r'' = -z \frac{d^2w}{dr^2}; \quad e_t'' = -z \frac{\varphi}{r} \dots \dots \dots [2]$$

The middle surface extensions give rise to the membrane stresses σ_r' and σ_t' which by Hooke's law are as follows:

$$\left. \begin{aligned} \sigma_r' &= \frac{E}{1 - \mu^2} \left(\frac{d\rho}{dr} + \frac{\varphi^2}{2} + \mu \frac{\rho}{r} \right) \\ \sigma_t' &= \frac{E}{1 - \mu^2} \left(\frac{\rho}{r} + \mu \frac{d\rho}{dr} + \mu \frac{\varphi^2}{2} \right) \end{aligned} \right\} \dots \dots \dots [3]$$

The extensions due to bending give rise to the following bending stresses

$$\left. \begin{aligned} \sigma_r'' &= \frac{E}{1 - \mu^2} \left(-z \frac{d^2w}{dr^2} - \mu z \frac{\varphi}{r} \right) \\ \sigma_t'' &= \frac{E}{1 - \mu^2} \left(-z \frac{\varphi}{r} - \mu z \frac{d^2w}{dr^2} \right) \end{aligned} \right\} \dots \dots \dots [4]$$

Summing the moments of σ_r'' and σ_t'' from $z = -h/2$ to $z = h/2$ the following are obtained:

$$\left. \begin{aligned} m_r &= -\frac{Eh^3}{12(1-\mu^2)} \left(\frac{d\varphi}{dr} + \mu \frac{\varphi}{r} \right) \\ m_t &= -\frac{Eh^3}{12(1-\mu^2)} \left(\frac{\varphi}{r} + \mu \frac{d\varphi}{dr} \right) \end{aligned} \right\} \dots\dots\dots [5]$$

Hereafter σ_r'' and σ_t'' will be used to denote the outer-surface bending stresses which are given by

$$\sigma_r'' = \frac{6}{h^2} m_r; \quad \sigma_t'' = \frac{6}{h^2} m_t \dots\dots\dots [6]$$

A useful relation between ρ and the membrane stresses is given by Hooke's law and is

$$\frac{\rho}{r} = \frac{1}{E} (\sigma_t' - \mu \sigma_r') \dots\dots\dots [7]$$

3 RELATIONS BETWEEN φ , σ_r' , AND σ_t' FOR EQUILIBRIUM AND COMPATIBILITY

In the preceding article, (2), expressions for the stresses in terms of the displacements were established. As the next step

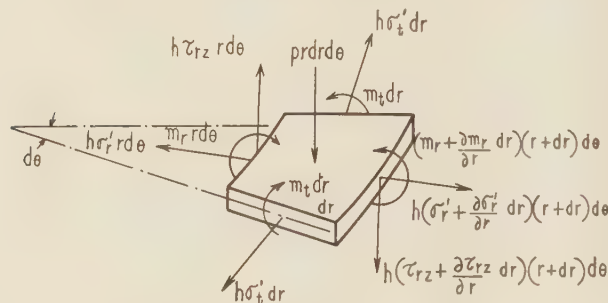


FIG. 1 CONDITION OF RADIAL EQUILIBRIUM

either two equations can be set up, which the displacements w and ρ must satisfy, or three equations can be constructed for φ , σ_r' , and σ_t' , and the radial displacement found from Equation [7]. Of these the latter course has been chosen.

The condition of vertical equilibrium of a disk of the plate of radius r results in

$$D \frac{d}{dr} \left(\frac{1}{r} \frac{d}{dr} (r\varphi) \right) = p \frac{r}{2} + h\sigma_r'\varphi \dots\dots\dots [8]$$

From the condition of radial equilibrium of the element shown in Fig. 1

$$\frac{d}{dr} (r\sigma_r') - \sigma_t' = 0 \dots\dots\dots [9]$$

Eliminating ρ and $d\rho/dr$ from Equations [1a] and [1b], and applying Hooke's law and the equilibrium Equation [9] results in

$$r \frac{d}{dr} (\sigma_r' + \sigma_t') + \frac{\varphi^2 E}{2} = 0 \dots\dots\dots [10]$$

Equations [8], [9], and [10] may be regarded as the fundamental equations for a circular plate bent to a figure of revolution.⁴ If the flexural rigidity is neglected, and D equals zero, the solution is known. This was developed by Hencky.⁵

⁴ Given in this form by A. Föppl, "Drang und Zwang," R. Oldenbourg, Berlin, 1924.

⁵ H. Hencky, *Zeitschrift für Math. und Phys.*, vol. 63 (1915), p. 311. Hencky found the maximum deflection to be

$$w_0 = 0.662 \sqrt{\frac{pa^4}{Eh^4}}$$

It will be noted that if deflections are small compared to the thickness the term involving φ^2 could be dropped from Equation [1a] and it would not appear in Equation [10]. Equations [9] and [10] would then show that the membrane stresses were constant, and Equation [8] would become a Bessel equation.

4 FUNDAMENTAL EQUATIONS IN DIMENSIONLESS FORM

The new variables q , S_r' , S_t' , S_r'' , S_t'' , and u are now introduced and are defined as follows:

$$\left. \begin{aligned} q &= p/E; & u &= r/h; & S_r' &= \sigma_r'/E \\ S_t' &= \sigma_t'/E; & S_r'' &= \sigma_r''/E; & S_t'' &= \sigma_t''/E \end{aligned} \right\} \dots\dots\dots [11a]$$

Also, the following dimensionless expressions

$$\frac{m_r h}{D}, \quad \frac{m_t h}{D}, \quad \frac{w}{h}, \quad \frac{\rho}{h}$$

shall be used hereafter to measure moments and displacements. It should be noted that the slope φ is

$$\frac{dw}{dr} = \frac{d}{du} \left(\frac{w}{h} \right)$$

The bending moments in terms of dimensionless quantities are

$$\frac{m_r h}{D} = - \left(\frac{d\varphi}{du} + \mu \frac{\varphi}{u} \right); \quad \frac{m_t h}{D} = - \left(\frac{\varphi}{u} + \mu \frac{d\varphi}{du} \right) \dots\dots [11b]$$

The fundamental Equations [8], [9], and [10] become

$$\frac{1}{12(1-\mu^2)} \frac{d}{du} \left(\frac{1}{u} \frac{d}{du} (u\varphi) \right) = q \frac{u}{2} + S_r'\varphi \dots\dots [12]$$

$$\frac{d}{du} (uS_r') - S_t' = 0 \dots\dots\dots [13]$$

$$u \frac{d}{du} (S_r' + S_t') + \frac{\varphi^2}{2} = 0 \dots\dots\dots [14]$$

5 BOUNDARY CONDITIONS

Boundary values shall be denoted by the subscript zero. For a plate with zero radial edge displacement Equation [7] results in

$$S_{t0}' = \mu S_{r0}' \dots\dots\dots [15]$$

For a plate with no tensile forces at the edge

$$S_{r0}' = 0 \dots\dots\dots [16]$$

For a plate with bending moment m_{r0} at the edge

$$- \left[\left(\frac{d\varphi}{du} \right)_0 + \mu \frac{\varphi_0}{u_0} \right] = \frac{m_{r0} h}{D} \dots\dots\dots [17]$$

For a plate with an edge clamped horizontally

$$\varphi_0 = 0 \dots\dots\dots [18]$$

For a plate with a simply supported edge

$$\left(\frac{d\varphi}{du} \right)_0 + \mu \frac{\varphi_0}{u_0} = 0 \dots\dots\dots [19]$$

In this paper two cases will be considered:

- (1) Plates with no load, with moment m_{r0} at the edge, and zero tensile force at the edge
- (2) Plates with a uniform load, clamped edge, and zero radial edge displacement.

GENERAL SOLUTION AND PARTICULAR SOLUTIONS

6 THE GENERAL SOLUTION

A solution for Equations [12], [13], and [14] is now desired. Either by successive differentiation of these equations or by a consideration⁶ of the basic assumptions of the theory of elasticity, it can be shown that all the derivatives of the displacements ρ and w will exist at all points in the plate. The displacements, extensions, and stresses may therefore be expanded in series of positive powers of u . Since S_r' is a symmetrical⁷ function of u it can be expanded in a series of even powers of u and since φ is an antisymmetrical function of u it can be expanded in a series of odd powers of u .

As the starting point, therefore, let

$$S_r' = B_0 + B_2 u^2 + B_4 u^4 + \dots \quad [20]$$

$$\varphi = \sqrt{8}(C_1 u + C_3 u^3 + C_5 u^5 + \dots) \quad [21]$$

From the equilibrium Equation [13]

$$S_t' = B_0 + 3B_2 u^2 + 5B_4 u^4 + \dots \quad [22]$$

By integrating the series expression for φ

$$\frac{w}{h} = \sqrt{8} \left(C_1 \frac{u^2}{2} + C_3 \frac{u^4}{4} + C_5 \frac{u^6}{6} + \dots \right) \quad [23]$$

and by differentiation of the φ series

$$\frac{d\varphi}{du} = \sqrt{8} (C_1 + 3C_3 u^2 + 5C_5 u^4 + \dots) \quad [24]$$

The moments are given in terms of φ and $d\varphi/du$ by Equation [11b]. The bending stresses are related to the moments by

$$S_r'' = \frac{m_r h}{2D(1-\mu^2)}; \quad S_t'' = \frac{m_t h}{2D(1-\mu^2)} \quad [25]$$

and the radial displacement from Equation [7] is

$$\frac{\rho}{h} = u (S_t' - \mu S_r') \quad [26]$$

All quantities in which we may be interested can be found therefore, if the constants C_k and B_k are known.

By substituting the series expressions for S_r' , S_t' , and φ in Equations [12] and [14], two sets of relations between the constants B_k and C_k are obtained:

$$B_k = - \frac{\sum_{m=1,3,5,\dots}^{k-1} C_m C_{k-m}}{k \left(\frac{k}{2} + 1 \right)}; \quad k = 2, 4, 6, \dots \quad [27]$$

$$\left. \begin{aligned} C_k &= 3(1-\mu^2) \frac{\sum_{m=0,2,4,\dots}^{k-3} B_m C_{k-2-m}}{k^2 - 1}; \quad k = 5, 7, 9, \dots \\ C_3 &= \frac{3(1-\mu^2) \left(\frac{q}{2\sqrt{8}} + B_0 C_1 \right)}{2} \end{aligned} \right\} \quad [28]$$

The series expressions [20] to [24] along with the Equations [27] and [28] constitute the general solution of the problem of a plate bent to a figure of revolution by a uniform load.

The two constants B_0 and C_1 are not determined. When they are assigned, all the other constants are determined by Equations [27] and [28], and the quantities S_r' , S_t' , and φ are determined by Equations [20], [21], and [22] for all points in the plate, including the boundary. Fixing B_0 and C_1 is thus equivalent to fixing the boundary conditions. It will be noted that B_0 is the value of S_r' at the center while C_1 is proportional to the bending moment at the center.

7 PARTICULAR SOLUTIONS FOR ZERO LOAD AND ZERO EDGE FORCE⁸

The following results apply to plates loaded by a distributed bending moment at the edge as shown in Fig. 2.

We assume the value $\mu = 1/4$ for Poisson's ratio. The method of obtaining the required values consists of assuming a pair of values for B_0 and C_1 and calculating all the other constants C_k and B_k by Equations [27] and [28]. The radius, u_0 , is then determined so as to make S_{r0}' zero, and w_0/h , $m_{r0}h/D$, $m_{t0}h/D$, $hm_{r0}(0)/D$, and $S_r'(0)$ are calculated from Equations [20] to [24], and [11b]. These calculations have been made for eleven plates with the results given in Table 1.

The values of $u_0^2 h m_{r0}/D$ are given in Table 1, because it can be shown from the general solution that all plates of the type considered, for which the values of $u_0^2 h m_{r0}/D$ are the same, will have the same deflection. In Fig. 3 is shown a curve for w_0/h for various values of $u_0^2 h m_{r0}/D$. This curve is ap-

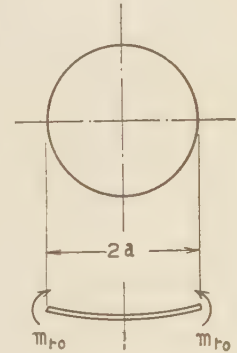


FIG. 2 DISTRIBUTED BENDING MOMENT AT EDGE OF CIRCULAR PLATE

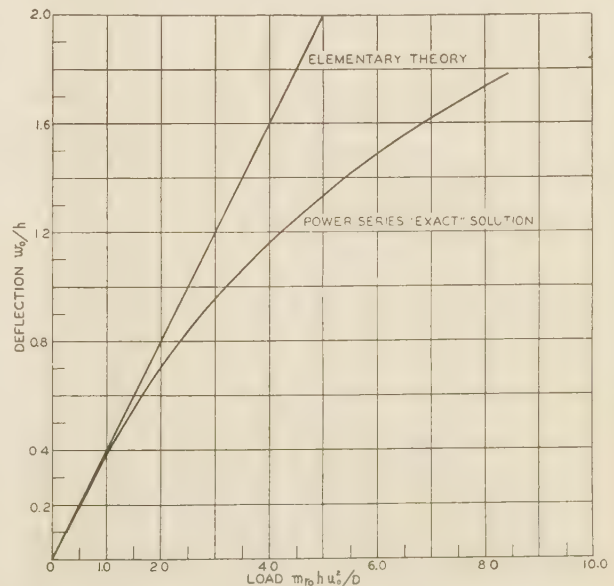


FIG. 3 DEFLECTION OF CIRCULAR PLATE WITH DISTRIBUTED BENDING MOMENT AT EDGE

⁶ E. Trefftz in the "Handbuch der Physik," vol. 6, p. 122.

⁷ That is $S_r'(u) = S_r'(-u)$. If φ is an antisymmetrical function $\varphi(u) = -\varphi(-u)$.

⁸ One such particular solution is given by S. Timoshenko, "Theory of Elasticity," St. Petersburg, Russia, 1916.

TABLE 1

Plate	u_0	w_0/h	$10^4 \frac{m_{r0}h}{D}$	$10^4 \frac{m_{\theta 0}h}{D}$	$10^4 \frac{m_{r\theta}(0)h}{D}$	$10^4 B_0 = 10^4 S_{r\theta}^{-1}(0)$	$10^4 C_1$	$10^4 \frac{h m_{r0}}{D}$
1	43.66	0.899	-14.43	-13.12	-10.61	1	3	-2.75
2	33.80	0.688	-17.07	-16.02	-14.16	1	4	-1.95
3	27.45	0.555	-20.03	-19.24	-17.69	1	5	-1.51
4	23.08	0.465	-23.18	-22.51	-21.23	1	6	-1.236
5	52.66	1.614	-25.21	-19.68	-10.61	2	3	-6.99
6	42.92	1.282	-25.47	-21.38	-14.16	2	4	-4.69
7	36.00	1.059	-26.87	-23.64	-17.69	2	5	-3.48
8	30.87	0.899	-28.36	-26.24	-21.23	2	6	-2.75
9	36.36	1.759	-38.3	-29.06	-14.16	3	4	-8.23
10	40.00	1.485	-37.3	-30.15	-17.69	3	5	-5.96
11	35.05	1.283	-38.2	-32.06	-21.23	3	6	-4.69

plicable to plates of all radii, all edge moments, and all materials of Poisson's ratio $1/4$.

The elementary theory gives

$$\frac{w_0}{h} = -\frac{1}{2(1+\mu)} \frac{m_{r0}h}{D} u_0^2 \dots [29]$$

This straight-line relation is shown in Fig. 3. For $w_0/h = 1$, the error in the elementary theory is seen to be 28 per cent.

8 PARTICULAR SOLUTIONS FOR PLATES WITH LATERAL LOAD AND BOUNDARY CONDITION $\varphi_0 = 0$

The following solutions apply to the case of plates with clamped edges and uniform lateral loading. It should be noted that the solutions obtained are not expected to satisfy the condition $\varphi_0 = 0$.

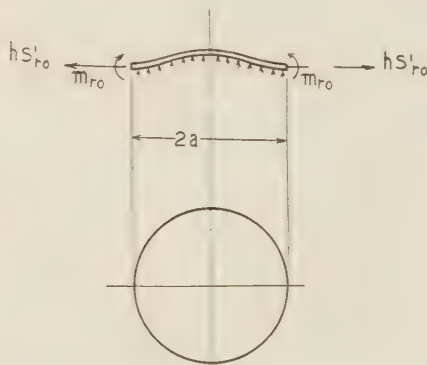


FIG. 4 CIRCULAR PLATE WITH CLAMPED EDGE AND UNIFORM LATERAL LOAD

The manner of loading is shown in Fig. 4. Values are first selected for μ and q :

$$\mu = 0.3; q = -2\sqrt{8} \times 0.117790 \times 10^{-6}$$

Values are then assumed for B_0 and C_1 , the remaining constants calculated, and the various quantities in which we are

TABLE 2

Plate	u_0	$10^4 S_{r\theta}'$	$10^4 S_{\theta r}'$	w_0/h	$10^4 \left(\frac{d\varphi}{du}\right)_0$	$10^4 B_0$	$10^4 C_1$
1	46.34	1.636	1.374	0.405	-16.89	2.0	2.5
2	52.20	1.319	0.8192	0.629	-21.15	2.0	3.0
3	57.27	0.8454	0.0025	0.905	-25.91	2.0	3.5
4	44.12	1.178	0.9539	0.360	-16.02	1.5	2.5
5	49.13	0.9153	0.4988	0.542	-19.71	1.5	3.0
6	53.44	0.5376	-0.1648	0.761	-23.41	1.5	3.5
7	42.23	0.7114	0.5155	0.324	-15.28	1.0	2.5
8	46.59	0.4878	0.1291	0.478	-18.56	1.0	3.0
9	36.20	0.3671	0.2775	0.187	-11.64	0.5	2.0
10	40.60	0.2377	0.0603	0.296	-14.66	0.5	2.5
11	44.44	0.0444	-0.2631	0.427	-17.71	0.5	3.0
12	41.81	2.311	2.177	0.263	-13.56	2.5	2.0
13	49.05	2.081	1.770	0.464	-18.00	2.5	2.5
14	56.08	1.680	1.062	0.745	-23.09	2.5	3.0
15	62.27	1.050	-0.1025	1.117	-28.39	2.5	3.5
16	43.79	2.789	2.635	0.294	-14.27	3.0	2.0
17	52.43	2.507	2.16	0.545	-19.44	3.0	2.5
18	61.23	1.965	1.143	0.933	-25.68	3.0	3.0
19	68.78	1.069	-0.563	1.453	-32.62	3.0	3.5

interested determined from the series expressions. In this case the radius is found from the condition that the right-hand member of Equation [21] vanishes when $u = u_0$. The results of these calculations for nineteen plates are given in Table 2.

The bending moment at the edge is given simply by

$$\frac{m_{r0}h}{D} = -\left(\frac{d\varphi}{du}\right)_0 \dots [30]$$

since in this case $\varphi_0 = 0$.

9 STRESSES AND DEFLECTIONS IN LATERALLY LOADED PLATES WITH BOTH BOUNDARY CONDITIONS, $\varphi_0 = 0$ AND $\rho_0 = 0$, SATISFIED

We group the plates in Table 2 according to common values of B_0 or C_1 as follows:

Group	Plates	Common Property
a	1, 2, 3	$10^4 B_0 = 2$
b	4, 5, 6	$10^4 B_0 = 1.5$
c	1, 4, 7, 10	$10^4 C_1 = 2.5$
d	2, 5, 8, 11	$10^4 C_1 = 3.0$
e	12, 13, 14, 15	$10^4 B_0 = 2.5$
f	16, 17, 18, 19	$10^4 B_0 = 3.0$

By interpolating between the results for the plates in any one group in such a manner as to make $S_{10} = \mu S_{r0}$, data for a plate having $\rho_0 = 0$ is obtained. From group a data for plate a is obtained, from group b data for plate b, etc. A typical set of interpolation curves is shown in Fig. 5.

TABLE 3

	a	b	c	d	e	f
qu_0^4	6.321	4.561	1.818	3.196	8.635	11.71
w_0/h	0.800	0.637	0.296	0.482	0.970	1.152
$u_0^2 S_{r0}'$	0.311	0.196	0.041	0.112	0.468	0.671
$u_0^2 S_{\theta r}''$	4.087	3.061	1.334	2.250	5.220	6.621
$u_0^2 S_{r\theta}'(0)$	0.616	0.392	0.085	0.226	0.900	1.258
$u_0^2 S_{r\theta}''(0)$	2.069	1.704	0.834	1.327	2.408	2.727

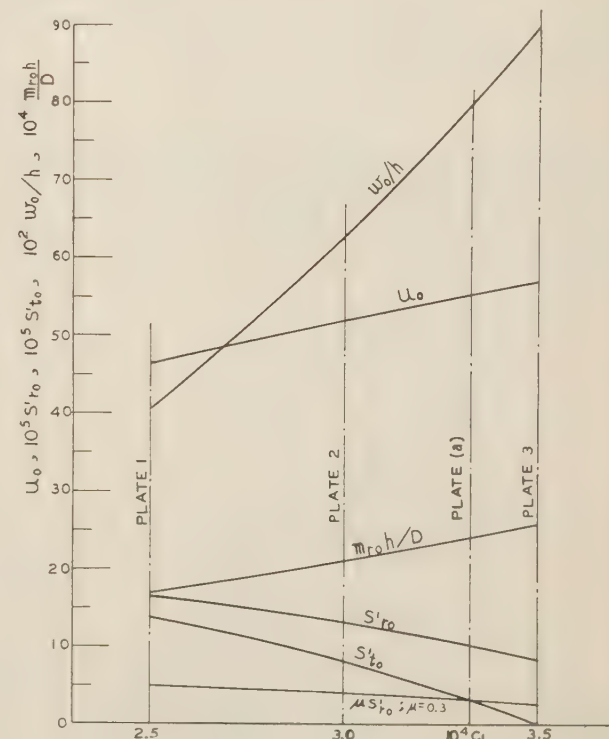


FIG. 5 INTERPOLATION CURVES—PLATES 1, 2, AND 3

The results for plates *a* to *f* are given in Table 3. The stresses at the center are given and, as has been noted, they depend on B_0 and C_1 . Stresses are multiplied by u_0^2 , for it can be shown that w/h and $u_0^2 S$ will have constant values at similarly situated points in all plates with constant qu_0^4 .

The curves in Fig. 6 show the relation of w_0/h to qu_0^4 and those in Fig. 7 show the membrane and bending stresses at the center and the edge for various values of w_0/h . By definition of q and u_0 , qu_0^4 is equivalent to pa^4/Eh^4 .

A numerical example will illustrate the use of these curves. Consider a plate of thickness 0.02 in., radius 2 in., and load 3 lb per sq in. Let $E = 30 \times 10^6$ lb per sq in. and let $\mu = 0.3$. For this plate $qu_0^4 = 10$. From Fig. 6 we see that $w_0/h = 1.055$ so that $w_0 = 0.0211$ in. From Fig. 7 the stresses are

$$\begin{aligned}\sigma_{r0}' u_0^2/E &= 0.56 \\ \sigma_{r0}' &= 1680 \text{ lb per sq in.} \\ \sigma_{r0}'' u_0^2/E &= 5.85 \\ \sigma_{r0}'' &= 17,550 \text{ lb per sq in.} \\ \sigma_r'(0) u_0^2/E &= 1.07 \\ \sigma_r'(0) &= 3210 \text{ lb per sq in.} \\ \sigma_r''(0) u_0^2/E &= 2.57 \quad \sigma_r''(0) = 7710 \text{ lb per sq in.}\end{aligned}$$

The figures given in Table 3 apply only for Poisson's ratio $\mu = 0.3$. For other values of μ values for qu_0^4 and w_0/h can be

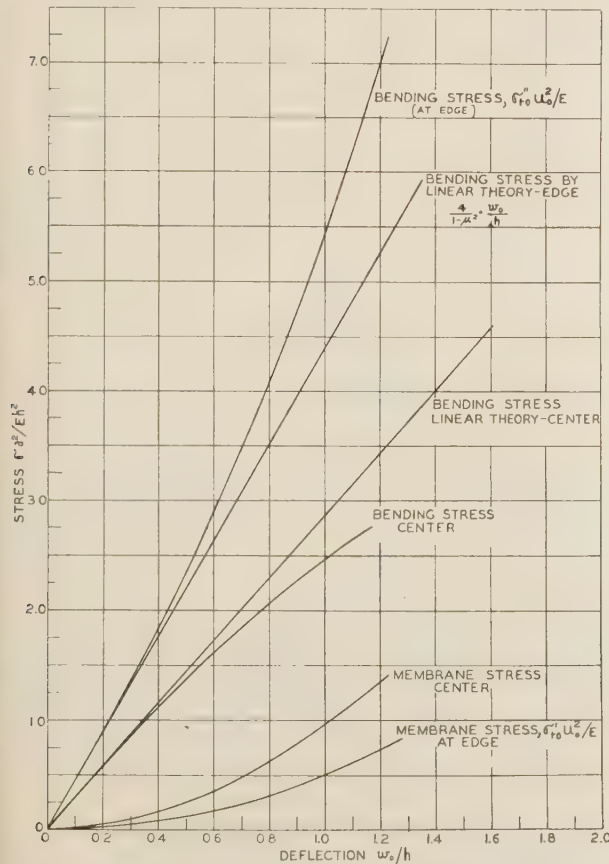


FIG. 7 STRESSES AT EDGE AND AT CENTER ($\mu = 0.3$)

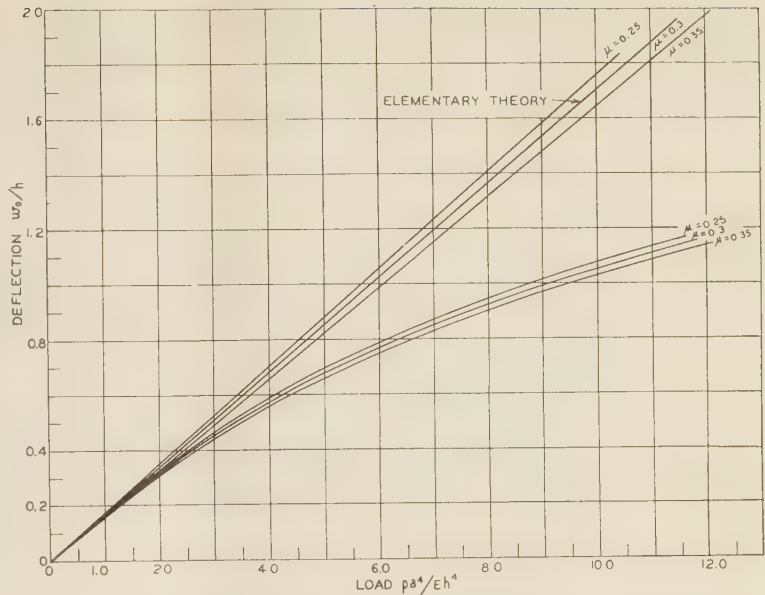


FIG. 6 DEFLECTION OF CIRCULAR PLATE WITH THE EDGE CLAMPED

found by making a suitable transformation of the results in Table 2. Space does not permit a discussion of this method but the deflection curves for $\mu = 0.25$ and $\mu = 0.35$ are shown in Fig. 6. It will be seen that variations in Poisson's ratio have very little effect on the behavior of the plate.

COMPARISON WITH APPROXIMATE FORMULAS

10 APPROXIMATE METHODS OF CONSIDERING MEMBRANE STRESSES

Nadai and Timoshenko have used approximate methods which seem to be reasonably accurate. Before discussing them, the basic equations will be restated in a different form:

$$\left. \begin{aligned}\frac{d}{dr} \left(\frac{1}{r} \frac{d}{dr} (r\varphi) \right) &= \frac{pr}{2D} + \frac{12\varphi}{h^2} \left(\frac{d\rho}{dr} + \frac{\varphi^2}{2} + \mu \frac{\rho}{r} \right) \\ \frac{d}{dr} \left(\frac{1}{r} \frac{d}{dr} (r\rho) \right) &= -\varphi \frac{d\varphi}{dr} - \frac{1-\mu}{2} \frac{\varphi^2}{r}\end{aligned} \right\} [31]$$

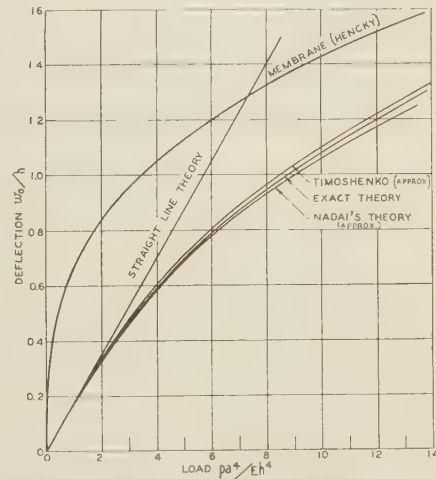


FIG. 8 COMPARISON OF NADAI'S THEORY AND THE MEMBRANE THEORY WITH THE "EXACT" OR POWER SERIES THEORY, LINEAR THEORY, AND TIMOSHENKO'S APPROXIMATE THEORY

The first is equivalent to Equation [8] and the second is Equation [9] with σ_r' and σ_t' replaced by their values in terms of ρ and φ .

Nadai⁹ assumes this expression for φ

$$\varphi = C \left[\frac{r}{a} - \left(\frac{r}{a} \right)^n \right] \dots \dots \dots [32]$$

and placing it in the second Equation [31], solves for ρ . The resulting expression for ρ and expression [32] are then placed in the first Equation [31] which is solved for p . The constants C and n are then determined so as to make p as nearly a constant as possible. Nadai gives the following equation for the maximum deflection:

$$\frac{w_0}{h} + 0.583 \left(\frac{w_0}{h} \right)^3 = \frac{3}{16} \frac{p}{E} \left(\frac{a}{h} \right)^4 (1 - \mu^2) \dots \dots [33]$$

This is obtained when $\mu = 0.25$. In Fig. 8 a curve is shown based on this formula and beside it a curve based on the power series solution discussed in this paper. The agreement is seen to be close.

The approximate method of Timoshenko¹⁰ is simpler. He assumes that the radial displacement is given by

$$\rho = r(a - r)(c_1 + c_2 r) \dots \dots \dots [34]$$

and that, for purposes of finding c_1 and c_2 , the deflection is of the same form as in the elementary theory. He then minimizes the potential energy of stretching to determine c_1 and c_2 , and arrives at the following equation for the deflection:

$$\frac{w_0}{h} + 0.488 \left(\frac{w_0}{h} \right)^3 = \frac{3}{16} \frac{p}{E} \left(\frac{a}{h} \right)^4 (1 - \mu^2) \dots \dots [35]$$

A curve for w_0/h based on this formula also is shown in Fig. 8. This approximation it will be seen errs on the safe side, while the formula [33] errs on the unsafe side.

In Fig. 8 the curve obtained from Hencky's membrane theory⁶ is shown also.

EXPERIMENTAL RESULTS

11 APPARATUS FOR TESTING

Experiments were made on circular plates of duralumin of $4\frac{1}{2}$ -in. diameter and various thicknesses. All plates were clamped at their edges and the method of clamping is shown in Fig. 9. The compartment beneath the plate was filled with water and the pressure controlled by means of a static head of mercury. An Ames dial directly above the center of the plate recorded the deflections.

Four plates of the following thicknesses were tested:

Plate 1.	$h = 0.064$ in.
Plate 2.	$h = 0.052$ in.
Plate 3.	$h = 0.0449$ in.
Plate 4.	$h = 0.032$ in.

In all cases it was assumed that the value of Poisson's ratio was 0.35.

12 RESULTS OF TESTS

As it was desirable to know the value of pa^4/Eh^4 for each measured deflection, a^4/Eh^4 had to be found for each plate. Now for very small deflections

$$\frac{a^4}{Eh^4} = \frac{16}{3} \frac{w_0}{h} \frac{1}{p(1 - \mu^2)} \dots \dots \dots [36]$$

Therefore, a fairly accurate method of finding a^4/Eh^4 was thought to be to determine $\text{Lim.}(p \rightarrow 0)w_0/ph$ by experiment at small pressures. For the various plates values of a^4/Eh^4 were found as follows:

Plate	1	2	3	4
a^4/Eh^4	0.172	0.359	0.711	2.747

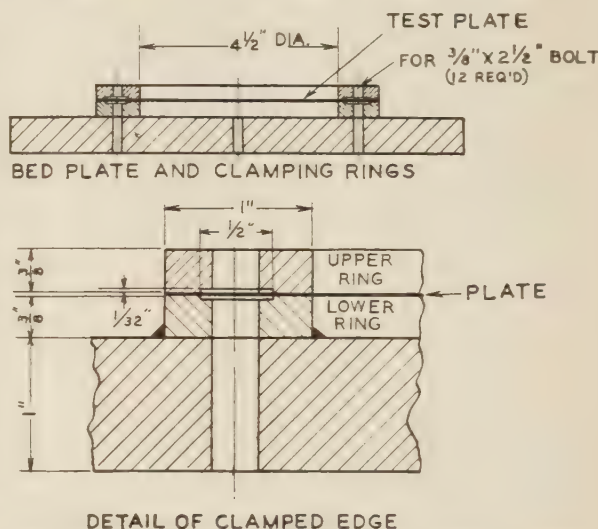


FIG. 9 METHOD OF CLAMPING EDGES OF CIRCULAR PLATES

The values of w_0/h and pa^4/Eh^4 obtained in the various tests are recorded in Table 4.

Plate 1		Plate 2		Plate 3		Plate 4	
w_0/h	$q_{w_0}^4$	w_0/h	$q_{w_0}^4$	w_0/h	$q_{w_0}^4$	w_0/h	$q_{w_0}^4$
0	0	0	0	0.002	0.01	0	0
0.075	0.437	0.067	0.42	0.002	0.98	0.387	2.51
0.153	0.939	0.138	0.84	0.376	2.36	0.527	3.58
0.234	1.440	0.229	1.40	0.550	3.75	0.649	4.64
0.308	1.842	0.333	2.09	0.697	5.13	0.793	6.24
0.377	2.443	0.432	2.79	0.826	6.51	0.980	8.91
0.445	2.946	0.529	3.49	0.931	7.89	1.135	11.58
0.507	3.447	0.611	4.19	1.022	9.27	1.263	14.25
...	...	0.687	4.89	1.108	10.66	1.375	16.92
...	...	0.752	5.59
...	...	0.821	6.28
...	...	0.883	6.98
...	...	0.937	7.68

13 COMPARISON WITH THEORY

In Fig. 10 the deflection curves found from the experiments have been plotted together with the theoretical curve for $\mu = 0.35$.

It will be noted that the difference between the values of w_0/h by theory and experiment is seldom more than 5 per cent. It will also be noted that the experimental curves always lie above the theoretical curve. This latter fact would indicate that part of the discrepancy is due to slipping and rotating at the edges of the test plate. The fact that there is no apparent relation between the plate thickness and the amount of disagreement shows, however, that edge slippage is not the only explanation. A much more likely source of error in the experimental curve lies in the determination of a^4/Eh^4 . To expect a determination of this quantity within 4 per cent accuracy would be very optimistic. On the whole, therefore, it must be concluded that the agreement found between experiment and theory is not at all bad.

14 SUGGESTIONS FOR DESIGN OF PLATES

For clamped circular plates with uniform loads the elementary theory is applicable for maximum deflections less than 0.4 of

⁹ A. Nadai, "Die Elastische Platten," Springer, Berlin, 1925, p. 288. Nadai actually uses the Equations [31] in dimensionless form.

¹⁰ S. Timoshenko, "Vibration Problems in Engineering," D. Van Nostrand Co., New York, 1928, p. 317.

the thickness. For such deflections the error in the deflection due to neglect of the middle surface stresses will be less than 10 per cent. (See Fig. 6.) For larger deflections the middle surface stresses should be considered, unless very rough results are permissible. The simplest method for the practical designer who wants to take account of the membrane stresses in his plate is to have at hand a set of curves such as those in Figs. 6 and 7. As reasonably close agreement was found between the power series solution and the approximate solution by Nadai, the curves in his book "Die Elastische Platten"⁹ (p. 288) should

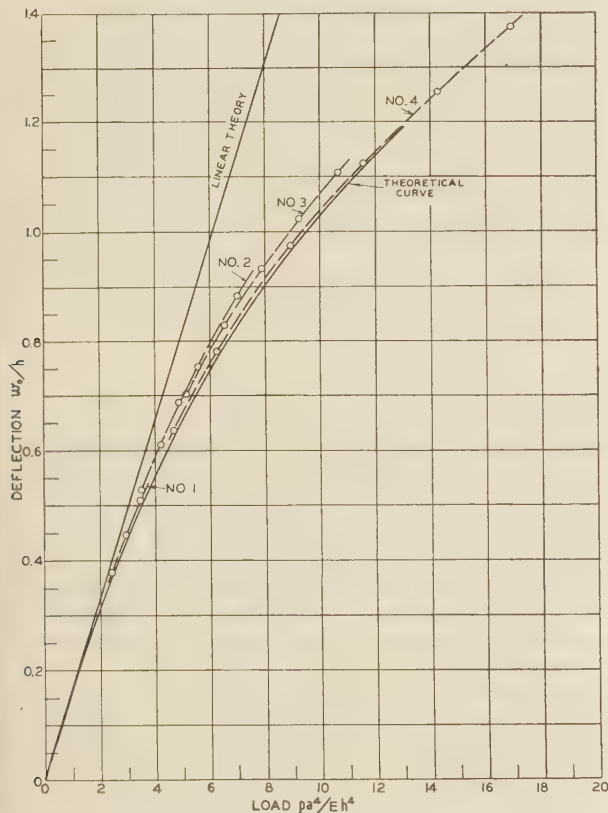


FIG. 10 DEFLECTIONS BY THEORY AND EXPERIMENT

also prove very satisfactory. The solution which offers the greatest ease of manipulation, if curves are not at hand, is the approximate solution by Timoshenko. It is presented on page 317 of his book, "Vibration Problems in Engineering."¹⁰ It seems to be quite as accurate as the method developed by Nadai and has the advantage of erring on the safe side.

Appendix

It has been stated in this paper that plates having the same values for qu_0^4 and the boundary conditions $\varphi_0 = 0$, $\rho_0 = 0$ fulfilled will have the same deflection. This property may be demonstrated in a more general form as follows.

Consider the basic Equations [12], [13], and [14]. Let us make the transformation

$$\left. \begin{aligned} q &= \frac{Q}{u_0^4}; \quad u/u_0 = v; \quad S_r' = s_r'/u_0^2; \quad S_t' = s_t'/u_0^2 \\ \varphi &= \Phi/u_0; \quad \int_0^u \varphi du = \int_0^v \Phi dv = \frac{w}{h}; \quad \frac{\rho u_0}{h} = \lambda \end{aligned} \right\} \dots [37]$$

We find that the form of the basic equations is unaltered:

$$\frac{1}{12(1-\mu^2)} \frac{d}{dv} \left(\frac{1}{v} \frac{d}{dv} (v\Phi) \right) = \frac{Qv}{2} + s_r'\Phi \dots [38]$$

$$\frac{d}{dv} (vs_r') - s_t' = 0 \dots [39]$$

$$v \frac{d}{dv} (s_r' + s_t') + \frac{\Phi^2}{2} = 0 \dots [40]$$

The general solution will contain two undetermined constants, fixing the values of which will determine Φ , s_r' , and s_t' at all values of v , and in particular at the boundary $v = 1$. Therefore the quantities w/h , s_r' , λ , s_t' , Φ , and $d\Phi/dv$ will have the same values at points similarly located in all plates having the same Q , the same μ and the same conditions at $v = 1$.

In particular, if $Q = 0$, w/h for any v will have the same values in all plates of the same μ and the same values of s_r' , Φ , and $d\Phi/dv$ at the boundary. It should be noted that

$$\frac{u_0^2 m_{ro} h}{D} = - \left(\frac{d\Phi}{dv} + \mu \frac{\Phi}{v} \right)_{v=1} \dots [41]$$

Discussion

WILLIAM HOVGAARD.¹¹ This paper is of considerable interest to engineers. It gives an application of the differential equations developed by von Kármán for a circular plate under normal load when the deflections are of the same order as the thickness of the plate. Here as in so many other cases engineers are confronted with differential equations, for the solution of which they have neither time nor, in general, sufficient mathematical preparation. In the present case good approximate solutions have been developed by Nadai and Timoshenko, but it is of great interest to obtain the results by a rigorous or quasi-rigorous solution. This is what the author has done by expanding the radial stress σ and the inclination of the middle surface φ in series of ascending powers of the radial coordinate. He obtains thus a general solution for a circular plate under a uniform load, but two unknown constants remain which were introduced in the serial expressions. The solution for particular boundary conditions is now found by a very ingenious and practical process, solving first for a number of assumed values of the unknown coefficients and then applying a method of interpolation.

The fact that plates, completely fixed and held horizontally at the rim and which have the same values for $q_0 u_0^4$, shall have the same deflection, might perhaps be readily tested by the use of different materials, such as copper, steel, etc., adjusting the pressures and the thickness so that this quantity remains unaltered.

The tables and curves given in Figs. 6 and 7, will be very useful to engineers dealing with thin circular plates under pressure. The curves in Fig. 8 give added confidence in the approximate solutions of Nadai and Timoshenko, especially as they are corroborated by experimental results. In fact the curves in Fig. 10 are a great triumph for the theory.

I would suggest that the author indicate in more detail the steps through which Equation [10] is derived.

L. H. DONNELL.¹² The author of this paper is to be congratulated, not only on an excellent paper, but for his choice of

¹¹ Professor, Massachusetts Institute of Technology, Cambridge, Mass.

¹² Engineering Department, Goodyear-Zeppelin Corp., Akron, Ohio. Mem. A.S.M.E.

a subject which is of much more practical importance than the attention it has hitherto received might indicate. In the case of the bending of beams, a large-deflection theory is needed only when the deflections are so great that the slope of the deflection curve is of the order of magnitude of one, that is, when the deflections are of the order of magnitude of the length of the beam. Such deflections are almost never experienced in practice, and engineers are thus prone to think of large-deflection theories as of academic interest only. But the situation is entirely different with flat or curved plates which are bent in such a way that stretching or compressing of the plate must accompany the flexure, as is the case when a developable surface is bent to a non-developable one. Then the simple theory of small deflections becomes inaccurate when the deflections are of the order of magnitude of the thickness, as is vividly illustrated by the results given in this paper. Such deflections are frequently met with in practice so that researches of this nature have great practical value.

The author develops an "exact" theory for his case and compares it with two previous more approximate large-deflection theories. The comparison shows that as far as deflections are concerned the approximate theories are sufficiently accurate for practical purposes. This is important, as it is advisable to have as many checks as possible on our approximate methods. However the author fails to give any comparison between the maximum stresses in the plate, as given by the exact and approximate methods, although such a comparison should be quite easy for him to make and would add greatly to the value of the paper. General experience has been that such approximate theories are less accurate in regard to stresses than deflections.

The writer believes that it will be necessary to use large deflection theories to satisfactorily explain and study a number of important phenomena in the buckling of flat and curved sheets. Thus it is well known that the ultimate strength of a flat sheet with clamped or supported edges, under edge compression, is usually much greater than the stability limit given by the well-known theories of Bryan and Timoshenko, based on small-deflection theory. Dr. von Kármán has explained most of this difference as an edge effect, due to the edges being artificially prevented from buckling. But there is an additional strengthening effect having no connection with this. This might be called a "disk-wheel" effect as it is due to the bulging out of the sheet to something like the shape and hence something of the strength of a disk wheel. This effect can only be studied by a large-deflection theory. It has practical importance in the case of very thin plates or plates of a material with a high elastic limit. Also, in the buckling of thin cylinders or curved sheets under axial load, experiments show many features which have never been satisfactorily explained by any theory based on small deflections. The writer has found that all these discrepancies can be explained by considering initial deviations from cylindrical shape and using large deflection theory.

H. HENCKY.¹³ The paper by Mr. Way is very valuable because the exact solution of his problem is very difficult and tedious to obtain and is nevertheless needed for a judgment on approximative methods. He discusses the methods of Nadai and Timoshenko and finds them fairly satisfactory.

It is perhaps of interest to remark that these methods are only special cases of a more general method which was developed 18 years ago by G. B. Galerkin, of Leningrad. The method of Galerkin is one of unlimited adaptability to the precision required in any special case and deserves therefore a greater amount of publicity than it has had.

The problem in question is a two-dimensional one, the two

dimensions being the displacement w perpendicular to the plate and the displacement ρ in the direction of the radius of the circular plate. Consequently we will have two equations of equilibrium to satisfy which we will call symbolically $E(w) = 0$ and $E(\rho) = 0$.

The first step is to substitute two integrations taken over the surface of the plate without changing anything essential.

This can be done by introducing two arbitrary variations δ and $\delta\rho$ corresponding to the displacements w and ρ and writing:

$$\begin{aligned}\int E(w)\delta w dA &= 0 \\ \int E(\rho)\delta\rho dA &= 0\end{aligned}$$

with the integrations taken over the whole area of the plate.

Until now we have not introduced anything of an approximate character. Galerkin substitutes for w and ρ two series of arbitrary functions and extends the variations only over the arbitrary constants to be determined in the case in question. Consequently, using the fact that the variations are absolutely arbitrary, the two integrations yield just the needed number of equations to determine the constants. Naturally the functions have to be chosen so that the boundary conditions are satisfied.

The advantage of this method lies in the fact that by increasing the number of constants the method can be employed even if the exact solution is impossible to obtain as the case of a rectangular plate.

E. O. WATERS.¹⁴ The author should be highly commended for giving to the engineering profession a simple, workable solution for a rather difficult problem. It is true that the general equations have been known for some time in differential form, but it is doubtful whether engineers have ever made much, if any, use of them. Now, thanks to the author's labor of setting up the power series and solving the coefficients, together with his ingenious method of adjusting the results so as to fit the prescribed boundary conditions, it is possible to find the maximum deflection and the important stresses in a circular plate clamped at the edges, simply by referring to the proper curve in Fig. 6 or Fig. 7.

It is interesting to note how nearly accurate are the two approximate solutions mentioned by the author, as far as maximum deflection is concerned. In this connection, it should be pointed out that the solution by Timoshenko, Equation [35], was evidently worked out for $\mu = 0.3$. If μ is changed to 0.25, the curve for this approximate solution would shift slightly to the left, in the manner indicated in Fig. 6, and the error on the side of safety would be greater. This, however, makes practically no difference as long as the proper value of μ^2 is used in the last term of Equation [35], as was apparently done in the paper.

The writer would like to place on record another approximate solution (not original) which gives practically the same maximum deflection as the Nadai and Timoshenko formulas, and in addition gives membrane stresses at the center and edge that agree substantially with the exact method. By multiplying equation [8] by r , differentiating and then dividing by r , the fundamental equation of equilibrium is obtained:

$$p = \frac{D}{r} \frac{d}{dr} \left\{ r \frac{d}{dr} \left[\frac{1}{r} \frac{d}{dr} \left(r \frac{dw}{dr} \right) \right] \right\} - \frac{h}{r} \frac{d}{dr} \left[r \sigma_r' \left(\frac{dw}{dr} \right) \right] \quad [42a]$$

After performing the differentiation indicated in the third term, and using the relation between σ_r' and σ_t' given by Equation [9], we have:

$$p = \frac{D}{r} \frac{d}{dr} \left\{ r \frac{d}{dr} \left[\frac{1}{r} \frac{d}{dr} \left(r \frac{dw}{dr} \right) \right] \right\} + h \left(\frac{\sigma_r'}{R_r} + \frac{\sigma_t'}{R_t} \right) \quad [42b]$$

¹⁴ Associate Professor of Mechanical Engineering, Yale University, New Haven, Conn. Assoc.-Mem. A.S.M.E.

¹³ Lisbon, N. H. Mem. A.S.M.E.

where R_r and R_t are the radial and tangential radii of curvature of the middle surface. If there were no membrane stresses, the third term would vanish, the external work would be

$$\pi p \int_0^a wrdr, \text{ and the equivalent strain energy of bending would be}$$

$$\pi D \int_0^a \frac{1}{r} \frac{d}{dr} \left\{ r \frac{d}{dr} \left[\frac{1}{r} \frac{d}{dr} \left(r \frac{dw}{dr} \right) \right] \right\} wrdr. \text{ Load is proportional}$$

to deflection. Now, if membrane stresses are considered, and we neglect all displacements except those normal to the middle surface, $e/w = 1/R$, and the strain energy of stretching may be expressed by multiplying the third term above by $1/2w$ and integrating over the entire plate. The total external work is

$$\text{no longer } \pi p \int_0^a wrdr, \text{ but, since the strain energy of stretching}$$

is only a small part of the total, about 20 per cent when the deflection at the center equals the plate thickness, we may assume as an approximation that the straight line relation still holds, giving

$$\pi p \int_0^a wrdr = \pi D \int_0^a \frac{1}{r} \frac{d}{dr} \left\{ r \frac{d}{dr} \left[\frac{1}{r} \frac{d}{dr} \left(r \frac{dw}{dr} \right) \right] \right\} wrdr - \pi h \int_0^a \frac{1}{r} \frac{d}{dr} \left[r \sigma_r' \left(\frac{dw}{dr} \right) \right] wrdr \dots [43]$$

Then we may assume a value for w in terms of r and a constant, perform the indicated operations, and solve for the constant or at least get a relation between it and p . The simplest assumption is $w = w_0 \left(1 - \frac{r^2}{a^2} \right)$, as this is the expression for w when the membrane stresses are neglected. Letting $r = aS$, we have from Equation [10]

$$S \frac{d}{dS} (\sigma_r' + \sigma_t') = - \frac{8Ew_0^2}{a^2} (S^6 - 2S^4 + S^2)$$

$$(\sigma_r' + \sigma_t') = - \frac{8Ew_0^2}{a^2} \left(\frac{1}{6} S^6 - \frac{1}{2} S^4 + \frac{1}{2} S^2 + A \right)$$

From Equation [9]

$$\sigma_r' + \sigma_t' = \sigma_r' + \frac{d}{dS} (S\sigma_r') = \frac{1}{S} \frac{d}{dS} (S^2\sigma_r')$$

From this relation, values for σ_r' and σ_t' may be obtained:

$$\sigma_r' = -E \frac{w_0^2}{a^2} \left(\frac{1}{2} A + \frac{B}{S^2} + \frac{1}{6} S^6 - \frac{2}{3} S^4 + S^2 \right)$$

$$\sigma_t' = -E \frac{w_0^2}{a^2} \left(\frac{1}{2} A - \frac{B}{S^2} + \frac{7}{6} S^6 - \frac{10}{3} S^4 + 3S^2 \right)$$

To determine the constants of integration, we have σ_r' and σ_t' finite when $S = 0$, and $\sigma_t' = \mu\sigma_r'$ when $S = 1$. Therefore

$$\sigma_r' = \frac{Ew_0^2}{6a^2} \left(\frac{5-3\mu}{1-\mu} - S^6 + 4S^4 - 6S^2 \right) \dots [44]$$

$$\sigma_t' = \frac{Ew_0^2}{6a^2} \left(\frac{5-3\mu}{1-\mu} - 7S^6 + 20S^4 - 18S^2 \right) \dots [45]$$

Returning to the approximate energy Equation [43], and substituting the values of w and σ_r' , the first term gives $\frac{\pi p a^2 b}{6}$; the

$$\text{second gives } \frac{32\pi b^2 D}{3a^2}; \text{ and the third gives } - \frac{2\pi b^4 h E}{3a^2} \left[\frac{23-9\mu}{42(1-\mu)} \right].$$

When these are equated and reduced to the same form as Equations [33] or [35], and μ is given the value 0.25, we have

$$\frac{w_0}{h} + 0.463 \left(\frac{w_0}{h} \right)^3 = \frac{3}{16} \frac{p}{E} \left(\frac{a}{h} \right)^4 (1 - \mu^2) \dots [46]$$

Furthermore, when S is given the values 0 and 1 in Equations [44] and [45], and $\mu = 0.3$, we have the membrane stress at the center

$$\frac{\sigma_{t0}^2}{E} = 0.976 \left(\frac{w_0}{h} \right)^2 \dots [47]$$

and the radial membrane stress at the edge

$$\frac{\sigma_{r0}^2}{E} = 0.476 \left(\frac{w_0}{h} \right)^2 \dots [48]$$

All three of these equations agree well with the exact curves in Figs. 7 and 8, up to deflections of the order of $w_0/h = 1.25$; both [46] and [47] err on the side of safety, and [48] is always less than [47] and is therefore not critical.

When we compare the bending stresses of the approximate method the agreement is very poor, and the reason is not hard to find. The approximate method gives the same bending stress as the linear theory, when expressed in terms of maximum deflection, because the approximate method assumes the same geometrical form for the bent plate as does the linear theory. Actually, the bent plate will tend to assume the form of a thin membrane, with very sharp curvature at the edge and fairly uniform curvature everywhere else. In consequence of this we have, by the exact method, extra large bending stresses at the edge and smaller bending stresses at the center. In this feature, if in no other, the exact solution developed by the author is clearly far superior to any approximate method which assumes a form for the bent plate similar to that given by the linear theory.

A close approximation to the true bending stress at the rim may be obtained by taking a slightly different form for the bent surface, say $w = w_0(1 - S^2)(1 + kS^2)$, and using the minimum energy principle for w_0 and k . Assuming that k is a small correction whose powers higher than the first may be neglected, we have approximately $k = 0.02 pa^4/Eh^4$, which when substituted in the appropriate formula for σ_{r0} gives good agreement with the upper curve in Fig. 7.

AUTHOR'S CLOSURE

Equation [10], the origin of which may seem mysterious, can be obtained from Equations [1a] and [1b] of the paper as follows:

$$e_r' = \frac{d\rho}{dr} + \frac{\varphi^2}{z} \dots [1a]; \quad e_t' = \frac{\rho}{r} \dots [1b]$$

From Equation [1b]

$$\frac{d\rho}{dr} = \frac{d}{dr} (re_t') \dots [49]$$

If we substitute for $\frac{d\rho}{dr}$ in Equation [1a] we obtain

$$e_r' = \frac{d}{dr} (re_t') + \frac{\varphi^2}{z} \dots [50]$$

Now replace the extensions by stresses, using Hooke's law

$$\frac{1}{E} (\sigma_r' - \mu\sigma_t') = \frac{1}{E} \frac{d}{dr} (r\sigma_t' - \mu r\sigma_r') + \frac{\varphi^2}{z}$$

or

$$-\sigma_r' + \frac{d}{dr}(r\sigma_t') + \frac{E\varphi^2}{z} = \mu \left[\frac{d}{dr}(r\sigma_r') - \sigma_t' \right] \dots [51]$$

By Equation [9] the right-hand member of Equation [51] is zero, and the left member can be transformed using Equation [9] to give

$$-\sigma_r' + r \frac{d}{dr} \sigma_t' + \frac{d}{dr}(r\sigma_r') + \frac{E\varphi^2}{z} = 0 \dots [52]$$

or

$$r \frac{d}{dr} (\sigma_r' + \sigma_t') + \frac{E\varphi^2}{z} = 0$$

Dr. Donnell brings up the question of the accuracy of the approximate methods in giving the stresses. The author recently made calculations for plates with Poisson's ratio $\mu = 1/4$ in order to make this comparison. For $pa^4/Eh^4 = 9.19$, stresses found by the "exact" theory and those found by Nadai are as follows:

	$u^2 S_{r0}'$	$u_0^2 S_r'(0)$	$u_0^2 S_{r0}''$	$u_0^2 S_r''(0)$
"Exact"	0.49	0.97	-5.46	2.35
Nadai	0.52	1.00	-5.55	2.32

It is seen that for the stresses, Nadai's method errs on the safe side, except in the case of the bending stress at the center.

Equation [33], which comes from Nadai's solution, does not make available the full accuracy of that solution, as it is only a first approximation of the results of the solution. If the values given in the table on page 297 of "Die Elastische Platten" had been used instead of Equation [33] in plotting the curve in Fig. 8, better agreement would have been found with the "exact" method. Furthermore, the error would have been on the safe side for $w_0/h \cong 1$.

Professor Waters has shown another interesting approximate method which gives expressions for the membrane stresses. He points out also that the numerical constant 0.488 in Equation [35] is based on an assumed Poisson's ratio $\mu = 0.3$, and the author regrets this oversight. For $\mu = 0.25$ this constant should be 0.477.

Studies in Photoelastic Stress Determination¹

By E. E. WEIBEL,² ANN ARBOR, MICH.

This paper covers three laboratory studies in photoelastic stress determination.

The first of these is an investigation of the strain-creep characteristics of bakelite and phenolite. It was undertaken in the belief that the information to be obtained would indicate how closely the behavior of these materials under load approached the theoretical proportionality of strain to stress; the significance of exact knowledge of the degree to which this relationship holds true being that the deduction of stress distribution in structural materials by photoelastic means is based on the assumption that the photoelastic specimen does conform to Hooke's law. The tests performed are described in detail and from the results it is concluded that with these materials the departure from the Hooke's law stress-strain relationship is exceedingly small and does not vary with time of loading within a two-hour period.

The second study was undertaken in the belief that more accurate information regarding stress concentration at points of sharp change in sections of machine parts could be obtained with bakelite and phenolite and the monochromatic fringe-photograph method than obtained previously with celluloid models. The paper describes the methods used in testing for both tension and bending and

includes fringe photographs illustrating the changes in stress distribution for different ratios of fillet radius to the width of the narrow section of the specimen. From these tests the author has established the values of the stress concentration factor, in both tension and bending, for a considerable range of the fillet-width ratio.

The third study as set forth in this paper is the application of the membrane analogy in conjunction with the photoelastic results to the determination of stresses in a specimen subjected to bending. A soap film, used as the membrane, was enclosed by a frame of same shape as the specimen being studied. Its boundary ordinates, measured perpendicularly, were made proportional to the corresponding boundary values of the sum of the principal stresses. Under these conditions the ordinates of all points of the membrane are proportional to the sum of the two principal stresses at the corresponding points on the stressed member. The lengths of the ordinates were measured by means of a depth micrometer and the stress values at the corresponding points on the stressed member determined from these. Because of the ease of application and accuracy of the results obtained it is believed that the membrane analogy will find increasing use in conjunction with photoelastic studies.

I—STRAIN CREEP IN BAKELITE AND PHENOLITE

THE high optical sensitivity of bakelite³ (1)⁴ and phenolite⁵ (2), which is four or five times that of celluloid (2, 3, 4), is chiefly responsible for their extensive use in photoelastic stress determination. Their proportional limit is about twice that of celluloid. This combination makes them particularly suitable for use in the monochromatic fringe-photograph method (5) in which a large number of black and white fringes permits increased accuracy of stress determination.

¹ From a dissertation submitted in partial fulfillment of the requirements for the degree of Doctor of Philosophy at the University of Michigan.

² Engaged in private research work. Dr. Weibel received the degree of B.Sc. in Mechanical Engineering at McGill University, Montreal, in 1918. During the summers, 1915 to 1917, he was employed as structural draftsman with the Dominion Bridge Company, Ltd., Montreal; and from 1918 to 1922 as mechanical designer and estimator on steam-turbine and electric-crane work. From 1922 to 1927 he was supervisor, under the mechanical engineer of the company, of the mechanical-design squad on cranes, hydroelectric regulating gates, etc. During 1928-29 he studied mathematics at the University of Toronto and in 1929 returned to the Dominion Bridge Company where he was employed on mechanical standardization and as field engineer on the installation of hydroelectric equipment. In 1931 Dr. Weibel received the M.S.E. degree and in 1932 the degree of Ph.D. in Engineering Mechanics from the University of Michigan where he specialized in photoelastic stress determination.

³ Type C-25 bakelite used in the present experiments was purchased from the Bakelite Corp. of America.

⁴ Numbers in parentheses refer to Bibliography at the end of the paper.

⁵ The phenolite used was purchased from the Institute for Physical and Chemical Research, Tokyo, Japan.

Contributed by the Applied Mechanics Division and presented at the Annual Meeting, New York, N. Y., December 4 to 8, 1933, of THE AMERICAN SOCIETY OF MECHANICAL ENGINEERS.

NOTE: Statements and opinions advanced in papers are to be understood as individual expressions of their authors, and not those of the Society.

The application of the photoelastic effect to the determination of stress distribution in plane stress problems is based upon the assumption that stress distribution in the photoelastic specimen is a true representation of that which would occur in a construction material which obeys Hooke's law of the proportionality of stress to strain. About 1923 Filon and Jessop studied strain creep in celluloid (6) and found that below a certain value of stress initial strain was proportional to stress and that strain creep was roughly proportional to stress squared. The implication in these results is that, at the moment of loading a celluloid specimen, the stress distribution is a true Hooke's law distribution but that the distribution changes with duration of load period, departing increasingly from the Hooke's law distribution.

A consideration of the amount of departure from a linear stress-strain relation in two actual samples of celluloid will perhaps suggest that the effect on stress distribution will not always be negligible. One sample of xylonite (celluloid) showed strain creep 12.8 per cent of initial strain⁶ in ten minutes under a constant stress of 1900 lb per sq in. The departure from a linear stress-strain relation in this case between 950 lb per sq in. and 1900 lb per sq in. can be shown to be 6.4 per cent, assuming creep proportional to the square of the stress. Edmonds and McMinn made extensive experiments on strain creep in celluloid in 1931 (7). One sample, Material G, Table 1, Fig. 3, of their paper, showed 6 per cent creep in ten minutes under a constant stress of 2000 lb per sq in. The departure from Hooke's law in this case between 1000 and 2000 lb per sq in. would be 3 per cent.

Bakelite and phenolite are finding increasing use as photoelastic materials, the former chiefly in this country and the latter in Japan. They are both known to exhibit the phenomenon of strain creep but published accounts of experiments on the stress-strain relation have not been found, other than the usual stress-

⁶ Calculated from values at 30 minutes given in "Photo-Elasticity," by Coker and Filon, Cambridge University Press, 1931, p. 271.

strain diagram obtained by loading and unloading a tension specimen at either a constant rate of deformation or a constant rate of loading. The present experiments on strain creep in type C-25 bakelite and phenolite were undertaken in the belief that the information to be obtained would indicate how closely the stress distribution in specimens of these materials approaches the Hooke's law distribution, both at the instant of loading and at later instants.

EQUIPMENT

Test Piece. The test piece shown in Fig. 1 was about $\frac{3}{4}$ in. square in the body with bushed pinholes at $3\frac{1}{4}$ in. centers. It

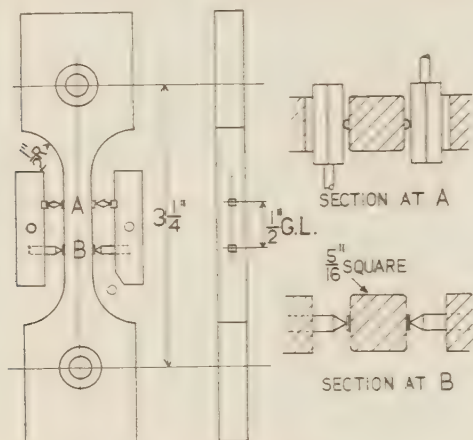


FIG. 1 TEST SPECIMEN

was carefully polished on all sides and the corners rounded to prevent nicking of the edges and consequent failure at a low average tensile stress. The test specimen was for use in tension and compression. Its dimensions were limited to some extent by the capacity of the loading frame available.

Extensometers. Martens mirror-type extensometers with a gage length of $\frac{1}{2}$ in. were used. A short gage length was originally used, as with it and the standard Martens knife edges the angularity of the light beam was so small that correction of readings was unnecessary. It also permitted the extensometers to be clamped at points well removed from the points of non-uniform stress at the fillets.

To protect the specimen from being scratched by the extensometer knife edges and to reduce friction small polished metal plates were attached at the gage points with Ambroid cement. In the earlier experiments the extensometer knife edges had a bearing across the full width of the specimen. This gave inconsistent results in the compression tests and was modified so that a point bearing at the center line of specimen was obtained. At the same time the distance members of the extensometer were made of bakelite of the same cross-section as the specimen so that strain readings would be virtually independent of small temperature changes. This detail is important as creep values are exceedingly small and the coefficient of expansion of phenolite, for example, is about sixteen times that of steel (8). The latter extensometer arrangement is shown in Fig. 3.

Loading Arrangement. Loading of the specimen was done by means of weights and a steel beam resting on a knife-edge attached to the loading frame of the photoelastic outfit. The change from tension to compression loading was effected by removing the specimen with extensometers attached, taking care not to disturb their setting, and shifting the position of the fulcrum. The photographs, Figs. 2 and 3 show these arrangements with extensometers, telescopes, and scales. The handle shown

was attached to an eccentric cam which permitted the load to be applied or removed quickly and smoothly.

TESTS AT CONSTANT LOADING AND UNLOADING RATE

These were tension tests in which a constant rate of loading was obtained by carefully adding equal load increments at precise intervals of time. Extensometer readings also were taken at precise time intervals. Unloading was carried out in a similar manner. Figs. 4 and 5 are two curves obtained for bakelite and phenolite at loading rates of 662 and 744 lb per sq in. per minute respectively. Proportional limits of about 4000 and 3500 lb per sq in. are obtained from the respective curves. The effect of strain creep is apparent in the relative displacement of the unloading curve. The displacement when the specimen is completely unloaded is not a permanent set but disappears almost

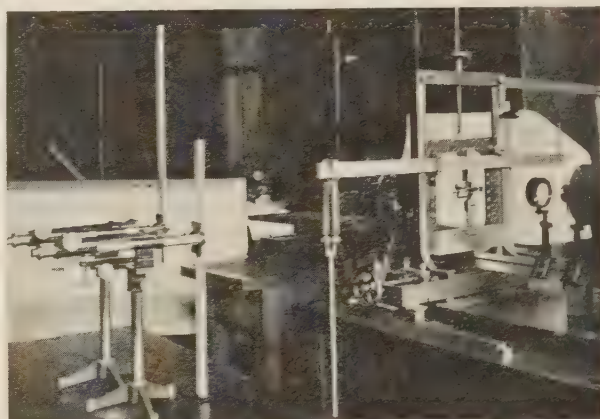


FIG. 2 LOADING ARRANGEMENT FOR TENSION TESTS SHOWING MARTENS MIRROR EXTENSOMETERS AND TELESCOPES

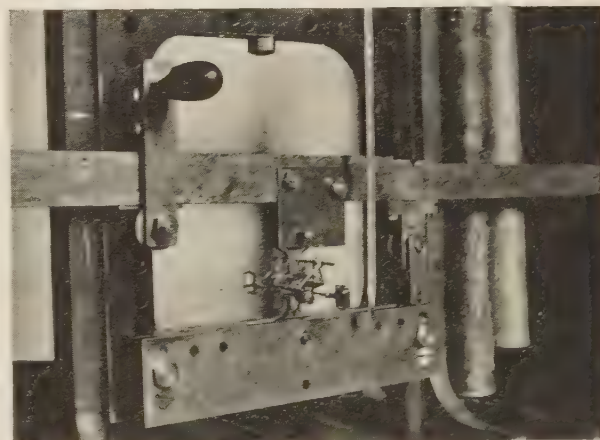


FIG. 3 LOADING ARRANGEMENT FOR COMPRESSION TESTS
(Distance members of extensometers are made of bakelite)

entirely in a length of time equal to the duration of the load period.

Different speeds of loading might result in different values of proportional limit, as was found by Edmonds and McMinn (7) for celluloid, but a large number of tests of this type were not carried out as the conditions of loading are too much unlike those of a photoelastic test for the results to be directly applicable.

Strain Creep Tests. The object of the strain creep tests was to obtain indirectly stress-strain curves which would truly repre-

sent the stress-strain relation in a photoelastic model at any time after the application of the load.

From a single strain-creep test at constant stress a curve of strain on a time base can be obtained. The value of strain at, say, five minutes after application of the load together with the value of stress used in that test would be a pair of values from which one point on the "five-minute stress-strain diagram" is obtained. If twelve points on the stress-strain diagram are arbitrarily demanded then twelve strain-creep tests must be run.

In the strain-creep tests the specimen was subjected to a tension or compression load which was applied quickly by means of the eccentric lever and which remained constant for a period of 15 minutes, during which strain readings were taken at suitable intervals. The load was then removed and the specimen was left unloaded for at least 15 minutes before starting another strain-creep test. A series of tests comprised six in tension and six in compression. In one series of tests on bakelite the following

sheet, strain on a time base, examples of which for bakelite and phenolite are shown in Figs. 6 and 7, respectively. The intersections of these curves with a vertical line drawn at a particular time after loading yield pairs of values of stress and strain each of which gives a point on the stress-strain curve. In Figs. 8 and 9 are shown the 15-minute stress-strain curves for bakelite and phenolite, respectively. The 5- and 10-minute curves were of the same type. Stress-strain curves for the instant of loading were not satisfactory as, due to the high initial rate of creep, accurate strain readings were obtained with difficulty.

The bakelite specimen used was one which had been completed a few months previously. It was tested before and after an annealing with little difference in the results. The phenolite specimen had been heat treated for 24 hours at 130 C and cooled slowly to room temperature. Heat treatment of this material for from 20 to 70 hours at 130 C⁷ reduces the amount of strain creep and raises the modulus of elasticity.

Curves. Examination of Figs. 6 and 7 shows that the creep rate is high immediately after application of the load and that it decreases rapidly with time of loading. Values of strain creep are discussed later in connection with strain-creep tests of two hours duration. Considering the tension portions of the stress-strain curves in Figs.

8 and 9 it is found that for bakelite the departure from linear between 2000 and 4000 lb per sq in. is 0.7 (± 0.2) per cent for the 5-, 10-, and 15-minute curves, and for the phenolite the corresponding figure is 0.8 (± 0.2) per cent. The differences in these figures were small and irregular, experimental errors probably masking the true values so that no conclusions could be drawn

⁷ Suggested in a personal letter from Dr. Z. Tuzi.

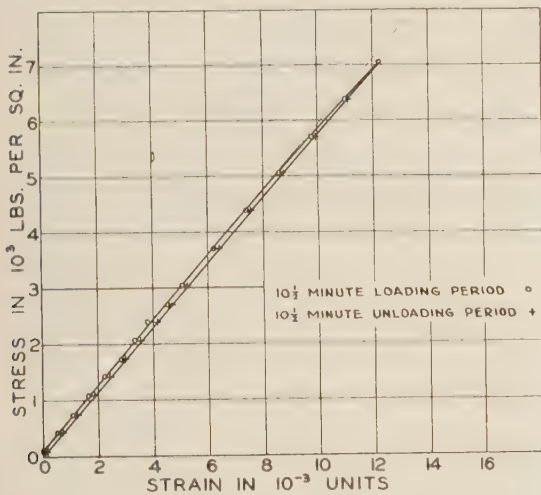


FIG. 4 LOAD-UNLOAD TEST WITH C-25 BAKELITE
(Loading rate: 662 lb per sq in. per min. $E = 595,000$ lb per sq in.)

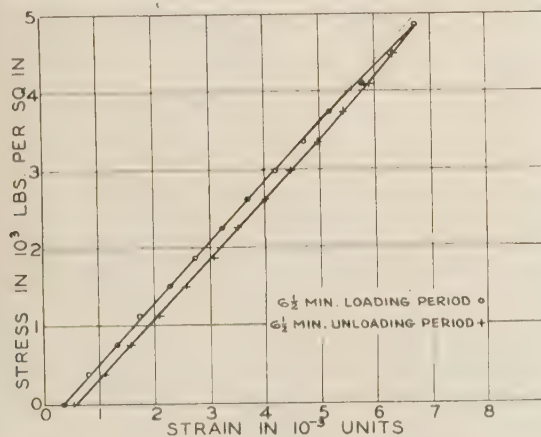


FIG. 5 LOAD-UNLOAD TEST WITH PHENOLITE
(Loading rate: 744 lb per sq in. per min. $E = 775,000$ lb per sq in.)

values of stress were used: tension, 1252, 2408, 3400, 4700, 5845, and 7000 lb per sq in.; compression, 1482, 2584, 3685, 4790, 5890, and 6980 lb per sq in. A number of series of tests of the above type were carried out on each material.

The results of such a group of tests were plotted on a single

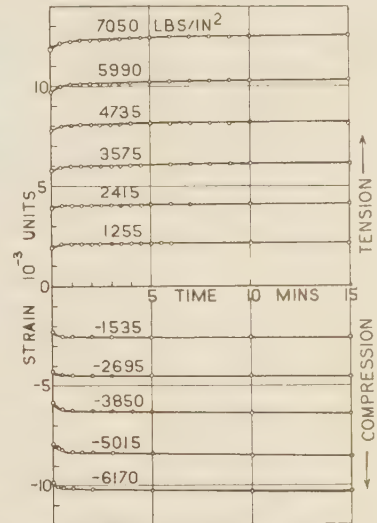


FIG. 6 STRAIN-TIME CURVES—C-25 BAKELITE

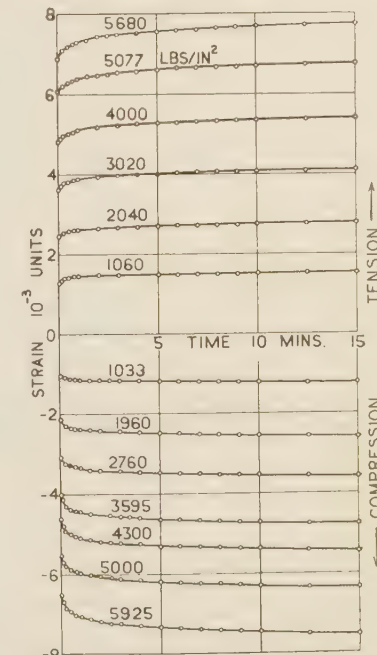


FIG. 7 STRAIN-TIME CURVES—PHENOLITE

as to whether the departure from linear increases with time of loading.

The compression portions of the curves in Figs. 8 and 9 were not drawn through the compression points but were an

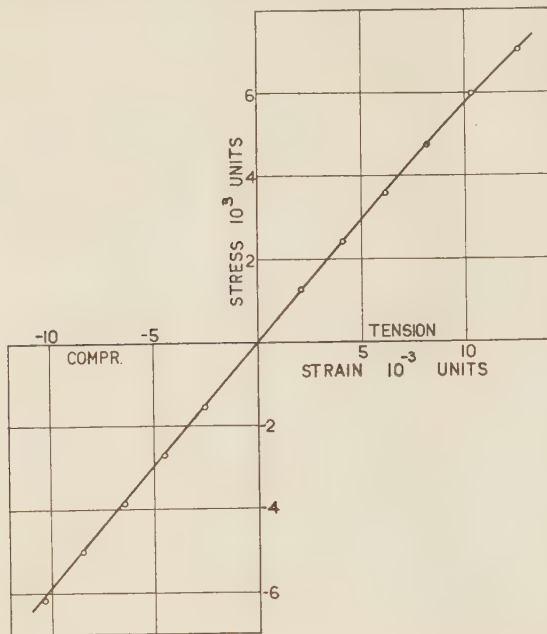


FIG. 8 STRESS-STRAIN RELATION FOR C-25 BAKELITE 15 MINUTES AFTER LOADING
($E = 590,000$ lb per sq in.)

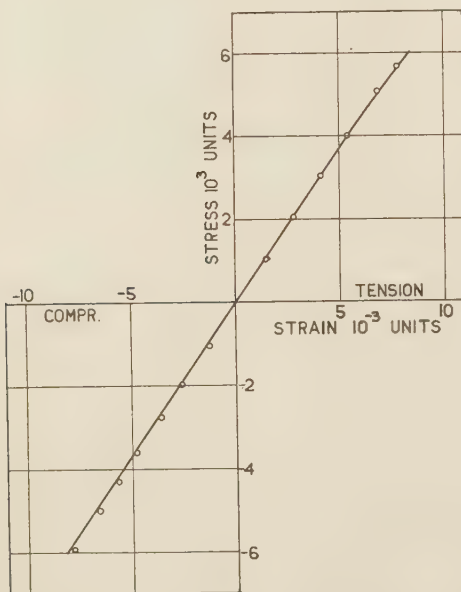


FIG. 9 STRESS-STRAIN RELATION FOR PHENOLITE 15 MINUTES AFTER LOADING
($E = 745,000$ lb per sq in.)

extension of the tension curves. Compression points in general lie slightly to the right of these extended lines which would indicate a modulus 0.5 to 1.2 per cent higher in compression than in tension, or that a slight slipping of the extensometer points had

occurred in changing over from tension to compression loading. The latter explanation is the more probable. An error of about 0.3 per cent may also be present due to inaccurate measurement of lever arms.

The departure from linear noted in the tension tests may be due largely to slipping of extensometers, which was difficult to control. In successive tests on a specimen at the same stress, strain readings could often be duplicated within 0.3 per cent, but only by exercising care in preventing the specimen from being jarred.

Two-Hour Strain-Creep Tests. The question as to whether the departure from a linear stress-strain relation varies with time

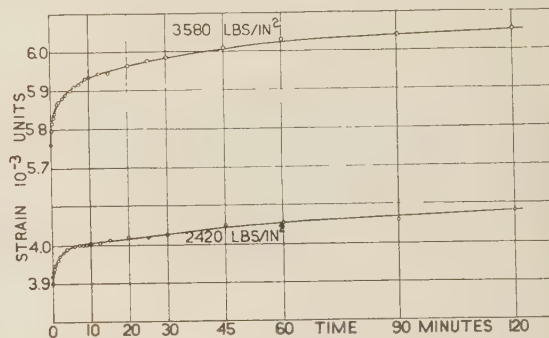


FIG. 10 STRAIN-TIME CURVES FOR C-25 BAKELITE—2-HOUR TEST

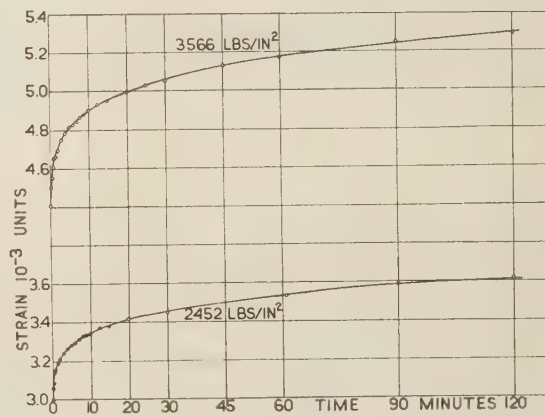


FIG. 11 STRAIN-TIME CURVES FOR PHENOLITE—2-HOUR TEST

could not be answered by the experiments just described as they were of too short duration. Consequently two two-hour strain-creep tests were run on the bakelite specimen at constant tension stresses of 2420 and 3580 lb per sq in., respectively, and two on the phenolite specimen at stresses of 2452 and 3566 lb per sq in. The strain-time curves are shown in Figs. 10 and 11.

For bakelite the strain creep in 15 minutes is 3 per cent of initial strain for both values of stress, and in 2 hours it is 5 per cent of initial strain, for both values of stress. For phenolite the corresponding figures are 16 and 24 per cent. Variations within the estimated experimental error of ± 0.3 per cent are neglected in presenting these results.

The fact that strain creep is the same percentage of initial strain for two different values of stress signifies that the stress-strain relation is unchanged with time of loading. This is shown also by a consideration of the departure from a linear relation at different times in these tests. For bakelite the departures from proportionality of stress to strain at 1, 15, and 120 minutes,

were 0.9, 0.9, and 1.0 per cent, respectively. For phenolite corresponding figures were 1.0, 0.6, and 0.6. Since the differences in these figures are within the experimental error it may be concluded that the departure from a linear stress-strain relation does not change within a two-hour load period.

Modulus of elasticity for bakelite in these tests varied from 620,000 lb per sq in. at the instant of loading to 591,000 lb per sq in. in two hours. For phenolite the modulus varied from 820,000 lb per sq in. at the beginning of the test to 675,000 lb per sq in. at the end. An error of 3 per cent due to inaccurate setting of gage length may be present in these figures which are mentioned only incidentally.

A phenolite specimen which had been heated 72 hours at 130 C was run through a two-hour strain-creep test and showed strain creep 10.8 per cent in 15 minutes and 14.3 per cent in two hours. Modulus of elasticity varied from 812,000 to 740,000 lb per sq in.

Comparison With Celluloid. In their paper on strain creep in Celluloid (6), Filon and Jessop, after rejecting a formula derived theoretically on the assumption of two constituents, one elastic, the other viscous, adopted the empirical formula:

$$e = e_0 + at^{1/2} + bt$$

in which e = strain at time, t minutes

e_0 = initial strain, roughly proportional to stress

a = a constant, roughly proportional to square of stress

b = a small constant, insignificant.

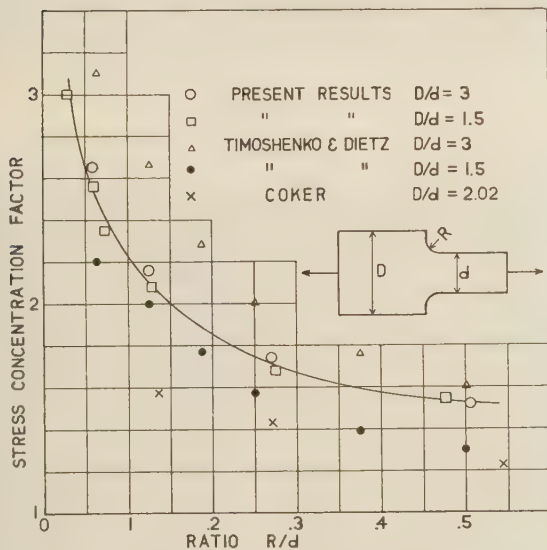


FIG. 12 STRESS-CONCENTRATION FACTORS—TENSION

In the present study a two-hour strain-creep test was made on the bakelite specimen at 2405 lb per sq in. tension stress. The fifteen strain-time points were fitted to the above type of formula by a method of least squares and found to agree remarkably well, the maximum residue being 0.26 per cent. The test was made with the early extensometer arrangement which was not independent of temperature variations, but as there has not been time to make a similar study of the later results it is included as being of interest. The temperature variation during this test could not be detected on a glass thermometer but it is believed to have been sufficient to affect the constant b in the formula.

If, as is probable, this formula applies to bakelite, the results of the two-hour tests mentioned earlier would indicate that for bakelite the constant a is proportional to the first power of stress.

This is of interest as an analogous result has been found for optical creep. Relative optical retardation in celluloid (6) follows the same law as that given above for strain, the coefficient of $t^{1/2}$ being again proportional to the stress squared. Arakawa (3) has shown that relative retardation in bakelite follows the same law, the coefficient of $t^{1/2}$ in the case of bakelite being closely proportional to the first power of stress.

A study of the agreement between the strain-time results for phenolite and the Filon and Jessop formula has not as yet been made.*

Conclusions. From the series of fifteen-minute tests it is concluded that for both C-25 bakelite and phenolite heat-treated as described, the stress-strain relation between 4000 lb per sq in.

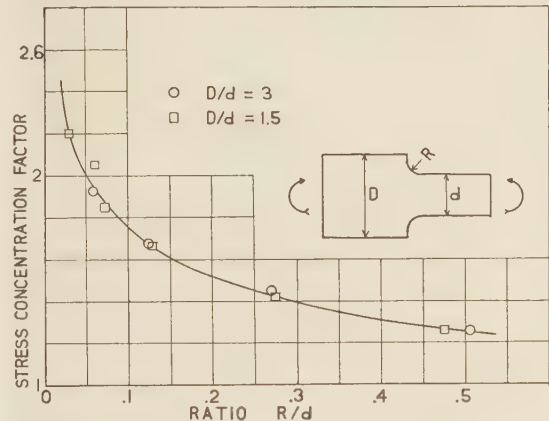


FIG. 13 STRESS-CONCENTRATION FACTORS—PURE BENDING

tension stress and 4000 lb per sq in. compression stress, during a fifteen-minute loading period, is linear within about one per cent.

From the two-hour tests it is concluded that the departure from a linear stress-strain relation does not vary in these materials with time of loading, within a two-hour period.

A tentative conclusion is that strain in bakelite follows the Filon and Jessop formula, the coefficient of $t^{1/2}$ being roughly proportional to stress.

Interpreting these results in their relation to the stress distribution in photoelastic models of bakelite or phenolite, we may conclude that the departure from the Hooke's law distribution will be very small and may be neglected.

Strain creep for phenolite is considerably greater than that for C-25 bakelite, but as creep is proportional to stress this has no effect on stress distribution which approximates closely the theoretical for both materials at all times within a two-hour period after loading.

II—STRESS-CONCENTRATION FACTORS FOR TENSION AND BENDING MEMBERS

It is usual to provide fillets of as large radius as convenient at sharp changes of section in machine parts because fatigue failures are known to begin at such points. Little accurate information is available as to the amount by which stress is increased for different proportions of a member.

Values for factors of maximum stress concentration for tension members of the form shown in Fig. 12 were determined photoelastically and tabulated in a paper by Timoshenko and Dietz (10) in 1925. In connection with his photoelastic studies on tensile-test specimens H. B. Maris (11) published in 1927 a table similar to that by Timoshenko and Dietz but covering a different

* The values of e_0 and a for the curves of Fig. 11 have since been found to be proportional to stress, within about two per cent.

range of proportions. Coker published four values of the same factor in some photoelastic studies on tensile test specimens⁸ (9). Reports of other experimental or of analytical work on this form of member have not been found in the literature.

All of the above mentioned photoelastic work was done using celluloid models and a compensating strip of the same material or a Babinet compensator. The present work was undertaken in the belief that more accurate results might be obtained by the use of the more sensitive photoelastic materials, bakelite and phenolite, and the monochromatic fringe-photograph method (5).

One purpose of the present study was to obtain factors of maximum stress concentration for tension members of the form shown in Fig. 12, for a range of values of D/d from 3 to 1.5, and of R/d from $1/32$ to $1/2$. This was roughly the range covered in the paper of Timoshenko and Dietz. In that paper it was concluded on

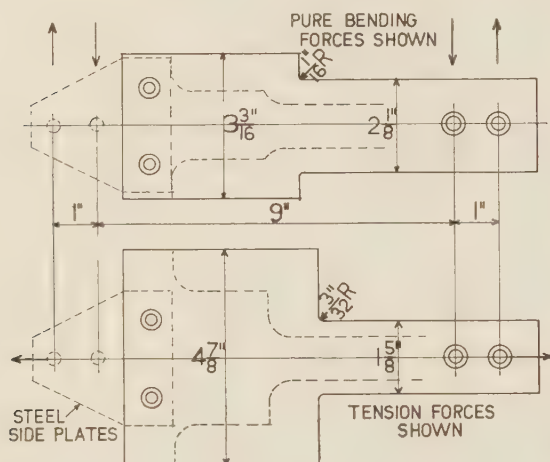


FIG. 14 FORM OF PHOTOELASTIC MODELS

rather limited experimental evidence that the values for factors in tension would hold also in bending. The present experiments were extended to include a study of concentration factors for members of the same form loaded by a pure bending moment as indicated in Fig. 13.

Acknowledgment is made of the use of Wahl and Beeuwkes' method⁹ of determining fringe order at the point of maximum stress concentration by extrapolation beyond the apparent boundary of the specimen. The curves of Figs. 12 and 13 were obtained by this means. Before learning of this method a set of curves had been obtained which agreed closely with the ones shown, but the uncertainty regarding individual points was of the order of plus or minus 5 per cent. More consistent results are possible using the extrapolation method; two subsequent experiments made to check the values of factors for R/d 0.2745 and 0.505, respectively, gave values which agreed with those shown in Figs. 12 and 13 within 1 per cent.

PHOTOELASTIC MODELS

The models were made from type C-25 bakelite or of phenolite of about $1/4$ in. thickness, polished on both faces and of initial dimensions as shown by the full lines of Fig. 14. All the points on the curves of Figs. 12 and 13 were obtained by the use of two models of bakelite which were filed and machined to a new

set of proportions after each test, the final shape of model being indicated by dotted lines in Fig. 14. Annealing of the model was done as has been described by Frocht (12) and Solakian and Karelitz (13). An automatic temperature regulator for the electric furnace was available and the dial of this was actuated by a clock and traveling-nut device to lower the temperature about $3\frac{1}{2}$ C per hr.

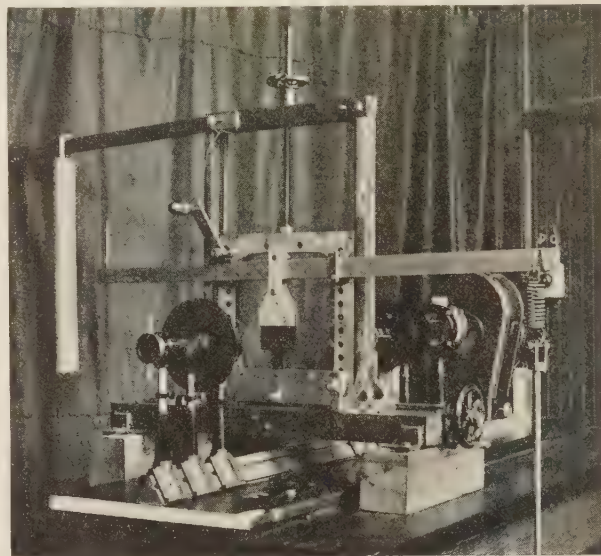


FIG. 15 TENSION-LOADING ARRANGEMENT IN STRESS-CONCENTRATION EXPERIMENTS
(Transparent yellow phenolite model appears black in photograph.)

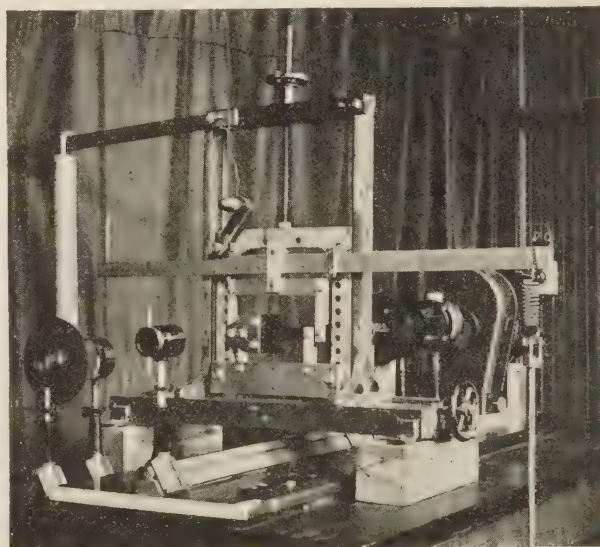


FIG. 16 LOADING ARRANGEMENT FOR PURE BENDING

Steel side plates attached to the model made it possible to apply a pure bending moment or tension forces as desired. The method of loading is indicated in Fig. 14 and in the photographs Figs. 15 and 16.

Considerable difficulty was experienced in obtaining accuracy of form in the region of the fillet, presumably due to the difference of cutting action along the straight portions of the contour and in

⁸ "Photo-Elasticity," by Coker and Filon, Cambridge University Press, 1931, pp. 564, 574.

⁹ "Stress Concentration Produced by Holes and Notches," by Wahl and Beeuwkes, A.S.M.E. Trans., 1934, paper APM-56-11.

the curve of the fillet. When cutting in the fillet, the milling cutters had a tendency to deflect or to bite in too deeply causing edge stresses where these were least desired. The method of obtaining the final contour was to lap the fillet by hand using a piece of drill rod of the correct diameter and fine emery powder. The straight portions were then milled to within about 0.0005 in. of the final shape using a cutter of smaller radius than the fillet radius, and were finished by hand lapping. A vise with fixture for guiding the lap made the lapping a simple and quick operation. Accuracy of form was checked by means of a microscope with a measuring head and magnification of about eighteen diameters.

TEST PROCEDURE AND METHOD

A preliminary study of optical creep in type C-25 bakelite and phenolite was made. The stress-optic relation at any time within 30 minutes after loading was found to be linear for values of stress up to at least 3500 lb per sq in. which was the maximum used in the stress concentration factor tests. Optical creep for C-25 bakelite in 30 minutes was approximately 4 per cent of initial optical retardation and for phenolite approximately 8 per cent. The presence of optical creep was allowed for in the loading tests by taking all photographs for one set of tests at the same number of minutes after applying the load, usually from 5 to 15 minutes.

Whenever possible the photoelastic tests were carried out immediately after completion of a model, as it was found that a delay of four hours caused edge stresses which introduced some uncertainty in estimating the fringe order at the point of maximum stress. In most cases complete elimination of internal stresses in the bakelite specimen by annealing was not obtained, but provided local edge stresses were not present, this is believed not to have affected the accuracy of the results obtained because of the method used in making the tests.

In two separate bending tests, moments of equal value but of opposite sign were applied to the specimen. The number of fringes at a fillet when it was on the tension side was different from the number of fringes in the same fillet when in compression. The average of these two values gave the true fringe order and half the difference gave the apparent initial stress at the point considered. Models were used in which this initial stress was as much as 0.35 fringe order. Non-uniformity of this initial stress condition would be indicated by a difference in the position of maximum stress in the two tests. If this difference is small the error introduced by the presence of initial stress is negligible. It is believed that the method of reversing the sign of external forces will increase the accuracy of results even in cases where apparently perfect annealing has been obtained, for the reason that an initial stress equivalent to about 0.1 fringe cannot be detected easily by examination of the unloaded model.

For the tension tests it was not practicable to run a corresponding set of compression tests because of the buckling-strength limitations of the models. The values of initial stress determined from the bending tests were used as a small correction however, and added algebraically to the fringe values obtained from the tension-test photographs. A single compression test was run in which the model was supported laterally by clamping metal rods on the two sides along its center line. The average of fringe orders observed in this test and the corresponding tension test checked closely with that obtained by making the correction mentioned.

The point of maximum stress was found to be about ten degrees from the point of tangency of the curve of the fillet and the straight side of the narrow portion of the model. As an adaptation of Wahl and Beeuwkes' method of extrapolation (14) three lines having an inclination of ten degrees with the center line of the model were scratched on one face near each fillet contour.

The distance between any two of these lines and the distance from one of them to the boundary were used in determining the true position of boundary on the fringe photograph.

To determine the fringe order in the straight part of the model in the pure-bending test a series of scratches was made across the width of the specimen. Any two of these could be used to measure the number of fringes in a known proportion of the total depth, from which the true fringe order at the straight boundary could be calculated. The fringe order in the straight portion in the tension tests was calculated from the known stress and the stress value per fringe obtained in the bending tests on the same model.

For each set of proportions four bending tests and two tension tests were made. In the first two bending tests, moments were used which gave maximum stresses of about 3200 and 3500 lb

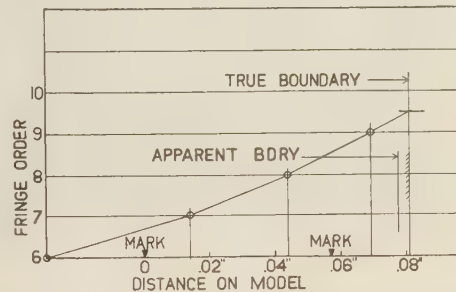


FIG. 17 TYPICAL EXTRAPOLATION CURVE

per sq in., respectively. Photographs were taken for these two loadings. The model was then reversed in the loading device so that the fillet originally in tension was put into compression and these same moments were again applied, a photograph being taken for each loading. The two tension tests were then made at maximum stresses of about 3200 and 3500 lb per sq in., a photograph being taken for each loading. From the six photographs obtained in this manner, extrapolation curves of the type shown in Fig. 17 were drawn; four for each value of bending moment and two for each value of tension load.

The stress-concentration factor in pure bending is defined as the ratio of maximum stress in the fillet to maximum stress in the straight part of the member where conditions are uniform. The same definition would apply to the case of tension, the stress in this case being uniform across a section of the straight portion. Values of the factors shown in Figs. 12 and 13 were calculated using the ratio of maximum fringe order in fillet to maximum fringe order in straight portion, allowance being made for initial stress as outlined above.

Fringe photographs for different ratios of fillet radius to width of narrow section are shown in Figs. 18 to 26.

CURVES AND DISCUSSION

In the curves of Figs. 12 and 13 stress-concentration factors are plotted against values of the ratio R/d ,

$$\frac{\text{Radius of Fillet}}{\text{Width of Narrow Portion}}$$

The large circles are for the case $D/d = 3$ and the large squares for $D/d = 1.5$. In Fig. 12 the triangles are the results obtained by Timoshenko and Dietz for the tension factor for $D/d = 3$ and the round dots their results for $D/d = 1.5$. The three crosses are Coker's results for the tension factor for $D/d = 2.03$.

The present results indicate that there is a negligible difference in either the tension or bending factor for values of D/d between

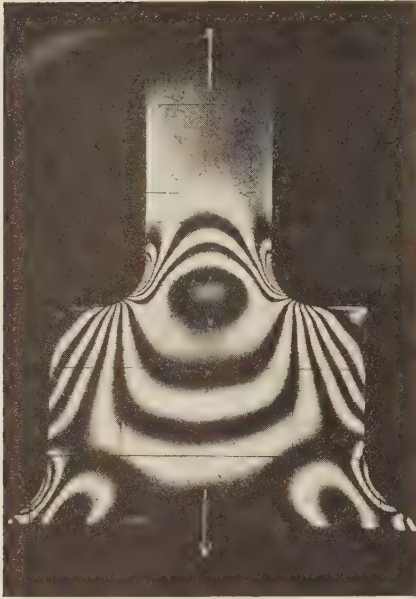


FIG. 18 FRINGE PHOTOGRAPH OF PHENOLITE MODEL UNDER TENSION LOADING
($D/d = 2.5$, $R/d = 0.34$.)

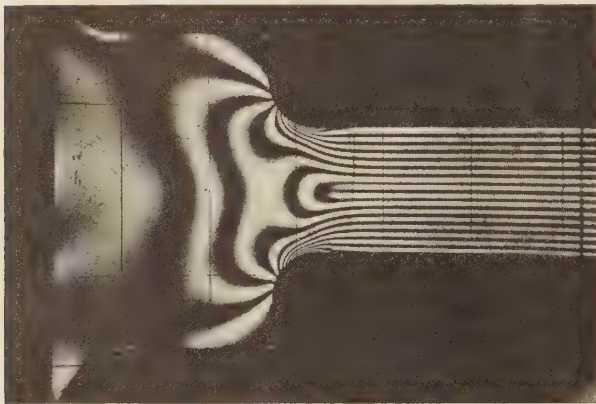


FIG. 19 PURE BENDING APPLIED TO MODEL SHOWN IN FIG. 18

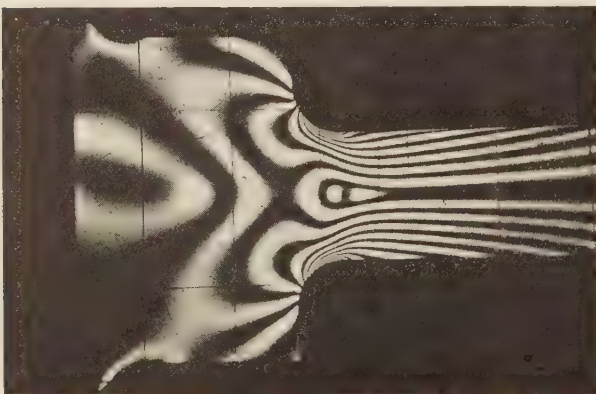


FIG. 20 CANTILEVER BENDING APPLIED TO MODEL SHOWN IN FIGS. 18 AND 19
(Lever arm is four times narrow width.)

1.5 and 3.0. This is in contrast with the values shown by Timoshenko and Dietz. Perhaps since the point of maximum stress is very near to the point of tangency of the fillet and the narrow portion of the member, and relatively distant from the wide

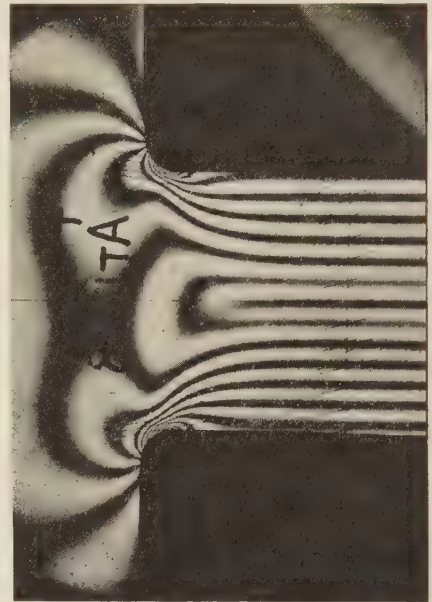


FIG. 21 PURE BENDING APPLIED TO A BAKELITE MODEL
($D/d = 3$, $R/d = 0.125$. Fillet A in tension.)

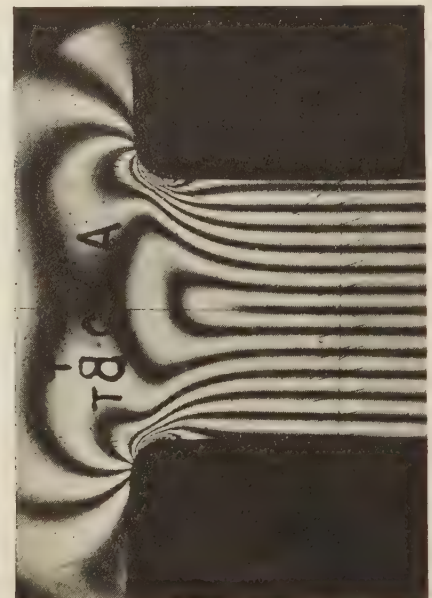


FIG. 22 MODEL SHOWN IN FIG. 21 WITH EQUAL MOMENT OF OPPOSITE SIGN
(Fillet B in Tension.)

portion, variations in shape of the wide portion will have little effect upon stream lines of stress at this point.

The factors for pure bending shown in Fig. 13 are also independent of the ratio D/d within the range studied. They are roughly 20 per cent lower than the tension factors for corresponding values

of R/d . This disagrees with the conclusion set forth in the paper by Timoshenko and Dietz, that tension factors might be used for the case of bending.

The factors for pure bending would be expected to apply almost exactly for cases of cantilever bending in which the ratio of lever arm to depth d is greater than 4, as the chief difference in such cases is the presence of a shear stress in the cantilever beam whose average value is not over $4\frac{1}{8}$ per cent of the value of maximum stress in the straight narrow portion of the member.

III—USE OF A SOAP FILM IN THE PLANE-STRESS PROBLEM

The fringes in a fringe photograph obtained by the photoelastic method are lines of constant maximum shear stress, or since

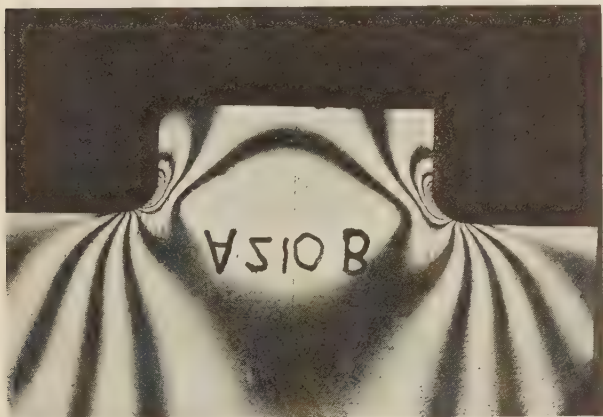


FIG. 23 TENSION LOADING APPLIED TO MODEL SHOWN IN FIGS. 21 AND 22



FIG. 24 PURE BENDING IN BAKELITE MODEL
($D/d = 1.5$, $R/d = 0.062$.)

in the case of two dimensional stress the maximum shear stress is half the difference of the principal stresses, usually denoted by P and Q , respectively, the fringes may be considered as lines of constant $(P - Q)$.

The directions of principal stresses are also obtained photoelastically by observing the loaded model in plane polarized light instead of in circularly polarized light as used for the fringe photograph. Lines of constant stress direction are known as isoclinics.

Since for a complete stress solution the value of each principal stress must be known at all points it is evident that the above in-

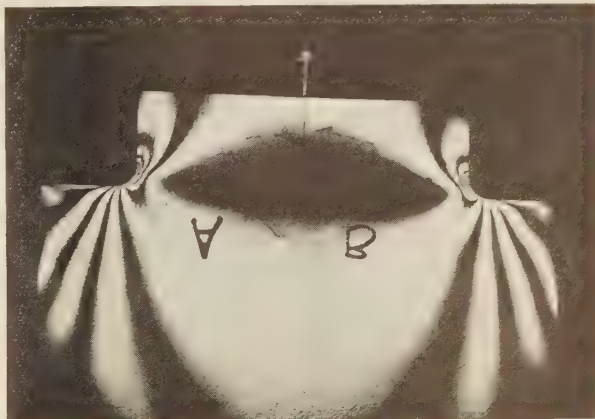


FIG. 25 TENSION APPLIED TO MODEL SHOWN IN FIG. 24

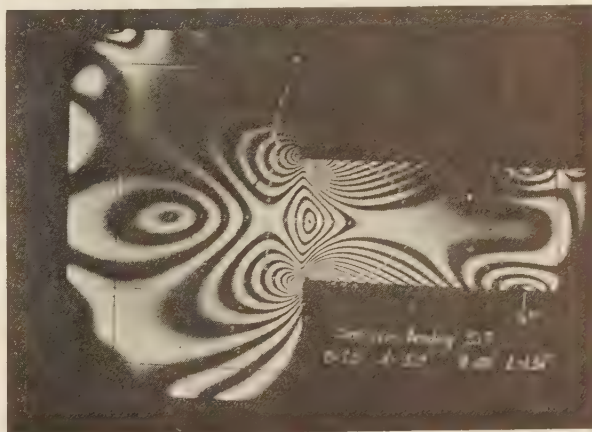


FIG. 26 CANTILEVER BENDING IN PHENOLITE MODEL WITH VERY SMALL FILLET RADIUS

(Material was overstressed accidentally providing a striking example of a photograph in which fringes could not be counted at point of maximum stress.)

formation obtained photoelastically is not sufficient. Several methods for completing the solution are in use, all of which require tedious measurements or calculations.

A purely mechanical method is the lateral extensometer method which was suggested by Mesnager and which was developed and used extensively by Coker.¹⁰ In this method very precise measurements of the change in thickness of the photoelastic model are made at different points. From these the value of the sum of the principal stresses, $(P + Q)$, is found. Combining these results with the known values of $(P - Q)$, the values of the individual principal stresses P and Q are obtained.

The graphical integration method of Filon (15, 16) is described as a purely optical method as it uses only data obtained photoelastically. Integration is carried out in steps along a stress

¹⁰ "Photo-Elasticity," by Coker and Filon, Cambridge University Press, 1931, p. 171.

trajectory, starting from a boundary free from external forces where one of the principal stresses is known. Each integration of this type provides values of one of the principal stresses at points along the line of integration. Considerable time is required and very often accuracy is far from satisfactory.

A wholly different method, that of Favre (17), which does not make use of the fringe photograph but obtains P and Q directly at any point by means of a delicate interferometer, is being developed abroad. A solution by this method would appear to involve a large amount of painstaking observation.

It was pointed out by Den Hartog (18) that the membrane analogy could be used in two dimensional stress problems for the determination of the sum of principal stresses ($P + Q$).¹¹ The

to forces distributed uniformly around the boundary and whose slope with the xy plane is not too large,

$$\left(\frac{\partial^2}{\partial x^2} + \frac{\partial^2}{\partial y^2} \right) z = 0$$

In order to solve a particular problem by means of the membrane analogy the boundary conditions for the membrane must be the same as those for the stresses. The shape of the opening over which the membrane is stretched must be the same as the shape of the member being studied, and boundary ordinates measured perpendicular to the plane of the opening must be proportional to corresponding boundary values of ($P + Q$). If these as well as the previously mentioned conditions are fulfilled the ordinates of the membrane at interior points will be proportional to the values of ($P + Q$) at corresponding points on the stressed member.

A soap film was used for the membrane. It automatically provides a uniformly distributed boundary force, as its surface

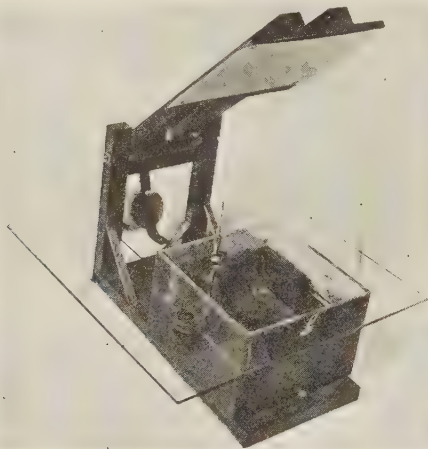


FIG. 27 SOAP-FILM EQUIPMENT

(A portion of the model is visible inside box. Pivoted sketch board can be brought into contact with pointer.)

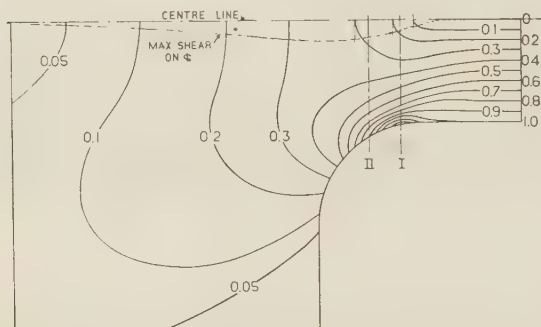


FIG. 28 LINES OF CONSTANT ($P - Q$) FROM FRINGE PHOTOGRAPH

following paragraphs describe an application of the membrane analogy in conjunction with the photoelastic results to the determination of stresses in one of the bending specimens of Section II of this paper; the case in which $D/d = 3$ and $R/d = 0.5$.

The analogy is a purely mathematical one and is based upon the fact that the equation, satisfied by the sum of principal stresses ($P + Q$),

$$\left(\frac{\partial^2}{\partial x^2} + \frac{\partial^2}{\partial y^2} \right) (P + Q) = 0$$

is satisfied also by the ordinates z of a membrane which is subject

¹¹ Independently noticed and worked on by M. Biot at California Institute of Technology.

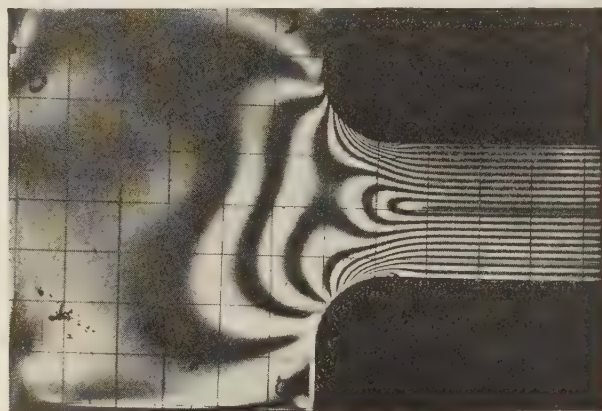


FIG. 29 PURE BENDING

(Presence of initial stress indicated by lack of symmetry in fringes and sudden change of direction at boundary. $D/d = 3.0$, $R/d = 0.5$.)

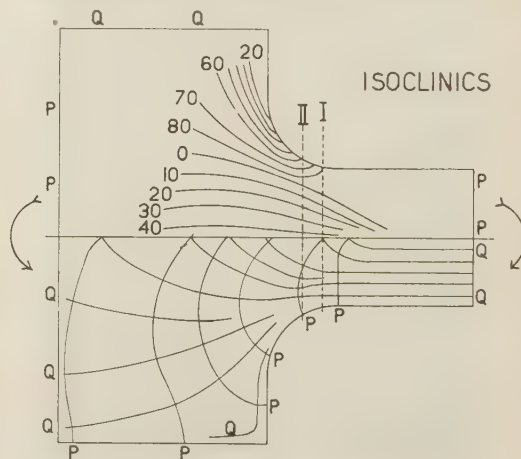


FIG. 30 ISOCLINICS AND STRESS TRAJECTORIES

tension is the same in all directions and at all points. The use of a soap film in the St. Venant torsion problem has been described by Griffith and Taylor (19) and later by P. A. Cushman (20) who applied it as well to the problem of lateral shearing stresses in beams. The equipment shown in Fig. 27 is that which was used in the experiments of P. A. Cushman, and follows closely

the original equipment of Griffith and Taylor. The soap-film model is clamped between the two halves of a square cast iron box with open top. An ordinary micrometer of the depth gage type is clamped to a glass plate which rests on the flat open top of the box, so that the elevation of any part of the film may be measured. In the present experiments holes through the base of the model permit equalization of pressure on two sides of the film. The positions of points on the film are transferred to a hinged sketch board above the box by bringing it into contact with the upper point of micrometer.

The lines of constant ($P - Q$), Fig. 28, were obtained as the average of a number of fringe photographs such as that shown in Fig. 29. Isoclinics and stress trajectories are sketched in Fig. 30. These two sets of lines are symmetrical about the center line but the notations of stress trajectories and of isoclinics are not symmetrical.

At a boundary which is free from external forces the principal stresses are parallel to and perpendicular to the boundary, the latter stress being zero. For this reason it is evident that at such a boundary ($P - Q$) = \pm ($P + Q$), and the boundary values of

ordinates proportional to these stress values, the ordinate corresponding to a stress value of 1.00 being 0.133 in., other dimensions as shown in Fig. 32. It was found that although the slope around the boundary nowhere exceeded 18 deg, the film surface when formed had a slope of about twice this angle in a small region around the point of maximum stress. A large slope introduces error in the use of the analogy as the assumption is made that the tangent of the angle of slope may be substituted for the sine, and that the cosine is approximately equal to unity.

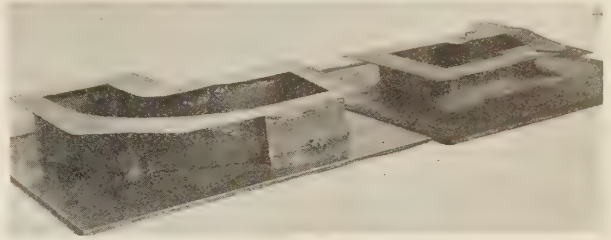


FIG. 33 SOAP-FILM MODELS

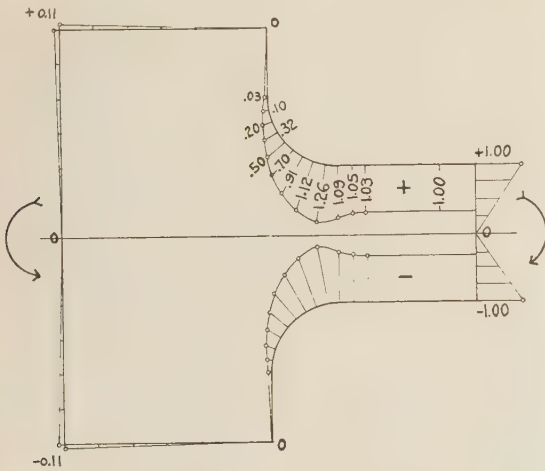


FIG. 31 BOUNDARY STRESSES

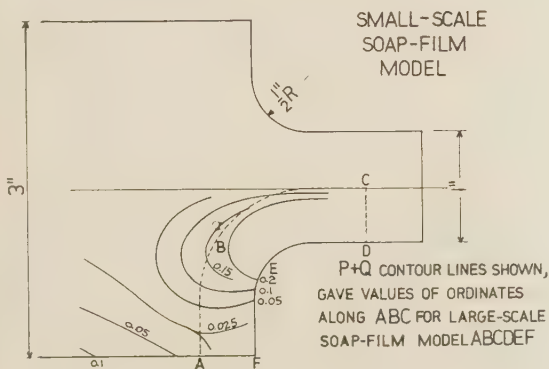
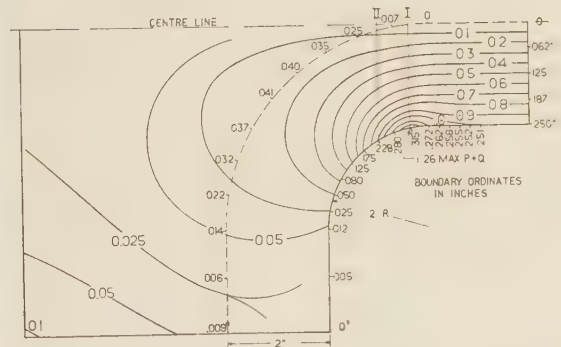


FIG. 32 SMALL SCALE SOAP-FILM MODEL

($P - Q$) in the fringe photograph may be used as boundary values of ($P + Q$) for the soap-film model.

These boundary stresses are shown in Fig. 31. Stresses in this as in all figures in this section are based upon a stress value of 1.00 at the boundary of the straight narrow portion of the member. Stresses are positive on those parts of the boundary which are above the center line and negative on those below the center line. A soap-film model was made with boundary ordi-

FIG. 34 ($P + Q$) CONTOUR LINES AND LARGE SCALE SOAP-FILM MODEL

It was assumed that at points removed from this localized region of steep slope the error would be negligible and a large scale model, $ABCDEF$ in Fig. 32, was made using as ordinates along ABC the values found from the first model. A photograph of the two models is shown in Fig. 33. Dimensions of the large model and ($P + Q$) contour lines obtained from both models are shown in Fig. 34. The maximum slope around the boundary of the large scale model was 8.5 deg and that of the soap-film surface about 17.5 degrees. The difference between sine and tangent of this angle is about 5 per cent and the cosine is about $4\frac{1}{2}$ per cent less than unity. The error introduced will be discussed later.

The normal and shearing stresses across two sections of the member are determined as shown in Figs. 35 and 36. Section I is taken through the point of maximum stress, about 11.2 deg from the beginning of the fillet. Section II is taken at 30 deg from the beginning of fillet. Values of ($P - Q$) are taken from Fig. 28. It will be seen that ($P - Q$) must be taken positive both above and below the center line in order to agree with the direction of couples and the notation in Fig. 30. Values of ($P + Q$) are taken from Fig. 34. The P and Q curves are obtained by successive addition and subtraction of ordinates of the ($P - Q$) and ($P + Q$) curves. The principal stresses are not in general perpendicular to the sections I and II. Their directions are found from the isoclinic curves of Fig. 30 and are shown above the caption "Angle ϕ ." Some of the values of ϕ shown are negative, others are greater than 90 deg. With the values of ϕ shown

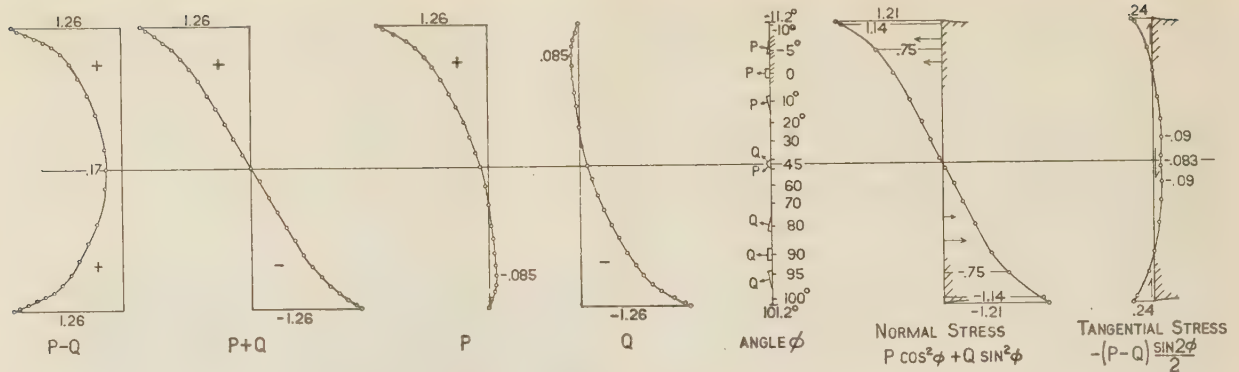


FIG. 35 STRESS VALUES AT SECTION I

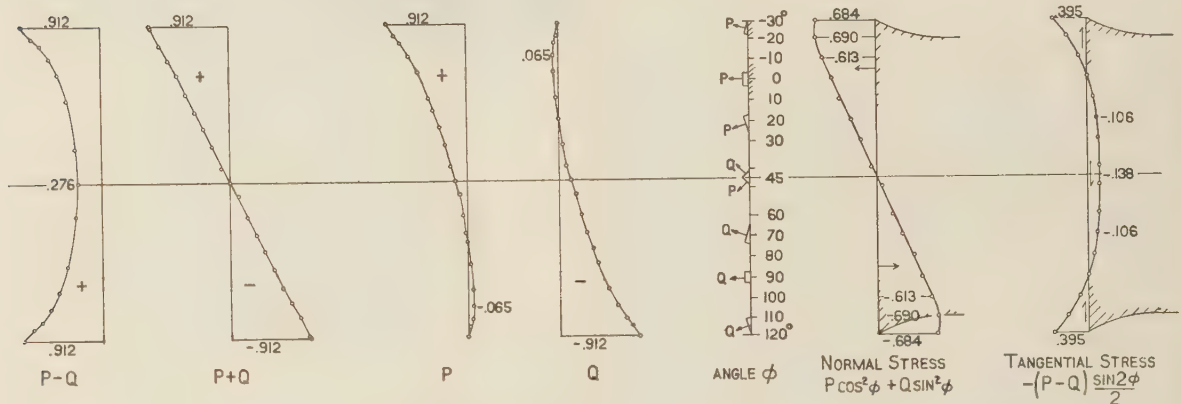


FIG. 36 STRESS VALUES AT SECTION II

the normal stress is $P \cos^2 \phi + Q \sin^2 \phi$ and ϕ tangential stress is $-(P - Q) \sin 2\phi / 2$.

The maximum value of stress along the boundary occurs at section I and is 1.26. Normal stresses on this section follow a linear law, as in bending of a straight beam, over the middle two-thirds of the depth of section and rise to a peak value of 1.21 at the boundary. At section II the effect of the greater width of section is already noticeable as here the stress falls away from a straight line as the boundary is approached and the maximum normal stress actually occurs inside the boundary.

Tangential components of stress are positive near the boundaries and negative in the middle portion. As the net shear is zero in pure bending these components must balance. The values of the tangential components along the center line can be taken directly from the fringe photograph as has been indicated in Fig. 28.

Errors introduced by the use of the membrane analogy as described above will not affect the values of normal or tangential components of stress at the center line and at the boundaries. Any errors must therefore affect only intermediate values and would cause a slight distortion of the curves. As a check upon the accuracy the total moment of normal forces across sections I and II was found from the curves, and in both cases was 1.9 per cent greater than it should have been. Assuming the small distortion of the normal stress curve to be parabolic and symmetrical about a point halfway between the centerline and the boundary, a rough calculation shows that the maximum error in normal stress is 1.9 per cent. If as is more probable, the maximum distortion occurs near the boundary, the maximum error would be nearer to 1 per cent.

A check of the tangential stresses for equilibrium showed an

unbalance of about 10 per cent of the total upward or total downward forces. These stresses are small however and the chief effect of the error is a shift of the point of zero stress.

Errors due to the effect of gravity on the soap film were corrected for in the following manner. On the small scale antisymmetrical model, the ordinates of the film along the center line were not zero as they should have been theoretically. In the one-inch wide portion the sag was negligible, but in the three-inch wide part a maximum sag of 0.006 in. was measured. Sag at other points was assumed to be parabolic, and corrected for accordingly. This was checked also by the fact that $(P + Q)$ contour lines on opposite sides of the center line must of necessity be symmetrical.

In the case of the large scale model it was found that, due to sag in the straight portion representing the narrow part of member where stress conditions are uniform, the contour lines were shifted slightly away from the edge representing the center line and toward that representing the outer boundary which was the higher edge. This shift at most was equivalent to 1.5 per cent of the boundary stress and contour lines in other parts of the film were corrected accordingly.

It is believed that the membrane analogy will find increasing use in conjunction with photoelastic studies. The errors introduced by its use can be reduced to a negligible amount by suitable proportioning of the boundaries and by making necessary corrections for the effect of sag. The errors in the results obtained from the present experiments which were done under the pressure of time are probably smaller than would be present in results obtained by means of the delicate lateral extensometer method or by the graphical integration method. The amount of time required

is surprisingly small when the soap-film equipment is already available. In the present instance the large scale model was completed, with about fifty points around the boundary set to within 0.001 in. of the desired value, in a day and a half. Tracing contour lines required only a few hours and working out of the curves in Figs. 35 and 36, another day and a half.

A limitation of the soap-film method is the size of opening which can be spanned without fear of the film breaking due to jarring or contact of the micrometer point. About 3 in. is a satisfactory maximum. By experimenting with the proportions of the ingredients of the soap solution, films composed of sodium oleate, glycerine, and water, can be made which will last twenty-four hours.

ACKNOWLEDGMENT

The author gratefully acknowledges the encouragement received in numerous contacts with Professor S. Timoshenko who suggested the problems treated in each of the three sections of the paper and whose comments during the progress of the work were invaluable.

BIBLIOGRAPHY

The numbers in parentheses appearing in the text refer to the following:

- 1 L. H. Baekeland, *Journal Ind. and Eng. Chem.*, vol. 5, no. 6, 506, 1913.
- 2 Z. Tuzi, "A New Material for the Study of Photoelasticity," *Sci. Paper No. 112*, Inst. for Phys. and Chem. Research, Tokyo, Japan, 1927.
- 3 I. Arakawa, "Determination of Stress-Optical Coefficient of Bakelite With Initial Stress," *Physics-Math. Soc., Japan, Ser. 3*, vol. 5, 1923, pp. 117-136.
- 4 J. Kuno, "Properties of Phenolite," "The Law of Photoelastic Extinction," *Phil. Mag.*, Ser. 7, vol. 12, 1931, p. 503.
- 5 Z. Tuzi, "On the Development of Experimental Methods in Photoelasticity," *Sci. Paper No. 209*, Inst. for Phys. and Chem. Research, Tokyo, Japan, vol. 12, 1929, pp. 21-36.
- 6 Filon and Jessop, "Stress-Optical Effect in Transparent Solids Strained Beyond the Elastic Limit," *Trans. Roy. Soc. Lond., Series A*, vol. 223, 1923, pp. 89-125.
- 7 Edmonds and McMinn, "Celluloid as a Medium for Photoelastic Investigation," *A.S.M.E. Trans.*, paper APM-54-8.
- 8 Z. Tuzi, *Sci. Paper No. 114*, Inst. for Phys. and Chem. Research, Tokyo, 1927.
- 9 E. G. Coker, "Tension Tests of Materials," *Engineering*, Jan. 7, 1921, p. 1.
- 10 Timoshenko and Dietz, "Stress Concentration Produced by Holes and Fillets," *A.S.M.E. Trans.*, 1925, pp. 199-237.
- 11 H. B. Maris, "Photoelastic Investigation of the Tensile Test Specimen," etc., *Journal Opt. Soc. Am.*, vol. 15, Oct., 1927, p. 203.
- 12 M. M. Frocht, *A.S.M.E. Trans.*, paper APM-53-11, 1931, and APM-54-9, 1932.
- 13 Solakian and Karelitz, *A.S.M.E. Trans.*, paper APM-54-10, 1932.
- 14 Wahl and Beeuwkes, *A.S.M.E. Trans.*, paper APM-56-11.
- 15 J. C. Maxwell, "On the Equilibrium of Elastic Solids," *Trans. Roy. Soc. Edinburgh*, vol. 20, 1853, p. 118.
- 16 L. N. G. Filon, "Graphical Determination of Stress From Photoelastic Observations," *Brit. Assoc. Report*, 1923, p. 350.
- 17 H. Favre, "Sur Une Nouvelle Methode Optique de Determination des Tensions Interieures," *Revue d'Optique*, vol. 8, Mai to Aout, 1929.
- 18 J. P. Den Hartog, *Zeitschrift. Angew. Math. and Mech.*, vol. 11, 1931, p. 156.
- 19 Griffith and Taylor, *Proc. Inst. Mech. Engineers*, 1917, p. 755.
- 20 P. A. Cushman, "Shearing Stresses in Torsion and Bending by Membrane Analogy," presented at meeting of A.S.M.E. Applied Mechanics Division, June, 1932.

Discussion

R. V. BAUD.¹² In the fall of 1932 the writer made compression and bending tests on glass models with fillets of circular shape, using true monochromatic light and a crossed Nicols and Babinet compensator. Some interesting results were obtained

from these tests which will soon be available in printed form. The conclusions drawn on the basis of these results with regard to stress concentration factors for bending appear to be confirmed by the results as related by the author. In this connection it may also be mentioned that the profile of constant edge stress for pure bending more recently investigated by the writer differs from that for compression in such a manner that the above statement regarding bending-stress-concentration factors is again confirmed.

As far as the method of investigation is concerned the writer is pleased to note that the fringe method suggested by him in a paper read before the Optical Society of America in February, 1929,¹³ is now in general use by several investigators in this country. The chief advantage of this method is the simplicity with which the complete shear stress distribution may be obtained but unfortunately this makes it possible for inexperienced investigators who do not know the physics nor the literature sufficiently well to work in this field as many recent photoelastic papers and discussions reveal. For instance, the directional effect when "white" light is used is discussed at length and in a manner as though the question were new. Yet the answer has been given in a paper read by the writer before the Optical Society of America in October, 1930.¹⁴ From this paper it can be

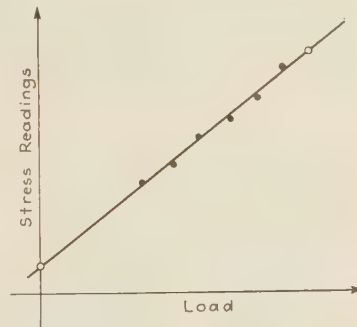


FIG. 37 LOAD-STRESS CURVE

seen that monochromatic light has no advantages unless the wave-length is such as to agree with the retardation produced in the mica plates. The two papers referred to really represent the scientific basis for the fringe method. The fact, that other investigators have shown some prettier pictures than the ones published by the writer does not detract from the above statement.

The statement, "A method of canceling the effect of small residual stresses is described which improves the accuracy of the results," is presumably the method devised by the writer in 1925 and used extensively ever since. It consists of taking various stress readings at various loads for every individual point and of plotting the values so obtained as indicated in Fig. 37. In this manner, by considering the slope of the straight line rather than taking one reading at a certain load or two readings at a certain load and zero load, we improve the accuracy by averaging as well as by excluding the initial edge stress. It should be observed that stress readings at comparatively large loads can be made more accurately and that in consequence the loads should be chosen accordingly, but always so that the stresses are below the yield point.

¹³ "Further Development in Photoelasticity," *Journal, Optical Society of America*, vol. 18, no. 5, May, 1929, p. 422.

¹⁴ "Contribution to Study of Effect of Elliptical Polarization Upon Energy Transmission," *Journal, Optical Society of America*, vol. 21, no. 2, Feb., 1931, p. 119.

¹² Westinghouse Research Laboratories, East Pittsburgh, Pa.

When a curve rapidly changes its curvature as is the case near the point of stress concentration, an extrapolation of the curve is unreliable to say the least and from a scientific view-point will be rejected. For my part thereof I cannot accept the "extrapolation method" as a satisfactory scheme to evaluate maximum edge stresses which exist in an infinitely small area only. The originators themselves admit that they devised it solely because they were unable to secure a sharp picture of the edge. Furthermore, the fact that consistent results were obtained is no proof of the value of a scheme. We can very well conceive of a set of results with consistent errors.

To solve the stress field problem by means of the membrane analogy the edge stresses from photoelastic tests are required as a basis. For known reasons these stresses are most likely the least accurate and consequently all results for points inside become inaccurate to the same extent. Furthermore, the problem must be such that for the complete contour both principal stresses are determinable, either photoelastically or on the basis of theoretical considerations. This restricts the field of application of the membrane-analogy method to a limited number of special cases.

J. P. DEN HARTOG.¹⁵ The author's investigation of the creep effect in phenolite is a valuable contribution to the technique of photoelastic research. This material is so decidedly superior for this purpose that it is gratifying to know that Hooke's law is completely satisfied for stresses up to 4000 lb per sq in., which means a sensitivity of 15 significant lines for a test specimen $1/4$ in. thickness.

The author is to be complimented on the care exercised in the execution of the tests, which is especially apparent by the complete absence of "edge" effects. Any one who has worked with photoelastic apparatus knows how extremely difficult it is to avoid the internal stresses that cause this trouble.

With respect to the membrane method employed for the determination of the sum of the principal stresses, the question of soap film versus stretched rubber sheet is of some interest. Whereas a soap-film surface can be made in a few minutes, it takes at least one or two hours to prepare a good rubber membrane. After this has been done, however, the rubber sheet presents several advantages.

In the first place, it can be easily made in a size ten times larger than that of a soap film. This means that the care with which the boundary space curve has to be made is very much less and it is by no means illogical to expect that the time saved in the preparation of the film is compensated for by the greater time it takes to make the boundaries with sufficient accuracy.

Secondly, on account of the greater size no correction for gravity deflection is necessary with a rubber membrane. In the third place, no drainage trouble occurs. However, either method seems to give more accurate results with comparatively little labor than any previous method known.

The writer has read with great interest a paper by Dr. M. M. Frocht in the *Journal of the Franklin Institute*, July, 1933, in which the lateral contraction of the test piece is not measured by mechanical means as suggested by Coker, but rather photographed directly on account of the properties of Newton's interference fringes. This method is of great interest since it furnishes a complete photograph of the $(P + Q)$ field. On the other hand, it requires grinding the test piece to an optically flat surface. If mercury green light is used, a deviation from flatness of one-hundredth of one mil in the specimen will produce a shift of one line in the $(P + Q)$ pattern. It seems, therefore, that the direct photography of such a field still requires instrument

makers' accuracy both in the preparation of the specimen as well as in the execution of the test.

R. H. G. EDMONDS¹⁶ AND B. T. MCMINN.¹⁷ The author of this paper deserves commendation for the correlation and advancement of the technique of photoelasticity. The experimental work is valuable especially that dealing with strain creep in bakelite and phenolite. It represents real progress toward making the photoelastic method a practical tool for engineering use.

It appears to the writers, however, that at least one of the conclusions, apparently lightly considered in the paper, should be given a critical review. This is the statement: "Strain creep for phenolite is considerably greater than that for C-25 bakelite, but this has no effect on stress distribution which approximates closely the theoretical for both materials at all times after loading."

The practical value of the photoelastic method lies in the parallelism of the stress distribution in the model with that of engineering materials, and the aptness of the comparison is of critical importance. Conceding that the fringe or color evidence in the photoelastic method is satisfactorily proportional to stress, the writers agree that where stress is normally uniform as in a simple tension member, the constancy of the stress-strain relation is unimportant. But where the stress is non-uniform, the strain non-uniform, and the stress-strain relation, therefore, non-uniform on a cross-section, it seems obvious to the writers that the load distribution in the model will not parallel the allied one in an engineering material. This proposition seems to be of an extremely fundamental nature and one to be thoroughly canvassed before attributing disagreeing results wholly to experimental error. This might easily account for some of the 20 per cent disagreement between tension and bending factors of concentration, referred to by the author.

The writers' experience with photoelastic materials leads them to question the advisability of using a gage length as short as $1/2$ in. and a compression specimen of the proportions of Fig. 1. The possibility of experimental error is further increased through the use of attached gage points. The data presented seem to be quite consistent. However, greater confidence could be placed in the results had they been obtained from more specimens and more tests.

The legitimacy of the scheme of correction for initial strains would be more thoroughly established if more data were presented. The method would seem to hold only for loadings with symmetrical isoclinic patterns, which narrows its usefulness.

The application of the membrane analogy and the use of the soap film in the determination of the sum of the principal stresses is unique and holds interesting possibilities in this rather difficult and unsatisfactory phase of the photoelastic method.

M. M. FROCHT.¹⁸ Of the three parts composing Dr. Weibel's paper, the writer is most interested in the part dealing with the soap-film method of determining the sum of the principal stresses, $(P + Q)$.

Dr. Weibel has used the soap film successfully for the problem of stresses at a fillet in a region of pure bending. He points out the simplicity of this method and predicts its wider acceptance in research.

The mathematical basis of the analogy, as the author points

¹⁶ Associate Professor of Mechanical Engineering, University of Washington, Seattle, Wash., Mem. A.S.M.E.

¹⁷ Associate Professor of Mechanical Engineering, University of Washington, Seattle, Wash.

¹⁸ Associate Professor of Mechanics, Carnegie Institute of Technology, Pittsburgh, Pa.

¹⁵ Asst. Professor of Applied Mechanics, Harvard Engineering School, Cambridge, Mass.

out, holds as long as the slopes at the boundary are small. When these become large, the analogy breaks down. It is here where the weakness of the method is found. It is clear that the success of its application depends on the nature of the boundary stresses. If these are small, as is the case in the author's problem, the soap film will yield good results. But, if the boundary be subjected to concentrated loads causing extremely large stresses, the method would in such a case break down.

The soap-film method, though not sufficient by itself, can



FIG. 38 SHOWING ISOPACHIC LINES BY MEANS OF INTERFERENCE FRINGES



FIG. 39 SMALLER LOADS



FIG. 40 LARGER LOADS

however, be effectively combined with another method to work satisfactorily, even in cases where concentrated loads act on the boundary. The principal stresses can be found, in such cases, by graphical integration, or lateral extensometer across a section or stress trajectory at a considerable distance from the region of the concentrated load, and the soap film can then be constructed for the new boundary. Such a combination of methods might prove useful.

In this connection the writer calls attention to two new methods in two-dimensional stress analysis; one by H. Neuber, published

in the August issue of the Royal Society Proceedings and dealing with what seems to be a simpler graphical procedure for the determination of principal stresses than the present graphical integration, and the other by the writer, published in the July issue of the *Journal* of the Franklin Institute and dealing with an application of interference fringes to stress analysis. We are not yet ready to appraise Mr. Neuber's method, but indications are that it is an improvement over present procedure. With regard to the interference fringes, it is not difficult to show that

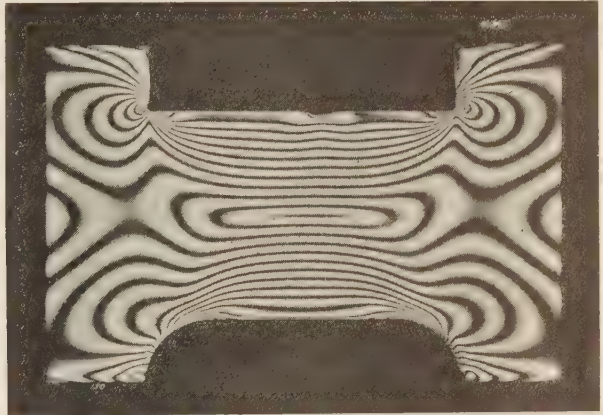


FIG. 41 PORTION OF BEAM IN PURE BENDING

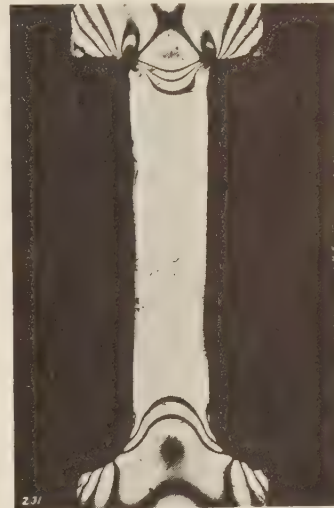


FIG. 42 MODEL WITH SHARP CORNERS AT UPPER END AND FILLETS AT LOWER

these fringes correspond to the contour lines in the soap film, and that they represent what Coker and Filon define as "isopachic lines." Interference fringes were successfully produced and photographed for the case of a pair of concentrated loads on a rectangular block and were found to agree with the theoretical predictions of this case, Figs. 38, 39, and 40. This method is of interest because it completes the optical method of two-dimensional stress analysis by providing the stress patterns of $(P + Q)$ exactly analogous to the ones furnished now by the polariscope for $(P - Q)$.¹⁹ However, much work is still to be done in the development of its technique.

¹⁹ "On the Application of Interference Fringes to Stress Analysis," by Max Mark Frocht, *Jour. Franklin Institute*, July, 1933.

Fig. 26, in which the fringes could not be counted because the material was overstressed, is of interest. This phenomenon can perhaps be seen more strikingly in a white-light celluloid color-photograph. Fig. 42 shows a black and white photograph of a celluloid tension model with fillets at one end and sharp corners at the other. When this model broke, the fracture ran from sharp corner to sharp corner. The appearance of the black zones shown in the sharp corners of the sketch, is due, in our opinion, not to any change in the optical properties of the material, but to a distortion in the surface of the model which prevents the light from reaching the lens. Thus at the sharp corner of the model there is a visible contraction of the material, the corner portions no longer being in the plane of the model. The same model also exhibits the paths of permanent sets. They are seen to follow the isochromatics, a phenomenon noted also by other observers. It is the formation of these black spots where the stresses are high that will explain the seeming paradox of the model shown in Fig. 41, which is supposed to show the effect of the fillet upon the factor of stress concentrations. For a time the writer was puzzled by the fact that there were no more fringes at the sharp corner than there were on the opposite side where the fillet was fairly large. This, however, is due to the existence of plastic formations causing the dark spots mentioned above.

As far as Dr. Weibel's work on stress concentrations is concerned the results seem quite reliable for fairly large values of r/d . For small values of r/d the writer's results do not agree with those obtained by Dr. Weibel. For r/d equal to 0.043 the writer finds that k equals 3.52 and for r/d equal to 0.0217 that $k = 4.49$. Both of these values are considerably greater than those found by Dr. Weibel.

Moreover, Dr. Weibel seems to have accepted the conventional assumption that the factors of stress concentration are determined by the ratio r/d alone. Our recent and as yet unpublished work definitely shows that this is not the case. It has been found

that the shape and the dimensions of the head as well as the manner of supporting the model contribute materially toward the determination of stress concentrations. Thus, for a compression model with an r/d equal to 0.281 and kept constant throughout the experiment, the factor k was varied from 1.9 to 6.77 by varying the dimensions of the head.

The whole subject is vastly more complicated than has been assumed and cannot be adequately covered in the space allotted for a discussion. However, the writer hopes to make available a more comprehensive study of this subject in a paper within the near future. The differences in the end conditions, shape, dimensions, and manner of loading—explain the rather wide discrepancies between results for pure tension and those for pure bending as obtained by Dr. Weibel.

R. E. PETERSON.²⁰ The paper by Dr. Weibel, as well as the paper by Dr. Wahl and Mr. Beeuwkes, serves to illustrate the progress made in the technique of photoelasticity in the past few years. Dr. Weibel's stress-concentration factors for fillets are shown in Fig. 43 in comparison with corresponding factors obtained eight years previously by Timoshenko and Dietz. Fatigue data are shown also in Fig. 43 and it will be noticed that the recent photoelastic results are considerably closer to the fatigue results. As a matter of fact larger specimens show higher fatigue stress-concentration factors and in the few cases tested the results are practically in agreement with the photoelastic values. This is important since not infrequently shafts fail, often with disastrous consequences, due to alternating stresses which are intensified at fillets. If by further research work a relation between photoelastic and fatigue results can be more firmly established, designers and engineers would have opened to them a vast amount of data which is not directly applicable in its present form.

ARSHAG G. SOLAKIAN.²¹ The three different problems investigated by Dr. Weibel are of equal interest and well presented by

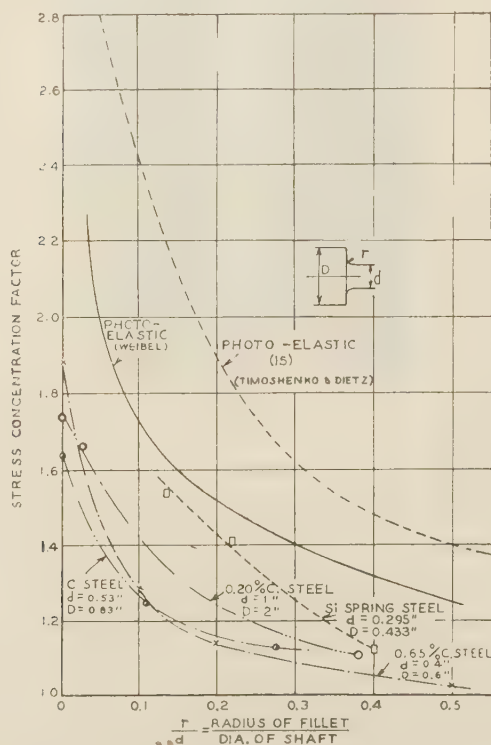


FIG. 43 STRESS-CONCENTRATION FACTORS FOR FILLETS

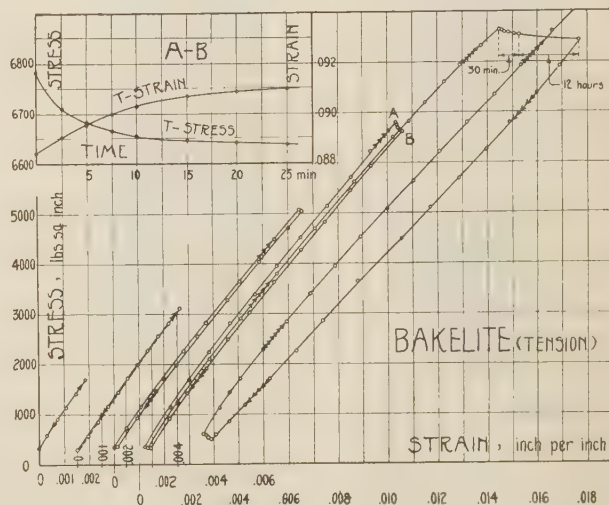


FIG. 44 BAKELITE UNDER A SERIES OF CYCLIC TENSILE STRESSES

the author. The writer will discuss each of them in the order as given.

(a) *Creep in Bakelite.* Creep action in bakelite under mod-

²⁰ Manager, Mechanics Division, Westinghouse Research Laboratories, East Pittsburgh, Pa., Assoc. Mem. A.S.M.E.

²¹ Lecturer, Civil Engineering, Columbia University, New York, N. Y.

erately high stresses is only one of the important phases in the study of physical properties of this material. A thorough study of the various characteristics of bakelite is being carried on at the Testing Laboratories of Columbia University and has been in progress for some time. Some work along this line has already been published by Arakawa,²² Carlton²³ and the writer.²⁴

The behavior of C-25 bakelite (No. BT 46-992) under tensile stresses is shown in Fig. 44. The specimen had a cross-section of 0.293 in. \times 0.309 in. and a gage length of 2 in. It was tested in an Amsler pendulum-type testing machine, using an Anderson extensometer reading to 1/10,000 in. The specimen was stressed to about $1/10$, $1/5$, $1/3$, $1/2$, and $3/5$ of its ultimate tensile strength (15,000 lb per sq in. approximately) with a rest of a half hour at each maximum limit before releasing the load gradually.

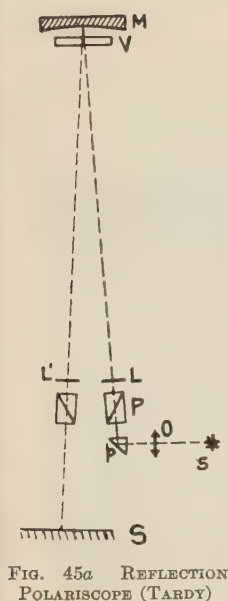


FIG. 45a REFLECTION POLARISCOPE (TARDY)

As is noticed in Fig. 44, creep action started at a stress of about 3000 lb per sq in. At a stress of 5000 lb per sq in. this effect is fairly appreciable. For engineering purposes, a stress of about

fringes produced. Fig. 45a is an outline of Tardy's reflection polariscope used in France. An improved type of such a polariscope as shown in Fig. 45b has been developed in the photoelastic laboratory of Columbia University by R. D. Mindlin in connection with the measurement of stresses in the individual plates of lap-welded connections. Another type of reflection polariscope which eliminates certain disadvantages of the two types mentioned is that developed by the writer and shown in Fig. 45c.

The effect of creep is represented by Dr. Weibel as an increase in strain only. It will be noticed from the stress-strain curve of Fig. 44 that it has a further effect—and one of great importance—of reducing the stress in the specimen. This reduction in stress for the portion A-B of the curve amounts, for an elapsed period of half an hour, to about 2.4 per cent of the stress in the specimen for this stage of intensity of loading. This effect of creep upon the change in stress as a matter of fact could not be detected by Dr. Weibel on account of the constant loading method adopted.

(b) *Stress Concentration at Circular Fillets.* To the designing

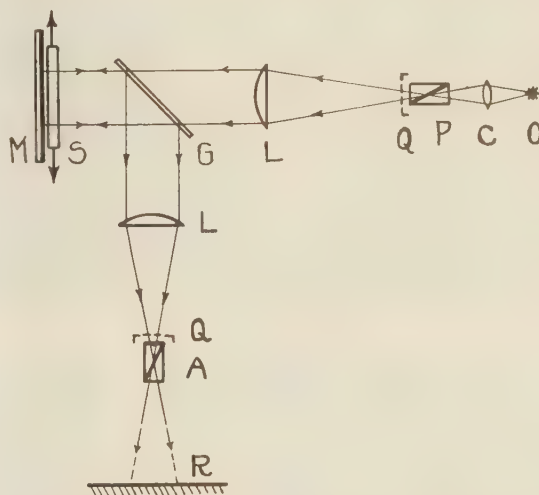


FIG. 45c REFLECTION POLARISCOPE (SOLAKIAN)

[O—light source; C—lens; G—glass plate; N—polarizer-analyzer; R—retardation plate ($\lambda/4$ for fringes and $\lambda/2$ for isoclinics); L—lens; S—specimen; M—mirror; P—screen.]

[O—light source; C—condenser; P—polarizer; Q—retardation plates ($\frac{\lambda}{4}$); L—lenses; G—glass plate; S—specimen; M—mirror; A—analyzer; R—screen.]

4000 lb per sq in. can be regarded quite safe. This stress in a specimen of $1/4$ in. in thickness corresponds to a fringe of about the eleventh order and can be used safely. As it is the custom of most investigators to produce a fringe pattern sometimes containing as high as twice this number of fringes, it is evident that the material under this maximum stress, and even for lower values develops considerable creep, as is evident from the last cycle of the stress-strain curve in Fig. 44.

An efficient way of eliminating the effect of creep and still producing an adequate number of fringes in a pattern is of that using a reflection type of polariscope instead of the ordinary transmission type. In the reflection type the polarized rays traverse through the specimen twice on their way back to the screen, thus doubling the relative phase difference of the refracted rays which in turn doubles the number of interference

fringes produced. Fig. 45a is an outline of Tardy's reflection polariscope used in France. An improved type of such a polariscope as shown in Fig. 45b has been developed in the photoelastic laboratory of Columbia University by R. D. Mindlin in connection with the measurement of stresses in the individual plates of lap-welded connections. Another type of reflection polariscope which eliminates certain disadvantages of the two types mentioned is that developed by the writer and shown in Fig. 45c.

engineer, the nature of stress distributions along certain sections in a machine part or structural element is of great importance. The stress-concentration effects of circular fillets between two adjacent members of unequal cross-sections has been an attractive field for photoelastic investigation. The results obtained by Dr. Weibel accurately show the stress distribution at circular fillets due to the use of bakelite and the refined testing methods employed. On the other hand, it is of greater importance to the engineer to know how to reduce or eliminate unduly high stresses. In an investigation (1932) of the stress distribution at the root of a helical spring made for the Westinghouse Electric & Manufacturing Co. (Philadelphia), the writer found that when the circular fillet is replaced by a suitable spiral or some form of multi-compound easement curve, as used in railroad practise, the stress concentrations at the fillets are materially reduced.

The fringe patterns in Figs. 46 and 47 clearly show the comparative effects of circular and spiral fillets upon the stress distributions. The specimen tested has ratios of $D/d = 3$ and $d/R = 1$ (using the author's notation) with circular fillets at one end and spiral fillets at the other. It was tested both in tension and in bending. In Figs. 46a and 47a the presence of an

²² "On the Determination of Stress-Optical Coefficient of Bakelite With Initial Stress," by I. Arakawa, Proc. Physico-Math. Society of Japan, October-December, 1923.

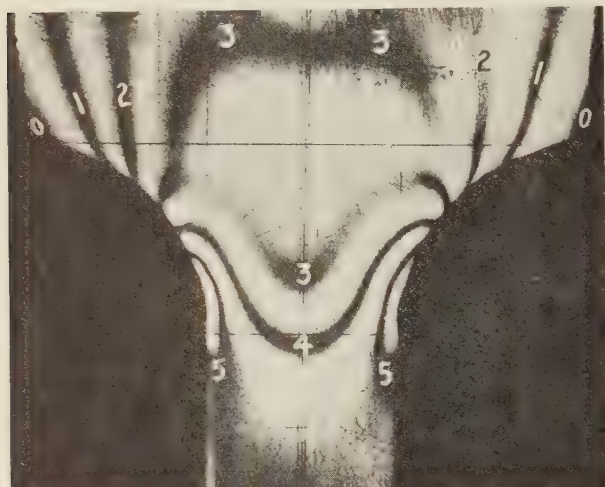
²³ "Suitability of Materials for Photoelastic Investigations," by R. B. Carleton, Review of Sci. Instruments, January, 1934.

²⁴ "Photoelastic Study of Shearing Stresses in Keys and Keyways," by A. G. Solakian and G. B. Karelitz, A.S.M.E. Trans., June, 1932.

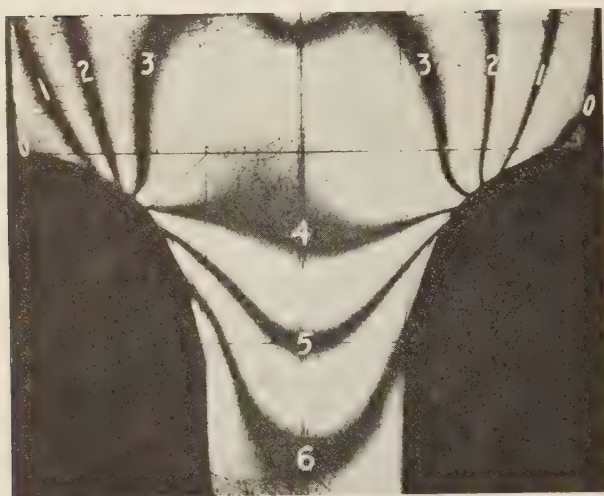
additional fringe at the circular fillets indicates a higher stress concentration at this locality. In the spiral fillet, the stress concentration is entirely eliminated.

The curves in Fig. 48 show the intensities of the boundary stresses for the two types of fillets investigated and bring out their relative merits. The fringe orders are marked on the ordinates to the curves and the relative intensities of the stresses, in terms of the average stress at the reduced sections, are given.

(c) *Soap-Film Method.* The adaptability of the soap-film method of measuring the sum of the principal stresses as advocated by Mr. Weibel and other investigators is of doubtful value



(a) Circular Fillets



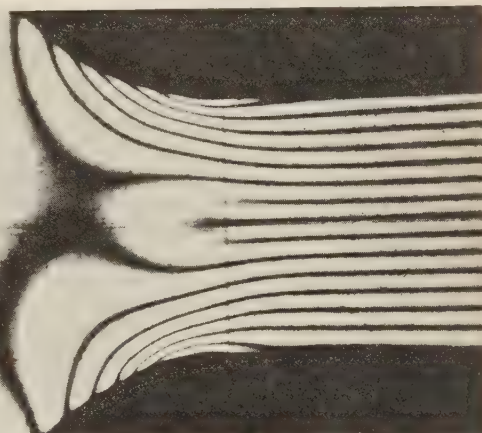
(b) Spiral Fillets

FIG. 46 FRINGE PATTERN FOR SPECIMEN IN TENSION

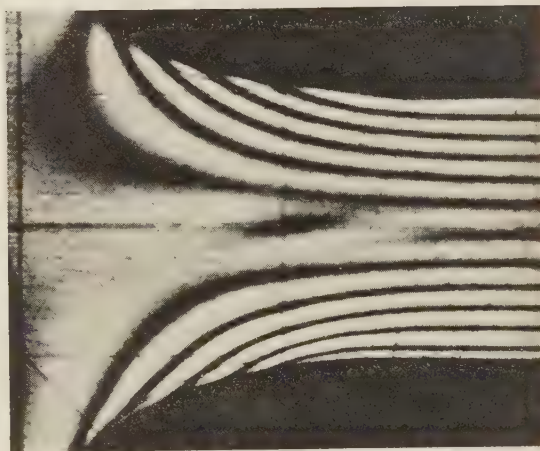
because of the many difficulties encountered in its use, namely, the limited span of the film, the sag formation and collection of water at the low regions, the errors in investigating large slope sections, etc.

In addition to the membrane-analogy method, the principle of which is similar to that of the soap-film method, there are two optical-mechanical methods for measuring the sum ($P + Q$), of the principal stresses: (1) Newton's fringe method and (2)

Coker's lateral extensometer method. Mesnager²⁵ first suggested the possibility of application of both methods to the evaluation of the ($P + Q$) stresses. A thorough analysis of Newton's fringe method with specimens having practical plane-parallel surface finishes was given in 1932 by V. Tesar.²⁶ In this country applications of this method to engineering problems



(a) Circular Fillets



(b) Spiral Fillets

FIG. 47 FRINGE PATTERN FOR SPECIMEN IN PURE BENDING

already have been made by Maris²⁷ in 1927 and Frocht²⁸ in 1933. Coker's lateral extensometer²⁹ has been widely used by the inventor in his numerous valuable researches. The writer³⁰ has found it a very convenient tool for the investigation of problems of an engineering nature on account of its simplicity of principle and dependability of results.

²⁵ "Contribution à l'Étude de la Déformation Élastique des Solides," by A. Mesnager, *Annales des Ponts et Chaussées*, 1901.

²⁶ "Méthode Purement Optique pour Déterminer les Déformations d'Épaisseurs des Modèles," by V. Tesar, *Revue d'Optique Théorique*, 1932, Tome 11.

²⁷ "Photoelastic Investigations of the Tensile Test Specimen, the Notched Bar, the Ship Propeller Strut and the Roller Path Ring," by H. B. Maris, *Journal, Optical Soc. Am.*, October, 1927.

²⁸ "On the Application of Interference Fringes to Stress Analysis," by Max M. Frocht, *Journal, Franklin Inst.*, July, 1933.

²⁹ "A Laboratory Apparatus for Measuring the Lateral Strains in Tension and Compression Members," by E. G. Coker, *Proc. Roy. Soc. Edin.*, vol. xxv, 1904-5.

³⁰ "Stresses in Transverse Fillet Welds by Photoelastic Methods," by A. G. Solakian, *Journal, Am. Welding Soc.*, February, 1934.

Filon's³¹ "graphical integration" method based upon the equations of equilibrium has quite frequently been used for determining the values of principal stresses from their algebraic differences and orientations. A revised "graphical" method, recently developed by A. Neuber,³² and based upon the elastic equations, offers greater accuracy. When results of high precision are required, undoubtedly Favre's³³ interferometer-polariscope method of optical measurement of the individual principal

In a transparent isotropic plate a point is said to have an optical thickness e_0 equal at any point to the product of the actual thickness of the plate and the refractive index of the unstressed material. On account of the double refracting property of the material under applied stress, any point possesses two optical thicknesses e' and e'' corresponding to the two principal vibrations. By measuring the values of $e' - e_0$ and $e'' - e_0$, the stresses P and Q can be evaluated.

The two surfaces of a plain-parallel plate of glass are silvered lightly. When monochromatic light is passed through the plate, very fine brilliant fringes will be observed in two different ways: (1) as lines of equal optical thickness with the parallel rays of the light normal to the plane of the plate and (2) as concentric circles situated at infinity, when a very small region of the model, less than a square millimeter, is observed. When the plate is stressed, the fringes are displaced and appear brighter. The two displacements relative to the initial fringes determine the two variations $e' - e_0$ and $e'' - e_0$ in the optical thicknesses. When these fringes are observed through an analyzing prism, it will be found that for each point, there will be found two rectangular orientations of the analyzer which will cause one or the other system of the fringes to disappear. These orientations correspond to the directions of the two principal stresses. The first method of "lines of equal optical thickness" is preferable, as photographic records of the fringe patterns can be obtained before and after the application of the stress.

With plates without silvered surfaces, the fringes can be observed with reflected light. However, the results will not be as accurate as those from a silvered plate.

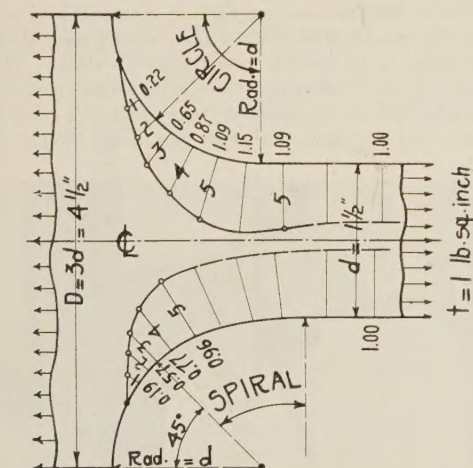
Still another simplified method is that now being developed by the writer. It consists of silvering only the surface of the specimen facing the polarizer and allowing a ray of plane-polarized monochromatic light from a reflecting polariscope to fall normally on a point in a stressed specimen, with the plane of polarization parallel to one of the principal stresses acting at that point. The principal stress at the point considered can be evaluated by measuring the absolute phase retardation between the original ray which is reflected from the silvered surface and the transmitted ray which in turn is reflected back from a mirror placed close to the nonsilvered surface of the specimen.

A. M. WAHL³⁵ AND R. BEEUWKES.³⁶ The author is to be commended for having made a very extensive and thorough study of various questions which frequently arise in photoelastic work and which are of importance in evaluating the results of such studies. It is gratifying to the writers to learn that the extrapolation method previously used by them has been found of value to other investigators.

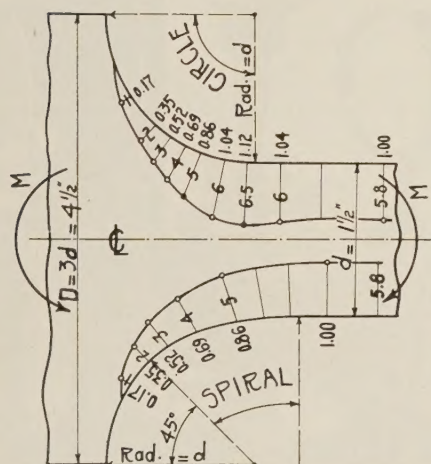
The writers have recently had occasion to make a few photoelastic tests on fillets in bending and tension similar to those carried out by the author. An arrangement using knife edges was used to obtain pure bending. One test with $D/d = 3$ and $R/d = 0.125$ gave a value of stress-concentration factor equal to 1.75, while another test with $D/d = 3$, $R/d = 0.187$ gave a value equal to 1.61. Care was taken not to stress the bakelite higher than 3500 lb per sq in. A similar test made under tension instead of under bending gave concentration factors equal to 2.20 for $D/d = 3.16$, $R/d = 0.132$ and 2.02 for $R/d = 0.198$ with D/d remaining the same. These values are around 4 to 5 per cent above those obtained by the author and check his findings that the value of stress concentration is considerably higher for tension than for bending. These small differences in the experi-

³⁵ Westinghouse Research Laboratories, East Pittsburgh, Pa., Mem. A.S.M.E.

³⁶ Westinghouse Research Laboratories, East Pittsburgh, Pa.



(a) Tension



(b) Bending

FIG. 48 CURVES SHOWING INTENSITY OF BOUNDARY STRESSES AT CIRCULAR AND SPIRAL FILLETS

stresses is unique. On account of the high cost of the apparatus and its delicacy, it has not as yet been widely introduced.

A method avoiding the use of a costly interferometer and hence more simple in its operation is that proposed by Fabry.³⁴ As there is no account of this method in American literature, it will be described here briefly.

³¹ "On the Graphical Determination of Stress From Photoelastic Observations," by L. N. G. Filon, *Engineering*, 1923, p. 116.

³² "New Method of Deriving Stresses Graphically From Photoelastic Observations," by A. Neuber, *Proc. Royal Society*, vol. 141, 1933.

³³ "Sur Une Nouvelle Méthode Optique de Détermination des Tensions Intérieures," by H. Favre, *Revue d'Optique Théorique*, 1929, Tome 8.

³⁴ "Sur une Nouvelle Méthode pour l'Étude Expérimentale des Tensions Élastiques," by C. Fabry, *Comptes Rendus l'Académie des Sciences*, 1930, p. 190.

mental values obtained by the author as compared with those obtained by the writers may probably be explained by slight differences in the experimental procedure.

One reason why the stress concentration is higher for tension than for bending lies in the fact that in tension there is a net contraction of the narrow portion of the specimen which is restrained by the wide portion. Tensile stresses in the fillets are thereby set up which are added to those due to the external load. In the case of bending, there is no net contraction of the narrow portion of the specimen (the compression side expanding as much as the tension side contracts) and consequently these stresses are not set up; hence the maximum stress is lower.

In photoelastic tests such as those under consideration, where the maximum stress is at an unknown location along the fillet, it should be more convenient to use a circular scratch concentric with the fillet, instead of a straight line. In order to insure concentricity with the edge, however, such a scratch would probably require the use of a special tool.

Attention is called to the very considerable difference between the results obtained by Timoshenko and Dietz or by Coker using the compensation method and those obtained by the more accurate fringe method used by the author (see Fig. 12). In most cases the values of stress concentration obtained by the latter method are higher than those obtained by the former. This was found true also by the writers in similar tests of tension bars with holes and notches.³⁷ In contrast to this, as will be seen from Fig. 12, the values of stress concentration obtained by Timoshenko and Dietz for $D/d = 3$ lie well above the author's curve. This seems rather unusual and the writers would be interested in an explanation of the difference.

The result, obtained by the author, namely, that values of stress concentration are practically the same for $D/d = 3$ as for $D/d = 1.5$ seems reasonable, since the point of maximum stress occurs in a portion of the fillet so close to the narrow portion of the bar that an increase in the width D should not have a large effect.

In connection with the study of photoelastic methods, the writers would like briefly to describe an interesting experiment made in connection with a study of thermal stresses. It was desired to determine the stress distribution resulting from the application of temperature to one edge of a thin square block in order to simulate certain conditions occurring in the cooling fins or brushes of electrical machines. The use of photoelasticity with a square specimen having one edge heated, immediately suggested itself. Bakelite, however, becomes soft and apparently unreliable at temperatures but little above room temperature, so it was decided to cool instead of heat the edge. Dry ice separated from the specimen by a thin piece of metal foil was used for this purpose. Beautiful stress patterns showing rather high stress concentrations at the two corners of the cold side were obtained. The transient conditions too were easily followed.

AUTHOR'S CLOSURE

The method of canceling residual stresses was not the same as that described by Dr. Baud. The extrapolation method is of value because of the extreme difficulty of adjusting parallelism of light beam and position of model so that, for example, a satisfactory image of both fillets is obtained at the same time. Extrapolation provides a correction for the small inaccuracies at the boundary which cannot be avoided.

Dr. Den Hartog's comments on the use of a rubber membrane are of considerable interest. A paper by two of his students,

describing an application of the rubber membrane has been published recently.³⁸

Messrs. Edmonds and McMinn suggest a critical review of the conclusion that strain creep in phenolite has no effect on stress distribution. The meaning of this statement is that, in a model of complex shape under constant load, the directions and values of principal stresses at any point will not vary with time even though the strain is steadily increasing. It is based upon the results of the tension-creep tests at constant load in which strain creep, and therefore total strain, at any time after loading was found to be directly proportional to stress. This is a necessary but not a sufficient condition for stress distribution to be invariable. It is also necessary that Poisson's ratio for the elastic strain be the same as that for the plastic strain. Kuno³⁹

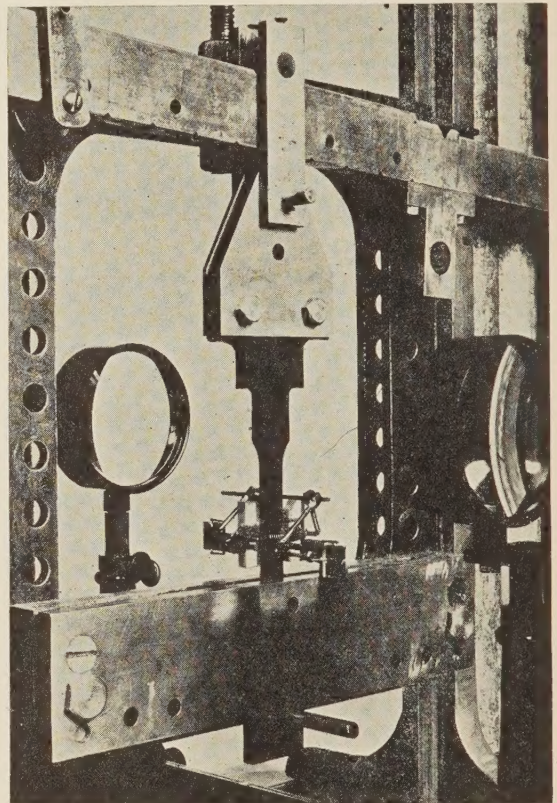


FIG. 49 PHENOLITE MODEL IN POSITION FOR STRESS REDISTRIBUTION TEST

finds Poisson's ratio for phenolite to be 0.356. If, according to our ordinary conception of plastic strain, we assume a value of 0.5 for Poisson's ratio for the plastic strain, the over-all value of Poisson's ratio would increase with time of loading from 0.356 to a limiting value 0.5. In the two-hour tests on phenolite, strain creep in two hours was 24 per cent of elastic strain. It can be shown readily on the basis of the above assumption that the overall value of Poisson's ratio increased from 0.356 to 0.383 or 7.6 per cent. This would have some effect on stress distribution and to this extent our conclusion would not be rigorous. One must discriminate between the law of strain creep in pheno-

³⁸ "A Membrane Analogy Supplementing Photoelasticity," by J. G. McGivern and H. L. Supper, A.S.M.E. Trans., 1934, paper APM-56-9. *Jl. Franklin Inst.*, April, 1934, vol. 217, no. 4, p. 491.

³⁹ "The Relation Between Strain and Photoelastic Effect in Phenolite," by J. Kuno, *London Phil. Mag.*, ser. 7, vol. 16, 1933, p. 353.

³⁷ "Stress Concentration Produced by Holes and Notches," by Wahl and Beeuwkes, A.S.M.E. Trans., 1934, paper APM-56-11.

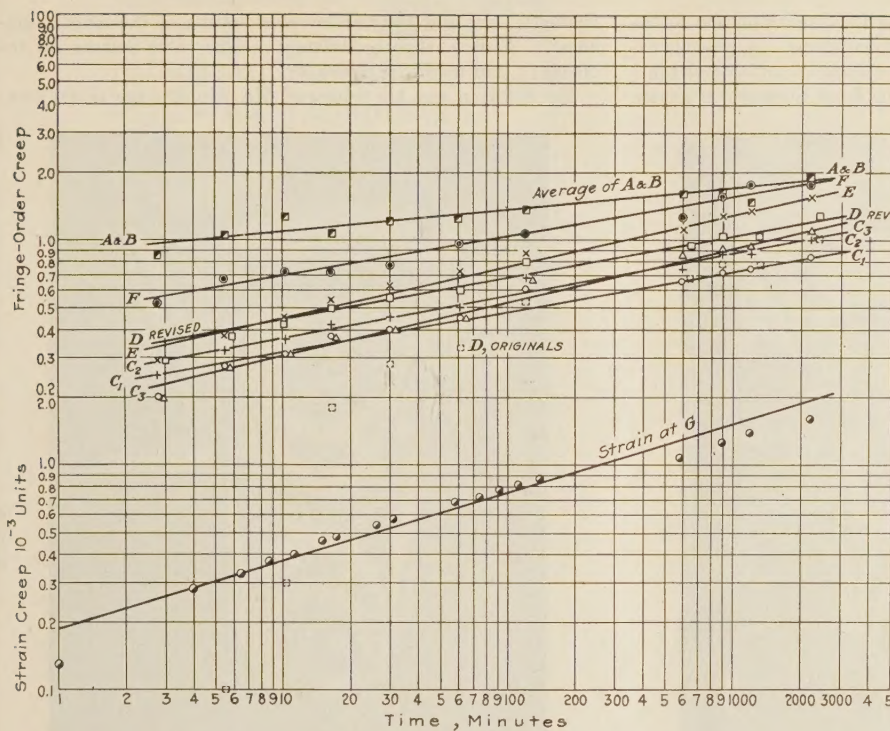
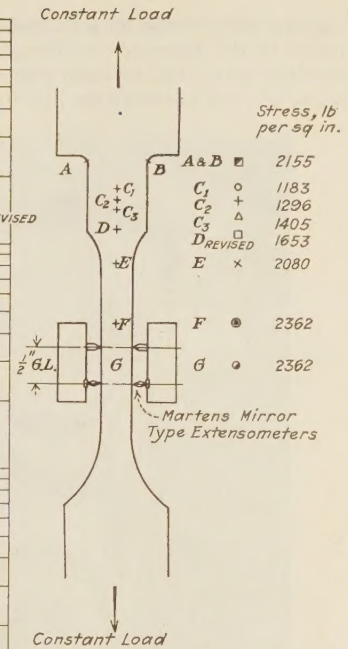


FIG. 50 STRAIN-TIME AND FRINGE ORDER-TIME CURVES FOR 36-Hr PERIOD



lite and that found by Filon and Jessop for celluloid (6). Strain creep in celluloid is not proportional to the stress but to the square of the stress, and consequently neither of the forementioned conditions necessary for unchanging stress distribution is fulfilled. It should be mentioned that in Kuno's experiments Poisson's ratio for phenolite was found to remain constant within about ± 2 per cent during a fifteen-minute load period. This result, if true, would provide the desired rigor to the conclusion in question, but it is to be viewed with caution as it implies a value of Poisson's ratio for plastic strain distinctly different from 0.5.

As a practical test for redistribution of stress, a phenolite model, Fig. 49, was subjected to a tension load which remained constant for 36 hours. Strain was measured at portion G, Fig. 50, which was in a state of uniform stress, of known constant value. In the 36-hour period strain creep of about 50 per cent of elastic strain was observed. Fringe order was observed at different points on the model during this period. The stress-concentration factor at points A and B had a value of about 2, and any redistribution of stress would be indicated by a reduction in peak value of stress at these points. During the period of the test, the fringe order increased an average of 12.9 per cent at points C₁, C₂, C₃, D, E, and F (optical creep), (see Figs. 51(a) and 51(b)), whereas the increase at points A and B was 9.7 per cent, a difference of only 3.2 per cent, which is believed to be within the experimental error. After 5 or 10 hours the aging effect at the boundary points A and B introduced some uncertainty into the extrapolation at these points. With the large value of strain creep observed, considerable reduction in fringe order at points A and B would be expected if redistribution of stress were taking place. The experiment, therefore, indicates that such redistribution does not occur. Objections to this conclusion may be found⁴⁰ as it assumes a simple stress-

optic relation, and it may be more satisfactory to reason that, since variations in Poisson's ratio with time of loading will probably be not greater than 8 per cent, considerations of superposition of elastic and plastic states of strain indicate that the system of stresses introduced to maintain continuity of the material is one in which values of stress will be about $\frac{1}{2} \times 0.356 \times (1 - 0.356) \times 8$ or about 1 per cent of original stress values, a negligible quantity.

The question of parallelism of stress distributions in transparent material and engineering material may now be considered entirely independently of the problem of strain creep. Michell has shown theoretically⁴¹ that stress distribution is independent of the elastic constants, Young's modulus, and Poisson's ratio, except for those members whose boundary consists of more than one closed curve and for which the external forces on any one of these closed boundaries are not in equilibrium. In a particular example worked by Bickley,⁴² stresses depended upon Poisson's ratio, but for values of 0.40 and 0.25, respectively, as for celluloid and steel, the difference in maximum stresses was only 1.4 per cent. The same order of discrepancy may be expected generally in members with multiple boundaries, loaded as described.

The applicability of the membrane method to the case of concentrated loads, questioned by Dr. Frocht, will depend largely upon the particular problem. In cases where St. Venant's principle may be applied the concentrated load may be replaced by an equal load distributed say parabolically over a small width, and the scale of ordinates for the membrane chosen so that slopes are not too great.

Dr. Frocht's photographs of interference fringes, Figs. 38, 39, and 40, are of interest. They illustrate some of the difficulties in this as well as in the lateral extensometer method in studying concentrated loads. It was pointed out at the December meet-

⁴¹ Michell, *Proc. Lond. Math. Soc.*, April, 1899, p. 100.

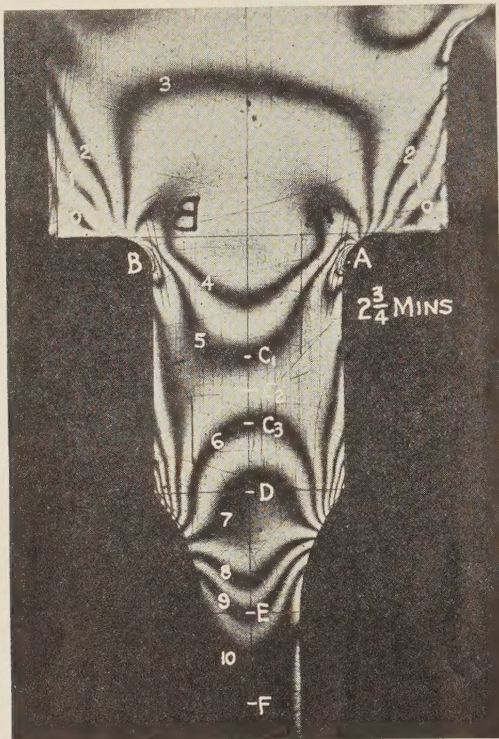
⁴⁰ "Photo-Elasticity," by Coker and Filon, Cambridge University Press, 1931, Pars. 3-36, p. 272.

⁴² "Photo-Elasticity," by Coker and Filon, Cambridge University Press, 1931, p. 501.

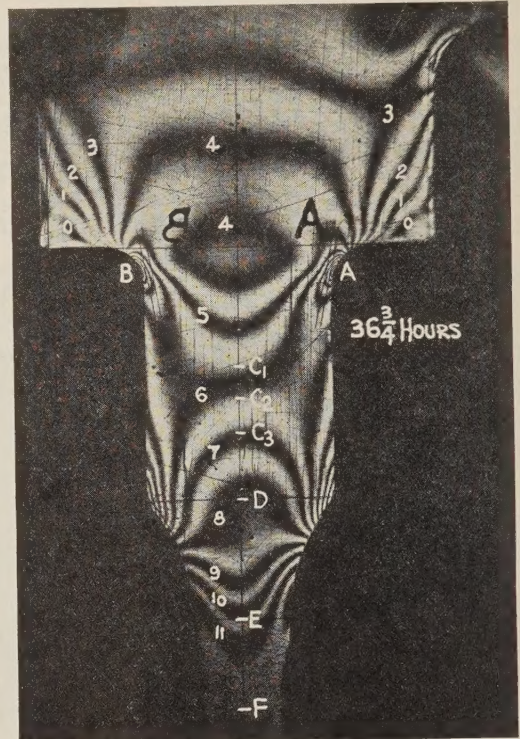
ing that these curves do not satisfy Laplace's equation as required by the theory of two-dimensional stress. A possible explanation is that true two-dimensional stress is not obtained in a region of stress concentration with the usual thickness of model,

characteristics and the needle-valve setting of the Amsler machine. With a slightly different needle-valve setting an increase in load might be obtained.

Mr. Solakian and his colleague Mr. Mindlin are to be com-



(a) $2\frac{3}{4}$ minutes after application of load.



(b) $36\frac{3}{4}$ hours after application of load.

FIG. 51 PHOTOGRAPH SHOWING OPTICAL CREEP DURING TEST

so that actual changes of thickness do not give true values of $(P + Q)$.

The end-loading conditions in the model will not affect stress-concentration factors if sufficient length is provided for stress conditions to become uniform. Dr. Frocht's results will be of interest in this connection.

The curves presented by Mr. Peterson show how the photoelastically determined stress-concentration factors may serve as a basis for comparison of fatigue-test results, and make it possible to assign numerical values to qualities such as susceptibility of the material to stress concentration in fatigue.

Mr. Solakian takes the view that creep in any photoelastic material is objectionable and finds a value of stress (3000 lb per sq in.) below which creep does not occur. The curves, Figs. 6 and 7, show creep for stresses as low as 1255 and 1060 lb per sq in., and the writer's attitude is that creep will not be objectionable if it is proportional to stress. Mr. Solakian refers to the portion A-B of the curve in Fig. 44 to show that stress in bakelite is reduced with time. From a consideration of the details of operation of the Amsler machine it is the writer's opinion that this reduction in load is not a characteristic of the material being tested, but is a function of the oil-pump and piston-leakage

mended for their efforts in the development of polariscopes. Doubling the number of fringes, apart from creep considerations will increase the adaptability of the equipment. The use of only one Nicol prism in the polariscope of Fig. 45(b) is an advantage where first cost is a factor. Considerable reduction in light intensity at the glass plates *G*, in Figs. 45(b) and 45(c) would be expected, and this might be a disadvantage when working with the usual types of mercury-vapor lamp.

Messrs. Wahl's and Beeuwkes' factors for the case of D/d about 3 are from 4 to 9 per cent higher than those given in Figs. 12 and 13. It is now the author's belief that in the present tests a greater length of the wide portion of specimen would have been preferable to that used, and this might affect values of factor for $D/d = 3$. From an analytical study by Bleich⁴³ the length necessary to obtain uniform distribution of load, for certain types of end loading, can be calculated. There has been no opportunity to go into this further but it should have a bearing on the differences mentioned. Friction in the pins used by the author was virtually eliminated in the bending tests by an up-and-down manipulation of the loading beam to give the mean fringe configuration.

⁴³ F. Bleich, *Bauingenieur*, vol. 9 (1923), pp. 255, 304, and 327.